

Applied Ecology and Environmental Research

International Scientific Journal



VOLUME 18 * NUMBER 1 * 2020

<http://www.aloki.hu>
ISSN 1589 1623 / ISSN 1785 0037
DOI: <http://dx.doi.org/10.15666/aecr>

A COMPARISON OF THE PHYSIOLOGICAL RESPONSES OF THREE PINE SPECIES IN DIFFERENT BIOCLIMATIC ZONES IN TUNISIA

CHERIF, S.^{1,2*} – EZZINE, O.³ – KHOUJA, M. L.³ – NASR, Z.²

¹*Faculty of Sciences of Bizerte (FSB), University of Carthage, 7021 Zarzouna, Tunisia*

²*LR161INRGREF01 Laboratory of Management and Valorization of Forest Resources, National Institute for Research in Rural Engineering Water and Forest (INRGREF), University of Carthage, Bp 10, 2080 Ariana, Tunisia*

³*LR161INRGREF03 Laboratory of Forest Ecology, National Institute for Research in Rural Engineering Water and Forest (INRGREF), University of Carthage, Bp 10, 2080 Ariana, Tunisia*
(phone: +216-97-135-047)

*Corresponding author
e-mail: sameh.cherif@gmail.com

(Received 12th Mar 2019; accepted 11th Jul 2019)

Abstract. Increasing aridity attributed to climate change is the main threat to the diversity and survival of Mediterranean forests including Tunisian pine species. The impact of this climatic condition in three pine species was examined in order to detect their responses to drought and guide their selection. Three Tunisian pine species: *Pinus halepensis*, *Pinus brutia* and *Pinus canariensis* growing in different climatic zones: humid, sub-humid, and semi-arid were studied in two months March and July 2016. Measurements carried out within this study are leaf gas exchange, twig water potential, and soil water content. The results showed a decrease in stomatal conductance and twig water potential in July in all pine species with increase in vapor pressure deficit and low soil water content. *Pinus halepensis*, *P. canariensis* and *P. brutia* had stronger stomatal control in semi-arid, sub-humid and humid climate, respectively (62, 95 and 63 mmol m⁻² s⁻¹) and had higher stem water potential; for *P. halepensis* (-2.04 MPa) in semi-arid climate; for *P. canariensis* and *P. brutia* (-2.21, -2.39 MPa) in sub-humid and humid climate, respectively. *Pinus halepensis*, *P. canariensis* and *P. brutia* are better adapted to semi-arid, sub-humid and humid climates, respectively. Nevertheless, *P. halepensis* is considered the most resistant species as that could maintain higher photosynthesis, stomatal control and water use efficiency particularly in semi-arid climate. These findings help to assess the interaction between species and climate on the physiological response of pine species in mid-summer water deficit, and to select among these species the most resistant for future reforestation programs.

Keywords: drought, leaf gas exchange, water potential, Mediterranean forest, genetic variability

Introduction

Mediterranean forest tree species are exposed to a range of pressures (Ramirez-Valiente et al., 2010) and are mainly vulnerable to drought (Allen et al., 2010; Choat et al., 2012). An increase in aridity is particularly expected in the Mediterranean regions and, is the main threat to the diversity and the survival of forest trees (Peñuelas et al., 2017). Pine forests are one of Mediterranean forest species that may be threatened by rising temperatures and reduced precipitations (Manzanera et al., 2016).

To resist to these hydric stress conditions (Rubio-Casal et al., 2010; Letts et al., 2011), *Pinus* species may develop mechanisms of tolerance or avoidance (David et al., 2007; Mittler, 2002). Resistance to high temperature and drought strongly differs among

plant species (Matías et al., 2012) being correlated to transpiration, hydraulic adaptations (Martínez-Vilalta et al., 2009) and water use efficiency (Warren et al., 2001). Plants protect themselves from excessive water losses (diffusion out of the leaf) under water-limited environments through a reduction of stomatal conductance (gs), which in turn leads to less carbon uptake (diffusion of CO₂ into the leaf) and possibly subsequent physiological stress (McDowell et al., 2008; Will et al., 2013), reduction of transpiration (Bréda et al., 1993; Granier et al., 2008), that has been recognized as the main environmental factor limiting plant photosynthesis on the global scale (Nemani et al., 2003).

This situation underlines the need to study leaf gas exchange as indicators of the ecophysiological tolerance of pine forests (Manzanera and Martinez-Chacon, 2007). Thus, pines species maintain rather constant leaf water potential in soils with low water status and/or under high evaporative demand (Martinez-Vilalta et al., 2004). Water use efficiency (WUE) is a critical metric parameter that quantifies the trade-off between photosynthetic carbon assimilation and transpiration at the leaf level (Farquhar et al., 1982). Leaf gas exchange and water potential variables were studied on three Mediterranean pine tree species located in three bioclimatic zones in Tunisia.

Aleppo pine (*Pinus halepensis* Mill.) is an important forest tree in the Mediterranean region (Klein et al., 2011). Its continental range extends from northern Africa and Middle East, up to southern Mediterranean Europe. It is native and the most abundant pine species in Tunisia (You et al., 2016). The majority of Aleppo pine forests are located in central and northwestern Tunisia, mainly in Kasserine, Kairouan, Kef, Seliana and Zaghouan (Ayari et al., 2012).

Calabrian pine (*Pinus brutia* Ten.), native to the eastern Mediterranean, can be found in many southern Mediterranean countries. It is the most pine specie that widely distributed in Turkey (Kucuk et al., 2012). Because of their drought tolerance, they are well adapted to dry summer conditions (López et al., 2016). In Tunisia, this species was introduced in 1960 in Souiniet, Tebaba, et Jebel Abderrahmane (Khouja et al., 2002).

Canary pine (*Pinus canariensis*) is an endemic species of the Canary Islands (de Nascimento et al., 2009). Despite its small distribution area (western islands, occupying much of La Palma, Tenerife, El Hierro and Gran Canaria, the species grows across a wide climate (from xeric conditions to mixed forest). In Tunisia, this species was introduced since 1965 in Souiniet, Henchir Naam, Jebel Abderrahmane (Khouja, 2001).

The purpose of this study was: (i) to assess drought tolerance of three pine species from the gas exchange data and water potential, (ii) to detect if climate has an effect on the degree of tolerance of species to drought, and (iii) to select the most droughts tolerant pine species. Therefore, our objective was to compare the physiological responses to drought in three pine species, Calabrian pine (*Pinus brutia*), Canary pine (*Pinus canariensis*) and Aleppo pine (*Pinus halepensis*), in different bioclimatic zones of Tunisia.

Materials and methods

Study sites

The study was carried out in three different arboretums (*Fig. 1*) on three pine species (*Pinus halepensis*, *P. brutia* and *P. canariensis*). The first, Souiniet “SNT”, is located in northwest Tunisia (*Table 1*). The shrub layer is composed of trees of *Arbutus unedo*,

Erica scoparia, *Erica arborea*, *Myrtus communis*, *Phillyrea media*, *Halimium halimofolium*, *Cistus salvifolius* and trees of *Quercus suber*

The second, Jebel Abderrahmane “JAB”, is located in northeast Tunisia. Vegetation consists of Mediterranean maquis with *Quercus coccifera*, *Erica arborea*, *Calycotome intermedia*, *Halimium halimofolium*, *Pistacia lentiscus*, and *Phillyrea media*.

The third arboretum, Henchir Naam “HNM”, is located in northwest Tunisia and is characterized by a semi-arid climate with moderate winters and hot dry summers. Pine trees: *P. halepensis*, *P. brutia* and *P. canariensis* are found in forest mosaics along with other tree species, including *Picris echioides*, *Phalaris truncata*, *Brassica amplexicaulis*, *Euscari comosum* and *Centaurea nicaensis*.

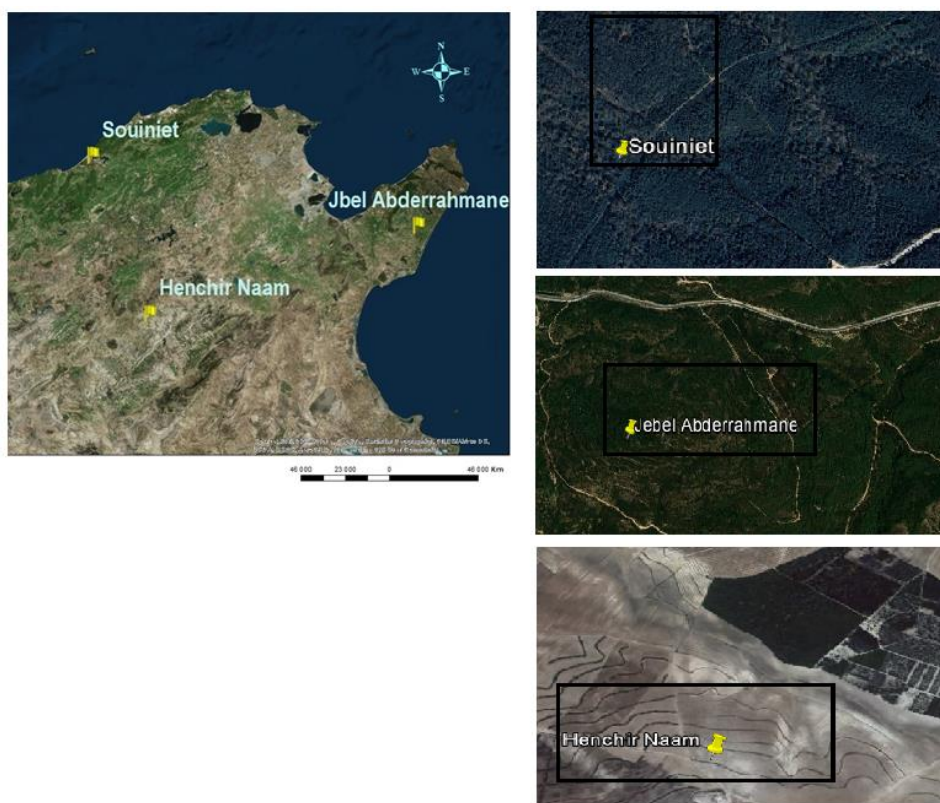


Figure 1. Localisation map of three experimental stations Souiniet, Jebel Abderrahmane and Henchir Naam Tunisia forest

Table 1. Geographical and climatic characteristics of three sites in which pine species grow

Sites	Climate	Latitude (N)	Longitude (E)	Altitude (m a.s.l)	Mean annual precipitation (mm) (1997-2016)
Souiniet	Humid	36°47'920"	8° 48'495"	492	1749.885
Jebel Abderrahmane	Sub-humid	36°40'086"	10°40'582"	255	611.751
Henchir Naam	Semi-arid	36°13'258"	9°10'374"	450	479.513

Figure 2 shows the monthly distribution of precipitation and temperature in 2016 at the three sites Souiniet, Jbel Abderrahmane and Henchir Naam.

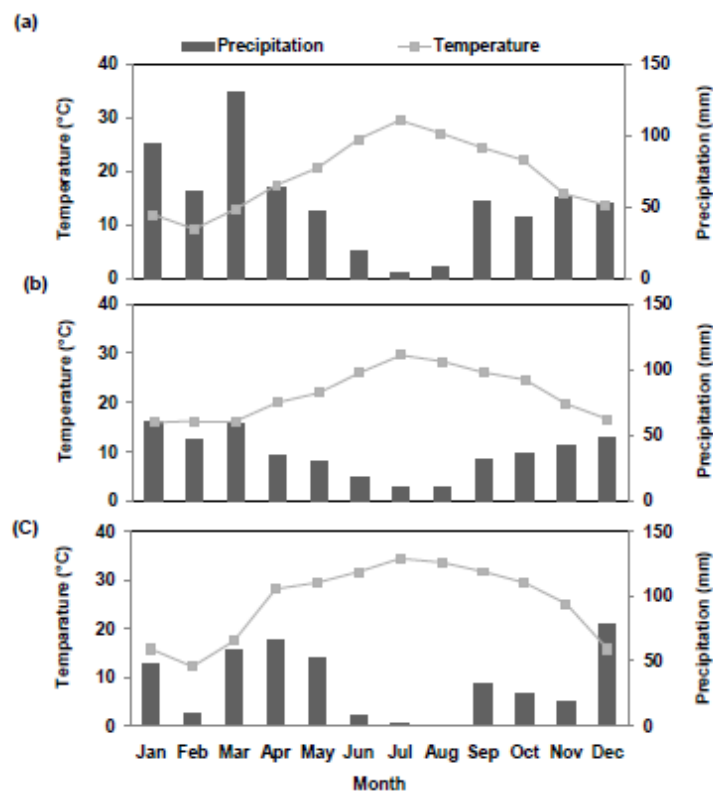


Figure 2. Climatograph of study site: (a) Souiniet site (humid climate), (b) Jbel Abderrahmane (sub-humid) and (c) Henchir Naam (semi-arid). The climatograph illustrates the monthly distribution of precipitation (P) and temperature (T) in 2016

Sampling

Three experiments were carried out in this study: leaf gas exchange, twig water potential, and soil water content on 11th in the month of March and July 2016 in SNT, JAB, and HNM.

Three different trees of each pine species were considered of a high of 13.5 ± 2.5 m and mean diameter at breast height (DBH) of 16 ± 0.3 cm. From each tree, three branches were collected. Thus, a total nine branches of each pine species were taken for leaf gas exchange (Santiago and Mulkey, 2003). The measurements of leaf gas exchange and twig water potential were taken immediately after the collection of branches.

Leaf gas exchange measurements

Leaf gas exchange were measured using a Licor 6400® (Li-Cor, Lincoln, NE, USA) on two-year old needles leaves. At the top of each tree, three lateral branches 90 cm in length were cut with pruning shears from three different trees of each pine species ($n = 27$) in the morning between 06:00 and 08:00 a.m, and immediately measured in the field. Branches placed in a bucket containing cold water during the measurements to maintain leaf gas exchange at a constant level. Photosynthetic rate of the leaves was measured at the ambient CO₂ concentration (400 ppm) with an open infrared gas analysis system (Li-Cor 6400-40 equipped with a red-blue LED source; Li-Cor Inc., Lincoln, NE, USA). Measurements for attached leaves were operated at 25 °C leaf

temperature and at an airflow rate of 300 cm³ min⁻¹. The vapor pressure deficit was kept at 1.2 ± 0.2 kPa. During the experiment, leaf temperature was maintained at 25 °C, photon flux density at 1500 μmol m⁻² s⁻¹, ambient CO₂ molar ratio (Ca) at 400 ppm and humidity of the incoming air were kept at 60%. The variables measured were: leaf stomatal conductance (gs, in mmol H₂O m⁻² s⁻¹), net carbon assimilation (An, in μmol CO₂ m⁻² s⁻¹), and transpiration (Tr, in mmol H₂O m⁻² s⁻¹). The instantaneous water use efficiency (WUE, in μmol CO₂ mol⁻¹ H₂O) was determined according to *Equation 1*:

$$WUE = \frac{An}{Tr} \quad (\text{Eq.1})$$

Twig water potential (TWP)

Water potential was measured at mid-day between 12:00 and 14:00 on three small twigs (5-7 cm long) from the considered trees using a Scholander pressure chamber (SKPM 1400®, Skye Instruments Ltd., Powys, UK) (Scholander et al., 1965).

Soil water content

Soil water content (SWC) was monitored using a time domain refractometry (TDR, Trase system I, Soil Moisture Equipment Corp., and USA) for the three sites.

Statistical analysis

Data analysis were done using Analysis of Variance ANOVA (SAS version 9.0) by GLM procedure and the mean values of species were compared using SNK test (Student-Newman-Keuls) tests at 95% confidence interval (P < 0.05). Pearson correlation coefficient was used to evaluate the correlations between physiological parameters studied.

Results

Gas exchange measurements at the leaf level

Drier conditions during the summer had a strong effect on gas exchange activity. Leaf gas exchange revealed significant differences in all variables (carbon net assimilation, transpiration and water use efficiency) between species (p < 0.001) and sites (p < 0.001), except for stomatal conductance where there was a significant difference between species (p < 0.05) but no difference between sites (p = 0.145). For any given species, there were differences among sites (p < 0.001) except for stomatal conductance in *Pinus canariensis* (p = 0.812). For any given site, there were differences among species (p < 0.001). The interaction between species x sites was significantly (p < 0.001) (*Table 2*).

At the leaf level, An was lower for all pine species in July compared to March, except for *P. halepensis*, which registered the highest values. Moreover, *P. halepensis* showed a sharp decrease (52%) in An from March to July in semi-arid climate (p < 0.001) than the other two species. For *P. canariensis*, there was a slight difference in reduction of An between humid, sub-humid and semi arid climates (44.07%, 41.77%

and 48.7%). While for *P. brutia*, the reduction of An was (51%, 47.56% and 46.23%) in humid, sub-humid and semi arid climates (Table 2).

Transpiration rate, (Tr) was significantly lower in July than in March ($p < 0.001$) and between sites ($p = 0.006$). *Pinus canariensis*, *P. halepensis* and *P. brutia* showed a sharp decrease from March to July ($p < 0.001$) in sub- humid, humid and in semi-arid climates. It was (77.72%, 77.5% and 82.30%, respectively) (Table 2).

Water use efficiency rate, (WUE) was significantly different between months and species ($p < 0.001$). Higher WUE values were measured in July in semi-arid climate. The overall means were (17.44 and 15.52 $\mu\text{mol CO}_2 \text{ mol}^{-1} \text{ H}_2\text{O}$), in *P. halepensis*, and *P. brutia*, respectively except for *P. canariensis* the highest value was measured in sub-humid climate (15.03 $\mu\text{mol CO}_2 \text{ mol}^{-1} \text{ H}_2\text{O}$).

There was also a difference in water use efficiency between climates for the same species however, in *P. canariensis* the difference was more pronounced between humid and semi-arid (7.71 $\mu\text{mol CO}_2 \text{ mol}^{-1} \text{ H}_2\text{O}$, 8.5 $\mu\text{mol CO}_2 \text{ mol}^{-1} \text{ H}_2\text{O}$) and JAB (15.03 $\mu\text{mol CO}_2 \text{ mol}^{-1} \text{ H}_2\text{O}$).

Table 2. Net assimilation rate ($\mu\text{mol CO}_2 \text{ m}^{-2} \text{ s}^{-1}$), transpiration rate ($\text{mmol H}_2\text{O m}^{-2} \text{ s}^{-1}$), stomatal conductance ($\text{mmol m}^{-2} \text{ s}^{-1}$), and water use efficiency ($\mu\text{mol CO}_2 \text{ mol}^{-1} \text{ H}_2\text{O}$) in March and July of *Pinus canariensis*, *Pinus halepensis*, *P. brutia* in Souiniet, Jebel Abderrahmane and Henchir Naam. Mean \pm SE with distinct letters are significantly different at 5% (SNK test)

Variable	Species	Site/month					
		SNT		JAB		HNM	
		March	July	March	July	March	July
An	PC	5.65 \pm 0.06 ^c	3.16 \pm 0.08 ^c	7.23 \pm 0.01 ^b	4.21 \pm 0.045 ^b	5.96 \pm 0.11 ^c	3.06 \pm 0.22 ^c
	PH	6.24 \pm 0.22 ^b	3.43 \pm 0.05 ^b	7.1 \pm 0.11 ^b	4.12 \pm 0.07 ^a	8.99 \pm 0.06 ^a	4.36 \pm 0.06 ^a
	PB	8.38 \pm 0.02 ^a	4.12 \pm 0.25 ^a	8.2 \pm 0.09 ^a	4.3 \pm 0.44 ^a	6.64 \pm 0.13 ^b	3.57 \pm 0.08 ^b
Tr	PC	1.42 \pm 0.03 ^a	0.41 \pm 0.02 ^a	1.23 \pm 0.12 ^b	0.28 \pm 0.01 ^c	1.53 \pm 0.05 ^a	0.36 \pm 0.03 ^a
	PH	1.2 \pm 0.11 ^b	0.27 \pm 0.01 ^c	1.18 \pm 0.12 ^b	0.33 \pm 0.01 ^a	0.82 \pm 0.01 ^c	0.25 \pm 0.01 ^b
	PB	1.45 \pm 0.04 ^a	0.32 \pm 0.05 ^b	1.4 \pm 0.21 ^a	0.31 \pm 0.01 ^b	1.3 \pm 0.21 ^b	0.23 \pm 0.02 ^b
gs	PC	450 \pm 0.04 ^b	106 \pm 0.00 ^a	440 \pm 0.03 ^c	95 \pm 0.00 ^b	510 \pm 0.02 ^b	116 \pm 0.07 ^a
	PH	410 \pm 0.01 ^b	82 \pm 0.00 ^b	620 \pm 0.04 ^b	96.6 \pm 0.00 ^b	410 \pm 0.01 ^c	62 \pm 0.00 ^a
	PB	550 \pm 0.08 ^a	63 \pm 0.00 ^c	720 \pm 0.06 ^a	102 \pm 0.00 ^a	630 \pm 0.06 ^a	110 \pm 0.04 ^a
WUE	PC	3.97 \pm 0.10 ^c	7.71 \pm 0.5 ^b	5.87 \pm 0.65 ^a	15.03 \pm 0.24 ^c	3.89 \pm 0.14 ^c	8.5 \pm 1.21 ^c
	PH	5.2 \pm 0.57 ^b	12.70 \pm 0.81 ^a	6.02 \pm 0.57 ^a	12.48 \pm 0.49 ^a	11 \pm 0.21 ^a	17.44 \pm 0.69 ^a
	PB	5.91 \pm 0.27 ^a	12.87 \pm 2.87 ^a	5.86 \pm 0.94 ^a	13.87 \pm 1.7 ^a	5.10 \pm 0.81 ^b	15.52 \pm 1.6 ^b

An: Net assimilation rate Tr: transpiration rate gs: stomatal conductance WUE: water use efficiency, Sp: species, PC: *Pinus canariensis*, PH: *P. halepensis* and PB: *P. brutia*

In July, there was a high positive correlation between An and gs: r^2 coefficient. The correlation was more important in *P. halepensis*, *P. brutia*, and *P. canariensis* in semi-arid climate than others climates. The coefficients were ($r^2 = 0.623$, $r^2 = 0.58$, $r^2 = 0.95$), respectively (Table 3).

Stomatal control and twig water potentials

Stomatal conductance was significantly lower in July than in March ($p < 0.001$) for all pine species. The highest rate of decline of stomatal conductance between the two months was recorded for *P. halepensis*, *P. canariensis* and *P. brutia* in semi-arid, sub-

humid and humid climates, respectively. The rate of loss was (84.87, 78.41 and 88.54%), respectively (Table 2).

Twig water potentials revealed a significant difference between species ($p < 0.001$), sites ($p < 0.001$) and months ($p < 0.001$). For any given species, there were differences among sites ($p < 0.001$) and for any given site; there were differences among species ($p < 0.001$). The interaction between species and sites was significantly ($p < 0.001$).

Table 3. Correlation coefficient r^2 of An and gs in July of *P. halepensis*, *P. brutia* and *P. canariensis* in Souiniet, Jebel Abderrahmane and Henchir Naam

Sites	<i>P. halepensis</i>	<i>P. brutia</i>	<i>P. canariensis</i>
Souiniet	0.49	0.46	0.42
Jebel Abderrahmane	0.53	0.56	0.65
Henchir Naam	0.62	0.58	0.95

An: Net assimilation rate, gs: stomatal conductance

The water potential decreases significantly from March to July in all pine species in different climates (sites). The lowest rates of decline of water potential between the two months were 17.91%, 31.40% for *P. halepensis* and *P. canariensis* in semi-arid climate. For *P. brutia* the lowest rate was 47.53% detected in humid climate (Table 4).

Table 4. Water potential (Ψ : MPa) of *P. canariensis*, *P. halepensis*, and *P. brutia* in two months March and July in Souiniet, Jebel Abderrahmane, and Henchir Naam. Mean \pm SE with distinct letters are significantly different at 5% (SNK test)

Pine species	Souiniet		Jebel Abderrahmane		Henchir Naam	
	March	July	March	July	March	July
PC	-1.54 \pm 0.01 ^a	-2.62 \pm 0.01 ^c	-1.68 \pm 0.01 ^a	-2.21 \pm 0.01 ^a	-2.42 \pm 0.01 ^c	-3.18 \pm 0.01 ^c
PH	-1.7 \pm 0.02 ^c	-2.58 \pm 0.01 ^b	-2.56 \pm 0.01 ^c	-3.47 \pm 0.02 ^c	-1.73 \pm 0.02 ^b	-2.04 \pm 0.00 ^a
PB	-1.62 \pm 0.01 ^b	-2.39 \pm 0.01 ^a	-1.92 \pm 0.00 ^b	-2.99 \pm 0.05 ^b	-1.57 \pm 0.00 ^a	-2.46 \pm 0.01 ^b

PC: *Pinus canariensis*, PH: *P. halepensis* and PB: *P. brutia*

Stomatal conductance (gs) decreased significantly as VPD increased in July in three sites (Fig. 3). In July and under semi-arid climate with (VPD = 2.4 kPa), the lowest minimum rate in gs was recorded in *Pinus halepensis* (62 mmol m⁻² s⁻¹). While in a sub-humid climate and with (VPD = 1.68 kPa), stomatal conductance was lower in *P. canariensis* (95 mmol m⁻² s⁻¹). In a humid climate and with (VPD = 1.9 kPa), *P. brutia* species recorded the lowest stomatal conductance value (63 mmol m⁻² s⁻¹).

Soil water content

Soil water content (SWC) showed significant differences between months ($p < 0.001$) and sites ($p = 0.017$). The interaction term was also significant ($p = 0.02$), being higher in March than in July (Table 5). In July, the correlation between soil water content and gs was high and positive for *P. brutia*, *P. canariensis*, and *P. halepensis* $r^2 = 0.916$, $r^2 = 0.798$ and $r^2 = 0.931$, respectively in all sites.

Soil water content was negatively correlated with WUE for all pine species under these climates: for *P. halepensis*, *P. brutia* and *P. canariensis* ($r = -0.84$; $r = -0.79$; $r = -0.78$), in a semi-arid, humid and sub-humid climate, respectively.

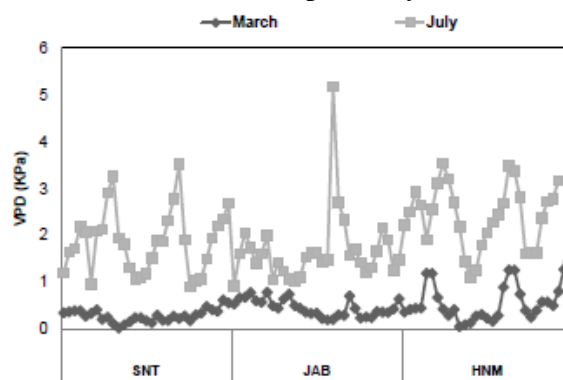


Figure 3. Vapor pressure deficit in kPa (VPD) in March and July 2016 in SNT (Souiniet), JAB (Jbel Abderrahmane), and HNM (Henchir Naam)

Table 5. Soil water content (%) for *P. canariensis*, *P. halepensis*, and *P. brutia* in three sites Souiniet, Jbel Abderrahmane, and Henchir Naam between March and July. Mean \pm SE with distinct letters are significantly different at 5% (SNK test)

Pine species	Souiniet		Jebel Abderrahmane		Henchir Naam	
	March	July	March	July	March	July
PC	34.63 \pm 0.02 ^c	17.43 \pm 0.01 ^b	47.80 \pm 0.01 ^a	19.23 \pm 0.01 ^{ab}	35 \pm 0.01 ^b	21.13 \pm 0.01 ^a
PH	58.43 \pm 0.01 ^a	21.93 \pm 0.03 ^a	45.90 \pm 0.02 ^{ab}	17.72 \pm 0.02 ^b	48.57 \pm 0.01 ^b	19.82 \pm 0.00 ^a
PB	48.43 \pm 0.01 ^b	19.46 \pm 0.01 ^b	44.67 \pm 0.02 ^{ab}	20.80 \pm 0.05 ^a	43.93 \pm 0.00 ^a	18.60 \pm 0.03 ^a

PC: *P. canariensis*; PH: *P. halepensis*, and PB: *P. brutia*

Discussion

Ecophysiological measurements and stomatal control

Drought may reduce leaf net carbon assimilation by both stomatal and metabolic limitations (Farquhar and Sharkey, 1982). In addition, the decrease in stomatal conductance is the main factor of photosynthesis inhibition during dehydration as previously reported (Cornic and Fresneau, 2002; Flexas and Medrano, 2002).

In this study, a significant decrease in “ g_s ” and “ A_n ” was found in July in *P. halepensis*, *P. canariensis* and *P. brutia* under different climates compared to results of March. Both parameters (g_s and A_n) plummeted concomitantly as aridity increased. In Spain, Manzanera et al. (2016) found the same results on *Pinus sylvestris*, *Pinus pinea* and *Pinus halepensis*.

In our study, *P. halepensis*, *P. canariensis* and *P. brutia* suggest a higher stomatal control and decreased their water potential in semi-arid, sub-humid and humid climate, respectively to a lesser in the other climates. Also a strong reduction of stomatal conductance under drought conditions slows transpiration allowing plants to keep high water potentials (Table 2).

In France, Lebourgeois et al. (1998) found that pine species were tolerant to drought and a significant decrease of stomatal conductance of *Pinus nigra* was not correlated

with obvious variation in water potential. They usually exhibit drought avoidance strategy with efficient stomatal control of transpiration loss, a decrease of stomatal conductance (up to 30%) and no change in water potential.

In July, our results (Table 2) revealed that the net carbon assimilation of *Pinus halepensis* was lower in humid climate ($3.43 \mu\text{mol m}^{-2} \text{s}^{-1}$) than sub-humid climate ($4.12 \mu\text{mol m}^{-2} \text{s}^{-1}$). However, Aleppo pine showed a higher assimilation rate than the other pine species in semi-arid climate ($4.36 \mu\text{mol m}^{-2} \text{s}^{-1}$). Similarly, in Spain, Salazar-Tortosa et al. (2018) found that net carbon assimilation in *P. halepensis* was ($3.4 \mu\text{mol m}^{-2} \text{s}^{-1}$) in the same season July 2014. It can maintain CO_2 uptake and photosynthesis by mean lower stomatal control.

The net carbon assimilation of *P. canariensis* was lower in July in semi-arid than humid climate but it maintain the high value in sub-humid climate. While, for *P. brutia* the net carbon assimilation was lower in semi arid climate but it can keep a high net assimilation in humid and sub-humid climates (Table 2).

Ecophysiological mechanisms driving WUE enhancement

In March and July, physiological activity and phenological development of the three pines species were critical. In March water availability in the soil was important and the radiation was not excessive, which leads to having a maximum value of photosynthesis, and the development of shoots and needles began. Whereas, in July water availability in the soil was limited; the radiation was excessive and lead to having minimal photosynthesis. The development of the shoots was complete and that of the needles was in progress.

For all studied pine species, the large fluctuations in WUE between March and July appear to be mainly related to changes in environmental conditions (soil water content, precipitation and temperature). Thus, soil water content was negatively correlated with WUE for all pine species under semi-arid, humid and sub-humid climate. These results revealed the degree of adaptation and resistance of three pine species particularly in these climates under drought conditions. The significant interaction observed between site (climate) and species clarify the behaviour of each pine species: *Pinus canariensis* have better water use efficiency in sub-humid than in humid and semi-arid. *Pinus brutia* have a high water use efficiency in the three sites with pronounced value in semi-arid. However, Aleppo pine showed higher water-use efficiency in different climates, supporting the notion that assimilation was less limited by climatic conditions (Table 1). As far as Klein et al. (2012) found that Aleppo pine has the ability to survive and grow in various environments indicates thus is a highly tolerant species. In contrary to previous study realized by Sardans and Peñuelas (2007) and Vila et al. (2008) confirmed that Aleppo pine is expected to suffer from changes in timing and duration of drought, particularly in spring and summer.

The effect of VPD and soil water content on stomatal response of pine species

Oren et al. (1999) emphasized that high VPD may be one of the signals that lead to stomatal closure. In our study, stomatal conductance decreased in July for all pine species in different climates with the increase of the VPD. Both high VPD and low SWC explained the reductions in stomatal conductance, transpiration and photosynthesis in all pine species under different climates (Table 2). The results were also in agreement with those reported in USA by Sulman et al. (2016) that worked on

Acer saccharum, *Liriodendron tulipifera*, *Sassafras albidum*, *Quercus alba*, *Quercus velutina*, and *Quercus rubra*. Under drought conditions and with low SWC or high VPD, these 5 plant species close stomata reduce transpiration and photosynthesis.

P. brutia was more resistant to drought in two climates humid and semi arid. Awada et al. (2003) showed that *P. brutia* was a drought-resistant species occupying the driest sites around the Mediterranean Basin. Furthermore, *P. canariensis* was resistant to drought in the three climates in Tunisia with less tolerance to humid climate. Jiménez et al. (2005) showed that *P. canariensis* was able to modulate its physiology (with a good stomatal control), depending of the site where it grows with. However, the performance of *P. halepensis* was much higher as much as this species exhibited higher stomatal control, higher photosynthesis and water use efficiency in a dry month (July) and under semi-arid climates. Salazar-Tortosa et al. (2018) showed that Aleppo pine would require less water in the carbon capture process when it is planted with limited water availability. This strategy allowed *P. halepensis* to be one of the more conservative species.

Conclusion

The findings showed significant differences in leaf water potential and gas exchange measurements among pine species. The responses are depending not only on species but also on the climate in which they grow.

Under dry conditions, *P. halepensis*, *P. canariensis* and *P. brutia* are better adapted to a semi-arid, sub-humid and humid climate, respectively. All pine species avoid drought by reducing stomatal conductance to water through conservation of soil water content at high VPD and thus avoiding future drought. While this strategy would result in a net increase in WUE, it would be at the expense of photosynthesis during periods of high VPD. The findings of these experiments may help to quantify the impact of mid-summer water deficit on Mediterranean pines and evaluate their potential responses to future climate regimes. Monitoring of these three species is required to reveal how ecological restoration is progressing and where management interventions are required.

Therefore, in Tunisia, it is highly recommended to plant *P. halepensis* in semi-arid climate, *P. brutia* was recommended to be planted in humid and semi-arid climates. While, it is recommended to plant *P. canariensis* in sub-humid and semi-arid climates.

Acknowledgements. This work was supported and funded by the INCREDIBLE project (funding from the European Union's Horizon 2020 research and innovation programme under grant agreement N° 774632). Thanks to Mokhtar Baraket for his considerable comments for manuscript and thanks to National Institute of Meteorology of Tunis for providing meteorological data from different regions.

REFERENCES

- [1] Allen, C. D., Macalady, A. K., Chenchouni, H., Bachelet, D., McDowell, N., Vennetier, M., Kitzberger, T., Rigling, A., Breshears, D. D., Hogg, E. H., Gonzalez, P., Fensham, R., Zhang, Z., Castro, J., Demidova, N., Lim, J. H., Allard, G., Running, S. W., Semerci, A., Cobb, N. (2010): A global overview of drought and heat-induced tree mortality reveals emerging climate change risks for forests. – *Forest Ecology and Management* 259: 660-684.

- [2] Awada, T., Radoglou, K., Fotelli, M. N., Constantinidou, H. I. (2003): Ecophysiology of seedlings of three Mediterranean pine species in contrasting light regimes. – *Tree Physiology* 23(1): 33-41.
- [3] Ayari, A., Moya, D., Zubizarreta-Gerendiain, A. (2012): Influence of Environmental Factors on Aleppo Pine Forest Production. – Nova Science Publishers, Inc., Hauppauge, NY.
- [4] Bréda, N., Cochard, H., Dreyer, E., Granier, A. (1993): Water transfer in a mature oak stands (*Quercus petraea*): seasonal evolution and effects of a severe drought. – *Canadian Journal of Forest Research* 23: 1136-1143.
- [5] Choat, B., Jansen, S., Brodribb, T. J., Cochard, H., Delzon, S., Bhaskar, R., Bucci, S. J., Field, T. S., Gleason, S. M., Hacke, U. G., Jacobsen, A. L., Lens, F., Maherali, H., Martinez-Vilalta, J., Mayr, S., Mencuccini, M., Mitchell, P. J., Nardini, A., Pittermann, J., Pratt, R. B., Sperry, J. S., Westoby, M., Wright, I. J., Zanne, A. E. (2012): Global convergence in the vulnerability of forests to drought. – *Nature* 491: 752-755.
- [6] Cornic, G., Fresneau, C. (2002): Photosynthetic carbon reduction and carbon oxidation cycles are the main electron sinks for photosystem II activity during a mild drought. – *Annals of Botany* 89: 887-894.
- [7] David, T. S., Henriques, M. O., Kurz-Besson, C., Nunes, J., Valente, F., Vaz, M., Pereira, J. S., Siegwolf, R., Chaves, M. M., Gazarini, L. C., David, J. S. (2007): Water-use strategies in two co-occurring Mediterranean evergreen oaks: surviving the summer drought. – *Tree Physiology* 27: 793-803.
- [8] de Nascimento, L., Willis, K. J., Fernández-Palacios, J. M., Criado, C., Whittaker, R. J. (2009): The long-term ecology of the lost forests of La Laguna, Tenerife (Canary Islands). – *Journal of Biogeography* 36: 499-514.
- [9] Khouja, M. L. (2001): Amélioration génétique: inventaire et bilan des recherches entreprises en Tunisie. – *Annales de l'INRGREF* 5: 1-44.
- [10] Khouja, M. L., Sghaier, T., Khaldi, A., Nouri, M., Souayah, N. (2002): Premiers résultats des essais de provenances de *Pinus brutia* TEN en Tunisie. – *Annales de l'INRGREF* 5: 57-70.
- [11] Farquhar, G. D., Sharkey, T. D. (1982): Stomatal conductance and photosynthesis. – *Annual Review of Plant Physiology* 33: 317-345.
- [12] Flexas, J., Medrano, H. (2002): Drought-inhibition of photosynthesis in C3 plants: stomatal and non-stomatal limitations revisited. – *Annals of Botany* 89(2): 183-9.
- [13] Granier, A., Bréda, N., Longdoz, B., Gross, P., Ngao, J. (2008): Ten years of fluxes and stand growth in a young beech forest at Hesse, North-eastern France. – *Annals of Forest Science* 64: 704.
- [14] Jiménez, M. S., Luis, V. C., Peters, J., González-Rodríguez, A., Morales, D. (2005): Ecophysiological studies on *Pinus canariensis* Phytol. – *Annales Rei Botanicae* 45(3): 169-177.
- [15] Klein, T., Cohen, S., Yakir, D. (2011): Hydraulic adjustments underlying drought resistance of *Pinus halepensis*. – *Tree Physiology* 31(6): 637-648.
- [16] Klein, T., Di Matteo, G., Rotenberg, E., Cohen, S., Yakir, D. (2012): Differential ecophysiological response of a major Mediterranean pine species across a climatic gradient. – *Tree Physiology* 33(1): 26-36.
- [17] Kucuk, O., Bilgili, E., Bulut, S., Fernandes, P. M. (2012): Rates of surface fire spread in a young calabrian pine (*pinus brutia* ten.) plantation – *Environmental Engineering and Management Journal* 11: 1475-148.
- [18] Lebourgeois, F., Levy, G., Aussenac, G., Clerc, B., Willm, F. (1998): Influence of soil drying on leaf water potential, photosynthesis, stomatal conductance and growth in two black pine varieties. – *Annals of Forest Science* 55: 287-299.
- [19] Letts, M. G., Rodriguez-Calcerrada, J., Rolo, V., Rambal, S. (2011): Long term physiological and morphological acclimation by the evergreen shrub *Buxus sempervirens* L. to understory and canopy gap light intensities. – *Trees* 26: 479-491.

- [20] López, R., Cano, F. G., Choat, B., Cochard, H., Gil, L. (2016): Plasticity in Vulnerability to cavitation of *Pinus canariensis* occurs only at the driest end of an aridity gradient. – *Frontiers in Plant Science* 3: 7-769.
- [21] Manzanera, J. A., Martínez-Chacon, M. F. (2007): Ecophysiological competence of *Populus alba* L., *Fraxinus angustifolia* Vahl. and *Crataegus monogyna* Jacq used in plantations for the recovery of riparian vegetation. – *Journal of Environmental Management* 40(6): 902-912.
- [22] Manzanera, J. A., Gómez-Garay, A., Pintos, B., Rodríguez-Rastrero, M., Moreda, E., Zazo, J., Martínez-Falero, E., García-Abril, A. (2016): Sap flow, leaf-level gas exchange and spectral responses to drought in *Pinus sylvestris*, *Pinus pinea* and *Pinus halepensis*. – *iForest* 10: 204-214.
- [23] Martínez-Vilalta, J., Sala, A., Piñol, J. (2004): The hydraulic architecture of Pinaceae—a review. – *Plant Ecology* 171(1): 3-13.
- [24] Martínez-Vilalta, J., Cochard, H., Mencuccini, M., Sterck, F., Herrero, A., Korhonen, J. F., Llorens, P., Nikinmaa, E., Nole, A., Poyatos, R., Ripullone, F., Sass-Klaassen, U., Zweifel, R. (2009): Hydraulic adjustment of scots pine across Europe. – *New Phytologist* 184(2): 353-64.
- [25] Matías, L., Jump, A. S. (2012): Interactions between growth, demography and biotic interactions in determining species range limits in a warming world: the case of *Pinus sylvestris*. – *Forest Ecology and Management* 282: 10-22.
- [26] McDowell, N., Pockman, W. T., Allen, C. D., Breshears, D. D., Cobb, N., Kolb, T., Plaut, J., Sperry, J., West, A., Williams, D. G., Yepez, E. A. (2008): Mechanisms of plant survival and mortality during drought: why do some plants survive while others succumb to drought? – *New Phytologist* 178: 719-739.
- [27] Mittler, R. (2002): Oxidative stress, antioxidants and stress tolerance. – *Trends in Plant Science* 7(9): 405-410.
- [28] Nemani, R. R., Keeling, C. D., Hashimoto, H., Jolly, W. M., Piper, S. C., Tucker, C. J., Myneni, R. B., Running, S. W. (2003): Climate-driven increases in global terrestrial net primary production from 1982 to 1999. – *Science* 300: 1560-1563.
- [29] Oren, R., Sperry, J. S., Katul, G. G., Pataki, D. E., Ewers, B. E., Phillips, N., Schaefer, K. V. R. (1999): Survey and synthesis of intra- and interspecific variation in stomatal sensitivity to vapour pressure deficit. – *Plant, Cell & Environment* 22: 1515-1526.
- [30] Peñuelas, J., Sardans, J., Filella, I., Estiarte, M., Llusà, J., Ogaya, R., Carnicer, J., Bartrons, M., Rivas-Ubach, A., Grau, O., Peguero, G., Margalef, O., Pla-Rabés, S., Stefanescu, C., Asensio, D., Preece, C., Liu, L., Verger, A., Barbeta, A., Achotegui-Castells, A., Gargallo-Garriga, A., Sperlich, D., Farré-Armengol, G., Fernández-Martínez, M., Liu, D., Zhang, C., Urbina, I., Camino-Serrano, M., Vives-Inglà, M. D., Stocker, B., Balzarolo, M., Guerrieri, R., Peaucelle, M., Marañón-Jiménez, S., Bórnez-Mejías, K., Mu, Z., Descals, A., Castellanos, A., Terradas, J. (2017): Impacts of global change on Mediterranean forests and their services. – *Forests* 8: 12-463.
- [31] Ramirez-Valiente, J. A., Sánchez-Gómez, D., Aranda, I., Valladarres, F. (2010): Phenotypic plasticity and local adaptation in leaf ecophysiological traits of 13 contrasting cork oak populations under different water availabilities. – *Tree Physiology* 30: 618-627.
- [32] Rubio-Casal, A. E., Leira-Doce, P., Figueroa, M. E., Castillo, J. M. (2010): Contrasted tolerance to low and high temperatures of three tree taxa co-occurring on coastal dune forests under Mediterranean climate. – *Journal of Arid Environments* 74: 429-439.
- [33] Santiago, L. S., Mulkey, S. S. (2003): A test of gas exchange measurements on excised canopy branches of ten tropical tree species. – *Photosynthetica* 41: 343-347.
- [34] Salazar-Tortosa, D., Castro, J., Rubio de Casas, R., Vīnegla, B., S´anchez-Cānete, E. P., Villar-Salvador, P. (2018): Gas exchange at whole plant level shows that a less conservative water use is linked to a higher performance in three ecologically distinct pine species. – *Environmental Research Letters* 13: 045004.

- [35] Sardans, J., Peñuelas, J. (2007): Drought changes the dynamics of trace element accumulation in a Mediterranean *Quercus ilex* forest. – *Environmental Pollution* 147(3): 567-583.
- [36] Scholander, P. F., Bradstreet, E. D., Hemmingsen, E. A., Hammel, H. T. (1965): Sap pressure in vascular plants: negative hydrostatic pressure can be measured in plants. – *Science* 148: 339-346.
- [37] Sulman, B. N., Roman, D. T., Yi, K., Wang, L., Phillips, R. P., Novick, K. A. (2016): High atmospheric demand for water can limit forest carbon uptake and transpiration as severely as dry soil. – *Geophysical Research Letters* 43: 9686-9695.
- [38] Vila, B., Vennetier, M., Ripert, C., Chandiooux, O., Liang, E., Guibal, F., Torre, F. (2008): Has global change induced opposite trends in radial growth of *Pinus sylvestris* and *Pinus halepensis* at their bioclimatic limit? The example of the Sainte-Baume forest (south-east France). – *Annals of Forest Science* 65: 709.
- [39] Warren, C. R., McGrath, J. F., Adams, M. A. (2001): Water availability and carbon isotope discrimination in conifers. – *Oecologia* 127: 476-486.
- [40] Will, R. E., Wilson, S. M., Zou, C. B., Hennessey, T. C. (2013): Increased vapor pressure deficit due to higher temperature leads to greater transpiration and faster mortality during drought for tree seedlings common to the forest–Grassland ecotone. – *New Phytologist* 200: 366-374.
- [41] You, H., Jinb, H., Khaldi, A., Kwaka, M., Lee, T., Khainea, I., Janga, J., Lee, H., Kim, I., Ahn, T., Song, J., Song, Y., Khorchani, A., Stiti, B., Woo, S. (2016): Plant diversity in different bioclimatic zones in Tunisia. – *Journal of Asia-Pacific Biodiversity* 9: 56-62.

ESTABLISHMENT AND VERIFICATION OF A NEW PREDICTION MODEL FOR DRY RUBBER YIELD

HUANG, H.^{2,3} – YANG, Z.^{1*} – WANG, C.³ – ZHANG, J.^{2,3} – LI, Y.¹ – HU, D.² – LIU, W.¹

¹*Collaborative Innovation Center on Forecast and Evaluation of Meteorological Disasters, Nanjing University of Information Science & Technology, Nanjing 210044, Jiangsu Province, P. R. China*

²*Hainan Climate Center, Haikou 570203, Hainan Province, P. R. China*

³*Key Laboratory of South China Sea Meteorological Disaster Prevention and Mitigation of Hainan Province, Haikou 570203, Hainan Province, P. R. China*

**Corresponding author*

e-mail: huanghai8815@163.com

(Received 15th Mar 2019; accepted 1st May 2019)

Abstract. The yield of rubber tree is influenced by environmental factors and its own variety characteristics. In this study, a simulation model for the stem volume of standing rubber trees was developed. Compared to the general model, the RMSE and R^2 values between the simulated and measured data were increased by 28.0% and 4.5%, respectively. Through analysis, the regression model Y_{dr1} (take the relative stem volume increment and climatic variables as independent variables), Y_{dr2} (take the climatic variables and disaster index as independent variables), and Y_{dr3} (take the relative stem volume increment, climatic variables and disaster index as independent variables) were established for the dry rubber yield prediction of a single plant. The result showed that, the RMSE and R^2 values of the yield prediction model Y_{dr3} were 0.0354 kg and 0.9862, they increased by 76.8% and 32.6% with respect to the model Y_{dr2} and rose 66.8% and 17.4% compared to the yield prediction model Y_{dr1} , respectively. In applying the prediction model Y_{dr3} to the yield prediction in different sub-compartments of a rubber plantations, the mean absolute error was 35.7 kg/ha. This study's newly established model could provide decision support for dry rubber yield prediction of rubber plantation over large areas.

Keywords: *climatic element, meteorological disaster, rubber tree, stem volume, yield prediction*

Introduction

The rubber tree (*Hevea brasiliensis*) is currently the main source of natural rubber. This species is native to the Amazon River Basin in South America, and is commonly found in a climatic environments with high temperature, high humidity, and abundant and evenly distributed rainfall, where it can avoid meteorological disasters hazards, such as typhoon, too-low temperature, and drought (Roberts, 1988; Yu et al., 2014).

China is now an important producer of natural rubber, with a yield is the fourth highest globally. In Hainan Province, the cultivated area is about 5.3×10^5 hm², and the rubber yield accounts for 53% of the national production, making it the largest production base of rubber in China (Xu et al., 2017). Rubber production is highly sensitive to various climatic factors. The locality in Hainan is prone to typhoons and chilling damage, which are mostly absent from rubber's native range (Chen et al., 2012; Liu et al., 2015; Roy et al., 2017). Against the background of global climate change, extreme weather events are more likely to occur than ever before. This raises a pressing question: How to quantitatively evaluate the effects of climatic element and disasters hazards on the rubber production. Predicting rubber yield is vital for promoting regional rubber production, so new models are presumably needed.

The theoretical yield of rubber tree is mainly determined by the species variety used (Lacote et al., 1998), while in its non-native range, annual fluctuations in yield are jointly affected by the market (Xu et al., 2017) and climate factors (Devakumar et al., 1998; Rao et al., 1998; Zomer et al., 2014; Golbon et al., 2015; Nguyen and Dang, 2016), in addition to meteorological disasters (Chen et al., 2012; Liu et al., 2015). The regular growth of rubber tree requires more than 2000 h of annual sunshine duration, over 1500 mm of annual precipitation, over 150 d of rainy days in a year, with an average relative humidity of more than 80% in the planting region. Additionally, the minimum limit temperature for its growth is 18 °C, while higher temperatures and stronger solar radiation are beneficial to this tree's photosynthesis. But if the temperature is < 10 °C and > 40 °C, then photosynthesis will cease. The range of 18–28 °C is the most suitable for rubber production, while that of 18–24 °C is the most suitable for rubber discharging temperatures (Yu et al., 2014; Yang, 1989; Priyadarshan et al., 2005; Kokmila et al., 2010; Carr, 2012).

In evaluating the relationships between climatic factors and rubber yield, much prior research has looked into various climatic factors to establish the yield prediction equation (Yu et al., 2014; Golbon et al., 2015; Nguyen and Dang, 2016; Zhang et al., 2014, 2017; Kim et al., 2017). For example, Yu et al. (2014) analyzed the relationship between the 5-d average yield of a single rubber tapping tree and the following: average temperature 1 day and 1 month before rubber tapping, day-night temperature difference, and sunshine duration 1 day and 1 month before the rubber tapping. They found that the day-night temperature difference was an important factor influencing the rubber yield, and established their yield prediction equation by using partial least squares regression and classification in a regression tree model. Golbon et al. (2015) considered the average value of rainfall, lowest temperature, highest temperature, and maximum relative humidity 30 days before the rubber tapping as the optimum yield predictors; using them, they established a prediction model of rubber yield by using a linear mixed model. Feng et al. (2016) reported that nine climatic factors influencing the rubber yield were ranked as follows: sunshine > highest temperature > average humidity > average temperature > lowest humidity > evaporation > wind speed > lowest temperature > precipitation; based on this they established a monthly rubber yield prediction model for Xishuangbanna, China. In other work, Nguyen and Dang (2016) analyzed the relationship between the yield and the average temperature, average highest temperature, and average lowest temperature, in the rubber tree varieties GT1 and PB235 in Vietnam for three consecutive years (during 2007~2009). Those rubber yields showed significant negative correlation with all three climatic factors. Earlier Liu et al. (2002) reported that a significant correlation between the diameter at breast height and dry rubber yield of two strains, RRIM600 and PR107. Some have researched the correlations among the laticifer differentiation capability of the rubber tree, the combined efficiency of rubber, and the rubber yield; this was then applied to early rubber yield predictions (Chen, 2014; Yu, 2007).

Until now, research on rubber yield prediction has mainly taken a single climatic factor or a physic-ecological index as the main predictor variable, thereby overlooking the effect of meteorological disasters and varietal characteristics on the predicted yield. In this study, the relative stem volume of rubber tree and a disaster index were introduced as the key predictors, and a new forecasting model for the dry rubber yield of rubber tree was developed, tested, and established. This work thus provides a theoretical basis for the accurate yield estimation in the rubber production over large areas of its cultivation in China.

Materials and methods

Study site

Hainan has a tropical oceanic monsoon climate. In this jurisdiction, the annual average temperature of various regions is 23.1~27.0 °C, with annual precipitation that is 940.8~2388.2 mm. The annual average sunshine duration is 1827.6~2810.6 h. During years of 2014–2017, rubber plantations differing in their stand ages were selected, as *Figure 1* shows, in Dongchang Farm of Dapo Town, Haikou City (Location: N19°36', E110°37'; Rubber cultivation: 1333.3 ha), Xinzhong Farm of Wanning City (Location: N18°51', E110°11'; Rubber cultivation: 5593.3 ha) and Xiqing Farm of Danzhou City (Location: N19°32', E109°28'; Rubber cultivation: 4573.3 ha). The sampling of the forest stand is the pure rubber plantation that has been tapped manually and the cultivated soil is red soil. The variety studied is RRIM600. The spatial position of the plantation sub-compartments is shown in *Figure 1*.

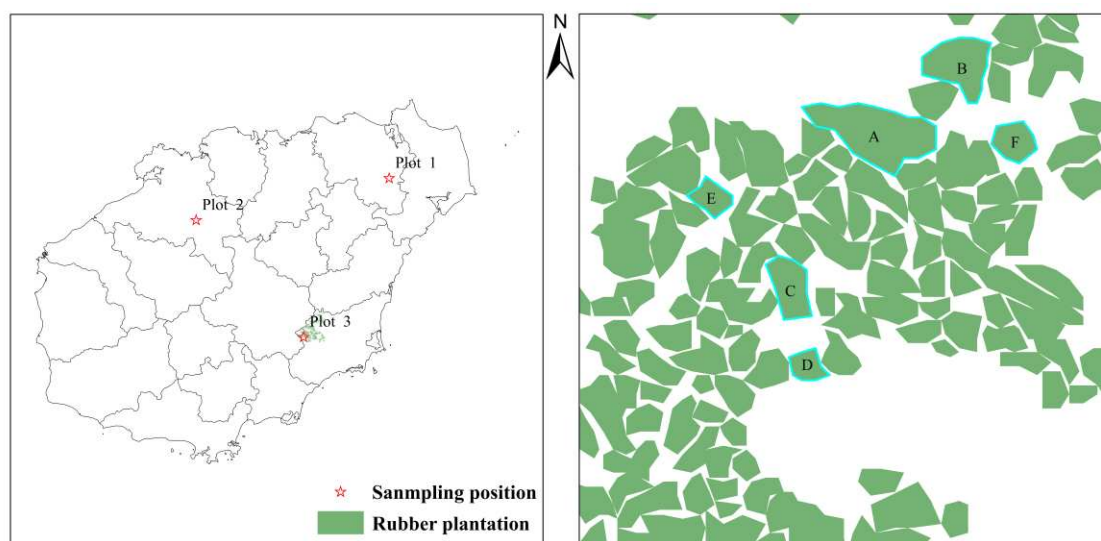


Figure 1. Distribution of sampling points in the study area. (Plot 1 is Dongchang Farm in Haikou City, Plot 2 is Xiqing Farm in Danzhou City, and Plot 3 is Xinzhong Farm in Wanning City. A, B, C, D, E, and F are the sub-compartments of a rubber plantation with different stand ages at the Xinzhong Farm)

Data sources

Forest characteristics collection

During 2014–2015, on December 20–31 every year, the sampling was carried out in differently aged stands in plot1 and 2. In the sampling rubber plantation of the farm, the tree height, diameter at breast height (at 1.3 m above the ground) and the thickness of the bark were measured, the crown area was calculated using elliptic area formula (the vertical projection width of the canopy from east to west and north to south was used as diameter). 100 trees were measured at each sampling point every year, a total of 400 samples were obtained until the end of 2015. The data sets applied for training.

During 2016–2017, on December 20–31 every year, the same sampling was carried out in differently aged stands in plot3. 100 trees were measured at this sampling point every year,

a total of 200 samples were obtained until the end of 2017. The data sets applied for validation.

Data for tree volume calculation

Differential planimetry is often used to calculate timber volume. In this method, the trunk is divided into several segments, and the volume of each segment is calculated respectively, and finally calculate the volume of the trunk. The precision of this method mainly depends on the number of segments. In this study, the trunk characteristics of rubber trees were comprehensively analyzed, and the number of trunk segments is determined to be 10. The trunk height of the sampled rubber tree was measured, and then the trunk was divided into 10 segments on average according to the height, and the diameter of each segment was measured.

The historical sequence data of tree diameter

In each plot, 20 rubber trees aged > 40 years with undamaged tree form were selected for destructive sampling (point 1: 45 years old, point 2: 47 years old, point 3: 46 years old). After being felled, a disk of the tree trunk at 1.3 m was removed and marked in the cardinal directions. The disk was polished until the annual ring boundary was clearly visible. Along the north-south direction of the disk, a section of 1 cm × 30 μm was cut by a slicer, and then made into a microsection of annual rings. Under a microscopic projector (XTL-2400), each annual ring width of the section from the pith to the bark was measured to the nearest 0.01 mm. The magnification used was 40x (Rahman et al., 2017). The annual tree wheel width of 20 rubber trees measured at each sampling point was averaged as the annual tree diameter (without bark). The annual tree diameter was multiplied by bark coefficient (bark coefficient = skin diameter/skin diameter) as the historical sequence of tree diameter (with bark).

Meteorological data

From the Hainan Meteorology Administration, the data of daily mean temperature, precipitation, wind speed and sunshine hours was obtained for the years 1960–2017. From the “tropical cyclone yearbook”, the data of maximum wind speed (m/s) and maximum instantaneous wind speed (m/s) in each process was obtained for the years 1960–2017.

Rubber production data

The data on rubber yields came from production records of farms (Dongchang, Xiqing, Xinzhong) during the same period (1960-2017), including the total production of dry rubber and plant cutting, and further calculate the dry rubber yield of single plant (total production of dry rubber/plant cutting).

Meteorological index

K_I is the heat-index, P_I is the precipitation-index, R_I is the sunshine-index, and D_I is the disaster-index, with their calculations made as follows (Eqs. 1-6):

$$K_I = 0.724 \sum_{i=1}^n (T_1 - 18) + 0.276 \sum_{j=1}^n (T_2 - 10) \quad (\text{Eq.1})$$

T_1 is the daily average temperature during April–November, T_2 is the daily average temperature from December in the last year to March in the next year ($^{\circ}\text{C}$), and n is the number of days of regular rubber tree growth. The critical temperature for this regular growth is 18°C and 10°C .

$$P_I = (P - 1500)/n \quad (\text{Eq.2})$$

P is the annual precipitation (mm), with 1500 mm being the minimum annual precipitation required by the rubber tree; n is the number of rainy days.

$$R_I = (R_i - 2000)/2000 \quad (\text{Eq.3})$$

The term R_i is the annual sunshine duration (h), with the rubber tree requiring 2000 h of annual sunshine duration for regular growth.

$$D_I = 0.724I_{tc} + 0.276I_c \quad (\text{Eq.4})$$

I_{tc} is the typhoon disaster index. V_{m1} , V_{m2} , R_i , and R_m are the standardized values of maximum wind speed (m/s), maximum instantaneous wind speed (m/s), total precipitation (mm), and daily maximum precipitation (mm), respectively; I_c is the chilling damage index, and X_1 – X_6 are the standardized values of yearly lowest extreme temperature ($^{\circ}\text{C}$), maximum temperature drop in degrees ($^{\circ}\text{C}$), sustained days of chilling damage, radiant accumulated coldness, advective accumulated coldness, and the sustained days of cold weather process with the longest advection. The coefficients in the formula are calculated by the analytic hierarchy process.

$$I_{tc} = 0.340 * \sum_{i=1}^n V_{m1}^2 + 0.280 * \sum_{i=1}^n V_{m2}^2 + 0.136 * \sum_{i=1}^n R_i + 0.244 * \sum_{i=1}^n R_m \quad (\text{Eq.5})$$

$$I_c = 0.064X_1 + 0.143X_2 + 0.282X_3 + 0.100X_4 + 0.207X_5 + 0.204X_6 \quad (\text{Eq.6})$$

Calculation of stem volume of felled rubber trees

The stem volume (V) of a sampled rubber tree was calculated using the average basal area quadrature method (Eq. 7; Zeng, 2011).

$$V = \frac{\pi}{4} \left(\frac{D_0^2 + D_{10}^2}{2} + \sum_{i=1}^9 D_i^2 \right) \theta \quad (\text{Eq.7})$$

In this formula, V is the stem volume of fallen tree (m^3); D_0 , D_n , and D_i are the cross-sectional diameters of the segment at the bottom, top and in the middle of the trunk (m), respectively; θ is the segment length; and the number of segments is 10.

Model construction

Model construction for the crown area and the height of tree

Referring to previous studies, it can be seen that the relation between tree height and the diameter at breast conforms to Richard equation, and the crown area and the diameter at breast conform to Weibull equation (Zeng et al., 1999; Bi et al., 2012). The

tree height model RH (Eq. 8) and crown area model RA (Eq. 9) was established respectively.

$$H_r = \lambda_1 * (1 + (\lambda_2 - 1) * \exp(-\lambda_3 * (D - \lambda_4)))^{1/(1 - \lambda_5)} \quad (\text{Eq.8})$$

$$A_r = \gamma_1 * (1 - \exp(-(\gamma_2 * (D - \gamma_3)))^{\gamma_4} \quad (\text{Eq.9})$$

where $\lambda_1, \lambda_2, \lambda_3, \lambda_4, \lambda_5, \gamma_1, \gamma_2, \gamma_3, \gamma_4$ are the model parameter, Hr is tree height (m), Ar is crown area (m²), and D is diameter at breast height (cm), respectively.

Stem volume of a single standing tree

A general model(V1) based on tree height and DBH is used to calculate the stem volume of standing tree (Eq. 10) (Gonzalez-Benecke et al., 2012, 2013, 2014; Zhou et al., 1995):

$$\text{LnV1} = \alpha_1 + \alpha_2 \text{Ln}(D^2H) \quad (\text{Eq.10})$$

where V is the living wood growing stock (m³), D is DBH (the diameter at breast height) (cm), H is the tree height (m), and α_1 and α_2 are the model parameters for estimation.

Since the crown area is an important factor influencing the stem volume of standing tree, by incorporating it into model V1, the stem volume model of a standing tree could potentially be improved. Thus, a prediction model V2 that includes three tree characteristics—namely diameter at breast height, tree height, and crown area—was established, which had the following form (Eq. 11):

$$\text{Ln}(V2) = \alpha_1 + \alpha_2 \cdot \text{Ln}(D^2H) + \alpha_3 \cdot \text{Ln}(CA) \quad (\text{Eq.11})$$

where α_1, α_2 , and α_3 are the model parameters, respectively, for the characteristics: D , diameter at breast height (cm); H , tree height (m); and CA , crown area (m²).

Model construction for dry rubber yield prediction

Under a scenario of reasonable growth management, the theoretical rubber yield is mainly affected by its own strain, while the actual yield is also jointly influenced by environmental factors including the climatic variables and disasters hazards (Zhang et al., 2017; Gouvea et al., 2013; Slipi et al., 2006). During the plantation of rubber trees in Hainan, the first 10 years are usually the non-economic production period, whereas the update and elimination are carried out when the stand age is over 35 years. Therefore, a subsection regression prediction equation was established to forecast the rubber yield of single plant in the economic production period. In this research, the yield model Y_{dr1} including the relative stem volume increment and climatic variables, Y_{dr2} including the climatic variables and disasters hazards, and Y_{dr3} including the relative stem volume increment, and both climatic and disaster factors, were established and compared and analyzed (Eqs. 12-14):

$$Y_{dr1} = \begin{cases} 0 & n \leq 10 \\ \beta_1 + \beta_2 \left(\frac{V_n - V_{n-1}}{V_{n-1}} \right) + \beta_3 T + \beta_4 K_I + \beta_5 P + \beta_6 R_I & 10 < n \leq 35 \\ 0 & 35 < n \end{cases} \quad (\text{Eq.12})$$

$$Y_{dr2} = \begin{cases} 0 & n \leq 10 \\ \beta_1 + \beta_2 T + \beta_3 K_I + \beta_4 P + \beta_5 R_I + \beta_6 D_I & 10 < n \leq 35 \\ 0 & 35 < n \end{cases} \quad (\text{Eq.13})$$

$$Y_{dr3} = \begin{cases} 0 & n \leq 10 \\ \beta_1 + \beta_2 \left(\frac{V_n - V_{n-1}}{V_{n-1}} \right) + \beta_3 T + \beta_4 K_I + \beta_5 P + \beta_6 R_I + \beta_7 D_I & 10 < n \leq 35 \\ 0 & 35 < n \end{cases} \quad (\text{Eq.14})$$

where $\beta_1, \beta_2, \beta_3, \beta_4, \beta_5, \beta_6,$ and β_7 are the model parameters, respectively. n is tree age.

Model testing

Using a separate validation dataset, the prediction precision ability of tree height, crown area, stem volume, and yield model were tested. Differences among the simulations in their precision were compared and analyzed by comparing precision differences of the yield models differing in their predictors between the conventional stem volume model and our newly proposed model. The simulation precision of all model variants was assessed by calculating the mean absolute error (MAE), the root-mean-square error (RMSE), and the determination coefficient (R^2) between the observed and simulated (predicted) values (Yu et al., 2014; Zhang et al., 2014).

$$\text{RMSE} = \sqrt{\frac{1}{N} \sum_{t=1}^N (d_{\text{observe}} - d_{\text{predict}})^2} \quad (\text{Eq.15})$$

$$\text{MAE} = \frac{1}{N} \sum_{t=1}^N |d_{\text{observe}} - d_{\text{predict}}| \quad (\text{Eq.16})$$

In *Equations 15-16*: d_{observe} and d_{predict} represent the empirically measured value and predicted value from the model simulations, respectively.

In this study, the statistical analysis of the data was done by programming in MATLAB2016, and the model fitting was done via equation parameter fitting in the software Origin v9.0.

Results

Model fitting

Model fitting for tree height and crown area

Using the sampled data of rubber tree from 2014–2015 (*Table 1*), the relationship of diameter at breast height (D) against tree height and crown was analyzed. Fitted curves were drawn as shown in *Figure 2*. Evidently these were non-linear correlations. There is an exponential relationship between the tree height as a function of diameter at breast height, as well as the crown and tree height (Bi et al., 2012; Zeng et al., 1999).

By the model fitting the data in *Table 1*, the fitting equations of tree height and crown with the diameter at breast height and tree height as variables were established, respectively, with the fitting results of the equation parameters given in *Table 2*. All parameters in the equations passed the significance threshold of $p < 0.001$. Based on the fitting results of the tree height and crown area models, we obtained corresponding R^2 , RMSE values that were 0.99, 0.84 m and 0.98, 0.77 m², respectively (as shown in *Fig. 3*).

Table 1. Summary of individual-tree and stand-level characteristics for rubber trees

Variable	Model fitting data (2014-2015)				Validation data (2016-2017)			
	Mean	SD	Min	Max	Mean	SD	Min	Max
A (year)	32.3	9.73	14	51	33	10.82	10	51
D (cm)	20.97	6.99	10.50	37.28	22.3	5.9	11.74	33.08
H (m)	14.1	7.06	3.2	25.3	16.2	6.67	3.5	24.7
CW (m)	4.5	1.23	2.2	6.1	4.9	1.09	2.2	5.8
CA (m ²)	14.7	7.55	3.8	23.2	15.8	6.12	3.7	20.9
V (m ³)	0.35	0.35	0.01	1.32	0.38	0.30	0.02	1.02

A – tree age; D – diameter at the height of 1.3 m; H – tree height; CW – crown width; CA – crown area; V – stem volume of rubber trees

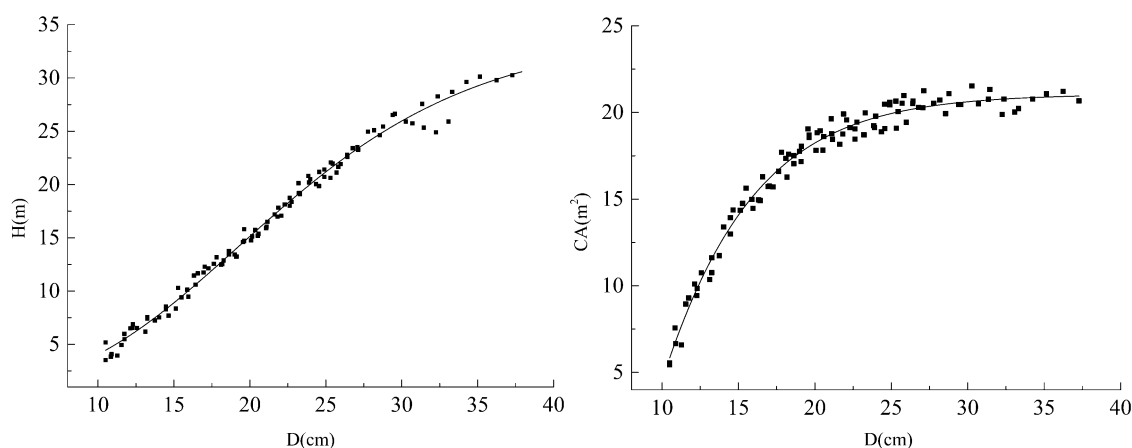


Figure 2. Fitting non-linear relationships between the diameter at breast height (D) against tree height (H) and crown area (CA)

Model fitting for stem volume of single standing tree

The correlations between the stem volume of single standing tree and its diameter at breast height, tree height, and crown area, were all clearly positive. A general model(V1) based on tree height and DBH is used to calculate the stem volume of standing tree (*Eq. 10*) (Gonzalez-Benecke et al., 2012, 2013, 2014; Zhou et al., 1995). In this research, the existing model has been improved, in that another remarkable factor in the stem volume response was added: crown area. According to *Table 1*, the binary stem volume model (*Eq. 10*) and the improved model equation of stem volume (*Eq. 11*) were established, and the fitting results of their equation parameters are shown in *Table 2*. These all passed the significance threshold of $p < 0.001$. By comparing the

binary fitting equation of stem volume (V1) to the improved fitting equation (V2), it can be seen that the fitting precision of two equations to the stem volume were both high: When compared with the binary volume model V1, for the improved model V2 added the crown area, RMSE decreases 0.0045, and reaches 0.0116 m³. Meanwhile, R² increases 0.0434, and is 0.9975. Hence, the model precision has been improved significantly (as shown in Fig. 3). Therefore, V2 was selected as the volume calculation model.

Table 2. Model parameters and precision statistics

Model	Parameter	Parameter estimate	Standard Error	R ²	RMSE
RH (m)	λ_1	34.6708	2.3361	0.9911	0.8424
	λ_2	0.1432	0.0032		
	λ_3	0.1071	0.0018		
	λ_4	18.7575	1.2257		
	λ_5	1.1432	0.2316		
CA (m ²)	γ_1	21.0405	2.0134	0.9832	0.7710
	γ_2	8.4217	1.1519		
	γ_3	1.0612	0.3513		
	γ_4	0.1672	0.0039		
V1 (m ³)	α_1	-10.0614	0.2030	0.9541	0.0161
	α_2	1.0352	0.0232		
V2 (m ³)	α_1	-9.9143	2.3016	0.9975	0.0116
	α_2	1.0125	0.0131		
	α_3	0.1739	0.0494		
Ydr1 (kg/plant)	β_1	-1.6276	1.6655	0.7439	0.1525
	β_2	19.7356**	3.2119		
	β_3	0.1319**	0.0729		
	β_4	0.0279**	0.1699		
	β_5	-0.0112*	0.0139		
	β_6	0.0588*	0.0328		
Ydr2 (kg/plant)	β_1	-3.0087*	1.0936	0.8397	0.1065
	β_2	0.2315**	0.0466		
	β_3	0.0244**	0.1181		
	β_4	-0.0110*	0.0095		
	β_5	0.0571**	0.0239		
	β_6	-0.3826**	0.0363		
Ydr3 (kg/plant)	β_1	-0.7201	0.4418	0.9862	0.0354
	β_2	13.2997**	0.8665		
	β_3	0.1150**	0.0184		
	β_4	0.0123**	0.0417		
	β_5	-0.0092*	0.0079		
	β_6	0.0571*	0.02152		
	β_7	-0.2975**	0.0136		

*Indicates the factor is significantly correlated with the yield ($p < 0.05$). **Indicates a significant correlation between the factor and yield ($p < 0.01$)

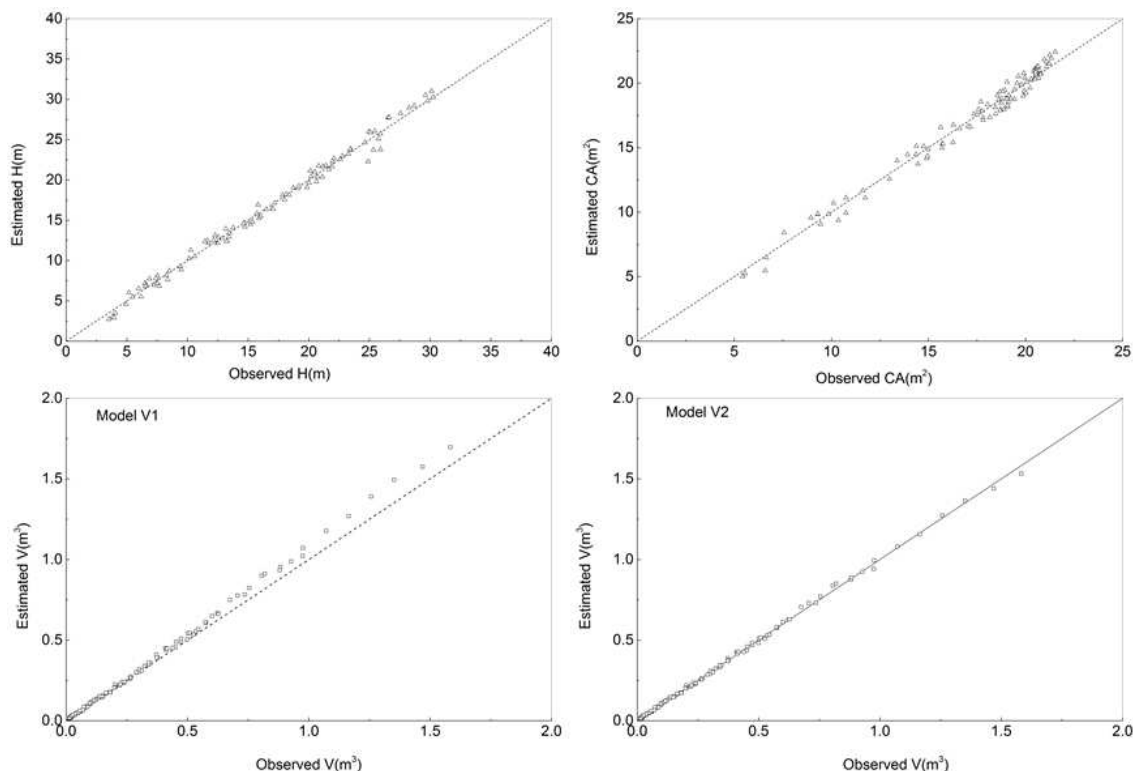


Figure 3. Comparison analysis of the estimated and observed values of tree height (H), crown area (CA), and stem volume (V)

Model fitting for yield of a single plant

By parsing the data of annual ring widths and using the stem volume equation (from the sampling farms of Dongchang and Xiqing), the annual stem volume produced is obtained, and the relative stem volume increment may be calculated. Based on the historical meteorological data of the sampling sites, we calculated the heat, precipitation, sunshine, and disaster indexes. Moreover, the annual average temperature was summarized. From the correlation analysis using the yield of a single plant in the sampling section, it can be seen that the precipitation index ($p < 0.05$) and disaster index ($p < 0.01$) are negatively correlated with the yield, while the sunshine index ($p < 0.05$) and other factors ($p < 0.01$) are all positively correlated with the yield.

Using the data from Dongchang Farm of Haikou City and Xiqing Farm in Danzhou City, fitting of the models of rubber tree yield Y_{dr1} , Y_{dr2} , and Y_{dr3} with the relative stem volume increment, annual average temperature, precipitation index, sunshine index and disaster index as the variables were performed, respectively. Through the follow-up comparison and analysis, the mode Y_{dr1} with relative stem volume increment, annual average temperature, heat index, precipitation index, and sunshine index as the predictor variables showed the lowest precision, having an RMSE and R^2 of 0.1525 and 0.7439, respectively. However, the rubber tree yield models Y_{dr2} and Y_{dr1} with annual average temperature, heat index, precipitation index, sunshine index, and disaster index as predictors showed increased RMSE and R^2 values, reaching 0.1065 and 0.8397, respectively. Nevertheless, it was the fitting of the model of rubber tree yield Y_{dr3} with the relative stem volume increment, annual average temperature, heat index, precipitation index, sunshine index, and disaster index as the predictors, which gave the

highest precision. Compared with Y_{dr1} , Y_{dr2} , the corresponding RMSE and R^2 values of Y_{dr3} were 76.8%, 32.6% and 0.9862, 0.0354, respectively (as shown in Fig. 4). Therefore, when trying to forecast the rubber plantation yield, the stem volume increasing as determined by the varietal characteristics is not the only condition affecting the yield. As demonstrated in these results, the climatic variables and disasters hazards are also significant factors that play a role in this prediction of rubber yield. Y_{dr3} was selected as the yield prediction model in this study.

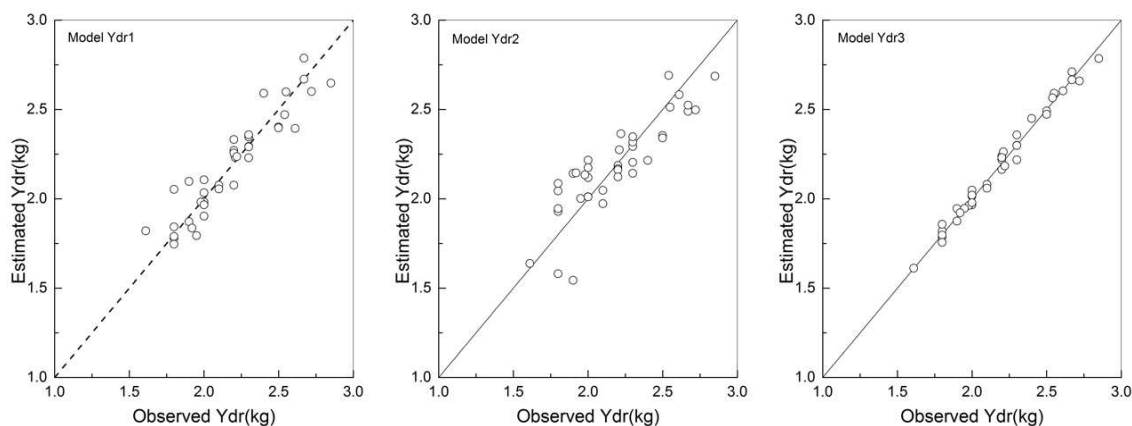


Figure 4. Comparison analysis of the estimated and observed values of dry rubber yield of a single rubber tree

Model validation

Validation of tree height and crown area

Based on model *RA* and *RH*, the sampled data from 2016–2017 (Table 1) in plot3 were used to calculate the tree height and crown area. The model settlement results were compared with the measured data of tree height and crown area for model verification. The results are shown in Table 3 and Figure 5. According to the error analysis of the observed and predicted values, these two models can be used to simulate tree height and canopy area.

Table 3. MAE and RMSE of the observed vs. predicted values verified by the independent data

	H (m)	CA (m ²)	V (m ³)	Ydr (kg/plant)
MAE	0.5045	0.4750	0.0150	0.0279
RMSE	0.5680	0.5464	0.0157	0.0528

Validation of stem volume

Based on model *V2*, the sampled data from 2016–2017 (Table 1) in plot3 were used to calculate the stem volume. The model settlement results were compared with the measured data of stem volume for model verification. The results are shown in Table 3 and Figure 5. According to the error analysis of the observed and predicted values, this model can be used to simulate stem volume.

Validation of dry rubber yield of a single tree

Based on model *Ydr3*, the sampled data and meteorological statistical data from 2016–2017 (Table 1) in plot3 were used to calculate the dry rubber yield of a single tree. The model settlement results were compared with the measured data of dry rubber yield. The results are shown in Table 3 and Figure 5. According to the error analysis of the observed and predicted values, this model can be used to simulate dry rubber yield of a single tree.

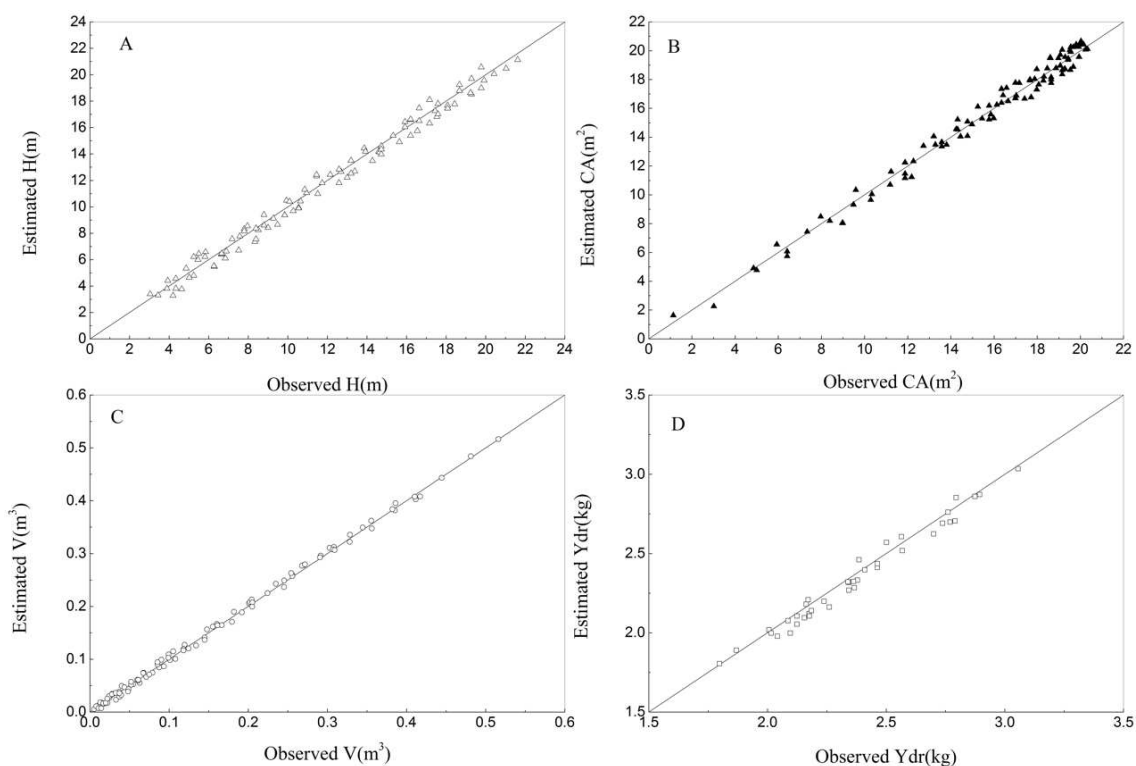


Figure 5. Comparison analysis of the estimated vs. observed values of the rubber tree height (A), crown area (B), stem volume (C), and yield (D)

Validation of sub-compartmental dry rubber yield

The stand-level plantation data (i.e., average diameter, density, and area of woodland) sampled randomly in six different stand sub-compartments (the variety is RRIM600) of Xinzhong Farm (refer to Fig. 1), and the rubber yield data in the sub-compartment during 2016-2017 (as shown in Table 4) were used to verify the application of model *Ydr3* in actual production. Based on the meteorological observation data, we calculated the heat, precipitation, sunshine, and disaster indexes. Using the established stem volume model *V2* and yield model *Ydr3*, the yield of rubber plantation in 2017 is estimated, and the results are shown in Table 4. This yield simulation shows that the average absolute error of the model in different sub-compartments is 35.7 kg/ha. When the accurate yield estimation is done on a large-scale the precision is high; hence, it can be applied to rubber production on an industrial scale.

Table 4. Forest stand, yield, and simulated yield of different sub-compartments in 2017

Woodland	Average diameter (cm)		Density (plants/ha)	Area (ha)	Observed yield (kg)	Simulate yield (kg)	MAE (kg/ha)
	2016	2017					
A	18.2	19.4	423	6.8	9015.0	8922.7	34.2
B	26.3	27.2	398	4.3	4706.4	4753.6	38.9
C	19.5	20.2	411	3.4	3675.2	3701.3	31.2
D	17.4	18.8	458	1.3	1711.7	1696.2	35.0
E	25.2	26.2	401	1.5	1870.7	1856.1	41.0
F	15.6	16.7	436	1.9	2144.9	2169.5	34.0

The average diameter is the mean value of 30 randomly trees in each sub-compartment, and the yield is the actual yield in the sub-compartment; the simulated yield is the product of the yield of single plant and the total number of rubber trees which can be tapped

Discussion

The general stem volume model of rubber trees is mainly based on DBH and tree height (Gonzalez-Benecke et al., 2012, 2013, 2014; Zhou et al., 1995). Previous studies have shown that the crown growth of trees is closely related to stem volume, which generally increases with the decrease of crown length (Liu et al., 2002). Therefore, this study improved the existing model by adding another important response factor of stem volume, canopy area, and significantly improved the model accuracy (see Fig. 3).

In this study, when establishing the prediction model of rubber yield per plant, we consider the actual growth of rubber trees and combine it with the actual production, and finally established the prediction model of yield at different stages. Although the volume of rubber tree will increase in seedling stage, it is not cut during production, so the yield is not considered. From the beginning to the flourishing stage is the main economic production period of rubber trees, and the yield fluctuates under the influence of volume increase, climatic factors and disasters. The economic value of the rubber tree in the aging period, will be greatly reduced, so the yield is not taken into account. Therefore, the establishment of a piecewise prediction model for the yield of rubber trees in the main economic production period is more practical than a single prediction model for the whole growth period, which can improve the prediction accuracy of the model.

Previous studies have found that the diameter of rubber trees, the laticifer differentiation capability and the yield of rubber trees are significantly correlated (Chen, 2014; Liu et al., 2002). In our study, the variation and trends analysis in the cumulative growth and annual growth in the stem volume of rubber tree show that (Fig. 6): the volume of rubber trees increased rapidly from seedling stage to sapling stage (1-10 years), and from primary stage to flourishing stage (11-35 years), and decreased significantly from aging stage (35 years), which was consistent with previous studies (Gonzalez-Benecke et al., 2012, 2013; Gouvea et al., 2013; Ohashi et al., 2001; Xu et al., 2002; Luo et al., 2015). The main explanation for this result is that stem volume increment reflects the increase of nutrients and resource capture by the tree's canopy area and the enhancement of the laticifer differentiation capability in the bark, which thus promotes the synthesis of photosynthate and the generation of latex. In the senescence stage, when the stem volume increment is reduced significantly, the diameter at breast height only increases slowly. This is mainly due to the gradual aging

of secondary phloem system and a gradual decrease in the laticifer differentiation capability, thus resulting in a yield reduction. Therefore, the yield prediction model with the annual volume increment of rubber tree as a variable has higher precision than the prediction equation with only meteorological elements as a variable.

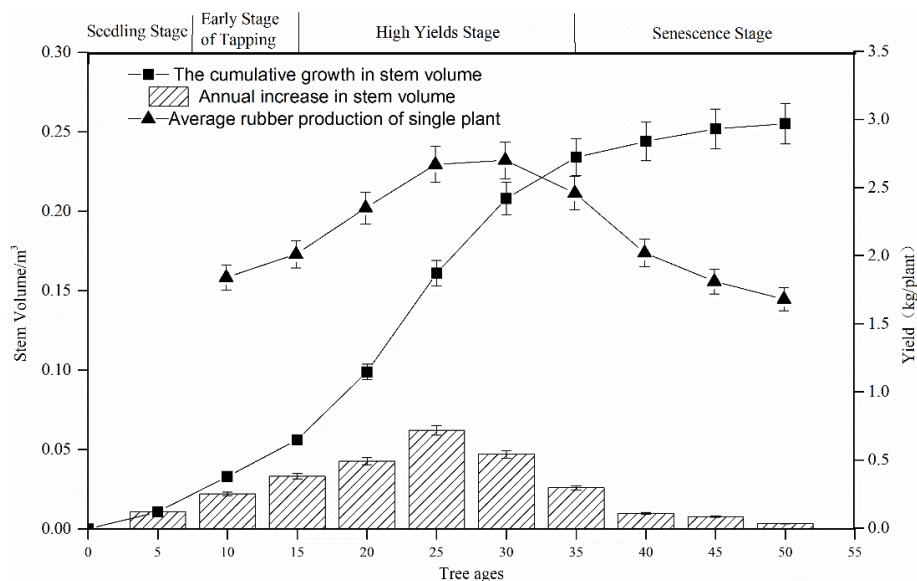


Figure 6. Cumulative growth and annual growth means for the stem volume of rubber tree

Under the condition of standardized and consistent management mode, the annual variation in the trends of the stem volume and yield of rubber tree are mainly determined by tree age and variety, while the differences in the interannual fluctuations is affected by the environmental factors among others, with the climatic variables and meteorological disaster hazard being the main factors influencing the yield of rubber trees. Published research has shown that climate variables, such as the temperature, precipitation, and sunshine, are all closely related to the photosynthesis rate in rubber trees (Roberts, 1988; Devakumar et al., 1998; Satheesan et al., 1984; Rao et al., 1990; Carr, 2012; Zhao et al., 2014), their respiration and transpiration (Zhao et al., 2014), and their synthesis of latex (Lacote et al., 1998; Zomer et al., 2014; Golbon et al., 2015). Therefore, in previous studies, meteorological factors such as temperature, precipitation, humidity and sunshine were often used as variables to establish yield prediction models (Yu et al., 2014; Zhang et al., 2014, 2017; Golbon, 2015; Nguyen and Dang, 2016; Kim et al., 2017). In our study, the heat indexes of effective accumulative temperature over 10 °C (after the tapping from December to March in the next year) and 18 °C (from April to November) had significant correlations with the dry rubber yield. The heat index can better reflect the demand for heat in the actual growth of rubber trees than the heat factor that only considers the daily average temperature, average maximum temperature and average minimum temperature (Yu et al., 2014; Nguyen and Dang, 2016). The precipitation index, which included not only the rainy days but also the minimum annual precipitation suitable for the growth of rubber, had a significant negative correlation with the yield. Compared with the previous prediction model of rubber tree yield only considering precipitation, the precipitation index eliminated the effect of cumulative precipitation caused by the increase in rainy days. In a region with

enough precipitation to meet the regular growth requirement, clearly moisture was not the limiting factor to a change in yield. The rainy days had more obvious effects on the yield (Rao, et al., 1990; Carr, et al., 2012; Zhao, et al., 2014). The disaster index reflected the combined effects of typhoon and chilling damage on the rubber yield. It was significantly positively correlated with the yield, thus suggesting it was also an important factor for the yield prediction. Until now, this important factor was always ignored in prior research publications. In our study, based on the previous prediction model simulating the rubber yield but only considering the climatic variables (average temperature, average maximum temperature, average relative humidity, sunshine duration, and precipitation) (Yu et al., 2014; Zhang et al., 2014, 2017; Golbon, 2015; Nguyen and Dang, 2016; Kim et al., 2017), the collective climate impact was corrected via inclusion of a heat index, precipitation index, and sunshine index. Meanwhile, the relative stem volume increment and disaster index were introduced as predictors to establish a novel model for rubber yield prediction. Compared to the prediction model that uses just a single influencing factor, the precision of our new model was elevated significantly. By applying this yield prediction in the sub-compartment of a rubber plantation, the results revealed that the newly established model was suitable for accurate yield estimation in the study region. As such, it could also provide technical support for the yield forecast or yield loss estimation of different forest sections in the production of rubber over time.

In rubber tree plantations, the stem volume and yield are often impacted by geographical conditions, such as altitude, slope aspect, and slope gradient, albeit to varying extent among sites (Liu et al., 2015; Nguyen, 2013). In our prediction model, these considerations were not further studied, since we sampled a single source. Nonetheless, the stand density did show a certain correlation with the rubber yield: as the stand density increased, the yield of single plant decreased. In our study, the effect of stand density on stand-levels yields was not considered (Naji et al., 2014; Rodrigo and Stirling, 1997). Additionally, the forecasting model for dry rubber in this paper was based on the species variety RRIM600 that was planted in Hainan Province. Hence, the applicability and adaptability of our forecasting to other Chinese regions and cultivated rubber tree varieties requires testing and verification.

Conclusion

In this study, a simulation model for the stem volume of standing rubber trees on the basis of tree diameter at breast height, tree height and, tree crown area was developed. Based on this result, the relative stem volume increment, annual average temperature, heat index, precipitation index, sunshine index, and disaster index were the main factors considered in a forecasting model for the dry rubber yield of single plant. In applying the prediction model to the yield prediction in the different sub-compartments of a rubber plantation, the mean absolute error was 35.7 kg/ha. This study's the newly established model could thus provide management with decision support for the dry rubber yield prediction of rubber plantation over large areas.

In the future, the morphological, yield, and meteorological features of rubber tree plantations could be sampled in the main rubber growing regions of China, which would enable a more suitable prediction model to be established. We plan to couple the model with satellite remote sensing technology for rubber plantations of different ages, so that research on the large-scale rubber yield prediction will be advanced.

Acknowledgements. The study was jointly funded by the NSFC (National Natural Science Foundation of China, Grant no. 41675113; 41765007; 41465005).

REFERENCES

- [1] Bi, H., Fox, J. C., Li, Y., Lei, Y., Pang, Y. (2012): Evaluation of nonlinear equations for predicting diameter from tree height. – *Canadian Journal of Forest Research* 42: 1-18.
- [2] Carr, M. K. V. (2012): The water relations of rubber (*Hevea brasiliensis*): a review. – *Experimental Agriculture* 48(2): 176-193.
- [3] Chen, B. Q., Cao, J. H., Wang, J. K., Wu, Z. X., Tao, Z. L., Chen, J. M., Yang, C., Xie, G. (2012): Estimation of rubber stand age in typhoon and chilling injury afflicted area with Landsat TM data: a case study in Hainan Island, China. – *Forest Ecology and Management* 274: 222-230.
- [4] Chen, Y. Y. (2014): Assessment of the Ability of Secondary Laticifer Differentiation and Efficiency of Rubber Biosynthesis in Relation to Rubber Yield of Rubber Tree. – Hainan University, Haikou.
- [5] Devakumar, A. S., Shayee, M. S., Udayakumar, M., Prasad, T. G. (1998): Effect of elevated CO₂ concentration on seedling growth rate and photosynthesis in *Hevea brasiliensis*. – *Journal of Biosciences* 23(1): 33-36.
- [6] Feng, F. F., Zhang, H. Y. (2016): Gray relevancy analysis and the stepwise regression analysis between latex yield and meteorological factors. – *Chinese Journal of Tropical Agriculture* 36: 57-60.
- [7] Golbon, R., Ogutu, J. O., Cotter, M., Sauerborn, J. (2015): Rubber yield prediction by meteorological conditions using mixed models and multi-model inference techniques. – *International Journal of Biometeorology* 59(12): 1747-1759.
- [8] Gonzalez-Benecke, C. A., Gezan, S. A., Leduc, D. J., Martin, T. A., Cropper, W. P., Samuelson, L. J. (2012): Modeling survival, yield, volume partitioning and their response to thinning for longleaf pine plantations. – *Forests* 3(4): 1104-1132.
- [9] Gonzalez-Benecke, C. A., Gezan, S. A., Martin, T. A., Cropper, W. P., Samuelson, L. J., Leduc, D. J. (2013): Individual tree diameter, height and volume functions for longleaf pine. – *Forest Science* 60(1): 43-56.
- [10] Gonzalez-Benecke, C. A., Gezan, S. A., Samuelson, L. J., Cropper, W. P., Leduc, D. J., Martin, T. A. (2014): Estimating *Pinus palustris* tree diameter and stem volume from tree height, crown area and stand-level parameters. – *Journal of Forestry Research* 25(1): 43-52.
- [11] Gouvêa, L. R. L., Silva, G. A. P., Verardi, C. K., Oliveira, A. L. B., de Souza Gonçalves, P. (2013): Simultaneous selection of rubber yield and girth growth in young rubber trees. – *Industrial Crops and Products* 50: 39-43.
- [12] Kim, O. S., Nugent, J. B., Yi, Z. F., Newell, J. P., Curtis, A. J. (2017): A mixed application of geographically weighted regression and unsupervised classification for analyzing latex yield variability in Yunnan, China. – *Forests* 8(5): 162.
- [13] Kokmila, K., Lee, W. K., Yoo, S., Byun, J. G., Lee, S. (2010): Selection of suitable areas for rubber tree (*Hevea brasiliensis*) plantation using GIS-data in Laos. – *Forest Science and Technology* 6(2): 55-66.
- [14] Lacote, R. C., D'Auzac, A., Gallois, J., Gohet, R., Joet, E., T Pujade Renaud, V. (1998): The biological mechanisms controlling *Hevea brasiliensis* rubber yield. – *Plant* 5: 5-17.
- [15] Liu, L. H., Chen, D. L., Zhen, H., Wang, Y., H., Yin, G. Y. (2002): The effect of the rate of crown length on the diameter and volume of a tree. – *Journal of Agricultural University of Hebei* 25(z): 149-150.
- [16] Liu, S. B., Lin, W. F. (2002): Correlation studies between tree growth, vessel structural characters and rubber yield in *Hevea brasiliensis*. – *Chinese Journal of Tropical Crops* 23(3): 7-11.

- [17] Liu, S. J., Zhang, J. H., Cai, D. X., Zhang, M. J., Tian, G. H., Zou, H. P. (2015): Risk regionalization of rubber plant yield loss in Hainan Island. – *Journal of Natural Disasters* 24(2): 235-241.
- [18] Luo, J. X., Lu, D., Qi, J. Q., Huang, X. Y., Li, F. (2015): Growth ring width and anatomical properties of *Toona sinensis* wood. – *Journal of Southwest Forestry University* 35(2): 95-99.
- [19] Naji, H. R., Bakar, E. S., Soltani, M., Ebadi, S. E., Abdul-Hamid, H., Javad, S. K. S., Sahri, M. H. (2014): Effect of initial planting density and tree features on growth, wood density, and anatomical properties from a *Hevea brasiliensis* trial plantation. – *Forest Products Journal* 64(1): 41-47.
- [20] Nguyen, B. T. (2013): Large-scale altitudinal gradient of natural rubber production in Vietnam. – *Industrial Crops and Products* 41: 31-40.
- [21] Nguyen, B. T., Dang, M. K. (2016): Temperature dependence of natural rubber productivity in the southeastern Vietnam. – *Industrial Crops and Products* 83: 24-30.
- [22] Ohashi, Y., Sahri, M. H., Yoshizawa, N., Itoh, T. (2001): Annual rhythm of xylem growth in rubberwood (*Hevea brasiliensis*) trees grown in Malaysia. – *Holzforschung* 55(2): 151-154.
- [23] Priyadarshan, P. M., Hoa, T. T. T., Huasun, H., De Gonçalves, P. (2005): Yielding potential of rubber (*Hevea brasiliensis*) in sub-optimal environments. – *Journal of Crop Improvement* 14(1-2): 221-247.
- [24] Rahman, M., Islam, M., Bräuning, A. (2017): Local and regional climatic signals recorded in tree-rings of *Chukrasia tabularis* in Bangladesh. – *Dendrochronologia* 45: 1-11.
- [25] Rao, G. G., Rao, P. S., Rajagopal, R., Devakumar, A. S., Vijayakumar, K. R., Sethuraj, M. R. (1990): Influence of soil, plant and meteorological factors on water relations and yield in *Hevea brasiliensis*. – *International Journal of Biometeorology* 34(3): 175-180.
- [26] Rao, P. S., Saraswathyamma, C. K., Sethuraj, M. R. (1998): Studies on the relationship between yield and meteorological parameters of para rubber tree (*Hevea brasiliensis*). – *Agricultural and Forest Meteorology* 90(3): 235-245.
- [27] Roberts, A. D. (1988): *Natural Rubber Science and Technology*. – Oxford University Press, New York.
- [28] Rodrigo, V. H. L., Stirling, C. M., Teklehaimanot, Z., Nugawela, A. (1997): The effect of planting density on growth and development of component crops in rubber/banana intercropping systems. – *Field Crops Research* 52(1): 95-108.
- [29] Roy, C. B., Newby, Z. J., Mathew, J., Guest, D. I. (2017): A climatic risk analysis of the threat posed by the South American leaf blight (SALB) pathogen *Microcyclus ulei* to major rubber producing countries. – *European Journal of Plant Pathology* 148(1): 129-138.
- [30] Satheesan, K. V., Rao, G. G., Sethuraj, M. R., Raghavendra, A. S. (1984): Canopy Photosynthesis in Rubber (*Hevea Brasiliensis*): Characteristics of Leaves in Relation to Light Interception. – In: Sybesma, C. (ed.) *Advances in Photosynthesis Research*. Springer Netherlands, pp. 125-128.
- [31] Silpi, U., Thaler, P., Kasemsap, P., Lacoite, A., Chantuma, A., Adam, B., Améglio, T. (2006): Effect of tapping activity on the dynamics of radial growth of *Hevea brasiliensis* trees. – *Tree Physiology* 26(12): 1579-1587.
- [32] Xu, C. G., Shi, L., Zhong, X. (2017): Analysis of natural rubber market in China in 2016. – *Chinese Journal of Tropical Agriculture* 36(12): 92-97.
- [33] Xu, Y. M., Jiang, Z. H., Ma, W., Yang, R. W. (2002): Variation of growth ring width and wood basic density of rubber tree and their modelling equations. – *Scientia Silvae Sinicae* 38(1): 95-102.
- [34] Yang, S. Q. (1989): The relationship between latex yield and several climatic factors. – *China. J. Agrometeorol.* 10: 42-44.

- [35] Yu, H., Hammond, J., Ling, S., Zhou, S., Mortimer, P. E., Xu, J. (2014): Greater diurnal temperature difference, an overlooked but important climatic driver of rubber yield. – *Industrial Crops and Products* 62(4): 14-21.
- [36] Yu, J. H. (2007): *Laticifer Differentiation in Adult Rubber Tree and Its Application to Rubber Yield Prediction*. – Hainan University, Haikou.
- [37] Zeng, Q. S., Luo, Q. B., He, D. B., Xiong, Z. P., Bao, T. H., Zhou, G. H. (1999): Establishment and application of relative tree height models for main tree species in Hainan. – *Central South Forest Inventory and Planning* 18(2): 1-7.
- [38] Zeng, W., S. (2011): *The Modeling Method for Single-Tree Biomass*. – China Forestry Press, Beijing.
- [39] Zhang, H. J., Hua, Y. F., Xu, Z. G., Zhang, L. H., Lan, Z. N., Huang, H. S. (2014): Correlation between latex yield from *Hevea brasiliensis* and meteorological factors. – *Chinese Journal of Tropical Agriculture* 34(3): 1-3.
- [40] Zhang, Y. Y., Wu, Z. X., Wang, X. J., Gao, X. S., Zhang, X. F., Wei, M. M., Huang, X., Li, W. G. (2017): Correlation between meteorological factors and early yield of different-clone rubber trees (*Hevea brasiliensis* Muell. Arg.) with various rubber production characteristics. – *Journal of Southern Agriculture* 48(8): 1427-1433.
- [41] Zhao, W., Zhang, Y. P., Song, Q. H., Zhang, X., Ji, H. L., Syed, M. N., Yu, L. (2014): Characteristics of transpiration of rubber trees (*Hevea brasiliensis*) and its relationship with environmental factors. – *Chinese Journal of Ecology* 33(7): 1803-1810.
- [42] Zhou, Z. Z., Zheng, H. S., Yin, G. T., Yang, Z. J., Chen, K. T. (1995): A volume table for *Hevea brasiliensis* in Leizhou Peninsula. – *Forest Research* 9(5): 486-491.
- [43] Zomer, R. J., Trabucco, A., Wang, M., Lang, R., Chen, H., Metzger, M. J., Xu, J. (2014): Environmental stratification to model climate change impacts on biodiversity and rubber production in Xishuangbanna, Yunnan, China. – *Biological Conservation* 170: 264-273.

REVIEW PAPER ON BEVERAGE AGRO- INDUSTRIAL WASTEWATER TREATMENT PLANT BIO-SLUDGE FOR FERTILIZER POTENTIAL IN ETHIOPIA

ENGIDA, T.^{1,2,3} – MEKONNEN, A.³ – WU, J. M.^{2*} – XU, D.² – WU, Z. B.^{2*}

¹*School of Resources and Environmental Engineering, Wuhan University of Technology, Wuhan, P.R. China
(e-mail: zewedenahomruhama@gmail.com)*

²*State Key Laboratory of Freshwater Ecology and Biotechnology, Institute of Hydrobiology, Chinese Academy of Sciences, Wuhan, P.R. China*

³*Department of Industrial Chemistry, Addis Ababa Science and Technology University, Addis Ababa, Ethiopia*

**Corresponding authors*

*e-mail: wuzb@ihb.ac.cn (Wu, Z. B.); wujunmei@ihb.ac.cn (Wu, J. M.)
phone: +86-027-6878-0020; fax: +86-027-6878-0675*

(Received 27th Mar 2019; accepted 19th Jun 2019)

Abstract. Agro-industrial sectors in Ethiopia are highly expanding sector and offers substantial challenges for the environment and public health. The brewery industries use large quantities of water for their production processes and at the end, they discharged large amount of effluents that contains a high strength organic waste. The main objective of this review paper is to discuss and summarize the characteristics, treatment techniques, fertilizer potential and other available management options of breweries sludge generated from wastewater treatment plants. Recent (2015) research finding indicated that the brewery sludge contains a very high nitrogen and potassium content, i.e., 420.25 kg ha⁻¹ and 840 kg ha⁻¹ respectively compared to the control. Scientific evidences indicated that brewery sludge amended soil they have the tendency to produce more yields (4081.6 kg ha⁻¹). Brewery sludge has also other beneficial advantages in production of biogas and building materials with co-digestion with other organic solid residues. The probable drawbacks of the use of sludge on agricultural land application is its pollutant loads including heavy metals, organic compounds and pathogens. Therefore, more research investigation has to be done on the possible sludge treatment mechanisms and the feasibility of sludge generated from brewery industries for agricultural recycling.

Keywords: *brewery sludge, nutrient, treatment plant, fertilizer and yield*

Introduction

Background information and justification

Rapid industrialization and urbanization in Ethiopia demanded huge increase in the extraction of resources and release of huge volume of wastes. Agro-industrial sectors in Ethiopia are a highly expanding sector and offers substantial challenges for the environment and public health (Tadese and Seyoum, 2015). Even if, the brewing sectors hold a planned economic position by increasing their production capacity (Fillaudeau et al., 2006). But, they also become one of the known industry by producing by-products such as effluent, spent grain, excess yeast and sludge from the wastewater treatment plant (Alemu et al., 2017). The brewery industry uses large quantities of water and lastly discharged large amount of effluents that contains a high strength organic wastes (Kanagachandran and Jayaratne, 2006).

Besides its advantage, at moderate and low temperatures, removal of Chemical oxygen demand (COD) by Up-flow Anaerobic Sludge Blanket (UASB) reactor is limited and long hydraulic retention time is needed to provide efficient hydrolysis. Therefore, anaerobic effluent requires post-treatment to remove the remaining Chemical oxygen demand (COD), nutrients and pathogens. Post-treatment of Up-flow Anaerobic Sludge Blanket (UASB) reactor effluent by aeration systems is one among the different techniques (Bodík, 2005). An aerobic treatment process oxidized organic substances to carbon dioxide, water, sulfate, phosphate and nitrate by different microbial communities dominated by heterotrophic bacteria and fungi. This aerobic process produces large volumes of sludge requiring further treatment and disposal (Stocks et al., 2002). According to Stocks et al. (2002) report, the UK breweries generates around 40-50 m³ of brewery sludge has been removed by tanker each weekday for application to local agricultural land. The 1991 reports also indicate that the beer Thai generates 100-120 m³/day of sludge as a waste (Babel et al., 2009).

There are different disposal methods of sludge such as landfilling, solidification, incineration, deep well injection and land application (Dolgen et al., 2004). Landfill is the common disposal method of brewery wastewater treatment plant sludge. Whereas, land application is an alternative option to avoid these high cost techniques, landfill cost and available of land space as well as public opposition on the offensive odor problems. Most research investigation shows that land application of agro-industrial wastewater treatment plant sludge for agricultural purposes can be recommended as an ultimate disposal alternative without any hazardous effect, since the presence of low heavy metal concentration and high organic carbon content are typical features of agro-industry sludge for soil conditioner. However, if it is not properly managed, potential risks to both environment and public health may occur from the accumulation of heavy metals (lead, cadmium, zinc and mercury), organic compounds, salts and pathogen contamination in soil and crops resulting such components entering in to the food chain (Dolgen et al., 2004; Babel et al., 2009; Olowu et al., 2012).

The application of sludge generated by industrial plants is limited due to fears of the accumulation of toxic matters in soils and plants. There are little scientific evidences in Ethiopia on the application of brewery wastewater sludge for increment of productivity of different crops through supplying nutrients and organic matter. Alemu et al. (2017) conducted a field trial in Daker, Harari regional state of eastern Ethiopia using different ratios of brewery sludge and commercial fertilizer to grow sorghum. Results demonstrated that 15 t ha⁻¹ of brewery wastewater sludge amended sorghum plots produce crop yields higher than that of commercial fertilizer. In line to this, Wendimagegn (2016) has also investigated similar results, i.e., addition of 2.5% BWS produced more number of tomato fruits (16.33) compared with addition of 200 mg of urea/kg of soil and control yields 13.0 and 7.67 tomato fruits respectively. However, these studies are not adequate enough to conclude on the feasibility of sludges generated from brewery industries for agricultural recycling. Brewery sludge is the easiest byproduct to handle but the most difficult due to its diverse in characteristics and variable composition that vary with the raw materials and product manufacturing process systems followed. Due to the increasing environmental issues and strict regulations, there should be further investigation on the feasibility, levels of application, economic benefits and assessing the environmental safety of brewery industrial wastewater treatment plant sludges to utilize it in an environmentally friendly approach (Erdem and Ok, 2002; Thomas and Rahman, 2006; Abushammala et al., 2009).

Review of literature

By amount, beer is the fifth highest consumed beverage in the world next to tea, carbonated drinks, milk, and coffee (Fillaudeau et al., 2006). The brewing steps for beer produce large volume of wastewater effluent and solid wastes that must be discarded without affecting in negative way the quality of water and soil. According to dos Santos Mathias et al. (2014), some of the solid waste that can come from the breweries are waste yeast, hot rub as well as the spent diatomite. This kind of wastes creates a residual sediment layer at the fermenter bottom. Every year in Ethiopia about 4 million hL of beer is usually produced. Since all Ethiopian breweries used diatomite for clarification used in the total amount of BWS produced each year is estimated to be about 69,000 metric tons (dos Santos Mathias et al., 2014).

Beverage and its wastewater treatment systems

Beer production process

Beer is a fermented beverage which has low alcohol content and made from barley, wheat, maize and other grains. The beer production steps include grinding of the malt to grist, mixing of grist with water to produce mash in the mash tun, wort production, separation of grist residues from liquid wort, boiling of wort with hops, separation of the wort from the trub/hot break, addition of yeast to cooled wort, fermentation, separation of spent yeast by filtration, centrifugation or settling and bottling or kegging (Ramya et al., 2015). In line to this production, wastewater management and waste disposal becomes a major cost factor and an important factor in the running of a brewery operation. Every brewery tries to keep waste disposal costs low whereas the legislation imposed for waste disposal by authorities becomes more stringent. Water consumption in a brewery is an economic parameter and a tool to determine its process performance in comparison with other breweries. Furthermore, the position of beer as a natural product leads the brewers to pay attention to their marketing image and to make waste treatment (wastewater, spent grain, Kieselguhr sludge, yeast surplus) into account as shown in *Figure 1* (Fillaudeau et al., 2006)

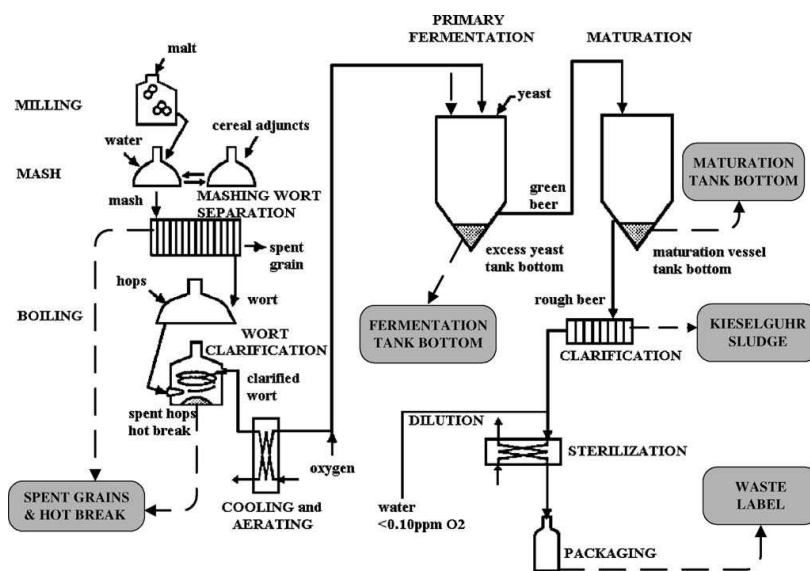


Figure 1. Brewing process and main wastes

Brewery wastewater treatment processes

Biological wastewater treatment works on the principle of activity of bacteria and microorganisms living in their own organic matter can occur in the presence of oxygen, called aerobic process and in the absence of oxygen called anaerobic process. Most commonly used treatment system of agro-industrial wastewater is summarized in *Figure 2* (Berni et al., 2014). Whatever the process or process combination is suitable for wastewater treatment methods are generally the following: Mechanical pre-treatment with removal of large particles using rakes, sieves, grit chambers and preliminary sedimentation; Chemical-physical pre-treatment using neutralization and metering of chemicals; and Biological wastewater treatment such as Anaerobic pre-treatment, Anaerobic-aerobic treatment and Aerobic treatment (Bodík, 2005; Asia et al., 2008). Anaerobic and aerobic biological treatment are widely applied. Previously, aerobic treatment has been applied for the treatment of brewery wastewater. However, recently anaerobic systems have become more attractive option. Because, the aerobic treatment of brewery effluent requires a comparatively large energy input compared to anaerobic treatment. During aerobic process, complex organic substances are completely oxidized to carbon dioxide, water, sulfate, phosphate and nitrate by a community of microorganisms dominated by heterotrophic bacteria and fungi. This produces large amounts of biomass (Kanagachandran and Jayaratne, 2006).

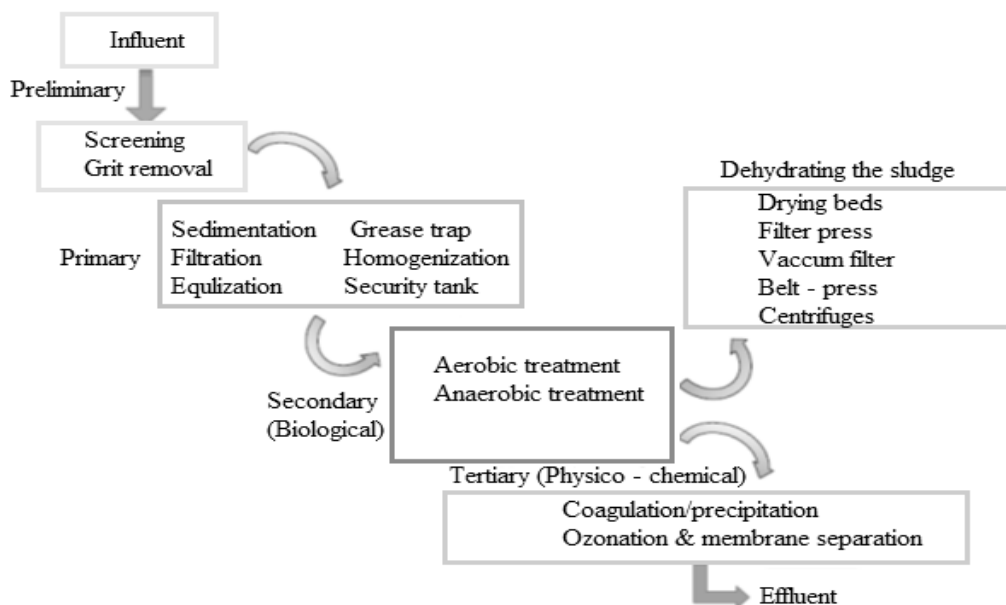


Figure 2. Scheme of agro-industrial wastewater treatment process

Brewery biomass (sludge) produced by aerobic, anaerobic, physicochemical, combined aerobic/physicochemical and combined anaerobic/physicochemical methods. Physicochemical method increases the quantity of sludge solids, thus making the sludge suitable for land reclamation. Whereas biological treatment methods (aerobic and anaerobic) can reduce the quantity of sludge before disposal. Processing and disposal of sludge is economic and environmentally friendly manner is currently of great importance to local authorities and industry. The disposal or reuse of sludge is a significant part of wastewater treatment program (Asia et al., 2008).

Sources of sludge

Bio-solids/sludge's are nutrient rich organic matter solid residues generated from wastewater treatment plant (Sampson, 2016). Sludge is most commonly produced from secondary wastewater treatment plants. However, half of the solids suspended in wastewater are removed through primary treatment. The residual material from this process is a concentrated suspension called primary sludge, which will undergo further treatment to become bio-solids. Preliminary wastewater treatment (extracts of coarse solids by screening and other filtering devices) and tertiary (mainly chemical addition to clean the final effluent are called chemical sludge) wastewater treatment processes are also produce solid byproducts which are not incorporated in sludge or bio-solids (Şengün, 2007).

Characteristics of sludge

Environmental concerns regarding to land disposal of sludge causes surface-water and ground water pollution, contamination of soil and crops with toxic substances and transmission of human and animal diseases. Chemical analysis of a sludge shows that sludge consists of nitrates, ammonium and organic nitrogen, soluble and organic phosphate, potassium, heavy metals of cadmium, copper, nickel, lead and zinc, and selected organic compounds such as polychlorinated biphenyls (PCB) (Wendimagegn, 2016). Other chemical analysis on brewery sludge also revealed that it has high nitrogen, phosphorus, potassium, volatile fatty acids and nutrients which are important requirements for plant growth. Brewery sludge is also consisting of various important organisms like heterotrophic fungi and actinomycetes (Ramya et al., 2015).

In the present scenario, there is an increasing interest of recycling sludge's for agricultural application due to their valuable components such organic matter, nitrogen, phosphorus and other plant nutrients. However, the chemical properties of the sludge may be affected by the treatment process applied to wastewater and sludge (i.e., extent of industrial pretreatment, primary, secondary or tertiary wastewater treatment and chemicals used in the treatment, and method of sludge stabilization) and the original pollution load of the wastewater (Şengün, 2007).

Characterization of sludge is extremely important prior to sludge disposal or application to farm land because of associated risks of toxic elements accumulation in soil and potential health hazard of pathogens. The sludge physicochemical and biological content depend on the original pollution load of the treated water, treatment process applied to wastewater and sludge (Usman et al., 2012). The physicochemical and biological composition of brewery wastewater sludge is presented in *Table 1*.

In sludge content of heavy metals

The results of the BWS selected heavy metals indicates that the sludge can be used in farming since they are well below the EU standards as shown in *Table 2*. Trace elements of heavy metals are toxic in the living organisms even if they are not in large amounts under the natural systems. With the existence of the soil-plant system that helps in the reducing of the toxicity of the trace elements, there is negligible issues of health in humans as well as animals. Nonetheless, if the amounts are high and the concentrations of these heavy metals are high, there could be some problems such as toxicity of the soil and harmful effects to humans and animals. Cadmium, selenium, mercury, nickel, zinc and copper are come the metals that gives a huge anxiety when it

comes to bio-solids. These trace elements are indispensable nutrients in the health of animals and plants and have less risks in small amounts due to their low solubility a sound aerated soil at 6.0 to 7.5 PH (Şengün, 2007).

Table 1. Physicochemical and biological characteristics of brewer wastewater sludge

Parameters	Babel et al. (2009)	Alemu et al. (2017)	(Ediget, 2016)	Kanagchandra and Jayarante (2006)	Erdem and Sozudogu (2002)	Olowu et al. (2012)	South Africa pollutant limits (class B)
pH	8.4	8.67	7.08	6.97	6.89	7.14	-
TS (%)	12.5	-	29.63	-	-	-	-
TN (%)	5.98	1.33	4.2	4.5	3.10	-	-
TP (%)	5.48	0.004	2.52	3.3	-	-	-
TK (%)	0.92	-	106.4	0.2	-	-	-
OC (%)	269	3.5	31.12	27.1	42.5	-	-
CEC (meq/100g)	-	-	-	-	47.4	-	-
Cd (mg/kg)	28	1.27	0.04	Not detected	-	1.23	85
Cr (mg/kg)	16	47	34.09	-	-	37.08	3000
Cu (mg/kg)	75	40	21.04	42	-	90.6	4300
Pb (mg/kg)	336	-	0.62	2.9	-	28.35	840
Ni (mg/kg)	7	31.33	13.93	17	-	-	420
Zn (mg/kg)	691	38.5	35.17	75	-	-	7500
Hg (mg/kg)	0.3	-	0.22	Not detected	-	-	55
Fe (mg/kg)	-	20.5	9642.14	-	-	-	Not set
Mn (mg/kg)	-	0.83	37.82	46	-	-	No set
Co (mg/kg)	-	33	0.77	-	-	7.10	No set
Se (mg/kg)	-	12.56	-	-	-	-	15
Mo (mg/kg)	-	0.45	-	-	-	-	12
Na (mg/kg)	-	-	101.08	-	-	-	-
Ca (mg/kg)	-	-	40.0	-	-	-	-
Mg (mg/kg)	-	-	11.34	1106	-	-	-
Pathogens (fecal coliforms), PN/g	5.6×10^2	-	5 cfu	-	-	-	< 10 ² MPN/g, EPA, class A standards

Table 2. Analysis result of heavy metal in BWS

Parameters	Lead, Pb (mg/kg)	Cadmium, Cd (mg/kg)	Mercury, Hg (mg/kg)	Nickel, Ni (mg/kg)	Chromium, Cr (mg/kg)	Cobalt, Co (mg/kg)
BWS	0.62_0.01	0.04_0.01	0.22_0.01	13.93_0.00	34.09_0.00	0.77_0.02

Brewery sludge nutrient content

In Table 3, the sludge of the brewery was seen to be virtually neutral. The normal range of the brewery sludge PH is between 6.5 and 11.5 (Luque et al., 1990). Various disparities in the treatment of the wastewater in the plants and the raw water attributes to the differences in the PH observed. The Organic carbon of the control soil was 1.5% while that of the sludge was 31.12% showing a great improvement. The BWS Soil parameters on the other hand attributes to the high-water holding capacity. Greater potential of cation exchange capacity, more organic matter, and other nutrients. has investigated that BWS amendments enhanced pH of acidic soils and improved the organic carbon, exchangeable cations, soluble cations and anions (Luque et al., 1990)

Table 3. Brewery sludge plant nutrient parameter results

Parameters	PH	Manganese mg/kg	Copper mg/kg	Magnesium mg/kg	Potassium mg/kg	Organic carbon %	Sodium mg/kg	Total P (as P ₂) %	Zinc	Total nitrogen %	Iron mg/kg	Volatile matter %	Calcium mg/kg	Total solid %
BWS	7.08± 0.06	37.82± 0.04	21.04± 0.04	11.34± 0.30	106.40± 1.41	31.12± 10.27	101.08± 0.25	2.52± 0.28	35.17± 0.01	4.20± 0.21	9642.14± 2.91	54.23± 0.96	40.00± 0.57	29.63± 0.68
Soil	7.15± 0.02	-	0.45± 0.01	12.72± 0.37	66.44± 0.37	1.56± 0.06	19.20± 00.28	0.56± 0.03	1.25± 00.00	1.96± 0.03	25.05± 0.22	-	33.13± 0.03	-

Sludge treatment methods

Sludge treatment techniques: Sludge must be processed for economic and hygienic reasons. Sludge processing reduces the volume, stabilize the sludge, remove water and kill pathogenic organisms. There are different sludge treatment techniques, such as thickening, conditioning, dewatering and stabilization. *Figure 3* shows that the possible sludge treatment processes, each treatment effect on the sludge and how that treatment techniques may affect the sludge application to land. Reducing sludge volume is an important thing which helps to limit its handling and transporting costs. There are series of constructive sludge treatment technologies possible to reduce sludge volume up to 2% of the initial volume. Mechanical and thermal dewatering increases the concentration of dry solids from 2% up to 90%, making the dried and stabilized sludge ready for easy storage and reuse as soil conditioner or fertilizer, depending on its composition. When sludge physicochemical composition does not allow for agricultural reuse, the best alternative option is sludge destruction by incineration. Since sludge contains energy which can be recovered either by digestion in anaerobic reactors to produce biogas or by incineration which generates heat and can be used as thermal energy for sludge drying process and transformed into steam for electricity production. Sludge treatment has generally the following advantages: Reduction of pathogens: Reduce the excess sludge mass and handling cost, improve rheological, mechanical and biological properties of the waste sludge, prevent fermentation and odor problems and Improve soil physical properties such as porosity, water retention and stability. (www.waterleav.com)

Thickening

Sludge generated from wastewater treatment plant contains lots of water and it has to be thickened to reduce the volume and make some of its water free. Thickening is the process of increasing solids content of sludge by the removal of a proportion of its liquid content. Gravity thickening is the simplest and least expensive process for thickening sludge (Garg and Tanyimboh, 2009). Sludge treatment systems are usually physical in nature. They include gravity settling, floatation, centrifugation, and gravity belts (Hänel, 1988).

Conditioning

This method involves modification of the sludge structure by removing more water from it. This method can improve thickening, and dewatering. Chemical method is one of the conditioning system which uses mineral agents like lime or salts or an organic

compound to remove the water content. Thermal method is another method in which sludge is heated to 150-200 °C for 30-60 min. It involves the chemical or physical treatment of sludge to enhance its dewatering characteristics. The most applied conditioning systems are the addition of chemicals and heat treatment. Other conditioning processes include freezing, irradiation and elutriation (Garg and Tanyimboh, 2009).

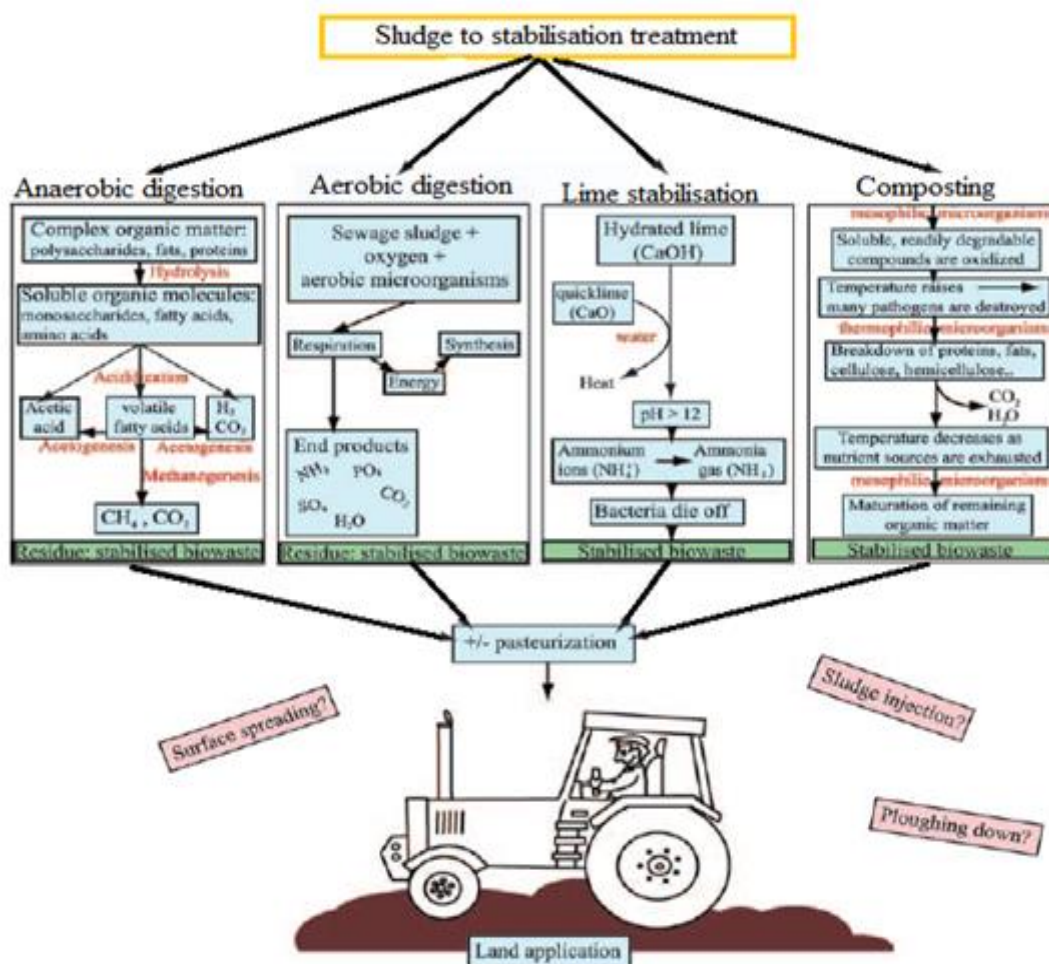


Figure 3. Flow chart of sludge treatment steps with the view to yield an end by product with high microbial quality for subsequent use as a crop fertilizer. (Source: Arthurson, 2008)

Stabilizing

Sludge stabilization is necessary to reduce pathogen content, eliminate offensive odors and reduce or eliminate the potential for putrefaction. Technologies that used for stabilization of sludge are liming, heat treatment aerobic digestion, anaerobic digestion and composting (Fig. 3) (Garg and Tanyimboh, 2009). Because, these treatment systems reduce the organic matter content, water content, emission of unpleasant odors and concentration of pathogenic micro-organisms. Anaerobic digestion of sludge at mesophilic (30-38 °C) and thermophilic (50-60 °C) is used to inactivate pathogens.

Thermophilic treatment is more efficient in minimizing the content of pathogenic bacteria and parasites than mesophilic. Thermophilic treatment sludge fulfills class A bio-solids results from sludge digestion at 60-75 °C which has low pathogen content compared to class B bio-solids, hence class A bio-solids can be used for unrestricted public contact. Whereas, class B results from mesophilic sludge digestion at 28-38 °C, contains fecal coliform density as an indication of pathogenic level. The major advantage of anaerobic digestion is to generate biogas as an end product that used for the treatment facility. Aerobic digestion process is performed by aerobic microorganisms and generates heat. However, this stabilization does not reduce the pathogen content to the acceptable standards for unrestricted use of sludge in agriculture. This indicates that sludge should be under go additional stabilization step to achieve a product with sufficiently high microbial quality to enable recycling of residues. Some of sludge stabilizing methods are pasteurization (heated at temperature 70-80 °C) (Arthurson, 2008).

Dewatering

This is mainly useful to reduce the volume of the sludge via water separation. In this process, it is possible to remove a certain proportion of free, adhered and capillary water with the technology available technology. Among these processes; drying beds, centrifuging, filter belt and filter press. All process except drying beds, other process requires addition of a chemical conditioning agent (Sullivan, 2015). Dewatering is a vital step in sludge treatment processes. In this process, belt filter press and/or a centrifuge are mostly applied (Evans, 2008). Dewatering process is a physical unit operation used in reducing the moisture content of sludge. This process is not incinerated, but achieved by applying sand beds or by mechanical dewatering equipment. Selection of appropriate sludge dewatering technique depends upon the nature/characteristics of the sludge to be dewatered, available space, and moisture content requirements of the sludge cake for ultimate disposal. Sludge dewatering may also be improved by chemical conditioning such as addition of polymer. However, if land is available and sludge quantity is small, natural dewatering techniques such as drying beds and drying lagoons are most attractive (Garg and Tanyimboh, 2009).

Sludge disposal methods

Sludge disposal without treatment changes public perceptions and legislation of worldwide to make disposal to landfill less popular. Due to this issue, in many countries agricultural use of sludge is becoming more attractive for sustainability. There are different sludge disposal methods such as landfill, incineration, and land application. Among these, incineration end product is not sustainable for beneficial use (Şengün, 2007).

Landfill

Landfill system is the simplest solution to handle sludge by concentrating the material in a single location. This disposal system causes bio-sludge borne pollutants and pathogens to ecosystems and humans if landfill is not properly constructed and maintained. Landfill is economically feasible disposal options, but it is risky. Buried organic matters undergo anaerobic decomposition which produces methane gas. This gas is a greenhouse gas and causes global warming. Therefore, there is a need to collect at some landfills and utilize the energy content. On the other hand, the chemicals and

nutrients can pose risk to local groundwater from older landfills if it does not have synthetic liners that protects seepage. Pathogen content in sludge has also a risk and additionally, the potential content of organic matter and plant nutrients in the sludge will be lost with landfilling (Şengün, 2007).

Incineration

This process is one of most expensive method and working by burning of sludge at high temperatures in a closed device in order to reduce the sludge volume, kills pathogens and destroys most organic chemicals, but this disposal method requires extra energy for safe disposal of the resulting ash. The end product of incineration, i.e., ash is a stable inorganic material containing 10-20% of the original solids. The associated problem with this method is that it does not destroy trace elements rather than concentrating them in the ash. Beside this, it also produces carbon dioxide which also a greenhouse gas causes global warming and lose of beneficial plant nutrients and organic matter for plant. The aim of integrated sludge treatment is to maximize the intrinsic value of sludge in its volume reduction processes. Depending on the type of sludge characteristics, one or more sludge treatment steps are used to optimize the sludge volume.

Land application

Land application of sludge is an alternative to landfilling or incineration because of the negative environmental impacts and high costs of sludge management practices. The high organic and nutrient content of the sludge makes it a valuable resource for farmers as it increases soil quality and crop yields and decreasing the need for expensive chemical fertilizer costs (Stout, 2002). Land application of sludge is less expensive and can improve the structure of the soil as fertilizer by supplying nutrients to crops and other vegetation's grown in the soil. Application of sludge that contains organic matter can improve the physical, chemical and biological properties of the soil. Because presence of organic matter can increase water infiltration, reduce soil erosion, increase water holding capacity, reduce soil compaction and increase soil granulation, increase the ability of soil to retain nutrients and provide nutrients for plant growth and food and energy for beneficial microorganisms. All of these beneficial properties make sludge considered a good choice for homeowners, landscapes, farmers and foresters. One type of sludge application as organic fertilizer is more commonly in the form of dried and/or pelletized. Producing sludge in this form is complex and expensive, however, dried sludge are often blended with other materials and marketed as an organic fertilizer with balanced nutrient levels. However, agricultural use of these sludge showed a great variability over time depending on weather conditions and crop type. Therefore, scheduling sludge transport and application are compatible with agricultural planting, harvesting and possible adverse climatic conditions requires careful management (www.waterleav.com, 2017).

Factors affecting land application of sludge

Bio-solids

Contain significant amounts of macro- and micronutrients which are economically attractive for land application. Bio-solids are rich in organic matter and essential plant nutrients which can be utilized as soil conditioner and fertilizer through the contribution of organic matter and as a fertilizer by supplying essential micro- (zinc, copper and iron)

and macronutrients (nitrogen, phosphorus and potassium) that increase the plant growth and productivity, improve soil quality, water holding capacity, air and water transport. The slow release of nutrients prevents leaching of excess plant available nutrients and possible contamination of ground and surface water (Wendimagegn, 2016). The only drawbacks of the use of sludge on agricultural land application is its pollutant load including heavy metals, organic compounds, and pathogens. The potential toxic elements such as cadmium, copper, nickel, lead, zinc, mercury and chromium concentrated in the sludge as a result of their association with settleable solids during primary and secondary treatment processes (Usman et al., 2012).

Heavy metals

Trace elements are elements that exist in natural systems in small amounts and when they present in excessive concentrations they become toxic to living organisms. The plant-soil system has its own protective mechanisms that limit the potential toxicity of trace elements in their areal portions and these minimize health problems of animals and humans. However, excessive accumulation of these trace elements in plants can cause either reduced yields or health problems to animals or humans that ingest the plants. Toxicity of heavy metals to plant species depends on their concentration in the soil. Some potentially toxic heavy metals may occur at increased levels in the food chain. There are two concerns regarding trace element additions to agricultural soil amendment might become toxic to crops and sufficiently concentrated in an edible crop to have harmful effects on an animal or human that consumes it. Cadmium, copper, mercury, molybdenum, nickel, selenium and zinc are the greatest concern in bio-solids. In fact, many of these trace elements are essential nutrients for plant and animal health. These metals cause little hazard to crop production or plant accumulation because of their low solubility at pH 6.0 to 7.5 in a well aerated soil where field crops are typically grown or are present in bio-solids in small quantities (Şengün, 2007).

Organic contaminants

In line with presence of beneficial organic matter, bio-sludge also may contain toxic organic contaminants. Particularly, those organic substances that do not decompose will likely be strongly adsorbed onto the organic matter particles present in bio-solids. Sludge does not only contain urine or feces from human but also contains hormones and pharmaceutical substances that could possibly constitute a risk of influencing the microflora of the land. Sludges may contain synthetic organic chemicals from industrial wastes, household products and pesticides. These chemicals may be volatilized, degraded, sorbed to sludge or discharged in the aqueous effluent. Degradation results in the formation of other products that can be toxic or less toxic than the original compounds (Şengün, 2007).

Salts

Different kinds of salts can be present in bio-solids which can cause an effect to seed germination or growth of young plants through accumulation in the root zone of the soils. Soluble salts are not expected to be a problem with agronomic rates of bio-solids that used for soil amendment of disturbed land, because leaching by rainfall will remove excess amount of salt from the root zones. However, large rate application of bio-solids is contributing high salt discharges to the sewer system (Şengün, 2007).

Pathogens

As sludge vary in quality and quantity of its organic and inorganic content, it also varies in the type and number of pathogens it contains. In sewage sludge and similar wastes, most of the pathogens will be hazard, but a few salmonella typhi, E. coli and some mycobacteria have a higher rating of hazard. Bacteria, viruses, protozoa and parasitic worms are disease causing pathogens. These pathogens can present a public health hazard if they are transferred to food crops grown on land to which bio-sludge are supplied and contained in runoff to surface waters from land supplied sites. Advanced and conventional sludge treatment systems produce a stabilized final product where such organisms are unlikely to multiply to large numbers and problems arising from bacterial toxins during sludge storage or application (Şengün, 2007).

Objective

The objective of this review paper is to discuss and summarize the characteristics, treatment techniques, fertilizer potential and other available management options of breweries sludge generated from wastewater treatment plants.

Materials and methods

This review paper was written using searching key phrases “Brewery sludge generation”, “Sludge chemical composition”, “Brewery sludge disposal”, “Brewery sludge treatment” and “Brewery sludge management” in Springer link, science direct, library genesis, jester, and www.nap.org searching web pages. From these searching, peer reviewed journals, review papers and MSc. Thesis were used. The interpretation of the result of each document was done using bar graphs, lines and scatter plot in a Microsoft excel. Result measurement units of sludge physicochemical parameters investigated by different scholars were reorganized and expressed in similar units for comparison.

Results and discussion

Characteristics of BWWS

BWWS amended with clay loamy soil

According Remya et al. (2015), the brewery wastewater sludge (BWWS) were characterized and tested for chilly seed germination. Plant growth trials were conducted to evaluate the application of BWWS as organic fertilizer. This brewery wastewater sludge was amended with clay loamy soil in different proportion of soil to BWWS with controls. The physicochemical characterization result showed that the pH of the sludge alone and its composite ranges almost neutral (i.e., 6.08-7.62).

The brewery sludge is also shows a rich source of nitrogen, and potassium were very high, i.e., 420.25 kg/ha and 840.0 kg/ha respectively as compared to the clay loamy soil. On the contrary to nitrogen and potassium increased application of sludge decreased the availability of phosphorus. *Figure 4a, b, c* and *d* indicates that the levels of nitrogen, phosphorus, potassium, organic carbon, electrical conductivity, and pH in clay loamy soil amended with brewery sludge (Remya et al., 2015).



Figure 4. a, b, c and d: Levels of N, P, K, OC, EC and pH in clay loamy soil amended with BWWS

From *Figure 4* the percentage of organic carbon of the sludge was 2.90, which is greater than all composite and control values (clay loamy soil). This may be due to addition of brewery sludge that improve the organic carbon content of the clay loamy soil significantly and the higher water retention capacity is linked to the high organic matter, high cation exchange capacity and other nutrients.

Analysis of heavy some selected heavy metals (Pb = 0.004%, Ni = 0.0024%, Hg = below detection limit, and Cd = traces) in BWWS were present below the standard levels and the sludge can be safely used for agricultural application (Ramya et al., 2015).

Similar research investigation by Erdem and Ok (2002) also proves that brewery sludge amendments improved the carbon and nitrogen content of the soil. Organic carbon content of the amended soil was increased as the BWWS loading rates were increased. The total nitrogen has also indicated the increasing trend with the addition of BWWS for all incubation periods. Whereas, the pH and salinity of soil shows fluctuations. The pH of amended and un-amended soil samples decreased with the incubation time. The decreased pH values could be explained by organic acids produced during nitrogen mineralization and release of soluble electrolytes such as nitrates and sulfates in the soil solution. While salinity increment arises from addition of BWWS, which does not at a level to affect the yield of sensitive crops. The increment of organic carbon and nitrogen content of the amended soil as brewery sludge loading rates increased was indicated in *Figure 5* (Erdem and Ok, 2002).

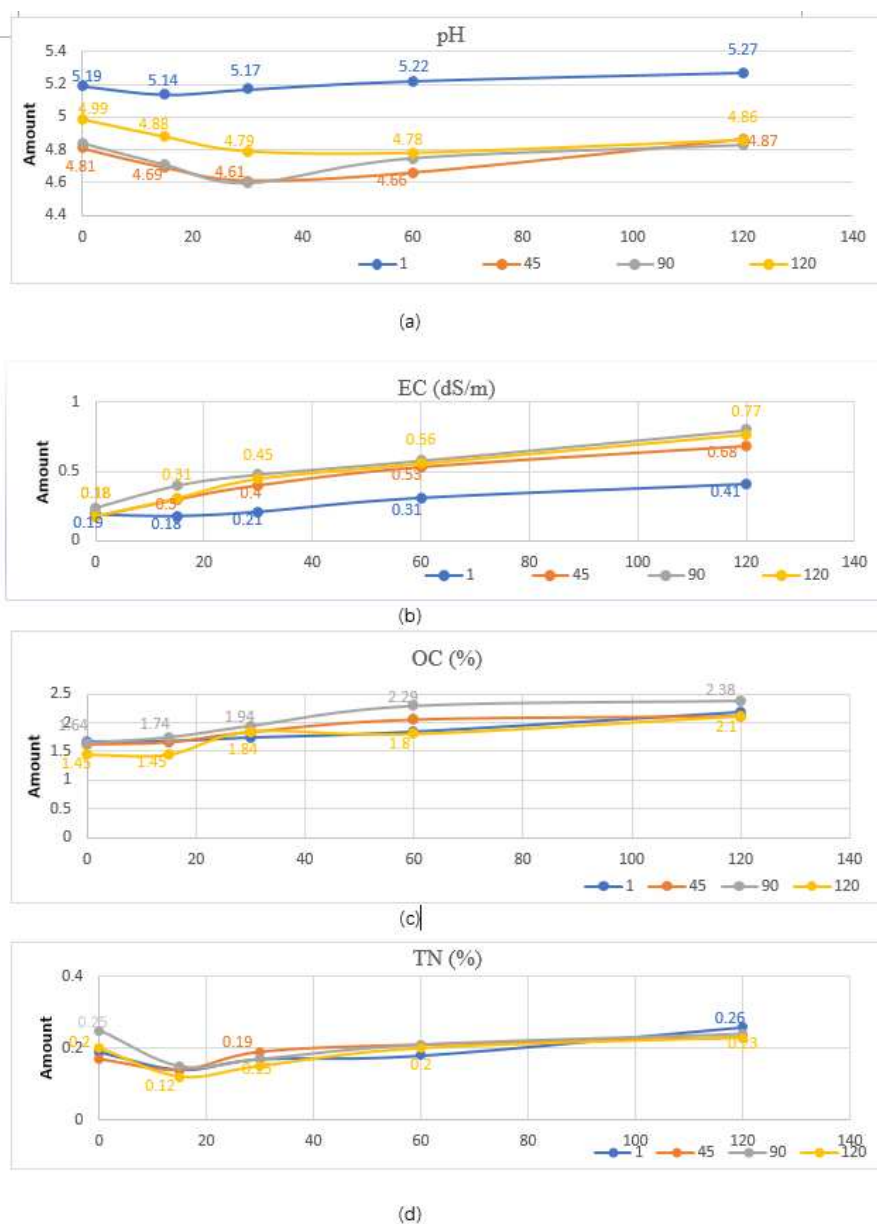


Figure 5. a, b, c and d: Changes in some chemical characteristics of BWWS addition on soil sample

Physicochemical properties of dried (brewery waste sludge) BWWS

Kanagachandran and Jayaratne (2006) investigates the brewery wastewater sludge potential application as an organic fertilizer alone and with combination of municipal solids and farm solids for germination of pumpkin seeds. Before the pilot scale trial was conducted, sun dried brewery wastewater sludge (denoted as BWS), mixtures of BWS with municipal solids (denoted as compost A) and farm solids (denoted as compost B) were analyzed for both chemical and physical parameters. The results of physicochemical characteristics of BWS, Compost A and Compost B are explained in graph (Fig. 6).

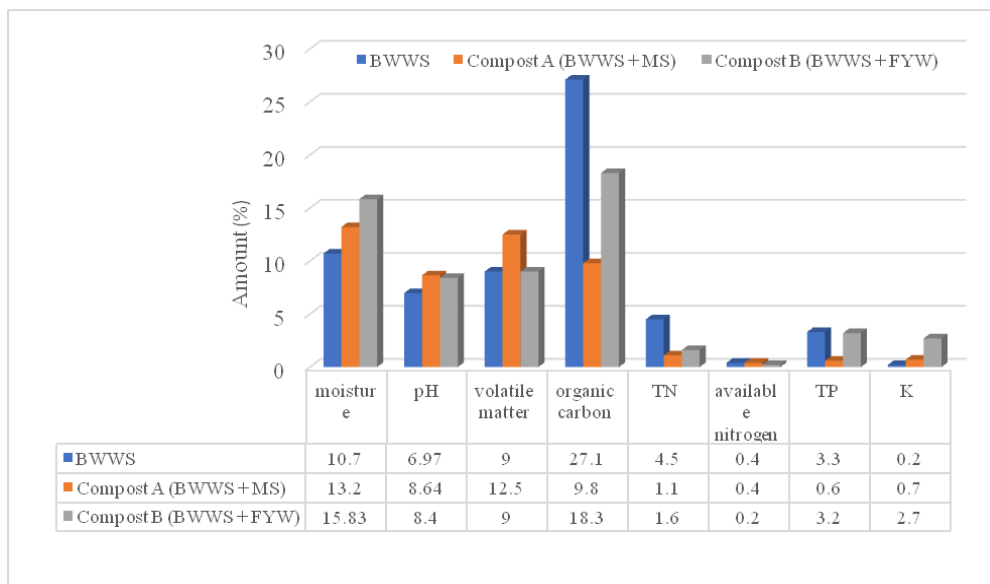


Figure 6. Physicochemical properties of dried BWWS, Compost A and Compost B

The pH of (Brewery waste sludge) BWWS investigated by Kanagachandran and Jayaratne (2006) was approaches to neutral whereas compost A and compost B appeared under alkaline conditions. This may be due to the differences in the presence of mixtures of other substrates in BWWS. The total nitrogen and organic content of BWWS was higher than compost A and compost B which are derived from municipal wastes and farm yard wastes. This has a vital role in plant nutrition and ecosystem functioning. The total phosphorus content of BWWS was equivalent to farm yard compost. While, potassium, and the micronutrients manganese, copper and zinc contents were lower in BWWS compared to both composts. Water holding capacity is one of the valuable property and important in soil for releasing humidity to the plants when they require. The water holding capacity of BWWS was the highest compared to compost A and compost B. This property may be linked to the high content of organic matter and nutrients. Presence of heavy metals is one of the main hurdle in the agricultural application of wastewater sludge because of their toxic effects on crops and soil and the leaching of heavy metals into the nearby water sources.

The concentration of metals in (Brewery waste sludge) BWWS, compost A and compost B are explained in *Figure 7*. The analysis of heavy metals in BWWS revealed that the level of lead and nickel were lower than the expected Sri Lankan standards for organic fertilizer which are 250 mg/kg and 100 mg/kg, respectively.

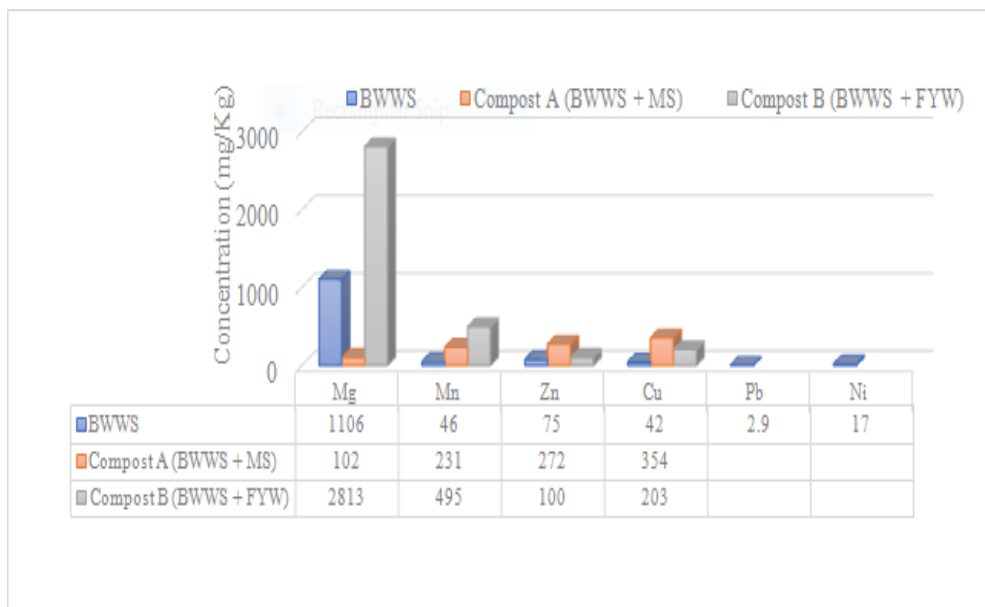


Figure 7. Content of minerals in BWWS, Compost A and Compost B

The effects and potential of brewery sludge (BWWS) as application of organic fertilizer

Effects on treatment of acidic soils and heavy metals

Dessalew et al. (2017) also tried to analyze the effect of BWSS on the treatment of acidic soils and their result showed that the PH of BS samples presented alkalinity that ranged from 8.79 in fresh BS to 8.37 in a two-year old sample as shown in *Table 4*. According to Luque et al. (1990), alterations in the source of water and processing method can create a difference in PH as shown from the South American breweries which gave their PH oscillating from 6.5 to 11.5. Using BS as a method of modifying the soil can alter the micronutrients and macronutrients availability. Therefore, combination of BS with some other compounds can help in lowering the PH values. Conversely plants that can endure alkalinity can be used in such cases.

Since about 40% of the cultivated land in Ethiopia have soils that are acidic (Mesfin, 2007), then BSDS can be utilized so as to make the fertility of the soil to be better. Additionally, since there is decline of PH of BS with age, then the aged BSDS can be useful in impartial or alkaline soils (Dessalew et al., 2017).

Table 4. Physicochemical analysis of the brewery waste sludge (BWWS)

Parameters		Organic carbon (g kg ⁻¹)	Total nitrogen (g kg ⁻¹)	P (mg kg ⁻¹)	Total P (mg kg ⁻¹)	k (mg kg ⁻¹)	Zn (PPM)	Cu (PPM)	Porosity (%)	pH
Age of brewery sludge	Fresh brewery sludge	309	22	415.91	1664.98	3296.88	33.19	25.19	71.61	8.79
	Two months	108	8	416.29	4069.76	1676.05	33.03	25.08	77.27	8.51
	Two years	106	7.	373.22	5475.43	882.58	33.02	25.01	72.83	8.37

Khan et al. (2014), found that the soil (control) and brewery sludge are slightly acidic in nature. Nitrogen, phosphorus, potassium and heavy metals (Zn, Cu, Cd, Pb, and Cr) content in brewery sludge were higher than the soil. The characteristics of soil and brewery sludge are presented in *Table 5*. Importantly, the content of heavy metals in both brewery sludge and soil are below the permissible limits of the United States Environmental Protection Agency (USEPA, 1997).

Table 5. Effect of brewery sludge on curd yields of cauliflower

Parameters	Brewery sludge	USEPA (1997) limit	Soil	USEPA (1997) limit
pH	6.2	-	6.01	-
OM (g/kg)	265.3	-	14.1	-
TN (g/kg)	25.3	-	0.9	-
TP (g/kg)	6.7	-	1.15	-
K (g/kg)	7.3	-	0.34	-
Zn (µg/kg)	558.47	3000	38.09	300
Cu (µg/kg)	75.23	1500	10.66	100
Pb (µg/kg)	33.88	1000	11.91	350
Cr (µg/kg)	34.98	1200	9.18	250
Cd (µg/kg)	2.25	20	0.73	0.6

Effect of brewery sludge on curd yields of cauliflower

The presence of heavy metals in BWWS affect the soil physicochemical characteristics. For example, soil zinc from 20 Mg ha⁻¹ BWWS application was significantly increased compared to 5 and 10 Mg ha⁻¹ sludge addition. Higher rate application of BWWS was also increased the accumulation of copper and lead in soil significantly as compared to the other treatments. The lowest copper and lead concentration was found in the control. This indicates that high loading rate of BWWS increases the accumulation of heavy metals in soil (see *Fig. 8*) (Khanal et al., 2014).

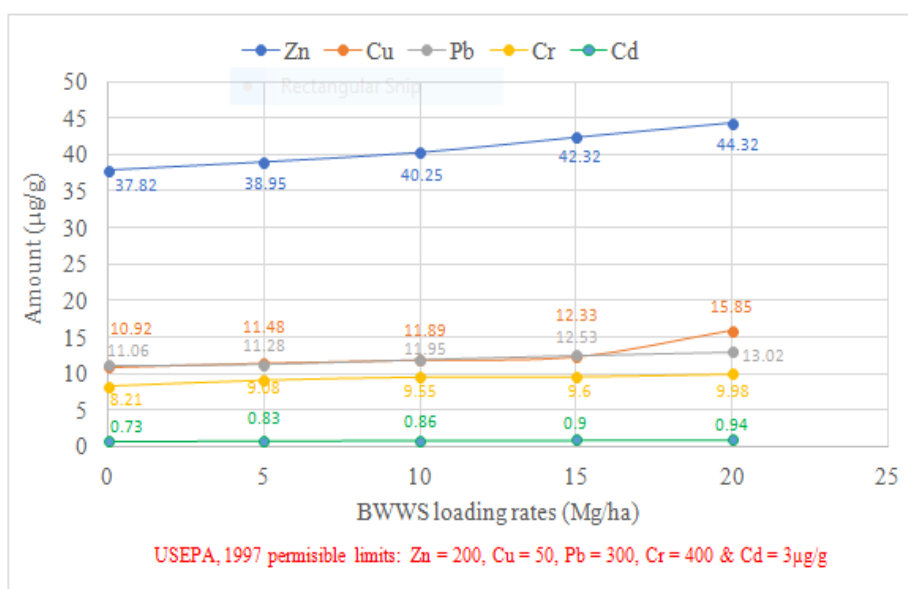


Figure 8. Effect of BWWS on heavy metals content of soil (control)

A good percentage of nitrogen, phosphorus and potassium in sludge also make them a valuable resource for agricultural production. Such sludge is spread on land surface and when they decompose can serve as a source of those minerals to plant growth.

The potential of BWSS as application of organic fertilizer

Grain protein content

BWSS role on grain protein content was investigated in Ethiopia and the research result can be seen in *Table 6*. From this table, the wheat and teff protein contents were also differing among the various treatments. RIF treated crops gave the highest grain protein of 12.53% teff and 12.09% wheat owing to better grain nitrogen acceptance by wheat and teff. Control treated crops gave the lowest grain protein of 10.25% teff and 9.98% wheat (Dessalew et al., 2017).

These results were in line with other researches by Lemon (2007), Blumenthal (2008) and also Mariani (1995). From all these researches, it can be seen that in addition to better performance in the biomass yields and grain of teff and wheat, BSDS also improves the grain protein content. In this regard, with BSDS as a substitute to RIF, it can greatly improve nutritional recompenses of low-contribution agroecosystems.

Table 6. Comparison of protein content of wheat and teff treated with BWSS (brewery spent sludge), FYM (farmyard manure) and RIF (recommended inorganic fertilizer) (Dessalew et al., 2017)

Treatment	Cereals									
	Teff					Wheat				
	Control	FYM	BSD	RIF		Control	FYM	BSD	RIF	
Protein content	-9.98	-11.4	-11.23	12.09	-	10.25	11.55	11.38	12.53	-
Comparison group	Control vs FYM	Control vs BS	Control vs RIF	BS vs FYM	BS vs RIF	Control vs FM	Control vs BS	Control vs RIF	BS vs FYM	BS vs RIF
Mean difference	-1.3	-1.25	-2.11	-0.18	-0.86	-1.3	-1.13	-2.28	0.17	-1.15
T-value	-25.2	-48.4	-71.7	13.7	-33.3	-33.9	-26.2	-66.8	3.7	-27.4
P-value	0.000	0.000	0.000	0.000	0.000	0.000	0.000	0.000	0.000	0.000

A good percentage of nitrogen, phosphorus and potassium in sludge also make them a valuable resource for agricultural production. Such sludge is spread on land surface and when they decompose can serve as a source of those minerals to plant growth. The fertilizer value of sludge is evaluated by the percentage concentrations of nitrogen, phosphorus and potassium (NPK) present in it. A typical NPK value of recommended fertilizer has NPK composition of 8% N, 8% P and 8% K. It may become difficult to achieve these compositions of NPK value in sludge. From the results of NPK concentrations definitely do have fertilizer values. The aerobically digested brewery and textile sludge's indicates that a nutrient composition of 4.1% N, 2.0% P, 0.6% K and 2.6% N, 0.5% P and 0.6% K. Whereas the results of anaerobically digested sludge indicate brewery sludge had 9.7% N, 0.9% P and 1.4% K. While textile processing sludge had a N, P, and K concentration of 9, 0.2 and 0.5% respectively. If these nutrients concentration are improved upon by a suitable complementary method such as composting, they can be used to fertilizer soil (Asia et al., 2008). The results of the fertilizer values (NPK) of the sludge are presented in *Figure 9*.

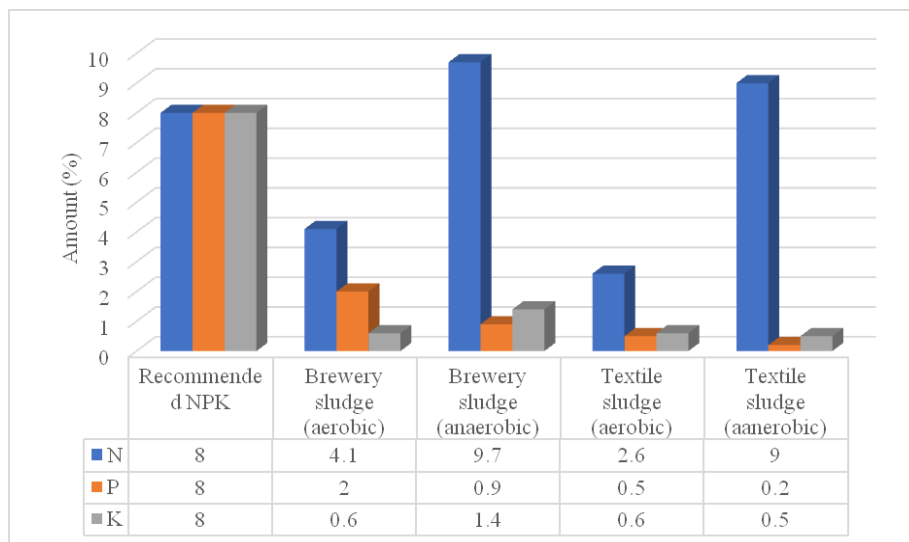


Figure 9. NPK value of anaerobically and aerobically processed brewery and textile sludge's

Brewery waste sludge (BWWS) for vegetable and crop cultivation

The pot experiment (500-g container germination study of chilly plant indicated that increased growth of the plants when compared to that controls (Fig. 10). However enhanced plant growth was observed with increasing proportions of brewery sludge in clay loamy soil. For example, plant height in 9:1, 8:2, and 7:3 amended with BWWS illustrates an increment in plant height (Ramya et al., 2015).

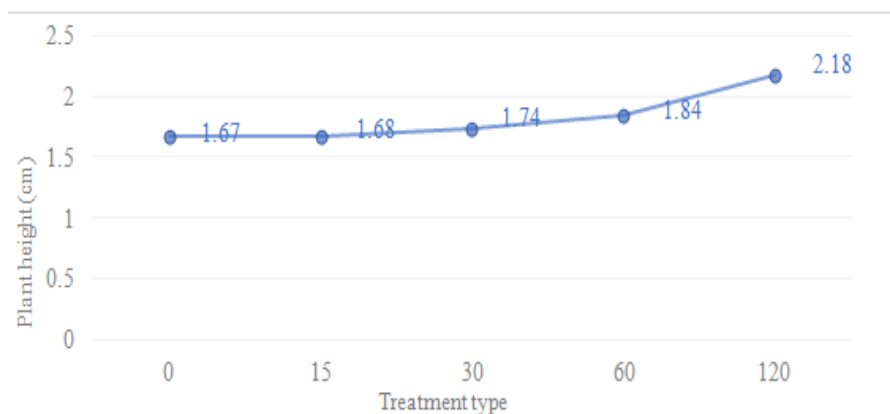


Figure 10. Comparison of plant height planted in clay loamy soil amended with brewery sludge

Beside this plant height increment, application of BWWS in river sand soil media has also shown a significant increase in yields. This confirms that brewery sludge would have a positive input for yield increase in relation to poor and semi-arid soils (Fig. 11).

Improvement on grain yield

Ramya et al. (2015) also agreed with Khan et al. (2014), in which the effect of brewery sludge (Fig. 12) on the yield of curd were shows an increasing trend with an increasing application of brewery sludge. The highest curd yield (i.e., 12.43 Mg ha⁻¹)

was obtained from 20 Mg ha⁻¹ brewery sludge application rate whereas the lowest curd yield (i.e., 7.0 Mg ha⁻¹) was obtained from the soil (control). This highest yield was also significantly higher compared to the control and 5 Mg ha⁻¹ brewery sludge application.

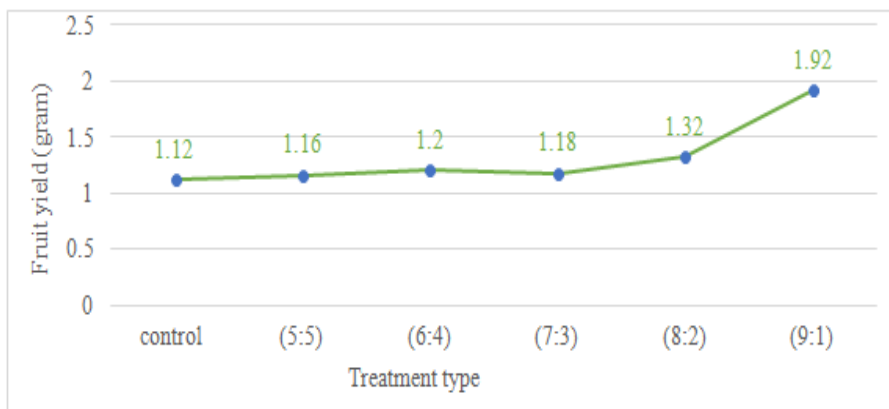


Figure 11. Comparison of fruit height cultivated in river sand amended with BWWS

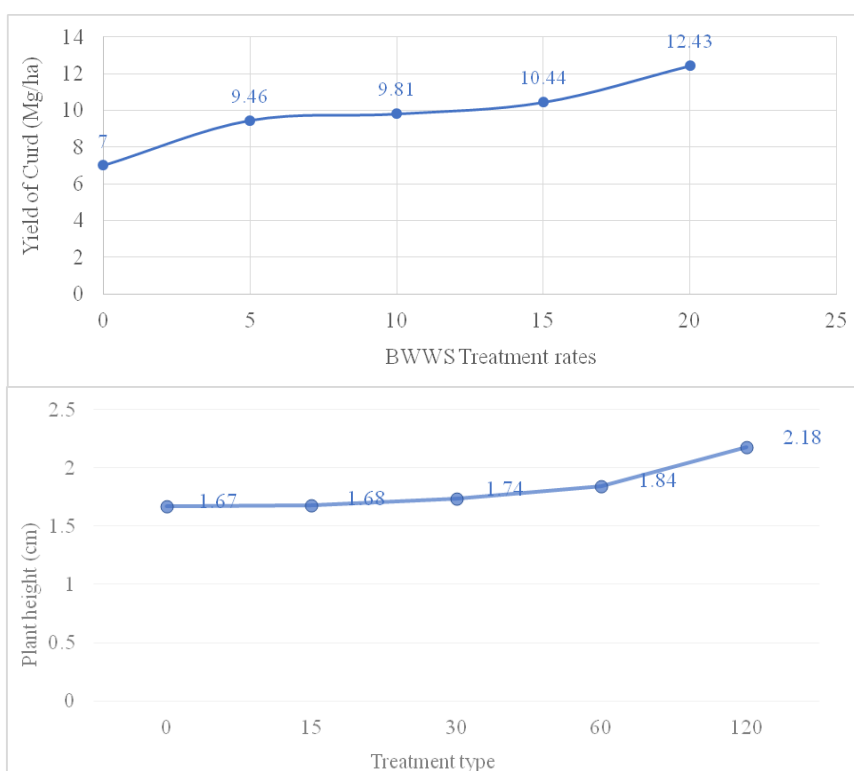


Figure 12. Role of BWWS on curd yields of cauliflower

However, Wendimagegn's (2016) research finding indicated that there was a negative effect on the yields of tomato fruit when brewery sludge loading rates was increased. According to Alemu et al.'s (2017) investigation, increased application from 0 to 15 t ha⁻¹ to 2.5 t ha⁻¹ increased plant height consistently. However, further increasing of sludge application from 2.5 t ha⁻¹ to 15 t ha⁻¹ not increased plant height

significantly indicating the application of brewery sludge beyond 2.5 t ha⁻¹ did not significantly increase plant height.

However, as compared to the control and NP fertilized plots, brewery sludge application at all levels showed significance difference and the increment ranged from 23 to 27% and 8 to 11% respectively. This increment in plant height is due to the increase in crop cell elongation and cell division improved as a result of application of brewery sludge that might enhanced availability of essential nutrients for the growth of plants. Similarly, total grain yield of sorghum crop was affected significantly by application of brewery sludge, where sludge at 15 t ha⁻¹ treated plot gave the highest (4081.6 kg/ha) mean grain yield. When averaged across the application levels, sorghum grain yield showed a significant variation due to the brewery sludge application. The sludge treated plots produced 261.7 and 75.6% more grain yield than that of control and NP applied plots, respectively. The low response to NP might have been due to the fact that part of the applied NP would not be available to plants, rather it tends to fixed by the soil and existing available nutrients reserve of the soil might be very low (*Fig. 13*).

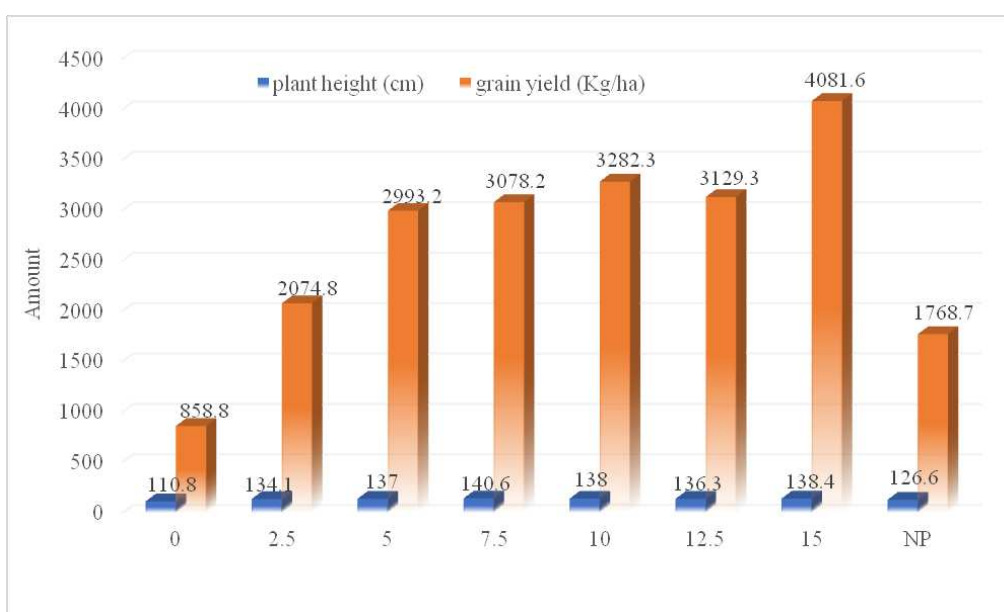


Figure 13. Plant height and grain yield of sorghum cultivated under different levels of BWWS and NP

In addition to this, the results of a research conducted in one of the city found in Ethiopia on Teff and wheat grain yield can be seen in *Figure 14* and *Table 7*. From these results, RIF gave the highest yields followed by soils that were added BWSS and lastly the soils where no was fertilizer added (control) and those for FYM. From the addition of BWSS for both teff and wheat, the yields were doubled in comparison with the yields from control; 1.5 times for teff and 1.3 for wheat in comparison with the yields from FYM. This gave a yield of 2.45 t/ha for teff and 2.65 t/ha for wheat in Ethiopia (Dessalew et al., 2017). This increase in yields goes hand in hand with other research works such as Luque et al. (1990) and Iliescu (2009). Therefore, BWSS can serve as a good organic fertilizer that can be applied in the farming areas which is cost effective and with lesser enduring undesirable significances for the quality of water and soil, along with the general public health.

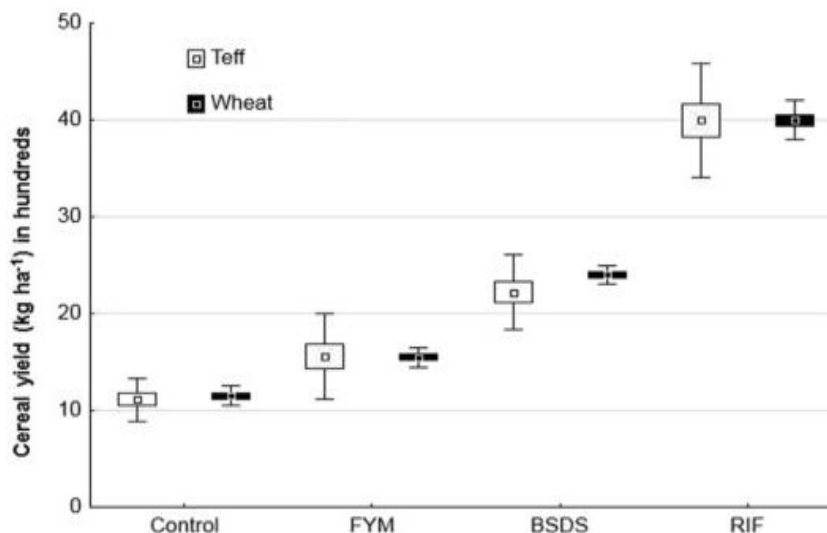


Figure 14. Box plot showing cereals yield among the different treatment groups (control, FYM ¼ farmyard manure, BWSS ¼ brewery spent sludge; RIF ¼ recommended inorganic fertilizer). Boxes represent the mean ± standard error and whiskers represent two standard deviations

Table 7. comparison of grain and biomass yields for wheat and teff treated with BWSS (brewery waste sludge), FYM (farmyard manure) and RIF (recommended inorganic fertilizer)

Treatment	Cereals									
	Teff					Wheat				
	Control	FYM	BWS	RIF		Control	FYM	BWS	RIF	
Grain yield (kg ha ⁻¹)	-1111.1	1555.6	2222.2	4000-		-1150.0	-155	2400	12496	
Comparison group	Control vs FYM	Control vs BWS	Control vs RIF	BWS vs FYM	BWS vs RIF	Control vs FM	Control vs BWS	Control vs RIF	BS vs FYM	BWS vs RIF
Mean difference	-0.0440	0.1111	-0.2889	0.066	0.1780	-0.158	-0.640	-0.640	0.112	-0.370
T-value	-3.11	-8.66	-15.92	3.928	-8.76	-6.72	-11.64	-26.9	6.95	-22.54
P-value	0.036	0.001	0.000	0.017	0.009	0.003	0.000	0.000	0.002	0.000
<i>Biomass yield (kg ha⁻¹)</i>										
Treatment	Cereals									
	Teff					Wheat				
	Control	FYM	BWS	RIF		Control	FYM	BWS	RIF	
Grain yield (kg ha ⁻¹)	2785	4852	6568	12460	-	2938	4876	7164	12496	
Comparison group	Control vs FYM	Control vs BWS	Control vs RIF	BWS vs FYM	BWS vs RIF	Control vs FM	Control vs BS	Control vs RIF	BWS vs FYM	BWS vs RIF
Mean difference	-2067	-3783	-9675	-1716	-5892	-1938	-4226	-9558	-2288	-5332
T-value	-2414	-547.9	-544.6	-204.6	-333.2	-281.7	-793.9	-1850.9	-348.9	-1128.3
P-value	0.000	0.000	0.000	0.000	0.000	0.000	0.000	0.000	0.000	0.000

(Source; G. Dessalew et al. 2017)

Biomass yield

As the result showed in Table 7, the treatments between biomass harvest showed substantial variances ($p < 0.05$) during the analysis of variance. BWSS usage gave far much better results than FYM (farmyard manure) but lower than RIF (recommended inorganic fertilizer). Like in the case of the grains, the addition of (Brewery waste

sludge) BWSS for biomass yields, were doubled in comparison with the yields from control; 1.5 times for teff and 1.3 for wheat in comparison with the yields from FYM; but lesser yields when compared to RIF due to the fast release of if RIF than BWSS (Dessalew et al., 2017).

Conclusions and recommendations

Conclusions

Brewery wastewater sludge is generated as the result of biological wastewater treatment process. Previously, this sludge is considered as a waste product, but now it can be substituted for fertilizers and avoid the need of costly inputs of chemical fertilizers because of its valuable nutrients for plant growth and high water retention capacity. To do this, cost effective and environmentally friendly treatment technique should be developed to convert brewery sludge into bio-fertilizer. Composting with other organic wastes like straw and paper generally offers a relatively cheap and environmentally sound method of recycling organic brewery by-products.

Currently, in Ethiopia there is an increased expansion of agro-industrial sectors mainly beverage industries. This expansion may increase sludge production along with increase in their beer productions. Therefore, it is inevitable to focus on the development of appropriate agro-industrial sludge waste management strategy enabling to reutilize the sludge in an environmentally friendly manner.

Recommendations

Most of the Ethiopian breweries have wastewater treatment plant and generates large amount of sludge which is disposed anywhere. Limited research evidences are available (i.e., only restricted to Harare sofi and Heineken breweries) on the possibility of recycling brewery wastewater sludge for land application at pilot scale levels. Therefore, more research has to be investigated on potential fertilizer values of Ethiopian breweries wastewater sludge's.

REFERENCES

- [1] Abushammala, M. F., Basri, N. E. A., Kadhum, A. A. H. (2009): Review on landfill gas emission to the atmosphere. – *European Journal of Scientific Research* 30: 427-436.
- [2] Alemu, D. N., Ahmed, A., Mohammed, M. (2017): Impact of Brewery waste sludge on sorghum (*Sorghum bicolor* L. Moench) productivity and soil fertility in Harari Regional State, Eastern Ethiopia. – *Turkish Journal of Agriculture, Food Science and Technology* 5: 366-372.
- [3] Arthurson, V. (2008): Proper sanitization of sewage sludge: a critical issue for a sustainable society. – *Appl. Environ. Microbiol.* 74: 5267-5275.
- [4] Asia, I. O., Ekpo, K., Chukwuedo, M. (2008): Economic importance and application options of some industrial sludge conditioned by different treatment methods. – *African Journal of Biotechnology* 7(14).
- [5] Babel, S., Sae-Tang, J., Pecharaply, A. (2009): Anaerobic co-digestion of sewage and brewery sludge for biogas production and land application. – *International Journal of Environmental Science & Technology* 6: 131-140.
- [6] Berni, M., Dorileo, I., Nathia, G., Forster-Carneiro, T., Lachos, D., Santos, B. G. (2014): Anaerobic digestion and biogas production: combine effluent treatment with energy

- generation in UASB reactor as biorefinery annex. – *International Journal of Chemical Engineering*. <http://dx.doi.org/10.1155/2014/543529>.
- [7] Blumenthal, J., Baltensperger, D., Cassman, K., Mason, S., Pavlista, A. (2008): Importance and Effect of Nitrogen on Crop Quality and Health. – *Agronomy & Horticulture - Faculty Publications*. <http://digitalcommons.unl.edu/agronomyfacpub/>, 200.
- [8] Bodík, E. G., Kapusta, Š., Derco, I. J. (2005): Evaluation of anaerobic-aerobic wastewater treatment plant operations. – *Polish Journal of Environmental Studies* 14: 29-34.
- [9] Dessalew, G., Beyene, A., Nebiyu, A., Ruelle, M. L. (2017): Use of industrial diatomite wastes from beer production to improve soil fertility and cereal yields. – *Journal of cleaner production* 157: 22-29.
- [10] Dolgen, D., Alpaslan, M. N., Delen, N. (2004): Use of an agro-industry treatment plant sludge on iceberg lettuce growth. – *Ecological Engineering* 23: 117-125.
- [11] Dos Santos Mathias, T. R., De Mello, P. P. M., Ervulo, E. F. C. (2014): Solid wastes in brewing process: A review. – *Journal of Brewing and Distilling* 5: 1-9.
- [12] Ediget, W. (2016): The Fertilizing Potential of Breweries Waste Water Sludge Compared to Urea on the Growth and Yield of Tomato Plant. – Center for Environmental Science Program. Addis Ababa University College Of Natural Sciences.
- [13] Erdem, N., Ok, S. S. (2002): Effect of brewery sludge amendments on some chemical properties of acid soil in pot experiments. – *Bioresource Technology* 84: 271-273.
- [14] Evans, T. D. (2008): An Independent Review of Sludge Treatment Processes and Innovations. – Australian Water Association Bio-Solids Conference, Adelaide.
- [15] Fillaudeau, L., Blanpain-Avet, P., Daufin, G. (2006): Water, wastewater and waste management in brewing industries. – *Journal of Cleaner Production* 14: 463-471.
- [16] Garg, N. K., Tanyimboh, T. (2009): Multi-criteria assessment of alternative sludge disposal methods. – Unpublished M. Sc. Thesis. Department of Mechanical Engineering, University of Strathclyde.
- [17] Hänel, K. (1988): Biological Treatment of Sewage by the Activated Sludge Process. – E. Horwood, Chichester.
- [18] Iliescu, M., Faraco, M., Popa, M., Cristea, M. (2009): Reuse of residual kieselguhr from beer filtration. – *J. Environ. Prot. Ecol.* 10: 156-162.
- [19] Kanagachandran, K., Jayaratne, R. (2006): Utilization potential of brewery waste water sludge as an organic fertilizer. – *Journal of the Institute of Brewing* 112: 92-96.
- [20] Khanal, B. R., Shah, S. C., Sah, S. K., Shrivastav, C. P., Acharya, B. S. (2014): Heavy metals accumulation in cauliflower (*Brassica oleracea* L. var. botrytis) grown in brewery sludge amended sandy loam soil. – *Int. J. Agric. Technol* 2: 87-92.
- [21] Lemon, J. (2007): Nitrogen Management for Wheat Protein and Yield in the Esperance Port Zone. – Department of Agriculture and Food, State of Western Australia.
- [22] Luque, O., Bracho, O., Maier, T. (1990): Utilization of Brewery Waste Water Sludge for Soil Improvement. – *Technical Quarterly, Master Brewers Association of the Americas, USA*.
- [23] Mariani, B. M., D'egido, M. G., Novaro, P. (1995): Durum wheat quality evaluation: influence of genotype and environment. – *Cereal Chem.* 72(2): 194-197.
- [24] Mesfin, A. (2007): Nature and Management of Acidic Soil in Ethiopia. – Addis Abeba, Ethiopia.
- [25] Olowu, R., Osundiya, M., Onwordi, C., Denloye, A., Okoro, C., Tovide, O., Majolagbe, A., Omoyeni, O., Moronkola, B. (2012): Pollution status of brewery sewage sludge in Lagos, Nigeria. – *International Journal of Research and Reviews in Applied Sciences* 10: 159-165.
- [26] Ramya, N., Srinivas, T., Lakshmi, K. A. (2015): Studies on effect of brewery waste water sludge (BWS) on morphology and yield of chilly (*Capsicum annum* L.) plant. – *International Journal of Pharmaceutical Sciences and Research* 6: 405.

- [27] Sampson, E. I. (2016): Fertilizer value of bio-solids produced from the treatment of wastewater sludge. – TLEP International Journal of Chemical Engineering Research 2: 14-24.
- [28] Şengün, T. (2007): Use of agro industry treatment plant sludge for agricultural purposes. – Dokuzeylül University. Master's thesis, environmental engineering.
- [29] Stocks, C., Barker, A., Guy, S. (2002): The composting of brewery sludge. – Journal of the Institute of Brewing 108: 452-458.
- [30] Stout, J. K. (2002): Sludge Management in Alfenas, Brazil. – Massachusetts Institute of Technology, Cambridge, MA.
- [31] Sullivan, D. M. (2015): Fertilizing with Biosolids. – Oregon State University, PNW 508.
- [32] Tadese, A., Seyoum, L. A. (2015): Evaluation of selected wetland plants for removal of chromium from tannery wastewater in constructed wetlands, Ethiopia. – African Journal of Environmental Science and Technology 9: 420-427.
- [33] Thomas, K., Rahman, P. (2006): Brewery wastes. Strategies for sustainability. A review. – Aspects of Applied Biology 80: 147-153.
- [34] USEPA (1997). Exposure Factors Handbook. – EPA, Washington, DC.
- [35] Usman, K., Khan, S., Ghulam, S., Khan, M. U., Khan, N., Khan, M. A., Khalil, S. K. (2012): Sewage sludge: an important biological resource for sustainable agriculture and its environmental implications. – American Journal of Plant Sciences 3: 1708.
- [36] Wendimagegn, E. (2016): The fertilizing potential of breweries waste water sludge compared to urea on the growth and yield of tomato plant. – Msc Thesis, Addis Ababa University College of Natural Sciences.
- [37] www.waterleav.com (2017): Integrated Sludge Treatment, Protecting the 4 Elements. – Herent (Leven), Belgium.

THE CORRELATION BETWEEN HAZE AND ECONOMIC GROWTH: BIBLIOMETRIC ANALYSIS BASED ON WOS DATABASE

XIONG, H.^{1*} – ZHAO, Z.²

¹*School of Management, Nanchang University, Nanchang 330031, China*

²*Institute of China's Science, Technology and Education Policy, Zhejiang University, Hangzhou 310058, China*

**Corresponding author
e-mail: xionghuanhuan@ncu.edu.cn*

(Received 6th May 2019; accepted 15th Nov 2019)

Abstract. This paper takes 4,225 articles on the relationship between haze and economic growth in the Web of Science database from 1992 to 2017 as the research object, and uses CiteSpace to explore the spatial and temporal distribution, research topics and hot trends of the literature. The results show that: (1) The relevant literature volume keeps growing at a high speed. (2) The cooperative group of high-yield authors represented by Huang GH and Streets DG is basically formed. (3) The research institutions are divided into the top international colleges and universities represented by Tsinghua University and the University of California, Berkeley, as well as the two major groups of international well-known scientific research institutes represented by the Chinese Academy of Sciences and the American Environmental Protection Agency. (4) The cited high literature is concentrated in the six international high level journals such as “Science”. (5) The two major cooperation bodies of “the United States–China” and “Holland–France–Italy–Spain” have been formed. (6) The research topics are mainly about the economic mechanism of haze formation, its relationship with economic growth, spatial spillover effects and countermeasures. (7) The research hotspots show trends from “air pollution” and “health” to “PM_{2.5}” and “CO₂ emission”.

Keywords: *PM_{2.5}, EKC, spatial spillover, knowledge map, CiteSpace, hot trend*

Introduction

In recent years, with the continuous expansion of China's population and rapid economic development, energy consumption has been increasing, and air pollution problems such as smog and haze have become increasingly serious. Haze will not only seriously affect people's physical and mental health, but also cause a certain degree of impact on traffic safety, agricultural production, ecological environment and economic development. According to the calculation results of official agencies such as the World Bank and the environmental protection administration, the annual loss due to environmental pollution in China is about 10% of GDP (Zhou, 2011). The high frequency of haze and the great influence have attracted the attention of people from all walks of life. In 2017, Premier Li Keqiang wrote the “resolutely fighting the blue sky defence war” into the government work report.

In addition to natural factors, serious haze pollution is largely attributed to extensive economic development mode and unbalanced industrial structure. Studying and exploring the internal relationship between haze and economic growth will help in finding out the root causes of frequent haze, and put forward the regulation mechanism of coordinating air pollution and economic development represented by haze, so as to provide scientific basis and policy suggestions for regional economic development and

ecological environmental protection, so as to achieve the goal of green development and ecological civilization construction.

The relevant research work in the world has been carried out relatively early. Many scholars have studied the relationship between haze pollution and economic growth from different perspectives, such as the formation mechanism of haze and the analysis of influencing factors, the health economic loss caused by regional particles (PM_{2.5}, PM₁₀, etc.), and environmental Kuznets curve test, etc. These documents reflect the research results of this field only in one way, but it is difficult to grasp the dynamic development and hot trend of the international research field in a comprehensive way. Through the method of knowledge map, the research dynamic and development trend of professional field can be presented in the form of visual atlas (Hou et al., 2009). At present, the map of science knowledge has made great achievements in many fields, such as management, pedagogy and so on (Feng et al., 2017). However, the academic circles still lack the bibliometric analysis of the relationship between haze and economic growth. Based on this, this paper selects the bibliography of haze and economic growth in the core collection database of Web of Science (hereinafter referred to as WoS) during 1992-2017 years as the analysis data. Through CiteSpace visualization software, using knowledge mapping method and related tools, this paper makes a holistic and multi-dimensional visualization analysis of the international research on the correlation effect of haze and economic growth. The aim is to sort out the research hot spots and trends of international literature, which not only helps domestic scholars to understand the research status of the correlation between haze and economic growth in the world, track its frontier hot spots, explore and grasp the development trend and potential of this field, but also provide some reference for the haze control and ecological environmental protection in China, whether for academic research or practical.

Materials and methods

Research methods

The development of information technology and bibliometrics provides a basis for the generation of visual software. The visualization software provides a new way for document processing and analysis (Shi and Li, 2016). Based on this, this paper chooses CiteSpace as the main measurement and visualization software, and Excel as an auxiliary measurement tool. Firstly, CiteSpace is used to describe the current research status and hot trend in the field of international haze and economic growth, and then the literature is read critically according to the analysis results provided by the software, so as to summarize the research topics in this field.

Data sources

In order to explore the status of international research in the area of haze and economic growth and ensure the integrity of the literature search, this paper searches relevant literature in the WoS database by means of TS = ((Economic OR Economy) AND (PM_{2.5} OR PM₁₀ OR haze OR smog OR air quality OR air pollution)). The time span is 1992-2017, and the literature types are pure scientific documents (ARTICLE), PROCEEDINGS PAPER and EDITORIAL MATERIAL, and a total of 4730 literature data are obtained. Later, using the Remove duplicates function in CiteSpace, the duplicate documents were filtered, and finally 4,225 effective records were obtained.

Results

Time distribution

The amount of document information can reflect the heat level and research process of a certain area to some extent, which is an important part of scientific bibliometrics. According to the statistical results in WoS, the time distribution map of the literature (*Fig. 1*) is drawn by Excel mapping in order to understand the time distribution and growth of the literature on the related effects of haze and economic growth in the world.

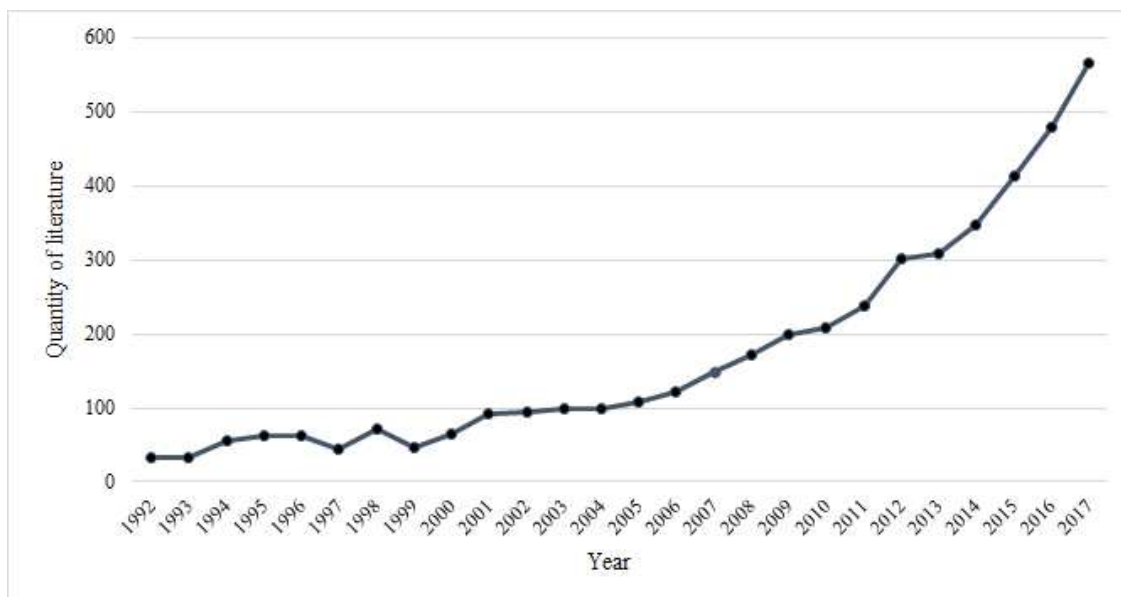


Figure 1. Time distribution of literature on correlation between haze and economic growth

As can be seen from *Figure 1*, the international literature on the correlation between haze and economic growth shows a relatively rapid growth trend. One of the reasons is that the number of journals on ecological environment and environmental economy is increasing, but the more important reason is that the problem of haze has become more and more serious in recent years, which has attracted extensive attention and research from scholars all over the world. According to *Figure 1*, the time distribution of relevant literature can be roughly divided into three stages: (1) Stage 1 (1992-2000 year): the number of literature is small, and the fluctuation range is not large, indicating that the international research in this field started very early, but the research progress is relatively slow. (2) Stage 2 (2001-2010 year): In the first half of this phase (2001-2005), the amount of literature fluctuated around 100, and it did not increase until 2006. (3) Stage 3 (2011-2017 year): the stage of rapid literature growth. Since 2011, the continuous broadcasting of PM_{2.5} by the US Embassy has aroused widespread social concern. Academic circles have also paid great attention to the correlation effect between haze and economic growth, and have done a lot of research on it, and achieved a lot of research results. It can be seen that the literature in this stage is gradually increasing, and the growth rate is gradually accelerating.

According to the law of the logical growth curve of literature, the growth of literature can be divided into four stages (Qiu JP, 2007). The first stage is the embryonic stage, the growth of literature is relatively slow; the second stage is the rapid growth stage, the

literature grows sharply; the third stage is the mature stage, the growth rate is slow; the fourth stage is the saturation stage, and the literature growth rate approaches zero. From the above theory, it can be inferred that the literature on the correlation between haze and economic growth is in a state of rapid growth, so it accords with the second stage of literature development, and it is predicted that the volume of literature will remain high growth in the next few years (Sun and Wang, 2016).

Spatial distribution

In this paper, we use the co-occurrence network of the provided by CiteSpace, the co-occurrence network of research institutions, the co-citation network of the periodicals, the shared network function of the country and the region, to analyze the scientific research cooperation network in the field of haze and economic growth in the world from the micro, meso and macro levels, thus showing the spatial distribution characteristics of the field (Liu et al., 2017).

Micro layer – author analysis

1) Author's analysis: initially formed a batch of high-yielding authors

Through the analysis of the amount of the author's publications, we can understand the author's scientific research ability and level, and make a quantitative analysis of the author's publications in the field of the correlation effect haze and economic growth, and can get the international high-yielding author group in this field (Liu et al., 2011).

According to *Table 1*, the most frequently published research topic in the field of haze and economic growth is the Huang GH of North China Electric Power University, who has published 32 articles. According to Price formula (*Eq. 1*):

$$M = 0.749 * (N_{\max})^{1/2} \quad (\text{Eq.1})$$

M is the number of papers, N_{\max} refers to the number of the highest producers, the authors who have published more than M are called high-yielding authors (Sun and Wang, 2016). This paper calculates the threshold of high-yielding authors in the field of correlation between haze and economic growth, which is 4.24. Therefore, this paper takes the author whose articles are more than or equal to 5 to be a high-yielding author. There are 46 high-yielding authors (*Table 1*). These high-yielding authors are relatively active in the research field, and have strong scientific research ability. Altogether 397 papers are published, accounting for 9.40% of the total. This indicates that a certain number of high-yielding authors have been formed to some extent in the field of international academia.

2) Author cooperation analysis: high-yielding authors gathered and the rest of the authors dispersed and coexist

In order to identify the core scholars in the research field and their mutual cooperation strength, the author analyzes the literature from the perspective of author's co-occurrence.

In CiteSpace, the time zone is selected from 1992-2017, the time slice is 2, the threshold is "Top N = 30", the other parameters use the default value, Node Types selects the Author, and generates *Figure 2*. *Figure 2* shows that there are 296 nodes and

303 connections in the map, and the density is 0.0069. The node in the map represents the author, the size of the node indicates the author's volume of publications, and the thickness and color of the connection indicate the strength of the cooperation relationship and the year in which the co-occurrence relationship first occurred (Chen et al., 2014).

Table 1. High-yielding author statistics (Number of documents ≥ 5)

Number of documents	Name	The year of the first paper	Number of documents	Name	The year of the first paper
32	Huang GH	2008	6	Carmichael GR	1999
25	Zhang Q	2010	6	Chen L	2006
21	Wang Y	2010	6	Li L	2016
18	Liu Y	2010	6	Beig G	2008
15	Zhang Y	2012	6	Hao Y	2016
13	Li Y	2006	6	Hao JM	2010
12	Zaman K	2014	6	Rojas-Rueda D	2016
12	Streets DG	1999	6	Chen JM	2016
12	Zhou Y	2010	5	Dincer I	1998
11	Brajer V	2004	5	Liu XJ	2016
10	Li YP	2008	5	An XQ	2010
9	Guan DB	2014	5	Li J	2016
9	Zhao Y	2010	5	Huo H	2014
9	Wang L	2014	5	Levy JI	2005
8	Wang SX	2014	5	Bi J	2010
8	Liao H	2012	5	Nam KM	2008
8	Li W	2012	5	Amann M	1999
8	Mead RW	2004	5	Zhang J	2014
7	Wang J	2013	5	Guttikunda SK	2014
7	Zhu Y	2014	5	He LY	2016
7	Smith KR	2004	5	Millimet DL	2003
7	He KB	2014	5	Scasny M	2010
6	Paltsev S	2008	5	List JA	2003

As shown in *Figure 2*, a number of nodes are concentrated in the center of the map, and there are many connections between these nodes; at the same time, many isolated nodes are dispersed around it. It shows that there are different degrees of cooperation between the authors of the central region, and the flow of knowledge between each other is better, but the authors in the scattered parts around them lack communication and cooperation and are in a state of isolation. At the same time, most of the node connections in the center of the original map are orange red (corresponding to 2012-2017 year). It shows that the cooperative group has been formed in the last five years. It is now in the stage of strengthening communication and deepening the cooperation. It is expected that the future part of the author will create more research results through cooperation.

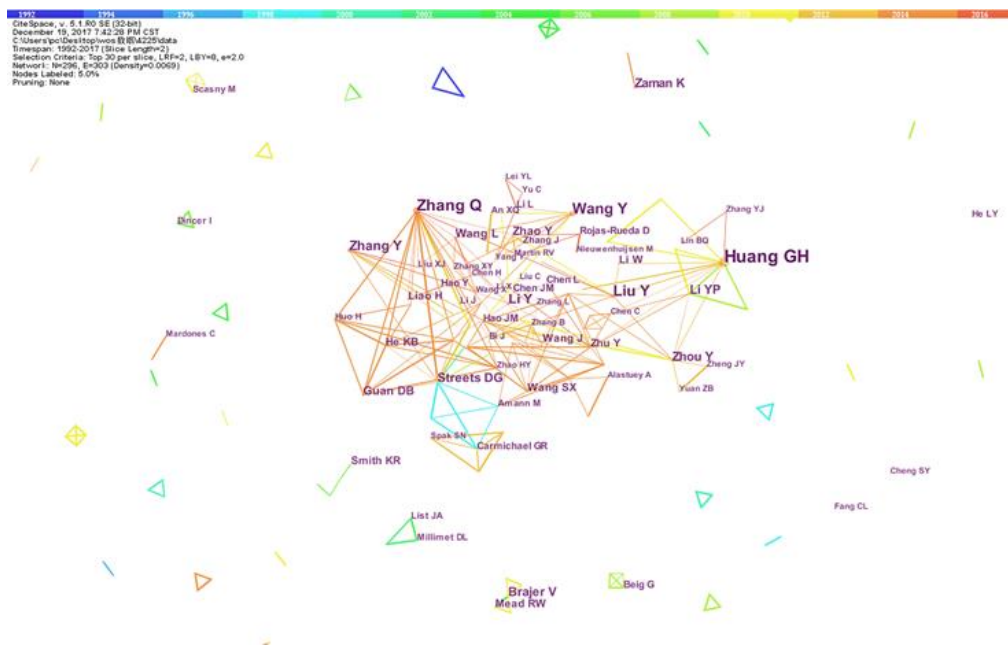


Figure 2. Co-occurrence map of scholars

Meso level – research institutions and periodicals analysis

1) Cooperation analysis of research institutions: focusing on top international universities and research institutes

Research institutes can identify the status and importance of each research institution in the field, and the degree of cooperation between them (Liu et al., 2017). In order to make the map display more concise and clear, the time slice is 4, the threshold “Top 5% per slice” is selected, and the image is “pruned” using the minimum spanning tree algorithm (MST), and *Figure 3* is obtained. As shown in the following figure, there are 165 nodes and 194 connections. The overall density of the network is 0.0143. *Table 2* lists the detailed information of the top 20 institutions.



Figure 3. Co-occurrence map of institutions

Combined with the analysis of *Figure 3* and *Table 2*, we can see: (a) the research power of the correlation between haze and economic growth is concentrated in universities and research institutes. Tsinghua University, Univ Calif Berkeley, Peking University and Harvard University are among the top international universities with environmental and economic advantages. The largest node is the Chinese Acad Sci. Its scientific research level is highly recognized both in China and internationally. (b) There are many connections in the central area of *Figure 3*, and there are scattered nodes in the non-central area. It shows that most of the research institutions in this field work closely, but there are still some institutions that lack cooperation, which should continue to strengthen exchanges and cooperation between institutions.

Table 2. Top 20 institutional information

Frequency	Institution	Country
124	Chinese Acad Sci	China
81	Tsinghua Univ	China
71	Univ Calif Berkeley	U.S.A
71	Peking Univ	China
64	Harvard Univ	U.S.A
55	US EPA	U.S.A
43	Beijing Normal Univ	China
37	Univ Maryland	U.S.A
36	Univ Calif Davis	U.S.A
34	Fudan Univ	China
31	Univ London Imperial Coll Sci Technol & Med	Britain
31	Nanjing Univ Informat Sci & Technol	China
31	North China Elect Power Univ	China
30	Univ N Carolina	U.S.A
29	Nanjing Univ	China
28	Univ Illinois	U.S.A
26	Univ Michigan	U.S.A
26	MIT	U.S.A
25	Univ Utrecht	Netherlands
25	Univ Chinese Acad Sci	China

2) Co-cited analysis of journals: research results concentrate on six high level journals

The “Cited Journal” function is selected to reflect the relevance between the various journals and disciplines by the phenomenon that the two journals are cited by the same document, so as to further analyze the knowledge base distribution in the area of haze and economic growth (Chen et al., 2014). The parameter is set to Top N = 10, and MST is selected for pruning to highlight its main components.

As shown in *Figure 4A*, the journal co citation map has 148 nodes and 355 connections. The density is 0.0326, and there are many nodes in the annual ring. Combined with the analysis of background data, the six journals of “Atmospheric Environment”, “Environmental Science & Technology”, “Environmental Health Perspectives”, “Energy Policy”, and “Science of the Total Environment” and “Science” have concentrated most of the research literature on the association effects of haze and

economic growth. The related papers are of academic value, data value and applied value, representing the research hotspots and frontiers in this field. Among the representative journals, the impact factors of “Science”, “Environmental Health Perspectives” and “Environmental Science & Technology” from 2016 to 2017 are larger, and the impact factor of Science is even as high as 37.205, which is one of the most authoritative academic journals in the world. All of these show that the correlation between haze and economic growth has received international attention.

Then, through the Spotlight function in CiteSpace, the nodes with high centrality (purple circle nodes) are highlighted (*Fig. 4B*). It can be found that the number of nodes with purple circles in the journal’s co-citation map is relatively large. Among them, the intermediary centrality of “Science” and “Energy Policy” is more than 0.2, indicating that these journals are in the key position in the network, which is the object that scholars in this field should focus on (Liu et al., 2017).



Figure 4. Co-citation map of journals

The macro level – national co-occurrence analysis: “USA–China”, “Holland–France–Italy–Spain” are two largest emerging cooperatives

At the macro level, through the analysis of the national cooperation network, we can understand whether there is a cooperation relationship and the intensity of cooperation among the countries in the field of the correlation effect between haze and economic growth. Therefore, the node selects “Country”, the parameter is set to Top N = 10, and the time slice is 2, the result is shown in *Figure 5*.

From the background data analysis of *Figure 5*, 28 countries have published more than 3 papers in the field of the correlation between haze and economic growth, but a large number of documents are obviously concentrated in a few countries. The data show that there are five countries with more than 200 papers, but the total number of papers in these five countries is up to 2941, that is, nearly 70% papers in this field are produced from these countries. Among them, the United States has a very obvious advantage, with a total of 1382 (32.71% of the total), and the centrality is as high as 0.55, indicating that the United States is in a key dominant position in the field of haze and economic growth, with a high achievement and outstanding contribution. China’s paper output ranks second, with a total of 770, followed by the UK (a total of 334 articles), Canada (a total of 247 articles) and Germany (a total of 208 articles). In *Figure 5*, the thickness of the connection indicates the strength of the cooperation. The color of the line in the original figure indicates the time of cooperation between

countries. Based on this, it can be concluded that “the United States-Canada” and “Canada-Germany” had close cooperation in the early period (1992-2000). “The United Kingdom-Canada-China” had strong cooperation in the medium term (2001-2008), while the two cooperation bodies of “the USA–China” and “Holland–France–Italy–Spain” were formed in recent years (2009-2017).

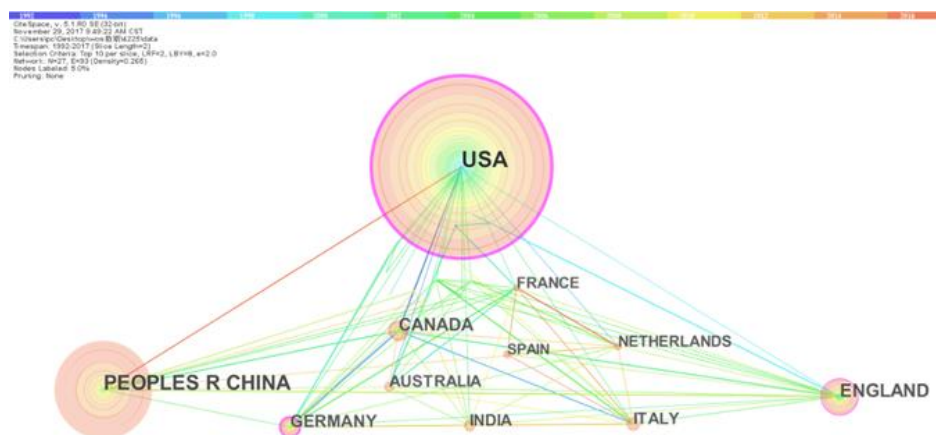


Figure 5. National cooperation network map

From the analysis of *Figure 5*, we can see that the research power in the field of the correlation effect between haze and economic growth in the world is mainly concentrated in the developed countries such as the USA and the UK, as well as the rapidly developing countries such as China, indicating that these countries are more concerned with the field relative to other countries and have corresponding researchers. At the same time, *Figure 5* shows that there are many links between countries, indicating that their cooperation and exchange are relatively close, which is conducive to the in-depth research in this field and the output of more scientific research results. However, the original map shows that the connection between some countries is a tone, indicating that the cooperation between these countries only existed for a period of time, and has not always maintained cooperation. In the future, countries should strengthen continuous contacts and exchanges, maintain long-term cooperation so as to further promote sustainable development in this field.

Discussion

Research topics

From the previous analysis, we can see that the research literature on the correlation between haze and economic growth is very rich, but the research topic is more scattered. Combined with the high-frequency keyword clustering processed by CiteSpace (*Table 3*), and reading and sorting out the existing literature, the author divides the research topics into four aspects: (1) the economic mechanism of haze formation; (2) the relationship between haze and economic growth; (3) the spatial spillover effect of haze; (4) the countermeasures of haze control.

The economic mechanism of haze formation

Some scholars believe that energy and industrial structure and other factors have led to the emergence of haze weather. Jessie (2006) found that when entering the heavy industry stage, the consumption of coal increased continuously, the PM_{2.5} concentration also increased, and the air pollution problem became more and more serious. Wang et al. (2015) found that the aggravation of haze pollution is mainly caused by the rising consumption of coal energy in industrial production. Improving industrial structure is an important way to control haze. Antonakakis (2017) analyzed the relationship between carbon emissions and economic growth, and found that the increase of global carbon emissions is accompanied by rapid economic growth.

However, some scholars have raised questions and conducted research: Antweiler (2001) established a theoretical model and used the data of SO₂ concentration to test the theory, and finally came to the conclusion that more free trade seems to be favorable to the environment. He (2012) analysed the impact of the three heavy transformation processes on the environment, such as marketization, globalization and decentralization, and concluded that the marketization and decentralization are harmful to the urban environment, while the economic globalization is beneficial to the urban air quality.

The relationship between haze and economic growth

1) Empirical research based on EKC

Panayotou (1993) applied the Kuznets curve to the analysis of the relationship between environmental quality and economic growth, and proposed the EKC hypothesis (an inverted U-shaped relationship between environmental pollution and economic growth) for the first time. Selden and Song (1994) analyzed and found that the per capita emissions of suspended particulate matter, SO₂, NO_x and CO had a reverse relationship with GDP per capita. They believed that although emissions would be reduced in the long run, it was expected that global emissions would continue to grow rapidly in the next few decades. Grossman and Krueger (1994) found that economic growth brought about environmental deterioration in the early stages of economic growth and improvement in the later stages; and the turning points of different pollutants were different.

With the deepening of research, different voices have emerged in academia: Ansuategi (2003), by analyzing the panel data of SO₂ emissions in Europe, proposed that EKC would be established only when the pollutants are semi-local and have medium-term effects. Stern (2004) pointed out that there are some problems in EKC hypothesis, such as omission of variable bias, heteroscedasticity and endogeneity. Dinda (2004) combed the related literature, background history and conceptual insights, and summarized two general explanations for the formation of EKC. At the same time, there were some doubts about EKC from the perspective of concept and method. However, Tamazian and Rao (2010) considered the questions raised by the predecessors and examined them again. The results still showed the environmental Kuznets hypothesis was valid.

Hao and Liu (2016) used spatial error model and spatial lag model to analyze the direct relationship between PM_{2.5} and economic development. The results show that the relationship between PM_{2.5} and per capita GDP is inverted U-shaped. Secondary industry has a significant positive impact on urban PM_{2.5} concentrations. Sarkodie et al. (2019) concluded that the per capita PM_{2.5} emissions and income levels showed an

inverted U-shaped curve, which confirmed the validity of the Kuznets curve hypothesis between air pollution and urbanization.

2) Theoretical research

Compared with empirical analysis, the theoretical research in this field is relatively weak: Bovenberg and Smulders (1993) explored the relationship between environmental quality and economic growth in the endogenous economic growth model under the technological change driven by pollution. Chichilnisky (1994) put the environment and pollution into the neoclassical production function and utility function to analyze, and believed that the different property rights created different regional trade motives.

The spatial spillover effect of haze

Many scholars in the world believe that the haze pollution in a certain region will affect the environmental quality of the surrounding areas, and its governance will also affect the surrounding areas. That is, there is a spatial spillover effect of haze. Therefore, it is necessary to explore the relationship between the environment and the economy in the space framework, although it will make the relationship more complex.

In the early twenty-first Century, Anselin (2001), a famous international econometric economist, applied the spatial econometric modeling method to the perspective of environment and resource economy, and studied the importance of spatial factor analysis. Maddison (2007) selected SO₂, NO₂ and other pollutants as the typical measure of air quality, and used the spatial econometric method to establish a model. It was found that there was a spillover effect on the pollution and governance of haze between countries under this model. Poon et al. took Chinese provinces as the research object. By simulating the impact of energy, transportation and trade on local air pollution emissions, it was confirmed that spillover effect did exist in Chinese provinces Poon et al. (2006). Hosseini and Kaneko (2013) used six kinds of weight matrices to create six spatial models, demonstrating that air pollution does have spillover effects between countries. Dimitriou and Kassomenos (2014) studied the origin of PM_{2.5} in Rome and its impact on air quality, indicating that pollutants have potential external spillover effects.

The countermeasures of haze control

According to the policy connotation reflected by EKC, economic growth will ultimately help improve environmental quality, and pollution is only a “by-product” on the growth path (Lu and Sun, 2015). However, accelerating economic growth is not a panacea for improving environmental quality (Arrow et al., 1995). Grossman and Krueger (1995) believed that the effective way to solve the environmental problems is to improve the technology and optimize the industrial structure. Based on the theory of sustainable development, Karki (2005), taking the ASEAN region as an example, believed that in order to maintain sustainable development under the condition of growing economy, comprehensive management of resources and energy was needed. Ma et al. (2019) analyzed haze in eastern and northern China, and believed that emission reduction and regional joint prevention and control would help improve air quality.

Some scholars use the Computable General Equilibrium (CGE) model to study the methods and countermeasures of haze control. Jie (2005) established a static CGE model, and found that under the policy of flue gas desulfurization, the economic growth rate will decrease, and clean energy will be used instead of polluting energy to achieve the purpose of reducing pollution. Based on the CGE model, scholars such as Xu (2009) and Allan (2014) have proposed the idea of using tax tools, including sulfur taxes and carbon taxes, to control haze. Chander (2018) proposed to strengthen the current policy system to solve the haze problem in Indonesia, including the implementation of various tax laws.

Research hotspots and trend analysis

Research hotspots

Keyword co-occurrence network can reflect the current research hotspots in a certain field. Based on this, the network node of CiteSpace is selected as “Keywords”, the time slice is 3, the threshold is set to “Top 10% per slice, up to 30”, and the Pathfinder algorithm is selected to be simplified. After that, the clustering analysis is carried out, and key words are extracted with LLR (logarithmic likelihood algorithm) as the clustering identifiers. The results are shown in *Figure 6* and *Table 3*.

The upper left corner of *Figure 6* shows that the Q value of the co-occurrence network of haze and economic growth is $0.5682 \geq 0.3$, and the S value is close to 0.5, which indicates that the network structure is significant and the result is basically reasonable. The graph has 221 nodes and 424 connections, with a density of 0.0174. The greater the node is, the higher the number of occurrences is. The nodes with purple outer ring will play an important role in the network. In this paper, the keywords with intermediary centrality (≥ 0.1) are selected to explore the research hotspots in various fields in the different periods, as shown in *Table 4*.

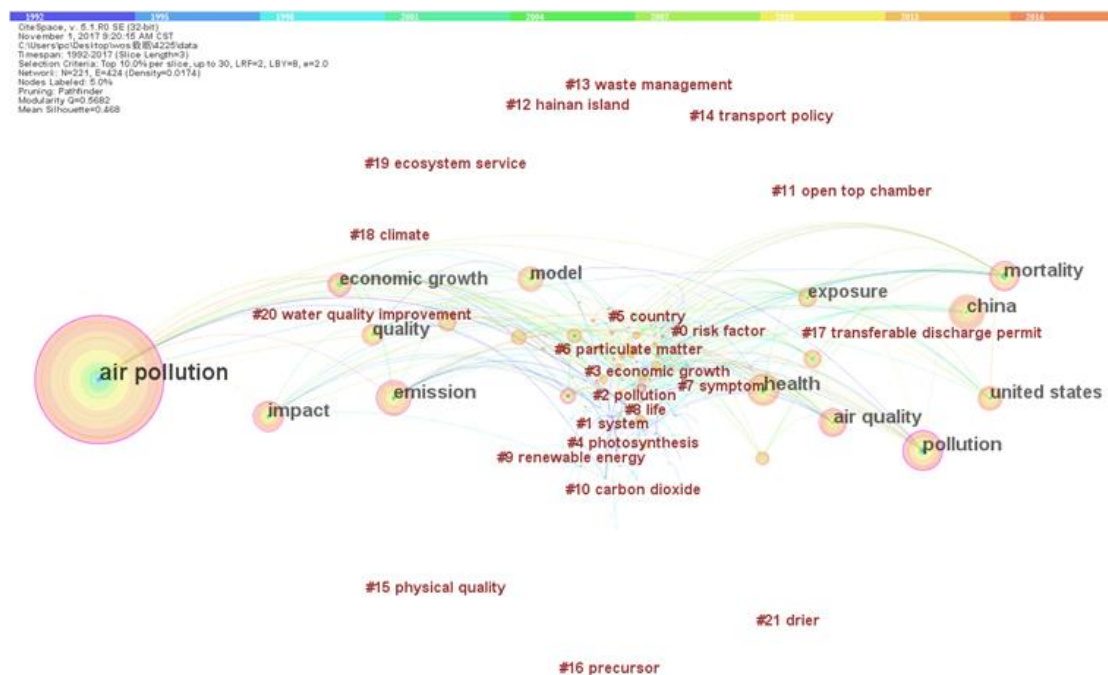


Figure 6. Keywords co-occurrence map

Table 3. Keywords clustering

Serial number	Cluster size	The tightness of clustering	Label	High frequency keywords
0	39	0.617	Risk factor	Health(313); mortality(275); exposure(203)
1	27	0.7	System	Climate change(179); energy(153) performance(112)
2	26	0.549	Pollution	China(330); impact(277); air quality(272)
3	24	0.723	Economy growth	Emission(328); policy(165) environmental Kuznets curve(113)
4	19	0.808	Photosynthesis	Acidification(14); deposition(8); critical load(7)
5	17	0.76	Country	CO ₂ emission(103); consumption(46); lead(15)
6	14	0.757	Particulate matter	Aerosol(94); pm ₁₀ (81); pm _{2.5} (65)
7	14	0.771	Symptom	Particle(40); water(15); respiratory health(14)
8	12	0.771	Life	Benefit(63); cost(50); industry(27)
9	11	0.865	Renewable energy	Plant(12); environmental impact(8); greenhouse effect(7)
10	5	0.976	Carbon dioxide	Abscisic acid(6); SO ₂ (5); transport policy(3)

Table 4. Keywords with intermediary centrality ≥ 0.1

Serial number	Frequency	Centrality	Key word	Serial number	Frequency	Centrality	Keywords
1	1076	0.45	Air pollution	8	228	0.14	Quality
2	365	0.23	Pollution	9	203	0.14	Exposure
3	328	0.22	Emission	10	313	0.13	Health
4	330	0.19	China	11	270	0.12	Air quality
5	275	0.18	Mortality	12	108	0.11	System
6	52	0.18	Children	13	175	0.1	Particulate matter
7	153	0.15	Energy	14	5	0.1	Acid rain

According to the map analysis, the keywords “air pollution”, “pollution”, “emission”, “mortality” and “China” are ranked in the top five, and their co-occurrence frequency is more than 200 times. These keywords with high frequency and centrality represent the issues that researchers have paid close attention to and conducted a lot of research during this period, and play a key pivotal role in the study of the correlation effect between haze and economic growth.

Trend analysis

Timezone view focuses on the evolution trend of research topics over time and their impact on each other. Therefore, the timezone view of keyword co-occurrence network can show the hot trends in the field of the correlation between haze and economic growth in the world. The network node is selected as “Keywords”, the time slice is 3, the threshold is set to “Top N = 20”, and the MST algorithm is selected for pruning to get the main hot trends in this field. Finally, the time map of the keyword evolution since 1992 is obtained (Fig. 7).

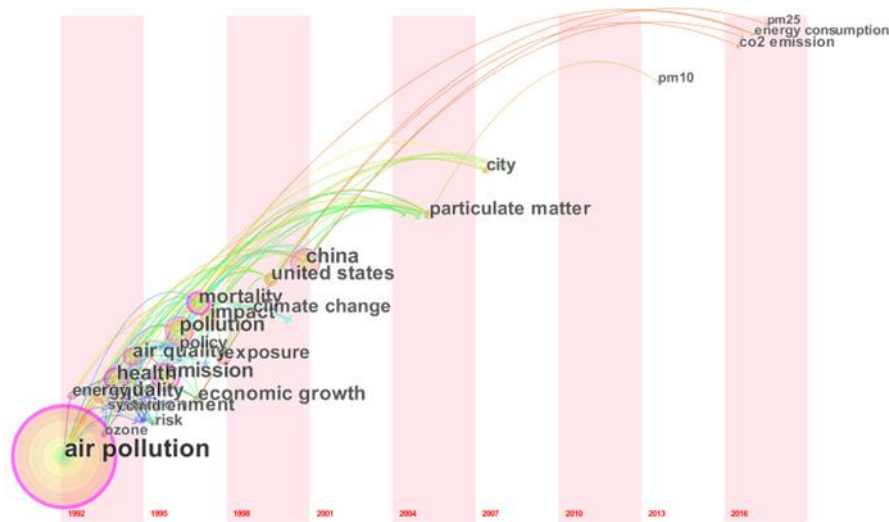


Figure 7. Keywords time zone map

Through the analysis of *Figure 7* and its background data, there are many key words in the early stage of the evolution of the correlation between haze and economic growth, such as “air pollution”, “health”, “economic growth” and “energy”. These keywords are the most important focus of the academic community on the correlation between smog and economic growth in the 1990s. Since the 21st century, keywords such as “China”, “particulate matter”, “city” and “PM_{2.5}” “CO₂ emission” have attracted wide attention and become the current research hotspot in this field, which may continue to be hot in the future. On the whole, *Figure 7* shows the trend of international research on haze and economic growth.

Conclusion

In view of the fact that the current research has not yet fully demonstrated the development of international research on the correlation between haze and economic growth, and the lack of scientific visual quantitative analysis, this paper systematically analyzed the research on the correlation effect between haze and economic growth by using knowledge map method and CiteSpace tool. The time distribution of the literature in this field is distributed. The author’s publications and cooperation in this field is analyzed by using the co-occurrence map of the author. Through the analysis of the research institutions, national co-occurrence and co-cited of journals, the main research forces in the field and the high level journals are found. The research hotspots and trends in this field are explored by using the keyword co-occurrence map and time zone map.

The main conclusions are as follows: (1) In the past sixteen years, the international academia has paid more and more attention to the correlation effect between haze and economic growth, and the literature in this field is increasing. According to the four stages of the logical growth curve of the literature, we can see that it is now in the T₁-T₂ period (rapid development stage), which has abundant research results, and the growth rate of the literature volume remains relatively high. (2) At the international level, a group of high-yielding authors headed by Huang Guohe of North China Electric Power

University, has been formed in this field, and the cooperation between these high-yielding authors is closer in the last five years and is in the stage of deepening cooperation. But the other authors lack communication and are in a state of isolation. (3) The main research forces in the field are concentrated in the international top universities and scientific research institutes. “The USA-China” and “Holland-France-Italy-Spain” are the main cooperation bodies in recent years. (4) Literature with great value in this field in the world is mainly concentrated on “Science”, “Environmental Health Perspectives” and “Environmental Science & Technology”. The related papers in these journals represent the hot and frontier research in this field, and have high academic value. (5) The research topics in this field mainly include the economic mechanism of haze formation, the relationship between haze and economic growth, the spatial spillover effect of haze and the countermeasures for haze control. (6) Keywords such as “air pollution”, “health”, “economic growth” and “energy” have been released in the early stage of the field. Since the 21st century, “China”, “particulate matter”, “city”, “PM_{2.5}” and “CO₂ emission” have become the research hotspots.

In short, from the perspective of economic growth, the phenomenon of haze can be studied in many aspects. However, from the perspective of system theory and scientific development concept, the existing research still has the following shortcomings: (1) In terms of research content, there are many studies on the causes and countermeasures of haze, but little attention has been paid to the transmission mechanism of haze and its relationship with economic growth, especially the lack of theoretical research on this issue; (2) In terms of research methods, the normative analysis of haze and economic activities is more, but the empirical analysis of spatial statistics and econometrics is relatively lacking. Therefore, as a hot research topic in the interdisciplinary field of environment and economy, the use of spatial statistics and econometric methods to study whether haze and economic growth are related, and what kind of correlation exists is a further research direction in the future.

Acknowledgements. This work is supported by the National Social Science Foundation of China (grant number 15CJL029).

REFERENCES

- [1] Allan, G., Lecca, P., Mcgregor, P., Swales, K. (2014): The economic and environmental impact of a carbon tax for Scotland: a computable general equilibrium analysis. – *Ecological Economics* 100: 40-50.
- [2] Anselin, L. (2001): Spatial effects in econometric practice in environmental and resource economics. – *American Journal of Agricultural Economics* 83: 705-710.
- [3] Ansuategi, A. (2003): Economic growth and transboundary pollution in Europe: an empirical analysis. – *Environmental & Resource Economics* 26: 305-328.
- [4] Antonakakis, N., Chatziantoniou, I., Filis, G. (2017): Energy consumption, CO₂, emissions, and economic growth: an ethical dilemma. – *Renewable & Sustainable Energy Reviews* 68: 808-824.
- [5] Antweiler, W., Copeland, B. R., Taylor, M. S. (2001): Is free trade good for the environment? – *American Economic Review* 91: 877-908.
- [6] Arrow, K., Bolin, B., Costanza, R., et al. (1995): Economic growth, carrying capacity, and the environment. – *Science* 268: 520.

- [7] Bovenberg, A. L., Smulders, S. (1993): Environmental quality and pollution-augmenting technological change in a two-sector endogenous growth model. – *Journal of Public Economics* 57: 369-391.
- [8] Chander, P. (2018): A political economy analysis of the Southeast Asian haze. – *Singapore Economic Review* 63: 1085-1100.
- [9] Chen, Y., Chen, C. M., Hu, Z. G. (2014): Principles and Applications of Analyzing a Citation Space. – Science Press, Beijing.
- [10] Chichilnisky, G. (1994): North-south trade and the global environment. – *American Economic Review* 84: 851-874.
- [11] Dimitriou, K., Kassomenos, P. (2014): Indicators reflecting local and transboundary sources of PM_{2.5} and PMCOARSE in Rome-impacts in air quality. – *Atmospheric Environment* 135: 69-86.
- [12] Dinda, S. (2004): Environmental Kuznets curve hypothesis: a survey. – *Ecological Economics* 49: 431-455.
- [13] Feng, X. L., He, S., Xiong, T. C., Wu, Q. H., L, Y. J. (2017): Comparison and analysis of mapping knowledge domain and Google knowledge graph; based on the theory of knowledge management. – *Journal of Intelligence* 36: 149-153.
- [14] Grossman, G. M., Krueger, A. B. (1994): Economic Growth and the Environment. – *Quarterly Journal of Economics* 110: 353-377.
- [15] Grossman, G. M., Krueger, A. B. (1995): Economic Growth and the Environment. – Springer, Netherlands.
- [16] Hao, Y., Liu, Y. (2016): The influential factors of urban PM_{2.5} concentrations in China: a spatial econometric analysis. – *Journal of Cleaner Production* 112: 65-80.
- [17] He, C., Pan, F., Yan, Y. (2012): Is economic transition harmful to China's urban environment? Evidence from industrial air pollution in Chinese cities. – *Urban Studies* 49: 1767-1790.
- [18] Hosseini, H. M., Kaneko, S. (2013): Can environmental quality spread through institutions? – *Energy Policy* 56: 312-321.
- [19] Hou, H. Y., Liu, Z. Y., Luan, C. J. (2009): Quantitative analysis on the research front of international scientometrics: based on mapping of knowledge. – *Science Research Management* 30: 164-170.
- [20] Jie, H. E. (2005): Estimating the economic cost of China's new desulfur policy during her gradual accession to WTO: the case of industrial SO₂ emission. – *China Economic Review* 16: 364-402.
- [21] Karki, S. K., Mann, M. D., Salehfar, H. (2005): Energy and environment in the ASEAN: challenges and opportunities. – *Energy Policy* 33: 499-509.
- [22] Liu, N. B., Ruan, X. P., Sun, L. Z. (2011): Bibliometrics analysis on information organization research in China. – *Journal of Modern Information* 31: 100-103.
- [23] Liu, X. X., Zhang, G. Y., Tan, R. J., Ma, W. C. (2017): Foreign sustainable transformation theory research context and hotspot detection: based on the perspective of scientific knowledge. – *Journal of South China Normal University (Social Science Edition)* 5: 86-97 + 190-191.
- [24] Lu, H., Sun, H. C. (2015): Spatial characteristics of smog pollution and associated effects on economic growth. – *Fujian Forum·Humanities and Social Sciences Edition* 9: 44-51.
- [25] Ma, T., Duan, F., He, K., Qin, Y., Tong, D., Geng, G. (2019): Air pollution characteristics and their relationship with emissions and meteorology in the Yangtze River Delta region during 2014-2016. – *Journal of environmental sciences* 83:8-20.
- [26] Maddison, D. (2007): Modelling sulphur emissions in Europe: a spatial econometric approach. – *Oxford Economic Papers* 59: 726-743.
- [27] Panayotou, T. (1993): Empirical tests and policy analysis of environmental degradation at different stages of economic development. – International Labour Organization.
- [28] Poon, J. H., Casas, I., He, C. F. (2006): The impact of energy, transport, and trade on air pollution in China. – *Eurasian Geography & Economics* 47: 568-584.

- [29] Qiu, J. P. (2007): *Information Metrology*. – Wuhan University Press, Wuhan.
- [30] Sarkodie, S. A., Strezov, V., Jiang, Y. (2019): Proximate determinants of particulate matter (PM_{2.5}) emission, mortality and life expectancy in Europe, Central Asia, Australia, Canada and the US. – *The Science of the Total Environment* 683:489-497.
- [31] Selden, T. M., Song, D. (1994): Environmental quality and development: is there a Kuznets curve for air pollution emissions? – *Journal of Environmental Economics & Management* 27: 147-162.
- [32] Shi, X. C., Li, M. L. (2016): The hotspots and trends of international literature research on MOOC from 2013-2015: a visualized analysis based on citespace. – *Open Education Research* 1: 90-99.
- [33] Stern, D. I. (2004): The rise and fall of the environmental Kuznets curve. – *World Development* 32: 1419-1439.
- [34] Sun, R. Y., Wang, X. (2016): Analysis on the status of the internet of things in China based on the bibliometrics statistical methods. – *Journal of Modern Information* 36: 153-159.
- [35] Tamazian, A., Rao, B. B. (2010): Do economic, financial and institutional developments matter for environmental degradation? Evidence from transitional economies. – *Energy Economics* 32: 137-145.
- [36] Wang, H. J., Chen, H. P., Liu, J. P. (2015): Arctic Sea ice decline intensified haze pollution in eastern China. – *Atmospheric and Oceanic Science Letters* 8(1):1-9.
- [37] Xu, Y., Masui, T. (2009): Local air pollutant emission reduction and ancillary carbon benefits of SO₂ control policies: application of AIM/CGE model to China. – *European Journal of Operational Research* 198(1): 315-325.
- [38] Zhou, Q. (2011): The effects of China's regional economic growth on the environmental quality: based on the empirical study of eastern central and western Kuznets curve. – *Statistics & Information Forum* 26: 45-51.

CONCENTRATION DISTRIBUTION OF HEAVY METALS IN MANILA CLAM (*RUDITAPES PHILIPPINARUM*) AND POTENTIAL HEALTH RISK IN THE COASTAL AREAS OF LIAODONG BAY, CHINA

LIU, Y.-H.^{1,2} – YANG, S.² – TANG, F.² – MA, W.² – LI, Y.-F.^{1*}

¹*College of Veterinary, Northeast Agricultural University
HarBin 150030, Hei Longjiang Province, China*

²*College of Animal Husbandry and Veterinary, Jinzhou Medical University
Jinzhou 121000, Liaoning Province, China*

**Corresponding author
e-mail: bdlyh@163.com*

(Received 24th May 2019; accepted 10th Oct 2019)

Abstract. Arsenic (As), Cadmium (Cd), Chromium (Cr), Copper (Cu), Lead (Pb), and Zinc (Zn) concentrations in Manila clam from Liaodong Bay (China) were determined by inductively coupled plasma mass spectrometry. Tissue-specific bioaccumulation, geographical variability (using metal pollution indices) and health risks (using target hazard quotients and maximum daily consumption values) were assessed. Cd concentrations were high at all sampling sites, particularly S6 and S7, where it reached Category III. Other metal concentrations were high at S7 (As), S1 (Cr), S5 (Pb), and S5 and S7 (Zn). As, Cr and Cu accumulated to a higher degree in the viscera than muscles, but Cd accumulated more in muscles than viscera. Heavy metal (HM) contamination was worse in the west than that in the east. The Cd target hazard quotients were greater than 1, but the other HM target hazard quotients were less than 1 at all sites, indicating Cd posed the greatest health risks to humans. The maximum daily consumption values also indicated Cd poses health risks.

Keywords: *heavy metals, clam, bioaccumulation, geographical variability, health risk estimate, Liaodong Bay*

Introduction

Liaodong Bay is one of the three main bays in the Bohai Sea. Water exchange between Liaodong Bay and the open sea is slow, so pollutants are not readily transported out of Liaodong Bay. Many rivers (e.g., the Dalinghe River, Liaohe River, and Xiaolinghe River) flow into the bay area. There are cities of different sizes around Liaodong Bay, and large parts of the coast are occupied by harbors, industrial areas and aquaculture facilities. Large amounts of domestic sewage and industrial effluent containing various pollutants are discharged into Liaodong Bay (Zhang et al., 2016; Naser, 2013; Gargouri et al., 2011; Wan et al., 2008a). These wastewaters also contain large amount of heavy metals (HMs). HM contamination is a serious issue around the world (Zhang et al., 2016; Gao and Chen, 2012; Hu et al., 2013).

HMs are persistent, stable, toxic, non-biodegradable, and bioaccumulative. HMs can accumulate in organisms and can cause many diseases (Li et al., 2015). HMs in the marine environment therefore pose health risks to aquatic organisms and humans consuming aquatic organisms. It is necessary to determine HM concentrations in aquatic media and organisms to gain an understanding of the health risks posed by contaminated seafood to humans consuming (Wei et al., 2014; Li et al., 2015).

Bivalves as benthic species can accumulate many pollutants, including HMs, to which they are very tolerant. Bivalves are therefore used as bioindicators of HM contamination in aquatic systems (Li and Gao, 2014; Won et al., 2016; Shoults-Wilson et al., 2015). The bivalve Manila clam (*Ruditapes philippinarum*, *Rud*) is generally found in sediment and tends to accumulate HMs present in the sediment (Zhao et al., 2012). *Rud* is easily collected in Liaodong Bay. *Rud* is considered to be delicious, and is consumed in large quantities. Determining the concentrations of HMs in *Rud* in Liaodong Bay will allow HM pollution of the aquatic environment and health risks posed to humans consuming contaminated seafood to be assessed (Liang et al., 2004).

In previous studies of HM in the Bohai Sea, most sampling sites were located along the Bohai Bay coast (Li et al., 2015; Zhang et al., 2016; Wang et al., 2005) and in Laizhou Bay (Liu et al., 2017). Few sampling sites in Liaodong Bay were used. In this study, we determined the concentrations of Arsenic (As), Cadmium (Cd), Chromium (Cr), Copper (Cu), Lead (Pb), and Zinc (Zn) in muscles and viscera from *Rud* collected from seven sites along the Liaodong Bay coast. The main objectives were 1) to determine HM concentrations in *Rud* from the different sampling sites, 2) to assess tissue-specific HM bioaccumulation by *Rud* 3) to assess geographical variability in HM concentrations in *Rud* using metal pollution indices (MPIs), and 4) to assess the risks posed by HMs in *Rud* to human health using national and international guidelines, target hazard quotients (THQs), and maximum daily consumption rates ($CR_{\max S}$).

Materials and methods

Samples were collected from seven sites along the coastal area of Liaodong Bay (China) in July and August 2017, which is the main fishing season (*Fig. 1*). Attached mud and debris was removed from the surface of each shell. The *Rud* weights and shell lengths were measured. Muscle and viscera tissue samples were collected. Muscle tissue from three individuals were combined and homogenized to form a single sample. Viscera from 15 individuals were combined and homogenized to form a single sample to provide sufficient analytes for analysis (Liu et al., 2017). Six mixed muscle samples and six viscera samples from each sampling site were analyzed. The samples were lyophilized and ground into powder. The samples were analyzed using a previously described method (Li et al., 2015). Briefly, 0.2 g of a dry sample was placed in a polytetrafluoroethylene tube containing 3 mL HNO₃ (65%) (Suprapur; Merck, Darmstadt, Germany) and 1 mL H₂O₂ (35%) (Suprapur; Merck). The tube was then placed in a Mars-5 microwave digestion instrument (CEM, Buckingham, UK) to digest the mixture. The digest was then diluted to 50 mL with ultrapure water and passed through a 0.45 μm membrane filter. The HM concentrations in the digest were determined using an Agilent 7500i inductively coupled plasma mass spectrometer (Agilent Technologies, Santa Clara, CA, USA). A standard reference material (GBW08571, mussel tissue) was analyzed to ensure the HM analysis method gave acceptable results. The mean recovery rates of the metals that were analyzed in the reference material samples were 82–112%.

The MPI was calculated for each sampling site to allow geographical variability in the HM concentrations in the *Rud* tissues to be assessed (Liu et al., 2017). The MPI was calculated using *Equation 1*:

$$MPI = (Cf_1 \times Cf_2 \times \dots \times Cf_n)^{\frac{1}{n}} \quad (\text{Eq.1})$$

where Cf_1 is the concentration of the first HM in muscle tissue (in this study) from the sampling site of interest, Cf_2 is the concentration of the second HM, Cf_n is the concentration of the n th HM, and n is the total number of HMs analyzed.

The risks posed by HMs in *Rud* to human health were assessed using THQs and $CR_{\max S}$ (US EPA, 2000; Li et al., 2015). The THQs and $CR_{\max S}$ were calculated from the HM concentrations in the muscle samples using *Equations 2 and 3*:

$$THQ = \frac{C \times W_{clam} \times ED \times EF}{BW \times RfD \times Atn} \times 10^{-3} \quad (\text{Eq.2})$$

and

$$CR_{\max} = \frac{RfD \times BW}{C} \quad (\text{Eq.3})$$

where C is the mean concentration of a HM in *Rud* muscle (in mg/kg wet weight (ww)), W_{clam} is the daily *Rud* ingestion rate for an adult (38.9 g/d) (National Bureau of Statistics of China, 2009), ED is the exposure duration (74.8 y, the expected average lifetime) (MEP, 2013), EF is the exposure frequency (365 d/y), BW is the average body weight (63 kg for an adult) (National Physique Monitoring Center of China, 2012), RfD is the average oral reference dose for the HM of interest (US EPA, 2014), Atn is the average exposure time for a non-carcinogen ($ED \times 365$ d/y), and 10^{-3} is the unit conversion factor.

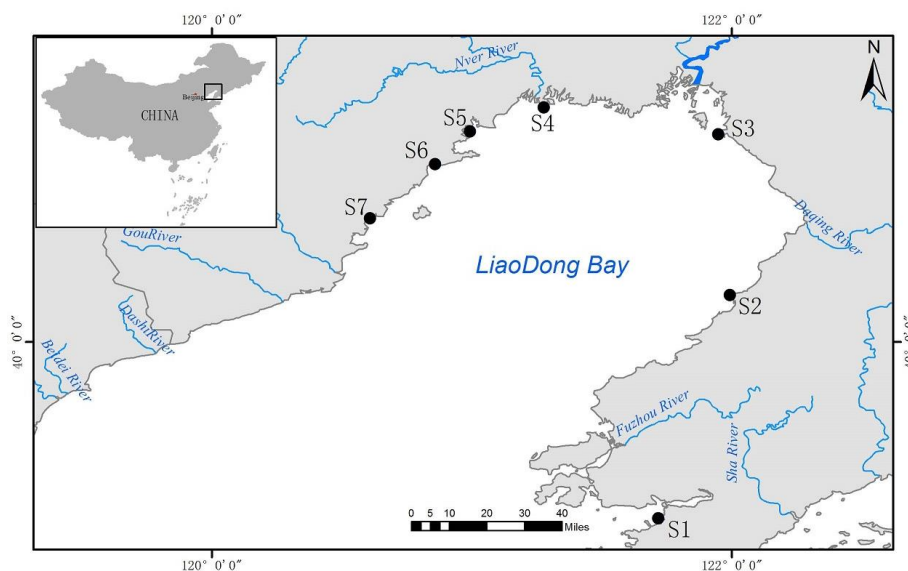


Figure 1. Map of sampling sites at the Liaodong Bay, China. S1, Puwan (39°19'16.15785"N, 121°42'59.84795"E); S2, Bayuquan (40°10'46.84870"N, 121°59'34.03441"E); S3, Erjiogou (40°47'49.44684"N, 121°56'54.37565"E); S4, Qilihekou (40°54'2.31809"N, 121°16'37.68160"E); S5, Laohekou (40°48'33.39360"N, 120°59'32.76576"E); S6, Huludao (40°41'0.69727"N, 120°51'31.40488"E); S7, Shahousuo (40°28'27.18772"N, 120°36'32.63602"E)

Data analyses were performed using SPSS 18.0 software (IBM, Armonk, NY, USA). Each result is expressed as the mean \pm standard deviation. ANOVA, SNK, and post hoc multiple comparisons, etc. were used to detect differences between groups. Differences between results for groups of samples were considered to be statistically significant at $P < 0.05$.

Results

Heavy metal concentrations in *Rud*

The HM concentrations found in the *Rud* muscle and viscera samples from each sampling site are shown in *Figure 2*. The Cd concentrations were quite high in the samples from all of the sites, particularly S6 and S7, the samples from which had Cd concentrations much higher than the Category III standard for Cd. The Cd concentrations in the samples from sites S1, S3, and S4 exceeded the Category II standard. The maximum permissible level for Cd, set by the World Health Organization in 1982, is 2 mg/kg ww, which is equivalent to the Category II standard. This indicated that attention needs to be paid to Cd pollution in Liaodong Bay. The As concentrations were higher in the samples from site S7 than in the samples from the other sites. The As concentration in the viscera samples from site S7 exceeded the Category II standard for As. The Cr concentrations were higher in the samples from site S1 than in the samples from the other sites but lower than the Category II standard for Cr. The Cu concentrations in all of the samples were low and were lower than the Category I standard for Cu. The Pb concentrations were higher in the samples from site S5 than in the samples from the other sites but were lower than the Category II standard for Pb. The Pb concentrations in the samples from the other sites were lower. The Zn concentrations in the samples from sites S5 and S7 exceeded the Category II standard.

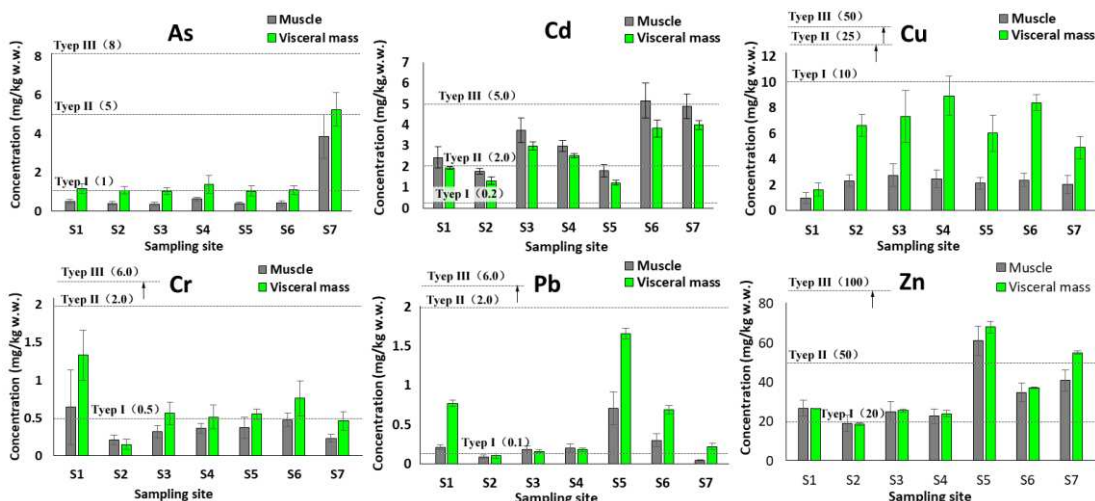


Figure 2. Concentration ranges of heavy metals in different tissues at different sampling sites

According to the standard (*Table 1*; *Fig. 2*), the concentrations of Cd, Pb and Zn in *Rud* have exceeded the allowable limits. Moreover, compared with previous studies (*Table 1*), the concentration of Cd was the highest and the others were present at a moderate level in the Liaodong Bay.

Table 1. Comparison of heavy metal concentrations in the soft tissues of shellfish from the Liaodong Bay, other areas in China, and world marine waters

Site	Species		Year	As	Cd	Cr	Cu	Pb	Zn	Reference
Liaodong Bay	<i>Ruditapes philippinarum</i>	w. w.	2017	0.92	3.27	0.37	2.15	0.25	32.82	This study
Shanghai	<i>Macra chinensis</i>	d. w.	2008 2009	0.2	0.03	0.1		0.13	14.8	Lei et al., 2013
A site of Bohai Bay	<i>Macra veneriformis</i>	w.w.	2008	1.44	0.27	1.37	2.34	0.37	11.57	Li et al., 2015
B site of Bohai Bay				1.51	0.45	1.95	1.98	0.56	14.56	
C site of Bohai Bay					2.51	0.47	0.49	1.05	0.17	
Laizhou Bay	Ark shell	w.w.	2011	30.4	1.3	0.25	1.17	0.1	17.53	Liu et al., 2017
	Surf clam			1.16	0.22	0.48	1.11	0.21	9.89	
	Manila clam			3.08	0.26	0.38	1.78	0.22	21.35	
Daya Bay	<i>Perna viridis</i>	w.w.	2015	0.54	0.006	1.07	0.69	0.07	10.76	Gu et al., 2016
Catania Gulf	<i>D. trunculus</i>	w.w.	2012	1.53	0.01	0.25		0.07	7.63	Copat et al., 2013
Adriatic coastal area	<i>Mytilus galloprovincialis</i>	d.w.	2009		1.72		5.31	3.79	111.2	Jovic and Stankovic, 2014
Venezuelan coast	<i>Crassostrea rhizophorae</i>	d.w.	2008 2009		2.5	1.2	50.4	2.6	563.3	Alfonso et al., 2013
Grade I.	Shellfish	w.w.		1.0	0.2	0.5	10	0.1	20	SEPA, 2001
Grade II.	Shellfish	w.w.		5.0	2.0	2.0	25	2.0	50	SEPA, 2001
Grade III.	Shellfish	w.w.		8.0	5.0	6.0	50	6.0	100	SEPA, 2001

w.w.: wet weight, d.w.: dry weight

Tissue-specific bioaccumulation of HMs in Rud

The results of one-way analyses of variance in the HM concentrations in the muscle and viscera samples are summarized in *Table 2*. The concentrations in the muscle and viscera samples were significantly different for As, Cd, Cr, and Cu ($p < 0.05$) but not for Zn and Pb ($p > 0.05$). Different tissue-specific bioaccumulation patterns were found for different metals (*Fig. 3*). The Cd concentrations were significantly higher in the muscle samples than the viscera samples ($p < 0.05$). The As, Cr, and Cu concentrations were significantly higher in the viscera samples than the muscle samples ($p < 0.05$).

Table 2. One-way ANOVA results running on the heavy metal concentrations (mg/kg wet wt) in the muscles and visceral masses of *Rud* from Liaodong Bay

HM	Cd	Cr	As	Cu	Zn	Pb
F	4.29	10.93	4.59	65.76	0.73	9.40
p	0.043	0.002	0.036	0.002	n.s.	n.s.

n.s.: no statistical difference

Geographical variability in the HM concentrations in Rud

HM concentrations in samples from different areas

Comparison of the HM concentrations (mg/kg dry wt) in the muscles of *Rud* in different sampling regions of Liaodong Bay are summarized in *Figure 4*. The west coast is S4–S7, and the east coast is S1–S3. The As, Cd, and Pb concentrations were significantly higher along the west coast than along the east coast ($p < 0.05$). The Cr, Cu, and Zn concentrations along the east and west coasts were not significantly different ($p > 0.05$).

Rud MPIs in different areas

MIPs were calculated according to *Equation 1*. The MPIs for the different sampling sites are summarized in *Table 3*. The MPIs for the sampling sites decreased in the order $S4 > S5 > S6 > S7 > S3 > S1 > S2$. The MPIs were higher for the west coast (sites S4–S7) than the east coast (sites S1–S3). These results indicated that HM contamination is more serious along the west coast than the east coast.

Table 3. MPI values of Rud in different sampling sites of Liaodong Bay

Eastern site	MPI	Western site	MPI
S1	3.36	S4	4.61
S2	2.70	S5	4.50
S3	3.71	S6	4.45
		S7	3.93
Mean value	3.26	Mean value	4.37

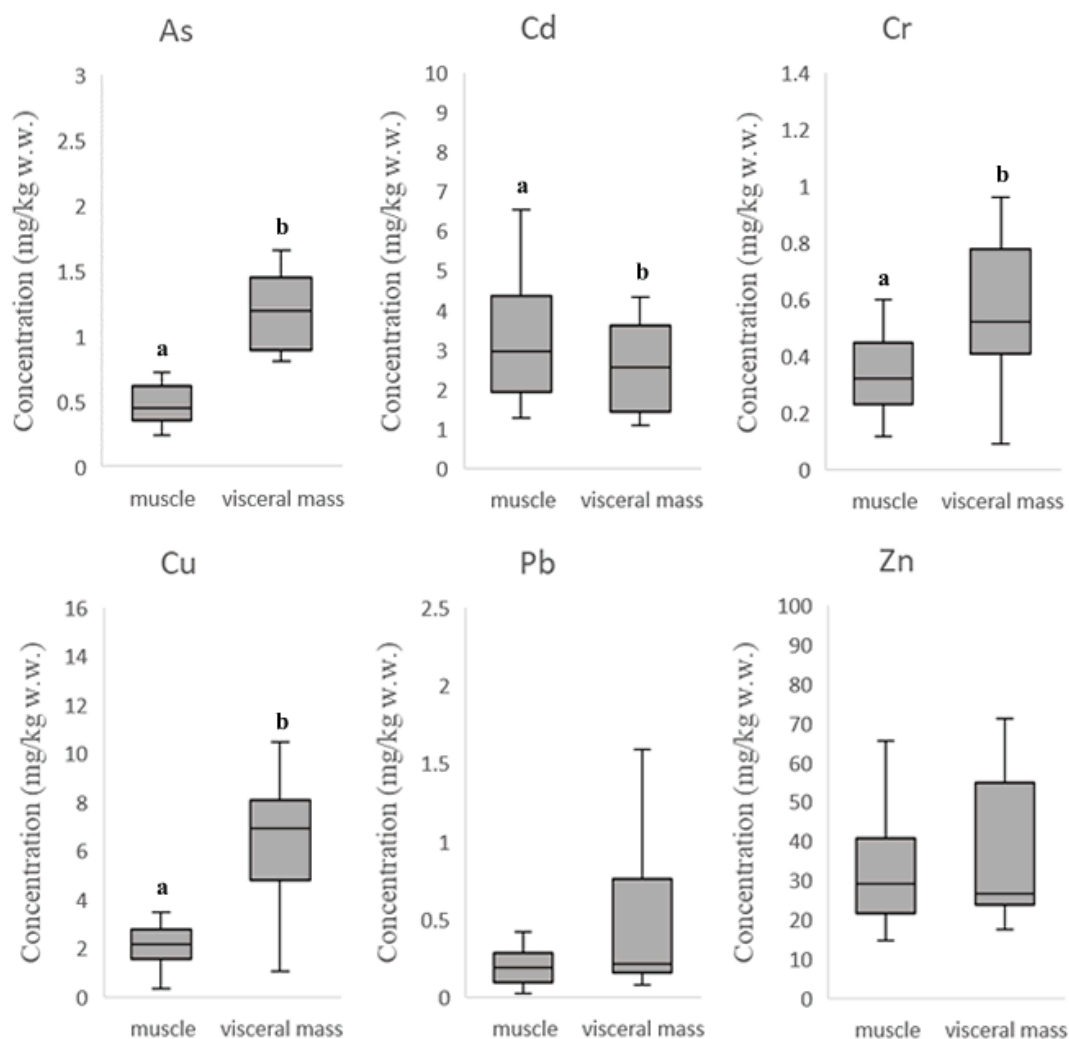


Figure 3. Boxing plotting of the heavy metal concentrations (mg/kg dry wt) in the tissues of Rud from Liaodong Bay. Different superscript letters indicate significant differences at $p < 0.05$ ($n = 6$)

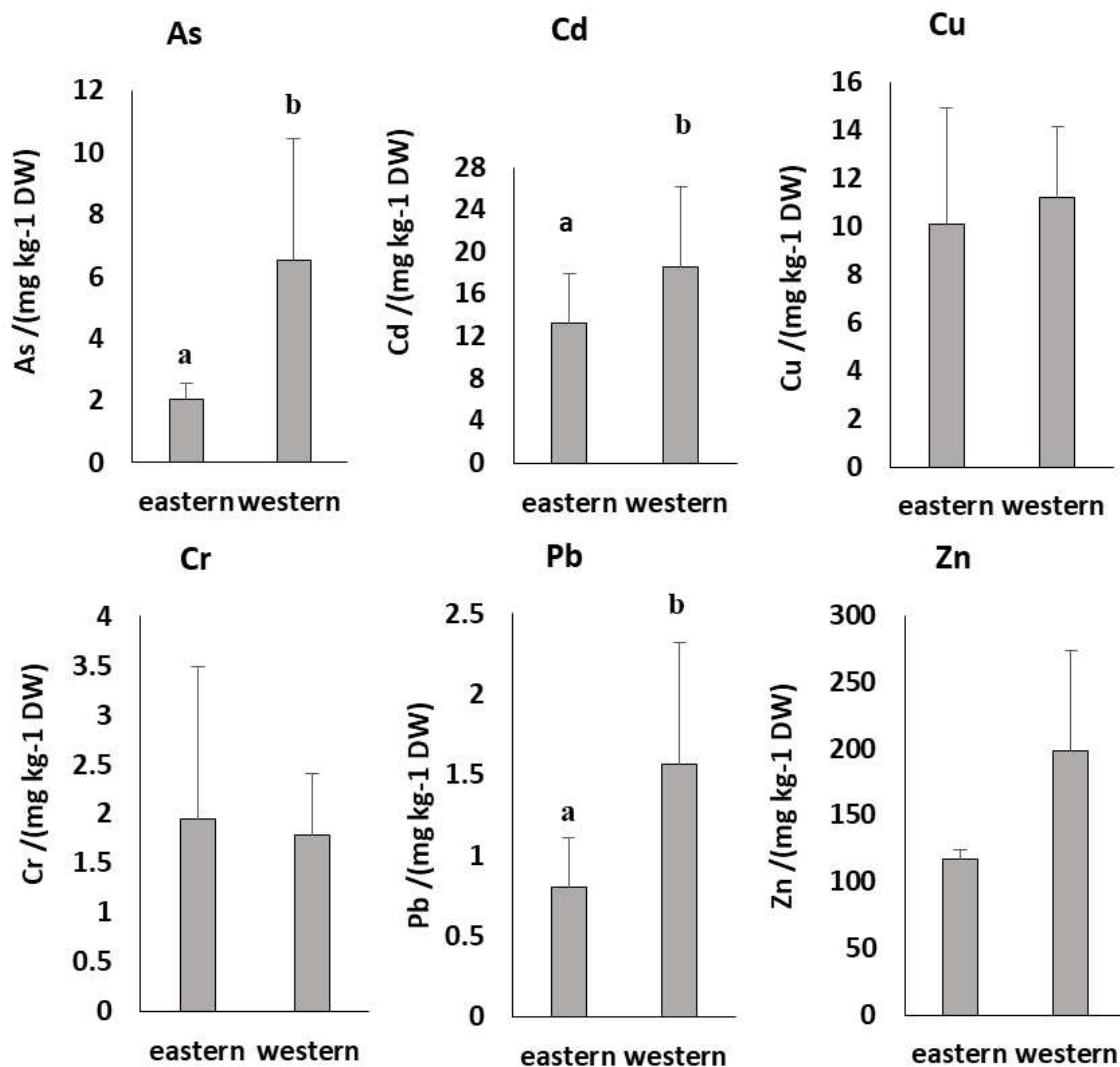


Figure 4. Comparison of the heavy metal concentrations (mg/kg dry wt) in the muscles of *Rud* in different sampling regions of Liaodong Bay. Different superscript letters indicate significant differences at $p < 0.05$ ($n = 6$)

Health risks posed to humans by HMs in *Rud*

The HM concentrations in the muscle tissues and national and international guidelines for the HMs are summarized in *Table 4*. The Cd concentrations in the muscle tissue samples from sites S1, S3, S4, S6, and S7 (2.45–5.18 mg/kg ww) exceeded the relevant limits for Cd (1–2 mg/kg ww). The As concentrations in the samples from sites S4 and S7 (0.6 and 3.84 mg/kg ww, respectively) exceeded the Chinese national guideline of 0.5 mg/kg ww. The Cr, Cu, Pb, and Zn concentrations (0.21–0.64, 0.98–2.76, 0.04–0.71, and 18.94–60.97 mg/kg ww, respectively) were within the relevant limits (2, 50, 1.0–1.5, and 100 mg/kg ww, respectively).

The potential health risks posed by HMs in *Rud* to humans were estimated by calculating THQs and CR_{maxS} according to *Equations 2* and *3*. The results are summarized in *Tables 5* and *6*. Inorganic As is more toxic than organic As, and the calculations were performed assuming that inorganic As contributed 3% of the total As concentrations (Li et al., 2015).

Table 4. Heavy metal concentrations in the muscle tissues of *Rud* from Liaodong Bay. (mg/kg w.w.)

	Safety guidelines	Heavy metal concentrations						
		S1	S2	S3	S4	S5	S6	S7
Cd	1 ^b ,2 ^d	2.45	1.78	3.74	3	1.82	5.18	4.91
Cr	2 ^{a,b}	0.64	0.21	0.32	0.36	0.37	0.47	0.23
As	0.5 ^{a,b}	0.49	0.39	0.35	0.61	0.38	0.4	3.84
Cu	50 ^b	0.98	2.33	2.76	2.45	2.13	2.38	2.04
Zn	150 ^e	26.75	18.94	24.87	22.66	60.97	34.79	40.79
Pb	1.0 ^{bd} ,1.5 ^c	0.21	0.09	0.18	0.2	0.71	0.3	0.04

Table 5. Estimated target hazard quotient (THQ) for *Rud*

HMs	RfD (mg/kg·day)	THQ						
		S1	S2	S3	S4	S5	S6	S7
Cd	5×10^{-4}	3.03	2.20	4.62	3.71	2.25	6.40	6.06
Cr	3×10^{-3}	0.13	0.04	0.07	0.07	0.08	0.09	0.05
As	3×10^{-4}	0.03	0.02	0.02	0.04	0.02	0.03	0.24
Cu	4×10^{-2}	0.02	0.04	0.04	0.04	0.03	0.04	0.03
Zn	3×10^{-1}	0.06	0.04	0.05	0.05	0.13	0.07	0.08
Pb	1×10^{-2}	0.01	0.01	0.01	0.01	0.04	0.02	0.00

Table 6. Estimated maximum consumption rates (CR_{max}) for *Rud*

HMs	CR_{max} (g w.w.)						
	S1	S2	S3	S4	S5	S6	S7
Cd	12.86	17.70	8.42	10.50	17.31	6.08	6.42
Cr	295.31	900.00	590.63	525.00	510.81	402.13	821.74
As	1285.71	1615.38	1800.00	1032.79	1657.89	1575.00	164.06
Cu	2571.43	1081.55	913.04	1028.57	1183.10	1058.82	1235.29
Zn	706.54	997.89	759.95	834.07	309.99	543.26	463.35
Pb	3000.00	7000.00	3500.00	3150.00	887.32	2100.00	15750.00

A $THQ \leq 1$ was taken to indicate no risks were posed to humans, and a $THQ > 1$ was taken to mean risks were posed to humans (Li et al., 2015). The Cd THQs (2.189–6.397) were higher than the other metal THQs for all the sampling sites. The concentrations of the HMs other than Cd in *Rud* from all of the sampling sites were found not to pose significant risks to humans ($THQ < 1$).

HMs can accumulate in *Rud*. Consuming certain amounts of contaminated *Rud* could therefore cause adverse health effects. CR_{max} s for the HMs in *Rud* were therefore calculated. The Pb CR_{max} s were relatively high, at 887.32–15750.00 g ww). The Cd CR_{max} s (6.08–17.70 g ww) were lower than the CR_{max} s for the other HMs, meaning the probability of health risks being posed to humans consuming *Rud* from Liaodong Bay was higher for Cd than the other HMs.

Discussion

HMs in Rud

Liaodong Bay is the largest bay in the Bohai Sea. A complete water exchange cycle in Liaodong Bay takes 15 y (Wan et al., 2008a). Many rivers (including the Cishanhe River, Dalinghe River, Liaohe River, Shuangtaizihe River, Xiaolinghe River, and Wulihe River) discharge into Liaodong Bay. These rivers are thought to be important sources of HMs to Liaodong Bay (Wan et al., 2008b). The Cd concentrations in the samples from all of the sampling sites were quite high, and the concentration in the muscle samples from site S6 exceeded the Category III standard for Cd. This indicated that attention needs to be paid to Cd pollution in Liaodong Bay. The Cr and Pb concentrations were higher in the samples from sites S1 and S5, respectively, than in the samples from the other sites but lower than the Category II standards. The As concentrations in the viscera samples from site S7 exceeded the Category II standard for As, and the Zn concentrations in the viscera samples from sites S5 and S7 exceeded the Category II standards. These results indicated that the sites mentioned may be contaminated with these HMs. The Pb concentrations were not high. Pb and its salts can cause kidney damage and negatively affect the nervous system. Even low Pb concentrations in food cannot be ignored (Gao et al., 2014).

Compared with other domestic and international bays, Liaodong Bay has higher Cd concentration in shellfish (Lei et al., 2013; Li et al., 2015; Liu et al., 2017; Gu et al., 2016; Copat et al., 2013; Jovic and Stankovic, 2014; Alfonso et al., 2013). Cd pollution is worthy of attention.

Tissue-specific differences in HM concentrations

In clams, HMs tend to accumulate more efficiently in viscera than muscles (Husmann et al., 2012; Sarkar et al., 2008; Liu et al., 2017). Viscera play important roles in metabolic processes related to HMs. The hepatopancreas and kidney play important roles in HM absorption, transport, storage, and excretion. HMs in muscle tissue can be removed relatively quickly. In this study, As, Cr, and Cu had similar tissue-specific accumulation characteristics. The concentrations of these HMs were higher in the viscera than the muscles. In contrast, the Cd concentrations were higher in the muscles than the viscera. Similar results have been found in previous studies (Liu et al., 2017; Tarque et al., 2012). Insufficient data were available to explain this. In aquatic environments, Cd is mainly in the dissolved phase. Cd may easily be absorbed by tissues it comes into contact with (e.g., the mantle) in *Rud*. Large amounts of Cd may therefore accumulate in the mantle (Liu et al., 2017). This could explain the Cd concentrations being higher in the muscle samples than the viscera samples. Zn is an essential element that is absorbed and eliminated through various physiological processes in different tissues. Excess Zn may accumulate in the mantle of a clam. These factors may affect Zn accumulation in the muscles and viscera and explain the Zn concentrations in the muscle and viscera samples not being different.

Geographical differences in HM concentrations

HM contamination of *Rud* was more severe in the west of Liaodong Bay (at sites S4–S7) than in the east (sites S1–S3). Geographical variations in HM concentrations in clams are generally considered to be related to the distributions and characteristics of

local sources of pollutants. The sampling sites along the west coast of Liaodong Bay were in Jinzhou Bay, a small cove in the northwestern part of Liaodong Bay. Jinzhou Bay has been contaminated by industrial effluent from chlor-alkali plants, petrochemical plants, the Huludao zinc plant, and the Bohai shipyard (Gao et al., 2014). Water in Liaodong Bay and the open sea is exchanged quite weakly, so HMs are not quickly transported from Liaodong Bay into the open sea. HMs released into Liaodong Bay can therefore accumulate in aquatic environmental media (e.g., sediment and clams).

Assessment of the risks posed by HMs in *Rud* to humans

The Cd concentrations in the muscle samples from sites S1, S3, S4, S6, and S7 exceeded the relevant limit. In particular, the Cd concentrations in the samples from site S6 exceeded the limit by a factor of ~2.5. The Cd THQs for all of the sampling sites were > 1 and were higher than the THQs for the other metals. The Cd CR_{maxS} (6.08–17.70 g ww) were lower than the CR_{maxS} for the other HMs that were analyzed. These results indicated that Cd would pose health risks to humans consuming *Rud* from the study area.

Industrial and other human activities are the main causes of Cd entering the environment. Cd can effectively accumulate in clams. Cd is very toxic to humans and can seriously affect the structures and functions of the bones, central nervous system (including the brain), kidneys, lungs, liver, and placenta. The *Rud* in the study area were heavily contaminated with Cd. Humans living around Liaodong Bay and consuming local *Rud* for a long period may be exposed to risks posed by Cd.

Rud was the only source of HMs to humans considered in the risk assessments performed in this study. Other sources include other types of seafood, rice, vegetables, and water, but these were not included in the risk assessments. The health risks found to be posed by HMs to humans in the risk assessments would have been stronger if all possible sources of HMs were considered.

Conclusions

The Cd concentrations were quite high in the samples from Liaodong Bay. The Cd concentrations in the samples from sites S6 and S7 were in the Category III standard for Cd. The concentrations of Cr in the samples from site S1, As in the samples from site S7, Pb in the samples from site S5, and Zn in the samples from sites S5 and S7 were also quite high. The *Rud* samples had typical tissue-specific heavy metal bioaccumulation patterns. Cd tended to accumulate more efficiently in muscle than viscera, whereas As, Cr and Cu tended to accumulate more efficiently in viscera than muscles. Pb and Zn were not significantly different in the muscle and viscera samples. Heavy metal contamination of *Rud* tended to be worse in the west than the east of Liaodong Bay. The heavy metal THQs and CR_{maxS} for the muscle samples and national and international guidelines indicated that Cd was the main source of health risks to humans through consuming *Rud* from Liaodong Bay.

In summary, Cd was found to have an impact on the local environment and human health. Effective measures should be taken to control Cd pollution. Distribution characteristics and the bioaccumulation of HMs in seawater, surface sediments and other marine organisms will be studied in the future in order to take effective measures to control the pollution of HMs.

Acknowledgements. This study was supported by grants from the National Natural Science Foundation of China (NSFC, No. 31601914), the Key Research and Development Guidance Project of Liaoning Province of China (2018225028).

REFERENCES

- [1] Alfonso, J. A., Handt, H., Mora, A., Vasquez, Y., Azocar, J., Marcano, E. (2013): Temporal distribution of heavy metal concentrations in oysters *Crassostrea rhizophorae* from the central Venezuelan coast. – *Mar. Pollut. Bull.* 73(1): 394-398.
- [2] Copat, C., Arena, G., Fiore, M., Ledda, C., Fallico, R., Sciacca, S., Ferrante, M. (2013): Heavy metals concentrations in fish and shellfish from eastern Mediterranean Sea: consumption advisories. – *Food Chem. Toxicol.* 53: 33-37.
- [3] Gao, X., Chen CTA (2012): Heavy metal pollution status in surface sediments of the coastal Bohai Bay. – *Water Res* 46: 1901-1911.
- [4] Gao, X., Zhou, F., Chen, C. T. (2014): Pollution status of the Bohai Sea: an overview of the environmental quality assessment related trace metals. – *Environment International* 62: 12-30.
- [5] Gargouri, D., Azri, C., Serbaji, M. M., Jedoui, Y., Montacer, M. (2011): Heavy metal concentrations in the surface marine sediments of Sfax Coast, Tunisia. – *Environ Monit Assess* 175: 519-530.
- [6] Gu, Y. G., Huang, H. H., Lin, Q. (2016): Concentrations and human health implications of heavy metals in wild aquatic organisms captured from the core area of Daya Bay's Fishery Resource Reserve, South China Sea. – *Environmental Toxicology and Pharmacology* 45: 90-94.
- [7] Hu, B. Q., Li, G. G., Li, J., Bi, J. Q., Zhao, J. T., Bu, R. Y. (2013): Spatial distribution and ecotoxicological risk assessment of heavy metals in surface sediments of the southern Bohai Bay, China. – *Environ. Sci. Pollut. Res.* 20(6): 4099-4110.
- [8] Husmann, G., Abele, D., Monien, P., Kriews, M., Philipp, E. E. R. (2012): The influence of sedimentation on metal accumulation and cellular oxidative stress markers in the Antarctic bivalve *Laternula elliptica*. – *Estrat. Coast. Sgelf Sci.* 111: 46-59.
- [9] Jovic, M., Stankovic, S. (2014): Human exposure to trace metals and possible public health risks via consumption of mussels *Mytilus galloprovincialis* from the Adriatic coastal area. – *Food Chem. Toxicol.* 70: 241-251.
- [10] Lei, B. L., Chen, L., Hao, Y., Cao, T. H., Zhang, X. Y., Yu, Y. G., Fu, J. M. (2013): Trace elements in animal-based food from Shanghai markets and associated human daily intake and uptake estimation considering bioaccessibility. – *Ecotoxicol. Environ. Saf.* 96: 160-167.
- [11] Li, P. M., Gao, X. L. (2014): Trace elements in major marketed marine bivalves from six northern coastal cities of China: concentrations and risk assessment for human health. – *Ecotoxicol. Environ. Saf.* 109: 1-9.
- [12] Li, Y. H., Liu, H., Zhou, H. L., Ma, W. D., Han, Q., Diao, X. P., Xue, Q. Z. (2015): Concentration distribution and potential health risk of heavy metals in *Macra veneriformis* from Bohai Bay, China. – *Marine Pollution Bulletin* 97: 528-534.
- [13] Liang, L. N., He, B., Jiang, G. B., Chen, D. Y., Yao, Z. W. (2004): Evaluation of mollusks as biomonitors to investigate heavy metal contaminations along the Chinese Bohai Sea. – *Sci Total Environ.* 324: 105-113.
- [14] Liu, J. H., Gao, L., Dou, S. Z. (2017): Bioaccumulation of heavy metals and health risk assessment in three benthic bivalves along the coast of Laizhou Bay, China. – *Marine Pollution Bulletin* 117: 98-110.
- [15] Liu, W. X., Chen, J. L., Lin, X. M., Fan, Y. S., Tao, S. (2007): Residual concentrations of micropollutants in benthic mussels in the coastal areas of Bohai Sea, North China. – *Environ Pollut.* 146: 470-477.

- [16] MEP (2013): Exposure Factors Handbook of Chinese Population (Adults). – Chinese Environment Press, Beijing (in Chinese).
- [17] Naser, H. A. (2013): Assessment and management of heavy metal pollution in the marine environment of the Arabian Gulf: a review. – *Mar Pollut Bull* 72: 6-13.
- [18] National Bureau of Statistics of China (2009): China Yearbook - 2009. – <http://www.stats.gov.cn/tjsj/ndsj/2009/indexch.htm>.
- [19] National Physique Monitoring Center of China (2012): Communique of national physical fitness monitoring. – <http://www.fitness.org.cn/w/791.html>.
- [20] Sarkar, S. K., Cabral, H., Chatterjee, M., Cardoso, I., Bhattacharya, A. K., Satpathy, K. K., Alam, M. A. (2008): Biomonitoring of heavy metals using the bivalve molluscs in Sunderban mangrove wetland, northeast coast of Bay of Bengal (India): possible risks to human health. – *Clean-Soil Air Water* 36: 187-194.
- [21] SEPA (State Environmental Protection Administration of China). (2001): Marine Biological Quality (GB 18421-2001). – Standards Press of China, Beijing.
- [22] Shoultz-Wilson, W. A., Elsayed, N., Leckrone, K., Unrine, J. (2015): Zebra mussels (*Dreissena polymorpha*) as a biomonitor of trace elements along the southern shoreline of Lake Michigan. – *Environ. Toxicol. Chem.* 34: 412-419.
- [23] Tarque, Q., Burger, J., Reinfelder, J. R. (2012): Metal concentrations in organs of the clam *Amiantis umbonella* and their use in monitoring metal contamination of coastal sediments. – *Water Air Soil Pollut.* 223: 2125-2136.
- [24] US EPA (2000): Risk-Based Concentration Table. Philadelphia PA. – United States Environmental Protection Agency, Washington, DC.
- [25] US EPA (United States Environmental Protection Agency) (2014): Risk-based concentration table. – <http://www.epa.gov/reg3hwmd/risk/human/index.htm>.
- [26] US EPA (2015): Integrated Risk Information System. – <http://www.epa.gov/iris>.
- [27] Wan, L., Wang, N. B., Li, Q. B., Zhou, Z. C., Sun, B., Xue, K., Ma, Z. Q., Tian, J., Du, N. (2008a): Estival distribution of dissolved metal concentrations in Liaodong Bay. – *Bull Environ Contam Toxicol.* 80: 311-314.
- [28] Wan, L., Wang, N. B., Li, Q. B., Sun, B., Zhou, Z. C., Xue, K., Ma, Z., Tian, J., Song, L. (2008b): Distribution of dissolved metals in seawater of Jinzhou Bay, China. – *Environ Toxicol Chem.* 27: 43-48.
- [29] Wang, Y. W., Liang, L., Shi, J. B., Jiang, G. B. (2005): Study on the contamination of heavy metals and their correlations in mollusks collected from coastal sites along the Chinese Bohai Sea. – *Environment International* 31: 1103-1113.
- [30] Wei, Y. H., Zhang, J. Y., Zhang, D. W., Tu, T. H., Luo, L. G. (2014): Metal concentrations in various fish organs of different fish species from Poyang Lake, China. – *Ecotoxicol. Environ. Saf.* 104: 182-188.
- [31] Won, E. J., Kim, K. T., Choi, J. Y., Kim, E. S., Ra, K. (2016): Target organs of the Manila clam *Ruditapes philippinarum* for studying metal accumulation and biomarkers in pollution monitoring: laboratory and in-situ transplantation experiments. – *Environ. Monit. Assess.* 188: 10.
- [32] Zhang, Y., Lu, X. Q., Wang, N. L., Xin, M. N., Geng, S. W., Jia, J., Meng, Q. H. (2016): Heavy metals in aquatic organisms of different trophic levels and their potential human health risk in Bohai Bay, China. – *Environ Sci Pollut Res.* 23: 17801-17810.
- [33] Zhao, L. Q., Yang, F., Yan, X. W., Huo, Z. M., Zhang, G. F. (2012): Heavy metal concentrations in surface sediments and Manila clams (*Ruditapes philippinarum*) from the Dalian coast, China after the Dalian port oil spill. – *Biol. Trace Elem. Res.* 149: 241-247.

PHYSIO-BIOCHEMICAL CHARACTERISTICS AND CORRELATION ANALYSIS OF THE SEEDS OF SOME COTTON (*GOSSYPIUM HIRSUTUM* L.) GENOTYPES UNDER COLD TEMPERATURE STRESS

XIA, J.^{1#} – KONG, X.^{2#} – SHI, X.¹ – HAO, X.¹ – LI, N.¹ – KHAN, A.¹ – LUO, H.^{1*}

¹Key Laboratory of Oasis Eco-Agriculture, Xinjiang Production and Construction Group, Shihezi University, 832003 Shihezi, Xinjiang, China

²Cotton Institute, Xinjiang Academy of Agricultural and Reclamation Science, 832003 Shihezi, Xinjiang, China

[#]These authors contributed equally to this work

*Corresponding author
e-mail: Luohonghai79@163.com

(Received 18th Jun 2019; accepted 14th Nov 2019)

Abstract. Cotton seed germination and seedling development is severely restricted, when the seed is exposed to low temperature stress. It is urgently needed to explore cotton seed germination characteristics and the mechanism involved in low temperature stress tolerance. Different cotton genotypes (Upland cotton Xinluzao65 and Island cotton Xinhai35), and three temperatures levels i.e. 12-15 °C, 18-21 °C and 25-28 °C (CK) were studied to explore germination characteristics, antioxidant enzymes activities and osmotic adjustment substances responses. The results show that with the decline of temperature, germination characteristics, cold resistance index and that water absorption of cotton seeds significantly decreased at ($P < 0.05$), and XH35 shows stronger resistance to cold. The activities of antioxidant enzymes and osmotic adjustment substances of cotton seeds were substantially increased under low temperature. Superoxide dismutase (SOD), peroxidase (POD), catalase (CAT) activities, soluble protein (SP), soluble sugar (SS) and free proline (FP) contents of XH35 were increased by 31.06%, 17.03%, 12.33%, 23.80%, 9.63%, and 5.36%, respectively than those of XLZ65. The principal component analysis revealed that SS and FP are the main drivers, hindering cotton seeds germination. Therefore, Island cotton shows a higher cold resistance by increasing water absorption rate, antioxidant enzyme activities and osmotic adjustment.

Keywords: seed germination characteristics, water absorption rate, correlation analysis, principle component analysis

Introduction

Cotton (*Gossypium hirsutum* L.) is the world's leading crop as it provides fiber and oil. Even though it has been introduced to temperate zones at high latitudes, it still shows sensitivity to low temperature stress (Barrero-Gil and Salinas, 2013). Xinjiang is rich in light and heat and is one of the major cotton planting areas in China, accounting for 19.77% of global cotton production (Chen et al., 2017). According to the meteorological data in the past years, damages caused by low temperature (7.72~10.52 °C) in the cotton seeding time (April-May) in Xinjiang occur frequently, and the area reseeded, destroyed and replanted each year accounts for 5 to 12% of the total cotton planting area (Wu et al., 2012). The low temperature has become one of the main factors affecting the efficient production of cotton (Khan et al., 2017; Wang et al., 2016a). Therefore, it has become one of the most important problems for sustainable

cotton production and cotton breeding program. It is essential to identify physiological responses of cotton seeds and the mechanism involved in low temperature tolerance.

The optimal growth temperature for cotton is 20~30 °C, however, when the daily temperature average is lower than 15 °C, the growth of cotton will be inhibited (Barrero-Gil and Salinas, 2013b; Ashraf, 2002), especially during the germination and seedling phases (Chen, 2003). Lauterbach (1999) concludes that the minimum temperature for germination of cotton seeds is 10.5~12 °C. Wang et al. (2016b) can effectively identify cotton cold resistance in its cotyledon stage according to the fact that the cotton can grow as normal when it undergoes low temperature treatment of 4 °C in its cotyledon stage. The response of cotton of different genotypes also differs largely in the seedling phases. Seedlings of high-cold-resistant cotton have more sensitive and efficient active oxygen scavenging capacity and osmotic adjustment response mechanism in low temperature. At the same time, the resistance to low temperature of cotton seedlings is enhanced by maintaining a high photosynthetic rate (Wu et al., 2014). Yan et al. (2016) used 17 cotton varieties in three major (Yangtze River, Yellow River and Northwest Inland) cotton growing areas as experimental materials, and it was found that low temperature stress could significantly weaken the correlation between seed vigor and physical characteristics. Therefore, it is important to know the physiological mechanism for responding to low temperature of cotton seeds of different cold-tolerant genotypes in terms of germination, which plays a pivotal role in working out cold-resistant cultivation measures and breeding cold-tolerant varieties.

Island cotton (*Gossypium barbadense*) has better comprehensive tolerance and excellent fiber properties, and is an important raw material for top-grade and special cotton textiles (Liu et al., 2015). Xinjiang is the only growing area for Island cotton in China due to its suitable light and heat conditions. The perennial planting area is 100,000 hm², and its total output accounts for about a quarter of the world's ELS (including Egyptian long-staple cotton with its velvet length ≤ 35mm) (Tian et al., 2014). At present, the research on cold tolerance of Island cotton in low temperature mainly focuses on seedling stage, flowering and boll stage (Sawan et al., 2011; Yan et al., 2019), and fiber quality (Mei et al., 2012; Avci et al., 2013). However, it has not been systematically studied to transform ingredients and physiological regulation mechanism in the germination of cotton seeds, especially the physiological mechanism for responding to low temperature of cotton seeds of different cold-tolerant genotypes (Island cotton and Upland cotton) in terms of germination.

Therefore, the objectives of this experiment are (i) to study the germination index of different genotypes (Island cotton and Upland cotton) under low temperature stress, (ii) to analyze the antioxidant enzyme activity, osmotic adjustment substance content and membrane lipid peroxidation products dynamic changes and intrinsic relationship under low temperature stress, and (iii) to clarify the intrinsic relationship between the germination characteristics, physiological indexes of cotton seeds and the cold tolerance of cotton varieties; it is expected to provide a theoretical basis for studying the cold resistance mechanism of cotton and the breeding of low temperature resistant cotton varieties.

Materials and methods

Plant materials

Cotton varieties of different genotypes: Xinluzao65 (Upland Cotton) and Xinhai35 (Island Cotton) were used. These materials were obtained from Cotton Institute of

Xinjiang (45°22'43.4"N, 84°50'32.5"E) Academy of Agricultural Sciences. The experiment was carried out in the artificial climate chamber (GXZ-208B, Ningbo Jiangnan Instrument Factory, China) of Shihezi University. The biological characteristics of cotton seeds of different genotypes are shown in *Table 1*. The content of protein, adipose, and starch in Xinhai35 (XH35, *Table 2*) is respectively 19.02%, 50.85% and 4.83% higher than those of Xinluzao65 (XLZ65), grain weight and seed vigor of XH35 are 20.02%, 6% higher than those of XLZ65, respectively, but water content of XH35 is 56.2% lower than that of XLZ65. Preliminary experiments showed that different genotypes of cotton had different germination effects under low temperature stress (*Fig. 1*).

Experimental design

Three temperature levels i.e. 12-15 °C, 18-21 °C and 25-28 °C (*Table 2*) were targeted. During the test, the environment of cotton seed germination under field conditions was simulated in the artificial climate chamber (GXZ-208B, Ningbo Manufacturing Factory, Zhejiang, China), where the relative humidity was 50%, the light/dark ratio was 14 h/10 h and the light intensity was 283 $\mu\text{mol m}^{-2} \text{s}^{-1}$. Cotton seeds with full grain, intact embryo, no mildew and of same size were selected for the experiment. Seeds were sterilized in 200 ml of 1% potassium permanganate for 3 to 5 min, and then rinsed with deionized water for 3 to 4 times. After that, seeds were placed neatly in Petri dishes ($\varphi = 15 \text{ cm}$) with 2 layers of filter paper (GB/T1914-93, Hangzhou Xinhua Paper Ltd., China), 50 seeds in each dish. The sterile distilled water was added until saturation. The dishes were placed in climatic chambers at 15/12 °C, 21/18 °C and 28/25 °C, respectively, to test germination. Each treatment was repeated 5 times, and every 24 h 5~10 ml distilled water was added.

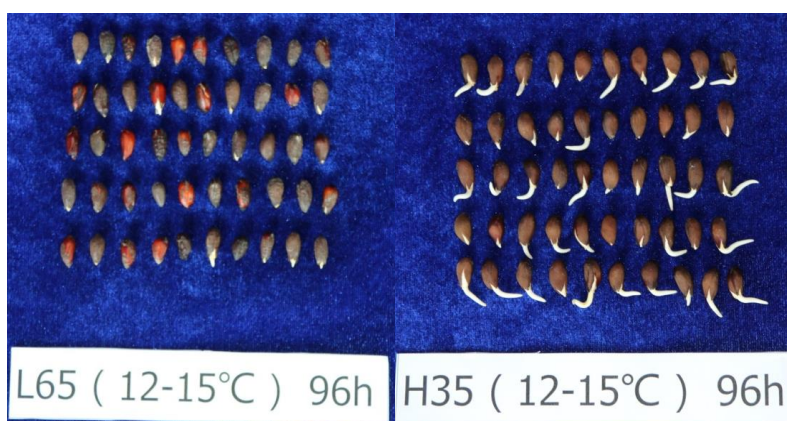


Figure 1. The picture of two cotton seeds germinations (Xinluzao65 seed on the left and Xinhai35 on the right)

Table 1. Biological characteristics of different genotypes of cotton seeds

Variety	Seed mass (g/100)	Water content (%)	Seed vigor (%)	Protein (mg/g)	Adipose (mg/g)	Starch (mg/g)
Xinluzao65 (XLZ65)	9.55 ± 0.38	8.17 ± 1.02	92	13.33 ± 0.44	0.29 ± 0.027	33.10 ± 5.76
Xinhai35 (XH35)	11.94 ± 0.48	5.23 ± 0.43	98	16.46 ± 0.49	0.59 ± 0.032	34.78 ± 1.92

Values are presented as means ± standard error (n ≥ 3)

Table 2. The abbreviations of the treatment

Temperature	Varieties	
	Xinluzao65 (XLZ65)	Xinhai35 (XH35)
12-15 °C	L12	H12
18-21 °C	L18	H18
25-28 °C (CK)	L25	H25

Test items and methods

Determination of germination index

It is taken as germination when germ is longer than 1/2 of the cotton seed. The number of germinated seeds was counted daily from the first day. The following parameters were determined: Germination rate (%) = (number of all germinated seeds during the germination test / number of cotton seeds tested) × 100%; Germination potential (%) = (number of normally germinated seeds within 96 h / number of cotton seeds tested) × 100%; Germination index (GI) = $\sum Gt/Dt$, Mean time of germination (MTG) = $\sum(GtDt)/\sum Gt$, while Gt refers to the germination rate at t and Dt refers to germination days; Water absorption rate (%) = (wet weight-dry weight)/dry weight × 100%; Germination index = $1.00 \times n_3 + 0.75 \times n_5 + 0.5 \times n_7 + 0.25 \times n_9$ (n_3, n_5, n_7, n_9 represent the seed germination rate on the 3rd, 5th, 7th and 9th day respectively); Seed germination cold resistance index = germination index in low temperature/control germination index.

Measurement of physiological index of germination

The sampling time was determined according to the water uptake rate of cotton seeds. At the temperature of 25~28 °C, seeds were sampled at: 2 h, 4 h, 6 h, 12 h (0.5 d), 24 h (1 d), 48 h (2 d); at the temperature of 18~21 °C, seeds were sampled at: 2 h, 4 h, 6 h, 12 h (0.5 d), 24 h (1 d), 48 h (2 d), 72 h (3 d), 96 h (4 d); at the temperature of 12~15 °C, seeds were sampled at: 2 h, 4 h, 6 h, 12 h (0.5 d), 24 h (1 d), 48 h (2 d), 72 h (3 d), 96 h (4 d), 120 h (5 d). About 50 cotton seeds weighing 4~6 g were taken and frozen with liquid nitrogen directly at -80 °C. With the seed coats removed, enzymes were extracted to test activity; the samples were put in 10 ml container and then ground using a freezing grinder for 45 s, and they were used to measure the content of soluble sugar (SS), soluble protein (SP), free proline (FP), malondialdehyde (MDA) and hydrogen peroxide (H₂O₂), as well as the activities of superoxide dismutase (SOD), peroxidase (POD) and catalase (CAT).

Antioxidant enzymes (SOD, POD, and CAT) activities in seed

The activities of enzymatic antioxidants viz., SOD, POD, and CAT in seed were assessed according to the standard procedure (Kochba et al., 1977; Kraus and Fletcher, 1994). The SOD activity was the amount of extract that gave 50% inhibition in nitrotetrazolium blue chloride (NBT) photoreduction detected at 560 nm (Q/YXLZ82, Shanghai Precision Science Instrument Co., Ltd. China). The POD activity was based on the determination of guaiacol oxidation at 470 nm by H₂O₂ and was presented as $\mu\text{mol H}_2\text{O}_2 \text{ g}^{-1} \text{ (FW)}$. The change in absorbance at 470 nm was recorded every min by a spectrophotometer. One unit of POD activity is the amount of enzyme that causes the decomposition of 1 μg substrate at 470 nm for 1 min in 1 g fresh sample at 37 °C. The

CAT activity was measured using the 0.5 g fresh seed sample. The CAT activity was defined as the amount of enzyme that causes the decomposition of 1 μmol H_2O_2 at 405 nm per min in 1 g fresh sample at 37 °C.

Osmotic adjustment substance (SS, SP, and FP) contents in seed

0.5 g seed germ powder was put in a 10 ml centrifuge tube, 5 ml 80% ethanol solution was added to it, and then it was kept in a water bath at 80 °C for 30 min, then cooled to room temperature and centrifuged at 4000 rpm for 10 min, and then 2 ml of supernatant was taken and mixed well with anthrone-sulfuric reagent. The mixture was heated in a boiling water bath at 100 °C for 10 min, and the absorbance was measured at 620 nm after cooling it to room temperature. SP was extracted by adding homogenized 0.5 g of seed germ powder in a 10 ml centrifuge tube. The homogenate was centrifuged at 5000 rpm for 10 min, and then 0.1 ml of the supernatant was thoroughly mixed with 0.9 ml of distilled water and 5 ml of Coomassie brilliant blue G-250 reagent; after 2 min, the absorbance was measured at 595 nm. Free proline content of cotton seed was assayed by the method (Bates et al., 1973). The samples were homogenized in 5 mL of 3% sulfosalicylic acid and centrifuged at 6000 rpm for 10 min. Supernatant was heated with 2 mL of ninhydrin and glacial acetic acid at 100 °C for 1 h. The reaction was further extracted with 4 ml of toluene by vigorous vortexing for 30 s. The absorption of the chromophore was determined at 520 nm (Tecan-infinite M200, Switzerland).

Lipid peroxidation (MDA and H_2O_2)

Lipid peroxidation in cotton seed was determined as MDA content using the thiobarbituric acid method (Bailly et al., 1996). A 1.0 ml aliquot of supernatant of tissue extract (seed) was mixed with 4 ml of 20% (v/v) trichloroacetic acid containing 0.5% (v/v) thiobarbituric acid. The mixture was heated at 100 °C for 30 min, and was cooled down and centrifuged at 10,000 rpm for 10 min. The absorbance of the supernatant was assayed at 532 and 600 nm. H_2O_2 content was determined according to Nakano and Asada (1987). H_2O_2 was extracted by homogenizing 0.5 g seed embryo powder in 3 ml cold acetone. The homogenate was centrifuged at 3000 rpm for 10 min, with the supernatant mixed with 0.1 mL 5% (w/v) TiSO_4 and 0.2 mL ammonia water. After centrifuging the solution at 10,000 rpm for 5 min, the precipitate was washed with acetone till the supernatant was colorless. The precipitate was solubilized in 3 ml 1 M H_2SO_4 , with the absorbance measured at 415 nm. H_2O_2 content was expressed as mmol g^{-1} FW.

Data analysis

Data were processed and mapped by Microsoft Excel 2010, R Studio, Origin and SigmaPlot 12.5. Single factor analysis of variance and correlation analysis were performed by SPSS 18.0. Significant difference examination was carried out using Duncan test at ($\alpha = 0.05$).

Results

Effect of low temperature on germination index of cotton seeds

The relative germination rate, relative germination potential, relative sprouting index, germination index and water absorption rate of the two cotton varieties decreased with

the decline of temperature (Table 3 and 4). The average germination time shows an increasing trend under low temperature treatment, with obvious differences existing in all control groups ($P < 0.05$). The germination rate, germination potential and germination index of XH35 are respectively 30.70%, 12.22% and 16.22% higher than those of XLZ65, and the water absorption rate of XH35 was significantly higher than that of XLZ65 ($P < 0.05$), which indicates that the water absorption rate is closely related to the germination of cotton seeds.

Table 3. Cotton seed germination temperature, germination time and cumulative germination rate

Germination time (t/h)	XLZ65 (%)			XH35 (%)		
	12-15 °C	18-21 °C	25-28 °C	12-15 °C	18-21 °C	25-28 °C
0	0	0	0	0	0	0
24	0	0	3.33	0	0	9.33
48	0	0	14.67	0	0	40.67
72	0	3.33	72	0	18	83.33
96	0	24	84	0	43.33	96
120	0	46.67	89.33	0	68.67	97.33
144	0	58.67	90.67	5.33	79.33	98
168	0	64	90.67	18.67	85.33	98.67
192	4	65.33	92	48	90	98.67
216	10.67	67.33	92	76	92.67	98.67
240	22	67.33	92	84.67	96.67	98.67
264	28.67	67.33	92	84.67	96.67	98.67
288	28.67	67.33	92	84.67	96.67	98.67
312	28.67	67.33	92	84.67	96.67	98.67

Table 4. Effect of low temperature stress on germination index of cotton seeds

Treatment	Germination percentages (%)	Germination (%)	MTG ± SE (d)	Germination index ± SE	Germination index	Cold resistance index	Water absorption rate (%)
L12	28.67 ^d	0.00 ^e	9.32 ± 0.80 ^a	1.49 ± 0.31 ^e	0.05668 ^c	0.0915 ^d	78.58 ^c
L18	67.33 ^c	24.00 ^d	5.12 ± 0.19 ^c	6.98 ± 0.78 ^d	1.1714 ^b	0.4287 ^b	83.3bb ^c
L25	92.00 ^{ab}	84.00 ^b	3.17 ± 0.09 ^d	16.28 ± 2 ^b	2.0733 ^a	-	86.14 ^b
H12	84.67 ^b	0.00 ^e	8.23 ± 0.42 ^b	5.27 ± 0.13 ^d	0.2834 ^c	0.2457 ^c	88.33 ^b
H18	96.67 ^a	48.67 ^c	4.73 ± 0.18 ^c	11.15 ± 0.42 ^c	1.3534 ^b	0.5204 ^a	99.84 ^a
H25	98.67 ^a	96.00 ^a	2.66 ± 0.32 ^d	21.43 ± 1.93 ^a	2.3033 ^a	-	102.7 ^a
Source of variance							
T	1.23×10 ^{-8***}	5.12×10 ^{-7***}	2.16×10 ^{-10***}	1.58×10 ^{-9***}	4.36×10 ^{-5***}	1.84×10 ^{-5***}	0.000896 ^{***}
V	3.92×10 ^{-9***}	0.00114 ^{**}	0.0119 [*]	3.98×10 ^{-5***}	ns	1.03×10 ^{-6***}	2.74×10 ^{-6***}
T×V	1.65×10 ^{-6***}	ns	ns	ns	0.0348 [*]	0.0011 ^{**}	ns

Values are presented as means ± standard error (n ≥ 3). Lowercase letters represent significant differences after the same column of data ($p < 0.05$). *, **or *** indicates a significant ($p < 0.05$), extremely significant ($p < 0.01$) or very significant difference ($p < 0.001$) between the treatments; “-” means none. The table below is the same. T: Temperature, V: Variety. L12 represents XLZ65 at the level of 12-15 °C, L18 represents XLZ65 at the level of 18-21 °C, L25 represents XLZ65 at the level of 25-28 °C (CK). H12 represents XH35 at the level of 12-15 °C, H18 represents XH35 at the level of 18-21 °C, H25 represents XH35 at the level of 25-28 °C (CK)

According to the results of variance analysis, cotton seed germination indices at different temperatures show great variations. The germination rate, germination index, cold resistance index and water absorption rate of different varieties show significant differences. Germination index, the interactions between temperatures and variations are significantly different ($P < 0.05$), but there is no significant difference between the varieties. With the decrease of temperature, the germination cold resistance indices of the two cotton varieties significantly decreased, and show significant differences in temperatures and variations and their interactions. This indicates that cotton seeds of different genotypes show different cold resistance abilities.

Effect of low temperature on protective enzyme activities in cotton seeds in process of imbibition

The activity of SOD in the cotton seed embryos of XH35 is 10.00% higher than those of XLZ65. With the decrease of temperature, the activities of SOD enzyme under low temperature are higher than those of control groups at normal temperature (Fig. 2). The activity of SOD in XLZ65 embryos decreased with the time of low temperature and stress intensity. However, after 4 h of stress treatment, the activity of SOD of L12 and L18 are respectively 22.83% and 10.92% higher than that of L25 (Fig. 2A). The SOD activity of XH35 reaches a peak after 4 h of stress treatment (rapid water absorption phase), and increases respectively by 13.00%, 9.44% and 3.10% at different temperatures, especially after 24 h of imbibition, the enzyme activities of H25, H18, H12 increase respectively by 18.66%, 27.19% and 29.10%, compared with those after 12 h of imbibitions (Fig. 2B).

Before imbibition, POD activity of XH35 (dry seeds) was 35.16% lower than that of XLZ65 (Fig. 2). Over imbibition time, the POD enzyme activity of XLZ65 treated by low temperature treatment was higher than that of control groups. After 12 h of imbibition, POD activity of L12 and L18 was 39.23% and 9.11% higher, respectively, than of L25 (Fig. 2C). The POD enzyme activity of XH35 increases starting from the initial imbibition phase. After 4 h of imbibition, the increase of POD enzyme activities of H12 and H18 are significantly different from that of H25, and 20.28% and 20.27% higher, respectively, than that of control groups. After 12 h of imbibition, no significant differences were observed among variations (Fig. 2D).

CAT activity was increased under low temperature during germination of cotton seeds, and the CAT activities between varieties showed significant differences (Fig. 2). After 2 h of stress treatment, the CAT activity of L12 increased, while that of L18 and L25 first decreased and then decreased. After 24 h of stress treatment (slow water absorption phase), the CAT activity of L12 and L18 was 26.83% and 33.98% higher than that of L25, which shows a significant difference (Fig. 2E). The CAT activity of XH35 greatly decreased at the initial stage of imbibition, and the decrease of that of H25, H18 and H12 were 47.23%, 46.59% and 37.64%, respectively. After 24 h of imbibition, the CAT activity of H12 and H18 peaked 34.84% and 22.80% higher respectively than H25 (Fig. 2F).

Effect of low temperature on osmotic adjustment substances in cotton imbibition process

The content of soluble sugar (SS) decreased with imbibition, but the differences between the varieties were obvious at 4 h (Fig. 3). The content of SS increased in

XLZ65 at 4 h under low temperature (Fig. 3A). The SS content of the XH35 decreased with the decline of temperature, that of H12, H18 and H25 increased at 6 h, 24 h and 4 h, respectively. Whilst a rapid reduction was observed in H25 after 12 h of imbibition (Fig. 3B).

Under low temperature treatment, soluble protein (SP) content in XH35 seed embryos was 19.04% higher than that in XLZ65's (Fig. 3). After imbibition for 2 to 4 h, the content of SP decreases rapidly, and L12 was 22.68% higher than that of L25. However, no significant differences were noted after 4 h of imbibition (Fig. 3C). H35 had similar trend in SPA content with no obvious differences (Fig. 3D).

The content of free proline (FP) shows significant differences between varieties; under low temperature FP content increased (Fig. 3). After 6 h of imbibition, the content of FP in H12 and H18 increased respectively by 40.31% and 31.97%, compared with that of H25 (Fig. 3F). The FP content of XLZ65 was significant, and after 6 h of imbibition, L12 and L18 resulted in the highest FP content (Fig. 3E).

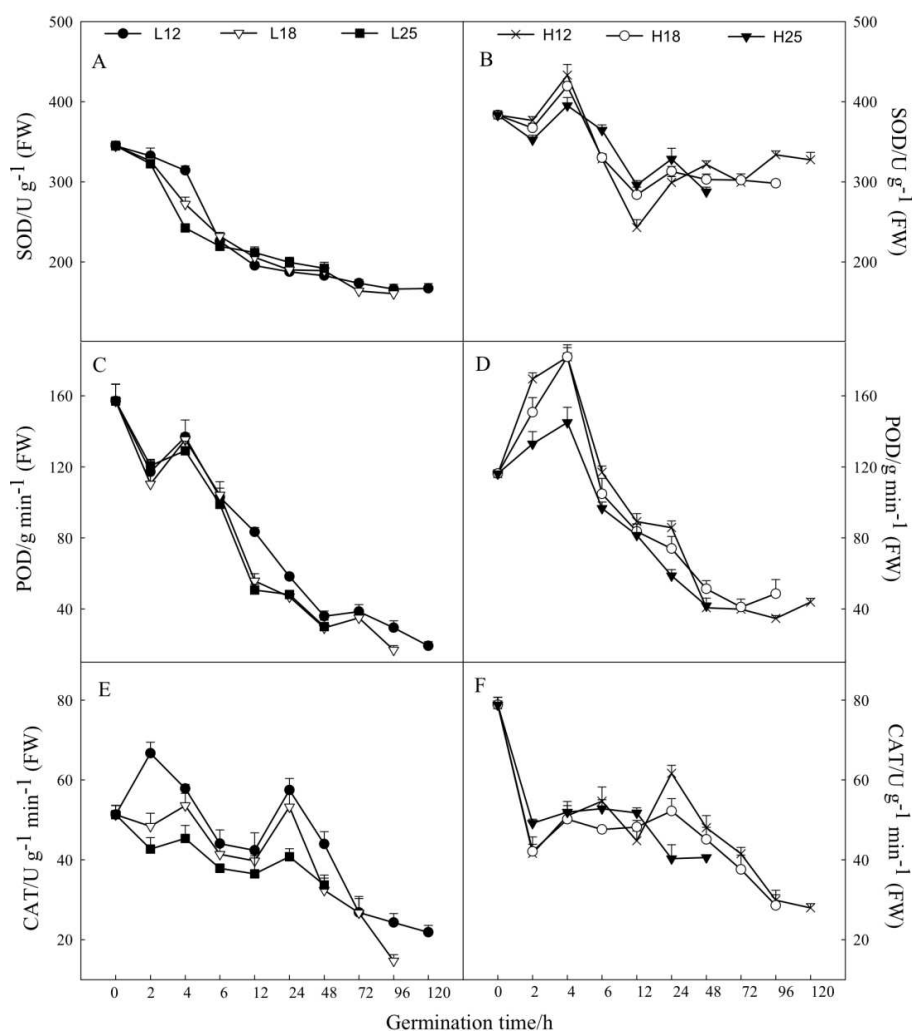


Figure 2. The dynamic change of low temperature stress on SOD, POD, CAT during cotton seed swelling. A, B, C, D, E, F represent respectively the changes of SOD, POD, CAT activities during the germination of XLZ65 and XH35 cotton. Bars indicate SD (n = 3). L12 represents XLZ65 at the level of 12-15 °C, L18 represents XLZ65 at the level of 18-21 °C, L25 represents XLZ65 at the level of 25-28 °C (CK). H12 represents XH35 at the level of 12-15 °C, H18 represents XH35 at the level of 18-21 °C, H25 represents XH35 at the level of 25-28 °C (CK)

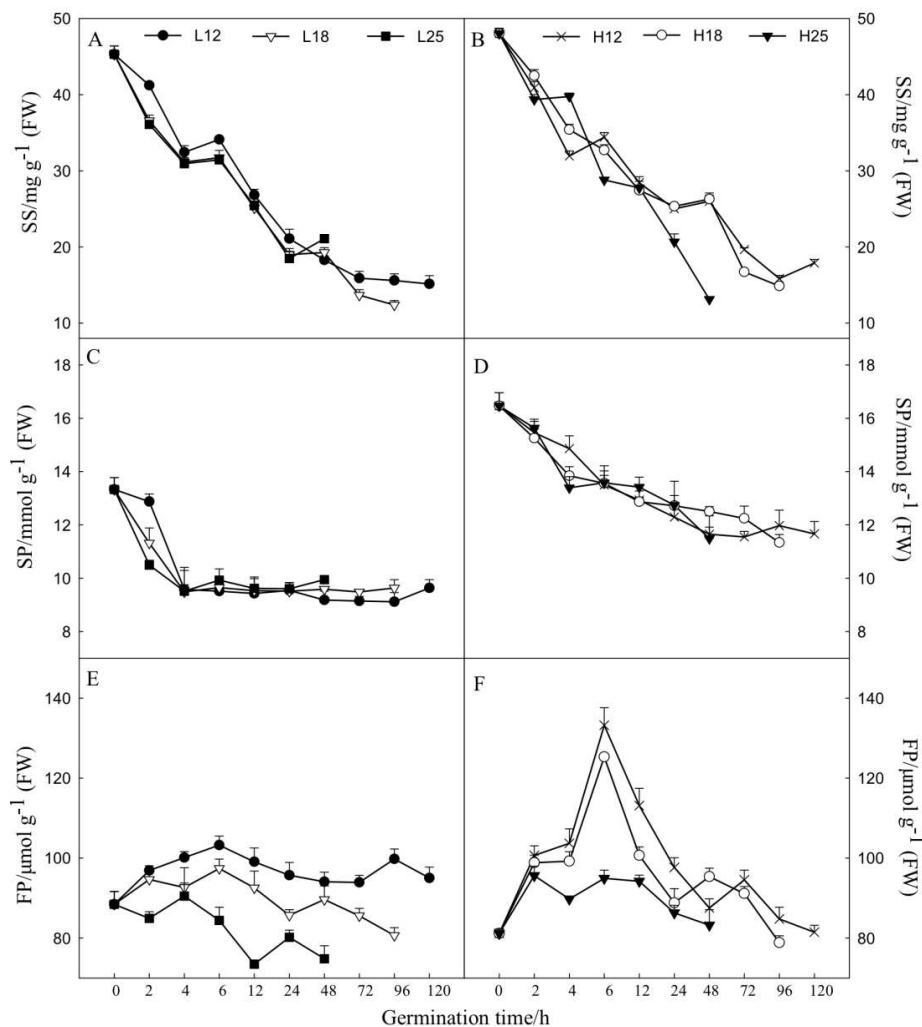


Figure 3. The dynamic change of low temperature stress on SS, SP, FP during cotton seed imbibition. A, B, C, D, E, F represent respectively the changes of SS, SP, FP contents during the germination of XLZ65 and XH35 cotton. Bars indicate SD ($n = 3$). L12 represents XLZ65 at the level of 12-15 °C, L18 represents XLZ65 at the level of 18-21 °C, L25 represents XLZ65 at the level of 25-28 °C (CK). H12 represents XH35 at the level of 12-15 °C, H18 represents XH35 at the level of 18-21 °C, H25 represents XH35 at the level of 25-28 °C (CK)

Effect of low temperature on the contents of hazardous substances (mda, h₂o₂) in cotton imbibition

With the decrease of temperature, the MDA content increased significantly compared with control (Fig. 4). After 2 h of imbibition, the MDA content of L12 and L18 increased by 64.83% and 62.15% respectively, while L25 increased by 15.09% (Fig. 4A). With the decrease of temperature, there is no significant increase in MDA content of XH35, and after 2 h of imbibition, the MDA content in its cotton seeds decreased significantly (Fig. 4B). Since the beginning of imbibition, the H₂O₂ content shows a significant decrease, and with the decrease of temperature, the H₂O₂ content was higher than that of control groups at normal temperature. At the initial stage of imbibition, the H₂O₂ content of XH35 was 28.55% higher than that of XLZ65 (Fig. 4).

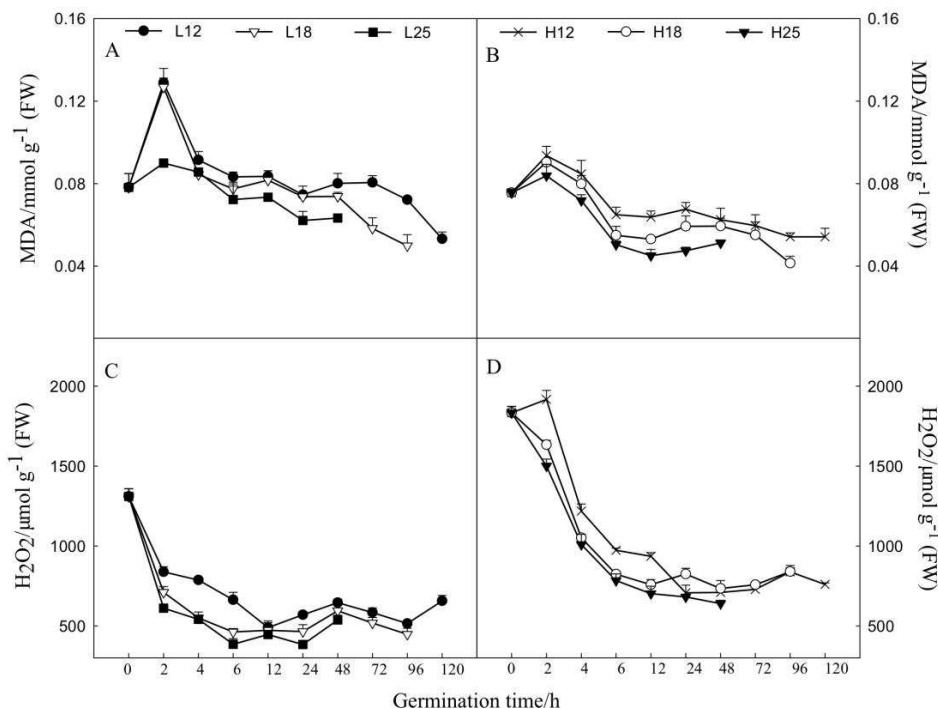


Figure 4. The dynamic change of low temperature stress on MDA, H₂O₂ during cotton seed imbibition. A, B, C, D represent respectively the changes of MDA, H₂O₂ contents during the germination of XLZ65 and XH35 cotton. Bars indicate SD (n = 3). L12 represents XLZ65 at the level of 12-15 °C, L18 represents XLZ65 at the level of 18-21 °C, L25 represents XLZ65 at the level of 25-28 °C (CK). H12 represents XH35 at the level of 12-15 °C, H18 represents XH35 at the level of 18-21 °C, H25 represents XH35 at the level of 25-28 °C (CK)

Correlation analysis on cotton seeds germination and their physiological and biochemical indices at low temperature

Correlation analysis of physiological parameters of cotton seeds germination are shown in Fig. 5. The activity of POD shows extremely significant and positive correlation to SOD, CAT, MDA, SP, H₂O₂, SS ($P < 0.001$), and significant and positive correlation to FP ($P < 0.05$). A significant and positive correlation between SOD and CAT, SP, H₂O₂ and SS ($P < 0.001$) was observed. CAT activity was highly positively with SP, H₂O₂ and SS ($P < 0.001$), and significantly correlated with MDA ($P < 0.05$). There is an extremely significant and positive correlation between MDA and SS ($P < 0.001$); SP extremely significantly and positively correlated with H₂O₂ and SS ($P < 0.001$); H₂O₂ had extremely significant and positive correlation with SS ($P < 0.001$).

Dry seed stage had a significant and positive correlation with SP, H₂O₂, SOD and CAT (Table 5), SS ($P < 0.05$), extremely and negatively correlated with POD ($P < 0.01$), and with FP ($P < 0.05$). The rapid water absorption stage was significantly positively correlated with SP ($P < 0.05$), but significantly negatively correlated with MDA and CAT ($P < 0.01$). The slow water absorption stage had a significantly positive correlation with SP and SOD ($P < 0.01$), but highly negatively correlated with CAT ($P < 0.05$) and MDA ($P < 0.01$). Germination stage was strongly positively correlated with SP, SOD, POD and CAT ($P < 0.01$), but is extremely negatively correlated with FP ($P < 0.01$).

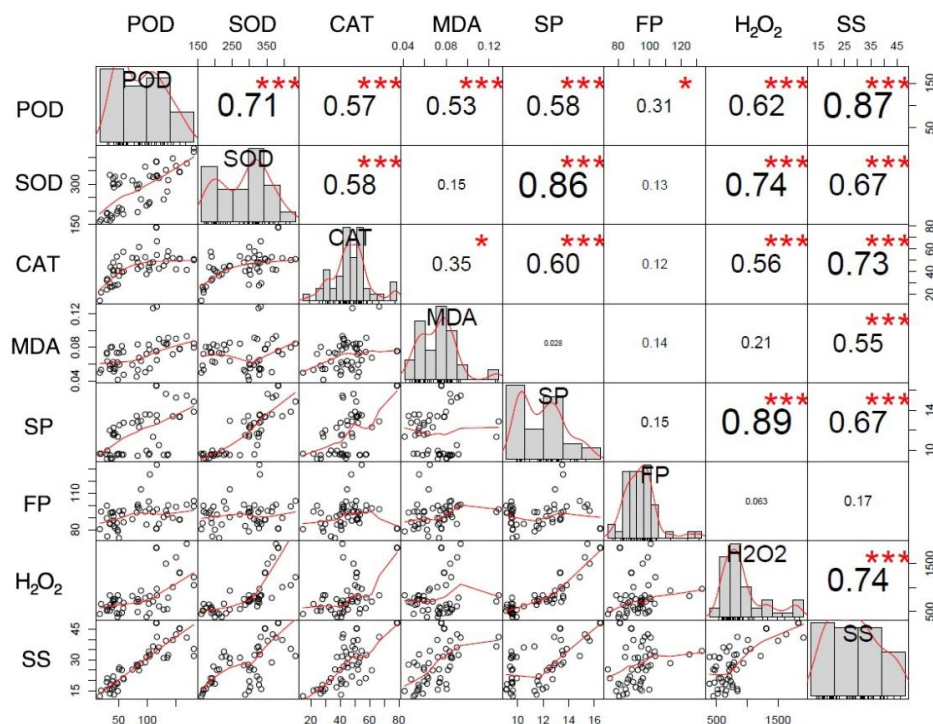


Figure 5. Correlation analysis of physiological index parameters during germination of different genotypes of cotton. The line and bars in the figure represent comparison values with a correlation coefficient of 1 ($r = 1$), where * represents significant ($P \leq 0.05$), ** represents highly significant ($P \leq 0.01$), and *** represents very significant ($P \leq 0.001$). MDA: malondialdehyde content; SS: soluble sugar content; SP: soluble protein content; FP: free proline content; H₂O₂: hydrogen peroxide; SOD: superoxide dismutase; POD: peroxidase; CAT: catalase

Table 5. Correlation coefficient between seed imbibition stage and physiological and biochemical indices

Imbibition stage	MDA	SS	SP	FP	H ₂ O ₂	SOD	POD	CAT
Dried seeds	0.053	0.520*	0.601**	-0.526*	0.617**	0.601**	-0.594**	0.621**
Rapid water absorption stage	-0.861**	-0.106	0.496*	-0.137	0.463	0.383	0.457	-0.857**
Slow water absorption stage	-0.716**	0.204	0.620**	-0.456	0.306	0.677**	0.229	-0.539*
White period	-0.103	0.181	0.666**	-0.755**	0.213	0.690**	0.746**	0.651**

**Significant at the 0.01 probability level (2-tailed); *significant at the 0.05 probability level (2-tailed). MDA: malondialdehyde content; SS: soluble sugar content; SP: soluble protein content; FP: free proline content; H₂O₂: hydrogen peroxide; SOD: superoxide dismutase; POD: peroxidase; CAT: catalase. Dried seeds showed seed imbibition initial time, Rapid water absorption stage showed start to absorb water to 12 h, Slow water absorption stage showed seed absorb water 12 h to revealing radicle, White period showed the growing radicle

Effect of low temperature on the variation of physiological parameters of cotton seeds germination

The principle component analysis of eight physiological parameters, i.e. SOD, POD and CAT in cotton seeds of different genotypes was conducted; the cumulative contribution rates of the first two principal components extracted are 81.49% and

80.46%, which are important in interpreting the total variation of the data set (Fig. 6). Principle component 1(PC1) explains the variations of 64.73% (XLZ65) and 65.59% (XH35), and can clearly distinguish different imbibition time. Principal component 2 (PC2) shows the variations of 16.76% and 14.87%, and can distinguish different low temperature treatments. In principle component 1, the weight coefficients of SP, SS and PSD of Xinluzao65 were higher than 0.400 (Table 6), indicating that the imbibition time has a significant effect on SOD, POD and SS of upland cotton and SP and SS of XH35. In principal component 2, the load values of MDA and FP of L65 and FP of XH35 are greater. This indicates that FP is obviously affected by temperature.

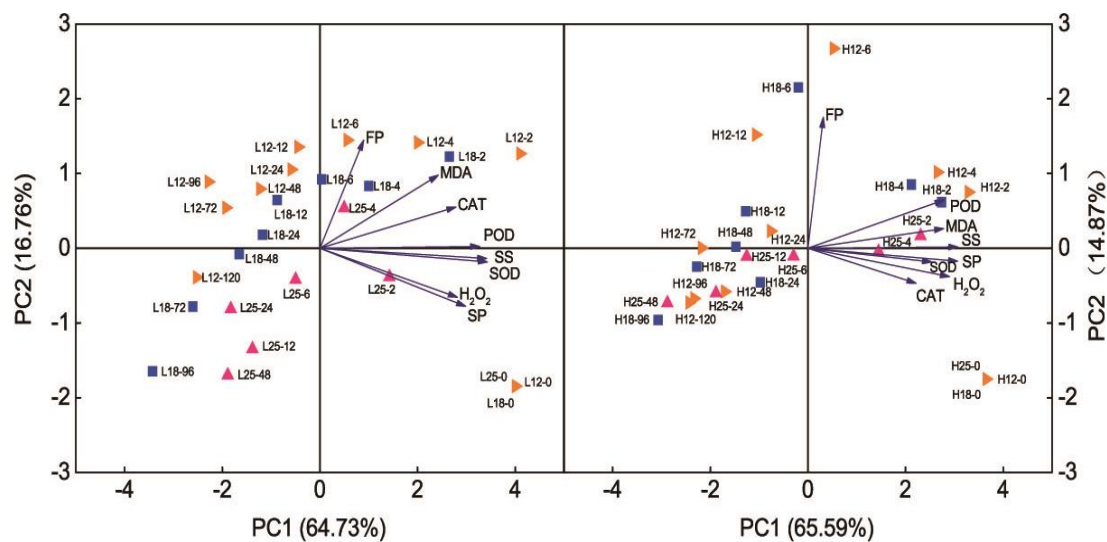


Figure 6. Principal component analysis showing the relationship of the couple of low temperature stress and genotypic differences on cotton germination parameters. The couple of seed imbibition time and physiological and biochemical indices. L showed XLZ65, H showed XH35, 12 showed temperature 12~15 °C; 18 showed temperature 18~21 °C; 25 showed temperature 25~28 °C (CK), 0, 2, 4, 6, 12, 24, 48, 72, 96, 120 showed the cotton seed imbibition time. Soluble Sugar (SS), Soluble Protein (SP), Free Proline (FP), Malondialdehyde (MDA) and Hydrogen Peroxide (H₂O₂), superoxide dismutase (SOD), peroxidase (POD) and catalase (CAT)

Table 6. Principal component loading matrix

Parameter	Extracted component (XLZ65)		Parameter	Extracted component (XH35)	
	PC1	PC2		PC1	PC2
POD	0.405	0.011	POD	0.379	0.323
SOD	0.424	-0.088	SOD	0.344	-0.091
CAT	0.344	0.261	CAT	0.301	-0.236
MDA	0.3	0.464	MDA	0.378	0.132
SP	0.369	-0.369	SP	0.416	-0.087
FP	0.111	0.686	FP	0.043	0.878
H ₂ O ₂	0.348	-0.312	H ₂ O ₂	0.394	-0.191
SS	0.422	-0.065	SS	0.417	0.009

MDA: malondialdehyde content; SS: soluble sugar content; SP: soluble protein content; FP: free proline content; H₂O₂: hydrogen peroxide; SOD: superoxide dismutase; POD: peroxidase; CAT: catalase

Discussion

Cotton seeds are susceptible to temperature in the early stages of germination. When the temperature is below 10 °C, cotton seeds fail to germinate (Kargiotidou et al., 2008). Yang (2015) shows that low temperature reduces the water absorption rate of wheat (*Triticum aestivum* L.) seeds, resulting in a decrease in their respiratory rate and delayed germination. This study shows that with the decrease of temperature, the water absorption rate, sprouting rate and germination index of cotton seeds of different genotypes shows a downward tendency. This indicates that low temperature influences the water absorption rate of seeds leading to reduced water intake and interferes with metabolic activities in seed embryos. As a result, germination ability of cotton seeds is decreased. Cutting watermelon (*Citrullus lanatus*) seed coat at low temperature can improve water absorption capacity, making it able to maintain high cold resistance and increase germination rate (Nerson et al., 1985). This study shows that with the decrease of temperature, water absorption, germination index and germination cold resistance index of XH35 were higher than those of XLZ65. Consequently, a high water absorption rate and capacity was the main reason for the strong cold resistance of Island cotton.

Active oxygen accumulation can cause chilling injuries in plants (Baek and Skinner, 2003; Xu et al., 2006). The antioxidant enzyme system plays an important role in the active oxygen injury caused by low temperature (Imahori et al., 2008; Ashraf, 2009). Zhang and Xie (2013) find that at low temperature, the activities of SOD, POD and CAT in cotton seedlings were significantly reduced, which inhibit the growth of cotton seedlings. In the current study, the activities of cotton seed enzymes under low temperatures were higher than those of control groups in normal temperature. It may be that low temperature inhibits the expression of enzyme activities in cotton seeds, delays the metabolism of storage materials and hinders the germination of cotton seeds. Ren et al. (2017) find that low temperature inhibits the enzymes involved in metabolism in peony (*Paeonia suffruticosa* Andr.) seeds, leading to delayed degradation of starch and other metabolites which affects glycolysis resulting in inhibition of seed germination. However, the contents of SOD and CAT in XH35 seed embryos were higher than those in XLZ65's, and after 4 h of low temperature treatment, the POD content of XH35 was higher than that in XLZ65, the water absorption capacity and rate of XH35 are higher than those of XLZ65, which accelerate the metabolism and transformation of substances at low temperature, increasing the germination rate of Island cotton.

Under stress conditions, soluble sugar, soluble protein and proline in plants can alleviate cell damage caused by low temperature and improve low temperature resistance of plants (Duncan and Widholm, 1987; Solomon et al., 1994). Chang et al. (2018) found that the contents of soluble sugar and soluble protein increased at low temperature, and the increase of proline in low temperature resistant varieties was large. This study shows that after low temperature treatment, the contents of soluble protein and soluble sugar were higher than those of control groups, which may delay the physiological metabolic reaction due to low temperature, causing the content to change more slowly than in normal temperature. This is consistent with previous studies (Liu et al., 2012). Soluble sugar, soluble protein and free proline contents of XH35 were higher than that of XLZ65, which is consistent with the results of the study by Mambetale et al. (2017). This is probably because of the adjustment capacity produced by the protection system of Upland cotton under stress conditions is lower than that of Island cotton. Therefore, the contents of soluble protein, soluble sugar and free proline in the embryo

after low temperature treatment can be used as physiological indices of cold resistance of cotton seed germination.

Malondialdehyde (MDA) reflects to some extent the degree of damage to the cell membrane (Velikova et al., 2000). Gao et al. (2018) found that at low temperature, the MDA content of low temperature resistant varieties remained almost unchanged, and low temperature resistant varieties were increased. The data from this study shows that higher MDA content of XH35 after low temperature treatment was lower than XLZ65, indicating that Island cotton was less damaged by low temperature compared with Upland cotton due to its poor membrane stability. Ou-yang et al. (2007) reported that increase of H₂O₂ content in tomato (*Solanum lycopersicum*) peel can induce the enhancement of cold resistance of tomato. This study shows that due to the high content of H₂O₂ in XH35, the activities of antioxidant enzymes were enhanced, and the damage caused by low temperature stress were alleviated, thereby improving cotton seeds germination ability under low temperature.

Correlation analysis of physiological indicators of cotton seedlings that the improvement of antioxidant enzyme activity provides a favorable metabolic environment for maintaining the normal physiological balance of cells and the accumulation of soluble substances (Wu et al., 2013). This experiment shows that there is an extreme significant or significant relationship between osmotic adjustment substances content and antioxidant enzyme activities exist under high stress conditions. This indicates that by adjusting SS, SP contents and POD, SOD and CAT activities to reduce oxidative damage and osmotic balance is maintained and cold resistance of cotton seeds is improved. Numerous researchers use principal component analysis to determine the strength of resistance of test varieties in stress resistance studies (Dai et al., 2014; Gulhane and Kolekar, 2014; Farshadfar et al., 2013). Wu et al. (2012) convert 12 individual items of cotton seedling leaves at low temperature into 7 independent comprehensive indicators by principal component analysis, and use cluster analysis to objectively obtain the cold resistance of the tested varieties. In this study, the principal component analysis of eight individual indicators in cotton embryos at low temperature shows that the imbibition time has a great influence on the physiological indices of cotton seed germination, i.e. the main component 1 in *Figure 5* explains variations of 64.73% (XLZ65) and 65.59% (XH35). With the increase of imbibition time, low temperature decreased SOD, POD activities and FP content. This might be of the low temperature that inhibits water absorption rate and capacity of cotton seeds, slows the transformation of metabolites, and increases content of harmful substances which depress cotton germination. However, the physiological traits of cotton seeds of different genotypes were significantly different. SOD and POD activities of Island cotton increased in the first 4 h of inhibition, which reduces MDA content, thus improving the cold tolerance of Island cotton.

Conclusions

Water absorption is critical in seeds germination and the absorbing speed and volume decide the speed of germination. With the decrease of temperature, a significant decrease in water absorption rate of cotton seeds of both genotypes was observed. However, water absorption rate of Xinhai35 was 14.29% higher than that of Xinluzao65. Germination rate, germination index and cold resistance index of Island Cotton rate are respectively 30.70%, 34.63% and 32.10% higher than those of Upland

Cotton. As a result, Island cotton shows low temperature tolerance. As the imbibition lasts, the activity of antioxidant enzymes and contents of osmotic adjustment substances were declined. Correlation analysis that there exists significant relation between the contents of osmotic adjustment substances and the activity of antioxidant enzymes. By coordinating the 8 indices in principle component analysis, it is found that SS and FP were the main factors affecting cotton seeds germination.

Therefore, under low temperature stress, it is required for seed to increase the water absorption and water absorption rate, and to quickly reach saturation state, thereby regulating metabolic pathways such as osmotic adjustment substances and antioxidant enzymes, and starting a corresponding anti-reverse response mechanism to maintain the metabolic balance and further enhance the low temperature resistance of cotton seedlings and avoid damage during germination.

Acknowledgements. This study was funded by the National Natural Science Foundation of China (No. 31760355), the Fok Ying Tung Education Foundation (No. 151030), and Program of Youth Science and Technology Innovation Leader of The Xinjiang Production and Construction Corps (No. 2017CB005).

REFERENCES

- [1] Ashraf, M. (2002): Salt tolerance of cotton: some new advances. – *Critical Reviews in Plant Sciences* 21(1): 1-30.
- [2] Ashraf, M. (2009): Biotechnological approach of improving plant salt tolerance using antioxidants as markers. – *Biotechnology Advances* 27(1): 84-93.
- [3] Avci, U., Pattathil, S., Singh, B., Brown, V. L., Hahn, M. G., Haigler, C. H. (2013): Cotton fiber cell walls of *Gossypium hirsutum* and *Gossypium barbadense* have differences related to loosely-bound xyloglucan. – *PloS One* 8(2): e56315.
- [4] Baek, K. H., Skinner, D. Z. (2003): Alteration of antioxidant enzyme gene expression during cold acclimation of near-isogenic wheat lines. – *Plant Science (Oxford)* 165(6): 1221-1227.
- [5] Bailly, C., Benamar, A., Corbineau, F., Dome, D. (1996): Changes in malondialdehyde contents and in superoxide dismutase, catalase, glutathione reductase activities in sunflower seeds related to accelerated seed aging. – *Plant Physiology* 97: 104-110.
- [6] Barrero-Gil, J., Salinas, J. (2013): Post-translational regulation of cold acclimation response. – *Plant Science - An International Journal of Experimental Plant Biology* 205-206(5): 48-54.
- [7] Bates, L. S., Waldren, R. P., Teare, I. D. (1973): Rapid determination of free proline for water stress studies. – *Plant Soil* 39: 205-207.
- [8] Chang, B. W., Zhong, P., Liu, J., Tang, Z. H., Gao, Y. B., Yu, H. J., Guo, W. (2019): Effect of low-temperature stress and gibberellin on seed germination and seedling physiological responses in peanut. – *Acta Agronomica Sinica* (1): 118-130.
- [9] Chen, Q. (2003): Studies of physiologic characteristics of reaction of cucumber to low temperature and poor light. – *Scientia Agricultura Sinica* 36(1): 77-81.
- [10] Chen, Z., Ma, H., Xia, J., Hou, F., Shi, X. J., Hao, X. Z., Abdul, H., Han, H., Luo, H. H. (2017): Optimal pre-plant irrigation and fertilization can improve biomass accumulation by maintaining the root and leaf productive capacity of cotton crop. – *Scientific Reports* 7(1): 17168.
- [11] Dai, H. F., Wu, H., Amanguli, M., Wang, L. H., Maimaiti, A., Zhang, J. S. (2014): Analysis of salt-tolerance and determination of salt-tolerant evaluation indicators in cotton seedlings of different genotypes. – *Scientia Agriculture Sinica* 47(7): 1290-1300.

- [12] Duncan, D. R., Widholm, J. M. (1987): Proline accumulation and its implication in cold tolerance of regenerable maize callus. – *Plant Physiology* 83(3): 703-708.
- [13] Farshadfar, E., Mohammadi, R., Farshadfar, M., Dabiri, S. (2013): Relationships and repeatability of drought tolerance indices in wheat-rye disomic addition lines. – *Australian Journal of Crop Science* 7(1): 130-138.
- [14] Gao, L. Y., Deng, Y. S., Han, Z. F., Kong, F. J., Shen, G. F., Li, R. Z., Yin, Y. P. (2018): Evaluation of the low-temperature tolerance of cotton varieties in the Huang-Huai region during seed germination. – *Cotton Science* 30(06): 36-44.
- [15] Gulhane, V. A., Kolekar, M. H. (2015): Diagnosis of diseases on cotton leaves using principal component analysis classifier. – 2014 Annual IEEE India Conference (INDICON), December 11-13, Pune, India.
- [16] Imahori, Y., Takemura, M., Bai, J. (2008): Chilling-induced oxidative stress and antioxidant responses in mume (*Prunus mume*) fruit during low temperature storage. – *Postharvest Biology and Technology* 49(1): 54-60.
- [17] Kargiotidou, A., Deli, D., Galanopoulou, D., Tsaftaris, A., Farmaki, T. (2008): Low temperature and light regulate delta 12 fatty acid desaturases (FAD2) at a transcriptional level in cotton (*Gossypium hirsutum*). – *Journal of Experimental Botany* 59(8): 2043-2056.
- [18] Khan, A., Tan, D. K., Afridi, M. Z., Luo, H. H., Tung, S. A., Ajab, M., Fahad, S. (2017): Nitrogen fertility and abiotic stresses management in cotton crop: a review. – *Environmental Science and Pollution Research* 24(17): 14551-14566.
- [19] Kochba, J., Lavee, S., Spiegel-Roy, P. (1977): Difference in peroxidase activity and isoenzymes in embryogenic and non-embryogenic ‘shamouti’ orange ovular callus lines. – *Plant and Cell Physiology* 18(2).
- [20] Kraus, T. E., Fletcher, A. R. (1994): Paclobutrazol protects wheat seedlings from heat and paraquat injury. Is detoxification of active oxygen involved? – *Plant and Cell Physiology* 35(1): 45-52.
- [21] Lauterbach, B., Krieg, D. R., Jividen, G. (1999): Fatty acid composition of lipid fractions in germinating cotton as affected by temperature. – *Proceedings of the Belt Wide Cotton Conference, Memphis, Tennessee, National Cotton Council of America*, pp. 564-565.
- [22] Liu, C. Y., Chen, D. Y., Gai, S. P., Zhang, Y. X., Zheng, G. S. (2012): Effects of high- and low temperature stress on the leaf PS II functions and physiological characteristics of tree peony. – *Chinese Journal of Applied Ecology* 23(01): 133-139.
- [23] Liu, X., Zhao, B., Zheng, H. J., Hu, Y., Lu, G., Yang, C. Q. (2015): *Gossypium barbadense* genome sequence provides insight into the evolution of extra-long staple fiber and specialized metabolites. – *Scientific Reports* 5: 14139.
- [24] Mambetale, A., Nurbulat, L., Gao, L. L., Zhang, J. S., Tian, L. W. (2017): Effect of salt stress on growth and physiological characteristics of sea island cotton and Upland cotton cultivars. – *Chin Bull Bot* 52: 465-473.
- [25] Mei, Y. J., Zhou, J. P., Xu, H. M., Zhu, S. J. (2012): Development of sea island cotton (*Gossypium barbadense* L.) core collection using genotypic values. – *Australian Journal of Crop Science* 6(4): 673-680.
- [26] Nakano, Y., Asada, K. (1987): Purification of ascorbate peroxidase in spinach chloroplasts; its inactivation in ascorbate-depleted medium and reactivation by monodehydroascorbate radical. – *Plant and Cell Physiology* 28(1): 131-140.
- [27] Nerson, H., Paris, H. S., Karchi, Z., Sachs, M. H. (1985): Seed treatment for improved germination of tetraploid watermelon. – *HortScience* 20: 897-899.
- [28] Ou-Yang, L. Z., Shen, L., Chen, H. R., Fan, B., Zhang, Y., Sun, J. J., Sheng, J. P. (2007): Effects of H₂O₂ on cold tolerance and antioxidant enzyme activities of tomato by cold-shock treatment. – *Food Science* 28(7): 31-35.
- [29] Ren, X. X., Xue, J. Q., Wang, S. L., Xue, Y. Q., Zhang, P., Jiang, H. D. (2017): Proteomic analysis of tree peony (*Paeonia ostii* ‘feng dan’) seed germination affected by low temperature. – *Journal of Plant Physiology* 224-225: S0176161717303127.

- [30] Sawan, Z. M., Fahmy, A. H., Yousef, S. E. (2011): Effect of potassium, zinc and phosphorus on seed yield, seed viability and seedling vigor of cotton (*Gossypium barbadense* L.). – Archives of Agronomy & Soil Science 57(1): 75-90.
- [31] Solomon, A., Beer, S., Waisel, Y., Jones, G. P., Paleg, L. G. (2010): Effects of nacl on the carboxylating activity of rubisco from *Tamarix jordanis* in the presence and absence of proline-related compatible solutes. – Physiologia Plantarum 90(1): 198-204.
- [32] Tian, L. W., Cui, J. P., Xu, H. J., Guo, R. S., Lin, T. (2013): Analysis of the current status of American long-staple cotton production. – World Agriculture (09): 105-110.
- [33] Velikova, V., Yordanov, I., Edreva, A. (2000): Oxidative stress and some antioxidant systems in acid rain-treated bean plants: protective role of exogenous polyamines. – Plant Science (Shannon) 151(1): 0-66.
- [34] Wang, J. J., Wang, D. L., Yin, Z. J., Wang, S., Fan, W. L., Lu, X. K., Mu, M., Guo, L. X., Ye, W. W., Shun, X. (2016b): Identification of the chilling resistance from germination stage to seedling stage in upland cotton. – Scientia Agricultura Sinica 49(17): 3332-3346.
- [35] Wang, Q., Liu, N., Yang, X., Tu, L., Zhang, X. (2016a): Small RNA-mediated responses to low- and high-temperature stresses in cotton. – Scientific Reports 6(1): 35558.
- [36] Wu, H., Hou, L. L., Shi, J. Y., Ali-yan, R. Z., Zhang, J. S. (2012): Analysis and evaluation indicator selection of chilling tolerance of different cotton genotypes. – Scientia Agricultura Sinica 45(9): 1703-1713.
- [37] Wu, H., Zhang, J. S., Shi, J. Y., Fan, Z. C., A, L. Y., Zhang, P., Zheng, S. (2013): Physiological responses of cotton seedlings under low temperature stress. – Acta Botanica Boreali-Occidentalia Sinica 33(1): 74-82.
- [38] Wu, H., Dai, H. F., Zhang, J. S., Jiao, X. L., Liu, C., Shi, J. Y., Fan, Z. C., Aliyan, R. Z. (2014): Responses of photosynthetic characteristics to low temperature stress and recovery treatment in cotton seedling leaves. – Chinese Journal of Plant Ecology 38(10): 1124-1134.
- [39] Xu, S., Li, J., Zhang, X., Wei, H., Cui, L. (2006): Effects of heat acclimation pretreatment on changes of membrane lipid peroxidation, antioxidant metabolites, and ultrastructure of chloroplasts in two cool-season turfgrass species under heat stress. – Environmental and Experimental Botany 56(3): 274-285.
- [40] Yan, Q., Zeng, Y. Q., Wang, L. R., Meng, Y. L. (2016): Response of seed vigor in different cotton cultivars under low temperature and artificial aging stress. – Cotton Science 28(2): 144-151.
- [41] Yan, Q. Q., Zhang, J. S., Li, X. X., Wang, Y. T. (2019): Effects of salinity stress on seed germination and root growth of seedlings in island cotton. – Acta Agronomica Sinica (1): 100-110.
- [42] Yang, W. S. (2015): Protein Expression and Respiratory Metabolism Response to Low Temperature during Wheat Seed Germination. – Shandong Agricultural University, Shandong (in Chinese).
- [43] Zhang, W., Xie, J. Z. (2013): Effects of low temperature stress on resistance indices of sympodial bamboo seedlings. – Advanced Materials Research 726-731: 4241-4247.

INDOOR SIMULATION OF REMEDIATION OF 2, 2', 4, 4'-TETRABROMODIPHENYL ETHER CONTAMINATED SOIL BY *BACILLUS LATEROSPORA*

GUAN, J. F.^{1*} – WANG, J. H.² – GUO, Y. N.² – ZENG, Q.²

¹*Mudanjiang Normal College, Mudanjiang 157000, China*

²*Harbin Normal University, Harbin 150025, China*

*Corresponding author

e-mail: bangeshiji@126.com; phone: +86-1881-0503-141

(Received 13th Jul 2019; accepted 25th Nov 2019)

Abstract. High-throughput sequencing and traditional microbial culturing were used to analyze the effects of the addition of free or immobilized degrading bacteria on the soil physicochemical properties and microbial community structure by simulating the pollution of 2, 2', 4, 4'-tetrabromo diphenyl ether (BDE-47), and to measure the degradation rates. The results showed that (1) The soil physicochemical properties including pH, organic matter, total nitrogen, total phosphorus and total potassium were not significantly affected by the addition of BDE-47, free or immobilized bacteria; (2) *Proteobacteria*, *Acidobacteria*, and *Actinobacteria* were the dominant phyla in the simulation systems, of which the relative abundance of *Proteobacteria* and *Acidobacteria* decreased whereas that of *Actinobacteria* increased through the simulation. *Firmicutes* was dominant in the simulation system B. Seven phyla, including *Bacteroidetes*, *Gemmatimonadetes*, and *Nitrospirae*, were shared by all simulation systems. The free degrading strain adapted well to the simulation system, and the cell count increased from $(5.0 \pm 0.1) \times 10^4$ Colony-forming unit (CFU) /g to $(1.0 \pm 0.2) \times 10^5$ CFU/g at the end of the simulation; (3) The degradation of BDE-47 occurred in the original soil used for the simulation, while the addition of the free degrading strain promoted the degradation of BDE-47 at a rate of 39.77%. The addition of the immobilized strain also promoted the degradation of BDE-47, but only at a rate of 36.94%, slightly lower than that of the free strain.

Keywords: BDE-47, microbial degradation, immobilization, high-throughput sequencing

Introduction

As persistent organic pollutants, polybrominated diphenyl ethers (PBDEs) are a class of brominated flame retardants (BFRs) widely used in the electronics industry, electrical appliances, household appliances, textile, oil and construction materials (Dewit, 2002). The general chemical formula of PBDEs is $C_{12}H_{(0-9)}Br_{(1-10)}O$, and there are 209 homologs with different numbers of bromine atoms (Costa et al., 2008). As of 2001, the market demand for the flame retardants PBDEs has exceeded 67,440 metric tons and keeps rising (Arias, 1992; Dewit, 2002). Due to a lack of chemical bonds, PBDEs added to products can easily enter their environment through volatilization and leaching, and with the migration to the atmosphere and water bodies, they may extensively pollute the atmosphere, water, sediments, soil, and biosphere. PBDEs are highly lipophilic,

chemically stable, and resistant to degradation. Numerous studies have found that PBDEs have endocrine disrupting toxicity (Walter et al., 2017), developmental neurotoxicity (Chen et al., 2014), and immunotoxicity (Talsness, 2008), all of which can be enriched, amplified along food chains (Zhou et al., 2016) and transferred to the next generation through breast milk, placenta, and cord blood (Chen et al., 2014; Xu et al., 2017), posing a potential threat to human and environmental health. Therefore, at the 4th Meeting of the Conference of the Parties (COP-4) of the Stockholm Convention on Persistent Organic Pollutants (POPs) in May 2009, tetrabromo and pentabromo diphenyl ethers in commercial pentabromide products, and the hexabromo and heptabromo diphenyl ethers in commercial octabromide products were added to the Annex A of the Convention as new POPs.

As the primary commercial, pentabromo diphenyl ether (Penta-BDE) monomer 2, 2', 4, 4'-tetrabromo diphenyl ether (BDE-47) is very toxic and can cause harm even at very low doses. Soil is one of the final destinations of BDE-47 and plays a very important role in the spatiotemporal distribution and geochemical cycling of BDE-47. The micro-ecological environment of the polluted soil is complex, where microbes play the central part and the abiotic and biotic factors interact with each other. As an essential biological component of the soil environment, microbes play a pivotal role in the migration and transformation of BDE-47. At present, physical, chemical and biological methods are mainly used for remediation of contaminated soil. Microbial remediation, as the main means of bioremediation, is widely used because of its economic and non-secondary pollution characteristics. One of the widely applied bioremediation techniques is microbial enhancement technology. It improves the pollutant degradation ability of soil or a system by adding bacterial strains screened from a natural source to the soil or biological treatment system for quickly removing the pollutants. As a microbial enhancement technology, microbial immobilization basically confines or localizes free cells or microorganisms to a defined spatial region by using chemical or physical methods to keep them active and reusable. The advantages of this technique include high microbial density, fast reaction rate, strong resistance to toxicity, and low microbial loss.

In the present study, the trends of the dominant bacteria in the simulation systems were dynamically tracked using high-throughput sequencing technology. Chen et al. (2006) reviewed the methods for determining the structural and functional diversities of microbial communities in polluted soils at China and abroad in recent years, and observed that the analysis and research on the microbial diversity of polluted soils were still not robust and conclusive. One of the reasons for this was the fact that the methods and techniques for determining microbial species had not yet considerably developed for comprehensive and accurate analysis of the soil microbial diversity, while the other was the high heterogeneity of the environment. The local spatial-temporal environment kept changing all the time (Vanelsas et al., 1997). In recent years, with the development of high-throughput sequencing technologies, more studies on the microbial structure changes in polluted soils are being conducted. Wang (2016) used high-throughput sequencing to analyze the response of various farmland soil microbial communities to oil spill pollution and planted black locusts. Likewise, the characteristics of the microbial

community structure and distribution in petroleum-contaminated soil were analyzed by Liang using high-throughput sequencing (Yang et al., 2013).

In this study, indoor simulation of BDE-47 contaminated soil environment was carried out; an immobilized degrading strain was used to simulate soil remediation, and the changes in microbial community structural during the restoration was analyzed. Our study provides a theoretical basis and technical support for the microbial remediation of BDE-47 polluted soil.

Materials and Methods

Immobilization of the degrading strain

A strain with a good aerobic degradation ability for BDE-47 was isolated and purified from the soil of an electronic waste dismantling site in Taizhou City, Zhejiang Province, China. The strain was identified as *Bacillus laterospora* of the genus *Bacillus* and is deposited in the China General Microbiological Culture Collection Center (deposition number CGMCC No. 8616). The optimum growth temperature for the strain is 30-37°C, with reddish brown colonies on the bacterial solid medium, having moist surface and uneven edges.

In this study, sodium alginate was used as the immobilization carrier for the bacteria, and the cells were embedded inside according to the embedding method discussed. In brief, before simulation, the degrading strain was acclimated in an inorganic liquid culture medium containing 500 µg/L BDE-47, for 10 d acclimation period and a total of four periods. The acclimated strain was enriched in liquid culture and the cells were collected by centrifugation and washed three times with sterilized water to prepare the bacterial suspension ($OD_{600} = 2.5$) for immobilization. The bacterial suspension was added to the sodium alginate sol, thoroughly stirred and mixed. The mixed solution was dropped into a calcium chloride solution using a syringe, to form beads which were fixed at 4°C. Then the beads were washed with 0.85% sterilized physiological saline and filtered. After drying on a sterilized filter paper, they were stored at 4°C. According to the comprehensive properties of the immobilized beads, the final immobilization conditions were set as bacteria (2 g/L), sodium alginate (4% w/v), calcium chloride (3% w/v), and fixation for 4 h.

Construction of the simulation systems

Taizhou, Zhejiang is a typical e-waste dismantling site in China. To explore the effect of the preliminary screened free strain and its immobilized form on the polluted soil, the soil sample for simulation in this study was collected from the surface (0-20 cm) at the Taizhou Park with no BDE-47 pollution. During the collection, the debris such as plant residues were removed. The soil sample was sealed in a sampling bag and transported to the laboratory in a sampling box with an ice pack. One part (about 15 kg) of the soil sample was directly filtered through a 10 mm sieve for indoor simulation experiments, the other part (about 2 kg) was ground and air-dried, filtered through a 60 mm sieve for

preparing the polluted mother soil, and the remaining part was stored at respective 4°C (about 1 kg) and -20°C (about 200 g) for further soil physicochemical analyses and high-throughput sequencing, respectively.

Construction of microbial remediation simulation system for BDE-47 contaminated soil: The vases of height 18 cm and an opening diameter of 21 cm were selected as the simulation containers. In system A the simulated soil and pollutant BDE-47 were added. In system B the simulated soil, pollutant BDE-47, and the free degrading bacteria were added, while the degrading bacteria were in the form of a bacterial suspension. In system C, the simulated soil, pollutant BDE-47 and the immobilized degrading bacteria, in the form of 100 g/kg immobilized beads were added. The soils were turned once every 30 days. The concentration of BDE-47 in the simulation systems were approximately 1,500 ng/g. A certain amount of sterilized water was added to the simulation systems regularly to maintain the water content of the tested soil. Each simulation system had two replicates and the simulation remediation time was 90 days.

Preparation of bacterial suspension: Before the simulation, the degrading strain was acclimated in the inorganic liquid culture medium containing 500 µg/L BDE-47, for 10 d as an acclimation period and four periods totally. The acclimated strain was enriched in the Luria-Bertani (LB) liquid medium, collected by centrifugation and washed three times with sterilized water to avoid the interference of nutrients in the bacterial liquid medium. Then the bacterial suspension was prepared for further simulation experiment with free degrading bacteria.

LB liquid medium: peptone, 10 g; yeast extract, 5 g; and NaCl, 10 g were added to 1 L water. The pH was adjusted to 7 and the medium was sterilized at 121°C for 20 min.

Determination of physicochemical properties of the soil sample

The soil pH, organic matter (OM), total nitrogen (TN), total phosphorus (TP) and total potassium (TK) were determined by the potentiometric method (NY/T1377-2007), potassium dichromate was determined by external heating method (NY/T1121.6-2006) and semi-micro Kjeldahl method (NY/T1121.24-2012), sulfuric acid was determined by perchloric acid digestion (NY/T88-1988) and flame photometric method (NY/T87-1988) (Bao et al., 2008).

Determination of microbial count and community structure

Determination of microbial count: Soil sample (10 g) was aseptically transferred to an Erlenmeyer flask containing 90 mL of sterilized water with an appropriate amount of glass beads in the flask, shaken for 2 h at 37°C and 120 rpm. Then, 1:10 dilution was prepared, which was further diluted 1:10 and a ten-fold serial dilution was made as described above. For each dilution, 1 mL of each dilution was plated on a sterilized LB plate, with three replicates for each dilution. The plates were cultured at 37°C for 36 h, and those with 30-300 total colonies were considered for determining the microbial count.

Determination of microbial community structure: Microbial community structure test analysis process as shown in the literature (Edgar et al., 2011; Knight et al., 2018).

Determination of BDE-47 content in the soil

The soil of each simulation system was collected, dried, ground, and filtered through a 100-mesh sieve. The soil sample (10 g) was added with an appropriate amount of diatomaceous earth, mixed, and extracted with an accelerated solvent extractor. The extraction tank was 34 mL, the solvent used was hexane/dichloromethane (1:1), and the static extraction was performed at 100°C and 1.03 kpa for five minutes and two cycles. The extract was transferred to a 100 mL rotary evaporator flask for rotary evaporation at 30°C to 1-2 mL, then 10 mL hexane was added to it and rotary evaporated to 1-2 mL again. The prepared sample was loaded on a silica gel alumina column and eluted with 75 mL hexane/dichloromethane (1:1) for purification. The eluent was collected and again rotary evaporated at 30°C to 1-2 mL, then 5 mL acetonitrile was added and concentrated again to approximately 1 mL. Next, it was transferred to a 2 mL sample vial, concentrated under nitrogen, fixed with 1 mL with acetonitrile, and filtered through a 0.22 µm membrane. Finally, it was loaded onto the Waters ACQUITY UPLC C18 column, sized 2.1 mm × 50 mm × 1.7 µm, with 100% acetonitrile as the mobile phase. The flow rate was set to 0.2 mL/min, the column temperature was 30°C, and the absorbance was measured at 226 nm.

Results and discussion

Changes in soil physicochemical properties

Compared with the original, natural soil, there was no significant change in the soil pH, OM, TN, TP or TK in the simulation systems, indicating that in the simulation processes, the addition of BDE-47, free or immobilized bacteria, had no significant effect on the soil physicochemical properties (*Table 1*). Liu et al. (2011) showed that the OM in soil could maintain soil water content and water availability, and thus, can be used as a routine indicator to measure soil water retention and availability. The increase of soil OM content may cause changes in soil aggregate structure to loosen the texture and increase the water permeability and water holding capacity (Guo, 2007). The nitrogen in the soil exists primarily in the surface soil and is closely related to the organic matter content. Nearly 80~97% of the total nitrogen in the surface soil comes from the decomposition of organic matter (Ros et al., 2004). Therefore, the changes in OM content change the soil nitrogen content (Huangshan, 1998). Total phosphorus is an index measuring the sum of various forms of phosphorus in soil. Its value is greatly impacted by the soil parent material and soil formation, and it is also related to soil texture and organic matter (Ding et al., 2010). While the changes in soil physicochemical properties directly affect the microbial community structure, various physicochemical properties synergistically affect the microbial community. As a result, none of the tested simulation systems demonstrated significant changes in physicochemical properties, thus, indicating that the simulation process does not significantly impact the microbial community structure.

Table 1. Soil Physical and Chemical Properties in Simulated System

Properties	Original soil	A-E	B-E	C-E
pH	7.2	7.3	7.2	7.1
OM (g/kg)	21.7±0.66a	21.80±0.757a	22.04±0.76a	20.4±0.7a
TN (g/kg)	2.18±0.023a	2.19±0.02a	2.23±0.07a	2.18±0.06a
TP (g/kg)	0.58±0.008a	0.58±0.008a	0.59±0.012a	0.61±0.002a
TK (g/kg)	10.53±0.55a	10.54±0.7a	10.80±0.2a	10.82±0.11a

A, B, and C represent the three simulation systems, and E represents the end of the simulation

Analysis of microbial structure changes

Changes in microbial community structure

As mentioned in Fig. 1, *Proteobacteria*, *Acidobacteria*, and *Actinobacteria* were the dominant phyla in the simulation systems. During the initial stage of the simulation, *Proteobacteria* accounted for 41.58%, 34.47% and 40.97% in systems A, B, and C, respectively. Along the simulation process, its percentages depleted, and accounted for 31.53%, 27.33%, and 29.35%, respectively, at the end of the simulation. The changes in *Acidobacteria* population was similar to that of *Proteobacteria*. The percentage of *Actinobacteria* went up along the simulation, changing from initial 18.62%, 12.27%, and 19.81% to the final 42.02%, 37.66%, and 43.34%, respectively, for the systems A, B, and C. *Firmicutes* were the dominant phylum in system B, and its percentages before and after simulation were 18.80% and 13.89%, respectively. The phyla *Bacteroidetes*, *Chloroflexi*, *Gemmatimonadetes*, *Verrucomicrobia*, *Nitrospirae*, *Planctomycetes*, and *Candidate_division_WS3* were common in all simulation systems, while the other bacteria were rarely found.

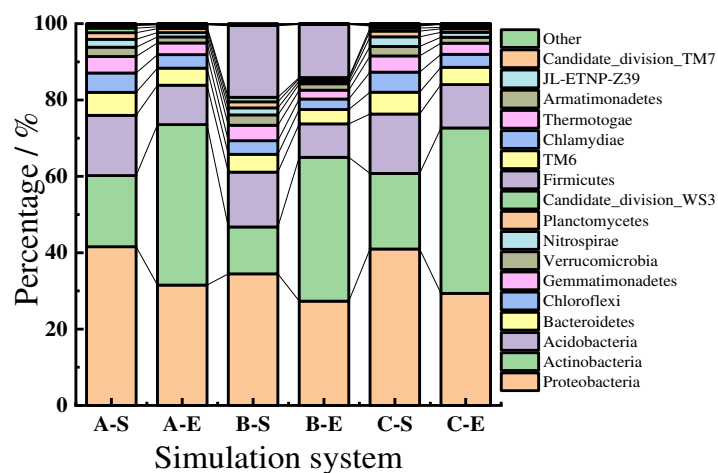


Figure 1. Analysis of microbial community structure at Phylum level start and end each simulation system. A: Soil + BDE-47; B: Soil + BDE-47 + free degradation bacteria; C: Soil + BDE-47 + immobilized strains; S: Simulation start; E: Simulation end

In system A and C, as the simulation progressed, the proportions and trends of the bacterial phyla were consistent, indicating that the addition of the immobilized degrading strain did not affect the microbial community structure in the soil significantly. Although, the addition of the free degrading strain actually impacted the original microbial community structure to some extent. For system B, the dominant role of *Firmicutes* was observed because the added free degrading bacteria belonged to this phylum. In summary, for the simulation systems, the change of the microbial community structure in the soil was related more closely to the addition of the degrading bacteria in the simulation process. The degrading strain was screened and isolated from the contaminated soil in Zhejiang and was more adaptable to the soil ecological environment in that province. Hence, when it was applied to remediate the soil polluted by BDE-47 in Zhejiang, it had less impact on the soil microbial community structure.

Analysis of the trend of the degrading strain

As per the high-throughput sequencing results (Figure 2), the dynamic tracking of the degrading strain which belonged to *Bacillus* showed that the relative abundance of *Bacillus* in system A dropped from 0.0062 at the initial stage to 0.0041 at the later stage. Whereas in system B, the addition of the degrading *Bacillus* strain directly caused its relative abundance to increase to 0.1857 at the initial stage, and decrease later to 0.13813, although it was still the dominant species. In the system C, the relative abundance of *Bacillus* at the initial stage was 0.00553, and with the simulated remediation, its relative abundance increased by 0.16% to the final 0.00714. The analysis of the free degrading strain count by the traditional microbial culturing technique in system B showed an initial count of $(5.0 \pm 0.1) \times 10^4$ CFU/g, which increased along the simulation to a final count of $(1.0 \pm 0.2) \times 10^5$ CFU/g (Fig. 3).

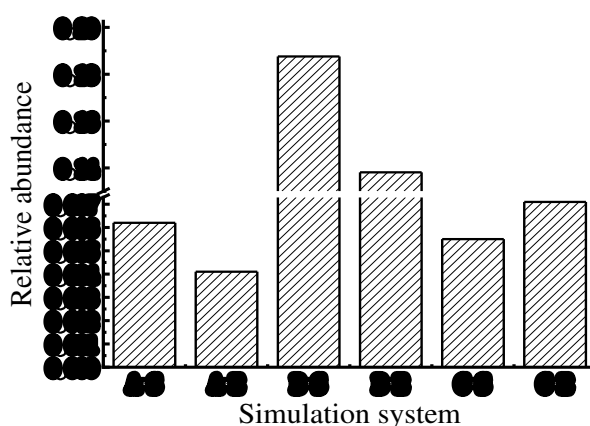


Figure 2. Analysis of relative abundance variation of *Bacillus* sp in each simulation system

The two approaches revealed that the free degrading strain adapted well to the simulated soil environment and that the decrease in *Bacillus* may be due to cell death and DNA degradation during the simulation process, resulting in a decline in final relative

abundance. At present, only about a dozen strains have been found capable of aerobic degradation of PBDEs, and the reported ones include *Sphingomonas* sp. (Schmidt et al., 1992, 1993; Hundt et al., 1999), *Rhodococcus* sp. RR1, *Seudonocardia dioxanivorans* CB1190 (Robrock et al., 2009), *Lysinibacillus fusiformis* strain DB-1 (Deng et al., 2011), *Bacillus cereus* JP12, *Acinetobacter*, *Pseudomonas*, and *Staphylococcus* (Wang et al., 2016). Currently, there are very limited reports on the application of free strains for environmental remediation.

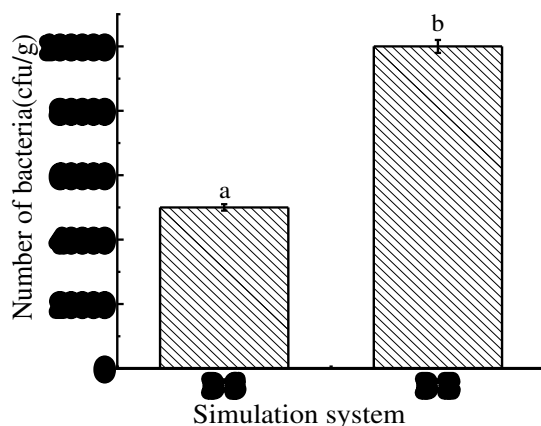


Figure 3. Change in the number of free bacteria in B simulation system

BDE-47 degradation analysis

As shown in Table 2, at the start of simulation, the BDE-47 concentrations were 1,504 ng/g in system A, 1,775 ng/g in system B, and 1,654 ng/g in system C. After 90 days of simulation remediation, the remaining BDE-47 concentrations were 1,135 ng/g in system A, 1,069 ng/g in system B, and 1,043 ng/g in system C. The degradation rate of BDE-47 in system A was 24.53%, demonstrating existence of BDE-47 degrading strain in the simulated original soil. The degradation rate in system B was 39.77%, indicating that the added free degrading strain potentially promoted the degradation of BDE-47. The degradation rate in system C was 36.94%, indicating that while the added immobilized strain could promote the degradation of BDE-47 as well, but it was inferior to the free strain. The micro-ecological environment of the polluted soil consists mostly of microorganisms, which are important biotic components of the soil environment. The soil used for simulations was collected from Taizhou, Zhejiang and the added degrading strain was also screened from a contaminated site in Taizhou, Zhejiang. Therefore, the free strain could adapt well to this soil environment, promoting the degradation of the pollutant BDE-47. Although studies show that the immobilization of degrading bacteria can increase the concentration of microorganisms, keep the strains highly active and repeatedly usable, and greatly enhance the environmental adaptability of the immobilized microbes and their ability to degrade organic matter (Karamanev et al., 1998; Su et al., 2006, 2008; Lu et al., 2015). In this present study, although the

immobilization increased the concentration of bacteria inside the immobilized beads, the bacteria could not diffuse. Therefore, it was not conducive to the degradation of pollutant in the soil.

Table 2. BDE-47 concentration chromatographic results

System	Simulation time (day)	Peak time (min)	Peak area ($\mu\text{A/s}$)	Peak height (μA)	BDE-47 concentration (ng/g)
A	0	1.106	264969	135094	1504
	90	1.104	204801	106061	1135
B	0	1.106	308973	154296	1775
	90	1.105	194046	100537	1069
C	0	1.104	289360	147979	1654
	90	1.104	189882	94948	1043

Conclusions

a) In all simulation systems, the addition of pollutant BDE-47, and the free or immobilized strain had little effect on the soil physicochemical properties such as pH, OM, TN, TP, and TK.

b) The dominant phyla in the simulation systems were *Proteobacteria*, *Acidobacteria*, and *Actinobacteria*. A total of seven phyla including *Bacteroidetes*, *Gemmatimonadetes*, and *Nitrospirae* were common bacteria shared by all three simulation systems. The *Firmicutes* became the dominant bacterial phylum because the added strain of free bacteria belonged to this phylum. The free degrading strain adapted well to the simulation system, and its count was increased in the later stages.

c) The original soil used for the simulation contained the BDE-47 degrading strain, and the addition of the free degrading strain could promote the degradation of BDE-47 at a rate of 39.77%. The addition of the immobilized strain also promoted the degradation of BDE-47, although the degradation rate was 36.94%, slightly below that of the free strain. The next research plan focuses on the degradation pathway of BDE-47, which lays the foundation for regulating the degradation process of BDE-47.

Acknowledgments. This work supported by PhD Research Foundation Project (MNUB201709) and Heilongjiang Provincial Department of Education Basic Research Project (1353MSYYB026).

REFERENCES

- [1] Arias, P. (1992): Brominated diphenyloxides as flame retardants: bromine based chemicals. – Consultant report to the OECD, Paris.
- [2] Bao, S. D. (2008): Soil agrochemical analysis. – China Agricultural Publishing board 2: 58-179.
- [3] Chen, C. L., Liao, M., Zeng, L. S. (2006): Methods to measure the microbial community structure and functional diversity in polluted soils. – Acta Ecologica Sinica 26(10): 3404-3412.

- [4] Chen, A., Yolton, K., Rauch, S. A., Webster, G. M., Hornung, R., Sjödin, A., Dietrich, K. N., Lanphear, B. P. (2014): Prenatal polybrominated diphenyl ether exposures and neurodevelopment in U.S. children through 5 years of age: the HOME study. – Environmental Health Perspectives 122(8): 856-862.
- [5] Costa, L. G., Giordano, G., Tagliaferri, S., Caglieri, A., Mutti, A. (2008): Polybrominated diphenyl ether (PBDE) flame retardants: environmental contamination, human body burden and Potential adverse health effects. – Aeta Biomed 79(3): 172-183.
- [6] Deng, D. Y., Guo, J., Sun, G. P., Chen, X. J., Qiu, M. D., Xu, M. Y. (2011): Aerobic debromination of deca-BDE: Isolation and characterization of an indigenous isolate from a PBDE contaminated sediment. – International Biodeterioration & Biodegradation 65(3): 465-469.
- [7] Dewit, C. A. (2002): An overview of brominated flame retardants in the environment. – Chemosphere 46(5): 583-674.
- [8] Ding, S. L., Yang, N. G., Zhao, C. C., Yang, Q. M., Wang, Y., Dong, X. (2010): Soil physical and chemical properties in water conservation forest in eastern Qinghai Province. – Bulletin of Soil and Water Conservation 30(6): 1-6.
- [9] Edgar, R. C., Haas, B. J., Clemente, J. C., Quince, C., Knight, R. (2011): UCHIME improves sensitivity and speed of chimera detection. – Bioinformatics 27(16): 2194-200.
- [10] Guan, J. F., Wang, J. H., Liu, X., Xin, J., Zhang, S. S., Zhu, D. (2013): Biodegradation of 2,2',4,4'-tetrabromodiphenyl ether in an aerobic environment by a novel strain of *Bacillus* sp. – Advanced Materials Research 771: 45-49.
- [11] Guo, B. L. (2007): Research on change of carbon pool of soda meadow sodic soil after biological rehabilitation. – Harbin: northeast agricultural university: 15-18.
- [12] Huangshan Soil editorial board (1998): Huangshan soil. – China University of Science and Technology Press 119.
- [13] Hundt, K., Jonas, U., Hammer, E., Schauer, F. (1999): Transformation of diphenyl ethers by *Trametes versicolor* and characterization of ring cleavage products. – Biodegradation 10(4): 279-286.
- [14] Karamanev, D. G., Chavarie, C., Samson, R. (1998): Soil Immobilization: Newconcept for Biotreatment of Soil Contaminants. – Biotechnol Bioeng 57: 471-476.
- [15] Kim, Y. M., Nam, I. H., Murugesan, K., Schmidt, S., Crowley, D. E., Chang, Y. S. (2007): Biodegradation of diphenyl ether and transformation of selected brominated congeners by *Sphingomonas* sp. PH-07. – Applied Microbiology and Biotechnology 77: 187-194.
- [16] Knight, R. (2018): Best practices for analysing microbiomes. – Nature Reviews Microbiology 16: 410-422.
- [17] Liu, X. D., Qiao Y., Zhou, G. Y. (2011): Controlling action of soil organic matter on soil moisture retention and its availability. – Chinese Journal of Plant Ecology 35(12): 1209-1218.
- [18] Lu, H., Guan, X. F., Wang, J., Zhou, J. T., Zhang, H. K. (2015): Enhanced biodecolorization of 1-amino-4-bromoanthraquinone-2-sulfonic acid by *Sphingomonas xenophaga* with nutrient amendment. – Journal of Environmental Sciences 27: 124-130.
- [19] Robrock, K. R., Coelhan, M., Sedlak, D. L., Alvarez-Cohen, L. (2009): Aerobic biotransformation of polybrominated diphenyl ethers (PBDEs) by bacterial isolates. – Environmental Science & Technology 43: 5705-5711.
- [20] Ros, M., Garcia, C., Hernandez, T., Andres, M., Barja, A. (2004): Short-term effects of human trampling on vegetation and soil microbial activity. – Communications in Soil Science and Plant Analysis 35(11/12): 1591-1603.
- [21] Schmidt, S., Wittich, R. M., Erdmann, D., Wilkes, H., Francke, W., Fortnagel, P. (1992): Biodegradation of diphenyl ether and its monohalogenated derivatives by *Sphingomonas* sp. strain SS3. – Applied and Environmental Microbiology 58(9): 2744-2750.

- [22] Schmidt, S., Fortnagel, P., Wittich, R. M. (1993): Biodegradation and transformation of 4,4-and 2,4-dihalodiphenyl ethers by *Sphingomonas* sp. strain SS33. – *Applied and Environmental Microbiology* 59: 3931-3933.
- [23] Su, D., Li, P. J., Stagnitti, R., Xiong, X. (2006): Biodegradation of Benzo α -pyrene in Soil by *Muco* sp. SF06 and *Bacillus* sp. SB02 Co-immobilized on Vermiculite. – *Journal of Environmental Sciences-China* 18(6): 1204-1209.
- [24] Su, D., Li, P. J., Wang, X., Stagnitti, F., Xiong, X. (2008): Biodegradation of Benzo α -Pyrene in Soil by immobilized Fungus. – *Environmental Engineering Science* 25(8): 1181-1188.
- [25] Talsness, C. E. (2008): Overview of toxicological aspects of polybrominated diphenyl ethers: A flame-retardant additive in several consumer products. – *Environmental Research* 108(2): 158-167.
- [26] Vanelsas, J. D., Mantynen, V., Wolters, A. (1997): Soil DNA Extraction and assessment of the Fate of mycobacterium *Chlorophenicum* Strain PCP-1 in different soils by 16S ribosomal RNA gene sequence based most-probable-number PCR and immunofluorescence. – *Biology and Fertility of Soils* 24: 188-195.
- [27] Walter, K. M., Lin, Y. P., Kass, P. H., Puschner, B. (2017): Association of Polybrominated Diphenyl Ethers (PBDEs) and Polychlorinated Biphenyls (PCBs) with Hyperthyroidism in Domestic Felines, Sentinels for Thyroid Hormone Disruption. – *BMC Veterinary Research* 13(1): 120.
- [28] Wang, J. M. (2016): The response of microbial community to petroleum pollution and planting robinia pseudoacacia in different agricultural soils. – Yangling: Northwest A&F University: 58-62.
- [29] Wang, L. Q., Li, Y., Zhang, W. L., Niu, L., Du, J., Cai, W., Wang, J. (2016): Isolation and characterization of two novel psychrotrophic decabromodiphenyl ether-degrading bacteria from river sediments. – *Environmental Science and Pollution Research* 23(11): 10371-10381.
- [30] Xu, B., Wu, M., Wang, M., Pan, C., Qiu, W., Tang, L., Xu, G. (2017): Polybrominated diphenyl ethers (PBDEs) and hydroxylated PBDEs in human serum from Shanghai, China: a study on their presence and correlations. – *Environmental Science Pollution Research* 25(4): 3518-3526. <https://doi.org/10.1007/s11356-017-0709-4>.
- [31] Yang, M. Q., Li, L. M., Li, C., Li, G. H. (2013): Microbial community structure and distribution characteristics in oil contaminated soil. – *Environmental Science* 34(2): 789-794.
- [32] Zhou, Y., Chen, Q., Du, X., Yin, G., Qiu, Y., Ye, L., Zhu, Z., Zhao, J. (2016): Occurrence and trophic magnification of polybrominated diphenyl ethers (PBDEs) and their methoxylated derivatives in freshwater fish from Dianshan Lake, Shanghai, China. – *Environmental Pollution* 219: 932-938.

EFFECTS OF BIOGAS SLURRY IRRIGATION ON TOMATO (*SOLANUM LYCOPERSICUM* L.) PHYSIOLOGICAL AND ECOLOGICAL INDEXES, YIELD AND QUALITY AS WELL AS SOIL ENVIRONMENT

ZHENG, J.^{1,2,3*} – MA, J.^{1,3} – FENG, Z. J.^{1,3} – ZHU, C. Y.^{1,3} – WANG, J.⁴ – WANG, Y.^{1,2}

¹*College of Energy and Power Engineering, Lanzhou University of Technology
Lanzhou 730050, China*

²*Western China Energy & Environment Research Center, Lanzhou University of Technology
Lanzhou 730050, China*

³*Key Laboratory of Complementary Energy System of Biomass and Solar Energy
Gansu Province, Lanzhou 730050, China*

⁴*College of Water Resources and Architectural Engineering, Northwest A&F University
Yangling 712100, China*

**Corresponding author*

e-mail: zhj16822@126.com; phone: +86-1391-9257-393

(Received 13th Jul 2019; accepted 25th Nov 2019)

Abstract. Replacement feasibility of inorganic fertilizer using biogas slurry was investigated via two-season pot culture experiments in greenhouse. Three biogas slurry treatments (treatment 1, T1; treatment 2, T2; treatment 3, T3) and a inorganic fertilizer treatment (CK) were set to explore the effects on tomato growth, yield, quality and root-zone soil environment. The volume concentrations of biogas slurry in T1, T2 and T3 treatments were 20, 15 and 10%, respectively. Results showed that T1 and CK treatments maintained a high leaf area index (LAI), photosynthetic rate and chlorophyll (a+b) contents during the whole growing period. T1 treatment can obtain an equivalent yield to CK, however, the yield of T2 and T3 treatments were inferior to that of CK. For the quality of tomato, T1 treatment can improve the soluble sugar and titratable acid contents for about 19.07 and 4.17% when compared to CK, and T2 treatment can improved about 7.55 and 4.17%. Furthermore, T1 and T2 treatment can get a better sugar-acid ratio and tastes. In comparison with inorganic fertilizer treatment, all biogas treatments could increase soil porosity and soil aggregate, decrease soil debris, in which the superior treatment is T1 and can be considered as a good organic fertilizer.

Keywords: *leaf area index, photosynthetic rate, chlorophyll, comprehensive benefit evaluation, soil saturated hydraulic conductivity, soil organic matter, soil total nitrogen, soil microstructures*

Introduction

Application of inorganic fertilizers has played a significant role in the development of food and other agricultural crop productions (Smith et al., 2015). However, recent researches showed that the production benefit did not increase proportionately with the quantity of fertilizer input (Liu et al., 2017). Application of fertilizer in excess, not only increased the cost of agricultural products, but also result environmental problems such as soil hardness and soil acidification of the cultivated lands. A reduction in the amount of applied fertilizer could bring the cost of agricultural production down, enhance efficiency, save energy and reduce emissions. As a result the national food security, agricultural product quality and agricultural ecological condition all become saved (Li et al., 2016). It has been verified that organic fertilizers could promote the healthy growth

of crops and enhance yield and quality of crops through improving soil structure of fungal community (Ding et al., 2017; Rong et al., 2018). Thus, the replacement of inorganic fertilizer with the organic ones could bring a safer food production system with adequate achievements of ecological and environmental safety of the cultivated lands.

Biogas slurry is the post-product of biogas production technology via anaerobic fermentation process. It is an effective organic fertilizer, which contains the most basic water soluble nutrients necessary for crop growth, such as N, P and K. Besides, it also contains microelements like Ca and Mg and some essential amino acids as well as growth stimulating and regulating materials including vitamins and growth hormones. Application of biogas slurry irrigation could enhance crop yield, optimize fruit quality, promote crop seed germination, prevent diseases and pests, and improve soil quality (Tambone et al., 2010; Ledda et al., 2013; Oh et al., 2014). Duan et al. (2011) applied biogas slurry as liquid fertilizer on greenhouse cucumber production. They obtained high yield and good quality of cucumber compared with inorganic fertilizer treatment. Their experiment had also achieved a reduction of greenhouse gas emission. Albuquerque et al. (2012) showed that the application of biogas slurry could effectively improve soil environment and obtain yield which was comparable with that obtained by traditional fertilizer application. Using biogas slurry in the field increased the population of microorganisms which contributed to the formation of soil organics (Coban et al., 2015). Nabel et al. (2017) carried out a comparative experiment of three years duration and showed that the application of biogas slurry as fertilizer could enhance carbon content, water holding capacity and fertility of soils. Lu et al. (2012) showed that irrigation by appropriate biogas slurry could enhance rice yield compared with traditional fertilizer use. Besides, the heavy metal concentration of underground water, soil and rice, determined after one week of biogas slurry irrigation were seen unaffected. Actually biogas slurry contains high water content and low fertilizer properties. However, in current researches, biogas slurry was treated simply as fertilizer and applied each time according to the calculated equivalent fertilizer application amounts. This had resulted in the loss of nutrient and a decrease of nutrient utilization efficiency. In addition, current researches did not consider comprehensively the effect of biogas slurry on crop growth elements, yield and quality, soil nutrient and micro-aggregation structure of roots over the whole growth period. Besides, there was a lack of study on the effect of application of biogas slurry as replacement of inorganic fertilizer. Considering the above mentioned knowledge gaps, it has been aimed in the present research to study the effect of application of biogas slurry in different concentrations on tomato cultivation. In the present research, physiological and ecological indexes, yield and quality, as well as the soil environment of root of tomato plant were considered to study over the entire growth period. Another objective of this research was to evaluate the tomato comprehensive benefit using the 'Technique for order preference by similarity to ideal solution' (TOPSIS). This would enable to obtain appropriate biogas slurry irrigation mode during the whole tomato growth period in realization of providing theoretical support for further field application as total replacement of inorganic fertilizer.

Materials and Methods

Experimental materials

In the present research, pot culture experiments were performed in the spring and autumn seasons of 2017. The experimental site was the greenhouse of the demonstration

site of integration of facilities, vegetables, water and fertilizer at Weiling Country, Qilihe District, Lanzhou City, Gansu Province of the People's Republic of China. The experimental criteria were: Daylight greenhouse with the type of ridge $50.0 \times 10.5 \times 4.0$ m (L×W×H) at $36^{\circ}03'$ N and $103^{\circ}40'$ E and with an average altitude of 1872 m (Figure 1). The study area is subjected to a temperate continental dry climate with sufficient sunlight and little rain. Average annual temperature was 8.9°C with a no-frost period of about 150 d. Average annual precipitation and evaporation were 310.5 and 1158.0 mm, respectively. There was a minimized automatic weather site in greenhouse to constantly monitor conventional meteorological data.

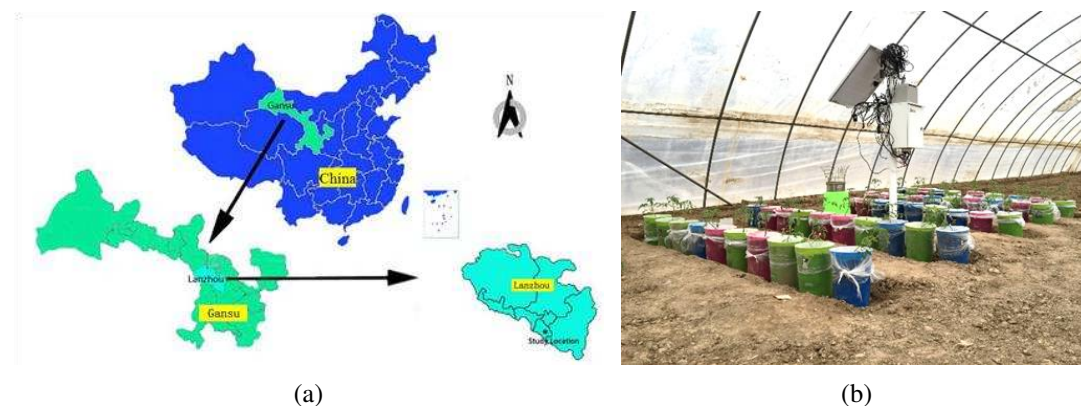


Figure 1. Research site location and pot culture experiment equipment in greenhouse. (a) The research site location; (b) the pot culture experiment equipment

Tomato (*Solanum lycopersicum* L.) cultivar “No.3 of Hongbao” was tested in pot culture experiments. The soil used in this experiment was collected from the indoor surface layer of 0-40 cm within the greenhouse complex. Soil particle size distribution was determined by laser particle size analyzer (MS2000). The calculated ratios of sand, silt and clay to total weight were 25.3, 64.6 and 10.1%, respectively. According to International soil texture classification standard, the tested soil was silt. Soil nutrient condition was determined before potting. Contents of total N, organic matter, and total P were 1.022, 9.08 and 1.616 g/kg, respectively. The bottom and top diameter of the cultivation container, the height of soil and the unit weight of soil were 16, 22 and 22 cm and 1.35 g/cm^3 , respectively. Field water holding content, namely, weight water fraction θ_f was 23.5%. A hole at the bottom of pot was drilled for ventilation. Gauze and filter paper were put at the bottom to prevent the leakage of soil. To monitor soil water fraction a hole was drilled at the wall of the pot. Tomato was permanently planted with a seedling of four big leaves and one heart. The growth period of tomato in the experiments was shown in Table 1. In the experiment 1500 ml slow seedling water in permanent planting was unifiedly irrigated. The plastic film was covered 5 d after permanent planting. Soil evaporation could be neglected. Other cropping management practices, such as pesticide and herbicide application, were consistent with those used by local farmers.

The tested biogas slurry was collected from the biogas tank with normal fermentation and normal gas production in Gansu Hesitan cows breeding center in Huazhuang Country, Lanzhou City. After two months of aeration and standing, the clear liquid was extracted for further use until the physicochemical properties stabilized. The biogas engineering perennially used cow dung as fermentation material. Nutritional status of the

biogas slurry were 10.75, 1.036, 0.533 and 1.186 g/L for organic matter, total N, P and K contents, respectively.

Table 1. *The growth period of tomato in the experiments*

Planting time	Growth period	Date	Days	Planting time	Growth period	Date	Days
Plant in spring	Seedling stage	12-28th May	16	Plant in autumn	Seedling stage	14-29th September	16
	Flowering stage	May 29th to June 9th	12		Flowering stage	September 30th to October 9th	10
	Fruit swelling stage	June 10th to July 3rd	24		Fruit swelling stage	October 10th to November 10th	31
	Fruit maturity stage	4-21st July	18		Fruit maturity stage	11-29th November	19

Experimental design

In the experimental trials, hole irrigation water-biogas slurry integration method was applied (Tan et al., 2015). Four treatments were set, wherein CK was the routine fertilizer treatment and T1, T2 and T3 were the biogas slurry treatments with volume concentrations of 20, 15 and 10%, respectively. Inorganic fertilizer application of CK treatment in tomato growth period was as follows: once in each of the seedling and flowering stage and twice in each of the fruit swelling stage and fruit maturity stage with urea, P and K fertilizer. The application amounts for NPK were 78, 94.5 and 97.5 kg/ha, respectively.

During the entire growth period, the biogas slurry treatment adopted integration irrigation of water and biogas slurry. Namely, irrigation was conducted with biogas slurry of different concentrations. The irrigation amount was calculated by the evaporation amount of the standard evaporating dish of $\Phi 20$ cm which was put at the height with a distance of 20 cm to tomato canopy. The evaporation amount of cumulative 2 d was set as the irrigation standard. The irrigation frequency was 1 time/2 d.

The calculation method was according to (Eq.1) (Azizi-Zohan et al., 2008)

$$M = K_p \times S \times E_p \quad (\text{Eq.1})$$

where, M was the irrigation water amount in mL; K_p was the crop-pan coefficient; S was the irrigation water amount control area with the unit of cm^2 ; E_p was the evaporation amount of the evaporating dish in the gap between two irrigation with the unit of mm.

To illustrate the difference between the integration irrigation of water and biogas slurry and traditional fertilizer treatment in tomato whole growth period as well as to obtain appropriate biogas slurry concentration, none of water deficit treatment was set in different growth periods of crop in experiment.

Thus, K_p value was set as 1.0 in the experiment. In addition, three replicates were set for each treatment.

The determination of indexes and methods

The determination of physiological and ecological indexes

Leaf area index (LAI) was determined by the image method using Photoshop software. Three plants in each treatment were chosen to measure and the final LAI are the average

value. In the seedling and flowering stages, the LAI for each treatment was measured once. However, in the fruit swelling and maturity stages this parameter was measured twice for the longer period of these two growth stages. The measurement of LAI followed the scanning of the leaf first with the help of a scanner and then the leaf area was calculated with the software of Photoshop. Finally, the value of LAI was obtained according to the equation (Eq.2):

$$\text{LAI} = A_l/A_s \quad (\text{Eq.2})$$

where, A_l is the total leaf area of a single plant, A_s is the irrigation water amount control area of a plant.

Soil water fraction was determined by WET three parameter calibrated tester. The determination was done at 2 days during the growth period. Chlorophyll was determined by the mixed solution method of acetate and ethanol (Liu et al., 2018) before and the third day after the first fertilizer application as well as before the second fertilizer application in the fruit swelling stage. The photosynthetic rate was determined by CIRAS-I portable photosynthesizer (made in UK) during 9:30 to 10:30 AM of sunny day in different tomato growth periods. The photosynthetic rate was determined on May 22 and September 21 in seedling stage, and measured on June 2 and October 6 in flowering stage, on June 24 and October 19 in the fruit swelling stage and on July 15 and November 20, 2017 for tomato planted in spring and autumn. Weights of dry materials were determined by the drying method. Samples were collected at the end of different tomato growth periods. For each treatment, three crops were determined separately, whose average value was reported as experimental final result.

Quality index determination

Soluble solids of tomato fruit contents were determined by WAY-2S Abbe refractometer. Vitamin C, soluble protein, total soluble sugar and the titrate acidity were determined by Molybdenum blue colorimetry, Coomassie brilliant blue G-250 staining method, Anthrone colorimetry method and the titration method (Liu et al., 2018), respectively.

Soil environment index determination

Soil saturated hydraulic conductivities were determined by the variable water level method with soil sampling by cutting ring after experiment. Total N content in soil was determined by Kjeldahl method. Soil microstructure was determined by imaging via scanning electron microscope (SEM), whose figure was treated by Photoshop CS6 software.

Data processing and analysis

Each data was the average of three replicate determinations. Turkey HSD of the variance analysis and the significance of difference were conducted by SPSS 19.0 statistical analysis software. Figures were drawn by Excel 2010 and Origin 8.0. Tomato comprehensive benefit was evaluated by TOPSIS analysis method.

Results and analysis

The response pattern of tomato physiological and ecological indexes on different treatments

LAI

Figure 2 showed the changing pattern of LAI of different treatments over the whole growth period. It showed that LAI of tomato which was planted in spring was significantly larger than that of autumn treatment. LAIs of different biogas slurry treatments in two growth periods were in a descending order of $T1 > T2 > T3$, whereas LAI of CK treatments in stages of seedling, blossoming and fruiting, and pre fruit swelling stage of tomato was the maximum among all, namely $CK > T1 > T2 > T3$, respectively. However, LAI of CK treatment in the late fruit swelling stage gradually decreased to be lower than that of T1 treatment. The pattern followed $T1 > CK > T2 > T3$. Besides, LAI in the late fruit maturity stage decreased dramatically. The changing trend of LAI illustrated that the fertilizer application in tomato nutritional growth period could provide optimum nutrient supply for tomato, whereas during the gradual transition of tomato from nutritional growth to reproductive growth, CK treatment on the aspect of sustainable support of crop growth was insufficient. In addition, LAI of T1 treatment demonstrated a much higher level in the entire tomato growth period, especially in the fruit swelling stage. During which period the value was far higher than those of other treatments. Thus, it demonstrated better growth persistence and illustrated that the water and fertilizer supply of T1 treatment could obtain better LAIs with the corresponding biogas slurry concentration and irrigation frequency.

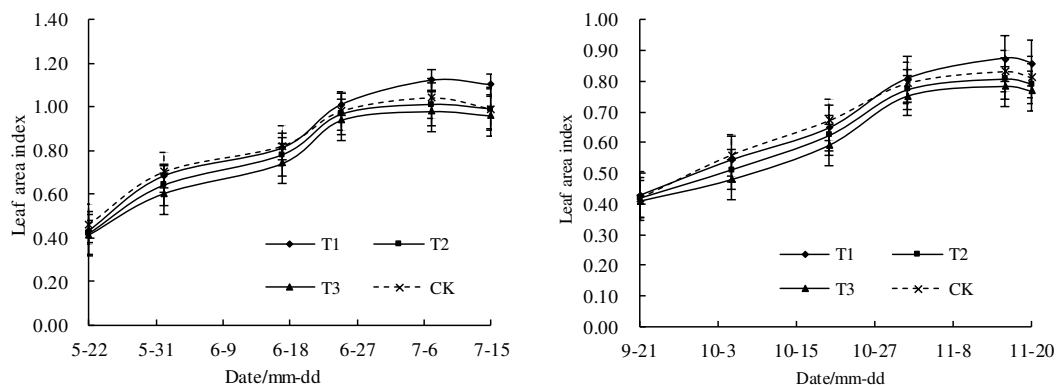


Figure 2. Growth stage variations of tomato leaf area index under different treatments. The error bars mean a 5% range of error. CK is the control treatment applied with inorganic fertilizer, T1, T2 and T3 are treatments applied with biogas slurry of 20, 15 and 10% in volume concentrations, respectively

The photosynthetic rate

From Table 2, leaf photosynthetic rates of CK treatment in tomato seedling as well as flowering stages in both spring and fall experiments were significantly higher than those of biogas slurry treatments (T1, T2 and T3) and with apparent advantages. Leaf photosynthetic rates of T1 treatment in fruit swelling and maturity stages were apparently higher than those of other treatments. It followed a descending order of $T1 > CK > T2 > T3$.

The leaf photosynthetic rates of T1 treatment were 0.06 and 0.07 $\mu\text{mol}/\text{m}^2/\text{s}$ as well as 0.10 and 0.09 $\mu\text{mol}/\text{m}^2/\text{s}$ higher than those of CK treatment in spring and fall cultivation, respectively.

Table 2. Leaf photosynthetic rate of tomato in different growth stages

Treatments	Planted in spring				Planted in autumn			
	Seeding stage ($\mu\text{mol m}^{-2}\text{s}^{-1}$)	Flowering stage ($\mu\text{mol m}^{-2}\text{s}^{-1}$)	Fruit swelling stage ($\mu\text{mol m}^{-2}\text{s}^{-1}$)	Fruit maturity stage ($\mu\text{mol m}^{-2}\text{s}^{-1}$)	Seeding stage ($\mu\text{mol m}^{-2}\text{s}^{-1}$)	Flowering stage ($\mu\text{mol m}^{-2}\text{s}^{-1}$)	Fruit swelling stage ($\mu\text{mol m}^{-2}\text{s}^{-1}$)	Fruit maturity stage ($\mu\text{mol m}^{-2}\text{s}^{-1}$)
CK	7.96aA	8.26aA	8.06abAB	8.12bA	8.16aA	7.86aA	7.46bB	6.76bB
T1	7.84bB	8.16bB	8.12aA	8.19aA	8.10bA	7.82aAB	7.56aA	6.85aA
T2	7.82bB	8.06cC	8.00bB	7.98cB	8.08bA	7.76bBC	7.42cC	6.66cC
T3	7.80bB	8.00cC	7.86cC	7.82dC	8.06bA	7.72bC	7.34dD	6.46dD

Lowercase a, b, c, d indicate significant differences among treatments at the level of $P < 0.05$; Capital letters A, B, C, D indicate significant differences among treatments at the level of $P < 0.01$. CK is the control treatment applied with inorganic fertilizer, T1, T2 and T3 are treatments applied with biogas slurry of 20, 15 and 10% in volume concentrations, respectively

In the two seasonal experiments namely, spring and autumn, leaf photosynthetic rates of T1, T2 and T3 treatments were 0.8 and 1.3%, 2.1 and 2.4%, as well as 4 and 4.5% higher than those of CK treatment, respectively. In tomato seedling stage, there was no significant variation among different biogas slurry treatments (T1, T2 and T3), e.g. the largest variance was only 0.5%. In the flowering stage of spring cultivation, there was significant difference between tomato leaf photosynthetic rate of T1 treatment and those of T2 and T3 treatments. But there were no significant difference between T2 and T3 treatment. In addition, rate of T1 treatment was 1.2 and 2.0% higher than those of T2 and T3 treatments, respectively. However, in the flowering stage of fall cultivation, rate of T1 treatment was 0.8 and 1.3% higher than those of T2 and T3 treatments, respectively. This means that there started a certain degree of differentiation between the nutrient supply of biogas slurry and the tomato growth demand at the time of gradual transition from tomato nutritional growth to reproductive growth. This also affected the leaf photosynthesis to some extent. In the stages of fruit swelling and fruit maturity, the photosynthetic rate of T1 treatment was significantly higher than those of T2 and T3 treatments. This indicates that T1 treatment could better promote leaf photosynthetic rate of tomato during tomato reproductive growth stages which promotes further the synthesis of photosynthetic products.

Chlorophyll

Chlorophyll in leaves could demonstrate the photosynthetic ability of leaf to some extent. *Figure 3* showed the variation of chlorophyll (a+b) content with different treatments. Chlorophyll (a+b) content of CK treatment before the first fertilizer application in the fruit swelling stage was 0.055 and 0.025 mg g/FW which was lower than that of T1 treatment in two seasonal experiments, respectively (*Figure 2*).

Leaf chlorophyll (a+b) contents at the 3rd-5th day after the fertilizer application which were 0.067 and 0.048 mg g/FW higher compared to the values before fertilizer application, respectively. The values were the highest among those of different treatments, namely, 0.045 and 0.028 mg g/FW higher than those of T1 treatment.

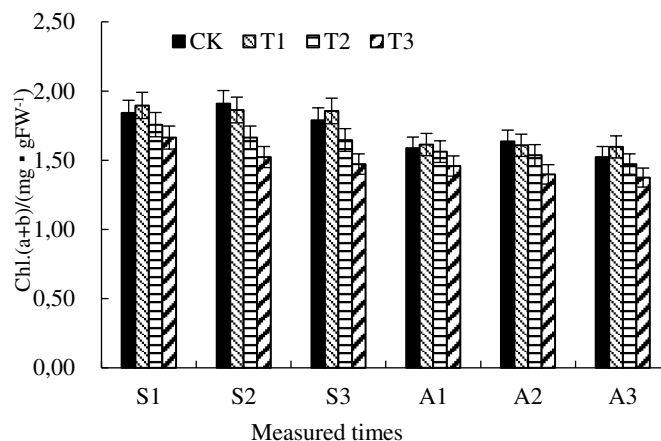


Figure 3. Chlorophyll (a+b) content in tomato leaves under different treatments. S1, S2 and S3 were the chlorophyll (a+b) in spring experiment, and A1, A2 and A3 were that in autumn experiment of 2017. CK is the control treatment applied with inorganic fertilizer, T1, T2 and T3 are treatments applied with biogas slurry of 20, 15 and 10% in volume concentrations, respectively. The error bars mean a 5% range of error. Chl., chlorophyll; FW, fresh weight

Leaf chlorophyll (a+b) content of CK treatment before the second fertilizer application in the fruit swelling stage decreased 0.119 and 0.113 mg g/FW compared with those of T1 treatment, respectively. Leaf chlorophyll (a+b) content of T2 and T3 treatments were lower than those of CK and T1 treatments and demonstrated a decreasing trend. The overall change of leaf chlorophyll (a+b) content of T1 treatment was the most stable among those of different treatments with respective changing amplitudes of only 0.04 and 0.017 mg g/FW of two seasonal experiments.

Besides, the changing amplitude of T3 treatment in two seasonal experiments was the largest i.e., 0.119 and 0.113 mg g/FW, respectively. The next largest changing amplitude was 0.111 and 0.09 mg g/FW of CK treatment. Thus, it showed that T1 treatment could maintain leaf chlorophyll (a+b) content at a stable level.

The response trend of tomato yield and quality

From Table 3, in 2017 spring experiment, the yield of T1 treatment was highest. The next was that of CK treatment. The yield of T1 treatment was 11.8 and 31.7% higher than those of T2 and T3 treatments, respectively. There was a significant difference between CK and T1 treatment at the level of $p=0.05$.

However, in 2017 autumn experiment, the yield of CK treatment was the highest. The next was that of T1 treatment. The yield of CK treatment was 15.5 and 18.2% higher than those of T2 and T3 treatments, respectively. However, there was no significant difference between the yield of CK treatment and that of T1 treatment at levels of $p=0.05$ and $p=0.01$. It illustrated that T1 treatment could not only replace fertilizer but also obtain the yield which was comparable with that of traditional fertilizer treatment. Different nutritional qualities of T1 and T2 treatments in two season experiments were higher than those of CK treatment, wherein total soluble sugar and titrate acid contents of T1 treatment were 19.07 and 16.30% as well as 4.17 and 10.32% higher than those of CK treatment, respectively.

Besides, total soluble sugar and titrate acid contents of T2 treatment were 75.5 and 7.70% as well as 2.24 and 7.54% higher than those of CK treatment, respectively.

Table 3. Effects of different treatments on tomato yield and nutritional quality

Planting time	Treatments	Yield/(g)	Nutritional quality				
			Titration acid/(%)	Total sugar/(%)	Sugar/Acid	Vitamin C/(mg•100g ⁻¹)	Soluble protein/(mg•g ⁻¹)
Planted in spring	CK	321bA	0.312abA	3.178cC	10.186cC	20.834cC	1.078cC
	T1	332aA	0.325aA	3.784aA	11.643aA	23.465aA	1.132aA
	T2	287cB	0.319abA	3.418bB	10.715bB	22.722bB	1.105bB
	T3	252dC	0.286bB	2.859dD	9.997dD	20.011dD	0.986dD
Planted in autumn	CK	268aA	0.252cB	2.626cC	10.421bB	18.847cC	0.912bB
	T1	259aA	0.278aA	3.054aA	10.986aA	19.973aA	0.967aA
	T2	232bB	0.271bA	2.828bB	10.435bB	19.077bB	0.923bB
	T3	219cB	0.244dB	2.311dD	9.471cC	18.376dD	0.881cC

Lowercase a, b, c, d indicate significantly differences among treatments at the level of P<0.05; Capital letters A, B, C, D indicate significantly differences among treatments at the level of P<0.01. CK is the control treatment applied with inorganic fertilizer, T1, T2 and T3 are treatments applied with biogas slurry of 20, 15 and 10% in volume concentrations, respectively

In addition, the sugar acid ratio of T1 treatment was 14.3, 8.6 and 16.5% higher than those of CK, T2 and T3 treatments, respectively in spring cultivation as well as 5.4, 5.2 and 16.0% higher in autumn cultivation, respectively. Besides, the sugar acid ratio of T2 treatment was 5.19 and 0.13% higher than those of CK treatment in spring and fall, respectively.

Vc contents of T1 and T2 treatment were 12.58 and 5.97% higher than those of CK treatment in spring cultivation as well as 9.02 and 1.02% higher in fall cultivation, respectively. Different nutritional quality indexes of T3 treatment was the lowest among those of different treatments.

Results showed that T1 and T2 treatments not only obtained a higher soluble sugar content and the titrate acidity but also increased the sugar acid ratio, Vc, and soluble protein contents. All these factors contributed to increase the nutritional value as well as the taste and flavor of tomato. However, T3 treatment was unfavourable to the formation of tomato nutritional quality, illustrating the effect of biogas slurry irrigation frequency and concentration on tomato yield and quality to some extent. Thus, the appropriate biogas slurry irrigation mode could effectively improve the nutritional quality of tomato.

Tomato comprehensive benefit evaluation by the TOPSIS method

To obtain the optimum biogas slurry irrigation mode over the whole growth period of tomato, seven indexes such as yield, soluble solids, the soluble sugar, the titrate acid, the sugar acid ratio, the soluble protein and vitamin C were chosen. Besides, as shown in Table 4, tomato comprehensive benefit was evaluated by the TOPSIS method. Thus, in 2017 spring and fall experiments, comprehensive benefit indexes (CIs) of different treatments as well as comprehensive sorting were in a descending order of T1>T2>CK>T3. In addition, CI value of T1 treatment was 31.21 and 40.86% higher than those of CK treatment, respectively. This illustrated that T1 treatment was better than traditional fertilizer treatment. So, on the comprehensive benefit aspects of tomato yield and nutritional quality, T1 could be recommended as reference mode for the replacement of fertilizer with biogas slurry.

Table 4. Tomato comprehensive benefit evaluated by TOPSIS

Planting time	Treatments	Yield	Titration acid	Total sugar	Sugar/Acid	Vitamin C	Soluble protein	D ⁺	D ⁻	CI	Rank
Planted in spring	CK	0.5356	0.5018	0.4776	0.4780	0.5207	0.5006	0.1367	0.3039	0.6897	3
	T1	0.5540	0.5227	0.5687	0.5464	0.5864	0.5257	0.0000	0.4058	1.0000	1
	T2	0.4789	0.5131	0.5137	0.5028	0.5678	0.5132	0.1056	0.3441	0.7651	2
	T3	0.4205	0.4600	0.4297	0.4691	0.2502	0.4579	0.4058	0.0000	0.0000	4
	A ⁺	0.5540	0.5227	0.5687	0.5464	0.5864	0.5257				
	A ⁻	0.4205	0.4600	0.4297	0.4691	0.2502	0.4579				
Planted in autumn	CK	0.5463	0.4816	0.4830	0.5038	0.4900	0.4950	0.1073	0.1265	0.5411	3
	T1	0.5279	0.5313	0.5617	0.5311	0.5248	0.5248	0.0183	0.1971	0.9149	1
	T2	0.4729	0.5179	0.5201	0.5045	0.5013	0.5009	0.0955	0.1242	0.5653	2
	T3	0.4464	0.4663	0.4250	0.4579	0.4829	0.4781	0.2054	0.0000	0.0000	4
	A ⁺	0.5463	0.5313	0.5617	0.5311	0.5248	0.5248				
	A ⁻	0.4464	0.4663	0.4250	0.4579	0.4829	0.4781				

D⁺ and D⁻ mean the weighted distances between each alternative and the optimal or inferior ideal solutions, respectively; A⁺ and A⁻ are the optimal and inferior ideal solutions, respectively. CK is the control treatment applied with inorganic fertilizer, T1, T2 and T3 are treatments applied with biogas slurry of 20, 15 and 10% in volume concentrations, respectively

The effect of different treatments on soil environment

Soil saturated hydraulic conductivity and soil organic matter

By studying the trend of soil saturated hydraulic conductivities of different treatments, it has been seen that T1 was apparently higher than other treatments (Figure 4). Soil saturated hydraulic conductivities (Ks) of different treatments was in a descending order of T1>T2>CK>T3. In the two experiments carried out in both the seasons, the values of T2 treatment were 0.002 and 0.005 cm/min higher than those of CK treatment, respectively. Besides, values of T3 treatment were the lowest, illustrating that T1 and T2 treatment could provide higher soil saturated hydraulic conductivities than CK treatment.

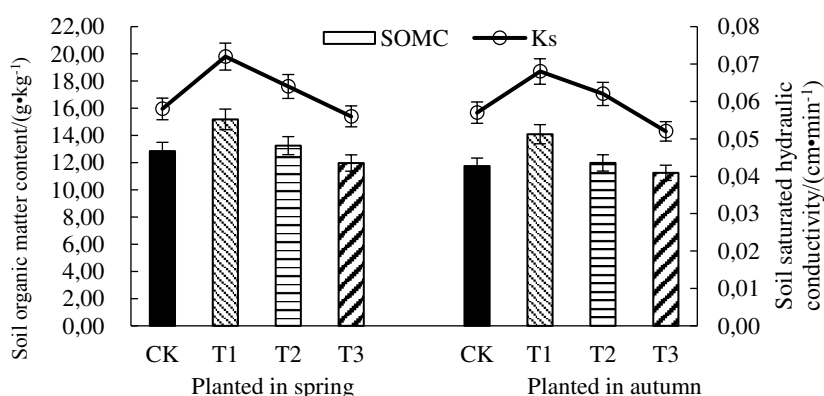


Figure 4. Soil organic matter and saturation conductivity under different treatments. CK is the control treatment applied with inorganic fertilizer, T1, T2 and T3 are treatments applied with biogas slurry of 20, 15 and 10% in volume concentrations, respectively. The error bars mean a 5% range of error

In 2017 spring and autumn experiments, soil organic matter content (SOMC) of all treatments increased compared with the original soil as shown in dashed line of *Figure 4*. Besides, values of CK treatment which were 22.80 and 18.39% higher than those of original soil, respectively, were lower than those of T1 and T2 biogas slurry treatments.

SOMC of different treatments related in a descending order $T1 > T2 > CK > T3$. Its content in T1 and T2 treatments were 18.13 and 19.91%, respectively which were 10.34 and 8.77% higher than CK treatment. However, the contents were 3.57 and 3.63% higher than those of T3 treatment, respectively, in spring and fall experiments. All these illustrated that T1 and T2 treatment were better than CK treatment on the aspect of increasing SOMC. Therefore, the finding supports that appropriate biogas slurry irrigation could increase SOMC.

Change of soil total N content

From *Table 4*, soil total N content of CK treatment was the highest in tomato different growth stages in spring and fall and the next was T1 treatment. On the other hand, the soil total N content was the lowest in T3 treatment. The soil total N contents of different treatments from the seedling to the flowering stages, increased to some extent. The increasing amplitudes of soil total N of T3 treatment were the smallest i.e., 0.007 and 0.002 g/kg, in spring and fall, respectively. This illustrates that N supply of different treatments from the seedling stage to the flowering stage was surplus. Thus, N fertilizer application amount or biogas slurry concentration could be proportionately decreased in the application process. T3 treatment could be used as reference for the application during the corresponding growth period. Considering soil N contents in stages of blossoming and fruiting, fruit swelling stage and fruit maturity stage, the change of T1 treatment was stable with the smallest changing amplitudes or increasing amounts of only 0.007 and 0.004 g/kg. On the other hand, the increased amounts of CK treatment were 0.117 and 0.216 g/kg, illustrating that N element provided by traditional fertilizer treatment has been accumulated to some extent in soil. However both the T2 and T3 treatments demonstrated the decreasing trend, especially T3 whose soil N content was already lower than that of original soil (1.022 g/kg) in stages of fruit swelling stage and fruit maturity stage. This clarifies that T3 treatment could not satisfy the N element demand of tomato growth. Values of T1 treatment were stable.

The influence of different treatments on soil microstructures

Soil microstructure reflects the original soil characteristics which is directly related to soil fertility and happens to be an important compositional part of soil quality (Kapur et al., 2007; Price et al., 2007). From *Figure 5*, soil of CK treatment was in debris aggregation state with the close contact between soil bone particles and soil matrix. Soil of T1 treatment was in the status of cementitious compactness with a microstructure distribution of flocculated mass as well as the loose contact of bone particles and soil matrix. Soil debris of T2 treatment was fewer than that of CK treatment with apparent better soil pore development than that of CK treatment.

There was a compacting contact between soil bone particles and soil matrix in T3 treatment as well as an apparent higher amount of soil debris than those of T1 and T2 treatments but lower amount than that of CK treatment. The pore area, average pore area and average pore size of T1 treatment, which were the highest among different treatments were 31.62, 55.39 and 14.51% higher than those of CK treatment, respectively (*Table 5*).

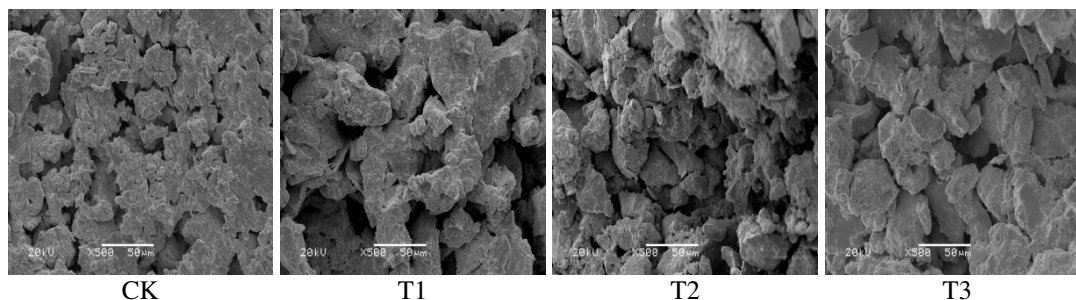


Figure 5. Comparison of soil microstructure under different treatments (500 times). CK is the control treatment applied with inorganic fertilizer, T1, T2 and T3 are treatments applied with biogas slurry of 20, 15 and 10% in volume concentrations, respectively

Table 5. Pore parameters of different treatments after image treatment

Treatments	The pore area (μm^2)	Average pore area (μm^2)	Average pore size (μm)	Area ratio
CK	4824.00c	19.93d	3.79b	0.071
T1	6349.21a	30.97a	4.34a	0.081
T2	5118.24b	21.24c	3.83b	0.073
T3	2859.68d	24.87b	3.70c	0.051

CK is the control treatment applied with inorganic fertilizer, T1, T2 and T3 are treatments applied with biogas slurry of 20, 15 and 10% in volume concentrations, respectively

It illustrated that the intensity of soil aggregation could be increased by biogas slurry application, leading the loose contact between bone particles and soil matrix which promoted the formation of different loose pores as well as the improvement of soil quality.

Discussions

LAI, photosynthetic rate as well as chlorophyll (a+b) were important indexes which demonstrated plant growth status and related to the sufficiency of N element supply to some extent (Inoue, 2003; Roca et al., 2018; Feng et al., 2018). In this work, LAIs of CK treatment in stages of seedling, blossoming and fruiting, and pre-fruit swelling stage were the highest. However, the value decreased gradually until a lower value than T1 treatment in the late fruit swelling stage is reached. The photosynthetic rate of CK treatment was the highest in stages of seedling as well as blossoming and fruiting.

T1 treatment was the best at key stages of the crop yield like fruit swelling stage and fruit maturity stage over the tomato reproductive periods. It also maintained stable chlorophyll (a+b) content of the crop. However, there was an apparent phase effect for current fertilizer application modes and methods. The promotion effect of which existed only for a short time period and after application decreased gradually with the increase of time. Thus it demonstrates a poor sustainability.

In the present experiment, biogas slurry concentration and irrigation frequency of T1 treatment could make tomato different physiological indexes over the growth period more stable compared with CK treatment. This indicates that a lot of inorganic N as well as many active materials which stimulated the growth of plants could be more easily absorbed by plants compared with inorganic fertilizer applications. Thus, it enhanced the nutrient absorption and utilization efficiency of crop plants (Wu et al., 2013; Rive et al.,

2016). In all the treatments of the present experiment same irrigation methods were adopted. This verified that the integration technology and fertilizer application were appropriate. Water availability and nutrient absorption by crops with the same irrigation methods were optimum, wherein the reasonable nutrient concentration in the integration of water and fertilizer (Liang et al., 2013; Abalos et al., 2014; Al-Qurashi et al., 2015) could better promote the growth of crops.

The reasonable utilization of water and fertilizer was the key factor to enhance crop yield, quality and utilization efficiency of water and fertilizer (Hebbar et al., 2004). Al-Qurashi et al. (2015) showed that nutrient concentration was the key factor which influenced the crop yield. In this study, yield of T1 treatment was higher in spring and lower in fall than that of CK treatment. On the other hand, there was no significant difference between those two, illustrating that T1 treatment could satisfy the water and nutritional condition of tomato yield. Thus, T1 treatment could be an alternative for the replacement of traditional fertilizer use. However, crop quality determined market competitiveness. With the improvement of people's living standard, crop fruit quality has been paid more and more attention (Luo and Li, 2018). Nutritional quality of vegetables usually depends upon their genetic characteristics and environmental factors such as irrigation, soil and fertility. Yue et al. (2003) proposed that whether or not, tomato was delicious and tasty, that depends on the soluble sugar content as well as absolute content of the titrate acid. In this study, soluble sugar content and absolute content of the titrate acid of T1 and T2 treatment were higher than those of CK. Whereas, those of T3 treatment were the lowest, illustrating that appropriate biogas slurry concentration could effectively improve nutritional quality of tomato. After analysis, various organic and inorganic salts, microelements and soluble materials of many amino acids, hydrolase, etc. were found to be present in biogas slurry (Wu et al., 2013). These were generated via fermentation process, wherein the microelements not only involved directly in many physiological metabolic processes of plant but also were the basis of dry material accumulation (Xing et al., 2014). Besides, those active materials of amino acids and hydrolase had important regulatory functions of crop growth and development. Thus, application of reasonable concentration of biogas slurry as well as the utilization water-biogas slurry integration provided better conditions for the formation of crop yield as well as the quality enhancement.

Soil saturated hydraulic conductivity was not only an important factor for the calculation of soil water movement but also a comprehensive ratio coefficient which described the permeability of porous media (Liang et al., 2009). In addition, organic matter was the main driving factor of increasing soil saturated hydraulic conductivity (Peng et al., 2010).

Results from the present study showed that every treatment could increase not only soil saturated hydraulic conductivity but also soil organic matter content. Current research showed that organic matter could absorb more cations and make soil nutrient preserving capability and the buffering capacity high. Parallel to this it could also loosen the soil, contributing to the formation of soil structure (Nabel et al., 2017). From the soil microstructure image obtained in this study, it was seen that there were more soil debris, less soil pores and more compact contact between soil bone particles and soil matrix in CK treatment.

However, there was a microstructure distribution of flocculated mass in soil of T1 treatment. Besides, soil of T1 treatment possessed a loose contact between bone particles and soil matrix, more pores with larger pore size. In addition, soil debris with T2 and T3

treatment were apparently lower than that of CK treatment. From initial analysis, there were a certain number of organic suspended particles in biogas slurry which entered into the soil with water during the irrigation process. Later on those were absorbed at the surface of soil particles and could be considered as input of exogenous organic matter. In the meantime, appropriate biogas slurry irrigation made microbial activities of crop root and enzyme catalyzed reactions active. This had contributed to the formation of soil aggregation and further enhanced water saturated water conductivity.

Application of fertilizer or CK treatment didn't possess the input of exogenous organic matters. In those, the enhancement of soil organic matter occurred due to rapid increase of soil effective nutrient content which quickly satisfied the nutritional demand of crop growth and development. Thus, a higher crop biomass as well as the resultant input of soil organic matter were obtained (Lee et al., 2009), which did not have a promotion effect for the formation of soil aggregation and pore.

Conclusions

(1) Compared with CK (the inorganic fertilizer) treatment, T1 (biogas slurry volume concentrations of 20%) treatment could provide more stable nutrient supply to tomato crop over the growth period, keeping LAI, photosynthetic rate, and leaf chlorophyll (a+b) content at a relatively stable level in tomato growth stage.

(2) T1 treatment could obtain yield which was comparable with that of CK treatment. T1 and T2 (biogas slurry volume concentrations of 15%) treatments could not only obtain higher absolute contents of soluble sugar and the titrate acid but also better coordinated the sugar acid ratio, whereas T3 treatment was adverse to the formation of tomato nutritional quality.

(3) In tomato seedling stage, N fertilizer application amount or biogas slurry concentration could be decreased appropriately. From the stage of blossoming and fruiting to fruit maturity stage, T1 and CK treatment could both increase N content in soil. The increase amplitude of T1 treatment was a little smaller (0.007 and 0.004 g/kg in spring and fall cultivation, respectively) than that of CK treatment (0.117 and 0.216 g/kg of CK treatment). This illustrates the much more stable trend which was appropriate for a long term application. N content in soil of T2 and T3 treatments decreased dramatically from the stage of blossoming and fruiting to fruit maturity stage.

(4) Each treatment could increase soil organic matter content, whereas the increase amplitudes of soil organic matter as well as soil saturated water hydraulic conductivities of T1 and T2 treatments were all higher than those of CK treatment. This illustrates that T1 and T2 treatment could be more effective to increase soil organic matter content and thus improve soil water holding capacity. Compared with CK treatment, different treatments with biogas slurry could increase the number of soil aggregates, decrease soil debris and increase the number of soil pores, wherein T1 treatment had the most apparent effect.

In all, T1 (biogas slurry volume concentrations of 20%) treatment could provide more stable nutrient supply for the growth and development of tomato. While not only obtaining the yield comparable with that of traditional fertilizer treatment but also improving tomato nutritional quality. T1 treatment improved soil environmental conditions, which could be used as reference for the replacement of fertilizer with biogas slurry.

The effects of different biogas slurry irrigation amounts on crop growth, fruit quality and soil environment, also the effects on other crops should be explored in future studies.

Acknowledgements. This study was funded by the National Natural Science of China (51969012) and Gansu Provincial Higher Education Science and Technology Achievements Transformation Project (2018D-04), Gansu Provincial Natural Science Foundation (18JR3RA154), Red Willow First-class Discipline Project of Lanzhou University of Technology (0807J1), Industry Supporting and Guiding Project of Gansu Higher Education Institutions (2019C-13) which are duly acknowledged here with thanks.

REFERENCES

- [1] Abalos, D., Sanchez-Martin, L., Garcia-Torres, L., van Groenigen, J. W., Vallejo, A. (2014): Management of irrigation frequency and nitrogen fertilization to mitigate GHG and NO emissions from drip-fertigated crops. – *Science of The Total Environment* 490: 880-888.
- [2] Albuquerque, J. A., de la Fuente, C., Campoy, M., Carrasco, L., Nájera, I., Baixauli, C., Caravaca, F., Roldán, A., Cegarra, J., Bernal, M. P. (2012): Agricultural use of digestate for horticultural crop production and improvement of soil properties. – *European Journal of Agronomy* 43: 119-128.
- [3] Al-Qurashi, A. D., Awad, M. A., Ismail, S. M. (2015): Growth, yield, fruit quality and nutrient uptake of tissue culture-regenerated 'Barhee' date palms grown in a newly established orchard as affected by NPK fertigation. – *Scientia Horticulturae* 184: 114-122.
- [4] Azizi-Zohan, A., Kamgar-Haghighi, A. A., Sepaskhah, A. R. (2008): Crop and pan coefficients for saffron in a semi-arid region of Iran. – *Journal of Arid Environments* 72(3): 270-278.
- [5] Coban, H., Miltner, A., Kästner, M. (2015): Fate of fatty acids derived from biogas residues in arable soil. – *Soil Biology and Biochemistry* 91: 58-64.
- [6] Ding, J., Jiang, X., Guan, D., Zhao, B. S., Ma, M. C., Zhou, B. K., Cao, F. M., Yang, X. H., Li, L., Li, J. (2017): Influence of inorganic fertilizer and organic manure application on fungal communities in a long-term field experiment of Chinese Mollisols. – *Applied Soil Ecology* 111: 114-122.
- [7] Duan, N., Lin, C., Gao, R. Y., Wang, Y., Wang, J. H., Hou, J. (2011): Ecological and economic analysis of planting greenhouse cucumbers with anaerobic fermentation residues. – *Procedia Environmental Sciences* (5): 71-76.
- [8] Feng, H. K., Yang, F. Q., Yang, G. J., Li, Z. H., Pei, H. J., Xing, H. M. (2018): Estimation of chlorophyll content in apple leaves base on spectral feature parameters. – *Transactions of the Chinese Society of Agricultural Engineering (Transactions of the CSAE)* 34(6): 182-188. (in Chinese with English abstract).
- [9] Hebbar, S. S., Ramachandrappa, B. K., Nanjappa, H. V., Prabhakar, M. (2004): Studies on NPK drip fertigation in field grown tomato (*Lycopersicon esculentum* Mill.). – *European Journal of agronomy* 21(1): 117-127.
- [10] Inoue, Y. (2003): Synergy of remote sensing and modeling for estimating ecophysiological processes in plant production. – *Plant Production Science* 6(1): 3-16.
- [11] Kapur, S., Ryan, J., Akça, E., Çelik, İ., Pagliai, M., Tülün, Y. (2007): Influence of mediterranean cereal-based rotations on soil micromorphological characteristics. – *Geoderma* 142(3/4): 318-324.
- [12] Ledda, C., Schievano, A., Salati, S., Adani, F. (2013): Nitrogen and water recovery from animal slurries by a new integrated ultrafiltration, reverse osmosis and cold stripping process: a case study. – *Water Res* 47(16): 6157-6166.
- [13] Lee, S. B., Lee, C. H. I., Jung, K. Y. (2009): Changes of soil organic carbon and its fractions in relation to soil physical properties in a long-term fertilized paddy. – *Soil & Tillage Research* 104(2): 227-232. (in Chinese with English abstract).

- [14] Li, X. H., Gong, Q. W. (2016): Trend and direction of China's development of regulatory policies preventing over-fertilization in farming: From "increasing yield by increasing fertilizer quantity" to "increasing efficacy by reducing fertilizer quantity". – *Research of Agricultural Modernization* 37(5): 877-884. (in Chinese with English abstract).
- [15] Liang, X. F., Zhao, S. W., Zhang, Y., Hua, J. (2009): Effects of vegetation rehabilitation on soil saturated hydraulic conductivity in Ziwuling Forest Area. – *Acta Ecologica Sinica* 29(2): 636-642. (in Chinese with English abstract).
- [16] Liang, H., Li, F., Nong, M. (2013): Effects of alternate partial root-zone irrigation on yield and water use of sticky maize with fertigation. – *Agricultural Water Management* 116: 242-247.
- [17] Liu, Q. P. (2017): Spatio-temporal changes of fertilization intensity and environmental safety threshold in China. – *Transactions of the Chinese Society of Agricultural Engineering (Transactions of the CSAE)* 33(6): 214-221. (in Chinese with English abstract).
- [18] Liu, X., Qi, Y., Li, F., Yang, Q., Yu, L. (2018): Impacts of regulated deficit irrigation on yield, quality and water use efficiency of Arabica coffee under different shading levels in dry and hot regions of southwest China. – *Agricultural Water Management* 204: 292-300.
- [19] Lu, J., Jiang, L., Chen, D., Toyota, K., Strong, P. J., Wang, H. L., Hirasawa, H. (2012): Decontamination of anaerobically digested slurry in a paddy field ecosystem in Jiaying region of China. – *Agriculture Ecosystems & Environment* 146(1): 13-22.
- [20] Luo, H., Li, F. S. (2018): Tomato yield, quality and water use efficiency under different drip fertigation strategies. – *Scientia Horticulturae* 235: 181-188.
- [21] Nabel, M., Schrey, S. D., Poorter, H., Koller, R., Jablonowski, N. D. (2017): Effects of digestate fertilization on *Sida hermaphrodita*: Boosting biomass yields on marginal soils by increasing soil fertility. – *Biomass and Bioenergy* 107: 207-13.
- [22] Oh, T. K., Shinogi, Y., Lee, S. J., Choi, B. (2014): Utilization of biochar impregnated with anaerobically digested slurry as slow-release fertilizer. – *J. Plant Nutr. Soil Sci* 177(1): 97-103.
- [23] Peng, S. L., You, W. H., Shen, H. T. (2010): Effect of syndynamic on soil saturated hydraulic conductivity. – *Transactions of the CSAE* 26(11): 78-84. (in Chinese with English abstract).
- [24] Price, K., Jackson, C. R., Parker, A. J. (2010): Variation of surficial soil hydraulic properties across land uses in the southern Blue Ridge Mountains, North Carolina, USA. – *Journal of hydrology* 383(3-4): 256-268.
- [25] Riva, C., Orzi, V., Carozzi, M., Acutis, M., Boccasile, G., Lonati, S., Tambone, F., D'Imporzano, G., Adani, F. (2016): Short-term experiments in using digestate products as substitutes for mineral (N) fertilizer: Agronomic performance, odours, and ammonia emission impacts. – *Science of The Total Environment* 547: 206-214.
- [26] Roca, L. F., Romero, J., Bohórquez, J. M., Alcántara, E., Fernández-Escobar, R., Trapero, A. (2018): Nitrogen status affects growth, chlorophyll content and infection by *Fusicladium oleagineum* in olive. – *Crop Protection* 109: 80-85.
- [27] Rong, Q. L., Li, R. N., Huang, S. W., Tang, I. W., Zhang, Y. C., Wang, L. Y. (2018): Soil microbial characteristics and yield response to partial substitution of chemical fertilizer with organic amendments in greenhouse vegetable production. – *Journal of Integrative Agriculture* 17(6): 1432-1444.
- [28] Smith, L. E. D., Siciliano, G. A. (2015): Comprehensive review of constraints to improved management of fertilizers in China and mitigation of diffuse water pollution from agriculture. – *Agriculture Ecosystems & Environment* 209: 15-25.
- [29] Tambone, F., Scaglia, B., D'Imporzano, G., Schievano, A., Orzi, V., Salati, S., Adani, F. (2010): Assessing amendment and fertilizing properties of digestates from anaerobic digestion through a comparative study with digested sludge and compost. – *Chemosphere* 81(5): 577-583.
- [30] Tan, Y., Zheng, J., Jia, S., Kang, Y. H. (2016): Interference Infiltration characteristics of the soil water movement under the hole Irrigation with Biogas slurry. – *Journal of Hunan*

- Agricultural University (Natural Science) 42(5): 573-578. (in Chinese with English abstract).
- [31] Wu, J., Yang, Q., Yang, G., Shen, F., Zhang, X. H., Zhang, Y. Z. (2013): Effects of biogas slurry on yield and quality of oil-seed rape. – *Journal of Plant Nutrition* 36(13): 2084-2098.
- [32] Wu, X., Wang, K. Y., Niu, X. L., Hu, T. T. (2014): Construction of comprehensive nutritional quality index for tomato and its response to water and fertilizer supply. – *Transactions of the Chinese Society of Agricultural Engineering (Transactions of the CSAE)* 30(7): 119-127. (in Chinese with English abstract).
- [33] Xing, Y. Y., Zhang, F. C., Zhang, Y., Li, J., Qiang, S. C., Li, Z. J., Gao, M. X. (2014): Irrigation and fertilization coupling of drip irrigation under plastic film promotes tomato's nutrient uptake and growth. – *Transactions of the Chinese Society of Agricultural Engineering (Transactions of the CSAE)* 30(21): 70-80. (in Chinese with English abstract).
- [34] Yue, S. J., Liu, H. C., Zhai, Y. F., Xie, Y. (2003): Studies on Flavor of Cherry Tomato Fruit. – *China Vegetables* 3: 15-17. (in Chinese with English abstract).

MAPPING PROTECTED AREAS BY GIS METHOD: A CASE STUDY OF IZMIR CITY, ÇEŞME DISTRICT (TURKEY)

ANKAYA, F.¹ – TÜRKYILMAZ, B.² – KÖSE, H.³

¹*Alaşehir Vocational School, Manisa Celal Bayar University, Alaşehir-Manisa, Turkey
(e-mail: fundaunalankaya@hotmail.com; phone: +90-531-425-3407; fax: +90-236-654-1200)*

²*Department of Landscape Architecture, Faculty of Agriculture, Ege University, İzmir, Turkey
(e-mail: turkyilmaz.bahar@hotmail.com; phone: +90-533-660-5740)*

³*Alaşehir Vocational School, Manisa Celal Bayar University, Alaşehir-Manisa, Turkey
(e-mail: mhkose@yahoo.com; phone: +90-534-612-7077)*

**Corresponding author
e-mail: fundaunalankaya@hotmail.com*

(Received 24th Jul 2019; accepted 25th Nov 2019)

Abstract. In Turkey, in order to protect nature, there are strategies and categories depending on differences between local environmental conditions as in many countries in the world. The term of “protected environments”, is also supported by laws as in other countries around the world. Natural protected environments are divided into the following three categories “Critical Environments under the Protection of Law” (SAPUL), “Natural Protected Environments with Qualifications” and “Sustainable Protection and Controlled Usage Environments”, according to the resolution Conditions of Protection and Use of Natural Protected Environments, dated 2017, of Turkish Republic Ministry of Environment and Urban Planning. A map of Natural Protected Environments has been generated as a result of evaluation of 81 polygons which have been specified as natural protected environment borders by the Protection Commission of the Turkish Republic Ministry of Environment and Urban Planning, the strategy for determining (SAPUL) is approached as this article’s subject. According to this strategy, in Çeşme (İzmir/Turkey) district, 20 polygons were specified to belong to the categories (SAPUL) among 81 polygons based on the terms and definition of the resolution of İzmir City and Çeşme district. Borders of natural protected environments, which were specified by the protection commission of the Turkish Republic Ministry of Environment and Urban Planning, each polygon is generated based on up-to-date land use information, have been formed based on the visuals taken from İKONOS satellite in 2017. The natural areas that carry the status of SAPUL were specified based on the specifications of the landscape and criteria of landscape assessment as the “use of the land”, “live natural landscape”, “historical landscape”, Hereat, each polygon has been evaluated and mapped according to their specifications of landscape. Primarily, sample map has been created by using quantitative evaluation, which is supported by geographical information system (GIS). It is thought that this strategy will be useful for the resolutions that will be taken by the Committee on Conservation of Cultural Assets in Turkey in the Ministry of Environment and Urban Planning.

Keywords: *natural protected areas, Çeşme Peninsula, İzmir City, Çeşme District, environments under the protection of the law, GIS*

Introduction

In general, when the topic is about the protection of nature the following factors are considered: plants, animals, their environment where they grow and live and some pieces of nature which are thought to be valuable according to some criteria for the guarantee of human life (Caner, 2007; Yücel, 1995). Protection of nature covers protection of wild animals, varieties of plants, their natural living environments, securing landscapes with natural conditions, pieces of landscape and protective

measurements (Çolak, 2001). The term of protection is shortly and newly defined as; the usage of the Earth's sources in a rationalist way (Mac Kinnon et al., 1986). The term "natural protected area", which is the main topic of this research, is known under different names in different countries. According to Gülez (1984) natural protected areas are defined as the environments that have topographical, hydrologic, biological, aesthetics- perceptive, cultural-historical values. In general, the environments that have historical and natural beauty, are considered as natural protected areas (Mumcu, 2009; Yenilmez Arpa, 2016). Nowadays, in so many countries, the necessity of protection of the inherited natural protected areas is accepted at national level. Thus, every nation participates in protecting biological diversity and resources with their own affords (Türkyılmaz, 1991).

Çesme District which is the research zone, is located in west of Anatolia and was a port town known as Ildiri. This port town was a part of Erythrai which was one of 12 Ion cities B.C. 1000. Erythrai was a very important city in 6th century B. C. Erythrai had good relations with Cyprus, Egypt and some western countries and developed its trade routes. Çesme was under the rule of Persians, Romans and Byzantium.

It is important to determine the characteristics of the area before taking it under protection because the land should have some required characteristics to be under the protection (Özer, 2004; Buchwald, 1980; Heydemann, 1981; Mac Kinon, 1986; Green, 1985; Yücel, 1995; Yazıcı et al., 2017). The strategies of evaluation and classification of the lands must suit to three conditions; 1) The strategy must be understandable for the planners, 2) Local people must take advise from naturalists, 3) Rational goals should be set to overcome the legal barriers (Frederic et al., 1988). Different kinds of grades are given to the areas according to the different criteria in the system of identifying priority of natural protection (Mackinnon et al., 1986). There are some measurements to specify and categorize the natural protected areas. Those measurements should be set with bio-ecologic (flora, fauna, habitat), geological, hydrogeological, geomorphologic characteristics of the landscape. In the evaluation made by the Ministry of Environment and Urban Planning in terms of specifications of landscape, it is considered if the field has the natural characteristics, manmade or not and it was supported by *GIS*. *GIS* is a database where bulky geographical data is collected, stored and processed. The data in *GIS* helps users during the period of decision for areas/locations to prevent planing problems of complex social, economic, environmental problems (Yazıcı et al., 2017; Yazıcı and Gülgün, 2018a). Geographical Information System is an important support base for the protection of natural protected areas (Yazıcı et al., 2018b).

Materials and methods

Çesme District, which has cultural values, is one of the tourist centers of our country as well as of the world. Therefore, it is needed to be managed effectively in order to keep the sustainability of natural and cultural values. The main material of the research is the research field. Research field İzmir city (Turkey) Cesme district (*Fig. 1*).

Cesme, is one of the districts of İzmir, it is located in the west of the country, in the Aegean Region, in the southwest of the Karaburun Peninsula. Cesme district is 94 km away from İzmir city at 38.32 North latitude and 26.30 East longitudes. The district is surrounded by Urla district in the east Karaburun district in the north, and the Aegean Sea in west and south. Square measure of Cesme district is 260 km². Cesme has one town (Alaçatı) and four villages. According to the census in 2017, the district has a

population of 41.278 (Anonymous, 2019b) However during the summer/tourism period it increases more than 20 times. Tourism designate the economic structure. Cesme is one of the few places in Turkey that are domestic and international tourism centers.



Figure 1. Cesme district general layout (Anonymous, 2019a)

Material

Main materials of the research are research field (Cesme District) images taken from Ikonos satellite in 2017, image analyst (Intergraph) program, 1/25000 scale map of current natural protected area, 1/25000 scale map of Cesme District's topographic map and Microstation (Bentley) program that provides the geometrical corrections, Geomedia 6.0 program, Ipad Air tablet. Table 1 shows the distinguishing specifications of "SAPUL" based on the conditions of Natural protected areas resolution dated 2017 by the Ministry of Environment and Urban Planning. In this chart, the explanations of "yes", "no", "partly" are quantitatively interpreted according to the specialists' opinions and evaluations. Specifications such as being *organic*, *inorganic*, *historical*, *renewable and sensitive*, specified 20 polygons out of 81 in the category of "SAPUL" (Fig. 2) based on the terms and definition of resolution of Izmir City, which was considered while scoring as seen in Tables 3–7. The methods in research studies of Green (1985), Mackinnon et al. (1986), Gülez (1990), Türkyılmaz (1991, 2005) and Uzun and Müderrisoğlu (2010) have been used while evaluating the specifications of the landscape.

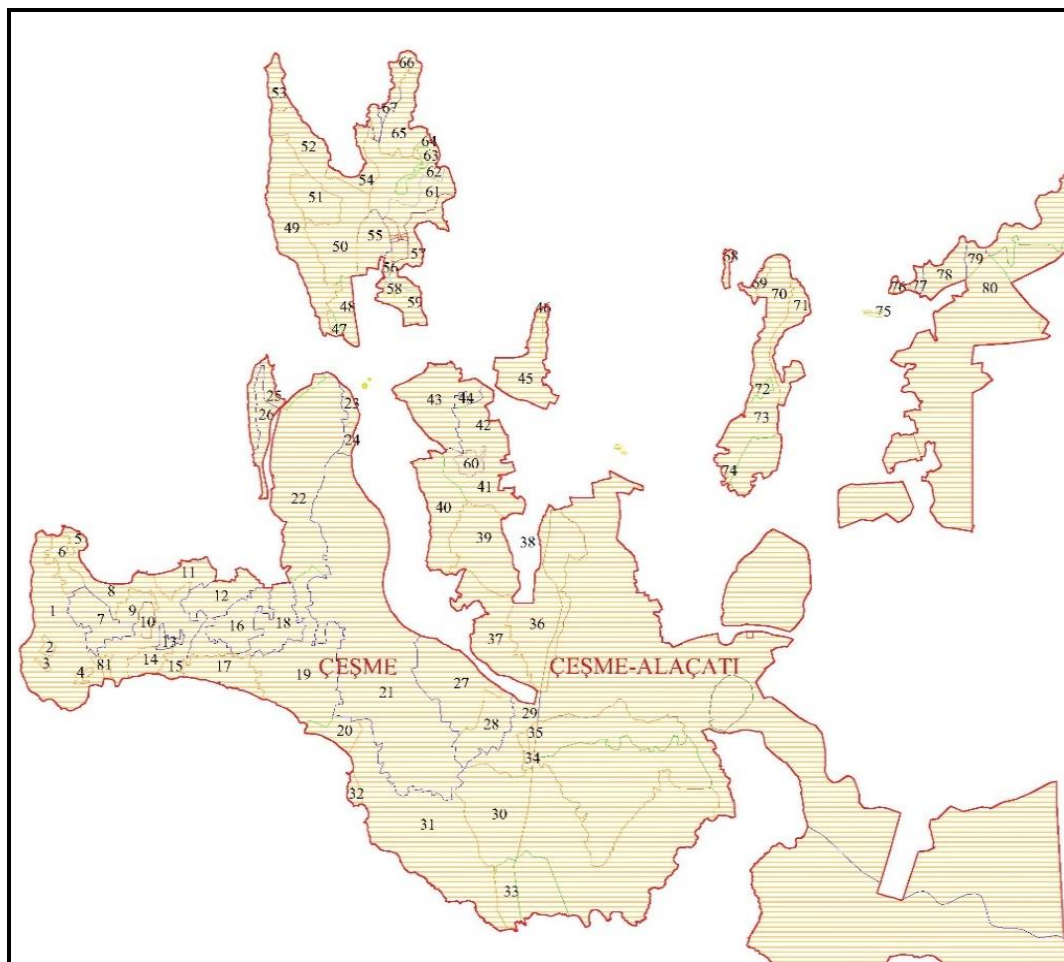


Figure 2. Borders of natural protected area polygons determined by Protection Commission of Cesme District. (The numbers seen in the figure, were given by the researchers so the polygons in Figure 2. shown in the map could be evaluated. Those numbers are used in Table 15 to create the result map)

Method

The research method was designed with the stages shown below.

First Stage: 6 tables, which show specifications of evaluation the research field, have been created in consideration of *Table 1* and each chart has been graded based on the matrix method in itself.

In the second stage, the materials, which show the distinguishing specifications, are questioned in consideration of *Table 2*. Border of cultural natural protected area polygons and status of each polygon given by protection commission was adapted with the grading method in the first stage. Qualitative evaluation such as “yes”, “no”, “partly” was quantified with GIS in order to create natural protected area map in terms of specifications of landscape.

The evaluating method has been approached based on the explanations given in *Table 2*.

Each polygon, which generates the map shown in *Figure 2*, was digitalized by using Ikonos satellite images with GIS program so the specifications of land use plan have been stated.

The land use map has been classified in four fields. These are:

1. Residential area
2. Agricultural areas
3. Tarsius spectrum + Garrigue + Forest areas
4. Litosolig + Garrigue areas

Table 1. Distinguishing specifications of “environments under the protection of the law

Distinguishing specifications of “environments under the protection of the law”		Yes	No	Partly	Opinions and evaluations of specialists
a	They have regional, national and global extraordinary ecosystems and species	12-13-14	7-8	9-10-11	Evaluated based on the specifications of organic natural landscape (Table 3)
b	Specifications of geologic, geomorphologic	7-8-9	2-3	4-5-6	Evaluated based on the specifications of Inorganic natural landscape (geologic-Table 4)
c	In general, came to existence without human effect	2-3-4	-2-(-3)	-1-0-1	Evaluated based on the specifications of cultural landscape
d	Because of human effect, it is under the risk of perishment	6-7-8	1-2	3-4-5	Evaluated based on the specifications of organic natural landscape (sensitivity Table 7)
e	The area does not contain human effect which is against its protection targets	18-19-20-21-22 (historical landscape)	9-10-11	12-13-14-15-16-17 (historical landscape)	Evaluated based on the specifications of (organic + inorganic) + historical landscape If there is touristic area, it is mentioned (Tables 3–5)
f	It contains large percentage of the local species that is expected to exist. It has the ability to transform itself to the intensity with natural process or limited interferences	19-20-21-22-23-24	10-11-12	13-14-15-16-17-18	Evaluated based on the specifications of (Natural organic landscape + renewable ability) (Tables 3 and 6)
g	In order to reach the aim of protection it has very vital and continuous interference	25-26-27-28-29-30-31-32	12-13-14-15	16-17-18-19-20-21-22-23-24	Evaluated based on the specifications of (Natural organic landscape + ability to renew itself + Natural inorganic landscape (Tables 3, 4 and 6)
h	It is surrounded by the use of areas that will help the area to reach the aims of protection when it is possible and necessary				It has been evaluated based on the natural zone around the polygon
i	It could be managed by application of simple interference	8-10	3-4	5-6-7	It has been interpreted based on the ability to renew itself (Table 6)
i	It contains the reproduction area for the species that are aimed to be protected				It has been evaluated based on the floristic evaluation report of the area

Table 2. Evaluation of acreage of the specifications of land use in polygons, which belong to “the natural areas protected under law” (SAPUL)

Polygon No	Status of natural protected areas	Land use	Area (m ²)	Area (%)
	(SAPUL)	1		
	(SAPUL)	2		
	(SAPUL)	3		
	(SAPUL)	4		
		Total		100.00

Cultural Landscape values of suitability, levels of suitability and abbreviations:

Suitability value	Suitability level	Abbreviation
4	Most suitable	M.S.
3	Suitable	S.
2	Partial suitable	P.S
1	Less suitable	L.S.
0	Least suitable	Lea. S.
-1	Not suitable	N.S
-2	Partially not suitable	P.N.S
-3	Not suitable at all	N.S.

Cultural landscape values of suitability in *Tables 3–7* have been set after considering the percentage of the 1 (residential) and 2 (agricultural) areas specifications. According to the given information in *Table 2*, if there is no residential area in the polygon the following calculations have been used; [$<1\%$) the least suitable] was given “0” point, if percentage of area (%) reached [$1-33\%$); not suitable] it was given “-1” point, if percentage of the area (%) reached [$34-66\%$); Partially not suitable] it was given “-2” points, if percentage of area (%) reached [$67-100\%$); Not suitable at all.] it was given “-3” points. According to the given information in *Table 2*, if there is no agricultural area in the polygon the following calculations have been used; [$<1\%$) The most suitable] “4” points were given, if the percentage of the area (%) reached [$1-33\%$); Suitable] “3” points were given, if percentage of the area (%) reached [$34-66\%$); Partial suitable] “2” points were given, if the percentage of the area (%) reached [$67-100\%$); Less suitable] “1” point was given. Thus, cultural landscape values of suitability have been set. 81 polygons have been evaluated separately by using GIS and 20 polygons have been determined as the areas will be under protection. Thus, the map of suggested natural protected areas has been created in *Table 15* and *Figure 10*.

Below it has been defined how the index values has been created in *Tables 3–7*.

According to the organic natural landscape index values (*Table 3*), each polygon is determined after considering the research studies on the field (each polygon has been checked and compared based on the 2017 satellite images and the actual area) and map of land use and listed according to their importance. According to this information; evaluation has been done as the followings. If the area is stony and rocky 1 point is given, if there is a Frigana-Maquis 2 points are given, if there is a forest 3 points are given, if there is an endemic and sensitive area 4 points are given.

Table 3. Combining of qualifications of organic natural landscape index values and cultural landscape of suitability

Organic natural landscape	Index value	Suitability value							Cult. lands.	
		Residential areas				Agricultural areas				
		N.S. at all 67-100%	P.N.S 34-66%	N.S 1-33%	Lea.S <1%	L.S 67-100%	P.S 34-66%	S 1-33%		M.S <1%
Stony-rocky	1	1	1	1	1	1	1	1	1	
Frigana-lemuroid	2	2	2	2	2	2	2	2	2	
Forest	3	3	3	3	3	3	3	3	3	
Endemic and sensitivity	4	4	4	4	4	4	4	4	4	
Total		7	8	9	10	11	12	13	14	
		“no” scale score (Table 1)		“partly” scale score (Table 1)			“yes” scale score (Table 1)			

In *Table 3* cultural landscape values of suitability points and organic natural landscape index points have been combined and total evaluation points have been created and organic natural landscape points have been created for each polygon.

In *Table 4* each polygon has been determined according to the map of land use and has been pointed based on their importance. Thus; Inorganic natural landscape specifications have been set based on the criteria given below.

Elevation from sea level: Accrue ment of the polygon positively according to sea level “0”. It has been evaluated as +1.

Ascending slope: The map with scale 1/25000 of Cesme district was evaluated and if the landscape has 12% and above slope, it is accepted that the landscape has an ascending slope and it is estimated as caterpillars cannot be operated on the landscape. (If the slope is 12% > on the area the caterpillars will not be able to work in the area.

Shore-Edge: The polygons which has edges to shore next to the sea, has been evaluated +1 points.

Dune: The polygons which has edges to shore and has dune areas, has been evaluated +1 points.

Geologic- geomorphologic: If the cultural landscape point is 3 or above, it has been evaluated +1 points.

In *Table 4*, cultural landscape values of suitability and inorganic natural landscape index points have been combined and evaluation points have been created. Considering this table for each polygon, inorganic natural landscape points have been created (those points can be seen in *Table 15*).

Table 4. Combining of inorganic natural landscape index values specifications and cultural landscape values of suitability

Inorganic natural landscape		Suitability value								Cult. lands.
		Residential areas				Agricultural areas				
		N.S. at all 67-100%	P.N.S 34-66%	N.S 1-33%	Lea.S <1%	L.S 67-100%	P.S 34-66%	S 1-33%	M.S <1%	
Index value		-3	-2	-1	0	1	2	3	4	
Height	1	1	1	1	1	1	1	1	1	
Slope	1	1	1	1	1	1	1	1	1	
Shore-edge	1	1	1	1	1	1	1	1	1	
Dune	1	1	1	1	1	1	1	1	1	
Geologic- geomorphologic	1	1	1	1	1	1	1	1	1	
		2	3	4	5	6	7	8	9	
		“no” scale score (Table 1)		“partly” scale score (Table 1)			“yes” scale score (Table 1)			

In *Table 5*, each polygon has been determined according to the observations on the field and considering map of land use. Thus, in addition to the cultural landscape score if there is an urban protected area, it has been evaluated + 1, if there is an archeological protected area it has been evaluated +2. In *Table 5* each polygon has been evaluated separately and historical landscape score has been set up based on combining each index value with the values of suitability that creates cultural landscape by using matrix method.

In the *Table 5*, each polygon has been evaluated separately and natural landscape score has been set up based on combining each values of suitability with qualification of use of terrain that creates cultural landscape.

Table 5. Combining of historical landscape specifications index values and cultural landscape values of suitability

Historical landscape		Suitability value								Cult. lands.
		Residential areas				Agricultural areas				
		N.S. at all 67-100%	P.N.S 34-66%	N.S 1-33%	Lea.S <1%	L.S 67-100%	P.S 34-66%	S 1-33%	M.S <1%	
Index value		-3	-2	-1	0	1	2	3	4	
Urban protected area	1	1	1	1	1	1	1	1	1	
Archeological prot. area	2	2	2	2	2	2	2	2	2	
		0	1	2	3	4	5	6	7	
		"no" scale score (Table 1)		"partly" scale score (Table 1)		"yes" scale score (Table 1)				

In *Table 6*, each polygon has been determined according to the observations on the field and considering map of land use. and they are listed based on their importance. Thus, forest areas are determined as 3 points, Frigana-Maquis areas are determined as 2 points and agricultural areas are determined as 1 point in each polygon.

In *Table 6*, each polygon has been evaluated separately based on combining index values of cultural landscape with values of suitability that has the ability of renewing itself.

Table 6. Combining the ability to renew itself index values and cultural landscape values of suitability

Ability of renewing itself		Suitability value								Cult. lands.
		Residential areas				Agricultural areas				
		N.S. at all 67-100%	P.N.S 34-66%	N.S 1-33%	Lea.S <1%	L.S 67-100%	P.S 34-66%	S 1-33%	M.S <1%	
Index value		-3	-2	-1	0	1	2	3	4	
Forest Area	3	3	3	3	3	3	3	3	3	
Frigana-maki	2	2	2	2	2	2	2	2	2	
Agricultural area	1	1	1	1	1	1	1	1	1	
		3	4	5	6	7	8	9	10	
		"no" scale score (Table 1)		"partly" scale score (Table 1)		"yes" scale score (Table 1)				

In *Table 7*, 4 points are added if there are endemic and sensitive areas specifications in organic natural landscape specifications (if there are only endemic or rare species). In *Table 7*, each polygon has been evaluated separately based on combining values of suitability cultural landscape with index values that creates sensibility characteristics by using matrix method.

Table 7. Combining sensibility characteristics index value and values of suitability of cultural landscape

Organic natural landscape		Suitability value								Cult. lands.
		Residential areas				Agricultural areas				
		N.S. at all 67-100%	P.N.S 34-66%	N.S 1-33%	Lea.S <1%	L.S 67-100%	P.S 34-66%	S 1-33%	M.S <1%	
Index value		-3	-2	-1	0	1	2	3	4	
Stony-rocky	1									
Frigana-maki	2									
Forest	3									
Endemic and sensibility	4	4	4	4	4	4	4	4	4	
		1	2	3	4	5	6	7	8	
		"no" scale score (Table 1)		"partly" scale score (Table 1)			"yes" scale score (Table 1)			

Main findings and argument

The reason for evaluation each Polygon separately on each table (Tables 9–14) that is determined as "Environments under the protection of the law" (SAPUL) is because each polygon is evaluated based on the scoring of different systems as a result of GIS examination which was explained in the above table.

- Turkish Republic Ministry of Environment and Urban Planning protection commission has specified and mapped 81 polygons as a result of a study. In this study they wanted to specify what kind of status the polygons would have. In order to do so, the polygons, which create sensitive areas that will be protected under GIS environment polling, have been set up based on the point scoring system in the Table 7 and the areas that polygon cover their percentages has been given in Table 8 and mapped in Figure 3.
- The map and the areas that polygons cover, which was specified as sensitive areas that will be protected by the law (SAPUL), are given in Table 9 and Figure 4 based on the point scoring system that belongs to forest areas that has qualifications of usage of landscape.
- The total scoring is given in Table 15, according to qualifications of the forest's ability to renew itself. The index value of the areas, which has the qualifications of forest zone, is given as "3" in Table 9.

Table 8. The total areas and the areas the polygons with the status of sensitive areas that will be definitely protected cover based on specifications of usage of landscape and their percentages

Usage of landscape	Area (m ²)	Area (%)
1	152 817.90	0.55%
2	3 609 881.10	12.9%
3	22 044 944.00	78.9%
4	2 133 453.70	7.6%
Total	27 941 096.70	100.0%

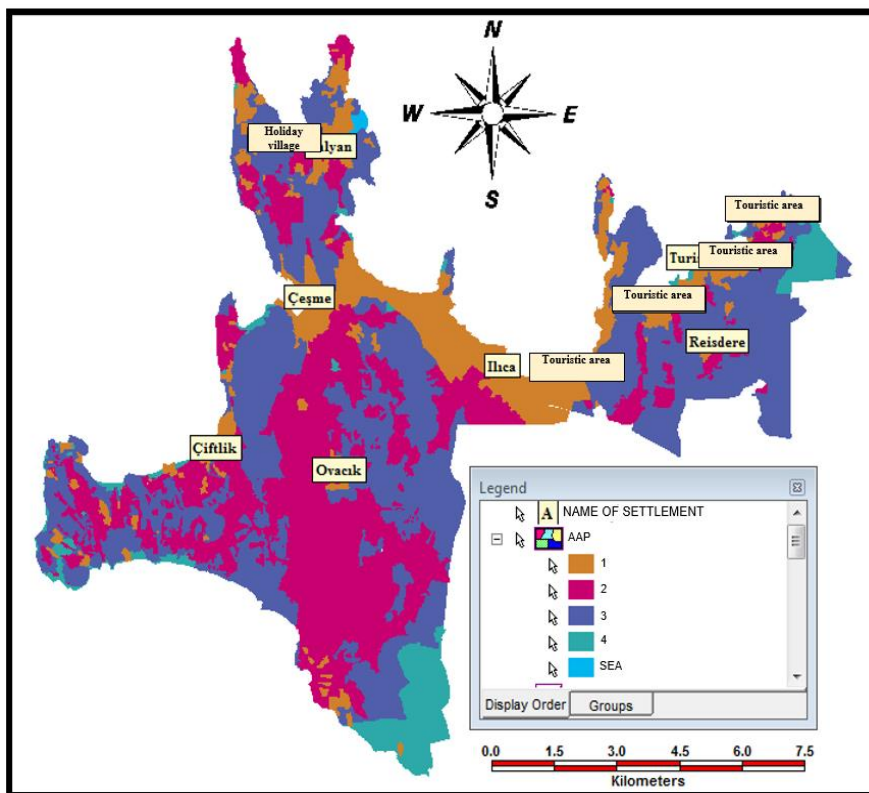


Figure 3. Map belonging to Table 8

Table 9. The areas which polygons with forest qualifications cover among sensitive areas that will be definitely protected

Polygon number	Protected area number	Area (m ²)
1	SAPUL	2 848 752.80
5	SAPUL	146 900.10
15	SAPUL	1 949 916.20
16	SAPUL	808 389.20
19	SAPUL	254 557 370.00
20	SAPUL	401 061.50
22	SAPUL	3 499 518.80
33	SAPUL	477 665.00
37	SAPUL	1 377 460.00
40	SAPUL	1 804 035.40
46	SAPUL	110 890.30
48	SAPUL	423 369.40
51	SAPUL	628 957.70
57	SAPUL	557 441.30
66	SAPUL	237 463.90
70	SAPUL	1 970 311.00
77	SAPUL	79 142.30
80	SAPUL	5 901 654.40
	Total	277 780 299.30

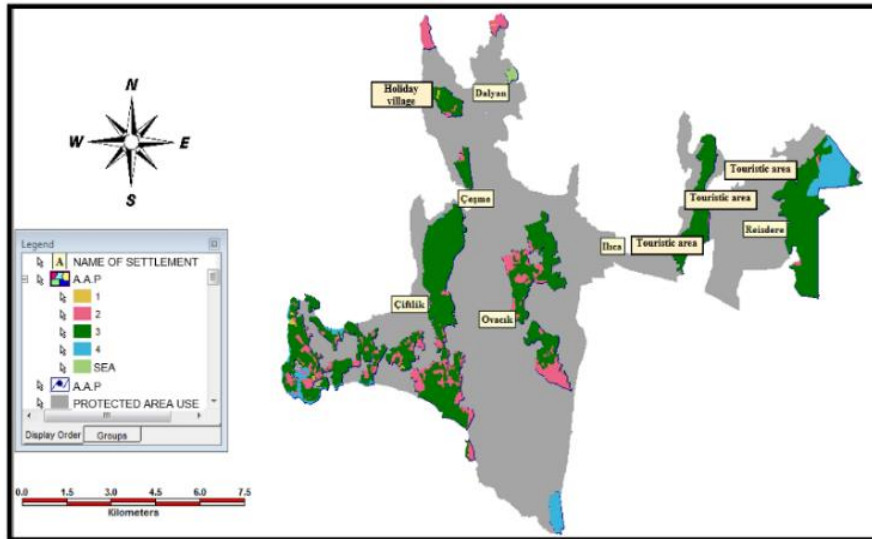


Figure 4. Map belonging to Table 9

- The map of the areas that polygons cover is shown in *Table 10* and *Figure 5*. Those polygons are known as sensitive areas that will be protected by the law according to rare species point scoring system. The total point scoring based on “sensitiveness” characteristic could be seen in *Table 15*. In *Table 10*, the index value has been taken as “4” for the polygons with “forest zone” qualification.
- The criterion score has been examined based on models that have been developed on CBS according to these sensitive areas that will be protected by the law. In *Table 15*:
 - Cultural landscape score is evaluated as ≥ 2 . (Considering *Table 2*: It was considered to make a decision for the index value if the residential areas are less than agricultural areas in polygons).
 - Organic landscape score is evaluated as ≥ 7 . (Considering *Table 3*: Forest formation and endemic-rare species were considered to make a decision for the index value).
 - Inorganic landscape score is evaluated as ≥ 3 . (Considering *Table 4*: At least 3 qualifications that set the criteria of inorganic landscape, were considered to make decision for index value).
 - Sensitiveness score is evaluated as ≥ 0 (Considering *Table 7*: because the Sensitiveness is evaluated separately, it is not necessary to look for rare endemic species in polygon).
 - Renewing itself score is evaluated as ≥ 3 (Considering *Table 6*: Forest formation is considered to make decision for the index value in polygons).
- The Map and the area coverage of polygons are shown in *Table 11* and *Figure 6*. Those areas are known as sensitive that will be protected by the law (SAPUL) based on the points of cultural landscape, organic landscape, inorganic landscape and ability of renewing itself on the GIS platform. According to the qualifications given above, the total scoring could be seen in *Table 15*. Polygons in *Table 11*, the scores given above are evaluated as index values.

Table 10. The areas that polygons with characteristic of “sensitivity” cover. Those areas have the sensitive areas that will have definitely protected characteristics

Polygon number	Protected area number	Area (m ²)
1	SAPUL	2 848 752.80
5	SAPUL	146 900.10
15	SAPUL	1 949 916.20
16	SAPUL	808 389.20
19	SAPUL	2 545 573.70
20	SAPUL	401 061.50
22	SAPUL	3 499 518.80
33	SAPUL	477 665.00
	Total	12 677 777.30

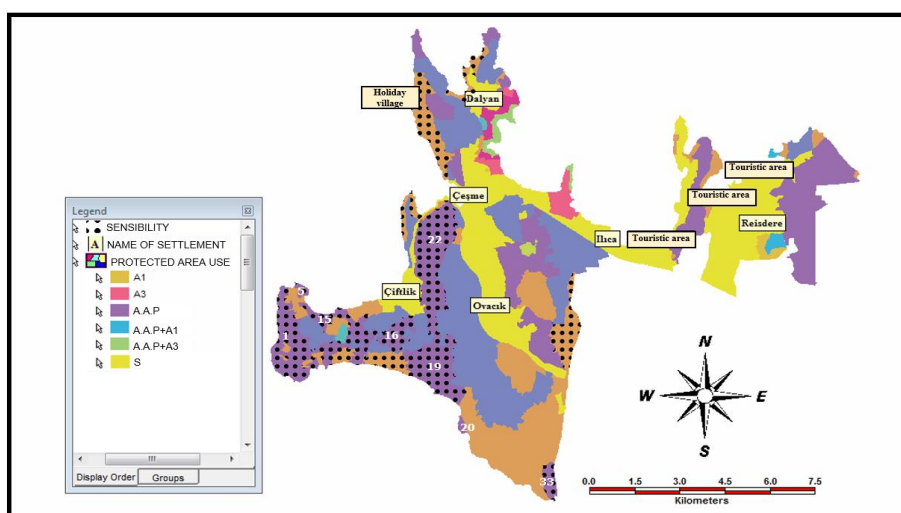


Figure 5. Map belonging to Table 10

Table 11. The areas of polygons with qualifications of cultural landscape, organic, inorganic and ability to renew itself among polygons that are in the areas that will be definitely protected

Polygon number	Protected area number	Area (m ²)
1	SAPUL	2 848 752.80
5	SAPUL	146 900.10
16	SAPUL	808 389.20
19	SAPUL	2 545 573.70
22	SAPUL	3 499 518.80
33	SAPUL	477 665.00
	Total	10 180 046.40

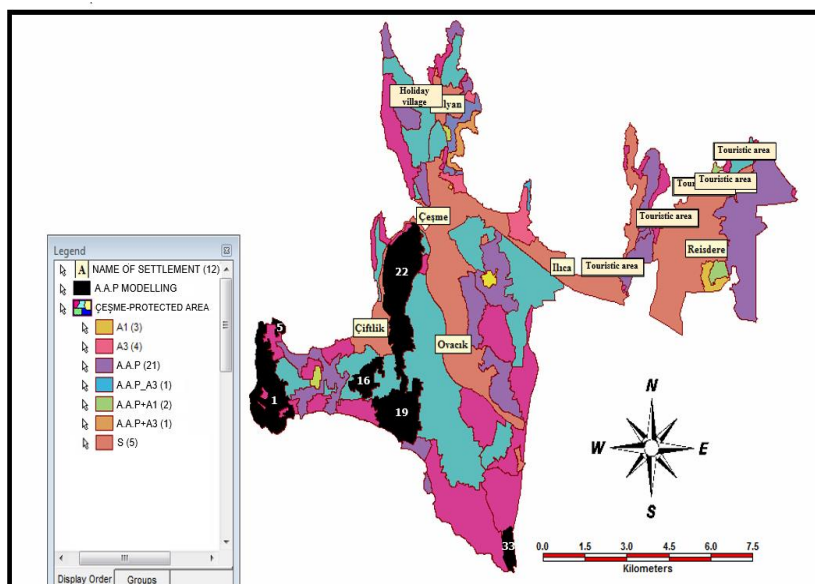


Figure 6. Map belongs to Table 11

- The criterion score has been examined based on models that have been developed on GIS according to these sensitive areas that will be protected by the law. In *Table 15*
 - Cultural landscape score is evaluated as ≥ 3 (Considering *Table 2*: residential areas' being so less and absence of agricultural areas are considered to make decision for the index value in polygons).
 - Organic landscape score is evaluated as ≥ 3 (Considering *Table 3*: forest formation existence is considered to make the decision for index value in polygons).
 - Inorganic landscape score is evaluated as ≥ 3 (Considering *Table 4*: at least 3 qualifications in inorganic landscape qualification table (*Table 4*) that set the criteria of inorganic landscape, were considered to make decision for index value).
 - Sensitiveness score is evaluated as ≥ 0 (Considering *Table 7*: it is not necessary to look for rare endemic species in polygon).
 - Historical landscape score is evaluated as ≥ 1 (Considering *Table 5*: at least 3 qualifications in historical landscape qualification table (*Table 5*) that set the criteria of historical landscape, were considered to make decision for index value).
 - Renewing itself score is evaluated as ≥ 3 (Considering *Table 6*: forest formation is considered to make decision for the index value in polygons).

The Map and the area coverage of polygons are shown in *Table 12* and *Figure 7*. Those areas are known as sensitive areas that will be protected by the law (SAPUL) based on the scores of cultural landscape, organic landscape, inorganic landscape, historical landscape and ability of renewing itself which has specifications of archeological protected areas on the GIS platform. According to the qualifications given above, the total scoring could be seen in *Table 15*. Polygons in *Table 12*, the scores given above are evaluated as index values.

Table 12. The areas of polygons with qualifications of cultural landscape, organic, inorganic, historical landscape and ability to renew itself among polygons that are in the areas that will be definitely protected

Polygon number	Protected area number	Area (m ²)
46	SAPUL	110 890.30
57	SAPUL	557 441.30
77	SAPUL	79 142.30
	Total	747 473.90

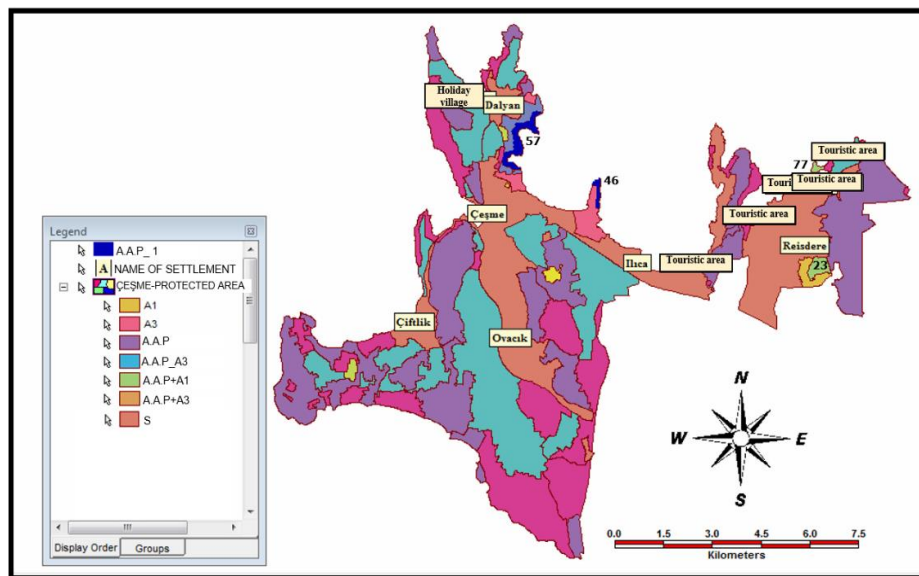


Figure 7. Map belonging to Table 12

- The criterion score has been examined based on models that have been developed on GIS according to these sensitive areas that will be protected by the law. In *Table 15*
 - Cultural landscape score is evaluated as ≥ 3 (Considering *Table 2*: residential areas' being so less and absence of agricultural areas are effective to make decision for the index value in polygons)
 - Organic landscape score is evaluated as ≥ 3 (Considering *Table 3*: forest formation existence is considered to make the decision for index value in polygons).
 - Inorganic landscape score is evaluated as ≥ 3 (Considering *Table 4*: at least 3 qualifications in inorganic landscape qualification table (*Table 4*) that set the criteria of inorganic landscape, were considered to make decision for index value).
 - Sensitiveness score is evaluated as ≥ 0 (Considering *Table 7*: it is not necessary to look for rare endemic species in polygon).
 - Renewing itself score is evaluated as ≥ 3 (Considering *Table 6*: forest formation is considered to make decision for the index value in polygons).

The Map and the area coverage of polygons are shown in *Table 13* and *Figure 8*. Those areas are known as sensitive areas that will be protected by the law (SAPUL) based on the scores of cultural landscape, organic landscape, inorganic landscape and ability of renewing itself on the GIS platform. According to the qualifications given above, the total scoring could be seen in *Table 15*. Polygons in *Table 13*, the scores given above are evaluated as index values.

Table 13. The areas of polygons with qualifications of cultural landscape, organic, inorganic, and ability to renew itself among polygons that are in the areas that will be definitely protected

Polygon number	Protected area number	Area (m ²)
5	SAPUL	146 900.10
15	SAPUL	1 949 916.20
19	SAPUL	2 545 573.70
20	SAPUL	401 061.50
33	SAPUL	477 665.00
40	SAPUL	1 804 035.40
46	SAPUL	110 890.30
48	SAPUL	423 369.40
53	SAPUL	304 164.50
57	SAPUL	557 441.30
77	SAPUL	79 142.30
80	SAPUL	5 901 654.40
	Total	14 701 814.10

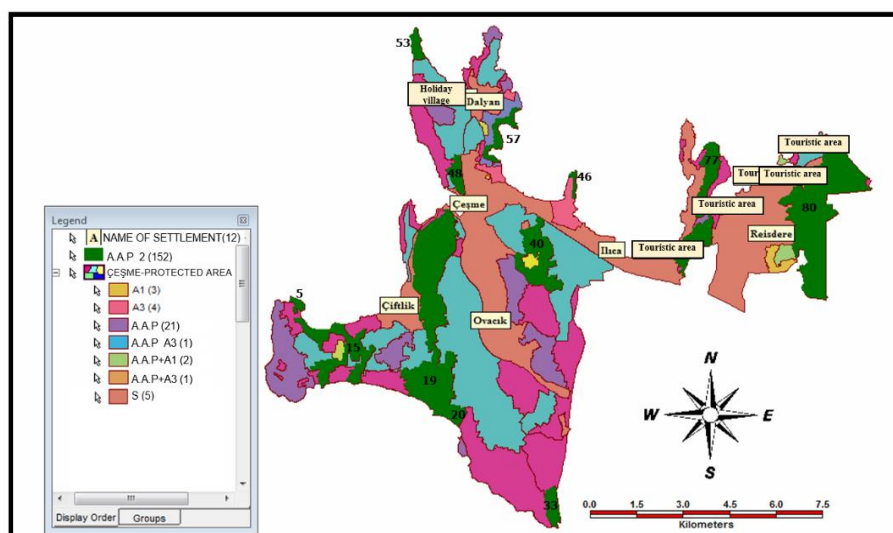


Figure 8. Map belonging to *Table 13*

- The criterion score has been examined based on models that have been developed on CBS according to these sensitive areas that will be protected by the law. In *Table 15*

- Cultural landscape score is evaluated as ≥ 3 (Considering *Table 2*: residential areas' being so less and absence of agricultural areas are considered to make decision for the index value in polygons)
- Organic landscape score is evaluated as ≥ 3 (Considering *Table 3*: forest formation existence considered to make the decision for index value in polygons).
- Inorganic landscape score is evaluated as ≥ 3 (Considering *Table 4*: at least 3 qualifications in inorganic landscape qualification table (*Table 4*) that set the criteria of inorganic landscape, were considered to make decision for index value).
- Sensitiveness score is evaluated as ≥ 4 (Considering *Table 7*: it was researched if there was rare endemic species in polygon).
- Ability of renewing itself score is evaluated as ≥ 3 (Considering *Table 6*: forest formation is considered to make decision for the index value in polygons).

The Map and the area coverage of polygons are shown in *Table 14* and *Figure 9*. Those areas are known as sensitive areas that will be protected by the law (SAPUL) based on the scores of cultural landscape, organic landscape, inorganic landscape, sensitiveness and ability of renewing itself on the GIS platform. According to the qualifications given above, the total scoring could be seen in *Table 15*. Polygons in *Table 14*, the scores given above are evaluated as index values.

Table 14. *The areas of polygons with qualifications of cultural landscape, organic, inorganic, sensitiveness and ability to renew itself among polygons that are in the areas that will be definitely protected*

Polygon number	Protected area number	Area (m ²)
5	SAPUL	146 900.10
15	SAPUL	1 949 916.20
19	SAPUL	2 545 573.70
20	SAPUL	401 061.50
22	SAPUL	3 499 518.80
33	SAPUL	477 665.00
Total		9 020 635.30

Table 15 has been generated by obtaining usage of areas according to satellite visuals and based on the tables above scoring qualifications of “cultural, organic, inorganic, historical landscape and ability of renewing itself. Landscape criteria values have been evaluated based on the database of GIS (Geomedia). As a result of modeling done above, polygons mentioned in *Tables 9–14* have come forth and *Table 15* has been created. *Table 15*, landscape criteria score mirrors landscape criteria scores of 20 polygons among 81 polygons that has been specified as sensitive areas and will be protected by the law (SAPUL) by Protection Commission of the Ministry of Environment and Urban Planning. As a result, the “suggested map of natural protected areas” has been created *Figure 10*.

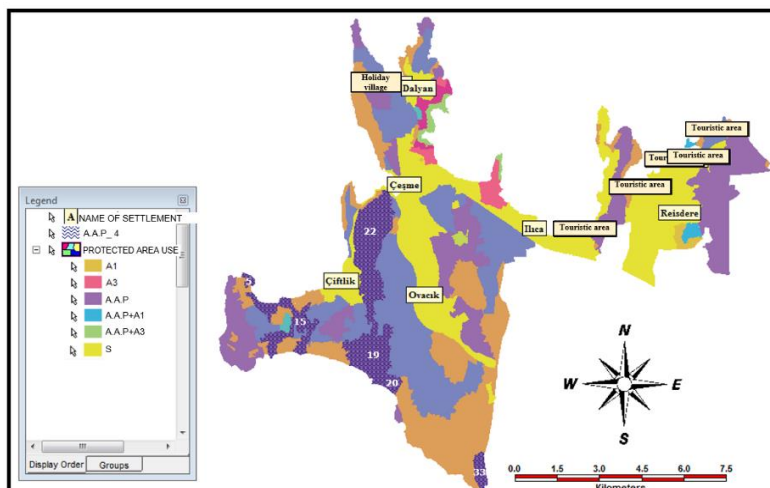


Figure 9. Map belonging to Table 14

Table 15. Distribution of landscape criteria scores of sensitivity of the areas that will be definitely protected

Landscape criteria	Polygon numbers																			
	1	5	15	16	19	20	22	33	37	40	46	48	51	53	57	66	70	73	77	80
Cultural landscape	2	4	3	2	3	3	3	4	2	3	3	3	2	4	3	2	4	4	4	4
Organic landscape	10	9	10	9	10	6	12	9	5	5	5	5	5	3	3	5	5	2	3	3
Inorganic landsc.	4	4	5	3	5	5	5	4	3	3	4	3	3	4	4	4	4	3	3	4
Historical landsc.	0	0	0	0	0	0	0	0	0	0	2	0	0	0	2	0	0	0	2	0
Ability to renew itself	6	5	6	6	6	3	8	5	6	6	5	6	6	3	3	6	6	2	2	3
Sensitiveness	4	4	4	4	4	4	4	4	0	0	0	0	0	0	0	0	0	0	0	0

Results and suggestions

The scores of cultural, organic, inorganic, historical landscape and ability of renewing itself and sensitivity of the areas that will be protected by the law has been presented based on the area usage status which has been evaluated on GIS platform by the Protection Commission of the Ministry of Environment and Urban Planning in order to finalize the legal decisions about natural protection fast and accurate. As a result of the examinations that have been made above (modellings), 20 polygons, which will be evaluated as sensitive areas that will be protected by the law in 5 different maps have been appeared. Those maps have been appeared based on the charts. The polygons known as sensitive areas that will be protected by the law (SAPUL) is classified based on their types of the area usage. According to this:

- Areas of Cesme district is covered by residential areas 0.54%, agricultural areas 12.82%, scrub + garrigue + forest 78.27%, lithosolic + garrigue 7.58%. Scrub + garrigue + forest areas are 22.044.944.00 m² which is 11.79% of Cesme district's square measure.
- According to the result map of ability to renew itself only in 73rd polygon there is no forest area. But this 73rd polygon establishes a buffer zone between other polygons that has the protection status.

- According to the sensitiveness map; in the forest areas in 1st, 5th, 15th, 16th, 19th, 20th, 22nd, 23rd polygons, there are “*Juniperus oxycedrus* subs. *Macrocarpa*” (large size fruited bushy juniper) and *Pistacia lentiscus*. Also there are *Chia* (gumwood) in enough quantity. According to this map the areas with sensitive qualifications covers 54.84% in the polygons that have been determined as scrub + garrigue + forest sensitive areas that will be protected by the law (SAPUL).
- In the given maps in *Figures 4–8* and examined models, according to the evaluation which has been done based on the landscape criteria scores, 20 polygons have been determined as sensitive areas that will be protected by the law (SAPUL) (*Fig. 10; Table 15*).

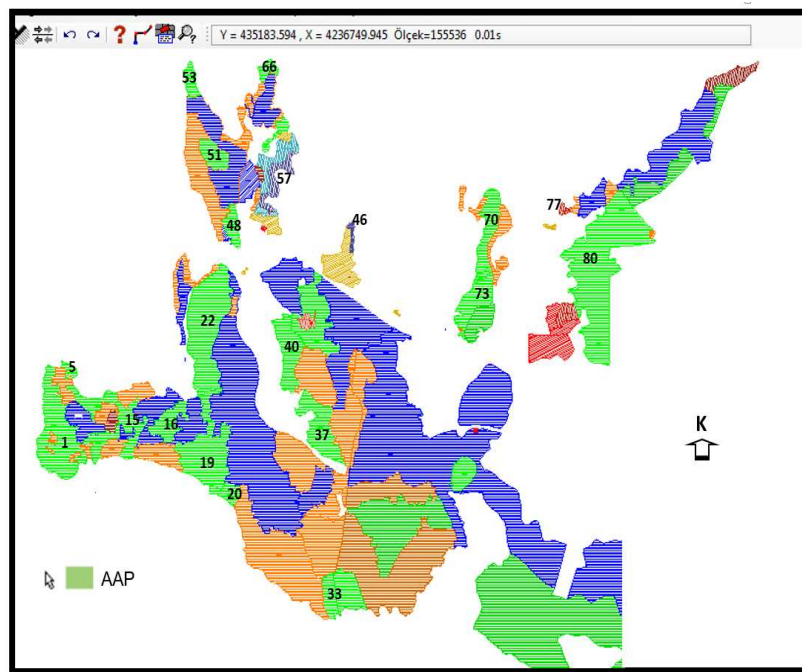


Figure 10. The map that shows the sensitive areas that will be protected by the law

It is aimed to suggest natural protected area mapping method supported by geographical information system which is based on true and scientific information in order to generate the maps of natural protected areas that are supposed to be prepared by the Cultural and Natural Heritage Preservation Board affiliated with the Ministry of Environment and Urban Planning. The results of the applications that will be obtained after the research studies are completed in Cesme district, will allow building a source and data to prevent disoperation which are still being applied. It is hoped that it will be an accurate and objective guiding method for the maps of natural protected areas that are supposed to be prepared by the Cultural and Natural Heritage Preservation Board affiliated with the Ministry of Environment and Urban Planning in Turkey as well as the other related institutions and organizations around the world.

Acknowledgements. This article has been produced based on Funda ANKAYA'S doctoral thesis “The analysis of the natural protected areas in terms of landscape criteria in Çeşme district, province of İzmir”.

REFERENCES

- [1] Anonymous (2019a): <https://www.google.com.tr/maps/search/%C3%A7e%C5%9Fme+s%C4%B1n%C4%B1rlar%C4%B1/@38.3208098,26.2268388,12z/data=!3m1!4b1>. – Date accessed: 30.09.2019.
- [2] Anonymous (2019b): https://www.nufusu.com/ilce/cesme_izmir-nufusu. – Date accessed: 30.09.2019.
- [3] Buchwald, K. (1980): Aufgabenstellung ökologisch-gestalterischer Planungen im Rahmen umfassender Umweltplanung. Handbuch für Planung, Gestaltung und Schutz der Umwelt. Band 3. – BLV, München, pp. 1-126.
- [4] Caner, G. (2007): National and International Nature Conservation Criteria and Natura 2000. – Master Thesis, Department of City and Regional Planning, Yıldız Teknik University, Graduate School of Science and Engineering, İstanbul.
- [5] Çolak, A. H. (2001): Nature Conservation in Forest. – National Parks Game and Wildlife General Directorate Publication, Ankara.
- [6] Frederic, O., et al. (1988): Classification of natural areas for planning. – Journal of Soil and Water Conservation, Department of Agricultural and Resource Economics, University of Vermont, Burlington.
- [7] Green, B. (1985): Countryside Conservation: The Protection and Management of Amenity Ecosystems. – George Allen & Unwin London.
- [8] Gülez, S. (1984): Classification of natural monuments. – Journal of Nature and Human 18(1).
- [9] Gülez, S. (1990): An Assessment Method Developed for the Determination of Forest Recreational Potential. Istanbul University Journal of the Faculty of Forestry, 40 (2).
- [10] Heydemann, B. (1981): Zur Frage der Flächengröße von Biotopbeständen für den Arten- und Ökosystemschutz. – Jahrbuch für Naturschutz und Landschaftspflege. Heft 31. Kilda Verlag, Greven, pp. 21-51.
- [11] Kinnon, M., et al. (1986): Managing Protected Areas in the Tropics. – International Union for Conservation of Nature and Natural Resources and the United Nations Environment Programme, Gland, Switzerland.
- [12] Mumcu, E. (2009): A Research on Landscape Planning in Protected Areas in Italy: The Case of Boretto. – Master Thesis. Ankara University, Institute of Natural and Applied Sciences, Ankara.
- [13] Özer, S. (2004): Investigation of Sarıkamış (Kars) Forests in Terms of Nature Conservation Criteria. – PhD Thesis, Department of Landscape Architecture. Atatürk University, Institute of Natural and Applied Sciences, Erzurum.
- [14] Türkyılmaz, B. (1991): Turkey in the field of nature conservation and natural sites of identifying and determining the criteria to be used in order to classify Izmir/Kemalpaşa research-based methods of sampling”. – Dissertation, Bornova-Izmir. Ege University, Institute of Natural and Applied Sciences, Department of Landscape Architecture, İzmir.
- [15] Türkyılmaz, B., Kurucu, Y., Altınbaş, Ü., Bolca, M., Esetlili, T., Özen, F., Gülgün, B., Gencer, G., Güney, A., Hepcan, Ş., Özden, N. (2005): Usability of Geographical Information System in Determination and Classification of Natural Sites and Researches on Creating a Database in a Sampling Area (Kaynaklar -Izmir). – Project No: 102 Y 046.
- [16] Uzun, O., Müderrisoğlu, H. (2010): Visual Landscape Quality in Landscape Planning: Examples of Kars and Ardahan Cities in Turkey. – Department of Landscape Architecture, Faculty of Forestry, Düzce University, Düzce, Turkey.
- [17] Yazıcı, K., Gülgün Aslan, B., Ankaya, F. (2017): Function of landscape scenery areas; a case study on Van Province. – Karabük University Journal of the Institute of Social Sciences Special Issue: 168-176.
- [18] Yazıcı, K., Gülgün Aslan, B. (2018a): GIS Using Multi-Criteria Decision Analysis for Assessment and Map-Based Indicators for Nursery Garden Management. – IJEES 8(2): 415-428.

- [19] Yazici, K., Kalaycı Önaç, A., Gülgün Aslan, B. (2018b): The Importance of UAV (Drone) Usage According to Landscape Architecture. – International Marmara Science and Social Sciences Congress 2018, Kocaeli, Turkey, pp. 1416-1426 (full text paper/oral presentation).
- [20] Yenilmez Arpa, N., Gülgün Aslan, B., Yazici, K. (2016): Designation of the trails and routs for visitor management in the protected areas case on Göreme Historical National Park in Turkey. – 6th International Conference of Ecosystems, Tirana, Albania, 2-6 June (ICE 2016).
- [21] Yücel, M. (1995): Nature Conservation Areas and Planning. – Ç. Ü. Faculty of Agriculture Publications, Adana.

REVIEW PAPER ON HORIZONTAL SUBSURFACE FLOW CONSTRUCTED WETLANDS: POTENTIAL FOR THEIR USE IN CLIMATE CHANGE MITIGATION AND TREATMENT OF WASTEWATER

ENGIDA, T.^{1,2}, – WU, J. M.^{2*} – XU, D.² – WU, Z. B.^{1,2*}

¹*School of Resources and Environmental Engineering, Wuhan University of Technology,
Wuhan, P. R. China
(e-mail: zewedenahomruhama@gmail.com)*

²*State Key Laboratory of Freshwater Ecology and Biotechnology, Institute of Hydrobiology,
Chinese Academy of Sciences, Wuhan, P. R. China*

**Corresponding authors*

*e-mail/phone/fax: wuzb@ihb.ac.cn/+86-27-6878-0020/+86-27-6878-0675 (Z. B. Wu);
wujunmei@ihb.ac.cn (J. M. Wu)*

(Received 25th Jul 2019; accepted 4th Dec 2019)

Abstract. The combination of rapid urbanization and industrialization expansion increased waste volumes. Most of the wastewaters generated from either domestic or industrial sources are still discharged without adequate treatment processes, and impact on the environment and public health. The objective of this paper was to provide a comprehensive literature review on the application of horizontal subsurface flow constructed wetlands in treating a variety of wastewaters, discussing its feasibility in pollutant removal efficiency and additional benefit in climate change mitigation through carbon sequestration. The following results were obtained: 98%, 96%, 85%, 90%, 92%, 88% for BOD₅, COD, TSS, TN, NH₄ –N, PO₄³⁻ respectively in Kenya; 98.46% and 98.55% for COD and BOD₅ in Indonesia; and ranges from 94-99.9%, 91.7-97.9% and 99.99% for BOD₅, COD and TFC respectively in Costa Rica. Whereas in Ethiopia, the HSSFCW achieved the following abatement efficiencies: COD ranges from 58 to 80%, BOD ranges from 66 to 77%, TKN ranges from 46-61%, sulfates ranges from 53 to 82%, and NH₄ – N range from 64 to 82.5% for tannery wastewater treatment. For domestic wastewater treatment; 99.3%, 89%, 85, 84.05%, 77.3%, 99% and 94.5% were achieved for BOD₅, COD, TSS, TN, PO₄³⁻, TP, Sulfate, and TFC, respectively. In addition to improving water quality, CWs have a CSP. For example, CWs showed CO₂ equivalent of 4119.54 g C/m²/yr CSP (carbon sequestration potential) which is 15118.7118 g CO₂. The methane equivalent to this amount of carbon sequestration is 604.748472 g/m²/yr. Generally, research results indicated that constructed wetlands are efficient wastewater treatment techniques and should be encouraged for wastewater management as a strategy to reduce wastewater pollution. However, constructed wetland performance efficiency sustainability is affected by the operational conditions of HSSFCW including plant species, media/substrate types, water depth, hydraulic loading, and hydraulic retention time and feeding mode.

Key words: *carbon sequestration potential, horizontal subsurface flow, climate mitigation, wastewater, constructed wetland, performance evaluation, and greenhouse gases, carbon cycle*

Introduction

Globally, wetland ecosystems are more and more being used for the treatment and disposal of wastewater because they have been known as low-cost and operative treatment schemes (Brix et al., 2001). Their potential to advance the quality of water from inflow to outflow has been recognized (Donald, 1989) Constructed wetland schemes use a conglomerate of biological physical, and chemical parameters. The combination of rapid urbanization and industrialization expansion increased waste

volumes. Most of the wastewater generated from either domestic or industrial sources are discharged still without adequate treatment processes. The discharging of untreated or partially treated wastewater by cities and industries causes an impact on the environment and public health resulting in the contaminated downstream water supplies becoming unfit for drinking, irrigation and recreational activities (Birhanu and Seyoum, 2007), due to the presence of nutrients, heavy metals, toxic organic pollutants and pathogens. Research reported by Bahri et al. (2008) also agreed that untreated wastewaters discharged into the freshwater bodies change the quality of freshwater. Besides deteriorating the freshwater bodies, the farmland soil characteristics are also changed due to using contaminated river waters or direct use of wastewater for irrigation. According to Bayrau et al. (2008) surveyed results in the case of Ethiopia outbreaks of waterborne diseases in addition to eutrophication of surface water and farmland resources are common.

The use of constructed wetlands for wastewater management is becoming more and more popular all over the world. This is due to its efficient wastewater management ability with cost-effective option in both developed and developing countries. Most of these systems are easy to operate, require low maintenance, and have low investment cost (Ballesteros et al., 2016; Langergraber, 2013). Today horizontal subsurface flow CWs (Constructed wetlands) are quite commonly used in many developed countries such as Germany, UK, France, Denmark, Australia, Poland and Italy. Constructed wetlands are also appropriate for developing countries but they are rarely investigated and implemented (Prasad et al., 2016). Water body deterioration is becoming a serious issue in developing countries due to indiscriminate discharge of wastewaters and lack of comprehensive management techniques. In developing countries constructed wetlands (CWs) are used to treat a wide variety of wastewaters such as domestic, municipal, industrial, landfill leachate as well as agricultural and highway runoff (Tilak et al., 2016). Wetland technologies are a reliable onsite wastewater treatment technology and work with a higher rate of biological activity which enables conversion of many of the pollutants that are contained in the wastewater into non-toxic byproducts and serve as secondary or tertiary treatment level that meets the regulatory standards. CWs have shown to successfully control macro (organic material, nutrients and pathogens) pollutants and provide high quality water used for irrigation, recreational and other reuse purposes. Generally, this technology serves as an active and low-cost alternative technology for the treatment of wastewater all over the world (Mustafa, 2013).

Treatment wetlands are technologies that are able to remove nutrients, toxic metals, organic pollutants, emerging contaminants and pathogenic organisms effectively (Belmont et al., 2009; Chen et al., 2012). Their effective pollutant removal is associated with several mechanisms involved in the constructed wetland systems. These are sedimentation, filtration, volatilization, adsorption, plant uptake and bacterial activity (Chazarenc et al., 2009; Ballesteros et al., 2016; Langergraber, 2013). The mechanisms of treatment in constructed wetland are complex processes which can happen simultaneously or sequentially involving microbial degradation, plant uptake, sorption, sedimentation, filtration and precipitation. In designing the good wetland, the main biological component in the CW is aquatic plants (macrophytes). However, it is important in determining the appropriate plant species that can survive in the wastewater environment, because only suitable plant species can treat a high concentration of pollutant in the waste water (Prasad et al., 2016). The selection of media type is also very important, because clogging problems are observed in subsurface flow constructed wetlands and linked hydraulic

retention time and hydraulic conductivity. Therefore, adequate selection of granular media could decrease the estimated wetland area and improve the removal efficiencies (Lopez-Lopez et al., 2015). The vegetation biomass from the constructed wetlands can provide economic importance to communities by harvesting it for biogas production, animal feed, fiber for paper making and compost (Lakshman, 1987).

They also have an important role in carbon sequestration (CS) and reports indicated that the highest CSP (carbon sequestration potential) was recorded for *Typha latifolia* (741.02 g m⁻²/yr) followed by *Phragmites australis* (740.5 g m⁻²/yr) and the lowest for *Carex sp.* (137.37 g m⁻²/yr) from wetlands (Maqubool et al., 2013). Generally, CW can provide economical on-site wastewater treatment that is both effective and aesthetically pleasing (El-Gohary, 2008), and become a popular subject among many community leaders, health officials, and home owners. However, in developing countries the use of CWs is certainly lower in comparison to their use in Europe or the United States, despite the enormous potential and the great necessity of these countries to implement low-cost treatment for better wastewater management strategy to achieve the required standards (Belmont et al., 2004; Zurita et al., 2006, 2008). In order to establish the performance of constructed wetland systems under different conditions various research studies have been carried out to investigate constructed wetland systems in the removal of pathogens, organic matter and nutrients. To date however, very limited research works on the performance of CW, especially under tropical conditions have been reported. Therefore, the purpose of this review paper was to provide a comprehensive literature review on the application of horizontal subsurface flow constructed wetlands in treating a variety of wastewaters, and to discuss its feasibility in pollutant removal efficiency and additional benefit in climate change mitigation through carbon sequestration.

Objective

This systematic review was aimed to assess and to provide a comprehensive literature review on the application of horizontal subsurface flow constructed wetlands in treating a variety of wastewaters, and to discuss its feasibility in pollutant removal efficiency and additional benefit in climate change mitigation through carbon sequestration.

Method

This review paper was written using searching key phrases “HSSF (Horizontal Sub Surface Flow) practice in the world”, “Factors affecting treatment efficiency and “benefits and limitation of Constructed wetland” in springer link, science direct, library genesis, jester, and www.nap.org searching web pages. From these search results, peer reviewed journals and review papers were used. The interpretation of the result of each document was done using bar graphs, lines and scatter plot in a Microsoft Excel. In view of the current demand of this review, the performance assessment assignment employed a range of tools to gather and analyze data from secondary sources. The review approach considered and used specific indicator parameters that are important for the environment. The parameters used include: Total suspended solids (TSS), Total phosphorus (TP), Total Kjeldahl nitrogen (TKN), Biological oxygen demand (BOD), Chemical oxygen demand (COD) and NH₄-N (ammonia nitrogen).

Constructed wetland historical background

Natural wetlands are usually found between water bodies and terrestrial areas. These systems naturally screen and collect pollutants such as silt and nutrients as they migrate towards water bodies. Natural wetlands were historically used as wastewater discharge sites (Kadlec, 2003). This system is still used for wastewater treatment under controlled conditions and the use of constructed wetlands has increased significantly. The purposeful construction and study of wetlands to treat wastewater was started at the Max Plank Institute in 1952 by Seidel (Vymazal, 2011).

Research in this area has accelerated since 1985 because of the simplicity of the systems regarding mechanical operation, biological complexity and high level of treatment. The other attractive advantage for developing countries is that construction may be completed using local materials and labor. The first full scale horizontal flow constructed wetland was constructed and used in the Netherlands in the 1975 but vertical flow wetlands dated back to the time of Seidel (Kadlec, 2008). Horizontal subsurface flow constructed wetland is the most widely used technology in Europe. This technology is designed typically in a rectangular bed form, and contains planted macrophytes and lined with an impermeable membrane or made from concrete. Mechanically raw or pretreated wastewater is fed in at the inlet and passes slowly through the filtration medium under the subsurface of the bed in a horizontal path until it reaches the outlet zone before discharging via level control arrangement at the outlet (Vymazal, 2005).

Constructed wetland classification

General classifications

Constructed wetlands for wastewater treatment are typically classified into two types according to the wetland hydrology, i.e. free water surface (FWS) constructed wetland and subsurface flow (SSF) constructed wetlands (Saeed and Sun, 2012).

In the FWS system, the water flowing through the system is exposed to the atmosphere, while in the SSF system, water is designed to flow through a granular media, without coming into contact with the atmosphere. FWS wetlands can be subdivided into four categories based on their dominant type of vegetation: emergent macrophyte, free floating macrophyte, free floating leaved macrophyte and submerged macrophyte. However, the subsurface flow wetlands (which by definition must be planted with emergent macrophytes) can be sub-classified according to their flow patterns: horizontal or vertical (Vymazal and Kröpfelová, 2008).

Surface flow systems are further subdivided based on the type of macrophytes that grow on them as free floating macrophytes (e.g. duck weed and water hyacinth), submerged macrophytes, free floating leaved macrophytes and floating mat macrophytes. FWS systems are similar to natural wetlands, with shallow flow of wastewater over saturated substrate. Whereas, in SSF systems, wastewater flows horizontally or vertically through the substrate which supports the growth of plants, and based on the flow direction, SSF constructed wetland is divided further into horizontal flow (HF) and vertical flow (VF) systems. A combination of various wetland systems was also introduced for the treatment of wastewater, and this design generally consisted of two stages of several parallel constructed wetlands in series, such as VF-HF CWs, HF-VF CWs, HF-FWS, CWs, and FWS-HF, CWs (Vymazal, 2013). In addition, the multiple-

stage constructed wetlands that were comprised of more than three stages were used (Kadlec, 2008). In the recent years, enhanced artificial constructed wetlands such as artificial aerated CWs, baffled flow CWs, Hybrid towers CWs, step feeding CWs and circular flow corridor CWs have been proposed to enhance the performance of the system for wastewater treatment (Wu et al., 2014). According to Haberl (1999) design configurations of constructed wetlands are classified on the basis of the following parameters, as illustrated in *Figure 1*.

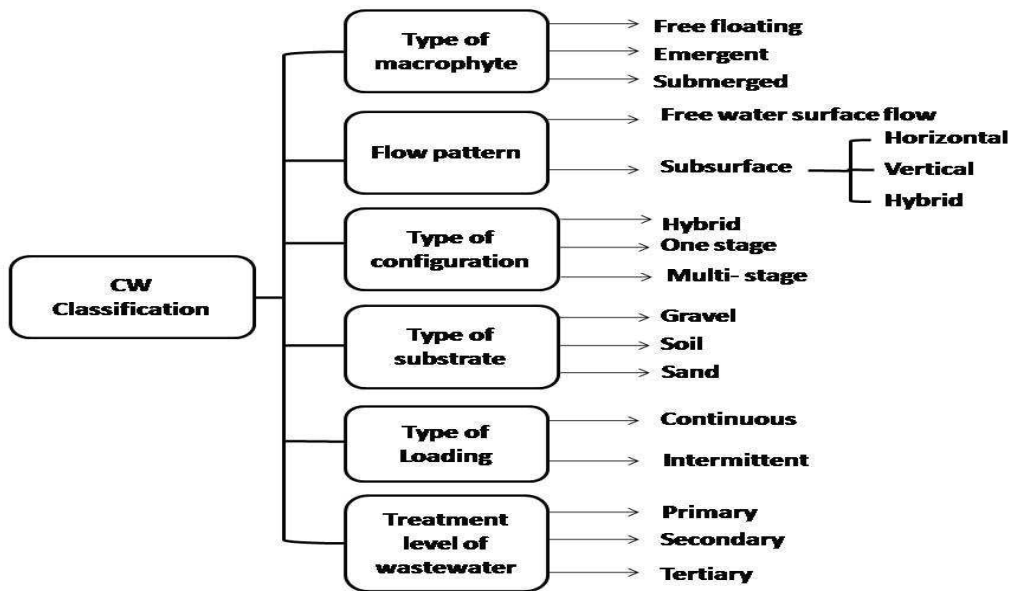


Figure 1. Classification and types of constructed wetland systems. Performance evaluation of constructed wetlands (Haberl, 1999)

Performance evaluation of constructed wetlands

Constructed wetlands are considered as natural treatment processes to stabilize, sequester, accumulate, degrade, metabolize and mineralize pollutants. They are used for a wide range of wastewater treatment such as municipal, domestic, agricultural, industrial, acid mine drainage, petroleum refinery wastes, compost and landfill leachates, and storm wastewaters (Vymazal, 2005). The treatment system involves macrophytes, substrates and microorganisms able to improve the water quality for reuse purposes. Macrophytes and Medias are an active component of horizontal subsurface flow constructed wetland (Vymazal, 2011). The selection of media type is also very important, because clogging problems are observed in subsurface flow constructed wetlands and linked hydraulic retention time and hydraulic conductivity (Lopez-Lopez et al., 2015).

Wastewater treatment is accomplished through the integrated combination of physical, biological and chemical interactions among biotic and abiotic components of the ecosystem and macrophytes cultivated in constructed wetlands make one of the basic components in the treatment process.

They influence plant microorganism's wastewater interactions by providing microbial attachment sites, sufficient wastewater residence time, trapping and settlement of suspended wastewater components as a result of resistance to hydraulic flow, surface area for pollutant adsorption, uptake and storage in plant tissue and diffusion of oxygen from aerial parts to the rhizosphere (Kyambadde et al., 2005). Wetlands remove metals using a

variety of processes such as filtration of solids, sorption onto organic matter, oxidation and hydrolysis, formation of carbonates, formation of insoluble sulfides, binding to iron and manganese oxides, reduction to immobile forms by bacterial activity, and uptake by plants and bacteria. Metal removal rates in both surface flow and subsurface flow wetlands can be high, but can vary greatly depending upon the influent concentrations and the mass-loading rate (Vymazal, 2005).

A study conducted in Kenya to assess the effectiveness of CW in treating domestic wastewater showed that the removal of BOD₅, TSS, COD, TN, NH₄-N and Orthophosphate were highly effective with a removal value of 98%, 85%, 96%, 90%, 92%, and 88%, respectively (Nyakango, 1999). This was mainly because this wetland consists of a combination of an SF system followed by three SSF wetland cells in a series adjacent to it. A case study conducted in Italy, to assess the treatment performance of an SSF CW by Pucci et al. (2000) showed high removal efficiencies for COD (93%), TSS (81%), hygienic parameters (TC 99%, FC 99.7%), but relatively low for nitrate (55%), total nitrogen (50%) and ammonium (30%), and very low for total phosphorus (20%). This is mainly due to poor nitrification and denitrification in the system. There is substantial evidence in the design of CW that a number of cells in series can consistently produce a higher quality effluent. Because this process minimizes the short-circuiting effects of any one unit and maximizes the contact area in the subsequent cell (Gearheart, 2004).

Constructed wetland contaminant removal mechanisms

Nitrogen removal mechanisms in wetland are nitrification in aerobic zone, denitrification in anaerobic zones which release N₂ and N₂O gases, plant uptake, sedimentation, decomposition, ammonia volatilization, and accumulation of organic nitrogen in gravels because of redox potential of hydric sediment conditions (Fig. 2).

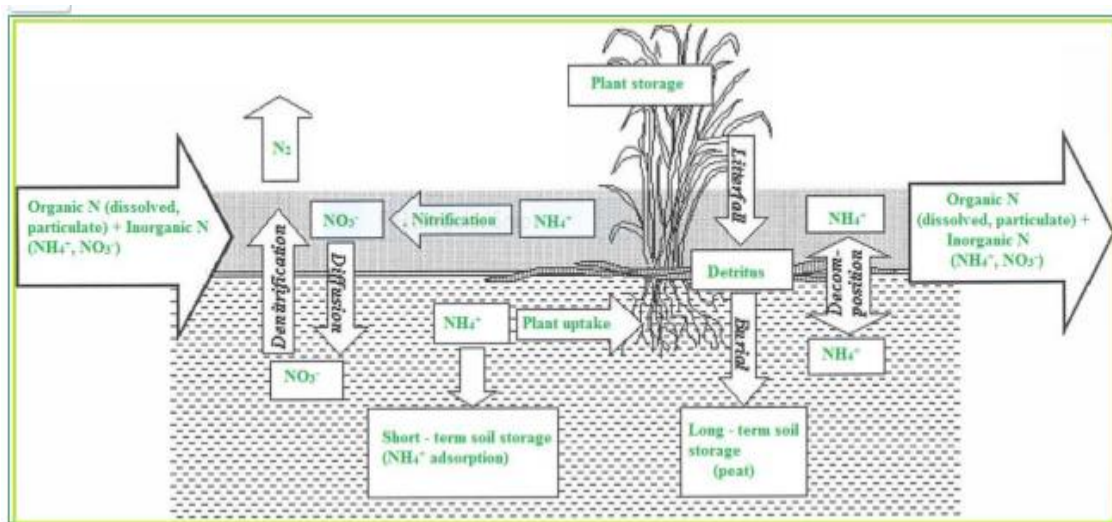


Figure 2. Nitrogen removal processes in wetland (Vymazal and Kröpfelová, 2008)

The fate of phosphorus is quite different in wetland soils, since there are no mechanisms comparable to de-nitrification as phosphorus has no gaseous phase.

Consequently, plant uptake, sorption, decomposition and long-term storage occur, and then phosphorus tends to accumulate in wetlands. Precipitation of phosphate minerals can provide a significant sink for phosphorus in wetlands with large stores or inputs of iron and aluminum or calcium (*Fig. 3*) (Vymazal and Kröpfelová, 2008).

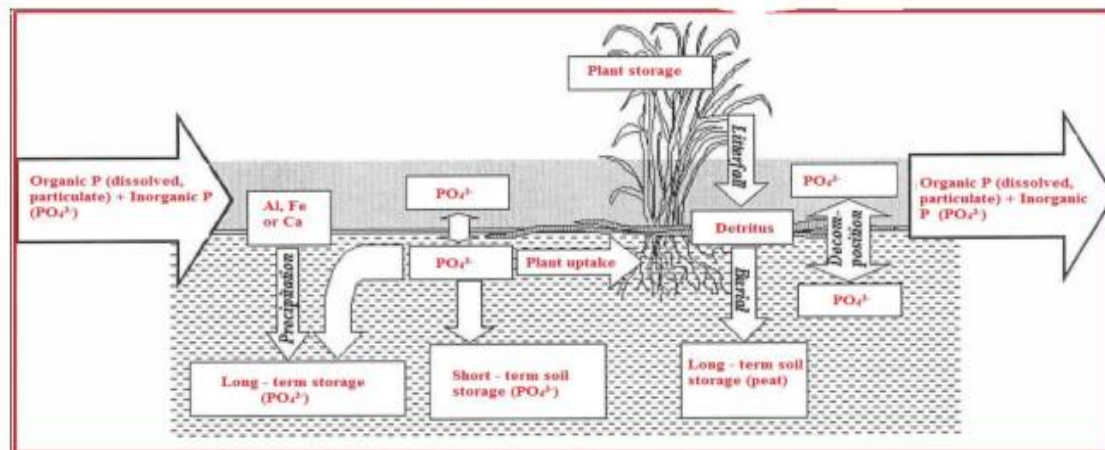


Figure 3. Phosphorus removal mechanisms (Vymazal and Kröpfelová, 2008)

The wetland treatment mechanism is a dynamic process acting wastewater purification under the cooperation of emergent macrophytes, substrates and attached microorganisms. In general, in constructed wetlands it is important to study biomass accumulation and nutrient flux in order to understand the dynamics of nutrients. The carbon cycle in wetlands has been investigated to understand the linkage between biomass generation and carbon sequestration (Kayranli et al., 2010). Wastewater treatment may also serve as a carbon sequestration offset (Rosso and Stenstrom, 2008). Wetland ecosystems are acting as a net carbon emission and sequestration systems depending on the time scale and hydrology operational strategies (Whiting et al., 2001), and as a component of a larger system treating wastewater (Rosso and Stenstrom, 2008). Constructed wetlands are passive natural processes and avoid carbon emission equivalent of 1.3 Mt C/yr for every 1.0 MGD as compared to conventional high rate treatment facilities such as activated sludge. There are many mechanisms for the capture and release of carbon in a wetland (*Fig. 4*). Pathways for the release of carbon in the constructed wetland system are slow decomposition, respiration, and physical removal. Photosynthesis is the process whereby a plant transforms atmospheric carbon in the form of CO₂ into the carbon of the plant tissue or biomass. The process of plant respiration releases some CO₂ to the atmosphere as a byproduct of cellular growth. In addition to respiration, plants release carbon as a byproduct of decomposition in the form of CO₂ and CH₄ (Burke, 2011).

Factors affecting the performance of constructed wetlands

Temperature

This is a key environmental factor that determines the activity of nitrifying bacteria and the de-nitrification potential in treatment wetlands (Langergraber, 2013). Nitrogen removal by biological means is most efficient at 20-25 °C and temperatures above this

affect both microbial activity and oxygen diffusion rates in the constructed wetlands. The microbial nitrification and de-nitrification activities can decrease considerably at water temperatures below 15 °C or above 30 °C, and most microbial communities for nitrogen removal function at temperatures greater than 15 °C (Kuschik et al., 2003). Literature revealed that the activity of de-nitrifying bacteria in constructed wetland sediments is generally more robust in spring and summer than in autumn and winter and the overall removal rate of nitrate is higher in the summer than in winter (Oostrom, 1994). De-nitrification is commonly believed to cease at temperatures below 15 °C, but some studies have demonstrated de-nitrification activity at 14 °C or lower temperatures. Richardson et al. (2004) reported that the optimum temperature range for nitrification is 30-40 °C in soils and the optimal ammonification is carried out at 40-60 °C at the optimal pH between 6.5 and 8.5. At low temperature, nitrification is insufficient to prevent a net increase in ammonia concentration due to ammonification (Akratos and Tsihrintzis, 2007).

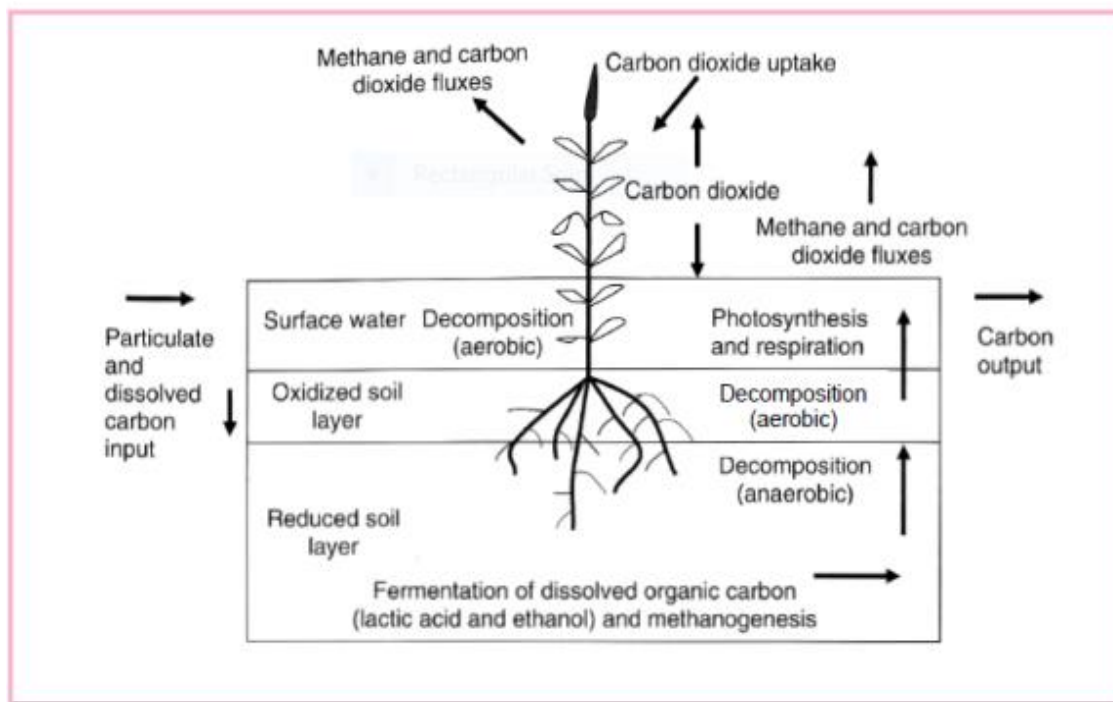


Figure 4. The carbon cycle (Kayranli, 2010)

HRT

The high purification efficiency of constructed wetlands can be achieved by choosing suitable growth media. Particle size, surface nature, bulk porosity and pore spaces of the growth media are important factors in selection of media type for wastewater treatment. Growth media provide not only physical support for plant growth but also additional sites for biofilm growth and the adsorption of nutrients, heavy metals and promote the sedimentation and filtration of pollutants. In general, the inconsistent treatment efficiency of constructed wetlands depends on the type of feeding mode, the plant types and type of media used (Abdelhakeem et al., 2016). According to Huang et al. (2000) explanation, ammonium and total Kjeldhal Nitrogen (TKN) concentrations in treated effluent decreased diagrammatically with increased wastewater retention time. In most

wetland systems, efficient nitrogen removal requires longer retention time compared with organic matter (COD and BOD) removal efficiency. Accordingly, nitrogen removal efficiency varies greatly with flow conditions and HRT (Taylor et al., 2006).

In subsurface constructed wetlands, media perform the function of rooting material for macrophytes surface for microbial biofilm growth, screen organic and inorganic suspended matter, and distribute inflow and collect outflow water (U.S. EPA, 1993). Keeping the water level below the surface of the bed, this reduces the risk of human contact with pathogens, and reduces the opportunities for breeding vector organisms such as mosquitoes. Media can also provide adsorption sites for phosphorus (Kadlec, 2003). According to this researcher, potentially active industrial byproduct substrates include blast furnace slag, crushed rock, fly ash, and crushed concrete, burnt oil shale, iron ochre and wood chips. The microorganisms responsible for the degradation of pollutants are located at the surface of the media and the smaller sized media has a larger surface area than the coarser media (Vymazal and Kröpfelová, 2008).

Well graded media (containing all gravel sizes in the selected range) is better than poorly graded media as it offers greater pore space and provides good removal of particulate matter. In general, the substrate alone also provides significant wastewater treatment, but vegetation further improves treatment efficiency (Abdelhakeem et al., 2016). Therefore, the high purification efficiency of constructed wetlands can be achieved by choosing suitable growth media.

Types of plant species

Plants are often grown in gravel beds to stimulate uptake and create suitable conditions for the oxidation of the substrate, thereby improving the ability of the system to treat the wastewater and create aesthetic value, exhibit several properties which enhance wastewater treatment processes and thus, make them an essential component of the treatment wetland. These properties influence wastewater treatment through physical effects such as filtration, provision of surface area for the growth and attachment of microorganisms and regulation of undesirable water temperature as well as surplus algal growth. Macrophytes are the main biological component of wetlands and their presence has been hypothesized to play a key role in wastewater remediation (Luckeydoo et al., 2002). Macrophytes are also play an important role in wastewater treatment through uptake of nutrients, surface bed stabilization and other mechanisms (Kadlec, 2008). Wetland plants must survive the potentially toxic effects of the effluent and enhance the treatment process of wetlands in several ways such as filtering wastes, regulating flow, providing surface area for microbiological treatment, providing shed and controlling algae growth, contributing oxygen to the cells, taking up and storing some metals and nutrients from the wastewater (Kyambadde et al., 2005).

Metabolically, plants take up pollutants; produce organic carbon and oxygen, thereby improve the water to varying extents. They are not only assimilating pollutants directly into their tissues, but also act as catalysts for purification reactions by increasing the environmental diversity in the rhizosphere, promoting a variety of chemical and biological reactions that enhance purification. Several studies have shown that plants enhance treatment efficiency by providing a favorable environment for the development of microbial populations and by oxygenating the system. The roots of macrophytes provide surface areas for microbial growth and aerobic zones in constructed wetlands. The root facilitates various physical and biochemical processes caused by the relationship of plants, microbial communities, soil and contaminants. Wetland systems with

vegetation typically remove greater amounts of total nitrogen than non-vegetated systems (Taylor et al., 2006). Nutrient removal by the emergent plants is achieved by two processes: absorption of the plant itself and microorganism activity around the rhizome (Cooper and Boon, 1987). In general, the main role of macrophytes in constructed wetlands is to promote microbial growth with the media surfaces, and to assist the permeation velocity of the wastewater for pollutant treatment efficiency (*Table 1*).

Table 1. Pollutant removal processes in surface flow constructed wetland (Tousignant and Fankhauser, 1999)

Pollutant type	Removal process
Organic material (COD and BOD)	Particular organic matter is removed by settling and filtration then converted to soluble BOD Soluble organic matter is fixed by biofilms and degraded by attached bacteria in the biofilm on stems, roots sand particles etc.
Suspended solids (TSS)	Filtration Decomposition by bacteria during long retention time
Nitrogen	Nitrification and de-nitrification in biofilm Plant and microbial uptake
Phosphorus	Adsorption (retention in the media) Precipitation with Ca, AL or Fe
Pathogens	Filtration, adsorption, predation (feeding) by protozoa Die-off due to long retention times
Heavy metals	Precipitation and adsorption Plant uptake
Organic contaminates	Adsorption by biofilm and clay particles Decomposition due to long retention time and by bacteria

Other factors

Other important factors are wetland depth, pH, and DO. The nitrification and denitrification process depend upon water pH, the presence or depletion of dissolved oxygen, hydraulic loading rate, and the hydrological period of the wetland. At low DO concentration, nitrification occurs in the aerobic zone but denitrification occurs in the anoxic zone (Kadlec, 2008). The biofilm may improve the denitrification; because of algae provide a desirable carbon source for denitrifies (Mariñelarena and Di Giorgi, 2001). In general, in order to maintain and improve nitrogen removal and water quality in constructed wetlands, attention should be given to factors that promote the growth rate of macrophytes and bacteria, such as planting depth, harvesting time, optimization of temperature, pH, DO and HRT.

Performance efficiency of horizontal sub surface flow constructed wetland (HSSFCW): a case in other countries

This section presents different macrophytes used for treatment of wastewater in constructed wetland and their effectiveness in treating wastewater pollutants. The focus of each case study is according to parameters related to the overall constructed wetland design, macrophyte species, hydraulic loading rates and the efficiency of pollutant removal. In order to evaluate the performance efficiency of a CW unit, the percentage of concentration reduction and mass removal is reported. The wetland effluent is being

irrigated on vegetation, nutrient levels in the effluent do not need to be as strict as for direct discharge into a water course (Tousignant and Fankhauser, 1999). These systems are highly effective at improving water quality have many benefits such as habitat creation and low-cost operations (Kadlec, 2008). According to Mustafa (2013), the monitoring of horizontal flow constructed wetland indicates that the general performance of the system was good and it successfully reduced pollutants even under fluctuating pollutant loading resulting from power breakdown. The average reduction of BOD concentration over the treatment periods was 50% with mean effluent concentration of 34 mg/L. Whereas, the average removal efficiency of the treatment system for COD, TSS, ammonia–nitrogen, orthophosphate and fecal coliform were 44%, 78%, 49%, 52% and 98% with mean effluent concentrations of 68.3 mg/L, 45 mg/L, 9.7 mg/L, 3.7 mg/L and 3.0×10^3 CFU (Colony-forming units)/100 ml respectively.

In general, the monitoring of horizontal flow constructed wetland indicates that it was good and successful in reducing pollutants from wastewater up to the required standards even under fluctuating pollutant loading. The outcomes revealed that if constructed wetlands are properly planned and operated, they can be used as secondary or tertiary treatment level under local conditions and finally delivers high value water that can be used for landscape irrigation and also for other helpful uses. The COD removal efficiency of HSSFCW even at low concentration which might be due to high degradation rate in the wastewater collection systems and in settling tank before entering the CWs. In overall, the results obtained in Indonesia, Thailand, and Costa Rica revealed that, the local macrophytes and local natural substrates can perform successfully in the treatment of domestic wastewater (Table 2). The organic contaminants and pathogens can be removed successfully, therefore, the treated water can be used safely for irrigation, fishery or out-door uses. In addition, the treated water can replace a part of the fresh water need supplied from the pipe distribution systems and be potential to protect surface and ground water reduces from the pollutants. Moreover, the use of macrophyte creates a green space in a single house yard or green public views for neighborhood (Qomariyah et al., 2017).

Table 2. The effective removal of pollutants in CWs with local macrophytes and natural substrates (Qomariyah et al., 2017)

Type and size of CW	Type plant	Type of substrate	Country	Removal efficiency (%)
HSSFCW (1.7 x 0.7 x 0.7 m)	C. papyrus	Sand & gravel	Indonesia	BOD=98.55% COD=98.46% TSS=88 – 96% Detergent=99.86%
HSSFCW (2 x 1 x 1 m)	Canna & Heliconia	Gravel	Thailand	BOD=94-99.9% COD=42-83% TSS=88%-96% TN=4 – 37% TP=6 – 35%
HSSFCW (14 x 1.2 x 0.6 m)	Coix lacrymajodi	Crushed rock	Costa Rica	BOD=94-99.9% COD=91.7-97.9% FC=99.99%

The performance efficiency of subsurface flow constructed wetland in Italy done by Pucci et al. (2000) indicates that it has high removal efficiency for COD (93%), TSS (81%) and total coliform (99%), but relatively less removal for nitrates (55%), total nitrogen (50%), ammonium (30%) and total phosphorus (20%). This is mainly due to poor nitrification and denitrification in the treatment system. A study done in Kenya also revealed that the effectiveness of the constructed wetland in treating domestic wastewater and indicated a removal efficiency of 98%, 85%, 96%, 90%, 92% and 88% for BOD₅, TSS, COD, TN, NH₄-N and PO₄ respectively (Nyakango, 1999). This achievement was due to the wetland design which consists of a combination of a surface flow system followed by three subsurface flow wetlands in a series adjacent to it.

The removal efficiency of constructed wetlands varies with hydraulic retention time, hydraulic loading, wetland design, temperature, substrate and vegetation. Although considerable number of reports has contributed to our understanding of the physical, chemical and biological processes that facilitate the removal process, inconsistency results suggest that further studies are required to optimize the system functioning. For example, many scholars show that, a wetland scheme with vegetation has advanced efficiency of removal than that without plants (Bwire et al., 2011) although others did not notice any significant change between planted and unplanted systems (Baldizon et al., 2002). Similarly, the percentages of nutrient (nitrates/nitrites and phosphates) removal obtained in the planted constructed wetland cell were higher than the averaged percentages of nutrient removal rates in the unplanted cell.

Thus, the average nitrate/nitrite percentage removal was 58.1% for planted cells and 21.6% for unplanted cell while the phosphate percentage removal averaged 40.1% for planted cells and 5.2% for unplanted cell (Mairi et al., 2012). Bacteria may be reduced by sedimentation, chemical reactions, natural die-off and predation by zooplankton, nematodes, lytic bacteria and attacks by bacteriophages (Denny, 1997). The role of plants related to the treatment of wastewater is the physical effects brought about by the presence of the plants. The macrophytes alleviate the surface of the beds, offer good condition for physical filtration and deliver enormous surface area for attached microbial growth (Brix and Schierup, 1989). Furthermore, macrophytes reduce the velocity of wastewater into the wetland system and also supply oxygen at the root zone which is used by aerobic microbes, thereby enhancing purification process of wastewater in addition to purification done by anaerobic microbes (Watson et al., 1989).

The performance efficiency of different constructed wetland systems that contain different HRT, substrate, plant species and wastewater type were reviewed in order to regulate the performance of constructed wetland parts in elimination of contaminants. The influent and effluent concentrations including percentage removal were summarized in *Table 3*.

Table 3. HSSFCW percentage abatement in different locations planted with *Phragmites australis*

Location	BOD ₅	COD	TSS	TN	NH ₄	TP	Reference
Egypt	93	91	92	60	57	63	Puigagut, 2007
Spain	74.2	66	87.8	56.5	45.7	45	Barbera, 2009
Italy	74	60	89	35	-	57	Kotti, 2010
Greece	76	64	-	55	43	48	El Hamouri, 2007

As indicated in *Table 4*, the nitrogen removal in constructed wetlands depends upon system design, environmental chemistry (roots, plants, water and sediments), plant uptake, available carbon and material type. The mean removal efficiency of the planted (reeds) and unplanted constructed wetlands during the three months of warm and cold study periods are indicated in *Figure 5*. In general, proper performance and high removal at the first treatment unit (septic tank) increases the efficiency of the treatment plant (Farzadkia et al., 2015).

Table 4. Treatment efficiency of HSSFCW in different countries

Type of waste water	Type of media	Plant type	HLRL/D	HRT/D	Removal efficiency	Country	Reference
Domestic	Soil	P. karka	1	9	COD 44% BOD 50% TSS 78% NH ₃ 49% Po ₄ 52% FC 98%	Pakistan	Mustafa, 2013
Domestic	Gravel	P. mauritianus	2	12	BOD 76% NO ₃ 58.1 Po ₄ 40.1 FC 93.9%	Tanzania	Mairi, 2012
		Unplanted			BOD 48% NH ₃ 21.6% Po ₄ 5.2% FC 58.7		
Raw domestic	Tezontile rock	Z. aethiopica	200	3	COD 64% BOD 80.6 TSS 80.1 Org-N 54.9% NO ₃ 53.6 NH ₄ 19.6%	Mexico	Zurita et al., 2014
		C. papyrus			TP 4.8% FC 92%		
Raw domestic	Gravel (10-15 mm)	C. zizanooides	40	0.92	TSS 90.2% TN 59.4% NH ₄ 51.8%	San midi Ganzaria	Maucieri et al., 2014
		M. giagnteus			TSS 81.2% TN 45.7% NH ₄ 40%		
		P. australis			TSS 90.3% TN 57.2% NH ₄ 54.3%		
Domestic	Gravel (5 cm), peat (35 cm)	P. australis	0.27	22.6	BOD 96.4 COD 84.6 TSS 94.8% TN 79.5% NH ₄ -N 98.8% TP 83.7%	Spain	Andero-martiuer et al., 2016

HLR = hydraulic loading rate, HRT = hydraulic retention time

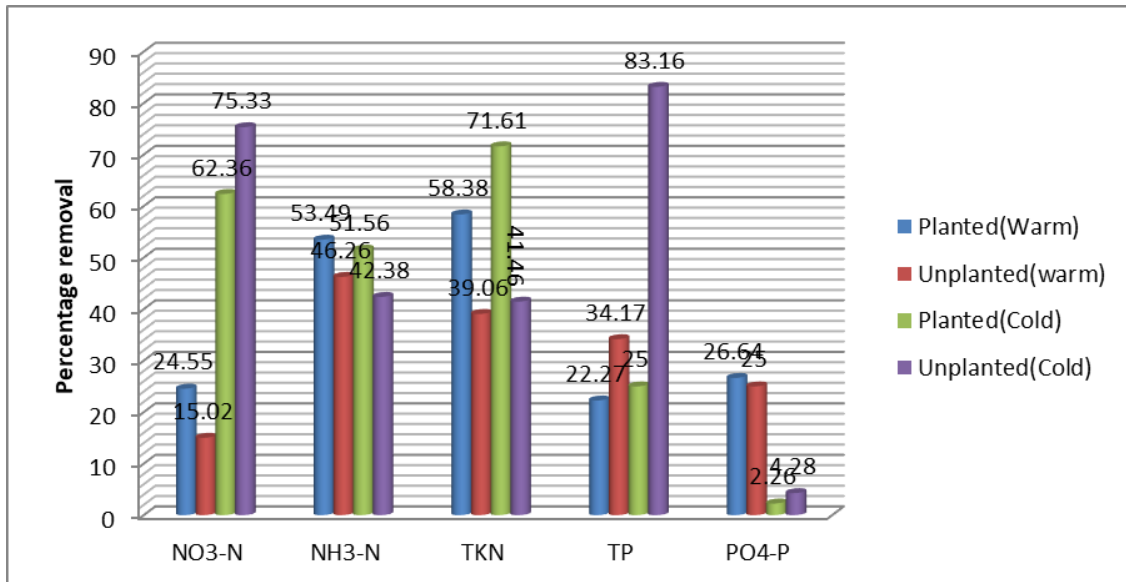


Figure 5. Effect of vegetation, climate and media on nutrient removal (Farzadkia et al., 2015)

The mean influent concentration of COD, TSS, NH₄-N, NO₃-N and PO₄-P in January were 144, 54, 96, 2.76 and 3.62 mg/L, respectively. The effluent concentrations after treating with constructed wetland were 64, 8, 62, 1.69 and 3.55 mg/L, respectively. The mean percentage removal reductions for COD, TSS, NH₄-N, NO₃-N and PO₄-P in this month were 55%, 85%, 35%, 39% and 2%, respectively. The mean influent concentrations of these pollutants in February were 192, 38, 63, 2.91 and 4.12 mg/L, respectively. The mean effluent concentrations were 64, 4, 28, 2.33 and 1.05 mg/L, respectively. The mean percentage removal efficiency of the wetland was reached 66%, 89%, 55%, 20%, and 75% for COD, TSS, NH₄-N, NO₃-N and PO₄-P, respectively. In hydrologic comparison in the constructed wetland indicated that the COD, TSS, NH₄-N, NO₃-N and PO₄-P reductions were considerably greater in February compared to January. This was due to the lower HLR and greater HRT in February compared to January. The major mechanisms of TSS and COD removals in constructed wetlands are sedimentation, filtration and physical entrapment in the void pores of the sand and gravel medias. The higher HRT also allows for greater physical settling of suspended particles, which reduces the TSS and the higher residence time allows wetland plants to uptake nutrients effectively thereby decreasing the effluent concentrations (Tilak et al., 2016). The nitrogen content of *Pistia stratiotes*, *Typha latifolia* and Lemon grass in the subsurface flow constructed wetland were 37.4 g/kg, 27.1 g/kg and 15.8 g/kg, respectively.

The phosphorus accumulation capacity of these plant species were also 8.4 g/kg, 2.96 g/kg and 2.29 g/kg, respectively for *Pistia stratiotes*, *Typha latifolia* and Lemon grass in the constructed wetland (Fig. 6) (Tilak et al., 2016). Subsurface flow constructed wetlands are good in utilizing pollutants in a symbiotic relation between aquatic plants and microorganisms in the media and the plant root system. Composite organic compounds confined in wastewater will be used up by plants as a nutrient, while the root structure of the aquatic plants will yield oxygen that can be used as energy or catalyst for a sequence of metabolic courses for heterotrophic aerobic microorganisms. Plants that are usually used include *Cyperus alternifolus*, *Canna indica*,

Phragmites australis, *Typha* spp., *Scirpus* spp., etc. these plants reduce the concentration of BOD, COD, ammonia, nitrites, phosphorus and bacterial contaminants (Wijaya et al., 2016).

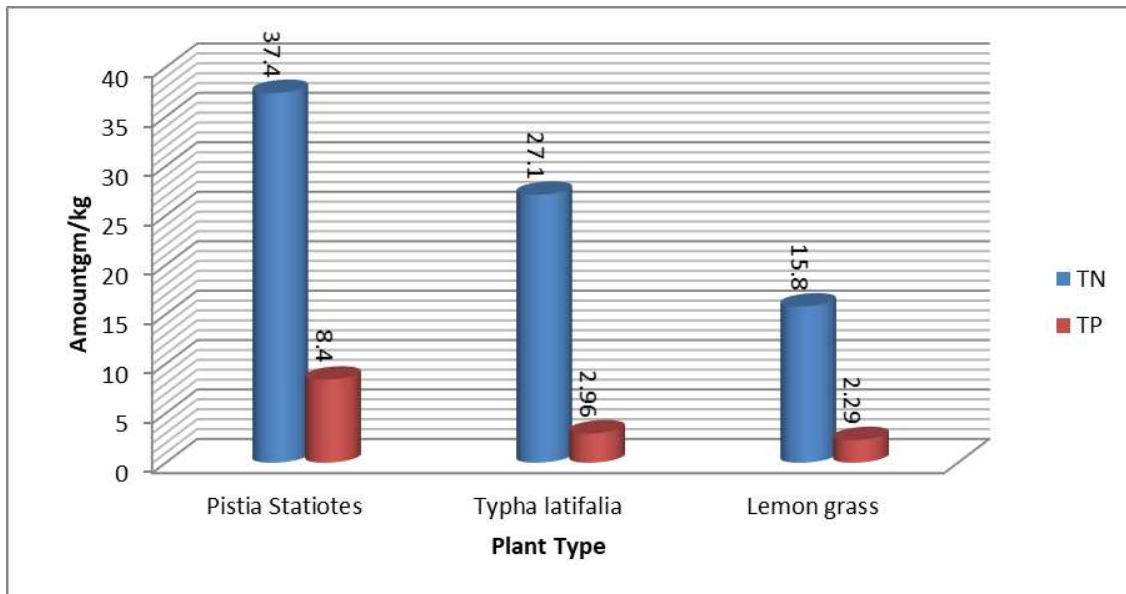


Figure 6. Nutrient accumulation in the wetland plants (Tilak et al., 2016)

The removal of nutrients from constructed wetlands are also dependent on the media types. The accumulation of total nitrogen and phosphorus in the constructed wetland media was also investigated by Tilak et al. (2016) as indicated in *Figure 7*.

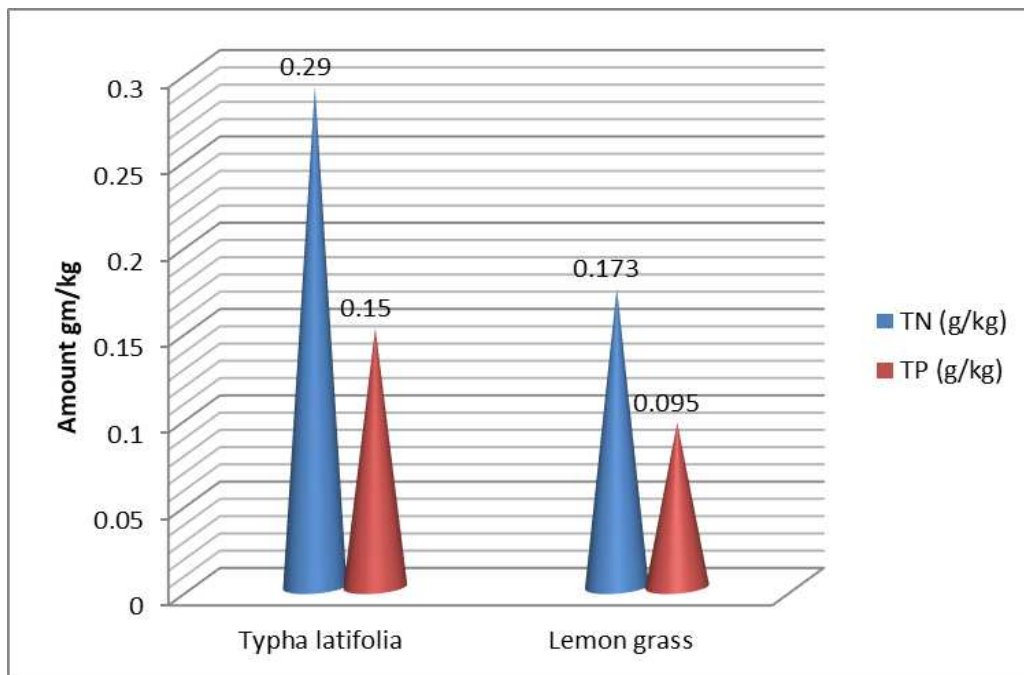


Figure 7. Nutrient accumulation in sand media (Tilak et al., 2016)

The effect of vegetation on the organic matter removal was better than (i.e., 5 to 15%) those of the unplanted. In general, the organic removal results suggest that control treatment influences wetland performance more than the type of macrophytes. The TSS removal efficiencies varied from 35 to 76% in both dry and nortes season. The organic matter (COD and BOD) removal showed similar pattern to that of TSS, which was varied from 36 to 68% and 28 to 69% for COD and BOD, respectively in the dry season, and whereas for the nortes season, they varied from 40 to 78% for COD and 49 to 74% for BOD. The nutrient removal efficiencies ranged from 47 to 66% and 59 to 79% for TN, 53 to 67% and 50 to 75% for $\text{NH}_4 +$ and 69 to 84% and 60 to 75% for NO_3^- respectively for dry and nortes seasons. In general, the performance efficiency of the horizontal subsurface flow constructed wetland in organic matter, nutrient and pathogens were shown in *Figures 8 and 9*. The overall result clearly indicates that HRT is a key factor in the removal of a wide variety of contaminants (COD, BOD, TSS, TN, $\text{NH}_4 + \text{NO}_3^-$ and TP) in horizontal subsurface flow constructed wetland treating swine wastewater. According to the findings, the *Typha latifolia* and *Eleocharis interstincta* are the most suitable macrophyte species to be used for the treatment of piggery wastewater. In spite of the fact that high contaminant concentrations in wastewater may have masked the macrophytes; contributing to the overall treatment efficiency of HSSFCW, vegetated beds usually provide better effluent quality than unplanted beds (Puigagut et al., 2007).

The above graph indicates that the local macrophytes and natural substrate can perform successfully in the treatment of domestic wastewater. The results demonstrated that removals of organics (COD and BOD) are high in the horizontal subsurface flow constructed wetlands. The treatment efficiency of BOD nan COD ranged between 76 and 99.4% and 76 and 8.46%, respectively except COD removal studied results in Thailand which varied between 42 and 83%.

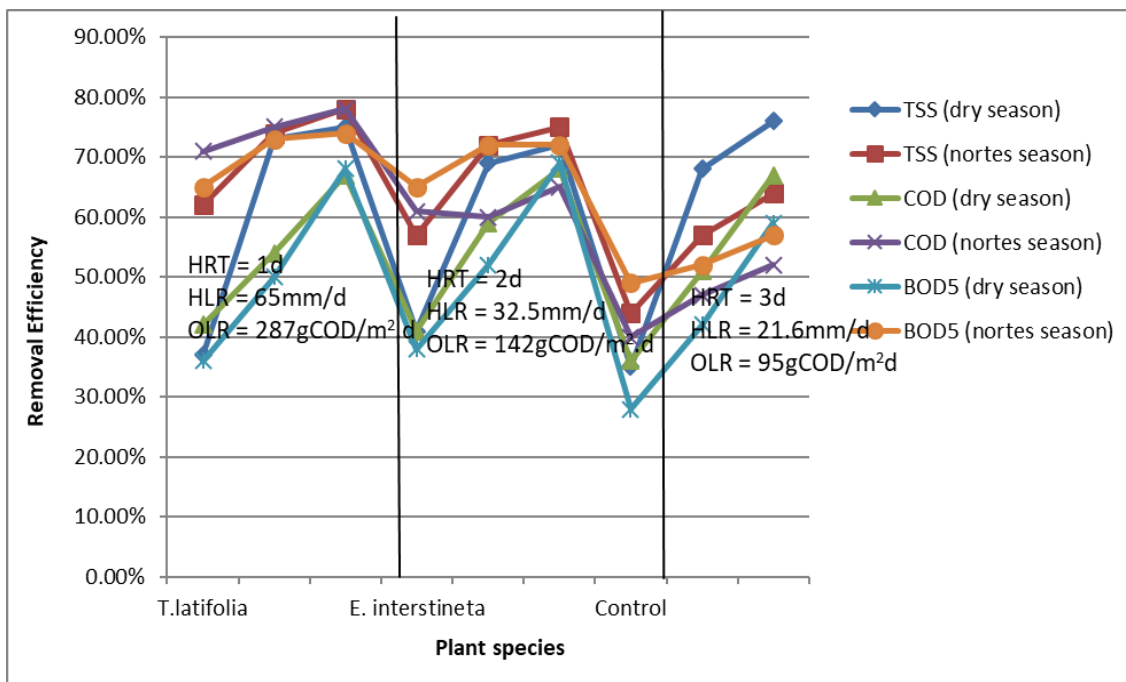


Figure 8. COD, BOD and TSS removal efficiency of HSSFCW at different seasons (Puigagut et al., 2007)

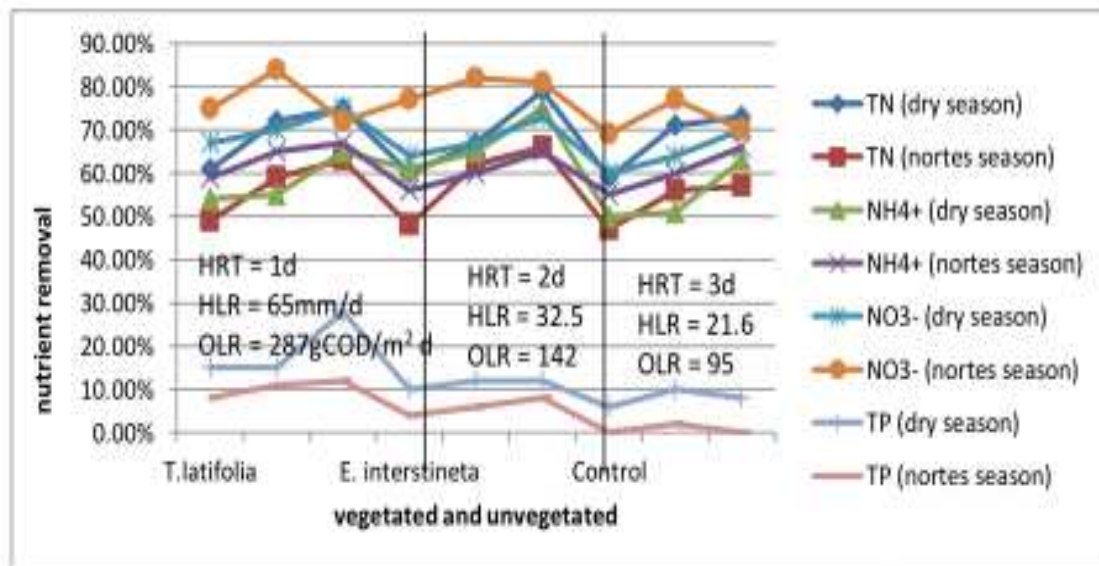


Figure 9. Influence of plant species and HRT on nutrient removal efficiency of HSSFCW (Gonzalez et al., 2009)

Performance efficiency of HSSFCW: a case in Ethiopia

In Ethiopia, environmental degradation within and downstream of cities has multiple consequences for public health, in particular through the use of untreated wastewater in irrigated agriculture. Significant wastewater treatment efforts are done by Addis Ababa Water Supply and Sewerage Authority (AAWSSA), but it remained limited. Due to the combination of poor sanitation and undulating topography, almost all wastewaters generated in the city finds its way through a dense network of streams into Akaki Rivers (Little and Great Akaki rivers). Several factories also discharge their untreated effluents into the rivers. Wastewater collection and treatment are limited and treated wastewater is also discharged into the same river. Discharges from industry, domestic, and agricultures can cause an impact on environmental condition in river and coastal waters. Eutrophication is an accelerated growth of algae on higher forms of plant life caused by the enrichment of water by nutrients, especially compounds of nitrogen and/or phosphorus and inducing an undesirable disturbance to the balance of organisms present in the water and to the quality of the water concerned. Eutrophication of fresh water ecosystem is one of the most prevalent environmental problems responsible for water quality degradation on a world-wide scale. At present hardly any infrastructure is available for the effective treatment of sewage in developing countries.

Municipal sewerage and the extent of domestic and industrial wastewater treatment are inadequate in most urban situations. When there is a municipal sewerage network in place, the coverage is usually incomplete and the treatment level is insufficient. Even when treatment facilities exist, poor maintenance and operation often results in failing treatment processes, causing pollution of the effluent receiving surface waters. The risk of water borne diseases may actually increase in developing countries as a result of the introduction of a conventional sewerage scheme, since it is usually not accompanied by effective end-of-pipe treatment (UNEP/GPA, 2004). Untreated effluent contains high concentrations of salts, total suspended solids, chemical oxygen

demand, nitrogen and phosphorous and toxic compounds, such as heavy metals and chlorinated organic compounds. Industrial effluents can seep into the aquifer and pollute groundwater or where it is discharged without proper treatment can affect the physico-chemical properties of the receiving water and consequently its biota (Kambole, 2003).

All this unregulated discharge of wastewater undermines biological diversity, natural resilience and has a significant impact on macro-invertebrates composition due to the water quality deterioration (Beyene et al., 2009). Addis Ababa City Rivers are highly affected by pollution of heavy metals, pathogens, organic compounds, synthetic chemicals, micro-plastics and nutrients (Aregawi, 2014). Study reports indicated that the city water bodies and surrounding agricultural soils are contaminated with heavy metals such as Hg, As, Pb, Sb, Ni, Sr, and Cd (Elias and Yohannes, 2017), which are extremely toxic even at low concentrations and cause gastrointestinal, skin, nerve damage, lung damage, cancer, nervous, immune system, and kidney damage, brain damage, liver damage, and etc. (Kassa, 2012). Beside these, water, soil and air pollution due to industrial and domestic waste discharges cause peculiar diseases. Study and literature report showed that most people found in Akaki Kality industrial zone are affected by peculiar diseases such as cough (76.5%), diarrhea (58.8%), typhoid (51%), typhus (45.1%), gastrointestinal (39.2%), skin problem (29.4%), asthma (33.3%), and bronchitis (3.9%) (Aregawi, 2014; Elias and Yohannes, 2017). This may be due to long term intake of food that contains high levels of heavy metals and pathogens, and contact with sediments containing heavy metals and pathogens, posing risks to human health (Itanna, 2002; Bekele, 2008) To protect water bodies from pollution, serious waste management implementation should be conducted. The main challenge mentioned by researchers is selecting the appropriate wastewater treatment techniques. Therefore, locally available effective pollution control systems are very important based on the country's economy. For this problem, constructed wetlands can be a good alternative options.

In Ethiopia, Terfie and Asfaw (2004) conducted a research on five pilot scale subsurface flows constructed wetlands; four units vegetated with *Cyprus altenifolius*, *Typha domingensis*, *Phragmites karka* and *Borassus aethiopum* and the fifth left as unvegetated (control). The performance efficiency of each cells in removing organic matter (COD & BOD5), ammonium and total nitrogen including total chromium under the 5-day hydraulic retention time and hydraulic loading of 120 L/day showed promising results. The wastewater analysis indicated that COD reduction by 58-80% for an inlet organic loading rate (OLR) ranged from 2202-8100 mg/L and BOD5 reduction by 66-77% for an inlet OLR ranged from 650-1950 mg/L. The removal of inorganic substances such as nitrates, sulfates, sulfides, total nitrogen and ammonia-nitrogen ranged from 30-57%, 82-92.4%, 53-82%, 46-61% and 64-82.5%, respectively (Table 5). Similarly, Kassa and Mengistou (2014) tested pilot scale HSSFCWs efficiency in treating domestic wastewater in vegetated and unvegetated conditions at HLR and HRT of 7 day and 26 L/day HLR. The results showed that the nutrient removal efficiency of HSSFCW was significantly higher in the planted species than in the unplanted treatment system. The average removal efficiency of orthophosphate in the treatment beds was 84.05% for *C. papyrus*, 65.29% for *P. Karaka* and 50.20% for the unplanted. She proved that the average removal efficiency of planted cells was higher than unplanted due to the macrophytes role to accumulate high biomass and remove nutrients.

Table 5. Pollutant removal efficiency of HSSFCW in Ethiopia

Types of waste water	Media type	Plant type	HLR (L/d)	HRT (day)	Removal efficiency (%)	Standards (EEPA, 2000)	Reference
Domestic	Gravel (40-80 mm) (20-30 mm)	C. papyrus	17.7	2.16	COD = 89.4. BOD = 97.8. TSS = 83.9. TN = 53.9. NH ₄ = 24.8. NO ₃ = 82.4. TP = 16.5. PO ₄ = 22.3		Genet, 2007
		C. alternifolia			COD = 87.3. BOD = 97.7. TSS = 82.3. TN = 54.8. NH ₄ = 24.6. NO ₃ = 78. TP = 12.5. PO ₄ = 16.2		
		P. canariensis			COD = 89.6. BOD = 98.1. TSS = 83.2. TN = 57. NH ₄ = 23. NO ₃ = 81. TP = 18.1. PO ₄ = 23.4		
Tannery	Clay (15 cm and gravel 45 cm)	C. alternifolius	120	5	COD = 64.8. BOD = 67.5. TN = 46. NH ₄ = 64.8	BOD=80% (200) COD = 500 TSS = 50% NH ₄ ⁺ =30% TN = 80% (60%) TP = 8% (10)	Terfie and Asfaw, 2014
		T. domingensis			COD = 56.6. BOD = 66. TN = 46.7. NH ₄ = 53		
		B. aethiopicum			COD = 58 BOD = 66 TN = 58 NH ₄ = 80		
		P. karka			COD = 81. BOD = 64. TN = 61. NH ₄ = 82.5		
		Unplanted			COD = 89.4. BOD = 64. TN = 40.3. NH ₄ = 62.7		
Domestic	Gravel (20-30 mm)	P. karka	26	7	NO ₃ -N = 58.3%. PO ₄ -P = 65.3%		Kassa and Mengistu, 2014
		P. Cyprus			NO ₃ -N = 56.4%. PO ₄ -P = 50.2%		
		Unplanted			NO ₃ -N = 36.1%. PO ₄ -P = 50.2%		
Domestic	Gravel (8-16 mm)	P. australis	18	6	BOD ₅ = 82. TSS = 78.3. TN = 27		Ayano, 2013
		Unplanted	18	6	BOD ₅ = 82. TSS = 78.3. TN = 27		

Jehovah Witnesses Branch Office (JWBO) full scale HSSFCW performance was evaluated by Birhanu (2007) and the result showed average removal efficiency of the constructed wetland system for BOD₅, COD, TSS, ammonium, nitrate, total nitrogen, orthophosphate, total phosphorus, sulfate, sulfide and total coliform was 99.3%, 89%, 85%, 28.1%, 64%, 61.5%, 28%, 22.7%, 77.3%, 99% and 94.5%, respectively. The individual cells removal efficiency indicated that the wetland planted with Cyprus papyrus showed higher removal efficiency for nitrate (82.4%), ammonium (24.8%), total nitrogen (54.8%), orthophosphate (23.5%), and total suspended solids (83.9%) as compared to the other wetland systems. In the same regard, wetland cells planted with Phoenix canariensis showed higher removal efficiency for total phosphorus (17%), sulfide (99%), BOD₅ (98%), COD (90%) and total coliform (94%). Whereas, the other wetland cells planted with Cyprus alternifolia showed higher removal efficiency only for sulfate ion (82.2%). The performance efficiency results indicated that, this wetland system has excellent removal capability for BOD₅, COD, TSS, sulfate, sulfide and total coliform bacteria. However, since the HRT of the constructed wetland system (2.16

days), the nutrient (nitrogen and phosphorus) removal efficiency was low. The organic matter removal efficiency of JWBO CW investigated by Brhanu (2007) was similar to that of the study done in the USA: i.e., BOD₅ (93%) (USEPA, 1993); in Kenya: BOD₅ (98%), COD (96%) and TSS (85%) (Nyakango, 1999); in Northern Alabama: BOD₅ (85%) (Kathleen, 2000); and in Italy: COD (93%) and TSS (81%) (Pucci, 2000). The higher removal of the planted treatment beds may be due to a combined biochemical reaction mechanism favored by plants, substrates and microorganisms. The most important effects of the macrophytes in relation to the wastewater treatment processes are the physical effects of the plant tissues that give rise to filtration effect and provide surface area for attached microorganisms. In addition to this, the media and macrophytes roots in SSF may provide a greater number of small surfaces, pores, and crevices which create the opportunity for the availability of a vast number of organic matter utilizing microorganisms adapted to the aerobic and anaerobic environment of wetland ecosystems which facilitate the organic matter removal process of CW more effectively (USEPA, 1993; Michael, 2006). On the other hand, the effectiveness may be associated with the presence of easily biodegradable organic matters in domestic wastewater by biological decomposition process within a short HRT (Reddy, 1991). According to Ayano' (2013) demonstration on the performance efficiency of horizontal subsurface flow constructed wetland at deferent depth with the same media type (gravel, 8-16 mm), wetland area and different hydraulic loading rate of 18 L/m²/day and 36 L/m²/day for depths 25 cm and 50 cm in planted and unplanted conditions, showed no significant difference in removal of pollutants at the same HLR. The removal of BOD₅ and TSS were not different between planted and unplanted beds. However, areal and volumetric rates for planted beds were significantly greater than the unplanted beds for TKN. Unplanted beds may be more anaerobic than planted beds to favor reducing bacteria. Garcia et al. (2004) reported that the removal of HSSFCW increased with decreasing depth and attributed high oxidation reduction potential which is responsible for increasing nitrification. The result showed that constructed wetlands are successful in removal of nutrients from domestic wastewater.

Heavy metal removal efficiency of HSSFCW

The toxicity nature of most heavy metals

Recently there has been an increase in the river pollution trend in Addis Ababa and other cities, due to the discharge of untreated wastewater from the industries and municipal wastes. Constructed wetlands have a good potential for the removal of heavy metals from wastewater (Sahu, 2014). According to Sahu report, the horizontal subsurface flow constructed wetland reduced the concentration of Hg, Cr, Fe and Ni from the initial concentrations by 43%, 54%, 46% and 49%, respectively. The potential heavy metal remediation of HSSFCW planted with *Phragmites australis* was investigated by Bahre (2013) and achieved high removal efficiency of 99.33%, 93.67%, 89.24%, 96.14% and 98.33%, respectively for Fe, Mn, Pb, Cu and Zn at hydraulic loading rate of 22 L d⁻¹ and hydraulic retention time of 28th days. In the same regard, the unplanted unit showed removal efficiency of 98.43%, 91.66%, 85.01%, 90.70% and 85.19% for Fe, Mn, Pb, Cu and Zn, respectively at the same conditions. The result indicates that uptake on roots for Pb and Cu was higher than the uptakes by plant leaves and stems. The soil media heavy metals accumulation also showed the highest adsorption capacity for the analyzed heavy metals from the planted and control systems.

This demonstrates that horizontal subsurface flow constructed wetland planted with *Phragmites australis* and red ash gravel can remove heavy metals from leachate.

This result is similar to the reported metal removal efficiency of subsurface flow constructed planted with *S. globulosus* and *E. sexangularis* in treating leachates, which were 81.33% and 94.19%, respectively for Cu and Pb; while 86.91% and 95.88% removal in *E. sexangularis*, respectively for Cu and Pb (Mohamed and Baskar, 2018). This finding also agrees with the result of Refidah (2002) who reported the removal efficiency of surface flow constructed planted with *S. sumantresisana* in treating leachate; which was 89%, 90% and 89%, respectively for Fe, Zn and Mn. The analysis of results showed that up to 99.3% of chromium was reduced from tannery wastewater for an inlet average Cr loading rate of 40 mg/L (Amenu, 2015). Similar values were reported by Terfie and Assfaw (2014) of total chromium in HSSFCW beds. The plant parts analysis on the accumulation of chromium showed similar results, more Cr was accumulated in root parts of the plants than in the shoot. This indicates that constructed wetland is a cost effective and environmentally friendly treatment method in removal of not only organic matters, nutrients and pathogens, but also heavy metals, and hence it can be used as an alternative treatment method for developing countries (Table 6).

Table 6. Heavy metal removal efficiency of HSSFCW in Ethiopia

Types of waste water	Media type	Plant type	HLR (L/d)	HRT (day)	Removal efficiency (%)	Standards (EEPA, 2000)	Reference
Leachates	Redish gravel (40-80 mm) (15-25 mm)	<i>P. australis</i>	22	28	Fe = 99.33. Mn = 93.6. Pb = 89.24. Cu = 96.14. Zn = 98.33		Bahre, 2008
		Unplanted			Fe = 99.33. Mn = 93.6. Pb = 89.24. Cu = 96.14. Zn = 98.33		
Tannery	Clay (15 cm and gravel 45 cm)	<i>C. alternifolius</i>	120	5	Cr = 35.84	Pb = 0.5 Ni = 2 Cu = 2 Hg = 0.001 Zn = 5 Cr = 2	Terfie and Asfaw, 2014
		<i>T. domingensis</i>			Cr = 48.68		
		<i>B. aethiopicum</i>			Cr = 26.96		
		<i>P. karka</i>			Cr = 30.26		
		Unplanted			Cr = 59.6 for clay, 38.15 for Gravel		
Syntatic	-	-	48.6	9	Cr = 51. Ni = 47 Fe = 45. Hg = 43		Sahu, 2014

Heavy metals in plant tissues and substrate media

The probable recognized biological processes for metal removal in wetlands are plant uptake and adsorption on the substrate media. The Pb and Cu uptake ability of *P. australis* by its roots may be due to the localized properties of the root, mainly predominated rhizofiltration mechanisms to accumulate heavy metals (Zhu et al., 1999). Similarly, Kadlec and Wallace (2009) reported that plants can accumulate higher concentrations of metals in their roots. This may be due to the slow mobility of metal transport from the root to shoot. In the same case, substrate media is also one of the important factors for the removal of heavy metals. Figures 10 and 11 indicate the role of substrate media for Pb and Cu removal from leachate. However, the retention time and the type of media have an effect on the treatment of wetland (Knox et al., 2004). Since media provides a viable

condition for maximum removal of pollutants, due to its diverse treatment mechanisms including sedimentation, adsorption, precipitation and microbial interaction (USEPA, 1993). In general, the control HSSFCW showed the higher removal efficiency of Pb and Cu than the planted wetland. Similar finding was observed in the removal of chromium from tannery wastewater (Terfie and Assfaw, 2014). This may be due to chemical precipitation and sorption of metals on substrate media.

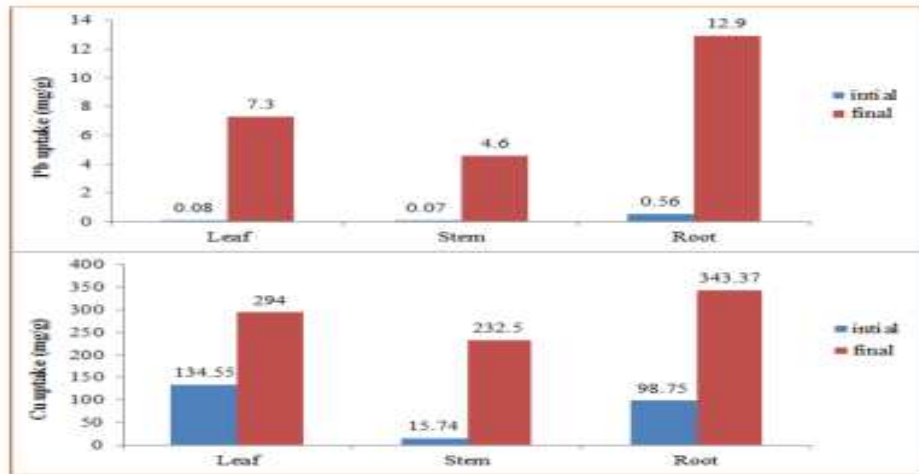


Figure 10. Pb and Cu uptake of different parts of *P. australis* in CW (Knox et al., 2004)

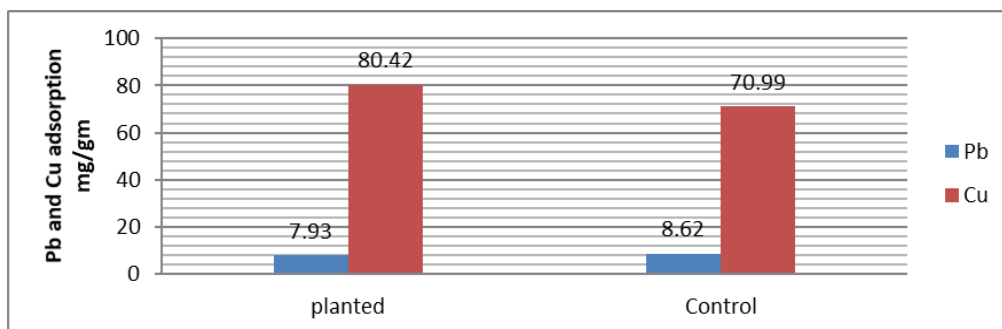


Figure 11. Pb and Cu adsorption in planted and control CW beds (substrate media, red ash gravel) (Knox et al., 2004)

Terfie and Assfaw (2014) investigation data indicates clearly the fate of total chromium in the horizontal subsurface flow constructed wetland (Fig. 12a). Whereas Kassa and Mengistou (2014) investigated data on the fate of total phosphorus is under question mark, where the fate of TP is in a constructed wetland (Fig. 12b).

However, the removal efficiency of heavy metals is dependent on the HRT, flow rate (Q) and pH. Sahu (2014) determined the effect of HRT on the reduction of different heavy metals. The treatment efficiency was observed increased as HRT increases from 1 to 7 days at a flow rate of 8 cm³/min (Fig. 13). As Fig. 13 showed the maximum removal of 54%, 49%, 46% and 43% were obtained respectively for Cr, Ni, Fe and Hg at 7 days HRT. The effect of HRT on the removal of heavy metals was also determined by Bahre (2013) and presented in Figure 14.

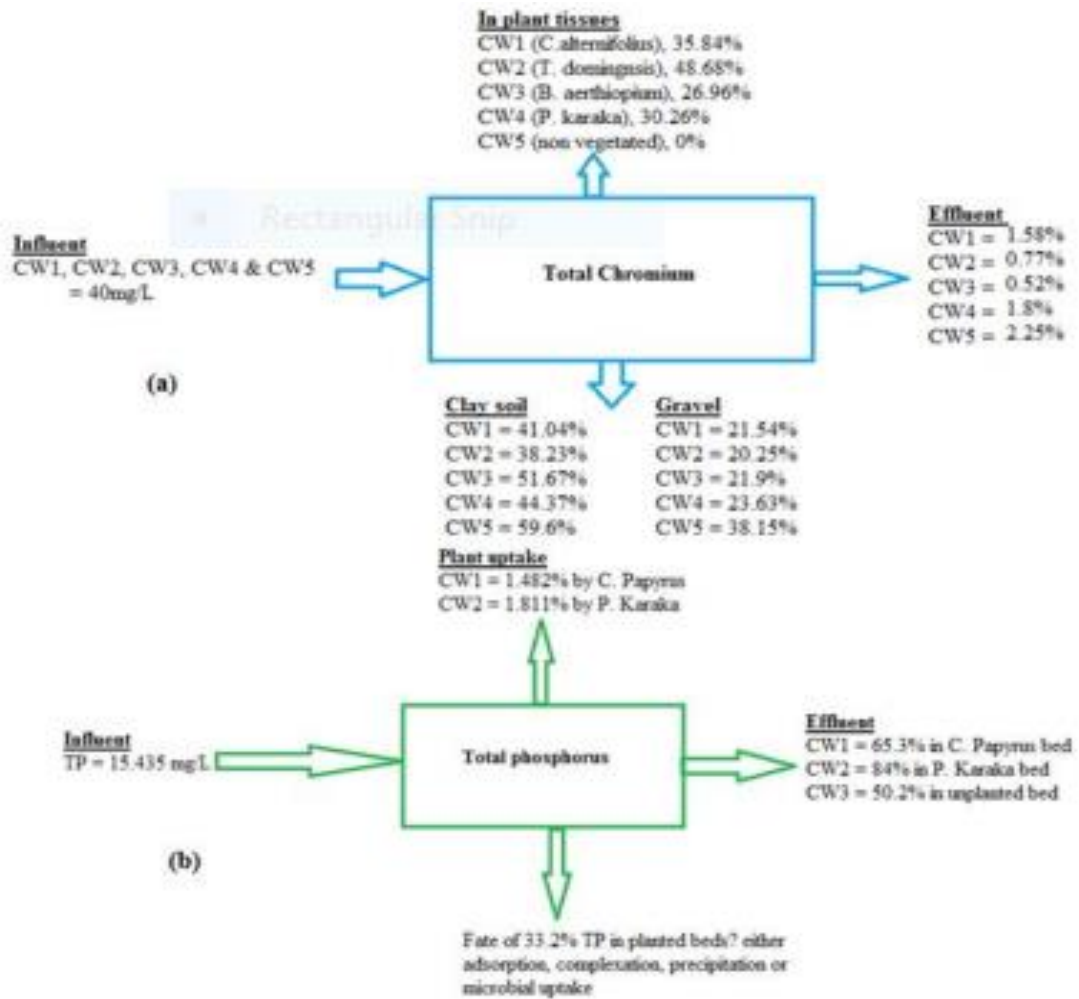


Figure 12. a Mass balance of chromium. b Mass balance of TP in HSSFCWs (Kassa and Mengistou, 2014)

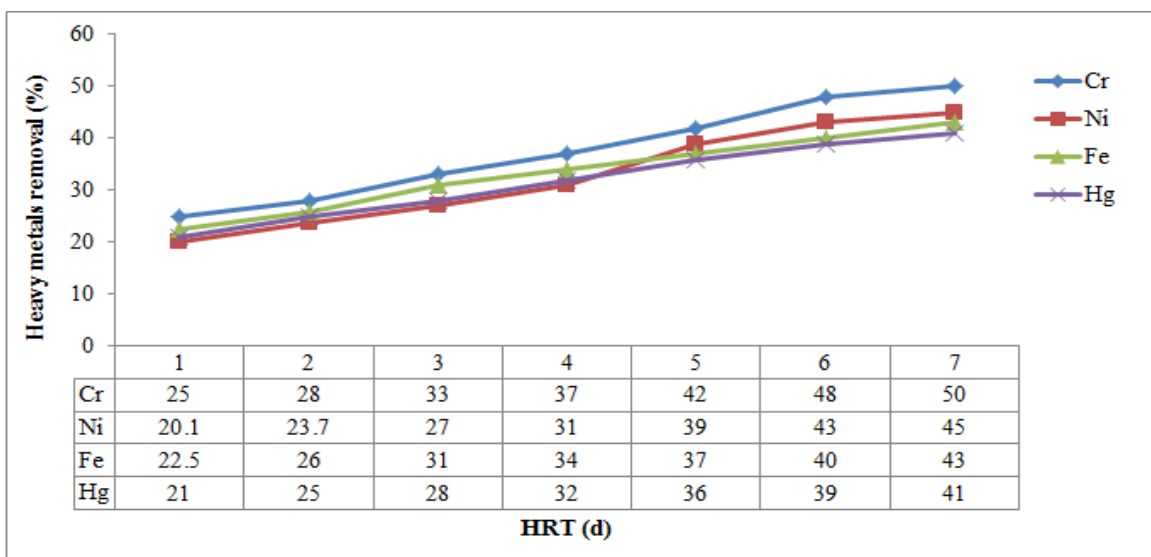


Figure 13. Effect of HRT on heavy metals removal from HSSFCW (Bahre, 2013)

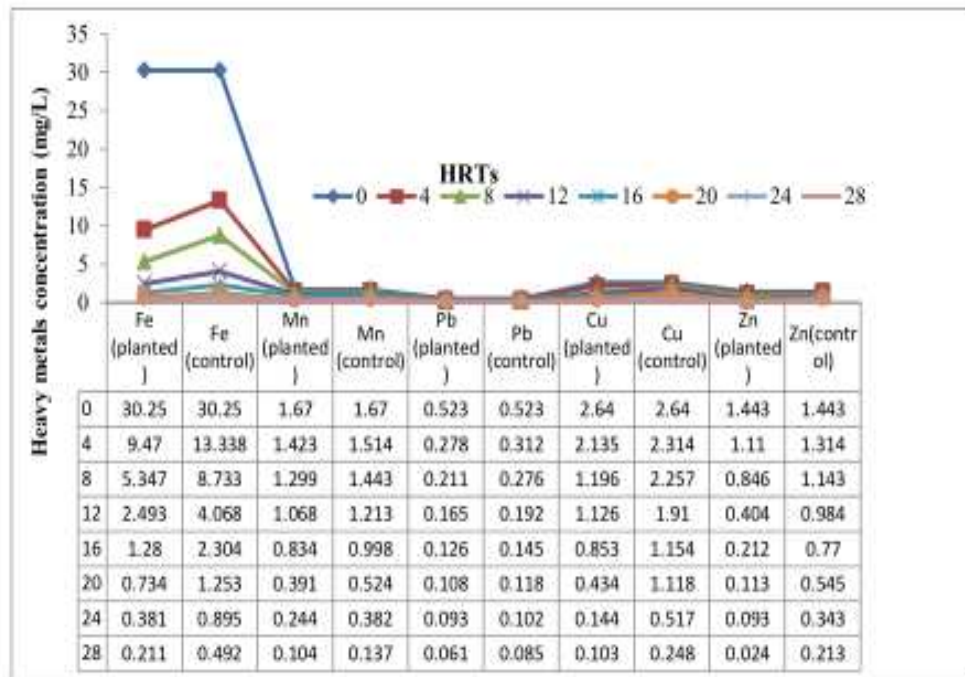


Figure 14. Effect of vegetation and HRT on the removal efficiency of heavy metals (Bahre, 2013)

Factors affecting the performance efficiency of constructed wetlands

Vegetation and HRT

The TSS removal efficiency of planted and unplanted constructed wetland at different HRT was significantly different. The initial TSS concentration was 106 mg/L. Some while after treatment under CW were reduced to 35.4 and 19.7 mg/L at 2 and 4 days HRT with a removal efficiency of 66.7% and 81.5%, respectively in the vegetated one. Whereas, for the unplanted CW, TSS were reduced to 62.3 and 49.8 mg/L for 2 and 4 days HRT with total removal efficiency of 41.5% and 53.2%, respectively. The planted CW had higher results in TSS removal than the unplanted one (Fig. 15). Increase of HRT resulted in better TSS removal efficiency even for the non-vegetated CW. The efficiency of BOD₅ removal was 52% and 73.4% at HRT of 2 and 4 days in the planted beds. Constructed wetland without plantation removed only 20-35% BOD₅ from the influent.

Constructed wetland planted with *Canna indica* L. gave higher BOD₅ removal efficiency than non-vegetated CW. The BOD₅ removal also increased at higher HRT (i.e., almost half BOD₅ removed at 4 days HRT) than shorter HRT (i.e. 2 days HRT). TKN removal in the vegetated CW also gave the maximum removal efficiency compared to the non-vegetated CW. This removal efficiency of TKN may be associated with addition of plant activity. CW planted with *Canna indica* L. removed TKN for 45.3% for 2 days HRT and 69.6% for 4 days HRT. TKN removal efficiency had increased at increasing HRT (Panrare et al., 2015). This TKN removal of the CW technique may be due to volatilization, plant uptake and bacterial assimilation (Vymazal, 2007). The vegetated CW at 4HRT also gave the highest phosphate removal efficiency (77.7%). This phosphate removal in CW could be normally by plant and bacterial uptake, adsorption at the media and sedimentation. The effect of vegetation and HRT on the performance efficiency of constructed wetland is indicated in Figure 15.

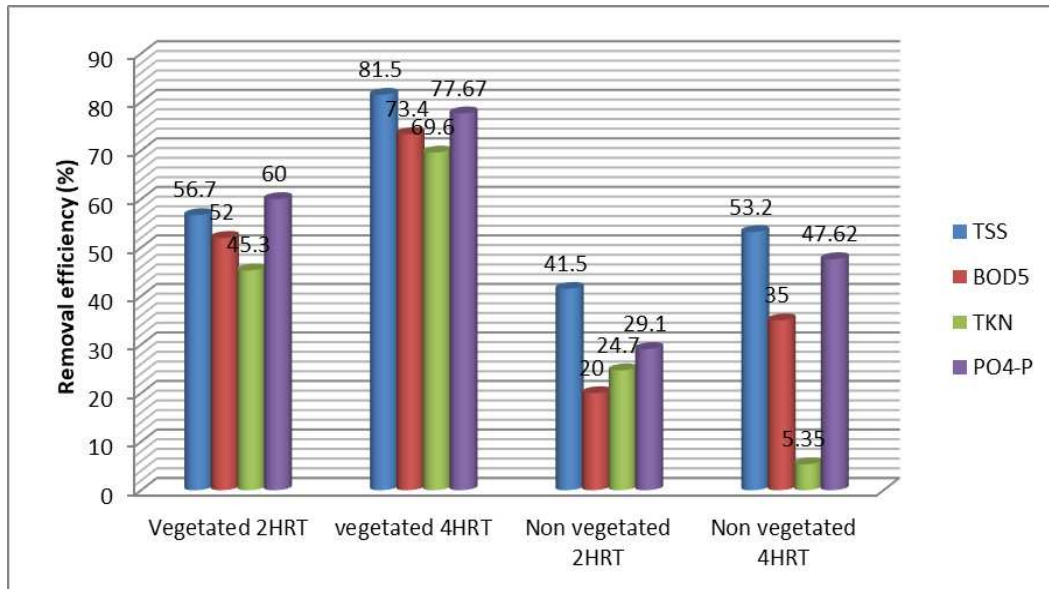


Figure 15. Effect of vegetation and HRT on pollutant removal efficiency of CW

Plant species

Plants used in constructed wetlands play a major role in absorbing nutrients from wastewater. Some of the most important plant species with nutrient absorbing ability is summarized in *Table 7*.

Table 7. Nutrient absorption capacity of macrophytes (Brix, 1994)

Media type		<i>Cyperus alternifolus</i>	<i>Typha latifolia</i>	<i>Eichornia crassipes</i>	<i>Pistia stratoites</i>	<i>Potamogeton pectinatus</i>	<i>Certophyllum demersum</i>
Absorption capacity kg/ha/h	N	1100	1000	2400	900	500	100
	P	50	180	350	40	40	10

Media type

The level of permeability and hydraulic conductivity of the media is very influential on the retention time of wastewater, in which the retention time is enough to give a chance to contact between microorganisms in wastewater and oxygen released by plant roots. The main function of the media in the constructed wetland is to provide places for plants to grow, microbial attachment for pollutant transformation process, and nutrient absorption (Dadan, 2016). The performance of subsurface flow constructed wetland based treatment can be shown in *Table 8*.

Microorganisms

Preferably heterotrophic aerobic microorganisms are present due to faster processing ability than anaerobic types. The oxygen content in the media will be supplied by plant roots, which is a byproduct of the process of photosynthesis of plants with the help of sunlight (Dadan et al., 2016).

Temperature

The temperature of wastewater affects the activity of microorganisms and plants, furthermore it will affect the performance of processing (Dadan et al., 2016).

Table 8. Performance of SSFCW media (Khatuddin, 2003)

Media type		Gravel	Soil	Sand	Clay
Percentage of removal efficiency (%)	BOD	55-96	62_85	96	92
	SS	51_98	49_85	94	91
	Coloforms	99	-	100	

Constructed wetland as climate change mitigation

Constructed wetlands are increasingly widespread for wastewater treatment in small communities and households where in addition to the fundamental purifying function, they also have decorative function that imposes the choice of plants characterized by high functional, amenity, and aesthetic values (Ghermandi et al., 2010). Constructed wetlands carbon cycles contribute to the global greenhouse gases (GHGs) balance through their CO₂ and CH₄ emissions. In particular, they can act as CO₂ sinks by photosynthetic CO₂ assimilation from the atmosphere or as a source of CO₂ through bed respiration (Barbera et al., 2009) and organic matter decomposition (Brix et al., 2001). The rate of carbon decomposition in constructed wetlands depends on the redox chemistry of the soil, the bioavailability of organic carbon and temperature. For example, in summer season, oxygen diffusion to the topsoil can reduce methanogenesis and stimulate methane oxidation (Grünfeld and Brix, 1999). However, an increase in temperature can decrease dissolved oxygen in deeper subsoil and enhance methane production. All biochemical reactions increase as temperature increases C and N turnover in constructed wetlands causing high variations in GHG emissions in different regions. Due to this more data and investigation are needed on constructed wetland types for better extrapolation of GHG emissions. Hence, organizing more information on nutrient removal efficiency and GHG emissions across CW in different CW types is necessary for better management. Emissions of GHG in CWs can vary across CW types, e.g., surface flow or subsurface flow (Tables 9 and 10).

Generally, methane emissions are higher in surface flow CWs (SFCWs) than subsurface flow constructed wetlands (Table 9), but may vary with season. Nitrous oxide and carbon dioxide emissions are higher in VSSFCWs than in HSSFCWs and SFCWs. Aquatic plants play an important role in GHG production and transport to the atmosphere by releasing GHG through their interconnected internal gas lacunas. Emergent plants can transport atmospheric oxygen to the rooting zone and contribute to increase the N₂O and CO₂ production and methane consumption (Brix, 1989). Release of low molecular weight organic matter that is labile in nature is more likely to produce GHGs than stable forms. A fluctuating water table in CWs has significant impacts on GHG dynamics (Mander, 2011). In aerobic and anaerobic conditions, incomplete nitrification and denitrification increase N₂O emissions (Healy et al., 2007). In general, assessment of GHG emissions in various types of CWs which are vegetated or unvegetated is necessary in the light of the national and global GHG budgets.

Table 9. Nitrous oxide emission from various CW types ($m g m^{-2} d^{-1}$)

CW type	Type of WW	N ₂ O emission ($m g m^{-2} d^{-1}$)	Reference
Surface flow	Municipal	2	Johansson, 2003
SF	Dairy	16.8	Van der Zaag, 2010
SF	Municipal	0.01	Søvik, 2006
SF	Agri runoff	0.4	Søvik, 2006
SF	Municipal	4	Søvik, 2006
All SF		4.642	
Horizontal sub surface flow	Domestic	8.6	Mander, 2005
HSSF	Municipal	7.1	Søvik, 2006
HSSF	Domestic	0.17	Liu et al., 2009
HSSF	Dairy	9.5	Van der Zaag, 2010)
HSSF	Domestic	0.17	Mander, 2011
All HSSF		5.108	
Vertical sub surface flow	Domestic	4.6	Mander, 2008
VSSF	Domestic	11	Mander, 2005
VSSF	Domestic	1.44	Mander, 2011
VSSF	Domestic	0.005	Gui et al., 2007
VSSF	Municipal	15	Søvik, 2006
All VSSF		6.409	

Table 10. Carbon dioxide and methane emission from various CW types ($m g m^{-2} d^{-1}$)

CW type	Type of WW	CO ₂ emission	CH ₄ emission	Reference
SF	Dairy	4250	223	Van der Zaag, 2010
SF	Municipal	1200	29	Søvik, 2006
SF	Agri runoff	3200	350	Søvik, 2006
SF	Municipal	1400	72	Søvik, 2006
ALL SF		2512.5	168.5	
HSSF	Domestic	5.33	0.001	Garcia, 2005
HSSF	Dairy	3475	118	Van der Zaag, 2010
HSSF	Domestic	600	0.48	Mander, 2011
HSSF	Municipal	3800	340	Søvik, 2006
ALL HSSF		1970.1	114.6	
VSSF	Municipal	2662	33.5	Mander, 2008
VSSF	Domestic	1080	3.36	Mander, 2011
VSSF	Municipal	8400	110	Søvik, 2006
VSSF	Municipal	22000	140	Søvik, 2006
ALL VSSF		8535.5	71.72	

Even if constructed wetlands are contributors of GHG, on the other hand, constructed wetlands present an important opportunity for carbon sequestration and greenhouse gas offsets by virtue of their potential for restoration using known and innovative land management methods. Because constructed wetlands are inherently highly productive and accumulate large below-ground stocks of organic carbon. Wetlands are major carbon sinks. While vegetation traps atmospheric carbon dioxide in wetlands and other ecosystems alike, the net-sink of wetlands is attributed to low decomposition rates in anaerobic zones. Recently, constructed wetlands used for wastewater treatment and

protecting wetland bodies clearly represent an immediate and large opportunity for enhancing carbon sequestration (Kanungo et al., 2017). The percentage of organic carbon (OC%) content of the 15 emergent macrophytes varied between 34.97 to 50.92, 34.98 to 52.04, 34.96 to 52.01 and 34.91 to 50.94. similarly, biomass (g/m^2) ranged from 104 to 687, 16 to 1382, 141 to 1493 and 122 to 635. The carbon sequestration potential (CSP) was determined by multiplying the OC in per gram of dry weight to the biomass of that species (Wang et al., 2011) and the total CSP of all the emergent macrophytes was obtained by the summation of individual CSP of all species. Based on this calculation, the highest CSP was recorded for *Typha latifolia* followed by *Phragmites australis* and the lowest for *Carex* sp. (Fig. 16) which exhibited from the highest carbon content of 53.62% which was greater than the 44% value reported by Wang et al. (2011) for *Typha orientalis*.

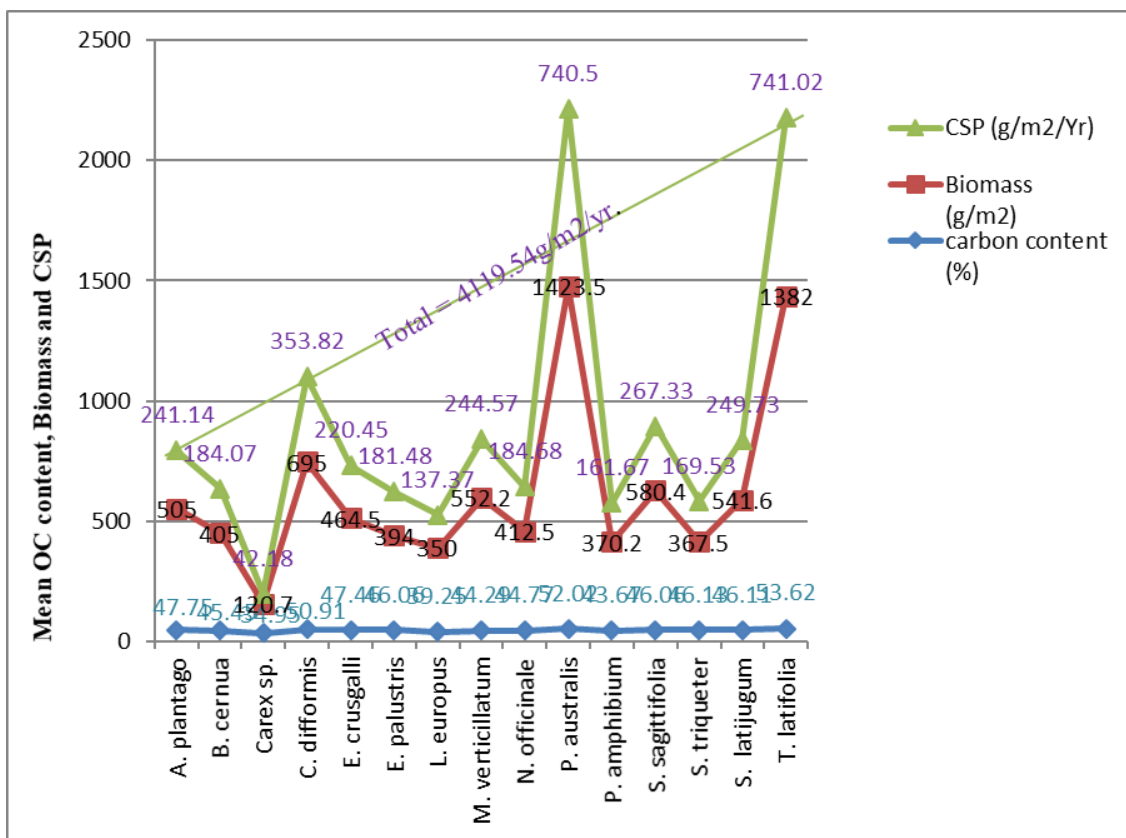


Figure 16. Mean carbon content, biomass and carbon sequestration of macrophytes (Mitsch et al., 2015)

Wang also reported 44.7%, 44.1% and 41.8% of carbon for *Phragmites communis*, *Cyperus malaccensis*, and *Eleocharis dulcis*, respectively which is lower than the values of *Phragmites australis*, *Cyperus difformis*, and *Eleocharis palustris*, respectively obtained by Khan and Maqubool (2014). These macrophytes species carbon content and hence their CSP was higher when compared with other reported results for *Scirpus lacustris* (44.12%), *Eleocharis palustris* (43%) (Fernández-Aláez et al., 1999); *Phragmites australis* (29.2%) and *Myriophyllum salicifolium* (15.8%) (Piola et al., 2008). Furthermore, Costa and Henry (2010) observed the highest carbon content for E.

azurea (43.7%), *Myriophyllum aquaticum* (43%), *Cyperus esculentus* (41.6%) and *Polygonumspectabile* (38%). Assuming 4119.54 gC/m²/yr as the rate of carbon sequestered in each year in this system, the limit for carbon emissions can be calculated to determine the point at which the system offsets carbon emission. To compare the physical sequestration and the gaseous emissions both are converted to carbon dioxide equivalents (CO₂e) (Forster et al., 2007). The CO₂e allows the comparison of different masses and gases as they relate to their greenhouse warming potential. Methane has 25 times the potential as CO₂. Each gram of carbon is equivalent to 3.67 g of CO₂. The CO₂ equivalent of 4119.54 gC/m²/yr. is 15118.7118 g CO₂. The methane equivalent to this amount of carbon sequestration is 604.748472 g/m²/yr. Constructed wetlands showing methane emission values less than 1,600 kg/ha/yr are considered as potential for carbon sequestration (Kayranli et al., 2010). Based on this argue, the above treatment plant has a carbon sequestration potential.

Constructed wetlands are purposely constructed in order to reduce input of nutrients and organic pollutants to water bodies. When these systems are used for wastewater treatment, microbial processes and gas dynamics are likely to be altered. With increased inputs of nutrients and organic pollutants, there is an increase in greenhouse gases production due to decomposition processes. Constructed wetlands therefore, can be sources of important greenhouse gases. The average CH₄, N₂O and CO₂ fluxes for surface flow constructed wetland were 2.9, 1.05, and 15.2 mg/m²/h, respectively. Whereas the average higher fluxes were found from free water surface constructed wetland with average CH₄, N₂O and CO₂ fluxes at 5.9, 1.8, and 29.6 mg/m²/h, respectively, corresponding to the average global warming potential (GWP) of 392 mg CO₂ equivalents/m²/h and 698 mg CO₂ equivalents/m²/h, respectively for SSFCW and FWSCW (Fig. 17) (Chuersuwan et al., 2014).

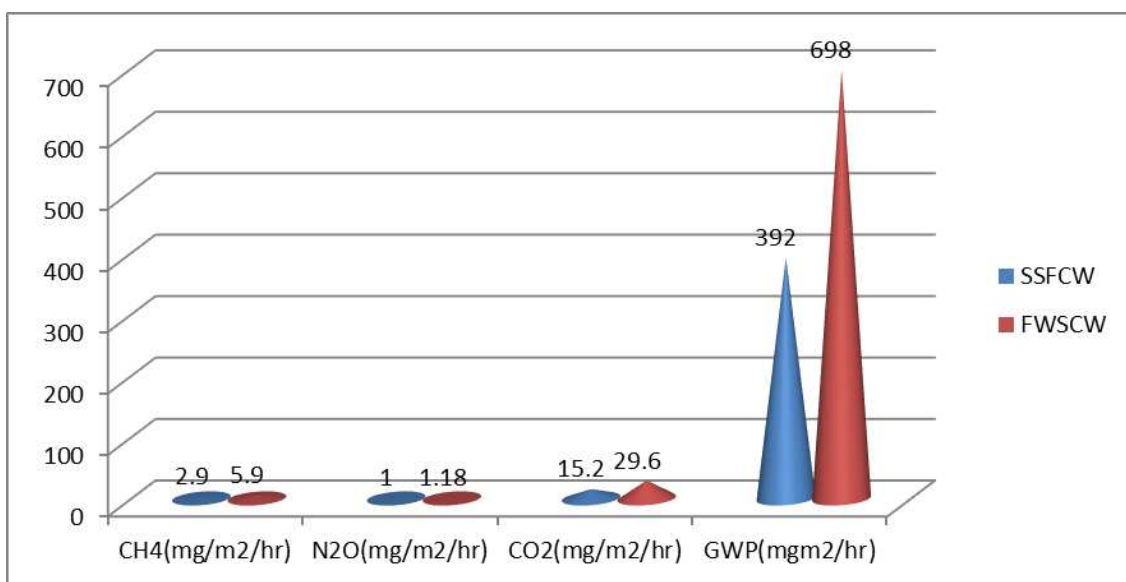


Figure 17. Comparison of greenhouse gas emissions and GWP of free water and subsurface flow CWs (Chuersuwan et al., 2014)

In another study by Maucieri et al. (2014), the comparison of vegetated and unvegetated horizontal subsurface flow constructed wetland effect on the CO₂ (eq)

balance showed a significant difference. The average CO₂ emission of the whole monitored period were 15.5, 15.1, and 3.6 g m⁻² d⁻¹ for *Arundox donax* L. *Phragmites australis* and unvegetated beds, respectively. Whereas, cumulative estimated CH₄ emissions during the study period were 159.5, 134.1 and 114.5 g m⁻² d⁻¹ for *A. donax*, *P. australis* and unvegetated beds, respectively. CO₂ (eq) balance showed that the two vegetated beds act as CO₂ (eq) sinks, while the unvegetated bed act as CO₂ (eq) source. Considering only the above-ground plant biomass in the CO₂ (eq) budgets, *P. australis* and *A. donax* determined uptakes of 1.3 and 8.35 kg CO₂ m⁻² d⁻¹, respectively, and generally the plant biomass carbon content and the bed biomass yield in the vegetated cell fixed 11.61 and 27.03 kgCO₂ (eq) m⁻² d⁻¹, respectively for *P. australis* and *A. donax*, showing a positive balance, while the unvegetated bed had a negative balance (Fig. 18). Carbon dioxide and methane emissions and carbon budgets in a horizontal subsurface flow pilot constructed wetland with vegetated with *C. papyrus* and *Chrysopogon zizanioides* Roberty and *Mischantus giganteus*, showed higher biomass accumulation in *M. giganteus* (7.4 kg m⁻²) followed by *C. zizanioides* (5.3 kg m⁻²) and *C. papyrus* (1.8 kg m⁻²).

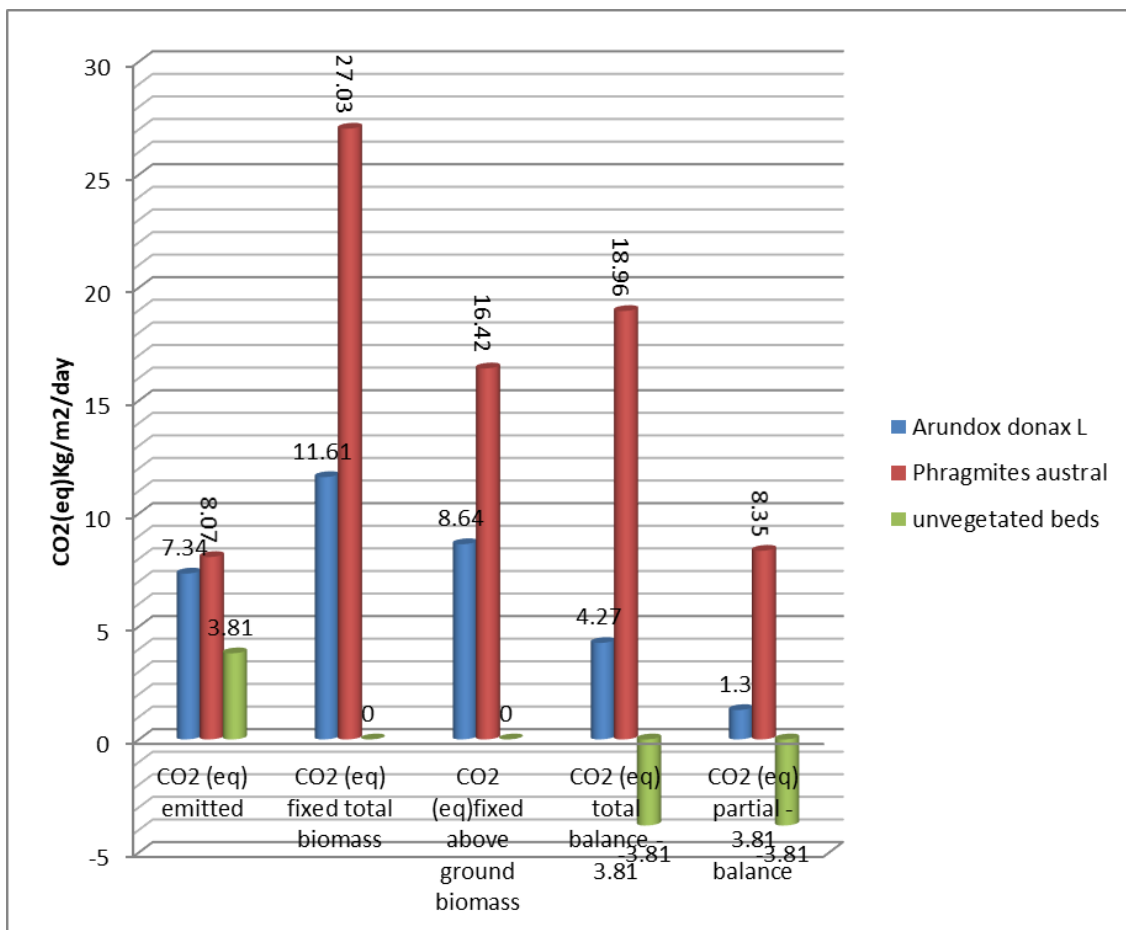


Figure 18. HSSFCW beds carbon dioxide equivalent balance (Maucieri et al., 2014)

The cumulative CO₂ emissions by *C. papyrus* and *C. zizanioides* during the 1-year monitoring period showed similar trends with final volumes of about 775 and 1074 g m⁻², respectively, whereas *M. giganteus* emitted 3,395 g m⁻². Cumulative methane emission

showed the greatest methane emission for *C. zizanioids* bed with 240.3 g m^{-2} followed by *C. papyrus* (12 g m^{-2}) and *M. giganteus*. The organic carbon abatement determined the carbon flux in the atmosphere. Gas fluxes were influenced both by plant species and monitored months with average carbon emitted to carbon removed ratio for *C. zizanioids*, *C. papyrus* and *M. giganteus* of 0.3, 0.5 and 0.9, respectively. The growing season carbon balances were positive for all vegetated beds with the highest carbon sequestered in the bed with *M. giganteus* (4.26 kg m^{-2}) followed by *C. zizanioids* (3.78 kg m^{-2}) and *C. papyrus* (1.89 kg m^{-2}) in *Figure 19*.

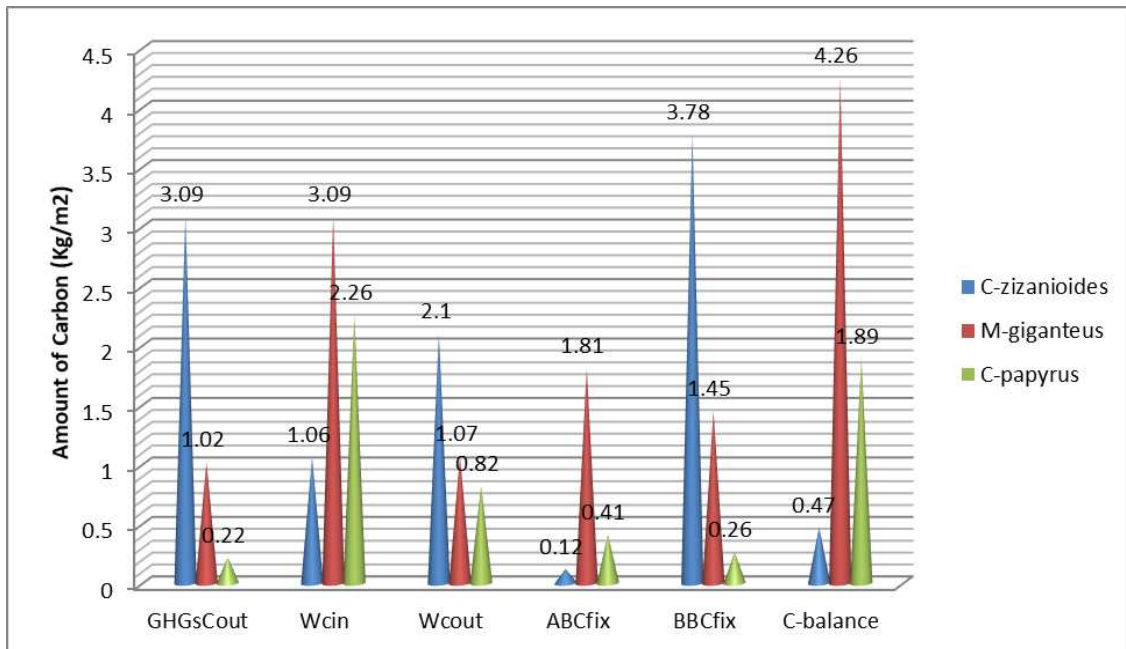


Figure 19. Carbon balance in HSSFCW

Conclusion

The reviewed results showed that the HSSFCWs perform good removal efficiencies for organic matter and SS under low C:N:P loading conditions. Nowadays, the strategies of treating domestic and municipal wastewaters by decentralized way become common in rural and urban areas using constructed wetland technologies. Besides this, constructed wetlands are accepted as a reliable wastewater technology as post treatment of effluents. Because they are low cost, easily operated and maintained and have a strong prospective for application in developing countries.

Most research investigation results revealed that use of a subsurface horizontal flow phytoremediation treatment system is a promising natural technology in the treatment of municipal or industrial wastewater. Because, CW treatment system was found to comply with WHO (1989) standards for treated effluent reuse. Globally, the following abatement efficiencies were achieved by HSSFCW treatment system: 98%, 96%, 85%, 90%, 92%, 88% for BOD₅, COD, TSS, TN, NH₄-N, PO₄³⁻, respectively in Kenya; 98.46% and 98.55% for COD and BOD₅ in Indonesia; and ranges from 94-99.9%, 91.7-97.9% and 99.99% for BOD₅, COD and TFC, respectively in Costa Rica. Whereas in Ethiopia, the HSSFCW achieved the following abatement efficiencies: COD ranges from 58 to 80%, BOD ranges from 66 to 77%, TKN ranges from 46 to 61%, sulfates ranges from 53 to

82%, and $\text{NH}_4\text{-N}$ ranges from 64 to 82.5% for tannery wastewater treatment. For domestic wastewater treatment; 99.3%, 89%, 855, 84.05%, 77.3%, 99% and 94.5% were determined for BOD₅, COD, TSS, TN, $\text{PO}_4^{3-}\text{-TP}$, Sulfate, and TFC, respectively.

The pollutant removal efficiencies and greenhouse gas emissions from the CWs increased with the rise in temperature. The HSSF CWs had the highest tendency to emit CH_4 and thus global warming potential of CWs, and the combined CWs by way of contrast showed low global warming potential. Due to the climate demonstrative of CW and periodic changes, further study to observe the seasonal fluctuations of CH_4 and N_2O emission is necessary. CWs have been found to be potential sinks of Carbon in terms of organic carbon. We face several significant questions regarding the potential for carbon sequestration in wetlands. Constructed wetlands can be managed as net carbon sinks over time. From the Reviewed results point of view, the net carbon gain and the biomass was comparatively higher, carbon storage in biomass and reduced CO_2 emissions. For example, the City of Arcata sequesters carbon in all three treatment units at a rate equivalent of 80,000 kg CO_2/yr . Most research investigation results revealed that horizontal subsurface flow constructed wetlands have been successfully employed to abate key contaminants from wastewater and able to meet the required standard discharge limits.

However, constructed wetland performance efficiency sustainability is affected by the operational conditions of HSSFCW including plant species, media/substrate types, water depth, hydraulic loading, and hydraulic retention time and feeding mode. Though the Total Carbon value at the CW is particularly beneficial for the growth of emergent macrophyte. CWs can be used to treat the wastewater from an industry or community development and also provide an additional benefit as green belts around the industries or the community development. By adopting these Biological CW treatment systems, we can not only achieve our plan of carbon emission reduction but also generate huge amount of savings and earn carbon credits too to ensure a Clean Development Mechanism.

Recommendations

In this paper, encouraging reviewed results were obtained on the role of HSSF CWs on the performance of climate mitigation and wastewater treatment. Based on this review, recommendations for the educational community and user of the technology are suggested. In order to obtain refined results for further long-term research on the performance of the wetlands with respect to all parameters using advanced sized wetland is essential. Besides, further analysis of carbon sequestration potential for climate mitigation and nitrification potential using the HSSF constructed wetlands is recommended for better results. For the user of the technology it can be chosen for application and their construction cost is evidently cheaper. However, evapotranspiration was peak and overstated during dry seasons in planted beds. Furthermore; it is worthwhile to use HSSFCW as one part of the treatment system to reduce GHG emission effect and infection before applying wastewater to recycle in irrigation.

REFERENCES

- [1] Abdelhakeem, S. G., Abouloos, S. A., Kamel, M. M. (2016): Performance of a vertical subsurface flow constructed wetland under different operational conditions. – *Journal of Advanced Research* 7: 803-814.

- [2] Akrotos, C. S., Tsihrintzis, V. A. (2007): effect of temperature, HRT, vegetation and porous media on removal efficiency of pilot-scale horizontal subsurface flow constructed wetlands. – *Ecological Engineering* 29: 173-191.
- [3] Andreo-Martínez, P., García-Martínez, N., Almela, L. (2016): Domestic wastewater depuration using a horizontal subsurface flow constructed wetland and theoretical surface optimization: a case study under dry Mediterranean climate. – *Water Science* 8: 434.
- [4] Amenu, D. (2015): Evaluation of selected wetland plants for the removal efficiency of pollutants from waste water. – *International Journal of Advanced Multidisciplinary Research - IJAMR* 2(7): 63-66.
- [5] Aregawi, T. (2014): Peculiar health problems due to industrial wastes In Addis Ababa City the case of Akaki Kality Industrial Zone. – M.Sc. Thesis, Addis Ababa University.
- [6] Ayano, K. K. (2013): Effect of depth and plants on pollutant removal in Horizontal Subsurface flow constructed wetlands and their application in Ethiopia. – PhD Published Dissertation, Technische Universität Berlin. DOI: 10.14279/depositonce-3931.
- [7] Bahri, A., Drechsel, P., Brissaud, F. (2008): Water reuse in Africa: challenges and opportunities. – CGIAR: A Repository of Agricultural Research Outputs, pp. 1-16. <https://hdl.handle.net/10568/38135>.
- [8] Bahre, A. M. (2013): Horizontal subsurface constructed wetland for removal of heavy metals from leachate using *Phragmites australis* (a case of Addis Ababa solid waste open dump). – Published MSc. Thesis, Addis Ababa University.
- [9] Baldizon, M., Dolmus, R., Quintana, J., et al. (2002): Comparison of conventional and macrophyte-based systems for the treatment of domestic wastewater. – *Water Science and Technology* 45: 111-116.
- [10] Ballesteros, J. F., Vuong, T. H., Secondes, M. F., Tuan, P. D. (2016): Removal efficiencies of constructed wetland and efficacy of plant on treating benzene. – *Sustainable Environment Research* 26(2): 93-96.
- [11] Barbera, A. C., Cirelli, G. L., Cavallaro, V., Di Silvestro, I., Pacifici, P., Castiglione, V., Toscano, A., Milani, M. (2009): Growth and biomass production of different plant species in two different constructed wetland systems in Sicily. – *Desalination* 246(1-3): 129-136.
- [12] Bayrau, A., Boelee, E., Drechsel, P., Dabbert, S. (2008): Health impact of wastewater use in crop production in peri-urban areas of Addis Ababa: implication for policy. – Paper submitted to *Environmental and Development Economics*.
- [13] Bekele, M. (2008): Determination of heavy metals concentration in the sediment cores, water hyacinths and water of Aba Samuel Lake. – M.Sc. thesis, Addis Ababa University.
- [14] Belmont, M. A., Cantellano, E., Thompson, S., Williamson, M., Sanchez, A., Metcalfe, C. D. (2004): Treatment of domestic wastewater in a pilot-scale natural treatment system in Central Mexico. – *Ecol. Eng.* 23(4-5): 299-311.
- [15] Belmont, M. A., Zurita, F., De Anda, J. (2009): Treatment of domestic wastewater and production of commercial flowers in vertical and horizontal subsurface-flow constructed wetlands. – *Ecological Engineering* 35(5): 861-869.
- [16] Beyene, A., Addis, T., Kifle, D. et al. (2009): Comparative study of diatoms and macroinvertebrates as indicators of severe water pollution: case study of the Kebena and Akaki Rivers in Addis Ababa, Ethiopia. – *Ecological Indicators* 9: 381-392.
- [17] Birhanu, G., Seyoum, L. (2007): Constructed wetland system for domestic wastewater treatment: a case study in Addis Ababa, Ethiopia. – <https://www.amazon.com/Constructed-Wetland-Domestic-Wastewater-Treatment/dp/3846504394>.
- [18] Brix, H., Schierup, H. H. (1989): The use of aquatic macrophytes in water-pollution control. – *Ambio. Stockholm* 18: 100-107.
- [19] Brix, H., Arias, C. A., Del Bubba, M. (2001): Media selection for sustainable phosphorus removal in subsurface flow constructed wetlands. – *Water Science and Technology* 44(11-12): 47-54.

- [20] Burke, C. M. (2011): An assessment of carbon, nitrogen and phosphorus storage and the carbon sequestration potential in Arcata's constructed wetland for wastewater treatment. – Published MSc Thesis, Humboldt State University.
- [21] Bwire, K., Njau, K., Minja, R. (2011): Use of vetiver grass constructed wetland for treatment of leachate. – *Water Science and Technology* 63: 924-930.
- [22] Chazarenc, F., Gagnon, V., Comeau, Y., Brisson, J. (2009): Effect of plant and artificial aeration on solids accumulation and biological activities in constructed wetlands. – *Eco. Eng* 35(6): 1005-1010.
- [23] Chen, Z., Wu, S., Braeckevelt, M., Paschke, H., Kästner, M., Köser, H., Kusch, P. (2012): Effect of vegetation in pilot-scale horizontal subsurface flow constructed wetlands treating sulphate rich groundwater contaminated with a low and high chlorinated hydrocarbon. – *Chemosphere* 89(6): 724-731.
- [24] Chuersuwan, S., Suwanwaree, P., Chuersuwan, N. (2014): Estimating greenhouse gas fluxes from constructed wetlands used for water quality improvement. – *Songklanakarın Journal of Science & Technology* 36(3): 46-55.
- [25] Costa, R. L. M., Raoul Henry, R. (2010): Phosphorus, nitrogen, and carbon contents of macrophytes in lakes lateral to a tropical river, Paranapanema River Paulo. – *Brazil Journal of Acta Limnologica Brasiliensia* 22(2): 122-132.
- [26] Cooper, F. P., Boon, G. A. (1987): The Use of Phragmites for Wastewater Treatment by Root Zone Method: The UK Approach. – In: Reddy, R. K., Smith, H. W. (eds.) *Aquatic Plants for Wastewater Treatment and Resource Recovery*. Mangnolia Publishing, Orlando, pp. 153-174.
- [27] Haberl, R. (1999): Constructed wetlands: a chance to solve wastewater problems in developing countries. – *Water Science and Technology* 40(3): 11-17.
- [28] Dadan, S. W., Taufiq, H., Dadan, S., Bento, K. T. B., Denny, K. (2016): A review on sub-surface flow constructed wetlands in tropical and sub-tropical countries. – *Open Science Journal*. <https://osjournal.org/ojs/index.php/OSJ/article/download/415/24>.
- [29] Denny, P. (1997): Implementation of constructed wetlands in developing countries. – *Water Science and Technology* 35(5): 27-34.
- [30] Donald, A. H. (1989): *Constructed Wetlands for Wastewater Treatment: Municipal, Industrial and Agricultural*. – Lewis Publishers, Chelsea, MI. <https://www.crcpress.com/Constructed-Wetlands-for-Wastewater-Treatment-Municipal-Industrial-and-Hammer/p/book/9780873711845>.
- [31] El Gohary, R. (2008): Restoration of chemical, bacteriological characterization for drainage water: case study. – *Ain Shams Engineering Journal* 1: 15-32.
- [32] El Hamouri, B., Nazih, J., Lahjouj, J. (2007): Subsurface-horizontal flow constructed wetland for sewage treatment under moroccan climate conditions. – *Desalination* 215(1-3): 153-158.
- [33] El-Khateeb, M. A., El-Bahraw, A. Z. (2013): Extensive post treatment using constructed wetland. – *Life Science Journal* 10(2): 560-568.
- [34] Elias, E., Yohannes, H. (2017): Contamination of rivers and water reservoirs in and around Addis Ababa City and actions to combat it. – *Environ Pollution and Climate Change* 1(2): 1-13.
- [35] Farzadkia, M., Ehrampoush, M. H., Mehrizi, E. A., Sadeghi, S., Talebi, P., Salehi, A., Kermani, M. (2015): Investigating the efficiency and kinetic coefficients of nutrient removal in the subsurface artificial wetland of yazd wastewater treatment plant, environmental. – *Health Engineering and Management* 2(1): 23-30.
- [36] Fernández-Aláez, C., Fernández-Aláez, M., Bécares, E. (1999): Influence of water level fluctuation on the structure and composition of the macrophyte vegetation in two small temporary lakes in the northwest of Spain. – *BMC Biology, Ecology and Management of Aquatic Plants* 415: 155-162.

- [37] Florentina, Z., John, R. W. (2014): Comparative study of three two-stage hybrid ecological wastewater treatment systems for producing high nutrient, reclaimed water for irrigation reuse in developing countries. – *Water* 6: 213-228.
- [38] Forster, P., et al. (2007): Changes in Atmospheric Constituents and in Radiative Forcing. – In: *Climate Change. The Physical Science Basis. Contribution of Working Group I to the Fourth Assessment Report of the Intergovernmental Panel on Climate Change.* Cambridge University Press, Cambridge.
- [39] Garcia, J., Chiva, J., Aguirre, P., Alvarez, E., Pau Sierra, J., Mujeriego, R. (2004): Hydraulic behaviour of horizontal subsurface flow constructed wetlands with different aspect ratio and granular medium size. – *Ecological Engineering* 23(3): 177-187.
- [40] Gearheart, R. (2004): planning and preliminary technical study for the application of a wetland treatment system at the city of Fort Bragg wastewater facility. – [https://city.fortbragg.com/DocumentCenter/View/3574/Mill-Pond-Marsh-Report?bidId=.](https://city.fortbragg.com/DocumentCenter/View/3574/Mill-Pond-Marsh-Report?bidId=)
- [41] Ghermandi, A., Van Den Bergh, J. C. J. M., Brander, L. M., de Groot, H. L. F., Nunes, P. L. A. D. (2010): Values of natural and human - made wetlands: a meta - analysis. – *Water Resources Research* 46(12): 1-12.
- [42] Gonzalez, T. F., Vallejos, G. G., Silveira, H. J., Franco, Q. C., Garcia, J., Puigagut, J. (2009): Treatment of swine wastewater with subsurface flow constructed wetlands in Yucatan, Mexico: influence of plant species and contact time. – *Water SA* 35: 333-341.
- [43] Grünfeld, S., Brix, H. (1999): Methanogenesis and methane emissions: effects of water table, substrate type and presence of *Phragmites australis*. – *Aquatic Botany* 64: 63-75.
- [44] Gui, P., Inamori, R., Matsumura, M., et al. (2007): Evaluation of constructed wetlands by wastewater purification ability and greenhouse gas emissions. – *Water Science and Technology* 56: 49-55.
- [45] Haberl, R., (1999): Constructed wetlands: a chance to solve wastewater problems in developing countries. – *Water Science and Technology* 40(3): 11-17.
- [46] Huang, J., Reneau, R., Hageborn, C. (2000): Nitrogen removal in constructed wetlands employed to treat domestic wastewater. – *Water Res.* 34: 2582-2588.
- [47] Itanna, F. (2002): metals in leafy vegetables grown in Addis Ababa and toxicological implications. – *Ethiopian Journal of Health Development* 16: 295-302.
- [48] Johansson, A. E., Kasimir-Klemedtsson, A., Klemedtsson, L., Svensson, B. H. (2003): nitrous oxide exchanges with the atmosphere of a constructed wetland treating wastewater. – *Tellus B* 55(3): 737-750.
- [49] Kadlec, R. H. (2003): Effects of pollutant speciation in treatment wetlands design. – *Ecological Engineering* 20: 1-16.
- [50] Kadlec, R. H., Wallace, S. (2008): *Treatment Wetlands*. 2nd Ed. – CRC Press, Boca Raton.
- [51] Kambole, M. S. (2003): Managing the water quality of the Kafue River. – *Physics and Chemistry of the earth, Parts A/B/C* 28: 1105-1109.
- [52] Kanungo, P., Kumawat, D. M., Billore, S. K. (2017): Potential of constructed wetlands to reduce and assimilate total organic carbon from municipal wastewaters. – *Indian Journal of Environmental Sciences* 21(1): 35-44.
- [53] Kassa, A. (2012): Challenges and opportunities of riverbank urban agriculture. – <http://localhost:80/xmlui/handle/123456789/885>.
- [54] Kassa, Y., Mengistou, S. (2014): Nutrient uptake efficiency and growth of two aquatic macrophyte species under constructed wetlands, Ethiopia. – *THIOP. J. Sci.* 37: 95-104.
- [55] Kathleen, L. M. (2000): Analysis of residential subsurface flow constructed wetlands performance in northern Alabama. – *Small Flows Quarterly* 1(3): 34-39.
- [56] Kayranli, B., Scholz, M., Mustafa, A., et al. (2010): Carbon storage and fluxes within freshwater wetlands: a critical review. – *Wetlands* 30: 111-124.

- [57] Khan, J., Maqbool, T. S., Lee, C.-H. (2014): Effects of filtration modes on membrane fouling behavior and treatment in submerged membrane bioreactor. – *Bioresource Technology* 172: 391-395.
- [58] Khatuddin, M. 2003. *Melestarikan Sumber Daya Air Dengan Teknologi Rawa Buatan*. – Gajah Mada University Press, Yogyakarta.
- [59] Knox, A. S. D., Nelson, E., Specht, W., Paller, M., Seaman, J. (2004): *Metals Retention in Constructed Wetland Sediments*. – Report WSRC-MS-2004-00444, U. S. Department of Energy, Oak Ridge, TN.
- [60] Kotti, I. P., Gikas, G. D., Tsihrintzis, V. A. (2010): Effect of operational and design parameters on removal efficiency of pilot-scale FWS constructed wetlands and comparison with HSF systems. – *Ecological Engineering* 36(7): 862-875.
- [61] Kröpfelová, L., Vymazal, J. (2008): *Wastewater Treatment in Constructed Wetlands with Horizontal Sub-Surface Flow*. – Springer Science & Business Media, Dordrecht.
- [62] Kuschik, P., Kappelmeyer, U., Weixbrodt, E., Kästner, M., Stottmeister, U. (2003): Annual cycle of nitrogen removal by a pilot-scale subsurface horizontal flow in a constructed wetland under moderate climate. – *Water Research* 37(17): 4236-4242.
- [63] Kyambadde, J., Kansime, F., Dalhammar, G. (2005): Nitrogen and phosphorus removal in substrate-free pilot constructed wetlands with horizontal surface flow in Uganda. – *Water, Air, and Soil Pollution* 165: 37-59.
- [64] Lakshman, G. 1987 *Ecotechnological Opportunities for Aquatic Plants: A Survey of Utilization Options*. – Saskatchewan Research Council, Saskatoon, Saskatchewan, Canada.
- [65] Langergraber, G. (2013): Constructed treatment wetlands sustainable sanitation solutions. – *Water Science and Technology* 67(10): 2133-2140.
- [66] Lopez-Lopez, A., Vallejo-Rodríguez, R., León-Becerril, E., López-Rivera, A. (2015): Effect of the organic loading rate in the stillage treatment in a constructed wetland with *Canna Indica*. – *Environmental Progress & Sustainable Energy* 35(2): 411-415.
- [67] Liu, C., Xu, K., Inamori, R., Ebie, Y., Liao, J. (2009): Pilot-scale studies of domestic wastewater treatment by typical constructed wetlands and their greenhouse gas emissions. – *Environ. Sci. Engin.* 3(4): 477-482.
- [68] Luckeydoo, L. M., Fausey, N., Brown, L. et al. (2002): Early development of vascular vegetation of constructed wetlands in Northwest Ohio receiving agricultural waters. – *Agriculture, Ecosystems & Environment* 88: 89-94.
- [69] Mahmoud, K., Baskar, G. (2018): Constructed wetlands for wastewater treatment. – *Journal of Modern Science and Technology* 6(1): 78-86.
- [70] Mairi, P. J., Lyimo, J. T., Njau, N. K. (2012): Performance of subsurface flow constructed wetland for domestic wastewater treatment. – *Tanz. J. Sci.* 38: 67-76.
- [71] Mander, Ü., Löhmus, K., Teiter, S., Nurk, K., Muring, T., Augustin, J. (2005): Gaseous fluxes from subsurface flow constructed wetlands for wastewater treatment. – *J. Environ. Sci. Health A.* 40(6-7): 1215-1226.
- [72] Mander, U., Löhmus, K., Teiter, S., Muring, T., Nurk, K., Augustin, J. (2008): Gaseous fluxes in the nitrogen and carbon budgets of subsurface flow constructed wetlands. – *Sci. Total Environ.* 404(2-3): 343-353.
- [73] Mander, Ü., Maddison, M., Soosaar, K., Karabelnik, K. (2011): The impact of intermittent hydrology and fluctuating water table on greenhouse gas emissions from subsurface flow constructed wetlands for wastewater treatment. – *Wetlands* 1023-1032.
- [74] Maqbool, T., Jamal Khan, S., Lee, C.-H. (2014): Effects of filtration modes on membrane fouling behavior and treatment in submerged membrane bioreactor. – *Bioresource Technology* 172: 391-395.
- [75] Mariñelarena, A. J., Di Giorgi, H. D. (2001): Nitrogen and phosphorus removal by periphyton from agricultural wastes in artificial streams. – *Journal of Freshwater Ecology* 16: 347-353.

- [76] Maucieri, C., Borin, M., Barbera, A. C. (2014): Role of C3 plant species on carbon dioxide and methane emissions in Mediterranean constructed wetland. – *Italian Journal of Agronomy* 9: 120-126.
- [77] Michael, J. C.; Lori, W., Kathleen, C. P. (2006): Patterns of vertical stratification in a subtropical constructed wetland in South Florida (USA). – *Ecological Engineering* 27(4): 322-330.
- [78] Mitsch, W. J., Bernal, B., Hernandez, M. E. (2015): Ecosystem services of wetlands. – *International Journal of Biodiversity Science, Ecosystem Services & Management* 11(1): 1-4.
- [79] Mustafa, A. (2013): Constructed wetland for wastewater treatment and reuse: a case study of developing country. – *International Journal of Environmental Science and Development* 4(1): 20-24.
- [80] Nyakango, J. J. (1999): Combination of a well-functioning constructed wetland with a pleasing landscape design in Nairobi, Kenya. – *J. Water Science and Technology* 40: 247-247.
- [81] Oostrom, J (1994): Denitrification in constructed wastewater wetlands receiving high concentrations of nitrate. – *Water Sci. Technol* 7-14.
- [82] Panrare, A., Prapa, S., Tusanee, T. (2015): Constructed wetland for sewage treatment and thermal transfer reduction. – *Energy Procedia* 79: 567-575.
- [83] Piola, R. F., Suthers, I. M., Rissik, D. (2008): Carbon and nitrogen stable isotope analysis indicates fresh water shrimp *Paratya australiensis* Kemp, 1917 (Atyidae) assimilate cyanobacterial accumulations. – *Hydrobiologia* 608(1): 121-132.
- [84] Prasad, B., Maiti, D. (2016): Comparative study of metal uptake by *Eichhornia crassipes* growing in ponds from mining and nonmining areas—a field study. – *Bioremediation Journal* 20(2): 144-152.
- [85] Prasad, R., Rangari, P. J., Jasutkar, D. (2016): Performance evaluation of constructed wetland in treating domestic wastewater. – *International Journal of Latest Research in Engineering and Technology* 2(5): 28-33.
- [86] Pucci, B., Conte, G., Martinuzzi, N., Giovannelli, L., Masi, F. (2000): Design and performance of a horizontal flow constructed wetland for treatment of dairy and agricultural wastewater in the Chianti countryside. – https://pdfs.semanticscholar.org/eeda/90e784d52cf07695cebfaa79399a9b7af9d5.pdf?_ga=2.126156365.1936323412.1579619295-814467461.1579619295.
- [87] Puigagut, J., Villaseñor, J., José Salas, J., Bécares, E., García, J. (2007): Subsurface-flow constructed wetlands in Spain for the sanitation of small communities: a comparative study. – *Ecological Engineering* 30(4): 312-319.
- [88] Qomariyah, S. Sobriyah, S., Ramelan, A. H., Setyono, P. (2017): Use of macrophyte plants, sand and gravel materials in constructed wetlands for greywater treatment. *IOP Conf. Series. – Materials Science and Engineering* 176: 1-7.
- [89] Reddy, K., Debusk, W. (1991): Decomposition of water hyacinth detritus in eutrophic lake water. – *Hydrobiologia* 211: 101-109.
- [90] Richardson, W. B., Strauss, E. A., Bartsch, L. A., Monroe, E. M., Cavanaugh, J. C., Vingum, L., Soballe, D. M. (2004): Denitrification in the upper Mississippi River: rate, controls, and contribution to nitrate flux. – *Can. J. Fish. Aquat. Sci.* 61: 1102-1112.
- [91] Rosso, D., Stenstrom, M. K. (2008): The carbon-sequestration potential of municipal Wastewater treatment. – *Chemosphere* 8: 1468-1475.
- [92] Saeed, T., Sun, G. (2012): A review on nitrogen and organics removal mechanisms in subsurface flow constructed wetlands: dependency on environmental parameters, operating conditions and supporting media. – *Journal of Environmental Management* 112: 429-448.
- [93] Sahu, O. (2014): Reduction of heavy metals from wastewater by wetland. – *International Letters of Natural Sciences* 12: 35-43. DOI: 10.18052/www.scipress.com/ILNS.12.35.

- [94] Sovik, A. K., Augustin, J., Hekkinen, K., Huttunen, J. (2006): Emission of the greenhouse gases nitrous oxide and methane from constructed wetlands in Europe. – *Journal of Environmental Quality* 35(6): 2360-2373.
- [95] Taylor, G. D., Fletcher, T. D., Wong, T. H. F., Duncan, H. P. (2006): Baseflow water quality behavior: implication for wetland performance monitoring. – *Aust. J. Water Resour* 10(3): 293-302.
- [96] Terfie, T. A., Asfaw, S. L. (2014): Evaluation of selected wetland plants for removal of chromium from tannery wastewater in constructed wetlands, Ethiopia. – *African Journal of Environmental science and technology* 9(5): 420-427.
- [97] Tilak, S. A., Wani, P. S., Patil, D. M., Datta, A. (2016): Evaluating wastewater treatment efficiency of two field scale subsurface flow constructed wetlands. – *Current Science* 110(9): 1764-1771.
- [98] Tousignant, E., Fankhauser, O., Hurd, S. (1999): Guidance manual for the design, construction and operations of constructed wetlands for rural applications in Ontario. – <http://hdl.handle.net/10214/15203>.
- [99] UNEP/GPA – UNESCO-IHE (2004): Train-Sea-Coast GPA. A Joint UNESCO-IHE – Improving Municipal Wastewater Management in Coastal Cities, The Netherlands. Version 01. – UNEP/GPA – UNESCO-IHE
- [100] USEPA (1993): Subsurface Flow Constructed Wetlands for Wastewater Treatment. – Technology Assessment. EPA 832-R-93-001.
- [101] Van Der Zaag, A. C., Gordon, R. J., Burton, D. L., Jamieson, R. C., Stratton, G. W. (2010): Greenhouse gas emissions from surface flow and subsurface flow constructed wetlands treating dairy wastewater. – *Journal of Environmental Quality* 39(2): 460-471.
- [102] Vymazal, J. (2005): Horizontal sub-surface flow and hybrid constructed wetlands systems for wastewater treatment. – *Ecological Engineering* 25: 478-490.
- [103] Vymazal, J. (2007): removal of nutrients in various types of constructed wetlands. – *Science of The Total Environment* 380(1-3): 48-65.
- [104] Vymazal, J. (2011): Plants used in constructed wetlands with horizontal subsurface flow: a review. – *Hydrobiologia* 674: 133-156.
- [105] Vymazal, J. (2013): The use of hybrid constructed wetlands for wastewater treatment with special attention to nitrogen removal: a review of a recent development. – *Water Research* 47: 4795-4811.
- [106] Vymazal, J., Kröpfelová, L. (2008): Wastewater treatment in constructed wetlands with horizontal sub-surface flow. – *Springer Science & Business Media* 14: 561.
- [107] Wang, Y. C., Ko, C. H., Chang, F. C., Chen, P. Y., Liu, T. F., Sheu, Y. S., Shih, T. L., Teng, C. J. (2011): Bioenergy production potential for aboveground biomass from a subtropical constructed wetland. – *Biomass and Bioenergy*. 35: 50-58.
- [108] Watson, J. T., Hobson, J. A. (1989): Hydraulic Design Considerations and Control Structures for Constructed Wetlands for Wastewater Treatment. – In: Hammer, D. A. (ed.) *Constructed Wetlands for Wastewater Treatment*. Lewis Publishers, Chelsea, MI.
- [109] Whiting, G. J., Chanton, J. P. 2001. Greenhouse carbon balance of wetlands: methane emission versus carbon sequestration. – *Tellus B* 5: 521-528.
- [110] Wijaya, S. D., Hidayat, T., Sumiarsa, D., Kurnaeni, B. T. B., Kurniadi, D. (2016): A Review on sub surface flow constructed wetlands in tropical and sub-tropical countries. – *Open Science Journal*. DOI: 10.23954/osj.v1i2.415.
- [111] Wu, S., Kusch, P., Hans, B. (2014): Development of constructed wetlands in performance intensification for wastewater treatment. A nitrogen and organic matter targeted. – *Water Resources Research* 57: 40-55.
- [112] Zhu, A. Z. M., Qian, J. M., De Souza, M., Terry, N. (1999): Phytoaccumulation of trace elements by wetland plants: II. Water hyacinth. – *Journal of Environmental Quality* 28: 339-344.

- [113] Zurita, F., John, R. W. (2014): Comparative study of three two-stage hybrid ecological wastewater treatment systems for producing high nutrient, reclaimed water for irrigation reuse in developing countries. – *Water* 6: 213-228.
- [114] Zurita, F., De Anda, J., Belmont, M. A. (2006): Performance of laboratory-scale wetlands planted with tropical ornamental plants to treat domestic wastewater. – *Water Quality Research Journal Canada* 41(4): 410-417.
- [115] Zurita, F., De Anda, J., Belmont, M. A., Cervantes-Martinez, J. (2008): Stress detection by laser-induced fluorescence in *Zantedeschia aethiopica* planted in subsurface-flow treatment wetlands. – *Ecological Engineering* 33: 110-118.

TREATMENT OF WASTEWATER WITH CONSTRUCTED WETLANDS SYSTEMS AND PLANTS USED IN THIS TECHNOLOGY – A REVIEW

SANJRANI, M. A. – ZHOU, B. – ZHAO, H. – ZHENG, Y. P. – WANG, Y. – XIA, S. B.*

School of Resources and Environmental Engineering, Wuhan University of Technology, Wuhan, P. R. China

(e-mails: manzoor.geo@gmail.com, boxunzhou@foxmail.com, zhaoheng0802@126.com, zhengyouping0614@163.com, wang569874@126.com)

**Corresponding author
e-mail: xiashibin@126.com*

(Received 24th Jun 2019; accepted 25th Oct 2019)

Abstract. Water issues are still here, urbanization and industries generate different types of wastes which then affect water. Many technologies have been introduced for water treatment and efforts are being made to improve and maintain water quality, while also providing easily available and low-cost technologies. Several methods which are easily available but due to high cost, they cannot be introduced everywhere, especially rural areas. Recently, constructed wetlands have been proven to be an efficient technology to treat water. With its biological, physical and chemical treatment, constructed wetland technology becomes the best choice by many countries around the world. Existing research shows that COD (Chemical Oxygen Demand), BOD5 (Biological Oxygen Demand), TKN (Total Kjeldahl Nitrogen), TSS (Total suspended solids) etc. have been removed to a significant degree by using constructed wetlands. This technology is a system of different materials, such as gravel, vegetation and recently introduced tool known as biochar. The combination of these makes the system efficient for water treatment but some factors such as area, weather conditions, type of wastes do matter. Selection of constructed wetland type and suitable plants is very important. In this paper, efficiency of constructed wetland system, its mechanism, the types of plants used in the system and role of plants to enhance the efficiency of the wetland system from all over the world are widely reviewed and discussed.

Keywords: *constructed wetlands, water treatment, removal mechanisms, removal of pollutants, plants in wetlands*

Introduction

Recent environmental issues and the discovery of their solutions have been increasing rapidly throughout the world. The discharge of wastewater from industries is a threat to nature creating water borne diseases. Recently, the lack of proper wastewater treatment, rapid urbanization is making the situation worse (Varga et al., 2017; Sanjrani et al., 2017; Brix et al., 2013). There are many options available for water treatment, but wetland technology is more efficient and less-cost. One of the valuable services given by natural, restored, or constructed wetlands is that they generally protect downstream waterways from the impact of nutrient pollution. This happens naturally because constructed wetlands are complex systems with a large number of active physical, chemical, and biological processes that mutually influence each other. Nutrient removal use some of the main physical processes such as particle settling known as sedimentation or volatilization, it releases as a gas into the atmosphere, and sorption which includes a nutrient adhering to a solid or diffusing into another liquid or solid. The chemical processes are involved with transformations and precipitation. The biological processes by plants, algae, and bacteria and further process of transformation are conducted by microbes. Wetland compartments have all of these processes with water; biota i.e. plants, algae, and bacteria; litter; and soil.

Around the world, wastewater treatment by constructed wetlands has become one of the efficient solutions (Varga et al., 2017; Sanjrani et al., 2019; Jácome, 2016).

CWs are applied to the treatment of varieties of wastewaters created either from industries or human settlements. Some of them are: food industry effluents (including dairy, abattoir, fruit, vegetables and meat industries), effluents of petrochemical and refinery industry, distillery and winery effluents, textile, aquaculture, tannery, steel and mixed industrial effluents, pulp and paper industry etc (Varga et al., 2017). CWs are planned engineered systems that are generally constructed and designed by natural processes such as wetland vegetation, soils, and their associated microbial assemblages (Vymazal, 2014). In this process, it also needs to create a specific environment for the growth of microorganisms and hydrophytes (aquatic and semi aquatic plants) which can live in aerobic, anaerobic and facultative anaerobic environmental systems. Their interactions bring many changes, such as the intensification of oxidation and reduction responsible for the removal and retention of pollutants. These processes are generally supported by sorption, sedimentation and assimilation (Skrzypiec and Gajewska, 2017).

Wastewater is being treated by different types of wetland, i.e. H.F and V.F and a combination of VF and HF systems, known as hybrid wetlands. They are also known as: horizontal subsurface flow constructed wetlands (HSSFCWs), vertical subsurface flow constructed wetlands (VSSFCWs) and free water surface constructed wetlands (FWSCW). Wetlands for the treatment of wastewater, sludge, storm-water, and leachate have been evaluated in laboratory, pilot, and full-scale studies. Due to the benefits acquired from wetlands, wetlands are now at the centres of human evolution and the development of this planet's diverse cultures. Without water we would not exist. In Europe countries, these constructed wetlands are treating water at several places, i.e. tourist resorts, farms and landfills. Various CWs systems show different results in treatment efficiency (Mander et al., 2000). Moreover, recent studies have shown that every country relies on some type of wetlands (Jiang et al., 2016; RAMSAR, 2016; Sirianuntapiboon and Jitvimolnimit, 2007).

Recently, the use of biochar to enhance constructed wetland performance in wastewater has highly appreciated. Different types of biochar have been used to promote wetlands activities. Combining both of these technologies can greatly augment the efficiency of the system. Pollutant removal performance was compared between the controlled and experimental wetland beds. Study reveals that the wetlands with biochar are more efficient as compared to the wetland with gravels alone, which had the average removal rate (Prabuddha et al., 2015). The present paper documents an overall review on the efficiency of wetland systems and common pollutant removal around the world. It also attempts about overall review on the role of the wetland plants in constructed wetlands, efficiency of constructed wetland system, its mechanism, and the types of plants used in the system. Recommendations for future studies have been recommended to improve the efficiency for better treatment.

The efficiency of wetland systems for wastewater treatment

The efficiency of wetland systems for Wastewater Treatment has been proved that it is the best technology around the world. The first experiment on the use of wetland plants for treatment of wastewater was carried in the early 1950s by Dr. Kathe Seidel in Germany. The first full scale systems were put in operation during the late 1960s and since then constructed wetland systems have been speeding throughout the world (Vymazal and Kröpfelová, 2009). Different types of wastes are being treated by wetland technology and

have shown promising results for the removal of pollutants (Newman et al., 2015). This is the reason; this technology is developing everywhere around the world. There are now more than 1,000 constructed wetland systems (CWs) in the UK (WRC UK, 2012). In Northeastern USA and Eastern Canada, 25 full-scale CWs treated agricultural wastewater and showed an average of good removal efficiencies: BOD₅, TKN, TSS, NH₄⁺-N, NO₃⁻-N and TP (Rozema and Andrew, 2016a; Rozema and Zheng, 2016b). In Russia, geographical conditions and the weather, depending on the possibilities for accommodation of certain types of CWs really need careful consideration. Recently, the use of constructed wetlands for xenobiotics removal in climatic conditions in Russia has been conducted. This project was both efficient and low-cost (Schegolkova et al., 2015).

In Korea, because of its lower construction cost and simplicity in operation and maintenance, many different types of wetland treatment systems have been built during the last 10 years, the efficiency of removal of pollutants is great. However, Kim et al. (2006) identified some issues; systems suffer from the reduced effectiveness in performance during the winter. And need to evaluate the partial treatment accomplished during six to seven months per year (Kim et al., 2006). In Pakistan, this technology was introduced relatively late, between 2009 and 2010, a small NGO Sindhica Reforms Society (Sindhica) initiated “Pakistan’s first community managed Constructed Wetland” with the support of Indus for All Programme-WWF Pakistan and the technical support of UN HABITAT water for Asian cities Programme, South Asia region. Constructed wetland Majeed Keerio was designed, with the realization that substrate of the wetland can rapidly fill up with debris, grit, and solids from raw waste water if these materials are not removed prior to the wetland. Therefore, Majeed Keerio was designed as: (1) Preliminary treatment: Removal of large contaminants, such as solid waste and grit to avoid operation and maintenance problems; (2) Primary treatment: Removal of suspended solids and organic matter; (3) Secondary treatment: Removal of biodegradable organic matter; (4) Tertiary treatment: Removal of specific pollutants such as nutrients. This wetland has brought good results in removing pollutants from water (Keryo, 2012).

In Egypt, there are two major challenges that affect the ecosystem and the urban environment: the first being water scarcity and the second being wastewater management. Egypt is an arid country; it is important that reusing wastewater be encouraged as it is documented that reused wastewater is safe and economically feasible. There are several available methods for wastewater treatment; however treatment by wetlands is the most effective method (ElZein et al., 2016). In Malaysia, Faculty of Engineering, Universiti Putra Malaysia has been trying to resolve water treatment issues in Malaysia. In their study (Katayon et al., 2008), results showed that the constructed wetlands have removed 27-96% of NH₄⁺, 50-88% of TSS, 56-77% of COD, 20-88% of TP, and 99% of total coliform numbers. In Kerala, India, a CW system made using a laboratory scale model; including plant ‘Reed’ has given good results for removal efficiencies for domestic wastewater treatment at a considerable level (Midhun et al., 2016).

In Ireland, 52 constructed wetland sites from 17 local authorities were aimed to identify the best performing types of constructed wetlands; some constructed wetland sites achieved long or frequent periods of zero effluent discharge and thus did not transfer any waterborne pollution to their receptors during these periods (Hickey et al., 2017).

Besides, there are very few disadvantages of this technology. Depending on design, constructed wetlands may possess a larger land-area than other technology. Mosquito populations increased because of wetlands and can be the reason for the diseases like malaria or other diseases caused by mosquitoes. Wetlands produce about one quarter of the

Earth's atmospheric methane through the anaerobic decomposition of organic matter. Sometimes nutrients are changed to harmless forms year-round by wetland bacteria. Constructed wetlands may not to treat highly toxic modern wastewater till it is pre-treated in special installations. In climates with cold winters, bacteria and plants living in the constructed wetland's soil die back and release their own nutrients back into the system. A constructed wetland's biological processes are not well understood. Residual pollutants may have a negative effect on the reserve's wildlife (Gutiérrez, 2011; Kielmas, 2018; Permaculture, 2015; Akers, 2012; Patil, 2016).

Removal of pollutants by wetlands

Various studies have documented that wetlands are the best and low-cost available option for removing several pollutants from water. It can be concluded that the use of constructed wetland is very effective in removing major nutrients and pollutants. Some recent studies from all over the world have been mentioned in *Table 1*, which prove that this technology is best option for pollutants removal up to 99%.

Table 1. Removal percentage of pollutants by wetlands

S.No.	COD	BOD ₅	TN	TKN	TSS	TDS	TP	References
1	99%			94%	98%		83%	Rozema and Andrew (2016a); Rozema and Zheng (2016b)
2	86.6	83.7%		36.66%		87.36%		Midhun et al. (2016)
3			69.96%				82.4%	Patil and Munavalli (2016)
4					83%	58%		Haukos et al. (2016)
5	97.2%		90.6%					Wu et al. (2016)
6	75%		75%				55%	Sartori et al. (2016)
7			67%					Khajah, and Babatunde (2016)
8	74.6-76.6%		60.1-84.7%				49.3-70.7%	Chyan et al. (2016c)
9		87.81%			86.10%	67.27%		Upadhyay et al. (2016)
10	89.2%		90.0%				50.3%	Maucieri et al. (2016)
11	91%							Sultana et al. (2016)
12			60% ± 12%				77% ± 4%	Mateus et al. (2016)
13	95.6%		85.8%					Fan et al. (2016)
14	91.3%		58.3%				79.5%	Prabuddha et al. (2015)
15					85%		68%	Niu et al. (2016)
16	83-88%	90-95%			89-93%			Carballeira et al. (2016)
17	66%		79%					Uggetti et al. (2016)
18	91 ± 7%	95 ± 5%	70 ± 10%				90 ± 6%	Yin et al. (2016)
19		81%		75%	83%		64%	Rozema and Andrew (2016a); Rozema and Zheng (2016b)
20	69%		69%					Wu et al. (2016)
21			43%	38%				Vymazal and Kröpfelová (2009)
22	65%		43%					Wang et al. (2016a)
23	68.1%			78.25%	86.5%		64.85%	Zhao et al. (2016)
24			71%					He et al. (2016)

The data shows that high levels of removal were detected for Total Phosphorus (TP) and Soluble Reactive Phosphorus (SRP), Total Nitrogen, ammonium/ammonia, nitrate and nitrite, Biological Oxygen Demand (BOD), Chemical Oxygen Demand

(COD), and Suspended Sediments (SS). Large amounts were reduced for all these parameters. It can be concluded that constructed wetland systems are effective for the reduction of several pollutants

Removal mechanisms and wastewater constituents

There are many mechanisms involved in the wetlands system which can remove BOD, COD, and Nitrogen, as shown in *Table 2*.

Table 2. Removal mechanisms and wastewater constituents. (Source: modified from: Newman et al., 2015; Keryo, 2012; FCN, 2014)

Removal mechanisms and wastewater constituents	
Wastewater constituents	Removal mechanisms
Heavy metals	Sedimentation, adsorption, plant uptake, chemical precipitation, infiltration
Bacteria/pathogens	Sedimentation, natural die off
Synthetic organics	Sedimentation, adsorption, oxidation, volatilization, infiltration
Hydrocarbons	Bio-filtration, microbial decomposition, oxidation, plant uptake metabolism
Total phosphorus	Matrix sorption, plant uptake, sedimentation bio-filtration
Nitrate	Denitrification
Nitrite	Denitrification
Ammonia	Nitrification
Biological oxygen demand	Sedimentation, bio-filtration,
Chemical oxygen demand	Sedimentation, bio-filtration, oxidation
Suspended solids	Sedimentation, filtration
Soluble organics	Aerobic microbial degradation, anaerobic microbial degradation
Total nitrogen	Ammonification followed by microbial nitrification, denitrification, plant uptake, matrix adsorption, ammonia volatilization

Efficiency of vegetation in wetlands for water treatment

Efficiency of wetland systems increases with different vegetation for common pollutant removal; it has been demonstrated in several studies around the world. Roy et al. (2016) described that the basin morphometry of constructed wetlands is not same as natural wetlands, which explains the difference in vegetation composition. Plants provide a substrate for microorganisms, and microorganisms, with a source of carbon, are the most important processors of wastewater contaminants. There are various processes through which plants can incorporate pollutants are: (i) Phyto-extraction: the process in which a plant's leaves and roots play a role in concentrating heavy metals. (ii) Rhizo-filtration: the process in which plants roots play role in absorption and precipitations of metals from contaminated liquid. They are also used to degrade organic compounds. (iii) Phyto-stabilization: the process in which metal-tolerant plants reduce the power of mobility of metals -- especially chlorinated compounds -- to air or groundwater. (iv) Phyto-stimulation: the process in which roots help bacterial and fungal development for biodegrading the compounds, i.e. petrochemical hydrocarbons, benzene, polyaromatic etc. (v) Phytovolatilization: the process in which plants take up heavy metals and some organic compounds via transpiration and place them into the atmosphere. (vi) Phyto-decomposition: the process in which both terrestrial and aquatic

plants get organic compounds to decompose and decrease toxicity at a considerable level (FCN, 2014; Leiva, 2018).

Sieben et al., (2016a) studied about the classification of the vegetation in specific type of wetland habitats in semi-arid regions of South Africa and presented the overview. There are two types of resilience (physical human disturbance and altered hydrology). From this, conclusion has been drawn that hydric species are not resilient to hydrological impacts than terrestrial species. Pretorius and Brown (2016) studied different types of wetlands while planting the main drivers of vegetation species in South Africa. This study suggested that vegetation composition vary with the wetland type so they should be evaluated individually for better results. In addition, the immoderate use of these wetlands may accelerate their deterioration because tall indigenous vegetation in wetlands can be used as fibers for traditional crafts and construction (Sieben et al., 2016b; Sieben and Nyambeni, 2016c). Vegetation in CWs also plays a vital role in the removal of nutrients from wastewater because the removal efficiency depends on the type of plants. As Leung et al. (2016) studied about efficiency of CWs on treating mangrove plants (*Bruguiera gymnorrhiza* and *Aegiceras corniculatum*) and non-mangrove plants (*Canna indica*, *Phragmites australis*, and *Acorus calamus*). Comparisons results showed that Mangrove CWs planted with *A. corniculatum* gave higher application values than the non-mangrove CWs to treat toxic wastewater. Additionally, water hyacinth plant has also efficiency to remove nutrients from wastewater (Patil and Munavalli, 2016). In Eastern Africa, Moges et al. (2016) developed a plant-based index of biological integrity with 122 plant species belonging to 37 families, aiming to evaluate the long term natural wetland conditions, also provide an effective tool, and therefore, facilitate the management of wetlands. In the United States, CWs got big problem due to erosion, which is degrading playa-wetlands in this semi-arid country, so Haukos et al. (2016) evaluated the role of vegetation surrounding playa-wetlands for removal of nutrients, metal, and dissolved/suspended solids from runoff. According to the results, vegetative Buffers removed about 78% of N, 70% P, 58% TDS and 83% TSS. It was suggested that vegetation buffers could be an economical conservation tool for playa-wetlands (Haukos et al., 2016). Ge et al., (2016) highlighted the influence on contaminants removal in the sense of seasonal change. In the study, efficiency of three plants was recorded. *Thalia dealbata* outperformed *C. indica* and *Lythrum salicaria* in the removal of total nitrogen (69.96%) and total phosphorus (82.4%) from urban storm-water runoff sewage. It is concluded that it is important to select most suitable plant communities for CWs. Wetland vegetations are important components of wetlands which play several roles in relation to the wastewater treatment processes.

Plants used in constructed wetlands around the world:

There are many plants planted in constructed wetlands (Wu, 2010; Polomski, 2007; Vymazal, 2007). Study (Oluseyi et al., 2011; Wang et al., 2016c) shows the result that three aquatic tropical plants (*Canna indica*, *Phragmites australis* and *Sacciolepis africana*) can be planted effectively. Some aquatic plants used in constructed wetlands are: *Lemna valdiviana*, *Spirodela sp.*, *Typha angustifolia*, *Typha domingensis*, *Typha latifolia*, *Cyperus involucratus*, *Cyperus giganteus*, *Thalia dealbata*, *Cyperus giganteus*, *Juncus effuses*, *Phragmites communis*, *Sagittaria lancifolia* (Appenroth et al., 2010; Sohsalam and Sirianuntapiboon, 2008; Vymazal, 2011).

Many studies have concluded that most commonly used species, which are given in Table 3, are robust species of emergent plants, such as the cattail (*Typha latifolia*), common reed (*Phragmites australis*), and bulrush (Appenroth et al., 2010; Sohsalam et al., 2008; Vymazal and Kröpfelová, 2011).

Table 3. Plants used in wetlands in different countries

Location	Types of plants	References
Australia, Logan, Queensland	A combination of banksia <i>intergrifolia</i> , <i>callistemon pachyphyllus</i> , <i>carpobrotusglaucescens</i> , <i>pennisetumalopecuroides</i>	Sievers et al. (2018)
Australia, Logan, Queensland	<i>Melaleuca quinquenervia</i> , <i>Melaleuca alternifolia</i>	Langergraber and Weissenbacher (2017)
Australia, Melbourne	<i>Phragmites australis</i>	Dotro et al. (2017)
Brazil	<i>Heliconia psittacorum</i>	Hu et al. (2016)
Brazil	<i>Alpinia purpurata</i> , <i>Arundina bambusifolia</i> , <i>Canna sp.</i> <i>Heliconia psittacorum L.F.</i>	Wang et al. (2016a)
Brazil	<i>Hedychium coronarium</i> , <i>Heliconia rostrata</i>	Gao et al. (2014)
Brazil	<i>Hemerocallis flava</i>	Prata et al. (2013)
Brazil	<i>Heliconia psittacorum L.F.</i>	Teodoro et al. (2014)
China	<i>Canna indica</i>	Shi et al. (2004)
China	<i>Canna indica mixed with other species</i>	Li et al. (2007)
China	<i>Canna indica Linn</i>	Yang et al. (2007)
China	<i>Canna indica</i>	Zhang et al. (2007a)
China	<i>R. carnea</i> , <i>I. pseudacorus</i> , <i>L. salicaria</i>	Zhang et al. (2007b)
China	<i>Canna sp</i>	Sun et al. (2009)
China	<i>Canna indica</i>	Cui et al. (2010)
China	<i>Canna indica mixed with other natural wetland plants</i>	Zhang et al. (2010)
China	<i>Canna indica mixed with other natural wetland plants</i>	Qiu et al. (2011)
China	<i>Canna indica and Hedychium coronarium</i>	Wen et al. (2011)
China	<i>Iris pseudacorus mixed with other natural wetland plants</i>	Wu et al. (2011)
China	<i>Iris pseudacorus, mixed with other plants of natural wetlands</i>	Xie et al. (2012)
China	<i>Canna indica</i>	Chang et al. (2012)
China	<i>Iris sibirica</i>	Gao et al. (2014)
China	<i>Canna sp</i>	Qiu et al. (2011)
China	<i>Iris sibirica</i>	Gao et al. (2015)
China	<i>Canna indica L.</i>	Hu et al. (2016)
China, Changping, Beijing	<i>Salix babylonica</i>	Gautam and Greenway (2014)
China, Guangzhou	<i>Pennisetumsineserob Pennisetum purpureum</i>	Bolton, and Greenway (1999)
China, Guangzhou	<i>Canna indica</i>	Saeed and Sun (2011)
China, Guangzhou	<i>Canna indica and windmill grass</i>	Wu et al. (2011)
China, Jinan	<i>Phragmites australis</i>	Cui et al. (2015)

China, Shanghai	<i>Phragmites australis Thypalatifolia</i>	Huang et al. (2016)
China, Shanghai	<i>Iris sibirica Thaliadealbata</i>	Peng et al. (2014)
China, Wuhan	<i>Thypaorientalis Canna indica</i>	Wu et al. (2015)
China, Wuhan	<i>Juncuseffusus</i>	Xu et al. (2015)
China, Xi'an	<i>Phragmites australis</i>	Li et al. (2008)
China, Xi'an	<i>Phragmitesaustralis, T orientalis</i>	Zhong et al. (2015)
China, Cuihua, Xi'an	<i>Thypalatifolia</i>	Chang et al. (2012)
Chile	<i>Zantedeschia aethiopica, Canna spp. and Iris spp</i>	Morales et al. (2013)
Chile	<i>Tulbaghia violácea, and Iris pseudacorus.</i>	Burgos et al. (2016)
Colombia	<i>Heliconia psittacorum</i>	Madera-Parra et al. (2015)
Colombia	<i>Alpinia purpurata</i>	Marrugo-Negrete et al. (2016)
Colombia	<i>Heliconia psitacorum</i>	Toro-Vélez et al. (2016)
Costa Rica	<i>Ludwigia inucta, Zantedechia aetiopica, Hedychium coronarium and Canna generalis</i>	León and Cháves (2010)
Cuba	<i>Cyperus alternifolius</i>	Zheng et al. (2016)
Czech republic, Trebon	<i>Phragmites australis Phalarisarundinacea</i>	Zheng et al. (2015)
Egypt, Giza	<i>Phragmites australis</i>	Wang et al., (2016b)
Egypt	<i>Canna sp</i>	Abou-Elela and Hellal (2012)
Egypt	<i>Canna sp</i>	Abou-Elela et al. (2013)
Egypt, Manzala lake	<i>Phragmites australis Thypalatifolia</i>	Perez et al. (2014)
Estonia, Paistu	<i>Phragmites australis</i>	Vymazal (2011)
Greece	<i>Phragmites australis Thypalatifolia</i>	Abou-Elela et al. (2013)
Greece, Pompia	<i>Phragmites australis Arundadonax</i>	El-Sheikh et al. (2010)
India, Nagpur	<i>Thypalatifolia</i>	Öovel et al. (2007)
India	<i>Canna indica</i>	Choudhary et al. (2010)
India	<i>Canna indica</i>	Yadav et al. (2012)
India	<i>Heliconia angusta</i>	Saumya et al. (2015)
India	<i>Canna generalis</i>	Ojoawo et al. (2015)
India	<i>Canna Lily</i>	Haritash et al. (2015)
India	<i>Canna indica</i>	Patil and Munavalli (2016)
India	<i>Polianthus tuberosa L.</i>	Singh and Srivastava (2016)
India, Patancheru	<i>Thypa Eichhorniacrassipes</i>	Akratos and Tsihrintzis (2007)
Indonesia, Bandung	<i>Phragmiteskarka</i>	Tsihrintzis et al. (2007)
Iran, Isfahan	<i>P. australis (PA) T. latifolia (TL) A. donax (AD)</i>	Kadaverugu et al. (2016)
Ireland	<i>Iris pseudacorus</i>	Gill and O'Luanaigh (2010)

Israel, Kiryat	<i>Lemnagibba L.</i>	Datta et al. (2016)
Italy, Florence	<i>Phragmites australis</i>	Kurniadie (2011)
Italy	<i>Zantedeschia aethiopica, Canna indica</i>	Macci et al. (2015)
Japan, Mito	<i>Zizania latifolia</i>	Haghshenas Adarmanabadi (2016)
Kenya, Nairobi	<i>Cyperus papyrus</i>	RAN et al. (2004)
Kenya	<i>Canna sp</i>	Kimani et al. (2012)
Mexico	<i>Zantedeschia aethiopica</i>	Belmont and Metcalfe (2003)
Mexico	<i>Zantedeschia Aethiopica and Canna flaccida</i>	Belmont et al. (2004)
Mexico	<i>Heliconia psittacorum</i>	Orozco et al. (2006)
Mexico	<i>Strelitzia reginae, Zantedeschia esthiopica, Canna hybrids, Anthurium andreanum, Hemerocallis Dumortieri</i>	Zurita et al. (2006)
Mexico	<i>Zantedeschia aethiopica</i>	Zurita et al. (2008)
Mexico	<i>Zantedeschia aethiopica</i>	Ramírez-Carrillo (2009)
Mexico	<i>Strelitzia reginae, Anthurium, andreanum.</i>	Zurita et al. (2009)
Mexico, Ocotlan, Jalisco	<i>Strelitzia reginae A combination of Strelitzia reginae, Anthurium andreanum and Agapanthus africanus</i>	Masi and Martinuzzi (2007)
Nepal	<i>Canna latifolia</i>	Singh et al. (2009)
Nigeria, Akure	<i>Azolla pinnata</i>	Abe et al. (2014)
Portugal	<i>Canna indica mixed with other plants</i>	Calheiros et al. (2007)
Portugal	<i>Canna flaccida, Zantedeschia aethiopica, Canna indica, Agapanthus africanus and Watsonia borbonica</i>	Calheiros et al. (2015)
Singapore, Nanyang	<i>Thyaaugustifolia</i>	Mburu et al. (2012)
Spain	<i>Iris sp</i>	García et al. (2007)
Spain	<i>Iris pseudacorus</i>	Ansola et al. (2003)
Spain, Santiago of Compostela	<i>Phragmites australis</i>	Akinbile et al. (2016)
Spain, Galicia, Boimorto	<i>Phragmites australis</i>	Zhang et al. (2012)
Spain, Valencia	<i>Cattail Phragmites australis</i>	Ávila et al. (2016)
Srilanka	<i>Canna iridiflora</i>	Weragoda et al. (2012)
Srilanka, Peradeniya	<i>Thyaaugustifolia</i>	Vazquez et al. (2013)
Taiwan	<i>Canna indica</i>	Chyan et al. (2016a)
Taiwan	<i>Canna indica</i>	Chyan et al. (2016b)
Thailand	<i>Canna sp</i>	Sirianuntapiboon and Jitvimolnimit (2007)
Thailand	<i>Canna siamensis, Heliconia spp and Hymenocallis littoralis</i>	Sohsalam et al. (2008)
Thailand	<i>Heliconia psittacorum L. f. and Canna generalis L. Bailey</i>	Konnerup et al. (2009)
Thailand	<i>Canna hybrida</i>	Kantawanichkul et al. (2009a)
Thailand	<i>Canna lilies, Heliconia</i>	Brix et al. (2011)

Thailand, Bangkok	<i>Typhaangustifolia Cyperusinvolucratus</i>	Martin et al. (2013a)
Thailand, Bangkok	<i>Canna</i>	Eerakoon et al. (2016)
Thailand, Chiang Mai	<i>Oryzasativa L</i>	Mayo and Bigambo (2005)
Thailand, Petchaburi	A combination of <i>Thyphaangustifolia</i> , <i>Cyperuscorymbosus</i> , <i>Brachiariamutica</i> , <i>Digitariabicornis</i> , <i>Vetiveriazizaniodes</i> , <i>spartina patents</i> , <i>Leptochloafusca</i> , <i>Echinodoruscordifulia</i>	Kantawanichkul et al. (2009b)
Tunisia, Joogar	<i>Phragmitesaustralis and thyphalatifolia</i>	Klomjek and Nitorisravut (2005)
Turkey	<i>Iris australis</i>	Tunçsiper (2009)
Turkey, Garip	<i>Thyphalatifolia</i>	Konnerup et al. (2009)
Uganda, Kampala	<i>Cyperus papyrus</i>	Kantawanichkul and Duangjaisak (2011)
USA	<i>Canna flaccida</i> , <i>Gladiolus sp.</i> , <i>Iris sp.</i>	Neralla et al. (2000)
USA	<i>Canna sp.</i>	Zachritz et al. (2008)
United Kingdom	<i>Iris pseudacorus</i>	McKinlay and Kasperek (1999)
Vietnam, Can Tho	<i>Phragmitessvillatoria</i>	Kouki et al. (2009)

Most commonly plants used in CW

Around the world, four most commonly genera plants used in CW are: *Canna*, *Iris*, *Heliconia*, *Zantedeschia*, *Phragmites* and *Typhas* have been recommended as the main species planted in constructed wetland due to their effectiveness, even though they are considered invasive and outside their native range. Common plants planted in constructed wetlands in North America are *cattails* (*Typha latifolia*). *Cattails* (*Typha latifolia*) have the ability to grow at different water depths, are easy to transport and transplant, and they have broad tolerance of water composition (including pH, dissolved oxygen, salinity, and contaminant concentrations), making them ideal plants for constructed wetlands. Another species known as Common Reed (*Phragmites australis*) is also commonly found in both black-water treatment and in grey-water treatment systems to clean wastewater. *Bulrush* is also known as effective species (Appenroth et al., 2010; Sohsalam and Sirianuntapiboon, 2008; Vymazal, 2011).

Conclusion

The overall finding of this review is that all wetland types are very effective at reducing major nutrients and suspended sediments. Constructed wetland is recommended for wastewater treatment because it treats water biologically, physically and chemically, making it the best option. It is no surprise that many countries around the world opt to use constructed wetlands. The data previously published have concluded that consistently high levels of removal were found for Total Nitrogen, nitrate and nitrite, ammonium/ammonia, Total Phosphorus (TP), Biological Oxygen Demand (BOD), Chemical Oxygen Demand (COD) and Suspended Sediments (SS). Therefore, it can be concluded that wetland systems are effective for the reduction of all of these parameters as they were reduced by large amounts. While reviewing, it was found that “Biochar” is being used in wetlands. The use of biochar to enhance

constructed wetland performance in wastewater has highly appreciated. Different types of biochar have been used to promote wetlands activities. Combining both of these technologies can greatly augment the efficiency of the system, so it is recommended that Biochar from different materials be considered for further improvement. With this change, societies around the world may get easy and sustainable way of water treatment, especially in the affected areas, while also keeping in mind of the social, cultural and economic status of the population. It is concluded that most of plants play a vital role to enhance the efficiency of wetlands to treat all the types of wastewater, either it is natural wetlands or constructed wetlands. Several studies around the world have proved that plants have ability to remove the contaminant at considerable level.

It is recommended that before selection of plants for wetlands; consider the condition such as weather of the area, type of wetlands, and type of water need to be treated so that removal percentage should be higher. Addition of biochar/ACF boosts efficiency of the system. It is recommended that select an efficient material for media. Wood biochar is less expensive than other synthetic materials like granular activated carbon. Therefore, use of wood biochar for removal efficiency is recommended as a simple, cost effective, and environmentally friendly solution for constructed wetland system especially in developing countries. Furthermore, future research is needed on combination of different advanced techniques to undertake stability and mechanism of things which are involved in the constructed wetland system for better solution during water treatment. Additionally, it is important to elucidate the possibility and efficiency of suitable approaches to treat and safely dispose of the resultant material after the treatment process. There is still gap and need to investigate as industrialization and urbanization is changing the world every day and creating different water issues.

Acknowledgements. This research was supported by the Demonstration of Integrated Management of Rocky Desertification and Enhancement of Ecological Service Function in Karst Peak-cluster Depression (grant no.:2016YFC0502400).

REFERENCES

- [1] Abe, K., Komada, M., Ookuma, A., Itahashi, S., Banzai, K. (2014): Purification performance of a shallow free-water-surface constructed wetland receiving secondary effluent for about 5 years. – *Ecological Engineering* 69: 126-133.
- [2] Abou Elela, S., Hellal, M. (2012): Municipal wastewater treatment using vertical flow constructed wetlands planted with *Canna*, *Phragmites* and *Cyperus*. – *Ecol Eng.* 47: 209-213.
- [3] Abou Elela, S., Golinielli, G., Abou Taleb, E., Hellal, M. (2013): Municipal wastewater treatment in horizontal and vertical flows constructed wetlands. – *Ecol Eng.* 61: 460-468. DOI: <https://doi.org/10.1016/j.ecoleng.2013.10.010>.
- [4] Akers, C. (2012): Constructed wetlands. – online available at: <https://sites.biology.colostate.edu/phytoremediation/2012/Constructed%20wetlands%20by%20Chris%20Akers.pdf>.
- [5] Akinbile, C. O., Ogunrinde, T. A., Che Bt Man, H., Aziz, H. A. (2016): Phytoremediation of domestic wastewaters in free water surface constructed wetlands using *Azollapinnata*. – *International Journal of Phytoremediation* 18: 54-61.
- [6] Akrotos, C. S., Tsihrantzis, V. A. (2007): Effect of temperature, HRT, vegetation and porous media on removal efficiency of pilot-scale horizontal subsurface flow constructed wetlands. – *Ecological Engineering* 29: 173-191.

- [7] Ansola, G., González, J. M., Cortijo, R., de Luis, E. (2003): Experimental and full-scale pilot plant constructed wetlands for municipal wastewaters treatment. – *Ecol. Eng* 21(1): 43-52. DOI: <https://doi.org/10.1016/j.ecoleng.2003.08.002>.
- [8] Appenroth, K. J., Krech, K., Keresztes, Á., Fischer, W., Koloczek, H. (2010): Effects of nickel on the chloroplasts of the duckweeds *Spirodela polyrhiza* and *Lemna minor* and their possible use in biomonitoring and phytoremediation. – *Chemosphere* 78: 216-223.
- [9] Ávila, C., García, J., Garfí, M. (2016): Influence of hydraulic loading rate, simulated storm events and seasonality on the treatment performance of an experimental three-stage hybrid CW system. – *Ecological Engineering* 87: 324-332.
- [10] Belmont, M. A., Metcalfe, C. D. (2003): Feasibility of using ornamental plants (*Zantedeschia aethiopica*) in subsurface flow treatment wetlands to remove nitrogen, chemical oxygen demand and nonylphenol ethoxylate surfactants – a laboratory-scale study. – *Ecol Eng* 21: 233-247. DOI: <https://doi.org/10.1016/j.ecoleng.2003.10.003>.
- [11] Belmont, M. A., Cantellano, E., Thompson, S., Williamson, M., Sánchez, A., Metcalfe, C. D. (2004): Treatment of domestic wastewater in a pilot scale natural treatment system in central Mexico. – *Ecol Eng* 23: 299-311. DOI: <https://doi.org/10.1016/j.ecoleng.2004.11.003>.
- [12] Bolton, K. G., Greenway, M. (1999): Pollutant removal capability of a constructed *Melaleuca* wetland receiving primary settled sewage. – *Water Science and Technology* 39: 199-206.
- [13] Brix, H., Koottatep, T., Fryd, O., Laugesen, C. H. (2011): The flower and the butterfly constructed wetland system at Koh Phi Phi - system design and lessons learned during implementation and operation. – *Ecol Eng* 37(5): 729-735, DOI: <https://doi.org/10.1016/j.ecoleng.2010.06.035>.
- [14] Brix, H., Currie, K. I., Mikaloff Fletcher, S. E. (2013): Seasonal variability of the carbon cycle in subantarctic surface water in the South West Pacific. – *Global Biogeochemical Cycles* 27:1: 200-211
- [15] Burgos, V., Araya, F., Reyes-Contreras, C., Vera, I., Vidal, G. (2016): Performance of ornamental 423 plants in mesocosm subsurface constructed wetlands under different organic sewage loading constructed wetlands under different organic sewage loading. – *Ecol Eng* 99: 246-255. DOI: <https://doi.org/10.1016/j.ecoleng.2016.11.058>.
- [16] Calheiros, C. S., Rangel, O. S. S., Castro, P. K. L. (2007): Constructed wetland systems vegetated with different plants applied to the treatment of tannery wastewater. – *Water Res.* 41: 1790-1798. DOI: <https://doi.org/10.1016/j.watres.2007.01.012>.
- [17] Calheiros, C., Bessa, V., Mesquita, R., Brix, H., Rangel, A., Castro, P. (2015): Constructed wetlands with a polyculture of ornamental plants for wastewater treatment at a rural tourism facility. – *Ecol Eng* 79: 1-7. DOI: <https://doi.org/10.1016/j.ecoleng.2015.03.001>.
- [18] Carballeira, T., Ruiz, I., Soto, M. (2016): Effect of plants and surface loading rate on the treatment efficiency of shallow subsurface constructed wetlands. – *Ecol. Eng.* 90: 203-214.
- [19] Chang, J.-J., Wu, S.-Q., Dai, Y.-R., Liang, W., Wu, Z.-B. (2012): Treatment performance of integrated vertical-flow constructed wetland plots for domestic wastewater. – *Ecological Engineering* 44: 152-159.
- [20] Choudhary, A. K., Kumar, S., Sharma, C. (2010): Removal of chlorinated resin and fatty acids from paper mill wastewater through constructed wetland. – *World Acad Sci Eng Technol.* 80: 67-71.
- [21] Chyan, J. M., Jhu, Y. X., Chen, I., Shiu, R. (2016a): Improvement of nitrogen removal by external aeration and intermittent circulation in a subsurface flow constructed wetland of landscape garden ponds. – *Proc Saf Environ Prot.* 104: 587-597. DOI: <https://doi.org/10.1016/j.psep.2016.02.016>.
- [22] Chyan, J. M., Lin, C. J., Lin, Y. C., Chou, Y. A. (2016b): Constructed wetland using corncob charcoal. – *Int. Biodeterior. Biodegrad.* 113: 146-154.

- [23] Chyan, J. M., Lu, C. C., Shiu, R. F., Bellotindos, L. (2016c): Purification of landscape water by using an innovative application of subsurface flow constructed wetlands. – *Environ Scie Pollut Res.* 23: 535-545. DOI: <https://doi.org/10.1007/s11356-015-5265>.
- [24] Cui, L., Ouyang, Y., Lou, Q., Yang, F., Chen, Y., Zhu, W., Luos, S. (2010): Removal of nutrients from wastewater with *Canna indica* L. under different vertical-flow constructed wetland conditions. – *Ecol Eng.* 36: 1083-1088. DOI: <https://doi.org/10.1016/j.ecoleng.2010.04.026>.
- [25] Cui, L., Ouyang, Y., Yang, W., Huang, Z., Xu, Q., Yu, G. (2015): Removal of nutrients from septic tank effluent with baffle subsurface-flow constructed wetlands. – *Journal of Environmental Management* 153: 33-39.
- [26] Datta, A., Wani, S., Patil, M., Tilak, A. (2016): Field scale evaluation of seasonal wastewater treatment efficiencies of free surface-constructed wetlands in ICRISAT, India. – *Current Science* 110: 1756-1763.
- [27] Dotro, G., Langergraber, G., Molle, P., Nivala, J., Puigagut Juárez, J., Stein, O. R., von Sperling, M. (2017): “Treatment wetlands”. Volume 7. *Biological Wastewater Treatment Series.* – IWA Publishing, London.
- [28] Eerakoon, W. G., Jinadasa, K., Herath, G., Mowjood, M., Zhang, D., Tan, S. K., Jern, N. W. (2016): Performance of tropical vertical subsurface flow constructed wetlands at different hydraulic loading rates. – *CLEAN - Soil, Air, Water* 44: 938-948.
- [29] El-Sheikh, M. A., Saleh, H. I., El-Quosy, D. E., Mahmoud, A. A. (2010): Improving water quality in polluted drains with free water surface constructed wetlands. – *Ecological Engineering* 36: 1478-1484.
- [30] ElZein, Z., Abdou, A., Abd ElGawad, I. (2016): Constructed wetlands as a sustainable wastewater. – *Procedia Environmental Sciences.* doi.org/10.1016/j.proenv.2016.04.053.
- [31] Fan, J., Zhang, J., Guo, W., Liang, S., Wu, H. (2016): Enhanced long-term organics and nitrogen removal and associated microbial community in intermittently aerated subsurface flow constructed wetlands. – *Bioresour. Technol.* 214: 871-875.
- [32] FCN (2014): Fourth Corner Nurseries. – <http://fourthcornernurseries.com/>.
- [33] Gao, J., Wang, W., Guo, X., Zhu, S. (2014): Nutrient removal capability and growth characteristics of *Iris sibirica* in subsurface vertical flow constructed wetlands in winter. – *Ecol Eng.* 70: 351-361. DOI: <https://doi.org/10.1016/j.ecoleng.2014.06.006>.
- [34] Gao, J., Zhang, J., Ma, N., Wang, W., Ma, C., Zhang, R. (2015): Cadmium removal capability and growth characteristics of *Iris sibirica* in subsurface vertical flow constructed wetlands. – *Ecol Eng.* 84: 443-450. DOI: <https://doi.org/10.1016/j.ecoleng.2015.07.024>.
- [35] García, M., Soto, F., González, J. M., Bécares, E. A. (2007): comparison of bacterial removal efficiencies in constructed wetlands and algae-based systems. – *Ecol. Eng.* 32(3): 238-243. DOI: <https://doi.org/10.1016/j.ecoleng.2007.11.012>.
- [36] Gautam, D., Greenway, M. (2014): Nutrient accumulation in five plant species grown in bioretention systems dosed with wastewater. – *Australasian Journal of Environmental Management* 21: 453-462.
- [37] Ge, Z., Feng, C., Wang, X., Zhang, J. (2016): Seasonal applicability of three vegetation constructed floating treatment wetlands for nutrient removal and harvesting strategy in urban stormwater retention pond. – *Int. Biodeterior. & Biodegrad.* 112: 80-87.
- [38] Gill, L., O’lunaigh, N. (2010): Nutrient removal from on-site wastewater in horizontal 473 subsurface flow constructed wetlands in Ireland. – *Water Pract Techn.* 6(3): 1-2. DOI: <https://doi.org/10.1016/j.ecoleng.2010.06.002>.
- [39] Gutiérrez Mosquera, H., Peña-Varón, M. (2011): Eliminación de nitrógeno en un humedal construido subsuperficial, plantado con *Heliconia psittacorum*. – *Tecnología Ciencias del Agua* 11(3): 49-60. http://www.scielo.org.mx/scielo.php?pid=S2007-24222011000300004&script=sci_arttext
- [40] Haghshenas Adarmanabadi, A., Heidarpour, M., Tarkesh-Esfahani, S. (2016): Evaluation of horizontal-vertical subsurface hybrid constructed wetlands for tertiary treatment of

- conventional treatment facilities effluents in developing countries. – *Water, Air, & Soil Pollution* 227: 1-18.
- [41] Haritash, A. K., Sharma, A., Bahel, K. (2015): The potential of Canna lily for wastewater treatment under Indian conditions. – *Int J Phytoremed.* 17(10): 999-1004. DOI: <https://doi.org/10.1080/15226514.2014.1003790>.
- [42] Haukos, D. A., Johnson, L. A., Smith, L. M., McMurry, S. T. (2016): Effectiveness of vegetation buffers surrounding playa wetlands at contaminant and sediment amelioration. – *J. Environ. Manage.* 181: 552-562.
- [43] He, K., Lv, T., Wu, S., Guo, L., Ajmal, Z., Luo, H. (2016): Treatment of alkaline stripped effluent in aerated constructed wetlands: feasibility evaluation and performance enhancement. – *Water.* <https://doi.org/10.3390/w8090386>.
- [44] Hickey, A., Arnscheidt, J., Joyce, E., O'Toole, J., Galvin, G., O' Callaghan, M., Conroy, K., Killian, D., Shryane, T., Hughes, F., Walsh, K., Kavanagh, E., (2017): An assessment of the performance of municipal constructed wetlands in Ireland. – *J Environ Manage.* 15(210): 263-272. DOI: 10.1016/j.jenvman.2017.12.079.
- [45] Hu, Y., He, F., Ma, L., Zhang, Y., Wu, Z. (2016): Microbial nitrogen removal pathways in integrated vertical-flow constructed wetland systems. – *Bioresou Technol.* 207: 339-345. DOI: <https://doi.org/10.1016/j.biortech.2016.01.106>.
- [46] Huang, Z., Zhang, X., Cui, L., Yu, G. (2016): Optimization of operating parameters of hybridvertical down-flow constructed wetland systems for domestic sewerage treatment. – *Journal of Environmental Management* 180: 384-389.
- [47] Jácome, J. A., Molina, J., Suárez, J., Mosqueira, G., Torres, D. (2016): Performance of constructed wetland applied for domestic wastewater treatment: case study at Boimorto (Galicia, Spain). – *Ecological Engineering* 95: 324-329.
- [48] Jiang, Y., Martinez-Guerra, E., Gneswar Gude, V., Magbanua, B., Truax, D. D., Martin, J. L. (2016): Constructed wetland for water treatment. – *Water Environment Research* 88(10): 1160-1191 DOI: 10.2175/106143016X14696400494650.
- [49] Kadaverugu, R., Shingare, R. P., Raghunathan, K., Juwarkar, A. A., Thawale, P. R., Singh, S. K. (2016): The role of sand, marble chips and *Typhalatifolia* in domestic wastewater treatment—a column study on constructed wetlands. – *Environmental Technology* 2016: 1-8.
- [50] Kantawanichkul, S., Duangjaisak, W. (2011): Domestic wastewater treatment by a constructed wetland system planted with rice. – *Water Science and Technology* 64: 2376-2380.
- [51] Kantawanichkul, S., Karnchanawong, S., Jing, S. H. (2009a): Treatment of fermented fishproduction wastewater by constructed wetland system in Thailand. – *Chiang MaiJ Sci.* 36(2): 149-157. <http://www.thaiscience.info/journals/Article/CMJS/10905526.pdf>.
- [52] Kantawanichkul, S., Kladprasert, S., Brix, H. (2009b): Treatment of high-strength wastewater in tropical vertical flow constructed wetlands planted with *Typhaangustifolia* and *Cyperus involucratus*. – *Ecological Engineering* 35: 238-247.
- [53] Katayon, S., Fiona, Z., Megat Mohd Noor, M. J., Abdul Halim, G., Ahmad, J. (2008): Treatment of mild domestic wastewater. – *International Journal of Environmental Studies* 65(1): 87-102: DOI: 10.1080/00207230601125192.
- [54] Keryo, M. A. (2012): Project completed report on community managed constructed wetland in Majid Keryo, Sindh province, Pakistan. – <http://sindhicapk.blogspot.com>.
- [55] Khajah, M., Babatunde, A. O. (2016): Wetlands for wastewater treatment. – *J. Water Sustain.* 2016: 43-52.
- [56] Kielmas, M. (2018): The disadvantages of wetland nature reserves. – <https://sciencing.com/info-8396288-disadvantages-wetland-nature-reserves.html>.
- [57] Kim, Y., Hwang, G., Lee, J.-W., Park, J.-C., Kim, D.-S., Kang, M.-G., Chang, I.-S. (2006): Experiences with constructed wetland systems in Korea. – *J Ocean Univ. China* 5: 345. <https://doi.org/10.1007/s11802-006-0027-9>.

- [58] Kimani, R. W., Mwangi, B. M., Gichuki, C. M. (2012): Treatment of flower farm wastewater effluents using constructed wetlands in lake Naivasha Kenya. – *Indian J Sci Technol.* 5: 1870-1878.
- [59] Klomjek, P., Nitorisavut, S. (2005): Constructed treatment wetland: a study of eight plantspecies under saline conditions. – *Chemosphere* 58: 585-593.
- [60] Konnerup, D., Koottatep, T., Brix, H. (2009): Treatment of domestic wastewater in tropical subsurface flow constructed wetlands planted with *Canna* and *Heliconia*. – *Ecol Eng.* 35(2): 248-257. DOI: <https://doi.org/10.1016/j.ecoleng.2008.04.018>.
- [61] Kouki, S., M'hiri, F., Saidi, N., Belaïd, S., Hassen, A. (2009): Performances of a constructed wetland treating domestic wastewaters during a macrophytes life cycle. – *Desalination* 246: 452-467.
- [62] Kurniadie, D. (2011): Wastewater treatment using vertical subsurface flow constructed wetland in Indonesia. – *American Journal of Environmental Sciences* 7(1): 15-19.
- [63] Langergraber, G., Weissenbacher, N. (2017): Constructed wetland. – *Water Science and Technology* 75(10): 2309-2315. DOI: 10.2166/wst.2017.112.
- [64] Leiva, A., Núñez, R., Gómez, G., López, D., Vidal, G. (2018): Performance of ornamental plants in monoculture and polyculture horizontal subsurface flow constructed wetlands for treating wastewater. – *Ecol. Eng.* 120: 116-125. DOI: <https://doi.org/10.1016/j.ecoleng.2018.05.023>.
- [65] León, C., Cháves, D. (2010): Tratamiento de residual vacuno utilizando microalgas, la lenteja de agua *Lemna* aequinoctiales y un humedal subsuperficial en Costa Rica. – *Rev Latinoam Biotecn Amb Alga* 1(2): 155-177. DOI: <https://doi.org/10.1016/j.scitotenv.2015.09.154>.
- [66] Leung, J. Y. S., Cai, Q., Tam, N. F. Y. (2016): Comparing subsurface flow constructed wetlands with mangrove plants and freshwater wetland plants for removing nutrients and toxic pollutants. – *Ecol. Eng.* 95: 129-137.
- [67] Li, G., Wu, Z., Cheng, S., Liang, W., He, F., Fu, G., Zhong, F. (2007): Application of constructed wetlands on wastewater treatment for aquaculture ponds. – *Wuhan University J Natur Sci* 12: 1131-1135. DOI: <https://doi.org/10.1007/s11859-007-0116-7>.
- [68] Li, J., Wen, Y., Zhou, Q., Xingjie, Z., Li, X., Yang, S., Lin, T. (2008): Influence of vegetation and substrate on the removal and transformation of dissolved organic matter in horizontal subsurface-flow constructed wetlands. – *Bioresource Technology* 99: 4990-4996.
- [69] Macci, C., Peruzzi, E., Doni, S., Iannelli, R., Masciandaro, G. (2015): Ornamental plants for micropollutant removal in wetland systems. – *Environ Sci Pollut Res.* 22: 2406-2415. DOI: <https://doi.org/10.1007/s11356-014-2949-x>.
- [70] Madera-Parra, C. A., Peña-Salamanca, E. J., Peña, M. R., Rousseau, D. P. L., Lens, P. N. (2015): Phytoremediation of landfill leachate with *Colocasia esculenta*, *Gynerum sagittatum* and *Heliconia psittacorum* in Constructed Wetlands. – *Int J Phytoreme.* 17: 16-24. DOI: <https://doi.org/10.1080/15226514.2013.828014>.
- [71] Mander, Ü., Kuusemets, V., Öövel, M., Ihme, R., Sevola, P., Pieterse, A. (2000): Experimentally constructed wetlands for wastewater treatment in Estonia. – *Journal of Environmental Science and Health, Part A: Toxic/Hazardous Substances and Environmental Engineering* 35(8): 1389-1401: DOI: 10.1080/10934520009377042.
- [72] Marrugo-Negrete, J., Ortega-Ruíz, J., Navarro-Frómata, A., Enamorado-Montes, G., Urango-Cárdenas, I., Pinedo-Hernández, J., Durango-Hernández, J., Estrada-Martínez, A. (2016): Remoción de cipermetrina presente en el baño de ganado utilizando humedales construidos. – *Corpoica Cienc Tecnol Agrop.* 17(2): 203-216.
- [73] Martin, M., Gargallo, S., Hernández-Crespo, C., Oliver, N. (2013a): Phosphorus and nitrogen removal from tertiary treated urban wastewaters by a vertical flow constructed wetland. – *Ecological Engineering* 61: 34-42.
- [74] Masi, F., Martinuzzi, N. (2007): Constructed wetlands for the Mediterranean countries: hybrid systems for water reuse and sustainable sanitation. – *Desalination* 215: 44-55.

- [75] Mateus, M. D., Vaz, M. M., Capela, I., Pinho, J. H. (2016): The potential growth of sugarcane in constructed wetlands designed for tertiary treatment of wastewater. – *Water* 8(3): 93. <https://doi.org/10.3390/w8030093>.
- [76] Maucieri, C., Mietto, A., Barbera, A. C., Borin, M. (2016): Emerging and eco-friendly approaches for waste management. – *Ecol. Eng.* 94: 406-417.
- [77] Mayo, A., Bigambo, T (2005): Nitrogen transformation in horizontal subsurface flow-constructed wetlands I: model development. – *Physics and Chemistry of the Earth Parts A/B/C* 30: 658-667.
- [78] Mburu, N., Tebitendwa, S. M., Rousseau, D. P., Van Bruggen, J., Lens, P. N. (2012): Performance evaluation of horizontal subsurface flow-constructed wetlands for the treatment of domestic wastewater in the tropics. – *Journal of Environmental Engineering* 139: 358-367.
- [79] McKinlay, R. G., Kasperek, K. (1999): Observations on decontamination of herbicide polluted water by marsh plant system. – *Water Res.* 33: 505-511. DOI: [https://doi.org/10.1016/S0043-1354\(98\)00244-9](https://doi.org/10.1016/S0043-1354(98)00244-9).
- [80] Midhun, G., Divya, L., George, J., Jayakumar, P., Suriyanarayanan, S. (2016): Wastewater Treatment Studies on Free Water Surface Constructed Wetland System. – In: Prashanthi, M., Sundaram, R. (eds.) *Integrated Waste Management in India. Environmental Science and Engineering*. Springer, Cham, pp. 97-109.
- [81] Moges, A., Beyene, A., Kelbessa, E., Mereta, S. T., Ambelu, A. (2016): Development of a multimetric plant-based index of biotic integrity for assessing the ecological stated of forested, urban and agricultural natural wetlands of Jimma Highlands, Ethiopia. – *Ecol. Indic.* 71: 208-217.
- [82] Morales, G., López, D., Vera, I., Vidal, G. (2013): Humedales construidos con plantas ornamentales para el tratamiento de materia orgánica y nutrientes contenidos en aguas servidas. – *Theoria*. 22(1): 33-46. <http://revistas.ubiobio.cl/index.php/RT/article/view/1188>.
- [83] Neralla, S., Weaver, R. W., Lesikar, B. J., Persyn, R. A. (2000): Improvement of domestic wastewater quality by subsurface flow constructed wetlands. – *Bioresour Technol.* 75(1): 19-25. DOI: [https://doi.org/10.1016/S0960-8524\(00\)00039-0](https://doi.org/10.1016/S0960-8524(00)00039-0).
- [84] Newman, J. R., Duenas-Lopez, M. A., Acreman, M. C., Palmer-Felgate, E. J., Verhoeven, J. T. A., Scholz, M., Maltby, E. (2015): A systematic review. Do on-farm natural, restored, managed and constructed wetlands mitigate agricultural pollution in Great Britain and Ireland. – www.defra.gov.uk.
- [85] Niu, S., Park, K., Cheng, J., Kim, Y. (2016): Percentile analysis of rainfall depth estimation on performance of constructed wetland. – *Water Sci. Technol* 73(6): 1483-1491.
- [86] Ojoawo, S., Udayakuman, G., Naik, P. (2015): Phytoremediation of phosphorus and nitrogen with *Canna x generalis* reeds in domestic wastewater through NMAMIT constructed wetlands. – *Aquatic Procedia* 4: 349-356. DOI: <https://doi.org/10.1016/j.aqpro.2015.02.047>.
- [87] Oluseyi, E., Abimbola, S., Thevenot, D. (2011): Urban Waters: Resource or Risks? 11th Ed. – World Wide Workshop for Young Environmental Scientists, France.
- [88] Öovel, M., Tooming, A., Muring, T., Mander, Ü. (2007): Schoolhouse wastewater purification in a LWA-filled hybrid constructed wetland in Estonia. – *Ecological Engineering* 29: 17-26.
- [89] Orozco, C., Cruz, A., Rodríguez, M., Pohlan, A. (2006): Humedal subsuperficial de flujo vertical como sistema de depuración terciaria en el proceso de beneficiado de café. – *Hig Sanid Ambient.* 6: 190-196.
- [90] Patil, S. S., Dhulap, V. P., Kaushik, G. (2016): Application of constructed wetland using *Eichhornia crassipes* for sewage treatment. – *J. Mater. Environ. Sci.* 7(9): 3256-3263.

- [91] Patil, Y. M., Munavalli, G. R. (2016): Performance evaluation of and integrated on-site greywater treatment system in a tropical region. – *Ecol Eng.* 95: 492-500. DOI: <https://doi.org/10.1016/j.ecoleng.2016.06.078>.
- [92] Peng, L., Hua, Y., Cai, J., Zhao, J., Zhou, W., Zhu, D. (2014): Effects of plants and temperature on nitrogen removal and microbiology in a pilot-scale integrated vertical-flow wetland treating primary domestic wastewater. – *Ecological Engineering* 64: 285-290.
- [93] Perez, M., Hernández, J., Bossens, J., Jiménez, T., Rosa, E., Tack, F. (2014): Vertical flow constructed wetlands: kinetics of nutrient and organic matter removal. – *Water Science and Technology* 70: 76-81.
- [94] Permaculture (2015): Wastewater treatment and constructed wetlands. Part One. – <http://www.permaculture-and-sanity.com/pcarticles/constructed-wetland-wastewater-treatment-part1.php>.
- [95] Polomski, R. F., Bielenberg, D. G., Whitwell, T. (2007): Nutrient recovery by seven aquatic garden plants in a laboratory-scale subsurface-constructed Wetland. – *Hortscience* 42(7): 1674-1680.
- [96] Prabuddha, G., Tae-woong, A., Seung-Mok, L. (2015): Use of biochar to enhance constructed wetland performance. – *Environ. Eng. Res.* <http://dx.doi.org/10.4491/eer.2015.067>.
- [97] Prata, R., Matos, A., Cecon, P., Monaco, P., Pimenta, L. (2013): Sewage treatment in wetlands cultivated with yellow lily. – *Eng. Agrícola* 33: 1144-1155. DOI: <http://dx.doi.org/10.1590/S0100-69162013000600007> (in Portuguese).
- [98] Pretorius, M. L., Brown, L. R. (2016): An investigation into the vegetation composition along the topographical gradients of various wetland types to inform wetland delineation in northern Kwazulu-Natal. – *South Africa J of Botany* 103: 345.
- [99] Qiu, Z., Wang, M., Lai, W., He, F., Chen, Z. (2011): Plant growth and nutrient removal in constructed monoculture and mixed wetlands related to stubble attributes. – *Hydrobiologia* 661: 251-260. DOI: <https://doi.org/10.1007/s10750-010-0530-2>.
- [100] Ramírez-Carrillo, H. F., Luna-Pabello, V. M., Arredondo-Figueroa, J. L. (2009): Evaluación de un humedal artificial de flujo vertical intermitente, para obtener agua de buena calidad para la acuicultura. – *Rev Mex Ing Quím.* 8(1): 500-93-99.
- [101] RAMSAR (2016): World wetlands. – <https://www.ramsar.org/activity/world-wetlands-day>.
- [102] Ran, N., Agami, M., Oron, G. (2004): A pilot study of constructed wetlands using duckweed (*Lemnagibba* L.) for treatment of domestic primary effluent in Israel. – *Water Research* 38: 2241-2248.
- [103] Roy, M. C., Foote, L., Ciborowski, J. J. H. (2016): Vegetation community composition in wetlands created following oil sand mining in Alberta, Canada. – *J Environ. Manage.* 172: 18-28.
- [104] Rozema, E. R., Andrew, C., VanderZaag, J., Wood, D., Drizo, A., Zheng, Y., Madani, A., Gordon, R. J. (2016a): Constructed wetlands for agricultural wastewater treatment. – *Water* 8: 173. DOI: 10.3390/w8050173.
- [105] Rozema, E. R., Rozema, L. R., Zheng, Y. (2016b): Controlled environment systems research facility. – *Ecol. Eng.* 86: 262-268.
- [106] Saeed, T., Sun, G. (2011): A comparative study on the removal of nutrients and organic matter in wetland reactors employing organic media. – *Chemical Engineering Journal* 171: 439-447.
- [107] Sanjrani, M. A., Mek, T., Sanjrani, N. D., Leghari, S. J., Moryani, H. T. (2017): Current situation of aqueous arsenic contamination in Pakistan, focused on Sindh and Punjab province, Pakistan: a review. – *J Pollut Eff Cont* 5: 207. DOI: 10.4176/2375-4397.1000207.
- [108] Sanjrani, M. A., Zhou, B., Zhao, H., Bhutto, S. A., Muneer, A. S., Xia, S. B. (2019): Arsenic contaminated groundwater in China and its treatment options. a review – *Applied*

- Ecology and Environmental Research 17(2): 1655-1683. DOI: http://dx.doi.org/10.15666/aeer/1702_16551683.
- [109] Sartori, L., Canobbio, S., Fornaroli, R., Cabrini, R., Marazzi, F., Mezzanotte, V. (2016): COD, nutrient removal and disinfection efficiency of a combined subsurface and surface flow constructed wetland: a case study. – *Int. J. Phytoremediation* 18(4): 416-422.
- [110] Saumya, S., Akansha, A., Rinaldo, J., Jayasri, M. A., Suthindhiran, K. (2015): Construction and evaluation of prototype subsurface flow wetland planted with *Heliconia angusta* for the treatment of synthetic greywater. – *J Cleaner Product*. 91: 235-240.
- [111] Schegolkova, N. M., Rybka, K. Y., Almashin, D. S., Skripchinskij, A. K. (2015): Use of constructed wetlands for xenobiotics removal in climatic conditions of Russia. – *Water: Chemistry and Ecology* 7: 32-42. <http://watchemec.ru/en/article/27436/>.
- [112] Shi, L., Wang, B. Z., Cao, X. D., Wang, J., Lei, Z. H., Wang, Z. R., Liu, Z. Y., Lu, B. N. (2004): Performance of a subsurface-flow constructed wetland in Southern China. – *J Environ Sci.* 16(3): 476-481. <https://content.iospress.com/articles/journal-of-environmental-sciences/jes16-3-27>.
- [113] Sieben, E. J. J., Collins, N. B., Corry, F. T. J., Kotze, D. C., Job, N., Muasya, A. M., Venter, C. E., Mtshali, H. (2016a): The vegetation of grass lawn wetlands of floodplains and pans in semi-arid region of South Africa: description, classification and explanatory environmental factors. – *S Afr J Bot.* 104: 215-224.
- [114] Sieben, E. J. J., Collins, N. B., Mtshali, H., Venter, C. E. (2016b): The vegetation of inland wetlands with salt-tolerant vegetation in South Africa: description, classification and explanatory environmental factors. – *S. Afr. J Bot.* 104: 199-207.
- [115] Sieben, E. J. J., Nyambeni, T., Mtshali, H., Corry, F. T. J., Venter, C. E., MacKenzie, D. R., Matela, T. E., Pretorius, L., Kotze, D. C. (2016c): The herbaceous vegetation of subtropical freshwater wetlands in South Africa: classification, description and explanatory environmental factors. – *S. Afr. J Bot.* 104: 158-166.
- [116] Sievers, M., Parris, K. M., Swearer, S. E., Hale, R. (2018): Stormwater wetlands can function as ecological traps for urban frogs. – *Ecological Applications* 28(4): 1106-1115. DOI: 10.1002/eap.1714.
- [117] Singh, M., Srivastava, R. (2016): Horizontal subsurface flow constructed wetland for heavy metal removal from domestic wastewater. – *Environ Progress Sustain Energy* 35(1): 125-132. DOI: <https://doi.org/10.1002/ep.12214>.
- [118] Singh, S., Haberl, R., Moog, O., Shrestha, R. R., Shrestha, P., Shrestha, R. (2009): Performance of an anaerobic baffled reactor and hybrid constructed wetland treating high-strength wastewater in Nepal—a model for DEWATs. – *Ecol Eng.* 35(5): 654-660. DOI: <https://doi.org/10.1016/j.ecoleng.2008.10.019>.
- [119] Sirianuntapiboon, S., Jitvimolnimit, S. (2007): Effect of plantation pattern on the efficiency of subsurface flow constructed wetland (SFCW) for sewage treatment. – *Afr J Agric Res.* 2: 447-454. DOI: 10.5897/AJAR.
- [120] Skrzypiec, K., Gajewska, M. H. (2017): the use of constructed wetlands for the treatment. – *Journal of Water and Land Development* 34: 233-240. DOI: 10.1515/jwld-2017-0058.
- [121] Sohsalam, P., Sirianuntapiboon, S. (2008): Feasibility of using constructed wetland treatment for molasses wastewater treatment. – *Bioresource Technol.* 99: 5610-5616.
- [122] Sohsalam, P., Englande, A., Sirianuntapiboon, S. (2008): Seafood wastewater treatment in constructed wetlands: tropical case. – *Bioresour Technol.* 99: 1218-1224. DOI: <https://doi.org/10.1016/j.biortech.2007.02.014>.
- [123] Sultana, M. Y., Mourti, C., Tatoulis, T., Akrotos, C. S., Tekerlekopoulou, A. G., Vayenas, D. V. (2016): Artificial or constructed wetlands: a suitable technology. – *J. Chem. Technol. Biotechnol.* 91(3): 726-732.
- [124] Sun, L. P., Liu, Y., Jin, H. (2009): Nitrogen removal from polluted river by enhanced floating bed grown canna. – *Ecol Eng.* 35(1): 135-140. DOI: <https://doi.org/10.1016/j.ecoleng.2008.09.016>.

- [125] Teodoro, A., Boncz, M., Júnior, A., Paulo, P. (2014): Disinfection of greywater pretreated by constructed wetlands using photo-fenton: influence of pH on the decay of *Pseudomonas aeruginosa*. – *J. Environ. Chem. Eng.* 2: 958-962.
- [126] Toro-Vélez, A. F., Madera-Parra, C. A., Peñón-Varón, M. R., Lee, W. Y., Bezares-Cruz, J. C., Walker, W. S., Cárdenas-Henao, H., Quesada-Calderón, S., García-Hernández, H., Lens, P. N. I. (2016): BPA and NP removal from municipal wastewater by tropical horizontal subsurface constructed wetlands. – *Sci Total Environ.* 542: 442-93-101.
- [127] Tsihrintzis, V., Akrotos, C., Gikas, G., Karamouzis, D., Angelakis, A. (2007): Performance and cost comparison of a FWS and a VSF constructed wetland system. – *Environmental Technology* 28: 621-628.
- [128] Tunçsiper, B. (2009): Nitrogen removal in a combined vertical and horizontal subsurface-flow constructed wetland system. – *Desalination.* 247(1-3): 466-475. DOI: <https://doi.org/10.1016/j.desal.2009.03.003>.
- [129] Uggetti, E., Hughes-Riley, T., Morris, R. H., Newton, M. I., Trabi, C. L., Hawes, P., Puigagut (2016): Treatment wetland aeration without electricity? – *J. Sci. Total Environ.* 559: 212-7.
- [130] Upadhyay, A. K., Singh, N. K., Bankoti, N. S., Rai, U. N (2016): Designing and construction of simulated constructed wetland for treatment of sewage containing metals. – *Environ. Technol.* 2016: 1-9.
- [131] Varga, D. de la, Soto M, Arias CA, van Oirschot D, Kilian R, Pascual A, Alvarez JA. 2017. Constructed Wetlands for Industrial Wastewater Treatment and Removal of Nutrients. – In: Val del Rio, A., Campos Gómez, J.L., Mosquera Corral, A. (Eds) *Technologies for the Treatment and Recovery of Nutrients from Industrial Wastewater.* IGI global. pp. 202-230. (Advances in Environmental Engineering and Green Technologies). <https://doi.org/10.4018/978-1-5225-1037-6.ch008>
- [132] Vazquez, M., De La Varga, D., Plana, R., Soto, M. (2013): Vertical flow constructed wetland treating high strength wastewater from swine slurry composting. – *Ecological Engineering* 50: 37-43.
- [133] Vymazal, J. (2007): Constructed Wetlands for Wastewater Treatment: A Review. – *Proceedings of Taal2007: The 12th World Lake Conference: 965-980*, Available online at: <https://pdfs.semanticscholar.org/74be/95cf6073691249fa2b9f45702a4a7f3f440e.pdf>
- [134] Vymazal, J. (2011): Constructed wetland for wastewater treatment, five decades. – *Environ. Sci. Technol.* 45: 61-69.
- [135] Vymazal, J. (2014): Constructed wetlands for treatment of industrial wastewaters: a review. – *Ecological Engineering* 73: 724-751. DOI: 10.1016/j.ecoleng.2014.09.034.
- [136] Vymazal, J., Kröpfelová, L. (2009): Removal of organics in constructed wetlands with horizontal sub-surface flow: a review of the field experience. – *Sci Total Environ* 15(13): 3911-22. DOI: 10.1016/j.scitotenv.2008.08.032.
- [137] Vymazal, J., Kröpfelová, L (2011): A three-stage experimental constructed wetland for treatment of domestic sewage: first 2 years of operation. – *Ecological Engineering* 37: 90-98.
- [138] Wang, W., Ding, Y., Ullman, J., Ambrose, R., Wang, Y., Song, X., Zhao, Z. (2016a): Nitrogen removal performance in planted and unplanted horizontal subsurface flow constructed wetlands treating different influent COD/N ratios. – *Environ Sci Pollut Res.* 23: 9012-9018. DOI: <https://doi.org/10.1007/s11356-016-6115-5>.
- [139] Wang, W., Ding, Y., Wang, Y., Song, X., Ambrose, R. F., Ullman, J. L., Winfrey, B. K. (2016c): Treatment of rich ammonia nitrogen wastewater with polyvinyl alcohol immobilized nitrifier biofortified constructed wetlands. – *Ecol. Eng.* 94: 7-11.
- [140] Wang, W., Wang, X., Zhou, L., Liu, H., Ding, Z., Liang, Y. (2016b): Wastewater treatment in a constructed wetland followed by an oxidation pond in a rural area of China. – *Environmental Engineering & Management Journal* 15(1): 199-205.

- [141] Wen, L., Hua, C., Ping, Z., Xiang, L. (2011): Removal of total phosphorus from septic tank effluent by the hybrid constructed wetland system. – *Procedia Environ Sci* 10: 2102-2107. DOI: <https://doi.org/10.1016/j.proenv.2011.09.328>.
- [142] Weragoda, S. K., Jinadasa, K. B. S. N., Zhang, D. Q., Gersberg, R. M., Tan, S. K., Ng, W. J. (2012): Tropical application of floating treatment wetlands. – *Wetlands* 32(5): 955-961. DOI: <https://doi.org/10.1007/s13157-012-0333-5>.
- [143] WRC UK (2012): Constructed wetland program. – <http://www.wrcplc.co.uk/>.
- [144] Wu, H., Zhang, J., Li, P., Zhang, J., Xie, H., Zhang, B. (2010): Nutrient removal in constructed microcosm wetlands for treating polluted river water in northern China. – *Ecol Eng.* 37: 560-568. DOI: <https://doi.org/10.1016/j.ecoleng.2010.11.020>.
- [145] Wu, H., Fan, J., Zhang, J., Ngo, H. H., Guo, W., Hu, Z., Liang, S. (2015): Decentralized domestic wastewater treatment using intermittently aerated vertical flow constructed wetlands: impact of influent strengths. – *Bioresource Technology* 176: 163-168.
- [146] Wu, H., Fan, J., Zhang, J., Ngo, H. H., Guo, W., Hu, Z., Lv, J. (2016): Optimization of organics and nitrogen removal in intermittently aerated vertical flow constructed wetlands: effects of aeration time and aeration rate. – *Int. Biodeterior. Biodegrad.* 113: 139-145.
- [147] Wu, S., Austin, D., Liu, L., Dong, R. (2011): Performance of integrated household constructed wetland for domestic wastewater treatment in rural areas. – *Ecological Engineering* 37: 948-954.
- [148] Xie, X., He, F., Xu, D., Dong, J., Cheng, S., Wu, Z. (2012): Application of large scale integrated vertical-flow constructed wetland in Beijing Olympic forest park: design, operation and performance. – *Water Environ J.* 26: 100-107.
- [149] Xu, Q., Hunag, Z., Wang, X., Cui, L. (2015): *Pennisetum sinense* Roxb and *Pennisetum purpureum* Schum. as vertical-flow constructed wetland vegetation for removal of N and P from domestic sewage. – *Ecological Engineering* 83: 120-124.
- [150] Yadav, A., Dash, P., Mohanty, A., Abbassi, R., Mishra, B. (2012): Performance assessment of innovative constructed wetland-microbial fuel cell for electricity production and dye removal. – *Ecol Eng.* 47: 126-131. DOI: <https://doi.org/10.1016/j.ecoleng.2012.06.029>.
- [151] Yang, Q., Chen, Z., Zhao, J., Gu, B. (2007): Contaminant removal of domestic wastewater by constructed wetlands: effects of plant species. – *J Integrat Plant Biol.* 49(4): 437-446. DOI: <https://doi.org/10.1111/j.1744-7909.2007.00389.x>.
- [152] Yin, X., Zhang, J., Hu, Z., Xie, H., Guo, W., Wang, Q., Ngo, H. H. (2016): Using the Dashu Old rail bridge constructed wetland system for polluted river water purification and ecosystem rehabilitation. – *Environ. Sci. Pollut. Res.* 23(15): 15524-15531.
- [153] Zachritz, W. H., Hanson, A. T., Saucedo, J. A., Fitzsimmons, K. M. (2008): Evaluation of submerged surface flow (SSF) constructed wetlands for recirculating tilapia production systems. – *Aquacult Eng.* 39: 16-23. DOI: <https://doi.org/10.1016/j.aquaeng.2008.05.001>.
- [154] Zhang, D. Q., Tan, S. K., Gersberg, R. M., Zhu, J., Sadreddini, S., Li, Y. (2012): Nutrient removal in tropical subsurface flow constructed wetlands under batch and continuous flow conditions. – *Journal of Environmental Management* 96: 1-6.
- [155] Zhang, S., Zhou, Q., Xu, D., He, F., Cheng, S., Liang, W., Du, C., Wu, Z. (2010): Vertical-flow constructed wetlands applied in a recirculating aquaculture system for channel catfish culture: effects on water quality and zooplankton. – *Polish J Environ Stud* 19: 1063-1070.
- [156] Zhang, X. B., Liu, P., Yang, Y. S., Chen, W. R. (2007a): Phytoremediation of urban wastewater by model wetlands with ornamental hydrophytes. – *J Environ Sci (China)*: 19(8): 902-909.
- [157] Zhang, Z. H., Rengel, Z., Meney, K. (2007b): Nutrient removal from simulated wastewater using *Canna indica* and *Schoenoplectus validus* in mono- and mixed culture in wetland microcosms? – *Water Air Soil Pollut.* 183(1-4): 95-105.

- [158] Zhao, J., Zhao, Y., Xu, Z., Doherty, L., Liu, R. (2016): Highway runoff treatment by hybrid adsorptive media-baffled subsurface flow constructed wetland. – *Ecol. Eng.* 91: 231-239.
- [159] Zheng, Y., Wang, X. C., Ge, Y., Dzakpasu, M., Zhao, Y., Xiong, J. (2015): Effects of annual harvesting on plants growth and nutrients removal in surface-flow constructed wetlands in northwestern China. – *Ecological Engineering* 83: 268-275.
- [160] Zheng, Y., Wang, X. C., Dzakpasu, M., Ge, Y., Zhao, Y., Xiong, J. (2016): Performance of a pilot demonstration-scale hybrid constructed wetland system for on-site treatment of polluted urban river water in Northwestern China. – *Environmental Science and Pollution Research* 23: 447-454.
- [161] Zhong, F., Wu, J., Dai, Y., Xiang, D., Cheng, S., Ji, H. (2015): Performance evaluation of wastewater treatment using horizontal subsurface flow constructed wetlands optimized by micro-aeration and substrate selection. – *Water Science and Technology* 71: 1317-1324.
- [162] Zurita, F., De Anda, J., Belmont, M. (2006): Performance of laboratory-scale wetlands planted with tropical ornamental plants to treat domestic wastewater. – *Water Qual Res J Canada* 41(4): 410-417. DOI: <https://doi.org/10.2166/wqrj.2006.044>.
- [163] Zurita, F., Belmont, M., De Anda, J., Cervantes-Martínez, J. (2008): Stress detection by laser-induced fluorescence in *Zantedeschia aethiopica* planted in subsurface-flow treatment wetlands. – *Ecol Eng.* 33: 110-118. DOI: <https://doi.org/10.1016/j.ecoleng.2008.02.004>.
- [164] Zurita, F., De Anda, J., Belmont, M. (2009): Treatment of domestic wastewater and production of commercial flowers in vertical and horizontal subsurface-flow constructed wetlands. – *Ecological Engineering*. 35: 861-869.

RELATIONSHIP BETWEEN BLUE CARBON AND METHANE AND THE HYDROCHEMISTRY OF MANGROVES IN SOUTHEAST MEXICO

AGRAZ-HERNÁNDEZ, C. M.¹ – CHAN-KEB, C. A.^{2*} – MUÑIZ-SALAZAR, R.³ – PÉREZ-BALAN, R. A.² – OSTI-SÁENZ, J.¹ – GUTIÉRREZ-ALCÁNTARA, E. J.² – REYES-CASTELLANO, J. E.¹ – MAY-COLLI, L. O.² – CONDE-MEDINA, K. P.² – RUIZ-HERNÁNDEZ, J.²

¹*Instituto EPOMEX, Universidad Autónoma de Campeche, Av. Agustín Melgar s/n entre Juan de la Barrera y Calle 20, Col. Buenavista, A.P. 24039, San Francisco de Campeche, Campeche, México*

²*Facultad de Ciencias Químico Biológicas, Universidad Autónoma de Campeche, Avenida Ing. Humberto Lanz Cárdenas S/N, Colonia Ex Hacienda Kalá, C.P. 24085 San Francisco de Campeche, Campeche, México*

³*Laboratorio de Epidemiología y Ecología Molecular, Escuela de Ciencias de la Salud, Universidad Autónoma de Baja California, Blvd. Zertuche y Blvd. de los Lagos s/n. Fracc. Valle Dorado C.P., Ensenada 22890, Baja California, México*

*Corresponding author

e-mail: carachan@uacam.mx; phone: +52-981-811-9800 (ext. 2010110)

(Received 25th Jul 2019; accepted 4th Dec 2019)

Abstract. The anthropogenic activities change hydrological pattern of mangrove ecosystems affecting their carbon accumulation and methane emissions. For this reason, the aim for this study was to estimate carbon and nitrogen quantity, in addition to methane emission associated with physicochemical parameters from sediment into three mangrove ecosystems (*Los petenes* Biosphere Reserve (BR), *Laguna de Términos* and *Champotón*) with different anthropic pressure and hydrological characteristics along the Campeche coast. Sampling was realized in rainy season and pH, Redox from interstitial water were measured, soil parameters, salinity, methane emissions and carbon concentration were determined simultaneously. Carbon sequestered average in the three study areas was 170 Mg ha⁻¹, significant differences were not observed ($F_{2,29}=0.02$, $p=0.97$). The highest methane emissions were found in *Laguna de Términos* (673.24±922 mg m⁻²h⁻¹), with significant differences ($F_{2,29}=3.55$, $p=0.042$) among the three ecosystems. Carbon sequestration in *Los Petenes* BR established an inverse relationship with methane emissions ($Y=482.4-2.245x$, $R^2=0.67$, $p<0.025$). In *Champotón* ecosystem, carbon sequestration presented a direct correlation with salinity ($Y=-116.3+11.53x$, $R^2=0.70$, $p<0.008$). Methane emissions in *Laguna de Términos* established an inverse relationship with soil pH ($Y=12027-2190x$, $R^2=0.77$, $p<0.0001$), attributed to different environmental conditions and different prevailing anthropic pressures in each ecosystem.

Keywords: redox potential, soil, greenhouse gases, interstitial water, elemental analyzer, environment

Introduction

Globally, mangroves cover approximately 13,776,000 ha (Giri et al., 2011), with Mexico being one of the four countries with the largest mangroves of the 125 countries and territories in which this ecosystem is found, comprising an estimated cover of 770,057 ha (Rodríguez-Zúñiga et al., 2013). Mexico's mangrove forests are found in the watersheds of the Pacific, the Gulf of Mexico and the Gulf of California (Sandoval-Castro et al., 2014). The state of Campeche contains the largest area of mangroves in the country (25.2%) (CONABIO, 2009). The mangroves on this coast are mainly located in the

Laguna de Términos Flora and Fauna Protection Area, the *Los Petenes* Biosphere Reserve and on the Champotón river (Agraz-Hernández et al., 2015).

With the mangroves contributing a great variety of goods and services, they are considered one of the most productive ecosystems of the biosphere (Mazda et al., 1997; Barbier, 2008). They are characterized by functions of great ecological, economic and social value, providing diverse ecosystem services, such as protection against hurricanes and the mitigation of the erosion caused by winds and tides, while also functioning as natural barriers against marine currents and flooding (Alongi et al., 2004). In turn, the mangroves contribute to the retention of sediments and act as a deposit, as well as processing, recycling and exporting organic material and nutrients, and producing oxygen (Vázquez-Lule et al., 2019). Over the last 50 years, approximately a third of the world's mangrove forests has been lost due to anthropogenic activities, such as tourism, badly developed or unsustainable aquaculture, unmoderated industrial and urban development, highway construction, and unsustainable livestock and agricultural practices (Alongi, 2014).

The carbon stock is one of the most important ecosystem services provided by the mangroves, given that it contributes to minimizing the effects of climate change (Kauffman et al., 2013). The efficiency of a mangrove forest in capturing atmospheric CO₂ mainly depends on its density and productivity, the basal area, height and age of the trees, and the photosynthetic efficiency of each species (Siteo et al., 2014), which are, in turn, influenced by the physicochemical characteristics of the water and soil, the topography, the hydroperiod, the sediment dynamics and the climate. The carbon capture capacity of mangroves varies greatly on a global, regional and local level (Mitsch and Gosselink, 2000; De la Peña et al., 2010; Adame et al., 2013).

Alongi (2014) describes how the soil plays an important role in the carbon cycle, also mentioning that carbon sequestration in the mangrove forests occurs due to their low pH values, salinity concentration and hypoxic conditions, which contribute to the accumulation of carbon. However, soil use change caused by anthropogenic activities has negative effects on the carbon cycle, due to the modification of the decomposition rate of litterfall, sedimentation, the loss of plant biomass, and increased methane emission, causing more reduced conditions due to the decreased redox potential. This thus indicates the depletion of oxygen in the soil, an effect which occurs with greater intensity in the presence of the discharge of urban, agricultural, livestock and industrial waste water into the wetlands (Zinn et al., 2005; Lal, 2005). The mangrove wetlands do not efficiently accumulate carbon via photosynthesis, requiring a large amount of nitrogen-based nutrients, such as the nitrites and nitrates produced by the biogeochemical cycle. In this regard, Alongi et al. (2004) mention that the recycling of nutrients, such as nitrogen (N) and carbon (C), in mangrove forests occurs via the decomposition of organic material through the production and defoliation of litterfall, for which reason, the concentration of nitrogen in the soil increases in line with carbon sequestration (Rivera-Monroy et al., 1995; Yimer et al., 2006).

The accumulation of nitrogen in the soil is also associated with the cover and the aerial plant biomass (Hooker and Compton, 2003; Liao, 2007).

The wetlands store carbon with a minimal release of greenhouse gases, due to the inhibition of methanogenesis by sulfates and salinity (Graham et al., 2005). However, various authors have demonstrated that the higher levels of nutrients of anthropic origin (eutrophication) found in mangrove forests generate higher methane emissions into the atmosphere by means of increased microbial activity (Kreuzwieser et al., 2003; Chen et

al., 2010). Abril and Iversen (2002) report that, within marine systems, estuaries are an important source of methane emitted into the atmosphere as a consequence of the constant supply of nutrients of anthropogenic origin. Given the foregoing, the measurement of greenhouse gases (GG), such as methane (CH₄) and nitrous oxide (N₂O), in mangrove ecosystems has generated great interest, at both a global and national level (IPCC, 2001). For years, global estimates of wetland GG levels have been inaccurate, due to the lack of either flow measurements or an understanding of the environmental factors that control them (Lu et al., 1999). The objective of the present study was to estimate the amount of carbon, nitrogen and methane emissions in the soils of four mangrove forests along the length of the Campeche coast and presenting differences in environmental conditions and anthropic activity. It also seeks to relate the capture of carbon and nitrogen and methane emissions to the physicochemical variables of the soil during the rainy season.

Material and methods

Study area and sample collection

The geographical area studied here comprises the southeastern and northeastern parts of the state of Campeche and is divided into three zones: the *Laguna de Términos* (LT) Protected Natural Area, with two sampling sites (Xibujá and Atasta); *Río Champotón* (RC), with one site; and, *Los Petenes* Biosphere Reserve (RBP), with one site (*Río Verde*) (Figures 1 and 2).

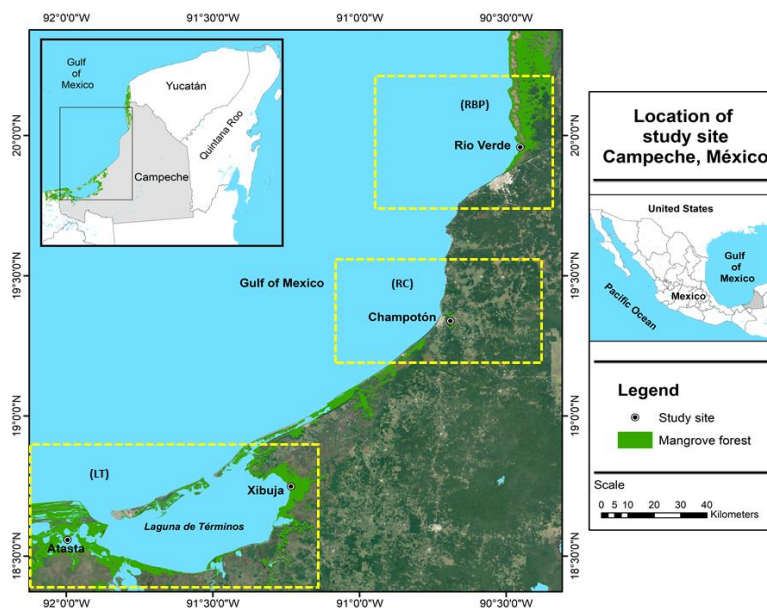


Figure 1. Geographical location established for three mangrove study areas in the southeast of Campeche: The Protected Natural Area Laguna de Términos (LT), Río Champotón (RC) and the Los Petenes Biosphere Reserve (RBP), Campeche

A sampling site was established within two plot of 0.01 hectares for each of three mangrove areas (RBP, RC and LT). Duplicate Samples of interstitial water and soil were obtained in each month of the rainy season (September and October, 2017) for every sampling site.



Site name	Coordinates	
	Latitude N	Longitude W
Río verde (RBP)	19°57'26.10"	90°26'59.40"
Champotón (RC)	19°20'59.87"	90°41'34.85"
Xibujá (LI)	18°44'56.74"	91°14'6.04"
Atasta (LI)	18°35'56.35"	91°57'24.05"

Figure 2. Measurement of the physicochemical parameters of the soil, interstitial water and sampling sites location

Located in the northern region of the state of Campeche, the *Los Petenes* Biosphere Reserve (*Reserva de la Biósfera Los Petenes*, or RBP) forms part of an ecoregion that includes the *Ría Celestún* Biosphere Reserve and the *El Palmar* Protected Natural Area in the state of Yucatán. These areas contain a high diversity of flora and fauna and unique ecosystems, particularly those found in *Los Petenes* and the seagrass beds, with the latter considered to be the largest in the country and in the best state of conservation. In 2004, the *Los Petenes* Biosphere Reserve was declared a RAMSAR site (named after the 1971 Ramsar Convention on Wetlands of International Importance especially as Waterfowl Habitat) in recognition of the peten (or hammock) ecosystems (complex habitats that develop as islands of varied vegetation). These ecosystems are found in only three parts of the world, the Yucatán Peninsula, Cuba and the Florida Peninsula, and are recognized as a wetland of international importance. The *Los Petenes* Biosphere Reserve is found within one of the regions of Mexico considered a priority under all existing categories: *Regiones Prioritarias Terrestres* (RPTs or Priority Terrestrial Regions) (*Petenes-Ría Celestún*, RPT No. 145); *Regiones Marinas Prioritarias* (RMPs or Priority Marine Regions) (*Anillo de Cenotes*, RMP No. 102.); and, *Áreas de Importancia para la Conservación de las Aves* (AICASs or Important Bird Conservation Areas) (*Petenes*, Clave SE-28). Considered the dominant vegetation, mangroves occupy approximately 50% of the terrestrial surface area of the *Los Petenes* Biosphere Reserve. Their principal components are the red mangrove (*Rhizophora mangle*), black mangrove (*Avicennia germinans*), white mangrove (*Laguncularia racemosa*) and the button mangrove (*Conocarpus erectus*). The mangroves of the *Río Verde* study area (located at coordinates Latitude North: 20.756793 and Longitude East: 90.551896) are characterized as fringe-type with riverine, fringe and scrub tendencies.

The municipality of Champotón is located in the central region of the state of Campeche.

The Champotón river, located in *Región Hidrológica Prioritaria* (RHP or Priority Hydrological Region) No. 31 (19°22'LN and 90°43'LN), is approximately 48 kilometers in length from its source close to the community of San Juan Carpizo to where it discharges into the Gulf of Mexico (*Figure 1*). The Champotón river basin is close to 650 km² in area, while the river's volume reaches an annual average of approximately 483.93 million m³. Its median discharge has been estimated at 0.2 x 10⁹ m³ year⁻¹, while its mouth is approximately 85 m wide with an median depth that varies from 2.5 to 4.5 m depending on the tides. The predominant climate is warm subtropical with rains in the summer, with a total annual precipitation of 1100-1500 mm, while the average annual temperature is between 26 and 28°C. The predominant soil types are mainly vertisol, gleysol and lithosol. The *Comisión Nacional para el Conocimiento y Uso de la Biodiversidad* (CONABIO or the Mexican National Commission for the Knowledge and Use of Biodiversity) identifies various types of vegetation in the Champotón river basin, such as tall semideciduous forests, medium subdeciduous forests, low floodable forests, low flood forest, mangroves, flood-prone palm groves, thorn scrub, savannah and cultivated grassland. Among the main anthropogenic activities undertaken in the Champotón river basin are agricultural practices and, to a lesser extent, livestock farming and tilapia aquaculture. Wastewater discharge from the *La Joya S.A de C.V.* sugar mill, based in the former ranch at Haltunchen, is carried by run-off into the river during the rainy season (Dzul-Caamal et al., 2016). The area of mangrove studied in the present research is found on the margin of the Champotón river, at the coordinates 19.35 Latitude and -90.7167 Longitude (*Figure 1*).

The *Laguna de Términos* Flora and Fauna Protection Area (*Área de Protección de Flora y Fauna de Laguna de Términos* or APFFLT) is located between 18°01'54" and 19°13'30" Latitude North and 92°32'33" and 90°59'15" Longitude West. Aquatic and terrestrial plant associations are found in the APFFLT, with high biodiversity, wherein 374 plant species and 1,468 fauna species are identified, the majority of which have been traditionally exploited since pre-hispanic times by the local communities. The surrounding vegetation mainly comprises four mangrove species: *R. mangle*; *A. germinans*; *L. racemose*; and *C. erectus*.

The trees of the *R. mangle* forests in the Atasta, Río San Pedro, and Sontecomapan areas and the mouth of the Grijalva river reach a height of 30 m. and above. In the northern part of the laguna, the *A. germinans* trees reach a height of up to 15 m., while, in the internal areas of the Sabancuy estuary that border the edge of the laguna, scrub-type mangroves, dominated by *R. mangle* and with a height of no higher than 1.5 m., can be found on an exposed soil on a karst topography (Agraz-Hernández et al., 2011 – *Figure 1*).

Chemistry of interstitial water

Two PVC tubes, with a diameter of 10 cm and a length of 1.5 m, were installed at each study site. Orifices, 1 cm in diameter, were made in the lower part of each tube up to the 30 cm mark (the depth at which the maximum root biomass is found). Each tube was installed at a depth of 50 cm from the surface of the soil. The sample was collected once the tube had been drained and the filtration of water into the interior of the tube had been stabilized. In order to determine the availability of the dissolved oxygen in the interstitial water (Chan-Keb et al., 2018), the redox potential was measured by means of the chemical activity of the electrons using a multi-parametric probe (HACH, model HQ40d) and an ORP (Oxidation Redox Potential) electrode. The salinity was determined with an A&O

refractometer, with a 0 to 100 PSU (Practical Salinity Units) measurement interval (Agraz-Hernández et al., 2011). The interstitial water collected during the rainy season in each piezometer was then transferred, via a vacuum pump, to 50 ml flasks, to enable sulfate concentration measurement, which was carried out based on the criteria proposed by Agraz-Hernández et al. (2018) using ion chromatography (IC advanced 861).

Determination of the physicochemical parameters of the mangrove sediments

The soil samples were extracted using corers constructed with PVC tubes 15.24 cm in diameter and 10 cm deep, following the criteria proposed by Satheeshkumar and Khan (2009). Two samples were taken from the first strip of mangrove forest. The pH and redox potential of the soil were taken *in situ* using a multiparametric IQ150. The samples were transported to the coastal wetlands laboratory for physicochemical analysis.

Determination of carbon and nitrogen

The organic carbon and total nitrogen (TN) analysis was conducted via the dry combustion method based on the Dumas principal described by Ruiz-Fernandez et al. (2018), using a FLASH 2000 elemental analyzer.

Between 5 and 10 mg of soil was weighed in silver capsules using a METLER TOLEDO XP6 micro balance with a 0.001 mg precision. The soil was then digested with HCl 1:1 until the inorganic carbon was eliminated, as indicated when the sample ceased bubbling, and then placed in the elemental analyzer. The samples were dried on a heating plate at 50°C and then sealed. In order to obtain precise results, the elemental analyzer was calibrated using both the known standard (sulfanilamide and methionine) and a target.

Soil bulk density

The Soil bulk density was determined via the known volume cylinder method (gcm^{-3}) (Rodríguez-Fuentes and Rodríguez-Absi, 2002). This method consists in introducing the cylinder (sampler) to a depth of 10 cm and a diameter of 15.2 cm, with the cylinder, now saturated with soil, then extracted and transferred to a receptacle and placed in an oven at 105°C until the constant dry weight is obtained. The Soil bulk density was then measured by dividing the dry soil weight by the volume of the cylinder.

Quantification of organic carbon sequestered in the soil

The carbon content in each 10 cm soil core was obtained by multiplying the carbon concentration per depth interval by its apparent density, the corresponding length, and the average amount of organic carbon in the cores extracted per parcel, giving, as a result, the subterranean carbon for each physiognomic type of mangrove identified (Mg C ha^{-1}).

Methane Emission

Methane emissions were determined using static cylindrical chambers manufactured from polyvinyl chloride (PVC) tubes, caps and couplings, which were closed prior to high tide, allowing the accumulation of gases in a minimum time period of three hours, with another sample extracted during low tide. The extraction of gas was undertaken, using a vacuum pump, via brass connectors with $\frac{1}{2}$ " hoses and a 1-liter Tedlar Bag manufactured with classic duPont ® film (SNC, cat No. 232 - 01). The bags were transported to the coastal wetland laboratory, to determine the methane (CH_4) level via a Trace 1310 gas

chromatograph fitted with a flame ionization detector (FID) and a Q 15 m x 0.32 x 10.0 µm TG-Bond column. The working temperatures were 225°C (FID), 230°C (SSL injector) and 60°C. Nitrogen (N₂) at 40 mL/min was used as a carrier gas, while the compressed air flow was 350 mL/min and H₂ was used as a catalyzer gas for the FID at 35 mL/min. The methane concentrations were calculated based on the criteria proposed by Mendoza-Mojica et al. (2013).

$$Flow = \frac{(C_f - C_i) \times Volume}{Time \times Area} \quad (\text{Eq.1})$$

where C_i is the initial concentration and C_f the final concentration of CH₄ gas in mg L⁻¹,
Volume = Volume of the static chamber in liters,
Time = Time in the emission of methane gas in hours,
Area = Area of the static camera in m²,
Flow = Flow of the emission of methane gas in CH₄ m⁻² h⁻¹.

Statistical analysis

A database was generated with the physicochemical parameters of the sediment (NT, Soil bulk density, pH, carbon sequestration and methane emission), as well as the chemical parameters of the interstitial water (salinity, redox potential and sulfates), in the mangrove forests of the coast of the state of Campeche.

A one-way analysis of variance was applied in order to determine the variation among the sites (mangrove areas). Subsequent post hoc analysis Fisher's Least Significant Difference test (LSD) was applied to determine significant differences among means at $p \leq 0.05$ level of significance. For this analysis, the normality of the physicochemical variables was validated by means with a significance level of $\alpha = 0.05$ on non-compliance with the supposed normal distribution. The data were transformed using the Box-Cox method as recommended in Zar (2010), while, principal component analysis (PCA) was applied in order to determine the environmental variables of greatest importance to the soil and interstitial water of the mangrove forests. A simple linear regression analysis was then performed in order establish the relationship among the physicochemical parameters of the interstitial water and sediment in terms of carbon sequestration, methane emission and total nitrogen concentration. The statistical analysis was undertaken with a significance level of $\alpha = 0.05$, using the Statgraphics Centurion XVII software (Statpoint, 2014).

Results

Physicochemical parameters of the interstitial water

In the rainy season, mesohaline conditions presented in the three mangrove areas under study (RBP, RC and LT), which comprise the large part of the cover found in the state of Campeche. The highest salinity levels were registered in RBP and LT (36.0 ± 8.7 and 33.5 ± 8.3 UPS), while the lowest levels were observed in RC (26.3 ± 8.3 UPS). On applying a one-way ANOVA, significant differences were established in the salinity levels measured in three study areas ($F_{2,29} = 3.8$, $p = 0.033$) (Figure 3a). Similar behavior was registered for sulfate concentration, with maximum levels found in RBP and LT (2976.2 ± 1255.2 mg L⁻¹ and $3,180 \pm 1580$ mg L⁻¹) and minimum levels in RC

($2,333 \pm 1,074 \text{ mg L}^{-1}$); however, significant differences were not found ($F_{2,29} = 0.99$, $p = 0.38$) (Figure 3b).

The oxido-reduction conditions established in the interstitial water in RBP were an oxic-hypoxic type of $-290 \pm 23 \text{ mV}$, while RC and LT presented hypoxic-type conditions, with values of -321 ± 27 and $-301 \pm 47 \text{ mV}$, respectively. Significant differences were not established during the rainy reason along the length of the Campeche coast ($F_{2,29} = 1.28$, $p = 0.29$) (Figure 3c).

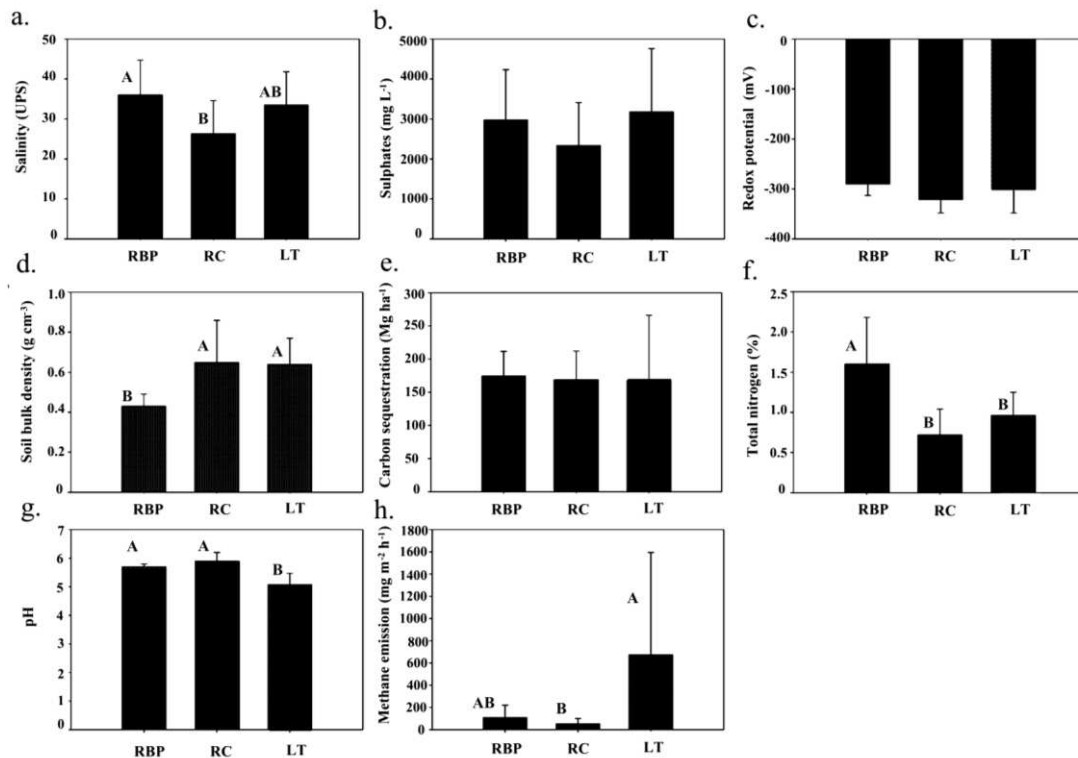


Figure 3. Physicochemical parameters of the interstitial water and soil in three mangrove ecosystems on the coast of the Campeche state. RBP: Reserva de la Biosfera de los Petenes (Los Petenes Biosphere Reserve); RC: Río Champotón (Champotón river); and, LT: Laguna de Términos. the site that do not share a letter are significantly different ($p \leq 0.05$). Error bars represent standard deviation

Physicochemical parameters of the soil

The highest Soil bulk density values were registered in RC and LT ($0.65 \pm 0.21 \text{ g cm}^{-3}$ and $0.64 \pm 0.13 \text{ g cm}^{-3}$), while they were lower in RBP ($0.43 \pm 0.06 \text{ g cm}^{-3}$), presenting significant differences ($F_{2,29} = 6.4$, $p = 0.005$) (Figure 3d).

The highest concentration of total nitrogen (NT) in the soil was $1.6 \pm 0.58\%$ in RBP, followed by $0.96 \pm 0.29\%$ for LT and, finally, $0.72 \pm 0.32\%$ in RC, with significant differences found among them ($F_{2,29} = 12.83$, $p = 0.0001$) (Figure 3f).

The pH conditions of the soil were acidic in the three mangrove areas studied: RC (5.9 ± 0.3); RBP (5.7 ± 0.1); and, LT (5.07 ± 0.40). The one-way ANOVA test revealed significant differences among these ecosystems, despite the minimal differences ($F_{2,29} = 20.29$, $p = 0.0001$) (Figure 3g).

Carbon sequestration

The highest carbon sequestration levels were observed in RBP ($174.6 \pm 37 \text{ Mg ha}^{-1}$), followed by RC and LT ($169 \pm 43 \text{ Mg ha}^{-1}$ and $168 \pm 98 \text{ Mg ha}^{-1}$, respectively), despite which, significant differences were not observed among the mangrove ecosystems in RBP, RC and LT ($F_{2,29} = 0.02$, $p = 0.97$) (Figure 3e).

Behavior of methane emissions

Average methane emissions were higher in LT, with a flow of $673.24 \pm 922 \text{ mg m}^2\text{h}^{-1}$, and lower in RBP and RC, with values of $109.80 \pm 111 \text{ mg m}^2 \text{ h}^{-1}$ and $51.73 \pm 48 \text{ mg m}^2 \text{ h}^{-1}$, respectively. These flows presented significant differences between the study areas ($F_{2,29} = 3.55$, $p = 0.042$) (Figure 3h).

Behavior of methane emissions, in terms of interstitial water conditions and the soil

The results of the PCA, considering the variables of methane emissions and the physicochemistry of the interstitial water and soil, presented three components that explain 71.01% of the total variance in the mangrove forests that border the coast of the state of Campeche. Thus, the first component (28.72%) describes the most important sulfates with a direct relationship with both the salinity and the redox potential of the interstitial water. The second component (22.02%) defines the pH of the soil as the most important factor, presenting an inverse correlation with the methane emissions, while the third component (20.27%) shows that carbon sequestration is the most important parameter, establishing a direct relationship with the TN (Table 1).

Table 1. PCA applied to chemical parameters in the soils of the mangrove forests, with an accumulated 71.01% of the total variance in the first three factors of the mangrove forests on the coast of the state of Campeche

Parameter	Component I (28.72%)	Component II (22.02%)	Component III (20.27%)
ECH ₄ (mg m ⁻² h ⁻¹)	-0.026	0.650	0.197
Soil bulk density (g cm ⁻³)	0.337	0.242	-0.315
CS (Mg ha ⁻¹)	-0.137	0.075	-0.735
TN (%) S	-0.268	-0.139	-0.474
pH S	-0.126	-0.671	0.146
Redox potential (mV) IW	0.450	-0.160	-0.199
Salinity (UPS) IW	0.513	-0.098	-0.147
SO ₄ ⁻² (mg L ⁻¹) IW	0.560	-0.097	0.120

CS: Carbon sequestration; TN: Total nitrogen; ECH₄: Methane emission; SO₄⁻²: sulfates; IW: Interstitial water; and, S: soil

Modeling of carbon sequestration and methane emissions, in relation to the chemical conditions of the interstitial water and soil

In general, the mangrove forests that border the northern (RBP), central (RC) and southern (LT) regions of the state of Campeche have established a direct relationship between carbon sequestration and the TN concentration in the soil (Table 2). The TN presented a direct relationship with carbon sequestration, while methane emissions registered an inverse relationship with the pH of the soil (Table 2).

Table 2. Simple linear regression analysis of carbon sequestration, total nitrogen and methane emissions using the physicochemical parameters of the mangrove forests on the edge of the three mangrove ecosystems found on the coast of the state of Campeche

Ecosystem/dependent variable (Y)	Equation	R ²	p
<i>Los Petenes Biosphere Reserve (RBP)</i>			
ECH ₄ (mg m ⁻² h ⁻¹)	Y = - 1064 - 4.091 X ₂	0.84	0.004
ECH ₄ (mg m ⁻² h ⁻¹)	Y = 482.4 - 2.245 X ₆	0.67	0.025
CS (Mg ha ⁻¹)	Y = 79.99 + 59.56 X ₇	0.76	0.01
<i>Champotón river</i>			
SC (Mg ha ⁻¹)	Y = - 116.3 + 11.53 X ₁	0.79	0.008
CS (Mg ha ⁻¹)	Y = - 23.34 + 264.4 X ₇	0.77	0.004
<i>Laguna de Términos (LT)</i>			
SO ₄ ⁻² (mg L ⁻¹)	Y = - 1946 + 155.1 X ₁	0.92	0.0001
TN _{suelo} (%)	Y = - 0.1744 + 0.0067 X ₆	0.67	0.001
ECH ₄ (mg m ⁻² h ⁻¹)	Y = 12027 - 2190 X ₅	0.77	0.0001
SO ₄ ⁻² (mg L ⁻¹)	Y = 9285 + 21.55 X ₂	0.69	0.001

CS: Carbon Sequestration; TN: Total nitrogen; ECH₄: Methane emissions; SO₄⁻²: sulfates.

Where: X₁ (Salinity in UPS); X₂ (IW redox potential in mV); X₃ (Sulfates in mg L⁻¹); X₄ (Soil bulk density in g cm⁻³); X₅ (pH); X₆ (CS in Mg ha⁻¹); and, X₇ (TN in %). Level of significance: α = 0.05

Specifically, methane emissions in RBP presented an inverse relationship in terms of the redox potential of the interstitial water and carbon sequestration, while the contrary was found for the RC wetlands, in which carbon sequestration presented a direct relationship with the salinity of the interstitial water and the concentration of TN in the soil. For LT, a direct correlation was found with the sulfate concentration, salinity and redox potential of the interstitial water. Similarly, the relationships were significant (p<0.05) (*Table 2*).

Discussion

Behavior of the physicochemical parameters of the interstitial water

The salinity and sulfate concentration varied among sites, increasing from south (LT) to north (RBP). This may be related to the level of ingress of seawater and the ingress from superficial and subterranean rivers, causing a dilution effect in the interstitial water (Chan-Keb et al., 2018) in each of the areas. The ingress of freshwater into the mangroves in this lagoon system is drawn from the Champotón river to the center, with a higher flow in the south (LT), from such sources as the San Pedro, San Pablo, Grijalva and Palizada rivers (Chan-Keb et al., 2018), and decreasing towards the north. The results of this study are similar to that reported by Barreto et al. (2016), who describe how sulfates originate in the seawater and are directly related to the salinity of the interstitial water. Moreover, in Zanzibar, Africa (Siteo et al., 2014), and in Florida, USA (Rivera-Monroy et al., 2007), the low salinity levels found in the mangroves are reported to indicate a higher level of freshwater ingress. Flores-Verdugo et al. (2007) establish that, in the mangrove forests, the interstitial salinity levels are caused by the hydrological pattern, variation in the level of the soil, the evaporation rate and, moreover, the ingress of salts of anthropic origin. The general tendency of the oxido-reduction conditions of the interstitial water in the mangrove areas (RBP, RC and LT) results from the different levels of ingress of freshwater (rivers) and seawater (tides). It is also a consequence of the intensity and

direction of the winds by season of the year ('northerlies' and 'southerlies') and, therefore, the circulation of the lagoon system and/or the marine front.

In turn, this tendency is defined by annual hydrometeorological cycles (precipitation) and the type of anthropic pressure exerted on each ecosystem. Gleason et al. (2003) state that the oxido-reduction conditions are related to hydrology (the residence time of the water, the frequency of flooding due to the effect of the tides, and the ingress of urban and/or industrial wastewater). The highest redox potential values were registered in RBP due to the lower water residence time caused by the continual ebb and flow of the tide, as well as the higher level of freshwater ingress (interstitial and subterranean) during the rainy season. In this regard, Chen et al. (2010) indicate that, during the rainy season, the redox potential increases, as a result of the runoff caused by the rain, the increased river flow and the effect of the tide.

The RC and LT study areas, despite receiving a higher level of freshwater ingress from the rivers than that received by the wetlands of RBP, receive large amounts of organic material resulting from anthropogenic activities, thus causing a greater demand for dissolved oxygen, due to the oxidation of organic material, and, thus, a decrease in redox potential. Mitsch and Gosselink (2000) describe how the hydrological pattern (hydroperiod) and the ingress of organic material are determinants of the oxido-reduction conditions in the mangrove forests, establishing changes in the redox potential. Similar redox potential values have been reported in both Campeche (Chan-Keb et al., 2018) and the Laguna de Términos Flora and Fauna Protection Area (Agraz-Hernandez et al., 2012).

Behavior of the physicochemical parameters of the soil

The variations found in Soil bulk density in the study areas are attributed to the variations in the organic and inorganic composition of the soil among these ecosystems (Agraz-Hernández et al., 2011). Specifically, RBP presents a lower apparent density, due to the high organic material content, the opposite of which was found in RC and LT. Similar behavior is described by Chen and Twilley (2005) in the soils of the mangroves of the state of Florida, USA, and by Moreno et al. (2002) in soils of the mangroves of the state of Tabasco, Mexico.

The general behavior of the pH registered in the three study areas (RBP, RC and LT) presented acidic conditions due to the production of hydrogen sulphide and the formation of humic and fulvic acids during the decomposition of the organic material caused by the ingress of sulfates originating in seawater. Moreover, this was also due to the discharge of wastewater from agricultural and livestock activities. This behavior is similar to that reported by Marchand et al. (2004) and Moreno et al. (2002).

Carbon sequestration

In general, similar carbon sequestration was found among the RBP, RC and LT study areas ($p > 0.05$), despite presenting differences in the physicochemical parameters of the interstitial water and the soil. The foregoing is attributed to the interaction among the hydroperiod, topography and ingress of organic material (Kristensen et al., 2008; Schmidt et al., 2011; Alongi, 2014; Lehmann and Kleber, 2015). The higher levels of carbon sequestration registered in the RBP and RC study areas may be attributed to the ingress of organic material resulting from the generation of *R. mangle* litterfall. *R. mangle* leaves contain a high concentration of lignin, cellulose and lipids, which are complex in structure, thus causing a slow decomposition speed and favoring carbon sequestration (Hogarth, 1999). Other influential factors are the mineralization of organic material and

the decrease in microbial activity in response to the high salinity concentrations (Kreuzwieser et al., 2003; Chen et al., 2010). The opposite was found in LT, where carbon sequestration was lower due to the greater dominance of *A. germinans* (Chan-Keb et al., 2018).

The lower water residence time in RC and LT has established hypoxic conditions in the interstitial water, thus limiting the degradation of organic material and generating carbon sequestration. However, the carbon sequestration results identified by this research are lower than those reported by Kauffman et al. (2011, 2013) in the mangroves of Micronesia (53.4 Mg ha⁻¹), Bangladesh (16.9 Mg ha⁻¹) and Indonesia (28 Mg ha⁻¹), at a depth of 10 cm.

Concentration of total nitrogen

The NT concentration in the three study areas (RBP, RC and LT) presented significant differences ($p < 0.05$), due to the ingress of organic material originating in both litterfall and anthropogenic activity (Rivera-Monroy et al., 1995, 2007). Similarly, the TN concentration in RC and LT may be attributed to the discharge of urban, agricultural and livestock wastewater. Adame et al. (2015) and Alongi et al. (2004) describe how the levels of carbon and nitrogen in the mangroves also originate in allochthonous sources, such as the discharge of urban, agricultural and livestock wastewater, as observed in this study.

Carbon sequestration presented a direct and significant relationship ($p < 0.05$) with the concentration of total nitrogen in the three study areas (RBP, RC and LT) (*Tables 1 and 2*).

In this regard, authors such as Yimer et al. (2006) and Xue and Shaoshan (2019) mention that mangrove forests are efficient in the accumulation of not only carbon, but also nitrogen (Vázquez-Lule et al., 2019).

This is due to the interaction that occurs during the biogeochemical cycle, with these authors emphasizing that nitrogen concentration increases along with increases in carbon sequestration.

Behavior of methane emissions

The variation in methane emissions ($p < 0.05$) in the three mangrove ecosystems on the coast of the state of Campeche results from the differences in the dynamics of the carbon present in first 10 cm of soil, influenced by the prevailing environmental conditions in each study area (Agraz-Hernández et al., 2015). According to the results obtained by the present study, the highest methane emissions are released in the mangrove forest of the LT study area.

The foregoing is a consequence of the constant ingress of terrigenous nutrients (from the Atasta and Palizada rivers), anthropogenic activity, topographic gradient, and, thus, the water residence time and the extent of the flooding, reducing oxido-reduction conditions, pH levels, and salinity, in contrast with the forests of RC and RBP.

Studies by various authors show that increased organic discharge into coastal ecosystems result in significant increases in methane gas emissions (Heyer and Berger, 2000; Purvaja and Ramesh, 2001; Muñoz-Hincapie et al., 2002; Chiu et al., 2004; Punshon and Moore, 2004), caused by the bacterial degradation of this organic material during the processes of methanogenesis. Authors such as Purvaja and Ramesh (2001) consider that mangrove soils are sources of the emission of CH₄, given that they are especially sensitive to methanogenesis and other biogeochemical processes. This increases considerably due to other factors, such as changes to the hydrological pattern,

the ingress of wastewater, or deforestation. However, the results of the present research indicate lower levels than those reported by Alongi et al. (2005), who report an emission level of $0.088 \text{ mg m}^{-2}\text{h}^{-1}$ in the Changning Estuary in China. Moreover, the results obtained by the present study are similar to that reported by Purvaja and Ramesh (2001), who reported emission levels of $15.41 \text{ mg m}^{-2}\text{h}^{-1}$ for the Adyar Estuary in India, while May-Herrera (2017) report methane emissions ranging from 45 to $948 \text{ mg m}^{-2}\text{h}^{-1}$ in the San Pedro river, in the state of Nayarit, Mexico.

Mukhopadhyay et al. (2002) report emissions of 15.4 to $32 \text{ mg m}^{-2}\text{h}^{-1}$ in mangrove forests receiving runoff from the Sundarban river in India.

Conclusions

The highest amount of sequestered carbon was registered in the *Los Petenes* Biosphere Reserve, while, in comparison, significant differences were not observed for the Champotón river and *Laguna de Términos*. In turn, the carbon sequestration presented a direct relationship with the concentration of total nitrogen in the three study areas. This may be due to the production of litterfall by the dominant species, with *R. mangle* dominating the northern and central areas of the Campeche coast, as well as the ingress of organic material and nitrogen of anthropogenic origin.

The highest methane emissions were registered in *Laguna de Términos* ($673.24 \pm 922 \text{ mg m}^{-2} \text{ h}^{-1}$), while the lowest were found in Champotón ($51.73 \pm 48 \text{ mg m}^{-2} \text{ h}^{-1}$), with significant differences found between the study areas ($p < 0.05$). The highest level of methane released in the mangrove forest in LT presented an inverse relationship with the pH of the soil.

This is a consequence of the constant ingress of terrigenous nutrients (from the Atasta and Palizada rivers), anthropogenic activity, topographic gradient, and, thus, the water residence time and the extent of the flooding, reducing oxido-reduction conditions, pH levels, and salinity, in contrast with the forests of RC and RBP.

The results of the present study demonstrate that the quantity of carbon and methane emitted on the coast of the state of Campeche depended on the hydrochemical variables of both the soil and the interstitial water, as well as the different prevailing anthropic pressures in each ecosystem.

The results in this study were obtained only in the rainy season, so carbon sequestration and methane emission could be different throughout year and to be influenced by other physicochemical parameters of interstitial water and soil. For further research on this topic it is necessary to include physicochemical parameters of interstitial water such as micronutrients and monitor the profiles (quantities) of sequestration and emission of methane at three different times of the year.

REFERENCES

- [1] Abril, G., Iversen, N. (2002): Methane dynamics in a Shallow, non-tidal estuary (Ramders Fjord, Denmark). – *Marine Ecology Progress Series* 230: 171-181.
- [2] Adame, M. F., Kauffman, J. B., Medina, I., Gamboa, J. N., Torres, O., Caamal, J. P., Reza, M., Herrera-Silveira, J. A. (2013): Carbon stocks of tropical coastal wetlands within the karstic landscape of the Mexican Caribbean. – *PloS One* 8(2): e56569.

- [3] Adame, M. F., Santini, N. S., Tovilla, C., Vázquez-Lule, A., Castro, L., Guevara, M. (2015): Carbon stocks and soil sequestration rates of tropical riverine wetlands. – *Biogeosciences* 12(12): 3805-3818.
- [4] Agraz-Hernández, C. M., García Zaragoza, C., Iriarte-Vivar, S., Flores-Verdugo, F. J., Moreno Casasola, P. (2011): Forest structure, productivity and species phenology of mangroves in the La Mancha lagoon in the Atlantic coast of Mexico. – *Wetlands Ecology Management* 19: 273-293.
- [5] Agraz-Hernández, C. M., Chan-Keb, C. A., Iriarte-Vivar, S., Posada-Vanegas, G., Vega-Serratos, B. E., Osti-Sáenz, J. (2015): Phenological variation of *Rhizophora mangle* L. and ground water chemistry associated to changes of the precipitation. – *Hydrobiológica* 25(1): 61-73.
- [6] Agraz-Hernández, C. M., del Río-Rodríguez, R., Chan-Keb, C. A., Osti-Saenz, J., Muñiz-Salazar, R. (2018): Nutrient Removal Efficiency of *Rhizophora mangle* (L.) Seedlings Exposed to Experimental Dumping of Municipal Waters. – *Diversity* 10(1): 1-16.
- [7] Alongi, D. M., Sasekumar, A., Chong, V. C. (2004): Sediment accumulation and organic material flux in a managed mangrove ecosystem: estimates of land–ocean– atmosphere exchange in peninsular Malaysia. – *Mar. Geol.* 208: 383-402.
- [8] Alongi, D. M., Pfitzner, J., Trott, L. A., Tirendi, F., Dixon, P., Klumpp, D. W. (2005): Rapid sediment accumulation and microbial mineralization in forests of the mangrove *Kandelia candel* in the Jiulongjiang Estuary, China. – *Estuar. Coast. Shelf Sci.* 63(4): 605-618.
- [9] Alongi, D. M. (2014): Carbon cycling and storage in mangrove forests. – *Annual review of marine science* 6: 195-219.
- [10] Barreto, M. B., Mónaco, S. L., Díaz, R., Barreto-Pittol, E., Lopez, L., Ruaro Peralba, M. do C. (2016): Soil organic carbon of mangrove forest (*Rhizophora* and *Avicennia*) of the Venezuelan Caribbean coast. – *Organic Geochemistry* 100: 51-61.
- [11] Chan-Keb, C. A., Agraz-Hernández, C. M., Muñiz-Salazar, R., Posada-Vanegas, G., Osti-Sáenz, J., Reyes Castellano, J. E., Conde-Medina, K. P., Vega-Serratos, B. E. (2018): Ecophysiological Response of *Rhizophora mangle* to the Variation in Hydrochemistry during Five Years along the Coast of Campeche, México. – *Diversity* 10(1): 1-9.
- [12] Chen, R., Twilley, R. (2005): A simulation model of organic matter and nutrient accumulation in mangrove wetland soils. – *Biogeochemistry* 44(1): 93-118.
- [13] Chen, G. C., Tam, N. F. Y., Ye, Y. (2010): Summer fluxes of atmospheric greenhouse gases N₂O, CH₄ and CO₂ from mangrove soil in South China. – *Sci Total Environ* 408: 2761-2767.
- [14] Chiu, C. Y., Lee, S. C., Chen, T. H., Tian, G. (2004): Denitrification associated N loss in mangrove soil. – *Nutrient Cycling in Agroecosystems* 69: 185-189.
- [15] CONABIO (2009): Manglares de México: Extensión y distribución. – Comisión Nacional para el Conocimiento y Uso de la Biodiversidad. Mexico D.F.
- [16] De la Peña, A., Rojas, C. A., De la Peña, M. (2010): Valoración económica del manglar por el almacenamiento de carbono, Ciénaga Grande de Santa Marta. – *Clío América* 4(7): 133-150.
- [17] Dzul-Caamal, R., Hernández-López, A., Gonzalez-Jáuregui, M., Padilla, S. E., Girón-Pérez, M. I., Vega-López, A. (2016): Usefulness of oxidative stress biomarkers evaluated in the snout scraping, serum and Peripheral Blood Cells of *Crocodylus moreletii* from Southeast Campeche for assessment of the toxic impact of PAHs, metals and total phenols. – *Comparative Biochemistry and Physiology, Part A.* 200: 35-46.
- [18] Flores-Verdugo, F., Casasola, P. M., Agraz-Hernández, C. M., Rosas, H. L., Pardo, D. B., Bello, A. C. T. (2007): La topografía y el hidroperiodo: dos factores que condicionan la restauración de los humedales costeros. – *Boletín de la Sociedad Botánica de México* 80: 33-47.

- [19] Giri, C., Ochieng, E., Tieszen, L. L., Zhu, Z., Singh, A., Loveland, T., Masek, J., Duke, N. (2011): Status and distribution of mangrove forests of the world using earth observation satellite data. – *Global Ecology and Biogeography* 20(1): 154-159.
- [20] Gleason, S. M., Ewel, K. C., Hue, N. (2003): Soil redox conditions and plant–soil relationships in a Micronesian mangrove forest. – *Estuarine, Coastal & Shelf Science* 56: 1065-1074.
- [21] Graham, S. A., Craft, C. B., McCornick, P. V., Aldous, A. (2005): Forms and accumulation of soil P in natural and recently restored peatlands-upper Klamath Lake, Oregon, USA. – *Wetlands* 25: 594-606.
- [22] Heyer, J., Berger, U. (2000): Methane emission from the coastal area in the Southern Baltic Sea. – *Estuarine, Coastal and Shelf Science* 51: 13-30.
- [23] Hogarth, P. J. (1999): *The biology of mangroves. Biology of habitats.* – Oxford University Press, 228 p.
- [24] Hooker, T. D., Compton, J. E. (2003): Forest ecosystem carbon and nitrogen accumulation during the first century after agricultural abandonment. – *Ecol. Appl.* 13: 299-313.
- [25] IPCC. (2001): Atmospheric chemistry and greenhouse gases. – In: Houghton, J. H., Ding, Y., Griggs, D. J., Noguer, M., van der Linden, P. J., Dai, X., Maskell, K., Johnson, C. A. (eds.) *Climate change 2001: The scientific basis.* pp 239-287. Cambridge University Press, Nueva York.
- [26] Kauffman, J. B., Heider, C., Cole, T. G., Dwire, K. A., Donato, D. C. (2011): Ecosystem carbon stocks of Micronesian mangrove forests. – *Wetlands* 31: 343-352.
- [27] Kauffman, J. B., Donato, D. C., Adame, M. F. (2013): Protocolo para la medición, monitoreo y reporte de la estructura, biomasa y reservas de carbono de los manglares. – Documento de Trabajo 117. Bogor, Indonesia: CIFOR.
- [28] Kreuzwieser, J., Buchholtz, J., Rennerberg, H. (2003): Emission of methane and nitrous oxide by Australian mangrove ecosystems. – *Plant Biol* 5: 423-43.
- [29] Kristensen, E., Bouillon, S., Dittmar, T., Marchand, C. (2008): Organic carbon dynamics in mangrove ecosystems: A review. – *Aquat. Bot.* 89: 201-219.
- [30] Lal, R. (2005): Soil carbon sequestration in natural and managed tropical forest ecosystems. – *J Sustain For* 21: 1-30.
- [31] Lehmann, J., Kleber, M. (2015): The contentious nature of soil organic matter. – *Nature* 528: 60-68.
- [32] Liao, C., Luo, Y., Jiang, L., Zhou, X., Fang, C., Chen, J., Li, B. (2007): Invasion of *Spartina alternifolia* enhanced ecosystem carbon and nitrogen stocks in the Yangtze Estuary, China. – *Ecosystems* 10: 1351-1361.
- [33] Marchand, C., Baltzer, F., Lallier-Vergès, E., Albéric, P. (2004): Pore water chemistry in mangrove sediments in relationship to species composition and developmental stage (French Guiana). – *Marine Geology* 208: 361-381.
- [34] May-Herrera, C. I. (2017): Respuesta morfofisiológica del manglar ante el cambio de las condiciones ambientales y emisiones de metano por influencia antrópica. – Tesis de maestría Instituto EPOMEX Universidad Autónoma de Campeche. Campeche, Mexico.
- [35] Mazda, Y., Magi, M., Kogo, M., Hong, P. N. (1997): Mangroves as a coastal protection from waves in the Tong King delta, Vietnam. – *Mangr. and Salt Marsh.* 1(2): 127-135.
- [36] Mendoza Mojica, M., Martínez Arroyo, A., Espinosa Fuentes, M. de la L., Peralta Rosales, Ó., Castro Romero, T. (2013): Caracterización de dos lagunas costeras del Pacífico tropical mexicano en relación con el contenido de carbono y la captura y emisión de CH₄ Y CO₂. – *Revista internacional de contaminación ambiental* 29(2): 145-154.
- [37] Mitsch, W. J., Gosselink, J. G. (2000): *Wetlands.* – 3rd edition, New York. John Wiley & Sons, 920 p.
- [38] Moreno-Cáliz, E., Guerrero-Peña, A., Gutiérrez- Castorena, M. C., Ortíz Solorio, C., Palma-López, D. J. (2002): Los manglares de Tabasco, una reserva natural de carbono. – *Maderas y bosques* 8: 115-128.

- [39] Mukhopadhyay, S. K., Biswas, H., De, T. K., Sen, B. K., Sen, S., Jana, T. K. (2002): Impact of Sundarban mangrove biosphere on the carbon dioxide and methane mixing ratios at the NE Coast of Bay of Bengal, India. – *Atmospheric Environment* 36(4): 629-638.
- [40] Muñoz-Hincapié, M., Morell, J. M., Corredor, J. E. (2002): Increase of nitrous oxide flux to the atmosphere upon nitrogen addition to red mangroves sediments. – *Marine Pollution Bulletin* 44: 992-996.
- [41] Punshon, S., Moore, R. (2004): Nitrous oxide production and consumption in a eutrophic coastal embayment. – *Marine Chemistry* 91(1-4): 37-51.
- [42] Purvaja, R., Ramesh, R. (2001): Natural and anthropogenic methane emission from coastal wetlands of South India. – *Environ. Manage.* 27(4): 547-557.
- [43] Rivera-Monroy, V. H., de Mutsert, K., Twilley, R. R., Castaneda-Moya, E., Romigh, M. M., Davis, S. E. (2007): Patterns of nutrient exchange in a riverine mangrove forest in the Shark River estuary, Florida, USA. – *Hydrobiologica* 17(2): 169-178.
- [44] Rodríguez-Fuentes, H., Rodríguez-Absi, J. (2000): Métodos de análisis de suelos y plantas: criterios de interpretación. – 1st ed., México D.F, Trillas, UANL.
- [45] Rodríguez-Zúñiga, M. T., Troche-Souza, C., Vázquez-Lule, A. D., Márquez-Mendoza, J. D., Vázquez-Balderas, B., Valderrama-Landeros, L., Velázquez-Salazar, S., Cruz-López, M. I., Ressler, R., Uribe-Martínez, A., Cerdeira-Estrada, S. (2013): Manglares de México/Extensión, distribución y monitoreo. – Comisión Nacional para el Conocimiento y Uso de la biodiversidad. México D.F.
- [46] Ruiz-Fernández, A. C., Agraz-Hernández, C. M., Sanchez-Cabeza, J. A., Díaz-Asencio, M., Pérez-Bernal, L. H., Keb, C. C., López-Mendoza, P. G., Correa, J. B., Ontiveros-Cuadras, J. F., Saenz, J. O., Castellanos, J. R. (2018): Sediment geochemistry, accumulation rates and forest structure in a large tropical mangrove ecosystem. – *Wetlands* 38(2): 307-325.
- [47] Sandoval-Castro, E., Dodd, R. S., Riosmena-Rodríguez, R., Enríquez-Paredes, L. M., Tovilla-Hernández, C., López-Vivas, J. M., Muñoz-Salazar, R. (2014): Post-glacial expansion and population genetic divergence of mangrove species *Avicennia germinans* (L.) Stearn and *Rhizophora mangle* L. along the Mexican coast. – *PLoS One* 9(4): e93358.
- [48] Satheeshkumar, P., Khan, B. A. (2009): Seasonal variations in physico-chemical parameters of water and sediment characteristics of Pondicherry mangroves. – *African Journal of Basic and Applied Sciences* 1(1-2): 36-43.
- [49] Schmidt, M. W. I., Torn, M. S., Abiven, S., Dittmar, T., Guggenberger, G., Janssens, I. A., Kleber, M., Kögel-Knabner, I., Lehmann, J., Manning, D. A. C., Nannipieri, P., Rasse, D. P., Weiner, S., Trumbore, S. E. (2011): Persistence of soil organic matter as an ecosystem property. – *Nature* 478: 49-56.
- [50] Siteo, A., Mandlate, L., Guedes, B. (2014): Biomass and carbon stocks of Sofala bay mangrove forests. – *Forests* 5(8): 1967-1981.
- [51] Vázquez-Lule, A., Colditz, R., Herrera-Silveira, J., Guevara, M., Rodríguez-Zúñiga, M. T., Cruz, I., Vargas, R. (2019): Greenness trends and carbon stocks of mangroves across Mexico. – *Environmental Research Letters* 14(7): 075010.
- [52] Xue, Z., An, S. (2018): Changes in soil organic carbon and total nitrogen in a small hydrographic basin scale as a result of the conversion of land use on the Loess Plateau. – *Sustainability* 10(12): 4757.
- [53] Yimer, F., Ledin, S., Abdelkair, A. (2006): Soil organic carbon and total nitrogen stocks affected by topographic aspect and vegetation in the Bale Mountains, Ethiopia. – *Geoderma* 135: 335-344.
- [54] Zar, J. H. (2010): *Biostatistical Analysis*. – 5th Edition. Pearson Prentice-Hall, Upper Saddle River, NJ.
- [55] Zinn, Y. L., Lal, R., Resck, D. V. S. (2005): Changes in soil organic carbon stocks under agriculture in Brazil. – *Soil Till. Res.* 84: 28-40.

PLASTIC FILM-MULCHING WITH APPROPRIATE SEEDING RATE ENHANCES YIELD AND WATER USE EFFICIENCY OF DRYLAND WINTER WHEAT IN LOESS PLATEAU, CHINA

ZHAO, J.¹ – KHAN, S.¹ – ANWAR, S.² – MO, F.¹ – MIN, S.^{1*} – YU, S.¹ – DONG, S.¹ – REN, A.¹ – LIN, W.¹ – YANG, Z.¹ – HOU, F.¹ – GAO, Z.^{1*}

¹College of Agriculture, Shanxi Agricultural University, Taigu 030801, Shanxi, PR China

²Institute of Molecular Biology and Biotechnology, The University of Lahore, Lahore, Pakistan

*Corresponding author

e-mail: sunmin@163.com; phone: +86-354-628-7226

(Received 23rd Jul 2019; accepted 31st Oct 2019)

Abstract. The arid and semi-arid regions of Loess Plateau in China are major winter wheat producing areas where water shortage is limiting wheat production. Present study was designed to analyzed the water consumption characteristics of plastic film-mulched wheat under different seeding rates in order to attain a high yield of dryland wheat. Wheat was sown in dryland areas of Shanxi province, China during the 2014-2016 growing seasons at different seeding rates (60, 75, 90, 105 and 120 kg h⁻¹) under ridged plastic film mulching and flat sowing without mulching. The results showed that the plastic film mulching had increased the total water consumption (7.8-11%), water use efficiency (7.6%-11.3%), number of tillers (8-16%), and grain yield (15.9-23.6%). Water use efficiency, water consumption, and yield were highest at 90 kg h⁻¹ under film mulching and 105 kg h⁻¹ under no mulching. Increasing seeding rate had increased the number of tillers per unit area and leaf area index, while reduced the number of grains per panicle and 1000 grains weight whereas, yield was increased first and then decreased. Therefore, film-mulching with appropriate seeding rate is an effective approach to enhance yield and water use efficiency of dryland wheat.

Keywords: dryland wheat, biomass, grain to leaf ratio, planting density, water consumption

Introduction

Insufficient precipitation during the growth stages of wheat and shortages of irrigation water in dryland wheat (*Triticum aestivum* L.) producing areas are major constraints to high yield (Li et al., 2017). The arid and semi-arid area of the Loess Plateau is typical rainfed and 60% of the dryland area is under wheat cultivation (Jin et al., 2007). Previous reports indicated that there is a potential to increase wheat yield in this region by sufficient irrigation (Mo et al., 2005; Liu et al., 2007). However, due to the distribution of the area and limited surface and ground water, an increase in irrigation is not possible, therefore, increasing water use efficiency is of great importance (Huang et al., 2003; Mo et al., 2005). The cropping system of the Loess Plateau is mainly a monocropping of winter wheat with a 3-month fallow during the rainy summer season (Deng et al., 2006). Even though the precipitation in this region is enough for the wheat requirement but most of rainfall (60-70%) falls during summer season which does not coincide with the growing season of winter wheat (Liu et al., 2007). Therefore, less soil water content severely limits the wheat yield (Sun et al., 2016). Conserving soil moisture at the summer fallow period and adjusting water consumption rate according to the growth stages of plant are the main objectives for sustainable wheat production in Loess Plateau (Zhang et al., 2013; Liang et al., 2019; Xue et al., 2019). Management practices which modulate the plant population density and conserve soil moisture can regulate the seasonal partitioning of water use (Zhang et al., 2013).

Reduction in grain yield also depends on the physiological stage of the plants under water stress (Destro et al., 2001). Grain yield could be expressed as the product of yield components such as grain weight, number of grains per spike and number of effective tillers. Tillering is important trait which effect yield as less tillers reduce yield by producing less spikes while too high tillering affect yield by reducing water use efficiency, competition for resource utilization and inducing lodging (Hou and Huang, 2009; Wang et al., 2009; Yang et al., 2019). Number of seeds planted and effective number of tillers significantly effect yield. Number of tillers survived until reproductive stage to contribute to yield (Yang et al., 2019). Water stress at the booting and stem elongation stage resulted in tillers mortality by restricting water and nutrient availability. Seeding rate also affect the yield by tillering and water consumption (Ren et al., 2019; Yang et al., 2019). Previous studies indicated that increasing seeding rate to a certain amount could increase the number of spikes and yield of dryland wheat (Ma et al., 2018; Yang et al., 2019). However, higher seeding rate could also increase the water consumption which could induce water shortage at later growth stages (Ren et al., 2019).

Using reasonable cultivation measures to maintain soil moisture and increase yield have always been the main objectives of research in dryland area (Yang and Chai, 2019). Film mulching is one of the effective measures to improving soil water storage and agronomic traits (Wang et al., 2009; Ren et al., 2017). Mulching can effectively conserve the rainwater by reducing evaporation and increase soil water content, promote the transfer of soil moisture from deep to the surface layer by vapor transfer, which can increase efficiency of water utilization during critical growth stage (Hou et al., 2014; Ma et al., 2018). Wang and Shagguan (2015) reported that ridge furrow mulching is the best practice for conserving soil moisture at planting and increasing yield of dryland wheat. It has been studied that the increase in yield by film mulching is based on the higher water consumption of crops, and the water consumption during the whole growth period of crops after mulching is significantly higher than that of open field (Gan et al., 2013; Hou et al., 2013). However, some studies have shown that the film mulching increased water consumption by higher vegetative growth which resulted in less soil moisture at the later stages of growth, leading to reduced yield (Li et al., 2000; Zhang et al., 2013). Du et al. (2005) reported that plastic film-mulching increased grain yield but reduced the reproductive allocation and increased the number of sterile tillers due to increased competition between the survived plants.

The water consumption process of crops is affected by many factors and change of soil hydrothermal conditions after film mulching will inevitably affect the growth and development process of crops, which in turn will affect the water consumption characteristics of crops, leading to changes in crop yield and water use efficiency (Huang et al., 2005). In order to reduce the problems caused by water shortage, balancing water consumption by adopting plastic film-mulching and adjusting plating density is one of the important cultivation measures to achieve high yield.

Although plastic film-mulching is being extensively applied in semi-arid and arid regions of North and Northwest China to increase yield, however the underlying mechanisms and impact of plastic film-mulching on crop yields is still under debate. At present only a few researches had focused the water consumption characteristics under plastic film-mulching. Therefore, we designed a two-year study with objectives (i) to analyze the difference in water utilization efficiency and biomass allocation of wheat between ridge-furrow plastic film-mulching and flat planting with no mulching condition, (ii) to optimize the effect of different sowing rates on the water consumption

and tiller formation, and (iii) to access the contribution of mulching and seeding rate to enhancing yield traits of dryland wheat.

Materials and methods

Site description

Subheading

The field experiment was performed in wheat growing season from 2014-2016 at the Agriculture Station of Shanxi Agricultural University, China. Experimental site is alongside a hill at the dryland area of Loess Plateau, located to the north of Yuncheng Basin, Shanxi province. This winter wheat planting area has semi-arid, monsoon climate with cold and dry winters and warm summers with the typical characteristics of the Loess Plateau. The average annual rainfall is 450-630 mm, average annual temperature is 11-13 °C, annual sunshine is 2,200-2,500 h, and 190-230 frost-free days. Experimental field has a flat terrain, and soil is clay loam with good permeability and pH of 20 cm soil was 7.5-8.0. Nutrient contents of soil are presented in *Table 1*.

Table 1. Soil properties in experimental location

Year	Organic matter (g kg ⁻¹)	Total nitrogen (g kg ⁻¹)	Alkaline hydrolysis nitrogen (mg kg ⁻¹)	Available phosphorus (mg kg ⁻¹)
2014-2015	10.55	0.68	37.65	17.64
2015-2016	9.27	0.86	41.31	10.25

In this experimental area, wheat is planted once a year without irrigation. Natural precipitation is the main source of water for crop cultivation in this area, and precipitation mainly concentrating in July-September, which is the fallow period of wheat. Precipitation during experimental years and long-term average of 10 years are given in *Table 2*. Total precipitation in 2014-2015 was 516.7 mm, from which 151.1 mm was during winter wheat growth period and 365.6 mm was in the fellow periods. In 2015, precipitation before flowering was more than average in 2015, but flowering to maturity was 73% less than the long-term average, and drought was during the grain filling period. In 2015-2016, total precipitation was 386.8 mm, and precipitation during growth and fallow period was 292.1 mm and 94.7 mm, respectively. Precipitation from sowing to wintering and jointing to maturity was abundant, but the fallow period and wintering to jointing precipitation was about 64% less than the average precipitation with severe drought during the early growth period.

Table 2. Precipitation at the experimental site in Wenxi (mm)

Year	Fallow period	S-W	W-J	J-A	A-M	Total
2005-2016 mean	265.0 ± 107.5	53.2 ± 35.9	30.2 ± 13.6	37.8 ± 15.8	64.4 ± 29.7	450.5 ± 96.7
2014-2015	365.6	21.5	50.8	61.2	17.6	516.7
2015-2016	94.7	101.2	11.0	57.1	122.8	386.8

Source: Meteorological Observation of Wenxi County, Shanxi Province, China

Fallow period: Jun 21 to Sep 30; S-W (sowing–wintering): Oct 1 to Nov 30; W-J (wintering–jointing): Dec 1 to Apr 10 in the following year; J-A (jointing–anthesis): Apr 11 to May 10; A-M (anthesis–maturity): May 11 to Jun 10

Experimental design and treatments

The wheat cultivar ‘Jinmai92’ used in this experiment was obtained from Wenxi Agriculture Bureau. The two factors split-plot design was adopted, the seeding method as the main factor and sowing density as sub-plot factor. The sowing methods were film mulching with ridges and no mulching without ridges. The seeding rates were 60, 75, 90, 105, and 120 kg h⁻¹ (D₆₀, D₇₅, D₉₀, D₁₀₅, D₁₂₀). All treatments were replicated 3 times. The area of each plot was 135 m² (9 m × 15 m).

Winter wheat was sown in October in 2014 and 2015 and harvested in June of the following year. Stubble (about 25 cm high) was left in field after harvesting wheat. In mid-July, deep ploughing was conducted at the depth of 25-30 cm and 1500 kg h⁻¹ of commercial organic fertilizer (containing 45% organic matter, 1.2% available N, 1% available P, 0.3% available K) was applied to the soil. In August, rotary tillage was used to crumble large lump and level the fields. Before sowing, 150 kg h⁻¹ of nitrogen (46% urea), phosphorous (16% P₂O₅) and potassium (52% K₂O) were applied to soil and no fertilizer was applied during growth seasons. Ridging, mulching and sowing are completed at one time. The width and height of ridge was 30 cm and 15 cm respectively and ridges were covered from top with plastic film (*Fig. 1*).

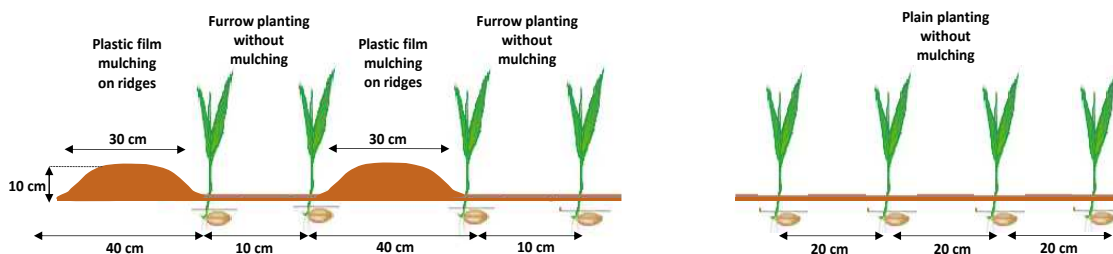


Figure 1. Schematic representation of ridged film-mulching and without mulching

The transparent plastic film with 0.008 mm thickness and 1.2 m width was used for mulching. Two rows of wheat were planted on the sides of the ridges at narrow row spacing of 20 cm and wide row spacing of 40 cm (*Fig. 2*). At three-leaf stage, planting density of 150×10^4 , 187.5×10^4 , 225×10^4 , 262.5×10^4 , 300×10^4 plants h⁻¹ was attained by thinning. Plastic film was removed 10-15 days after anthesis (mid-May of the next year). In no mulching plots, seeds were sown at 3-5 cm soil depth at a row spacing of 20 cm. Crop phenology was recorded when half of the plants reached the wintering (GS23), jointing (GS31), anthesis (GS61), and maturity stage (GS92), using the Zadoks scale (Zadoks, 1974). Weeds were controlled by hand.

Plant sampling and analysis

The plants and soil samples were collected for analysis, according to the phenology of wheat crop (Zadoks, 1974) when 50% of the wheat plants reached at the corresponding jointing (GS30), anthesis (GS60), and maturity (GS100) stage.

Determination of total stem and tiller and effective tillers rate

The total number of stems or tillers was investigated at the jointing stage and the number of fertile tillers were counted at late grain filling stage. The number of tillers was calculated from the area of 1 m² at 3 random points from each plot and average at

each plot was the number of stem and tillers. The effective tiller rate was calculated as the proportion of main stem and tiller at jointing stage to the number of effective panicles at maturity.



Figure 2. Field preparation at experimental site of Shanxi Agricultural University

Biomass and yield

At maturity, the number of panicles per unit area, the average number of grains per panicle and weight of 1000 grains were investigated from 50 plants per plot, and plants from 20 m² area were harvested to calculate economic yield. For determining the aboveground dry biomass, plants samples were kept at 105 °C for 30 min, and then oven dried at 75 °C for 12 h until constant weight.

Leaf area index

For the determination of leaf area, the length and width of the second leaf and total number of leaves were calculated. Leaf area was measured using the following formula:

$$\text{Leaf area} = \text{length} \times \text{width} \times \text{number of green leaves} \times 0.85 \quad (\text{Eq.1})$$

where 0.85 was the adjustment factor. Then leaf area index (LAI) was calculated by dividing the leaf area (cm²) by the ground surface area.

Grain to leaf area ratio

Grain to leaf ratio was calculated according to Feng et al. (1999), using *Equations 2* and *3*:

$$\text{Grain number to leaf area ratio} = \frac{\text{total number of grain per unit area}}{\text{total leaf area on the same plot at booting stage}} \quad (\text{Eq.2})$$

$$\text{Grain weight to leaf ratio} = \frac{\text{grain weight (mg) per unit area}}{\text{total leaf area on the same plot at booting stage}} \quad (\text{Eq.3})$$

Total leaf area was taken from the same plot at booting stage (cm²).

Soil sampling and analysis

Determination of soil moisture

Soil was drilled from 0-300 cm depth were with soil drill at sowing, wintering, jointing, flowering and maturity stages. The soil was divided into 20 cm layers and soil water content and soil water storage were determined.

The soil water storage was calculated by methods as described by He et al. (2009):

$$SWS_i = W_i \times D_i \times H_i \times \frac{10}{100} \quad (\text{Eq.4})$$

where SWS_i is the soil water storage capacity (mm) of the i -th soil layer; W_i is the soil water content (%) of the i -th soil layer; D_i is the soil bulk density (g cm^{-3}) of the i -th soil layer; H_i is the thickness of soil layer (cm). The soil water content and soil bulk density were both measured using the oven-drying method (Gardner et al., 1986).

Water consumption

Water consumption in wheat fields was measured using simplified formula as described by Xue et al. (2019):

$$ET = P - \Delta S \quad (\text{Eq.5})$$

where P is the effective precipitation (mm) during that stage and ΔS is reduction of soil water storage at each stage and was measured as $\Delta S = S_1 - S_2$, where S_1 and S_2 were the soil water content at the beginning and end of the stage, respectively. Whereas, runoff and drainage were considered negligible.

The water consumption intensity (CWR , mm d^{-1}) was calculated as:

$$CWR = \frac{ET_i}{d} \quad (\text{Eq.6})$$

where ET_i is the water consumption (mm) of wheat in each growth stage and d is the number of days in the growth stage.

Water use efficiency (WUE)

The yield water use efficiency (WUE_y) was calculated as:

$$WUE_y = \frac{Y}{ET} \quad (\text{Eq.7})$$

where: Y is the output, and ET is the total water consumption calculated from Equation 5.

Data processing

Two-way analysis of variance (ANOVA) was performed to determine the significance of sowing rate and mulching and statistical analysis was carried out using DPS7.05 software and the significant difference among treatments were calculated by least significant difference test (LSD) at the significance level of $p \leq 0.05$. Graphs were

constructed using Microsoft Excel 2010. Pearson correlation coefficients between water consumption and yield related components were assessed at $p \leq 0.05$.

Results

Soil water content

Soil water content of 0-300 cm soil layer was recorded at the wintering, jointing, anthesis and maturity stages under film-mulching and no-mulching (Fig. 3).

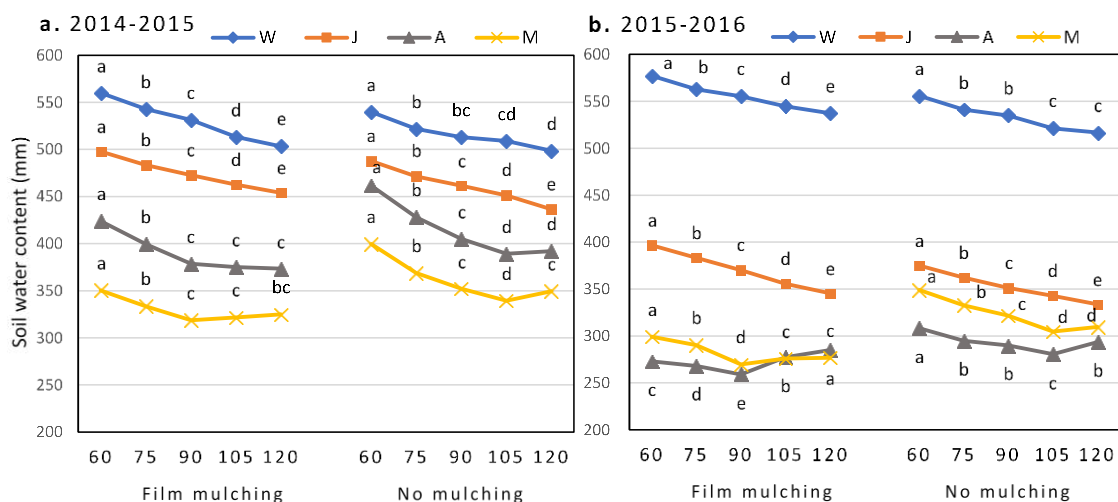


Figure 3. Effects of sowing methods and sowing rates on water content in 0-300 cm soil layer at different growth stages of dryland wheat. W, J, A and M indicate wintering, jointing, anthesis and maturity stages of winter wheat represented by GS23, GS31, GS61 and GS92 respectively, according to Zadoks system. Different letters indicate significant difference among treatments at the significance level of $p \leq 0.05$

At wintering and jointing stages, soil water content of film-mulching treatment was higher than no mulching whereas at the anthesis and maturity stages, water content of no-mulching was higher than the film-mulching. Soil water content was significantly decreased with increasing the seeding rate at wintering and jointing stage. At anthesis and maturity stage, the soil water content was first decreased by increasing the seeding rate and then did not further decreased. Soil water content was also affected by the stages with maximum at wintering, whereas minimum soil water content in 2014-2015 was at maturity and in 2015-2016 was at anthesis stage.

Water consumption at different stages of plastic film mulched wheat

The total water consumption of plastic film mulched dryland wheat was significantly increased as compared to no mulched during all the growth stages (Fig. 4). By increasing the seeding rate, water consumption was increased first and then decreased, and the highest water consumption was observed at 90 kg h⁻¹ under the conditions of film mulching, and at 105 kg h⁻¹ under conventional sowing without mulching.

The water consumption of sowing-jointing stage was increased with the increase of sowing quantity (Fig. 4). By increasing the sowing amount, the water consumption at

jointing-flowering was increased first and then decreased in 2014-2015 with highest at 90 kg h⁻¹ under film-mulching and 105 kg h⁻¹ under conventional sowing. Whereas in 2015-2016 water consumption at jointing-flowering was reduced with increasing the seeding rate. At flowering to maturity stage, water consumption was decreased in 2014-2015 whereas increased in 2015-2016 with increasing the seeding rate. It can be seen that the total water consumption of dryland wheat was increased by film mulching, but the difference of precipitation during the growth stages also have a great influence on the water consumption of each stage.

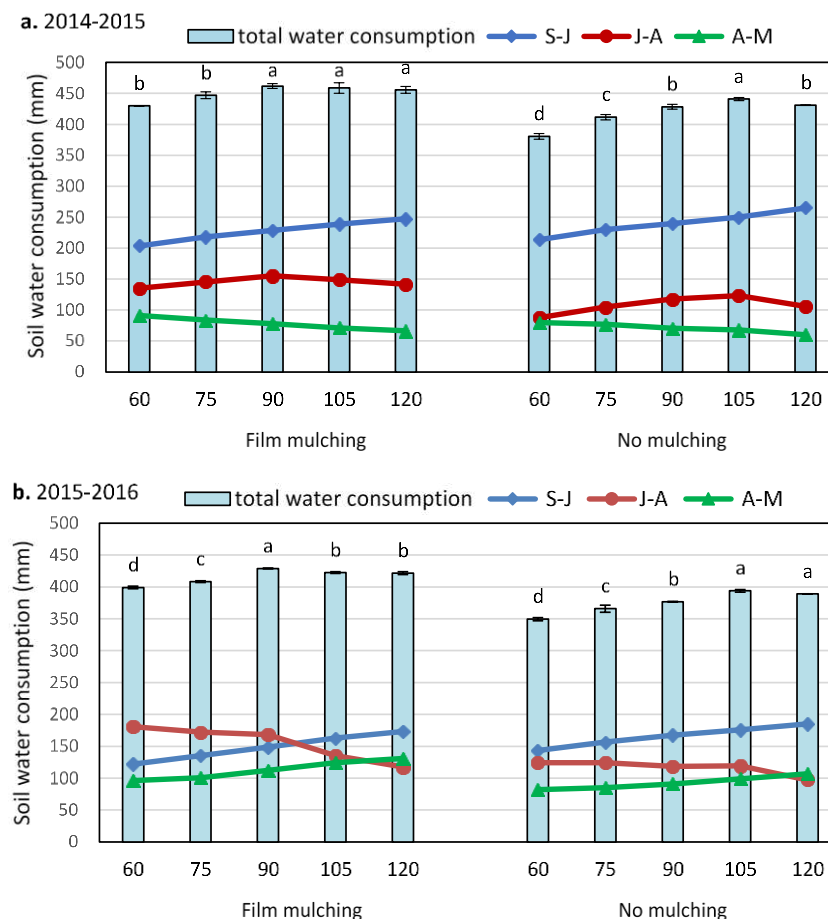


Figure 4. Effects of sowing methods and sowing rates on water consumption of 0-300 cm soil layer at different growth stages of dryland wheat. S-J: Sowing stage to jointing stage, Oct 1 to Apr 10 in the following year; J-A: Jointing stage to anthesis, Apr 11 to May 10; A-M: Anthesis to maturity, May 11 to Jun 10. Different letters indicate significant difference among treatments at the significance level of $p \leq 0.05$

Water consumption rate

Film mulching reduced the water consumption rate from the sowing-jointing stage compared with no mulching, whereas water consumption rate from jointing to anthesis and anthesis to maturity stage was increased by film mulching (Fig. 5). The water consumption rate of the jointing to anthesis stage was increased first and then decreased with the increasing seeding rate in 2014-2015 and lowest water consumption rate was observed at 90 kg h⁻¹ under no-mulching and at 105 kg h⁻¹ under film-mulching,

whereas, in 2015-2016, water consumption rate from jointing to anthesis was decreased with increasing seeding rate. The water consumption rate during the flowering to maturity stage was decreased by increasing the seeding rate in 2014-2015 while in 2015-2016 the water consumption was increased with increasing seeding rate.

Effect of sowing rate and mulching on leaf area and dry biomass

Film mulching had significantly increased the leaf area index and dry biomass in both years (*Table 3*).

Table 3. *Effect of sowing rate on dry matter formation of wheat covered with plastic film*

Treatment		2014-2015				2015-2016			
		LAI	Grain to leaf area ratio		Dry biomass (t ha ⁻¹)	LAI	Grain to leaf area ratio		Dry biomass (t h ⁻¹)
			GW/leaf (mg cm ⁻²)	GN/leaf (no. cm ⁻²)			GW/leaf (mg cm ⁻²)	GN/leaf (no. cm ⁻²)	
Film mulching	D ₆₀	7.53 ^c	5.6 ^b	0.133 ^{bc}	13.07 ^e	7.01 ^e	4.07 ^b	0.0963 ^b	8.87 ^e
	D ₇₅	7.98 ^d	5.93 ^a	0.143 ^a	14.01 ^d	7.25 ^d	4.04 ^b	0.0958 ^{bc}	9.25 ^d
	D ₉₀	9.11 ^c	6.04 ^a	0.146 ^a	14.65 ^c	8.04 ^c	4.46 ^a	0.1057 ^a	10.08 ^c
	D ₁₀₅	9.25 ^b	5.65 ^b	0.138 ^b	15.44 ^b	8.12 ^b	4.14 ^{ab}	0.1002 ^{bc}	10.36 ^b
	D ₁₂₀	9.27 ^a	5.25 ^c	0.132 ^c	16.26 ^a	8.58 ^a	3.52 ^c	0.0875 ^c	11.74 ^a
	Mean	8.63 ^A	5.70 ^A	0.139 ^A	14.68 ^A	7.80 ^A	4.05 ^A	0.0971 ^A	9.86 ^A
No mulching	D ₆₀	6.21 ^d	5.80 ^a	0.138 ^{ab}	11.53 ^e	4.87 ^e	4.81 ^a	0.1141 ^a	6.68 ^e
	D ₇₅	7.49 ^c	5.53 ^{ab}	0.136 ^b	12.82 ^d	6.00 ^d	4.09 ^b	0.0986 ^b	7.87 ^d
	D ₉₀	8.00 ^b	5.46 ^{bc}	0.135 ^b	13.72 ^c	6.47 ^c	3.93 ^b	0.0955 ^b	8.52 ^c
	D ₁₀₅	8.11 ^b	5.76 ^{ab}	0.145 ^a	14.72 ^b	8.01 ^b	3.52 ^c	0.0860 ^c	9.25 ^b
	D ₁₂₀	8.49 ^a	5.20 ^c	0.135 ^b	15.37 ^a	8.18 ^a	3.17 ^c	0.0788 ^c	9.40 ^a
	Mean	7.66 ^B	5.55 ^B	0.138 ^A	13.63 ^B	6.71 ^B	3.90 ^B	0.0946 ^B	8.34 ^B
ANOVA	M	2349.2 ^{***}	20.8 ^{***}	0.93 ^{ns}	1.92 ^{***}	2430.6 ^{***}	12.5 ^{**}	6.2 [*]	36.9 ^{***}
	D	1387.8 ^{***}	38.7 ^{***}	14.2 ^{***}	2.64 ^{***}	1596.5 ^{***}	81.9 ^{***}	55.6 ^{***}	67.8 ^{***}
	M×D	56.7 ^{***}	21.3 ^{***}	20.9 ^{***}	0.03 ^{***}	326.9 ^{***}	36.4 ^{***}	33.4 ^{***}	4.06 ^{***}

Means followed by different small letters indicate significant difference among treatments within seeding method, and capital letters indicate difference among seeding method at 0.05 level. D₆₀, D₇₅, D₉₀, D₁₀₅, and D₁₂₀ are 60, 75, 90, 105 and 120 kg seeds h⁻¹; GW: grain weight; GN: grain numbers per spike

In film mulched plants, the leaf area index was increased by 13-16%, the grain weight to leaf area ratio was increased by 2.7-3.8%, the grain number to leaf area ratio was increased by 0.6-3%, and grain yield was increased by 4.9-7.5% as compared to no mulching. It can be seen that the film mulching treatment has improved the balance of source reservoir relationship and increased grain yield of wheat during the growth and development of wheat as compared to no mulching.

The leaf area index was gradually increased with the increase in seeding rate and leaf area index at 120 kg h⁻¹ was significantly higher than the lower rates. Grain to leaf ratio was first increased and then decreased under film-mulching with maximum grain to leaf area observed at 90 kg h⁻¹. The dry biomass was minimum at the lowest seeding rate and was increased by increasing seeding rate reaching maximum at 120 kg h⁻¹. Without

mulching, increasing seeding rate did not significantly enhanced the grain to leaf area ratio. Therefore, the yield could be effectively increased by improving the grain to leaf ratio in the suitable range of leaf area index.

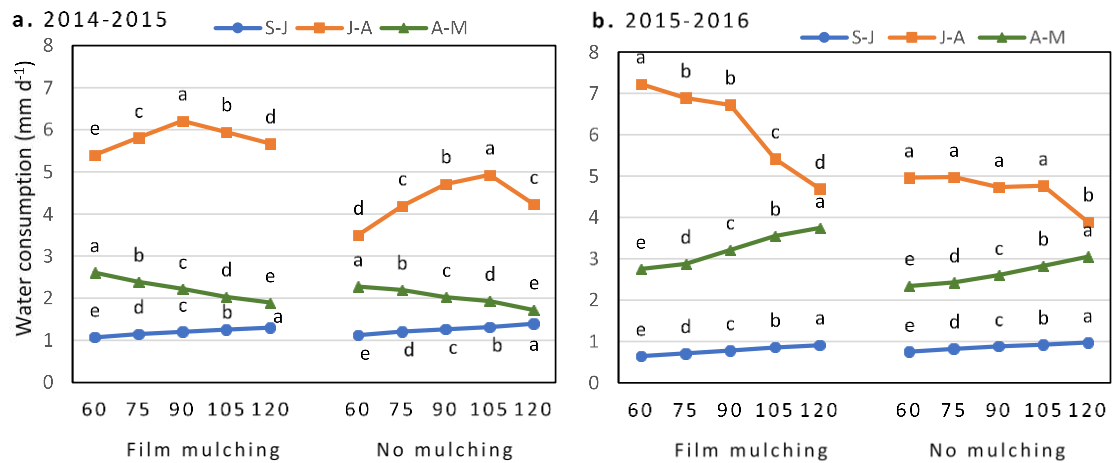


Figure 5. Effects of sowing rate on daily water consumption amount of dryland wheat at different growth stages under different sowing patterns. S-J: Sowing stage to jointing stage, Oct 1 to Apr 10 in the following year; J-A: Jointing stage to anthesis, Apr 11 to May 10; A-M: Anthesis to maturity, May 11 to Jun 10. Different letters indicate significant difference among treatments at the significance level of $p \leq 0.05$

Effect of sowing rate and mulching on tillers formation of wheat

The mulching has effectively increased the number of tillers at jointing by 3-4% and the effective number of panicles by 8-16% as compared to the conventional sowing (Fig. 6).

The number of tillers at the jointing stage was increased by increasing the amount of sowing rate, whereas, the effective number of tillers at maturity was first increased and then decreased at higher sowing rates. The highest number of effective tillers were recorded at seeding rate of 105 kg h⁻¹. Under the same sowing rate, the number of effective tillers were increased by 0.83-7.02% in film mulched as compared with no mulching.

Effect of sowing rate and mulching on yield

The grain yield and yield related traits were significantly increased by film mulching as compared to no-mulching (Table 4). The number of grains per pod were increased by 4.25-7.04%, the 1000-grains weight were increased by 1.2-2.0%, the grain yield was increased by 16-24%, and water use efficiency was improved by 8-11% as compared to no mulching. With the increase of sowing rate, the 1000-grain weight was decreased gradually and lowest grain weight was observed at the highest density (120 kg h⁻¹). In film-mulched plants, the number of grains were not increased by increasing the seeding rate whereas in no-mulching treatment, number of grains were firstly increased by increasing seeding rate reaching maximum at 105 kg h⁻¹ and then decreased by further increasing seeding rate to 120 kg h⁻¹.

The yield and water use efficiency were increased by increasing seed rate with maximum at 90 kg h⁻¹ under film mulching and 105 kg h⁻¹ without mulching (Table 4).

However further increasing seeding rate had significantly decreased the yield and water use efficiency. The conventional treatment with 105 kg h⁻¹ was the highest, and the yield increased by 5.4-30.4% compared with other treatments. Mulching has increased yield by 5.4-30.4%, 5.8-29.5% in 2014-2015 and 2015-2016 respectively as compared to without mulching. The water use efficiency was improved by 4.7-21.4% and 3.4-11.8% by plastic film mulching in 2014-2015 and 2015-2016 respectively as compared to without mulching.

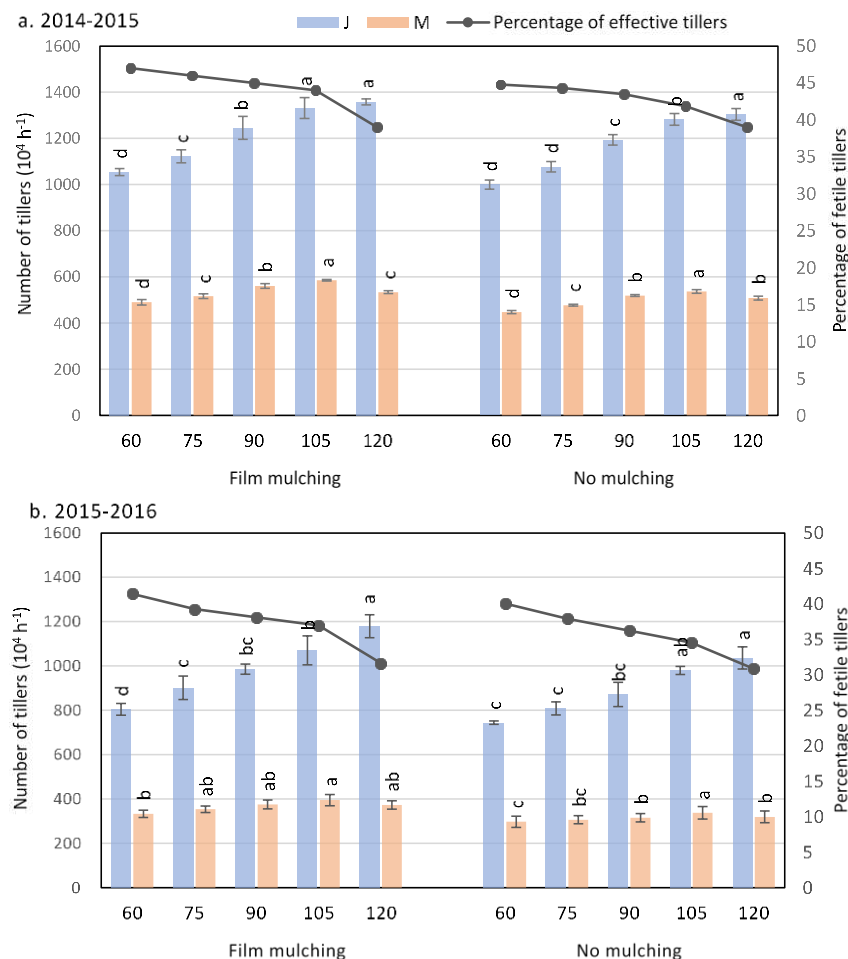


Figure 6. Effects of different sowing rates and mulching on number of tillers at jointing and maturity stage and percentage of effective tillers. Different letters indicate significant difference among treatments at the significance level of $p \leq 0.05$

Correlation analysis of water consumption from soil at different growth stages and yield and yield related components of wheat

The correlation between water consumption from soil at sowing to jointing, jointing to anthesis and anthesis to maturity stage and yield components were determined (Table 5). It can be seen that the water consumption during different stages have different impact on biomass and yield traits. There was a significant and positive correlation between the leaf area index, grain yield and number of grain and spikes and the amount of water consumed in sowing-jointing and jointing-anthesis stage, and the

influence of water consumption in the stage of sowing to jointing was higher than that in jointing to anthesis. Water consumption in the anthesis-maturity stage was positively correlated with 1000-grain weight, whereas, negatively related with aboveground biomass, LAI, number of spikes, number of grains and grain yield.

Table 4. Effects of different sowing rates on yield formation of wheat covered with plastic film

Treatment		2014-2015				2015-2016			
		GN (spike ⁻¹)	GW (g)	GY (t h ⁻¹)	WUEy (kg h ⁻¹ mm ⁻¹)	GN (spike ⁻¹)	GW (g)	GY (t h ⁻¹)	WUEy (kg h ⁻¹ mm ⁻¹)
Film mulching	D ₆₀	33.3 ^a	42.0 ^a	4.22 ^c	9.83 ^d	30.41 ^{ab}	42.3 ^a	2.85 ^b	7.15 ^c
	D ₇₅	32.5 ^{ab}	41.4 ^{ab}	4.74 ^d	10.6 ^c	28.9 ^{bc}	42.2 ^{ab}	2.93 ^b	7.18 ^c
	D ₉₀	33.0 ^a	41.3 ^{ab}	5.51 ^a	11.9 ^a	32.5 ^a	42.2 ^{ab}	3.59 ^a	8.37 ^a
	D ₁₀₅	31.6 ^{ab}	40.9 ^{ab}	5.23 ^b	11.4 ^b	27.8 ^{cd}	41.3 ^b	3.36 ^a	7.95 ^b
	D ₁₂₀	30.1 ^b	39.7 ^b	4.86 ^c	10.7 ^c	26.1 ^d	40.2 ^c	3.02 ^b	7.15 ^c
	mean	32.1 ^A	41.1 ^A	4.91 ^A	10.9 ^A	30.8 ^A	41.6 ^A	3.10 ^A	7.56 ^A
No mulching	D ₆₀	30.4 ^b	41.9 ^a	3.60 ^d	9.46 ^c	28.4 ^{ab}	42.1 ^a	2.34 ^b	6.70 ^a
	D ₇₅	30.0 ^b	40.7 ^b	4.14 ^c	10.1 ^b	28.6 ^{ab}	41.5 ^{ab}	2.46 ^b	6.72 ^a
	D ₉₀	31.2 ^{ab}	40.5 ^b	4.37 ^{bc}	10.2 ^{ab}	28.1 ^{ab}	41.1 ^{ab}	2.54 ^b	6.74 ^a
	D ₁₀₅	32.7 ^a	39.6 ^c	4.67 ^a	10.6 ^a	29.1 ^a	40.9 ^{ab}	2.82 ^a	7.16 ^a
	D ₁₂₀	29.7 ^b	38.5 ^d	4.41 ^b	10.2 ^{ab}	27.9 ^b	40.2 ^b	2.59 ^{ab}	6.66 ^a
	mean	30.8 ^B	40.2 ^B	4.24 ^B	10.1 ^B	28.4 ^B	41.2 ^B	2.55 ^B	6.79 ^B
ANOVA	M	15.7 ^{***}	15.4 ^{***}	627.1 ^{***}	196.6 ^{***}	6.02 [*]	7.5 [*]	383.6 ^{***}	94.4 ^{***}
	D	6.51 ^{**}	14.3 ^{***}	201.9 ^{***}	86.6 ^{***}	13.7 ^{***}	9.4 ^{***}	41.0 ^{***}	15.2 ^{***}
	M×D	4.9 ^{**}	7.9 ^{***}	20.0 ^{***}	20.9 ^{***}	14.6 ^{***}	7.7 ^{***}	13.8 ^{***}	9.3 ^{***}

Means followed by different small letters indicate significant difference among treatments within seeding method, and capital letters indicate difference among seeding method at 0.05 level. D₆₀, D₇₅, D₉₀, D₁₀₅, and D₁₂₀ are 60, 75, 90, 105 and 120 kg seeds h⁻¹; GN: number of grains per spike; GW: 1000 grains weight; GY: grain yield; WUEy: yield water use efficiency

Table 5. Correlation coefficients between water consumption from soil and yield components at different growth stage in dryland wheat

Water consumption	Aboveground biomass	LAI	SN	GN	GW	GY
S-J	0.913 ^{**}	0.536 ^{**}	0.862 ^{**}	0.400 ^{**}	-0.386 ^{**}	0.818 ^{**}
J-A	-0.065	0.511 [*]	0.528 [*]	0.323 [*]	0.074	0.543 [*]
A-M	-0.547 ^{**}	-0.026	-0.603 ^{**}	-0.422 ^{**}	0.598 ^{**}	-0.566 ^{**}

S-J: sowing to jointing; J-A: jointing to anthesis; A-M: anthesis to maturity; S-M: sowing to maturity; LAI: leaf area index; WUEy: yield water use efficiency; SN: number of spikes per panicle; GN: grain number per spike; GW: 1000 grain weight; GY: grain yield ha⁻¹; *, ** and *** indicate significance at 0.05, 0.01 and 0.001 probability level

Discussion

Water stress is the main limiting factor for wheat production in Loess Plateau and other arid and semiarid regions (Liu et al., 2007). The growth of winter wheat plants

depends on the soil water stored by rainfall during summer fallow season (60-70%) and growing season (30-40%). The roots of rainfed winter wheat are not able to utilize water from deeper soil layers and ground water in Loess Plateau is below 5 m (Li et al., 2017). Hence, the limiting precipitation during growth season means that winter wheat must utilize soil water stored from precipitation during fallow season (Xue et al., 2019).

Soil water availability and water use efficiency by ridge plastic mulching

Mulching is an effective measure to increase soil moisture in arid and semiarid areas. Film mulching can reduce soil surface evaporation and thus improve soil moisture content and promote crop growth and yield (Li et al., 2013). Ridge mulching is one of the main measures to increase agricultural production in arid regions (Zhang et al., 2013). In the present study soil water content of 0-300 cm depth was higher by plastic film mulching at the wintering and jointing stages. Thus, our study indicated that plastic film mulching effectively relieved the drought stress at early stages of winter wheat growth as similar with Zhao et al. (2016) and Yang et al. (2018). Zhang et al. (2013) reported that ridges mulched with plastic film was better than the straw mulching and other conservation practices in conserving rainfall of summer fallow periods by reducing soil water evaporation.

However, soil water content at anthesis and maturity was higher under no-mulching than the film mulching. This might be because plastic mulching reduces soil surface evaporation at early stages and promote the accumulation of biomass at the vegetative growth with more leaf area which increase transpiration rate (Li et al., 2001). The results of present study also indicated that the biomass and leaf area index of mulched wheat was higher than in no mulching (*Table 3*). Positive effect of plastic film mulching on leaf area index and biomass of wheat was also previously reported (Li et al., 2013; Xie et al., 2005).

Therefore, more vegetative growth and high transpiration rate increases utilization of soil water content and manifested by less soil water at late growth stages. Yang et al. (2018) also reported that plastic film mulching conserve soil water in top layers at the early growth stages of spring wheat by decreasing evaporation rate while plants consumed more water from the soil at the middle growth stage under film mulching.

The present study showed that the plastic film-mulching had increased water consumption by 8.4-11%. The plastic film mulch also increased the development and production of biomass by improving the water consumption, similar as previously reported by Niu et al. (2004). Furthermore, increasing water absorption and water consumption by plant also lessen water loss by evaporation (Li et al., 2013).

The water use efficiency of plastic film mulched plants was increased by 7.6-11.3%, which was consistent to Hou et al. (2013). Water use efficiency was 10.9 kg ha⁻¹ mm⁻¹ and 7.6 kg ha⁻¹ mm⁻¹ under film mulching and 10 kg ha⁻¹ mm⁻¹ and 6.8 kg ha⁻¹ mm⁻¹ under no mulching in 2014-2015 and 2015-2016 respectively, as compared with the globally measured average water use efficiency of 6-17 kg ha⁻¹ mm⁻¹ for wheat (Zwart and Bastiaanssen, 2004) and 7-10 kg ha⁻¹ mm⁻¹ for rainfed wheat in Loess Plateau (Huang et al., 2003; Deng et al., 2006). WUE indicates the relationship of production of grain yield and water consumption of the crop (Mo et al., 2005; Jin et al., 2018).

The water for evapotranspiration during the early growth stage comes from stored soil water before sowing and rest from precipitation during growth season (Huang et al., 2003). Soil water conserved at early growth stages is utilized to accumulate biomass and yield formation at the later growth stages and thus improve water use efficiency of

the crop by changing the pattern of water consumption. Huang et al. (2003) reported that almost 68% of total water consumed was derived from seasonal precipitation and 32% derived from the soil water stored from rainfall before planting. The variation in water use efficiency is also attributable to yearly variation in rainfall.

The daily water consumption varied with the growth period of winter wheat and was minimum at sowing to jointing stage and then increased to maximum at jointing to anthesis stage and then decreased at anthesis to maturity. The higher water consumption is at the active growth stage of wheat (Hou et al., 2016). It can be seen that the film mulching reduced the water consumption rate of the initial growth stage (sowing to jointing) and increase the water consumption rate at the late growth stage (jointing to anthesis and anthesis to maturity).

Effect of mulching on yield and relationship between water consumption and yield

This study showed that both seeding rate and film mulching had significant effects on wheat yield and its components. The number of panicles per unit area was increased by 8-16%, the number of grains per spike were increased by 4.25-7.04%, and the 1000-grain weight were increased by 1.2-2.0%, and the yield was increased by 16-24% in film mulched plants as compared to no mulching and this increase in yield was more prominent in the dry years. Increase in yield of wheat covered by plastic film is mainly to increase the number of spikes per unit area and number of grains per plant. This is because the film mulching can effectively reduce the evaporation of soil moisture, enhance the soil moisture in deep soil layer and improve the growth and development and water use efficiency (Li et al., 2013; Zhang et al., 2013, 2018b).

Zhang et al. (2019) reported a 31% reduction in soil evaporation and 28% increase in transpiration rate by plastic film mulching, improving water use efficiency. Similarly, Zhang et al. (2018b) reported 16.1% increased of grain yield by plastic film mulching and attributed this increase of yield to increase in number of spikes per area and number of grains per spike. However, some contrary studies have shown that mulching resulted in reduced grain yield due to vigorous growth at early stages and lack of soil moisture at the later stages (Li et al., 2001). Zhang et al. (2013) reported that ridge plastic mulching caused increased yield in 20% cases under different tillage treatments, while 8% reduction in yield is due to fast depletion of soil water at the early growth stage of wheat due to favorable water conditions under plastic film mulching, which caused water stress at the grain filling stages. Li et al. (2017) reported that grain yield of dryland wheat is mainly limited by soil water content at sowing and increasing soil water at sowing could improve yield.

Previous research indicated that the high yield of the film mulched wheat is based on high water consumption and water utilization efficiency (Hou et al., 2014, 2016; Yang et al., 2015). Plastic film mulching increased the available water content and water consumption during the whole growth period of wheat. This study showed that the number of spikes, grain number and grain yield were significantly positively correlated with water consumption from sowing to jointing and jointing to flowering stage, while negatively correlated with water consumption from flowering to maturity stage (Table 5). The effect on the number of effective panicles was higher than that in jointing-flowering stage. This might be because the number of spikes and grain numbers were determined at early reproductive stage and higher water consumption at jointing to flowering stage resulted in more spikes and grain numbers but with less water content at grain filling stage. In contrast to other yield traits, 1000 grain weight was positively

related to water consumption from flowering to maturity, showing the importance of available soil water after anthesis on grain filling. Yang et al. (2018) showed that there was a significant positive correlation between yield and water consumption.

Higher soil moisture contents under film mulching also improved the absorption of N and other nutrients and thus improve the nutrient use efficiency. Studies have shown that the mulching had improved the N translocation rate before anthesis, N accumulation to grains after anthesis and nitrogen use efficiency of dryland wheat (Zhang et al., 2016).

The grain yield in 2014-2015 season was higher than in 2015-2016 under both plastic film mulching and no mulching condition. The fluctuation of rainfall in Loess Plateau in different years causes variation in grain yield of dryland wheat (Ren et al., 2019). The total precipitation in 2014-2015 was higher, while in 2015-2016 was less than the long-term average precipitation of the site. Grain yield of wheat is not only influenced by variation in total water content available from seasonal rainfall but also by the pattern of water consumption with growth stages of wheat (O'Leary and Connor, 1997; Ren et al., 2019). Huang et al. (2003) reported a significant relationship between yield of wheat and water consumption during fallow or precipitation during growing season precipitation.

Modulating water consumption and water use efficiency with seeding rate

Establishing a population structure with high light use efficiency and low water consumption is the fundamental content of high water-saving cultivation of wheat. The water consumption of wheat in dryland is closely related to planting methods and seeding rate. A large number of studies have shown that the amount of seeding rate had a significant impact on wheat growth and water use efficiency (Wang et al., 2017; Ren et al., 2019); therefore, appropriate seeding rate is conducive to increasing soil water storage capacity and water use efficiency in dryland wheat planting areas where soil moisture is the most limiting factor at various growth stages (Ren et al., 2019). Therefore, in the present study wheat was sown at different seeding rates in a ridge and furrow planting method using plastic film mulching whereas, no mulching and plain field was used as a control.

The experimental study showed that the total water consumption during the whole growth period of wheat increased first and then decreased with the increase of the seeding rate and total water consumption was highest at 90 kg h⁻¹ under film mulching and 105 kg h⁻¹ under no mulching. This indicated that too high or small seeding rate could reduce the water consumption of winter wheat, which is consistent with the results of Wang et al. (2017). However, some studies have shown that water consumption during the whole growth period increases with the increasing seeding rate (Zhang et al., 2018a; Ren et al., 2019). This may be because the water consumption gradually increases from vegetative to reproductive stage. Water consumption at the early stage of wheat from sowing to jointing was increased with increasing the seeding rate due to increase in the amount of evaporation in the wheat field by increasing plant population. Whereas, reduction in field water consumption at jointing to anthesis and anthesis to maturity by increasing seeding rate up to a certain limit might be due to the inhibited growth and premature senescence of high seeded population due to the lack of soil moisture. Therefore, it is necessary to regulate the amount of seeding rate to improve the utilization of water resources and effectively increase crop yield.

Soil water content was decreased with increasing the seeding rate at wintering, jointing and anthesis stages whereas at maturity stage, soil water content was lowest at 90 kg h⁻¹ and 105 kg h⁻¹ under film mulching and no mulching respectively. In present study, the pre-anthesis water consumption ratio is higher than the post-anthesis. Ratio of pre-anthesis to post anthesis water consumption varies with the pattern of rainfall, from 3:1, when post-anthesis precipitation was less, to 6:1 with high post-anthesis rainfall. It has been reported that water used by wheat in a ratio of 2:1 before and after anthesis favors yield (Passioura, 1983; Zhang et al., 2013).

Effect of sowing rate on tillering and yield formation

Population density could influence the ratio of water used and thus yield (Wang, 2010; Zhang et al., 2013). Increasing the amount of seeding rate improves the efficiency of radiation utilization efficiency, and ultimately have a positive effect on formation of grain yield. However, increasing the amount of seeding rate will increase the competition of wheat for resources such as water and nutrients, which will further reduce the grain yield of wheat, accelerate leaf senescence and even reduce the final yield of wheat (Liu et al., 2016). This study showed that the seeding rate had significant effects on wheat yield and its components. Grain yield was first increased with increasing seed rate and reached maximum at 90 kg h⁻¹ under mulching and 105 kg h⁻¹ under no mulching and then decreased by further increasing seeding rate. Grain yield was maximum at seeding rates where maximum water consumption was observed. Similarly, Ren et al. (2019) also reported that the highest water consumption during the growth stage of winter wheat resulted in highest grain yield in Loess Plateau both in years with low and high rainfall.

Tillering is a key component in determining wheat yield by influencing the photosynthesis rate, plant canopy size and fertile tillers bearing grains. Results from present study indicated that the number of tillers were increased by increasing the seeding rate from 60 to 120 kg h⁻¹ at jointing stage whereas at maturity was increased first and then decreased. However, the percentage of fertile tillers were decreased gradually by increasing seeding rate indicating that the number of unproductive tillers were increased at high seeding rate. Generally, from the total tiller initiated, only a proportion of tillers survive to become fertile and others are destined to abort (Xie et al., 2016). The number of aborted tillers varies with the seeding rate and most of previous studies indicated that the effective number of tillers were decreased with increasing the seeding rate (Evers et al., 2006; Kondić et al., 2017). Increasing numbers of unproductive tillers also resulted in high water consumption (Wang et al., 2017). Therefore, seeding rate should be properly optimized because higher number of non-surviving tiller are detrimental for yield due to the loss of dry matter especially in a condition where increase in water use efficiency and yield is most important (Berry et al., 2003).

Number of tillers are determined by the tillers produced and tillers survived. Percentage of effective tillers was highest at the lowest seeding rate but the grain yield was minimum. Because if the seeding rate is too low, the number of tillers per area will be also low due to smaller population resulting in less grain yield per area. This is also indicated by our results as the minimum number of tillers at the jointing and maturity stages were produced at the lowest seeding rate. Increasing seeding rate up to optimum rate at which increasing the number of tillers balance the competition among plants and transfer of photosynthetic products to the grain, and harvest index and the yield per plant are highest. However, if the seeding rate is too high, the grain weight, tillering and

number of effective tillers are reduced due to the competition for nutrient and light resulting in low yield per plant (Ren et al., 2019). It was obvious from the present results that under film mulching, the maximum yield was attained at relatively low seeding rate (90 kg h^{-1}) as compared to without mulching at which the highest yield was attained at 105 kg h^{-1} . The high yield at relatively less seeding rate might be related to higher number of effective and survived tillers and increased competition between tillers for resource allocation.

The grain-to-leaf ratio is an effective indicator reflecting the coordination of source and sink relationship and related to density (Serrago et al., 2013). The grain number to leaf area ratio reflects the storage capacity per unit leaf area, while the grain weight to leaf area ratio shows the contribution of unit leaf area to yield, which is used to explain the source quality level and transfer capacity of the source (Wang et al., 2016). Studies have shown that within the range of suitable leaf area index, expanding the total storage capacity and increasing the ratio of grain to leaf is conducive for high yield (Bijan-zadeh and Emam, 2010).

This study showed that by increasing the sowing amount, the grain weight-to-leaf ratio and the grain number-to-leaf ratio were increased first and then decreased. The ratio of leaf area to grain weight and number was positively correlated with grain number per spike and 1000 grain weight. Therefore, increasing the ratio of grain to leaf can effectively increase the yield, which is consistent with the results of Yu et al. (2005). Maximum grain weight to leaf area ratio and grain number to leaf area ratio was attained at 90 kg h^{-1} under film mulching and at 105 kg h^{-1} for plants without mulching.

Conclusion

The water consumption at different growth stages of dryland wheat field is closely related to wheat yield. The water consumption from sowing to jointing and jointing to anthesis stage was positively related with the spike number, grain number, and grain yield whereas higher water consumption from anthesis to maturity stage was positively related with 1000 grain weight. Plastic film mulching with ridge and furrow planting significantly increased water use efficiency and wheat yield by improving the effective tillers per unit area and number of spikes. Under film mulching, maximum yield was attained at relatively lower seeding rate (90 kg h^{-1}) as compared to no mulching at which maximum yield was attained at 105 kg h^{-1} . Thus, for the dryland wheat production in Shanxi, seeding rate of 90 kg h^{-1} under film mulching improved the grain to leaf area ratio and relationship between source and sink, increase the number of grains per panicle and 1000-grain weight, increase yield and moisture under the premise of ensuring water use efficiency. Furthermore, in future the effect of different mulching methods on water consumption could be compared.

Acknowledgements. This research work was funded by ‘Modern Agriculture Industry Technology System Construction (CARS-03-01-24), The National Key Research and Development Program of China (2018YFD020040105), NSFC (Natural Science Foundation of China) (31771727), Sanjin Scholar Support Special Funds Projects, Research Project Supported by Shanxi Scholarship Council of China (2017-068), Crop Ecology and Dry Cultivation Physiology Key Laboratory of Shanxi Province (201705D111007), Shanxi Provincial Key Research and Development Program (201703D211001), Shanxi Agricultural Valley Construction Research Project (SXNGJSKYZX2017) “1331” Engineering Key Innovation Cultivation Team- Organic Dry Cultivation and Cultivation Physiology Innovation Team and The excellent talents come to Shanxi to reward scientific research projects (SX YBKY201733)’.

REFERENCES

- [1] Berry, P. M., Spink, J. H., Foulkes, M. J., Wade, A. (2003): Quantifying the contributions and losses of dry matter from non-surviving shoots in four cultivars of winter wheat. – *Field Crops Research* 80: 111-121.
- [2] Bijanzadeh, E., Emam, Y. (2010): Effect of source-sink manipulation on yield components and photosynthetic characteristic of wheat cultivars (*Triticum aestivum* and *T. durum* L.). – *Journal of Applied Sciences* 10(7): 564-569.
- [3] Deng, X. P., Shan, L., Zhang, H., Turner, N. C. (2006): Improving agricultural water use efficiency in arid and semiarid areas of China. – *Agricultural Water Management* 80(1-3): 23-40.
- [4] Destro, D., Miglioranza, É., Arias, C. A. A., Vendrame, J. M., Almeida, J. C. V. D. (2001): Main stem and tiller contribution to wheat cultivars yield under different irrigation regimes. – *Brazilian Archives of Biology and Technology* 44(4): 325-330.
- [5] Du, Y. J., Li, Z. Z., Li, W. L. (2005): Effect of water control and plastic-film mulch on growth and the range of size inequalities in spring wheat (*Triticum aestivum*) populations. – *New Zealand Journal of Crop and Horticultural Science* 33(3): 251-260.
- [6] Evers, J. B., Vos, J., Andrieu, B., Struik, P. C. (2006): Cessation of tillering in spring wheat in relation to light interception and red: far-red ratio. – *Annals of Botany* 97(4): 649-658.
- [7] Feng, C. N., Guo, W. S., Wang, F. T., Zhu, X. K., Peng, Y. X. (1999): Mechanism of the population formation with high grain-leaf ratio in wheat. – *Scientia Agricultura Sinica* 32(6): 47-55.
- [8] Gan, Y. T., Siddique, Kadambot, H. M. (2013): Ridge-furrow mulching systems-an innovative technique for boosting crop productivity in semiarid rain-fed environments. – *Advances in Agronomy* 118: 429-476.
- [9] Gardner, W. H. (1986): Water Content. – In: Klute, A. (ed.) *Methods of Soil Analysis, Part 1-Physical and mineralogical methods*. Soil Science Society of America, Inc. Madison, WI, pp. 493-544.
- [10] He, J., Kuhn, N. J., Zhang, X. M., Zhang, X. R., Li, H. W. (2009): Effects of 10 years of conservation tillage on soil properties and productivity in the farming–pastoral ecotone of Inner Mongolia, China. – *Soil Use and Management* 25(2): 201-209.
- [11] Hou, H., Huang, G. (2009): Tiller redundancy in winter wheat in irrigated arid areas. – *Chinese Journal of Eco-Agriculture* 17(3): 522-526.
- [12] Hou, H. Z., Gao, S., Zhang, X., Wang, D. (2013): Effect of micro ridge-furrow with whole field plastic film mulching and bunching seeding on water consumption characteristics and water use efficiency of winter wheat in semiarid areas of northwest Loess Plateau. – *Scientia Agricultura Sinica* 49(24): 4701-4713.
- [13] Hou, H. Z., Lü, J. F., Guo, T. W., Zhang, G. P., Dong, B., Zhang, X. C. (2014): Effects of whole field soil-plastic mulching on spring wheat water consumption, yield, and soil water balance in semiarid region. – *Scientia Agricultura Sinica* 47: 4392-4404.
- [14] Hou, H. Z., Gao, S. M., Zhang, X. C., Wang, D. G. (2016): Effects of micro ridge-furrow with plastic film mulching and bunching seeding on water consumption characteristics and water use efficiency of winter wheat in semiarid areas of Northwest Loess Plateau. – *Scientia Agricultura Sinica* 49(24): 4701-4713.
- [15] Huang, M., Shao, M., Zhang, L., Li, Y. (2003): Water use efficiency and sustainability of different long-term crop rotation systems in the Loess Plateau of China. – *Soil and Tillage Research* 72(1): 95-104.
- [16] Huang, Y., Chen, L., Fu, B., Huang, Z., Gong, J. (2005): The wheat yields and water-use efficiency in the Loess Plateau: straw mulch and irrigation effects. – *Agricultural Water Management* 72(3): 0-222.
- [17] Jin, K., Cornelis, W. M., Schiettecatte, W., Lu, J., Yao, Y., Wu, H. J., Gabriels, D., Neve, S. D., Cai, D. X., Jin, J. Y., Hartmann, R. (2007): Effects of different management

- practices on the soil–water balance and crop yield for improved dryland farming in the Chinese Loess Plateau. – *Soil & Tillage Research* 96(1-2): 131-144.
- [18] Jin, N., Ren, W., Tao, B., He, L., Ren, Q., Li, S., Yu, Q. (2018): Effects of water stress on water use efficiency of irrigated and rainfed wheat in the Loess Plateau, China. – *Science of the Total Environment* 642: 1-11. DOI: 10.1016/j.scitotenv.2018.06.028.
- [19] Kondić, D., Bajić, M., Hajder, Đ., Bosančić, B. (2017): The rate of productive tillers per plant of winter wheat (*Triticum aestivum* L.) cultivars under different sowing densities. – *Agro-knowledge Journal* 17(4): 345-357.
- [20] Li, F. M., Yan, X., Wang, J., Li, S. Q., Wang, T. C. (2001): The mechanism of yield decrease of spring wheat resulted from plastic film mulching. – *Scientia Agricultura Sinica* 34(3): 330-333.
- [21] Li, H., Xun, J. F., Gao, Z. Q., Xue, N. W., Yang, Z. P. (2017): Response of yield increase for dryland winter wheat to tillage practices during summer fallow and sowing method in the Loess Plateau. – *Journal of Integrative Agriculture* 16: 60345-7.
- [22] Li, J., Zhou, D., Wang, P., Lan, L. (2000): *The Principals of Winter Wheat Cultivation for High Use Efficiencies of Water and Fertilizers*. – Publishing House of China Agricultural University, Beijing, pp. 3-18.
- [23] Li, S. X., Wang, Z. H., Li, S. Q., Gao, Y. J., Tian, X. H. (2013): Effect of plastic sheet mulch, wheat straw mulch, and maize growth on water loss by evaporation in dryland areas of China. – *Agriculture Water Management* 116: 39-49.
- [24] Liang, Y. F., Khan, S., Ren, A. X., Lin, W., Anwar, S., Sun, M., Gao, Z. Q. (2019): Subsoiling and sowing time influence soil water content, nitrogen translocation and yield of dryland winter wheat. – *Agronomy* 9(1): p.37.
- [25] Liu, L., Xu, B. C., Li, F. M. (2007): Effects of limited irrigation on yield and water use efficiency of two sequence-replaced winter wheat in Loess Plateau, China. – *African Journal of Biotechnology* 6(13): 1493-1497.
- [26] Liu, T., Wang, Z., Cai, T. (2016): Canopy apparent photosynthetic characteristics and yield of two spike-type wheat cultivars in response to row spacing under high plant density. – *PloS One* 11(2): e0148582.
- [27] Ma, D., Chen, L., Qu, H., Wang, Y., Misselbrook, T., Jiang, R. (2018): Impacts of plastic film mulching on crop yields, soil water, nitrate, and organic carbon in Northwestern China: a meta-analysis. – *Agricultural Water Management* 202: 166-173.
- [28] Ma, S., Yu, Z., Zhang, Y., Zhao, J., Shi, Y., Wang, D. (2014): Effect of field border width for irrigation on water consumption characteristics, yield and water use efficiency of wheat. – *Scientia Agricultura Sinica* 47(8): 1531D1540.
- [29] Ma, S. C., Wang, T. C., Guan, X. K., Zhang, X. (2018): Effect of sowing time and seeding rate on yield components and water use efficiency of winter wheat by regulating the growth redundancy and physiological traits of root and shoot. – *Field Crops Research* 221: 166-174.
- [30] Mo, X., Liu, S., Lin, Z., Xu, Y., Xiang, Y., McVicar, T. R. (2005): Prediction of crop yield, water consumption and water use efficiency with a SVAT-crop growth model using remotely sensed data on the North China Plain. – *Ecological Modelling* 183(2-3): 301-322.
- [31] Niu, J. Y., Gan, Y. T., Huang, G. B. (2004): Dynamics of root growth in spring wheat mulched with plastic film. – *Crop Science* 44: 1682-1688.
- [32] O’Leary, G. J., Connor, D. J. (1997): Stubble retention and tillage in a semi-arid environment: 3. Response of wheat. – *Field Crops Research* 54: 39-50.
- [33] Passioura, J. B. (1983): Roots and drought resistance. – *Agriculture Water Management* 7: 265-280.
- [34] Ren, A. X., Sun, M., Wang, P. R., Xue, L. Z., Lei, M. M., Xue, J. F., Gao, Z. Q., Yang, Z. P. (2019): Optimization of sowing date and seeding rate for high winter wheat yield based on pre-winter plant development and soil water usage in the Loess Plateau, China. – *Journal of Integrative Agriculture* 18(1): 33-42.

- [35] Ren, X., Chen, X., Cai, T., Wei, T., Wu, Y., Ali, S., Zhang, P., Jia, Z. (2017): Effects of ridge-furrow system combined with different degradable mulching materials on soil water conservation and crop production in semi-humid areas of China. – *Frontiers in Plant Science* 8: 1877.
- [36] Serrago, R. A., Alzueta, I., Savin, R., Slafer, G. A. (2013): Understanding grain yield responses to source-sink ratios during grain filling in wheat and barley under contrasting environments. – *Field Crops Research* 150: 42-51.
- [37] Sun, S., Wang, Y., Engel, B. A., Wu, P. (2016): Effects of virtual water flow on regional water resources stress: a case study of grain in China. – *Science of Total Environment* 550: 871-879. DOI: 10.1016/j.scitotenv.2016.01.016.
- [38] Wang, B., Zhang, Y., Hao, B., Han, M., Zhao, Z., Wang, Z., Xue, Q. (2017): Late sowing with high seeding rate increases wheat water use efficiency under deficit irrigation. – *Journal of Soil and Water Conservation* 72(6): 629-638.
- [39] Wang, L. F., Shangguan, Z. P. (2015): Water-use efficiency of dryland wheat in response to mulching and tillage practices on the Loess Plateau. – *Scientific Reports* 5: 12225.
- [40] Wang, X., Huang, G., Li, Q., Ma, J., Gao, Y., Liu, B. (2010): Characteristics of the evapo-transpiration and its yield performance of rainfed spring wheat and peas fields. – *Journal of Arid Land Resources and Environment* 24: 172-177 (in Chinese).
- [41] Wang, Y., Xie, Z., Malhi, S., Vera, C., Zhang, Y., Wang, J. (2009): Effects of rainfall harvesting and mulching technologies on water use efficiency and crop yield in the semi-arid Loess Plateau, China. – *Agriculture Water Management* 96: 374-382. DOI: 10.1016/j.agwat.2008.09.012.
- [42] Wang, Y. Q., Xi, W. X., Wang, Z. M., Bin, W. A. N. G., Xu, X. X., Han, M. K., Zhou, S. L., Zhang, Y. H. (2016): Contribution of ear photosynthesis to grain yield under rainfed and irrigation conditions for winter wheat cultivars released in the past 30 years in North China Plain. – *Journal of Integrative Agriculture* 15(10): 2247-2256.
- [43] Xie, Z., Wang, Y., Li, F. (2005): Effect of plastic mulching on soil water use and spring wheat yield in arid region of northwest China. – *Agriculture Water Management* 75: 71-83.
- [44] Xie, Q., Mayes, S., Sparkes, D. L. (2016): Optimizing tiller production and survival for grain yield improvement in a bread wheat × spelt mapping population. – *Annals of Botany* 117(1): 51-66.
- [45] Xue, L., Khan, S., Sun, M., Anwar, S., Ren, A., Gao, Z., Lin, W., Xue, J., Yang, Z., Deng, Y. (2019): Effects of tillage practices on water consumption and grain yield of dryland winter wheat under different precipitation distribution in the loess plateau of China. – *Soil and Tillage Research* 191: 66-74.
- [46] Yang, C. G., Chai, S. X. (2019): Regulatory effects of bundled straw covering on winter wheat yield and soil thermal-moisture utilization in dryland. – *Chinese Journal of Applied Ecology* 29(10): 3245-3255.
- [47] Yang, C. G., Chai, S. X., Chang, L. (2015): Influences of different plastic film mulches on soil water use and yield of winter wheat in semiarid rain-fed region. – *Acta Ecologica Sinica* 35(8): 2676-2685. DOI: 10.5846/stxb201406051158.
- [48] Yang, D., Cai, T., Luo, Y., Wang, Z. (2019): Optimizing plant density and nitrogen application to manipulate tiller growth and increase grain yield and nitrogen-use efficiency in winter wheat. – *Peer J* 7: e6484.
- [49] Yang, J., Mao, X., Wang, K., Yang, W. (2018): The coupled impact of plastic film mulching and deficit irrigation on soil water/heat transfer and water use efficiency of spring wheat in Northwest China. – *Agricultural Water Management* 201: 232-245.
- [50] Yu, J., Liu, Z., Gao, H., Han, Q. (2005): Relationships between the ratios of GNPS/FLA and SGW/FLA with yield in wheat. – *Journal of Triticeae Crops* 25(1): 61-64.
- [51] Zadoks, J. C., Chang, T. T., Konzak, C. F. (1974): A decimal code for the growth stages of cereals. – *Weed Research* 14: 415-421.

- [52] Zhang, L. L., Sun, S. J., Chen, Z. J., Jiang, H., Zhang, X. D., Chi, D. C. (2018a): Effects of different colored plastic film mulching and planting density on dry matter accumulation and yield of spring maize. – *Chinese Journal of Applied Ecology* 29(1): 113-124.
- [53] Zhang, M., Sun, M., Gao, Z. Q., Zhao, H. M., Li, G., Ren, A. X., Hao, X. Y., Yang, Z. P. (2016): Relationships of water conservation through mulching in fallow period with wheat nitrogen transpiration and crop yield in dryland. – *Chinese Journal of Applied Ecology* 27(1): 117-124.
- [54] Zhang, M., Dong, B., Qiao, Y., Yang, H., Wang, Y., Liu, M. (2018b): Effects of sub-soil plastic film mulch on soil water and salt content and water utilization by winter wheat under different soil salinities. – *Field Crops Research* 225: 130-140.
- [55] Zhang, M., Baodi, D., Yunzhou, Q., Hong, Y., Yakai, W., Mengyu, L. (2019): Effects of subsoil plastic film mulch on yield and water use of rainfed winter wheat. – *Crop and Pasture Science* 69(12): 1197-1207.
- [56] Zhang, S., Sadras, V., Chen, X., Zhang, F. (2013): Water use efficiency of dryland wheat in the Loess Plateau in response to soil and crop management. – *Field Crop Research* 151: 9-18.
- [57] Zhao, Y. G., Li, Y. Y., Wang, J., Pang, H. C., Li, Y. (2016): Buried straw layer plus plastic mulching reduces soil salinity and increases sunflower yield in saline soils. – *Soil and Tillage Research* 155: 363-370.
- [58] Zwart, S. J., Bastiaanssen, W. G. M. (2004): Review of measured crop water productivity values for irrigated wheat, rice, cotton and maize. – *Agricultural Water Management* 69: 115-133.

EFFECT OF CULTURE FILTRATE OF *SINORHIZOBIUM FREDII* SNEB183 ON THE ACTIVITY AND BEHAVIOR OF SOYBEAN CYST NEMATODE (*HETERODERA GLYCINES* ICHINOHE, 1952)

WANG, Y. Y.¹ – SIKANDAR, A.² – ZHAO, Y. S.² – ZHAO, J.² – LIU, D.² – ZHU, X. F.² – LIU, X. Y.³
– FAN, H. Y.² – CHEN, L. J.² – DUAN, Y. X.^{2*}

¹College of Biological Science and Technology, Shenyang Agricultural University
Shenyang, China

²Nematology Institute of Northern China, Shenyang Agricultural University, Shenyang, China

³College of Sciences, Shenyang Agricultural University, Shenyang, China

*Corresponding author

e-mail: duanyx6407@163.com; phone: +86-139-9825-3910

(Received 30th Jul 2019; accepted 15th Nov 2019)

Abstract. *Rhizobium* species and the soybean cyst nematode (SCN, *Heterodera glycines*) are attracted by the root exudates of soybean and colonize its roots. There is complicated relationship between the soybean, *Rhizobium* species, and SCN. This study intended to discover the effect of *Sinorhizobium fredii* Sneb183 culture filtrate on SCN second-stage larvae (J2), egg hatching and J2 chemotaxis. The mortality of J2 treated with *S. fredii* Sneb183 culture filtrate increased with the exposure duration. Additionally, *S. fredii* Sneb183 culture filtrate reduced egg hatching within cysts, neutralized the positive effect of a susceptible soybean cultivar root exudate on hatching, and postponed the peak of hatching, thereby revealing other mechanisms for reducing nematode infection and J2 numbers. *Heterodera glycines* J2 were repelled by the culture supernatant of *S. fredii* Sneb183, the movement of J2 towards the susceptible cultivar root exudate and soybean roots was disrupted by a mixture of susceptible cultivar root exudate with *S. fredii* Sneb183 culture filtrate or by dipping the root into culture filtrate. These results indicate that *S. fredii* Sneb183 may be a potential economic, eco-friendly and effective biocontrol microorganism against SCN.

Keywords: root exudate, biocontrol, chemotaxis, mortality, susceptible

Introduction

Plant-parasitic nematodes pose a serious threat the food production of many economically important crops. Soybean cyst nematode (SCN) (*Heterodera glycines* Ichinohe) was first reported as a pest of soybean in 1899. Currently it is one of the most damaging pathogen for soybean, causing more than 30% yield losses annually in the United States (Allen et al., 2017). The combination of the use of SCN-resistant cultivars and non-host crop rotation are important means of managing the pest population levels in the field. Nevertheless, an overdependence on resistant cultivars coupled with genetic variation in SCN field populations has led to population shifts (Mitchum et al., 2007; Niblack et al., 2008). Meanwhile, public concern over environmental hazards evoked by chemical pesticides has steadily increased (Pimentel and Burgess, 2014). Therefore, alternative control strategies are highly desirable for the control of SCN. Biological control of plant diseases is usually an eco-friendly and potential component of integrated disease management; biological control of SCN has been studied for more than 40 years (Davies and Spiegel, 2011). Zhou et al. (2017) Demonstrated that combination of multiple rhizobacterial strains applied through seed coating may be a better management method for SCN.

Rhizobia are the best known beneficial plant-associated bacteria because they can fix nitrogen, which occurs during the *Rhizobium*-legume symbiosis (Zahran, 1999; Long, 2001). Several strains of *Rhizobium* spp. inhibit the growth of several root-infecting fungi to various degrees. For example, reports determined that *Rhizobium* could inhibit spore germination, and hyphae growth of some plant pathogens, including *Phoma medicaginis*, *Macrophomina phaseolina* and *Rhizoctonia solani* (Omar and Abd-Alla, 1998; Dileep Kumar et al., 2001). Drapeau et al. (1973) isolated *Rhizobium* strain TL-3 with obviously suppressive effects on *Pyrenochaeta terrestris*, *Colletotrichum destructivum* and *Coniothyrium* sp. Antagonism toward the potato cyst nematode *Globodera pallida* and the root-knot nematode *Meloidogyne incognita* by *Rhizobium etli* G12 is associated with its ability to induce systemic resistance (Hallmann et al., 2001; Martinuz et al., 2013). Numerous observations confirm that rhizobia may function as potential inducers of plant disease resistance.

Sinorhizobium fredii Sneb183, isolated from soybean nodules, could induce systemic resistance in soybean against SCN; the number of juveniles and cysts significantly decreased as a result of Sneb183 inoculation (Tian et al., 2014). The oxygen consumption rate of J2 was decreased by 93.1% after 24 h treated with Sneb183 culture filtrate, while after 48 h treatment, J2 body fluids exuded and the conductivity was increased by 62.4% (Tian et al., 2014). The present study is conducted to evaluate the effect of *S. fredii* Sneb183 fermentation filtrate on the activity of J2, the hatching rate of eggs within cysts, and J2 chemotaxis, with the goal being to expand the potential of this strain as a new agent for biological control of soybean cyst nematode.

Materials and methods

Experimental Design

Current study has been conducted to evaluate efficacy of *S. fredii* Sneb183 against *H. glycine* at Nematology Institute of Northern China, Shenyang Agricultural University, Liaoning, China during 2018.

Isolation of cysts and J2 of SCN

H. glycine was first reported as pest of soybean in 1899. Surface soil samples (2 cm depth) were removed from the rhizosphere of soybean (*Glycine max* cv Liaodou 15, a SCN-susceptible cultivar). *H. glycine* was first reported as pest of soybean in 1899. Cysts were obtained from experimental field of Nematology Institute of Northern China, and collected by following elutriation and hand-picking under a stereomicroscope. Cysts were surface-sterilized by immersion in 0.1% HgCl₂ solution for 1 minute followed by rinsing three times with sterile distilled water. The cysts were then placed in Baermann funnel at 25°C. J2 were collected from the bottom of the Baermann funnel every two or three days (Liu, 1995).

Preparation of soybean roots and root exudates

Soybean seeds ('Liaodou 15') were rinsed with distilled water, sterilized in 75% ethanol for 1 min, and rinsed several times with sterilized water. After the seeds were swollen for 4 h in Petri dish covered with sterile moist filter paper, then they were placed in sterile petri dishes filled with sand sterilized (160°C for 1 h). After one week, apical

1 cm segments of roots were rinsed with sterilized water and stored in 4°C for subsequent use.

The sterilized sand and soil (V:V=2:1) in pots 25 cm in diameter was seeded with one of the surface-sterilized soybean seeds, and plants were watered with N-free Hoagland's solution on alternate days, in which Ca(NO₃)₂ and KNO₃ were replaced with CaCl₂, K₂HPO₄ and KH₂PO₄, as recommended (Hoagland and Arnon, 1950). The soybeans were grown in a greenhouse at 28 ± 2°C with a 16/8 h light/dark photoperiod. Soybean root exudates were obtained via a slightly modified procedure of Tefft and Bone (1985) and Levene et al. (1998) such as five soybean seedlings were used for root exudate. The soybean seedling roots after grown 20 d were rinsed with tap water and distilled water, placed in sterile 50 mL centrifuge tubes containing sterile water of volume sufficient to submerge the roots, incubated in a dark room at room temperature for 24 h, one soybean seedling in each centrifuge tube. Some root exudates was stored at 4°C for subsequent egg hatch bioassays and 50 mL exudate was placed in a rotary evaporator, concentrated to 5 mL under reduced pressure at 50°C, and stored at 4°C for chemo-attraction experiments.

Preparation of Rhizobium Sneb183 fermentation filtrate

Sinorhizobium fredii Sneb183 was originally isolated from pine rhizosphere and identified by Zhao et al. (2009). Strain was stored at -80°C at Nematology Institute of Northern China, Shenyang Agricultural University, Liaoning, China. *S. fredii* Sneb183 was suspended in sterilized water and adjusted to 1.0×10⁸ cfu/ml with a hemocytometer under a microscope, then 1.0 mL of this suspension was added to 50 mL sterilized TY liquid medium (Duelli and Noel, 1997). Cultures were maintained at 28°C and 150 rpm for 168 h, and were then centrifuged at 5590 g for 20 min. The fermentation filtrate through 0.22 µm filter was used for the impact of J2 lethality and chemotaxis assays and egg hatching bioassays (Hasky-Guenther et al., 1998; Reitz et al., 2000).

J2 lethality assay

100 J2 was transferred into a 5 ml glass petri dishes containing 2.0 ml Sneb183 fermentation filtrate (Sneb183F) and sterilized TY liquid medium (TY), respectively. After that dishes were incubated at 25°C and covered by coverslip. The number of dead nematodes was determined at 12 h, 24 h, 48 h, and 72 h. Three independent experiments were done and each experiment has three replicates. J2 treated with sterilized water was used in the control treatment. The J2 were regarded dead when they were remained static once touched with hair-needle (Cayrol et al., 1989). The lethality (L) of J2 was calculated by Eq.1.

$$L = \frac{L_t}{100} \times 100 \quad (\text{Eq.1})$$

where, L_t stands for the number of dead J2 in assay.

Cyst hatching inhibition assay

Plump and brown cysts were crushed and 1000 eggs were picked into glass petri dish under room temperature to test the hatching rate. The experiment included four treatments with nine replicates per treatment: 10 ml soybean root exudate (SRE), 10 ml Sneb183

fermentation filtrate (Sneb183F), a mixture of 5.0 mL soybean root exudate and 5.0 mL Sneb183 fermentation filtrate (SRE+Sneb183F), 10 mL Sterile water (Control). The treatment solution was replaced and numbers of hatched J2 were determined every three days until no additional J2s were observed in the control treatment. The hatching rate (HR) was calculated by (Eq.2).

$$HR = \frac{T.N.H.J2}{1000} \times 100 \quad (\text{Eq.2})$$

where, *T.N.H.J2* stands for the total number of hatched J2.

Chemotaxis assays

Indirect method with filter paper

The effect of *S. fredii* Sneb183 fermentation filtrate on nematode movement and chemotaxis was studied on Pluronic F-127 gel in 60 mm diameter petri dishes (Wang et al., 2009), with the bottom engraved with concentric circles of radii 1.0 and 2.0 cm (Hewlett et al., 1997; Schroeder and MacGuidwin, 2010). Filter paper ($r = 0.5$ cm) was soaked with soybean root exudate (SRE), Sneb183 fermentation filtrate (Sneb183F), an equal proportional mixture of soybean root exudate and Sneb183 fermentation filtrate (SRE+Sneb183F) was placed in the center of the dish. 50 freshly hatched J2 in 1 ml sterile water were uniformly distributed in the radius of 1-2 cm along the circumference of dish. After 24 h at 25°C, the number of J2 distributed in the different sections was counted. Sterile water was used as a control. Three independent experiments were done and each experiment has three replicates. The distribution rate, regarded as an index of chemotaxis, was calculated as follows: $DR_s = DN_s/50$. DR_s represents the distribution rate in each section and DN_s represents the distribution number in each section.

Direct method with in vitro root

A direct method for observing chemotaxis utilized 5 cm young soybean roots at the growing point instead of filter paper. Roots were soaked in Sneb183 fermentation filtrate and sterile water, respectively. The remaining operations are the same as indirect method with filter paper. After 24 h at 25°C, counted the number of J2 distribute in different sections of Petri dish and their distribution rate.

Statistical analysis

Data were analyzed using one-way analysis of variance (ANOVA). Means for each trial in each assay were separated by the Duncan multiple range test.

Results

J2 activity assay

This result strongly indicates that Sneb183 has biocontrol potential against SCN. The fermentation filtrate of *S. fredii* Sneb183 showed high nematicidal activity (*Fig. 1* and *Table 1*). When exposed to Sneb183 fermentation filtrate, J2s of *H. glycines* displayed significant time-dependent mortality. Treatment with Sneb183 fermentation filtrate for 24 h and 72 h, the lethality (L) of J2 reached to 46.66% and 86.66%, respectively. These

results indicated that *S. fredii* Sneb183 can produce some extracellular substances to kill nematodes.

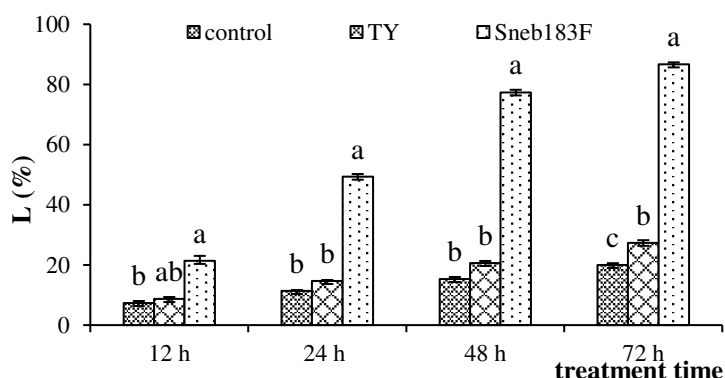


Figure 1. Lethality of *Sinorhizobium fredii* Sneb183 fermentation supernatant to J2 of *Heterodera glycines*. Different letters on bar indicates that values are significantly different according to Duncan multiple range test at $P > 0.05$. Whereas; Control (Sterile water), TY (Fermentation liquid without bacteria), Sneb183F (Sneb183 Fermentation filtrate)

Table 1. Effects of treatments on lethality of second stage juveniles of *H. glycines*

Treatments	Time of exposure			
	12-h	24-h	48-h	72-h
Control	7.33±2.31 ^c	11.33±1.15 ^b	15.33±2.31 ^b	20.0±2.0 ^c
TY	12.0±7.21 ^{ab}	14.67±1.15 ^b	20.67±2.31 ^b	27.33±3.06 ^b
Sneb183	21.33±6.11 ^a	49.33±3.06 ^a	77.33±3.06 ^a	86.67±2.31 ^a
ANOVA Test				
SS	304.889	2656.889	7083.556	8018.667
Df	2	2	2	2
MS	152.444	1328.444	3541.778	4009.333
F	4.831	332.111	531.267	644.357
P	0.056	0.000	0.000	0.000

Data represent the Mean±Standard deviation of lethality of J2 of *H. glycines*. Whereas; SS (Sum of square); Df (Degree of freedom); MS (Mean square); F (F-value); P (Significant value). The different letter within columns are significantly different according to Duncan's multiple range test ($P > 0.05$). Whereas; Control (Sterile water), TY (Fermentation liquid without bacteria), Sneb183F (Sneb183 Fermentation filtrate)

Egg hatching assay

The effects of the four treatments on the hatching of soybean cyst nematode eggs were determined. The results showed that SRE significantly promoted the hatching of soybean cyst nematode eggs compared with the control, the hatching rate reached to 56%. Treatment Sneb183F significantly inhibited the hatching of soybean cyst nematode eggs, the hatching rate was only 0.63%, and the inhibition rate was 98.75%. SRE+Sneb183F also showed inhibition of egg hatching, with an inhibition rate of 39.04% (Fig. 2 and Table 2), the inhibition effect is lower than that of Sneb183F. According to Fig. 3, treated with Sneb183F, J2 were not hatched out until 18d, it was almost the deadline of other treatments. It could be seen that all the treatments containing Sneb183F can significantly reduce the hatching rate of soybean cyst nematode eggs as well as delay the peak period of egg hatching (Fig. 3).

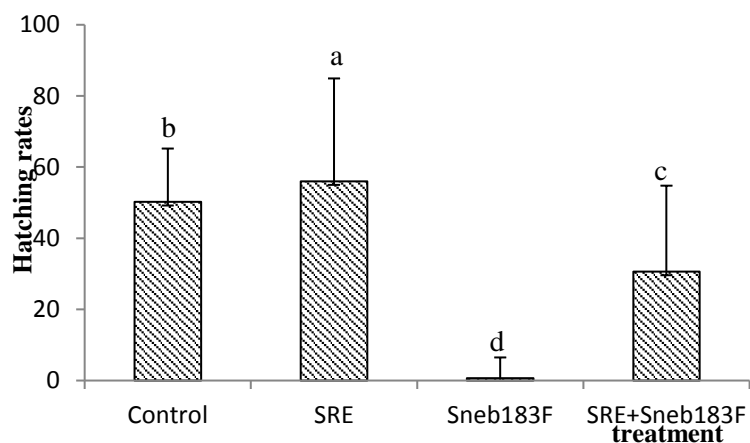


Figure 2. Effect of treatments with 4 treatments on eggs of *Heterodera glycines* hatching rate. Different letters on bar indicates that values are significantly different according to Duncan multiple range test at $P > 0.05$. Whereas; Control (Sterile water), SRE (Soybean root exudate), Sneb183F (Sneb183 Fermentation filtrate), SRE+Sneb183F (Soybean root exudate + Sneb183 fermentation filtrate)

Table 2. Effects of treatments on egg hatching of *H. glycines*

Treatments	Hatching
Control	49.67±1.50 ^b
SRE	55.27±2.89 ^a
Sneb183F	0.5±0.56 ^d
SRE+Sneb183F	30.07±2.42 ^c
ANOVA Test	
SS	5506.123
Df	3
MS	1835.374
F	437.776
P	0.000

Data represent the Mean±Standard deviation egg hatching of *H. glycines*. Whereas; SS (Sum of square); MS (Mean square); Df (Degree of freedom); F (F-value); P (Significant value). The different letter within columns are significantly different according to Duncan's multiple range test ($P > 0.05$). Whereas; Control (Sterile water), SRE (Soybean root exudate), Sneb183F (Sneb183 Fermentation filtrate), SRE+Sneb183F (Soybean root exudate + Sneb183 fermentation filtrate)

Chemotaxis assays

The influence of fermentation filtrate of *S. fredii* Sneb183 on the chemotaxis of J2 was determined by an indirect method utilizing filter paper. The distribution rate of J2 in different region of dish varied in different treatment (Fig. 4 and Table 3). In the control treatment, the nematodes placed within 1-2 cm area originally were evenly distributed in three sections after 24 h. At 0-1 cm, the distribution rates of J2 in the root exudate and in the *S. fredii* fermentation filtrate treatments were the highest and the lowest, respectively. The majority of J2 were attracted to the central area where soybean root exudate-impregnated filter paper was placed. The opposite happened at 2-3 cm, treatment with fermentation filtrate of *S. fredii* Sneb183 or in the equal mixture of fermentation filtrate and root exudate, most J2 were repelled to the region of 2-3 cm. Overall, the effect of J2

attracted by root exudate was remarkably reduced with the addition of fermentation filtrate. Therefore, *S. fredii* Sneb183 fermentation filtrate is repellent to *H. glycines* J2.

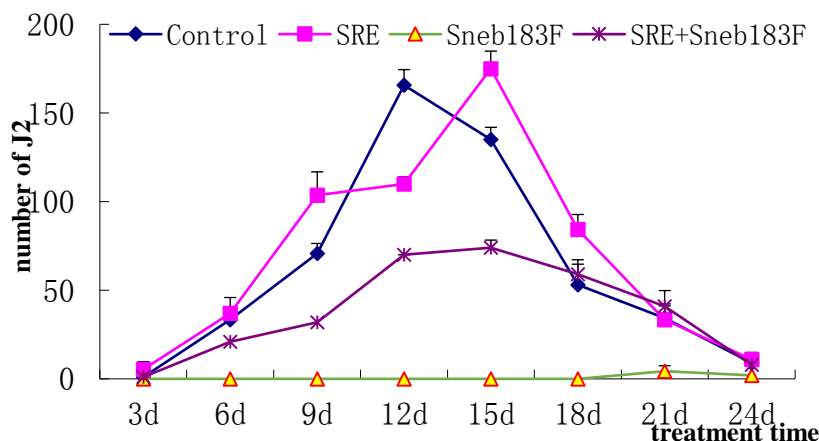


Figure 3. Effects of 4 treatments on the number of *Heterodera glycines* eggs hatching at different treatment times. Whereas; Control (Sterile water), SRE (Soybean root exudate), Sneb183F (Sneb183 Fermentation filtrate), SRE+Sneb183F (Soybean root exudate + Sneb183 fermentation filtrate)

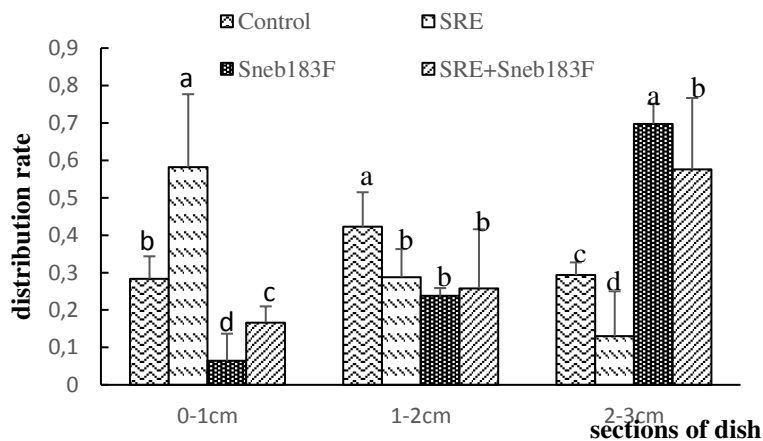


Figure 4. Effect on chemotaxis of *Heterodera glycines* J2 to filter paper treated with four treatments. Different letters on bar indicates that values are significantly different according to Duncan multiple test at $P > 0.05$. Whereas; Control (Sterile water), SRE (Soybean root exudate), Sneb183F (Sneb183 Fermentation filtrate), SRE+Sneb183F (Soybean root exudate + Sneb183 fermentation filtrate)

In the direct method of chemotaxis with roots in vivo, the distribution rates of J2 significantly differed among treatments with Sneb183F and sterile water. At original region (1-2 cm), the distribution rate of J2 in the two treatments is not much different. The young root treated with sterile water strongly attracted J2, the distribution rate of J2 in the sterile water reached 0.6 in the region of 0-1 cm, whereas the treatments with fermentation filtrate was only 0.15, which was significantly different from that in the control treatments (Fig. 5 and Table 4).

Table 3. Effect filter paper chemotaxis assay of second stage juveniles of *H. glycines*

Treatments	Filter paper Chemotaxis assay		
	0-1cm	1-2cm	2-3cm
Control	0.29±0.05 ^b	0.42±0.03 ^b	0.29±0.03 ^c
SRE	0.58±0.05 ^a	0.29±0.01 ^a	0.13±0.05 ^d
Sneb183F	0.06±0.00 ^d	0.24±0.03 ^b	0.70±0.03 ^a
SRE+Sneb183F	0.17±0.03 ^c	0.26±0.07 ^b	0.57±0.10 ^b
ANOVA Test			
SS	0.453	0.059	0.600
Df	3	3	3
MS	0.151	0.020	0.200
F	96.454	10.224	57.152
P	0.000	0.004	0.000

Data represent the Mean±Standard deviation of filter paper chemotaxis assay of *Heterodera glycines* J2. Whereas; SS (Sum of square); Df (Degree of freedom); MS (Mean square); F (F-value); P (Significant value). The different letter within columns are significantly different according to Duncan's multiple range test (P>0.05). Whereas; Control (Sterile water), SRE (Soybean root exudate), Sneb183F (Sneb183 Fermentation filtrate), SRE+Sneb183F (Soybean root exudate + Sneb183 fermentation filtrate)

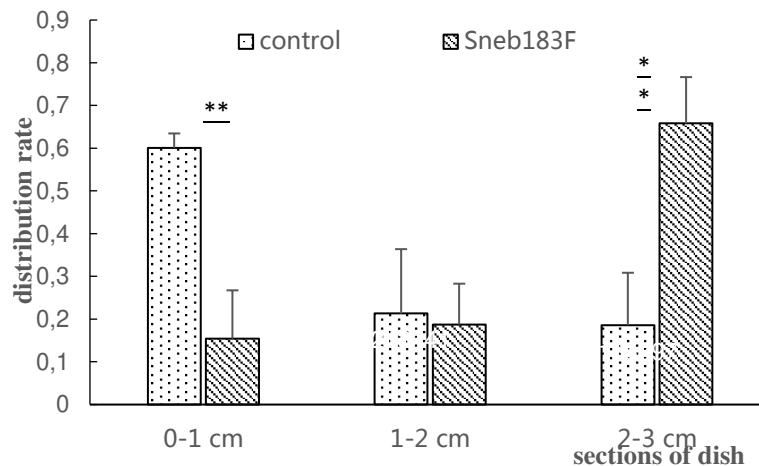


Figure 5. Effect on chemotaxis of *Heterodera glycines* J2 to *Glycine max* root treated with sterile water or *S. fredii* Sneb183 fermentation filtrate. Different letters on bar indicates that values are significantly different according to Waller-Duncan test at P>0.05. Whereas; Control (Sterile water), Sneb183F (Sneb183 Fermentation filtrate)

Table 4. Effect of In-vivo Chemotaxis assay of second stage juveniles of *H. glycines*

Treatments	In-vivo Chemotaxis assay		
	0-1cm	1-2cm	2-3cm
Control	0.60±0.33	0.21±0.15	0.19±0.12
Sneb183F	0.15±0.11	0.19±0.10	0.66±0.10
ANOVA Test			
SS	0.299	0.01	0.334
Df	1	1	1
MS	0.299	0.01	0.334
F	43.037	0.062	24.950
P	0.03	0.816	0.008

Data represent the Mean±Standard deviation of in-vivo chemotaxis assay of second stage juveniles of *H. glycines*. Whereas; SS (Sum of square); Df (Degree of freedom); MS (Mean square); F (F-value); P (Significant value). Whereas; Control (Sterile water), Sneb183F (Sneb183 Fermentation filtrate)

Discussion

The *Rhizobium*-legume symbiosis is a special mutualistic relationship (Hirsch et al., 2001). In which beneficial bacterial symbionts provide the nitrogen source for soybean as a result of rhizobia-soybean coevolution (Coba de la Peña et al., 2018). Using *Rhizobium* as a biocontrol agent against *H. glycines* should not only provide nitrogen for soybean plants but also ease to colonize the rhizosphere of soybean. Some studies on the use of *Rhizobium* strains to control nematodes and other pathogens indicate that rhizobia may become excellent biological control agents for disease control. We obtained *Sinorhizobium fredii* Sneb183 out of more than 300 rhizobial strains isolated from the roots of different plants and rhizosphere soils to study their potential against *H. glycines*. A mixture of *Sinorhizobium fredii* Sneb183 and other strains greatly reduced SCN reproduction and significantly promoted plant growth (Zhou et al., 2017).

In this study, we evaluated *S. fredii* Sneb183 action against *H. glycines* by investigating its suppression of juvenile survival and egg hatching and its disruption of host-finding behavior. The fermentation filtrate from *S. fredii* Sneb183 had obvious nematicidal activity against J2, with lethality directly correlated with the duration of exposure, reaching a maximum of 84% at 72 h. Although numerous in vitro studies have discovered the antibiotic or nematicidal activity of bacterial culture filtrates (Sikora, 1992; Li et al., 2005), reported the production of rhizobial compounds that inhibit the growth of other organisms are few. Chakraborty and Purkayastha (1984) discovered toxic substances in the fermentation liquid of *R. japonicum*, and identified one as rhizobitoxine; fermentation liquid of *R. japonicum* inhibited *Macrophomina phaseolina* at 48 h.

Nematode egg hatching in soil is known to be affected by host root exudate, as well as by some chemicals, enzymes, toxins and metabolic by-products of microorganisms (Schmitt and Riggs, 1991; Hu et al., 2017). Previous studies have shown that egg hatching may be stimulated by exudates from roots of susceptible cultivars (Yang et al., 2016). In our current study, the root exudate of soybean 'Liaodou 15' stimulated egg hatching, but the supernatant from *S. fredii* Sneb183 culture inhibited egg hatching strongly and reduced the stimulatory effect of Liaodou 15 root exudate on egg hatchability, thereby possibly reducing the speed at which nematode populations can establish within a root. Using microorganisms to inhibit egg hatching may be an effective strategy resulting in reduced nematode populations in soils and lowered disease severity in infected plants.

Plant-parasitic nematodes were attracted by root exudates to search, locate, penetrate and establish a feeding site in host roots (Yang et al., 2016). Their movement toward host roots may be disturbed by regulating their behaviour. We found that the attraction of J2 to host roots significantly declined during treatment with supernatant from *S. fredii* Sneb183 culture. Whether an indirect or direct assay was employed, the fermentation filtrate not only strongly repelled J2 but also effectively weakened J2 chemotaxis to root exudate and soybean roots.

Nematodes dwelled in soils containing millions of soil microbes. Inevitably, nematodes exposed to fungi and bacteria interacted with them (Tian et al., 2007), including rhizobia. In general, plant-parasitic nematodes inhibit nodulation and nitrogen fixation of roots of leguminous plants (Hussey and Barker, 1976). Horiuchi et al. (2005) reported that the microbivorous nematode *Caenorhabditis elegans* mediates the interaction between roots and rhizobia positively, leading to nodulation through transfer of the rhizobial species *Sinorhizobium meliloti* to the roots of the legume *Medicago truncatula*. Some plant-pathogenic nematodes like *Meloidogyne* spp. have positive

effects on the symbiosis between rhizobia-legume interactions by enhancing the number of nodules and the amount of nitrogen fixed (Baldwin et al., 1979).

Conclusion

It is concluded that *Sinorhizobium fredii* Sneb183 culture filtrate showed nematicidal potential toward soybean cyst nematode (*Heterodera glycines*). The results of current research reveal a unique interaction between *S. fredii* Sneb183 and *H. glycines*, possibly providing a foundation as a biocontrol agent for new prospects of future utilization of rhizobia. However, further study is needed to determinants of *S. fredii* Sneb183 responsible for the activity of nematicide, mechanism of action and screening of active components.

Acknowledgements. Special Fund for Agro-scientific Research in the Public Interest (201503114), National Natural Science Foundation of China (31330063), and China Agriculture Research System CARS-04-PS13.

Conflict of interests. The authors have no conflict of interests.

REFERENCES

- [1] Allen, T. W., Bradley, C. A., Sisson, A. J., Byamukama, E., Chilvers, M. I., Coker, C. M., Collins, A. A., Damicone, J. P., Dorrance, A. E., Dufault, N. S. (2017): Soybean yield loss estimates due to diseases in the United States and Ontario, Canada, from 2010 to 2014. – *Plant Health Progress* 18: 19-27.
- [2] Baldwin, J., Barker, K., Nelson, L. (1979): Effects of *Meloidogyne incognita* on nitrogen fixation in soybean. – *Journal of Nematology* 11: 156-161.
- [3] Cayrol, J.-C., Djian, C., Pijarowski, L. (1989): Study of the nematicidal properties of the culture filtrate of the nematophagous fungus *Paecilomyces lilacinus*. – *Revue de Nematologie* 12: 331-336.
- [4] Chakraborty, U., Purkayastha, R. (1984): Role of rhizobitoxine in protecting soybean roots from *Macrophomina phaseolina* infection. – *Canadian Journal of Microbiology* 30: 285-289.
- [5] Coba de la Peña, T., Fedorova, E., Pueyo, J. J., Lucas, M. M. (2018): The symbiosome: legume and rhizobia co-evolution toward a nitrogen-fixing organelle? – *Frontiers in plant science* 8: 2229.
- [6] Davies, K., Spiegel, Y. (2011): *Biological Control of Plant-Parasitic Nematodes: Building Coherence between Microbial Ecology and Molecular Mechanisms*. – Springer Science & Business Media.
- [7] Dileep Kumar, B., Berggren, I., Mårtensson, A. (2001): Potential for improving pea production by co-inoculation with fluorescent *Pseudomonas* and *Rhizobium*. – *Plant and soil* 229: 25-34.
- [8] Drapeau, R., Fortin, J., Gagnon, C. (1973): Antifungal activity of *Rhizobium*. – *Canadian Journal of Botany* 51: 681-682.
- [9] Duelli, D. M., Noel, K. D. (1997): Compounds exuded by *Phaseolus vulgaris* that induce a modification of *Rhizobium etli* lipopolysaccharide. – *Molecular plant-microbe interactions* 10: 903-910.
- [10] Hallmann, J., Quadt-Hallmann, A., Miller, W., Sikora, R., Lindow, S. (2001): Endophytic colonization of plants by the biocontrol agent *Rhizobium etli* G12 in relation to *Meloidogyne incognita* infection. – *Phytopathology* 91: 415-422.

- [11] Hasky-Guenther, K., Hoffmann-Hergarten, S., Sikora, R. A. (1998): Resistance against the potato cyst nematode *Globodera pallida* systemically induced by the rhizobacteria *Agrobacterium radiobacter* (G12) and *Bacillus sphaericus* (B43). – *Fundamental and Applied Nematology* 21: 511-517.
- [12] Hewlett, T., Hewlett, E., Dickson, D. (1997): Response of *Meloidogyne* spp., *Heterodera glycines*, and *Radopholus similis* to tannic acid. – *Journal of Nematology* 29: 737.
- [13] Hirsch, A. M., Lum, M. R., Downie, J. A. (2001): What makes the rhizobia-legume symbiosis so special? – *Plant physiology* 127: 1484-1492.
- [14] Hoagland, D. R., Arnon, D. I. (1950): The water-culture method for growing plants without soil. – Circular 347. California agricultural experiment station.
- [15] Horiuchi, J.-I., Prithiviraj, B., Bais, H. P., Kimball, B. A., Vivanco, J. M. (2005): Soil nematodes mediate positive interactions between legume plants and rhizobium bacteria. – *Planta* 222: 848-857.
- [16] Hu, Y., You, J., Li, C., Williamson, V. M., Wang, C. (2017): Ethylene response pathway modulates attractiveness of plant roots to soybean cyst nematode *Heterodera glycines*. – *Scientific Reports* 7: 41282.
- [17] Hussey, R., Barker, K. (1976): Influence of nematodes and light sources on growth and nodulation of soybean. – *Journal of Nematology* 8: 48-52.
- [18] Levene, B. C., Owen, M. D., Tylka, G. L. (1998): Influence of herbicide application to soybeans on soybean cyst nematode egg hatching. – *Journal of nematology* 30: 347-352.
- [19] Li, B., Xie, G.-I., Soad, A., Coosemans, J. (2005): Suppression of *Meloidogyne javanica* by antagonistic and plant growth-promoting rhizobacteria. – *Journal of Zhejiang University. Science. B* 6: 496.
- [20] Liu, W. (1995): The Research Technique of Plant Pathogenic Nematodes. – *Screen Method of Nematodes in Soil and Plants*. Liaoning Science and Technology Press, Shenyang, China 47-49.
- [21] Long, S. R. (2001): Genes and signals in the rhizobium-legume symbiosis. – *Plant Physiology* 125: 69-72.
- [22] Martinuz, A., Schouten, A., Sikora, R. A. (2013): Post-infection development of *Meloidogyne incognita* on tomato treated with the endophytes *Fusarium oxysporum* strain Fo162 and *Rhizobium etli* strain G12. – *BioControl* 58: 95-104.
- [23] Mitchum, M. G., Wrather, J. A., Heinz, R. D., Shannon, J. G., Danekas, G. (2007): Variability in distribution and virulence phenotypes of *Heterodera glycines* in Missouri during 2005. – *Plant disease* 91: 1473-1476.
- [24] Niblack, T., Colgrove, A., Colgrove, K., Bond, J. (2008): Shift in virulence of soybean cyst nematode is associated with use of resistance from PI 88788. – *Plant Health Progress* 9: 29.
- [25] Omar, S., Abd-Alla, M. (1998): Biocontrol of fungal root rot diseases of crop plants by the use of rhizobia and bradyrhizobia. – *Folia Microbiologica* 43: 431-437.
- [26] Pimentel, D., Burgess, M. (2014): Environmental and economic costs of the application of pesticides primarily in the United States. – In: Peshin, R., Dhawan, A. K. (eds.) *Integrated Pest Management: Innovation-Development Process*. Springer, Dordrecht.
- [27] Reitz, M., Rudolph, K., Schröder, I., Hoffmann-Hergarten, S., Hallmann, J., Sikora, R. (2000): Lipopolysaccharides of *Rhizobium etli* Strain G12 Act in Potato Roots as an Inducing Agent of Systemic Resistance to Infection by the Cyst Nematode *Globodera pallida*. – *Applied and Environmental Microbiology* 66: 3515-3518.
- [28] Schmitt, D., Riggs, R. (1991): Influence of selected plant species on hatching of eggs and development of juveniles of *Heterodera glycines*. – *Journal of Nematology* 23: 1.
- [29] Schroeder, N. E., MacGuidwin, A. E. (2010): Mortality and behavior in *Heterodera glycines* juveniles following exposure to isothiocyanate compounds. – *Journal of nematology* 42: 194.
- [30] Sikora, R. A. (1992): Management of the antagonistic potential in agricultural ecosystems for the biological control of plant parasitic nematodes. – *Annual Review of Phytopathology* 30: 245-270.

- [31] Tefft, P. M., Bone, L. W. (1985): Plant-induced hatching of eggs of the soybean cyst nematode *Heterodera glycines*. – Journal of Nematology 17: 275.
- [32] Tian, B., Yang, J., Zhang, K.-Q. (2007): Bacteria used in the biological control of plant-parasitic nematodes: populations, mechanisms of action, and future prospects. – FEMS Microbiology Ecology 61: 197-213.
- [33] Tian, F., Chen, L., Wang, Y., Zhu, X., Duan, Y. (2014): Action mode of *Sinorhizobium fredii* Sneb183 on the activity of soybean cyst nematode. – Chinese Journal of Biological Control 30: 540-545.
- [34] Wang, C., Lower, S., Williamson, V. M. (2009): Application of Pluronic gel to the study of root-knot nematode behaviour. – Nematology 11: 453-464.
- [35] Yang, G., Zhou, B., Zhang, X., Zhang, Z., Wu, Y., Zhang, Y., Lü, S., Zou, Q., Gao, Y., Teng, L. (2016): Effects of tomato root exudates on *Meloidogyne incognita*. – PloS one 11: e0154675.
- [36] Zahran, H. H. (1999): Rhizobium-legume symbiosis and nitrogen fixation under severe conditions and in an arid climate. – Microbiol. Mol. Biol. Rev. 63: 968-989.
- [37] Zhao, Y.-s., Duan, Y.-x., Wang, Y.-y., Chen, L.-j., YIN, L.-n. (2009): Stress resistance and biocontrol potential of soybean rhizobia resources isolated from Liaoning Province. – Soybean Science 28: 114-117.
- [38] Zhou, Y., Wang, Y., Zhu, X., Liu, R., Xiang, P., Chen, J., Liu, X., Duan, Y., Chen, L. (2017): Management of the soybean cyst nematode *Heterodera glycines* with combinations of different rhizobacterial strains on soybean. – PloS one 12: e0182654.

GENETIC RELATIONSHIP AND POLYMORPHISM OF TURKISH MYRTLES (*MYRTUS COMMUNIS* L.) AS REVEALED BY INTER SIMPLE SEQUENCE REPEAT (ISSR)

SIMSEK, O.^{1*} – DONMEZ, D.² – SARIDAS, M. A.³ – PAYDAS-KARGI, S.³ – AKA-KACAR, Y.³

¹*Horticulture Department, Agriculture Faculty, Erciyes University, Kayseri, Turkey*

²*Biotechnology Research and Application Center, Çukurova University, Adana, Turkey*

³*Horticulture Department, Agriculture Faculty, Çukurova University, Adana, Turkey*

**Corresponding author
e-mail: ozhan12@gmail.com*

(Received 30th Jul 2019; accepted 25th Nov 2019)

Abstract. Myrtle is known native to Southern Europe and North Africa and was naturally grown in tropical and subtropical regions. Myrtle could be grown successfully in soils under hot, arid environments. Myrtle has several genotypes with yellowish-white or bluish-black colored fruits. The present study aimed to investigate genetic diversity among myrtle genotypes with different fruit colors from different parts of Turkey. A total of 28 myrtle genotypes were collected from Adana, Mersin, Hatay provinces of Turkey. 19 ISSR primers were used for the characterization of the 28 myrtle genotypes. In total, 19 ISSR primers produced 99 clear and reproducible DNA band profiles, 89 of which were polymorphic. Therefore, the average polymorphic was 89.90%. In conclusion, we determined that the ISSR molecular markers could differentiate the white and dark-fruited myrtle genotypes. Myrtle genotypes were also separated according to their geographical origin.

Keywords: *molecular marker, PCR, genetic diversity, plant genetic resources, different fruit-colored*

Introduction

Myrtus communis L., commonly called Myrtle, is one of the significant medicinal and aromatic species (Wannes et al., 2010; Dahmoune et al., 2015). Myrtle is a diploid ($2n = 2x = 22$) plant known to be native to Southern Europe and North Africa (Serce et al., 2008). Myrtle is known to be a member under the Myrtaceae family, which contains 3,000 species were naturally grown in tropical and subtropical regions. Myrtle is largely consumed as spice having several practices in the food, pharmaceutical, and industries (Sumbul et al., 2011; Casaburi et al., 2015). Myrtle plant could also be used as ornamental purposes such as fencing, roadsides, and green cutting (Skekafandeh, 2007; Danial, 2009). Myrtle grows roughly at an altitude of 500–600 m, most particularly in pine forests and riversides in the Taurus Mountains of Turkey (Aydin and Ozcan, 2007). Myrtle is also called as “hambeles,” “mersin,” or “murt” in Turkish. It can be grown successfully in soils under hot, arid environments. Myrtle has several genotypes with yellowish-white or bluish-black colored fruits (San et al., 2015; Simsek et al., 2017a).

Many different biotechnological methods could be performed to fruit crops to get better ones during plant breeding strategies. One of significant application of biotechnology is known to be molecular markers in fruit science (Donmez et al., 2016). In recent years, it has been observed that biotechnology studies have been adapted to the breeding activities carried out in many plant species together with classical breeding. Especially, it is possible to shorten the breeding process by adapting the molecular

techniques to the breeding processes and make a selection in terms of some features in the early period by using molecular markers (Simsek et al., 2017b). In recent years, molecular techniques in plant breeding can be beneficial in many ways. Among these molecular techniques, ISSR markers having high usage rates have an important place. Molecular markers overcoming the limitations of morphological and biochemical markers avoid the influence of the environment on the performance of genotypes (Madadi et al., 2017). There are several studies on molecular characterization of myrtle genotypes having different origins in literature by various molecular markers (Bruna et al., 2004, 2007; Messaoud et al., 2007, 2011; Serce et al., 2008; Albaladejo et al., 2009; Melito et al., 2013, 2016, 2017; Nora et al., 2015; Ghafouri et al., 2018; Mele et al., 2019). The present study aimed to investigate genetic diversity among different fruit-colored myrtle genotypes from different parts of Turkey. Especially fruit color was chosen as phenotypic trait besides plant materials were collected from different locations of Turkey to ensure that ISSR markers could discriminate myrtle genotypes.

Materials and methods

Plant material

A total of 28 myrtle genotypes were collected from Adana, Mersin, Hatay provinces of Turkey (Table 1). A map with the sampling sites is presented in Figure 1.

DNA extraction

Total genomic DNA was extracted from leaves tissues by CTAB method (Simsek et al., 2008). The quality and quantity of DNA were detected by NanoDrop (ND 100) spectrophotometer (NanoDrop Technologies, Inc., Wilmington, DE, USA) and agarose gel electrophoresis. DNA samples were subsequently diluted to 10 ng/ μ l for ISSR-PCR reactions and stored at -20 °C.

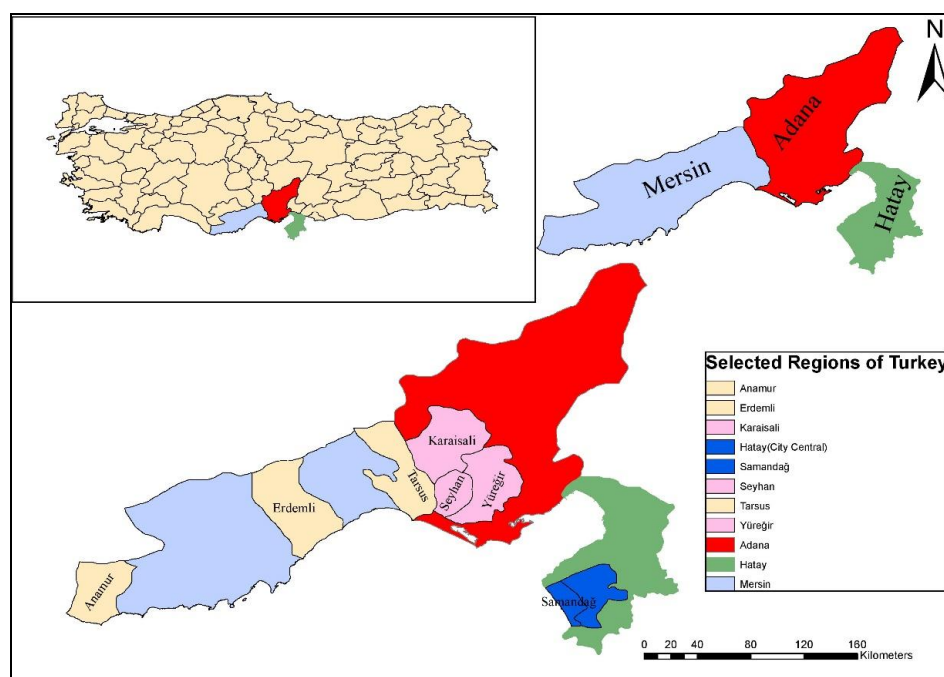


Figure 1. Map with the sampling sites

Table 1. *Myrtle genotypes and their sampling locations*

Name	Sampling location province/city	Fruit color
Çelemlı1	Çelemlı/Yüreğir/Adana	Dark-fruited
Akpınar1	Akpınar/Yüreğir/Adana	Dark-fruited
Akpınar2	Akpınar/Yüreğir/Adana	Dark-fruited
Zıyanlı1	Zıyanlı/Yüreğir/Adana	Dark-fruited
Zıyanlı2	Zıyanlı/Yüreğir/Adana	Dark-fruited
Zıyanlı3	Zıyanlı/Yüreğir/Adana	Dark-fruited
Seyhan1	Çaputçu/Seyhan/Adana	White-fruited
Seyhan2	Mıdık/Seyhan/Adana	White-fruited
Tarsus1	Kefeli/Tarsus/Mersin	Dark-fruited
Seyhan3	Kayışlı/Seyhan/Adana	White-fruited
Erdemli1	Tömük/Erdemli/Mersin	White-fruited
Tarsus2	Tarsus/Mersin	Dark-fruited
Karaisalı	Karaisalı/Adana	Dark-fruited
Erdemli2	Erdemli/Mersin	Dark-fruited
Seyhan4	Gölbaşı/Seyhan/Adana	White-fruited
Seyhan5	Gölbaşı/Seyhan/Adana	White-fruited
Seyhan6	Gölbaşı/Seyhan/Adana	White-fruited
Antakya	Antakya/Hatay	White-fruited
Samandağ	Samandağ/Hatay	White-fruited
Baltacık	Baltacık/Hatay	White-fruited
Harbiye1	Harbiye/Hatay	White-fruited
Harbiye2	Harbiye/Hatay	Dark-fruited
Kozan	Kozan/Adana	White-fruited
Anamur	Anamur/Mersin	White-fruited
Sarıçam1	Sarıçam/Adana	White-fruited
Sarıçam2	Sarıçam/Adana	White-fruited

ISSR-PCR analysis

19 ISSR primers were used for characterization of the 28 myrtle genotypes (Table 2). All ISSR-PCR reactions were carried in a reaction containing 2X PCR Mastermix (Fermentas K0171, Waltham, MA, USA), 1 U Taq DNA polymerase (Fermentas EP0402), 25 mM MgCl₂, 10 µM primer, and 10 ng of myrtle DNA. Mixtures were assembled at 0 °C, transferred to a thermal cycler, and then precooled to 4 °C. The amplification was carried out in a model Master Gradient thermal cycler (Eppendorf, Hauppauge, NY, USA) using an optimized in-house program consisting of an initial denaturation step of 3 min at 95 °C, and then 35 cycles of 45 s at 94 °C, 1 min at 55 °C, 45 s at 72 °C, followed by a 7-min elongation step at 72 °C. ISSR-PCR amplification products were separated by agarose gel electrophoresis on 1.5% agarose gels and 0.5 g/mL ethidium bromide in 1X TAE buffer (40 mM Tris-acetate, 1 mM EDTA, pH 8.0) for 3.5 h at 80 V. The fragment patterns were photographed under UV light for further analysis. A 1-kb DNA ladder (Fermentas) was used to determine the fragment size.

Table 2. ISSR primer list

No	ISSR primers	DNA sequences (5'-3')
1	UBC 807	AGA GAG AGA GAG AGA GT
2	UBC 808	AGA GAG AGA GAG AGA GC
3	UBC 810	GAG AGA GAG AGA GAG AT
4	UBC 811	GAG AGA GAG AGA GAG AC
5	UBC 814	CTC TCT CTC TCT CTC TA
6	UBC 815	CTC TCT CTC TCT CTC TG
7	UBC 816	CAC ACA CAC ACA CAC AT
8	UBC 818	CAC ACA CAC ACA CAC AG
9	UBC 820	GTG TGT GTG TGT GTG TC
10	UBC 823	GTG TGT GTG TGT GTG TC
11	UBC 824	TCT CTC TCT CTC TCT CG
12	UBC 825	ACA CAC ACA CAC ACA CT
13	UBC 827	ACA CAC ACA CAC ACA CG
14	UBC 828	TGT GTG TGT GTG TGT GA
15	UBC 834	AGA GAG AGA GAG AGA GT
16	UBC 835	AGA GAG AGA GAG AGA GC
17	UBC 843	CTC TCT CTC TCT CTC TA
18	UBC 845	CTC TCT CTC TCT CTC TG
19	UBC 850	GTG TGT GTG TGT GTG TC

Data analysis

ISSR data were recorded as 1 for the presence of a band and 0 for its absence to generate a binary matrix. Only reproducible bands were scored for all the accessions tested. All data were analyzed by Principle Coordinate (PCoA) and Cluster analyses using PAST program (Hammer et al., 2001). First, a similarity matrix was generated using Jaccard coefficients. This matrix was then used for PCO. For cluster analyses, the UPGMA (Unweighted Pair Group Method using Arithmetic Average) method was used to construct dendrogram. The bootstrap values for the clusters were calculated by 1000 replicates using PAST program. The representativeness of dendrogram was evaluated by estimating cophenetic correlation for the dendrogram and comparing it with the similarity matrix, using Mantel's matrix correspondence test (Mantel, 1967). The result of this test is a cophenetic correlation coefficient, r , indicating how well dendrogram represents similarity data.

Results

In total, 19 ISSR primers produced 99 clear and reproducible DNA band profiles, 89 of which were polymorphic. Therefore, the average polymorphic was 89.90%. The results of the ISSR analyses for myrtle genotypes are presented in *Table 3*. The number of alleles determined by each primer ranged from 4 to 7, with an average of 5.2. In terms of the total number of alleles, UBC811, and UBC824 loci produced the highest number of alleles (7), PIC values ranged between 0.41 (UBC835) and 0.90 (UBC824).

Table 3. Results of the ISSR analyses for myrtle genotypes

No	ISSR primers	Size (bp) (min-max)	Number of alleles	Monomorphic bands	Polymorphic bands	Polymorphism rate (%)	PIC
1	UBC807	630-2000	4	0	4	100	0.59
2	UBC808	750-2200	5	1	4	80	0.47
3	UBC810	600-2000	5	0	5	100	0.87
4	UBC811	250-2200	7	0	7	100	0.89
5	UBC814	740-2000	6	1	5	83.33	0.74
6	UBC815	400-1500	5	0	5	100	0.69
7	UBC816	500-1250	5	0	5	100	0.79
8	UBC818	500-2100	6	0	6	100	0.78
9	UBC820	1100-2000	4	1	3	75	0.90
10	UBC823	1200-2050	4	1	3	75	0.75
11	UBC824	500-2100	7	0	7	100	0.90
12	UBC825	450-1600	5	0	5	100	0.95
13	UBC827	700-1900	4	0	4	100	0.66
14	UBC828	750-1950	6	0	6	100	0.87
15	UBC834	300-1750	6	0	6	100	0.76
16	UBC835	300-2500	6	4	2	33.33	0.41
17	UBC843	750-2150	5	1	4	80	0.84
18	UBC845	500-2150	5	0	5	100	0.47
19	UBC850	1100-1900	4	1	3	75	0.70
Total		250-2500	99	10	89	33.33-100.00	

The dendrogram generated from the UPGMA algorithm based on ISSR data is presented in *Figure 2*. The validity of the dendrogram in reflecting the genetic relationships among the myrtle genotypes was indicated by a high cophenetic correlation coefficient (r) of 0.88. Genetic similarity coefficients ranged from 0.37 to 0.97. The UPGMA clustering pattern grouped all the genotypes into two major clusters (*Fig. 1*). Principle coordinate analysis (PCoA) was also performed using the similarity matrix, and the two-dimensional dendrogram corroborated UPGMA analyses (*Fig. 3*). While the first axis (Coordinate 1) explained 55.95% of the total molecular variance, the second axis (Coordinate 2) explained 13.56%.

Genetic similarities among all myrtle genotypes ranged from 0.37 to 0.97. The highest similarity rate (1.00) was among Antakya, Samandağ, Baltacık, Harbiye1 genotypes collected from the city of Hatay in southern Turkey, on the eastern Mediterranean coast and they all are white-fruited. The lowest similarity rate was 0.27, and it was obtained between dark-fruited Akpınar1 collected from Adana and white-fruited Antakya, Samandağ, Baltacık, Harbiye1 collected from Adana.

Based on the similarity index, a clustering dendrogram was constructed using UPGMA. The dendrogram separated all genotypes except Antakya, Samandağ, Baltacık, Harbiye1. The dendrogram grouped all genotypes into two main clusters. The first main cluster included all dark-fruited genotypes except Harbiye2. The second main cluster included all white-fruited genotypes and dark-fruited genotypes (Harbiye2).

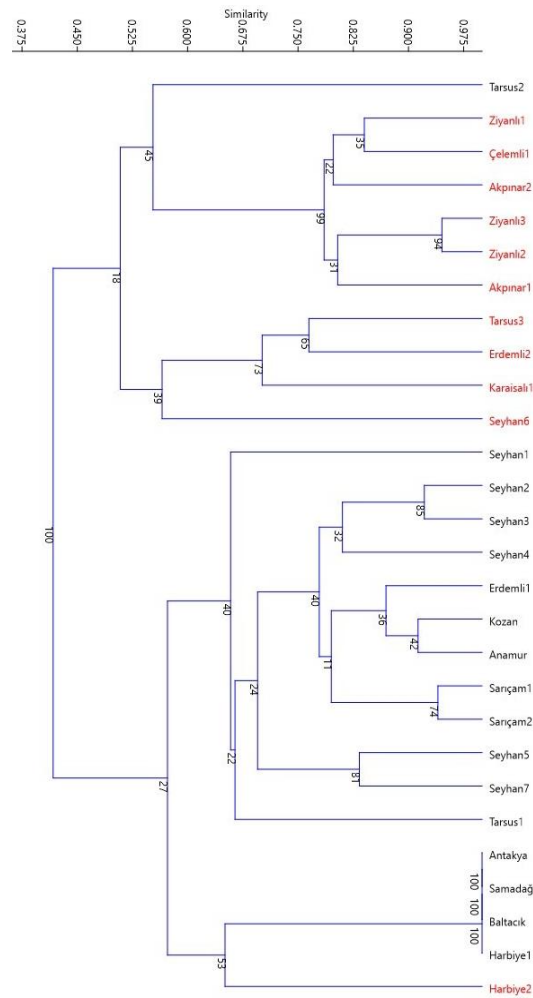


Figure 2. ISSR dendrogram of myrtle genotypes. (Red colors present dark-fruited genotypes, black colors white fruited genotypes)

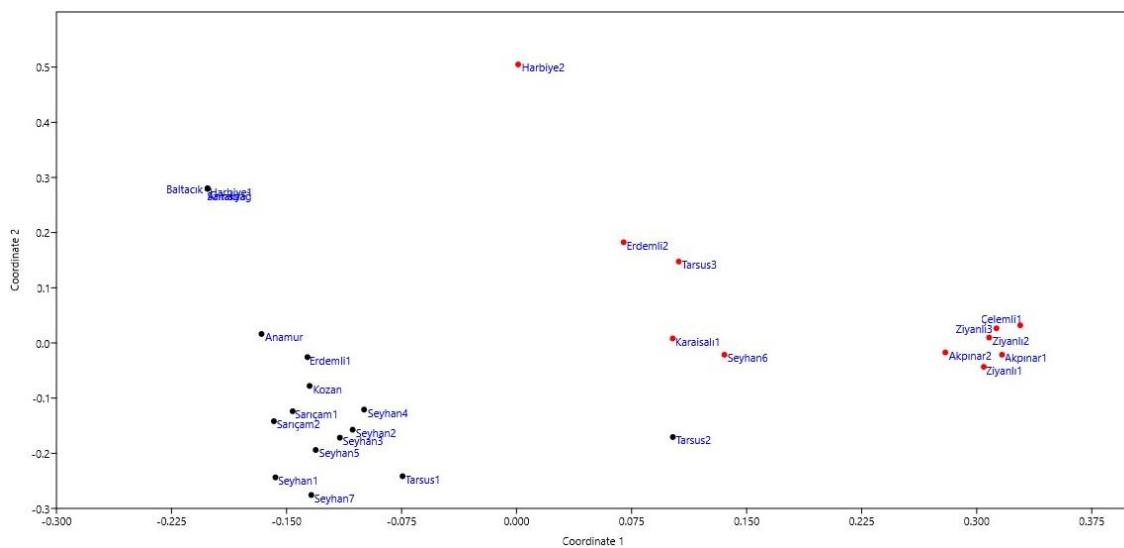


Figure 3. Principle coordinate analysis of 28 myrtle genotypes generated by the data from ISSR analyses. (Red colors present dark-fruited genotypes, black colors white fruited genotypes)

Discussion

Plant genetic resources are significant plant materials for breeders. The collection and identification of these plants is the first and important step of plant breeding. The assessment of genetic diversity is a necessary step to protect natural myrtle populations. We examined the genetic diversity among Turkish myrtle genotypes in comparison with fruit color and geography origin. 19 ISSRs produced 89.90% polymorphism; this result was higher than the results of previous genetic diversity studies (AFLP 56%: Bruna et al., 2007; RAPD 51.9%; Messaoud et al., 2007; RAPD 72.9%: Serce et al., 2008) conducted by different molecular markers.

The evolutionary relationships between the wild and cultivated myrtle types are not well-known. The large-fruited, cultivated type was likely domesticated from the white-colored, wild types. The fact that all the cultivated myrtle accessions are white-fruited, and the dark-fruited form is prevalent in nature indicates that the white color was preferred during the domestication process (Serce et al., 2008). In our study, we used white and dark-fruited genotypes to estimate evolutionary relationships between white and dark-fruited genotypes. Based on the results, all dark-fruited myrtle genotypes were clustered together except Harbiye2. Harbiye2 is also dark-fruited genotype; however, it is collected from different provinces of Turkey. Totally five different genotypes (one of them is dark-fruited) were collected from the city of Hatay. They were clustered together, but the only one dark-fruited genotype Harbiye2 from Hatay was different from the other white-fruited genotypes from Hatay. This result showed that dark-fruited genotypes are certainly different from white-fruited genotypes; however, the differences were also related to geographical origin. Serce et al. (2008) used two sets of myrtle accessions from Hatay, Turkey. Set 1 consisted of two wild accessions, dark- and white-colored forms, and six cultivated selections, while Set 2 contained three open-pollinated individuals from each accession of Set 1. The researcher examined genotypic variation of Sets 1 and 2 using RAPD markers. According to results, the molecular analysis clearly separated the cultivated types from the wild accessions. In the present study, we used different white and dark-fruited myrtle genotypes from Hatay, Adana and Mersin provinces of Turkey. We confirmed that ISSR analysis separated the cultivated white-fruited types from the wild dark-fruited genotypes. Melito et al. (2013) investigated genetic diversity of 80 wild accessions of Sardinian myrtle collected from four different localities (Corsica, Asinara, Surigheddu and Oristano) via ISSR markers. The researchers used totally 17 ISSR primers and among them 12 ISSR primers were informative. Based on the results, there was no convincing evidence of a correlation between genotype and geographical origin. In another study Melito et al. (2016) explored the morphological, chemical, and genetic diversity of wild myrtle populations in Sicily, with the aim to provide a first characterization of a core collection of 36 accessions from 7 localities (Ispica, M. Pellegrino, Misilmeri, R. Zingaro, Scopello, Ribera, Sciacca) for future domestication programs. AFLP fingerprinting generated 152 polymorphic fragments. Structure analysis identified three genetic clusters (cluster A: most of the Misilmeri samples, cluster B: Scopello, Ribera, Sciacca, and M. Pellegrino, cluster C: Ispica and Ribera) corresponding to specific geographical origin. In our study; we used 19 ISSR primers and all ISSR primers proved to be informative. PIC values obtained from ISSR primers were ranged from 0.41-0.90. In the present study, myrtle genotypes collected from different parts of Turkey were used and genotypes were clustered by geographic origin.

Conclusions

In conclusion, we determined that the white and dark-fruited myrtle genotypes could be differentiated by the ISSR molecular markers. Myrtle genotypes were separated according to their geographical origin. It is shown that there are significant myrtle genetic resources that are genetically and morphologically different from each other in Turkey.

REFERENCES

- [1] Albaladejo, R. G., Carrillo, L. F., Aparicio, A., Fernández-Manjarrés, J. F., González-Varo, J. P. (2009): Population genetic structure in *Myrtus communis* L. in a chronically fragmented landscape in the Mediterranean: can gene flow counteract habitat perturbation? – *Plant Biology* 11(3): 442-453.
- [2] Aydin, C., Ozcan, M. M. (2007): Determination of nutritional and physical properties of myrtle (*Myrtus communis* L.) fruits growing wild in Turkey. – *Journal of Food Engineering* 79(2): 453-458.
- [3] Bruna, S., Mercuri, A., Cervelli, C., Braglia, L., Benedetti, L. D., Schiva, T. (2004): Genetic characterization of *Myrtus communis* L. populations using AFLP markers [Amplified Fragment Length Polymorphism; Italy]. – *Italus Hortus (Italy)* 11(4): 332-335.
- [4] Bruna, S., Portis, E., Cervelli, C., De Benedetti, L., Schiva, T., Mercuri, A. (2007): AFLP-based genetic relationships in the Mediterranean myrtle (*Myrtus communis* L.). – *Scientia Horticulturae* 113(4): 370-375.
- [5] Casaburi, A., Di Martino, V., Ercolini, D., Parente, E., Villani, F. (2015): Antimicrobial activity of *Myrtus communis* L. water-ethanol extract against meat spoilage strains of *Brochothrix thermosphacta* and *Pseudomonas fragi* *in vitro* and in meat. – *Annals of Microbiology* 65(2): 841-850.
- [6] Dahmoune, F., Nayak, B., Moussi, K., Remini, H., Madani, K. (2015): Optimization of microwave-assisted extraction of polyphenols from *Myrtus communis* L. leaves. – *Food Chemistry* 166: 585-595.
- [7] Danial, G. H. (2009): Propagation of *Myrtus communis* L. *in vitro*. – *Journal of Duhok University* 12(1): 80-84.
- [8] Donmez, D., Simsek, O., Aka Kacar, Y. (2016): Genetic engineering techniques in fruit science. – *International Journal of Environmental Research* 2(12): 115-128.
- [9] Ghafouri, F., Rahimmalek, M. (2018): Genetic structure and variation in different Iranian myrtle (*Myrtus communis* L.) populations based on morphological, phytochemical and molecular markers. – *Industrial Crops and Products* 123: 489-499.
- [10] Hammer, Ø., Harper, D. A., Ryan, P. D. (2001): PAST: paleontological statistics software package for education and data analysis. – *Palaeontologia Electronica* 4(1): 9.
- [11] Madadi, M., Zamani, Z., Fatahi, R. (2017): Assessment of Genetic Variation within Commercial Iranian Pomegranate (*Punica granatum* L.) Cultivars, Using ISSR and SSR Markers. – *Turkish Journal of Agriculture-Food Science and Technology* 5(6): 622-628.
- [12] Mantel, N. (1967): The detection of disease clustering and a generalized regression approach. – *Cancer Research* 27: 209-220.
- [13] Mele, C., Corona, L., Melito, S., Raggi, L., Mulas, M. (2019): The genetic diversity of selections and wild populations of myrtle revealed by molecular geographic contexts. – *Industrial Crops and Products* 132: 168-176.
- [14] Melito, S., Chessa, I., Erre, P., Podani, J., Mulas, M. (2013): The genetic diversity of Sardinian myrtle (*Myrtus communis* L.) populations. – *Electronic Journal of Biotechnology* 16(6): 7-7.

- [15] Melito, S., Dessena, L., Sale, L., Mulas, M. (2017): Genetic diversity and population structure of wild Sardinian myrtle (*Myrtus communis* L.) genotypes from different microclimatic areas. – Australian Journal of Crop Science 11: 1488-1496.
- [16] Melito, S., La Bella, S., Martinelli, F., Cammalleri, I., Tuttolomondo, T., Leto, C., Fadda, A., Molinu, M. G., Mulas, M. (2016): Morphological, chemical, and genetic diversity of wild myrtle (*Myrtus communis* L.) populations in Sicily. – Turkish Journal of Agriculture and Forestry 40(2): 249-261.
- [17] Messaoud, C., Afif, M., Boulila, A., Rejeb, M. N., Boussaid, M. (2007): Genetic variation of Tunisian *Myrtus communis* L. (Myrtaceae) populations assessed by isozymes and RAPDs. – Annals of Forest Science 64(8): 845-853.
- [18] Messaoud, C., Béjaoui, A., Boussaid, M. (2011): Fruit color, chemical and genetic diversity and structure of *Myrtus communis* L. var. *italica* Mill. morph populations. – Biochemical Systematics and Ecology 39(4-6): 570-580.
- [19] Nora, S., Albaladejo, R. G., Aparicio, A. (2015): Genetic variation and structure in the Mediterranean shrubs *Myrtus communis* and *Pistacia lentiscus* in different landscape contexts. – Plant Biology 17(2): 311-319.
- [20] San, B., Yildirim, A. N., Polat, M., Yildirim, F. (2015): Chemical compositions of myrtle (*Myrtus communis* L.) genotypes having bluish-black and yellowish-white fruits. – Erwerbsobstbau 57(4): 203-210.
- [21] Serce, S., Simsek, O., Gunduz, K., Aka-Kacar, Y., Ercisli, S. (2008): Relationships among myrtle accessions from Turkey as revealed by fruit characteristics and RAPD. – Roumanian Biotechnology Letters 13(6): 4054-4065.
- [22] Shekafandeh, A. (2007): Effect of different growth regulators and source of carbohydrates on in and ex vitro rooting of Iranian Myrtle. – International Journal of Agricultural Research 2: 152-158.
- [23] Simsek, O., Kanat, F. E., Serce, S., Kacar, Y. A. (2008): Comparisons of DNA isolation methods for some fruit species. – Derim 25(1): 59-69.
- [24] Simsek, O., Bicen, B., Donmez, D., Aka Kacar, Y. (2017a): Effects of different media on micropropagation and rooting of myrtle (*Myrtus communis* L.) in *in vitro* conditions. – International Journal of Environmental & Agriculture Research 3(10): 54-59.
- [25] Simsek, O., Donmez, D., Aka Kacar, Y. (2017b): RNA-seq analysis in fruit science: A review. – American Journal of Plant Biology 2: 1-7.
- [26] Sumbul, S., Ahmad, M. A., Asif, M., Akhtar, M. (2011): *Myrtus communis* Linn.-A review. – Indian Journal of Natural Products and Resources 395-402.
- [27] Wannes, W. A., Mhamdi, B., Sriti, J., Jemia, M. B., Ouchikh, O., Hamdaoui, G., Kchouk, M. E., Marzouk, B. (2010): Antioxidant activities of the essential oils and methanol extracts from myrtle (*Myrtus communis* var. *italica* L.) leaf, stem and flower. – Food and Chemical Toxicology 48(5): 1362-1370.

MOLECULAR MECHANISM OF GROWTH DIVERSITY FOR THE FIRST HYBRID GENERATION INDIVIDUALS OF GRASS CARP (*CTENOPHARYNGODON IDELLUS*) (♀) × BARBEL CHUB (*SQUALIOBARBUS CURRICULUS*) (♂)

LV, L. G.^{1,2#} – XU, Y.^{1,2#} – XU, B. H.^{1,2*} – LIU, Q. L.^{1,2*} – XIAO, T. Y.^{1,2} – LIU, Y.^{1,2} – SU, H.^{1,2}

¹Hunan Engineering Technology Research Center of Featured Aquatic Resources Utilization, Hunan Agricultural University, Changsha 410128, China

²Collaborative Innovation Center for Efficient and Health Production of Fisheries in Hunan Province, Changde, Hunan 415000, China

[#]The authors contributed equally to this work

*Corresponding authors

e-mail: xbht568@126.com; phone: +86 15802616494 (Xu, B. H.)

e-mail: qiaolinliu2017@hunau.edu.cn; phone: +86 18374893286 (Liu, Q. L.)

(Received 1st Aug 2019; accepted 28th Nov 2019)

Abstract. The first hybrid generation (F1) individuals of grass carp (*Ctenopharyngodon idellus*, ♀) × barbel chub (*Squaliobarbus curriculus*, ♂) commonly show obvious growth diversity, even though they are from the same parents and cultured in the same environment. To characterize the molecular mechanism of the growth diversity, the present study compared the expressions of growth-related genes of the fast-growth population (FGP) and slow-growth population (SGP). The expression of growth-inhibiting *SRIF* gene was significantly higher in the SGP hypophysis than in the FGP. The expressions of growth-promoting *GHR* and *IGF-I* genes in blood, *GHR*, *IGF-I* and *IGF-II* genes in liver, and *IGF-I* and *IGF-II* genes in muscle of the FGP were significantly higher than those of the SGP in liver. The results implied that hypernomic-expression of *SRIF* gene in hypophysis caused the expressions of *GHR* and *IGF-I* genes in blood, *GHR*, *IGF-I* and *IGF-II* genes in liver, and *IGF-I* and *IGF-II* genes in muscle of the SGP to be significantly lower than those in the FGP, which caused the lower growth of the SGP. These results provided valuable reference for studying the relationship between growth-related genes and fish growth, and the molecular mechanism of fish growth.

Keywords: fish, growth axis, quantitative reverse transcriptional PCR, growth-inhibiting gene, *GHR* gene, expression analysis

Introduction

Grass carp (*Ctenopharyngodon idellus*) is already the largest freshwater aquaculture product worldwide (Ni and Yu, 2013; Ni et al., 2014) and it is an important aquaculture species in Asia. Approximately 5.90 million tons of grass carp was produced ever year only in China (Department of Fisheries of Ministry of Agriculture of China, 2017). However, frequent occurrence of diseases in grass carp culture has caused serious loss and severely restricts sustained development of grass carp culture (Nie and Pan, 1985; Chen et al., 2012). Hybridization between different fish species is extensively used as their offspring exhibit growth and disease-resistant superiority compared to their parents. For instance, the first hybrid generation (F1) of Kaluga sturgeon (*Huso dauricus*, ♀) × sterlet (*Acipenser ruthenus*, ♂) exhibits fast-growth and disease-resistant superiority (Yin

et al., 2004). The hybrid offspring of rainbow trout (*Oncorhynchus mykiss*, ♀) × speckled trout (*Salvelinus fontinalis*, ♂) exhibit disease-resistant superiority (Wu et al., 2014). The F1 of grass carp (♀) × topmouth culter (*Erythroculter ilishaeFormis*, ♂) also exhibits disease-resistant superiority (Aquaculture Research Group of Jianhu County of Jiangsu Province, 1974).

Barbel chub (*Squaliobarbus curriculus*) as well as grass carp belongs to the Leuciscinae subfamily of fish. The shape of barbel chub is similar to grass carp, and barbel chub exhibits strong adaptability and disease-resistant superiority (Liu et al., 2012). In addition, a previous study has showed that disease resistance of the F1 of grass carp (♀) × barbel chub (♂) was significantly higher than that of grass carp (He et al., 2015). However, the F1 individuals of grass carp (♀) × barbel chub (♂) commonly emerge obvious individual difference in size during culture process, even though they are from the same parents and cultured in the same environment (Zhou et al., 2017).

Fish growth is influenced by various internal (such as incretion) and external factors (such as environment and nutrition) (Su et al., 2012; Valente et al., 2013). The incretion factors regulate fish growth through *GH/IGF-I* axis, which involves the hypothalamus, the hypophysis, and the liver (Lin, 1996; Peng and Peter, 1997). Hypothalamus secretes stimulators and inhibitors. The stimulators, such as growth hormone releasing factor (*GRF*), gonadotropin-releasing hormone (*GnRH*), pituitary adenylate cyclase activating polypeptide (*PACAP*), dopamine (*DA*) and neuropeptide Y (*NPY*), stimulate the release of growth hormone (*GH*) in the hypophysis (Parker et al., 1997; Montero et al., 1998), while the inhibitors, such as somatostatin (*SRIF* or *SS*), 5-serotonin (*5-HT*), norepinephrine (*NE*) and glutamate (*Glu*), inhibit the release of *GH* that induces the secretion of *GRF*, *GnRH*, *PACAP*, and *NPY* (Peter and Marchant, 1995; Peng and Peter, 1997). Secretion of stimulators and inhibitors regulates the secretion of *GH*, and *GH* is transmitted to the surface of liver cell membrane through the circulation system and then it binds to growth hormone receptor (*GHR*) to trigger the transduction of insulin-like growth factors (*IGFs*). Then *IGFs* are transmitted to each tissue through the circulation system to promote fish growth.

Considering the F1 individuals of grass carp (♀) × barbel chub (♂) commonly emerge obvious individual difference in size during culture process, to characterize the molecular mechanism of the growth diversity of the F1 populations, the present study compared the expressions of growth-related genes of the fast-growth population (FGP) and slow-growth population (SGP) using fluorescence quantitative reverse transcriptional PCR (qRT-PCR). The results provided valuable reference for studying the relationship between growth-related genes and fish growth, and the molecular mechanism of fish growth.

Materials and Methods

Sample collection

The F1 samples were collected from Wulong Fishing Ground located at Beisheng Town, Liuyang City of China (28.295 N, 113.436 E). The F1 fish were cultured 150 days from 1⁺ years of F1 offspring with the same parents. They were fed with commercial puffed compound feed-8110 (Dabeinong, China), which contains equal more than 36.0% of crude protein, equal more than 4.0% of crude fat, and equal more than 15.0% of crude ash. The F1 samples were distinguished to two populations, i.e. the FGP (their body weights were more than 500 g) and the SGP (their body weights were equal or less than

500 g), according to their body weight. Each population was collected 7 healthy samples, and the samples were anaesthetized using an overdose of neutralized MS222 (ethyl 3-aminobenzoate methane-sulfonic acid). Then the samples were dissected as approximately 80 mg of their hypothalamus, hypophysis, liver and muscle, and 2 ml of blood was collected and stored in liquid nitrogen.

RNA extraction and synthesis of cDNA

The tissues stored in liquid nitrogen were put in homogenizing pipe with 1 ml TRK lysis buffer and homogenized three times (15 s per time with 6000 rpm/min, 5 s of interval between homogenizing). Subsequently, RNAs were extracted from the homogenates using an E.Z.N.A. total RNA kit I (OMEGA, USA) according to the manufacturer instructions. The RNAs were used to synthesize the first strand of cDNA by a RevertAid first strand cDNA synthesis kit (Thermo, USA), with Oligo(dT)₁₈ and random primers.

qRT-PCR

To design the primers for qRT-PCR, fragments of *GH*, *GHR*, *IGF-I*, *IGF-II*, *PACAP*, *SRIF*, *MSTN-1* and *MYOG* genes of the F1 were cloned and sequenced. To clone these gene fragments, the primers (*Appendix 1*) were designed using primer 6.0 referenced cDNA sequences of these genes from Cyprinidae in GenBank. The fragments were amplified using the first strand of cDNA of the F1 as templet. Each 50 µl of the PCR reaction mixture contained 1×Ex Taq Buffer (TaKaRa, China), 1.25 U of Ex Taq polymerase (TaKaRa, China), 10 nmol of each primer, 40 nmol of each NTP, and 2 µl of cDNA. The PCR amplified procedure was carried out at 94°C for 5 min; at 94°C for 30 s, at 52~56°C (β-actin: 54°C; EF-1α: 54°C; GH: 56°C; GHR: 54°C; *IGF-I*: 55°C; *IGF-II*: 55°C; *PACAP*: 52°C; *SRIF*: 52°C) for 30 s, at 72°C for 90 s, in 30 cycles; and finalized at 72°C for 5 min. Then the fragments were sequenced using AB3730 sequencer at Beijing Aokedingsheng Bio-Science Ltd., China (*Appendix 2*). Finally, the primers that used to qRT-PCR were designed based on these fragments using primer 6.0 (*Table 1*).

Table 1. Primers for gene expression of growth-related genes

Gene name	Primer name	Primer sequence (5'-3')	Length of target sequence (bp)	Amplification efficiency
β-actin	β-actin-RT-F	GCTATGTGGCTCTTGACTTCG	124	95~97
	β-actin -RT-R	GGGCACCTGAACCTCTCATT		
EF-1α	EF-1α-RT-F	GCTATGTGGCTCTTGACTTCG	124	96~99
	EF-1α-RT-R	GGGCACCTGAACCTCTCATT		
GH	GH-RT-F	ACAGTTTGACCGTCGGGAACCC	131	95~99.8
	GH-RT-R	CAGCGGCAGGGAGTCGTTATCA		
GHR	GHR-RT-F	TGTGTGGAAACGGACTGGTGTCTG	115	101~105
	GHR-RT-R	CAGCAACGGAAGGTCTCCTGTTCT		
IGF-I	IGF-I-RT-F	ACATTGCCCCGATCTCATCCTCT	114	95~97.7
	IGF-I-RT-R	CCCTGGAAGAAATGACCGCTAGAC		
IGF-II	IGF-II-RT-F	GTTTCAGCCACATCCCTACAGGTCA	108	97~99.6
	IGF-II-RT-R	CCGTTGCCACCGTCATATTTGGA		
PACAP	PACAP-RT-F	AGCCTTGAGGGACATCCTGGTTCA	101	96~98.6
	PACAP-RT-R	CCGATTTCGTTCTTCCTCGCTGCTT		
SRIF	SRIF-RT-F	TGCTTGGACGAGGTCTGTGAGC	108	95~97.1
	SRIF-RT-R	ACGCCAAACTCCGCCAACTTCT		
MSTN-1	MSTN-1-RT-F	AGGACTTCGGCTGGGACTGGATTA	126	95~96.5
	MSTN-1-RT-R	GCGGATTGGCCTTGTTACCAGAT		
MYOG	MYOG-RT-F	AAGCCGCCACATTGAGGGAGAAG	100	98~101.5
	MYOG-RT-R	GGCAGCCTCTGGTTGGGATTCAT		

The expressions of *PACAP* and *SRIF* genes in the hypothalamus, *PACAP*, *SRIF* and *GH* genes in the hypophysis, *GH*, *GHR*, *IGF-I* and *IGF-II* genes in the blood, *GHR*, *IGF-I* and *IGF-II* in the liver, and *IGF-I*, *IGF-II*, *MYOG* and *MSTN-1* genes in the muscle were tested through qRT-PCR using a SYBR Premix Ex Taq™ II kit (TaKaRa, China). The first strand cDNA from the tissues was used as template. The β -actin and EF-1 α genes were used as internal controls. The qRT-PCR was conducted using a CFX96Touch™ real-time PCR detection system (Bio-Rad, USA). Each 10 μ l of the qRT-PCR reaction mixture contained 5 μ l of SYBR Green PCR master mix (CW BIO, China), 0.4 μ l of each primer (10 μ M), 1 μ l of cDNA, and 3.2 μ l of ddH₂O. The PCR amplified procedure was carried out at 94°C for 10 min, followed by 35 cycles of 95°C for 10 s, 60°C for 10 s, and 72°C for 15 s. The solubility curve was obtained by raising 0.5°C per 5 s from 65°C to 95°C. Seven samples in each group and triplicate of each sample were analyzed. Data were collected and analyzed using CFX manager software 3.1 (Bio-Rad, USA).

Data analysis

The results are presented as the mean \pm standard error (S.E.) for each group. One-way ANOVA and t-test was conducted using R 3.5.1 (R Core Team, 2014). Differences for which *P* values were < 0.05 were considered statistically significant.

Results and Discussion

The body lengths of the FGP and the SGP were 38.043 ± 0.44 and 26.243 ± 0.48 cm, respectively (Fig. 1A). The body weights of the FGP and the SGP were 932.86 ± 50.41 and 312.43 ± 22.70 g, respectively (Fig. 1B). The average body length and body weight of the FGP were significantly higher than those of the SGP, respectively (independent t-test, $p < 0.001$).

Expressions of *PACAP* (Welch two sample t-test, $t = 1.393$, $P = 0.230$) and *SRIF* (Welch two sample t-test, $t = 0.448$, $P = 0.670$) genes in the hypothalamus of the FGP were not detected significantly different to the SGP (Fig. 2A). However, the relative expression of the *SRIF* gene in the hypophysis was significantly increased in the SGP than those in the FGP (Welch two sample t-test, $t = -13.818$, $P < 0.001$; Fig. 2B). The results implied that the high expression of *SRIF* gene in the SGP hypophysis was probably the major reason that caused the slow growth of the SGP, as *SRIF* is considered as an inhibitor that inhibits secretion of *GH* in the hypophysis (Peter and Marchant, 1995; Peng and Peter, 1997; Lin and Peter, 2001). Meanwhile, *SRIF* also reduces the combination of *GHR* to *GH* and transcriptional level of *IGF-I* gene in the liver (Tanaka et al., 1995; Masini et al., 1999). The *GH* gene was rarely expressed in the hypophysis and in the blood, and its expressions were not detected significantly different between the hypophysis of FGP and SGP (Welch two sample t-test, $t = 1.266$, $P = 0.250$; Fig. 2B) and in the blood (Welch two sample t-test, $t = -0.576$, $P = 0.605$; Fig. 2C). However, the expressions of *GHR* (Welch two sample t-test, $t = 3.162$, $P = 0.014$) and *IGF-I* genes (Welch two sample t-test, $t = 5.663$, $P = 0.002$) in the FGP blood were significantly higher than those in the SGP (Fig. 2C).

The expressions of *GHR* (Welch two sample t-test, $t = 3.334$, $P = 0.039$), *IGF-I* (Welch two sample t-test, $t = 5.157$, $P < 0.001$) and *IGF-II* (Welch two sample t-test, $t = 5.995$, $P = 0.004$) genes in the FGP liver were significantly higher than those in the SGP liver (Fig. 2D). In addition, the expressions of *IGF-I* (Welch two sample t-test,

$t = 7.744$, $P < 0.001$) and *IGF-II* (Welch two sample t-test, $t = 3.594$, $P = 0.012$) genes in the FGP muscle were significantly higher than those in the SGP muscle. *IGF-I* and *IGF-II* genes are mainly expressed in the liver. Therefore, these genes were higher expressed in the liver than in the muscle (Fig. 2E). Fish growth mainly shows as fast growth of muscle. The growth of muscle was regulated by *GH-IGF* axis. *GH* regulates expression of genes that promote muscle growth, such as myostatin and muscular atrophy genes. *IGFs* mainly regulate expression of genes that regulate muscle form (Fuentes et al., 2013). In addition, the external factors, such as environment and nutrition, also influence fish growth through the *GH/IGF-I* axis (Reinecke, 2010; Su et al., 2012). However, the expressions of *MYOG* and *MSTN-1* genes in the muscle were not significantly different between the FGP and the SGP (Welch two sample t-test, $t = 0.569$, $P = 0.589$ for *MYOG* gene, and $t = -2.006$, $P = 0.090$ for *MSTN-1* gene).

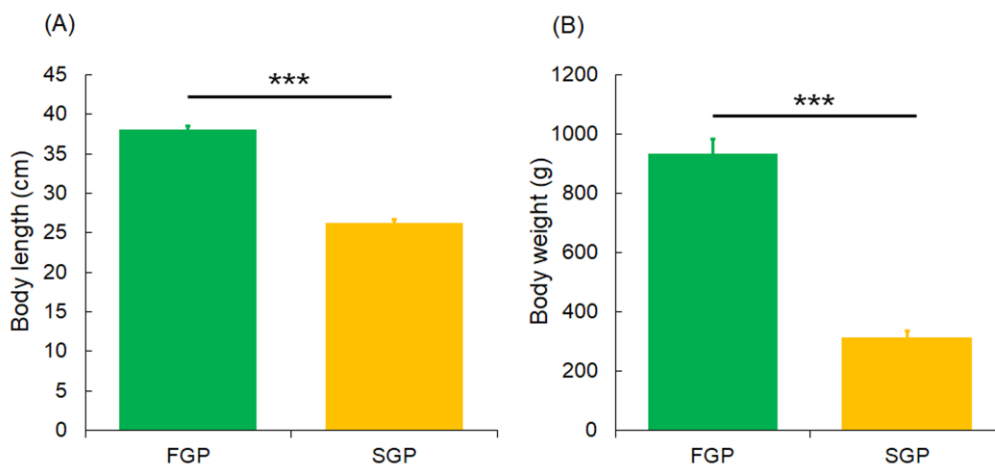


Figure 1. Body length (A) and body weight (B) of the samples. ***, $P < 0.001$

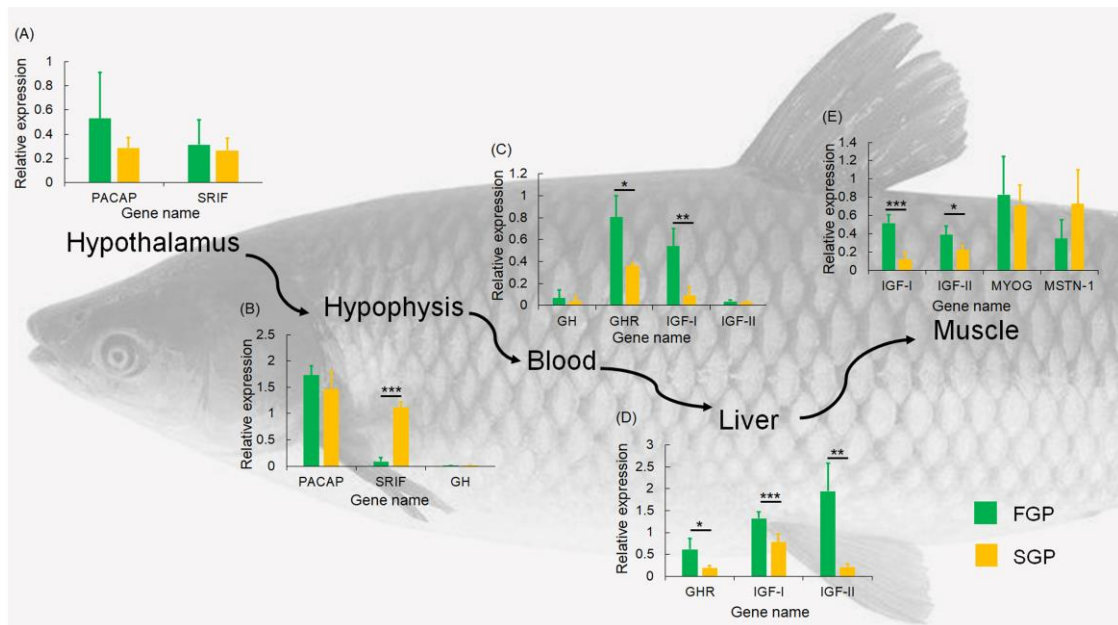


Figure 2. Expression analysis of genes in growth axis of direct cross F1. *: $P < 0.05$; **: $P < 0.01$; ***: $P < 0.001$

GH is synthesized in the hypophysis and transported to target tissues through the circulatory system. The growth-promoting performance of *GH* is vitally needed to mediate *GHR* and *IGFs*. Therefore, fish growth could not be expressed only by the expression of *GH* gene, but the expressions of *GHR* and *IGF* genes are also vital. In the present study, the expressions of *GHR*, *IGF-I* and *IGF-II* genes in the FGP liver were significantly higher than those in the SGP, consistent with previous studies in goldfish (*Carassius auratus*) (Zhong et al., 2012), Japanese pufferfish (*Takifugu rubripes*) (Kaneko et al., 2011), mud carp (*Cirrhinus molitorella*) (Zhang et al., 2006), Nile tilapia (*Oreochromis niloticus*) (Cruz et al., 2006), European eel (*Anguilla anguilla*) and half-smooth tongue sole (*Cynoglossus semilaevis*) (Degani et al., 2003; Ma et al., 2012). In addition, *GH* also regulates muscle growth through regulating the expressions of myogenic factors. For instance, expressions of *MYOG*, *MYOD2*, *MYF5V* and *MEF2A* genes in the muscle of the fast-growth transgenic fish were significantly higher than those of wildtype fish (Devlin et al., 2013). However, we did not detect significant difference between the expression of *MYOG* and *MSTN-1* genes in the muscle of the FGP and the SGP.

Conclusion

The significantly higher expression of *SRIF* gene in the SGP hypophysis than in the FGP hypophysis caused the expressions of *GHR* and *IGF-I* genes in the blood, *GHR*, *IGF-I* and *IGF-II* genes in the liver, and *IGF-I* and *IGF-II* genes in the muscle of the SGP to be significantly lower than those in the FGP, which caused the lower growth of the SGP than the FGP. However, whether increasing the expression of *SRIF* gene in the hypophysis could increase growth in other fishes still needs further study.

Acknowledgments. This study was funded by the National Natural Science Foundation of China (No. 31702335) and the Natural Science Foundation of Human Province (No. 2019JJ50265) and the Natural Science Foundation of Human Province (2018JJ3221). We would like to thank anonymous technicians at Guangdong Meilikang Bio-Science Ltd., China for assistance with figure preparation.

REFERENCES

- [1] Aquaculture Research Group of Jianhu County of Jiangsu Province. (1974): Hybrid test report of *Ctenopharyngodon idellus* (♀) × *Erythroculter ilishae* Formis (♂). – *Freshwater Fisheries* 4(3): 22-23.
- [2] Chen, J., Li, C., Huang, R., Du, F., Liao, L., Zhu, Z., Wang, Y. (2012): Transcriptome analysis of head kidney in grass carp and discovery of immune-related genes. – *BMC Veterinary Research* 8: 108.
- [3] Cruz, E. M. V., Brown, C. L., Luckenbach, J. A., Picha, M. E., Bolivar, R. B., Borski, R. J. (2006): Insulin-like growth factor-I cDNA cloning, gene expression and potential use as a growth rate indicator in Nile tilapia, *Oreochromis niloticus*. – *Aquaculture* 251(2-4): 585-595.
- [4] Degani, G., Tzchori, I., Yom-Din, S., Goldberg, D., Jackson, K. (2003): Growth differences and growth hormone expression in male and female European eels (*Anguilla anguilla*). – *General and Comparative Endocrinology* 134(1): 88-93.
- [5] Department of Fisheries of Ministry of Agriculture of China. (2017): *China Fisheries Yearbook 2017*. – Beijing, China Agricultural Press.

- [6] Devlin, R. H., Sakhrani, D., White, S., Overturf, K. (2013): Effects of domestication and growth hormone transgenesis on mRNA profiles in rainbow trout (*Oncorhynchus mykiss*). – *Journal of Animal Science* 91(11): 5247-5258.
- [7] Fuentes, E. N., Valdes, J. A., Molina, A., Björnsson, B. T. (2013): Regulation of skeletal muscle growth in fish by the growth hormone-insulin-like growth factor system. – *General and Comparative Endocrinology* 192(9): 136-148.
- [8] He, M., Xiao, T., Liu, Q., Li, D., Li, W., Deng, Y. (2015): Morphological characteristics analysis of *Ctenopharyngodon idellus*, *Squaliobarbus curriculus* and their reciprocal hybrids F1. – *Journal of Hunan University of Arts and Sciences (Science and Technology)* 27(4): 36-42.
- [9] Kaneko, G., Furukawa, S., Kurosu, Y., Yamada, T., Takeshima, H., Nishida, M., Mitsuboshi, T., Otaka, T., Shirasu, K., Koda, T., Takemasa, Y., Aki, S., Mochizuki, T., Fukushima, H., Fukuda, Y., Kinoshita, S., Asakawa, S., Watabe, S. (2011): Correlation with larval body size of mRNA levels of growth hormone, growth hormone receptor I and insulin-like growth factor I in larval torafugu *Takifugu rubripes*. – *Journal of Fish Biology* 79(4): 854-874.
- [10] Lin, H. (1996): The regulation of growth and growth hormone secretion in fish. – *Acta Zoologica Sinica* 42(1): 69-79.
- [11] Lin, X., Peter, R. E. (2001): Somatostatins and their receptors in fish. – *Comparative Biochemistry and Physiology Part B: Biochemistry and Molecular Biology* 129(2-3): 543-545.
- [12] Liu, Q., Xiao, T., Liu, M., Zhou, W. (2012): Research progress of biology in *Squaliobarbus curriculus*. – *Fisheries Science* 31(11): 687-691.
- [13] Ma, Q., Liu, S., Zhuang, Z., Lin, L., Sun, Z., Liu, C., Ma, H., Su, Y., Tang, Q. (2012): Genomic structure, polymorphism and expression analysis of the growth hormone (GH) gene in female and male Half-smooth tongue sole (*Cynoglossus semilaevis*). – *Gene* 493(1): 92-104.
- [14] Masini, M. A., Sturla, M., Uva, B. (1999): Somatostatin in the ovary of an African lungfish (*Protopterus annectens*): an in situ hybridisation, immunohistochemical, and autoradiographical study. – *General and Comparative Endocrinology* 114(2): 287-292.
- [15] Montero, M., Yon, L., Rousseau, K., Arimura, A., Fournier, A., Dufour, S., Vaudry, H. (1998): Distribution, characterization, and growth hormone-releasing activity of pituitary adenylate cyclase-activating polypeptide in the European eel, *Anguilla anguilla*. – *Endocrinology* 139(10): 4300-4310.
- [16] Ni, J., Yu, Y. (2013): Intestinal microbiota changes of grass carp (*Ctenopharyngodon idellus*) in different months. – *Journal of Fisheries of China* 37(10): 1558-1563.
- [17] Ni, J., Yan, Q., Yu, Y., Zhang, T. (2014): Factors influencing the grass carp gut microbiome and its effect on metabolism. – *FEMS Microbiology Ecology* 87(3): 704-714.
- [18] Nie, D., Pan, J. (1985): Diseases of grass carp (*Ctenopharyngodon idellus* Valenciennes, 1844) in China, a review from 1953-1983. – *Fish Pathology* 20(2/3): 323-330.
- [19] Parker, D. B., Power, M. E., Swanson, P., Rivier, J., Sherwood, N. M. (1997): Exon skipping in the gene encoding pituitary adenylate cyclase-activating polypeptide in salmon alters the expression of two hormones that stimulate growth hormone release. – *Endocrinology* 138(1): 414-423.
- [20] Peng, C., Peter, R. E. (1997): Neuroendocrine regulation of growth hormone secretion and growth in fish. – *Zoological Studies* 36(2): 79-89.
- [21] Peter, R. E., Marchant, T. A. (1995): The endocrinology of growth in carp and related species. – *Aquaculture* 129(1): 299-321.
- [22] R Core Team. (2014): R: A language and environment for statistical computing. – R Foundation for Statistical Computing, Vienna, Austria. <http://www.r-project.org/>.

- [23] Reinecke, M. (2010): Influences of the environment on the endocrine and paracrine fish growth hormone-insulin-like growth factor-I system. – *Journal of Fish Biology* 76(6): 1233-1254.
- [24] Su, J., Zhang, Y., Lou, Z., Jiao, W., Yang, J., Wei, Y. (2012): Progress on fish growth traits improvement and its regulation. – *Sichuan Journal of Zoology* 31(1): 165-169.
- [25] Tanaka, M., Hayashida, Y., Wakita, M., Hoshino, S., Nakashima, K. (1995): Expression of aberrantly spliced growth hormone receptor mRNA in the sex-linked dwarf chicken, Gifu 20. – *Growth Regulation* 5(4): 218-223.
- [26] Valente, L. M. P., Moutou, K. A., Conceição, L. E. C., Engrola, S., Fernandes, J. M. O., Johnston, I. A. (2013): What determines growth potential and juvenile quality of farmed fish species. – *Reviews in Aquaculture* 5(s1): S168-S193.
- [27] Wu, S., Li, J., Ou, Y., Lv, G., Liu, J. (2014): Allometric growth of hybrid grouper (*Epinephelus coioides* ♀ × *E. lanceolatus* ♂) larvae and juveniles. – *Journal of Fishery Sciences of China* 21(3): 503-510.
- [28] Yin, H., Sun, Z., Sun, D., Qiu, L. (2004): Comparison of nutritive composition in muscles among six farmed sturgeon species. – *Journal of Dalian Fisheries University* 19(2): 92-96.
- [29] Zhang, D. C., Huang, Y. Q., Shao, Y. Q., Jiang, S. G. (2006): Molecular cloning, recombinant expression, and growth-promoting effect of mud carp (*Cirrhinus molitorella*) insulin-like growth factor-I. – *General and Comparative Endocrinology* 148(2): 203-212.
- [30] Zhong, H., Zhou, Y., Liu, S., Tao, M., Long, Y., Liu, Z., Zhang, C., Duan, W., Hu, J., Song, C., Liu, Y. (2012): Elevated expressions of GH/IGF axis genes in triploid crucian carp. – *General and Comparative Endocrinology* 178(2): 291-300.
- [31] Zhou, Z., Li, X., Wang, R., Jin, S., Xiao, T. (2017): Growth test report of 1+ year hybrid F₁ of grass carp (*Ctenopharyngodon idellus* ♀) × barbel chub (*Squaliobarbus curriculus* ♂). – *Scientific Fish Farming* 33(6): 79-80.

APPENDIX

Appendix 1. Primers used for partial fragment cloning of growth-related genes

Primers	Sequences (5'-3')
GH-F	GGATGGGAGTTGGAGGAGAAA
GH-R	GGCTGACCGTCTGACACAA
GHR-F	GCCATTTCAGGACGAGGAGATA
GHR-R	TGGTTGGGATTACAGGGAGATG
IGF-I-F	TCTCACTTCTCCACAACGA
IGF-I-R	CTTCTGATGAACCTCCTTACA
IGF-II-F	GTCGAACAGTCGGCGTCTCTCAA
IGF-II-R	CTGTGGTGGTGCAGTTGCTCCT
PACAP-F	AGAATGGCTRYRCAAACCYTGG
SRIF-F	GTCCGAGCAAAGAGAACT
SRIF-R	GGTTAGGATGGAGAATGTGA
MSTN-1-F	GTGTTGCTTTTTCTCCTTCAGTC
MSTN-1-R	CACAGCGGTCTACTACCATCG
MYOG-F	AGGCGGCGATAACTTCTCCA
MYOG-R	CTTGCTCATGTTCTGCTGGTT

Appendix 2. Partial target fragment used for cloning

Gene name	Sequences (5'-3')
IGF-I	CCACAACGAGCCTGCGCAATGGAACAAAGTCGGAATATTGAGATGTGACATTGCCCGCATCTCATCCTC TTTCCTCGCTTTTTAATGACTTCAAACAAGTTCAATTTTTGCTGGGCTTTTGTGGAGACCCAAGGGGATGT CTAGCGGTCAATTTCTCCAGGGGCAYTGGTGTGATGTCTTTAAGTGTACCATGCGCTGTCTCTCGTGAC CCACACCTCTCACTGGTGTGCTGTGCGTCTCGCGTTGACTCCCGCGACACTGGAGGCRGGGCCGAGAG CGCTGTGCGGGGGCGGAGCTGTAGACACGCTGCGAGTTTGTGTGTGGAGACAGGGCTTTTATTTCAGCA AACCAACAGGATATGGGCTAGTTCGAGRCGGTGCACAAACCGCGGCAATGTGGACGAATGCTGCTTTC AGAGCTGCGAACTGCGGCGCCTCGAGATGTAAGTGTGACCCGTGAAAACCGGCAAAWCTCCACGATCC CTACGAGCGCAACGGCACACAGATATCACCAGGACAGCAAAGAA
IGF-II	GACGCGCTACAGTTTGTGTGCGAAGACAGAGGCTTCTATTTCAAGTCGACCAACTAGTAGGTGCAACAGT CGGCGTCTCAAATCGTGGGATGTGGAAGAGTGTGTTTTAGCAGTTGTAACCTAGCTCTACTAGAAC AATACTGCGCTAAACCTGCCAAGTCAGAGAGGGACGTTTACGCCACATCCCTACAGGTCATCCCGGTGA TGCCCGCATTAACAGGAGGTCCCAAGAAAACATGTGACCGTGAAAATATTCAAAATATGACGTGTGGC AACGGAAGGCCGCACAGAGGCTACGAAGGGGCTCCCTGCCATCCTGCGGGCCAAGAAGTTTAGGCG GCAGGGGAGAGAATCAAGGCCAGGAGCAACTGCACCACACAGGCCTCTCATCACGCTTCCCAGCA A
PACAP	GCAGGGCAAGGTCTAGTAGAGCGACTTTAGCGTTGCTCATCTACGGAATCATGATGCATTACAGCGCCTA CTGCACGCCTATTGGGATGGCTTTTCTAAGATGAGACTAGACAACGATGTATTTGACGAAGACGGAAA CTCTGTAAGCGACCTGGCTTTTGGCACGGATCAAATGTCTATACGAAGTCCCTCTTCTTACGGATGAC CTATACACGCTATACTATCCTCCAGAGAAAAGAACGGAAAGGCATGCGAGATGGATTATTAGATAGAGCCT TGAGGGACATCCTGGTTTCAGTTATCAGCACGAAAATATCTGCATTCTCTGATGGCAGTTCCGCTAGGCGG AGGAAGCAGCGAGGAAGACGAATCGGAACCATATCAAAAAGGCATTCCGGATGGGATCTTACCAGCA TTTACAGTCGCTACCGAAAACAGATGGCCGTCAAGAAGTATTTAGCAGCCGCTCTGGGAAGAAGGTACA GACAGAGAATTAACAAAGGACG
SRIF	GACGTAACGGTAAGTTTCAGAGAGTTCTTGCATCCGGCTTTGCGCTCGCGAGGTGCCAGCATGGGACCG GCGGCGCGCTCGAGCTCAAACGAACGTCATCTTCTCCACAGCGCGAGACAGATCCTCGGGCTCCAG CACCTCGTTTTCTGCTTGGACGAGGTCTGTGAGCAAATCTGCAAGTGTGTATCTTGGAGTTCTGTTTT CCAGCCGGTTGAGGAGAGATCTCTGCAGAAGTTGGCGGAGTTTGGCGTA
MSTN-1	GTGTTGCTTTTTCTCCTCAGTCCGAAAATCCAAGCGAACCGGATCGTAAGAGCGCAGCTCTGGGTTCA TCTGAGACCGGGCGAAGAAGCGACCCGCTTCTTACAGATATCACGGCTGATGCCGTTTACGGACGG AGGAAGACACATACGAATACGATCCCTGAAGATCGATGTGAACGCAGGAGTCACGTCTTGGCAGAGTAT AGACGTAAGCAGGTGCTCTCGGTGTGGTTAAGACAACCGGAGACCAACTGGGGCATCGAGATAAACG CGTATGACGCGAAGGGAAACGACTTGGCCGTACCTCAGCTGAGGCTGGAGAGGATGGACTGTCCCC TTTATGGAGGTGAAAATCTCAGAGGGCCAAAGCGAATCCGGAGGGACTCCGGACTGGACTGCGACGA GAATTCCTCAGAGTCTCGATGCTGCAGATACCCTCTCACTGTGGACTTCGAGGACTTCGGC
MYOG	AGGATATCAGGACAGAAGCTCCATGATGGGCTTGTGTGGAGACGGACGGCTGCTGTCTAATGGAGTGGG GTTGGAGGACAAACCGTCTCCATCATCTAGCCTCGGTCTGTCCATGTCTCCTCACCAGGAGCAGCAGCA CTGTCCGGGTCAAGTGTGCTTGGGCTGCAAGGTGTGTAAGCGCAAGTCCGGTACCATGGACCGAC GGAAAGCCGCCACATTGAGGGAGAAGAGGAGTTGAAGAAGGTCAACGAGGCCTTTGAGGCTCTTAA GAGGAG

TEMPORAL AND SPATIAL DISTRIBUTIONS OF NUTRIENTS AND POLLUTION RISK ASSESSMENT OF TAXODIUM 'ZHONGSHANSHAN' WETLAND OF DIANCHI LAKESIDE, SOUTHWEST OF CHINA

LING, Z.^{1,2} – SHI, Z.^{1*} – XU, S.³ – DONG, M.²

¹*College of Tourism and Geographic Sciences, Yunnan Normal University, 650500 Yunnan, China*

²*Kunming University, Kunming, 650214 Yunnan, China*

³*Kunming Dianchi Lake Pollution Prevention and Control Cooperative Research Center, 650214 Yunnan, China*

**Corresponding author
e-mail: shizhengtao@163.com*

(Received 5th Aug 2019; accepted 25th Nov 2019)

Abstract. The *Taxodium 'zhongshanshan'* is one of the main wetland plants of lakeside of a plateau Dianchi Lake, in Southwest of China. The sediments and overlying water samples of the *T. 'zhongshanshan'* wetland were collected. The temporal and spatial distributions of the total nitrogen (TN), total phosphorus (TP) and total organic matter (OM) were analyzed by principal component analysis (PCA) and correlation coefficient method. The pollution risk assessment of *T. 'zhongshanshan'* in Wetland. The results showed that: (1) There were differences in the temporal and spatial distributions of nutrients in the dynamic groundwater of *T. 'zhongshanshan'* wetland. In overlying water, the TP, TN and SS were higher in rainy season than in dry season. The removal rates of TN and TP were higher in dry season than in rainy season. The pollutant in the upstream were higher than the downstream. (2) The sediment pollution sources of nitrogen and phosphorus in wetland were also different in the rainy and dry seasons. The TP in sediment were higher in rainy season than in dry season. (3) The comprehensive pollution index was combined with the organic index to provide an evaluation method. The TN and TP content reached a heavy pollution level and the organic contaminants were at a medium level.

Keywords: *Taxodium 'zhongshanshan'* wetland, nutrients distribution characteristics, pollution index, organic matter index, organic nitrogen index

Introduction

Dianchi Lake Basin is a region with the highest level of urbanization in Yunnan Province, Southwest of China. The deterioration of the water environment and eutrophication in Dianchi Lake seriously restrict the sustainable development of the region (Xue and Lu, 2015; Li et al., 2015). It is the key watershed of “Three rivers and three lakes” management project in China. People have paid close attention to the temporal and spatial distribution characteristics and environmental significance of nutrient elements, assessment pollution risk of nutrients in lakeside wetlands of Dianchi.

The Lakeside wetlands could intercept pollution into lakes, restore the function of terrestrial and aquatic ecosystems and maintain water quality of lakes and improve the ecological landscape of lakes, which play an important role as barrier for eutrophic lakes (Wondie, 2018; Reeves et al., 2018). Also the lakeside wetlands control the lake eutrophication. To restore the ecosystem of eutrophic lakes, a 54,000 ha of lakeside ecological rehabilitation zone and 800,000 plants of *T. 'zhongshanshan'* ecoregion have

been constructed in the lakeside wetland of Dianchi Lake. There are many studies have shown that the *T. 'zhongshanshan'* have a good capacity to purify different concentration of eutrophic water (Hua et al., 2013; Han et al., 2015) and reduce the concentration of nitrogen and phosphorus in the ecological rehabilitation zone of wetland (Mayo et al., 2018; Oldenborg and Steinman, 2018).

Although, there are many related research reports in the Take Griffin Lake Wetland, Louisiana Rainy Land, Caohai Typical Plateau Wetland and Typical Lakes of Qinghai-Tibet Plateau (Zhang et al., 2013; Marton et al., 2014; Fulton et al., 2015). These results indicated that the spatial distribution and release potential of pollutant indicator have the obvious differences in lakeside wetlands. Temporal and spatial of nutrients has important impact on wetland ecosystem restoration and further affected the restoration of eutrophic lakes. However, combined nutrient distribution and assessment risk of pollutant has rarely been reported, especially in the lakeside wetland of plateau eutrophic lake.

The Laoyuhe River is one of the 35 main rivers input Dianchi Lake, which is typical contaminated non-point source pollution. During 2002 and 2004, the water quality of the Laoyuhe River was worse than Grade V due to lack of protection and management, and the main pollution index were the TN and TP. According to Laoyuhe River pollutants characteristics, a 20 hm² of the *T. 'zhongshanshan'* ecological restoration area was constructed near the estuary of Laoyuhe River. The removal rate of TP and TN respectively reached 37.1% and 67.5% in ecological restoration wetland of the Laoyuhe River. The annual COD reduction of the pollution load was 473.2 t, TP 1.703 t, TN 79.1 t and SS 483.7 t by the ecological restoration wetland of the Laoyuhe River (Ma et al., 2007). Laoyuhe River wetland is the largest, last biological barrier in the lakeside of Dianchi Lake where *T. 'zhongshanshan'* is the typical and main trees. It plays an important roles in reduce pollution from the agricultural non-point source.

This research is aim to systematically analyze the temporal and spatial distributions characteristics and ecological effects of sediments in the ecological restoration area of the *T. 'zhongshanshan'* in the lakeside wetland. It is contained the temporal and spatial distribution characteristics of TP, TN and OM in sediments and the interaction between sediment-overlying water and the evaluation of pollution level in *T. 'zhongshanshan'* wetland.

Materials and methods

Study area and Sampling sites as shown in *Figure 1*. The Laoyuhe River wetlands about 53.34 hm²(108°48'46"-108°52'09"E,22°56'28"-23°0'49"N) has formed a wetland ecosystem in the River-Lake interaction area. In addition, plenty of *T. 'zhongshanshan'* has been planted in that wetland area which plays an important role in purifying water quality, intercepting pollutants, controlling soil loss and improving lakeside landscape.

Moreover, the study area forms the unique regional precipitation unit in the dry season during October to April and rainy seasons during May to September in the Yunnan-Guizhou Plateau. So that the hydrological processes (Weyer et al., 2018), wetland vegetation suitability (Pan et al., 2012), nutrient transport and transformation in sediments (Naranjo et al., 2019) of the Laoyuhe River are mainly affected by dry and rainy seasons.

Sediment and water sample treatment and statistical analysis

In this study, 27 sample sites (A1-A9, B1-B9, C1-C9) as marked in *Figure 1* were located in the central of *T. 'zhongshanshan'* ecological restoration area in Laoyuhe River wetland near Dianchi Lake. A1-A9 were located at downstream, B1-B9 were

located at midstream, C1-C9 were located at upstream. Surface sediment (0-10 cm) and overlying water are collected by using a home-made core Plexiglas sampler (Zhang, 2014) in May 27, 2018 (rainy season) and November 27, 2018 (dry season). The samples collected from each site consisted of three parallel samples. Following collection, the sediment and overlying samples were sealed in plastic bags and bottles were transported to the laboratory in cooled boxes at 4 °C. Each sediment sample was freeze-dried, ground, and passed through a 0.15-mm sieve.

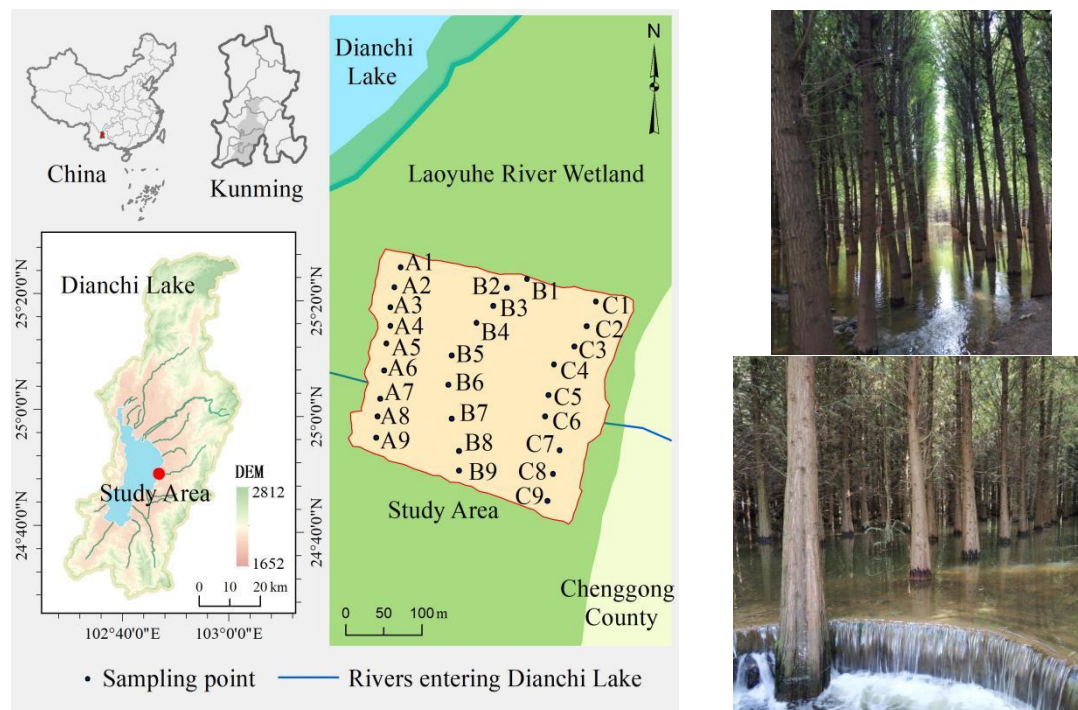


Figure 1. Locations of sampling sites and pictures of Laoyuhe River wetlands around Dianchi

To measure TP in the sediment samples, TP in acid-digested extract was determined by the ascorbic acid method using a Shimadzu UV-3600 spectrophotometer. TN was determined using an elemental analyzer (CE-440, Exeter Analytical, Inc., North Chelmsford, MA, USA). To measure OM which were analyzed by potassium dichromate oxidation-external heating (Zhang et al., 2014).

Suspended Solids (SS), Total nitrogen (TN) and Total phosphorus (TP) were tested and analyzed in overlying water. The parameters of water samples were determined according to the *Monitoring Method for Water and Wastewater* (4th Edition). SS was filtered by centrifuge and filter paper. National Standards HJ 636- 2012 and GB 11893-89 illustrated that TN was determined by alkaline potassium persulfate oxidation-ultraviolet spectrophotometry and that TP was determined by ammonium molybdate spectrophotometry. The average of three parallel samples for each index is tested for reduce error, and the laboratory error is controlled within 5%. The data were analyzed by SPSS20.0 and Excel 2013 software for the principal components of TN, TP, OM in sediments and SS, TN and TP in the overlying water of each sampling point in the research area. Then the correlation between different index also be studied.

The nutrient element distribution diagram of the study area was drawn by GraphPad.Prism5 software in order to compare and analyze the distribution characteristics of different nutrient elements in the sediment-overlying water in the dry and rainy season.

Pollution assessment method of T. 'zhongshanshan' ecoregion

Comprehensive pollution index evaluation

The assessment criteria of TN and TP (0.55 and 0.60 g/kg) used in this paper. They are consistent with the contents of TN and TP in sediments that can cause the lowest level of ecological risk effects issued by the Department of Environment and Energy, Ontario, Canada (1992) (Li et al., 2016). The formula for calculating single pollution index is (Kapelewska et al., 2018):

$$S_i = \frac{C_i}{C_s} \quad (\text{Eq.1})$$

$$FF = \frac{\sqrt{F^2 + F_{max}^2}}{\sqrt{2}} \quad (\text{Eq.2})$$

where S_i is a single evaluation index or standard index, $S_i > 1$ indicates that the content exceeds the evaluation standard value; C_i is the measured value of evaluation factor i (g/kg); C_s is the evaluation standard value of evaluation factor i (g/kg). The C_s of TN is 0.55 g/kg, the C_s of TP is 0.60 g/kg; FF is the comprehensive pollution index; F is the average value of n pollutant pollution indices (average of STN and STP); F_{max} is the maximum single pollution index (maximum of STN and STP). The comprehensive pollution for the surface sediments of Laoyuhe wetland shown in *Table 1*.

Table 1. Classification of comprehensive pollution degree of surface sediments in Laoyuhe River wetland

Grade	STN	STP	FF	Pollution Level
1	STN < 1.0	STP < 0.5	FF < 1.0	Non-pollution
2	1.0 ≤ STN < 1.5	0.5 ≤ STP < 1.0	1.0 ≤ FF < 1.5	Mild pollution
3	1.5 ≤ STN < 2.0	1.0 ≤ STP < 1.5	1.5 ≤ FF < 2.0	Moderate pollution
4	STN > 2.0	STP > 1.5	FF > 2.0	Heavy pollution

Organic pollution index evaluation

The sediment pollution in *T. 'zhongshanshan'* wetland of Dianchi Lakeside was further evaluated by organic pollution index method for improve the evaluation results (Zhang et al., 2015; Yang et al., 2017). It is output of comprehensive information (Zhu et al., 2019) then it has advantages over the comprehensive pollution index evaluation.

According to *Equations 3–5* and *Table 2*, the evaluation results of organic pollution of surface sediments in *T. 'zhongshanshan' ecoregion* around Dianchi Lake are shown in *Table 4*.

$$IO = OC(\%) \times ON(\%) \quad (\text{Eq.3})$$

$$ON = TN(\%) \times 0.95 \quad (\text{Eq.4})$$

$$OC = OM(\%) / 1.724 \quad (\text{Eq.5})$$

where *OC* is organic carbon.

Table2. Evaluation criteria of organic index of surface sediments in Laoyuhe wetland

Project	OI < 0.05	0.05 ≤ OI < 0.20	0.20 ≤ OI < 0.5	OI ≥ 0.5
Level	Non-pollution	Mild pollution	Moderate pollution	Heavy pollution
Type	I	II	III	IV

Results and analysis

Spatial distribution characteristics of nutrients in the ecological restoration area of the T. 'zhongshanshan'

The Distribution characteristics of TN, TP and SS of the overlying water is shown in *Figure 2* and TN, TP and OM contents in surface sediments of Laoyuhe River wetland during dry and rainy seasons is shown in *Figure 3*.

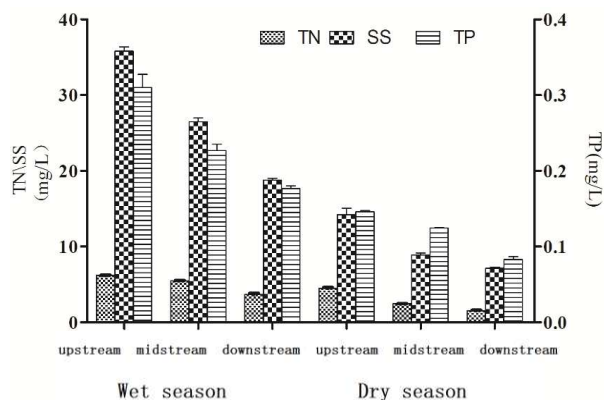


Figure 2. Distribution characteristics of TN, TP and SS of the overlying water in the ecological restoration area

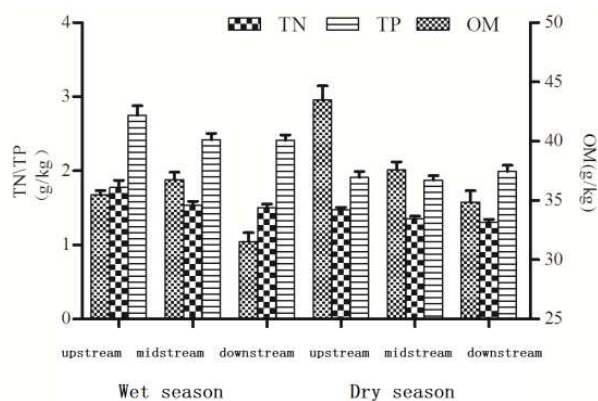


Figure 3. Distribution characteristics of TN, TP and OM contents in surface sediments of Laoyuhe river wetland during dry and rainy seasons

In the research area overlying water, the average values of TN was 5.13 mg/L and TP was 0.24 mg/L in rainy season, while TN is 2.83 mg/L and TP is 0.12 mg/L in dry season. The TN and TP in rainy season were nearly twice higher than in dry season.

All of TN, TP and SS decreases when the water flow through the ecological restoration area. The TN removal rate was 40.3% in rainy season and 65.9% in dry season. The TP removal rate was 43.0% in rainy season and 43.2% in dry season. The removal rates of TP and TN in dry season are higher than in rainy season. The removal efficiency of TN is higher than TP. The removal rates of SS in the overlying water 47.58% in rainy season and 49.88% in dry season.

Distribution of nutrients in sediments of ecological restoration area was obviously different. The OM was 38.64 g/kg in dry season and 34.58 g/kg in rainy season. Moreover, it was 33.19 g/kg in downstream and 39.48 g/kg in upstream. But the TN in sediment was 2.53 g/kg in rainy season and 1.92 g/kg in dry season. It was 0.21 g/kg higher in upstream than that in downstream. The TP was 1.61 g/kg in rainy season and 1.38 g/kg in dry season. It was 0.22 g/kg higher in upstream than that in downstream.

Correlation analysis of nitrogen, phosphorus and organic matter in sediment and overlying water

The correlation coefficient matrix of TN and TP in sediment-overlying water of *T. 'zhongshanshan'* ecoregion in rainy and dry season in Laoyuhe River was shown in Table 3. The correlation coefficient between TP and TN in sediment was 0.943 in rainy season and 0.757 in dry season ($P < 0.01$). There was a significant positive correlation between TN and OM in overlying water in rainy season ($P < 0.05$) with a correlation coefficient of 0.808. There was a significant positive correlation between TN and TP in water and TP in sediment in dry season ($P < 0.05$) with a correlation coefficient of 0.540 and 0.662. In dry season, TP and OM in sediments were positively correlated with TN and TP in overlying water ($P < 0.05$).

Table 3. Correlation analysis of surface sediment-water nitrogen, phosphorus and organic matter in dry and rainy seasons of Laoyuhe river wetland

Rainy season	Sediment TN	Sediment TP	Sediment OM	Overlying water TN	Overlying water TP
Sediment TN	1	0.943**	0.360	0.465	0.594*
Sediment TP		1	0.364	0.540*	0.662*
Sediment OM			1	0.808*	0.511
Overlying water TN				1	0.879**
Overlying water TP					1
Dry season	Sediment TN	Sediment TP	Sediment OM	Overlying water TN	Overlying water TP
Sediment TN	1	0.287	0.020	-0.116	-0.202
Sediment TP		1	0.757**	0.668**	0.687**
Sediment OM			1	0.848**	0.816**
Overlying water TN				1	0.914**
Overlying water TP					1

**Significant correlation at 0.01.*Significant correlation at 0.05

Assessment pollution risk of the ecological restoration area of the T. 'zhongshanshan'

This paper used the comprehensive pollution index evaluation method and organic index evaluation method to evaluate the pollution status of surface sediments in the T. 'zhongshanshan' wetland of Dianchi Lake. It based on the distribution characteristics of TN, TP and OM in the surface sediments. The results were shown in the *Table 4*. The results showed that the comprehensive pollution index which all of them belong to severe pollution is as follows: upstream > midstream > downstream (rainy season); downstream > upstream > midstream (dry season).

Table 4. *Comprehensive assessment pollution risk of surface sediments in dry and rainy seasons of assessment pollution risk*

	Area	STP	Grade	STN	Grade	FF	Level
Rainy season	Upstream	2.96	4	5.00	4	4.52	Heavy
	Midstream	2.56	4	4.40	4	3.97	Heavy
	Downstream	2.51	4	4.38	4	3.94	Heavy
	Area	STP	Grade	STN	Grade	FF	Level
Dry season	Upstream	2.45	4	3.47	4	3.23	Heavy
	Midstream	2.26	4	3.40	4	3.13	Heavy
	Downstream	2.18	4	3.62	4	3.28	Heavy

Applying the organic pollution index to evaluate the organic pollution of surface sediments of *T. 'zhongshanshan'* *ecoregion* is shown in *Table 5*. The distribution of organic pollution in the rainy or dry seasons of *T. 'zhongshanshan'* *ecoregion* along the lakeside is as follows: upstream > midstream > downstream. The organic pollution was moderate except water inlet in rainy season that was level III (heavily polluted).

Table 5. *Assessment of organic pollution in surface sediments of Laoyuhe river wetland in dry and rainy seasons*

	Area	OC/%	ON/%	OI/%	Level
Rainy season	Upstream	2.06	0.26	0.54	IV
	Midstream	2.13	0.23	0.49	III
	Downstream	1.83	0.23	0.42	III
	Area	OC/%	ON/%	OI/%	Level
Dry season	Upstream	2.52	0.18	0.46	III
	Midstream	2.18	0.18	0.39	III
	Downstream	2.02	0.19	0.38	III

Discussion

Spatial distribution characteristics of nutrients elements in the ecological restoration area of the T. 'zhongshanshan' in Dianchi Lakeside wetland

(1) There are differences in nutrient elements in overlying water between rainy season and dry season. Compare with dry season, the average content of TN in rainy season was 2.3 mg/L higher than in dry season, while TP in rainy season was 0.12 mg/L

also higher than in dry season. Dianchi Lake Basin is a phosphorus-rich area, the lakeside wetland of the Laoyuhe River is located in the East Bank of the Dianchi Lake (Zeng et al., 2017) where agricultural non-point sources have become the main pollution sources.

According to research, crops such as flowers and vegetables in dry season are widely planted which were the main causes of agricultural non-point source pollution in the basin. These crops require large amounts of fertilizer and have high nutrient surpluses (Zeng et al., 2017). Therefore, the loss and migration of phosphorus have become an important source of water pollution in the phosphorus-rich area, Dianchi Lake, with the increase of precipitation in rainy season. The nitrogenous and phosphorus fertilizer in the soil with the heavy rain washed into the river channel and finally entered the *T. 'zhongshanshan'* wetland. Then, it makes the content of nutrients in the overlying water in rainy season are much higher than those in dry season.

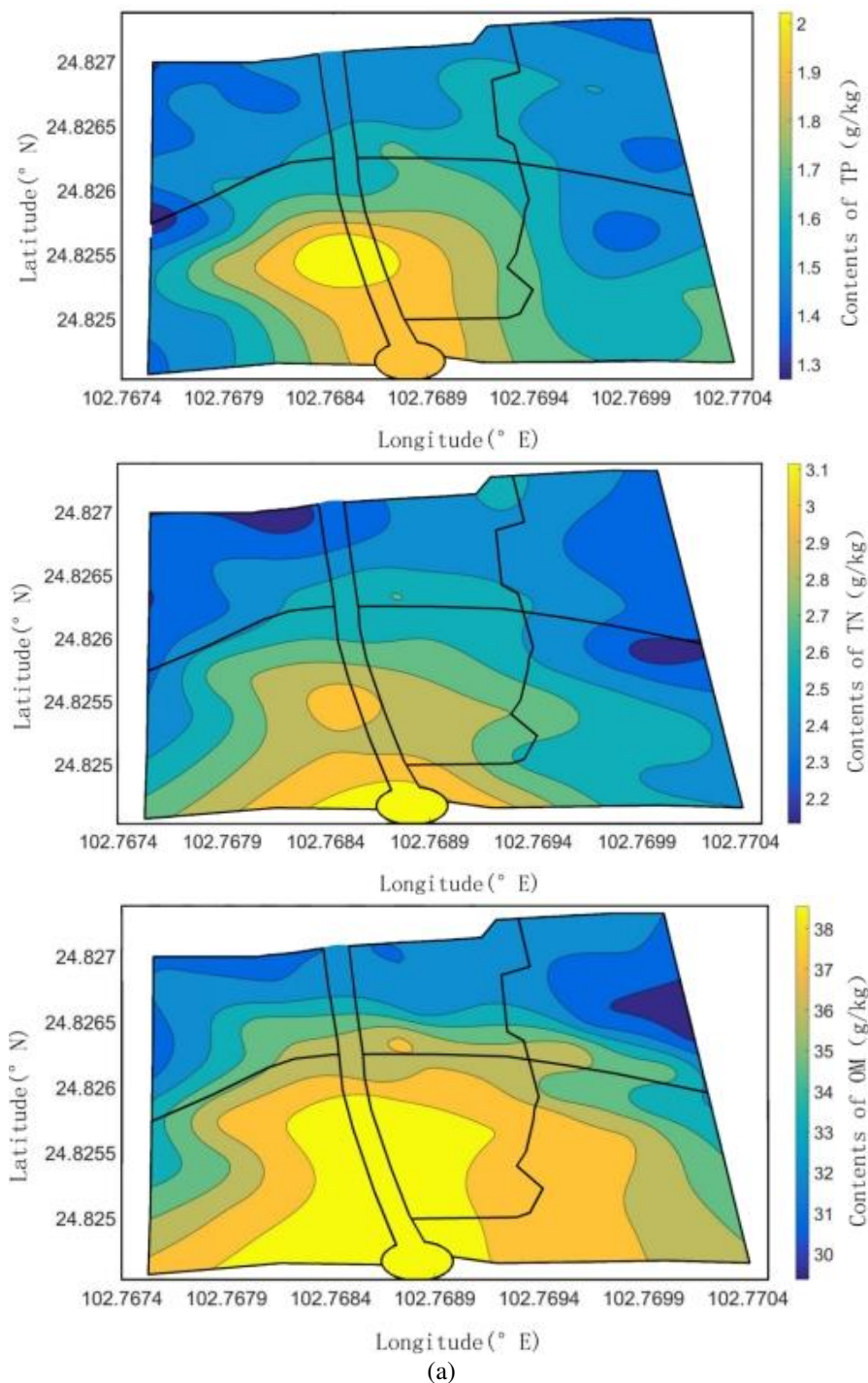
(2) In *T. 'zhongshanshan'* wetland, the removal rate of TN and TP in overlying water in dry season is higher than that in rainy season. The removal rate of TN was 25.6% higher in dry season than in rainy season. The removal rate of TP in dry season was 0.2% higher than in rainy season. The first reason is that the content of TN, TP and other nutrients in the overlying water is higher in rainy season than those in dry season. Secondly, the higher hydraulic load and longer hydraulic residence time can makes higher removal efficiency. There are an amount of water, fast flow rate and short hydraulic retention time in *T. 'zhongshanshan'* ecoregion in rainy season. That is consistent with that the purification effect of *T. 'zhongshanshan'* on mild and moderate eutrophic wastewater was better than heavy (Hua et al., 2013; Han et al., 2015). Meanwhile, that the growth of *T. 'zhongshanshan'* is stable in the dry season causes the unique climatic conditions of Kunming (Ma et al., 2011). So the nutrient elements removal rate such as TN and TP are kept at a certain rate to promote TN and TP reduction in dry season.

(3) The content of TP in sediment is higher in rainy season than in dry season. Also it is higher in upstream than downstream in research area. The spatial and temporal distribution of nutrient elements such as TN, TP and OM in sediments are mainly affected by many reasons such as exogenous inputs, sedimentary environment, human factors, hydrodynamic conditions and pollution conditions (Marton et al., 2014). The content of TP in the sediment in rainy season is higher than that in dry season because of a large amount of phosphorus entered the *T. 'zhongshanshan'* wetland with soil erosion in rainy season especially Dianchi Lake which is located a phosphorus-rich area (Ma et al., 2015). The particulate phosphorus in the soil is intercepted and settled into the sediment by the roots of *T. 'zhongshanshan'* and other plants. The absorption of phosphorus nutrients in the roots of plants plays a certain role in reducing the pollution of total phosphorus in sediments. Therefore, the content of TP in the sediment in upstream of *T. 'zhongshanshan'* ecological restoration area was higher than that in the downstream which is consistent with Varol's (2013) and Dzakpasu et al.'s (2015) studies.

(4) The effect of *T. 'zhongshanshan'* on the TN removal efficiency in overlying water and sediment are not consistent which mainly due to the different morphology of N in water-sediment system (Hossain et al., 2016). The TN in overlying water was 3.98 mg/L with the removal efficiency of 41.65%, while the TN in sediment was 1.99 g/kg with the removal efficiency of 27.29%. The average content of TN in surface sediment of *T. 'zhongshanshan'* wetland was higher than many other lakeside wetlands.

such as Taihu Lake, Chaohu Lake, Hongze Lake, the nitrogen substances also was mainly absorbed from the overlying water in the growth process of *T. 'zhongshanshan'* which played indispensable role (Stottmeister et al., 2003). Furthermore, nitrogen is released and returned to the sediment because the dense *T. 'zhongshanshan'* restoration area produced a large amount of litters which degrade. It increased the content of TN in the sediment (Jacobson et al., 2014).

Based on the monitoring results of TP, TN, OM at the 27 sampling sites, the spatial distribution of average TP, TN, OM in the surface sediment of *T. 'zhongshanshan'* wetland is shown in Figure 4a, b.



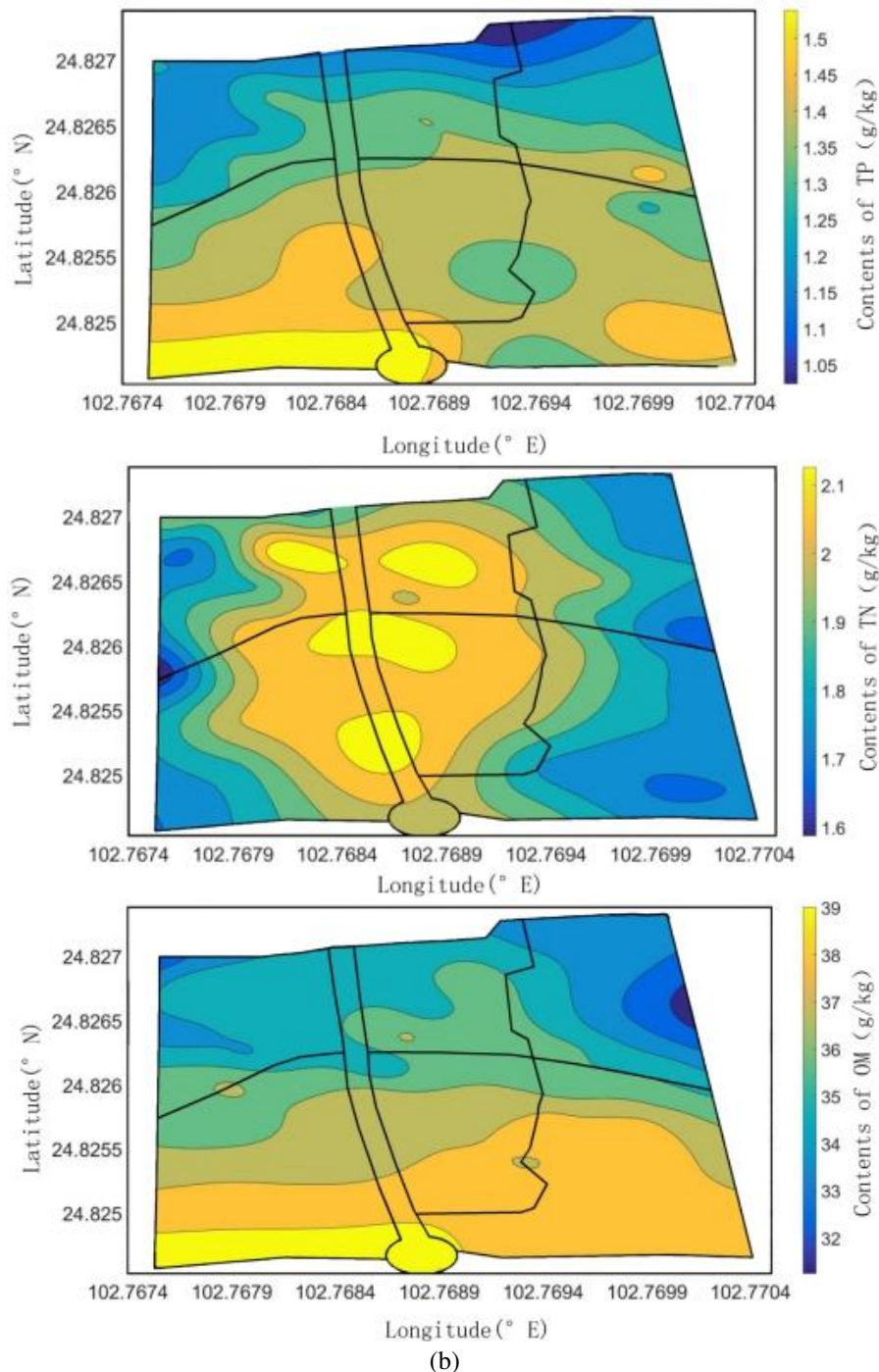


Figure 4. The spatial distribution of average TP, TN, OM in the surface sediment of research area in rainy season (a) and in dry season (b). Abscissa axis is Longitude, ordinate axis is Latitude, black lines in colourful area (our research area) are the boundary of different units *T. 'zhongshanshan'* forests in Laoyuhe River wetland

Correlation of nutrient elements in Sediment- Overlying water

According to correlation analysis, the TP in sediments was a significant positive correlation with TN in sediments ($P < 0.01$), but no correlation with OM in rainy season. The TP in sediments was positively correlated with OM ($P < 0.01$) but not with the TN in

sediments in dry season. It indicated that there are differences in the sources of nitrogen and phosphorus pollution in the sediments of the Laoyuhe River wetland in the different seasons. Compared with the research of Sediments in Tigris river basin, lake mouth wetland of Erhai Lake and Taihu Lake basin (Yang et al., 2014; Wang et al., 2016; Ouyang et al., 2018) the reduction of N and P in the rainy season is significantly correlated, while the OM in the dry season was a significant source of TP in sediments. The TN and TP mainly affect by exogenous factors while OM affect by endogenous factors. Also, the source of pollution is mainly exogenous in rainy season and endogenous in dry season.

In addition, the OM play an important role on the release of nitrogen and phosphorus. For example, Wang et al. (2011) and Di Luca et al. (2017) found that the larger variation range of nitrogen and phosphorus release in sediments when it under heavy organic pollution. So it can be inferred that the potential release risk of nitrogen and phosphorus from surface sediments of *T. 'zhongshanshan'* wetland around Dianchi Lake during rainy season is higher. It was more likely to cause secondary pollution to overlying water.

Pollution assessment of T. 'zhongshanshan' ecoregion on the lakeside of Dianchi Lake

Currently, there is no report on the methods and standards for evaluated the pollution status in shallow lake sediments. The research is mainly focused on the Organic Index (OI) and Organic Nitrogen (ON) evaluation methods which that only considered the OM and ON, but ignored the presence of phosphorus (Qiu et al., 2016). Some researchers adopted the method developed by Ontario Department of Environment and Energy in Canada since 1992, for the environmental quality assessment standard (Li et al., 2016). Although the method has derived from the ecological toxicity analysis of marine sediments, it takes the phosphorus into account.

The comprehensive and organic pollution levels were between moderate and severe levels in the sediments of *T. 'zhongshanshan'* wetland which has consistent results on the FF and OI. The pollution level of surface sediment of *T. 'zhongshanshan'* wetland around Dianchi Lake is at a high level which showed a difference with the plain wetland such as Sundarbans mangrove forest wetlands, Hongkong coastal wetland and Min River Estuary Wetland's evaluation results of sediment pollution (Mustafa et al., 2011; Hossain et al., 2016; Hu et al., 2014).

Sediment is a reservoir of nitrogen and phosphorus nutrients in wetlands (Zhang et al., 2013). The release of nitrogen and phosphorus from sediments will gradually become the focus of eutrophication control of water after the control of exogenous sources. Although not all forms of nitrogen and phosphorus can be released into water, the TN and TP forms of sediments represent the pollution degree and potential release risk of nitrogen and phosphorus in sediments (Wang et al., 2012).

The FF and OI indices of sediments from *T. 'zhongshanshan'* wetland in the lakeside of Dianchi were higher in rainy season than in dry season.

It is easy to cause sediment of *T. 'zhongshanshan'* wetland disturbance and resuspension under the action of hydraulic force when an amount of increased water enter in rainy season. It is helpful for the release or regeneration of nutrients.

Conclusion

This study quantitatively assessed the spatial distribution of nutrient levels as indicated by TP, OM, TN and SS in sediment and overlying water of *T. 'zhongshanshan'* wetland of Dianchi Lakeside to lay the groundwork for further

sedimentary remediation and pollution prevention. The contents of nutrients were higher in water inlet than in water outlet. The removal rates of TN and TP in water are higher in upstream than in downstream. Meanwhile, the reduction of TN was significantly different in water and sediments. TP and TN in the rainy season were significantly higher than in the dry season. TN were mainly from agricultural non-point source pollution. TP were mainly from rich phosphorus around Dianchi ((Zeng et al., 2017); Ma et al., 2015). They washed into wetlands as exogenous pollutants in rainy season, then they settled and released into wetlands as endogenous pollutants in the dry season. The nitrogen and phosphorus pollution of sediments were all severe pollution both in dry and rainy season of *T. 'zhongshanshan'* ecoregion, but the organic pollution was basically moderate.

The *T. 'zhongshanshan'* lakeside wetland is the first ecological restoration area around Dianchi. Non-point resource pollutants are rapidly and efficiently absorbed, degraded and converted. Although the reduction effect of this single plant is efficient, there is still a part of the pollutants flowing into the next ecological restoration area along with surface runoff. Therefore, other wetland plants such as *Typha orientalis presl* and *Phragmites communis* in the downstream restoration areas should be mainly constructed. These repair strategies should form a complementary function and strengthen the interception of pollutants in the lakeside wetland of Dianchi Lake.

Acknowledgments. We thank reviewers from Kunming Dianchi Lake Pollution Prevention and Control Cooperative Research Center, China. This study was financial supported by Yunnan Provincial Fund project (2019J0573).

REFERENCES

- [1] Di Luca, G. A., Maine, M. A., Mufarrege, M. M., Hadad, H. R., Pedro, M. C., Sánchez, G. C., Caffaratti, S. E. (2017): Phosphorus distribution pattern in sediments of natural and constructed wetlands. – *Ecological Engineering* 108: 227-233. DOI: 10.1016/j.ecoleng.2017.08.038.
- [2] Dzakpasu, M., Wang, X., Zheng, Y., Ge, Y., Xiong, J., Zhao, Y. (2015): Characteristics of nitrogen and phosphorus removal by a surface-flow constructed wetland for polluted river water treatment. – *Water Science and Technology* 71(6): 904-912. DOI: 10.2166/wst.2015.049.
- [3] Fulton, R. S., Godwin, W. F., Schaus, M. H. (2015): Water quality changes following nutrient loading reduction and biomanipulation in a large shallow subtropical lake, Lake Griffin, Florida, USA. – *Hydrobiologia* 753(1): 243-263. DOI: 10.1007/s10750-015-2210-8.
- [4] Han, L. W., Hua, J. F., Yin, Y. L., Yu, C. G., Shi, Q. (2015): Purification of eutrophic water by four Chinese cedar varieties. – *Chinese Journal of Environmental Engineering*. 9 3311-3318.
- [5] Hossain, G. M., Bhuiyan, M. A. H. (2015): Spatial and temporal variations of organic matter contents and potential sediment nutrient index in the Sundarbans mangrove forest, Bangladesh. – *KSCE Journal of Civil Engineering* 20(1): 163-174. DOI: 10.1007/s12205-015-0333-0.
- [6] Hu, M. J., Zou, F. F., Tong, C., Hu, W. F., Ji, Q. Y. (2014): Contents and ecological risk assessment of biogenic elements in estuary wetland sediments of Min River. – *Journal of Soil & Water Conservation*. 28(3) 121-126.
- [7] Hua, J. F., Yin, Y. L. (2013): Application potential of *T. zhongshanshan* in wetland construction. *Botany in ecological civilization construction: present and future*. – The 15th Annual Congress of the Chinese Botanical Society and the 80th Anniversary Academic Year Will.
- [8] Jacobson, T. K. B., Bustamante, M. M. C. (2014): Leaf Litter Decomposition and Nutrient Release Under Nitrogen, Phosphorus and Nitrogen Plus Phosphorus Additions in

- a Savanna in Central Brazil. – Sutton, M. A. et al. (eds.) Nitrogen Deposition, Critical Loads and Biodiversity. Springer, Dordrecht, pp. 155-163. DOI: 10.1007/978-94-007-7939-6_17.
- [9] Kapelewska, J., Kotowska, U., Karpińska, J., Astel, A., Zieliński, P., Suchta, J., Algrzym, K. (2018): Water pollution indicators and chemometric expertise for the assessment of the impact of municipal solid waste landfills on groundwater located in their area. – Chemical Engineering Journal. DOI: 10.1016/j.cej.2018.11.137.
- [10] Li, J. L., Zheng, B. H., Zhang, L. S., Jin, X. W., Hu, X. P., Liu, F., Shao, J. (2016): Characteristics and differences of eutrophication in the main estuary of China. – China Environmental Science 36(2) 506-516.
- [11] Li, L. P., Liu, L., Wang, S. R., Liu, W. B., Jiao, L. X., Yang, Y., Yang, R. (2015): Spatial distribution of phosphorus fractions in sediment and the potential mobility of phosphorus in Dianchi Lake. – Environ Earth Sci. DOI: 10.1007/s12665-015-4151-y.
- [12] Zeng, X. L., Wang, T.T., Luo, W. S., Liu, D., Ding, W. C., Wang, S. S. (2017): Characteristics and simulation of rainfall runoff and nitrogen & phosphorus outputs in facility agricultural area: A case study of flower greenhouse region in the East Coast of Lake Dianchi – J.Lake Sci. 29(5) : 1061-1069. DOI 10. 18307 / 2017. 0504.
- [13] Ma, G., Wang, S. (2015): Temporal and spatial distribution changing characteristics of exogenous pollution load into Dianchi Lake, Southwest of China. – Environmental Earth Sciences 74(5): 3781-3793. DOI: 10.1007/s12665-015-4721-z.
- [14] Ma, M. J., Yang, W., Li, B. (2007): Measures and effects of ecological restoration engineering in the lakeside of Yuyu River. – Environmental Science Guide 26 26-28.
- [15] Marton, J. M., Roberts, B. J. (2014): Spatial variability of phosphorus sorption dynamics in Louisiana salt marshes. – Journal of Geophysical Research: Biogeosciences 119(3): 451-465. DOI: 10.1002/2013jg002486.
- [16] Mayo, A. W., Muraza, M., Norbert, J. (2018): Modelling nitrogen transformation and removal in Mara River basin wetlands upstream of Lake Victoria. – Physics and Chemistry of the Earth, Parts A/B/C 105: 136-146. DOI: 10.1016/j.pce.2018.03.005.
- [17] Mustafa, A., Scholz, M. (2011): Nutrient accumulation in *Typha latifolia* Land sediment of a representative integrated constructed wetland. – Water, Air, & Soil Pollution 219 329-341.
- [18] Naranjo, R. C., Niswonger, R. G., Smith, D., Rosenberry, D., Chandra, S. (2018): Linkages between hydrology and seasonal variations of nutrients and periphyton in a large oligotrophic subalpine lake. – Journal of Hydrology. DOI: 10.1016/j.jhydrol.2018.11.033.
- [19] Oldenborg, K. A., Steinman, A. D. (2019): Impact of sediment dredging on sediment phosphorus flux in a restored riparian wetland. – Science of the Total Environment 650: 1969-1979. DOI: 10.1016/j.scitotenv.2018.09.298.
- [20] Ouyang, W., Yang, W., Tysklind, M., Xu, Y., Lin, C., Gao, X., Hao, Z. (2018): Using river sediments to analyze the driving force difference for non-point source pollution dynamics between two scales of watersheds. – Water Research 139: 311-320. DOI: 10.1016/j.watres.2018.04.020.
- [21] Pan, K., Wang, W. X. (2012): Trace metal contamination in estuarine and coastal environments in China. – Science of the Total Environment 421-422 3-16.
- [22] Qiu, Z. K., Hu, X. Z., Yao, C., Zhang, W. H., Xu, Q. J., Huang, T. Y. (2016): Pollution characteristics and evaluation of nitrogen, phosphorus and organic matter in sediments of Shanmei Reservoir in Fujian, China. – Environmental Science 37(4) 1389-1396.
- [23] Reeves, R. R., Wilke, M., Cashmore, P., Macdonald, N., Thompson, K. (2018): Physical and ecological effects of rehabilitating the geothermally influenced Waikite Wetland, New Zealand. – Journal of Environmental Management 228: 279-291. DOI: 10.1016/j.jenvman.2018.09.027.
- [24] Stottmeister, U., Wießner, A., Kuschik, P., Kappelmeyer, U., Kästner, M., Bederski, O., Moormann, H. (2003): Effects of plants and microorganisms in constructed wetlands for

- wastewater treatment. – *Biotechnology Advances* 22(1-2): 93-117. DOI: 10.1016/j.biotechadv.2003.08.010.
- [25] Varol, M. (2013): Temporal and spatial dynamics of nitrogen and phosphorus in surface water and sediments of a transboundary river located in the semi-arid region of Turkey. – *Catena* 100: 1-9. DOI: 10.1016/j.catena.2012.08.003.
- [26] Wang, L. Z., Wang, G. X., Yu, Z. F., Zhou, B. B., Ge, X. G. (2011): Study on simulation of phosphorus release from lake sediments caused by wind and waves disturbance. – *Journal of Soil and Water Conservation* 25(2): 121-124, 129.
- [27] Wang, S., Jiao, L. X., Yang, S., Jin, X., Yi, W. (2012): Effects of organic matter and submerged macrophytes on variations of alkaline phosphatase activity and phosphorus fractions in lake sediment. – *Journal of Environmental Management* 113: 355-360. DOI: 10.1016/j.jenvman.2012.09.007.
- [28] Wang, S. J., Liu, Y. G., Wang, Y., Hou, L., Zhang, C. (2016): Vertical distribution and pollution risk assessment of nitrogen, phosphorus, and organic matter in sediment of inflowing rivers of Erhai Lake estuarine wetland in wet and dry seasons. – *Environmental Science* 12 4615-4625.
- [29] Weyer, C., Peiffer, S., Lischeid, G. (2018): Stream water quality affected by interacting hydrological and biogeochemical processes in a riparian wetland. – *Journal of Hydrology* 563: 260-272. DOI: 10.1016/j.jhydrol.2018.05.067.
- [30] Wondie, A. (2018): Ecological conditions and ecosystem services of wetlands in the Lake Tana Area, Ethiopia. – *Ecohydrology & Hydrobiology* 18(2): 231-244. DOI: 10.1016/j.ecohyd.2018.02.002.
- [31] Xue, W., Lu, S. Y. (2015): Effects of inactivation agents and temperature on phosphorus release from sediment in Dianchi Lake. – *Environ Earth Sci, China*. DOI: 10.1007/s12665-014-3910-5.
- [32] Yang, Y., Liu, Q. G., Hu, Z. J., Zhang, Y. M., Gao, Y. X. (2014): Spatial distribution of sediment carbon, nitrogen and phosphorus and pollution evaluation of sediment in Taihu Lake Basin. – *Acta Scientiae Circumstantiae* 34: 3057-3064.
- [33] Yang, Y., Gao, B., Hao, H., Zhou, H. D., Lu, J. (2017): Nitrogen and phosphorus in sediments in China: a national-scale assessment and review. – *Science of the Total Environment* 576 840-849.
- [34] Zhang, B., Fang, F., Guo, J., Chen, Y., Li, Z., Guo, S. (2012): Phosphorus fractions and phosphate sorption-release characteristics relevant to the soil composition of water-level-fluctuating zone of Three Gorges Reservoir. – *Ecological Engineering* 40: 153-159. DOI: 10.1016/j.ecoleng.2011.12.024.
- [35] Zhang, Z. M., Lin, S. X., Zhang, Q. H., Guo, Y., Lin, C. H. (2013): Distribution characteristics of soil carbon, nitrogen and phosphorus in Caohai Plateau wetland under different land use patterns. – *Journal of Soil and Water Conservation* 27(6) 199-204.
- [36] Zhang, Z., Lv, Y., Zhang, W., Zhang, Y., Sun, C., Marhaba, T. (2014): Phosphorus, organic matter and nitrogen distribution characteristics of the surface sediments in Nansi Lake, China. – *Environmental Earth Sciences* 73(9): 5669-5675. DOI: 10.1007/s12665-014-3821-5.
- [37] Zhu, Y., Jin, X., Tang, W., Meng, X., Shan, B. (2018): Comprehensive analysis of nitrogen distributions and ammonia nitrogen release fluxes in the sediments of Baiyangdian Lake, China. – *Journal of Environmental Sciences* DOI: 10.1016/j.jes.2018.05.024.

ANALYSIS OF HEAVY METAL CONCENTRATION USING TRANSPLANTED LICHEN *USNEA MISAMINENSIS* AT KOTA KINABALU, SABAH (MALAYSIA)

ABAS, A.* – AWANG, A. – AIYUB, K.

Centre for Development, Social and Environmental Studies, Faculty of Social Sciences and Humanities, Universiti Kebangsaan Malaysia, 43600 UKM Bangi, Selangor, Malaysia

**Corresponding author
e-mail: azlanabas@ukm.edu.my*

(Received 5th Aug 2019; accepted 15th Nov 2019)

Abstract. Heavy metals were emitted from motor vehicles and industries as part of the effects of rapid urbanization. This study aims to measure the heavy metal concentrations (Cu, Fe, Zn, Pb, Mn, Cr) at Kota Kinabalu, Sabah using transplanted lichen. Samples of *Usnea misaminensis* were transplanted to the environment of the urban area. The lichen was collected from Mt. Kinabalu Park which is a remote area. Fifteen sampling stations were selected and transplanted lichens were exposed to heavy metals in those stations for about 4-6 weeks. Exposed lichens were analyzed using the inductively coupled plasma mass spectrometry (ICP-MS) to determine the concentration of heavy metals in each sample. One-way ANOVA also has been used to test whether there is significant variation between heavy metals concentration at Kota Kinabalu, Sabah. The result showed that iron (Fe) has the highest concentration with 84.43 µg/g and chromium (Cr) has the lowest concentration with 0.66 µg/g. A statistical One-way ANOVA test showed that there is a significant variation between heavy metal frequency with P-value is $0.0000 < 0.05$. A Tukey test also revealed that Fe has significantly higher concentration compare to the others. These findings prove that the increasing number of motor vehicles will also elevate the concentration of heavy metals in the atmosphere. Transplanted lichen can be the alternative approach in assessing air pollution in Malaysia's urban area.

Keywords: *lichen, air pollution, urban ecosystem, applied ecology, environmental management, Malaysia*

Introduction

Human well-being has been degrading tremendously due to the air pollution that caused by industrialization and urbanization in the city. In Malaysia, strategies to tackle environmental issues have been enacted by enforcing several policies such as National Policy on Environment (DASN) and the ratification of multi-lateral environmental agreement for example Paris Agreement 2015 (Sulaiman et al., 2018). These strategies were designed in order to sustain the human well-being in the city and also actions have been taken to create a liveable vicinity. One of the most common causes of the degradation of human well-being in Malaysia is air pollution according to statistics 54% of Malaysia's happiness disturbance was from air pollution. The Department of Environment has outlined a few protocols to be followed. But, in terms of the measurement it still not sufficient. The three major causes of air pollution are transportation, stationary sources and open burning. The problem they face now is that the quality of air in areas far away from their air monitoring stations is difficult to determine, hence lichen has been selected as a potential bio-indicator for this purpose.

Heavy metals can be measured and analyzed using two approaches which are sampling directly from the atmosphere and sampling using biological indicator. According to Carreras and Pignata (2002), High volume air samplers and glass fiber

filters were used to collect the samples containing heavy metals. Collected samples were digested using a mixture of analytical grade nitric acid and analytical grade hydrochloric acid, and analyzed to evaluate the levels of heavy metals by atomic absorption spectrophotometry. Heavy metals also can be sampled from lichen where selected lichen from specific sampling location brought to the lab and analyzed using atomic absorption spectrophotometry (Samsudin et al., 2013a). Heavy metals also can be found from the dust inside a building as studied by Abas et al. (2017) where they stated heavy metals such as Fe, Pb, Zn, Cu and as are existed inside the university building which can bring harm to the occupant health.

Lichen has been used as bio-indicator for air pollution for decades ago. In Italy, a standard called Lichen Biodiversity Index been developed and used to monitor air pollution in the district of Faenza, Italy (Cioffi, 2009). Also, Loppi and Frati (2006) conducted research in Central Italy measuring the nitrogen compounds in foliose lichen. Foliose-type lichen *Hypogymnia physodes* also been used and collected to analyse the heavy metals contents due to traffic pollutants (Blicharska et al., 2016; Koroleva and Revunkov, 2017). Transplanting foliose type lichen from remote and clean air area to much more polluted area is widely used to monitor the air pollution in certain vicinity. As examples, in Thailand they used *Parmotrema tinctorum* to monitor airborne trace elements near a petrochemical industry complex (Boonpeng et al., 2017). Apart of assessing outdoor pollution, transplanted lichen also used to indicate the level of indoor air quality where heavy metals such as As, Cd, Cr, Cu, Hg, Ni, and Pb also 12 Polycyclic Aromatic Hydrocarbon (PAH) been recorded (Abas, 2015; Protano et al., 2017). In Malaysia, research on lichens more focused on lichens dwelling in the highland such as Gunung Machincang, Cameron Highland, Genting Highland, Fraser Hills, Pulau Pangkor and Bukit Larut (Sulaiman et al., 2018; Abas et al., 2019). In addition, these researches only touched about the ecological and chemical part of the lichen (Din et al., 2010; Zulkifly et al., 2011). None of them studied the relationship between lichen and its vicinity, not until 2015 where a study on lichen diversity distribution in Kuala Lumpur (Abas and Awang, 2017). The research found that lichen diversity distributions are much related to the population density in Kuala Lumpur.

The study of monitoring air pollution using lichen in Malaysia is still based on lichen diversity and frequency. There is still lacking in using transplanting method to monitor air pollution in Malaysia especially in an urban area. Therefore, the aims of this study are; to analyze the heavy metals contents using transplanted lichen (*Usnea minaminensis*) as the alternative approach in air quality measurement and to determine the relationship between motor vehicles frequency and heavy metals concentration.

Methodology

Area of study

The City of Kota Kinabalu, Sabah (5.9804° N 116.0735° E) is situated at the west coast of Sabah, part of Borneo Island. As one of the largest city in Malaysia, Kota Kinabalu has a total population of 457,326 people with density of 1,463/km² according to census in 2018. Kota Kinabalu has developed into an over-concentrated urban area where recent studies showed the air quality in Kota Kinabalu has depleted.

Sampling procedures

Lichen *Usnea minaminensis* samples were collected from remote area (unexposed from excessive air pollution) of Mt. Kinabalu Park, Sabah, Malaysia (6.0192 N 116.5369 E). All samples were segregated into 45 samples for 15 sampling locations and only one sample was excluded from the segregation to be the control sample. *Table 1* and *Figure 1* show the location of 15 sampling stations that have been selected randomly around the City Centre of Kota Kinabalu, Sabah. This research was conducted using lichen transplanting method where lichen *Usnea minaminensis* was taken from remote area then placed on selected stations for approximately 1 month (from 20th Aug 2018 to 20th Sept 2018). About 50g of lichen samples were put in a punctured paper bags and placed on trees 1.5 m above ground facing the source of air pollution. After that, all samples were collected and brought to the lab for heavy metals concentration analysis (Nimis et al., 2002; Abas et al., 2016).

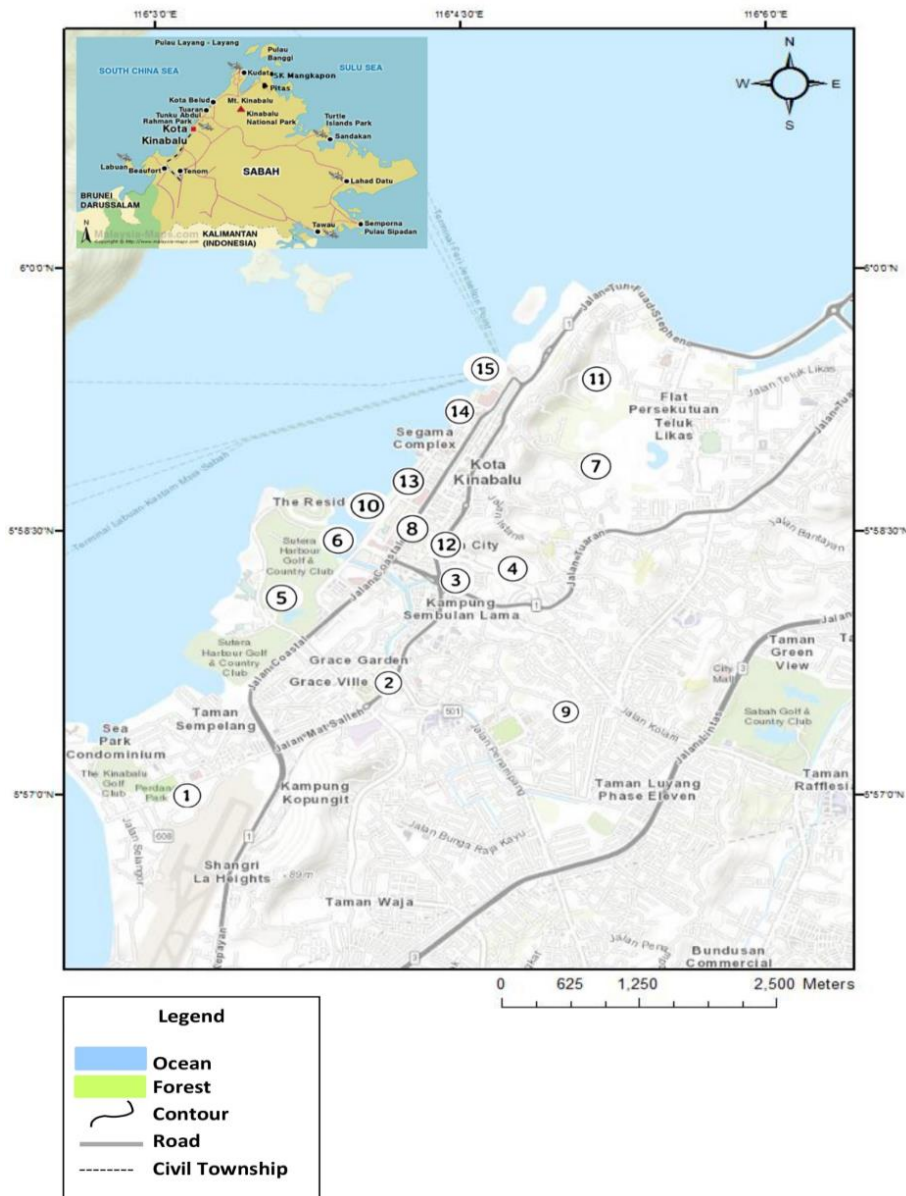


Figure 1. Location of the sampling stations

Table 1. Coordinate for sampling locations

Sampling location	Location name	Coordinates
1	Perdana Park, Tanjung Aru	5.9518N 116.0531E
2	Sabah State Mosque	5.9588N 116.0673E
3	Karamunsing Flyover	5.9698N 116.0740E
4	Nenas Hill Road	5.9693N 116.0808E
5	Sutera Harbour	5.9635N 116.0611E
6	Imago Mall & The Loft	5.9708N 116.0647E
7	Anjung Senja	5.9745N 116.0674E
8	Sinsuran	5.9793N 116.0732E
9	Gaya Street	5.9842N 116.0773E
10	KK Sky City	5.9706N 116.0806E
11	Signal Hill	5.9823N 116.0822E
12	Bandaran Berjaya	5.9768N 116.0753E
13	KK Central Market	5.9826N 116.0729E
14	Suria Sabah	5.9870N 116.0778E
15	Jesselton Point	5.9905N 116.0813E

Laboratory analysis

After about 2-4 weeks, those samples were collected and placed in sealed containers and were taken to the laboratory to be analysed. In the lab, the samples were air dried for about two days in the open air. Then, those samples were heated in the oven for another two days at about 50 °C in order to remove any excessive moisture. Any debris or dust on the samples was then picked out using clean tweezers before it then has been crushed into powder form. 1.0 g of each samples from the control area and all sampling stations later were weighed for the digestion process. After that, the digestion process was carried out by mixing 5 mL concentrated nitric acid and 15 mL perchloric acid into one conical flask. The samples were then heated on a hot plate until the initial volume was reduced into half. Then, the samples were then cooled off and later rinsed using 5 mL concentrated nitric acid before filtered into the 150 mL conical flask using Whatman No. 42 filter papers. During the filtration process, the samples were rinsed with 5% nitric acid and the filtrates were diluted to 50 mL using 5% nitric acid. The dilution later placed in Inductively Coupled Plasma Mass Spectrometry (ICP-MS) to detect heavy metals such as copper (Cu), manganese (Mn), lead (Pb), zinc (Zn), iron (Fe) and chromium (Cr).

Statistical analysis

One-way ANOVA been used in this research to determine whether there are any statistically significant differences between heavy metals concentration among all sampling stations. Tukey Test was also performed to check significant comparisons between each of the heavy metals.

Results and discussion

Table 2 shows the concentration of heavy metals determined in the lichen samples transplanted and collected from all 15 sampling stations including a control sample.

Table 2. Concentration of heavy metals

Sample	Concentration of heavy metals in lichen <i>Usnea minaminensis</i> (µg/g)					
	Fe	Zn	Mn	Cu	Pb	Cr
Control	14.96 ± 0.11	1.77 ± 0.23	0.93 ± 0.14	0.51 ± 0.12	0.40 ± 0.03	0.38 ± 0.09
1	68.54 ± 0.08	17.02 ± 0.12	16.73 ± 0.07	1.54 ± 0.21	1.41 ± 0.13	1.48 ± 0.14
2	64.30 ± 0.12	18.55 ± 0.11	15.33 ± 0.18	1.47 ± 0.03	1.29 ± 0.21	1.39 ± 0.34
3	64.57 ± 0.33	15.81 ± 0.23	15.69 ± 0.02	1.61 ± 0.28	1.37 ± 0.14	1.51 ± 0.11
4	57.66 ± 0.34	15.63 ± 0.34	16.43 ± 0.33	1.44 ± 0.16	1.22 ± 0.06	1.43 ± 0.17
5	60.12 ± 0.15	16.57 ± 0.19	12.85 ± 0.24	1.51 ± 0.16	1.40 ± 0.15	1.33 ± 0.18
6	71.47 ± 0.27	19.29 ± 0.02	22.61 ± 0.18	2.42 ± 0.14	3.02 ± 0.27	1.87 ± 0.03
7	82.09 ± 0.19	20.38 ± 0.16	24.75 ± 0.21	2.39 ± 0.08	4.11 ± 0.24	1.90 ± 0.16
8	76.32 ± 0.26	18.44 ± 0.08	19.68 ± 0.04	2.50 ± 0.12	3.67 ± 0.34	2.22 ± 0.25
9	84.43 ± 0.04	18.07 ± 0.21	20.28 ± 0.25	2.22 ± 0.32	3.73 ± 0.03	2.38 ± 0.09
10	44.55 ± 0.06	9.54 ± 0.34	6.49 ± 0.27	0.98 ± 0.21	1.08 ± 0.17	0.66 ± 0.09
11	32.78 ± 0.13	13.66 ± 0.23	10.70 ± 0.14	1.33 ± 0.20	1.19 ± 0.16	0.91 ± 0.33
12	63.17 ± 0.21	14.91 ± 0.09	17.19 ± 0.11	1.49 ± 0.10	2.62 ± 0.24	1.67 ± 0.22
13	79.89 ± 0.14	15.31 ± 0.10	18.87 ± 0.31	1.64 ± 0.31	1.31 ± 0.24	1.93 ± 0.17
14	69.51 ± 0.11	16.83 ± 0.11	14.61 ± 0.01	1.71 ± 0.04	2.77 ± 0.30	1.47 ± 0.13
15	63.73 ± 0.26	15.72 ± 0.12	15.79 ± 0.07	1.39 ± 0.03	1.84 ± 0.09	1.55 ± 0.06

The table shows that the heavy metals' concentration in all of the lichen samples from sampling stations are higher compared to the control sample. Iron (Fe) has the highest concentration in all lichen samples with sampling station number 9 has the highest concentration and number 11 has the lowest concentration, followed by manganese (Mn) (highest is number 7 and the lowest is number 10), zinc (Zn) (the highest is number 7 and the lowest is number 10), lead (Pb) (the highest is number 7 and the lowest is number 10), copper (Cu) (the highest is number 8 and the lowest is number 10) and the lowest is chromium (Cr) (the highest is number 9 and the lowest is number 10). Among all sampling stations, sampling station number 7 have the highest accumulation of heavy metals in the lichen samples, followed by number 8, number 9, number 6, number 13, number 14, number 1, number 2, number 15, number 3, number 4, number 5, number 11 and the lowest is sampling station number 10.

Table 3 shows the one-way ANOVA analysis result. Based on the table, it has been shown that p-value is < 0.05 meaning that there is significant variation between heavy metal groups. A Tukey post hoc test has revealed that the concentration of Fe in the transplanted lichen is significantly higher compare to the other heavy metals, while Zn and Mn has lower significant differences in concentration but higher compare to the other 4 and Cu, Pb and Cr also has lower significant difference in concentration but higher towards the other heavy metals as shown in Table 4.

Table 3. One-way ANOVA result

Source of variation	SS	df	MS	F	P-value	F crit
Between groups	44196.1640	5	8839.2328	135.5519	0.0000	2.3157
Within groups	5868.8303	90	65.209225			
Total	50064.9943	95				

Table 4. Post hoc test (Tukey HSD) result

Heavy metal		Sig. value
Fe	Zn	.000
	Mn	.000
	Cu	.000
	Pb	.000
	Cr	.000
Zn	Fe	.000
	Mn	1.000
	Cu	.000
	Pb	.000
	Cr	.000
Mn	Fe	.000
	Zn	1.000
	Cu	.000
	Pb	.000
	Cr	.000
Cu	Fe	.000
	Zn	.000
	Mn	.000
	Pb	1.000
	Cr	1.000
Pb	Fe	.000
	Zn	.000
	Mn	.000
	Cu	1.000
	Cr	1.000
Cr	Fe	.000
	Zn	.000
	Mn	.000
	Cu	1.000
	Pb	1.000

Our results demonstrate that heavy metals concentration in lichen *Usnea minaminensis* closely reflected the heavy metals deposition in the City Centre of Kota Kinabalu, Sabah. We presumed that heavy metals accumulation in lichen samples were due to automobile traffic pollution. Based on previous studies in the urban area of Malaysia, there was a high correlation between heavy metals accumulation in lichen and automobile traffic (Abas and Awang, 2015; Abas and Awang, 2017; Abas et al., 2018). A similar pattern has been found in many other areas of the world, that is, that air pollution caused by heavy metal deposition generally tends to be higher in urban zones with more traffic, than in rural areas with less traffic (Benitez et al., 2019). All those heavy metals usually come from anthropogenic activities such as industrial activity and motor vehicles emission. In addition, in densely populated urban area heavy metals are

trapped by buildings and prevent it from flew away from the urban vicinity (Samsudin et al., 2013b; Amil et al., 2016).

Iron (Fe), zinc (Zn), manganese (Mn) and copper (Cu) are categorized as an essential nutrient for organism as those metals are needed for growth and body development. Whereas, lead (Pb) and chromium (Cr) are known as non-essential heavy metal to living things and only exist in the surroundings due to industrial activity and automobile traffic emission. All of the heavy metals showed a similar pattern, with higher concentration was found in lichen samples of highly dense urban area than in nearby forest or highland. We also found that the heavy metals concentration varied depending on the location of the sampling station. Sampling stations that nearby the city centre such as Anjung Senja, Sinsuran and Gaya Street showed higher heavy metals concentration than sampling stations that located in rural areas such as Signal Hill and KK Sky City.

All the heavy metals are so much related to the density of automobile traffic where Zn deposition in lichens typically related to increases of traffic along traffic routes serving inner city urban areas. Air pollution from Zn can typically be ascribed to tyre wear, and this metal is also a common component of antioxidants used as dispersants to improve lubricating oils. Lead was originated from the fuel combustion of automobile traffic and its concentration is much higher in diesel oil.

Conclusion

This research shows that lichen *Usnea minaminensis* can be used to determine the heavy metal deposition in urban area. Besides that, there is significant variation between heavy metals in Kota Kinabalu. The concentration of heavy metals in Kota Kinabalu is varied, where location nearby to the city centre has higher concentration than nearby the rural or forest area.

Acknowledgements. We would like to thanks to Universiti Kebangsaan Malaysia (UKM) for funding this research by awarding the research grant of GUP-2018-032.

REFERENCES

- [1] Abas, A. (2015): Lichen as air pollution bio-indicator in the federal territory of Kuala Lumpur. – PhD Thesis. Universiti Kebangsaan Malaysia, Malaysia.
- [2] Abas, A., Awang, A. (2015): Penentuan tahap pencemaran udara di Malaysia Menggunakan pendekatan penunjuk bio (Liken): Kajian kes Bandar Baru Bangi. – Geografia: Malaysian Journal of Society and Space 11(9): 67-74.
- [3] Abas, A., Awang, A. (2017): Air pollution assessment using lichen biodiversity index (LBI) in Kuala Lumpur, Malaysia. – Pollution Research 36(2): 242-249
- [4] Abas, A., Nizam, M. S., Aqiff, M. W. (2016): Elevated CO₂ effects on lichen frequencies and diversity distribution in free-air CO₂ enrichment (FACE) station. – Journal of Environmental Protection 7: 1192-1997.
- [5] Abas, A., Khalid, R. M., Rosandy, A. R., Sulaiman, N. (2019): Lichens of Pulau Pangkor, Perak. – The Malaysian Forester 82(1): 59-66.
- [6] Amil, N., Latif, M. T., Khan, M. F., and Mohamad, M. (2016): Seasonal variability of PM_{2.5} composition and sources in the Klang Valley urban-industrial environment. – Atmos. Chem. Phys. 16: 5357-5381. DOI: 10.5194/acp-16-5357-2016

- [7] Benitez, A., Medina, J., Vasquez, C., Loaiza, T., Luzuriga, Y., Calva, J. (2019): Lichens and bromeliads as bioindicators of heavy metal deposition in Ecuador. – *Diversity* 1(28). DOI: 10.3390/d11020028
- [8] Boonpeng, C., Polyiam, W., Sriviboon, C., Sangiamdee, D., Watthana, S., Nimis, P. L., Boonpragob, K. (2017): Airborne trace elements near petrochemical industry complex in Thailand assessed by the lichen *Parmotrema tinctorum* (despr. Ex Nyl.) Hale. – *Environmental Science and Pollution Research* 24(13): 1-8.
- [9] Carreras, H. A., Pignata, M. L. (2002): Biomonitoring of heavy metals and air quality in Cordoba City, Argentina, using transplant lichens. – *Environmental Pollution* 117: 77-87.
- [10] Cioffi, M. (2009): Air quality monitoring with the lichen biodiversity index (LBI) in the district of Faenza (Italy). – *EQA-Environmental Quality* 1: 1-6.
- [11] Din, L. B., Zakaria, Z., Samsudin, M. W., Elix, J. A. (2010): Chemical profile of compounds from lichens of Bukit Larut Peninsular Malaysia. – *Sains Malaysiana* 39(6): 901-908.
- [12] Koroleva, Y., Revunkova, V. (2017): Air pollution monitoring in the South-East Baltic using the epiphytic lichen *Hypogymnia physodes*. – *Atmosphere* 8(19): 1-12.
- [13] Blicharska, M., Andersson, J., Bergsten, J., Bjelke, U., Hilding-Rydevik, T., Johansson, F. (2016): Effects of management, function and vegetation on the biodiversity in urban ponds. – *Urban For Urban Green* 20: 103-112.
- [14] Loppi, S., Frati, L. (2006): Lichen diversity and lichen transplants as monitors of air pollution in a rural area of Central Italy. – *Environmental Monitoring and Assessment* 114: 361-375.
- [15] Muhamad, N., Hashim, N. H., Khairuddin, N. A., Yusof, H., Jusoh, H., Abas, A., Talip, B. A., Abdullah, N., Din, L. (2018): Identification of most tolerant lichen species to vehicular traffic's pollutants: A case study at Batu Pahat. – *Journal of Advanced Research in Fluid Mechanics and Thermal Sciences* 42(1): 57-64.
- [16] Nash, T. H. (2008): *Lichen Biology*. 4th Ed. – Cambridge University Press, Cambridge, UK.
- [17] Nimis, P. L., Scheidegger, C., Wolseley, P. A. (2002): *Monitoring with Lichens*. – Springer, Dordrecht.
- [18] Protano, C., Owczarek, M., Antonucci, A., Guidotti, M., Vitali, M. (2017): Assessing indoor air quality of school environments: transplanted lichen *Pseudovernia furfuracea* as a new tool for biomonitoring and bioaccumulation. – *Environmental Monitoring Assessment* 189: 358.
- [19] Samsudin, M. W., Azahar, H., Abas, A., Zakaria, Z. (2013a): Determination of heavy metals and polycyclic aromatic hydrocarbon (UKM) contents using Lichen *dirinariapicta* in Universiti Kebangsaan Malaysia. – *Journal of Environmental Protection* 4: 760-765.
- [20] Samsudin, M. W., Daik, R., Abas, A., Meerah, T. S. M., Halim, L. (2013b): Environmental learning workshop: lichen as biological indicator of air quality and impact on secondary student's performance. – *International Education Studies* 6(6): 28-34.
- [21] Shukla, V., Upreti, D. K., Patel, D. K., Yunus, M. (2012): Lichens reveal air PAH fractionation in the Himalaya. – *Environmental Chemistry Letters* 11: 19-23.
- [22] Sipman, H. (2009): Tropical urban lichens: observations from Singapore. – *Blumea* 54: 297-299.
- [23] Sulaiman, N., Mohd Fuzy, S. F. F., Abdul Muis, S. I. N., Sulaiman, N., Ismail, B. S. (2018): Use of lichens as bioindicators for determining atmospheric heavy metals concentration in Malaysia. – *Pakistan Journal of Botany* 50(1): 421-428.
- [24] Zulkifli, S., Kim, Y. S., Abdul Majid, M., Merican, A. F. (2011): Distribution of lichen flora at different altitudes of Gunung Machincang, Langkawi Islands, Malaysia. – *Sains Malaysiana* 40(11): 1201-1208.

BIOLOGICAL REMEDIATION OF AMMONIA IN THE RIVER NILE BY USING EFFICIENT BACILLUS ISOLATES UNDER STATIC CULTURE CONDITIONS

SHALABY, M. E.¹ – EL-KHATEEB, N. M. M.¹ – EL-GREMI, SH.M.¹ – EL-SAYED, I. E.^{2*}

¹*Agricultural Botany Dept., (Agric. Microbiology), Fac. of Agric., Kafrelsheikh Univ. Kafr El-sheikh, Egypt*

²*Water and Wastewater Company, Main laboratory of Sidi Salem city, Kafr El-sheikh, Egypt*

**Corresponding author*
e-mail: Ibrahimelsayedahmed@yahoo.com

(Received 8th Aug 2019; accepted 25th Nov 2019)

Abstract. Applicability of ammonia bioremediation by efficient bacterial isolates was investigated under static batch culture conditions. *Bacillus aerius* (M.1), *Bacillus bingmayongensis* (M.2) and *Bacillus toyonensis* (M.3) were isolated from the Inlet of El-Bahr El-Saedy drinking water treatment plant, Rosetta Branch, Egypt and identified based on their morphological, cultural and biochemical characteristics. Identification of these isolates via genomic 16S rRNA sequencing technique was also performed. To optimize ammonia removing process, effect of some environmental conditions (pH, temperature and ammonia concentrations) were tested. Results indicated that a pH of 6.5 and 7.0, and the temperature between 30 and 35°C were the most optimal values for removing ammonia by the three tested isolates. Ammonia was consumed effectively during the first five incubation days, indicating maximum consumption rate, but it was reduced to its lowest level 25 days after incubation. Ammonia consumption rates were increased by increasing its concentration for all tested isolates, indicating growth activation and no substrate inhibition. Ammonia consumption rate by the ternary mixture reached its maximum of 1.60 mg L⁻¹day⁻¹ five days after incubation, and then reduced slowly to 0.38 mg L⁻¹day⁻¹ 25 days after incubation. It indicated sequential and synergistic effects between the isolates in their ternary mixture during the removal of ammonia.

Keywords: *aquatic system, bacillus isolates, consumption rate, genomic sequences, pollution*

Introduction

Nile River is the main source of fresh water used for drinking, agricultural activities, industry, navigation, recreation and fish production in Egypt. So, it is of dominating influence on the economic, cultural, public health, social and political aspects of the country (Ibrahim et al., 2018). Nile receives enormous amounts of environmental pollutants including fertilizers, fishing activities, pesticides and great amounts of industrial wastes, municipal and domestic materials which drained directly or indirectly into it. Due to their limitation, fresh water resources worldwide required more attention, especially in Egypt, to overcome the harmful effects of such pollutions against all vital activities. Nile pollutants are derived from sources such as industrial wastewater, oil pollution, municipal wastewater and agricultural drainage (Abou-Elela et al., 2017). The pollution status of the water of Nile River is an important indicator of water quality (Ibrahim et al., 2018). In this aspect Abdel-Satar et al. (2017) reported that the problem of Nile pollution will increase in Egypt, if Nile's low water level was done; especially after completing the Ethiopia Dam building.

The cost needed for environmental degradation due to water pollution is relatively high with serious health and quality of life consequences; as well as increasing the severity of water scarcity problems (Zenhom et al., 2017). Hence, increasing water pollution causes not only the deterioration of water quality, but also threatens human health and the balance of

aquatic ecosystems, economic development and social prosperity (Fawzy et al., 2012). Nitrogen is one of the most common element appearing in wastewater as ammonia, nitrite, nitrate and organic nitrogen. Organic nitrogen is decomposed to ammonia which has effects on human health (Nieder et al., 2018). Ammonia is a common pollutant in Nile River where it increases in winter because of the winter block which causes low water levels and the leaching of fertilizer residues used on the agriculture into the aquatic environment (Al-Rashedy et al., 2018). The maximum acceptable concentration of ammonia in the drinking water is equal to 0.5 mg/dm³ according to WHO Guidelines for drinking water and Egyptian standards (WHO, 2006). Bioremediation of ammonia using microorganisms shows great potential for future development due to its environmental compatibility and possible cost-effectiveness (Belal et al., 2017). Microorganisms, such as *Burkholderia cepacia* G4, are effectively used in bioremediation processes due to their natural capacity to oxidize toxic hazardous substances such as phenol and benzoate as a sole source of carbon (Shalaby, 2007). Chemosynthetic autotrophic bacteria, Ammonia Oxidizing Bacteria (AOB) and Nitrite Oxidizing Bacteria (NOB) can convert ammonia to nitrate, and heterotrophic bacteria converts ammonia directly to microbial biomass. Microbes like chemolitho-autotrophic bacteria converts ammonia into nitrite and nitrates. These nitrates are again converted to nitrogen gas by denitrification process (Holmes et al., 2019).

Therefore, this study was carried out to isolate and identify some ammonia-degrading bacterial isolates from the Nile River and to evaluate their substrate consumption rates at different ammonia concentrations from the aquatic samples. As well as, ability of the tested bacterial isolates to remove ammonia at different levels of pH, temperature and ammonia concentrations was also aimed to be described. As well as, removing of ammonia by a ternary mixture of isolates was also evaluated under static batch culture conditions.

Materials and methods

Sampling

Thirty samples were collected in bottles reached their total volume 1000 ml according to APHA (2005) at the end of December 2017 from Inlet of El-Bahr El-Saedy drinking water treatment plant, Rosetta Branch River Nile, Sidi-Salem, Kafr El-Sheikh Governorate, Egypt. Location of the studied area based on GPS information was done (*Table 1*). As well as, overview of the sampling site by GPS was recorded and a photo was taken as shown in *Figure 1*.

Media

For screening, isolation and enrichment of the microbial population, plate count agar media containing 5.0 g tryptone, 2.5 g yeast extracts, 1.0 g glucose, 9.0 g agar and 1.0 L reagent-grade water was used (APHA, 2005). Nutrient agar (NA) media (1 L; pH 6.3-6.8) contained 5.0 g peptone, 3.0 g beef extract and 15.0 g agar was also used for bacterial cultivation and purification after Vincent (1970). The shaking flask culture media namely Minimal Salt Broth (MSB) media containing different ammonia (NH₃) concentrations as a sole source of Nitrogen were used instead of (NH₄)₂SO₄ to determine efficiency of the tested three selected bacterial isolates in removing ammonia. MSB media containing 3.5 g Na₂HPO₄·2H₂O, 1.0 g KH₂PO₄, 0.1 g MgCl₂·6H₂O, 0.05 g Ca (NO₃)₂·4H₂O was added to the tested NH₃ doses (Belal et al., 2017). For biochemical tests, different media were also used. To determine catalase activity, Mannitol Salt Agar media (MSA) containing 75.0 g

NaCl, 10.0 g D-Mannitol, 0.025 g Phenol Red, 15.0 g agar as described by Gerhardt et al. (1981) were used. All media were autoclaved at 121°C for 30 min before use.

Table 1. Sampling site location of the studied drinking water treatment plant by GPS

Treatment Plant (GPS)	X	Y
El-Bahr El-Saedy	281022.66	3463930.43

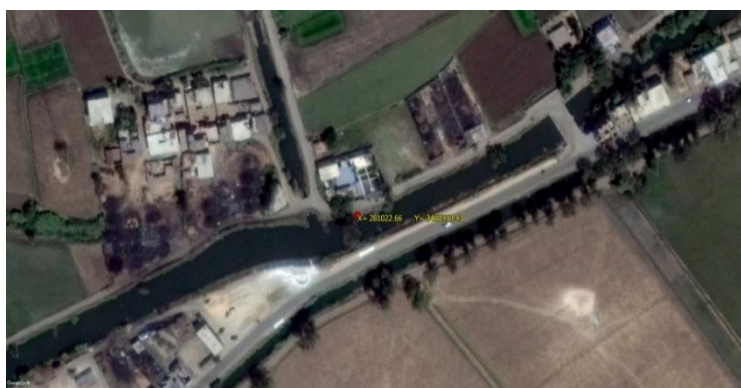


Figure 1. Sampling site location (inlet of El-Bahr El-Saedy drinking water treatment Plant, Rosetta Branch, Nile River)

Isolation of ammonia-degrading bacteria

Screening of the microbial population and isolation of ammonia-degrading bacteria from site El-Bahr El-Saedy drinking water treatment plant by cultivation on plate count agar media at 35±0.5°C for 48 h was done by enrichment technique. Bacterial isolates were purified on nutrient agar media using the standard spatial streaking method. Based on their morphological characteristics, ten isolates were transferred into Minimal salt broth (MSB) media containing 5 mg L⁻¹ ammonia (NH₃) as a sole source of Nitrogen, instead of (NH₄)₂ SO₄ as in the preliminary test. Cultures were incubated at 35±0.5°C for 25 days. To detect their performance in degradation of ammonia, absorbance degree of the cultures was assayed by using spectrophotometer (CECIL of CECIL INSTRUMENTS, CAMBRIDGE, ENGLAND) at 420 nm as described by APHA (2005) and consumption rates were considered. Based on their preliminary test, three bacterial isolates (M.1, M.2 and M.3) were selected to evaluate their efficiency in removing ammonia in MSB media.

Identification

The efficient isolates were identified on the basis of morphological, cultural and biochemical characteristics. Data were optimized with those described based on Bergey's Manual of Systematic Bacteriology (1984) and then confirmed genetically using 16S rRNA by Boye et al. (1999). The molecular techniques were performed by sigma, Cairo, Egypt.

Morphological, cultural and biochemical tests

Samples were examined microscopically to investigate shape of cells, formation of endospores, gram staining reaction and motility. Starch hydrolysis, growth on 5% NaCl and at 40°C were tested as recommended. Catalase activity was determined using a 3%

H₂O₂ solution on MSA slant media as described by Gerhardt et al. (1981). Oxidase test was carried out by observing color change of trypticase soy agar (TSA) medium (containing 15.0 g Pancreatic Digest of Casein, 5.0 g Peptic Digest of Soybean Meal, 5.0 g Sodium Chloride, 15.0 g Agar) from pink to maroon and finally to purple within 30 sec after adding 2-3 drops of 1% of P-aminodimethyl aniline oxalate solution on the cultures (Cappuccino and Sherman, 1996). Urease test was performed on 5 ml of urea broth (20 g L⁻¹) (containing 20 g of urea, 9.5 g of Na₂HPO₄, 9.1 g of KH₂PO₄, 0.1 g of yeast extract) at pH 6.8 in test tubes containing phenol red (0.012 g L⁻¹) as the pH indicator. The cultures were transferred into the sterilized urea broth and incubated for 24 h. The development of red color indicates a positive reaction for the test (Cappuccino and Sherman, 1996). Citrate utilization test was carried out by changing coloration of Simmons citrate agar medium (containing 5.0 NaCl, 2.0 g Sodium Citrate dehydrate, 1.0 g Ammonium Dihydrogen Phosphate) from green to blue due to pH change, which indicated positive reaction, according to Seeley and Vandemark (1981). To test indole production, isolates were inoculated into sterilized glucose tryptone broth (containing 2% (w/v) tryptone, 0.5% (w/v) yeast extract, 10 mM NaCl, 2.5 mM KCl, 10 mM MgCl₂, 10 mM MgSO₄, and 20 mM glucose, pH 7.0.) in test tubes. After 48 h of incubation, 0.3 ml of Kovac's reagent was added (10 gm of p-dimethyl aminobenzaldehyde were dissolved in 150 ml of isoamylalcohol and then slowly 50 ml of concentrated HCL were added) and mixed well. The reddening of the alcohol layer within few minutes indicated indole production (Seeley and Vandemark, 1981).

16S rRNA sequencing tests

To confirm their identification, genomic 16S rRNA sequencing technique was carried out for the selected bacterial isolates. This technique was performed by Sigma, Cairo, Egypt and GATC Company, Germany. Genomic DNA of the tested bacterial antagonists was extracted according to use protocol of GeneJET™ genomic DNA purification Kit (Thermo K0721). The 16S rRNA gene was amplified through the recommended 37 thermal cycling conditions using Maxima Hot Start PCR (Polymerase Chain Reaction) Master Mix (Thermo K1051) according to Eden et al. (1991) were used. PCR reaction set-up (5 µL DNA Template + 1 µl (20 µM) Forward Primer + 1 µl (20 µM) Reverse Primers (of each 8 primers) + 25 µL Maxima® Hot Start PCR Master Mix (2X) + 18 µL Nuclease Free Water) to complete total volume of 25 µL was adjusted. Then, PCR products of 16S rRNA using GeneJET™ PCR Purification Kit (Thermo K0701) were purified. PCR products were then sequenced and analyzed using ABI 3730x1 DNA sequencer via forward and reverse primers (GATC Company, Germany) by combining the traditional Sanger technology with the new 454 technology as follows:

F: 5 — AGA GTT TGA TCC TGG CTC AG — 3

R: 5 — GGT TAC CTT GTT ACG ACT T — 3

Phylogenetic analysis in MEGA6 was conducted (Tamura et al., 2013). For the phylogenetic analysis, maximum parsimony and neighbor-joining trees were constructed from 1000 bootstrap replicates.

Cultivations

As classical batch, cultivations of the selected three bacterial isolates on ammonia as a sole source of Nitrogen were carried out. Prior to the batch experiment, a studied

substrate (ammonia, NH₃) was added to the culture through a sterile Cellulose Nitrate filter membrane of 0.45 μm (Sartorius Stedim, Biotech GmbH, 37070 Gottingen, Germany) by a syringe. All cultivations were carried out in flasks containing MSB media, with replacing NH₃ instead of (NH₄)₂ SO₄. The working volume was 200 ml. Cultures were supplied with 0.0, 5.0, 10.0 and 20.0 mg L⁻¹ ammonia as a sole source of nitrogen for each isolate. All cultivations were carried out in three replicates. Cultures were shaking incubated on 150 rpm at 35±0.5°C (Shaking Incubator, INCUCELL-V-55, Einrichtungen GmbH, D-82166 Gräfelfing, Germany) for 25 days. After that, removing of ammonia was assayed in the incubated cultures by a spectrophotometer at 420 nm as described by APHA (2005) and substrate consumption rates at the tested substrate concentrations, pH, temperature and ammonia concentrations were determined.

Based on a material balance for substrate (ammonia) in the batch cultivation, absolute substrate consumption rate (*Rs*) can be expressed as mg L⁻¹ day⁻¹ according to Shalaby (2007) and the modified equation of Curtis et al. (2018) as follows:

$$rs = \frac{dCs}{dt} \quad (\text{Eq.1})$$

where:

rs - ammonia consumption rate (mg L⁻¹ day⁻¹),

dCs - difference between Initial ammonia and remaining ammonia concentrations (mg L⁻¹),

dt - difference between end and start incubation time (day).

Effect of pH, temperature and ammonia concentrations on the biodegradation of ammonia

To determine the effect of temperature, pH and ammonia concentrations on the biodegradation of ammonia, a volume of 200 ml MSB media containing 5.0 mg L⁻¹ ammonia and inoculating with 1.0 ml bacterial cell suspension 10⁵ CFU ml⁻¹. To determine the optimum pH, experiments were carried out at pH 5.5, 6.5, 7.0, 7.5 and 8.0. Cultures were incubated on a rotary shaker at 35±0.5°C and 150 rpm up to 25 days. To determine the effect of temperature, MSB media with pH 7.0 was incubated at 20, 25, 30, 32 and 35°C under 150 rpm for 25 days. To determine the effect of ammonia concentration, MSB media replaced their nitrogen source with 0.0, 5.0, 10.0 and 20.0 mg L⁻¹ ammonia adjusted their pH at 7.0 and incubated at 35±0.5°C under 150 rpm for 25 days. Bioremediation of ammonia based on the absorbance measured by a spectrophotometer was determined and substrate consumption rate was calculated according to Shalaby (2007) and Curtis et al. (2018).

Bioremediation of ammonia by mixtures of the tested bacterial isolates

To test interaction behavior between them, antagonism test of the three bacterial isolates were inoculated in dual and in ternary bacterial mixtures in the same media as preliminary experiment. Nutrient agar (NA) media were liquefied, allowed to cool to about 45°C, homogenized and inoculated with the initial test organism. These were then poured into sterile petri dishes and allowed to cool at room temperature before streaking with the second bacteria in the dual mixture or with the second and third bacteria in the

ternary mixture. Observations and cultural relations were recorded 48 h after incubation of the plates at 37°C as described by Herbert et al. (2009).

Based on the observations of the antagonism test between the three isolates, applicability of the ternary bacterial mixtures in removal or degradation of ammonia was tested. To achieve the purpose mentioned, 1.0 ml bacterial cell suspension containing 10^5 CFU ml⁻¹ of each isolate was cultivated immediately with 200 ml raw water from El-Bahr El-Saedy drinking water treatment plant in shake flasks containing 10.0 mg L⁻¹ of ammonia. The cultures were shaking incubated under 150 rpm at 35±0.5°C for 5.0, 10.0, 15.0, 20.0 and 25 days. Un-inoculated shake flasks were acted as control. The experiment was carried out in three replicates. Bioremediation of ammonia by the bacterial mixture was determined after the incubation period based on the absorbance measured by a spectrophotometer and substrate consumption rate was calculated according to the well-known formula of Shalaby (2007) and the modified equation of Curtis et al. (2018) previously used.

Statistical analysis

The statistical results were calculated by one-way analysis using the SPSS statistical software. A *P*-value < 0.05 indicated statistical significance. The means were compared according to Duncan's multiple range test (Snedecor and Cochran, 1980).

Results and discussion

Isolation of the ammonia-removing isolates

From the microbial source (El-Bahr El-Saedy drinking water treatment plant) a total of 10 morphologically different ammonia-degrading bacterial isolates were obtained. Based on their efficiencies, three bacterial isolates designated as (M.1), (M.2) and (M.3) achieved higher ammonia consumption rates and were selected for further tests comparing with the other isolates, and the differences between treatment were significant at *P* < 0.05 (Table 2).

Identification of the ammonia-removing isolates

Based on their cultural, morphological and biochemical properties, M.1, M.2 and M.3 isolates were identified as *Bacillus aerius*, *Bacillus bingmayongensis* and *Bacillus toyonensis* (Table 3). They were rods in shape, white color colonies, gram-positive, motile, had positive ability to form endospores and grew on 5% NaCl. It was found also that all tested bacteria gave positive of oxidase, citrate utilization, catalase activity and starch hydrolysis. On the contrary, negative reactions of both urease and indole production were obtained.

Identification of such isolates was confirmed by using molecular genomic technique (Boye et al., 1999). According to the 16S rRNA analysis, the phylogenetic tree of the ammonia degrading *Bacillus* isolate (M.1) was done. It can be clearly seen that the M.1 *Bacillus* isolate was closely related to the species *aerius*. It showed the highest sequence similarities with *Bacillus aerius* strain 24K (76%) (Figure 2).

Although *Falsibacillus pallidus* strain has ident (77%), the identification confirms that the tested isolate belongs to *Bacillus aerius* (76%) based on total score of it (315) in comparison with total score of *Falsibacillus pallidus* (280). As well as, the second isolate (M.2) was found to be included in the genus *Bacillus* and closely related to the

species *bingmayogensis*. It showed the highest sequence similarities with *Bacillus bingmayongensis* strain FJAT-13831 (89%) (Figure 3). Although all strains have the same ident (89%), the identification confirms that the tested isolate belongs to *Bacillus bingmayongensis* based on total score of it (547) which is higher total score than that of other strains.

Table 2. Ammonia consumption rates of 10 bacterial isolates cultivated in MSB media under batch conditions

Isolate	Ammonia consumption rate (mg L ⁻¹ day ⁻¹)
M.1	0.206 a
M.2	0.197 c
M.3	0.202 b
M.4	0.012 i
M.5	0.070 d
M.6	0.020 fg
M.7	0.015 hi
M.8	0.035 e
M.9	0.017 gh
M.10	0.022 f

Ammonia consumption rate followed by different letters within a column are significantly different at ($P < 0.05$), Duncan's multiple range test

Table 3. Morphological, cultural and some biochemical characteristics of the three bacterial isolates coded as M.1, M.2 and M.3

Characteristics	M.1	M.2	M.3
Shape of cell	Rods	Rods	Rods
Formation of endospore	+	+	+
Motility	+	+	+
Gram reaction	+	+	+
Growth on 5 % NaCl	+	+	+
Growth at 40 °C	-	+	+
Starch hydrolysis	+	+	+
Catalase reaction	+	+	+
Oxidase test	+	+	+
Urease test	-	-	-
Citrate utilization	+	+	+
Indole production	-	-	-

+ Positive; - Negative

For the third isolate (M.3), it was found that it also belonged to genus *Bacillus* and was closely related to the species *toyonensis*. It showed the highest sequence similarities with *Bacillus toyonensis* strain BCT-7112 (99%) (Figure 4). Although all strains have the same ident (99%), the identification confirms that the tested isolate belongs to *Bacillus toyonensis* based on total score of it (1437) which is a higher total score than in other strains.

As well as, results recorded in Figure 5 showed that 1500 bp DNA fragment was obtained by PCR amplification of the 16S rRNA gene of the three tested *Bacillus* isolates.

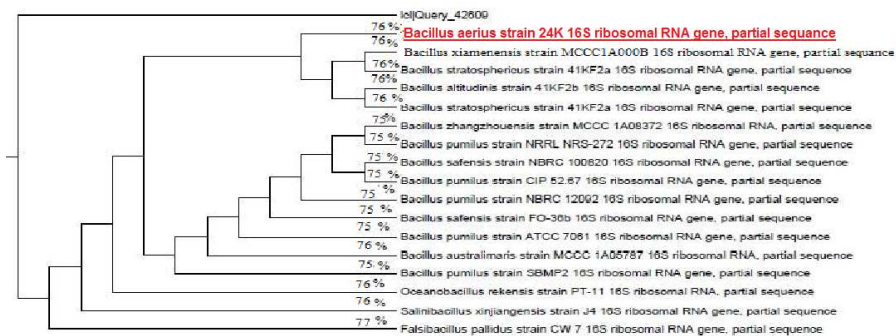


Figure 2. The phylogenetic tree of the ammonia-degrading bacterium isolate M.1 was identified as *Bacillus aerius*

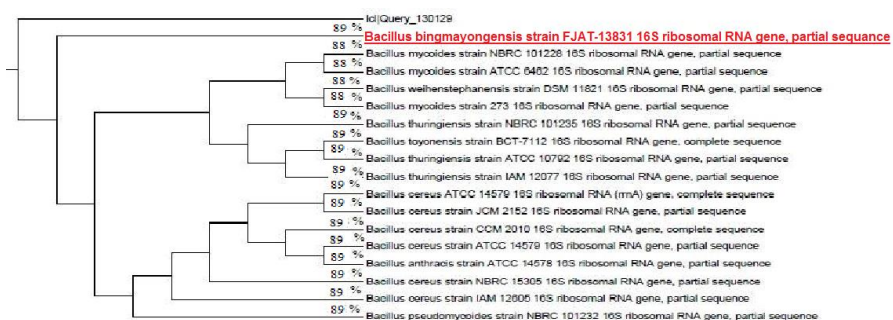


Figure 3. The phylogenetic tree of the ammonia-degrading bacterium isolate M.2 was identified as *Bacillus bingmayongensis* (M.2)

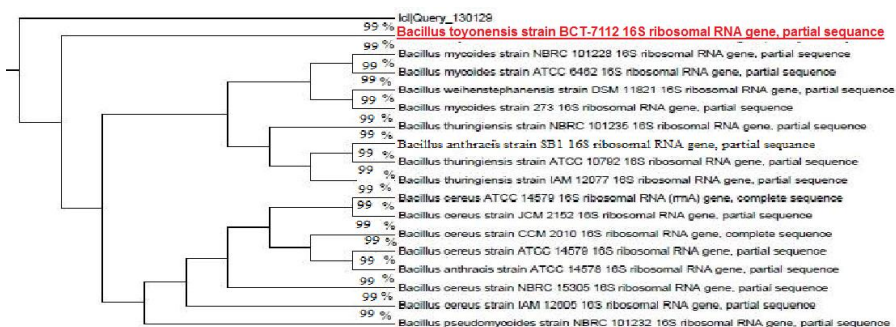


Figure 4. The phylogenetic tree of the ammonia-degrading bacterium isolate M.3 was identified as *Bacillus toyonensis* (M.3)

Isolation of such ammonia-degrading *Bacillus* isolates from the studied aquatic inlet site on Rosetta branch, River Nile indicated high capacity and variation of the microbial populations. It was in full agreement with Belal et al. (2017), who isolated *Ralstonia pickettii* (ST.1) and *Chryseobacterium gambrini* (ST.2) from River Nile during increasing ammonia concentration and identified it morphologically using enrichment technique then molecularly using 16S rDNA gene. While Kundu et al. (2014) pointed that *Chryseobacterium gambrini* is capable of simultaneous removal of organic carbon and nitrogen from wastewater.

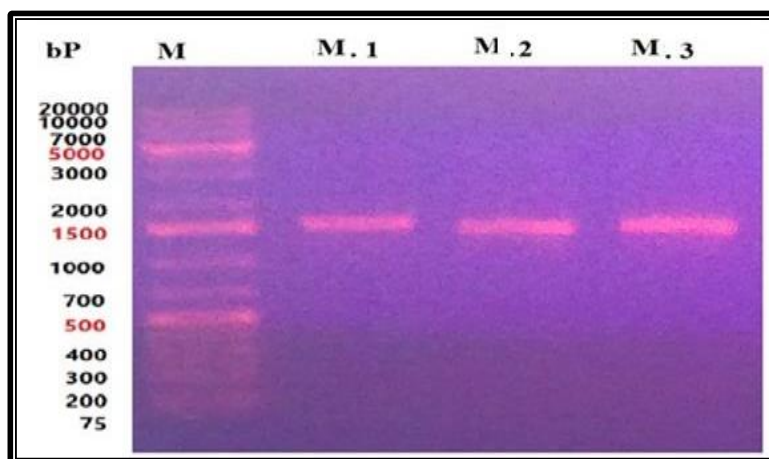


Figure 5. Agarose gel electrophoresis showing 16S rRNA sequencing patterns of the three tested *Bacillus* isolates. M: marker, M.1: *Bacillus aeri*us, M.2: *bingmayongensis* and M.3: *Bacillus toyonensis*

Effect of pH and temperature on the biodegradation of ammonia

Effect of pH

Influence of pH on ammonia consumption rate in cultures inoculated separately with *B. aeri*us (M.1), *B. bingmayongensis* (M.2) and *B. toyonensis* (M.3) each was obtained and presented in Table 4. Results indicated that pH values of 6.5 and 7.0 were the most suitable range for removing ammonia by the three tested isolates. On the other hand, no consumption of ammonia in the control cultures free from any biomass was noticed, indicating no chemical degradation. For *B. aeri*us (M.1) and *B. toyonensis* (M.3), the highest consumption rates of 0.160 and 0.157 mg L⁻¹ day⁻¹ at pH 6.5 was achieved. In the case of *B. aeri*us (M.1), the differences between treatment are significant at $P < 0.05$, as well as in the case of *B. toyonensis* (M.3) at pH values 6.5, 7.5 and 8, the differences between treatments are significant at $P < 0.05$, but at pH values 5.5 and 7, the differences between treatments are not significant.

Table 4. Effect of different pH values on ammonia consumption rates by *B. aeri*us (M.1), *B. bingmayongensis* (M.2) and *B. toyonensis* (M.3) under batch culture conditions

pH	Ammonia consumption rate (mg L ⁻¹ day ⁻¹)			
	Control	<i>B. aeri</i> us (M.1)	<i>B. bingmayongensis</i> (M.2)	<i>B. toyonensis</i> (M.3)
5.5	00.0	0.143 b	0.114 e	0.138 b
6.5	00.0	0.160 a	0.136 b	0.157 a
7.0	00.0	0.130 c	0.158 a	0.140 b
7.5	00.0	0.120 d	0.130 c	0.110 c
8.0	00.0	0.118 e	0.124 d	0.100 d

It was in full agreement with Shafi et al. (2017), who suggested that the pH value has a critical role in the production of secondary metabolites and that its maintenance at medium levels is optimal for neutrophils such as *B. aeri*us and confirmed that activity achieved at range pH 4-10 and the highest activity for bioremediation was observed at

pH 6.5. As well as, Tallur et al. (2016) confirmed that *B. toyonensis* (PNTB1) can grow at pH ranged between 5.5 – 10.0 and its optimal value at pH 7.1 was obtained. While, the highest consumption rate due to use of *B. bingmayongensis* (M.2) was achieved at pH 7.0, and the differences between treatments are significant at $P < 0.05$. Such result was given by Liu et al. (2014). They reported that *B. bingmayongensis* can grow at pH ranged between 4.0 – 10.0 and its optimal value was recorded at pH 7.0.

Effect of temperature

Influence of temperature degrees on ammonia consumption rate in cultures inoculated separately with *B. aerius* (M.1), *B. bingmayongensis* (M.2) and *B. toyonensis* (M.3) each was obtained and presented in Table 5. Data illustrated that temperature degrees of 30, 32 and 35°C were the most optimal for removing ammonia by the three tested isolates. On the other hand, no consumption of ammonia in the control cultures was noticed, indicating no chemical degradation. In the case of *B. aerius* (M.1), the optimal temperature degree recorded for ammonia bioremediation was 32°C, at which ammonia consumption rate to its maximum of 0.168 mg L⁻¹day⁻¹ was reached, and the differences between treatments are significant at $P < 0.05$. This result was in full agreement with Shafi et al. (2017), who confirmed that *B. aerius* can grow at temperature ranging between 8.0 and 40.0°C and the optimal was reached at 32°C under the experimental conditions. For *B. bingmayongensis* (M.2), the corresponding optimal temperature degree at 30°C was done and ammonia consumption rate of 0.164 mg L⁻¹day⁻¹ were given, but the differences between treatments are not significant.

Table 5. Effect of different temperature degrees on ammonia consumption rates by *B. aerius* (M.1), *B. bingmayongensis* (M.2) and *B. toyonensis* (M.3) under batch culture conditions

Temp. (°C)	Ammonia consumption rate (mg L ⁻¹ day ⁻¹)			
	Control	<i>B. aerius</i> (M.1)	<i>B. bingmayongensis</i> (M.2)	<i>B. toyonensis</i> (M.3)
20	00.0	0.116 e	0.132	0.124 e
25	00.0	0.130 d	0.148	0.138 d
30	00.0	0.158 b	0.164	0.150 c
32	00.0	0.168 a	0.140	0.156 b
35	00.0	0.156 c	0.130	0.168 a

Temp. (°C): Temperature

Liu et al. (2014) agreed with these results and stated that *B. bingmayongensis* can be grown very well at range varied between 15.0 and 45.0°C and 30.0°C was the optimum. On the other hand, *B. toyonensis* (M.3) was the most thermo-tolerant isolate in comparison with the others; by its ammonia consumption rate reached to its maximum of 0.164 mg L⁻¹day⁻¹ at 35.0°C, and the differences between treatments are significant at $P < 0.05$. These results agreed by Tallur et al. (2016), who confirmed that *B. toyonensis* (PNTB1) has a great ability to grow at temperature range between 10.0 and 45.0°C and its optimum degree is 37.0°C.

Effect of ammonia concentrations

To investigate the effect of high ammonia concentrations accumulated in the aquatic system on the microbial activity and their ability to remove the excess of its doses,

relationship between ammonia concentrations and its consumption rates by the tested isolates were recorded in *Table 6*. Results illustrated increase in ammonia consumption rates by increasing its concentration in the cultivation media due to the tested bacterial isolates, indicating growth activation and no substrate limitation. It seems to note that substrate consumption rates at both 5.0 and 10.0 mg L⁻¹ ammonia were found to be identical and located at similar line for all isolates. At 20.0 mg L⁻¹, efficiencies of the three isolates in removing ammonia varied. The greatest ability to overcome and remove the excess of ammonia concentrations (20.0 mg L⁻¹) was obtained by the superior isolate *B. toyonensis* (M.3), by which its consumption rate to its maximum of 0.684 mg L⁻¹day⁻¹ was reached. It was followed by *B. bingmayongensis* (M.2) and *B. aerius* (M.1), by which consumption rates of ammonia to 0.635 and 0.595 mg L⁻¹day⁻¹ at the highest dose were obtained, respectively. On the other hand, no ammonia was consumed in control cultures, indicating no chemical degradation, and the differences between treatments are significant at $P < 0.05$. These results were in agreement with Leejeerajumnean et al. (2000), who found that bacteria particularly sensitive to ammonia (inhibited by 25 mmol l⁻¹) or specially tolerant to ammonia (growth in the presence of 300 mmol l⁻¹) included both Gram-positive and Gram-negative strains and there was no evidence for sensitivity or tolerance being associated with any specific bacterial genera.

Table 6. Effect of different ammonia concentrations on its consumption rates by *B. aerius* (M.1), *B. bingmayongensis* (M.2) and *B. toyonensis* (M.3) under batch culture conditions

Ammonia concentration (mg L ⁻¹)	Ammonia consumption rate (mg L ⁻¹ day ⁻¹)			
	Control	<i>B. aerius</i> (M.1)	<i>B. bingmayongensis</i> (M.2)	<i>B. toyonensis</i> (M.3)
0.0	0.0	0.000 d	0.000 d	0.000 d
5.0	0.0	0.206 c	0.197 c	0.202 c
10.0	0.0	0.364 b	0.351 b	0.359 b
20.0	0.0	0.595 a	0.635 a	0.684 a

Bioremediation of ammonia by mixtures of the tested bacterial isolates

One of the major problems of the biological degradation of environmental pollutants in an aquatic environment is the co-existence of substrate compounds or/and microbial mixtures. In the aquatic ecosystems, the microorganisms grow under complex conditions. Therefore, occurrence of the microbes in mixtures is an important problem, because removal or degradation of one component by a microbe can be prevented or inhibited by the other microbe in the mixture, and different conditions may be required.

Accordingly, and based on their cultural observations, growth and microbial relations, results showed no antagonistic reaction between isolates *B. aerius* (M.1), *B. bingmayongensis* (M.2) and *B. toyonensis* (M.3) in both dual and ternary culture mixtures. Microbes of the tested cultural mixtures were in their normal states without any disorders, disruption or competition between each other. Microbe may compete with another microbe for place or nutrients. Competitions often led to inhibit growth of the other microbe(s) in the same media via production of toxic metabolites, indicating antagonistic effect (Talaro et al., 2002).

Based on the results of antagonism test, efficiency of the ternary bacterial mixture composed of *B. aerius* (M.1), *B. bingmayongensis* (M.2) and *B. toyonensis* (M.3) in

removal or degradation of 10.0 mg L⁻¹ ammonia in MSB media free from any other nitrogen source at 35±0.5°C for different incubation periods was evaluated (Figure 6).

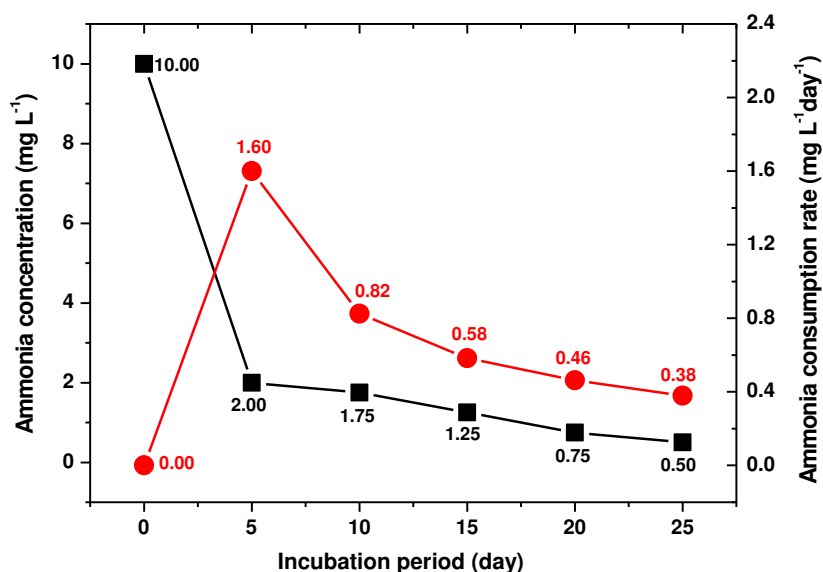


Figure 6. Remaining ammonia concentrations and their consumption rates by ternary bacterial mixtures composed of *B. aerius* (M.1), *B. bingmayongensis* (M.2) and *B. toyonensis* (M.3) at 35±0.5°C for different incubation periods. Curve with different letters are significantly different at 0.05 level based on Duncan's multiple range test

Results showed sharp reduction of ammonia concentration by the ternary bacterial mixture five days after incubation from 10.0 to 2.0 mg L⁻¹, and consumption rate to its maximum of 1.60 mg L⁻¹day⁻¹ was reached, and then reduced slowly. After 25 incubation days, only 0.50 mg L⁻¹ of ammonia were remained and its consumption to its minimal rate of 0.38 mg L⁻¹day⁻¹ was given, and the differences between treatments were significant at $P < 0.05$. These results were in agreement with the findings of Hemida et al. (2018), who reported that the co-inoculation of the two selected endophytic bacteria strains *B. aerius* (M.1) and *B. toyonensis* could successfully enhance salt tolerance and nitrogen fixation, ammonia utilization, inorganic phosphate solubilization. To investigate ammonia utilization pattern by the ternary mixture (simultaneous or sequential), its consumption rates by the individual isolates were compared with those obtained by the ternary mixture. In the presence of 10 mg L⁻¹ ammonia, its consumption rate reached to 0.46 mg L⁻¹ day⁻¹ by the ternary mixture 20.0 days after incubation, compared with 0.36, 0.35 and 0.36 mg L⁻¹ day⁻¹ by single isolates of *B. aerius* (M.1), *B. bingmayongensis* (M.2) and *B. toyonensis* (M.3), respectively. It means increasing efficiency of the ternary mixture in removing ammonia compared with the individual treatment. So, ammonia utilization pattern by the ternary bacterial mixture was sequential, indicating activation not antagonism between isolates in the ternary mixture.

Conclusion

From the obtained results it can be concluded that the cultivation of a ternary tested bacterial mixture of ammonia can be expressed by substrate consumption rates obtained

from the individually cultivations. In general, it can be stated that the removal of different ammonia concentrations from the aquatic systems was successfully done via both individual and ternary mixture composed of *B. aerius* (M.1), *B. bingmayongensis* (M.2) and *B. toyonensis* (M.3) under static batch cultivation.

We must keep River Nile as a sole source of drinking water in Egypt healthy. Complete optimization of such tested bacterial isolates used successfully for removing pollutants of aquatic systems, especially at a temperature range more than 35°C and high concentrations of ammonia more than 20 mg L⁻¹ is necessary in the future.

Acknowledgments. The author highly acknowledges, Agriculture Botany Department, Fac. of Agric., Kafr El-sheikh Univ., Kafr El-Sheikh, Egypt; water and wastewater Company, Main laboratory of Sidi Salem city, Kafr El-sheikh, Egypt.

REFERENCES

- [1] Abdel-Satar, A. M., Ali, M. H., Goher, M. E. (2017): Indices of water quality and metal pollution of Nile River, Egypt. – The Egyptian Journal of Aquatic Research 43(1): 21-29.
- [2] Abou-Elela, S. I. (2017): Constructed Wetlands: The Green Technology for Municipal Wastewater Treatment and Reuse in Agriculture. – Unconventional water Resources and agriculture in Egypt: 1-51.
- [3] Al-Rashedy, A. H., Youssef, R. A., Farfour, S. A., Mousa, I. E. (2018): Seasonal Variation Of Water Resources And Its Suitability For Drinking Water Production. – The 9th Int. Conf. for Develop. and the Env. in the Arab world: 15-17.
- [4] APHA. (2005): Standard methods for the examination of water and waste water, 21st ed. – American Public Health Association, Washington, D.C.
- [5] Belal, E. B., Shalaby, M. E., El-Khateeb, N. M., Maksoud, Y. M. A., Gad, M. A. (2017): Bioremediation of ammonia in river Nile by *Ralstonia pickettii* and *Chryseobacterium gambrini*. – Research Journal of Pharmaceutical, Biological and Chemical Sciences (RJPBCS) 8(3): 497-505.
- [6] Bergey, D. H., Holt, J. G., Krieg, N. R., Sneath, P. H. A., Mair, N. S., Sharpe, M. E., Williams, S. T. (1984): Bergey's manual of systematic bacteriology. – Williams and Wilkins, Baltimore, USA.
- [7] Boye, K., Høgdall, E., Borre, M. (1999): Identification of bacteria using two degenerate 16S rDNA sequencing primers. – Microbiological research 154(1): 23-26.
- [8] Cappuccino, J. G., Sherman, N. (1996): In Microbiology: A Laboratory Manual. – The Benjamin/Cummings Publishing Company Inc. (4th Edition), Menlo Park, California, USA.
- [9] Curtis, B., Giorgi, S., Buffone, A. E., Ungar, L. H., Ashford, R. D., Hemmons, J., Schwartz, H. A. (2018): Can Twitter be used to predict county excessive alcohol consumption rates? – PLoS One 13(4): e0194290.
- [10] Eden, P. A., Schmidt, T. M., Blakemore, R. P., Pace, N. R. (1991): Phylogenetic analysis of *Aquaspirillum magnetotacticum* using polymerase chain reaction-amplified 16S rRNA-specific DNA. – International Journal of Systematic and Evolutionary Microbiology 41(2): 324-325.
- [11] Fawzy, M. A., Badr, N. E. S., El-Khatib, A., Abo-El-Kassem, A. (2012): Heavy metal biomonitoring and phytoremediation potentialities of aquatic macrophytes in River Nile. – Environmental monitoring and assessment 184(3): 1753-1771.
- [12] Gerhardt, P., Murray, R. G. E., Costilow, R. N., Nester, E. W., Wood, W. A., Krieg, N. R., Phillips, G. B. (1981): Manual of methods for general bacteriology. – Washington, D.C., American Society for Microbiology.

- [13] Hemida, K. A., Reyad, A. M. (2018): Improvement salt tolerance of safflower plants by endophytic bacteria. – J Horticult Plant Res 5: 38-56.
- [14] Herbert, J., Santos, D., Jefty, J. R., Garcera, A., Zuniega, R. R. (2009): Synergistic and Antagonistic Relationships of *Escherichia coli*, *Bacillus cereus*, *Bacillus subtilis*, *Staphylococcus aureus* and *Penicillium notatum*, BIO120. – General Microbiology (Laboratory).
- [15] Holmes, D. E., Dang, Y., Smith, J. A. (2019): Nitrogen cycling during wastewater treatment. – Advances in applied microbiology 106: 113.
- [16] Ibrahim, M., Al-Zyoud, S., Elhaddad, E. (2018): Surface Water Quality Monitoring for River Nile, Egypt Using GIS-Techniques. – Open Journal of Geology 8(02): 161.
- [17] Kundu, P., Pramanik, A., Dasgupta, A., Mukherjee, S., Mukherjee, J. (2014): Simultaneous heterotrophic nitrification and aerobic denitrification by *Chryseobacterium* sp. R31 isolated from abattoir wastewater. – BioMed research international: 1-12.
- [18] Leejeerajumnean, A., Ames, J. M., Owens, J. D. (2000): Effect of ammonia on the growth of *Bacillus* species and some other bacteria. – Letters in applied microbiology 30(5): 385-389.
- [19] Liu, B., Liu, G. H., Hu, G. P., Cetin, S., Lin, N. Q., Tang, J. Y., Lin, Y. Z. (2014): *Bacillus bingmayongensis* sp. nov., isolated from the pit soil of Emperor Qin's Terracotta warriors in China. – Antonie Van Leeuwenhoek 105(3): 501-510.
- [20] Nieder, R., Dinesh, K. B., Franz, X. R. (2018): Reactive Water-Soluble Forms of Nitrogen and Phosphorus and Their Impacts on Environment and Human Health. – Soil Components and Human Health. Springer, Dordrecht: 223-255.
- [21] Seeley, H. W., Van Demark, P. J. (1981): Microbes in Action. – Laboratory Manual of Microbiology, 3rd Ed, WH Freeman and Company USA.6.
- [22] Shafi, J., Mingshan, J., Zhiqiu, Q., Xiuwei, L., Zumin, G., Xinghai, L., Kai, W. (2017): Optimization of *Bacillus aerius* strain JS-786 cell dry mass and its antifungal activity against *Botrytis cinerea* using response surface methodology. – Archives of Biological Sciences 69(3): 469-480.
- [23] Shalaby, M. E. (2007): Kinetics of phenol and benzoate biodegradation in static cultivation system by *Burkholderia cepacia* G4. J. – Agric. Sci. Mansoura Univ. 32(4): 3007-3019.
- [24] Snedecor, G. W., Cochran, W. G. (1980): Statistical methods. 7th Ed. – Iowa State Univ. press, Ames, Iowa.
- [25] Talaro, K. P., Talaro, A. (2002): Foundations in Microbiology 4th Edition. – Mc Graw Hill Publishing, USA.
- [26] Tallur, P. N., Sajjan, D. B., Mulla, S. I., Talwar, M. P., Pragasam, A., Nayak, V. M., Bhat, S. S. (2016): Characterization of antibiotic resistant and enzyme producing bacterial strains isolated from the Arabian Sea. – 3 Biotech 6(1): 28.
- [27] Tamura, K., Stecher, G., Peterson, D., Filipinski, A., Kumar, S. (2013): MEGA6: molecular evolutionary genetics analysis version 6.0. – Molecular biology and evolution 30(12): 2725-2729.
- [28] Vincent, J. M. (1970): A manual for the practical study of root-nodule bacteria. – IBP handbook, Blackwell Scientific Publications, Oxford and Edinburgh 15: 54-58.
- [29] WHO. (2006): Guidelines for the Safe Use of Wastewater, Excreta and Greywater: Policy and regulatory aspects. – World Health Organization.
- [30] Zenhom, S. E., Elsaiedy, G., El-Nahrawy, A. (2017): Assessment of the Groundwater Quality for Drinking and Irrigation Purposes in the Central Nile Delta Region, Egypt. – Groundwater in the Nile Delta: 1-38.

PREDICTION OF ECOLOGICAL IMPORTANCE OF *CARABIDAE* BIOTOPES USING COMMUNITY INDEX OF THE GROUND BEETLES (IKS) IN THE SOUTHERN PART OF CENTRAL SLOVAKIA

LANGRAF, V.^{1*} – PETROVIČOVÁ, K.² – DAVID, S.³ – SVORADOVÁ, A.⁴ – SCHLARMANNOVÁ, J.⁵

¹*Ludovita Okánika 14, 949 01 Nitra, Slovak Republic*

²*Department of Environment and Zoology, Faculty of Agrobiological and Food Resources Slovak University of Agriculture in Nitra, Tr. A. Hlinku 2, 949 76 Nitra, Slovak Republic*

³*Department of Ecology and Environmental Sciences, Faculty of Natural Sciences, Constantine the Philosopher University in Nitra, Tr. A. Hlinku 1, Nitra, Slovak Republic*

⁴*Research Institute for Animal Production in Nitra, National Agricultural and Food Centre Hlohovecká 2, 951 41 Lužianky, Slovak Republic*

⁵*Department of Zoology and Anthropology, Faculty of Natural Sciences, Constantine the Philosopher University in Nitra, Tr. A. Hlinku 1, Nitra, Slovak Republic*

*Corresponding author

e-mail: langrafvladimir@gmail.com

(Received 13th Aug 2019; accepted 25th Nov 2019)

Abstract. Using the community index of the ground beetles (IKS) the quality status of 4 habitat types in 6 localities of, Stolické vrchy and Juhoslovenská kotlina basin (The Southern Part Of Central Slovakia) were evaluated. In the 2015-2017 period we noticed 2,379 individuals (1,030 ♂, 1,349 ♀) belonging to 52 species. Friedman's test showed a significant difference in IKS values in years 2015-2017 between study areas. By calculating IKS we found a greater number of adaptable species in areas with lower habitat disturbance (quality class III) compared to higher disturbance (quality class I), where eurytopic species predominated. We predicted an increase in IKS values for 2020 and 2022 for the habitats including meadow (area 1), nitrophilous waterside vegetation (areas 2, 6) and a decrease for pasture habitat (area 3), nitrophilous waterside vegetation (area 4) and fallow field (area 5) using the regression polynomial and exponential distribution models.

Keywords: *Carabidae*, *Stolické vrchy*, *Juhoslovenská kotlina*, *assessment of habitats quality*, *bioindication classes (A,E,R)*

Introduction

For the bioindication and monitoring changes in the quality of the environment, the *Carabidae* family (Coleoptera) is the most commonly used (Nietupski et al., 2015; Burgio et al., 2015). *Carabidae* inhabit different habitat types, especially meadow, field and forest habitats (Heydemán, 1955; Hürka, 1996). Most species have a narrow ecological valence and therefore respond sensitively to changes in habitat conditions (pH, soil moisture changes) as well as the presence of toxic substances including herbicides and insecticides. Changes in the species structure of the short-lived communities reflect various long-term environmental changes. Bioindicative use is based on assessing the impact of human economic activities (Cardamo and Spence, 1994; Porhajašová et al., 2008, 2009).

We have already conducted similar faunistic research, the results of which can be found in the following references: Langraf et al., 2016b, 2018a. We processed data of 54 species (N = 4,675 individuals) serving as an input dataset for the calculation of indexes for ellipsoid biovolume (EV), flight ability and community index of the ground beetles (IKS). Pilot results (Langraf et al., 2016a) confirm a negative anthropogenic impact on the forest ecosystem, which means the worsening of living conditions for adaptable and relict species. We found out the prevalence of eurytopic species (IKS - bioindication group E) in intensively influenced forest and meadow habitats of the Juhoslovenská kotlina basin. Langraf et al. (2017, 2018b) assessed the ellipsoid biovolume (EV) and flight ability indices on 5 habitat types (forest, fallow field, meadow, pasture, nitrophilic waterside vegetation). The results confirm a decrease in EV index values and an increase in the number of flight ability (eurytopic) species on habitats with higher anthropogenic disturbance. On the contrary, with decreasing anthropic intervention, the value of the EV index and thus the number of apteric and brachypterous species increases. In the last study (Langraf et al., 2019) we evaluated all 3 bioindication methods in forest ecosystems. We confirmed the correlation of the decrease of IKS, EV index values and increase of eurytopic species due to anthropogenic disturbance of forest ecosystems by cutting.

Monitoring of gradual successive changes and the impact of management on agricultural land is also important for bioindicative evaluation. Compared to natural ecosystems, biodiversity is reduced in agricultural areas. Typical *Carabidae* bound to arable land reported Vician et al. (2010, 2011) as follows: *Amara aenea*, *Anchomenus dorsalis*, *Calathus fuscipes*, *Clivina fossor*, *Harpalus affinis*, *H. distinguendus* and *Pseudoophonus rufipes*. Šťastná and Bezděk (2004), Purchart and Kula (2005), Baranová et al. (2013), Lemic et al. (2017) recorded the predominance of eurytopic species over adaptable (terminology used in IKS assessment) in the agricultural areas of the family *Carabidae* as a consequence of habitat disturbance. The species represented by a high number of individuals were: *Anchomenus dorsalis*, *Poecilus cupreus*, *Pseudoophonus rufipes* and *Pterostichus melanarius*. Igondová and Majzlan (2015) confirmed the lowest IKS values at the field-meadow edge and the meadow playground. The highest IKS values were recorded in forest areas and peatbogs. The prevalence of eurytopic species over adaptable to Permanent grassland has been reported by Jaďud'ová et al. (2016). Stluka (2013) investigated the *Carabidae* on three habitats: spruce forest, spruce nursery and glade.

The IKS index in the glade found a strong anthropogenic impact with a predominance of group E (see chapter Methodology) and the lowest in the spruce forest with a predominance of group A species. It is clear that the intensity of management influences the biodiversity of the forest ecosystem. Rajová (2007) found in 10 localities of Klánovice forest in 2000 and 2001 a higher proportion of adaptable species compared to eurytopic, but significant decrease of stenotopic (relict) species. This fact points to anthropogenic influence of forest and worsening of living conditions of stenotopic (relict) species. The lowest value of IKS was recorded by the author at 2 marginal forest localities the remaining forest areas had higher IKS values.

The destruction of the microorganism environment due to forest cutting leads to the loss of specific forest species of *Carabidae* and their replacement by eurytopic species, which are typically found in open habitats, ruderal habitats and fields (Elek et al., 2001; Finch, 2005; Wiezik et al., 2007). According to Niemelä et al. (2002), urbanization

causes a decrease in the biodiversity of *Carabidae* species and in most cases increases the number of small species belonging to bioindication group E towards the city center.

In this study we continue with the bioindicative evaluation of the *Carabidae* obtained during the years 2015-2017 in Stolické vrchy and Juhoslovenská kotlina basin for prediction models.

The aim of the paper is to set habitat quality using IKS on 6 study areas representing 4 habitat types with different intensity of anthropogenic activity (habitat management). We evaluated the working hypotheses: (1) IKS value decreases in the direction from anthropically less disturbed habitats to anthropically more disturbed; (2) in unstable habitats disturbed by anthropic activity, there is a predominance of species from bioindication group E; (3) in more stable habitats less disturbed by anthropic activity, the predominance of species from bioindication group A is predominant.

Material and methods

Ground beetles were collected from April to October 2015-2017 in 6 localities (Fig. 1) representing 4 types of biotopes, classified according to Ružičková et al. (1996). The following crops were grown in the contact area of sites 4, 5 and 6: wheat, barley, sunflower, maize and rape. We used pitfall traps (750 ml), yellow pan trap (1,500 ml) (Novák et al., 1969) which were arranged at each biotope in a trap line, and each trap line consisted of five pitfall traps (at 10 m intervals). The material was collected in eat regular three-week intervals. As a killing agent, 4% saline solution was used.



Figure 1. Study localities (1 – 6) (photos: Langraf, 2015)

Study area

The study localities are located in the geomorphological units Stolické vrchy and Juhoslovenská kotlina basin (The Southern Part Of Central Slovakia) (Fig. 2). Location data and habitat characteristics of the areas are shown in Table 1.

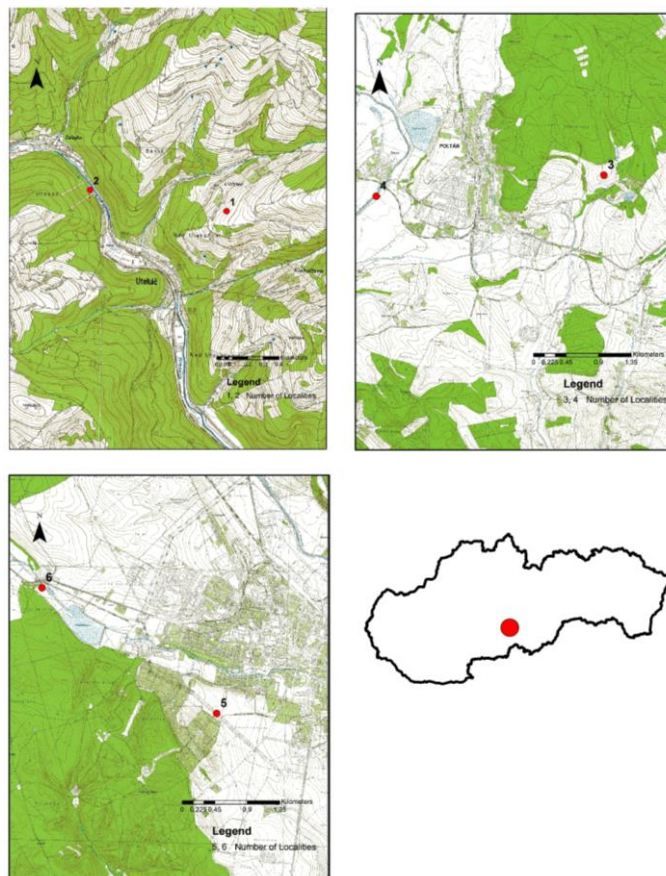


Figure 2. A map indicating the location of sampling sites

Table 1. Location data of the study localities

Geomorphological unit	Study area	C. a.	m a.s.l.	biotope	G.C.
Stolické vrchy	1 Lichovo	Utekáč	556	meadow	48°36'30"S 19°48'35"V
	2 Farkaška	Utekáč	446	nitrophilous waterside vegetation	48°36'34"S 19°47'52"V
Juhoslovenská kotlina basin	3 Prievranka	Poltár	272	pasture	48°25'52"S 19°49'08"V
	4 Pažiť	Poltár	218	nitrophilous waterside vegetation	48°25'41"S 19°46'35"V
	5 Zajačie brehy	Lučene c	208	fallow field	48°19'017"S 19°39'05"V
	6 Ladovo	Lučene c	207	nitrophilous waterside vegetation	48°20'12"S 19°37'06"V

C. a. – Cadastral area; m a.s.l. – metres above sea level; G.C. - geographic coordinates

Computation community index of the ground beetles (IKS)

Ground beetles we divided into three bioindication classes according to Farkač et al. (2006):

Group R – relicts, stenotopic species, narrow ecological valence – mostly rare and endangered species of natural ecosystems.

Group A – adaptable species which colonize semi-natural habitats, they occur in secondary, good regenerating biotopes and its ecotones.

Group E – eurytopic species without special requirements on the character and quality of environment. They occur in unstable and changing biotopes with strong anthropogenic influence.

The Index of Community of ground beetles (IKS) is calculated according to Nenadál (1998) based on the division of the *Carabidae* into bioindication groups (A, E, R). We use the following formula:

$$\text{IKS} = 100 - (\Sigma E + 0.5 \times \Sigma A) \quad (\text{Eq.1})$$

where E = percentage of individuals in group E (E%), A = percentage of individuals in group A (%).

The IKS index includes the values ranging from zero to 100. In cases where the index value is close to zero, we identified mostly species of group E. Conversely, when the value of index is close to 100; there are mostly species from group R. The final values included five classes according to the Nenadál's (1998) classification scale of human influence on habitat: I (0–15) strongly influenced, II (10–35) significantly influenced, III (30–50) influenced, IV (45–65) marginally influenced and V (65–100) not influenced.

Data analyses

Statistical analysis of IKS data on the study areas in years 2015-2017 using the programs Statistica Cz. Ver. 7.0 (StatSoft, 2004; Ter Brak and Šmilauer, 2002), CanoDraw 4.5 (Ter Brak and Šmilauer, 2002) and the Excel 2016 Analysis Program (Barrila et al., 2016) were evaluated.

For data assessment Detrended Correspondence Analysis (DCA), Redundancy Analysis (RDA), normality distribution (Shapiro-Willksov W test), testing of variance from mean values Friedman test (ANOVA), testing of selected correlation relations (polynomial regression, exponential distribution) were used. Statistical significance of the environment (luminance, humidity and pH) was tested by the Monte Carlo permutation test.

Results

In the study area of Stolické vrchy and Juhoslovenská kotlina basin using both methods (pitfall traps, yellow pan trap) we recorded 2,379 individuals (1,030 ♂, 1,349 ♀) belonging to 52 species. Based on the division of the *Carabidae* into bioindication groups (A, E, R) to tolerate anthropogenic effects, we calculated the *Carabidae* IKS for each area examined. We recorded the highest species distribution in the localities in group A (31 species; 66.62%). To a lesser extent, group E species (18 species; 32.45%) were represented. Group R was represented by 3 species (0.92%) (Table 2).

Table 2. Distribution of the *Carabids* based on bioindication groups in the study areas

Species	IKS	Study areas					
		1	2	3	4	5	6
<i>Abax ovalis</i> (Duftschmid, 1812)	A	1	1	-	-	-	1
<i>Abax parallelepipedus</i> (Pill. & Mitt.,1783)	A	15	28	1	44	1	139
<i>Abax parallelus</i> (Duftschmid, 1812)	A	20	43	-	3	-	73
<i>Agonum viduum</i> (Panzer, 1797)	A	-	-	-	-	-	1
<i>Amara aenea</i> (DeGeer, 1774)	A	1	-	2	-	2	-
<i>Amara aulica</i> (Panzer, 1797)	A	-	2	-	-	-	-
<i>Amara erratica</i> (Duftschmid, 1812)	R	8	-	-	-	-	-
<i>Amara familiaris</i> (Duftschmid, 1812)	E	-	-	6	-	-	1
<i>Amara saphyrea</i> (Dejean, 1828)	A	-	-	-	-	-	2
<i>Amara similata</i> (Gyllenhal, 1810)	E	-	-	1	-	-	1
<i>Anchomenus dorsalis</i> (Pontopp, 1763)	E	-	-	3	1	2	10
<i>Brachinus crepitans</i> (Linnaeus, 1758)	E	-	-	6	1	2	-
<i>Brachinus explodens</i> (Duftschmid, 1812)	E	-	-	-	1	-	-
<i>Calathus fuscipes</i> (Goeze, 1777)	E	7	-	12	-	-	-
<i>Calathus melanocephalus</i> (Linnaeus, 1758)	E	-	-	2	-	-	-
<i>Callistus lunatus</i> (Fabricius, 1775)	A	-	-	-	-	3	-
<i>Carabus cancellatus</i> (Illiger, 1798)	A	28	36	-	-	-	-
<i>Carabus convexus</i> (Fabricius, 1775)	A	4	9	-	-	-	-
<i>Carabus coriaceus</i> (Linnaeus, 1758)	A	-	3	5	11	2	9
<i>Carabus glabratus</i> (Paykull, 1790)	A	6	10	-	-	1	-
<i>Carabus granulatus</i> (Linnaeus, 1758)	E	1	29	-	-	-	9
<i>Carabus hortensis</i> (Linnaeus, 1758)	A	2	20	-	-	-	2
<i>Carabus intricatus</i> (Linnaeus, 1761)	A	-	4	-	-	-	6
<i>Carabus nemoralis</i> (O.F.Müller, 1764)	A	36	4	-	-	1	-
<i>Carabus scheidleri</i> (Panzer, 1799)	A	2	-	3	5	255	1
<i>Carabus ullrichi</i> (Germar, 1824)	A	-	39	-	-	46	-
<i>Carabus violaceus</i> (Linnaeus, 1758)	A	81	4	12	-	98	16
<i>Cicindela germanica</i> (Linnaeus, 1758)	A	-	-	9	-	17	-
<i>Cychrus caraboides</i> (Linnaeus, 1758)	A	-	1	-	-	-	-
<i>Cymindis humeralis</i> (Fourcroy, 1785)	A	-	-	-	-	1	2
<i>Drypta dentata</i> (Rossi, 1790)	E	-	-	3	-	3	-
<i>Elaphrus aureus</i> (P. Müller, 1821)	R	-	-	-	3	-	5
<i>Harpalus affinis</i> (Schränk, 1781)	E	6	-	350	-	4	-
<i>Harpalus froelichi</i> (Sturm, 1818)	A	-	-	-	7	-	-
<i>Harpalus rubripes</i> (Duftschmid, 1812)	E	39	-	5	3	1	-
<i>Lebia chlorocephala</i> (Hoffm. a kol., 1803)	A	2	-	1	-	-	-
<i>Leistus rufomarginatus</i> (Duftschmid, 1812)	R	-	-	-	-	-	6
<i>Molops piceus</i> (Fabricius, 1801)	A	9	3	-	-	-	-
<i>Nebria brevicollis</i> (Fabricius, 1792)	A	6	9	-	17	1	94
<i>Notiophilus biguttatus</i> (Fabricius, 1799)	A	-	-	-	1	-	-
<i>Ophonus azureus</i> (Fabricius, 1775)	E	-	-	-	-	3	-
<i>Ophonus nitidulus</i> (Stephens, 1828)	A	-	2	-	-	-	-
<i>Platynus assimilis</i> (Paykull, 1790)	A	-	16	-	74	-	109
<i>Poecilus cupreus</i> (Linnaeus, 1758)	E	13	1	36	-	34	-
<i>Poecilus versicolor</i> (Sturm, 1824)	E	-	-	2	-	-	-
<i>Pseudoophonus rufipes</i> (DeGeer, 1774)	E	11	-	58	34	28	4
<i>Pterostichus melanarius</i> (Illiger, 1798)	E	-	17	-	13	2	4
<i>Pterostichus melas</i> (Creutzer, 1799)	A	1	-	-	-	-	-
<i>Pterostichus niger</i> (Schaller, 1783)	A	9	1	-	11	3	5
<i>Pterostichus nigrita</i> (Paykull, 1790)	E	-	-	-	2	-	-
<i>Pterostichus oblongopunctatus</i> (Fab., 1787)	A	-	19	-	7	3	1
<i>Zabrus tenebrioides</i> (Goeze, 1777)	E	-	-	1	-	-	-
∑ individuals	-	308	301	518	238	513	501
∑ species IKS -A	-	16	20	7	10	14	15
∑ species IKS -E	-	6	3	13	7	9	6
∑ species IKS -R	-	1	-	-	1	-	2
IKS 2015	-	34,21	42,31	3,795	40,19	45,77	46,94
IKS 2016	-	40,64	41,5	4,715	39,785	39,455	47,045
IKS 2017	-	41,385	50	0	34,21	42,16	50,275
Total value IKS for years 2015 - 2017	-	38,8	42,195	3,185	39,075	42,3	48,2
Class/quality of habitat	-	III	III	I	III	III	III

Class I (0-15) very influenced, Class II (10-35) heavily influenced, Class III (30-50) influenced, Class IV (45-65) not influenced, Class V (65-100) not affected

The lowest value of IKS was observed in the area of 3 (pastures), which shows the highest anthropogenic interference in the study areas. There were 4 species preferring arable land find in the area 1: *Amara aenea*, *Calathus fuscipes*, *Harpalus affinis* and *Pseudoophonus rufipes*, which were represented by a low number of individuals. The arable land (areas 3 and 5) species were represented by a higher number of individuals *Amara aenea*, *Anchomenus dorsalis*, *Calathus fuscipes*, *Harpalus affinis* and *Pseudoophonus rufipes*. Indeed, the intensive agricultural use of the landscape prevails around areas 3 and 5. Fallow field of the watercourses of the locality had different IKS values. The lowest value was recorded in area 4, where 2 species *Anchomenus dorsalis* and *Pseudoophonus rufipes* favoring arable land. Areas 2 and 6 were connected with forest fields, therefore adaptable species predominated and IKS values were higher than in area 4.

We evaluated the difference in representation of bioindication groups A, E, R and IKS values between areas from 2015 to 2017 by RDA analysis (the highest value of lengths of gradient = 2.51). The RDA analysis has values of explained variability of species data of the first ordination axis (45.3%) and the second ordination axis (68.4%). The variability of the species set explained by environmental variables represent by the ordinal axis is 46.3%, while the second axis represents 70.5% (Fig. 3).

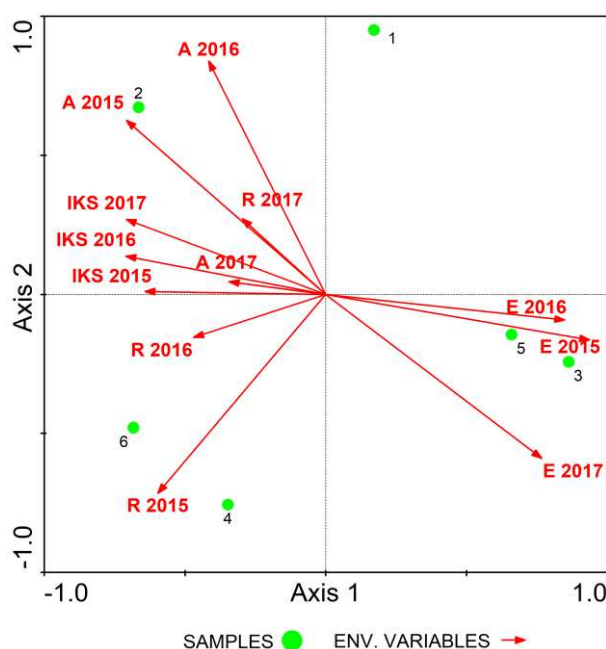


Figure 3. Representation of groups A, E, R and IKS values 2015 - 2017. Explanatory notes: A - Group A, E - Group E, R - Group R, IKS – Carabidae Community Index

Ordination graph showed correlation between the group A species with the nitrophilous waterside vegetation (area 2) with their highest representation. Vectors showing individual years (2015-2017) for this group did not differ significantly, suggesting only small variations in the number of species for group A. Open spaced areas 3 and 5 were abundantly represented by group E species, as illustrated by the correlation of this group over the years 2015-2017. Vectors did not differ significantly between 2015-2016, until 2017 indicating a change in the number of group E species.

The following fact indicates an intensification of agricultural land use. Area 1 (meadow) is ordained away from the vectors, indicating a slight variation in the proportion of bioindication groups and IKS values. Group R species correlated in 2015 with areas 4 and 6 (nitrophilic herbaceous vegetation) where they were recorded. In 2016 and 2017 there was a significant delay in vectors, which was influenced by the occurrence of R group species also in area 1. The vectors for IKS values did not significantly diverge in years 2015-2017. The following fact shows that there have been minor changes in IKS values over the years 2015-2017. The correlation with forest areas 2 and 6 was influenced by high IKS values during all 3 years.

For normality distribution in years 2015-2017 for all areas the Shapiro-Wilks W-test was used. We tested the hypothesis H_0 : random selection comes from a set with normal distribution, if $p > p\alpha \Rightarrow$ we do not reject H_0 at the level of selected statistical significance $p\alpha = 0.05$. As a result, the normal distribution of IKS data across all areas in 2015-2017 was disrupted (p -value = 0.00).

A non-parametric Friedman test for testing H_0 hypothesis was used because of distribution normality data disruption, which verified the H_0 hypothesis: IKS values do not differ in areas in 2015-2017. This means if $p > p\alpha \Rightarrow$ do not reject H_0 at the level of statistical significance chosen by us $p\alpha = 0.05$. The result of the testing is the rejection of the H_0 hypothesis ($p=0.00$), which means that IKS values are significantly different in all areas in 2015-2017 (Fig. 4). The gradual increase in the IKS value caused by the succession and non-mowed meadow was recorded. The same increase in IKS was also observed in area 6, where waterside vegetation was not treated for 3 years and naturally overgrown with trees. Species of group R were found in the study areas, their presence indicates a low anthropic interference in the environment. In 2016, the waterside vegetation of area 2 was modified by tree and shrubs cutting and therefore the value of IKS decreased. No changes were made in the following year and the area was overgrown, which also affected the increase in the IKS value for 2017. The same progress was also recorded in the area 5, where shrubs were removed and frequent mowing during 2016 and subsequent succession in 2017. Area 3 was grazed by cattle, which was more intense in 2017 reflected in IKS 0. The waterside vegetation of area 4 was treated during all 3 years by removing shrubs and trees causing annual IKS values to fall.

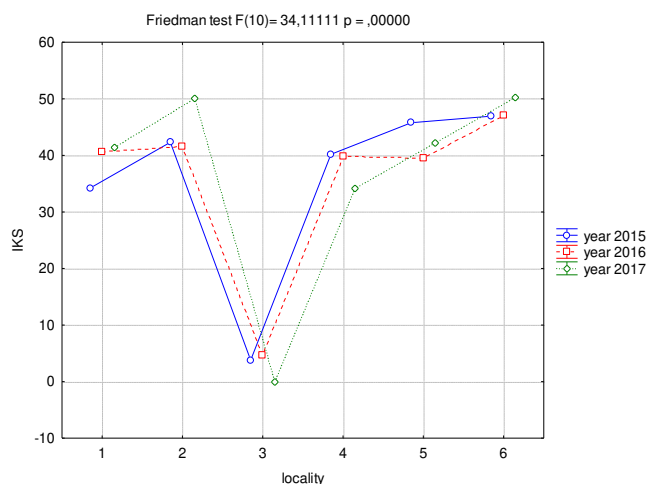


Figure 4. Analysis of IKS variation of individual areas by Friedman test (ANOVA) from 2015 to 2017

Polynomial regression (quadratic distribution) for evaluation of IKS change in 2015-2017 was used. Using the regression model we expressed the relationship (correlation) between IKS at the areas to the harvest years. The value of the correlation coefficient for area 1 is ($r = 0.90$), which indicates an almost perfect relationship. For areas 2 ($r = 0.81$), 3 ($r = 0.75$), 4 ($r = 0.89$) and 6 ($r = 0.87$) the relationship is very large. For area 5 ($r = 0.56$) the relationship is large. The overall suitability of the regression model is statistically significant for all areas. The results are as follow: area 1 (p-value = 0.02), 2 (p-value = 0.03), 3 (p-value = 0.04), 4 (p-value = 0.02), 5 (p-value = 0.01) and 6 (p-value = 0.03) thus confirms the effect of years on the IKS values of the study areas. Based on the regression equations shown in *Fig. 5* we can predict the IKS value of individual areas for year 2020: for area 1 (IKS = 53), area 2 (IKS = 59), area 3 (IKS = 0), area 4 (IKS = 26), area 5 (IKS = 35) and area 6 (IKS = 54). The predicted results may be fulfilled in areas 1, 2 and 6 in the case of continued spontaneous succession in which the areas are overgrown by vegetation (areas not managed). For areas 3, 4 and 5 the trend will be reversed and areas will be modified by anthropogenic activity. From the above results we can conclude, that the quality of habitats and class will change as follows. Areas 1, 2 and 6 rise from Class III (affected) to Class IV (little affected). For area 3 the quality and habitat class will remain unchanged I (very strongly affected). In areas 4 and 5 there will be a decline from Class III (affected) to Class II (heavily affected).

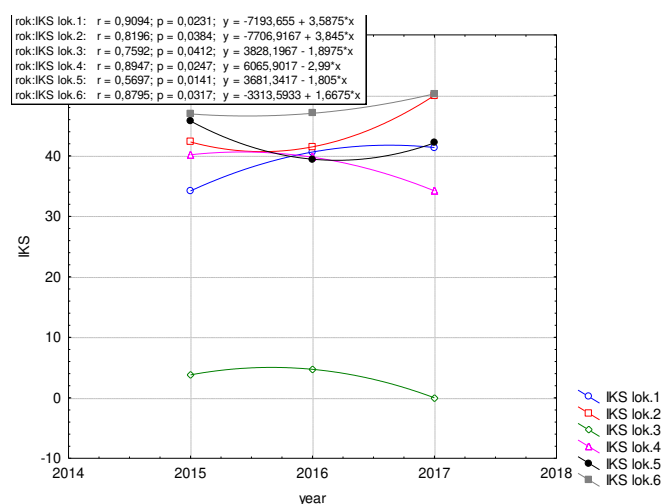


Figure 5. Polynomial regression of IKS values 2015 - 2019

Using the exponential distribution we predicted that IKS = 70 would be 5 years later (with 99% probability) in areas 1, 2 and 6. In the same way we predicted IKS = 10 by 5 years (with 57% probability) in areas 4 and 5.

The correlation of luminous intensity, moisture, pH was determined by redundancy analysis (RDA), which points out on values of explained variability of species data of the first ordination axis 43.7% and on the second ordination axis 64.5%. The variability of the species set explained by the environmental variables captured by the first ordinate axis 57%, the second axis captured by 84.2%. *Carabidae* are ordained into 4 clusters (*Fig. 6*), the first cluster (I) consisted of species correlating with luminous intensity. The second cluster (II) was represented by pH-binding species. The third (III) cluster was

represented by species correlating with moisture. The last cluster (IV) consisted of species that were not ordained in any cluster and are not influenced by the investigated factors (luminous intensity, moisture and pH). The Monte Carlo permutation test verified the H0 hypothesis: environmental factors (luminous intensity, moisture and pH) did not affect the species of the *Carabidae* family, if $p > p_{\alpha} \Rightarrow$ do not reject H0 at the stated level of statistical significance $p_{\alpha} = 0.05$. As statistically significant factor (p-value = 0.002) we confirmed luminous intensity, in others we did not confirm statistical significance: moisture (p-value = 0.378) and pH (p-value = 0.268). Factors were not correlated with each other, maximum inflation factor = 4.247.

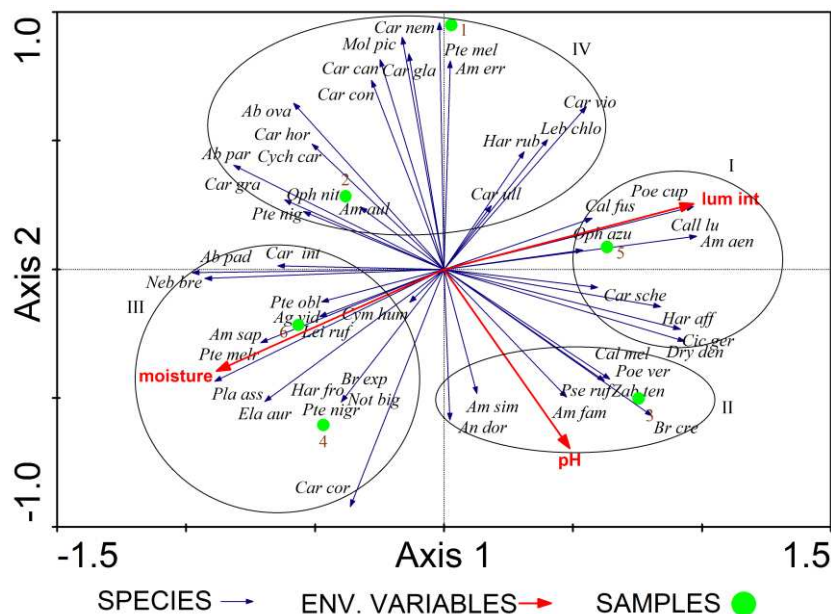


Figure 6. RDA analysis of ground beetles and environment variables (luminous intensity, moisture, pH). Explanatory notes: lum int - luminous intensity

Discussion

Our research evaluated the anthropogenic effect (agriculture, treatment of waterside vegetation, mowing meadows) on the *Carabidae* cenosis. The species were divided into bioindication groups according to Farkač et al. (2006) and the subsequently calculated Index of the *Carabidae* IKS according to Nenadál (1998).

The lowest IKS value was recorded in area 3 (IKS = 0) with the prevalence of eurytopic species (IKS) over adaptable (IKS). This fact confirms a very strong disruption of the area (habitat quality class I). The same fact was pointed out by Langraf et al. (2016), Igondová and Majzlan (2015), Št'astná and Bezděk (2004), Purchart and Kula (2005), Baranová et al. (2013) and Lemic et al. (2017) whose in their work have noticed the prevalence of eurytopic species (IKS) over adaptable (IKS) in agricultural areas and Jaďud'ová et al. (2016) in permanent grassland. Other areas had a habitat quality class III, indicating a moderate disturbance with adaptable species predominating over eurytopic species. The same fact was noted in their works Stluka (2013), and Rajová (2007).

A gradual increase in IKS over 3 years was observed in areas 1 and 6, which was influenced by succession. Area 1 (meadow) was not mowed and area 6 (nitrophilic

waterside) had no treated waterside vegetation. Species from group R were also recorded in the areas. The decrease in IKS values over the study period was found in the areas 3 and 4 in which significant anthropic activity took place. A higher number of E group species was also recorded. Area 3 (pasture) was grazed by cattle and area 4 (nitrophilic waterside vegetation) had trimmed waterside vegetation by cutting trees and shrubs. Areas 2 (nitrophilic waterside vegetation) and 5 (fallow field) had a decrease in IKS values and an increase in group E species during 2016, in the following 2017 IKS values increased. With increasing anthropic intervention IKS values decreased and the number of eurytopic species that replaced adaptable increased. As a result of decreasing interventions IKS values increased and the number of group A and R species increased as well. The same was found by Langraf et al. (2019), Niemel et al. (2002), Elek et al. (2001), Finch (2005) and Wiezik et al. (2007).

Polynomial regression models assume the continuing trend of succession (areas 1, 2 and 6), where we predicted by exponential distribution 99% probability of IKS increase to 70 in 2022. For areas 3, 4 and 5 we predicted a higher impact of anthropogenic activity. Exponential distribution predicted 57% probability of reducing IKS to 10 for 2022.

Vician et al. (2010, 2011) cited as typical species mainly associated with arable land *Clivina fossor*, *Calathus fuscipes*, *Amara aenea*, *Anchomenus dorsalis*, *Harpalus affinis*, *H. distinguendus* and *Pseudoophonus rufipes*. The presence of these species with a higher number of individuals was recorded in areas 3 and 5 adjacent to the farmed land.

Conclusion

The different intensity of anthropogenic impacts (developed agriculture, treatment of waterside vegetation, mowing meadows) on *Carabidae* species in six study areas representing 4 habitat types was evaluated.

We confirmed statistically significant changes in values in years 2015-2017 for all study areas using the IKS index. We found a low IKS value = 0 with a predominance of eurytopic species on habitat quality class 3 = I, indicating a very strong disturbance. Other areas had habitat quality class III, indicating moderate disturbance with the prevalence of adaptable species. The above facts have confirmed our first working hypothesis.

Significant differences in the number of bioindicating species (groups A, E, R) were observed for eurytopic species in years 2016-2017, indicating a more intensive agricultural use of the landscape (cattle grazing, expansion of fields at area 5). Bioindication group R also increased in years 2016-2017, which was influenced by the spread of group R species to area 1. Species belonging to group A showed year-on-year changes, but not so significant. It follows from the above that the second and third working hypotheses are confirmed. The arable land species were represented by a higher number of individuals: *Amara aenea*, *Anchomenus dorsalis*, *Calathus fuscipes*, *Harpalus affinis* and *Pseudoophonus rufipes* on areas 3 and 5.

The regression models predicted the continuation of succession on areas 1, 2 and 6, where we predict a 99% probability of IKS to rise to 70 in 2022 at exponential distribution. The above facts confirm the reduction of anthropic activity in these localities. We predicted a higher impact of anthropogenic activity and a decrease in IKS

values by the regression polynomial model on areas 3, 4 and 5. We also pointed on the 57% probability of reducing IKS with a value of 10 in 2022 by exponential distribution.

In order to maintain the original biodiversity of the carabidae family, it is possible to adjust the management and management of the investigated sites. Verification of the success of the introduced changes during the continuation of the results in the years referring to the forecast.

Acknowledgements. This research is supported by the project VEGA 1/0496/16: Assessment of natural capital, biodiversity and ecosystem services in Slovakia – basis for practical implementation of integrated environmental policy.

REFERENCES

- [1] Baranová, B., Fazekašová, D., Jászay, T., Manko, P. (2013): Ground beetle (Coleoptera: Carabidae) community of arable land with different crops. – *Folia faunistica Slovaca* 18(1): 21-29.
- [2] Barilla, J., Simr, P., Sýkorová, K. (2016): Microsoft excel 2016 podrobná uživatelská příručka. – In: Computer Press, Brno.
- [3] Burgio, G., Campanelli, G., Leteo, F., Ramilli, F., Depalo, L., Fabbri, R., Sgolastra, F. (2015): Ecological Sustainability of an Organic Four-Year Vegetable Rotation System: Carabids and Other Soil Arthropods as Bioindicators. – *Agroecology and Sustainable Food Systems* 39(3): 295-316.
- [4] Cardamo, H. A., Spence, J. R. (1994): Crop type effects on the activity and distribution of ground beetles (Coleoptera, Carabidae). – *Environmental entomology* 23(3): 123-140.
- [5] Elek, Z., Magura, T., Tóthmérész, B. (2001): Impacts of non-native Norway spruce plantation on abundance and species richness of ground beetles (Coleoptera: Carabidae). – *Web Ecology* 2: 32-37.
- [6] Farkač, J., Kopecký, T., Veselý, P. (2006): Využitie střeblíkovitých (Coleoptera, Carabidae) fauny Slovenska k indikaci kvality prostredí. – *Ochrana Přírody* 25: 226-242.
- [7] Finch, O. D. (2005): Evaluation of mature conifer plantations as secondary habitat for epigeic forest arthropods (Coleoptera: Carabidae; Aranae). – *For. Ecol. Manag.* 204: 23-36.
- [8] Heydeman, B. (1955): Carabiden de Kulturfelder ökologische Indikatoren. – *Wanderversammlung Deut. Ent. Ber.* 7: 172-185.
- [9] Hůrka, K. (1996): Carabidae České a Slovenské republiky. – Zlin, Czech Republic: Kabourek.
- [10] Igondová, E., Majzlan, O. (2015): Assemblages of ground beetles (Carabidae, Coleoptera) in peatland habitat, surrounding dry pine forests and meadows. – *Folia Oecologica* 42(1): 21-28.
- [11] Jaďud'ová, J., Kanianska, R., Kizeková, M., Makovníková, J. (2016): Evaluation of Habitat Provision On the Basis of Carabidae Diversity in Slovak Permanent Grasslands. – *World Multidisciplinary Earth Sciences Symposium (WMESS 2016)*, Earth and Environmental Science 44: 1-5.
- [12] Langraf, V., Petrovičová, K., David, S., Schlarmannová, J. (2016a): The bioindication importance of the Carabidae communities of Veporské vrchy and Juhoslovenská kotlina. – *Ekológia (Bratislava)* 35(2): 126-135.
- [13] Langraf, V., Petrovičová, K., David, S., Schlarmannová, J. (2016b): Bystruškovité (Carabidae) Veporských vrchov a Juhoslovenskej kotliny. – *Ochrana prírody* 28: 29-38.
- [14] Langraf, V., Petrovičová, K., David, S., Ábelová, M., Schlarmannová, J. (2017): Body volume in ground beetles (Carabidae) reflects biotope disturbance. – *Folia Oecologica* 44(2): 114-120.

- [15] Langraf, V., David, S., Schlarmannová, J. (2018a): Ekologická charakteristika bystruškovitých (Coleoptera: Carabidae) Stolických vrchov a lučenskej Kotliny. – Ochrana prírody 31: 13-19.
- [16] Langraf, V., Petrovičová, K., David, S., Kanská, M., Nozdrovická, J., Schlarmannová, J. (2018b): Change Phenotypic Traits in Ground Beetles (Carabidae) Reflects Biotope Disturbance in Central Europe. – Journal of the Entomological Research Society 20(2): 119-129.
- [17] Langraf, V., Petrovičová, K., David, S., Nozdrovická, J., Petrovič, F., Schlarmannová, J. (2019): The Bioindication Evaluation of Ground Beetles (Coleoptera: Carabidae) in Three Forest Biotops in the Southern Part of Central Slovakia. – Ekológia (Bratislava) 38(1): 25-36.
- [18] Lemic, D., Čačija, M., Viric, G. H., Drmic, Z., Bažok, R., Pajac, Ž. I. (2017): The Ground Beetle (Coleoptera: Carabidae) Community in an Intensively Managed Agricultural Landscape. – Applied Ecology and Environmental Research 15(4): 661-674.
- [19] Nenadál, S. (1998): Využití indexu komunity střevlíkovitých (Coleoptera, Carabidae) pro posouzení antropogenních vlivů na kvalitu přírodního prostředí. – Vlastivědný Sborník Vysočiny 13: 293-312.
- [20] Niemelä, J., Kotz, J. D., Venn, S., Penev, L., Stoyanov, I., Spence, J., Hartley, D., Oca, M. E. (2002): Carabid beetle assemblages (Coleoptera, Carabidae) across urban-rural gradients: an international comparison. – Landscape Ecology 17: 387-401.
- [21] Nietupski, M., Kosewska, A., Markuszewski, B., Sadej, W. (2015): Soil management system in hazelnut groves (*Corylus* sp.) versus the presence of ground beetles (Coleoptera: Carabidae). – Journal of Plant Protection Research 55(1): 26-34.
- [22] Novák, K. (1969): Metody sběru a preparace hmyzu. – Academia, Praha, 243 p.
- [23] Porhajašová, J., Petřvalský, V., Macák, M., Urmínská, J., Ondříšek, P. (2008): Occurrence of species family Carabidae (Coleoptera) independence on the input of organic matter into soil. – Journal Central European Agriculture 9(3): 557-565.
- [24] Porhajašová, J. (2009): The evaluation of bioindicators abilities of selected zoocenosis (Carabidae, Coleoptera) in dependence on different farming systems. – Environmental protection and food safety in crop production 262-266.
- [25] Purchat, L., Kula, E. (2005): Ground beetles (Coleoptera, Carabidae) agrocenoses of spring and winter wheat. – Acta univ. agric. et silvic. Mendel. Brun., 2005, LIII, No. 5: 125-132.
- [26] Rajová, Š. (2007): Využití hmyzu k výuce biologie. Střevlíkovití (Coleoptera: Carabidae) Klánovického lesa a posouzení stavu jeho zachovalosti metodou bioindikace. – PhD thesis, Katedra biologie a ekologické výchovy Pedagogické fakulty Univerzity Karlovy.
- [27] Ružičková, H., Halada, L., Jedlička, L., Kalivodová, E. (1996): Biotopy Slovenska. – Bratislava, Ústav krajinné ekológie Slovenskej Akadémie Vied.
- [28] Statsoft, inc. (2004): Statistica Cz [Softwarový systém na anlyzu dat], verze 7. – Www.StatSoft.Cz.
- [29] Stluka, P. (2013): Vliv managementu na biodiverzitu lesních ekosystémů- epigeičtí brouci na vybraných biotopech Písecka. – Diploma thesis, Zemědělská fakulta, Jihočeská Univerzita v Českých Budějovicích.
- [30] Šťastná, P., Bezděk, J. (2004): Carabidae a ostatní čeledi brouků (Coleoptera) zjištění v zemních pastech v polní agrocenóze v Sivicích. – Zoologické dny Brno 2004: 104-105.
- [31] Ter Brak, C. J. F., Šmilauer, P. (2002): CANOCO Reference Manual and User's Guide to Canoco for Windows. – Centre for Biometry, Wageningen. Ithaca NY, USA.
- [32] Vician, V., Stašiov, S., Kočík, K., Hazuchová, L. (2010): Carabidae (Coleoptera) Structure on Variously Managed Agricultural Land of Podpoľanie area. – Acta facultatis ecologiae, Zvolen 22: 133-146.
- [33] Vician, V., Stašiov, S., Kočík, K., Hazuchová, L. (2011): Structure of the Carabids (Coleoptera: Carabidae) Associations on Variously Managed Agricultural Land of Podpoľanie area and their bioindication. – Acta facultatis ecologiae: 123-131.

- [34] Wiezik, M., Svitok, M., Dovčiak, M. (2007): Conifer introductions decrease richness and alter composition of litter-dwelling beetles (Coleoptera) in Carpathian oak forests. – For. Ecol. Manag. 247: 61-71.

EFFECT OF SEAWEED APPLICATION ON THE VEGETATIVE GROWTH OF STRAWBERRY CV. ALBION GROWN UNDER IRAQ ECOLOGICAL CONDITIONS

AL-SHATRI, A. H. N.¹ – PAKYÜREK, M.^{1*} – YAVIÇ, A.²

¹*Siirt University Faculty of Agriculture, Department of Horticulture, 56100 Siirt, Turkey*

²*Yüzüncü Yıl University Faculty of Agriculture, Department of Horticulture, 65080 Van, Turkey*

*Corresponding author

e-mail: mine.pakyurek@siirt.edu.tr

(Received 15th Aug 2019; accepted 14th Nov 2019)

Abstract. This experiment was established in pots during the vegetative period of 2017, in Kalar Sulaymaniyah, Northern Iraq, to investigate the effect of seaweed extracts (Alga 600) of four concentrations (0, 2, 4, 8 g.L⁻¹) applied with fertigation system on growth, flowering, yield and quality properties of strawberry cv. Albion. Drip irrigation system was used in this experiment. According to the results in terms of the vegetative growth characteristics, increasing seaweed extract (Alga 600) amounts had significantly different effects on plants with a different number of crowns. The results concerning flower properties show that increasing seaweed extract applications had significant effects on the number of flowers per plant, yielding 16.55-21.77 units/plant. The results in point of fruit properties show that increasing Alga 600 amounts caused a significant increase of 11.81-17.7 units/plant in terms of fruit number, 211.74-329.37 ml in terms of fruit volume, and an increase of 191.7-295.03 g in terms of yield, compared to the control treatment. The results show that increasing seaweed extract caused a significant increase in fruit quality (TSS/TA ratio from 8.29 to 13.35) compared to the control treatment and increasing seaweed application caused a significant decrease in the TA of the fruit.

Keywords: *Fragaria x ananassa* Duch, organic fertigation, cv. Albion, morphological properties, pomological properties, algae extract

Introduction

Strawberry (*Fragaria x ananassa* Duch) is small fruit that planted in a wide range in the world, it belongs to family Rosaceae. Before the relatively modernity development of *Fragaria x ananassa*, wood strawberries (*Fragaria vesca*) and Musky strawberries (*Fragaria moschata*) were cultivated in Europe and Russia for centuries. These species were in generally supplanted by the cultivation of *Fragaria x ananassa* over the last 250 years. In the early 1700s, inter-planting of *Fragaria virginiana* (male) with *Fragaria chiloensis* (female) in France led to the production of hybrid seedlings that bring to be known as Pineapple or Pine strawberry plants, progenitors of the new cultivated strawberry plant (*Fragaria x ananassa* Duch) (Darrow, 1966). It is a rich source of vitamins and minerals with delicate flavor (Sharma, 2002).

It is one of the most delicious and refreshing temperate fruits of the world. It gives early and very high returns per unit area compared to other fruits because its crop is ready for harvesting within six months after planting (Katiyar et al., 2009). Being a non-climacteric, it matures only on the plant (Cordenunsi et al., 2003). Its fruits are appealing with a distinct, enjoyable and refreshing aroma. It also contains a higher percentage of other components including phenolic and flavonoids (Häkkinen and Törrönen, 2000). Strawberry is a perfect source of Vitamin C (30-100 mg/100 g of fruit) as well as a foliate and photochemical compound such as the Alganic acid. Consuming

strawberries can reduce the risk of increasing cancer by 50% due to higher levels of Vitamin C can increase the flow of blood and oxygen to the muscles by 7% due to nitrates (Kumar et al., 2013). Strawberry contains 90% water and 37% calories, 0.7 grams of protein, 0.5 g of oil, 10 g of carbohydrate, 1.3 g fiber and vitamins, contain vitamin A (0.07 mg), vitamin B1, B2 (0.3 mg), niacin (28 mg) and calcium (27 mg) (Watt et al., 1963).

Strawberry can be cultivated in almost all regions from arctic to tropic regions (Hancock, 1999). Including sub-tropical areas like North of Iraq. Country's weather is favorable for the production of high quality strawberries though it is normally produced in countries having cold weather, particularly in the north. Strawberry cultivation technique is fairly new in North of Iraq whereas cultivation area is increasing bit by bit. Strawberry can be grown during the month of October to April in North of Iraq. A sustainable variety is needed for continuous production from year to year. Screening of strawberry variety is needed for a suitable variety for continuous production and some varieties screening has also done. Today, strawberries are produced in almost every country in the world, most notably, Turkey, America, and Iran. This wide distribution suggests that the strawberry plant is well adapted, and as a genus. However, a lot of individual genotypes or cultivars of strawberries are accurately adapted to local conditions, and so choosing cultivars that are proven to perform well in your specific region is important and key of the work. Strawberry reproduction, fruit quality and yield depends on a lot of factors, for example; weather conditions during the growing stage, the cultivar and all agronomic practices such as fertilization, irrigation or crop protection (Gülsoy and Yılmaz, 2004).

Cultivated strawberry (*Fragaria x ananassa*) and wild strawberry (*Fragaria virginiana*) are plants in the family of Rosaceae. The fruit of the strawberry plant is composed of several tiny fruits that together produce the whole fruit, where every small fruit has one seed called achene. Seaweed extracts are the cheap source of naturally occurring plant development regulators which have better potential as bio stimulants in horticulture. The plant growth regulators available in the seaweed extracts and concentrates is thought to be involved in the enhancing plant growth and yield. Different plant phytohormones and growth regulators available in seaweed extracts are known to promote the yield and yield attributes of crops. Because the extract contains natural plant hormones and different natural nutrient material, vitamins, carbohydrates such as Algalic acid, polysaccharide, trace minerals (Panda et al., 2012).

The aim of this study, to investigate the effect of seaweed extract (Alga 600) on the vegetative growth, flowering quantitative and qualitative parameter of yield on strawberry cv. Albion under Iraq ecological conditions.

Literature Review

Seaweed extract is an organic substance that is concentrated and can be found in liquid or soluble granule form. It is mixed with water and added to seeds, transplant, and plant to fertilize it. Accordingly, as it has been remarked by Aitken and Senn (1965) it can also replace nutrition deficiencies of plant development. This material is an important substance because it is safe to use. It does not have a dangerous side effect on human being, animal and land. In addition to that it reduces land pollution and the rate of soil salt inside the soil (El-Moniem and Abd-Allah, 2008). It is also economical to

use since it won't cast too much. For the above-mentioned reason, it has been a preferred fertilizer throughout centuries (Temple and Bomke, 1988).

Seaweed extract, in its different types and methods of application, has been a catalyst for plant growth and productivity. As it has been concluded in different studies, seaweed has led to the active development of plants through improving photosynthesis, activating flower, leaves, promoting shoots, leaf minerals, and carbohydrates, vegetative weights. As it has been remarked by Masny et al. (2004) in a study leaves activity improves and photosynthesis will be in better quality when seaweed (Kelpak SL and Goemar BM86®) with three treatments (0, 0.5 and 1 ml.L⁻¹) is sprayed on the leaves of strawberry. It also promotes an increase in the number of flowers in each plant. This experiment is done on strawberry plants cv. Elkat and Salut in 2001-2003. It is also stated it stimulates shoot growth, the area of leaves a long with the chemical components of leave such as carbohydrates and minerals of the leaf. As it is mentioned by Mansour et al. (2006) in an experiment when algae extract added to the sandy soil of thirty Anna apple trees aged 12 years on MM106 rootstock cultivated at 3.5x3.5 m. The effect of the extract is shown in other studies again remarks its positive effect on plant growth. El-Moniem and Abd-Allah (2008) in a study show the positive effect of the extract. The result of spraying green alga cells extract on the grapevine is shown in comparison with other nutrition fertilizers. The use of algae extract at 25 to 100% had improved on the growth characters, including the leaf area, shoot length and promoted leaves number in each shoot rather than check treatment.

The development and activation of leaves noticed when algae extract concentration was under 50%. But with a concentration above 50%, its effect on increasing percentage N, P, and K in the leaves is less than under 50%. Other studies also indicate the positive effect of the extract on plant production and leaf improvement. Taha (2008) in a study exposes the influence of spraying three seaweed extracts (Algren, Soluamine, Mannarine) in two types of Strawberry (Hapil and Kaiser's sampling). It is concluded that spraying cv. Kaiser's sampling with seaweed (Algren) stimulates an increase in the total chlorophyll content and obvious enhance in pollen viability ratio, whereas spraying extracts Soluamine has boosted flower in each plant more than negative controls, as for the cv. Hapil when using Algren extract, there was an increase in dry weight of shoots and leaf area and important superiority of crown diameter. However, spraying extract Soluamine there was an increase in the rate of fresh weight of shoot and dry weight of the root system.

Algae extract increases productivity in strawberry as found by Al-Hermizy (2011) in a study. That deals with the effect of sea algae extract (Alga 600) in two levels (0 and 3 ml.L⁻¹) on strawberry growth as far as productivity concerned. The outcome of the study shows that spraying with sea algae extract (Alga 600) caused a significant increase in all vegetative growth characteristics (crown diameter, total leaf area, fresh and dry weight of vegetative growth, number of runner and number of leaflet per plant). Accordingly, Mac et al. (2008) studied the influence of Alga Green (cold process seaweed liquid extract), as foliar fertilization on the plots of mature "Bramley's seedling" apple trees in comparison of other non-applicant trees. It is found that seaweed caused a significant increase in leaf mineral content.

Seaweed can be defined as a fertilizer that makes plant prolific in terms of quantity and quality. As it has been proved in different studies seaweed extract has helped the increase in the rate of fruit weight, size, number. It promotes them to be prolific. As affirmed by Kivijarvi et al. (2002) in a study done on strawberry (Jonsock, Ruukki, and Bounty) with different concentrations of seaweed extract that resulted in the

improvement of the rate of fruit weight and size, the quantity of yield. There is also a positive outcome of studies done by Al-Hermizy (2011) in search of the impact of seaweed (Alga 600) in two-scale (Zero, and 3 mL.L⁻¹) on yield properties of strawberry. The outcome indicated that Spraying with seaweed Alga 600 caused a significant increase in every yield characteristic (fruit weight, size, yield per plant, total yield). Again in other studies like Eshghi et al. (2013), there is a prolific result of using a foliar application of seaweed extracts including Algren at 0, 3, 6 and 9 g.L⁻¹, Drin at 0, 0.5, 1 and 2 g.L⁻¹ focus on quality fruits of strawberry cv. Selva. The results show that the Algren at 9 g.L⁻¹ focus produces better chlorophyll content.

Material and Methods

This study was carried out during the vegetation periods of 2016-2017 with pots in open area in Kalar, Sulaymaniyah, North of Iraq located between latitude N 34.62131°, longitude E 45.31961° and on elevation 200 m above sea level. During the vegetation period, in Kalar, the minimum temperature was -3°C; max. the temperature started to increase in the middle of April, more than 35°C. No field trials have been established to protect plants from low temperatures seen in winter due to continental climatic conditions. When the temperature dropped below zero during the experiment, a plastic sheet was drawn over the plants. Effect of high temperature was seen on strawberry fruit size and weight in our experiment at the beginning of May (it was the last harvest time) as shown in *Table 1* (Anonymous, 2017).

Table 1. The weather of Kalar - Sulaymaniyah / Iraq, from January/2017 to June/2017.

Date	Average temperature /month	Maximum temperature /month	Minimum temperature /month	Average relative humidity /month	Maximum relative humidity /month	Minimum relative humidity /month
mm/yy	°C	°C	°C	%	%	%
Jan-17	8.72	20.3	-2.98	88.19	100	0.89
Feb-17	12.62	25.73	0.92	73.59	100	0.9
Mar-17	15.7	28.22	2.47	65.59	100	0.9
Apr-17	21.01	38.4	5.53	9.71	100	0.89
May-17	27.49	41.91	13.66	15.27	100	0.92
Jun-17	33.51	46.95	17.49	21.13	56.45	7.33

Experimental Details

Albion variety was used as plant material in our experiment. Seedlings were brought at 1st January 2017 from Antalya, Turkey (*Figure 1*). The experiment was established in pots with capacity 5 kg in open area on 15 January 2017 in Kalar. Four concentrations of fertigation solutions (0, 2, 4 and 8 g.L⁻¹) were prepared from seaweed (Alga 600). The prepared solutions were applied to the plants twice with fertigation. The first application was in the flowering stage (after the formation of first fruiting) and the second application was twenty days later. The seaweed was dissolved in 22°C of water for better fixing. Fertigation was applied in the morning. Components of seaweed are shown in *Table 2*.

Plant Growth Observations and Pomological Properties

After full flowering (15th February 2017) and two harvesting times (20th March and 12th May 2017) some vegetative growth parameters and pomological properties such as

single leaf area, total leaf area of per plant, number of leaves per plant, vegetative fresh weight, vegetative dry weight, root dry weight, chlorophyll (total =chlorophyll A + chlorophyll B) content in the plants, strawberry runner properties (daughter plant), strawberry runner properties (stolon), strawberry crown, number of flowers per plant, flower setting percentage, number of fruits of per plant, average fruit weight, average fruit volume, average total fruit volume, yield of per plant, yield per unit area (kg/hectare), fruit total soluble solid percentage (TSS %), fruit total acidity (TA %), TSS/TA ratio (ripening index) were measured. For measurements of root weight, after second harvest time, the roots of plants were washed to remove the soil particles under tap water very well. Then roots of plants were dried at 70°C in the oven.

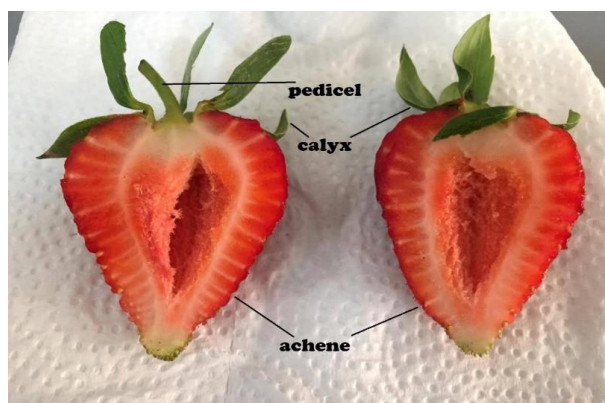


Figure 1. Fruit of Strawberry cv. Albion.

Table 2. Components of seaweed (Alga 600).

1	Nitrogen N	0.5-1.0%
2	Alganic acid	6-9%
3	Sulfur (S)	1.0-1.5%
4	Phosphorus pentoxide (P ₂ O ₅)	6-9%
5	Calcium oxide (CaO)	0.4-1.6%
6	Iron (Fe)	0.15-0.3%
7	Magnesium oxide (MgO)	0.06%
8	Potassium oxide (K ₂ O)	21-24%
9	Amino acid	4%
10	PH	9-11
11	Organic matter	40-50%

Statistical Calculations

Data were analyzed by the analysis of variance method for randomized plot design. Four treatments (0, 2, 4, and 8 g.L⁻¹), with three replications and each experimental unit, contains nine plants. LSD multiple comparison test was used for determination of the differences between of the means. Significance threshold were set as $\alpha = 0.05$ and $\alpha = 0.01$. Descriptive statistics, like mean and standard errors, were presented for the investigated features. Statistical calculations of findings are presented under the tables as **: p<0.01, significant at 0,01 level; *: p<0.05, significant at 0.05 level and NS: not significant.

Results and Discussion

Plant Growth Observations and Pomological Properties

Single Leaf Area Per Plant

As shown in *Table 3*, compared to the negative control seaweed (Alga 600) showed an increase in single leaf area per plant. However, it is not a statistically significant result. Measurements gave the maximum value of the single leaf area as 127.88 cm² in seaweed (Alga 600) in 8 g.L⁻¹ treatment group. Owing to seaweed (Alga 600) including more vitamins, amino acids, and some trace elements, these results were expected. However, the past studies have demonstrated that seaweed extracts indirectly or directly, effects on the physiological performance of the plants. Previous studies were concluded to be stemming from the content properties of seaweed (Alga 600), which contains auxin and cytokines. Accordingly, cell division and elongation proposed to be affected by the content (El-Yazied et al., 2012; El-Miniawy et al., 2014; Saif Eldeen et al., 2014).

Table 3. *The effect of fertigation of seaweed on single leaf area.*

Name	Single leaf area per plant (cm ²) ^{NS}
T1 (Control)	102.87
T2 (2 g.L ⁻¹)	106.52
T3 (4 g.L ⁻¹)	116.35
T4 (8 g.L ⁻¹)	127.88

NS: not significantly different.

Total Leaf Area Per Plant

Data in *Table 4* shows the effect of seaweed (Alga 600) on the total leaf area per plant. There is an increase compared with control treatment yet it was not significant, and it shows the fertigation of seaweed (Alga 600) in 8 g.L⁻¹ give the maximum value of total leaf area per plant is (1464.44 cm²) and lowest value recorded by control treatment (1038.21 cm²). These results are plausibly observed because of the incentive effect of Seaweed (Alga 600) on the single leaf area as previously mentioned.

Table 4. *The effect of fertigation of seaweed on total leaf area of per plant.*

Name	Total leaf area (cm ²) ^{NS}
T1 (Control)	1038.21
T2 (2 g.L ⁻¹)	1088.56
T3 (4 g.L ⁻¹)	1167.29
T4 (8 g.L ⁻¹)	1464.44

NS: not significantly different.

The Number of Leaves Per Plant

The results in *Table 5* reveal fertigation levels and their combinations. There is an increasing trend in the number of leaves per plant notwithstanding there is no statistically significant difference among the groups. The highest measurement recorded by fertigation with seaweed (Alga 600) in 8 g.L⁻¹ (11.33 unit), and the lowest one recorded by the control group (9.48 unit).

Table 5. The effect of fertigation of seaweed on leaves number of per plant.

Name	Number of leaf per plant ^{NS}
T1 (Control)	9.48
T2 (2 g.L ⁻¹)	9.74
T3 (4 g.L ⁻¹)	10.59
T4 (8 g.L ⁻¹)	11.33

NS: not significantly different.

Vegetative Fresh Weight

Table 6 shows that the effect of seaweed (Alga 600) on vegetative fresh weight. Despite there is an increasing trend on vegetative fresh weight compared with control, this increase is not significant. The fertigation of seaweed (Alga 600) in 8 g.L⁻¹ gives the maximum value of vegetative fresh weight (65.95 g) and the lowest value recorded by control (53.02 g). These result can be explained by the favorable effects of seaweed for the increase in the parameters such as single leaf area and leaf number per plant (El-Miniawy et al., 2014; Saif Eldeen et al., 2014).

Table 6. The effect of fertigation of seaweed on vegetative fresh weight.

Name	Vegetative fresh weight (g) ^{NS}
T1 (Control)	53.02
T2 (2 g.L ⁻¹)	58.12
T3 (4 g.L ⁻¹)	62.23
T4 (8 g.L ⁻¹)	65.95

NS: not significantly different.

Vegetative Dry Weight

As shown in Table 7, the effect of seaweed (Alga 600) on vegetative dry weight, there is a raise compared with control, and it shows the fertigation of seaweed (Alga 600) in 8 g.L⁻¹ gives the maximum value of vegetative dry weight (23.96 g) and the lowest value read by control (17.74 g). The reason behind this observation might be caused by seaweed (Alga 600) components, as discussed before. Besides, our records revealed that there is an increasing trend for single leaf area, the number of leaves per plant and vegetative fresh weight. Previous studies reported that seaweed extracts lead to the spectacular physiological performance of the plants (El-Yazied et al., 2012; El-Miniawy et al., 2014; Saif Eldeen et al., 2014).

Table 7. The effect of fertigation of seaweed on Vegetative dry weigh.

Name	Vegetative dry weight (g) ^{NS}
T1 (Control)	17.74
T2 (2 g.L ⁻¹)	20.50
T3 (4 g.L ⁻¹)	21.87
T4 (8 g.L ⁻¹)	23.96

NS: not significantly different.

Root Dry Weight

Data in *Table 8* shows the effect of seaweed (Alga 600) on root dry weight. The fertigation of seaweed (Alga 600) in 8 g.L⁻¹ give the maximum value of root dry weight (12.31 g) and the lowest value recorded by the control group (8.36 g). Again, we observed an improvement in dry root weight with seaweed (Alga 600) treatment yet it is not significant. Vitamins, minerals and some trace elements might have caused this observation. Our records are compatible with previous studies (Abdel-Mawgoud et al., 2010; Shehata et al., 2011; El-Yazied et al., 2012).

Table 8. The effect of fertigation of seaweed on root dry weight.

Name	Root dry weight (g) ^{NS}
T1 (Control)	8.36
T2 (2 g.L ⁻¹)	8.62
T3 (4 g.L ⁻¹)	11.96
T4 (8 g.L ⁻¹)	12.31

NS: not significantly different.

Chlorophyll Content in Plant

As shown in *Table 9*, seaweed (Alga 600) augments total chlorophyll content despite the statistically significant difference. The fertigation of seaweed (Alga 600) in 8 g.L⁻¹ resulted with the maximum value of total chlorophyll content in the leaf (41.09 unit) and the lowest value recorded by the control (38.41 unit). This observation can be grounded by the amino acid content of seaweed. Seaweed treatment eases amino acid accession of the plant which culminates in provoked protein synthesis and this leads to the higher amount of photosynthetic pigment production, the total chlorophyll in the leaves. Previous studies also approve this observation (Thirumaran et al., 2009; Shehata et al., 2011; El-Miniawy et al., 2014; Mohamed, 2015).

Table 9. The effect of seaweed fertigation on total chlorophyll in leaves.

Name	Total Chlorophyll in leaf (Unit) ^{NS}
T1 (Control)	38.41
T2 (2 g.L ⁻¹)	38.81
T3 (4 g.L ⁻¹)	39.72
T4 (8 g.L ⁻¹)	41.09

NS: not significantly different.

Plant Runner Properties

Data has shown in *Table 10*, the effect of seaweed (Alga 600) on number daughter plant and number of stolon that there is an increase compared with control. However, it is not significant, and it pointed that the fertigation of seaweed (Alga 600) in 8 g.L⁻¹ give the maximum value of number daughter plant (4.55 unit) and for number of stolon (7.29 unit) and lowest value recorded by control treatment for daughter plant (3.44 unit) and number of stolons is (5.85 unit). These results suggest that the physiological and biological activity of seaweed extract, containing high levels of auxin and cytokinins, stimulates the cell division in the plant. Another parameter can be GA₃ which causes an

increase of the number of the runners, growth in length of the cell, and elongation of internodes. Our results are coherent with previous papers by Hytönen et al. (2009), Ragab et al. (2010), Abo Sedera et al. (2014) and Mohamed (2015).

Table 10. The effect of fertigation of seaweed on plant runner properties.

Name	Number of runner (daughter plant) ^{NS}	Number of stolon ^{NS}
T1 (Control)	3.44	5.85
T2 (2 g.L ⁻¹)	3.71	6.66
T3 (4 g.L ⁻¹)	3.70	6.70
T4 (8 g.L ⁻¹)	4.55	7.29

NS: not significantly different.

The Number of Crowns

Data in *Table 11* has showed that the effect of seaweed (Alga 600) on the number of crowns. We observed that there is a significant increase in the number of crowns of treatment groups compared with control. The fertigation of seaweed (Alga 600) in 4 g.L⁻¹ and 8 g.L⁻¹ given rise to the maximum value of the number of crowns (T3=3.64 unit) and (T4=3.5 unit) and the lowest value recorded by control (2.75 unit). These records are thought to be driven by the physiological and biological activity of seaweed extract, which is rich in terms of auxin and cytokinins. Hence, cell division on the plant must be triggered. These results are coherent with studies of Khalid et al. (2013) and Mohamed (2015).

Table 11. The effect of seaweed fertigation on the number of crowns.

Name	Number of crown ^{**}
T1 (Control)	2.75b
T2 (2 g.L ⁻¹)	2.719b
T3 (4 g.L ⁻¹)	3.64a
T4 (8 g.L ⁻¹)	3.50a

** : p<0.01, significant at 0.01 level.

Fruit Setting Percentage

As shown in *Table 12*, the effect of seaweed (Alga 600) on fruit setting percentage is not significant but an increasing trend is detected (T4=8 g.L⁻¹) compared with control. The fertigation of seaweed (Alga 600) in 8 g.L⁻¹ culminated in the maximum value of setting percentage (T4=80%) and the lowest value recorded by control treatment (T1=70%). These results are consistent with previous studies of Khalid et al. (2013) and Mohamed (2015).

Table 12. The effect of seaweed fertigation on fruit setting percentage.

Name	Fruit Setting percentage ^{NS}
T1 (Control)	70%
T2 (2 g.L ⁻¹)	74%
T3 (4 g.L ⁻¹)	78%
T4 (8 g.L ⁻¹)	80%

NS: not significantly different.

The number of fruits per plant

Records of the number of fruits per plant are shown in *Table 13*. The significant effect of seaweed (Alga 600) is observed in the number of fruits per plant. Specifically, there was a significant increase in T4 and T3 compared with control (T1). The fertigation of seaweed (Alga 600) in 8 g.L⁻¹ resulted in the maximum value of the number of fruits per plant (T4-17.70 unit) and the lowest value recorded by control treatment (T1-11.81 unit). Increasing the vegetative growth or the number of crowns per plant might be the cause of this finding.

Table 13. *The effect of seaweed fertigation on number of fruits per plant.*

Name	Number of fruits per plant**
T1 (Control)	11.81b
T2 (2 g.L ⁻¹)	13.40ab
T3 (4 g.L ⁻¹)	17.22a
T4 (8 g.L ⁻¹)	17.70a

** : p<0.01, significant at 0.01 level.

The average weight of the fruit

The effect of seaweed (Alga 600) is shown in *Table 14*. Seaweed does not have a significant effect on the average weight of the fruit. On the other hand, we observed an increase in T4 compared with T3 and T2. The maximum value of the average weight of fruit (g) was T4=16.85 g and the lowest value recorded by T3=14.65 g. The seaweed extract improves some vegetative characteristics. It also stimulates production quality and quantity through the enhancement of photosynthetic process. Accordingly, Abdurraheem (2009) has affirmed that seaweed application leads to the improvement in the development of fruit diameter, strength, and length in addition to a better rate of fruit production. In spite of there is no direct correlation between treatment groups, this finding might be caused by increasing the vegetative growth or the number of the crown.

Table 14. *The effect of seaweed f fertigation on Average weight of fruit.*

Name	Average weight of fruit (g) ^{NS}
T1 (Control)	15.80
T2 (2 g.L ⁻¹)	15.11
T3 (4 g.L ⁻¹)	14.65
T4 (8 g.L ⁻¹)	16.85

NS: not significantly different.

Average and Total volume of fruit per plant

In *Table 15*, data showed the effect of seaweed (Alga 600) on the average volume of fruit (ml³). There is no significant effect but there is an increasing trend in T4 compared with other treatments T1 and T2. The fertigation of seaweed (Alga 600) in 8 g.L⁻¹ gave the maximum value of the average volume of fruit (ml³) (T4=18.88 ml³) and total volume of fruit (ml³) (T4=329.37 ml³) and the lowest value recorded by control treatment. This records can be explained by the fact that seaweed application leads to

the improvement in the development of fruit diameter, strength, and length in addition to a better rate of fruit production (Abdulraheem, 2009).

Table 15. The effect of seaweed fertigation on average and total volume of fruit.

Name	Average volume of fruit (ml ³) ^{NS}	Total volume of fruit (ml ³) [*]
T1 (Control)	17.50	211.74b
T2 (2 g.L ⁻¹)	16.89	228.14b
T3 (4 g.L ⁻¹)	16.60	285.92ab
T4 (8 g.L ⁻¹)	18.88	329.37a

NS: not significantly different, *: p<0.05, significant at 0.05 level.

Plant yield and yield per area unit

The influence of seaweed (Alga 600) on yield per plant (g) and per hectare (kg/ha) are shown in *Table 16*. There is a significant increase in T4 compared with control (T1) and T2. The fertigation with seaweed (Alga 600) in and 8 g.L⁻¹ resulted in the maximum value of yield per plant (g) T4-295.03 g and per hectare T4-3278.18 kg/ha. The lowest value belongs to the negative control. This results can be explained as seaweed extract improves some vegetative characteristics. It also stimulates the quality and quantity of production through the augmentation of the photosynthetic process. Accordingly, Abdulraheem (2009) has affirmed that seaweed application leads to the improvement in the development of fruit diameter, strength, and length in addition to a better rate of fruit production. This increase leads to improved vegetative growth or number of the crowns.

Table 16. The effect of seaweed fertigation on yield per plant and yield per hectare.

Name	Yield per plant (g) [*]	Yield per hectare (kg/hectare) [*]
T1 (Control)	191.70b	2130.04b
T2 (2 g.L ⁻¹)	204.11b	2267.90b
T3 (4 g.L ⁻¹)	254.11ab	2823.45ab
T4 (8 g.L ⁻¹)	295.03a	3278.18a

*: p<0.05, significant at 0.05 level.

Total soluble solid (TSS)

According to the findings in *Table 17*, the effect of seaweed (Alga 600) on total soluble solid (TSS) that there is an increase compared with control. However, it was not significant and it has shown the fertigation of seaweed (Alga 600) in 8 g.L⁻¹ resulted in the maximum value of total soluble solid (TSS) (7.46 unit) and lowest value recorded by control (6.85 unit). These results are compatible with reports from El-Moniem and Abd-Allah (2008) and Taha (2008).

Total acidity (TA)

In *Table 18* the effect of seaweed (Alga 600) on total acidity (TA), there are significant differences among the treatment groups. Increasing of levels of seaweed extract (Alga 600) decreases the TA, control treatment has significantly different than T2 and higher than T4 but it is not significant, and it showed the maximum value in

control treatment and lowest value recorded by fertigation of seaweed (Alga 600) in 2 g.L^{-1} , because while TSS increase, the TA decrease.

Table 17. The effect of seaweed fertigation on total soluble solid.

Name	Total soluble solid (TSS) ^{NS}
T1 (Control)	6.85
T2 (2 g.L^{-1})	7.39
T3 (4 g.L^{-1})	7.05
T4 (8 g.L^{-1})	7.46

NS: not significantly different.

Table 18. The effect of seaweed fertigation on Total acidity.

Name	Total acidity* (TA)
T1 (Control)	0.88a
T2 (2 g.L^{-1})	0.69b
T3 (4 g.L^{-1})	0.74ab
T4 (8 g.L^{-1})	0.80ab

*: $p < 0.05$, significant at 0.05 level.

TSS/TA ratio (ripening index)

The findings have shown in *Table 19*, the effect of seaweed (Alga 600) on TSS/TA ratio in T4 and T2 significantly increased compared with control. It showed the fertigation of seaweed (Alga 600) in 8 g.L^{-1} gave the maximum value of TSS/TA ratio (13.35 unit) and the lowest value recorded by control treatment (8.29 unit). These results are coherent with that information by El-Moniem and Abd-Allah (2008) and Taha (2008).

Table 19. The effect of seaweed fertigation on TSS/TA ratio.

Name	TSS/TA ratio**
T1 (Control)	8.29b
T2 (2 g.L^{-1})	13.11a
T3 (4 g.L^{-1})	11.81ab
T4 (8 g.L^{-1})	13.35a

** : $p < 0.01$, significant at 0.01 level.

Conclusion

According to the results of our study the effect of seaweed (Alga 600) on the flowering, vegetative growth and fruiting of strawberry cv. Albion, the following conclusion can be drawn. The seaweed extract at 2 g.L^{-1} is less effective on strawberry vegetative properties, flowering and yield properties and chemical characteristics of fruit than other treatment. The seaweed extract (Alga 600) at 4 g.L^{-1} is more effective than 2 g.L^{-1} and it has a significant effect on the number of the crowns, number of flowers, number of the fruits at 0.01 level, and total volume of the fruit, yield per plant, yield per hectare, TA and TSS/TA ratio at 0.05 level. The seaweed extract at a higher

concentration (8 g.L⁻¹) has the more effective to increase the vegetative growth, flowering and yield properties. Organic fertigation (Alga 600) has a significant effect on the number of the crown, number of flowers, number of the fruit at 0.01 level, and total volume of fruit, yield per plant, yield per hectare, TA and TSS/TA ratio.

Seaweed fertilizers are an important alternative organic fertilizing to increase yield and to achieve a better quality product. The use of seaweed as support for fertilization in production increases the yield and quality while ensuring the sustainability of the soil due to its ecological nature. Strawberry, with high economic returns; rich in taste, aroma and antioxidant substances and no marketing problems, is a fruit. Strawberry cultivation is not common in Iraq yet. In this sense, the result of our study is a guide for those who want to cultivate strawberry in Iraq. In conclusion, as the amount of seaweed extract applied increased, vegetative growth rate and flowering rate increased in our experiment. For this reason, in particular, we believe that the application of doses above 8 g.L⁻¹ will significantly increase the productivity and quality of yield.

Acknowledgements. This article is produced from the MSc Thesis belongs to A.H.N. AL-SHATRI and the thesis has been funded with the project (2017-SIÜFEB-90) by Scientific Research Projects Council, Siirt University.

REFERENCES

- [1] Abdel-Mawgoud, A. M. R., Tantawy, A. S., Hafez, M. M., Habib, H. A. M. (2010): Seaweed extract improves growth, yield and quality of different watermelon hybrids. – Res. J. Agric. & Biol. Sci. 6(2): 161-186.
- [2] Abdulraheem, S. M. (2009): Effect of nitrogen fertilizer and seaweed extracts on vegetative growth and yield of cucumber. – Diyala Agric. Sci. J. 1: 134-145.
- [3] Abo Sedera, F. A., Bader, L. A., Abd El-Latif, A. A., Rezk, S. M. (2014): Effect of mineral N, P plus P Bio-fertilizer levels and foliar spray with calcium and seaweed extract on strawberry productivity. – J. Biol. Chem. Environ. Sci. 9(3): 343-366.
- [4] Aitken, J. B., Senn, T. L. (1965): Seaweed products as a fertilizer and soil conditioner for horticultural crops. – Botanica Marina 8(1): 144-147.
- [5] Al-Hermizy, S. M. M. (2011): Study the effect of Cyanobacteria Inoculation and Spraying of Sea Alga (Alga 600) in growth and yield and chemical properties of strawberry plants (*Fragaria x ananass* Duch). – Journal of Tikrit Univ. for Agric. Sci. 11(3): 40-50.
- [6] Anonymous (2017): Statistical data. – Agrometeorology Directorate, Sulaymaniyah / Iraq.
- [7] Cordenunsi, B. R., Nascimento, J. D., Lajolo, F. M. (2003): Physico-chemical changes related to quality of five strawberry fruit cultivars during cool-storage. – Food Chemistry 83(2): 167-173.
- [8] Darrow, G. (1966): The Strawberry: history, breeding and physiology. – Holt, Rinehart and Winston, New York, Chicago, 447 p.
- [9] El-Miniawy, S. M., Ragab, M. E., Youssef, S. M., Metwally, A. A. (2014): Influence of foliar spraying of seaweed extract on growth, yield and quality of strawberry plants. – Journal of Applied Sciences Research 10: 88-94.

- [10] El-Moniem, E. A. A., Abd-Allah, A. S. E. (2008): Effect of green Alga cells extract as foliar spray on vegetative growth, yield and berries quality of superior grapevines. – J. Amer. Eur. Agric. and Environ. Sci. 4(4): 427-33.
- [11] El-Yazied, A. A., El-Gizawy, A. M., Ragab, M. I., Hamed, E. (2012): Effect of seaweed extract and compost treatments on growth, yield and quality of snap bean. – Journal of American Science 8(6): 1-20.
- [12] Eshghi, S., Zare, M., Jamali, B., Gharaghani, A., Farahi, M. H. (2013): Vegetative and Reproductive Parameters of Selva Strawberry as Influenced by Algren, Drin and Green Hum Foliar Application. – Agricultural Communications 1(1): 27-32.
- [13] Gülsoy, E., Yılmaz, H. (2004): The effects on adaptation of some strawberry cultivars grown under different tunnels in Van ecological conditions. – YYU. J. Inst. Natural Applied Sci. 9(1): 50-57.
- [14] Hancock, J. F. (1999): Strawberries. – CABI Publishing, Wallingford, Oxon OX10 8DE, UK. 237 p.
- [15] Häkkinen, S. H., Törrönen, A. R. (2000): Content of flavonols and selected phenolic acids in strawberries and Vaccinium species: influence of cultivar, cultivation site and technique. – Food research international 33(6): 517-524.
- [16] Hytönen, T., Elomaa, P., Moritz, T., Junttila, O. (2009): Gibberellin mediates daylength-controlled differentiation of vegetative meristems in strawberry (*Fragaria* × *ananassa* Duch). – BMC Plant Biology 9(1): 18.
- [17] Katiyar, P. N., Singh, J. P., Singh, P. C. (2009): Effect of mulching on plant growth, yield and quality of strawberry under agro-climatic conditions of Central Uttar Pradesh. – International Journal of Agricultural Sciences 5(1): 85-86.
- [18] Khalid, S., Qureshi, K. M., Hafiz, I. A., Khan, K. S., Qureshi, U. S. (2013): Effect of organic amendments on vegetative growth, fruit and yield quality of strawberry. – Pakistan Journal of Agricultural Research 26(2).
- [19] Kivijärvi, P., Prokkola, S., Aflatuni, A., Parikka, P., Tuovinen, T. (2002): Cultivation techniques for organic strawberry production in Finland. – Proceedings of the fourth international strawberry symposium: volume 2/ed. International Society for Horticultural Science.
- [20] Kumar, R., Saravanan, S., Bakshi, P., Sharma, R. M. (2013): Influence of Gibberellic Acid and Blossom Removal on Fruit Quality of Strawberry (*Fragaria* × *ananassa* Duch.) CV. Belrubi. Vegetos. – An International Journal of Plant Research 26(1): 107-110.
- [21] Macant-Saoir, S., Archer, J. (2008): The effect of Alga green 200 (cold-process seaweed liquid extract) on the mineral content of 'Bramley's Seedling' apple leaves and fruit. – VI International Symposium on Mineral Nutrition of Fruit Crops 868: 301-306.
- [22] Mae, H., Ooi, J., Takahashi, S., Tomonari, A., Tsukada, N., Konumai, T. (2008): Early renal injury after myeloablative cord blood transplantation in adults. – Leuk Lymphoma 49: 538-42.
- [23] Mansour, A. E., Cimpoies, G., Ahmed, F. F. (2006): Application of Alga extract and boric acid for obtaining higher yield and better fruit quality of Anna apple. – Stiinta agricola (Republic of Moldova) 2: 14-20.
- [24] Masny, A., Basak, A., Zurawicz, E. (2004): Effects of foliar applications of Kelpak SL and Goëmar BM 86® preparations on yield and fruit quality in two strawberry cultivars. – Journal of fruit and ornamental plant research (12): 23-27.

- [25] Mohamed, M. (2015): Effect of some growth stimulants on production and quality of strawberry transplants. – *Annals of Agric. Sci. Moshtohor* 53(4): 693-708. ISSN 1110-0419.
- [26] Panda, D., Pramanik, K. B., Naya, R. (2012): Use of sea weed extracts as plant growth regulators for sustainable agriculture. – *Int. J. Biores. Stress Manage.* 3(3): 404-411.
- [27] Ragab, M. E., Omran, A. E., Youssef, S. M., Sabt, W. M. (2010): Effect of some application and agricultural practices on runner formation and transplant production in strawberry nurseries. – *J. Biol. Chem. Environ. Sci.* 5(4): 247-261.
- [28] Saif Eldeen, U. M., Shokr, M. M., Shotoury, R. S. (2014): Effect of foliar spray with seaweeds extract and chitozan on earliness and productivity of globe artichoke. – *Journal of Plant protection, Mansoura Univ.* 5(7): 1197-1207.
- [29] Sharma, R. R. (2002): *Growing strawberry*. – Int. Book Distributing Co., India 1: 01-02.
- [30] Shehata, S. M., Abdel-Azim, H. S., El-Yazied, A. A., El-Gizawy, A. M. (2011): Effect of foliar spraying with amino acids and seaweed extract on growth chemical constituents, yield and its quality of celeriac. – *Plant. Euro. J. Sci. Res.* 58(2): 257-265.
- [31] Taha, S. M. (2008): Effect of foliar spray of gibberellic acid, Cycocel and three of seaweed extract in some characters of vegetative growth, flower and yield components characteristics of two varieties of strawberry (*Fragaria × ananassa* Duch.). – PhD Thesis. Dept of Hort. and Forest. College of Agric. Uni. Salah Eldin – Erbil.
- [32] Temple, W. D., Bomke, A. A. (1988): Effects of kelp (*Macrocystis integrifolia*) on soil chemical properties and crop responses. – *Plant Soil* 105: 213-222.
- [33] Thirumaran, G., Arumugam, M., Arumugam, R., Anantharaman, P. (2009): Effect of seaweed liquid fertilizer on growth and pigment concentration of *Abelmoschus esculentus* (l) medikus. – *American-Eurasian Journal of Agronomy* 2(2): 57-66.
- [34] Watt, B. K., Merrill, A. L., Pecot, R. K. (1963): *Composition of Foods: Raws, Processed, Prepared*. – Agriculture Handbook No: 8. Washington, DC. US Department of Agriculture.

PHYSIOLOGICAL AND MOLECULAR BASIS OF THE EFFECTS OF EXOGENOUS SELENIUM APPLICATION ON WHEAT SEEDLING PERFORMANCE UNDER DROUGHT STRESS

CHEN, R. J.¹ – WANG, L. X.^{2*} – ZHANG, X. J.³ – WANG, S. L.¹ – LI, H.¹ – GAO, S. J.¹

¹*Agricultural and Rural Bureau of Dingtao District, Heze City, Shandong Province 274100, PR China*

²*Academy of Agricultural Sciences, Heze City, Shandong Province 27400, PR China*

³*Caozhou Agricultural Chemistry Co., Ltd., Heze City, Shandong Province 27400, PR China*

*Corresponding author
e-mail: twidh1611@163.com

(Received 17th Aug 2019; accepted 15th Nov 2019)

Abstract. Drought stress is a severe problem for wheat production. The purpose of the present experiment was to study the effects of the exogenous sodium selenite application at different concentrations on wheat seedlings performance under drought stress. Two wheat varieties, ‘*Shunmai-1718*’ and ‘*Jintai-102*’ were used as materials in this study and four selenium concentration levels were prepared from distilled water (CK), and 20 mg/L (Se1), 40 mg/L (Se2) and 60 mg/L (Se3) of sodium selenite. 7 days after the sowing, the sodium selenite solutions were foliarly applied to wheat seedlings. 9 days after the sowing, 20% PEG-6000 was used to simulate drought conditions for 7 days. The results showed that exogenous selenium significantly increased the plant height, root length, root number, fresh weight and dry weight of wheat seedlings under drought stress. Foliar application of sodium selenite under drought stress also increased antioxidant enzyme activity and the osmoprotectant contents while reducing the content of MDA and O₂⁻. Furthermore, the application of sodium selenite under drought stress up-regulated the levels of transcriptional expression in some genes related to antioxidative enzymes and osmo-protectants such as Plant peroxidase, Class III peroxidase, Glutathione S-transferase and Catalase immune-responsive.

Keyword: *wheat, selenite, drought resistance, gene expression, antioxidant*

Introduction

China is a big wheat (*Triticum aestivum* L.) planting country reaching 10.5% of the global planting area, but around 70% of it is distributed over arid and semiarid regions (Xuan et al., 2017). Many studies had showed that drought stress could severely affect the growth and development of crops (Clauw et al., 2015; Hatmi et al., 2015). The study of Hao et al. (2015) indicated that the problems of wheat yield reduction and poor grain quality caused by drought always exist in the process of wheat cultivation. Thus, effective ways to relieve the drought stress are required to achieve the goal of ensuring the stability of wheat productivity and exogenous plant growth regulators might come in handy.

Selenium (Se) is a necessary chemical element for human body. It exists in nature in two forms: inorganic Se and organic Se. Selenium has the functions of anti-cancer, anti-oxidation and improving human immunity (Broghamer et al., 1976; Scott et al., 1998). Coronary heart disease, hypertension, Kashin-Beck disease and other diseases are all related to selenium deficiency, and low selenium environment is one of the main factors for the occurrence of these diseases (Rayman, 2012). Although selenium is not an essential element in plants, it has a significant effect on the physiological characteristics of plants. A number of studies showed that Se application could enhance the crops

performance. For example, He et al. (2019) demonstrated that foliar application of sodium selenate at low concentration could enhance the antioxidant enzymes activities and increase the chlorophyll content of rice. The study of Duan et al. (2019) revealed that exogenous Se application at heading stage could delay the senescence of rice leaves at grain filling stage. Some early studies have shown selenium can improve the drought resistance of wheat or alleviate the damage caused by drought stress (Yao et al., 2009a,b). However, the physiological and molecular basis for effects of exogenous selenium on wheat seedlings performance under drought stress remained largely unexplored.

Hence, present study was conducted with four concentration of exogenous selenite in order to explore the effect of foliar application of sodium selenite on wheat seedling under drought stress and the related physiological and molecular basis.

Materials and Methods

Plant materials and experimental details

Present experiment was conducted in the College of Agriculture with two wheat cultivars, *Yangmai9023* and *Zhengmai20*, which are widely planted in Central China. Before sowing, the selected seeds were soaked with 0.1% HgCl₂ for 15 minutes for sterilization, and then washed by distilled water, shade dried, the seeds were sowed into culture dish (9 cm in diameter and 50 seeds for each dish). 7 days after the sowing, the sodium selenite solutions (0 (CK), 10 (Se1), 20 (Se2), 30 (Se3) mg L⁻¹ and 40 (Se4) mg L⁻¹) were foliar applied to wheat seedlings. 9 days after the sowing, 20% PEG-6000 was used to simulate drought conditions for 7 days.

Seedling quality

After 7 days of cultivation under drought stress, 15 wheat seedlings with the same growth status were selected in each dish, and their plant height, root length, root number, fresh weight and dry weight were measured.

Estimation of superoxide anion (O₂⁻), malondialdehyde (MDA) and anti-oxidant responses

The MDA content and activities of peroxidase (POD), superoxide (SOD) and catalase (CAT) were detected according to the methods of Kong et al. (2017). After MDA reacted with thiobarbituric acid, the absorbance was read at the 532, 600 and 450 nm. The MDA content in the reaction solution was calculated as: MDA content (μmol/L) = 6.45 (OD₅₃₂ – OD₆₀₀) – 0.56OD₄₅₀, and finally expressed as μmol/g FW. POD (EC 1.11.1.7) activity was estimated after the reaction in the solution including enzyme extract (50 μl), 1 ml of 0.3% H₂O₂, 0.95 ml of 0.2% guaiacol, and 1 ml of 50 mM·l⁻¹ sodium phosphate buffer (SPB, pH 7.0). One POD unit of enzyme activity was expressed as the absorbance increase by 0.01 (U/g FW) due to guaiacol oxidation. SOD (EC 1.15.1.1) activity was measured by using nitro blue tetrazolium (NBT). In brief, 0.05 ml of an enzyme extract was added into the reaction mixture which contained 1.75 ml of SPB (pH 7.8), 0.3 ml of 130 mM methionine buffer, 0.3 ml of 750 μmol·L⁻¹ NBT buffer, 0.3 ml of 100 μmol·L⁻¹ ethylene diamine tetraacetic acid (EDTA)-2Na buffer and 0.3 ml of 20 μmol·L⁻¹ lactoflavin. After the reaction, the absorbance was recorded at 560 nm. One unit of SOD activity was equal to the volume of the extract needed to cause 50% inhibition of the color reaction. CAT (EC 1.11.1.6) activity was estimated by adding an aliquot of enzyme

extract (50 µl) to the reaction solution containing 1 ml of 0.3% H₂O₂ and 1.95 ml of SPB and then the absorbance was read at 240 nm. One CAT unit of enzyme activity was defined as the absorbance decrease by 0.01 (U/g FW). Ascorbate peroxidase (APX, EC 1.11.1.11) activity was estimated by using “APX determination kit” purchased from Nanjing Jiancheng Bioengineering Institute, China (Ashraf et al., 2017). The estimation of superoxide anion (O₂⁻) was according to the method of Shah et al. (2001) and the content of O₂⁻ was expressed as nmol g⁻¹ FW.

Estimation of soluble protein, proline, reduced glutathione (GSH) and ascorbic acid (AsA)

The contents of soluble protein and proline were detected according to the methods of Li et al. (2016). In brief, the reaction mixture of 2-ml proline and 4 ml of 1.25% ninhydrin in glacial acetic acid was bathed at 100°C for 30 min, and then the absorbance of the reaction mixture was recorded at 508 nm. Protein concentration was measured based on the standard curve of bovine serum albumin after reaction with Coomassie Brilliant Blue G250 Reagent. The measurement of GSH was described by Ashraf et al. (2018) and the instructions were strictly followed and the absorbance was read at 420 and 412 nm. The determination of AsA was according to Yu et al. (2017). About 0.1 g of fresh flag leaves or endosperms were homogenized in 1 mL 6% trichloroacetic acid (TCA) solution in an ice bath, and the homogenate was centrifuged at 12 000 rpm and 4°C for 10 min and the supernatant was used for AsA analysis.

Real-time quantitative RT-PCR

Fresh leaves (0.03 g) were collected for total RNA extraction. Total RNA was extracted using HiPure Plant RNA Mini Kit (Magen, Guangzhou, China). The quality and quantity of RNA was assessed by Nanodrop 2000. The Hiscript II QRT SuperMix for qPCR (+gDNA wiper) (Vazyme, Nanjing, China) was used to synthesize cDNA from 500 ng of total RNA. The following mixtures were prepared in qPCR tubes: 4.4 µl cDNA, 0.2 µl each for forward and reverse primers, 5 µl 2*chamQ SYBR qPCR Master MiX and 0.2 µl ROX reference Dye 1, ddH₂O to 20 µl (Vazyme, Nanjing, China). Real-time quantitative RTPCR (qRT-PCR) was conducted in CFX96 real-time PCR System (Bio-Rad, Hercules, CA, USA). Each RNA sample was performed in triplicate. A negative control without cDNA template was always included. Primers used for qRT-PCR were listed in *Table 1*. All primers were designed using the software tool Primer 5.

Table 1. Primer sequences of genes encoding enzymes involved in 2-AP synthesis in rice grains

Gene name	Primer sequences
<i>Plant peroxidase</i>	F 5'-TGATTCGTCCATCGTCTCG-3' R 5'-CGTGTAGCATTGCCGCTTA-3'
<i>ClassIII peroxidase</i>	F 5'-TTTGCCTCCGACTTCGTG-3' R 5'-TGCAGTTGCGCCTAATCT-3'
<i>Glutathione S-transferase</i>	F 5'-GCATCATCATTCCCTTCATC-3' R 5'-GCATCATCATTCCCTTCATC-3'
<i>Catalase immune-responsive</i>	F 5'-GTCTCAACGTGAAGCCAAGC-3' R 5'-GCACAGTAGGTAATCGACCACA-3'

Statistical analysis

Data were analyzed using statistical software 'Statistix 8.1' (Analytical Software, Tallahassee, FL, USA) while differences amongst means were separated by using least significant difference (LSD) test at 5% probability level. Graphical representation was conducted via Sigma Plot 14.0 (Systat Software Inc., California, USA).

Result

Seedling quality

Analysis of variance showed that foliar application of sodium selenite treatments significantly affected the wheat seedling quality (plant height, root length, root number, fresh weight and dry weight) under drought stress (*Table 2*). Comparing CK, Se1, Se2, Se3 and Se4 treatment all significantly increased plant height of rice seedling for *Zhengmai9023* and *Yangmai20*. The higher root lengths were recorded in Se1, Se2, Se3 and Se4 than CK for both cultivars. Similar trends were also observed in fresh weight and dry weight.

Table 2. The effect of exogenous sodium selenite on wheat seedling quality under drought stress

Cultivar	Treatment	Plant height (cm)	Root length (cm)	Root number	Fresh weight (g)	Dry weight (g)
<i>Zhengmai9023</i>						
	CK	16.37±0.20b	10.10±0.15b	5.13±0.24b	2.05±0.03b	0.23±0.00b
	Se1	17.52±0.25a	11.02±0.13a	5.40±0.13ab	2.15±0.02a	0.28±0.00a
	Se2	17.45±0.27a	11.12±0.16a	5.40±0.13ab	2.14±0.02a	0.28±0.01a
	Se3	17.48±0.25a	10.87±0.15a	5.47±0.13ab	2.16±0.02	0.27±0.01a
	Se4	17.56±0.25a	11.18±0.14a	5.67±0.13a	2.11±0.02a	0.27±0.00a
<i>Yangmai20</i>						
	CK	15.71±0.20b	8.53±0.23b	4.93±0.13b	1.90±0.02b	0.21±0.00b
	Se1	17.54±0.29a	10.48±0.24a	5.53±0.13a	2.07±0.02a	0.25±0.01a
	Se2	17.70±0.22a	10.22±0.22a	5.47±0.13a	2.06±0.02a	0.24±0.00a
	Se3	17.80±0.25a	10.29±0.29a	5.33±0.13a	2.06±0.02a	0.24±0.00a
	Se4	17.28±0.22a	10.59±0.25a	5.40±0.13a	2.08±0.02a	0.25±0.01a
Analysis of variance						
	Cultivar (C)	ns	**	ns	**	**
	Treatment (T)	**	**	**	**	**
	C × T	ns	ns	ns	*	ns

Values ± SE sharing a common letter within a column don't differ significantly at ($P \leq 0.05$) according to least significant difference (LSD) test. The same as below

MDA and O_2^- content

Analysis of variance showed that sodium selenite treatments significantly influenced the contents of MDA and O_2^- in wheat seedling under drought stress (*Figure 1*). For *Zhengmai9023* CK, Se1, Se2, Se3 and Se4 treatments significantly decreased the O_2^- content by 7.47, 6.68, 12.06 and 16.82% while 16.53, 16.67, 20.51 and 22.97% lower MDA contents were recorded in Se1, Se2, Se3 and Se4 than in CK. For *Yangmai20* CK, Se1, Se2, Se3 and Se4 treatments significantly decreased the O_2^- content by 12.33, 16.04, 20.75 and 27.22% while 14.74, 24.30, 26.82 and 35.56% lower MDA contents were recorded in Se1, Se2, Se3 and Se4 than in CK.

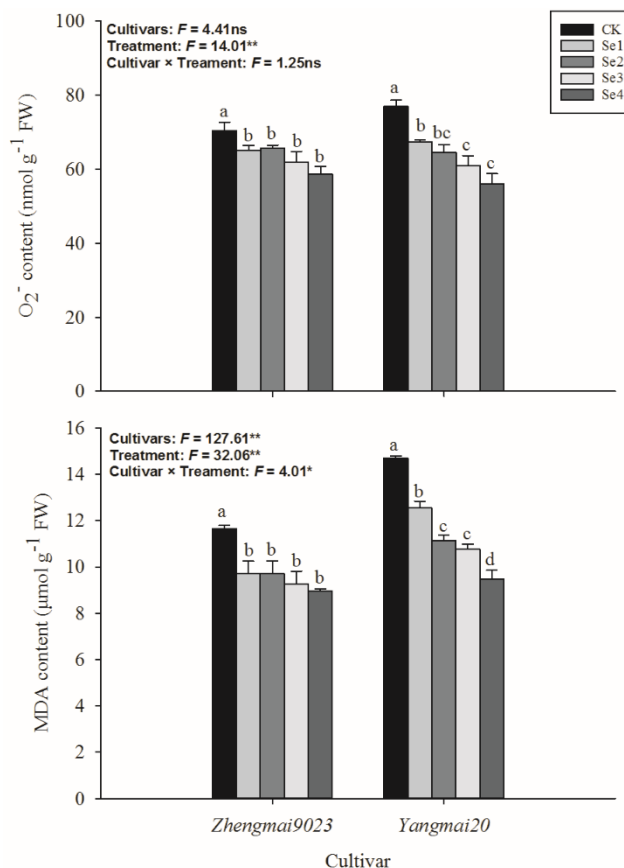


Figure 1. Effect of exogenous sodium selenite on MDA and O₂⁻ content of wheat seedling under drought stress (Bars within the same cultivar followed by a different letter are significantly different at $P < 0.05$ probability level)

Anti-oxidant enzymes activity

As shown in *Figure 2*, foliar application of sodium selenite significantly increased the anti-oxidant enzymes activities of wheat seedling under drought stress. Higher POD activities were recorded in Se1, Se2, Se3 and Se4 treatments than in CK in both cultivars and similar trends were also recorded in SOD activities. For CAT activities, Se1, Se2, Se3 and Se4 all significantly increased CAT activities compared to CK in *Yangmai20* whilst only Se3 and Se4 remarkably increased CAT activities in *Zhengmai9023*. For APX activities, comparing CK, Se2, Se3 and Se4 significantly increased APX activities were observed in *Zhengmai9023* while for *Yangmai20*, higher APX activities were recorded in Se1, Se2, Se3 and Se4 treatments than in CK.

Osmo-protectants

As shown in analysis of variance, exogenous selenium induced dynamics in soluble protein, proline, GSH and AsA accumulation under drought stress (*Figure 3*). For *Zhengmai9023* CK, Se2, Se3 and Se4 treatments increased the soluble protein, proline, GSH and AsA contents by 10.22-19.93, 6.54-10.98, 13.40-24.92 and 12.32-22.82%, respectively. For *Yangmai20* CK, Se2, Se3 and Se4 treatments increased the soluble protein, proline, GSH and AsA contents by 23.70-25.16, 10.89-26.95, 23.41-23.94 and 21.28-31.15%, respectively.

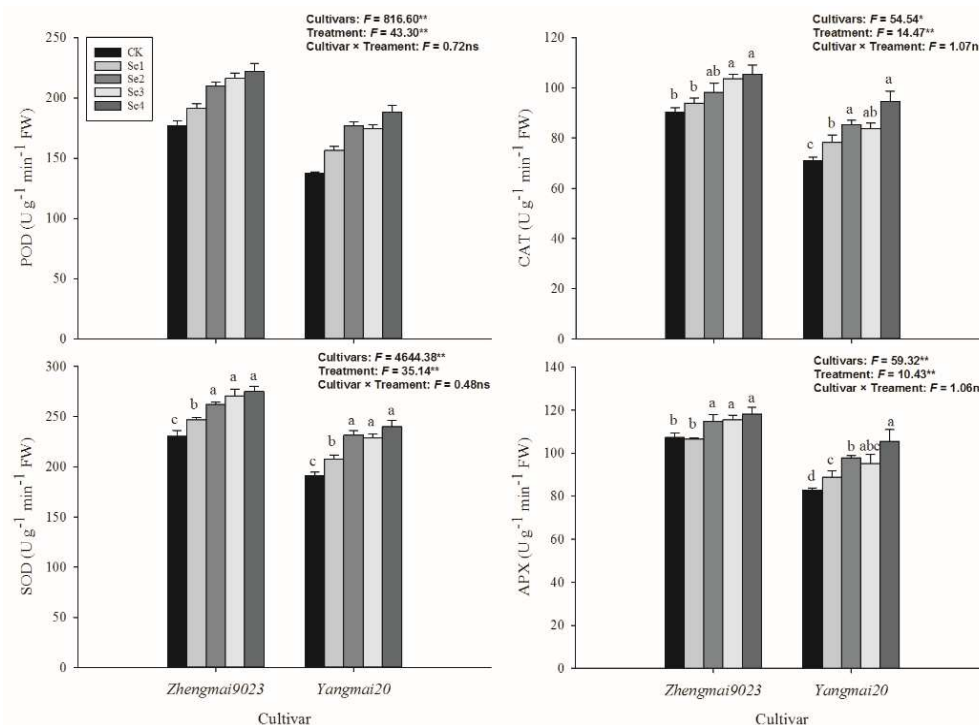


Figure 2. Effect of exogenous sodium selenite on anti-oxidant enzymes activities of wheat seedling under drought stress (Bars within the same cultivar followed by a different letter are significantly different at $P < 0.05$ probability level)

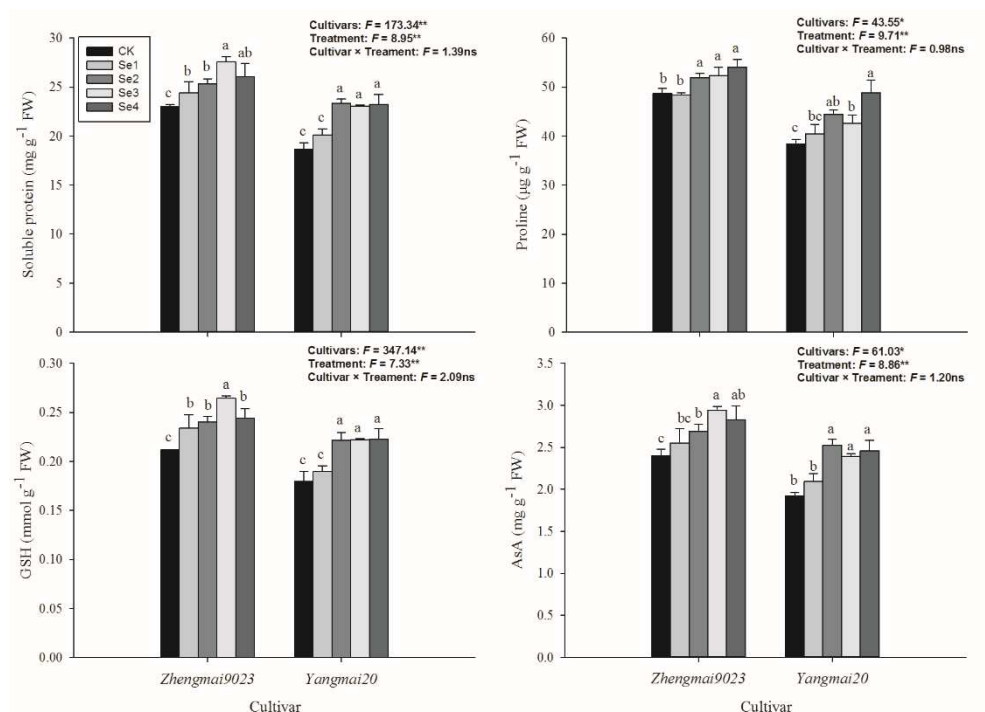


Figure 3. Effect of exogenous sodium selenite on contents of soluble protein, proline, GSH and AsA in wheat seedling under drought stress (Bars within the same cultivar followed by a different letter are significantly different at $P < 0.05$ probability level)

Real-time PCR analyses

As depicted in Figure 4, compared to CK, higher levels of *Plant peroxidase*, *Class III peroxidase*, *Glutathione S-transferase* and *Catalase immune-responsive* transcripts were found in Se2, Se3 and Se4 treatments for *Zhengmai9023* and *Yangmai20*.

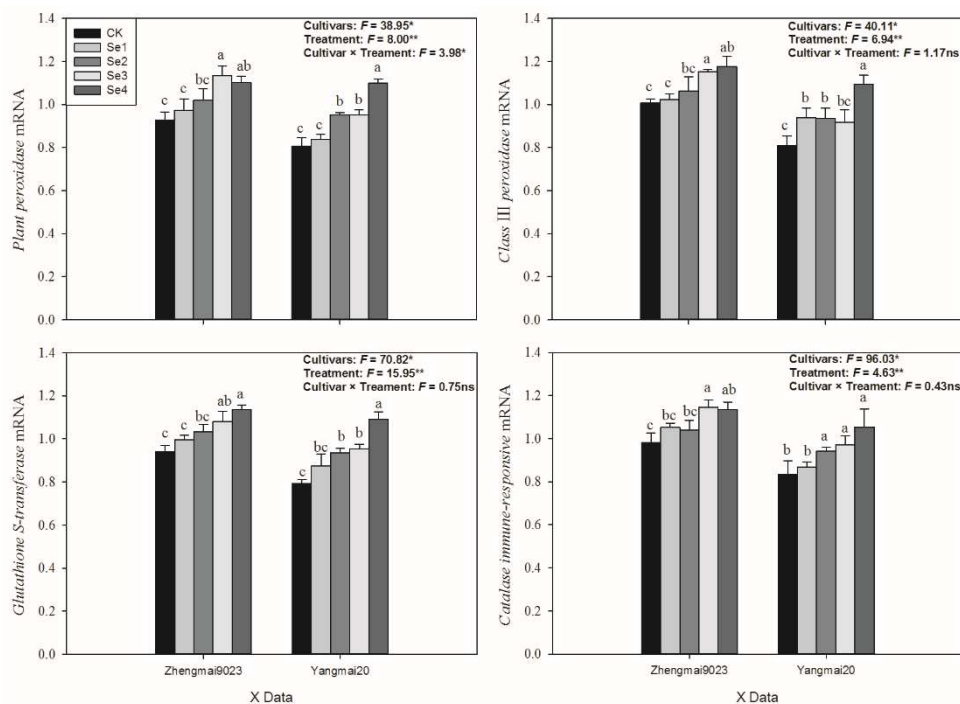


Figure 4. Analysis of transcript levels of *Plant peroxidase*, *Class III peroxidase*, *Glutathione S-transferase* and *Catalase immune-responsive* in wheat seedling under drought stress (Bars within the same cultivar followed by a different letter are significantly different at $P < 0.05$ probability level)

Discussion

Water is the main limiting factor for wheat growth and yield formation (Li et al., 2015). In recent years, due to climate change, frequent drought weather is one of the main natural disasters affecting wheat production in China (Wang et al., 2014). The tillering and root growth of wheat were mainly carried out at seedling stage and hence, the growth and development of seedling significantly affected the formation of effective panicle and grain number per panicle which are the yield components of wheat. Previous study revealed that drought stress in wheat seedling stage will seriously affect tillering and spikelet differentiation, and ultimately lead to yield reduction (Leilah and Al-Khateeb, 2005). Present study revealed the alleviative effect of Se application on wheat seedling to drought stress in two wheat cultivars. Foliar applications of Se improved the wheat seedling quality under drought stress in terms of plant height, root length, fresh weight and dry weight. This result agreed with the study of Yao et al. (2009b) who indicated that treatments with selenium was able to promote the biomass accumulation of wheat seedlings under drought stress.

When the plant is under drought stress, it will affect the metabolism of reactive oxygen species (ROS) in the plant, leading to the increase of the content of reactive oxygen

species in the plant (Kong et al., 2017). A large number of ROS can peroxidise the membrane lipids in plants to produce MDA which can damage the membrane structure of plant cells (Ashraf et al., 2017). Normally, plant itself has an antioxidant enzyme system to reduce the damage of cell membrane lipids in arid environment (Ashraf et al., 2018). Present study observed that foliar application of sodium selenite could regulated the anti-oxidative enzymatic activities in terms of SOD, POD, CAT and APX while reducing the oxidative damage by lowering the MDA and O_2^- production. The increase of O_2^- in plants will lead to the oxidation of polyunsaturated fatty acids, which will lead to the excessive accumulation of MDA. The anti-oxidative enzymes have significant roles in osmo-regulations and often help in maintaining cellular structures and functions under stress condition (Luo et al., 2018). For example, SOD dismutates superoxide radical whereas POD and CAT involved in scavenging H_2O_2 (Pan et al., 2013). In our study, the activities of SOD, POD, CAT and APX in wheat seedlings of two cultivars were significantly increased after applying exogenous selenium (Figure 2), and the contents of O_2^- and MDA were decreased (Figure 1) under PEG simulated drought stress. On the other hand, Se treatments also induced regulation in proline, soluble protein, GSH and AsA accumulation. Proteins and proline have significant roles in osmo-regulations and often help in maintaining cellular structures and functions while anti-oxidants help to quench ROS (Luo et al., 2018). Previous studies also indicated that both GSH and AsA are the most abundant non-enzymatic anti-oxidants in plants and also provide protection in plant cells from ROS-generated free radicals and serve as redox buffer (Ashraf et al., 2017). The regulations in anti-oxidative enzymatic activities and non-enzymatic antioxidants due to Se applications under drought stress may be attributed to higher levels of transcriptional expression of *Plant peroxidase*, *Class III peroxidase*, *Glutathione S-transferase* and *Catalase immune-responsive* genes. Our results indicated that the foliar application of Se in the appropriate concentration could increase the activities of antioxidant enzymes in wheat seedlings, enhance the ability of scavenging active oxygen free radicals and reduce the degree of membrane lipid peroxidation to alleviate the adverse effects of drought stress on crops.

As far as sodium selenite concentration was concerned, the highest activities of antioxidative enzyme and the highest content of osmo-protectants were all recorded in Se2, Se3 and Se4 for both cultivars while the lowest MDA and O_2^- was also recorded in Se2, Se3 and Se4 treatments for both cultivars. Thus, the optimized selenium amendment for wheat seedlings under drought stress might be the foliar application of 20-40 mg L⁻¹ sodium selenite.

Conclusion

Foliar application of sodium selenite under drought stress can promote root growth of wheat seedlings, maintain water content and biomass of plant tissues, increase activities of antioxidant enzymes and the contents of osmo-protectants while reducing the content of MDA and O_2^- . Furthermore, the application of sodium selenite under drought stress up-regulated the levels of transcriptional expression in some genes related to anti-oxidative enzyme and osmo-protectants such as *Plant peroxidase*, *Class III peroxidase*, *Glutathione S-transferase* and *Catalase immune-responsive*. More field experiments should be conducted in the future.

Acknowledgements. This study was supported by Shandong province key research and development project (2019GNC106121).

REFERENCES

- [1] Ashraf, U., Kanu, A. S., Deng, Q. Q., Mo, Z. W., Pan, S. G., Tian, H., Tang, X. R. (2017): Lead (Pb) Toxicity; Physio-Biochemical Mechanisms, Grain Yield, Quality, and Pb Distribution Proportions in Scented Rice. – *Frontiers in Plant Science* 8: 259.
- [2] Ashraf, U., Hussain, S., Akbar, N., Anjum, S. A., Hassan, W., Tang, X. R. (2018): Water management regimes alter Pb uptake and translocation in fragrant rice. – *Ecotoxicology and Environmental Safety* 149: 128-134.
- [3] Broghamer, W. L., McConnell, K. P., Blotcky, A. L. (1976): Relationship between serum selenium levels and patients with carcinoma. – *Cancer* 37: 1384-8.
- [4] Clauw, P., Coppens, F., De Beuf, K., Dhondt, S., Van Daele, T., Maleux, K., Storme, V., Clement, L., Gonzalez, N., Inzé, D. (2015): Leaf Responses to Mild Drought Stress in Natural Variants of Arabidopsis. – *Plant Physiology* 167(3): 800-16.
- [5] Duan, M. Y., Cheng, S. R., Lu, R. H., Lai, R. F., Zheng, A. X., Ashraf, U., Fan, P. S., Du, B., Luo, H. W., Tang, X. R. (2019): Effect of foliar sodium selenate on leaf senescence of fragrant rice in South China. – *Applied Ecology and Environmental Research* 17: 3343-3351.
- [6] Hao, P., Zhu, J., Gu, A., Lv, D., Ge, P., Chen, G., Li, X., Yan, Y. (2015): An integrative proteome analysis of different seedling organs in tolerant and sensitive wheat cultivars under drought stress and recovery. – *Proteomics* 15: 1544-1563.
- [7] Hatmi, S., Gruau, C., Trotel-Aziz, P., Villaume, S., Rabenoelina, F., Baillieul, F., Eullaffroy, P., Clement, C., Ferchichi, A., Aziz, A. (2015): Drought stress tolerance in grapevine involves activation of polyamine oxidation contributing to improved immune response and low susceptibility to *Botrytis cinerea*. – *Journal of Experimental Botany* 66: 775-787.
- [8] He, L. X., Zheng, A. X., Du, B., Luo, H. W., Lu, R. H., Du, P., Chen, Y. L., Zhang, T. T., Lai, R. F., Tang, X. R. (2019): Low-concentration sodium selenite applications improve oxidation resistance of filling-stage rice. – *Applied Ecology and Environmental Research* 17: 989-998.
- [9] Kong, L. L., Ashraf, U., Cheng, S. R., Rao, G. S., Mo, Z. W., Tian, H., Pan, S. G., Tang, X. R. (2017): Short-term water management at early filling stage improves early-season rice performance under high temperature stress in South China. – *European Journal of Agronomy* 90: 117-126.
- [10] Leilah, A. A., Al-Khateeb, S. A. (2005): Statistical analysis of wheat yield under drought conditions. – *Journal of arid environments* 61: 483-496.
- [11] Li, X., Xia, X., Xiao, Y., He, Z., Wang, D., Trethowan, R., Wang, H., Chen, X. (2015): QTL mapping for plant height and yield components in common wheat under water-limited and full irrigation environments. – *Crop & Pasture Science* 66: 660-670.
- [12] Li, M., Ashraf, U., Tian, H., Mo, Z., Pan, S., Anjum, S. A., Duan, M., Tang, X. (2016): Manganese-induced regulations in growth, yield formation, quality characters, rice aroma and enzyme involved in 2-acetyl-1-pyrroline biosynthesis in fragrant rice. – *Plant Physiology and Biochemistry* 103: 167-175.
- [13] Luo, H. W., Du, B., Zheng, A. X., Lai, R. F., You, Z. S., Wang, M., Wang, Z. M., He, L. X., Zhang, T. T., Tang, X. R. (2018): Flooding treatment restrains volunteer rice germination and seedling growth. – *Applied Ecology and Environmental Research* 16: 7231-7242.
- [14] Pan, S., Rasul, F., Li, W., Tian, H., Mo, Z., Duan, M., Tang, X. (2013): Roles of plant growth regulators on yield, grain qualities and antioxidant enzyme activities in super hybrid rice (*Oryza sativa* L.). – *Rice* 6: 1-10.

- [15] Rayman, M. P. (2012): Selenium and human health. – *Lancet* 379: 1256-1268.
- [16] Scott, R., Macpherson, A., Yates, R. W. S., Hussain, B., Dixon, J. (1998): The effect of oral selenium supplementation on human sperm motility. – *BJU* 82: 76-80.
- [17] Shah, K., Kumar, R. G., Verma, S., Dubey, R. S. (2001): Effect of cadmium on lipid peroxidation, superoxide anion generation and activities of antioxidant enzymes in growing rice seedlings. – *Plant Science (Shannon)* 161: 1135-1144.
- [18] Wang, Y., Huang, J., Wang, J. (2014): Household and Community Assets and Farmers' Adaptation to Extreme Weather Event: the Case of Drought in China. – *Journal of Integrative Agriculture* 13: 687-697.
- [19] Xuan, Y., Zhan, T., Sun, L., Chen, B., Tubiello, F. N., Xu, Y. (2017): The impacts of increased heat stress events on wheat yield under climate change in China. – *Climatic Change* 140: 605-620.
- [20] Yao, X., Chu, J., Wang, G. (2009a): Effects of drought stress and selenium supply on growth and physiological characteristics of wheat seedlings. – *Acta Physiologiae Plantarum* 31: 1031-1036.
- [21] Yao, X. Q., Chu, J. Z., Wang, G. Y. (2009b): Effects of Selenium on Wheat Seedlings Under Drought Stress. – *Biological trace element research* 130: 283-290.
- [22] Yu, L., Liu, Y., Lu, L., Zhang, Q., Chen, Y., Zhou, L., Chen, H., Peng, C. (2017): Ascorbic acid deficiency leads to increased grain chalkiness in transgenic rice for suppressed of L-GallDH. – *Journal of Plant Physiology* 211: 13-26.

GGE BILOT ANALYSIS IN WILD (*PISUM SATIVUM* L. SUBSP. *ELATIUS* AND SUBSP. *SATIVUM*) AND CULTIVATED PEA (*PISUM SATIVUM* L.) GENOTYPES IN NORTHERN AND SOUTHERN TURKEY

GIRGEL, U.¹ – COKKIZGIN, A.^{2*}

¹Bayburt University, Aydıntepe Vocational School, 69500 Bayburt, Turkey
(phone: +90-458-311-4426; fax: +90-458-311-4466)

²Gaziantep University, Nurdagi Vocational School, 27840 Gaziantep, Turkey
(phone: +90-342-671-3382; fax: +90-342-671-3384)

*Corresponding author

e-mail: acokkizgin@gantep.edu.tr, acokkizgin@hotmail.com

(Received 18th Aug 2019; accepted 25th Nov 2019)

Abstract. This research was carried out in the multiple-environment trials (MET) which one is in Bayburt (40°24'05.7"N 40°08'31.3"E) where the Black Sea geographical region located in the north of Turkey and in the Kahramanmaraş (37°35'24.8"N 36°48'49.4"E) where the Mediterranean geographical region located in the south of Turkey in 2016 and 2017 years. In this investigation, 6 registered pea cultivars (Bolero, Jof, Karina, Nihal, Reyna and Utrillo) and 2 wild pea genotypes (*Pisum sativum* L. subsp. *elatius* and *P. sativum* L. subsp. *sativum*) were used. The variance analysis showed a significant difference among Location (L), genotypes (G), genotypes×locations interaction (GL), genotypes×year interaction (GY), year×location interaction (YL) (all significant at P<0.01 level) and genotype×location×year interaction (GLY) (significant at P<0.05 level) interaction in terms of seed yield. Main effect genotypes (G) is explained 24.42% of total variation. This is followed by 18.78% (L), 17.87% (YL) 7.04% (GL), 4.91% (GY), 2.71% (GLY) and 1.12% (Y), respectively. Graphs were drawn according to the results of GGE biplot analysis and yield data of genotypes were evaluated according to these graphs. In accordance with GGE biplot analysis the seed yield first principal component explained 82.81% of the total variation and second principal component explained 17.19% of the total variation.

Keywords: multi environment (MET), stability, yield, *Pisum sativum*

Introduction

Dry pea cultivation was carried out on 8.141.031 hectare area in the world and it has 16.205.448 tons production and 1990,6 kg/ha yield value. On the other hand green pea cultivation has 2.669.305 hectare area value, 20.699.736 tons production and 7754,7 kg/ha yield value worldwide (FAO, 2018).

Peas are the second most produced legumes in worldwide (FAO, 2018). The number of diploid chromosomes in pea is 14 (Murtaza et al., 2005) and it is a legume crops which origin is near east (Abbo et al., 2017). This region is also the source of wild pea subspecies (Symkal et al., 2015). On the other hand for further pea crop improvement the wild peas are important sources of genetic diversity in climate change context (Symkal et al., 2018).

It is known that Biplot concept started with Descartes. Also Ptolemy used to map cities in ancient times (Gower et al., 2011). Also “Biplot” is a term used by Gabriel (1971), but the first using of biplots in agricultural data was Bradu and Gabriel (1978), as popular versions of variables which were represented by directed vectors and Gower and Hand (1996), emphasized its advantages of biplots with calibrated axes.

Genotype×Environment interaction is a complicated source of variation and also makes the selection of genotype(s) difficult (Magari and Kang, 1993). Genotype by environment (GE) interaction may vary according to crops and years (Milligan, 1994). When G×E interaction is statistically significant, its nature, reason and results must be carefully examined (Magari and Kang, 1993). On the other hand, genotype environment interaction is very effective on seed yield to reveal the effectiveness of interaction; trials should have multiple years and multiple locations (Rao et al., 2011; Luo et al., 2015).

It is reported that the best method for revealing Genotype×Environment interaction is GGE-biplot analysis (Samonte et al., 2005; Fan et al., 2007). Using the graphs, GE interaction could be better understandable (Luo et al., 2015). GGE biplot technique has been used by many researchers to determine product performance such as rapeseed (Shang et al., 2006), peanut (Chen et al., 2009), millet (Zhang et al., 2016), barley (Kendal et al., 2014; Kizilgeci, 2019), oat (Zhang et al., 2010), rice (Sharifi and Motlagh, 2011), sugarcane (Luo et al., 2015), wheat (Akbarzai et al., 2017), maize (Fan et al., 2007), bean (Kang et al., 2006), chickpea (Farshadfar, 2013).

The objectives of the study were to (1) reveal genotype, location, year values, (2) determine genotype by location interaction, (3) determine genotype by year interaction, (4) determine year×location interaction, (5) determine genotype×location×year interaction, (6) reveal the stability of wild and cultivated pea genotypes in Bayburt and Kahramanmaras locations (in northern and southern part of Turkey) via GGE biplot analysis. As a result, more compatible genotypes will be obtained in future breeding studies.

Material and Methods

Research areas

This research was carried out in the multiple-environment trials (MET). The locations were Bayburt/Turkey (Bayburt University, Food and Agriculture and Livestock Application and Research Center area) (40°24'05.7"N 40°08'31.3"E) and Kahramanmaras/Turkey (Kahramanmaras Sutcu Imam University, Field Crops Department Treatment area) (37°35'24.8"N 36°48'49.4"E). The study was conducted at the locations in 2016 and 2017 years. These locations are located in the northern and the southern of Turkey (Table 1). Climate data of the research areas are given in Table 2. In the research, each plot consists of 5 rows, the distance between rows was 50 cm and the plot length was 5 m, total plot area is determined as 12.5 m² and plant density was 40 plant m⁻².

Table 1. Global positions and soil properties of the research areas

Location	Soil feature	Altitude	Global position
Bayburt	Loamy soil	1650	40°24'05.7"N 40°08'31.3"E
Kahramanmaras	Loamy soil	507	37°35'24.8"N 36°48'49.4"E

Seed materials

Two wild pea genotypes (*Pisum sativum* L. subsp. *elatius* and *P. sativum* L. subsp. *sativum*) in which they were gained from natural vegetation in Turkey and six registered pea cultivars (Bolero, Jof, Karina, Nihal, Reyna and Utrillo) were used and the study

was used in the study. The selection criterion was considered to be the genotype that can adapt to both regions.

Before the seed yield was obtained, one row on each side of the plot and 0.5 m from both ends of the plot which was evaluated as side effect were excluded from the evaluation and the central rows harvested by hand, according to Girgel (2013).

Table 2. Some climatical datas for research areas (Bayburt and Kahramanmaras)

Long time period (1959 - 2018) climatical datas in growing period for Bayburt Province					
Parameters	May	Jun	July	Aug	Sep
Average Temp. (°C)	11.8	15.5	19.2	19.0	14.8
Average Highest Temp. (°C)	18.2	22.7	27.1	27.6	23.5
Average Lowest Temp. (°C)	5.7	8.3	11.2	11.0	7.3
Average Rainy Days	16.0	10.7	5.0	4.4	5.0
Average Monthly Total Rainfall (mm)	71.8	50.5	20.2	13.9	20.5
Highest Temp.(°C)	29.6	32.9	37.0	37.2	33.7
Lowest Temp. (°C)	-4.4	-1.6	0.2	2.4	-2.1
Long time period (1930-2018) climatical datas in growing period for Kahramanmaras province					
Parameters	Feb	Mar	Apr	May	Jun
Average Temp. (°C)	6.6	10.8	15.5	20.3	25.2
Average Highest Temp. (°C)	11.0	15.9	21.2	26.7	31.9
Average Lowest Temp. (°C)	2.4	5.7	9.8	13.9	18.6
Average Rainy Days	11.3	11.1	9.9	7.4	2.2
Average Monthly Total Rainfall (mm)	109.9	96.3	72.8	41.9	7.4
Highest Temp.(°C)	25.3	29.8	36.0	38.0	42.0
Lowest Temp. (°C)	-9.6	-7.6	-1.8	4.7	4.9

*(TSMS, 2019)

Statistical analysis

In the research, for the phenotypic variation, $P = E + G + GE$ formula was used. In the formula, the phenotype P represents the environment, the G genotype, and GE represents the genotype×environment interaction (Yan and Kang, 2003). Also, year and location factors are within environment (E).

In addition to being a multiple-environment trials (MET), the factors could be divided because it was conducted for two years (2016 and 2017). For a more detailed variance analysis (E) is divided year (Y) and location (L) factors also all interactions between G, L and Y factors were evaluated according to Comstock and Moll (1963).

The experiment was established with 3 replications in according to randomized complete block design (RCBD). Statistical analysis was performed with GenStat Release 12.1 (VSN International Ltd.) according to Gomez and Gomez (1984) and Rao (2007). And GGE biplot graphs and analysis was performed according to Gabriel (1971), Yan et al. (2000), Yan and Tinker (2006) and Kang et al. (2006) by using GenStat software (VSNI, 2009).

Results and Discussion

Analysis of variance

In the study, genotype, locaiton, year and their interactions were examined. The variance analysis showed a significant difference among genotypes (G), locations (L), genotypes×location interaction (GL), genotypes×year interaction (GY), year×location interaction (YL) (all significant at $P < 0.01$ level) and genotype×location×year interaction

(GLY) (significant at $P < 0.05$ level) in terms of seed yield (Table 3). Luo et al. (2015) reports that the factors of genotype, location, year, and all interactions between them were found to be statistically significant. And similar statistical results reported by Kan et al. (2010).

Table 3. Variance analysis for seed yield of pea genotypes in two years (2016 and 2017) and two locations (Bayburt and Kahramanmaraş)

Source of Variation	DF	SS	MS	F pr.	Explained (%)
G	7	45612.4	6516.1	<.001	24.42
Y	1	299.3	299.3	0.294	1.12
L	1	5009.8	5009.8	<.001	18.78
GY	7	9162.3	1308.9	<.001	4.91
GL	7	13142.9	1877.6	<.001	7.04
YL	1	4767.2	4767.2	<.001	17.87
GLY	7	5056.3	722.3	0.016	2.71
Residual	64	17891.2	940.9		
Total	95	100941.5			

DF: Degree of freedom, SS: Sum of square, MS: Mean square, F pr.: Probability

In the investigation, variance analysis showed that the genotypes had greater effect on seed yield than the factors location or year. Genotype, environment and year factors and their interactions explain 76.85% of the total variance (Table 3). In here the greatest variance value is due to main effect genotypes (G) and it is explained 24.42% of total variation. This is followed by 18.78% (L), 17.87% (YL) 7.04% (GL), 4.91% (GY), 2.71% (GLY) and 1.12% (Y), respectively. On the other hand, least significant difference statistical groups (LSD) for all measurement interactions and factors were determined with the help of MSTAT-C software package program (v2.10) (MSTAT-C, 1994) (Table 4).

Environmental factors and primarily genetic structure are the main factors in determining the phenotype. As a result of the interactions of these factors reveals the amount of seed yield. Yan and Kang (2003) reported that phenotypic variation consists of genotype and environment and their interaction. Sabaghnia et al. (2011) reported that when there are no different locations, the year factor explained the large proportion of the total variation. On the other hand, similar results gained by Noerwijati et al. (2014).

According to GGE biplot analysis results for the seed yield first principal component explained 82.81% of the total variation and second principal component explained 17.19% of the total variation. The PCA (Principle Component Analysis) model based on the GGE biplot explains further variation (Yan and Kang, 2003).

Scatter plot results

According to the scatter plot graph for ranking of locations and genotypes, it can be said that there is almost none correlation the between Bayburt and Kahramanmaraş locations due to the acute angle value is very close to the right angle (Fig. 1). In the analysis, the cosine of the angle between vectors shows that correlation between vectors i.e. obtuse angles shows that negative association and acute angle indicate positive association and at right angles there is no relationship between vectors (Yan, 2014; Dallo et al., 2019).

Table 4. Means and the least significant difference (LSD) groups for all measurement interactions and factors*

Location	Genotype**	Year		Location×Genotype Interaction	Means of Location
		2016	2017		
Bayburt	1	106.0 ^{b-f}	86.00 ^{c-i}	96.00 ^{BC}	88.56 ^A
	2	67.00 ^{g-l}	59.00 ^{i-l}		
	3	89.00 ^{c-i}	82.00 ^{d-j}		
	4	99.00 ^{c-h}	80.00 ^{e-k}		
	5	138.0 ^{ab}	110.00 ^{a-e}		
	6	101.0 ^{c-h}	78.00 ^{e-k}		
	7	61.00 ^{i-l}	54.00 ^{i-m}		
	8	118.0 ^{a-c}	89.00 ^{c-i}		
	Location×Year Interaction	97.38 ^A	79.75 ^B		
Kahramanmaras	1	66.00 ^{h-l}	67.53 ^{g-l}	66.77 ^{DEF}	74.12 ^B
	2	45.00 ^{k-n}	86.67 ^{c-i}		
	3	17.67 ⁿ	72.67 ^{f-k}		
	4	115.70 ^{a-d}	107.50 ^{a-f}		
	5	107.00 ^{a-f}	72.87 ^{f-k}		
	6	74.80 ^{f-k}	36.67 ^{l-n}		
	7	23.27 ^{mn}	49.43 ^{j-n}		
	8	101.30 ^{e-g}	141.80 ^a		
	Location×Year Interaction	68.83 ^B	79.40 ^B		
Year×Genotype Interaction	1	86.00 ^{CD}	76.77 ^{DE}	Means of Genotype	
	2	56.00 ^{EFG}	72.83 ^{DEF}	1	81.38 ^B
	3	53.33 ^{EFG}	77.33 ^{DE}	2	64.42 ^{BC}
	4	107.30 ^{ABC}	93.75 ^{BCD}	3	65.33 ^B
	5	122.50 ^A	91.43 ^{BCD}	4	100.50 ^A
	6	87.90 ^{CD}	57.33 ^{EFG}	5	107.00 ^A
	7	42.13 ^G	51.72 ^{FG}	6	72.62 ^B
	8	109.60 ^{ABC}	115.4 ^{AB}	7	46.92 ^C
	Means of Year	83.10 ^{NS}	79.57 ^{NS}	8	112.50 ^A

* Differences between means that share same letter was not statistically significant.

** 1. Bolero, 2. Jof, 3. Karina, 4. Nihal, 5. Reyna, 6. ssp. sativum, 7. ssp. elatius, 8. Utrillo

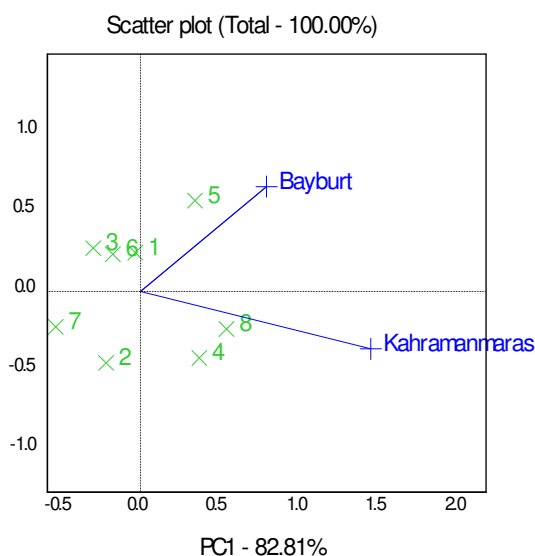


Figure 1. GGE scatter biplot graph shows that ranking of genotypes over the environments (x: shows wild and cultivated genotype scores and +: shows environment scores) (1. Bolero, 2. Jof, 3. Karina, 4. Nihal, 5. Reyna, 6. ssp. sativum, 7. ssp. elatius, 8. Utrillo)

Narrow angle, indicates a correlation between genotypes. Similar opinions have been reported by Yan (2002) and Kang et al. (2006). Utrillo cv. was found to be most yielding genotype but *Pisum sativum* subsp. *elatius* was determined as the lowest yielding but the most stable genotype.

In terms of the years the first principal components (PC1) and second principal components (PC2) of the seed yield accounted as 87.65 and 12.35, respectively (Fig. 2). The years was similar to each other due to the narrow angle and there is a very small amount positive correlation. In other words, the conditions of the years are similar. It is reported that in such graphs, there is a correlation between the parameters examined when there is a narrow angle (Yan, 2002).

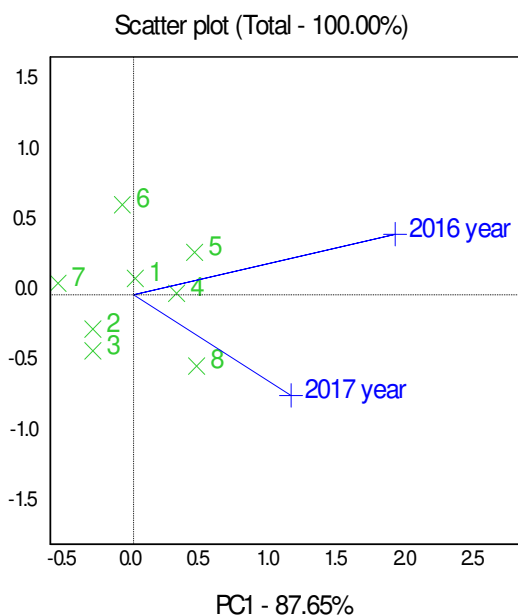


Figure 2. GGE scatter biplot graph shows that ranking of genotypes over the years (x: shows wild and cultivated genotype scores and +: shows year scores) (1.Bolero, 2.Jof, 3.Karina, 4.Nihal, 5.Reyna, 6.ssp.sativum, 7.ssp.elatius, 8.Utrillo)

Pea plants showed better adaptation under the first year environmental conditions and the first year point was close to the stability line than second year. On the other hand, the Nihal variety was determined as the genotype closest to the stability line (Fig. 2). Snoad and Arthur (1974), point out that repeated trials for many years reveal genotype-environment interaction in a more understandable way.

According to polygonal Genotype×Environment interaction scatter biplot graph, under the conditions of Kahramanmaras, Utrillo genotype is environmentally compatible and under the Bayburt conditions, Reyna and bolero genotypes are located in the same sectors and emerged as high performance varieties that are compatible with this environment (Fig. 3). Genotype×Environment interaction is very important for genotype selection and therefore, repeating the experiments at different years and locations provides accurate genotypic results. Similar opinions reported by Weber et al. (1996). On the other hand, Yan and Kang (2003) recommended a biplot polygon graph to better understanding the genotype environment interaction.

According to polygonal Genotype×Year interaction scatter biplot graph, in the first year Reyna and Nihal, in the second year, Utrillo and Nihal varieties appeared as the

highest performance genotypes (Fig. 4). In the graph, the polygon was divided into 5 parts and the years had taken place in different sections. As a rule, polygon edges and axes were at right angles to each other. If the locations are not taken into consideration, in terms of years, the cv. Bolero was located at the center of the axis in the graph and had been the least affected by the environmental conditions of that year. However, this genotype had less seed yield. On the other hand, cv. Nihal was determined to be stable regardless of locations and it had higher seed yield from cv. Bolero.

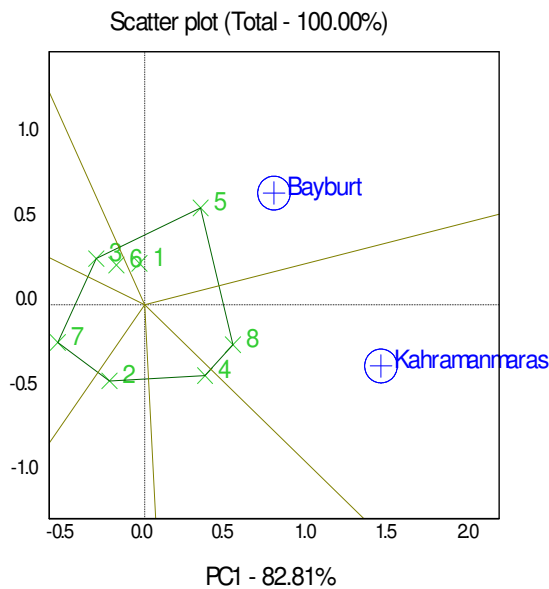


Figure 3. Polygon graph of Genotype×Environment interaction for genotypes over the environments (x: shows wild and cultivated genotype scores and +: shows environment scores) (1.Bolero, 2.Jof, 3.Karina, 4.Nihal, 5.Reyna, 6.ssp.sativum, 7.ssp.elatius, 8.Utrillo)

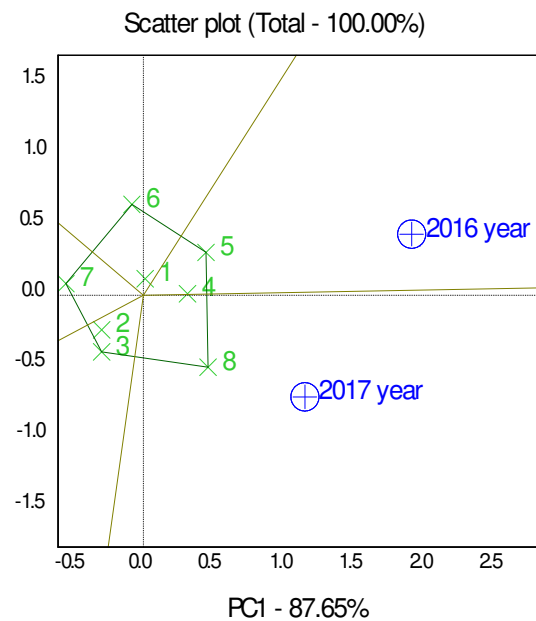


Figure 4. Polygon graph of Genotype×Year interaction for genotypes over the years (x: shows wild and cultivated genotype scores and +: shows year scores)

Ranking biplot results

GGE ranking biplot graph shows the status of genotypes by Bayburt location (Fig. 5). In the graph a line representing the province of Bayburt was drawn through the biplot origin and another a line perpendicular to the Bayburt axis was drawn from each genotype. The Bayburt line represented the axis for the Bayburt province. Yan and Tinker (2006) reported that the seed yield in the direction of the arrow increases and genotypes closer to the arrow line are more stable. When the GGE ranking biplot graph was examined, Reyna variety showed the highest performance in Bayburt province, followed by Utrillo variety, but it was found that Reyna, which is close to the axis in terms of stability, was more convenient (Fig. 5).

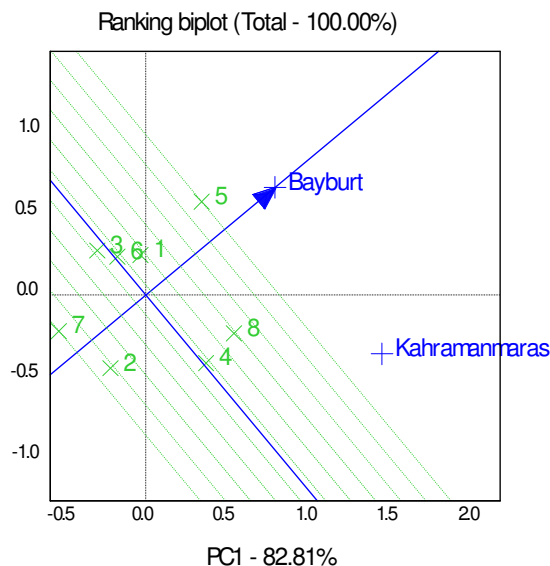


Figure 5. GGE ranking biplot graph showed according to Bayburt province the ranking of the genotypes yield (x: shows wild and cultivated genotype scores and +: shows environment scores) (1.Bolero, 2.Jof, 3.Karina, 4.Nihal, 5.Reyna, 6.ssp.sativum, 7.ssp.elatius, 8.Utrillo)

In the GGE ranking biplot graph the Kahramanmaraş line represented the axis for the Kahramanmaraş province. Yan and Tinker (2006) pointed that the seed yield in the direction of the arrow increases and genotypes closer to the arrow line are more stable. When the GGE ranking biplot graph was examined, under the Kahramanmaraş conditions, the Utrillo variety was determined as highest seed yield and the most stable genotype in terms of seed yield (Fig. 6).

Comparison biplot results

By using the ideal environment as the center in order to visualize the distance between Bayburt and Kahramanmaraş locations concentric circles were drawn (Yan et al., 2000; Yan and Rajcan, 2002).

The comparison biplot graph assumes that the province of Bayburt has ideal environmental conditions and draws from the center towards the outer ring suitability for genotypes. Concentric circles were drawn so that the ideal environment is in the center (Yan et al., 2000; Yan and Rajcan, 2002). Bayburt ecological conditions were considered as an ideal environment; Reyna variety was found to be most suitable. In

addition, Bolero and Utrillo varieties and wild genotype *Pisum sativum* subsp. *sativum* can be evaluated. Jof cultivar and *Pisum sativum* subsp. *elatius* wild cultivar were not suitable for the region (Fig. 7). Our results are in agreement with other observational study of Yihunie and Gesesse (2018).

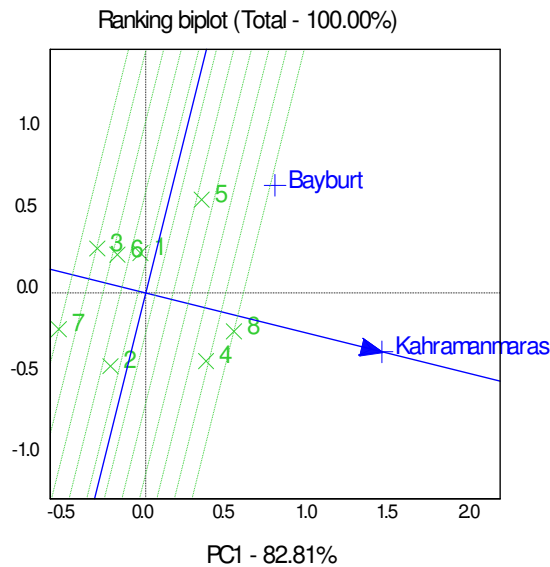


Figure 6. GGE ranking biplot graph shows according to Kahramanmaras province the ranking of the genotypes yield (x: shows wild and cultivated genotype scores and +: shows environment scores) (1.Bolero, 2.Jof, 3.Karina, 4.Nihal, 5.Reyna, 6.ssp.sativum, 7.ssp.elatius, 8.Utrillo)

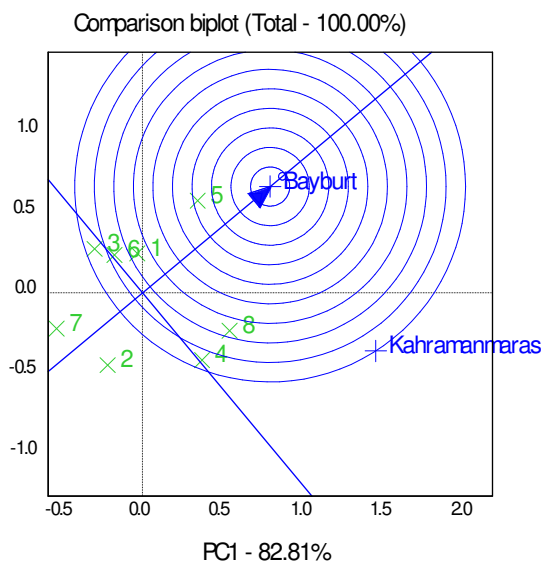


Figure 7. GGE Comparison biplot graph shows the ranking of the genotypes as an ideal environment Bayburt province (x: shows wild and cultivated genotype scores and +: shows environment scores) (1.Bolero, 2.Jof, 3.Karina, 4.Nihal, 5.Reyna, 6.ssp.sativum, 7.ssp.elatius, 8.Utrillo)

Kahramanmaras as the ideal environment according to the comparison biplot graph, Utrillo and Nihal varieties are found to be appropriate (Fig. 8). The rings moving away

from the center of Kahramanmaras in the comparison biplot graph show that the genotype is less suitable for the province.

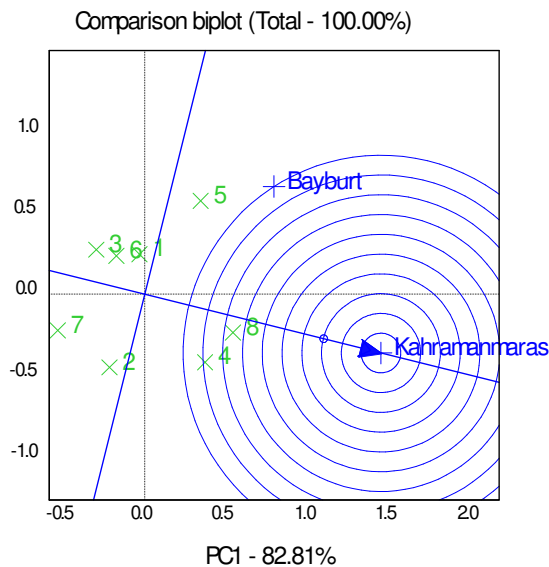


Figure 8. GGE Comparison biplot graph shows the ranking of the genotypes as an ideal environment Kahramanmaras province (x: shows wild and cultivated genotype scores and +: shows environment scores) (1.Bolero, 2.Jof, 3.Karina, 4.Nihal, 5.Reyna, 6.ssp.sativum, 7.ssp.elatius, 8.Utrillo)

Joint biplot results

When the provinces were evaluated together according to the joint biplot graph, it was determined that Utrillo was a more stable variety on the other hand Reyna showed higher yield differences (Fig. 9).

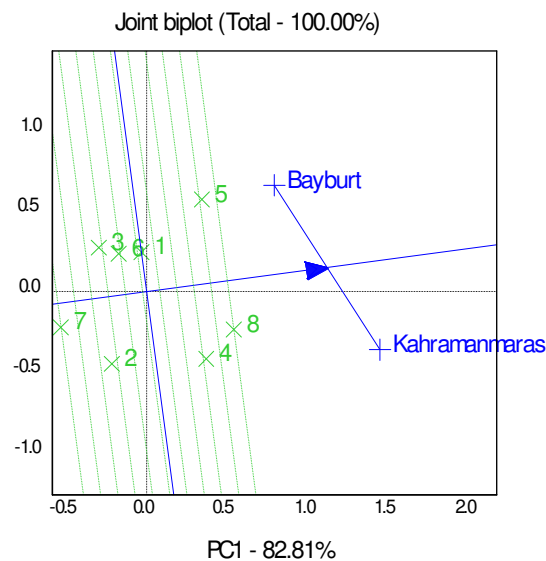


Figure 9. GGE Joint biplot graph shows stability of genotypes according to evaluation of two provinces (x: shows wild and cultivated genotype scores and +: shows environment scores) (1.Bolero, 2.Jof, 3.Karina, 4.Nihal, 5.Reyna, 6.ssp.sativum, 7.ssp.elatius, 8.Utrillo)

Two genotype or two locations can be visually compared by connecting them with a linear line in a GGE biplot (Yan and Tinker, 2006). When the two provinces are evaluated together, the yield ranking of the varieties is as follows; Utrillo > Reyna > Nihal > Bolero > *Pisum sativum* subsp. *sativum* > Karina > Jof > *Pisum sativum* subsp. *elatius*. However, Reyna Jof and Nihal varieties were located further away from the stability line.

Considering the biplot graph based on an average of two years, genotypes showed as follows ranking; Utrillo > Reyna > Nihal > Bolero > *Pisum sativum* subsp. *sativum* > Karina > Jof > *Pisum sativum* subsp. *elatius* (Fig. 10). Subsp. *sativum* was the closest wild species to the cultivars, so yield levels were higher than some cultivars. Nihal, *Pisum sativum* subsp. *elatius* ve Bolero genotypes were determined to be highly stable, regardless of locations, according to two year averages. Repeated trials for many years reveal GEI in a more understandable way (Snoad and Arthur, 1974).

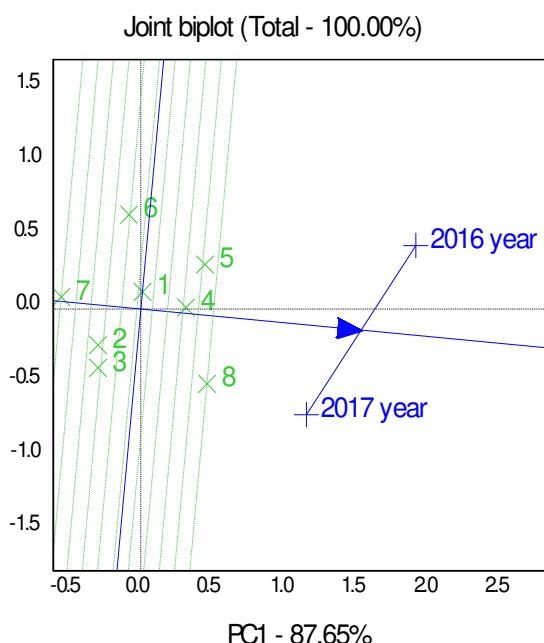


Figure 10. GGE Joint biplot graph shows stability of genotypes according to evaluation of two years (2016 and 2017) (x: shows wild and cultivated genotype scores and +: shows year scores) (1.Bolero, 2.Jof, 3.Karina, 4.Nihal, 5.Reyna, 6.ssp.sativum, 7.ssp.elatius, 8.Utrillo)

Environment-centered data results

According to environment-centered data graphs, when two locations were taken into consideration, Utrillo, Jof, Nihal performed better in Kahramanmaras, while Reyna, Bolero, *Pisum sativum* L. subsp. *sativum*, Karina and *Pisum sativum* L. subsp. *elatius* had better performance in Bayburt province (Fig. 11). Subsp.*sativum* was the closest wild species to the cultivars, so yield levels were higher than some cultivars. To select superior genotypes and increase efficiency in selection, the biplot analysis is a good method (Dallo et al., 2019).

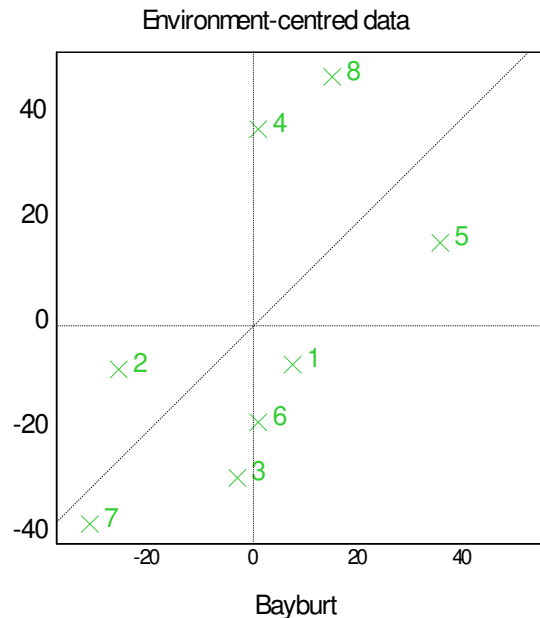


Figure 11. Environment-centered data graph shows that sorting genotypes by environment (x: shows wild and cultivated genotype scores) (The right side of the diagonal represents Bayburt province and the left side of the diagonal represents Kahramanmaras province) (1.Bolero, 2.Jof, 3.Karina, 4.Nihal, 5.Reyna, 6.ssp.sativum, 7.ssp.elatius, 8.Utrillo)

Conclusion

Biplot analysis is an important technique in crop improvement and agricultural research. GGE biplot is an appropriate method for genotype selection and data analysis for agronomists, geneticists and breeders of the plant.

According to variance analysis main effect genotypes (G) explained 24.42%, main effect locations 18.78% (L) and main effect year 1.12% (Y). On the other hand, year×location interaction explained 17.87% (YL) of total variation and it is followed by other interactions 7.04% (GY), 4.91% (GY), 2.71% (GLY) and respectively.

According to GGE biplot analysis results for the seed yield first principal component explained 82.81% of the total variation and second principal component explained 17.19% of the total variation.

In Bayburt province Reyna cultivar was highest yielding and most stable genotype, in Kahramanmaras province Utrillo cv. highest yielding and most stable genotype. When evaluated together for two years, ranking of the wild and cultivated pea genotypes such as Utrillo > Reyna > Nihal > Bolero > *Pisum sativum* subsp. *sativum* > Carina > Jof > subsp. *elatius*. Considering the two-year results obtained from Bayburt and Kahramanmaras, ranking of the genotypes such as Utrillo > Reyna > Nihal > Bolero > *Pisum sativum* subsp. *sativum* > Carina > Jof > *Pisum sativum* subsp. *elatius*.

According to all these results, it would be more appropriate to use Utrillo variety. On the other hand, wild genotype *Pisum sativum* subsp. *sativum* has higher seed yield from some standard varieties (Karina and Jof) and as an important result it can be used to provide gene in breeding studies.

REFERENCES

- [1] Abbo, S., Gopher, A., Lev-Yadun, S. (2017): The Domestication of Crop Plants. – Encyclopedia of Applied Plant Sciences (2nd edition) 3: 50-54. <http://dx.doi.org/10.1016/B978-0-12-394807-6.00066-6>.
- [2] Akbarzai, D. K., Saharawat, Y., Mohammadi, L., Manan, A. R., Habibi, A., Tavva, S., Nigamananda, S., Singh, M. (2017): Genotype×Environment Interaction And Identification Of High Yielding Wheat Genotypes For Afghanistan. – Journal of Experimental Biology and Agricultural Sciences 5(2): 225-234. DOI: [http://dx.doi.org/10.18006/2017.5\(2\).225.234](http://dx.doi.org/10.18006/2017.5(2).225.234).
- [3] Bradu, D., Gabriel, K. R. (1978): The Biplot as a Diagnostic Tool for Models of Two-Way Tables. – Technometrics 20(1): 47-68.
- [4] Chen, S. L., Li, Y. R., Cheng, Z. S., Liu, J. S. (2009): GGE-Biplot Analysis of Effects of Planting Density on Growth and Yield Components of High Oil Peanut. – Acta Agron. Sin. 35: 1328-1335. doi:10.3724/SP.J.1006.2009.01328.
- [5] Comstock, R. E., Moll, R. H. (1963): Genotype-Environment Interactions. – In: Hanson, W. D., Robinson, H. F. (eds.) Statistical Genetics and Plant Breeding. National Academy of Science - National Research Council Publishing NAS-NRC, Washington, D.C. pp. 164-196.
- [6] Dallo, S. C., Zdziarski, A. D., Woyann, L. G., Milioli, A. S., Zanella, R., Conte, J., Benin, G. (2019): Across year and year-by-year GGE biplot analysis to evaluate soybean performance and stability in multienvironment trials. – Euphytica 215: 113. <https://doi.org/10.1007/s10681-019-2438-x>.
- [7] Fan, X. M., Kang, M. S., Chen, H., Zhang, Y., Tan, J., Xu, C. (2007): Yield Stability of Maize Hybrids Evaluated in Multi-Environment Trials in Yunnan, China. – Agron. J. 99: 220-228. doi:10.2134/agronj2006.0144.
- [8] FAO (2018): The Food and Agriculture Organization Statistical Database. – www.fao.org.
- [9] Farshadfar, E. (2013): Simultaneous Selection Of Yield And Yield Stability In Chickpea Genotypes Using The Gge Biplot Technique. – Acta Agronomica Hungarica 61(3): 185-194. DOI: 10.1556/AAgr.61.2013.3.2.
- [10] Gabriel, K. R. (1971): The Biplot Graphic Display of Matrices with Application to Principal Component Analysis. – Biometrika 58(3): 453-467.
- [11] Girgel, U. (2013): The Determination Of Agronomic And Biological Properties Of Some Culture And Wild Pea Genotypes In Kahramanmaraş Conditions. – Kahramanmaraş, Sutcu Imam University, Graduate School of Natural and Applied Sciences, PhD Thesis, 123 p.
- [12] Gomez, K. A., Gomez, A. A. (1984): Statistical Procedures for Agricultural Research. – A Wiley-interscience Publication, USA, 680 p.
- [13] Gower, J. C., Hand, D. J. (1996): BIPLOTS. – Chapman & Hall, London, 277 p. ISBN 0-412-71630-5.
- [14] Gower, J. C., Lubbe, S. G., Le Roux, N. J. (2011): Understanding Biplots. – John Wiley & Sons, Ltd. ISBN 978-0-470-01255-0.
- [15] Kan, A., Kaya, M., Gurbuz, A., Sanli, A., Ozcan, K., Ciftci, C. Y. (2010): A study on genotype x environment interaction in chickpea cultivars (*Cicer arietinum* L.) grown in arid and semi-arid conditions. – Scientific Research and Essays 5(10): 1164-1171.
- [16] Kang, M. S., Aggarwal, V. D., Chirwa, R. M. (2006): Adaptability and Stability of Bean Cultivars as Determined via Yield-Stability Statistic and GGE Biplot Analysis. – Journal of Crop Improvement 15: 1, 97-120. https://doi.org/10.1300/J411v15n01_08.
- [17] Kendal, E., Tekdal, S., Aktas, H., Karaman, M., Berekatoglu, K., Dogan, H. (2014): Determination of Yield and Yield Components of Spring Barley Genotypes Using Biplot Analysis. – Trakya University Journal of Natural Sciences 15(2): 95-103.

- [18] Kizilgeci, F., Yildirim, M., Akinci, C., Albayrak, O. (2019): Genotype and Environment Effects on the Grain Yield and Quality Traits of Some in Barley Genotypes. – *KSU J. Agric Nat* 22(3): 346-353. DOI:10.18016/ksutarimdog.vi.499013.
- [19] Luo, J., Pan, Y. B., Que, Y., Zhang, H., Grisham, M. P., Xu, L. (2015): Biplot Evaluation of Test Environments and Identification of Mega-Environment for Sugarcane Cultivars in China. – *Scientific Reports* 5: 15505. DOI: 10.1038/srep15505.
- [20] Magari, R., Kang, M. (1993): Genotype Selection Via a New Yield-Stability Statistic in maize Yield Trials. – *Euphytica* 70: 105-111.
- [21] Milligan, S. B. (1994): Test Site Allocation within and among Stages of a Sugarcane Breeding Program. – *Crop Science* 34(5): 1184-1190. doi:10.2135/cropsci1994.0011183X003400050008x.
- [22] MSTAT-C (1994): A software package for the design, management, and analysis of agronomic experiments. – V2.10. Michigan State University.
- [23] Murtaza, G., Ahmed, N., Majid, S. A. (2005): Karyotype Analysis of *Pisum sativum* L. – *International Journal Of Agriculture & Biology* 7(1): 118-120.
- [24] Noerwijati, K., Taryono, N., Prajitno, D. (2014): Fresh Tuber Yield Stability Analysis of Fifteen Cassava Genotypes Across Five Environments in East Java (Indonesia) Using GGE Biplot. – *Energy Procedia* 47: 156-165. doi: 10.1016/j.egypro.2014.01.209.
- [25] Rao, G. N. (2007): *Statistics for Agricultural Sciences*, Second Edition. – BS Publications, Hyderabad, India, 466 p. ISBN 987-81-7800-141-8.
- [26] Rao, P. S., Reddy, P. S., Rathore, A., Reddy, B. V. S., Panwar, S. (2011): Application GGE biplot and AMMI Model to Evaluate Sweet Sorghum (*Sorghum bicolor*) Hybrids for Genotype x Environment Interaction and Seasonal Adaptation. – *Indian Journal of Agricultural Sciences* 81(5): 438-444.
- [27] Sabaghnia, N., Dehghani, H., Alizadeh, B., Moghaddam, M. (2011): Yield Analysis of Rapeseed (*Brassica napus* L.) Under Water-stress Conditions Using GGE Biplot Methodology. – *Journal of Crop Improvement* 25(1): 26-45. DOI: 10.1080/15427528.2011.521919.
- [28] Samonte, S. O. P. B., Wilson, L. T., McClung, A. M., Medley, J. C. (2005): Targeting Cultivars onto Rice Growing Environments Using AMMI and SREG GGE Biplot Analyses. – *Crop Sci.* 45: 2414-2424. doi:10.2135/cropsci2004.0627.
- [29] Shang, Y., Li, S. Q., Li, D. R., Tian, J. H. (2006): GGE biplot analysis of diallel cross of *B. napus* L. – *Acta Agron. Sin.* 32: 243-248.
- [30] Sharifi, P., Motlagh, M. R. S. (2011): Biplot Analysis of Diallel Crosses for Cold Tolerance in Rice at the Germination Stage. – *Crop & Pasture Science* 62(2): 169-176. <https://doi.org/10.1071/CP10207>.
- [31] Smykal, P., Coyneb, C. J., Ambrose, M. J., Maxted, N., Schaefer, H., Blair, M. W., Berger, J., Greene, S. L., Nelson, M. N., Besharat, N., Vymyslicky, T., Toker, C., Saxena, R. K., Roorkiwal, M., Pandey, M. K., Hu, J., Li, Y. H., Wang, L. X., Guo, Y., Qiu, L. J., Redden, R. J., Varshney, R. K. (2015): Legume Crops Phylogeny and Genetic Diversity for Science and Breeding 34: 1-3, 43-104. DOI: 10.1080/07352689.2014.897904.
- [32] Smykal, P., Trneny, O., Brus, J., Hanacek, P., Rathore, A., Roma, R. D., Pechanec, V., Duchoslav, M., Bhattacharyya, D., Bariotakis, M., Pirtinos, S., Berger, J., Toker, C. (2018): Genetic Structure of Wild Pea (*Pisum sativum* subsp. *elatus*) Populations in the Northern Part of the Fertile Crescent Reflects Moderate Cross-Pollination and Strong Effect of Geographic but not Environmental Distance. – *PLoS ONE* 13(3): e0194056. <https://doi.org/10.1371/journal.pone.0194056>.
- [33] Snoad, B., Arthur, A. E. (1974): Genotype-Environment Interactions in Peas. – *Theoretical and Applied Genetics* 44: 222-231.
- [34] TSMS (2019): The Turkish State Meteorological Service, Long-term rainfall and temperature data. – www.mgm.gov.tr.
- [35] VSNI (2009): GenStat Release 12.1. – VSN International Ltd. www.vsni.co.uk.

- [36] Weber, W. E., Wricke, G., Westermann, T. (1996): Selection of Genotypes and Prediction of Performance by Analyzing Genotype-by-Environment Interactions. – In: Kang, M. S., Gauch, Jr. H. G. (eds.) Genotype-by-Environment Interaction, 1st edition pp. 353-371.
- [37] Yan, W., Hunt, L. A., Sheng, Q., Szlavics, Z. (2000): Cultivar Evaluation and Mega-Environment Investigation Based on the GGE Biplot. – Crop Sci. 40(3): 597-605. doi:10.2135/cropsci2000.403597x.
- [38] Yan, W. (2002): Singular-Value Partitioning in Biplot Analysis of Multi-environment Trial Data. – Agron. J. 94: 990-996. doi:10.2134/agronj2002.9900.
- [39] Yan, W., Rajcan, I. (2002): Biplot Analysis of Test Sites and Trait Relations of Soybean in Ontario. – Crop Sci. 42: 11-20. doi:10.2135/cropsci2002.1100.
- [40] Yan, W., Kang, M. S. (2003): GGE Biplot Analysis, A Graphical Tool for Breeders, Geneticists, and Agronomists. – CRC Press LLC, Florida, USA, 267 p. ISBN 0-8493-1338-4.
- [41] Yan, W., Tinker, N. A. (2006): Biplot Analysis of Multi-Environment Trial Data: Principles and Applications. – Can. J. Plant Sci. 86: 623-645.
- [42] Yan, W. (2014): Crop Variety Trials: Data Management and Analysis. – John Wiley & Sons, Inc. 351 p. ISBN 978-1-118-68855-7.
- [43] Yihunie, T. A., Gesesse, C. A. (2018): GGE Biplot Analysis of Genotype by Environment Interaction in Field Pea (*Pisum sativum* L.) Genotypes in Northwestern Ethiopia. – J. Crop Sci. Biotech. 21(1): 67-74. DOI No. 10.1007/s12892-017-0099-0.
- [44] Zhang, Z. F., Fu, X. F., Liu, J. Q., Yang, H. S. (2010): Yield Stability and Testing-Site Representativeness in National Regional Trials for Oat Variety Based on GGE-Biplot Analysis. – Acta Agron. Sin. 36: 1377-1385. doi:10.3724/SP.J.1006.2010.01377.
- [45] Zhang, P. P., Song, H., Ke, X. W., Jin, X. J., Yin, L. H., Liu, Y., Qu, Y., Su, W., Feng, N. J., Zheng, D. F., Feng, B. L. (2016): GGE Biplot Analysis of Yield Stability and Test Location Representativeness in Proso Millet (*Panicum miliaceum* L.) Genotypes. – Journal of Integrative Agriculture 15(6): 1218-1227.

DISTRIBUTION AND POTENTIAL ECOLOGICAL RISK ASSESSMENT OF HEAVY METALS IN THE YELLOW RIVER BEACH REGION, SHAANXI, CHINA

LI, G.^{1,2,3,4,5} – LU, N.^{1,2,3,4,5} – HAN, J. C.^{1,2,3,4,5*} – WANG, N.^{1,2,3,4,5}
– WEI, Y.^{1,2,3,4,5} – SUN, Y. Y.^{1,2,3,4,5}

¹*Shaanxi Provincial Land Engineering Construction Group Co., Ltd. Xi'an 710075, China*

²*Institute of Land Engineering and Technology, Shaanxi Provincial Land Engineering
Construction Group Co., Ltd. Xi'an 710075, China*

³*Key Laboratory of Degraded and Unused Land Consolidation Engineering, the Ministry of
Natural Resources, Xi'an 710075, China*

⁴*Shaanxi Provincial Land Consolidation Engineering Technology Research Center, Xi'an
710075, China*

⁵*Shaanxi Key Laboratory of Land Consolidation, Xi'an 710075, China*

*Corresponding author

e-mail: hanjc_sxdj@126.com; phone: +86-029-8848-9545

(Received 19th Aug 2019; accepted 25th Nov 2019)

Abstract. This study investigated the distribution of heavy metals in the soil layer from 0 to 30 cm in the Yellow River beaches of Hancheng, Heyang and Tongguan section, China. The results showed that: (1) In the soil of the study area, the average Zn content was highest, and the average contents of As and Cd were lowest. Except for Ni, the coefficient of variation of other heavy metals is relatively large. (2) Pb and Cd of Hancheng beach showed significant positive correlations between Cr and Cu ($p < 0.01$). The correlations among Cr-Cd, Pb-Ni, Zn-Cr, and Zn-Cu of Tongguan beach were significant ($p < 0.01$). (3) Single factor pollution index and Nemerlo pollution index identified a certain degree of Zn pollution in the soil of Hancheng beach, and the overall heavy metal content of the soil of both Heyang and Tongguan beaches reached the level I safety level. (4) According to the Hakanson potential ecological hazard index, the average potential ecological risk index of the soil in the study area is $83.36 < 135$. The comprehensive potential risk of soil in different river sections follows: Hancheng > Heyang > Tongguan.

Keywords: heavy metal pollution, floodplain, pollution assessment, soil

Introduction

Over recent years, due to the rapid development of mining and transportation industries, compound pollution of inorganic and organic pollutants has gradually intensified (Chakraborty and Das, 2016). Especially in coastal areas, soil heavy metal pollution is gradually appearing. Due to the persistence and high toxicity of heavy metals in soil, the ecotoxicological risks induced by heavy metals have been gradually received increasing attention (Mi et al., 2015; Fan et al., 2019; Li et al., 2017). The problems of soil environmental quality and soil environmental safety related to agriculture have received particular attention (Crnkovic et al., 2006; Douay et al., 2007; Tume et al., 2008). All countries conducted research on the distribution laws of heavy metals in soil, their migration characteristics, enrichment characteristics, their forms, and phytoremediation. Starting from the idea of soil organic reconstruction,

Shaanxi Land Engineering Construction Group carry out soil heavy metal repair by the means of the soil materials and soil structure, and achieved notable results. At present, research on heavy metals in soils mainly explores their migration, transformation, enrichment, morphology, and bioremediation. The study area is dominated by farmland, urban land, and mining areas; however, river beaches and wetlands have not received sufficient attention (Islam et al., 2015; Fan et al., 2008; Li et al., 2015; Cheng et al., 2012).

The Yellow River Hancheng to Tongguan section is located at the junction between central Shaanxi and southern Shanxi, and is commonly known as the Xiaobei River, with a total length of 132.5 km. It forms an important section that integrates natural resources, humanities, agriculture, water resources, and tourism resources. This study focused on the distribution of heavy metals in the Yellow River beaches, beginning at the Hancheng-Tongguan section of the Yellow River. The sampling points include three regions, they are Xiayukou of Hancheng, Bailiang of Heyang and Qindong of Tongguan, Shaanxi, China. The risk and harm for the ecological protection of the Yellow River beaches and the development and utilization of the Yellow River beaches were investigated. The results of this study have practical significance for the alleviation of heavy metal pollution in this region.

Materials and methods

Description of the research area

The section between Hancheng and Tongguan in the Yellow River is located at the junction between central Shaanxi and southern Shanxi. To the west of the Yellow River, Hancheng, Heyang, and Tongguan are located, and Hejin and Yongji in Shanxi Province form the main areas to the east of the Yellow River. The project covers a total length of 132.5 km from Yumenkou to the Tongguan Railway Bridge on the west bank of the Yellow River. It includes four cities and counties, such as Hancheng, Heyang, Dali, and Tongguan in Weinan City, as well as 12 towns and 54 administrative villages with a total population of 57,500. Sampling points of Hangcheng range between $110^{\circ}5'50''$ - $108^{\circ}36'29''$ E and $34^{\circ}36'59''$ - $35^{\circ}39'34''$ N; sampling points of Heyang range between $109^{\circ}58'33''$ - $110^{\circ}27'00''$ E and $34^{\circ}59'16''$ - $35^{\circ}26'07''$ N; sampling points of Tongguan range between $110^{\circ}09'13''$ - $110^{\circ}25'26''$ E and $34^{\circ}23'38''$ - $34^{\circ}40'17''$ N (Fig. 1).

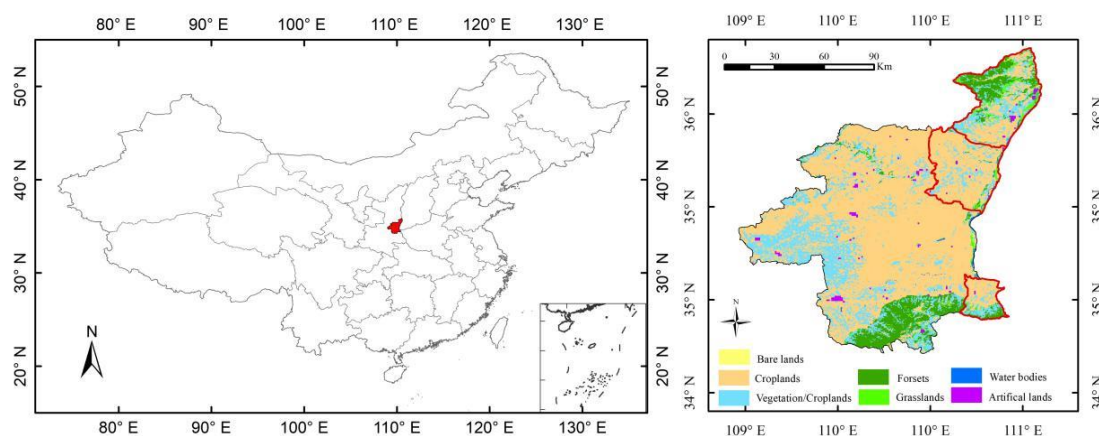


Figure 1. The sample distribution from Hancheng to Heyang

The study area has a warm temperate semi-humid and semi-arid monsoon climate, with four seasons. The frost-free period lasts 199-255 days, and the area has a changing spring climate, with hot and rainy summers, cool autumns, and dry and sunny winters. The average annual temperature is 12-14 °C, the annual rainfall is 600 mm, and the sun shines for 2200-2500 h annually. Climatic conditions are conducive to the development of agriculture; however, droughts, autumn floods, and dry and hot summer winds are more harmful for crops. *Figure 2* shows the average temperature and precipitation for each month. The economy of this region is mainly based on agricultural production and transportation hubs.

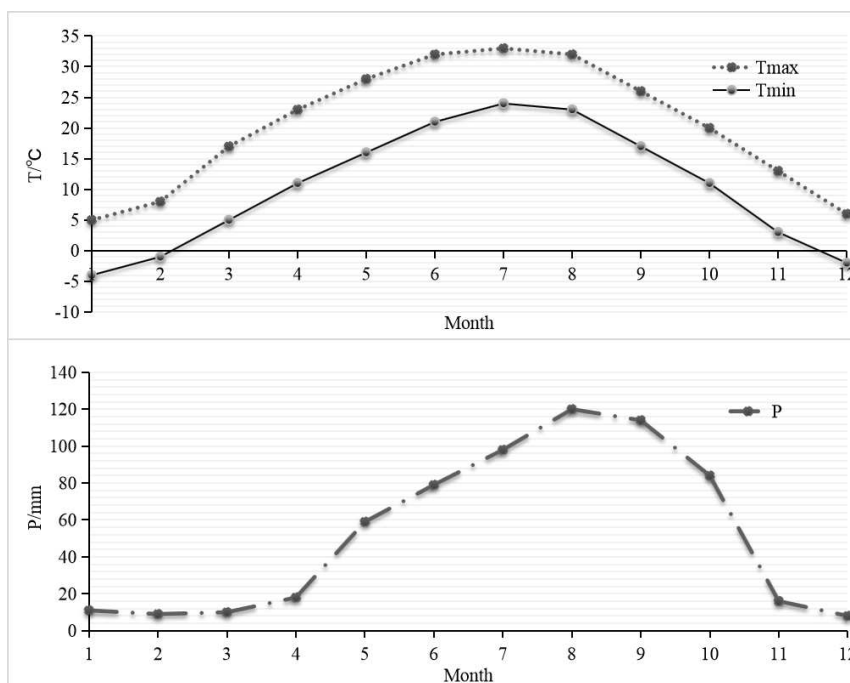


Figure 2. An average temperature and rainfall in the study area from January to December of the year 2016 (*Tmax*, *Tmin* and *P* are represent the an average maximum temperature, anaverage minimum temperature and precipitation of every month)

Sample collection

Soil samples were collected in May 2016. Sampling spots were distributed throughout Hancheng, Heyang, and Tongguan Yellow River floodplains and were collected from the Yellow River beach 0-30 cm surface soil layer. 300 samples were collected, 120 of which were collected from the Xiayukou in Hancheng section of the Yellow River. 80 samples were collected from Bailiang Town in Heyang. 100 samples were collected from Tongguan; the sampling point distribution is shown in *Figure 1*.

Each sample is a mixture of five points and consists of mixed samples. At each sampling spot, approximately 1 kg of soil was taken, stored in a sample bag, and returned to the laboratory to determine heavy metals in the soil.

Sample processing and determination

The soil samples (50 g) were air-dried, debris was removed, and samples were ground through a 0.149 mm nylon mesh (Hu et al., 2014; Xu et al., 2014). The soil total

Pb-Zn was determined according to GB/T 17141-1997, "Determination of Pb and Cd in Soil Quality: Graphite Furnace Atomic Absorption Spectrometry" (GB/T-22105.1-2008), "Determination of Cr: Flame atomic absorption spectrophotometry" (HJ 491-2009), "Determination of soil quality Ni: Flame atomic absorption spectrophotometry" (GB/T 17139-1997), "Determination of soil quality of Cu, Zn: Flame atomic absorption spectrophotometry" (GB/T 17138-1997), "Determination of total mercury in soil quality, total As, total Pb by atomic fluorescence spectrometry Part 1: Determination of total mercury in soil" (GB/T 22105.1-2008), and "Determination of total mercury, total As and total Pb in soil quality: atomic fluorescence spectrometry Part 2: Determination of total As in soil" (GB/T 22105.2-2008). The pH was determined potentiometrically and the heavy metal contents in soils were determined by Inductively Coupled Plasma-Mass Spectrometry (ICP-MS).

Hakanson potential ecological risk index

This study used the Hakanson potential ecological risk index method (Hakanson, 1980) to evaluate the degree of heavy metal risk in the soils of Yellow River beaches. The equations are as follows:

$$C_f^i = \frac{C^i}{C_n^i} \quad (\text{Eq.1})$$

$$E_r^i = T_r^i \times C_f^i \quad (\text{Eq.2})$$

$$RI = \sum_{i=1}^m E_r^i \quad (\text{Eq.3})$$

where C_f^i represents the individual pollution coefficient, C^i represents the actual content of pollutant i in the soil sample, and C_n^i represents the reference value of pollutant i . E_r^i represents the single potential ecological risk index of pollutant i , in which T_r^i represents the toxicity coefficient of pollutant i , and RI represents the potential ecological risk index. E_r^i and RI can be used to evaluate the degree of the potential ecological risk of single pollutants and multiple pollutants, respectively. *Tables 1, 2, and 3* are the toxicity coefficients of pollutants, the potential ecological risk classification criteria according to Hankanson, and the grading standards, respectively.

Results

Descriptive statistics of the data

According to the national soil environmental quality standard (GB 15618-2018), the soil environmental quality was divided into three grades (Yuan et al., 2008) (*Table 4*). As an important section of the middle and lower reaches of the Yellow River, the Hancheng-Tongguan section forms an important demarcation line between Shaanxi Province and Shanxi Province. A wide range of agricultural cultivation areas are distributed throughout both sides of the Yellow River. The environmental quality of the

Yellow River soil is directly related to the broad masses. In addition, the Yellow River beach area also forms a very important wetland system in this region. Therefore, this study used the soil background value of Grade I standard of the national soil environmental quality standard to evaluate the soil of the Yellow River beach land. The main evaluation index includes As, Ni, Pb, Cd, Cr, Cu, and Zn.

Table 1. Toxicoefficients of heavy metals and reference values

Elements	As	Pb	Cd	Cr	Cu	Zn	Ni
Toxicoefficient	10	5	30	2	5	1	5
Reference value	9.7	21.9	0.1	66.6	26	65.2	30.2

Table 2. Grading standards of Hakanson potential ecological risk

Ecological damage	Slight	Medium	Strong
E_r^i	< 30	30~60	> 60
RI	< 135	135~265	> 265

Table 3. Grading standards for evaluation factors of C_f^i

Pollution degree	Slight	Medium	Strong	Very strong
C_f^i	< 1	1~3	3~6	> 6

Table 4. National Soil Environmental Quality Standard (GB 15618-2018)

Level	1 st	2 nd			3 rd
	Background	< 6.5	6.5~7.5	> 7.5	> 6.5
pH					
As	15	40	30	25	40
Ni	40	40	50	60	200
Pb	35	250	300	350	500
Cd	0.20	0.30	0.30	0.60	1.0
Cr	90	150	200	250	300
Cu	35	50	100	100	400
Zn	100	200	250	300	500
Hg	0.15	0.30	0.50	1.0	1.5

Descriptive statistical analysis of the heavy metals As, Hg, Pb, Cr, Cd, Cu, and Zn in soils from the Hancheng to Tongguan section of the Yellow River (Table 5) showed that the mean value of Zn was highest in the Yellow River beach soil, which was followed by Cr, and the average value of Cd was lowest. The average level of Cr was highest in Heyang and Tongguan, where the average Cd was lowest. Coefficients of variation of heavy metals of Hancheng exceeded 10%. Coefficients of variation for heavy metals such as Cr, Cu, Zn, and Ni were highest in Heyang and Tongguan. The sources of soil heavy metal pollution are very complex and other sources may add

pollution based on the siltation of the Yellow River beach soil. The status of heavy metal pollution in this soil is similar in that of the section of Heyang and Tongguan. As, Pb, Cd, and other heavy metals have a small variation coefficient, which may be mainly related to the formation and deposition of soils on the Yellow River beaches. Heavy metal elements such as Cr, Cu, Zn, and Ni may be affected by other sources of pollution. Among these, the coefficient of variation of Cu was highest in all reaches. The coefficient of variation of Cu was 40.1% in the lower reaches of Hancheng, the coefficient of variation of Cu in Heyang was 49.4%, and the coefficient of variation of Cu in Tongguan was 56.9%. Although the average content of Cu met the national standard, the Cu content of several samples reached the national standard. This shows that Cu in the Yellow River beach soil is particularly affected by external disturbances. The main origin may lie in the heavy use of pesticides and the emission of smelting gases around the Yellow River. The study area is located at the junction between Shaanxi, Shanxi, and Henan provinces, where the main modes of transportation include cars and trains, especially large trucks, according to the data on the official website of 12306 (the official website of China Railway), there are more than 40 trains through this area, which introduce a significant volume of tail gases and heavy metal pollution. The main pesticides used include *butacarb*, *bensultap*, *bismerthiazol*, *bromacil*, and *2,4,5-TB*. Farmers use these pesticides about two to three times every year to reduce pests and weeds. Furthermore, this area features a large number of coal and gold mines, which also introduce severe heavy metal pollution, such as Pb, Cd, and Hg.

Table 5. Descriptive statistics of soil heavy metal contents in the Yellow River region between Hancheng to Tongguan

Sites	Sample types	As	Pb	Cd	Cr	Cu	Zn	Ni
Hancheng	Maximum	9.8	23.3	0.5	79.3	76.2	307.8	52.6
	Minimum	3.4	7.0	0.2	36.4	19.4	205.5	21.3
	Average value	5.8	12.4	0.3	55.8	43.7	265.8	41.2
	Standard deviation	1.8	4.0	0.1	12.5	17.5	31.0	9.2
	Coefficient of variation	31.8	32.2	30.6	22.4	40.1	11.7	22.3
Heyang	Maximum	12.8	27.6	0.2	89.7	45.7	62.9	40.1
	Minimum	7.9	19.9	0.1	33.6	11.2	32.7	17.3
	Average value	11.1	23.5	0.1	57.7	21.9	50.4	25.7
	Standard deviation	1.4	2.5	0.0	16.9	10.8	9.3	6.0
	Coefficient of variation	12.5	10.6	11.5	29.4	49.4	18.5	23.5
Tongguan	Maximum	12.3	27.6	0.132	120	54.3	95.4	40.1
	Minimum	8.6	19.9	0.11	23.9	10.1	42	22.5
	Average value	10.8	23.0	0.1	62.5	23.0	59.6	30.3
	Standard deviation	1.0	2.5	0.0	23.4	13.1	15.6	4.1
	Coefficient of variation	9.2	10.7	5.0	37.4	56.9	26.2	13.6
Overall characteristics	Maximum	12.8	27.6	0.5	120.0	76.2	307.8	52.6
	Minimum	3.4	7.0	0.1	23.9	10.1	32.7	17.3
	Average value	9.0	18.8	0.2	58.4	30.3	137.3	33.2
	Standard deviation	3.0	6.3	0.1	17.6	17.7	106.4	9.8
	Coefficient of variation	33.7	33.3	45.3	30.2	58.5	77.5	29.6

Table 5 and Figure 3 show that the As content in the soils of the Yellow River Hancheng to Tongguan section ranged within 3.4-12.8 mg·kg⁻¹, with an average content of 9.0 mg·kg⁻¹. The As content in the soil of the floodplain in various regions follows a distribution of Heyang > Tongguan > Hancheng. The As content of the river beaches of Heyang was highest, with an average of 11.1 mg·kg⁻¹, and lowest in Hancheng. As content in the soil of the floodplain of Tongguan is more than Hancheng significantly ($p < 0.05$). The soil As content in the estuary was 5.8 mg·kg⁻¹. These results showed that the average As content in the floodplain of the Yellow River Hancheng to Tongguan section remained below the national soil environmental quality standard.

The Pb level in the soil of the Yellow River Hancheng to Tongguan section was 7.0-27.6 mg·kg⁻¹, at an average content of 18.8 mg·kg⁻¹. The average Pb content in the soil of the Yellow River beach in Hancheng was significantly lower compared with the whole area ($p < 0.05$). Here, the average content was 12.4 mg·kg⁻¹, and the average Pb content of the soil in the Yellow River beaches of Heyang County and Tongguan County were 23.5 mg·kg⁻¹ and 23 mg·kg⁻¹, respectively. However, the value was lower than that of the first-level standard for soil environmental quality. These levels remain below the national first-level standard for soil environmental quality.

The Cd content in the soil of the Yellow River Hancheng to Tongguan section was 0.1-0.5 mg·kg⁻¹, with an average of 0.2 mg·kg⁻¹. The Cd content in the floodplains of each region can be ordered according to: Hancheng > Heyang and Tongguan. Cd content in the soil of the floodplain of Hancheng is more than Heyang and Tongguan significantly ($p < 0.05$). The average Cd content in the Yellow River beach in Hancheng was 0.3 mg·kg⁻¹, which basically met the national secondary standard for soil environmental quality.

The Cr content in the soil of the Yellow River Hancheng to Tongguan section was 23.9-120.0 mg·kg⁻¹, with an average of 58.4 mg·kg⁻¹. The average content of Cr in the Yellow River beach of Hancheng was lowest at 55.8 mg·kg⁻¹ and the Cr content in the Yellow River beach of Tongguan County was highest, with an average value of 62.5 mg·kg⁻¹. Both levels remain far below the national first-level standard for soil environmental quality.

The Cu content in the soil of the Yellow River Hancheng to Tongguan section was 10.1-76.2 mg·kg⁻¹, with an average of 30.3 mg·kg⁻¹. The Cu content in the soil of Hancheng was about twice as high as that of Heyang and Tongguan ($p < 0.05$), with an average value of 43.7 mg·kg⁻¹. This exceeds the national first-level standard for soil environmental quality.

The Zn content in the soil of the Yellow River Hancheng to Tongguan section was 32.7-307.8 mg·kg⁻¹, with an average of 137.3 mg·kg⁻¹. The Zn content in the soil of the Yellow River beach in Hancheng was highest, reaching 265.8 mg·kg⁻¹, which slightly exceeded the national secondary standards for soil environmental quality.

The Ni content in the soil of the Yellow River Hancheng to Tongguan section was 17.3-52.6 mg·kg⁻¹, with an average content of 33.2 mg·kg⁻¹. The Ni content in the soil of each region followed: Hancheng > Tongguan > Heyang. Ni content in the soil of the floodplain of Hancheng is more than Tongguan significantly ($p < 0.05$), while Ni content of Tongguan and Heyang is not significantly ($p > 0.05$). The average Ni content in the soil of the Yellow River beach in Hancheng was 41.2 mg·kg⁻¹, which exceeds the national first-level standard for soil environmental quality.

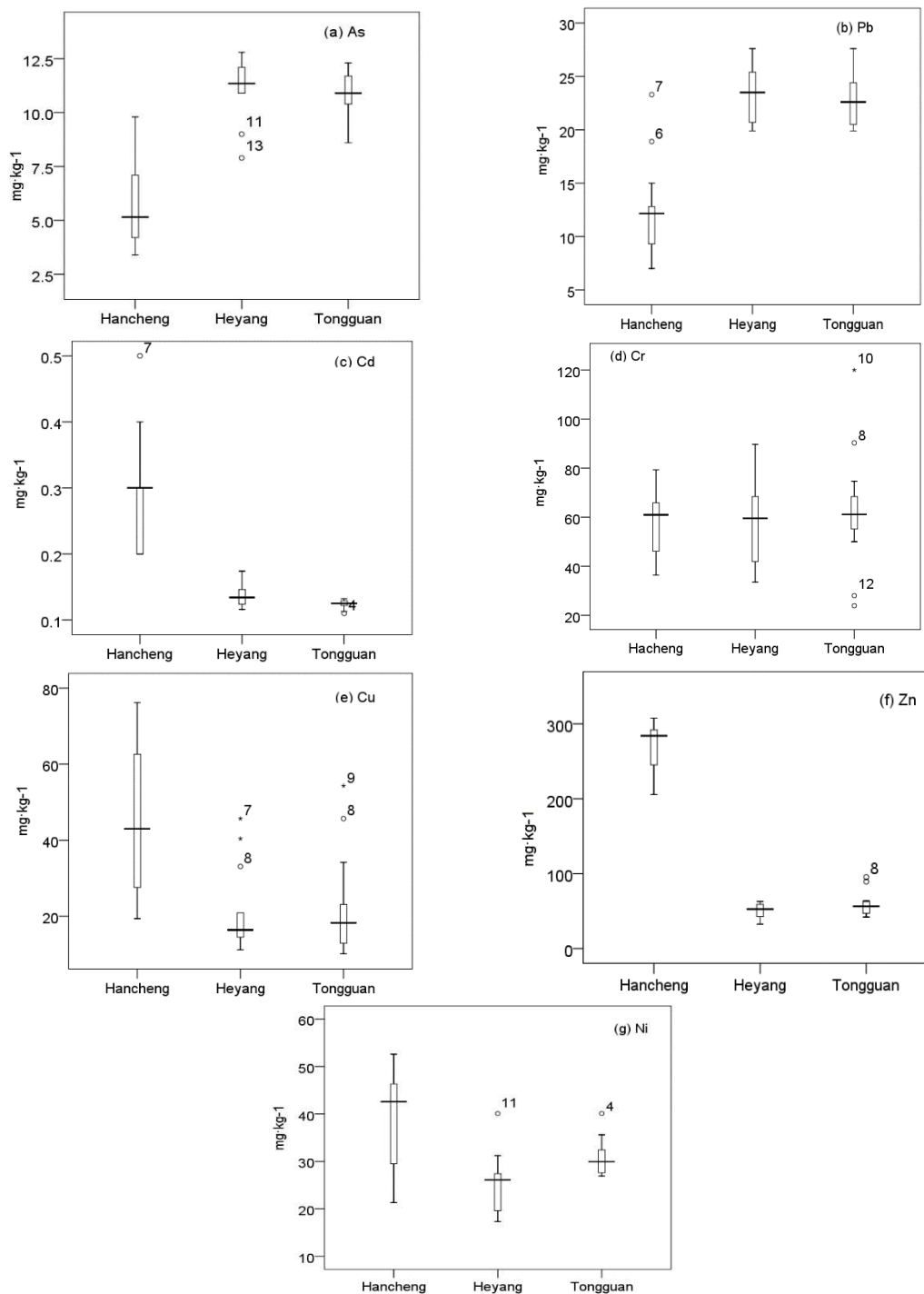


Figure 3. Boxplots of heavy metals concentration in the Yellow River region between Hancheng to Tongguan

Discussion

Correlation analysis of soil heavy metals

Correlation analysis of the soil heavy metal contents in the floodplain from Hancheng to Tongguan section of the Yellow River identified Pb, Cd, Cr, and Cu in

soils of the Yellow River beach at the Lower Xiayukou section of Hancheng (Table 6). A significant positive correlation was found between heavy metals ($p < 0.01$), indicating that these heavy metals have similar sources, which may mainly originate from the region's automobile exhaust and large-scale pesticide use. The correlation between Cr, Cd, Pb-Ni, Zn-Cr, Zn-Cu, and other heavy metals was significant ($p < 0.01$) in the Yellow River beach of Tongguan. This is likely due to the large-scale gold development in Tongguan.

Table 6. Correlation coefficient for heavy metals in the Yellow River region between Hancheng to Tongguan

Sites	Elements	As	Pb	Cd	Cr	Cu	Zn	Ni
Hancheng	As	1	.599**	.691**	.592**	.654**	0.311	0.214
	Pb		1	.660**	.777**	0.352	0.218	-0.075
	Cd			1	0.347	.573*	0.36	0.217
	Cr				1	.499*	0.139	-0.026
	Cu					1	0.373	-0.128
	Zn						1	-0.084
	Ni							1
Heyang	As	1	-0.259	0.253	0.287	0.177	-0.003	-0.361
	Pb		1	-0.126	-0.145	0.034	-0.055	0.013
	Cd			1	-0.377	0.007	-0.243	0.223
	Cr				1	0.151	.643*	-0.206
	Cu					1	0.116	-0.254
	Zn						1	-0.088
	Ni							1
Tongguan	As	1	-0.499	0.067	0.216	0.1	-0.022	0.181
	Pb		1	-0.083	0.371	0.184	0.493	-.643**
	Cd			1	-.589*	-0.269	-0.401	-0.221
	Cr				1	0.494	.755**	-0.24
	Cu					1	.756**	0.031
	Zn						1	-0.142
	Ni							1

Soil ecological risk assessment of heavy metals

The results of Equations 1–3 were calculated for each heavy metal, and the values are listed in Table 7. With regard to the average single pollution coefficient of heavy metals, the soil of Hancheng had strong Zn pollution. Cd, Cu, and Ni caused moderate pollution, and other elements caused slight pollution. The pollution degree of the heavy metals followed $Zn > Cd > Cu > Ni > Cr > As > Pb$. As shown in Table 8, the percentage of samples with strong Zn pollution in soil reached 100%, the percentage of samples with strongly contaminated soil Cd was 11.11%, and 88.89% of samples were moderately contaminated. With regard to the single potential ecological risk index of heavy metals, the potential ecological risk of Cd in the soil of Hancheng in the Yellow River reached a strong level (=80), while the ecological potential risks of other heavy metal elements were slight. The contribution of Cd to the potential ecological risk of heavy metals reached as high as 50%, which therefore is the heavy metal with the most

important ecological risk. This is consistent with the study of Yuan et al. (2008), Ye et al. (2010) and Davidson et al. (1994). The order of the ecological hazards of heavy metals followed Cd > Cu > Ni > As > Zn > Pb > Cr.

Table 7. Assessment of potential ecological risks of soil heavy metals in the Yellow River region between Hancheng to Tongguan

Sites	Statistics items	C_f^i							E_r^i						RI	
		As	Pb	Cd	Cr	Cu	Zn	Ni	As	Pb	Cd	Cr	Cu	Zn		Ni
Hancheng	Max	1.01	1.06	5.00	1.19	2.93	4.72	1.74	10.10	5.32	150.00	2.38	14.65	4.72	8.71	195.89
	Min	0.35	0.32	2.00	0.55	0.75	3.15	0.71	3.51	1.60	60.00	1.09	3.73	3.15	3.53	76.61
	Ave	0.58	0.55	2.67	0.84	1.66	4.09	1.38	5.84	2.75	80.00	1.67	8.31	4.09	6.89	109.56
Heyang	Max	1.32	1.26	1.74	1.35	1.76	0.96	1.33	13.20	6.30	52.20	2.69	8.79	0.96	6.64	90.78
	Min	0.81	0.91	1.16	0.50	0.43	0.50	0.57	8.14	4.54	34.80	1.01	2.15	0.50	2.86	54.02
	Ave	1.16	1.07	1.37	0.86	0.81	0.78	0.84	11.52	5.34	41.08	1.72	4.03	0.78	4.19	68.66
Tongguan	Max	1.27	1.26	1.32	1.80	2.09	1.46	1.33	12.68	6.30	39.60	3.60	10.44	1.46	6.64	80.73
	Min	0.89	0.91	1.10	0.36	0.39	0.64	0.75	8.87	4.54	33.00	0.72	1.94	0.64	3.73	53.44
	Ave	1.12	1.05	1.24	0.92	0.84	0.90	1.00	11.20	5.24	37.22	1.84	4.18	0.90	5.00	65.58
Overall characteristics	Max	1.32	1.26	5.00	1.80	2.93	4.72	1.74	13.20	6.30	150.00	3.60	14.65	4.72	8.71	201.18
	Min	0.35	0.32	1.10	0.36	0.39	0.50	0.57	3.51	1.60	33.00	0.72	1.94	0.50	2.86	44.13
	Ave	0.93	0.86	1.83	0.87	1.14	2.08	1.10	9.27	4.32	54.75	1.74	5.72	2.08	5.48	83.36

Table 7 shows the average individual pollution coefficients of heavy metals. Cd, As, and Pb in Heyang cause moderate pollution, and soil was slightly polluted with other heavy metals. Their degree of pollution followed Cd > As > Pb > Cr > Ni > Cu > Zn. As shown in Table 8, 100% of Cd reached a moderate level of pollution, and the percentages of samples with moderate pollution of As and Pb were 85.71% and 64.29%, respectively. With regard to the average single potential ecological risk index of heavy metals in soils (Tables 7 and 8), all heavy metals in the soils of riverside beaches in Heyang, except for medium pollution (=41.08), reached a contribution rate of Cd to soil potential ecological risk in the floodplain of Heyang of 100%.

With regard to the average individual pollution coefficient of heavy metals, the contents of Cd, As, Pb, Ni, and other elements in the soil of Yellow River beach in Tongguan caused moderate pollution. The contents of heavy metals in other soils caused slight pollution. The levels follow Cd, As, Pb > Cr > Ni > Cr > Zn > Cu. This is similar to the heavy metal pollution in the soil of the Yellow River beach in Heyang. The average single potential ecological risk index of heavy metals in Tonglian and Heyang followed a similar trend. Except for the moderate pollution (37.22), all other heavy metal elements caused slight pollution. Among these, the contribution of Cd to soil potential ecological risk of the Yellow River beach in Tongguan was 100%, which agreed with the results of Heyang.

In general, Cd was identified as the main pollutant in the Yellow River beaches of the Hancheng-Tongguan section of the Yellow River. The contribution rate of Cd to soil potential ecological risk was 82.98%, while that to the soil potential strong ecological risk was 17.02%. This study showed that the overall potential ecological risk index of soils in Hancheng-Tongguan section of Yellow River was 83.36 < 135; therefore, the

potential risk of soils in the Yellow River beach is slight. The comprehensive potential risks of soil in different reaches of the river follow: Hancheng > Heyang > Tongguan. The comprehensive potential ecological risk index of soils in Hancheng was $109.5 < 135$, indicating slight risks.

Table 8. Percentage of the samples in different C_f^i and E_r^i grades for different metals in the Yellow River region between Hancheng to Tongguan/%

Sites	Elements	C_f^i				E_r^i		
		Slight pollution	Moderately polluted	Strongly contaminated	Strong pollution	Slight risk	Medium risk	Strong risk
Hancheng	As	94.44	5.56			100		
	Pb	94.44	5.56			100		
	Cd		88.89	11.11			50	50
	Cr	88.89	11.11			100		
	Cu	22.22	77.78			100		
	Zn			100		100		
	Ni	22.22	77.78			100		
Heyang	As	14.29	85.71			100		
	Pb	35.71	64.29			100		
	Cd		100				100	
	Cr	71.43	28.57			100		
	Cu	78.57	21.43			100		
	Zn	100				100		
	Ni	14.29	85.71			100		
Tongguan	As	6.67	93.33			100		
	Pb	46.67	53.33			100		
	Cd		100				100	
	Cr	73.33	26.67			100		
	Cu	80.00	20.00			100		
	Zn	86.67	13.33			100		
	Ni	60.00	40.00			100		
Overall characteristics	As	42.55	57.45			100		
	Pb	89.36	10.64			100		
	Cd		95.74	4.26			82.98	17.02
	Cr	95.74	4.26			100		
	Cu	17.02	82.98			100		
	Zn	10.64		89.36		100		
	Ni	17.02	82.98			100		

Conclusions

(1) The contents of As, Ni, Pb, Cd, Cr, Cu, Zn in the soil samples of the Hancheng to Tongguan section of the Yellow River were assessed. The average Zn content was highest, arrived $137.3 \text{ mg}\cdot\text{kg}^{-1}$. The average As and Cd contents were smallest, and with the exception of Ni, the coefficients of variation of all other tested heavy metals were large, indicating a notable difference between these heavy metals.

(2) A significant positive correlation ($p < 0.01$) was found between heavy metals such as Pb, Cd, Cr, and Cu in the Yellow River floodplain of Hancheng ($p < 0.01$). This

indicates that these heavy metals have similar origins and are most likely the result of car exhaust emissions and large-scale pesticide use. The correlation between Cr, Cd, Pb-Ni, Zn-Cr, Zn-Cu, and other heavy metals was significant ($p < 0.01$) in the Yellow River beach of Tongguan, which is likely due to the large-scale gold development in Tongguan.

(3) According to the Hakanson potential ecological risk index, the overall potential ecological risk index of soil in the Yellow River from Hancheng to Tongguan section is $83.36 < 135$; therefore, the potential risk of soils in the Yellow River beach is slight. The results follow: Hancheng > Heyang > Tongguan. The comprehensive potential ecological risk index of the soil of the Yellow River beach in Hancheng is $109.5 < 135$, which also indicates slight risk.

(4) The impact of human activities on heavy metal pollution in the Yellow River beaches is relatively minor; however, to avoid intensification of the potential ecological hazards in the soil, attention should be directed to the treatment of heavy metal pollution in the Yellow River beach at their source.

Acknowledgements. Financial support was supported by Research Project of Shaanxi Provincial Land Engineering Construction Group in China (DJNY2018-16 & DJNY2018-19) and the Fund Project of Shaanxi Key Laboratory of Land Consolidation (2019-JC05 & 2019-JC04).

REFERENCES

- [1] Chakraborty, J., Das, S. (2016): Molecular perspectives and recent advances in microbial remediation of persistent organic pollutants. – *Environ Sci Pollut Res Int* 23(17): 16883-16903.
- [2] Cheng, Q., et al. (2012): Investigation of the heavy metal contamination of the sediments from the Yellow River Wetland Nature Reserve of Zhengzhou, China. – *Iranian Journal of Public Health* 41(3): 26-35.
- [3] Crnkovic, D., Ristic, M., Antonovic, D. (2006): Distribution of heavy metals and As in soils of Belgrade (Serbia and Montenegro). – *Soil and Sediment Contamination* 15: 581-589.
- [4] Davidson, C. M., et al. (1994): Evaluation of a sequential extraction procedure for the speciation of heavy metals in sediments. – *Analytica Chimica Acta* 291(3): 277-286.
- [5] Douay, F., Roussel, H., Fourier, H. (2007): Investigation of heavy metal concentrations on urban soils, dust and vegetables nearby a former smelter site in Mortagne du Nord, Northern France. – *Journal of Soils and Sediments* 7: 143-146.
- [6] Fan, Q., et al. (2008): Heavy metal pollution in the Baotou section of the Yellow River, China. – *Chemical Speciation & Bioavailability* 20(2): 65-76.
- [7] Fan, S., Wang, X., Lei, J., et al. (2019): Spatial distribution and source identification of heavy metals in a typical Pb/Zn smelter in an arid area of northwest China. – *Human and Ecological Risk Assessment an International Journal* 25(7): 1-27.
- [8] Hakanson, L. (1980): An ecological risk index for aquatic pollution control: a sedimentological approach. – *Water Research* 14: 975-1001.
- [9] Hu, M., Wu, J. Q., Peng, P. Q., et al. (2014): Assessment model of heavy metal pollution for arable soils and a case study in a mining area. – *Acta Scientiae Circumstantiae* 34: 423-430.
- [10] Islam, M. S., et al. (2015): Heavy metal pollution in surface water and sediment: A preliminary assessment of an urban river in a developing country. – *Ecological Indicators* 48(48): 282-291.

- [11] Li, K., Gu, Y., Li, M., et al. (2017): Spatial analysis, source identification and risk assessment of heavy metals in a coal mining area in Henan, Central China. – *International Biodeterioration & Biodegradation* 128: S0964830517304766.
- [12] Li, P., et al. (2015): Heavy metal contamination of Yellow River alluvial sediments, Northwest China. – *Environmental Earth Sciences* 73(7): 3403-3415.
- [13] Mi, Z., Liao, B., Shu, W., et al. (2015): Pollution Assessment and Potential Sources of Heavy Metals in Agricultural Soils around Four Pb/Zn Mines of Tongguan City, China. – *Journal of Soil Contamination* 24(1): 76-89.
- [14] Tume, P., Bech, J., Sepulveda, B. (2008): Concentrations of heavy metals in urban soils of Talcahuano (Chile): a preliminary study. – *Environmental Monitoring and Assessment* 140: 91-98.
- [15] Xu, Y. N., Zhang, J. H., Ke, H. L., et al. (2014): Human health risk under the condition of farmland soil in a gold mining area. – *Geological Bulletin of China* 33: 1239-1252.
- [16] Ye, C. et al. (2010): Heavy metals in soil of the ebb-tide zone of the Three-Gorges research and their ecological risks. – *Acta Pedologica Sinica* 47(6): 1264-1269.
- [17] Yuan, H., et al. (2008): Chemical forms and pollution characteristics of heavy metals in Yellow River sediments. – *Chinese Journal of Ecology* 27(11): 1966-1971.

EFFECT OF SEAWEED APPLICATION ON NUTRIENT UPTAKE OF STRAWBERRY CV. ALBION GROWN UNDER THE ENVIRONMENTAL CONDITIONS OF NORTHERN IRAQ

AL-SHATRI, A. H. N.¹ – PAKYÜREK, M.^{1*} – YAVIÇ, A.²

¹*Siirt University Faculty of Agriculture, Department of Horticulture, 56100 Siirt, Turkey*

²*Yüzüncü Yıl University Faculty of Agriculture, Department of Horticulture, 65080 Van, Turkey*

*Corresponding author

e-mail: mine.pakyurek@siirt.edu.tr

(Received 22nd Aug 2019; accepted 15th Nov 2019)

Abstract. This pot experiment was carried out to investigate the effects of four doses (0, 2, 4 and 8 g.L⁻¹) of seaweed extract (Alga 600) application with fertigation on nutrient uptake of strawberry cv. Albion during the 2016-2017 vegetation period in Kalar city located in Northern Iraq. The results of leaf analysis indicated significant ($p < 0.01$) differences at the nitrogen (N), phosphorus (P), potassium (K), magnesium (Mg), calcium (Ca), manganese (Mn) and iron (Fe) concentrations between two sampling periods. In contrast, copper (Cu) and zinc (Zn) concentrations of plants leaves did not significantly differed between the sampling periods. According to the statistical analysis, the effect of seaweed doses on nutrients were statistically insignificant for all nutrients except Mn ($p > 0.05$). While for the Mn element, the highest value (223.70 ± 11.59 mg kg⁻¹) obtained from T4 (8 g.L⁻¹) seaweed dose; the lowest one (164.91 ± 11.59 mg kg⁻¹) obtained from control dose. The effect of interaction between seaweed doses and periods on nutrients was also not found statistically significant ($p > 0.05$). In general, seaweed extract of 8 g.L⁻¹ was more effective on macro and micro nutrient contents of strawberry leaves.

Keywords: *Fragaria x ananassa* Duch, cv. Albion, organic fertigation, algae extract, plant nutrients

Introduction

Strawberry (*Fragaria x ananassa* Duch) belonging to family Rosaceae, is one of the most delicious and refreshing temperate fruits of the world. It has rich source of vitamins and minerals with delicate flavor (Sharma, 2002) and gives early and very high returns per unit area compared to the other fruits because the fruits are ready for harvest within six months of the planting (Katiyar et al., 2009). Wood strawberry (*Fragaria vesca*) and musky strawberry (*Fragaria moschata*) had been cultivated in Europe and Russia for centuries before the breeding of *Fragaria x ananassa*. In the early 1700s, inter-planting of *Fragaria virginiana* (male) with *Fragaria chiloensis* (female) in France led to the production of hybrid seedlings known as Pineapple or Pine strawberry plants, which are the progenitors of the new cultivated strawberry plant (*Fragaria x ananassa* Duch) (Darrow, 1966).

Several factors constrain agricultural production by negatively affecting the plant growth. Soil characteristics determining the fertility of soils on which the plant is grown and the climatic characteristics such as temperature and humidity positively or negatively affect the crop production. Seaweed is used in many countries as liquid extract or mixing directly with the soil. The seaweed, an organic amendment regulates the soil structure when mixed directly into the soil and sustains the productivity for a long time. Some seaweeds have been used as fertilizers in the production areas for many years (Güner and Aysel, 1996). Seaweed extracts have been used extensively in organic

farming especially in developed countries due to the reducing storage losses, increasing the production, uptake of inorganic nutrients from soil, seed germination, resistance to stress conditions, diseases and pests (Blunden, 1991). Seaweed increases nutrient and water uptake by providing strong root development of plants and encourages vegetative growth by accelerating the formation of chlorophyll. In addition, yield and quality of the products are improved by increasing the balanced and long-term uptake of macro and micro nutrients from the soil; thus, the market and export value of the product are increased (Blunden et al., 1992; Hong et al., 1995). Seaweed extracts increase the uptake of micro elements by chelating the micronutrients. Side branching and fruit formation in fruit trees also have been increased with seaweed application. In addition, flower and fruit losses have been decreased and yield increased up to 30%. Seaweeds also have been reported to increase the impacts of pesticides by 25% (Blunden et al., 1992).

Seas are generally covered with various qualities and numbers of seaweeds from the surface to a depth of 1000 m. The distribution of seaweeds, whose nutritional and other economic values have been documented, in the seas vary greatly depending on the water compositions of seas and the climate characteristics of the region (Blunden, 1991). Several types of compounds such as macro and micro elements (N, Ca, Mg, Mn, B, Br, I, Zn, Cu and Co), plant growth regulators (auxin, cytokinin, gibberellin and abscisic acid) and betaines are responsible from the positive effects of seaweeds (Hong et al., 1995).

In this study, a potting experiment with four different doses of seaweed extract, including the control treatment, was carried out to investigate the effect of seaweed, an organic fertilizer, on plant growth and nutrient uptake of Albion strawberry cultivar. This is a pioneering study that will serve to expand the production of strawberry which has not yet been cultivated widespread in Iraq.

Materials and Methods

The study was carried out during the vegetation period of 2016-2017 with pots in an open area of Kalar city located at Sulaymaniyah governate in Northern Iraq. The experimental site is situated between 34.62131° north latitude and 45.31961° east longitude at 200 m above sea level. The minimum and the maximum temperatures in Kalar during the vegetation period were -3°C and 35°C (Anonymous, 2017). The temperature started to increase in the middle of the April; thus, the effects of high temperature on size and weight of strawberry fruits appeared at the beginning of May, which was the last harvest time (*Table 1*).

Table 1. Climate data of Kalar-Sulaymaniyah, Iraq from January to June 2017.

Months	Temperature (°C)			Relative Humidity (%)		
	Average	Maximum	Minimum	Average	Maximum	Minimum
January	8.72	20.3	-2.98	88.19	100	0.89
February	12.62	25.73	0.92	73.59	100	0.9
March	15.7	28.22	2.47	65.59	100	0.9
April	21.01	38.4	5.53	9.71	100	0.89
May	27.49	41.91	13.66	15.27	100	0.92
June	33.51	46.95	17.49	21.13	56.45	7.33

Experimental Details

The plant material used in the experiment was Albion variety which was registered in 2006 by the University of California and sent out to the world. Despite the low yield of the Albion variety, the farmers report from the Mid-Atlantic on fruit quality are positive. The Albion variety has firm fruits with a high marketable yield percentage due to the shape and volume of the fruits. The ideal color and acceptable flavor of strawberry fruits are obtained at maturity. The Albion variety is very strong, and produces a high number of daughter plants and stolons (Lantz et al., 2010) (*Figure 1*).



Figure 1. Strawberry plants and fruits of cv. Albion.

The seedlings used in the experiment were obtained on January 1st, 2017 from Antalya province, Turkey. The pot experiment laid out based on the randomized plot design with three replicates. The pots were filled with 5 kg peat moss, watered with drip system and placed to an open area on January 15th, 2017 in Kalar district. Full flowering time was on 15th February 2017, first harvesting time was on 20th March and second one was on 12th May 2017 in our experiment. Four different doses (0, 2, 4 and 8 g.L⁻¹) of fertigation solutions were prepared from the seaweed (Alga 600). Based on the literature information, we applied three different doses (except control) starting from 2 g.L⁻¹ and increasing in double doses thought to will be obtained effective results in the study. The seaweed was dissolved in 22°C water for better absorption. The prepared solutions were applied to the plants twice. First application was applied in the full flowering stage (after the formation of first fruits) and second one was applied 20 days later then previous one, in other words, after the first harvesting time. The fertigation was applied in the morning. Components of seaweed were shown in *Table 2*.

Nutrient Analysis of Strawberry Leaves

Twelve (Four seaweed applications with three repetitions) leaf sample bags (each bag contains three leaves) with two replications (two fertigation times) were prepared during the flowering stage and after the first harvest to determine the plant nutrient concentrations. Leaves were washed in tap water and rinsed with distilled water then left for drying in oven at 60°C for 48 hours. The dried samples were ground by milling and stored in pouch papers until the chemical analysis. Plant nutrient concentration of

samples was determined by using the methods reported by Kaçar and İnal (2008). Nitrogen (N) concentration was determined by Kjeldahl method. Phosphorus (P), potassium (K), magnesium (Mg), calcium (Ca), manganese (Mn) and iron (Fe) copper (Cu) and zinc (Zn) concentrations were analyzed by microwave method using an ICP-MS instrument (Thermo Scientific, ICAP Q model).

Table 2. Chemical composition of seaweed (*Alga 600*) used in the experiment.

Chemical Composition	Unit	Content
Nitrogen (N)		0.5-1.0
Alganic acid		6.0-9.0
Sulfur (S)		1.0-1.5
Phosphorus pentoxide (P ₂ O ₅)		6.0-9.0
Calcium oxide (CaO)		0.4-1.6
Iron (Fe)	%	0.15-0.3
Magnesium oxide (MgO)		0.06
Potassium oxide (K ₂ O)		21-24
Amino acid		4.0
pH		9-11
Organic matter		40-50

Statistical Analysis

The effects of seaweed doses and application periods on nutrient concentrations of strawberry leaves were assessed by the two-way analysis of variance test conducted according to the randomized plot design (ANOVA). Significance threshold was set to 0.05 and 0.01 levels. Paired samples t test was used to test the difference between the periods. Descriptive statistics such as mean and standard errors of nutrient contents were presented.

Results and Discussion

According to the results obtained in our study, increasing seaweed doses (0, 2, 4 and 8 g.L⁻¹) were increased the yield and fruit quality of the product. There is a significant increase in T4 (8 g.L⁻¹) compared with control (T1) and T2 treatment. The fertigation with seaweed (*Alga 600*) in T4 treatment resulted in the maximum value of yield per plant (g) 295.03 g and per hectare 3278.18 kg/ha. The lowest value belongs to the control treatment. Moreover, the T4 dose (8 g.L⁻¹) gave the maximum value of the average volume of fruit (18.88 ml³) and total volume of fruit (329.37 ml³) and the lowest value recorded by control treatment. This records can be explained by the fact that seaweed application leads to the improvement in the development of fruit diameter, strength, and length in addition to a better rate of fruit production (Abdulraheem, 2009).

The essential elements are divided in two groups as macro and micro plant nutrients. Macro nutrients consist of N, P, K, Ca and Mg which are used in large quantities; therefore, macro nutrients are very important for plant growth supplied by fertilizers. Micro nutrients are Fe, Cu, Cl, Bo, Mn and Zn which are used in small quantities by the plants though are necessary for plant essential. As a result of two-way analysis of variance, the effect of seaweed doses on nutrients was statistically insignificant for all nutrients except Mn (p>0.05) (*Table 3*). The results of nutrient concentrations of

strawberry leaf samples in flowering time and after the first harvest were given in *Table 4*. The effect of interaction between seaweed doses and periods on nutrients was also not found statistically significant ($p>0.05$).

Table 3. Nutrient concentrations of plant leaves get from four several seaweed doses.

Dose	N	P	K	Mg	Ca	Mn	Fe	Cu	Zn
	mg kg ⁻¹ (ppm)								
T1	3.13± 0.13	4329.42± 258.25	17877.93± 1106.18	5259.78± 300.60	921.16± 49.64	164.91± 11.59 b	380.13± 18.41	3.61± 0.20	31.99± 2.34
T2	2.87± 0.13	3945.21± 258.25	18258.25± 1106.18	4818.04± 300.60	882.59± 49.64	178.01± 11.59 ab	359.32± 18.41	3.12± 0.20	30.54± 2.34
T3	3.14± 0.13	3814.78± 258.25	17327.27± 1106.18	4805.63± 300.60	853.96± 49.64	180.17± 11.59 ab	379.59± 18.41	3.01± 0.20	30.21± 2.34
T4	2.94± 0.13	4277.42± 258.25	17857.60± 1106.18	4851.53± 300.60	887.16± 49.64	223.70± 11.59 a	385.73± 18.41	3.05± 0.20	30.46± 2.34
Sig. (P value)	NS	NS	NS	NS	NS	p<0.05	NS	NS	NS

p<0.05: significant at 0.05 level; ns: not significantly different.

Table 4. Nutrient concentrations of plant leaves get from two fertigation periods.

Periods	N	P	K	Mg	Ca	Mn	Fe	Cu	Zn
	mg kg ⁻¹ (ppm)								
Flowering Stage	3.73± 0.09 a	5657.78± 182.61 a	20155.3± 782.19 a	3380.43± 212.56 b	490.88± 35.10 b	131.30± 8.19 b	267.62± 13.02 b	3.17± 0.14	31.90± 1.65
After the first harvest	2.31± 0.09 b	2525.63± 182.61 b	15505.2± 782.19 b	6487.06± 212.56 a	1281.56± 35.10 a	242.09± 8.19 a	484.77± 13.02 a	3.22± 0.14	29.70± 1.65
Sig. (P value)	p<0.01	p<0.01	p<0.01	p<0.01	p<0.01	p<0.01	p<0.01	NS	NS

p<0.01: significant at 0.01 level; NS: not significantly different.

Macronutrient Contents of Strawberry Leaves

The effect of different fertigation doses of seaweed (Alga 600) treatments on N concentration of strawberry leaves were presented in *Figure 2*. The highest N concentration was obtained with T3 seaweed treatment (4 g.L⁻¹), while the N concentration was sharply decreased with T4 treatment (8 g.L⁻¹) which caused to the lowest N concentration in leaves. The N concentration of leaves in the seaweed treatments after the second harvest was lower than the control treatment (T1). Sampling time had a significant effect on N concentration of leaves (*Table 4*). The N concentration recorded in the flowering stage (3.73 ± 0.09 mg kg⁻¹) was significantly higher than that obtained after the first harvest (2.31 ± 0.09 mg kg⁻¹). The differences in N concentration between the sampling periods was related to the higher consumption of N in fruiting stage compared to the flowering stage (Rathore et al., 2009). The results indicated that seaweed was not able to supply adequate N required by strawberry plants (Schmidt et al., 2003), though it may improve the root growth of plants. The results obtained were in agreement with those reported by Shehata et al. (2011).

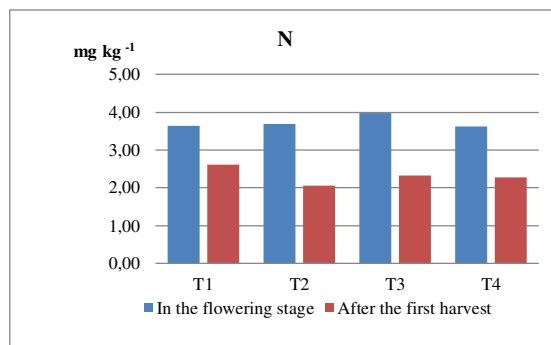


Figure 2. Nitrogen concentrations of strawberry leaves at two different sampling times for 4 different seaweed doses.

Phosphorus has several key plant functions, including energy transfer, photosynthesis, transformation of sugars and starches, nutrient movement within the plant and transfer of genetic characteristics between the generations (Blevins, 1999). Plants with high P content in leaves need high P supply for fruit production (Margarida et al., 2014). The effects of different doses of seaweed fertigation on P concentration of strawberry leaves were shown in *Figure 3*. The P concentration in T2, T3 and T4 treatments did not significantly differ from the control treatment. The highest P concentration of strawberry leaves was recorded in T4 treatment at flowering stage and the lowest P concentration was in T3 treatment at flowering stage. The highest P value in the second sampling period was obtained in T1, while the lowest P value was in T4 treatment. The P concentration between two sampling periods was significantly different ($p < 0.01$). The concentration of P in the flowering stage was significantly higher ($5657.78 \pm 182.61 \text{ mg kg}^{-1}$) than the P concentration recorded after the first harvest ($2525.63 \pm 182.61 \text{ mg kg}^{-1}$).

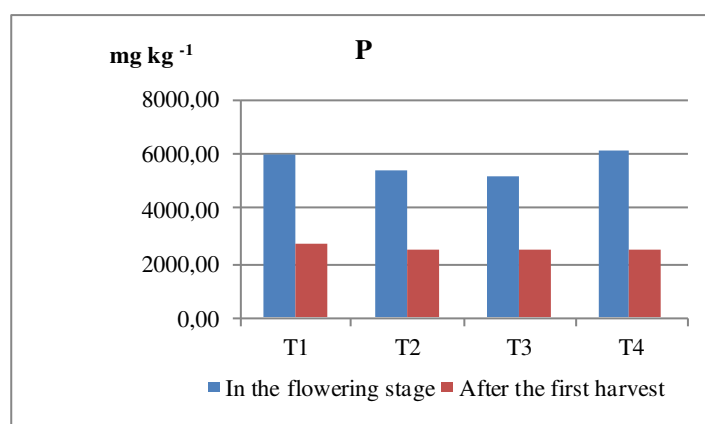


Figure 3. Phosphorus content of strawberry leaves at two different sampling times for 4 different seaweed doses.

Potassium is one of the major nutrients for plant survival and is involved in activation of the meristematic tissue growth, water transport and photosynthesis (Mengel and Kirkby, 1987). The results of ANOVA indicated that seaweed doses did not have significant affect on K concentrations of strawberry leaves (*Figure 4*). The highest K concentration was obtained in T4 at flowering stage and the lowest K value was in T3 treatment at flowering stage. The highest K content in the second sampling was recorded in T3, while the lowest value was in T4 treatment. The K content of strawberry leaves was significantly different ($p < 0.01$) between the sampling periods. The K concentration of leaves in the flowering stage ($20155.3 \pm 782.19 \text{ mg kg}^{-1}$) was higher compared to K content recorded after the first harvest ($15505.2 \pm 782.19 \text{ mg kg}^{-1}$). Battacharyya et al. (2015), had been found similar results to our results in their experiment.

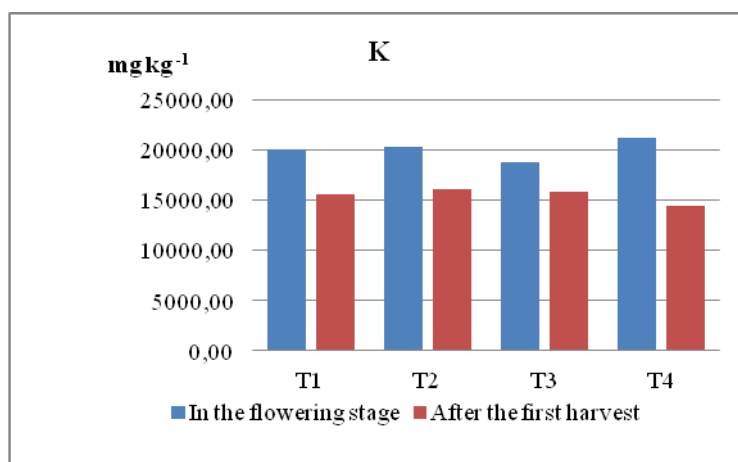


Figure 4. Potassium content of strawberry leaves at two different sampling times for 4 different seaweed doses.

Magnesium is the key nutrient of chlorophyll production, improves the mobility of P, increases the activity and components of some plant hormones; influences earliness and uniformity of the fruit maturity. Tavasoli et al. (2010) showed that Mg increases the fruit yield due to the influence on the intensity of photosynthesis different doses of seaweed (Alga 600) had no significant effect on Mg concentration of strawberry leaves as similar to our study in *Figure 5*. The concentration of Mg in T4 and T2 treatments were higher compared with the control, and the highest value was recorded in T4 treatment at flowering stage. The highest Mg content in the second sampling was obtained in T3 treatment while the lowest value was in T4 treatment. The concentration of Mg was significantly different ($p < 0.01$) between the sampling periods (*Table 3*). The highest Mg value was recorded after the first harvest ($6487.06 \pm 212.56 \text{ mg kg}^{-1}$) and the lowest value was in the flowering stage ($3380.43 \pm 212.56 \text{ mg kg}^{-1}$).

The effects of different doses of seaweed extracts on Ca concentration of strawberry leaves was presented in *Figure 6*. The seaweed doses had no significant effect on Ca concentration of leaves. The concentration of Ca in T2 and T4 treatments was higher compared with the control. The highest Ca concentration was recorded in T4 treatment at flowering stage while the lowest value in control at flowering stage. In the second sampling, the highest value was obtained in control and the lowest value was in T2 treatment. The concentration of Ca was significantly different ($p < 0.01$) between the

sampling periods. The highest Ca concentration was recorded after the first harvest ($1281.56 \pm 35.10 \text{ mg kg}^{-1}$) and the lowest value was at the flowering stage ($490.88 \pm 35.10 \text{ mg kg}^{-1}$). Rathore et al. (2009), had also been determined close results to ours in their research.

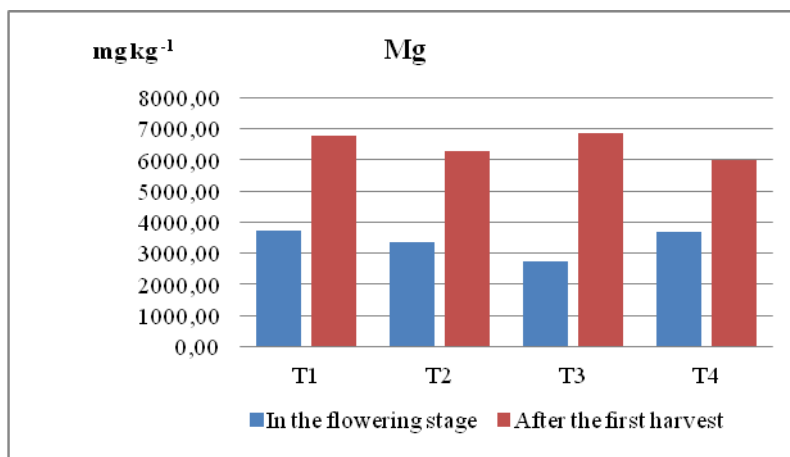


Figure 5. Magnesium content of strawberry leaves at two different sampling times for 4 different seaweed doses.

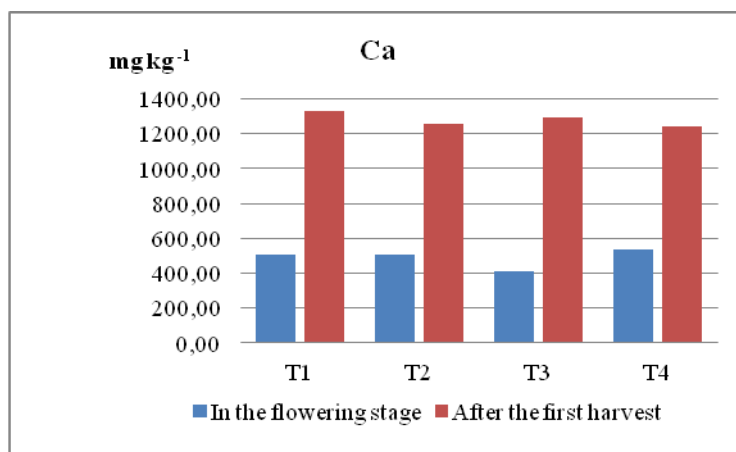


Figure 6. Calcium content in strawberry leaves at two different sampling times for 4 different seaweed doses.

Micronutrient Concentrations of Strawberry Leaves

The results of ANOVA test conducted to determine the effects of seaweed treatments on Mn concentration of strawberry leaves were given in *Figure 7*. The seaweed application significantly ($p < 0.05$) increased the Mn concentration of leaves and the Mn concentrations of leaves increased with increasing doses of seaweed. The highest Mn value was recorded in T4 while the lowest value was in T1 at flowering stage. In the first harvest, the Mn concentration of leaves increased with higher doses of seaweed though the changes were not significant. The highest Mn content after the first harvest was obtained with T4 treatment and the lowest value was in T1 treatment. Statistically significant difference ($p < 0.01$) was observed in Mn concentration of leaves between the

sampling periods. The concentration of leaves after the first harvest was significantly higher ($242.09 \pm 8.19 \text{ mg kg}^{-1}$) than the Mn concentration recorded in the flowering stage ($131.30 \pm 8.19 \text{ mg kg}^{-1}$). The increase in Mn concentration of leaves can be attributed to the high micronutrient concentration of seaweed used in this study. Fertilization of seaweed improved the Mn uptake by root system. Kumari et al. (2011) reported higher vegetative growth, yield and pest resistance with liquid spray application of seaweed. Similarly, Crouch and Staden (1992) showed that seaweed enhanced the root growth and had positive effect on nutrient uptake such as Mn.

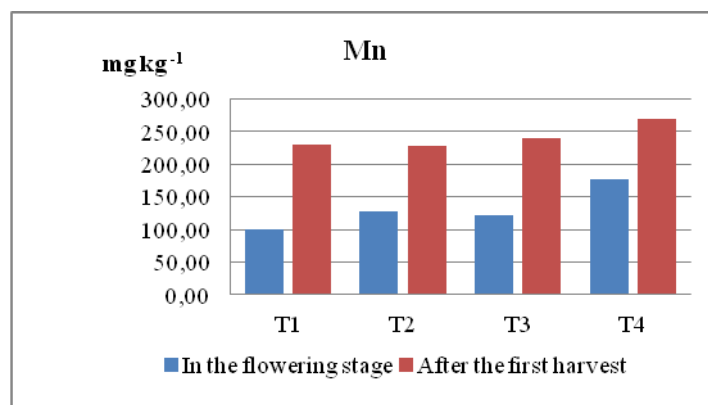


Figure 7. Manganese content in strawberry leaves at two different sampling times for 4 different seaweed doses.

The effect of seaweed doses on Fe concentration of strawberry plants were shown in *Figure 8*. The seaweed doses did not have a significant effect on Fe concentration of leaves. The concentration of Fe in T1 and T4 treatments were higher compare to the T2 and T3 treatments. The highest value was recorded in control at the flowering stage and the lowest value was in T2 treatment at flowering stage. In second sampling, the highest value was obtained with T4 treatment and the lowest value was in control. The concentration of Fe recorded after the first harvest ($484.77 \pm 13.02 \text{ mg kg}^{-1}$) was significantly ($p < 0.01$) higher than the Fe concentration obtained in the flowering stage ($267.62 \pm 13.02 \text{ mg kg}^{-1}$). Similarly, Rathore et al. (2009), had been highlighted close results to our study.

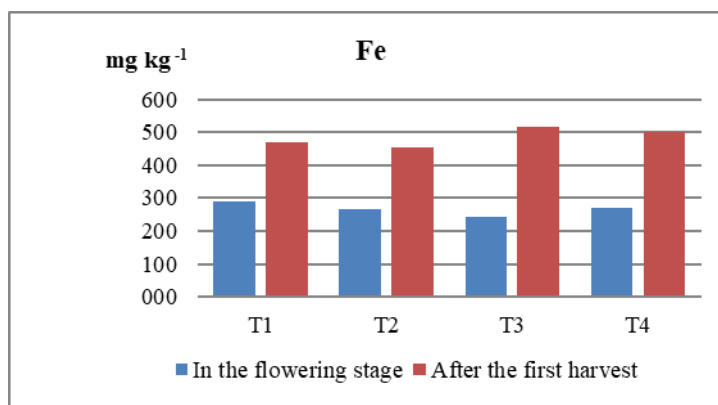


Figure 8. Iron content in leaf of strawberry leaves at two different sampling times for 4 different seaweed doses.

The seaweed treatments had no significant effect on Cu concentrations of strawberry leaves (*Figure 9*). The concentration of Cu in control treatment was higher than the Cu contents recorded in seaweed applications. The highest Cu concentration in flowering stage was recorded in control and the lowest value was obtained in T2 at the flowering stage. Similarly, the highest Cu concentration in the second sampling was recorded in T1 treatment. The Cu concentration of strawberry leaves recorded in flowering stage ($3.17 \pm 0.14 \text{ mg kg}^{-1}$) was slightly lower compared to the Cu concentration recorded after the first harvest ($3.22 \pm 0.14 \text{ mg kg}^{-1}$). Shehata et al. (2011), had also been found similar findings to our experiment.

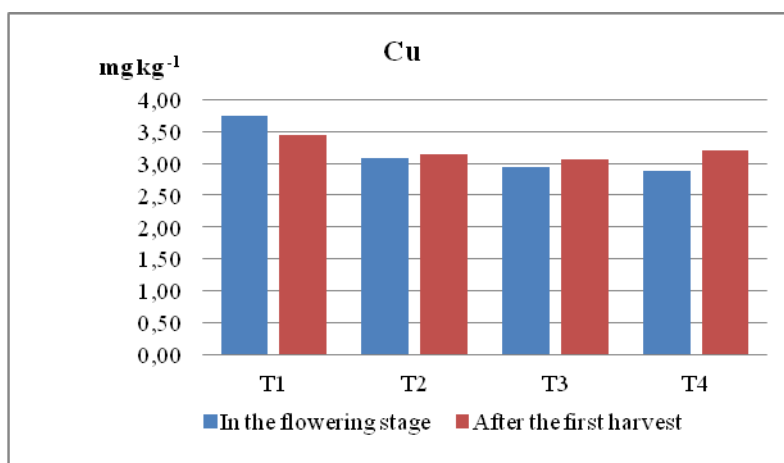


Figure 9. Copper content in leaf of strawberry leaves at two different sampling times for 4 different seaweed doses.

Zn has been reported causing higher fruit yield due to the positive effects on the intensity of photosynthesis (Tavasoli et al., 2010). The seaweed treatment did not significantly affect the Zn concentration of strawberry leaves. The lowest Zn concentration was obtained with T3 treatment, while the highest value was recorded in T4 at flowering stage. In contrast to the flowering stage, the highest Zn concentration after the first harvest was obtained with T3 and the lowest value was in T2 treatment. The concentration of Zn at two different sampling periods was significantly different ($p < 0.01$). The Zn concentration in flowering stage ($31.90 \pm 1.65 \text{ mg kg}^{-1}$) was higher than the Zn concentration recorded after the first harvest ($29.70 \pm 1.65 \text{ mg kg}^{-1}$), though the difference was not statistically significant (*Figure 10*).

Soil quality in undeveloped and developing countries deteriorates due to the lack of proper fertilization techniques or over-fertilization. In appropriate fertilization causes losing the fertility of agricultural lands and the sustainability of soils and nature. In some cases, a lack of sufficient fertilization results in low yield in agricultural lands. Fertilization and productivity have a close relationship in agriculture. For healthy plant growth, sufficient and balanced amount of plant nutrients must be present in soils. On the other hand, the availability of nutrients for plant uptake is extremely important for the plants to benefit sufficiently from the nutrients in the soil. Several factors such as soil structure, plant type, and climate affect the ability of plants to benefit from fertilizers applied to soil (Özbek, 1970). The use of organic fertilizers such as seaweed instead of chemical inputs should be expanded to maintain a sustainable production

system that protects the environment and natural resources in the long term. Recent scientific studies also support these views (Khan et al., 2009; Craigie, 2011; Calvo et al., 2014; Arioli et al., 2015).

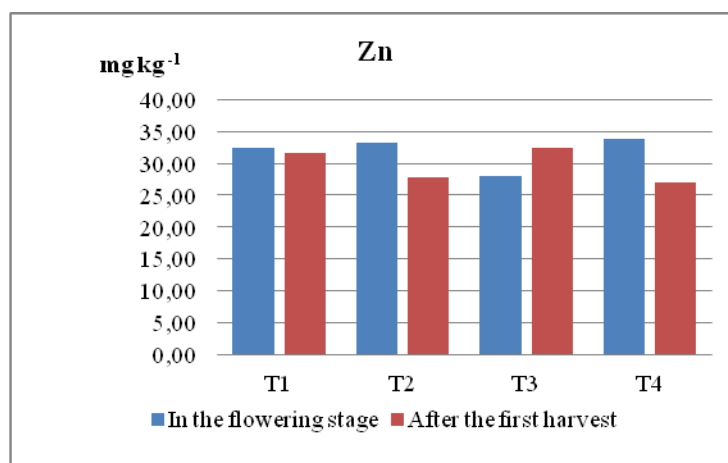


Figure 10. Zinc content in leaf of strawberry leaves at two different sampling times for 4 different seaweed doses.

Conclusion

This study was conducted to investigate the effects of seaweed (Alga 600) on nutrient uptake of strawberry cv. Albion. Following conclusions can be drawn from the results obtained in this study. The concentrations of N, P, K, Mg, Ca, Mn and Fe in strawberry leaves recorded in two different sampling periods (flowering and after the first harvest) were significantly different from each other. Consequently, it was pointed according to the result of the two-way analysis of variance, the effect of seaweed doses on nutrients were statistically insignificant for all nutrients except Mn ($p > 0.05$) (Table 3). While the Mn element, the highest value ($223.70 \pm 11.59 \text{ mg kg}^{-1}$) obtained from T4 (8 g.L^{-1}) seaweed dose; the lowest value ($164.91 \pm 11.59 \text{ mg kg}^{-1}$) obtained from control dose. The effect of interaction between seaweed doses and periods on nutrients was also not found statistically significant ($p > 0.05$). As shown in Table 4, the effect of fertilizer application periods on N, P, K, Mg, Ca, Mn and Fe elements were significant statistically except Cu and Zn elements. In general, the seaweed (Alga 600) do not have a significant effect on macro and micro nutrient contents of leaves. Seaweed fertigation significantly increased the Mn contents of leaves at both application periods. In general, seaweed extract of 8 g.L^{-1} was more effective on macro and micro nutrient contents of strawberry leaves. Higher N, P, K, Mg, Ca, Mn and Fe concentrations were recorded respectively; $2.94 \pm 0.13 \text{ mg kg}^{-1}$, $4277.42 \pm 258.25 \text{ mg kg}^{-1}$, $17857.60 \pm 1106.18 \text{ mg kg}^{-1}$, $4851.53 \pm 300.60 \text{ mg kg}^{-1}$, $887.16 \pm 49.64 \text{ mg kg}^{-1}$, $223.70 \pm 11.59 \text{ mg kg}^{-1}$, $385.73 \pm 18.41 \text{ mg kg}^{-1}$ in T4 treatment after the first seaweed application.

As a result of this study carried out in Iraq, which tries to strengthen agriculture, industry, and economy after the war, is thought to lead the expanding of strawberry production in the region, improving the strawberry cultivation with superior yield and quality characteristics and adopting the environmentally friendly production techniques.

Acknowledgement. This article is produced from the MSc Thesis belongs to A.H.N. AL-SHATRI and the thesis has been funded with the project (2017-SIÜFEB-90) by Scientific Research Projects Council, Siirt University.

REFERENCES

- [1] Abdulraheem, S. M. (2009): Effect of nitrogen fertilizer and seaweed extracts on vegetative growth and yield of cucumber. – *Diyala Agric. Sci. J.* 1: 134-145.
- [2] Anonymous (2017): Statistical data. – Agrometeorology Directorate, Sulaymaniyah/Iraq. Access Date: August 10, 2017.
- [3] Arioli, T., Mattner, S. W., Winberg, P. C. (2015): Applications of seaweed extracts in Australian agriculture: past, present and future. – *J Appl Phycol* 27: 2007-2015.
- [4] Battacharyya, D., Babgohari, M. Z., Rathor, P., Prithiviraj, B. (2015): Seaweed extracts as biostimulants in horticulture. – *Scientia Horticulturae* 196: 39-48.
- [5] Blevins, J. P. (1999): Productivity and exponent. – *Behavioral and Brain Sciences* 22(6): 1015-1016.
- [6] Blunden, G. (1991): Agricultural Uses of Seaweeds and Seaweed Extracts. – In: Guiry, M. D., Blunden, G. (eds.) *Seaweed Resources in Europe: Uses and Potential*. John Wiley and Sons. p. 65-81.
- [7] Blunden, G., Whapham, C., Jenkins, T. (1992): *Seaweed Extracts in Agriculture and Horticulture: Their Origins, Uses and Modes of Action*. School of Pharmacy and Biomedical Science and School of Biological Sciences. – University of Portsmouth, King Henry John Street, Portsmouth, Hampshire P01 202, U.K.
- [8] Calvo, P., Nelson, L., Kloepper, J. W. (2014): Agricultural uses of plant biostimulants. – *Plant Soil* 383: 3-41.
- [9] Craigie, J. S. (2011): Seaweed extract stimuli in plant science and agriculture. – *J Appl Phycol* 23: 371-393.
- [10] Crouch, I. J., Staden, J. V. (1992): Effect of seaweed concentrate on the establishment and yield of greenhouse tomato plants. – *Journal of Applied Phycology* 4(4): 291-296.
- [11] Darrow, G. M. (1966): *The Strawberry: history, breeding and physiology*. – Holt, Rinehart and Winston, New York, Chicago. 447 p.
- [12] Güner, H., Aysel, V. (1996): *Systematics of seedless plants. Vol. 1 Algae*. – Ege University Science Faculty Books Series. No. 108. Bornova, İzmir. (in Turkish).
- [13] Hong, Y. P., Chen, C. C., Cheng, H. L., Lin, C. H. (1995): Analysis of Auxin and Cytokinin Activity of Commercial Aqueous Seaweed Extract. – *Gartenbauwissenschaft* 60(4): 191-194.
- [14] Kaçar, B., İnal, A. (2008): *Plant analysis*. – Nobel publication No: 1241. (in Turkish).
- [15] Katiyar, P. N., Singh, J. P., Singh, P.C. (2009): Effect of mulching on plant growth, yield and quality of strawberry under agro-climatic conditions of Central Uttar Pradesh. – *International Journal of Agricultural Sciences* 5(1): 85-86.
- [16] Khan, W., Rayirath, U. P., Subramanian, S., Jithesh, M. N., Rayorath, P., Hodges, D. M., Critchley, A. T., Craigie, J. S., Norrie, J., Prithiviraj, B. (2009): Seaweed extracts as biostimulants of plant growth and development. – *J Plant Growth Regul* 28: 386-399.

- [17] Kumari, R., Kaur, I., Bhatnagar, A. K. (2011): Effect of aqueous extract of *Sargassum johnstonii* Setchell & Gardner on growth, yield and quality of *Lycopersicon esculentum* Mill. – *Journal of Applied Phycology* 23(3): 623-633.
- [18] Lantz, W., Swartz, H., Demchak, K., Frick, S. (2010): Season-long strawberry production with ever bearers for northeastern producers. – *University of Maryland Extension*, p.11.
- [19] Margarida, C. A., Villas Boas, T. M., Mota, V. S., Silva, C. K. M., Poveda, V. B. (2014): Microbial Contamination of Jackets Firsts During Health Care. – *Brazilian Journal of Nursing* 67. (In French).
- [20] Mengel, K., Kirkby, E. A. (1987): Potassium. – In: *Principles of Plant Nutrition*. Intern. Potash Institute: 427-446. Basel, Switzerland.
- [21] Rathore, S. S., Chaudhary, D. R., Boricha, G. N., Ghosh, A., Bhatt, B. P., Zodape, S. T., Patolia, J. S. (2009): Effect of seaweed extract on the growth, yield and nutrient uptake of soybean (*Glycine max*) under rain fed conditions. – *South African Journal of Botany* 75(2): 351-355.
- [22] Schmidt, R. E., Ervin, E. H., Zhang, X. (2003): Questions and answers about biostimulants. – *Golf Course Management* 71: 91-94.
- [23] Sharma, R. R. (2002): Growing strawberry. – *Int. Book Distributing Co., India* 1: 01-02.
- [24] Shehata, S. M., Abdel-Azim, H. S., El-Yazied, A. A., El-Gizawy, A. M. (2011): Effect of foliar spraying with amino acids and seaweed extract on growth chemical constitutes, yield and its quality of celeriac. – *Plant. Euro. J. Sci. Res.* 58(2): 257-265.
- [25] Tavasoli, A., Ghanbari, A., Ahmadian, A. (2010): The effect of magnesium and zinc nutrition on the fruit yield and nutrient concentrations in greenhouse tomato Hydroponic cultivation. – *J. Sci. Technol. Greenhouse Plantation* 1: 1-5.

INTEGRATION OF MIXED-CROPPING AND RICE-DUCK CO-CULTURE HAS ADVANTAGE ON ALLEVIATING THE NONPOINT SOURCE POLLUTION FROM RICE (*ORYZA SATIVA* L.) PRODUCTION

LI, M. J.¹ – LI, R. H.^{1,4} – ZHANG, J. E.^{1,2,3,4*} – GUO, J.¹ – ZHANG, C. X.¹ – LIU, S. W.¹ – HEI, Z. W.¹ – QIU, S. Q.¹

¹*Department of Ecology, College of Natural Resources and Environment, South China Agricultural University, Wushan Road, Tianhe District, Guangzhou 510642, Guangdong province, P.R. China*

²*Guangdong Engineering Technology Research Centre of Modern Eco-agriculture and Circular Agriculture, Guangzhou 510642, Guangdong province, P.R. China*

³*Key Laboratory of Agro-Environment in the Tropics, Ministry of Agriculture, Guangzhou 510642, Guangdong province, P.R. China*

⁴*Guangdong Province Key Laboratory of Eco-Circular Agriculture, Guangzhou 510642, Guangdong province, P.R. China*

*Corresponding author

e-mail: jeanzh@scau.edu.cn; phone: +86-020-8528-0211; fax: +86-020-8528-1885

(Received 25th Aug 2019; accepted 25th Nov 2019)

Abstract. With the rapid development of agricultural industrialization, agricultural nonpoint source pollution, which occurs when synthetic chemical additives (e.g. fertilizer, pesticides, and herbicides) runoff into rivers or lakes, has become a major concern. To explore the approaches of reducing the application of chemical additives, we conducted a field experiment to test whether the integrated farming systems would alleviate the nonpoint source pollution. Specifically, we tested whether mixed-cropping or mixed-cropping plus duck co-culture (MCDC) systems with optimized rice (*Oryza sativa* L.) cultivars could reduce nutrients runoff or leaching from paddy field. We found that compared to the mono-cropping systems, the electrical conductance (EC), oxidation-reduction potential (ORP), the contents of dissolved oxygen (DO), nitrates (NO₃⁻), ammonium (NH₄⁺), total nitrogen (TN), total phosphorus (TP) and total potassium (TK) of paddy water in MCDC systems all increased during the rice-growing stages. The contents of the TN, TP, and TK of paddy water in MCDC systems were 45.35%, 52.43% and 40.47% higher than those in the mono-cropping systems, respectively. Compared to the conventional mono-cropping, the mixed-cropping systems could alleviate nonpoint source pollution by decreasing the application of synthetic chemicals to rice paddies, the rice-duck co-culture system had significantly lower additions of agro-chemicals to paddy fields, which decreased the loss/runoff/leaching rates of nitrogen, phosphorus and potassium from paddy fields into the surrounding water areas by 32.73%, 8.72% and 31.88%, respectively. Considering that the MCDC systems exerted similar/even better performances as/than the rice-duck co-culture system and the rice mixed-cropping system, we deduced that the MCDC systems could also could alleviate nonpoint source pollution to a certain extent.

Keywords: *mixed-cropping, rice-duck co-culture, rice cultivars, nutrient runoff, paddy water, nonpoint source pollution*

Introduction

Nonpoint source pollution is a serious problem that degrades surface waters and aquatic ecosystems (Dodds et al., 2008). Nutrients, sediment, and other pollutants from human-altered landscapes can damage the integrity of freshwater systems (Hunsaker et

al., 1995). Technologies and techniques to prevent and control industrial point source pollution are becoming more mature and widely implemented, but agricultural nonpoint source pollution has become the main cause of eutrophication in the world's aquatic environments (Ma et al., 2012). Water pollution has become an increasingly serious problem in China since the 1970s (Jusi, 1989). Literature reviews have highlighted concerns of agricultural nonpoint pollution in China entailing excessive inputs of fertilizers, pesticides, herbicides, and heavy metals into waters and soils (Smil, 1997; Schwarzenbach et al., 2010; Sun et al., 2012; Kale, 2013; Moldes et al., 2013).

At present, China is the largest rice growing and consuming country in the world (Thomas et al., 2011). In 2017, China accounted for 15.7% of the world's rice planting area and 28.8% of the world's total rice output. However, the area of cultivated land available for rice cultivation in China is gradually decreasing, while the population and demand for food are increasing (Cheng et al., 2007; Chen et al., 2019; Yin et al., 2019). Studies have shown that the farmers in the country currently use chemical fertilizers at very high rates (Wu, 2011; Yin et al., 2018; Wang et al., 2019). For instance, Li et al. (2019a) reported that the average rates of nitrogen (N), phosphorus (P) and potassium (K) fertilizers runoffs in orchards of major citrus producing regions of China were as high as 485 kg ha⁻¹ (N), 198 kg ha⁻¹ (P₂O₅), and 254 kg ha⁻¹ (K₂O), respectively. Sun et al. (2019) found that more than 85% of sampled farming households used complex fertilizers in rice production, and that complex fertilizers account for more than half of the total use of chemical fertilizers. These overuse of chemical fertilizers could damage streams and rivers (Liu et al., 2018; Qiu, 2018; Reddy et al., 2018), pollute groundwater (Cui et al., 2018), and lead to declines in biodiversity (Asai et al., 2011; Sun et al., 2015). Nonpoint source pollution from rice farms is becoming particularly bad in southern China, a region with relatively high precipitation.

To reduce nonpoint source pollution and improve water quality, it is important to adopt techniques that reduce the use of synthetic chemical additives, such as chemical fertilizers, pesticides and herbicides (Saraswat et al., 2016). Ecological agriculture technologies, including livestock farming, intercropping and mixed farming, show promise for improving water quality and increasing biodiversity in rice paddy fields (Wu et al., 2013; Li et al., 2019b). Teng et al. (2019) found that rice-duck integrated organic farming protected water quality in Dianshan Lake and raised the incomes of local farmers. Another study found that hedgerow intercropping could fix nitrogen, reducing the need for chemical fertilizers, hedgerows also, prevented soil erosion, took up soil nutrients, and filtered pollutants (Zhang et al., 2008).

Rice-duck co-culture, in particular, is an integrated farming technology that helps control rice pests and weeds, and improve rice production, grain quality, and ecological sustainability (Zhang et al., 2008; Luo, 2018; Yang et al., 2018; Li et al., 2019c). Also, there is a mixed-cropping system, which cultivates multiple crop species or cultivars simultaneously in the same field for a significant part of their life cycles, using the space more efficiently and spreading risks more uniformly (Vandermeer et al., 1998; Lithourgidis et al., 2011). Numerous studies have reported that intensive integrated cropping systems, like rice-duck co-culture, have advantages over mono-cropping systems, largely due to reductions in pest incidence (Gold, 1993; Pridham et al., 2007) and more efficient use of nutrients, water, and solar radiation (Mason et al., 1988).

However, the relative effectiveness of different integrated cropping approaches for reducing nutrients loss, runoff, or leaching is still unknown. In this study, we compared the effects of rice mono-cropping system, mixed-cropping system with different rice

cultivars, and mixed-cropping of different rice cultivars plus duck co-culture (MCDC) on paddy water nutrients in paddy fields in southern China. We hypothesized that mixed-cropping system and mixed-cropping plus duck co-culture system with optimized rice cultivars would have more ecological benefits to improve the absorption of nutrients by rice plants and reduce nutrients loss, runoff, and leaching from the paddy fields.

Material and methods

Site description

We conducted our field experiment at Zengcheng Teaching and Research Farm (23°14'N, 113°38'E), South China Agricultural University, Guangzhou, China in 2018, where subtropical monsoonal climate was characterized by warm winter and hot summer, with an annual rainfall of 1,738 mm and an average temperature of 22.75°C (Fig. 1). The soil in the experimental site was sandy loam. The nutrients of the soil were determined at epipedon prior to the experiment. The soil contained organic matter of 15.62 g·kg⁻¹, total nitrogen of 0.81 g·kg⁻¹, total phosphorous of 0.55 g·kg⁻¹, total potassium of 12.84 g·kg⁻¹, available nitrogen of 61.62 mg·kg⁻¹, available phosphorus of 39.11 mg·kg⁻¹, and available potassium of 69.19 mg·kg⁻¹. The soil had a pH value of 4.88.

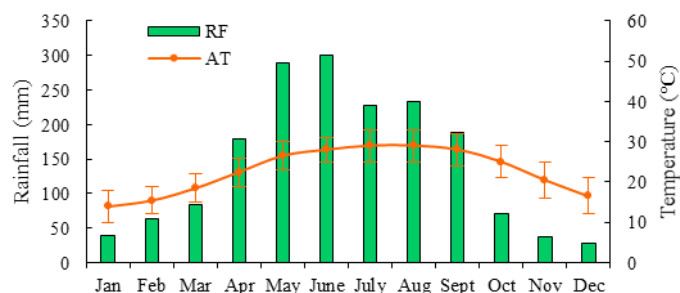


Figure 1. Monthly rainfall (RF) and average temperature (AT) during 2018, the year of the experiment, in Zengcheng, Guangzhou, Guangdong, China. Temperature errorbars indicate the highest and lowest recorded temperatures.

Experimental design and treatment

The experiment used completely random design with thirteen treatments and three replicates for each treatment (see Appendix Fig. S1). Each plot covered an area of 35 m² (5.0 m × 7.0 m). In this study, we used five traditional *indica* rice cultivars, including four from Rice Research Institute of Guangdong Academy of Agricultural Sciences (*Yuenongsimiao*, *Meixiangzhan 2*, *Huangguangyouzhan*, and *Huanghuazhan*) and one from National Engineering Research Centre of Plant Breeding at South China Agricultural University (*Huahang 31*) (Table S1), here labelled as A, B, C, D, and E, respectively. We selected four combinations of cultivars (BC, ACD, BDE, and ABDE) according to their growth period, plant height, grain yield and quality, and resistance to diseases of the five rice cultivars (Table S1), and also according to the screening of combinations optimized by pot experiments (Li et al., 2019b). Seeds were mixed for all combinations with the rice cultivars at equal weight ratios. Each mixed-cropping combination had six plots, three with and three without co-culture of ducks. The five

rice cultivars were also mono-cropped in pure plots as the corresponding controls of the three replicates, but without duck co-culture.

Agronomic management

All seeds were soaked in water for 48 h at room temperature and germinated under suitable conditions. Germinated seeds of each combination were sown on 15th March 2018 in the fields of Zengcheng Teaching and Research Farm. Seedlings of all combinations were transplanted to the field plots on 21th April 2018 at the normal spacing of 20 cm × 20 cm. In each plot, we applied organic fertilizer (6,750 kg·ha⁻¹, among which N ≥ 1.63%, P₂O₅ ≥ 3.53%, K₂O ≥ 1.92% and organic matter ≥ 46%) by broadcasting before rice transplanting.

Seven days after transplanting rice seedlings, we released ducklings into the specified plots at a density of 3 ducks per plot, based on the recommended population of Zhang et al. (2005). Each paddy field plot was surrounded by 50 cm high nylon mesh fencing to prevent ducks from escaping. The ducks were kept in the fields until rice reached its heading stage on 18th June in 2018. Water was kept at 6-8 cm deep while ducks were in the fields, but irrigation was stopped one week before the rice harvest. Photos of different growth periods in the paddy field of this study were shown in Fig. 2.



Figure 2. Photos of different growth periods in the paddy field of this study. (a): Returning green stage; (b): Full heading stage

Trait measurements

Physical and chemical parameters of paddy water, such as pH value, temperature (Temp), electrical conductivity (EC), oxidation-reduction potential (ORP), and dissolved oxygen content (DO), were analyzed using pH meter, EC meter, ORP meter (KEDIDA, Shenzhen, China), and DO meter (LEICI JPB-607A, Shanghai, China). Measurements were made at 10:00h-11:30h with three repetitions in each plot. Water samples were randomly collected as composites of 5 sub-samples from the surface water (0-5 cm) within a 2-m-diameter circular area centered in each plot on 5th April (one week before rice seedlings were transplanted), 27th May, 22nd June, and 18th July in 2018 correspondingly. The impurities of all water samples were filtrated with filter papers (d12.5 cm). We measured nitrates (NO₃⁻), ammonium (NH₄⁺), total nitrogen (TN), total phosphorus (TP) and total potassium (TK).

Data analyses

All data were expressed as means ± standard errors. To compare the effects of rice mono-cropping, mixed-cropping with different rice cultivars, and mixed-cropping of different rice cultivars with duck co-culture on paddy water physical and chemical

properties, we compared the experimental treatments using one-way ANOVA followed by Fisher's least significant difference post-hoc tests. For example, the data from B and C mono-cropping systems were pooled, and then compared with the results from BC mixed-cropping and BC mixed-cropping with duck co-culture. All statistical analyses were performed with R 3.20 (R Development Core Team 2015).

Results

Environmental background before ducklings released in paddy fields

Prior to releasing ducklings, the treatment plots did not differ significantly in water physical and chemical characteristics (pH, water temperature, electrical conductance, oxidation-reduction potential, and dissolved oxygen content) (Fig. 3), and also in the contents of nutrients (nitrate, ammonium, total nitrogen, total phosphorus, and total potassium) of paddy water (Fig. 4). These included plots for mono-cropping, mixed-cropping and MCDC systems for all combinations of rice cultivars (BC, ACD, BDE, and ABDE).

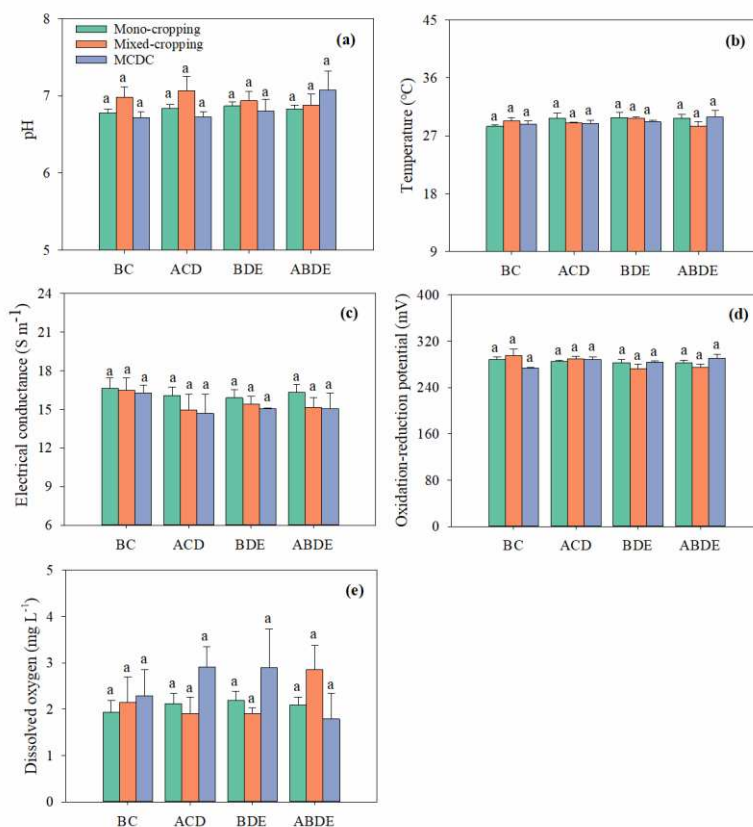


Figure 3. pH value (a), temperature (b), electrical conductance (c), oxidation-reduction potential (d), and dissolved oxygen content (e) of paddy water for mono-cropping, mixed-cropping, and MCDC systems before ducklings were released in the paddy fields. MCDC refers to rice mixed-cropping with duck co-culture. Labels on the x-axes represent combinations of rice cultivars, with A=Yuenongsimiao, B=Meixiangzhan 2, C=Huangguangyouzhan, D=Huanghuazhan, E=Huahang 31. The error terms above bars indicates SEs. Different lowercase letters above bars indicate significant differences between the mean values of treatments (Fisher's LSD; $P < 0.05$)

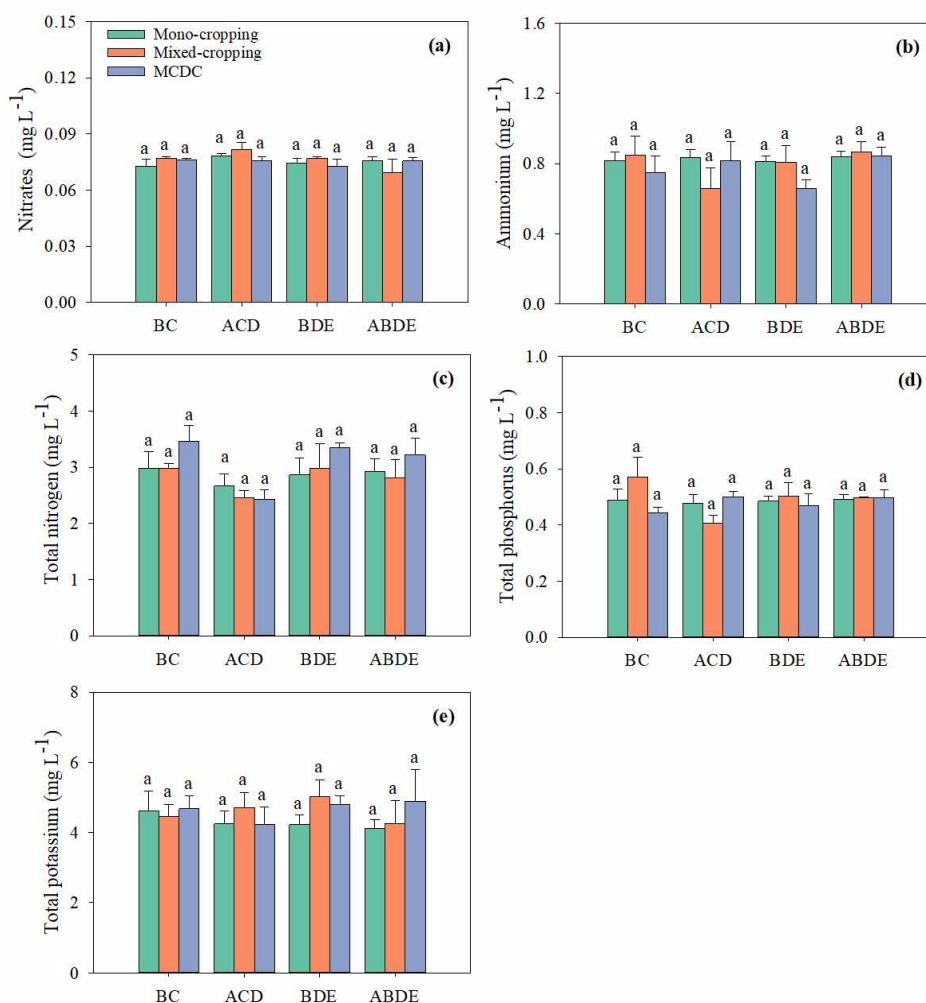


Figure 4. Concentrations of nitrates (a), ammonium (b), total nitrogen (c), total phosphorus (d), and total potassium (e) of paddy water for mono-cropping, mixed-cropping, and MCDC systems before ducklings were released in the paddy fields. MCDC refers to rice mixed-cropping with duck co-culture. Labels on the x-axes represent combinations of rice cultivars, with A=Yuenongsimiao, B=Meixiangzhan 2, C=Huangguangyouzhan, D=Huanghuazhan, E=Huahang 31. The error terms above bars indicates SEs. Different lowercase letters above bars indicate significant differences between the mean values of treatments (Fisher's LSD; $P < 0.05$)

Physical and chemical properties of paddy water

According to ANOVA analyses, the pH of MCDC treatments was significantly higher than that of the mono-cropping and mixed-cropping systems on 22nd June and 18th July (Fig. 5). Compared to the mono-cropping and mixed-cropping systems, the MCDC treatments had lower paddy water temperatures on 22nd June and 18th July. The electrical conductance, oxidation-reduction potential, and dissolved oxygen content were all significantly higher in the MCDC systems than in the mono-cropping and mixed-cropping systems on 27th May, 22nd June and 18th July, respectively (Fig. 5).

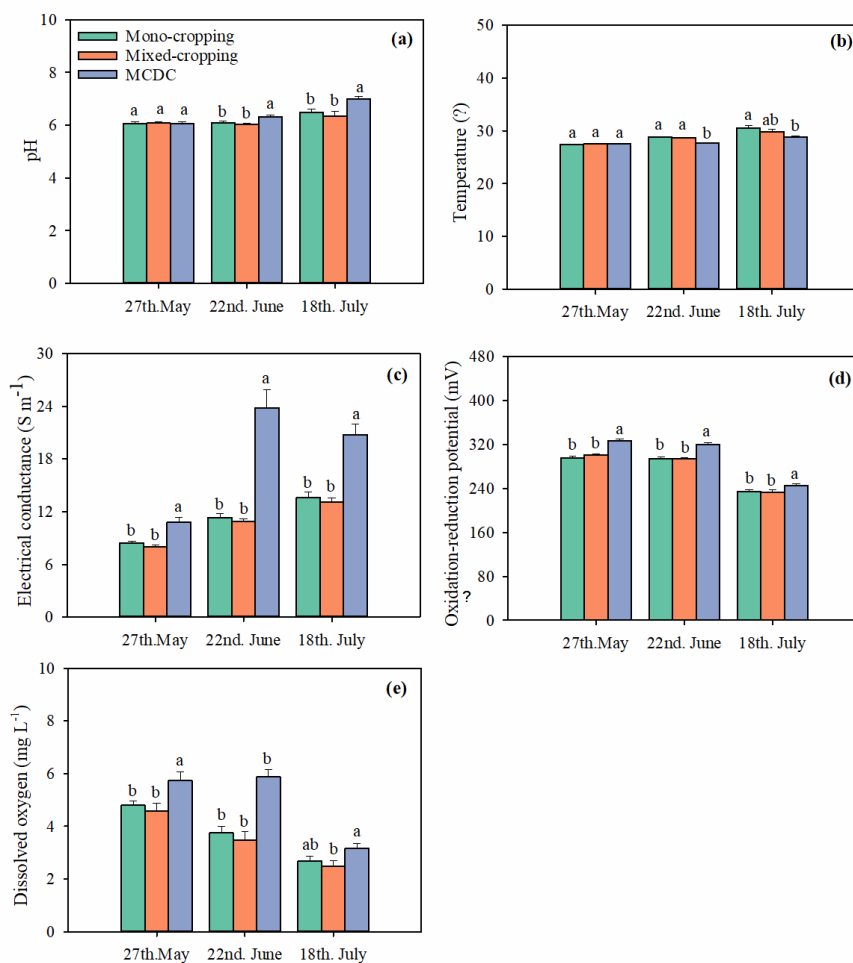


Figure 5. Differences in the water pH value (a), water temperature (b), electrical conductance (c), oxidation-reduction potential (d), and dissolved oxygen (e) for mono-cropping, mixed-cropping, and MCDC systems after ducklings were released in the paddy fields in 2018. MCDC refers to rice mixed-cropping plus duck co-culture system. Different letters above bars indicate significant differences between the mean values of treatments (Fisher's LSD; $P < 0.05$)

Nutrient concentration of paddy water

Compared to the mono-cropping and mixed-cropping systems, the nitrate concentrations of paddy water in MCDC systems were higher at all stages (except 18th July) of rice growth, which exerted an increase status (from 8.67 to 33.39%, and from 6.53 to 27.97%, respectively) (Fig. 6). The ammonium concentration of paddy water in MCDC systems was also significantly higher than that in the other two systems. Similarly, compared to the mono-cropping systems, the concentrations of total nitrogen, total phosphorus, and total potassium of paddy water all improved (39.51-45.35%, 18.23-52.43%, 34.09-40.47%) obviously in MCDC systems. Moreover, the concentrations of total nitrogen, total phosphorus, and total potassium of paddy water all significantly increased (22.96-36.99%, 19.14-40.27%, 35.03-40.94%) in the MCDC systems than the mixed-cropping systems.

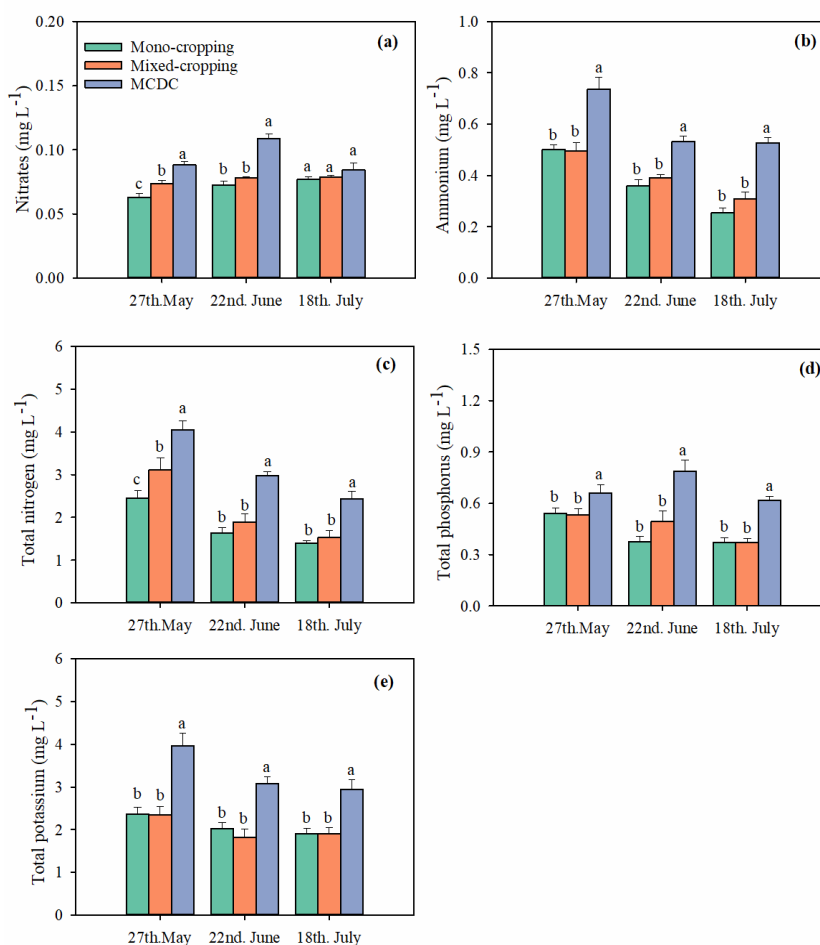


Figure 6. Differences in concentrations of water nitrates (a), water ammonium (b), total nitrogen (c), total phosphorus (d), and total potassium (e) for mono-cropping, mixed-cropping, and MCDC systems after ducklings were released in the paddy fields in 2018. MCDC refers to rice mixed-cropping plus duck co-culture system. Different letters above bars indicate significant differences between the mean values of treatments (Fisher's LSD; $P < 0.05$)

Nutrients loss/runoff/leaching from paddy fields

Both the mixed-cropping and the rice-duck co-culture required almost no use of chemical fertilizers and pesticides, or other chemical additives (Table 1), but the conventional mono-cropping required much more application of chemical pesticides to protect the rice from being attacked by pests, and required much more compound fertilizers to increase rice production. Compared to the conventional mono-cropping rice system, the rice-duck co-culture systems showed lower rates of nitrogen, phosphorus and potassium loss, runoff, and leaching, which dropped to 32.73%, 8.72%, and 31.88%, respectively (Table 1).

Table 1. The rate of the nutrients loss/runoff/leakage among the conventional mono-cropping, mixed-cropping system, and rice-duck co-culture

Farming systems	N/P/K	Before rice harvest					After rice harvest				Water nutrients / (soil nutrients + rice plant nutrients) (%)	Rates of nutrients loss/runoff/leaching (%)	References
		①Soil nutrients of background (g·kg ⁻¹)	②Water nutrients of background (mg L ⁻¹)	Input chemical or organic fertilizers (kg ha ⁻¹)	Input pesticides /herbicides	Ducks feces nutrients (kg ha ⁻¹)	①Soil nutrients (kg ha ⁻¹)	②Water nutrients (mg L ⁻¹)	Plants nutrients (%)	Biomass of rice plant (kg ha ⁻¹)			
③Conventional mono-cropping	N	62.81	0.87	231.30	1800g L ⁻¹ of Butachlor	-	65.45	1.34	1.01	13600	0.38	39.82	(Qin et al., 2010; Quan et al., 2008; Wang et al., 2004; Xiang et al., 2013)
	P	40.54	0.07	219.15	(3 times); w = 50% of Carbendazim	-	38.45	0.32	0.34				
	K	68.97	2.45	226.00	WP; 250 g L ⁻¹ of Bisultap	-	42.53	3.17	1.08				
③Mixed-cropping system	N	63.98	3.37	110.03		-	65.47	1.54	1.02	9290	0.57	13.89	(Qin et al., 2010; Wang et al., 2004)
	P	39.75	0.74	104.03	No or less	-	38.93	0.37	0.35				
	K	69.06	4.61	107.54		-	42.63	1.91	1.08				
③Rice-duck co-culture	N	61.29	3.74	110.03		14.1	68.06	2.44	1.08	10490	0.81	7.09	(Qin et al., 2010; Wang et al., 2004)
	P	41.39	0.72	104.03	No	21.0	43.56	0.62	0.48				
	K	69.60	4.65	107.54		9.0	45.76	2.94	1.14				

Rates of nutrients loss/runoff/leaching (%) = (The total amount of N/P/K before rice harvest – The total amount of N/P/K after rice harvest) ÷ (The total amount of N/P/K before rice harvest) × 100%;

① Soil bulk density of the conventional mono-cropping, mixed-cropping system, and rice-duck co-culture were 1.21g cm⁻¹, 1.21g cm⁻¹, and 1.09g cm⁻¹, respectively;

② Paddy water density of the conventional mono-cropping, mixed-cropping system, and rice-duck co-culture were considered the same.

③The data of the conventional mono-cropping was taken from the references, and the data of the mixed-cropping system and rice-duck co-culture were measured in this study (except for the indexes of nutrients from duck feces and plants)

Discussion

Few studies evaluated the effect of the mixed-cropping or mixed-cropping plus duck co-culture systems (MCDC) on nutrient leaching or runoff. In this study, we investigated whether this two new agroecosystems could reduce nonpoint source pollution. And we found that integrated rice-duck coculture in paddy fields could reduce nonpoint source pollution. In a previous study, Quan et al. (2008) illustrated that rice-duck co-culture improved the paddy water nutrient supply. Wang et al. (2004) indicated that rice-duck co-culture reduced the cardinal numbers of plant diseases and insect pests, and increased N and P uptake by rice crops. In this study, we found that the electrical conductance, oxidation-reduction potential, the contents of dissolved oxygen, nitrates, ammonium, total nitrogen, total phosphorus and total potassium in paddy water of MCDC systems were all higher than those of the mono-cropping and mixed-cropping systems, but there was no significant difference between the rice mono-cropping and mixed-cropping systems (*Fig. 4* and *Fig. 5*).

Rice-duck co-culture system is a typical farmland ecosystem, in which rice plants or weeds are producers, ducks are top consumers, bacteria and fungi are decomposers, and other animals (e.g. spiders, locusts, rice planthoppers, etc.) are consumers as well (*Fig. 7*). In this ecosystem, ducks play an important role to help rice to grow by eradicating the insect pests and weeds, trampling the paddy soil, stirring the paddy water, and excreting the feces to produce the nutrients absorbed by rice plants. This highly cycling and efficient utilization of nutrients by crops in the rice-duck co-culture system with less water drainage and without chemical pesticide and herbicide additions would help to reduce nutrients (such as TN and TP) loss and runoff and other pollutants from paddy field and hence may alleviate agricultural nonpoint source pollution (*Fig. 7*).

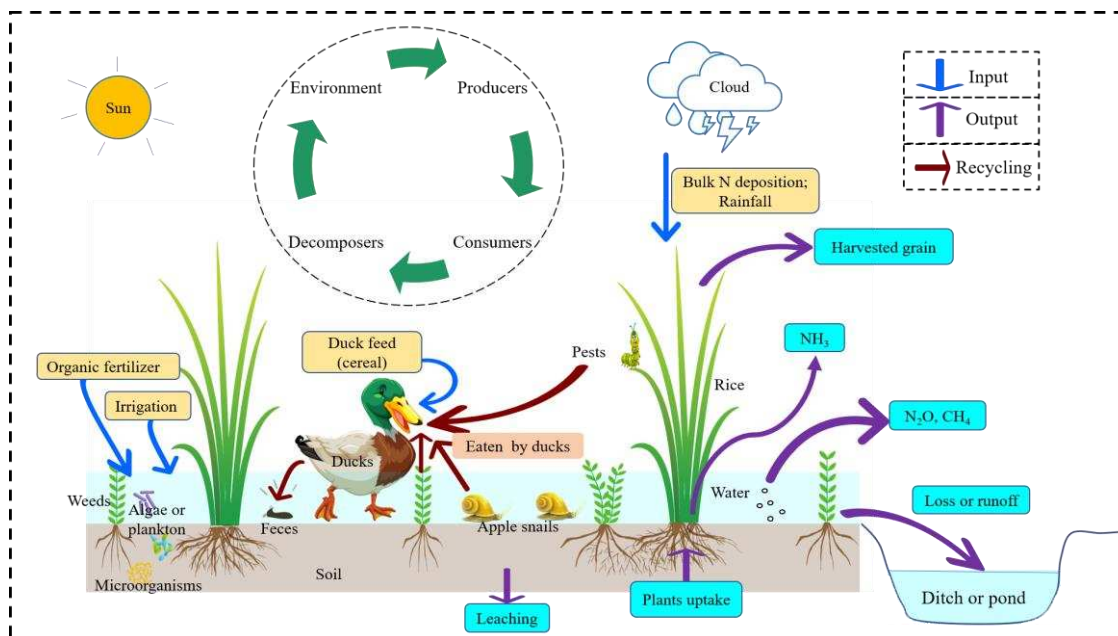


Figure 7. Outline of nutrients flows in rice-duck co-culture paddy fields. NH_3 , ammonia volatilization; N_2O , nitrous oxide; CH_4 , methane

Our study is consistent with previous researches that have shown increases in the soil nutrients, paddy water nutrients, and the efficiency with which rice plants could use nutrients under oxidation reaction by increasing dissolved oxygen, strengthening oxidation-reduction potential, and improving electrical conductance. These effects resulted from ducks activities in rice paddy fields, such as touching, pecking or shaking rice plants, eating weeds, pests, apple snails and other consumable organisms, depositing fecal matter, and agitating and stirring paddy water (Zhang, 2013; Yang et al., 2018). In this study, we kept the same irrigation or drainage in each plot. But in the rice-duck co-culture system, ducks could mix paddy water in the rice fields to play a role in evenly spreading nutrients, stirring paddy water to increase dissolved oxygen and electrical conductance, and then to activate nutrients pool of paddy water and soils for rice plants to absorb available and greatly.

Studies reported that keeping ducks in the paddy fields all day and night until rice reached the heading stage could increase the economic value of rice grains and ducks, and reduce the loss of nutrients that could potentially lead to nonpoint source pollution (Zhang et al., 2011; Zhang, 2013; Sheng et al., 2018). Moreover, some researches indicated that rice-duck co-culture system could reduce the risk of N and P runoff and leaching, and could improve the use efficiency of N and P by the growth of rice under the ducks agitating or stirring the water in paddy fields (Li et al., 2008; Zhang et al., 2011; Yang et al., 2018; Teng et al., 2019). In addition, Zhang et al. (2008) found that emissions of heat-trapping gasses which contributed to global warming potential (CH₄ and N₂O) decreased when rice-duck co-culture was implemented.

Furthermore, rice-duck co-culture systems, especially those that use green or organic production techniques, could reduce or limit the use of chemical fertilizers, pesticides (Teng et al., 2016), and herbicides (Zhang et al., 2009; Teng et al., 2016), and then to decrease the nonpoint source pollution. Likewise, mixed-cropping systems are commonly used in marginal agroecological environments, where they fulfill a variety of functions, such as supplementing the use of growth factors (e.g. soil nutrients, light, and water), reducing pests and diseases incidence, reducing soil erosion, and improving total biomass production, yield stability, and household food security (Weltzien et al., 2017). Mixed-cropping systems, with different genetic diversity and species diversity from different crops or varieties, could alleviate pests and diseases and avoid the applications of chemical pesticides and herbicides. For example, Zhu et al. (2000) found that multiple cropping systems with different disease-susceptible rice cultivars could control rice disease effectively by genetic diversity of rice cultivars. Paulsen et al. (2006) also found that mixed-cropping systems could suppress weeds in linseed and reduce pests infestation in cereals or legumes. In our study, the concentrations of nitrates, ammonium, nitrogen, phosphorus, and potassium in paddy water were not significantly differed between the mixed-cropping and mono-cropping systems. However, the mixed-cropping systems might reduce the pests or weeds by integrating diverse characteristics possessed by different rice cultivars (e.g. growing period, height, genotype, resistance for pests and diseases, and so on), and changing the microclimate (i.e. light, moisture, air, and temperature).

On the contrary, the conventional mono-cropping system had more applications of chemical fertilizers, pesticides and herbicides, and the nutrients were not completely absorbed by plants and then the stagnant water in rice fields could be discharged into rivers or lakes. Usually, in the rice mono-cropping systems, different kinds of chemical pesticides are overused to kill insects pests and diseases to protect crops in paddy fields,

and they have negative impact on the environment and biodiversity (Mahmood et al., 2016; Larsen et al., 2017). Some researchers have found that only 10-20% of the chemical pesticides applied to crops remain on the plants for a long time; 1-4% directly act on target pests, and the rest go into the atmosphere, soil, and water (Nascimento et al., 2017). Mao et al. (2002) also reported that about 9.22% of pesticides are lost into water while those were applied to rice paddy fields. Our findings reinforce that mixed-cropping system which does not require synthetic chemical pesticides can reduce pollution of these chemicals.

In our study, the MCDC systems also increased electrical conductance, oxidation-reduction potential, the concentrations of dissolved oxygen, nitrates, ammonium, total nitrogen, total phosphorus and total potassium of paddy water, and reduce the external inputs of synthetic chemical additives (chemical fertilizers, pesticides and herbicides). The MCDC systems showed similar/even better performances as/than the rice-duck co-culture systems and the rice mixed-cropping systems. Based on the above comparative analysis, although we didn't measure and calculate the nutrient loss/runoff/leaching from the MCDC systems, we may estimate that the MCDC system could reduce total loss of N, P, and K, and hence decrease agricultural nonpoint source pollution, because this farming approach maintains a virtuous circle within the ecosystem and without chemical pesticide and herbicide inputs, and then ensure the ecological balance of the farmland.

However, further detailed studies are needed in the future. For example, in order to know better and more accurately about the nonpoint pollution status in the MCDC and mixed cropping systems, the water quality of large-scale paddy fields and its surrounding water bodies should be monitored, and the quantity of the nutrients loss/runoff/leaching outside the paddy fields should also be measured, finally the nutrients balance analysis in paddy ecosystem should be studied as well.

Conclusion

We found that the MCDC systems increased the electrical conductance, oxidation-reduction potential, contents of dissolved oxygen, nitrates, ammonium, total nitrogen, total phosphorus, and total potassium of paddy water. The mixed-cropping systems had no differences from the mono-cropping systems in terms of their effects on physical and chemical properties of paddy water. Nevertheless, compared to the conventional rice mono-cropping system, both of the rice-duck co-culture and mixed-cropping systems could prevent pollution of the water environment by reducing or eliminating inputs of chemical fertilizers, herbicides and pesticides that would otherwise be applied to rice paddy fields, and lower the total loss of nutrients, pesticides and herbicides from paddy fields. Moreover, we deduced and pointed out that the MCDC systems, which exerted similar/even better performances as/than the rice-duck co-culture systems and the rice mixed-cropping systems, could reduce the application and transportation of chemical fertilizers, pesticides and herbicides into the nearby rivers or lakes, and hence could also alleviate nonpoint source pollution to a certain extent from rice production.

Acknowledgements. This study was supported by grants from the Science and Technology Project of Guangdong Province (2015B090903077, 2016A020210094, 2017A090905030), the Science and Technology Project of Guangzhou (201604020062), the Innovation Team Construction Project of Modern Agricultural Industry Technology System of Guangdong Province (2018LM1100, 2019KJ105),

the Guangdong Provincial Key Laboratory of Eco-Circular Agriculture (2019B030301007), and the Overseas Joint Doctoral Training Program of South China Agricultural University (2018LHPY010). We would like also to thank Dr. Abe Miller-Rushing for his evaluable comments on our early manuscript, and for his assistance with English language and grammatical editing of the manuscript.

REFERENCES

- [1] Asai, M., Reidsma, P., Feng, S. (2011): Impacts of agricultural land-use changes on biodiversity in Taihu Lake Basin, China: a multi-scale cause–effect approach considering multiple land-use functions. – *International Journal of Biodiversity Science, Ecosystem Services & Management* 6: 119-30.
- [2] Chen, Z., Wang, L., Wei, A., Gao, J., Lu, Y., Zhou, J. (2019): Land-use change from arable lands to orchards reduced soil erosion and increased nutrient loss in a small catchment. – *Science of the Total Environment* 648: 1097-104.
- [3] Cheng, S., Zhuang, J.-Y., Fan, Y., Du, J., Cao, L. (2007): Progress in research and development on hybrid rice: a super-domesticated in China. – *Annals of Botany* 100: 959-66.
- [4] Cui, Z., Zhang, H., Chen, X., Zhang, C., Ma, W., Huang, C., Zhang, W., Mi, G., Miao, Y., Li, X. (2018): Pursuing sustainable productivity with millions of smallholder farmers. – *Nature* 555: 363.
- [5] Dodds, W., Oakes, R. (2008): Headwater influences on downstream water quality. – *Environmental Management* 41: 367-77.
- [6] Gold, C. S. (1993): Effects of Cassava Intercropping and Varietal Mixtures on Herbivore Load, Plant Growth, and Yields: Applications for Small Farmers in Latin America. – *Crop-protection Strategies for Subsistence Farmers*, London: Intermediate Technology Publications.
- [7] Hunsaker, C. T., Levine, D. A. (1995): Hierarchical approaches to the study of water quality in rivers. – *BioScience* 45: 193-203.
- [8] Jusi, W. (1989): Water pollution and water shortage problems in China. – *Journal of Applied Ecology* 26(3): 851-7.
- [9] Kale, A. A. (2013): Evaluation of sieved biomass of *Cicer arietinum* (horse bean) for removal of methylene blue: batch study. – *International Journal Of Recycling of Organic Waste in Agriculture* 2: 18.
- [10] Larsen, A. E., Gaines, S. D., Deschenes, O. (2017): Agricultural pesticide use and adverse birth outcomes in the San Joaquin Valley of California. – *Nature Communication* 8: 302.
- [11] Li, C., Cao, C., Wang, J., Zhan, M., Yuan, W., Shahrear, A. (2008): Nitrogen losses from integrated rice–duck and rice–fish ecosystems in southern China. – *Plant and Soil* 307: 207-17.
- [12] Li, Y., Yang, M., Zhang, Z., Li, W., Guo, C., Chen, X., Shi, X., Zhou, P., Tang, X., Zhang, Y. (2019a): An Ecological Research on Potential for Zero-growth of Chemical Fertilizer Use in Citrus Production in China. – *Ekoloji* 28: 1049-59.
- [13] Li, M., Zhang, J., Liu, S., Ashraf, U., Zhao, B., Qiu, S. (2019b): Mixed-cropping systems of different rice cultivars have grain yield and quality advantages over mono-cropping systems. – *Journal of Science of Food Agricultural* 99: 3326-34.
- [14] Li, M., Li, R., Liu, S., Zhang, J., Luo, H., Qiu, S. (2019c): Rice-duck co-culture farming benefits grain 2-acetyl-1-pyrroline accumulation and quality and yield enhancement of fragrant rice. – *The Crop Journal* 7(4): 419-30.
- [15] Lithourgidis, A., Dordas, C., Damalas, C. A., Vlachostergios, D. (2011): Annual intercrops: an alternative pathway for sustainable agriculture. – *Australian journal of crop science* 5: 396.
- [16] Liu, X., Beusen, A., Van Beek, L., Mogollon, J., Ran, X., Bouwman, A. (2018): Exploring spatiotemporal changes of the Yangtze River (Changjiang) nitrogen and

- phosphorus sources, retention and export to the East China Sea and Yellow Sea. – *Water Research* 142: 246-55.
- [17] Luo, S. (2018): *Agroecological Rice Production In China*. – FAO and South China Agricultural University, 116 p.
- [18] Ma, J., Chen, X., Shi, Y. (2012): Distinguishing the main pollution source an efficient way in agricultural non-point source pollution control. – *Advanced Materials Research* 347: 2195-9.
- [19] Mahmood, I., Imadi, S. R., Shazadi, K., Gul, A., Hakeem, K. R. (2016): Effects of pesticides on environment. – In: Hakeem, K. R. (ed.) *Plant, soil and microbes*: 253-69. Springer.
- [20] Mao, G., Wang, H., Gu, Y. (2002): Current situation of non-point source pollution of chemical fertilizer and pesticide in Shanghai and approach to controlling ways. – *Acta Agriculturae Shanghai* 18: 56-60.
- [21] Mason, S., Leihner, D. (1988): Yield and land-use efficiency of a cassava/cowpea intercropping system grown at different phosphorus rates. – *Field Crops Research* 18: 215-26.
- [22] Moldes, A., González, J. M. D., Rodrigues, L. R. M., Converti, A. (2013): New trends in biotechnological processes to increase the environmental protection. – *BioMed research international* 2013: 138018.
- [23] Nascimento, M., da Rocha, G., de Andrade, J. (2017): Pesticides in fine airborne particles: from a green analysis method to atmospheric characterization and risk assessment. – *Scientific Reports* 7: 2267.
- [24] Paulsen, H. M., Schochow, M., Ulber, B., Kuhne, S., Rahmann, G. (2006): Mixed cropping systems for control of weeds and pests in organic oilseed crops. – *COR 2006, Aspects of Applied Biology* 79: 215-9.
- [25] Pridham, J. C., Entz, M. H., Martin, R. C., Hucl, P. J. (2007): Weed, disease and grain yield effects of cultivar mixtures in organically managed spring wheat. – *Canadian journal of plant science* 87: 855-9.
- [26] Qin, Z., Zhang, J., Luo, S., Xu, H., Zhang, J. (2010): Estimation of ecological services value for the rice-duck farming system. – *Resources Science* 32: 864-72.
- [27] Qiu, J. (2018): Safeguarding China's water resources. – *National Science Review* 5: 102-7.
- [28] Quan, G., Zhang, J., Chen, R., Xu, R. (2008): Effects of rice-duck farming on paddy field water environment. – *Chinese Journal of Applied Ecology* 19: 2023-8.
- [29] Reddy, V., Cunha, D., Kurian, M. (2018): A Water–Energy–Food Nexus Perspective on the Challenge of Eutrophication. – *Water* 10: 101.
- [30] Saraswat, C., Kumar, P., Mishra, B. K. (2016): Assessment of stormwater runoff management practices and governance under climate change and urbanization: An analysis of Bangkok, Hanoi and Tokyo. – *Environmental Science & Policy* 64: 101-17.
- [31] Schwarzenbach, R. P., Egli, T., Hofstetter, T. B., Von Gunten, U., Wehrli, B. (2010): Global water pollution and human health. – *Annual Review of Environment and Resources* 35: 109-36.
- [32] Sheng, F., Cao, C., Li, C. (2018): Integrated rice-duck farming decreases global warming potential and increases net ecosystem economic budget in central China. – *Environmental Science and Pollution Research* 25: 22744-53.
- [33] Smil, V. (1997): Global population and the nitrogen cycle. – *Scientific American* 277: 76-81.
- [34] Sun, B., Zhang, L., Yang, L., Zhang, F., Norse, D., Zhu, Z. (2012): Agricultural non-point source pollution in China: causes and mitigation measures. – *Ambio* 41: 370-9.
- [35] Sun, R., Zhang, X., Guo, X., Wang, D., Chu, H. (2015): Bacterial diversity in soils subjected to long-term chemical fertilization can be more stably maintained with the addition of livestock manure than wheat straw. – *Soil Biology and Biochemistry* 88: 9-18.

- [36] Sun, Y., Hu, R., Zhang, C. (2019): Does the adoption of complex fertilizers contribute to fertilizer overuse? Evidence from rice production in China. – *Journal of Cleaner Production* 219: 677-85.
- [37] Teng, Q., Hu, X., Cheng, C., Luo, Z., Luo, F., Xue, Y., Jiang, Y., Mu, Z., Liu, L., Yang, M. (2016): Ecological effects of rice-duck integrated farming on soil fertility and weed and pest control. – *Journal of Soils and Sediments* 16: 2395-407.
- [38] Teng, Q., Hu, X., Luo, F., Wang, J., Zhang, D. (2019): Promotion of rice-duck integrated farming in the water source areas of Shanghai: its positive effects on reducing agricultural diffuse pollution. – *Environmental Earth Sciences* 78: 171.
- [39] Thomas, C. S., Nelson, N. P., Jahn, G. C., Niu, T., Hartley, D. M. (2011): Use of media and public-domain Internet sources for detection and assessment of plant health threats. – *Emerging Health Threats Journal* 4: 7157.
- [40] Vandermeer, J., van Noordwijk, M., Anderson, J., Ong, C., Perfecto, I. (1998): Global change and multi-species agroecosystems: concepts and issues. – *Agriculture, Ecosystems & Environment* 67: 1-22.
- [41] Wang, Q., Huang, P., Zhen, R., Jing, L., Tang, H., Zhang, C. (2004): Effect of rice-duck mutualism on nutrition ecology of paddy field and rice quality. – *The journal of applied ecology* 15: 639-45.
- [42] Wang, P., Zhang, W., Li, M., Han, Y. (2019): Does Fertilizer Education Program Increase the Technical Efficiency of Chemical Fertilizer Use? Evidence from Wheat Production in China. – *Sustainability* 11: 543.
- [43] Weltzien, E., Christinck, A. (2017): Participatory breeding: developing improved and relevant crop varieties with farmers. – *Agricultural Systems, Agroecology and rural innovation for development*: 259-301.
- [44] Wu, Y. (2011): Chemical fertilizer use efficiency and its determinants in China's farming sector. – *China Agricultural Economic Review* 3: 117-30.
- [45] Wu, M., Tang, X., Li, Q., Yang, W., Jin, F., Tang, M., Scholz, M. (2013): Review of Ecological Engineering Solutions for Rural Non-Point Source Water Pollution Control in Hubei Province, China. – *Water, Air, & Soil Pollution* 224: 1561.
- [46] Xiang, H., Zhang, J., Luo, M., Zhao, B., Quan, G. (2013): Effects of intercropping rice with *Oenanthe javanica* on diseases, pests and weeds hazards and yield of rice. – *Journal of Ecology and Rural Environment* 29: 58-63.
- [47] Yang, H., Yu, D., Zhou, J., Zhai, S., Bian, X., Weih, M. (2018): Rice-duck co-culture for reducing negative impacts of biogas slurry application in rice production systems. – *Journal of Environmental Management* 213: 142-50.
- [48] Yin, H., Zhao, W., Li, T., Cheng, X., Liu, Q. (2018): Balancing straw returning and chemical fertilizers in China: Role of straw nutrient resources. – *Renewable and Sustainable Energy Reviews* 81: 2695-702.
- [49] Yin, G., Lin, Z., Jiang, X., Yan, H., Wang, X. (2019): Spatiotemporal differentiations of arable land use intensity — A comparative study of two typical grain producing regions in northern and southern China. – *Journal of Cleaner Production* 208: 1159-70.
- [50] Zhang, J., Lu, J., Huang, Z., Zhang, G. (2005): Discussion on practical and theoretic issues of integrated rice-duck farming system. – *Ecologic Science* 24: 49-51.
- [51] Zhang, J., Ouyang, Y., Huang, Z. (2008): Characterization of nitrous oxide emission from a rice-duck farming system in South China. – *Archives of Environmental Contamination and Toxicology* 54: 167-72.
- [52] Zhang, J., Shan, Q., Qian, H., Xu, Y.-h., Cao, M.-j. (2008): Effects and planting techniques of hedgerow intercropping on sloping lands in agricultural non-point source pollution control. – *Bulletin of Soil and Water Conservation* 5: 180-5.
- [53] Zhang, J., Xu, R., Chen, X., Quan, G. (2009): Effects of duck activities on a weed community under a transplanted rice-duck farming system in southern China. – *Weed Biology and Management* 9: 250-7.

- [54] Zhang, J., Zhang, F., Yang, J., Wang, J., Cai, M., Li, C., Cao, C. (2011): Emissions of N₂O and NH₃, and nitrogen leaching from direct seeded rice under different tillage practices in central China. – *Agriculture, ecosystems & environment* 140: 164-73.
- [55] Zhang, J. (2013): Progresses and perspective on research and practice of rice-duck farming in China. – *Chinese Journal of Eco-Agriculture* 21: 70-9.
- [56] Zhu, Y., Chen, H., Fan, J., Wang, Y., Li, Y., Chen, J., Fan, J., Yang, S., Hu, L., Leung, H. (2000): Genetic diversity and disease control in rice. – *Nature* 406: 718.

APPENDIX

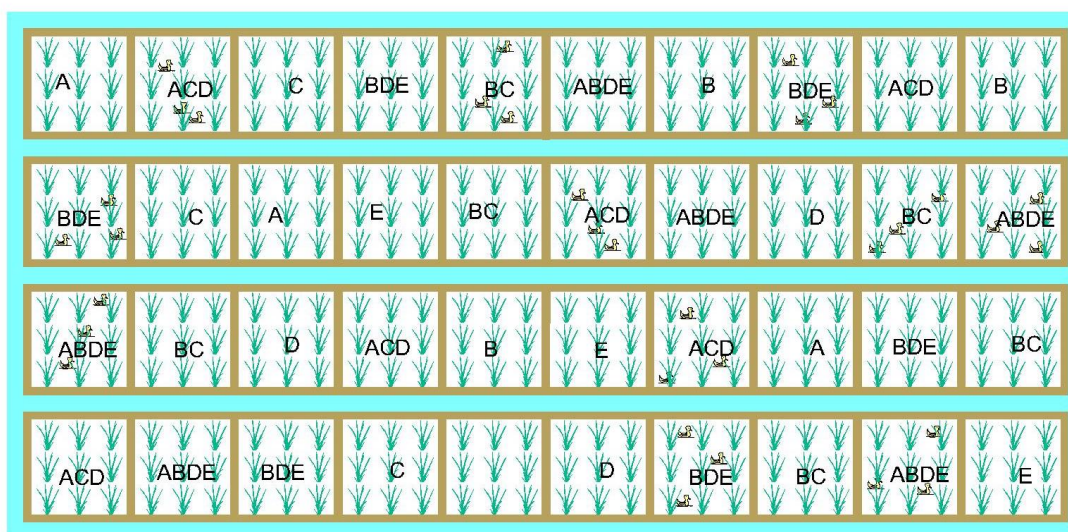


Figure S1. Design of mono-cropping, mixed-cropping, and MCDC treatments in the paddy field. The A, B, C, D, and E stand for Yuenongsimiao, Meixiangzhan 2, Huangguangyouzhan, Huanghuazhan and Huahang31, respectively. Two or more letters indicate the treatments of mixed-cropping systems or MCDC systems (with duck in the plots). For example, BC stands for the treatment of mixed-cropping system with the rice cultivars of Meixiangzhan 2 and Huangguangyouzhan or stands for the treatments of rice-duck co-culture with different rice cultivars (MCDC) of Meixiangzhan 2 and Huangguangyouzhan. Other treatments are labelled similarly. In the figure, one plot was one replication of one treatment

Table S1. Traits of the five rice varieties that accessed from the China Rice Data Center

Rice cultivars	Period (d)	Height (cm)	Spikelet per panicle (10 ⁴ ha ⁻¹)	Seed setting rate (%)	1000-grain weight (g)	Head rice rate (%)	Chalky rice rate (%)	Chalkiness degree (%)	Amylose content (%)	Length/width	Yield (t ha ⁻¹)
Yuenongsimiao (A)	111~113	97.0~97.9	122~124	87.1~88.0	22.0~22.6	71.8~73.0	3~6	0.5~0.9	17.3~18.2	3.3~3.5	6.57
Meixiangzhan 2 (B)	112~113	90.5~96.6	145.1	83.9~87.7	18.1~18.5	63.7~67	8~20	0.8~1.4	15~17.6	-	5.31
Huangguangyouzhan (C)	128~132	107.7~110.1	133~144	84.9~87.2	24.5~24.6	44.0	8~11	1.0~2.5	13.7~15.9	3.1	7.62
Huanghuazhan (D)	129~131	93.8~102.8	118.3~123	80.5~86.8	22.2~23.1	40.0~55.2	4~6	0.6~3.2	13.8~14.0	-	7.20
Huahang 31 (E)	110~111	109.5~110.6	132.1~132	83.5~85.8	22~22.3	70.4~72.5	4~18	0.8~6.9	16.2~16.5	-	6.31

Data from: <http://www.ricedata.cn/>

Table S2. ANOVA analysis for the water physical and chemical properties of the treatments before ducklings were released in the paddy fields

Indexes	Treatments	Df	Sum Sq	Mean Sq	F value	Pr(>F)
pH	BC	2	0.1225	0.06125	2.670	0.123
		9	0.2064	0.02294		
	ACD	2	0.1818	0.0909	2.451	0.128
		12	0.445	0.03708		
	BDE	2	0.0275	0.01374	0.347	0.714
		12	0.4751	0.03959		
	ABDE	2	0.1435	0.07173	1.401	0.277
15		0.7682	0.05121			
Temp	BC	2	1.352	0.6758	1.284	0.323
		9	4.737	0.5264		
	ACD	2	2.45	1.226	0.292	0.752
		12	50.45	4.204		
	BDE	2	0.98	0.488	0.134	0.876
		12	43.62	3.635		
	ABDE	2	3.95	1.977	0.548	0.589
15		54.1	3.607			
EC	BC	2	0.262	0.1308	0.045	0.957
		9	26.375	2.9306		
	ACD	2	5.91	2.954	0.648	0.540
		12	54.69	4.558		
	BDE	2	1.767	0.8833	0.343	0.716
		12	30.87	2.5725		
	ABDE	2	5.86	2.929	0.766	0.482
15		57.38	3.825			
ORP	BC	2	760.7	380.4	2.623	0.127
		9	1305.4	145		
	ACD	2	73.9	36.97	0.557	0.587
		12	796.1	66.34		
	BDE	2	291.2	145.6	0.656	0.537
		12	2664.1	222		
	ABDE	2	373.4	186.7	0.960	0.405
15		2916.1	194.4			
DO	BC	2	0.272	0.1361	0.215	0.811
		9	5.704	0.6337		
	ACD	2	1.8	0.9002	2.080	0.168
		12	5.193	0.4327		
	BDE	2	1.66	0.8302	1.427	0.278
		12	6.98	0.5817		
	ABDE	2	1.93	0.9648	1.950	0.177
15		7.423	0.4948			

Table S3. ANOVA analysis for the water nutrient concentration of the treatments before ducklings were released in the paddy fields

Indexes	Treatments	Df	Sum Sq	Mean Sq	F value	Pr(>F)
NO ₃ ⁻	BC	2	0.0000419	0.00002097	0.428	0.664
		9	0.0004409	0.00004898		
	ACD	2	0.00005356	0.00002678	1.160	0.346
		12	0.0002769	0.00002308		
	BDE	2	0.0000269	0.00001346	0.281	0.760
		12	0.0005742	0.00004785		
	ABDE	2	0.0001017	0.00005083	0.738	0.495
15		0.0010329	0.00006886			
NH ₄ ⁺	BC	2	0.01626	0.008132	0.371	0.700
		9	0.1971	0.0219		
	ACD	2	0.07208	0.03604	1.467	0.269
		12	0.29491	0.02458		
	BDE	2	0.05649	0.02824	2.431	0.130
		12	0.13942	0.01162		
	ABDE	2	0.00178	0.000889	0.091	0.914
15		0.14665	0.009776			
TN	BC	2	0.5209	0.2604	0.757	0.497
		9	3.0947	0.3439		
	ACD	2	0.173	0.08661	0.282	0.759
		12	3.68	0.30667		
	BDE	2	0.535	0.2675	0.412	0.672
		12	7.797	0.6497		
	ABDE	2	0.281	0.1403	0.247	0.785
15		8.531	0.5687			
TP	BC	2	0.02526	0.01263	1.403	0.295
		9	0.08105	0.009005		
	ACD	2	0.01489	0.007445	1.278	0.314
		12	0.06988	0.005823		
	BDE	2	0.00193	0.000966	0.253	0.781
		12	0.04585	0.00382		
	ABDE	2	0.00011	0.0000534	0.021	0.979
15		0.03831	0.0025542			
TK	BC	2	0.079	0.0393	0.033	0.968
		9	10.748	1.1943		
	ACD	2	0.526	0.263	0.237	0.792
		12	13.299	1.108		
	BDE	2	1.716	0.8581	1.356	0.294
		12	7.593	0.6328		
	ABDE	2	1.464	0.7322	0.715	0.505
15		15.354	1.0236			

Table S4. ANOVA analysis for the water physical and chemical properties of the treatments after ducklings were released in the paddy fields

Indexes	Time	Df	Sum Sq	Mean Sq	F value	Pr(>F)
Ph	27th May	2	0.0049	0.00245	0.054	0.948
		36	1.6424	0.04562		
	22nd June	2	0.6204	0.31019	6.708	0.00334
		36	1.6647	0.04624		
	18th July	2	2.684	1.3419	5.559	0.00787
		36	8.69	0.2414		
Temp	27th May	2	0.433	0.2167	1.194	0.315
		36	6.536	0.1815		
	22nd June	2	9.774	4.887	90.79	8.64E-15
		36	1.938	0.054		
	18th July	2	19.29	9.646	6.283	0.00456
		36	55.27	1.535		
EC	27th May	2	56.02	28.009	17.54	4.81E-06
		36	57.49	1.597		
	22nd June	2	1334.9	667.4	38.32	1.21E-09
		36	627.1	17.4		
	18th July	2	454.2	227.09	28.22	4.25E-08
		36	289.7	8.05		
ORP	27th May	2	7364	3682	18.5	2.97E-06
		36	7163	199		
	22nd June	2	5625	2812.4	16.4	8.63E-06
		36	6172	171.5		
	18th July	2	1118	559.2	3.918	0.0289
		36	5139	142.7		
DO	27th May	2	8.989	4.495	5.22	0.0102
		36	31	0.861		
	22nd June	2	42.22	21.112	20.17	1.33E-06
		36	37.69	1.047		
	18th July	2	2.981	1.4903	2.821	0.0727
		36	19.016	0.5282		

Table S5. ANOVA analysis for the water nutrient concentration of the treatments after ducklings were released in the paddy fields

Indexes	Time	Df	Sum Sq	Mean Sq	F value	Pr(>F)
NO ₃ ⁻	27th May	2	0.2392	0.1196	4.004	0.0269
		36	1.0755	0.02987		
	22nd June	2	0.3218	0.1609	323.8	<2e-16
		36	0.0179	0.0005		
	18th July	2	0.14638	0.07319	97.7	2.85E-15
		36	0.02697	0.00075		
NH ₄ ⁺	27th May	2	6.272	3.1362	146.4	<2e-16
		36	0.771	0.0214		
	22nd June	2	25.658	12.829	473.4	<2e-16
		36	0.976	0.027		
	18th July	2	1.1982	0.5991	42.06	3.81E-10
		36	0.5128	0.0142		
TN	27th May	2	317.8	158.89	126.6	<2e-16
		36	45.2	1.26		
	22nd June	2	669.9	334.9	543	<2e-16
		36	22.2	0.6		
	18th July	2	23.39	11.694	18.84	2.52E-06
		36	22.35	0.621		
TP	27th May	2	80.43	40.22	158	<2e-16
		36	9.16	0.25		
	22nd June	2	214.22	107.1	133.7	<2e-16
		36	28.84	0.8		
	18th July	2	1.1367	0.5684	29.88	2.25E-08
		36	0.6848	0.019		
TK	27th May	2	1516.9	758.5	153.3	<2e-16
		36	178.1	4.9		
	22nd June	2	6775	3387	75.73	1.26E-13
		36	1610	45		
	18th July	2	12.06	6.028	14.36	2.60E-05
		36	15.12	0.42		

APPENDIX-1

HUMAN-GREY WOLF INTERACTION SURVEY

Enumerator Name: _____ Date: _____
 Respondent Name: _____ Village Name: _____
 Education: _____ Age: _____
 Ethnic background: _____ Occupation _____
 How many earning members are there in the household? _____
 Home much agricultural land your family own? _____ HH Size _____

Predator Status:

Did you sight Grey wolf in your area in the past 1 year (Jan-Dec 2016)?

Wolf Sighting/observation	Response		Nubmer of observations	Status		
	Yes	No		Common	Rare	Absent

Population of wolf you wish to increase/maintain/reduce /eliminate from your area:

↑ / → / ↓/x

Increase	Maintain	Reduce	Eliminate	No response

Do you consider wolf dangerous for your livestock? Pelase rate it from not dangerou to extermly dangreous

Not dangerous	Dangerous	Slightly dangerous	Very dangerous	Extremly dangerous

Livestock

How many livestock your family own?

Livestock	Goats	Sheep	Cattle	Other
Number				
Vaccinated				

Other: Donkey, Horse etc.

Mortality due to Disease in 1 year (January – December 2016):

Livestock	Goats	Sheep	Cattle	Yak	Other
Number					

Livestock sold in 1 year:

Livestock	Goats	Sheep	Cattle	Yak	Other
Number					
Total Income in Rs					
Slaughtered for domestic consumption					

Predation Losses

Predation in 1 year:

Predator	Season/ month	Location	Prey type	Prey sex	Prey Age	Guarded (Y/N)	Circumstances

Seasons: Winter (Dec-Feb), Spring (Mar-May), Summer (Jun-Aug), Autumn (Sep-Nov)

Any other Damage by wildlife: _____

STATUS AND ATTITUDE OF LOCAL COMMUNITIES TOWARDS THE GREY WOLF (*CANIS LUPUS* LINNAEUS, 1758) IN LOWER DIR DISTRICT, KHYBER PAKHTUNKHWA, PAKISTAN

KHAN, T. U.¹ – LUAN, X.^{1*} – KHAN, W.⁷ – AHMAD, S.⁸ – MANNAN, A.² – AHMAD, S.¹ – SHAH, S.³ – IQBAL, A.⁴ – AMMARA, U.⁵ – DIN, E. U.⁶ – KHAN, H.⁴

¹*School of Nature Conservation, Beijing Forestry University, No. 35, Tsinghua East Road, Haidian District, China*

²*Forest, Wildlife and Fisheries Department, Government of Punjab, Lahore 54500, Pakistan*

³*College of Forestry, Beijing Forestry University, Beijing 100083, China*

⁴*Center for Biotechnology and Microbiology, University of Swat, Swat 19200, Pakistan*

⁵*Department of Environmental Science, International Islamic University, Islamabad, Pakistan*

⁶*College of Environmental Sciences and Engineering, Beijing Forestry University, Beijing 100083, China*

⁷*Department of Zoology, Shaheed Benazir Bhutto University, Sheringal, Dir Upper, KP, Pakistan*

⁸*Carnivores Conservation Lab, Department of Animal Sciences, Faculty of Biological Sciences, Quaid-I-Azam University, Islamabad, Pakistan*

**Corresponding author*

e-mail: luanxiaofeng@bjfu.edu.cn; phone/fax: + 86-139-1009-0393

(Received 28th Jun 2019; accepted 10th Sep 2019)

Abstract. Human-wolf conflict is a major factor contributing to the decline of grey wolf population both locally and globally. This study was carried out in December 2016 to determine the status and nature of human-wolf conflict in the study area. A total 80 locals from all walks of life were interviewed using a semi-structured questionnaire. The grey wolf was declared as a common species by 50% of the locals with an annual sighting rate of 0.3 each. During the year, a total of 256 livestock were lost to grey wolf predation and disease. Of the total, grey wolf was held responsible for a total 71 livestock losses. Goat was the most vulnerable domestic prey as it accounted for 60.5% of the total reported depredations. Out of the total economic loss (USD 27562, USD 344.525/household), grey wolf was accountable for USD 6244 (USD 78.05/household), while disease contributed USD 21318 (USD 266/household). High depredation was observed during the summer season (54%) followed by spring and autumn. The unattended livestock grazing in forest were more prone to grey wolf attack. Most of the respondents (71%) displayed a negative attitude towards grey wolf. Reported human-wolf conflict in the area can be reduced by initiating wildlife importance related awareness programs, livestock vaccination and depredation compensation schemes. Active herding technique is also recommended to reduce chances of wolf attacks on livestock.

Keywords: *human-wolf conflict, predation, diseases, economical loss, live stock*

Introduction

Generally, the large carnivores are known as keystone species in an ecosystem, due to their top position in the food chain. They are considered as the important population regulators of different species especially their prey. Therefore, they play an impactful role in maintaining the quality of a habitat and eventually of the whole ecosystem

(Meyer and Terborgh, 2011; Ripple and Beschta, 2012). Human-wildlife conflict has its roots in the human history and it has intensified many folds over the time. Due to this conflict a large number of species especially, large carnivores have become extinct and threatened or their population is rapidly decreasing in most part of the world (Qamar et al., 2010; Ripple et al., 2014; Van et al., 2018; Jamtsho and Katel, 2019)

Human and wildlife conflict cases are represented by snow leopards (*Panthera uncia*) in the rugged mountains of central Asia (Bagchi and Mishra, 2006), grey wolf (*Canis lupus*) (Linnaeus, 1758) in the North America (Musiani et al., 2003), hyenas (*Crocuta crocuta*) and lions (*Panthera leo*) in Africa (Kolowski and Holekamp, 2006; Kissui, 2008) jaguars (*Panthera onca*) and pumas (*Puma concolor*) in South America (Mazzoli et al., 2002; Polisar et al., 2003), brown bear (*Ursus arctos*) in Tibetan Plateau of northwest China (Tsering et al., 2006) and dingoes (*Canis lupus dingo*) in Australia (Allen and Sparkes, 2001).

Human-wolf conflict is a major issue in various parts of the world (Ali & Usman, et al., 2016). Primarily, it occurs for two main reasons, first wolf predation on domestic livestock which is the primary source of income in the pastoral communities. Secondly, sometime wolf also attacks on human causing injuries or even death (Krithivasan et al., 2009). There has been 3-18% annual economic loss to the pastoral communities that holds livestock in trans-Himalaya due to snow leopard and wolf (Namgail et al., 2007). The other perception held by livestock owners that contributes to the conflict is surplus killings of livestock by wolf that is beyond its food requirement. It causes a huge economic loss in short time thus negatively influencing the opinion of livestock owners (Gipson et al., 1998; Short et al., 2002; Din et al., 2019). The grey wolf may have occasional attacks on human beings and may cause mortalities and injuries (Shahi, 1982). But these incidences are rare and often because of human interference like destroying dens, traps and persecution of pups (Linnell et al., 2002).

Wolves have traditionally inhabited much of the northern hemisphere and conflicts between them and pastoralists were common and this was primary cause of extirpation of wolves from the western world (Jhala, 2003). Although there are sanctions on wolf hunting but it is killed within its range in retaliatory killings using mostly firearms (Fritts et al., 1997). The other methods used for killing wolves include blocking or smoking out dens containing pups or adults inside them (Kumar and Rahmani, 2000; Singh and Kumara, 2006) and poisoning which is recently come in practice (Jhala, 2003).

The other issues beside retaliatory killings with wolf include habitat loss, degradation and fragmentation, disease, decrease in natural prey population and competition with other carnivore species (Irshad, 2010). Peaceful coexistence between people and wolves is very challenging due to high rate of predation of livestock (Eshete et al., 2018), most of livestock herders perceived wolves as dangerous to livestock and wanted to reduce or eliminate their population from the area. Greater number of livestock density and high predation of wolves led to negative attitude by the local communities (Din et al., 2013). The grey wolf living closer to an urbanized area where plentiful food sources, livestock and garbage are abundantly available, the chances of predation and human wolf conflict are higher (Timm et al., 2004). A recent study conducted in Karakoram suggested that livestock made about 66-75% of the diet of wolf and snow leopard (Bocci et al., 2017) while, in the Himalayas livestock constituted about 24-27% their diet (Chetri et al., 2017). Besides, spatial trend in livestock depredation by wolf can also be subjected to habitat preference and suitability, abundance of predator in that area (Wielgus and

Peebles, 2014), population of natural prey and competition with livestock over available resources and livestock grazing pattern (Johansson et al., 2015).

Pastoralist-predator conflict is a major social-ecological concern that can affect community attitudes and tolerance towards carnivores (Din et al., 2017). The coexistence predator and livestock can be attained by incorporating livestock management into conservation planning and initiation of predation mitigation and compensation schemes in the sensitive mountain ecosystem where pastoral communities live (Tyrrell et al., 2017). A very few research studies have been conducted in Pakistan in order to evaluate the status and magnitude of grey wolf conflict with locals. However, there was no single record of grey wolf status, nature of conflict and perception of local communities about the species from the study area. Hence, considering the importance grey wolf ecological role, we conducted this study to explore status, magnitude and nature of grey wolf conflict with resident communities of the area.

Methodology

Field survey

Our study area named Timergara is located in District Lower Dir, Khyber Pakhtunkhwa (KP) province, Pakistan (35°10'N, 72°00'E). During 2016, we interviewed male participants from the selected villages of the study area. We interviewed only male participants because in our study area, only males are engaged in outdoor activities related to livestock grazing and selling, fodder collection and agriculture, while on the other hand females stay at home doing household jobs. These households represent about 5% of the total households within each village (Shakeel et al., 2016). The questionnaire surveys are considered as an important tool to gather information about presence, tolerance and perception of local communities towards the wildlife species present in an area (White et al., 2005). Moreover, the local people can be a valuable and a reliable source of information about the presence of wildlife species in their area (Lunney et al., 2001; Shima et al., 2019). The participants were selected based on their pre-existing knowledge about different wildlife species in general and grey wolf in specific. The main proportion of the participants included the herders, farmers, locals engaged in different businesses, school/college teachers and local hunters of the study area. The interviews were taken from the respondents in the study area (*Fig. 1*) with the help of written semi-structured questionnaires designed with open ended questions following (Dar et al., 2009; Din et al., 2013).

In addition, color printed photographs of the species (grey wolf and other carnivores) were shown to the local respondents to evaluate their level of species identification. This was helpful to get credible information during the interview. These types of surveys are considered as an important tool for evaluating attitude, tolerance and perception of local people towards the wildlife species present in an area.

The sequence of questions asked were varied in different interviews, and depended on the response flow of respondents during interviewing. The questionnaire topics mainly covered; the number of grey wolves sighted by the respondents in one year, perceptions about the grey wolf and human attitude towards grey wolf (current). The attitudes of the respondents who wanted to increase or maintain wolf population in the study area were categorized as a positive while those who desired to decrease or eradicate wolf were grouped as a negative attitude category. Intensity of wolf danger for

livestock was categorized into five main categories; not dangerous, dangerous, slightly dangerous, very dangerous, and extremely dangerous (following L & Rensis 1932). Moreover, we also recorded the primary demographic respondent's data including earning members, age, agriculture land, household (HH) size, occupation, education level, numbers of livestock, and their dependency (L & Rensis 1932) on livestock. All the collected data was put and analyzed in the Microsoft Excel (2016). The map of the study area was developed using Arc Global Positioning System in (ArcGIS, 10.2)

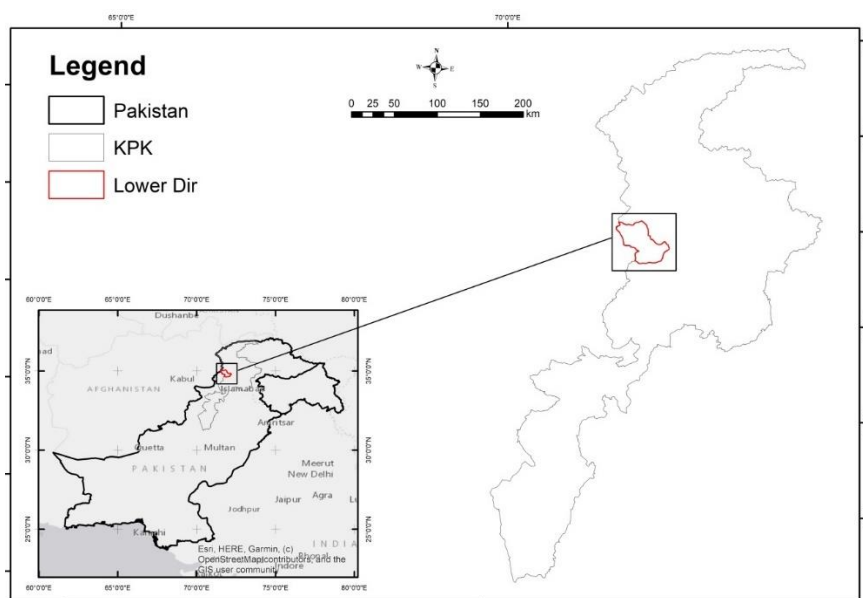


Figure 1. Location of our study area where the questionnaire surveys were done

Results

Demography of local people

During 2016 we interviewed 80 male respondents with an average age of 38 years (range 20-76 years). Most respondents (63.5%) were farmers and herders, followed by business men (19.3%) while the remaining (17.2%) were mainly school teachers, engineers and doctors. Most of the respondent (55.5%) in study sites were also highly dependent on livestock, 20.22% showed medium dependency and 20.22% showed low dependency on the livestock. Only 10% of interviewers poorly recognized the occurrence or absence of wolves in the study sites (i.e., their information's about the presence or absence of wolves was low); whereas, 35.5% of people were at average knowledge level and 54.4% were remarkably knowledgeable.

Wolf damage and people response

In the study area livestock rearing was the main source of income. In the study area, our surveyed households ($n = 80$) owned 1745 livestock with an average herd size of 21.8/household. Goats accounted for the largest percentage of livestock (56%), followed by sheep (24%), cattle (17%), and others (mules, horses and donkeys) (3%). We interviewed a total of 80 respondents to document sighting records of grey wolf in the study area. Respondent reported a total of 31 sighting records of grey wolf with an average sighting of 0.3 during the past one year. About the status of grey wolf in the

study area, our respondents shared mix views. Most (n = 43, 50%) of the respondents claimed that wolf is a common species in the area, while 46% and 4% respondents declared its status as a rare (n = 31) and absent (n = 6) respectively in the area (Fig. 2).

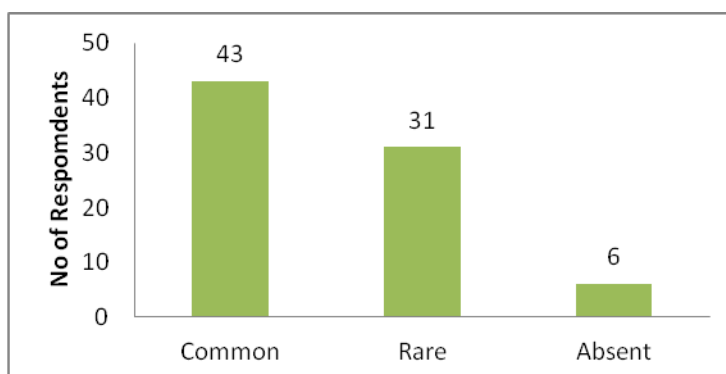


Figure 2. Status of grey wolf in the study area

Respondent reported a total loss of 256 livestock diseases and wolf predation and disease during the year 2016 (Table 1). Among the total 71 livestock losses were caused by wolves, while different disease accounted for 185 livestock losses. Goats were the largely victimized prey species, which accounted 43 (60.5%) of wolf killings, followed by sheep 23 (32.3%), cattle 2 (2.8%) and other 3 (4.2%). The reported figure of 256 livestock losses to grey wolf and diseases constitute an economic loss of USD 27562 (USD 344.525 per household).

Livestock depredation by grey wolf was reported at peak in the summer season, where more than half (54%) of the total livestock depredation occurred. Attack of wolf on the livestock was lowest in spring and winter (4% each) (Fig. 3). During the last year, a total of two attacks of wolf were reported on the human in the study area. The victims were attacked in nearby forest. In the attacks, the victims revived injuries that were not fatal, but it ended in the killing of wolf. Most (71%) of the respondents shared negative views about wolf (Fig. 4). The entire respondents declared the intensity of wolf danger as extremely high for their livestock as compared to rest of the wildlife species found in their area. Locals reported that all livestock depredation occurred inside the forest. Majority (55%) of the livestock depredation occurred when livestock were grazing in the nearby forest unattended by guard.

Table 1. Economic losses due to grey wolf predation and diseases

Livestock	UV (\$)	Wolf		Disease		Total (\$)
		No	Loss in \$	No	Loss in \$	
Goat	80	43	3440	95	7600	11040
Sheep	80	23	1840	59	4720	6560
Cattle	302	2	604	29	8758	9362
Other	120	3	360	2	240	600
		71	6244	185	21318	27562
			78.05		266.475	344.525

UV: unit value, 1 US Dollar = 149, hh: households

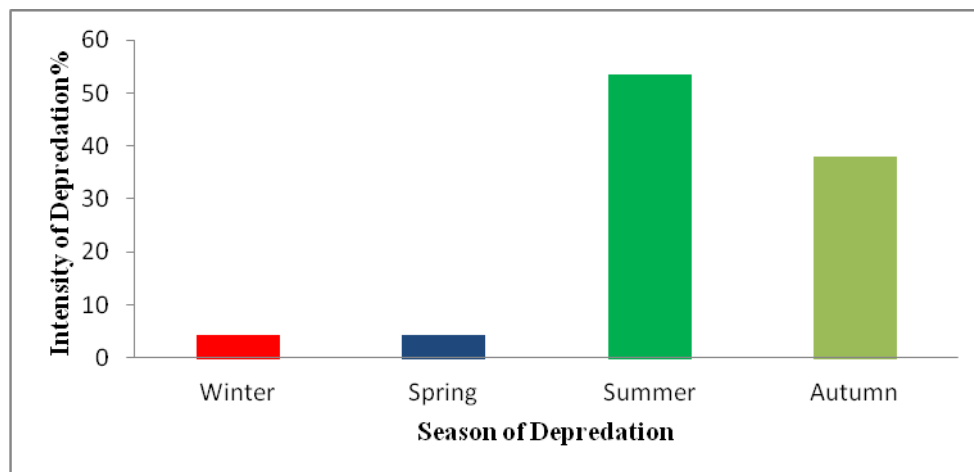


Figure 3. Depredation of livestock in different season of the year

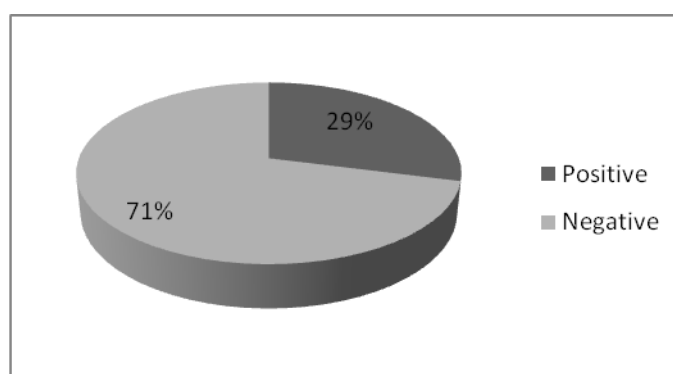


Figure 4. Attitude of locals towards grey wolf

Discussion

The grey wolf is known to the remote and rugged mountainous terrains of the district Lower Dir (KPK). This study was aimed to explore the statues and conflict of grey wolf with the local people of the selected villages of study area. Roberts (1977) and Dar et al. (2009) stated that the northern areas are the intrinsic habitats for the grey wolf. The human population inhabiting the study area is scattered and the presence of pastures and greenery accompanied by rugged terrains makes the area an appropriate habitat for the species. According to Divisional forest officer (Waqif, personal communication, December 27, 2016) locals were attack by an animal that resulted in the certain death of the animals and injuries to victims. The animal was thoroughly examined later one and was identified as a grey wolf.

Due to the unavailability of the veterinary service and high rate of livestock per household in the study area, a high rate of mortalities due to different diseases was observed. In the year 2016 a total of 256 livestock losses were reported by the locals. Due to diseases locals bear an economic loss of USD 21318 (USD 266 per household), that was higher than the economic loss occurred due to wolf depredation USD 6244 (USD 78.05 per household). Similar results (Ahmad et al., 2016; Dar et al., 2009) stated that the diseases in the livestock are the major cause of losses in stocks in the northern part of Pakistan. It is always argued that the carnivore predators are the prime suspects

and responsible factor of livestock losses and paired economic losses. In a recent study, it was concluded that the disease had resulted in the economic loss twice more than the loss caused by carnivore's predators, which was higher than each household's income by selling livestock.

Moreover, a research study carried in Sanjiangyuan part of China by Li et al. (2013) showed 809 livestock mortality cases related to loss due to disease accounting for a money loss of 375,031 USD per annum, which makes 2604 UDS per family yearly. It was evident from the interviews conducted from the affected locals that these economic losses were primarily caused by the livestock disease that were easily curable but were not treated well in time due to unavailability of the veterinary services in the study area, see (Table 1).

Livestock depredation is one of the main causes of human-carnivores conflict, which resulted in the retaliated killings of wildlife both locally and globally. The human-wildlife conflict is prevailing in its severe form in the developing countries where locals are highly dependent on livestock rearing. In the Himalayas and Hindu Kush mountain regions the higher rate livestock depredations by large carnivores has been linked with higher population of livestock per household (Jackson and Hunter, 1996; Mishra, 1997; Hussain, 2003; Distefano, 2005). Additionally, the areas having small population of carnivore's natural prey and large livestock population have higher depredation rates (Meriggi and Lovari, 1996; Kolowski and Holekamp, 2006). In our study, the respondent's stated that a total of 71 livestock depredation were caused due to wolf predation last year.

Current study showed that medium size prey including goats and sheep were more vulnerable to grey wolf attacks. The most vulnerable livestock to depredation is the medium-sized livestock weighing 25–45 kg, because predators can easily capture and eat them with ease safety (Dar et al., 2009; Bibi et al., 2013). Similar results were concluded in studies carried out in Musk Deer National Park (Ahmad et al., 2016), Machiara National Park Azad Jammu and Kashmir (Dar et al., 2009; Kabir et al., 2014) and India (Suryawanshi et al., 2013).

Livestock depredation by wolf was found at its peak during summer season, followed by autumn, spring and winter respectively. Livestock depredation normally follows some seasonal patterns. During summer and autumn season the pasture and other grazing grounds of the study area are the suitable locations for livestock grazing. This makes the unattended livestock more vulnerable to predator attack. While during winter season locals usually keep livestock at home nourishing them with the stocked fodders (Dar et al., 2009; Sogbohossou et al., 2011)

The local respondents shared negative perception and attitude towards the grey wolf (Fig. 4). Due to conflict over livestock depredation most of our respondents wanted to see the grey wolf population decreases or even eliminated from their area. Usually livestock losses due to carnivores, when coupled with restricting locals from using the naturally resources found in their area like forest, develop negative and aggressive attitude among the locals towards wildlife (Conforti and de Azevedo, 2003). The interviewed locals reported that the wolves were the major predators found in their area, and they consider them the most dangerous to livestock. Moreover, it was also considered to be a threat to local people too. The species is depicted as a sign of viciousness and tyranny in the study.

Most of the depredation was reported when the livestock were grazing inside the near forest in the absence of guard. Herd guarding mechanism and active defense is

important and necessary against the carnivore's attack. Low predation rate was observed in presence of herdsman (Breitenmoser, 1998). Studies conducted in Europe, Italy and France reveal high depredation in the areas where domestic livestock graze freely or rarely guarded (Sillero-Zubiri and Laurenson, 2001; Espuno et al., 2004). Our study also helps to conclude that livestock depredation is much lower when herds were guarded, showing the effectiveness of active guarding.

Conclusion and recommendations

Most of the respondents of the area consider the grey wolf as a common carnivore found in the area. The species was blamed for a high rate of livestock depredation and faced a severe negative attitude of locals as it caused them economic loss. To ensure the grey wolf conservation and reduce the economic losses of the local communities, it is recommended to initiate a vaccination program as the area is lacking any animal care center. Livestock compensation scheme is also recommended because it will shift the negative perception of the local to positive. Proper guarding of livestock is recommended to reduce chances of wolf attacks. Moreover, intensive sign and camera trap surveys are recommended to be carried out in order to determine the abundance and habitat preference of the species in the area.

Acknowledgements. We are grateful to the locals in general and our respondents of the area for specific for giving us time and sharing their views about the species. This study was jointly supported by grants from The Ministry of Science and Technology of the People's Republic of China (research and application of key techniques on endangered species conservation and prediction of forest fire and pests in response to climate change, 2013BAC09B00) and National forestry and grassland administration, (management and improvement of monitoring in national park, 2018HWFQBHQLXF-01).

REFERENCES

- [1] Ahmad, S., Hameed, S., Ali, H., Khan, T. U., Mehmood, T., Nawaz, M. A. (2016): Carnivores' diversity and conflicts with humans in Musk Deer National Park, Azad Jammu and Kashmir, Pakistan. – *European Journal of Wildlife Research* 62(5): 565-76.
- [2] Ali, U., Minhas, R. A., Awan, M. S., Ahmed, K. B., Qamar, Q. Z., Dar, N. I. (2016): Human-Grey Wolf (*Canis lupus* Linnaeus, 1758) Conflict in Shouther Valley, District Neelum, Azad Jammu and Kashmir, Pakistan. – *Pakistan Journal of Zoology* 48(3).
- [3] Allen, L., Sparkes, E. (2001): The effect of dingo control on sheep and beef cattle in Queensland. – *Journal of Applied Ecology* 38(1): 76-87.
- [4] Bagchi, S., Mishra, C. (2006): Living with large carnivores: predation on livestock by the snow leopard (*Uncia uncia*). – *Journal of Zoology* 268(3): 217-24.
- [5] Bibi, S., Minhas, R., Awan, M., Ali, U., Dar, N. (2013): Study of ethno-carnivore relationship on Dhirkot, Azad Jammu and Kashmir (Pakistan). – *Journal of Animal and Plant Sciences* 23: 854-59.
- [6] Bocci, A., Lovari, S., Khan, M. Z., Mori, E. (2017): Sympatric snow leopards and Tibetan wolves: coexistence of large carnivores with human-driven potential competition. – *European Journal of Wildlife Research* 63(6): 92.
- [7] Breitenmoser, U. (1998): Large predators in the Alps: the fall and rise of man's competitors. – *Biological Conservation* 83(3): 279-89.
- [8] Chetri, M., Odden, M., Devineau, O., Wegge, P. (2019): Patterns of livestock depredation by snow leopards and other large carnivores in the Central Himalayas, Nepal. – *Global Ecology and Conservation* 17: e00536.

- [9] Conforti, V. A., de Azevedo, F. C. C. (2003): Local perceptions of jaguars (*Panthera onca*) and pumas (*Puma concolor*) in the Iguaçú National Park area, South Brazil. – *Biological Conservation* 111(2): 215-21.
- [10] Dar, N. I., Minhas, R. A., Zaman, Q., Linkie, M. (2009): Predicting the patterns, perceptions and causes of human–carnivore conflict in and around Machiara National Park, Pakistan. – *Biological Conservation* 142(10): 2076-82.
- [11] Din, J. U., Hameed, S., Shah, K. A., Khan, M. A., Khan, S., Ali, M., Nawaz, M. A. (2013): Abundance of canids and human canid conflict in the Hindu Kush Mountain range of Pakistan. – *Wildlife Biology in Practice* 9(2): 20-29.
- [12] Din, J. U., Ali, H., Ali, A., Younus, M., Mehmood, T., Norma-Rashid, Y., Nawaz, M. A. (2017): Pastoralist-predator interaction at the roof of the world: Conflict dynamics and implications for conservation. – *Ecology and Society* 22(2).
- [13] Din, J. U., Nawaz, M. A., Mehmood, T., Ali, H., Ali, A., Adli, D. S. H., Norma-Rashid, Y. (2019): A transboundary study of spatiotemporal patterns of livestock predation and prey preferences by snow leopard and wolf in the Pamir. – *Global Ecology and Conservation* 20: e00719.
- [14] Distefano, E. (2005): Human-Wildlife Conflict worldwide: collection of case studies, analysis of management strategies and good practices. – Food and Agricultural Organization of the United Nations (FAO), Sustainable Agriculture and Rural Development Initiative (SARDI), Rome, Italy. Available from: FAO Corporate Document repository <http://www.fao.org/documents>.
- [15] Eshete, G., Marino, J., Sillero-Zubiri, C. (2018): Ethiopian wolves conflict with pastoralists in small Afroalpine relicts. – *African Journal of Ecology* 56(2): 368-374.
- [16] Espuno, N., Lequette, B., Poulle, M. L., Migot, P., Lebreton, J. D. (2004): Heterogeneous response to preventive sheep husbandry during wolf recolonization of the French Alps. – *Wildlife Society Bulletin* 32(4): 1195-208.
- [17] Fritts, S. H., Bangs, E. E., Fontaine, J. A., Johnson, M. R., Phillips, M. K., Koch, E. D., Gunson, J. R. (1997): Planning and implementing a reintroduction of wolves to Yellowstone National Park and central Idaho. – *Restoration Ecology* 5(1): 7-27.
- [18] Gipson, P. S., Ballard, W. B., Nowak, R. M. (1998): Famous North American wolves and the credibility of early wildlife literature. – *Wildlife Society Bulletin* 1988: 808-16.
- [19] Hussain, S. (2003): The status of the snow leopard in Pakistan and its conflict with local farmers. – *Oryx* 37(1): 26-33.
- [20] Irshad, R. (2010): Ecology and Conservation of Wild Canids in the Salt Range Pakistan with Focus on Indian Wolf (*Canis Lupus Pallipes*). – Quaid-i-Azam University, Islamabad.
- [21] Jackson, R. M., Hunter, D. O. (1996): Snow Leopard Survey and Conservation Handbook. – International Snow Leopard Trust, Seattle, WA.
- [22] Jamtsho, Y., Katel, O. (2019): Livestock depredation by snow leopard and Tibetan wolf: Implications for herders' livelihoods in Wangchuck Centennial National Park, Bhutan. – *Pastoralism* 9(1): 1.
- [23] Jhala, Y. (2003): Status, ecology and conservation of the Indian wolf *Canis lupus pallipes* Sykes. – *J. Bombay Natural History Society* 100(2): 3.
- [24] Johansson, O., Rauset, G. R., Samelius, G., McCarthy, T., Andren, H., Tumursukh, L., Mishra, C. (2015): Land sharing is essential for snow leopard conservation. – *Biological Conservation* 203: 1-7.
- [25] Kabir, M., Ghoddousi, A., Awan, M. S., Awan, M. N. (2014): Assessment of human–leopard conflict in Machiara National Park, Azad Jammu and Kashmir, Pakistan. – *European Journal of Wildlife Research* 60(2): 291-96.
- [26] Kissui, B. (2008): Livestock predation by lions, leopards, spotted hyenas, and their vulnerability to retaliatory killing in the Maasai steppe, Tanzania. – *Animal Conservation* 11(5): 422-32.

- [27] Kolowski, J., Holekamp, K. (2006): Spatial, temporal, and physical characteristics of livestock depredations by large carnivores along a Kenyan reserve border. – *Biological Conservation* 128(4): 529-41.
- [28] Krithivasan, R., Athreya, V., Odden, M. (2009): Human-Wolf Conflict in Human Dominated Landscapes of Ahmednagar District, Maharashtra. – Rufford Small Grants Foundation for Nature Conservation, London, pp. 1-53.
- [29] Kumar, S., Rahmani, A. R. (2000): Livestock depredation by wolves in the Great Indian Bustard Sanctuary, Nannaj (Maharashtra), India (with three text-figures). – *Journal - Bombay Natural History Society* 97(3): 340-48.
- [30] Li, J., Yin, H., Wang, D., Jiagong, Z., Lu, Z. (2013): Human-snow leopard conflicts in the Sanjiangyuan Region of the Tibetan Plateau. – *Biological Conservation* 166: 118-23.
- [31] Likert, R. (1932): A technique for the measurement of attitudes. – *Archives of Psychology* 22: 140-55.
- [32] Linnell, J., Andersen, R., Andersone, Z., Balciauskas, L., Blanco, J. C., Boitani, L., Liberg, O. (2002): The Fear of Wolves: A Review of Wolf Attacks on Humans. – NINA Oppdragsmelding 731, Trondheim.
- [33] Lunney, D., Matthews, A. (2001): The contribution of the community to defining the distribution of a vulnerable species, the spotted-tailed quoll, *Dasyurus maculatus*. – *Wildlife Research* 28: 537-545. DOI: 10.1071/WR00018.
- [34] Mazzolli, M., Graipel, M. E., Dunstone, N. (2002): Mountain lion depredation in southern Brazil. – *Biological Conservation* 105(1): 43-51.
- [35] Meriggi, A., Lovari, S. (1996): A review of wolf predation in southern Europe: does the wolf prefer wild prey to livestock? – *Journal of Applied Ecology* 33(6): 1561-71.
- [36] Meyer, W. M., Terborgh, J. A. (2011): Trophic cascades: predators, prey, and the changing dynamics of nature. – *Oryx* 45(1): 151.
- [37] Mishra, C. (1997): Livestock depredation by large carnivores in the Indian trans-Himalaya: conflict perceptions and conservation prospects. – *Environmental Conservation* 24(4): 338-43.
- [38] Musiani, M., Mamo, C., Boitani, L., Callaghan, C., Gates, C. C., Mattei, L., Volpi, G. (2003): Wolf depredation trends and the use of fladry barriers to protect livestock in western North America. – *Conservation Biology* 17(6): 1538-47.
- [39] Namgail, T., Fox, J. L., Bhatnagar, Y. V. (2007): Carnivore-caused livestock mortality in Trans-Himalaya. – *Environmental Management* 39(4): 490-96.
- [40] Polisar, J., Maxit, I., Scognamillo, D., Farrell, L., Sunquist, M. E., Eisenberg, J. F. (2003): Jaguars, pumas, their prey base, and cattle ranching: ecological interpretations of a management problem. – *Biological Conservation* 109(2): 297-310.
- [41] Qamar, Q., Dar, N., Ali, U., Minhas, R., Ayub, J., Anwar, M. (2010): Human-leopard conflict: an emerging issue of common leopard conservation in Machiara National Park, Azad Jammu and Kashmir, Pakistan. – *Pakistan J Wildlife* 1(2): 50-56.
- [42] Ripple, W. J., Beschta, R. L. (2012): Trophic cascades in Yellowstone: the first 15 years after wolf reintroduction. – *Biological Conservation* 145(1): 205-13.
- [43] Ripple, W. J., Estes, J. A., Beschta, R. L., Wilmers, C. C., Ritchie, E. G., Hebblewhite, M., Berger, J., Elmhagen, B., Letnic, M., Nelson, M. P. (2014): Status and ecological effects of the world's largest carnivores. – *Science* 343(6167). DOI: 10.1126/science.1241484.
- [44] Roberts, T. J. (1977): *The Mammals of Pakistan*. – E. Benn, London.
- [45] Shahi, S. (1982): Status of the grey wolf (*Canis lupus pallipes* Sykes) in India - a preliminary survey. – *Journal of the Bombay Natural History Society* 79(3): 493-502.
- [46] Shima, A. L., Berger, L., Skerratt, L. F. (2019): Conservation and health of Lumholtz's tree-kangaroo. – *Australian Journal of Mammal* 41: 57-64. <https://doi.org/10.1071/AM17030>.

- [47] Short, J., Kinnear, J., Robley, A. (2002): Surplus killing by introduced predators in Australia—evidence for ineffective anti-predator adaptations in native prey species? – *Biological Conservation* 103(3): 283-301.
- [48] Sillero-Zubiri, C., Laurenson, M. K. (2001): Interactions between Carnivores and Local Communities: Conflict or Co-existence? – *Conservation Biology Series*. Cambridge University Press, Cambridge, pp. 282-312.
- [49] Singh, M., Kumara, H. (2006): Distribution, status and conservation of Indian gray wolf (*Canis lupus pallipes*) in Karnataka, India. – *Journal of Zoology* 270(1): 164-69.
- [50] Sogbohossou, E. A., de Iongh, H. H., Sinsin, B., de Snoo, G. R., Funston, P. J. (2011): Human–carnivore conflict around Pendjari Biosphere Reserve, northern Benin. – *Oryx* 45(4): 569-78.
- [51] Suryawanshi, K. R., Bhatnagar, Y. V., Redpath, S., Mishra, C. (2013): People, predators and perceptions: patterns of livestock depredation by snow leopards and wolves. – *Journal of Applied Ecology* 50(3): 550-560.
- [52] Timm, R. M., Baker, R. O., Bennett, J. R., Coolahan, C. C. (2004): Coyote attacks: an increasing suburban problem. – *Proceedings of the Twenty-First Vertebrate Pest Conference*. University of California, Davis, pp. 47-57.
- [53] Tsering, D., Farrington, J., Norbu, K. (2006): Human–Wildlife Conflict in the Chang Tang Region of Tibet. – *World Wide Fund for Nature (WWF) China–Tibet Program*, Lhasa, Tibet, China.
- [54] Tyrrell, P., Russell, S., Western, D. (2017): Seasonal movements of wildlife and livestock in a heterogeneous pastoral landscape: implications for coexistence and community based conservation. – *Global Ecology and Conservation* 12: 59-72.
- [55] Van Eeden, L. M., Crowther, M. S., Dickman, C. R., Macdonald, D. W., Ripple, W. J., Ritchie, E. G., Newsome, T. M. (2018): Managing conflict between large carnivores and livestock. – *Conservation Biology* 32(1): 26-34.
- [56] White, P. C., Jennings, N. V., Renwick, A. R., Barker, N. H. (2005): Questionnaires in ecology: a review of past use and recommendations for best practice. – *Journal of Applied Ecology* 42(3): 421-430.
- [57] Wielgus, R. B., Peebles, K. A. (2014): Effects of wolf mortality on livestock depredations. – *PLoS One* 9(12): e113505, 10.1371.

CYTOTOXICITY AND IN-VITRO ANTIVIRAL ACTIVITY OF LECTIN FROM *CROCUS VERNUS* L. AGAINST POTATO VIRUS Y

BILAL, M.^{1,2*} – NASIR, I. A.¹ – TABASSUM, B.¹ – AKREM, A.³ – AHMAD, A.⁴ – ALI, Q.⁵

¹*Centre of Excellence in Molecular Biology, University of the Punjab, 87-West Canal Road Thokar Niaz Baig, Lahore 53700, Pakistan*

²*Centre for Applied Molecular Biology, University of the Punjab, 87-West Canal Bank Road, Thokar Niaz Baig, Lahore 53700, Pakistan*

³*Department of Botany, Institute of Pure and Applied Biology, Bahauddin Zakariya University, Multan, Pakistan*

⁴*Institute of Genetics and Developmental Biology, University of Chinese Academy of Sciences, Beijing, China*

⁵*Institute of Molecular Biology and Biotechnology, University of Lahore, Lahore, Pakistan*

**Corresponding author*

e-mail: bilal.camb@pu.edu.pk

(Received 2nd Sep 2019; accepted 4th Dec 2019)

Abstract. Plant lectins are the potential proteins that specifically bound and cross linked with carbohydrates and target particular glycans present on the cell surface of viruses through a pathway termed as a lectin activation pathway. They have a role in plant defense system. In this study, we evaluated anti-*PVY* (potato virus Y) activity of plant derived lectin in in-vitro assay. A tetramer lectin was isolated from the corms of *Crocus vernus* and purified to sub fractions through ammonium sulfate precipitation, dialysis, filtration on the PD 10 column, cation exchange chromatography on SP-Sepharose gel. In-silico studies predicted stable interaction between *Crocus vernus* lectin (CVL) and targeted protein of *PVY*. Cytotoxicity tests performed on HepG2 cells indicated IC₅₀ value for CVL was 770 µg/ml. The IC₅₀ values indicated the safe limit and non-cytotoxic effect of the CVL extract and worth for further testing. The hemagglutination activity of CVL against the rabbit erythrocytes was revealed to be 100 µg/ml. The anti-*PVY* activity displayed in the CVL lectin was evaluated through quantitative real-time PCR assay. It was revealed that CVL was effective against targeted gene of *PVY* at 30, 60 and 90 µg/ml concentration and up to 100% inhibition of the *PVY* mRNA was achieved in all three tested concentrations in comparison with control. Our results clearly indicate the CVL gene can be a used for transformation studies in potato to control the potato virus Y as an effective tool, in the future.

Keywords: *Crocus vernus* lectin (CVL), potato virus Y, real time PCR, coat protein, antiviral activity, in silico analysis

Introduction

Mannose-binding lectins prove to be of immense importance and potency in preventing and treating virus-mediated infections as they specifically target particular glycans present on the cell surface which are required by virus for entry (Balzarini et al., 2007). A variety of lectins have already been reported from different organisms belonging to a wide range of taxonomical groups, including plants, animals, bacteria, fungus and algae (Golotin et al., 2019; Singh et al., 2018; Sreeramulu et al., 2018; Muslim et al., 2018; Zhang et al., 2017a). The structure, efficacy and specificity of these lectins may vary from source to source. Till to date, lectins have been published from different plant families, including *Alliaceae*, *Amaryllidaceae*, *Araceae*, *Bromeliaceae*,

Iridaceae, *Liliaceae*, and *Orchidaceae* and their activity has been reported against Human Immunodeficiency Virus, Simian Immunodeficiency Virus and Feline Immunodeficiency Virus (Lam and Ng, 2001; Davidson et al., 2000).

Potato virus Y (PVY) belongs to the genus *Potyvirus* of the *Potyviridae* family (Kitajima et al., 1997). Worldwide a number of crops are affected in a severe damaging way by this virus, especially solanaceous plants like potato (*Solanum tuberosum* L.), tobacco (*Nicotiana glauca* L.) and pepper (*Capsicum annuum* L.). PVY symptoms vary from barely visible mosaic patterns to an extreme necrosis and premature death of plants (Tabassum et al., 2016). PVY infection is difficult to control because it is vegetatively propagated, making primary viral infection more destructive and consistent generations after generations (Gargouri-Bouزيد et al., 2005). In Pakistan, due to early infection of PVY loss is about 70% (Abbas et al., 2017). Among the crucial genes of PVY, capsid protein (CP) gene is involved in the encapsulation, in replication of the viral genome, movement across host cells, and transfer from infected to uninfected plants using mobile biological vectors (Callaway et al., 2001).

Several approaches have been tested to date to produce high yielding commercial varieties with advance levels of resistance, including genetic amendments of the PVY coat protein (CP) gene or P1 gene (Gargouri-Bouزيد et al., 2005; Mäki-Valkama et al., 2000). Resistance exhibited by gene silencing is more effective as compared to protein mediated resistance (Mäki-Valkama et al., 2007).

In Pakistan, commercially offered high yielding potato lines fail to show resistance against viruses, especially the potato virus Y. In the current study, we aimed to find out the effect of mannose-binding lectin from the bulbs of *C. vernus* activity against the PVY coat protein gene.

Materials and methods

Sequence retrieval and modeling of CP protein

The full-length amino acid sequence of potato virus Y, coat protein (Accession # ABK13679.1) was retrieved from the NCBI database and functional domains of Coat Protein (CP) were determined using an online InterPro server (www.ebi.ac.uk/interpro/).

Crocus vernus lectin (CVL) molecular structure, coordinate information (PDB ID: 3MEZ) was downloaded from the protein database (<http://www.rcsb.org/structure/3MEZ>) and the CP structure was generated using the online tool (<http://zhanglab.ccmb.med.umich.edu/I-TASSER/>). The validity of the predicted model was checked by calculating the Ramachandran plot which was produced by online tool RAMPAGE (<http://mordred.bioc.cam.ac.uk/~rapper/rampage.php>).

Refinement, evaluation, and validation of CP protein model

Using the ModRefiner online tool (<https://zhanglab.ccmb.med.umich.edu/ModRefiner/>), the CP model was further refined. Using Ramachandran plot and by determining the physiochemical properties of the CP protein through ProtScale, the model was evaluated and authenticated.

Protein-protein docking analysis of CP and CVL

Online server Z-DOCK (<http://zdock.umassmed.edu/>) was used for docking of receptor model to fusion protein and ten coordinate files were obtained. PDBePISA

online tool (<http://www.ebi.ac.uk/pdbe/pisa/>) was used to find the interactions between the CP and CVL. For the visualization of structures showing the interactions between the two proteins the PDB viewer was used.

Protein source, extraction and fractionation of extract

Crocus vernus (L.) Hill corms were kindly provided by Dr. Ahmed Akrem (Institute of Pure and Applied Biology, Bahauddin Zakariya University, Multan-Pakistan). Briefly, 10 g of corms were reduced to powder and homogenized in 0.1 M phosphate buffer (pH 6.5). The slurry was stirred continuously at 4 °C for 2 h. Further, the suspension was filtered through the muslin cloth and centrifuged at 15000 × g for 15 min at 4 °C. Supernatant was collected and subjected to 60% ammonium sulfate precipitation. The pellet was re-suspended in 20 mM phosphate buffer (pH 6.5) and dialyzed overnight by dialyzing tube (Spectra/Por RC Biotech membrane, 6-8 kDa MWCO) against 10 mM phosphate buffer (pH 6.5).

Crude protein extracts were fractionated through cation exchange chromatography where desalted protein was subjected to Hi Trap SP FF column (GE Healthcare). The column was equilibrated with 5 cv of 50 mM of phosphate buffer (pH 6.5) and then partially purified protein was loaded onto the column. Protein was eluted with 0.5 M NaCl gradient and different fractions were obtained which were analyzed by SDS-PAGE. The protein was quantified through the Bradford method (Bradford, 1976).

Construction of pCP-PVY clone

Full length coat protein (CP) gene of potato virus Y (PVY) was amplified from PVY infected potato samples. A fragment of full-length CP gene 807 bp was amplified with specific forward 5'-ATGGCAAATGACACAATCGAT-3' and reverse primer 5'-ATCACCTGCCACCTCTATC-3' and the deduced sequence was submitted in NCBI database under accession # MK130988. For directional cloning in pCDNA3.1 (+) (mammalian expression vector), the amplified fragments were generated with *HindIII* and *EcoRI* restriction sites at 5 and 3 ends. The recombinant vector was named as pCP-PVY.

Cell line

The HepG2 cell line was grown and maintained in Dulbecco's modified Eagle medium (DMEM) containing 100 U/ml penicillin, 100 µg/ml streptomycin and 10% Fetal Bovine Serum (FBS) at 37 °C in 5% CO₂ atmosphere at 37 °C.

Cytotoxicity assay for CVL

Cell survival and proliferation was quantified by using the MTT assay kit (Millipore, USA). Using the HepG2 cell model, Cell viability and proliferation was evaluated. HepG2 cells were cultured in 96 well plate containing DMEM supplemented with 10% FBS, 100 µg/ml streptomycin and 100 IU/ml penicillin. CVL protein was diluted in different concentration ranges (110 to 770 µg/ml, 3 wells per concentration) in 96-well plates and incubated at 37 °C in the humidified CO₂ incubator.

After incubation, the concentration range of CVL drawn from 110 to 770 µg/ml and were added to the wells of the plate in triplicates and the plate was again incubated at 37 °C for 24 h in CO₂ incubator. After incubation, the exhausted media was discarded

and fresh media along with MTT reagent (5 mg/ml in PBS) were added to each well according to the manufacturer's instructions. The plate was then incubated at 37 °C in a CO₂ incubator for 4 h. To dissolve the formazan crystals produced after incubation, DMSO was added in the wells. To quantify the MTT formazan product, the optical density of contents of plate was analyzed through ELISA plate reader as per described protocol.

Cell viability was attained by means of following formula (Rehman et al., 2011):

$$\text{Percent cell viability} = (\text{Test } 570 \text{ nm} - 620 \text{ nm} / \text{Control } 570 \text{ nm} - 620 \text{ nm}) \times 100.$$

Hemagglutinating activity

The hemagglutinating activity of the CVL was evaluated against the rabbit erythrocytes using the U-shaped bottom 96 wells microtiter plate as described by Ynalvez et al. (2015). Briefly, twofold serial dilutions of the CVL were made in phosphate buffer saline (PBS) and was incubated with 2% erythrocytes suspension in equal volume and kept at room temperature for 1 h, while control contains the PBS in spite of the CVL. Positive results indicated the red-carpet layer while negative results show the red button formation in the well.

Co-transfection

The HepG2 cells were cultured at a cell density of 1×10^6 cells per well in a 6-well plate. CVL protein extract and pCP-PVY plasmid DNA were co-transfected at 50-70% cell confluence. Lipofectamine 2000 (Invitrogen, CA) was used as transfection reagent. For the down regulation of CP-PVY mRNA, 50 ng – 1 µg construct DNA was used along with three different CVL concentrations; 30, 60 and 90 µg/ml. Experiments were carried out in triplicate.

Real-time PCR analysis

To measure the anti-PVY potential of CVL, the mRNA expression of CP gene was revealed through real time PCR assay. Post co-transfection, total RNA was isolated from HepG2 cells by using TRIzol reagent (Invitrogen) and 1 µg was used to synthesize complementary DNA (cDNA) by using the cDNA synthesis kit (Thermo Scientific, Lithuania). Specific forward 5'-TGTGGGTTTAGCGCGTTATG-3' and reverse 5'-GTGCCTCTCTGTGTTCTCCT -3' were used to amplify 172 bp amplicon. The assay was run in triplicate in the PikoReal™ Real-Time PCR system (Thermo Scientific). Reactions were prepared in a total volume of 10 µl containing: 1 µl cDNA, 0.5 µl of each 10 pmoles primer, 5 µl of Maxima SYBR Green qPCR Master Mix (2X) (Thermo scientific) and 2.5 µl RNase/DNase-free sterile water. The cycle profile comprised of 30 cycles with denaturation at 94 °C for 30 s, annealing at 54 °C for 30 s and extension at 72 °C for 30 s after an initial denaturation at 94 °C for 10 min. For normalization, β-actin was used as a control. The relative gene expression analysis was measured by using C_q values in different samples. Each real-time PCR assay was performed in triplicate.

Statistical analysis

Statistical analysis was carried out using GraphPad Prism 7. Triplicate studies were performed. Descriptive statistics were used to evaluate the mean and standard deviation

of the results. One-way ANOVA was used to investigate a significant reduction in the cell viability and mRNA expression of the CP gene at $P \leq 0.05$.

Results

In silico modeling, refinement, evaluation, and validation of CP gene was performed with online available tools as indicated in *Figure 1A* and *B*. The verified in silico model of CP was used for docking analysis.

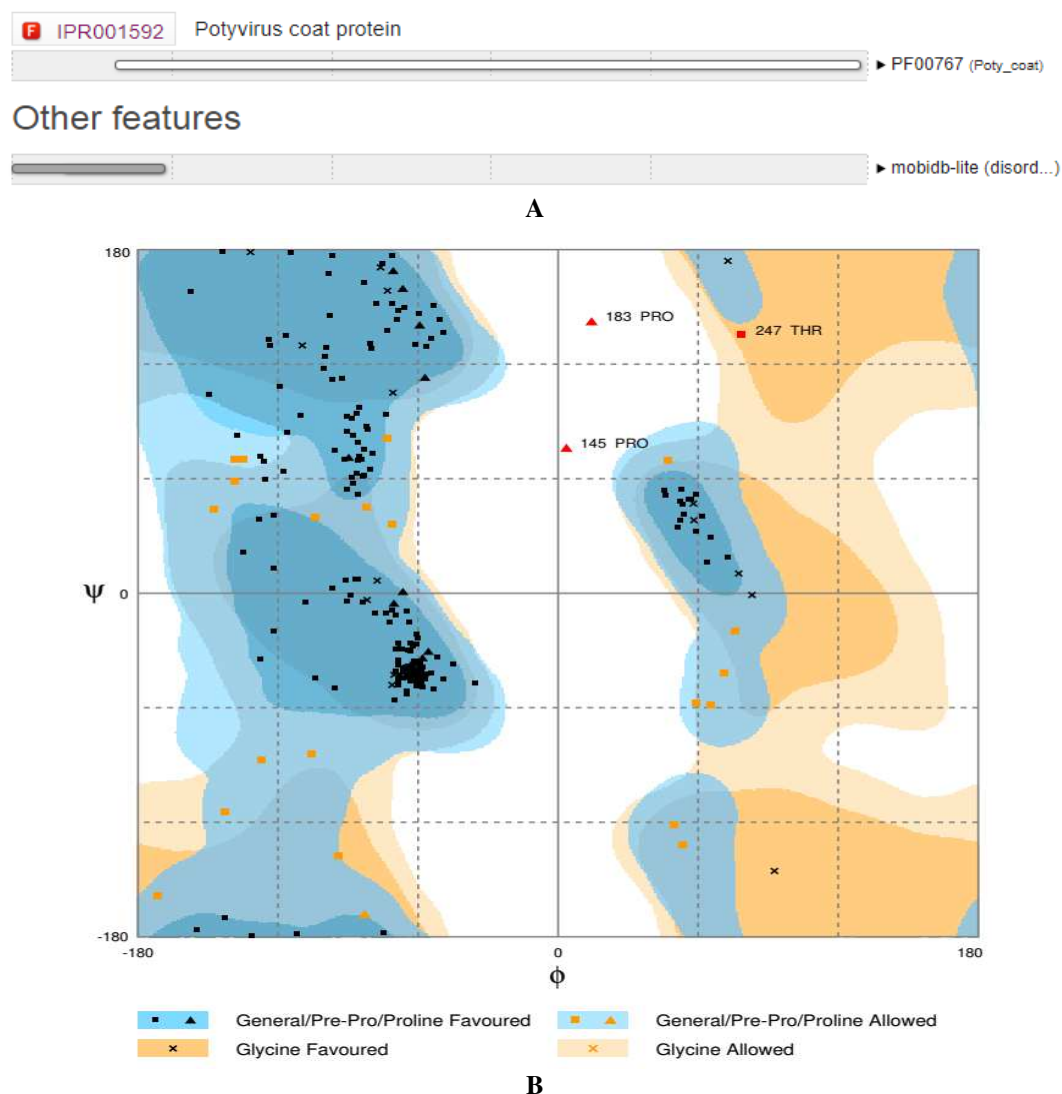


Figure 1. *A* Functional domains analysis of CP sequence through InterPro is showing Potyvirus CP domain. *B* Ramachandran plot analysis of Capsid protein model to visualize dihedral angles; ϕ against ψ . Only two residues indicated with a red triangle in the figure are in the outlier region except these two, all other residues are in favored and allowed regions

Primary structure examination of the CP model was executed utilizing ProtParam (<https://web.expasy.org/protparam/>). It was found that the CP has an aggregate length of 267 amino acids and hypothetical *pI* of 6.61. The instability index was 43.03, ordering it

as not steady protein. The evaluated half-life in mammalian reticulocytes was 30 h, whereas in yeast and *Escherichia coli* is over twenty and 10 h, on an individual basis (Fig. 2A). Similarly, the CVL protein model was taken as a PDB format from the online protein data bank. CVL protein contains four chains in which chain 1 and 3 were the same and chain 2 and 4 were same as given with the amino acid details (Fig. 2B).

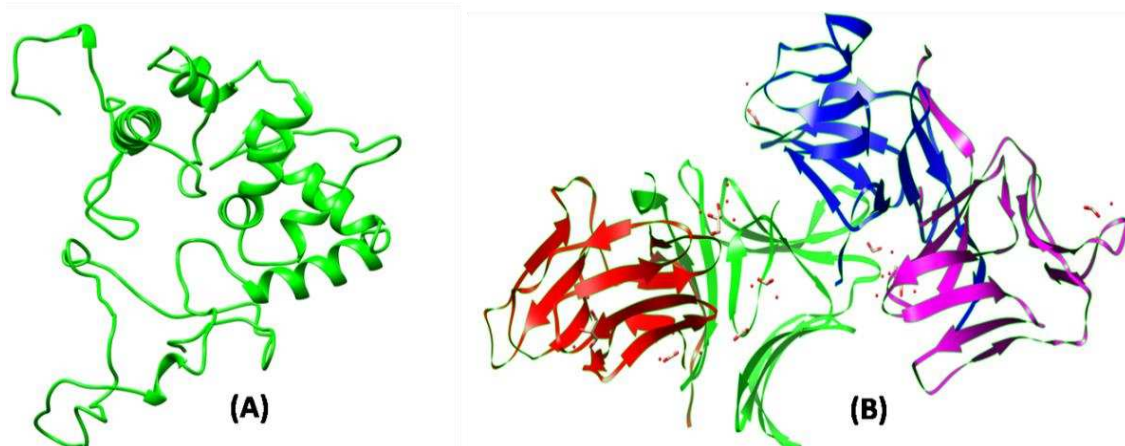


Figure 2. Three-dimensional protein models of (A) PVY coat protein and (B) CVL protein, predicted by I-TASSER. In (B), the red color chains present A chain, green shows B, magenta C and blue presenting D chain

Docking analysis of coat protein with CVL

The amino acids and molecules concerned in interchain H bonds, while not choosing any residue within the CP, were assessed utilizing the ZDOCK server. The interactions created through the ZDOCK server between CP and CVL protein are shown by the hydrogen bonds between the two proteins. Details of hydrogen bonds are given as in Tables 1 and 2.

Table 1. Hydrogen bonds between CP and CVL (A and C domain) obtained from PDBePisa. Interactions with a value less than 3.0 were considered to have highlighted bond distances

Sr. No.	CP	Dist. [Å]	CVL
1	:GLY 131 [N]	3.16	A: Tyr 76 [OH]
2	:Asn 130 [N]	2.94	A: Tyr 76 [OH]
3	:Tyr 185 [OH]	3.09	A: Ser 79 [O]
4	:Tyr 181 [OH]	2.73	A: Val 97 [O]
5	:Arg 184 [NH1]	3.83	A: Val 97 [O]
6	:Tyr 181 [N]	3.79	A: Tyr 100 [OH]
7	:Arg 189 [N]	3.03	A: Gly 101 [O]
8	:Tyr 181 [OH]	3.47	A: Val 97[N]
9	:Leu 187 [O]	3.11	A: Gly 101 [N]
10	:Ile 188 [O]	3.00	A: Tyr 87 [OH]
11	:Ala 224 [O]	3.20	A: Asn 81 [ND2]
12	:Ala 225 [O]	2.94	A: Asn 81 [ND2]
13	:Asp 254 [OD2]	2.56	A: Arg 84 [NH2]

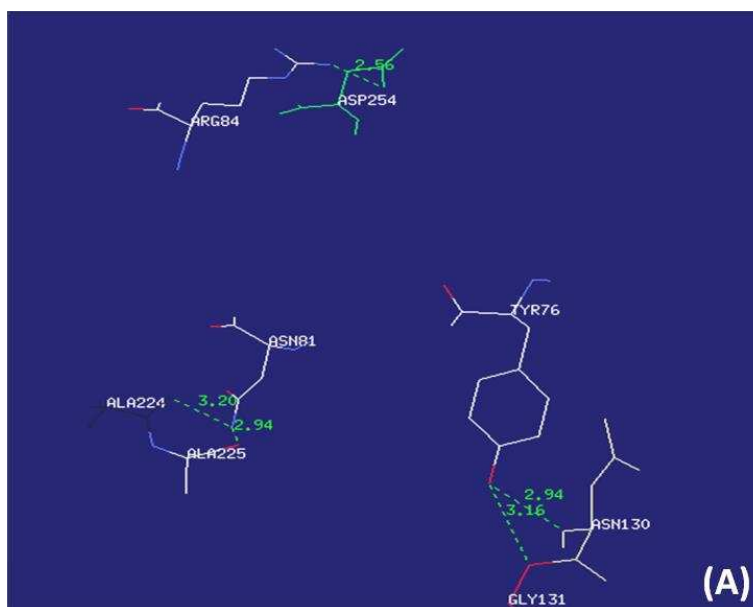
Table 2. Hydrogen bonds between CP and CVL (B and D domain) obtained from PDBePisa. Highlighted bond distances were considered as an interaction whose value was less than 3.0

Sr. No.	CP	Dist. [Å]	CVL
1	:Lys 177 [NZ]	3.76	B: Asn 1 [O]
2	:Lys 147 [NZ]	3.16	B: Asp 17 [OD2]
3	:Tyr 144 [OH]	2.58	B: Gln 57 [O]
4	:Val 134 [O]	3.84	B: Asn 1 [ND2]
5	:Tyr 181 [OH]	3.17	B: Arg 4 [N]
6	:Gly 138 [O]	3.71	B: Ser 12 [OG]
7	:Gly 138 [O]	3.61	B: Arg 62 [NH2]
8	:Glu 140 [[OE1]	3.72	B: Thr 72 [OG1]
9	:Asp 103 [OD1]	3.86	B: Leu 76 [N]

The two proteins interacted only through hydrogen bonds and no disulphide or covalent bonds were observed. The PDBePISA tool was utilized to locate the most effective interaction between coat protein and the two chains, i.e. chain A and B of CVL as mentioned before as CVL has four chains and chain 1 and 3 are same as chain 2 and 4. The outcomes demonstrated that various residues of the CP are predictable to act with the chain of CVL. In the case of A and C domain of CVL interaction with CP, totally 13 hydrogen bonds were observed from which three bonds, which are highlighted in *Table 1* has been shown in *Figure 3A*. In the case of B and D domain of CVL interacting with CP, totally 9 hydrogen bonds were observed from which two bonds, which are highlighted in *Table 2* has been shown in *Figure 3B*.

CVL protein purification and cytotoxic activity

CVL protein was purified through cation exchange chromatography using the column Hi Trap SP FF (GE Healthcare). On SDS-PAGE, two final fractions were obtained with their exchange profiles; one was of 10.5 kDa and the other fraction was about 11.5 kDa (*Fig. 4A and B*).



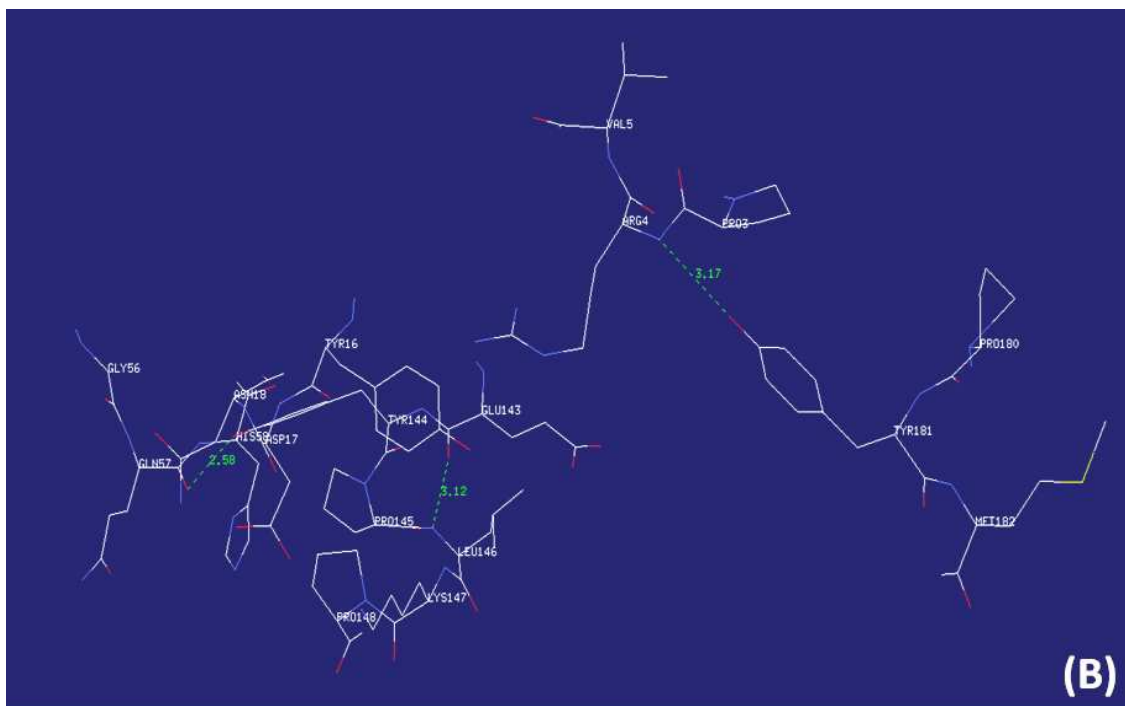


Figure 3. In-silico protein-protein docking analysis. **A** Interactions of CVL A and C chains with CP visualized by PDBViewer. Asn 130, Ala 225 and Asp 254 residues of CP were interacting with Tyr 76, Asn 81 and Arg84 residues of CVL. **B** Interactions of B and D chains of CVL with CP visualized by PDBViewer. Lys 147, Tyr 144 and Tyr 181 residues of CP were interacting with Asp 17, Gln 57 and Arg 4 residues of CVL

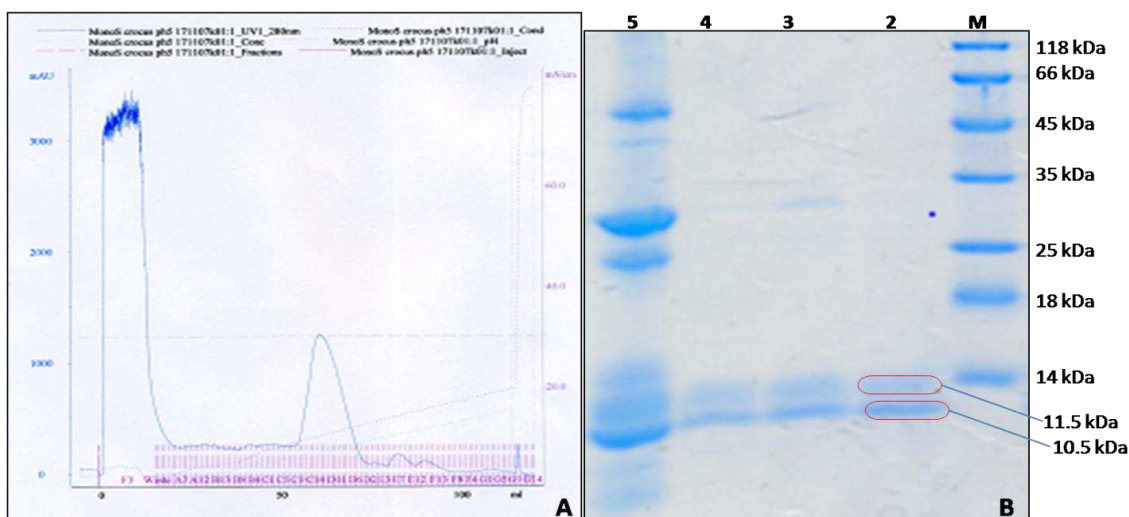


Figure 4. SDS PAGE shows purified fractions of the CVL. Lane 1: PageRuler™ unstained Protein Ladder (Catalog number: 26610); lane 2, 3 and 4: purified CVL fractions obtained after cation exchange chromatography; lane 5: crude CVL protein after desalting

The cytotoxic concentration that inhibited 50% of cell growth (CC50) showed that the CVL protein extract had the highest cytotoxicity with CC50 value of 770 µg/ml (Fig. 4). It was found that at 110 µg/ml CVL concentration, the cytotoxicity was

111.47%. Similarly, at 220, 330, 440, 550, 660 $\mu\text{g/ml}$ CVL concentrations, the cytotoxicity was recorded as 71.87, 62.39, 65.13 and 54.00% as compared to the control (Fig. 5).

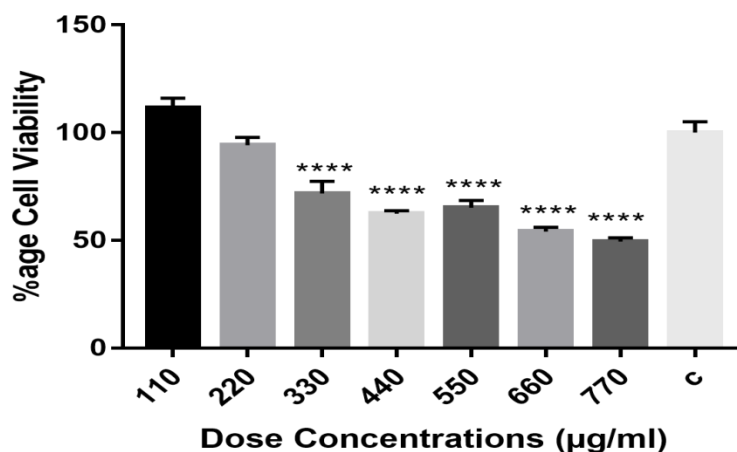


Figure 5. Cytotoxicity of CVL to reveal a safe dose limit. The dose concentration of CVL purified protein extracts was ranging between 110 - 770 $\mu\text{g/ml}$. Percentage cell survivals were calculated for each dose. Bars indicate the standard deviation. One-way ANOVA (see tables in the Appendix) shows the significant reduction of cell viability at the concentrations 330, 440, 550, 660 and 770 $\mu\text{g/ml}$ at $P < 0.0001$. Three biological replicated were processed to obtain data

Hemagglutination activity

The minimum concentration of purified CVL was observed at the end of the 1-h incubation period, which shows hemagglutination activity against the rabbit erythrocytes was high approximately 100 $\mu\text{g/ml}$ as described by Van Dam et al. (2000).

Antiviral activity of CVL purified fractions against CP-PVY

In the antiviral screening assay, the CVL purified fractions were found to be active against the CP-PVY in in-vitro assays. Briefly, 30 $\mu\text{g/ml}$ CVL displayed 98% inhibition of CP-PVY, 99% inhibition at 60 $\mu\text{g/ml}$, while up to 100% inhibition at 90 $\mu\text{g/ml}$ CVL concentration (Fig. 6). However, the control sample did not exhibit any inhibition of CP-PVY expression.

Discussion

Potato is central crop and it is rigorously affected by Potato Virus Y (PVY). The essential point of the present work was to utilize CVL to effectively build firm PVY-resistance in in-vitro assays. Lectins derived from different plants have shown the antiviral activity against different plant viruses (Lusvarghi and Bewley, 2016; Liu et al., 2014). CVL is a tetrameric protein comprising of four subunits with two chains of 10.5 kDa, while other two of 11.5 kDa and is capable of agglutinating the rabbit erythrocytes. Previous studies have shown that CVL and lectin from *C. sativus* has identical N-terminal sequences and moreover, CVL showed reasonable similarity with respect to the two domain lectins of tulip and *Arum maculatum*, which reinforce that the

CVL belongs to monocot mannose-binding lectins (Van Dam et al., 2000). There are numbers of pathogens, including bacteria, fungi, viruses and parasites through, which mannose binding lectins interact and provide protection against these to the host (Kilpatrick, 2002).

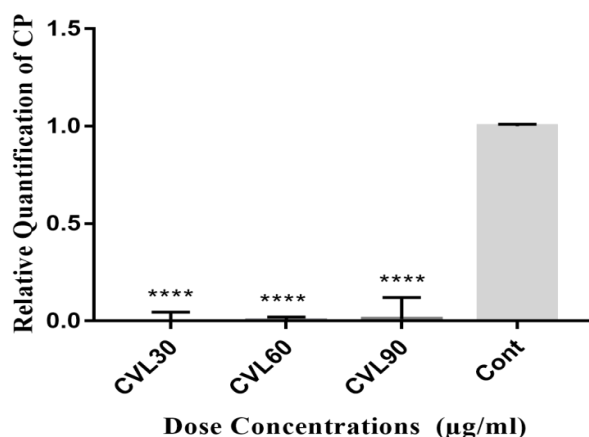


Figure 6. Real time PCR study of down regulation of CP-PVY against CVL. Antiviral activity of CVL dose against CP-PVY. Three dose concentrations of CVL were tested; 30, 60 and 90 µg/ml. Percent inhibition of CP-PVY mRNA was measured, bars in the graph depict the standard deviation, while a significant decrease in CP gene expression was observed in 30, 60 and 90 µg/ml at $P < 0.0001$

Protein docking refers to the scheming of three-dimensional (3D) structure of a protein initiating with the separate structures of protein subunits. The aim of protein docking is to know how proteins interact (Vitkup et al., 2001). Aloy and Russell stated that an estimate of 9 interaction partners are present for each protein and these interactions are one of around 10000 basic types, out of which only 2000 are known till date (Aloy and Russell, 2004) protein docking has emerged as a distinct computational field which make use of techniques and knowledge from diverse spectrum of science with the intention of formulating in silico how macromolecules like proteins act (Camacho et al., 2000). The in-silico protein-protein interaction showed that CP interact with the chain C and chain B of CVL. Our findings correlate with of Zhang et al. (2017b) who reported that Arg90 of *TMV* (tobacco mosaic virus) has a major role of interaction with the antiviral enantiomeric α -aminophosphonate derivatives for the loss of virus ability to cause infection. In a similar study, mannose binding lectin from *Lycoris radiata* indicated that Gln80, Asp82, Asn84 and Tyr88 are the main residues which are involved in the interaction with mannose (Zhu et al., 2013).

We adopted in-vitro assay to reveal the antiviral effect of CVL, which is based on transient expression of the CP gene in the mammalian cell line. Several reports support the adoption of in-vitro assay to screen potential plant extracts against plant viruses like Li et al. (2012) showed that tobacco mosaic virus (*TMV*) virions were transfected into HeLa cells to generate the expression of the CP gene of *TMV*. The possibility of plant capsid uptake and release in mammalian cells has been proposed in case of clover necrotic mosaic virus (*RCNMV*) by Lockney et al. (2011). In another study, 480 bp of CP from *PVY* was transfected into CHO cells and its mRNA knockdown assay was conducted with siRNA (Tabassum et al., 2011). Furthermore, plant viral capsids have

been used as vectors in mammalian cells for gene delivery and expression studies (Azizgolshani et al., 2013). More recently, *Arabidopsis* cryptochrome was successfully expressed in the HEK293T cells to produce a photochemically active product (Yang et al., 2016).

To reveal the activity of lectin (CVL), instead of full PVY virus particles, we cloned the CP gene as it is involved in the number of virus infection events like, uncoating and translation of the viral RNA, targeting the site of replication and in the transmission of potyviruses by vectors/aphids (Bol, 2008). There are some studies which clearly indicate involvement of CP transgene in creating resistance in transgenic potato crops (Bukovinszki et al., 2007; Gargouri-Bouzid et al., 2005).

The high antiviral effect of CVL protein fractions (up to 100% in our study) attributed the effectiveness of plant derived lectins in preventing notorious plant viruses like PVY. Plant lectins might show involvement in recognition of pathogenic microorganisms. Lectin from a soybean show high affinity for binding to β -glucan, which is a powerful PAMP of *Phytophthora* (Mithöfer et al., 2000). Similarly, spread of tobacco etch virus (TEV), a single-stranded RNA plant virus belonging to the genus Potyvirus is restricted by, the *Arabidopsis thaliana* restricted TEV movement 1 (RTM1) lectin gene (Whitham et al., 2000). Moreover, a jacalin-type lectin gene exhibits resistance to potexviruses which belong to family Potexviridae. This resistance is conferred in the early stage of infection caused by plant viruses as compared to another lectin RTM1 which shows resistance at an advanced stage of viral infection, implementing the vital role of lectin-mediated resistance in a multiplicity of plant-virus relation (Yamaji et al., 2012). Conclusively, we have reported the antiviral activity of lectin derived from *C. vernus* against potato virus Y. The purified fractions of CVL exhibited the strong antiviral effect against PVY. To the best of our knowledge, this is the first report on the antiviral activity of CVL against PVY. Furthermore, as results showing the maximum down regulation of the CP gene due to CVL, which clearly indicate that efficiency of the CVL against PVY. The genetic integration of lectin in the potato genome could provide complete protection from PVY in transgenic potato plants.

Conclusion

Lectins obtained from different plants have been shown to have antiviral activity against various plant viruses. The purified *Crocus vernus* lectin exhibited the strong antiviral effect against PVY. This is the first study of CVL's antiviral activity against PVY, as far as we know. Genetic incorporation of lectin into the genome of potatoes could provide comprehensive defense against PVY in transgenic potato plants.

Conflict of interests. The authors have no conflict of interests.

REFERENCES

- [1] Abbas, A., Amrao, L. (2017): Potato virus Y: an evolving pathogen of potato worldwide. – *Pakistan Journal of Phytopathology* 29: 187-191.
- [2] Aloy, P., Russell, R. B. (2004): Ten thousand interactions for the molecular biologist. – *Nature biotechnology* 22: 1317.

- [3] Azizgolshani, O., Garmann, R. F., Cadena-Nava, R., Knobler, C. M., Gelbart, W. M. (2013): Reconstituted plant viral capsids can release genes to mammalian cells. – *Virology* 441: 12-17.
- [4] Balzarini, J. (2007): Targeting the glycans of glycoproteins: a novel paradigm for antiviral therapy. – *Nature Reviews Microbiology* 5: 583.
- [5] Bol, J. F. (2008): Role of Capsid Proteins. – In: Uyeda, I., Masuta C. (eds.) *Plant Virology Protocols*. Humana Press, Totowa, NJ, pp. 21-31.
- [6] Bradford, M. M. (1976): A rapid and sensitive method for the quantitation of microgram quantities of protein utilizing the principle of protein-dye binding. – *Analytical Biochemistry* 72: 248-254.
- [7] Bukovinszki, Á., Divéki, Z., Csányi, M., Palkovics, L., Balázs, E. (2007): Engineering resistance to PVY in different potato cultivars in a marker-free transformation system using a ‘shooter mutant’ *A. tumefaciens*. – *Plant Cell Reports* 26: 459-465.
- [8] Callaway, A., Giesman-Cookmeyer, D., Gillock, E. T., Sit, T. L., Lommel, S. A. (2001): The multifunctional capsid proteins of plant RNA viruses. – *Annual Review of Phytopathology* 39: 419-460.
- [9] Camacho, C. J., Gatchell, D. W., Kimura, S. R., Vajda, S. (2000): Scoring docked conformations generated by rigid-body protein-protein docking. – *Proteins: Structure, Function, and Bioinformatics* 40: 525-537.
- [10] Davidson, E., Forrest, J. M. S., Morrison, I. M., Stewart, D. (1999): Mannose-specific plant lectins from plants as diagnostics, vaccines and tools for the elucidation of viral infection mechanisms in animals. – *Annual Report for the Scottish Crop Research Institute for 2000*, pp. 125-128.
- [11] Gargouri-Bouزيد, R., Jaoua, L., Mansour, R. B., Yemna, H., Malika, A., Radhouane, E. (2005): PVY resistant transgenic potato plants (cv Claustar) expressing the viral coat protein. – *Journal of Plant Biotechnology* 7: 1-6.
- [12] Golotin, V. A., Filshtein, A. P., Chikalovets, I. V., Kim, N. Y., Molchanova, V. I., Chernikov, O. V. (2019): Expression and purification of a new lectin from mussel *Mytilus trossulus*. – *Protein Expression and Purification* 154: 62-65.
- [13] Kilpatrick, D. C. (2002): Mannan-binding lectin: clinical significance and applications. – *Biochimica et Biophysica Acta (BBA)-General Subjects* 1572: 401-413.
- [14] Kitajima, E. W., De Ávila, A. C., Resende, R. O. (1997): Taxonomia de vírus de plantas. – *Fitopatologia Brasileira* 22: 5-24.
- [15] Lam, Y. W., Ng, T. B. (2001): A monomeric mannose-binding lectin from inner shoots of the edible chive (*Allium tuberosum*). – *Journal of protein chemistry* 20: 361-366.
- [16] Li, L. I., Wang, L., Xiao, R., Zhu, G., Li, Y., Liu, C., Yang, R., Tang, Z., Li, J., Huang, W., Chen, L. (2012): The invasion of tobacco mosaic virus RNA induces endoplasmic reticulum stress-related autophagy in HeLa cells. – *Bioscience Reports* 32: 171-184.
- [17] Liu, X. Y., Li, H., Zhang, W. (2014): The lectin from *Musa paradisiaca* binds with the capsid protein of tobacco mosaic virus and prevents viral infection. – *Biotechnology & Biotechnological Equipment* 28: 408-416.
- [18] Lockney, D. M., Guenther, R. N., Loo, L., Overton, W., Antonelli, R., Clark, J., Hu, M., Luft, C., Lommel, S. A., Franzen, S. (2010): The Red clover necrotic mosaic virus capsid as a multifunctional cell targeting plant viral nanoparticle. – *Bioconjugate Chemistry* 22: 67-73.
- [19] Lusvardi, S., Bewley, C. (2016): Griffithsin: an antiviral lectin with outstanding therapeutic potential. – *Viruses* 8: 296.
- [20] Mäki-Valkama, T., Pehu, T., Santala, A., Valkonen, J. P., Koivu, K., Lehto, K., Pehu, E. (2000): High level of resistance to potato virus Y by expressing P1 sequence in antisense orientation in transgenic potato. – *Molecular Breeding* 6: 95-104.
- [21] Mithöfer, A., Fliegmann, J., Neuhaus-Url, G., Schwarz, H., Ebel, J. (2000): The Hepta-?- Glucoside elicitor-binding proteins from legumes represent a putative receptor family. – *Biological Chemistry* 381: 705-713.

- [22] Muslim, S. N., Al-Kadmy, I., Auda, I. G., Ali, M., Naseer, A., Al-Jubori, S. S. (2018): A novel genetic determination of a lectin gene in Iraqi *Acinetobacter baumannii* isolates and use of purified lectin as an antibiofilm agent. – *Journal of AOAC International* 101: 1623-1630.
- [23] Rehman, S., Ashfaq, U. A., Riaz, S., Javed, T., Riazuddin, S. (2011): Antiviral activity of *Acacia nilotica* against Hepatitis C Virus in liver infected cells. – *Virology journal* 8: 220.
- [24] Singh, R. S., Walia, A. K., Kennedy, J. F. (2018): Purification and characterization of a mitogenic lectin from *Penicillium duclauxii*. – *International Journal of Biological Macromolecules* 116: 426-433.
- [25] Sreeramulu, B., Arumugam, G., Paulchamy, R., Karuppiyah, H., Sundaram, J. (2018): β -Galactoside binding lectin from caddisfly larvae, *Stenopsyche kodaikanalensis* with selective modes of antibacterial activity: purification and characterization. – *International Journal of Biological Macromolecules* 115: 1033-1045.
- [26] Tabassum, B., Nasir, I. A., Husnain, T. (2011): Potato virus Y mRNA expression knockdown mediated by siRNAs in cultured mammalian cell line. – *Virologica Sinica* 26: 105-113.
- [27] Tabassum, B., Nasir, I. A., Khan, A., Aslam, U., Tariq, M., Shahid, N., Husnain, T. (2016): Short hairpin RNA engineering: in planta gene silencing of potato virus Y. – *Crop Protection* 86: 1-8.
- [28] Van Damme, E. J., Astoul, C. H., Barre, A., Rougé, P., Peumans, W. J. (2000): Cloning and characterization of a monocot mannose-binding lectin from *Crocus vernus* (family Iridaceae). – *European Journal of Biochemistry* 267: 5067-5077.
- [29] Vitkup, D., Melamud, E., Moul, J., Sander, C. (2001): Completeness in structural genomics. – *Nature Structural & Molecular Biology* 8: 559.
- [30] Whitham, S. A., Anderberg, R. J., Chisholm, S. T., Carrington, J. C. (2000): Arabidopsis RTM2 gene is necessary for specific restriction of tobacco etch virus and encodes an unusual small heat shock-like protein. – *The Plant Cell* 12: 569-582.
- [31] Yamaji, Y., Maejima, K., Komatsu, K., Shiraiishi, T., Okano, Y., Himeno, M., Sugawara, K., Neriya, Y., Minato, N., Miura, C., Hashimoto. (2012): Lectin-mediated resistance impairs plant virus infection at the cellular level. – *The Plant Cell* 24: 778-793.
- [32] Yang, L., Wang, X., Deng, W., Mo, W., Gao, J., Liu, Q., Zhang, C., Wang, Q., Lin, C., Zuo, Z. (2016): Using HEK293T expression system to study photoactive plant cryptochromes. – *Frontiers in Plant Science* 7: 940.
- [33] Ynalvez, R. A., Cruz, C. G., Ynalvez, M. A. (2015): Isolation, partial purification and characterization of Texas live oak (*Quercus fusiformis*) lectin. – *Advances in Bioscience and Biotechnology* 6: 470.
- [34] Zhang, W., van Eijk, M., Guo, H., van Dijk, A., Bleijerveld, O. B., Verheije, M. H., Wang, G., Haagsman, H. P., Veldhuizen, E. J. (2017a): Expression and characterization of recombinant chicken mannose binding lectin. – *Immunobiology* 222: 518-528.
- [35] Zhang, W., Li, X., Zhang, G., Ding, Y., Ran, L., Luo, L., Wu, J., Hu, D., Song, B. (2017b): Binding interactions between enantiomeric α -aminophosphonate derivatives and tobacco mosaic virus coat protein. – *International Journal of Biological Macromolecules* 94: 603-610.
- [36] Zhu, Q. K., Zhu, M. L., Zou, J. X., Feng, P. C., Fan, G. T., Liu, Z. B., Wang, W. J. (2013): Molecular modeling and docking of mannose-binding lectin from *Lycoris radiata*. – *Chemical Research in Chinese Universities* 29: 1153-1158.

APPENDIX

Table Analyzed	Data 1									
Data sets analyzed	A : CVL30	B : CVL60	C : CVL90	D : Cont						
ANOVA summary										
F	207.9									
P value	<0.0001									
P value summary	****									
Significant diff. among means (P < 0.05)?	Yes									
R square	0.9873									
Brown-Forsythe test										
F (DFn, DFd)										
P value										
P value summary										
Are SDs significantly different (P < 0.05)?										
Bartlett's test										
Bartlett's statistic (corrected)										
P value										
P value summary										
Are SDs significantly different (P < 0.05)?										
ANOVA table										
	SS	DF	MS	F (DFn, DFd)	P value					
Treatment (between columns)	2.23	3	0.7432	F (3, 8) = 207.9	P<0.0001					
Residual (within columns)	0.0286	8	0.003575							
Total	2.258	11								
Data summary										
Number of treatments (columns)	4									
Number of values (total)	12									
Number of families	1									
Number of comparisons per family	3									
Alpha	0.05									
Dunnett's multiple comparisons test										
	Mean Diff.		95.00% CI of diff.		Significant?	Summary		Adjusted P Value		D-?
Cont vs. CVL30	0.9988		0.8582 to 1.139		Yes	****	0.0001	A	CVL30	
Cont vs. CVL60	0.9986		0.858 to 1.139		Yes	****	0.0001	B	CVL60	
Cont vs. CVL90	0.9889		0.8483 to 1.129		Yes	****	0.0001	C	CVL90	
Test details										
	Mean 1	Mean 2	Mean Diff.	SE of diff.	n1	n2	q	DF		
Cont vs. CVL30	1	0.001217	0.9988	0.04882	3	3	20.46	8		
Cont vs. CVL60	1	0.001426	0.9986	0.04882	3	3	20.45	8		
Cont vs. CVL90	1	0.01111	0.9889	0.04882	3	3	20.26	8		

Table Analyzed Data 1

Data sets analyzed A : 110 B : 220 C : 330 D : 440 E : 550

ANOVA summary

F 113.8
 P value <0.0001
 P value summary ****
 Significant diff. among means (P < 0.05)? Yes
 R square 0.9803

Brown-Forsythe test

F (DFn, DFd)
 P value
 P value summary
 Are SDs significantly different (P < 0.05)?

Bartlett's test

Bartlett's statistic (corrected)
 P value
 P value summary
 Are SDs significantly different (P < 0.05)?

ANOVA table	SS	DF	MS	F (DFn, DFd)	P value
Treatment (between columns)	11026	7	1575	F (7, 16) = 113.8	P<0.0001
Residual (within columns)	221.5	16	13.84		
Total	11247	23			

Data summary

Number of treatments (columns) 8
 Number of values (total) 24
 Number of families 1
 Number of comparisons per family 7
 Alpha 0.05

Dunnnett's multiple comparisons test

	Mean Diff.	95.00% CI of diff.	Significant?	Summary	Adjusted P Value	H-?
c vs. 110	-11.48	-20.36 to -2.593	Yes	**	0.0091 A	110
c vs. 220	5.825	-3.058 to 14.71	No	ns	0.2967 B	220
c vs. 330	28.13	19.24 to 37.01	Yes	****	0.0001 C	330
c vs. 440	37.61	28.72 to 46.49	Yes	****	0.0001 D	440
c vs. 550	34.86	25.98 to 43.75	Yes	****	0.0001 E	550
c vs. 660	45.99	37.11 to 54.88	Yes	****	0.0001 F	660
c vs. 770	50.58	41.7 to 59.46	Yes	****	0.0001 G	770

Test details	Mean 1	Mean 2	Mean Diff.	SE of diff.	n1	n2	q	DF
c vs. 110	100	111.5	-11.48	3.038	3	3	3.778	16
c vs. 220	100	94.17	5.825	3.038	3	3	1.917	16
c vs. 330	100	71.87	28.13	3.038	3	3	9.258	16
c vs. 440	100	62.39	37.61	3.038	3	3	12.38	16
c vs. 550	100	65.14	34.86	3.038	3	3	11.47	16
c vs. 660	100	54.01	45.99	3.038	3	3	15.14	16
c vs. 770	100	49.42	50.58	3.038	3	3	16.65	16

DIFFERENTIAL ROLES FOR DOPAMINE D1-LIKE AND D2-LIKE RECEPTORS IN LEARNING AND BEHAVIOR OF HONEYBEE AND OTHER INSECTS

RAZA, M. F.^{1,2} – SU, S.^{1*}

¹*College of Animal Sciences (College of Bee Science), Fujian Agriculture and Forestry University, Fuzhou, China*

²*College of Life Sciences, Fujian Agriculture and Forestry University, Fuzhou 35002, China*

**Corresponding author*

e-mail: susongkun@zju.edu.cn; phone: +86-136-6500-5782

(Received 9th Sep 2019; accepted 4th Dec 2019)

Abstract. Biogenic amines and neuropeptides are important neurotransmitters and modulators in the peripheral and central nervous systems of several invertebrate species. Biogenic amines play essential roles in modulating physiological and behavioral processes as neuromodulators, neurotransmitters, and neurohormones. Biogenic amines such as octopamine, dopamine, tyramine, or even serotonin can act as slow neuromodulator or fast transmitters. In both invertebrates and vertebrates, dopamine found in the central nervous system. Dopamine receptors (D1-like family - D1, D5) and (D2-like family- D2, D3, D4) directly modulate and regulate other neurotransmitters, the release of cyclic adenosine monophosphate (cAMP), differentiation, and cell proliferation. Here, we highlighted the essential role of dopamine and dopamine receptors in the control of cognition, locomotion, attention, memory formation, and behavioral plasticity in the central nervous system (CNS). In CNS, D1-like and D2-like are the most abundant dopamine receptors. Dopamine receptors contribution in several aspects of motor function, cognition besides reinforcement/reward and complex behavior. Behavioral and mental diseases associated with major neurotransmission disruptions of dopamine as well as hyperactivity/attention-deficit disorder, schizophrenia, substance abuse, and Huntington's disease cause a major neuropsychological deficiency in attention, memory, and learning besides to other major symptoms.

Keywords: *biogenic amines, honeybee, memory, receptors, olfactory learning*

Introduction

In numerous social insects, such as bees and ants, biogenic amines perform decisive roles in the regulation of sociality. How biogenic amines (BA) and their receptors in ancestral, most of the solitary species have been chosen during the change to control different behaviors in complex social species are discussed by Kamhi et al. (2017). Biogenic amines are vital messenger elements in the central nervous system (CNS) and the peripheral area of invertebrates and vertebrates. Honeybee, *A. mellifera*, is outstandingly appropriated to reveal the biogenic amines functions in behavior, as long as it has wide-ranging behavioral capabilities, in this insect, there are a lot of biogenic amine receptors (Scheiner et al., 2006). Biogenic amines are involved in coordinating responses related to metabolic reactions, for instance, starvation. Whenever there exist starve d rate-limiting enzyme tyrosine- β -hydroxylase mutant fruit flies, octopamine cannot be synthesized, having higher concentrations of glucose level in their hemolymph compared to controls, as revealed by Li et al. (2017). Damrau et al. (2018) investigated starvation or fat deposition resistance by using fruit flies defective in the expression of tyramine and octopamine receptors. Their tissue-specific RNAi experiments showed a very complicated interorgan transmission resulting in various

metabolic phenotypes in tyramine and octopamine lacking fruit flies. Stocker et al. (2018) reported the comparison of the axon terminals of octopaminergic efferent ventral and dorsal median unpaired neurons in whether fruit flies or desert locusts throughout skeletal muscles, exposing numerous similarities. For both octopamine and tyramine, type II terminals are immunopositive and dissimilar to the type I terminals that have visible synaptic blades, and they comprise of dense-core vesicles. They revealed that hunger modulates the neuromuscular-branched morphology in a time-based manner. In this mini-review, we discuss the role of dopamine (DA) receptors to regulate the behavior in honeybee and other insects and summarize the role of dopamine, types, physiology, and genes of dopamine receptors.

Moreover, the authors confirmed that the delivery of octopamine from axonal and dendritic type II terminals applies parallel to synaptic machinery to glutamate allow from excitatory motor neurons (type I terminals). Buckemüller et al. (2017) examined changes in glucose concentration level in hemolymph, feeding, and survival behaviors after hunger and studied the role of octopamine on these pharmacological experiments. Their experiments confirmed that octopamine in honeybee performs similarly to noradrenalin and adrenalin in mammals in modulating an animal's counter-regulatory response. The study evaluates different types of octopamine and tyramine receptors that might be involved in energy homeostasis. Many neurons that mediate the release of octopamine belong to the class median dorsal unpaired neurons, and their electrical qualities in cockroaches have been widely investigated by Lapied et al. (2017). Scheiner et al. (2017) reported the role of the fat body in regulating gustatory sensitivity accomplished by tyramine signaling in many behavioral races of the honeybee. Their findings proposed that distinctive tyramine signaling in the fat body play an essential role in the adaptability of labor division by modulating gustatory responsiveness (*Fig. 1*).

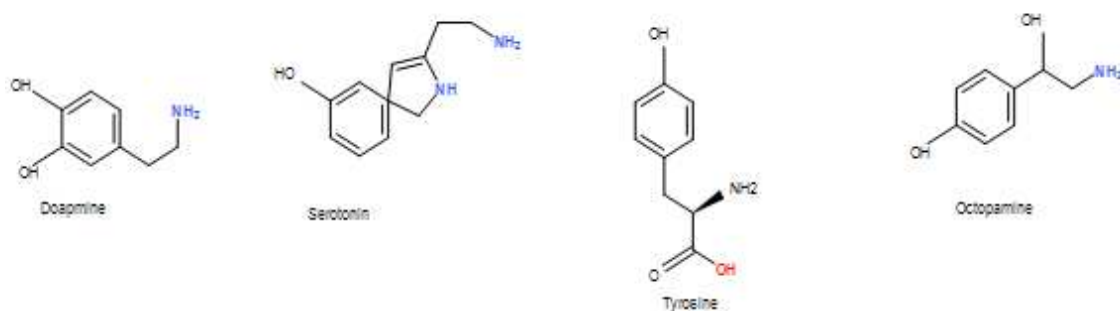


Figure 1. Chemical structure of each monoamine

Blenau et al. (2017) disclosed the fifth serotonin receptor in *Drosophila melanogaster* that is Dm5-HT2B. Besides that, three Dm5-HT7, Dm5-HT1B, and Dm5-HT1 along with the Dm5-HT2A and cyclic adenosine monophosphate (cAMP) signaling cascades directing toward Ca²⁺ signaling mechanism through ITP. Authors also reported that this important fifth receptor is concerned with immune system function and controlling heartbeat, and it can be aggravated by mianserin and metoclopramide. The circulation of immune reactivity for receptor molecules-AmTyr1 and tyramine has been reported by Sinakevitch et al. (2017) for the brain of the honeybee, and specific significance is positioned on neuropils related to olfactory sensation learning and memory (*Fig. 2*). They emphasized two important Ventral (Unpaired) median neurons of the suboesophageal ganglion belong to axons that arise to the bee's brain and stimulate the

antennal lobe (AL) and mushroom body (MB) calyx. Remarkably, AmTyr1 expression was initiated in pre-synaptic positions of olfactory receptor neurons (ORN) and projection neurons, maximum prospective to apply for the inhibitory mechanism of neurotransmitter (Chemical messenger) release.

There is adding confirmation that octopamine and tyramine use opposite performances in insects. Their investigation upon *Drosophila melanogaster* (fruit fly) flight behavior, revealed the role and importance of tyramine and an enzyme-dehydrogenase/reductase for tyramine catabolism. This enzyme is found in the specific glial cells group, which is placed near the border of motor neuropil and through continuations toward the motor neuropil of flight. Whenever RNAi knocks down this enzyme, flight time is decreased, which is distinctive for high tyramine levels and blocked octopamine. This study also explores critical signaling pathways for tyramine (Ryglewski et al., 2017).

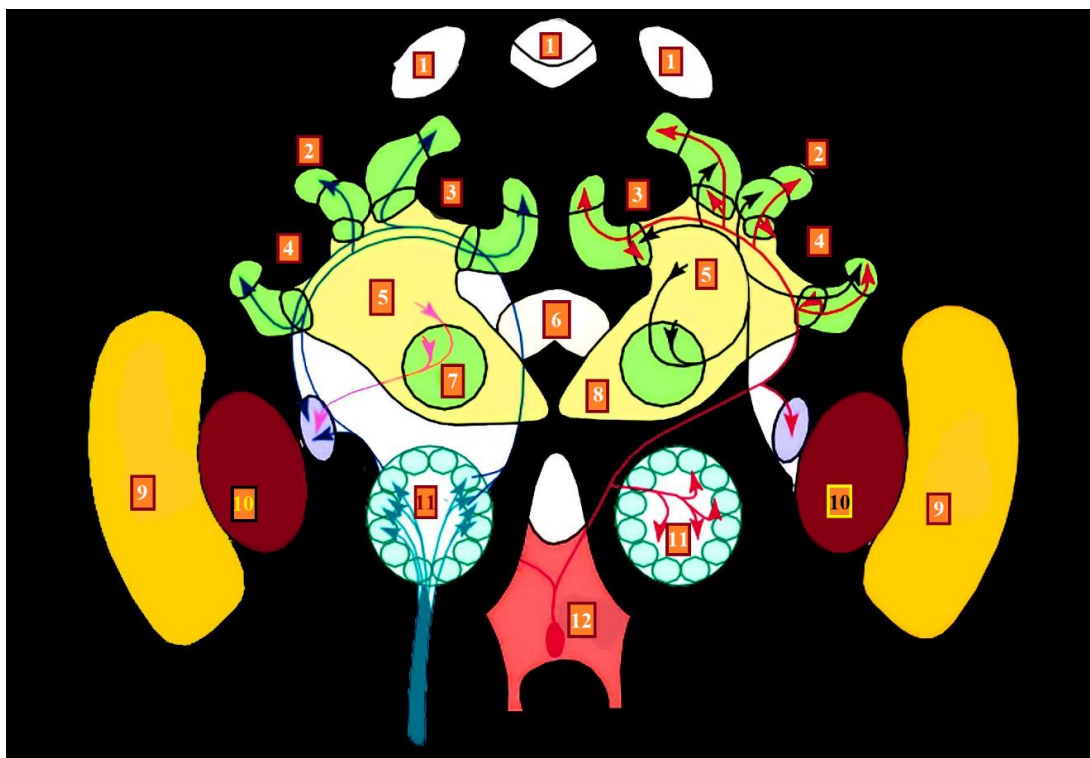


Figure 2. Schematic diagram of adult honeybee brain (frontal view). (1) Ocelli, (2) Mushroom bodies, (3) medial calyx, (4) lateral calyx, (5) peduncle, (6) central brain, (7) alpha lobe (α ; vertical lobe), (8) beta lobe (β); medial lobe), (9) medulla, (10) lobula, (11) antennal lobe, (12) suboesophageal ganglion., projection neurons (blue), VUMmx1 (red), an inhibitory feedback loop (black), indirect input from the mushroom body to lateral protocerebrum (also called lateral horn, violet). (Source: Grünewald, 1999; Barron et al., 2015)

Role of dopamine and dopamine receptors

Berke (2018) described that dopamine transfer's motivational significance and encourages movement activity even at seconds time scales. They also reported that, is dopamine a signal for motivation or signal for learning, or both? Our knowledge about dopamine has modulated in the previous and is fluctuating once again. One essential and distinctive is between dopamine effects on future learning behavior and current

performance behavior. Both kinds of behavior are significant and real, but sometimes one was in favor, and other was not. DA is a critical vital learning and motivation modulator. Dopamine receptors (D1-like, D2-like) are classified into two significant subfamilies. Dopamine is a major neurotransmitter that facilitates physiological tasks in both the peripheral and central nervous system (CNS) via relating to DA cell surface receptors. Dopamine receptors (D1-like, D2-like) are classified into two significant subfamilies. Dopamine is a major neurotransmitter that facilitates physiological tasks in both the peripheral and central nervous system (CNS) via relating to DA cell surface receptors. DA receptors are G-protein coupled receptors (GPCRS) that are categorized into (D1-like, D2-like) receptors based on their physiological, pharmacological, and biochemical effects (Fig. 3).

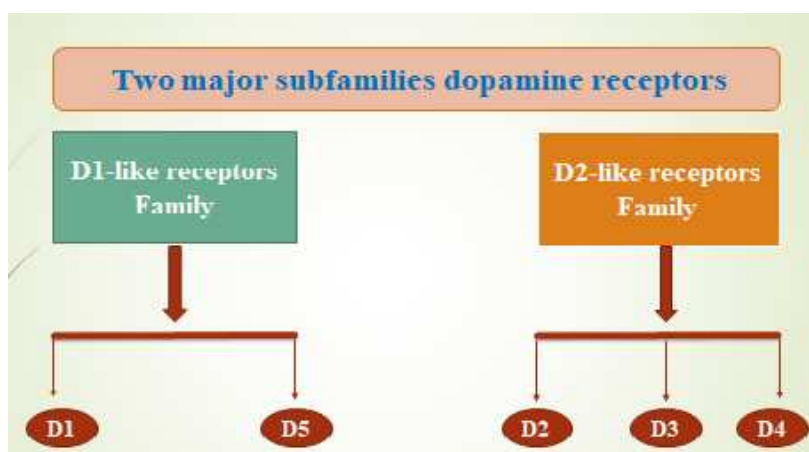


Figure 3. Dopamine receptors are divided in to two major subfamilies: D1-like and D2-like

Physiology of dopamine receptors

The biogenic amines (BA) of serotonin, dopamine, tyramine, and octopamine in the honeybee modify neuronal tasks in numerous ways. Serotonin and dopamine are present in the bee brain at high concentrations. Additionally, tyramine and octopamine are a small quantity. Octopamine is a critical molecule to regulate the behavior of honeybee. It usually has a stimulating effect and results in increasing the sensitivity of sensory inputs, improve learning efficacy, and better foraging behavior. Tyramine has been recommended to act as an inhibitor to octopamine, but only limited experimental data are available for this amine. Serotonin and Dopamine often have inhibitory effects in comparison with octopamine. Scheiner et al. (2006) reported the role of BA and biogenic amines receptor-mediated cellular responses regulating distinct behavior involved in learning performance and labor division. Biogenic amines (BA) bind to membrane receptors that belong primarily to big GTP-binding (G) protein gene family combined with receptors. The behavioral function, the regional brain expression, selective antagonists, selective agonists, and mechanism of action of various types of dopamine receptors are outlined in (Table 1; Mishra et al., 2018).

Significant differences are produced in the concentration of Inositol trisphosphate receptor (IP3), (cAMP), and Ca²⁺ in intracellular Second messenger levels. Besides, several honeybee (BA) receptors have been characterized and cloned recently; still, several genes remained to be recognized. The approachability of the fully sequenced *Apis mellifera* genome will make a significant contribution in bridging this gap in Table 2.

Table 1. Perspective and knowledge of different dopamine receptors

Receptors	Location	Type	Mechanism	Function	Selective agonist	Selective antagonist
D1	Olfactory bulb Nucleus accumbens Striatum Amygdala Hippocampus Frontal cortex Substantia nigra Hypothalamus	Gs-coupled	Enhanced intracellular cAMP through activated adenylate cyclase	Attention Learning Locomotion Sleep Impulse control Regulation of renal function Memory	SKF-81297 SKF-38393 Fenoldopa (SKF-82526)	SCH-39166 SKF-83566 SCH-23390
D5	Hypothalamus Substantia nigra Cortex	Gs-coupled	Adenylate cyclase	Motor Learning Cognition Decision Making Renin Secretion		
D2	VTA Olfactory bulb Striatum Cerebral cortex	Gi-coupled	Increased level of cAMP intracellular by activating adenylate cyclase	Reproductive behavior Locomotion Sleep Attention	Bromocriptine Pergolide Cabergoline Ropinirole	Haloperidol Raclopride Sulpiride Spiperone Risperidone
D3	Cortex Islands of Calleja Striatum	Gi-coupled		Locomotion Regulation of food intake Impulse control Cognition	Nafadotride GR-103691 GR-218231 SB-277011A NGB-2904 PG-01037 ABT-127	7-OH-DPAT Pramipexole Rotigotine PD-128907
D4	Hypothalamus Amygdala Frontal cortex Nucleus accumbens	1- Gi-coupled		Attention Impulse control Reproductive behavior	A-381393 FAUC213L-745870L-750667	A-412997 ABT-670 PD-168077

Table 2. The role of dopamine receptors genes of vertebrate and invertebrate

Gene ID	Gene name	Organisms	Function	References
1621	Dopamine beta-hydroxylase	<i>Homo sapiens</i>	Plays a dominant role in the process of converting dopamine into norepinephrine (NE)	Tang et al., 2018
37867	Dopamine N acetyltransferase	<i>Drosophila melanogaster</i>	Encodes an enzyme that is identified to show a part in the insect pigmentation pathway	Ahmed-Braimah and Sweigart, 2015
406111	Dopamine receptor, D1	<i>Apis mellifera</i>	Regulating behavioral plasticity in the honey bee	McQuillan et al., 2012 a; Elsik et al., 2014
408995	D2-like dopamine receptor	<i>Apis mellifera</i>	Cognition, impulse, locomotion, control, attention	Mishra et al., 2018
41726	Dopamine 1-like receptor 1	<i>Drosophila melanogaster</i>	Memory formation for aversive and appetitive learning	Swenson et al., 2016
25432	Dopamine receptor D4	<i>Rattus norvegicus</i>	Modulates fear expression	Vergara et al., 2017
43484	Dopamine 1-like receptor 2	<i>Drosophila melanogaster</i>	For initiating biochemical cascades underlying olfactory learning.	Swenson et al., 2016
1816	Dopamine receptor D5	<i>Homo sapiens</i>	Tumor and cancer treatment	Leng et al., 2017
13491	Dopamine receptor D4, Drd4	<i>Mus musculus</i>	Social interaction, novelty-seeking, increased anxiolytic and exploratory behavior, alcohol binge	Thanos et al., 2015

Types of dopamine receptors

Dopamine receptors are five distinct kinds (D1, D2, D3, D4, and D5), all receptors, coupled with G-proteins. These subtypes are categorized into two significant classes

(D1 like receptors and D2 like receptors). D1 like receptors are excitatory and post-synaptic. D2 like receptors are inhibitory, pre-synaptic, and post-synaptic. (Rang HP, 2006) summarized the overview of activation of each receptor type, follow the comparison of kinds and function of dopamine receptors, and Under comparison of the kinds and tasks of dopamine receptors, it is possible to determine how the dopaminergic system unique built-in phyla. Ferreri et al. (2019) demonstrated that dopamine role is related to the pleasure of music experience. They orally controlled each contributor, a dopamine antagonist (risperidone), a placebo (lactose), and a dopamine precursor (levodopa) in three separate sessions, according to their results, risperidone and levodopa led to a conflicting response in trials of motivation and musical pleasure. Although the placebo compared with dopamine precursor levodopa, improved the cognitive experience and motivational responses associated with music, but risperidone result decreased in both. Shows a vital function musical pleasure of dopamine and specifies that dopaminergic transmission could play a distinct role.

In recent studies, (Beggs and Mercer (2009) found that Queen mandibular pheromone produced by the queen is used to control the physiology and behaviors of their colony individual. Homovanillyl alcohol is one of the significant components of Queen mandibular pheromone QMP in blocking aversive learning in young working bees. Homovanillyl alcohol (HVA) was found to reduce the concentration of brain dopamine and modify the intracellular cAMP concentration in the centers of the brain concerned with learning and memory. They investigated that HVA directly interacts with the bee's dopamine receptor, also HVA activates AmDOP3 (D2-like dopamine receptor) selectively. They suggested a specific molecular system through which dopamine signaling pathways can be modulated. *Apis mellifera* dopamine receptor (DOP3) induced blockage of aversive learning in worker bees is caused by HVA (Beggs and Mercer, 2009).

In a study on *Apis mellifera* brain, Lerner et al. (1995) observed that expression of amino-receptors varies significantly throughout Kenyon cell subpopulations. In present models of mushroom body function, differential expression of amine-receptor genes in neurons and plasticity that exists at this stage are mainly ignored characteristics. Their findings are consistent with confirmation that short-term and long-term sensory memories formed in distinct parts of the brain's mushroom bodies and there are efficient parts of the brain center (McQuillan et al., 2012 b). They illustrated the role of gene expression in reproductive organisms of male honeybee are throughout the sexual development and maturation. Dopamine is a distinct operator between three reproductive systems and CNS. They also suggested that in seminal vesical of honeybee brain, 20 dopamine receptors can be used to drive dopamine (DA) for reproduction and 21 receptors involved in storage and sperm transfer in the reproductive organ of males (Matsushima et al., 2019).

In these studies, they investigated specific caste development of the dopaminergic system in female honeybees during metamorphosis. Caste-specific changes by dopaminergic systems in social insects help to continue caste-specific behavior. Their findings showed that the developmental procedure of caste-specific dopaminergic systems in honey bee during metamorphosis recommends caste-specific behavior and reproduction division in this greatly eusocial species (Sasaki et al., 2018).

Mustard et al. (2010) investigated that dopamine and D1-like receptors (AmDOP2) cause regulation of motor behavior in the honeybee. Assessing the particular molecular pathways by which dopamine impacts behavior complexed by the involvement of

various subtypes of dopamine receptors linking distinct second messenger pathways. Spontaneous movements of adult bees in the field were used to explore the role of dopamine signaling in modulating the behavior of honeybee. A significant difference between control and treated bees was observed for many behaviors such as flying, grooming, fanning, stopped walking and upside down. Finally, their findings established that DA plays a significant role in modulating the motor behavior of the *Apis mellifera* (Mustard et al., 2010).

Kokay and Mercer (1997) found the developmental changes in densities of dopamine receptors and the measurement of dopamine levels in the honeybee brain. Their findings confirmed the expression of dopamine receptor subtype-specific patterns in insect brain and illustrated that D1 and D2-like receptors are not only expressed in the adult bees CNS, as well as during bee's brain developmental stages (Fig. 4)

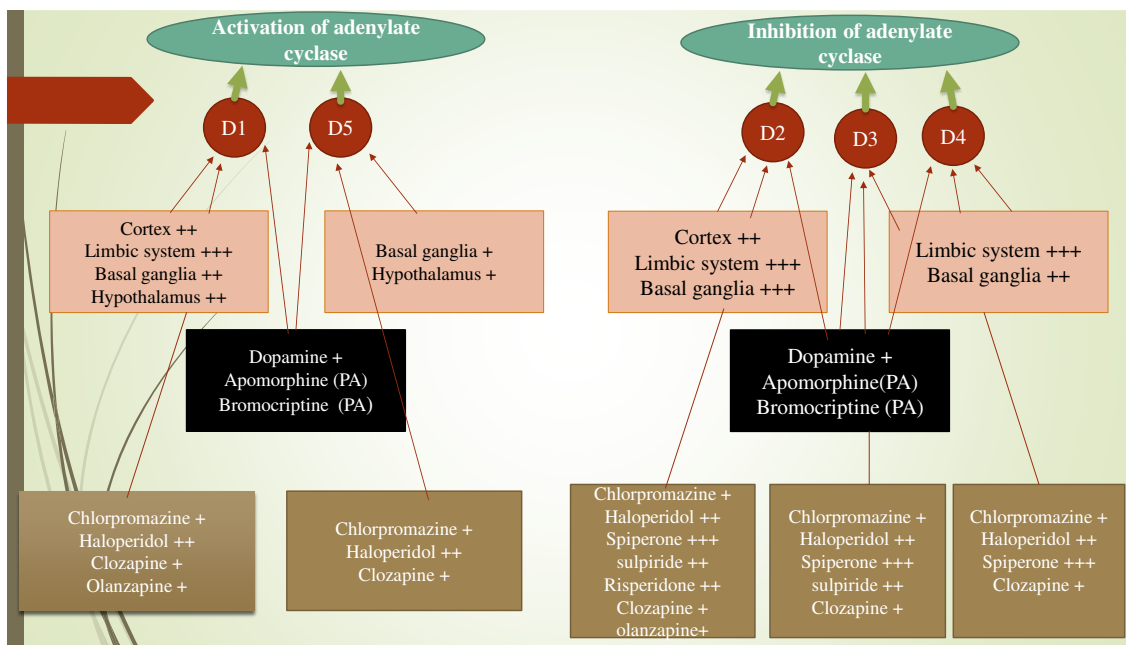


Figure 4. Expression of dopamine receptor

Role of dopamine in insects

Locusta migratoria (migratory locust), showed incredible phenotypic adaptability in response to the population density variation at morphological, physiological, and cognitive levels. In migratory locust, two dopamine (Dop1 and Dop2) receptors play distinct roles in developmental changes. DA and dopamine genes in metabolic pathways facilitate phase modification in *L. migratoria*. They proved that dopamine (Dop1 and Dop2) controlled locust phase variation in two various directions (Guo et al., 2015).

The significant role of dopamine being strengthening and processing is applied in a range of species varying from *Homo sapiens* to *Drosophila melanogaster*, while D1 receptors have been recognized to make a significant contribution to fruit flies' aversive odor sensitivity learning. Scholz-Kornehl and Schwartzel (2016) revealed that D2 receptors endorsed to facilitate a combined type of odor memory referred to as anesthesia-resistant learning and memory. Observing the distinct role of dopamine and dopamine receptor (D2R) in "forgetting"(retroactive role of dopamine), balancing,

acquisition of memory (the proactive task of dopamine) and dopamine release, their findings recommended D2R as the crucial player of each process (Scholz-Kornehl and Schwärzel, 2016). Ichinose et al. (2017) analyzed the function of dopaminergic neurons in the fruit fly brain, and how they influence the animal's internal condition/cognitive behavior. Dopamine might play both roles, a slow neuromodulator, a fast neurotransmitter. It depends on the postsynaptic neuron. Genetic modification of dopamine neuron activity resulted in differences in the fly's behavior. Behaviors such as learning and memory, sexual drive, sleep, and hunger were affected (Ichinose et al., 2017).

Zhukovskaya and Polyanovsky (2017) studied the effects of various amines such as octopamine, tyramine, dopamine, and serotonin on olfactory and gustatory receptor neurons in insect antennae. Many amines systemically released into the hemolymph, an open circulatory system in insects, supplied different body compartments, the dorsal or ventral cavity, the muscles, the central nervous system, and so on.. The authors suggest that the antenna may be a partially autonomous hemolymph compartment separated from other body parts. An important aspect of chemical signaling is that all transmitters, whether they be classical transmitters, neuromodulators, or hormones, can only act through their respective receptor molecules. Depending on which receptor type activated, different signaling cascades can be triggered. In this issue, some articles devoted to receptors. Niens et al. (2017) showed that in the fruit fly, imbalances between dopamine and serotonin are modeled. Like in rodents, a lack of dopamine leads to increased levels of 5-HT and arborizations in specific brain neuropils.

Conversely, increased dopamine levels lead to reduced connectivity of 5-HT neurons., both neurons, dopamine, and 5-HT play an essential role in learning behavior. Dopamine signaling is critical for mediating reinforcing properties of unconditioned stimuli during associative learning. Tedjakumala et al. (2017) characterized dopaminergic neurons in the honeybee brain by immune reactivity distribution of dopamine precursor enzyme, tyrosine-hydroxylase. They also describe new clusters of dopaminergic neurons. Sun et al. (2018) studied startle-induced locomotion and the activity of specific clusters of dopaminergic neurons afferent to the mushroom bodies.

Conclusion

Receptors of dopamine (DA) have a crucial role in a broad range of behavior, such as motor function, sensory processing, arousal, and reward. In this way, abnormal dopamine signaling is correlated with many psychiatric and neurological disorders. Comprehension of the pathways through which DA neurotransmission motivates intracellular signaling mechanisms, that behavior modulation can provide essential insights for the development of specific therapeutics. Since these general themes begin to emerge, a lot of work needs to be done to distinguish the particular signaling mechanisms of DA receptors in simple model organisms.

This mini review also contributes toward an emerging picture of the brain circuits modulating locomotor reactivity that appear to both overlaps and differ from those mediating associative learning and memory, sleep/wake state, and stress-induced hyperactivity. Further, requires more investigation on the molecular, pharmacological, functional, and physiological basis of dopamine receptors and functions in modulating phase change will improve our understanding of the molecular mechanism underlying phenotypic plasticity in honeybee and model insects.

REFERENCES

- [1] Ahmed-Braimah, Y. H., Sweigart, A. L. (2015): A single gene causes an interspecific difference in pigmentation in *Drosophila*. – *Genetics* 200(1): 331-342.
- [2] Barron, A. B., Gurney, K. N., Meah, L. F., Vasilaki, E., Marshall, J. A. (2015): Decision-making and action selection in insects: inspiration from vertebrate-based theories. – *Frontiers in Behavioral Neuroscience* 9: 216.
- [3] Beggs, K. T., Mercer, A. R. (2009): Dopamine receptor activation by honey bee queen pheromone. – *Current Biology* 19(14): 1206-1209.
- [4] Berke, J. D. (2018): What does dopamine mean? – *Nature neuroscience* 21(6): 787-793.
- [5] Blenau, W., Daniel, S., Balfanz, S., Thamm, M., Baumann, A. (2017): Dm5-ht2b: pharmacological characterization of the fifth serotonin receptor subtype of *drosophila melanogaster*. – *Frontiers in Systems Neuroscience* 11: 28.
- [6] Buckemüller, C., Siehler, O., Göbel, J., Zeumer, R., Ölschläger, A., Eisenhardt, D. (2017): Octopamine underlies the counter-regulatory response to a glucose deficit in honeybees (*Apis mellifera*). – *Frontiers in Systems Neuroscience* 11: 63.
- [7] Damrau, C., Toshima, N., Tanimura, T., Brembs, B., Colomb, J. (2018): Octopamine and tyramine contribute separately to the counter-regulatory response to sugar deficit in *Drosophila*. – *Frontiers in Systems Neuroscience* 11: 100.
- [8] Elsik, C. G., Worley, K. C., Bennett, A. K., Beye, M., Camara, F., Childers, C. P., de Graaf, D. C., Debyser, G., Deng, J., Devreese, B., Elhaik, E. (2014): Finding the missing honey bee genes: lessons learned from a genome upgrade. – *BMC Genomics* 15(1): 86.
- [9] Ferreri, L., Mas-Herrero, E., Zatorre, R. J., Ripollés, P., Gomez-Andres, A., Alicart, H., Olivé, G., Marco-Pallarés, J., Antonijoan, R. M., Valle, M., Riba, J. (2019): Dopamine modulates the reward experiences elicited by music. – *Proceedings of the National Academy of Sciences* 116(9): 3793-3798.
- [10] Grünewald, B. (1999): Morphology of feedback neurons in the mushroom body of the honeybee, *Apis mellifera*. – *Journal of Comparative Neurology* 404(1): 114-126.
- [11] Guo, X., Ma, Z., Kang, L. (2015): Two dopamine receptors play different roles in phase change of the migratory locust. – *Frontiers in Behavioral Neuroscience* 9: 80.
- [12] Ichinose, T., Tanimoto, H., Yamagata, N. (2017): Behavioral modulation by spontaneous activity of dopamine neurons. – *Frontiers in Systems Neuroscience* 11: 88.
- [13] Kamhi, J. F., Arganda, S., Moreau, C. S., Traniello, J. F. (2017): Origins of aminergic regulation of behavior in complex insect social systems. – *Frontiers in Systems Neuroscience* 11: 74.
- [14] Kokay, I. C., Mercer, A. R. (1997): Age-related changes in dopamine receptor densities in the brain of the honey bee, *Apis mellifera*. – *Journal of Comparative Physiology A* 181(4): 415-423.
- [15] Lapiéd, B., Defaix, A., Stankiewicz, M., Moreau, E., Raymond, V. (2017): Modulation of low-voltage-activated inward current permeable to sodium and calcium by DARPP-32 drives spontaneous firing of insect octopaminergic neurosecretory cells. – *Frontiers in Systems Neuroscience* 11: 31.
- [16] Leng, Z. G., Lin, S. J., Wu, Z. R., Guo, Y. H., Cai, L., Shang, H. B., Tang, H., Xue, Y. J., Lou, M. Q., Zhao, W., Le, W. D. (2017): Activation of DRD5 (dopamine receptor D5) inhibits tumor growth by autophagic cell death. – *Autophagy* 13(8): 1404-1419.
- [17] Lerner, T. J., Boustany, R. M. N., Anderson, J. W., D'Arigo, K. L., Schlumpf, K., Buckler, A. J., Gusella, J. F., Haines, J. L. (1995): Isolation of a novel gene underlying Batten disease, CLN3. – *Cell* 82(6): 949-957.
- [18] Li, Y., Tiedemann, L., von Frieling, J., Nolte, S., El-Kholy, S., Stephano, F., Gelhaus, C., Bruchhaus, I., Fink, C., Roeder, T. (2017): The role of monoaminergic neurotransmission for metabolic control in the fruit fly *Drosophila melanogaster*. – *Frontiers in Systems Neuroscience* 11: 60.

- [19] Matsushima, K., Watanabe, T., Sasaki, K. (2019): Functional gene expression of dopamine receptors in the male reproductive organ during sexual maturation in the honey bee (*Apis mellifera* L.). – *Journal of Insect Physiology* 112: 9-14.
- [20] McQuillan, H. J., Barron, A. B., Mercer, A. R. (2012a): Age- and behaviour-related changes in the expression of biogenic amine receptor genes in the antennae of honey bees (*Apis mellifera*). – *Journal of Comparative Physiology A* 198(10): 753-761.
- [21] McQuillan, H. J., Nakagawa, S., Mercer, A. R. (2012b): Mushroom bodies of the honeybee brain show cell population-specific plasticity in expression of amine-receptor genes. – *Learning & Memory* 19(4): 151-158.
- [22] Mishra, A., Singh, S., Shukla, S. (2018): Physiological and functional basis of dopamine receptors and their role in neurogenesis: possible implication for Parkinson's disease. – *Journal of Experimental Neuroscience* 12: 1179069518779829.
- [23] Mustard, J. A., Pham, P. M., Smith, B. H. (2010): Modulation of motor behavior by dopamine and the D1-like dopamine receptor AmDOP2 in the honey bee. – *Journal of Insect Physiology* 56(4): 422-430.
- [24] Niens, J., Reh, F., Çoban, B., Cichewicz, K., Eckardt, J., Liu, Y. T., Hirsh, J., Riemensperger, T. D. (2017): Dopamine modulates serotonin innervation in the *Drosophila* brain. – *Frontiers in Systems Neuroscience* 11: 76.
- [25] Rang, H. P., Dale, M. M., Ritter, J. M., Moore, P. K. (2006): *Pharmacology* 5th Ed. – Churchill Livingstone, London.
- [26] Ryglewski, S., Duch, C., Altenhein, B. (2017): Tyramine actions on *Drosophila* flight behavior are affected by a glial dehydrogenase/reductase. – *Frontiers in Systems Neuroscience* 11: 68.
- [27] Sasaki, K., Ugajin, A., Harano, K. I. (2018): Caste-specific development of the dopaminergic system during metamorphosis in female honey bees. – *PloS One* 13(10).
- [28] Scheiner, R., Baumann, A., Blenau, W. (2006): Aminergic control and modulation of honeybee behaviour. – *Current Neuropharmacology* 4(4): 259-276.
- [29] Scheiner, R., Entler, B. V., Barron, A. B., Scholl, C., Thamm, M. (2017): The effects of fat body tyramine level on gustatory responsiveness of honeybees (*Apis mellifera*) differ between behavioral castes. – *Frontiers in Systems Neuroscience* 11: 55.
- [30] Scholz-Kornehl, S., Schwärzel, M. (2016): Circuit analysis of a *Drosophila* dopamine type 2 receptor that supports anesthesia-resistant memory. – *Journal of Neuroscience* 36(30): 7936-7945.
- [31] Sinakevitch, I. T., Daskalova, S. M., Smith, B. H. (2017): The biogenic amine tyramine and its receptor (AmTyr1) in olfactory neuropils in the honey bee (*Apis mellifera*) brain. – *Frontiers in Systems Neuroscience* 11: 77.
- [32] Stocker, B., Bochow, C., Damrau, C., Mathejczyk, T., Wolfenberger, H., Colomb, J., Weber, C., Ramesh, N., Duch, C., Biserova, N. M., Sigrist, S. (2018): Structural and molecular properties of insect type II motor axon terminals. – *Frontiers in Systems Neuroscience* 12: 5.
- [33] Sun, J., Xu, A. Q., Giraud, J., Poppinga, H., Riemensperger, T., Fiala, A., Birman, S. (2018): Neural control of startle-induced locomotion by the mushroom bodies and associated neurons in *Drosophila*. – *Frontiers in Systems Neuroscience* 12: 6.
- [34] Swenson, J. M., Colmenares, S. U., Strom, A. R., Costes, S. V., Karpen, G. H. (2016): The composition and organization of *Drosophila* heterochromatin are heterogeneous and dynamic. – *Elife* 5: e16096.
- [35] Tang, S., Yao, B., Li, N., Lin, S., Huang, Z. (2018): Association of dopamine beta-hydroxylase polymorphisms with Alzheimer's disease, Parkinson's disease and schizophrenia: evidence based on currently available loci. – *Cellular Physiology and Biochemistry* 51(1): 411-428.
- [36] Tedjakumala, S. R., Rouquette, J., Boizeau, M. L., Mesce, K. A., Hotier, L., Massou, I., Giurfa, M. (2017): A tyrosine-hydroxylase characterization of dopaminergic neurons in the honey bee brain. – *Frontiers in Systems Neuroscience* 11: 47.

- [37] Thanos, P. K., Roushdy, K., Sarwar, Z., Rice, O., Ashby Jr, C. R., Grandy, D. K. (2015): The effect of dopamine D 4 receptor density on novelty seeking, activity, social interaction, and alcohol binge drinking in adult mice. – *Synapse* 69(7): 356-364.
- [38] Vergara, M. D., Keller, V. N., Fuentealba, J. A., Gysling, K. (2017): Activation of type 4 dopaminergic receptors in the prelimbic area of medial prefrontal cortex is necessary for the expression of innate fear behavior. – *Behavioural Brain Research* 324: 130-137.
- [39] Zhukovskaya, M. I., Polyanovsky, A. D. (2017): Biogenic amines in insect antennae. – *Frontiers in Systems Neuroscience* 11: 45.

PHYSIOLOGICAL AND BIOCHEMICAL RESPONSES OF (*APTENIA CORDIFOLIA*) TO SALT STRESS AND ITS REMEDIATIVE EFFECT ON SALINE SOILS

KARAKAS, S.^{1*} – DIKILITAS, M.² – ALMACA, A.¹ – TIPIRDAMAZ, R.³

¹Department of Soil Science and Plant Nutrition, Faculty of Agriculture, Harran University, Sanliurfa, Turkey

²Department of Plant Protection, Faculty of Agriculture, Harran University, Sanliurfa, Turkey

³Department of Biology, Faculty of Science, Hacettepe University, Ankara, Turkey

*Corresponding author

e-mail: skarakas@harran.edu.tr; phone: +90-414-318-3679

(Received 9th Sep 2019; accepted 21st Jan 2020)

Abstract. Salinization is one of the most significant environmental problems in the world. Salinity negatively affects the physicochemical properties of the soil and reduces crop production. This study aimed to investigate the potential use of *Aptenia cordifolia* L. for the phytoremediation of salt-affected soils. Three salt levels; non-saline (NS, EC: 1.38 dS m⁻¹), slightly saline (SS, EC: 3.54 dS m⁻¹) and highly saline (HS, EC: 9.58 dS m⁻¹) soils were collected from Harran Plain-Turkey and used to cultivate *A. cordifolia* in pots. To assess the salt tolerance of the plants, physiological and biochemical parameters as well as the accumulation of leaf Na⁺ and Cl⁻ ions were determined. In the meantime, soils were evaluated in terms of electrical conductivity, pH, organic matter and soil enzymes (dehydrogenase, urease, phosphatase and protease) before and after the cultivation. A significant increase in shoot fresh weight and dry weight were obtained from *A. cordifolia* cultivated-SS soils. No significant differences were determined in terms of crop yield in NS and HS soils. A decrease in total chlorophyll content was evident only in plants growing in HS soils. Proline and malondialdehyde contents and the activity of catalase and peroxidase enzymes were found significantly higher ($P \leq 0.05$) in plants growing in HS as compared to those growing in SS and NS soils. *A. cordifolia* plants, accumulated more Na⁺ and Cl⁻ ions in their leaves as the salinity levels increased. Soil pH levels under all soil conditions were not affected although slight increases were observed. However, soil electrical conductivity were decreased 2 and 2.5 times in SS and HS soil types, respectively. Soil organic matter were significantly increased along with the increase in the activity of soil enzymes in all soil types. We suggest that cultivation *A. cordifolia* in SS and HS soils will improve the condition of soil physicochemical properties in an environmentally-friendly manner.

Keywords: abiotic stress, phytoremediation, soil enzymes, halophytes, ameliorate

Introduction

Salinization is a worldwide problem in which salts gradually accumulate in the soil. In this process, water-soluble salts in the soils are dissolved via irrigation or rain and transferred to upper part of the soil and can then be accumulated when irrigation or rain ceased in semi-arid or arid environments (Panta et al., 2018). This negatively affects the crop productivity, quality and microbial community thus affects soil health (FAO, 2016). Due to soil salinization, soil infertility has been in an increasing trend (Slama et al., 2015). If serious measurements have not been taken, salt stress not only negatively affects the physical and chemical properties of the soil but also reduces the concentration of microorganisms and decrease the soil fertility. On the other hand, salinity reduces the quality and quantity of crops and in severe cases, it would not allow any seeds to germinate in which the standing point of agriculture (Yuan et al., 2007;

Negrao et al., 2017). Salt stress also leads to the production of reactive oxygen species (ROS) in crop plants that disrupt the membrane functionality and damages protein, lipid and nucleic acids. Although plants are able to develop a series of ROS detoxification mechanisms to minimize the impact of ROS via antioxidative enzyme systems including catalase (CAT), glutathione reductase (GR), superoxide dismutase (SOD), ascorbate peroxidase (APX) and non-enzymatic metabolites (ascorbate, proline, glutathione etc.), this may not be enough for plants to function under harsh conditions. Even resistant plants may not cope with the ongoing stress such as salinity and heavy metal stress (Gill and Tuteja, 2010; Hossain et al., 2017).

In nature, plants develop various physiological and biochemical mechanisms in order to survive in soils characterized with salinity. General salt tolerance mechanisms include ion homeostasis and compartmentalization, ion transport and uptake and synthesis of osmoprotectants via compatible solutes (Gupta and Huang, 2014). Halophytes are plants that can tolerate and grow in soils characterized with high salt concentration. They, in general, are known to accumulate salts in various plant parts such as leaf, root etc. (Grigore et al., 2014; Flowers and Colmer).

Various physical, chemical and biological techniques can be used to remediate salt contaminated soils. The use of halophytes is one of the most promising and cost-effective methods for phytoremediation. It is a strategy where plants are used to remove, immobilize, degrade the soil contaminants such as salt and heavy metals (Kaushal et al., 2015). Phytoremediation has been used to manage wastes, especially petroleum hydrocarbons, polycyclic aromatic hydrocarbon, organic matter, and nutrients. So far a number of plants have been identified in use of phytoremediation purposes. Reclamation of salt-affected soils could be achieved and crop plants could grow in less stressed soils. Glycophyte plants could be grown together with the halophytes as companion plants in such soils. Also, the harvested above-ground biomass of halophytes can be used as animal feed (Ammari et al., 2013; Karakas et al., 2013).

A. cordifolia (L. f.) Schwant, also known as *Mesembryanthemum cordifolium*, is a species of succulent plant from the Aizoaceae family and has a Crassulacean acid metabolism (CAM) (Herppich and Peckmann, 1997; Tripodi and Modesta, 2003). In this study, we aimed to determine the performance of *A. cordifolia* against salt stress and to evaluate its performance under saline conditions for phytoremediation purposes. We determined the shoot fresh and dry weight, total chlorophyll, proline, malondialdehyde (MDA), Na⁺ and Cl⁻ ions levels and catalase (CAT, E.C.1.11.1.6) and peroxidase (POX, E.C.1.11.1.7) enzyme responses of *A. cordifolia*. We also elucidated the physical and chemical properties of the soil in the vicinity of root area of *A. cordifolia* to determine the remediation capacity of the halophyte through measurement of soil electrical conductivity (EC), pH, organic matter (OM), ion (Na⁺, Cl⁻) contents and soil enzyme activities (dehydrogenase, urease and protease) prior to and following cultivation with *A. cordifolia*.

Materials and methods

Experimental design and plant growth

Treatments consisted of three different soil salinity levels; non-saline (NS, EC: 1.38 dS m⁻¹), slightly saline (SS, EC: 3.54 dS m⁻¹) and highly saline (HS, EC: 9.58 dS m⁻¹) soils collected from Harran Plain-Turkey. Trials were performed in a randomized block design with three replicates. Before trial, soil samples were carefully air-dried to

allow sieving with a 2-mm mesh sieve. Three-week-old *A. cordifolia* seedlings were planted into 8-L pots containing 6 kg air-dried soil from each category in greenhouse ($35\text{ }^{\circ}\text{C} \pm 1$) conditions. The seedlings were planted on (April 2016) at a rate of 6 plants per pot. Pots were irrigated with full field capacity. Plants were then harvested on (July 2016) 100 days after onset of treatments. For the plant analysis, the shoot fresh weight (FW) and shoot dry weight (DW) were determined following harvest (Fig. 1).

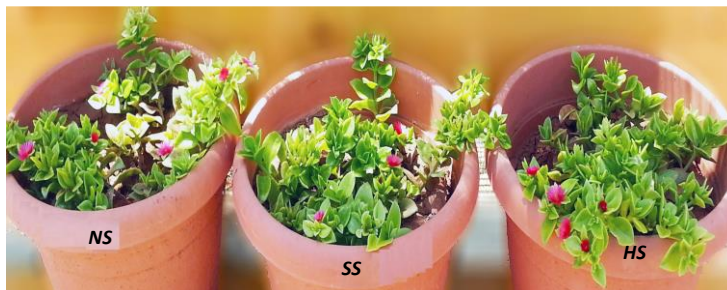


Figure 1. Growth of *A. cordifolia* at three different salinity levels

Total chlorophyll contents were determined according to the method of Arnon (1949) with slight modifications (Dikilitas, 2003). For the analysis, a 0.5 g leaf sample was homogenized in a 5 mL acetone: water (80:20% v/v) mixture. After filtration through Whatman No. 2 filter paper, a reading was made against 80% acetone blank for total chlorophyll at 652 nm using a UV spectrophotometer (UV-1700, Shimadzu). The results were then expressed as mg g^{-1} FW for total chlorophyll.

The proline measurement was conducted according to the method of Bates et al. (1973). Acid-ninhydrin was employed as a reagent, which was made by dissolving (warming and agitating) 1.25 g of ninhydrin in 30 mL of glacial acetic acid and 20 mL of 6 M phosphoric acid. A quantity of 0.5 g of leaf material was homogenized in 10 mL of 3% w/v sulphosalicylic acid then the homogenate was filtered through Whatman No. 2 filter paper. A 2-mL of filtrate was mixed in a test tube with 2 mL of acid ninhydrin reagent and boiled at $100\text{ }^{\circ}\text{C}$ for 1 h. The reaction was terminated in an ice bath. The reaction mixture was extracted with 5 mL of toluene. Tubes were thoroughly shaken for 15-20 s and left for further 20 min in order to achieve separation of the two layers. The chromophore containing toluene was removed and allowed to warm to room temperature. Absorbance of the solution was measured at 515 nm using a toluene blank as a reference in a spectrophotometry (UV-1700, Shimadzu). The results were expressed as $\mu\text{mol g}^{-1}$ fresh tissue.

The malondialdehyde (MDA) content was determined according to the method of Sairam and Sexena (2003). A 0.5 g leaf tissue sample was homogenized using 10 mL of a 0.1% trichloroacetic acid (TCA) and the homogenate was centrifuged at 10,000 g for 5 min. Four mL of 20% v/v TCA containing 0.5% v/v thiobarbituric acid (TBA) was added to 1 mL of the supernatant. The solution was heated at $95\text{ }^{\circ}\text{C}$ for 30 min and then quickly cooled on ice. The mixture was centrifuged once again at 10,000 g for 5 min and the absorbance of the clean supernatant was determined at 532 and 600 nm. The MDA content was calculated using Equation 1.

$$MDA (\text{nmol g}^{-1}) = \frac{\text{Extract volume (ml)} \times [(A_{532} - A_{600}) / (155 \text{ mM}^{-1} \text{ cm}^{-1})]}{\text{Sample amount (g)}} \times 10^3 \text{ (Eq.1)}$$

Catalase enzyme activity (CAT, E.C.1.11.1.6) was determined by monitoring the decomposition of H₂O₂ according to the method of Aebi (1984), with slight modifications (Karakas et al., 2016). For the analysis, 0.5 g of plant material was homogenized in 10 mL of a 50 mM Na-phosphate buffer solution then 50 µL of plant extract was added to a 2.95 mL (10 mM H₂O₂, 50 mM Na-phosphate buffer and 4 mM Na₂EDTA) reaction mixture and measured for 30 s at 240 nm with a UV spectrometer (UV-1700, Shimadzu). One CAT activity unit (U) is defined as a change of 0.1 absorbance unit per minute. Activity is expressed as enzyme units per gram fresh weight.

Peroxidase enzyme activity (POX, E.C.1.11.1.7) was determined by monitoring the increase in absorbance due to the tetraguaiacol formation at 470 nm according to the method of Cvikrova et al. (1994) with slight modifications (Karakas et al., 2016). For the analysis, 100 µL of extract (obtained as above) was added to 3 mL of the reaction mixture (13 mM guaiacol, 5 mM H₂O₂, and 50 mM Na-phosphate, pH 6.5). The reaction was initiated with an H₂O₂ addition and was measured at 470 nm using a UV spectrophotometer (UV-1700, Shimadzu) at 1-min interval until 3rd minute. One unit of POX activity is defined as a change of 0.1 absorbance unit per minute at 470 nm. Activity is expressed as enzyme units per gram of fresh weight.

The Na⁺ ion content of leaves was determined according to the method of Chapman and Pratt (1961). with slight modifications (Karakas et al., 2016). Samples burned at 500 °C were homogenized in 5 mL of a 2N HCl. For quantification of Na⁺ ions, the homogenate obtained following filtration was analyzed via Inductively Coupled Plasma (ICP, Perkin Elmer).

Chloride determination of plant samples was made according to the Mohr method using indicator (Johnson and Ulrich, 1959; Kacar and Inal, 2008).

Soil samples electrical conductivity (EC), pH, organic matter (OM) content and soil enzymes were determined before and after the trial. Soil EC and pH were determined using a saturated soil paste extraction (Soil Conservation Service, 1972; Thomas, 1996). OM content was determined according to Walkley (1947) and FAO (1974). One gram soil, 10 mL 1 N Cr₂O₇ solution and 20 mL concentrated H₂SO₄ were poured into 500 mL beaker and mixed and allowed to stand for 30 min at room temperature. Then, 200 mL dH₂O and 10 mL concentrated orthophosphoric acid was added to the solution. The mixture was then cooled down to room temperature and 10-15 drops of diphenylamine indicator were added. The mixture was then titrated with 0.5 M FeH₈N₂O₈S₂ solution until the color changes from violet-blue to green. A reagent blank using the above procedure without soil was employed. The blank is used to standardize the Fe²⁺ solution daily. OM was calculated with *Equation 2*.

$$Total\ C(\%) = ((A - S) \times Fe^{+2} \times (0.003) \times (100 / B)) \quad (Eq.2)$$

To convert total C, the results were multiplied by 1.30 into the correction factor, OM, *Equation 3* was used.

$$OM(\%) = TotalC \times 1.72 / 0.58 \quad (Eq.3)$$

where A: blank titration ml ferrous solution, B: sample titration ml ferrous solution, 0.003: milliequivalent weight of C in g, factor of 1.72.

Dehydrogenase activity was measured using triphenyl tetrazolium chloride (TTC) colorimetric analysis according to Tabatabai (1994). The principle of dehydrogenase assay is that when metabolizing cells come in contact with an aqueous solution of 2,3,5-triphenyl tetrazolium chloride (TTC) under anaerobic conditions, it is converted into triphenylformazan (TPF) and can be measured colorimetrically. Soil sample (5 g) was taken in 70 × 150 mm screw cap tubes. To each tube, 1 ml of 3% TTC and 5 ml of deionized water were added. Then the samples were mixed on a vortex, the tubes were stoppered and incubated in the dark for 24 h at 37 °C. After incubation, 10 ml of methanol were added, the samples were shaken and filtered Whatman filter paper No.1. After filtration, the optical reading was made at 485 nm with a UV spectrophotometer using methanol extract as the blank. The results were expressed as $\mu\text{mol TPF g}^{-1} \text{ soil h}^{-1}$.

The urease activity was determined following the method of Guan (1986) with some modifications. Briefly, 0.5 ml toluene, 20 ml of 0.1 M Na-citrate buffer (pH 6.7) and 10 ml of 10 % urea were added to 5.0 g soil and then the mixture was incubated at 37 °C for 24 h. One milliliter from the filtrate was obtained and added to 9 ml dH₂O and mixed with 4 ml Na-phenolate and 3 ml NaClO. The releasing ammonium was measured with a UV spectrophotometer at 578 nm. A control without urea was prepared with each sample. The results were expressed as $\text{mg urease-N kg}^{-1} \text{ h}^{-1}$.

Phosphatase activities were measured based on the colorimetric estimation of the *p*-nitrophenol release from *p*-nitrophenyl phosphate (Tabatabai, 1994). One gram soil was placed in a 50-mL Erlenmeyer flask and then 0.2 mL toluene, 0.1 M modified universal buffer (pH 6.5), 1 ml 0.1 M *p*-nitrophenyl phosphate (PNP) solution was added to the flask. The flask was swirled for a few seconds and incubated at 37 °C for 1 h in the incubator with a stopper. After removing the stopper, 1 ml of 0.5 M CaCl₂ and 4 ml of 0.5 M NaOH were added to the mixture. The soil suspension was filtered through Whatman No. 1 filter paper. The optical density of the filtrate was then measured at 420 nm in a spectrophotometer (UV-1700, Shimadzu). Blank was maintained similarly without soil. The results were expressed as $\text{mg P-nitrophenyl kg}^{-1} \text{ h}^{-1}$.

Protease activity was determined according to the method of Girard and Michaud (2002). Air-dried soil (0.1 g) was placed into 1.5 mL Eppendorf tube and then 500 μL of 1% (w/v) azocasein in 50 mmol L⁻¹ Tris-HCl, pH 8.8. Azocasein hydrolysis was initiated by incubating the tubes 2 h at room temperature. Proteolysis was stopped by adding 300 μl of 10 (w/v) cold trichloroacetic acid (TCA). After centrifugation for 10 min at 15000 g, 350 μl of the supernatant was collected and mixed with of 300 μl of 1 N NaOH. Protease activity was then determined by reading the optical density of the resulting solution at 440 nm using a UV spectrophotometer. A change of 0.01 units per minute in absorbance was considered to be equal to one unit protease activity, which was expressed as U (unit) mg^{-1} protein.

Data were subjected to an analysis of variance (ANOVA) at a significance level of $P \leq 0.05$ using Duncan's Multiple Range Test (DMRT) from the SPSS software program (Version 22.0). Data are presented as a mean value \pm the standard error.

Results

Plant analysis of A. cordifolia under salinity levels

A. cordifolia plants were harvested after 100 days of cultivation from the soils differing in salinity levels. Growth of shoots was followed by measuring FW and DW

of the plants. At SS soil conditions, FW and DW of the plants significantly increased. At HS soil conditions, FW and DW of the plants did not significantly differ from those of control plants cultivated in NS soil conditions (*Fig. 2A and B; Table 1*).

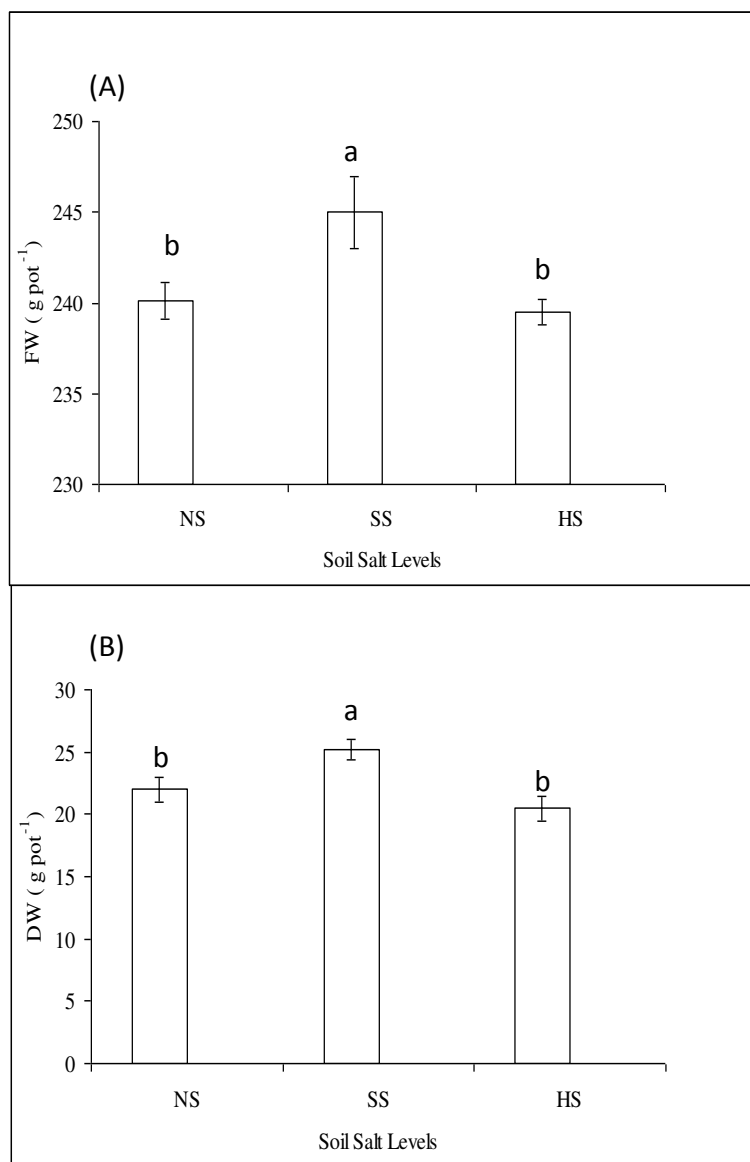


Figure 2. A) FW, B) DW of *A. cordifolia* plants at three different salinity levels: non-saline (NS), slightly saline (SS), and highly saline (HS) soils. Bars indicate the means of the three replicates \pm standard error. Bars with different letters indicate significant differences from one another according to Duncan's Multiple Range Test at $P \leq 0.05$

When salinity levels increased, the accumulation of NaCl ions, Na⁺ and Cl⁻, in leaves of *A. cordifolia* also increased. The accumulation of both ions was more prominent of HS soil conditions. *A. cordifolia* plants accumulated approximately 16 g Na⁺ and 19 g Cl⁻ ions per kg leaf at SS soil conditions. On the other hand, *A. cordifolia* plants at HS soils accumulated almost 28 g kg⁻¹ and 32 g kg⁻¹ Na⁺ and Cl⁻ ions, respectively their leaves (*Fig. 3A and B; Table 1*).

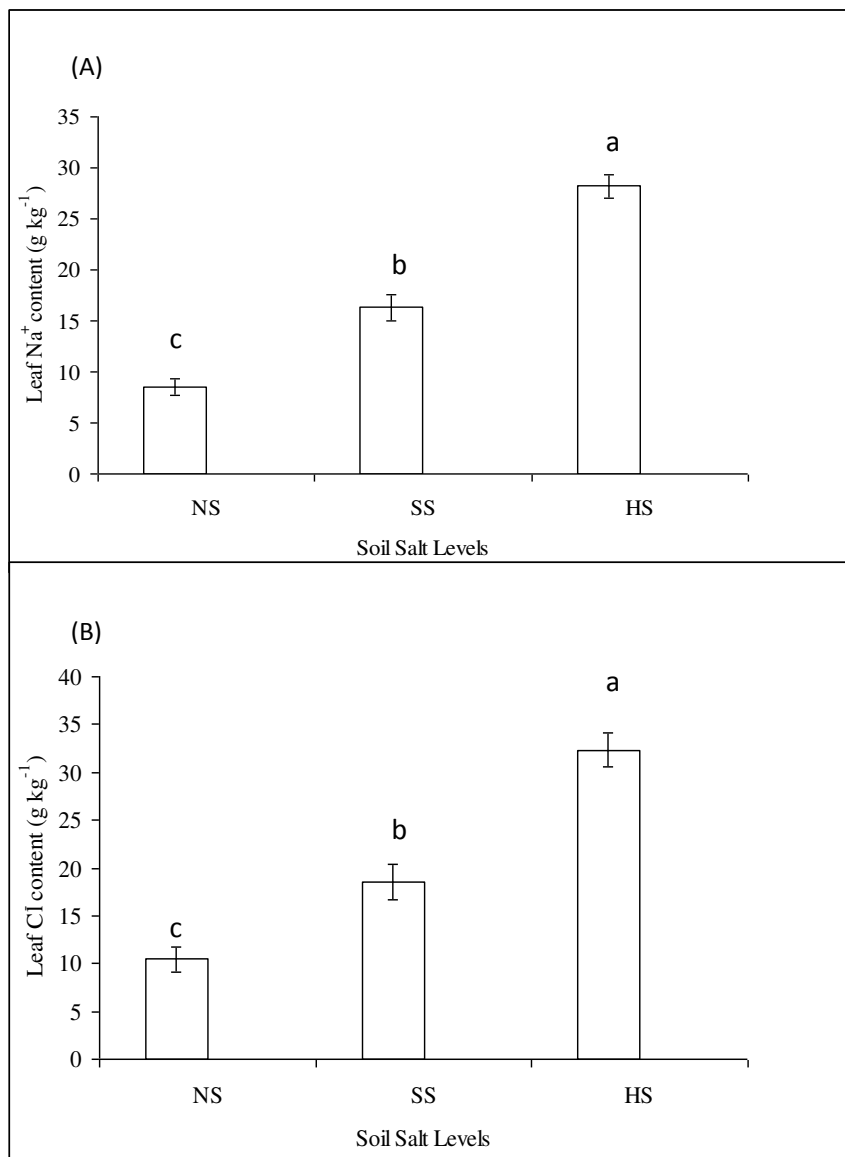


Figure 3. A) leaf Na⁺ content, B) leaf Cl⁻ content of *A. cordifolia* plants at three different salinity levels: non-saline (NS), slightly saline (SS), and highly saline (HS) soils. Bars indicate the means of the three replicates ± standard error. Bars with different letters indicate significant differences from one another according to Duncan's Multiple Range Test at $P \leq 0.05$

When biochemical parameters were examined under saline conditions, total chlorophyll contents were not statistically significant at all saline conditions (Fig. 3A). Both proline and MDA contents increased in plants subjected to HS soil conditions. The proline content was $1.9 \mu\text{mol g}^{-1}$ at HS conditions doubling the levels of NS and SS soil conditions. Again, MDA contents were at the highest levels at HS conditions (Fig. 4B and C).

As a response to salinity stress, both enzymes, POX and CAT, showed increasing trend as the concentration of NaCl increased in the soil. A significant increase was evident at HS soil conditions *A. cordifolia* plants did not exhibit significant enzyme responses at SS soil conditions (Fig. 4D and E; Table 1).

Table 1. Analyses of plant parameters using ANOVA

Plant parameters	Soil salt levels	n	Mean ± S.E	F	P
FW	NS	3	240.12 ± 1.15	9.07	0.02
	SS	3	245.11 ± 2.01		
	HS	3	239.43 ± 0.61		
	Total	9	241.55 ± 1.37		
DW	NS	3	21.99 ± 0.97	5.69	0.04
	SS	3	25.19 ± 0.87		
	HS	3	20.85 ± 0.98		
	Total	9	22.68 ± 0.80		
Leaf Na ⁺	NS	3	8.47 ± 0.55	86.20	0.00
	SS	3	16.33 ± 1.23		
	HS	3	28.20 ± 1.27		
	Total	9	17.67 ± 2.92		
Leaf Cl ⁻	NS	3	10.47 ± 1.35	41.41	0.00
	SS	3	18.54 ± 1.98		
	HS	3	32.35 ± 1.77		
	Total	9	20.46 ± 3.31		
Total chlorophyll	NS	3	1.51 ± 0.29	0.05	0.95
	SS	3	1.46 ± 0.14		
	HS	3	1.41 ± 0.28		
	Total	9	1.46 ± 0.12		
Proline	NS	3	0.96 ± 0.07	48.87	0.00
	SS	3	1.07 ± 0.09		
	HS	3	1.91 ± 0.06		
	Total	9	1.310.15		
MDA	NS	3	1.40 ± 0.21	49.40	0.00
	SS	3	1.71 ± 0.29		
	HS	3	5.25 ± 0.38		
	Total	9	2.79 ± 0.64		
CAT	NS	3	0.43 ± 0.08	6.09	0.04
	SS	3	0.52 ± 0.10		
	HS	3	0.96 ± 0.16		
	Total	9	0.64 ± 0.10		
POX	NS	3	2.41 ± 0.23	26.31	0.00
	SS	3	2.72 ± 0.25		
	HS	3	6.28 ± 0.64		
	Total	9	3.80 ± 0.65		

Soil analysis of *A. cordifolia* under salinity levels

Soil characteristics such as soil pH, EC and OM contents were evaluated bare soil before (control) and after cultivation with *A. cordifolia*. To make a comprehensive evaluation, bare soil (not cultivated with any plants) was also employed when pH, EC and OM contents were measured. In this trial, physical soil parameters were determined and recorded in all soil conditions before and after 100-days cultivation with *A.*

cordifolia. The same parameters were-remeasured to see the differences in measured soil parameters. According to our findings, soil pH levels measured at different salinity conditions did not change throughout the course of the experiment. Cultivation of saline soils with *A. cordifolia* plants increased soil pH levels, however, this was not significant as compared to those of soils with no-cultivation (Fig. 5A; Table 2).

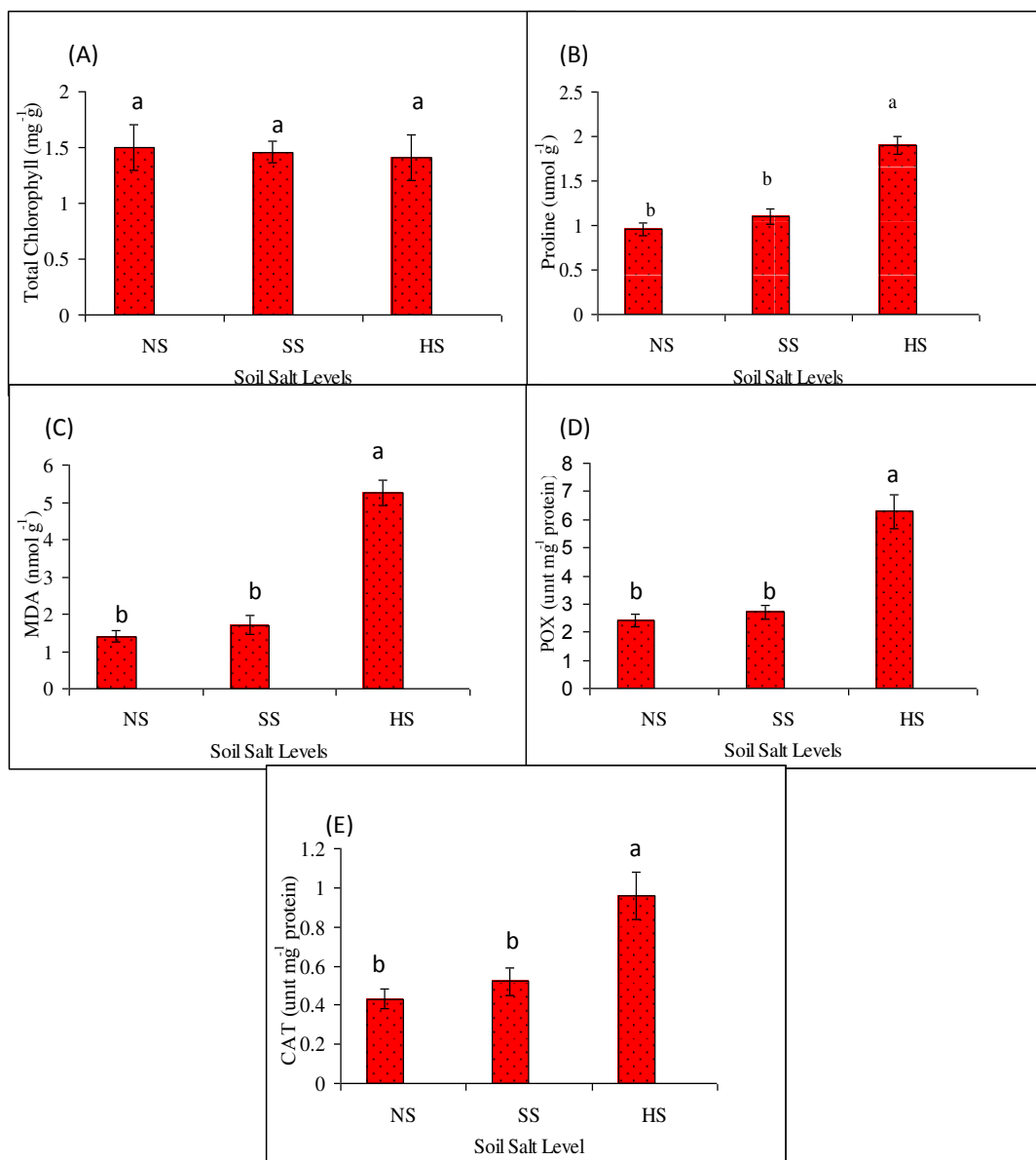


Figure 4. A) Total chlorophyll; B) proline; C) MDA; D) POX and E) CAT of *A. cordifolia* plants at three different salinity levels: non-saline (NS), slightly saline (SS), and highly saline (HS) soils. Bars indicate the means of the three replicates \pm standard error. Bars with different letters indicate significant differences from one another according to Duncan's Multiple Range Test at $P \leq 0.05$

Use of *A. cordifolia* also affected the contents of OM in all soil conditions including SS soil conditions. Cultivation with *A. cordifolia* improved the soil OM significantly

meaning that cultivation with *A. cordifolia* contributed soil OM by secreting organic materials from their root systems (Fig. 5B; Table 2).

When soil EC levels were measured, it was determined that soil EC levels were significantly decreased in all conditions after 100-days cultivation with *A. cordifolia* (Fig. 5C; Table 2). Decrease in soil EC level was more remarkable in HS soil conditions.

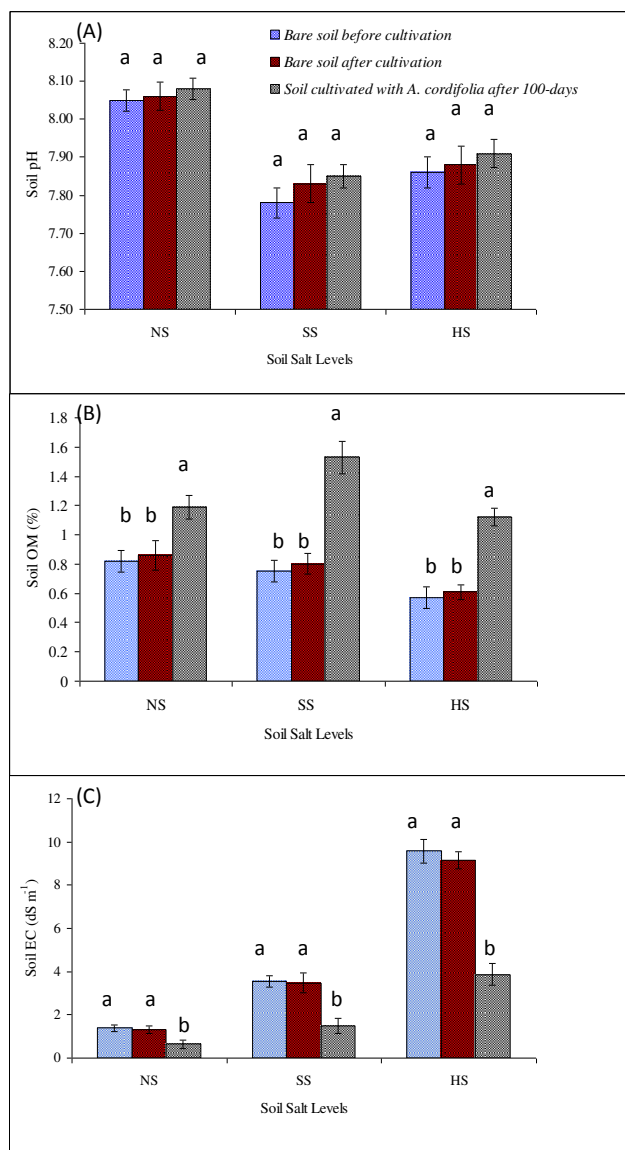


Figure 5. A) soil pH; B) soil OM; C) soil EC values of before and after cultivation with *A. cordifolia* at three different salinity levels: non-saline (NS), slightly saline (SS), and highly saline (HS) soils. Bars with different letters indicate significant differences from one another according to Duncan's Multiple Range Test at $P \leq 0.05$

Finally, soil enzymes were measured in all soil conditions to see if *A. cordifolia* plants contributed to soil health through increase in soil enzymes. Accordingly, cultivation with *A. cordifolia* significantly increased the soil enzymes such as dehydrogenase, urease, phosphatase and protease.

Table 2. Analyses of soil characteristics (pH, EC and OM) using ANOVA before and after cultivation with *A. cordifolia*

Soil salt levels	Application	pH				OM				EC			
		n	Mean ± S.E	F	P	n	Mean ± S.E	F	P	n	Mean ± S.E	F	P
NS	Bare soil before cultivated	3	8.05 ± 0.03	0.24	0.80	3	0.82 ± 0.07	5.76	0.04*	3	1.38 ± 0.15	6.82	0.02
	Bare soil after cultivated	3	8.06 ± 0.04			3	0.87 ± 0.10			3	1.34 ± 0.21		
	Soil cultivated with <i>A. cordifolia</i> after 100 days	3	8.08 ± 0.03			3	1.19 ± 0.08			3	0.65 ± 0.13		
	Total	9	8.06 ± 0.02			9	0.96 ± 0.07			9	1.12 ± 0.13		
SS	Bare soil before cultivated	3	7.78 ± 0.05	0.58	0.59	3	0.75 ± 0.10	16.43	0.00**	3	3.54 ± 0.35	7.29	0.03
	Bare soil after cultivated	3	7.83 ± 0.06			3	0.80 ± 0.08			3	3.46 ± 0.53		
	Soil cultivated with <i>A. cordifolia</i> after 100 days	3	7.85 ± 0.03			3	1.53 ± 0.14			3	1.48 ± 0.40		
	Total	9	7.82 ± 0.03			9	1.03 ± 0.14			9	2.83 ± 0.40		
HS	Bare soil before cultivated	3	7.86 ± 0.04	0.31	0.74	3	0.57 ± 0.15	9.88	0.01**	3	9.58 ± 0.64	34.41	0.00
	Bare soil after cultivated	3	7.88 ± 0.05			3	0.61 ± 0.06			3	9.14 ± 0.47		
	Soil cultivated with <i>A. cordifolia</i> after 100 days	3	7.91 ± 0.04			3	1.13 ± 0.05			3	3.87 ± 0.49		
	Total	9	7.88 ± 0.02			9	0.77 ± 0.10			9	7.53 ± 0.96		

A. cordifolia plants contributed to soil enzyme activities in NS soil conditions an indicating that soil health could be improved via cultivation with this plant (Figs. 6A, B, C and D; Table 3). Also, *A. cordifolia* plants improved soil enzyme levels in saline conditions. For example, soil dehydrogenase activity 1.5, soil urease activity 1.4, soil phosphatase activity 1.2 and soil protease activity 1.8 times increased after cultivation with *A. cordifolia* plants in HS soil conditions when compared to control soil (bare soil before cultivated). The increase in soil enzyme levels were more prominent in SS and HS soil conditions indicating that *A. cordifolia* plants played significant roles under saline stress conditions.

Table 3. Analyses of soil enzymes (dehydrogenase, urease, phosphatase, and protease) using ANOVA before and after cultivation with *A. cordifolia*

Soil salt levels	Application	Dehydrogenase				Urease				Phosphatase				Protease			
		n	Mean ± S.E.	F	P	n	Mean ± S.E.	F	P	n	Mean ± S.E.	F	P	n	Mean ± S.E.	F	P
NS	Bare soil before cultivated	3	19.10 ± 1.58	7.50	0.02	3	67.67 ± 0.88	11.45	0.01	3	142.33 ± 5.04	20.58	0.00	3	37.60 ± 3.75	5.03	0.05
	Bare soil after cultivated	3	20.10 ± 1.58			3	69.33 ± 1.45			3	150.00 ± 5.29			3	40.17 ± 0.73		
	Soil cultivated with <i>A. cordifolia</i> after 100 days	3	25.95 ± 0.69			3	78.10 ± 2.31			3	180.00 ± 2.08			3	48.50 ± 2.18		
	Total	9	21.72 ± 1.26			9	71.70 ± 1.82			9	157.44 ± 6.15			9	42.09 ± 2.08		
SS	Bare soil before cultivated	3	11.23 ± 1.40	17.70	0.00	3	54.73 ± 1.97	6.35	0.03	3	110.33 ± 3.76	24.35	0.00	3	26.10 ± 2.74	10.79	0.01
	Bare soil after cultivated	3	12.20 ± 1.01			3	58.46 ± 1.13			3	120.00 ± 7.64			3	27.00 ± 3.28		
	Soil cultivated with <i>A. cordifolia</i> after 100 days	3	19.28 ± 0.55			3	69.17 ± 4.62			3	160.00 ± 3.61			3	46.57 ± 4.35		
	Total	9	14.24 ± 1.37			9	60.79 ± 2.62			9	130.11 ± 8.06			9	33.22 ± 3.77		
HS	Bare soil before cultivated	3	4.28 ± 0.19	9.25	0.02	3	51.20 ± 1.61	10.99	0.01	3	81.00 ± 5.13	6.54	0.03	3	21.50 ± 1.59	7.06	0.03
	Bare soil after cultivated	3	4.07 ± 0.37			3	50.46 ± 1.96			3	85.00 ± 2.89			3	23.29 ± 1.09		
	Soil cultivated with <i>A. cordifolia</i> after 100 days	3	6.31 ± 0.57			3	68.90 ± 2.27			3	102.00 ± 4.73			3	37.54 ± 2.46		
	Total	9	4.89 ± 0.65			9	56.89 ± 2.12			9	89.33 ± 3.89			9	27.44 ± 1.65		

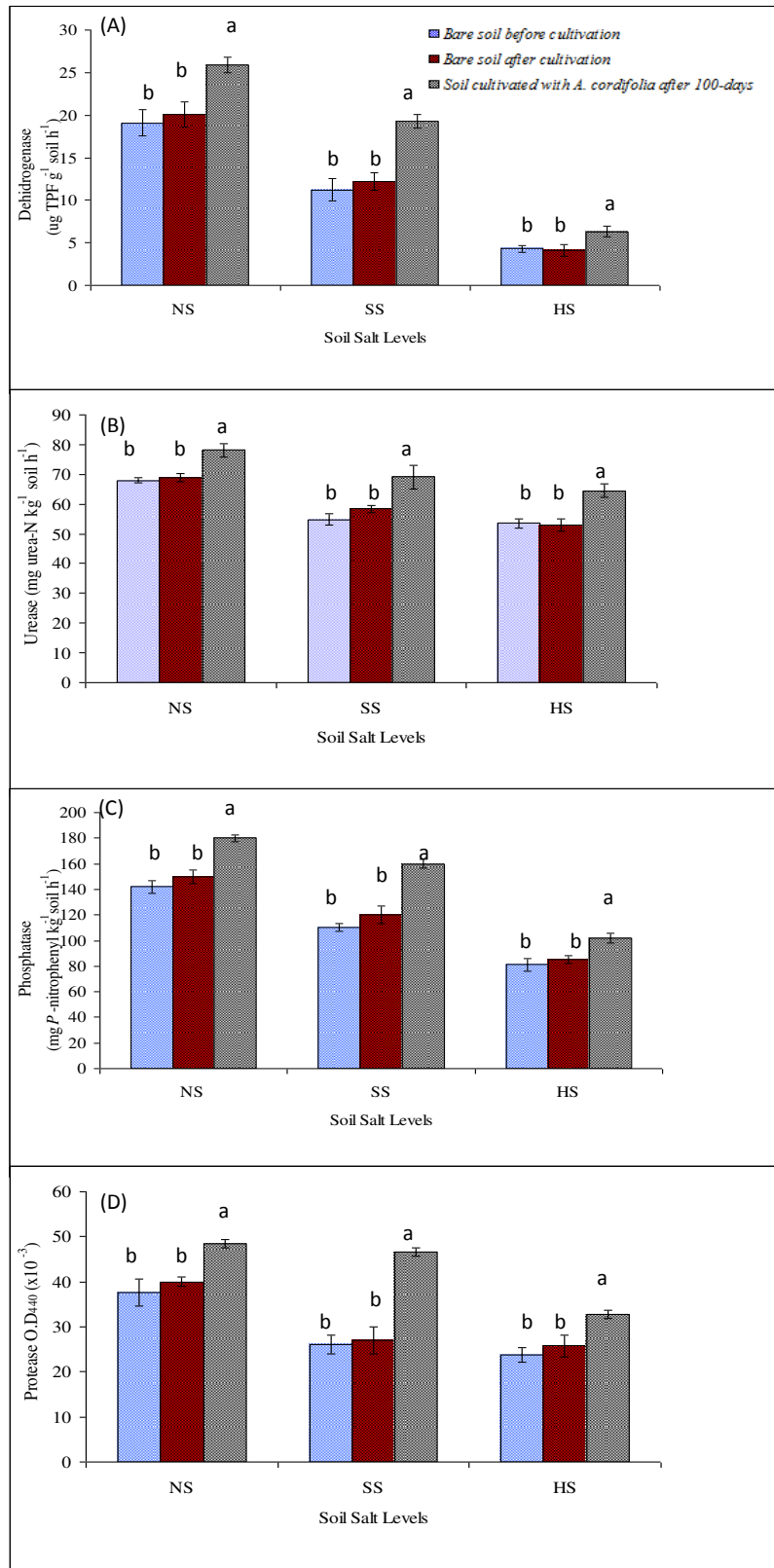


Figure 6. A) The soil dehydrogenase; B) urease; C) phosphatase; and D) protease values before and after cultivation with *A. cordifolia* at three different salinity levels: non-saline (NS), slightly saline (SS), and highly saline (HS) soils. Bars with different letters indicate significant differences from one another according to Duncan's Multiple Range Test at $P \leq 0.05$

Discussion

This study assessed the capacity of *A. cordifolia* to withstand salt stress. Phytoremediation and production potentials (biomass production and ion uptake) of *A. cordifolia* was evaluated at three different salinity levels in a 100-day pot experiment under controlled greenhouse conditions. Measurement was made in terms of growth, total chlorophyll, proline, malondialdehyde (MDA), mineral content, CAT and POX antioxidant enzyme changes as well as with the determination of soil EC, pH, OM, ion (Na^+ , Cl^-) contents and soil enzyme activities (dehydrogenase, urease, phosphatase and protease) before and after cultivation of such soils with *A. cordifolia*.

The results of this study showed that *A. cordifolia* plant was tolerant to both slight and high salinity. Accumulation of Na^+ and Cl^- ions increased in the leaves at both salinity levels. Therefore, this plant would be promising in reducing the electrical conductivity (EC) of such soils. The plants displayed great tolerance to the deleterious influence of salinity by preserving the integrity of their cell membranes by their proline and enzyme levels. During the growth period, proline contents and enzyme activities increased in the leaves under increasing saline levels. The accumulation of organic osmolytes such as proline, glycine betaine, sugar, alcohols, polyamines and proteins plays a key role in maintaining the low intracellular osmotic potential of plants and in preventing the harmful effects of salinity stress (Hýskova and Ryslava, 2018; Dutta et al., 2018). In our study, lipid peroxidation (MDA), POX and CAT activities increased significantly in *A. cordifolia* under salt stress. Salt stress, in general, increases lipid peroxidation and induces oxidative stress in plant tissues (Kim et al., 2016; Taibi et al., 2016). However, antioxidants such as POX and CAT tend to increase in tolerant cultivars, which scavenge H_2O_2 and other reactive oxygen species (ROS). These enzymes play significant roles in preventing cellular damages. We noticed that *A. cordifolia* plants were able to increase their organic metabolites upon stress exposure. It is important to note that those parameters were measured after 100 days in saline conditions. At SS conditions, FW and DW of the plants significantly increased. It is possible that SS might exert hormonal activity on *A. cordifolia* plants. This might have increased the FW and DW contents of the plants. Similar findings were stated that by Cela and Munné-Bosch (2012) on *A. cordifolia* was able to adapt to salt stress by increasing fresh biomass production. Therefore, tolerance of this plant after relatively long time under saline conditions is quite remarkable when compared to short-time stress of glycophytes in saline conditions under salinity stress. A plant with high tolerance to salinity with high capacity to accumulate Na^+ and Cl^- ions in their leaf or other parts including fruits is a good candidate for phytoremediation purposes (Bhuiyan et al., 2017; Karakas et al., 2017). *A. cordifolia* also improved the conditions of saline soils without spoiling the physical and chemical properties of such soils. Soil enzyme levels significantly increased along with the increase of OM contents and decrease in EC levels without changing pH balance of such soils. In most cases, changes in physical and chemical properties result in changes in pH levels (Miltner et al., 2012; Shrivastava and Kumar, 2015; Yang et al., 2018).

Soil enzyme activity is closely related to the carbon inputs, crop growth stages, organic matter content, microbial community structure, soil ecology, physical and chemical properties, vegetation, fertility, soil pH, soil quality and abiotic soil environment (Jin et al., 2009; Rout et al., 2017). Microbial population and decomposition of organic matter result in increased activity of soil enzymes. For example, high urease activity was observed during the active growth of maize (Jin et al.,

2009). The present study suggests that *A. cordifolia* can be used for soil improvement in saline areas. *A. cordifolia* could remediate structure of soil where salinity is predicted to occur. Indeed, this species behaves similarly to those of halophytes that tolerate moderate and high doses of salt. The use of this species over halophytes has a great advantage since its vegetative life is longer than halophytes, therefore, it has significantly more time to improve soil conditions under saline threat. Its ecological competence via rapid colonization in soils and accumulation of toxic ions in over those of other species could be considered as a good remediative plant. Our next approach is to investigate other properties of this plant if it is to be used as a good companion plant with other glycophytes to improve the potential vegetative and fruiting performance under saline stress conditions. It is important to note that the performance of *A. cordifolia* plants under heavy metal polluted soils would increase the popularity and use of this plant.

Conclusions

Salinity is one of the most significant environmental problems in arid and semi-arid regions. One of the alternate ways is to use of arable lands efficiently and to include the marginal quality of areas or non-agricultural lands into agricultural areas. These areas should be remediated via physical, chemical and biological approaches. Phytoremediation, in this aspect, has many advantageous; its major advantages are the low cost and environmentally-friendly sites. In this respect use of one of salt-tolerant (halophyte) plants is one of the cost-effective methods. Although salt-tolerant plants are less affected than their non-salt tolerant counterparts to the effect of salinity, however, the generation of salt-tolerant plants is very difficult and not cost-effective as planned. Those plants might possess salt tolerance properties unlike exhibiting disease susceptibility, therefore, the generation of salt-tolerant plants might not be good solution as its own. However, this could be achieved via the use of halophyte plants if they are used for phytoremediation purposes. Phytoremediation process not only remediate the conditions of soil but also reduces the stress level on crop plants. This approach could be practiced in all soil types in differing soil salinity levels and in all plant species when co-cultivated. With this approach, much cheaper and faster improvements could be achieved. Instead of developing salt-tolerance mechanisms via expensive arrays directly on crop plants, use of phytoremediation in saline stressed soils would reduce the impact of salinity indirectly via much safer ways.

This study assessed salt tolerance capacity of the *A. cordifolia* in three salt levels (NS, SS and HS). Its adaptation mechanisms and performances were assessed in terms of plant growth, total chlorophyll, accumulation of osmolyte proline, MDA, and antioxidative system (POX, CAT). *A. cordifolia* significantly increased soil OM and soil enzymes (dehydrogenase, urease, phosphatase and protease). We suggest that cultivation of *A. cordifolia* in slightly and highly saline soils would improve the condition of soil physicochemical and soil enzymes properties in an environmentally-friendly manner. *A. cordifolia* could be used in phytoremediation studies.

Acknowledgments. This study was financially supported by Harran University Scientific Research Project (HUBAP) no: 14077. We thank Dr. Murat Dikilitas for the biochemical analyses.

REFERENCES

- [1] Aebi, H. (1984): Catalase in Švitro. – Methods in Enzymology 105: 121-126.
- [2] Ammari, T. G., Al-Hiary, S., Al-Dabbas, M. (2013): Reclamation of saline calcareous soils using vegetative bioremediation as a potential approach. – Archives of Agronomy and Soil Science 59: 367-375.
- [3] Arnon, D. I. (1949): Copper enzymes in isolated chloroplasts, polyphenol oxidase in *Beta vulgaris* L. – Plant Physiology 24: 1-15.
- [4] Bates, L. S., Waldren, R. P., Teare, I. D. (1973): Rapid determination of free proline for water-stress studies. – Plant Soil 39: 205-207.
- [5] Bhuiyan, M. S. I., Raman, A., Hodgkins, D. S. (2017): Plants in remediating salinity-affected agricultural and landscapes. – Proceedings of the Indian National Science Academy 83: 51-66.
- [6] Cela, J., Munné-Bosch, S. (2012): Acclimation to high salinity in the invasive CAM plant *Aptenia cordifolia*. – Plant Ecology and Diversity 5(3): 403-410.
- [7] Chapman, H. D., Pratt, P. F. (1961): Methods of Analysis for Soils, Plants, and Waters. – Division of Agricultural Sciences, University of California, Berkeley.
- [8] Cvikrova, M., Hrubcova, M., Vagner, M., Machackova, I., Eder, J. (1994): Phenolic acids and peroxidase activity in Alfalfa (*Medicago sativa*) embryogenic cultures after ethephon treatment. – Plant Physiology 91(2): 226-233.
- [9] Dikilitas, M. (2003): Effect of Salinity and Its Interactions with *Verticillium Albo-Atrum* on the Disease Development in Tomato (*Lycopersicon Esculentum* Mill.) and Lucerne (*Medicago Sativa* & *M. Media*) Plants. – University of Wales, Swansea.
- [10] Dutta, T., Neelapu, N.R.R., Wani, S. H., Challa, S. (2018): Compatible Solute Engineering of Crop Plants for Improved Tolerance toward Abiotic Stresses. – In: Wani, S. H. (ed.) Biochemical, Physiological and Molecular Avenues for Combating Abiotic Stress Tolerance in Plants. Elsevier, Amsterdam.
- [11] FAO (1974): The Euphrates Pilot Irrigation Project. Methods of Soil Analysis, Gadeb Soil Laboratory (A Laboratory Manual). – FAO, Rome.
- [12] FAO (2016): Food and Agriculture: Key to Achieving the 2030, Agenda for Sustainable Development. – Food and Agriculture Organization of the United Nations, Rome, 23, I5499, <http://www.fao.org/3/a-i5499e>.
- [13] Flowers, T. J., Colmer, T. D. (2015): Plant salt tolerance: adaptations in halophytes. – Annals of Botany 115: 327-331.
- [14] Gill, S. S., Tuteja, N. (2010): Reactive oxygen species and antioxidant machinery in abiotic stress tolerance in crop plants. – Plant Physiology and Biochemistry 48: 909-930.
- [15] Girard, C., Michaud, D. (2002): Direct monitoring of extracellular protease activities in microbial cultures. – Analytical Biochemistry 308(2): 388-391.
- [16] Grigore, M. N., Ivanescu, L., Toma, C. (2014): Halophyte Definitions and Classifications. – In: Grigore, M. N., Ivanescu, L., Toma, C. (eds.) An Integrative Anatomical Study. Springer, New York.
- [17] Guan, S. Y. (1986): Soil Enzymes and Their Research Methods. – Agricultural Sciencetech Press, Beijing, pp. 273-339.
- [18] Gupta, B., Huang, B. (2014): Mechanism of salinity tolerance in plants: physiological, biochemical, and molecular characterization. – International Journal of Genomics. <http://dx.doi.org/10.1155/2014/701596>.
- [19] Herppich, W. B., Peckmann, K. (1997): Responses of gas exchange, photosynthesis, nocturnal acid accumulation and water relations of *Aptenia cordifolia* to short-term drought and rewatering. – Journal of Plant Physiology 150: 467-474.
- [20] Hossain, M. D., Inafuku, M., Iwasaki, H., Taira, N., Mostofa, M. G., Oku, H. (2017): Differential enzymatic defense mechanisms in leaves and root of two true mangrove species under long-term salt stress. – Aquatic Botany 142: 32-40.

- [21] Hýskova, V., Ryslava, H. (2018): Hyperosmotic versus hypoosmotic stress in plants. – *Biochemistry and Analytical Biochemistry* 7(1): 170.
- [22] Jin, K., Sleutel, S., Buchan, D., De Neve, S., Cai, D., Gabriels, D., Jin, J. (2009): Changes of soil enzyme activities under different tillage practices in the Chinese Loess Plateau. – *Soil and Tillage Research* 104(1): 115-120.
- [23] Johnson, C. M., Ulrich, A. (1959): II. Analytical methods for use in plant analysis. – *Calif Agric Exp Stat Bull* 766.
- [24] Kacar, B., Inal, A. (2008): *Plant Analysis*. – Nobel Publication and Distribution, Ankara.
- [25] Karakas, S. (2013): Development of tomato growing in soil differing in salt levels and effects of companion plants on same physiological parameters and soil remediation. – PhD, University of Harran, Sanliurfa.
- [26] Karakas, S., Cullu, M. A., Kaya, C., Dikilitas, M. (2016): Halophytic companion plants improve growth and physiological parameters of tomato plants grown under salinity. – *Pakistan Journal of Botany* 48: 21-28.
- [27] Karakas, S., Cullu, M. A., Dikilitas, M. (2017): Comparison of two halophyte species (*Salsola soda* and *Portulaca oleracea*) for salt removal potential under different soil salinity conditions. – *Turkish Journal of Agriculture and Forestry* 41: 183-190.
- [28] Kaushal, J., Bhasin, S. K., and Bhardwaj, P. (2015): Phytoremediation: a review focusing on phytoremediation mechanisms. – *International Journal of Research* 5: 1-9.
- [29] Kim, J., Liu, Y., Zhang, X., Zhao, B., Childs, K. (2016): Analysis of salt-induced physiological and proline changes in 46 switchgrass (*Panicum virgatum*) lines indicates multiple responses modes. – *Plant Physiology Biochemistry* 105: 203-212.
- [30] Miltner, A., Bombach, P., Schmidt-Brücken, B., Kästner, M. (2012): SOM genesis: microbial biomass as a significant source. – *Biogeochemistry* 111: 41-55.
- [31] Negrao, S., Schmockel, S. M., Tester, M. (2017): Evaluating physiological responses of plants to salinity stress. – *Annals of Botany* 119: 1-11.
- [32] Panta, S., Doyle, R., Hardie, M., Lane, P., Flowers, T., Haros, G., Shabala, S. (2018): Can highly saline irrigation water improve sodicity and alkalinity in sodic clayey subsoils? – *Journal of Soils and Sediments*. DOI: 10.1007/s11368-018-1986-3.
- [33] Rout, P. P., Chandrasekaran, N., Padhan, D. (2017): Soil enzyme activity as influenced by seasonal rainfall and crop growth stages under long-term fertilization and intensive cropping with hybrid maize. – *International Journal of Plant and Soil Science*. 18(2): 1-9.
- [34] Sairam, R. K., Sexena, D. (2000): Oxidative stress and antioxidants in wheat genotypes: a possible mechanism of water stress tolerance. – *Journal of Agronomy and Crop Science* 184: 55-61.
- [35] Shrivastava, P., Kumar, R. (2015): Soil salinity: a serious environmental issue and plant growth promoting bacteria as one of the tools for its alleviation. – *Saudi Journal of Biological Sciences* 22: 123-131.
- [36] Slama, I., Abdelly, C., Bouchereau, A., Flowers, T., Savoure, A. (2015): Diversity, distribution and roles of osmoprotective compounds accumulated in halophytes under abiotic stress. – *Annals of Botany* 115: 433-447.
- [37] Soil Conservation Service (1972): *Soil Survey Laboratory Methods and Procedures for Collecting Soil Samples*. – Soil Survey Invest Rep No. 1. US Gov Print Office, Washington, DC.
- [38] Tabatabai, M. A. (1994): Soil Enzymes. – In: Weaver, W., Angel, J. S., Bottomley, P. S. (eds.) *Methods of Soil Analysis. Part 2. Microbiological and Biochemical Properties*. SSSA Book Series 5, Soil Science Society of America, Madison, WI.
- [39] Taibi, K., Taibi, F., Abderrahim, L. A., Ennajah, A., Belkhdja, M., Mulet, J. M. (2016): Effect of salt stress on growth, chlorophyll content, lipid peroxidation and antioxidant defense systems in *Phaseolus vulgaris* L. – *South African Journal of Botany* 105: 306-312.
- [40] Thomas, G. W. (1996): Soil pH and Soil Acidity. – In: Sparks, D. L. (ed.) *Methods of Soil Analysis: Part 3. Chemical Methods*. Soil Science Society of America, Madison, WI.

- [41] Tripodi, K. E. J., Modesta, F. E. (2003): Purification and characterization of an NAD-dependent malate dehydrogenase from leaves of the crassulacean acid metabolism plant *Aptenia cordifolia*. – *Plant Physiology and Biochemistry* 41: 97-105.
- [42] Walkley, A. (1947): A critical examination of a rapid method for determining organic carbon in soils: effects of variations in digestion conditions and of inorganic soil constituents. – *Soil Sciences* 37: 29-38.
- [43] Yang, M., Yang, D., Yu, X (2018): Soil microbial communities and enzyme activities in sea-buckthorn (*Hippophae rhamnoides*) plantation at different ages. – *PLoS One* 13(1).
- [44] Yuan, B. C., Li, Z. Z., Liu, H., Gao, M., Zhang, Y. Y. (2007): Microbial biomass and activity in salt-affected soils under arid conditions. – *Applied Soil Ecology* 35: 319-328.

SELECTION OF BARLEY (*HORDEUM VULGARE*) GENOTYPES BY GYT (GENOTYPE × YIELD × TRAIT) BILOT TECHNIQUE AND ITS COMPARISON WITH GT (GENOTYPE × TRAIT)

KARAHAN, T.^{1*} – AKGÜN, I.²

¹Field Crops Department, Institute of Natural Sciences, Isparta University of Applied Sciences, Isparta, Turkey

²Department of Field Crops, Faculty of Agricultural Sciences and Technologies, Isparta University of Applied Sciences, Isparta, Turkey

*Corresponding author

e-mail: turan_karahan@hotmail.com

(Received 11th Sep 2019; accepted 28th Nov 2019)

Abstract. The selection of genotypes based on multiple traits and multiple environments is very important to improve stable varieties for breeding programs. Since climatic conditions are very variable and unpredictable, they are very effective in the selection of genotypes based on multiple traits in multiple environmental conditions. Thus, the genotype by yield*trait (GYT) biplot approach was used to determine the best barley candidate from 12 barley genotypes based on multiple (four) environment and multiple (six) traits. In this study, the strengths and weaknesses of each genotype was determined by combining yield and other target traits with GYT biplot method and it was compared with GT (genotype*trait). The stability and general adaptability of each genotype showed differences with between GYT and GT biplot techniques. According to the GT biplot method, advanced lines (3, 9, 12) and Altikat variety were good genotypes, whereas in the GYT biplot method only Altikat variety was the best genotype based on yield × traits combinations. In addition, it was concluded that the best genotype was not fully determined in the GT biplot method, whereas Altikat variety was the best genotype and based on combined traits by GYT biplot. The study showed that GYT biplot is a very good technique, the ideal and stable genotypes can be detected visually with it, and it can be used to define the best candidate based on combining yield and traits selection in breeding programs.

Keywords: *physiological traits, genotype, Turkey, multiple traits, yield*

Introduction

Barley (*Hordeum vulgare* L.) is used by animal feed, malt industries, human food and biodiesel industries and it has been the fourth most produced cereal plant after corn, wheat and rice in the world. The production of barley, ranged between 5.4 and 7.4 million tons depending on the growing seasons and it is the most produced after wheat in Turkey (<http://www.fao.org/faostat/en/#data/QC>; Kendal et al., 2019; Oral et al., 2019). Therefore, it is very important to develop high yield varieties which are physiologically and morphologically compatible with different environmental conditions.

Barley breeders have been conducting studies in all fields for many years in order to develop high yielding varieties for multi-environments. It is very difficult to develop varieties which are high-yielding in multi-environments. In addition, many ecological and agronomic problems encountered during breeding process, limiting the success of plant breeders and so they have been struggling to develop different models to overcome these problems. The breeder process is confronted with two problems. The

first is the negative interaction between the genotype and the environmental interaction (GEI) and the second is genotype yield traits interaction (Yan and Frégeau-Reid, 2018).

The breeders have studied for many years the first subjects (genotype x environment interactions). The candidate and new varieties have been tested under different environmental conditions by many developed methods (GE, GEI, AMMI) in order to characterize their behavior. In the breeder programs, many researchers who work with cereals in different years and environments (Dogan et al., 2016; Kendal and Tekdal, 2016; Kilic, 2014; Mohammadi et al., 2014) reported that the interaction of genotype x year x location (GYL) is very important. The second subjects is to develop varieties that can give good results (high efficiency and quality, resistant to diseases, hospitalization, and drought and temperature stress and frost risk) in different environmental conditions. It is very difficult to improve the best varieties in terms of all traits studied in different environments. Therefore, the breeder has the responsibility for identifying if a trait is positively or negatively associated with grain yield, i.e., identifying if grain yield should be multiplied or divided by a specific trait (Mohammadi, 2019). From this, indices are generated by multiplying the grain yield by the magnitudes of traits in question (positive selection) or by dividing the magnitude of traits by the grain yield (negative selection).

The value of crop cultivars for growers increases, when the breeding is done based on multiple traits. For this purpose, a genotype by yield*trait (GYT) biplot approach recently improved by different researchers (Yan and Frégeau-Reid, 2018; Mohammadi, 2019; Kendal, 2019) and this method provide useful information for genotype evaluation on multiple traits. This methodology identifies strengths and weaknesses of each genotype and provides a superiority index (SI) which allows evaluating genotypes in relation to multi-traits.

The aims of this study are to use GYT biplot and identify which traits are associated with grain yield in barley breeding materials to develop new barley cultivars determined in terms of high yielding, agronomic and physiological traits in different environmental conditions.

Materials and methods

Twelve spring barley genotypes (two checks) were evaluated in two locations in 2013-2014 and 2014-2015 growing seasons in Turkey. The information on genotypes are presented in *Table 1* and the information about locations are presented in *Table 2*. The locations and trial pictures are given in *Appendix* as *Photos 1, 2* and *3*. The standards used in the research are widely cultivated in the region. Therefore, these varieties were selected as standard. *Altikat* cultivar is used in the study as control; because this cultivar was released in 2011 in the research area. So, it is very stable among cultivars which used in research on grain yield, because it is regional and majority barley growers prefer the 6 rows cultivar in this area. *Şahin 91* cultivar was used in the study as control; because this cultivar is a national cultivar, and it is a facultative type and used in common in the north part of the region, because it is resistant to cold damage which sometimes occur in spring time. The advanced lines used in the research are genotypes generally developed by ICARDA and recommended to the regions with moderate precipitation. These genotypes are suitable for the conditions of Southeastern Anatolia Region since the temperature values are high and average rainfall areas are suggested during the development period. For this reason, detailed studies on these genotypes will be made and registered as appropriate for the region.

Table 1. The code, name/pedigree, origin, and spike type of barley genotypes

Code	Name of cultivar and pedigree of lines	Origin	Spike type
G5	ŞAHİN 91 (YEA 1553-1/Eskişehir)	GAPIARTC	2 rows
G1	NK1272/Moroc 9-75/6/ ..SEA01 04-OS.0S-0SD-0SD-0SD-0SD-	AARI	2 rows
G4	ARUPO/K8755//MORA/3.. CBSS00M00098S.0S-0SD-0SD-1SD-0SD-0SD-0SD-0SD	ICARDA	2 rows
G6	ARUPO/K8755//.. CBSS00M00098S.0S-0SD-0SD-2SD-..	ICARDA	2 rows
G7	ARUPO/K8755//.. CBSS00M00098S.0S-0SD-0SD-4SD-0SD-0SD-	ICARDA	2 rows
G8	RECLA 78/SHYRI 2000..CBSS00M00122S.0S-0SD-0SD-4SD-	ICARDA	2 rows
G10	ALTIKAT (Arta/4/Arta/3/Hml-.. (ICB96-0601-0AP-10AP-0AP)	GAPIARTC	6 rows
G2	ROBUST//GLORIA-..CBSS00M00027S.0S-0SD-0SD-1SD-0SD--	ICARDA	6 rows
G3	CABUYA/JUGL ..CBSS00M00060S.0S-0SD-0SD-01SD-0SD-	ICARDA	6 rows
G9	CUCAPAH/PUEBLA/.. CBSS00M00206S.0S--0SD-0SD-5SD-0SD-	ICARDA	6 rows
G11	TAPIR-BAR/PETUNIA 1...CBWS00WM00056S.0S-0SD-0SD-1SD-	ICARDA	6 rows
G12	UNKONOWN	AARI	6 rows

G: Cultivar, ICARDA: International Center for Agricultural Research in the Dry Areas, GAPIARTC: GAP International Agricultural Research and Training Center; AARI: Aegean Agricultural Research Institute

Table 2. Years, sites, codes and coordinate status of environment

Years	Sites	Altitude (m)	Latitude	Longitude	Soil properties	Average of pers. (mm)
2013-2014	Diyarbakır	612	37° 55' N	40°14' E	pH = 7.30 clay-silt	483.5
2014-2015	Adiyaman	685	37° 46' N	38° 17' E	pH = 7.50 clay-silt	704.3

The trials were carried out in a randomized block design with four replications and sowing density was used 450 seeds per m⁻². Plot size was 7.2 m⁻² in sowing time (6 m long × 1.2 m wide) spacing was 20 cm and they composed of a total of 6 rows. Sowing of trials were done in November. The fertilizing percentages were used 60 kg N ha⁻¹ and 60 kg P ha⁻¹ with planting and 60 kg N ha⁻¹ was used to each plots at tillering time for all plots. Harvesting was done using a Hege 140 harvester in an area of 6 m² in each plot.

Moreover, grain yield, agronomic traits (plant height, heading time), physiological traits (canopy temperature depression, SPAD chlorophyll meter (Minolta Co. Ltd., Tokyo, Japan) morphological traits (seed number per spike and yield per spike) gathered for each genotype in each plot. The investigated traits were measured as follows.

Plant height: While the plants were yellow, they were obtained by measuring between the bottom of the plants and the peak.

Heading time: It was obtained by calculating between the period of tillering and the period in which 50 percent of the plants in the parcel were spiked.

Canopy temperature depression: Measurements were measured with Rothenbenger precision infrared thermometer when plants were in spike flowering time (50%). Measurements were performed by Fisher et al. (1998) and the measurement method and time was measured at an angle of 30° in the middle of the plot, 50 cm above the plant height, in the afternoon, in open and windless weather.

SPAD measurement: While the plants were in the grain filling period, the middle parts of the flag leaf of 10 plants which were randomly selected were determined in SPAD unit by measuring with the SPAD-502 Plus (Minolta SPAD-502, Osaka, Japan) device which is used to measure the chlorophyll amount of the plants. Measurements were measured when plants were in spike flowering time (50%).

Seed number per spike: The 10 ears randomly taken from each parcel were blended and the values were obtained by counting grains.

Yield per spike: The 10 ears randomly taken from each parcel were blended and the values were obtained by weighing grains.

Sowing and harvesting time: All test plots were sown in the fall (November), which is the optimal sowing time for barley in the trial areas. Harvesting was carried out in July, when the plants were in the harvesting period. The soil properties of the trials area, pH = 7.30 and soil is clay-silt. All agronomic application such as weed control and fertilization were practiced uniformly.

Statistical analysis (GT and GYT)

The data of twelve barley genotypes in multi-location and multi-year trials were analyzed by GT biplot method, as recommended by Yan and Thinker (2005), GYT biplot method, as recommended by Yan and Frégeau-Reid (2018) and Mohammadi (2019). A superiority index (SI) combining all yield-trait integrations were calculated based on the standardized GYT (Yan and Frégeau-Reid 2018). Biplot method was built for all scored traits of genotypes using Genstat 14 release software program. The data were graphically analyzed for interpretation of GT and GYT using the GGE biplot software. *Figure 1A-E* was produced based on the performance of each genotype for each trait (GT), *Figure 2A-E* was generated based on the performance of genotypes by yield*traits (GYT).

Results

The biplot of genotype by trait (GT) and yield trait combination (GYT)

The mean data of traits across two years in two location of 12 barley genotypes are shown in *Table 3*. The pairwise correlations among traits of 12 spring barley genotypes are shown in *Table 4*. These two table data were used to generate a GT biplot *Figure 1*, although the genotype is compatible with biplot, it represents only 69.01% of the variation. The genotype by yield*trait (GYT) data for 12 spring barley genotypes across two years in two locations are shown in (*Table 5*). The data in the GYT table (*Table 5*) was generated from the GT table (*Table 3*) and in GYT table. The data in each column consists of a combination of yield-trait. The standardized genotype by yield*trait (GYT) data and superiority index for 12 spring barley genotypes across two years in two locations are shown in *Table 6*. The genotypes are quite compatible with biplot, they represent 91.58% of the total variation (PC1 74.96%, PC2 16.60%).

Figure 1A visualize the relationships between properties and trait by genotype profiles. Considering the observations on this figure indicated that grain yield was positively correlated with (GY, CTD, SPAD, SNS and YS), while negative corelated with especially quality traits (HT and PH). However, On the other hand the explanations are confirmed by the correlation values in (*Table 2*). Based on these principles

described in the GYT biplot technique, the following observations can be made about relationships between yield trait combinations in *Figure 2A*. Considering the observations on this figure indicated that all yield-trait combinations tend to correlate positively with each other because they have yields as a component, as shown by the triangular angles between the vectors (*Fig. 2A*). This is an important feature of the GYT biplot (*Fig. 2*) technique, in contrast to the GT biplot (*Fig. 1*); According to the yield-trait combinations (below), graphically, it provides the opportunity for genotypes to be ranking in a more meaningful way. However, as shown the strong relationships between the two traits in the GT biplot technique (*Fig. 1A*), for exam, there is a positive correlation between GY*CTD and a negative correlation between GY*HT and GY*PH (*Fig. 1A; Table 3*). In GYT biplot technique there is a positive correlation among GY and all traits. Therefore, it is better to select genotypes based on different analysis output.

Table 3. The mean data of tarits across two years in three location of 12 barley genotypes

Genotype	GY (kg/ha ⁻¹)	SPAD	CTD (°C)	SNS	YS	HT (date)	PH (cm)
G5-Şahin 91	4759	41.3	27.3	28.3	1.24	100	108
G1	6478	42.9	28.6	33.3	1.31	95	93
G4	6464	42.3	27.2	35.8	1.51	100	103
G6	6359	39.6	27.7	30.6	1.45	97	93
G7	6297	40.8	28.2	39.2	1.43	100	103
G8	6076	42.1	28.4	28.3	1.27	96	95
G10-Altıkat	6978	47.1	29.4	57.5	1.93	97	98
G2	5559	40.3	27.5	50.4	1.65	98	108
G3	5891	40.3	28.1	51.9	1.88	101	95
G9	5660	44.7	28.2	50.0	1.94	112	105
G11	5228	45.7	27.1	51.0	1.69	97	108
G12	6052	41.7	28.0	58.5	2.17	97	110
Mean	5983	42.4	28.0	42.9	1.62	99	101
SD	609.1	2.33	0.66	11.46	0.30	4.35	6.45
LSD (0.05)	140.5	2.2	1.8	6.8	0.3	1.2	13.3
CV (%)	15.17	5.18	2.78	13.8	15.5	5.80	3.95

SD: Standard Deviation, GY: Grain Yield, SPAD: Soil-Plant Analysis Development, CTD: Canopy Temperature Depression, SNS: Seed Number of per Spike, YS: Yield of per Spike, HT: heading time, PH: plant height

Table 4. Pairwise correlations among traits of 12 spring barley genotypes

	GY	SPAD	CTD	SNS	YS	HT
SPAD	0.16					
CTD	0.66*	0.37				
SNS	0.08	0.42	0.22			
YS	0.13	0.33	0.22	0.94**		
HT	-0.28	0.12	-0.02	0.17	0.29	
PH	-0.60*	0.11	-0.51	0.40	0.35	0.26

*Value significant for 0.05, ** for 0.01 probability level

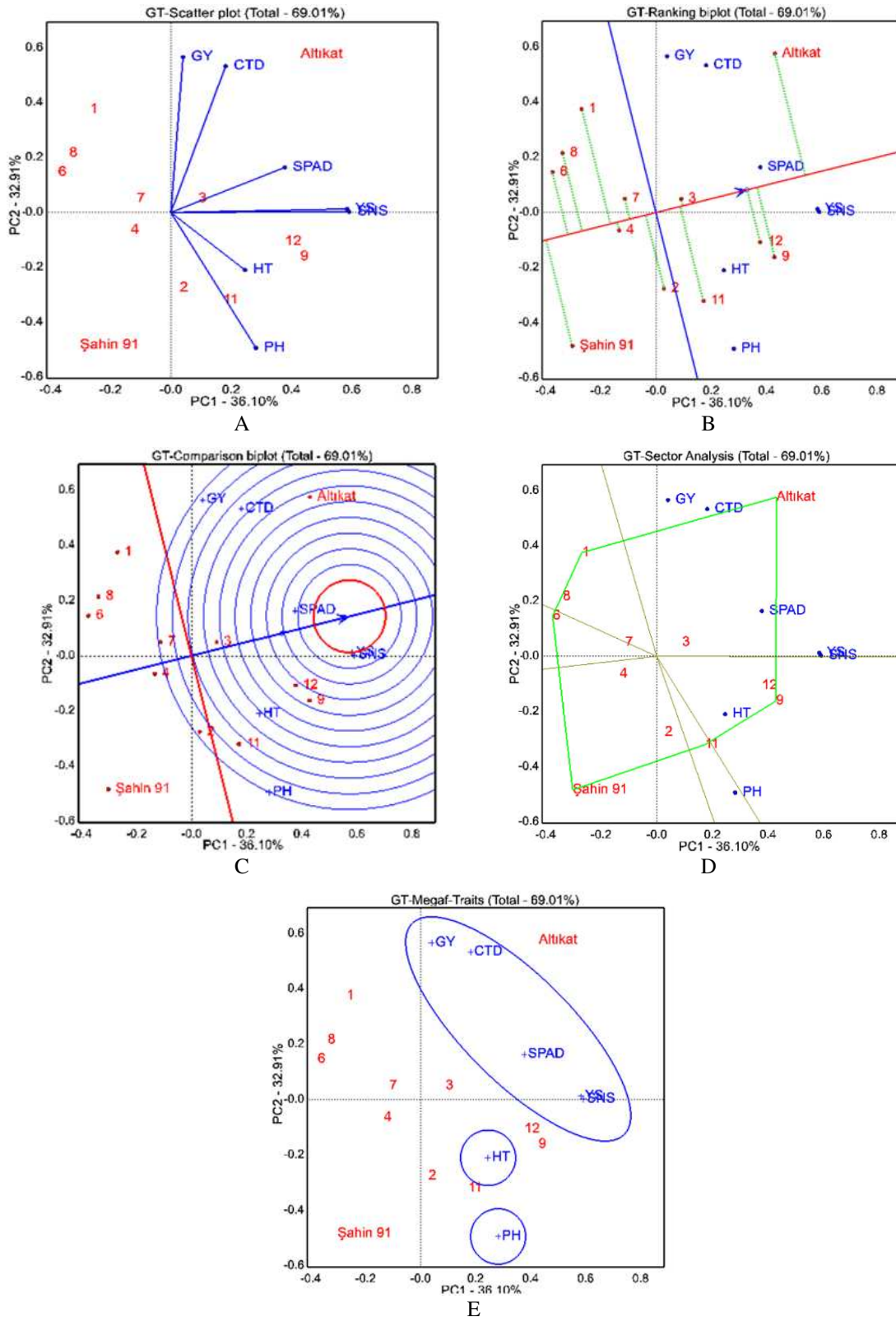


Figure 1. This figure was generated based on genotype by trait mean values across two locations and two growing seasons (Tables 3 and 4). **A** The relationship genotypes and traits. **B** The stability of genotypes based on traits data. **C** The comparison of genotypes based on traits data. **D** Which-won-where/what of GT biplot based on traits data. **E** The mega-traits based on two seasons and locations data

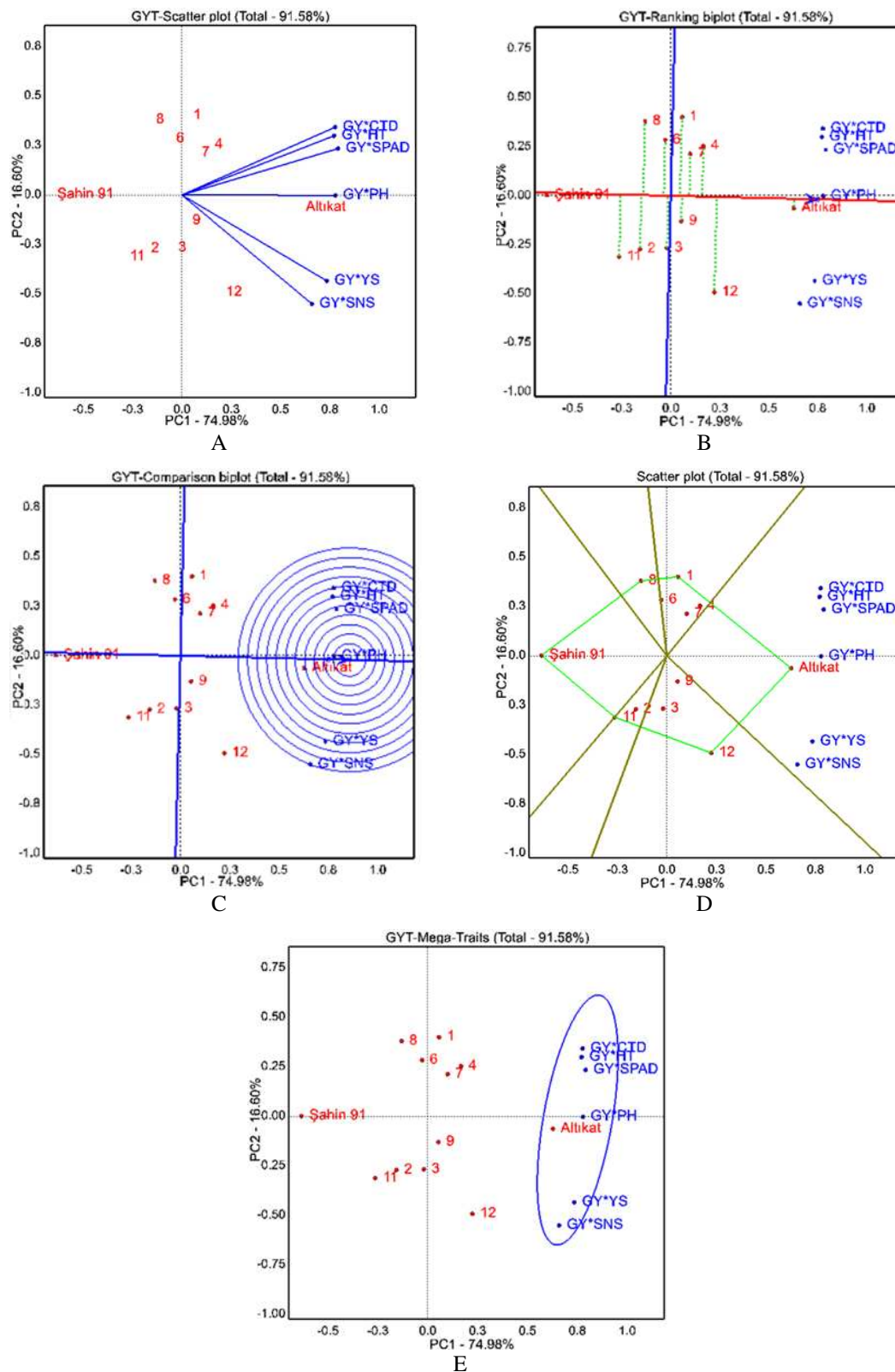


Figure 2. This figure was generated from genotype by yield*trait values across two locations and two growing seasons (Tables 5 and 6). **A** The relationship based on GYT combination data. **B** The stability based on GYT combination data. **C** the comparison based on GYT combination data. **D** Which-won-where/what based on of GYT combination data. **E** The mega-traits based on GYT combination data

Table 5. Genotype by yield*trait (GYT) data for 12 spring barley genotypes across two years in two locations

Genotypes	GY*SPAD	GY*CTD	GY*SNS	GY*YS	GY*HT	GY*PH
G5-Şahin 91	19631	12974	13447	588	47768	51159
G1	27767	18495	21546	849	61623	59923
G4	27326	17566	23168	973	64316	66256
G6	25149	17610	19474	919	61600	58818
G7	25707	17773	24709	900	63047	64543
G8	25566	17272	17208	769	58408	57724
G-10 Altıkat	32849	20489	40096	1349	67686	68035
G2	22381	15287	28013	917	54406	59757
G3	23710	16531	30583	1107	59569	55961
G9	25312	15985	28313	1095	63104	59426
G11	23872	14148	26672	881	50515	56200
G12	25207	16923	35426	1313	58554	66573
Mean	25373	16754	25721	972	59216	60364

Table 6. Standardized genotype by yield*trait (GYT) data and superiority index for 12 barley genotypes across two years in two locations

Genotype	GY*SPAD	GY*CTD	GY*SNS	GY*YS	GY*HT	GY*PH	YLD*SPAD	Mean (SI)
G5-Şahin 91	0.77	0.77	0.52	0.60	0.81	0.85	0.98	0.72
G1	1.09	1.10	0.84	0.87	1.04	0.99	0.96	1.09
G4	1.08	1.05	0.90	1.00	1.09	1.10	0.99	1.08
G6	0.99	1.05	0.76	0.95	1.04	0.97	1.12	0.99
G7	1.01	1.06	0.96	0.93	1.06	1.07	1.20	1.01
G8	1.01	1.03	0.67	0.79	0.99	0.96	1.01	1.00
G10-Altıkat	1.29	1.22	1.56	1.39	1.14	1.13	0.99	1.29
G2	0.88	0.91	1.09	0.94	0.92	0.99	1.01	0.88
G3	0.93	0.99	1.19	1.14	1.01	0.93	0.95	0.93
G9	1.00	0.95	1.10	1.13	1.07	0.98	0.89	0.99
G11	0.94	0.84	1.04	0.91	0.85	0.93	0.93	0.94
G12	0.99	1.01	1.38	1.35	0.99	1.10	0.96	0.72
SD	1.00	1.00	1.00	1.00	1.00	1.00	1.00	1.00

Figure 1B visualizes the stability of genotypes based on trait, and in the figure, a horizontal stability axis and a vertical mean axis are created over the average values and the genotypes are evaluated according to these axes. If the genotypes are located under of vertical axis, it means that they are unpreferable if they located above vertical axis, it means that they are preferable genotypes. On the other hand; the genotypes are located near or in the center of the horizontal line it means that these genotypes are stable, and if they move away from the horizontal line, it means that they are unstable (Yan and Rajcan, 2002). Considering Figure 1B with this prediction;

the advanced line (3) is quite stable because this genotype is located in the center of horizontal axis, and advanced line 12 is stable because this genotype is located near the center of the horizontal axis; Altıkat variety and advanced line 9,11 etc. are unstable, because they are located far from the center of the horizontal axis. While, Şahin 91(control), advanced line 1 and 8 are unpreferable genotypes because they are located under the vertical axis line, other genotypes (Altıkat variety, etc), which are located above the axis vertical line, are preferable genotypes based on trait profiles. The effect of GYT to stability and superiority of genotypes are presented in *Figure 2B*. The stability and superiority analysis of GYT indicated that Altıkat (control) variety is quite stable because this genotype is located in the center of the horizontal axis, and advanced line 4 is stable because this genotype is located near the center of the horizontal axis; advanced line 12, 11 etc. are unstable, because they are located far from the center of the horizontal axis. While, Şahin 91 (control), advanced line 11 and 8 are unpreferable genotypes because of they located under the vertical axis line, other genotypes (advanced line 1, etc), in which located above the vertical axis line, are preferable genotypes based on trait profiles. The result showed that we have to select different genotypes based on GT and GYT biplot analysis and GYT biplot allows us to make a much clear and more efficient selection in the breeding program.

Figure 1C visualizes the discrimination and representativeness of genotypes based traits, and it provides a representative “ideal center” over the mean values of the properties and offers the opportunity to evaluate genotypes according to their proximity or distance to this center (Yan and Tinker, 2005; Oral, 2018). If the genotypes are located in the center, they are the most ideal, if they are located on the average vertical axis, but far from the center, it means that they are ideal, if they are located below the vertical axis, it means that they are undesirable. Considering *Figure 1C* with this prediction; advanced line 9 and 12 are more ideal than 3, 11 and Altıkat variety, because it is nearest to the “ideal center”, while Şahin 91(control) and advanced lines 1, 6, 8 are located under the vertical axis, and also far from the ideal center, so these genotypes are undesirable. Discrimination and representativeness of genotypes based on GYT combination are presented in *Figure 2C* and it provides a representative “ideal center” over the mean values of GYT. Considering *Figure 2C* with this prediction; Altıkat variety is the most ideal genotype, because it was located nearest to the “ideal center” and advanced lines 12, 9, 4, 7, 6, 1 and 3 are desirable for GYT combination. while Şahin 91 and advanced lines 11, 2, 8 are undesirable genotypes, because these genotypes are located under the mean values of the vertical line. The results of GYT biplot analysis were found to be more clear and stable than GT.

Figure 1D visualizes the polygon of GT biplot (which-won-where/what) based on across season data. The figure divided by thick axis from center figure, and each zone separated by two thick lines is referred to as the “sector” and is indicated by numbers 1, 2, 3 etc., starting from the lower right part of the graph, and if the genotypes and properties located the same sector it means they are closely related to each other (Yan and Tinker, 2006; Dogan et al., 2016). Considering *Figure 1D* with this prediction; figure is divided into 6 sectors and different traits are associated with different genotypes in each sector. Genotype 11 is the winner of the sector 1 correlated to PH trait, advanced line 9 is the winner of the sector 2 located in the same sector with line 12 and correlated to HT. The Altıkat variety is the winner of the sector 3 located and correlated to GY, CTD, SPAD, SNS and YS. The other genotypes (2, 3, 4, 6, 7, 8, Şahin 91 variety) are located in other sectors and did not correlate with any traits. The GYT

biplot of sector analysis “which-won-where” can be seen in *Figure 2D*. The most effective genotype associated with trait profiles in each sector is indicated by a polygon peak. In the sector analysis, the figure was divided into 6 sectors and all combinations were in the same sector. Altıkat (control) variety located in sector 1 with all combining (GY*CTD, GY*SPAD, GY*SNS, GY*YS, GY*HT, GY*PH). Other genotypes except Altıkat variety did not correlated with any combinations. The result showed that Altıkat is the best based on combining of all traits with GY. The result showed that GYT is more effective on the selection of genotypes which is the best based on all traits with grain yield than GT biplot method.

Figure 1E visualizes the group of GT based on across season data and in the figure, the traits and genotypes have relationship, they are located in the center of a circle, it means that there are positive correlation among them (Kendal and Dogan, 2016). Considering *Figure 1E* in the light of these explanations; features were separated to 3 different mega-traits. The mega-trait 1 were included only (HT) trait, the mega-trait 2 included only (PH) trait, and other traits (GY, CTD, SPAD, SNS, YS) included mega-trait 3. The mega- traits based on yield-traits combination across season data are presented in *Figure 2E*, which visualizes to yield-trait combinations, which are in a close relationship, are shown in the same circle. Considering *Figure 2E* in the light of these explanations; all yield-trait combinations (GY*CTD, GY*SPAD, GY*SNS, GY*YS, GY*HT and GY*PH) were located in only one mega-trait and Altıkat variety was located in the center of this mega-trait. It means that there is correlation among all trait with yield combination. On the other hand, the figure showed that Altıkat variety is the best genotype based on grain yield with combining traits. The results showed that in a possible selection, the GYT biplot method explained the results more clearly and formally than the GT method.

Discussion

The GT biplot technique has been used successfully by many researchers for a long time to see the relationship between genotype by trait in different plants, and effective selections were made in breeding programs according to the interaction between genotype by trait. However, GYT biplot technique was designed to complete the deficiencies encountered in the GT biplot technique and to enable more efficient selection of plant breeders. GYT biplot is used to sort genotypes according to their general advantages over yield by trait combinations and to show profiles of traits.

The result showed that the selection of genotypes is based on mega-traits, the use of GYT biplot has more advantages instead of GT biplot in breeding studies. In fact, in barley breeding studies, yield is the only trait that can determine the effectiveness of a genotype alone; other traits (agronomic, morphological and physiological characteristics) are valuable only for the breeders when combined with high yield levels, and these properties alone do not mean anything to growers. For example; a barley genotype is not valuable for breeders if it is resistant to temperature stress and the yield is low. However, if the genotype yield is high, it makes the genotype valuable if it has good agronomic and morphological and physiological characteristics as well as. Therefore, the selection of the best genotypes based on the combination effects of yield-trait are more meaningful than the effects of individual traits. In the GT biplot technique, a great value (*Table 3; Fig. 1B*) makes the ATC appearance insignificant in

some cases (Dehghani et al., 2006; Yan and Tinker, 2006; Kendal and Dogan, 2016; Oral et al., 2018), while in the GYT biplot technique it makes the ATC appearance a meaningful and effective tool (Yan and Frégeau Reid, 2018; Mohammadi, 2019; Kendal, 2019), because it ranks genotypes based on various yield-trait combinations and indicates the strengths and weaknesses of genotypes (Fig. 2B; Table 5). The GT biplot technique was used to construct Figure 1A-E using the data in Table 3, while the GYT biplot technique was used in Figure 2A-E using the data given in Table 5, and genotypes were examined with different graphs according to both techniques. The genotypes examined depend on the superiority index (SI) and yield-trait combination (GYT) and the result of Figure 2 showed that the genotypes can be select easy than GT biplot in Figure 1. On the other hand, in GT biplot it is not clear which is the best genotype that is very stable for all traits, while the Altıkat is stable and advanced line 4 and 12 for all combination in GYT biplot. Therefore, it was found in this study that GYT biplot technique is a suitable method for determining the most suitable genotype for all properties in barley breeding studies. GYT biplot, in combination with the yield and any trait, is used to measure how the grain yield is combined with that trait in genotypes. When both the grain yield and the values of any trait are low or high, the values will be either low or high and the genotypes will be evaluated accordingly. On the other hand, the GYT biplot technique was developed to determine when the value of a trait of any genotype is low, grain yield is high or vice versa, whether the results are affected from the combination or is there any changing in the ranking of them. As a result, when the values of the traits and the yield values enter the combination, the data changes and the ranking of the genotypes changes. GYT biplot approach has been reported to be a comprehensive and effective method since it classifies genotypes according to their levels in combination with target characteristics and graphically rank the genotypes with their strengths and weaknesses and in different plants (Yan and Frégeau-Reid, 2018).

Conclusion

The results of this study showed that GYT approach puts too much weight on yield relative to other traits. However, this approach can be used in other crops which is studied based on multi-location, multi-years with multi-traits. The study also verified that there is a potential for simultaneous genetic improvement of the characteristics (SPAD-reading, CTD) in barley. In terms of all traits, the stability of the genotypes and the best genotype is clearly can be seen in the GYT biplot technique (Altıkat), while the best genotypes cannot be seen, because of the GT biplot technique is more complex. Therefore, GYT technique can be used in different plants and traits by researchers for breeding studies.

REFERENCES

- [1] Dehghani, H., Ebadi, A., Yousefi, A. (2006): Biplot analysis of genotype by environment interaction for barley yield in Iran. – *Agronomy Journal* 98(2): 388-393.
- [2] Dogan, Y., Kendal, E., Oral, E. (2016): Identifying of relationship between traits and grain yield in spring barley by GGE Biplot analysis. – *Agriculture & Forestry/Poljoprivreda i Sumarstvo* 62(4): 239-252.

- [3] Kendal, E. (2019): Comparing durum wheat cultivars with genotype×yield×trait (GYT) and genotype× trait (GT) by biplot method. – Chilean Journal of Agricultural Research 79(4): 512-522.
- [4] Kendal, E., Dogan, Y. (2015): Stability of a candidate and cultivars (*Hordeum vulgare* L) by GGE Biplot analysis of multi-environment yield trials in spring barley. – Agriculture & Forestry 61(4): 307-318.
- [5] Kendal, E., Karaman, M., Tekdal, S., Doğan, S. (2019): Analysis of promising barley (*Hordeum vulgare* L.) lines performance by AMMI and GGE biplot in multiple traits and environment. – Applied Ecology and Environmental Research 17(2): 5219-5233.
- [6] Kendal, E., & Tekdal, S. (2016). Application of AMMI model for evaluation spring barley genotypes in multi-environment trials. Bangladesh Journal of Botany, 45(3), 613-620.
- [7] Kilic, H. (2014): Additive main effect and multiplicative interactions (AMMI) Analysis of grain yield in barley genotypes across environments, J. – Agr. Sc. 20: 337-344.
- [8] Mohammadi, R. (2019): Genotype by yield*trait biplot for genotype evaluation and trait profiles in durum wheat. – Cereal Research Communications 47(3): 541-551.
- [9] Mohammadi, R., Haghparast, R., Sadeghzadeh, B., Ahmadi, H., Solimani, K., Amri, A. (2014): Adaptation patterns and yield stability of durum wheat landraces to highland cold rainfed areas of Iran. – Crop Science 54: 944-954.
- [10] Oral, E. (2018): Effect of nitrogen fertilization levels on grain yield and yield components in triticale based on AMMI and GGE biplot analysis. – Applied Ecology and Environmental Research 16(4): 4865-4878.
- [11] Oral, E., Kendal, E., Dogan, Y. (2018): Selection the best barley genotypes to multi and special environments by AMMI and GGE biplot models. – Fresenius Environmental Bulletin 27(7): 5179-5187.
- [12] Oral, E., Kendal, E., Kilic, H., Dogan, Y. (2019): Evolution barley genotypes in multi-environment trials by AMMI model and GGE biplot analysis. – Fresenius Environmental Bulletin 28(4A): 3186-3196.
- [13] Solonechnyi, P., Kozachenko, M., Vasko, N., Gudzenko, V., Ishenko, V., Kozelets, G., Vinyukov, A. (2018): AMMI and GGE biplot analysis of yield performance of spring barley (*Hordeum vulgare* L.) varieties in multi environment trials. – Poljoprivreda i Sumarstvo 64(1): 121-132.
- [14] Yan, W., Tinker, N. A. (2005): An integrated biplot analysis system for displaying, interpreting, and exploring genotype × environment interaction. – Crop Science 45(3): 1004-1016.
- [15] Yan, W., Tinker, N. A. (2006): Biplot analysis of multi-environment trial data: Principles and applications. – Canadian Journal of Plant Science 86(3): 623-645.
- [16] Yan, W., Frégeau-Reid, J. (2018): Genotype by yield * trait (GYT) biplot: a novel approach for genotype selection based on multiple traits. – Sci Rep. 8: 1-10.
- [17] Yan, W., Rajcan, I. R. (2002): Biplot analysis of test sites and trait relations of soybean in Ontario. – Can. J. Plant Sci. 42: 11-20.

APPENDIX

Photo 1. The locations of research in Southeast Anatolia of Turkey



Photo 2. Before and after maturity time of genotypes in the trials in Adiyaman



Photo 3. Maturity time of genotypes in the trials in Diyarbakir



CALIBRATION AND VALIDATION OF REFERENCE EVAPOTRANSPIRATION MODELS IN SEMI-ARID CONDITIONS

ISLAM, S.^{1*} – ABDULLAH, R. A. B.¹ – BADRUDDIN, I. A.² – ALGAHTANI, A.^{2,3} – SHAHID, S.¹ –
IRSHAD, K.⁴ – MALLICK, J.⁵ – HIROL, H.¹ – ALSUBIH, M.⁵ – ELOUNI, M. H.^{5,6} – KAHLA, N. B.^{5,6}

¹*Department of Civil Engineering, University Teknologi Malaysia, P.O. Box 81310 Johor Bahru, Johor, Malaysia*

²*Department of Mechanical Engineering, College of Engineering, King Khalid University, Abha 61413 Asir, Kingdom of Saudi Arabia*

³*Research Centre for Advanced Materials Science (RCAMS), King Khalid University, P.O. Box 9004, Abha-61413, Asir, Kingdom of Saudi Arabia*

⁴*Center of Research Excellence in Renewable Energy (CoRERE), King Fahd University of Petroleum & Minerals, Dhahran, Saudi Arabia*

⁵*Department of Civil Engineering, College of Engineering, King Khalid University, Abha 61413, Asir, Kingdom of Saudi Arabia*

⁶*Laboratory of Systems and Applied Mechanics, Tunisia Polytechnic School, University of Carthage La Marsa, Tunis 2078, Tunisia.*

**Corresponding author*

e-mail: isaiful2@graduate.utm.my; phone: +966-59-521-9933; fax: +966-17-241-8816

(Received 13th Sep 2019; accepted 4th Dec 2019)

Abstract. Reference evapotranspiration (ET_o) is an important parameter for climatological, hydrological and agricultural management. The FAO56 Penman-Monteith (FAO56-PM) model is one of the most accurate models. But it needs a detailed climate dataset from weather stations. Therefore, empirical reference evapotranspiration models (ET_o) that need a reduced set of climate data can become an alternative approach. In this study, nine different evapotranspiration models were calibrated for the 1978-2000 period and validated based on the period between 2001-2017 with respect to standard FAO56-PM method based on the real climatic data obtained from Aseer metrological department, Saudi Arabia. The ranking of all the evaluated models based on the multi-criteria decision making was done in order to get the best alternative to the FAO56-PM Model. The result showed that Mahringer and Trabert models are the most appropriate with RMSE values of 2.13 mm/day and 2.47 mm/day, respectively and the value of percent error were 77.27% and 89.43%, respectively. Moreover, the values of mean bias error were found to be -2.03 mm/day and -2.35 mm/day, respectively. The calibration and validation of different ET_o equations tend to increase their performance. Thus, the validated evapotranspiration model that used less climatic parameters could predict the ET_o condition accurately for any region.

Keywords: *water management, agricultural management, climate, ranking, entropy, AHP*

Introduction

Having an accurate estimation of crop water requirements is crucial for good planning so that water resources can be utilized efficiently (Jin et al., 2018). The most important factors for water resource planning and irrigation scheduling is the determination of reference evapotranspiration ET_o (Jiang et al., 2017; Tie et al., 2018). Therefore, precise estimation of ET_o is essential for net irrigation water requirement, regional water management,

environmental studies and climate change impacts (Wei et al., 2016; Gabri et al., 2019). The method of estimating the evapotranspiration is using a lysimeter. It can provide high accuracy while measuring the evapotranspiration (Hausler et al., 2018). However, these methods are very costly and require much expensive and sophisticated equipment for measurement. As a result, the FAO56-PM Model which bears the high correlation with lysimeter measurement is used for the estimation of evapotranspiration (Allen et al., 1998). Although FAO56-PM method is rigorously used in different part of the world, it still requires various climatic parameters as an input to compute the reference evapotranspiration. Hence, based on the limited climatic parameters, researchers have developed and estimated numerous ETo equations around the world (Djaman et al., 2015, 2016a). Therefore, empirical methods, including mass transfer, radiation, temperature and pan evaporation-based methods have been developed to estimate the reference crop evapotranspiration using the limited data. Although different ETo methods can provide the estimated ETo with relatively good accuracy, they fail to adapt to all the climatic conditions. As a result, the performance of these ETo equations needs to improve under various weather conditions (Li et al., 2018). During the past few years, many studies have been conducted to evaluate various evapotranspiration model but very few studies are focusing on the calibration and validation of evapotranspiration model (Table 1) with respect to the standard FAO56-PM model. Considerable effort has been exerted to evaluate other methods using FAO56-PM as the standard (Hu et al., 2009). Trajkovic and Kolakovic (2009) evaluated five evapotranspiration equations under the humid conditions and concluded that the Turc equation is suitable to estimate the reference evapotranspiration at humid locations, especially when the weather data are limited. Calibration and validation of six evapotranspiration model were performed in the Senegal river delta and it can be concluded that the preciseness of the result can be enhanced substantially as the error was decreased after calibration (Djaman et al., 2016a). Besides that, eleven equations to calculate the monthly ETo were calibrated (Zhai et al., 2010). After calibration, the differences of the regional suitability disappeared or even reversed. In addition, the ETo equations with lysimeter results and found radiation-based method can perform much better as compared to the temperature-based model after calibration (Xu et al., 2013). Pandey and Pandey (2018) performed the calibration and ranking of seven Valiantzas reference evapotranspiration equations for the study period of 2006-2016 under the humid climate at North India. The result showed that Valiantzas model 7 has the best performance. However, the study is lacking the validation of calibrated equation. Djaman et al. (2017a) performed the validation of Valiantzas' reference evapotranspiration equation under humid, sub-humid and semiarid conditions in Africa. The analysis showed that the Valiantzas' ETo equation could become an alternative to the FAO56-PM equation without calibration to follow the local humid, sub-humid and semiarid climatic conditions. However, the analysis is lacking evaluation of different ETo equations. Djaman et al. (2016b) performed the evaluation of the FAO56-PM model with limited data and the Valiantzas models for estimating evapotranspiration in agro-ecological zones of Burkina Faso, West Africa. The result showed that Valiantzas 2 equation with full climatic data has resulted in good ETo estimates relative to the FAO56-PM. However, the calibration and validation are not incorporated in the study. Djaman et al. (2016a) performed the calibration and validation of six ETo model in Senegal river basin, West Africa and concluded that the Valiantzas 2 equation was the best model for the Senegal river delta. However, the ranking operation is not performed in the equation. Albelewi et al. (2015) assessed six evapotranspiration models in the hyper-arid environment in Saudi Arabia. The study concluded that FAO56-PM is the most accurate ETo model to estimate crop water irrigation needs in hyper-arid environments.

However, the validation of the model is not incorporated in the study. Djaman et al. (2015) evaluated sixteen reference evapotranspiration methods under the sahelian conditions in the Senegal river valley. The study showed that Valiantaz is the most promising model that can be used as an alternative to the FAO56-PM model. However, the ranking of the equation is lacking in this study. Pandey et al. (2016) evaluated eighteen reference evapotranspiration methods for the northeastern region of India. The findings revealed that Irmak3 and Turc models performed equally well and are the best among the selected models for the majority of stations. However, the validation of the calibrated equation is not performed in the study. Cadro et al. (2017) performed the validation and calibration of eleven reference evapotranspiration alternative methods under the climate conditions of Bosnia and Herzegovina and concluded that Trajkovic method is the best model. Djaman et al. (2017b) evaluated eleven reference evapotranspiration models in semiarid conditions and concluded that the Abteu equation showed the best performance among the selected ETo equations but the validation and ranking are lacking in the analysis. Bogawski and Bednorz (2014) made comparison and validation of selected evapotranspiration models for conditions in Poland (Central Europe). This approach could substantially decrease the errors produced by the recommended non-calibrated equations. However, there is no ranking procedure involved in the analysis. Lang et al. (2017) make a comparative study of evapotranspiration estimation by eight methods with FAO56-PM method in Southwestern China. The result showed that the radiation-based methods performed better than temperature-based methods among the selected methods in the study area. Among the radiation-based methods, Makking performed the best while Hargreaves and Samani showed the best performance among the temperature-based methods. However, the calibration and ranking are lacking in the study.

The past studies were basically assessed different ETo models against the FAO56-PM model based on the Central and Eastern region and few in southern region of Saudi Arabia (Salih and Sendil, 1984; Saeed, 1986; Mustafa et al., 1989; Al-Omran and Shalaby, 1992; Abo-Ghobar and Mohammad, 1995; Elnesr et al., 2010; Islam et al., 2019a,b). However, in high mountain environments, such as the Abha Asir region, Saudi Arabia, meteorological monitoring is limited and high-quality data are scarce. Moreover, measurements of relative humidity by electronic sensors are commonly plagued by hysteresis, nonlinearity and calibration errors (Allen, 1996). There is no significant work related to the calibration and validation of different evapotranspiration model with respect to standard FAO56-PM in Abha city of Asia region. Based on an extensive literature review, it can be concluded that there are no comprehensive studies being conducted to evaluate the performance of empirical models in the semi-arid region, Abha Aseer, Kingdom of Saudi Arabia on the basis of calibration validation and ranking, especially on a monthly timescale. To fill in this research gap, in this study, an effort was made to estimate the evapotranspiration from a different model based on the availability of meteorological data for the period 1978-2017 and ranking has been done using multi-criteria decision making method. This can aid in recognizing the suitable method that can be used as an alternative equation to standard FAO56-PM method. The finding of the research work is helpful in reducing the error during the evapotranspiration computation. Moreover, the best-evaluated model equation the for evapotranspiration could assist in computing the evapotranspiration in future in the field of water management system, climate change studies, irrigation and water resource planning.

Table 1. Summarization of the previous studies

Sno	Methods/Region	Performance indicator	Remarks	Reference
1	Valiantaz Equation (1 to 7) (Humid-subtropical, Northern India)	R ² (Coefficient of determination), D (Index of agreement), MAE (Mean absolute error), MBE (Mean bias error), Weighted root mean square error (WRMSE)	Valiantaz 2 can be Recommended for daily ETo estimation under conditions of missing data in northeast India. With R ² (0.95), D (0.988), MAE (0.151), MBE (-0.026), WRMSE (0.206)	(Pandey and Pandey, 2018)
2	12 alternative ETo model (Bosnia and Herzegovina region)	Mean bias error (MBE), Root mean square difference (RMSD), Mean Absolute error (MAE), Coefficient of determination (R ²)	Trajkovic method best model RMSD (from 0.157 to 0.243 mm/day), MAE (0.121 to 0.173 mm/day), MBE (0.266 to 0.080) R ² (0.952 to 0.980)	(Cadro et al., 2017)
3	Valiantzas equation using 61 weather stations across 10 African countries (humid, sub-humid and semiarid conditions in Africa)	Root mean squared error (RMSE), Percent error (PE), Mean bias error (MBE), and Mean absolute error (MAE)	The Valiantzas' ETo equation could be an alternative to the Penman-Monteith equation without calibration, RMSE values that varied from 0.03 to 0.27 mm/day, percent error PE from 0.87 to 5.46%, MBE from -0.09 to 0.23 mm/day and MAE from 0.03 to 0.23 mm/day	(Djaman et al., 2017a)
4	Jensen and Haise, Hansen method, Abteu Christiansen, Droogers and Allen, Hargreaves and Allen Irmak method, Tabari 1 and 2 (Semi Arid region, Mali West Africa)	Root mean squared error (RMSE), relative error (RE), mean bias error (MBE), and the absolute mean error (AME)	The Abteu ETo equation is best one, RMSE varying from 0.20 to 0.58 mm/day and average RE, MBE and MAE of 6.7%, -0.25 mm/day and 0.30 mm/day.	(Djaman et al., 2017b)
5	Makkink (Mak), Abteu (Abt), and Priestley-Taylor (PT), Hargreaves-Samani (HS), Thornthwaite (Tho), Hamon (Ham), Linacre (Lin), and Blaney-Criddle (BC) (Southwestern China)	Nash-Sutcliffe efficiency, (NSE), relative error (Re), normalized root mean squared error (NRMSE) and linear regression	NSE (0.34-0.86), Re (-0.10 to -0.13), NRMSE (0.12-0.14), R2 (0.96-0.98) Radiation-based Makkink methods shows better performance	(Lang et al., 2017)
6	Trabert, Mahringer, Penman1948, Albrecht, Valiantzas1 and Valiantzas2 (Senegal River Basin, West Africa)	Root mean squared error (RMSE), Mean bias error (MBE), Percentage Error (PE)	Valiantzas2 equation was the best-performing model for the Senegal River-Delta and had the lowest root mean squared difference (RMSE) of 0.45 mm/day, MBE of -0.05 mm/day and the lowest percent error of estimate (PE) about 7.1%.	(Djaman et al., 2016a)
7	Valiantaz 1 and 2 equation (Agro-ecological zones of Burkina Faso, West Africa)	Root mean squared error (RMSE), Mean bias error (MBE)	ETo-Val 1 method, RMSE varied from 0.43 to 0.57 mm/day and the MBE varied from -0.05 to 0.04 mm/day whereas the ETo-Val-2 method had the RMSE ranging from 0.59 to 2.11 mm/day and the MBE ranging from 0.26 to 1.90 mm/day. (The Valiantzas 2 equation with full climatic data resulted in good ETo estimates)	(Djaman et al., 2016b)
8	12 Radiation based,6 temperature based (Humid Region,North India)	Index of agreement (d), Mean absolute error (MAE),Standard Error of estimates (SEE), Weighted root mean square difference RMSD (WRMSD)	Radiation-based equations of IRMAK3, TURC, 1957MAKK, and MODTURC had superior and consistent performance d(0.88-0.96), MAE(0.15-0.28 mm/day), SEE (0.13-0.38 mm/day), WRMSD (0.23-0.35 mm/day)	(Pandey et al., 2016)
9	FAO-56 Penman-Monteith, Priestly Taylor, Hargreaves-Samani, Makkink (MK), Turc (hyper-arid condition,Saudi Arabia)	Coefficient of determination (R ²), Coefficient of efficiency (E), Modified coefficient of efficiency (E1), Root mean square error (RMSE), Coefficient of residual mass (CRM)	R ² (0.64-0.97), E(0.73-0.95), E1 (0.47-0.78), RMSE (0.33-0.77), CRM (-0.02-0.13) FAO-56 PM is the most accurate , ETo model.	(Ablewi et al., 2015)

Sno	Methods/Region	Performance indicator	Remarks	Reference
10	Hargreaves and Samani , Trajkovic, Ravazzani et al, Modified Hargreaves, Schendel, Trabert, Penman (1948,1963), Romanenko, Romanenko's modified equation, Mahringer, Turc, Makkink, Makkink modified, Valiantzas 1 method, Valiantzas 2 method (Senegal River Valley)	Root mean squared error (RMSE), Mean absolute error (MAE), Percentage error (PE) and Mean ratio (MR)	Valiantzas 2 most promising model with RMSE (0.79 mm/day), MAE (0.63 mm/day) PE (2.47%),MR(1)	(Djaman et al., 2015)

Material and Methods

Site Description

The research work deals with Abha mountainous region of Aseer province, Kingdom of Saudi Arabia having an area of 370 km² located between the latitude of 18°10'12.39"N and 18°23'33.05"N and longitude of 42°21'41.58"E and 42°39'36.09"E as shown in Fig. 1.

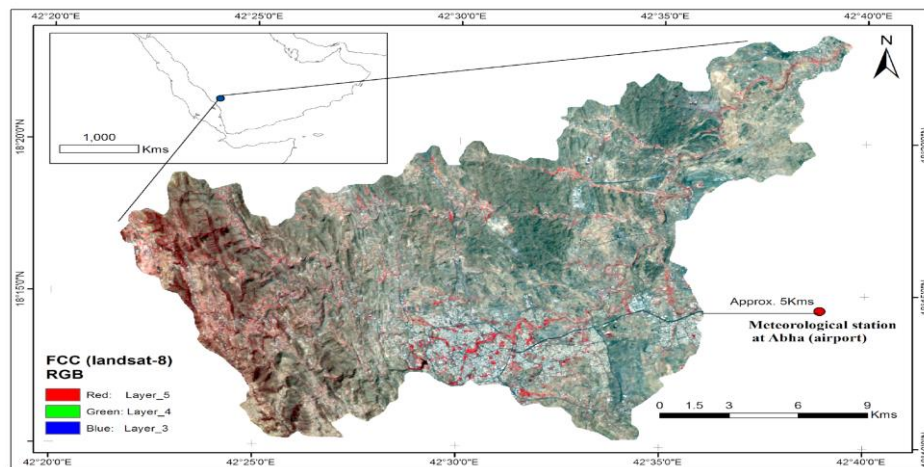


Figure 1. Location map of Abha Asir region, Kingdom of Saudi Arabia

The zone is prone to heavy rainfall as compared to other parts of Saudi Arabia. The elevation varies from 1951 to 2991 m (msl) with average precipitation of 355 mm which mainly occurs between June and October. According to the topographical features of the investigation region, it is found to have weak geology because of the precipitation and slope nature during the past few years. It was observed that this area is facing problem-related to the soil disintegration which influences the efficiency of agriculture, especially water characteristics of catchment zones.

Data Availability

In this research work, primary (raw) weather parameters were collected from Abha meteorological weather station for the period between 1978–2017 (40 years) which includes wind velocity, maximum and minimum temperature, mean temperature, mean relative humidity and solar radiation as well. The data collected were checked by Allen (1996). The weather data are shown in Table 2.

Table 2. Characteristics of Abha weather parameters during the study period

	U2(m/s)	Tmax(°C)	Tmin(°C)	Tmean(°C)	RH mean%	SR (MJm ⁻² d ⁻¹)	Vapour Pressure Deficit (kPa)
Min	0.75	20.3	-0.4	11.9	14	16.8	0.2
Max	5.23	35.1	21.4	25.1	88	25.5	2.9
Mean	2.36	28.5	9.2	18.7	54.7	21.9	1.2
ST-Dev	0.64	3.7	4.4	3.73	12.9	2.5	0.5

Methodology

Various ETo estimation techniques taking into account distinctive data prerequisites are available in the literature. In this research work ETo were estimated by nine reference evapotranspiration model based on available climatic data. Among nine model four model were mass transfer based i.e., Trabert (1896), Mahringer (1970), Penman (1948), Albrecht (1950). Four model were radiation based i.e., Priestley and Taylor (1972), Turc (1961), Makkink modified (1967), Makkink (1957) and one combination based Valiantzas (2013) model. Moreover, the reference ETo values were estimated using standardized FAO56-PM. The values estimated from different equations were compared with the reference value obtained from FAO56-PM for the period between 1978-2017. Further all nine equations were calibrated for the period between 1978-2000 then validation of calibrated equation for the period between 2001-2017 with respect to FAO56-PM model. The performance of equations was evaluated by utilizing several statistical measures such as root mean square value, mean bias error, standard error of estimates, percentage error respectively and finally based on evaluation criteria the ranking was done in order to get most promising model which can be used alternative to FAO56-PM model. The flowchart as shown in Fig. 2 described the stepwise procedure to compute most promising model among nine model to be used as alternate of FAO56-PM model.

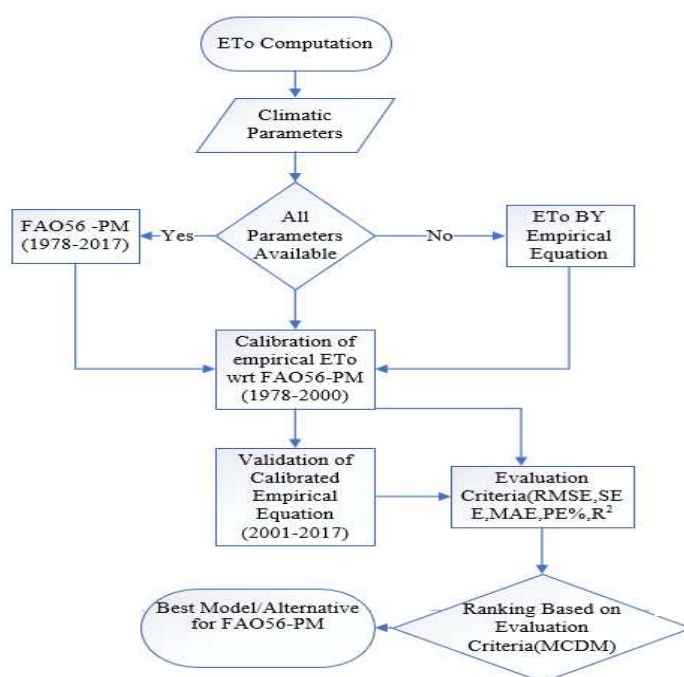


Figure 2. Flowchart showing stepwise computation of ETo

Reference Evapotranspiration (ET_o) Model

This study work aims to analyze trends of the monthly ET_o calculated by the Standard FAO56-PM model (Eq. 1) in the Abha Asir region, Kingdom of Saudi Arabia. However, the use of the FAO56-PM is limited by the insufficiency of climatic input parameters, and the alternative is to employ simple empirical models. The following mass transfer combination and temperature based alternative methods (Eq. 2-11) for estimating ET_o have been chosen for this study. The selection of methods was based on their wide acceptance, simple calculation procedure and applicability in present conditions.

FAO Penman -Monteith (Allen et al., 1998)

$$ET_o = \frac{0.408 \times \Delta \times (R_n - G) + \gamma \times \left(\frac{900}{T + 273}\right) \times u_2 \times (e_s - e_a)}{\Delta + \gamma \times (1 + 0.34u_2)} \quad (\text{Eq.1})$$

Trabert (1896)

$$ET_o = 0.408 \times 0.3075 \times \sqrt{u_2} \times (e_s - e_a) \quad (\text{Eq.2})$$

Mahringer (1970)

$$ET_o = 0.15072 \times \sqrt{3.6u_2} \times (e_s - e_a) \quad (\text{Eq.3})$$

Penman (1948)

$$ET_o = 0.35 \times (1 + 0.24u_2) \times (e_s - e_a) \quad (\text{Eq.4})$$

Albrecht (1950)

$$ET_o = (0.1005 + 0.297u_2) \times (e_s - e_a) \quad (\text{Eq.5})$$

Priestley and Taylor (1972)

$$ET_o = 1.26 \times \left(\frac{\Delta}{\Delta + \gamma}\right) \times \left(\frac{R_n - G}{\lambda}\right) \quad (\text{Eq.6})$$

Turc (1961)

$$ET_o = 0.013 \times \left(\frac{T}{T + 15}\right) \times (R_s + 50) \times \left(1 - \frac{50 - RH}{70}\right) \quad RH < 50 \quad (\text{Eq.7})$$

$$ET_o = 0.013 \times \left(\frac{T}{T + 15}\right) \times (R_s + 50) \quad RH < 50 \quad (\text{Eq.8})$$

Makkink (1967) modified Hansen (1984)

$$ET_o = 0.7 \times \left(\frac{\Delta}{\Delta + \gamma}\right) \times \left(\frac{R_s}{\lambda}\right) \quad (\text{Eq.9})$$

Makkink (1957)

$$ET_o = 0.61 \times \left(\frac{\Delta}{\Delta + \gamma} \right) \times \left(\frac{R_s}{\lambda} \right) - 0.12 \quad (\text{Eq.10})$$

Valiantaz (2013)

$$\begin{aligned} ET_o = & 0.00668 \times R_a \times (T_{mean} + 9.5) \times (T_{max}- \\ & T_{min})^{0.5} - 0.0696 \\ & \times (T_{max}-T_{min}) - 0.024 \times (T_{mean} + 20) \times \left(1 - \frac{RH}{100} \right) - \\ & 0.00455 \times R_a \times (T_{max}-T_{dew})^{0.5} \\ & + 0.0984 \times (T_{mean} + 20) \times (1.03 + 0.00055 \times (T_{max}- \\ & T_{min})^2 - (RH/100)) \end{aligned} \quad (\text{Eq.11})$$

where ET_o = reference evapotranspiration (mm day^{-1}); R_n = net radiation at the crop surface ($\text{MJm}^{-2} \text{day}^{-1}$); G = soil heat flux density ($\text{MJm}^{-2} \text{day}^{-1}$) that is taken as zero for daily ET_o estimation; u_2 = wind speed at 2 m height (m s^{-1}); e_s = saturation vapor pressure (kPa); e_a = actual vapor pressure (kPa); T = temperature at 2 m height ($^{\circ}\text{C}$); $(e_s - e_a)$ = vapor pressure deficit (kPa); Δ = slope of vapor pressure curve ($\text{kPa } ^{\circ}\text{C}^{-1}$); and γ = psychrometric constant ($\text{kPa } ^{\circ}\text{C}^{-1}$); T_{max} = Maximum Temperature ($^{\circ}\text{C}$); T_{min} = Minimum Temperature ($^{\circ}\text{C}$); T_{mean} = Mean Temperature ($^{\circ}\text{C}$); RH_{mean} = Mean Relative Humidity (%); RH_{max} = Maximum Relative Humidity (%); RH_{min} = Minimum Relative Humidity (%).

Model Validation

For the validation of FAO56-PM ET_o model, the estimated result of FAO56-PM were compared with value measured from Davis Vantage Pro2 weather stations installed in Abha region. The instrument provides real-time data for weather conditions. It uses air temperature, relative humidity, average wind speed, and solar radiation data to estimate ET_o , which is calculated once an hour. Validation of FAO56-PM with measured value as represented by Fig. 3. After evaluating FAO56-PM with measure ET_o the RMSE and MBE value found to be 0.144 and 0.011 mm while coefficient of determination found to be 0.987 with slope and intercept of 1.013 and -0.032, respectively.

Calibration and Validation of ET_o Equations

The linear regression model was employed to calibrate and validate the empirical models against the FAO56-PM model (Allen et al., 1998). The specific expression is as shown in Eq. 12.

$$ET_{FAO56-PM} = a \cdot ET_{EMP} + b \quad (\text{Eq.12})$$

where $ET_{FAO56-PM}$ and ET_{EMP} represent the daily reference evapotranspiration estimated by the FAO56-PM model and the nine empirical models respectively whereby a and b are calibrated empirical coefficients. In this research work, the climatic data from 1978-2000 were used for the development of the calibrated equations and data from

2000-2017 were applied for validation purpose. This partitioning is important as more data is required for the models' training.

The main objective of calibrating ETo was to make the slope equally inclined to both x and y axis and intercept reaching zero. For this purpose, a linear regression was done in between Standard PM-ETo and values were obtained through the nine ETo equations. To accomplish this, calibration coefficients need to be determined which can be obtained by applying product operation to the slope of a regression line between the FAO56-PM-ETo and ETo equation by inverting the slope. This will get a new slope so that the new equation will be closer to unity. Moreover, opposite sign value of the intercept was added to get a new intercept close to zero for new regression equation. The calibration and validation of ETo estimates were performed as suggested by (Xu et al., 2013).

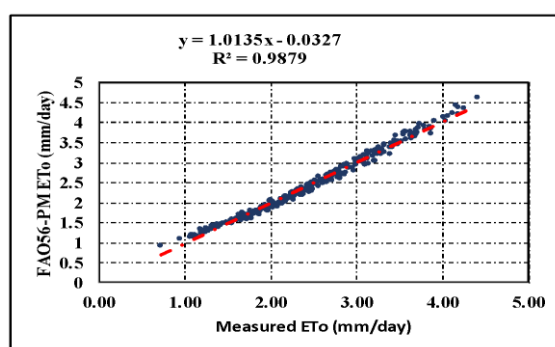


Figure 3. Validation of Standard FAO56-PM ETo with Measured ETo

Comparison of the Performance of Different ETo Methods

The comparative study was performed for the FAO56-PM model and the rest of the local nine ETo equations by making use of the scatter plot. The linear regression line was plotted to get the the coefficient of determination. The high value of coefficient shows the best sign of goodness of fit for the observations (Djaman et al., 2016a). Moreover, the performance indicator such as root mean squared error (RMSE) (Eq. 13), mean bias error (MBE) (Eq. 14), percent error of estimate (PE) (Eq. 15), the standard error of estimate (SEE) (Eq. 16), Correlation Coefficient (R^2) (Eq. 17) were used to compare the nine ETo models. A comprehensive statistical analysis was used to analyze the model results against the observed data. Moreover, it can also be employed to test the agronomical models. The significance of root mean square error is that it is an absolute measure of the overall error in the estimates relative to the observed values which are expressed in the same units and scale as the data itself. It can take any positive value with zero indicating a perfect lack of error.

Root Mean Square Error

$$RMSE = \sqrt{\frac{\sum_{i=1}^n (ET_{Eq} - ET_{PM-FAO})^2}{n}} \quad (Eq.13)$$

Similarly, the mean bias error (MBE) measures the extent to which the estimated value deviates from the observed value. It can take any value with negative values

indicating the systematic under-estimation and positive values, over-estimation and zero indicating a perfect lack of bias.

Mean Bias Error

$$MBE = \sum_{i=1}^n \frac{(ET_{Eq} - ET_{PM-FAO})}{n} \quad (Eq.14)$$

$$PE = \left| \frac{(ET_{Eq_{av}} - ET_{PM-FAO_{av}})}{ET_{PM-FAO_{av}}} \right| \times 100 \quad (Eq.15)$$

The SEE was computed following the equation as shown below:

$$SEE = \sqrt{\frac{1}{n(n-2)} \left[n \sum_{i=1}^n ET_{eq}^2 - \left(\sum_{i=1}^n ET_{eq} \right)^2 - \frac{[n \sum_{i=1}^n ET_{FAO56-PM} \times ET_{eq} - \sum_{i=1}^n ET_{FAO56-PM} \times \sum_{i=1}^n ET_{eq}]^2}{n \sum_{i=1}^n ET_{FAO56-PM}^2 - (\sum_{i=1}^n ET_{FAO56-PM})^2} \right]} \quad (Eq.16)$$

Correlation Coefficient

$$R^2 = 1 - \frac{\sum_{i=1}^n (ET_{O,Mi} - ET_{O,FAO56-PM})^2}{\sum_{i=1}^n (ET_{O,Mi} - ET_{O,Mi_{av}})^2} \quad (Eq.17)$$

where, $ET_{O,Mi}$ = Reference evapotranspiration by *i*th model; $ET_{O,FAO56-PM}$ = Reference evapotranspiration by Standard model 1; SD = Standard Deviation.

Ranking

Many researchers employ multi-criteria decision making (MCDM) methods to cope with water-related problems in their studies (Makropoulos et al., 2008) such as river basin planning (Qin et al., 2008), water supply reservoir (e.g. Srdjevic et al., 2004), urban water management (Zarghami et al., 2008), groundwater management (Petersen, 2006), wetland management (Janssen et al., 2005), and irrigation planning (Gupta et al., 2000). Senent-Aparicio et al. (2017) uses SWAT and Fuzzy TOPSIS to assess the Impact of Climate Change in Segura River Basin (SE Spain). The present study deals MCDM technique (Entropy for weightage and TOPSIS for performance) for ranking ETo models (alternatives) using statistical indices (criterias), coefficient of determination, standard error of estimate, mean bias error, root mean square error and percent error. The value of SEE, RMSE, MBE and PE is indirectly proportional to the rank called as non-beneficial criteria. Moreover, R^2 value is directly proportional to the rank called as beneficial criteria. The performance value (greater the value better will be the model) of different ETo models will decide the promising model in Abha region which is one of the novelty in this research work.

Entropy Method

Objective Weight

The objective weight is determined by Entropy method by making use of probability theory (Vinogradova et al., 2018).

The decision matrix *A* with *m* alternatives and *n* criteria is shown by Eq. 18.

$$A = \begin{bmatrix} x_{11} & \cdots & x_{1n} \\ \vdots & \ddots & \vdots \\ x_{m1} & \cdots & x_{mn} \end{bmatrix} \quad (\text{Eq.18})$$

where x_{ij} ($i = 1, 2, \dots, m; j = 1, 2, \dots, n$) shows the performance value of the i^{th} alternative to the j^{th} criteria.

The normalized decision matrix is calculated using *Eq. 19*.

$$P_{ij} = \frac{x_{ij}}{\sqrt{\sum_{i=1}^m x_{ij}^2}} \quad (\text{Eq.19})$$

The entropy E_j of the j^{th} criteria is computed by *Eq. 20*.

$$E_j = -k \sum_{i=1}^m P_{ij} \ln(P_{ij}) \quad j = 1, 2, \dots, n \quad (\text{Eq.20})$$

A constant that ensures $0 \leq E_j \leq 1$ in the $k = 1/\ln m$ where m presents the number of choices.

The degree of divergence (d_j) computed by *Eq. 21*.

$$d_j = |1 - E_j| \quad (\text{Eq.21})$$

The j^{th} criteria entropy weight is computed by *Eq. 22*.

$$\beta_j = \frac{d_j}{\sum_{j=1}^n d_j} \quad (\text{Eq.22})$$

Topsis Method

The TOPSIS method (Alamanos et al., 2018) is expressed in a succession of six steps as follows:

Step 1: The normalized value of matrix as in *Equation 18* is calculated by *Eq. 23*.

$$\overline{X}_{ij} = \frac{x_{ij}}{\sqrt{\sum_{j=1}^n x_{ij}^2}} \quad (\text{Eq.23})$$

where $i = 1, 2, \dots, m$ and $j = 1, 2, \dots, n$.

Step 2: The weighted normalized value is computed by multiplying the normalized value by weightage of criterios obtained by *Eq. 22*.

Step 3: Determine the ideal best value (V_j^+) and ideal negative value (V_j^-) from weightage normalized value.

Step 4: The Euclidean distance of each alternative from the ideal best solution (*Eq. 24*) and the ideal worst solution (*Eq. 25*), respectively, are as follows:

$$S_i^+ = \left[\sum_{j=1}^m (V_{ij} - V_j^+)^2 \right]^{0.5} \quad (\text{Eq.24})$$

$$S_i^- = \left[\sum_{j=1}^m (V_{ij} - V_j^-)^2 \right]^{0.5} \quad (\text{Eq.25})$$

Step 5: The performance score is computed by Eq. 26.

$$P_i = \frac{S_i^-}{S_i^+ + S_i^-} \quad (\text{Eq.26})$$

Step 6: Rank the alternatives (greater the P_i value better will be rank).

Results

Evaluation of Reference Evapotranspiration Equations for the 1978–2017 Period

The comparative study of all reference evapotranspiration equation with Standard Penman-Monteith equation is shown in Fig. 4a-i. The plot clearly stated that the Evapotranspiration value from all the nine equations has a high correlation with the PM-ETo with the coefficient of determination R^2 range from 0.54 to 0.96. The highest correlation was shown by Albrecht model while the lowest correlation was Makkink method. The best fit of a model is measured by the linear regression line slope close to unity and the intercept to zero. The variation of slope and intercept of the Trabert model were found to be 0.114 and -0.053, respectively and the value of the coefficient of determination was 0.944 (Fig. 4a). Similarly, slope and intercept of the Mahringer model (Fig. 4b) were found to be 0.261 and -0.12, respectively and the value of the coefficient of determination was 0.944. Moreover, slope and intercept of the Penman model (Fig. 4c) were found to be 0.421 and -0.81, respectively and the value of the coefficient of determination was 0.941. Meanwhile, slope and intercept of the Albrecht model (Fig. 4d) were found to be 0.473 and -0.225 and the value of the coefficient of determination was 0.963. The slope and intercept of the Priestly Taylor model (Fig. 4e) were found to be 1.126 and 1.039, respectively and the value of the coefficient of determination was 0.733. From Fig. 4f, it can be seen that the slope and intercept of the Turc model were found to be 0.287 and 0.981, respectively and the value of the coefficient of determination was 0.659. In Fig. 4g, the slope and intercept of the Makkink Modified Hansen model were found to be 0.63 and 2.958, respectively and the value of the coefficient of determination was 0.54. The slope and intercept of the Makkink (1957) model (Fig. 4h) were found to be 0.549 and 2.459, respectively and the value of the coefficient of determination was 0.54. Similarly, the slope and intercept of the Valiantaz model (Fig. 4i) were found to be 0.457 and 0.511 and the value of the coefficient of determination was 0.673. The slope that was closer to one was observed in Priestly Taylor method. On the other hand, the intercept that was closer to zero was shown by Trabert model. The regression equation for evaluation, calibration and validation are shown in Table 3) The accuracy of the result was performed using evaluation criteria like RMSE, SEE, MBE and PE values as shown in Table 4. Statistical analysis showed that all the selected equations underestimated ETo. The RMSE values were ranging from 0.98 to 2.36 mm/day with the minimum error shown by Valiantaz model and maximum error shown by Trabert model. The MBE values were ranging from 0.78 to 2.24 mm/day with the minimum error shown by Turc model.

The SEE values were ranging from 0.023 to 0.571 with the minimum error shown by Trabert and the maximum error shown by the Priestly Taylor method. The PE% were ranging from 90.70 to 33.53 with minimum error shown by the Valiantaz model.

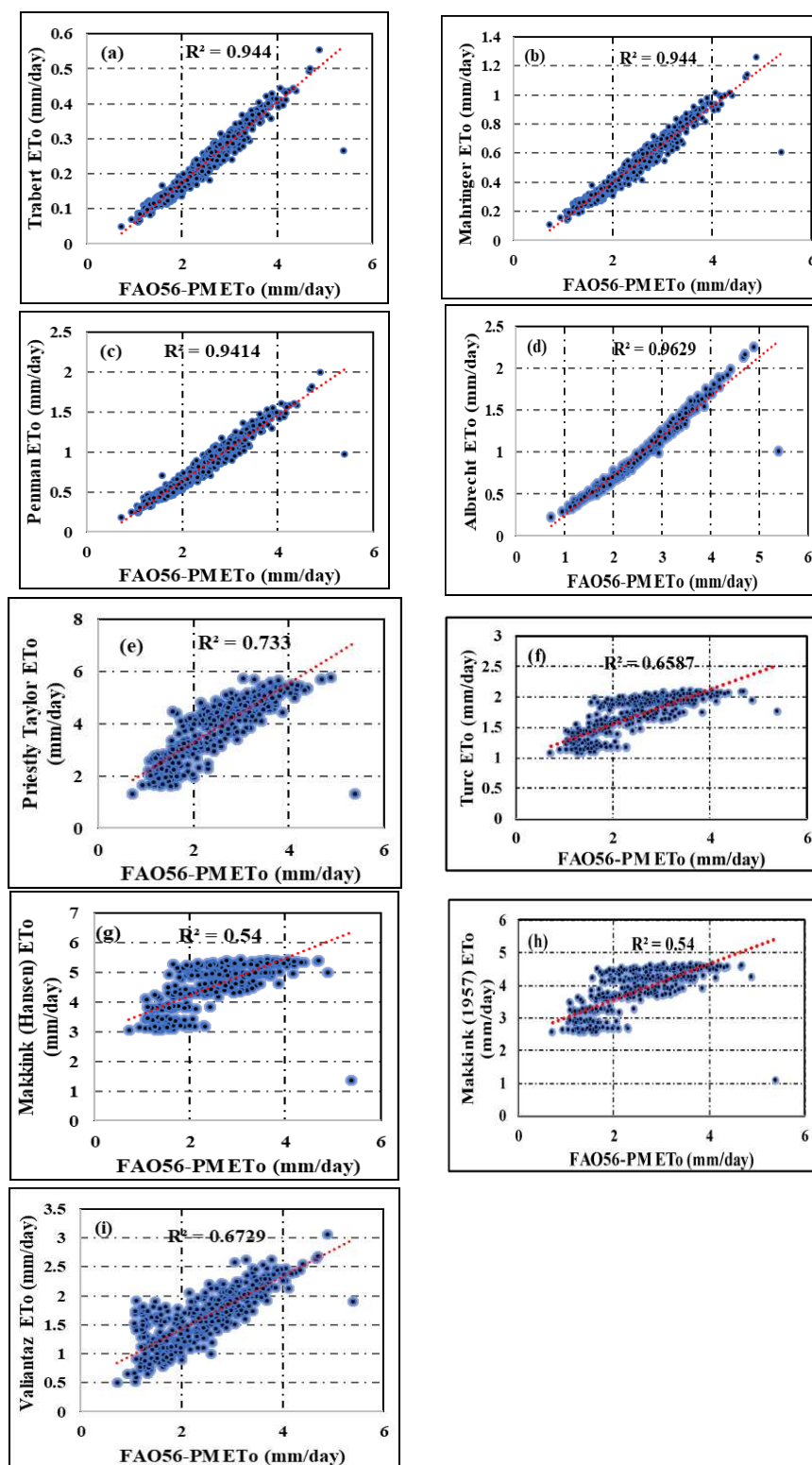


Figure 4. Relationship between the daily ETo estimates of each method versus the FAO56-PM at Abha for the 1978–2017 period

Table 3. Regression equation for Evaluation, Calibration and validation

SN	Method	Evaluation	Calibration	Validation
1	Trabert	$y=0.114x-0.0528$	$y=1.0149x-0.0326$	$y=0.1108x-0.0136$
2	Mahringer	$y=0.2607x-0.1203$	$y=1.0105x-0.0355$	$y=0.2539x-0.0699$
3	Penman	$y=0.412x-0.1813$	$y=1.0114x-0.0332$	$y=0.4012x-0.127$
4	Albrecht	$y=0.473x-0.225$	$y=1.0132x-0.0314$	$y=0.4599x-0.0.1726$
5	Priestly-Taylor	$y=1.1258x+1.0394$	$y=1.0588x-0.0894$	$y=1.0189x+1.1118$
6	Turc	$y=0.2869x+0.9811$	$y=1.0587x-0.0803$	$y=0.2609x+1.0072$
7	Makkink (Hansen)	$y=0.63x+2.9573$	$y=1.0963x-0.1422$	$y=0.5373x+2.8613$
8	Makkink(1957)	$y=0.549x+2.4574$	$y=1.0963x-0.1409$	$y=0.4681x+2.4252$
9	Valiantaz	$y=0.4575x+0.5107$	$y=1.048x+0.1694$	$y=0.4012x+0.7759$

Table 4. Evaluation of criteria parameters for ET estimate between 1978-2017

	R ²	SEE	RMSE	MBE	PE
Trabert-ET0(mm)	0.94	0.023	2.36	2.24	90.70
Mahringer-ET0(mm)	0.94	0.053	2.04	1.94	78.81
Penman-ET0(mm)	0.94	0.086	1.71	1.63	66.15
Albrecht-ET0(mm)	0.96	0.078	1.59	1.52	61.82
Priestly Taylor-ET0(mm)	0.73	0.571	1.47	1.35	54.75
Turc -ET0(mm)	0.66	0.174	1.00	0.78	31.50
Makkink-Modified Hansen ET0(mm)	0.54	0.489	2.13	2.05	83.00
Makkink 1957 ET0(mm)	0.54	0.426	1.46	2.17	54.60
Valiantaz ET0 (mm)	0.67	0.268	0.98	0.83	33.53

Calibration of the Reference Evapotranspiration Equations between 1978-2000

The main objective of the model calibration is to improve the performance of all equations. The computed result from the year 1978 to 2000 was used to calibrate the evapotranspiration equation. Based on the calibration procedure as shown in *Fig. 5a-i*, it can be observed that the coefficient for determination improved substantially with values of R² ranges from 0.61 to 0.99 whereby high correlation was shown by Albrecht model and lower value by Makkink method. The slope and intercept of the Trabert model were found to be 1.015 and -0.033, respectively and the value of the coefficient of determination was 0.963 (*Fig. 5a*). Similarly, the slope and intercept of the Mahringer model (*Fig. 5b*) were found to be 1.01 and -0.036, respectively and the value of the coefficient of determination was 0.963. In *Fig. 5c*, the slope and intercept of the Penman model were found to be 1.011 and -0.033, respectively and the value of the coefficient of determination was 0.961. The slope and intercept of the Albrecht model (*Fig. 5d*) were found to be 1.013 and -0.031, respectively and the value of the coefficient of determination was 0.985. In *Fig. 5e* the slope and intercept of the Priestly Taylor model were found to be 1.059 and -0.089, respectively and the value of the coefficient of determination was 0.77. Similarly, in *Fig. 5f*, the slope and intercept of the Turc model were found to be 1.059 and -0.08, respectively and the value of the coefficient of determination was 0.66. The slope and intercept of the Makkink Modified Hansen model (*Fig. 5g*) were found to be 1.096 and -0.142, respectively and the value of the coefficient of determination was 0.609. In *Fig. 5h* the slope and intercept of the Makkink (1957) model were found to be 1.096 and -0.169, respectively and the value of the coefficient of determination was 0.609. Similarly, in *Fig. 5i* the slope and intercept

of the Valiantaz were found to be 1.048 and -0.169, respectively and the value of the coefficient of determination was 0.681. The slope that was closer to one was observed in Mahringer model while the intercept that was closer to zero was shown by Albrecht model.

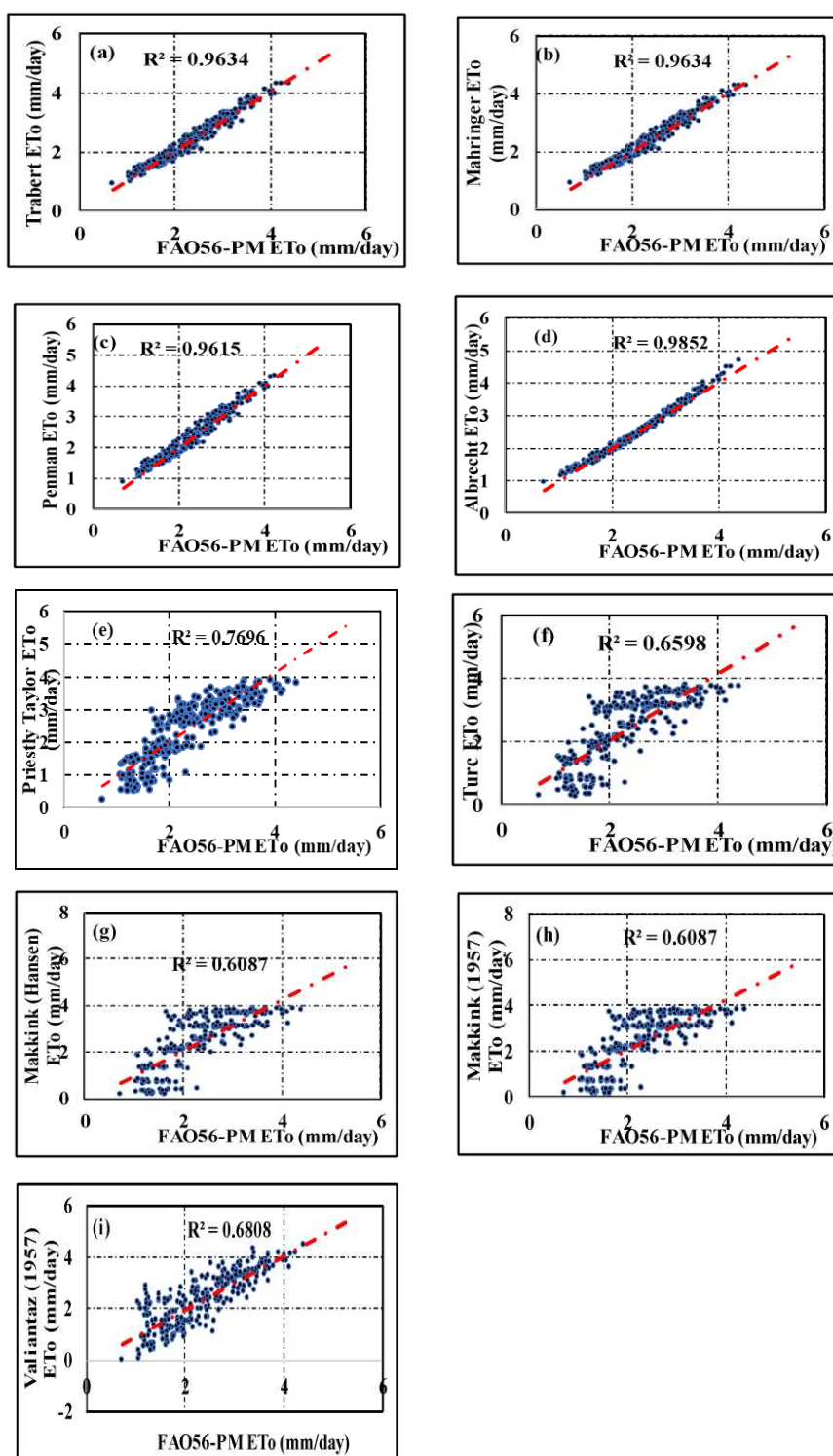


Figure 5. Relationship between the calibrated daily ETo estimates of each method versus the FAO56-PM at Abha for the 1978-2000 period

The RMSE values were ranging from 0.1 to 0.71 mm/day with the minimum error shown by Albrecht model and maximum error is shown by Makkink model. The MBE values were ranging from -0.14 to 0.09 mm/day with the minimum error shown by Albrecht and Trabert. The SEE values were ranging from 0.1 to 0.7 with the minimum error shown by Albrecht and Maximum error shown by Makkink method. The PE% were ranging from 3.63 to 0.01 with minimum error shown by Albrecht model. There was considerable a reduction in RMSE and MBE values for all the equations after calibration as shown in *Table 5*. The percentage error also reduced significantly whereby the maximum reduction in error percentage was found to be in Trabert Model in which the error reduced from 90.70 to 0.1%. However, there was no improvement in SEE values as the error increased slightly in Priestly Taylor method whereby the error reduced from 0.57 to 0.46.

Table 5. Evaluation of criteria parameters for calibrated ET estimate between 1978-2000

	R²	SEE	RMSE	MBE	PE
Trabert-ET0(mm)	0.96	0.16	0.16	0.00	0.10
Mahringer-ET0(mm)	0.96	0.16	0.16	-0.01	0.47
Penman-ET0(mm)	0.96	0.16	0.16	-0.01	0.28
Albrecht-ET0(mm)	0.99	0.10	0.10	0.00	0.01
Priestly Taylor-ET0(mm)	0.77	0.46	0.46	0.05	2.07
Turc -ET0(mm)	0.66	0.60	0.61	0.00	2.44
Makkink-Modified Hansen ET0(mm)	0.61	0.70	0.71	0.09	3.57
Makkink 1957 ET0(mm)	0.61	0.70	0.71	0.09	3.63
Valiantaz ET0 (mm)	0.68	0.57	0.57	-0.14	2.42

Validation of ET Model from Calibrated Equation for Period between 2001-2017

Nine calibrated evapotranspiration equations have been validated for the period of 2001–2017 in order to show which calibrated equation perform well and can be further employed as an alternative to Standard FAO Penman Monteith model.

From the validation procedure as shown in *Fig. 6a-i*, it can be observed that the coefficient of determination improved substantially with values of R² ranges from 0.48 to 0.936 with high correlation shown by Albrecht model and lower value by Makkink method. The slope and intercept of the Trabert model were found to be 0.111 and -0.014, respectively and the value of the coefficient of determination was 0.919 (*Fig. 6a*). Similarly, the slope and intercept of the Mahringer model (*Fig. 6b*) were found to be 0.254 and -0.07, respectively and the value of the coefficient of determination was 0.919. In *Fig. 6c* the slope and intercept of the Penman model were found to be 0.401 and -0.127, respectively and the value of the coefficient of determination was 0.916. The slope and intercept of the Albrecht model (*Fig. 6d*) were found to be 0.46 and -0.173, respectively and the value of the coefficient of determination was 0.936. In *Fig. 6e* the slope and intercept of the Priestly Taylor model were found to be 1.019 and 1.112, respectively and the value of the coefficient of determination was 0.696. In *Fig. 6f* the slope and intercept of the Turc model were found to be 0.261 and 1.007, respectively and the value of the coefficient of determination was 0.667. Similarly, in *Fig. 6g* the slope and intercept of the Makkink Modified Hansen model were found to be 0.537 and 2.86, respectively and the value of the coefficient of determination was 0.48. The slope and intercept of the Makkink (1957) model (*Fig. 6h*) were found to be 0.468 and 2.425, respectively and the value of the coefficient of determination was 0.48. In *Fig. 6i* the slope and intercept of the Valiantaz model were found to be 0.4 and 0.776,

respectively and the value of the coefficient of determination was 0.647. The slope that was closer to one was observed in the Priestly Taylor model while the intercept closer to zero was shown by Trabert model.

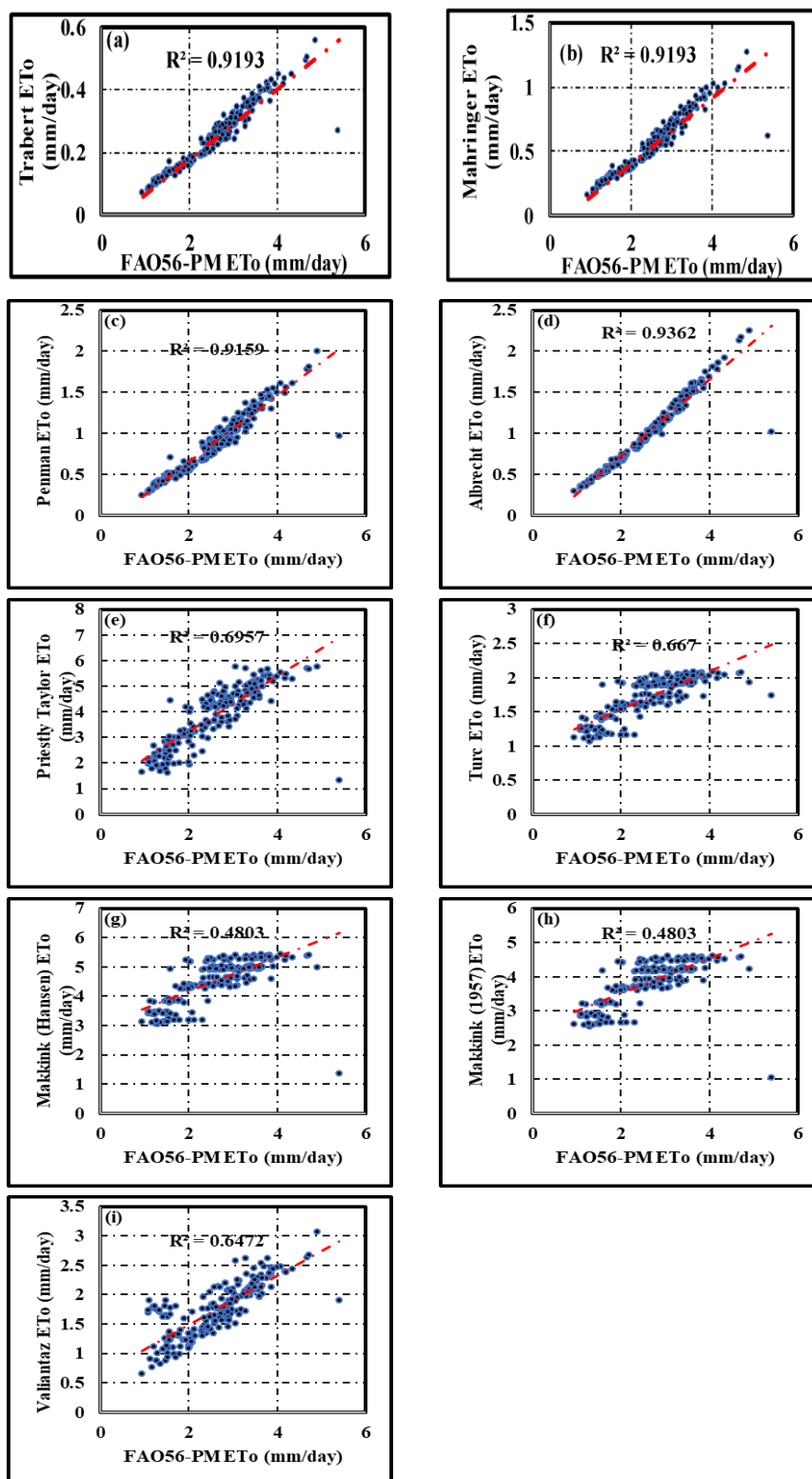


Figure 6. Validating the calibrated equation for the period between 2001-2017

The statistical analysis as shown in *Table 6* illustrates that there is a close relationship between the validated equation result with the Penman Monteith estimates. Similar to the output of the calibrated equation, the result obtained from SEE, RMSE, MB and PE showed a similar pattern with only slightly decrease in R^2 . The value of SEE, RMSE, MBE and PE is acceptable for ETo estimation with any of the nine ETo equations at Abha station. However, Validated Valiantzas equation ($R^2=0.65$, the lowest RMSE 0.99 mm/day and the lowest PE of 30.32%) should be the first option to estimate ETo in the Abha Region followed by Turc then Albrecht. The worst performance was given by Makkink modified method.

Table 6. Evaluation of criteria parameters for validating ET estimate between 2001-2017

Method	R2	SEE	RMSE	MBE	PE
Trabert-ET0(mm)	0.92	0.03	2.47	-2.35	89.43
Mahringer-ET0(mm)	0.92	0.07	2.13	-2.03	77.27
Penman-ET0(mm)	0.92	0.11	1.78	-1.70	64.71
Albrecht-ET0(mm)	0.94	0.11	1.66	-1.59	60.58
Priestly Taylor-ET0(mm)	0.70	0.59	1.30	1.16	44.25
Turc -ET0(mm)	0.67	0.16	1.15	-0.93	35.53
Makkink-Modified Hansen ET0(mm)	0.48	0.49	1.76	1.65	62.73
Makkink 1957 ET0(mm)	0.48	0.43	1.21	1.03	39.21
Valiantaz ET0 (mm)	0.65	0.26	0.99	-0.80	30.32

Ranking of ETo Estimation

The primary requirement of ranking is to get weightage for statistical indices which is computed by Entropy method (*Table 7*). The values depicted as shown in *Table 8* below describes the ranking of ETo Estimate of nine models for the period between 1978-2017. It was observed that the Mahringer model ranked number 1 while Makkink Modified model was in the last position for the case of without calibrating the ETo equation. Also, the ranking of ETo Estimate of nine models after calibrating for the period between 1978-2000 are shown in *Table 9*, Albrecht model ranked number 1 and Valiantaz model was in the last position. Moreover, the ranking as shown in *Table 10* gives the ETo Estimate of nine models for Validating the Calibrated equation for the period between 2001-2017. Mahringer model ranked number 1 and Priestly Taylor was in the last position. Hence, it is quite clear that Mahringer method is the most promising model which can be used as an alternative to FAO56-PM model. The comparative study of Ranking is shown in *Fig. 7*. From the whole ranking analysis, it can be observed that the ranks' results did not exactly match with each other and in some cases considerably differs from the other.

Table 7. Weightage by Entropy Method

Criteria	R ²	SEE	RMSE	MBE	PE	Sum
Weightage Evaluation	0.05	0.67	0.08	0.11	0.10	1.00
Weightage Calibration	0.01	0.13	0.13	0.44	0.29	1.00
Weightage Validation	0.06	0.62	0.08	0.12	0.12	1.00

Table 8. Ranking of ETo estimate of nine models for period between 1978-2017

Sn	Method	Si+	Si-	Si++si-	Ci	Rank
1	Trabert-ET0(mm)	0.048558	0.393007	0.441566	0.890032	2
2	Mahringer-ET0(mm)	0.036844	0.373905	0.41075	0.9103	1
3	Penman-ET0(mm)	0.060846	0.349965	0.410811	0.851888	5
4	Albrecht-ET0(mm)	0.054297	0.355604	0.4099	0.867537	3
5	Priestly Taylor-ET0(mm)	0.394267	0.037161	0.431427	0.086134	4
6	Turc -ET0(mm)	0.109701	0.287544	0.397245	0.723845	6
7	Makkink-Modified Hansen ET0(mm)	0.338601	0.0735	0.412101	0.178354	9
8	Makkink 1957 ET0(mm)	0.292096	0.10872	0.400815	0.271246	8
9	Valiantaz ET0 (mm)	0.176656	0.220993	0.397648	0.555749	7

Table 9. Ranking of ETo estimate of nine models after calibrating for period between 1978-2000

Sn	Method	Si+	Si-	Si++si-	Ci	Rank
1	Trabert-ET0(mm)	0.008826	0.355287	0.364113	0.97576	2
2	Mahringer-ET0(mm)	0.140201	0.300896	0.441096	0.682154	5
3	Penman-ET0(mm)	0.024904	0.30044	0.325345	0.923453	3
4	Albrecht-ET0(mm)	0.000438	0.321685	0.322123	0.998639	1
5	Priestly Taylor-ET0(mm)	0.150164	0.223602	0.373766	0.598241	6
6	Turc -ET0(mm)	0.125925	0.329778	0.455703	0.723669	4
7	Makkink-Modified Hansen ET0(mm)	0.265806	0.192504	0.45831	0.42003	8
8	Makkink 1957 ET0(mm)	0.267363	0.194648	0.462011	0.421306	7
9	Valiantaz ET0 (mm)	0.334992	0.107558	0.44255	0.243042	9

Table 10. Ranking of ETo estimate of nine models for validating the calibrated equation for period between 2001-2017

Sn	Method	Si+	Si-	Si++si-	Ci	Rank
1	Trabert-ET0(mm)	0.060765	0.366145	0.42691	0.857663	2
2	Mahringer-ET0(mm)	0.045617	0.344014	0.389631	0.882922	1
3	Penman-ET0(mm)	0.07262	0.317463	0.390083	0.813835	4
4	Albrecht-ET0(mm)	0.069836	0.31736	0.387196	0.819637	3
5	Priestly Taylor-ET0(mm)	0.367337	0.046783	0.414119	0.112969	9
6	Turc -ET0(mm)	0.088572	0.28517	0.373742	0.763012	5
7	Makkink-Modified Hansen ET0(mm)	0.304764	0.08038	0.385144	0.208702	8
8	Makkink 1957 ET0(mm)	0.263072	0.114761	0.377833	0.303735	7
9	Valiantaz ET0 (mm)	0.151847	0.221546	0.373392	0.593332	6

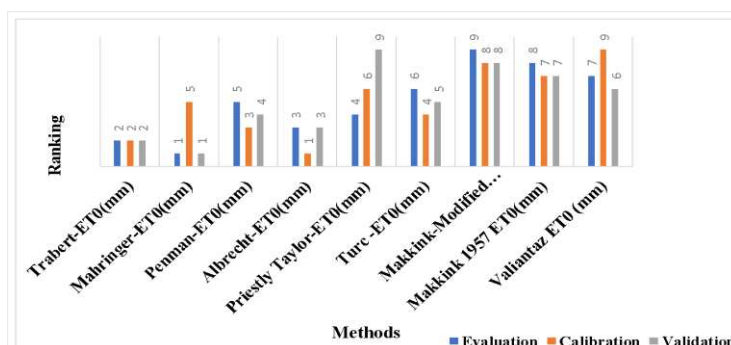


Figure 7. Comparison of ranking of ETo estimates based on ETo equation, Calibrated equation and Validating the calibrated equation

Discussions

Different ETo models were used around the world to compute the reference evapotranspiration by using the climatic parameters such as mean temperature, relative humidity, solar radiation and wind speed. FAO56-PM model recommended by the Food and Agricultural Organization (FAO) has been recognized as the most accurate model for estimating the ETo over the past few decades. But due to the constraint of limited climatic parameters, FAO56-PM is not suitable to be implemented. Thus, to find an alternative technique of accurate prediction of ETo, the performance of the nine empirical models were evaluated against the FAO56-PM model by using the four common statistical approaches: root-mean-square error (RMSE), mean bias error (MBE), standard error of estimates (SEE) and percent error (PE). Additionally, a linear regression model was adopted to calibrate and validate the performance of the empirical models during the 1978–2000 and 2001–2017 time periods, respectively. The current study compared four mass transfer methods (Trabert, Mahringer, Penman and Albrecht), four radiation-based methods (Priestly Taylor, Turc, Makkink and Makkink Modified) and one combination-based method against the FAO56-PM method.

The result evaluated from 1978-2017 showed that the mass transfer method performed better without calibration with the highest the coefficient of determination was the Albrecht ($R^2=0.96$) followed by the combined method and lastly was the radiation method. The statistical output showed that the combined model (Valiantzas equation) performed better as compared to the other model with an RMSE value of 0.98 mm/day, MBE=0.83, PE%=33.53 and SEE=0.268 mm/day. The higher precision of the combined models might be due to the combination of the most suitable and important meteorological parameters being incorporated. Similar results were also obtained previously after evaluating six ETo equations (Trabert, Mahringer, Penman (1948), Albrecht, Valiantzas1 and Valiantzas2) for the Senegal River Delta (Djaman et al., 2016a). The result is in agreement with the present work with $R^2 > 0.60$ for the daily ETo estimates. The Valiantzas2 equation was the best model for the Senegal River Delta and had the lowest root mean squared difference (RMSE) of 0.45 mm/day and the lowest percent error of estimate (PE) about 7.1%. The findings of the research are in agreement with the study conducted by other researchers (Djaman et al., 2015) after evaluating the sixteen reference evapotranspiration methods under sahelian conditions in the Senegal River Valley. However, Valiantzas equation was found to be the promising equations that could be used for the reference evapotranspiration estimation in the Senegal River Valley. After calibrating the empirical equation from (1978-2000), it was observed that there was a remarkable improvement in the performance of these nine equations. Additionally, the findings revealed that the calibration improved the reliability and consistency of different ETo equations. The correlation value significantly increased. Moreover, the statistical measures such as RMSE, SEE, MBE and PE significantly reduced for all the models but both the Albrecht and Makkink models gave the least correlation. However, no improvement was seen in Turc model with its SEE. But, there was a remarkable improvement in the performance of equations. Additionally, the findings revealed that calibration improved the reliability and consistency of different Valiantzas equations. Valipour (2015) reported that there was an improvement in the calibrated Trabert and Mahringer equations in Iran with MBE as low as 0.02 mm/day. He indicated that the Trabert model can skip the calibration process to generate the best performance in Iran. Meanwhile, Valiantzas equations were suitable for ETo estimation as compared to PM-ETo in the Pilbara

region of Western Australia. But, their performance can be further improved through calibration (Ahooghalandari et al., 2017).

The calibrated Valiantzas equation showed the best performance using the limited data in Guizhou Province, China (Gao et al., 2015). This phenomenon was similar to the performance's results of the calibrated Valiantzas equation at Adana Station in Turkey (Kisi and Zounemat-Kermani, 2014). The calibrated Trabert, Albrecht and the Mahringer equations showed different performance relative to the PM-ET_o, depending on the region. But, the better performance was observed at Ndiaye 35 km inland than Saint-Louis at the coast. The dependency of mass transfer equation on the vapor pressure was too small. It was reported that better performance of the Trabert and Mahringer equations were in inland area than at the coastal area in the Senegal River Valley (Djaman et al., 2015). The climate variables in a coastal area like Saint-Louis located near the mouth of the Senegal river might be influenced by surrounding water (Hargreaves, 1994). These results were contradicted with the findings of Valipour (2015) who reported that the calibrated mass transfer ETo equation had better performance near the Caspian Sea and the Persian Gulf in Iran with RH higher than 65% than the other area. The validation of the nine ETo equations for the 2001–2017 shows a strong correlation between the calibrated equations to the PM estimates. Similar RMSE, MBE and PE were obtained from the calibration and validation with only slightly decrease in R². The magnitude of RMSE, MBE and PE were acceptable for ETo estimation for any nine ETo equation at Abha.

From the ranking of evaluated model and during validation of calibrating ETo model, it was observed that Mahringer ranked number 1 and Makkink modified gives worst performance during evaluation and Priestly Taylor was in the last position during the validation of the calibrated equation. Hence, Mahringer method is the most promising model which can be used as an alternative to the FAO Penman-Monteith method. Moreover, during calibration the Albrecht model is found to be best one and Valiantzas shows the worst result. The overall improvement result after calibration and during validation against the evaluated evapotranspiration for the first three rank model is as shown in Fig. 8. It clearly shows that the evaluation criteria significantly improved with respect to the evaluated equation after calibration and validation. However, there is no considerable improvement in the coefficient of determination in some cases. The outcomes of the study will provide meaningful guidance for agricultural production, hydrological planning and management in the vital region as well as other regions with similar climates.

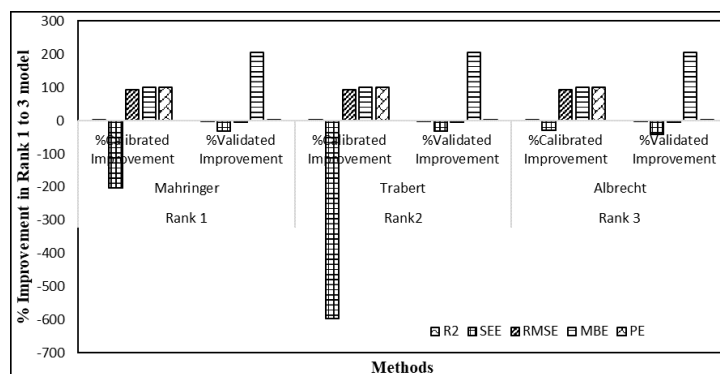


Figure 8. Comparative study of rank 1 to 3 evaluation criteria

Conclusions

The current study was performed with an aim to evaluate the nine reference evapotranspiration models with respect to standard FAO56-PM model in the semi-arid region of Kingdom of Saudi Arabia. The nine evapotranspiration models have been successfully evaluated (period: 1978-2017), calibrated (period: 1978-2000) and further validated (period: 2001-2017). Based on the statistical indices as criteria, the ranking was performed using multi criteria decision making (weightage by Entropy and performance score by TOPSIS) in order to observe the performance against the FAO56-PM equation under the available climatic conditions in Abha city. Based on the analysis result following inference can be made

- There was a remarkable improvement in the performance of calibrated equation. Moreover, the calibration approach improves the reliability and consistency of different evapotranspiration equation.
- The ranking of evaluated evapotranspiration models (1978-2017) and during validation (2001-2017) shows that the Mahringer model performed very well. While during calibration (1978-2000), Albrecht model shows better performance. Hence Mahringer model was the most promising model and can be used as an alternative approach to Standard FAO56-PM model.
- In the case of data limitations, the equations calibrated in this study are recommended for ETo estimation in the Abha region.
- The Use of multiple criterion decision-making methods (MCDM) allows a researcher to choose the best alternative out of a number of the considered alternatives.
- The findings, are likely to help in diminishing the error associated with ETo estimation, and the recognized models in this study could be utilized as part of further examinations in the related field.
- To some extent, it is expected that the conclusions of this study can be used in regions with similar topography and climatic conditions in the world.
- The results of this study could be used by the water management system, crop cultivators, crop advisors, researchers and students from universities and research centres. Moreover, it is beneficial for the decision maker in the vast field of agriculture, hydrology and environment.
- Further research is required in order to assess the effect of using reduced set of data for daily hourly ETo estimation. Moreover, the seasonal changes in ETo is also need to be investigated in future.

Acknowledgments. The authors extend their appreciation to the Deanship of Scientific Research at King Khalid University for funding this work through research group program under grant number (R.G.P.1/85/40). The authors of current work wish to thank Universiti Tecknologi Malaysia, Johor Bahru for their facilities and Lab support. The outcome of this research paper is based on the excerpts of current ongoing Ph.D research study. We would also like to thank general authority of the meteorological department, Abha, Asir region, Saudi Arabia for providing the weather data.

Conflict of interests. The authors declare no conflict of interests.

REFERENCES

- [1] Abo-Ghobar, H. M., Mohammad, S. (1995): Evapotranspiration measurement by lysimeters in a desert climate. – Arab Gulf Journal of Scientific Research 13(1): 109-122.
- [2] Ahooghalandari, M., Khiadani, M., Jahromi, M. E. (2017): Calibration of Valiantzas' reference evapotranspiration equations for the Pilbara region, Western Australia. – Theoretical and applied climatology 128(3-4): 845-856.
- [3] Alamanos, A., Mylopoulos, N., Loukas, A., Gaitanaros, D. (2018): An integrated multicriteria analysis tool for evaluating water resource management strategies. – Water 10(12): 1795.
- [4] Ablewi, B., Gharabaghi, B., Alazba, A. A., Mahboubi, A. A. (2015): Evapotranspiration models assessment under hyper-arid environment. – Arabian Journal of Geosciences 8(11): 9905-9912.
- [5] Albrecht, F. (1950): Die methoden zur bestimmung der verdunstung der natürlichen erdoberfläche. – Archiv für Meteorologie, Geophysik und Bioklimatologie, Serie B 2(1-2): 1-38.
- [6] Allen, R. G. (1996): Assessing integrity of weather data for reference evapotranspiration estimation. – Journal of irrigation and drainage engineering 122(2): 97-106.
- [7] Allen, R. G., Pereira, L. S., Raes, D., Smith, M. (1998): Crop Evapotranspiration-Guidelines for computing crop water requirements. – FAO Irrigation and drainage paper 56. FAO, Rome 300(9): D05109.
- [8] Al-Omran, A. M., Al-Ghobari, H. M., Alazba, A. A. (2004): Determination of evapotranspiration of tomato and squash. – International Agricultural Engineering Journal 13(142): 27-36.
- [9] Bogawski, P., Bednorz, E. (2014): Comparison and validation of selected evapotranspiration models for conditions in Poland (Central Europe). – Water Resources Management 28(14): 5021-5038.
- [10] Ćadro, S., Uzunoviæ, M., Žurovec, J., Žurovec, O. (2017): Validation and calibration of various reference evapotranspiration alternative methods under the climate conditions of Bosnia and Herzegovina. – International Soil and Water Conservation Research 5(4): 309-324.
- [11] Djaman, K., Balde, A. B., Sow, A., Muller, B., Irmak, S., N'Diaye, M. K., Manneh, B., Moukoumbi, Y. D., Futakuchi, K., Saito, K. (2015): Evaluation of sixteen reference evapotranspiration methods under sahelian conditions in the Senegal River Valley. – Journal of Hydrology: Regional studies 3: 139-159.
- [12] Djaman, K., Tabari, H., Balde, A. B., Diop, L., Futakuchi, K., Irmak, S. (2016a): Analyses, calibration and validation of evapotranspiration models to predict grass-reference evapotranspiration in the Senegal river delta. – Journal of Hydrology: Regional Studies 8: 82-94.
- [13] Djaman, K., Irmak, S., Kabenge, I., Futakuchi, K. (2016b): Evaluation of FAO-56 penman-monteith model with limited data and the valiantzas models for estimating grass-reference evapotranspiration in Sahelian conditions. – Journal of Irrigation and Drainage Engineering 142(11): 04016044.
- [14] Djaman, K., Koudahe, K., Allen, S., O'Neill, M., Irmak, S. (2017a): Validation of Valiantzas' reference evapotranspiration equation under different climatic conditions. – Irrigation & Drainage Systems Engineering 6(3): 196.
- [15] Djaman, K., Koudahe, K., Akinbile, C. O., Irmak, S. (2017b): Evaluation of eleven reference evapotranspiration models in semiarid conditions. – Journal of Water Resource and Protection 9(12): 1469.
- [16] ElNesr, M., Alazba, A., Abu-Zreig, M. (2010): Spatio-temporal variability of evapotranspiration over the Kingdom of Saudi Arabia. – Applied engineering in agriculture 26(5): 833-842.

- [17] Gabiri, G., Leemhuis, C., Diekkrüger, B., Näschen, K., Steinbach, S., Thonfeld, F. (2019): Modelling the impact of land use management on water resources in a tropical inland valley catchment of central Uganda, East Africa. – *Science of the Total Environment* 653: 1052-1066.
- [18] Gao, X., Peng, S., Xu, J., Yang, S., Wang, W. (2015): Proper methods and its calibration for estimating reference evapotranspiration using limited climatic data in Southwestern China. – *Archives of Agronomy and Soil Science* 61(3): 415-426.
- [19] Gupta, A. P., Harboe, R., Tabucanon, M. T. (2000): Fuzzy multiple-criteria decision making for crop area planning in Narmada river basin. – *Agricultural Systems* 63(1): 1-18.
- [20] Hansen, S. (1984): Estimation of potential and actual evapotranspiration. – *Nordic Hydrol.* 15: 205-212.
- [21] Hargreaves, G. H. (1994): Simplified coefficients for estimating monthly solar radiation in North America and Europe. – Utah State Univ, Logan, Utah.
- [22] Häusler, M., Conceição, N., Tezza, L., Sánchez, J. M., Campagnolo, M. L., Häusler, A. J., Ferreira, M. I. (2018): Estimation and partitioning of actual daily evapotranspiration at an intensive olive grove using the STSEB model based on remote sensing. – *Agricultural water management* 201: 188-198.
- [23] Hu, Z., Yu, G., Zhou, Y., Sun, X., Li, Y., Shi, P., Li, S. (2009): Partitioning of evapotranspiration and its controls in four grassland ecosystems: Application of a two-source model. – *Agricultural and Forest Meteorology* 149(9): 1410-1420.
- [24] Islam, S., Abdullah, R. A. B., Algahtani, A., Irshad, K., Hirol, H. (2019a): Performance of vapour pressure models in the computation of vapour pressure and evapotranspiration in Abha, Asir region, Saudi Arabia. – *Applied Ecology and Environmental Research* 17(4): 9691-9715.
- [25] Islam, S., Abdullah, R. A. B., Algahtani, A., Irshad, K., Hirol, H. (2019b): Performance evaluation off mass transfer-based method using global performance index in semi-arid region, Saudi Arabia. – *Applied Ecology and Environmental Research* 17(5): 11121-11141.
- [26] Janssen, R., Goosen, H., Verhoeven, M. L., Verhoeven, J. T., Omtzigt, A. Q. A., Maltby, E. (2005): Decision support for integrated wetland management. – *Environmental Modelling & Software* 20(2): 215-229.
- [27] Jiang, S., Wang, J., Zhao, Y., Shang, Y., Gao, X., Li, H., Wang, Q., Zhu, Y. (2017): Sustainability of water resources for agriculture considering grain production, trade and consumption in China from 2004 to 2013. – *Journal of Cleaner Production* 149: 1210-1218.
- [28] Jin, N., Ren, W., Tao, B., He, L., Ren, Q., Li, S., Yu, Q. (2018): Effects of water stress on water use efficiency of irrigated and rainfed wheat in the Loess Plateau, China. – *Science of the total environment* 642: 1-11.
- [29] Kisi, O., Zounemat-Kermani, M. (2014): Comparison of two different adaptive neuro-fuzzy inference systems in modelling daily reference evapotranspiration. – *Water resources management* 28(9): 2655-2675.
- [30] Lang, D., Zheng, J., Shi, J., Liao, F., Ma, X., Wang, W., Chen, X., Zhang, M. (2017): A comparative study of potential evapotranspiration estimation by eight methods with FAO Penman–Monteith method in southwestern China. – *Water* 9(10): 734.
- [31] Mahringer, W. (1970): Verdunstungsstudien am neusiedler See. – *Archiv für Meteorologie, Geophysik und Bioklimatologie, Serie B* 18(1): 1-20.
- [32] Makkink, G. F. (1957): Testing the Penman formula by means of lysimeters. – *Journal of the Institution of Water Engineers* 11: 277-288.
- [33] Makropoulos, C. K., Natsis, K., Liu, S., Mittas, K., Butler, D. (2008): Decision support for sustainable option selection in integrated urban water management. – *Environmental modelling and software* 23(12): 1448-1460.

- [34] Mustafa, M. A., Akabawi, K. A., Zoghet, M. F. (1989): Estimation of reference crop evapotranspiration for the life zones of Saudi Arabia. – *Journal of arid environments* 17(3): 293-300.
- [35] Pandey, P. K., Dabral, P. P., Pandey, V. (2016): Evaluation of reference evapotranspiration methods for the northeastern region of India. – *International Soil and Water Conservation Research* 4(1): 52-63.
- [36] Pandey, V., Pandey, P. K. (2018): Calibration and ranking of Valiantzas reference evapotranspiration equations under the humid climate of northeast India. – *Journal of Water and Climate Change: jwc2018305*.
- [37] Penman, H. L. (1948): Natural evaporation from open water, bare soil and grass. – *Proceedings of the Royal Society of London. Series A. Mathematical and Physical Sciences* 193(1032): 120-145.
- [38] Pietersen, K. (2006): Multiple criteria decision analysis (MCDA): A tool to support sustainable management of groundwater resources in South Africa. – *Water SA* 32(2): 119-128.
- [39] Priestley, C. H. B., Taylor, R. J. (1972): On the assessment of surface heat flux and evaporation using large-scale parameters. – *Monthly weather review* 100(2): 81-92.
- [40] Qin, X. S., Huang, G. H., Chakma, A., Nie, X. H., Lin, Q. G. (2008): A MCDM-based expert system for climate-change impact assessment and adaptation planning—A case study for the Georgia Basin, Canada. – *Expert Systems with Applications* 34(3): 2164-2179.
- [41] Saeed, M. (1986): The estimation of evapotranspiration by some equations under hot and arid conditions. – *Transactions of the ASAE* 29(2): 434-0438.
- [42] Salih, A. M., Sendil, U. (1984): Evapotranspiration under extremely arid climates. – *Journal of irrigation and drainage engineering* 110(3): 289-303.
- [43] Senent-Aparicio, J., Pérez-Sánchez, J., Carrillo-García, J., Soto, J. (2017): Using SWAT and Fuzzy TOPSIS to assess the impact of climate change in the headwaters of the Segura River Basin (SE Spain). – *Water* 9(2): 149.
- [44] Srdjevic, B., Medeiros, Y. D. P., Faria, A. S. (2004): An objective multi-criteria evaluation of water management scenarios. – *Water resources management* 18(1): 35-54.
- [45] Tie, Q., Hu, H., Tian, F., Holbrook, N. M. (2018): Comparing different methods for determining forest evapotranspiration and its components at multiple temporal scales. – *Science of the Total Environment* 633: 12-29.
- [46] Trabert, W. (1896): Neue beobachtungen über verdampfungsgeschwindigkeiten. – *Meteorol Z* 13: 261-263.
- [47] Trajkovic, S., Kolakovic, S. (2009): Evaluation of reference evapotranspiration equations under humid conditions. – *Water Resource Management* 23: 3057.
- [48] Turc, L. (1961): Water requirements assessment of irrigation, potential evapotranspiration: simplified and updated climatic formula. – *Annales Agronomiques* 12: 13-49.
- [49] Valiantzas, J. D. (2013): Simplified forms for the standardized FAO-56 Penman–Monteith reference evapotranspiration using limited weather data. – *Journal of Hydrology* 505: 13-23.
- [50] Valipour, M. (2015): Investigation of Valiantzas' evapotranspiration equation in Iran. – *Theoretical and applied climatology* 121(1-2): 267-278.
- [51] Vinogradova, I., Podvezko, V., Zavadskas, E. (2018): The recalculation of the weights of criteria in MCDM methods using the bayes approach. – *Symmetry* 10(6): 205.
- [52] Wei, Y., Tang, D., Ding, Y., Agoramoorthy, G. (2016): Incorporating water consumption into crop water footprint: A case study of China's South–North Water Diversion Project. – *Science of The Total Environment* 545: 601-608.
- [53] Xu, J., Peng, S., Ding, J., Wei, Q., Yu, Y. (2013): Evaluation and calibration of simple methods for daily reference evapotranspiration estimation in humid East China. – *Archives of Agronomy and Soil Science* 59(6): 845-858.

- [54] Zarghami, M., Abrishamchi, A., Ardakanian, R. (2008): Multi-criteria decision making for integrated urban water management. – *Water Resources Management* 22(8): 1017-1029.
- [55] Zhai, L., Feng, Q., Li, Q., Xu, C. (2010): Comparison and modification of equations for calculating evapotranspiration (ET) with data from Gansu Province, Northwest China. – *Irrigation and drainage* 59(4): 477-490.

ISOLATION AND IDENTIFICATION OF HEAVY METAL TOLERANT BACTERIA FROM SUGARCANE INDUSTRIAL WASTEWATER

ABD ELHADY, M. A. E.¹ – ELSAYED, A. I.² – MOHAMED, S. H.² – ABOELLIL, A. H.³ – AHMAD, M. S.³

¹*Department of Agricultural Microbiology (Mallawy Agric. Res. Station), Soil, Water and Environmental Research Institute, Agricultural Research Centre, P.O. Box, 12619, Giza, Egypt*

²*Department of Agricultural Microbiology, Soil, Water and Environmental Research Institute, Agricultural Research Centre, P.O. Box, 12619, Giza, Egypt*

³*Department of Botany and Microbiology, Faculty of Science, Beni Suef University, Beni Suef, Egypt*

*Corresponding author

e-mail: dr.mohamed334455@gmail.com

(Received 14th Sep 2019; accepted 4th Dec 2019)

Abstract. One of the most serious problems of the environment is heavy metal toxicity originating from the industrial activities even in traces which harm the ecosystems. Initially a total of 30 isolates were screened on nutrient agar medium containing heavy metals: zinc, iron, cobalt, cadmium, copper and lead at four different concentrations (25, 50, 75 and 100 µg/mL in their salt form). Three isolates of *Bacillus* sp. were isolated from effluent industrial wastewater of Abu Kerqas Sugar Factory (27°55' 28.8" N 30°49' 00.4" E), identified by using 16S rRNA gene and documented in GenBank as *Bacillus* spp. SMMAA-1 (LC472522), *Bacillus cereus* SMMAA-3 (LC472523), *Bacillus altitudinis* SMMAA-4 (LC472524). The bacterial isolates were selected based on their growth curve; IAA reaction and antibiosis effect were identified based on their morphological, biochemical characterization and utilization of carbohydrates as carbon sources. These isolates were evaluated for their abilities to bioremediate the toxic heavy metals. Results showed that bacteria present resistance to six heavy metals. *B. cereus* is more effective concerning its removal efficiency percentage for six heavy metals (Zn⁺², Fe⁺², Co⁺², Cd⁺², Cu⁺² and Pb⁺²) (94.77%) from Industrial Wastewater than *Bacillus* spp. (83.19%) and *B. altitudinis* (83.21%). The highest removal efficiencies by Bacterial isolates were found with Co⁺², Cd⁺² and Cu⁺² and the lowest removal biosorption were recorded with Fe⁺².

Keywords: *Bacillus* spp., *Bacillus cereus*, *Bacillus altitudinis*, bioremediation, effluent wastewater, 16S rRNA gene, GenBank

Introduction

Many organizations and scientists from various disciplines mentioned that the bioremediation can be used to break down the metal availability below the permissible limit. Most of them are in their advanced stages of developing different protocols and identifying a plethora of bacterial species to solve the issue (Kielak et al., 2017; Sardar et al., 2018). Exceedingly higher concentrations of heavy metals are a menace to human health due to their harmful effects such as genotoxicity towards the DNA and immunotoxicity as they are major irritants to the body. The genomic instability by these metals induces cancer (Leonard et al., 2004).

Heavy metals toxicity is significant environmental pollutants problem of increased significance for ecological, evolutionary, nutritional and environmental reasons (Nagajyoti et al., 2010; Jaishankar et al., 2014). Heavy metals water pollution one of serious important problems in world and Egypt. Heavy metals accumulations were observed in Egyptian

cultivated such as soil, Nile River and air (Abbas and Kamel, 2004). Today, the quality of Nile water is a matter of serious concern due to exposure to increasing at an alarming rate multiple sources of heavy metals pollution including industrial, agricultural and domestic effluents. Effluent industrial wastewater is the main source of Nile pollution by heavy metals. The most commonly found heavy metals in wastewater include arsenic, cobalt, iron, cadmium, chromium, copper, lead, nickel, and zinc, all of which cause risks for human health and the environment (Lambert et al., 2000).

So, quick and easy removal and recovery of heavy metals from industrial wastewater at low cost are needed. Several conventional methods include precipitation, membrane filtration, ion exchange, electrochemical recovery; biological separation and adsorption are used to remove heavy metals from wastewater. Nevertheless, these methods unfriendly environmental, long processing times and high costs (Carolin et al., 2017). Nowadays, in light of this necessary for attractive alternative strategies low-cost, efficient and environmentally friendly methods instead of traditional to recover heavy metals from wastewater are needed (Moradi et al., 2015). The growing industrialization has spread worldwide and has left persistent toxic heavy metals, like chromium, nickel, lead, zinc, cadmium and copper in our ecosystem. These heavy metals tend to accumulate and deteriorate the environment. This is especially true for developing countries like China and India (Raja et al., 2008; Chauhan et al., 2017).

The bioremediation methods for reducing more of heavy metals in the environment have attracted importance. Living organisms were reported to able to absorb pollutants and remove heavy metals from the environment. Plants, fungi and microorganisms such as yeasts, bacteria, algae, and cyanobacteria are usually used for the bioremediation of heavy metals and recorded to be the best acceptable ones because they are easier to work with (Massoud et al., 2018). Several studies reported that bioremediation is the most effective management tool to manage the polluted environment and recover contaminated environment (Ahemad, 2012). Since heavy metals are ubiquitously present in our environment, microorganisms such as bacteria, yeast or fungi have developed mechanisms to removal contaminated soil and water via heavy metals (Kumar et al., 2011). Bioremediation includes some methods such as phytoremediation, biodegradation, bioventing (Dupont, 1993).

Assessment of microbes for their remediation potential in dealing with industrial pollutants is another point of interest where a bacterium or a fungus produces metabolites as their weapon of degradation (Pathak et al., 2017). Many bacterial strains contain genetic determinants of resistance to heavy metals such as Hg^{2+} , Ag^{2+} , Cu^{2+} , Ni^{2+} , Cd^{2+} and others (Karellova et al., 2011; Chauhan et al., 2017).

Several investigators have used different bacterial strains like *Bacillus* sp., *Bacillus licheniformis*, *Bacillus thuringiensis*, *Pseudomonas* sp., *Staphylococcus aureus* to for the biosorption as well as bioaccumulation of various metal ions like Cr(VI), Ni(II), Zn(II), Pb(II) etc. (Şahin and Ozturk, 2005; Tunali et al., 2006; Zhou et al., 2007; Ziagova et al., 2007; Wang et al., 2010; Akhter et al., 2017). Thus, the overall objective of the study is to enhance production of bacterial strains with high ability to uptake of heavy metals by different concentrations to helping in the reduction of Industrial wastewater effluent pollution of heavy metal. This emphasizes the importance and needs of carrying out extended testing for the compatibility of biosorption to heavy metals toxicity. It is more effective, cheap than traditional technologies of treating contaminated water with heavy metals, including precipitation, ion exchange or reverse osmosis still generate too large costs.

This study aimed to isolation and identification of bacterial isolates that have ability to heavy metals biosorption and the role of bioremediation as technological method for uptake of six heavy metal ions from industrial wastewater effluent in Egypt to reduce the environmental pollutions.

Materials and methods

This study was conducted at both of Laboratory of Microbiology, Malloway Agric. Res. Station, Dept. of Agric. Microbiology., Soil, Water and Environmental Research Institute, Agric. Res. Center, Giza, Egypt, and Central Lab., Faculty of Postgraduate Studies for Advanced Sciences, Beni Suf University. Molecular identification of the bacterial isolates was done in Microbiological Laboratory, Faculty of Agriculture, Zhejiang University, Hangzhou City, and East China during the period of 2017-2018.

Industrial wastewater samples collection and preparation

In this study, effluent industrial wastewater samples were collected from the site of the main drain of Abu Kerqas Sugar Factory (27°55' 28.8" N 30°49' 00.4" E) (Fig. 1), El-Minia Governorate, March, 2017. Three samples of wastewater each 10 L per sample were collected in plastic jerry cans. Cans were previously sterilized by 75% ethanol, washed three times with wastewater to remove the residual effect of ethanol, and filled with the samples and then transferred immediately to the Microbiology Lab of Malloway Agric. Res. Station. The three samples were mixed gently to obtain the main sample and kept in the refrigerator (6 ± 2 °C) for the further studies.



Figure 1. The main drain of Abu Kerqas Sugar Factory (27°55' 28.8" N30°49' 00.4" E)

Determination of heavy metal concentrations in the wastewater samples

Samples were taken from the main sample and sent to the Central Lab., Faculty of Postgraduate Studies for Advanced Sciences, Beni Suf University. The concentrations of heavy metals (Zn^{+2} , Fe^{+2} , Co^{+2} , Cd^{+2} , Cu^{+2} and Pb^{+2}) in samples were analyzed and determined by the Atomic Absorption Spectroscopy (Model: Agilent Technologies 200 series AA System) according to the method of EPA (2005).

Bacteria isolation via streak plate technique

Three dilutions (1.00, 0.50 and 0.25) of each of the main sample and collected samples containing heavy metals, was done as described by Azad et al. (2013) to isolate

the desired bacteria that have more tolerance to high concentration of heavy metals. This technique was applied to isolate some bacterial colonies able to grow in the presence of heavy metals. Two loops from the best dilution of the wastewater samples was taken and streaked onto sterile petri plates containing nutrient agar medium (NAM) as recorded by Marzan et al. (2017). Single colonies were selected, picked, purified and inoculated on NAM slant and coded as T1 up to T30. These single colonies were purified on NAM, and preserved on different plates or slants for further experiments.

Tolerance of bacterial isolates to six heavy metals

Six heavy metals: zinc (Zn^{+2}), iron (Fe^{+2}), cobalt (Co^{+2}), cadmium (Cd^{+2}), copper (Cu^{+2}) and lead (Pb^{+2}) were used in their salt structures as: $ZnSO_4$, $FeSO_4 \cdot 7H_2O$, $CoCl_2$, $CdSO_4 \cdot 3H_2O$, $CuSO_4 \cdot 5H_2O$ and $PbSO_4$. According to the method of Vijayadeep and Sastry (2014) heavy metals salt solutions (25, 50, 75, 100 $\mu g/mL$) were prepared in distilled water to obtain concentrations and sterilized by 0.2 μm pore-size Millipore sterile filters. The bacterial isolates (T1, T2 and T3.....T30) were checked for the heavy metals tolerance using the agar well diffusion method as reported by Collins et al. (1985) in sterile NAM plates. On incubation of plates at 35-37 °C for 72 h, the inhibition zones (the distance between the end of the zone and the edge of the well, mm) were measured. Isolates showing a clear zone of 1 mm or less was considered as resistance (R) isolate according to Rani and Moreira (2010). The bacterial isolates which appeared resistance to the heavy metal ions at the all tested concentrations were recorded as (T1, T2, T3, T4, T5, T6, T7, T8, T10 and T18).

Effect of industrial wastewater (IWW) toxicity on each of bacterial growth and indole acetic acid (IAA) production (color change) by the ten bacterial isolates

The effects of IWW on the growth of the selected isolates (T1, T2, T3, T4, T5, T6, T7, T8, T10 and T18) were determined by growing the bacteria in nutrient broth medium (NBM) supplemented with sterile IWW (SIWW). IWW was sterilized by 0.2 μm pore-size Millipore sterile filters. The cultures of bacterial isolates were grown in the presence of SIWW, and as a blank SIWW were taken out. One loop from each isolate culture was taken and inoculated in 100 mL NBM and incubated under shaking condition (180 rpm) for 24 h at 30 °C as described by Priyadarshini and Kumar (2016). Then, 3.0 mL of the bacterial culture were added to each flask contained 100 mL of SIWW, mixed well and incubated as mentioned before. Bacterial growth was measured using a spectrophotometer (Spectronic 20 BauTchandLomp) at 620 nm as optical density (OD). The recorded data were taken after 1, 2, 3, 4, 5, 6 and 7 days from the incubation.

In case of effect of IWW on IAA produced by the bacterial isolates under investigation, the ten bacterial isolates were grown overnight in sterilized NB medium at 30 °C for 24 h, and then 2.0 mL from each isolate were taken and inoculated with 5 mL SIWW to determine the degree of IAA by change of color visually as described by Glickmann and Dessaux (1995).

Methods to determine the antibiosis activities of the ten bacterial isolates

The antagonism of the bacterial isolates against *F. solani*, *S. rolfsii* and *E. coli* was performed using well diffusion method of Nedialkova and Naidenova (2005). The filtrate of *E. coli* was dropped (1-2 mL) in prepared holes of the NAM inoculated with

ten bacterial isolates and incubated at 30 °C for 24-48 h. Concerning to the antagonistic effect against *F. solani* and *S. rolfsii*, disc from each fungus growing on potato dextrose agar medium (PDA) was taken, and inoculated with the tested bacterial isolates. Three petri dishes per each of isolate and pathogen were used as replicates. The plates were incubated at 28 °C for 6 days, and the antagonistic activities were then recorded.

Biological and molecular identification of the selected bacterial isolates

The three bacterial isolates (T1, T3, and T4) which selected based on their tolerance to heavy metals; growth curve, IAA production and antagonistic effects were identified according to the methods described by Juni (1986) reported in Bergey's Manual of Systematic Bacteriology (1986, 2012).

Using 16S rRNA gene the identification of the three bacterial isolates was confirmed. NAM slants of the isolates were sent to Microbiology Laboratory, Faculty of Agriculture, Zhejiang University, Hangzhou City and East China. The genomic DNA of isolates was extracted using a Gene JET extraction kit (Thermo K0721) according to the Manufacturer's instructions. 16S rRNA region was amplified with the following bacterial primers (F: 5'AGA GTT TGA TCC TGG CTC AG3' and R: 5'GGT TAC CTT GTT ACG ACTT3'). Thermal cycling consisted of initial denaturation at 94 °C for 2-5 min, followed by a cycle of denaturation at 95°C for 30 s, annealing at 55-60 °C for 1 min and elongation at 72 °C for 60 s, and finally, at 72 °C for 5-10 min for completion. The PCR amplification was performed using Gene JET Gel Extraction (ThermoK0701). Sequencing was performed using the ABI PRISM BigDye™ Terminator Cycle Sequencing Kits, ABI PRISM 3730XL Analyzer (96 capillary type) sequencer (Applied Biosystems), MJ Research PTC-225 Peltier Thermal Cycler, DNA polymerase (FS enzyme) (Applied Biosystems). The DNA sequences of the PCR product of the 16S rRNA gene of the three bacterial isolates were through the BLAST P program which available on the National Center for Biotechnology Information website http://blast.ncbi.nlm.nih.gov/Blast.cgi?PROGRAM=blast_p and PAGE – TYPE=BLAST Search and LINK – LOC=blast home (Altschul et al., 1990).

Selected bacterial isolates (T1) Bacillus spp., (T3) B. cereus and (T4) B. altitudinis effects

The effects of the selected isolates (*Bacillus* spp., *B. cereus* and *B. altitudinis*) were tested for their ability to alleviate or eliminate the heavy metal concentrations for industrial wastewater effluent.

1 ml from each bacterial isolate that growing in nutrient broth medium was inoculated to flasks contained 100 ml of sterilized industrial wastewater (SIWW). The flasks were incubated in a shaker for 24 h at 30 ± 2 °C under static conditions as mentioned by Priyadharshini and Kumar (2016). The flasks were filtered (Whatman filter paper No.1) then the samples were received to the Central Lab., Faculty of Postgraduate Studies for Advanced Sciences, Beni Suef University to determinate the heavy metals concentrations for each sample. The percentage of removal heavy metals (Zn^{+2} , Fe^{+2} , Co^{+2} , Cd^{+2} , Cu^{+2} and Pb^{+2}) was calculated as *Equation 1* and that recoded by Bakar et al. (2013) as follows:

$$\text{Removal efficiency\%} = \frac{\text{Initial metal conc.} - \text{Final metal conc.}}{\text{Initial metal conc.}} \times 100 \quad (\text{Eq.1})$$

Statistical analysis

The data were prepared by mean \pm standard deviation ($n = 3$) and carried out as a randomized complete design (Snedecor and Cochran, 1980) using LSD test to compare means of treatments in investigation. Statistical significance was defined as $P < 0.05$. Mean values of three replicates followed by the same letters in each column are not significantly different ($P > 0.05$) (Duncan multiple range test).

Results and discussion

This study was designed to isolate some promising bacteria able to tolerate the high levels of heavy metals in EIWW in a trail to decrease or remove the heavy metals present in the EIWW. Therefore, determination of heavy metals concentration in EIWW samples was conducted for the six heavy metal ions (Zn^{+2} , Fe^{+2} , Co^{+2} , Cd^{+2} , Cu^{+2} and Pb^{+2}) that threatening the environments, human, plants and animals.

Heavy metal concentrations in the EIWW samples

Data illustrated in *Table 1*, showed that the concentrations of the six selected heavy metal ions in EIWW samples. The concentrations were ranged from 6 ppm (Zn^{+2}) to 1.4 ppm (Co^{+2}). It was noted that all tested heavy metals presented in high concentration compared to permissible limits excepted for Fe^{+2} ion which was the lowest one (2.1 ppm) compared to permissible rate (3.0 ppm). Also, the concentrations of Co^{+2} , Cd^{+2} and Pb^{+2} heavy metals were more folds than the guidelines and standers of WHO, therefore, these ions were considered as the highest toxic ions. This notes in harmony with that reported by Rajendran and Gunasekaran (2007) and Murthy et al. (2012).

Table 1. Heavy metals concentrations in the main EIWW sample collected from Abu Kerqas Sugar Factory, El-Minia, Egypt, compared to permissible rate (ppm) according the guidelines and standers of WHO

Metals	Conc. (ppm)	Permissible rate (ppm)	References
Zn^{+2}	6.0	5.000	WHO (1984)
Fe^{+2}	2.1	3.000	WHO (2006)
Co^{+2}	1.4	0.010	WHO (2003)
Cd^{+2}	1.8	0.005	WHO (1984)
Cu^{+2}	1.5	0.003	WHO (2003)
Pb^{+2}	1.9	1.000	WHO (1984, 2003)
		1.300	WHO (2006)
		0.050	WHO (1984, 2003)

WHO = World Health Organization

Bacteria isolation via streak plate technique using NA media supplemented with different dilutions of EIWW

Data represented in *Figure 2* show the presence of single colonies exhibited Bacillus-like species cultural properties grown on NAM inoculated with different dilutions of EIWW. The lowest concentration (0.25 mL) from (EIWW) have purified single separated colonies compared that of 0.50 and 1.00 mL. The last two dilutions showed crowded, compacted and irregular colonies on the NAM which are not easily

distinguished. Therefore, it has been observed that of the dilution of 0.25 mL was considered the best dilution to obtain the single separated colonies which were easily selected, picked, purified and easily distinguished. A number of 30 isolates were picked, purified and coded symbols of T1, T2, T3 and T4 ...to T30.

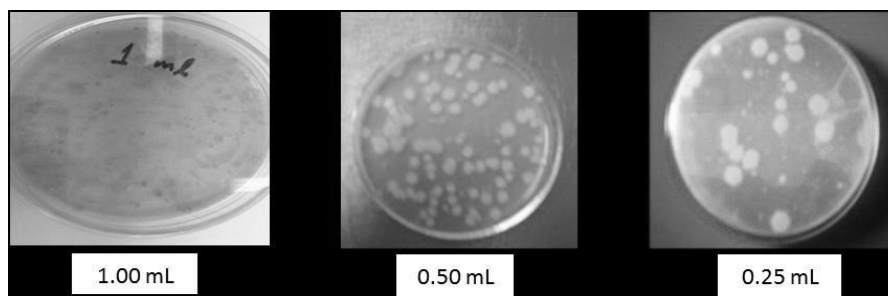


Figure 2. Cultural properties of the isolated bacteria grown on different dilutions of EIWW

Tolerance of bacterial isolates to six heavy metals

The bacterial isolates were coded as T1 up to T30, and evaluated for their abilities to tolerant a number of six heavy metals (Zn^{+2} , Fe^{+2} , Co^{+2} , Cd^{+2} , Cu^{+2} and Pb^{+2}) at four concentrations (25, 50, 75 and 100 $\mu\text{g/mL}$) as shown in *Table 2*. Based on the diameter of inhibition zones, the isolates were classified as sensitive or tolerant to each heavy metal ion and its concentration. The isolates were varied in their abilities to tolerant the heavy metal concentrations. The isolates that able to grow at concentrations of metal ions at 25, 50, 75 and 100 ($\mu\text{g/mL}$) were considered as tolerant as they showed a clear inhibition zone of 1 mm (*Fig. 3*) or less according to (Rani et al., 2010). Data in *Table 2*, showed that T10 isolate appeared tolerance to Cd^{+2} , Cu^{+2} and Pb^{+2} , while T18 isolate were tolerant to Zn^{+2} , Fe^{+2} and Co^{+2} . Results also showed that the highest tolerant bacterial isolates to the four concentrations of the six for heavy metal ions were T1, T2, T3, T4, T5, T6, T7, and T8. On the other direction, T23 isolate appeared sensitivity to all tested heavy metal ions except for with Pb, as it was tolerant (*Table 2*).

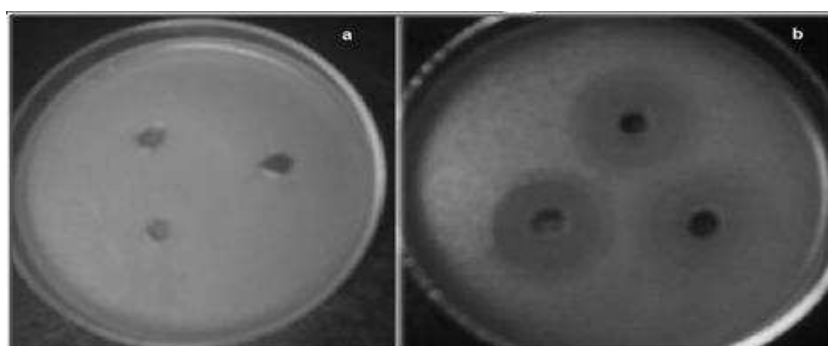


Figure 3. Tolerance of the bacterial isolate to heavy metals [resistant (a) and clear of inhibition zone as sensitive (b)]

At the lowest concentration (25 $\mu\text{g/mL}$) of all six heavy metal ions, all bacterial isolates were tolerant except for the heavy metal ion (Pb^{+2}). These results are in agreed with that reported by Malik and Jaiswal (2000), who showed that acceptable

concentration of metal ions, which could be used for distinguishing metal tolerant and metal-sensitive bacteria, strains able to grow at concentrations of metal ions at and above 1.0 mM were considered resistant. Based on the experimental findings, the heavy metal-tolerant bacteria could be selected as especially promising microorganisms for bioremediation application of heavy metals polluted places.

Effect of EIWW toxicity on each of bacterial growth and indole acetic acid (IAA) produced by bacterial isolates

Effects of SIWW on bacterial growth, representing in each of growth curve [expressed as optical density (OD) ($\lambda = 620$ nm) as recommended by Priyadharshini and Kumar (2016), and bacterial growth periods [1, 2, 3, 4, 5, 6 and 7 days] of ten isolates (T1, T2, T3, T4, T5, T6, T7, T8, T10 and T18) was carried out.

Table 2. Tolerance of bacterial isolates to six heavy metals expressed as zone of inhibition

ICs	Heavy metal concentrations ($\mu\text{g/mL}$)											
	25	50	75	100	25	50	75	100	25	50	75	100
	Zn^{+2}				Fe^{+2}				Co^{+2}			
T1	R	R	R	R	R	R	R	R	R	R	R	R
T2	R	R	R	R	R	R	R	R	R	R	R	R
T3	R	R	R	R	R	R	R	R	R	R	R	R
T4	R	R	R	R	R	R	R	R	R	R	R	R
T5	R	R	R	R	R	R	R	R	R	R	R	R
T6	R	R	R	R	R	R	R	R	R	R	R	R
T7	R	R	R	R	R	R	R	R	R	R	R	R
T8	R	R	R	R	R	R	R	R	R	R	R	R
T9	R	R	R	R	3.5 (S)*	3.7 (S)	3.5 (S)	3.9 (S)	R	R	R	R
T10	R	R	R	R	3.5 (S)	4 (S)	3.5 (S)	3.7 (S)	R	R	R	R
T11	R	R	1, (S)	1, (S)	R	R	R	0.5 (S)	1 (S)	1 (S)	1 (S)	1 (S)
T12	R	R	R	0.5 (S)	R	R	R	1, (S)	R	R	R	R
T13	2,(S)	2 (S)	2 (S)	2.6 (S)	1.6 (S)	1.6 (S)	1.6 (S)	1.6 (S)	R	R	R	R
T14	R	R	R	R	1.4 (S)	2.6 (S)	2.6 (S)	2.6 (S)	1.6 (S)	1.6 (S)	1.6 (S)	1.6 (S)
T15	R	2 (S)	1.3 (S)	1.9 (S)	1.8 (S)	2.1 (S)	1.8 (S)	2.5 (S)	R	2 (S)	1 (S)	1.3 (S)
T16	R	0.9 (R)	1.2 (S)	1.3 (S)	2.2 (S)	3.1 (S)	2, (S)	2.3 (S)	R	0.9 (S)	0.9 (S)	1.1 (S)
T17	R	R	R	R	R	R	R	R	1.2 (S)	1.2 (S)	1.2 (S)	1.2 (S)
T18	R	R	R	R	R	R	R	R	R	R	R	R
T19	1(S)	1, (S)	1, (S)	1, (S)	R	R	0.7 (S)	0.7 (S)	1.9 (S)	1.9 (S)	1.9 (S)	1.9 (S)
T20	R	R	1, (S)	2, (S)	1.3 (S)	1.7 (S)	1.1 (S)	2.5 (S)	1.5 (S)	1.5 (S)	1.9 (S)	2, (S)
T21	R	R	0.9 (S)	1.8 (S)	R	R	0.5 (S)	0.5 (S)	R	R	1 (S)	1 (S)
T22	R	R	R	0.9 (S)	R	R	R	1.6 (S)	R	R	R	1 (S)
T23	1.9(S)	1.9 (S)	2, (S)	2, (S)	1.2 (S)	1.2 (S)	1.5 (S)	1.7 (S)	1.2 (S)	1.2 (S)	1.8 (S)	1.8 (S)
T24	R	R	R	R	2.6 (S)	3.6 (S)	3.6 (S)	3.6 (S)	1.1 (S)	1.1 (S)	1.1 (S)	1.1 (S)
T25	R	R	1.9 (S)	1.9 (S)	R	R	0.5 (R)	0.5 (R)	1.8 (S)	1.8 (S)	2.8 (S)	2.8 (S)
T26	R	R	R	R	R	R	1.7 (S)	1.7 (S)	R	R	1.5 (S)	1.5 (S)
T27	R	R	R	2.8 (S)	R	R	R	R	R	R	R	1.9 (S)
T28	R	R	R	3.8 (S)	R	R	0.1 (R)	0.1 (R)	R	R	R	3.9 (S)
T29	R	R	R	2, (S)	R	R	1.6 (S)	1.6 (S)	R	R	R	0.5 (S)
T30	R	R	R	3.2 (S)	R	1 (S)	1 (S)	1 (S)	R	R	R	2.6 (S)

	Cd ⁺²				Cu ⁺²				Pb ⁺²			
T1	R	R	R	R	R	R	R	R	R	R	R	R
T2	R	R	R	R	R	R	R	R	R	R	R	R
T3	R	R	R	R	R	R	R	R	R	R	R	R
T4	R	R	R	R	R	R	R	R	R	R	R	R
T5	R	R	R	R	R	R	R	R	R	R	R	R
T6	R	R	R	R	R	R	R	R	R	R	R	R
T7	R	R	R	R	R	R	R	R	R	R	R	R
T8	R	R	R	R	R	R	R	R	R	R	R	R
T9	R	R	R	0.9 (S)	R	R	R	R	R	R	R	R
T10	R	R	R	R	R	R	R	R	R	R	R	R
T11	R	R	1 (S)	1 (S)	R	R	R	2 (S)	R	R	R	R
T12	R	R	R	R	R	R	R	1.8 (S)	R	R	R	2, (S)
T13	R	R	R	R	R	R	R	2.2 (S)	R	R	R	3.2 (S)
T14	3 (S)	3.2 (S)	3.2 (S)	3.2 (S)	3, (S)	3.9 (S)	3.9 (S)	3.9 (S)	R	R	R	R
T15	R	R	R	R	R	0.9 (S)	2, (S)	2, (S)	R	R	R	R
T16	R	R	R	0.7 (S)	R	1 (S)	1, (S)	1.3 (S)	R	R	R	R
T17	R	R	R	R	1.3 (S)	1.3 (S)	2.3 (S)	2.3 (S)	R	R	R	R
T18	R	R	R	R	1.4 (S)	1.4 (S)	1.6 (S)	1.6 (S)	R	R	R	R
T19	R	R	1 (S)	1 (S)	1 (S)	1 (S)	1 (S)	1 (S)	R	R	R	R
T20	R	0.8 (S)	1 (S)	1.6 (S)	R	0.1 (R)	1.2 (S)	1.9 (S)	R	1, (S)	1.9 (S)	2.9 (S)
T21	1.4 (S)	1.9 (S)	1.9 (S)	1.9 (S)	2.6 (S)	3.6 (S)	3.6 (S)	3.6 (S)	R	R	0.5 (S)	1.3 (S)
T22	R	R	R	1, (S)	2.7 (S)	3.7 (S)	4 (S)	4 (S)	R	R	R	0.9 (S)
T23	0.8 (S)	0.8 (S)	1.8 (S)	1.9 (S)	2.3 (S)	2.6 (S)	2.8 (S)	2.8 (S)	R	R	R	R
T24	2.5 (S)	3.9 (S)	3.9 (S)	3.9 (S)	2.8 (S)	3.8 (S)	3.8 (S)	3.8 (S)	R	R	R	R
T25	2 (S)	2 (S)	2, (S)	2, (S)	4.9 (S)	4.9 (S)	4.9 (S)	4.9 (S)	R	R	R	R
T26	R	R	0.8 (S)	0.8 (S)	R	R	0.1 (R)	0.1 (R)	R	R	1, (S)	1, (S)
T27	R	R	1.9 (S)	1.9 (S)	R	R	3.6 (S)	3.6 (S)	R	R	R	R
T28	R	R	R	R	R	R	3.7 (S)	3.7 (S)	R	R	R	R
T29	R	R	R	1.9 (S)	R	R	R	2.8 (S)	R	R	R	R
T30	R	R	R	3.9 (S)	R	R	R	3.8 (S)	R	1.3 (S)	1 (S)	1 (S)

ICs: Isolate codes. R: Resistance. S: sensitive. *: Inhibition zone dimension

Results in *Figures 4 and 5* revealed that the lag phase growth started in the 1st day of bacterial isolates (T1, T2, T3, T4 and T5) and in the 2nd day for the isolates (T6, T7, T8, T10 and T18). Four recognizable phases are seen when the increase in cell number was determined in relation to time by lag phase, log phase, stationary phase and decline phase (Priyadarshini and Kumar, 2016).

The lag phase continuously in the growth for the 3rd day and the highest OD (0.61 nm) was recorded with isolates T10 and T18. Regarding to the log phase, the three isolates coded T1, T3 and T4 registered the highest values (0.41, 0.40 and 0.46 nm) respectively. The stationary phase was observed in the 5th day and the high value was recorded for T3 isolate (0.42 nm) and T6 isolate (0.41 nm). From the 6th day all the tested bacterial isolates started in the decline phase. The obtained data indicated that the selected bacterial isolates (T1, T3 and T4) were continuously to the growth from the 1st day until the 5th day and the optimum growth period was registered in the 4th day. These

results considering that the selected bacterial isolates (T1, T3 and T4) are promising bacteria for up taking the heavy metal ions from EIWW.

Effect of EIWW toxicity on the abilities of the selected bacterial isolates to produce IAA was studied. Results in *Table 3* (illustrated by *Fig. 6*) showed that the selected bacterial isolates were varied in their production of IAA affected by EIWW.

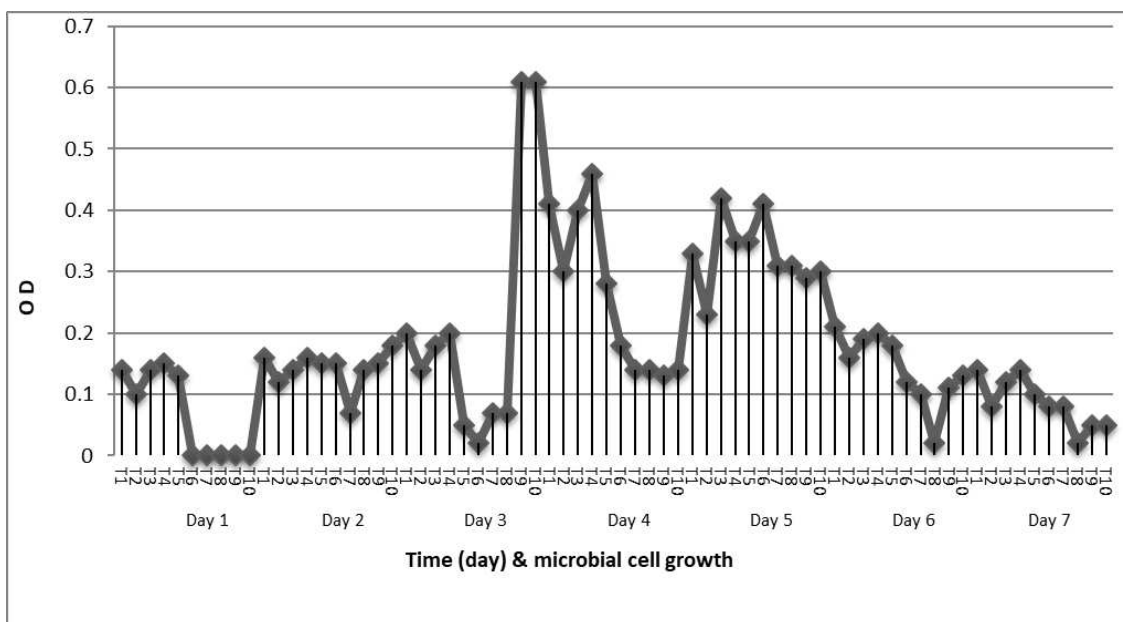


Figure 4. Optical density ($\lambda = 620 \text{ nm}$) of ten selected bacterial isolates (T1, T2, T3, T4, T5, T6, T7, T8, T10 and T18) as affected by growth periods

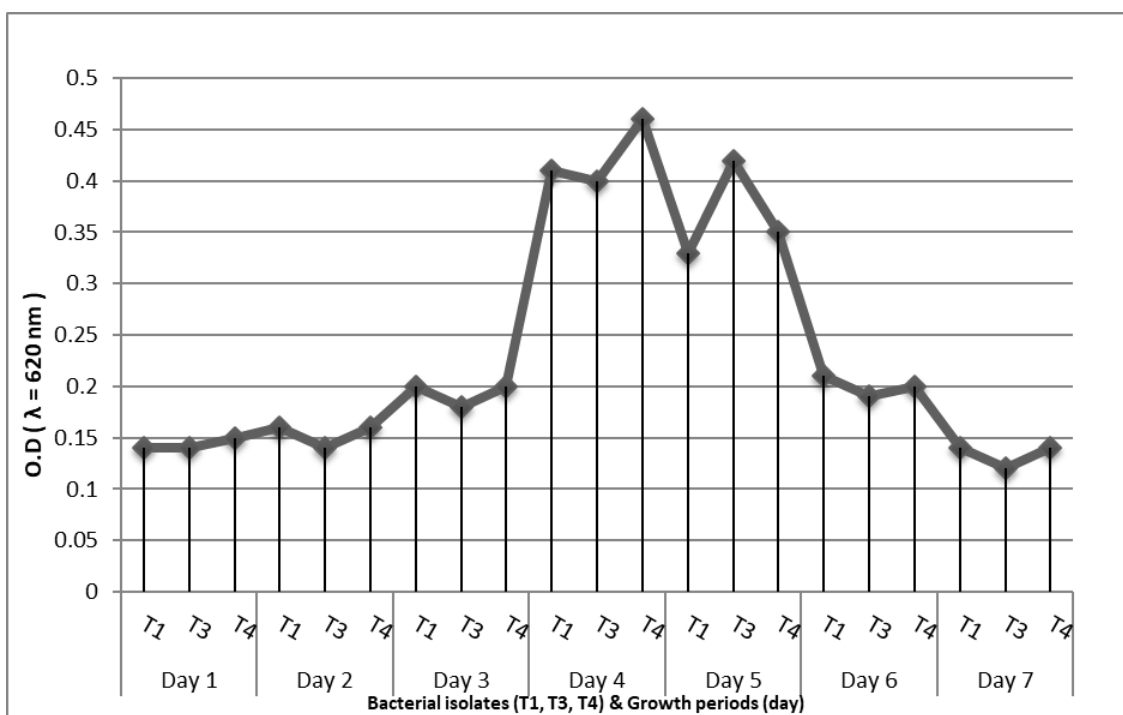


Figure 5. Optical density ($\lambda = 620 \text{ nm}$) of three selected bacterial isolates (T1, T3, and T4) as affected by growth periods

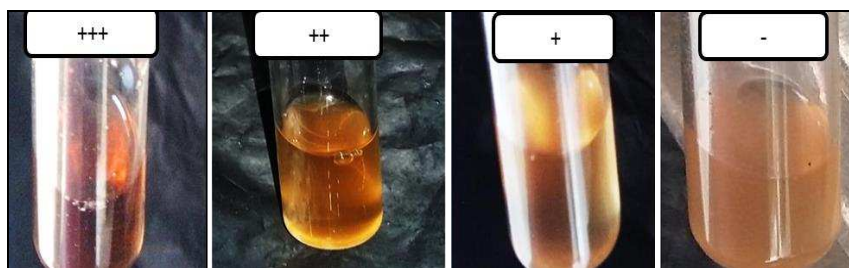


Figure 6. Photos shows the IAA visual reaction degrees of a bacterial isolate for IAA production, [high (+++), moderate (++) , low (+), no reaction (-)]

Table 3. Degree of color changes of bacterial isolates (T1, T2, T3, T4, T5, T6, T7, T8, T10 and T18) to producing IAA on NBM containing SIWW, and L-tryptophan (0.1%, v/w)

Bacterial isolates code	IAA visual reaction degrees
T1	Moderate
T2	High
T3	Moderate
T4	Moderate
T5	Moderate
T6	Moderate
T7	Low
T8	Low
T10	Low
T18	Low

These results are harmony with that reported by Özdal et al. (2016) who reported that the production of IAA dependence on the Bacillus spp. isolates and fermentation time. Isolate (T2) gave the highest degree of color change that evidence on its high ability for the consumption of L-tryptophan and IAA production, while, the T1, T3, T4, T5 and T6 isolates gave the moderate degree of color change. The lowest degree for color change was noticed by T7, T8, T10 and T18 isolates. From these results three bacterial isolates coded T1, T3 and T4 were selected and subjected to biological and molecular identification.

Determination of antibiosis activities of the ten bacterial isolates

Data presented in Table 4 and Figure 7 revealed that the all tested bacterial isolates gave antibiosis reaction against *E. coli* when growing on NAM. Similar results were obtained by Yilmaz et al. (2006), who mentioned that *B. cereus* has inhibitory affect both against Gram-positive and Gram-negative bacteria. Negative reaction was recorded with T2 and T6 isolates against *F. solani* and *S. rellsii*. The rest of bacterial isolates, T1, T3, T4, T5, T7, T8, T10 and T18 have positive reaction against the three tested pathogens (*F. solani*, *S. rellsii* and *E. coli*).

These results are in harmony with that of Kim et al. (2015), who showed that the Bacillus spp. had broad-spectrum antifungal activity against *F. solani* and *F. oxysporum*. Results of Ghai et al. (2007) also supported this study, as they recorded that the more strains of Bacillus spp. had antagonistic activities against some fungal

pathogens, e.g. *Clerotium rolfsii*, *Fusarium oxysporum* and *Rhizoctonia solani*. Based on these results it has been observed that, three isolates coded T1, T3 and T4 were selected and subjected to biological and molecular identification.

Table 4. Antibiosis activities of bacterial isolates (T1, T2, T3, T4, T5, T6, T7, T8, T10 and T18) against *F. solani*, *S. rolfsii* and *E. coli*

Bacterial isolates code	Antibiosis reaction		
	<i>F. solani</i>	<i>S. rolfsii</i>	<i>E. coli</i>
T1	+	+	+
T2	-	-	+
T3	+	+	+
T4	+	+	+
T5	+	+	+
T6	-	-	+
T7	+	+	+
T8	+	+	+
T10	+	+	+
T18	+	+	+

+: Antibiosis, -: Non antibiosis

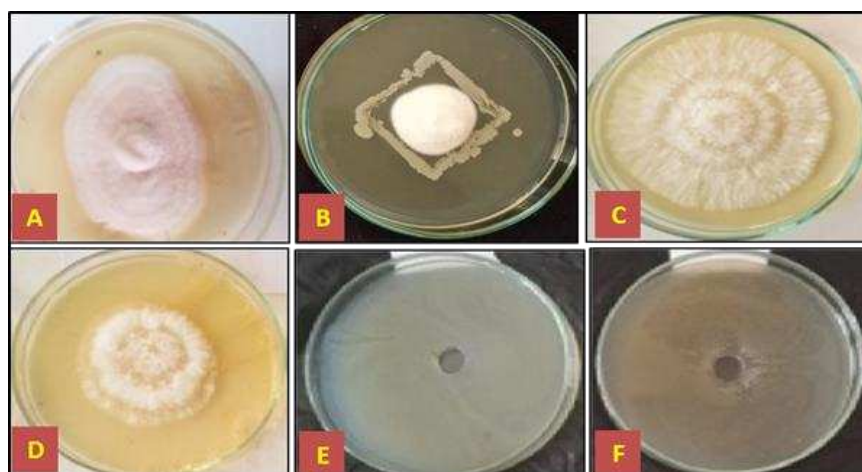


Figure 7. Antibiosis activities of abacterial isolate against *F. solani* (A), *S. rolfsii* (C) and *E. coli* (E) compared to the growth alone to every one (B, D and F), respectively

Biological identification of the selected bacterial isolates

The bacterial isolates which were selected based on their growth curve; IAA reaction (color change) and antibiosis effect were identified according to (Juni 1986) mentioned in Bergey's Manual of Systematic Bacteriology (1986, 2012) and Barrow and Felltham (1993).

Morphological, biochemical characterization and utilization of carbohydrates as carbon sources via the bacterial isolates which coded with T1, T3 and T4 are presented in Table 5. On NAM, all 48 h-old cultures of tested isolates were positive to Gram stain, motile, rod shaped with white colony for T3, T4 isolates and yellowish colony for T1

isolate. Furthermore, all bacterial isolates were positive effect on both catalase and Indole tests. The coded isolates T1 and T3 were negative with oxidase, Methyl-red and citrate tests. All isolates utilized sucrose and lactose as carbon sources, while, T1 failed to utilize glucose, maltose and xylose. From the obtained data and classifying bacterial isolates in accordance to Claus and Berkeley (1986) that identified the coded (T1, T3 and T4) as *Bacillus spp.*, *Bacillus cereus* and *Bacillus altitudinis*, respectively.

Table 5. Morphological and biochemical characterization, utilization of carbohydrate test of Bacterial isolates (Claus and Berkeley, 1986; Barrow and Felltham, 1993)

Characters	Bacterial isolates		
	T1	T3	T4
Morphological characteristics			
Colony color on agar	Yellowish	White	White
Gram stain	Positive	Positive	Positive
Cell shape	Rod	Rod	Rod
Motility	Motile	Motile	Motile
Biochemical test results			
Oxidase	+	+	+
Catalase	+	+	+
Indole	+	+	+
Methyl-Red	-	+	+
Citrate	-	+	+
Utilization of carbohydrate			
Glucose	-	+	+
Sucrose	+	+	+
Maltose	-	+	+
Xylose	-	+	+
Lactose	+	+	+
Nomenclatures	<i>Bacillus spp.</i>	<i>Bacillus cereus</i>	<i>Bacillus altitudinis</i>

+: Positive, -: Negative

Molecular identification of the selected bacterial isolates

Biological identification of the three bacterial isolates alone was not completely enough, and these tests consume a lot of time and chemicals. Due to the advanced technology such as 16SrRNA gene, primers had been developed by investigators to target specifically the 16S rRNA sequence of the bacteria. In this search, the three bacterial isolates obtained from EIWW samples were also identified using primers targeting their 16S rRNA sequence (Jeffrey, 2008). The nucleotide sequences of 16S rRNA gene were partially determined using the DNA template of the three bacterial isolates (T1, T3, and T4). Results showed that partial sequences of 985, 997 and 983 nts were obtained for the three isolates, respectively. These sequences were compared with four universal bacterial isolates as mentioned in Table 5. These bacteria were classified as *Bacillus sp.* SMMAA-1, *Bacillus cereus* SMMAA-3 and *Bacillus altitudinis* SMMAA-4 and documented in GenBank under the accession numbers of LC472522, LC472523 and LC472524, respectively. Results in Table 6 showed that the percent

identities between the three bacterial strains and those similar strains recorded in GenBank ranged from 84.85% to 100.00%. Phylogenetic trees of the three bacterial strains compared to that similar strain in GenBank confirmed the biological identification of these strains as illustrated in *Figure 8*.

Table 6. Sequences producing significant alignments of the three bacterial strains compared to those similar strains in GenBank with E-value (0.0)

Description	Query cover (%)	Identities (%)	Accession
T1 isolate (LC472522)			
<i>Bacillus altitudinis</i> strain P-10 chromosome, complete genome	91	84.97	CP024204.1
<i>Bacillus aerophilus</i> strain 232 chromosome, complete genome	91	84.85	CP026008.1
<i>Bacillus altitudinis</i> strain SGAir0031 chromosome, complete genome	91	84.85	CP022319.2
<i>Bacillus cellulasensis</i> strain GLB197, complete genome	91	84.85	CP018574.1
T3 isolate (LC472523)			
<i>Bacillus cereus</i> strain ATCC 14579 16S ribosomal RNA (rrnA), partial sequence	98	100.00	NR_074540.1
<i>Bacillus thuringiensis</i> 16S rRNA gene and 16S-23S IGS, strain SBS-BT6	98	99.73	AM779002.1
<i>Bacillus mycoides</i> 16S rRNA gene, strain MWS5303-1-4	98	99.46	Z84591.1
<i>Bacillus thuringiensis</i> 16S rRNA gene and 16S-23S IGS, strain SBS-BT3	98	99.46	AM778999.1
T4 isolate (LC472524)			
<i>Bacillus altitudinis</i> strain P-10 chromosome, complete genome	99	99.08	CP024204.1
<i>Bacillus cellulasensis</i> strain GLB197, complete genome	99	98.98	CP018574.1
<i>Bacillus aerophilus</i> strain 232 chromosome, complete genome	99	99.08	CP026008.1
<i>Bacillus altitudinis</i> strain SGAir0031 chromosome, complete genome	99	99.08	CP022319.2

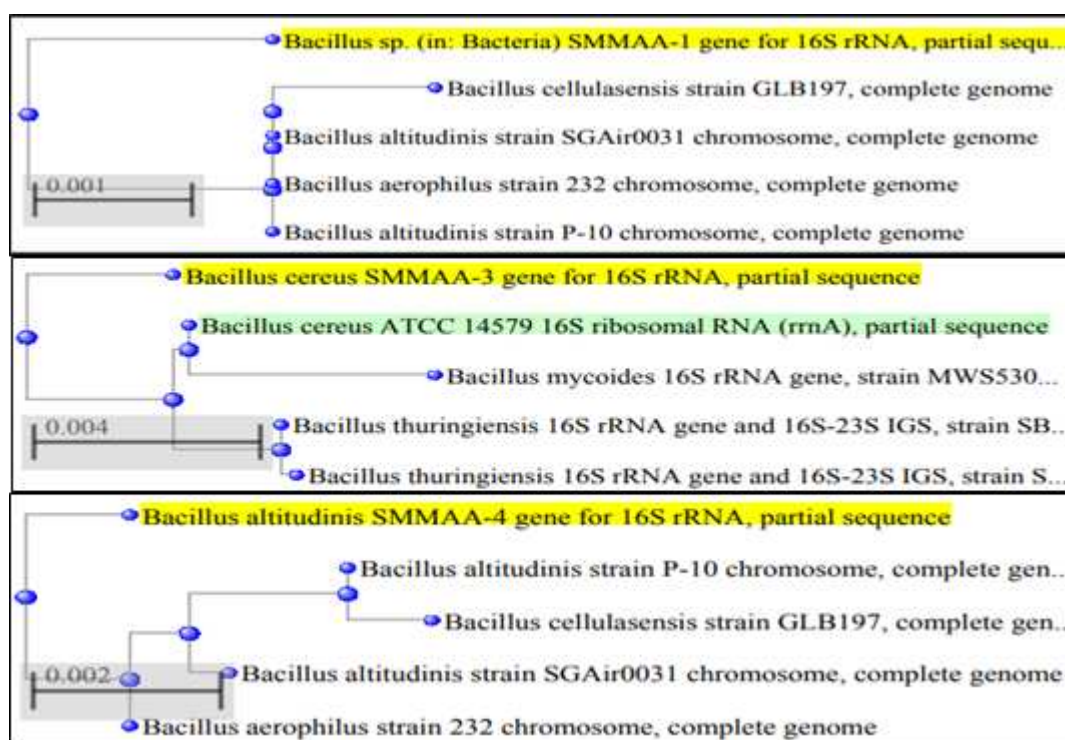


Figure 8. Phylogenetic trees of the three bacterial strains compared to those similar strains in GenBank

Role of selected bacterial isolates (*Bacillus* spp., *B. cereus* and *B. altitudinis*) on the biosorption of six heavy metals (Zn^{+2} , Fe^{+2} , Co^{+2} , Cd^{+2} , Cu^{+2} and Pb^{+2}) from industrial wastewater (IWW)

Biosorption efficiency of heavy metals from SIWW by *Bacillus* spp., *B. cereus* and *B. altitudinis* is depicted in *Table 7* and *Figure 9*. Data showed that the initial values of six heavy metals (ppm) were founded by diversity in IWW and wide ranged from 1.4 ppm to 6 ppm. The maximum conc. was found with Zn^{+2} (6 ppm) while, the minimum conc. was found with Co^{+2} (1.4 ppm). The values of final metal conc. of heavy metals in SIWW were reduced as result of biosorption occurred by bacteria and ranged from 0.109 ppm to 0.409 ppm compared to the initial metal conc. (2.450 ppm). The ability of bacterial isolates tested (*Bacillus* spp., *B. cereus* and *B. altitudinis*) for biosorption of the six heavy metals were differed among them.

Table 7. Initial and residual values of heavy metals (ppm) in IWW as affected by SIWW inoculated with the selected bacteria (*Bacillus* spp., *B. cereus* and *B. altitudinis*)

Heavy metals	Initial metal conc.(ppm)	Residual values of heavy metals (ppm)			Mean
		SIWW + <i>Bacillus</i> spp.	SIWW + <i>B. cereus</i>	SIWW + <i>B. altitudinis</i>	
Zn	6.000	0.551	0.016	0.490	0.352
Fe	2.100	1.782	0.552	1.782	1.372
Co	1.400	0.002	0.004	0.008	0.004
Cd	1.800	0.017	0.016	0.019	0.017
Cu	1.500	0.017	0.004	0.014	0.011
Pb	1.900	0.087	0.063	0.097	0.082
Mean	2.450	0.409	0.109	0.401	

IWW = Industrial Wastewater, SIWW = Sterile Industrial Wastewater

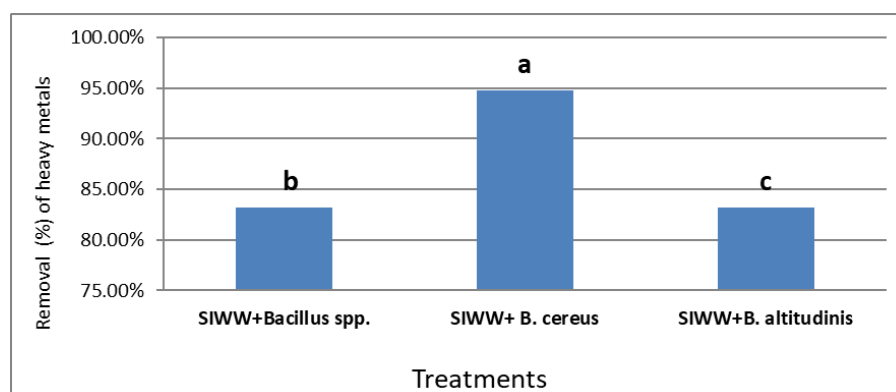


Figure 9. Average of the mean values (A) of the heavy metals removal % of IWW as affected by SIWW inoculated with the selected bacteria (*Bacillus* spp, *B. cereus* and *B. altitudinis*). Values having the same alphabetical letter within each column are not significantly different at the 0.05 level according to (Duncan multiple range test)

Data exhibited that *B. cereus* was more effected than *B. altitudinis* and *Bacillus* spp. for biosorption final metal conc. (0.109, 0.401 and 0.409 ppm) respectively. Also, the data indicated that (Co^{+2}) ion was more biosorption by the three bacterial isolates and gave the

little values compared to (Fe⁺²) which gave the highest values in IWW. The ions (Co⁺² and Cu⁺²) recorded the highest biosorption by the three bacterial isolates followed by the (Zn⁺², Pb⁺² and Cd⁺²) but the lowest biosorption recorded with Fe⁺² metal.

From the obtained result data revealed that the all bacterial isolates play an important role in detoxification of heavy metals founded in the IWW of Abu-kerqas sugar factory-El-Minia, Egypt. The all studied bacteria were more effective for the biosorption of the heavy metal contents in SIWW. Co⁺² ion was more absorbed by *Bacillus spp.* (0.002 ppm) followed by *B. cereus* (0.004 ppm) and *B. altitudinis* (0.008 ppm).

The results presented in *Table 8* and *Figure 9* show the biosorption ability of *B. cereus* is significantly effective for removal efficiency percentage of six heavy metals (Zn⁺², Fe⁺², Co⁺², Cd⁺², Cu⁺² and Pb⁺²) (94.77%) from IWW. However, the removal efficiency % of it is heavy metals using *Bacillus spp.* and *B. altitudinis* recorded 83.19% and 83.21% with insignificant difference between them. This indicated that *B. cereus* has a higher capability of biosorption potentiality of heavy metals compared to the others. Similar results are recorded by Huang et al. (2013).

Regarding to the effects of the different heavy metals tested for the removal efficiency %, the results in *Table 8* and *Figure 10* show significant effects. Available data revealed that higher removal efficiencies of 99.66% for Co⁺², 99.22% for Cu⁺² and 99.03% for Cd⁺² and lower removal efficiencies 34.66% for Fe⁺² were recorded as Mullen et al. (1989).

Table 8. Removal efficiency % of heavy metals from IWWs affected by SIWW inoculated with the selected bacteria (*Bacillus spp.*, *B. cereus* and *B. altitudinis*)

Treatments	Removal efficiency % of heavy metals						Mean of A
	Zn ⁺²	Fe ⁺²	Co ⁺²	Cd ⁺²	Cu ⁺²	Pb ⁺²	
Bacillus spp. + SIWW	90.83 d	15.14 f	99.86 a	99.06 a	98.87 a	95.42 bc	83.19 b
<i>B. cereus</i> + SIWW	99.73 a	73.71 e	99.71 a	99.11 a	99.73 a	96.68 b	94.77 a
<i>B. altitudinis</i> + SIWW	91.83 c	15.14 f	99.42 a	98.94 a	99.06 a	94.89 bc	83.21 b
Mean of B	94.13 b	34.66 c	99.66 a	99.03 a	99.22 a	95.66 b	

Mean values of three replicates followed by the same letters in each column are not significantly different (P > 0.05) (Duncan multiple range test). LSD at (0.05%) for A = 0.0715, B = 1.012, AB = 1.753

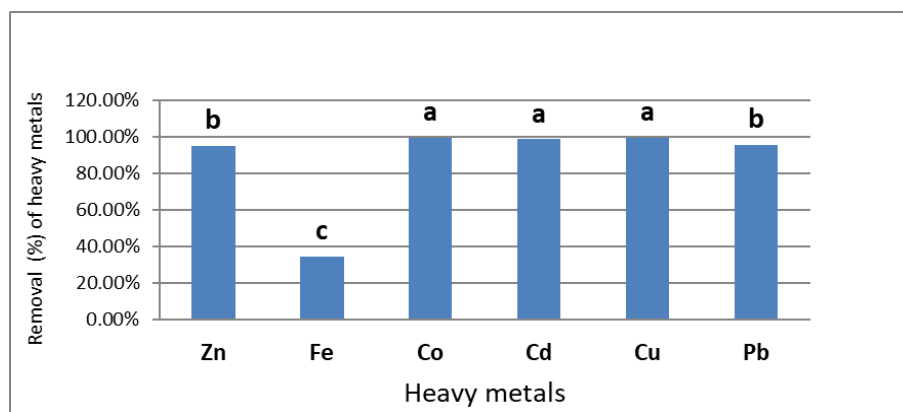


Figure 10. Average of the mean values (B) of the different six heavy metals removal % from IWW). Values having the same alphabetical letter within each column are not significantly different at the 0.05 level according to (Duncan multiple range test)

Also, similar data in *Table 8* and *Figure 11* revealed that a significantly higher removal efficiencies for Co^{+2} , Cd^{+2} and Cu^{+2} when combined with bacterial isolates (*Bacillus spp.*, *B. cereus* and *B. altitudinis*) without significant differences among them. The highest residual values and the lowest removal biosorption by bacterial isolates were recorded with Fe^{+2} similar results are recorded by Tuzen et al. (2007).

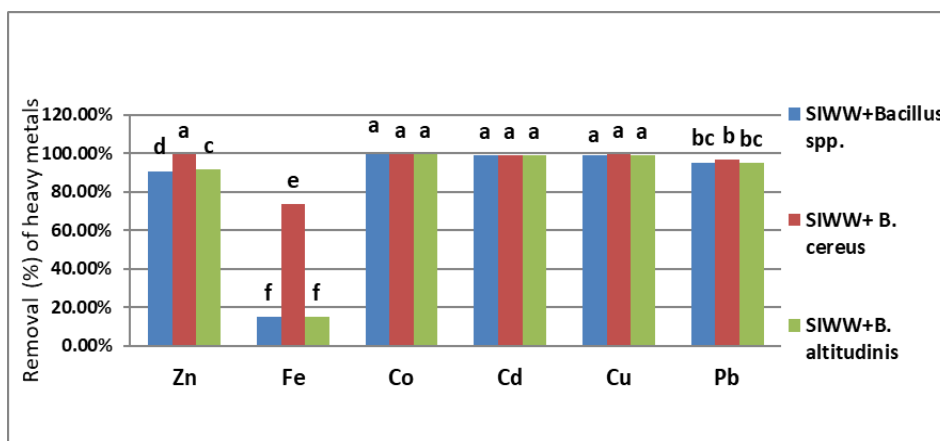


Figure 11. The interaction (AB) effect between the treatments (SIWW + *Bacillus spp.*, SIWW + *B. cereus*, SIWW + *B. altitudinis*) and six heavy metals removal % of IWW. Values having the same alphabetical letter within each column are not significantly different at the 0.05 level according to (Duncan multiple range test). IWW = Industrial Wastewater, SIWW = Sterile Industrial Wastewater

Conclusion

The isolation and identification of tolerant bacteria against six heavy metals (Zn^{+2} , Fe^{+2} , Co^{+2} , Cd^{+2} , Cu^{+2} and Pb^{+2}) give the new technology of bioremediation method. Among 30 isolates of *Bacillus spp.*, 3 isolates exhibited more resistance effect against 6 heavy metals. These isolates were identified by morphological, biochemical characterization, molecular identification by using 16S rRNA gene and documented in GenBank as *Bacillus sp.* SMMAA-1 (LC472522), *Bacillus cereus* SMMAA-3 (LC472523), and *Bacillus altitudinis* SMMAA-4 (LC472524). These isolates are promising for further studies and can be used in bioremediation. The findings showed that bacteria present resistance of six heavy metals. *B. cereus* is more effective for removal efficiency percentage of six heavy metals (Zn^{+2} , Fe^{+2} , Co^{+2} , Cd^{+2} , Cu^{+2} and Pb^{+2}) (94.77%) from IWW than *Bacillus spp.* (83.19%) and *B. altitudinis* (83.21%). The highest removal efficiencies by Bacterial isolates were found with Co^{+2} , Cd^{+2} and Cu^{+2} and the lowest removal biosorption were recorded with Fe^{+2} . Data recommended to using of *Bacillus cereus* in bioremediation of heavy metals from industrial wastewater effluent especially with Co^{+2} , Cd^{+2} and Cu^{+2} metals.

Acknowledgements. A special thank is paid to Prof. Dr. Nasser Sayed Youssef professor of Vegetables, Horticulture Research Institute, Agriculture Research Centre for his valuable continuous helpful, discussing the results, fruitful discussions, encouragement and necessary guidance during the long tenure of my study.

REFERENCES

- [1] Abbas, S. M., Kamel, E. A. (2004): Rhizobium as a biological agent for preventing heavy metal stress. – *Asian J Plant Sci* 3(4): 416-424.
- [2] Ahemad, M., Khan, M. S. (2012): Effect of fungicides on plant growth promoting activities of phosphate solubilizing *Pseudomona sputida* isolated from mustard (*Brassica compestris*) rhizosphere. – *Chemosphere* 86(9): 945-950.
- [3] Akhter, K., Ghous, T., Andleeb, S., Ejaz, S., Khan, B. A., Ahmed, M. N. (2017): Bioaccumulation of heavy metals by metal-resistant bacteria isolated from *Tagetes minuta* rhizosphere, growing in soil adjoining automobile workshops. – *Pakistan Journal of Zoology* 49(5).
- [4] Altschul, S. F., Gish, W., Miller, W., Myers, E. W., Lipman, D. J. (1990): Basic local alignment search tool. – *Journal of Molecular Biology* 215(3): 403-410.
- [5] Azad, A. K., Nahar, A., Hasan, M. M., Islam, K., Azim, M. F., Hossain, M. S., Rahman, M., Ojha, R. K., Mahmud, G. M. S., Kayes, R. (2013): Fermentation of municipal solid wastes by bacterial isolates for production of raw protein degrading proteases. – *Asian J. Microbiol. Biotechnol. Environ. Sci.* 15: 365-374.
- [6] Bakar, A., Farid, A., Yusoff, I., Fatt, N. T., Othman, F., Ashraf, M. A. (2013): Arsenic, zinc, and aluminium removal from gold mine wastewater effluents and accumulation by submerged aquatic plants (*Cabomba piauhyensis*, *Egeriadensa*, and *Hydrillaverticillata*). – *Biomed Research International*. <https://doi.org/10.1155/2013/890803>.
- [7] Barrow, G. I. I., Feltham, R. K. A. (1993): *Cowan and Steel's Manual for the Identification of Medical Bacteria*. – Cambridge University Press, Cambridge.
- [8] Carolin, C. F., Kumar, P. S., Saravanan, A., Joshiba, G. J., Naushad, M. (2017): Efficient techniques for the removal of toxic heavy metals from aquatic environment: a review. – *Journal of Environmental Chemical Engineering* 5(3): 2782-2799.
- [9] Chauhan, M., Solanki, M., Nehra, K. (2017): Putative mechanism of cadmium bioremediation employed by resistant bacteria. – *Jordan Journal of Biological Sciences* 10(2).
- [10] Claus, D., Berkeley, R. C. W. (1986): Genus *pseudomonas*. – *Bergey's Manual of Systematic Bacteriology* 1: 140-219.
- [11] Collins, C. H., Lyne, P. M., Grange, J. (1985): *Microbiological Methods*. – Butterworths, London.
- [12] Dupont, W. D., Parl, F. F., Hartmann, W. H., Brinton, L. A., Winfield, A. C., Worrell, J. A., Plummer, W. D. (1993): Breast cancer risk associated with proliferative breast disease and atypical hyperplasia. – *Cancer* 71(4): 1258-1265.
- [13] EPA (2005): *Lead in Paint, Dust and Soil*. – U.S. Environmental Protection Agency, Washington.
- [14] Ghai, S., Sood, S. S., Jain, R. K. (2007): Antagonistic and antimicrobial activities of some bacterial isolates collected from soil samples. – *Indian Journal of Microbiology* 47(1): 77.
- [15] Glickmann, E., Dessaux, Y. (1995): A critical examination of the specificity of the Salkowski reagent for indolic compounds produced by phytopathogenic bacteria. – *Appl. Environ. Microbiol.* 61(2): 793-796.
- [16] Huang, F., Dang, Z., Guo, C. L., Lu, G. N., Gu, R. R., Liu, H. J., Zhang, H. (2013): Biosorption of Cd (II) by live and dead cells of *Bacillus cereus* RC-1 isolated from cadmium-contaminated soil. – *Colloids and Surfaces B: Biointerfaces* 107: 11-18.
- [17] Jaishankar, M., Tseten, T., Anbalagan, N., Mathew, B. B., Beeregowda, K. N. (2014): Toxicity, mechanism and health effects of some heavy metals. – *Interdisciplinary Toxicology* 7(2): 60-72.
- [18] Jeffery, G. I., Ley, R. E., Hamady, M., Lozupone, C., Turnbaugh, P. J., Ramey, R. R., Bircher, J. S. (2008): Evolution of mammals and their gut microbes. – *Science* 320(5883): 1647-1651.

- [19] Juni, E., Heym, G. A. (1986): *Psychrobacter immobilis* gen. nov., sp. nov.: genospecies composed of gram-negative, aerobic, oxidase-positive coccobacilli. – *International Journal of Systematic and Evolutionary Microbiology* 36(3): 388-391.
- [20] Karelova, E., Harichova, J., Stojnev, T., Pangallo, D., Ferienc, P. (2011): The isolation of heavy-metal resistant culturable bacteria and resistance determinants from a heavy-metal contaminated site. – *Biologia* 66: 18-26.
- [21] Kielak, A. M., Castellane, T. C., Campanharo, J. C., Colnago, L. A., Costa, O. Y., Da Silva, M. L. C. (2017): Characterization of novel *Acidobacteria* exopolysaccharides with potential industrial and ecological applications. – *Scientific Reports* 7: 41193.
- [22] Kim, Y. G., Kang, H. K., Kwon, K. D., Seo, C. H., Lee, H. B., Park, Y. (2015): Antagonistic activities of novel peptides from *Bacillus amyloliquefaciens* PT14 against *Fusarium solani* and *Fusarium oxysporum*. – *Journal of Agricultural and Food Chemistry* 63(48): 10380-10387.
- [23] Kumar, A. (2011): Mental health services in rural India: challenges and prospects. – *Health* 3(12): 757-761.
- [24] Lambert, M., Leven, B. A., Green, R. M. (2000): *New Methods of Cleaning Up Heavy Metal in Soils and Water. Environmental Science and Technology Briefs for Citizens.* – Kansas State University, Manhattan, KS.
- [25] Leonard, S. S., Bower, J. J., Shi, X. (2004): Metal-induced toxicity, carcinogenesis, mechanisms and cellular responses. – *Molecular and Cellular Biochemistry* 255(1-2): 3-10.
- [26] Malik, A., Jaiswal, R. (2000): Metal resistance in *Pseudomonas* strains isolated from soil treated with industrial wastewater. – *World J Microbiol Biotechnol* 16: 177-182.
- [27] Marzan, L. W., Hossain, M., Mina, S. A., Akter, Y., Chowdhury, A. M. A. (2017): Isolation and biochemical characterization of heavy-metal resistant bacteria from tannery effluent in Chittagong city, Bangladesh: bioremediation viewpoint. – *The Egyptian Journal of Aquatic Research* 43(1): 65-74.
- [28] Massoud, R., Hadiani, M. R., Darani, K. K., Hamzehlou, P. (2018): Bioremediation of heavy metals in food industry: application of *Saccharomyces cerevisiae*. – *Electronic Journal of Biotechnology*. <https://doi.org/10.1016/j.ejbt.2018.11.003>.
- [29] Moradi, M. H., Eskandari, M., Hosseini, S. M. (2015): Operational strategy optimization in an optimal sized smart microgrid. – *IEEE Transactions on Smart Grid* 6(3): 1087-1095.
- [30] Murthy, S., Bali, G., Sarangi, S. K. (2012): Lead biosorption by a bacterium isolated from industrial effluents. – *International Journal of Microbiology Research* 4(3): 192-196.
- [31] Mullen, M. D., Wolf, D. C., Ferris, F. G., Beveridge, T. J., Flemming, C. A., Bailey, G. W. (1989): Bacterial sorption of heavy metals. – *Appl. Environ. Microbiol.* 55(12): 3143-3149.
- [32] Nagajyoti, P. C., Lee, K. D., Sreekanth, T. V. M. (2010): Heavy metals, occurrence and toxicity for plants: a review. – *Environmental Chemistry Letters* 8(3): 199-216.
- [33] Nedialkova, D., Naidenova, M. (2005): Screening the antimicrobial activity of actinomycetes strains isolated from Antarctica. – *Journal of Culture Collections* 4: 29-35.
- [34] Özdal, M., Özdal, O. G., Sezen, A., Algur, O. F. (2016): Biosynthesis of indole-3-acetic acid by *Bacillus cereus* immobilized cells. – *Cumhuriyet Science Journal* 37: 212-222.
- [35] Pathak, M., Sarma, H. K., Bhattacharyya, K. G., Subudhi, S., Bisht, V., Lal, B. (2017): Characterization of a novel polymeric bioflocculant produced from bacterial utilization of n-hexadecane and its application in removal of heavy metals. – *Frontiers in Microbiology* 8: 170.
- [36] Priyadarshini, M., Kumar, S. R. (2016): Biodegradation of dairy wastewater using bacterial isolates. – *International Journal of Modern Trends in Engineering and Science* 3(7): 133-138.

- [37] Raja, S., Ravikrishna, R., Yua, X. Y., Leea, T., Chenc, J., Murugesand, K., Xinhua, S., Qingzhongc, Y., Kalliat, T., Collett, J. L. (2008): Fog chemistry in Texas-Louisiana Gulf Coast corridor. – *Atmosph Environ J* 42(9): 2048-2061.
- [38] Rajendran, P., Gunasekaran, P. (2007): Nanotechnology for Bioremediation of Heavy Metals. – In: Singh, S. N., Tripathi, R. D. (eds.) *Environmental Bioremediation Technologies*. Springer, Berlin, Heidelberg, pp. 211-221.
- [39] Rani, D., Moreira, M. M. (2010): Simulation–optimization modeling: a survey and potential application in reservoir systems operation. – *Water Resources Management* 24(6): 1107-1138.
- [40] Şahin, Y., Öztürk, A. (2005): Biosorption of chromium (VI) ions from aqueous solution by the bacterium *Bacillus thuringiensis*. – *Process Biochemistry* 40(5): 1895-1901.
- [41] Sardar, U. R., Bhargavi, E., Devi, I., Bhunia, B., Tiwari, O. N. (2018): Advances in exopolysaccharides based bioremediation of heavy metals in soil and water: A critical review. – *Carbohydrate Polymers* 199: 353-364.
- [42] Sneath, P. H., Mair, N. S., Sharpe, M. E., Holt, J. G. (1986): *Bergey's Manual of Systematic Bacteriology*. Vol. 2. – Williams & Wilkins, Philadelphia, PA.
- [43] Snedecor, G. W., Cochran, W. G. (1980): *Statistical Methods*. 7th Ed. – The Iowa State University Press, Ames.
- [43] Tuzen, M., Uluozlu, O. D., Usta, C., Soylak, M. (2007): Biosorption of copper (II), lead (II), iron (III) and cobalt (II) on *Bacillus sphaericus*-loaded Diaion SP-850 resin. – *AnalyticaChimicaActa* 581(2): 241-246.
- [44] Vijayadeep, C., Sastry, P. S. (2014): Effect of heavy metal uptake by *E. coli* and *Bacillus* spp. – *Journal of Bioremediation & Biodegradation* 5: 238.
- [45] Wang, K., Li, M., Hakonarson, H. (2010): ANNOVAR: functional annotation of genetic variants from high-throughput sequencing data. – *Nucleic Acids Research* 38(16): 164-164.
- [46] WHO (2003): *The World Health Report: Shaping the Future*. – World Health Organization, Geneva.
- [47] World Health Organisation WHO (1984): *Guidelines for Drinking Water Quality*. – WHO, Geneva, No.111.
- [48] World Health Organization WHO (2006): *Guidelines for the Safe Use of Wastewater, Excreta and Greywater: Wastewater Use in Agriculture (Volume II)*. – WHO, Geneva.
- [49] Yilmaz, M., Soran, H., Beyatli, Y. (2006): Antimicrobial activities of some *Bacillus* spp. strains isolated from the soil. – *Microbiological Research* 161(2): 127-131.
- [50] Zhou, X., Borén, J., Akyürek, L. M. (2007): Filamins in cardiovascular development. – *Trends in Cardiovascular Medicine* 17(7): 222-229.
- [51] Ziağova, M., Dimitriadis, G., Aslanidou, D., Papaioannou, X., Tzannetaki, E. L. (2007): Comparative study of Cd (II) and Cr (VI) biosorption on *Staphylococcus xylosus* and *Pseudomonas* sp. in single and binary mixtures. – *Bioresour. Technol.* 98: 2859-2865.

ISOLATION AND CHARACTERIZATION OF MULTIDRUG RESISTANT BETA-LACTAMASE PRODUCING *SALMONELLA ENTERICA* FROM WILD MIGRATORY BIRDS

SHARIF, M.¹ – ALAM, S.^{1*} – FAZAL, S.¹ – KABIR, M.² – SHAH, A.¹ – KHAN, W.³ – KHAN, M. M.¹ – KHURSHID, A.⁴

¹Department of Microbiology, The University of Haripur, Haripur, Pakistan

²Department of Forestry and Wildlife Management, The University of Haripur, Haripur, Pakistan

³Department of Biotechnology, COMSATS University Islamabad, Abbottabad Campus, Abbottabad, Pakistan

⁴Department of Biochemistry, Hazara University, Mansehra, Pakistan

*Corresponding author

e-mail: sadia.alam2004@gmail.com

(Received 14th Sep 2019; accepted 8th Jan 2020)

Abstract. A multidrug resistant, an enteric pathogen, *Salmonella enterica* is the most frequent cause of food poisoning. They are gram negative, aerobic or facultative anaerobic bacteria belonging to the family *Enterobacteriaceae*. Migratory birds serve as key factor, may disseminate *Salmonella* to the susceptible people through shared environment, fecal shedding and by mean of direct contact. The aim of present study was to investigate the occurrence of beta-lactamase genes (CTX-M and TEM) within antibiotic resistant strains of *Salmonella enterica* isolated from migratory birds. Present study incorporated isolation of 60 samples of *Salmonella enterica* from saliva, intestinal fluid and blood of different migratory birds. They are catalase positive, oxidase negative and H₂S gas producer. The antibiotic resistance of all isolated strains (29) was tested against 10 antibiotics by Kirby-Bauer disc diffusion method. The antibiotics that were used include ciprofloxacin (5 µg), ceftriaxone (30 µg), meropenam (10 µg), aztreonam (30 µg), penicillin (10 µg), erythromycin (15 µg), streptomycin (10 µg), gentamycin (10 µg), vancomycin (10 µg) and imipenem (10 µg). These strains indicated more resistance towards penicillin (93%), streptomycin (100%), erythromycin (93%), aztreonam (62%) and vancomycin (90%) and low resistance towards ciprofloxacin (21%), ceftriaxone (54%) and imepenam (45%). For the detection of CTX-M and TEM gene in ciprofloxacin and ceftriaxone resistant strains, DNA was obtained through chemical method. These strains were further checked for the presence of CTX-M and TEM gene by polymerase chain reaction (PCR). PCR results demonstrated that all the strains contain TEM gene but CTX-M gene was not identified in any of these strains. PCR amplified product was sequenced, followed by BLAST, which confirmed the presence of TEM gene giving resistance to beta-lactam antibiotics.

Keywords: *Salmonella enterica*, TEM gene, antimicrobial resistance, CTX-M gene, polymerase chain reaction (PCR), BLAST

Abbreviations: SS agar: *Salmonella Sheila* agar, DNA: Deoxyribonucleic acid, STE buffer: Sodium Chloride-Tries-EDTA, TE buffer: Tries-EDTA, PCR: Polymerase Chain Reaction, CIP: Ciprofloxacin, CRO: Ceftriaxone, MEM: Meropenam, ATM: Aztreonam, S: Streptomycin, E: Erythromycin, P: Penicillin, CN: Gentamicin, VA: Vancomycin, IPM: Imipenem, BLAST: Basic Local Alignment Search Tool

Introduction

The bacterial genus *Salmonella* which is an enteric pathogen causes a wide spectrum of disease (Acheson and Hohmann, 2001). *Salmonella enterica* is mostly responsible for food poisoning (Herikstad et al., 2002). *Salmonella* is an exceptionally assorted family,

which contain two species that are *S. bongori* and *S. enterica* (Tindall et al., 2005). *S. bongori* infects mostly ectotherms and unusually humans while *S. enterica* incorporates around 2500 serovars (Brenner et al., 2000). It is subdivided into 6 subspecies *enterica*, *arizonae*, *diarizonae*, *salamae*, *indica* and *houtenae* dependent on biochemistry and genomics (Malorny et al., 2011). The normal characteristic environment for subspecies *enterica* is endotherms while for the subspecies *salamae*, *arizonae*, *diari zonae*, *houtenae*, *indica* and *S. bongori* is ectotherms and environment. Migratory birds may serve as vehicle for the transmission of various extrinsic microorganisms (Maeda et al., 2001). *Salmonella* have been isolated from wildlife including exotic birds (Refsum et al., 2002). Gourmelon et al. (2010) have also observed that aquatic system gets polluted by fecal material of these exotic species can lead to human infection. During annual migration, migratory birds move from one place to another in search of suitable weather and food and play an important role in causing infections in humans and animals (Foti et al., 2011). They can easily be transmitted through contaminated food and water, improper hygienic conditions and improper disposal of sewage. Antimicrobial resistance in *Salmonella* takes place due to horizontal and vertical transference of antimicrobial gene, inappropriate self-medication which leads to resistance in microorganisms against chemical, therapeutic agents (White et al., 2002). The excessive use of antimicrobials has brought about a development of antibiotic resistance in humans, animals and environment (Berendonk et al., 2015; Radhouani et al., 2014). Majority of ceftriaxone and ciprofloxacin resistance was because of the action of β -lactamase gene. The horizontal gene transfer plays an important part in expanding ceftriaxone and ciprofloxacin resistance.

The main objective of present study was to isolate different strains of *Salmonella* from oral, intestinal and blood samples of migratory birds and to investigate the occurrence of beta-lactamase genes (CTX-M and TEM) which give antibiotic resistance against beta-lactam antibiotics (ciprofloxacin and ceftriaxone).

Material and methods

Study design

This study involved biochemical identification of *Salmonella enterica* from blood, nasal and intestinal fluid of migratory birds and molecular characterization and PCR detection of β -lactamase (CTX-M and TEM) genes.

Sample collection

Oral, intestinal and blood samples were collected from different seasonal avian species at watery sites of Hazara division (Tarbela Lake, Chakai, Siran Valley, and Khanpur). During period from September 2018 till February 2019, migratory birds were captured for study by licensed hunters from different watery sites of Hazara division. A sterile culturette was used to collect samples. A total of 60 samples were collected by rubbing swabs to oral, intestine and blood of different migratory birds. 47 blood samples were obtained through sterile syringes while 6 swabs from saliva and 7 swabs from intestinal fluid were obtained. After sampling, the culturettes were placed in their plastic sheath having nutrient broth and kept in refrigerator at 4 °C. Then the samples were enriched by adding peptone water and incubated at 37 °C for 24 h. After incubation, the pre-enriched samples were examined for the presence of *Salmonella*.

Isolation and identification

The samples were inoculated on sterile petri plates containing *Salmonella Shigella* agar and incubated at 37 °C for 24 h. The isolated colonies were picked up and again streaked on SS agar medium to obtain a pure culture. Purified bacterial colonies were exposed to cultural, colony morphology and biochemical identification by using catalase, oxidase and citrate test.

Antibiotic sensitivity

Antibiotic Sensitivity of 29 positive isolates of *Salmonella enterica* to 10 antibiotics was checked on Muller Hinton agar by Kirby-Bauer disc diffusion method. A fresh colony of *Salmonella* was picked up from the culture plate and spread over the entire petri plate containing Muller Hinton agar by using sterile cotton swab. Ten antibiotics with different concentrations were used which included ciprofloxacin, ceftriaxone, penicillin, erythromycin, streptomycin, vancomycin, gentamicin, imipenem, meropenam and aztreonam. The antimicrobial disks were placed on the surface of agar with the help of forceps and plates were incubated overnight at a temperature of 37 °C. After incubation, the zone diameters were measured to nearest millimeter and classified as sensitive (S), intermediate (I) and resistant (R) according to European Committee on Antimicrobial Susceptibility Testing (EUCAST) (Table 1).

Table 1. Concentration (μg) and breakpoints (mm) of antibiotics

Antibiotics	Disc code	Potency (μg)	Zone diameter breakpoint (mm)	
			S \geq	R <
Ciprofloxacin	CIP	5	22	19
Ceftriaxone	CRO	30	23	20
Penicillin	P	10	14	15
Erythromycin	E	15	21	15
Streptomycin	S	10	15	11
Vancomycin	VA	10	17	14
Gentamicin	CN	10	17	14
Imipenem	IPM	10	22	16
Meropenam	MEM	10	22	16
Aztreonam	ATM	30	24	21

DNA extraction

DNA was extracted by chemical method (Ausubel et al., 1994). The 1 ml growth culture of bacterial suspension was incubated overnight and centrifuged at 8000 g for 2 min. Supernatant was removed. 400 μl STE buffer was added twice and cells were centrifuged at 8000 g for 2 min. Supernatant was discarded again and 200 μl TE buffer was added to the pellets. Then, 100 μl Tris-saturated phenol was added and tubes were vortexed for 1 min. Samples were centrifuged at 13,000 g for 5 min at 4 °C so that the aqueous phase is separated from organic phase. Then 40 μl TE buffer was added to 160 μl upper aqueous phase and mixed with 100 μl chloroform and centrifuged at 13,000 g for 5 min at 4 °C. 150 μl upper aqueous phase was taken into clean eppendorf tube and that contained the required purified DNA.

Polymerase chain reaction (PCR)

PCR was performed for DNA amplification on thermocycler (Multigene Optimax, USA). Two sets of primer pairs specific for TEM and CTX-M gene were used (Table 2). The reactions were performed in final volume of 25 µL that involved 3 µL of DNA template, 1 µL of forward primer, 1 µL of reverse primer, 10 µL of 5X FIREPol® master mix (FIREPol® DNA Polymerase, 5X reaction buffer B (0.4 M Tris-HCl, 0.1 M (NH₄)₂SO₄, 0.1% w/v Tween 20), 7.5 mM MgCl₂, 1 mM dNTPs of each dATP, dGTP, dCTP, dTTP) (Solis BioDyne) and 10 µL of distilled water. Amplification was carried out using optimum conditions as follows: 1 cycle of 5 min for initial denaturation at 94 °C, 35 cycles of 45 s for final denaturation at 94 °C, 45 s for annealing at 54 °C, 1 min for initial extension at 72 °C and 1 cycle of 10 min for final extension at 72 °C in case of CTX-M gene. TEM gene was amplified using the same thermocycler with the exception of annealing at 52 °C for 45 s.

The amplification products were interpreted by gel electrophoresis. The samples were loaded in 1.2% gel stained with ethidium bromide (2 µg/mL) with the help of micro pipette and run at 90 V for 45 min. A 100-bp ladder (Solis BioDyne) was used as molecular weight marker. Gel was placed in Cleaver Scientific UV transilluminator (CSLUVTL312) to visualize the DNA bands under UV light for the presence of target gene.

Table 2. Primers sequence of CTX-M and TEM gene

Primers	Target gene	Length	Sequence (5'-3')	References
TEM F_5 TEM R_5	TEM	20 20	5' TTGGGTGCACGAGTGGGTTA 3' 5' TAATTGTTGCCGGGAAGCTA 3'	Gangoue-Pieboji et al., 2005
CTX-M F_5 CTX-M R_5	CTX-M	20 22	5' ACCGCCGATAATTCGCAGAT 3' 5' GATATCGTTGGTGGTGCCATAA 3'	Kaftandzieva et al., 2011

Statistical analysis

The Vassar Stats.net was used for *Chi Square* test (χ^2) to estimate significance level between sources of *S. enterica* isolates.

Genome sequencing and BLAST

Identification of resistant gene was confirmed by genome sequencing. The DNA of isolated strains was sequenced by Sanger sequencing method. The nucleotide sequence was analyzed and compared with sequences available on databases by using Basic Local Alignment Search Tool (BLAST).

Results

For the isolation of *Salmonella enterica*, *Salmonella Shigella* agar was used. Out of 60 samples 29 samples were positive for different serovars of *Salmonella enterica* and 31 samples were negative. Total isolation frequency of *Salmonella enterica* was found to be 29/60 (48%) (Fig. 1).

Out of these 29 samples, 22 (30%) samples were positive from blood, 3 (27%) from intestinal fluid and 4 (43%) from saliva (Fig. 2).

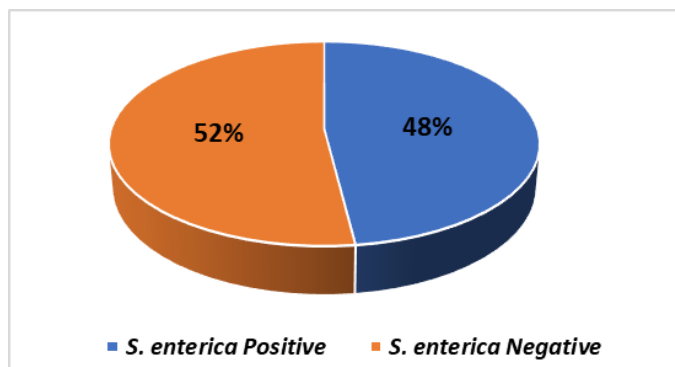


Figure 1. Isolation frequency of *Salmonella enterica* from migratory birds

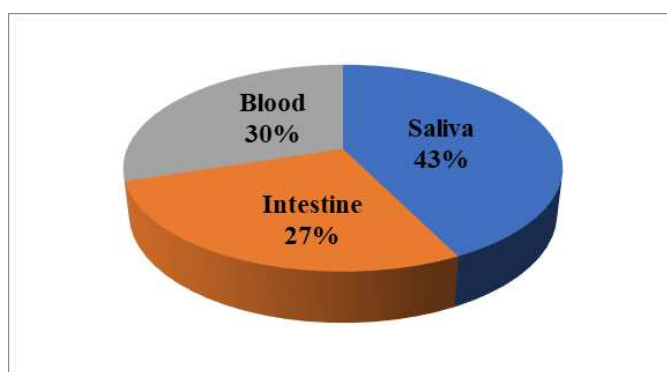


Figure 2. Percentage comparison of migratory birds positive for *S. enterica*

The chi square test (χ) revealed a non-significant difference between sources of *S. enterica* for all antibiotics tested except meropenem where a significant difference was observed ($p < 0.3$) (Table 3). The pink or yellow with black centered, flat and irregular/smooth colonies were observed on SS agar. The isolated colonies were stained with Gram's stain and appeared as rod shaped and pink in color under microscope (100X) (Fig. 3).

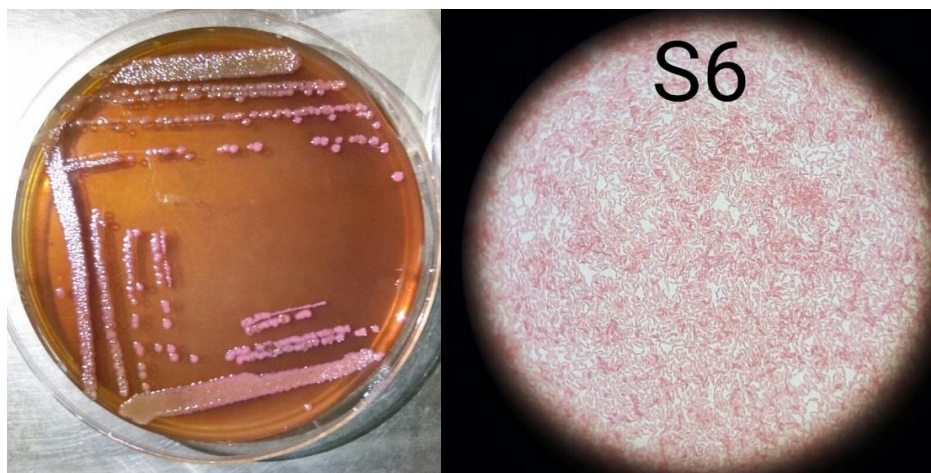


Figure 3. Cultural and microscopic (100X) identification of *S. enterica* isolated from migratory birds

All the positive isolates were catalase positive and oxidase negative (Fig. 4).

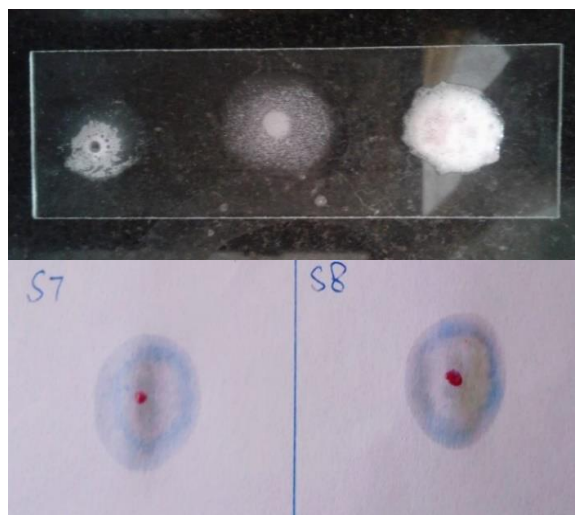


Figure 4. Biochemical identification of *Salmonella enterica* isolated from migratory birds

The *Salmonella enterica* serotypes were confirmed by citrate test. *Salmonella enterica* is citrate positive except *S. typhimurium* (Fig. 5).



Figure 5. Citrate test for the detection of *Salmonella enterica*

Antibiotic sensitivity of 29 isolates of *Salmonella enterica* obtained from saliva (n = 4), intestine (n = 3) and blood (n = 22) was checked against the ten antibiotics. In this study, *Salmonella enterica* showed resistance towards most antibiotics. The isolated strains showed more resistance against penicillin (93%), streptomycin (100%), erythromycin (93%), vancomycin (90%), aztreonam (59%) and meropenam (59%). They showed low resistance against ciprofloxacin (21%), ceftriaxone (52%), imipenem (45%) and gentamycin (55%). 25% (1/4) resistance was observed against ciprofloxacin and ceftriaxone in saliva samples, 33% (1/3) resistance against ciprofloxacin and 100% (3/3) resistance against ceftriaxone was noticed in intestinal fluid and 18% (4/22) resistance against ciprofloxacin and 50% (11/22) resistance against ceftriaxone were recognized in blood samples of migratory birds (Figs. 6, 7 and 8).

Statistical analysis was performed by chi-square test (Vassarstats.net) with P values for the comparison of difference between resistance rates of *S. enterica* to different antibiotics among the three sample sources (blood, intestine, saliva) (Table 3). The P values showed that there were no significant differences in antibiotic prescription patterns between blood, intestine and saliva sample except meropenam (0.03) (P value < 0.05 = significantly different).

Table 3. Chi-square test for comparison of *S. enterica* resistance rate (%) to various antibiotics among different sources

Antibiotics	Blood	Intestine	Saliva	X ²	P value
Ciprofloxacin	4/22 (18%)	1/3 (33%)	1/4 (25%)	0.42	0.81
Ceftriaxone	11/22 (50%)	3/3 (100%)	1/4 (25%)	3.97	0.13
Meropenam	10/22 (45%)	3/3 (100%)	4/4 (100%)	6.51	0.03
Aztreonam	11/22 (50%)	3/3 (100%)	3/4 (75%)	3.23	0.19
Penicillin	20/22 (91%)	3/3 (100%)	4/4 (100%)	0.68	0.71
Erythromycin	20/22 (91%)	3/3 (100%)	4/4 (100%)	0.68	0.71
Streptomycin	22/22 (100%)	3/3 (100%)	4/4 (100%)	0.00	1.00
Gentamycin	10/22 (45%)	2/3 (67%)	4/4 (100%)	4.25	0.11
Vancomycin	19/22 (86%)	3/3 (100%)	4/4 (100%)	1.06	0.58
Imipenem	8/22 (36%)	2/3 (67%)	3/4 (75%)	2.69	0.26

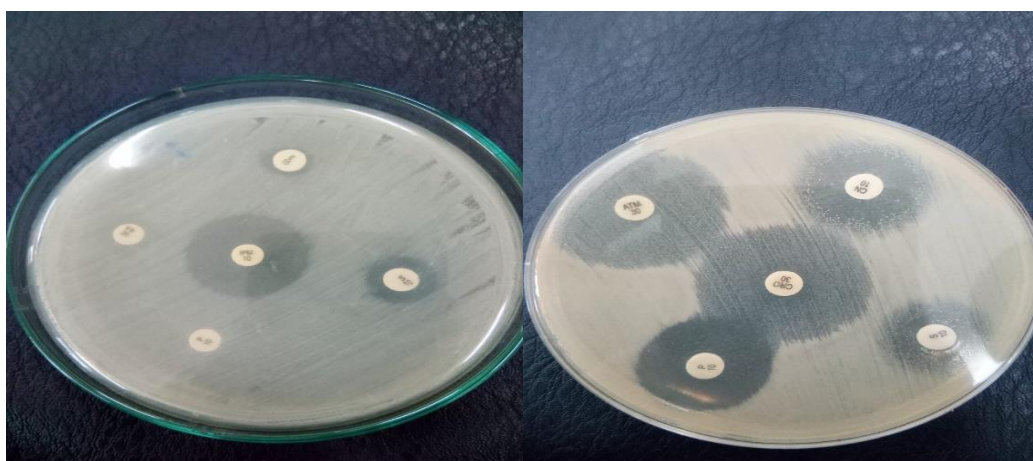


Figure 6. Antibiotic sensitivity of different antibiotics against *S. enterica* isolates

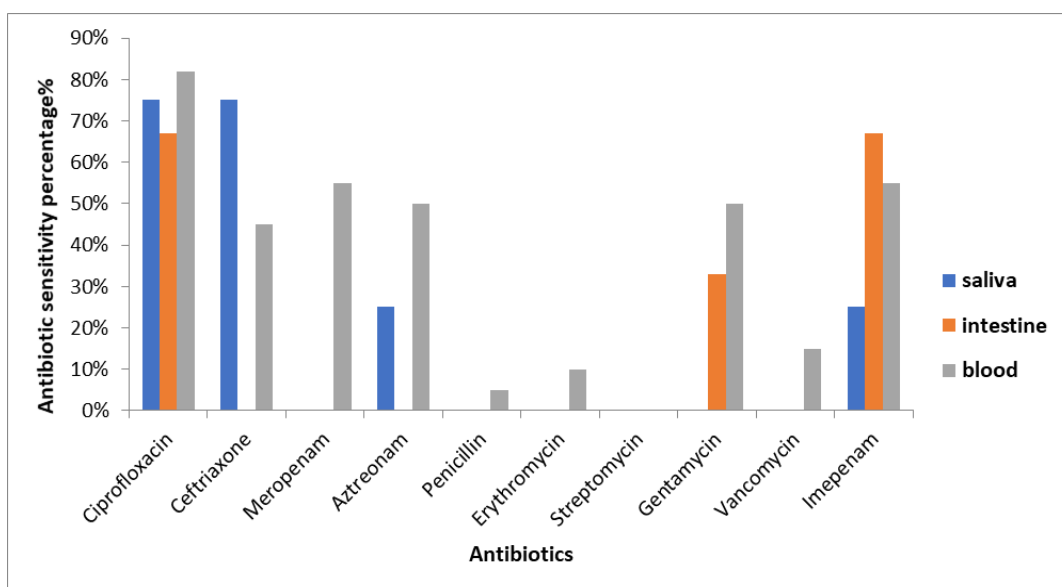


Figure 7. Antibiotic sensitivity pattern of isolates obtained from migratory birds

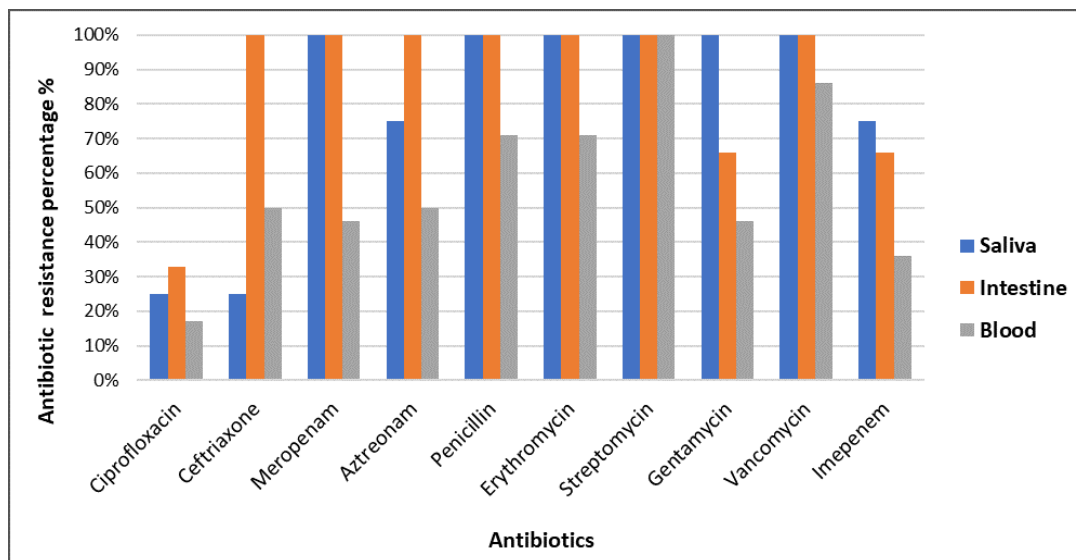


Figure 8. Antibiotic resistance pattern of isolates obtained from migratory birds

The extracted DNA of isolated strains was visualized by using gel electrophoresis (Fig. 9).

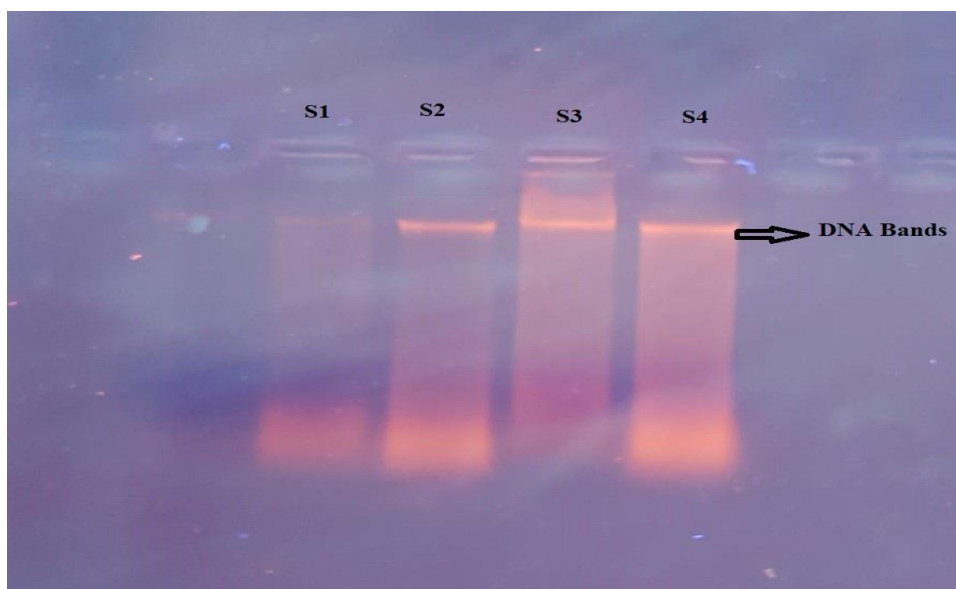


Figure 9. Gel electrophoresis of extracted DNA of isolated strains

Amplified PCR samples were analyzed by using gel electrophoresis. TEM gene was amplified in 100% strains of *S. enterica* tested for the presence of antibiotic resistant gene, yielding a strong band as dictated by correlation with size markers keep running on similar gel while no one isolates have CTX-M gene and its presence is 0% (Fig. 10).

Sample numbers S1, S2, S3, S4 and S5 showed a 508 bp fragment of TEM gene and L (Ladder) showed a 100 bp DNA size marker. Genome sequencing, followed by BLAST, confirmed the presence of TEM gene. The BLAST analysis showed highest similarity (88% identity) with *Klebsiella oxytoca*, which also harbors TEM gene (Fig. 11).

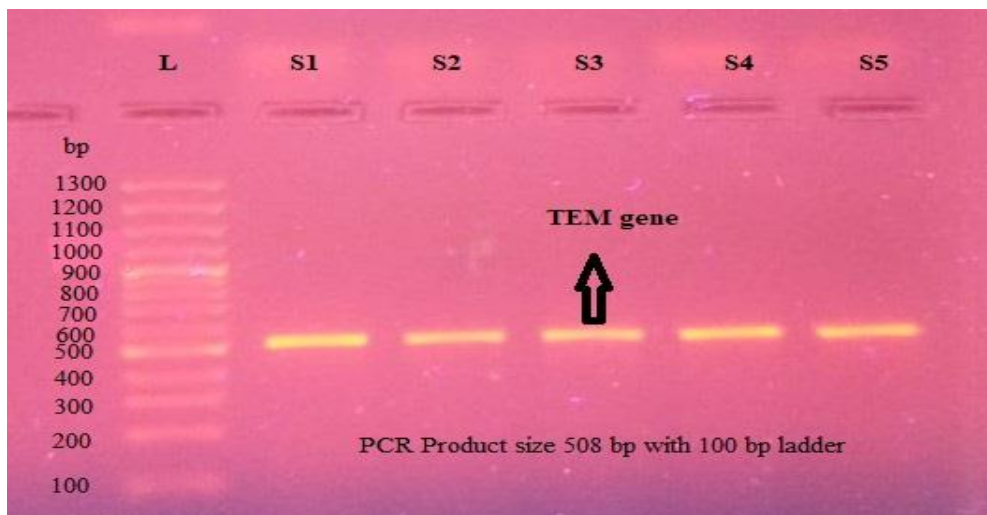


Figure 10. Amplification of TEM gene through polymerase chain reaction (PCR)

Klebsiella oxytoca extended-spectrum beta-lactamase (blaTEM1) gene, partial cds					
Sequence ID: KU991932.1 Length: 621 Number of Matches: 1					
Range 1: 121 to 535 GenBank Graphics ▼ Next Match ▲ P					
Score	Expect	Identities	Gaps	Strand	
510 bits(276)	2e-140	369/417(88%)	6/417(1%)	Plus/Plus	
Query 56	AGCACTGTT-ATGTTGTGCTATGTGTRTGCGGYATTATCAGTTATTGACGCC-GGCAAGA	113			
Sbjct 121	AGCACTTTTAAAGTTCGCTATGTG-GTGCGGTATTATCCCGTATTGACGCCGGGCAAGA	179			
Query 114	TCAACTCGGTCGCCGCGTACACTATTTCGCACAA-GACTGGGCTGATTATTGRCCAGCGTC	172			
Sbjct 180	GCAACTCGGTCGCCGCATACACTATTCTCAGAATGACTTGTTGAGTACTACACAGTCAC	239			
Query 173	AGAAGAGCATCTTACGCATGGGGTGCCAGCMGGAGAATTATGCMGGGCTGCTGTAACCCA	232			
Sbjct 240	AGAAAAGCATCTTACGGATGGCATGACAGTAAGAGAATTATGCAAGTCTGCCATAACC-A	298			
Query 233	CTCKTG-CACCCCAACGGCCAACTTACTTCTGACAACGATCGGAGGACCGAAGGAGCTAA	291			
Sbjct 299	TGAGTGATAAACACTGCGGCCAACTTACTTCTGACAACGATCGGAGGACCGAAGGAGCTAA	358			
Query 292	CCGCTTTTTTGCAACAACATGGGGGATCATGTAACCTCGCCTTGATCGTTGGGAACCGGAGC	351			
Sbjct 359	CCGCTTTTTTGCAACAACATGGGGGATCATGTAACCTCGCCTTGATCGTTGGGAACCGGAGC	418			
Query 352	TGAATGAAGCCATACCAAACGACGAGCGTGACACCACGATGCCCTGTAGCAATGGCAACAA	411			
Sbjct 419	TGAATGAAGCCATACCAAACGACGAGCGTGACACCACGATGCCCTGTAGCAATGGCAACAA	478			
Query 412	CGTTGCGCAAACTATTAACGGCGAACTACTTACTCTAGCTTCCCGGCAACAATTAA	468			
Sbjct 479	CGTTGCGCAAACTATTAACGGCGAACTACTTACTCTAGCTTCCCGGCAACAATTAA	535			

Figure 11. Sequence analysis of TEM gene showing similarity with Gene bank database sequence. Vertical lines represent identical nucleotides

Discussion

The *S. enterica* was found higher in oral cavity (43%) followed by blood (30%) and intestinal fluid (27%). The different isolation frequency of *Salmonella* was due to reason that it was found in oral cavity by eating contaminated food and its presence in blood indicates bacteremia. Experimental studies have demonstrated that gastrointestinal carriage of *Salmonella* take place in wild birds after disease; hence it is conceivable that healthy birds could be persisting carriers. Samad (2011) declared that *Salmonella* was transmitted through birds which obtain this infection from their surrounding environment. Present data was identical to the findings of Samad that

infected birds can play a main role in the transmission of diseases in humans and animals. In current study, among the ten antibiotics used a high rate of antibiotic resistance was observed against penicillin (93%), streptomycin (100%), erythromycin (93%) and vancomycin (90%). Thung et al. (2018) have also discovered comparable outcomes, who found higher prevalence of *Salmonella* in retail beef meat from different retail markets of Selangor, Malaysia. Antibiotic susceptibility was checked against 15 antibiotics. They also found that all the isolates showed resistance towards penicillin, erythromycin and vancomycin but sensitivity was observed for tetracycline, gentamicin and amoxicillin/clavulanic acid.

TEM gene was present in all positive strains (100%) tested for the presence of antibiotic resistant gene but CTX-M was absent in these strains and its presence is (0%). The presence of TEM gene was further confirmed by genome sequencing which showed 88% similarity with database sequence of *Klebsiella oxytoca* by using BLAST. This indicates that *S. enterica* might have acquired TEM gene from *K. oxytoca*. Threfall et al. (2002) reported *Salmonella* from India and different locations of Asia. They presumed that one of the primary factors of failure of treating *Salmonella* is because of resistance to ciprofloxacin. Majority of ceftriaxone and ciprofloxacin resistance was the result of activity of β -lactamase gene which includes CTX-M and TEM gene (Elumalai et al., 2014). Beta-lactamases producing *Enterobacteriaceae* have progressively developed because of widespread utilization of cephalosporin and represent a major challenge in disease control (Chong et al., 2018). The horizontal gene transfer through wild birds plays an important role in expanding ciprofloxacin and ceftriaxone resistance.

CTX-M gene was not amplified in any *S. enterica* isolate. This is due to the reason that the universal CTX-M primer used in current study was unable to recognize all positive strains even though showing positive results of resistance to beta lactam drugs. The primers for one group of CTX-M gene were unable to recognize the other groups of CTX-M gene, which results in no amplification of DNA. Pitout et al. (2004) also demonstrated a high level of specificity for the group specific primers.

Wild migratory birds have been recommended as reservoir of beta-lactamase producing pathogenic bacteria in various studies around the world (Bonnedahl et al., 2015; Atterby et al., 2016). Mohsin et al. (2017) indicated beta-lactamase producing *E. coli* in migratory birds along the Indus migration in Pakistan. He revealed that all ESBL-producing *E. coli* have CTX-M gene as the most prevailing genotype. Study carried out in Korea by Kang et al. (2015) declared that *Salmonella enterica* subsp. were the infectious agent mostly found in wild birds and brings about mortality in certain species of birds.

Conclusion

The increase in antimicrobial resistance has turned into a serious issue around the world. It has also been found that migratory birds are playing a main role in the transmission of multidrug resistant pathogens from one place to another. It presents potential risk around the world since these species can easily be utilized as expected and unexpected agents of serious foodborne disease. To avoid the occurrence of antibiotic resistance and MDR *Salmonella*, it is basic to keep up the continuous checking of antimicrobial resistance and pursue an objective remedy of antimicrobials dependent on local antimicrobial pattern.

REFERENCES

- [1] Acheson, D., Hohmann, E. L. (2001): Nontyphoidal salmonellosis. – *Clinical Infectious Diseases* 32(2): 263-269.
- [2] Ausubel, F. M., Brent, R., Kingston, R. E., Moore, D. D., Seidman, J. G., Smith, J. A., Struhl, K. (1994): *Current Protocols in Molecular Biology*. – John Wiley & Sons, Inc., Chichester.
- [3] Atterby, C., Ramey, A. M., Hall, G. G., Järhult, J., Börjesson, S., Bonnedahl, J. (2016): Increased prevalence of antibiotic-resistant *E. coli* in gulls sampled in Southcentral Alaska is associated with urban environments. – *Infection Ecology & Epidemiology* 6(1): 32334.
- [4] Berendonk, T. U., Manaia, C. M., Merlin, C., Fatta-Kassinos, D., Cytryn, E., Walsh, F., Bürgmann, H., Sørum, H., Norström, M., Pons, M. N., Kreuzinger, N. (2015): Tackling antibiotic resistance: the environmental framework. – *Nature Reviews Microbiology* 13(5): 310.
- [5] Bonnedahl, J., Stedt, J., Waldenström, J., Svensson, L., Drobni, M., Olsen, B. (2015): Comparison of extended-spectrum β -lactamase (ESBL) CTX-M genotypes in Franklin Gulls from Canada and Chile. – *PLoS One* 10(10): e0141315.
- [6] Brenner, F. W., Villar, R. G., Angulo, F. J., Tauxe, R., Swaminathan, B. (2000): *Salmonella* nomenclature. – *Journal of Clinical Microbiology* 38(7): 2465-2467.
- [7] Chong, Y., Shimoda, S., Shimono, N. (2018): Current epidemiology, genetic evolution and clinical impact of extended-spectrum β -lactamase-producing *Escherichia coli* and *Klebsiella pneumoniae*. – *Infection, Genetics and Evolution* 61: 185-188
- [8] Elumalai, S., Muthu, G., Selvam, R. E. M., Ramesh, S. (2014): Detection of TEM-, SHV- and CTX-M-type β -lactamase production among clinical isolates of *Salmonella* species. – *Journal of Medical Microbiology* 63(7): 962-967.
- [9] Foti, M., Rinaldo, D., Guercio, A., Giacobello, C., Aleo, A., De Leo, F., Fisichella, V., Mammina, C. (2011): Pathogenic microorganisms carried by migratory birds passing through the territory of the island of Ustica, Sicily (Italy). – *Avian Pathology* 40(4): 405-409.
- [10] Gangoué-Piéboji, J., Bedenic, B., Koulla-Shiro, S., Randegger, C., Adiogo, D., Ngassam, P., Ndumbe, P., Hächler, H. (2005): Extended-spectrum- β -lactamase-producing *Enterobacteriaceae* in Yaounde, Cameroon. – *Journal of Clinical Microbiology* 43(7): 3273-3277.
- [11] Gourmelon, M., Caprais, M. P., Mieszkin, S., Marti, R., Wery, N., Jardé, E., Derrien, M., Jadas-Hécart, A., Communal, P. Y., Jaffrezic, A., Pourcher, A. M. (2010): Development of microbial and chemical MST tools to identify the origin of the faecal pollution in bathing and shellfish harvesting waters in France. – *Water Research* 44(16): 4812-4824.
- [12] Herikstad, H., Motarjemi, Y., Tauxe, R. V. (2002): *Salmonella* surveillance: a global survey of public health serotyping. – *Epidemiology & Infection* 129(1): 1-8
- [13] Kaftandzieva, A., Trajkovska-Dokic, E., Panovski, N. (2011): Prevalence and molecular characterization of extended spectrum beta-lactamases (ESBLs) producing *Escherichia coli* and *Klebsiella pneumoniae*. – *Prilozi* 32(2): 129-41
- [14] Kang, M. S., Jeong, O. M., Kim, H. R., Jang, I., Lee, H. S., Kwon, Y. K. (2015): Arthritis in an egret (*Egretta intermedia*) caused by *Salmonella* Typhimurium and its potential risk to poultry health. – *Journal of Wildlife Diseases* 51(2): 534-537.
- [15] Maeda, Y., Tohya, Y., Nakagami, Y., Yamashita, M., Sugimura, T. (2001): An occurrence of *Salmonella* infection in cranes at the Izumi Plains, Japan. – *Journal of Veterinary Medical Science* 63(8): 943-944.
- [16] Malorny, B., Hauser, E., Dieckmann, R. (2011): *New Approaches in Subspecies-Level Salmonella Classification*. – *Salmonella - From Genome to Function*. Caister Academic Press, Norfolk, pp.1-23

- [17] Mohsin, M., Raza, S., Schaufler, K., Roschanski, N., Sarwar, F., Semmler, T., Schierack, P., Guenther, S. (2017): High prevalence of CTX-M-15-Type ESBL-producing *E. coli* from migratory avian species in Pakistan. – *Frontiers in Microbiology* 8: 2476.
- [18] Pitout, J. D., Hossain, A., Hanson, N. D. (2004): Phenotypic and molecular detection of CTX-M- β -lactamases produced by *Escherichia coli* and *Klebsiella* spp. – *Journal of Clinical Microbiology* 42(12): 5715-5721.
- [19] Radhouani, H., Silva, N., Poeta, P., Torres, C., Correia, S., Igrejas, G. (2014): Potential impact of antimicrobial resistance in wildlife, environment and human health. – *Frontiers in Microbiology* 5: 23.
- [20] Refsum, T., Handeland, K., Baggesen, D. L., Holstad, G., Kapperud, G. (2002): *Salmonellae* in avian wildlife in Norway from 1969 to 2000. – *Appl. Environ. Microbiol.* 68(11): 5595-5599.
- [21] Samad, M. A. (2011): Public health threat caused by zoonotic diseases in Bangladesh. – *Bangladesh Journal of Veterinary Medicine* 9(2): 95-120.
- [22] Threlfall, E. J. (2002): Antimicrobial drug resistance in *Salmonella*: problems and perspectives in food-and water-borne infections. – *FEMS Microbiology Reviews* 26(2): 141-148.
- [23] Thung, T. Y., Radu, S., Mahyudin, N. A., Rukayadi, Y., Zakaria, Z., Mazlan, N., Tan, B. H., Lee, E., Yeoh, S. L., Chin, Y. Z., Tan, C. W. (2018): Prevalence, virulence genes and antimicrobial resistance profiles of *Salmonella* serovars from retail beef in Selangor, Malaysia. – *Frontiers in Microbiology* 8.
- [24] Tindall, B. J., Grimont, P. A. D., Garrity, G. M., Euzeby, J. P. (2005): Nomenclature and taxonomy of the genus *Salmonella*. – *International Journal of Systematic and Evolutionary Microbiology* 55(1): 521-524.
- [25] White, D. G., Zhao, S., Simjee, S., Wagner, D. D., McDermott, P. F. (2002): Antimicrobial resistance of foodborne pathogens. – *Microbes and Infection* 4(4): 405-412.

A COMPARATIVE STUDY ON APPLE CHLOROTIC LEAFSPOT VIRUS (ACLSV) ISOLATES FROM DIFFERENT HOSTS IN THE EAST MEDITERRANEAN REGION OF TURKEY

KOÇ, G.^{1*} – FIDAN, H.² – SARI, N.² – ÇALIŞ, O.²

¹*Biotechnology Research and Application Centre, Cukurova University, Adana, Turkey*

²*Plant Protection Dept., Akdeniz University, Antalya, Turkey*

**Corresponding author*

e-mail: gkmnkoc@hotmail.com

(Received 19th Jul 2019; accepted 15th Nov 2019)

Abstract. The study was conducted on ACLSV (Apple Chlorotic Leafspot Virus) isolates found in samples collected from temperate zone fruit orchards in Adana and Mersin provinces and districts in the Eastern Mediterranean region of Turkey. Reported as a natural host, *Styrax officinalis* bush was included in the study as a different host isolate (Kayseri). Leaf and cortical samples have been tested with commercial ELISA kits for the presence of common viruses. In order to verify DAS-ELISA results, the total RNAs were used in RT-PCR test and only positive responses were obtained from ACLSV-specific antiserum and primers. ACLSV isolates obtained from different hosts in the Eastern Mediterranean region were subjected to molecular variation analyses. Possible recombination sites of ACLSV were identified in the partial sequences of coat protein genes via comparison of ACLSV sequences from the GenBank database. As a result, for the first time recombinant or variant ACLSV isolates were reported in the region. Coat Protein Nucleotide sequences based on phylogenetic trees showed that these isolates were grouped and conserved signatures of type B6 clusters. This paper confirmed that *Styrax officinalis* as a natural ACLSV reservoir.

Keywords: *ACLSV, Rosacea and wild hosts, genetic variability, CP, East Mediterranean region of Turkey,*

Introduction

ACLSV, found in the morphological subgroup A in the trichovirus group of family Betaflexiviridae, is a member of the stone and pome fruit infecting virus species leading to significant losses (Dunez, 1988; Martelli et al., 1994). ACLSV is known to have a convoluted filamentous particle of 600-740 × 12 nm, and the RNA of the virus is known to be single-helical and one-part (Lister, 1970; German et al., 1990). Many strains of ACLSV are reported to have changed due to a high proportion of virus strains in their emerging symptoms; many of the strains are able to infect all hosts, but some Apple strains are difficult to transmit to stone fruits (Chairez and Lister, 1973; Smith et al., 1998; Brunt et al., 1996). ACLSV's hosts are found all over the world where they are grown and the virus is often carried without symptoms in pome fruit trees, while stone-core fruit trees suffer from very serious diseases (Nemeth, 1986; Poul and Dunez, 1988; Smith et al., 1998; Brunt et al., 1996). ACLSV, in cherry and sour cherry, are also found as latent in many varieties (Dosba et al., 1986; Desvignes and Boye, 1989). Martelli et al. (1994) thought that ACLSV was one of the most economically dangerous viruses and ACLSV is transmitted by mechanically and grafting. Flegg and Clark (1979) noted that ELISA (Enzyme Linked Immuno Sorbent Assay) is a very convenient method for diagnosing viruses in broad indexing programs and epidemiological studies, and that the classical DAS (Double Antibody Sandwich)-ELISA method can identify ACLSV from time to time, and they have developed a different procedure. Barba and Clark (1986)

stated that the virus dispersed irregularly in trees, in a way that the leaves at the bottom of the tree contained more viruses, and that bark tissues were the most suitable material for ELISA, especially towards the end of the vegetation period. However, because of the low concentration problem of the virus is known to infect plants even with ELISA negative results.

Candresse et al. (1995) reported variability in nucleotide sequences between different isolates despite being of the same plant origin. In addition, Niu et al. (2012) underlined that ACLSV genomes are relatively variable. They analyzed ten complete genome sequences from different hosts and reported a variation percentage between 67.2 and 95.1%. Moreover, Kuzmitskaya et al. (2016) when they compared ACLSV isolates in Belarus, Apple interpreted divergence levels of chlorotic leaf spot virus that varied in different genomic regions.

The presence of ACLSV in stone fruit trees grown in Turkey was first identified in Yalova by Yürektürk (1984) with biological indexing using GF305 peach rootstocks. The agent has been reported by different researchers in stone and pome fruits of different species, varieties and geographical origin (Dunez, 1986; Çağlayan and Çalı, 1994; Elibüyük, 1998; Fidan and Özdemir, 1998; Sipahioğlu et al., 1999; Ulubaş and Ertunç, 2004; Ulubas Serce and Rosner, 2006; Koç and Bakoglu, 2007; Koç et al., 2008; Öztürk, 2012; Değirmenci and Akbaş, 2013). But the background about the genetic variability of Apple Chlorotic Leaf Spot Virus in the East Mediterranean region and Turkey, still has influence. Therefore, we have investigated molecular variability of ACLSV isolates in Pome and Stone fruit orchard isolates from the East Mediterranean Region of Turkey (EMT) to forecast genetic relationships by analysing the nucleotide sequences of ACLSV genome via BootScan and Sisscan pro.

Materials and methods

Sources of ACLSV isolates

Temperate zone fruit orchards in the East Mediterranean region of Turkey (EMT) is generally maintained between low and high altitude (50 to 1360 m) in two different condition levels. Five ACLSV isolates from samples of different plant species have been collected from commercial gardens in the area to establish genbank accession numbers.

The isolates compared in the study were selected according to host type and geographical differences and distances. In addition, these isolates originated from the samples that have been collected and tested by the same investigator team during the surveys conducted in the region in the last fifteen years. The studied isolates represent 379 samples collected from the surveys followed in the region between 2005 and 2019 (*Fig. 1*).

Therefore, five isolates were stepped forward as representative for the virus comparison and the region. A nectarine isolate of ACLSV was collected from Yenice/Adana (2019) and an apple isolate from Fındıklı/Adana (2011), a pear isolate from Kamışlı/Adana (2006), a sweet cherry isolate from Çamardı/Nigde (2013) and an *Strax officinalis* isolate supplied from Kayseri (by Dr. H. Fidan; 2018), Fresh shoots of systemically infected isolates were used as samples within nucleic acid extraction and RT-PCR assays. Collected plantlets were stored at 4 °C before when DAS-ELISA tests and nucleic acid extractions were run. All positive samples were eradicated according to national interests, internal quarantine rules and sanctions. Studies were only carried out on isolated nucleic acids.

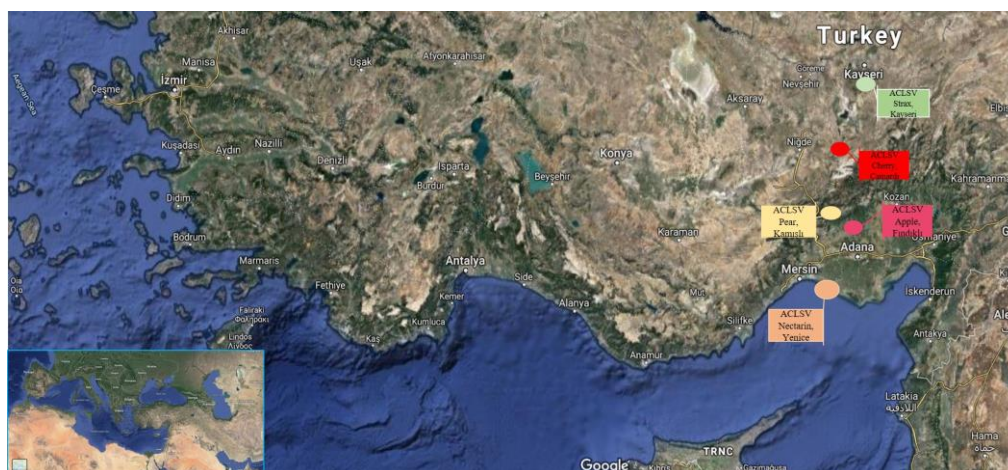


Figure 1. Isolate sources and locations of ACLSV in the East Mediterranean region of Turkey. (<https://www.google.com/maps/@37.5034496,33.2747851,395256m/data=!3m1!1e3>)

Serological tests

The plantlets were labelled and placed in isolated transparent bags, which were put in ice pail and transported to the virology laboratory and maintained at 4 °C. All samples were tested within a day.

Enzyme linked immunosorbent assay (ELISA)

To distinguish their infection in the specimens, the leaves were tested through ELISA using polyclonal antiserum against various virus species that could possibly be found in temperate zone plants given in *Table 1*. Antiserums provided by Agdia (USA) and Bioreba AG, (Switzerland) were diluted in accordance with suppliers' instructions and tested according to Clark and Adams (1977). PNRSV, PDV, PPV and other possible mixed infections common in Pome and Prunus were tested by ELISA with virus-specific antibodies.

Results were made by photometric measurement of absorption values at 405 nm wavelength and yellow color formation in ELISA reader. At photometric absorbance values read at a wavelength of 405 nm, samples that yielded at least twice the healthy control value and a higher reading value were considered positive or contaminated.

Nucleic acid based assays, total RNA extraction and RT-PCR

Samples with serologically positive results with ACLSV specific antibodies (Bioreba) were concentrated in molecular studies. Moreover, Nucleic acid isolations, RT-PCR and sequence analyses were performed to detect possible recombinations or variations of ACLSV isolates from the East Mediterranean in Turkey (EMT). In Molecular Studies, a pair of primers specific to the conserved regions containing some or all of the CP genes belonging to ACLSV, and identified as a result of DAS-ELISA and RT-PCR, were used.

Total nucleic acid extraction (NAE) and reverse transcription polymerase chain reaction (RT-PCR)

Extracted Nucleic Acid (NA) from infected plants were processed in Dellaporta et al. (1983). RT-PCR Assay; The cDNAs were generated by sense primer

5'TTCATGGAAAGACAGGGGCAA 3' and antisense primer 5'AAGTCTACAGGCTATTTATTATAAGTCTAA3' which were described before by Menzel et al. (2002), to obtain 677 bp fragment related to the partial CP for screening of ACLSV isolates. cDNAs were obtained from ACLSV NAs with Thermo Science Verso 1 Step RT-PCR Kit package in accordance with manufacturer's manual. The amplification process and conditions were described at Menzel et al. (2002). Therefore, ACLSV thermal cycling parameters were, reverse transcription at 42 °C for 30 min; one cycle for activation of *Taq* polymerase at 95 °C for 15 min chained by 34 cycles of denaturation at 94 °C for 30 s, annealing at 62 °C for 30 s, and extension at 72 °C for 1 min. The final extension step was carried out at 72 °C for 7 min.

The amplified PCR products were run in 1.5% agarose gel, stained with ethidium bromide and visualized under UV illumination.

Table 1. Results obtained from plant samples as a result of serological and molecular analyses

Virus species	Result and assays	
	ELISA	RT-PCR
Arabis mosaic virus (ArMV)	-	-
Strawberry latent ringspot virus (SLRSV)	-	-
Apple stem pitting virus (ASPV)	-	-
Apple stem grooving virus (ASGV)	-	-
Tobacco blackring virus (TBRV)	-	-
Cherry leafroll virus (CLRV)	-	-
Strawberry latent ringspot virus (SLRSV)	-	-
Prune dwarf virus (PDV)	+ <i>Strax sp.</i>	-na
Prunus necrotic ringspot virus (PNRSV)	-	-
Plum pox virus (PPV)		
Apple mosaic virus (ApMV)	+ <i>Strax sp.</i>	- na
Apple chlorotic leaf spot virus (ACLSV)	+ apple, pear, Sw. cherry, Strax sp., nectarine	+ apple, pear, Sw. cherry, Strax sp., nectarine

-Negative (not infected); +Positive (infected); na: non assayed by RT-PCR

RT-PCR products analysis

10 ul of PCR item was used with gel loading buffer and analyzed on a 1.5% agarose gel containing 0.5 mg/ml of ethidium bromide (Sambrook et al., 1989). 100 bp DNA ladder (thermo) was used on each gel to analyze PCR items.

Phylogenetic analysis

The ACLSV RT-PCR products obtained according to Menzel et al. (2002) primers, were sequenced by a commercial sequencing company and dnasp5 program was conducted. Phylogeny and evolutionary analyses were made by MEGA 7 (Molecular Evolutionary Genetics Analysis) software and neighbour joining process, according to convention analysis. Occurred sequences were compared with different isolates of ACLSV originated by host and geographical locations from gen bank (NCBI, National

Center for Biotechnology Information). Sequences from the accessions (Table 2) had been considered. Sequence alignment of the ACLSV isolates and homology between sequences were acted in accordance with to Thompson et al. (1994). The present ACLSV isolates in the study compared with those of 23 ACLSV isolates were available in the NCBI GenBank. A sequence identity matrix of the partial CP gene of the ACLSV isolates were configured using the BIOEDIT with worldwide ACLSV sequences obtained in the GenBank.

Table 2. Accession numbers, Isolate origin, hosts and name of ACLSV isolates subjected to this molecular comparisons analysis (1-5 as bold from East Mediterranean of Turkey)

No	Accession No	Country	Host	Isolate name	Identity
1	MK986792	Turkey	Nectarine	ACLSV_Nectarine	96.12
2	MK986793	Turkey	Cherry	ACLSV_Cherry	96.61
3	MK986794	Turkey	Pear	ACLSV_Pear	96.92
4	MK986795	Turkey	Apple	ACLSV_Apple	97.09
5	MK986796	Turkey	<i>Strax officinalis</i>	ACLSV_Strax officinalis	96.77
6	AM498050.1	India:Solan	Peach		97.42
7	GQ334201.1	Canada	Pear	Pyrus0167	92.89
8	AJ586630.1	Italya	Apricot	Apr 20	91.92
9	KU749434.1	Afghanistan	European Plum cv. Alu Bokhara Shalili	364/10	
10	JQ866622.1	Ukraine	Pear	ACLSV-43	85.58
11	LC475152.1	South Korea	<i>Pyrus Pyrifolia</i>	ACLSV_WH	89.09
12	AM498048.1	India:Kullu	Wild Apricot (Chuli)		86.01
13	GQ334210.1	China	Pear	SMJ	85.44
14	AJ586634.1	Spain	Apricot	Apr 62	
15	X99752.1		Cherry	Balaton1	
16	AJ586644.1	Italy	Peach	PE-FC	
17	MF069041.1_	Czech Republic	Cherry	Lambert 43	
18	AY730560.1	Turkey	Sweet Cherry	ASwC43	83.19
19	AJ586654.1	Jordan	Plum	PL111	91.92
20	AJ586653.1	Italy	Plum	PL110	80.22
21	JN849004.1	China		Y2	69.83
22	EU223295.1	USA			70.27
23	JN848998.1	China		Z2	71.46
24	GQ334195.1	Canada	Apple	Malus0582	93.70
25	FJ952176.1	Belgium	Apple	5Be	90.21
26	FJ952177.1	Serbia	Apple Cultivar Granny S.	11Sr	90.38
27	DQ329162.1	Bulgaria	Apple	P10R1D3	86.24
28	KC244768.1	Belarus	Malus X Domestica	Sakavita-1	86.22

Recombination event analysis

The Recombination Detection Program v4.16 (RDP4) was performed (Martin et al., 2010), by utilizing the RDP, GENECONV, Chimaera, MaxChi, BOOTSCAN, SISCAN and 3SEQ methods implemented in the RDP 4 program with default settings. These

recombination determinations have been accepted if determined as “clear” recombination by more than four methods with a p-value $> 1 \times 10^{-6}$ (Martin and Rybicki, 2000).

Genetic diversity analysis for ACLSV population of EMR

The estimate of nucleotide diversity values of EMR ACLSV isolates is structured by DNASP version 5.0 (Librado and Rozas, 2009).

The Pi value, including nucleotide diversity, was estimated by Tajima, [1983], with the average number of nucleotide differences between two random sequences in a population.

The frequency and number of haplotypes in a population of haplotype diversity (Hd) was conducted by Watterson (1975) according to the θ Estimator from the number of segregated sites (S), while the average ratio of non-synonymous and synonym substitutes (Tajima's d'si) was conducted by Tajima (1989), and the D and F analyses of Fu and Li were conducted by Fu and Li (1993) neutrality tests.

Results and discussion

Serology (DAS-ELISA)

Commercially available ELISA kits have been used to serologically detect virus diseases that are harmful in stone fruit trees. ACLSV, ApMV, PPV, PNRSV, PDV and other important temperate zone fruit viruses (*Table 1*) commercially available kits have been used in accordance with the procedures reported by the companies. As a result of the ELISA tests, mostly non-mixed infections were determined from samples collected from important temperate climate fruits such as quince, pear, apple, cherry, apricot, cherry peach and nectarine. Only one example showed multiple mixed infections. The number of viral infections detected is summarized in *Table 1* according to fruit species. Accordingly, it was also tested for verification of previous serological studies, one Nectarine isolate of ACLSV was collected from Yenice/Adana (2019) and one Apple isolate from Fındıklı/Adana (2011), one Pear isolate from Kamışlı/Adana (2006), one Sweet cherry isolate from Çamardı/Nigde (2013) and one *Strax officinalis* isolate supplied from Kayseri (by Dr. H. Fidan; 2018) in the samples, ACLSV infection was confirmed by giving at least twice the healthy control value and a higher reading value. Only *Strax officinalis* has been identified with a triple mixed viral infection. This mixed infection was found to be caused by ACLSV, PDV and ApMV.

In contrast to having positive results against to ACLSV, ApMV and PDV, ELISA did not give positive results for all samples for the rest of among all 12 tested different viruses (*Table 1*).

However, serological techniques, although very widely used costs are high, each phenological period of plants and different organs of the delicate results can not stand as techniques. For these reasons, molecular techniques are applied to verify the results. In particular, low costs, high sensitivity and detailed characterization possibilities can be provided in part, as well as an easy-to-implement technique can be considered as an advantage.

RT-PCR, sequence analysis and phylogenetic analysis

In addition, reverse transcription-polymerase chain reaction (RT-PCR) method was used to obtain the complementary DNA (cDNA) from the RNAs obtained as a result of

Total RNA isolation. In the next stage, approximately 677 bp-sized compounds containing conserved regions associated with the ACLSV CP gene parts by means of forward and reverse primers were observed in 1.5% agarose gel containing 0.5 mg/ml of ethidium bromide (Fig. 2).

DAS-ELISA positive results of isolates obtained from different production areas of the Eastern Mediterranean region were confirmed in this way. Phylogenetic tree was created based on sequence analyses of amplicons or RT-PCR products obtained.

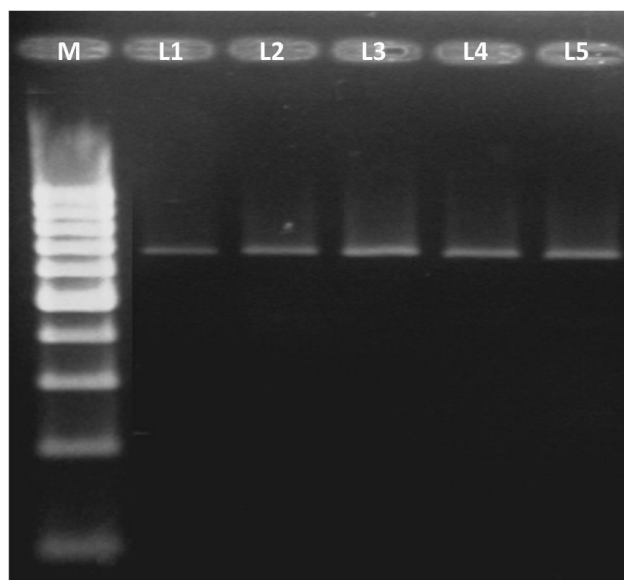


Figure 2. First lane M DNA ladder; RT-PCR products of 677 bp of ACLSV CP on agarose gel (1.5%) (Lane1 nectarine isolate of ACLSV; Lane2 apple isolate; Lane3 pear isolate; Lane4 *Strax officinalis* isolate; Lane5 sweet cherry isolate from Mediterranean Coast in Turkey)

Phylogenetic analysis

Designated sequences have been compared with different isolates' sequences of ACLSV from the accessions (Table 2). Phylogeny was conducted by Mega7, as indicated by entered ACLSV sequences (Fig. 3). The evolutionary history was inferred using the Neighbor-Joining method. The optimal tree with the sum of branch length = 22,06180530 is shown. The percentage of replicate trees in which the associated taxa clustered together in the bootstrap test (1000 replicates) are shown next to the branches.

The Phylogenetic tree is drawn to scale, with branch lengths in the same units as those of the evolutionary distances used to infer the phylogenetic tree. The computed evolutionary distances using the Maximum Composite Likelihood method, are in the units of the number of base substitutions per site. The analysis had been involved 28 nucleotide sequences. All positions containing gaps and missing data were eliminated. There were a total of 237 positions in the final dataset. Evolutionary analyses were conducted in MEGA7. The *Stone Ansd Pome Fruit* Samples from East Mediterranean of Turkey in Genbank with accession Number (Table 2) MK986792 Nectarine, MK986793 Cherry, MK986794 Pear, MK986795 Apple and MK986796 *Strax officinalis* were accessed as to NCBI system (Fig. 3) and listed below with other isolates from worldwide in Table 2 and matrixed in Table 3.

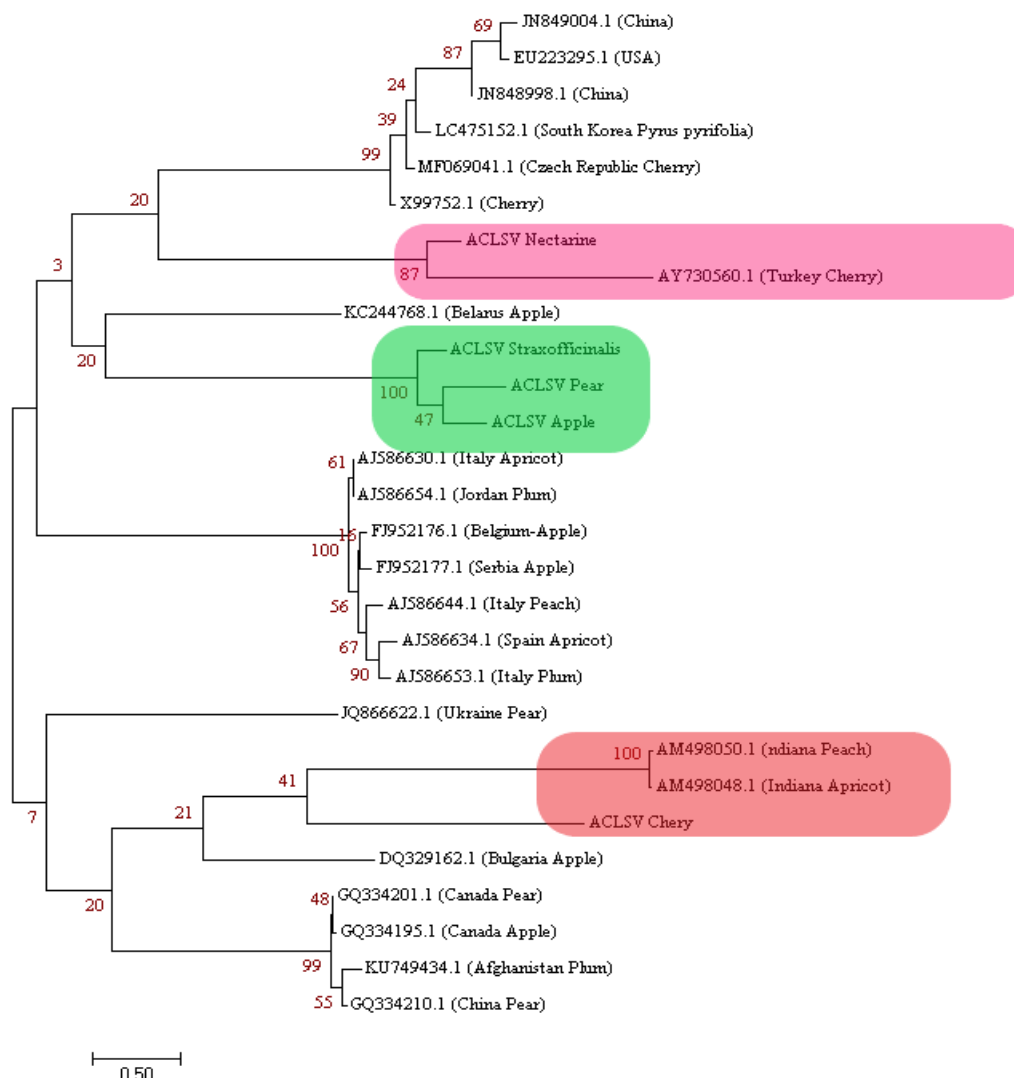
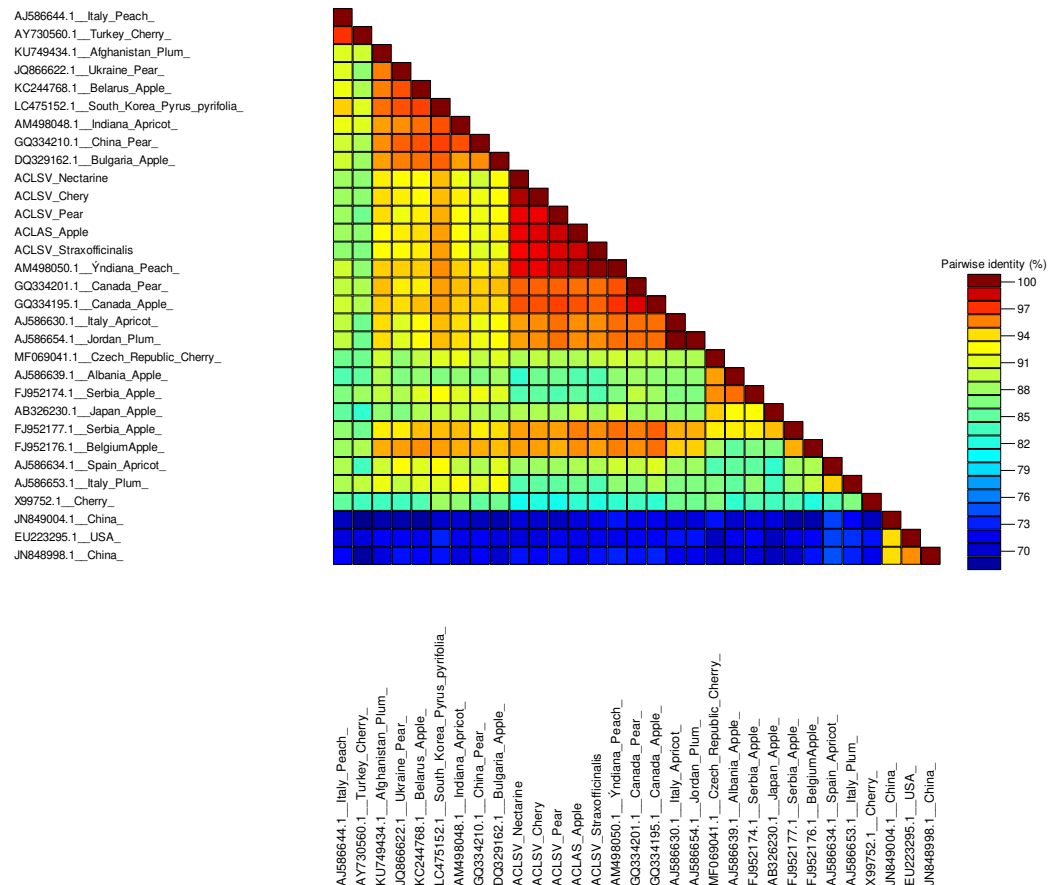


Figure 3. Phylogenetic tree of five different ACLSV isolates from Mediterranean coast of Turkey and 23 of gene bank, were clustered within the GenBank database

Despite of having approximately 97.09 %similarity with each other isolates from Turkey there are three clades among *Stone and Pome Fruit* isolates from East Mediterranean Turkey (EMT). It may be caused by material origin. The sequences were clarified with Accession Num. MK986792 Nectarine isolates (96.12%) from EMT have similar homology with Accession Num. AY730560.1 Sweet Cherry isolate (83.19%) from Turkey (in pink cloud at tree). While Accession Num. MK986794 Pear (96.92%), Accession Num. MK986795 Apple (97.09%) and Accession Num. MK986796 *Strax officinalis* (96.77%) from EMT were in cluster with Accession Num. KC244768.1 Malus X Domestica from Belarus isolate (86.22%) (in green cloud at tree).

The third cluster which is covering Accession Num. MK986793 ACLSV Chery (96.61%) (in coral orange cloud at tree) has two more isolates, with Accession Num. AM498048.1 Wild Apricot (Chuli) (86.01%) from India: Kullu and Accession Num. AM498050.1 Peach from India: Solan (97.42%). This cluster next to other branch, has Accession Num. DQ329162.1 Apple isolates (86.24%) from Bulgaria (*Tables 2 and 3; Fig. 3*).

Table 3. Pairwise distances have matrixed according to the accession numbers (also in Table 2), of ACLSV isolates which are MK986792 Nectarine, MK986793 Cherry, MK986794 Pear, MK986795 Apple and MK986796 *Strax officinalis* in this study for molecular comparisons analysis (1-5) from EMT. It compares the degree of proximity between red and blue



Dark Red indicates the closest kinship level. While Dark Blue is the opposite

According to Liu et al. (2014) specifications, isolates P205, B6 and Ta Tao 5 can be determined based on some amino acid points on the Capsid protein. According to this analysis, ACLSV-Pear, ACLSV-Nectarine, ACLSV-Apple, ACLSV-Cherry, ACLSV-*Strax officinalis* isolates from Turkey all have amino acid alignment within the B6 group isolates (Table 4). In our result CP based classification for ACLSV was proposed likely on the covariation analysis of the five amino acids at positions 40, 59, 75, 130 and 184, which are highly conserved within two clusters recently described by Yaegashi et al. [2007). The Amino acid clusters of East Mediterranean ACLSV isolates were designated as ‘B6 type’ due to the isolates containing Ser40, Leu59, Tyr75, Ala86, Thr130 and Leu184 series.

Table 4. Protein-based amino acid sequence of ACLSV isolates

Group name	40	59	75	86	130	184
Group I P205	Ala	Val	Phe	Ile	Ser	Met
Group II B6	Ser	Leu	Tyr	Ala	Thr	Leu
Group III Ta Tao 5	Ser	Val	Tyr	Leu	Lys	Ile

MK986794>ACLSV_Pear (B6 type) nucleotide and amino acid sequence

-----ggggcaatcctggaacagatggttgag**tcc**
-----G A I L E Q M L E **S**
atcttcgcgtacatagcgatacaggggacgtcggagcaaacggagttcctggat**ctg**gtg
I F A Y I A I Q G T S E Q T E F L D **L** V
gtggaagtgaagatcaatggaggacaaaagtgatcgggtca**taca**acctgaaggaggtg
V E V K I N G G P K V I G S **Y** N L K E V
gtcaatatgatcaag**gcc**ttcaagactacatcttcggacccaaacatcagcaacatgact
V N M I K **A** F K T T S S D P N I S N M T
taccgccaggtatgtgaggccttcgcacctgaggcgaggaaccgggttggttaaattgaag
Y R Q V C E A F A P E A R N R L V K L K
tataaaggggttttaactaacctcttt**aca**accatgccggaagtaggaagtaagtaccg
Y K G V L T N L F **T** T M P E V G S K Y P
gagctgatgttcgacttcaataagggccttaatatggttatcatgaataaggcccaacia
E L M F D F N K G L N M F I M N K A Q Q
aaggtcattactaatatgaatcggcgctcttttacagactgaatttgcaaaaagcgagaac
K V I T N M N R R L L Q T E F A K S E N
gaggcgaaa**ctg**tcgtctgttacgactgatctttgcatttag
E A K **L** S S V T T D L C I -

MK986795>ACLSV_Apple (B6 type) nucleotide and amino acid sequence

-----ggggcaatcctggaacagatattggag**tcc**
- - - - - G A I L E Q I L E **S**
atcttcgcgaacatagcgatacaagggacatcggagcaaacggagttcctggat**ctg**gtg
I F A N I A I Q G T S E Q T E F L D **L** V
gtggaagtgaagatcaatggaggaccaattgggtgatcgggtca**taca**acctgaaggaggtg
V E V K S M E D Q L V I G S **Y** N L K E V
gtcaatatgatcaag**gcc**ttcaagactacatcttcggacccaaacatcagcaacatgact
V N M I K **A** F K T T S S D P N I S N M T
ttccgccaggtgtgtgaggccttcgcacctgaggcgaggaaccgggttggttaaactgaag
F R Q V C E A F A P E A R N G L V K L K
tataaaggggttttactaacctcttt**aca**accatgccggaagtaggaagtaagtaccg
Y K G V F T N L F **T** T M P E V G S K Y P
gagctgatgttcgacttcaataagggccttaatatggttatcatgaataaggcccaacia
E L M F D F N K G L N M F I M N K A Q Q
aaggtcattactaacatgaatcggcgctcttttacagactgaatttgcaaaaagcgagaac
K V I T N M N R R L L Q T E F A K S E N
gaggcgaaa**ctg**tcgtctgttacaactgatctttgcatttag
E A K **L** S S V T T D L C I -

MK986796>ACLSV__Strax_officinalis (B6 type) nucleotide and amino acid sequence

-----ggggcaaacctggaacagatggttgag**tcc**
- - - - - G A N L E Q M L E **S**
atcatcgcgaacatagcgatacaagggacgtcgcagcaaacggagttcctggat**ctg**gtg
I I A N I A I Q G T S Q Q T E F L D **L** V
gtggaagtgaagatcaatggaggacaaaaggtgatcgggtca**taca**acctgaaggaggtg
V E V K S M E D Q K V I G S **Y** N L K E V
gtcaatatgatcaagccttcaagactacatcttcggacccaaacatcagcaacatgact
V N M I K A F K T T S S D P N I S N M T
ttccgccaggtgtgtgag**gcc**ttcgcacctgaggcgaggaaccgggttggttaaactgaag
F R Q V C E **A** F A P E A R N G L V K L K
tataaaggggttttactaacctcttt**aca**accatgccggaagtaggaagtaagtaccg
Y K G V F T N L F **T** T M P E V G S K Y P
gagctgatgttcgacttcaataagggccttaatatggttatcatgaataaggcccaacia
E L M F D F N K G L N M F I M N K A Q Q
aaggtcattactaacatgaatcggcgctcttttacagactgaatttgcaaaaagcgagaac
K V I T N M N R R L L Q T E F A K S E N
gaggcgaaa**ctg**tcgtctgttacaactgatctttgcatttag
E A K **L** S S V T T D L C I -

MK986792>ACLSV_Nectarine (B6 type) nucleotide and amino acid sequence

```
-----  
-----ggggcaatcctggaacagatggttgagtcc  
- - - - - - - - - - G A I L E Q M L E S  
atcttcgcgaacatagcgatagcaggggacatcgagcaaacggagtttctggatctggtg  
I F A N I A I Q G T S E Q T E F L D L V  
gtggaagtgaagtcaatggaggatcaaaaggatcggtcatacaatctgaaggaggtg  
V E V K S M E D Q K V I G S Y N L K E V  
gtcaatatgatcaaggccttcttgactacatcttcggaccgaaacatcagcaacatgact  
V N M I K A F L T T S S D R N I S N M T  
ttccgccaggtgtgtgaggccttcgcacctgaggcgaggaacgggttggttaaactgaag  
F R Q V C E AF A P E A R N G L V K L K  
tataaaggggttttactaacctctttacaaccatgccggaagttaggaagtaagtaccg  
Y K G V F T N L F T T M P E V G S K Y P  
gagctgatgttcgacttcaataagggccttaatatgttcacatgaataaggccaacaa  
E L M F D F N K G L N M F I M N K A Q Q  
atggtcattaccaatatgaatcggcgtctttacagactgaatttgcaaaaagcgagaac  
M V I T N M N R R L L Q T E F A K S E N  
gaggcgaaactgtcgtctgttacaactgatctttgcatttag  
E A K L S S V T T D L C I -
```

MK986793>ACLSV_Chery (B6 type) nucleotide and amino acid sequence

```
-----  
-----ggggcaatcctggaacagatggttgagtcc  
- - - - - - - - - - G A I L E Q M L E S  
atcttcgcgtacatagcgatagcaggggacgtcgagcaaacggagtttctggatctggtg  
I F A Y I A I Q G T S E Q T E F L D L V  
gtggaagtgaagatcaatggaggacaaaagtatcggtcatacaacctgaaggaggtg  
V E V K I N G G P K V I G S Y N L K E V  
gtcaatatgatcaagggccttcaagactacatcttcggaccgaaacatcagcaacatgact  
V N M I K A F K T T S S D P N I S N M T  
taccgccaggtatgtgaggccttcgcacctgaggcgaggaaccgggttggttaaattgaag  
Y R Q V C E A F A P E A R N R L V K L K  
tataaaggggttttaactaacctctttacaaccatgccggaagttaggaagtaagtaccg  
Y K G V L T N L F T T M P E V G S K Y P  
gagctgatgttcgacttcaataagggccttaatatgtttatcatgaataaggccaacaa  
E L M F D F N K G L N M F I M N K A Q Q  
aaggtcattactaatatgaatcggcgtctttacagactgaatttgcaaaaagcgagaac  
K V I T N M N R R L L Q T E F A K S E N  
gaggcgaaactgtcgtctgttacgactgatctttgcatttag  
E A K L S S V T T D L C I -
```

Recombination analysis by RPD4

In order to determine recombination events with each other of the 5 isolates used in the phylogenetic tree, “the Recombination Detection Program v4.16 RDP4” was used. RPD 4 (Martin et al., 2010) according to the program given 7 algorithms; recombination events were analyzed.

The presence of recombination signal on ACLSV_Pear isolate was determined according to BootScan and SisCan algorithms from 7 algorithms used. When the RDP4 program data was examined, the ACLSV_pear isolate was determined to be a potential recombinant (Table 5). Because the nucleotide variation value ($p > 0.1$) was determined in two algorithms.

In analyses performed using RDP4, recombinations must be determined by at least three of the methods in the program (Martin and Rybicki, 2000; Martin et al., 2010). However, in this study the discovery of recombination signals in only two algorithms established the general belief that recombination events were not detected in the 5 isolates in the study (Table 5; Figs 4 and 5).

Table 5. CP genes based “The Recombination Detection Program” v4.16 algorithms (BootScan and SiScan) of the ACLSV Pear isolate

Methods	Time elapsed	Unique events (Rec. signals)	Av. P. Val
RDP	0,00s	0(0)	--
GENECONV	0,00s	0(0)	--
BootScan	0,12s	1(0)	1,126x1002
MaxChi	0,00s	0(0)	--
Chimera	0,20s	0(0)	--
SisCan	0,00s	1(0)	1,591x1003
3Seq	0,00s	0(0)	--
TOTAL	0,41s	1(2)	

Rec. Signal ACLSV-Pear/Major Parent:ACLSV Apple/Minor Parent unknown



Figure 4. SISCan Model analyses were identified possible recombination sites within the fragment of ACLSV movement protein gene sequences at approximately positions 75 and 86, respectively only for ACLSV pear isolates

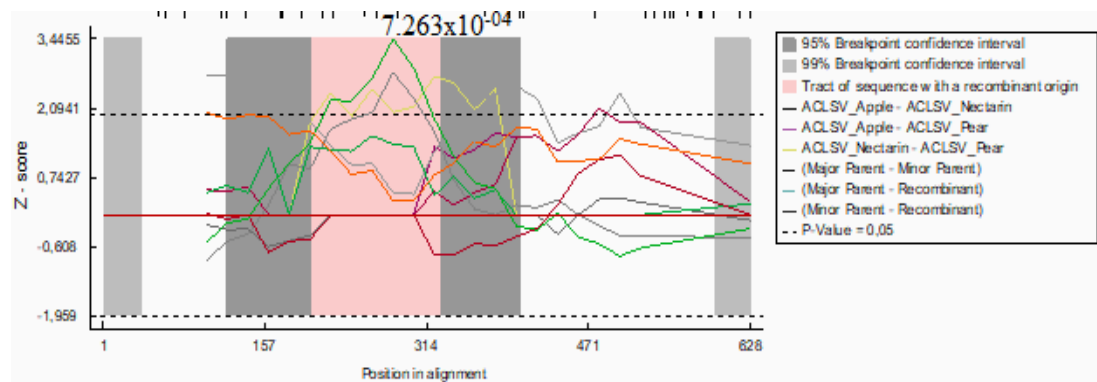


Figure 5. BootSCAN Model analyses identified possible recombination sites within the fragment of ACLSV movement protein gene sequences at positions 75 and 86, respectively only for ACLSV pear isolates

Population diversity data according to DNAsp6

ACSLV isolates obtained from different regions were subjected to recombination analysis using the DNAsp6 program. According to this analysis, S:41 fields were

identified in Segregation (polymorphic). According to Hudson (1987) data, recombination parameters have been estimated. The distribution variance of the samples was determined as K_{ij} , Sk^2 : 72,838. Theta estimate data for each gene: 18,800, functional data $g(C,n)$ 0.1798, estimated value of R for each gene: 368 was determined.

The number of minimum recombination events was determined according to Hudson and Kaplan (1985). According to this analysis, the number of binary comparisons analyzed was determined as 820. The number of minimum recombination activity was found to be at (54.61) (61,407) points as $Rm:2$ (Table 6).

Table 6. Population diversity data according to DNAsp6 of the ACLSV pear isolate

Region	Population statics							Tests of neutrality		
	n	S	Hd	Pi:	dS	dN	dN/dS	Tajima's D	Fu & Li's D	Fu & Li's F
CP	5	41	1.000	0.03072	0.59633	-0.17175	0.288	-0.6543	-0.3364	-0.3364

n: Number of sequences; S: number of segregating sites; Hd: haplotype diversity; Pi: Nucleotide diversity; dS: rate of synonymous substitutions per site; dN: rate of non-synonymous substitutions per site

Conclusion

The East Mediterranean region is a unique area for many varieties of plants grown in Turkey. The viruses similarly with the other plant diseases can restrict the production via reducing fruitfulness all through the Mediterranean region of Turkey. But in practice, there is no chemical suggestion to control virus diseases unlike the others. Consequently, their epidemiology and molecular bases have to be well decoded to apply control measures. Additionally, resistant cultivars and sanitation should be used for controlling the many viruses in practices.

Natural distribution and occurrence of Temperate Zone viruses in the studied area have determined in Turkey. Our results showed as it has already mentioned above that sanitary situations in stone and pome fruits growing regions are very vitally important in Turkey.

Therefore, molecular epidemiology of ACLSV should be well understood for the prevention. The insufficient of ecologically more important agrochemical disease management strategy, has been increased the jeopardy of infection spread. As well, it can also originate progressively from different annual species and occurs after infection with infected saplings or contamination sources (herbaceous and woody plants) if the insufficient level is suppressed. This is the first preliminarily recombination event report of ACLSV pear isolate among the other isolates from different hosts in the Mediterranean region of Turkey. Our results have shown that reliable laboratory molecular methods with immunological ELISA and molecular RT-PCR analyses have to be used. Further advanced statistical techniques such as RPD4 etc. could be used to confirm our results and other possible recombination events. Because the new recombinant isolates, may become economically dangerous in time, it can cause aggressive breeds to form. Likewise, Fidan (2016) has reported new TSWV isolates that break down the durability of peppers.

Presumably it may more easy transmitted by infected material and cuttings. In response to this "Certified plant materials, destruction of the source of disease and prevention of vectors" are powerful strategies to overcome the disease. Recognition of new strains or isolates will help sustain disease management on the right track. Genetic

changes due to recombination events can be very important for RNA viruses. Isolate due to point mutations in virus structures are changing so that the emergence of new isolates is realized (Fidan and Sari, 2019). Cultural methods used for preventing virus infections are not enough. Virus vectors and host weeds need to be managed.

Durable/tolerant as possible varieties should be preferred (Öztürk Keleş and Baloğlu, 2019). It is possible that the new isolates may cause severe virus diseases even in mixed or different isolates in the host plants. It is not possible to predict this without observing or experiencing the negative effects and epidemiology of recombinants in agricultural ecology and natural ecology (Fidan et al., 2019).

This paper might additionally indicate that broadened distribution of infected host species between countries and regions will allow the spread of plant's viruses. In the present paper RT-PCR was used as a standardized method for reliable detection of local ACLSV isolates. The analyses performed in this study revealed the variability between ACLSV pear and other isolates in the Eastern Mediterranean region. Molecular variability analysis of 5 ACLSV isolates in the Eastern Mediterranean region, were detected comparable. The phylogenetic tree separated the 5 ACLSV isolates into only 3 subgroups (but not the main group). In addition, our results highlighted possible relationships between ACLSV clusters and host resources. Viruses with large host sequences such as ACLSV are highly likely to undergo recombination.

In addition, isolates resulting from mutation and recombination with high adaptation or adaptability will be able to reach a wider host sequence. This may have severe ecological consequences. In order to detect and identify measures, race and isolate variations should be better analyzed with detailed research. Vertical transmission of ACLSV and many viral agents among different plant species may be the result of recombination or mutation delivery.

Variation analysis will be better understood over time as more advanced technologies emerge and the analysis width of these methods increases. Applicable and facilitated algorithms will be able to reveal wider host sequences and variations in geographic area. Thus, threat risks on agricultural and environmental ecologies will have the potential to be proactively resolved. Moreover, full and true decoding of recombination may open new accessions to the management against ACLSV and others. Deep impacts on the ecological environment can be prevented by well understanding of virus relationships. As well, the detailed and multidisciplinary projects should be acted. All isolates in the study were eradicated on behalf of the country's interests.

Acknowledgements. Thanks to Prof. M. Asil YILMAZ for critical review of the publication.

Conflict of interests. The authors declare that they have no conflict of interests.

Ethical approval. This article does not contain any studies with human participants or animals performed by any of the authors.

REFERENCES

- [1] Barba, M., Clark, M. F. (1986): Detection of strains of apple chlorotic leafspot virus by F(ab)₂-based indirect ELISA. – Arch. Phytopathol. Pflanzenschutz 22: 279-282.
- [2] Brunt, H. A., Crabtree, K., Dallawitz, M. J., Gibbs, A. J., Watson, L. (1996): Viruses of Plants. – CAB International, Cambridge, UK.

- [3] Çağlayan, Y. K., Çalı, S. (1994): Occurrence and detection of virus and virus like diseases of plum and apricot trees in the East Mediterranean. – Proc. of 9th Cong. of the Mediter. Phytopath. Union. Sept. 18-24, Kuşadası-Aydın, Türkiye, pp. 551-553.
- [4] Candresse, T., Lanneau, M., Revers, F., Grasseau, N., Macquaire, G., German, S., Malinowski, T., Dunez, J. (1995): An immuno-capture PCR assay adapted to the detection and the analysis of the molecular variability of the Apple chlorotic leaf spot virus. – Acta Horticult. 386: 136-147.
- [5] Chairez, R., Lister, R. M., (1973): A comparison of two strains of apple chlorotic leaf spot virus. – Phytopathology 63: 1458-1464.
- [6] Clark, M., Adams, A. M. (1977): Characteristics of microplate method of enzymelinked immunosorbent assay for the detection of plant viruses. – J. Gen. Virol. 34: 475-483.
- [7] Değirmenci, K., Akbaş, B. (2013): Molecular detection of apple chlorotic leaf spot virus in different host in the Central Anatolia Integrated protection of fruit crops. – IOBC-WPRS Bulletin 91: 337-343.
- [8] Dellaporta, S. L., Wood, J., Hicks, J. B. (1983): A plant DNA mini-preparation: version 2. – Plant Mol Biol Rep. 1(4): 19-21. DOI: 10.1007.
- [9] Desvignes, J. C., Boye, R. (1989): Different diseases caused by chlorotic leaf spot virus on the fruit trees. – Acta Hort. 235: 31-38.
- [10] Dosba, F., Lansac, M., Pêcheur, G., Teyssier, B., Piquemal, J. P., Michel, M., (1986): Plum pox virus detection by ELISA technique in peach and apricot infected trees at different growing stage. – Acta Horticulturae 193: 187-191.
- [11] Dunez, J. (1986): Preliminary observations on virus and virus like diseases of stone fruit trees in Mediterranean and Near East countries. – FAO Plant Protection Bulletin 34: 43-48.
- [12] Dunez, J., Delbos, R. (1988): Closteroviruses. – In: Smith, I. M., Dunez, J., Lelliot, R. A., Phillips, D. A., Archer, S. A. (eds.) European Handbook of Plant Diseases. Blackwell, Oxford, pp. 5-7.
- [13] Elibüyük, İ. Ö. (1998): Malatya ilinde yetiştirilen sert çekirdekli meyve ağaçlarındaki viruslerin tanımlanması üzerinde araştırmalar. – Doktora tezi, Ankara Üniversitesi, Fen Bilimleri Enstitüsü.
- [14] Fidan, H. (2016): Antalya’da Örtü Altı Domates ve Biber Alanlarında Dayanıklılık Kıran Tomato spotted wilt virus (TSWV) İzolatların Genetik Kıyaslanması. – VI. Türkiye Bitki Koruma Kongresi KONYA, Türkiye, pp. 560-560.
- [15] Fidan, Ü., Özdemir, S. (1998): Kiraz ağaçlarında görülen virüslerin DAS-ELISA ile belirlenmesi. – Zirai Mücadele Araştırma Enstitüsü, Bornova/İzmir. www.tagem.gov.tr/yeni%20web/projeler/uygulamaya%20aktarilan/projeler00/bsad00/11.HTM.
- [16] Fidan, H., Sari, N. (2019): Molecular characterization of resistance-breaking tomato spotted wilt virus (TSWV) isolate medium segment in tomato. – Applied Ecology and Environmental Research 17(2): 5321-5339.
- [17] Fidan, H., Karacaoğlu, M., Koç, G., Çağlar, B. K. (2019): Tomato yellow leaf curl virus (TYLCV) strains and epidemiological role of Bemisia tabaci (Hemiptera: Aleyrodidae) biotypes on tomato agroecology in Turkey. – Applied Ecology and Environmental Research 17(4): 9131-9144.
- [18] Flegg, H. C., Clark, M. F. (1979): The detection of apple chlorotic leaf spot virus by a modified procedure of enzyme-linked immunosorbent assay (ELISA). – Annals of Applied Biology 91: 61-65.
- [19] Fu, Y.-X., Li, W.-H. (1993): Statistical tests of neutrality of mutations. – Genetics 133: 693-709.
- [20] German, S., Candresse, T., Lanneau, M., Huet, J. C., Pernollet, J. C. Dunez, J. (1990): Nucleotide sequence and genomic organisation of apple chlorotic leaf spot virus. – Virology 179: 104-112.

- [21] Hudson, R. R. (1987): Estimating the recombination parameter of a finite population model without selection. (Reprinted). – *Genetics Research* 89(5-6): 427-32. DOI: 10.1017/S0016672308009610.
- [22] Hudson, R. R., Kaplan, N. L. (1985): Statistical properties of the number of recombination events in the history of a sample of DNA sequences. – *Genetics* 111(1): 147-164.
- [23] Koç, G., Baloğlu, S., (2007): Çukurova’da Sharka (PPV; Plum Pox Potyvirus). – *Türkiye II. Bitki Koruma Kongresi Bildirileri*.
- [24] Koç, G., Bayırdar, L., Baloglu, S. (2008): Pear, a new host of Apple chlorotic leaf spot virus in Turkey. – *Journal of Plant Pathology* 90(2): 397-400.
- [25] Kuzmitskaya, P., Titok, V., Anoshenko, B., Urbanovich, O. (2016): Molecular variability of Apple chlorotic leaf spot virus isolated in Belarus. – *Environmental and Experimental Biology* 14: 121-126.
- [26] Librado, P., Rozas, J. (2009): DnaSP v5: a software for comprehensive analysis of DNA polymorphism data. – *Bioinformatics* 25: 1451-1452.
- [27] Lister, R. M. (1970): Apple Chlorotic Leaf Spot Virus. – No. 30 in CMI AAB Description of Plant Viruses. CMI/AAB, Kew, UK.
- [28] Liu, P., Li, Z., Song, S., Wu, Y. Y. (2014): Molecular variability of Apple chlorotic leaf spot virus in Shaanxi, China. – *Phytoparasitica* 42: 445-454.
- [29] Martelli, G. P., Candresse, T., Namba, S. (1994): Trichovirus, a new genus of plant viruses. – *Arch. Virology* 134: 451-455.
- [30] Martin, D., Rybicki, E. (2000): RDP: detection of recombination amongst aligned sequences. – *Bioinformatics* 16: 562-563.
- [31] Martin, D. P., Lemey, P., Lott, M., Moulton, V., Posada, D., Lefevre, P. (2010): RDP3: a flexible and fast computer program for analyzing recombination. – *Bioinformatics* 26: 2462-2463.
- [32] Menzel, W., Jelkmann, W., Maiss, E. (2002): Detection of four apple viruses by multiplex RT-PCR assays with coamplification of plant mRNA as internal control. – *Journal of Virological Methods* 99: 81-92.
- [33] Nemeth, M. (1986): Virus, Mycoplasma and Rickettsia Diseases of Fruit Trees. – Akademiai Kiado, Budapest.
- [34] Niu, F. Q., Pan, S., Wu, Z. J., Jiang, D. M. Li, S. F. (2012): Complete nucleotide sequences of the genomes of two isolates of apple chlorotic leaf spot virus from peach (*Prunus persica*) in China. – *Arch Virol* 157:783-786.
- [35] Öztürk, Y. (2012): Isparta Kiraz Üretim Alanlarında Görülen Önemli Virüslerin Serolojik Ve Moleküler Yöntemlerle Teşhisi Ve Kılıf Protein Gen Dizilimlerinin Belirlenmesi. – T. C. Süleyman Demirel Üniversitesi Fen Bilimleri Enstitüsü, Yüksek Lisans Tezi Bitki Koruma Ana Bilim Dalı Isparta.
- [36] Öztürk Keleş, P., Baloğlu, S., (2019): Doğu Akdeniz Bölgesi’nde Açık Alanda Yetiştirilen Biberlerde Bazı Virüslerin Serolojik ve Moleküler Tanısı. – *Alatarım* 18(1): 1-11.
- [37] Poul, F., Dunez, J. (1988): Use of monoclonal antibodies for the detection of the apple chlorotic leaf spot virus. – *Acta Hort.* 235: 49-56.
- [38] Sambrook, J., Fritsch, E. F., Maniatis, T. (1989): *Molecular Cloning: A Laboratory Manual*. 2nd Ed. – Cold Spring Harbor Laboratory, New York.
- [39] Sipahioğlu, H. M., Myrta, A., Abou-Ghanem, N., Di Terlizzi, B., Savino, V. (1999): Sanitary status of stone fruit trees in East Anatolia (Turkey) with particular reference to apricot. – *Bull. OEPP/EPPO* 29(4): 439-442.
- [40] Smith, I. M., Dunez, J., Philips, D. H., Lelliot, R. A., Archer, S. A. (1998): *European Handbook of Plant Diseases*. – Blackwell Scientific Publ., Oxford, UK.
- [41] Tajima, F. (1983): Evolutionary relationship of DNA sequences in finite populations. – *Genetics* 105: 437-460.

- [42] Tajima, F. (1989): Statistical method for testing the neutral mutation hypothesis by DNA polymorphism. – *Genetics* 123: 585-595.
- [43] Thompson, J. D., Higgins, D. G., Gibson, T. J. (1994): CLUSTAL W: improving the sensitivity of progressive multiple sequence alignment through sequence weighting, position-specific gap penalties and weight matrix choice. – *Nucl. Acids Res.* 22: 4673-4680.
- [44] Ulubaş, Ç., Ertunç, F. (2004): RT-PCR Detection and Molecular Characterization of *Prunus necrotic ringspot virus* Isolates Occurring in Turkey. – *Journal of Phytopathology* 152: 498-502.
- [45] Ulubas Serce, Ç., Rosner, A., (2006): Molecular typing of Turkish Apple chlorotic leaf spot virus isolates based on partial coat protein gene. – *Phytopathologia Mediterranea* 45: 117-125.
- [46] Watterson, G. (1975): On the number of segregating sites in genetical models without recombination. – *Theoretical Population Biology* 7: 256-276.
- [47] Yaegashi, H., Isogai, M., Tajima, H., Sano, T., Yoshikawa, N. (2007): Combinations of two amino acids (Ala40 and Phe75 or Ser40 and Tyr75) in the coat protein of apple chlorotic leaf spot virus are crucial for infectivity. – *Journal of General Virology* 88: 2611-2618.
- [48] Yürektürk, M. (1984): Marmara Bölgesi'nde sert çekirdekli meyvelerde görülen Sharka virüs hastalığı üzerine çalışmalar. – Atatürk Bahçe Kùltürleri Araştırma Enstitüsü.

BIOLOGICAL CONTROL OF NATURAL HERBIVORES ON AMBROSIA SPECIES AT LIAONING PROVINCE IN NORTHEAST CHINA

IQBAL, M. F.¹ – FENG, W.-W.¹ – GUAN, M.^{1,2} – XIANG, L.-Z.¹ – FENG, Y.-L.^{1*}

¹*Liaoning Key Laboratory for Biological Invasions and Global Changes, College of Bioscience and Biotechnology, Shenyang Agricultural University, Shenyang 110866, Liaoning Province, China*

²*School of Life Sciences, Taizhou University, Taizhou 318000, Zhejiang Province, China*

*Corresponding author

e-mail: yl_feng@tom.com; phone: +86-24-8848-7163; fax: +86-24-8849-2799

(Received 16th Sep 2019; accepted 15th Nov 2019)

Abstract. Giant ragweed (*Ambrosia trifida* L.) and Common ragweed (*Ambrosia artemisifolia* L.) are well known species native to North America and can now be found in China. These weeds are ecologically important and have the ability to spread into agricultural areas and can create future risks. This study is an attempt to investigate the control potential of the root, a pathogen and a gall forming stem insect herbivore for *Ambrosia* species at different locations of Liaoning Province in Northeast China. Significantly ($P < 0.05$) high pathogen herbivore (*Puccinia xanthii*) abundance was investigated in sites IV and II (16.76%; 14.04%) with 58-66% humidity at site temperature ranges between minimum-maximum (20-30°C). Significant abundance ($P < 0.05$) in stem gall insect herbivore (*Epiblema strenuana*) were recorded in site IV (12.49%) and site I (12.34%). This herbivore displayed a steep asymptotic curve decrease significantly from upper to lower position gave positive relationship. The value of co-efficient of determination ($R^2 = 0.52$) as depicted gave the indication of model fitness. Pathogen herbivore displayed also a steep asymptotic curve investigated moderate positive relationship with $R^2 = 0.45$ followed by site I ($R^2 = 0.36$) form parabola curve. Stem galling insect and pathogen herbivores were diversified significantly with Simpson's index of diversity (SID). Similarly, root herbivore (fire ant) demonstrated its biological control potential on invasive *Ambrosia artemisifolia* at site I recorded significant ($P < 0.05$) reduction in plant height (30.62%); diameter (43.21%) and number of leave (73.60%) compared to gall forming stem herbivore.

Keywords: damage level, *Epiblema strenuana*, invasiveness, potential, *Puccinia xanthii*, *Solenopsis invicta*

Introduction

Invasive alien species (IAS) create hazard and develop a key pressure on biodiversity of the world that alter ecosystem, reduce native species abundance and cause economic loss (Butchart et al., 2010; Vilà et al., 2011; Hejda et al., 2009; Buttenschøn et al., 2010). However, there is a dire need to react and develop strategies against this hazard should be a basic goal (Lambertini et al., 2011).

Common ragweed (*Ambrosia artemisifolia* L.) is an annual invasive weed belongs to family asteraceae native to North America and Mexico present all over the world (*Fig. 1*) and also in China (Zhou et al., 2017). This weed unintentionally introduced in south east coastal areas in China in 1930's (Chen et al., 2007; Wan et al., 1995). Invasive weeds can affect ecosystem processes, alter community structure and resulting in loss of native weeds populations (Hejda et al., 2009; Powell et al., 2011). *Ambrosia* species introduced as noxious invasive weed in southern area of European Russia, Europe that extends into Georgia and westwards into Ukraine (Moskalenko, 2002; Reznik, 2009; Bullock et al., 2012; Essl et al., 2015; Protopopova et al., 2006; Ustinova and Sizovenko, 2006). This weed infested on agricultural crops (oilseed, rapeseed crop,

sunflower and soybean) as well as on fallow land resulted significant yield losses (Kazinczi et al., 2008; Buttenschön et al., 2010; Tóth et al., 2004; Kőmives et al., 2006; Chollet, 1999; Moskalenko, 2002).

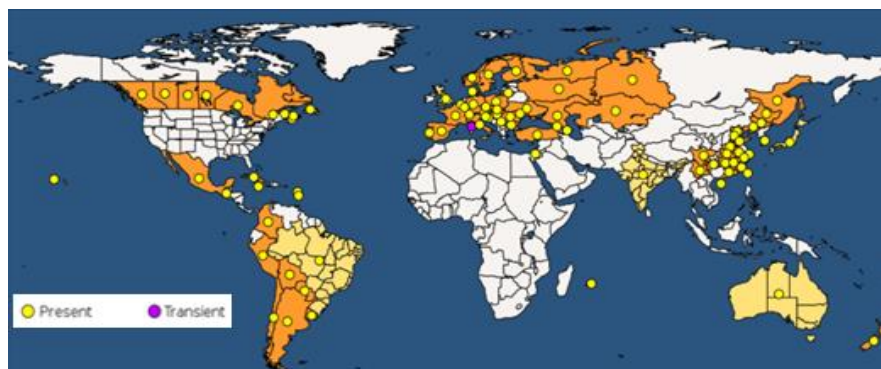


Figure 1. Distributional map and invasion status of Common ragweed (*Ambrosia artemisiifolia*) around the globe (EPPO, 2008)

Giant ragweed (*Ambrosia trifida* L.) is an annual herb with branched, erect stems with 30 - 150 cm in height which prolong up to 400 cm. Their leaves were mostly opposite, slightly scabrous, elliptical, 3-5 lobes, margins usually dentate, petioles with 10-30 mm in size (Strother, 2006). This is the most competitive weed in row crops which evolved resistance against multiple herbicides (Goplen et al., 2016). *Ambrosia* species dispersed in 21 provinces in eastern part of China including Jiangxi, Hunan, Hubei, Anhui, Fujian, Zhejiang, Nanjing, Jiangsu (Zhou et al., 2014; Zhou et al., 2010; Meng and Li, 2005) and this weed is polymorphism in nature (Bassett and Crompton, 1975). There is extensive history of biological control against *Ambrosia* species in Eastern Europe, Australia, China and Kazakhstan (Fig. 2).



Figure 2. Distributional map and invasion status of Giant ragweed (*Ambrosia trifida*) around the globe (GBIF, 2018; Committee, 2011)

Epiblema strenuana (Walker) (Lepidoptera: Tortricidae) is an endemic and widely distributed in North America, Canada, Mexico and USA, Arkansas, California, Colorado, Connecticut, Columbia, Florida, Illinois, Maryland, New Jersey, New York, North Carolina, Ohio, Pennsylvania, Tennessee, Virginia (Heinrich, 1923), Iowa, Mississippi, Dakota (Brown, 1973) and Israel (Yaacoby and Seplyarsky, 2011).

Rust is a pathogen herbivore (*Puccinia xanthii*), the most promising candidate for biological control of *Ambrosia* species (Hennen et al., 2005). *P. xanthii* collected on *A. trifida* in North America recorded high level of specificity to its original host named *P. xanthii* f. sp. *ambrosiae-trifidae* (Batra, 1981), however, this pathogen did not show its infection on *A. artemisiifolia* (Kiss, 2007; Morin et al., 1993). The significant impact of *P. xanthii* having its host documented in China on *Ambrosia trifida* caused serious die-back of infected plants (Lu et al., 2004a).

Fire ants (Formicidae: Hymenoptera) are social insects reside in colonies that habitually fabricate hills/mounds/tunnels within the soil like pastures and arable lands. Their nests are present within the soil, under stones, or in trees.

The stem galling insect herbivore (*Epiblema strenuana*) was introduced from Australia to China and host specificity tests were conducted on sunflower crops (Zhao et al., 2014; Wan et al., 1995), however, insect herbivore was introduced in 1990 to control *A. artemisiifolia*. The insect release in a small-scale in Hunan Province, and later the insect established its population and began to spread. Host specificity and feeding studies indicated that there are four host plants (*A. artemisiifolia*, *A. trifida*, *Xanthium sibiricum* and *Parthenium hysterophorus*) were discovered in China (Ma et al., 2003).

There is an intensive need to locate and develop eco-friendly solutions regarding biological control agents (BCA's) for the proper management of invasive weeds (McFadyen, 1998). These weeds produced allergic pollens that cause pollution and considered significant possible hazard to human beings and the natural diversity (Qureshi et al., 2014). The most important key provoking strategies to control these invasive weeds are chemicals. The chemical industry of China has taken one of the most re-known positions in global village. Many broad, narrow and sedges type of invasive and non invasive weeds were controlled by herbicides. These chemical herbicides create negative impacts on the natural ecosystem may cause toxicity to human beings (Bastiaans et al., 2008; Wilson and Tisdell, 2001; Zhang et al., 2011b).

To overcome the problem of excessive usage of chemicals; biological control agents are the best option without posing contamination to environment and naturally growing populations. The study hypothesis is that the damage level of pathogen herbivore (*Puccinia xanthii*) may vary with locations depend upon the prevailing environmental conditions and to find out insects having biological control efficiency against invasive weeds. The study comprised the relationship between root and stem galling insect herbivores against *Ambrosia artemisiifolia* in relation to plant growth parameters. However, the survey was conducted to point out coefficient of determination (R^2) of natural herbivores associated with *Ambrosia trifida* and to study diversity of natural herbivores with Ecological Indices on *Ambrosia trifida* at four locations. This survey was planned under Liaoning Key Laboratory for Biological Invasions and Global Changes, College of Bioscience and Biotechnology, Shenyang Agricultural University (SYAU), Shenyang, Liaoning Province, People Republic of China during 2018.

Materials and Methods

The field survey was conducted to evaluate root herbivore fire ant (*Solenopsis invicta*); gall forming stem herbivore (*Epiblema strenuana*) and pathogen herbivore (*Puccinia xanthii*) studied as biological control agents (BCA's) on invasive ragweed species (*Ambrosia artemisiifolia* and *A. trifida*) at different sites. However, minimum and maximum temperature was recorded on the spot site having site I (22-31°C & 69% humidity); site II (21-30°C &

66% humidity); site III (21-34°C with 62% RH) and site IV (20-30°C with 58% RH) as shown (Fig. 3). The study was conducted in peak season keeping in view the pressure of the herbivores are maximum in July-August during 2018 (Fig. 4).

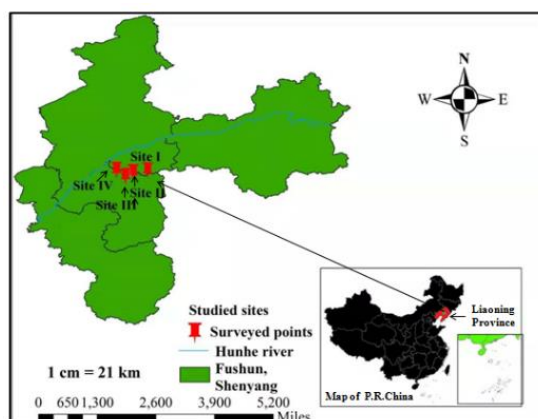


Figure 3. Mapping location of biological control agents (*Epiblema*, *Puccinia* and *Solenopsis*) using ArcGIS software (Kumar et al., 2014)

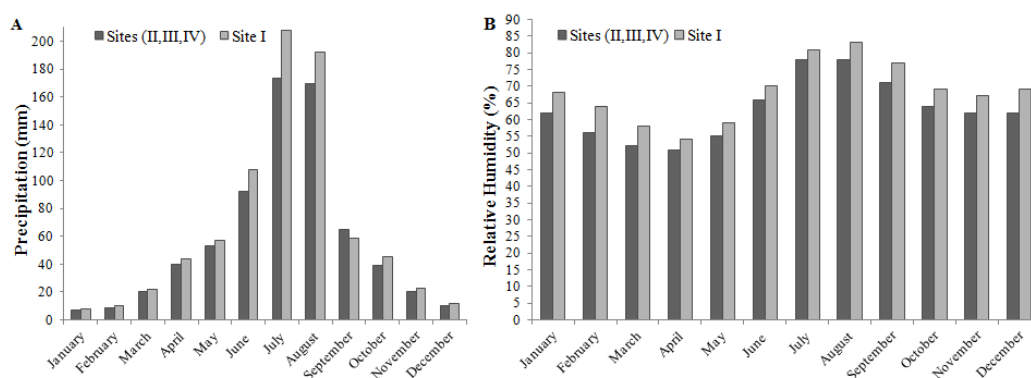


Figure 4. The climatic data showing mean monthly precipitation (A); Monthly mean Relative Humidity (B) of four sites (data sourced from Chinese meteorological data base)

The studied area is a northeastern part in China having hilly area at the boarder of South Korea. The average annual rainfall of site I was recorded 786.8 mm with range of annual relative humidity 54-83%. However, the site II, III, IV having annual rainfall were recorded 698.5 mm with range of annual relative humidity 51-78% (Fig. 4A,B).

The approach used was a simple random sampling technique designed through extensive field survey (Iqbal et al., 2019). The transect line was eighty meter long parallel to the roadside or riverside; however, we collected four different points twenty meters in one side of transect and data were recorded using quadratic ring (Murphy et al., 2015; Riaz and Javaid, 2011; Zereen et al., 2018; Iqbal et al., 2019) having (100 x 100 cm) following standard protocol (Andersen et al., 2015). Our sampling focused on stem galling insect and pathogen herbivores consumed directly on the leaf and stem on *Ambrosia trifida* at four locations. The data of root with gall forming herbivore were recorded in site I on *Ambrosia artemisifolia* due to the availability of both herbivores at this site. The root herbivore of common ragweed plants present in each quadratic ring

was collected and same procedure was adopted for control for proper comparison. The nine damaged leaves collected randomly from the upper, middle and lower portions of *A. trifida*, and repeat this procedure three times. The insect galled stems in *A. artemisifolia* were also collected in a quadratic ring counted the number of galls and repeated thrice. The *A. trifida* leaf spread fully on the hardboard with white background and cover it by transparent flexible plastic cover for digital image analysis. We evaluated and quantify herbivore damage on *A. trifida* leaves by Adobe Photoshop and ImageJ at maximum entropy (MaxEnt) threshold (Moles and Westoby, 2000; Lowman, 1984; Goodwin and Hsiang, 2010; O'Neal et al., 2002). Then leaf area fed/consumed (%) by natural herbivores were assessed (Balami and Thapa, 2017).

At the end, total number of healthy and damaged leaf were counted for the calculation of damage percentage (Balami and Thapa, 2017). Simpson index of Diversity (SID), evenness and abundance values were calculated (Magurran, 1988; Qureshi et al., 2018; Mahajan and Fatima, 2017; Chao et al., 2005; Letourneau et al., 2009; Kilewa and Rashid, 2014; El-Azazi et al., 2013).

The consumed area by *Puccinia xanthii* recorded on *A. trifida* leaves collected from these locations and examined under microscope (Iqbal et al., 2019) with 40 μm and 100 μm magnifications. The root, stem and pathogen herbivore were identified by morphometric characteristics (McClay, 1987; Bincheng, 1994; Yaacoby and Seplyarsky, 2011; Wahyuno, 2012; Batra, 1981).

Re-modification of the evolving model

The regression-type relationship carried out for developing the model comparison between mean of natural herbivore fed sites with root mean square error (RMSE). The regression model was set out to determine the effect natural herbivores consumed plant/leave parts investigated different parameters, gave the information about how far away the predicted line is from the observed line. The researchers previously exposed how scattered the observed points around the predicted line, which alternatively revealed about the validity of the model fitness (Hossain et al., 2017; Debaeke et al., 1997; Ahmed et al., 2019). RMSE gave magnitude of the characteristic variation between predicted and observed data (Mayer and Butler, 1993) resulted to assess the precision of the model (Royo-Esnal et al., 2010; Iqbal et al., 2019).

Statistical analysis

The growth parameter analyzed by one-way analysis of variance with Tukey's HSD test keeping in view $P > 0.05$; however, coefficients of determinations (R^2) were calculated by means of respective sites. The geographic coordinates during survey site was recorded using GPS navigator (GPS-Hollox, Taiwan) and map was drawn on ArcGIS version 10.2 software (ESRI) (ArcGis, 2013).

Results

Response of natural herbivores on Giant Ragweed (Ambrosia trifida L.)

Validation of the model fitness

The gall forming stem herbivore (*Epiblema strenuana*) after emergence fed on *A. trifida* leaf at four different sites gave indication that site II and IV displayed a steep asymptotic curve decrease significantly from upper to lower position. This curvature

went in upward direction investigated moderate strength of the variables that gave positive relationship. However, *coefficient of determination* was recorded in site II ($R^2 = 0.52$) followed by site I ($R^2 = 0.49$) showed linear line. In site IV, *coefficient of determination* ($R^2 = 0.43$) was recorded polynomial positive interactions of the model fitness as depicted (Fig. 5A,B) compared to site III ($R^2 = 0.02$) having line parallel to x-axis recorded no relationship of herbivore with its calculated consumed leaf (%).

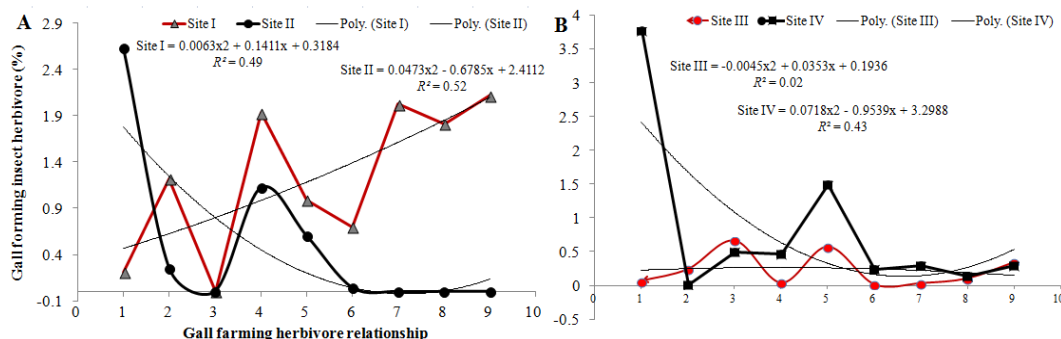


Figure 5. Power relationship of gall forming stem herbivores feeding (%) on *A. trifida* leaf with different sites; whereas Site I and II (A); III and IV (B); $R^2 =$ Co-efficient of determinations; Poly means Polynomial

The affect of natural insect herbivore feeding (%) on *A. trifida* leaves were investigated non significant ($P > 0.05$) relationship at all four sites, therefore the value of root mean square error (RMSE) < 5 recorded in our experiment gave the indication of model fitness (Table 1). The pathogen herbivore recorded significant ($P < 0.05$) effect in site II on *A. trifida* leaf with the leaf feeding rate (7.78%) with RMSE (3.15) compared to the rest of the studied sites.

Table 1. Relationship of RMSE with affect of natural stem galling and pathogen herbivore (%) on *A. trifida* leaf at different locations during 2018

Locations	GFSH±SE	RMSE	PH±SE	RMSE
Site I	1.22±0.27*	0.30	3.25±1.89	3.13
Site II	0.52±0.29*	0.27	7.78±1.55*	3.15
Site III	0.23±0.08*	0.25	1.17±0.20	3.12
Site IV	0.80±0.40*	0.28	5.98±1.27	3.14

Whereas level of significance was $P < 0.05$, RMSE – root mean square error; GFSH – means gall forming stem insect herbivore (%); PH – means pathogen herbivore (%); SE – standard error

The pathogen herbivore investigated on *A. trifida* leaf described that site II and I displayed a steep asymptotic curve decrease significantly from upper to lower side. At the end of the streak curvature went in upward direction investigated moderate positive relationship with the value of *coefficient of determination* ($R^2 = 0.45$) followed by site I ($R^2 = 0.36$) and falls this polynomial curve on the ground like parabola. Same trend line was recorded in Site IV with $R^2 = 0.14$ described polynomial positive weak interactions of the studied model soundness as illustrated (Fig. 6A,B) compared to site III ($R^2 = 0.03$) have no significant relationship with herbivore feeding or consumed (%).

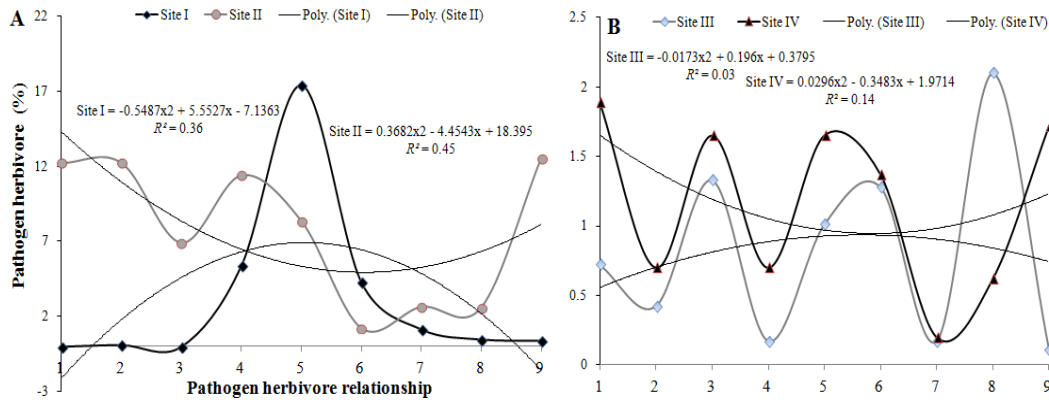


Figure 6. Power relationship of pathogen herbivore feeding (%) on *A. trifida* with different sites whereas site I and II (A); III and IV (B); R^2 (Co-efficient of determinations); Poly (Polynomial)

Ecological indices

Maximum evenness of gall forming insect (*Epiblema strenuana*) herbivore was investigated on site I & IV (0.15 & 0.15) recorded more stable in the community followed by site II (0.13) and site III (0.08). Similarly this herbivore was also more diversified in site I and IV (0.86 and 0.85) compared to other sites.

Maximum evenness of pathogen herbivore was investigated on site II & IV (0.15 & 0.15) recorded maximum stability in the community followed by site I (0.13) and site III (0.12). Pathogen herbivore was more diversified in site II and IV produced simpson's index of diversity 0.91 and 0.88 respectively (Fig. 7).

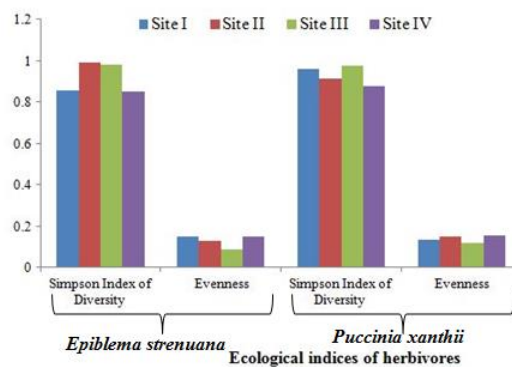


Figure 7. Ecological indices of gall forming insect and pathogen herbivores on *A. trifida*

The maximum pathogen herbivore abundance (%) per plant recorded in site IV (16.76%) followed by site II (14.04%). Similarly, highly significant ($P < 0.05$) abundance in leaf consumed was determined by gall forming stem herbivore at site IV (12.49%) followed by site I (12.34%) which was comparable to the other sites (Fig. 8A). Further more high number of leaves (12.22 and 14.56) consumed by gall forming insect and *Puccinia xanthii* herbivores respectively at location IV which differed significantly ($P < 0.01$) compared to all other sites (Fig. 8B).

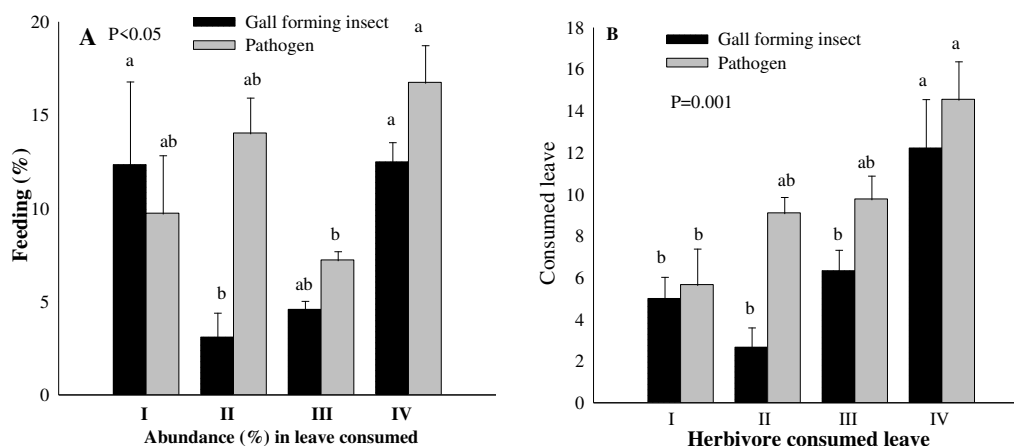


Figure 8. Comparison of abundance (%) in leaf consumed/plant by gall forming insect (*Epiblema strenuana*) and pathogen (*Puccinia xanthii*) herbivores (A), number of leaf consumed by herbivores (B) at four locations during 2018. Whereas level of significance was $P < 0.05$ by Tukey's HSD test for each response variable; the mean having different lettering differ statistically from each other

Response of natural herbivores on common ragweed (*Ambrosia artemisifolia* L.)

Plant growth parameters

The result of this study recorded significant ($P < 0.05$) increase in total number of leaves (74.70%) with $F = 138.416$; $SS = 9202.722$ in control treatment comparable to the root herbivore in quadratic rings. However, significant ($P < 0.05$) increase in plant height (cm) with ($F = 74.729$ and $SS = 4461.976$); diameter (mm) were (34.16%) with ($F = 55.106$; $SS = 26.451$) and (33.90%) with in control compared to root herbivore (Fig. 9A,B,C).

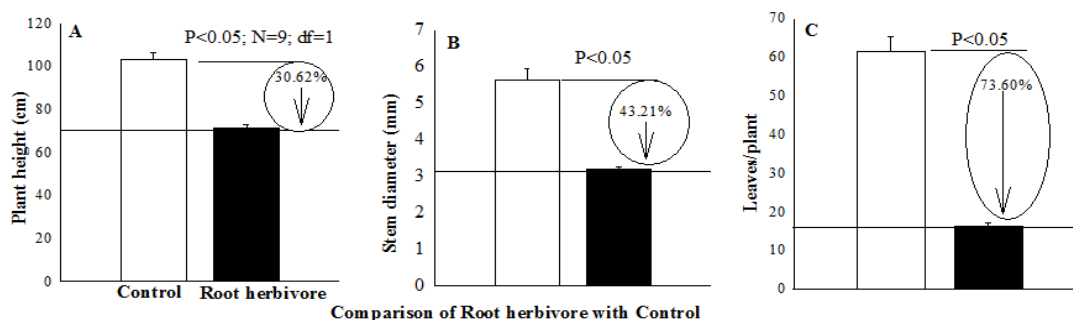


Figure 9. Comparative efficiency of root herbivore affected on growth parameters of *Ambrosia artemisifolia* L. during 2018 whereas (A) plant height (cm), (B) stem diameter (mm), (C) total number of leaves per plant. Whereas level of significance was $P < 0.05$ by Tukey's HSD test

The analysis showed that root herbivore distributed at site I showed its biological control potential against common ragweed. These results suggested that the trend of plant height (30.62%), stem diameter (43.21%) and the number of leaves (73.60%) of *A. artemisifolia* decreased significantly due to biting behavior of root herbivores on the roots zone compared to control.

Comparative efficacy of herbivores

The data regarding root herbivore showed non significant ($P>0.05$) result on replicated plots at three different sub locations in site I with each other but recorded significant ($P<0.05$) result with gall forming stem herbivore. The data described that root herbivore reduced the plant height significantly ($P<0.05$) of the invasive *A. artemisifolia* compared to stem feeding herbivore (Fig. 10A). Furthermore, the same significant ($P<0.05$) trend was investigated in case of stem diameter (mm) to control *A. artemisifolia* (Fig. 10B). Multivariate analysis suggested that biological control herbivores recorded significant ($P<0.05$) reduction in growth parameters of invasive weed compared to control.

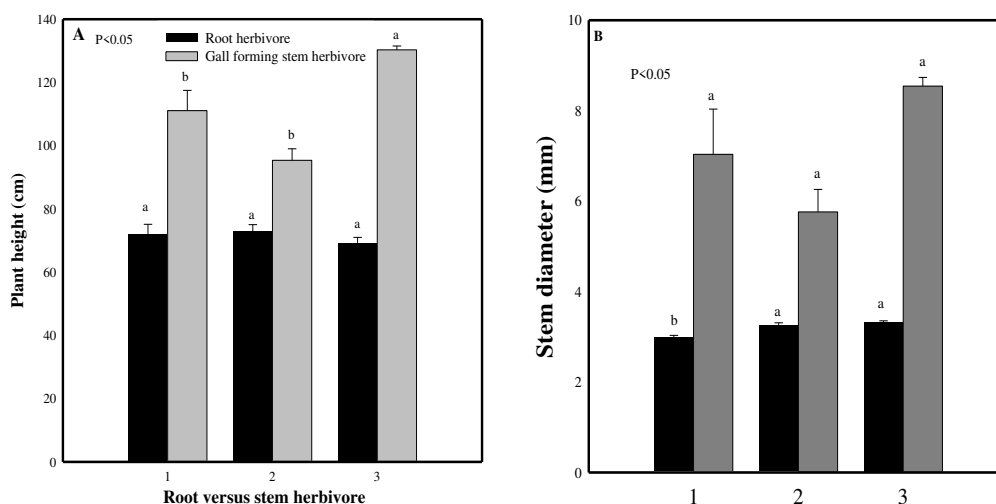


Figure 10. Comparative efficacy of root and gall forming stem herbivore on plant height (A); stem diameter (B) of *Ambrosia artemisifolia* at $\alpha = 0.05$ (Tukey's HSD test), for each response variable at site I; the mean having different lettering differed statistically from each other

Discussion

Relationship of gall forming herbivore with *Ambrosia trifida* L.

The infestation of gall forming insect herbivore used as biological control agent on *A. trifida* displayed a steep asymptotic curve decrease significantly gave polynomial positive and moderate relationship of coefficient of determination (R^2) indicated model fitness as depicted. This insect herbivore fed on leaf tissues (%) was produced statistically non significant ($P>0.05$) relationship (Table 1) with root mean square error (RMSE = 0.30). These results were supported to the researchers who reported that the value of RMSE investigated less than 5 gave the indication of awesome model fitness (Royo-Esnal et al., 2010; Iqbal et al., 2019).

Significant evenness was recorded by gall insect herbivore investigated on site I & IV (0.15 & 0.15). This herbivore was more diversified in site I and IV (0.86, 0.85) compareable to the other sites. These results are in accordance to the researchers who reported that *A. trifida* L. occurred in Northeast China, in heavily infested areas, ragweeds were often found in dense monospecific communities with an average diversity index of 0.19 (Wan et al., 1995). *Ambrosia* species an annual weed plant present almost everywhere in China and prefers open and sunny habitats where its

competition with other native weed is comparatively low. *Ambrosia* species reduced the natural species abundance in arable land and thus it investigated negative impacts on the agriculture and biodiversity (Pinke et al., 2011; Pál, 2004). The present investigation stated that stem insect herbivore larvae after hatching fed initially on *Ambrosia trifida* leave. After that the larvae enter on the terminal meristem, thickens the stem thus creating elongated galls in plants live there until it pupates. Highly significant ($P < 0.05$) abundance in leave consumed by stem gall forming herbivore investigated 12.49% and 12.34% in plant. Gall forming stem herbivore consumed high number of leaves 12.22 per plant at site IV differed significantly ($P < 0.01$) with all other rest of the sites. These results are agreed with the scientists who reported that gall herbivore is a nocturnal moth, with a life span of 7-11 days that feed on the invasive weed (Bincheng, 1994; McFadyen, 1992; Dhilepan and McFadyen, 2001; Dhilepan et al., 2018).

Biological characteristics of gall forming stem herbivore

The stem-galling herbivore (*Epiblema strenuana* Walker; Lepidoptera: Tortricidae) lay very small pale color eggs on the leaves (Dhilepan et al., 2018). After hatching eggs, the larvae emerged and fed directly on leave. The length of the larva is about 10 mm straight, but the length of 3rd instar larva is 14 mm, yellow or creamy, with brown heads with light brown genitalia. The larva of this herbivore make small hole on the top meristem and branches, enter into plant tissues. The developmental stages completed within the gall and pupate. The color of the pupa is brown, 8-9 mm long. Pupal stage converted into adult moth under favorable environmental conditions within 5-7 days, however this period prolonged upto 13 days under unfavorable environmental conditions. The open wing span of caterpillar was 15-18 mm in male and 12-15 mm wide in females. Adult moths have 10-8 mm (male-female) long grayish wings with pale glitery wingtips (Fig. 11). There are 3-4 generations of this herbivore that start from the end of April to early October in Southern China and each generation prolong upto 30–40 days (Feng-feng et al., 2002) and the survival time of the adult was 3-5 days under natural environmental conditions at Shenyang.

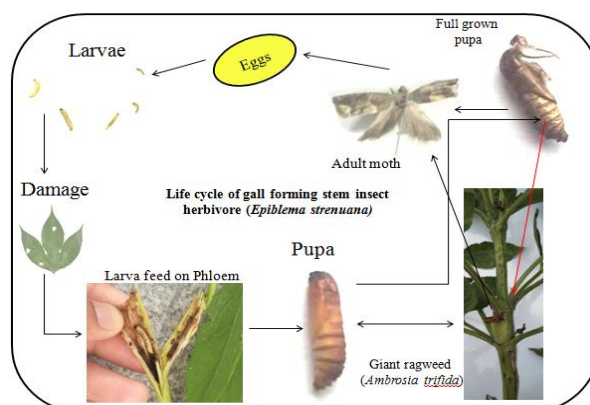


Figure 11. Biological characteristics of gall forming stem herbivore on *Ambrosia trifida* plant

Relationship of pathogen herbivore with *Ambrosia trifida* L.

The pathogen herbivore described moderate positive co-efficient of determinations (R^2) in site II (0.45) and site I (0.36), however, weak relationship was recorded in site

IV and no relationship was determined in site III having its almost line parallel to X-axis. Maximum evenness of pathogen herbivore (*Puccinia xanthii*) was investigated on site II & IV (0.15 & 0.15) and more diversified in site II (0.91) and IV (0.88) compared to site I and III, respectively. These results are in line with the previously studied field investigations in Liaoning and Jilin provinces reported that pathogen herbivore caused considerable destruction to giant ragweed. The fungus of pathogen herbivore feed on the leaves cause plant death on a large scale and may serve as an effective biological control agent of *A. trifida* (Zhang et al., 2011a; Lu et al., 2004b).

Significantly ($P < 0.05$) high pathogen herbivore (*Puccinia xanthii*) abundance was investigated in sites IV and II (16.76%; 14.04%) with 58-66% humidity at site temperature ranges minimum 20°C and maximum 30°C. These results are in accordance to the researchers who reported that this pathogen herbivore (giant ragweed rust) significantly favored high humidity and high temperature for its development. This pathogen was flourished in June-September in Shenyang area (Liaoning Province), so due to its obligate parasitic behavior and strong pathogenicity, this herbivore expected as biocontrol agent for the control of *Ambrosia trifida* (Qu et al., 2009; Guozhong et al., 2018). *Puccinia xanthii* herbivore consumed high number of leaves (14.56/plant) at location IV differed significantly ($P < 0.01$) with all other sites. These results gave the indications that favorable humidity played a significant positive role for spread of pathogen herbivore pressure. These findings support our hypothesis that significant infection of rust herbivore (*Puccinia xanthii*) on invasive weed may vary with locations depending upon the favorable environmental conditions. The favorable temperature for the germination of teliospore was 20-30°C and optimum temperature for the production and germination of basidiospores was 20°C but the temperature required for high infection was 20-25°C (Morin et al., 1992). The researchers reported in their field experiment that pathogen herbivore (*Puccinia xanthii* Schwein. f. sp. *Ambrosiae-trifidae* S.W.T. Batra) is an obligate parasitic rust fungus recorded an effective biocontrol agent against giant ragweed (Zhang et al., 2011a; Lu et al., 2004c; Seier et al., 2009; Batra, 1981) used as mycoherbicides against *Ambrosia* species (Wilson, 1969; Hasan, 1974; Barreto and Evans, 1995).

Life stages of pathogen herbivore

The pathogen herbivore (*Puccinia xanthii*) is an obligate parasite overwinters in the form of yellow powder of spores in dead plants at high humidity (Dhileepan, 2001; Qu et al., 2009). Its initial symptoms are clearly identified on leaves and its infection causes reduced plant growth rates and, dark brown telia appears clearly, easily identified on the whole leaves (Fig. 12).

Response of root herbivore on common ragweed (*Ambrosia artemisifolia* L.)

The present study suggested that root herbivore (Fire ants) is a biological control agent on common ragweed (*A. artemisifolia*) present in site I at 26°C (22-31°C) near Hanhe River. These results are in line with the researchers who reported that environmental conditions played a vital role for the development of root herbivore, however optimum temperature required for its foraging was between 25–35°C (Drees et al., 2007). Multivariate analysis suggested that biological control herbivores recorded significant ($P < 0.05$) reduction in growth parameters of invasive weed compared to control treatment. This herbivore affected root portion resulted in significant ($P < 0.05$) reduction of growth parameters of invasive weed compared to control. The experiment

suggested that the trend of plant height (30.62%), stem diameter (43.21%) and number of leaves (73.60%) of the *A. artemisifolia* decreased significantly ($P < 0.05$) due to biting behaviour of root herbivores compared to control. Scientists studied plant mortality up to 12.5-17.2% in grooves (Smittle et al., 1988), calyx feeding resulted in reduction of 50% flowers (Adams, 1986) due to root herbivores. Root herbivores constructed furrows/holes in the stem, hypocotyls portion and reduced plants height. The results of this study are in line with the researchers who reported that root herbivore reduced plant height significantly ($P < 0.05$) having potential to feed on carbohydrates and polysaccharides from the root tissues (Stewart and Vinson, 1991).

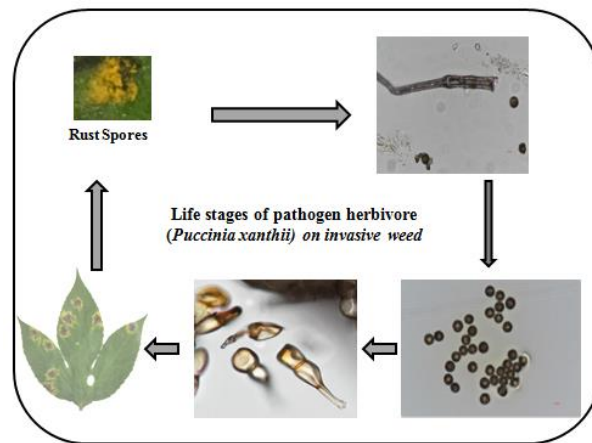


Figure 12. Life stages of pathogen herbivore completed on *Ambrosia trifida* leaves identified with 40 μm and 100 μm magnification under microscope

Our results are also in accordance with the researchers who reported that polyphagous ant (Hymenoptera: Formicidae) thinning the root collars that interrupt nutrient supply between shoots and roots (Niu et al., 2010; Vörös and Gallé, 2002) recorded significant damage to the plants. Root herbivores have high reproductive and distribution capabilities, toxic and non-toxic belongings of stings and forceful scavenging performance (Allen et al., 2004; Parris et al., 2002). Root herbivores store small portion of food material to the nest but also assist to crash bigger food item along its transportation (Tschinkel, 2006). These results are in accordance to the researchers who reported that growth and plant height reduced significantly by feeding of fire ant root herbivore (Adams, 1983). Oil contents and carbohydrates (polysaccharides, glucose, and fructose) are necessary ingredients in the diet of ants (root herbivores). Therefore, these herbivores scratch the sap from root portion may be associated with their necessary nutritional carbohydrates (Vander Meer et al., 1995) from plant tissues. The researchers investigated that root herbivore feed on the bark and cambium to obtain sap resulting the death of orange and grapefruit plants in Florida (Banks et al., 1991). Root herbivore (ants) attack on the stems of sunflower at ground level, removed phloem tissue leaving the woody cortex however, 40–50% of the crop was infested (Stewart and Vinson, 1991). In our experiment root herbivore significantly ($P < 0.05$) reduced the plant growth characteristics of *A. artemisifolia* compared to gall forming stem herbivore. The hypothesis was proved that root herbivore having capability to injure the roots of invasive *A. artemisifolia* resulting in significant reduction in plant growth characteristics.

This study shows that gall forming stem insect and pathogen herbivores have potential biological control agent against *Ambrosia trifida* recorded significant abundance (%) regarding leave area consumption. During field survey it had observed that plant hoppers suck the cell sap from the basal portions of stem tissues of *A. Artemisifolia* plant. In future, it may become a biological control agent (BCA's) of this invasive weed. The study also described that root herbivore significantly reduced the growth characteristics of *A. artemisifolia* may become a promising candidate for BCA's in future.

Conclusion

The present study concluded that pathogen herbivores deliberated and caused significant effect on giant ragweed (*Ambrosia trifida* L.). The root, stem galling insect and pathogen herbivores having biologically effective and helpful in reducing the growth characteristics of the *Ambrosia* species in natural ecosystems. In future, there is a dire need to find out more natural enemies having biologically control efficiency against invasive weeds. In the light of our study, we encouraged the entomologists, plant pathologists and ecologists to explore the mode of action of these herbivores along with phyto-chemical screening and their interactions mechanism on invasive weeds. However, reciprocal relationship of root herbivores with roots of the invasive weeds would be studied in future.

Acknowledgements. This study was supported by the National Key R&D Program of China (2017YFC1200101), the National Natural Science Foundation of China (31470575, 31670545 and 31971557).

Author's contributions. All authors have contributed equally to this paper.

Conflict of interests. All authors declare no conflict of interests.

REFERENCES

- [1] Adams, C. T. (1983): Destruction of eggplants in Marion County, Florida by red imported fire ants (Hymenoptera: Formicidae). – *The Florida Entomologist* 66: 518-520.
- [2] Adams, C. T. (1986): Agricultural and medical impact of the imported fire ants. – *Fire ants and leaf cutting ants: biology and management*. Westview Press, Boulder, CO 435: 48-57.
- [3] Ahmed, M., Ji, M., Qin, P., Gu, Z., Liu, Y., Sikandar, A., Iqbal, M. F., Javeed, A. (2019): Phytochemical screening, total phenolic and flavonoids contents and antioxidant activities of *Citrullus colocynthis* L. and *Cannabis sativa* L. – *Applied Ecology and Environmental Research* 17: 6961-6979.
- [4] Allen, C. R., Epperson, D. M., Garmestani, A. S. (2004): Red imported fire ant impacts on wildlife: a decade of research. – *The American Midland Naturalist* 152: 88-104.
- [5] Andersen, K. M., Naylor, B. J., Endress, B. A., Parks, C. G. (2015): Contrasting distribution patterns of invasive and naturalized non-native species along environmental gradients in a semi-arid montane ecosystem. – *Applied Vegetation Science* 18: 683-693.
- [6] ArcGis, E. (2013): Version 10.2. 0. – Redlands: Environmental Systems Research Institute
- [7] Balami, S., Thapa, L. B. (2017): Herbivory damage in native *Alnus nepalensis* and invasive *Ageratina adenophora*. – *Botanica Orientalis: Journal of Plant Science* 11: 7-11.

- [8] Banks, W. A., Adams, C. T., Lofgren, C. S. (1991): Damage to young citrus trees by the red imported fire ant (Hymenoptera: Formicidae). – *Journal of Economic Entomology* 84: 241-246.
- [9] Barreto, R. W., Evans, H. C. (1995): The mycobiota of the weed *Mikania micrantha* in southern Brazil with particular reference to fungal pathogens for biological control. – *Mycological Research* 99: 343-352.
- [10] Bassett, I. J., Crompton, C. W. (1975): The biology of Canadian weeds.: 11. *Ambrosia artemisiifolia* L. and *A. psilostachya* DC. – *Canadian Journal of Plant Science* 55: 463-476.
- [11] Bastiaans, L., Paolini, R., Baumann, D. T. (2008): Focus on ecological weed management: what is hindering adoption? – *Weed Research* 48: 481-491.
- [12] Batra, S. W. T. (1981): *Puccinia xanthii* forma specialis *ambrosia-trifidae*. – *Mycopathologia* 73: 61-64.
- [13] Bincheng, Z. (1994): Index of economically important Lepidoptera. – CAB International 599 p.
- [14] Brown, R. L. (1973): Phylogenetic systematics: its application to the genus *Epiblema* (Lepidoptera). Fayetteville, AR: University of Arkansas; 1973. 179 p. –
- [15] Bullock, J. M., Chapman, D., Schafer, S., Roy, D., Girardello, M., Haynes, T., Beal, S., Wheeler, B., Dickie, I., Phang, Z. (2012): Assessing and controlling the spread and the effects of common ragweed in Europe. – Final Report to the European Commission, DG Environment. Wallington, UK: Centre for Ecology and Hydrology.
- [16] Butchart, S. H. M., Walpole, M., Collen, B., Van Strien, A., Scharlemann, J. P. W., Almond, R. E. A., Baillie, J. E. M., Bomhard, B., Brown, C., Bruno, J. (2010): Global biodiversity: indicators of recent declines. – *Science* 328: 1164-1168.
- [17] Buttenschön, R. M., Waldispühl, S., Bohren, C. (2010): Guidelines for management of common ragweed, *Ambrosia artemisiifolia*. – Technical report, <http://www.EUPHRESCO.org>
- [18] Chao, A., Chazdon, R. L., Colwell, R. K., Shen, T. J. (2005): A new statistical approach for assessing similarity of species composition with incidence and abundance data. – *Ecology letters* 8: 148-159.
- [19] Chen, H., Chen, L., Albright, T. P. (2007): Developing habitat-suitability maps of invasive ragweed (*Ambrosia artemisiifolia*. L) in China using GIS and statistical methods.- GIS for Health and the Environment, Springer, In: International Conference in GIS and Health; GIS for health and the environment: development in the Asia-Pacific region, Springer, Berlin, pp. 105-121,
- [20] Chollet, D. (1999): Lutte contre l'ambrosie a feuille d'armoise. – *Perspect. Agric.* 250: 78-82.
- [21] Committee, F. O. C. E. (2011): *Ambrosia trifida* Linnaeus. – Accessed online February 13 2018.
- [22] Debaeke, P., Caussanel, J. P., Kiniry, J. R., Kafiz, B., Mondragon, G. (1997): Modelling crop: weed interactions in wheat with ALMANAC. – *Weed Research* 37: 325-341.
- [23] Dhileepan, K. (2001): Effectiveness of introduced biocontrol insects on the weed *Parthenium hysterophorus* (Asteraceae) in Australia. – *Bulletin of entomological research* 91: 167-176.
- [24] Dhileepan, K., Callander, J., Shi, B., Osunkoya, O. O. (2018): Biological control of parthenium (*Parthenium hysterophorus*): the Australian experience. – *Biocontrol science and technology* 28: 970-988.
- [25] Dhileepan, K., McFadyen, R. E. C. (2001): Effects of gall damage by the introduced biocontrol agent *Epiblema strenuana* (Lep., Tortricidae) on the weed *Parthenium hysterophorus* (Asteraceae). – *Journal of Applied Entomology* 125: 1-8.
- [26] Drees, B. M., Summerlin, B., Vinson, S. B. (2007): Foraging activity and temperature relationship for the red imported fire ant. – *Southwestern Entomologist* 32:

- [27] El-Azazi, E.-S., Khalifa, E. A., Belal, M. M. S. A. H., Eltanger, N. A. (2013): Ecological studies of some Acacia species grown in Egyptian Deserts. – *Earth* 7: 3-8542.
- [28] EPPO (2008): *Ambrosia artemisiifolia* (AMBEL). – *Bulletin OEPP/EPPO Bulletin* 38: 414–418.
- [29] Essl, F., Biró, K., Brandes, D., Broennimann, O., Bullock, J. M., Chapman, D. S., Chauvel, B., Dullinger, S., Fumanal, B., Guisan, A. (2015): Biological flora of the British Isles: *Ambrosia artemisiifolia*. – *Journal of Ecology* 103: 1069-1098.
- [30] Feng-feng, D. A. I., Zao-hong, Z., You-gang, H. E., Zao-fa, J. (2002): Preliminary Investigation on Occurrence Law of *Epiblema strenuana* A Natural Enemy of *Ambrosia artemisiifolia* [J]. – *Acta Agriculturae Jiangxi* 4:
- [31] GBIF (2018): *Ambrosia trifida* L. – Accessed online January 29 2018. <https://www.gbif.org/species/3110588>:
- [32] Goodwin, P. H., Hsiang, T. (2010): Quantification of fungal infection of leaves with digital images and Scion Image software.- *Molecular and Cell Biology Methods for Fungi*, Springer,
- [33] Goplen, J. J., Sheaffer, C. C., Becker, R. L., Coulter, J. A., Breitenbach, F. R., Behnken, L. M., Johnson, G. A., Gunsolus, J. L. (2016): Giant ragweed (*Ambrosia trifida*) seed production and retention in soybean and field margins. – *Weed Technology* 30: 246-253.
- [34] Guozhong, L., Fengxuan, G., Xinran, S., Xiaodong, S., Hua, J. (2018): The rust fungus of *Puccinia Xanthii* f. sp. *Ambrosiae-trifidae* being a good biocontrol agent of giant ragweed. – *Applied Microbiology* 4: 67.
- [35] Hasan, S. (1974): Recent advances in the use of plant pathogens as biocontrol agents of weeds. – *PANS Pest Articles & News Summaries* 20: 437-443.
- [36] Heinrich, C. (1923): Revision of the North American moths of the subfamily Eucosminae of the family Olethreutidae.-US Government Printing Office,
- [37] Hejda, M., Pyšek, P., Pergl, J., Sádlo, J., Chytrý, M., Jarošík, V. (2009): Invasion success of alien plants: do habitat affinities in the native distribution range matter? – *Global Ecology and Biogeography* 18: 372-382.
- [38] Hennen, J. F., Figueiredo, M. B., Carvalho Jr, A. A., Hennen, P. G. (2005): Catalogue of the species of plant rust fungi (Uredinales) of Brazil. – *Jardim Botanico do Rio de Janeiro: Rio de Janeiro, Brazil*
- [39] Hossain, S. A. A. M., Wang, L., Chen, T., Li, Z. (2017): Leaf area index assessment for tomato and cucumber growing period under different water treatments. – *Plant, Soil and Environment* 63: 461-467.
- [40] Iqbal, M. F., Feng, Y. L., Liu, M. C., Lu, X. R., Nasir, M., Sikandar, A. (2019): Parasitic activity of powdery mildew (Pathogen strain HMLAC 226) on prostrate knotweed (*Polygonum aviculare* L.) at various locations of Shenyang, Northeast China. – *Applied Ecology and Environmental Research* 17: 13383-13394.
- [41] Kazinczi, G., Béres, I., Novák, R., Biró, K., Pathy, Z. (2008): Common ragweed (*Ambrosia artemisiifolia*): a review with special regards to the results in Hungary. I. Taxonomy, origin and distribution, morphology, life cycle and reproduction strategy. – *Herbologia* 9: 55-91.
- [42] Kilewa, R., Rashid, A. (2014): Distribution of invasive weed *Parthenium hysterophorus* in natural and agro-ecosystems in Arusha Tanzania. – *International Journal of Science and Research* 3: 1-4.
- [43] Kiss, L. (2007): Why is biocontrol of common ragweed, the most allergenic weed in Eastern Europe, still only a hope. – *Biological control: A global perspective* 80-91.
- [44] Kórmives, T., Béres, I., Reisinger, P., Lehoczky, E., Berke, J., Tamás, J., Páldy, A., Csornai, G., Nádor, G., Kardeván, P. (2006): New strategy of the integrated protection against common ragweed (*Ambrosia artemisiifolia* L.). – *Magyar Gyomkutatás és Technológia* 7: 5-49.

- [45] Kumar, S., Graham, J., West, A. M., Evangelista, P. H. (2014): Using district-level occurrences in MaxEnt for predicting the invasion potential of an exotic insect pest in India. – *Computers and Electronics in Agriculture* 103: 55-62.
- [46] Lambertini, M., Leape, J., Marton-Lefevre, J., Mittermeier, R. A., Rose, M., Robinson, J. G., Stuart, S. N., Waldman, B., Genovesi, P. (2011): Invasives: a major conservation threat. – *Science* 333: 404-405.
- [47] Letourneau, D. K., Jedlicka, J. A., Bothwell, S. G., Moreno, C. R. (2009): Effects of Natural Enemy Biodiversity on the Suppression of Arthropod Herbivores in Terrestrial Ecosystems. – *Annual Review of Ecology, Evolution, and Systematics* 40: 573-592.
- [48] Lowman, M. D. (1984): An assessment of techniques for measuring herbivory: is rainforest defoliation more intense than we thought? – *Biotropica* 264-268.
- [49] Lu, G., Yang, H., Sun, X., Yang, R., Zhao, Z. (2004a): *Puccinia xanthii* f. sp. ambrosiae-trifidae, a newly recorded rust taxon on *Ambrosia* in China. – *Mycosystema* 23: 310-311.
- [50] Lu, G. Z., Yang, H., Qu, B., Huang, G. K., Chen, W. Z., Cannon, P. (2004b): Ultrastructure observation of *Puccinia xanthii* Schwein. f. sp. ambrosiae-trifidae SWT Batra. – *J. Fung. Res* 2: 14-16.
- [51] Lu, G. Z., Yang, H., Sun, X. D., Yang, Y. X., Zhao, Z. H. (2004c): *Puccinia xanthii* Schwein. f. sp. ambrosiae-trifidae SWT Batra, a newly recorded rust taxon on *Ambrosia* in China. – *Mycosystema* 23: 612-614.
- [52] Ma, J., Wan, F.-H., Guo, J.-Y., You, L.-S. (2003): Bio-climatic matching analysis for *Epiblema strenuana* (Lepidoptera: Tortricidae) in China. – *Scientia Agricultura Sinica* 10:
- [53] Magurran, A. E. (1988): *Why diversity? - Ecological diversity and its measurement*, Springer,
- [54] Mahajan, M., Fatima, S. (2017): Frequency, abundance, and density of plant species by list count quadrat method. – *International Journal of Multidisciplinary Research* 3: 1-8.
- [55] Mayer, D. G., Butler, D. G. (1993): Statistical validation. – *Ecological modelling* 68: 21-32.
- [56] McClay, A. S. (1987): Observations on the biology and host specificity of *Epiblema strenuana* (Lepidoptera, Tortricidae), a potential biocontrol agent for *Parthenium hysterophorus* (Compositae). – *Entomophaga* 32: 23-34.
- [57] McFadyen, R. C. (1992): Biological control against parthenium weed in Australia. – *Crop protection* 11: 400-407.
- [58] McFadyen, R. E. C. (1998): Biological control of weeds. – *Annual review of entomology* 43: 369-393.
- [59] Meng, L., Li, B. P. (2005): Advances on biology and host specificity of the newly introduced beetle, *Ophraella communa* Lesage (Coleoptera: Chrysomelidae), attacking *Ambrosia artemisiifolia* (Compositae) in continent of China. – *Chinese Journal of Biological Control* 21: 65-69.
- [60] Moles, A. T., Westoby, M. (2000): Do small leaves expand faster than large leaves, and do shorter expansion times reduce herbivore damage? – *Oikos* 90: 517-524.
- [61] Morin, L., Auld, B. A., Brown, J. F. (1993): Host range of *Puccinia xanthii* and postpenetration development on *Xanthium occidentale*. – *Canadian Journal of Botany* 71: 959-965.
- [62] Morin, L., Brown, J. F., Auld, B. A. (1992): Teliospore germination, basidiospore formation and the infection process of *Puccinia xanthii* on *Xanthium occidentale*. – *Mycological Research* 96: 661-669.
- [63] Moskalenko, G. P. (2002): Common ragweed. – *Zashchita i Karantin Rastenii* 2: 38-41.
- [64] Murphy, S. J., Audino, L. D., Whitacre, J., Eck, J. L., Wenzel, J. W., Queenborough, S. A., Comita, L. S. (2015): Species associations structured by environment and land-use history promote beta-diversity in a temperate forest. – *Ecology* 96: 705-715.

- [65] Niu, Y., Feng, Y.-L., Xie, J., Luo, F. (2010): Noxious invasive *Eupatorium adenophorum* may be a moving target: Implications of the finding of a native natural enemy, *Dorylus orientalis*. – Chinese Science Bulletin 55: 3743-3745.
- [66] O’Neal, M. E., Landis, D. A., Isaacs, R. (2002): An inexpensive, accurate method for measuring leaf area and defoliation through digital image analysis. – Journal of Economic Entomology 95: 1190-1194.
- [67] Pál, R. (2004): Invasive plants threaten segetal weed vegetation of South Hungary. – Weed technology 18: 1314-1319.
- [68] Parris, L. B., Lamont, M. M., Carthy, R. R. (2002): Increased incidence of red imported fire ant (Hymenoptera: Formicidae) presence in loggerhead sea turtle (Testudines: Cheloniidae) nests and observations of hatchling mortality. – Florida Entomologist 85: 514-518.
- [69] Pinke, G., Karácsony, P., Czúcz, B., Botta-Dukat, Z. (2011): Environmental and land-use variables determining the abundance of *Ambrosia artemisiifolia* in arable fields in Hungary. – Preslia 83: 219-235.
- [70] Powell, K. I., Chase, J. M., Knight, T. M. (2011): A synthesis of plant invasion effects on biodiversity across spatial scales. – American Journal of Botany 98: 539-548.
- [71] Protopopova, V. V., Shevera, M. V., Mosyakin, S. L. (2006): Deliberate and unintentional introduction of invasive weeds: A case study of the alien flora of Ukraine. – Euphytica 148: 17-33.
- [72] Qu, B., Yang, H., Dong, S. (2009): Incidence and epidemics of giant ragweed rust (*Puccinia xanthii* f. sp. *ambrosiae-trifidae*). – Journal of Fungal Research 7: 180-184.
- [73] Qureshi, H., Arshad, M., Bibi, Y. (2014): Invasive flora of Pakistan: a critical analysis. – International Journal of Biosciences 4: 407-424.
- [74] Qureshi, H., Arshad, M., Bibi, Y., Osunkoya, O. O., Adkins, S. W. (2018): Multivariate impact analysis of *Parthenium hysterophorus* invasion on above-ground plant diversity of Pothwar region of Pakistan. – Applied Ecology and Environmental Research 16: 5799-5813.
- [75] Reznik, S. Y. (2009): Common ragweed (*Ambrosia artemisiifolia* L.) in Russia: spread, distribution, abundance, harmfulness and control measures. – Ambrosie, The first international ragweed review 200926:
- [76] Riaz, T., Javaid, A. (2011): Prevalence of alien weed *Parthenium hysterophorus* L. in grazing and wastelands of District attock, Pakistan. – Journal of Animal and Plant Science 21: 542-545.
- [77] Royo-Esnal, A., Torra, J., Conesa, J. A., Forcella, F., Recasens, J. (2010): Modeling the emergence of three arable bedstraw (*Galium*) species. – Weed Science 58: 10-15.
- [78] Seier, M. K., Morin, L., Evans, H. C., Romero, Á. (2009): Are the microcyclic rust species *Puccinia melampodii* and *Puccinia xanthii* conspecific? – Mycological Research 113: 1271-1282.
- [79] Smittle, B. J., Adams, C. T., Banks, W. A., Lofgren, C. S. (1988): Red imported fire ants: feeding on radiolabeled citrus trees. – Journal of economic entomology 81: 1019-1021.
- [80] Stewart, J. W., Vinson, S. B. (1991): Red imported fire ant damage to commercial cucumber and sunflower plants. – Southwestern Entomologist 16: 168-1760.
- [81] Strother, J. L. (2006): *Ambrosia* Linnaeus, pp. 10-18. In Flora of North America Editorial Committee (ed.), Flora of North America: North of Mexico vol 21 Magnoliophyta: Asteridae, Part 8: Asteraceae, Part 3. Oxford University Press. –
- [82] Tóth, Á., Hoffmanné, P. Z., Szentey, L. (2004): A parlagfű (*Ambrosia elatior*) helyzet 2003-ban Magyarországon. – A levegő pollenzám csökkentésének nehézségei 14:
- [83] Tschinkel, W. R. (2006): The fire ants.-Harvard University Press,
- [84] Ustinova, A. F., Sizovenko, L. E. (2006): Invasive weeds in Ukraine. – Zashchita i Karantin Rastenii 9: 27-29.

- [85] Vander Meer, R. K., Lofgren, C. S., Seawright, J. A. (1995): Specificity of the red imported fire ant (Hymenoptera: Formicidae) phagostimulant response to carbohydrates. – Florida Entomologist 144-154.
- [86] Vilà, M., Espinar, J. L., Hejda, M., Hulme, P. E., Jarošík, V., Maron, J. L., Pergl, J., Schaffner, U., Sun, Y., Pyšek, P. (2011): Ecological impacts of invasive alien plants: a meta-analysis of their effects on species, communities and ecosystems. – Ecology letters 14: 702-708.
- [87] Vörös, G., Gallé, L. (2002): Ants (Hymenoptera: Formicidae) as primary pests in Hungary: recent observations. – Tiscia 33: 31-35.
- [88] Wahyuno, D. (2012): *Puccinia xanthii* Penyebab Bercak Daun pada *Xanthium* sp. di Indonesia. – Jurnal Fitopatologi Indonesia 8: 116-119.
- [89] Wan, F. H., Wang, R., Ding, J. 1995: Biological control of *Ambrosia artemisiifolia* with introduced insect agents, *Zygogramma suturalis* and *Epiblema strenuana*. – Proceedings of the eighth international symposium on biological control on weeds. 193-200.
- [90] Wilson, C., Tisdell, C. (2001): Why farmers continue to use pesticides despite environmental, health and sustainability costs. – Ecological economics 39: 449-462.
- [91] Wilson, C. L. (1969): Use of plant pathogens in weed control. – Annual Review of Phytopathology 7: 411-434.
- [92] Yaacoby, T., Seplyarsky, V. (2011): *Epiblema strenuana* (Walker, 1863)(Lepidoptera: Tortricidae), a new species in Israel. – EPPO Bulletin 41: 243-246.
- [93] Zereen, A., Ahmad, S. S., Jahan, A. (2018): Determination of correlation between plant distribution and ecological factors in Narowal district Punjab, Pakistan. – Bangladesh Journal of Botany 47: 451-458.
- [94] Zhang, P., Lu, G.-z., Sun, X.-d., Zhang, W., Qu, B., Tian, X.-l. (2011a): The infection process of *Puccinia xanthii* f. sp. *Ambrosiae-trifidae* on *Ambrosia trifida*. – Botany 89: 771-777.
- [95] Zhang, W., Jiang, F., Ou, J. (2011b): Global pesticide consumption and pollution: with China as a focus. – Proceedings of the International Academy of Ecology and Environmental Sciences 1: 125.
- [96] Zhao, Y. Z., Feng, Y. L., Liu, M. C., Liu, Z. H. (2014): First Report of Rust Caused by *Puccinia xanthii* on *Xanthium orientale* subsp. *italicum* in China. – Plant disease 98: 1582-1582.
- [97] Zhou, Z.-S., Chen, H.-S., Zheng, X.-W., Guo, J.-Y., Guo, W., Li, M., Luo, M., Wan, F.-H. (2014): Control of the invasive weed *Ambrosia artemisiifolia* with *Ophraella communa* and *Epiblema strenuana*. – Biocontrol Science and Technology 24: 950-964.
- [98] Zhou, Z.-S., Guo, J.-Y., Chen, H.-S., Wan, F.-H. (2010): Effects of temperature on survival, development, longevity, and fecundity of *Ophraella communa* (Coleoptera: Chrysomelidae), a potential biological control agent against *Ambrosia artemisiifolia* (Asterales: Asteraceae). – Environmental Entomology 39: 1021-1027.
- [99] Zhou, Z., Wan, F., Guo, J. (2017): Common Ragweed *Ambrosia artemisiifolia* L. – Biological Invasions and Its Management in China, Springer 2:99-109.

EFFECTS OF GENOTYPE-BY-ENVIRONMENT INTERACTION ON THE MAIN AGRONOMIC TRAITS OF MAIZE HYBRIDS

YUE, H. W.¹ – WANG, Y. B.² – WEI, J. W.¹ – MENG, Q. M.² – YANG, B. L.³ – CHEN, S. P.¹ – XIE,
J. L.¹ – PENG, H. C.¹ – JIANG, X. W.^{4*}

¹*Dryland Farming Institute, Hebei Academy of Agriculture and Forestry Sciences, Hebei Provincial Key Laboratory of Crops Drought Resistance Research, Hengshui 053000, China*

²*Institute of Cereal and Oil Crops of Hebei Academy of Agriculture and Forestry Sciences, Shijiazhuang 050051, China*

³*Hebei Banghao Agricultural Development Co., Ltd., Shijiazhuang 050051, China*

⁴*College of Agronomy, Qingdao Agricultural University, Qingdao 266109, China*

(Received 16th Sep 2019; accepted 4th Dec 2019)

Abstract. The additive main effects and multiplicative interaction (AMMI) model and genotype main effects and genotype-by-environment interaction (GGE) biplot are commonly used to analyze multi environmental trial data. This study adopted the AMMI model and GGE biplot to comprehensively analyze the data on genotypes tested in the 2016–2017 Zhongcheng combined regional maize trial in China. Results showed that the traits highly and significantly differed across different genotypes (G) and environments (E). Significant or very significant genotype-by-environment interactions (GEI) were also found. With the exception of 100-kernel weight, the ratio of GEI for the remaining three traits was lower than that of E and higher than that of G. GEI was decomposed, and the interaction information of PCA1 and PCA2 in the interaction of four traits was significant. Hengyu1587 and Shiyu 1503 performed better than the other hybrids and were identified as excellent varieties across locations because of their outstanding performances according to a 2-year observation. The comprehensive utilization of the AMMI model and GGE biplot can enable the scientific and objective judgment of the high yield, stability, and adaptability of tested maize hybrids and provides theoretical support for the rational layout of maize hybrids in the environments of Hebei Province.

Keywords: *yield, stability, adaptability, AMMI model, GGE biplot*

Introduction

Maize (*Zea mays* L.) is an important industrial, feed, and food crop in China and plays an important role in the national economy (Yue et al., 2018a). The three major maize-producing areas in China are northeast spring, southwest mountainous, and Huanghuaihai summer, which has the largest maize concentration. The wheat–maize double cropping system is the planting mode in this region which accounts for approximately 1/3 of the planting area and output of the country and frequently experiences natural disasters, such as high winds, heavy rainfall, drought, mites, high temperatures, and low temperatures during the filling period (Zhang et al., 2015; Zhao and Yang, 2018). In addition, the continued occurrence of maize pests and diseases destabilizes the production from this area and results in a massive difference between the actual field yield and genetic yield potential of maize hybrids (Yue et al., 2018b). These problems have seriously hindered the healthy development of the maize industry. Breeding high-yielding and stable hybrids suitable for environmental conditions in various regions is necessary to achieve high and stable maize yields.

The combined regional trial of crop varieties is an important form of national and provincial regional trial that has emerged in the past 2 years and is an inevitable outcome of the modern seed industry. The combined regional trial of maize hybrids is the comprehensive evaluation of the yield, adaptability, stress resistance, quality, and representativeness of newly cultivated hybrids according to standard specifications (Bao et al., 2017; Zhao et al., 2018). Combined regional trials are performed to screen out genotypes with excellent performance, determine the best adaptation areas for the tested varieties, and maximize the yield potential in accordance with local conditions. Discriminative analysis between locations is an important aspect of combined regional trials. The scientific and effective selection of locations and the improvement of screening services for new hybrids are difficult problems encountered by agricultural researchers (Zhang et al., 2016; Blanche and Myers, 2016).

Yield and other important agronomic traits of maize hybrids are represented by genotype (G), environment (E), and genotype main effects and genotype–environment interaction effects (GEI). The GEI effect occurs when different hybrids face different Es. E affects G because of the GEI effect, which in turn causes changes in different hybrids (Ma’ali, 2008; Abakemal et al., 2016). A high interaction effect degrades the stability of maize hybrids. In general, maize hybrids that exhibit high and stable yields under different environmental conditions have good adaptability, a large promotion value, and an outstanding productivity but poor stability in local areas. Genotypes with special adaptability also have a high production promotion. Therefore, understanding the connotation and essence of the interaction effect is helpful for studying the stability of maize yields and agronomic traits under different environmental conditions.

Agricultural researchers have proposed numerous research methods, including ANOVA (Lin et al., 1992), principal component analysis (Perkins, 1972), high stability coefficient (Berzsenyi and Dang, 2008), coefficient of variation (Döring and Reckling, 2018), additive main effects and multiplicative interaction (AMMI model) (Zobel et al., 1988), and genotype main effects and GEI effect (GGE) biplot (Yan et al., 2000), for the analysis of crop genotype and environment interaction. The AMMI model and the GGE biplot have been commonly used for GEI analysis. The AMMI model, also known as the additive main effect product interaction model, is the combination of ANOVA and principal component analysis for maximizing the interaction between G and E and separating the sum of product terms with different values from additive model interactions. This technique can also maximize assessment accuracy (Thillainathan and Fernandez, 2001; Dehghani et al., 2016). The results of AMMI model analysis can be intuitively and concisely expressed and interpreted, thus aiding the stability analysis of varieties and the screening of G with special GEI effects and providing valuable information for the breeding of special varieties adapted for a particular environment (Lal, 2012). Several scholars have used the AMMI model for the GEI analysis of crops, such as maize (Ndhlela et al., 2014), wheat (Sareen et al., 2012), rice (Suwaero and Nasrullah, 2011), millet (Bashir et al., 2014), barley (Bocianowski et al., 2019) and potato (Thiyagu et al., 2012). The genotype main effect plus GEI (GGE) biplot method was first proposed by Yan to analyze the regional test data of wheat varieties (Yan et al., 2000). This method analyzes the data in the regional experiment in a 2D map, and the results only show the G effect and GEI related to variety evaluation. This technique has become an ideal tool for studying crop genotype stability and location discrimination (Kaya et al., 2006; Baxevanos et al., 2008; Laurie and Booyse, 2015; Rea et al., 2016; Dehghani et al., 2017). Nevertheless, any analytical method is

imperfect and has its own shortcomings. The AMMI model mainly considers the interaction between G and E. Comprehensively evaluating the G effect in the breeding and promotion of genotypes is necessary. Analysis results often focus on genotypes that are stable and high yielding or stable and low yielding while ignoring genotypes with high yields but poor stability and thus are subjected to certain restrictions during application (Akinwale et al., 2014). The GGE biplot reveals the GEI information in the form of maps and reflects the cultivar's environmental adaptability. Relying only on 2D plane mapping in the analysis will lead to a loss of a part of the GE's mutation information. Therefore, this approach has a certain risk. The AMMI model and the GGE biplot method can be combined for the regional trials of crop genotypes, to screen out genotypes with good yield and poor stability and apply them in specific regions, thus greatly improving the accuracy of results (Muthoni, 2015; Erdemci, 2018).

Here, the AMMI model and the GGE biplot were used to comprehensively evaluate the stability, adaptability, and discrimination in the Zhongcheng combined regional maize trial in Hebei province from 2016 to 2017. This work aims to provide a theoretical basis for the selection and utilization of maize hybrids in the Huanghuaihai summer maize area of China.

Materials and methods

Experimental data were derived from the Zhongcheng combined regional maize trial of Hebei Province, China. Thirteen hybrids from private and public companies were tested in 2016 and 2017, and Zhengdan 958 was used as a control hybrid. Information on the tested hybrids is shown in *Table 1*. The numbers of locations in 2016 and 2017 were 13 and 16, respectively. The latitude, longitude, altitude, and annual rainfall differed between locations as shown in *Table 2*.

Experimental design

Each location was designed by randomized complete block design (RCBD) with three repetitions. Each experimental plot contained 5 rows with dimensions of 6.7 m for each genotype, 6–8 rows were surrounded by protected areas, and 3 rows of each plot were harvested on time. The field management of each plot was slightly more intense than the field level and involved timely chemical weeding and pest control. Field management and measurements were completed on the same day in case of special weather. Integrated pest management methods, including the use of bait to trap rats. Thrips and armyworm are the most important pests in maize seedling stage, and the control measure is to use 4.5% high efficiency cypermethrin 15000 times liquid spray per hectare. The control of weeds is carried out in two stages. In the first stage, weeds are controlled by chemical agents (methalamin 3000 ml/ha plus 450 kg/ha) at pre-emergence stage. The second stage is to use 225 ml/ha of nitrocellulose at a concentration of 225 kg/ha of nitrocellulose in the 3-5 leaves of the post-emergence stage. Both pre-emergence and post-emergence weeding are directed sprayed under windless conditions. The sowing date was carried out on 10th-20th of June of each location, and the harvest period was controlled from 1th to 10th of October during 2016-2017. Each location was reasonably arranged for fertilizer application according to the respective soil measurement conditions, 150-200 kg N ha⁻¹ and 100-130 kg P₂O₅ ha⁻¹ were applied at the time of sowing date. The plant height and ear position of the hybrid were investigated during the milk maturity period, and lodging and folding were

investigated during the waxy stage. The traits of 100-grain weight, ear length, and kernel weight were investigated after harvest and the grain yield has been corrected for 14% moisture at each location.

Table 1. Basic information of the hybrids in the Zhongcheng maize combined regional trial in 2016–2017

Hybrid	Abbreviation	Growth period (d)	Breeding institute	Year
Jiyu 974	J974	106	Institute of Cereal and Oil Crops, Hebei Academy of Agriculture and Forestry Sciences	2016
Jiyu 610	J610	108	Institute of Cereal and Oil Crops, Hebei Academy of Agriculture and Forestry Sciences	2016
Jiyu 906	J906	106	Institute of Cereal and Oil Crops, Hebei Academy of Agriculture and Forestry Sciences	2016-2017
JL 658	JL658	105	Jifeng Seed Industry, Hebei	2016
Xingyu 26	X26	105	Xingtai Agricultural Science Research Institute	2016
Xingyu 375	X375	108	Xingtai Agricultural Science Research Institute	2016
Hengyu 1587	H1587	106	Dryland Farming Institute, Hebei Academy of Agriculture and Forestry Sciences	2016-2017
Hengyu 12	H12	106	Dryland Farming Institute, Hebei Academy of Agriculture and Forestry Sciences	2016
Shiyu 1501	S1501	108	Shijiazhuang Academy of Agricultural and Forestry Sciences	2016
Shiyu 1503	S1503	107	Shijiazhuang Academy of Agricultural and Forestry Sciences	2016-2017
Cangkeyu 1	C1	106	Cangzhou Academy of Agriculture and Forestry Sciences	2016
Tangyu 5115	T5115	108	Tangshan Academy of Agricultural and Forestry Sciences	2016
Zhengdan 958 CK	Z958	108	Henan Academy of Agriculture and Forestry Sciences	2016-2017
RT 3321	RT3321	107	Hebei Banghao Agricultural Development Co., Ltd.	2017
Cangyu 168	C168	108	Cangzhou Academy of Agriculture and Forestry Sciences	2017
Cangyu 268	C268	107	Cangzhou Academy of Agriculture and Forestry Sciences	2017
Hengyu 6084	H6084	106	Dryland Farming Institute, Hebei Academy of Agriculture and Forestry Sciences	2017
Jiyu 202	J202	107	Institute of Cereal and Oil Crops, Hebei Academy of Agriculture and Forestry Sciences	2017
Jiyu 7176	J7176	106	Institute of Cereal and Oil Crops, Hebei Academy of Agriculture and Forestry Sciences	2017
Tangyu 6925	T6925	108	Tangshan Academy of Agricultural and Forestry Sciences	2017
Xingyu 1511	X1511	106	Xingtai Agricultural Science Research Institute	2017
Xingyu 1799	X1799	106	Xingtai Agricultural Science Research Institute	2017

Table 2. Basic information of the locations and its code in the trials in 2016-2017

Location	Abbreviation	Longitude E	Latitude N	Altitude (m)	Annual rainfall (mm)	Year
Mancheng	MC	114°48'	38°52'	137	547	2016-2017
Handan	HD	114°54'	36°63'	55	515	2016-2017
Gaocheng	GC	114°85'	38°02'	59	494	2016-2017
Dingxing	DX	115°80'	39°20'	28	551	2016-2017
Shenzhou	SZ	115°56'	38°01'	29	482	2016-2017
Botou	BT	115°91'	38°09'	16	547	2016-2017
Luquan	LQ	114°20'	38°05'	90	540	2016-2017
Zhaoxian	ZX	114°76'	37°48'	42	351	2016-2017
Renxian	RX	114°40'	37°15'	33	498	2016-2017
Longyao	LY	114°46'	37°22'	35	524	2016-2017
Cangzhou	CZ	116°49'	38°18'	78	581	2016
Qingxian	QX	116°79'	38°58'	6	618	2016
Fengnan	FN	118°08'	39°34'	20	675	2016-2017
Qianying	QY	116°26'	38°21'	10	620	2017
Houying	HY	116°38'	38°44'	15	617	2017
Luanxian	LX	118°42'	39°45'	33	697	2017
Langfang	LF	116°42'	39°34'	27	554	2017
Yongnian	YN	114°38'	36°44'	48	583	2017

Data analysis

AMMI model

The formula for the AMMI model is as follows:

$$y_{ge} = \mu + \alpha_g + \beta_e + \sum_{n=1}^N \lambda_n \gamma_{gn} \delta_{en} + \theta_{ge} \quad (\text{Eq.1})$$

where y_{ge} represents the yield of genotype (g) in the environment (e), μ is the grand mean, α_g represents the average deviation of g from μ , β_e represents the average deviation of e from μ , λ_n is the n th eigenvalue of interaction effect principal component axis, γ_{gn} is the G principal component score representing the n th principal component, δ_{en} represents the environmental principal component score of the n th principal component, and θ_{ge} is the error term.

GGE biplot method

The yield and ear trait data in the regional trials of the Zhongcheng combined regional maize trial were compiled into a two-way table with G and E . Each test value was the average value of each hybrid in the corresponding location, and the calculation formula is as follows:

$$Y_{ge} - y_e = \lambda_1 \xi_{g1} \eta_{e1} + \lambda_2 \xi_{g2} \eta_{e2} + \varepsilon_{ge} \quad (\text{Eq.2})$$

where Y_{ge} is the yield of genotype g in environment e ; y_e is the yield performance of all varieties in environment e ; $\lambda_1\xi_{g1}\eta_{e1}$ and $\lambda_2\xi_{g2}\eta_{e2}$ represent the first and second principal component scores of genotype g in the environment e , respectively; λ_1 and λ_2 are the eigenvectors of the first and second principal components, respectively; ξ_{g1} and ξ_{g2} are the first and second eigenvector scores of environment e , respectively; and ε_{ge} represents the residuals in the model (Balestre et al., 2009). AMMI model and GGE biplot analyses were performed using DPSV18.0 edition (Tang and Zhao, 2013).

Results

Ear traits and yield performance of maize hybrids

100 kernel weight

As shown in *Figure 1*, in 2016, the average 100-kernel weight was 39.03 g for Xingyu 26 and 38.85 g for Hengyu 12. These values were significantly higher than that of the control hybrid Zhengdan 958. The 100-kernel weight of Shiyu 1501 had a minimum value of 31.89, which was significantly lower than that of Zhengdan 958.

In the 2017 Zhongcheng combined regional maize trial, the average 100-kernel weights of Xingyu 1799, Jiyu 7176, Hengyu 6084, Tangyu 6925 and Hengyu 1587 were 39.21, 39.20, 37.38, 35.99, and 35.89 g, respectively. These values were significantly higher than that of Zhengdan 958. The average of 100-kernel weights of Jiyu 906, Jiyu 202, and RT3321 were lower than those of Zhengdan 958, but the differences between these values were not significant. The 100-kernel weights of other varieties were significantly lower than that of Zhengdan 958.

Grain yield

In the 2016 Zhongcheng combined regional maize trial, the highest average grain yield of Shiyu 1501 was 10.44 t ha⁻¹. The average grain yields of Shiyu 1502 and Hengyu 1587 were 10.41 and 10.33 t ha⁻¹, respectively, which ranked second and third, respectively. The highest average grain yields of Xingyu 26 and Jiyu 906 were 10.10 and 10.01 t ha⁻¹, respectively. The average grain yields of the above hybrids increased significantly compared with those of the control hybrid Zhengdan 958. JL658 and the control Zhengdan 958 had the same yield, and the average grain yields of other hybrids were significantly reduced compared with those of the control.

In the 2017 Zhongcheng combined regional maize trial, the grain yields of Hengyu 1587, Shiyu 1503, Tangyu 6925 and Jiyu 906 were higher than those of Zhengdan 958 and were 10.53, 10.50, 10.40, and 10.26 t ha⁻¹, respectively. No significant differences existed between these varieties and Zhengdan 958. The yields of Hengyu 6084, Jiyu 202 and Xingyu 1511 were 10.14, 10.12, and 10.06 t ha⁻¹, respectively, and were insignificantly lower than those of the control. The grain yield of the other varieties was significantly lower than that of Zhengdan 958.

Grain weight per ear

In 2016, Jiyu 974 had the highest average grain weight per ear of 167.96 g, followed by Xingyu 375 (164.53 g) and Hengyu 1587. The average grain weight per ear of Xingyu 26 and Shiyu 1503 was 164.48 g. The average grain weights per ear of JL658 and Shiyu 1501 ranked fourth and seventh, respectively, and were insignificantly higher

than those of the control. The average grain weights per ear of Jiayu 906, Hengyu 12, Tangyu 5115, and Cangkeyu 1 were lower than those of control hybrid. The average grain weight per ear of Cangkeyu 1 was the lowest (141.59 g) and was significantly different from that of Zhengdan 958.

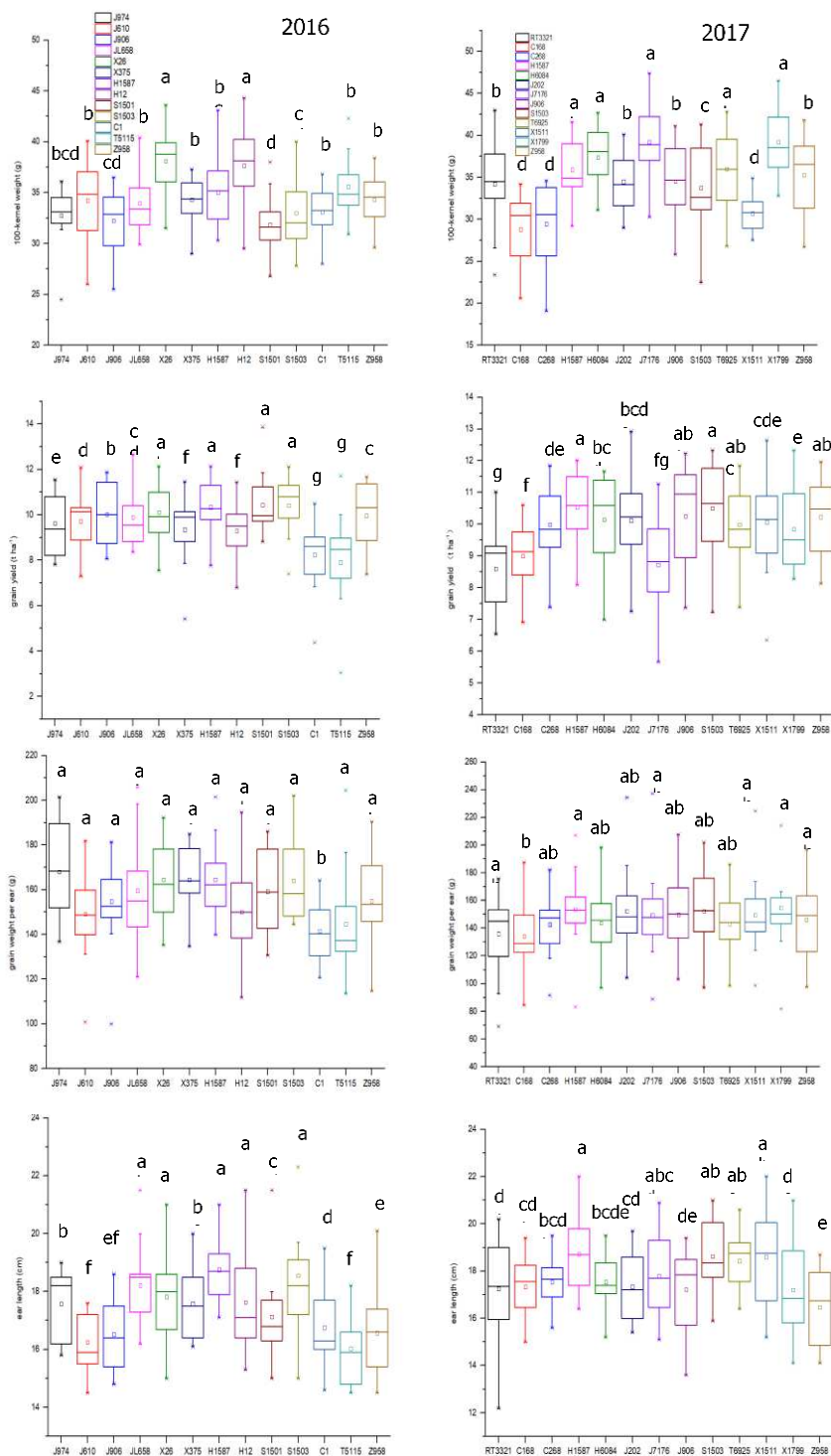


Figure 1. Traits average performance of maize hybrids in 2016-2017. The lowercase letters indicate significant difference at the 0.05 level

In the 2017 test, Xingyu 1799 had the highest average grain weight per ear of 154.96 g, followed by Hengyu 1587 at 153.58 g and Jiyu 202 at 152.53 g. The average grain weights per ear of Hengyu 6084, Tangyu 6925, Cangyu 268, RT3321, and Cangyu 168 were lower than that of the control hybrid Zhengdan 958.

Ear length

In 2016, Hengyu 1587 had the highest average ear length of 18.75 cm, followed by Shiyu 1503 and JL 658. The average ear lengths of Xingyu 26, Hengyu 12, Shiyu 1501, and Cangkeyu 1 ranked fourth, fifth, sixth, and seventh, respectively, and were significantly higher than that of the control. The average ear lengths of Jiyu 906, Jiyu 610, and Tangyu 5115 were lower than that of the control. Significant difference was found between Jiyu 906 and Zhengdan 958 but not between the two hybrids and the control hybrid Zhengdan 958.

In 2017, the average ear length of all tested hybrids was higher than that of the control. Among them, Hengyu 1587 had the highest with 18.72 cm, followed by Shiyu 1503, Xingyu 1511, and Jiyu 7176 with 18.62, 18.61, and 17.78 cm, respectively. The differences between the above hybrids and the control were significant. The values for other hybrids did not reach significant levels.

Analysis of AMMI model for various traits of maize hybrids

100-kernel weight

Variance analysis for 100-kernel weight in 2016 showed that G, E, and GEI were extremely significant (*Table 3*). The squared sum of G accounted for 39.39% of the sum of squares. The square of the GEI had a total squared sum of 36.40%. The ratio of square sum to the sum of squares for E was the smallest at 24.21%. The interaction between G and GEI had a greater impact on 100-kernel weight than E. GEI was 1.5 times higher than E, indicating that the former is crucial for the reasonable evaluation of 100-kernel weight. GEI was decomposed by the AMMI model, and the interaction effects of the first two principal component axes (PCA1 and PCA2) reached extremely significant levels. The square sums of PCA1 and PCA2 accounted for 33.01% and 21.34% of the sum of the interaction effects, respectively.

Variance analysis for 100-grain weight in the 2017 trial showed that the squared sum of G and E accounted for 36.19% and 35.66% of the sum of squares, respectively (*Table 4*). GEI squared accounted for 28.15% of the sum of squares, and G effects and E effects reached extremely significant levels. However, GEI effect was not significant. AMMI model analysis showed that the *P*-value of the GEI effect expressed by PCA1 and PCA2 was less than 0.01 and reached a very significant level, and the sum of the squares accounted for 31.02% and 20.77% of the square of the interaction effect.

Grain yield

Variance analysis of grain yield in the 2016 regional trial showed that the square sum of the E accounted for 46.67% of the total squared sum, that of GEI accounted for 31.06%, and the square of G accounted for 22.26%. G, E, and GEI effects reached a very significant level. E effect accounted for the largest proportion of the total effect. The variations of E and GEI were 2.10 times and 1.40 times that of genotype variation,

respectively. Therefore, analyzing the stability of grain yield was necessary. PCA1 and PCA2 accounted for 41.04% and 23.55% of the sum of the GEI effects, respectively, and both reached extremely significant levels.

Table 3. Results of each trait analysis of variance and AMMI model analysis in 2016

Items	Source of variation	Degree of freedom	Sum of squares	Mean square	F value	P value	Percentage of total sum of squares (%)
100-kernel weight	Total	168	1907.70	11.36			
	Genotype	12	751.35	62.61	17.60**	< 0.0001	39.39
	Environment	12	461.95	38.50	10.82**	< 0.0001	24.21
	Genotype and environment interaction (G×E)	144	694.39	4.82	1.36*	0.0431	36.40
	PCA1	23	229.21	9.97	2.80**	0.0002	33.01
	PCA2	21	148.20	7.06	1.98*	0.0114	21.34
	Error	119	423.33	3.56			
Grain yield	Total	168	433.20	2.58			
	Genotype	12	96.45	8.04	14.53**	< 0.0001	22.26
	Environment	12	202.19	16.85	30.45**	< 0.0001	46.67
	Genotype and environment interaction (G×E)	144	134.56	0.93	1.69**	0.0016	31.06
	PCA1	23	55.22	2.40	4.34**	< 0.0001	41.04
	PCA2	21	31.69	1.51	2.73**	0.0003	23.55
	Error	119	65.84	0.55			
Grain weight per ear	Total	168	76763.01	456.92			
	Genotype	12	11106.85	925.57	4.94**	< 0.0001	14.47
	Environment	12	35443.89	2953.66	15.75**	< 0.0001	46.17
	Genotype and environment interaction (G×E)	144	30212.27	209.81	1.12	0.2636	39.36
	PCA1	23	7530.63	327.42	1.75*	0.0286	24.93
	PCA2	21	5992.86	285.37	1.52	0.0827	19.84
	Error	119	22317.71	187.54			
Ear length	Total	168	449.73	2.68			
	Genotype	12	120.15	10.01	12.79**	< 0.0001	26.72
	Environment	12	169.18	14.10	18.02**	< 0.0001	37.62
	Genotype and environment interaction (G×E)	144	160.41	1.11	1.42*	0.0233	35.67
	PCA1	23	53.34	2.32	2.96**	0.0001	33.25
	PCA2	21	36.94	1.76	2.25**	0.0033	23.03
	Error	119	93.13	0.78			

Table 4. Results of each trait analysis of variance and AMMI model analysis in 2017

Items	Source of variation	Degree of freedom	Sum of squares	Mean square	F value	P value	Percentage of total sum of squares (%)
100-kernel weight	Total	207	5761.09	27.83			
	Genotype	12	2084.88	173.74	26.05**	< 0.0001	36.19
	Environment	15	2054.31	136.95	20.54**	< 0.0001	35.66
	Genotype and environment interaction (G×E)	180	1621.90	9.01	1.35*	0.0278	28.15
	PCA1	26	503.11	19.35	2.90**	< 0.0001	31.02
	PCA2	24	336.86	14.04	2.10**	0.0037	20.77
	Error	152	1013.58	6.67			
Grain yield	Total	207	433.36	2.09			
	Genotype	12	79.77	6.65	14.32**	< 0.0001	18.41
	Environment	15	208.74	13.92	29.97**	< 0.0001	48.17
	Genotype and environment interaction (G×E)	180	144.86	0.80	1.73**	0.0003	33.43
	PCA1	26	58.51	2.25	4.85**	< 0.0001	40.39
	PCA2	24	33.12	1.38	2.97**	< 0.0001	22.87
	Error	152	70.58	0.46			
Grain weight per ear	Total	207	153812.95	743.06			
	Genotype	12	8316.55	693.05	3.58**	0.0001	5.41
	Environment	15	99346.57	6623.10	34.24**	< 0.0001	64.59
	Genotype and environment interaction (G×E)	180	46149.83	256.39	1.33*	0.0366	30.00
	PCA1	26	15342.13	590.08	3.05**	< 0.0001	33.24
	PCA2	24	8937.10	372.38	1.93**	0.0095	19.37
	Error	152	29399.43	193.42			
Ear length	Total	207	581.60	2.81			
	Genotype	12	92.25	7.69	9.01**	< 0.0001	15.86
	Environment	15	296.43	19.76	23.15**	< 0.0001	50.97
	Genotype and environment interaction (G×E)	180	192.92	1.07	1.26	0.0738	33.17
	PCA1	26	49.37	1.90	2.22**	0.0015	25.59
	PCA2	24	47.94	2.00	2.34**	0.0010	24.85
	Error	152	129.76	0.85			

Variance analysis for 2017 showed that G, E, and GEI accounted for 18.41%, 48.17% and 33.43% of the total squared sum, respectively, and all of them reached extremely significant levels. The variations in E and GEI were 2.62 and 1.82 times

higher than those of G. GEI was decomposed by the AMMI model, and the interaction information between PCA1 and PCA2 reached a very significant level. PCA1 and PCA2 accounted for 40.39% and 22.87% of the sum of square effects, respectively.

Grain weight ear

Variance analysis of regional trials in 2016 and 2017 showed that G and E differences reached extremely significant levels. GEI did not reach significant levels in 2016 but was significantly different in 2017. Environmental variation accounted for the majority of the variation in the 2-year regional trial. In 2016 and 2017, the sum of the squared environmental variances accounted for 46.17% and 64.59% of the total squared sum, respectively. The variations in GE and GEI were 2.72 and 5.55 times those of G effects, respectively. In 2016, PCA1 and PCA2 explained 44.77% and 52.61% of the square of the interaction effect. In 2016, the PCA1 interaction information reached a significant level, and PCA2 did not reach a significant level. PCA1 and PCA2 reached a very significant level in 2017.

The ear length

The variance analysis of ear length in 2016 showed that the squared sums of G, E, and GEI accounted for 26.72%, 37.62%, and 35.67%, respectively. G and E reached extremely significant differences. GEI effect reached a significant difference. AMMI model analysis showed that the square sum of PCA1 and PCA2 accounted for 33.25% and 23.03% of the sum of the square effects of the interaction, respectively. Both reached extremely significant levels. The AMMI model provided a thorough analysis of GEI effects.

Variance analysis revealed a significant difference between G and E in 2017. The sum of the squares accounted for 15.86% and 50.97% of the total squared sum, respectively, and the square of the interactions accounted for 33.17% of the total square but did not reach a significant level. The results of AMMI model analysis showed that PCA1 and PCA2 accounted for 50.44% of the sum of squares of interactions and reached extremely significant differences.

Adaptability analysis of tested varieties based on GGE biplot

The GGE biplot visually represents the varieties with outstanding performance in different environments with different traits. Each of the “vertex” hybrid in the biplot is sequentially connected by a straight line to form a polygon, which is divided into a plurality of sectors from its origin. Each test environment is embedded in the sector. The “top angle” hybrid in each sector is the best-performing genotype in a certain environment (Yue et al., 2019a).

100-kernel weight

Adaptive analysis showed that the biplot map for 100-kernel weight in 2016 was divided into six sectors (*Fig. 2-A1*). Shenzhou, Fengnan, and Renxian were in the first sector. Xingyu 26 performed best in this sector. The remaining locations were divided into the second sector, and Hengyu 12 was the best performing hybrid. Adaptive analysis showed that the biplot map for 100-kernel weight in 2017, and the biplot map was divided into four sectors (*Fig. 2-B1*). The first sector included three locations in Shenzhou, Gaocheng, and Dingxing. Tangyu 6925 performed best in this sector. Hengyu 6084 had

good adaptability in Zhaoxian, Botou, Qixian, and Luquan, and Hengyu 6084 showed the best performance in the second sector. The remaining locations were distributed in the third sector, wherein Xingyu 1799 and Jiyu 7176 showed the best performance. The fourth sector did not show a location, indicating that Cangyu 168, Cangyu 268, and Xingyu 1511 in this sector were not satisfactory in all locations.

Grain yield

The 13 locations of the 2016 regional trial were divided into three sectors (*Fig. 2-A2*). Only Botou was located in the first sector, and Cangkeyu 1 showed the best performance. Zhaoxian, Longyao, Luquan, Mancheng, Dingxing, Cangzhou, Shenzhou, Gaocheng, Fengnan, and Qingxian were located in the second sector. Hengyu 1587 and Shiyu 1501 performed well in these locations. The third sector did not contain a location and included only Tangyu 5115. This result showed that Tangyu 5115 performed poorly in all locations. In 2017, the 16 plots of regional trial were divided into four sectors (*Fig. 2-B2*). Jiyu 202 exhibited outstanding performance in Botou, Shenzhou, Qianying, Gaocheng, Dingxing, and Longyao. Shiyu 1503 performed best in the remaining locations, and Hengyu 1587, Xingyu 1511, and Xingyu 1799 had strong adaptability.

Grain weight per ear

In 2016, 13 plots were divided into five sectors (*Fig. 2-A3*). Luquan, Cangzhou, Shenzhou, Qingxian, and Fengnan were classified as the first sector, and Hengyu 1587 had good adaptability in the above locations. The second sector had four locations, namely, Handan, Gaocheng, Mancheng, and Longyao. Jiyu 974 performed best in this sector. Renxian, Zhaoxian, and Botou were located in the third sector, and Xingyu 26 performed best. The fourth sector had only one location, and Cangkeyu 1 and Hengyu12 performed well in the Dingxing location. A location drop was not observed in the fifth sector, indicating that Tangyu 5115 and Jiyu 610 in this sector did not perform well in all locations. In 2017, 16 plots of the regional trial were divided into four sectors (*Fig. 2-B3*). The first sector only had one location in Zhaoxian, and RT3321 performed best in this sector. Botou, Dingxing, Langfang, Fengnan, Houying, and Luquan belonged to the second sector, and Xingyu 1799 had good adaptability in these locations. Mancheng, Yucheng, and Qianying belonged to the third sector, and Jiyu 7176 performed best. The remaining locations belonged to the fourth sector, and Jiyu 202 performed best.

Ear length

The adaptation analysis of the 2016 regional trial based on ear length showed that Shiyu 1503 performed best in the locations of Dingxing, Qingxian, Handan, and Zhaoxian. Hengyu 1587 had strong adaptability in Luquan, Zhangzhou, Yucheng, Shenzhou, Botou, Mancheng, and Renxian. Jiyu 974, Jiyu 906, Jiyu 610, Tangyu 5115, Shiyu 1501, and Cangkeyu 1 had unsatisfactory performances in all locations (*Fig. 2-A4*). The results of the adaptation analysis of the 2017 regional trial based on ear length were obtained (*Fig. 2-B4*). Xingyu 1511 showed good adaptability in Langfang, Longyan, Renxian, Zhaoxian, Qixian, Shenzhou, Luquan, and Botou locations. Shiyu 1503 and Hengyu 1587 had good adaptability in different locations, such as Gaocheng, Dingxing, Handan, Mancheng, Houying, and Yongnian. The performance of all varieties in Qianying was not satisfactory, and the performances of Zhengdan 958 and Xingyu 1799 were not satisfactory in all the locations.

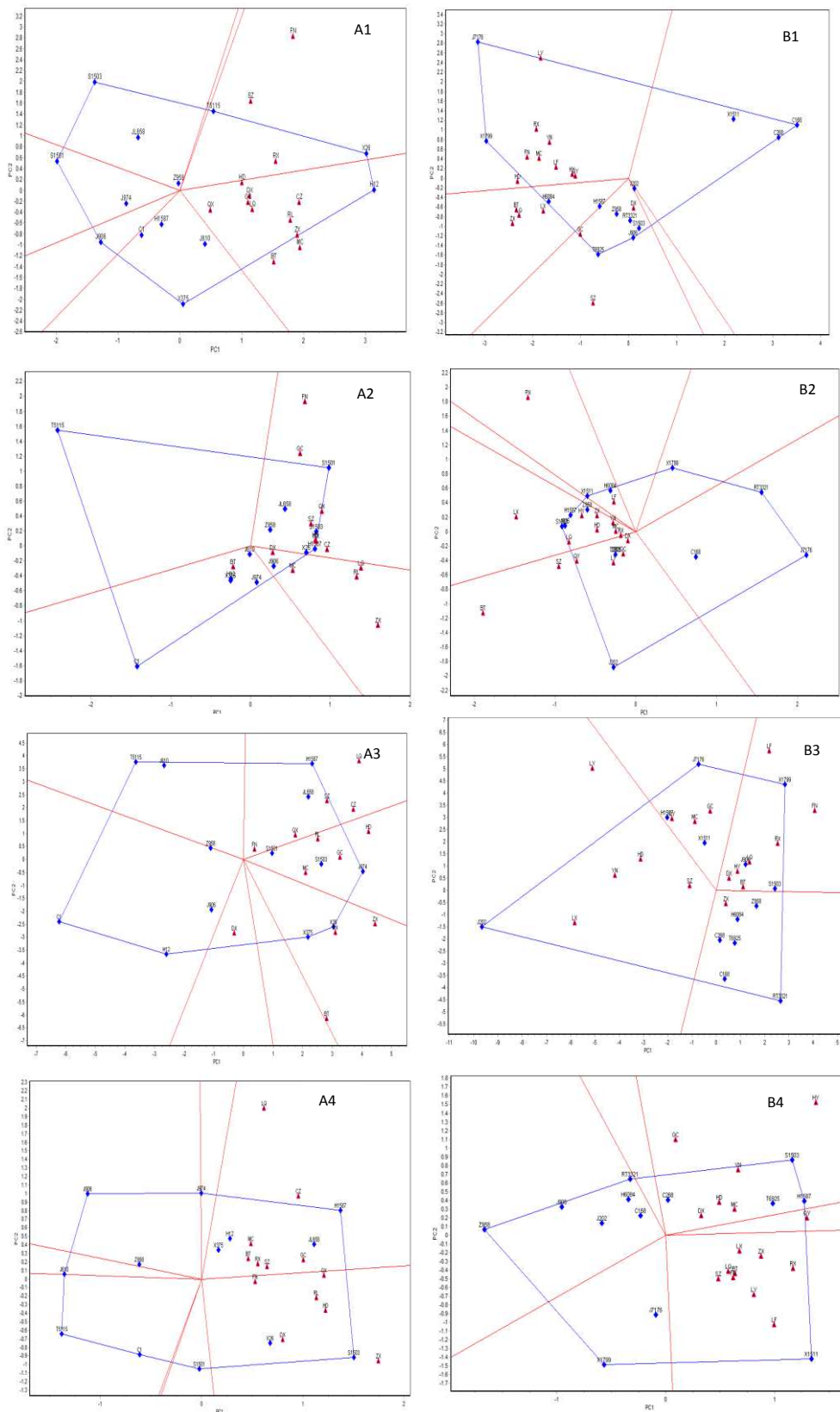


Figure 2. Adaptability analysis of maize hybrids based on GGE-biplot analysis. A: field data in 2016; B: field data in 2017; 1: 100-kernel weight; 2: grain yield; 3: grain weight per ear; 4: ear length (similarly hereinafter, the same below)

Analysis of the high yield and stability of the tested varieties based on GGE biplot

The small diamond in *Figure 3* represents the average environment, and the central straight line represents the average environmental axis. The genotypes in the double plot is perpendicular to the average environmental axis, and the high yield of the hybrids can be determined in accordance with the position and length of the vertical line. Vertical lines close to the average environment indicate that traits have high average values and are superior. Short vertical lines are indicative of small deviations from the average environmental axis and high trait stability (Sujay et al., 2012).

100-kernel weight

The analysis of 100-kernel weight and stability in the 2016 Zhongcheng combined regional maize trial revealed that Hengyu 12 had the highest weight, followed by Xingyu 26, Tangyu 5115, and Jiyu 610. Jiyu 906, Shiyu 1503, and Shiyu 1501 had poor performances in terms of 100-kernel weight. Hengyu 12, Zhengdan 958, Jiyu 974, Hengyu 1587, and Cangkeyu 1 had good stability, and Tangyu 5115, Xingyu 375, and Shiyu 1503 had poor performances (*Fig. 3-A1*). In the 2017 regional trial, Jiyu 7176 and Xingyu 1799 were closer to the average environment than other varieties. These two varieties had good 100-kernel weight performance. The performances of these varieties were followed by those of Hengyu 6084, Tangyu 6925, and Hengyu 1587. Xingyu 1511, Cangyu 268, and Cangyu 168 had low average 100-kernel weight. The stabilities of the 100-kernel weights of Jiyu 7176, Xingyu 1799, and Tangyu 6925 were poor, and those of the 100-kernel weights of Jiyu 202, Hengyu 6084, and Hengyu 1587 were good (*Fig. 3-B1*).

Grain yield

The grain yield in 2016 was analyzed (*Fig. 3-A2*). The yields of Shiyu 1501, Shiyu 1503, Hengyu 1587, and Xingyu 26 exceeded those of the control Zhengdan 958, Tang 5115, Cangkeyu 1, and Shiyu 1501, and the stability of the three varieties was significantly lower than that of the remaining varieties. In the 2017 regional trial, the yields of Shiyu 1503, Hengyu 1587, and Jiyu 906 were superior to those of Zhengdan 958. Cangyu 168, Cangyu 268, Hengyu 1587, and Shiyu 1503 had good stability (*Fig. 3-B2*).

Grain weight per ear

In the 2016 regional trial, the average grain weights per ear of Jiyu 974 were the highest, followed by those of Xingyu 26, Shiyu 1503, Xingyu 375, and Hengyu 1587. Cangkeyu1 had the lowest average grain weight per ear. The grain weight stabilities of Jiyu 974, Shiyu 1501, Shiyu 1503, and Zhengdan 958 were high, and those of other varieties were low (*Fig. 3-A3*). In the 2017 regional trial, the average grain weights of Jiyu 7176 were the highest, followed by those of Hengyu 1587, Xingyu 1799, Xingyu 1511, Jiyu 202, Jiyu 906, and Shiyu 1503. The average grain weights of the remaining varieties were lower than those of the control variety Zhengdan 958. The grain weight stabilities of Tangyu 6925, Xingyu 1511, Cangyu 268, and Hengyu 6084 were high, and those of Jiyu 202, Xingyu 1799, and Shiyu 1503 were poor (*Fig. 3-B3*).

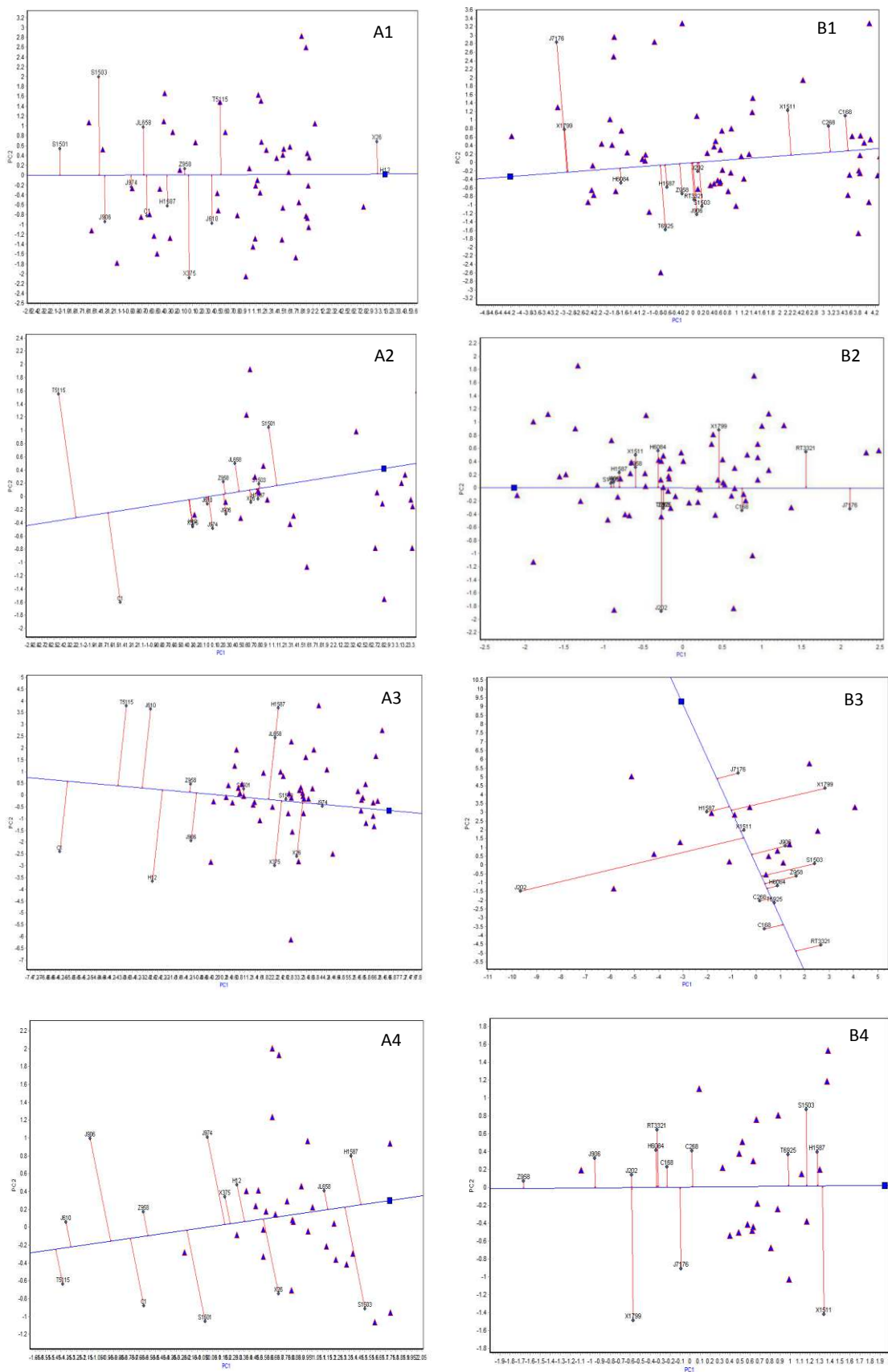


Figure 3. The yielding and stability of each trait of maize hybrids based on GGE-biplot analysis

Ear length

In the 2016 regional trial, the average ear length of Hengyu 1587 was the highest, and those of Shiyu 1503 and JL658 were ranked second and third, respectively. Those of Cangkeyu 1, Jiyu 906, Jiyu 610, and Tang 5115 were lower than those of the control. The ear lengths of Jiyu 658, Xingyu 375, Hengyu 12, Hengyu 1587, Tangyu 5115, and Zhengdan 958 were stable, and those of other varieties were unstable (*Fig. 3-A4*). In the 2017 regional trial, the average ear lengths of Xingyu 1511, Hengyu 1587, Shiyu 1503, and Tangyu 6925 were high, and Zhengdan 958 had the lowest average ear length. Zhengdan 958, Jiyu 202, Cangyu 168, and Hengyu 1587 had high stability, and Shiyu 1503, Jiyu 7176, Xingyu 1511, and Xingyu 1799 had poor stability (*Fig. 3-B4*).

Analysis of ideal varieties based on GGE biplot

The GGE biplot can be used to visually and clearly determine the position of an ideal genotype. The ideal hybrid is the genotype with the highest average yield and the best stability in all test environments. The ideal hybrid is presented as the center of a multilayered concentric circle, and the pros and cons of the tested hybrids are judged on the basis of their distance from the ideal hybrid. Genotypes close to the center of the concentric circle have good performance, and those far from the center of the circle have poor performance (Kendal and Tekdal, 2019).

100-kernel weight

As shown in *Figure 4-A1*, Hengyu 12 and Xingyu 26 were closer to the center of the concentric circle than other hybrids. These two hybrids had high 100-kernel weights and were stable. Jiyu 906, Shiyu 1503, and Shiyu 1501 were far from the center of the concentric circle and had low 100-kernel weights and poor stability. As shown in *Figure 4-B1*, Xingyu 1799 was closest to the center of the concentric circle, indicating that this hybrid had a high kernel weight and good stability. Xingyu 1511, Cangyu 268, and Cangyu 168 were far from the center of the concentric circle and had low 100-grain weights and poor stability.

Grain yield

As illustrated in *Figure 4-A2*, Shiyu 1501, Shiyu 1503, and Hengyu 1587 were close to the center of the concentric circle, indicating that these genotypes had good yield and stability. Cangkeyu 1 and Tangyu 5115 were far from the center of the circle and had low yield and poor stability. *Figure 4-B2* shows that Shiyu 1503, Jiyu 906, and Hengyu 1587 were closest to the center, indicating that these three varieties were high yielding and stable. Jiyu 202, Xingyu 1799, Cangyu 168, RT3321, and Xingyu 7176 were far from the center and had poor yield and stability.

Grain weight per ear

In 2016, Jiyu 974 was the closest to the center of concentric circles, indicating that its grain weight per ear was the highest and its stability was the best. The grain weight per ear of Cangkeyu 1 was opposite to that of Jiyu 974 and was the worst (*Fig. 4-A3*). In the 2017 regional trial, the grain weight per ear of Jiyu 7176 was the closest to the ideal value. Jiyu 7176 was a genotype with high grain weight per ear and good stability. The

grain weights per ear of Hengyu 1587, Xingyu 1511, and Xingyu 1799 were ideal, and the comprehensive performances of Cangyu 168 and RT3321 were poor (Fig. 4-B3).

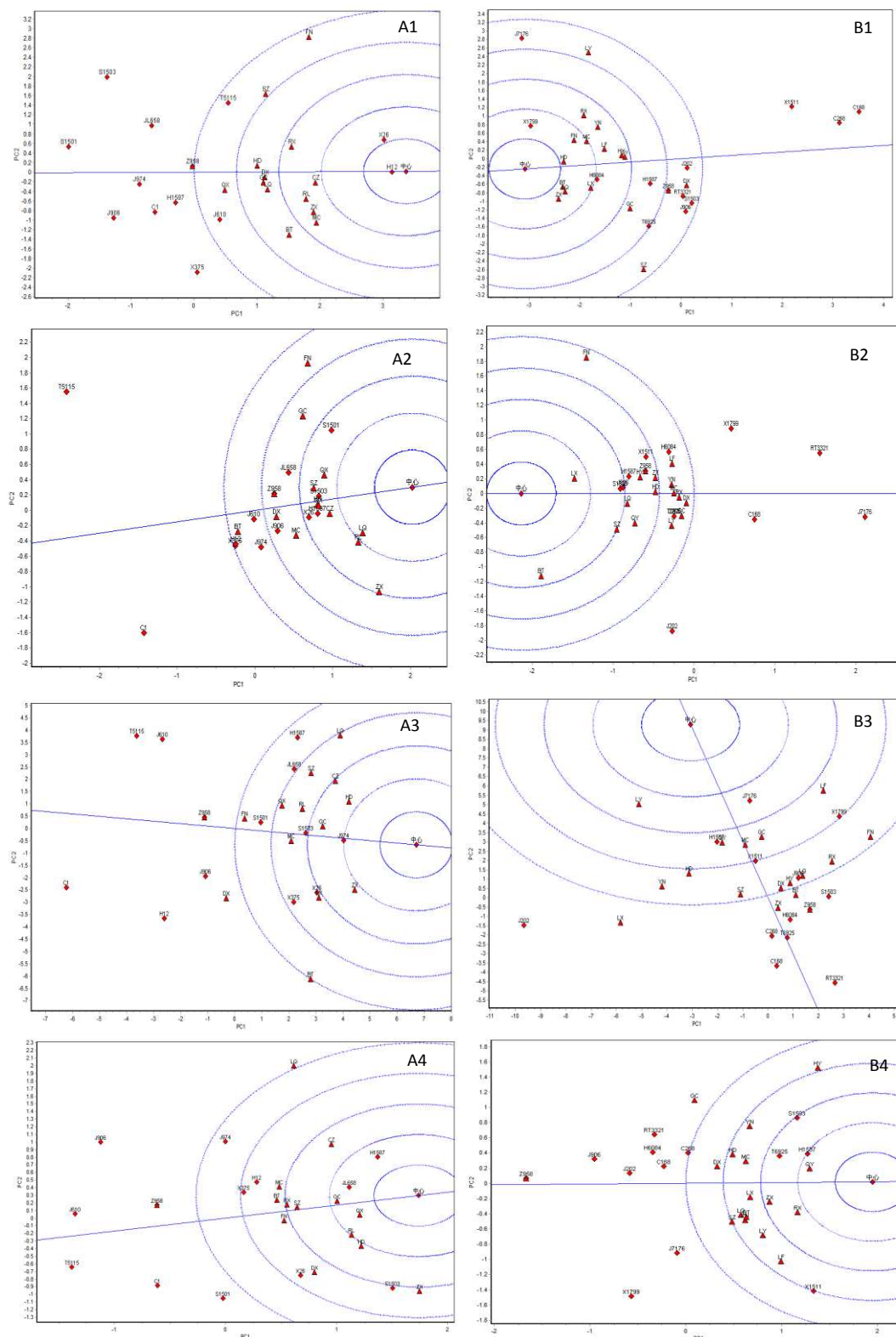


Figure 4. Comparisons of maize tested varieties with the ideal cultivar for each trait based on GGE biplot

Ear length

It can be seen from *Figure 4-A4* that the closest ideal genotypes in 2016 were Hengyu 1587 and JL 658, and the overall performance of the ear length was better. Genotypes such as Shiyu 1501, Cangkeyu 1, Zhengdan 958, Jiyu 906, Jiyu 610 and Tang 5115 had poor overall performance and are not ideal genotype. In the 2017 regional trial, Hengyu 1587 was the closest to the center of concentric circles, indicating that its overall ear length was excellent and belongs to the ideal genotype. Jiyu 202, Xingyu 1799, Jiyu 906 and Zhengdan 958 were far away from the center of concentric circles. Among them, Zhengdan 958 was the farthest from the center, and the overall performance of ear length was the worst (*Fig. 4-B4*).

Discussion

The traits of crop varieties are the results of G, E, and GEI. GEI directly affects the stability of varietal traits (Tekdal and Kendal, 2018). This study showed that in addition to 100-kernel weight, the effects of GEI on three agronomic traits were less than those of E, but had significant effects on traits that were greater than those of G. The GEI effect of three traits, such as grain yield, grain weight per ear, and ear length in 2016–2017 was 1.3–5.5 times that of G (Balestre et al., 2009; Badu-Apraku et al., 2012; Yue et al., 2019b). This result is consistent with previous results. Trait differences caused by crop G changes and GEI effects must be considered in the regional trial analysis of crop varieties. Only by fully studying and utilizing the effects of GEI can breeding efficiency be considerably improved. This requires us to promote corn production and rationally distribute of varieties. First, the appropriate promotion area must be selected in accordance with local light and heat resources. Then, suitable varieties must be screened on the basis of characteristics. The influence of GEI on varietal traits must be emphasized (Kandus et al., 2010). The 2-year analysis of variance showed that the 100-kernel weight of the tested varieties was less affected by external E and GEI. This indicates that 100-kernel weight is an inherent characteristic of the hybrid and is not easily affected by environmental changes. The expression of this trait is dominated by genotype effects.

The research and mastery of the variation in maize panicle traits are important bases for the breeding of high-yielding and stable maize hybrids and developing supporting cultivation techniques. Therefore, the stability analysis of important panicle traits and grain yield of maize genotypes can help fully understand the variation factors of varietal traits. The AMMI model can be used to calculate the AMMI stability value of the tested varieties in the form of a table and judge whether a genotype is high yielding and stable. The model focuses on GEI and enables the stability analysis of the genotypes. However, it fails to fully describe the adaptability of the varieties. The GGE biplot analysis compensates for this shortcoming. The GGE biplot map is a visual representation of the adapted area of the tested genotypes in a polygonal manner. This method focuses on the evaluation of varietal adaptability and yield (Erdemci, 2018; Malik et al., 2019). The GGE biplot analysis of the 2016 regional trial showed the adaptability of varieties on the basis of 100-kernel weight performance. Xingyu 26 and Hengyu 12 showed wide adaptability. The analysis of grain yield revealed that Hengyu 1587 and Shiyu 1501 had wide adaptability in 10 locations. The analysis of grain weight per ear revealed that Hengyu 1587, Jiyu 974, and Xingyu 26 had good adaptability in their respective regions. The analysis of ear length performance indicated that Shiyu 1503 and Hengyu

1587 had wide adaptability. According to the 100-kernel weight adaptation analysis of the GGE biplot of the regional trial in 2017, Tangyu 6925, Hengyu 6084, Xingyu 199 and Jiyu 7176 had strong adaptability. The analysis of grain yield showed that Jiyu 202, Shiyu 1503, Hengyu 1587, Xingyu 1511, and Xingyu 1799 were widely adaptable. The analysis of grain weight per ear indicated that Xingyu 1799, Jiyu 7176, and Jiyu 202 had wide adaptability. Ear length analysis revealed that Shiyu 1503 and Xingyu 1511 had wide adaptability.

Ideal genotypes have high yield, stability, and wide adaptability in different environments. In fact, this is an ideal assumption and is rare in actual agricultural production. The high yield, stability, and adaptability of crop varieties are important indicators in breeding. Breeders tend to focus on genotypes with good yield stability but often overlook varieties with high yield and outstanding stability but limited adaptability (Jain et al., 2019). The rational use of maize hybrids should be based on the premise of high yield, and some varieties with good stability and adaptability should be selected. Selecting hybrids with good stability and adaptability from genotypes with poor yield is inadvisable. The stability of maize hybrids must be based on the premise of high yield. The regional trials of maize hybrids revealed that some genotypes are suitable for specific regions. For example, in 2016, Cangkeyu 1 exhibited the best grain yield in the environment of Botou but showed general performance at other locations. It had the highest grain weight per ear in the Dingxing environment. In 2017, the grain yield of Jiyu 202 ranked first in the environments of Botou, Shenzhou, Qianying, Gaocheng, Dingxing, and Longyao but had general overall performance in the remaining locations. Cangkeyu 1 and Jiyu 202 had special adaptability and can be planted in suitable areas. Therefore, we should not only pay attention to genotypes with perfect characteristics, but also to the identification and utilization of special adaptive hybrids in production practice (Rakshit et al., 2012; Yue et al., 2019). Through the analysis of the results of AMMI and GGE in this study, the two analytical methods had similar results considering the specific adaptability to environmental conditions. Due to the GEI, both AMMI and GGE can effectively explore the variability in multi environmental trials (Mets) data, and both methods have been shown to be approximately equivalent, thus screening for genotypes with the highest yield and high stability (Neisse et al., 2018; Kendal et al., 2019).

Conclusion

Multi environmental trials are an effective means to identify good or bad maize hybrids. The scientific evaluation of the stability, yield, and adaptability of maize genotypes is an important link before the promotion of hybrids. We evaluated important agronomic traits, such as 100-kernel weight, grain yield, grain weight per ear and ear length of maize hybrids using the AMMI model and GGE biplot analysis. We observed significant differences in agronomic traits between different genotypes and environments and significant or extremely significant GEIs. Combined with the performance of 2 years of experiments, Hengyu 1587 and Shiyu 1503 presented good comprehensive performance, while Cangkeyu 1 and Jiyu 202 showed special adaptability. The comprehensive application of AMMI and GGE biplot can more accurately and intuitively evaluate the high yield, stability and adaptability of each hybrid as well as the resolution and representativeness of each location. This research can provide valuable theoretical reference for the identification and promotion of new maize hybrids.

Acknowledgements. This research was supported by the Appropriate Mechanization of New Summer Maize Variety Breeding, Demonstration and Promotion in North Huanghuaihai (Beijing-Tianjin-Hebei) (2017YFD0101202), the National Natural Science Foundation of China (31601386), the Special Fund for National System (Maize) of Modern Industrial Technology (nycyt-02), Science and Technology Support Program of Hebei Province (16226323D-X), the Special Fund for Agro-scientific Research in the Public Interest (201303002), the National Key Research and Development Program of China (2017YFD0701203), Shandong Key Research and Development Plan (Public Welfare Special Project, 2017GNC11103), A Project of Shandong Province Higher Educational Science and Technology Program (J18KA121).

REFERENCES

- [1] Abakemal, D., Shimelis, H., Derera, J. (2016): Genotype-by-environment interaction and yield stability of quality protein maize hybrids developed from tropical-highland adapted inbred lines. – *Euphytica* 209(3): 757-769.
- [2] Akinwale, R. O., Fakorede, M. A. B. Badu-Apraku, B. Oluwaranti, A. (2014): Assessing the usefulness of GGE biplot as a statistical tool for plant breeders and agronomists. – *Cereal Research Communications* 42(3): 534-546.
- [3] Badu-Apraku, B., Oyekunle, M., Obeng-Antwi, K., Osuman, A. S., Didjeira, A. (2012): Performance of extra-early maize cultivars based on GGE biplot and AMMI analysis. – *Journal of Agricultural Science* 150(4): 473-483.
- [4] Balestre, M., Von Pinho, R. G., Souza, J. C., Oliveira, R. L. (2009): Genotypic stability and adaptability in tropical maize based on AMMI and GGE biplot analysis. – *Genetics and Molecular Research* 8(4): 1311-1322.
- [5] Bao, Y., Hoogenboom, G., McClendon, R. Vellidis, G. (2017): A comparison of the performance of the CSM-CERES-Maize and EPIC models using maize variety trial data. – *Agricultural Systems* 150: 109-119.
- [6] Bashir, E. M. A., Ali, A. M., Ismail, M. I., Parzies, H. K., Haussmann, B. I. G. (2014): Patterns of pearl millet genotype-by-environment interaction for yield performance and grain iron (Fe) and zinc (Zn) concentrations in Sudan. – *Field Crop Research* 166: 82-91.
- [7] Baxevanos, D., Goulas, C., Rossi, J., Braojos, E. (2008): Separation of cotton cultivar testing sites based on representativeness and discriminating ability using GGE biplots. – *Agronomy Journal* 100: 1230-1236.
- [8] Berzsenyi, Z., Dang, Q. L. (2008): Effect of various crop production factors on the yield and yield stability of maize in a long-term experiment. – *Cereal Research Communications* 36(1): 167-176.
- [9] Blanche, S. B., Myers, G. O. (2016): Identifying discriminating locations for cultivar selection in Louisiana. – *Crop Science* 46: 946-949.
- [10] Bocianowski, J., Warzecha, T., Nowosad, K., Bathelt, R. (2019): Genotype by environment interaction using AMMI model and estimation of additive and epistasis gene effects for 1000-kernel weight in spring barley (*Hordeum vulgare* L.). – *Journal of Applied Genetics* 60: 127-135.
- [11] Dehghani, M. R., Majidi, M. M., Mirlohi, A., Saeidi, G. (2016): Study of genotype by environment interaction in tall fescue genotypes and their polycross progenies in Iran based on AMMI model analysis. – *Crop Pasture Science* 67: 792-799.
- [12] Dehghani, M. R., Majidi, M. M., Saeidi, G., Mirlohi, A., Amiri, R., Sorkhilalehloo, B. (2017): Application of GGE biplot to analyse stability of Iranian tall fescue (*Lolium arundinaceum*) genotypes. – *Crop Pasture Science* 66: 963-972.
- [13] Döring, T. F., Reckling, M. (2018): Detecting global trends of cereal yield stability by adjusting the coefficient of variation. – *European journal Agronomy* 99: 30-36.
- [14] Erdemci, I. (2018): Investigation of genotype×environment interaction in chickpea genotypes using AMMI and GGE biplot analysis. – *Turkish Journal of Field Crops* 23(1): 20-26.

- [15] Jain, B. T., Sarial, A. K., Kaushik, P. (2019): Understanding $G \times E$ interaction of elite basmati rice (*Oryza sativa* L.) genotypes under north Indian conditions using stability models. – *Applied Ecology and Environmental Research* 17(3): 5863-5885.
- [16] Kandus, M., Almorza, D. R., Salerno, J. C. (2010): Statistical models for evaluating the genotype-environment interaction in maize (*Zea mays* L.). – *Phyton* 79(1): 39-46.
- [17] Kaya, Y., Akcura, M., Taner, S. (2006): GGE-biplot analysis of multi-environment yield trials in bread wheat. – *Turkish Journal of Agriculture and Forestry* 30: 325-337.
- [18] Kendal, E., Tekdal, S. (2019): Proficiency of biplot methods (AMMI and GGE) in the appraisal of triticale genotypes in multiple environments. – *Applied Ecology and Environmental Research* 17(3): 5995-6007.
- [19] Lal, R. K. (2012): Stability for oil yield and variety recommendations' using AMMI (additive main effects and multiplicative interactions) model in Lemongrass (*Cymbopogon* species). – *Industrial Crops and Products* 40: 296-301.
- [20] Laurie, S. M., Booyse, M. (2015): Employing the GGE SREG model plus Elston index values for multiple trait selection in sweet potato. – *Euphytica* 204(2): 433-442.
- [21] Lin, C. S., Butler, G., Hall, I., Nault, C. (1992): Program for investigating genotype-environment interaction. – *Agronomy Journal* 84(1): 121-124.
- [22] Ma'ali, S. H. (2008): Additive mean effects and multiplicative interaction analysis of maize yield trials in South Africa. – *South African Journal of Plant and Soil* 25(4): 185-193.
- [23] Malik, W. A., Forkman, J., Hans-Peter, P. (2019): Testing multiplicative terms in AMMI and GGE models for multi-environment trials with replicates. – *Theoretical and Applied Genetics* 132: 2087-2096.
- [24] Muthoni, J., Shimelis, H., Melis, R. (2015): Genotype \times environment interaction and stability of potato tuber yield and bacterial wilt resistance in Kenya. – *American Journal of Potato Research* 92(3): 367-378.
- [25] Neisse, A. C., Kirch, J. L., Hongyu, K. (2018): AMMI and GGE biplot for genotype \times environment interaction: a medoid-based hierarchical cluster analysis approach for high-dimensional data. – *Biometrical Letters* 55(2): 97-121.
- [26] Ndhlela, T., Herselman, L., Magorokosho, C., Labuschagne, M. (2014): Genotype \times environment interaction of maize grain yield using AMMI biplots. – *Crop Science* 54: 1992-1999.
- [27] Perkins, J. M. (1972): The principal component analysis of genotype-environmental interactions and physical measures of the environment. – *Heredity*. 64: 51-70.
- [28] Rakshit, S., Ganapathy, K. N., Gomashe, S. S. (2012): GGE biplot analysis to evaluate genotype, environment and their interactions in sorghum multi-location data. – *Euphytica* 185(3): 465-479.
- [29] Rea, R., Sousa-Vieira, O. D., Díaz, A., Ramón, M., Briceño, R., George, J. (2016): Genotype-environment interaction, megaenvironments and two-table coupling methods for sugarcane yield studies in Venezuela. – *Sugar Tech* 18(4): 354-364.
- [30] Sareen, S., Munjal, R., Singh, B. N., Verma, R. S., Meena, B. K. (2012): Genotype \times environment interaction and AMMI analysis for heat tolerance in wheat. – *Cereal Research Communications* 45(2): 267-276.
- [31] Sujay, R., Ganapathy, K. N., Gomashe, S. S., Rathore, A., Ghorade, R. B., Kumar, N., Ganesmurthy, K., Jain, S., Kamtar, M. Y., Sachan, J. S., Ambekar, S. S., Ranwa, B. R., Kanawade, D. G., Balusamy, M., Kadam, D., Sarkar, A., Tonapi, V. A., Patil, J. V. (2012): GGE biplot analysis to evaluate genotype, environment and their interactions in sorghum multi-location data. – *Euphytica* 185(3): 465-479.
- [32] Suwaero, N. (2011): Genotype \times environment interaction for iron concentration of rice in central java of Indonesia. – *Rice Science* 18: 75-78.

- [33] Tang, Q. Y., Zhang, C. X. (2013): Data Processing System (DPS) software with experimental design, statistical analysis and data mining developed for use in entomological research. – *Insect Science* 20: 254-260.
- [34] Thillainathan, M., Fernandez, G. C. J. (2001): Sas applications for tai's stability analysis and ammi model in genotype \times environmental interaction (GEI) effects. – *Journal of Heredity* 92(4): 367-371.
- [35] Thiyagu, D., Rafii, M. Y., Mahmud, T. M. M., Latif, M. A. (2012): Stability analysis of sweetpotato (*Ipomoea batatas* Lam.) shoot tips yield for leafy vegetable across agro-ecologies using AMMI. – *Australian Journal of Crop Science* 6: 1522-1526.
- [36] Tekdal, S., Kendal, E. (2018): AMMI model to assess durum wheat genotypes in multi-environment trials. – *Journal of Agricultural Science and Technology* 20(1): 153-156.
- [37] Yan, W. K., Hunt, L. A., Sheng, Q., Szlavnics, Z. (2000): Cultivar evaluation and mega-environment investigation based on the GGE biplot. – *Crop Science* 40: 597-605.
- [38] Yue, H. W., Wei, J. W., Bu, J. Z., Li, J., Wang, X. G., Zheng, S. H., Xie, J. X., Chen, S. P., Peng, H. C., Jiang, X. W., Xie, J. L. (2019a): Comprehensive analysis of genotype by environment interaction of maize cultivars under multi-environment conditions in North China. – *International Journal of Agriculture and Biology* 21(6): 289-299.
- [39] Yue, H. W., Bu, J. Z., Wei, J. W., Zhang, Y. L., Chen, S. P., Peng, H. C., Xie, J. L., Jiang, X. W. (2019b): Evaluation of the adaptability and stability of maize cultivars through GGE biplot analysis. – *Fresenius Environmental Bulletin* 28(9): 6719-6732.
- [40] Yue, H. W., Li, Y., Li, C. J., Guo, A. Q., Chen, S. P., Peng, H. C., Xie, J. L., Jiang, X. W. (2018a): Grain filling characteristics of maize hybrids with different maturity periods. – *International Journal of Agriculture and Biology* 20(7): 1650-1656.
- [41] Yue, H. W., Bu, J. Z., Wei, J. W., Chen, S. P., Peng, H. C., Xie, J. X., Zheng, S. H., Jiang, X. W., Xie, J. L. (2018b): Effect of planting density on grain-filling and mechanized harvest grain characteristics of summer maize varieties in Huang-Huai-Hai plain. – *International Journal of Agriculture and Biology* 20(6): 1365-1374.
- [42] Zhang, X., Wang, Q., Xu, J., Gilliam, F. S., Tremblay, N., Li, C. (2015): In situ nitrogen mineralization, nitrification, and ammonia volatilization in maize field fertilized with urea in Huanghuaihai region of northern China. – *Plos One* 10(1): e0115649.
- [43] Zhao, J., Yang, X. (2018): Average amount and stability of available agro-climate resources in the main maize cropping regions in China during 1981-2010. – *Journal of Meteorological Research* 32: 146-156.
- [44] Zhao, Z. L., Liu, Z., Zhang, X. D., Zan, X. L., Yao, X. C., Wang, S. J., Ye, S. J., Li, S. M., Zhu, D. H. (2018): Spatial layout of multi-environment test sites: a case study of maize in Jilin province. – *Sustainability*. 10: 1424.
- [45] Zhang, P. P., Song, H., Ke, X. W., Jin, X. J., Yin, L. H., Liu, Y. (2016): GGE biplot analysis of yield stability and test location representativeness in proso millet (*Panicum miliaceum* L.) genotypes. – *Journal of Integrative Agriculture* 15(6): 1218-1227.
- [46] Zobel, R. W., Wright, M. J., Gauch, H. G. (1988): Statistical analysis of a yield trial. – *Agronomy Journal* 80(3): 388-393.

RESEARCH AND EVALUATION OF GROWTH RATE MODEL FOR NATIVE CHINESE MOSO BAMBOO

SHEN, C.^{1,2} – FENG, Z.^{1*} – CHEN, P.¹ – CHEN, S.¹ – ULLAH, T.³

¹*Beijing Key Laboratory of Precision Forestry, Beijing Forestry University
Beijing 100083, China*

²*The Third Surveying and Mapping Institute of Guizhou Province, Guiyang 550004, China*

³*School of Nature Conservation, Beijing Forestry University, Beijing 100083, China*

**Corresponding author*

e-mail: fengzhongke@126.com; phone/fax: +86-138-1030-5579

(Received 17th Sep 2019; accepted 8th Jan 2020)

Abstract. Tree height growth assessment is important to understand forest dynamics that can reflect the health, productivity, and sustainability of a forest. Tree growth models are important tools to provide a reliable set of information for forest management. Accurate prediction of plant height from time is important for estimating future production. In this study, we used 80 native Moso bamboo and fit 9 models to predict bamboo height as a function of time since sprouting. Our results showed that Logistic growth model was the most suitable for predicting bamboo height ($r=0.969$), and can be used for predicting the growth and yield of mature native Moso bamboo, and provide a basis for the calculating biomass and carbon storage.

Keywords: *Phyllostachys heterocycla, tree growth, height, growth time, optimal model*

Introduction

Forest ecosystems account for 30% of the global terrestrial ecosystem. It is the most biologically and genetically diverse ecosystem providing not only habitat to more than 50% of the world's flora and fauna (Aerts and Honnay, 2011; Keenan et al., 2015; Miura et al., 2015), but also served human all through human history by providing food, water resources and other valuable timber products (Morales et al., 2015; Miura et al., 2015). Forest ecosystems also play an irreplaceable role in curbing global climate change, carbon cycle, soil and water conservation, and sustainable supply and regulation of forest products (Piao et al., 2018). The research and development of the forest growth model can timely and accurately understand the quantity, quality and dynamic changes of forest resources, and provide a basis for the analysis and assessment of forest growth, biomass and forest yield (Köhl et al., 2015).

Tree growth is an important facet of forest dynamics and can reflect the health, productivity, and sustainability of the forest (Zhang et al., 2019), therefore, it is very important to measure it on a regular basis. Tree growth models are important tools in providing reliable information for decision making regarding forest management (Liu et al., 2017). Many tree growth models that can effectively project changes in forest resources have been developed (Cortini et al., 2011; McCullagh et al., 2017). Tree height is the most important factor in forest resource inventory surveys, production and management of forest resources and for research on forest ecosystems (Vargas-Larreta et al., 2009; Xuan et al., 2016). Accurate estimation of tree height is important in the

development of forest growth models and can be used to estimate stock volume, biomass and carbon stocks (Li et al., 2015).

Tree growth is a complex process that depends on multiple and interacting factors. It is influenced by site conditions (Lévesque et al., 2016), climatic variables (Zell, 2018), and management (Biging and Dobbertin, 1995). Observation of tree height (H) from the ground is usually affected by the complexity of the distribution of understory vegetation, forest density and topography of the terrain (Temesgen et al., 2014). Moreover, the procedure to measure H is both time and cost expansive. Due to these reasons estimation of H is relatively more tricky and difficult than DBH (D) measurement. Because of this difficulty and to reduce the costs associated with field inventories, it is common practice to fit tree models based on D to predict H (Saunders and Wagner, 2008; Paulo et al., 2011). Further, an improved understanding of the H–D relationship is needed for reliable regional and global estimates of forest biomass and carbon storage. An allometric power relationship between H and D is often assumed in estimating H, although this approach neglects the possible large deviation in estimating biomass by allometry (Feldpausch et al., 2011; Stark et al., 2013). Besides this, non-linear theoretical functions are often used, such as the Chapman-Richards (Song et al., 2011), Hossfeld (Yen et al., 2010), Logistic, and Gompertz (Richards, 1959; Huang et al., 1992; Zeide, 1993; Cieszewski, 2001).

Bamboo is an important forest resource in many parts of the world. There are more than 70 genera of bamboo that are mainly distributed in tropical and subtropical regions (Zhou, 1992). Bamboo is particularly important in China, which is known as the "kingdom of bamboo". There are more than 40 genera and 400 species of bamboo in China. The Chinese bamboo forest covers 6.01 million ha, mainly distributed in Fujian, Jiangxi, Zhejiang, Hunan, Sichuan, Guangdong, Guangxi, and Anhui provinces (State Forestry Administration, 2014).

Bamboo is the main food for giant pandas, which are a unique and protected species in China (Mertens et al., 2008). Bamboo provides food for humans too. Further, it is a green material that can be used as a substitute and supplement for wood where it is widely used in construction, transportation, papermaking, furniture, and handicraft manufacturing (Tang et al., 2016). *Phyllostachys heterocycla* (Moso bamboo), which is characterized by its fast growth and rapid biomass accumulation is an important forest type in Southern China (Zhao et al., 2016). These forests cover 4.43 million ha in China, accounting for about 70% of the national bamboo forest area. The main forest products from Moso bamboo forests are timber and shoots for human consumption. Moso bamboo can reach a height of 20 m when mature and can grow between 30 and 100 cm per day during the growing season (Jiang et al., 2002; Chen, 2011). Thus, it has a higher annual carbon sequestration than other common timber trees (Song et al., 2011), suggesting a high potential for carbon storage (Yen et al., 2010).

For these reasons, there is a need to monitor and accurately estimate the biomass of Moso bamboo forests in China. The growth patterns of bamboo are different from trees; its unique characteristics include fast growth, high production and rapid maturation from shoot to culm (Scurlock et al., 2000). Few researchers have addressed the H–D relationship of bamboo using an allometric power equation (Inoue et al., 2011). The H–D relationship of Moso bamboo has only been studied by Inoue (2013), who used reduced major axis regression. Previous studies have mostly focused on biomass and carbon storage, and did not systematically study bamboo height. In this paper we use the bamboo height data to develop a growth model for Moso bamboo. Such an equation is useful for quantifying bamboo biomass and carbon storage.

Materials and methods

Study area

The study area is located near Yixing City and Wuxi City in southwest Jiangsu Province, adjacent to the Zhuhai Scenic Area (N 31°25' and E 119°73'). The area has a higher elevation and mountainous in the south and lower in elevation and relatively flat in the north, the range of the DEM is -137~614 m (Fig. 1). The area called “the ocean of bamboo” in Chinese. The area falls within the subtropical monsoon climate region, with abundant rainfall all year round. The average annual number of rainy days is 136.6, and the annual average precipitation is 1177 mm (Wu and Ming, 2007). The rainfall is concentrated in spring and summer, although it is warm and humid throughout much of the year. The annual average temperature is 15.7°C, the average frost-free period is more than 240 days, and the growth period is up to 250 days. The rivers criss-cross the study area and the average annual precipitation is 1177 mm. The soil is mainly yellow in colour with abundant organic matter providing excellent conditions for the growth of bamboo (Peng and Zou, 2011).

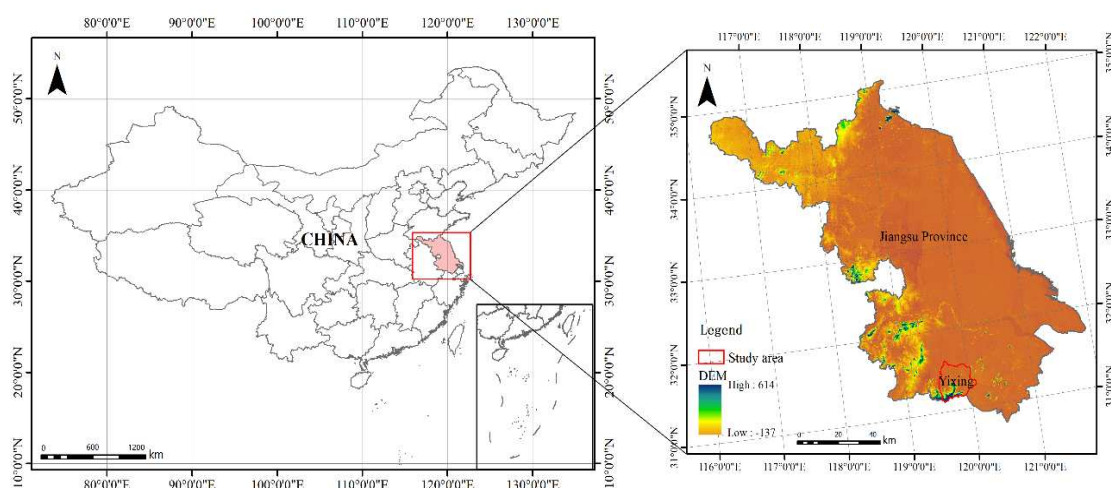


Figure 1. Location and digital elevation model (DEM) of the study area

Data acquisition

Five plots (15*15 m) were set up in the study area, and 20 bamboo shoots were randomly selected from each sample plots. Shoots that died or which were damaged by animal foraging or vandalism were removed from the data set, eighty bamboo shoots were left from sample plots in the study area as measurement samples, shoots were identified for measurement on March 26, 2015, and visited at regular intervals. By May 22, the shoots began to grow in height. Height growth was completed after 56 days. When the shoot height was less than 2 m, height was measured by a tape; when the shoot height exceeded 2 m, the height references were accurately measured by total station (Leica Flexline TS06plus Total Station) with accuracy to the millimetre level. The complete height recorded after the growth ranged from 10.71m to 16.06 m.

The models used were nonlinear and fit using the statistical package SPSS 20.0 (SPSS for Windows version 20.0) and the Levenberg-Marquardt (LM) method.

Tree height models assessment

We selected nonlinear models such as tree growth empirical equations and theoretical equations to compare the performance of the model. All model formulas refer to the reference (Meng, 2006). The model formulas were shown in Table 1.

Table 1. Selected tree height models

Number	Model	Formula
Model 1	Logistic	$h = \frac{A}{1 + be^{-ct}}$
Model 2	Richard	$h = A(1 - e^{-bt})^c$
Model 3	Gompertz	$h = Ae^{-be^{-t}}$
Model 4	Schumacher	$h = Ae^{-b/t}$
Model 5	Sloboda	$h = Ae^{-be^{-ct^d}}$
Model 6	Роляср	$h = At^b e^{-ct}$
Model 7	Weibull	$h = A(1 - e^{-bt})^c$
Model 8	Power function	$h = At^b$
Model 9	Korf	$h = Ae^{-bt^{-c}}$

H: Moso bamboo's height, m; t: time, day; a-d are parameters

Model evaluation

In order to verify the accuracy of the forecasting accuracy of the above methods, we validated the models. Usually the model is validated by independent data sets, which is the best way to validate the model at present (Zhang et al., 2019). The majority of the data (80%) was used for model calibration, and the remaining (20%) data was used for verifying the consistency of the models. At present, this method of model validation has been applied in many model validation, such as the biomass model, DBH growth model and carbon storage model (Zhang et al., 2019). Model evaluation mainly used the following indicators: root mean squared error (RMSE), adjusted coefficient of determination (R^2_{adj}), and other criteria (Montgomery, 2013). RMSE combines the variation of mean deviation and deviation, and can directly and clearly evaluate the accuracy of the model. RMSE and R^2 are important evaluation factors in this paper. The closer the R^2 value is to 1, the better the fitness of the model is (Peng et al., 2001). However, Cameron and Windmeijer (1997) suggested that the coefficient of determination (R^2) is not suitable for model evaluation of non-linear functions. Therefore, this paper uses six indicators to evaluate it comprehensively (Burnham and Anderson, 2002) including: root of mean square error (RMSE), coefficient of determination (R^2) and adjusted coefficient of determination (R^2_{adj}), bias (BIAS) and relative bias ($BIAS_{rel}$), residual sum of squares (RSS), Akaike's Information Criterion (AIC). The smaller the RMSE value, the higher the predicted accuracy. The large of R^2 and R^2_{adj} value, and correlation is stronger. AIC is an information standard commonly used to choose the best model. The expressions of the statistics are shown as follows:

$$RMSE = \sqrt{\frac{\sum_{i=1}^n (h_i - \hat{h}_i)^2}{n - p - 1}} \quad (\text{Eq.1})$$

$$R^2 = 1 - \frac{\sum_{i=1}^n (h_i - \hat{h}_i)^2}{\sum_{i=1}^n (h_i - \bar{h}_i)^2} \quad (\text{Eq.2})$$

$$R_{\text{adj}}^2 = 1 - (1 - R^2) \times \frac{n - 1}{n - p - 1} \quad (\text{Eq.3})$$

$$\text{Bias} = \frac{\sum_{i=1}^n (\hat{h}_i - h_i)}{n} \quad (\text{Eq.4})$$

$$\text{Bias}_{\text{rel}} = \frac{\sum_{i=1}^n (\hat{h}_i - h_i) / h_i}{n} \times 100 \quad (\text{Eq.5})$$

$$RSS = \sum_{i=1}^n (h_i - \hat{h}_i)^2 \quad (\text{Eq.6})$$

$$AIC = n \ln(RSS) + 2(p + 1) - n \ln(n) \quad (\text{Eq.7})$$

where h_i is the observation value; \hat{h}_i is the forecast value and \bar{h}_i is the average value; n is the total number of data used to the fitted model; and p is the number of independent variables.

Results

Non-linear regression analysis was performed by SPSS. The model estimated all the parameters by using the calibration data, and obtained the parameters and R^2 values of each model (Table 2). Except for model 9, all of them showed relatively satisfying results. Therefore, it can be seen that model 9 is not suitable for this data. As shown in Table 2, Model 1-8 uses all the data to estimate the parameters by nonlinear regression. All parameters are significant ($p < 0.05$), and the parameters of each model are easily obtained by calculation except model 9.

Table 2. Parameter estimates and fitting statistics of the models using all data

Parameter	a	b	c	d	R ²
Model 1	1553.94	142.43	0.135		0.969
Model 2	1946.97	7.73	0.06		0.964
Model 3	1891.38	10.05	0.066		0.965
Model 4	5506.07	72.04			0.961
Model 5	2181.55	51.33	0.596	0.523	0.963
Model 6	0.389	2.206	0.011		0.953
Model 7	2357.07	0.000	2.482		0.960
Model 8	0.893	1.859			0.949
Model 9	605.285	4.867	1637.086		0.06

a-d are model's parameters

According to the above test formula, each test index value is calculated using the calibration data and the verification data, and the results are shown in *Table 3*.

Table 3. Calibration data and validation data adaptive statistics for models

No.	Variables	Fitting data				Validation data			
		bias(m)	RMSE(m)	AIC	Adj. R ²	bias(m)	RMSE(m)	AIC	Adj. R ²
1	h,t	-0.66	4.26	187.55	0.9689	-0.96	3.05	38.73	0.9836
2	h,t	-2.38	4.57	196.42	0.9643	-2.68	3.52	43.25	0.9782
3	h,t	-2.88	4.52	195.07	0.965	-3.17	3.44	42.55	0.9792
4	h,t	-1.37	4.75	201.54	0.9613	-1.66	3.72	45.04	0.9757
5	h,t	-2.61	4.63	198.03	0.9634	-2.90	3.60	44.01	0.9772
6	h,t	-0.45	4.75	215.40	0.9613	-0.75	4.34	50.01	0.9668
7	h,t	-0.22	4.63	204.26	0.9634	-0.07	3.75	45.33	0.9752
8	h,t	1.80	5.3	219.08	0.9519	1.50	4.45	50.77	0.9652

Model fitting and evaluation

Using the Origin8.1, the growth model was fitted by the Levenberg-Marquardt (LM) method. The fitting effects of Model 1, Model 2, Model 3, Model 4 and Model 8 were good (*Fig. 2*). Other models adopt nonlinear regression, and the fitting results werenon-convergence, which was not suitable for the prediction of this data. In the subsequent statistics, the statistical results of the unconverging model were removed.

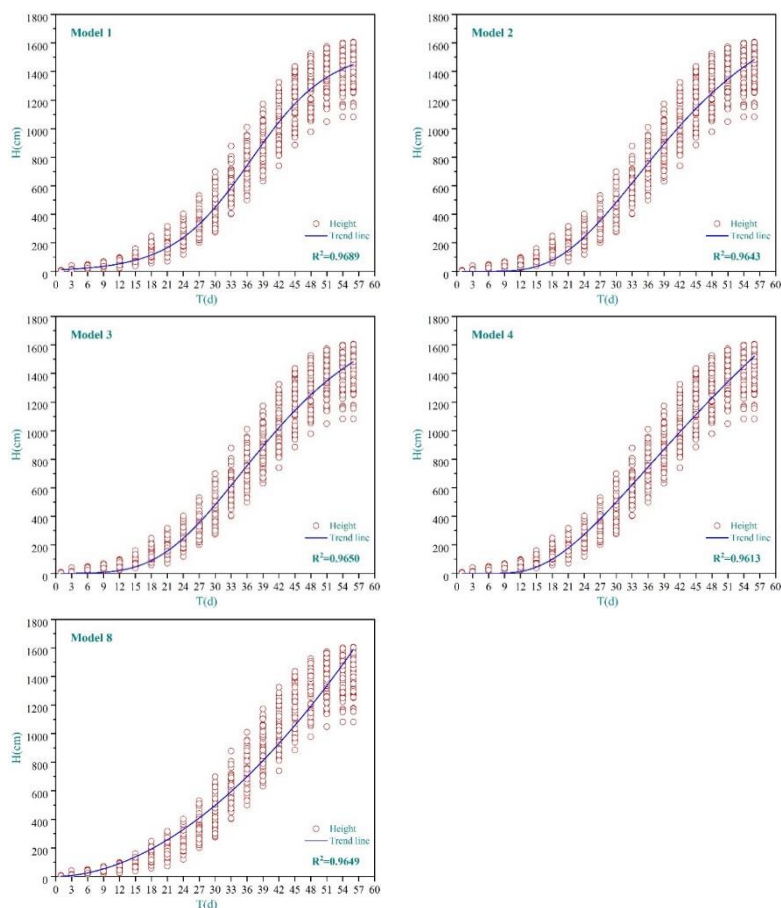


Figure 2. Models fitting trend line

It can be seen from the above trend graph that bamboo's height and the growth time have a high correlation, and models 1, 2, 3, 4 and 8 have higher R^2 values: 0.9689, 0.9643, 0.9650, 0.9613 and 0.9649, respectively. The correlation coefficient of Model 1 was the highest observed, and the result obtained in the fitting of the calibration data has the highest precision, which is suitable for the estimation of bamboo's height growth and conforms to the law of tree growth curve.

As shown in *Fig. 3*, the models 1, 2, 3, 4, and 8, respectively, use the calibration data to obtain the residual of the predicted height, and most of the data points are distributed around $y=0$. These models show the full uniformity of the predicted values and the independence of the residuals. The residual distribution of model 1 in the figure is relatively small, which reveals model 1 is the best model in the study.

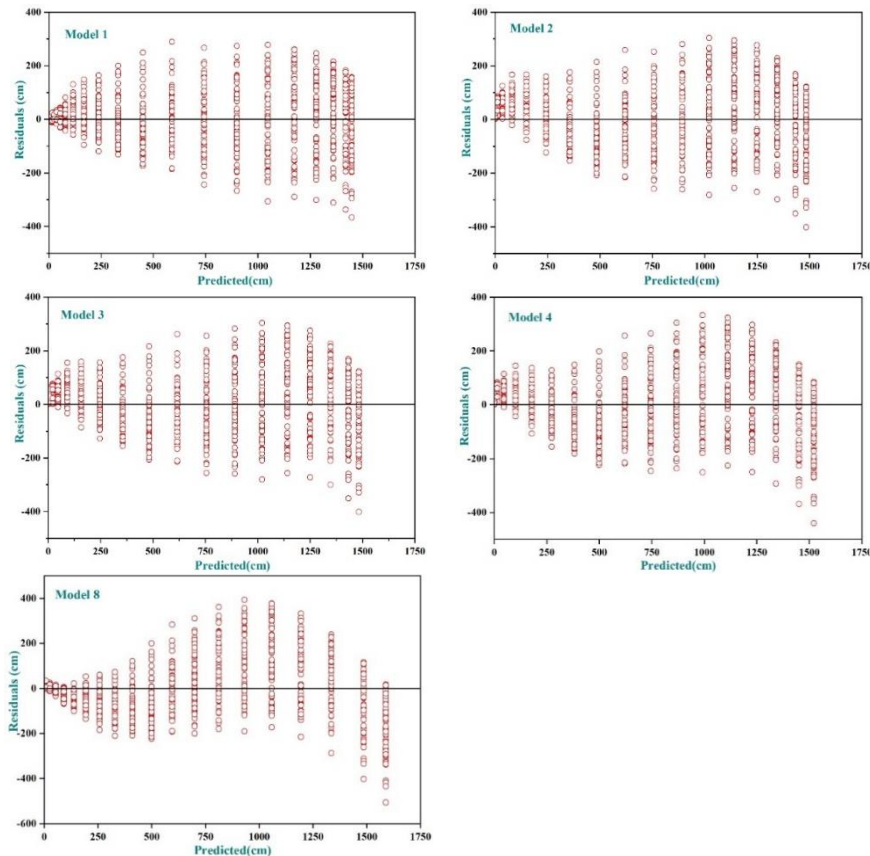


Figure 3. Residual plots in the calibration dataset for the models (Model 1; Model 2; Model 3; Model 4; Model 8)

As shown in *Fig. 4*, the models 1, 2, 3, 4, and 8 use the verification data to obtain the average deviation value and RMSE of the bamboo height through the growth period. The standard deviations of models 1, 2, 3, 4 and 8 are mainly distributed around $y=0$, in which the standard deviation of model 8 is 1.61 m, and deviations of most model are less than 1 m, accounting for 93% of all deviations. The RMSE values of models 1, 2, 3, 4 and 8 are between 0.049-1.86, the RMSE of model 8 varies greatly, the RMSE value of model 1 changes little, and the model is relatively stable. According to the above analysis, the model 1 is the most suitable model in the calibration data and the verification data among the five models.

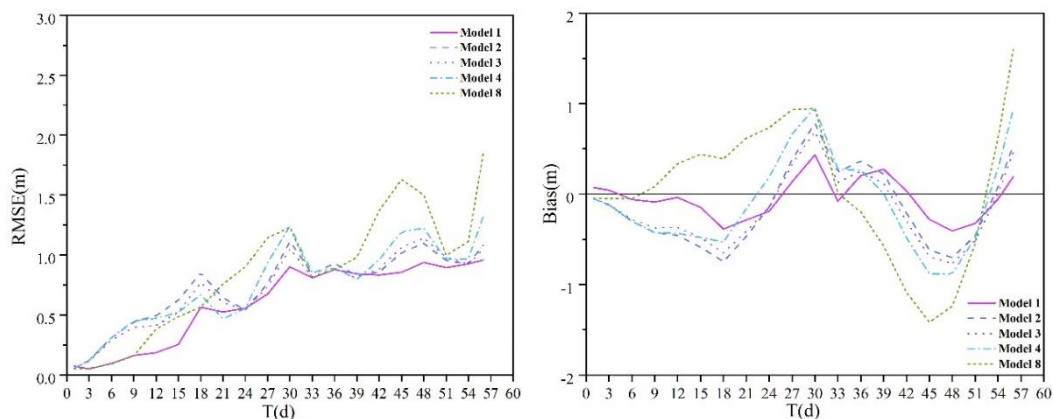


Figure 4. Values of average RMSE and Bias in relation to T in the calibration and validation datasets for the models (Model 1; Model 2; Model 3; Model 4; Model 8)

Discussion

In this study, based on the tree-based growth model, a model suitable for bamboo height and time was selected, which is very important for predicting the change of bamboo growth height with time. Tree growth is an important manifestation of the dynamic changes of forests, which can provide a basis for forest productivity and temporal and spatial changes in forests. The tree height and DBH models are the most basic and effective models in the growth model. The choice of models should be based on the arrangement of the expression of models with calibration data and validation data (the adjusted R^2 , R^2 , RMSE, the absolute deviation, the relative deviation and the AIC). The model with the adjusted R^2 , R^2 value closest to the highest value and a deviation (absolute and relative deviation) closest to zero is thought to be the best. The lower the value of RMSE and AIC, the higher the ranking of the model. For each model, its final ranking is the sum of the statistics of the five evaluation values. The model with the minimum sum (i.e., the highest ranking) is considered to be the functional model that is most suitable for estimating the growth of Moso bamboo. According to this analysis, the calibration data and the validation data show that model 1 is the most suitable for estimating the growth rate.

In comparison with previous studies, Huang et al., (1992) developed the HT-DBH functional model of the main tree species from 20 weighted nonlinear equations. It was observed that Weibull, Modified Logistic, Chapman-Richards and Schnute functions generally provided the most satisfactory results. Zhang (1997) concluded that the Schnute, Weibull and Chapman-Richards models provided the best predictive performance for 10 conifer species in the inland regions of the United States in the six nonlinear growth functions selected for HT-DBH. Peng et al. (2001) and Sharma and Parton (2007) recommended Chapman-Richards, Weibull, and Schnute nonlinear growth functions as the most satisfactory models in total height predictions in Canada. Ahmadi et al. (2013) reported that Chapman-Richards, Weibull and Schnute functions in predicting accurate total height predictions in Iranian Hyrcanian forests have shown excellent predictive performance, based on mathematical features, biological interpretation of parameters.

Furthermore, Lumbres et al. (2013) reported that the Modified Logistic nonlinear growth function was the best model for the *Pinus kesiya* Royle ex Gordon of Benguet in

Philippines. Based on the result of the researchers, nonlinear growth functions are reliable in the prediction of total height of trees. In the latest study of Lumbres et al. (2015) entitled DBH-height modeling and validation for *Acacia mangium* and *Eucalyptus pellita*, the Weibull and Chapman-Richards models were observed as the best nonlinear growth functions for *Acacia mangium*. However, the result of our study suggested that the Logistic regression model has the highest accuracy in predicting the growth of bamboo among the nine models we selected, which is obviously different from the previous research results.

Conclusion

In this study, the bamboo was used as the object, and the measured data of the fixed sample plots were used. The nonlinear regression method was used to model 80 bamboo shoots randomly selected in five different study plots. Considering the interrelation between the growth time of bamboo and bamboo's height, the tree growth and empirical equations were used to establish a height growth model of bamboo. From the modeling results, the conclusions are showed as follow. Using the models 1, 2, 3, 4 and 8 to predict the bamboo height, the majority of the bamboo height determination coefficient R^2 can reach 0.9 or more, and in terms of accuracy the model 1 performance was the best. The methods and the models recommended in this study are based on statistics, which provide a reliable basis for the estimation of forest growth and survival and planting management for Chinese native Moso bamboo.

Acknowledgements. The research reported in this manuscript is funded by the Fundamental Research Funds for the Central Universities (Grant No. 2015ZCQ-LX-01), the National Natural Science Foundation of China (Grant No. U1710123).

REFERENCES

- [1] Aerts, R., Honnay, O. (2011): Forest restoration, biodiversity and ecosystem functioning. – *Annals of Occupational and Environmental Medicine* 11: 1-10.
- [2] Ahmadi, K., Alavi, S. J., Kouchaksaraei, M. T., Aertsen, W. (2013): Non-linear height-diameter models for oriental beech (*Fagus orientalis* Lipsky) in the Hyrcanian forests, Iran. – *Biotechnologie Agronomie Société Et Environnement* 17: 431-440.
- [3] Biging, G. S., Dobbertin, M. (1995): Evaluation of Competition Indices in Individual Tree Growth Models. – *Forest Science* 41: 360-377.
- [4] Burnham, K. P., Anderson, D. R. (2002): Model selection and multimodel inference: A practical. – Springer Berlin Heidelberg. doi:10.1088/1751-8113/44/8/085201.
- [5] Cameron, A. C., Windmeijer, F. A. G. (1997): An R-squared measure of goodness of fit for some common nonlinear regression models. – *Journal of Econometrics* 77: 329-342.
- [6] Chen, S. L. (2011): Thoughts on related problems of mulched technique with organic materials in moso bamboo forest for early shooting. – *Journal of Zhejiang A & F University* 28: 799-804.
- [7] Cieszewski, C. J. (2001): Three methods of deriving advanced dynamic site equations demonstrated. – *Canadian Journal of Forest Research* 31: 165-173.
- [8] Cortini, F., Filipescu, C. N., Groot, A., Dan, A. M., Nunifu, T. (2011): Regional Models of Diameter as a Function of Individual Tree Attributes, Climate and Site Characteristics for Six Major Tree Species in Alberta, Canada. – *Forests* 2: 814-831.

- [9] Feldpausch, T. R., Banin, L., Phillips, O. L., Baker, T. R., Lewis, S. L., Quesada, C. A., Affum-Baffoe, K., Arets, E. J. M. M., Berry, N. J., Bird, M. (2011): Height-diameter allometry of tropical forest trees. – *Biogeosciences* 8(5): 7727-7793.
- [10] Huang, S. M., Titus, S. J., Wiens, D. P. (1992): Comparison of Nonlinear Height Diameter Functions for Major Alberta Tree Species. – *Canadian Journal of Forest Research* 22: 1297-1304.
- [11] Inoue, A., Sakamoto, S., Suga, H., Kitahara, F. (2011): Estimation of culm volume for bamboo, *Phyllostachys bambusoides*, by two-way volume equation. – *Biomass and Bioenergy* 35: 2666-2673.
- [12] Inoue, A. (2013): Culm form analysis for bamboo, *Phyllostachys pubescens*. – *Journal of Forestry Research* 24: 525-530.
- [13] Jiang, Z. H., Wang, G., Fei, B. H., Yu, W. J. (2002): The Research and Development on Bamboo/Wood Composite Materials. – *Forest Research* 15: 712-718.
- [14] Keenan, R. J., Reams, G. A., Achard, F., Freitas, J. V. D., Grainger, A., Lindquist, E. (2015): Dynamics of global forest area: Results from the FAO Global Forest Resources Assessment 2015. – *Forest Ecology and Management* 352: 9-20.
- [15] Köhl, M., Lasco, R., Cifuentes, M., Jonsson, Ö., Korhonen, K. T., Mundhenk, P., Navar, J. D. J., Stinson, G. (2015): Changes in forest production, biomass and carbon: Results from the 2015 UN FAO Global Forest Resource Assessment. – *Forest Ecology and Management* 352: 21-34.
- [16] Lévesque, M., Walthert, L., Weber, P. (2016): Soil nutrients influence growth response of temperate tree species to drought. – *Journal of Ecology* 104: 377-387.
- [17] Li, Y. Q., Deng, X. W., Huang, Z. H., Xiang, W. H., Yan, W. D., Lei, P. F., Zhou, X. L., Peng, C. H. (2015): Development and Evaluation of Models for the Relationship between Tree Height and Diameter at Breast Height for Chinese-Fir Plantations in Subtropical China. – *Plos One* 10: e0125118.
- [18] Liu, M., Feng, Z., Zhang, Z., Ma, C., Wang, M., Lian, B.-l., Sun, R., Zhang, L. (2017): Development and evaluation of height diameter at breast models for native Chinese *Metasequoia*. – *Plos One* 12: e0182170.
- [19] Lumbres, R. I., Lee, Y. J., Calorajr, F., Parao, M. (2013): Model fitting and validation of six height-DBH equations for *Pinus kesiya* Royle ex Gordon in Benguet Province, Philippines. – *Forest Science and Technology* 9: 6.
- [20] Lumbres, R. I. C., Lee, Y. J., Yun, C. W., Chang, D. K., Kim, S. B., Son, Y. M., Lee, K. H., Won, H. K., Jung, S. C., Seo, Y. O. (2015): DBH-height modeling and validation for *Acacia mangium* and *Eucalyptus pellita* in Korintiga Hutani Plantation, Kalimantan, Indonesia. – *Forest Science and Technology* 11: 119-125.
- [21] McCullagh, A., Black, K., Nieuwenhuis, M. (2017): Evaluation of tree and stand-level growth models using national forest inventory data. – *European Journal of Forest Research* 136: 251-258.
- [22] Meng, X. Y. (2006): *Forest Mensuration*. – China Forestry Publishing House: 179-187.
- [23] Mertens, B., Hua, L., Belcher, B., Ruiz, M. (2008): Spatial patterns and processes of bamboo expansion in Southern China. – *Applied Geography* 28: 16-31.
- [24] Miura, S., Amacher, M., Hofer, T., San-Miguel-Ayanz, J., Ernowati, Thackway, R. (2015): Protective functions and ecosystem services of global forests in the past quarter-century. – *Forest Ecology and Management* 352: 35-46.
- [25] Montgomery, D. C. (2013): *Introduction to Linear Regression Analysis*. – Fifth Edition Set, *American Statistician* 57: 67-67.
- [26] Morales-Hidalgo, D., Oswalt, S. N., Somanathan, E. (2015): Status and trends in global primary forest, protected areas, and areas designated for conservation of biodiversity from the Global Forest Resources Assessment 2015. – *Forest Ecology and Management* 352: 68-77.
- [27] Paulo, J. A., Tomé, J., Tomé, M. (2011): Nonlinear fixed and random generalized height-diameter models for Portuguese cork oak stands. – *Annals of Forest Science* 68: 295-309.

- [28] Peng, C., Zhang, L., Liu, J. (2001): Developing and Validating Nonlinear Height Diameter Models for Major Tree Species of Ontario's Boreal Forests. – Northern Journal of Applied Forestry 18: 87-94.
- [29] Peng, J. Y., Zou, S. M. (2011): Feasibility research on karst cave national geopark construction in Yixing of Jiangsu. – Journal of Geology 2011-01.
- [30] Piao, S., Huang, M., Zhuo, L., Wang, X., Ciais, P., Canadell, J. G., Kai, W., Bastos, A., Friedlingstein, P., Houghton, R. A. (2018): Lower land-use emissions responsible for increased net land carbon sink during the slow warming period. – Nature Geoscience 11: 739-743.
- [31] Richards, F. J. (1959): A Flexible Growth Model for Empirical Use. – Journal of Experimental Botany 10: 290-301.
- [32] Saunders, M. R., Wagner, R. G. (2008): Height-diameter models with random coefficients and site variables for tree species of Central Maine. – Annals of Forest Science 65: 203-203.
- [33] Scurlock, J. M. O., Dayton, D. C., Hames, B. (2000): Bamboo: An Overlooked Biomass Resource? – Biomass and Bioenergy 19: 229-244.
- [34] Sharma, M., Parton, J. (2007): Height–diameter equations for boreal tree species in Ontario using a mixed-effects modeling approach. – Forest Ecology and Management 249(3): 187-198.
- [35] Song, X., Zhou, G., Hong, J., Yu, S., Fu, S., Li, W., Wang, W., Ma, Z., Peng, C. (2011): Carbon sequestration by Chinese bamboo forests and their ecological benefits: Assessment of potential, problems, and future challenges. – Environmental Reviews 19(1): 418-428.
- [36] Stark, H., Nothdurft, A., Bauhus, J. (2013): Allometries for Widely Spaced *Populus* ssp. and *Betula* ssp. in Nurse Crop Systems. – Forests 4: 1003-1031.
- [37] State Forestry Administration (2014): China Forest Resources Report (2009-2013). – China Forestry Publishing House, Beijing: 6-8.
- [38] Tang, X., Fan, S., Qi, L., Guan, F., Manyi, D., Zhang, H. (2016): Soil respiration and net ecosystem production in relation to intensive management in Moso bamboo forests. – Catena 137: 219-228.
- [39] Temesgen, H., Zhang, C., Zhao, X. H. (2014): Modelling tree height–diameter relationships in multi-species and multi-layered forests: A large observational study from Northeast China. – Forest Ecology and Management 316: 78-89.
- [40] Vargas-Larreta, B., Castedo-Dorado, F., Álvarez-González, J. G., Barrio-Anta, M., Cruz-Cobos, F. (2009): A generalized height–diameter model with random coefficients for uneven-aged stands in El Salto, Durango (Mexico). – Forestry 84: 445-462.
- [41] Wu, S. J., Ming, W. W. (2007): Preliminary study on surface pollen flora in the Longchi Mountain nature reserve, Yixing, Jiangsu Province. – Acta Palaeontologica Sinica 46: 340-346.
- [42] Xu, H., Sun, Y., Wang, X., Fu, Y., Dong, Y., Li, Y. (2014): Nonlinear mixed-effects (NLME) diameter growth models for individual China-Fir (*Cunninghamia lanceolata*) trees in Southeast China. – Plos One 9(8): e104012.
- [43] Xuan, G., Li, Z., Yu, H., Jiang, Z., Chen, W., Yu, Z., Qi, L., Lei, S. (2016): Modeling of the height–diameter relationship using an allometric equation model: a case study of stands of *Phyllostachys edulis*: ecosystem management. – Journal of Forestry Research 27: 339-347.
- [44] Yen, T. M., Ji, Y. J., Lee, J. S. (2010): Estimating biomass production and carbon storage for a fast-growing makino bamboo (*Phyllostachys makinoi*) plant based on the diameter distribution model. – Forest Ecology and Management 260: 339-344.
- [45] Zeide, B. (1993): Analysis of Growth Equations. – Forest Science 39: 594-616.
- [46] Zell, J. (2018): Climate Sensitive Tree Growth Functions and the Role of Transformations. – Forests 9: 382.
- [47] Zhang, L. J. (1997): Cross-validation of non-linear growth functions for modelling tree height-diameter relationships. – Annals of Botany 79: 251-257.

- [48] Zhang, H., Feng, Z., Chen, P., Chen, X. (2019): Development of a Tree Growth Difference Equation and Its Application in Forecasting the Biomass Carbon Stocks of Chinese Forests in 2050. – *Forests* 10: 582.
- [49] Zhao, J. C., Su, W. H., Fan, S. H., Cai, C. J., Zhu, X. W., Peng, C., Tang, X. L. (2016): Effects of various fertilization depths on ammonia volatilization in Moso bamboo (*Phyllostachys edulis*) forests. – *Plant Soil and Environment* 62: 128-134.
- [50] Zhou, F. C. (1992): The State of Utilization, Trend and strategies for the World Bamboo Industry. – *World Forestry Research* 1992-01.

ECOLOGICAL CHARACTERISTICS AND HABITAT PREFERENCES OF OSTRACODA (CRUSTACEA) WITH A NEW BISEXUAL POPULATION RECORD (MUĞLA, TURKEY)

AKDEMİR, D.^{1*} – KÜLKÖYLÜOĞLU, O.² – YAVUZATMACA, M.¹ – TANYERI, M.² – GÜRER, M.² – ALPER, A.³ – DERE, Ş.⁴ – ÇELEN, E.¹ – YILMAZ, O.¹ – ÖZCAN, G.¹

¹*Institute for Geology and Mineralogy, University of Cologne, Zùlpicher Str. 49a, 50674 Cologne, Germany*

²*Department of Biology, Faculty of Arts and Science, Bolu Abant İzzet Baysal University, 14030 Bolu, Turkey*

³*Department of Biology, Faculty of Arts and Science, Balıkesir University, 10440 Balıkesir, Turkey*

⁴*Department of Biology, Faculty of Arts and Science, Bursa Uludağ University, 16059 Bursa, Turkey*

**Corresponding author*

e-mail: dakdemir@uni-koeln.de; phone: +49-221-470-5784; fax: +49-221-470-1663

(Received 17th Sep 2019; accepted 8th Jan 2020)

Abstract. In order to compare the ecological characteristics of non-marine ostracods with different reproductive modes, 68 sites including 11 different habitat types were examined in the province of Muğla during July of 2014. A total of 28 taxa were found and 11 of them were new reports for Muğla. Sexual populations of *Psychrodromus olivaceus* and *P. fontinalis* were encountered from the same sampling site. Males of the latter species were reported for the first time from Turkey. The female/male ratio of these species was higher at low altitudes while it was about the same at medium altitudes. Numbers of species in sexual and/or parthenogenetic populations with/without swimming setae and individuals in natural and artificial habitats did not show significant difference ($P > 0.05$). Troughs were described as the richest habitats for ostracods. The first two axes of Canonical Correspondence Analysis explained 66.2% of the relationships between species and environmental variables when the water temperature was the most effective factor on species composition ($P < 0.01$). Results suggest that type of reproductive modes did not show significant relationship with species distribution among different water bodies. Hence, it seems distribution of species is most probably affected by several biotic and abiotic factors.

Keywords: *non-marine species, distribution, natural-artificial habitats, altitudes, swimming ability*

Introduction

Although, freshwater habitats occupy only small parts of the Earth's surface with a ratio of 0.8%, they host approximately 6% of species known in the world (Dudgeon et al., 2006). In this respect, freshwaters are considered to be one of the main sources of biological diversity on the Earth. However, these habitats are known to be affected at global (e.g. climate changes) and local (e.g. species invasion, habitat degradation, water pollution) scales by a variety of biotic and abiotic factors (Dudgeon et al., 2006). Thus, different kinds of habitat destruction lead to changes in species composition, their geographic distribution, and also cause a decrease in species diversity (Finlayson et al., 2013). However, some features of the organisms including (i) morphological characteristics (e.g., to occupy different ecological niches with different movement types (Wiens, 2011), (ii) phenotypic plasticity (e.g., fitting ability of the size and shape

as a response to the changes in environmental conditions (Carbonel et al., 1988)), (iii) biological characteristics (e.g., to tolerate rapid or great environmental changes with different reproductive modes (Cohuo et al., 2015)), and (iv) ecological characteristics (e.g., to endure unpredictable environmental conditions with high ecological tolerance levels (Külköylüoğlu, 2004)) allow species to cope with the changes and elevate their survival chances in a variety of habitats. These biological and ecological features of the species also determine the degree of their distribution and abundance at spatiotemporal scale in relation to habitat conditions (Heino and Tolonen, 2018).

Ostracods, small bivalved crustaceans, are an important part of biological diversity in freshwater habitats with approximately 2330 extant species (Meisch et al., 2019). They can be fossilized due to their carapace (two valves) which consists of low Mg-calcite. The first record of fossil ostracods dates back to Early Ordovician (ca. 485 Ma), and thus ostracods are known as one of the oldest groups in microfauna (Williams et al., 2008). Besides, they have different reproductive modes of sexual, parthenogenetic (asexual) and/or mixed populations, and exhibit specific ecological requirements and species-specific tolerance levels. The different types of reproductive modes of the ostracods can be related to taxonomic and ecological features of particular species (Gülen, 1985a; Cohen and Morin, 1990; Martens et al., 2008) and may depend on geographical and/or ecological isolation (Mayr and Ashlock, 1991). All these features contribute to their widespread geographic distribution and high species diversity and also make them a particularly valuable group for a number of purposes in palaeo- and neoenvironmental studies. If the ostracod species' morphological features and ecological preferences are known, they can be used to estimate water quality conditions and rate of environmental changes (Wagner, 1964; Mezquita et al., 1999; Külköylüoğlu, 2004). In addition, the knowledge of the present-day distributional patterns of ostracods according to their reproductive modes in different region and/or environmental conditions can also be used as an informative marker for non-marine ostracods in the ecological sense.

Studies on ostracods in Turkey exhibited that distribution of both parthenogenetic and sexual populations were widespread throughout the country (Külköylüoğlu et al., 2015; Yavuzatmaca et al., 2017). Nevertheless, the distributional pattern and habitat preferences of species according to their reproductive modes have not been discussed and explained the Muğla province in the south-western part of Anatolia. Therefore, the main aim of the study is to investigate ecological preferences and distribution of species with different reproductive modes among the different aquatic bodies of the region.

Materials and methods

Site description

The province of Muğla, which is located on the south-west corner of Turkey, was chosen as a research area because of the possibility to find a variety of aquatic habitats and the lack of extensive studies on ostracods in this area. It represents typical Mediterranean climatic conditions where summers are very hot, long and dry, winters are cool and rainy. In total, 68 sites containing 11 habitat types (lake, reservoir, pond, pool, ditch, canal, creek, stream, spring water, trough, and waterfall) were randomly chosen from sea level to 1093 m of altitude between the 12 and 15 of July 2014 (*Fig. 1*).

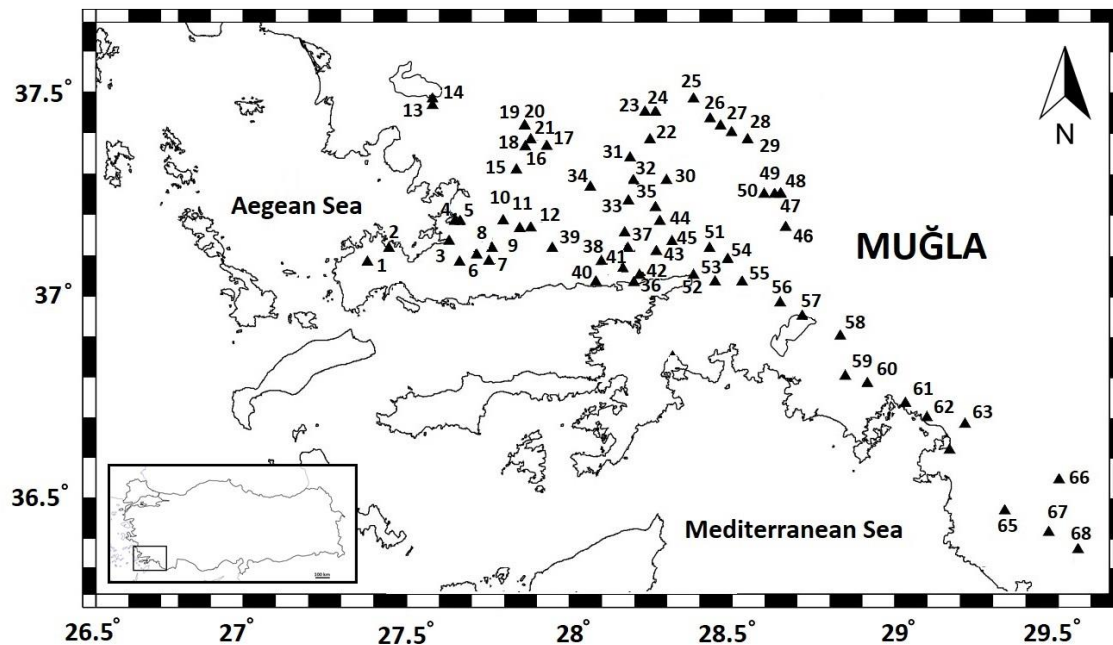


Figure 1. Distribution of the 68 sampling sites in the Muğla province

Sampling and measurements

Ostracod samples were collected with a standard sized hand net (200 μm mesh size) from the surface of sediments within an area of approximately 100 cm^2 and a depth of up to 100 cm. At each site, approximately 100 g of sediments were gathered and fixed with 70% ethanol in 250 ml plastic containers *in situ*. In the laboratory, sediments including ostracods were washed and filtered through 4 standard sized sieves (1.00, 0.25, 0.16, 0.08 mm mesh size) under tap water and fixed in 70% ethanol for long term storage. Ostracod samples were sorted from sediments by using fine needles and Pasteur pipettes under a stereo microscope (Meiji-Techno). Soft body parts of ostracods were separated from the carapace and dissected in Lactophenol – Orange G solution. The carapace and valves were preserved in micropaleontological slides. Subsequently, species identification was carried out under a binocular microscope (Olympus-CX41) based on the dissected soft body parts and carapace structures by using the standard taxonomic works of Broodbaker and Danielopol (1982), Gonzalez Mozo et al. (1996), Meisch (2000) and Karanovic (2012). However, some species were identified at the genus-level because of damaged individuals, lack of soft body parts or only the presence of juveniles.

Environmental variables were measured *in situ* before sampling to avoid possible results of Pseudoreplication (Hurlbert, 1984). Dissolved oxygen (DO, mg L^{-1}), oxygen saturation (S, %), electrical conductivity (EC, $\mu\text{S cm}^{-1}$), water temperature (T_w , $^{\circ}\text{C}$), salinity (Sal, ppt) and total dissolved solids (TDS, mg L^{-1}) of aquatic habitats were measured with a YSI professional plus device (Table A1 in the Appendix). Geographical data (latitude, longitude, elevation) from each sampling site were determined with a Garmin GPS 45 XL (Fig. 1) while air temperature (T_a , $^{\circ}\text{C}$), moisture (Moi, %), wind (m s^{-1}) and atmospheric pressure (Atm, mmHg) were measured with a Testo 410-2 anemometer (Table A1 in the Appendix).

A 100 ml of water was taken from each sampling site in plastic bottles and preserved in a container at 4 °C for the analyses of cations (sodium (Na⁺), potassium (K⁺), magnesium (Mg²⁺), calcium (Ca²⁺)), and anions (fluoride (F⁻), chloride (Cl⁻), sulphate (SO₄²⁻)). Analyses of these major ions were conducted in the laboratory of the Engineering Department of Bolu Abant İzzet Baysal University. The standard method no: 4110 using Ion Chromatography (Dionex 1100) was followed during the analyses. Also, sediment samples were collected from each site in eppendorf tubes for in/organic phosphate and total phosphate (mg kg⁻¹) analyses. In the laboratory, sediment samples were dried in oven at 40 °C (at least 24 h) and were subsequently analyzed according to Ruban et al. (1999) with a sequential extraction procedure (*Table A1* in the *Appendix*).

Statistical analyses

A Detrended Correspondence Analysis (DCA) was applied to confirm the suitability of the data for Canonical Correspondence Analysis (CCA) (ter Braak, 1986). The length of gradient in DCA was calculated as 3.64 referring the suitability of our data for CCA. CCA was performed to estimate most effective environmental variable(s) on species composition by using the CANOCO version 5 program (ter Braak and Šmilauer, 2012). The significance of the environmental variables used in CCA was tested by Monte Carlo permutation test (499 permutations). To eliminate possible multicollinearity, rare species were not used during the analyses. Shannon-Wiener (or Shannon, H') index values were calculated by using a Species Diversity and Richness 4 software (Seaby and Henderson, 2006) to determine the species diversity in different habitat types where the values of H' (1.5 and 3.5) for ecological data suggest poor to rich diversity, respectively. In order to understand possible correlations among species and environmental variables measured here, Spearman Correlation Analyses were conducted in the SPSS program version 6.0. The C2 Software was used to measure ecological tolerance (t_k) and optimum (u_k) estimates of individual species along with Hill's coefficient (measure of effective number of occurrences) (Juggins, 2003). The chi-square test was used to determine whether there was a significant difference between the numbers/abundances of species in sexual and parthenogenetic populations with or without swimming setae in natural and artificial habitats. During the analyses, only adult individuals, occurred at least three or more times in different habitats, were used. The ostracod materials were deposited at the Limnology Laboratory of the Department of Biology, Bolu Abant İzzet Baysal University, Bolu, Turkey. Additional information about the sampling sites and species reported here can be available upon request from the authors.

Results

During this study, a total of 28 taxa (24 living and 4 sub-fossil) were reported among 11 habitat types while 11 of the living species (*Candona weltneri*, *Psychrodromus fontinalis*, *Heterocypris barbara*, *Ilyocypris gibba*, *I. hartmanni*, *Limnocythere inopinata*, *Potamocypris arcuata*, *P. producta*, *P. unicaudata*, *P. villosa* and *Trajancypris leavis*) were new for Muğla. The sexual population of *P. fontinalis* was found for the first time, while *P. producta* was recorded for the second time in Turkey.

The first two axes of the CCA explained about 66.2% of the relationship between 12 species and 5 environmental variables (F = 2.9, P = 0.04) (*Table 1*). According to CCA,

the water temperature ($P = 0.008$, $F = 1.8$) showed a significant effect on the ordination of species (Fig. 2). Except *L. inopinata*, four species (*C. neglecta*, *I. bradyi* and *P. olivaceus*, *P. fontinalis*) without (reduced or short) swimming setae on A2 were located on the left side of the CCA diagram, while species with swimming setae were situated on the right side of the diagram. However, one of the species with reduced swimming setae, *Cyprideis torosa*, was placed separately from other species on the CCA diagram (Fig. 2).

Table 1. Summary table of CCA. Test of significance of first axis, $F = 2.9$, $P = 0.04$; and all canonical axes, $F = 1.5$, $P = 0.028$.

	Axis 1	Axis 2	Axis 3	Axis 4	Total inertia
Eigenvalues	0.483	0.186	0.173	0.116	7.699
Species-environment correlations	0.763	0.464	0.514	0.413	
Cumulative percentage variance of species data	6.3	8.7	10.9	12.4	
Cumulative percentage variance of species-environment relation	47.8	66.2	83.3	94.8	
	Sum of all eigenvalues				7.699
	Sum of all canonical eigenvalues				1.010

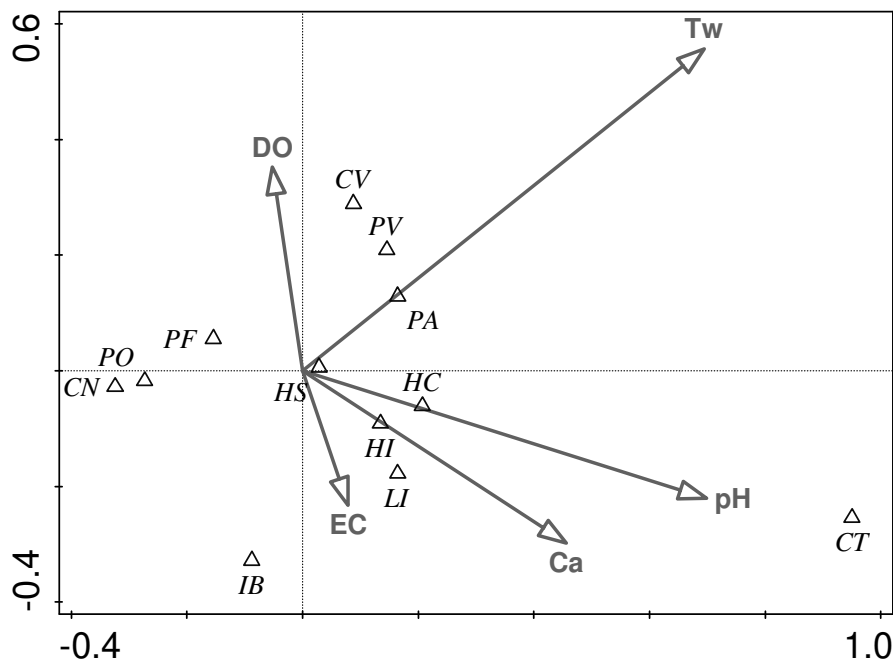


Figure 2. CCA diagram of five environmental variables (arrows) and 12 species (triangle). Abbreviations are given in Tables 4 and A1 in the Appendix

According to the results of Spearman Correlation Analyses, *H. salina* showed negatively significant correlations with *P. olivaceus* and *P. fontinalis* while the correlation was positive with *I. bradyi* ($P < 0.01$). *P. fontinalis* exhibited a negative correlation with *L. inopinata* ($P < 0.01$). Among the species, *C. torosa* indicated strong

and significant positive correlations with Ca^{+2} and Mg^{+2} values of the water bodies, when *P. variegata* showed negative correlation to Ca^{+2} and electrical conductivity ($P < 0.01$). *Potamocypris variegata* displayed low ecological tolerance values for dissolved oxygen, electrical conductivity, Na^+ , Mg^{+2} , and Ca^{+2} when *C. torosa* showed the highest tolerances for total phosphates in the sediment, and several other major ions of the water bodies. Also, *I. bradyi* had the lowest tolerance levels for pH but the highest tolerances for conductivity and water temperature. *Heterocypris salina* displayed the highest tolerance levels for dissolved oxygen and pH (for more details see Table 2).

Table 2. Ecological tolerance (t_k) and optimum (u_k) levels of the 11 species occurred at least three times

Species	Count	Max	N2	DO		pH		Tw		EC		Na		Mg	
				u_k	t_k	u_k	t_k	u_k	t_k	u_k	t_k	u_k	t_k	u_k	t_k
<i>C. neglecta</i>	3	6	1.68	3.68	1.39	7.24	0.77	18.14	6.98	297.75	235.62	10.16	9.44	3.96	4.15
<i>C. vidua</i>	7	46	3.11	4.45	2.27	7.98	0.41	26.99	5.20	408.68	196.94	4.89	3.47	2.43	2.98
<i>P. olivaceus</i>	15	172	6.63	5.15	2.23	7.44	0.57	17.50	2.98	296.25	211.68	11.29	11.33	4.27	6.52
<i>P. fontinalis</i>	10	146	3.39	7.32	2.94	7.98	0.52	23.57	4.61	567.02	205.16	4.21	6.43	41.75	25.44
<i>H. incongruens</i>	6	265	2.16	5.10	1.94	8.69	0.56	25.82	1.93	563.31	227.39	39.82	38.39	13.93	9.98
<i>H. salina</i>	13	320	3.77	5.18	3.06	7.45	0.82	21.90	3.83	555.33	234.71	12.45	7.38	18.58	19.61
<i>H. chevreuxi</i>	4	105	1.22	3.83	1.82	7.99	0.70	22.66	7.03	339.60	216.42	5.99	19.88	5.51	1.92
<i>I. bradyi</i>	6	67	1.73	9.24	3.04	8.07	0.26	13.10	7.64	328.66	303.95	4.58	8.36	9.01	12.12
<i>L. inopinata</i>	7	60	3.70	6.34	1.28	8.29	0.46	22.96	4.51	549.13	258.97	8.60	6.47	24.55	20.03
<i>P. arcuata</i>	4	85	2.30	4.62	2.85	8.01	0.81	26.84	4.87	374.41	225.98	26.90	12.85	5.18	2.53
<i>P. variegata</i>	4	804	1.24	6.61	0.48	8.15	0.31	31.09	2.88	252.55	43.80	5.22	1.56	2.48	1.45
			Mean	5.59	2.12	7.94	0.56	22.78	4.77	412.06	214.60	12.19	11.41	11.97	9.70
			Min.	3.68	0.48	7.24	0.26	13.10	1.93	252.55	43.80	4.21	1.56	2.43	1.45
			Max.	9.24	3.06	8.69	0.82	31.09	7.64	567.02	303.95	39.82	38.39	41.75	25.44

Abbreviations: Count, numbers of species occurrence; Max, maximum numbers of individuals; N2, Hill's coefficient (measure of effective number of occurrences); u_k , optimum values; t_k , ecological tolerance values. See Tables 4 and A1 in the Appendix for the other abbreviations

Numbers of species with (17 spp.) and without (20 spp.) swimming setae on A2 were not significantly different ($P > 0.05$) between artificial (e.g., trough, reservoir, canal etc.) and natural (e.g., lake, spring, creek etc.) habitats (Table 3). Among the species, 13 species were commonly found in both natural and artificial habitats. Parthenogenetic populations herein were encountered from all of the habitat types, while only five sexual populations (*Candona neglecta*, *C. weltneri*, *N. monacha*, *P. olivaceus* and *P. fontinalis*) were obtained from four natural habitats (spring water, pool, ditch, waterfall), and one artificial habitat (trough). A total of 17 species were represented with parthenogenetic populations but bisexual populations of two (*P. olivaceus* and *P. fontinalis*) of them were also reported in artificial habitats. 12 of 17 species carried swimming setae when five species had reduced setae. All of the obtained specimens of *Potamocypris* spp. have long swimming setae and three of them (*P. producta*, *P. unicaudata* and *P. villosa*) were reported only from the artificial habitats (troughs) with an accompanying swimming species (*Heterocypris barbara*). In contrast, 4 sexual and 17 parthenogenetic species were encountered in natural habitats. Among them, 11 and 9 species were with and without swimming setae, respectively. The species *C. neglecta*, *C. weltneri*, *C. torosa*, and *P. zenkeri* are non-swimmers while *I. decipiens*, *N. monacho* and *T. leavis* are known as swimmers established solely in natural habitats (Table 3).

Table 3. Species occurrences based on their swimming ability and types of reproduction in artificial and natural habitats. Note that sexual and parthenogenetic populations of *P. olivaceus*, also parthenogenetic populations of *P. fontinalis* were found in artificial and natural habitats. On the other hand, sexual population of *P. fontinalis* was found in only artificial habitats. This situation was taken into consideration for total numbers of species

		Artificial habitat	Natural habitat	Total
Sexual species	Without swimming setae	2	3	4
	With swimming setae	-	1	1
Parthenogenetic species	Without swimming setae	5	7	7
	With swimming setae	12	10	14
	Numbers of species	17	20	24
	Numbers of individuals	2388	2081	4469

According to Shannon-Wiener index results, among the habitat types, troughs were shown as the richest habitats with regards to species diversity (up to 14 spp.) (Table 4) and numbers of individuals (2147 of 4469 ind.). On the other hand, numbers of species per site (ca. 0.54) were almost the lowest in troughs in comparison to the other habitats. In addition, although the number of troughs (26) was significantly higher than the creeks (12) and ponds (9), Shannon-Wiener (H') values for troughs ($H' = 2.34$), creeks ($H' = 2.33$) and ponds ($H' = 2.11$) were very close to each other (Table 4). H' values of the other habitats were relatively low and close to or less than 1.5 degree, which implies to be poor in diversity.

Although sexual populations of *P. olivaceus* and *P. fontinalis* are less-known in the literature, sexual population of them were found herein from a trough (Site 37) but individual populations of both species with different reproductive modes were also found from other habitats (Table 5). The dominance of females against males (female-biased sex ratio) was especially remarkable at low altitudes (Sites 15, 16, 33) while the ratio was almost equal at medium altitudes (Table 5).

Discussion

Along with the 28 ostracod taxa herein, the number of recent freshwater ostracod species of the Muğla province is now increased to 49 with the addition of previous reports (e.g. Gülen, 1985a; Aygen et al., 2004).

According to CCA and Spearman correlation analyses, the water temperature was the most effective factor on species occurrences and composition (Fig. 2). Especially, the ecological tolerance and optimum values of the commonly occurring species were found relatively higher than the other species. For example, common occurrences of *P. olivaceus* in many aquatic habitats (with 15 independent occurrences) agree with the literature (Meisch, 2000) that pinpointed the relatively high ecological tolerance levels of this species for many ecological variables. Also, Külköylüoğlu and Yılmaz (2006) suggested that *P. olivaceus* have a broader geographical distribution as long as habitat conditions are suitable.

In the present study, there was no statistical difference between the population density or the number of species in the natural or the artificial habitats. On the other hand, while the number of the swimming and non-swimming species were close to each other in the natural habitats with 11 and 10 spp., respectively, the number of the

swimming species (12 spp.) was higher than the numbers of non-swimmers (7 spp.) in the artificial habitats (Table 3). Species in such habitats can alter their location faster in active way (using swimming setae) than passive one due to unpredictable ecological conditions of artificial habitats (e.g., troughs). Thus, such ability of active movement may increase their survival chances by finding new location. Along with these movement abilities, the importance of ecological fitting abilities of species and habitat suitability should not be ignored for the survival success of species in different niches or wider range of habitats.

Table 4. Species diversity and population density of different habitat types

Habitat type	N.St	N.Sp	N.Ind	Spp/St	Obs	Obs/St	Var H'	Exp H'	H'	Species
Canal	4	5	168	1.25	3	0.75	0.08	5.00	1.61	<i>PO, HS, HC, IB, LI</i>
Creek	12	11	254	0.92	9	0.75	0.02	10.31	2.33	<i>CT, PO, PF, HI, HS, IB, LI, PZ, Asp*, Cysp, Psp</i>
Ditch	2	3	11	1.50	2	1.00	0.11	3.00	1.10	<i>CV, HC, NM</i>
Lake	2	1	7	0.50	2	1.00	0.00	1.00	0.00	<i>CT</i>
Pond	9	9	1154	1.00	5	0.56	0.03	8.22	2.11	<i>CN, CV, HC, IG, IH, PA, PV, TL, Csp</i>
Pool	1	1	6	1.00	1	1.00	0.00	1.00	0.00	<i>CN</i>
Reservoir	3	6	73	2.00	3	1.00	0.07	5.74	1.75	<i>CV, PF, IH, LI, Csp, Psp</i>
Spring water	6	6	578	1.00	6	1.00	0.05	4.87	1.58	<i>CN, PO, PF, HS, HBr, IB</i>
Stream	2	3	19	1.50	1	0.05	0.11	3.00	1.10	<i>IB, ID, LI</i>
Waterfall	1	4	52	4.00	1	1.00	0.09	4.00	1.39	<i>CW, PO, PF, IB</i>
Trough	26	14	2147	0.54	22	0.85	0.02	10.37	2.34	<i>CV, PO, PF, HB, HI, HS, HC, HBr, IG, PA, PP, PU, PV, Pvi</i>
All sample index	28								2.97	
Jackknife standard error	4.05								0.14	

Abbreviations: N.St., number of site; N.Sp., number of species; N.Ind., number of individual; Spp/st, ratio of number of species per site; Obs., number of observation; Obs/St, ratio of number of observations per site; H', Shannon-Wiener Index value; Var. H', variance H'; Exp H', expected value of H'. Species codes: *CN*: *Candona neglecta*, *CW*: *Candona weltneri*, *CT*: *Cyprideis torosa*, *CV*: *Cypridopsis vidua*, *PO*: *Psychrodromus olivaceus*, *PF*: *Psychrodromus fontinalis*, *HB*: *Heterocypris barbara*, *HI*: *Heterocypris incongruens*, *HS*: *Heterocypris salina*, *HC*: *Herpetocypris chevreuxi*, *HBr*: *Herpetocypris brevicaudata*, *IB*: *Ilyocypris bradyi*, *ID*: *Ilyocypris decipiens*, *IG*: *Ilyocypris gibba*, *IH*: *Ilyocypris hartmanni*, *LI*: *Limnocythere inopinata*, *NM*: *Notodromas monacha*, *PA*: *Potamocypris arcuata*, *PP*: *Potamocypris producta*, *PU*: *Potamocypris unicaudata*, *PV*: *Potamocypris variegata*, *Pvi*: *Potamocypris villosa*, *PZ*: *Prionocypris zenkeri*, *TL*: *Trajancypris leavis*, *Csp*: *Cypris* sp., *Psp*: *Pseudocandona* sp., *Csp*: *Cypridopsis* sp., *Asp*: *Aurila* sp. *brackish water taxon

Among habitats, troughs are generally located in/near villages to provide water for drinking, cleaning and/or irrigation purposes and they are used as microhabitats by ostracods (Külköylüoğlu et al., 2013). Such kind of artificial habitats (e.g., troughs) can open new possibilities for other species, although the establishment of troughs from natural sources can cause irreversible changes in species diversity and habitats. Because, waters of troughs come from underground sources, springs and/or surface waters, and these connections with those of natural habitats may influence species diversity (Külköylüoğlu et al., 2013). Except these water connections, different transportation vectors (e.g., air, insect, fish, birds, humans) may enrich species diversity

since ostracods can be distributed passively between different aquatic habitats by such kind of vectors (Mezquita et al., 1999). All of these explain the high Shannon-Wiener index value of troughs among habitats.

Table 5. The distribution of sexual and parthenogenetic populations of *P. olivaceus* and *P. fontinalis* at different habitats from 14 m to 1093 m of altitude

Species			<i>Psychrodromus olivaceus</i>		<i>Psychrodromus fontinalis</i>		<i>Candona neglecta</i>		<i>Candona weltneri</i>		<i>Notodromas monacho</i>	
St. No.	Alt. (m)	Habitat type	♀	♂	♀	♂	♀	♂	♀	♂	♀	♂
62	14	Creek	6									
65	114	Creek	35		15							
63	136	Trough	5									
17	294	Spring water	3		6							
66	296	Canal	126									
39	351	Spring water	36		14							
33	362	Spring water	80	15			1					
19	484	Reservoir			3							
20	490	Trough	1									
47	504	Creek			2							
49	540	Trough			146							
35	609	Ditch									3	4
18	656	Trough	85									
68	656	Pond	30		14				5	2		
15	669	Spring water	152	20								
16	669	Spring water	146	10								
36	699	Pool					3	3				
50	769	Trough			124							
46	799	Trough	3		7							
38	808	Trough	1									
42	839	Pond					1					
37	1093	Trough	12	6	21	8						
		Total	721	51	352	8	5	3	5	2	3	4

Potamocypris producta was commonly found in Africa (see e.g., Sars, 1924; Martens, 1984) but it was also reported from Europe (Macedonia, Petkovski, 1964), Japan (Okubo, 1976), and Turkey. Males of the species were only reported from South Africa by Sars (1924). 48 female individuals of *P. producta* in a trough along with *P. olivaceus* and *H. Barbara* were found. This record of *P. producta* herein makes an important contribution to the distribution and ecological preferences of species. This indicates that the species can also be found in artificial habitats.

The occurrence of parthenogenetic and sexual populations of *P. olivaceus* and *P. fontinalis* in troughs (Table 5) contribute to the knowledge of the habitat preferences of these species with different reproduction modes. This situation probably signals to a passive dispersal of them by subaquatic/nearby springs or underground waters, since these two species are known to prefer spring waters, flowing waters and pond fed by springs (Meisch, 2000). Fox (1965) claimed that males of *P. fontinalis* were found in northern Italy but later, Baltanás et al. (1993) stated that these specimens belong to another species, *P. betharrami*, collected from a subterranean stream in the Cave of Betharram (France). Sexual populations of *P. fontinalis* were described for the first time

in Macedonia by Petkovski and Meisch (1995). Until now, there is no any report of the sexual populations of these species from Turkey. Therefore, the sexual population of *P. fontinalis* herein is the first report from Turkey. However, males of *P. olivaceus* are already known from different countries of Europe (Petkovski, 1959, 1966; Järvekülg, 1959; Petkovski and Meisch, 1995). In Turkey, the male of *P. olivaceus* was found for the first time by Gülen (1985b) in the Lake Karamık (Afyon) and followed by other studies (Külköylüoğlu and Yılmaz, 2006; Rasouli et al., 2014; Külköylüoğlu et al., 2015; the present study).

Among these records, similar distribution patterns of *P. producta* and *P. fontinalis* were recorded from Macedonia and Turkey, and this may be explained with different passive dispersion ways. For instance, it is well known that Anatolia is an important migration route and works as a bridge between the Balkans and Africa for some migratory birds (Deinet et al., 2013). Ostracods can attach to the external surface of the birds, and so they are transported passively among the different geographic regions. Additionally, the record of *P. producta* from Japan is an interesting finding and might signal a human-mediated dispersal. Considering that the success of the species transported is related to the habitat suitability, and the ecological and biological features of the species, these records show the fitting ability under suitable environmental conditions of these two species.

Although troughs have relatively high ostracod diversity, the numbers of species per trough is not the highest among habitats (Table 4). Comparing to other sites, this situation may be explained with more samplings from these artificial habitats. However, another interesting point here is that although the number of individuals in troughs was prominently high, most of the individuals (1111 of 2147) collected from troughs belonged to two well-known cosmopolitan species (*H. incongruens* and *H. salina*). Moreover, finding at least two other species (e.g., *P. olivaceus*, *Potamocypris unicaudata*) with high densities in these habitats suggests that such artificial habitats can provide some chance of survival mainly for species with relatively high ecological tolerance ranges. Actually, troughs are routinely cleaned out and emptied by local people. Eventually, such process can cause a huge impact on the populations. In such case, ostracods may leave their desiccation resistant eggs until troughs are filled by water again. It means that the species with their cosmopolitan features as well as their adaptive values to harsh environmental conditions can easily colonize in the troughs. If troughs are accepted as newly development habitat after habitat degradation, in the case of recolonization, high ostracod richness and strong dominance of cosmopolitan species in troughs are inevitable. Therefore, this situation indicates the “primer succession” of species with high ecological tolerance levels as transitional and/or opportunistic populations. Additionally, most of the species found from troughs were parthenogens, even though some species were represented with sexual populations in a trough. A similar case observed in a newly developed spring in Turkey (Külköylüoğlu, 2009) supports this previous statement. The dominance of the parthenogens in following colonization may be the sign of the transition to stability or predictability in the environmental conditions, because it is known that if environmental deterioration continues as a result of stochastic and drastic changes, such kind of habitats can be established by sexual populations (Hewitt, 1999; Horne and Martens, 1999). Thus, it can be argued that the different reproduction modes of species can be effective as well as their relatively wide ecological tolerance levels for the initial colonization of the habitats.

As seen in *Table 5*, sexual populations of *P. olivaceus* and *P. fontinalis* co-occurred in a trough (St. 37) and there is a difference in the sex ratio of the individuals of both species. Generally, one of the reasons of female-biased sex ratio can be explained by the presence of the females of species with both reproductive modes from the same sampling site. On the other hand, although it is not the scope of this study, some genetic factors can play a role such as the greater longevity of females that lead to the skewed sex ratio in the population (Butlin et al., 1998). Thus, the possible reasons of the skewed sex ratio can be better understood by means of genetic data to determine the proportion of the fully sexual and parthenogenetic females.

In contrast to Gülen (1985b) who reported the sex ratio of *P. olivaceus* as about 1/2 favoring males (16 females and 33 males), the ratio in our study was almost about 1/8 favoring the females. The dominance of females against males (female-biased sex ratio) was especially remarkable at low altitudes (e.g., cf. stations 15, 16, 33) where the population densities were high. However, both the numbers of female and male became close to each other, and population densities were low at medium altitude (st. 37, 1093 m). In addition, the first record of the sexual forms of *P. olivaceus* was given by Petkovski (1959) from the moderately medium altitudes (1300 m) to high altitudes (ca. 2200 m) favoring the females. In the present study, a sexual population of *P. olivaceus* was found from two spring waters and one trough located at different altitudes that put into the previously known altitudinal ranges. Unlike *P. olivaceus*, the sexual populations of *P. fontinalis* were only found from a trough at 1093 m in Muğla. Males of *P. fontinalis* were also known from a small mountain spring water at 1600 m a.s.l (Petkovski and Meisch, 1995). The ranges of altitude (312-1262 m, Külköylüoğlu et al., (2012b) where species occur in literature reinforce the statement of Külköylüoğlu et al. (2012a) as parthenogenetic populations of *P. fontinalis* had the highest tolerance values for altitude. Similarly, parthenogenetic populations of *P. fontinalis* were found at various altitudes ranging from 114 m to 1093 m a.s.l. in the present study.

Parthenogenetic populations of the species were found from sea level to 1093 m, while sexual populations were obtained in a limited number of habitats located between 327 and 1093 m a.s.l. Külköylüoğlu et al. (2012b) showed no relationship between occurrence of sexual and parthenogenetic forms at different altitudes, although Peck et al. (1998) suggested that population densities of parthenogens exhibited the tendency to occur in northern areas at high altitudes.

According to the hypotheses of the distributional patterns of ostracods in terms of reproduction modes, both circum-Mediterranean shelters staying after the Pleistocene glaciation, and the fluctuating environmental conditions of the early Holocene, persisted some sexual populations in southern regions (i.e., post glacial invasion/re-colonization hypothesis). The following Holocene climatic stability provided more common dispersion and increase of frequencies of the parthenogens (Holocene stability hypothesis) (Horne and Martens, 1999). Similarly (but not in the same way), during this glaciation period, Anatolia played a critical role for the survival of both sexual and parthenogens providing opportunity to recolonize species in the other regions (Gülen, 1985a; Hewitt, 1999; Külköylüoğlu et al., 2012b). Additionally, as stated above, since Anatolia is an important route for the migration of birds, the ostracods species can be transported via passive dispersion from different regions to Anatolia. Then, other factors, such as different climatic conditions, latitudes in Anatolia, allow the colonization of the species in new locations. Thus, finding the males of *P. fontinalis*

along with *P. olivaceus* supports the idea that “there are so many sexual populations in Turkey” (Külköylüoğlu et al., 2012b).

Conclusion

Overall, along with ecological preferences and tolerance levels of the species, if it is created the distributional patterns of ostracods according to their reproductive modes, ostracods can be used as an informative marker for monitoring environmental changes for the neo-studies. On the other hand, to know (i) how species diversity is affected when species faced with changes in habitat degradation, (ii) which species are the first members of the new colonization or (iii) that there is any remarkable alteration favoring the parthenogens or sexual in time after the dramatic environmental changes provides useful information for invisible environmental shifts (e.g. volcanic eruptions, drought) in the palaeo-studies. Due to short sampling time, our results, however, cannot be generalized at the moment but they support the idea that parthenogenetic species (and populations as well) clearly show a much wider geographical distribution than their sexual counterparts. Therefore, different factors and/or combination of them that affect this distribution (ecological, historical, and biological) should be investigated comprehensively.

Acknowledgements. The work was supported by the Scientific and Technological Research Council of Turkey (TUBITAK) (Project no: 213O172). We thank the anonymous reviewers for their comments and suggestions on our manuscript.

REFERENCES

- [1] Aygen, C., Balık, S., Ustaoglu, R. M. (2004): Two new records for the non-marine ostracod fauna of Turkey: *Humphycypris subterranea* (Hartmann, 1964) and *Herpetocypris brevicaudata* Kaufmann, 1900. – Zoology in the Middle East 31(1): 77-82.
- [2] Baltanás, A., Danielopol, D. L., Roca, J. R., Marmonier, P. (1993): *Psychodromus betharrami* n. sp. (Crustacea, Ostracoda): morphology, ecology and biogeography. – Zoologischer Anzeiger 231(1-2): 39-57.
- [3] Broodbaker, N., Danielopol, D. L. (1982): The Chaetotaxy of Cypridacea (Crustacea, Ostracoda) limbs: proposals for a descriptive model. – Bijdragen tot de Dierkunde 52(2): 103-120.
- [4] Butlin, R., Schön, I., Martens, K. (1998): Asexual reproduction in nonmarine ostracods. – Journal of Heredity 81(5): 473-480.
- [5] Carbonel, P., Colin, J. P., Danielopol, D. L., Löffler, H., Neustrueva, I. (1988): Paleocology of limnic ostracodes: a review of some major topics. – Palaeogeography, Palaeoclimatology, Palaeoecology 62(1-4): 413-461.
- [6] Cohen, A. C., Morin, J. G. (1990): Patterns of Reproduction in Ostracodes: a review. – Journal of Crustacean Biology 10(2): 184-211.
- [7] Cohuo, S., Macario, L., Pérez, L., Naumann, K., Schwalb, A. (2015): Effects of Altitudinal Gradients in Neotropical Ostracod Species Composition and Distribution: An Example from North-Central Guatemala. – In: Perrier, V., Meidla, T. (eds.) Abstracts, 8th European Ostracodologists Meeting, Tartu, Estonia, 22-30 July 2015.
- [8] Deinet, S., Ieronymidou, C., McRae, L., Bureld, I. J., Foppen, R. P., Collen, B., Böhm, M. (2013): Wildlife Comeback in Europe: The Recovery of Selected Mammal and Bird Species.

- Final Report to Rewilding Europe by ZSL, BirdLife International and the European Bird Census Council. ZSL, London.
- [9] Dudgeon, D., Arthington, A. H., Gessner, M. O., Kawabata, Z. I., Knowler, D. J., Lévêque, C., Naiman, R. J., Prieur-Richard, A. H., Soto, D., Staissny, M. L. J., Sullivan, C. A. (2006): Freshwater biodiversity: importance, threats, status and conservation challenges. – *Biological Reviews* 81(2): 163-182.
- [10] Finlayson, C. M., Davis, J. A., Gell, P. A., Kingsford, R. T., Parton, K. A. (2013): The status of wetlands and the predicted effects of global climate change: the situation in Australia. – *Aquatic Sciences* 75(1): 73-93.
- [11] Fox, H. M. (1965): Discovery of a male *Ilyodromus fontinalis* (Wolf) (Crustacea, Ostracoda). – *Memorie dell'Istituto Italiano di Idrobiologia* 18: 197-201.
- [12] Gonzalez Mozo, M. E., Martens, K., Baltanás, A. (1996): A Taxonomic Revision of European *Herpetocypris* Brady and Norman, 1889 (Crustacea, Ostracoda). – *Biologie* 66: 93-132.
- [13] Gülen, D. (1985a): The species and distribution of the group of Podocopa (Ostracoda-Crustacea) in freshwaters of western Anatolia. – *İstanbul Üniversitesi Fen Fakültesi Mecmuası* 50: 65-80.
- [14] Gülen, D. (1985b): Bisexual ostracoda (Crustacea) populations in Anatolia. – *İstanbul Üniversitesi Fen Fakültesi Mecmuası* 50: 81-86.
- [15] Heino, J., Tolonen, K. T. (2018): Ecological niche features override biological traits and taxonomic relatedness as predictors of occupancy and abundance in lake littoral macroinvertebrates. – *Ecography* 41(12): 2092-2103.
- [16] Hewitt, G. M. (1999): Post-glacial re-colonization of European biota. – *Biological Journal of the Linnean Society* 68(1-2): 87-112.
- [17] Horne, D. J., Martens, K. (1999): Geographical parthenogenesis in European non-marine ostracods (Crustacea: Ostracoda): post-glacial invasion or Holocene stability? – *Hydrobiologia* 391: 1-7.
- [18] Hurlbert, S. H. (1984): Pseudoreplication and the design of ecological field experiments. – *Ecological Monographs* 54(2): 187-211.
- [19] Järvekülg, A. (1959): The finding of a male *Ilyodromus olivaceus* (Brady and Norman) (Ostracoda, Cypridae). *Eesti NSV Teaduste Akadeemia Toimetised*. – *Biologia* 8: 242.
- [20] Juggins, S. (2003): Software for ecological and palaeoecological data analysis and visualization, *C² User Guide*. – University of Newcastle, Newcastle-Upon-Tyne.
- [21] Karanovic, I. (2012): *Recent Freshwater Ostracods of the World*. – Springer, Heidelberg.
- [22] Külköylüoğlu, O. (2004): On the usage of ostracods (Crustacea) as bioindicator species in different aquatic habitats in the Bolu region, Turkey. – *Ecological Indicators* 4: 139-147.
- [23] Külköylüoğlu, O. (2009): Ecological succession of freshwater Ostracoda (Crustacea) in a newly developed rheocrene spring (Bolu, Turkey). – *Turkish Journal of Zoology* 33(2): 115-123.
- [24] Külköylüoğlu, O., Yılmaz, F. (2006): Ecological requirements of Ostracoda (Crustacea) in three types of springs in Turkey. – *Limnologica-Ecology and Management of Inland Waters* 36(3): 172-180.
- [25] Külköylüoğlu, O., Akdemir, D., Yüce, R. (2012a): Distribution, ecological tolerance and optimum levels of freshwater Ostracoda (Crustacea) from Diyarbakır, Turkey. – *Limnology* 13(1): 73-80.
- [26] Külköylüoğlu, O., Sarı, N., Akdemir, D., Yavuzatmaca, M., Altınbaş, C. (2012b): Distribution of sexual and asexual Ostracoda (Crustacea) from different altitudinal ranges in the Ordu region of Turkey: testing the rapoport rule. – *High Altitude Medicine and Biology* 13(2): 126-137.
- [27] Külköylüoğlu, O., Akdemir, D., Sarı, N., Yavuzatmaca, M., Oral, C., Başak, E. (2013): Distribution and ecology of Ostracoda (Crustacea) from troughs in Turkey. – *Turkish Journal of Zoology* 37(3): 277-287.
- [28] Külköylüoğlu, O., Akdemir, D., Yavuzatmaca, M., Yılmaz, O. (2015): A checklist of recent non-marine Ostracoda (Crustacea) of Turkey with three new records. – *Review of Hydrobiology* 8(2): 77-90.

- [29] Martens, K. (1984): Annotated checklist of non-marine ostracods (Crustacea, Ostracoda) from African inland waters. – Zoologische Documentatie - N20-Koninklijk Museum voor Midden-Afrika.
- [30] Martens, K., Schön, I., Meisch, C., Horne, D. J. (2008): Global diversity of ostracods (Ostracoda, Crustacea) in freshwater. – *Hydrobiologia* 595(1): 185-193.
- [31] Mayr, E., Ashlock, P. D. (1991): Principles of Systematic Zoology. 2nd Ed. – McGraw-Hill, New York.
- [32] Meisch, C. (2000): Freshwater Ostracoda of Western and Central Europe (Süßwasserfauna von Mitteleuropa 8/3). – Spektrum Akademischer Verlag, Heidelberg.
- [33] Meisch, C., Smith, R. J., Martens, K. (2019): A subjective global checklist of the extant non-marine Ostracoda (Crustacea). – *European Journal of Taxonomy* 492: 1-135.
- [34] Mezquita, F., Griffiths, H. I., Sanz, S., Soria, J. M., Piñón, A. (1999): Ecology and distribution of ostracods associated with flowing waters in the eastern Iberian Peninsula. – *Journal of Crustacean Biology* 19(2): 344-354.
- [35] Okubo, I. (1976): *Potamocypris producta* (Sars, 1924) from Japan (Ostracoda, Cyprididae). – *Researches on Crustacea* 7: 52-56.
- [36] Peck, J. R., Yearsley, J. M., Waxman, D. (1998): Explaining the geographic distributions of sexual and asexual populations. – *Nature* 391: 889-892.
- [37] Petkovski, T. K. (1959): Beitrag zur Kenntnis der Ostracodenfauna Jugoslawiens (V). – *Hidrobiologi. Publications of the Hydrobiological Research Institute, Faculty of Science, University of Istanbul, Seri B* 4(4): 158-165.
- [38] Petkovski, T. K. (1964): Bemerkenswerte Entomostraken aus Jugoslavien. – *Acta Musei Macedonici Scientiarum Naturalium* 9: 147-182.
- [39] Petkovski, T. K. (1966): Ostracoden aus einigen Quellen der Slowakei. – *Acta Musei Macedonici Scientiarum Naturalium* 10: 91-168.
- [40] Petkovski, T. K., Meisch, C. (1995): Interesting freshwater Ostracoda (Crustacea) from Macedonia. – *Bulletin de la Societe des Naturalistes Luxembourgeois* 96: 176-183.
- [41] Rasouli, H., Aygen, C., Külköylüoğlu, O. (2014): Contribution to the Freshwater Ostracoda (Crustacea) Fauna of Turkey: Distribution and Ecological Notes. – *Turkish Journal of Fisheries and Aquatic Sciences* 14: 11-20.
- [42] Ruban, V., López-Sánchez, J. F., Pardo, P., Rauret, G., Muntau, H., Quevauviller, P. (1999): Selection and evaluation of sequential extraction procedures for the determination of phosphorus forms in lake sediment. – *Journal of Environmental Monitoring* 1: 51-56.
- [43] Sars, G. O. (1924): The freshwater Entomostraca of the Cape Province. – *Annals of the South African Museum* 20: 105-193.
- [44] Seaby, R. M., Henderson, P. A. (2006): Species Diversity and Richness Version IV. – Pisces Conservation Ltd, Lymington.
- [45] ter Braak, C. J. F. (1986): Canonical correspondence analysis: a new eigenvector technique for multivariate direct gradient analysis. – *Ecology* 67: 1167-1179.
- [46] ter Braak, C. J. F., Šmilauer, P. (2012): Canoco Reference Manual and User's Guide: Software for Ordination, Version 5.0. – Microcomputer Power, Ithaca.
- [47] Yavuzatmaca, M., Külköylüoğlu, O., Yılmaz, O., Akdemir, D. (2017): On the relationship of ostracod species (crustacea) to shallow water ion and sediment phosphate concentration across different elevational range (Sinop, Turkey). – *Turkish Journal of Fisheries and Aquatic Sciences* 17(7): 1333-1346.
- [48] Wagner, C. W. (1964): Ostracods as environmental indicators in recent and holocene estuarine deposits of the Netherlands. – *Publicazioni della Stazione Zoologica di Napoli* 33: 480-495.
- [49] Wiens, J. J. (2011): The niche, biogeography and species interactions. – *Philosophical Transactions of the Royal Society of London B: Biological Sciences* 366(1576): 2336-2350.
- [50] Williams, M., Siveter, D. J., Salas, M. J., Vannier, J., Popov, L. E., Pour, M. G. (2008): The earliest ostracods: The geological evidence. – *Senckenbergiana Lethaea* 88(1): 11-21.

APPENDIX

Table A1. Minimum–maximum values of the geographical data and physicochemical variables from 11 different aquatic habitat types with station numbers in Muğla province

		Ta	Atm	Moi	Wind	Alt	pH	DO	S
Canal	Min	21.700	727.300	34.700	0.000	17.000	8.220	3.260	42.400
	Max	33.800	754.800	63.600	6.400	296.000	8.520	7.360	83.600
	Mean	30.275	745.500	45.200	3.075	110.500	8.353	5.538	63.025
	St dev	3.139	26.103	11.020	4.506	308.349	0.638	2.352	22.683
Creek	Min	23.600	702.600	27.500	0.000	5.000	7.090	2.000	22.500
	Max	33.200	757.400	67.400	7.700	790.000	8.820	8.060	83.800
	Mean	30.275	735.175	46.917	2.783	272.750	7.893	4.761	56.308
	St dev	2.800	25.877	11.099	4.413	308.862	0.639	2.351	22.918
Ditch	Min	29.500	705.300	38.700	2.200	19.000	8.150	3.020	37.500
	Max	31.500	755.600	49.200	4.200	609.000	8.330	6.630	86.000
	Mean	30.500	730.450	43.950	3.200	314.000	8.240	4.825	61.750
	St dev	2.797	26.454	10.740	4.594	310.429	0.652	2.406	23.301
Lake	Min	28.500	752.900	44.500	3.200	17.000	8.690	4.840	65.900
	Max	32.800	759.100	52.600	9.500	17.000	8.760	4.870	68.500
	Mean	30.650	756.000	48.550	6.350	17.000	8.725	4.855	67.200
	St dev	2.816	26.636	10.782	4.630	311.697	0.662	2.386	22.953
Pond	Min	23.100	685.000	26.300	0.000	40.000	7.810	2.140	5.980
	Max	33.900	754.000	55.900	15.700	839.000	9.810	7.420	97.600
	Mean	30.122	719.722	41.678	5.556	434.000	8.772	5.984	69.531
	St dev	2.884	26.536	10.812	4.611	310.229	0.700	2.335	24.465
Pool*	Mean	29.200	697.500	35.400	8.900	699.000	7.080	3.300	33.400
Spring water	Min	27.700	701.000	28.800	0.000	294.000	6.450	3.300	37.500
	Max	33.500	773.500	49.100	4.800	669.000	8.040	10.340	93.700
	Mean	32.100	722.600	35.900	3.533	493.500	7.313	5.643	57.150
	St dev	2.808	26.412	10.675	4.489	301.974	0.677	2.428	23.166
Stream	Min	30.900	750.100	47.500	2.700	0.000	8.390	5.120	59.000
	Max	32.100	751.700	51.800	3.900	43.000	8.390	5.360	60.400
	Mean	31.500	750.900	49.650	3.300	21.500	8.390	5.240	59.700
	St dev	2.798	26.472	10.788	4.591	313.260	0.654	2.384	22.919
Reservoir	Min	22.200	708.800	32.400	0.000	57.000	8.320	2.500	29.700
	Max	32.600	752.400	55.400	7.500	574.000	9.250	5.750	75.400
	Mean	28.733	726.533	45.937	4.267	371.667	8.657	4.307	54.500
	St dev	2.961	26.189	10.849	4.600	307.379	0.665	2.394	23.120
Trough	Min	26.000	665.700	23.400	1.400	11.000	6.490	2.450	29.000
	Max	35.300	758.600	64.400	34.000	1093.000	8.980	14.450	112.700
	Mean	30.900	713.942	37.920	5.252	504.731	7.761	5.579	58.238
	St dev	2.679	26.801	10.926	5.181	315.476	0.629	2.587	23.185
Waterfall*	Mean	29.700	698.800	42.100	0.000	656.000	7.380	10.400	91.700

Abbreviations: Ta, air temperature (°C); Atm, atmospheric pressure (mmHg); Moi, moisture (%); Wind, (m s⁻¹); Alt, Altitude (m); DO, dissolved oxygen (mg L⁻¹); S, oxygen saturation (%); Tw, water temperature (°C); Sal, salinity (ppt); EC, electrical conductivity (µS cm⁻¹); TDS, total dissolved solids (mg L⁻¹); Na⁺, sodium (mg L⁻¹); K⁺, potassium (mg L⁻¹); Mg²⁺, magnesium (mg L⁻¹); Ca²⁺, calcium (mg L⁻¹); F⁻, fluoride (mg L⁻¹); Cl⁻, chloride (mg L⁻¹); SO₄²⁻, sulphate (mg L⁻¹); Tot-Ph; total phosphate (mg kg⁻¹); In-Ph, inorganic phosphate (mg kg⁻¹); Or-Ph; organic phosphate (mg kg⁻¹), b.d.l. below detectable limits; *single sampling

Table A1. Continuation

		Tw	Sal	EC	TDS	Na⁺¹	K⁺¹	Mg⁺²	Ca⁺²
Canal	Min	16.900	0.030	271.400	0.209	2.195	0.313	6.913	10.884
	Max	28.900	0.380	736.000	0.410	18.152	3.898	40.088	93.513
	Mean	22.450	0.203	538.350	0.319	7.542	1.671	17.153	52.465
	St dev	5.261	8.701	247.021	8.113	67.140	22.478	30.256	50.092
Creek	Min	16.300	0.060	148.600	0.089	0.378	0.409	1.444	0.487
	Max	32.200	73.180	1150.860	65.780	35.002	113.541	195.433	237.959
	Mean	22.008	7.789	593.498	6.931	8.595	18.062	49.252	80.255
	St dev	5.243	11.696	265.480	10.931	66.260	25.952	37.440	55.475
Ditch	Min	20.100	0.090	62.100	0.131	9.998	0.656	1.619	44.557
	Max	29.800	0.270	185.000	0.364	34.042	17.408	9.395	72.609
	Mean	24.950	0.180	123.550	0.248	22.020	9.032	5.507	58.583
	St dev	5.312	9.006	252.891	8.360	69.616	23.324	31.175	50.961
Lake	Min	29.600	2.230	254.510	2.756	554.518	18.293	50.098	29.502
	Max	30.300	14.070	466.900	15.210	554.518	140.824	58.081	200.468
	Mean	29.950	8.150	360.705	8.983	554.518	79.558	54.090	114.985
	St dev	5.351	9.121	248.412	8.526	97.051	28.672	31.566	54.076
Pond	Min	23.600	0.100	83.700	0.145	3.252	0.361	1.207	12.546
	Max	34.100	0.700	399.300	0.910	34.068	19.395	20.041	238.423
	Mean	29.211	0.201	254.167	0.271	11.062	7.652	7.854	49.126
	St dev	5.416	8.588	244.248	7.942	66.192	22.158	29.928	53.863
Pool*	Mean	16.400	0.140	0.184	236.300	8.507	0.329	3.291	b.d.1
Spring water	Min	10.300	0.090	165.000	0.133	2.067	0.587	1.068	4.722
	Max	21.900	0.410	694.000	0.533	29.259	4.009	10.727	46.601
	Mean	16.683	0.198	345.750	0.267	19.072	1.757	4.704	25.391
	St dev	5.525	8.759	249.534	8.113	68.557	22.962	30.852	50.758
Stream	Min	21.200	0.240	481.300	0.329	5.687	0.424	14.705	37.110
	Max	22.400	0.300	564.000	0.397	5.935	0.980	30.134	37.993
	Mean	21.800	0.270	522.650	0.363	5.811	0.702	22.419	37.551
	St dev	5.252	9.005	248.131	8.360	69.641	23.312	31.080	50.964
Reservoir	Min	24.200	0.080	183.600	0.115	4.372	0.597	2.122	14.346
	Max	29.700	0.170	369.100	0.226	17.790	2.267	6.258	46.339
	Mean	27.033	0.137	298.233	0.170	11.150	1.558	3.833	30.153
	St dev	5.272	8.943	247.683	8.361	69.086	23.132	31.029	50.811
Trough	Min	15.800	0.070	113.200	0.093	2.060	0.100	0.495	3.258
	Max	32.100	0.650	913.000	0.845	108.242	12.396	68.254	126.984
	Mean	24.054	0.321	462.350	0.432	16.715	2.149	19.002	48.008
	St dev	4.951	7.811	250.365	7.217	60.527	20.357	29.113	47.648
Waterfall*	Mean	9.800	0.140	0.184	200.800	1.776	0.336	5.860	b.d.1

Table A1. Continuation

		F⁻¹	Cl⁻¹	SO₄⁻²	Tot-Ph	In-Ph	Or-Ph	Station numbers
Canal	Min	0.056	2.564	1.943	0.239	0.269	0.054	64, 66, 11, 56
	Max	0.140	38.574	146.011	0.598	0.737	0.126	
	Mean	0.098	13.143	40.965	0.429	0.468	0.089	
	St dev	0.485	39.211	110.086	0.267	0.206	0.066	
Creek	Min	0.026	0.721	0.324	0.051	0.096	0.008	2, 5, 10, 21, 25, 31, 47, 48, 52, 58, 62, 65
	Max	0.183	69.199	356.561	0.629	0.892	0.190	
	Mean	0.110	14.055	80.035	0.330	0.282	0.067	
	St dev	0.498	39.077	114.608	0.257	0.196	0.067	
Ditch	Min	0.036	8.526	13.864	0.648	0.336	0.356	4, 35
	Max	0.917	53.448	13.864	0.648	0.336	0.356	
	Mean	0.477	30.987	13.864	0.648	0.336	0.356	
	St dev	0.517	40.564	113.620	0.280	0.187	0.083	
Lake	Min	1.603	0.000	0.000	0.314	0.100	0.003	14, 57
	Max	1.603	0.000	0.000	0.314	0.171	0.027	
	Mean	1.603	0.000	0.000	0.314	0.136	0.015	
	St dev	0.561	41.012	114.528	0.276	0.185	0.069	
Pond	Min	0.060	4.676	0.491	0.040	0.001	0.010	3, 7, 8, 12, 41, 42, 44, 45, 51
	Max	0.406	64.564	799.695	0.612	0.351	0.214	
	Mean	0.216	17.382	104.214	0.293	0.145	0.058	
	St dev	0.472	38.838	142.439	0.269	0.185	0.070	
Pool*	Mean	9.170	b.d.l.	10.291	3.837	0.160	0.257	36
Spring water	Min	0.025	2.605	2.030	0.170	0.100	0.019	15, 16, 17, 33, 39, 67
	Max	2.563	45.591	70.574	1.720	0.314	0.064	
	Mean	0.903	25.669	29.196	0.610	0.190	0.036	
	St dev	0.632	39.909	111.036	0.338	0.184	0.068	
Stream	Min	0.117	6.171	9.430	0.153	0.100	0.006	59, 61
	Max	0.117	9.341	43.900	0.657	0.549	0.046	
	Mean	0.117	7.756	26.665	0.405	0.324	0.026	
	St dev	0.511	40.450	112.690	0.278	0.191	0.069	
Reservoir	Min	0.046	7.004	10.279	0.083	0.045	0.003	19, 30
	Max	0.081	36.789	28.626	0.197	0.129	0.063	
	Mean	0.063	19.040	17.301	0.123	0.084	0.024	
	St dev	0.505	40.136	111.841	0.276	0.187	0.068	
Trough	Min	0.010	2.330	1.880	0.213	0.138	0.040	1, 9, 13, 18, 20, 22, 23, 24, 26, 27, 28, 29, 32, 34, 37, 38, 40, 43, 46, 49, 50, 53, 54, 55, 60, 63
	Max	0.266	285.837	152.303	0.464	0.448	0.160	
	Mean	0.101	34.196	24.818	0.345	0.305	0.064	
	St dev	0.454	46.757	96.951	0.262	0.180	0.067	
Waterfall*	Mean	45.792	b.d.l.	2.229	1.648	0.219	0.156	68

CARCASS COMPOSITION, SPERMATOGENESIS PROCESSES AND PATHOGENIC THREATS OF MALE MALLARD DUCKS (*ANAS PLATYRHYNCHOS* L.)

FLIS, M.¹ – BRODZKI, P.^{2*}

¹*Department of Animal Ethology and Wildlife Management, Faculty of Animal Sciences and Bioeconomy, University of Life Sciences in Lublin, 20-950 Lublin, Poland*
ORCID: 0000-0001-7429-3158

²*Department of Andrology and Biotechnology of Reproduction, Faculty of Veterinary Medicine, University of Life Sciences in Lublin, 20-950 Lublin, Poland*

*Corresponding autor
e-mail: wetdoc@interia.pl

(Received 23rd Sep 2019; accepted 8th Jan 2020)

Abstract. The paper presents the characteristics of slaughter efficiency and chemical composition of carcasses, the course of spermatogenesis processes as well as epizootic and epidemiological threats of male mallard ducks (*Anas platyrhynchos* L.). Tests and analyses carried out indicate a high slaughter output of 64.5% and a decrease in body weight during the winter months and the subsequent turning period. Muscles of male crosses were characterized by high protein content (23.54-23.58%) and low fat content (0.65-0.84%). In addition, a high level of unsaturated fatty acids, including those in the C 20 group, and a favorable UFA to SFA ratio of 1.5 were found. Organoleptic and bacteriological evaluation showed the presence of intestinal parasites of the *Hymenolepididae* family and muscle parasites of the *Sarcocystis* genus, as well as *E. coli* and *Staphylococcus aureus*, which were mostly resistant to the antibiotics used. The assessment of the advancement of the spermatogenesis process during the reproductive season showed the correct development of reproductive capacity in drakes. In addition, it has been shown that fully developed sperm capable of fertilization is produced at the turn of March and April, despite the fact that pairing occurs much earlier. The described composition of fatty acids indicates high pro-health values of mallard meat. At the same time, the parasites and bacteria found indicate that mallard duck meat may pose a risk to human health, and therefore carcasses must be tested before being intended for consumption.

Keywords: mallard duck, body mass, venison, slaughter efficiency, natural selection, bacterial diseases, Lublin Upland

Introduction

Mallard duck (*Anas platyrhynchos* L.) is one of the most common species of wild duck in many European, Asian and North American countries. They are also the ancestor of most domestic duck breeds. Can also be found in Australia and New Zealand (Tracey et al., 2008; Söderquist, 2012). In the United States, breeding crosses settled hunting grounds for hunting (Smith and Rohwer, 1997). In Poland, the mallard is the most huntable species among the four huntable of wild ducks that can be hunted and has been one of the most important game birds for many years. Despite the continuing downward trend over the past decade, approximately 100,000 wild ducks are acquired annually, of which around 95% are mallards (Książkiewicz, 2006; List of hunting reporting data, 2018). As the reason for the decline in the population, the most frequently mentioned are transformations in aquatic ecosystems and the related reproduction processes of these birds. Therefore, an important element of knowledge about the population is to learn the principles of natural selection during the mating

season and the timeliness of its course. It is also important to learn about male spermatogenesis processes, which directly affect breeding success, and thus natural growth. Although climate change and improvement of habitat conditions affect the increase of duck weight and survival in winter, it is not known whether these changes cannot have a negative effect on the spermatogenesis process and reproduction rates of mallard ducks (Guillemain et al., 2010). Guillemain et al. (2013) reported that climate change may have an impact on the course of many population processes such as: migration distance, mortality rates as well as reproductive distribution and success. In addition, climate change significantly affects the shift towards the north of the optimal winter refuges, as well as earlier migrations to the southern areas. Climate change also leads to the impoverishment of habitat and hence breeding areas. Consequently, the described elements may affect the course of reproductive processes as well as the raising of chicks, and thus the complete reproductive success (Gaston et al., 2009).

Hunting is one of the areas of social activity that is quite important in terms of culture and recreation. In addition, they allow the regulation of the size of individual populations on the principles of sustainable development. By hunting, it is possible to regulate the population structures of individual species that affect reproduction and survival rates, while optimizing the functioning of the population (Borman and Mattson, 2012). Not without significance is the fact that high-quality meat is provided, commonly referred to as venison, which is characterized by both taste and health benefits. Despite the fact that the global production of poultry meat shows an upward trend, many consumers are looking for an alternative in terms of meat quality, hence there is an increasing interest in meat from wild animals, in particular from wild game (Hoffman and Wiklund, 2006; Górecka and Szmańko, 2010; Nuernberg et al., 2011; Siminska et al., 2011; Kasprzyk, 2013; Ljung et al., 2015; Żmijewski et al., 2018; Flis et al., 2019).

On average in Europe, in total meat production, venison accounts for a small percentage of 0.2-0.4% (Siminska et al., 2011; Popczyk, 2012). According to research carried out in Sweden, venison consumption also depends on the social perception of hunting in a given region and is characterized by quite considerable variation. Nevertheless, only 2% of the total consumption of this type of meat comes from sales in shops, while the remaining consumption is conditioned by the fact of hunting or the purchase of it is related to social networks (Ljung et al., 2015).

Among game meat from game birds, pheasant meat definitely prevails, which has very high taste and dietary values (Kuźniacka et al., 2007; Biesiada-Drzazga et al., 2011; Kokoszyński et al., 2014; Flis et al., 2019), nevertheless meat from mallard ducks is most often considered a culinary delicacy, but it is most often consumed in hunters' environment. This is conditioned by its periodic supply related to the hunting season, as well as the limited accessibility resulting from meat trade regulations, and thus the lack of companies distributing this type of game (Bertolini et al., 2005; Nuernberg et al., 2011; Popczyk, 2012; Janiszewski et al., 2018).

In the nutritional aspect, a fairly important element is the fatty acid profile, in particular the share of polyunsaturated acids. Meat from wild birds is usually characterized by an increased share of these acids, mainly omega-3, which is why it is referred to as dietary and health-promoting. The taste characteristics, high digestibility and quality of meat deserve emphasis, which is also largely determined by the content of polyunsaturated acids - n-3 and n-6 PUFA in an appropriate proportion (Mishra et al., 1993; Cobos et al., 2000; Janiszewski et al., 2018; Flis et al., 2019). In addition, meat

from wild ducks is a valuable source of iron, zinc, copper and manganese (Lorenzo et al., 2011).

At the same time, one of the consumers' concerns about the possibility of consuming venison is the fact related to the common opinion about the possibility of contracting diseases (Nagalska and Rejman, 2014; Kwiecińska et al., 2016). Avian influenza is mentioned as the most dangerous in the mallard, which is a migratory species (Gunnarsson et al., 2012; Wille et al., 2018), however, other viral or bacterial diseases and quite often parasitic diseases, as well as mycoses are also found (Betlejewska et al., 2002; Żbikowski et al., 2006; Haščík et al., 2010; Dynowska et al., 2013; Flis and Grela, 2018).

Despite the fact that when consuming meat derived from carcasses of small animals, as a rule no research is carried out in terms of epidemiological risk, organoleptic assessment of carcasses and internal organs is carried out during post-mortem inspection and preparation of meat for consumption.

The aim of the study was to evaluate the composition of the carcasses, their slaughter performance and the chemical composition of the pectoral muscles in the aspect of healthy properties of wild duck meat. In addition, bacteriological and macroscopic evaluation (presence of sarcocysts) of carcasses was aimed at determining a possible threat to human health. The aim was also to assess the correct development of male reproduction capacity of male mallard ducks during the breeding period in terms of climate change.

Materials and methods

Material

The materials for work were male mallard ducks obtained by hunting, in accordance with applicable law in the hunting season in Poland, from October to December 2017 years. In addition, with the consent of the Minister of the Environment (decision DL-III.6713.21.2017.JC), five drakes were shot per month in the period from January to April 2018 years, i.e. during the protection period, in order to determine possible changes in the winter and spring, when the birds are exposed to increased pressure of environmental factors, and furthermore a lekking site is taking place. Thus, seven periods of one month were identified in which the material for research was obtained. In total, 35 subjects constituted the research material. Male mallard ducks were shot in water reservoirs (fish ponds, small ponds and rivers) in the south-western part of the Lublin region (*Figure 1*).

Preparation of tests

In each case, after obtaining the birds, they were cooled down. Then, after being transported to the laboratory, each of them was weighed. The next weighing was performed after decapitation of the head. The next step was to nibble and weigh the carcass without feathers and lower legs. Then the birds were gutted and weighed again. Weighing also included edible intestines (heart, liver and muscle stomach after cleansing of gastrointestinal content). Each weighing was carried out on a laboratory scale with an accuracy of 1 gram. The entrails were stored in a refrigerator at 4°C for 24 hours, after which they were sent for bacteriological and parasitological tests.



Figure 1. Location of the research area

Then the pectoral muscle (*m. pectoralis*) of the birds was prepared, minced and stored one day at 4°C, after which the crude fat content was determined according to the method of Folch et al. (1957). The fatty acid profile was determined by gas chromatography in the obtained fat. Fatty acid methyl esters were determined in a Varian CP 3800 gas chromatograph under the following assay conditions: CP WAX 52CB DF 0.25 UM capillary column, 100 m long, carrier gas - helium, flow - 1.4 ml/min, column operating temperature - 120°C with a gradual increase of 2°C/min. up to 210°C, determination time - 157 min, dispenser temperature - 160°C, detector temperature - 160°C, supporting gases - hydrogen and air.

Also after evisceration, the testicles were dissected, which were stored in string bags for a period of 24 hours also at 4°C, after which they were transferred to laboratory tests covering the course of spermatogenesis processes.

Organoleptical, bacteriological research

The macroscopic evaluation included the examination of each bird directly after shooting, plucking the carcass and skinning it. Its purpose was to capture possible lesions or occurrence of parasites.

Various multiplication and differentiation media were used to identify individual microbial species. The solid medium was agar with the addition of 5% sheep blood to multiply aerobic microorganisms and possibly determine hemolysis. As a liquid medium, sugar broth was used to propagate aerobic bacteria. Other media, including Chapman, MacConkey, and Sabouard media were also used to identify possibly occurring organ mycoses. The cetrimid medium for the identification of *Pseudomonas* microorganisms and the D-coccosel medium for the identification of fecal bacteria were also used for the tests. Further identification of individual types of bacteria was carried out using bioMerieux API (Analytical Profile Index) biochemical tests. Media fertility control was carried out using standard strains. After determining the bacterial strain, the growth rate of bacterial flora was assessed using the criteria of fairly low (+), intensive

(++) and very intensive (+++). An analysis of the sensitivity of isolated bacterial strains to 7 commonly used antibiotics was also carried out. The analysis was performed using the diffusion-disk method (Kirby-Bauer) based on the diffusion of the antibiotic in the disk into the medium using the created concentration gradient. Based on the size of the bacterial inhibition zone, its sensitivity to a given antibiotic is determined by defining it as sensitive, moderately sensitive and resistant (Borowska et al., 2014). The sensitivity scale was determined on the basis of the tables of the "European Committee on Antimicrobial Susceptibility Testing" (EUCAST).

The following antibiotics were used for the analyzes in doses: Doxycycline DO30 - 30µg, Amoxicilin AML25/AX25 - 25µg, Ampicillin AMP10/AM10 - 10µg, Amoxicillin/clavulanic acid Synulox AMC30 - 30µg, Lincomycin/Spectinomycin LS109 - 5µg, Colistin CT50 - 50µg.

Spermatogenesis process

The prepared nuclei were weighed on a laboratory scale with an accuracy of 0.001 gram. Then microscopic preparations were made. The epididymis and testes were incised with a scalpel, followed by several imprint preparations on microscope slides. The preparations were dried, fixed and stained by several methods to obtain the best-quality microscopic image. The best preparations were obtained using the Hemacolor rapid staining method (Merck KGaA, Darmstadt, Germany). After preparation, the slides were evaluated on an Olympus CX4 light microscope with an attached Bassler A312 camera (Olympus Corporation, Japan) at 1000-fold magnification, under immersion. The image from the camera was read on a computer monitor, which facilitated the work and significantly improved the accuracy of the examination and allowed documentation of the preparations.

Statistical analysis

To determine the differences between the average values of the analyzed slaughter performance traits and testicles weight analyzed, between test periods, a one-way analysis of variance was performed. Considering equal sample sizes ($n = 5/\text{period}$), in order to verify the possible occurrence of differences between the means, calculations were made using the Newman Keuls test in Statistica 10.0. The impact of the study period was considered significant at a significance level of $P \leq 0.05$. The value and significance of correlation coefficients between the weight of internal organs and the body weight and weight of duck carcasses were also calculated.

Results

Body weight and characteristics of carcasses

During the study period, despite slight fluctuations, weight loss occurred (*Table 1*). Between October and April this decrease was 10.3% ($y = -25.643x + 1316.9$). This indicates a high impact of environmental factors on the body weight of birds, which is confirmed by the value of the determination coefficient of $R^2 = 0.7303$. The average weight of drakes during the study period was 1214.3 grams. The carcass weight decrease was slightly larger and amounted to 11.4% ($y = -19.771x + 865.03$), which indicates the utilization of fat reserves in the winter period. The average carcass weight was 785.9 grams.

Table 1. Weight characteristics (g) carcasses of male mallard ducks during the testing period

Item	Period research													
	I		II		III		IV		V		VI		VII	
	x	SD	x	SD	x	SD	x	SD	x	SD	x	SD	x	SD
Body weight	1278.0 _a	13.03	1246.0 _{a,b}	48.27	1308.0 _a	38.34	1208.0 _{a,b}	84.97	1150.0 _b	76.48	1164.0 _b	68.04	1146.0 _b	49.79
Body weight after decapitation of the head	1220.0 _a	21.21	1145.0 _{a,b}	66.70	1226.6 _a	41.30	1125.4 _{a,b}	81.47	1067.6 _b	75.10	1073.4 _b	79.93	1061.4 _b	44.68
Body weight after plucking	1066.0 _a	16.73	1082.6 _a	71.76	1104.0 _a	56.83	1002.8 _{a,b}	86.05	955.2 _b	66.19	938.8 _b	71.98	919.2 _b	42.97
Weight of the carcass after evisceration	806.0 _{a,c}	15.16	849.2 _a	45.72	841.0 _a	21.41	784.2 _{a,b}	81.65	752.4 _{b,c}	53.29	755.0 _{a,b}	45.13	713.8 _b	22.67

a, b, c - means denoted by the same letter between individual study periods do not differ statistically significantly ($p \leq 0.05$)

In the analyzed period, slaughter performance was at an average level of 64.5% with a differentiation from 60.4 to 69.1% in individual study periods. In terms of body weight, the heart was 1.0%, the liver 2.1% and the muscle stomach 2.9%. The remaining part (29%) were inedible guts (*Figure 2*). A statistically significant relationship between the mass of internal organs (heart, liver, stomach) and the body weight of birds was shown (*Table 2*). The relationship between the mass of organs described and the carcass weight was significant only for the heart and stomach.

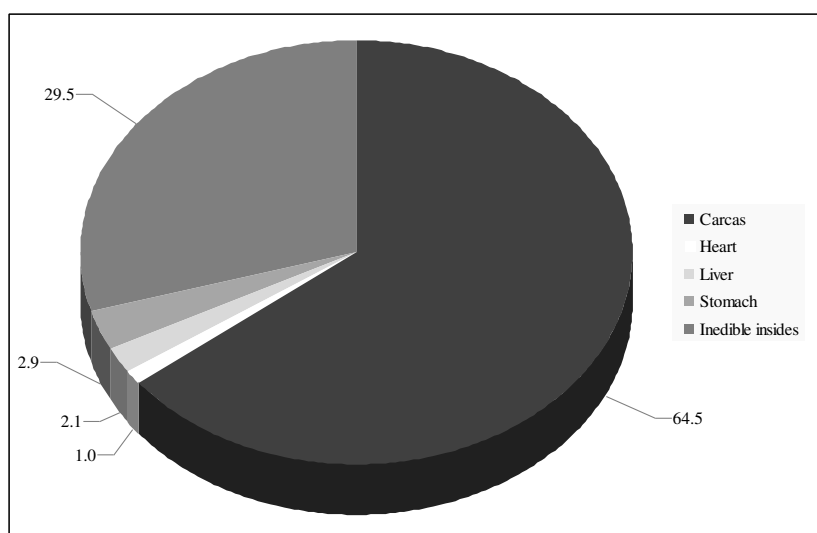


Figure 2. Percentage shares of carcass components in the total body weight male mallard

The chemical composition of the pectoral muscle showed slight variation in individual periods of the study (*Table 3*). Muscles contained 23.54 to 23.58% protein. The fat content showed a downward trend from 0.84 to 0.65% but these differences were not statistically significant ($p > 0.05$). The highest heart weight (12.6 g) was found

in drakes obtained in October. In the following months, until February, the mass of this body decreased, but in the last two study periods it increased to 11.8 grams in the last study period. The mean values of individual components of the breast muscle chemical composition did not differ statistically significantly between the study periods ($p > 0.05$). In contrast, the average values of the mass of internal organs showed differentiation between some periods of the study and some differences proved to be statistically significant ($p \leq 0.05$). During the seven-month study period, liver mass showed quite significant variations. The drakes shot in December had the highest average weight of this organ, while the lightest livers were found in drakes obtained in April. The average values of this trait between some periods of research were statistically significantly different ($p \leq 0.05$). Ducks from the first study period had the highest and statistically significantly different ($p \leq 0.05$) muscle mass.

Table 2. Correlation coefficients between body weight and carcass weight and weight of edible guts (offal)

Item	Type of guts (offal)		
	Heart weight	Liver weight	Stomach weight
Body weight	0.459*	0.381*	0.465*
Carcass weight	0.363*	0.212	0.343*

*- significant correlations at $p \leq 0.05$

Table 3. Chemical composition of mallard meat and mass of internal organs

Item	Period research						
	I	II	III	IV	V	VI	VII
Water, %	74.13	74.15	74.20	74.22	74.23	74.23	74.25
Total protein, %	23.58	23.57	23.56	23.56	23.54	23.55	23.54
Crude fat, %	0.84	0.85	0.83	0.79	0.77	0.73	0.65
Crude ash, %	1.36	1.43	1.41	1.43	1.46	1.49	1.56
Heart, g	12.6 _a	11.8 _a	12.2 _a	10.4 _{a,b}	10.0 _b	11.6 _a	11.8 _a
Liver, g	26.6 _{a,b}	25.4 _{a,b}	29.2 _a	23.0 _{b,c}	24.2 _{a,b}	25.4 _{a,b}	21.0 _c
Stomach, g	60.8 _a	37.0 _b	33.4 _b	34.8 _b	35.8 _b	26.6 _c	24.4 _c

a, b, c - means denoted by the same letter between individual study periods do not differ statistically significantly ($p \leq 0.05$)

In the next four periods, the mass was similar, while in the last two it dropped to an average level of 25.5 grams and these values differed significantly ($p \leq 0.05$) from the average for this feature from all other periods.

Analysis of the fatty acid profile indicates that the pectoral muscles of the crosses had an average of 38.28% content of saturated SFA fatty acids (Table 4). There were no significant differences during the study period. The share of MUFA monounsaturated acids was 17.24%, and polyunsaturated at the average level of 40.35%. In both cases, no significant differences were found between study periods ($p \leq 0.05$). The share of unsaturated acids in total accounted for over 57%, while their ratio to saturated acids was at the level of 1.5. On the other hand, the ratio of omega 6 to omega 3 polyunsaturated acids was not very differentiated in particular periods of the study and averaged 4.40.

Table 4. Profile of fatty acids [%] of breast muscle fat of the mallards

Specification	Period research							Mean
	I	II	III	IV	V	VI	VII	
Lauric acid C 12:0	0.13	0.12	0.11	0.12	0.13	0.14	0.12	0.12
Myristic acid C 14:0	0.57	0.58	0.55	0.54	0.54	0.56	0.55	0.56
Palmitic acid C 16:0	20.28	20.25	20.27	20.30	20.29	20.30	20.28	20.28
Pahnitoic acid C 16:1	2.38	2.38	2.41	2.44	2.43	2.41	2.44	2.41
Margaric acid C 17:0	0.86	0.84	0.89	0.95	0.99	0.91	0.93	0.91
Margaroleic acid C 17:1	0.58	0.60	0.62	0.61	0.59	0.58	0.59	0.60
Stearic acid C 18:0	15.62	15.65	16.21	16.05	15.92	16.09	15.86	15.91
Oleic acid C 18:1	13.90	14.05	14.09	14.11	14.08	14.05	14.10	14.05
Linoleic acid C 18:2	19.27	19.43	19.38	19.54	19.41	19.44	19.53	19.43
α -linoleic acid C 18:3	7.35	7.39	7.41	7.44	7.41	7.39	7.40	7.40
Arachidic acid C 20:0	0.49	0.48	0.51	0.50	0.51	0.53	0.47	0.50
Gadoleic acid C 20:1	0.16	0.18	0.17	0.19	0.20	0.17	0.18	0.18
Eicosadienoic acid C 20:2	0.39	0.40	0.42	0.39	0.41	0.40	0.41	0.40
Arachidonic acid C 20:4	13.19	13.14	13.11	13.12	13.08	13.07	13.11	13.12
Other acids	4.83	4.51	3.85	3.70	4.01	3.96	4.03	4.13
SFA	37.95	37.92	38.54	38.46	38.38	38.53	38.21	38.28
MUFA	17.02	17.21	17.29	17.35	17.30	17.21	17.31	17.24
PUFA	40.20	40.36	40.32	40.49	40.31	40.30	40.50	40.50
UFA (MUFA + PUFA)	57.22	57.57	57.61	57.84	57.61	57.51	57.76	57.59
UFA/SFA	1.51	1.52	1.49	1.50	1.50	1.49	1.51	1.50
PUFA <i>n</i> -3	7.35	7.39	7.41	7.44	7.41	7.39	7.40	7.40
PUFA <i>n</i> -6	32.46	32.57	32.49	32.66	32.49	32.51	32.64	32.55
<i>n</i> -6/ <i>n</i> -3	4.42	4.41	4.38	4.39	4.38	4.40	4.41	4.40

Organoleptic and bacteriological analysis

The organoleptic analyzes carried out showed the presence of four drakees in the breast muscles of *Sarcocystis* protozoan cysts (Table 5). One case occurred in a drake shot in November, another case was shot in March, and two cases were found in drake obtained in April. In the case of one drake, the invasion was defined as very numerous (Figure 3), while in the remaining three cases the occurrence was less numerous.

Bacteriological analyzes of internal organs showed the presence of three groups of bacteria. *Escherichia coli* were found to be abundant in three drakes in the stomach and liver. They were specimens obtained in February and March, in the same complex of water reservoirs. One drake obtained in December and one in January found numerous occurrences of *Aeromonas veronii*. In one case, the bacterium was found in all internal organs, while in the other only in the liver. *Staphylococcus aureus* has also been found to be quite abundant in the livers of two drakes. In the small intestines of the individuals examined both organoleptically and using a stereoscopic microscope, tapeworms from the *Hymenolepididae* family were found. These parasites were found in all drakes with varying degrees of severity, from a few to several animals.

Table 5. Results of macroscopics and bacteriological evaluation

Rated element		Period research						
		I	II	III	IV	V	VI	VII
Macroscopic and microscopic evaluation	Carcass	-	<i>Sarcocystosis</i> 1 cases	-	-	-	<i>Sarcocystosis</i> 1 case	<i>Sarcocystosis</i> 2 cases
	Intestines	Tapeworms from the <i>Hymenolepididae</i> family	Tapeworms from the <i>Hymenolepididae</i> family	Tapeworms from the <i>Hymenolepididae</i> family	Tapeworms from the <i>Hymenolepididae</i> family	Tapeworms from the <i>Hymenolepididae</i> family	Tapeworms from the <i>Hymenolepididae</i> family	Tapeworms from the <i>Hymenolepididae</i> family
Bacteriological evaluation	Heart	-	-	<i>Aeromonas veronii</i> 1 case (++)	-	-	-	-
	Liver	<i>Staphylococcus aureus</i> 1 case (+)	-	<i>Aeromonas veronii</i> 1 case (++)	<i>Aeromonas veronii</i> 1 case (++)	<i>Escherichia coli</i> 1 case (++)	<i>Escherichia coli</i> 2 cases (++)	<i>Staphylococcus aureus</i> 1 case (+)
	Stomach	-	-	<i>Aeromonas veronii</i> 1 case (++)	-	<i>Escherichia coli</i> 1 case (++)	<i>Escherichia coli</i> 2 cases (++)	-



Figure 3. Numerous sarcocysts in the pectoral muscles of a male mallard duck

Resistance to antibiotics

As part of the study, an assessment of the sensitivity of isolated bacterial strains to antibiotics in vitro was performed (Table 6). The isolated *Escherichia coli* strain was found to be resistant to most of the antibiotics used, moderately sensitive to one and sensitive to Colistin and Doxycycline. The *Aeromonas veronii* strain was resistant to 4 antibiotics and sensitive to Colistin, Doxycycline and Enrofloxacin. In turn, the *Staphylococcus aureus* strain was also resistant to 4 of the antibiotics used, moderately sensitive to Enrofloxacin, and sensitive to Doxycycline and Lincomycin/Spectinomycin.

Table 6. Sensitivity of isolated bacterial strains to antibiotics

Antibiotic used	Type of bacterial strain		
	<i>Escherichia coli</i>	<i>Aeromonas veronii</i>	<i>Staphylococcus aureus</i>
Doxycycline DO30	W	W	W
Amoxycilin AML25/AX25	O	O	O
Ampicillin AMP10/AM10	O	O	O
Amoxycillin/clavulanic acid Synulox AMC30	O	O	O
Lincomycin/Spectinomycin LS109	O	O	W
Enrofloxacin ENR5	ŚW	W	ŚW
Colistin CT50	W	W	O

Description: W - sensitive; ŚW - moderately sensitive; O - resistant

Spermatogenesis process

The analysis of the spermatogenesis process was carried out based on the mass of the testicles and epididymis and the cytological evaluation of testicular and epididymal imprints. The analysis was carried out until the presence of correctly formed sperm was observed. During the seven-month period of research for the period from October to January, the testicular mass was quite stable and ranged from 0.205 to 0.414 grams (Figure 4). In duck shot in February, testis weight was 0.712 g, and this value did not differ significantly from those of previous months. In drakes obtained in March, the average testis weight was 2,572 g and was significantly higher than the values obtained in previous months, and lower than the last test ($p \leq 0.05$). The average mass of drake

testicles shot in April was 14.140 g and was significantly higher ($p \leq 0.05$) than the values obtained in all earlier months of the study. The correlation coefficient between body weight and testicular weight was negative and statistically insignificant, $r_{xy} = -0.400$.

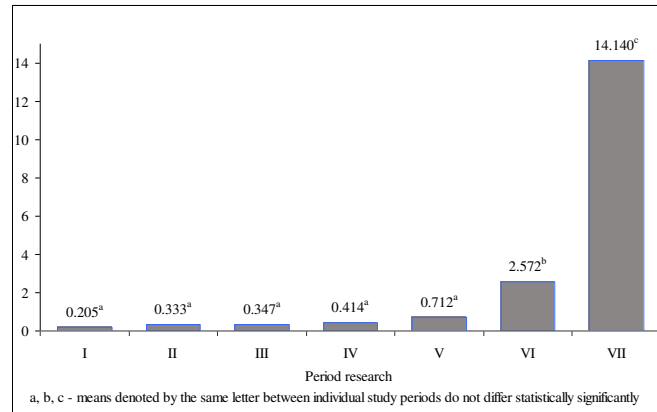


Figure 4. Shaping the weight of testes (g) drakes during the study period

In the evaluated microscopic preparations, in the initial period of research, i.e. October, proper germ cells were not shown, but only sperm-forming epithelial cells difficult to identify, in the initial period of development presumably spermatogonies (Figure 5). Later, from November to the end of February, characteristic cells were observed in the preparations - oval with a wide, clear layer of cytoplasm and the nucleus in the central part of the cell, reminiscent of spermatocytes. It was observed that the shape of the cell changed from oval to round with time, and the shape of the nucleus from cylindrical to oval (Figure 6). From the first half of March, correctly formed spermatozoa were visible in the preparations, but spermatocytes were also visible (Figure 7). In addition, spermatides in the less advanced - early spermatid (WS) and the more advanced - late spermatid (PS) stage of transformation into mature germ cells - spermatozoa were also seen in preparations from this period (Figure 8). Duck sperm had a very large head in the shape of an elongated cone and a thinly visible thin withe, reminiscent of hot pepper Peperoni (Figure 9).

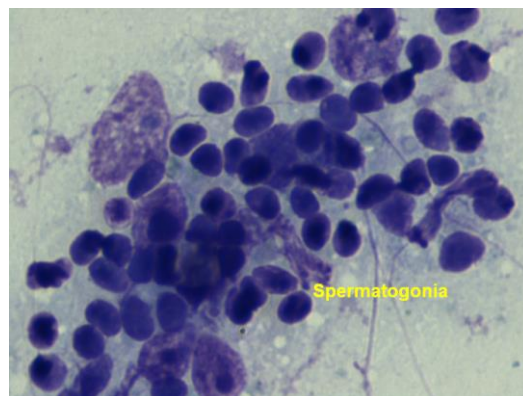


Figure 5. Cytological preparation, formed by impressing on a microscope slide, the epididymis and testis of the drake, made in October, visible germ cells in the initial period of development - spermatogonia. Hemacolor staining (1000 x)

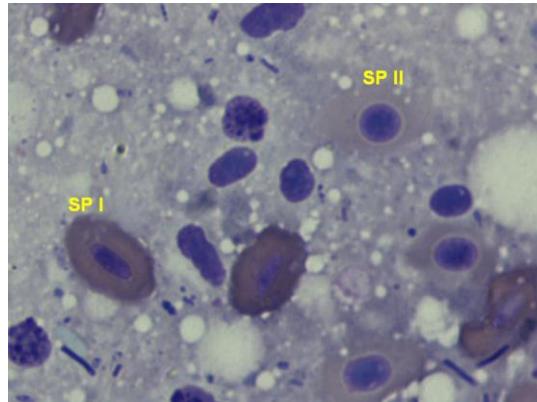


Figure 6. Cytological preparation, formed by impressing on a microscope slide, the epididymis and testis of the drake, made at the turn of November and December, visible germ cells of first order spermatocytes (SP I) and second order spermatocytes (SP II). Hemacolor staining (1000 x)

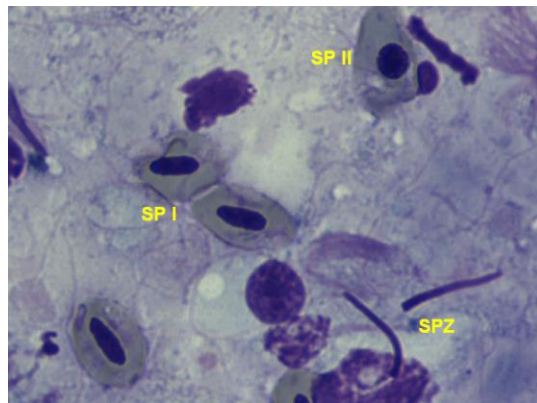


Figure 7. Cytological preparation, formed by impressing on a microscope slide, the epididymis and testis of the drake, made in the first half of March. Visible germ cells of first order spermatocytes (SP I), second order spermatocytes (SP II) and spermatozoa (SPZ). Hemacolor staining (1000 x)



Figure 8. Cytological preparation, formed by impressing on a microscope slide, the epididymis and testis of the drake, made in the second half of March. Visible early spermatids (ES), late spermatids (LS) and spermatozoa (SPE). Hemacolor staining (1000 x)



Figure 9. Cytological preparation, formed by impressing on a microscope slide, the epididymis and testis of the drake, made in the first half of April. Visible mature spermatozoa. Hemacolor staining (1000 x)

Discussion

The obtained weight results of mallard ducks, despite the differences in the 7-month research cycle, indicate that it was higher than that in studies conducted in north-eastern Poland, despite the fact that these studies covered the winter period and matings, which is associated with more than 10% decrease in body weight compared to the initial weight (Janiszewski et al., 2018). The average value of this trait is similar to that of research conducted in Hungary and in the case of males it is only less than 14 grams lower (Szász et al., 2006), while compared to the results of research from north-eastern France, it was 49 grams lower (Boos et al., 2002). The carcass weight was also higher than that in research conducted in north-eastern Poland, which resulted in slaughter efficiency higher by 7.7%. On the other hand, the share of heart and liver weight was similar, and the stomach weight was significantly lower compared to ducks from north-eastern Poland (Janiszewski et al., 2018). Also the chemical composition of the carcass was similar to that of research conducted in north-eastern Poland, and slight differences were due to the date of hunting and the habitat from which the birds came. At the same time, the pectoral muscles were characterized by a high protein content, with a low fat content, whose share decreased with the time of shooting (Lorenzo et al., 2011; Janiszewski et al., 2018). In turn, the results of other authors indicate lower protein content and definitely higher fat in meat from mallard ducks (Cobos et al., 2000).

The content of 14 fatty acids was found in the pectoral muscles of male crosses. The occurrence of saturated fatty acids (SFA) as well as monounsaturated (MUFA) and polyunsaturated (PUFA) was similar to that of other authors. However, the content of individual acids showed slight variation, which may be due to the composition of the diet of birds from different environments and the date of their shooting (Cobos et al., 2000; Nuernberg et al., 2011; Janiszewski et al., 2018). Quite a high level of C 20 PUFA acids, especially C 20:4, was conditioned by the diet of birds, because these acids come only from exogenous sources and cannot be synthesized in the body of birds. High levels of these acids in mallard meat have also been confirmed in studies by other authors (Mishra et al., 1993; Nuernberg et al., 2011). Such a high level of PUFA acids, as well as the UFA to SFA ratio of 1.50 means that the meat of the crosses has enormous health benefits,

especially for people suffering from hypertension, which has been confirmed in experimental and clinical studies (Appel et al., 1993).

The demonstrated occurrence of protozoan cysts of the *Sarcocystis* genus in 4 ducks, with varying severity, indicates that there is a fairly serious threat from this pathogen. Based on the data obtained, it can be assumed that every 5 ducks may have sarcocysts. Until now, reports of sarcocystosis in ducks have been few, which were explained by the fact that duck hunters did not pay attention especially to the rare sarcocysts (Stenzel and Koncicki, 2007; Śmiałek et al., 2014; Flis and Grela, 2018). Intestinal parasites, including those found in the *Hymenolepididae* family, are quite common in both wild and domestic ducks, and although they have a destabilizing effect on the host organism, they do not affect the meat's utility (Raś-Noryńska et al., 2016; Sokół et al., 2016). Studies conducted in three different places in Poland have shown the occurrence of 22 nematode species from the family *Hymenolepididae* (Nowak et al., 2012). Also Ukrainian studies indicate the presence of parasites of this family with varying severity (Syrota et al., 2018).

The finding in some internal organs of *Escherichia coli* indicates that the crossbreeds can be an important reservoir of zoonotic strains of this bacterium, as well as a bioindicator of the state of the environment, mainly of the water reservoirs in which they reside. This is confirmed by studies of other authors indicating that crosses can be an important source of *E. coli* strains capable of causing intestinal diseases (Ewers et al., 2009). Slovak studies have shown that in fresh meat of crosses no *E. Coli* bacteria were found, and they were found after a 7-day meat maturation period (Haščík et al., 2010). Gram negative rods of the genus *Aeromonas* are widespread in the aquatic environment, thus they are quite common in birds inhabiting these habitats. They may also be responsible for infection in humans (Mencacci et al., 2003). The finding of two cases of *Staphylococcus aureus* is a confirmation that this highly widespread bacterium can also occur in mallards, and thus may be a potential source of infection for people who have contact with hunted ducks as well as eating meat derived from them. In addition, duck droppings can also be a source of infection, as well as a vector of the spread of bacteria in the natural environment, and thus may pose a threat to public health (Adegunloye and Adejumo, 2014).

Our own research shows that reproductive processes in male mallard ducks are normal. Outside of the October and November breeding season, inhibition of sexual activity in drakes was observed. This is evidenced by both the very low testicular mass and the presence in the cytological preparations of the testicles from this period, only the basic germ cells - spermatogonia. Although the ducks are already mating at this time of year, the spermatogenesis process is still stopped. Bonding of both sexes in pairs is dictated, as Davis studies (2002) show, by a periodic increase in testosterone levels in drakes. After pairing, the level of this hormone decreases, and during the reproductive period it gradually increases again and also gradually stimulates the process of spermatogenesis. A slight increase in testosterone levels causes mating of ducks and mating behavior, but it is too low to activate spermatogenesis. That is why, in the initial studies, no increase in testicular mass and germ cell development was demonstrated. Similar relationships were observed in guinea fowls (*Numida meleagris*), which also show seasonal reproduction (Abdul-Rahman et al., 2016). In the following months of December, January and February, the spermatogenesis process, which was already beginning, was observed, since the first and second order spermatocytes and second order spermatocytes were visible in the preparations. Although the testicular mass was still low, it increased steadily (from October to February it increased more than threefold). Similar increase in testicular

weight and development of reproductive cells in the beginning reproductive season was demonstrated by other authors in drakes and pheasants (Bauchinger et al., 2007; Górska et al., 2015). In March, the process of spermatogenesis was already developed; fully developed spermatozoa appeared in cytological preparations. However, it seems that the drakes obtained full fertility at the beginning of April, which is visible both in the highest testis mass obtained (increase 69 times since the beginning of the study) and the presence of a large number of spermatozoa in cytological preparations. The proper intensification of the spermatogenesis process is a very important factor in the reproduction of ducks, but equally important is the shift associated with global warming during the breeding period in wild birds (Virkkala and Lehikoinen, 2017). Research carried out on the capercaillie and the black grouse has shown acceleration of the breeding period, but for the benefit of reproduction rates in these bird species (Wegge and Rolstad, 2017). It is not known, however, whether this effect can also be expected in ducks.

Conclusions

The conducted research authorizes to formulate the following statements and conclusions:

Body weight and cross carcass weight were similar to the results of other authors, and its 10% decrease occurred only in the winter and spring months, which should be associated with the climatic conditions and course of mating in this species. The crosswords were characterized by high slaughter efficiency at the level of 64.5%. A statistically significant relationship between the mass of internal organs (heart, liver, stomach) and the body weight of birds was demonstrated.

The chemical composition of cross carcasses was characterized by high protein content and low fat content. At the same time, the fatty acid profile indicates a high content of unsaturated fatty acids, including those from the C 20 group, which can only come from exogenous sources. The high content of the described acids in connection with the favorable ratio of UFA to SFA at 1.5, confirms the high health benefits of these birds, which should be an important component of the diet, especially for people with hypertension.

Organoleptic and bacteriological evaluation of carcasses showed the occurrence of protozoan cysts of the *Sarcocystis* genus and intestinal parasites of the *Hymenolepididae* family. These groups of parasites, despite having an impact on the host, do not play a major epidemiological significance. At the same time, it should be emphasized that the presence of *E. coli* and *Staphylococcus aureus* in some internal organs is of some concern, especially since these bacteria showed sensitivity to only two of the seven antibiotics used. This is due to the fact that crosswords can be a potential source of human infection as well as a reservoir, and also a vector for the spread of these bacteria, and thus pose a threat to public health.

Assessment of both testicular weight and cytological imprints made of testicles and epididymis allows confirmation of the correct development of the spermatogenesis process in mallard ducks during the breeding season. Despite the fact that pairing takes place already in winter, the fullness of matings, and thus the fertilization of females, takes place in April, which is confirmed by the results obtained. However, it is not possible to determine from conducted studies whether there were shifts during the breeding season, this requires furthermore focused research.

Funding. This research received no external funding.

Conflicts of Interests. The authors declare no conflict of interests.

REFERENCES

- [1] Abdul-Rahman, I. I., Robinson, J. E., Obese, F. Y., Jeffcoate, I. A., Awumbila, B. (2016): Effects of season on the reproductive organ and plasma testosterone concentrations in guinea cocks (*Numida meleagris*). – *Poultry Science* 95: 636-644. doi.org/10.3382/ps/pev342.
- [2] Adegunloye, D. V., Adejumo, F. A. (2014): Microbial assessment of Turkey (*Meleagris ocellata* L.) and Duck (*Anas platyrhynchos* L.) Faeces (Droppings) in Akure Metropolis. – *Advances Microbiology* 4: 774-779. doi.org/10.4236/aim.2014.412085.
- [3] Appel, L. J., Miller, E. R., Seidler, A. J., Whelton, P. K. (1993): Does supplementation of diet with „fish oil” reduce blood pressure? A meta-analysis of controlled clinical trial. – *Archives Internal Medicine* 153: 1429-1438.
- [4] Bauchinger, U., Van't Hof, T., Biebach, H. (2007): Testicular development during long-distance spring migration. – *Hormones Behavior* 51: 295-305.
- [5] Bertolini, R., Zgrablic, G., Cuffolo, E. (2005): Wild game meat: Products, market, legislation and processing controls. – *Veterinary Research Communication* 29(2): 97-100.
- [6] Betlejewska, K., Kalisińska, E., Korniyushin, V., Salamatin, R. (2002): *Eucolus* contours (Creplin, 1839) nematode in mallard (*Anas platyrhynchos* Linnaeus, 1758) from North-Western Poland. – *Electronic Journal Polish Agricultural Universities - Veterinary Medicine* 5: 03.
- [7] Biesiada-Drzazga, B., Socha, S., Janocha, A., Banaszkiwicz, T., Koncerewicz, A. (2011): Assessment of slaughter value and quality of meat in common game pheasants (*Phasianus colchicus*). – *Żywność Nauka Technologia Jakość* 1: 79-86.
- [8] Boos, M., Zorn, T., Le Maho, Y., Groscolas, R., Robin, J. P. (2002): Sex differences in body composition of wintering Mallards (*Anas platyrhynchos*): possible implications for survival and reproductive. – *Bird Study* 49: 212-218.
- [9] Borman, M., Mattsson, L. (2012): The hunting value of game in Sweden: Have changes occurred over recent decades? – *Scandinavian Journal Forest Research* 27(7): 1-6.
- [10] Borowska, D., Jabłoński, A., Pejsak, Z. (2014): Disk diffusion method in veterinary diagnostics - practical data. – *Życie Weterynaryjne* 89(2): 116-120.
- [11] Cobos, A., Veiga, A., Díaz, O. (2000): Chemical and fatty acid composition of meat and liver of wild ducks (*Anas platyrhynchos*). – *Food Chemistry* 68(1): 77-79.
- [12] Davis, E. S. (2002): Female choice and the benefits of mate guarding by male mallards. – *Animal Behaviour* 64(4): 619-628.
- [13] Dynowska, M., Meissner, W., Pacyńska, J. (2013): Mallard duck (*Anas platyrhynchos*) as a potential link in the epidemiological chain mycoses originating from water reservoirs. – *Bulletin Veterinary Institute Pulawy* 57(3): 323-328.
- [14] Ewers, C., Guenther, S., Wieler, L. H., Schierack, P. (2009): Mallard duck - a waterfowl species with high risk of distributing *Escherichia coli* pathogenic for humans. – *Environmental Microbiology Reports* 1(6): 510-517. doi:10.1111/j.1758-2229.2009.00058.x.
- [15] Flis, M., Magdziak, K., Rataj, B. (2017): Social and economic determinants meat of game animals consumption. – *Przegląd Leśniczy* 8(314/XXVII): 12-14.
- [16] Flis, M., Grela, E. R. (2018): Sarcocystosis in a male of the Mallard *Anas platyrhynchos*. – *Ornis Polonica* 59: 81-87.
- [17] Flis, M., Grela, E. R., Gugęła, D., Kołodziejski, A. (2019): Carcass composition and fatty acid profile of pectoral muscle of male and female pheasants (*Phasianus colchicus*). – *Żywność Nauka Technologia Jakość* 26(1): 111-124.

- [18] Folch, J., Less, M., Stanley, G. H. (1957): A simple method for the isolation and purification of total lipids from animal tissues. – *Journal Biological Chemistry* 226(1): 497-509.
- [19] Gaston, A. J., Gilchrist, H. G., Mallory, M. L., Smith, P. A. (2009): Changes in seasonal events, peak food availability, and consequent breeding adjustment in a marine bird: a case of progressive mismatching. – *Condor* 111: 111-119.
- [20] Górecka, J., Szymańko, T. (2010): Nutritional values of venison (Original in Polish: Walory żywieniowe dziczyzny). – *Magazyn Przemysłu Mięsnego* 1-2: 20-21.
- [21] Górska, M., Wojciechowska, J., Wojtyśiak, D. (2015): Seasonal changes in steroidogenic activity and pheasant testicular microstructure (Original in Polish: Sezonowe zmiany w aktywności steroidogennej oraz mikrostrukturze jąder bażanta). – *Roczniki Naukowe Zootechniki* 42(2): 147-154.
- [22] Guillemain, M., Elmberg, J., Gauthier-Clerc, M., Massez, G., Hearn, R., Champagnon, J., Simon, G. (2010): Wintering French Mallard and Teal are heavier and in better body condition than 30 years ago: Effects of a changing environment? – *Ambio* 39(2): 170-180.
- [23] Guillemain, M., Pöysä, H., Fox, A. D., Arzel, C., Dessborn, L., Ekroos, J., Gunnarsson, G., Holm, T. E., Christensen, T. K., Lehtikoinen, A., Mitchell, C., Rintala, J., Møller, A. P. (2013): Effect of climate change on European ducks: what do we know and what do we need to know? – *Wildlife Biology* 19: 404-419.
- [24] Gunnarsson, G., Latorre-Margalef, N., Hobson, K. A., Van Wilgenburg, S. L., Almberg, J., Olsen, B., Fouchier, R. A. M., Waldenström, J. (2012): Disease dynamics and bird migration – linking mallards *Anas platyrhynchos* and subtype diversity of the influenza A virus in time and space. – *PLoS One* 7(4): e35679. doi:10.1371/journal.pone.0035679.
- [25] Haščik, P., Nováková, I., Kačániová, M., Fikselová, M., Kuwová, S. (2010): Microbiological quality of the *Anas platyrhynchos* and the *Fulica atra* meat. – *Ecological Chemistry Engineering A* 17(1): 81-87.
- [26] Hoffman, L. C., Wiklund, E. (2006): Game and venison - Meat for the modern consumer. – *Meat Science* 74(1): 197-208.
- [27] Janiszewski, P., Murawska, D., Hanzal, V., Gesek, M., Michalik, D., Zawadka, M. (2018): Carcass characteristics, meat quality, and fatty acid composition of wild-living mallards (*Anas platyrhynchos* L.). – *Poultry Science* 97(2): 709-715.
- [28] Kasprzyk, A. (2013): Meat in the human diet - history, present and future (Original in Polish: Mięso w diecie człowieka – historia, terażniejszość i przyszłość). – *Produkcja zwierzęca w warunkach zrównoważonego rolnictwa. Materiały LXXVIII Zjazdu Naukowego Polskiego Towarzystwa Zootechnicznego, Kraków*: 133-145.
- [29] Kokoszyński, D., Bernacki, Z., Pieczewski, W. (2014): Carcass composition and quality of meat from game pheasants (*P. colchicus*) depending on age and sex. – *Europ. Poultry Science* 78. DOI: 10.1399/eps.2014.16.
- [30] Książkiewicz, J. (2006): A mallard duck – *Anas platyrhynchos* L. means a flat-billed duck. – *Wiadomości Zootechniczne* 1: 25-30.
- [31] Kuźniacka, J., Adamski, M., Bernacki, Z. (2007): Effect of age and sex of pheasants (*Phasianus colchicus* L.) on selected physical properties and chemical composition of meat. – *Annals Animals Science* 1(7): 45-53.
- [32] Kwiecińska, K., Kosicka-Gębska, M., Gębski, J. (2016): Assessment of consumer preferences related to game selection (Original in Polish: Ocena preferencji konsumentów związanych z wyborem dziczyzny). – *Handel Wewnętrzny* 1: 53-64.
- [33] List of hunting reporting data 2018. (2019): Zestawienie danych sprawozdawczości łowieckiej 2018 rok (in Polish). – *Stacja Badawcza Polskiego Związku Łowieckiego w Czempiniu, Biuletyn Czempin*.
- [34] Ljung, P. E., Riley, S. J., Ericsson, G. (2015): Game meat consumption feeds urban support of traditional use of natural resources. – *Journal Society Natural Resources* 28(6): 657-669.

- [35] Lorenzo, J. M., Purrinos, L., Temperan, S., Bermudez, R., Tallon, S., Franco, D. (2011): Physicochemical and nutritional composition of dry-cured duck breast. – Poultry Science 90(4): 931-940.
- [36] Mencacci, A., Cenci, E., Mazzolla, R., Farinelli, S., D'Alò, F., Vitali, M., Bistoni, F. (2003): *Aeromonas veronii* biovar *veronii* septicaemia and acute suppurative cholangitis in a patient with hepatitis B. – Journal Medical Microbiologu 52(8): 727-730.
- [37] Mishra, V. K., Temelli, F., Ooraikul, B. (1993): Extraction and purification of ω -3 fatty acids with an emphasis on supercritical fluid extraction - A review. – Food Research International 26(3): 217-226.
- [38] Nagalska, H. M., Rejman, K. (2014): Consumer knowledge of venison and purchasing behavior on the meat market (Original in Polish: Wiedza konsumentów o dziczyźnie i zachowania nabywcze na rynku tego mięsa). – Marketing i Rynek 6: 488-500.
- [39] Nowak, M., Kavetska, K., Królaczyk, K., Stapf, A., Korna, S., Wajdzik, M., Basiaga, M. (2012): Comparative study of Cestode and Nematode fauna of the gastrointestinal tract of mallard (*Anas platyrhynchos* L. 1758) from three different Polish ecosystem. – Acta Scientiarum Polonorum Zootechnica 11(4): 99-106.
- [40] Nuernberg, K., Slamecka, J., Mojto, J., Gasparik, J., Nuernberg, G. (2011): Muscle fat composition of pheasants (*Phasianus colchicus*), wild ducks (*Anas platyrhynchos*) and black coots (*Fulica atra*). – European Journal Wildlife Research 57(4): 795-803.
- [41] Popczyk, B. (2012): Game trading problems (Original in Polish: Problemy handlu dziczyzną). – In: Gwiazdowicz, D. J. (ed.) Problemy współczesnego łowiectwa w Polsce.. Polskie Towarzystwo Leśne. Regionalna Dyrekcja Lasów Państwowych w Poznaniu. Poznań: 137-150.
- [42] Raś-Noryńska, M., Sokół, R., Michalczyk, M., Koziątek-Sadłowska, S. (2016): Parasites of the captive mallard duck (*Anas platyrhynchos*). – Annals Parasitology 62(128).
- [43] Siminska, E., Bernacka, H., Sadowski, T. (2011): The global and domestic venison market situation. – Annals Warsaw University Life Science - SGGW Animal Science 50: 89-96.
- [44] Smith, D. B., Rohwer, F. C. (1997): Perceptions of releases of captive-read mallards with emphasis on an intensive program in Maryland. – In: Proceedings of the Transactions of the North American Wildlife and Natural Resources Conference 62: 403-411.
- [45] Sokół, R., Raś-Noryńska, M. A., Gesek, M. A., Murawska, D., Hanzal, V., Janiszewski, P. E. (2016): The parasites of the mallard duck (*Anas platyrhynchos*) as an indicator of health status and quality of the environment. – Annals Parasitology 62(4): 351-353.
- [46] Söderquist, P. (2012): Ecological and genetic consequences of introductions of native species: The mallard as a model system. – Introductory Research Essay No. 15 Department of Wildlife, Fish, and Environmental Studies Swedish University of Agricultural Sciences 901 83 Umeå, Sweden.
- [47] Stenzel, T., Koncicki, A. (2007): A case of sarcocystosis in wild duck. – Medycyna Weterynaryjna 63(11): 1361-1362.
- [48] Syrota, Y. Y., Greben, O. B., Poluda, A. M., Maleha, O. M., Lisitsyna, O. I., Kornushin, V. V. (2018): Helminths of the mallard, *Anas platyrhynchos* (Aves, Anatidae), in Ukraine: Analysis of the diversity in mixed forest zone and the Black Sea region. – UDC 595.1:598.252.1: 267-278.
- [49] Szász, S., Sugár, L., Pócz, O., Ujvári, J., Taraszenkó, Z. (2006): Some slaughter characteristics of the mallard (*Anas p. platyrhynchos* L. 1758). – Acta Agraria Kaposváriensis 10(2): 321-323.
- [50] Śmiałek, M., Stenzel, T., Śmiałek, A., Koncicki, A. (2014): Clinical cases of sarcocystosis in duck. – Życie Weterynaryjne 89(7): 594-596.
- [51] Tracey, J., Lukins, B., Haselden, C. (2008): Lord Howe Island Duck: Abundance, Impact and Management Options. – A report to the World Heritage Unit. Lord Howe Island Board. Invasive Animals Cooperative Research Centre, Canberra: 1-35.

- [52] Virkkala, R., Lehtikoinen, A. (2017): Birds on the move in the face of climate change: High species turnover in northern Europe. – *Ecology Evolution* 7(20): 8201-8209. doi: 10.1002/ece3.3328.
- [53] Wegge, P., Rolstad, J. (2017): Climate change and bird reproduction: warmer springs benefit breeding success in boreal forest grouse. – *Proceedings Biological Sciences* 284(1866). pii: 20171528. doi: 10.1098/rspb.2017.1528.
- [54] Wille, M., Bröjer, C., Lundkvist, A., Järhult, J. D. (2018): Alternate routes of influenza A virus infection in mallard (*Anas platyrhynchos*). – *Veterinary Research* 49(110): doi.org/10.1186/s13567-018-0604-0.
- [55] Żbikowski, A., Szeleszczuk, P., Karpińska, E., Rzewulska, M., Malicka, E., Biniek, M. (2006): Epidemic deaths of mallard ducks after *Aeromonas hydrophila* infection. – *Medycyna Weterynaryjna* 62(6): 720-722.
- [56] Żmijewski, T., Mozolewski, W., Rybaczek, S. (2018): Characteristics and directions of wild game meat usage. – *Przemysł Spożywczy* 72(3): 32-35.

ANTIOXIDANT AND ANTIDIABETIC POTENTIAL VALUES OF *FARSETIA JACQUEMONTII* FROM BANNU DISTRICT, PAKISTAN

KHAN, A.¹ – MUHAMMAD, Z.² – ULLSH, I.² – KHAN, S.² – KHAN, S. U.² – KHAN, S.³ – ABBAS, S.²
– WAZIR, S. M.² – HAYAT, M.¹ – ZHANG, K.^{1*}

¹*School of Soil and Water Conservation, Beijing Forestry University, Beijing 100083, China*
(e-mails: alamgir.forester@gmail.com – A. Khan, muhammadhayat66@gmail.com – M. Hayat)

²*Department of Botany, University of Science and Technology, Bannu 28100, Pakistan*
(e-mails: sagarwazir03078@gmail.com – Z. Muhammad, iukwazir@gmail.com – I. Ullah,
sami84196@gmail.com – S. Khan, saadwazir99@yahoo.com – S. U. Khan,
sairaabbas07@gmail.com – S. Abbas, sultanwazir@outlook.com – S. M. Wazir)

³*College of Life Science and Technology, Beijing University of Chemical Technology, Beijing 100029, China*
(e-mail: uomians@yahoo.com – S. Khan)

*Corresponding author

e-mail: ctccd@126.com, phone: +86-133-6665-5775

(Received 25th Sep 2019; accepted 8th Jan 2020)

Abstract. Traditional medicine has a great contribution to the treatment of many chronic diseases. Therefore, the main purpose of this study was to evaluate the antioxidant and antidiabetic values and the α -amylase and α -glucosidase inhibiting potential of *Farsetia jacquemontii* in Bannu district, Pakistan. Antioxidant activity was assessed by using reagents; 1, 1-diphenyl-2-picrylhydrazyl (DPPH) stable free radicals, 2, 2'-azino-bis (3-ethylbenzthiazoline-6-sulfonic acid) (ABTS) radical cation, hydrogen peroxide (H_2O_2) and sodium molybdate (Na_2MoO_4). The antidiabetic activity was analyzed through the inhibition of α -amylase and α -galactosidase with IC_{50} values of 290 $\mu g/ml$ and 240 $\mu g/ml$ respectively. The extract was found to possess antioxidant potential depending on concentration in a cell-free system. Antioxidant potential was highest against ABTS with 98 $\mu g/mL$ IC_{50} , followed by MoO_4 100 $\mu g/mL$, DPPH 149 $\mu g/mL$ and H_2O_2 250 $\mu g/mL$ respectively. The antidiabetic activity was a result of the inhibition of α -amylase and α -galactosidase with IC_{50} values of 290 $\mu g/ml$ and 240 $\mu g/ml$ respectively. The methanolic extract possessed electron donating ability and reduced the free radicals in a cell free system. *F. jacquemontii* exhibited highest antioxidant potential against ABTS with IC_{50} 98 $\mu g/mL$ $IC_{50} > MoO_4$ 100 $\mu g/mL > DPPH$ 149 $\mu g/mL > H_2O_2$ 250 $\mu g/mL$. Based on the results, it can be concluded that *Farsetia jacquemontii* has antioxidant and antidiabetic potential as it contains vital phytochemicals with aforementioned properties.

Keywords: DPPH, ABTS, H_2O_2 , Na_2MoO_4 , α -amylase

Abbreviations: DPPH: 1, 1-diphenyl-2-picrylhydrazyl stable free radicals; ABTS: 2, 2'-azino-bis (3-ethylbenzthiazoline-6-sulfonic acid); ROS: Reactive oxygen species; UOP: University of Peshawar; Na_2MoO_4 : sodium molybdate; IC_{50} : Half maximal inhibitory concentration; H_2O_2 : Hydrogen peroxide; H_2SO_4 : Sulphuric acid; HCl: Hydrochloric acid; MV: Concentration and volume; Abs: Absorbance; AC: Absorbance of control; AS: Absorbance of sample; FJME: *Farsetia jacquemontii* methanolic extract; DNA: Deoxyribonucleic acid

Introduction

Antioxidants are substances that possess free radical chain reaction breaking properties (Pourmorad et al., 2006). The reactive derivatives of O_2 recognized as reactive oxygen species (ROS) are constantly produced in the human body that encourages oxidative damage of many biomolecules (Farber, 1994). Oxidative stress is

a common factor of many chronic diseases such as cardiovascular disease, diabetes, cancer, liver diseases, Alzheimer's disease and cataracts (Lü et al., 2010). Nowadays, research is focused on natural antioxidants used in food for health promotion and disease prevention (Finkel and Holbrook, 2000; Gorinstein et al., 2003; Valko et al., 2007; Pham-Huy et al., 2008). Many plants species have been recognized for their antioxidant activities and their consumption is recommended (Tiwari, 2001; Lee et al., 2003; Alali et al., 2007; Gan et al., 2010; Spiridon et al., 2011). Phenols are mostly found in plants and heaving antioxidant activity (Foti, 2007). Their antioxidant activity is mainly due to the fact that they can act as a reducing agent and hydrogen donators. Several studies had been conducted in order to correlate the number of compounds in plants and antioxidant activity (Alali et al., 2007; Gan et al., 2010; Spiridon et al., 2011).

Diabetes mellitus is a chronic disease attributed by hyperglycemia, glycosuria, negative nitrogen balance and insufficient production of insulin hormone. Three types of diabetes mellitus have been recognized; insulin dependent, noninsulin-dependent and gestational diabetes (Devi et al., 2016). It is the prevailing disorder throughout the globe affecting about 25% world population (Grover et al., 2002). According to WHO report in 2012, 1.5 million deceases worldwide were due to diabetes mellitus and 80% of deaths occurred in poor countries due to these diseases (WHO, 2012). Statistics show that this disease will affect more people, which will increase the death ratio up to 347 million in 2030 (Boyle et al., 2001; Shaw et al., 2010). In the world, Pakistan is considered among the top ten countries in which diabetes occur with high frequency. There were 5.2 million people in 2000 that would increase to 13.9 million in 2030 (Wild et al., 2004).

Presently, type II diabetes mellitus is a common type of diabetes, which is managed by a combination of diet, exercise, oral hypoglycemic drugs and sometimes insulin injections. However, these drugs have adverse side effect and high secondary failure rate (Bailey, 2000; Dormandy et al., 2005; Colhoun et al., 2012). In these patients, there is the main focus on blood glucose level (Stratton et al., 2000). Herbal drugs play important role in traditional medicine with many plant species showing antidiabetic activity (Arulrayan et al., 2007).

F. jacquemontii (Hook.f. & Thoms.) Jafri belongs to family Brassicaceae, a small shrub usually with a woody base. Ethnobotanical studies conducted indicate that this plant possesses medicinal properties i.e. root of the plant is used as carminative, colic, heartburns, dyspepsia (Ullah et al., 2014), anti-rheumatic agent (Ajaib et al., 2014), in piles, abdominal/stomach problems and pain (Shaheen et al., 2014). Ethnomedicinal information of this plant was collected from district Bannu, Pakistan (Fig. 1), where inhabitants use this plant as a household remedy for diabetes, ulcer, febrifuge, antidropsical, diuretic, in piles, and dyspepsia. Even though the plant is used for medicinal purposes but lacks pharmacological indication. From this perspective, the current study was conducted; to assess the antioxidant and antidiabetic potential of *F. jacquemontii* and their potential of inhibiting α -amylase and α -glucosidase.

Materials Methods

Identification and extraction

F. jacquemontii plant was collected in March, 2018 from Bannu District, union council Asperka, (Pakistan) and identified with the help of available literature (Ali and

Qaisar, 1995-2009; Nasir and Ali, 1971-2007), assigned with herbarium voucher number no# Bot. 20131(PUP) and placed in herbarium, Department of Botany, University of Peshawar.

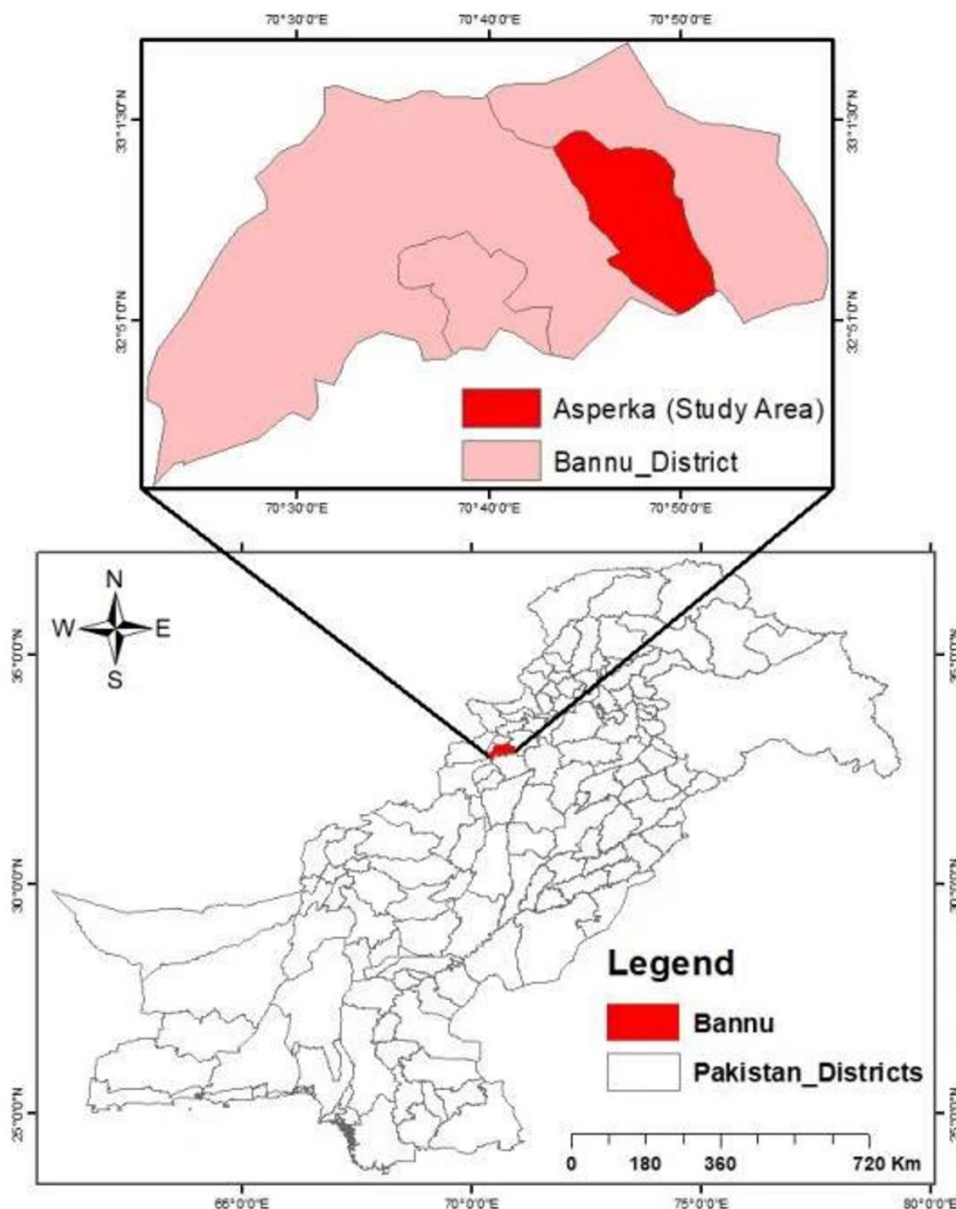


Figure 1. Map of the study area

The plant was washed with distilled water and the material was dried in shade, mechanically grounded into fine powder using Digitran grinder. The extract was provided gentle agitation through magnetic stirrer (Utech-Schenectady, USA) for 12 h then the extract of 100 g powder was obtained by keeping for 7 days in methanol (Ahmad et al., 2100). The extract was then filtered by Whatman no. 1 filter paper (125 mm) (Whatman Ltd., England). Phytochemical analysis of the extract for saponins, flavonoids, phenols, tannins and phlobatannins were made according to Trease and Evans (1989) with some amendments accordingly.

Screening procedure

Test for tannins and phenols

An extract of 5 mg was dissolved in 5 ml distilled water and then filtered. The filtrate was mixed with the FeCl₃ solution. A greenish-black precipitate was an indicator of tannins and phenols in the extract.

Test for saponins

An extract of 5 mg was mixed with distilled water and shake gently. Then the mixture was kept on heating Wisd Lab and foaming appearance was the indication of saponins.

Test for terpenoids

Chloroform (2 ml) was added with 5 ml methanolic extract and then added a small amount of H₂SO₄. The solution color was changed to blue-green with ring formation that confirmed terpenoids in the extract.

Test for flavonoids

Plant powder was boiled using Wiseven in 5 ml ethanol and an insufficient amount of concentrated HCl with a combination of magnesium. Then the solution color was changed to red that indicated the flavonoids.

Antioxidant activity

In this study, four procedures of antioxidant evaluation, ABTS, DPPH, H₂O₂ and Na₂MoO₄ were carried out to check the antioxidant potential of methanolic extract of *F. jacquemontii* (Hook.f. & Thoms.) Jafri.

Standard and sample solutions

An extract of 3 mg was dissolved in 3 ml methanol as a stock solution. Further dilutions were prepared by dissolving stock in methanol i.e. 50-500 µg/ml concentration (M1V1 = M2V2). Ascorbic acid served as a control and prepared accordingly as mentioned above i.e. 4 mg/1000 mL.

Diphenyl picrylhydrazyl radical scavenging activity

The DPPH (1, 1-diphenyl-2-picrylhydrazyl) assay was carried according to the method described by Gyamfi et al. (1999) with some amendments. The absorbance of DPPH was measured via spectrophotometer (UV-1602 BMS) at 517 nm which was 0.854 (<1). The reaction was performed at 37 °C in darkness. 200 µL extract from each sample solution and 800 µL DPPH were mixed and allowed to react at 25 °C for 30 min in darkness and checked its absorbance. The same procedure was repeated with an ascorbic acid solution. The potential of methanolic extract scavenging free radicals was articulated as IC₅₀. Ascorbic acid served as a control. The experiment was repeated three times. Extract potential was calculated on the basis of % DPPH radicals scavenged:

$$\% \text{ DPPH scavenging} = 1 - \frac{\text{Abs of DPPH} - \text{Abs of sample}}{\text{DPPH Abs}} \times 100 \quad (\text{Eq.1})$$

where: Abs of DPPH means an absorbance of 1, 1-diphenyl-2-picrylhydrazyl.

ABTS⁺ radical cation (potassium persulfate) bioassay

Arnao et al. (2001) procedure with modification was borrowed for ABTS⁺ radical cation (potassium persulfate) bioassay. The basic theme of ABTS bioassay was the capability of extract to scavenge 2, 2'-azino-bis (3-ethylbenzthiazoline-6-sulfonic acid) radical cation. Seven millimolar ABTS were mixed with 2.45 mM potassium persulfate and allowed to react for 30 min. Next 0.2 mL extract was added to 1.8 mL ABTS⁺ potassium persulfate solution. Absorbance (ABTS⁺ Potassium persulfate) were taken in comparison to control (ascorbic acid) at 745 nm using (UV-1602 BMS). The scavenging potential of the extract was calculated at various concentrations:

$$\% \text{ antioxidant capacity} = 1 - \frac{\text{Abs of test sample}}{\text{Abs of ascorbic acid}} \times 100 \quad (\text{Eq.2})$$

where Abs means absorbance.

Hydrogen peroxide scavenging activity

Dehpour method with some modification was employed to determine extract scavenging activity of hydrogen peroxide radical (Ruch et al., 1989). Forty millimolar hydrogen peroxide solution in phosphate buffer of pH 7.4 was measured at 230 nm to determine its concentration. Methanolic extract of 200 µL extract from each concentration (50-500 µg/ml) was added to 1.8 mL of hydrogen peroxide solution, incubated for 10 min at room temperature and the measured absorbance at 230 nm against a blank, with phosphate buffer only. Scavenging of hydrogen peroxide radical was calculated:

$$\% \text{ antioxidant capacity} = 1 - \frac{\text{Abs of test sample}}{\text{Abs of ascorbic acid}} \times 100 \quad (\text{Eq.3})$$

where Abs means absorbance.

Sodium molybdate reduction assay

The methanolic extract antioxidant ability against sodium molybdate radical was determined by mixing 3 mL solution (0.6 M sulphuric acid, 28 mM sodium phosphate and 4 mM sodium molybdate) with various concentrations of extract. The mixture was incubated (DAIHAN Scientific) (Ahmad et al., 2011) at 95 °C for 90 min. The mixture was cool down and measured its absorbance at 765 nm via digital spectrophotometer against a blank containing methanol. Ascorbic acid served as standard. Reduction power of the extract was calculated as the number of the equivalent of ascorbic acid. The comparative antioxidant capacity of *F. jacquemontii* (Hook.f. & Thoms.) Jafri extract was calculated:

$$\% \text{ Sodium molybdate reduction} = \frac{\text{Abs of test sample}}{\text{Abs of ascorbic acid}} \times 100 \quad (\text{Eq.4})$$

where Abs means absorbance.

Anti-diabetic assay

Test for alpha-amylase

0.1 g of potato starch and 100 mL of sodium acetate buffer were taken and mixed them to obtain a solution of starch (0.1% w/v). 27.5 mg of α -amylase was dissolved in 100 mL distilled water to prepare enzyme solution. 96 mM of 3, 5 di-nitro salicylic acid solution was prepared and mixed with sodium potassium Tartarate to obtain colorimetric reagent. Plant extract was mixed with the starch solution and then added α -amylase and left for some time. The condition was basic for reaction and temperature was 25 °C. The measurement was taken after 3 min. The maltoses generated were calculated by the production of 3-amino-5-nitro salicylic acid which was formed from the reduction of 3, 5 dinitro salicylic acid. The absorbance was measured at 540 nm with the help of spectrophotometer.

Test for alpha-glucosidase

The inhibitory activity of alpha-glucosidase was performed by taking starch solution as a substrate (2% w/v). The starch used in this assay was sucrose. 0.2 M Tris buffer (pH 8.0) was prepared. Plant extracts (200-800 μ g/ml), starch solution and Tris buffer were incubated at 37 °C for 5 min and 1mL of α -glucosidase (1 U/mL) was then added and incubated for 40 min at 35 °C using (DAIHAN Scientific) and then 2 ml of 6N HCl was added to the solution to stop the reaction. The color intensity was measured at 540 nm with the help of spectrophotometer.

Calculation of IC₅₀

The concentration of *F. jacquemontii* (Hook.f. & Thoms.) Jafri extracts required for 50% inhibition of the activity of the enzyme (IC₅₀) was calculated by using % inhibition at five different concentrations of the extract. Percentage inhibition (I %) was calculated:

$$\% \text{ Inhibition} = \frac{Ac - As}{Ac} \times 100 \quad (\text{Eq.5})$$

where: Ac means absorbance of the control and As means absorbance of the sample.

Statistical analysis

All calculations and art work presentation were performed in ORIGIN Pro 8. Percentages of inhibition were expressed as Mean \pm Standard deviation from three observations in each case.

Results

DPPH

The methanolic extract of *F. jacquemontii* scavenges the DPPH (1, 1-diphenyl-2-picrylhydrazyl) radicals at all tested concentrations (50-500 μ g/ml). Extract declared

highest scavenging potential at 500 $\mu\text{g/ml}$ (70%). The IC_{50} calculated in this case was 147 $\mu\text{g/ml}$. The effect was detected with reduced scavenging activity. The antioxidant effect of FJME against DPPH free radicals presented is in *Figure 2*.

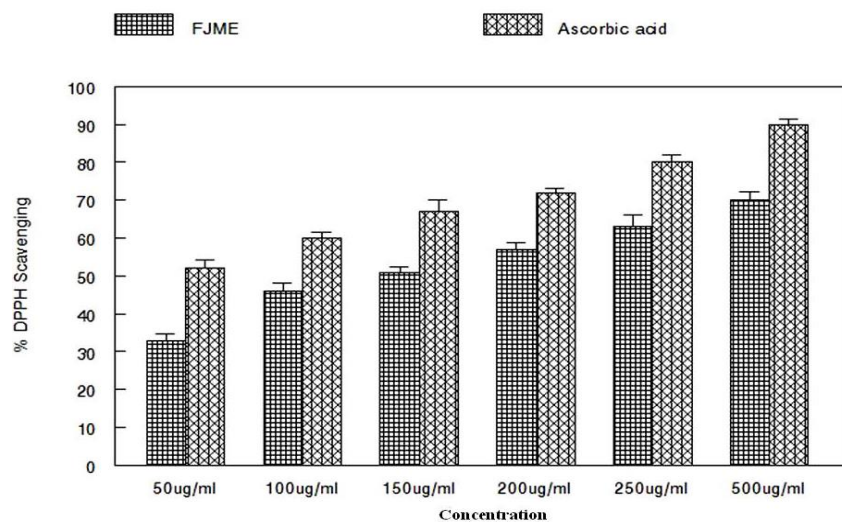


Figure 2. 1, 1- diphenyl-2-picrylhydrazyl stable free radicals (DPPH) scavenging at various concentrations by *Farsetia jacquemontii*. Error bars show the standard deviation. FJME is *Farsetia jacquemontii* methanolic extract ($n = 3$)

ABTS

Scavenging capacities of tested samples were measured spectrophotometrically with ABTS (2, 2'- azino-bis ethylbenzthiazoline-6-sulfonic acid) free radical. The extract showed the highest scavenging at 500 $\mu\text{g/ml}$ (85%), while at the same concentration, control exhibited (92%) antioxidant property. IC_{50} calculated in this case was 80 $\mu\text{g/mL}$ (*Fig. 3*).

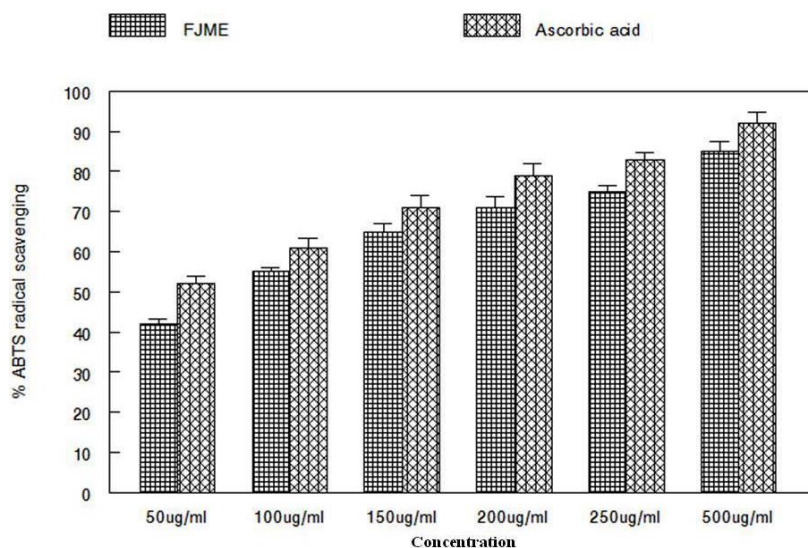


Figure 3. Interaction of *Farsetia jacquemontii* with 2'- azino-bis ethylbenzthiazoline-6-sulfonic acid (ABTS) radical cation. Error bars show the standard deviation. FJME is *Farsetia jacquemontii* methanolic extract ($n = 3$)

H₂O₂ reducing activity

H₂O₂ radicals reducing the power of FJME was tested at various concentrations (50-500 µg/ml). The extract showed significant radical scavenging activity (61%) at 500 µg/mL and declined with the decrease in extract concentration. While control showed the highest antioxidant activity (90%) at 500 µg/ml. IC₅₀ in this case was 215 µg/mL (Fig. 4).

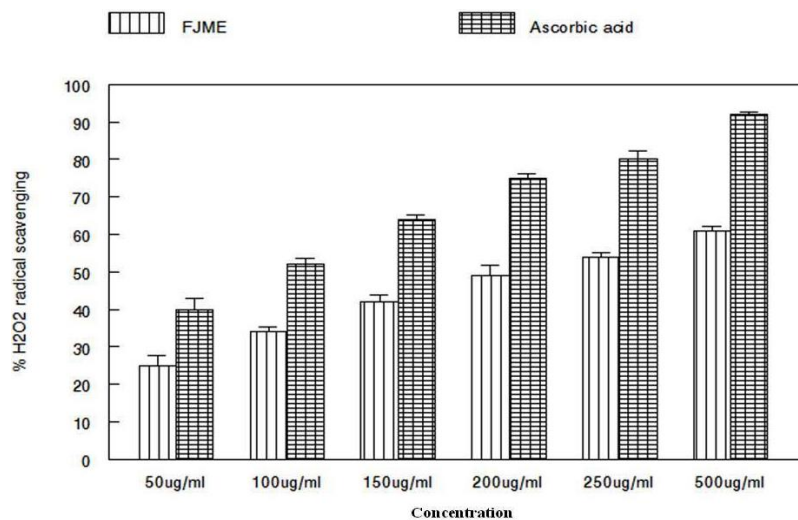


Figure 4. Reduction of hydrogen peroxide (H₂O₂) by *Farsetia jacquemontii* methanolic extract. Error bars show the standard deviation. FJME is *Farsetia jacquemontii* methanolic extract (n = 3)

Sodium molybdate reduction activity

It was found that FJME reduced molybdate radicals in a concentration-dependent manner. Results indicate that 78% molybdate radicals were reduced at 500 µg/ml comparative to control 95% at the same concentration, shown in Figure 5. IC₅₀ for molybdate activity was 101 µg/ml.

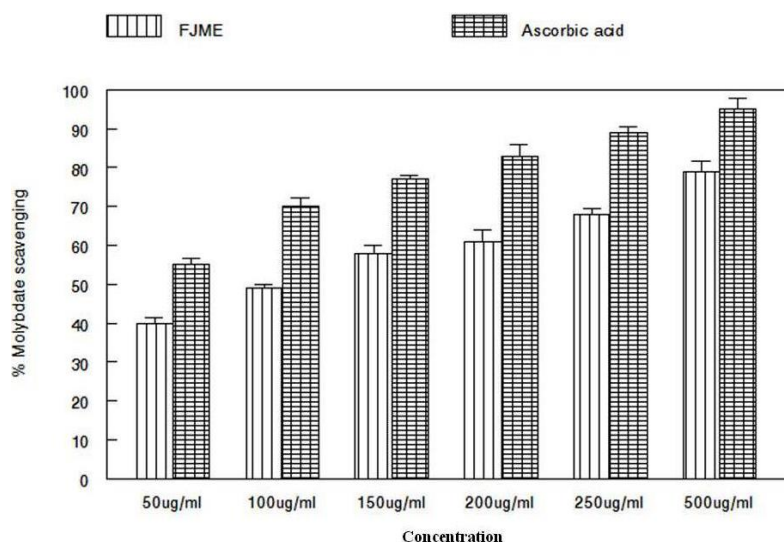


Figure 5. Reduction potential of *Farsetia jacquemontii* methanolic extract (FJME) against sodium molybdate free-radicals. Error bars show the standard deviation (n = 3)

α -amylase inhibitor effectiveness of FJME

Various concentrations (200-1000 $\mu\text{g/ml}$) of FJME were analyzed for α -amylase inhibitory activity. Fair increase in the percentage of α -amylase inhibition was observed. IC_{50} was 520 $\mu\text{g/ml}$ for α -amylase. Among the extracts tested, 1000 $\mu\text{g/ml}$ revealed the highest percentage of inhibition (82%). The concentration of Glimepiride (reference standard antidiabetic) employed in the test was similar to that of extract. Glimepiride (10 $\mu\text{g/ml}$) showed 98% inhibition with IC_{50} of 1.3 $\mu\text{g/ml}$ (Table 1).

Table 1. Inhibition of α -amylase enzyme activity by FJME

Sample	Concentrations ($\mu\text{g/ml}$)	α -amylase inhibition (%)	IC_{50}
FJME	200	41 \pm 1.45	290 $\mu\text{g/ml}$
	400	60 \pm 0.88	
	600	67 \pm 1.26	
	800	76 \pm 2.02	
	1000	82 \pm 1.71	
Glimepiride	2	75 \pm 0.74	1.3 $\mu\text{g/ml}$
	4	81 \pm 2.91	
	6	89 \pm 0.97	
	8	95 \pm 1.86	
	10	98 \pm 1.50	

FJME is *Farsetia jacquemontii* methanolic extract. Percentages of inhibition expressed as mean \pm standard deviation, IC_{50} is the half maximal inhibitory concentration

α -glucosidase inhibitor effectiveness of FJME

A dose-dependent and gradual increase in the percentage inhibition of α -glucosidase was observed with FJME. Highest percentage inhibition (87%) was observed at 1000 $\mu\text{g/ml}$. The IC_{50} values were found to be 250 $\mu\text{g/ml}$. Glimepiride at a concentration of 2 to 10 $\mu\text{g/ml}$ was employed and served as reference standard drug for α -glucosidase inhibitory activity. The lowest dose (2 $\mu\text{g/ml}$) produced an inhibitory percentage of (60%) and the highest dose (10 $\mu\text{g/ml}$) produced 96% inhibition with IC_{50} of 1.7 $\mu\text{g/ml}$. Like FJME, a dose-dependent increase in the percentage of inhibition was observed (Table 2).

Table 2. Inhibition of α -glucosidase enzyme activity by FJME

Sample	Concentrations ($\mu\text{g/ml}$)	α -glucosidase inhibition (%)	IC_{50}
FJME	200	40 \pm 0.92	240 $\mu\text{g/ml}$
	400	62 \pm 1.83	
	600	74 \pm 2.80	
	800	82 \pm 2.67	
	1000	87 \pm 1.73	
Glimepiride	2	60 \pm 0.74	1.7 $\mu\text{g/ml}$
	4	74 \pm 2.91	
	6	84 \pm 0.97	
	8	91 \pm 1.86	
	10	96 \pm 1.50	

FJME is *Farsetia jacquemontii* methanolic extract. Percentages of inhibition expressed as mean \pm standard deviation, IC_{50} is the half maximal inhibitory concentration

Discussion

Free radicals have been focused on notable concern amongst researchers due to their potential role in human diseases (Maxwell, 1995; Finkel and Holbrook, 2000). They are atoms or group of atoms with free electrons while antioxidants neutralize these toxins by providing electron (Jovanovic and M.G, 2000). These include mitochondrial radicals that initiate series of reaction in a living organism. In normal conditions, the production of pro-oxidants in the form of reactive oxygen species is efficiently checked and maintained by various levels of antioxidant defense mechanism like enzymes. Our dietary supplement contains antioxidants that effectively neutralizing these ROS during various disease conditions. Oxidative stress has been concerned with the consequence of free radical that attacks lipids, proteins and DNA. To investigate the characteristics of phenolic and anthocyanin as an antioxidant, MoO₄, DPPH and H₂O₂ radicals were used as a model in this study.

Mostly plants are investigated for their antioxidant effects that conventionally used in folk medicine. For the evaluation of antioxidant activity, various methods and modifications have been used (Aksoy et al., 2013). Our study revealed the presence of bioactive polyphenolic flavonoids, which might play an important role in improving of oxidative stress. Other studies documented the presence of phytochemicals during chemical characterization of medicinal plants (Aksoy et al., 2013). The data of the present study concluded that FJME contained good amount of phenolic compounds gifted with high antioxidant. The results provide a good pharmacological proof for this plant in diabetes, ulcer, febrifuge, antidropsical, and anti-rheumatic as well as its use in traditional medicine in Pakistan.

Phenolic compounds with one cyclic ring along with one or more OH functional moiety are the major group of phytochemicals in plants. Antioxidant activity which is one of the valuable activity among biological function exists in different phenolic compounds. Phenolic compounds have a unique structure and high affinity for metal chelating. Their electron donating/accepting ability let them play various potential roles to scavenge free radicals (Huang et al., 2009; Huda-Faujan et al., 2009; Bhatt and Negi, 2012; Khoddami et al., 2013). They are well predicted on the basis of their involvement in a large number of pathogenic diseases. Effective scavenger of free radicals acts as a potential antioxidant candidate (Ebrahimzadeh et al., 2008).

In the current research work, FJME in all cases showed equivalent scavenging ability to the standard compounds. Its phytochemical forage stable radicals and may exercise a defensive protection against oxidative damage to DNA, proteins etc. *F. jacquemontii* (Hook.f. & Thoms.) Jafri is a rich source of phenolic compounds and therefore strongly showed antioxidant properties in each case. So in food industries and other pharmaceutical planning *F. jacquemontii* (Hook.f. & Thoms.) Jafri is the best candidate because of its effective antioxidant properties.

On the other hand, diabetes results in huge oxidative damage by means of the creation of reactive oxygen free radicals, which leads to the pathogenesis of various diabetic complications. Insulin is a foremost participant in the management of glucose concentration. Deficiency or absence of insulin indicates very low or no carbohydrate metabolism (Gandhi and Sasikumar, 2012). Diabetes management still challenges the medical community. It was documented that inhibition of α -amylase and α -glucosidase would defer carbohydrate breakdown, which in turn results in reduced absorption of glucose, as a consequence blood glucose level becomes reduced (Chiasson and Rabasa-Lhoret, 2004).

Current research has been conducted to assess FJME in inhibiting α -amylase and α -glucosidase. The inhibitory effectiveness indicates that FJME acquires the potential to inhibit the gastrointestinal enzymes α -amylase and α -glucosidase. Possible inhibition mechanism disclosed that FJME exerts action on carbohydrate linking sites in starch and glycogen, delayed their breakdown to oligosaccharides and considered targets for inhibition of postprandial hyperglycemia. Dietary starch is hydrolyzed into maltose which in turn breaks down to glucose by the action of amylase. Since delayed and even weakened starch digestion, such inhibitors in foodstuff could be accountable to play a significant role in the starch breakdown (Jaffé and Vega Lette, 1968; Marshal, 1975). For the first time, we have explored FJME as a potent antidiabetic agent against gastrointestinal enzymes that are mainly accountable for hyperglycemia in diabetes and hope that this study will help researchers for further investigation in isolating the target compounds.

Conclusion

In the present study *Farsetia jacquemontii* methanolic extract showed the presence of various phytochemicals. These bioactive constituents are considered the medicinal efficacy of *F. jacquemontii*. Furthermore, the phenols and flavonoids of *F. jacquemontii* methanolic extract might be able to manage oxidative stress.

Acknowledgments. We are thankful to the funding institutions Chinese Scholarship Council (CSC) and Beijing Forestry University, Beijing, China for their financial support under the grant number 2160284. We are thankful to CSC and BFU for encouragement and support regarding this article.

REFERENCES

- [1] Ahmad, M., Khan, R. A., Khan, F. U., Khan, N. A., Shah, M. S., Khan, M. R. (2011): Antioxidant and antibacterial activity of crude methanolic extract of *Euphorbia prostrata* collected from District Bannu (Pakistan). – *African Journal of Pharmacy and Pharmacology* 5: 1175-1178.
- [2] Ajaib, M., Ashraf, Z., Riaz, F., Siddiqui, M. F. (2014): Ethnobotanical studies of some plants of Tehsil Kharian, District Gujrat. – *FUUAST Journal of Biology* 4: 65.
- [3] Aksoy, L., Kolay, E., Ağılönü, Y., Aslan, Z., Kargıoğlu, M. (2013): Free radical scavenging activity, total phenolic content, total antioxidant status, and total oxidant status of endemic *Thermopsis turcica*. – *Saudi journal of biological sciences* 20: 235-239.
- [4] Alali, F. Q., Tawaha, K., El-Elimat, T., Syouf, M., El-Fayad, M., Abulaila, K., Oberlies, N.H. (2007): Antioxidant activity and total phenolic content of aqueous and methanolic extracts of Jordanian plants: an ICBG project. – *Natural Product Research* 21(12): 1121-1131.
- [5] Ali, S. I., Qaisar, M. (1915-2009) *Flora of Pakistan*, Islamabad. – Pakistan Agricultural Research Council, Islamabad.
- [6] Arnao, M. B., Cano, A., Acosta, M. (2001): The hydrophilic and lipophilic contribution to total antioxidant activity. – *Food Chemistry* 73: 239-244.
- [7] Arulrayan, N., Rangasamy, S., James, E., Pitchai, D. (2007): A database for medicinal plants used in the treatment of diabetes and its secondary complications. – *Bioinformation* 2: 22-23.
- [8] Bailey, C. J. (2000): Potential new treatments for type 2 diabetes. – *Trends In Pharmacological Sciences* 21: 259-265.

- [9] Bhatt, P., Negi, P. S. (2012): Antioxidant and antibacterial activities in the leaf extracts of Indian borage (*Plectranthus amboinicus*). – Food and Nutrition Sciences 3: 146.
- [10] Boyle, J. P., Honeycutt, A. A., Narayan, K. V., Hoerger, T. J., Geiss, L. S., Chen, H., Thompson, T. J. (2001): Projection of diabetes burden through 2050: impact of changing demography and disease prevalence in the US. – Diabetes care 24(11): 1936-1940.
- [11] Chiasson, J-L., Rabasa-Lhoret, R. (2004): Prevention of type 2 diabetes: insulin resistance and beta-cell function. – Diabetes 53: S34-S38.
- [12] Colhoun, H. M., Livingstone, S. J., Looker, H. C., Morris, A. D., Wild, S. H., Lindsay, R. S., Reed, C., Donnan, P. T., Guthrie, B., Leese, G. P., McKnight, J. (2012): Hospitalised hip fracture risk with rosiglitazone and pioglitazone use compared with other glucose-lowering drugs. – Diabetologia 55(11): 2929-2937.
- [13] Devi, S., Kumar, D., Kumar, M. (2016): Ethnobotanical values of antidiabetic plants of MP region India. – Journal Medicinal Plants Studies 4: 26-28.
- [14] Dormandy, J. A., Charbonnel, B., Eckland, D. J., Erdmann, E., Massi-Benedetti, M., Moules, I. K., Skene, A. M., Tan, M. H., Lefèbvre, P. J., Murray, G. D., Standl, E. (2005): Secondary prevention of macrovascular events in patients with type 2 diabetes in the PROactive Study (PROspective pioglitAzone Clinical Trial In macroVascular Events): a randomised controlled trial. – The Lancet 366(9493): 1279-1289.
- [15] Ebrahimzadeh, M. A., Pourmorad, F., Hafezi, S. (2008): Antioxidant activities of Iranian corn silk. – Turkish Journal of Biology 32: 43-49.
- [16] Farber, J. L. (1994): Mechanisms of cell injury by activated oxygen species. – Environmental Health Perspectives 102: 17.
- [17] Finkel, T., Holbrook, N. J. (2000): Oxidants. Oxidative stress and the biology of aging. – Nature 408: 239.
- [18] Foti, M. C. (2007): Antioxidant properties of phenols. – Journal of Pharmacy and Pharmacology 59: 1673-1685.
- [19] Gan, R-Y., Xu, X-R., Song, F-L., Kuang, L., Li, H-B. (2010): Antioxidant activity and total phenolic content of medicinal plants associated with prevention and treatment of cardiovascular and cerebrovascular diseases. – Journal of Medicinal Plants Research 4: 2438-2444.
- [20] Gandhi, G. R., Sasikumar, P. (2012): Antidiabetic effect of *Merremia emarginata* Burm. F. in streptozotocin-induced diabetic rats. – Asian Pacific Journal of Tropical Biomedicine 2: 281-286.
- [21] Gorinstein, S., Yamamoto, K., Katrich, E., Leontowicz, H., Lojek, A., Leontowicz, M., Ciz, M., Goshev, I., Shalev, U., Trakhtenberg, S. (2003): Antioxidative properties of Jaffa sweets and grapefruit and their influence on lipid metabolism and plasma antioxidative potential in rats. – Bioscience, Biotechnology, and Biochemistry 67: 907-910.
- [22] Grover, J., Yadav, S., Vats, V. (2002): Medicinal plants of India with anti-diabetic potential. – Journal of Ethnopharmacology 81: 81-100.
- [23] Gyamfi, M. A., Yonamine, M., Aniya, Y. (1999): Free-radical scavenging action of medicinal herbs from Ghana: *Thonningia sanguinea* on experimentally-induced liver injuries. *General Pharmacology*. – The Vascular System 32(6): 661-667.
- [24] Huang, W-Y., Cai, Y-Z., Zhang, Y. (2009): Natural phenolic compounds from medicinal herbs and dietary plants: potential use for cancer prevention. – Nutrition and Cancer 62: 1-20.
- [25] Huda-Faujan, N., Noriham, A., Norrakiah, A., Babji, A. S. (2009): Antioxidant activity of plants methanolic extracts containing phenolic compounds. – African Journal of Biotechnology 8: 3.
- [26] Jaffé, W. G., Vega Lette, C. L. (1968): Heat-labile growth-inhibiting factors in beans (*Phaseolus vulgaris*). – The Journal of Nutrition 94: 203-210.
- [27] Jovanovic, S. V., Simic, M. G. (2000): Antioxidants in nutrition. – Annals of the New York Academy of Sciences 899(1): 326-334.

- [28] Khoddami, A., Wilkes, M. A., Robrets, T. H. (2013): Techniques for analysis of plant phenolic compounds. – *Molecules* 18: 2328-2375.
- [29] Lee, S. E., Hwang, H. J., Ha, J-S., Jeong, H-S., Kim, J. H. (2003): Screening of medicinal plant extracts for antioxidant activity. – *Life Sciences* 73: 167-179.
- [30] Lü, J. M., Lin, P. H., Yao, Q., Chen, C. (2010): Chemical and molecular mechanisms of antioxidants: experimental approaches and model systems. – *Journal of Cellular and Molecular Medicine* 4: 840-860.
- [31] Marshal, J. (1975): Hypothesized that negatively charged residues of pilaic acid from the membrane. – *International American Chemical Society Symposium Series* 1975(15): 244-266.
- [32] Maxwell, S. R. (1995): Prospects for the use of antioxidant therapies. – *Drugs* 49(3): 345-361.
- [33] Nasir, E., Ali, S. I. (1971-2007): *Flora of West Pakistan*. – Department of Botany, University of Karachi, Karachi.
- [34] Pham-Huy, L. A., He, H., Pham-Huy, C. (2008): Free radicals, antioxidants in disease and health. – *International journal of biomedical Science* 4: 89.
- [35] Pourmorad, F., Hosseinimehr, S., Shahabimajd, N. (2006): Antioxidant activity, phenol and flavonoid contents of some selected Iranian medicinal plants. – *African Journal of Biotechnology* 5: 11.
- [36] Ruch, R. J., Cheng, S-j., Klaunig, J. E. (1989): Prevention of cytotoxicity and inhibition of intercellular communication by antioxidant catechins isolated from Chinese green tea. – *Carcinogenesis* 10: 1003-1008.
- [37] Shaheen, H., Qureshi, R., Akram, A., Gulfraz, M. (2014): Inventory of medicinal flora from Thal desert, Punjab, Pakistan. – *African Journal of Traditional, Complementary and Alternative Medicines* 11: 282-290.
- [38] Shaw, J. E., Sicree, R. A., Zimmet, P. Z. (2010): Global estimates of the prevalence of diabetes for 2010 and 2030. – *Diabetes Research and Clinical Practice* 87: 4-14.
- [39] Spiridon, I., Bodirlau, R., Teaca, C-A. (2011): Total phenolic content and antioxidant activity of plants used in traditional Romanian herbal medicine. – *Central European Journal of Biology* 6: 388-396.
- [40] Stratton, I. M., Adler, A. I., Neil, H. A. W., Matthews, D. R., Manley, S. E., Cull, C. A., Hadden, D., Turner, R. C., Holman, R. R. (2000): Association of glycaemia with macrovascular and microvascular complications of type 2 diabetes (UKPDS 35): prospective observational study. – *BMJ* 321(7258): 405-412.
- [41] Tiwari, A. K. (2001): Imbalance in antioxidant defense and human diseases: multiple approaches of natural antioxidants therapy. – *Current Science* 81(9): 1179-1187.
- [42] Trease, G. E., Evans, W. C. (1989): *Pharmacology*. 11th Ed. – Bailliere Tindall Ltd., London, pp. 60-75.
- [43] Ullah, S., Khan, M. R., Shah, N. A., Shah, S. A., Majid, M., Farooq, M. A. (2014): Ethnomedicinal plant use value in the Lakki Marwat District of Pakistan. – *Journal of Ethnopharmacology* 158: 412-422.
- [44] Valko, M., Leibfritz, D., Moncol, J., Cronin, M. T., Mazur, M., Telser, J. (2007): Free radicals and antioxidants in normal physiological functions and human disease. – *The International Journal of Biochemistry & Cell Biology* 39: 44-84.
- [45] WHO (2012): *Global Status Report on Non-communicable Diseases*. – World Health Organization, Geneva.
- [46] Wild, S., Roglic, G., Green, A., Sicree, R., King, H. (2004): Global prevalence of diabetes: estimates for the year 2000 and projections for 2030. – *Diabetes Care* 27: 1047-1053.

IMPACTS OF LEAF AREA ON THE PHYSIOLOGICAL ACTIVITY AND BERRY MATURATION OF MERLOT (*VITIS VINIFERA* L.)

CANDAR, S.¹ – BAHAR, E.² – KORKUTAL, I.^{2*}

¹*Tekirdag Viticulture Research Institute, Tekirdag, Turkey*

²*Department of Horticulture, Agricultural Faculty, Tekirdag Namik Kemal University
59030 Tekirdag, Turkey*

**Corresponding author*

e-mail: ikorkutal@nku.edu.tr; +90-282-250-2059

(Received 26th Sep 2019; accepted 8th Jan 2020)

Abstract. The aim of this research was to understand some physiological and agronomical behaviors of the Merlot grapevine subjected to different canopy management practices under the climatic conditions of different growing seasons in Tekirdag, Turkey. The resulting must composition and berry maturation were also determined. Adult vines of *Vitis vinifera* L. cv. Merlot, grafted onto 5BB were applied to different leaf areas (various levels of leaf removal from main and lateral shoots) during the growing season. Leaf photosynthesis (A) and transpiration (E), stomatal conductance (g_s), yield parameters, maturation indices and berry composition at harvest were analyzed over a period of three consecutive years between 2013 and 2015. In the vegetation periods of 2013 and 2015 when there is less precipitation, proportional humidity is relatively low and temperatures are high, positive results were obtained in terms of quality criteria in half lateral shoots (3-4 leaves= HLS) application. Under extreme rainfall and high relative humidity conditions as in 2014, none lateral shoots (NLS) application increased physiological activity and relative quality. The main factor controlling the physiological behavior and grape ripening in Merlot vines was largely dependent on the meso-climatic conditions during the growing season. However, the total effect of small differences in the canopy microclimates created by different leaf area reduction applications affected the indicators of industrial maturity at the end of vegetation. Planning of canopy management practices should be done by taking into consideration long- and medium-term meteorological evaluations, and short-term planning within vegetation should be considered by weighing weekly and monthly meteorological risks.

Keywords: *canopy management, green pruning, climate, leaf gas exchange, quality*

Introduction

Climate, especially temperature is the major component of wine grape terroirs, with a number of other factors including soil characteristics and soil water reserves, grape variety and rootstock, cultivation techniques such as cover crops and leaf fruit ratio. Grape berry maturation is generally associated with all of these factors.

The negative effects of the current climate crisis are getting worse every year. Early and accelerated berry ripening (Petrie and Sadras, 2008; Keller, 2010a), changing of usual wine styles due to unexpected seasonal precipitation (Mira de Orduña, 2010; Schultz and Stoll, 2010), problems like higher alcohol ratios with lower acidity and reduced varietal aroma compounds due to high sugar in berries (Keller, 2010a) are the troubles that stand out to be solved by winemakers. It is very important for the wine industry to adapt to alternative viticulture and winemaking methods to get used to these new climatic conditions (Clingeffer, 2010). As Carbonneau and Bahar (2009) stated global warming is inevitable, a couple of new strategies should be tried like breeding of new varieties and rootstocks, soil management and more important for short term vine

canopy management for sustainable viticulture. Canopy management treatments, such as pruning, trimming and leaf removal, can be certainly utilize to organize vine source-sink balance (Santesteban et al., 2011; Moran et al., 2017). There are a lot of researches indicating that the early maturation or postponement of the industrial maturity may occur when the leaf removal is applied in the proper style and time (Poni et al., 2013; Caccavello et al., 2017).

Another factor which is as effective as the climate in determining berry maturity is the genetic infrastructure of the variety that determines the physiological activity. Young leaves generally start to produce excess photo assimilates, translocated afterwards to the other parts of the vine after they reach one third of their full sizes, approximately 5 or 6 weeks after leaf unfolding (Keller, 2010b). As the leaves age, their photosynthetic capacity and their contribution to organic matter production increase to some point, then fall. Depending on leaf age, regardless of whether they come from the lateral or main shoot, individual photosynthetic activities are effective in berry ripening and in sugar accumulation in grape juice (Hirano et al., 1994). Due to this phenomenon it is important to point out the role of leaf removal practices about ripening processes. The lack of proper canopy management promotes the occurrence of unbalanced vineyards with intense vegetative growth (Zalamena et al., 2013; Bem et al., 2016) and results unbalanced wines.

The aim of the study was to have a better understanding about the impact of leaf removal practices on physiological activities and berry maturation of grapes under the monitored climate conditions.

Materials and Methods

Location, vine material and experimental set-up

The experimental study was conducted in 2013, 2014 and 2015 in an experimental vineyard, in Tekirdağ Viticulture Research Institute, Turkey (40.96 °N-40.97 °N latitudes, 27.46 °E-27.47 °E longitudes) with *Vitis vinifera* cv. Merlot which is grown in large quantities in the Thrace region and preferred because it has high adaptability to the region climate and gives high wine quality. However, Merlot which showed more anisohydric characters (Collins and Loveys, 2010).

The grapevines, grafted on 5BB rootstock were 14 years old. Double Guyot training vines loaded 16-18 buds per vine, with distances of 2.5 m between rows and 1.5 m between plants. The vineyard is planted on North-South at 40 m altitude on a high groundwater and, flat land with no significant soil variations. Analyses in 0-90 cm soil depth observed that in the clay-loam structure, slightly alkaline and calcareous, in at a depth of 60-90 cm highly calcareous with no salinity problem. Agrotechnical applications were done 3 consecutive years which were given *Table 1*. All plant protection procedures were done routinely in vineyard.

Different leaf areas of vines were created by the limitations of main shoot lengths 1 m, 1.25 m and 1.5 m while they reached 170-180 cm (EL 31-33). Lateral shoots also limited as full lateral shoots (6-7 leaves: FLS), half lateral shoots (3-4 leaves: HLS) and none lateral shoots (no leaf: NLS) performed in veraison (Eichhorn-Lorenz growing stages 35) according to Lorenz et al. (1995). Both applications were kept at the same length until the harvest period.

Descriptive meso-climatic weather data such as temperature, relative humidity, light intensity, wind speed and total precipitation at two meters high from ground were

monitored during for 3 consecutive years with a weather station installed within the experimental area (*Table 2*).

Table 1. Agrotechnical applications and dates in years of 2013, 2014 and 2015

Applications	2013	2014	2015	EL stages
Equalization of buds	06.03.2013	15.03.2014	09.03.2015 10.03.2015	16 buds (EL 5-7)
Equalization of shoots	07.05.2013	15.05.2014 20.05.2014	14.05.2015 15.05.2015	30-40 cm shoot length (EL 12-15-17)
Equalization of cluster numbers	18.06.2013 19.06.2013	18.06.2014 19.06.2014	-	Clusters visible (EL 15-17).
Topping	01.07.2013 03.07.2013	19.06.2014 23.06.2014	22.06.2015 26.06.2015	170-180 cm main shoot length (EL 31-33)
Lateral shoot removal	08.07.2013 10.07.2013	28.07.2014 01.08.2014	27.07.2015 05.08.2015	Veraison and post veraison (EL 35)
Control of top and lateral shoots	22.07.2013 05.08.2013	21.08.2014 22.08.2014 01.09.2014 02.09.2014 08.09.2014 09.09.2014	24.08.2015 28.08.2015	

Table 2. The climatic data of Tekirdag during the vegetation period in years of 2013, 2014 and 2015

Years	Months	Mean Temp. (°C)	Precipitation (mm)	Relative humidity (%)	Wind speed. (m s ⁻¹)	Light intensity (μmol m ⁻² s ⁻¹)
2013	April	13.50	16.00	84.80	2.20	1026.82
	May	19.50	8.00	69.70	2.40	1244.67
	June	22.40	35.00	68.70	2.60	1189.14
	July	24.70	0.00	61.40	3.20	1307.08
	August	25.90	0.00	62.30	3.50	1128.17
	September	21.60	10.20	61.40	2.60	854.82
	October	14.30	96.40	76.20	2.30	573.62
2014	April	13.37	46.80	83.27	2.43	408.98
	May	17.53	72.10	80.29	2.36	560.41
	June	21.8	69.6	76.2	No data	No data
	July	24.81	107.70	73.03	2.50	800.19
	August	25.28	80.50	74.52	2.72	1154.46
	September	20.77	98.50	77.90	2.58	1027.51
2015	October	15.61	136.10	79.84	2.92	684.94
	April	11.4	58.6	74.3	2.8	1179.36
	May	18.6	32.0	76.3	2.5	1172.86
	June	21.3	63.6	73.3	2.8	1167.01
	July	24.9	1.8	70.6	3.0	1760.77
	August	26.1	1.6	68.9	3.3	1289.66
	September	22.7	29.8	77.2	2.7	891.70
October	16.4	80.4	80.1	3.2	621.58	

Despite the equal number of (16) buds left in the winter pruning, the plants that disrupt homogeneity in the number of shoots and bunches were balanced when the shoots reached an average length of 30-40 cm (EL 15-17) or excluded from the trial. Standard cultural practices in the region were applied to all treatments during research. The vines data taken were selected from the same development period and with the approximate charge and those without spaces.

Total leaf area and leaf area per kg of grapes

Leaf areas of each application were calculated by, multiplying the number of shoots per vine and the number of leaves per shoot which were scanned with CI-202 Portable Laser Leaf Area Meter (CID Bio-Science, Washington, USA), from four shoots in each vine of every application.

Ratio of total leaf area ($\text{m}^2 \text{vine}^{-1}$) to yield (kg vine^{-1}) was calculated for determining leaf area per kg of grapes according to Sanchez-de-Miguel et al. (2010).

Leaf gas exchange measurements

Leaf gas exchange [net photosynthesis (A , $\mu\text{mol CO}_2 \text{m}^{-2} \text{s}^{-1}$) and transpiration (E , $\text{mmol H}_2\text{O m}^{-2} \text{s}^{-1}$)], stomatal conductance (g_s , $\mu\text{mol m}^{-2} \text{s}^{-1}$) were measured on healthy, fully expanded, mature and non-senescent leaves by using LI-6400XT (Li-Cor Inc., Nebraska, USA) portable photosynthesis system, between 10:00-12:00 AM. During the measurements, the device was calibrated to $400 \mu\text{mol CO}_2 \text{m}^{-2} \text{s}^{-1}$ atmospheric CO_2 and 25°C block temperature. In each application, 10 measurements were performed on one leaf of each of the four grapevines, and these measurements were used as the average of repetitions.

Must composition and berry maturation

At harvest, two hundred berries per replicate were selected to determine primary juice compounds as total soluble solids (% TSS; $^\circ\text{Brix}$) with handheld refractometer (ATAGO Co. Ltd., Tokyo, Japan), pH with digital pH meter (Mettler Toledo FE20, Switzerland), total acidity (g L^{-1} of tartaric acid) in must at the harvest date using the official methods of the Organisation Internationale de la Vigne et du Vin (OIV, 2012).

In addition, the amount of sugar per gram of grapes (mg g-berry^{-1}) was calculated by dividing the amount of sugar in the berry by the fresh weight (Ferrer et al., 2014). Maturity indicators; $^\circ\text{Brix}$ /titratable acid, and $\text{pH}^2 \times ^\circ\text{Brix}$ values were calculated and evaluated according to Blouin and Guimberteau (2000).

Statistical analysis

Results were subjected to variance analysis with JMP 13.2.0 statistical software according to split-plots trail design for determining of differences in applications and years. LSD test was used at 5% significance level to identify differences between significant means.

Results and Discussion

Climatic conditions and grapevine phenology

In the 3 years that the study was carried out, 2014 was distinguished from 2013 and 2015 in terms of temperature and especially precipitation amount, as well as climatic characteristics such as light intensity, relative humidity and wind speed. While the mean of total annual precipitation for the 1939-2018 period is 582.90 mm; the total precipitation was 443.80 mm in 2013, 770.50 mm in 2014 and 507.90 mm in 2015 (Table 2).

As a result of the phenological observations made throughout the trial, the day green shoot tips seen clearly in the buds was 05.04.2013 in 2013 (94th calendar day),

02.04.2014 (91st calendar day) for the year 2014, for 2015 it was observed as 12.04.2015 (101st calendar day). The date of the veraison was determined as 22.07.2013 (202th calendar day) for the year 2013, 30.07.2014 (210th calendar day) for the year 2014 and 01.08.2015 (212th calendar day) for the year 2015. Harvest was done at %22-23 TSS excluding 2014. It was held on 26.08.2013 (237th calendar day) in 2013, 16.09.2014 (258th calendar day) in 2014 and 05.10.2015 (277th calendar day) in 2015.

Climatic data were also recorded on the days of physiological activity measurement at 10.00-12.00 during the experiment (*Table 3*).

Table 3. The climatic data of physiological activity measurement days in years of 2013, 2014 and 2015

Dates	Calendar days	Mean temp. (°C)	Max. temp. (°C)	Min. temp. (°C)	Wind speed (m s ⁻¹)	Relative humidity (%)	Light intensity (μmol m ² s ⁻¹)
11.06.2013	161	23.46	27.70	17.30	1.70	73.90	1466.47
04.07.2013	184	24.56	25.20	16.30	1.65	53.00	1202.07
12.07.2013	192	27.73	28.30	19.40	1.90	52.00	1559.96
26.07.2013	206	28.65	28.90	19.70	1.85	37.70	1496.46
31.07.2013	211	27.58	29.30	23.10	2.90	59.00	966.06
15.08.2013	226	28.37	31.50	23.20	3.00	60.80	1063.89
27.08.2013	238	25.17	29.10	18.80	1.70	79.80	1293.80
24.06.2014	174	23.69	28.12	18.68	2.54	70.37	1163.02
01.07.2014	181	23.30	26.50	18.20	2.10	78.00	723.24
08.07.2014	188	24.70	29.30	19.30	2.30	65.00	1144.04
15.07.2014	195	25.30	30.20	20.10	3.50	73.00	725.67
19.08.2014	230	23.60	28.30	17.90	3.60	66.00	1318.75
26.08.2014	237	25.00	29.90	20.40	3.10	72.00	1743.94
02.09.2014	244	24.00	28.30	19.90	2.10	80.00	1496.11
07.07.2015	187	24.60	29.50	18.40	2.30	70.10	1902.26
21.07.2015	201	25.00	31.10	18.40	2.80	74.20	1841.68
28.07.2015	208	27.70	32.30	21.80	1.70	69.30	1677.26
04.08.2015	215	26.50	30.20	21.70	2.20	76.20	1894.88
11.08.2015	222	25.90	29.40	21.00	2.90	74.50	1589.56
18.08.2015	229	27.30	32.00	22.80	3.30	74.90	1159.53
25.08.2015	236	25.50	30.40	19.80	4.30	61.40	1583.40
11.09.2015	253	25.20	29.20	22.20	2.80	82.40	939.32
02.10.2015	274	16.30	19.90	13.00	3.20	77.30	44.37

Yield (kg vine⁻¹)

In both years, 16 buds per vine were left in winter pruning, and shoots and clusters were equalized when the shoots reached 30-40 cm length. Thus, the differences between the yield values were not statistically significant. Yield values were seen the lowest for NLS application with 4.60 kg vine⁻¹ and highest for FLS application with 5.00 kg vine⁻¹.

Due to 16 buds per vine were left in winter pruning and the equalization of shoots and clusters, in every three years the differences between the yield values were not statistically significant and ranged between 5.20 kg vine⁻¹ and 5.43 kg vine⁻¹. The lowest yield was seen for 1 m main shoot length and the highest were seen for 1.5 m main shoot length treatment for the mean of years.

Total leaf area and leaf area per kg of grapes (m² vine⁻¹)

In accordance with the method, different total leaf areas and different canopy microclimates were tried to be created in each year. The result that the interventions on

the total leaf areas per vine were found to be statistically significant when the mean of the three years and were each year individually, showed that the desired different canopy architecture and differentiation of the canopies were achieved (*Table 4*).

Table 4. Effects of main shoot and lateral shoot treatments on total leaf area (m^2 per vine) and leaf area (m^2 per kg grape)

Treatments	2013		2014		2015		Mean of years	
	TLA (m^2 per vine)	LA (m^2 per kg grape)	TLA (m^2 per vine)	LA (m^2 per kg grape)	TLA (m^2 per vine)	LA (m^2 per kg grape)	TLA (m^2 per vine)	LA (m^2 per kg grape)
1 m	4.55 ^b	0.73 ^b	3.50	5.55	4.10	0.46	4.05 ^b	2.25
1.25 m	4.66 ^b	0.76 ^b	3.94	6.39	4.22	0.46	4.27 ^b	2.54
1.5 m	5.43 ^a	0.89 ^a	4.41	7.25	4.72	0.51	4.85 ^a	2.88
NLS	2.10 ^c	0.33 ^c	1.79 ^c	2.89 ^c	1.83 ^c	0.21 ^c	1.92 ^c	1.14 ^c
HLS	5.70 ^b	0.92 ^b	3.95 ^b	6.23 ^b	4.55 ^b	0.51 ^b	4.73 ^b	2.55 ^b
FLS	6.83 ^a	1.14 ^a	6.11 ^a	10.08 ^a	6.67 ^a	0.71 ^a	6.54 ^a	3.98 ^a
YME	4.88 ^A	0.79 ^B	3.95 ^B	6.40 ^A	4.35 ^B	0.48 ^B		
MSME LSD _{0.05}	0.412	0.151	n.s.	n.s.	n.s.	n.s.	0.282	n.s.
LSME LSD _{0.05}	0.554	0.083	0.729	1.738	0.453	0.045	0.401	0.432
YME LSD _{0.05}	0.401	0.432	0.401	0.432	0.401	0.432		

TLA and LA represent total leaf area (m^2 per vine) and leaf area (m^2 per kg grape). NLS, HLS, and FLS represent none lateral shoots (no leaf), half lateral shoots (3-4 leaves) full lateral shoots (6-7 leaves), MSME means main shoot main effect, LSME means lateral shoot main effect and YME means year main effect. Different lowercase superscript letters in same column and uppercase letters in same line represent statistically significant differences between means at $p < 0.05$ according to least significant difference test. n.s. means not significant

Values for leaf area per kg of grapes resulting from unusually low yields in 2014, due to severe *Plasmopara viticola* epidemic caused extraordinary rainfall, increased average values for both lateral and main shoot treatments. When the year 2014 is ignored, it is seen that $0.73 m^2$ leaf area for kg grape⁻¹ of vine for 1 m main shoot length for 2013 year is sufficient and statistically significant. Also, lateral shoot treatments were found statistically significant in terms of each year and mean of years (*Table 4*).

In our study, it is seen that the targeted yield can be achieved, without quality loss, with some delay in industrial maturity even when the leaf areas are reduced more than regional standards. Therefore, it is considered that the decrease in leaf areas can be compensated for in terms of yield by arrangements in the internal metabolism of the vine. This shows that unusual canopy management practices that can be applied against unusual climatic conditions (high relative humidity, high temperature fluctuations, extreme rainy periods, etc.) can be used in certain periods, but not every year. However, to obtain the quality and optimum yield without excessive vegetative growth, interventions to the clusters and canopy should be considered carefully in order to optimize the leaf/crop ratio at different stages of development.

Net photosynthesis (A), transpiration (E) and stomatal conductance (g_s) measurements

When the measurement days are examined one by one in 2013; it is seen that photosynthesis (A) values vary between $18.03 - 7.62 \mu\text{mol CO}_2 m^{-2} s^{-1}$. HLS showed the highest rate of photosynthesis (A) in 4 of 7 days. In terms of main shoot lengths, 1.25 m treatment showed the highest rates of photosynthesis in 4 of 7 days. As can be seen in

Figure 1 transpiration (E) measurements also show parallelism with photosynthesis (A) rates. In general, the highest transpiration rates were observed in the measurements performed in July. Although there were no significant differences between the applications, highest transpiration values were measured in NLS and 1.25 m applications after the completion of the lateral shoot applications and the creation of the desired leaf area formations.

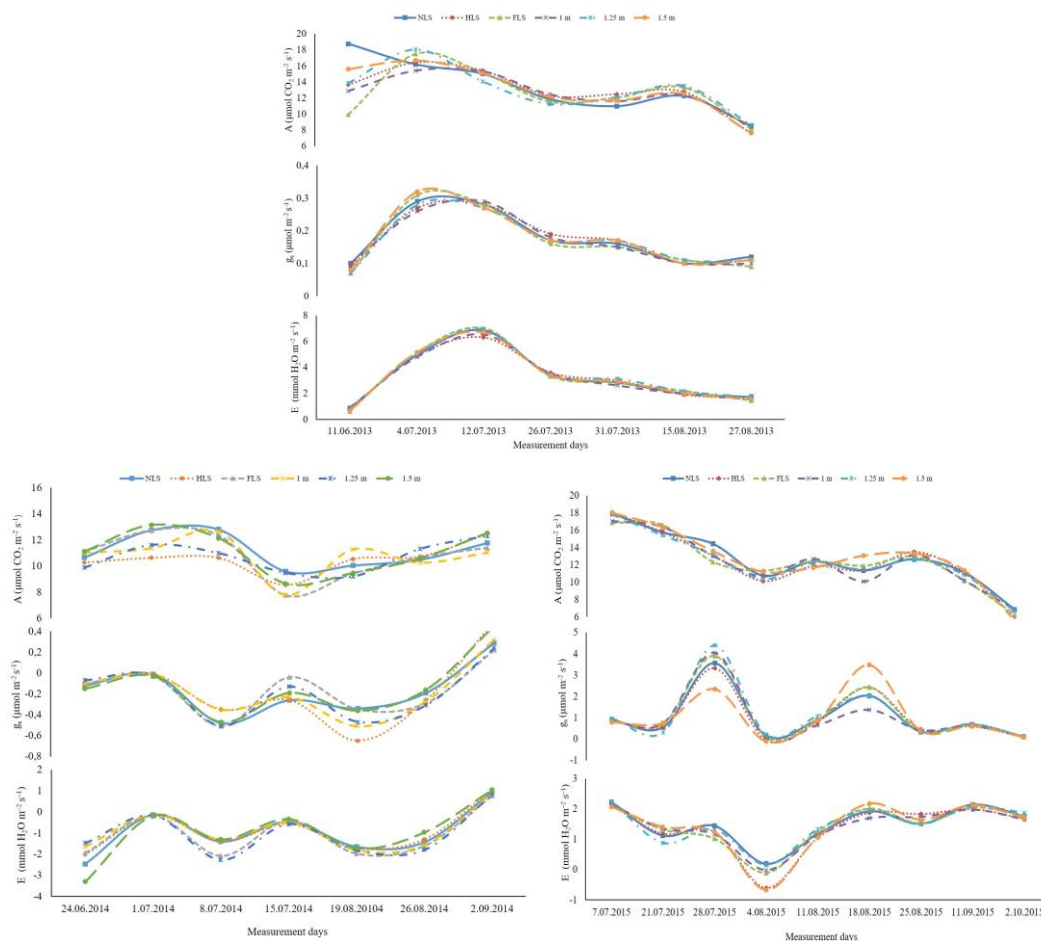


Figure 1. Net photosynthesis (A), transpiration (E) and stomatal conductance (g_s) measurements in years of 2013, 2014 and 2015. NLS, HLS, and FLS represent none lateral shoots (no leaf), half lateral shoots (3-4 leaves) full lateral shoots (6-7 leaves). 1 m, 1.25 m and 1.5 m also represent main shoot lengths

In many literature examining the relationship between photosynthesis (A), transpiration (E), stoma conductivity (g_s) (Motzer et al., 2005; Miyashita et al., 2005; Greer, 2012) and in the previous year measurements at the same vineyard (Candar et al., 2017), high correlation between stoma conductivity (g_s), photosynthesis (A) and transpiration (E) in other varieties and grapevines was also observed in 2013 measurements. The highest values in the measurements made after completion of canopy interventions were seen in NLS and 1.25 m applications.

In 2014 when the photosynthesis averages of the measurement days are evaluated as a whole without leaving the treatments, it is seen that the measurements taken on 181st calendar day of 2014 have a higher rate of photosynthesis than the other days with

12.05 $\mu\text{mol CO}_2 \text{ m}^{-2} \text{ s}^{-1}$ ratio. In the meso-climatic measurements made between 10:00-12:00 on the same day, the average temperature was 23.30°C, the highest temperature was 26.50°C and the lowest temperature was 18.20°C. The average wind speed was 2.10 m sec^{-1} and relative humidity was 78%, while the light intensity was 723.24 $\mu\text{mol m}^2 / \text{sec}$. The lowest photosynthesis rate for all days in 2014 was measured as 7.76 $\mu\text{mol CO}_2 \text{ m}^{-2} \text{ s}^{-1}$ on 195th calendar day of 2014. On 195th calendar day of 2014 the maximum air temperature was 30.20°C and the relative humidity 73.00%. Light intensity recorded at 725.67 $\mu\text{mol m}^2 \text{ sec}^{-1}$. The lowest photosynthesis rate for all days was measured as 7.76 $\mu\text{mol CO}_2 \text{ m}^{-2} \text{ s}^{-1}$ on 195th calendar day of 2014. On the same calendar day maximum air temperature was 30.20°C and the relative humidity 73.00%. Light intensity recorded at 725.67 $\mu\text{mol m}^2 / \text{sec}^{-1}$.

In 2014, NLS was the first in 3 of 7 days and in 4 days, it was seen that the second place. When the measurement days are evaluated together, NLS application stands out with the highest photosynthesis rate with the average of 11.16 $\mu\text{mol CO}_2 \text{ m}^{-2} \text{ s}^{-1}$.

Transpiration (E) measurements in 2014 recorded less than zero results in six of the seven measurement days. Although this situation is not encountered in the literature in terms of vine varieties, it is seen in the studies made for perennial woody plants (Vesala et al., 2017).

In terms of the monitored climate characteristics, the average, low and high temperature values at 2 m level for 2014 and 2015 are very close to each other; the relative humidity is 72.33% in 2014 and 73.36% in 2015; It can be said that the sub-zero transpiration values in 2014 were due to the average wind speed of 2.78 m s^{-1} and the light intensity values measured as 1191.955 $\text{mol m}^2 \text{ s}^{-1}$ which is slow than 2015.

Escalona et al. (2013) reported that water vapor can condense on the leaf surface and enter through the stoma openings, especially on humid nights where the vapor pressure difference is very low in coastal areas. This prevents transpiration at night and therefore reduces water loss and increases the water usage efficiency of the next day.

As expected, stoma conductivity (g_s) values are also largely negative measurements. When stoma conductivity (g_s) measurements are examined by subjects, it is seen that there are no significant differences between applications. However, the variation between the measurements is higher than the transpiration (E) values.

Both transpiration (E) and stoma conductivity (g_s) produce similar curves. In terms of shoot length applications, 1.25 m application showed high values in vegetation average, albeit with very small differences. The main factor controlling these physiological variables appears to be meso-climatic conditions rather than applications. However, the cumulative effect of small canopy management manipulations becomes more significant when evaluated throughout phenological periods or when the all vegetation period is evaluated as whole.

When photosynthesis (A), transpiration (E) and stoma conductance (g_s) measurements were evaluated on the basis of applications, although there were no significant differences between the applications, the removal of the entire lateral shoots in 2014 positively affected the vine microclimate in terms of these criteria.

Figure 1 shows the measurement values of 2015 photosynthesis (A). When the averages of the measurement days are evaluated as a whole without separating the applications, it is seen that the measurements made on 187th calendar day of 2015 have a higher rate of photosynthesis than the other days with a ratio of 17.63 $\mu\text{mol CO}_2 \text{ m}^{-2} \text{ s}^{-1}$. On the same calendar day between 10:00-14:00 meso-climatic measurements mean temperature of 24.60°C; The highest temperature was 29.50°C and

the lowest temperature was 18.40°C. The average wind speed was 2.30 m sec⁻¹ and relative humidity was recorded as 70.10%, while the illumination intensity is 1902.26 μmol m² s⁻¹. The lowest photosynthesis rate for all days on 02.10.2015 was measured as 6.40 μmol CO₂ m⁻² s⁻¹. On 274th calendar day of 2015, the maximum air temperature was 19.90°C and the relative humidity was 77.30%. Light intensity was recorded as 44.37 μmol m² s⁻¹.

In terms of photosynthesis values, HLS was in the first place in 5 of 9 days in 2015; and in the second place in 2 days. When all measurement days average is evaluated together, this time. FLS application has the highest photosynthesis rate, with a small difference of 12.70 μmol CO₂ m⁻² s⁻¹.

The highest transpiration (E) value in all days in 2015 was measured as 2.15 mmol m⁻² s⁻¹ under the average temperature of 24.60°C, average wind speed of 2.30 m s⁻¹, 70.10% relative humidity and 1902.26 μmol m² s⁻¹ light intensity conditions.

Furthermore, the lowest transpiration (E) value was measured as -0.18 mmol m⁻² s⁻¹ on 215th calendar day of 2015. Today's average temperature was 30.20°C and the relative humidity was 76.20%. The average wind speed was recorded as 2.20 m s⁻¹.

Although some researchers report that transpiration decreases due to wind speed (Kuiper, 1961; Drake et al., 1970; Dixon and Grace, 1984). General acceptance, evaporation also increased due to the increasing wind speed that increased atmospheric evaporative demand (Mcvicar et al., 2012; Ben Neriah et al., 2014; Schymanski and Or, 2015).

In terms of general application averages, the highest transpiration rate was 1.49 mmol m⁻² s⁻¹ with NLS application which all lateral leaves were taken.

When stoma conductivity (g_s) measurements of 2015 are examined according to the subjects, it is seen that there are no significant differences between the applications and create similar curves with transpiration (E).

Greer (2012) reported that transpiration is strongly related to temperature. It is stated that the rates increase exponentially, especially at temperatures above 35°C, and it is 4 times more than 20°C at 45°C. In our study, when the data for 3 years are examined, it can be said that the relative humidity above 75% decreases the transpiration and increases between 65-70% the relative humidity.

Many studies on grapevine have focused on seeking answers to questions about water use efficiency through photosynthesis (A), transpiration (E), and stoma conductivity (g_s) by different levels of drought stress (Bota et al., 2001; Flexas et al., 2002; Souza et al., 2003; Pou et al., 2008; Zsófi et al., 2009), variety differences (Gibberd et al., 2001; Gaudillère et al., 2002; Tomás et al., 2012) and the effects of rootstocks (Satisha et al., 2006). However, attempting to interpret results over total biomass is problematic due to measurements made from a single leaf.

Photosynthesis is the source of carbohydrate gain in plants; transpiration is also the biggest source of water losses under normal conditions. Discrepancies between WUE leaf and WUE plant may occur due to water losses during the night and daily carbon losses through respiration (Flexas et al., 2010; Schultz and Stoll, 2010).

Must composition and berry maturation

In terms of total soluble solids (TSS) content NLS treatment differs from other lateral shoot applications every 3 years. While the lowest data were obtained from this application with 21.18% in 2013 and 22.42% in 2015, the highest TSS content was observed in 2014 with 21.31% (*Table 5*).

Table 5. Effects of main shoot and lateral shoot treatments on total soluble solids and total acidity

Treatments	2013		2014		2015		Mean of years	
	TSS (%)	Total acid (g/L)	TSS (%)	Total acid (g/L)	TSS (%)	Total acid (g/L)	TSS (%)	Total acid (g/L)
1 m	21.90 ^c	5.85	20.97	7.45	22.42	5.85	21.76 ^b	6.38
1.25 m	22.23 ^b	5.83	20.97	7.53	22.80	5.83	22.00 ^a	6.40
1.5 m	22.56 ^a	5.93	20.86	7.56	22.75	5.90	22.06 ^a	6.46
NLS	21.18 ^b	5.96	21.31 ^a	7.13 ^b	22.42 ^b	5.78	21.64 ^b	6.29
HLS	22.65 ^a	5.85	20.84 ^b	7.61 ^a	22.86 ^a	5.86	22.12 ^a	6.42
FLS	22.85 ^a	5.80	20.66 ^b	7.80 ^a	22.68 ^{ab}	5.93	22.07 ^a	6.52
YME	22.28 ^B	5.87 ^B	20.94 ^C	7.51 ^A	22.65 ^A	5.86 ^B		
MSME LSD _{0.05}	0.299	n.s.	n.s.	n.s.	n.s.	n.s.	0.209	n.s.
LSME LSD _{0.05}	0.629	n.s.	0.383	0.273	0.343	n.s.	0.342	n.s.
YME LSD _{0.05}	0.342	0.378	0.342	0.378	0.342	0.378		

NLS, HLS, and FLS represent none lateral shoots (no leaf), half lateral shoots (3-4 leaves) full lateral shoots (6-7 leaves), MSME means main shoot main effect, LSME means lateral shoot main effect and YME means year main effect. Different lowercase superscript letters in same column and uppercase letters in same line represent statistically significant differences between means at $p < 0.05$ according to least significant difference test. n.s. means not significant

As NLS application stands out with the highest photosynthesis rate in 2014, during the vegetation period, excessive precipitation and high proportional humidity conditions positively affected the physiological activity of the NLS application and accelerated the photosynthetic efficiency and thus the accumulation of dry matter. Therefore, it was seen that the effects of negative climate characteristics can be reduced by manipulations on the canopy at the right time and in the right way.

The results obtained in 2013 and 2015 suggest that increased photosynthesis rates in HLS application also increase the accumulation of TSS.

Korkutal et al. (2017) reported that the complete removal of the lateral leaves increases the total acidity. In our study, the same results were observed in NLS application in 2013, but it was seen in 2014 and 2015 and the mean of all years caused lower total acidity (Table 5).

One of the most significant relationships between temperature and berry quality is that high temperatures reduce the concentration of organic acid in the berry (Kliewer, 1973). Organic acid accumulation and degradation at different stages of berry development also show different characteristics (Ford, 2012). Tartaric and malic acids are predominant organic acids in all stages of berry maturation and cause significant effects on must acidity and pH (Morris et al., 1983). In particular, malate is deposited in the berry until the veraison and stored as a potential source for the carbon requirement that occurs during the ripening process (Ruffner, 1982). During this period, the reduction of total acidity due to consumed malic acid balances sugar and acid ratios (Kliewer, 1965).

A similar situation was observed in 2013, NLS application reduced the usefulness of photosynthesis, thus reducing the use of malic acid as a carbon source and the total acidity remained high. Apart from this, no statistical significance was found between the applications and total acidity level for the mean of years. On the other hand, the increase in the length of the main shoot caused an increase of titratable acid in the average of years, but not statistically. Likewise, according to Yasasin et al. (2018), the

increase in main shoot length causes a decrease in total acidity, although this is not statistically significant.

pH is a measure of active acidity in must and wine. Therefore, there is a dynamic relationship between pH and acidity. The pH of grape must be one of the critical determinants of wine quality. The exchange of tartaric acid compounds with potassium cations produces water-insoluble potassium bi-tartrates. This leads to a reduction of free acids and tartaric/malic acid ratios and an increase in pH (Kodur, 2011).

In our study, pH values increased in 2013 and 2014 with the decrease of leaf area under the main effect of lateral shoot applications. This change in 2014 is also statistically significant. Although this relationship between manipulations and pH did not occur in the mean of years, it is important to reflect the relationship between variables such as titratable acidity, potassium and the amount of precipitation to which they depend. Lateral shoot manipulations have a statistically significant effect on the amount of sugar per gram every 3 years. The NLS application reached its highest value in 2014 and took the last place in the other years (Table 6).

Table 6. Effects of main shoot and lateral shoot treatments on pH and sugar

Treatments	2013		2014		2015		Mean of years	
	pH	Sugar (mg g-berry ⁻¹)	pH	Sugar (mg g-berry ⁻¹)	pH	Sugar (mg g-berry ⁻¹)	pH	Sugar (mg g-berry ⁻¹)
1 m	3.85	164.41c	3.54	156.22	3.75	169.00	3.71	163.21b
1.25 m	3.74	167.35b	3.54	156.22	3.73	172.40	3.67	165.32a
1.5 m	3.79	170.29a	3.53	155.26	3.77	171.99	3.70	165.84a
NLS	3.90	158.11b	3.58a	159.15a	3.75	169.03b	3.74	162.09b
HLS	3.84	171.10a	3.54b	155.05b	3.75	172.96a	3.65	166.37a
FLS	3.65	172.85a	3.50c	153.48b	3.75	171.40ab	3.70	165.91a
YME	3.79A	167.35 A	3.54B	155.90C	3.75A	171.13A		
MSME LSD _{0.05}	n.s.	5.615	n.s.	3.386	n.s.	3.076	n.s.	3.035
LSME LSD _{0.05}	n.s.	2.659	0.034	n.s.	n.s.	n.s.	n.s.	1.866
YME LSD _{0.05}	0.197	3.035	0.197	3.035	0.197	3.035		

NLS, HLS, and FLS represent none lateral shoots (no leaf), half lateral shoots (3-4 leaves) full lateral shoots (6-7 leaves), MSME means main shoot main effect, LSME means lateral shoot main effect and YME means year main effect. Different lowercase superscript letters in same column and uppercase letters in same line represent statistically significant differences between means at $p < 0.05$ according to least significant difference test, n.s. means not significant

The ideal °Brix/titratable acid ratio range was expressed as 3-4 g L⁻¹ by Blouin and Guimberteau (2000). Except for 2014, these values were observed in other years and in different main and lateral shoot applications. 2013 and 2015 were the years with the highest °Brix/titratable acid ratios of 3.87 g L⁻¹ and 3.82 g L⁻¹. In 2014 °Brix/titratable acid ratio was calculated as 2.79 g L⁻¹. The mean of years was statistically significant at LSD level of 5%. The main effects of lateral and main shoot applications were not statistically significant except for 2014. In 2014, the NLS application differs from HLS and FLS (Table 7).

The mean of years was statistically significant at LSD level of 5% for pH² × °Brix, maturity index. However, the main effects of the applications in 2014 were statistically significant and it is seen that NLS application has brought maturity to an early stage when compared to other two. In 2014, the pH² × °Brix was calculated as 262.98.

According to the maturity index of pH² × °Brix, berries over 260 reach full maturity (Blouin and Guimberteau, 2000). According to this indicator, maturity was reached

every three years and in all applications. The difference between the applications is low and statistically insignificant, but it is determined that small changes in maturity level can be created with different canopy management techniques.

Table 7. Effects of main shoot and lateral shoot treatments on maturity indices

Treatments	2013		2014		2015		Mean of years	
	°Brix/ T.A	pH ² ×°Brix	°Brix/ T.A	pH ² ×°Brix	°Brix/ T.A	pH ² ×°Brix	°Brix/ T.A	pH ² ×°Brix
1 m	3.78	324.63	2.82	264.38	3.83	310.01	3.48	301.67
1.25 m	3.86	316.05	2.79	263.26	3.91	317.99	3.52	299.10
1.5 m	3.82	327.16	2.76	261.31	3.86	324.53	3.48	304.33
NLS	3.57	323.85	2.98 _a	273.52 _a	3.88	315.78	3.48	304.38
HLS	3.94	302.45	2.74 _b	261.91 _b	3.90	322.52	3.53	295.63
FLS	3.94	341.54	2.65 _b	253.52 _c	3.83	320.22	3.47	305.09
YME	3.82 _A	322.61 A	2.79 _B	262.98 B	3.87 _A	319.51 _A		
MSME LSD _{0.05}	<i>n.s.</i>	<i>n.s.</i>	<i>n.s.</i>	<i>n.s.</i>	<i>n.s.</i>	<i>n.s.</i>	<i>n.s.</i>	<i>n.s.</i>
LSME LSD _{0.05}	<i>n.s.</i>	<i>n.s.</i>	0.121	8.036	<i>n.s.</i>	<i>n.s.</i>	<i>n.s.</i>	<i>n.s.</i>
YME LSD _{0.05}	0.272	33.184	0.272	33.184	0.272	33.184		

NLS, HLS, and FLS represent none lateral shoots (no leaf), half lateral shoots (3-4 leaves) full lateral shoots (6-7 leaves), MSME means main shoot main effect, LSME means lateral shoot main effect and YME means year main effect, T.A. Titratable acid, Different lowercase superscript letters in same column and uppercase letters in same line represent statistically significant differences between means at $p < 0.05$ according to least significant difference test, *n.s.* means not significant

Conclusion

When photosynthesis (A), transpiration (E) and stoma conductivity (g_s) measurements were evaluated together with the climatic conditions of lateral shoot applications; It can be said that the significant differences between the applications are mostly seen in the criteria of average light intensity, relative humidity and average wind speed on some days.

In this sense, the main factor controlling these physiological variables appears to be the meso-climatic climatic conditions. However, the cumulative effect of small microclimatic differences becomes more significant when compared to phenological periods or when the vegetation period is evaluated as a whole.

Relative humidity is more effective than temperature in terms of physiological activity. It can be said that proportional humidity above 75% decreases transpiration and increases proportional humidity between 65-70%. The potential importance of night-time transpiration and the interaction of water use efficiency with regard to plant quality are emerging as new research topics.

It can be said that keeping the leaf areas under control in order to provide sufficient yield/quality balance under the conditions which the experiment is carried out may be a solution. Even in cases where leaf areas are reduced more than normal, there is no shortage of the desired yield with delay in industrial maturity.

Therefore, it is considered that the decrease in leaf areas can be compensated for in terms of yield by arrangements in the internal metabolism of the vine. This shows that unusual canopy management practices that can be performed against unusual climatic conditions (high proportional humidity, high temperature fluctuations, heavy rainy periods, etc.) can be used at certain periods even if not every year.

It is seen that NLS application is separated from the others in total soluble solids content every 3 years. While the lowest data were obtained from this application with 21.18% in 2013 and 22.42%. In 2015, the highest TSS was observed in 2014 with 21.31%. In 2014, excessive rainfall and high proportional humidity during the vegetation period positively affected the physiological activity of NLS vines, accelerating the efficiency of photosynthesis and thus the accumulation of dry matter throughout the vine.

In terms of the main shoot lengths, as the shoot length increases, stress and some quality criteria tend to increase, but these effects are generally not statistically significant. Even when the main shoot length is kept at 1m, leaf areas can reach a sufficient level in terms of yield and quality.

Although the applications are effective in terms of quality and physiological activity, seasonal effects of each vegetation period are the main determining factors.

Acknowledgements. This study is based on a part of the doctoral thesis of the corresponding author and supported by Republic of Turkey Ministry of Agriculture and Forestry General Directorate of Agricultural Research and Policies with the project number TAGEM / BBAD / 2013 / A08 / P04-08.

REFERENCES

- [1] Bem, B. P., Bogo, A., Everhart, S. E., Casa, R. T., Gonçalves, M. J., Macron Filho, J. L., Rufato, L., Silva, F. N., Allebrandt, R., Cunha, I. C. (2016): Effect of four training systems on the temporal dynamics of downy mildew in two grapevine cultivars in Southern Brazil. – *Tropical Plant Pathology* 41: 370-379. doi.org/10.1007/s40858-016-0110-8.
- [2] Ben Neriah, A., Assouline, S., Shavit, U., Weisbrod, N. (2014): Impact of ambient conditions on evaporation from porous media. – *Water Resources Research* 50(8): 6696-6712. doi.org/10.1002/2014WR015523.
- [3] Blouin, J., Guimberteau, G. (2000): *Maturation et Maturite des Raisins*. – Feret. Bordeaux. 151 p. ISBN: 2-902416-49-0.
- [4] Bota, J., Flexas, J., Medrano, H. (2001): Genetic variability of photosynthesis and water use in Balearic grapevine cultivars. – *Annals of Applied Biology* 138(3): 353-361. doi.org/10.1111/j.1744-7348.2001.tb00120.x.
- [5] Caccavello, G., Giaccone, M., Scognamiglio, P., Forlani, M., Basile, B. (2017): Influence of intensity of post-veraison defoliation or shoot trimming on vine physiology, yield components, berry and wine composition in Aglianico grapevines. – *Australian Journal of Grape and Wine Research* 23: 226-239. doi.org/10.1111/ajgw.12263.
- [6] Candar, S., Yasasin, A. S., Alco, T., Bahar, E., Korkutal, I. (2017): Interactions of Some Environmental Factors on Physiological Parameters in cv. Merlot (*Vitis vinifera* L.). – 2nd International Balkan Agriculture Congress 16-18 May 2017. Abstract Book, pp: 328. Tekirdag.
- [7] Carbonneau, A., Bahar, E. (2009): Vine and Berry Responses to Contrasted Water Fluxes in Ecotron Around 'Veraison'. Manipulation of Berry Shrivelling and Consequences on Berry Growth. Sugar Loading and Maturation. – *Proceedings of the 16th International GiESCO Symposium*. July 12-15. Univ. of California. Davis, pp. 145-155.
- [8] Clingeleffer, P. R. (2010): Plant management research: status and what it can offer to address challenges and limitations. – *Australian Journal of Grape and Wine Research* 16(1): 25-32. doi.org/10.1111/j.1755-0238.2009.00075.x.

- [9] Collins, M., Loveys, B. (2010): Optimizing irrigation for different cultivars. – Final Report to Grape and Wine Research & Development Corporation, Project Number: CSP 05/02. CSIRO Plant Industry.
- [10] Dixon, M., Grace, J. (1984): Effect of wind on the transpiration of young trees. – *Annals of Botany* 53(6): 811-819. doi.org/10.1093/oxfordjournals.aob.a086751.
- [11] Drake, B. G., Raschke, K., Salisbury, F. B. (1970): Temperature and transpiration resistances of *Xanthium* leaves as affected by air temperature, humidity, and wind speed. – *Plant Physiology* 46: 324-330. doi.org/10.1104/pp.46.2.324.
- [12] Escalona, J., Fuentes, S., Tomas, M., Martorella, S., Flexas, J., Medrano, H. (2013): Responses of leaf night transpiration to drought stress in *Vitis vinifera* L. – *Agricultural Water Management* 118: 50-58. doi.org/10.1016/j.agwat.2012.11.018.
- [13] Ferrer, M., Echeverría, G., Carbonneau, A. (2014): Effect of berry weight and its components on the contents of sugars and anthocyanins of three varieties of *Vitis vinifera* L. under different water supply conditions. – *South African Journal of Enology and Viticulture* 35(1): 103-113.
- [14] Flexas, J., Medrano, H., Escalona, J. M., Bota, J., Gulias, J. (2002): Regulation of photosynthesis of C3 plants in response to progressive drought: Stomatal conductance as a reference parameter. – *Annals of Botany* 89(7): 895-905. doi.org/10.1093/aob/mcf079.
- [15] Flexas, J., Galmés, J., Gallé, A., Gulías, J., Pou, A., Ribas-Carbo, M., Tomás, M., Medrano, H. (2010): Improving water use efficiency in grapevines: Potential physiological targets for biotechnological improvement. – *Australian Journal Grape Wine Research* 16(1s): 106-121. doi.org/10.1111/j.1755-0238.2009.00057.x.
- [16] Ford, C. M. (2012): *The Biochemistry of Organic Acids in the Grape. The Biochemistry of the Grape Berry.* – Bentham Science Publishers, 67-88. doi: 10.2174/978160805360511201010067.
- [17] Gaudillère, J. P., van Leeuwen, C., Ollat, N. (2002): Carbon isotope composition of sugars in grapevine and integrated indicator of vineyard water status. – *Journal of Experimental Botany* 53(369): 757-763. doi.org/10.1093/jexbot/53.369.757.
- [18] Gibberd, M. R., Walker, R. R., Blackmore, D. H., Condon, A. G. (2001): Transpiration efficiency and carbon-isotope discrimination of grapevines grown under well-watered conditions in either glasshouse or vineyard. – *Australian Journal Grape and Wine Research* 7(3): 110-117. doi.org/10.1111/j.1755-0238.2001.tb00197.x.
- [19] Greer, D. H. (2012): Modelling leaf photosynthetic and transpiration temperature dependent responses in *Vitis vinifera* cv. Semillon grapevines growing in hot, irrigated vineyard conditions. – *AoB Plants* pls009. doi: 10.1093/aobpla/pls009.
- [20] Hirano, K., Noda, M., Hasegawa, S., Okamoto, G. (1994): Contribution of lateral and primary leaves to the development and quality of Kyoho grape berry. – *Journal of Japan Society Horticultural Science* 63(3): 515-521. doi.org/10.2503/jjshs.63.515.
- [21] Keller, M. (2010a): Managing grapevines to optimise fruit development in a challenging environment: a climate change primer for viticulturists. – *Australian Journal of Grape and Wine Research* 16: 56-69. doi:10.1111/j.1755 0238.2009.00077.x.
- [22] Keller, M. (2010b): *The Science of Grapevines: Anatomy and Physiology* 1st Edition. – Academic Press, 400 p. ISBN: 9780123748812.
- [23] Kliewer, W. M. (1965): Changes in the concentration of malates, tartrates, and total free acids in flowers and berries of *Vitis vinifera*. – *American Journal of Enology and Viticulture* 16: 92-100.
- [24] Kliewer, W. M. (1973): Berry composition of *Vitis vinifera* cultivars as influenced by photo temperatures and nycto-temperatures during maturation. – *Journal of the American Society for Horticultural Science* 98: 153-159.
- [25] Kodur, S. (2011): Effects of juice pH and potassium on juice and wine quality, and regulation of potassium in grapevines through rootstocks (*Vitis*): a short review. – *Vitis* 50(1): 1-6.

- [26] Korkutal, İ., Bahar, E., Bayram, S. (2017): Farklı toprak işleme ve yaprak alma uygulamalarının Syrah üzüm çeşidinde su stresi, salkım ve tane özellikleri üzerine etkileri. – Ege Üniversitesi, Ziraat Fakültesi Dergisi 54(4): 397-407.
- [27] Kuiper, P. (1961): The Effects of Environmental Factors on the Transpiration of Leaves, With Special Reference to Stomatal Light Response. – Ph.D. Thesis. Veenman, Wageningen, Proefschriftwageningen.
- [28] McVicar, T. R., Roderick, M. L., Donohue, R. J., Li, L. T., Van Niel T. G., Thomas, A. (2012): Global review and synthesis of trends in observed terrestrial near-surface wind speeds: Implications for evaporation. – Journal of Hydrology 416-417: 182-205. doi.org/10.1016/j.jhydrol.2011.10.024.
- [29] Mira de Orduña, R. (2010): Climate change associated effects on grape and wine quality and production. – Food Research International 43(7): 1844-1855. doi.org/10.1016/j.foodres.2010.05.001.
- [30] Miyashita, K., Shigemi, T., Toshihiko, M., Kazuyoshi, K. (2005): Recovery responses of photosynthesis, transpiration and stomatal conductance in kidney bean following drought stress. – Environmental and Experimental Botany 53(2): 205-214. doi: 10.1016/j.envexpbot.2004.03.015.
- [31] Moran, M. A., Sadras, V. O., Petrie, P. R. (2017): Late pruning and carry-over effects on phenology, yield components and berry traits in Shiraz. – Australian Journal of Grape and Wine Research 23(3): 390-398. doi.org/10.1111/ajgw.12298.
- [32] Morris, J. R., Sims, C. A., Cawthon, D. L. (1983): Effects of excessive potassium levels on pH, acidity and color of fresh and stored grape juice. – American Journal of Enology and Viticulture 34(1): 35-39.
- [33] Motzer, T., Nicole, M., Manfred, K., Dieter, S., Dieter, A. (2005): Stomatal conductance, transpiration and sap flow of tropical Montane rain forest trees in the Southern Ecuadorian Andes. – Tree Physiology 25(10): 1283-1293. doi.org/10.1093/treephys/25.10.1283.
- [34] OIV (2012): Compendium of International Methods of Wine and Musts. – Ed. 2012. v: 1-2.
- [35] Petrie, P., Sadras, V. (2008): Advancement of grapevine maturity in Australia between 1993 and 2006: putative causes, magnitude of trends and viticultural consequences. – Australian Journal of Grape and Wine Research 14: 33-45. doi:10.1111/j.1755-0238.2008.00005.x.
- [36] Poni, S., Gatti, M., Bernizzoni, F., Civardi, S., Bobeica, N., Magnanini, E., Palliotti, A. (2013): Late leaf removal aimed at delaying ripening in cv. Sangiovese: physiological assessment and vine performance. – Australian Journal of Grape and Wine Research 19(3): 378-387. doi.org/10.1111/ajgw.12040.
- [37] Pou, A., Flexas, J., Alsina, M., Bota, J., Carambula, C., Herralde, F., Galmes, J., Lovisoló, C., Jimenez, M., Carbo, M. R., Rusjan, D., Secchi, F., Tomas, M., Zsófi, Z., Medrano, H. (2008): Adjustments of water use efficiency by stomatal regulation during drought and recovery in the drought-adapted *Vitis* hybrid Richter-110 (*V. berlandieri* x *V. rupestris*). – Physiologia Plantarum 134(2): 313-323. doi: 10.1111/j.1399-3054.2008.01138.x.
- [38] Ruffner, H. P. (1982): Metabolism of tartaric and malic acids in *Vitis*-A review. – Vitis 21: 346-358.
- [39] Sanchez-de-Miguel, P., Bazea, P., Junquera, P., Lissarrague, J. R. (2010): Vegetative Development: Total Leaf Area and Surface Area Indexes. – In: Delrot, S., Medrano, H., Or, E., Bavaresco, L., Grando, S. (eds.) Methodologies and Results in Grapevine Research. Springer Science. 448 p. ISBN: 904819282X.
- [40] Santesteban, L. G., Miranda, C., Royo, J. B. (2011): Regulated deficit irrigation effects on growth, yield, grape quality and individual anthocyanin composition in *Vitis vinifera* L. cv. 'Tempranillo'. – Agricultural Water Management 98(7): 1171-1179.

- [41] Satisha, J., Prakash, G. S., Venugopalan, R. (2006): Statistical modeling of the effect of physio-biochemical parameters on water use efficiency of grape cultivars. rootstocks and their stionic combinations under moisture stress conditions. – Turkish Journal of Agriculture and Forestry 30(4): 261-271.
- [42] Schultz, H. R., Stoll, M. (2010): Some critical issues in environmental physiology of grapevines: future challenges and current limitations. – Australian Journal of Grape and Wine Research 16: 4-24. doi:10.1111/j.1755-0238.2009.00074.x.
- [43] Schymanski, S. J., Or, D. (2015): Wind increases leaf water use efficiency. – Plant, Cell & Environment 39(7): 1448-1459. doi.org/10.1111/pce.12700.
- [44] Souza, C. R., Maroco, J. P., Santos, T. P., Rodrigues, M. L., Lopes, C. M., Pereira, J. S., Chaves, M. M. (2003): Partial root zone drying: Regulation of stomatal aperture and carbon assimilation in field-grown grapevines (*Vitis vinifera* cv. Moscatel). – Functional Plant Biology 30: 653-662.
- [45] Tomás, M., Medrano, H., Pou, A., Escalona, J. M., Martorell, S., Ribas-Carbo, M., Flexas, J. (2012): Water use efficiency in grapevine cultivars grown under controlled conditions: Effects of water stress at the leaf and whole plant level. – Australian Journal of Grape Wine Research 18(2): 164-172. doi.org/10.1111/j.1755-0238.2012.00184.x.
- [46] Vesala, T., Sevanto, S., Grönholm, T., Salmon, Y., Nikinmaa, E., Hari, P., Hölttä, T. (2017): Effect of leaf water potential on internal humidity and CO₂ dissolution: Reverse transpiration and improved water use efficiency under negative pressure. – Frontiers in Plant Science 6(8): 54. doi: 10.3389/Fpls.2017.00054.
- [47] Yasasin, A. S., Bahar, E., Boz, Y., Kiraci, M. A., Gunduz, A., Avci, G. G., Gulcu, M. (2018): Different soil tillage and shoot length effects on vegetative growth, water stress and yield in cv. Cabernet Sauvignon (*Vitis vinifera* L.). – I. International Agricultural Science Congress, 9-12 May 2018, Van-Turkey, p 408.
- [48] Zalamena, J., Cassol, P. C., Brunetto, G., Grohskopf, M. A., Mafra, M. S. H. (2013): Estado nutricional, vigor e produção em videiras cultivadas com plantas de cobertura. – Revista Brasileira de Fruticultura 35: 1190-1200. doi: 10.1590/S0100-29452013000400030.
- [49] Zsófi, Z., Gál, L., Szilágy, Z., Szücs, E., Marschall, M., Nagy, Z., Bál, B. (2009): Use of stomatal conductance and pre-dawn water potential to classify terroir for the grape variety Kékfrankos. – Australian Journal of Grape Wine Research 15(1): 36-47. doi.org/10.1111/j.1755-0238.2008.00036.x.

DISCRIMINATION OF SEXUAL DIMORPHISM THROUGH EXTERNAL MORPHOLOGY OF SPOTTED STEED (*HEMIBARBUS MACULATUS*) IN THE YUANHE RIVER, CHINA

TUO, Y.^{1,2} – XIAO, T.^{1*} – WANG, H.¹

¹Hunan Engineering Technology Research Center of Featured Aquatic Resources Utilization, Hunan Agricultural University, Changsha 410128, China

²College of Life Science and Resources Environment, Yichun University, Yichun 336000, China

*Corresponding author

e-mail: tyxiao1128@163.com; phone: +86-1397-3195-105

(Received 27th Sep 2019; accepted 4th Dec 2019)

Abstract. Sex identification and composition analysis is an important research topic in fish population ecology, and the results have important implications concerning the conservation of wild fish resources and artificial propagation. However, since the individual morphological differences between male and female spotted steed (*Hemibarbus maculatus*) are not obvious, it is usually difficult to identify sex by direct observation. Thus, it is usually done by observing the reproductive system after dissection. However, this method results in the death of the identified fish and cannot be used for later reproduction. To establish a method for sex identification of *H. maculatus* by morphological quantitative indicators, 36 directly measured traits and 35 standardized traits from 68 *H. maculatus* individuals collected from the Yuanzhuo section of the Yuanhe River, China, were measured and analyzed. Based on the data, 13 personalities were screened from the 35 standardized traits by stepwise discriminant method and used to establish discriminant equations. The rate of correctly identifying the male and female individuals was 92.65%. In addition, the condition factor, D_{7-9} , the dorsal fin long-throated length, the post-orbital length, D_{7-10} , the head length, and the body length were significantly different between male and female *H. maculatus* (t-test, $P < 0.05$). These results implied that the male and female individuals of *H. maculatus* could be identified using our established discriminant equations.

Keywords: aquaculture, artificial propagation, fish, multivariate analysis, morphological discrimination

Introduction

Sex identification and composition analysis is an important research content in fish population ecology, and the results have important guidance to conservation of wild fish resources and artificial propagation (Chang et al., 2015; Lombardi-Carlson and Andrews, 2015; An et al., 2017). Sex can be distinguished by the differences of body size and secondary sexual characteristics for fish with obvious heteromorphism. However, it is very hard to distinguish the sex for fish that do not have obvious heteromorphism, such as *Acrossocheilus wenchowensis* (Xu et al., 2006), Khanka spiny bitterling (*Acanthorhodeus chankaensi* Dybowski) (Chen et al., 2013a), and top-mouth culter (*Erythroculter ilishaeformis*) (Chen et al., 2013b). There are a lot of limitations in the use of anatomical and other sex identification methods, which are not conducive to the protection of studied fish and the implementation of artificial reproduction. Methods that identify male and female individuals by quantitative indicators of body shape characteristics has been successfully applied in many fish, such as elongate ilisha (*Ilisha elongata*) (Ni and Chen, 2003), Japanese eel (*Aniguilla japonica*) (Guo et al., 2011) and spotted scat (*Scatophagus argus*) (Wu et al., 2014). Though the application of

discriminant equation that is established according to fish morphological indexes, the accuracy of sex identification can be as high as 85%.

Spotted steed (*Hemibarbus maculatus* Bleeker) is a small freshwater Cyprinidae fish, which is an endemic fish in China. Morphology and population ecology of *H. maculatus* living in different rivers have been studied (Wu et al., 1979; Miao and Yin, 1983; Xie et al., 1988; Fu and Qiao, 2008; Li et al., 2012; Tuo, 2012, 2013; Sun et al., 2014). Lin et al. (2005) report that there is no significant difference in individual size between male and female *H. maculatus* in the Oujiang River. Our previous investigation to *H. maculatus* in the Ganjiang River also shows that there is no obvious difference in individual size between male and female individuals of wild *H. maculatus*. Sexual maturity of male and female *H. maculatus* is not synchronous. Generally, the male fish reach sexual maturity in March, while the female fish reach sexual maturity in April or May. The parasexual characteristics of mature male fish lasted for a short time, and were obvious in March, but not in April and May. In addition, the abdominal bulge of the male fish is similar to that of females due to a large amount of food intake. Therefore, sex of *H. maculatus* cannot be identified directly from its morphological characteristics, which is not conducive to carrying out population ecology investigation and artificial reproduction. Therefore, to solve the problem of sex identification and provide reference for the study of population ecology and artificial reproduction of *H. maculatus*, in the present study, we systematically analyzed the morphological indexes of *H. maculatus* in the Ganjiang River, and established a sex identification model of *H. maculatus*.

Materials and Methods

Sample collection

H. maculatus samples were collected from the Yuanzhou section of the Yuanhe River using screen meshes and floor cages from December 2010 to June 2012 (113°54'-114°37' E, 27°33'-28°05' N; Fig. 1). The Yuanhe River is a breach of the Ganjiang River. Fresh samples were placed in containers with oxygen pump, which can continuously oxygenate, and were quickly transport to the laboratory. The fish samples were anaesthetized using anesthetic MS-222 (50 mg/L) for 3-5 min before morphological measure and dissecting for sex identification. All experiments were carried out in accordance with the Animal Ethics Committee of Hunan Agricultural University.

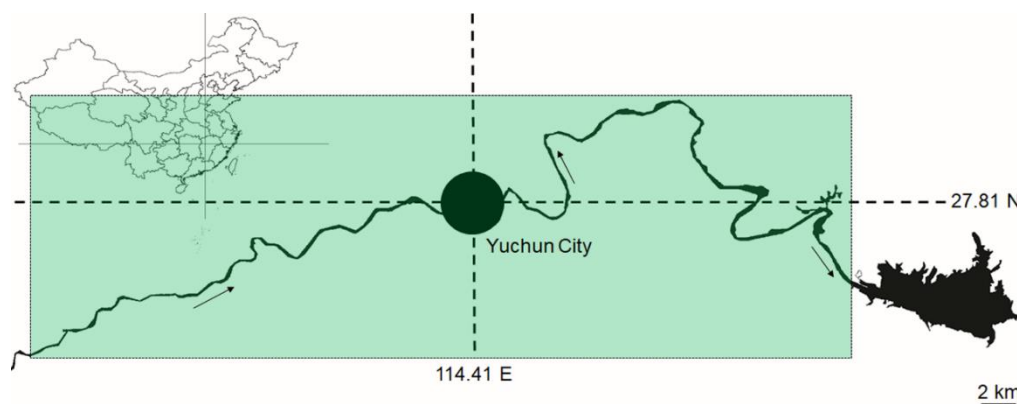


Figure 1. Map shows sampling area. The green rectangular area shows the range of sampling section of the river. The black arrows indicate the direction of water flow

Measurement of morphological indicators

Body length (*BL*), head length (*HL*), head width (*HW*), head height (*HH*), snout length (*SL*), post-orbital length (*PL*), eye diameter (*ED*), interorbital width (*IW*), mouth width (*MW*), mouth length (*ML*), body highness (*BH*), pectoral fin length (*PFL*), Caudal fin length (*CFL*), distance between pelvic fin and anal fin (*PAFD*), and dorsal fin long-throned length (*DFL*) were measured using rulers and vernier calipers according to previous description (Fish Research Laboratory of Hubei Institute of Hydrobiology, 1976; Lin et al., 2005). The lengths were accurate to two decimal places. Sex glands were dissected and sex was identified by naked eyes. Fish body weight (*W*), gonad weight (*W_g*), and shell weight (*W₀*) were weighed by an electronic balance. The weights were accurate to two decimal places. The condition factor (*K*) was calculated as follows,

$$K = 100 \times (W/BL^3) \quad (\text{Eq.1})$$

where *W* was body weight, and *BL* was body length.

Ten coordinate points were set up on the surface of fish based on the truss network theory (Fig. 2A), according to previous reports (Strauss and Bookstein, 1982; Corti et al., 1988; Bookstein, 1997). A total of 21 truss network measurement traits were measured, including *D*₁₋₂, ..., and *D*₉₋₁₀. The measured distance of truss network structure was the straight-line distance between two points (Fig. 2B).

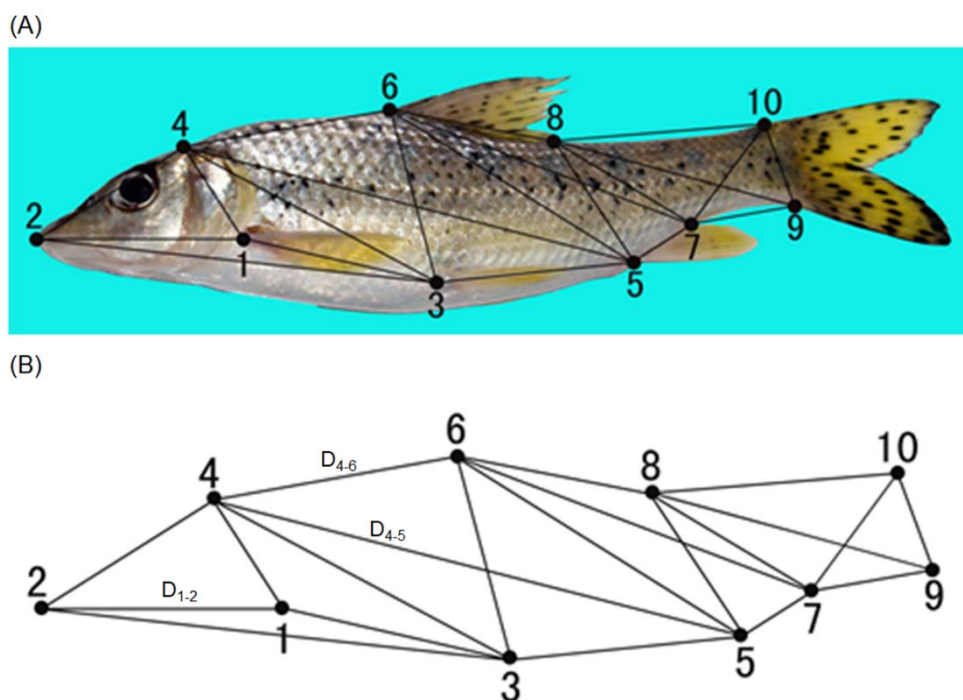


Figure 2. Schematic measuring points based on the truss network (A) and representation examples of the distances between points (B)

Data analysis

Data were recorded using Excel 2003 and analyzed using Statistica 10. Data are expressed as mean \pm standard deviation (S.D.). In the present study, we analyzed three

types of data, i.e. (1) data from traditional morphological indices, (2) data from truss network indices, and (3) data combining traditional morphological indices with truss network indices. Considering fish size is influenced by the age of fish, we also analyzed the traditional morphological data and truss network indices using three data transformed modes, i.e., ratio:

$$M_{adj} = M/SL \quad (\text{Eq.2})$$

logarithmic ratio:

$$M_{adj} = \log M / \log SL \quad (\text{Eq.3})$$

and logarithmic heterocorrelation index (*ALLOM*):

$$M_{adj} = \log M - b(\log SL - \log SL_{mean}) \quad (\text{Eq.4})$$

according to previous reports (Turan, 1999; Turan et al., 2004; Pinheiro et al., 2005). Where M is the local characteristic measurements of each specimen, SL is the body length of each specimen, SL_{mean} is the mean body length of male or female fish, and b is the slope of linear regression of $\log_{10}M$ and $\log_{10}SL$.

Index of sexual heteromorphism (I_{sh}) was calculated as follows (Gibbons and Lovich, 1990; Shou et al., 2005),

$$I_{sh} = 1 - BL_{mean.sbs} / BL_{mean.lbs} \quad (\text{Eq.5})$$

where I_{sh} is the index of sexual heteromorphism, $BL_{mean.sbs}$ is mean body length of the gender with smaller body size, and $BL_{mean.lbs}$ is mean body length of the gender with larger body size. *Student's t* test was used to compare the body length and 35 morphological parameters of male and female individuals. The significant level was set to $p = 0.05$.

A comprehensive index with the largest eigenvalue vector was selected from 35 directly measured characteristic parameters, and the principal component with a larger contribution rate was determined, then the principal component analysis (PCA) profile was drawn. R-cluster analysis was conducted based on the Pearson correlation coefficient. Stepwise regression method was used to further analyze and screen the characteristics with significant differences between male and female individuals, and the discriminant equations of male and female *H. maculatus* were established.

Results

Heteromorphism of male and female H. maculatus

A total of 68 *H. maculatus* samples were collected. The BL s of female *H. maculatus* were range from 11.00 to 26.90 cm (17.88 ± 3.91 cm), which were larger than those of male *H. maculatus* (range from 11.60 to 21.60 cm, 15.82 ± 3.25 cm; *Table 1*). The I_{sh} was 0.126. The individual size of male and female *H. maculatus* samples were significantly different (t-test, $t = -2.36$, $P=0.021$; *Table 1*). The morphological parameters were positively correlated with the body length (*Appendix 1*). The correlation coefficients were range from 0.278 to 0.903. After logarithmic heterodyne transformation according to the

equation Eq.4, the D_{7-9} , and D_{7-10} of males were significantly higher than those of females (t-test, $P < 0.05$). The K , HL , PL , and DFL of females were significantly higher than those of males (t-test, $P < 0.05$). There was no significant difference in other local characteristics between the sexes (Table 1).

Table 1. Descriptive statistics of morphological traits of *H. maculatus* (cm)

Characters	Female		Male		t-value	p-value
	Sampling size	Mean \pm S.D.	Sampling size	Mean \pm S.D.		
BL	33	17.88 \pm 3.91	35	15.82 \pm 3.25	-2.36	0.021
D ₁₋₂	33	0.63 \pm 0.03	35	0.63 \pm 0.03	0.20	0.844
D ₁₋₃	33	0.64 \pm 0.05	35	0.64 \pm 0.04	-0.06	0.953
D ₂₋₃	33	0.93 \pm 0.04	35	0.93 \pm 0.04	-0.07	0.944
D ₂₋₄	33	0.56 \pm 0.05	35	0.56 \pm 0.05	-0.21	0.832
D ₁₋₄	33	0.41 \pm 0.06	35	0.41 \pm 0.07	0.44	0.658
D ₃₋₄	33	0.77 \pm 0.05	35	0.78 \pm 0.04	0.69	0.490
D ₃₋₅	33	0.63 \pm 0.05	35	0.65 \pm 0.07	0.84	0.407
D ₄₋₆	33	0.63 \pm 0.05	35	0.64 \pm 0.05	1.04	0.301
D ₃₋₆	33	0.60 \pm 0.04	35	0.58 \pm 0.09	-0.91	0.369
D ₄₋₅	33	0.99 \pm 0.05	35	1.00 \pm 0.03	1.16	0.252
D ₅₋₆	33	0.79 \pm 0.04	35	0.79 \pm 0.05	0.03	0.974
D ₅₋₇	33	0.12 \pm 0.08	35	0.11 \pm 0.06	-0.31	0.758
D ₆₋₈	33	0.35 \pm 0.05	35	0.37 \pm 0.04	1.37	0.177
D ₅₋₈	33	0.62 \pm 0.05	35	0.62 \pm 0.04	0.14	0.885
D ₆₋₇	33	0.85 \pm 0.05	35	0.84 \pm 0.04	-0.03	0.977
D ₇₋₈	33	0.69 \pm 0.05	35	0.69 \pm 0.04	-0.09	0.928
D ₇₋₉	33	0.36 \pm 0.08	35	0.40 \pm 0.05	2.77	0.008
D ₈₋₁₀	33	0.82 \pm 0.04	35	0.83 \pm 0.03	1.60	0.116
D ₈₋₉	33	0.85 \pm 0.06	35	0.85 \pm 0.06	0.18	0.885
D ₇₋₁₀	33	0.47 \pm 0.05	35	0.49 \pm 0.04	2.02	0.048
D ₉₋₁₀	33	0.25 \pm 0.04	35	0.26 \pm 0.03	0.83	0.412
HL	33	0.64 \pm 0.02	35	0.63 \pm 0.03	-2.51	0.015
PL	33	0.23 \pm 0.05	35	0.21 \pm 0.03	-2.92	0.005
DFL	33	0.57 \pm 0.03	35	0.55 \pm 0.03	-2.89	0.005
K	33	1.51 \pm 0.31	35	1.79 \pm 0.24	4.01	< 0.001
HH	33	0.38 \pm 0.03	35	0.38 \pm 0.04	-0.30	0.762
HW	33	0.35 \pm 0.06	35	0.35 \pm 0.07	0.09	0.925
SL	33	0.23 \pm 0.18	35	0.18 \pm 0.05	-1.61	0.116
ED	33	0.00 \pm 0.04	35	0.00 \pm 0.04	0.30	0.768
IW	33	0.18 \pm 0.11	35	0.18 \pm 0.07	0.0004	1.000
BH	33	0.55 \pm 0.04	35	0.57 \pm 0.04	1.84	0.071
ML	33	-0.01 \pm 0.08	35	-0.01 \pm 0.05	-0.17	0.867
PFL	33	0.53 \pm 0.05	35	0.51 \pm 0.04	-1.47	0.148
CFL	33	0.55 \pm 0.05	35	0.54 \pm 0.04	-1.63	0.108
PAFD	33	0.63 \pm 0.04	35	0.63 \pm 0.03	0.40	0.692

Except BL, other morphological parameters were logarithmically heterodyne transformed. Data are expressed as mean \pm S.D. (cm). Transformation variables are compared with t-test. BL, body length; HL, head length; ED, eye diameter; PL, post-orbital length; DFL, dorsal fin long-throned length; K, condition factor; HH, head height; HW, head width; SL, snout length; IW, interorbital width; BH, body highness; ML, mouth length; PFL, pectoral fin length; CFL, caudal fin length; PAFD, Distance between pelvic fin and anal fin

Correlations between morphological characteristic variables of *H. maculatus*

The first three principal components of 35 morphological characteristics of *H. maculatus* explained 85.17% of variation (Table 2). BL , D_{1-2} , D_{1-3} , D_{2-3} , D_{5-6} , D_{9-10} , D_{4-6} , D_{6-7} , and HL had higher positive load coefficients in the first principal component (explaining 75.93% of variation). K had a higher positive load coefficient in the second principal component (explaining 6.40% of variation). HL had a higher positive load

coefficient in the third principal component (explaining 2.85% of variation; *Table 2*). The morphological features overlapped greatly, and some local features were significantly separated (*Fig. 3A*).

Table 2. Factor loadings of principal components extracted from 35 morphological characters in male and female *H. maculatus*

Character	Component		
	1	2	3
<i>BL</i>	0.98	0.02	0.00
<i>D</i> ₁₋₂	0.97	0.00	0.03
<i>D</i> ₁₋₃	0.95	0.05	-0.03
<i>D</i> ₂₋₃	0.97	0.02	-0.02
<i>D</i> ₂₋₄	0.92	0.03	-0.01
<i>D</i> ₁₋₄	0.80	-0.03	-0.03
<i>D</i> ₃₋₄	0.97	0.03	-0.07
<i>D</i> ₃₋₅	0.82	-0.07	0.02
<i>D</i> ₄₋₆	0.96	-0.01	-0.05
<i>D</i> ₃₋₆	0.77	0.12	-0.06
<i>D</i> ₄₋₅	0.98	-0.02	0.01
<i>D</i> ₅₋₆	0.97	0.01	0.02
<i>D</i> ₅₋₇	0.91	0.10	0.00
<i>D</i> ₆₋₈	0.95	-0.02	-0.01
<i>D</i> ₅₋₈	0.94	-0.03	0.15
<i>D</i> ₆₋₇	0.96	0.04	0.01
<i>D</i> ₇₋₈	0.94	0.00	0.10
<i>D</i> ₇₋₉	0.81	-0.29	0.16
<i>D</i> ₈₋₁₀	0.96	-0.10	0.09
<i>D</i> ₈₋₉	0.86	-0.03	0.14
<i>D</i> ₇₋₁₀	0.90	-0.19	0.08
<i>D</i> ₉₋₁₀	0.96	-0.05	0.02
<i>HL</i>	0.97	-0.05	-0.05
<i>HH</i>	0.94	0.00	-0.04
<i>HW</i>	0.88	0.11	-0.27
<i>SL</i>	0.27	-0.35	0.76
<i>PL</i>	0.95	-0.08	-0.02
<i>ED</i>	0.78	0.01	-0.20
<i>IW</i>	0.86	0.08	-0.10
<i>ML</i>	0.92	0.08	-0.01
<i>BH</i>	0.93	0.14	-0.04
<i>PFL</i>	0.92	-0.11	-0.13
<i>CFL</i>	0.91	-0.13	-0.04
<i>PAFD</i>	0.92	0.02	-0.02
<i>DFL</i>	0.92	-0.12	-0.03
<i>K</i>	0.06	0.69	-0.23
Eigenvalues	28.85	2.43	1.08
Contribution rate (%)	75.93	6.40	2.85
Cumulative contribution rate (%)	75.93	82.33	85.18

Variables with major contributions from each principal component are indicated in bold. *BL*, body length; *HL*, head length; *ED*, eye diameter; *PL*, post-orbital length; *DFL*, dorsal fin long-throated length; *K*, condition factor; *HH*, head height; *HW*, head width; *SL*, snout length; *IW*, interorbital width; *BH*, body highness; *ML*, mouth length; *PFL*, pectoral fin length; *CFL*, caudal fin length; *PAFD*, Distance between pelvic fin and anal fin

The results of R-cluster analysis of 35 morphological parameters by heterocorrelation transformation showed that the standardized relative traits were divided into two branches. The first branch contained *D*₁₋₂, ..., *D*₉₋₁₀, and *K*, which represented body shape and lean characteristic parameters; and the second branch contained *HL*, *HH*, *HW*, *SL*, *IW*, *ED*, and *IDL*, which mainly represented the head traits of *H. maculatus* (*Fig. 3B*).

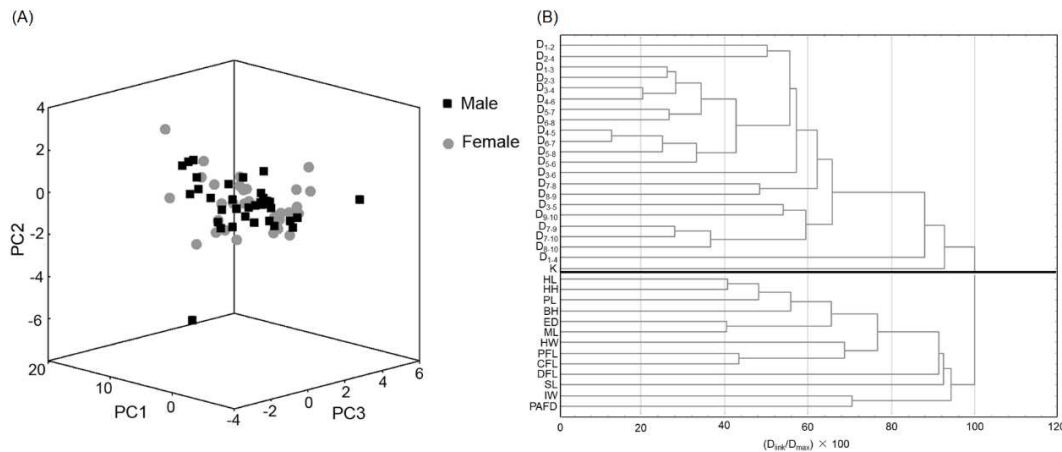


Figure 3. Principal component analysis (PCA) profile based on standardized morphological indexes (A) and R-cluster dendrogram of standardized morphological indexes (B) of *H. maculatus*. BL, body length; HL, head length; ED, eye diameter; PL, post-orbital length; DFL, dorsal fin long-throated length; K, condition factor; HH, head height; HW, head width; SL, snout length; IW, interorbital width; BH, body highness; ML, mouth length; PFL, pectoral fin length; CFL, caudal fin length; PAFD, Distance between pelvic fin and anal fin

Sex discrimination based on quantitatively morphological characteristics

The comprehensive discriminant rate based on the traditionally morphological data was 83.82%. (Male: 88.57%; Female: 78.79%). The comprehensive discriminant rate based on the truss network data was 91.18% (Male: 97.14%; Female: 84.85%). The comprehensive discriminant rate based on the integrated data of traditionally morphological characteristics and truss network characteristics was 98.53% (Male: 100%; Female: 96.97%). The comprehensive discriminant rates based on the three data transfer methods of the integrated data of traditionally morphological characteristics and truss network characteristics was 82.35% for ratio (Male: 80%; Female: 84.85%), 88.24% for logarithmic ratio (Male: 94.29%; Female: 81.82%), and 92.65% for ALLOM (Male: 1.43%; Female: 93.94%), respectively.

The discriminant formulas for male and female of *H. maculatus* were constructed as follows based on the 13 morphological parameters (i.e. *K*, *DFL*, *D₇₋₉*, *IW*, *D₃₋₆*, *D₄₋₆*, *BH*, *HL*, *D₈₋₉*, *D₆₋₈*, *D₃₋₄*, *D₅₋₈*, and *D₃₋₅*) after the logarithmic heterocorrelation transformation that were screened by stepwise regression,

$$\begin{aligned}
 Y_1 = & -1857.66 - 27.39K - 320.14DFL + 860.03D_{7-9} \\
 & - 385.12IW + 235.83D_{3-6} - 436.43D_{4-6} \\
 & - 21.39BH + 3527.74HL + 582.19D_{8-9} \\
 & - 1391.47D_{6-8} + 1491.79D_{3-4} + 717.05D_{5-8} \\
 & - 232.48D_{3-5}
 \end{aligned} \tag{Eq.6}$$

$$\begin{aligned}
 Y_2 = & -1960.26 - 33.16K - 355.13DFL + 904.87D_{7-9} \\
 & - 350.58IW + 258.83D_{3-6} - 474.59D_{4-6} \\
 & - 58.20BH + 3644.81HL + 603.11D_{8-9} \\
 & - 1446.06D_{6-8} + 1538.12D_{3-4} + 757.36D_{5-8} \\
 & - 246.62D_{3-5}
 \end{aligned} \tag{Eq.7}$$

If $Y_1 > Y_2$, the fish was male, otherwise it was female. The significance test of the discriminant function shows that the discriminant function has reached the extremely significant level ($F_{(13, 54)} = 9.2441, P < 0.001$). The frequency distribution of each individual's discriminant scores also showed that the model could distinguish male and female *H. maculatus* (Fig. 4). The sixty-eight individuals were judged by the sex discrimination equations (Eq.6 and Eq.7), and anatomical verification, only 5 (7.35%) fish individuals had misjudged sex by the sex discrimination equations. The accuracy rate was 92.65% (Table 3).

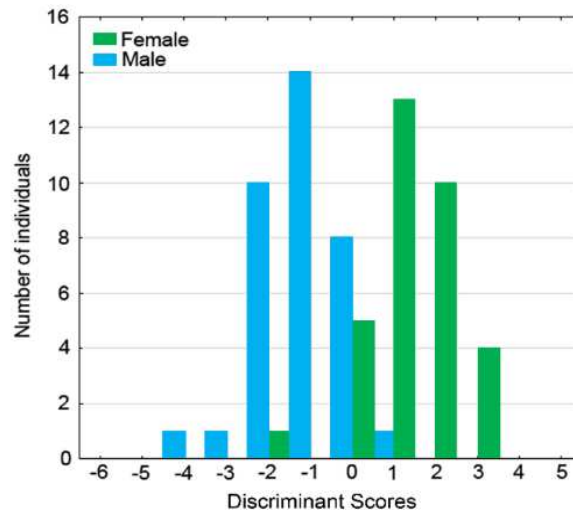


Figure 4. Frequency distribution of discriminant scores of male and female *H. maculatus*

Table 3. Discriminant analysis results of the stepwise discriminant function analysis based on the standardized morphological data of *H. maculatus*

Sex	Histologic identification	Predicted result		Accuracy of discrimination (%)	Total discrimination accuracy (%)	Transformations*
		Male	Female			
Male	35	28	7	80	82.35	M / SL
Female	33	5	28	84.85		
Male	35	33	2	94.29	88.24	$\log M / \log SL$
Female	33	6	27	81.82		
Male	35	32	3	91.43	92.65	$\log M - b(\log SL - \log SL_{mean})$
Female	33	2	31	93.94		

* M is the local characteristic measurements of each specimen, SL is the body length of each specimen, SL_{mean} is the mean body length of male or female fish, and b is the slope of linear regression of $\log_{10}M$ and $\log_{10}SL$

Discussion

Sexual heteromorphism of individuals is generally interpreted as the result of a combination of sexual selection, fertility selection, and ecological selection (Emlen and Oring, 1977; Lande, 1980; Hedrick and Temeles, 1989). There are three main types of sexual heteromorphism of fish individual size, i.e. female adult is larger than male adult, female adult is smaller than male adult, and the size of male and female individuals is similar (Parker, 1992; Pyron, 1996; Erlandsson and Ribbink, 1997). Lin et al. (2005)

report that the individual size of *H. maculatus* in the Oujiang River is no significant difference between male and female individuals, while female adults of *H. maculatus* in the Yuanhe River are significantly larger than male adults. This result indicates that the ecological factors from different habitats could influence the heteromorphism of individual size of *H. maculatus*. The difference of local morphological characteristics between males and females showed that the male of *H. maculatus* in the Yuanhe River had larger tail stalk than female, in consistent with eleotrid goby (*Odontobutis obscurus*) (Fan et al., 2009), and catfish (*Clarias fuscus*) (Fan et al., 2014).

The results of PCA and R-cluster analysis showed that the morphologic differences of male and female *H. maculatus* in the Yuanhe River mainly concentrated in three aspects: fish body shape, *K*, and head shape, which was basically consistent with the results of *I. Elongata* (Ni and Chen, 2003) and *S. argus* (Wu et al., 2014).

Integration of the traditionally morphological indicators and the truss network data could significantly improve the accuracy of sex discrimination of *H. maculatus*, which was consistent with the reports of blunt snout bream (*Megalobrama amblycephala*) (Li et al., 1991). The *ALLOM* data transformation method has the highest accuracy for male and female discrimination of *H. maculatus* in Yuanhe River, with a comprehensive recognition rate of 92.65%. It should be further verified whether the transformation method could improve the accuracy in other fish.

Conclusion

In conclusion, a quantitatively morphological discriminant model for identifying male and female *H. maculates* was established in the present study. The accuracy rate of *H. maculates* discrimination between male and female was 92.65% using logarithmic heterocorrelation method to transform the quantitatively morphological data. However, automatic identification system based on the model needs to further develop to speed up the identification of male and female *H. machlates*. The best sex ration for artificial propagation of *H. machlates* also needs to further study.

Acknowledgements. The authors thank anonymous technicians at Guangdong Meilikang Bio-Science Ltd., China for assistance with data re-analysis and figure preparation.

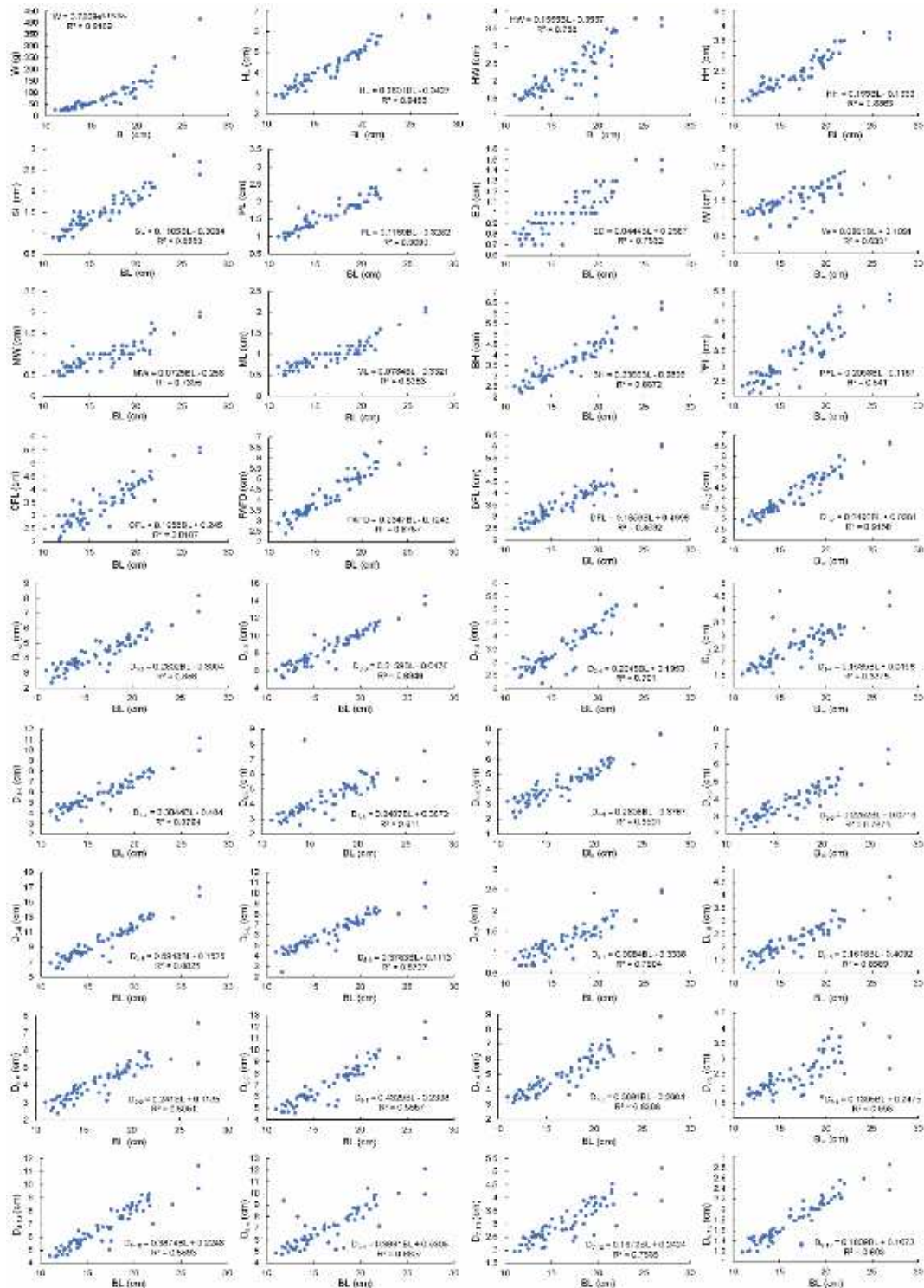
REFERENCES

- [1] An, L., Meng, Q., Zhang, L., Dong, X., Li, X., Li, W., Zhu, S. (2017): Analysis of morphological indexes and discrimination of male and female *Eryghroculter ilishaeformis*. – *Freshwater Fisheries* 47(2): 36-41.
- [2] Bookstein, F. L. (1997): *Morphometric tools for landmark data: geometry and biology* Cambridge. – New York: Cambridge University Press.
- [3] Chang, C.-H., Shao, Y. T., Fu, W.-C., Anraku, K., Lin, Y.-S., Yan, H. Y. (2015): Differentiation of visual spectra and nuptial colorations of two *Paratanakia himantegus* subspecies (Cyprinoidea: Acheilognathidae) in response to the distinct photic conditions of their habitats. – *Zoological Studies* 54: 43.
- [4] Chen, S., Zhao, R., Qi, D., Fan, X., Lei, H., Lin, Z. (2013a): Sexual dimorphism in morphological traits and female individual fecundity of *Acanthorhodeus chankaensis* Dybowsky. – *Journal of Shanghai Jiaotong University (Agricultural Science)* 31(5): 61-66, 78.

- [5] Chen, S., Zhao, R., Zhang, Y., Fan, X., Ding, G., Lin, Z. (2013b): Sexual dimorphism in morphology and female fecundity of *Erythroculter ilishaeformis* from rivers in Yuyao. – Journal of Lishui University 35(2): 11-15.
- [6] Corti, M., Thorpe, R. S., Sola, L., Sbordoni, V., Cataudella, S. (1988): Multivariate morphometrics in aquaculture: a case study of six stocks of the common carp (*Cyprinus carpio*) from Italy. – Canadian Journal of Fisheries and Aquatic Sciences 45: 1548-1554.
- [7] Emlen, S. T., Oring, L. W. (1977): Ecology, sexual selection, and the evolution of mating system. – Science 197: 215-223.
- [8] Erlandsson, A., Ribbink, A. J. (1997): Patterns of sexual size dimorphism in African cichlid fishes. – South African Journal of Science 93(11-12): 498-508.
- [9] Fan, X., Lin, Z., Lu, J., Qiu, Y., Chen, C., Cao, Y., Qi, D. (2009): Sexual dimorphism in morphological traits and female individual fecundity of *Odontobutis obscurus*. – Journal of Shanghai Jiaotong University (Agricultural Science) 28(6): 587-591,623.
- [10] Fan, X., Lin, Z., Ding, X., Zhu, J. (2014): Sexual size dimorphism and female individual fecundity of *Silurus asotus* and *Clarias fuscus*. – Acta Ecologica Sinica 34(3): 555-563.
- [11] Fish Research Laboratory of Hubei Institute of Hydrobiology. (1976): Yangtze River fishes. – Beijing: Science Press, 79-80.
- [12] Fu, L., Qiao, D. (2008): Studies on the morphology and biology of *Hemibarbus maculatus*. – Reservoir Fisheries 28(1): 53-55.
- [13] Gibbons, J. W., Lovich, J. E. (1990): Sexual dimorphism in turtles with emphasis on the slider turtle (*Trachemys scripta*). – Herpetological Monographs 4: 1-29.
- [14] Guo, H., Wei, K., Xie, Z., Tang, W., Shen, L., Gu, S., Wu, J., Chen, W. (2011): Analysis of morphological index system and discrimination of male and female silver eels (*Anguilla japonica*) collected at the Yangtze River Estuary. – Journal of Fisheries of China 35(1): 1-9.
- [15] Hedrick, A. V., Temeles, E. J. (1989): The evolution of sexual dimorphism in animals: hypotheses and tests. – Trends in Ecology & Evolution 4: 136-138.
- [16] Lande, R. (1980): Sexual dimorphism, sexual selection, and adaptation in polygenic characters. – Evolution 34: 292-305.
- [17] Li, S., Cai, W., Zhou, B. (1991): Morphological and biochemical genetic variations among populations of blunt snout bream (*Megalobrama amblycephala*). – Journal of Fisheries of China 15(3): 204-211.
- [18] Li, P., Xu, D., Peng, Z., Zhang, Y. (2012): The complete mitochondrial genome of the spotted steed, *Hemibarbus maculatus* (Teleostei, Cypriniformes). – Mitochondrial DNA 23(1): 34-36.
- [19] Lin, Z., Lei, H., Lin, Z., Hua, H. (2005): Sexual dimorphism and female reproductive output of *Hemibarbus maculatus*. – Journal of Shanghai Jiaotong University (Agricultural Science) 23(3): 284-288.
- [20] Lombardi-Carlson, L. A., Andrews, A. H. (2015): Age estimation and lead-radium dating of golden tilefish, *Lopholatilus chamaeleonticeps*. – Environmental Biology of Fishes 98(7): 1787-1801.
- [21] Miao, X., Yin, M. (1983): A study on the biology of spotted-carp (*Hemibarbus maculatus* Bleeker) in Tai Hu. – Journal of Fisheries of China 7(1): 31-44.
- [22] Ni, H., Chen, X. (2003): Analysis of shape index system and discriminant of male and female of *Ilisha elongata*. – Journal of Biomathematics 18(2): 224-228.
- [23] Parker, G. A. (1992): The evolution of sexual size dimorphism in fish. – Journal of Fish Biology 41 (supplement): 1-20.
- [24] Pinheiro, A., Teixeira, C. M., Rego, A. L., Marques, J. F., Cabral, H. N. (2005): Genetic and morphological variation of *Solea lascaris* (Risso, 1810) along the Portuguese coast. – Fisheries Research 73(1-2): 67-78.
- [25] Pyron, M. (1996): Sexual size dimorphism and phylogeny in North American minnows. – Biological Journal of the Linnean Society 57: 327-341.

- [26] Shou, L., Du, W. G., Shu, L. (2005): Sexual dimorphism and fecundity in the gold-stripe pond frog (*Pelophylax plancyi*) and the terrestrial frog (*Fejervarya limnocharis*). – *Acta Ecologica Sinica* 25(4): 664-668.
- [27] Strauss, R. E., Bookstein, F. L. (1982): The truss: body form reconstruction in morphometrics. – *Systematic Zoology* 31(2): 113-135.
- [28] Sun, L., Liu, J., Yang, Y. (2014): Primarily study on fish community structure of *Hemibarbus maculatus* in Tonglu area of the Qiantang River. – *Journal of Biology* 31(6): 46-50.
- [29] Tuo, Y. (2012): Population characteristics of *Hemibarbus maculatus* in Yuanhe River. – *Journal of Hydroecology* 33(6): 109-113.
- [30] Tuo, Y. (2013): Fecundity of *Hemibarbus maculatus* in the Yuanhe River of Jiangxi, China. – *Sichuan Journal of Zoology* 32(3): 375-379.
- [31] Turan, C. (1999): A note on the examination of morphometric differentiation among fish populations: the truss system. – *Turkish Journal of Zoology* 23(3): 259-263.
- [32] Turan, C., Ergüden, D., Gürlek, M., Basusta, N., Turan, F. (2004): Morphometric structuring of the anchovy (*Engraulis encrasicolus* L.) in the Black, Aegean and northeastern Mediterranean seas. – *Turkish Journal of Veterinary and Animal Sciences* 28: 865-871.
- [33] Wu, X., Yang, Q., Yue, P., Huang, H. (1979): *Economic Animals in China - Freshwater Fish*. – Beijing: Science Press, 86-87.
- [34] Wu, B., Zhang, M., Deng, S., Shi, S., Li, G., Zhu, C. (2014): Analysis of morphological index and discrimination of male and female *Scatophagus argus*. – *Journal of Shanghai Ocean University* 23(1): 64-69.
- [35] Xie, C., Gong, S., Yang, Z., Zhang, Q. (1988): The growth of *Hemibarbus maculatus* Bleeker in Nanhu Lake, Wuchang. – *Oceanologia et Limnologia Sinica* 19(3): 225-231.
- [36] Xu, D., Lin, Z., Lei, H. (2006): Sexual dimorphism in morphological traits and female individual fecundity of *Acrossocheilus wenchowensis*. – *Journal of Shanghai Jiaotong University (Agricultural Science)* 24(4): 335-340.

APPENDIX



Appendix 1. Correlation between body length (BL) and other morphological parameters. BL, body length; HL, head length; ED, eye diameter; PL, post-orbital length; DFL, dorsal fin long-throned length; K, condition factor; HH, head height; HW, head width; SL, snout length; IW, interorbital width; BH, body highness; ML, mouth length; PFL, pectoral fin length; CFL, caudal fin length; PAFD, Distance between pelvic fin and anal fin

ENVIRONMENTAL KUZNETS CURVE DERIVED EMPIRICAL EVIDENCE FROM THE MAIN GRAIN-PRODUCING REGION IN HEILONGJIANG PROVINCE OF NORTHEASTERN CHINA FROM 2005 TO 2017

CHAI, Q. Y.¹ – CHAI, F. Y.² – SUN, X.³ – MWAGONA, P. C.³ – CHAI, Y. H.⁴ – SUN, Z. L.^{5*}

¹*College of Economics and Management, Northeast Forestry University, Harbin 150040, China*

²*School of Management, Heilongjiang University of Science and Technology, Harbin 150020, China*

³*College of Wildlife and Protected Area, Northeast Forestry University, Harbin 150040, China*

⁴*Aulin College, Northeast Forestry University, Harbin 150040, China*

⁵*Northeastern University at Qinhuangdao, Qinhuangdao 066004, China*

**Corresponding author*

e-mail: sunzhenglin@neuq.edu.cn

(Received 28th Sep 2019; accepted 4th Dec 2019)

Abstract. In Heilongjiang of China, the income of farmers affects the consumption of chemical agricultural products. This study simulated the relationships between chemical fertilizers, pesticides, agricultural film, and farmers' income growth for Heilongjiang (2005–2017) using Environmental Kuznets Curve (EKC) models. The results show that the total agricultural output value and the per capita income of farmers showed a decreasing trend, respectively. However, influenced by economic and policy factors, both chemical fertilizers and pesticides showed an N-shaped curve. The total agricultural output value and farmers' income growth in Heilongjiang had been at the “fast-growing” stage, with low environmental pollution according to the agricultural pollution level. Thus, the control of agricultural non-point source pollution has been quite effective, and as a result the agricultural environment improved significantly. The EKC models provided scientific evidence for estimating agricultural non-point source pollution load as well as their changeable trends for Heilongjiang from an economic perspective.

Keywords: *agricultural non-point pollution, chemical fertilizers, pesticides, per capita income of farmers, Heilongjiang*

Introduction

For a long time, China's grain output has increased greatly mainly as a result of the use of chemicals, such as fertilizers, pesticides and agricultural film. The input of chemical agricultural means has increased annually, and the scale has been expanding (*Fig. 1*). The low utilization rate of agricultural chemical means has led to the increasingly prominent problem of agricultural non-point source pollution, which has become a hot issue of social and public concern (Ongley et al., 2010; Huang et al., 2013; Li et al., 2014; Wang et al., 2019).

Grossman and Krueger (1995) introduced the EKC hypothesis, suggesting the existence of an inverse U-shaped relationship between pollutants and economy growth/income. It is reflected in the Environmental Kuznets Curve hypothesis which argues that as per capital income increases, environmental damages also rise to the maximum point at the beginning stage of economic development and eventually declines

with the increase in income level (Barbier et al., 1996). The hypothesis is represented by an inverted U-shaped diagram that depicts the relationship between the level of environmental degradation and the economic growth (Grossman and Kruger, 1995).

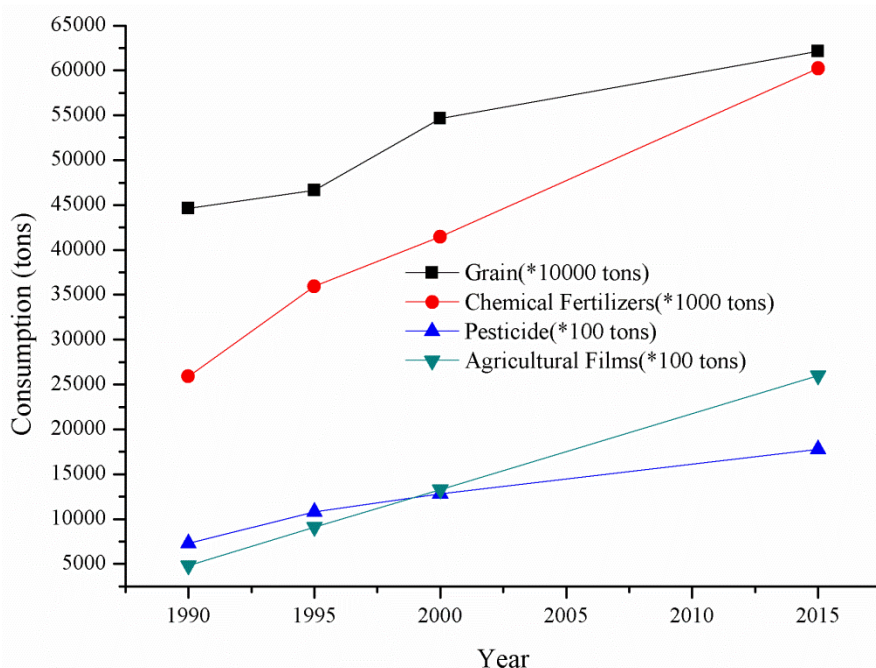


Figure 1. The relation between grain growth and consumption of chemical agricultural production material in China. (Source: Department of Rural Socio-Economic Survey, National Bureau of Statistics)

Empirical evidence on environmental risks in the US agricultural sector since 1970 supports the existence of increasing returns. Managi (2006) estimated the productivity of pesticide pollution abatement using refined empirical productivity measurement methods and explicitly control the level of technology. Their study showed the importance of including an environmental productivity variable in the EKC frame work. Jin et al. (2016) used time series data from 2000 to 2013 to verify the Environmental Kuznets Curve of pesticide use and economic growth in China, and to analyze the reasons for the increase of pesticide use in order to provide basis for the realization of pesticide reduction and sustainable agricultural development. Their results revealed that there is a significant inverted U-shaped curve relationship between pesticide use and per capita GDP and per capita gross agricultural output growth. That is, with economic growth, pesticide use increased first and then decreased. At present, China is still in the left half of the EKC curve, indicating that the use of pesticides is still in the rising stage (Zhang et al., 2019; Tzeremes, 2019). In order to achieve zero or even negative growth of pesticide use in China, it is necessary to formulate relevant policies for pesticide reduction and increase the promotion of advanced technology. Zhou et al. (2017) studied the provincial level data of 31 provinces (cities and districts) in China from 1993 to 2013, quantitatively analyzed the relationship between pesticide use and economic growth, and qualitatively explored the driving factors. The results show that there is a significant inverted U-shaped relationship between pesticide use and economic growth in China and other 24 provinces (cities and districts), except 7

provinces (cities and districts). Among them, the use of pesticides in seven provinces (cities and districts) is still in the rising stage, and has not reached the peak; the use of pesticides in eight provinces (cities and districts) has reached the peak and showed a downward trend; the EKC curve of nine provinces (cities and districts) is in the “N” shape, and the use of pesticides is still in the rising stage.

The emission of non-point source pollutants from fertilizers in China shows an increasing trend (Shi et al., 2019). Mao et al. (2013) estimated the loss of phosphorus and nitrogen fertilizer in Ningxia irrigation area, and tested the relationship between agricultural non-point source pollution and farmers’ per capita income. The results also supported the EKC hypothesis. Based on the provincial panel data from 1988 to 2016, Jie et al. (2018) examined the relationship between agricultural growth and non-point source pollution of fertilizers in China. On this basis, he used LMDI method to further investigate the internal causes of EKC formation. The results show that there is a significant “inverted U” EKC relationship between non-point source pollution of fertilizer and agricultural growth in China. The addition of space-time factors does not change the shape of EKC curve, but changes the time of inflection point. Wei et al. (2017) studied the effects of fertilizer input on water resources of Nanpanjiang River basin in Guizhou Province, taking fertilizer input and per capita income of rural residents in Guizhou Province from 2006 to 2015 as samples. Their results show that there is an Environmental Kuznets Curve between fertilizer input and environment, and the government and relevant departments should control the non-point source pollution caused by fertilizer input.

Shang et al. (2017) selected agricultural pollutants such as the intensity of agricultural film application as the evaluation index of agricultural non-point source pollution in Heilongjiang Province to verify the relationship between per capita agricultural output value and Environmental Kuznets Curve of agricultural non-point source pollution. Through research and analysis, the following conclusions are drawn: There is an EKC relationship between agricultural film and per capita agricultural output value in agricultural non-point source pollution sources in Heilongjiang Province, and the Environmental Kuznets Curve is inverted “N” type. On this basis, countermeasures and suggestions for non-point source pollution control in Heilongjiang Province are put forward. Combined with the first national census data of China, Dai et al. (2019) calculated agricultural non-point source pollution indexes based on the basic data of statistical yearbook. The results show that the overall trend of agricultural non-point source pollution is increasing yearly. From the EKC fitting curve test of agricultural non-point source pollution and per capita agricultural output value, it can be seen that the density of agricultural film use and per capita agricultural output value have a significant inverted u-shaped relationship. Combined with the results of empirical analysis, the paper puts forward some suggestions and measures to improve the situation of non-point source pollution in agriculture, increase agricultural economic growth and promote coordinated green development of agricultural environmental protection.

Materials and methods

Study area

Heilongjiang province (121°11'-135°05'E, 43°26'-53°33'N), located in the northeast of China, adjacent to Russia, is the world’s famous major grain producing area (*Fig. 2*).

It consists of thirteen municipalities and sixty-seven counties. The province covers a total area of 4.73×10^5 km², which accounts for 4.9% of China. Heilongjiang Province has been the main grain-producing area in China. In 2016, the cultivated land area was 1.24×10^7 ha, accounting for 7.5% of the whole country and 56.1% of the three northeastern provinces (Department of Rural Socio-economic Survey, National Bureau of Statistics, 2017). From the initial stage of the founding of the People's Republic of China, the annual output of grain has been increasing steadily reaching a breakthrough of 5×10^{10} kg in 2010. In 2018, the Province's total grain output reached 7.5×10^{10} kg, achieving a "15-years of bumper harvest" and ranking first in the country for eight consecutive years. In 2017, Heilongjiang's grain output accounted for 9.7% of the total national grain output and 51% of the three northeastern provinces (Department of Rural Socio-economic Survey, National Bureau of Statistics, 2018). Therefore, After the Sino-US Trade Dispute in 2018, the issue of agricultural resources and environmental security in Heilongjiang Province is of great significance in China.

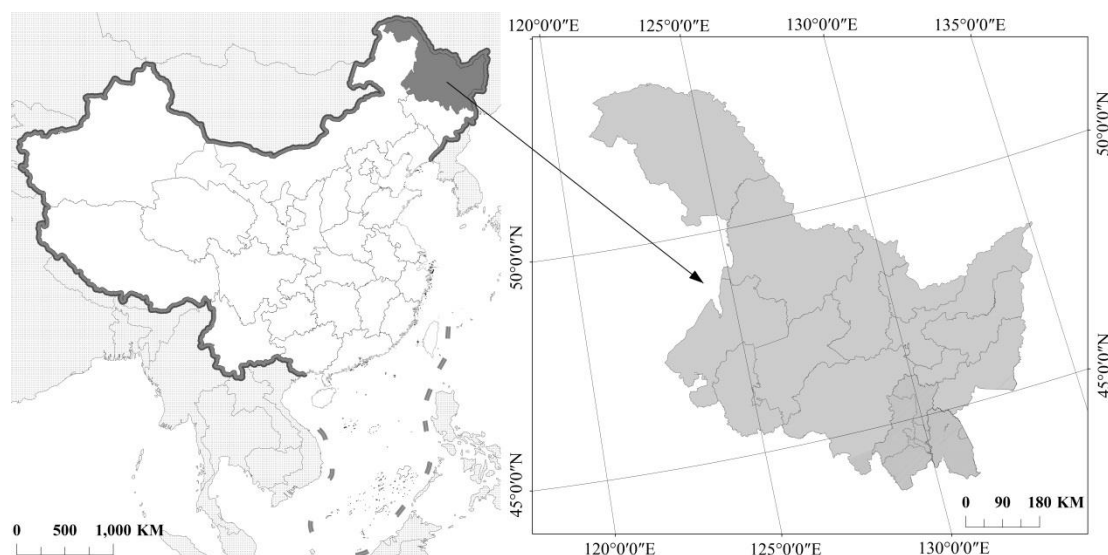


Figure 2. Location sketch map of Heilongjiang Province

Data and model

Data sources and processing

In order to analyze the relationship between farmers' income growth and agricultural non-point pollution in Heilongjiang, China, our empirical research used time series of consumption of chemical fertilizers, pesticides and agricultural films for the period 2005-2017 (Table 1). Data of farmers' income, consumption of chemical fertilizers, pesticides and agricultural films were obtained from the Heilongjiang Statistical Yearbook. The Data were processed using Excel 2016 and SPSS 20.

Model

On the basis of Environmental Kuznets Curve theory, the theoretical equation of the EKC between agricultural non-point pollution and farmers' income is

$$y = \beta_0 + \beta_1 X + \beta_2 X^2 + \beta_3 X^3 + \varepsilon$$

where y is the environmental indicators, x is the per capita annual Net Income of farmers, β_0 is a constant, β_1, β_2 and β_3 is the estimated coefficient, ε is the error term.

Table 1. Empirical research data in 2005-2017

Year	Consumption of chemical fertilizers (10000 tons)	Consumption of pesticide (10000 tons)	Consumption of agricultural films (10000 tons)	Per capita annual net income of farmers (yuan)
2005	121.6	2.9	5.3	3221
2006	150.9	4.8	5.7	3552
2007	175.2	6	6.4	4132
2008	180.7	6.2	6.6	4856
2009	198.9	6.7	6.5	5207
2010	214.9	7.4	6.9	6211
2011	228.4	7.8	7.6	7591
2012	240.3	8.1	8.5	8604
2013	245	8.4	8.5	9634
2014	251.9	8.7	8.4	10453
2015	255.3	8.3	8.3	11095
2016	252.8	8.3	8.3	11832
2017	251.2	8.3	7.9	12665

The relationship between economic development and environment quality can be very complicated. From the above formula, we can draw seven relationships between environmental pollution and economic growth in the model.

1. If $\beta_1 > 0, \beta_2 = 0, \beta_3 = 0$, it shows that the relationship between economic growth and environmental pollution is a simple incremental one, which satisfies the first-order function relationship. The bigger the first-term coefficient is, the more serious the pollution will be with economic growth, as shown in the straight line *a* of Figure 3.

2. If $\beta_1 < 0, \beta_2 = 0, \beta_3 = 0$, it shows that the relationship between economic growth and environmental pollution is simple and decreasing, which satisfies the first-order function relationship, and the smaller the first-term coefficient, the better the environmental quality will be with the rapid economic growth, as shown in the straight line *b* below.

3. If $\beta_1 < 0, \beta_2 > 0, \beta_3 = 0$, it shows that the relationship between environmental quality and economic growth is a normal U-shaped relationship, which first improves and then deteriorates. Unlike the traditional inverted U-shaped Environmental Kuznets Curve (EKC), the environmental condition first improves and then deteriorates, as shown in Figure 3c.

4. If $\beta_1 > 0, \beta_2 < 0, \beta_3 = 0$, it shows that the relationship between environmental quality and economic growth is an inverted U-shaped relationship that deteriorates first and then improves. This is also a typical shape in international experience. The deterioration of environmental quality has a turning point, which is the highest or extreme point of environmental pollution, as shown in Figure 3d.

5. If $\beta_1 > 0, \beta_2 < 0, \beta_3 > 0$, it shows that the relationship between environmental pollution and economic growth is an N-type relationship, which first deteriorates, then

improves, and finally deteriorates. The Environmental Kuznets Curve is shown in *Figure 3e*.

6. If $\beta_1 < 0$, $\beta_2 > 0$ and $\beta_3 < 0$, it shows that the relationship between environmental pollution and economic growth is an inverted N-type relationship, which first improves, then deteriorates, and then improves. The Environmental Kuznets Curve is shown in *Figure 3f*.

7. If $\beta_1 = 0$, $\beta_2 = 0$, $\beta_3 = 0$, it shows that there is no linear relationship between environmental pollution and economic growth, and there is no Environmental Kuznets Curve.

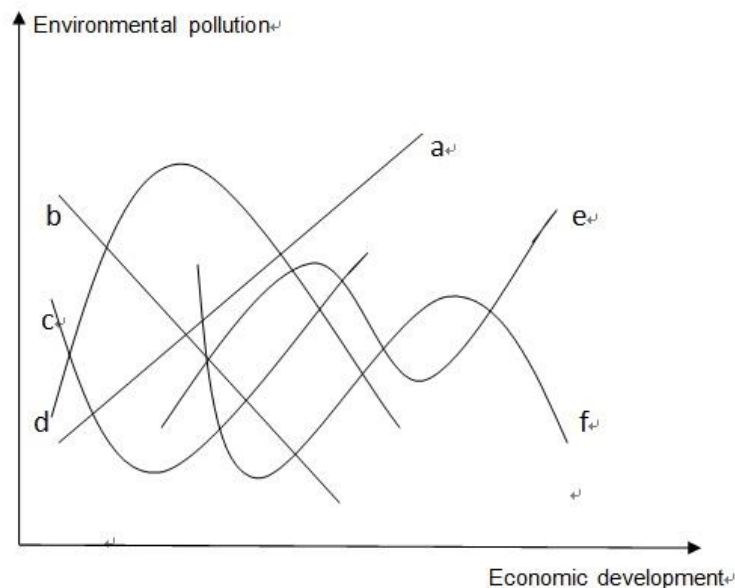


Figure 3. Shape diagram of Environmental Kuznets Curve

In this study, the per capita annual income of farmers was selected as the indicator which reflected the agricultural economic growth of Heilongjiang. Heilongjiang is a major agricultural province, agriculture is an important economic base. Therefore, the consumption of chemical fertilizers, pesticides and agricultural films was selected as the indicator which responded to pollution level of Heilongjiang.

With the help of SPSS software, income of farmers (as the horizontal axis) and agricultural production means (as the vertical axis) were fitted by linear, quadratic and cubic models. The results indicate that the cubic model can better reflect the relationship between consumption of chemical fertilizers, pesticides and income of farmers. The quadratic model can better reflect the fitting relationship between consumption of agricultural films and per capita income of farmers. For this reason, the relationship between income of farmers and agricultural environmental quality were fitted by the quadratic and cubic regression curve model (*Table 2*).

From the regression model of farmers' income of Heilongjiang with consumption of agricultural production means, it can be seen that the regression coefficient (R^2) of income with consumption of chemical fertilizer, pesticides and agricultural films was over 0.7. The fitting effect of per capita annual income of farmers and agricultural pollution index was ideal.

Table 2. The analysis results of regression model

Agricultural pollution index (Y)	Model summary					Regression equation
	R ²	F	df1	df2	Sig.	
Chemical fertilizers consumption	0.962	76.278	3	9	0.026	$Y = (1.728e - 10)X^3 + (-5.360e-06)X^2 + 0.0545X - 9.889$
Pesticides consumption	0.891	24.643	3	9	0.036	$Y = (1.245e - 11)X^3 + (-3.630e-07)X^2 + 0.003X - 4.357$
Agricultural films consumption	0.792	19.023	2	10	0.003	$Y = (-2.956e - 08)X^2 + 0.001X + 3.250$

Results and analysis

Agricultural development of Heilongjiang

From 2005 to 2017, the economy of Heilongjiang has grown rapidly. The Gross Domestic Product (GDP) increased from 554.28 billion yuan to 1590.27 billion yuan, an increase of approximately threefold, with an average annual growth rate of 15.58%. In addition, the per capita GDP increased from 14516 yuan to 41916 yuan, a 2.89-fold increase, with an average annual growth rate of 15.73%, and the per capita income of farmers increased from 3221 yuan to 12665 yuan, increased by 3.93 times, with an average annual growth rate of 24.43%, which exceeded the growth rate of GDP and per capita GDP (Fig. 4).

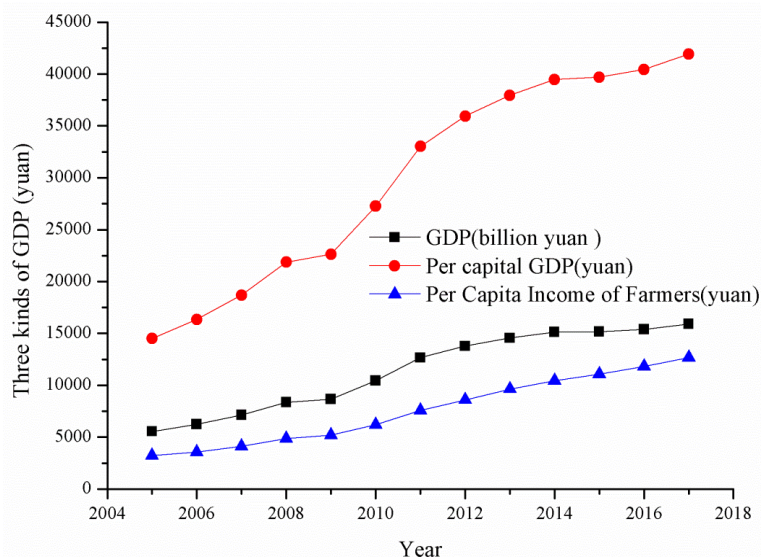


Figure 4. The growth trend of GDP, per capita GDP and farmers' income in Heilongjiang during 2005~2017

From 2005 to 2017, the growth rate of Heilongjiang's total agricultural output value is ahead of the whole country. China's agricultural output value increased 2.77 times, Heilongjiang's agricultural output value increased 4.32 times, and the growth rate exceeded China's agricultural output value by 1.56 times (Fig. 5). The average annual growth rate of China's total agricultural output value is 14.76%, while that of Heilongjiang Province is 27.63%, which is 1.87 times higher than the growth rate of China's total agricultural output value.

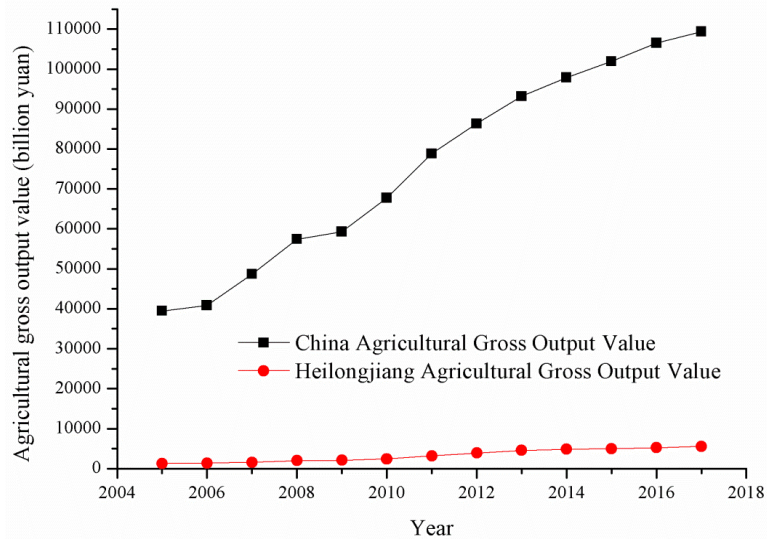


Figure 5. The agricultural gross output value of China and Heilongjiang 2005~2017

In the 13 years period (from 2005 to 2017), China's grain output has increased by 1.37 times, while Heilongjiang's grain output has increased by 2.06 times, and the grain growth rate is 1.5 times that of the whole country (Fig. 6). The average annual grain growth in China is 3.1%, compared with 8.8% in Heilongjiang, which is 2.84 times higher than that of the whole country. Heilongjiang accounted for 7.4% of the country's grain output in 2005, and increased to 11.2% in 2017.

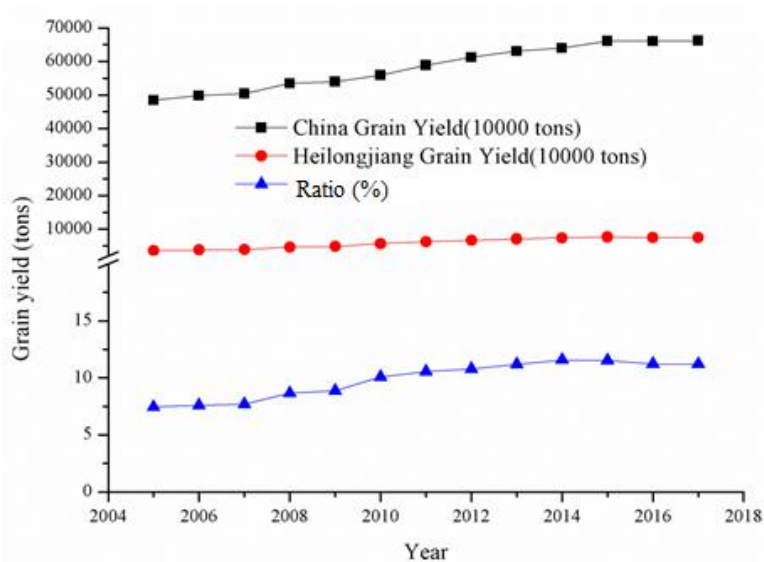


Figure 6. The grain yield of China and Heilongjiang during 2005~2017

In summary, the annual income growth rate of farmers exceeded the regional GDP and per capita GDP growth in Heilongjiang. The growth rate of Heilongjiang's total agricultural output value is obviously faster than that of the whole country. Heilongjiang is the most important major grain producing area in China, which is of great significance for ensuring national food security (Qi and Wu, 2017).

Agro-eco-environmental changes from 2005 to 2017 in Heilongjiang

With the growing demand of grain in China, the use of chemical fertilizers has also increased yearly. Until 2017, the intensity of fertilizer application in Heilongjiang Province was 170.10 kg/hm², which was 1.58 times higher than that in 2005, but still less than the world's recognized safety limit of 225 kg/hm² (Shi et al., 2016). The cubic model can better reflect the relationship between consumption of chemical fertilizers and income of farmers.

$$Y = (1.728e - 10)X^3 + (-5.360e - 06)X^2 + 0.0545X - 9.889 \quad (\text{Eq.1})$$

As we can see, from the result of curve fitting, it is roughly “N” type, and the per capita income of farmers at inflection point was 9634 yuan (*Fig. 7*). Before the inflection point, the intensity of fertilizer application increased with the increase of income. When the inflection point approached, the growth rate decreased significantly. After the inflection point exceeded 12665 yuan, the intensity of fertilizer application increased significantly. The result was similar to that of Hebei, Jilin, Jiangsu, Jiangxi, Guangdong, Hainan, Sichuan, Yunnan, Shanxi, Gansu and other 10 provinces (Liu et al., 2009). The relationship of fertilizer consumption and agricultural economic growth matched the N-shape EKC in Heilongjiang province (Shang et al., 2017). Without control, the input of fertilizer will continue to increase. Generally speaking, there is an EKC relationship between fertilizer application intensity and per capita income of farmers, and it is on the left side of the EKC curve. It can be understood that agricultural economic growth brings farmers' income. On the other hand, the rising demand for grain in China promotes the development of grain production, and the application of fertilizer also increases. This is consistent with the conclusion of some scholars (Bruyn and Opschoor, 1997; Opschoor, 1997) that the N-shaped curve is caused by economic factors.

The cubic model can better reflect the relationship between consumption of chemical pesticides and income of farmers.

$$Y = (1.245e - 11)X^3 + (-3.630e - 07)X^2 + 0.003X - 4.357 \quad (\text{Eq.2})$$

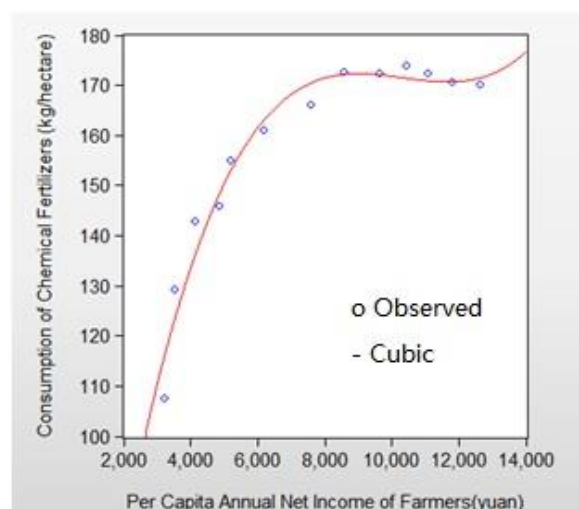


Figure 7. The fitting curve of fertilizer consumption and per capita income of farmers in Heilongjiang during 2005~2017

From the fitting income curve results of pesticides and farmers, it presented N-type EKC curve (Fig. 8), and the turning point was 7591 yuan per capita income of farmers. Before the turning point, the intensity of pesticide application increased with the increase of agricultural economy, and the growth rate of pesticide use decreased significantly near the turning point, while the intensity of pesticide application increased significantly after exceeding 11832 yuan. The intensity of pesticide application in Heilongjiang Province decreased with the increase of per capita agricultural income from 2014, because the overall planting structure of Heilongjiang Province has changed in recent years. There has been witnessed reduction of planting area of some cash crops and increase of planting area of Maize with lower pesticide consumption. This therefore has attributed reduction in the use of chemical herbicides. On the other hand, the production technology of pesticides has improved. Farmers are opting for the use of foliar spray hence the utilization rate of pesticides has been more efficiently Appeal causes led to the development of the right side of the EKC curve. Friedl and Getzner (2003) believed that the N-shaped curve is caused by policy factors. The application of pesticides in Heilongjiang validates this conclusion. There are about 232 million pesticide waste packages (bottles, bags and barrels) in Heilongjiang Province each year. The total weight of these packages is about 7,000 tons, and the residual pesticides in the packages are about 180 tons (Lin, 2017). The main causes of pesticide pollution in Heilongjiang Province is attributed to the weak awareness of environmental protection of farmers and safe use of pesticides; the lack of effective recovery methods and harmless treatment technology in the field of pesticides; and the lack of effective supervision mechanism for the use of pesticides.

The quadratic model can better reflect the fitting relationship between consumption of agricultural films and per capita income of farmers.

$$Y = (-2.956e - 08)X^2 + 0.001X + 3.250 \quad (\text{Eq.3})$$

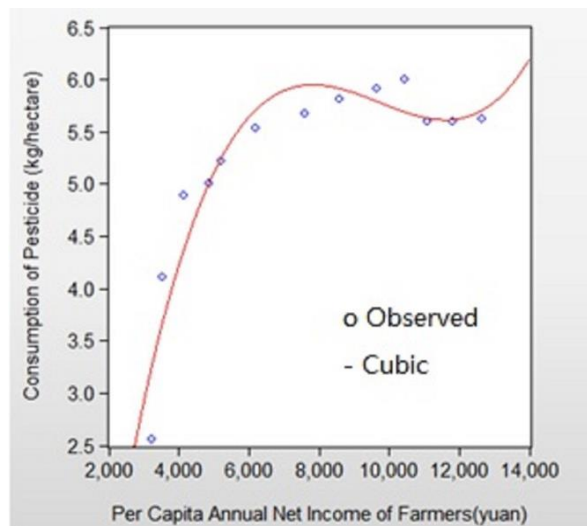


Figure 8. The fitting curve of pesticide consumption and per capita income of farmers in Heilongjiang during 2005~2017

According to the fitting curve results of agricultural film and income of farmers, it was a typical inverted U-shaped curve. The turning point of EKC occurred at 9634 yuan

of per capita income of farmers. Before the turning point, the intensity of agricultural film application increased with agricultural economic growth, and then increased slowly when approaching the turning point. After exceeding 9634 yuan, the intensity of agricultural film application decreased sharply. As we can see from *Figure 9*, the agricultural film consumption showed a fluctuation from 2005 to 2017. The year 2012 was a turning point. Before 2012, the agricultural film consumption showed an increasing tendency, an increase of about 1.3 times, with an average annual growth rate of 20.29%. After 2012, the agricultural film consumption started to decrease gradually, with a decline of 12.23% in 2017 compared with 2012, which has confirmed the results of the EKC of agricultural film consumption and per capita income of farmers.

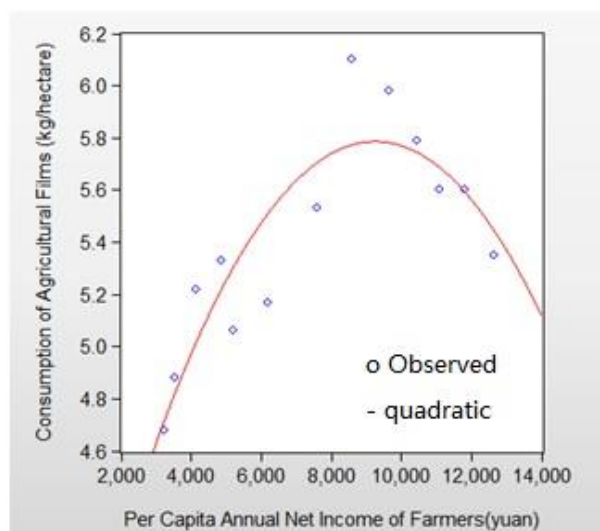


Figure 9. The fitting curve of agricultural film consumption and per capita income of farmers in Heilongjiang during 2005~2017

Control of agricultural non-point source pollution

A case study in north China showed that the amount of rural pollution source control reduced significantly, so as to protect and improve the environmental quality (Meng et al., 2014). In order to develop modern ecological agriculture, promote the transformation of China's grain base into a green granary and ensure food safety, Heilongjiang Province has implemented the "Three Reductions" of chemical fertilizers, chemical pesticides and chemical herbicides, and issued the "Opinions on the Implementation of the 'Three Reductions' of Agriculture in-depth". The opinions put forward that by 2020, the average application amount of chemical fertilizer per hectare should be reduced by more than 10%, the utilization rate of chemical fertilizer should be increased by 6.7%, the utilization rate of pesticides should be increased by 9%, and the use of herbicides should be reduced by more than 14,000 tons, or by 20%.

In controlling agricultural non-point source pollution, Heilongjiang Province has taken seven key measures.

Firstly, precise fertilization can be achieved by popularizing the technology of soil testing and formula fertilization and adjusting the structure of chemical fertilizer use.

Secondly, adhere to the combination of agriculture and animal husbandry, support large-scale aquaculture enterprises and large-scale farms, build fecal treatment facilities, encourage social capital to invest in the construction of organic fertilizer treatment plants, and promote harmless fermentation technology of livestock and poultry manure.

The third is to promote the technology of deep mechanical fertilization, water and fertilizer integration, foliar spraying and other effective fertilization techniques to reduce chemical fertilizer and improve fertilizer utilization rate.

The fourth is to demonstrate and popularize bio-pharmaceuticals and environmental protection agents, replacing low-activity pesticides and chemical additives with high-activity pesticides and environmental protection additives.

Fifth, to develop and improve the information management and prediction system of on-line monitoring of pests and diseases, establish a regional early warning and network management platform system above county level, and comprehensively enhance the ability of monitoring and early warning of major pests and diseases.

Sixth, through the national public welfare investment, the construction of centralized dispensing service stations, the precise allocation of pesticides, packaging and residual liquid recovery and treatment.

Lastly is to continue to implement subsidy policies for subsidy of subsistence land consolidation, so that all suitable cultivated land will be subsidized once every three years to improve land output capacity.

In 2018, the provincial high standard demonstration area of “Three Reductions” in agriculture reached 2.7 million ha. Tieli City carried out the “three-reduction” agricultural action, reducing the application of chemical fertilizer by more than 30 kg/ha, pesticide by 5% and herbicide by 5%. Nenjiang County completed the “three-reduction” agricultural demonstration area of 300,000 ha in 2018, with the application of organic fertilizer and farm manure reaching 648,000 tons, with an average reduction of 18% in the three indicators.

Agricultural non-point source pollution control in Heilongjiang has achieved results. From *Figure 10*, it can be seen that the application intensity of fertilizer and pesticide in Heilongjiang reached the highest value in 2014 from 2005 to 2017, which was 173.75 kg/ha and 6.0 kg/ha respectively, and showed a decreasing trend yearly. The application intensity of agricultural film reached the highest value of 6.10 kg/ha in 2012, and then decreased afterwards.

Conclusion and suggestions

In summary, the relationship between agricultural environment and agricultural economic growth was harmonious in Heilongjiang. While maintaining 24.43% annual growth of farmers’ income during the period from 2005 to 2017, Heilongjiang has managed to significantly reduce agricultural non-point source pollution. Analysis of a quadratic polynomial fit to the Environmental Kuznets Curve demonstrates that the environmental turning points for agricultural film consumption have occurred. This finding indicates that Heilongjiang has been at the stage of fast agricultural economic growth with low environmental pollution. Heilongjiang has established a green-oriented system forming a pattern of agricultural development that matches the carrying capacity of resources and environment and coordinates with the production of living ecology. Non-point source pollution in agriculture has been effectively controlled to achieve sustainable agricultural development.

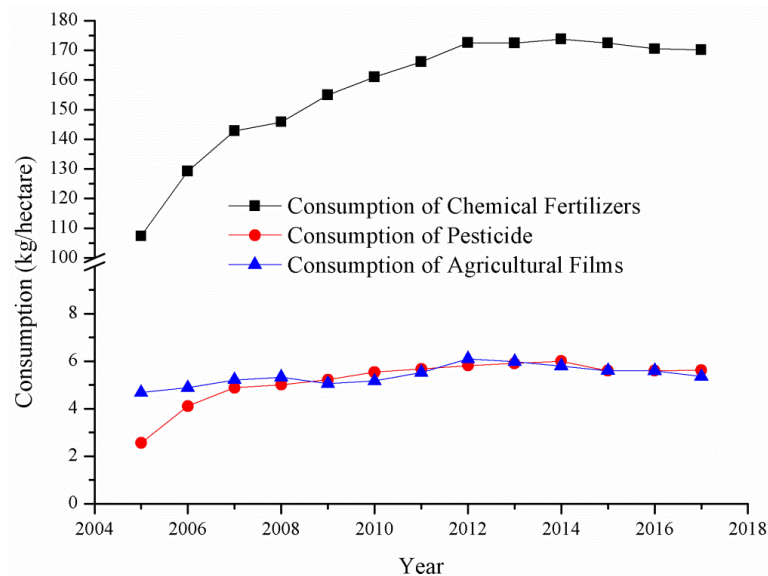


Figure 10. Growth trend of agricultural non-point source pollution indicators in Heilongjiang during 2005~2017

Although the quality of agricultural environment in Heilongjiang Province has been greatly improved, there are still many researches to be done in controlling agricultural comprehensive pollution and realizing ecological agriculture. In the future, the research work of increasing agricultural output value and controlling agricultural pollution will focus on three aspects.

First, give full play to regional comparative advantages and optimize the distribution structure of planting industry, in order to reduce the use of chemical fertilizers, pesticides and agricultural film. We should combine market demand orientation with farmers' traditional agriculture habits and accelerate the construction of a ternary planting structure featuring coordinated development of grain, economy and fodder. We will create an advantage zone for special agricultural products, and vigorously develop high value and high efficiency cash crops such as vegetables, fresh corn, edible fungi and potatoes with obvious supply advantages. As well as the special agricultural products such as selenium-rich ones, high green and organic food, and customized agricultural products. The corn industrial belt is mainly distributed in the cities of the first, second and third accumulative temperate zone in Songnen plain. The rice industrial belt is mainly distributed in the cities along the Nenjiang river, the Songhua river and the Sanjiang plain, as well as farms under the bureau of agricultural reclamation. The soybean industrial belt is mainly distributed in low limit of three accumulative temperate zones along the foothills of great and less Khingan mountains area and in the cities and farms under the bureau of agricultural reclamation in the fourth and fifth accumulative temperate zones. The belt is mainly distributed in arid and semi-arid areas such as Daqing, Qiqihar and Heihe. Potato industry belt is mainly distributed in Qiqihar, Harbin, Suihua, Heihe and other regions.

Secondly, to accelerate the open sharing and comprehensive utilization of large agricultural and rural data, in order to design and develop provincial-level agricultural Internet of Things (IoT) systems and related standards, and promote the application of Internet of Things technology. Through IoT, data sharing in the main business areas

such as agricultural planting and production, agricultural machinery management, green food, soil testing and fertilization, plant protection, and agricultural products safety is realized, which effectively solves the problem of agricultural comprehensive pollution and continuously increases the income of farmers.

Lastly, we should coordinate the development of urban and rural integration, improve laws, regulations and policies related to non-point source pollution prevention and control in rural areas, such as straw burning and utilization, pollution prevention and control of agricultural film, pollution prevention and control of poultry and livestock breeding, and soil pollution prevention and control.

Acknowledgements. The authors would like to thank the assistance of staff at the Heilongjiang Statistical Bureau and Heilongjiang Agricultural Commission. This work was financially supported by Heilongjiang Province Philosophy and Social Science Planning Youth Fund Project (16GLC04).

REFERENCES

- [1] Barbier, E. B., Stern, D. I., Common, M. S. (1996): Economic growth and environmental degradation: the environmental Kuznets curve and sustainable development. – *World Development* 24(7): 1151-1160.
- [2] Bruyn, S. M. D., Opschoor, J. B. (1997): Developments in the throughput-income relationship: theoretical and empirical observations. – *Ecological Economics* 20(3): 0-268.
- [3] Dai, Q. X., Wang, P. C. (2019): Verification and analysis of environmental Kuznets fitting curve of agricultural non-point source pollution-a province in Northwest China is taken as an example. – *Sustainable Development* 09(03): 362-373.
- [4] Department of Rural Socio-economic Survey, National Bureau of Statistics (2017): *China Rural Statistics Yearbook 2017*. – China Statistics Publishing Press, Beijing (in Chinese).
- [5] Department of Rural Socio-economic Survey, National Bureau of Statistics (2018): *China Rural Statistics Yearbook 2018*. – China Statistics Publishing Press, Beijing (in Chinese).
- [6] Friedl, B., Getzner, M. (2003): Determinants of CO₂ emissions in a small open economy. – *Ecological Economics* 45(1): 133-148.
- [7] Grossman, G. M., Krueger, A. B. (1995): *Economic Growth and the Environment*. – Nber Work. Pap. 110: 353-377.
- [8] Huang, L., Ban, J., Han, Y. T., Yang, J., Bi, J. (2013): Multi-angle indicators system of non-point pollution source assessment in rural areas: a case study near Taihu Lake. – *Environmental Management* 51(4): 939-950.
- [9] Jie, C. L., Wang, J. L., Pang, Y. N. (2018): Agricultural growth and non-point source pollution of chemical fertilizers in China: does the Environmental Kuznets Curve exist? – *Rural Economy* 11: 110-117 (in Chinese with English abstract).
- [10] Jin, S. T., Zhou, F. (2016): Research on the relationship between pesticide use and economic growth in China: based on Environmental Kuznets Curve. – *Journal of Jinan University (Social Science Edition)* 26(06): 87-92 (in Chinese with English abstract).
- [11] Li, C., Zhao, Y., Yang, J. (2014): Agricultural pollution hazard to soil and its control measures. – *Chinese Journal of Environmental Management* 6(03): 22-25.
- [12] Lin, Z. P. (2017): The present situation of pesticide pollution faced by Heilongjiang Province and measures taken. – *Pesticide Science and Administration* 38(12): 9-10 + 14.
- [13] Liu, Y., Chen, S. F., Zhang, Y. F. (2009): Study on Chinese agricultural EKC: evidence from fertilizer. – *China Agricultural Bulletin* 25(16): 263-267 (in Chinese with English abstract).

- [14] Managi, S. (2006): Are there increasing returns to pollution abatement? Empirical analytics of the environmental Kuznets curve in pesticides. – *Ecological Economics* 58(3): 617-636.
- [15] Mao C., Zhai N., Yang J., Feng, Y., Meng, Q. X. (2013): Environmental Kuznets curve analysis of the economic development and nonpoint source pollution in the Ningxia Yellow River irrigation districts in China. – *BioMed Research International* 1: 267968.
- [16] Meng, C., Yin, H., Kong, F. L., Li, Y. (2014): Roles of rural contiguous improvement measures on the non-point source pollution control in rural area in China. – *Advanced Materials Research* 1030-1032: 687-691.
- [17] Ongley, E. D., Xiaolan. Z., Tao, Y. (2010): Current status of agricultural and rural non-point source pollution assessment in China. – *Environmental Pollution* 158(5): 1159-1168.
- [18] Opschoor, J. B. (1997): The hope, faith and love of neoclassical environmental economics. – *Ecological Economics* 22(3): 0-283.
- [19] Qi, H., Wu, L. (2017): Analysis of the coordination degree between grain production and income level in the main grain-producing areas of China. – *Economic Geography* 37(06): 156-163 (in Chinese with English abstract).
- [20] Shang, J., Li, X., Deng, Y. Y. (2017): Analysis of the relationship between agricultural economic growth and agricultural non-point source pollution based on EKC: taking Heilongjiang province as an example. – *Ecological Economy* 33(06): 157-160 + 166 (in Chinese with English abstract).
- [21] Shi, C. L., Guo, Y., Zhu, J. F. (2016): Evaluation of excessive fertilizer application and its influencing factors in China's grain production. – *Study on Agricultural Modernization* 37(04): 671-679 (in Chinese with English abstract).
- [22] Shi, W. X., Chen, S. W. (2019): The drivers of fertilizer non-point source pollution in China and the Environmental Kuznets Curve characteristics. – *Resources and Environment in Arid Areas* 33(05): 1-7 (in Chinese with English abstract).
- [23] Tzeremes, P. (2019): Does the Environmental Kuznets Curve exist in the Chinese regions? – *Global Economic Review* 4: 1-15.
- [24] Wang, H. L., He, P., Shen, C. Y., Wu, Z. N. (2019): Effect of irrigation amount and fertilization on agriculture non-point source pollution in the paddy field. – *Environmental science and pollution research international* 26(10): 10363-10373.
- [25] Wei, J. N., Li, X. Y. (2017): Examination and analysis of the relation between fertilizer input and Environmental Kuznets Curve: a case study of Nanpanjiang River basin in Guizhou province. – *Hubei Agricultural Science* 56(05): 996-1001 (in Chinese with English abstract).
- [26] Zhang, S. (2019): Environmental Kuznets Curve revisit in central Asia: the roles of urbanization and renewable energy. – *Environmental Science and Pollution Research* 26(23): 23386-23398.
- [27] Zhou, F., Jin, S. T., Shen, G. Y. (2017): Study on Environmental Kuznets Curve of pesticide use in china based on provincial level. – *Jiangsu Agricultural Sciences* 45(13): 260-263 (in Chinese with English abstract).

FOREST FIRE RISK ASSESSMENT USING GIS AND AHP INTEGRATION IN BUCAK FOREST ENTERPRISE, TURKEY

ÇOBAN, H. O.^{1*} – ERDIN, C.²

¹*Department of Forest Engineering, Faculty of Forestry, Isparta University of Applied Sciences, 32260 Isparta, Turkey*

²*Department of Business Administration, Faculty of Economic and Administrative Sciences, Yıldız Technical University, İstanbul, Turkey*

**Corresponding author*

e-mail: oguzcoban@isparta.edu.tr

(Received 2nd Oct 2019; accepted 8th Jan 2020)

Abstract. Forest fires create an increasingly severe and negative impact on ecosystem services such as carbon storage, climate balancing and water supply as a result of global warming threatening our planet. One of the steps to fight forest fires is to perform a risk assessment. Forest fire risk assessment allows the identification of locations at high risk of forest fire and estimate its sphere of influence. In this way, it provides decision-making support to the fire-fighting organization. The purpose of this study was to conduct a forest fire risk assessment in forests located in Bucak Forest Enterprise in Turkey that is vulnerable to fire at the first degree. In the study, the weights of the criteria that lead to fire risk were computed with Analytic Hierarchy Process (AHP). The risk classes of the criteria were exported to the raster layer of the Geographical Information System (GIS). The results showed that 25% of forests in Bucak region were at high risk, while 32% were at medium fire risk. We believe that the approach adopted in this study may contribute to forest fire risk assessments and risk mapping of Mediterranean forest ecosystems that have similar climate, topographic structure and vegetation.

Keywords: *Mediterranean forests, fire risk factors, fire risk mapping, spatial analysis, fire sensitivity*

Introduction

Fire is an incident that leads to very severe changes in forest ecosystems (Naderpour et al., 2019). Forest fire poses a great danger to human life and environment (McKenzie et al., 2014; Garbolino et al., 2017). The European statistics demonstrate that 500 thousand hectares of forests are destroyed on average every year due to fire (EC, 2017). It is argued that the number of forest fires will increase in the future owing to climate change, changes in land use and forestry policies (González-De Vega et al., 2016; García-Llamas et al., 2019).

The Mediterranean forest ecosystems are resistant to fire (Pausas and Vallejo, 1999; Calvo et al., 2008); nevertheless, it is important to prevent fire before it reaches a dramatic point and fight against fire for social life and economy. We hope that forest fire risk assessments and organization of the efforts according to the risk levels identified will provide positive inputs for success in anti-forest fire efforts.

The forests located in the Mediterranean Region in the south of Turkey are vulnerable to fire; therefore, fire occurs very frequently in the forest ecosystems in this region. The statistics of the General Directorate for Forestry (GDF, 2019) reveal that on average more than 500 forest fire on average occur every year as a result of which more than 10000 hectares of forests are destroyed (*Figure 1*). As regards the causes of these fires, almost 90% of them are manmade (*Figure 2*).

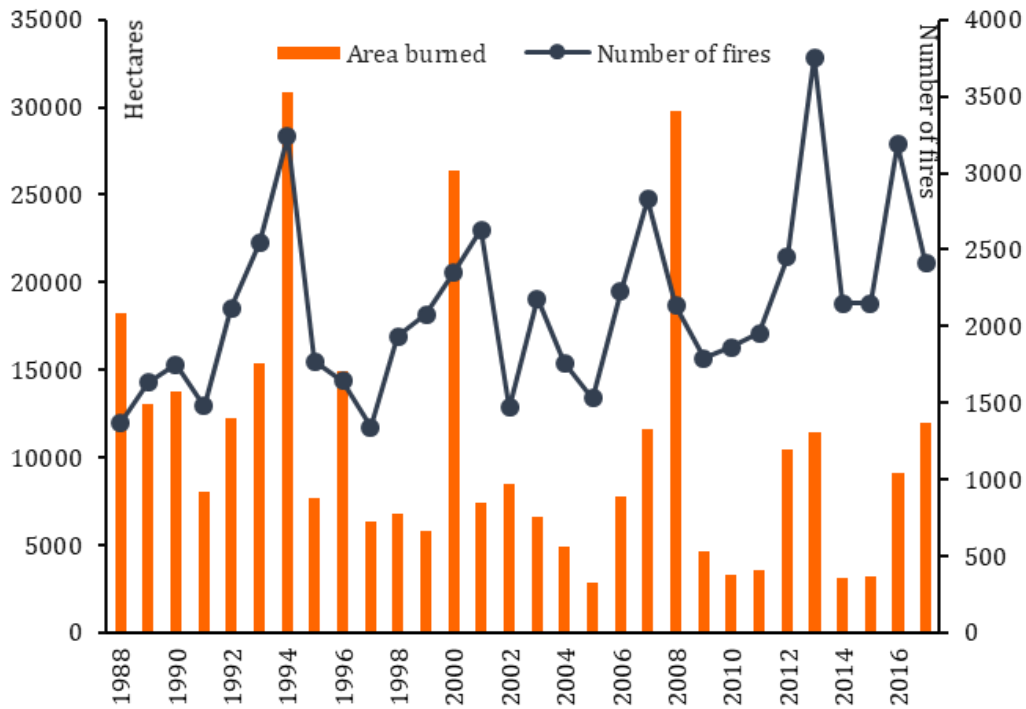


Figure 1. The number of forest fires in Turkey between years 1988-2017 and the area of forests burned (GDF, 2019)

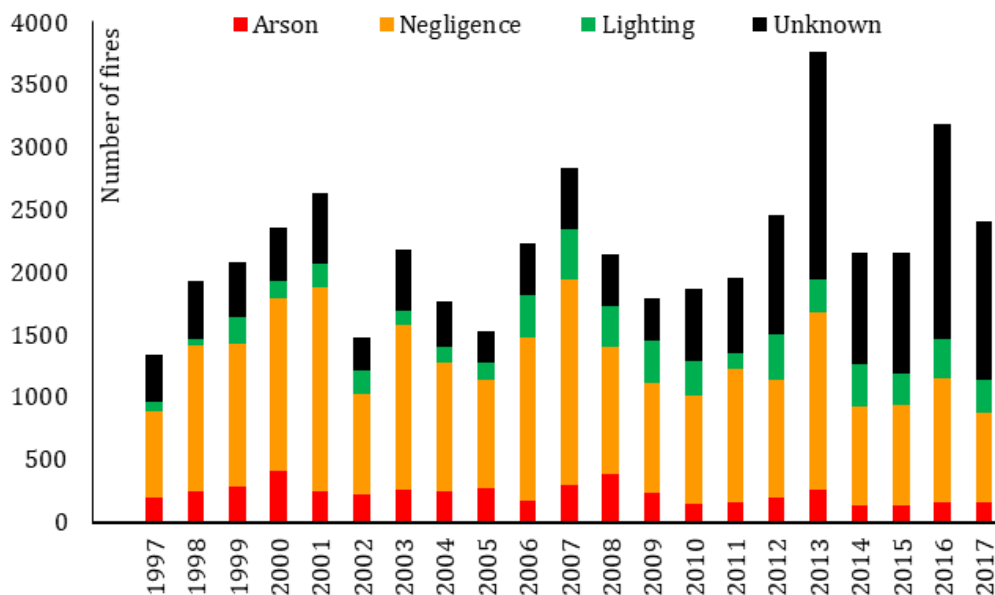


Figure 2. The causes of forest fires in Turkey between years 1997-2017 (GDF, 2019)

Forest lands are managed according to the decisions based on multiple criteria decision making (MCDM) methods. Particularly, decisions taken to prevent, fight and monitor forest fires are the most important ones. The location of fire lookout towers as well as

deployment area and number of first response teams are also decided with MCDM methods alone or MCDM in combination with GIS (Fisher and Keida, 1990; Korkmaz, 2004; Akay and Şakar, 2009; Akay and Şahin, 2019).

The objective of this study was to determine and map the fire risk zones of a forest ecosystem in Bucak Forest Enterprise in Turkey that is vulnerable to fire at the first degree. We are of the opinion that the best method to fight forest fires is to use the experts' knowledge, experience and predictions. In this context, the weights of the criteria for forest risk were determined with Analytic Hierarchy Process (AHP). GIS was also used as a support to determine the fire risk zones in the study area because one of the main goals of GIS is to support spatial decision making process (Simon, 1960). In this way, the spatial analysis of the criteria related to human behaviours, climate, vegetation and topography was conducted in GIS by using the risks computed for the study area with AHP. As a result, the "forest fire risk zones" of the forests in Bucak region were determined and mapped.

Multi-criteria decision making and AHP

Multi-criteria decision analysis is defined as a matrix to choose the best alternative from several potential candidates and in case of conflicting criteria to solve problems, which is called decision matrix. Various MCDM methods have been developed since 1960 for solving decision making problems (Malczewski and Rinner, 2015). What is important at this point is to determine which multiple-criteria decision-making method is the best to solve a certain multiple-criteria decision making problem (Guarini et al., 2018).

AHP is one of the most comprehensive methods of multi-criteria decision analysis, which is a digital approach (Kumar and Garg, 2017). It is a powerful and flexible decision-making theory to rank different features (Belhadi et al., 2017). AHP is a measurement theory based on pairwise comparison. In its comparisons, it uses absolute judgment scale to represent the measurement of a scale for a feature whereas the linguistic judgments related to the assessment of people are usually uncertain in real life and it is not realistic to represent them with exact values (Ishizaka and Nguyen, 2013). This method developed by Saaty (1980) is widely used to solve multiple-criteria decision making problems. It allows modelling in a hierarchical structure that describes the relationship between the main target of the criterion, sub-criteria and alternatives in solving a complex decision making problem. In another word, AHP is a method that synthesizes knowledge, experience, views and feelings of an individual (Kuruüzüm and Altan, 2001).

A priority vector is obtained in the pairwise comparison matrix. The priority vector is the "eigenvector" of the matrix. The decision priorities called as weights attributed to the qualitative features are determined in the form of eigenvector of the pairwise comparison matrix (Jain and Naq, 1996). The "relative importance" of the criteria is determined from the lowest ranking criteria to the highest criteria using the eigenvector. The stages of solving a multi-criteria decision making problem with AHP include the identification of the problem, observation of the system, creation of the hierarchical structure, control of consistency, determination of the priority values and conclusion (Saaty and Vargas, 2012).

GIS-based approach

GIS is a valuable tool that collects, processes and analyses spatial data with its structural and functional components and offers support to the decision-making process

(Chang, 2016). While it is commonly used in disciplines examining spatial data, many users in forestry sector also prefer it. The GIS-based studies regarding the identification of forest fire risk zones showed that the interactive structure of GIS was a powerful source (Jaiswal et al., 2002; Yomralıoğlu, 2015). A formulation was developed to calculate the fire risk index values using vegetation type, proximity to settlements, proximity to roads and gradient variables. The variables were categorized according to their vulnerability to fire and every category was given a specific value (You et al., 2017). To determine the fire risk zones, the factors and sub-factors were determined using AHP, while spatial distribution of the risk categories were produced using GIS computation in proportion to the weights of these factors.

In Turkey, there are studies that have determined fire risk categories based on GIS (Sağlam et al., 2008; Küçük et al., 2017) and combined use of GIS and AHP (Güngöroğlu, 2017; Akbulak et al., 2018). AHP appears to be a method used for determining factors and their weights as regards fire risk. The determination of weights of main factors and sub-factors, determination of risk categories of the sub factors and setting values for those categories are all done by consulting an expert opinion. Besides using multi-criteria decision-making methods when determining these factors, the fire statistics observed for many years are also relevant. It is therefore possible to adapt the information from the relevant literature to the special characteristics of the field.

Materials and Methods

Study area

This study was conducted in Bucak Department of Forestry located in Western Mediterranean Region of Turkey with coordinates of 37°12'08" - 37°34'20" North latitude and 30°14'02" - 30°50'53" East longitude (*Figure 3*). As for the topographic structure of the region; the minimum, maximum and average altitudes are 72 m, 2317 m and 900 m, respectively. Average slope is 26%. In addition to the Mediterranean climate, continental climate can also be observed. In this region, the mean temperature was 15°C, the average maximum temperature was 21°C and the average minimum temperature was 9°C from 1932 to 2018. Summer is arid and warm (maximum temperature 43°C) and winter is cold and rainy (minimum temperature -14°C). The annual mean precipitation is 450 mm whereas it is 15 mm on average in summer. The relative mean humidity in summer is 40% and while the dominant wind direction is south (GDF, 2019; Worldclim, 2019).

The size of the field is 141,057 ha, and 71% is forestland. 38.64% of the forestland is unproductive with crown closure under 10%. In the region's forests, 73013 ha of land consist of coniferous species, while 19621 ha consist of deciduous species. Approximately 72% of the coniferous species consists of *Pinus brutia* Ten. and *Pinus nigra* Arnold which are relatively sensitive to fire.

Bucak Department of Forestry under Isparta Regional Directorate of Forestry is highly sensitive regarding forest fires. From 2008 to 2018 when the forest fires were investigated in the region, the highest number of fires was observed in this region with 0.9×10^{-3} per hectare. According to the same statistics, 85% of the forest fires in the region started during daytime, from 7:00 to 19:00 (IRDF, 2019). Within the fire-fighting organization, there are 4 lookout towers, 5 fire first response teams, 11 water trucks, 1 grader, 1 dozer and 10 fire pools.

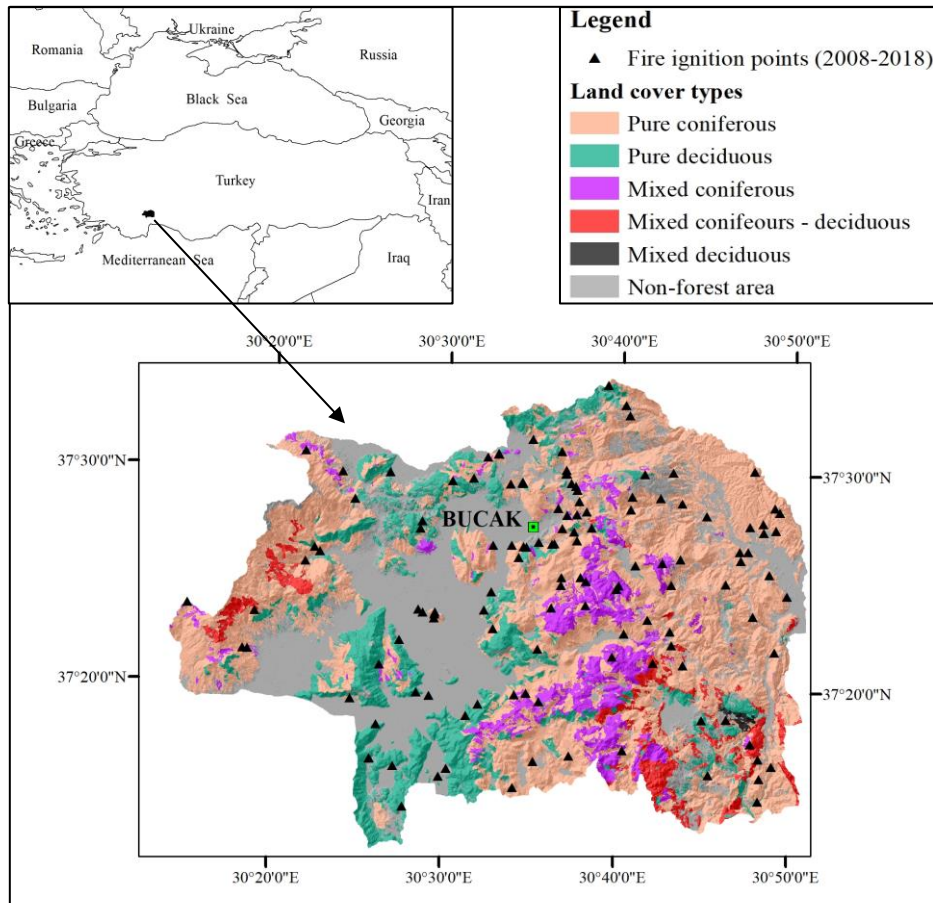


Figure 3. Spatial location of the study area

Dataset

Shuttle Radar Topography Mission (SRTM; version 3) data was used to create digital elevation model of the study field. This data was downloaded from <https://gdex.cr.usgs.gov/gdex/> at a resolution of 1 arc-second (30 meters) from a global dataset (USGS, 2019). Altitude, slope and aspect maps were produced from the digital elevation data. Forest management plan maps for the years 2007 to 2017 of Bucak Forest State Enterprise were geographically categorized in ArcGIS environment into vegetation type, stand development period, crown closure, cultivated areas and settlements. Digital vector data of power lines and roads were provided by GIS department of Isparta Regional Directorate of Forestry. Climate data from 1970 to 2000 was obtained from <http://worldclim.org/>. In this platform where global climate data are presented, raster data with a resolution of approximately 1 km × 1 km was used. ArcGIS (version 10.2.2) software was used for GIS applications.

Methods

Computing the criteria weights using AHP

In the first stage of AHP, the decision problem was structured hierarchically. In the second step of AHP, pairwise comparisons and the option matrix were established. The pairwise comparison is an innate human ability and focuses on the relationship between

pairwise data groups, thereby significantly reducing the complexity of decision-making (Saaty and Saaty, 2019). Pairwise comparison method consists of three steps: a) Forming the pairwise comparison matrix in all steps of the hierarchy, b) Computing the weights for each hierarchy, c) Determining the consistency index.

Hierarchically structuring the decision problem:

- Determining the criteria: Criteria are determined by expert opinion, relevant data sources and experiences of forest fire experts (Criteria and their definitions are shown in *Table 1*).
- The hierarchical structure of the decision problem was created (Saaty and Vargas, 2012).
- For pairwise comparisons to be evaluated by decision-makers to determine the criteria weights, pairwise comparison tables were formed (Saaty and Saaty, 2019).
- In pairwise comparisons, experts perform comparisons using the fundamental scale (Saaty, 1990).

Decisions are made by agreement based on two comparison scales or the geometric mean method can be used in the event of three different scales (Van den Honert and Lootsma, 1996; Bolloju, 2001).

Table 1. Criteria and definitions

Criteria	Sub-criteria	Definition
K ₁ : Human behaviour	K ₁₁ : Proximity to settlements K ₁₂ : Proximity to the road network K ₁₃ : Proximity to the cultivated areas K ₁₄ : Proximity to the power lines	Settlements in and around the forest Roads in and around the forest Cultivated areas in and around the forest Power lines in and around the forest
K ₂ : Structural characteristics of forests	K ₂₁ : Vegetation type K ₂₂ : Age of stand development K ₂₃ : Crown closure	Fire sensitivity of tree species Forest texture which is sensitive to fire Shading rate of forest trees
K ₃ : Topographic structure of forests	K ₃₁ : Altitude K ₃₂ : Slope K ₃₃ : Aspect	Elevations of the forest Forest slope Dominant aspect of forest areas
K ₄ : Climate data	K ₄₁ : Mean temperature of warmest quarter K ₄₂ : Precipitation of warmest quarter K ₄₃ : Mean wind speed of warmest quarter	Mean temperature during fire season Precipitation during fire season Mean wind speed during fire season

After determining the criteria and completing pairwise comparisons, the comparison matrices of criteria and sub criteria are formed. By evaluating the comparison matrices, weights of criteria are computed. Consistency tests were applied to check the reliability of the matrices. In order to check the consistency of the matrix, consistency index and consistency rate are calculated (Saaty, 1980). The consistency index (CI) of the comparison matrix is calculated with the following formulation:

$$CI = \frac{\lambda_{max} - n}{n - 1} \quad (\text{Eq.1})$$

where CI is consistency index, λ_{max} is the largest eigenvalue, n is the number of criteria compare.

The consistency rate (CR) is calculated with the following formulation:

$$CR = \frac{CI}{RI} \quad (\text{Eq.2})$$

where, CI is consistency index, RI is random index which depends on the number of criteria being compared. For example, for $n = 2, 3, 4,$ and 5 , $RI = 0.00, 0.52, 0.89$ and 1.11 , respectively. $CR < 0.10$ indicates a reasonable consistency level for pairwise comparisons. $CR \geq 0.10$, however, indicates that the values in the pairwise comparison matrix should be reviewed and revise (Saaty, 1980).

GIS-based evaluation and mapping

The relevant literature for determining the risk categories of the sub criteria used to identify the fire risk zones was reviewed (Jaiswal et al., 2002; Sağlam et al., 2008; You et al., 2017). Jaiswal et al. (2002) developed a formulation for fire risk index, which is also suitable for the field's conditions. The special conditions of the field require customisation of the variables related to the fire risk values. For example, variables of latitude and vegetation differ considerably. The risk values of vegetation cover were listed by examining the fire sensitivity status of the target stands, which were distributed in the region. After defining the risk values for all stand types in the geographic database, the stands with the same risk values were combined and clustered.

The most fire sensitive tree species in the region were red pine and black pine stands (Neyişçi et al., 1996). The highest risk values were assigned to these stands. The variables of the distance between the road and the power lines and the distance between the settlements and the cultivated areas were determined according to the approach described by You et al. (2017) and values proposed by Şentürk (2018). Additionally, the distribution of 130 fire exit points in the zones which were produced at intervals of 0-25 m, 25-50 m, 50-100 m and 100 m farther from the road, power lines, settlements and cultivated areas were also evaluated. The climate data was calculated according to the approach proposed by You et al. (2017).

Raster layers were prepared and categorized according to the classes in *Table 2*. These raster layers were multiplied by their own criteria weight using the “raster calculator” available at ArcGIS software and fire risk values were achieved. These values were categorized (Jenks and Caspall, 1971) and fire risk zones were mapped.

Results and Discussion

Forming of the comparison matrices of criteria and sub criteria in AHP

The criteria indicated in *Table 1* were evaluated by the experts according to the AHP comparison scale specified in *Table 3* and the comparison scheme in *Table 2*. Comparison matrix of the criteria was formed (*Table 3*).

Similarly, the same steps were applied for the sub criteria and as a result, the comparison matrices of the sub criteria of the K_1, K_2, K_3, K_4 criteria were calculated (*Tables 4-7*).

Evaluation of comparison matrices

To normalize the pairwise comparisons of the criteria,

- All columns are summed up (*Table 3*).
- Each column element in *Table 3* is divided into column sum (*Table 8*).
- Total rows are calculated (*Table 8*).
- Average of row sum (w) is found (*Table 8*).

Table 2. Variables and risk values to be used in the calculation and mapping of fire risk

Structural characteristics of forests							
Criterion	Class			Risk	Value		
Vegetation type	Pinus brutia and P. nigra stands			Very high	1.0		
	Pinus brutia / P. nigra – coniferous mixed stands			High	0.7		
	Other pure coniferous stands			Moderate	0.5		
	Coniferous- deciduous mixed stands			Low	0.3		
	Deciduous stands			Very low	0.1		
Age of stand development	Young forest			Very high	1.0		
	Medium age forest			High	0.7		
	Old-growth forest			Moderate	0.5		
	Mature forest			Low	0.3		
Crown closure	%10-%40			Very high	1.0		
	%40-%70			High	0.7		
	>%70			Moderate	0.5		
	<%10 coniferous –deciduous mixed stands			Low	0.3		
	<%10 deciduous mixed stands			Very low	0.1		
Human behavior				Topographic structure of forests			
Criterion	Class	Risk	Value	Criterion	Class	Risk	Value
Proximity to settlements (meter)	0-25	Very high	1.0	Altitude (meter)	<700	Moderate	0.5
	25-50	High	0.7		700-1000	Very high	1.0
	50-75	Moderate	0.5		1000-1300	High	0.7
	75-100	Low	0.3		1300-1600	Low	0.3
	>100	Very low	0.1		>1600	Very low	0.1
Proximity to the road network (meter)	0-25	Very high	1.0	Slope (%)	1-15	Moderate	0.5
	25-50	High	0.7		15-30	High	1.0
	50-75	Moderate	0.5		30-40	High	0.7
	75-100	Low	0.3		40-50	Low	0.3
	>100	Very low	0.1		>50	Very low	0.1
Proximity to the cultivated areas (meter)	0-25	Very high	1.0	Aspect	Sunny (S,SW)	Very high	1.0
	25-50	High	0.7		Semi sunny (W,SE)	High	0.7
	50-75	Moderate	0.5		Flat	Moderate	0.5
	75-100	Low	0.3		Semi shady (NW,E)	Low	0.3
	>100	Very low	0.1		Shady (N,NE)	Very low	0.1
Proximity to the power lines (meter)	0-25	Very high	1.0				
	25-50	High	0.7				
	50-75	Moderate	0.5				
	75-100	Low	0.3				
	>100	Very low	0.1				
Climate data							
Criterion	Class	Risk	Value	Criterion	Class	Risk	Value
Mean temperature of warmest quarter (°C)	>24	Very high	1.0	Precipitation of warmest quarter (millimeter)	<40	Very high	1.0
	22-24	High	0.7		40-50	High	0.7
	21-22	Moderate	0.5		50-60	Moderate	0.5
	20-21	Low	0.3		60-70	Low	0.3
	>20	Very low	0.1		>70	Very low	0.1
Mean wind speed of warmest quarter (meter second ⁻¹)	>2.1	Very high	1.0				
	2.0-2.1	High	0.7				
	1.95-2.0	Moderate	0.5				
	1.90-1.95	Low	0.3				
	>1.90	Very low	0.1				

Table 3. Comparison matrix of the criteria

	K ₁	K ₂	K ₃	K ₄
K ₁	1	3	5	7
K ₂	0.333	1	3	5
K ₃	0.200	0.333	1	1
K ₄	0.143	0.200	1	1
Total	1.676	4.533	10	14

K₁: Human behaviour, K₂: Structural characteristics of forests, K₃: Topographic structure of forests, K₄: Climate data

Table 4. Comparison matrix of the sub-criteria of K_1

	K_{11}	K_{12}	K_{13}	K_{14}
K_{11}	1	0.2	3	4
K_{12}	5	1	9	7
K_{13}	0.333	0.111	1	2
K_{14}	0.25	0.143	0.5	1

K_{11} : Proximity of settlement, K_{12} : Proximity of road network, K_{13} : Proximity of cultivated areas, K_{14} : Proximity of power lines

Table 5. Comparison matrix of the sub-criteria of K_2

	K_{21}	K_{22}	K_{23}
K_{21}	1	3	5
K_{22}	0.333	1	4
K_{23}	0.2	0.25	1

K_{21} : Vegetation type, K_{22} : Age of stand development, K_{23} : Crown closure

Table 6. Comparison matrix of the sub-criteria of K_3

	K_{31}	K_{32}	K_{33}
K_{31}	1	5	3
K_{32}	0.2	1	0.333
K_{33}	0.333	3	1

K_{31} : Altitude, K_{32} : Slope, K_{33} : Aspect

Table 7. Comparison matrix of the sub-criteria of K_4

	K_{41}	K_{42}	K_{43}
K_{41}	1	3	4
K_{42}	0.333	1	2
K_{43}	0.25	0.5	1

K_{41} : Mean temperature, K_{42} : Precipitation, K_{43} : Mean wind speed

Table 8. Calculation of criterion weights

	K_1	K_2	K_3	K_4	Row total	w
K_1	0.596659	0.661813	0.5	0.5	2.258472	0.564618
K_2	0.198687	0.220604	0.3	0.357143	1.076436	0.269109
K_3	0.119332	0.073461	0.1	0.071429	0.364220	0.091055
K_4	0.085322	0.044121	0.1	0.091055	0.300872	0.075218

w: the matrix's eigenvector

“w” in the last column of *Table 8* is the matrix's eigenvector and gives the weight of the criteria by percentage (%). It is necessary to calculate the consistency of the comparison matrix of the criteria. For a comparison matrix to be consistent, the maximum eigenvalue (λ_{max}) must be equal to the dimensions of the matrix (*Table 9*). Consistency rate greater than 10% shows that some evaluations are contradictory in the comparisons (Partovi and Hopton, 1994).

Table 9. Calculation of the consistency of the comparison matrix of criteria

	K₁	K₂	K₃	K₄	w	v	v/w
K₁	1	3	5	7	0.564618	2.353746	4.168741
K₂	0.333	1	3	5	0.269109	1.106382	4.111278
K₃	0.200	0.333	1	1	0.091055	0.368810	4.050408
K₄	0.143	0.200	1	1	0.075218	0.300835	3.999510

w: the matrix's eigenvector, v: column vector

The previously calculated column vector (eigenvector/priority vector) is obtained by multiplying each row of the comparison criterion. The calculated column vector (v) is divided by the corresponding elements of the column vector (w) to obtain v/w values. The arithmetic mean of the v/w column vector gives the largest eigenvalue ($\lambda_{max} = 4.082484$).

$$\text{Consistency Indicator} = (\lambda_{max} - n) / (n - 1) = (4.082484 - 4) / (4 - 1) = 0.27495$$

$$\text{Consistency Ratio} = \text{Consistency Indicator} / \text{Random index}$$

Random Index for matrices with sizes of 1 to 15, in the table of random index, n = 4 is 0.89 (Saaty, 1990). According to this;

$$\text{Consistency Ratio} = 0.027495 / 0.9 = 0.03055$$

Since the consistency ratio is <0.1, the matrix can be considered consistent. For the other comparison matrices, the same steps were taken, and the criteria weights and consistency of the criteria were calculated and shown in *Table 10*.

Table 10. Consistency ratios and weights of criteria and sub-criteria

CR	Criteria	Weights	CR	Sub-criteria	Local weight	Overall weight
0.03	Human behaviour	0.5646	0.058	Proximity to settlements	0.1993	0.1125
				Proximity to the roads	0.6535	0.3690
				Proximity to the cultivated areas	0.0860	0.0486
				Proximity to the power lines	0.0612	0.0345
	Structural characteristics of forests	0.2691	0.075	Vegetation type	0.6194	0.1667
				Age of stand development	0.2842	0.0765
				Crown closure	0.0964	0.0259
	Topographic structure of forests	0.0911	0.033	Altitude	0.6334	0.0557
				Slope	0.1061	0.0097
				Aspect	0.2605	0.0237
	Climate data	0.0752	0.016	Mean temperature of warmest quarter	0.6233	0.0469
				Precipitation of warmest quarter	0.2394	0.0180
Mean wind speed of warmest quarter				0.1373	0.0103	

CR: consistency ratio

Pairwise comparison method is frequently used to estimate the weights of the criteria in the GIS-based multiple-criteria decision-making applications (Malczewski and Rinner, 2015). This method has been tested and applied in land suitability analyses (Stoms et al., 2002; Hamzeh et al., 2016; Bozdağ et al., 2016), environmental impact assessment studies (Bojórquez-Tapia et al., 2002; Rikhtegar et al., 2014) and natural resource management (Hessburg et al., 2013).

In this study, it was concluded that the contribution of human behaviour to fire risk was over 50% (Table 10). In a study conducted by You et al. (2017), the weight of human activities used to calculate fire risk was found to be the first one among other factors. It is also known that proximity to the road increases the risk of fire. Şentürk (2018) examined the relationship between the locations of forest fire starting points and the roads in Istanbul and found that 427 (~ 65%) of the 660 fire starting points were located at 0-100 meters from the road. Although climate seems to have a primary effect, it is proposed that it is important to know the proximity of forests to roads and settlements (Sağlam et al., 2008; Wu et al., 2014).

The mapping of fire risk zones

All geographic layers of the sub criteria in the GIS database were recorded as raster data, and the risk classifications shown in Table 2 were identified. Thus, the spatial distribution of the risk zones belonging to 13 sub criteria was mapped (Figure 4). The criteria and weights determined by AHP were formulated with the help of ArcGIS software's spatial analysis tool and applied to the related geographical layers. The resulting fire risk map was created by using ArcGIS and is presented in Figure 5.

When the spatial distribution of fire risk zones is examined, it is understood that only 0.49% of forest lands in the field was ranked as very high risk (Table 11). Given that the ratio of the areas with medium and high fire risk is close to 60% in total, it is possible to suggest that the fire risk of forestlands in the region is relatively high.

The risk assessment conducted for the study area can possibly be used for the Mediterranean forest ecosystems that have similar forest cover, climate and topographic features. However, it should also be remembered that risk value may change as climate and forest cover change (Jaiswal et al., 2002; Sağlam et al., 2008; Neyişçi, 2009; Küçük et al., 2017). Moreover, we suggest that risk assessment can be performed and risk zones can be mapped for any forest ecosystem if the approach and methodology developed in this study are applied.

In terms of forest fire risks, coniferous species that account for about 80% of the forests in the field are at higher risk than broad-leaved species. However, it should not be overlooked that broad-leaved forests are also susceptible to fire in the dry season (Kodandapani et al., 2009).

In this study, human behaviour was found to have the highest weight for fire risk. The importance of human behaviours for fire risk has been reported by several studies (Vadrevu et al., 2009; Eskandari and Chuvieco, 2015; Eskandari, 2017). Proximity to forest roads, which is one of the sub-criteria of human behaviours has the highest weight in terms of fire risk (You et al., 2017; Şentürk, 2018). Other researchers also confirmed that vegetation composition (Sağlam et al., 2008; Chuvieco et al., 2012; You et al., 2017), topographic structure (Vadrevu et al., 2009; Çoban and Özdamar, 2014; Eskandari, 2017) and climate (Zumbrunnen et al., 2011; Eskandari, 2017) were important criteria for fire risk.

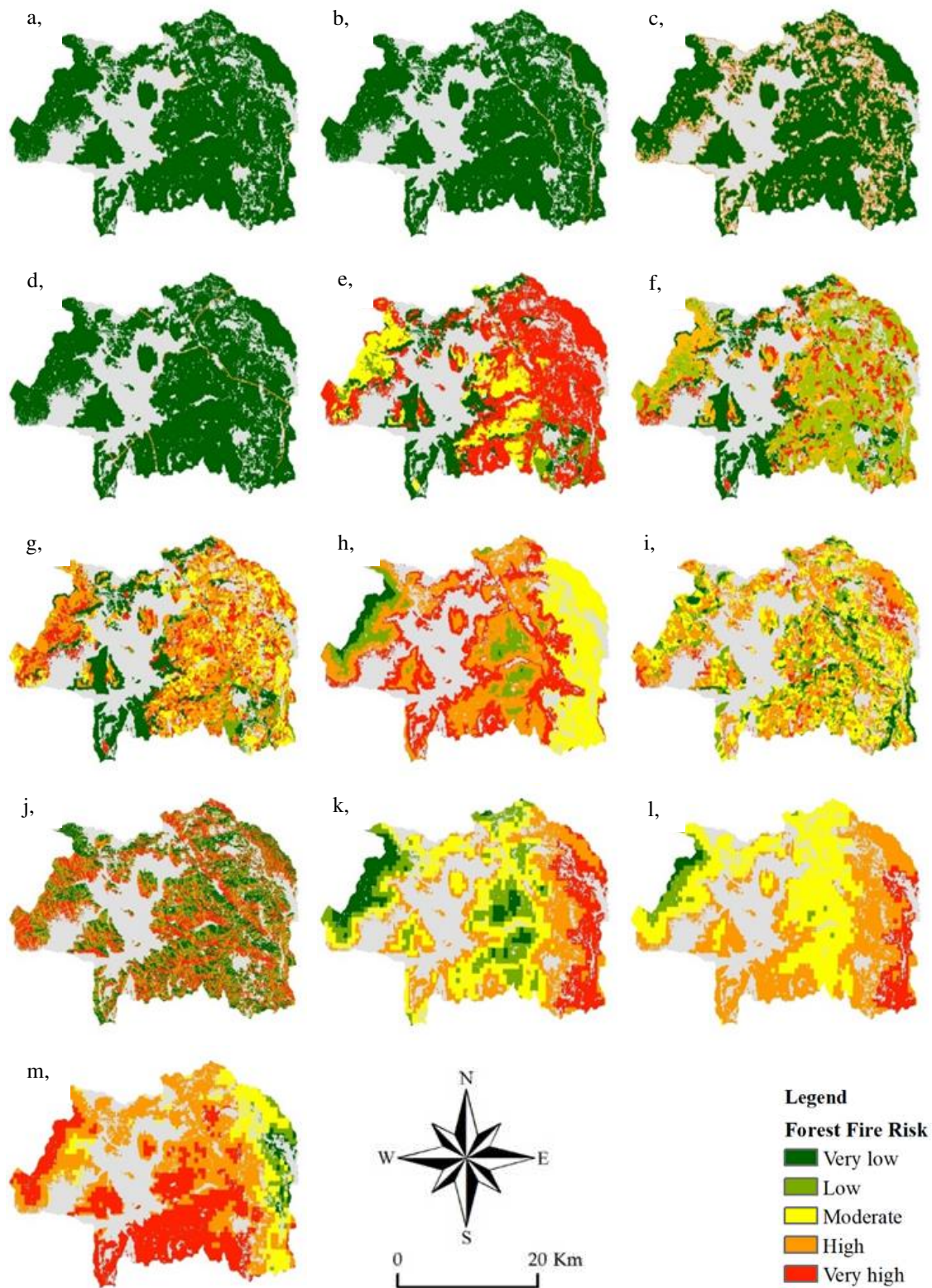


Figure 4. Fire risk zones of the sub-criteria, a) Proximity to settlements, b) Proximity to the road network, c) Proximity to the cultivated areas, d) Proximity to the power lines, e) Vegetation type, f) Age of stand development, g) Crown closure, h) Altitude, i) Slope, j) Aspect, k) Mean temperature of the warmest quarter, l) Precipitation of the warmest quarter, m) Mean wind speed of the warmest quarter

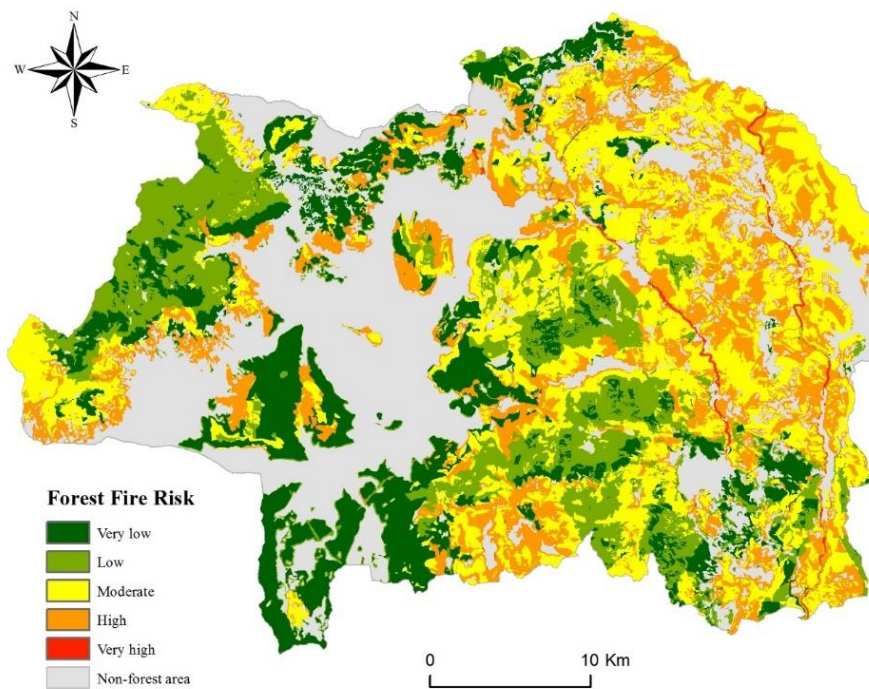


Figure 5. Spatial distribution of fire risk zones

Table 11. Spatial distribution of forest fire risk

Vegetation type	Forest Fire Risk										
	Very high		High		Moderate		Low		Very low		Total (ha)
	ha	%	ha	%	ha	%	ha	%	ha	%	
Calabrian and black pine	431.10	0.82	24107.93	46.10	27242.04	52.10	192.13	0.37	317.93	0.61	52291.13
Coniferous	17.09	0.08	418.80	2.02	4082.92	19.70	15186.35	73.29	1016.87	4.91	20722.03
Mixed coniferous-deciduous	1.73	0.03	16.14	0.31	48.80	0.95	3059.65	59.39	2025.74	39.32	5152.06
Deciduous	3.68	0.02	49.02	0.25	78.30	0.40	1949.93	9.92	17575.70	89.41	19656.62
Shrub grassland	31.27	2.09	107.14	7.17	903.40	60.48	421.62	28.23	30.32	2.03	1493.77
Other lands in forest area	8.57	0.79	80.18	7.39	45.22	4.17	37.08	3.42	914.31	84.24	1085.36
Total (ha)	493.44		24779.21		32400.68		20846.76		21880.88		100400.97

Conclusion

The nature has the power to find ways to compensate the damage caused by horrible catastrophes. Mediterranean forest ecosystems also have the power to cope with fire. Despite that, measures should be taken to fight forest fires as they threaten human life and lead to devastating economic loses, which may in turn lead to extremely dangerous consequence. In addition to several natural variables such as climate, topography, bedrock, vegetation cover, human factor also is also a dominant and adverse factors as regards forest fire. Therefore, it is ideal to manage so many processes from setting forestry

policies to fight forest fires to planning land use, preserving the structural features of the natural forests, establishing forests suitable for the relevant degraded area and under extreme conditions, ensuring social and cultural development and in this way raising environmental awareness. One of the crucial elements of fight against forest fire is to create fire risk maps. In this way, fire risk zones may provide decision support in planning the fire-fighting organization. Areas at higher fire risk and thus areas where fire may potentially spread and grow can be determined and necessary measures can be taken.

In this study, the fire risk zones of first-degree fire sensitive Mediterranean forest ecosystems in Bucak were identified and mapped. In the total forestland in the study area, 0.5% of the forests were at a very high fire risk, 25% were at high risk, while 32% were at medium risk. This shows that around 60% of the forestlands are at medium and high forest fire risk. Accordingly, we can say that it is important that forest authority should take measures to prevent forest fires during fire season in this region and raise awareness of people through media and other means of communication. In addition, forest fire reports should contain accurate and detailed information about fire ignition point location and records of all events from the beginning to the end of the fire. We recommend that fire risk maps should be compared with the real fire records and fire risk assessment should be keep up to date.

REFERENCES

- [1] Akay, A. E., Şakar, D. (2009): Using GIS-based decision support system to determine the optimum route to the fire site as soon as possible (in Turkish). – Chamber of Survey and Cadastre Engineers GIS Congress, 02-06, November, İzmir.
- [2] Akay, E. E., Şahin, H. (2019): Forest Fire Risk Mapping by using GIS Techniques and AHP Method: A Case Study in Bodrum (Turkey). – *European Journal of Forest Engineering* 5(1): 25-35.
- [3] Akbulak, C., Tatlı, H., Aygün, G., Sağlam, B. (2018): Forest fire risk analysis via integration of GIS, RS and AHP: The Case of Çanakkale, Turkey. – *International Journal of Human Sciences* 15(4): 2127-2143.
- [4] Belhadi, A., Touriki, F. E., El fezazi, S. (2017): Prioritizing the solutions of lean implementation SMEs to overcome its barriers: an intergrated fuzzy, AHP-TOPSIS approach. – *Journal of Manufacturing Technology Management* 28(8): 1115-1139.
- [5] Bojórquez-Tapia, L. A., Juarez, L., Cruz-Bello, G. (2002): Integrating fuzzy logic, optimization, and GIS for ecological impact assessments. – *Environmental Management* 30(3): 418-433.
- [6] Bolloju, N. (2001): Aggregation of analytic hierarchy process models based on similarities in decision makers' preferences. – *European Journal of Operational Research* 128: 499-508.
- [7] Bozdağ, A., Yavuz, F., Günay, A. S. (2016): AHP and GIS based land suitability analysis for Cihanbeyli (Turkey) County. – *Environ Earth Sciences* 75(813): 1-15.
- [8] Calvo, L., Santalla, S., Valbuena, L., Marcos, E., Tarrega, R., Luis-Calabuig, E. (2008): Post-fire natural regeneration of a *Pinus pinaster* forest in NW Spain. – *Plant Ecology* 197: 81-90.
- [9] Chang, K. T. (2016): *Introduction to geographic information systems* (eight edition). – McGraw-Hill Education, New York, pp. 10-85.
- [10] Chuvieco, E., Aguado, I., Jurdao, S., Pettinari, M. L., Yebra, M., Salas, J., Hantson, S., de la Riva, J., Ibarra, P., Rodrigues, M., Echeverria, M., Azqueta, D., Roman, M. V., Bastarrika, A., Martinez, S., Recondo, C., Zapico, E., Martinez-Vega, F. J. (2012):

- Integrating geospatial information into firerisk assessment. – *International Journal of Wildland Fire* 23: 606-619.
- [11] Çoban, H. O., Özdamar, S. (2014): Mapping forest fire in relation to land-cover and topographic characteristics. – *Journal of Environmental Biology* 35(1): 217-224.
- [12] EC (2017): Forest Fires in Europe 2017. – European Commission, Joint Research Centre (JRC) Technical Reports, Forest Fires in Europe, Middle East and North Africa 2017, 10. EUR 29318 EN.
- [13] Eskandari, S., Chuvieco, E. (2015): Fire danger assessment in Iran based on geospatial information. – *International Journal of Applied Earth Observation and Geoinformation* 42: 57-64.
- [14] Eskandari, S. (2017): A new approach for forest fire risk modeling using fuzzy AHP and GIS in Hyrcanian forests of Iran. – *Arabian Journal of Geosciences* 10(190): 1-13.
- [15] Fisher, M. L., Keida, P. (1990): Optimal solution of set covering/partitioning problems using dual heuristics. – *Management Science* 36(6): 674-688.
- [16] Garbolino, E., Sanseverino-Godfrin, V., Hinojos-Mendoza, G. (2017): Reprint of: Describing and predicting of the vegetation development of Corsica due to expected climate change and its impact on forest fire risk evolution. – *Safety Science* 97: 81-87.
- [17] García-Llamas, P., Suárez-Seoane, S., Taboada, A., Fernández-Manso, A., Quintano, C., Fernández-García, V., Fernández-Guisuruga, J. M., Marcos, E., Calvo, L. (2019): Environmental drivers of fire severity in extreme fire events that affect Mediterranean pine forest ecosystems. – *Forest Ecology and Management* 433: 24-32.
- [18] GDF (2019): Forestry statistics. – Publications of General Directorate of Forestry. <https://www.ogm.gov.tr/ekutuphane/Istatistikler/Forms/AllItems.aspx>. (accessed 09.06.2019). (in Turkish).
- [19] González-De Vega, S., De las Heras, J., Moya, D. (2016): Resilience of Mediterranean terrestrial ecosystems and fire severity in semiarid areas: Responses of Aleppo pine forests in the short, mid and long term. – *Science of the Total Environment* 573: 1171-1177.
- [20] Guarini, M. R., Battisti, F., Chiovitti, A. A. (2018): Methodology for the Selection of Multi-Criteria Decision Analysis Methods in Real Estate and Land Management Processes. – *Sustainability* 10(507): 1-28.
- [21] Güngöroğlu, C. (2017): Determination of forest fire risk with fuzzy analytic hierarchy process and its mapping with the application of GIS: The case of Turkey/Çakırlar. – *Human and Ecological Risk Assessment: An International Journal* 23(2): 388-406.
- [22] Hamzeh, S., Mokarram, M., Haratian, A., Bartholomeus, H., Ligtenberg, A., Bregt, A. K. (2016): Feature Selection as a Time and Cost-Saving Approach for Land Suitability Classification (Case Study of Shavur Plain, Iran). – *Agriculture* 6(52): 1-13.
- [23] Hessburg, P. F., Reynolds, K. M., Salter, R. B., Dickinson, J. D., Gaines, W. L., Harrod, R. J. (2013): Landscape evaluation for restoration planning on the Okanogan-Wenatchee National Forest USA. – *Sustainability* 5: 805-840.
- [24] IRDF (2019): Forest fire statistics (unpublished fire inventory forms, 2008-2018). – Isparta Regional Directorate of Forestry, Isparta, Turkey.
- [25] Ishizaka, A., Nguyen, N. H. (2013): Calibrated Fuzzy AHP for current bank account selection. – *Expert Systems with Applications* 40(9): 3375-3783.
- [26] Jain, B. A., Nag, B. N. (1996): A Decision-Support Model For Investment Decisions in New Ventures. – *European Journal of Operational Research* 90(3): 473-486.
- [27] Jaiswal, R. K., Mukherjee, S., Raju, D. K., Saxena, R. (2002): Forest fire risk zone mapping from satellite imagery and GIS. – *International Journal of Applied Earth Observation and Geoinformation* 4: 1-10.
- [28] Jenks, G. F., Caspall, F. C. (1971): Error on choroplethic maps: definition, measurement, reduction. – *Annals of the Association of American Geographers* 61(2): 217-244.
- [29] Kodandapani, N., Cochrane, M. A., Sukumar, R. (2009): Forest fire regimes and their ecological effects in seasonally dry tropical ecosystems in the Western Ghats, India. – In:

- Cochrane, M. A. (ed.) Tropical Fire Ecology: Climate change, Land use and Ecosystem Dynamics. Springer Praxis Books, 335-354.
- [30] Korkmaz, M. (2004): Determination of optimum fire observation points using cluster covering model. – Süleyman Demirel University, Journal of Forestry Faculty A(1): 37-49. (in Turkish).
- [31] Kumar, D., Gark, C. P. (2017): Evaluating Sustainable Supply Chain Indicators Using Fuzzy AHP Case of Indian Automotive Industry. – Benchmarking: An International Journal 24(6): 1742-1766.
- [32] Kuruüzüm, A., Atsan, N. (2001): Analytical Hierarchy Method and Applications in Business. – Akdeniz İ.İ.B.F. Journal 1: 83-105. (in Turkish).
- [33] Küçük, Ö., Topaloğlu, Ö., Altunel, A. O., Çetin, M. (2017): Visibility analysis of fire lookout towers in the Boyabat State Forest Enterprise in Turkey. – Environmental Monitoring and Assessment 189(329): 2-18.
- [34] Malczewski, J., Rinner, C. (2015): Multicriteria Decision Analysis in Geographic Information Science. – Springer-Verlag Berlin Heidelberg. pp. 23-50.
- [35] McKenzie, D., Shankar, U., Keane, R. E., Stavros, E. N., Heilman, W. E., Fox, D. G., Riebau, A. C. (2014): Smoke consequences of new wildfire regimes driven by climate change. – Earth's Future 2: 35-59.
- [36] Naderpour, M., Rizeei, H. M., Khakzad, N., Pradhan, B. (2019): Forest fire induced Natech risk assessment: A survey of geospatial technologies. – Reliability Engineering and System Safety 191: 106558.
- [37] Neyişçi, T., Ayaşlıgil, Y., Ayaşlıgil, T., Sönmezşık, S. (1996): Principles of afforestation for fire resistant forests. – Project report, The Scientific and Technological Research Council of Turkey, Project number: TOGTAG-1342, Antalya. (in Turkish).
- [38] Neyişçi, T. (2009): Flammable management as a means of forest fire management. – 1st Forest Fire Fighting Symposium, 07-10 January, Antalya, pp. 249-255. (in Turkish).
- [39] Partovi, F. Y., Hopton, W. E. (1994): The analytic hierarchy process as applied to two types of inventory problems. – Productions and Inventory Management Journal 35(1): 13-19.
- [40] Pausas, J. G., Vallejo, V. R. (1999): The role of fire in European Mediterranean ecosystems. – In: Chuvieco, E. (ed.) Remote Sensing of large wildfires in the European Mediterranean basin. Berlin, Springer-Verlag, pp. 3-16.
- [41] Rikhtegar, N., Mansouri, N., Oroumieh, A. A., Yazdani-Chamzini, A., Zavadskas, E. K., Kildienė, S. (2014): Environmental impact assessment based on group decision-making methods in mining projects. – Economic Research-Ekonomska Istraživanja 27(1): 378-392.
- [42] Saaty, T. L. (1980): The Analytic Hierarchy Process. – McGraw-Hill, New York, pp. 50-70.
- [43] Saaty, T. L. (1990): How to make a decision: The Analytic Hierarchy Process. – European Journal of Operation Research 48: 9-26.
- [44] Saaty, T. L., Vargas, L. G. (2012): Models, Methods, Concepts & Applications of the Analytic Hierarchy Process. – 2nd Edition, Springer Science+Business Media New York, pp. 63-70.
- [45] Saaty, R. W., Saaty, T. L. (2019): Decision Making in Complex Environments. – Available online: https://superdecisions.com/sd_resources/v28_man02.pdf (Accessed 29.08.2019).
- [46] Sağlam, B., Bilgili, E., Durmaz, B. D., Kadioğulları, A., Küçük, Ö. (2008): Spatio-Temporal analysis of forest fire risk and danger using LANDSAT imagery. – Sensors 8: 3970-3987.
- [47] Simon, H. A. (1960): The New Science of Management Decisions. – New York: Harper and Row, pp. 3-21.
- [48] Stoms, D. M., McDonald, J. M., Davis, F. W. (2002): Fuzzy assessment of land suitability for scientific research reserves. – Environmental Management 29(4): 545-558.
- [49] Şentürk, N. (2018): Assessment of relationship between locations and distances to roadside of forest fires in Istanbul, Turkey. – Applied Ecology and Environmental Research 16(5): 6195-6204.

- [50] USGS (2019): NASA SRTM Version 3.0 “1 Arc second” data. – United States Geological Survey, 2017, <https://gdex.cr.usgs.gov/gdex/> (accessed 07.06.2019).
- [51] Vadrevu, K. P., Eaturu, A., Badarinath, K. V. S. (2010): Fire risk evaluation using multicriteria analysis-a case study. *Environment Monitoring and Assessment* 166: 223-239.
- [52] Van den Honert, R. C., Lootsma, F. A. (1996): Group preference aggregation in the multiplicative AHP - the model of the group decision process and Pareto optimality. – *European Journal of Operational Research* 96: 363-370.
- [53] Worldclim (2019): Global Climate Data, Version 2 (Free climate data for ecological modeling and GIS). – <http://worldclim.org/version2> (accessed 07.06.2019).
- [54] Wu, Z., He, H. S., Yang, J., Liu, Z., Liang, Y. (2014): Relative effects of climatic and local factors on fire occurrence in boreal forest landscapes of northeastern China. – *Science of The Total Environment* 493: 472-480.
- [55] Yomralioğlu, T. (2015): *Geographic Information Systems*. – 6th Edition, Akademi Press, Trabzon, Turkey, pp. 45-61. (in Turkish).
- [56] You, W., Lin, L., Wu, L., Ji, Z., Yu, J., Zhu, J., Fan, Y., He, D. (2017): Geographical information system-based forest fire risk assessment integrating national forest inventory data and analysis of its spatiotemporal variability. – *Ecological Indicators* 77: 176-184.
- [57] Zumbrunnen, T., Pezzatti, G. B., Menéndez, P., Bugmann, H., Bürgi, M., Conedera, M. (2011): Weather and human impacts on forest fires: 100 years of fire history in two climatic regions of Switzerland. – *Forest Ecology and Management* 261: 2188-2199.

INFLUENCE OF NITROGEN FERTILIZER AND STRAW RETURNING ON CH₄ EMISSION FROM A PADDY FIELD IN CHAO LAKE BASIN, CHINA

SHAKOOR, A.^{1,2} – GAN, M. Q.¹ – YIN, H. X.¹ – YANG, W.¹ – HE, F.¹ – ZUO, H. F.¹ – MA, Y. H.^{1*} – YANG, S. Y.^{1*}

¹*School of Resources and Environment, Anhui Agricultural University, Hefei 230036, China*

²*Department of Environment and Soil Sciences, University of Lleida, Avinguda Alcalde Rovira Roure 191, 25198 Lleida, Spain*

**Corresponding authors*

e-mail: yhma@ahau.edu.cn; yangshy@ahau.edu.cn

(Received 3rd Oct 2019; accepted 8th Jan 2020)

Abstract. In the rice paddy ecosystem, application of nitrogen fertilizer and straw to soil methanogenic bacteria provides abundant methanogenic substrates, which significantly influences methane (CH₄) emission from paddy fields. The effects of nitrogen fertilizer and straw returning on CH₄ emissions in rice paddy fields were studied during a two year of the field experiment in Chao lake basin, China. The experiment consisted of 4 treatments: Control (CK), Traditional fertilizer (CT), Optimized fertilizer (CO) and CO with straw-return (CO + SR). The cumulative effects of straw-returning practices on greenhouse gas emission in a rice-wheat rotation system were determined, along with an estimation of CH₄ in a rice growing season. According to our results, The CH₄ emission fluxes from paddy field showed three different peak trends; Compared to CK, CT, CO, and CO + SR increased seasonal CH₄ emission by 36.6%, 45.8% and 42.0% in 2013 and by 42.0%, 48.5% and 80.1% in 2014, respectively. Anaerobic decomposition of wheat straw accelerates the decline of soil redox potential (Eh) after flooding, thereby providing suitable environmental conditions for the growth of methanogens and promoting CH₄ production in the subsequent rice season. The CH₄ emission fluxes of CK, CT, CO, and CO + SR were significantly correlated with soil temperatures at 5 cm depth. Therefore, our findings show that application rates of nitrogen fertilizer and straw returning to a paddy field could significantly affect the CH₄ emissions in China.

Keywords: CH₄ flux, rice paddy, chemical fertilizer, straw application, nitrogen use efficiency

Introduction

Since the industrial revolution, concentrations of atmospheric carbon dioxide (CO₂), methane (CH₄) and nitrous oxide (N₂O) have been increasing year after year; thus, global climate change caused by greenhouse gas emissions has become a common concern in the international community (Lubbers et al., 2013; Hussain et al., 2015; Xuejun and Fusuo, 2011; Shakoor et al., 2018). CH₄ is the smallest hydrocarbon and is a potent greenhouse gas (IPCC, 2013). It is mainly produced through the decomposition of organic waste and is also one of the main causes of global warming (Zhang et al., 2015b). Although its atmospheric concentration is much lower than that of CO₂, the rate of its emission is increasing at a much higher rate. The greenhouse effect of CH₄ is 27 times larger than that of CO₂, and its current contribution to the rate of global warming is about 15% (Liu et al., 2015; Hofmann et al., 2016).

The main sources of CH₄ in the atmosphere are natural wetlands, paddy fields, termites, ruminants, fossil fuel production processes, waste disposal and shallow water lakes (Karakurt et al., 2011; Musenze et al., 2014). It is estimated that 40 to 52% of

yearly CH₄ emissions are from soil, and farmlands are an important source of greenhouse gas emissions from soil ecosystems (Montzka et al., 2011; Linnquist et al., 2012). Paddy fields are the main source of farmland soil CH₄ emissions. Globally, the total yearly amount of CH₄ emissions from paddy fields is between 35 and 150 Tg, which accounts for about 12% of global CH₄ emissions (Le Mer and Roger, 2001; Hofmann et al., 2016). Rice is one of the most important cereal crops in China, and its planting area accounts for 17.8% of the world total. CH₄ emitted from paddy fields accounts for 17.9% of the total CH₄ emissions in China, and is the second largest source after livestock farming (Yan et al., 2009; Hoben et al., 2011). Therefore, the studies on CH₄ emission characteristics are of great significance for the reduction of CH₄ emissions from paddy fields.

There are many factors affecting CH₄ emissions from farmland, which can be summarized into three categories: climatic factors such as temperature, precipitation, solar radiation intensity, and atmospheric CO₂ concentration (Walter et al., 2001); soil factors, such as soil organic matter and oxide content, texture, pH value (Wagner et al., 2005); Human factors include water management, application of organic manure and fertilizer amounts, types and dosage (Zou et al., 2005; Mohanty et al., 2017). Straw-return is one of the most important measures for improvement of farmland ecological environment. It improves soil structure, increases soil organic matter content and promotes a virtuous circle of ecosystem health (Lou et al., 2011; Nyamadzawo et al., 2015; Wang et al., 2017). In the rice paddy ecosystem, the use of straw provides a rich substrate for soil methanogenic bacteria, which significantly promotes CH₄ emissions from rice paddies (Ma et al., 2009; Qin et al., 2016; Koga and Tajima, 2011). The choice of straw type (Wassmann et al., 2000), adjustment of the application pattern (Zhu et al., 2014) and application time (Zhang et al., 2015a) maintain soil fertility while reducing CH₄ emissions to a certain extent. Bao et al. (2016) demonstrate that addition of nitrate influences transcriptional and functionally active methanogens, and can alleviate CH₄ production associated with a straw amendment in paddy soil incubations; this could occur through competition for common substrates between nitrate-utilizing organisms and methanogens (Shakoor et al., 2016). Hu et al. (2016) indicated that returning wheat straw prior to rice transplantation significantly increased seasonal CH₄ emissions during both the rice seasons and wheat seasons, compared to no straw-return. At the same time, annual CH₄ emissions were lower under ditch-buried wheat straw-return than that under wheat straw returned with rotary tillage and plowing. Zhang et al. (2015c) determined that compared with straw removal, straw-return significantly increased annual CH₄ emissions by 35.0%, annual GWP by 32.0%, and annual GHGI by 31.1%.

As a typical traditional agricultural region of China, the Chao Lake Basin has problems with excessive fertilizer application, low fertilizer utilization rates, and serious agricultural non-point source pollution. Beyond that, Chaohu's agriculture had not implemented continuous straw-return before 2013. Therefore, there are no systematic studies on the effect of straw-return on production, oxidation, and emission of CH₄ in the subsequent rice cropping season. To define the contribution of straw-return and fertilization practices on CH₄ emissions, this experiment was designed to test plots with and without the application of wheat straw. The CH₄ emission flux was observed in situ throughout the following rice season; the CH₄ production potential and soil oxidation potential of paddy soils were studied to explore the effect of wheat straw application on CH₄ production, oxidation, and emission during the subsequent rice season.

Materials and methods

Experimental site

The field experiments were performed on the rice crop from a rice-wheat rotation system at the Chaochu Experiment Station of Anhui Agriculture University, Hefei, China between June 2013 and October 2014 (117° 40' E, 31° 39' N, altitude 17 m). The research site is situated in the north subtropical humid monsoon climate zone and it is within the Chao lake water regulation zone, which makes it suitable for the growth of crops (*Fig. 1*).

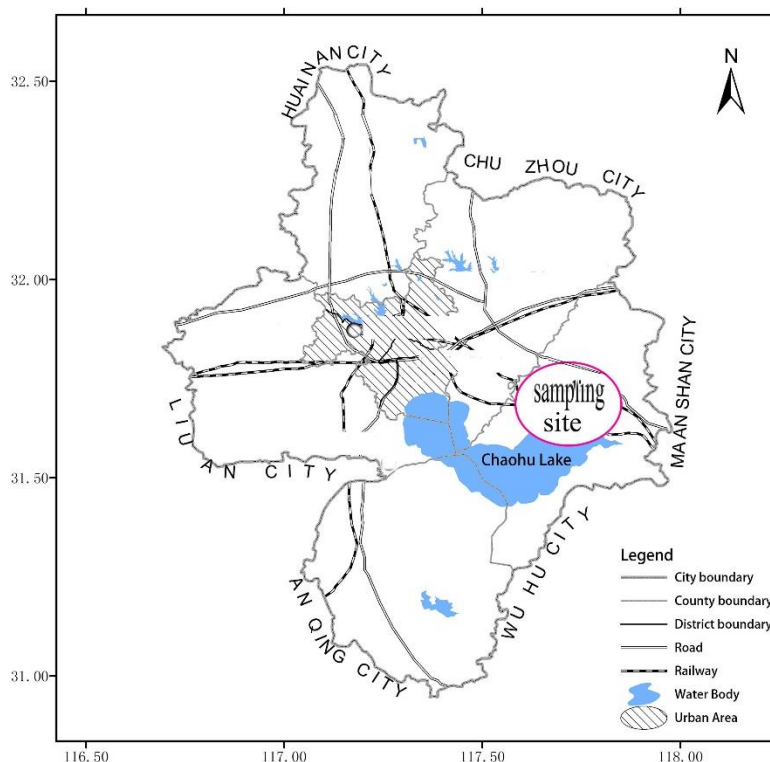


Figure 1. Localization of the study area in Chaochu, China. (ArcGIS, ArcMap 10.2 version; <http://www.esri.com/arcgis/about-arcgis>; <http://desktop.arcgis.com/en/arcmap/>)

The subtropical monsoon climate prevailed in the area with mean annual temperature and precipitation of 16.8 °C and 1358.3 mm, respectively. From 1986 to 2005, the mean seasonal temperature was 16.29 °C, which was similar to our findings (Shi et al., 2008). The soil type at the monitoring site is clay loamy soil with maximum water holding capacity. The specific physical and chemical properties of soil (0-10 cm) were: pH (H₂O) 6.18; Organic matter 23.64 g kg⁻¹; Total nitrogen 1.30 g kg⁻¹; clay content (particle size < 0.01 mm) 490 g kg⁻¹, respectively.

Treatment design and field management

The two phases of experiments included effects of different fertilization techniques and tillage patterns. The experiment consisted of 4 treatments, and each treatment was repeated 3 times; each experimental plot was 30 m², and the field was randomly sectorized. Four treatments were adopted as follows:

1. Control treatment (CK): no fertilization during the rice season.
2. Traditional treatment (CT): traditional fertilization during the rice season.
3. Optimized fertilization (CO): fertilization optimized for maximum local economic output.
4. Optimized fertilization with straw-return (CO + SR): all straw produced in the wheat season is returned to the field and an additional 2 kg of the decomposing agent is applied per acre in conjunction with a 20% reduction in application of the optimized fertilizer amount.

Fertilizer application methods were application after sowing, rice base fertilizer application after seedling transplantation, and two top-dressing applications during the tillering and heading stages. The total amount of applied fertilizer and the amount of applied nitrogen for each stage are shown in *Table 1*.

Table 1. Fertilization scheme of 2013 and 2014 rice season. (kg/hm²)

Rice season	Treatments	Total amount of the fertilizer			Base fertilizer			Tillering fertilizer	Panicle fertilizer	
		N	P ₂ O ₅	K ₂ O	N	P ₂ O ₅	K ₂ O	N	N	K ₂ O
	CK	0	0	0	0	0	0	0	0	0
	CT	180	67.5	67.5	67.5	67.5	67.5	67.5	45	0
	CO	225	67.5	120	90	67.5	84	90	45	36
	CO + SR	180	54	96	72	54	67.2	72	36	28.8

Management of all the fields was maintained at the same times, and in accordance with local routine management practices. During the rice growing period, irrigation was needed between 4 and 5 times. Fields were irrigated to a depth of 6-7 cm, 1 to 2 days prior to fertilizer application and at the end of the land sunning period. The amount of irrigation water was 822.7 mm. The rice crop was planted in May and harvested in early October. Rice plants were transplanted to the main field at a density of 20 hills per m² on May 25/26 and harvested on October 10/11 for the entire experimental period. The rice paddy field was regularly weeded to ensure the healthy growth of rice under normal conditions. Data was gathered for the individual cropping periods, which were June 13th, 2013 – September 27th, 2013 and June 21st, 2014 – October 10th, 2014, respectively (*Table 2*).

Table 2. Fertilization scheme for the 2013 and 2014 rice seasons. (kg/hm²)

Management practice	2013	2014
Field management		
Transplanting	Jun 13	Jun 20
Basal fertilizer	Jun 12	Jun 21
Tilling fertilizer	Jun 28	Jul 8
Panicle initiation fertilizer	Jul 27	Aug 5
Harvest	Sept 27	Oct 10

Gas sampling and measurements

A static closed chamber was constructed with polyester material, and was used to measure the CH₄ fluxes (Chadwicka, 2014; Roche et al., 2016) and the sample box was

made of 5 mm thick transparent organic glass. The sampling box was divided into upper and lower layers. In 2013, the box height was 1.2 m, and the dimensions of each layer were 0.5 m × 0.5 m × 0.6 m with an area of 0.25 m². In 2014, the height of the box is 1.0 m, and the dimensions of each layer were 0.5 m × 0.5 m × 0.5 m with an area of 0.25 m² (0.5 m × 0.5 m). A single-layer static box was used during the early growth stage, and a two-layer static box was used later when plants were higher than 0.6 m. The chamber was equipped with a thermometer on the top to measure the internal temperature. When taking samples, the chamber was placed into the base of the tank above. CH₄ gas samples were taken between 8:00 am and 11:00 am from the paddy fields, and 60 mL of the gas sample was extracted with a syringe 0, 10, 20, and 30-min interval after closing the chamber, respectively. At the same time, air temperature surface soil temperature and soil Eh at depths of 0, 5 and 10 cm were also measured. Daily precipitation and temperature were monitored with an automatic meteorological station approximately 500 m from the experimental plots.

Gas samples were collected from the first day of rice cultivation, and once every seven days thereafter. Samples were collected more frequently during the fertilization and land sunning periods. In the rice season, the conventional sampling frequency was every 3 to 5 days, but sampling was occasionally delayed in the event of precipitation. From 1 to 9 days after fertilization, data were collected every two days. In addition, sample analysis frequency increased during the land sunning period.

Data processing and statistical analysis

The samples were analyzed within 24 h. Gas chromatography (GC) was performed on a 450-GC system (Bruker Daltonics Inc., U.S.A.). CH₄ was detected by a flame ionization detector, and the emission flux was calculated using the following formula: $F = \rho \times V / A \times dc / dt \times 273 / T$, where F is the emission flux in units of mg.m⁻².h⁻¹ for CH₄, ρ is the density of CH₄ under standard conditions (0.714 kg.m⁻³ for CH₄), V is the effective volume of the sampling chamber (m³), A is the area covered by the sampling chamber (m²), dc/dt is the change of CH₄ concentration (μL.L⁻¹.h⁻¹) in the sampling chamber per unit of time (positive value: gas emission; negative value: gas absorption), T is the temperature inside the chamber (K) and 273/T is the temperature impact factor. CH₄ emissions were calculated using a trapezoidal method according to the following formula: $Q = (F1 + F2) \times (t2-t1)/2 \times 24$, where Q is the total emission amount of CH₄ (mg.m⁻²) and F1 and F2 are the corresponding emission fluxes at days t1 and t2. The temperature inside the chamber was measured simultaneously for the standardized correction of the volume of gas. Soil Eh was measured using a FJA-6 automated oxidation-reduction potential (ORP) analyzer (Nanjing Chuan-Di Instrument & Equipment CO., LTD. Nanjing, China).

All statistical analyses were performed using SPSS 17.0 (SPSS, Inc., USA) and EXCEL 2010 for Windows. Average fluxes and standard deviations of CH₄ were calculated based on data from triplicate plots. Differences in seasonal CH₄ emissions and grain yields between treatments were analyzed with two-way analysis of variance (ANOVA) and least significant difference (LSD) test. To determine correlation, Pearson's correlation test was applied at 5% level of significance. The map of study site was generated by using ArcGIS software (ArcMap 10.2 version; <https://www.esri.com/en-us/arcgis/about-arcgis/overview>). Finally, Origin 8.0 (Origin Lab Corporation, USA) was employed for figure preparation.

Results

Environmental conditions and crop productions

Chao Lake has a subtropical moist monsoon climate, and this region is dominated by both westerly circulation and subtropical circulation. Annual mean air temperatures were 15.8 °C and 16.3 °C for the 2013–2014 and 2014–2015 cropping years, respectively (*Fig. 2*). The respective annual precipitation values were 1065.6 mm and 1077.4 mm for the cropping years of 2013–2014 and 2014–2015, respectively (*Fig. 2*). The magnitudes and seasonal patterns of soil temperatures correlated with air temperatures during the two experimental years.

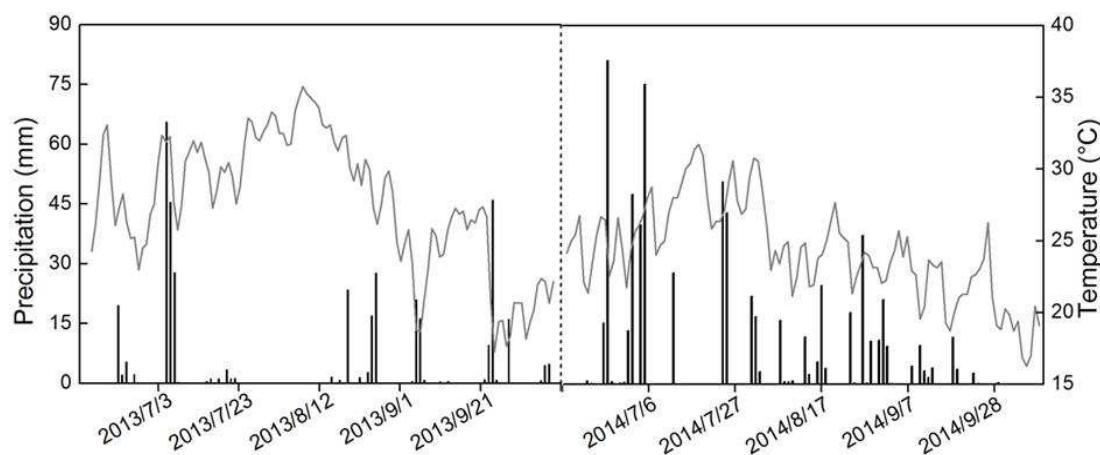


Figure 2. Daily precipitation and mean air temperatures during the three rice growing seasons from 2013 to 2014

CH₄ emissions during the rice-growing season

CH₄ emissions not only correlated with the influencing factors of substrate, environment, and fertilization but were also highly correlated with rice growth stage. Over the whole rice seasons from 2013 to 2014, the variable seasonal pattern of CH₄ emissions from rice paddies consisted of “three peaks”, as shown in *Figure 3*.

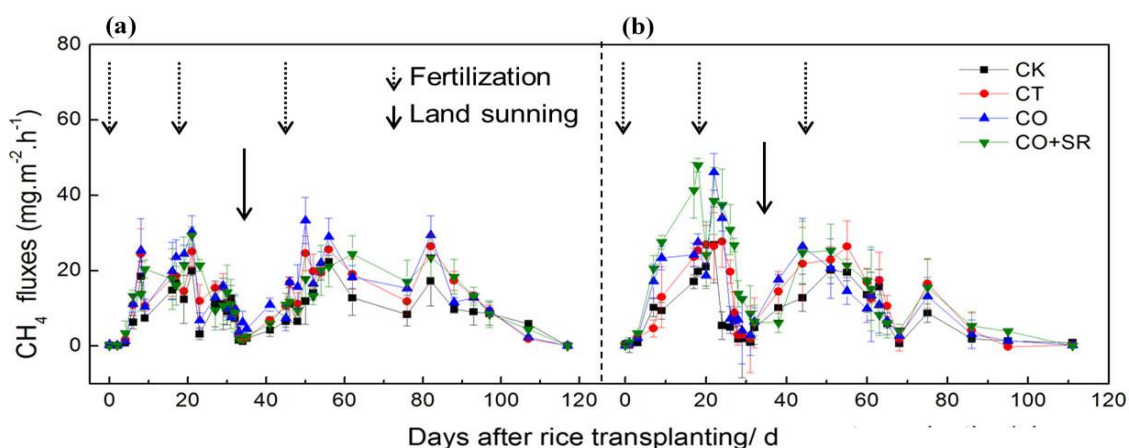


Figure 3. Variation in methane emissions during the rice growing seasons of (a) 2013 and (b) 2014. The vertical bars represent standard errors of the means ($n = 3$)

Due to the dry farming system in non-rice growing years, the soil environment had shifted to a state of oxidation; thus, CH₄ emissions did not appear during the early rice transplantation or with the latter fertilizer application. After a period of flooding, the soil state gradually shifted to a reducing environment, which directly resulted in gradual decreases in soil Eh and gradual increases in CH₄ emissions.

The first CH₄ emission peak appeared on the 22nd day after transplanting under the combined effects of fertilizer, substrate, and environmental factors. The order of CH₄ emission fluxes under each treatment were CO > CO + SR > CT > CK in 2013, and CO + SR > CO > CT > CK in 2014. During the drying of paddy fields in the sunshine (Days 23-31 in 2013 and days 27-35 in 2014), there were reductions in CH₄ production from methanogens, and the activity of methane-oxidizing bacteria was increased; thus, the CH₄ emissions from rice fields were very low during this period. After the re-flooding, the CH₄ emission flux of CK, CT, CO, and CO + SR increased slowly. With the application of panicle fertilizer on the 45th day, CH₄ emissions reached a high level and attained its second peak between days 50 and 55 both in 2013 and 2014. After 5 days of drying the paddy fields in the sunshine, the CH₄ emission flux decreased to a low level, but there were still measurable amounts of CH₄ emissions, and sixth-day observations showed a recovery of CH₄ emission fluxes. This may have been due to precipitation during the latter stages of drying. Even after the disappearance of field water, the soil retained a certain amount of moisture, and the added rainfall also contributed to the CH₄ emission flux recovery. The third CH₄ emission peak appeared during the blooming stage. The peak of CH₄ emissions was higher from CT, CO and CO + SR relative to CK, which was because the CK treatment lacked fertilizer; thus, the CT, CO, and CO + SR emission peaks were mainly caused by the input of nitrogen fertilizer.

Annual CH₄ emissions and global warming potential

The different fertilization treatments of the Chao Lake Basin experimental plots resulted in differential CH₄ emission fluxes (*Fig. 4*).

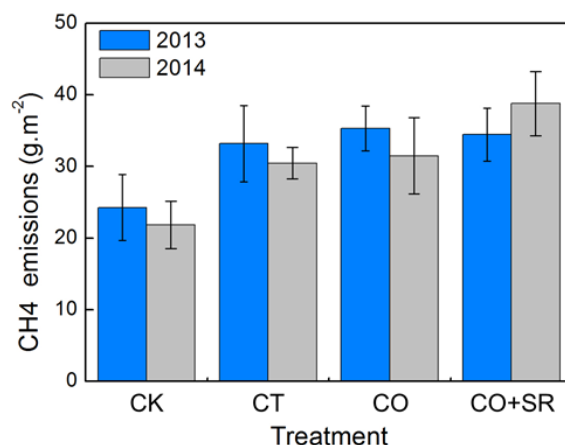


Figure 4. CH₄ emissions under different fertilizer practices throughout the experimental period in 2013 and 2014. The vertical bars indicate standard errors of three replicates

The total seasonal CH₄ emissions from all fertilization treatments were higher than the total CH₄ emissions from the CK treatment, indicating that application of chemical

nitrogen fertilizer could increase CH₄ emissions from single-cropping paddy fields. Different fertilization and straw-return practices had different effects on the seasonal CH₄ emission accumulations; the seasonal CH₄ emission accumulation was calculated and significant differences were determined ($P < 0.05$) by LSD analysis of significant differences (Table 3). During the entire 2013 rice growth period, the total CH₄ emissions in CO treatments were the highest. The total CH₄ emitted was $35.3 \pm 3.3 \text{ gm}^{-2}$ (Table 3), which indicated that there was a certain relationship between CH₄ emission and the applied amounts of chemical nitrogen fertilizer. Compared with the CK treatment, CH₄ emissions from the CT, CO, and CO + SR treatments were increased by 36.6%, 45.8% and 42.0%, respectively. Although the optimized fertilization treatment CH₄ emission was 3.8% higher than that of the Optimized fertilization plus straw-return treatment, the difference in CH₄ emissions was not significant. During the entire 2014 rice growing period, the total CH₄ emitted from the CO + SR treatment was the highest and amounted to $38.8 \pm 4.5 \text{ g m}^{-2}$ (Table 3).

Table 3. Average annual yields and emissions of CH₄ expressed as CO₂-equivalents for the rice growing seasons in 2013 and 2014

Year	Treatment	CH ₄ emission (g·m ⁻²)	Rice yield (kg·hm ⁻²)	Total E-CO ₂ (kgCO ₂ ·hm ⁻²)
2013	CK	24.3 ± 4.6a	5888.9 ± 146.9b	6063.6
	CT	33.2 ± 5.4a	7250.0 ± 127.3ab	8292.3
	CO	35.3 ± 3.3b	7611.1 ± 111.1a	8826.7
	CO + SR	34.5 ± 3.7b	7333.3 ± 364.3b	8613.7
2014	CK	21.8 ± 3.4c	5966.7 ± 135.6c	5456.6
	CT	30.4 ± 2.2b	8376.7 ± 189.6b	7612.5
	CO	31.5 ± 5.3a	8670.3 ± 111.1a	7870.5
	CO + SR	38.8 ± 4.5a	8273.4 ± 140.1a	9690.3

Data in the first two columns are expressed as Means ± SD; different letters within the same column denote significant differences in variable means among treatments over the 2013-2014 seasons based on the LSD multiple-range test ($P < 0.05$).

Compared with the CK treatment, the CT, CO, CO + SR treatments had increases in CH₄ emissions of 42.0%, 48.5%, and 80.1%, respectively. The maximum CH₄ fluxes were different between the two the rice growing season. The CH₄ emissions in 2014 from CK, CT and CO treatments showed a similar pattern as those of 2013, but were all lower than those in 2013; this was probably due to the inter-annual climate, rice growth conditions and other variability's, which led to differences in CH₄emission flux. There was a significant increase inCH₄ emission in the treatment of straw returning to the field in 2013 and 2014. The cumulative 2013 CH₄ emitted from straw-return was 1.42 times that of CK treatment, which increased to 1.80 in 2014; this indicated that straw-return increased the CH₄emissions in Chao Lake rice paddies.

Effects of soil Eh during the rice-growing season on CH₄ emissions

Since methanogenesis requires substrates and extreme reducing conditions, sufficient methane-producing substrates and a suitable methanogenic growth environment are

prerequisites for CH₄ production. During the early stage of rice growth, soil Eh was still high (Fig. 5), which hindered CH₄ production in the soil, resulting in almost no CH₄ production after the first two treatments (Fig. 3). During the first four days after transplanting, CH₄ fluxes remained at 0 mg m⁻² h⁻¹ and began to increase rapidly for 8 days starting on day 6 to reach the first peak. These changes correlated well with increases in soil Eh. In the middle stage of rice growth, the soil Eh had decreased levels suitable for methanogenesis, and there was un-degraded straw remaining from the straw-return CO + SR treatment; this provided a rich methanogenic substrate and appropriate environment for CH₄ production, thereby promoting the production of CH₄ in paddy fields.

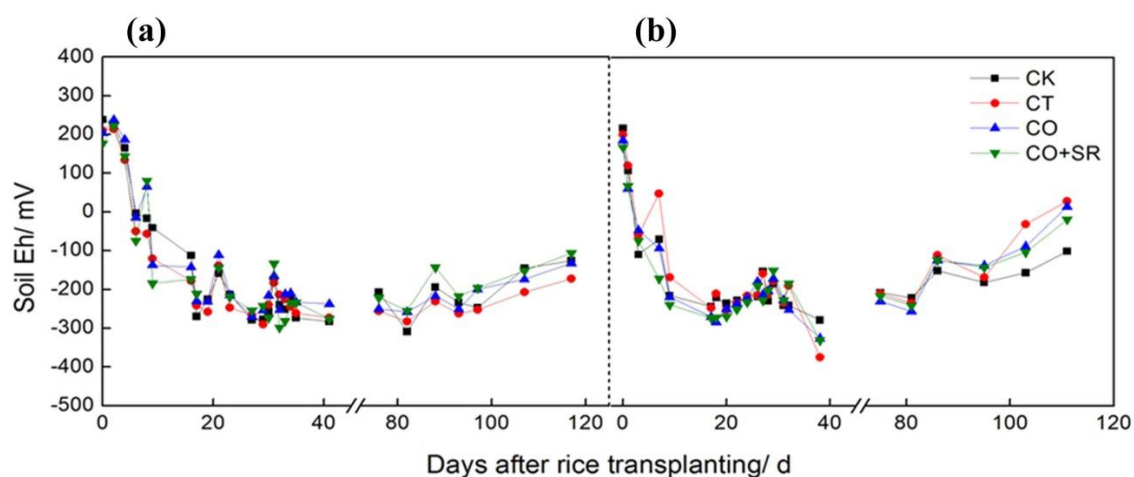


Figure 5. Seasonal dynamic of soil Eh during the rice growing seasons of (a) 2013 and (b) 2014

During the first four days after transplanting, CH₄ fluxes remained at 0 mg m⁻² h⁻¹ and began to increase rapidly for 8 days starting on day 6 to reach the first peak. These changes correlated well with increases in soil Eh. In the middle stage of rice growth, the soil Eh had decreased levels suitable for methanogenesis, and there was un-degraded straw remaining from the straw-return CO + SR treatment; this provided a rich methanogenic substrate and appropriate environment for CH₄ production, thereby promoting the production of CH₄ in paddy fields. The CH₄ production potential of the two treatments increased markedly from 35 to 66 days after transplanting. During the later stage of rice growth, soil Eh was not the limiting factor for CH₄ production. With the consumption of straw, CH₄ production potential gradually decreased and eventually stabilized. The straw mulch did not decompose because of the absence of straw organic matter supplement until the soil Eh decreased to levels suited for CH₄ production. The correlation between CH₄ emission flux and soil Eh is shown in Table 4.

Table 4. Correlations of the variations in CH₄ emission flux with soil Eh

Treatment	CK	CT	CO	CO + SR
E _h	-0.536	-0.652*	-0.571*	-0.736**

*At the P > 0.05 level significantly correlated (bilateral). **At the 0.01 level significantly correlated (bilateral)

Effects of temperature on CH₄ emissions during the rice-growing season

Temperature affects both CH₄ production and emission, and the CH₄ emission flux from paddy field closely correlates with air and soil temperature. Correlation analysis was performed for CH₄ emission flux and surface temperatures at depths of 5 and 10 cm during the sampling period, and the correlation coefficients are shown in *Table 5*.

Table 5. *The correlation of the variations of the CH₄ emission flux with soil temperature*

Treatment	Soil surface temperature	5 cm depth temperature	10 cm depth temperature
CK	0.074	0.320*	0.169
CT	0.128	0.308*	0.116
CO	0.290*	0.335**	0.135
CO + SR	0.270*	0.312*	0.196

*Significantly correlated at the $P > 0.05$ level (bilateral); **significantly correlated at the $P > 0.01$ level (bilateral)

CH₄ emission fluxes were significantly correlated with soil temperatures at 5 cm depth ($P < 0.05$) for all treatments and with surface temperatures (0 cm depth) for the CO and CO + SR treatments; the land surface temperatures failed to correlate with CH₄ emission fluxes for CK and CT, whereas temperatures at a depth of 10 cm failed to correlate with CH₄ emission fluxes for any treatments. A large number of studies have shown that CH₄ emissions from rice fields are affected by many factors, such as soil properties, rice growth, tillage measures and climatic factors. Under the conditions of continuous flooding and with an adequate supply of organic matter, soil Eh was non-limiting and changes of CH₄ emission fluxes were mainly affected by the factors such as soil temperature. Compared with the surface temperatures and soil temperatures at a depth of 10 cm, CH₄ fluxes were more closely related to soil temperature at 5 cm depth; this may be because the soil CH₄ activity mainly occurred in 0 ~ 5 cm soil layer and decreased significantly thereafter. In addition, straw mulching had a significant effect on the surface temperature, which could increase the soil temperature at 5 cm to a certain extent, thus promoting the activity of methane-producing bacteria.

Relationship between CH₄ flux and soil temperature at 5 cm depth

The soil temperature at 5 cm depth was the main environmental factor affecting the CH₄ flux in paddy fields, and the regression equation was obtained by regression analysis between the CH₄ flux and the corresponding of 5 cm soil temperature values: CK: $Y = -17.30573 + 0.84321X$ ($R^2 = 0.14732$, $P < 0.05$); CT: $Y = -24.27339 + 1.19103X$ ($R^2 = 0.16676$, $P < 0.01$); CO: $Y = -28.48551 + 1.35211X$ ($R^2 = 0.17485$, $P < 0.05$); CO + SR: $Y = -24.55386 + 1.17238X$ ($R^2 = 0.14732$, $P < 0.05$), where x is the temperature and y is the CH₄ emission flux (*Fig. 6*). According to the equation, CH₄ emission fluxes were positively correlated with temperature, and the methanogenic activity of the 0~5 cm soil layer was higher than that of deeper soils.

Discussion

Numerous latest studies have shown that application of nitrogen fertilizer positively correlates with CH₄ emissions from agricultural soils (Parkin and Hatfield, 2013;

Halvorson et al., 2014). CH₄ emission fluxes from rice cropping fields ranged between 35.3 and 38.8 g m⁻² over the experimental period, which agreed with results from previous studies (25.9 gm⁻² to 41.9 gm⁻²) conducted in different regions (Ku et al., 2017; Aulakh et al., 2001; Hu et al., 2016). In a terrestrial environment, there are numerous factors affecting CH₄ emissions such as denitrification, nitrification, chemodenitrification, heterotrophic nitrification, codenitrification and oxidation of ammonia; these processes are directly affected by the application of nitrogen fertilizer in the soil (Shurpali et al., 2016; Zhang et al., 2016; Luo et al., 2016; Shakoor et al., 2016). The results of this study also support this conclusion. In the same way, we analyzed the effects of nitrogen application on CH₄ emissions and emission peaks during the rice cropping seasons. In this study, the CK control treatment did not use nitrogen fertilizer application, and both its seasonal and annual CH₄ accumulated emissions were significantly lower than the other fertilization treatments. Seasonal CH₄ emissions fluxes observed by Ku et al. (2017) averaged a very low 15 gm⁻² with nitrogen fertilizer applied at 150 kg ha⁻¹. Similarly, with reduced nitrogen fertilizer application to different agricultural fields (Molodovskaya et al., 2011; Ussiri et al., 2009; Deng et al., 2015), lower CH₄ emissions fluxes were reported. This study found that increasing the application of nitrogen fertilizer could promote CH₄ emission from soil into the atmospheric environment. This study confirmed that the straw returning significantly affected the CH₄ emission in the soil, whereas reduced application of nitrogen fertilizer can decrease CH₄ emissions. In 2014 rice growing period, the total CH₄ emitted from the CO + SR treatment was the highest among all the treatments and amounted to 38.8 gm⁻² (Table 3). Similarly, previous studies also reported that the application of straw returning can significantly increase CH₄ emissions (Wang et al., 2017, 2016, 2015).

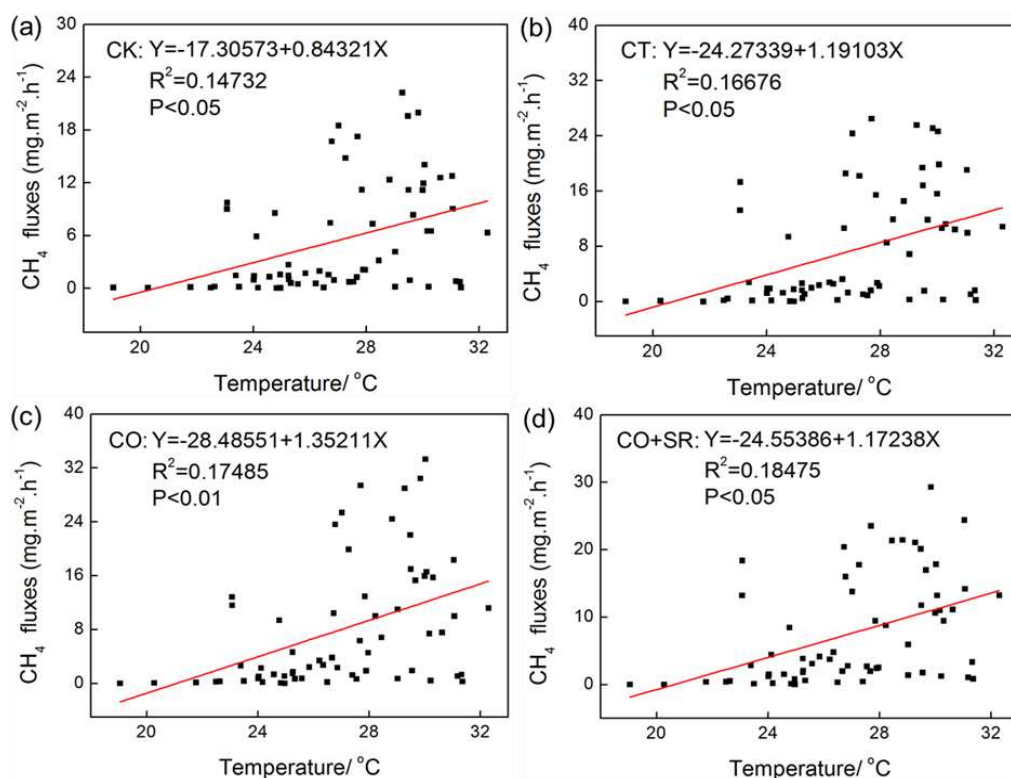


Figure 6. Relationship between methane fluxes and soil temperatures of the 5 cm soil layer, (a) CK, (b) CT, (c) CO, (d) CO + SR

Generally, CH₄ is emitted during soil denitrification and nitrification processes (Shakoor et al., 2016; Smith et al., 1997), which are highly related to soil temperature (Smith et al., 1997; Sun et al., 2016; Aulakh et al., 2001); thus, soil temperature can greatly influence CH₄ emissions. Increased emissions of CH₄ as soil temperature increased from 25 °C to 30 °C showed that production of CH₄ was sensitive to soil temperature (Liu et al., 2017). In this study, the average soil temperature was 15.6 °C with a range of -3.1 °C to 34.5 °C. Maximum CH₄ emissions were observed at 27.5 °C, which was similar to results from recent studies (Maljanen et al., 2017; Liu et al., 2017). Gaihre et al. (2013) also studied that higher temperature could be responsible for elevated CH₄ emission, which was further increased by the application of straw returning.

Soil Eh is a key factor of CH₄ emission from paddy fields and it does not only affect methanogens activities but also involved in gas transformation through the aerenchyma (Le Mer and Roger, 2001). At a lower value of soil Eh, methanogens activities and formation of aerenchyma were increased (Kludze et al., 1993). Significant emissions of CH₄ occur once soil Eh is < -100 mV (Hou et al., 2016; Gaihre et al., 2013). So, the emission of CH₄ is negatively correlated to soil Eh. In our findings, the value of soil Eh was very high during the early stage of rice growth (*Fig. 5*), which delayed CH₄ production and emissions, which was similar to previous recent studies (Charles et al., 2017; Xu et al., 2017; Gaihre et al., 2013; Wang et al., 2017).

Conclusions

The experimental results of two - year farmland in Chao lake single-cropping rice fields showed that: CH₄ emission pattern from rice field consisted of “three peaks”, which appeared before land sunning and after the re-flooding period; the seasonal variation pattern was consistent. CH₄ seasonal emissions were lowest under the CK treatment for both years and were highest under the CO treatment during 2013 and the CO + SR treatment in 2014. The CO + SR treatment may have produced less CH₄ in 2013 due to a large number of stalks initially returned to the field, resulting in an excessive C/N ratio which inhibited soil respiration and affected microbial activities. A year later, the physical and chemical properties of the land had reached a balance, which could better reflect the effect of straw return on CH₄ emissions. The CO + SR treatment increased the total CH₄ emissions by 42.0% and 80.1% in 2013 and 2014, respectively. There was a significant correlation between CH₄ emissions from CO + SR treatment and soil temperatures at depths of 0 and 5 cm, but not at 10 cm. In addition, there was a significant negative correlation between CH₄ emissions and soil E_h. We estimated total CH₄ emissions from the rice growing periods of the two years, and emissions of the different treatments were CO + SR > CO > CT > CK. Straw return to soil can improve soil fertility, increase rice yield, but also increases the CH₄ emissions from rice fields. Therefore, it is necessary to consider the problem of straw returning from no-tillage paddy fields to effectively realize the carbon sequestration potential and reduce the emission of greenhouse gases.

Acknowledgments. This work was financially supported by the Non-profit Research Foundation for Agriculture, China (201103039). The authors are grateful to them for providing the financial support, and Anhui Agro-ecological Environment Centre is acknowledged for organizing the field work.

REFERENCES

- [1] Aulakh, M. S., Khera, T. S., Doran, J. W., Bronson, K. F. (2001): Denitrification, N₂O and CO₂ fluxes in rice-wheat cropping system as affected by crop residues, fertilizer N and legume green manure. – *Biology and Fertility of Soils* 34(6): 375-389. DOI: 10.1007/s003740100420.
- [2] Bao, Q., Huang, Y., Wang, F., Nie, S., Nicol, G. W., Yao, H., Ding, L. (2016): Effect of nitrogen fertilizer and/or rice straw amendment on methanogenic archaeal communities and methane production from a rice paddy soil. – *Applied Microbiology and Biotechnology* 100(13): 5989-5998. DOI: 10.1007/s00253-016-7377-z.
- [3] Chadwick, D. R. (2014): Optimizing chamber methods for measuring nitrous oxide emissions from plot-based agricultural experiments. – *European Journal of Soil Science*. DOI: 10.1111/ejss.12117.
- [4] Charles, A., Rochette, P., Whalen, J. K., Angers, D. A., Chantigny, M. H., Bertrand, N. (2017): Global nitrous oxide emission factors from agricultural soils after addition of organic amendments: a meta-analysis. – *Agriculture, Ecosystems and Environment* 236(3): 88-98. DOI: 10.1016/j.agee.2016.11.021.
- [5] Deng, Q., Hui, D., Wang, J., Iwuzo, S., Yu, C. L., Jima, T., Smart, D., Reddy, C., Dennis, S. (2015): Corn yield and soil nitrous oxide emission under different fertilizer and soil management: a three-year field experiment in middle Tennessee. – *PLoS ONE* 10(4): 1-14. DOI: 10.1371/journal.pone.0125406.
- [6] Gaihre, Y. K., Wassmann, R., Villegas-Pangga, G. (2013): Impact of elevated temperatures on greenhouse gas emissions in rice systems: interaction with straw incorporation studied in a growth chamber experiment. – *Plant and Soil* 373(1-2): 857-875. DOI: 10.1007/s11104-013-1852-4.
- [7] Halvorson, A. D., Snyder, C. S., Blaylock, A. D., Del Grosso, S. J. (2014): Enhanced-efficiency nitrogen fertilizers: potential role in nitrous oxide emission mitigation. – *Agronomy Journal*. DOI: 10.2134/agronj2013.0081.
- [8] Hofmann, K., Farbmacher, S., Illmer, P. (2016): Methane flux in montane and subalpine soils of the Central and Northern Alps. – *Geoderma* 281: 83-89. DOI: 10.1016/j.geoderma.2016.06.030.
- [9] Hou, Y., Velthof, G. L., Lesschen, J. P., Staritsky, I. G., Oenema, O. – *Environmental Science & Technology*. DOI: 10.1021/acs.est.6b04524.
- [10] Hu, N., Wang, B., Gu, Z., Tao, B., Zhang, Z., Hu, S., Zhu, L., Meng, Y. (2016): Effects of different straw returning modes on greenhouse gas emissions and crop yields in a rice-wheat rotation system. – *Agriculture, Ecosystems and Environment* 223: 115-122. DOI: 10.1016/j.agee.2016.02.027.
- [11] Hussain, S., Peng, S., Fahad, S., Khaliq, A., Huang, J., Cui, K., Nie, L. (2015): Rice management interventions to mitigate greenhouse gas emissions: a review. – *Environmental Science and Pollution Research* 22(5): 3342-3360. DOI: 10.1007/s11356-014-3760-4.
- [12] IPCC (2013): *Climate Change 2013: The Physical Science Basis*. – IPCC, Geneva. DOI: 10.1017/CBO9781107415324.
- [13] Hoben, J. P., Gehl, R. J., Miller, N. Grace, P. R., Robertson, G. P. (2011): Nonlinear nitrous oxide (N₂O) response to nitrogen fertilizer in on-farm corn crops of the US Midwest. – pp.1140-1152. DOI: 10.1111/j.1365-2486.2010.02349.x.
- [14] Karakurt, I., Aydin, G., Aydiner, K. (2011): Mine ventilation air methane as a sustainable energy source. – *Renewable and Sustainable Energy Reviews* 15(2): 1042-1049. DOI: 10.1016/j.rser.2010.11.030.
- [15] Kludze, H. K., DeLaune, R. D., Patrick, W. H. (1993): Aerenchyma formation and methane and oxygen exchange in rice. – *Soil Science Society of America Journal* 57(2): 386-391. DOI: 10.2136/sssaj1993.03615995005700020017x.

- [16] Koga, N., Tajima, R. (2011): Assessing energy efficiencies and greenhouse gas emissions under bioethanol-oriented paddy rice production in northern Japan. – *Journal of Environmental Management* 92(3): 967-973. DOI: 10.1016/j.jenvman.2010.11.008.
- [17] Ku, H.-H., Hayashi, K., Agbisit, R., Villegas-Pangga, G. (2017): Effect of rates and sources of nitrogen on rice yield, nitrogen efficiency, and methane emission from irrigated rice cultivation. – *Archives of Agronomy and Soil Science* 63(7). DOI: 10.1080/03650340.2016.1255327.
- [18] Linquist, B. A., Adviento-Borbe, M. A., Pittelkow, C. M., van Kessel, C., van Groenigen, K. J. (2012): Fertilizer management practices and greenhouse gas emissions from rice systems: a quantitative review and analysis. – *Field Crops Research* 135: 10-21. DOI: 10.1016/j.fcr.2012.06.007.
- [19] Liu, G., Yu, H., Ma, J., Xu, H., Wu, Q., Yang, J., Zhuang, Y. (2015): Effects of straw incorporation along with microbial inoculant on methane and nitrous oxide emissions from rice fields. – *Science of the Total Environment* 518-519: 209-216. DOI: 10.1016/j.scitotenv.2015.02.028.
- [20] Liu, R., Hayden, H. L., Suter, H., Hu, H., Lam, S. K., He, J., Mele, P. M., Chen, D. (2017): The effect of temperature and moisture on the source of N₂O and contributions from ammonia oxidizers in an agricultural soil. – *Biology and Fertility of Soils* 53(1): 141-152. DOI: 10.1007/s00374-016-1167-8.
- [21] Lou, Y., Xu, M., Wang, W., Sun, X., Zhao, K. (2011): Return rate of straw residue affects soil organic C sequestration by chemical fertilization. – *Soil and Tillage Research* 113(1): 70-73. DOI: 10.1016/j.still.2011.01.007.
- [22] Lubbers, I. M., van Groenigen, K. J., Fonte, S. J., Six, J., Brussaard, L., van Groenigen, J. W. (2013): Greenhouse-gas emissions from soils increased by earthworms. – *Nature Climate Change* 3(3): 187-194. DOI: 10.1038/nclimate1692.
- [23] Luo, S., Yu, L., Liu, Y., Zhang, Y., Yang, W., Li, Z. (2016): Effects of reduced nitrogen input on productivity and N₂O emissions in a sugarcane/soybean intercropping system. – *European Journal of Agronomy* 81: 78-85. DOI: 10.1016/j.eja.2016.09.002.
- [24] Ma, J., Ma, E., Xu, H., Yagi, K., Cai, Z. (2009): Wheat straw management affects CH₄ and N₂O emissions from rice fields. – *Soil Biology and Biochemistry* 41(5): 1022-1028. DOI: 10.1016/j.soilbio.2009.01.024.
- [25] Maljanen, M., Yli-Moijala, H., Biasi, C., Leblans, N. I. W., De Boeck, H. J., Bjarnadóttir, B., Sigurdsson, B. D. (2017): The emissions of nitrous oxide and methane from natural soil temperature gradients in a volcanic area in southwest Iceland. – *Soil Biology and Biochemistry* 109: 70-80. DOI: 10.1016/j.soilbio.2017.01.021.
- [26] Le Mer, J., Roger, P. (2001): Production, oxidation, emission and consumption of methane by soils: a review. – *European Journal of Soil Biology* 37(1): 25-50. DOI: 10.1016/S1164-5563(01)01067-6.
- [27] Mohanty, S., Swain, C. K., Tripathi, R., Sethi, S. K., Bhattacharyya, P., Kumar, A., Raja, R., Shahid, M., Panda, B. B., Lal, B., et al. (2017): Nitrate leaching, nitrous oxide emission and N use efficiency of aerobic rice under different N application strategy. – *Archives of Agronomy and Soil Science*. DOI: 10.1080/03650340.2017.1359414.
- [28] Molodovskaya, M., Warland, J., Richards, B. K., Öberg, G., Steenhuis, T. S. (2011): Nitrous oxide from heterogeneous agricultural landscapes: source contribution analysis by eddy covariance and chambers. – *Soil Science Society of America Journal* 75(5): 1829. DOI: 10.2136/sssaj2010.0415.
- [29] Montzka, S. A., Dlugokencky, E. J., Butler, J. H. (2011): Non-CO₂ greenhouse gases and climate change. – *Nature* 476(7358): 43-50. DOI: 10.1038/nature10322.
- [30] Musenze, R. S., Grinham, A., Werner, U., Gale, D., Katrin Sturm, J. U., Yuan, Z. (2014): Assessing the spatial and temporal variability of diffusive methane and nitrous oxide emissions from subtropical freshwater reservoirs. – *Environmental Science & Technology* 48: 14499-14507. DOI: 10.1021/es505324h.

- [31] Nyamadzawo, G., Wuta, M., Nyamangara, J., Rees, R. M., Smith, J. L. (2015): The effects of catena positions on greenhouse gas emissions along a seasonal wetland (dambo) transect in tropical Zimbabwe. – *Archives of Agronomy and Soil Science* 61(2): 203-221. DOI: 10.1080/03650340.2014.926332.
- [32] Parkin, T. B., Hatfield, J. L. (2013): Enhanced efficiency fertilizers: effect on nitrous oxide emissions in Iowa. – *Agronomy Journal*. DOI: 10.2134/agronj2013.0219.
- [33] Qin, X., Li, Y., Wang, H., Liu, C., Li, J., Wan, Y., Gao, Q., Fan, F., Liao, Y. (2016): Long-term effect of biochar application on yield-scaled greenhouse gas emissions in a rice paddy cropping system: a four-year case study in south China. – *Science of the Total Environment* 569-570: 1390-1401. DOI: 10.1016/j.scitotenv.2016.06.222.
- [34] Roche, L., Forrestal, P. J., Lanigan, G. J., Richards, K. G., Shaw, L. J., Wall, D. P. (2016): Agriculture, ecosystems and environment impact of fertiliser nitrogen formulation, and N stabilisers on nitrous oxide emissions in spring barley. – *Agriculture, Ecosystems and Environment* 233: 229-237. DOI: 10.1016/j.agee.2016.08.031.
- [35] Shakoor, A., Abdullah, M., Yousaf, B., Amina, Ma, Y. (2016): Atmospheric emission of nitric oxide and processes involved in its biogeochemical transformation in terrestrial environment. – *Environmental Science and Pollution Research*. DOI: 10.1007/s11356-016-7823-6.
- [36] Shakoor, A., Xu, Y., Wang, Q., Chen, N., He, F., Zuo, H., Yin, H., Yan, X., Ma, Y., Yang, S. (2018): Effects of fertilizer application schemes and soil environmental factors on nitrous oxide emission fluxes in a rice-wheat cropping system, east China. – *PLoS ONE* 13(8): 1-16. DOI: 10.1371/journal.pone.0202016.
- [37] Shi, C., Roth, M., Zhang, H., Li, Z. (2008): Impacts of urbanization on long-term fog variation in Anhui Province, China. – *Atmospheric Environment* 42(36): 8484-8492. DOI: 10.1016/j.atmosenv.2008.08.002.
- [38] Shurpali, N. J., Rannik, Ü., Jokinen, S., Lind, S., Biasi, C., Mammarella, I., Peltola, O., Pihlatie, M., Hyvönen, N., Rätty, M., et al. (2016): Neglecting diurnal variations leads to uncertainties in terrestrial nitrous oxide emissions. – *Sci. Rep.* 6. DOI: 10.1038/srep25739.
- [39] Smith, K. A., McTaggart, I. P., Tsuruta, H. (1997): Emissions of N₂O and NO associated with nitrogen fertilization in intensive agriculture, and the potential for mitigation. – *Soil Use and Management* 13: 296-304. DOI: 10.1111/j.1475-2743.1997.tb00601.x.
- [40] Sun, H., Zhou, S., Fu, Z., Chen, G., Zou, G., Song, X. (2016): A two-year field measurement of methane and nitrous oxide fluxes from rice paddies under contrasting climate conditions. – *Scientific Reports* 6(February): 28255. DOI: 10.1038/srep28255.
- [41] Ussiri, D. A. N., Lal, R., Jarecki, M. K. (2009): Nitrous oxide and methane emissions from long-term tillage under a continuous corn cropping system in Ohio. – *Soil and Tillage Research* 104(2): 247-255. DOI: 10.1016/j.still.2009.03.001.
- [42] Wagner, D., Lipski, A., Embacher, A., Gattinger, A. (2005): Methane fluxes in permafrost habitats of the Lena Delta: effects of microbial community structure and organic matter quality. – *Environmental Microbiology* 7(10): 1582-1592. DOI: 10.1111/j.1462-2920.2005.00849.x.
- [43] Walter, B. P., Heimann, M., Matthews, E. (2001): Modeling modern methane emissions from natural wetlands 1. Model description and results. – *J. Geophys. Res.* 106(D24): 34189-34206.
- [44] Wang, C., Shen, J., Tang, H., Inubushi, K., Guggenberger, G., Li, Y., Wu, J. (2017): Greenhouse gas emissions in response to straw incorporation, water management and their interaction in a paddy field in subtropical central China. – *Archives of Agronomy and Soil Science* 63(2): 171-184. DOI: 10.1080/03650340.2016.1193163.
- [45] Wang, W., Lai, D. Y. F., Sardans, J., Wang, C., Datta, A., Pan, T., Zeng, C., Bartrons, M., Peñuelas, J. (2015): Rice straw incorporation affects global warming potential differently in early vs. late cropping seasons in Southeastern China. – *Field Crops Research* 181: 42-51. DOI: 10.1016/j.fcr.2015.07.007.

- [46] Wang, W., Wu, X., Chen, A., Xie, X., Wang, Y., Yin, C. (2016): Mitigating effects of ex situ application of rice straw on CH₄ and N₂O emissions from paddy-upland coexisting system. – *Scientific Reports* 6. DOI: 10.1038/srep37402.
- [47] Wassmann, R., Buendia, L. V., Lantin, R. S., Bueno, C. S., Lubigan, L. A., Umali, A., Nocon, N. N., Javellana, A. M., Neue, H. U. (2000): Mechanisms of crop management impact on methane emissions from rice fields in Los Banos, Philippines. – *Nutrient Cycling in Agroecosystems* 58(1-3): 107-119. DOI: 10.1023/A: 1009838401699.
- [48] Xu, G., Liu, X., Wang, Q., Yu, X., Hang, Y. (2017): Integrated rice-duck farming mitigates the global warming potential in rice season. – *Science of the Total Environment* 575: 58-66. DOI: 10.1016/j.scitotenv.2016.09.233.
- [49] Xuejun, L., Fusuo, Z. (2011): Nitrogen fertilizer induced greenhouse gas emissions in China. – *Current Opinion in Environmental Sustainability* 3(5): 407-413. DOI: 10.1016/j.cosust.2011.08.006.
- [50] Yan, X., Akiyama, H., Yagi, K., Akimoto, H. (2009): Global estimations of the inventory and mitigation potential of methane emissions from rice cultivation conducted using the 2006 Intergovernmental Panel on Climate Change guidelines. – *Global Biogeochemical Cycles* 23(2). DOI: 10.1029/2008GB003299.
- [51] Zhang, G., Zhang, W., Yu, H., Ma, J., Xu, H., Yagi, K. (2015a): Increase in CH₄ emission due to weeds incorporation prior to rice transplanting in a rice-wheat rotation system. – *Atmospheric Environment* 116: 83-91. DOI: 10.1016/j.atmosenv.2015.01.018.
- [52] Zhang, X., Xu, M., Liu, J., Sun, N., Wang, B., Wu, L. (2016): Greenhouse gas emissions and stocks of soil carbon and nitrogen from a 20-year fertilised wheat-maize intercropping system: a model approach. – *Journal of Environmental Management* 167: 105-114. DOI: 10.1016/j.jenvman.2015.11.014.
- [53] Zhang, Y., Sheng, J., Wang, Z., Chen, L., Zheng, J. (2015b): Nitrous oxide and methane emissions from a chinese wheat-rice cropping system under different tillage practices during the wheat-growing season. – *Soil and Tillage Research* 146(PB): 261-269. DOI: 10.1016/j.still.2014.09.019.
- [54] Zhang, Z. S., Guo, L. J., Liu, T. Q., Li, C. F., Cao, C. G. (2015c): Effects of tillage practices and straw returning methods on greenhouse gas emissions and net ecosystem economic budget in rice-wheat cropping systems in central China. – *Atmospheric Environment* 122: 636-644. DOI: 10.1016/j.atmosenv.2015.09.065.
- [55] Zhu, L., Hu, N., Yang, M., Zhan, X., Zhang, Z. (2014): Effects of different tillage and straw return on soil organic carbon in a rice-wheat rotation system. – *PLoS ONE* 9(2): 56-63. DOI: 10.1371/journal.pone.0088900.
- [56] Zou, J., Huang, Y., Jiang, J., Zheng, X., Sass, R. L. (2005): A 3-year field measurement of methane and nitrous oxide emissions from rice paddies in China: effects of water regime, crop residue, and fertilizer application. – *Global Biogeochemical Cycles* 19(2): 1-9. DOI: 10.1029/2004GB002401.

CHARACTERISTICS OF ORGANOCHLORINE POLLUTION IN THE TOPSOIL OF THE DAWEN RIVER WATERSHED AND POTENTIAL RISK ASSESSMENT IN CHINA

DING, M.^{1,2} – ZHAO, W.¹ – XU, X.¹ – TANG, J.¹ – FAN, T.¹ – ZHANG, L.¹ – ZHANG, Z.¹ – PENG, S.^{*1} – XU, L.¹

¹*Tourism College, Taishan University, Tai'an 271000, China*

²*Laboratory for Marine Geology, Qingdao National Laboratory for Marine Science and Technology, Qingdao 266000, China*

**Corresponding author
e-mail: shuzhenpeng@sohu.com*

(Received 22nd Jul 2019; accepted 15th Nov 2019)

Abstract. We detected presence of 23 types of organochlorine pesticides (OCPs) in 21 mixed samples obtained along the banks of Dawen River in China by gas chromatography. we analyzed the spatial distribution of OC residues, potential source, and the ecological and health risks. The results show that OCPs were detected in all the 21 sampling sites, and 86.6% of the 23 types of OCPs had a detection rate above 90%. Furthermore, the analysis of the single-factor pollution index shows that 14% of the sampling sites were mildly polluted, whereas 4.8% had medium-level pollution. Analysis of the Nemerow's multi-factor index shows that 9.5% of the sampling sites were mildly polluted. We found that Dawenkou Town and Wenyang Town are severely polluted, whereas Ciyao Town and Jiangji Town are less polluted by arcgis12.0 spatial analysis. Compared to other regions in China, the HCHs content is at a low level but DDTs at a high level in the study area. Assessment of health risks of OCP residues shows that the carcinogenic risk and the non-carcinogenic risk caused by exposure to OCPs is negligible. OCPs are primarily obtained from previous residues and recent use of lindane.

Keywords: *OCPs residues, DDT, HCHs, health risks*

Introduction

Chlorine in organic compounds is referred to as organochlorine. Organochlorine pesticides (OCPs), a type of persistent organic pollutants, have been drawn considerable research attention because of the pollution and environmental harm they have caused. Once OCPs enter the soil, the soil is contaminated, and because OCPs are hard to decompose and accumulate, they will enter the human body through the food chain and cause intoxication. OCPs are harmful to both the ecological system and human health, resulting in nervous system disorders, cancer, reproductive abnormalities, and congenital defects (Chen et al., 2017). Although the Chinese government banned OCPs in the 1980s, studies in recent years have revealed that HCHs and DDTs were still found in the soil and water in many regions across China (An et al., 2005; Cheng, 2014; Cui et al., 2014; Cheng et al., 2018; Cui et al., 2012, 2014; Chen et al., 2011; Dai et al., 2012).

Dawen River watershed, which is famous for high and stable crop yields, has been included in the ecological restoration program of the Mount Tai area in Shandong province of China. As an important part of the urban environment, the suburban soil has significant influence over the quality of the environment and ecological functions of a city. Note that OCPs residues in soil will affect the safety of crops and may cause food scarcity in cities and threaten human health (Cui et al., 2014).

Using the topsoil in Wenyang Field as the research object, we performed pollution analysis, health risk analysis, and ecological risk analysis to identify the pollution condition and potential risks in Wenyang Field. We believe this study will provide effective solutions for soil restoration and provide a scientific basis for sustainable soil utilization and the protection of human health.

Materials and methods

Study area description

Wenyang Field (*Fig. 1*), the fertile land along the banks of Dawen River in its middle and lower reaches in China, was selected as the research area. Wenyang Field has a flat terrain and covers an area of 14 km². Feicheng City, Ningyang County, and Daiyue District located in Wenyang Field. It is subject to the warm temperate continental monsoon climate with high temperature coinciding with high precipitation, which facilitates the growth of crops. The major soil types of soil in this area include cinnamon soil and brown soil. The soil layer is thick and the soil is fertile. Dawen River, the largest branch of Yellow River in its lower reach, flows through Wenyang Field, while the underground water level is three to four meters deep. These natural conditions provide Wenyang Field with abundant water and fertile soil. As an important crop-yielding area in Taiwan, Wenyang Field is known as the “bread basket of Mount Tai” and supplies over 10,000 tons of corns and wheat to China; it is also rich in mineral resources such as gypsum and halite.

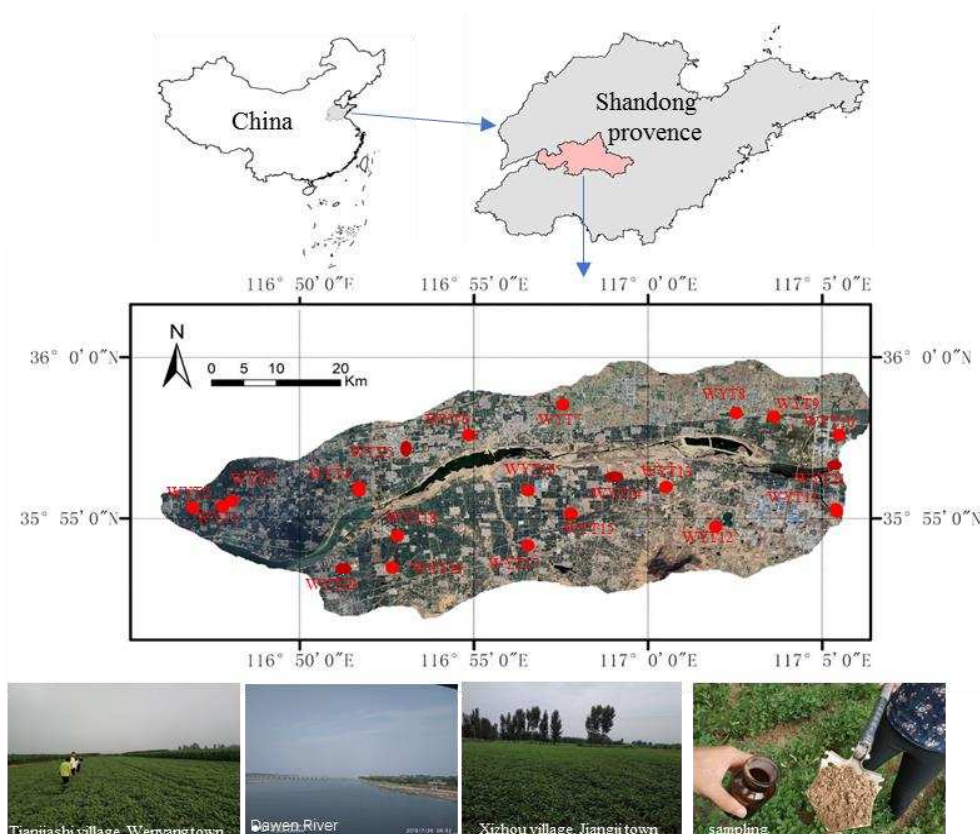


Figure 1. Location of study area, distribution of sampling sites and photos of the Dawen River Basin in China

Sample collection

The sampling points are located at 21 locations on both sides of the Dawen River (Table 1, Fig. 1). Preliminary surveys of the Dawen River watershed were conducted using GPS, and 21 mixed soil samples were collected according to “Technical Guidelines for Environmental Site Investigation” (HJ25.1-2014) in July 2018. Five-point sampling method was used to collect the samples, 5 samples are collected at each location to be mixed into one sample. and the sampling depth was from 0 to 20 cm. Details of specific sampling point locations and vegetation. The 200 g soil was sealed in brown wild-mouth bottles (250 ml) after being collected and stored in lab freezers at 4 °C. To test the physical and chemical indicators of the soil, a soil sample of 1 kg was collected and packed in the sampling bag. The collected soil samples were transported to the Lunan Institute of Geo-engineering Investigation of Shandong for additional tests.

In this paper, SPSS 12.0 software is used for data statistical analysis, and arcgis12.0 Kriging difference method is used for spatial analysis (Ma et al. 2015).

Table 1. Sampling sites, number of the samples and land use of soil sampling in Dawen River Basin in China

Samples	No.	Sampling point (n)	Longitude	Latitude	Land cover
WYT1	5	Sihechakou village, Wenyang town	116.79648°E	35.92304°N	Corn field
WYT2	5	Sanjiakou new village, Anjiazhuang town	116.78217°E	35.92241°N	Soybean field
WYT3	5	Donggaoyu village, Wenyang town	116.80101°E	35.92575°N	sorghum field
WYT4	5	Maidongshi village, Wenyang town	116.86177°E	35.93099°N	Vegetable plot
WYT5	5	Tianjiashi village, Wenyang town	116.86170°E	35.93279°N	Peanut field
WYT6	5	Beidian village, Wenyang town	116.91425°E	35.95981°N	Okra field
WYT7	5	Xiama village, Mazhuang town	116.95935°E	35.97548°N	Soybean field
WYT8	5	West of Yuejiazhuang, Dawenkou town	117.04230°E	35.97117°N	Corn field
WYT9	5	East Yuejia, Dawenkou town	117.06027°E	35.96941°N	Celery field
WYT10	5	Xinghua village, Wenkou town	117.09148°E	35.95994°N	Corn field
WYT11	5	Qijiazhuang, Ciyao town	117.08991°E	35.92143°N	Peanut field
WYT12	5	Lujiahuaguan village, Ciyao town	117.03247°E	35.91231°N	Peanut field
WYT13	5	Xizhou village, Jiangji town	117.00872°E	35.93303°N	Peanut field
WYT14	5	Dahuzhuang village, Jiangji town	117.00859°E	35.93293°N	Ginger field
WYT15	5	Hengjiazhuang, Jiangji town	116.96325°E	35.91915°N	Corn field
WYT16	5	Tianfu Village, Jiangji town	116.94264°E	35.93113°N	Corn field
WYT17	5	Zhangjiadian, Gucheng	116.94264°E	35.90261°N	Corn field
WYT18	5	Chenjiadian, Gucheng	116.880110°E	35.90768°N	Peanut field
WYT19	5	Xingquan village, Gucheng town	116.87773°E	35.89111°N	Corn field
WYT20	5	Panxinzhuang, Gucheng town	116.83494°E	35.87919°N	Corn field
WYT21	5	Zhengjia village, Ciyao town	117.09045°E	35.82018°N	Wetland

Methods

The samples were tested at the Lunan Institute of Geo-engineering Investigation of Shandong and 23 types of OC compounds were analyzed. The GC-ECD method was used to detect OCPs in the soil. The detection and testing tools included the Agilent 7890B-5977B mass spectrometer, the Thermo ASE 350 pressurized fluid extractor, the SUPELCO VISIPREP 24TM DL solid-phase extraction device, and the HP-5

chromatographic column. The reagents used included 20 types of standard mixtures of OC solvents, and the testing procedure was as follows. The samples were dried and grinded before being screened through a 250- μm sieve (No. 60 sieve). The sample was mixed with diatomaceous earth (1 g) and the mixture was added to the extraction cell (22 ml) before pressurized fluid extraction was conducted according to the HJ783-2016 standards. After extraction, n-hexane was used to wash the tube wall of the concentrator exposed during the nitrogen blowing process to concentrate n-hexane to 1 ml. The eluent was then transferred to the column and 2 ml of n-hexane was used to wash the concentrator several times, and then all the eluent was transferred into the column (if desulfurization was required, the solvent would be sunk in copper sheets for ~5 min). The eluents were collected and concentrated before the internal standard was added for testing. When drawing the curves, five sample bottles of 1.5 ml were used to prepare solvents of five different concentrations by mixing the OCPs standard intermediate solution, the substitute intermediate solution, internal standard intermediate solution, and n-hexane solution extracted by the pipette. The mass concentrations of OCPs and substitutes for the five solvents were 20, 50, 100, 200 and 500 ng/ml, and the internal standard mass concentration was 20.0 ng/ml.

Results

Characteristics of OCPs residues

Table 2 shows the conditions of OCPs residues in the soil of Wenyang Field in china. The total content of OCPs residues (ΣOCPs) is between *nd* and 197.01 ng/g. The detection rate of OCPs in the 21 sampling sites in Wenyang Field reached 100%, and 23 types of OCPs were detected. The most prevalent OCPs detected in the soil of Wenyang Field measured by the average content are DDTs (53.84 ng/g), endrin aldehyde (18.47 ng/g), and heptachlor epoxide (17.07 ng/g).

HCHs

The detection rate of HCHs (such as α -, β -, γ -, and δ -HCH) is 100% with the residue content between 1.58 and 15.95 ng/g (average of 4.23 ng/g). The largest content of HCHs was observed at WYT10 (near the glass manufacturing plant), while the content of HCHs in the topsoil of Wenyang Field was far below 100 ng/g, which is the threshold value for agricultural land pollution as stipulated in “Soil Environment Quality Standard” (GB15618-2018). The content of HCHs in the topsoil of Wenyang Field is below that at Jining in Shandong (5.73 ng/g) (Pang et al., 2009), Henan province (12.55 ng/g) (Cheng et al., 2018), Baotou (8.37 ng/g) (Meng et al., 2017a), Inner Mongolia (8.63 ng/g) (Meng et al., 2017b), Changchun (10.95 ng/g) (Xiao, 2017), and Yangtze River Delta (7.73 ng/g) (Shi et al., 2016); however, the content of HCHs is above that in Shanghai (2.19 ng/g) (Cheng et al., 2018). This comparison indicates that the HCHs pollution in the soil of Wenyang Field is still at a low level. The HCH isomers have different physical, chemical, and toxic properties; furthermore, in terms of the dichlorination and degradation rate, γ -HCH > α -HCH > δ -HCH > β -HCH. However, the results of this study show that the detection rate of β -HCH is the highest, and β -HCH > γ -HCH > α -HCH > δ -HCH in terms of the average residue of HCHs. According to Figure 2a, which shows the distribution of HCHs content, the HCH content is high in Wenkou Town and Ciyao Town but relatively low in the western area.

Table 2. Summary of OCPs concentrations in topsoil in Dawen River Basin in China (n = 21) (units for soil samples are ng g⁻¹ dw)

Compounds	Mean	Standard deviation	Minimum	Maximum	Coefficient of variation	Detection rate
HCB	0.06	0.03	0.03	0.16	0.52	100%
α-HCH	0.76	0.78	0.12	3.75	1.02	100%
β-HCH	2.18	2.25	0.75	8.76	1.03	100%
γ-HCH	0.98	0.87	0.25	3.40	0.89	100%
δ-HCH	0.31	0.33	0.10	1.43	1.07	100%
HCHs	4.23	3.95	1.58	15.95	0.93	100%
Heptachlor	1.89	1.17	0.75	5.83	0.62	100%
Aldrin	0.07	0.05	0.00	0.26	0.77	95.24%
Dicofol	3.69	3.74	0.40	15.79	1.01	100%
Epoxyheptachloride	17.07	4187.00	0.00	194.39	2.45	90.48%
γ-chlordane	0.02	0.02	0.00	0.09	0.66	95.24%
α-chlordane	0.02	0.01	0.00	0.05	0.52	90.48%
dieldrin	1.93	3.35	0.59	16.45	1.74	100%
Isodrin	0.78	1.44	0.00	5.58	1.84	38.10%
Endosulfan 2	0.56	1.08	0.00	4.30	1.19	95.27%
p,p'-DDD	2.04	3.49	0.26	15.58	1.71	100%
o,p'-DDT	0.44	0.40	0.08	1.71	0.90	100%
p,p'-DDT	47.53	48.21	5.83	192.65	1.01	100%
DDTs	53.84	50.08	8.40	197.01	0.93	100%
Endrin aldehyde	18.47	12.01	3.85	52.98	0.65	100%
Endosulfan sulphate	0.91	3.27	0.00	15.13	3.59	61.90%
Isodiazone	0.25	0.94	0.00	4.29	3.75	76.19%
methoxychlor	1.18	1.08	0.08	3.33	0.92	100%
Mirex	0.44	0.70	0.00	3.39	1.60	100%

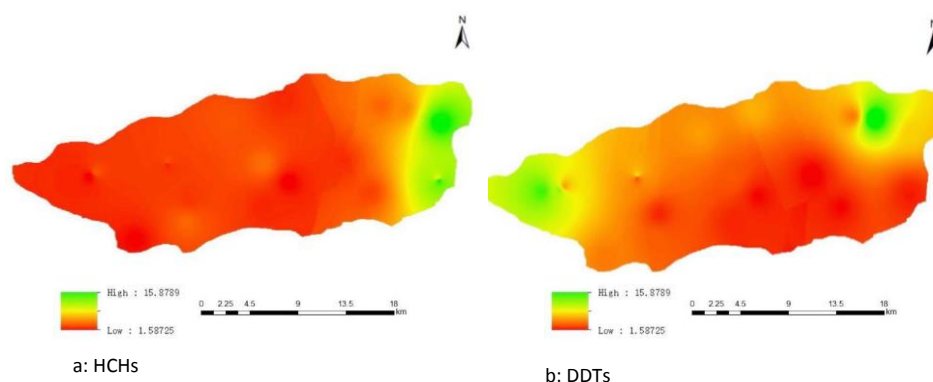


Figure 2. Distribution of HCHs and DDTs content in Dawen River Basin in China

DDTs

The detection rate of DDTs, including DD, DDE, and DDT, is 100% in the study area, and the residue content is between 8.4 and 197.01 ng/g (average of 53.84 ng/g).

The highest content occurs at WYT9 (a celery-growing field). Note that the residue content of DDTs is higher than that of HCHs, and HCHs and DDTs have the same variable coefficient of 0.93. The average content of DDTs in the topsoil of Wenyang Field is 51% of the average content of all organic pollutants. The DDTs content in the topsoil of some sampling sites is already > 100 ng/g, which is the threshold value for agricultural land pollution risks stipulated in “Soil Environment Quality Standard” (GB15618-2018). Note that the content of DDTs in the topsoil of Wenyang Field is higher than that at Jining (17 ng/g) (Pang et al., 2009), Shanghai (13.15 ng/g) (Jiang et al., 2010), Henan (8.97 ng/g) (Cheng et al., 2018), Baotou (9.51 ng/g) (Meng et al., 2017a), Inner Mongolia (9.71 ng/g) (Meng et al., 2017b) and Yangtze River Delta (Shi Lei et al., 2016); however, it is below that at Yantai (160 ng/g) (Dai et al., 2012) and Songhuajiang in Jilin (92 ng/g) (Liu et al., 2013). The comparison indicates that the DDT pollution in the soil of Wenyang Field is at a high level. The four derivatives of DDTs by average content are ranked as follows: p,p'-DDT > p,p'-DDE > p,p'-DDD > o,p'-DDT, and the content of p,p'-DDT is the highest. *Figure 2b* shows that the content of DDTs is high in Anjiazhuang Town and Dawenkou Town, but relatively low in Jiangji Town and Ciyao Town.

Discussion

OCPs pollution analysis

Single-factor pollution index analysis

The single-factor index method (Chen et al., 2011; Wu, 2012) and the equation $P_i = C_i/S_i$ were used to calculate the single-factor pollution index P_i of the pollutant i :

$$P_i = \frac{C_i}{S_i} \quad (\text{Eq.1})$$

Figure 3 shows the calculation results, and the single-factor pollution index of HCHs is generally seen to be lesser than that of DDTs. The curve for DDTs in *Figure 3* shows sharp fluctuation, which indicates the pollution level of DDTs varies considerably from one region to another. While 14% of sampling sites showed mild pollution, Xiaohou Village showed the highest single-factor pollution index of ~1.9; hence, it is considered under medium-level pollution. *Figure 4* shows that the level of pollution is high in Dawen Town and Wenyang Town, but relatively low in Ciyao Town and Jiangji Town.

Nemerow's pollution index analysis

According to the Nemerow's pollution index method, we used the equation to calculate the composite soil pollution index P_N :

$$P_N = \sqrt{\frac{P_i^2 + P_{i(\max)}^2}{2}} \quad (\text{Eq.2})$$

Figure 5 shows the calculation results in which 9.5% of sampling sites are mildly polluted with the highest index in Xiaohou Village. As shown in *Figure 6*, the pollution level in Dawenkou Town and Wenyang Town is high, but it is relatively low in Ciyao Town and Jiangji Town.

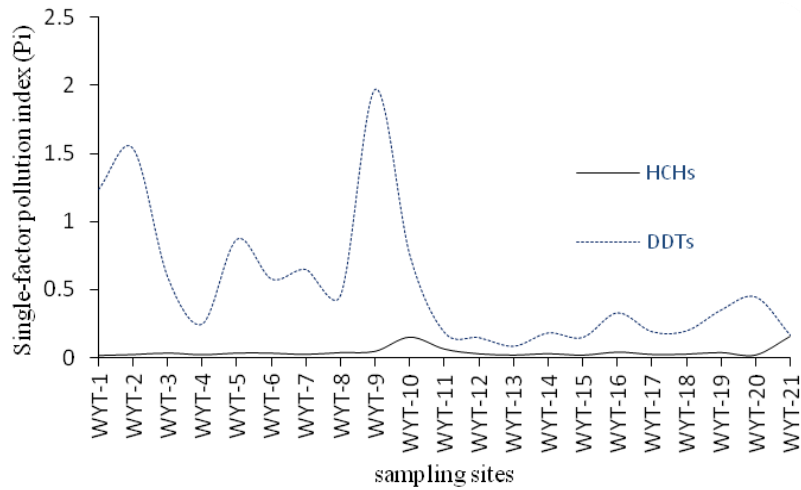


Figure 3. Single-factor indices of OCPs in the topsoil of Wenyang Field in China

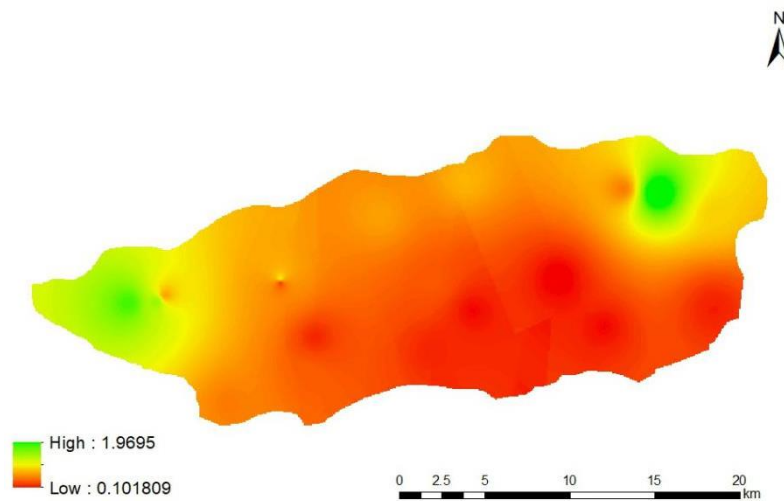


Figure 4. Spatial interpolation of DDT single-factor pollution in Dawen River Basin in China

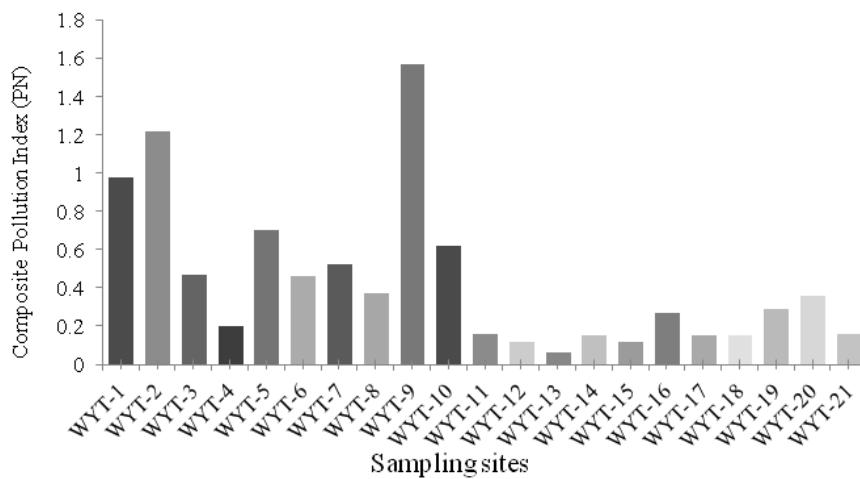


Figure 5. Composite OCPs pollution index in the topsoil of Wenyang Field in China

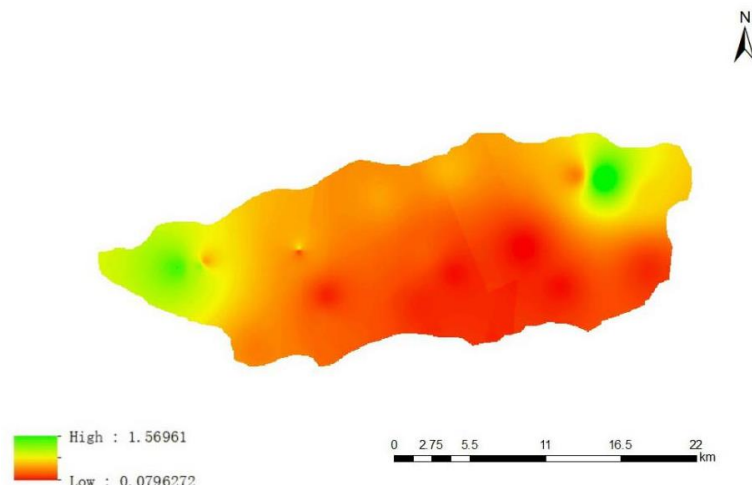


Figure 6. Interpolation of Nemerow's pollution index in Dawen River Basin in China

Assessment of ecological risks of OCPs

We assessed the ecological risks of OCPs according to the concept of adverse biological effects proposed (Long et al., 1995). Effect range low (ERL) and effect range median (ERM), proposed in the study by Long et al., are used as threshold values to identify the level of ecological risks of pollutants. If the value of a pollutant is lesser than ERL, it has no obvious biological toxicity and the ecological risk is < 10%; if the value falls between ERL and ERM, the pollutant has potential toxic effects; and if the value is higher than ERM, it is biologically toxic and its ecological risk is > 75% (Zhu et al., 2012; Lin et al., 2011).

The data obtained in tests in this study are compared with ERL and ERM. Note that in 20 of the 21 samples, i.e., ~95.24% of samples, the value of p,p'-DDT is higher than ERM, which indicates that it has a very high level of ecological risk. Among the 21 samples, the value of p,p'-DDE is lower than ERL in nine samples; however, the value of p,p'-DDE in the other 12 is between ERL and ERM, i.e., 42.86% and 57.14% of samples, respectively, which indicates that p,p'-DDE has a relatively high level of ecological risk. Note that in 16 of the 21 samples, i.e., 76.19% of samples, the value of p,p'-DDD is lower than ERL. Thus, the ecological risks posed by OCPs in the soil of Wenyang Field needs to be examined.

Assessment of ecological risks of DDTs is based on studies (Jongbloed et al., 1996). By designing a simplified food web, Jongbloed et al. identified the threshold content of DDTs in soil, which would cause secondary poisoning: 10 µg/kg for soil worms, 11 µg/kg for birds, and 190 µg/kg for mammals (Jongbloed et al., 1996). In most of the sampling sites, the content of DDT in soil is higher than the maximum allowable content of DDTs residues for soil worms and birds; therefore, the ecological risk they pose to soil worms and birds is high. However, the content of DDTs in most of the sampling sites is below the maximum allowable content of DDTs residues for mammals; therefore, the ecological risk DDTs pose to mammals is relatively low.

Assessment of health risks of OCPs

Human health risk research is an important content of organic pollution research, and the risk can be used as an important basis for the next soil use. Most of them use the

health risk model recommended by the EPA of the United States for evaluation, and the results show that the health risk in most regions is relatively small (Liu et al., 2017; Zhang, 2016; Cheng, 2014).

Based on the health risk assessment model proposed by United States Environmental Protection Agency (USEPA), this study assesses the human health risks of OCPs residues in soil. The human body can be exposed to OCPs in soil via three channels: ingestion through the mouth, dermal contact, and inhaling of dust or volatile gases. The parameters for calculating the average daily dosage are determined from the guiding documents issued by USEPA (USEPA, 1997, 2002, 2010) and the studies by Niu, et al. (Niu et al., 2013). The equations to calculate the average daily dosage (ADD, $\text{mg}/\text{kg}^{-1} \text{day}^{-1}$) of OCPs that the human body is exposed to by the three pathways are listed as Equations 3–5 (USEPA, 1996):

$$ADD_{\text{ingest}} = \frac{C_{\text{soil}} \times \text{IngR} \times \text{EF} \times \text{ED}}{\text{PEF} \times \text{BW} \times \text{AT}} \times CF \quad (\text{Eq.3})$$

$$ADD_{\text{dermal}} = \frac{C_{\text{soil}} \times \text{SA} \times \text{AF} \times \text{ABS} \times \text{EF} \times \text{ED}}{\text{BW} \times \text{AT}} \times CF \quad (\text{Eq.4})$$

$$ADD_{\text{inhale}} = \frac{C_{\text{soil}} \times \text{InhR} \times \text{EF} \times \text{ED}}{\text{PEF} \times \text{BW} \times \text{AT}} \quad (\text{Eq.5})$$

Using the hazard index (HI) method, this study evaluates the non-carcinogenic risk of OCPs; moreover, by dividing the reference daily dosage from each exposure channel (ADD_{ing} , ADD_{dermal} , and ADD_{inh}) by the actual daily dosage from each channel, this study calculates the hazard quotient (HQ) of each channel of exposure (Zhang Jingjing, 2016). By multiplying the life average daily dosage (LADD) and the cancer slope factor (SF), this study calculates the carcinogenic risk (Risk). The calculation equations are as follows (Eqs. 6–9) (USEPA, 2002):

$$HQ = \frac{ADD}{RFD} \quad (\text{Eq.6})$$

$$HI = \sum HQ_i \quad (\text{Eq.7})$$

$$Risk_i = LADD \times SF_i \quad (\text{Eq.8})$$

$$Risk = \sum Risk_i \quad (\text{Eq.9})$$

HI means the overall non-carcinogenic risk of exposure to OCPs via all three channels. When *HI* or *HQ* is < 1 , the risk is considered low or negligible; however, when *HI* or *HQ* is > 1 , it is considered that there are non-carcinogenic risks. *Risk* refers to the level of carcinogenic risk, i.e., the probability of developing cancer. *SF* refers to the cancer slope factor, which indicates the maximum possibility of developing cancer associated with exposure to a certain dosage of a pollutant. When *Risk* is $< 10^{-6}$, the risk of cancer is considered very low; when *Risk* is between 10^{-6} and 10^{-4} , the risk of cancer is considered low; and when *Risk* is $> 10^{-1}$, the risk of cancer is considered high (Niu et al., 2013). The reference dosage and carcinogenic slope factor for each channel are obtained from the Supplemental Guidance for Developing Soil Screening Levels for Superfund Sites issued by USEPA in 2010 (USEPA, 2010).

According to the calculation results, both among children and adults, the three exposure channels are ranked as follows by the dosage of OCPs that enter the human body: ingestion through the mouth > the dosage from inhaling > the dosage from dermal contact. Ingestion is the major channel of exposure to OCPs. By ranking the detected daily dosage of OCPs, the dosage in children from all these three channels is higher than that in adults. In terms of the dosage of exposure, leading to non-carcinogenic risks, the different types of OCPs are ranked as follows: DDT, HCHs, p,p'-DDE, β -HCH, p,p'-DDD, γ -HCH, α -HCH. Table 3 shows the average daily dosages of these OCPs.

Table 3. Average daily exposure of three pathways ($\text{mg}\cdot\text{kg}^{-1}\text{ day}^{-1}$)

	ADD _{ing}	ADD _{dermal}	ADD _{inh}	ADD _{ing}	ADD _{dermal}	ADD _{inh}
DDTs	5.26E-08	1.47E-08	2.32E-08	2.25E-08	8.99E-09	2.19E-08
HCHs	4.64E-09	1.30E-09	2.04E-09	1.99E-09	7.93E-10	1.94E-09
p,p'-DDE	4.21E-09	1.18E-09	1.86E-09	1.80E-09	7.19E-10	1.76E-09
β -HCH	2.39E-09	6.69E-10	1.05E-09	1.02E-09	4.08E-10	9.97E-10
p,p'-DDD	2.23E-09	6.25E-10	9.85E-10	9.57E-10	3.82E-10	9.33E-10
γ -HCH	1.08E-09	3.02E-10	4.76E-10	4.62E-10	1.84E-10	4.50E-10
α -HCH	8.36E-10	2.34E-10	3.69E-10	3.58E-10	1.43E-10	3.49E-10

According to equations and relevant parameters of the three channels, the different types of OCPs are ranked as DDTs > HCHs > α -HCH > β -HCH > p, p'-DDE > p,p'-DDD > γ -HCH in terms of the carcinogenic risk they incur. The carcinogenic risk associated with exposure to OCPs through all the three channels among children is higher than that among adults. As shown by the calculation result, the value of carcinogenic risks associated with exposure to OCPs through different channels is far below 10^{-6} , which indicates that the carcinogenic risk of OCPs in the topsoil of Wenyang Field is small and negligible; hence, it will not pose a threat to human health.

According to certain parameters and calculation of the equations, both among children and adults, the value of non-carcinogenic risk associated with exposure to OCPs via the ingestion channel is higher than that through the dermal contact channel. Note that the value of non-carcinogenic risk associated with exposure to OCPs through the inhaling channel has not been obtained because of the lack of corresponding parameters. In terms of the non-carcinogenic risk associated with exposure through the channels of ingestion and dermal contact, the different types of OCPs are ranked as DDTs > HCHs > β -HCH > γ -HCH > α -HCH. The non-carcinogenic risk (represented by HI) of each type of OCPs is far below 1, which indicates that the non-carcinogenic risk posed by OCPs in the topsoil of Wenyang Field is small and almost negligible.

Pollution source analysis

DDTs have two biodegradation mechanisms in soil, i.e. either DDT is degraded to DDD through reductive dichlorination in anaerobic conditions or it is degraded to DDE through dehydrochlorination in aerobiotic conditions. Note that DDD and DDE are less toxic than DDT, and DDE is very stable. Generally, in the soil contaminated by DDTs, the ratio of (DDE + DDD)/DDT will exceed 1, which indicates that the DDTs have not been used for a long time and that there is no new source of DDT pollution (Cui et al.,

2014). Thus, the ratio of (DDE + DDD)/DDT can be used to identify whether DDTs are used in the study area. In this study, the ratio (*Table 4*) of the 21 sampling sites is below 1(0-0.6), which means DDTs are used recently. If the ratio of (p,p'-DDT + o,p'-DDT)/DDTs is below 0.5, it indicates that the DDT pesticides are used long ago and there is no new source of pollution. The calculated ratio (*Table 4*) in the 21 sampling sites is above 0.5(0.6-1.0), which means that it has not been long since usage of DDTs in most areas of the Dawen River watershed, and DDTs are recently used in the 21 sampling sites (Cui et al., 2014). These two ratios lead to the same conclusion that it has not been long since DDTs are used in the topsoil of the Dawen River watershed.

Table 4. Proportions of DDTs for source identification in surface soil of the study area (ng g⁻¹)

Samples	p,p'-DDE	p,p'-DDD	p,p'-DDT	o,p'-DDT	DDTs	(p,p'-DDD+p,p'-DDE)/DDTs	(p,p'-DDT+o,p'-DDT)/DDTs
WYT-1	9.9	0.9	112.3	0.4	123.5	0.1	0.9
WYT-2	7.4	1.3	143.8	0.9	153.4	0.1	0.9
WYT-3	3.7	0.5	53.8	0.9	58.9	0.1	0.9
WYT-4	0.6	0.3	23.6	0.3	24.8	0.0	1.0
WYT-5	9.5	2.0	75.0	0.4	86.9	0.2	0.9
WYT-6	9.1	2.7	45.1	0.8	57.8	0.3	0.8
WYT-7	3.0	0.8	60.7	0.2	64.7	0.1	0.9
WYT-8	2.7	0.7	42.2	0.3	45.9	0.1	0.9
WYT-9	2.7	0.9	192.7	0.8	197.0	0.0	1.0
WYT-10	12.8	15.6	45.1	1.7	75.2	0.6	0.6
WYT-11	1.3	0.7	16.5	0.1	18.5	0.1	0.9
WYT-12	2.2	0.7	11.7	0.1	14.7	0.3	0.8
WYT-13	1.7	0.8	5.8	0.1	8.4	0.4	0.7
WYT-14	1.6	0.3	16.2	0.1	18.2	0.1	0.9
WYT-15	3.3	1.3	10.0	0.2	14.9	0.5	0.7
WYT-16	1.3	7.1	24.4	0.2	33.0	0.3	0.7
WYT-17	1.1	0.7	16.7	0.5	19.1	0.1	0.9
WYT-18	1.8	0.4	17.1	0.3	19.6	0.1	0.9
WYT-19	2.4	0.5	31.9	0.2	35.0	0.1	0.9
WYT-20	1.6	0.5	42.4	0.1	44.6	0.0	1.0
WYT-21	0.8	4.2	11.0	0.6	16.5	0.1	0.7

HCHs pollution is mainly caused by the usage of HCHs and lindane. In China, after HCHs were banned, lindane has been extensively used in agricultural production; therefore, the components of HCH isomers have been used as indicators for environmental pollution (USEPA, 2010). The components of HCHs include α -HCH (55%–60%), β -HCH (5%–14%), γ -HCH (12%–16%), δ -HCH (6%–8%), ϵ -HCH (2%–9%), heptachlorocyclohexane (4%), and octochlorocyclohexane (0.6%). In lindane, the content of γ -HCH is > 90%. Among the four HCH isomers, β -HCH is the easily absorbed by the soil but is the most difficult to be degraded by microorganisms in the soil. In the natural environment, α -HCH and γ -HCH can be converted to β -HCH. The average percentage of α -HCH, β -HCH, γ -HCH, and δ -HCH detected in this study is 9%,

26.33%, 11.90%, and 3.6% of the average content of HCH. Previously, studies have shown that the ratio of α -HCH/ γ -HCH can be used to analyze the source of HCHs. In particular, when the ratio is < 1 , HCHs are mainly derived from the usage of lindane; when the ratio is near 0, it indicates that lindane has been used recently (Cui et al., 2014); when the ratio of HCH/ γ -HCH falls between 3.44 and 5.00, the source of HCHs may be industrial production; and when the ratio exceeds 5.00, the HCHs may be the previous use of HCHs or biodegradation reactions (Cui et al., 2014). The results (Table 5) show that 33% of the sampling sites have a ratio that approaches 0 (α -HCH/ γ -HCH is below 0.4) and 57% of the sampling sites have a ratio below 1 (0.2-1.0), which indicates that lindane has been recently used in some areas around Wenyang Field. Most areas have no recent use of lindane.

Table 5. Proportions of HCHs for source identification in surface soil of the study area ($\text{ng}\cdot\text{g}^{-1}$)

Samples	α -HCH	γ -HCH	β -HCH	δ -HCH	α -HCH/ γ -HCH	Samples	α -HCH	γ -HCH	β -HCH	δ -HCH	α -HCH/ γ -HCH
WYT-1	0.1	0.3	0.9	0.3	0.4	WYT-12	0.1	0.4	1.7	0.6	0.3
WYT-2	0.6	0.5	1.1	0.1	1.1	WYT-13	0.5	0.3	0.8	0.3	2.1
WYT-3	1.0	0.8	1.5	0.2	1.3	WYT-14	0.4	0.7	1.7	0.1	0.6
WYT-4	0.2	0.8	1.1	0.1	0.2	WYT-15	0.5	0.4	0.7	0.1	1.3
WYT-5	0.7	0.7	1.9	0.1	1.1	WYT-16	0.6	2.2	1.2	0.1	0.3
WYT-6	0.6	1.3	1.3	0.1	0.4	WYT-17	0.6	0.5	1.2	0.1	1.2
WYT-7	0.3	0.6	1.4	0.1	0.4	WYT-18	0.6	0.4	1.0	0.6	1.7
WYT-8	0.7	1.1	1.9	0.1	0.6	WYT-19	1.1	0.7	1.7	0.3	1.7
WYT-9	1.1	0.6	2.7	0.3	1.9	WYT-20	0.4	0.4	1.0	0.1	1.0
WYT-10	1.7	3.4	8.8	1.4	0.5	WYT-21	3.8	3.0	8.5	0.7	1.3
WYT-11	0.4	1.6	3.8	0.6	0.3						

Conclusion

Using gas chromatography, we detected the content of OCPs in 21 topsoil samples of Wenyang Field and analyzed the residue characteristics, health risks, ecological risks, and potential sources of OCPs. We obtained the following results. First, the major components of the 23 types of OC pollutants are DDTs (6.76–222.76 ng/g), endrin aldehyde, heptachlor epoxide, and HCHs (1.22–17.34 ng/g). Note that the detection rates of HCHs and DDTs in the topsoil of the study area can reach 100%. As shown by the map of distribution of OCPs, the pollution level is high in Dawenkou Town and Wenyang Town, while the pollution is relatively low in Ciyao Town and Jiangji Town. Second, when analyzing the ecological risks of OCPs, it is revealed that OCPs pose high ecological risk to soil worms and birds but pose no obvious threats to mammals. Third, the analysis of health risks of OCPs shows that the carcinogenic risk associated with exposure to OCPs through different channels is below 10^{-6} , which indicates that the carcinogenic risk of OCPs in the soil of Wenyang Field is small and negligible. Note that the value of non-carcinogenic risk (represented by hazard index) of each type of OCPs is far below 1, which indicates that the non-carcinogenic risk associated with exposure to OCPs in the soil of Wenyang Field is small and almost negligible. Fourth, the analysis of the sources of OCPs in the study area reveals that OCPs are mainly

derived from residues of OCPs used previously and because of the recent use of lindane. To conclude, the development of biological agents that can clean the soil is important reduction in the usage of pesticides and fertilizers should be encouraged.

Follow-up research can be carried out, (1) A total of 21 samples were collected on the north and south of Dawen River this time, and the number of samples can be increased in the later. (2) Some organic pollutions, such as DDTs and HCHs, are hard to be degraded. In addition to the influence of natural and cultural environment, we can take samples and test in the same place several years later to see whether the pollution concentration will change significantly with time.(3) we can increase humanistic survey to know the changes of frequency, brand and efficacy of pesticides used by local farmers in recent years, Deeply understand the source of organic pollution.

Acknowledgements. This study was supported by National Natural Science Foundation of China (41402319), Supported by the Laboratory for Marine Geology, Qingdao National Laboratory for Marine Science and Technology(MGQNL201802),Shandong Social Science Fund (18CLYJ55), Project of Shandong Natural Science Foundation (ZR2014DL002, ZR2013DL010), Scientific Research Program of Shandong Universities (J18KA197), and Taishan University Talent Research Fund (Y-01-2016001).

REFERENCES

- [1] An, Q., Dong, Y., Wang, H., Ge, C. (2005): OCP residues in soil in Nanjing and distribution characteristics. – *Acta Scientiae Circumstantiae* 25(4): 470-474.
- [2] Chen, F., Wang, J., You, Y., Wang, C. (2011): Characteristics of OCP pollution in soil of vegetable-growing bases in Fuzhou and risk assessment. – *Chinese Journal of Tropical Crops* 6: 1185-1189.
- [3] Chen, L., Feng, Q., He, Q., Huang, Y., Zhang, Y., Jiang, G., Zhao, W., Gao, B., Lin, K., Xu, Z. (2017): Sources, atmospheric transport and deposition mechanism of organochlorine pesticides in soils of the Tibetan Plateau. – *Science of the Total Environment* 577: 405-412.
- [4] Cheng, H., Ding, P., Zhang, M. (2018): Characteristics of pollution of OCP residues in farmland soil in Henan. – *Jiangsu Agricultural Sciences* 46(14): 247-252.
- [5] Cheng, T. (2014): Spatial Distribution of OCP in Soil of Agricultural Areas in Suburban Shenyang and Risk Assessment. – Shenyang University, Shenyang.
- [6] Cui, J., Du, J. Z., Ma, H., Wang, X. (2012): Organic pollution assessment of soil in suburban Shenyang. – *Acta Ecologica Sinica* 34(24): 7874-7882.
- [7] Cui, J., Wang, X., Du, J., Yang, Z., Yue, M., Li, X., Ma, H. (2014): Characteristics of OCP residues of surface soil in suburban Shenyang and risk assessment. – *Geology in China* 41(5): 1705-1715.
- [8] Dai, J., Zhang, J., Yu, C., Pang, X. (2012): Research on OCP residues and sources in soil of Yantai of Shandong. – *Earth and Environment* 40(1): 50-56.
- [9] Jiang, Y., Wang, X., Sun, Y., Sheng, G., Fu, J. (2010): Research on OCP residues in soil of urban areas of Shanghai. – *Environmental Science* 31(2): 409-414.
- [10] Jongbloed, R. H., Traas, T. P., Luttik, R. (1996): A probabilistic model for deriving soil quality criteria based on secondary poisoning of top predators: calculations for DDT and Cadmium. – *Ecotoxicology and Environmental Safety* 34(3): 279-306.
- [11] Lin, T., Qin, Y., Zhang, L., Zheng, B., Li, Y., Guo, Z. (2011): Distribution, sources and risk assessment of OCP and PCB residues in sediments of Dahuofang Reservoir in Niaoning. – *Environmental Science* 23(11): 3294-3299.

- [12] Liu, H., Liu, M., Wu, D., Zheng, J., Zhan, C., Zhang, J., Yao, R. (2013): Characteristics of OCP residues in central and northern farmland in Jilin. – *Journal of Jilin University (Science Edition)* 51(6): 1187-1192.
- [13] Liu, H., Liu, M., Wu, D., Zheng, J., Zhan, C., Zhang, J., Yao, R. (2017): Characteristics of OCP pollution in eastern Hubei province and health risk assessment. – *Journal of Hubei Polytechnic University* 33(3): 19-23.
- [14] Long, E. R., Macdonald, D. D., Smith, S. L., Calder, F. D. (1995): Incidence of adverse biological effects within ranges of chemical concentrations in marine estuarine sediment. – *Environ. Manag.* 19(1): 81-97.
- [15] Ma, J., Qiu, Y., Zhou, H., Zhu, T. (2015): Research on spatial distribution of OCP residues in typical areas of Pearl River Delta based on multivariate geostatistics and GIS - a case study of Huizhou. – *Acta Pedologica Sinica* 47(3): 339-450.
- [16] Meng, P., Li, R., He, Y., Zhang, A., Zhang, L., Jin, M., Liang, Q., Zhang, L. (2017a): Characteristics of pollution of OCP in soil of pastoral areas of Baotou and health risk assessment. – *Modern Preventive Medicine* 44(1): 32-36, 56.
- [17] Meng, P., Li, R., He, Y., Zhang, A., Zhang, L., Jin, M., Liang, Q., Zhang, L. (2017b): Distribution characteristics of OCP in soil of pastoral areas in Inner Mongolia and health risk assessment. – *Journal of Agro-Environment Science* 36(3): 539-546.
- [18] Niu, L., Xu, C., Yao, Y., Liu, K., Yang, F., Tang, M., Liu, W. (2013): Status, influences and risk assessment of hexachlorocyclohexanes in agricultural soils across China. – *Environmental Science & Technology* 47: 12140-12147.
- [19] Pang, X., Zhang, F., Wang, H., Hu, X., Zeng, X. (2009): OCP residues and distribution characteristics in soil in southwestern Shandong province. – *Geological Bulletin of China* 28(5): 667-670.
- [20] Shi, L., Sun, Y., Lv, A., Cai, X., Shen, X., Shen, J. (2016): Distribution characteristics of 22 OCP in soil in Yangtze River Delta. – *Rock and Mineral Analysis* 35(1): 75-81.
- [21] United States Environmental Protection Agency (USEPA) (1996): *Soil Screening Guidance: Technical Background Document*. – EPA/540/R-95/128. Office of Solid Waste and Emergency Response, Washington, DC.
- [22] United States Environmental Protection Agency (USEPA) (1997): *Exposure Factors Handbook*. – EPA/600/P-95/002F; Environmental Protection Agency, Office of Research and Development, Washington, DC.
- [23] United States Environmental Protection Agency (USEPA) (2002): *Supplemental Guidance for Developing Soil Screening Levels for Superfund Sites*. – OSWER 9355.4-24, Washington, DC.
- [24] United States Environmental Protection Agency (USEPA) (2010): *Mid Atlantic Risk Assessment. – Regional Screening Level (RSL) Summary Table*, Washington, DC.
- [25] Wu, J. (2012): *Classification and Evaluation of Buffering and Filtering Functions of Regional Soil - A Case Study of Suburban Areas of Zhengzhou*. – China University of Geosciences, Beijing, pp. 11-13.
- [26] Xiao, P. (2017): Research advances on OCP pollution in soil of Jilin province. – *Heilongjiang Science and Technology Information* 17.
- [27] Zhang, H., Gao, R., Jiang, S., Huang Y (2006): Spatial distribution of OCP residues in farmland soil in Beijing. – *Scientia Agricultura Sinica* 39(7): 1403-1410.
- [28] Zhang, J. (2016): *OCP Residues in Soil-Vegetable System in Suburban Areas of Jilin and Risk Assessment*. – University of Chinese Academy of Sciences, Beijing, pp. 63-77.
- [29] Zhao, X., Lu, H., Luo, H., Li, R., Zhu, Y. (2006): Research on OCP residues in farmland in Cixi City. – *Journal of Ningbo University (Natural Science & Engineering)* 19(1): 98-100.
- [30] Zhu, Y., You, Z., Shen, T., Zhong, H., Chai, L. (2012): OCP and PCB residues in sediments in shellfish culturing areas of intertidal zones in Ningbo and ecological risk assessment. – *Chinese Journal of Applied Ecology* 23(6): 1689-1694.

EFFECTS OF HYDROPONIC MEDIA ON FORAGE AND SILAGE QUALITY OF BARLEY (*HORDEUM VULGARE* L.)

YURTSEVEN, S.^{1*} – GÜLER, A.¹ – SAKAR, E.²

¹*Department of Animal Science, Faculty of Agriculture, Harran University
63300 Şanlıurfa, Turkey*

²*Department of Horticulture, Faculty of Agriculture, Harran University
63300 Şanlıurfa, Turkey*

**Corresponding author*

e-mail: syurtseven@harran.edu.tr; phone: +90-414-318-3474; fax: +90-414-318-3274

(Received 3rd Oct 2019; accepted 8th Jan 2020)

Abstract. This study was carried out to investigate the effects of different substrates (barley+straw and barley+dry olive pulp) on the feed value of barley plants produced in a hydroponic system. In addition, germination of barley was tested in experiment 2 for silage quality. For this purpose, barley was harvested on the 7th day of the experiment. Nutrient contents of plant samples were determined. Dry matter content of the fodders increased significantly with the addition of straw ($P<0.01$), while the ash, ADF and NDF contents significantly increased ($P<0.01$) with the addition of dry olive pulp (prina) ratio. In trial 2, the addition of straw and dry olive pulp increased the dry matter content of the silage while the straw increased the pH of silage ($P<0.01$). The contribution of dry olive pulp increased total ash, ADF and NDF values in silage. Protein levels did not differ in either trials ($P>0.05$). The results revealed that the use of straw is useful in preventing the negative effect of excess water in germination environment. In addition, relative feed value (RFV) and digestible dry matter (DDM) criteria of feeds were quite satisfactory. Nutrient content and other quality criteria of feed indicated that hydroponic barley is a favorable silage material with base materials, though wheat straw was superior to dry olive pulp.

Keywords: *olive pulp, hydroponic farming, germination, animal feed, straw*

Introduction

Supply of quality fresh green feed is one of the major challenges for animal breeders in hot summer months. Traditional fresh green forage production requires land, labor and a significant amount of water. Hydroponic feed production technique converts an energy feed such as barley grain into a green feed and requires less soil, water and labor, and enables production at any time of the year. In addition, the fresh forage produced in hydroponic systems are claimed to have high digestibility (Chung et al., 1989; Islam and Jalal, 2016). Hydroponic systems, unlike other production systems, are based on the reuse of water; thus, consumes 87% less water for the same amount of feed production (Al-Karaki and Al-Moani, 2011). Corn is less preferred because it does not germinate as easily as barley. Wheat and rye are not preferred compared to barley because wheat is consumed as human food. Rye seeds are very small, an efficient germination cannot be achieved in one week and is more suitable for grazing on pasture. Rye grass is not also preferred because it is not a plant that is consumed as grain like barley. This production model is suitable and economical for some annual plants consumed as grain. Barley is most commonly used cheap source in hydroponic systems and can be obtained easily. The harvest is very easy and practical, so it is possible to harvest every day of the year and there is no need for stocking.

Studies conducted on the hydroponic feed production revealed no loss of dry matter or no significant changes in nutrient content (Peer and Leeson, 1985). In contrast, some reports indicated that high humidity in hydroponic fodder adversely affects the feed consumption of animals and excessive moisture causes mold problems in hydroponic production. Therefore, Tudor et al. (2003) recommended the addition of straw during consumption to decrease the moisture and increase dry matter content.

Total of 4500 tons of olive was produced in Sanliurfa province, Turkey in 2016 (TUIK, 2016). Olive pulp is a major byproduct and environmental pollutant of oil extraction process and approximately 70-80% of processed olives turns into olive pulp which corresponds to 3500 tons per year. Olive pulp consists of shell, seed and crushed fruit and can be utilized as a germination medium due to the high nutrient contents. Sansoucy (1985) reported that olive pulp may contain as high as 75 to 80% dry matter, 3 to 5% crude ash, 35 to 50% crude cellulose, 5 to 10% crude protein and 8 to 15% crude oil as dry matter basis (Sansoucy, 1985).

Moisture content of hydroponic feed can be reduced, and nutrient losses can be minimized using agricultural wastes such as straw or dry olive pulp in hydroponic plant production. Dry olive pulp can also provide some nutrients to the germination environment. This study was aimed to cope with high moisture problem in soilless barley production and to reduce nutrient losses in germinated barley by using olive pulp and straw.

Material and Method

The experiment was conducted during April 2014 at the Faculty of Agriculture, Harran University, Turkey. The study consisted of two different germination experiments in controlled room conditions under natural lighting at temperatures varying between 16 and 35°C throughout the experiments.

Experiment 1

The seeds of barley (*Hordeum vulgare* L.), with 88% dry matter and 11% crude protein used as the material in the experiments were purchased from a local grain market and kept in a cold environment (4°C) to ensure the germination (*vernalization*) a day before the start of the experiment. The barley used was the local *Ayhan* variety of malting barley in this study. The germination system was adapted from the system applied by Al-Karaki and Al-Hashimi (2012). Germination experiment was conducted in aluminum trays with the dimensions of 19 × 9 × 3 cm. The first experiment comprised only of the germination of barley and the second experiment was on quality of silage prepared by the germinated barley.

The barley grains, which were kept in the cold for one day, were washed and filtered to remove dust and dirt. In this way, seeds were thoroughly cleaned and disinfected. Barley grains were kept in water for one day to soften the seeds; thus, facilitated the germination. The soften seeds were scattered on trays for the germination.

The effect of three different treatments on germination of barley seeds was investigated. The treatments were control (C, only barley), wheat straw (WB) and dry olive pulp (PB). In control treatment, barley seeds were placed in the trays without any supportive material. Barley seeds were covered with wheat straw in WB and with dry olive pulp in PB treatments. WB and PB were taken up to cover the barley seeds and approximately 15 g for straw and 50 g for dry olive pulp. The aim of experiment 1 was

to investigate the germination power and the effects of wheat straw and dry olive pulp on nutritional value of germinated barley. Wet weight of barley was used to determine the amount of seeds to be sown. Accordingly, 60 g of wet barley seeds were weighed into 0.017 m² trays and left for germination. The amount of seeds corresponded to 3550 g wet barley per m², which was equivalent to 1000 g dry barley grain per m² (Fig. 1).



Figure 1. Barley germination patterns in hydroponics (top right: with dry olive pulp (PB); top left: with wheat straw (WB) and bottom: barley (Control; C))

The seeds were carefully placed into floor of the germination trays up to a height corresponding to finger thickness and covered the whole floor of the trays. Seeds were covered by straw and dry olive pulp to reduce the moisture in hydroponic feed. The trays were placed close to the windows for natural lighting throughout the germination. Temperature and humidity of the environment were recorded during the germination. The temperature varied between 16 and 35°C and humidity ranged from 20 to 66% during the trial. Since water accumulation in the system causes the formation of mold, excess water had to be drained. Therefore, the trays were placed with 1-2% inclination to discharge the excess water. Plants were watered twice a day (morning and afternoon) during the germination process, avoiding over watering and providing good drainage. Irrigation was continued until the water covered all the seeds.

Dense green cover and matted/entangled root accumulation in the tray were the criteria of germination success. The experiment 1 was terminated after 7 days, and the trays were weighed on the morning of 8th day. The biomass harvested in each treatment was measured and green fodder yield was determined. After the germination, straw and dry olive pulp was removed. Plant yield/seed ratio, grass yield, crude protein ratio, protein yield, plant height and root structure were determined. Fresh and dry weights of harvested plants were recorded. Plant samples were dried to a constant weight in an oven at 55°C for two 48 hours. The dried samples were ground to pass through 1 mm sieve for crude protein ratio and protein yield analysis.

Experiment 2

Barley seedlings of C, WB and PB treatments were harvested on day 7 and silage of each treatment was prepared in air tight nylon bags to determine quality traits of silages (Fig. 2). Silage bags were kept for 60 days, and the bags were opened, and samples were analyzed for quality traits. The pH, color, odor and appearance of silage samples were determined, and dry matter contents were measured. Dry matter yield, crude ash, acid detergent fiber (ADF), neutral detergent fiber (NDF) and protein contents were analyzed in air dried silage samples. The NDF and ADF contents were determined by ANKOM-200 fiber analyzer using the method of Van Soest et al. (1991). Nitrogen content was analyzed by Kjeldahl method. Flieg score was calculated using the relationship between pH of silage and dry matter content. There is a high correlation between the silo feed and quality calculated according to following equation (Kara et al., 2009).

$$\text{Flieg score} := 205 + (2 * \text{silage dry matter, \%}) - 40 * \text{pH of silage feed} \text{ (Eq.1)}$$



Figure 2. Making silage of germinated hydroponic product in nylon bags

Estimating the Relative Feed Value, Digestible Dry Matter and Dry Matter Intake

Relative Feed Value (RFV) is an index that estimates the digestible dry matter (DDM) of samples from the ADF and calculates the dry matter intake (DMI) potential (as a percentage of body weight, BW) from NDF. The index is then calculated as DDM multiplied by DMI and divided by 1.29 (Stallings, 2006).

$$\text{Digestible Dry Matter (DDM)} = 88.9 - (0.779 * \% \text{ ADF}) \quad \text{(Eq.2)}$$

$$\text{Dry matter intake (DMI)(\% of BW)} = 120 / (\% \text{ NDF}) \quad \text{(Eq.3)}$$

$$\text{Relative feed value (RFV)} = (\text{DDM} * \text{DMI}) / 1.29 \quad \text{(Eq.4)}$$

Statistical Analysis

The data were analyzed by one-way analysis of variance (ANOVA) test according to the randomized plot design with three treatments (SPSS, 2003). Experiment 1 and 2 were evaluated under 3 different groups by drying in trial 1 and silage in trial 2. Each experiment was analyzed separately; each treatment (C, WB and PB) had three replications. However, RFV, DDM and DMI values of the experiment 1 and 2 were analyzed together. Thus, the effects of different treatments (such as silage application) on feed value were assessed together.

Results

The images of green parts and root formation one week after the germination were shown in *Fig. 3*. Yield and some characteristics of germinated barley in experiment 1 were presented in *Table 1*. Forage yield barley with different hydroponic medium treatments ranged from 1056 to 1315 g m⁻² and the highest green yield was obtained in WB treatment (P<0.01).

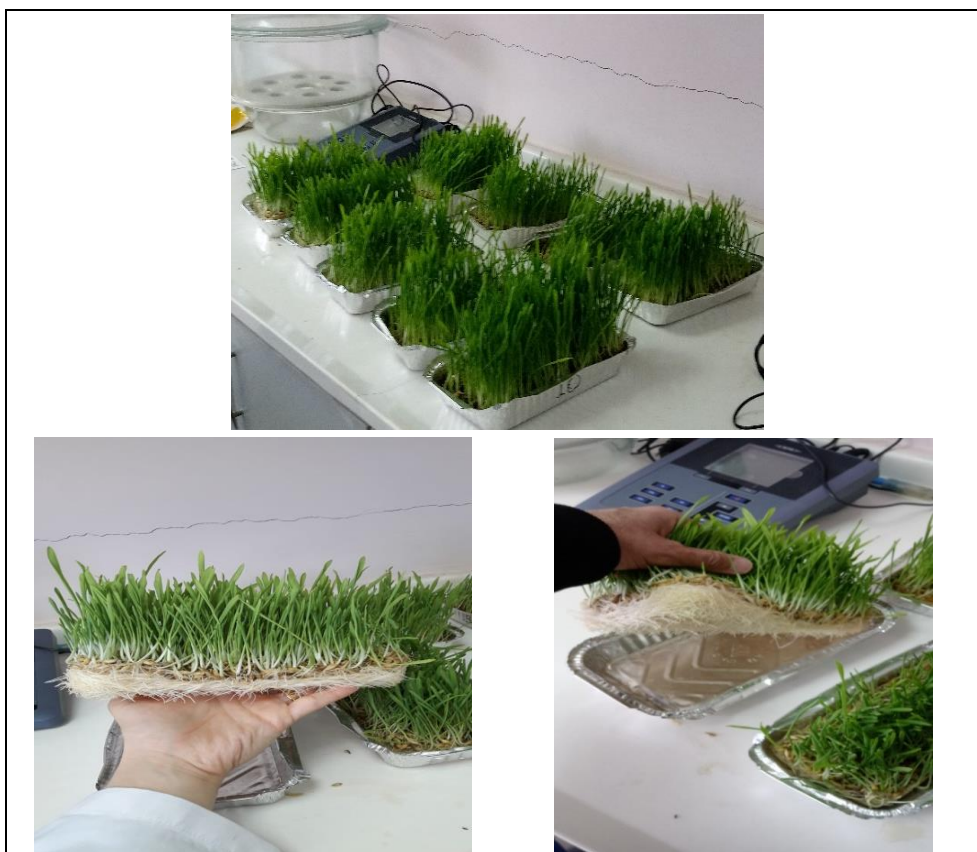


Figure 3. Green parts and root formation of barley plants one week after the germination

Mean dry matter content in WB treatment was significantly (P<0.01) higher than that in C and PB treatments. Total ash, ADF and NDF in PB treatment were higher than those in C and WB (P<0.01). Dry matter yield, total N and crude protein content were not significantly different among different treatments (*Table 1*).

Table 1. Some nutrient contents of barley grown in the hydroponic system (Experiment 1)

		Average	Standard dev.	Standard error	Sig.
Dry matter-biomass, [%]	C	21.25 ^{ab} ^β	3.29	0.92	0.006
	WB	25.75^b	3.45	0.99	
	PB	16.52 ^a	0.44	0.06	
Dry matter, in air-dried biomass [%]*	C	94.05 ^b	2.16	0.72	0.001
	WB	89.88 ^a	1.59	0.50	
	PB	96.02 ^c	1.26	0.39	
Productivity-dry yield [g m ⁻²]	C	1084.7 ^a	141.3	63.2	0.01
	WB	1315.3 ^b	151.9	67.9	
	PB	1056.1 ^a	53.1	23.9	
Dry matter yield, [g per g dry seed]	C	2.56	0.70	0.40	0.22
	WB	3.12	0.33	0.19	
	PB	2.28	0.49	0.28	
Total ash, [%]	C	4.21 ^{ab}	2.00	0.66	0.02
	WB	3.12 ^a	2.28	0.72	
	PB	5.94^b	1.81	0.57	
ADF-dry matter basis, [%]	C	16.53 ^a	0.86	0.43	0.001
	WB	14.77 ^a	1.46	0.73	
	PB	29.81^b	1.37	0.68	
NDF-dry matter basis, [%]	C	33.83 ^b	0.80	0.40	0.001
	WB	40.46 ^a	2.37	1.18	
	PB	47.77^c	1.83	0.91	
N- dry matter basis, [%]	C	1.72	0.14	0.10	0.32
	WB	1.12	0.07	0.06	
	PB	1.73	0.64	0.45	
Crude protein-dry matter basis, [%]	C	10.77	0.91	0.64	0.32
	WB	8.05	0.50	0.35	
	PB	10.85	4.00	2.83	
Germination plant length, [cm]	C	11.46	1.26	0.73	0.21
	WB	11.0	0.45	0.26	
	PB	12.46	0.83	0.48	

*: Determined in air dried samples after reaching to a constant weight.

C: Control (only barley), WB: barley covered with wheat straw, PB: barley covered with dry olive pulp, ADF: Acid detergent fiber, NDF: Neutral detergent fiber, Sig: significance level, ^β: Means followed by different letters are significantly different by each other at P<0.05 level of significance

Some characteristics of barley silage produced in hydroponic system with different cover materials in experiment 2 were presented in *Table 2*. Mean pH value and dry matter content of silage were higher in WB treatment than that in C and PB treatments (P<0.01). ADF and NDF content of silage samples were significantly higher (P<0.01) in PB treatment than that in C and WB treatments. Total N and crude protein content of silage samples were not significantly different among different treatments (*Table 2*).

The RFV values of both experiments were analyzed together in experiment 1 and 2 to assess the overall effect of cover materials and feed value of silage. The lowest DMI, DDM and RFV values were obtained in the PB treatments (P<0.01), while the highest values of RFV and DMI were observed in the WB treatments.

Table 2. Some characteristics of barley silage produced in hydroponic system with different cover materials (Experiment 2)

		Average	Standard dev.	Standard error	Sig.
pH	C	4.11 ^{aβ}	0.19	0.11	0.02
	WB	4.70^b	0.15	0.09	
	PB	4.11 ^a	0.26	0.15	
Flieg score	C	80.15 ^a	8.04	4.64	0.06
	WB	83.39 ^{ab}	8.43	4.86	
	PB	97.09 ^b	5.96	3.44	
Dry matter-biomass, [%]	C	19.16 ^a	8.69	4.34	0.02
	WB	33.86^b	1.83	1.05	
	PB	32.98 ^b	2.58	1.49	
Total ash, [%]	C	0.97	1.37	0.79	0.52
	WB	1.42	1.60	1.13	
	PB	10.57	16.83	9.71	
ADF-dry matter basis, [%]	C	17.49 ^a	2.19	1.09	0.001
	WB	18.29 ^a	1.54	0.77	
	PB	30.94^b	3.86	1.93	
NDF-dry matter basis, [%]	C	34.77 ^a	2.53	1.26	0.001
	WB	33.67 ^a	0.85	0.42	
	PB	40.99^b	1.22	0.61	
N-dry matter basis, [%]	C	1.44	0.26	0.19	0.92
	WB	1.13	0.06	0.07	
	PB	1.46	0.007	0.005	
Crude protein-dry matter basis, [%]	C	9.04	1.68	1.18	0.92
	WB	8.15	0.52	0.35	
	PB	9.17	0.04	0.03	

C: Control, barley only, WB: Barley covered with wheat straw, PB: Barley covered with dry olive pulp, Sig: significance level, ^β: Means followed by different letters are significantly different by each other at P<0.05 level of significance

Discussion

In contrast to Fazaeli et al. (2012) and Kılıç (2016) who stated that dry matter content of the hydroponic green feed does not substantially change compared to the grain form of the same feed (88%), the results showed that dry matter production was significantly improved in a short period of time (7 days). This is one of the important outcomes of our study. Although the cover materials were removed after the germination, dry matter content (90 and 96%, respectively) in WB and PB treatments was higher than that in control (barley-only) treatment (89.8%). The improvement in dry matter content was even more pronounced in the PB treatment. The highest dry matter yield was obtained in straw supported hydroponic barley; however, no significant change was observed in dry matter yield of control and PB treatments. The results revealed that contribution of straw cover on germination and subsequent growth of barley as indicated by the dry matter yield was greater compared to that of olive pulp.

Straw-supported hydroponic forage production improved the efficiency of water use. The productivity was higher in WB treatment compared to control and PB treatments. This result could be attributed to the high level of dry matter content in WB treatment

which absorbed higher water and provided a more suitable environment for germination. The results showed that straw can be an important cover material to eliminate the mold problem caused by high humidity in hydroponic forage production.

Crude protein content of fodder in all treatments was similar that could be related to the removal of straw cover material from the medium after the germination, and low protein content of olive pulp. Although the cover materials were removed from the environment after the germination, some of the dry olive pulp may have remained in the environment as dust or thinner form. Total ash, ADF and NDF contents in PB treatment were higher compared to the control. This could be ascribed by the high level of ash, ADF and NDF contents in dry olive pulp. Therefore, total ash content of dry olive pulp caused an increase in ash level of hydroponic barley fodder.

Plant height and root development were not significantly different among the treatments. The highest plant height during the 7-day of germination period was 12 cm. The results showed that the cover materials did not affect the growth rate, however, they could suppress the excess moisture occurring in the hydroponic environment. Gunasekaran et al. (2018) used plastic trays with cover materials to germinate barley seeds in hydroponic barley cultivation. Like the results on growth rate reported in our study, Gunasekaran et al. (2018) stated that the cover material did not affect the growth rate. However, they found that paddy husk and bagasse provided the highest forage yield. The researchers placed the cover materials on the floor of trays and stated that the entangled structure between the roots and the base material caused the waste of feed. However, the cover materials were used to cover the barley seeds in the trays (*Fig. 1*); thus, matted structure problem between the roots and the cover material was not observed in our study.

The study did not focus on measuring seed density per square meter. However, the seeding rate used was about 1000 g m⁻² which resulted in a certain amount of dry yield increase and no fungal contamination. Naik et al. (2015) reported that high seed density increased the chances of microbial contamination in the root mat, which in turn affected the growth of the sprouts. The fodder yield obtained from 1000 g dry seed m⁻² density for 7 days was 1315 g. Al-Karaki and Al-Hashimi (2012) used 400 g m⁻² seeding rate for barley and obtained 1122 g dry yield m⁻² for 8 days not 7 days.

The pH value and dry matter content in WB treatment were significantly increased during silage making, and this was quite favorable for silage quality (*Table 2*). The results revealed that the use of straw cover material during germination caused drier germination environment which had an effect on pH increase. The changes ADF and NDF contents were significantly important and related to the use of dry olive pulp as the cover material. The cell wall components of dry olive pulp increased the cell wall of the silage produced in PB treatments. The ash content of barley silages was increased in PB treatments during silage due to the high ash content of dry olive pulp (*Table 2*). The cell wall deposition, such as the percentage of NDF and ADF probably, increased the ash content of silage in PB treatment. Reasonable silages in terms of Flieg score were produced in WB and PB treatments due to the contribution of straw or dry olive pulp to ambient pH and dry matter level.

The highest RFV and DMI values were observed in the WB treatments where straw was used as the cover material (*Table 3*). The animal consumption of some fodders may negatively be affected due to the high moisture content of the fodders. Therefore, Fazaeli et al. (2012) and Tudor et al. (2003) suggested adding some hay to decrease the moisture and raise the dry matter contents of fodder. Mean DMI value of green feed in WB

treatment was higher in our study. The RFV value is used generally to compare similar forages for the consumption and digestion (Wettstein et al., 2000). The RFV values were found as “Prime” for all fodders according to the Quality Grading Standard assigned by the Hay Market Task Force of American Forage and Grassland Council. Since DDM value is affected from ADF content of feeds, higher DDM value in WB treatments can also be attributed to the lower ADF content (Robinson, 2005).

Table 3. The RFV, DDM and DMI values of samples from Experiment 1 and 2

Parameters of feed evaluation	Samples						SEM	Sig.
	Experiment 1			Experiment 2				
	C	WB	PB	CS	WB	PB		
DDM, [%]	77.4 ^{cβ}	76.0 ^{bc}	65.7 ^a	75.3 ^{bc}	74.6 ^b	64.8 ^a	0.7	0.01
DMI, [% BW]	3.0 ^b	3.5 ^c	2.5 ^a	3.5 ^c	3.6 ^c	2.9 ^b	0.1	0.01
RFV	178.5 ^c	209.1 ^d	128.0 ^a	202.2 ^d	206.3 ^d	147.1 ^b	4.4	0.01

RFV: Relative feed value, DDM: Digestible dry matter (% of body weight), DMI: Dry matter intake (% of body weight, C: Control (only barley germination), WB: barley covered with wheat straw, PB: barley covered with dry olive pulp, ^β: Means followed by different letters are significantly different by each other at P<0.05 level of significance

Conclusion

Feed analysis showed that dry matter protein content of the barley fodder produced in hydroponic system increased; however, the protein value did not significantly differ from the barley grain seeds as a percent of dry matter. The results concluded that barley is a good grain for fodder and silage production under hydroponic conditions. In addition, the green and silage feed values obtained are satisfactory and better-quality hydroponics can be produced in the germination environments supported by cover materials (straw and dry olive pulp). The results revealed that wheat straw was more effective than dry olive pulp which had no significant effect on all parameters compared to control in experiment 1 and 2. This production model is suitable for some annual plants consumed as grain and it is not a suitable production method for plants with very small seed. On the other hand, since this type of production is not effective and economical for perennial plants, it would be useful to conduct studies on some other annual forage plants.

Acknowledgements. This work was supported by the Harran University Research Committee under Grant [HUBAB-Research Projects Unit, Şanlıurfa, Turkey. Project no. -2018/17253].

REFERENCES

- [1] Al-Karaki, G. N., Al-Momani, N. (2011): Evaluation of some barley cultivars for green fodder production and water use efficiency under hydroponic conditions. – Jordan Journal of Agricultural Sciences 7: 448-456.
- [2] Al-Karaki, G. N., Al-Hashimi, M. (2012): Green fodder production and water use efficiency of some forage crops under hydroponic conditions. – International Scholarly Research Network ISRN Agronomy 2012: 1-5.
- [3] Chung, T. Y., Nwokolo, E. N., Sim, J. S. (1989): Compositional and digestibility changes in sprouted barley and canola seeds. – Plant Foods for Human Nutrition 39: 267-278.

- [4] Fazaeli, A., Golmohammadi, H. A., Tabatabayee, S. N., Asghari-Tabrizi, M. (2012): Productivity and nutritive value of barley green fodder yield in hydroponic system. – *World Applied Sciences Journal* 16(4): 531-539.
- [5] Gunasekaran, S., Bandeswaran, C., Valli, C. (2018): Low-cost hydroponic fodder production technology for sustainable livestock farming during fodder scarcity. – *Current Science* 116: 526-528.
- [6] Islam, R., Jalal, N. (2016): Effect of seed rate and water level on production and chemical analysis of hydroponic fodder. – *European Academic Research* 4(8): 6724-6753.
- [7] Kara, B., Ayhan, V., Akman, Z., Adıyaman, E. (2009): Determination of silage quality, herbage and hay yield of different triticale cultivars. – *Asian Journal Animal Veterinary Advances* 4(3): 167-171.
- [8] Kılıç, U. (2016): Kaba yem üretiminde hidroponik tarım sistemleri. – *Türk Tarım Gıda Bilim ve Teknoloji Dergisi* 4: 793-799.
- [9] Naik, P. K., Swain, B. K., Swain, N. P., Singh, N. P. (2015): Review-production and utilisation of hydroponics fodder. – *Indian Journal Animal Nutrition* 32(1): 1-9.
- [10] Peer, D. J., Leeson, S. (1985): Nutrient content of hydroponically sprouted barley. – *Animal Feed Science and Technology* 13: 191-202.
- [11] Robinson, P. H. (2005): Estimating alfalfa hay and corn silage energy levels, UC Davis Equations using NDF, ADF. – *Proceedings, 31st California Alfalfa and Forage Symposium, 12-13 December, 2001, Modesto, CA, UC.*
- [12] Sansoucy, R. (1985): Olive by-products for animal feed. Review. – *FAO Animal Production and Health Paper 43, Food and Agriculture Organization of the United Nations, Rome.*
- [13] Stallings, C. C. (2006): Relative Feed Value (RFV) and Relative Forage Quality (RFQ). – *Nutrition & Forage Quality* 540: 231-3066.
- [14] Tudor, G., Darcy, T., Smith, P., Shallcross, F. (2003): The intake and live weight change of drought master steers fed hydroponically grown, young sprouted barley fodder (Auto Grass). – *Department of Agriculture Western Australia.*
- [15] TUIK (2016): Plant production statistics. – *Agricultural Statistics Database. Turkish Statistical Institute, Ankara.*
- [16] Van Soest, P., Robertson, J., Lewis, B. A. (1991): Methods for dietary fiber, Neutral Detergent Fiber and Non-starch Polysaccharides in relation to animal nutrition. – *Journal of Dairy Science* 74(10): 3583-3597.
- [17] Wettstein, H. R., Machmuller, A., Kreuzer, M. (2000): Effects of raw and modified canola lecithins compared to canola oil, canola seed and soy lecithin on ruminal fermentation measured with rumen simulation technique. – *Animal Feed Science and Technology* 85: 153-169.

EVALUATION AND COMPARISON OF A NEW TYPE OF TEMPORARY IMMERSION SYSTEM (TIS) BIOREACTORS FOR MYRTLE (*MYRTUS COMMUNIS* L.)

AKA KAÇAR, Y.^{1,2*} – BIÇEN, B.² – ŞİMŞEK, Ö.³ – DÖNMEZ, D.² – EROL, M. H.²

¹*Horticulture Department, Agriculture Faculty, Çukurova University, Adana 01330, Turkey*

²*Biotechnology Research and Application Center, Çukurova University, Adana 01330, Turkey*

³*Horticulture Department, Agriculture Faculty, Erciyes University, Kayseri 38280, Turkey*

**Corresponding author*

e-mail: ykacar@cu.edu.tr; phone: +90-322-338-6084(2146)

(Received 4th Oct 2019; accepted 4th Dec 2019)

Abstract. Myrtle is known to be an important aromatic and medicinal plant species. Myrtle plant is consumed mainly as spice having several uses in the perfumery, food and pharmaceutical industries. It is also widely used for ornamental purposes such as fencing, roadsides, and green cutting. Plant tissue culture techniques are an essential tool to micropropagate for the plant producer. TIS (Temporary immersion systems) is an alternative plant tissue culture technique for micropropagation mechanism in plant species. A new culture vessel named PlantForm TIS bioreactor has been recently developed. In the present study, we aimed to evaluate and compare a new type of TIS bioreactors with agar media for myrtle. MS (Murashige and Skoog) medium supplemented with 1 mg l⁻¹ BAP (benzylaminopurine) was used for multiplication, with 1 mg l⁻¹ IBA (indole-3-butyric acid) for rooting. Two different immersion times (4 h and 8 h) were compared with the solid agar medium. Plantlets growing in PlantForm systems performed better than those in the solid medium. All data recorded at micropropagation and rooting treatments were much more successful. In conclusion, PlantForm TIS bioreactor presents a valid alternative to traditional in vitro micropropagation and rooting systems, resulting in a reduction of cost, labor, and time for the mass propagation.

Keywords: *benzylaminopurine, micropropagation, PlantForm, plant tissue culture, bioreactor*

Introduction

Myrtus communis L., commonly named myrtle, a valuable medicinal and aromatic species (Wannes et al., 2010; Dahmoune et al., 2015). Myrtle is known to be a member of the Myrtaceae family, which contains 3,000 species naturally growing in tropical and subtropical regions. Myrtle is mostly consumed as spice having several practices in the food, pharmaceutical, and industries (Sumbul et al., 2011; Casaburi et al., 2015). Myrtle plant could also be used as ornamental purposes such as fencing, roadsides, and green cutting (Shekafandeh, 2007; Danial, 2009). Myrtle broadly grows in 500-600 m altitude, most notably in pine forests and riversides in the Taurus Mountains of Turkey (Aydın and Özcan, 2007). Myrtle has several genotypes with yellowish-white or bluish-black colored fruits (Şan et al., 2015).

Many different biotechnological methods could be performed to fruit crops to get better ones during plant breeding strategies. One of the critical applications of biotechnology is known to be plant tissue culture in fruit science. Plant tissue culture techniques include several processes of clonal propagation and micropropagation. Known technologies in plant biotechnology have been expanded to contain virus elimination, somatic embryogenesis, organogenesis, production of haploid plants and

somatic hybridization as well as bioreactors (Idowu, 2009; Donmez et al., 2016). Bioreactors containing liquid media for micropropagation and rooting started to become more popular thanks to the low production costs (Paek et al., 2001) and the ease of scaling-up (Preil, 1991). Several bioreactor systems have been published (membrane raft system, nutrient mist bioreactor, and temporary immersion bioreactor) (Akita and Takayama, 1994). Among these systems, temporary immersion bioreactor has become more popular. TIS is simple to use and gives mass production rate with minimum physiological disorders (Afreen, 2008).

In practice, TIS wetting the entire culture or plant tissue used as explant with a nutrient medium, and then draining away of the excess nutrient medium under gravity consequently, the plant material has access to air defined as temporary immersion system. TIS usually involves two different cycles; one of them is a wetting, and the other is the drying cycle occurring periodically (Afreen, 2008). Various temporary immersion systems have been developed like RITA, RALM, PLANTIMA, SETIS as well as PlantForm. The RITA system has been found to increase root development in *Hevea brasiliensis* (Etienne et al., 1997). The bioreactor RALM (Biorreatores RALM, Ralm Industria e Comercio Ltda., Brazil) is a TIS, operating on the Twin-Flask principle. The SETIS system (Vervit, Belgium, distributed by Duchefa Biochemie, The Netherlands) operates similarly as the Ebb-and-Flow TIS system. PLANTIMA (A-Tech Bioscientific Co., Ltd., Taiwan) is a small volume TIS, operated on the RITA principle and has been used for plantlet propagation (Yan et al., 2010, 2011). Box-in-Bag is a disposable TIS, operating on the principle of the Ebb-and-Flow TIS. The WAVE bioreactor is a mechanical rocking platform that uses disposable pre-sterilized cultivation bags (Eibl and Eibl, 2006, 2008; Eibl et al., 2009; Georgiev et al., 2014).

An immersion cycle consists of the frequency and duration of immersion. It means immersion should be applied with a planned time and frequency. Immersion cycles directly affect the plant micropropagation by influencing water and nutrient uptake and in addition to that hyperhydricity of the cultured plant tissue (Albarran et al., 2005).

Liquid-based systems have been known to be much more suitable to automation and, consequently, appropriate for the reducing of costs and labor, as a liquid medium could be changed readily during scaling-up, and the cleaning of boxes is simplified compared to agar-based systems (Preil, 1991).

The present study is the first report for myrtle micropropagation with TIS. We aimed to determine the effects of the traditional tissue culture method and PlantForm Temporary Immersion System at in vitro propagation and rooting on Myrtle.

Materials and methods

Plant material

Myrtle, *Myrtus communis* L., genotype was used for in vitro micropropagation and rooting both PlantForm temporary immersion system and traditional solid medium. Plant material was obtained from a commercial seedling company in Adana, Turkey.

Surface sterilization

Shoot tips of Myrtle plants were cut from donor plants and washed firstly under running tap water about 10 min and then the plant material plunged in 70% ethanol for 2 min, and dipped in 10% solution of sodium hypochlorite (commercial bleach solution

with 4.5% active chlorine, v/v, NaOCl; Domestos®) together with 1–2 drops of Tween-20 for 20 min afterward, the plant material was washed three-four times with sterile distilled water.

Multiplication medium

MS (Murashige and Skoog, 1962) medium were used for multiplication. MS supplemented with 1 mg l⁻¹ BAP (benzylaminopurine), 30 g l⁻¹ sucrose, 8 g l⁻¹ agar, pH 5.8 were prepared and autoclaved at 121 °C for 15 min. Shoot tips of myrtle were cultured and propagated on MS medium, and incubated in a growth chamber at 25 ± 2 °C under cool white fluorescent light at 16 h photoperiod condition. Plants were propagated until we have enough plant material to experiment with PlantForm system (Fig. 1) and solid medium at the same time.

Micropropagation on PlantForm and solid medium

MS medium supplemented with 1 mg l⁻¹ BAP, 30 g l⁻¹ sucrose with 8 g l⁻¹ agar (all Sigma-Aldrich, St. Louis, USA) were prepared in magentas [(9 plantlets/magenta) (76.20 x 76.20 x 10.16 mm)] for solid medium, without agar for PlantForm bioreactor system [120 plantlets/box (180 x 150 x 150 mm)]. pH of media was adjusted to 5.8 and autoclaved at 121 °C for 15 min. The plantlets that developed were subcultured onto fresh MS media in Magenta and PlantForm boxes for three times in every six weeks. Two different immersion time were performed in PlantForm bioreactor system: 15 min/4 h and 15 min/8 h. The air was renewed for 15 min/4 h with a pumping system adjusted by an automatic timer for the regulation of aeration and medium supply to the plant material in the temporary immersion system for both treatments. At the end of the three subculture, micropropagation rate, average plant length (cm), number of leaves, fresh weight (g) and dry weight (g) were recorded.

Rooting medium

Shoots coming from micropropagation were moved to MS medium supplemented with the same components with multiplication medium except for BAP. For rooting 1 mg l⁻¹ IBA were used. The cultures were maintained incubated in a growth chamber at 25 °C under cool white fluorescent light at 16 h photoperiod condition. Six weeks later rooting rate, numbers of roots, fresh weight (g), dry weight (g), length of roots, and plants (cm) were recorded.

The plants were weighed on a precision balance and this was recorded as fresh weight. The plants that fresh weight was determined were weighed after being kept in 70 °C drying-oven for 3 days and the results were recorded as dry weight. Plant and root lengths were measured with a ruler.

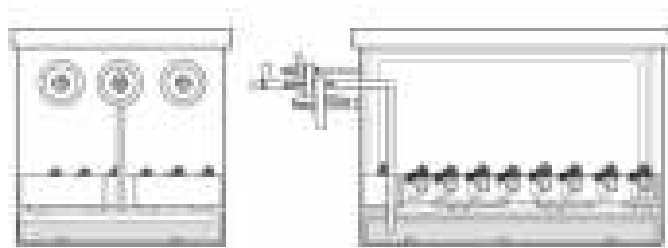


Figure 1. PlantForm TIS bioreactor system (the size is 180 x 150 x 150 mm)

Acclimatization

Plantlets well-developed in PlantForm bioreactor and magenta boxes were removed and roots of the plant material were gently washed under running tap water and plunged in a liquid including 50% (w/v) of a 2.5 g l⁻¹ fungicide (Captan 50WP, Fruit&Ornamental, NY, USA) for 10-15 s and afterward moved to plastic pots (7 cm × 7 cm width and length) including autoclaved peat (Klasmann, KTS-1) and perlite (1:1, v/v). Then, myrtle plants were replaced in a controlled greenhouse under natural light at 95-98% relative humidity and 22-24 °C.

Data analysis

All studies were performed according to a completely randomized design. Experiments were repeated twice with three replicates. Micropropagation rate was calculated as the number of shoots having after culture/total number of plants. The rooting rate was calculated by dividing the number of rooted plants by the number of total plantlets in rooting assays. All quantitative data calculated as percentage value were subjected to arcsine transformation before variance analysis. All data were expressed as means, and analysis of variance was performed. Means detected the statistically different were separated by least significant difference test (LSD) to evaluate differences among PlantForm 4h-8h immersion time and solid medium in Myrtle. Statistical analysis was performed by using JMP® software (SAS Institute, Cary, NC) ver. 8.00.

Results and discussion

Micropropagation on PlantForm and solid medium

The effects of PlantForm TIS bioreactor for myrtle were evaluated and compared with the traditional solid medium. Plantlets growing in PlantForm system were better than the solid medium. All data recorded at micropropagation treatments are much more successful. Micropropagation rate (%), plant length (cm), number of leaves, fresh weight (g) and dry weight (g) coming from PlantForm 4 h and 8 h immersion time and solid medium were presented *Table 1*. Micropropagation rate was detected statistically significant and calculated as 11.40 (PlantForm 8 h immersion), 8.55 (PlantForm 4 h immersion), and 6.25 (Solid medium). Similarly, there were important differences in plant length. The average plant length (cm) was detected only 3.12 cm in solid medium. However, plantlets coming from PlantForm 8 h immersion time 8.80 cm, PlantForm 4 h immersion time 7.95 cm. When compared to PlantForm 8 h, PlantForm 4 h immersion and solid medium, PlantForm systems were effective in plant mass. The mean fresh weight is 1.00, 0.59, and 0.17 g, and dry weight is 0.26, 0.11, 0.02 g, the number of leaves is 66.70, 51.85, and 38.80, respectively. Apparent differences between the agar medium and PlantForm were shown in *Figure 2*.

Rooting medium

The effects of PlantForm TIS bioreactor for rooting in myrtle were evaluated and compared with the traditional solid medium. Plantlets coming from PlantForm and Solid micropropagation media were transferred to rooting media. Rooting rate was calculated as 100% for PlantForm system in different two immersion time, but in the

solid medium, only 70% of plantlets were rooted. The roots were initiated in the media about after 10-15 days of inoculation. All data recorded at rooting treatments are much more successful similar to micropropagation data. Plant length (cm), root length, number of the root, fresh weight (g), and dry weight (g) at PlantForm 4 h and 8 h immersion time, and solid medium were presented *Table 2*. Plant length was calculated the highest in PlantForm 8 h immersion (15.10 cm), the lowest in solid medium (4.59 cm). The results of root length were also similar to plant length. The most successful treatment was detected PlantForm 8 h immersion time with 8.10 cm. It is only 1.45 cm in solid medium. It is about 6 times more in PlantForm system than a solid medium. PlantForm system (8 h immersion) was much more effective in root mass when compared to PlantForm 8 h, PlantForm 4 h immersion time and solid medium. The mean fresh weight is 1.54, 0.59, and 0.44 g, and dry weight is 0.068, 0.660, 0.018 g, the number of roots is 5.40, 4.10, and 2.01, respectively.

Acclimatization

Plantlets with shoots and roots from PlantForm bioreactor and magenta boxes were transferred to plastic pots. Plants were successfully acclimatized in a greenhouse. There were no statistical differences among the treatments on survival. However, plants from PlantForm bioreactor systems showed better performance on survival (*Fig. 2F*).

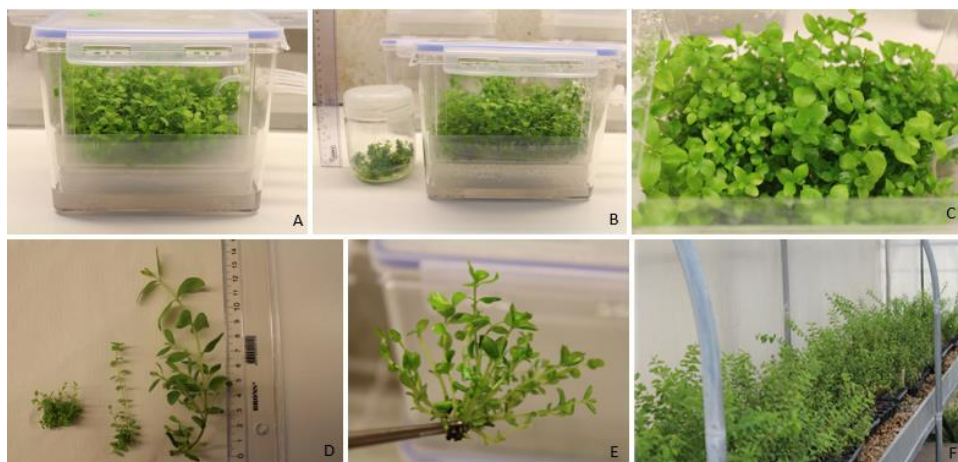


Figure 2. *A* PlantForm box with myrtle plantlets. *B* Agar medium and PlantForm. *C* Plantlets in the PlantForm box. *D* Myrtle plantlets from PlantForm and agar medium. *E* A plant from PlantForm. *F* Acclimatized plants in the greenhouse

Table 1. Data of micropropagation treatments in PlantForm and solid media for myrtle

Medium	Micropropagation rate	Plant length (cm)	Number of leaves	Fresh weight (g)	Dry weight (g)
PlantForm 8 h immersion time	11.40a	8.80a	66.70a	1.00a	0.26a
PlantForm 4 h immersion time	8.55ab	7.95a	51.85ab	0.59b	0.11b
Solid medium	6.25b	3.12b	38.80b	0.17c	0.02b

LSD_{Micropropagationrate} = 4.41, LSD_{Plantlength} = 1.71, LSD_{Numberofleaf} = 19.17, LSD_{Freshweight} = 0.30, LSD_{Dryweight} = 0.12

Table 2. Data on rooting treatments in PlantForm and solid media for myrtle

Medium	Plant length (cm)	Number of roots	Root length (cm)	Fresh weight (g)	Dry weight (g)
PlantForm 8 h immersion time	15.10a	5.40a	8.10a	1.54	0.068a
PlantForm 4 h immersion time	11.20b	4.10a	3.80b	0.59	0.660a
Solid medium	4.90c	2.01b	1.45c	0.44	0.018b

LSD_{Plantlength} = 1.99, LSD_{Numberofroot} = 1.66, LSD_{Rootlength} = 1.75, LSD_{Freshweight} = N.S, LSD_{Dryweight} = 0.01

TIS bioreactors are an alternative in vitro micropropagation mechanism for plant species. There are several different TIS systems; Gravity Immersion Bioreactors (BIG), Temporary Immersion Bioreactors (BIT®), Recipient for Automated Temporary Immersion (RITA®). However, these bioreactors are either too small or too heavy to handle with a small interior bottom, which often leads to disorders of cultures due to high density (Welander et al., 2007). In order to solve the problems of TIS, a new culture vessel named PlantForm TIS bioreactor has been recently produced (Welander et al., 2014). Since the first report of a liquid culture in TIS of about 30 years ago, numerous prototypes have been developed. Among these, PlantForm, a recently-developed TIS device, allowing periodic medium immersion and independent ventilation of containers (Lambardi et al., 2015). Immersion frequency could affect micropropagation and rooting in TIS cultures. Therefore, it is a critical issue to adjust optimum immersion time. The effect of immersion frequency (6, 8 and 12 h) for in vitro propagation of *Gerbera jamesonii* were investigated by Frómeta et al. (2017) in BIT system. They reported that immersion every 8 h with additional ventilation produced more shoots with better morphology than the control. However, when shoots were immersed every 6 h, shoots had higher fresh and dry weight. In the present study, we applied two different immersion time (4 h and 8 h) for myrtle. It was observed the better result in both micropropagation and rooting at 8 h immersion time. Damiano et al. (2007) investigated that growth performances of *Rubus fruticosus*, *Arbutus unedo* and *M. communis* plants by using a TIS composed of two glass bottles connected with a silicone tube; one of the bottles was used to contain explants which layed on glass beads. Immersion time was adjusted to 120 min/day. They compared to those in solid and stationary liquid conditions and, determined much higher multiplication rates in the TIS: *Rubus fruticosus* (x9.3), *M. communis* (x8.4), *Arbutus unedo* (x3.6). We also had a higher multiplication rate from PlantForm TIS for myrtle. Here, we detect a better multiplication rate in myrtle; it is high because PlantForm was positively affected the development of plants. Another reason could be the immersion time. Multiplication rate is higher in the 8 h immersion time than 4 h.

In different plant species, several TIS were used and tested. Ramírez-Mosqueda and Iglesias-Andreu (2016) compared BIT, BIG and RITA systems for multiplication and rooting of *Vanilla planifolia*. They found that a higher number of shoots/explant were observed in the multiplication phase in BIT systems (18.06 shoots/explant), followed by RITA (12.77) and BIG (6.83). In the rooting phase, a higher number of longer roots were obtained in BIT compared with BIG and RITA. It is clear that different systems could show conflicting results in the same genotype. PlantForm, in our study, gave high

positive results for micropropagation and rooting on myrtle. The success of PlantForm also was reported by Lambardi et al. (2015). Its performance with ornamental (*Carex oshimensis* 'Evergreen' and *Chrysanthemum morifolium*) and fruit species (*Ficus carica* and *Ribes rubrum*) is critically analyzed. The results confirmed the convenience of the PlantForm-based TIS for the proliferation of high-quality shoot clusters; moreover, with some species, the system stimulated the contemporary proliferation and rooting of shoots, which can be maintained in proliferation or directly transferred to the acclimatization phase. In another study, the effectiveness of the PlantForm bioreactor in micropropagation of myrtle and olive was examined through measurements of biomass production during the subcultured period in comparison to semi-solid medium culture. The results showed that both species are well adapted to growth in the bioreactor, with survival rates and quality of the crops higher than those obtained under standard culture conditions. Furthermore, the case of myrtle shoot cultures demonstrated the possibility to reduce the concentration of macro and micronutrients in the liquid medium without compromising the growth rates (Benelli et al., 2014).

Temporary immersion bioreactor system could also use for obtaining somatic embryos. Albarran et al. (2005) obtained somatic embryos in *Coffea arabica* L. using a temporary immersion bioreactor system. They optimized the immersion cycles to increased production and quality of embryos. Researches revealed that increasing the frequency of short immersions (1 min immersion every 24, 12 and 4 h) affected embryo production (480, 2,094 and 3,081 embryos/1-l bioreactor, respectively) and improved quality (60, 79 and 85% of torpedo-shaped embryos, respectively).

In tissue culture, cytokinins and auxins are remarkable medium contents in detecting the developmental pathways of the plant cells. Cytokinins induce adventitious bud formation in cultures (Rajbhar et al., 2016). Auxins play significant roles in the growth and differentiation of cultured cells and tissues (Alexandrova et al., 1996; Bohidar et al., 2008; Ngomuo et al., 2013). There are some reports that different cytokinins and auxins were used and compared for myrtle micropropagation and rooting in agar media. Rezaee and Kamali (2014) investigated the effect of different media and different plant growth regulations and the concentration of shoot proliferation in myrtle. The results indicated that between, MS and WPM, media, WPM showed better results rather than MS. In shoot proliferation stage were used BA at levels of 0, 0.5, 1, 2, 3, 4, 5 and 6 mg l⁻¹ and IBA at levels of 0 and 0.1 mg l⁻¹, then three traits containing: leaf number, shoot length and shoot proliferation were examined. The best result was obtained by using of modified WPM medium with BA in 4 and IBA in 0.1 mg l⁻¹. In the present study, we also used 1 mg l⁻¹ BAP, and we had positive results on the multiplication rate. Different auxins can be used for rooting of plants in in vitro cultures. Auxins such as NAA, IBA, IAA routinely use for plant rooting in vitro cultures. Scarpa et al. (2000) evaluated the influence of two IAA concentrations (0.5 mg l⁻¹ and 1 mg l⁻¹) and different medium to induce root induction of Myrtle. Researchers found that the best rooting results (61%) were obtained with O13 medium containing 1 mg l⁻¹ IAA. Hatzilazarou et al. (2001) investigated the rooting capability of two myrtle clones, with large (clone A) and small (clone B) leaves. Shoots transferred to WPM medium containing several concentrations (0, 0.5, 1 or 2 µM) of IBA, IAA or NAA in rooting assays. According to this study, the best rooting was achieved with the application of 0.5 µM IBA (96% rooting) and 1 µM IAA (100% rooting) for clone A and B, respectively. Ruffoni et al. (2010) determined that IAA and IBA at 0.5 mg/L increased the rooting percentage and evidenced a difference in the shape and length of the roots in myrtle plant. Aka Kacar et al. (2017)

investigated the effects of different IBA (0, 1, 2, 4 mg l⁻¹) and activated charcoal (AC) (0, 0.5, 1, 2 g l⁻¹) concentrations on myrtle rooting in in vitro conditions. They used agar MS medium for rooting and reported that the best combination was detected 2 mg l⁻¹ IBA without AC in terms of rooting rate. Similarly, root length, root number, and plant length were recorded less than PlantForm vessels of our study. In the present study, we used IBA for rooting, and it was successful for rooting both in PlantForm and agar media. However, there were apparent differences among the treatments in term of the rooting data. Plants coming from PlantForm were much more at high quality.

Conclusion

In conclusion, the PlantForm TIS bioreactor represents a valid alternative to conventional systems in vitro micropropagation and rooting, resulting in a reduction of cost, labor, and time for the mass propagation. Comparative investigations between semi-solid medium and bioreactor culture revealed that shoot proliferation and growth were more efficient in the temporary immersion bioreactor system.

Acknowledgments. This research was supported by Çukurova University, Scientific Research Project Unit (Project No: FBA-2015-4865).

REFERENCES

- [1] Afreen, F. (2008): Temporary Immersion Bioreactor. – In: Gupta, S. D., Ibaraki, Y. (eds.) Plant Tissue Culture Engineering. Springer. Netherlands, pp. 187-201.
- [2] Aka Kaçar, Y., Şimşek, Ö., Biçen, B., Dal, B. (2017): *In vitro* rooting of micropropagated shoots from *Myrtus communis* Linn: influence of activated charcoal and indole-3-butyric acid (IBA). – Acta Horticulture 1155: 531-536.
- [3] Akita, M., Takayama, S. (1994): Stimulation of potato (*Solanum tuberosum* L.) tuberization by semi continuous liquid medium surface level control. – Plant Cell Report 13: 184-187.
- [4] Albarran, J., Bertrand, B., Lartaud, M., Etienne, H. (2005): Cycle characteristics in a temporary immersion bioreactor affect regeneration, morphology, water and mineral status of coffee (*Coffea arabica*) somatic embryos. – Plant Cell, Tissue and Organ Culture 81(1): 27-36.
- [5] Alexandrova, K. S., Denchev, P. D., Conger, B. Y. (1996): Micropropagation of switch grass by node culture. – Crop Science 36(6): 1709-1711.
- [6] Aydın, C., Özcan, M. M. (2007): Determination of nutritional and physical properties of Myrtle (*Myrtus communis* L.) fruits growing wild in Turkey. – Journal of Food Engineering 79: 453-458.
- [7] Benelli, C., Fernanda, C. M., De Carlo, A. (2015): Plant Form. A Temporary immersion system, for *in vitro* propagation of *M. communis* and *Olea europae*. – 6th International Symposium on Production and Establishment of Micropropagated Plants, Sanremo, Italy, Abstract Book.
- [8] Bohidar, S., Thirunavoukkarasu, M., Roa, T. V. (2008): Effect of plant growth regulators on *in vitro* micropropagation of ‘Garden Rue’ (*R. graveolens* L.). – International Journal of Integrative Biology 3(1): 36-43.
- [9] Casaburi, A., Di Martino, V., Ercolini, D., Parente, E., Villani, F. (2015): Antimicrobial activity of *Myrtus communis* L. water-ethanol extract against meat spoilage strains of

- Brochothrix thermosphacta* and *Pseudomonas fragi* *in vitro* and in meat. – Annals of Microbiology 65(2): 841-850.
- [10] Dahmoune, F., Nayak, B., Moussi, K., Remini, H., Madani, K. (2015): Optimization of microwave-assisted extraction of polyphenols from *Myrtus communis* L. leaves. – Food Chemistry 166: 585-595.
- [11] Damiano, C., Arias, P. M. D., La Starza, S. R., Frattarelli, A. (2007): Temporary immersion system for temperate fruit trees. – Acta Horticulture 748: 87-90.
- [12] Danial, G. H. (2009): Propagation of *Myrtus communis* L. *in vitro*. – Journal of Duhok University 12(1): 80-84.
- [13] Dönmez, D., Şimşek, Ö., Aka Kaçar, Y. (2016): Genetic engineering techniques in fruit science. – International Journal of Environment, Agriculture and Biotechnology 2(12): 115-128.
- [14] Eibl, R., Eibl, D. (2006): Design and Use of the Wave Bioreactor for Plant Cell Culture. – In: Gupta, S. D., Ibaraki, Y. (eds.) Plant Tissue Culture Engineering. Springer, The Netherlands, pp. 203-227.
- [15] Eibl, R., Eibl, D. (2008): Design of bioreactors suitable for plant cell and tissue cultures. – Phytochemistry Reviews 7(3): 593-598.
- [16] Eibl, R., Werner, S., Eibl, D. (2009): Disposable bioreactors for plant liquid cultures at Litre-scale. – Engineering in Life Sciences 9(3): 156-164.
- [17] Etienne, H., Lartaud, M., Michaux-Ferrière, N., Carron, M. P., Berthouly, M., Teisson, C. (1997): Improvement of somatic embryogenesis in *Hevea brasiliensis* (Müll. Arg) using the temporary immersion techniques. – In Vitro Cellular & Developmental Biology-Plant 33(2): 81-87.
- [18] Frómeta, O. M., Morgado, M. M. E., Da Silva, J. A. T., Morgado, D. T. P., Gradaille, M. A. D. (2017): *In vitro* propagation of *Gerbera jamesonii* Bolus ex Hooker f. in a temporary immersion bioreactor. – Plant Cell, Tissue and Organ Culture 129(3): 543-551.
- [19] Georgiev, V., Schumann, A., Pavlov, A., Bley, T. (2014): Temporary immersion systems in plant biotechnology. – Engineering in Life Sciences 14(6): 607-621.
- [20] Hatzilazarou, S., Grammatikos, H., Economou, A. S., Rifaki, N., Ralli, P. (2001): Rooting *in vitro* and acclimatization of *Myrtus communis* microcuttings. – 1st International Symposium on Acclimatization and Establishment of Micropropagated Plants 616: 259-264.
- [21] Idowu, P. E., Ibitoye, D. O., Ademoyegun, O. T. (2009): Tissue culture as a plant production technique for horticultural crops. – African Journal of Biotechnology 8(16): 3782-3788.
- [22] Lambardi, M., Roncasaglia, R., Bujazha, D., Baileiro, F., Correia Da Silva, D. P., Özüdoğru, E. A. (2015): Improvement of shoot proliferation by liquid culture in temporary immersion. – 6th International Symposium on Production and Establishment of Micropropagated Plants, Sanremo, Italy, Abstract Book.
- [23] Murashige, T., Skoog, F. (1962): A revised medium for rapid growth and bio assays with tobacco tissue cultures. – Physiologia Plantarum 15(3): 473-497.
- [24] Ngomuo, M., Mneney, E., Ndadikemi, P. (2013): The effects of auxins and cytokinin on growth and development of (*Musa* sp.) var. “Yangambi” explants in tissue culture. – American Journal of Plant Sciences 4(11): 2174-2180.
- [25] Paek, K. Y., Hahn, E. J., Son, S. H. (2001): Application of bioreactors for large-scale micropropagation system of plants. – In Vitro Cellular & Developmental Biology - Plant 37: 149-157.
- [26] Preil, W. (1991): Application of Bioreactors in Plant Propagation. – In: Debergh, P. C., Zimmerman, R. H. (eds.) Micropropagation. Kluwer Academic Publishers, Dordrecht, pp. 425-445.
- [27] Rajbhar, Y. P., Sumit, T., Hariom, K., Mukesh, K., Anil, K., Govind, R. (2016): Effect of cytokinin and auxin on callus formation and shoot multiplication of strawberry (*Fragaria*

- × *ananassa* Duch.) under *in vitro* condition. – HortFlora Research Spectrum 5(3): 206-212.
- [28] Ramírez-Mosqueda, M. A., Iglesias-Andreu, L. G. (2016): Evaluation of different temporary immersion systems (BIT®, BIG, and RITA®) in the micropropagation of *Vanilla planifolia* Jacks. – In Vitro Cellular & Developmental Biology - Plant 52(2): 154-160.
- [29] Rezaee, A., Kamali, K. (2014): A New commercial protocol for micropropagation of myrtle tree. – Advances in Bioresearch 5(4): 73-79.
- [30] Ruffoni, B., Mascarello, C., Savona, M. (2010): *In Vitro* Propagation of Ornamental Myrtle (*Myrtus Communis*). – In: Jain, S. M., Ochatt, S. J. (eds.) Protocols for *In Vitro* Propagation of Ornamental Plants. Humana Press, Totowa, NJ, pp. 257-269.
- [31] San, B., Yildirim, A. N., Polat, M., Yildirim, F. (2015): Chemical compositions of myrtle (*Myrtus communis* L.) genotypes having bluish-black and yellowish-white fruits. – Erwerbs-Obstbau 57(4): 203-210.
- [32] Scarpa, G. M., Milia, M., Satta, M. (2000): The influence of growth regulators on proliferation and rooting of *in vitro* propagated myrtle. – Plant Cell, Tissue and Organ Culture 62(3): 175-179.
- [33] Shekafandeh, A. (2007): Effect of different growth regulators and source of carbohydrates on *in* and *ex vitro* rooting of Iranian Myrtle. – International Journal of Agricultural Research 2: 152-158.
- [34] Sumbul, S., Ahmad, M. A., Asif, M., Akhtar, M. (2011): *Myrtus communis* Linn. A review. – Indian Journal of Natural Products and Resources 2: 395-402.
- [35] Wannes, W. A., Mhamdi, B., Sriti, J., Marzouk, B. (2010): Glycerolipid and fatty acid distribution in pericarp, seed and whole fruit oils of *Myrtus communis* var. *italica*. – Industrial Crops and Products 31(1): 77-83.
- [36] Welander, M., Zhu, L. H., Li, X. Y. (2007): Factors influencing conventional and semi-automated micropropagation. – Propagation of Ornamental Plants 7(3): 103-111.
- [37] Welander, M., Persson, J., Asp, H., Zhu, L. H. (2014): Evaluation of a new vessel system based on temporary immersion system for micropropagation. – Scientia Horticulturae 179: 227-232.
- [38] Yan, H., Liang, C., Li, Y. (2010): Improved growth and quality of *Siraitia grosvenorii* plantlets using a temporary immersion system. – Plant Cell, Tissue and Organ Culture (PCTOC) 103(1): 131-135.
- [39] Yan, H., Yang, L., Li, Y. (2011): Improved growth and quality of *Dioscorea fordii* Prain et Burk and *Dioscorea alata* plantlets using a temporary immersion system. – African Journal of Biotechnology 10(83): 19444-19448.

BENTHIC MACROINVERTEBRATES AS BIOINDICATORS OF WATER QUALITY IN THE BLYDE RIVER OF THE OLIFANTS RIVER SYSTEM, SOUTH AFRICA

MALAKANE, K. – ADDO-BEDIAKO, A.* – KEKANA, M.

*Department of Biodiversity, University of Limpopo
Private Bag X1106, Sovenga 0727, South Africa*

**Corresponding author*

e-mail: abe.addo-bediako@ul.ac.za; ORCID: 0000-0002-5055-8315

(Received 4th Oct 2019; accepted 8th Jan 2020)

Abstract. The Olifants River System and its catchment have been exposed to prolonged and cumulative ecosystem stress as a result of human settlements, mining, agricultural and industrial activities. The Blyde River is known to supply the Olifants River with water of good quality and quantity. However, the intensive farming and human settlements in the catchment could threaten the river. The aim of the study was to assess the water quality of the Blyde River in South Africa using aquatic macroinvertebrates as bioindicators. Seven sites along the river were selected for sampling. The family composition, based on abundance and diversity was evaluated in relation to environmental variables. The results of some measured physicochemical parameters revealed that water quality of the Blyde River is not significantly altered and the presence of ecologically sensitive macroinvertebrates was an indication of good water quality as this benthic fauna was well represented in all seasons and most parts of the river. The study therefore has indicated that the river was inhabited by a healthy macroinvertebrate community suggesting that the water is still of good quality.

Keywords: *anthropogenic activities, bioassessment, environmental factors, spatial distribution, water pollution*

Introduction

Many river systems have been subjected to a range of disturbances due to the fast growing human population and increasing human activities, and leading to water quality degradation (Jun et al., 2016; Ferreira et al., 2017; Santos et al., 2017; Niba and Sakwe, 2018). The effluents from activities such as, industries, mining, agriculture, domestic and urban development contain various pollutants, which often end up in water bodies and may affect the ecological status of the river (Dalu and Froneman, 2016; Hunt et al., 2017).

Benthic macroinvertebrates respond differentially to biotic and abiotic factors in their environment and therefore, the structure of macroinvertebrates has long been used as bio-indicators to assess the water quality of water bodies (Li et al., 2010; Wolmarans et al., 2014; Jun et al., 2016). Benthic macroinvertebrates are the most common faunal assemblages for bio-assessment and provide more reliable assessment of long-term ecological changes in the quality of aquatic systems compared to its rapidly changing physicochemical characteristics. Their multiple life stages, sedentary nature, and varying tolerance levels to environmental stressors render them useful in assessing temporal and spatial changes within an aquatic ecosystem (Rosenberg and Resh, 1993). However, specific preferences for certain ranges of abiotic and biotic characteristics, mean that changes in these factors often create large differences in benthic community structure even over small spatial scales (Grönroos and Heino, 2012). Different groups of

macroinvertebrates have different environmental requirements and respond to changes in environmental factors, such as temperature, dissolved oxygen, conductivity and salinity (Külköylüoğlu, 2004; Grab, 2014; Masese et al., 2014). Thus, the degree of tolerance of these factors vary among different organisms, and information gathered from such studies reflect the quality of water in the river.

The Olifants River System provides water for industrial, mining, agricultural and domestic uses (Machete et al., 2004). Along the Olifants River, pollution arising from intensive and subsistence agriculture practices in all the sub-catchment and the numerous point- and non-point-sources (diffuse), including mining and industrial pollution in the Upper Olifants catchment area contain complex mixtures of chemicals, many of which may have deleterious effects on aquatic systems. Due to these various activities in its catchment, the river has become one of the most polluted rivers in South Africa (Grobler et al., 1994; Addo-Bediako et al., 2018). Many of the impoundments and tributaries of the Olifants River System are said to be contaminated with heavy metals, inorganic nutrients such as, sulphates and nitrates from agricultural areas, mine drainages and wastewater treatment (WWT) plant (Oberholster et al., 2013). The Blyde River is an important tributary of the Olifants River (Ashton et al., 2001). It is known for its continuous flow and good water quality (Raven, 2004). However, the recent human activities in the catchment may be impacting the quality of the water and the biota e.g. macroinvertebrates. Thus, the study assessed the water quality of the Blyde River using aquatic macroinvertebrate communities. The objectives of this study were: (i) to describe the spatial distribution and assemblage structures of macroinvertebrates; (ii) to determine major environmental variables that affect their distribution. We hypothesize that: environmental conditions play important role in the distribution and abundance of aquatic macroinvertebrates.

Materials and methods

Study area

The Blyde River rises on the western slopes of the Drakensberg Mountains (Mpumalanga) and flows northwards to join the Olifants River in Limpopo Province, South Africa (Raven, 2004). The catchment is approximately 2000 km² in size. The mean annual precipitation is about 1000 mm and it is considerably higher than the other sub-catchment areas in the Olifants River Basin (Raven, 2004). Seven sampling sites were selected along the river (*Fig. 1*). S1 (24°30'59.46"S 30°47'56.14"E), S2 (24°30'14.42"S 30°50'08.49"E), S3 (24°25'52.45"S 30°50'03.59"E), S4 (24°24'19.03"S 30°47'54.19"E), S5 (24°19'30.90"S 30°49'52.00"E), S6 (24°23'04.94"S 30°48'22.09"E) and S7 (24°15'30.38"S 30°50'13.22"E). The sites represent four different groups of land use; domestic (S1 & S2), agriculture (S3 & S5), industrial (S4) and nature reserves (S6 & S7).

Physicochemical parameters

This study was conducted in winter (July) and spring (October) of 2017, summer (January) and autumn (April) of 2018. Seasonal water samples were collected in 1000 ml polyethylene bottles (acid pre-treated) and stored at 4°C prior to analysis. Seasonal environmental variables, such as pH, water temperature, dissolved oxygen, (DO), total dissolved solids (TDS) and electrical conductivity were recorded at the

sampling sites using a YSI Model 554 Data logger, for the characterization of each sample point. Water current (flow velocity) was measured using a portable flowmeter Model 2000 (Marsh McBirney, Maryland, US). Channel width and water depth were measured using a tape measure and graduated measuring rod, respectively. Laboratory analysis was conducted to determine the nutrients (NH_4 , NO_2 , NO_3 and PO_4), turbidity, sulphates using a spectrophotometer (Merck Pharo 100 Spectroquant™) with Merck cell test kits in the Biodiversity Water Laboratory, University of Limpopo.

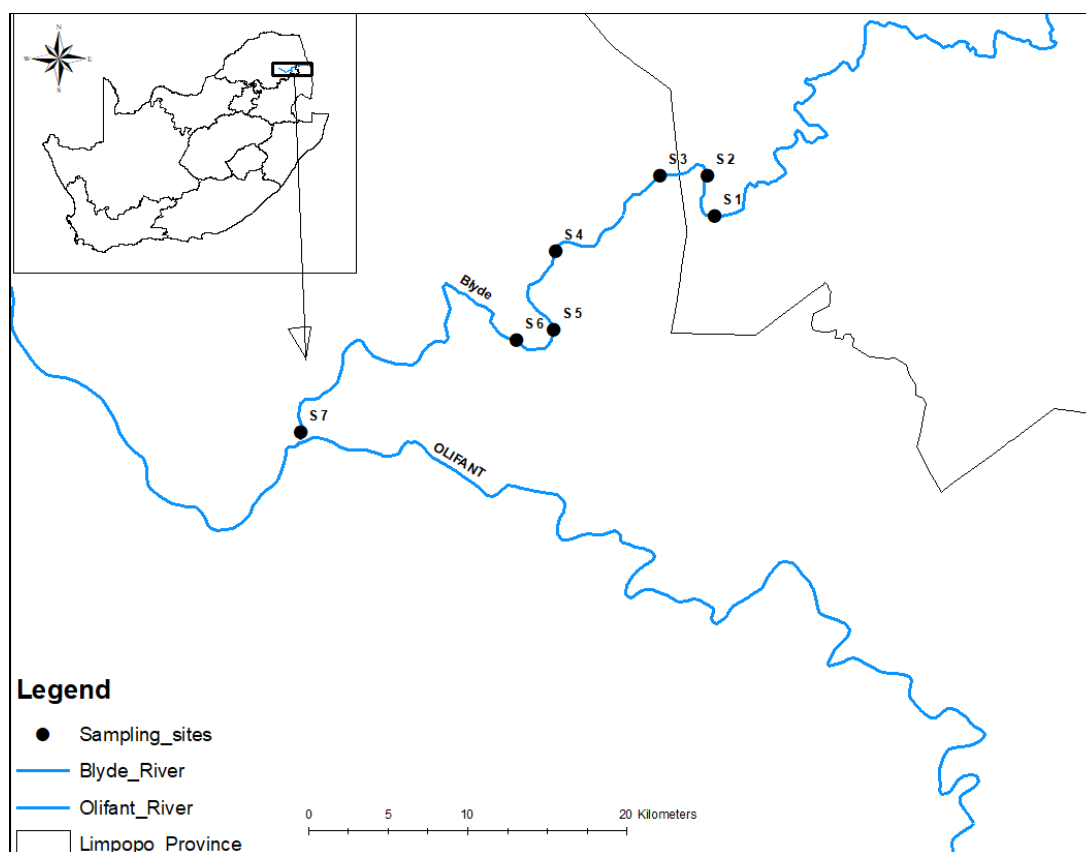


Figure 1. Map of the study area, showing the locations of the seven sampling sites of the Blyde River

Sampling of macroinvertebrates

Seasonal benthic macroinvertebrate samples were collected at seven sites (S1, S2, S3, S4, S5, S6 and S7) of the river. The samples were collected within a 100-m stretch of the study sites, with substrata of biotypes consisting mainly of mud, sand, gravel or stones. Samples were collected using a 30 cm by 30 cm sampling net with a 500 μm mesh size. Benthic macroinvertebrates were collected using the kick sampling method described by Dickens and Graham (2002), whereby the substrate was disturbed by kicking for a period of 5 min to free macroinvertebrates. The samples were collected per site from all aquatic habitats (i.e. riffles, pools and vegetated margins). For the vegetation biotopes, macroinvertebrates were sampled by scraping the net back and forth through vegetation (approximately 2 m). The macroinvertebrates were then separated from organic and mineral matter, counted, after identification to the family

level using Gerber and Gabriel's field guide manual (2002)), and released back into the river. Where specimens could not be identified in the field, the samples were preserved in 70% ethanol and transported to the University of Limpopo's Biodiversity laboratory for further identification, with an aid of a stereomicroscope (Leica EZ4) and a magnifying glass. The South African Scoring System (SASS 5) were further used to classify the macroinvertebrates collected into three groups, namely tolerant (scores 1–5), moderately tolerant (scores 6–10) and sensitive (scores 11–15) to pollution (Dickens and Graham, 2002).

Statistical analysis

The mean and standard deviation of the respective water variables were calculated. Data were first tested for normality and homogeneity of variance using the Kolmogorov-Smirnov and Levene's tests respectively. The analysis of variance (ANOVA) was performed to determine whether there were significant differences among the different sites and seasons (winter, spring, summer and autumn) in water variables. Canonical correspondence analysis (CCA) was used to relate macroinvertebrate assemblages to environmental variables and to identify which environmental variables could best differentiate them (Jun et al., 2016). Monte Carlo simulations were carried out to verify whether the variables exerted a significant effect ($p < 0.05$) on macroinvertebrate distributions. Taxa abundance data were transformed to $\log(x + 1)$ in both analyses to down-weight the effects of dominant taxa. Square-root-transformation was used for the environmental parameters and were transformed to $\log(x + 1)$ except pH. CCA were conducted using CANOCO version 5.1 software (ter Braak and Šmilauer, 2002). Spearman correlation coefficients between macroinvertebrates and environmental variables were calculated to assist interpretation of changes in community profile using STATISTICA software (StatSoft, Inc., version 10, Tulsa, OK, USA).

Results

Physicochemical parameters

The physicochemical parameters of the water are summarised in *Table 1*. The lowest mean temperature (22.3 °C) was recorded at Site 1 and the highest mean temperature at S7 (24.90 °C). The highest mean dissolved oxygen (DO) was recorded at S2 (11.85 mg/l) and the lowest was recorded at S5 (8.70 mg/l). The pH was slightly alkaline at all sites and showed little variation. The pH ranged from 8.3 at S5 to 8.7 at S1. The lowest mean EC (270.85 mS/m) was recorded at S1 and the highest (442.20 mS/m) was recorded at S5, while the lowest mean TDS (132.9 mg/l) was recorded at S1 and the highest (252.80 mg/l) was recorded at S7. The mean salinity ranged from 0.25‰ at S1 to 0.49‰ at S7. There was a very strong positive correlation between pH and DO ($r = 0.92$, $p < 0.05$). There were no significant differences in the above physicochemical parameters among the sites and seasons ($p > 0.05$), except seasonal variation in temperature and salinity ($p < 0.05$). However, S3 and S5 had the highest TDS and EC values but low DO values. Whilst S1, S2 and S6 exhibited low TDS and EC values but high DO values. Turbidity levels were within the recommended values. The nutrients levels were generally low except ortho-phosphate.

Table 1. Average values of physicochemical variables measured at different sites along the Blyde River

Water quality parameters	S1		S2		S3		S4		S5		S6		S7		F	p-value	Water quality guidelines
	AVE	±SD	AVE	±SD	AVE	±SD	AVE	±SD	AVE	±SD	AVE	±SD	AVE	±SD			
pH	8.4-9.0	—	8.4-8.9	—	8.3-8.7	—	8.2-8.8	—	8.1-8.5	—	8.2-8.8	—	8.2-8.8	—	0.63	0.372	6.5-9.0 ²
Temp (°C)	22.33	2.01	22.28	2.30	23.53	1.71	22.88	2.54	23.65	2.58	23.95	3.49	24.90	3.49	4.87	0.042	
EC (mS/m)	270.85	346.6	274.9	361.8	341.4	260.6	338.9	449.8	442.2	547.0	366.7	357.8	333.7	357.8	0.83	0.321	-
TDS (mg/l)	132.9	32.2	138.5	35.4	147.2	43.7	250.9	158.0	241.2	79.4	158.6	76.64	252.8	76.64	0.46	0.315	
DO (mg/l)	11.045	1.35	11.85	2.45	9.93	2.45	10.7	1.33	8.70	1.85	9.38	1.31	10.63	0.15	0.742	0.156	-
Salinity (‰)	0.25	0.34	0.27	0.37	0.35	0.47	0.38	0.51	0.46	0.59	0.38	0.51	0.49	0.63	18.29	<0.001	<0.5‰ ¹
NO ₂ (mg/l)	0.02	0.01	0.01	0.00	0.01	0.00	0.00	0.00	0.01	0.01	0.00	0.00	0.005	0.00	0.76	0.216	0.06 ³
NO ₃ (mg/l)	0.65	0.50	0.55	0.10	0.00	0.00	0.15	0.00	0.25	0.00	0.33	0.05	0.375	0.05	1.32	0.112	10.0 ³
NH ₃ (mg/l)	0.06	0.00	0.05	0.00	0.04	0.00	0.05	0.00	0.03	0.00	0.03	0.03	0.065	0.03	1.89	0.065	<0.007 ¹
Ortho-PO ₄ (mg/l)	0.22	0.0	0.16	0.32	0.40	0.00	0.25	0.00	0.03	0.00	0.18	0.20	0.13	0.20	5.24	0.421	-
SO ₄ (mg/l)	17.35	5.27	16.90	4.75	18.03	4.92	17.05	4.14	24.00	3.92	14.93	6.27	25.95	6.27	4.41	0.037	-
Turbidity NTU	14.00	8.69	14.00	12.88	6.75	2.05	7.50	2.69	13.25	10.99	7.75	5.24	10.25	3.34	1.69	0.072	8 -<50 ²

¹DWAF (1996)

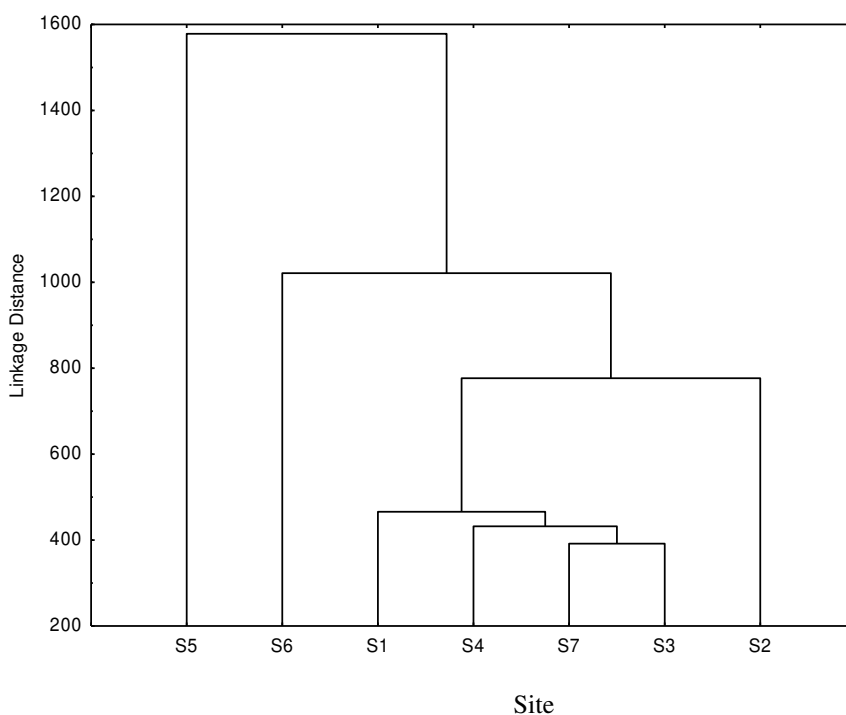
²BC-MECCS (2019)

³CCME (2012)

Macroinvertebrates

A total of 19 832 individuals belonging to 11 orders and 36 families were collected at the various sampling sites and seasons. The total number of specimens collected per site for the seasons ranged from 1 053 at S3 to 6 876 at S5 (*Table 2a*). The highest number of families (32) was found at S6 and the lowest (23) was found at S7. The dominant taxa were Hydropsychidae (3 683), followed by Caenidae (2 519), Baetidae (2 483), Simuliidae (2 218), Chironomidae (1 499), Elmidae (1 160) and Corbiculidae (1 079). S1 was dominated by generalist Caenidae, sensitive Hydropsychidae and Baetidae, S2 by generalist Caenidae, sensitive Baetidae and Hydropsychidae, S3 by sensitive Hydropsychidae, Baetidae and Heptageniidae, S4 by sensitive Baetidae, Hydropsychida and Hydropsychidae, S5 by sensitive Hydropsychidae and tolerant Chironomidae and Simuliidae, S6 by tolerant Simuliidae, sensitive Hydropsychidae and generalist Caenidae, and S7 by tolerant Thiaridae, sensitive Hydropsychidae and sensitive Baetidae. The highest macroinvertebrate diversity (32 families) was recorded at S6 and the lowest (23 families) was recorded at S7. S7 had low diversity but high numbers of certain taxa e.g. Thiaridae. Taxa richness ranged between 24 during summer and 33 in spring (*Table 2b*). Taxa richness differed among seasons ($p < 0.05$). The lowest number of individual macroinvertebrates were recorded during summer and the highest during winter, about ten times higher than that of summer.

Cluster analysis produced three main clusters of sites based on macroinvertebrate taxa (*Fig. 2a*). The first cluster was S5, the second was S6, and the third was a cluster of S1, S2, S3, S4 and S7. Spearman correlation was used to show the relationships among the sites (*Table 3*). The correlation yielded positive correlations among all the sites with respect to the macroinvertebrate families. The strongest correlations were between S1 and S2 ($r = 0.813$), S3 and S4 ($r = 0.812$), and the weakest correlation was between S1 and S5 ($r = 0.431$). Furthermore, even the seasonal variation across the sites rarely indicated any variation (*Fig. 2b*).



a

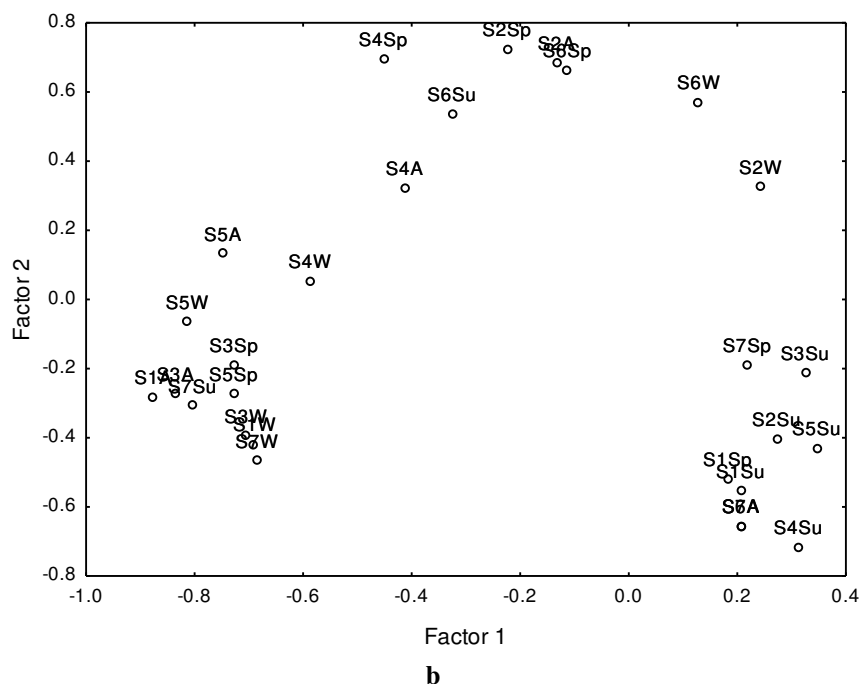


Figure 2. a Cluster analysis based on macroinvertebrates taxa collected at seven sampling sites along the Blyde River. **b** Seasonal macroinvertebrates distribution across the seven of the Blyde River (W = winter, Sp = spring, Su = summer and A = autumn)

The number of tolerant families ranged from 10 at S7 to 13 at S6, while the number of moderately tolerant families ranged from 11 at S1 and S7 to 15 at S2 and S3, and the sensitive families ranged from two at S7 to five at S6 (Fig. 3). There were more numbers of tolerant, moderate tolerant and sensitive families collected in winter and spring (low flow seasons) than in summer and autumn (high flow seasons). The highest numbers of families were recorded in spring (32), followed by winter (27), autumn (25) and then summer (22). Thus, 12 more families were collected in the low-flow season than in the high-flow season. More than 7 tolerant families, 2 moderate tolerant families and 3 sensitive families were recorded at low-flow than high-flow seasons.

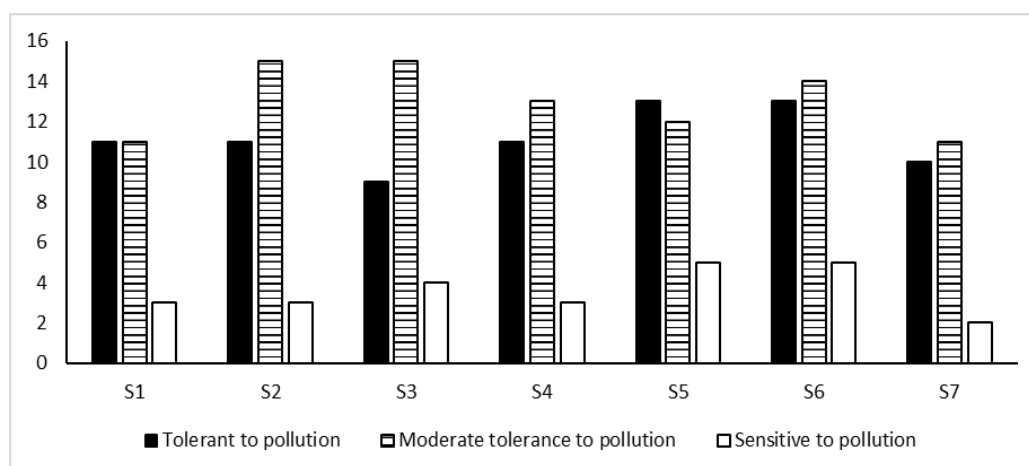


Figure 3. Tolerant, moderate tolerant and sensitive macroinvertebrate taxa recorded at the different sampling sites

Table 2a. Taxonomic profile (order, family) and number of macroinvertebrate individuals recorded at different sites along the Blyde River

Order	Family	Code	S1	S2	S3	S4	S5	S6	S7	Total
Ephemeroptera	Baetidae	BAE	227	594	138	417	501	330	276	2483
	Caenidae	CAE	490	722	91	85	612	396	123	2519
	Heptageniidae	HEP	7	123	95	272	103	267	40	907
	Teloganodidae	TEL	139	98	23	30	139	151	95	675
	Leptophlebiidae	LEP	1	3	20	3		53	76	156
	Tricorythidae	TRI	104	103	25	77	182	124	128	743
Trichoptera	Hydropsychidae	HYD	407	754	392	131	1108	631	260	3683
	Philopotamidae	PHI		11	17	15	226	2	2	273
	Leptoceridae	LEPC		3	3					6
Coleoptera	Gyrinidae	GYR	1	8	1	3	1	8	1	23
	Elmidae	ELM	23	72	31	52	917	52	13	1160
	Helodidae	HEL			2		9	1		12
	Psephenidae	PSE	24	12	38	21	1	17		113
Hemiptera	Naucoridae	NAU		1					1	2
Odonata	Libellulidae	LIB	10	12	6	5	50	4	10	97
	Aeshnidae	AES	8	8		2	1	1		20
	Gomphidae	GOM	68	21	3	2	2	1	15	112
Zygoptera	Chlorocyphidae	CHL	50	192	53	89	1	75	3	463
	Platycnemididae	PLA		3	2			1		6
	Coenagrionidae	COE	1		1	4	5	3	3	17
	Protoneuridae	PRO			1					1
Diptera	Athericidae	ATH	4	79	7	25	13	40	1	169
	Blephariceridae	BLE					2	8		10
	Tabanidae	TAB	11	8	5	7	79	19	11	140
	Dixidae	DIX			1	2	5	3		11
	Chironomidae	CHI	59	65	36	57	974	246	62	1499
	Muscidae	MUS		1			3	2		6
	Simuliidae	SIM	11	26	11	80	1223	855	12	2218
Plecoptera	Perlidae	PER	1	5	2	3	9	6		26
Crustacea	Potamonautidae	POT	2	3		8	11	8		32
Annelida	Hirudinea	HIR					36	57		93
	Oligochaeta	OLI	18	7	3	2	4	32	42	108
Mollusca	Physidae	PHY					1		2	3
	Planorbidae	PLA	1	3		2		17		23
	Thiaridae	THI	38	45	41	3	23	152	642	944
	Corbiculidae	COR	3	14	5	43	635	239	140	1079
Total number of individuals			1708	2996	1053	1440	6876	3801	1958	19832

Table 2b. Abundance of macroinvertebrate families recorded over the four seasons in the Blyde River

Order	Family		Autumn	Winter	Spring	Summer
Ephemeroptera	Baetidae	BAE	727	1386	191	179
	Caenidae	CAE	181	1708	587	43
	Heptageniidae	HEP	299	432	72	104
	Teloganodidae	TEL	0	669	6	0
	Leptophlebiidae	LEP	0	0	35	121
	Tricorythidae	TRI	584	0	5	154
Trichoptera	Hydropsychidae	HYD	862	1740	666	415
	Philopotamidae	PHI	273	0	0	0
	Leptoceridae	LEPC	3	0	3	0
Coleoptera	Gyrinidae	GYR	0	11	11	1
	Elmidae	ELM	511	340	293	16
	Helodidae	HEL	2	0	10	0
	Psephenidae	PSE	43	6	41	23
Hemiptera	Naucoridae	NAU	0	0	1	1
Odonata	Libellulidae	LIB	35	40	7	15
	Aeshnidae	AES	12	0	8	0
	Gomphidae	GOM	32	42	31	7
Zygoptera	Chlorocyphidae	CHL	67	166	222	8
	Platycnemididae	PLA	0	6	0	0
	Coenagrionidae	COE	1	1	6	9
	Protoneuridae	PRO	0	1	0	0
Diptera	Athericidae	ATH	16	53	95	5
	Blephariceridae	BLE	1	3	5	1
	Tabanidae	TAB	64	56	17	3
	Dixidae	DIX	0	9	2	0
	Chironomidae	CHI	299	1084	59	57
	Muscidae	MUS	0	4	2	0
	Simuliidae	SIM	82	1819	18	299
Plecoptera	Perlidae	PER	13	6	7	0
Crustacea	Potamonautidae	POT	16	5	4	7
Annelida	Hirudinea	HIR	0	90	3	0
	Oligochaeta	OLI	46	22	17	23
Mollusca	Physidae	PHY	0	0	2	1
	Planorbidae	PLA	0	5	18	0
	Thiaridae	THI	18	111	585	230
	Corbiculidae	COR	407	365	211	96
Total number of individuals			4594	10180	3240	1818

Table 3. Spearman correlation of macroinvertebrate taxa at the sampling sites

Site	S1	S2	S3	S4	S5	S6	S7
S1	1.000						
S2	0.813	1.000					
S3	0.639	0.768	1.000				
S4	0.603	0.804	0.812	1.000			
S5	0.405	0.519	0.431	0.624	1.000		
S6	0.608	0.674	0.640	0.781	0.576	1.000	
S7	0.705	0.593	0.544	0.554	0.515	0.697	1.000

The Canonical correspondence analysis (CCA) showed a correlation between some of the taxa and environmental variables (Fig. 4). The families Aeshnidae, Caenidae, Chlorocyphidae, Leptoceridae, Platynemididae, Protoneuridae and Psephenidae were associated with high pH and dissolved oxygen. The TDS, temperature, salinity and electrical conductivity, affected the families Coenagrionidae, Corbiculidae, Chironomidae, Physidae and Tricorythidae. The taxa-environment correlations for first and second axes were 0.99, and the cumulative percentage variance of taxa-environment relation for first and second axes combination was 65.5% (Table 4).

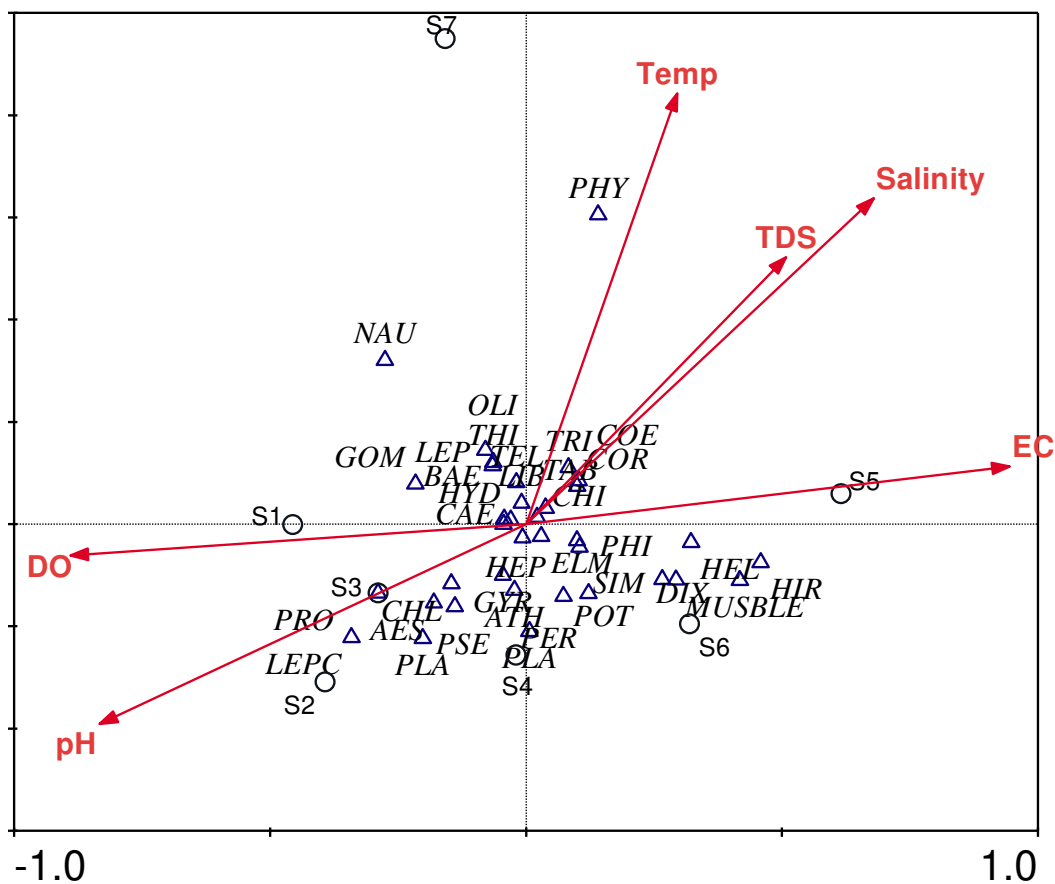


Figure 4. Canonical correspondence analysis (CCA) ordination of the macroinvertebrates collected at the sampling sites (arrows indicate environmental variables; circles denote sites; triangles denote family code names)

Table 4. Eigenvalues of the correlation matrix of the taxa-environment relation

Macroinvertebrates and water parameters	Axis 1	Axis 2	Axis 3	Axis 4	Total inertia
Eigenvalues	0.084	0.056	0.033	0.025	0.250
Taxa-environment correlations	0.994	0.990	0.993	0.923	
Cumulative percentage variance of					
- taxa data	33.5	56.1	69.5	79.6	
- taxa-environment relation	39.1	65.5	81.1	92.9	
Sum of all eigenvalues					0.250
Sum of all canonical eigenvalues					0.214
F-ratio	3.99				
<i>p</i> -value of CCA axis 1	0.002				

Discussion

Physicochemical parameters

The physicochemical parameters showed relatively little changes across sites and seasons. There was a strong positive correlation between pH and DO, and could be due to the fact that both pH and DO are affected by algal photosynthesis, respiration, temperature and oxidative decomposition of organic matter (Zang et al., 2011). Rivers in less disturbed areas are frequently characterised by low conductivity, turbidity and silt load, hence good water quality. In the Blyde River, the sites generally had moderate temperatures, TDS and conductivity values. However, TDS, salinity and sulphate were relatively high at S7 (the confluence of the Blyde and Olifants rivers), and could be due to increased runoff from human activities along the river to downstream or from the Olifants River. The DO levels were high throughout the sampling periods and the sites, with the highest level recorded in winter, as dissolved oxygen is temperature dependent. Nutrients levels were not too high despite the intensive agricultural activities in the catchment (DWAF, 1996; de Villiers and Thiart, 2007).

Macroinvertebrates

The macroinvertebrate assemblages in the Blyde River were rich in Ephemeroptera, Diptera and Trichoptera (Table 2a), and this trend is in support of other studies in both temperate and tropical rivers and streams (Al-Shami et al., 2013a, b; Jun et al., 2016). Taxa diversity is said to be variable in rivers in response to disturbance, suitable habitat availability and resource availability. Higher diversity is an indication of equal or close to equal opportunity of co-existence (Olomukoro and Ezemonye, 2007). A decreased diversity with corresponding increased abundance of few taxa is an indication of community disturbance and imbalance (Morphin-Kani and Murugesan, 2014). The low number of sensitive families at S7 and high numbers of tolerant species, could be due to poor water quality from the Olifants River. Furthermore, the low number of taxa at S3 could be due to the high-water current throughout the sampling period, resulting in less favourable conditions for many macroinvertebrates to survive in such an environment.

The high number of individuals and families of Ephemeroptera could be due to high oxygen concentration and fast flowing waters (Jun et al., 2016; Rasifudi et al., 2018). The presence of these taxa at all the sites indicates a high level of water quality at most parts of the river (Griffin et al., 2015). In addition, the high number of individuals from

the family Hydropsychidae (Tricoptera), at all the sites could further confirm the good quality of the water. The presence of sensitive taxa is an indication of good habitat structure and good water quality (Lopez-Doval et al., 2010; Matlou et al., 2017). The cluster analysis shows only three main groupings, an indication that the conditions of most of the sites are similar. This is confirmed by the Spearman correlation which shows positive relationship among all the sampling sites, with high correlation among the third cluster group (S1, S2, S3, S4 and S7). The seasonal macroinvertebrate distribution among the sites rarely showed any variation (*Fig. 2b*). While seasonality can be a driven force of river community dynamics, its effect is regulated by the likelihood of its recurrence (Tonkin et al., 2017). The lack of seasonality effect is an indication of the relative lack of a significant variability in environmental conditions of the river. The high number of macroinvertebrates recorded at S5 from different tolerant groups such as, Hydropsychidae, Simuliidae, Chironomidae and Elmidae could be attributed to good biotope diversity (higher habitat heterogeneity), as this site was characterised by bedrock, sand, areas of high current, pools and sparse vegetation. Furthermore, the high abundance of Simuliidae at S5 could be due to the presence of the Weir above the sampling site. High presence of Simuliidae has been reported below many impoundments, and their abundance is linked to reservoir outflows (Boon, 1998; Marchetti et al., 2014; Rasifudi et al., 2018).

There was seasonal variation in the composition of macroinvertebrates in the Blyde River. The high number of taxa and abundance during winter could be due to relatively good water quality as a result of less discharge from the catchment. During raining season, which usually starts in spring through to autumn in the area of the study, the river receives a lot of discharge from the catchment which may destroy the microhabitat of the macroinvertebrates. Furthermore, high flows which normally occur in raining season are known to affect aquatic macroinvertebrates both directly and indirectly through changes to habitat. Substrates of macroinvertebrates can be moved down-stream (Piniewski et al., 2017).

Most taxa sampled clumped at the centre of the CCA ordination plot, suggesting that no particular measured environmental variable defined the taxa distribution (Niba and Sakwe, 2018). It also confirms the fact that the conditions at most of the sites are similar and therefore may support similar macroinvertebrate communities. The taxa-environmental correlation for both axes 1 and 2 was 0.99, which indicates high predictive power of the selected environmental variables. Many of the pollution intolerant taxa could live in areas with high DO and pH and many of the pollution tolerant taxa could group in areas with high EC, TDS, salinity and temperature. Thus, interactions of macroinvertebrate communities may be influenced by abiotic factors in the environment (Florencio et al., 2013; Heino, 2013).

Conclusion

Despite the active agricultural activities in the Blyde River catchment, the aquatic community was indicative of good water quality. The high diversity and the presence of high abundance of sensitive taxa confirm the good quality or/and habitat heterogeneity of most parts of the river. However, the water from the Olifants River might have affected the quality of the water at S7 (the confluence of the Blyde and the Olifants River), hence the distribution of the macroinvertebrate communities was characterised by high number of pollutant taxa, Mollusca, especially Thiaridae. Seasonal variation of

the distribution of macroinvertebrates was also observed. The results suggest that currently the human activities along the Blyde River has little impact on the integrity of the river system. Though the current activities may not pose a threat to the water quality and benthic macroinvertebrates in the river, further monitoring is necessary due to increasing human activities in the catchment of the river. The study revealed that combination of physicochemical and biological measures in water quality assessment provides positive and promising results as they show sensitivity to environmental changes hence, aquatic macroinvertebrates are good biological indicators of pollution.

Acknowledgements. We are grateful to the Flemish Interuniversity Council (VLIR-UOS), Belgium for providing financial support for the study.

REFERENCES

- [1] Addo-Bediako, A., Matlou, K., Makushu, E. (2018): Heavy metal concentrations in water and sediment of the Steelpoort River, Olifants River System, South Africa. – *African Journal of Aquatic Science* 43(4): 413-416. DOI: 10.2989/16085914.2018.1524745.
- [2] Al-Shami, S. A., Heino, J., Che Salmah, M. R., Abu Hassan, A., Suhaila, A. H., Madziatul, R. M. (2013a): Drivers of beta diversity of macroinvertebrate communities in tropical forest streams. – *Freshwater Biology* 58: 1126-1137.
- [3] Al-Shami, S. A., Che Salmah, R., Abu Hassan, A., Madziatul, R. M. (2013b): Biodiversity of stream insects in the Malaysian Peninsula: spatial patterns and environmental constraints. – *Ecological Entomology* 38: 238-249.
- [4] Ashton, P. J., Love, D., Mahachi, H., Dirks, P. H. G. M. (2001): An overview of the impact of mining and mineral processing operations on water resources and water quality in the Zambezi, Limpopo and Olifants Catchments in Southern Africa. – Contract Report to the Mining, Minerals and Sustainable Development (Southern Africa) Project, by CSIR-Environmentek, Pretoria, South Africa and Geology Department, University of Zimbabwe-Harare. Report No. ENV-P-C 2001-042.xvi.
- [5] Boon, P. I. (1988): The impact of river regulation on invertebrate communities in the U. K. regulated rivers. – *Research and Management* 2: 389-409.
- [6] British Columbia-Ministry of Environment and Climate Change Strategy (BC-MECCS) (2019): British Columbia Approved Water Quality guidelines: Aquatic life, Wildlife and Agriculture. <https://www2.gov.bc.ca/gov/content/environment/air-land-water/water/water-quality/water-quality-reference-documents>. Accessed on 20/20/2020.
- [7] Canadian Council of Ministers of the Environment (CCME) (2012): Environmental Quality Guidelines: Water Quality Guidelines for the Protection of Aquatic Life and Sediment Quality Guidelines for the Protection of Aquatic Life. – Canadian Council of Ministers of the Environment, Winnipeg. <http://ceqg-rcqe.ccme.ca/> (accessed 05-05-2012).
- [8] Dalu, T., Froneman, P. W. (2016): Diatom based water quality monitoring in Africa: challenges and future prospects. – *Water SA* 42: 551-559.
- [9] De Villiers, S., Thiart, C. (2007): The nutrient status of South African rivers: concentrations, trends and fluxes from the 1970s to 2005. – *South African Journal of Science* 103: 343-349.
- [10] Department of Water Affairs and Forestry (DWAF) (1996): South African Water Quality Guidelines. Volume 7: Aquatic Ecosystems. Second Ed. – DWAF, Pretoria, South Africa.
- [11] Dickens, C. W., Graham, P. (2002): The South African Scoring System (SASS) version 5 rapid bio-assessment method for rivers. – *African Journal of Aquatic Science* 27: 1-10.

- [12] Ferreira, A. R. L., Sanches Fernandes, L. F., Cortes, R. M. V., Pacheco, F. A. L. (2017): Assessing anthropogenic impacts on riverine ecosystems using nested partial least squares regression. – *Science of the Total Environment* 583: 466-477.
- [13] Florencio, M., Gómez-Rodríguez, C., Serrano, L., Díaz-Paniagua, C. (2013): Competitive exclusion and habitat segregation in seasonal macroinvertebrate assemblages in temporary ponds. – *Freshwater Science* 32: 650-662.
- [14] Gerber, A., Gabriel, M. J. M. (2002): *Aquatic Invertebrates of South African Rivers: Field Guide*. – Department of Water Affairs and Forestry, Pretoria, South Africa.
- [15] Grab, S. (2014): Spatio-temporal attributes of water temperature and macroinvertebrate assemblages in the headwaters of the Bushmans River, southern Drakensberg. – *Water SA* 40: 19-26.
- [16] Griffin, D., Myers, S., Sloan, S. (2015): Implications on distribution and abundance of benthic macroinvertebrates in the Maple River based on water quality and habitat type. – *General Ecology* 381: 1-17.
- [17] Grobler, D. F. (1994): A note on the occurrence of metals in the Olifants River, Eastern Transvaal, South Africa. – *Water SA* 20: 195-205.
- [18] Grönroos, M., Heino, J. (2012): Species richness at the guild level: effects of species pool and local environmental conditions on stream macroinvertebrate communities. – *Journal of Animal Ecology* 81: 679-691.
- [19] Heino, J. (2009): Biodiversity of aquatic insects: spatial gradients and environmental correlates assemblage-level measures at large scales. – *Freshwater Review* 2: 1-29.
- [20] Hunt, L., Bonetto, C., Marrochi, N., Scalise, A., Fanelli, S., Liess, M., Lydy, M. J., Chiu, M. C., Resh, V. H. (2017): Species at Risk (SPEAR) index indicates effects of insecticides on stream invertebrate communities in soy production regions of the Argentine Pampas. – *Science of the Total Environment* 580: 699-709.
- [21] Jun, Y-C., Kim, N-Y., Kim, S-H., Park, S-H., Kong, D-S., Hwang, S-J. (2016): Spatial distribution of benthic macroinvertebrate assemblages in relation to environmental variables in Korean nationwide streams. – *Water* 8: 1-20.
- [22] Külköylüoğlu, O. (2004): On the usage of ostracods (Crustacea) as bioindicator species in different aquatic habitats in the Bolu region, Turkey. – *Ecological Indicators* 4: 139-147.
- [23] Li, L., Zheng, B., Liu, L. (2010): Biomonitoring and bioindicators used for river ecosystems: definitions, approaches and trends. – *Procedia Environmental Sciences* 2: 1510-1524.
- [24] Lopez-Doval, J. C., Großschartner, M., Höss, S., Orendt, C., Traunspurger, W., Wolfram, G., Munoz, I. (2010): Invertebrate communities in soft sediments along a pollution gradient in a Mediterranean river (Llobregat, NE Spain). – *Limnetica* 29: 311-322.
- [25] Machethe, C. L., Mollel, N., Ayisi, K., Mashatola, M., Anim, F., Vanasche, F. (2004): *Smallholder Irrigation and Agricultural Development in the Olifants River Basin of Limpopo Province: Management Transfer, Productivity, Profitability and Food Security Issues*. – Water Research Commission, Pretoria.
- [26] Marchetti, M. P., Esteban, E., Smith, A. N. H., Pickard, D., Richards, A. B., Slusark, J. (2014): Measuring the ecological impact of long term flow disturbance on the macroinvertebrate community in a large Mediterranean climate river. – *Journal of Freshwater Ecology* 26: 459-480.
- [27] Masese, F. O., Kitaka, N., Kipkembo, J., Gettel, G. M., Irvine, K., McClain, M. E. (2014): Macroinvertebrate functional feeding groups in Kenyan highland streams: evidence for a diverse shredder guild. – *Freshwater Science* 33(2): 435-450.
- [28] Matlou, K., Addo-Bediako, A., Jooste, A. (2017): Benthic macroinvertebrate assemblage along a pollution gradient in the Steelpoort River, Olifants River System. – *African Entomology* 25: 445-453.
- [29] Morphin-Kani, K., Murugesan, A. G. (2014): Assessment of River Water Quality Using Macroinvertebrate Organisms as Pollution Indicators of Tamirabarani River Basin, Tamil Nadu, India. – *International journal of Environmental Protection* 4: 1-14.

- [30] Niba, A., Sakwe, S. (2018): Turnover of benthic macroinvertebrates along the Mthatha River, Eastern Cape, South Africa. Implications for water quality biomonitoring using indicator species. – *Journal of Freshwater Ecology* 33: 157-171.
- [31] Oberholster, P. J., Botha, A., Chamier, J., De Klerk, A. R. (2013): Longitudinal trends in water chemistry and phytoplankton assemblage downstream of the rivers WWTP in the upper Olifants River. – *Eco hydrology and Hydrobiology* 13: 41-51.
- [32] Olomukoro, J. O., Ezemonye, L. I. N. (2007): Assessment of the macro-invertebrate fauna of rivers in Southern Nigeria. – *African Zoology* 42(1): 1-11.
- [33] Piniewski, M., Prudhomme, C., Acreman, M. C., Tylec, L., Ogłęcki, P., Okruszko, T. (2017): Responses of fish and invertebrates to floods and droughts in Europe. – *Ecohydrology* 10: 1-17. doi.org/10.1002/eco.1793.
- [34] Rasifudi, L., Addo-Bediako, A., Bal, K., Swemmer, A. (2018): Distribution of benthic macroinvertebrates in the Selati River of the Olifants River System, South Africa. – *African Entomology* 26(2): 398-406.
- [35] Raven, B. W. (2004): Water Affairs in the Lower Blyde River: The Role of DWAF in Local Water Management. – IMWI Working Paper. IMWI, Wageningen.
- [36] Rosenberg, D. M., Resh, V. H. (eds.) (1993): *Freshwater Biomonitoring and Benthic Macroinvertebrates*. – Chapman & Hall, New York.
- [37] Santos, R. M. B., Sanches Fernandes, L. F., Cortes, R. M. V., Varandas, S. G. P., Jesus, J. J. B., Pacheco, F. A. L. (2017): Integrative assessment of river damming impacts on aquatic fauna in a Portuguese reservoir. – *Science of the Total Environment* 601-602: 1108-1118.
- [38] Ter Braak, C. J. F., Smilauer, P. (2012): *Canoco Reference Manual and User's Guide: Software for Canonical Community Ordination (version 5)*. – Microcomputer Power, New York.
- [39] Tonkin, J. D., Bogan, M. T., Bonada, N., Rios-Touma, B., Lytle, D. A. (2017): Seasonality and predictability shape temporal species diversity. – *Ecology* 98: 1201-1216.
- [40] Wolmarans, C. T., Kemp, M., De Kock, K. N., Roets, W., Van Rensburg, L., Quinn, L. (2014): A semi-quantitative survey of macroinvertebrates at selected sites to evaluate the ecosystem health of the Olifants River. – *Water SA* 40(2): 245-254.
- [41] Zang, C., Huang, S., Wu, M., Du, S., Scholz, M., Gao, F., Lin, C., Guo, Y., Dong, Y. (2011): Comparison of relationships between pH, dissolved oxygen and chlorophyll a for aquaculture and non-aquaculture waters. – *Water Air Soil Pollution* 219: 157-174.

MAXENT MODELLING FOR PREDICTING IMPACTS OF CLIMATE CHANGE ON THE POTENTIAL DISTRIBUTION OF *ANABASIS APHYLLA* IN NORTHWESTERN CHINA

CHANG, Y. L. – XIA, Y. – PENG, M. W. – CHU, G. M.* – WANG, M.*

*Department of Forestry, Agricultural College, Shihezi University
Road of North 4th, Shihezi City, Xinjiang 832003, China*

*Corresponding authors

e-mail: chgmjx@163.com, wangm1205@163.com

(Received 4th Oct 2019; accepted 8th Jan 2020)

Abstract. Detailed and reliable information about the suitable distribution of species provides important knowledge for species protection management. The objectives of the study were to predict and analyze the potential distribution, driving factors and niche parameters of *Anabasis aphylla* under different scenarios. We combined the distribution data of *A. aphylla*, maximum entropy model and ArcGIS to predict the potential distribution of the plant in northwestern China under Paleoclimate, current and future (RCP4.5 2050 and RCP4.5 2070) climatic scenarios. The results showed the highly suitable distribution areas of *A. aphylla* were mainly concentrated in the southern margin of the Junggar Basin and the west side of the Tarim Basin. The primary environmental variable limit for the distribution of *A. aphylla* was precipitation seasonality. Precipitation and temperature have an important influence on the distribution of *A. aphylla*. According to the prediction of Palaeoclimate scenario, unsuitable areas of *A. aphylla* under the current, 2050 and 2070 climatic scenarios all increased, while the barely suitable areas of *A. aphylla* decreased. This study provides an important theoretical basis for the management, protection and restoration of *A. aphylla*.

Keywords: *Anabasis aphylla*, AUC, environmental variables, ecological niche, suitable area

Introduction

The study of the relationship between plant geographical distribution, climate and the prediction of plant spatial distribution pattern, is not only a research hot spot of traditional plant ecology and biogeography, but also an important research field of global ecology and global geography (Wang and Ni, 2009). Climate change research has noted that due to the increasing of CO₂ concentration in the earth's atmosphere, the global average temperature has increased over the past 100 years (Houghton et al., 2001). Climate change affected many ecosystems and biotas worldwide, it may accelerate the loss of biodiversity (Parmesan, 2006) and threaten the current distribution of species in the future (Araújo et al., 2011). In recent years, climate change and human activities have had a strong impact on the distribution of plant species in the arid northwest. Therefore, it is very necessary to study the future dynamics of vegetation in arid regions, which can provide better guidance for ecological protection and restoration in the arid regions of northwest China.

Anabasis aphylla is a chenopodiaceous shrub with high capabilities to endure salt-alkali, resist drought and prevent sand drift. It is also a constructive species for desert soil and plays a vital role in maintaining ecological stability and preventing natural disasters like desertification (Chu et al., 2014). Zhang et al. (2003) found that in areas with high groundwater level, easy to accumulate water and high salt content, *A. aphylla* occupied an absolute advantage. There were few studies on the correlation

between the geographical distribution and environmental variables in a large area of *A. aphylla*. Jiang (2003) predicted the potential geographical distribution of *Anabasis* plants, and indicated that the distribution of *Anabasis* plants in China was concentrated in the arid regions of northwest. Based on 19 environmental variables and Maxent (maximum entropy model), Wang (2018) studied the distribution center of *Anabasis* plants in China, and found that these plants have higher adaptability to the arid and semi-arid climate than the warm temperate continental arid climate. All of these studies can provide a reference for the research in this paper. In china, *A. aphylla* is mainly distributed in northwest region, in diluvial fans, lowlands among dunes, in the Gobi desert and on hillsides (Chu et al., 2014). However, due to the influence of agricultural development, oil exploitation, harsh environmental conditions and other activities, the habitat of *A. aphylla* populations in Xinjiang was severely fragmented. All of this caused the self-renewal ability of *A. aphylla* population was poor, and most of the areas were in a recession trend (Chu et al., 2014). Therefore, it is of great practical significance for the management and protection of the plant to study the potential distribution range and spatial distribution pattern of *A. aphylla* under climate change scenarios.

In previous studies, Species Distribution Models (SDMs) have been used to model the potential geographic distribution of species in areas where the known distribution of species is lacking (Stockwell and Peters, 1999), and have also been used to estimate species distribution patterns and propose conservation strategies (Ortega-Huerta and Peterson, 2004). There are many different SDMs to choose from when predicting the potential distribution of species. This study selected the maximum entropy model (Maxent) as a predictive tool, as recent studies have shown that this method has a stronger ability to distinguish between the suitable and unsuitable regions of the species than other model methods (Phillips et al., 2006; Hernandez et al., 2008; Ma et al., 2017). Maxent has been demonstrated to be a powerful function when modelling rare species with narrow ranges and available scarce presence only occurrence data (Phillips et al., 2006; Elith et al., 2006, 2015; Pearson et al., 2007; Wisz et al., 2008; Rebelo and Jones, 2010; Sardà-Palomera et al., 2012; Garcia et al., 2013; Marcer et al., 2013). The advantages of Maxent including (1) the input species data can be presence only data; (2) both continuous and categorical data can be used as input variables; (3) its prediction accuracy is always stable and reliable, even with incomplete data, small sample sizes and gaps; (4) a spatially explicit habitat suitability map can be directly produced; and (5) the importance of individual environmental variables can be evaluated using a built in jackknife test (Yi et al., 2016). Studies using the Maxent model to predict the extent of species in different areas are concentrated on rare or endangered plants (Wilson et al., 2011; Babar et al., 2012; Marcer et al., 2013; Yi et al., 2016), invasive plants (Padalia et al., 2014) and insects (Santos et al., 2017; Wang et al., 2017). Maxent also has been successfully applied to the potential distribution of desert plant species in arid regions. Wang and Ni (2009) predicted the potential geographical distribution of five *Caragana* species in temperate arid and semi-arid regions of northern China. Ma et al. (2010) predicted the potential distribution and pattern of *Gymnocarpos przewalskii* in the desert area of Northwest China.

This study is based on the new scenario of the Fifth Interval Panel on Climate Change (IPCC): climatic factor data obtained from the RCP (Representative concentration pathways) 4.5 (medium emission scenario). Combined with the distribution data of *A. aphylla*, Maxent model and ArcGIS tools were used to predict the

potential distribution, spatial pattern and changes of *A. aphylla* in northwestern China under Paleoclimate, current and future climatic scenarios. We aim to answer the following questions: (1) What is the distribution potential of *A. aphylla* in northwestern China under paleoclimate and current climate scenarios? (2) How will climate change affect the suitable distribution range and spatial pattern of *A. aphylla* in the future? (3) Which environmental factors and niche parameters that mainly restrict the distribution of *A. aphylla*?

Materials

Study area

In China, *A. aphylla* mainly distributed in the northwestern region. We attempted to find all possible habitats of *A. aphylla* in northwestern China, extending a certain distance to the surrounding area of the known geographical distribution of *A. aphylla* as the study area (31°09' N-53°23' N and 73°40' E-126°04' E). The specific geographical scope of the administrative division of this area mainly includes the whole territory of Xinjiang, Inner Mongolia, Qinghai and Gansu. A geographic base map of China was obtained from the National Fundamental Geographic Information System (<http://nfgis.nsd.gov.cn>). Most of the study area is arid and semi-arid and has a typical continental climate. The climate is dry all year with strong evaporation. Specifically, the dryness is greater than 4 (Ma et al., 2010), and the evaporation is basically more than 1000 mm (Wei et al., 2003). The study area is characterized by complex topography, fragile ecosystems, and long-term disturbance by human activities.

Occurrence collection of A. aphylla

The occurrence locations of *A. aphylla* were collected from databases, including the including the 1:1000000 vegetation atlas of China, the Chinese Virtual Herbarium dataset (CVH, <http://www.cvh.org.cn/>), Plant Photo Bank of China dataset (<http://plantphoto.cn>), Global Biodiversity Information Facility dataset (GBIF, <https://www.gbif.org/>) and some related references (Xu, 2003; Liu and Yang, 2006). Based on the occurrence location *A. aphylla*, we conducted extensive field investigations in Xinjiang, Badan Jaran Desert in Inner Mongolia and Jiuquan in Gansu during the summer (June to September) of 2017 and 2018. Xinjiang is the most distributed area of *A. aphylla*, the surveyed areas included Bole, Changji, Kashi, Atushi, Karamay and Shihezi. We found those areas where previously distributed with *A. aphylla* due to disturbances and disruptions of human activity are now less distributed, such as Karamay, Bole and Fukang of Changji. The distribution of *A. aphylla* in the core area was patchy. After removing repetitive occurrences and updating the distribution of *A. aphylla*, we obtained 99 data records for constructing the models. With the help of ArcGIS 10.4, a distribution of *A. aphylla* map was developed (Fig. 1).

Environmental variables

The 19 bioclimatic variables and one biophysical variable (altitude) with a 30s (ca. 1 km) spatial resolution, downloaded from World Bioclimatic Database (<http://www.worldclim.org>). The current climate data (1961-1990) and Paleoclimate data for the Mid-Holocene (about 6000 years ago) were derived from CCSM4 (Collins et al., 2006). The future climate data for RCP4.5 for carbon dioxide for 2050

(2041-2060 average climate) and 2070 (2061-2080 average climate) were included. Mid-Holocene is the most recent climate suitable period. Its radiation intensity and the increase of modern atmospheric CO₂ have similar warming effects on the climate, so the Mid-Holocene climate simulation is of great significance for the prediction of climate scenarios for future global warming (Joussaume et al., 1995). This data set describes annual trends in climate, seasonality, and extreme environmental conditions and is often used for the prediction of niche models.

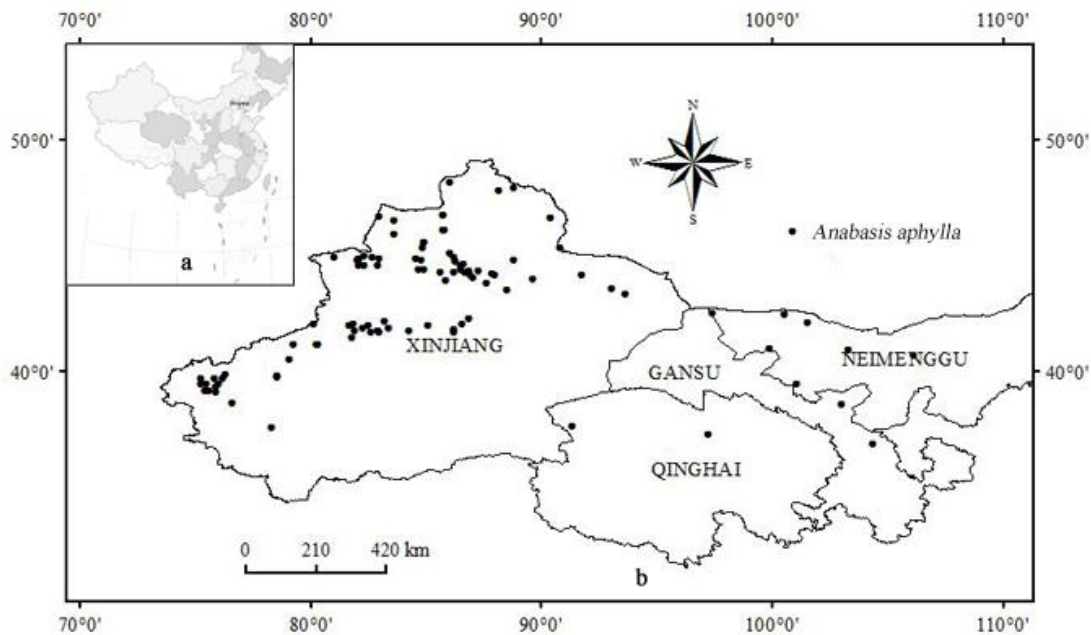


Figure 1. Distribution of *A. aphylla* used in this study (a) Map of China; (b) Distribution of *A. aphylla* in northwestern China

To avoid the collinearity between environmental variables, Maxent's jackknife was used to sort the 20 environmental variables according to their contribution rate. Environmental factors with a sum of 10 cumulative contribution rates >90% were selected for models (Wei et al., 2019), including 9 bioclimatic variables and altitude data (Table 1). These variables included annual mean temperature (bio1), isothermality (bio3, Eq.1), minimum temperature of coldest month (bio6), temperature annual range (bio7, Eq.2), annual precipitation (bio12), precipitation of wettest month (bio13), precipitation of seasonality (bio15), precipitation of driest quarter (bio17), precipitation of warmest quarter (bio18) and altitude.

$$\text{Isothermality (\%)} = (P2 / P7) \times 100 \quad (\text{Eq.1})$$

$$\text{Temperature Annual Range (}^\circ\text{C)} = P5 - P6 \quad (\text{Eq.2})$$

where P2 is mean diurnal range; P5 is maximum temperature of warmest month; P6 is minimum temperature of coldest month; P7 is temperature annual range.

Table 1. Environmental variables used in this study

Environmental variables	Description	Unit	Contribution (%)
Bio 1	Annual Mean Temperature	°C	8.8
Bio 2	Mean Diurnal Range	°C	
Bio 3	Isothermality	-	3.5
Bio 4	Temperature Seasonality	C of V	
Bio 5	Maximum Temperature of Warmest Month	°C	
Bio 6	Minimum Temperature of Coldest Month	°C	9.2
Bio 7	Temperature Annual Range	°C	4.9
Bio 8	Mean Temperature of Wettest Quarter	°C	
Bio 9	Mean Temperature of Driest Quarter	°C	
Bio 10	Mean Temperature of Coldest Quarter	°C	
Bio 11	Mean Temperature of Coldest Quarter	°C	
Bio 12	Annual Precipitation	mm	10
Bio 13	Precipitation of Wettest Month	mm	18.1
Bio 14	Precipitation of Driest Month	mm	
Bio 15	Precipitation of Seasonality (Coefficient of Variation)	CV	31
Bio 16	Precipitation of Wettest Quarter	mm	
Bio 17	Precipitation of Driest Quarter	mm	6.1
Bio 18	Precipitation of Warmest Quarter	mm	7.6
Bio 19	Precipitation of Coldest Quarter	mm	
Alt	Altitude	m	0.9

Species distribution modelling

This study used Maxent v3.3.3 software for analysis. We randomly selected 75% data for model training and 25% for model test. Selected the jackknife method in the environmental parameter settings, the remaining parameter settings selected the default parameters (Ma et al., 2017) and set 10 repetitions. The analysis results were output in logical format and ASCII type. For the 10 replicate results in different climate scenarios, used ArcGIS 10.4 to find the mean value as the final model result (Ma et al., 2017).

A Jackknife test was used to measure the variable importance in the model development, and receiver operating curve analysis (ROC) was used for model quality (Wang et al., 2017). The Jackknife test to examine the importance of individual variables for Maxent predictions. The receiver operating characteristic area under curve (AUC) method is a widely used procedure for comparing species distribution model performance of Maxent models (Lobo et al., 2010; Babar et al., 2012). The ROC plots the sensitivity values and the false positive fraction for all available probability thresholds (Manel et al., 2001). AUC provides a single measure of model performance independent of any particular choice of threshold. The AUC measures model performance ranging from 0 to 1. Accuracy classification for AUC is: 1>excellent>0.9>good>0.8>fair>0.7>poor>0.6>fail (Swets, 1988).

For display and further analysis, we imported the results of the Maxent models predicting the presence of *A. aphylla* (0-1 range) into Arc GIS 10.4. Five classes of potential habitats were regrouped (Yang et al., 2013): unsuitable habitat (0-0.2); barely suitable habitat (0.2-0.4); suitable habitat (0.4-0.6); highly suitable habitat (0.6-0.7); very highly suitable habitat (0.7-1.0). For each model, we calculated the areas of *A. aphylla* under different climatic scenarios.

Results

Model performance and variables' contribution

In this study, models predictive accuracy of *A. aphylla* habitat was assessed as a good level. Specifically, under the current and the RCP4.5 2050 period, the AUC values verified by the model results were 0.901. Under the Paleoclimate and the RCP4.5 2070 climate scenarios the value of AUC were 0.877 and 0.898, respectively. This indicated that the potential growth area and ecological suitability of *A. aphylla* modelled by this study were highly accurate and reliable.

Under different climatic scenarios, the environmental variables that contributed most to the construction of the potential distribution model of *A. aphylla* with the Maxent algorithm were Bio15 (31% of the variation), followed by bio13 (18.1% of the variation), bio12 (10% of the variation), bio6 (9.2% of the variation), bio1 (8.8% of the variation), bio18 (7.6% of the variation), bio17 (6.1% of the variation), bio7 (4.9% of the variation), bio3 (3.5% of the variation) and alt (0.9% of the variation) (Table 1, Fig. 2). The cumulative contributions of these factors reached values as high as 90.8%. *A. aphylla* is highly adaptable to low temperature environments (Peng et al., 2018). Our previous studies showed that the seeds of *A. aphylla* can germinate in early spring when the ground is moist due to melting snow (Peng et al., 2018). In the Junggar Basin with more *A. aphylla* distributed, the annual extreme maximum temperature can reach 42.9°C (Chu et al., 2014). Therefore, *A. aphylla* has a strong adaptability to temperature.

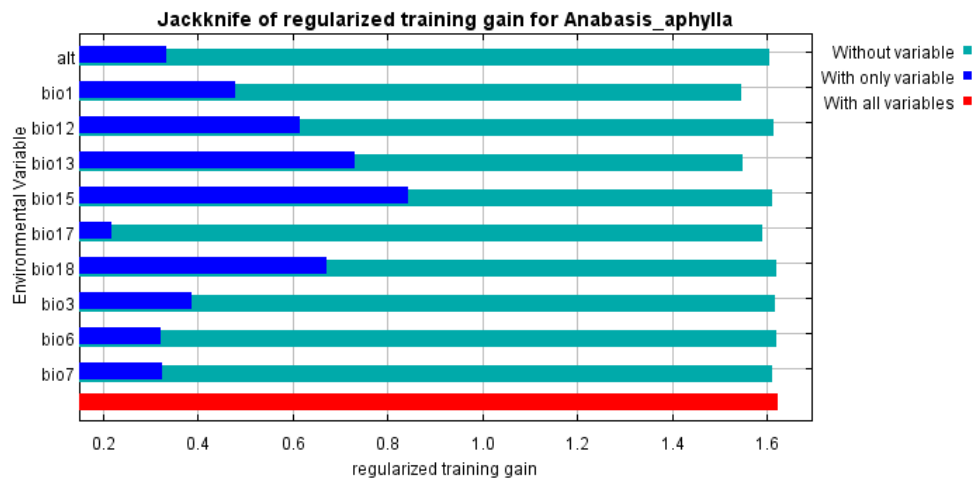


Figure 2. Results of the jackknife test of variables' contribution in modelling *A. aphylla*'s habitat distribution (The regularized training gain describes how much better the Maxent distribution fits the occurrence data compared to a uniform distribution. The dark blue bars indicate the gain from using each variable in isolation, the light blue bars indicate the gain lost by removing the single variable from the full model, and the red bar indicates the gain using all of the variables)

Response curves

Response curves showed the quantitative relationship between environmental variables and the logistic probability of occurrence, which deepen our understanding of the ecological niche of species (Yi et al., 2016). This curves can provide useful

information about the required environmental threshold (existence probability >0.4) for optimal growth of plant species. According to the response curve (Fig. 3), the probability of occurrence of *A. aphylla* decreases considerably in regions in which the precipitation of seasonality (bio15) is above 80% (Fig. 3A). The optimal growth annual precipitation of *A. aphylla* (bio12) was approximately 140 mm (Fig. 3B). The probability of occurrence of *A. aphylla* increases in areas with an annual mean temperature (bio1) between 5°C and 13°C (Fig. 3C).

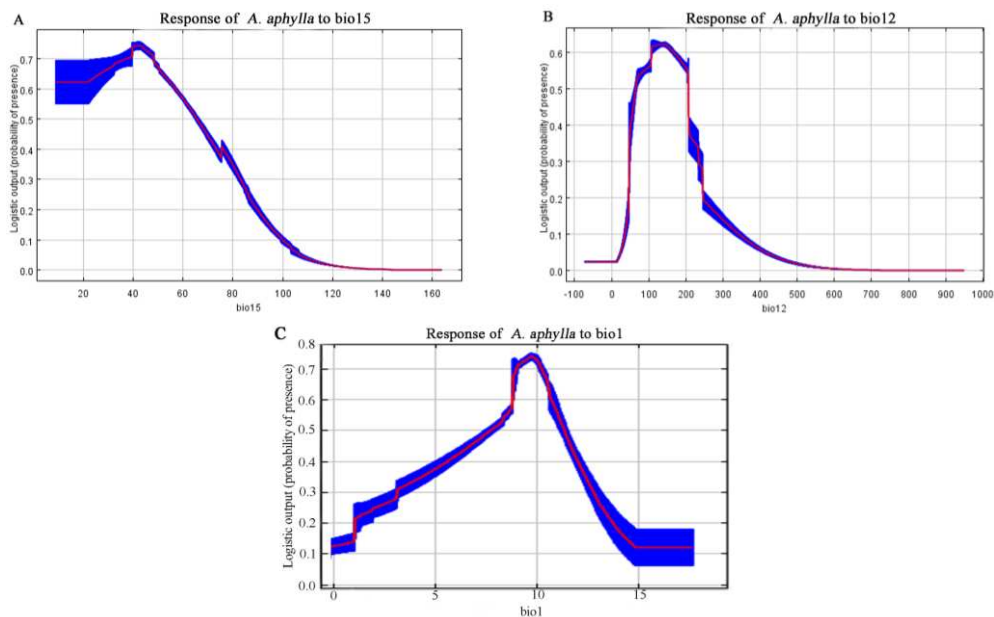


Figure 3. Response curves of the main environmental variables in *A. aphylla*'s habitat distribution model (A) bio15: precipitation of seasonality (C of V); (B) bio12: annual precipitation (mm); (C) bio1: annual mean temperature (°C)

Predicted geographical distribution of *A. aphylla*

According to the predicted geographical distribution under different climatic scenarios (Fig. 4), the highly and very highly suitable distribution areas of *A. aphylla* were mainly concentrated in Xinjiang, of which the southern margin of the Junggar Basin and the western side of Tarim Basin were the very highly suitable areas. As far as the Xinjiang region was concerned, the distribution of *A. aphylla* in northern was more than in southern. In addition, *A. aphylla* also had a suitable distribution in some areas of the Hexi Corridor. The suitable distribution value of *A. aphylla* in Inner Mongolia and Qinghai was low. In Inner Mongolia, the expansion of the Badain Jaran Desert area may be one of the reasons for the reduced distribution area of *A. aphylla*. Compared with the Palaeoclimate scenario, the suitable areas of *A. aphylla* in the central part of Qinghai were reduced under the current and RCP4.5 2050 climatic scenarios.

According to the prediction of Palaeoclimate scenario, the total unsuitable areas of *A. aphylla* under the current, 2050 and 2070 climatic scenarios were increased, while the barely suitable areas of *A. aphylla* decreased (Table 2). The reduction of barely suitable area was mainly concentrated in central Inner Mongolia (Fig. 4). Compared with the current climate scenario, the very highly suitable distribution area of *A. aphylla* will decrease by 10.5% and 13.9% respectively in 2050 and 2070 (Table 2).

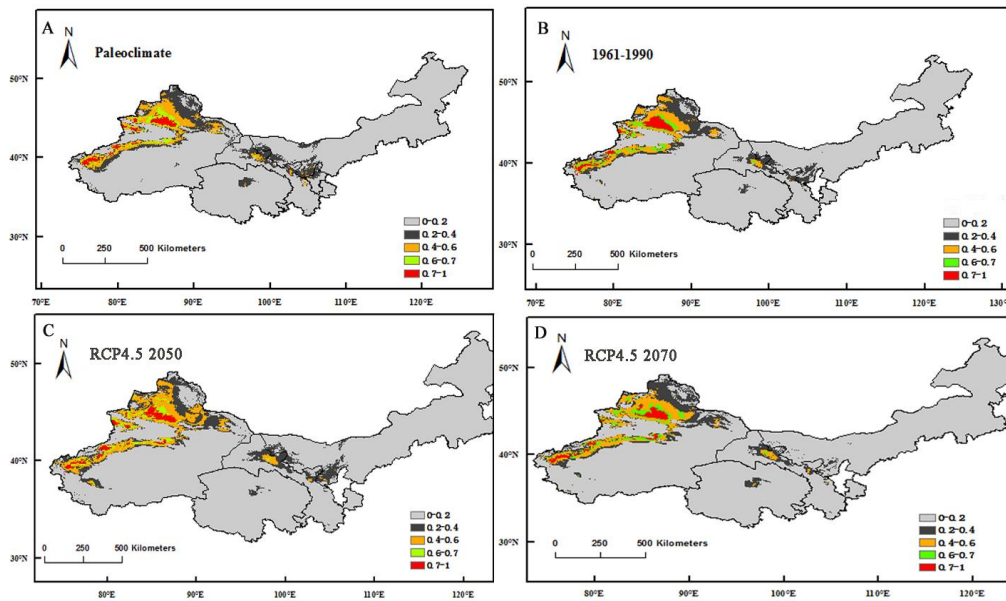


Figure 4. Predicted distribution of *A. aphylla* under different climatic scenarios (A) under Paleoclimate scenario; (B) under current scenario; (C) under RCP4.5 2050 scenario; (D) under RCP4.5 2070 scenario

Table 2. Areas in unsuitable, barely suitable, suitable, highly suitable and very highly suitable of *A. aphylla* under different climatic scenarios

Suitable grade	Palaeoclimate	1961-1990	2050 (RCP4.5)	2070 (RCP4.5)
Very highly suitable	5.7345	6.1109	5.4680	5.2587
Highly suitable	7.5168	6.3237	6.2516	6.9788
Suitable	20.0639	19.9467	21.6785	21.5845
Barely suitable	43.8072	35.7691	35.6073	34.3596
Unsuitable	345.7246	354.6966	353.8416	354.6654

Discussion

Based on the Maxent model and GIS tools, this study predicted the potential distribution of *A. aphylla* in northwestern China under Paleoclimate, current and future climatic scenarios (Fig. 3). The *A. aphylla*'s distribution points used for models were derived from the Chinese Plant Image Database, Vegetation Atlas, GBIF, CHV and published articles, these covered all distribution of *A. aphylla* in China. According to the ROC curve, the potential distribution model prediction results of *A. aphylla* during different climatic backgrounds showed that AUC values were higher than 0.877, indicating that the model prediction results were accurate and credible.

Under the Palaeoclimate and current climatic scenarios, the highly suitable distribution area of *A. aphylla* was mainly along the southern margin of the Junggar Basin and the west side of the Tarim Basin. In addition, the fitness value was higher in some areas of the Hexi Corridor, but low in most areas of Inner Mongolia and Qinghai. The highly suitable distribution area of *A. aphylla* found in this study was consistent with the findings of Wang et al. (2018). *A. aphylla* has a sporadic distribution in the Hexi Corridor area, and fragmentation is more serious. This finding may be related to the increase in evaporation caused by climatic warming in the Hexi Corridor, which has

led to aggravation of drought in this part of the region and increased desertification trends (Ren and Yang, 2008). Under climatic scenarios in the future, the total suitable areas of *A. aphylla* will be increased. As the global climate continues to warm because of the increase in CO₂, China's climate will accordingly change. According to the regional climatic model, annual precipitation in most parts of northwestern China will increase by more than 20% under a doubling of the CO₂ concentration, with Xinjiang and Hexi increasing the most, reaching 20%-50% (Gao et al., 2001). Climate change has different effects on the distribution patterns of different species. Some species are threatened by climate change and are endangered or even extinct; others will benefit from climate change (Ma et al., 2017). In this study, it was determined that *A. aphylla* belongs to the latter case according to the change in its distribution area. At large spatial scales, climatic factors are key factors limiting the plant's potential distribution (Ma et al., 2017). However, in addition to the influence of abiotic factors on the distribution range of plants, human activities, interactions between species and the limitation of groundwater level all affect the geographical distribution pattern of species and their relationship with climate (Wang and Ni, 2009).

The Maxent prediction results in this study showed that the suitable distribution area of *A. aphylla* was mainly along the southern margin of the Junggar Basin, the west side of the Tarim Basin and parts of the Hexi Corridor. *A. aphylla* often grows in gravel and saline soils in the desert at the front of diluvial fans, intermontane platforms and arid hillsides of low mountain (Chu et al., 2014); these areas were found to be more disturbed by human activities during the field investigation. Because of agricultural reclamation, oil exploitation and other human activities, the actual distribution of *A. aphylla* was mostly in patches with serious fragmentation. Particularly since the 1960s, the continuous increased population and the blind development of agricultural reclamation land resulted in a rapid expansion of desertification area. For example, along the southern margin of the Gurbantunggut Desert, the cultivated area increased from 818 km² to 5500 km², increasing the cultivated area nearly 7 times (Wei et al., 2003). Therefore, in view of the serious fragmentation caused by human activities, it is suggested to add *A. aphylla* to the list of endangered species for protection.

Conclusions

A. aphylla as one of the dominant species in the desert area of China, has strong drought tolerance. In this study, the highly and very highly suitable areas of *A. aphylla* were mainly concentrated in the southern margin of the Junggar Basin and the western side of Tarim Basin. The Maxent model's jackknife test of environmental variables showed that precipitation of seasonality (31%) contributed most to the model. The models obtained in this study indicated that climate change had different effects on different suitable distribution areas. By calculating the area of the very highly suitable of *A. aphylla*, it will decrease in the future climate scenarios (Table 2). Therefore, by modelling the potential suitable area of *A. aphylla* and studying its niche requirements, it is of great significance for its protection in the future.

In this study, the potential distribution prediction of *A. aphylla* was only based on environmental variables, without considering the influence of human factors and ecological niche overlap between different species. In the actual distribution, *A. aphylla* was distributed in patches in the core area due to the influence of land use. *Haloxyylon ammodendron* and other *Anabasis* plants have similar ecological characteristics to *A.*

aphylla, so its geographical distribution is also affected by these plants. It is very necessary to study the geographical distribution of vegetation in combination with human disturbance and the overlap of niche between different species, so as to provide protection suggestions. Such as the establishment of core reserves. At the same time, *A. aphylla* is more affected by the topography in the distribution area. For example, it is separated by Tianshan mountain in Xinjiang and influenced by Hexi Corridor in Gansu. Due to the effects of reproductive isolation and environmental differences, genetic differentiation among populations of the same species distributed in different regions will occur (Guo, 2010). Therefore, it is of great significance to study the species evolution and genetic diversity of *A. aphylla*.

Acknowledgements. This work was supported by the Program of the National Natural Science Foundation of China (31460187), General Financial Grant of the China Postdoctoral Science Foundation (2017M613253) and Scientific Research Foundation of Shihezi University for Advanced Talents (RCZX201518, RCZX201521).

REFERENCES

- [1] Araújo, M. B., Alagador, D., Cabeza, M., Thuiller, W. (2011): Climate change threatens European conservation areas. – *Ecology letters* 14: 484-492.
- [2] Babar, S., Amarnath, G., Reddy, C. S., Jentsch, A., Sudhakar, S. (2012): Species distribution models: ecological explanation and prediction of an endemic and endangered plant species (*Pterocarpus santalinus* L.f.). – *Current Science* 102: 1157-1165.
- [3] Chu, G. M., Wang, M., Zhang, S. X. (2014): Spatial point patterns of *Anabasis aphylla* populations in the Proluvial Fan of South Junggar Basin. – *Scientia Silvae Sinicae* 50: 8-14.
- [4] Collins, W. D., Bitz, C. M., Blackmon, M. L., Bonan, G. B., Bretherton, C. S., Carton, J. A., Chang, P., Doney, S. C., Hack, J. J., Henderson, T. B., Kiehl, J. T., Large, W. G., McKenna, D. S., Santer, B. D., Smith, R. D. (2006): The community climate system model version 3 (CCSM3). – *J. Clim* 19: 2122-2143.
- [5] Santos, L. A. D., Mendes, M. F., Krüger, A. P., Blauth, M. L., Gottschalk, M. S., Garcia, F. R. M. (2017): Global potential distribution of *Drosophila suzukii* (Diptera, *Drosophilidae*). – *Plos One* 12: e0174318.
- [6] Elith, J., Graham, C. H., Anderson, R. P., Dudik, M., Ferrier, S., Guisan, A., Hijmans, R. J., Huettmann, F., Leathwick, J. R., Lehmann, A. (2006): Novel methods improve prediction of species' distributions from occurrence data. – *Ecography* 29: 129-151.
- [7] Elith, J., Phillips, S. J., Hastie, T., Dudik, M., Chee, Y. E., Yates, C. J. (2015): A statistical explanation of Maxent for ecologists. – *Diversity and Distributions* 17: 43-57.
- [8] Gao, X. J., Zhao, Z. C., Ding, Y. H., Huang, R. H., Giorgi, F. (2001): Climate change due to greenhouse effects in China as simulated by regional climate model. – *Advances in Atmospheric Sciences* 18: 1224-1230.
- [9] Garcia, K., Lasco, R., Ines, A., Lyon, B., Pulhin, F. (2013): Predicting geographic distribution and habitat suitability due to climate change of selected threatened forest tree species in the Philippines. – *Applied Geography* 44: 12-22.
- [10] Guo, N. (2010): Genetic diversity of natural populations of *Rosa Laxa* Retz. and *Rosa platyacantha* Schrenk in Tianshan mountains of Xinjiang. – China Academy of Agricultural Science, Beijing, China.
- [11] Hernandez, P. A., Franke, I., Herzog, S. K. (2008): Predicting species distributions in poorly studied landscapes. – *Biodiversity and Conservation* 17: 1353-1366.

- [12] Houghton, J. T., Ding, Y., Griggs, D. J., Noguier, M., Dai, X., Maskell, K., Johnson, C. A. (2001): Climate change 2001: the scientific basis. – Cambridge: Cambridge University Press.
- [13] Jiang, X. (2003): Relationship between climate and geographic distribution of some plant species and prediction of species potential distribution in the arid land, northwest China. – Chinese Academy of Science, Beijing, China.
- [14] Joussaume, S., Taylor, K. E. (1995): Status of the Paleoclimate modeling intercomparison project (PMIP). – Proceedings of the First International AMIP Scientific Conference, WCRP Report. Monterey, California, USA 5: 425-430.
- [15] Liu, X. C., Yang, Q. (2006): The Analysis on the Control Index of the Desert Vegetation in Dynamics and Restoring Strategy in Arid Area. – Research of Soil and Water Conservation 13: 99-103.
- [16] Lobo, J. M., Alberto, J. V., Real, R. (2010): AUC: a misleading measure of the performance of predictive distribution models. – Global Ecology Biogeography 17: 145-151.
- [17] Ma, S. M., Zhang, M. L., Zhang, H. X., Meng, H. H., Chen, X. (2010): Predicting potential geographical distributions and patterns of the relic plant *Gymnocarpus przewalskii* using Maximum Entropy and Genetic Algorithm for rule-set prediction. – Chinese Journal of Plant Ecology 34: 1327-1335.
- [18] Ma, S. M., Wei, B., Li, X. C., Luo, C. H., Sun, F. F. (2017): The impacts of climate change on the potential distribution of *Haloxylon ammodendron*. – Chinese Journal of Ecology 36: 1243-1250.
- [19] Manel, S., Williams, H. C., Ormerod, S. J. (2001): Evaluating presence-absence models in ecology: the need to account for prevalence. – Journal of Applied Ecology 38: 92-931.
- [20] Marcer, A., Sáez, L., Molowny-Horas, R., Pons, X., Pino, J. (2013): Using species distribution modelling to disentangle realised versus potential distributions for rare species conservation. – Biological Conservation 166: 221-230.
- [21] Ortega-Huerta, M. A., Peterson, A. T. (2004): Modelling Spatial Patterns of Biodiversity for Conservation Prioritization in North-Eastern Mexico. – Diversity & Distributions 10: 39-54.
- [22] Padalia, H., Srivastava, V., Kushwaha, S. P. S. (2014): Modeling potential invasion range of alien invasive species, *Hyptis suaveolens* (L.) Poit. in India: comparison of MaxEnt and GARP. – Ecological Informatics 22: 36-43.
- [23] Parmesan, C. (2006): Ecological and evolutionary responses to recent climate change. Annual Review of Ecology. – Evolution and Systematics 37: 637-669.
- [24] Pearson, R. G., Raxworthy, C. J., Nakamura, M., Peterson, A. T. (2007): Predicting species distributions from small numbers of occurrence records: a test case using cryptic geckos in Madagascar. – Journal of Biogeography 34: 102-117.
- [25] Peng, M. W., Wang, M., Jiang, P., Chang, Y. L., Chu, G. M. (2018): The impact of low temperature on seed germination of two desert species in Junggar Basin of China. – Applied ecology and environmental research 16: 5771-5780.
- [26] Phillips, S. J., Anderson, R. P., Schapire, R. E. (2006): Maximum entropy modeling of species geographic distributions. – Ecological Modeling 190: 231-259.
- [27] Rebelo, H., Jones, G. (2010): Ground validation of presence only modelling with rare species: a case study on barbastelles *Barbastella barbastellus* (Chiroptera: Vespertilionidae). – Journal of Applied Ecology 47: 410-420.
- [28] Ren, Z. X., Yang, D. Y. (2008): Climate change and surface run off change impact on desertification in the arid area of northwest China in recent 50 years. – Journal of Arid Land Resources and Environment 22: 91-95.
- [29] Sardà-Palomera, F., Brotons, L., Villero, D., Sierdsema, H., Newson, S. E., Jiguet, F. (2012): Mapping from heterogeneous biodiversity monitoring data sources. – Biodiversity Conservation 21: 2927-2948.

- [30] Stockwell, D., Peters, D. (1999): The GARP modelling system: problems and solutions to automated spatial prediction. – *International Journal of Geographical Information Science* 13: 143-158.
- [31] Swets, J. A. (1988): Measuring the accuracy of diagnostic systems. – *Science* 240: 1285-1293.
- [32] Wang, J., Ni, J. (2009): Modelling the distribution of five *Caragana* species in temperate northern China. – *Chinese Journal of Plant Ecology* 33: 12-24.
- [33] Wang, T. T., Chu, G. M., Jiang, P., Niu, P. X., Wang, M. (2017): Influences of Different Treatments on the Germination of *Anabasis aphylla* Seeds. – *Journal of Northwest Forestry University* 32: 125-129, 207.
- [34] Wang, Y., Wen, Z. B., Zhang, H. X., Zhang, M. L. (2018): Geographical Distribution and Prediction on Potential Distribution Areas of *Anabasis* in China. – *Journal of Desert Research* 38: 1033-1039.
- [35] Wei, W. S., He, Q., Liu, M. Z., Gao, W. D. (2003): Study on climate change and desert environment in Junggar Basin. – *Journal of Desert Research* 2(2): 101-105.
- [36] Wei, W. S., He, Q., Liu, M. Z., Gao, W. D. (2003): Climate Change and the Desert Environment in Junggar Basin, Xinjiang, China. – *Journal of Desert Research* 23: 3-7.
- [37] Wei, B., Ma, S. M., Song, J., He, L. Y., Li, X. C. (2019): Prediction of the potential distribution and ecological suitability of *Fritillaria walujewii*. – *Acta Ecologica Sinica* 39: 228-234.
- [38] Wilson, C. D., Roberts, D., Reid, N. (2011): Applying species distribution modelling to identify areas of high conservation value for endangered species: a case study using *Margaritifera margaritifera* (L.). – *Biol. Cons* 144: 821-829.
- [39] Wisz, M. S., Hijmans, R. J., Li, J., Peterson, A. T., Graham, C. H., Guisan, A. (2008): Effects of sample size on the performance of species distribution models. – *Diversity Distribution* 14: 763-773.
- [40] Xu, L. (2003): Studies on ecological genetics of the important desert plants natural populations in Fukang, Xinjiang. – Northwest University, Shanxi, China.
- [41] Yang, X. Q., Kushwaha, S. P. S., Saran, S., Xu, J., Roy, P. S. (2013): Maxent modeling for predicting the potential distribution of medicinal plant, *Justicia adhatoda* L. in Lesser Himalayan foothills. – *Ecological Engineering* 51: 83-87.
- [42] Yi, Y. J., Cheng, X., Yang, Z. F., Zhang, S. H. (2016): Maxent modeling for predicting the potential distribution of endangered medicinal plant (*H. riparia* Lour) in Yunnan, China. – *Ecological Engineering* 92: 260-269.
- [43] Zhang, L. J., Yue, M., Zhang, Y. D., Gu, X. F., Pan, X. L., Zhao, G. F. (2003): Characteristics of plant community species diversity of oasis desert ecotone in Fukang, Xinjiang. – *Scientia Geographica Sinica* 23(3): 229-333.

EVALUATION OF SOME FRUIT CHARACTERISTICS OF JUJUBE (*ZIZIPHUS JUJUBA* MILL) GENOTYPES IN MANISA, TURKEY

ACARSOY BILGIN, N.

Department of Horticulture, Faculty of Agriculture, Ege University, İzmir, Turkey
(Orcid ID: 0000-0002-5018-6347; e-mail: nihalacarsoy@yahoo.com)

(Received 4th Oct 2019; accepted 8th Jan 2020)

Abstract. Jujube fruits are widely consumed all over the world as food and herbal medicine due to their health benefits. It is known as a species with a wide variety of products. It can be found naturally throughout the world, including Turkey. Jujube is particularly popular nowadays for its high antioxidant activity and phenolic content. In this study conducted on 10 genotypes selected in Manisa/Demirci (Turkey) pomological, biochemical and organoleptic properties of fruit genotypes were investigated. The results stated, the characteristics examined differed according to genotypes. The highest TSS, phenol and antioxidant content were 45.34%, 322.39 mg GAE/g fw and 96.75 μ mol TE/g fw, respectively. Some genotypes are thought to be beneficial for public health as well as for table use due to their phytochemical contents.

Keywords: selection, pomological, biochemical, organoleptic, statistical

Introduction

Jujube (*Ziziphus jujuba* Mill) is one of the temperate fruit species. This plant is resistant to extreme rain fall and is not affected by drought can survive at heights up to 1700 m above sea level (Ecevit et al., 2002). Jujube is widely grown in almost all over the world (Mukhtar et al., 2004; Gozlekci et al., 2015). In China, it has been cultivated in for many years. It is naturally found in Russia, India, Middle East, Anatolia, Southern Europe and North Africa. There are 6 genus including *Colletia*, *Frangula*, *Hovenia*, *Paliurus*, *Rhamnus*, *Ziziphus* and 25 species in the native flora of Turkey (Anşın and Özkan, 1997). Among them, *Ziziphus jujuba* and *Ziziphus mauritiana* are grown for fruits (İslam et al., 2006).

Jujube is usually growing home gardens and as a border tree in a field edge. It grows in Marmara, Western and Southern Anatolia in Turkey (Yücel, 2005). In this respect, Isparta, Hatay, Iskenderun, Antalya, Kayseri, Bursa, Çanakkale are important production centers (Karıncalı, 2003). Also besides, Çoruh Valley, Manisa/Demirci and Denizli/Çivril noteworthy. In this area, there is abundant natural flora and different species are observed (Yaşa, 2016).

In recent years, fruit species with high antioxidant activity, phenolic and vitamin contents are of great interest (Wojdylo et al., 2016). Thereby, jujube has a significant impact on human nutrition all over the world. Fruits are delicious and eaten as fresh, dried, candy, jam, juice, wine, syrup, tea bag sand compotes (Liu, 2006).

The bioactive components show large variations according to genotypes and growing, and ripening (Choi et al., 2011; Koley et al., 2016). Total phenol contents and antioxidant activity of jujube fruits were found to be high in previous study (Kamiloglu et al., 2009). They have significant levels of vitamin A, B, C and content many minerals (Wojdylo et al., 2016). Accordingly, it is an excellent source of nutrients and phytochemicals and can also contribute to a healthy diet. In this way, it also has a protective feature against various diseases with its composition. Because of these properties, the fruit is well-known as a nourishing food also seeds; roots and leaves are

known as folk medicine (Mukhtar et al., 2004; Abdel-Zaher et al., 2005; Li et al., 2005). Additionally, fruits contain sugar, tannin and mucilage substances. For this reason, it is recommended that diabetics consume fruit directly. This further increases the importance of the product.

Determining genetic diversity is a prerequisite for conservation of genetic resources, due to the loss of many features of gene erosion. This is important for the sustainability of biodiversity. In this economically valuable species, breeders are researching their genetic resources (Ahmad et al., 2019; Dahlia et al., 2019; Sharif et al., 2019). In the development of new varieties, hybridization breeding takes place over a long period and is difficult. Thanks to the genetic diversity in nature, selection breeding is preferred. Morphological and molecular markers are used to determine genotypes in the population (Ahmad et al., 2019; Chen et al., 2019; Dahlia et al., 2019). As is known, morphological evaluation is easy and inexpensive (Zhang et al., 2015). In this way, breeders can identify elite genotypes by investigating plant, fruit and sensory characteristics (Uddin and Hussain, 2012; Godi and Joshi, 2016).

In Turkey, similarly to many other fruits, this species has a gene pool. The characteristics of jujube genotypes have been determined in different locations in our country but there is no standard variety. This will contribute to breeding programs which new genotypes with different characteristics will be developed. Considering these explanations in the current study, pomological, biochemical and organoleptic properties of 10 genotypes were identified in Manisa/Demirci location.

Materials and methods

In this study, 10 local jujube genotypes selected from Manisa/Demirci were used as material (*Fig. 1*). Sampling was performed to represent genetic diversity in the experimental area. In phenotypic observations, individuals with different fruit characteristics such as fruit size, color and taste were selected. For each genotype, 30 fruits were analyzed. Samples were collected during the commercial maturation period (September 2018).



Figure 1. The location of the experimental area

Fruit and stone weights of the harvested samples were determined, and average flesh/stone ratios were calculated. The fruit width and length were measured. Fruit ground colors were stated twice at the equatorial regions of both cheeks for five fruits

with “CR300 model Minolta Colorimeter”. The values of L^* , a^* , b^* were measured and chrome (C^*) and hue angle (h°) were determined based on these values (Karaçalı, 2012). TA values (%) were measured such that 5 ml of fruit juice was completed to 100 ml with distilled water and 0.1 N of NaOH was added to reach a pH of 8.00-8.10. TSS content in fruit juice was found by a digital refractometer (%), and the pH values were read by a pH meter (Karaçalı, 2012). Total phenol content and antioxidant activity were determined in the fruit samples prepared by Thaipong et al. (2006) method. Total phenol content was determined by the Folin-Ciocalteu method (Swain and Hillis, 1959). The results were expressed as mg gallic acid equivalent (GAE)/100 g fresh weight (FW). The FRAP method was used to determine the antioxidant activities. The results were given as Trolox equivalent (TE)/g dm (Benzie and Strain, 1996).

Jujube fruits were evaluated regarding flavor, texture and general acceptability by Meligaared et al. (1991) and Uddin and Hussain (2012). According to this, flavor: no taste (1), elaeagnus-apple (3), apple-pear (5), elaeagnus (7), apple (9); texture: soft (3), medium (5), hard (7) and acceptability: poor (1), fair (3), medium (5), good (7), very good (9) were evaluated with scale ranged from dislike (1) to like (9). At this stage, each genotype was tasted by 10 panelists.

Results were subjected to a variance analysis by using SPSS Statistics 20 statistical package program. Significant differences between averages were defined by Duncan test at the $P < 0.05$ significant level. The mean, minimum, maximum, and standard deviation values of the properties examined were determined. Moreover, the relationship among these values was revealed by conducting Pearson’s correlation analysis. Differences or similarities of genotypes were evaluated according to their analyzed properties by applying PCA to the findings obtained. Moreover, cluster analysis (CA) was utilized to create a dendrogram showing similarities and differences between genotypes.

Results and discussion

Some pomological properties of 10 jujube genotypes are shown in *Table 1*. There was a statistically significant difference in fruit weight, flesh/stone ratio, fruit width and length among genotypes ($P \leq 0.05$). In terms of the investigated characteristics, genotype 10 was the first, followed by genotype 9. On the other hand, the values of genotype 8 were found to be low, in general. Differences in fruit weight (2.73 g to 24.33 g) caused a higher standard deviation. Thus, genotypes exhibited heterogeneity for this trait. The flesh/stone ratio ranged from 4.93 to 27.63. Similar to average fruit weight, higher standard deviation occurred. Minimum and maximum values of fruit width and length were determined as 17.55-34.83 and 18.64-37.48 mm, respectively. Jujube genotypes (*Ziziphus mauritiana*) with large fruits are reported to have a fruit weight range of 4 g (Gorh) to 36 g (Foladi) under the climatic conditions of Pakistan. The highest and lowest stone weight were found in the same genotype (Abbas et al., 2012). Confirming our results, fruit weight, width, and length were noticed as 23 g, 37 mm and 40 mm, respectively by Galindo et al. (2015). Furthermore, for three different jujube genotypes, Kavas and Dalkılıç (2015) explained the variation range of fruit weight (8.21-28.85 g), fruit width (24.02-37.35 mm) and fruit length (29.47-43.73 mm) in Kızılcaköy, Aydın. The change of data based on genotypes was also revealed in the earlier findings of Gao et al. (2012). These findings are synchronized with our study.

Table 1. Pomological properties of jujube genotypes

Genotypes number	Fruit weight (g)	Stone weight (g)	Flesh/stone ratio	Fruit width (mm)	Fruit length (mm)
1	5.37 c	0.78 ^a	5.88 f	22.62 b	21.80 c
2	4.72 e	0.41	10.47 c	19.17 cd	19.88 def
3	5.03 d	0.76	5.62 g	19.92 c	20.45 cde
4	3.26 h	0.32	9.19 d	19.16 cd	18.64 f
5	4.31 f	0.64	5.74 fg	19.08 cd	19.22 ef
6	4.30 f	0.68	5.32 h	18.17 d	21.43 cd
7	3.59 g	0.43	7.35 e	17.55 d	18.95 ef
8	2.73 i	0.46	4.93 i	17.68 d	18.76 ef
9	7.16 b	0.55	12.00 b	23.76 b	25.68 b
10	24.33 a	0.85	27.63 a	34.83 a	37.48 a
Min.	2.73	0.32	4.93	17.55	18.64
Max.	24.33	0.85	27.63	34.83	37.48
Avg.	6.48	0.59	9.41	21.19	22.23
St. dev.	6.17	0.17	6.60	5.07	5.61

The differences in the means were determined by the Duncan test according to $P \leq 0.05$. ^a: Not significant

For all color variables, significant differences among genotypes occurred (Table 2). Generally, the highest values were obtained in genotype 6, except a* value. In genotype 5, the a* value, which expresses the red color, was the maximum. At the same time, it has a darker color owing to the L* value is low. Moreover, the hue value was found low. Thus, this genotype has come to the fore in terms of color. The b* (5.62) and h° (5.71) values identified a high level of variation. As compared with Galindo et al. (2015), it was seen that h° value was lower in our study. This emphasizes that the red color is dominant. In contrast to this research, Kavas and Dalkılıç (2015) did not find any difference in this matter. The color values were influenced by many factors such as genotype, harvest time, cultural practices, crop load, etc. (Wang et al., 2012; Gündüz and Saraçoğlu, 2014).

Biochemical properties (pH, TSS, TA, total phenol and antioxidant activity) significantly differed depending on genotypes (Table 3). No variation was observed in terms of pH and TA. The average value of pH was 5.11 and the TA value was 0.45%. Genotypes are similar in this respect. In this trial, minimum TSS content was found to be 19.20% while a maximum of 45.34%. The high standard deviation indicates a high variation in the population on account of phenol content and antioxidant activity. This diversity is desirable for plant breeders. Total phenol content and antioxidant activity were detected to be 239.90-322.39 mg GAE/g FW and 43.86-96.75 µmol TE/g FW, respectively. Jujube contains much higher TSS than many fruit species (Yao, 2013). While the TSS content of jujube fruits was determined as 24% (Abbas et al., 2012), 32% (Kavas and Dalkılıç, 2015), 19% (Koley et al., 2016), 30% (Gao et al., 2012) and 32% (Ecevit et al., 2008) in previous research, this value was found to be extremely high as 45.34% by ours. Godi and Joshi (2016) stated that the variation in TSS among the jujube genotype may vary mainly due to different harvest periods or genotype. As it is known, if the product load decreases, TSS and TA values increase but not the pH. Compared with the previous study (Galindo et al., 2015), TA content was found to be lower, pH was similar in our study. It is pointed out that jujube fruits are rich in total

phenol contents and antioxidant activity (Yao, 2013). In Indian jujube commercial cultivars (*Z. mauritiana*), the range of total phenol was 172-328.6 mg GAE/100 g (Koley et al., 2016). Our findings are supported by this study. Many external factors may influence the change of the phenol content (Imamoglu, 2016). Although fruits such as strawberry (Zheng et al., 2007), grapes (İşçi et al., 2014), black mulberry (Özgen et al., 2009) contain high phenol, *Ziziphus* contains much more phenol than these fruit species. When compared to cherry and grapefruits with high antioxidant activity, jujube genotypes are superior in this respect (Çağlar and Demirci, 2017; Beyhan et al., 2018).

Table 2. Color values of jujube genotypes

Genotypes number	L*	a*	b*	C*	h°
1	37.54 e	25.94 ef	31.46 e	40.78 d	50.49 c
2	36.40 f	26.67 de	30.71 e	40.66 d	49.03 d
3	42.94 b	27.34 c	38.55 b	47.24 b	54.56 a
4	40.24 c	26.95 d	33.22 d	42.78 c	50.95 c
5	33.40 g	30.27 a	22.55 h	37.75 e	36.68 f
6	45.70 a	28.63 b	41.58 a	50.48 a	55.45 a
7	38.53 d	21.56 h	26.46 g	34.13 f	50.83 c
8	33.78 g	30.05 a	26.34 g	39.96 d	41.24 e
9	37.36 e	24.98 g	28.67 f	38.03 e	48.93 d
10	38.92 d	25.54 fg	34.18 c	42.67 c	53.23 b
Min.	33.40	21.56	22.55	34.13	36.68
Max.	45.70	30.27	41.58	50.48	55.45
Avg.	38.48	26.79	31.37	41.45	49.14
St. dev.	3.71	2.55	5.62	4.59	5.71

The differences in the means were determined by the Duncan test according to $P \leq 0.05$

Table 3. Some biochemical properties of jujube genotypes

Genotypes number	pH	TSS (%)	TA (%)	Total phenol (mg GAE/g fw)	Antioxidant activity ($\mu\text{mol TE/g fw}$)
1	5.03 d	20.67 d	0.50 c	259.13 ab	96.75 a
2	4.97 d	22.81 cd	0.58 b	251.59 ab	71.73 ab
3	4.76 e	23.47 cd	0.71 a	253.87 ab	75.59 ab
4	5.27 b	28.94 bc	0.49 c	239.90 b	63.38 bc
5	5.58 a	30.00 b	0.36 d	242.33 b	53.29 bc
6	4.71 e	19.20 d	0.71 a	322.39 a	73.52 ab
7	5.16 c	25.20 bcd	0.34 d	241.52 b	74.68 ab
8	5.22 bc	45.34 a	0.35 d	247.56 ab	67.24 bc
9	5.21 bc	24.00 bcd	0.34 d	206.04 b	43.86 c
10	5.22 bc	22.67 cd	0.17 e	237.99 b	54.91 bc
Min.	4.71	19.20	0.17	239.90	43.86
Max.	5.58	45.34	0.71	322.39	96.75
Avg.	5.11	26.23	0.45	250.23	67.50
St. dev.	0.25	7.76	0.17	43.24	18.32

The differences in the means were determined by the Duncan test according to $P \leq 0.05$

Results presented in *Table 4* display the organoleptic features of jujube genotypes. The difference between genotypes was statistically significant for flavor (1.00 to 9.00). The best flavor has been identified in genotypes 10 and 7, and there were also remarkable by texture. Considering general acceptability, genotypes 10 (9.00) and 8 (1.67) ranked first and last, respectively. The flavor of fruit was generally described as apple by Kavas and Dalkılıç (2015). It was reported that the product load and fruit flavor were not related to Grande de Albaterra variety (Galindo et al., 2015). The variation observed in these characteristics was also demonstrated in 19 genotypes evaluated by Godi and Joshi (2016). In addition to fresh consumption, fruits are also evaluated in different forms such as gel, pickle, and jelly. For this purpose, sensory evaluations are also important (Uddin and Hussain, 2012).

Table 4. Organoleptic evaluation of jujube genotypes

Genotypes number	Flavor	Texture	General acceptability
1	1.00 e	6.33 ab	5.67 bc
2	5.67 bc	4.33 bc	4.33 cd
3	3.00 d	4.33 bc	5.00 c
4	6.33 bc	4.33 bc	2.33 de
5	7.00 b	3.67 c	5.67 bc
6	5.00 c	4.33 bc	2.33 de
7	9.00 a	6.33 ab	2.33 de
8	7.00 b	3.67 c	1.67 e
9	5.00 c	6.33 ab	7.67 ab
10	9.00 a	7.00 a	9.00 a
Min.	1.00	3.67	1.67
Max.	9.00	7.00	9.00
Avg.	5.80	5.07	4.53
St. dev.	2.49	1.53	2.60

The differences in the means were determined by the Duncan test according to $P \leq 0.05$. Flavor: no taste (1), elaeagnus-apple (3), apple-pear (5), elaeagnus (7), apple (9); Texture: soft (3), medium (5), hard (7); General acceptability: poor (1), fair (3), medium (5), good (7), very good (9)

The correlation coefficients between the features examined of jujube genotypes are seen in *Table 5*. Accordingly, the highest correlation was determined between fruit width and length ($r = 0.976$; $p < 0.01$). Further, fruit width and length showed a significantly positive and strong correlation to fruit weight ($r = 0.960$ and 0.968 ; $p < 0.01$), stone weight ($r = 0.591$ and 0.589 ; $p < 0.01$) and flesh/stone ratio ($r = 0.918$ and 0.923 ; $p < 0.01$). Fruit weight had a positive correlation with stone weight and flesh/stone ratio but a negative correlation with total acidity. L^* , b^* , h° and C^* color of the fruit were also found to be correlated. As L^* increased, b^* ($r = 0.91$), h° ($r = 0.780$), C^* ($r = 0.861$) and total acidity ($r = 0.592$) increased; however, pH ($r = -0.757$) and TSS ($r = -0.556$) decreased. Fruit a^* value showed a positive correlation to h° value and TSS, but negative correlation to C^* value. A positive correlation was observed between fruit b^* color and total acidity, stone weight while pH negatively affected TSS. Fruit h° color had a positive and strong correlation with total acidity ($r = 0.659$) but weak correlation with stone weight ($r = 0.404$). Fruit C^* value showed a positive correlation

to total acidity ($r = 0.392$; $p < 0.05$), but negative correlation to pH ($r = 0.754$; $p < 0.01$) and TSS ($r = 0.653$; $p < 0.01$). A negative correlation was observed between antioxidant activity and pH ($r = -0.474$; $p < 0.01$). Total phenol had a positive correlation with L^* ($r = 0.407$; $p < 0.05$), b^* ($r = 0.412$; $p < 0.05$), h° ($r = 0.468$; $p < 0.01$) and total acidity ($r = 0.431$; $p < 0.05$). From the other side, a negative correlation appeared between total phenol and pH ($r = -0.436$; $p < 0.05$). In jujube with an apple-like flavor; pH and flesh/stone ratio were higher, whereas h° value, total acidity and antioxidant activity decreased. In jujube with hard flesh; fruit weight, flesh/stone ratio, fruit width and length were higher, whereas color a^* was lower than soft flesh. Fruit acceptability had a positive and strong correlation with fruit and stone weight, fruit width and length, flesh/stone ratio and texture while weak, and negative correlation with TSS. Positive correlation between phenolic content and antioxidant activity is mentioned (Gao et al., 2012; Imamoglu, 2016; Koley et al., 2016) however, a correlation was not found in our results. This is also confirmed by Li et al. (2005, 2007).

Principal component analysis (PCA) defined 88.850% of the genotypes with 18 properties and was explained by four principal components (Table 6). PC1, PC2, PC3 and PC4 accounted for 30.905%, 30.703%, 14.883% and 12.359% respectively of the variability. Consequently, PC1 constituted mainly fruit width, length, weight, acceptability, flesh/stone ratio and stone weight; PC2 included mainly ground color b^* , L^* , h° , C^* , pH, antioxidant activity, and total acidity; PC3 show mainly ground color a^* , texture and TSS; PC4 represents mainly flavor and total phenol.

Figure 2 shows biplot based on PCA for fruit quality traits in jujube genotypes in rotated space. PC1 explained fruit width, length, weight, acceptability, flesh/stone ratio, and stone weight. Positive values for PC2 indicated ground color b^* , L^* , h° , C^* , antioxidant activity, and total acidity, while negative PC2 values display pH. Positive values for PC3 represent ground color a^* and TSS, while negative PC3 values point out the texture. PCA was performed to study the correlation between fruit quality parameters (Koley et al., 2016).

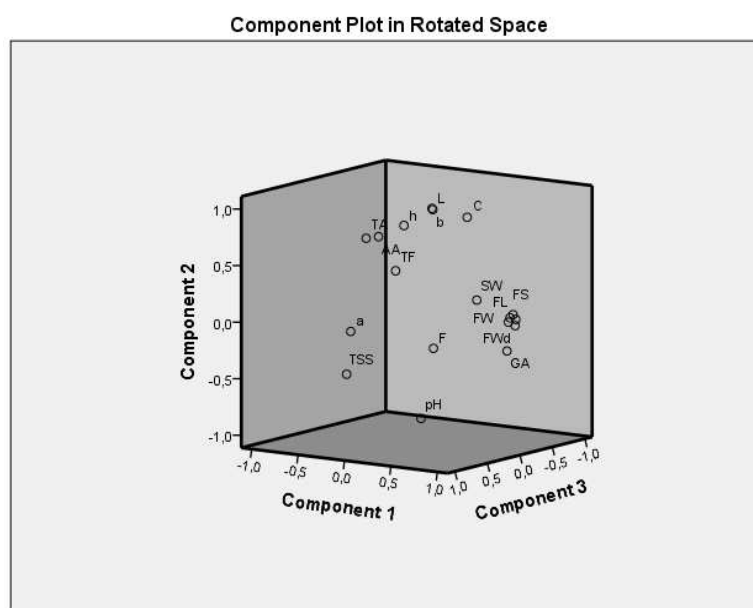


Figure 2. Biplot based on principal components analysis (PCA) for fruit quality traits in rotated space

Table 5. Pearson correlation coefficients among traits of jujube genotypes

	FW	SW	FS	FWd	FL	L	a	b	h	C	pH	TSS	TA	TF	AA	F	T
SW	0.577**																
FS	0.952**	0.318															
FWd	0.960**	0.591**	0.918**														
FL	0.968**	0.589**	0.923**	0.976**													
L	0.056	0.267	-0.006	0.004	0.090												
a	-0.213	0.104	-0.316	-0.242	-0.244	-0.127											
b	0.188	0.385*	0.107	0.152	0.217	0.921**	0.046										
h	0.088	0.404*	-0.033	0.042	0.102	0.780**	0.435*	0.917**									
C	0.282	0.261	0.273	0.263	0.316	0.861**	-0.473**	0.846**	0.566**								
pH	0.111	-0.248	0.189	0.134	0.054	-0.757**	0.083	-0.819**	-0.700**	-0.754**							
TSS	-0.258	-0.406*	-0.228	-0.266	-0.291	-0.556**	0.416*	-0.508**	-0.296	-0.653**	0.465**						
TA	-0.539**	0.000	-0.589**	-0.542**	-0.517**	0.592**	0.242	0.621**	0.659**	0.392*	-0.731**	-0.294					
TF	-0.131	0.159	-0.225	-0.187	-0.120	0.407*	0.229	0.412*	0.468**	0.223	-0.436*	-0.190	0.431*				
AA	-0.258	0.113	-0.343	-0.212	-0.263	0.202	-0.087	0.233	0.171	0.257	-0.474**	-0.133	0.338	0.210			
F	0.335	-0.310	0.438*	0.172	0.246	-0.241	-0.162	-0.359	-0.382*	-0.228	0.490**	0.307	-0.590**	-0.137	-0.427*		
T	0.492**	0.293	0.489**	0.544**	0.537**	0.093	-0.592**	0.036	-0.217	0.350	-0.001	-0.310	-0.336	-0.083	-0.096	0.058	
GA	0.691**	0.587**	0.638**	0.749**	0.708**	-0.114	-0.140	-0.017	-0.074	0.065	0.180	-0.379*	-0.358	-0.202	-0.352	-0.034	0.493**

*Significant at P < 0.05, **Significant at P < 0.01, ns: Non-significance

FW: fruit weight; SW: stone weight; FS: flesh/stone ratio; FWd: fruit width; FL: fruit length; L: L*; a: a*; b: b*; h: h°; C: C*; pH; TSS: total solids soluble; TA: total acidity; TF: total phenol; AA: antioxidant activity; F: flavor; T: texture; GA: general acceptability

Table 6. Component loading in principle component analysis (PCA)

Traits	PC1	PC2	PC3	PC4
W	0.956	-0.004	-0.150	0.141
L	0.942	0.094	-0.137	0.240
FW	0.933	0.070	-0.101	0.280
A	0.874	-0.235	-0.139	-0.163
FS	0.841	0.006	-0.210	0.434
SW	0.734	0.239	0.124	-0.461
Gb	0.178	0.965	0.006	-0.122
GL	0.028	0.932	-0.193	-0.047
Gh	0.141	0.878	0.398	-0.170
pH	0.136	-0.868	0.129	0.277
GC	0.187	0.825	-0.508	-0.018
AA	-0.204	0.730	0.296	-0.209
TA	-0.448	0.669	0.140	-0.494
Ga	-0.022	0.009	0.984	-0.128
T	0.497	-0.091	-0.814	-0.175
TSS	-0.368	-0.466	0.554	0.414
F	0.163	-0.267	-0.024	0.833
TF	-0.355	0.344	-0.182	-0.564
Eigenvalue	5.563	5.527	2.679	2.225
Proportion (%)	30.905	30.703	14.883	12.359
Cumulative (%)	30.905	61.608	76.491	88.850

Extraction method: principal component analysis. Rotation method: Varimax with Kaiser normalization

Clustering analysis (CA) was used to determine the degree of similarity of jujube genotypes, is shown in *Figure 3* as dendrograms. Thus, the genotypes were categorized under two main groups. 6th genotype formed a separate group from the others. The similarities or differences among the jujube genotypes examined with CA showed a correlation with those examined with PCA in terms of investigated characteristics.

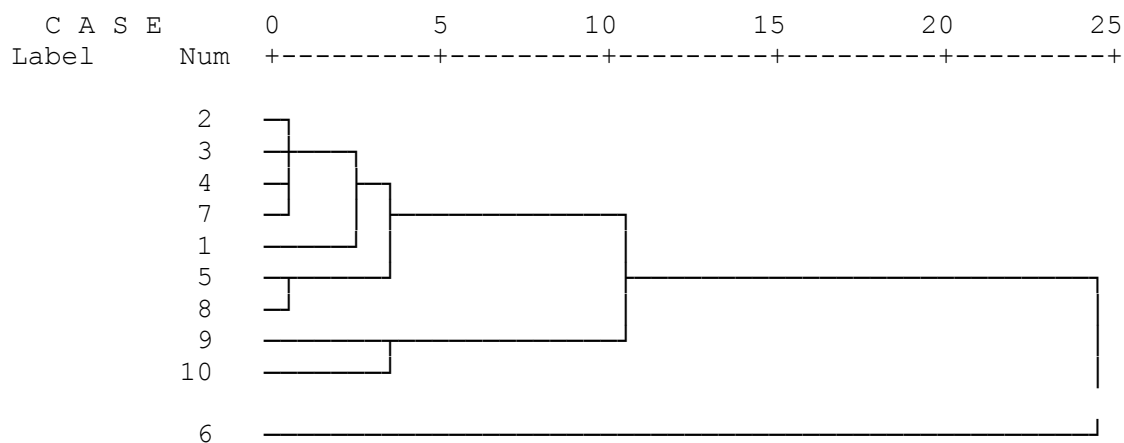


Figure 3. Dendrogram of hierarchical cluster analysis obtained by Ward's clustering method

Conclusion

This study was planned to evaluate some fruit characteristics of 10 jujube genotypes collected from the Demirci location in Turkey. In terms of TSS content, especially genotype 8 is very important and this value is also high in genotype 5. Besides, the fruits of these two genotypes are dark red, high phenol content, elaeagnus taste, and soft texture. Genotype 1 is prominent because of its rich antioxidant content. In this respect, it is a natural antioxidant source and can be considered as an alternative healthy food. On the other hand, genotype 6 is a different group from other genotypes due to its high phenol content and light color. Also, the fruits of genotype 10 are large and taste like apple and their acceptability is good. The jujubes mentioned above are suitable for table consumption. They seem to have a beneficial effect on folk medicine due to their phytochemical contents. The identified genotypes show variation under the same ecological conditions. In this context, they are valuable as a genetic resource. These genotypes are promising. In future studies, a patent may be granted for any genotypes. They can also be used as parents in breeding programs. Furthermore, molecular studies can be performed to determine the genetic relationship. For jujube, this study is essential because there is little information in Turkey. It is important to continue such studies in terms of evaluating the present population in nature and identifying genotypes for different purposes.

REFERENCES

- [1] Abbas, M. M., Sharif, N., Mohar, T. A. (2012): Quality evaluation of promising ber (*Ziziphus mauritiana*) varieties under climatic conditions of Faisalabad. – J. Agric. Res. 50(3): 401-409.
- [2] Abdel-Zaher, A. O., Salim, S. Y., Assaf, M. H., Abdel Hady, R. H. (2005): Anti diabetic activity and toxicity of *Ziziphus spina-christi* leaves. – Journal of Ethnopharmacology 101(1-3): 129-138.
- [3] Ahmad, R., Malik, W., Anjum, M. A. (2019): Genetic diversity and selection of suitable molecular markers for characterization of indigenous *Ziziphus* germplasm. – Erwerbs-Obstbau 61: 345-353.
- [4] Anşın, R., Özkan, Z. C. (1997): Tohumlu Bitkiler: (*Spermatophyta*) Odunsu Taksonlar. – Karadeniz Teknik Üniversitesi Basımevi, Trabzon, pp. 465-466 (in Turkish).
- [5] Benzie, I. F. F., Strain, J. J. (1996): Ferric reducing ability of plasma (FRAP) as a measure of antioxidant power: the FRAP assay. – Anal. Biochem. 239: 70-76.
- [6] Beyhan, Ö., Demir, T., Yurt, B. (2018): Determination of antioxidant activity, phenolic compounds and biochemical properties of cherry laurel (*Laurocerasus officinalis* R.) grown in Sakarya/Turkey. – Bahçe 47(1): 17-22.
- [7] Çağlar, M. Y., Demirci, M. (2017): Üzümsü Meyvelerde Bulunan Fenolik Bileşikler ve Beslenme Önemleri. – Avrupa Bilim ve Teknoloji Dergisi Cilt. 7(11): 18-26 (in Turkish).
- [8] Chen, X., Chen, R., Wang, Y., Wu, C., Huang, J. (2019): Genome-wide identification of WRKY transcription factors in Chinese jujube (*Ziziphus jujuba* Mill.) and their involvement in fruit developing, ripening, and abiotic stress. – Genes. 10: 360. DOI: 10.3390/genes10050360.
- [9] Choi, S. H., Ahn, J. B., Kozukue, N., Levin, C. E., Friedman, M. (2011): Distribution of free amino acids, flavonoids, total phenolics, and antioxidative activities of jujube (*Ziziphus jujuba*) fruits and seeds harvested from plants grown in Korea. – Journal of Agricultural and Food Chemistry 59: 6594-6604.

- [10] Dahlia, F., Benito, C., Boussaid, M. (2019): Genetic diversity of fruits in wild jujube (*Ziziphus lotus* L. Desf.) natural populations from Algeria. – Agriculture & Forestry 65(1): 165-183. DOI: 10.17707/AgricultForest.65.1.17.
- [11] Ecevit, M. F., Hallaç, F., Dilmaç Ünal, T. (2002): Denizli ili Çivril İlçesi Gümüşsu Yöresinde Yetişmekte Olan Ünnap (*Ziziphus jujuba* Mill.)'ın Seleksiyon Yoluyla Islahı Üzerinde Araştırmalar. – Tübitak Togtag Tarp-1988, Ankara (in Turkish).
- [12] Ecevit, M. F., Şan, B., Dilmaç, Ünal, T., Hallaç, Türk, F., Yıldırım, A. N., Polat, M., Yıldırım, F. (2008): Selection of superior ber (*Ziziphus jujuba* L.) genotypes in çivril region. – Tarım Bilimleri Dergisi 14(1): 51-56. (in Turkish).
- [13] Galindo, A., Noguera-Artiaga, L., Cruz, Z. N., Burlo, F., Hernandez, F., Torrecillas, A., Carbonell-Barrachina, A. A. (2015): Sensory and physico-chemical quality attributes of jujube fruits as affected by crop load. – LWT - Food Science and Technology 63: 899-905.
- [14] Gao, Q. H., Wu, C. S., Yu, J. G., Wang, M., Ma, Y. J., Li, C. L. (2012): Textural characteristic, antioxidant activity, sugar, organic acid, and phenolic profiles of 10 promising jujube (*Ziziphus jujuba* Mill.) selections. – Journal of Food Science 77(11): 1218-1225.
- [15] Godi, N. F., Joshi, V. R. (2016): Studies on biochemical and organoleptic characters of different ber (*Zizyphus mauritiana* Lamk) genotypes. – Advances in Life Sciences 5(6).
- [16] Gozlekci, S., Zarifi Khosroshahi, M., Kafkas, E. (2015): Some physical and chemical properties of two jujube (*Ziziphus jujuba* Mill.) genotypes grown in western Turkey. – DOI: 10.17660/ActaHortic.2015.1074.11.
- [17] Gündüz, K., Saraçoğlu, O. (2014): Changes in chemical composition, total phenolic content and antioxidant activities of jujube (*Ziziphus jujuba* Mill.) fruits at different maturation stages. – Acta Sci. Pol., Hortorum Cultus 13(2): 187-195.
- [18] Imamoglu, H. (2016): Total antioxidant capacity, phenolic compounds and sugar content of Turkey *Ziziphus jujubes*. – Acta Sci. Pol. Hortorum Cultus 15(5): 93-108.
- [19] İşçi, B., Şen, F., Güçlü Özdemir, A., Kaçar, E., Altun, A. (2014): Effects of modified atmosphere packing (MAP) and cold treatment on organically grown table grape cultivars. – Journal of Agriculture Faculty of Ege University 51(2): 191-199.
- [20] İslam, M. B., Simmons, M. P. (2006): A thorny dilemma: testing alternative intrageneric classifications within *Ziziphus* (*Rhamnaceae*). – Sistematic Botany 31: 826842.
- [21] Kamiloglu, O., Ericisli, S., Sengul, M., Toplu, C., Serce, S. (2009): Total phenolics and antioxidant activity of jujube (*Zizyphus jujuba* Mill.) genotypes selected from Turkey. – Afr. J. Biotechnol. 8: 303-307.
- [22] Karaçalı, İ. (2012): Bahçe Ürünlerinin Muhafaza ve Pazarlanması. – Ege Üniversitesi Ziraat Fakültesi Yayınları Bornova, İzmir (in Turkish).
- [23] Karıncalı, M. (2003): *Ziziphus jujuba* Mill. (Hünnap) Bitkisinin Morfolojik, Anatomik, Ekolojik ve Polen Özelliklerinin Araştırılması, – Pamukkale Üniversitesi Fen Bilimleri enstitüsü Biyoloji Anabilim Dalı, Yüksek Lisans Tezi, Denizli (in Turkish).
- [24] Kavas, İ., Dalkılıç, Z. (2015): Bazı Hünnap Genotiplerinin Morfolojik, Fenolojik Ve Pomolojik Özelliklerinin Belirlenmesi ve Melezleme Olanaklarının Araştırılması. – Journal of Adnan Menderes University Agricultural Faculty 12(1): 57-72 (in Turkish).
- [25] Koley, T. K., Kaur, C., Nagal, S., Walia, S., Jaggi, S. (2016): Antioxidant activity and phenolic content in genotypes of Indian jujube (*Zizyphus mauritiana* Lamk.). – Arabian Journal of Chemistry 9: S1044–S1052. <http://dx.doi.org/10.1016/j.arabjc.2011.11.005>.
- [26] Li, J. W., Ding, S., Ding, X. (2005): Comparison of antioxidant capacities of extracts from five cultivars of Chinese jujube. – Process Biochem. 40: 3607-3613.
- [27] Li, J. W., Fan, L. P., Ding, S. D., Ding, X. L. (2007): Nutritional composition of five cultivars of Chinese jujube. – Food Chem. 100(2): 454-460.
- [28] Liu, M. (2006): Chinese jujube: botany and horticulture. – Horticultural Reviews 32: 229-298.

- [29] Meligaared, M., Civille, G. V., Carr, B. T. (1991): Sensory Evaluation Techniques. 2nd Ed. – CRC Press, Boca Raton, FL.
- [30] Mukhtar, H. M., Ansari, S. H., Ali, M., Naved, T. (2004): New compounds from *Ziziphus vulgaris*. – *Pharmaceutical Biology* 42(7): 508-511.
- [31] Özgen, M., Serçe, S., Kaya, C. (2009): Phytochemical and antioxidant properties of anthocyanin *Morus nigra* and *Morus rubra* fruits. – *Scientia Horticulturae* 119: 275-279.
- [32] Sharifa, N., Jaskania, M. J., Naqvia, S. A., Awa, F. S. (2019): Exploitation of diversity in domesticated and wild ber (*Ziziphus mauritiana* Lam.) germplasm for conservation and breeding in Pakistan. – *Scientia Horticulturae* 249: 228-239.
- [33] Swain, T., Hillis, W. E. (1959): The phenolic constituents of *Prunus domestica* L.—the quantitative analysis of phenolic constituents. – *J Sci Food Agric* 10: 63-68.
- [34] Thaipong, K., Boonprakob, U., Crosby, K., Cisneros-Zevallos, L., Byrne, D. H. (2006): Comparison of ABTS, DPPH, FRAP, and ORAC assays for estimating antioxidant activity from guava fruit extracts. – *J Food Composit Anal* 19: 669-675.
- [35] Uddin, M. B., Hussai, I. (2012): Development of diversified technology for jujube (*Ziziphus jujuba* L) processing and preservation. – *World Journal of Dairy & Food Sciences* 7(1): 74-78. DOI: 10.5829/idosi.wjdfs.2012.7.1.62115.
- [36] Wang, H., Chen, F., Yang, H., Chen, Y., Zhang, L., An, H. (2012): Effects of ripening stage and cultivar on physicochemical properties and pectin nanostructures of jujubes. – *Carbohydrate Polymers* 89: 1180-1188.
- [37] Wojdylo, A., Carbonell-Barrachina, A. A., Legua, P., Hernandez, F. (2016): Phenolic composition, ascorbic acid content, and antioxidant capacity of Spanish jujube (*Ziziphus jujube* Mill.) fruits. – *Food Chemistry* 201: 307-314.
- [38] Yao, S. (2013): Past, present, and future of jujubes—Chinese dates in the United States. – *HortScience* 48(6): 672-680.
- [39] Yaşa, F. (2016): Türkiye’de Yetiştirilen Hünnap Meyvesinin Bileşimi Ve Meyvenin Kurutulması Sırasında Bileşiminde Meydana Gelen Değişimler. – Pamukkale Üniversitesi Fen Bilimleri Enstitüsü Gıda Mühendisliği Anabilim Dalı Gıda Teknolojisi Bilim Dalı. Yüksek Lisans Tezi, Denizli (in Turkish).
- [40] Yücel, E. (2005): Ağaçlar ve Çalılar. – Eskişehir (in Turkish).
- [41] Zhang, Z., Gao, J., Kong, D., Wang, A., Tang, S., Li, Y., Pang, X. (2015): Assessing genetic diversity in *Ziziphus jujuba* ‘Jinsixiaozao’ using morphological and microsatellite (SSR) markers. – *Biochemical Systematics and Ecology* 61: 196-202. <https://doi.org/10.1016/j.bse.2015.06.021>.
- [42] Zheng, Y., Wang, S. Y., Wang, C. Y., Zheng, W. (2007): Changes in strawberry phenolics, anthocyanins, and antioxidant capacity in response to high oxygen treatments. – *LWT-Food Science and Technology* 40(1): 49-57.

INFLUENCE OF GRASSLAND RENOVATION METHODS ON DRY MATTER AND PROTEIN YIELDS AND NUTRITIVE VALUE

GAWEL, E.^{1*} – GRZELAK, M.²

¹*Institute of Soil Science and Plant Cultivation-State Research Institute
Czartoryskich 8, 24-100 Puławy, Poland
(phone: + 48-81-4786-794, + 48-81-4786-900, <http://orcid.org/0000-0001-9050-4509>)*

²*Poznań University of Life Science, Department of Grassland and Natural Landscape
Dojazd 11, 60-656 Poznań, Poland
(phone: + 48 61-848-7423, + 48 61-848-7612, <http://orcid.org/0000-0002-7579-6117>)*

*Corresponding author
e-mail: eliza.gawel@iung.pulawy.pl

(Received 8th Oct 2019; accepted 21st Jan 2020)

Abstract. The aim of the research conducted in 2013–2016 at Grabów, Mazowieckie Province, Poland was to compare the yield and nutritive value of a fodder after the renovation of sward and to assess the usefulness of certain legume-grass mixtures for undersowing. A two-factor experiment was established in which the first factor included 3 methods of renovating grassland: 1 - after ploughing; 2 - after the compact disc harrow; 3 - after destroying the old sward with herbicide, sowing with the slit seed drill for direct sowing (Moore type). The second factor was 3 legume-grass mixtures: Krasula, Cent 4 and original. Similar fodder dry matter yields and nutritive values. Along with the increasing percentage of legumes in the sward (under conditions of rainfall deficiency), the protein value of feed (PDI), protein yield and feed filling value (LFU) increased in subsequent years of use. A tendency to lower yields after sowing grassland sward with a mixture Cent 4, containing short-lived grass species (*Lolium perenne* L. and *Lolium multiflorum* Lam.), was observed. The mean nutritive value was suitable for use for meat cattle, dried dairy cows, while in the first year after undersowing, for good beef cattle, older heifers, marginally for dairy cows.

Keywords: compact harrow, direct sowing, legume-grasses mixtures, ploughing, relative nutritional value

Abbreviations: RSD, residual standard deviation; v%, coefficient of variation; NDF, neutral detergent fibre (g·kg⁻¹); ADF, acid detergent fibre (g·kg⁻¹); ADL, acid detergent lignin's (g·kg⁻¹); UFL, feed unit for lactation; PDI, protein digested in small intestine (g·kg⁻¹); LFU, value of the filling units for lactation; RFV, relative nutritional value

Introduction

Grassland is a source of low-cost and valuable roughage for grasslands animals, mainly ruminants. The high percentage of green forage and fodder processed from grasslands increases the profitability of milk and beef production, ensuring a stable income for farmers (Donnellan et al., 2012). Proper grassland management, productivity, and species and chemical composition play an important role in animal nutrition.

Worldwide, grassland produces food for about one billion people (De Vlieghe et al., 2014). In Europe, they occupy about a third of the agricultural area (Lesschen et al., 2014) and are important not only for the production of animal feed and human food, but also for environmental functions which are now more important than economic functions. Grasslands have a positive impact on the natural environment, preventing soil erosion and carbon and nitrogen losses, constituting water reservoirs, maintaining the biodiversity of flora and fauna, increasing soil biological activity, limiting the effects of climate change (by collecting water), protecting nature, as well as providing biomass for energy purposes

(Velthof et al., 2010; Zając et al., 2010; De Vliegher et al., 2014; Lesschen et al., 2014; Reinsch et al., 2018). In the recent 30 years, the grassland area has decreased, among other things, due to a decrease in the cattle population, deterioration in the quality of feed, and the introduction of protein concentrates and low-cost soya beans in animal feed, as well as the abandonment of certain grassland (De Vliegher et al., 2014).

In Europe there is a large regional variation in grassland productivity, where the highest productivity, of about $10 \text{ t}\cdot\text{ha}^{-1}$, is observed in the regions of north-western Spain, the Netherlands, western France, northern Germany, Ireland (Lesschen et al., 2014). In Poland, according to the Central Statistical Office (GUS) data, in 2017 the yields obtained on permanent meadows amounted to $5.42 \text{ t}\cdot\text{ha}^{-1}$, while on pastures they were even lower (GUS, 2018).

Decrease in yield levels, weed infestation of sward, and its simplified species composition, as well as errors in pratotechniques (i.e., improper use, inadequate fertilization, or one-sided fertilization with nitrogen only), appearance of grass species of low economic value in sward, lack of legumes, inadequate climatic conditions, and in particular, the shortage of precipitation, all lead to the degradation, as a result of which grasslands have to be renovated (Kulik, 2010; Terlikowski and Barszczewski, 2015). This can be carried out by different methods including: fertilization and rational use; reseeding of low-cut sward in a traditional way or with machines constructed for this purpose after mechanical, or chemical destruction of a part of the sward with a heavy harrow or a tiller and applying the method of full tillage after ploughing to completely destruct the old sward (Mocanu and Hermenean, 2009; Kulik, 2010; Zając et al., 2010; Elsaesser, 2012; Reheul et al., 2017). Renovation by full tillage after ploughing, consisting of ploughing up, inverting the furrow-slice and carrying out a set of pre-sowing tillage, is considered the most radical, unfavourable for the environment and costly type of renovation, because it destroys the soil structure. The aerated soil organic matter releases nitrogen and phosphorus and washes out in the form of soluble forms of these components (Kulik, 2010; Velthof et al., 2010; Zając et al., 2010; De Vliegher et al., 2014). McDonald et al. (2011a,b) showed higher mineralization and loss of N_2O and higher leaching of soluble carbon by 10-30% both in manure fertilization and manure-free fertilization after the application of herbicide for the renovation of grassland than after the ploughing and a full set of pre-sowing procedures. Grasslands retain more greenhouse gases than arable land, so their ploughing and conversion to arable land has more drastic environmental consequences. Fewer side effects accompany the renovation of grassland with less invasive methods such as: direct sowing, tillage using rotary tillers and undersowing (Mocanu and Hermenean, 2009; Kulik, 2010; Łyszczarz et al., 2010; Velthof et al., 2010; Zając et al., 2010; Golka et al., 2016). The rate of organic matter mineralization on permanent grassland. On mineral soil can be reduced by ploughing in autumn, and on organic soil - in spring. Studies by Reheul et al. (2017) and Reinsch et al. (2018) did not confirm the effect of the ploughing date (autumn, spring) on yields and N_2O emissions, as similar yields were obtained after ploughing in autumn and spring. According to these authors, N_2O emissions are affected by quality of fodder after grassland renovation (Rehel et al., 2017; Reinsch et al., 2018).

In literature, there are different opinions regarding the increase in the level of yield and the improvement of the feed quality after the renovation of greenery. Mocanu and Hermenean (2009), who renovated the sward by direct sowing with a special seed drill, achieved an increase in dry matter yield by 48.5% to 134% in of protein yield by 105-129% in relation to the control (degraded meadow). Kayser et al. (2018) believe that

all renovation techniques lead to an increased productivity and that the renewed sward should be used properly to maintain valuable grass and legume species. Łyszczarz et al. (2010), in turn, describe the re-degradation of sward already after about three years after renovation, when the yield of the renovated sward became equal to that obtained on meadows not fertilized for 20 years. The effects of the renovation are not always positive, as there is often no increase in yield and quality of the forage and no guarantee of a long-term renovation effect (Elsaesser, 2012).

It was decided to evaluate the effect of grassland renovation methods on the yield of dry matter and protein as well as the relative nutritional value of fodder in conventional conditions. The usefulness for reseeded of several legume-grass mixtures available on the Polish market was also checked.

Material and methods

Site, location, and climate

A two-factor field experiment was carried out at the Agricultural Experimental Station of the Institute of Soil Science and Plant Cultivation in Grabów, Mazowieckie Voivodeship (51°21' N; 21°40' E), Poland in the years of 2013–2016. It was established on according to FAO – WRB classification system 2014, Umbrisols and Phaeozems. It was characterized by a neutral reaction (pH in 1 M KCl 6.6) the available nutrient content of the soil was as follows (mg·100 g⁻¹ soil): phosphorus 10.8 (average content), potassium 6.02 (low content) and magnesium 12.3 (high content).

Meteorological conditions

The field experiment was located in a temperate continental climate zone. Meteorological conditions during the study period were varied (*Fig. 1*). In Polish condition, for permanent meadows, optimal rainfall during the growing season is 420 mm, slightly larger are characterized by permanent pastures – 450 mm, rainfall distribution in individual months is also important (Grabarczyk, 1989). According to this author (Grabarczyk, 1989), optimal rainfall in meadows and pastures grasslands and average air temperature should be: in April - precipitation - 50 mm, average air temperature - 8°C; in May - rainfall of 65 mm (meadows) and 70 mm (pastures), air temperature - 13°C; in June - rainfall - 80 mm (meadows) and 90 mm (pastures), air temperature - 16°C; in July - rainfall 90 mm (meadows) and 100 mm, air temperature - 18°C; in August - precipitation is 80 mm of precipitation, air temperature - 17°C; in September - rainfall 55 mm (meadows) and 60 mm (pastures), air temperature 14°C. Optimal rainfall for grassland was recorded in May 2014 (120 mm precipitation), June 2013 (115 mm precipitation), July and August 2014 (100 mm and 80 mm, respectively) and in September 2015 (93,9 mm). In the remaining research period, and especially in 2016, the lack of rainfall was significant, therefore in the second and third years of use (2015 and 2016) the efficiency of thinned sward was estimated only in the first three shoots. The last revival of sward was grazed without prior crop evaluation or botanical mass analysis.

The mixtures were sown under good humidity and thermal conditions, after heavy but uneven rainfall. Favourable conditions promoted the germination, initial growth and development of crops and weeds. In summer, weather conditions deteriorated during the sowing year. In 2014, the average monthly precipitation was above the long-term average

for this period, with the highest storm precipitation in May (Fig. 1). In 2015, May, June and September, humidity conditions were conducive to the development of the sward. In the remaining period, the deficiency of precipitation and temperatures higher than the long-term average, resulted in poor regrowth, therefore only three sward harvests were carried out. The year of 2016 was the driest and warmest year compared to the other years, so the growth of the sward in this period was limited. As in the previous year, only 3 harvests were carried out, and the fourth sward regrowth was grazed upon by cows. Habitat and climate conditions determine the success of the renovation. Of special importance are humidity conditions in the year of sowing, not only during the procedure but also within a few days after sowing (Bélanger and Tremblay, 2010).

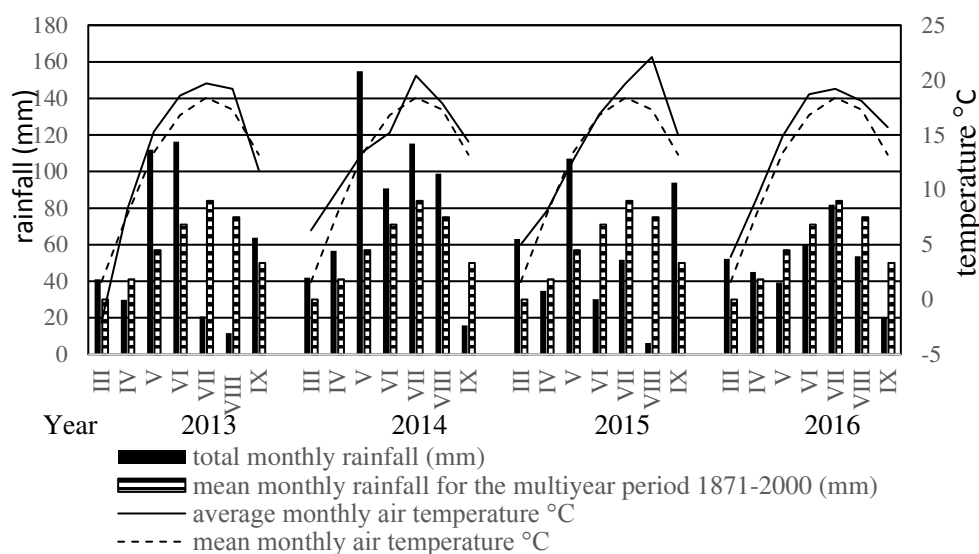


Figure 1. Meteorological condition in the years 2013–2016 Grabów, Poland during the growing season

Experimental treatments and design

Studies on the effect of grassland renovation on dry matter, protein yield, and nutritive value of the renovated sward were carried out in a two-factor experiment sown in the split-block system, in four replicates, on a gross area of 0.6 ha. The factors studied were three methods of renovating grassland:

1) ploughing and full tillage, plus sowing of legume-grass mixtures with a grain seed drill;

2) destruction of the sward with a compact disc harrow and sowing of seeds with a grain seed drill;

3) destruction of the old sward with a herbicide and sowing of seeds with a seed drill (Moore type). The second factor were three mixtures of legumes and grasses:

K - Krasula + 3.5 kg white clover (*Trifolium repens* L.) ‘Romena’ consisting of: perennial ryegrass (*Lolium perenne* L.) (25.7%), Italian ryegrass (*Lolium multiflorum* Lam.) (9.19%), meadow timothy (*Phleum pratense* L.) (13.79%), orchard grass (*Dactylis glomerata* L.) (9.19%), red fescue (*Festuca rubra* L.) (9.19%), tall fescue (*Festuca arundinacea* Schreb.) (9.19%), sheep’s fescue (*Festuca ovina* L.) (4.59%), red clover (*Trifolium pratense* L.) (4.59%), lucerne (*Medicago sativa* L.) (4.59%), bent grass

(*Agrostis alba* L.) (1.83%) + 3.5 kg·ha⁻¹ white clover (*Trifolium repens* L.) ('Romena', 8.11%); seed sowing rate – 40 kg·ha⁻¹.

C - Cent 4 consisting of: perennial ryegrass (*Lolium perenne* L.) (40.0%), Italian ryegrass (*Lolium multiflorum* Lam.) (10.0%), tall fescue (*Festuca arundinacea* Schreb.) (15.0%), meadow fescue (*Festuca pratensis* Huds.) (5.0%), meadow timothy (*Phleum pratense* L.) (5.0%), meadow bluegrass (*Poa pratensis* L.) (5.0%), festulolium (*Festulolium braunii* (K. Richt.) A. Camus) (5.0%), lucerne (*Medicago sativa* L.) (10.0%) and white clover (*Trifolium repens* L.) (5.0%); see sowing rate – 35 kg·ha⁻¹.

O - original mixtures consisting of: of white clover (*Trifolium repens* L.) 'Barda' (10.0%), hybrid lucerne (*Medicago x varia* Martyn Fl. Rust.) 'Radius' (20.0%), red clover (*Trifolium pratense* L.) 'Milena' (20.0%) (legumes accounting for 50.0% in total), perennial ryegrass (*Lolium perenne* L.) 'Artemis' (15.0%), orchard grass (*Dactylis glomerata* L.) 'Amila' (15.0%), meadow fescue (*Festuca pratensis* Huds.) 'Anturka' (10.0%), festulolium (*Festulolium braunii* (K. Richt.) A. Camus) 'Agula' 10.0% in pure sowing; seed sowing rate - 23 kg·ha⁻¹.

In the spring of 2013, the necessary cultivation procedures were carried out on the grassland to be renovated in accordance with the experiment scheme. The ploughing was carried out to a depth of 30 cm (treatment 1). Under the conditions of the renovation, the top layer of soil was loosened to the depth of 5 cm with a compact disc harrow (treatment 2) by a simplified method. On the treatments with direct sowing, the development of degraded sward was inhibited with Roundup 360 SL at a dose of 6 l per hectare (treatment 3). Legume-grass mixtures were sown in the second decade of June. In the summer, the sward was mowed twice in order to inhibit the development of weeds. In October the whole area of the experiment was grazed upon by cows. A total of 6 cuts of sward for haylage were carried out during the study and 9 short term grazing's (2–3 days of grazing) of 79–85 productive cows, were carried out. In the sowing year, two swaths were made for the mechanical weeding of sward mixtures and one grazing of cows on the surface of the entire experiment (2013 year). In the first year of use (2014 year), the first and second regrowth of sward was cutting, while in the second and third year of use (2015 and 2016 year) only first sward regrowth was intended for silage. Cows were grazed on the remaining sward regrowth. During the period of field research in the years 2013-2016 no chemical protection of sward mixtures was carried out.

Pre-sowing and top dressing fertilization

Superphosphate (40% P₂O₅) in the amount of 60 kg ha⁻¹ P₂O₅ and potassium salt (60% K₂O) in the dose of 60 kg ha⁻¹ were used before the sowing.

In each year of full use, during the spring start of the mixture's growing season, it was fertilized with phosphorus – 80 kg ha⁻¹ P₂O₅, potassium – 36 kg ha⁻¹ P₂O₅ and nitrogen (ammonium nitrate) - 34 kg ha⁻¹ N. After the first regrowth was harvested, the sward was fertilized with potassium - 60 kg ha⁻¹ K₂O in the first year of use, 40 kg ha⁻¹ K₂O in the following years, and with nitrogen 31 kg ha⁻¹ N. In the second year of use, phosphorus in the dose of 40 kg ha⁻¹ P₂O₅ was also applied. In all years of use, after the second and third harvest / grazing, the sward was fertilised with nitrogen in the amount of 31 kg ha⁻¹ N.

Measurements

Green matter yield was determined on the basis of green forage samples taken from the area of 10 m² from each plot. During harvesting, two samples of green forage weighing 0.5 kg were taken to calculate the drying rate (%) and to perform a simplified

botanical analysis of sward (grass of all species together, lucerne, white and red clover together, weeds). An analysis of the botanical composition of sward was carried out in each regrowth, and the percentage of a given plant fraction (lucerne; clover; grasses) in the total dry matter of the sample, was calculated.

Chemical analysis

The assessment of the chemical composition and feed value of the sward was carried out in an accredited IUNG-PIB laboratory in Puławy, Poland. Plant material from the first sward regrowth, in each of the 3 years of full use, was analysed. For chemical analyses, a sample of 0.5 kg of green fodder was taken from each plot. After drying, the plant material was combined into object tests and ground. Chemical analysis was carried out in some of the prepared plant material. The dry matter content of mixtures was determined by weight method according to test procedure PB 35.1 - first edition -10.05. 2013, total nitrogen - flow analysis (CFA) (PB 33.1- second edition -05.03.2014); while the contents of crude fibre and fibre fraction (Neutral Detergent Fibre -NDF; Acid Detergent Fibre - ADF; Acid Detergent Lignin's - ADL) - according to test procedure PB 51. 1 - second edition - 01.08.2013. The results of chemical analyses were used for the nutritional assessment of biomass according to the Linn and Martin (1989) based on the fibre fraction content. The evaluated classification parameter was relative feed value calculated on the basis of fibre fraction content according to the formula (*Eq. 1*) (Linn and Martin, 1989):

$$\text{RFV} = [\text{DDM} \times \text{DMI}] : 1.29 \quad (\text{Eq.1})$$

where,

DDM (dry matter digestibility in %) = $88.9 - 0.779 \times \text{ADF}$,

DMI (dry matter intake in % body weight) = $(\text{DMI}=120 : \text{NDF})$,

NDF – neutral detergent fibre,

ADF – acid detergent fibre.

The relative feed value (RFV) obtained from the calculation was compared with feed quality classes and the ranges of RFV developed by Jeranyama and Garcia (2004) for cattle.

Statistical analysis

For comparison of dry matter yields and total protein yields in the first cut, the content of total protein, crude fibre in mixtures' dry matter, digestibility of organic mass, content of neutral and acid detergent fibre (NDF, ADF and ADL), as well as relative nutritional value, the analysis of variance was applied. Calculations were performed in the program Statistica (Stat Soft Inc., USA). The Tukey's test ($P \leq 0.05$) compared the mean values for the factors tested in the field experiment; the 1st factor – three methods of grassland renovation; the 2nd factor – three legume-grass mixtures.

Results and discussion

Botanical composition

In the sward renovated with the full tillage method after ploughing (1), after disc harrow (2) and after the application of herbicide and direct sowing (3), in all years of use, grasses dominated in spring regrowth (*Fig. 2*). Their percentage was varied and amounted

to about 72% to 93% of the sward. The percentage of legumes in the sward increased in summer and autumn, and in the second and third year of use, there were more legumes than grasses in the sward. Among legumes, in the first two years of use of mixtures, there were more clovers (white clover and red clover in total) than lucerne in the sward. However, the situation changed due to a shortage of precipitation. In the third year of use, lucerne prevailed in the sward, as this plant tolerated the deepening drought, while part of clover and grass plants receded from the sward during this period.

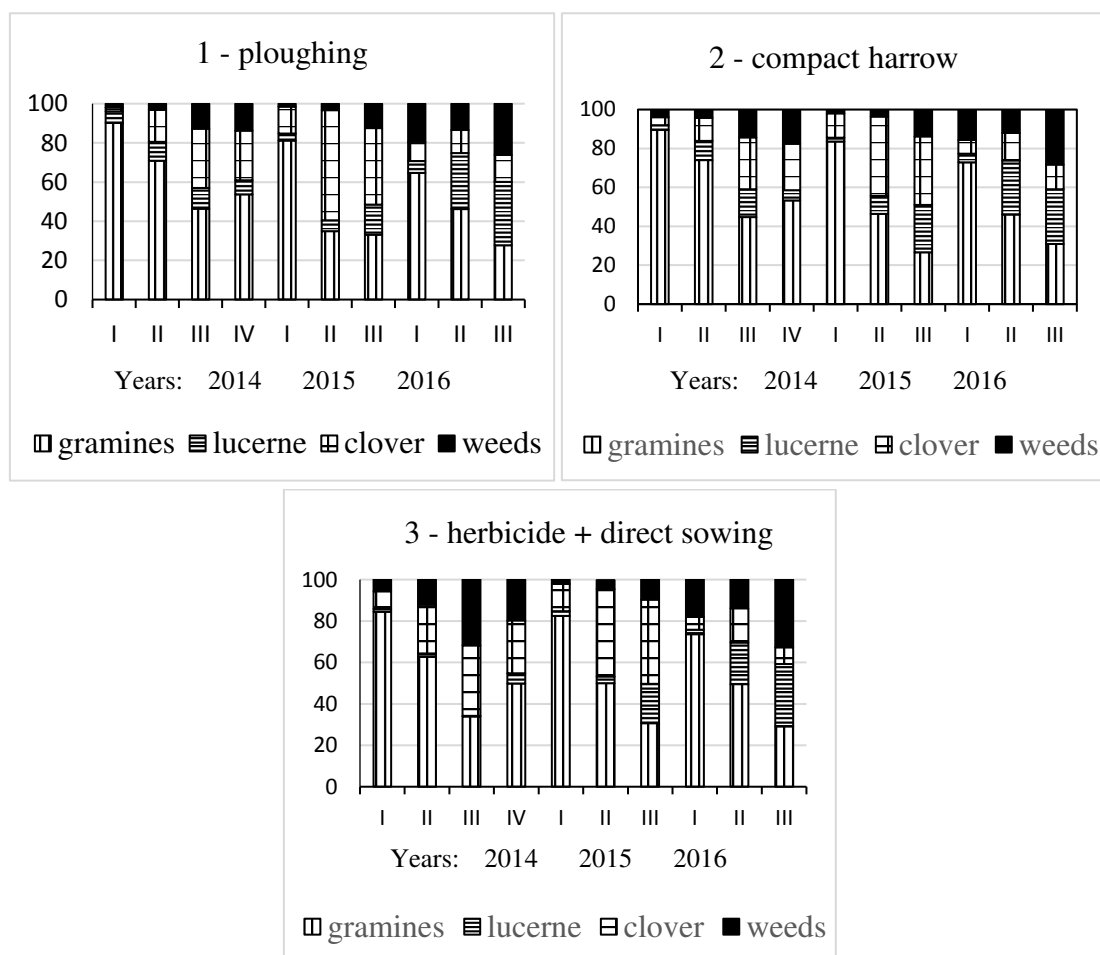


Figure 2. Percentage of components in the dry matter yield of legume-grass mixtures depending on the method of sward renovation in 2014–2016 (%)

Due to different sensitivity to drought, multi-species mixtures of legumes and grasses should be used for the renovation of grasslands as their varied development in subsequent years of use and different water needs may increase the sward longevity and success of this procedure (Łyszczarz et al., 2010; Isselstein and Kayser, 2015). Under non-precipitation conditions, weed infestation of the sward increased, especially in the second and third year of use (Fig. 2), being particularly high at the end of the third year of use. The sward weeded faster on the treatment with the use of herbicide to inhibit the development of sward and with direct sowing with a special slit seed drill (treatment 3). In this research treatment, part of the weeds was not completely destroyed by herbicide spraying and regenerated quite quickly. The same was true for the simplified tillage,

which involved moving the topsoil to a depth of 5 cm with a compact disc harrow (treatment 2), where some legumes and weeds with a deep root system (such as *Taraxacum officinale* Wep.) grew back quickly.

There were 18% of legumes (including red clover, lucerne and white clover) in the sown mixture Krasula seeds, 15% – in the mixture Cent 4 (lucerne, white clover), and 50% in the original mixture (white clover, hybrid clover and red clover). The percentage of components in the sward of mixtures changed dynamically in the years of use, and varied significantly from the species composition of seed mixtures (*Fig. 3*). In the spring of the first year of use, grasses dominated in the sward of the compared mixtures (from about 80% to 92% of the sward yield). However, already in the third growth of sward, their percentage was only about 40% of dry matter yield. In this period the percentage of clovers and weeds increased as well. In every year of use, in summer and autumn, when the lack of moisture in the soil was significant, legumes dominated in sward (especially in 2015 and 2016). In the second year (2015), these were clovers, while in the drier third year of use (2016) - lucerne. The weed infestation of the sward increased as well, with the highest weed infestation during the whole period of use being recorded for mixture Cent 4. At the end of the third year of use, weeds accounted for as much as 47% of the dry matter yield of this mixture. At that time, the sward of the original mixture was the least weeded (about 17% of weeds).

A small number of herbs and weeds in the sward (especially when used for grazing) is attractive for animals, as it improves the taste of the sward, and in the case of legumes, also the quality of feed, because the rate of decrease in the nutritive value of this group of plants is lower than that of grasses (Peyraude et al., 2009). Factors that make it possible to maintain biodiversity in the sward include proper use, proper fertilization, and grazing upon by a small number of animals, as well as proper selection of legume and grass species for mixtures (Klimek et al., 2007; De Vliegher et al., 2014; Głąb et al., 2016).

Dry matter production

During the three-year period of use, the method of renovation (full tillage after ploughing - treatment 1; surface soil disturbance to a depth of 5 cm with a compact disc harrow - treatment 2; sward spraying with herbicide and direct sowing - treatment 3) had no significant effect on dry matter yields (*Table 1*). In the years of use, no interaction was found between the factors investigated, i.e. the method of renovation of green use and mixtures used for renovation. The coefficient of variation (v%) indicates a small differentiation of dry matter yields in the first and second year of use of mixtures (2014 and 2015 years) and average yield changes in the third year of use of mixtures (2016 years; v% = 24.9).

The highest yields were harvested in the first year of use (from 10.65 to 11.21 t ha⁻¹). In the following years, the yield decreased due to deteriorating humidity conditions and summer drought. The lowest yields (about 8.4 t ha⁻¹) were obtained in the second year of full use (2015), when the deficit of precipitation in relation to the long-term average was the highest (*Table 1*). Good pluviometric conditions before sowing and in the year following the renovation were conducive to the development and yield of the mixtures. Similar observations on this subject are presented by Bélanger and Tremblay (2010). Literature contains various contradictory information about the yields of the renovated sward. Terlikowski and Barszczewski (2015) and Golka et al. (2016), after the renovation, achieved improved yield and use value of sward. However, Velthof et al. (2010), Reheul et al. (2017), Grace et al. (2018) and Kayser et al. (2018) argue that renovation does not

always lead to higher sward yields. Kulik (2010) considered the resowing performed directly into the old sward (without earlier inhibition of sward development) to be the most unreliable method of renovation in comparison with the use of herbicide or a tiller to limit the growth of the degraded sward. In turn, in the studies of Łyszczarz et al. (2010), the use of herbicide and disc harrow before resowing turned out to be the most effective method of renovation, while direct sowing into the sward with special seeders was completely unsuccessful.

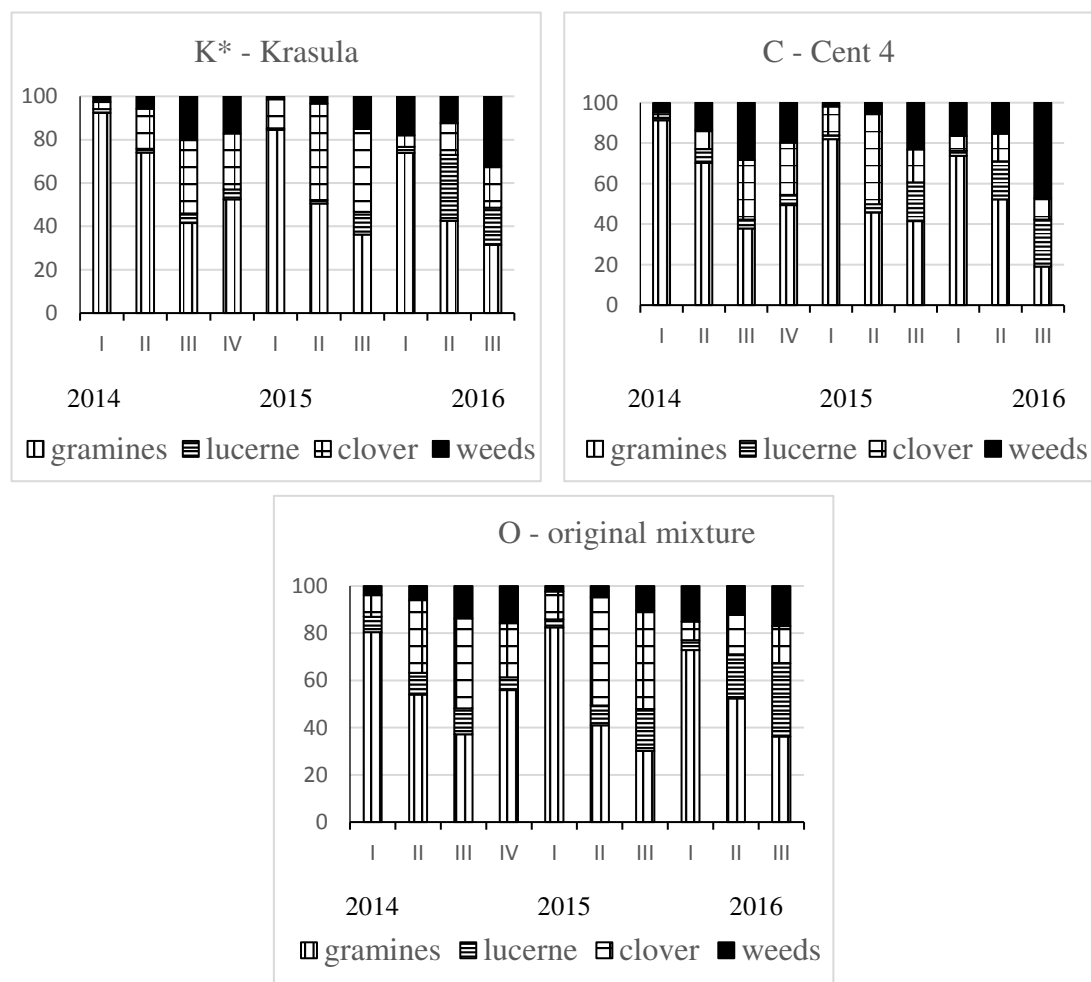


Figure 3. Influence of mixture species composition on the percentage of components in the dry matter yield (%).

K* – Krasula: *Lolium perenne* L. (25.7%), *Lolium multiflorum* Lam. (9.19%), *Phleum pratense* L. (13.79%), *Dactylis glomerata* L. (9.19%), *Festuca rubra* L. (9.19%), *Festuca arundinacea* Schreb. (9.19%), *Festuca ovina* L. (4.59%), *Trifolium pratense* L. (4.59%), *Medicago sativa* L. (4.59%), *Agrostis alba* L. (1.83%) + 3.5 kg *Trifolium repens* L. 'Romena' (8.11%)

C - Cent 4: *Lolium perenne* L. (40.0%), *Lolium multiflorum* Lam. (10.0%), *Festuca arundinacea* Schreb. (15.0%), *Festuca pratensis* Huds. (5.0%), *Phleum pratense* L. (5.0%), *Poa pratensis* L. (5.0%), *Festulolium braunii* (K. Richt.) A. Camus (5.0%), *Medicago sativa* L. (10.0%), *Trifolium repens* L. (5.0% %);

O - original mixtures: *Trifolium repens* L. 'Barda' (10.0%), *Medicago x varia* Martyn Fl. Rust. 'Radius' (20.0%), *Trifolium pratense* L. 'Milena' (20.0%), *Lolium perenne* L. 'Artemis' (15.0%), *Dactylis glomerata* L. 'Amila' (15.0%), *Festuca pratensis* Huds. 'Anturka' (10.0%), *Festulolium braunii* (K. Richt.) A Camus 'Agula' 10.0% in pure sowing

Table 1. Influence of the usage of the renovation of the grassland and species composition of legume-grass mixtures on the annual yield of dry matter

Usage of the renovation of the grassland (A)	Mixtures (B)			
	K**	C	O	Means
2014 years				
1*	11.56	10.09	11.98	11.21
2	9.94	10.22	12.82	10.99
3	11.36	9.40	11.20	10.65
Means	10.95	9.90	11.99	-
LSD_{0.05} for A- n.s.; B- 1.70; B/A - n.s.; A/B - n.s.; RSD = 2.78; v% - 15.2				
2015 years				
1	9.35	8.17	7.81	8.44
2	8.31	8.02	8.84	8.39
3	8.57	7.56	10.14	8.75
Means	8.74	7.91	8.93	-
LSD_{0.05} for A- n.s.; B - n.s.; B/A - n.s.; A/B - n.s.; RSD - 1.73; v% - 15.4				
2016 years				
1	10.32	9.39	9.10	9.60
2	8.67	8.41	8.95	8.68
3	7.05	7.00	8.36	7.47
Means	8.68	8.26	8.80	-
LSD_{0.05} for A- n.s.; B - n.s.; B/A - n.s.; A/B - n.s.; RSD - 4.58; v% - 24.9				

Usage of the renovation of the grassland: 1* – ploughing, 2 - compact disc harrow, 3 – herbicide + direct sowing. Mixtures: K** – see *Figure 3*, RSD – Residual Standard Deviation, v% – coefficient of variation. Values in bold are statistically significant ($P \leq 0.05$)

The species composition of legume-grass mixtures used for resowing the sward had a significant impact on the yields only in the first year of use (2014) (*Table 1*). Statistical analysis showed that the original mixture (treatment A) produced significantly higher yields (about 12 t·ha⁻¹) in comparison of with mixture Cent 4 (9.90 t ha⁻¹). The original mixture (treatment A) consisted of 3 species of legumes: white clover (10%), hybrid lucerne (20%) and red clover (20%), while the mixture Cent 4 was composed of two species of legumes in smaller amounts: lucerne (10%) and white clover (5%). Earlier studies confirmed the effect of the percentage and species of legumes on the yield and quality of feed obtained from legume-grass mixtures (Elgersma and Søegaard, 2016, 2018). In other studies, the lack of common cocksfoot in the mixture used for sowing and the high proportion of perennial and Italian ryegrass were found to be the cause of low yields of dry matter, energy, and protein per unit area (Gawel et al., 2018). Legumes from the mixtures enter into symbiosis with nitrogen-binding bacteria from the air, which in different amounts, depending on the species or even the cultivar of legume, is transferred to the grasses in the mixtures. Therefore, the longevity and frost resistance of this group of plants affects the quality of feed from the mixtures (Bélanger and Tremblay, 2010). In addition, the grasses absorb nitrogen from the soil by absorbing the biologically-bound nitrogen. Isselstein and Kayser (2015) recommend multispecies legume-grass mixtures for renovation of sward, but their opinion is not always confirmed in practice, as evidenced by similar yields of multispecies and simplified mixtures described by Grace et al. (2018).

In the second and third year of use (2015 and 2016), when humidity conditions deteriorated, the dry matter yield of the compared mixtures did not differ significantly, amounting to 7.91–8.86 t ha⁻¹ (*Table 1*). In this period, the lowest yield was obtained from a mixture the Cent 4, in which perennial ryegrass and Italian ryegrass accounted for 50%,

while the common cocksfoot did not occur at all. This type of grass, according to our own research, determines the durability and productivity of sward after resowing (Gaweł, 2017; Gaweł et al., 2018) (*Table 1*).

Organic components

In the period of three years of use, no significant differences were found in the concentration of total protein, crude fibre and organic matter digestibility in the sward renewed with comparable methods: full tillage after ploughing (treatment 1) and simplified tillage after surface soil disturbance to the depth of 5 cm (treatment 2), as well as after the inhibition of sward development with herbicide and direct sowing (treatment 3) (*Table 2*). Different results were obtained under ecological conditions, where the sward renovated using the simplified method after the compact harrow (treatment 2) had a higher content of total protein than the sward after ploughing (treatment 1) (Gaweł, 2017). There was no significant effect of the percentage and species of legumes in the sown mixtures on the abundance of the first cut in total protein. Vasiljević et al. (2011) describes seasonal changes and significant differences among cultivars of red clover in total protein concentration. In our own studies, the total protein content of sward increased in the third year of use, as legumes were better able to withstand the lack of moisture in the soil and their percentage in the sward was higher than that of grasses. In Mediterranean conditions, Mantino et al. (2016) also showed a positive correlation of the share of lucerne in the sward with the protein content in the dry matter of the mixtures and negative with the concentration of the neutral fibre fraction (NDF). Tremblay et al. (2015) believe that correctly selected species of legumes and grasses for mixtures offer an opportunity to balance energy and protein in feed.

Table 2. Content of organic components and digestibility of feed in the first cut (g kg^{-1})

Specification	Total protein			Crude fibre			Digestibility of organic mass		
	Year of utilization								
	1 st	2 nd	3 rd	1 st	2 nd	3 rd	1 st	2 nd	3 rd
Usage of the renovation of the grassland									
1 - ploughing	79.58	62.73	118.75	300.6	349.0	296.3	711.4	707.3	517.5
2 - compact harrow	104.37	80.63	102.08	277.0	318.7	311.0	710.9	709.1	536.5
3 - herbicide + direct sowing	80.62	67.93	114.58	296.7	335.7	314.7	710.3	713.5	511.1
Mixtures									
K - Krasula + 3.5 kg white clover	71.87	73.80	108.33	301.0	331.7	331.0	713.5	711.2	530.5
C - Cent 4	91.05	58.33	118.75	284.7	346.0	276.7	711.2	709.9	516.5
O - Original mixture	101.65	79.17	108.33	288.7	326.3	314.3	707.9	708.7	518.1

Usage of the renovation of the grassland: 1* – ploughing, 2 - compact disc harrow, 3 – herbicide + direct sowing. Mixtures: K** – see *Figure 3*. Values in bold are statistically significant ($P \leq 0.05$)

In the second year of use, in the conditions of the renovation with the simplified method, after surface soil disturbance to the depth of 5 cm (treatment 2), the abundance of dry matter in fibre was significantly lower in comparison to the one obtained on the treatment with the renovation after ploughing (treatment 1) (*Table 2*). The species composition of mixtures used for resowing had no effect on the crude fibre content, which

ranged from 276.67 to 346.00 g kg⁻¹ dry matter. The method of renovation and species composition of mixtures for resowing of the sward did not significantly affect the digestibility of organic matter. A significant decrease in organic matter digestibility in the third year of use was probably due to high weed infestation and the predominance of legumes in the sward of mixtures (*Figs. 1 and 2*). It is known from the literature that legume plants are characterized by a high concentration of crude fibre, especially of lignin fraction (Montino et al., 2016; Elgersma and Søegaard, 2018).

The method of renovation and species composition of legume-grass mixtures had no significant effect on the content of neutral and acid fractions of fibre and lignin in dry matter (*Table 3*). Most often, the fibre content increased in the third year of use of sward. It is known from the literature about the high abundance of legumes (especially lucerne) in fibre fractions (Elgersma and Søegaard, 2016). According to Bélenger and Tremblay (2010), lucerne contains more neutral fibre fraction (NDF), and the organic matter digestibility of this species is lower than that of grasses. In addition to the age of the plants, weather conditions (warmth, good sunshine) also increase the concentration of fibre in the sward. This is confirmed by the Elgersma and Søegaard (2018) study, which showed that in dry years the contents of NDF and ADF in the dry matter of sward increased. Vasiljević et al. (2011) emphasize the importance of the development stage of plants at harvest time in the evaluation of feed quality.

Table 3. Content of neutral and acid detergent fibre (NDF, ADF, ADL) (g kg⁻¹)

Specification	NDF			ADF			ADL		
	Year of utilization								
	1 st	2 nd	3 rd	1 st	2 nd	3 rd	1 st	2 nd	3 rd
Usage of the renovation of the grassland									
1 - ploughing	572.0	630.0	590.0	325.0	387.0	362.0	33.2	51.1	65.3
2 - compact harrow	535.3	639.0	626.0	304.3	379.3	378.3	34.7	54.6	66.7
3 - herbicide + direct sowing	564.7	622.7	634.3	319.3	318.0	366.3	35.2	58.0	69.6
Mixtures									
K - Krasula + 3.5 kg white clover	576.7	636.3	662.3	324.3	376.7	404.7	35.2	52.2	79.3
C - Cent 4	560.3	629.7	566.7	311.7	387.3	339.0	31.1	55.2	57.9
O - Original mixture	535.0	625.7	621.3	312.7	383.3	363.0	36.7	56.3	64.3

NDF – neutral fibre fraction, ADF – acid fraction fibre, ADL – lignin's fraction fibre. Usage of the renovation of the grassland: 1* – ploughing, 2 - compact disc harrow, 3 – herbicide + direct sowing. Mixtures: – see *Figure 3*

Nutritive value

There was no effect of sward renovation method and species composition of mixtures used for resowing on the nutritive quality of feed (*Table 4*). Lack of significant differences in nutritive value may be associated with the analysis of chemical composition only in the first growth of sward. As Vasiljević et al. (2011) have shown, the abundance of sward in minerals increases during the growing season, while spring regrowth is characterized by a low concentration of nutrients, energy, and protein. The 3-year average economic and production analysis carried out in this experiment also did not show any influence of the examined factors on the content and net production of energy units and kilograms of total protein produced from one hectare (Gaweł et al., 2018).

Table 4. Value energy (UFL), protein value of the feed expressed in units of protein digested in the small intestine of dry matter (g kg^{-1} ; PDI) and value of the filling units for lactation (LFU)

Specification	UFL			PDI ($\text{g}\cdot\text{kg}^{-1}$)			LFU		
	Year of utilization								
	1 st	2 nd	3 rd	1 st	2 nd	3 rd	1 st	2 nd	3 rd
Usage of the renovation of the grassland									
1- ploughing	0.95	0.92	0.67	17.9	14.10	26.7	0.84	0.72	0.84
2- compact harrow	0.94	0.93	0.67	23.5	18.12	22.9	0.80	0.71	0.83
3- herbicide + direct sowing	0.94	0.93	0.66	18.1	15.27	25.8	0.80	0.71	0.83
Mixtures									
K** - Krasula + 3.5 kg white clover	0.95	0.93	0.69	16.2	16.59	24.3	0.80	0.69	0.84
C - Cent 4	0.94	0.93	0.65	20.5	13.11	26.7	0.82	0.75	0.83
O - Original mixture	0.93	0.93	0.67	22.8	17.79	24.4	0.82	0.69	0.84

UFL – feed unit for lactation, PDI – protein digested in small intestine, LFU – value of the filling units for lactation. Usage of the renovation of the grassland: 1* – ploughing, 2 - compact disc harrow, 3 – herbicide + direct sowing. Mixtures: K** – see Figure 3

The experiment calculated the value of filling units (LFU) to evaluate the ability of animals to consume roughage with the lowest possible consumption of concentrates (Table 4). The influence of the sward renovation method and the species composition of mixtures on this parameter of feed quality were not found. It is believed that the nutritive value is influenced by the proportion of legumes in sward, which age slower than grasses (Peyraud et al., 2009). Rook and Yarrow (2002) obtained a higher filling value in the case of legumes than in the case of grasses, despite the high content of lignin fractions in the dry matter of these plants.

Yield of total protein and relative nutritional value

The compared methods of grassland renovation and species composition of mixtures had no significant effect on the total protein yield in the first year of use from 370.4 to 578.1 kg ha^{-1} , and in the third year of use 716.3 to 773.8 kg ha^{-1} (Table 5). The observed increase in protein yield in the third year of use resulted from the high percentage of legumes in the sward of mixtures in this period (Figs. 2 and 3). Renovation of permanent grassland carried out in north-eastern Poland by direct resowing and full tillage showed an increase in protein yield by an average of 300 kg ha^{-1} in relation to the control (Terlikowski and Barszczewski, 2015). On the other hand, after renovation by direct sowing with a slit seed drill, Mocanu and Hermenean (2009) recorded an increase in protein yield by 105–129% in relation to the control.

In the three-year period of use, no significant influence of the method of renovation of grassland and species composition of mixtures on relative feed value (Table 5) was found. The best-quality relative nutritional value, of class III, was obtained in the first year of use of the mixtures, due to the achieved compartments value of 103.42-114.93. According to Jeranyama and Garcia (2004), quality grading tables, good beef cattle, older heifers and marginally, dairy cows may be consumers of this feed. In the following years of use, the obtained fodder was classified to the class IV quality, intended for feeding meat cattle or dried dairy cows.

Table 5. Yield of total protein and relative nutritional value in first cut of the mixtures

Specification	Yields of total protein in the first cut (kg ha ⁻¹)			Relative nutritional Value (RFV)		
	Year of utilization					
	1 st	2 nd	3 rd	1 st	2 nd	3 rd
Usage of the renovation of the grassland						
1 - ploughing	446.11	387.79	739.33	103.42	86.79	97.06
2 - compact harrow	578.12	542.71	678.11	114.93	86.47	90.51
3 - herbicide + direct sowing	370.37	456.86	773.88	106.21	88.52	88.59
Mixtures						
K** - Krasula + 3.5 kg white clover	376.02	487.19	716.39	103.29	87.17	80.61
C - Cent 4	458.87	363.79	737.38	107.33	86.80	103.28
O - Original mixture	559.71	536.38	737.54	113.94	87.81	92.27

RFV– relative nutritional value. Usage of the renovation of the grassland: 1* – ploughing, 2 - compact disc harrow, 3 – herbicide + direct sowing. Mixtures: K** – see *Figure 3*

Conclusions

1. The compared methods of renovation of grassland sward (full tillage method after ploughing - treatment 1); simplified tillage after surface soil disturbance to the depth of 5 cm with a compact disc harrow - treatment 2); destruction of degraded sward with herbicide and sowing of mixtures with Moore slit seed drill - treatment 3), gave similar production results, therefore all of them are considered useful in conditions of research for renovation of degraded grassland.

2. In the three-year period of use, characterized by a periodic precipitation deficiency, a tendency to weaker yields for the mixture Cent 4, with short-lived species of grasses, including perennial and Italian ryegrass, was recorded compared to the mixture Krasula and the original mixture.

3. Regardless of the method of renovation and species composition of mixtures used to renovate the sward, legumes withstood moisture deficiency better than grasses, and their percentage in the sward increased in subsequent years of use. Increasing percentage of legumes in the sward positively influenced the content of protein value (PDI), value of the filling units for lactation (LFU) and protein yield (kg ha⁻¹).

4. Good beef cattle, older heifers, and marginally, dairy cows can be fed with fodder obtained in the first year after the renovation of the sward because of range of the relative nutritive value achieved. In the following years, the relative nutritional value worsened, which is why the feed should be used to feed animals with lower nutritional requirements, i.e., meat cattle or dried dairy cows.

5. In the years characterized by rainfall deficiency, renovation of grassland can be carried out by the method of destruction of the sward with a compact disc harrow and sowing of seeds with a grain seed drill. Under these conditions, reseeding should be used, among others, for species that tolerate soil moisture deficiency, such as alfalfa and cocksfoot.

Acknowledgements. The research did not receive any specific grant from funding agencies in the public, commercial, or not-for-profit sectors.

REFERENCES

- [1] Bélanger, G., Tremblay, G. F. (2010): Fodder quality of legume-based pastures. – NJF Seminar 432. The potential of forage legumes to sustain a high agricultural productivity-A Nordic perspective. NJF Report 6(3): 97-112. Hvanneyri, Iceland.
- [2] De Vliegher, A., Van Gils, B., van den Pol-van Dasselaar, A. (2014): Roles and utility of grasslands in Europe. – *Grassland Science in Europe* 19: 753-755. https://pure.ilvo.be/portal/files/3304733/A_De_Vliegher_3_Multisward_WP1.pdf.
- [3] Donnellan, T., Hennessy, T., Keane, M., Thorne, F. (2012): Competitiveness of the dairy sector at farm level un the EU. – Proceedings of the of 24th General Meeting of the European Grassland Federation 3-7 June 2012. Lublin, Poland, *Grassland Science in Europe* 17: 719-732.
- [4] Elgersma, A., Søegaard, K. (2016): Effect of species diversity on seasonal variation in herbage yield and nutritive value of seven binary grass-legume mixtures and pure grass under cutting. – *European Journal of Agronomy* 78: 73-83. <https://doi.org/10.1016/j.eja.2016.04.011>.
- [5] Elgersma, A., Søegaard, K. (2018): Changes in nutritive value and herbage yield during extended growth intervals in grass-legume mixtures: effects of species, maturity at harvest, and relationships between productivity and components of feed quality. – *Grass and Forage Science* 73(1): 78-93. <https://doi.org/10.1111/gfs.1228>.
- [6] Elsaesser, M. (2012): Grassland renovation as a possibility for increasing nitrogen efficiency. – *Grassland Science in Europe* 17: 607-609. <http://www.europeangrassland.org/fileadmin/media/EGF2012.pdf>.
- [7] Gaweł, E. (2017): Influence of renovation of grassland on sward yields in the condition of organic farming. – *Journal of Research and Applications Agricultural Engineering* 62(3): 105-111. http://www.pimr.poznan.pl/biul/2017_3_EG.pdf.
- [8] Gaweł, E., Madej, A., Grzelak, M. (2018): The effect of renovation of the permanent grassland on some economic evaluation parameters in conventional condition. – *Roczniki Naukowe Stowarzyszenia Ekonomistów Rolnictwa i Agrobiznesu XX* (6): 61-69. (in Polish). doi:10.5604/01.3001.0012.7733.
- [9] Głąb, T., Żabiński, A., Sadowska, U. (2016): Tractor traffic and nitrogen fertilization affect the herbage production of the red clover/grass sward. – *Zemdirbyste-Agriculture* 103(4): 347-354. Doi. 10.13080/z-a.2016.103.044.
- [10] Golka, W., Żurek, G., Kamiński, J. R. (2016): Permanent grassland restoration techniques – an overview. – *Agricultural Engineering* 20(4): 51-58. <https://doi.org/10.1515/agriceng-2016-0063>.
- [11] Grabarczyk, S. (1989): Potrzeby wodne użytków zielonych i traw. – *Zeszyty Problemowe Postępów Nauk Rolniczych i Leśnych* 343: 43-56.
- [12] Grace, C., Boland, T. M., Sheridan, H., Lott, S., Brennan, E., Fritch, R., Lynch, M. B. (2018): The effect of increasing pasture species on herbage production, chemical composition and utilization under intensive sheep grazing. – *Grass and Forage Science* 73: 852-864. <https://doi.org/10.1111/gfs.12379>.
- [13] GUS. (2018): Production of agricultural and horticultural crops in 2017. – Warszawa. [https://produkcja_upraw_rolnych_i_ogrodniczych_w_2017%20\(14\).pdf](https://produkcja_upraw_rolnych_i_ogrodniczych_w_2017%20(14).pdf).
- [14] Isselstein, J., Kayser, M. (2015): Grassland renovation and consequences for nutrient management. – Proceedings of 23rd International Grassland Congress 2015 - Keynote Lectures. New Delhi, India, Grassland production and utilization: 105-116. <https://www.internationalgrasslands.org/files/igc/publications/2015/Isselstein,%20Johannes.pdf>.
- [15] Jeranyama, P., Garcia, A. D. (2004): Understanding relative feed value (RFV) and relative forage quality (RFQ). – *Extension Extra*. Paper 352. http://openprairie.sdstate.edu/extension_extra.

- [16] Kayser, M., Müller, J., Isselstein, J. (2018): Grassland renovation has important consequences for C and N cycling and losses. – *Food and Energy Security* 7: e00146. <https://onlinelibrary.wiley.com/doi/10.1002/fes3.146>.
- [17] Klimek, S., Kemmermann, A. R., Hofmann, M., Isselstein, J. (2007): Plant species richness and composition in management and environmental factor. – *Biological Conservation* 134: 559-570. <http://doi:10.1016/j.biocon.2006.09.007>.
- [18] Kulik, M. A. (2010): The effect of regeneration technology of meadow sward on its species composition. – *Annales Universitatis Mariae Curie-Skłodowska Lublin- Polonia Sectio EE* 65(4): 95-104. (in Polish). <http://wydawnictwo-old.up.lublin.pl/Annales/Agricultura/2010/4/11.pdf>.
- [19] Lesschen, J. P., Elbersen, B., Hazeu, G., van Doorn, A., Mucher, S., Velthof, G. (2014): Defining and classifying grasslands in Europe. – Final report, Alterra, part of Wageningen UR, Wageningen. https://ec.europa.eu/eurostat/documents/2393397/8259002/Grassland_2014_Task+1.pdf/8b27c17b-b250-4692-9a58-f38a2ed59edb.
- [20] Linn, J. G., Martin, N. P. (1989): Forage quality test and interpretation. St Paul. – University of Minnesota, Extension Service Publ. AG-FO 2637: 1-5.
- [21] Łyszczarz, R., Dembek, R., Suś, R., Zimmer-Grajewska, M., Kornacki, P. (2010): The overdrilling of degraded grass communities as an environmentally-friendly method of their regeneration. – *Woda-Środowisko-Obszary Wiejskie* 10 z. 4(32): 129-148. (in Polish). http://www.itep.edu.pl/wydawnictwo/woda/zeszyt_32_2010/artykuly/Lyszczarz%20i%20in.pdf.
- [22] MacDonald, J. D., Chantigny, M. H., Angers, D. A., Rochette, P., Royer, I., Gasser, M. O. (2011): Soil soluble carbon dynamics of manured and unmanured grassland following chemical kill and ploughing. – *Geoderma* 164(1-2): 64-72. doi.org/10.1016/j.geoderma.2011.05.011.
- [23] MacDonald, J. D., Rochette, P., Chantigny, M. H., Angers, D. A., Royer, I., Gasser, M. O. (2011): Ploughing a poorly drained grassland reduced N₂O emissions compared to chemical fallow. – *Soil Tillage Research* 111: 123-132. [doi:10.1016/j.still.2010.09.005](https://doi.org/10.1016/j.still.2010.09.005).
- [24] Mantino, A., Ragolini, G., Nasso, N., Tozzini, C., Taccini, F., Bonari, E. (2016): Alfa (*Medicago sativa* L.) overseeding on mature switchgrass (*Panicum virgatum* L.) stand: biomass yield and nutritive value after the establishment year. – *Italian Journal of Agronomy* 11: 747. [doi:10.4081/ija.2016.747](https://doi.org/10.4081/ija.2016.747).
- [25] Mocanu, V., Hermenean, I. (2009): Restoration of grassland multifunctionality by direct drilling method – a solution for sustainable farming system. – Research-Development Institute for Grassland. ICDP Braşov, Romania 26: 71-74. <http://www.incdfundulea.ro/rar/nr26/rar26.14.pdf>.
- [26] Peyraud, J. L., Le Gall, A., Lüscher, A. (2009): Potential food production from forage legume-based-systems in Europe: an overview. – *Irish Journal of Agricultural and Food Research* 48: 115-135. <https://doi.org/10.1111/gfs.12124>.
- [27] Reheul, D., Cougnon, M., Kayser, M., Pannecouque, J., Swanckaert, J., De Cauwer, B., van den Pol-van Dassel, A., De Vlieghe, A. (2017): Sustainable intensification in the production of grass and forage crops in the Low Countries of north-west Europe. – *Grass and Forage Science* 72: 369-381. doi.org/10.1111/gfs.12285.
- [28] Reinsch, T., Loges, R., Kluß, C., Taube, F. (2018): Renovation and conversion of permanent grass-clover swards to pasture or crops: Effects on annual N₂O emissions in the year after ploughing. – *Soil and Tillage Research* 175: 119-129. <https://doi.org/10.1016/j.still.2017.08.009>.
- [29] Rook, A. J., Yarrow, N. H. (2002): Incorporating grazing behaviour measurements in models to predict herbage intake by grazing dairy cows. – *Grass and Forage Science* 57: 19-24. <https://doi.org/10.1046/j.1365-2494.2002.00297.x>.

- [30] Terlikowski, J., Barszczewski, J. (2015): The effectiveness of permanent grassland renovation under different soil and climatic conditions. – Journal of Research and Applications Agricultural Engineering 60(4): 112-119.
http://www.pimr.poznan.pl/biul/2015_4_TB.pdf.
- [31] Tremblay, G. E., Bélanger, G., Simili da Silva, M., Lajeunesse, J., Papadopoulos, Y. A., Filmore, S. A. E., Jobim, C. C. (2015): Herbage energy to protein ratio of binary and complex legume-grass mixtures. Grassland and forages in high output dairy farming systems. – Proceedings of the 18th Symposium of the European Grassland Wageningen. The Netherlands, Grassland Science in Europe 20: 328-330.
<http://www.europeangrassland.org/fileadmin/media/EGF2015.pdf>.
- [32] Vasiljević, S., Čupina, B., Krstić, Đ., Pataki, I., Katanski, S., Milošević, B. (2011): Seasonal changes of proteins, structural carbohydrates, fats and minerals in herbage dry matter of red clover (*Trifolium pretense* L.). – Biotechnology in Animal Husbandry 27(4): 1543-1550. DOI: 10.2298/BAH1104543V.
- [33] Velthof, G. L., Hoving, I. E., Dolfing, J., Smit, A., Kuikman, P. J., Oenema, O. (2010): Methode and timing of grassland renovation affects herbage yield, nitrate leaching, and nitrous oxide emission in intensively managed grasslands. – Nutrient Cycling in Agroecosystems 86: 401-412. <https://doi.org/10.1007/s10705-009-9302-7>.
- [34] Zajac, M., Spsychalski, W., Goliński, P. (2010): Effect of different methods of sward renovation on selected physical and chemical soil properties. – Grassland Science in Europe 15: 226-228.
http://www.europeangrassland.org/fileadmin/media/EGF2010_GSE_vol15.pdf.

REVIEW ARTICLE: *MELOIDOGYNE INCOGNITA* (ROOT-KNOT NEMATODE) A RISK TO AGRICULTURE

SIKANDAR, A.¹ – ZHANG, M. Y.¹ – WANG, Y. Y.² – ZHU, X. F.¹ – LIU, X. Y.³ – FAN, H. Y.¹ –
XUAN, Y. H.⁴ – CHEN, L. J.¹ – DUAN, Y. X.^{1*}

¹*Nematology Institute of Northern China, Shenyang Agricultural University
120 Dongling road, Shenyang 110866, China*

²*College of Biosciences and Biotechnology, Shenyang Agricultural University
120 Dongling road, Shenyang 110866, China*

³*College of Sciences, Shenyang Agricultural University
120 Dongling road, Shenyang 110866, China*

⁴*College of Plant Protection, Shenyang Agricultural University
120 Dongling road, Shenyang 110866, China*

**Corresponding author
e-mail: duanyx6407@163.com; phone: +86-13-99825-3910*

(Received 9th Oct 2019; accepted 8th Jan 2020)

Abstract. Phylum Nematoda is one of the most abundant group of metazoans. Root-knot nematodes (*Meloidogyne* spp.) pose a risk to agricultural crops in the world. The *Meloidogyne* genus comprises about 100 species and their host range includes more than 3000 plant species. *Meloidogyne incognita* is one of the most predominant species of this genus damaging a variety of field crops and vegetables. It is very difficult for farmers to diagnose its symptoms due to similarities with nutritional deficiencies. However to overcome this issue, the literature review of researches on the identification, classification, life cycle, symptoms, economic impact and management strategies of *M. incognita* was planned. The literature review provides an overview and useful information regarding decisions about management of this nematode species in the future.

Keywords: *Nematoda, Metazoan, economic impact, management, deficiencies*

Introduction

Phylum “Nematoda” is an abundant collection of metazoan on earth (Ahmed et al., 2016; Kergunteuil et al., 2016). Nematodes are common, extensively distributed and well adaptable group of organism that directly impact economy due to massive losses to crops. Nematodes covered about 90% of all multicellular organisms (Çetintaş et al., 2017). Nematodes are usually rounded in cross-section, both ends tapering and elongated in shape. They are heterosexual and possess all systems of higher organisms excluding the circulatory or respiratory systems. They are parasites of animals, insects, humans, and plants. Some of them feed upon decaying matters, bacteria and on other micro-organisms.

Plant parasitic nematodes caused lesions in plants and produced secondary infection in them by facilitating other organisms such as fungus, bacteria and viruses (Smant et al., 2018). However, damage caused by nematodes is frequently not easy to differentiate from other reasons because of their microscopic size. They are usually live in soil, roots and in leaves and cause enormous threat to agriculture, about upto US \$ 157 billion

annual losses (Youssef et al., 2013). Some of them are migratory in nature whereas others are sedentary (Kihika et al., 2017; Palomares-Rius et al., 2017).

The most destructive nematodes genera are *Heterodera*; *Meloidogyne*; *Rotylenchulus*; *Helicotylenchus*; *Tylenchorhynchus*; *Pratylenchus*; *Ditylenchus*; *Xiphinema*; *Longidorus*. Most of plant parasitic nematodes belong to order Tylenchida while *Xiphinema* and *Longidorus* belong to order Dorylaimida. They caused extensive losses to the crops because a number of them are vectors of some viruses (Lizanne and Pai, 2014).

Meloidogyne genus is one of the most destructive pathogen (Kamran et al., 2014; Xiang et al., 2017). They are economically important parasites and one of the most damaging pests of vegetables and others crops (Anwar and McKenry, 2010; Kamran et al., 2012; Castagnone-Sereno et al., 2013). They are cosmopolitan and recorded from Africa, Asia, Caribbean, Central, North and South America, Europe and Oceania. They are obligate parasites of woody plants, monocotyledonous and dicotyledonous herbaceous plants. This genus has approximately 100 species while four major species are *M. arenaria*; *M. heplia*; *M. incognita* and *M. javanica* (Hunt and Handoo, 2009; Lunt et al., 2014).

The major four species of Root-knot nematodes (RKN) are present in People's Republic of China but *M. incognita* is one of the most predominant (Dong et al., 2014). It has wide host range and cause dramatic yield loss in China (Naranjo and Ellsworth, 2001; Shun-xiang et al., 2001). It directly and indirectly damages the crop like toppling, loss of yield, poor quality, delay in maturity and also causes losses of economic importance etc. (Yan et al., 2011; Onkendi et al., 2014).

They have been controlled by synthetic chemicals but pose risks to soil environment, costly, highly toxic. Some of them are a carcinogenic agent, that's why most nematicide chemicals have been withdrawn from market for example methyl bromide, ethylene dibromide (EDB) and dibromochloropropane (Onkendi et al., 2014; Nicol et al., 2011). Nowadays scientists are mainly focused on crop rotation, plant resistance, bio-control and cultural practices to overcome this problematic issue (Chitwood, 2002). Bio-control is safe and eco-friendly in application compared to chemicals because it has no residual effects on food (Cetintas et al., 2018).

Identification of *Meloidogyne incognita*

For identification of *M. incognita* mostly morphological, molecular and isoenzymatic characters are used. Morphological study of perineal patterns of female has been most commonly used character for the identification. Whereas, sometimes morphological characters of different species overlap with each other that is why molecular identification is used for accurate diagnosis. Different methods have been employed for molecular identification like DNA Marker; ribosomal Large Subunits (LSU) D2/D3 expansion segments (Rius et al., 2007), Small Subunits (SSL) (Powers, 2004), Mitochondrial DNA (Xu et al., 2004; Jeyaprakash et al., 2006), intergenic spacer (IGS) (Wishart et al., 2002), Random amplified polymorphic DNA (RAPD) (Adam et al., 2007), internal transcribe spacers (ITS) (Skantar et al., 2008) and Sequence-Characterized-Amplified Regions (SCAR) (Randig et al., 2002). Isoenzyme phenotyping is based upon relative mobility of enzymes extracted from mature females of *M. incognita* on gel electrophoresis (Cunha et al., 2018). Morphological, molecular and biochemical data should be combined to improve the determination and reliability of diagnosis.

Life cycle of *Meloidogyne incognita*

The life cycle of *M. incognita* consists of five different stages; egg, J2, J3, J4 and adults (*Figure 1*). The female present in plant roots laid eggs, that developed into J2 juveniles. Hatching of eggs are temperature driven usually without requiring any stimulus from plants (Karssen et al., 2013). J2 infecting host roots and complete further developmental stages on feeding sites however J3 and J4 juveniles have sedentary nature and J4 molt into female or male adult. After fertilization females remained in plant roots and produced egg masses. Usually females reproduce through mitotic parthenogenesis (Hussey and Janssen, 2002).

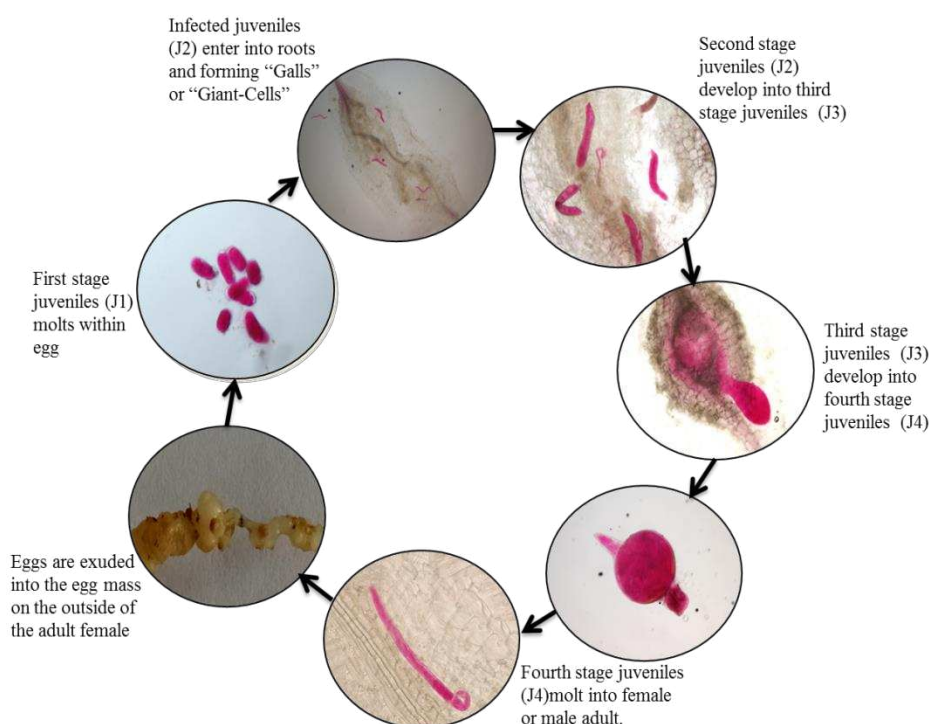


Figure 1. Life cycle of *Meloidogyne incognita*

Symptoms produced by *Meloidogyne incognita*

Plants infected by *M. incognita* showed nutritional deficiency i.e. yellowing of leaves, stunted growth, wilting and plant death (Priya et al., 2011). The farmers did not diagnose its damage due to similarities with nutritional deficiencies like chlorosis (Zeng et al., 2018; Ye et al., 2015). It developed the gall or swelling and cell expansion in roots of infected plant. Infected roots showed bushier and shorter length compared with healthy roots (Miyashita et al., 2014; Ma et al., 2013). The host range of root knot nematodes included more than 3000 plant species (Abdellatif et al., 2016). That's why it is difficult to find any common crop which was not parasitized by it (Castagnone-Sereno et al., 2013). They directly feed upon plants and cause the lesion in it which helps secondary pathogens such as pathogenic bacteria, fungus and viruses that cause secondary infections (Smant et al., 2018; Palomares-Rius et al., 2017).

Management strategies

The main objective of controlling *M. incognita* in soil is to secure crops from its attack to obtain maximum yield (Norshie et al., 2011). Different approaches have been implemented to control *M. incognita* such as chemical control, biological control, cultural control and use of resistant cultivars.

Chemical control

Nematicides are the most effective method to control the *Meloidogyne* spp. but they contain active components of Aldi-carb (Temik), methyl bromide and some other compounds which are prohibited. Chemical nematicides contain usually harmful agents which severely damage the ecosystem (Onkendi et al., 2014). Nematicides can reduced the high populations of root knot nematodes but unable to eliminate completely and accumulate in plant tissues (Sirias, 2011). Chemical nematicides are grouped into non-fumigant and fumigant and non-fumigant depend upon their volatility in soil. The first commercial non-fumigant active ingredient was *O*-2,4-dichlorophenyl *O,O*-diethyl phosphorothioate (Taylor, 2003). A few non-fumigant nematicidal active ingredients are ethoprop, fluazaindolizine, fluensulfone, fluopyram, oxamyl, spirotetramata and terbufos (Wram and Zasada, 2019; Hajihassani et al., 2019; Giannakou and Panopoulou, 2019). Chemical fumigant type nematicides are highly effective in controlling root-knot nematodes. Some common nematicidal active ingredients of fumigants are allyl isothiocyanate, chloropicrin, dimethyl disulfide, metam potassium, metam sodium and 1,3 dichloropropene (1,3-D) (Desaeger et al., 2017; Sikora and Roberts, 2018). They are very toxic for animals and human beings because its residues may be present in food chain (Walters and Heil, 2007).

Biological control

Biological control is usually safer than chemical. Fungi belong to genera *Acremonium*, *Chaetomium*, *Paecilomyces* and *Trichoderma* have been known as antagonistic to plant parasitic nematodes (Govinden-Soulange and Levantard, 2008; Sharon et al., 2009). Colonization of these genera of fungus showed that seedling on cucumber was very low because they suppressed plant parasitic nematodes before penetration into host (Kiewnick and Sikora, 2006). Saprophytic fungi demonstrated to reduce rate of penetration of root knot nematodes in tomato roots (Dababat and Sikora, 2007). Obligate symbiotic arbuscular mycorrhizal fungi can alter the finding host behavior in *Meloidogyne* spp. (Reimann et al., 2008). Roots colonization by *Fusarium oxysporum* led to accumulation of root that showed repelling effect on *M. incognita* in tomato (Selim, 2010). Nonpathogenic *Fusarium* strains were capable in reducing *M. incognita* on tomato (Terra et al., 2018). Certain endophytes can be used as controlling nematodes (Zabalgogezcoa, 2008). *Penicillium chrysogenum* is one of the most important fungi to control *M. incognita* (Yao et al., 2014). However level of inoculums can be reduced by seed treatment (Athman, 2006). (Dababat and Sikora, 2007) reported that systemic resistance against *M. incognita* was induced by changing chemical composition through nonpathogenic *Fusarium* Fo162. Arbuscular mycorrhizal (AM) fungi reduced severity of diseases in plants due to plant parasitic nematodes (Akköprü and Demir, 2005). Different mutualistic endophytes were used as antagonists against plant parasitic nematodes. Microorganisms such as fungi and rhizobacteria show

efficiency to control *Meloidogyne* spp. (Vos et al., 2013). The endophytic bacteria reduce root-knot nematodes penetration in plants (Padgham and Sikora, 2007).

Cultural control

The use and development of resistant crop cultivars and the use of cleaning of farm implements, intercropping, clean planting materials and crop rotation showed influence on cultural practices (Briar et al., 2016). Heat solarization and treatment of the soil before cultivation of seed played role for controlling *Meloidogyne incognita* (Ioannou, 2000). Egg infectivity of *M. incognita* can be reduced through solarization of soil for 3 weeks (Nicol et al., 2011).

Resistant cultivars

Several studies are going on throughout the world to extend the crops with resistance against root knot nematodes (Norshie et al., 2011). Resistance gene Rmc-1 located on chromosome 11 of wild potato was found resistant against *Meloidogyne* spp. (Brown et al., 2006). In isogenic tomato cultivars resistance gene Mi-1.2 confers best for huge nematode pressure (200,000 eggs/plant) (Corbett et al., 2011). The Me and N genes from pepper and the Mi2 through Mi8 genes from *Lycopersicon* identified against root knot nematodes (Mitkowski and Abawi, 2003). Some crops have been rendered susceptible with entering resistance breaking *Meloidogyne* spp. (Brown et al., 2009; Kiewnick et al., 2009).

Mode of reduction of Meloidogyne incognita

Four possible mode of action can reduce the *M. incognita* (i) inhibition (ii) development of antagonistic microbiota (iii) altered or enhanced plant growth, nutrition and morphology (iv) induced resistance (Whipps, 2004). Resistance is a safer and economically more important method than other disease controlling strategies (cultural or chemical control) due to its environmental friendly nature and disease controlling potential (Ibrahim et al., 2016).

Induced resistance

Induced resistance can be defined as a development of defensive capacity of plant against broad-spectrum of pests and pathogens that are attained after appropriate stimulation. The resulting evaluated resistance due to inducer upon infection or disease by a pathogen or pest is called systemic acquired resistance (SAR) or induced systemic resistance (ISR) (Ramamoorthy et al., 2001). The resistance in Nematology can be defined as the ability of a plant to inhibit the reproduction of nematode species relative to reproduction on plant lacking such resistance. There is a great potential in managing *M. incognita* because it is economically highly effective (Starr and Roberts, 2004). At least two forms of induced resistance, induced systemic resistance (ISR) and Systemic acquired resistance (SAR) have similar phenomenon responses but involve different pathways (Vallad and Goodman, 2004). The downstream components are similar but upstream components are usually different, mainly involving the ethylene (Et) or jasmonic acid (JA) pathways for induced systemic resistance and Salicylic acid (SA) for systemic acquired resistance (Pieterse and Van Loon, 2007). Systemic acquired resistance is usually triggered by local infections and disease, provides long-lasting

systemic resistance to successive pathogen or pest attack, and it is associated with PR genes activation and requires involvement of signaling molecules such as salicylic acid (Shoresh et al., 2010).

Induced resistance may be local or systemic. Local induced resistance response is local whereas systemic induced resistance is induced in a part of the plant that is separated spatially from the point of induction. When protection from disease is specific to a plant region which is treated with inducing agents is called local induced resistance. Whereas systemic induced resistance occurs when the plant is protected systemically due to the application of inducers to a single part of the plant. Induced systemic resistance is not necessarily confined to roots only (Vos et al., 2012), its extension towards aerial parts of plant seems possible (Fritz et al., 2006). Plant immune system proposes two pathogen induced defense responses such as effector-triggered immunity (ETI) and pattern-triggered immunity (PTI) (Shukla et al., 2018).

Inducers

Plant resistance against nematodes could be successfully induced by the application of different biotic and abiotic inducers resulting in broad-spectrum responses (Nikoo et al., 2014). These agents involve jasmonic acid (JA) and salicylic acid (SA) as key signaling molecules (Pieterse et al., 2012). Induced disease resistance is the process of an active resistance which depends upon host's barriers, activated by abiotic or biotic agents called elicitors (Fatma et al., 2014).

Abiotic inducer

Chemical defense activators can efficiently protect the crops against pests and pathogens such as *M. incognita* but they are rarely used in practice due to various reasons such as chemical induced resistance slowing down the progression of disease rather than completely eliminating it (Walters and Heil, 2007). Whereas when these chemicals applied in higher concentration negative effects are imposed on seed, plant growth and vigor (van Hulten et al., 2006). Chemicals can adversely affect the plant growth promoting microorganisms (de Roman et al., 2011).

Biotic inducer

Microorganisms such as fungi and rhizobacteria are efficient to control *Meloidogyne* spp. (Vos et al., 2013). These microorganisms are able to induce resistance through activation of jasmonic acid, salicylic acid and ethylene pathways which promote the production of PR proteins, reactive oxygen species and phenolic compounds (Hao et al., 2012). Fungi have the potential to induce resistance against *M. incognita* (Mascarin and Junior, 2012). *Trichoderma harzianum* have the ability to increase enzymatic activities against root-knot nematodes (Naserinasab et al., 2011). It has been reported that *T. harzianum* induces resistance against *M. incognita* in tomato (Harman et al., 2004) adopts priming of JA and SA related defense responses according to the stages of nematode (de Medeirosa et al., 2015; Martínez-Medina et al., 2017). Non-pathogenic *Fusarium oxysporum* changed the chemical composition of root exudates so it reduced invasion and attraction of *M. incognita* and thus induced systemic resistance in plants (Dababat and Sikora, 2007). Induced systemic resistance by plant growth promoting rhizobacteria (PGPR) has been successfully achieved in large number of agricultural crops including cucumber, potato, Arabidopsis, tomato, chili, sugarcane, rice, mango

and carnation against broad-spectrum of pathogens including bacteria, viruses, fungi and nematodes etc. (Reddy, 2012; Alizadeh et al., 2013).

Seed coating

Seed coating with resistance biotic inducing agents efficiently protected the plants against pathogens and pests (Paudel et al., 2014; Worrall et al., 2012). It is a common technique to improve seed germination and conservation while protecting the emerging seedling against pathogens (Govinden-Soulange and Levantard, 2008). Fermentation liquid of *Penicillium chrysogenum* induced resistance to *M. incognita* in *Solanum lycopersicum* and *Cucumis sativus* (Yao et al., 2014; Sikandar et al., 2019).

Conclusion

It is concluded that *M. incognita* is a great risk to agriculture because its above ground symptoms are usually similar with nutrition deficiencies. Although, chemical control is effective they contain harmful agents that rigorously damage any ecosystem. However, biological control and induced resistance in crop plants are safer strategies because of their eco-friendly nature. Thus, it is recommended to adopt biological control strategies rather than utilizing synthetic chemical agents.

Acknowledgements. The financial support provided by the Special Fund for Agro-scientific Research in the Public Interest (201503114) and China Agriculture Research System CARS-04-PS13.

Conflict of interests. All authors have no conflict of interests.

REFERENCES

- [1] Abdellatif, K. F., Abdelfattah, R. H., El-Ansary, M. S. M. (2016): Green Nanoparticles Engineering on Root-knot Nematode Infecting Eggplants and Their Effect on Plant DNA Modification. – Iranian Journal of Biotechnology 14: 250.
- [2] Adam, M. A. M., Phillips, M. S., Blok, V. C. (2007): Molecular diagnostic key for identification of single juveniles of seven common and economically important species of root-knot nematode (*Meloidogyne* spp.). – Plant Pathology 56: 190-197.
- [3] Ahmed, M., Sapp, M., Prior, T., Karssen, G., Back, M. A. (2016): Technological advancements and their importance for nematode identification. – Soil 2: 257-270.
- [4] Akköprü, A., Demir, S. (2005): Biological control of *Fusarium* wilt in tomato caused by *Fusarium oxysporum* f. sp. *lycopersici* by AMF *Glomus intraradices* and some rhizobacteria. – Journal of Phytopathology 153: 544-550.
- [5] Alizadeh, O., Azarpanah, A., Ariana, L. (2013): Induction and modulation of resistance in crop plants against disease by bioagent fungi (*Arbuscular mycorrhiza*) and hormonal elicitors and Plant Growth Promoting Bacteria. – International Journal of Farming and Allied Sciences 2: 982-998.
- [6] Anwar, S. A., McKenry, M. V. (2010): Incidence and reproduction of *Meloidogyne incognita* on vegetable crop genotypes. – Pakistan Journal of Zoology 42: 135-141.
- [7] Athman, S. Y. 2006. Host-endophyte-pest interactions of endophytic *Fusarium oxysporum* antagonistic to *Radopholus similis* in banana (*Musa* spp.). PhD, University of Pretoria
- [8] Briar, S. S., Wichman, D., Reddy, G. V. P. (2016): Plant-Parasitic Nematode Problems in Organic Agriculture.- In: Nandwani, D. (ed.) (eds.) Organic Farming for Sustainable

- Agriculture. Sustainable Development and Biodiversity, Springer International Publishing, Cham, Springer
- [9] Brown, C. R., Mojtahedi, H., James, S., Novy, R. G., Love, S. (2006): Development and evaluation of potato breeding lines with introgressed resistance to Columbia root-knot nematode (*Meloidogyne chitwoodi*). – American Journal of Potato Research 83: 1-8.
- [10] Brown, C. R., Mojtahedi, H., Zhang, L. H., Riga, E. (2009): Independent resistant reactions expressed in root and tuber of potato breeding lines with introgressed resistance to *Meloidogyne chitwoodi*. – Phytopathology 99: 1085-1089.
- [11] Castagnone-Sereno, P., Danchin, E. G. J., Perfus-Barbeoch, L., Abad, P. (2013): Diversity and evolution of root-knot nematodes, genus *Meloidogyne*: new insights from the genomic era. – Annual Review of Phytopathology 51: 203-220.
- [12] Çetintaş, R., Kareem, K. H., Nassar, H. A. (2017): Diagnosis of Nematode Populations Found in Chard, Barley and Onion Grown in North of Iraq and South of Turkey. – Doga Bilimleri Dergisi 20: 28.
- [13] Cetintas, R., Kusek, M., Fateh, S. A. (2018): Effect of some plant growth-promoting rhizobacteria strains on root-knot nematode, *Meloidogyne incognita*, on tomatoes. – Egyptian Journal of Biological Pest Control 28: 7.
- [14] Chitwood, D. J. (2002): Phytochemical based strategies for nematode control. – Annual Review of Phytopathology 40: 221-249.
- [15] Corbett, B. P., Jia, L., Saylor, R. J., Arevalo-Soliz, L. M., Goggin, F. (2011): The effects of root-knot nematode infection and mi-mediated nematode resistance in tomato on plant fitness. – Journal of Nematology 43: 82-89.
- [16] Cunha, T. G. d., Visôto, L. E., Lopes, E. A., Oliveira, C. M. G., God, P. I. V. G. (2018): Diagnostic methods for identification of root-knot nematodes species from Brazil. – Ciência Rural 48:
- [17] Dababat, A. E.-F. A., Sikora, R. A. (2007): Influence of the mutualistic endophyte *Fusarium oxysporum* 162 on *Meloidogyne incognita* attraction and invasion. – Nematology 9: 771-776.
- [18] de Medeirosa, H. A., Resendea, R. S., Ferreira, F. C., Freitas, L. G., Rodrigues, F. Á. 2015. Induction of resistance in tomato against *Meloidogyne javanica* by *Pochonia chlamydosporia*. Nematoda. ed.: Brazilian Nematological Society.
- [19] de Roman, M., Fernandez, I., Wyatt, T., Sahrawy, M., Heil, M., Pozo, M. J. (2011): Elicitation of foliar resistance mechanisms transiently impairs root association with arbuscular mycorrhizal fungi. – Journal of Ecology 99: 36-45.
- [20] Desaegeer, J., Dickson, D. W., Locascio, S. (2017): Methyl bromide alternatives for control of root-knot nematode (*Meloidogyne* spp.) in tomato production in Florida. – Journal of Nematology 49: 140-149.
- [21] Dong, S., Qiao, K., Zhu, Y., Wang, H., Xia, X., Wang, K. (2014): Managing *Meloidogyne incognita* and *Bemisia tabaci* with thiacloprid in cucumber crops in China. – Crop Protection 58: 1-5.
- [22] Fatma, M. A. M., Khalil, A. E., El Deen, N. A. H., Dina, S. (2014): Induction of Systemic Resistance in Sugar-Beet against Root-Knot Nematode with Commercial Products. – Journal of Plant Pathology and Microbiology 5: 1.
- [23] Fritz, M., Jakobsen, I., Lyngkjær, M. F., Thordal-Christensen, H., Pons-Kühnemann, J. (2006): Arbuscular mycorrhiza reduces susceptibility of tomato to *Alternaria solani*. – Mycorrhiza 16: 413.
- [24] Giannakou, I. O., Panopoulou, S. (2019): The use of fluensulfone for the control of root-knot nematodes in greenhouse cultivated crops: Efficacy and phytotoxicity effects. – Cogent Food & Agriculture 5: 1643819.
- [25] Govinden-Soulange, J., Levantard, M. (2008): Comparative studies of seed priming and pelleting on percentage and meantime to germination of seeds of tomato (*Lycopersicon esculentum* Mill.). – African Journal of Agricultural Research 3: 725-731.

- [26] Hajihassani, A., Davis, R. F., Timper, P. (2019): Evaluation of selected nonfumigant nematicides on increasing inoculation densities of *Meloidogyne incognita* on cucumber. – *Plant Disease* 103: 3161-3165.
- [27] Hao, Z., Fayolle, L., van Tuinen, D., Chatagnier, O., Li, X., Gianinazzi, S., Gianinazzi-Pearson, V. (2012): Local and systemic mycorrhiza-induced protection against the ectoparasitic nematode *Xiphinema index* involves priming of defence gene responses in grapevine. – *Journal of Experimental Botany* 63: 3657-3672.
- [28] Harman, G. E., Howell, C. R., Viterbo, A., Chet, I., Lorito, M. (2004): *Trichoderma* species—opportunistic, avirulent plant symbionts. – *Nature Reviews Microbiology* 2: 43.
- [29] Hunt, D. J., Handoo, Z. A. (2009): Taxonomy, identification and principal species.- In: Perry, R. N., Moens, M., J.L., S. (eds.) *Root-knot nematodes*, CABI, Wallingford, UK
- [30] Hussey, R. S., Janssen, G. J. W. (2002): *Root-knot nematodes: Meloidogyne* species.- In: Starr, J. L., Cook, R., Bridge, J. (eds.) *Plant resistance to parasitic nematodes*, CABI Wallingford, UK
- [31] Ibrahim, A., Shahid, A. A., Noreen, S., Ahmad, A. (2016): Physiological changes against *Meloidogyne incognita* in rhizobacterial treated eggplant under organic condition. – *JAPS, Journal of Animal and Plant Sciences* 26: 805-813.
- [32] Ioannou, N. (2000): Soil solarization as a substitute for methyl bromide fumigation in greenhouse tomato production in Cyprus. – *Phytoparasitica* 28: 248-256.
- [33] Jeyaprakash, A., Tigano, M. S., Brito, J., Carneiro, R., Dickson, D. W. (2006): Differentiation of *Meloidogyne floridensis* from *M. arenaria* using high-fidelity PCR amplified mitochondrial AT-rich sequences. – *Nematropica* 36: 1-12.
- [34] Kamran, M., Anwar, S. A., Javed, N., Khan, S. A., ul Haq, I., Ullah, I. (2012): Field evaluation of tomato genotypes for resistance to *Meloidogyne incognita*. – *Pakistan Journal of Zoology* 44: 1355-1359.
- [35] Kamran, M., Javed, N., Khan, S. A., Jaskani, M. J., Ullah, I. (2014): Efficacy of *Pasteuria penetrans* on *Meloidogyne incognita* reproduction and growth of tomato. – *Pakistan Journal of Zoology* 46: 1651-1655.
- [36] Karssen, G., Wesemael, W. M. L., Moens, M. (2013): *Root-knot nematodes*.- In: Perry, R. N., Moens, M. (eds.) *Plant nematology*, CABI, Wallingford, UK
- [37] Kergunteuil, A., Campos-Herrera, R., Sánchez-Moreno, S., Vittoz, P., Rasmann, S. (2016): The abundance, diversity, and metabolic footprint of soil nematodes is highest in high elevation alpine grasslands. – *Frontiers in Ecology and Evolution* 4: 84.
- [38] Kiewnick, S., Dessimoz, M., Franck, L. (2009): Effects of the Mi-1 and the N root-knot nematode-resistance gene on infection and reproduction of *Meloidogyne enterolobii* on tomato and pepper cultivars. – *Journal of Nematology* 41: 134-9.
- [39] Kiewnick, S., Sikora, R. A. (2006): Biological control of the root-knot nematode *Meloidogyne incognita* by *Paecilomyces lilacinus* strain 251. – *Biological Control* 38: 179-187.
- [40] Kihika, R., Murungi, L. K., Coyne, D., Hassanali, A., Teal, P. E. A., Torto, B. (2017): Parasitic nematode *Meloidogyne incognita* interactions with different *Capsicum annum* cultivars reveal the chemical constituents modulating root herbivory. – *Scientific Reports* 7: 2903.
- [41] Lizanne, A. C. M., Pai, I. K. (2014): A preliminary survey on soil and plant parasitic nematodes of southern Goa, India. – *Journal of Threatened Taxa* 6: 5400-5412.
- [42] Lunt, D. H., Kumar, S., Koutsovoulos, G., Blaxter, M. L. (2014): The complex hybrid origins of the root knot nematodes revealed through comparative genomics. – *PeerJ* 2: e356.
- [43] Ma, J., Kirkpatrick, T. L., Rothrock, C. S., Brye, K. (2013): Effects of soil compaction and *Meloidogyne incognita* on cotton root architecture and plant growth. – *Journal of Nematology* 45: 112-121.
- [44] Martínez-Medina, A., Fernandez, I., Lok, G. B., Pozo, M. J., Pieterse, C. M. J., Van Wees, S. (2017): Shifting from priming of salicylic acid-to jasmonic acid-regulated

- defences by *Trichoderma* protects tomato against the root knot nematode *Meloidogyne incognita*. – *New Phytologist* 213: 1363-1377.
- [45] Mascarin, G. M., Junior, M. F. B. (2012): *Trichoderma harzianum* reduces population of *Meloidogyne incognita* in cucumber plants under greenhouse conditions. – *Journal of Entomology and Nematology* 4: 54-57.
- [46] Mitkowski, N., Abawi, G. (2003): Root-knot nematodes. The Plant Health Instructor. – <http://www.apsnet.org/edcenter/intropp/lessons/nematodes/pages/rootknotnematode.aspx>:
- [47] Miyashita, N., Yabu, T., Kurihara, T., Koga, H. (2014): The feeding behavior of adult root-knot nematodes (*Meloidogyne incognita*) in rose balsam and tomato. – *Journal of Nematology* 46: 296-301.
- [48] Naranjo, S. E., Ellsworth, P. C. 2001. Special issue: Challenges and opportunities for pest management of *Bemisia tabaci* in the new century. Elsevier.
- [49] Naserinasab, F., Sahebani, N., Etebarian, H. R. (2011): Biological control of *Meloidogyne javanica* by *Trichoderma harzianum* BI and salicylic acid on tomato. – *African Journal of Food Science* 5: 276-280.
- [50] Nicol, J. M., Turner, S. J., Coyne, D. L., Nijs, L. D., Hockland, S., Maafi, Z. T. (2011): Current Nematode Threats to World Agriculture.- In: Jones, J., Gheysen, G., Fenoll, C. (eds.) *Genomics and molecular genetics of plant-nematode interactions*, Springer, London,
- [51] Nikoo, F. S., Sahebani, N., Aminian, H., Mokhtarnejad, L., Ghaderi, R. (2014): Induction of systemic resistance and defense-related enzymes in tomato plants using *Pseudomonas fluorescens* CHAO and salicylic acid against root-knot nematode *Meloidogyne javanica*. – *Journal of Plant Protection Research* 54: 383-389.
- [52] Norshie, P. M., Been, T. H., Schomaker, C. H. (2011): Estimation of partial resistance in potato genotypes against *Meloidogyne chitwoodi*. – *Nematology* 13: 477-489.
- [53] Onkendi, E. M., Kariuki, G. M., Marais, M., Moleleki, L. N. (2014): The threat of root-knot nematodes (*Meloidogyne* spp.) in Africa: a review. – *Plant Pathology* 63: 727-737.
- [54] Padgham, J. L., Sikora, R. A. (2007): Biological control potential and modes of action of *Bacillus megaterium* against *Meloidogyne graminicola* on rice. – *Crop Protection* 26: 971-977.
- [55] Palomares-Rius, J. E., Escobar, C., Cabrera, J., Vovlas, A., Castillo, P. (2017): Anatomical alterations in plant tissues induced by plant-parasitic nematodes. – *Frontiers in plant science* 8: 1987.
- [56] Paudel, S., Rajotte, E. G., Felton, G. W. (2014): Benefits and costs of tomato seed treatment with plant defense elicitors for insect resistance. – *Arthropod-Plant Interactions* 8: 539-545.
- [57] Pieterse, C. M., Van Loon, L. 2007. Signalling cascades involved in induced resistance. In: Walters, D., Newton, A. C., Lyon, G. (eds.) *Induced resistance for plant defense: A sustainable approach to crop protection*. ed. Oxford, UK.: Blackwell.
- [58] Pieterse, C. M. J., Van der Does, D., Zamioudis, C., Leon-Reyes, A., Van Wees, S. C. M. (2012): Hormonal modulation of plant immunity. – *Annual Review of Cell and Developmental Biology* 28:
- [59] Powers, T. (2004): Nematode molecular diagnostics: from bands to barcodes. – *Annual Review of Phytopathology* 42: 367-383.
- [60] Priya, D. B., Somasekhar, N., Prasad, J. S., Kirti, P. B. (2011): Transgenic tobacco plants constitutively expressing Arabidopsis NPR1 show enhanced resistance to root-knot nematode, *Meloidogyne incognita*. – *BMC Research Notes* 4: 231.
- [61] Ramamoorthy, V., Viswanathan, R., Raguchander, T., Prakasam, V., Samiyappan, R. (2001): Induction of systemic resistance by plant growth promoting rhizobacteria in crop plants against pests and diseases. – *Crop protection* 20: 1-11.
- [62] Randig, O., Bongiovanni, M., Carneiro, R. M. D. G., Castagnone-Sereno, P. (2002): Genetic diversity of root-knot nematodes from Brazil and development of SCAR markers specific for the coffee-damaging species. – *Genome* 45: 862-870.

- [63] Reddy, P. P. (2012): Plant Growth-Promoting Rhizobacteria (PGPR).- In: Reddy, P. P. (ed.) (eds.) Recent advances in crop protection, Springer India, New Delhi, India
- [64] Reimann, S., Hauschild, R., Hildebrandt, U., Sikora, R. A. (2008): Interrelationships between *Rhizobium etli* G12 and *Glomus intraradices* and multitrophic effects in the biological control of the root-knot nematode *Meloidogyne incognita* on tomato. – Journal of Plant Diseases and Protection 115: 108-113.
- [65] Rius, J. E. P., Vovlas, N., Troccoli, A., Liébanas, G., Landa, B. B., Castillo, P. (2007): A new root-knot nematode parasitizing sea rocket from Spanish Mediterranean coastal dunes: *Meloidogyne dunensis* n. sp. (Nematoda: Meloidogynidae). – Journal of Nematology 39: 190.
- [66] Selim, M. E. M. 2010. Biological, chemical and molecular studies on the systemic induced resistance in tomato against *Meloidogyne incognita* caused by the endophytic *Fusarium oxysporum*, Fo162. PH.D., University of Bonn.
- [67] Sharon, E., Chet, I., Spiegel, Y. (2009): Improved attachment and parasitism of Trichoderma on *Meloidogyne javanica* in vitro. – European Journal of Plant Pathology 123: 291-299.
- [68] Shores, M., Harman, G. E., Mastouri, F. (2010): Induced systemic resistance and plant responses to fungal biocontrol agents. – Annual Review of Phytopathology 48: 21-43.
- [69] Shukla, N., Yadav, R., Kaur, P., Rasmussen, S., Goel, S., Agarwal, M., Jagannath, A., Gupta, R., Kumar, A. (2018): Transcriptome analysis of root-knot nematode (*Meloidogyne incognita*)-infected tomato (*Solanum lycopersicum*) roots reveals complex gene expression profiles and metabolic networks of both host and nematode during susceptible and resistance responses. – Molecular plant pathology 19: 615-633.
- [70] Shun-xiang, R., Zhen-zhong, W., Bao-li, Q., Yuan, X. (2001): The pest status of *Bemisia tabaci* in China and non-chemical control strategies. – Insect Science 8: 279-288.
- [71] Sikandar, A., Zhang, M. Y., Zhu, X. F., Wang, Y. Y., Ahmed, M., Iqbal, M. F., Javeed, A., Xuan, Y. H., Fan, H. Y., Liu, X. Y., Chen, L. J., Duan, Y. X. (2019): Effects of *Penicillium chrysogenum* strain Sneh1216 against root-knot nematodes (*Meloidogyne incognita*) in cucumber (*Cucumis sativus* L.) under greenhouse conditions. – Applied Ecology and Environmental Research 17: 12451-12464.
- [72] Sikora, R. A., Roberts, P. A. (2018): Management Practices: An overview of integrated nematode management technologies.- In: Sikora, R. A., Coyne, D., Hallmann, J., Timper, P. (eds.) Plant parasitic nematodes in subtropical and tropical agriculture, CABI, Wallingford, UK
- [73] Sirias, H. C. I. 2011. Root-knot nematodes and coffee in Nicaragua: management systems, species identification and genetic diversity. PH.D., Swedish University of Agricultural Sciences.
- [74] Skantar, A. M., Carta, L. K., Handoo, Z. A. (2008): Molecular and Morphological Characterization of an Unusual *Meloidogyne arenaria* Population from Traveler's Tree, *Ravenala madagascariensis*. – Journal of Nematology 40: 179.
- [75] Smant, G., Helder, J., Govers, A. (2018): Parallel adaptations and common host cell responses enabling feeding of obligate and facultative plant parasitic nematodes. – The Plant Journal 93: 686-702.
- [76] Starr, J. L., Roberts, P. A. (2004): Resistance to plants parasitic nematodes.- In: Chen, Z. X., Chen, S. Y., Dickson, D. W. (eds.) Nematology: advances and perspectives, CABI, Wallingford, UK
- [77] Taylor, A. (2003): Nematocides and nematicides-a history. – Nematropica 33: 225-232.
- [78] Terra, W. C., Campos, V. P., Martins, S. J., Costa, L. S. A. S., da Silva, J. C. P., Barros, A. F., Lopez, L. E., Santos, T. C. N., Smant, G., Oliveira, D. F. (2018): Volatile organic molecules from *Fusarium oxysporum* strain 21 with nematicidal activity against *Meloidogyne incognita*. – Crop Protection 106: 125-131.
- [79] Vallad, G. E., Goodman, R. M. (2004): Systemic acquired resistance and induced systemic resistance in conventional agriculture. – Crop science 44: 1920-1934.

- [80] van Hulten, M., Pelsler, M., Van Loon, L. C., Pieterse, C. M. J., Ton, J. (2006): Costs and benefits of priming for defense in *Arabidopsis*. – Proceedings of the National Academy of Sciences 103: 5602-5607.
- [81] Vos, C., Schouteden, N., Van Tuinen, D., Chatagnier, O., Elsen, A., De Waele, D., Panis, B., Gianinazzi-Pearson, V. (2013): Mycorrhiza-induced resistance against the root-knot nematode *Meloidogyne incognita* involves priming of defense gene responses in tomato. – Soil Biology and Biochemistry 60: 45-54.
- [82] Vos, C. M., Tesfahun, A. N., Panis, B., De Waele, D., Elsen, A. (2012): Arbuscular mycorrhizal fungi induce systemic resistance in tomato against the sedentary nematode *Meloidogyne incognita* and the migratory nematode *Pratylenchus penetrans*. – Applied Soil Ecology 61: 1-6.
- [83] Walters, D., Heil, M. (2007): Costs and trade-offs associated with induced resistance. – Physiological and Molecular Plant Pathology 71: 3-17.
- [84] Whipps, J. M. (2004): Prospects and limitations for mycorrhizas in biocontrol of root pathogens. – Canadian journal of botany 82: 1198-1227.
- [85] Wishart, J., Phillips, M. S., Blok, V. C. (2002): Ribosomal intergenic spacer: a polymerase chain reaction diagnostic for *Meloidogyne chitwoodi*, *M. fallax* and *M. hapla*. – Phytopathology 92: 884-892.
- [86] Worrall, D., Holroyd, G. H., Moore, J. P., Glowacz, M., Croft, P., Taylor, J. E., Paul, N. D., Roberts, M. R. (2012): Treating seeds with activators of plant defence generates long-lasting priming of resistance to pests and pathogens. – New Phytologist 193: 770-778.
- [87] Wram, C., Zasada, I. A. (2019): Short-term effects of sub-lethal doses of nematicides on *Meloidogyne incognita*. – Phytopathology 109: 1605-1613.
- [88] Xiang, N., Lawrence, K. S., Kloepper, J. W., Donald, P. A., McInroy, J. A., Lawrence, G. W. (2017): Biological control of *Meloidogyne incognita* by spore-forming plant growth-promoting rhizobacteria on cotton. – Plant Disease 101: 774-784.
- [89] Xu, J., Liu, P., Meng, Q., Long, H. (2004): Characterisation of *Meloidogyne* species from China using isozyme phenotypes and amplified mitochondrial DNA restriction fragment length polymorphism. – European Journal of Plant Pathology 110: 309-315.
- [90] Yan, X.-n., Sikora, R. A., Zheng, J.-w. (2011): Potential use of cucumber (*Cucumis sativus* L.) endophytic fungi as seed treatment agents against root-knot nematode *Meloidogyne incognita*. – Journal of Zhejiang University Science B 12: 219-225.
- [91] Yao, Q., Lu, X., Zhu, X., Wang, Y., Chen, L., Duan, Y. (2014): Resistance against *Meloidogyne incognita* in tomato induced by fermentation liquid of *Penicillium chrysogenum* strain 1216. – Acta Phytopathologica Sinica 44: 693-699
- [92] Ye, W., Zeng, Y., Kerns, J. (2015): Molecular characterisation and diagnosis of root-knot nematodes (*Meloidogyne* spp.) from turfgrasses in North Carolina, USA. – PloS one 10: e0143556.
- [93] Youssef, R. M., Kim, K.-H., Haroon, S. A., Matthews, B. F. (2013): Post-transcriptional gene silencing of the gene encoding aldolase from soybean cyst nematode by transformed soybean roots. – Experimental Parasitology 134: 266-274.
- [94] Zabalgoceazcoa, I. (2008): Fungal endophytes and their interaction with plant pathogens: a review. – Spanish Journal of Agricultural Research 6: 138-146.
- [95] Zeng, J., Zhang, Z., Li, M., Wu, X., Zeng, Y., Li, Y. (2018): Distribution and Molecular Identification of *Meloidogyne* spp. Parasitising Flue-cured Tobacco in Yunnan, China. – Plant Protection Science 1-7.

NOTEWORTHY RECORDS OF THE LICHENIZED AND LICHENICOLOUS FUNGI FROM ALACADAĞ NATURE RESERVE (FİNİKE-ANTALYA) IN THE MEDITERRANEAN REGION OF TURKEY

KARAGÜNLÜ, G.¹ – TUFAN-ÇETİN, Ö.^{2*}

¹*Institute of Natural and Applied Sciences, Akdeniz University, Antalya, Turkey*

²*Program of Environmental Protection and Control, Department of Environmental Protection Technology, Vocational School of Technical Sciences, Akdeniz University, Antalya, Turkey
(phone: +90-242-310-6758; fax: +90-242-227-4785)*

*Corresponding author
e-mail: ozgetufan@akdeniz.edu.tr

(Received 9th Oct 2019; accepted 30th Jan 2020)

Abstract. Alacadağ, due its different vegetation composition, has been declared as Nature Protection Area in Antalya in Turkey. The special vegetation composition may sign that special lichen taxa can be found in the area. Therefore, the richness of the lichenized and lichenicolous fungi of the area was determined. According to results, a total of 125 taxa belonging to 9 orders, 27 families and 66 genera were identified. Three of these taxa are lichenicolous fungi living parasitically on lichens. Of these three, *Abrothallus welwitschii* Tul. ex Mont. is newly recorded from Turkey. In addition, lichenized fungi *Calicium pinicola* (Tibell) M. Prieto & Wedin, *Catapyrenium psoromoides* (Borrer) R. Sant., *Parmelia ernstiae* Feuerer & A. Thell., *Sticta limbata* (Sm.) Ach. were reported firstly in Turkey with this research. Of all determined taxa for the area and thirty-three taxa for Antalya Province are new. Fourteen taxa that had been known as specific to different geographical regions of Turkey before, were first record from Mediterranean region of the country. In addition, it is concluded that the species richness composition of Alacadağ Nature Protection Area showed low similarity to nearby compared areas. It was determined that many of these dissimilar taxa are only species that can live in good environmental conditions.

Keywords: biodiversity, lichen, lichen systematic, systematic

Introduction

Lichens are symbiotic association of fungi and algae and/or cyanobacteria (Hawksworth, 1991; Yuan et al., 2005; Tripp, 2017). This complex association makes it difficult to classify these organisms. However, photobiont partners have their own classifications. For this reason, the identification of “lichen species” is carried out by the classification of the fungus that can form lichen (lichenized fungi). In the world and Turkey, many studies on the classification of these interesting organisms have been done. In addition, parasitic fungi taxa on lichens (lichenicolous fungi) were also included in these studies. Feuerer and Hawksworth (2007) reported that a total of 18.882 lichenized and lichenicolous fungi were recorded worldwide. A book entitled “Türkiye Likenleri Listesi- A Checklist of the Lichens of Turkey” (John and Turk, 2017), based on previous studies, reported that totally 1898 taxa of lichenized and lichenicolous fungi had been determined in Turkey.

Lichens are highly diverse in protected areas without human intervention (Hilmo and Sâstad, 2001; Gauslaa et al., 2007; Knapp et al., 2008). Therefore, protected areas are very valuable in terms of lichens. Protected areas in Turkey are divided into four statuses: national parks, nature parks, nature monuments and nature protection area

(MPK, 1983). Nature protection areas are the least destructed of these areas by human intervention. Nature protection areas are defined as;

- A part of nature which contains rare examples of ecosystems.
- Species and natural phenomena that are rare.
- Endangered ecosystems which are important for science and education.
- Require absolute protection and are reserved for science use only and educational purposes (MPK, 1983).

Of the IUCN protected area categories (Dudley, 2008; Mitchell et al., 2018), the Absolute Nature Reserve and Wilderness category is equivalent to the Nature Protection Area (Eroğlu, 2014). Alacadağ Nature Protection Area is one of the rare areas that is located in Antalya Province in the Mediterranean Region of Anatolia. It is a special forest formed of more than 20 tree species that are rare, old and/or monumental. *Cedrus libani* A. Rich., *Pinus brutia* Ten., *Juniperus oxycedrus* L., *Quercus coccifera* L., *Fraxinus angustifolia* Wahl., *Acer platanoides* L., *Pistacia terebinthus* L., *Ostrya carpinifolia* Scop., *Fraxinus ornus* L., *Sorbus torminalis* (L.) Crantz. are some of these tree species. The vegetation composition of the area is even different than its near surroundings. Due to this feature, the area was declared a nature protection area in 01.10.1990. This special vegetation composition suggests that the area is rich in terms of lichen richness. Thus, the lichenized and lichenicolous fungi richness of the Alacadağ Nature Protection Area is found to be worth investigating and this formed the purpose of this study.

Materials and methods

Study area

Alacadağ Nature Protection Area is located in the Mediterranean Region of Anatolia at the western slopes of Alacadağ Mountain, with the Neighborhood of Alacadağ, District of Finike, Antalya Province Area which is 15 km away from the district of Finike and 128 km away from Antalya, between the coordinates: 36°21'31"N 30°02'14"E, 36°21'24"N 30°03'04"E - 36°23'27"N 30°03'04"E, 36°23'41"N 30°03'49"E. The total area is 427 hectares and the altitude varies between 884 - 1809 m (*Figure 1*).

Collecting of samples

The lichen samples had been collected from all substrates in Alacadağ Nature Protection Area in 2016 and deposited in the private fungarium Dr. Özge Tufan-Çetin. 398 lichen samples were collected. Field studies were carried out in selected 8 random localities that have different vegetation cover types, topographic structure, micro-climate characteristics and altitudes (*Table 1, Figure 1, Figure 2, Figure 3*).

Identification of samples

Dried samples were examined by using a light microscope (Nikon Eclipse E100) for microscopic characters; and a stereoscopic zoom microscope (Nikon SMZ745T) for macroscopic characters. For identification of the species, the following literature has been used: Clauzade and Roux (1985), Wirth et al. (1995), Smith et al. (2009), Moberg (1977), Tucker and Thiers (1998), Ihlen and Wedin (2008), Arup et al. (2013), Otálora et al. (2014). When required, spot tests, UV tests and TLC has also been carried out. Index Fungorum (2018) website was used in order to update the names of lichens taxa.

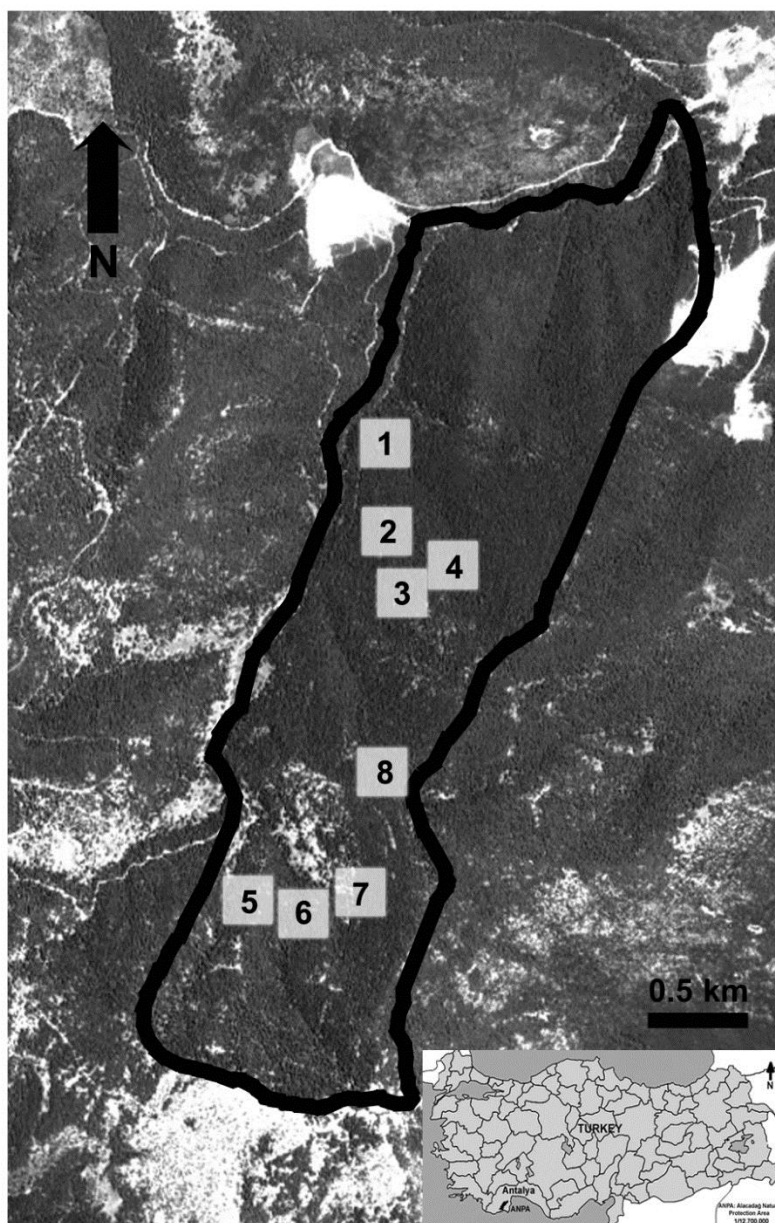


Figure 1. The map of Alacadağ Nature Area and the localities where the fieldwork was performed (The map was created with Adobe Photoshop 7.0 via data obtained from Google Earth Pro 7.3 program)

Table 1. Information about localities in Alacadağ Nature Protection Area

Localites	Coordinates	Altitudes	Dates
Loc 1	36°22,855' N 30°02,822' E	1185 m	18.6.2016
Loc 2	36°22,667' N 30°02,854' E	1343 m	18.6.2016
Loc 3	36°22,577' N 30°03,008' E	1494 m	18.6.2016
Loc 4	36°22,533' N 30°02,915' E	1449 m	18.6.2016
Loc 5	36°21,868' N 30°02,490' E	1547 m	19.6.2016
Loc 6	36°21,862' N 30°02,638' E	1516 m	19.6.2016
Loc 7	36°21,895' N 30°02,781' E	1528 m	19.6.2016
Loc 8	36°22,153' N 30°02,855' E	1609 m	19.6.2016



Figure 2. Entrance of Alacadağ Nature Protection Area (Nature Reserve) Finike-Antalya

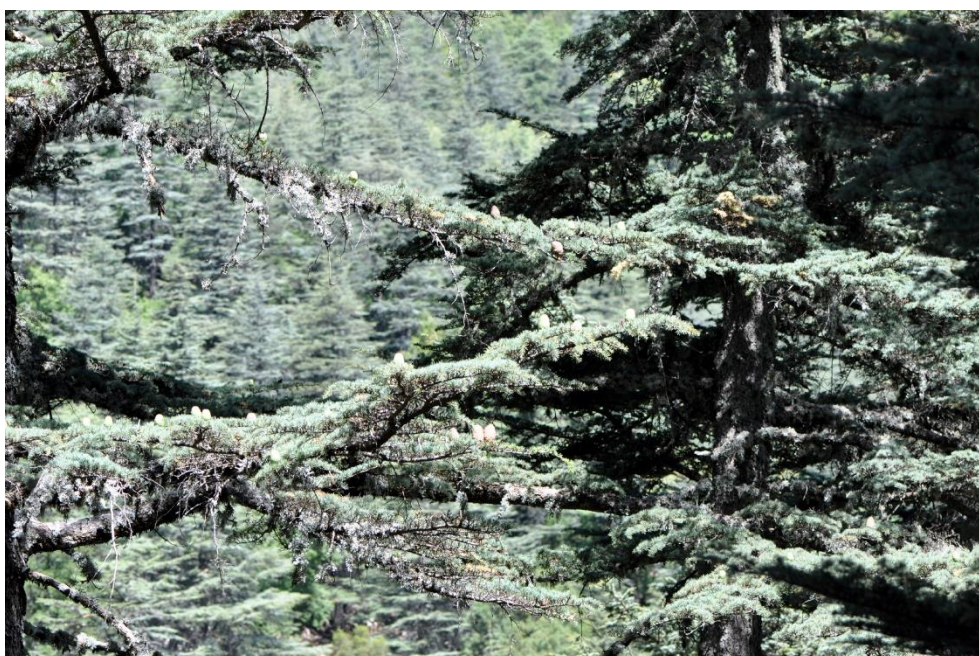


Figure 3. A view from Alacadağ Nature Protection Area (Nature Reserve) Finike-Antalya

Data analysis

The lichen richness data obtained from Alacadağ Nature Protection Area and the data obtained from near and previously studied areas were compared. These areas are the Elmalı Cedar Research Forest and Termessos National Park. The data from Elmalı Cedar Research Forest with altitudes from 1300 to 1880, approximately 23 km away from Alacadağ, were recorded by Çobanoğlu and Sevgi (2006). Data of Termessos

National Park with altitudes from 360 to 1665 m, approximately 75 km away from Alacadağ, were determined by Tufan et al. (2005). The similarities of these three areas were calculated using Sorensen similarity index (Sørensen, 1948) with PAST 3.14. Since the richness of lichenicolous fungi had not been found in previous studies, these taxa were not included in the similarity assessment. In addition by Çobanoğlu and Sevgi (2006), the richness of epiphytic lichens had been investigated in the Elmalı Cedar Research Forest. Therefore, the similarity study for this area was applied only for epiphytic lichens.

Results

Results of taxa identification

This study is the first comprehensive study to determine the lichenized and the lichenicolous fungi species in the Alacadağ Nature Protection Area (Antalya-Finike). As a result of the field studies, 398 specimens collected and identified. A total of 125 taxa belonging to 9 orders, 27 families and 66 genera were determined with laboratory studies. They are listed in alphabetic order below. Taxa new for Turkey are marked by a plus (+) and taxa new for Antalya province are highlighted by an asterisk (*) in the list. In addition, lichenicolous fungi are indicated with a hash (#):

Abrothallus parmeliarum (Sommerf.) Arnold, Loc 3 on lichen on *Cedrus libani*.

+ # * *Abrothallus welwitschii* Tul. ex Mont, Loc 1 on lichen on *Acer* sp.

Acarospora cervina A.Massal., Loc 5 on calcareous rock.

Acarospora glaucocarpa (Ach.) Körb., Loc 5 on calcareous rock.

Acarospora macrospora (Hepp) Bagl., Loc 5 on calcareous rock.

Amandinea punctata (Hoffm.) Coppins & Scheid., Loc 2 on *Cedrus libani*.

Anaptychia ciliaris (L.) Körb. ex A.Massal., Loc 1, Loc 2, Loc 3 on *Cedrus libani*; Loc 3, Loc 8 on *Juniperus excelsa*; Loc 8 on *Acer* sp.; Loc 4 on dead tree.

* *Arthonia didyma* Körb., Loc 2 on *Acer* sp.

* *Arthonia mediella* Nyl., Loc 2 on *Cedrus libani*.

Bagliettoa calciseda (DC.) Gueidan & Cl.Roux, Loc 4, Loc 5 on calcareous rock.

Bagliettoa cazzae (Zahlbr.) Vězda & Poelt, Loc 2 on calcareous rock.

Bagliettoa marmorea (Scop.) Gueidan & Cl.Roux, Loc 5 on calcareous rock.

Bagliettoa parmigera (J.Steiner) Vězda & Poelt, Loc 4, Loc 5 on calcareous rock.

Bagliettoa parmigerella (Zahlbr.) Vězda & Poelt, Loc 5 on calcareous rock.

Bilimbia sabuletorum (Schreb.) Arnold, Loc 4 on moss on calcareous rock.

Blastenia ferruginea (Huds.) A.Massal., Loc 3 on *Cedrus libani*.

Bryoria fuscescens (Gyelnik) Brodo & D.Hawksw., Loc 5, Loc 6, Loc 7 on *Cedrus libani*.

* *Bryoria nadvornikiana* (Gyeln.) Brodo & D.Hawksw., Loc 1 on *Cedrus libani*.

+ * *Calicium pinicola* (Tibell) M. Prieto & Wedin, Loc 3 on death tree.

* *Calicium trabinellum* (Ach.) Ach, Loc 3 on dead tree.

Caloplaca adriatica (Zahlbr.) Servit, Loc 5 on calcareous rock.

Caloplaca cerina (Ehrh. ex Hedw.) Th.Fr., Loc 1 on *Fraxinus ornus*, on *Juniperus oxycedrus*; Loc 4, Loc 5 on *Sorbus torminalis*; Loc 8 on *Acer* sp.

Candelariella aurella (Hoffm.) Zahlbr., Loc 1 on *Fraxinus ornus*.

Candelariella vitellina (Hoffm.) Müll.Arg., Loc 1 on *Fraxinus ornus*.

+ * *Catapyrenium psoromoides* (Borrer) R. Sant., Loc 3 on moss on calcareous rock.

Circinaria calcarea (L.) Mudd, Loc 1, Loc 5 on calcareous rock.

Circinaria contorta subsp. *hoffmanniana* S.Ekman & Fröberg ex R.Sant., Loc 4, Loc 5 on calcareous rock.

Cladonia fimbriata (L.) Fr., Loc 1, Loc 5 on dead tree; Loc 2 on moss on dead tree; Loc 7 on soil.

* *Cladonia parasitica* (Hoffm.) Hoffm., Loc 1 on dead tree; on *Cedrus libani*.

* *Clauzadea chondrodes* (A.Massal.) Clauzade & Cl.Roux, Loc 2 on calcareous rock.

Clauzadea immersa (Weber) Hafellner & Bellem., Loc 1, Loc 2 on calcareous rock.

* *Clauzadea monticola* (Ach.) Hafellner & Bellem., Loc 5 on calcareous rock.

Collema furfuraceum (Arnold) Du Rietz, Loc 4 on *Sorbus torminalis*.

Collema nigrescens (Huds.) DC., Loc 1 on *Acer* sp.; Loc 5 on *Sorbus torminalis*; Loc 8 on *Cedrus libani*.

Evernia prunastri (L.) Ach., Loc 1, Loc 5 on *Cedrus libani*.

* *Fuscopannaria mediterranea* (C.Tav.) P.M.Jørg., Loc 5 on *Acer* sp.

Fuscopannaria olivacea (P.M.Jørg.) P.M.Jørg., Loc 4 on dead tree.

Gyalolechia flavorubescens (Huds.) Søchting, Frödén & Arup, Loc 1 on *Fraxinus ornus*; Loc 5 on *Sorbus torminalis*.

Hypocenyce scalaris (Ach. ex Lilj.) M.Choisy, Loc 3 on dead tree.

Hypogymnia tubulosa (Schaer.) Hav., Loc 1, Loc 2, Loc 3, Loc 4, Loc 7 on *Cedrus libani*; Loc 1 on dead tree.

* *Hypogymnia vittata* (Ach.) Parrique, Loc 2 on *Cedrus libani*.

* *Lathagrium auriforme* (With.) Otálora, P.M.Jørg. & Wedin, Loc 4 on moss on calcareous rock.

Lathagrium cristatum (L.) Otálora, P.M.Jørg. & Wedin, Loc 5 on calcareous rock.

* *Lecania cuprea* (A.Massal.) van den Boom & Coppins, Loc 2 on calcareous rock.

Lecania cyrtella (Ach.) Th.Fr., Loc 1 on *Cedrus libani*.

* *Lecania naegelii* (Hepp) Diederich & P. Boom, Loc 1 on *Cedrus libani*; on *Juniperus oxycedrus*.

Lecanora carpinea (L.) Vain., Loc 1 on *Fraxinus ornus*; Loc 2 on *Cedrus libani*; Loc 5 on *Sorbus torminalis*; Loc 6 on *Acer* sp..

Lecanora chlarotera Nyl., Loc 1 on *Fraxinus ornus*; Loc 2 on *Cedrus libani*; Loc 4, Loc 5 on *Sorbus torminalis*; Loc 6 on *Acer* sp.

Lecanora pulicaris (Pers.) Ach., Loc 2 on *Cedrus libani*.

Lecanora saligna (Schr.) Zahlbr., Loc 1 on *Fraxinus ornus*.

Lecanora varia (Hoffm.) Ach., Loc 3 on dead tree.

Lecidella carpathica Körb., Loc 3 on calcareous rock.

Lecidella elaeochroma (Ach.) M.Choisy, Loc 1 on *Fraxinus ornus*; Loc 1, Loc 2, Loc 6 on *Cedrus libani*; Loc 3 on *Juniperus excelsa*; Loc 5, Loc 6 on *Acer* sp.; Loc 8 on *Juniperus excelsa*, on *Fraxinus ornus*, on *Acer* sp; Loc 4, Loc 5 on *Sorbus torminalis*.

* *Lecidella scabra* (Taylor) Hertel & Leuckert, Loc 5 on dead tree.

Lecidella stigmatea (Ach.) Hertel & Leuckert, Loc 2, Loc 4, Loc 5 on calcareous rock.

Lepra albescens (Huds.) Choisy & Werner, Loc 1 on dead tree, Loc 1, Loc 3, Loc 4, Loc 5, Loc 6, Loc 7 on *Cedrus libani*; Loc 1 on *Juniperus oxycedrus*; Loc 3 on *Juniperus excelsa*; Loc 5 on *Fraxinus ornus*, on *Acer* sp; Loc 5 on *Sorbus torminalis*.

* *Lepraria umbricola* Tønsberg, Loc 3 on dead tree.

Lepraria vouauxii (Hue) R.C.Harris, Loc 5 on moss on calcareous rock.

Leproplaca xantholyta (Nyl.) Hue, Loc 2, Loc 5 on calcareous rock.

Leptogium saturninum (Dicks.) Nyl., Loc 1 on *Acer* sp.

- Letharia vulpina* (L.) Hue, Loc 1 on dead tree; Loc 3, Loc 6, Loc 7 on *Cedrus libani*, on dead tree.
* *Lobaria pulmonaria* (L.) Hoffm., Loc 1 on *Cedrus libani*.
Lobothallia radiosus (Hoffm.) Hafellner, Loc 5 on calcareous rock.
Megaspora verrucosa (Ach.) Hafellner & V. Wirth, Loc 3 on *Juniperus excelsa*; Loc 8 on *Acer* sp., on *Cedrus libani*.
Melanohalea elegantula (Zahlbr.) O. Blanco, A. Crespo, Divakar, Essl., D. Hawksw. & Lumbsch, Loc 1, Loc 2, Loc 3 on *Cedrus libani*, on *Juniperus excelsa*.
Melanohalea exasperata (De Not.) O. Blanco et al., Loc 4 on *Sorbus torminalis*, Loc 6 on *Acer* sp.
Melanohalea exasperatula (Nyl.) O. Blanco et al., Loc 8 on *Acer* sp.
* *Mycobilimbia tetramera* (De Not.) Vitik., Ahti, Kuusinen, Lommi & T. Ulvinen, Loc 5 on moss on calcareous rock.
Myriolecis pruinosa (Chaub.) Sliwa, Zhao Xin & Lumbsch Loc 5 on calcareous rock.
Nephroma laevigatum Ach., Loc 4 on *Cedrus libani*; Loc 5 on *Acer* sp., on dead tree.
Nephroma tangeriense (Maheu & A. Gillet) Zahlbr., Loc 1 on *Acer* sp.
Ochrolechia balcanica Vers., Loc 1, Loc 2, Loc 3 on *Cedrus libani*; Loc 4 on dead tree; Loc 4, Loc 5 on *Sorbus torminalis*; Loc 5, Loc 8 on *Acer* sp.
Ochrolechia pallescens (L.) A. Massal., Loc 2, Loc 3, Loc 8 on *Cedrus libani*; Loc 5, Loc 8 on *Acer* sp.
* *Ochrolechia parella* (L.) A. Massal., Loc 1 on *Acer* sp.; Loc 8 on *Cedrus libani*.
* *Ochrolechia tartarea* (L.) A. Massal., Loc 5 on *Acer* sp.
Ochrolechia turneri (Sm.) Hasselrot, Loc 3 on *Cedrus libani*; Loc 8 on *Juniperus excelsa*.
* *Pannaria conoplea* (Ach.) Bory, Loc 8 on *Cedrus libani*.
+ * *Parmelia ernstiae* Feuerer & A. Thell., Loc 3 on *Cedrus libani*.
Parmelia saxatilis (L.) Ach., Loc 1, Loc 2, Loc 4, Loc 5 on *Cedrus libani*; Loc 1, Loc 4, Loc 5 on dead tree; Loc 1, Loc 5 on *Acer* sp.
Parmelia sp. (young individual), Loc 1 on *Juniperus oxycedrus*.
Parmelia submontana Nadv. ex Hale, Loc 2, Loc 8 on *Cedrus libani*; Loc 4 on *Sorbus torminalis*.
Parmelia sulcata Taylor, Loc 1, Loc 6 on *Cedrus libani*.
Parmelina pastillifera (Harm.) Hale, Loc 1 on *Cedrus libani*, on *Fraxinus ornus*; Loc 5 on *Acer* sp.
Parmelina tiliacea (Hoffm.) Hale, Loc 1 on *Cedrus libani*; Loc 5 on dead tree.
Pectenia atlantica (Degel.) P.M. Jørg., L. Lindblom, Wedin & S. Ekman, Loc 1, Loc 8 on *Acer* sp; Loc 3, Loc 8 on *Cedrus libani*, Loc 4 on dead tree.
Peltigera canina (L.) Willd., Loc 4, Loc 5 on moss on calcareous rock, Loc 5 on dead tree, on moss on *Acer* sp.
Peltigera collina (Ach.) Schrad., Loc 2 on moss on dead tree; Loc 4 on moss on soil; Loc 5 on dead tree, on *Acer* sp; Loc 8 on *Cedrus libani*.
Peltigera membranacea (Ach.) Nyl. Loc 1 on on soil on moss
Peltigera rufescens (Weiss) Humb., Loc 1 on dead tree.
Pertusaria pertusa (Weigel) Tuck., Loc 1 on *Acer* sp.
Phlyctis agelaea (Ach.) Flot., Loc 1 on *Acer* sp, on *Cedrus libani*.
Phlyctis argena (Sprengel) Flot., Loc 1, Loc 8 on *Fraxinus ornus*, on *Juniperus oxycedrus*; Loc 2, Loc 6, Loc 8 on *Cedrus libani*.
Physcia adscendens (Fr.) H. Olivier, Loc 1 on *Fraxinus ornus*; Loc 1, Loc 8 on

- Cedrus libani*; Loc 8 on *Acer* sp.; Loc 3 on *Juniperus excelsa*.
Physconia distorta (With.) J.R.Laundon, Loc 1, Loc 3 on *Cedrus libani*; Loc 1 on *Fraxinus ornus*; Loc 3 on *Juniperus excelsa*; Loc 4, Loc 5 on *Sorbus torminalis*, Loc 5, Loc 8 on *Acer* sp.; Loc 4 on dead tree.
Physconia venusta (Ach.) Poelt, Loc 3 on *Cedrus libani*, on *Juniperus excelsa*; Loc 4 on dead tree.
Placynthium nigrum (Huds.) Gray, Loc 3, Loc 5 on calcareous rock.
Platismatia glauca (L.) W.L.Culb. & C.F.Culb., Loc 1, Loc 2, Loc 3, Loc 4, Loc 5, Loc 6, Loc 7 on *Cedrus libani*; Loc 1, Loc 5 on dead tree; Loc 1 on *Acer* sp.
* *Protoblastenia calva* (Dicks.) Zahlbr., Loc 2 on calcareous rock.
Pseudevernia furfuracea (L.) Zopf var. *ceratea*, Loc 1 on *Acer* sp.; Loc 8 on *Juniperus excelsa*; Loc 2, Loc 3 on *Cedrus libani*.
* *Pseudevernia furfuracea* (L.) Zopf var. *furfuracea*, Loc 1 on *Juniperus oxycedrus*; Loc 1, Loc 2, Loc 3, Loc 4, Loc 5, Loc 6, Loc 7 on *Cedrus libani*; Loc 6 on *Acer* sp.
Psora vallesiaca (Schaer.) Timdal, Loc 5 on calcareous rock.
Pyrenodesmia chalybaea (Fr.) A.Massal., Loc 4 on calcareous rock.
Pyrenodesmia variabilis (Pers.) A.Massal., Loc 1, Loc 4 on calcareous rock.
* *Ramalina calicaris* (L.) Fr., Loc 1 on *Fraxinus ornus*; Loc 5 on *Acer* sp.
Ramalina farinacea (L.) Ach., Loc 1 on *Acer* sp., on *Cedrus libani*, on *Juniperus oxycedrus*, on *Fraxinus ornus*; Loc 2 on *Cedrus libani*.
Ramalina fastigiata (Pers.) Ach., Loc 1 on *Fraxinus ornus*.
Ramalina fraxinea (L.) Ach., Loc 1 on *Acer* sp., on *Fraxinus ornus*; Loc 2, Loc 3 on *Cedrus libani*.
* *Ricasolia amplissima* (Scop.) De Not., Loc 1 on *Cedrus libani*.
Rinodina capensis Hampe in A.Massal., Loc 1 on *Fraxinus ornus*.
* *Rinodina oleae* Bagl., Loc 4 on *Sorbus torminalis*; Loc 8 on *Acer* sp.
* *Rinodina pyrina* (Ach.) Arnold, Loc 6 on *Acer* sp.
* *Rinodina sophodes* (Ach.) A.Massal., Loc 4 on *Sorbus torminalis*.
Scytinium gelatinosum (With.) Otálora, P.M.Jørg. & Wedin, Loc 4, Loc 5 on moss on calcareous rock; Loc 5 on calcareous rock.
Scytinium lichenoides (L.) Otálora, P.M.Jørg. & Wedin, Loc 5 on moss on calcareous rock.
Scytinium teretiusculum (Wallr.) Otálora, P.M.Jørg. & Wedin, Loc 8 on *Cedrus libani*.
Squamarina cartilaginea (With.) P.James, Loc 3, Loc 5 on calcareous rock.
Squamarina gypsacea (Sm.) Poelt, Loc 3 on calcareous rock.
+ * *Sticta limbata* (Sm.) Ach., Loc 1 on *Cedrus libani*.
* *Toninia subfuscae* (Arnold) Timdal, Loc 5 on *Lecidella scabra*.
Variospora aurantia (Pers.) Arup, Frödén & Söchting, Loc 2 on calcareous rock.
Variospora flavescens (Huds.) Arup, Söchting & Frödén, Loc 2 on calcareous rock.
Variospora velana (A.Massal.) Arup, Söchting & Frödén, Loc 2 on calcareous rock.
Verrucaria nigrescens Pers., Loc 3, Loc 4, Loc 5 on calcareous rock.
Verruculopsis lecideoides (A.Massal.) Gueidan & Cl. Roux, Loc 2 on calcareous rock.
Xanthocarpia lactea (A.Massal.) A.Massal., Loc 5 on calcareous rock.
* *Xanthoria isidioidea* (Beltram.) Szatala, Loc 4 on *Cedrus libani*.

Results of data analysis

The results obtained from this study and the results obtained from Elmalı Cedar Research Forest (Çobanoğlu and Sevgi, 2006) and Termessos National Park (Tufan et al., 2005) were compared. In Elmalı Cedar Research Forest (Çobanoğlu and Sevgi, 2006), only the richness of epiphytic lichenized fungi had been investigated. Therefore, the similarity study for this area was applied only for epiphytic lichens. 54 epiphytic lichenized fungi taxa had been determined from Elmalı Cedar Research Forest and 77 epiphytic lichenized fungi taxa (without lichenicolous fungi) were identified in the Alacadağ Nature Protection Area. The epiphytic lichenized fungi taxa of the Elmalı Cedar Research Forest and the Alacadağ Nature Protection Area were found to be 0.4122% similar (27 common taxa) according to the Sorensen similarity index. 160 lichenized fungi taxa had been determined from Termessos National Park (Tufan et al., 2005). 39.007% similarity (55 common taxa) was determined between the lichenized fungi richness of Alacadağ Nature Protection Area and the lichenized fungi richness of Termessos National Park.

Discussion

Antalya, in Southern-west of Turkey, has been visited many times by lichen systematic researchers. A total of 402 lichenized and lichenicolous fungi taxa had been identified including the center city and districts of Antalya (Fellows, 1841; Pišút, 1970; Ayaşlıgil, 1987; Lumbsch, 1989; John, 1992, 1995, 1996, 2000, 2007; Zeybek et al., 1993; Vězda, 1996; Nimis and John, 1998; Schindler, 1998; Litterski and Otte, 2002; Meyer, 2002; Halda, 2003; Breuss and John, 2004; Çobanoğlu, 2005; Tufan et al., 2005; Schiefelbein, 2006; Mayrhofer and Sheard, 2007; Yavuz and Çobanoğlu, 2007; Pišút and Guttová, 2008; Kocakaya et al., 2009; Tufan-Cetin and Sümbül, 2011; Halici et al., 2012; Kocakaya et al., 2014; Özdemir Turk et al., 2015; Tufan-Çetin, 2015, 2019; Vondrák et al., 2016; John and Turk, 2017). In this study, 124 taxa belong to 9 orders, 27 families and 66 genera were determined. 33 of these were recorded for the first time in Antalya and the number of lichenized and lichenicolous fungi taxa of Antalya reach to 435.

Three of the taxa identified in the research area are lichenicolous fungi that live parasitically on lichens. A lichenicolous fungus species, *Abrothallus welwitschia*, is newly recorded for Turkey. *Abrotallus* is a genus that does not have a clear similarity to other genera of Ascomycetes and has many hypotheses about its phylogenetic relations (Pérez-Ortega et al., 2014). It is mostly composed of parasitic fungi living on lichens. World distribution of *Abrothallus welwitschii* is Europe (France, England, Ireland, Spain, Portugal), New Zealand, Africa (Kenya), North America (America), South America (Chile). *Abrothallus welwitschii* mostly chooses species belonging to the genus *Sticta* as host (Suija et al., 2015). In this study, this species was determined over *Sticta limbata*. *Sticta limbata* was determined first time in Turkey from Alacadağ Nature Protection Area. Also *Sticta limbata* is found in the Northern Hemisphere, South Africa, South America, Australia, New Zealand and East Asia (Japan, China, Korea) (Jayalal et al., 2014). Also the taxon in red list was categorized as “vulnerable” in Italy (Nascimbene et al., 2013). This species was reported living on mossy tree bark in the old forests by Smith et al. (2009). Similarly, in our research area, the species was identified from old *Cedrus libani* trees.

Calicium pinicola which had been defined as new combination with *Cyphelium pinicola* Tibell, Svensk Bot. Tidskr by Prieto et al. (2016), was reported as a new record for Turkey from this research area. This species which is located in Austria, Macedonia, USA (Obermayer, 1998) and the Swiss Alps (Nimis et al., 2018), is threatened with extinction in Switzerland (Bürgi-Meyer and Dietrich, 2011), categorized as “vulnerable” in Italy (Nascimbene et al., 2013).

Of the new records for Turkey *Catapyrenium psoromoides* is a species found in the Southwest of Asia Temperate, East Africa, Europe, New Zealand and North America. It is near threatened with extinction in Italy according to Nascimbene et al. (2013). The taxon lives on trees or on mosses (Breuss, 2002; Prieto et al., 2010). In our study, it was determined also over the moss.

Parmelia ernstia which has a wide distribution in Europe (Austria, Belgium, Bosnia and Herzegovina, Britain, Bulgaria, Czechia, Denmark, Estonia, France, Germany, Greece, Ireland, Lithuania, Luxembourg, Netherlands, Slovenia, Spain, Poland, Sweden), have been recorded from Turkey for the first time by this research. This species is also distributed in Algeria and Canary Islands in Africa (Kukwa et al., 2012). According to Kukwa et al. (2012) this species is rarely seen in coniferous deciduous trees. In Italy, *Parmelia ernstia* was identified from *Quercus* and *Pinus* species (Nimis and Martellos, 2017). Also in this study, the species was recorded on *Cedrus libani*.

In the Italian red list of epiphytic lichens *Calicium pinicola*, *Hypogymnia vittata*, *Sticta limbata* are categorized as “vulnerable” and *Catapyrenium psoromoides*; *Pannaria conoplea*; *Ricasolia amplissima* are classified as “near threatened” (Nascimbene et al., 2013). The Alacadağ Nature Protection Area is home to these sensitive species.

Most of the new records for Antalya in this study, have limited distribution in Turkey. In *Figure 4*, Turkey distribution maps of some taxa are given. The maps were created using the information of John and Türk (2017). There are also maps showing the biogeographical regions and phytogeographical regions of Turkey in *Figure 4g and 4h*. *Arthonia didyma* (*Figure 4a*), *Arthonia medulla*, *Lecania cuprea*, *Lepraria umbiricola*, *Mycobilimbia tetramera* (*Figure 4c*), *Ramalina calicaris*, *Ricasolia amplissima* (*Figure 4e*), that had been defined as specific to the Euro-Siberian Phytogeographical Region (P.R.) (Black Sea Biogeographical Region (B.R.)) of Turkey (John and Türk, 2017), have been found newly in Mediterranean Region of Turkey with this study. *Protoblastenia calva* that was defined only from Irano-Turanian P.R. (Anatolian B.R.) of Turkey have been found in our research area (John and Türk, 2017). Similarly, *Bryoria nadvornikiana*, *Calicium trabinellum*, *Hypogymnia vittata* (*Figure 4b*), *Pannaria conoplea* (*Figure 4d*), *Ochrolechia tartarea*, *Xanthoria isidioidea* were known in both Euro-Siberian P.R. (Black Sea B.R.) and Iran-Turanian P.R. (Anatolia B.R.) of Turkey (John and Türk, 2017). With our study these taxa have been recorded in Turkey's Mediterranean B.R. (Mediterranean P.R.). In addition, *Cladonia parasitica* which was defined as a lichen of the Euro-Siberian P.R. (Black Sea B.R.) in Turkey, had been found before in the south of Anatolia (in Hatay) same as with our study (John and Türk, 2017). The reason for this species to be found in Hatay may be due to the fact that this region is an enclave of Euro-Siberian P.R. (Black Sea B.R.) (Atalay, 1986). The presence of this species also in the research area may show that the area has a special ecological structure. On the other hand, *Rinodina oleae* (*Figure 4f*), *Lathagrium auriforme*, *Lobaria pulmonaria* (*Figure 5*), *Ochrolechia parella*, *Rinodina pyrina* which

are the new record taxa for Antalya, have a wide geographical distribution in Turkey and have been found in this research area.

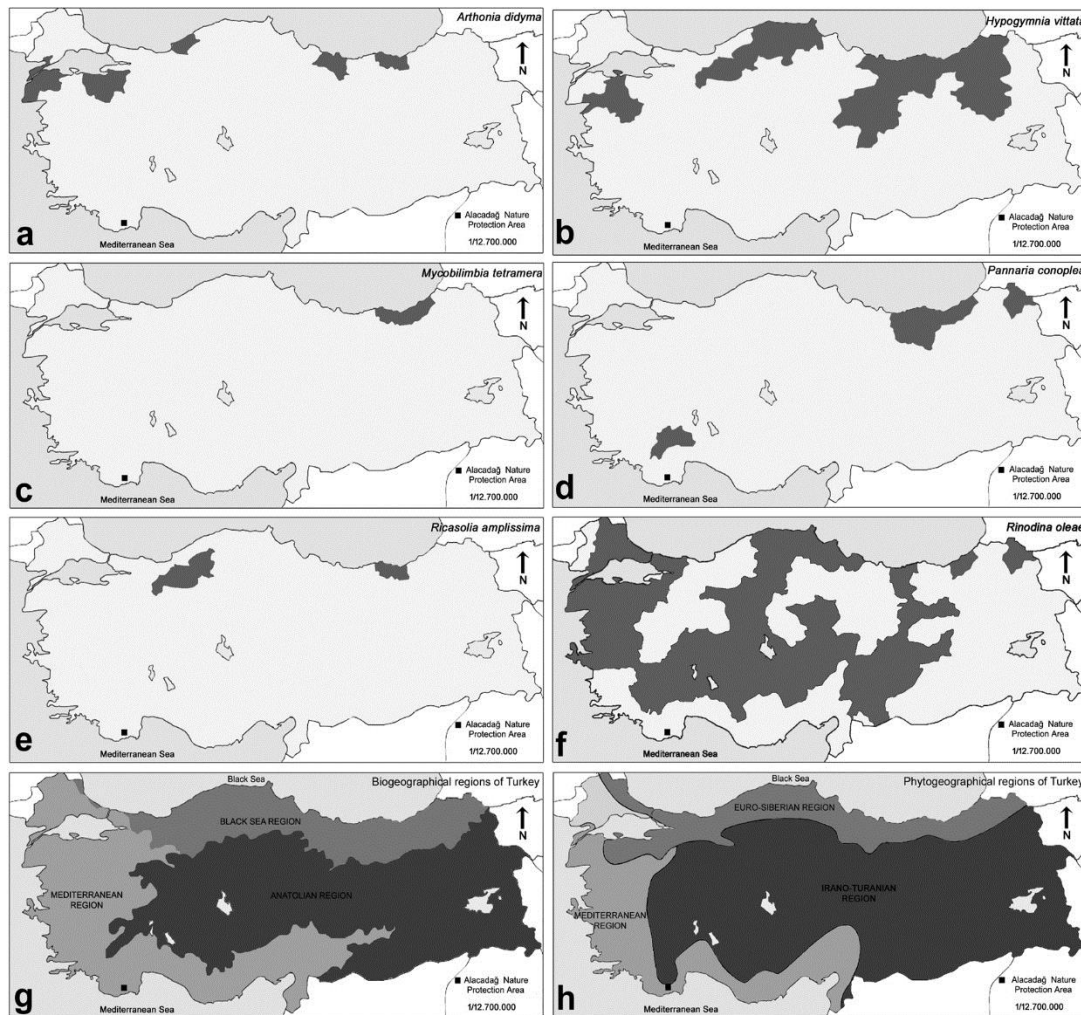


Figure 4. a-f. Turkey distribution map of some lichen taxa from Alacadağ Nature Protection Area (a. *Arthonia didyma*, b. *Hypogymnia vittata*, c. *Mycobilimbia tetramera*, d. *Pannaria conoplea*, e. *Ricasolia amplissima*, f. *Rinodina oleae*) g. Biogeographical regions of Turkey h. Phytogeographical regions of Turkey

When our richness data were compared with data of the nearby areas, with data of Termessos National Park, one of the compared area, 39.007% similarity rate were found. In addition, the epiphytic lichenized fungi richness data of the Alacadağ Nature Protection Area were found 0.4122% similarity with data of Elmalı Cedar Research Forest according to the Sorensen similarity index. However, according to Tufan-Çetin (2019), the richness of Termessos National Park is 55.52% (according to Sorensen similarity index) similar with the richness of Altınbeşik Cave National Park which is one of the protected areas of Antalya. In addition, Tufan-Çetin and Sumbul (2011) reported that Köprülü Canyon, another national park of Antalya, showed 58.29% similarity with Termessos National Park (according to Sorensen similarity index). According to these reference comparisons, it is concluded that the species richness

composition of Alacadağ Nature Protection Area showed low similarity to other areas. Furthermore, it was determined that many of dissimilar taxa (according to compared area) are only species that can live in good environmental conditions and in old forests (Figure 6) (Nimis and Martellos, 2017). Comparison area data dating back 13-14 years before may be the result of the better environmental quality than today. But the fact that these dissimilar taxa in the area can live in good environmental quality may indicate that the environmental change has not occurred in the area.



Figure 5. Some lichenized fungi taxa on *Cedrus libani* stem in Alacadağ Nature Protection Area (Nature Reserve) Finike-Antalya



Figure 6. Some old forest lichenized fungi taxa on dead tree in Alacadağ Nature Protection Area (Nature Reserve) Finike-Antalya

Conclusion

This study is the first comprehensive study to determine the lichenized and lichenicolous fungi taxa in the Alacadağ Nature Protection Area (Nature Reserve). Many taxa were newly recorded from Turkey, Turkey's Mediterranean region and Antalya Province with this study. Taxa that had been known as specific to different geographical regions of Turkey before, were firstly determined from the area. Furthermore, species richness composition of Alacadağ Nature Protection Area was found low similarity to other areas. All these noteworthy species findings indicate a different species composition structure in the Alacadağ Nature Protection Area compared to the Mediterranean lichen composition. In fact, Alacadağ has been declared as nature protection area (Nature Reserve) due to its rich plant diversity. In this study, it was also determined that the area has a different ecological structure in terms of lichens like plant diversity.

Nowadays, on three sides of Alacadağ Nature Protection Area are surrounded by marble quarries (*Figure 1*). It is obligatory to protect the area, which is emphasized as having a special structure also in this study, from the pressure of marble quarries. It has been observed that the density of sensitive species (*Catapyrenium psoromoides*, *Calicium pinicola*, *Hypogymnia vittata*; *Sticta limbata*, *Pannaria conoplea*; *Ricasolia amplissima*) in the area decreases when it was approached the marble quarries. For this reason, the density of the species in the area should be examined with a further study.

REFERENCES

- [1] Arup, U., Söchting, U., Frödén, P. (2013): A new taxonomy of the family Teloschistaceae. – *Nordic Journal of Botany* 31(1): 016-083.
- [2] Atalay, İ. (1986): Vegetation formations of Turkey. – *Travaux de l'Institut Géographique de Reims* 65-66: 17-30.
- [3] Ayaşlıgil, Y. (1987): Der Köprülü Kanyon Nationalpark. – *Landschaftsökologie Weihenstephan* 5: I-XIV, 1-307.
- [4] Breuss, O. (2002): *Catapyrenium*. – In: Nash, T. H., Ryan, B. D., Gries, C., Bungartz, F. (eds.) *Lichen Flora of the Greater Sonoran Desert Region*. Volume I: 125-128.
- [5] Breuss, O., John, V. (2004): New and interesting records of lichens from Turkey. – *Österreichische Zeitschrift für Pilzkunde* 13: 281-294.
- [6] Bürgi-Meyer, K., Dietrich, M. (2011): *Cyphelium pinicola* Tibell in den Nordalpen der Zentralschweiz. Einblicke in den Flechtenreichtum der subalpinen Altwälder am Fusse des Gugels in der UNESCO Biosphäre Entlebuch, Kanton Luzern. – *Meylania* 7: 11-17.
- [7] Clauzade, G., Roux, C. (1985): *Likenoj De Okcidenta Eŭropo Ilustrita Determinlibro*. – *Bulletin de la Société Botanique du Centre-Ouest Nouvelle série- Numéro Spécial*, Royan, France, 893 p.
- [8] Çobanoğlu, G. (2005): Lichen collection in the herbarium of the University of Istanbul (ISTF). – *Turkish Journal of Botany* 29: 69-74.
- [9] Çobanoğlu, G., Sevgi, O. (2006): Elmalı Sedir Araştırma Ormanı (Antalya) Epifitik Liken Florası. – *İstanbul Üniversitesi Orman Fakültesi Dergisi Seri A* 56(1): 81-88.
- [10] Dudley, N. (2008): *IUCN Guidelines for Applying Protected Area Management Categories*. – Gland, Switzerland.
- [11] Eroğlu, S. (2014): Milli Parklar Kanununda Belirlenen Korunan Alan Metodolojisi. – *Denetim* 13: 85-90.
- [12] Fellows, C. (1841): *An account of discoveries in Lycia: Being a journal kept during a second excursion in Asia Minor*. – London, 290 p.

- [13] Feuerer, T., Hawksworth, D. L. (2007): Biodiversity of lichens, including a world-wide analysis of checklist data based on Takhtajan's floristic regions. – *Biodiversity and Conservation* 16(1): 85-98.
- [14] Gauslaa, Y., Palmqvist, K., Solhaug, K. A., Holien, H., Hilmo, O., Nybakken, L., Ohlson, M. (2007): Growth of epiphytic old forest lichens across climatic and successional gradients. – *Canadian Journal of Forest Research* 37(10): 1832-1845.
- [15] Halda, J. (2003): A taxonomic study of the calcicolous endolithic species of the genus *Verrucaria* (Ascomycotina, Verrucariales) with the lid-like and radiately opening involucrellum. – *Acta Musei Richnoviensis Sect. Nat.* 10(1): 1-148.
- [16] Halici, M. G., Kocakaya, M., Kılıç, E. (2012): New *Candelariella* records for Turkey. – *Mycotaxon* 121: 313-318.
- [17] Hawksworth, D. L. (1991): The fungal dimension of biodiversity: magnitude, significance, and conservation. – *Mycological research* 95(6): 641-655.
- [18] Hilmo, O., Sæstad, S. M. (2001): Colonization of old-forest lichens in a young and an old boreal *Picea abies* forest: an experimental approach. – *Biological Conservation* 102(3): 251-259.
- [19] Ihlen, P. G., Wedin, M. (2008): An annotated key to the lichenicolous Ascomycota (including mitosporic morphs) of Sweden. – *Nova Hedwigia* 86:(3-4): 275-365.
- [20] Index Fungorum (2018): <http://www.indexfungorum.org>. – Son erişim tarihi: 14.07.2018.
- [21] Jayalal, U., Sohsokim, J. A., Koh, Y. J., Crişan, F., Hur, J. S. (2014): The Lichen Genus *Sticta* in South Korea. – *Mycobiology* 42(1): 6-11.
- [22] John, V. (1992): Das die Türkei betreffende lichenologische Schrifttum / Türkiye likenleri ile ilgili literatür. – *Pfalzmuseum für Naturkunde, Bad Dürkheim*, 1-14.
- [23] John, V. (1995): Ergänzungen zum die Türkei betreffenden lichenologischen Schrifttum / Türkiye likenleri ile ilgili literatüre ilaveler. – *Pfalzmuseum für Naturkunde, Bad Dürkheim*, 1-8.
- [24] John, V. (1996): Preliminary catalogue of lichenized and lichenicolous fungi of Mediterranean Turkey. – *Bocconea* 6: 173-216.
- [25] John, V. (2000): *Lichenes Anatolici Exsiccati*. Fasc. 4-5 (no. 76-125). – *Arnoldia* 19: 1-27.
- [26] John, V. (2007): Lichenological studies in Turkey and their relevance to environmental interpretation. – *Bocconea* 21: 85-93.
- [27] John, V., Turk, A. (2017): Türkiye Likenleri Listesi. – *Nezahat Gökyiğit Botanik Bahçesi Yayını, İstanbul*, 666 s.
- [28] Knapp, S., Kühn, I., Mosbrugger, V., Klotz, S. (2008): Do protected areas in urban and rural landscapes differ in species diversity? – *Biodiversity and Conservation* 17(7): 1595-1612.
- [29] Kocakaya, M., Halici, M. G., Aksoy, A. (2009): Lichens and lichenicolous fungi of Kızıldağ (Derebucak, Konya). – *Turkish Journal of Botany* 33: 105-112.
- [30] Kocakaya, M., Halici, M. G., Aksoy, A. (2014): Lichenized and lichenicolous fungi of Gevne valley (Konya, Antalya). – *Turkish Journal of Botany* 38(2): 358-369.
- [31] Kukwa, M., Łubek, A., Szymczyk, R., Zalewska, A. (2012): Seven lichen species new to Poland. – *Mycotaxon* 120(1): 105-118.
- [32] Litterski, B., Otte, V. (2002): Biogeographical research on european species of selected lichen genera. – *Bibliotheca Lichenologica* 82: 83-90.
- [33] Lumbsch, H. T. (1989): Die holarktischen Vertreter der Flechtengattung *Diploschistes* (Thelotremataceae). – *Journal of the Hattori Botanical Laboratory* 66: 133-196.
- [34] Mayrhofer, H., Sheard, J. W. (2007): *Rinodina archaea* (Phyciaceae, lichenized Ascomycetes) and related species. – *Bibliotheca Lichenologica* 96: 229-246.
- [35] Meyer, B. (2002): Die Flechtengattung *Clauzadea*. – *Sendtnera* 8: 85-154.
- [36] Mitchell, B. A., Stolton, S., Bezaury-Creel, J., Bingham, H. C., Cumming, T. L., Dudley, N., Fitzsimons, J. A., Malleret-King, D., Redford, K. H., Solano, P. (2018): Guidelines

- for privately protected areas. – Best Practice Protected Area Guidelines Series No. 29. Gland, Switzerland: IUCN. xii + 100 pp.
- [37] Moberg, R. (1977): The lichen genus *Physcia* and allied genera in Fennoscandia, Stockholm. – *Symbolae Botanicae Upsaliensis* 22(1): 1-108.
- [38] MPK (1983): Milli Parklar Kanunu. – Resmi Gazete (National Park Law, official newspaper) 5: 508-530.
- [39] Nascimbene, J., Nimis, P. L., Ravera, S. (2013): Evaluating the conservation status of epiphytic lichens of Italy: a red list. – *Plant Biosystems-An International Journal Dealing with all Aspects of Plant Biology* 147(4): 898-904.
- [40] Nimis, P. L., John, V. (1998): A contribution to the lichen flora of Mediterranean Turkey. – *Cryptogamie: Bryologie, Lichénologie* 19: 35-58.
- [41] Nimis, P. L., Martellos, S. (2017): ITALIC - The Information System on Italian Lichens. Version 5.0. – University of Trieste, Dept. of Biology, <http://dryades.units.it/italic>, [Son erişim tarihi: 20.11.2019].
- [42] Nimis, P. L., Hafellner, J., Roux, C., Clerc, P., Mayrhofer, H., Martellos, S., Bilovitz, P. O. (2018): The lichens of the Alps—an annotated checklist. – *MycKeys* 31: 1.
- [43] Obermayer, W. (1998): *Dupla Graecensia Lichenum* 1998. – *Fritschiana* 6: 7-14.
- [44] Otálora, M. A., Jørgensen, P. M., Wedin, M. (2014): A revised generic classification of the jelly lichens, Collemataceae. – *Fungal diversity* 64(1): 275-293.
- [45] Özdemir Türk, A., Halici, M. G., Candan, M., Yavuz, Y. (2015): The lichenized fungus genus *Peltigera* in Turkey. – *Biological Diversity and Conservation* 8(2): 146-156.
- [46] Pérez-Ortega, S., Suija, A., Crespo, A., De los Ríos, A. (2014): Lichenicolous fungi of the genus *Abrothallus* (Dothideomycetes: Abrothallales ordo nov.) are sister to the predominantly aquatic Janhulales. – *Fungal Diversity* 64(1): 295-304.
- [47] Pišút, I. (1970): Interessante Flechtenfunde aus der Türkei. – *Preslia, Praha* 42: 370-383.
- [48] Pišút, I., Guttová, A. (2008): Contribution to the lichen flora of Anatolia, Turkey. – *Sauteria* 15: 403-415.
- [49] Prieto, M., Gregorio, A., Isabel, M. (2010): The genus *Catapyrenium* s. lat. (Verrucariaceae) in the Iberian Peninsula and the Balearic Islands. – *The Lichenologist* 42(6): 637-684.
- [50] Prieto, M., Mats, W. (2016): Phylogeny, taxonomy and diversification events in the Caliciaceae. – *Fungal Diversity* 82: 221-238.
- [51] Schiefelbein, U. (2006): Ökologische und naturschutzfachliche Aspekte der Flechtenflora des Landkreises Uecker-Randow (Mecklenburg-Vorpommern). – *Archiv naturwissenschaftlicher Dissertationen* 16: 1-216.
- [52] Schindler, H. (1998): Beitrag zur Flechtenflora von Westanatolien, Türkei. – *Herzogia* 13: 234-237.
- [53] Smith, C. W., Aptroot, A., Coppins, B. J., Fletcher, A., Gilbert, O. L., James, P. W., Wolseley, P. A. (2009): *The Lichens of Great Britain and Ireland*. – British Lichen Society, London, 1046 p.
- [54] Sørensen, T. (1948): A method of establishing groups of equal amplitude in plant sociology based on similarity of species and its application to analyses of the vegetation on Danish commons. – *Kongelige Danske Videnskabernes Selskab Biologiske Skrifter* 5: 1-34.
- [55] Suija, A., Pérez-Ortega, S. (2015): A molecular reappraisal of *Abrothallus* species growing on lichens of the order Peltigerales. – *Phytotaxa* 195(3): 201-226.
- [56] Tripp, E. (2017): *Field Guide to the Lichens of White Rocks: (Boulder, Colorado)*. – University Press of Colorado.
- [57] Tucker, S., Thiers, H. (1998): Key to crustose lichen genera of California. – *Bulletin of the California Lichen Society* 5(1): 1-18.
- [58] Tufan, Ö., Sümbül, H., Özdemir Türk, A. (2005): The lichen flora of the Termessos National Park in southwestern Turkey. – *Mycotaxon* 94: 43-46.
www.mycotaxon.com/resources/weblists.html

- [59] Tufan-Cetin, Ö., Sümbül, H. (2011): Lichens of the Köprülü Canyon National Park in Turkey. – Mycotaxon 115: 534-536. (in Regional annotated mycobiotas new to www.mycotaxon.com).
- [60] Tufan-Çetin, Ö. (2015): Phaselis Antik Kenti (Antalya) Likenleri I. – Phaselis 1: 133-141.
- [61] Tufan-Çetin, Ö. (2019): Determination of lichen diversity variations in habitat type of Mediterranean maquis and arborescent matorral. – Applied Ecology and Environmental Research 17: 10173-10193.
- [62] Vězda, A. (1996): Lichenes Rariores Exsiccati. Fasc. 22 (No 211-220). – Brno: 1-4.
- [63] Vondrák, J., Halici, M. G., Güllü, M., Demirel, R. (2016): Taxonomy of the genus *Athallia* and its diversity in Turkey. – Turkish Journal of Botany 40(3): 319-328.
- [64] Wirth, V. (1995): Die Flechten Baden-Württembergs. Teil: 1-2. – Eugen GmbH & Co. Stuttgart, 1006 p.
- [65] Yavuz, M., Çobanoğlu, G. (2007): Kozalak likenleri, TLT Antalya araştırma gezisinden liken kayıtları. – TLT bülteni 4: 5-6.
- [66] Yuan, X., Xiao, S., Taylor, T. N. (2005): Lichen-like symbiosis 600 million years ago. – Science 308(5724): 1017-1020.
- [67] Zeybek, U., John, V., Lumbsch, H. T. (1993): Türkiye likenlerinden *Hypogymnia* (Nyl.) Nyl. cinsi üzerinde taksonomik araştırma. – Doğa, Tr. J. of Botany 17: 109-116.

GENOTYPE × ENVIRONMENT INTERACTION OF SOME TRAITS IN SUNFLOWER (*HELIANTHUS ANNUUS* L.) LINES

RADIĆ, V.* – BALALIĆ, I. – MILADINOV, Z. – ĆIRIĆ, M. – VASILJEVIĆ, M. – JOCIĆ, S. – MARJANOVIĆ-JEROMELA, A.

*Institute of Field and Vegetable Crops, Maksima Gorkog 30, Novi Sad 21000, Serbia
(phone: +381-21-489-8100, fax: +381-21-641-3833)*

**Corresponding author*

e-mail: velimir.radic@nsseme.com; phone: +381-64-820-5743; fax: +381-21-641-3833

(Received 9th Oct 2019; accepted 4th Dec 2019)

Abstract. The evaluation of genotype × environment interaction (G×E) is an important component of the selection process in multi-environment trials. The objective of this study was to analyze the G×E interaction for seed yield (SY), germination rate (GR), thousand seed weight (TSW) and protein content (PC) of 18 sunflower parental lines through the application of AMMI analysis, as well as to identify suitable sunflower parental lines with both high performance and high stability. Highly significant differences for SY, GR, TSW and PC were found for main effects (genotypes, years). For all investigated traits G×E interaction was also highly significant, suggesting a different response of genotypes across testing environments. Highest SY was shown by genotypes G12, G14 and G17. Most stable lines for seed yield were G1, G2, G18 and G17. High stability in terms of GR showed the genotypes G3, G11 and G15, with average values higher than the general average. In the three-year experiment environment E3 was most stable for GR. Genotypes G2, G4, G5, G6 and G7 were stable for TSW. Similar average values and stability for TSW showed E2 and E3. The lines with the most stable reaction in the examined environmental conditions for PC were G7 and G10. The most stable environment for PC was E3.

Keywords: *AMMI analysis, germination rate, protein content, 1000 seed weight, seed yield*

Introduction

Sunflower (*Helianthus annuus* L.), with soybean (*Glycine max* (L.) Merr.) and rapeseed (*Brassica napus* L.), are some of the most important crops grown in the world and used as edible oil (Rauf et al., 2017; Kaya et al., 2019; Mahmood et al., 2019). It is arousing the interest of the producers, due to the possibility of using its oil as human food or as raw material for industrial purposes (Sabaghnia et al., 2016). High and stable yields are characteristics of greatest importance in commercial production. In the production of sunflower seed despite the yield, seed quality is very important. The primary goal of sunflower seed production is the production of genetically and physically pure seeds which are physiologically mature and healthy and have high germination rate as well as tolerance to agro-ecological stress (Miklić et al., 2011). Success in sunflower growing and production depends not only on the genetic potential of the genotype but also on environmental conditions (Denčić et al., 2011). Knowing how environmental factors impact plant growth and development would reduce the possibility of sustaining significant yield and seed quality losses (Marjanović-Jeromela et al., 2011). The use of genotype main effect plus genotype-by-environment interaction biplot analysis by plant breeders and other agricultural researchers has increased dramatically during the past decade for analyzing multi-environment trial data (Yan et al., 2007).

The researchers very often ignore interaction in the recommendation for growing some hybrids. As the interaction is present in agriculture, it is necessary to use

corresponding statistical methods for the efficient evaluation of interaction (Ceretta and van Eeuwijk, 2008). The key question of adaptive selection is how to treat mutual relations between genotype and the environment. Basic aspects of this relation concern the assessment of adaptive capacity and stability of phenotypes in different environments and the assessment of the environment's suitability as a background for selection (Marinković et al., 2011).

In multi-environment trials, it is common to measure several response variables or attributes to determine the genotypes with the best characteristics. Thus, it is important to have techniques to analyze multivariate multi-environment trial data (García-Peña et al., 2016). AMMI (additive main effects and multiplicative interaction) model can be used to analyze multiple yield trials (Oliveira et al., 2014). It is one of the most often used model (Ceretta and van Eeuwijk, 2008). This hybrid statistical model incorporates both ANOVA for the additive component and PCA (principal component analysis) for the multiplicative component (Balalić et al., 2010). Since ANOVA and PCA are part of the AMMI model, this model is more suitable for characterizing the G×E interaction (Oliveira et al., 2006). The other advantage of AMMI analysis is to identify the presence of crossover GE Interaction (Kadhem, 2014). The magnitude of interaction shows the influence of environmental factors on adaptability and stability, which is a desired character only when it is connected with a yield above average (Yan and Hunt, 2003). AMMI model can provide an accurate estimation of the true performance potential of genotypes to determinate the effect of different environment (Musavi et al., 2016). Multi-environment trials (MET) are an important part of breeding programs in order to select superior genotypes for the specific region, as reported by Branković et al. (2012).

This study was conducted to give more accurate investigation about the performance of 18 different sunflower parental lines in order to identify those which are most promising for better exploitation. AMMI analysis will give information on stability and genotype by environment interaction for seed yield, germination rate, thousand seed weight and protein content of sunflower lines.

Materials and methods

Field experiments were conducted during three seasons on plots where seed production of sunflower parental lines was established. Ten of them were lines based on CMS (G1-G10) and eight of them were restorer lines (G11-G18). All examined genotypes represent parental components of the best-selling sunflower hybrids of the Institute of Field and Vegetable Crops, Novi Sad, Serbia.

The test environments are not typically environments for sunflower commercial production, since idea of successful sunflower seed production can be arranged only on locations where commercial sunflower is not producing (isolation and genetic purity of parental lines are one the most important factors for good seed production). Because of these facts (conditions), in many cases, the locations where the sunflower seed production (especially in cases of sunflower parental line seed production) are characterized by worse conditions (mainly refers to the quality of the soil and weather conditions). The average temperature and rainfall for both locations are presented in *Table 1*.

Plants were produced on two different soil types: pseudogley (location 1; pH is 5.9-6.5) and degraded chernozem (Location 2; pH 6.2-6.6); the soil is fertilized with 400 kg of complex fertilizer NPK (15:15:15) and 250 kg of KAN (27% N) given during crop cultivation.

Table 1. Average temperature (°C) and rainfall (mm) per month

Temperature (°C)		Location 1				
Year/month	April	May	June	July	August	September
2013	11.6	20.5	24.8	23.2	24.9	16.8
2014	11.5	18.8	22.2	23.3	21.7	16.3
2015	12.6	15.4	20.3	22.6	22.0	16.4
Perennial average	10.9	15.9	19.4	21.0	20.5	16.1
		Location 2				
2013	10.9	18.8	23.5	22.3	23.6	15.6
2014	10.9	17.6	20.8	22.4	20.5	15.2
2015	12.1	14.5	19.5	21.3	20.6	15.6
Perennial average	11.1	16.3	19.89	21.3	20.9	16.1
Rainfall (mm)		Location 1				
Year/month	April	May	June	July	August	September
2013	9.5	36.9	43.6	62.3	15.9	43.7
2014	62.8	143.7	47.3	37.8	55.3	71.9
2015	98.6	116.1	87.7	97.9	91	46.7
Perennial average	78.8	86.5	115.2	105.1	70.2	91.6
		Location 2				
2013	35.9	42.6	65.6	100.9	30	53.4
2014	114.7	194.2	59.8	54.1	160.8	87.4
2015	189.9	104.8	129.5	148.6	68.7	60.5
Perennial average	80.0	85.3	120.3	104.7	78.2	94.2

The experiments were arranged in a randomized complete block design (RCBD) with three replications. The following parameters were studied:

Seed yield (SY): Upon maturity, 10 plants were picked manually, from different locations on the plot, and seed yield per plant was determined. By the application of previously determined plant density ($50.000 \text{ plants ha}^{-1}$), obtained seed yield per plant was determined in kg ha^{-1} with 9% of moisture.

Samples from each replication were taken to laboratory and following parameters were studied:

Germination rate (G): Standard method. Examination of seed germination was repeated 4 times. Each time 100 seeds were used. Germination was determined after 10 days. Only naturally formed seeds were used for determination of this parameter. Germination was expressed in relative values (ISTA rules, 2014).

1000 seed weight (TSW): Examination of 1000 seed weight was repeated 4 times. Each time 100 seeds were used. The obtained value was applied to 1000 seed weight and was specified in grams.

Protein content (PC): Determined by standard Kjeldahl method with the help of VAP-50-Gerhardt apparatus. This parameter is also expressed in relative value.

Data were analyzed using two-way analysis of variance (ANOVA). The AMMI model was used to analyze the $G \times E$ interaction (Gauch, 1988). AMMI analysis of variance and AMMI1 biplot were done using GENSTAT computer program.

To analyze the $G \times E$ interaction, the AMMI model was used (Gauch, 1988). The AMMI statistical model is a combination of customary analysis of variance (ANOVA) and principal component analysis (PCA). The equation (Eq. 1) of this model is:

$$Y_{ge} = \mu + \alpha_g + \beta_e + \sum_n \lambda_n \gamma_{gn} \delta_{en} + \rho_{ge} + \varepsilon_{ger} \quad (\text{Eq.1})$$

with Y_{ge} is the trait of genotype g in environment e ; μ is the grand mean, α_g is the genotypes deviation from grand mean and the environment deviation β_e , λ_n is the eigenvalue of PCA axis n ; γ_{gn} and δ_{en} are the genotype and environment PCA scores for PCA axis n ; ρ_{ge} is the residual of AMMI model and ε_{ger} is the random error. AMMI uses ordinary ANOVA to analyze main effects and principal component to analyze the non-additive residual (interaction) left over by the ANOVA model. PCA decomposes the interaction into PCA axes 1 to N and residual remains if all axes are not used. If most of the $G \times E$ interaction sum of squares (SS) can be captured in the first N PCA axes, a reduced AMMI model, incorporating only the first N axes, can be used. The interaction between any genotype and environment can be estimated by multiplying the score of the interaction principal component axis (IPCA) of genotype by an environment IPCA score.

Results and discussion

Seed yield (SY)

Breeders are mainly concerned with crop yield and yield stability and this performance depends on the genetic yield potential; all those desirable genes that have been incorporated into a cultivar in the course of the breeding process (Marinković et al., 2011). According to these authors yield stability depends on the cultivar's capacity to react to environmental conditions.

On the basis of ANOVA, it can be seen that both main effects (G and Y) and interaction ($G \times Y$) had a highly significant effect on SY. For SY, main effects and interaction were highly significant. SY was predominantly influenced by the genotype (81.62%). Year amounted to SY with 0.38%, and interaction with 18.00% (Table 2). This interaction (sums of squares) showed different performance of genotypes in the year of growing. According to Marinković et al. (2011), the results of the AMMI analysis of variance for the seed yield showed that both additive effects (genotype and environmental conditions) as well as their interaction had highly significant proportions in the total variance of the experiment.

The SY varied between 253.3 kg (G4) and 1415.9 kg (G12). The general mean germination rate of the trial was 664.07 kg (Table 3). Some of the genotypes had mean values over this average value. Concerning years (E) the highest mean value for SY was stated in E3 (696.4 kg), while the lowest in E2 (645.2 kg), as shown in Table 3. According to Sial and Ahmad (2000) high seed yield should not be the only criterion for stability of a genotype unless its high performance is established over the different environmental conditions. The AMMI1 graph for SY shows the difference between the lines (G) and the years (E) in the main effects and interaction. Most stable are lines G1, G2, G18 and G17 and they had also seed yield over average. There are some other stable lines, but with lowest seed yield concerning the average which was 664.7 kg/ha. E1 (the year 2013) was most stable because its value was nearest to the line of stability

and had seed yield on the average value. E3 (the year 2015) contributed most to $G \times E$ interaction, having value farthest away from stability axes (*Fig. 1*).

Table 2. AMMI analysis of variance for seed yield (SY), germination (GR), 1000 seed weight (TSW) and protein content (PC) in sunflower

Source	DF	SY		GR		TSW		PC	
		SS	% SS	SS	% SS	SS	% SS	SS	% SS
Treatments	53	22484625		3478		38889		1178.3	
Genotypes (G)	17	18350901**	81.62	1294**	37.21	35597**	91.53	657.7**	55.82
Environments (E)	2	85643**	0.38	430**	12.36	412**	1.1	109.1**	9.26
Block	6	402		28		2		0.3	
Interaction (GEI)	34	4048081**	18.00	1754**	50.43	2880**	7.41	411.5**	34.92
IPCA1	18	2702041**	66.75	1393**	79.42	1661**	57.67	363.1**	88.24
IPCA2	16	1346040**	33.25	361**	20.58	1218**	42.29	48.4**	11.76
Residuals	0	0		0		0		0	
Error	102	3174		380		54		2.7	

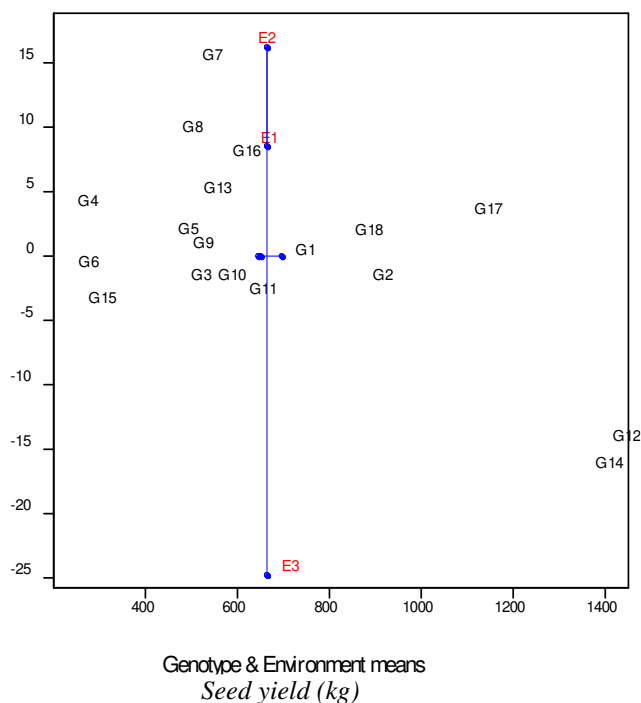


Figure 1. AMMI 1 biplot of 18 sunflower lines over three growing environments for seed yield

Germination rate (GR)

Understanding of $G \times E$ interaction in plant species is important because it has implications for economic yield and seed quality (Thangavel et al., 2011). The size of the genotype interaction × external environment ($G \times E$) is the result of variation of uncontrolled factors, such as climate factors that are varying from year to year (Adugna and Labuschagne, 2002). Germination seed under various environmental conditions and represents a critical component of the plant life cycle that is of eminent ecological and

agronomic importance (He et al., 2014). It has been observed that a change of temperature, photoperiod, or nutrient or drought stress, during seed development, maturation, and after dispersal, may strongly affect seed performance (Donohue, 2009). On the basis of ANOVA, it can be seen that both main effects (G and Y) and interaction (G × Y) had a highly significant effect on GR. From the main effects, genotype contributed mostly to the GR (37.21%), and then environment (12.36%). The interaction effect accounted for most of the sum of squares (50.43%) indicating the substantial effect of interaction on the GR performance of the eighteen sunflower genotypes evaluated in this study. Interaction showed that the performance of genotypes responded differently to variations in the year of growing (Table 2).

Table 3. Average values for seed yield (SY) and germination rate (GR) and first IPCA (interaction principal component axis) in sunflower lines

Genotype	SY (kg)	IPCA[1]	GR (%)	IPCA[1]
G1	726.3	-0.21	89.00	1.81
G2	894.0	-2.13	80.22	1.74
G3	499.3	-2.13	89.33	-0.13
G4	253.3	3.62	88.00	0.61
G5	471.3	1.40	84.00	1.29
G6	255.3	-1.11	87.22	-1.27
G7	523.9	14.94	86.44	0.84
G8	481.3	9.37	88.44	0.47
G9	504.3	0.36	88.00	-1.95
G10	558.0	-2.16	84.33	-1.65
G11	626.3	-3.26	88.89	0.16
G12	1415.9	-14.64	88.67	-0.95
G13	526.7	4.64	91.33	-1.23
G14	1378.7	-16.69	83.33	0.39
G15	276.7	-3.91	87.67	-0.37
G16	590.3	7.53	92.00	0.49
G17	1115.6	2.97	85.00	0.62
G18	856.0	1.38	87.78	-0.89
E1	650.6	8.54	85.44	-3.70
E2	645.2	16.22	89.37	2.58
E3	696.4	-24.76	86.80	1.12

It is very important that sunflower seed quality be maintained at a high level in different production conditions (Mrđa et al., 2012). The same finding was obtained by Pacheco et al. (2005), who reported that sunflower seed is greatly influenced by environmental factors, which most often results in high variability, both among different years in a single location and among different locations in a single year as well as among different locations and years. The GR varied between 80.22% (G2) and 92.00% (G16). The general mean germination rate of the trial was 87.2% (Table 3). Some of the genotypes had mean values over this average value. Concerning years (E) the highest mean value for GR was stated in E2 (89.37%), while the lowest in E1 (85.44%), as shown in Table 3. The same finding was obtained by Pacheco et al. (2005), who reported that

sunflower seed is greatly influenced by environmental factors, which most often results in high variability, both among different years in a single location and among different locations in a single year as well as among different locations and years.

AMMI is the best model in multi-environmental experiments. It provides an understanding of complex genotype by environment interactions (Gauch, 2006). AMMI1 biplot in our experiment showed that the sunflower genotypes were grouped on the basis of their reaction to environmental conditions which prevailed in the three-year period. From the AMMI1 biplot, it can be seen that it was a significant difference in GR for main effects (G, E) and for the interaction (G×E). Lower IPCA values for genotypes (lines) and environments (years) suggest lower interaction level and therefore higher stability (Gauch, 2006). The genotypes G3, G11 and G15, with mean values higher than the general average (87.2%) showed high stability for GR. Their position in relation to the abscissa indicates that it had similar GR in all environments. These genotypes contributed least to the G×E interaction, as they were closer to the center of origin of the axes. Genotypes G16 and G13, had the highest mean values for GR but had less stability. The genotypes farthest away from the graphic's origin contributed most to increase the G×E interaction for GR, such as G1, G2, G9 and G10 (Fig. 2).

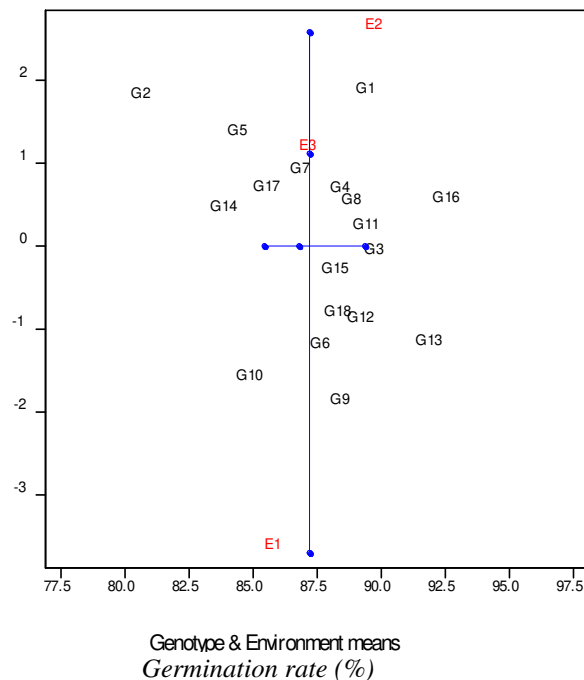


Figure 2. AMMI 1 biplot of 18 sunflower lines over three growing environments for germination rate

The lowest interaction effect was registered in E3, which was most stable in the three-year investigation. Genotypes with mean values on the average (G7) and over average (G4, G8) showed positive interaction with E3. G1 showed highest interaction effect on the positive side of IPCA. The highest interaction on the negative side of IPCA was evident in G9. Negative interaction with E2 had genotype G10, with mean values lower than average. G10 showed positive interaction with the first year of the experiment. Close positions on the graph of the lines G4, G8 and G11 suggest that they require similar environmental conditions which can be used in seed production. Similar

associations can be found between genotypes G6, G12 and G18. Among the environments, the highest level of stability was found in the E3, while the positions E1 and E2 at the ends of the graph suggest that they can be marked as very unstable for the trait of germination rate. Opposite positions of the environments E1 and E2 suggest that these environments have very different growing conditions for the examined trait.

1000 seed weight (TSW)

It is very important that the sunflower hybrid seed, which is used for sowing, has a high value of thousand seed mass. Such seed conserve more food reserves and plants that develop from embryos grow faster, which is often very important in unfavorable agro-ecological conditions (Balalić et al., 2012). Considering the fact that there is a significant positive correlation between the mass of 1000 seeds and yield (Kaya et al., 2007), it is in interest to use hybrids with as high values of this trait. All sources of variation, main effects and interaction, for TSW were highly significant. TSW was predominantly influenced by the genotype (91.53%). Year amounted to TSW with 1.10%, and interaction with 7.41% (Table 2). The TSW varied from 28.3 g (G12) to 79.10 g (G2), with a mean average of 55.7 g. The environment with highest TSW was E2 (57.9 g), while the E1 had the lowest average of TSW (53.9 g) (Table 4). Based on experiment carried out under Iranian conditions, the mass of 1000 seeds ranged between 36.0 g and 50.0 g (Beg et al., 2007), while the values obtained by Nel (2001) during the two-year experiment in the conditions of South Africa ranged between 59.4 g 78.5 g. Based on a test of 13 hybrids during a four-year experiment in the conditions of central Italy, Laureti et al. (2007) obtained that the 1000 seeds average mass was 45.2 g. Values closer to the stability line (0) indicate stabile genotypes or stable years in relation to genotypes. Genotypes G2, G4, G5, G6 and G7 were stable for TSW because their values are nearest to the line of stability (Fig. 3).

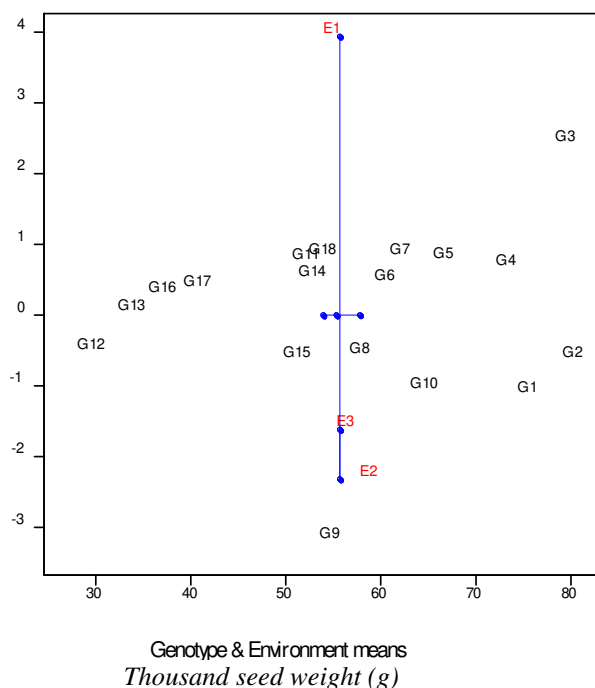


Figure 3. AMMI 1 biplot of 18 sunflower lines over three growing environments for thousand seed weight

Table 4. Average values for 1000 seed weight (TSW) and protein content (PC) and first IPCA (interaction principal component axis) in sunflower lines

Genotype	TSW (g)	IPCA[1]	PC (%)	IPCA[1]
G1	74.37	-1.14	21.94	0.80
G2	79.10	-0.65	20.47	0.64
G3	78.33	2.42	17.99	0.36
G4	72.10	0.66	20.64	0.42
G5	65.50	0.76	20.32	0.60
G6	59.34	0.45	20.40	0.50
G7	60.97	0.81	19.66	0.30
G8	56.71	-0.58	20.51	0.52
G9	53.52	-3.20	20.50	0.57
G10	63.10	-1.08	20.01	0.35
G11	50.69	0.75	17.98	-2.32
G12	28.03	-0.53	17.27	-1.19
G13	32.30	0.02	15.32	0.14
G14	51.33	0.50	15.85	-0.08
G15	49.70	-0.65	15.81	0.23
G16	35.57	0.28	18.03	-0.36
G17	39.23	0.37	16.49	-0.92
G18	52.42	0.81	16.51	-0.59
E1	53.94	3.94	19.71	-2.67
E2	57.79	-2.32	18.54	1.74
E3	55.32	-1.62	17.71	0.92

They had also higher average values in relation to the general average (55.7 g). G3 showed high mean value for TSW, but it was unstable. The lines with the high levels of IPCA scores (Table 4) were G3, G9 and G12 which is in accordance with their positions on the graph. Genotypes G13 and G12 had very high stability for this trait, but the lowest mean values for TSW. Positive interaction for TSW was stated for G3, which had the highest value for this trait, but was very unstable. Genotypes G10, G8, G15 on the negative side of IPCA were in interaction with E2 and E3. E1 had the highest IPCA score and was highly unstable environment from the aspect of TSW. It had the highest positive interaction effect for TSW, and mean value on the average level. Environments E2 and E3 had similar mean values and stability. Values of all environments varied around the average TSW axis. Also, lines with similar IPCA results can be separated into specific groups such as lines G6, G7 and G5, also lines G14, G11 and G18 create another distinct association.

Protein content (PC)

The protein content ranges from 13-20% in sunflower. Majority of existing proteins in fully developed seeds have structural or metabolic roles. Besides these roles, proteins in seeds also serve to provide a store of amino acids needed for germination and early seedling growth (Shewry et al., 1995). Results of ANOVA indicated that the main

effects and interaction were highly significant for PC. The influence of genotype on PC amounted to 55.82%, of the year to 9.26% and of interaction to 34.92% (Table 2). The values of the protein content were between 15.3% (G13) and 21.9% (G1). The general average value of the trial was 18.7%. The environment with the highest protein content was E1 (19.7%), while E3 (17.7%) has the lowest average value for this trait (Table 4).

From the aspect of protein content, the lines with the most stable reaction in the examined environmental conditions were G7 and G10. They had a PC over general average (18.7%) and were stable for this trait. High stability showed also G14, G15 and G13, but they had lowest mean values for PC. Genotype with the highest protein content was G1, but it was unstable. The environment with the lowest IPCA score for PC was E3. IPCA value of E2 was similar to E3 while the E1 had diametrically opposite reaction. It was the most unstable environment because it was furthest from the line of stability (0). G3 was in the positive interaction with E3. The most unstable environment was E1 because it was furthest from the line of stability (0). E2 had an average value on the general average. Specific groups of lines with similar IPCA scores such as G13, G15 and G14, also G2, G6, G8 and G9 can be marked out for they similar reaction to environmental conditions (Fig. 4).

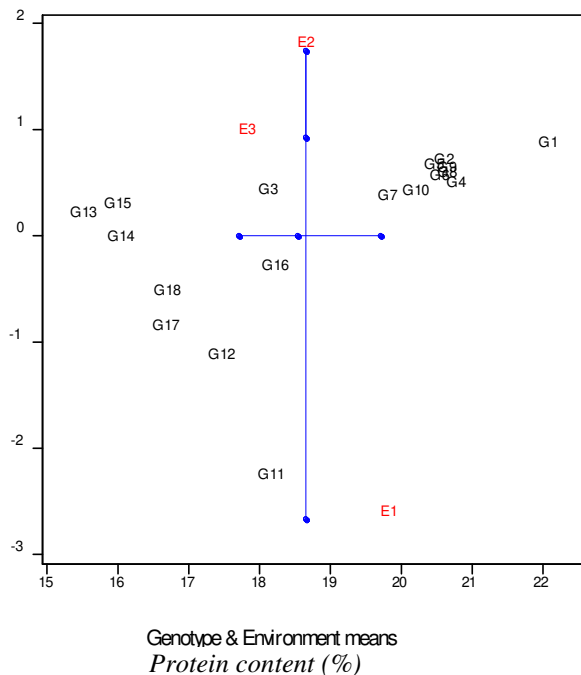


Figure 4. AMMI 1 biplot of 18 sunflower lines over three growing environments for protein content

An ideal genotype is defined as one that is the highest yielding across all test environments and is absolutely stable in performance, namely one that ranks the highest in all test environments (Yan et al., 2003; Pourdad and Moghaddam, 2013). Although such an ideal cultivar may not exist in reality, it can be used as a reference for cultivar evaluation. A genotype is more desirable if it is located closer to the ideal cultivar. Thus, using the ideal cultivar as the center, concentric circles were drawn to help visualize the distance between each genotype and the ideal cultivar (Yan, 2002; Pourdad and Moghaddam, 2013).

Conclusion

On the basis of the analyses of seed yield, germination rate, thousand seeds weight:

The AMMI ANOVA indicated that main effects (G, E) were highly significant for SY, GR, TSW and PC. G × E interaction also was highly significant for all investigated traits, suggesting a differential response of genotypes (lines) across testing environments (years).

Highest mean values for yield and stability had genotypes G12, G14 and G17. The genotypes G3, G11 and G15, with mean values higher than the general average showed high stability for GR. Environment E3 was most stable for GR in the three-year investigation. Genotypes G2, G4, G5, G6 and G7 were stable for TSW because their values were nearest to the line of stability. Environments E2 and E3 had similar mean values and stability for TSW. From the aspect of protein content, the lines with the most stable reaction in the examined environmental conditions were G7 and G10. For PC the environment E3 was most stable. The method successfully integrate the attributes measured in the multi-environment trial. The analysis helps the breeder make decisions in favor of moderate to high seed yield, 1000 seed weight and protein content with good seed germination to moderate sunflower hybrids in general or in selected environments. The combination of analysis of variance and principal component analysis in the AMMI model, along with the prediction assessment, is a valuable approach for understanding genotype × environment interaction.

Based on the obtained results we can conclude that sunflower lines G2, G12 and G14 developed at Institute of Field and Vegetable Crops Novi Sad are suitable for high yield production and all other observed parameters. Crossing this lines Institute created new hybrids NS FELIKS and NS KRUNA (both hybrids were registered in the EU and Serbia). The seeds of these hybrids Institute of Field and Vegetable Crops sales in the domestic and foreign markets. A further objective of this research will be observation of new created lines and their behavior in different years of production.

Acknowledgements. This research is part of the project 31025: Development of new varieties and production technology improvement of oil crops for different purposes, sponsored by the Ministry of Education, Science and Technological Development of the Republic of Serbia.

REFERENCES

- [1] Adugna, W., Labushange, M. T. (2002): Genotype-environment interactions and phenotypic stability analysis of linseed in Ethiopia. – *Plant Breeding* 121(1): 66-71.
- [2] Balalić, I., Crnobarac, J., Miklič, V. (2010): Interaction hybrid × planting date for oil yield in sunflower. – *Journal of Agricultural Science* 55(1): 9-16.
- [3] Balalić, I., Zorić, M., Crnobarac, J. (2012): Interpretacija interakcije hibrida i roka setve za masu 1000 semena suncokreta. – *Ratarstvo i povrtarstvo* 49(3): 229-235.
- [4] Beg, A., Pourdad, S. S., Pala, M., Oweist, T. (2007): Effect of supplementary irrigation and variety on yield and some agronomic characters of sunflower grown under rainfed conditions in northern Syria. – *Helia* 30(47): 87-98.
- [5] Branković, G., Balalić, I., Zorić, M., Miklič, V., Jocić, S., Šurlan Momirović, G. (2012): Characterization of sunflower testing environments in Serbia. – *Turkish Journal of Agriculture and Forestry* 36(3): 275-283.

- [6] Ceretta, S., van Eeuwijk, F. (2008): Grain yield variation in malting barley cultivars in Uruguay and its consequences for the design of a trials network. – *Crop Science* 48(1): 167-180.
- [7] Denčić, S., Mladenov, N., Kobiljski, B. (2011): Effects of genotype and environment on breadmaking quality in wheat. – *International Journal of Plant Production* 5(1): 71-82.
- [8] Donohue, K. (2009): Completing the cycle: maternal effects as the missing link in plant life histories. – *Philosophical Transactions of the Royal Society B: Biological Sciences* 364(1520): 1059-1074.
- [9] García-Peña, M., Arciniegas-Alarcón, S., Basford, K., dos Santos Dias, C. T. (2016): Analysis of sunflower data from a multi-attribute genotype × environment trial in Brazil. – *International Journal of Agricultural and Biological Sciences* 11(2): 127-139.
- [10] Gauch, H. G. (1988): Model selection and validation for yield trials with interaction. – *Biometrics* 44(3): 705-715.
- [11] Gauch, H. G. Jr. (2006): Statistical analysis of yield trials by AMMI and GGE. – *Crop Science* 46(4): 1488-1500.
- [12] He, H., de Souza Vidigal, D., Snoek, L. B., Schnabel, S., Nijveen, H., Hilhorst, H., Bentsink, L. (2014): Interaction between parental environment and genotype affects plant and seed performance in *Arabidopsis*. – *Journal of Experimental Botany* 65(22): 6603-6615.
- [13] ISTA Rules (2014): International Rules for Seed Testing. – International Seed Testing Association, Zurich.
- [14] Kadhem, F. A. (2014): Additive main effect and multiplicative interaction analysis of yield stability performance in sunflower genotypes grown in Iraqi environment. – *The Iraqi Journal of Agriculture Science* 45(8): 932-939.
- [15] Kaya, Y., Evcı, G., Durak, S., Pekcan, V., Gücer, T. (2007): Determining the relationships between yield and yield attributes in sunflower. – *Turkish Journal of Agriculture and Forestry* 31(4): 237-244.
- [16] Kaya, M. D., Akdogan, G., Kulan, E. G., Dağhan, H., Sari, A. (2019): Salinity tolerance classification of sunflower and safflower. – *Applied Ecology and Environmental Research* 17(2): 3849-3857.
- [17] Laureti, D., Del Gatto, A., Pieri, S. (2007): Commercial sunflower hybrid evaluation in east central Italy. – *Helia* 30(47): 141-144.
- [18] Mahmood, H. N., Towfiq, S. I., Rashid, K. A. (2019): The sensitivity of different growth stages of sunflower (*Helianthus annuum*) under deficit irrigation. – *Applied Ecology and Environmental Research* 17(2): 7605-7623.
- [19] Marinković, R., Jocković, M., Marjanović-Jeromela, A., Jocić, S., Ćirić, M., Balalić, I., Sakač, Z. (2011): Genotype by environment interactions for seed yield and oil content in sunflower (*H. annuum*) using AMMI model. – *Helia* 34(54): 79-88.
- [20] Marjanović-Jeromela, A., Nagl, N., Gvozdanović-Varga, J., Hristov, N., Kondić-Špika, A., Vasić, M., Marinković, R. (2011): Genotype by environment interaction for seed yield per plant in rapeseed using AMMI model. – *Pesquisa Agropecuaria Brasileira* 46(2): 174-181.
- [21] Miklič, V., Dušanić, N., Jocić, S. (2011): Sunflower Seed Production. – In: Milošević, M., Kobiljski, B. (eds.) Seed Production. Vol 2. Institute of Field and Vegetable Crops, Novi Sad, pp. 196-264 (in Serbian).
- [22] Mrđa, J., Crnobarac, J., Radić, V., Miklič, V. (2012): Sunflower seed quality and yield in relation to environment conditions of production region. – *Helia* 35(57): 123-134.
- [23] Musavi, S. M. N., Hejazi, P., Khalkhali, S. K. Z. (2016): Study on stability of grain yield sunflower cultivars by AMMI and GGE bi plot in Iran. – *Molecular Plant Breeding* 7(2): 1-6.
- [24] Nel, A. A. (2001): Determinants of sunflower seed quality for processing. – Ph. D. Diss. Univ. of Pretoria, Pretoria, Republic of South Africa. <http://upetd.up.ac.za/thesis/available/etd-09012001-132144/> (accessed on 21 Aug 2014).

- [25] Oliveira, E. J., Godoy, I. J. (2006): Pod yield stability analysis of runner peanut lines using AMMI. – *Crop Breeding and Applied Biotechnology* 6(4): 311-317.
- [26] Oliveira, E. J., Xavier de Freitas, J. P., Nunes de Jesus, O. (2014): AMMI analysis of the adaptability and yield stability of yellow passion fruit varieties. – *Scientia Agricola* 71(2): 139-145.
- [27] Pacheco, R. M., Duarte, J. B., Vencovsky, R., Pinheiro, J. B., Oliviera, A. B. (2005): Use of supplementary genotypes in AMMI analysis. – *Theoretical and Applied Genetics* 110(5): 812-818.
- [28] Pourdad, S. S., Moghaddam, M. J. (2013): Study on seed yield stability of sunflower inbred lines through GGE biplot. – *Helia* 36(58): 19-28.
- [29] Rauf, S., Jamil, N., Tariq, S. A., Khan, M., Kausar, M., Kaya, Y. (2017): Progress in modification of sunflower oil to expand its industrial value. – *Journal of the Science of Food and Agriculture* 97(7): 1997-2006.
- [30] Sabaghnia, N., Janmohammadi, M. (2016): Biplot analysis of silicon dioxide on early growth of sunflower. – *Plant Breeding and Seed Science* 73(1): 87-98.
- [31] Shewry, R. P., Napier, A. J., Tatham, S. A. (1995): Seed storage proteins: structures and biosynthesis. – *The Plant Cell* 7(7): 945-956.
- [32] Sial, M. M., Arain, M., Ahmad (2000): Genotype × environment interaction on bread wheat grown over multiple sites and years in Pakistan. – *Pakistan Journal of Botany* 32(1): 85-92.
- [33] Thangavel, P., Anandan, A., Eswaran, R. (2011): AMMI analysis to comprehend genotype-by-environment ($G \times E$) interactions in rainfed grown mungbean (*Vigna radiata* L.). – *Australian Journal of Crop Science* 5(13): 1767-1775.
- [34] Yan, W. (2002): Singular- value partitioning for biplot analysis of multienvironment trial data. – *Agronomy Journal* 94(5): 990-996.
- [35] Yan, W., Hunt, L. A. (2003): Biplot Analysis of Multienvironment Trial Data. – In: Kang, M. S. (ed.) *Quantitative Genetics, Genomics, and Plant Breeding*. CAB International, Wallingford, Oxon, UK, pp. 289-313.
- [36] Yan, W., Kang, M. S. (2003): *GGE Biplot Analysis: A Graphical Tool for Breeders, Geneticists and Agronomists*. 1st Ed. – CRC Press, Boca Raton, FL.
- [37] Yan, W., Kang, M. S., Ma, B., Woods, S., Cornelius, P. L. (2007): GGE Biplot vs. AMMI analysis of genotype-by-environment data. – *Crop Science* 47(2): 641-653.

HEAVY METAL RESISTANCE AND METALLOTHIONEIN INDUCTION IN BACTERIA ISOLATED FROM SEYBOUSE RIVER, ALGERIA

BENHALIMA, L.^{1*} – AMRI, S.¹ – BENSOUILAH, M.² – OUZROUT, R.²

¹*Department of Biology, Faculty of the Nature and the Life Sciences and the Earth and the Univers Sciences, Université 8 Mai 1945 Guelma, Algeria*

²*Laboratory of Ecobiology of Marine Environment and Coastlines, Faculty of Science, Badji Mokhtar University, Annaba, Algeria*

*Corresponding author

e-mail: lamia-kos1@hotmail.fr, benhalima.lamia@univ-guelma.dz; phone: +213-663-479-379

(Received 10th Oct 2019; accepted 23rd Jan 2020)

Abstract. Heavy metal pollution is a serious and widespread environmental problem that destroys microbial ecology. In this study, determination of copper and cadmium concentrations and heavy metal-resistant bacteria identification in water samples obtained from four sites at Seybouse River in Algeria were carried out. The minimum inhibition concentration (MIC) and minimum bactericidal concentration (MBC) were determined in culture media with 12.5-3600 µg/mL of cadmium and copper salts. Metallothionein (MT) production was evaluated by spectrophotometry methodology. Trace metal element concentrations determined in the water samples revealed spatial variations for Cu and Cd. A total of 12 copper- and cadmium-resistant bacteria (KZ1-KZ12) were isolated from surface water in Seybouse River. Five isolates KZ2, KZ5, KZ8, KZ10 and KZ11 showed high values of minimum inhibitory concentration (MIC = 3600 µg/mL) for each heavy metal. High MBC of the strain toward Cu and Cd was found to be >3600 µg/mL. The MT concentration in five best isolates which showed high resistances increased with increasing metal concentration ($r = 0.936$, $p = 0.006$). High levels of MT are detected in bacterial strains exposed to Cd (51.66-90.53 nmol MT/g bacterial biomass). These indicated that the isolates can be used efficiently in removal of heavy metals in contaminated sites.

Keywords: *cadmium, copper, MIC, MBC, protein-binding*

Introduction

Heavy metals are the main group of inorganic pollutants which are continuously accumulating in our environment (Manasi and Rajesh, 2016). In many developed and developing countries the heavy metal pollution has risen due to rapid industrialization, mining operations, discharge of industrial wastes, long term use of poor quality waters for irrigation and intensive agricultural practices (Rizvi et al., 2019). In recent years, heavy metal pollution in rivers, estuaries, and near-shore waters has become a serious problem (Li et al., 2015). At high concentrations, cadmium and copper which are major contaminants found in the environment, are extremely poisonous to human(s), animals, plants and microbes which can damage cell membranes, alter particularity of enzymes, destroy the structure of DNA, bind the vital protein and cause further discrepancies (Jaishankar et al., 2014; Marzan et al., 2017). In regards to bacteria cells, pollution by heavy metals affects every aspect of bacterial metabolism and activity, structural inconsistency of the cytoplasmic membrane, retardation of the onset of growth, extending the lag phase of cultures, various structural abnormalities, decrease in the respiratory activity and death of the cells are some of the predominant ones (Aljerf and Almasri, 2018).

Selective pressures from metal containing environments have led to the development of resistance systems in microorganisms to virtually all toxic metals. Bacteria strains have an array of mechanisms to deal with elevated concentrations of heavy metals and are often precise for one or few metals. This is achieved in different ways either through biological, physical, or chemical systems which include precipitation, complexation, adsorption, transport, product excretion, pigments, polysaccharides, enzymes, and specific metal binding proteins (Gupta and Diwan, 2017; Mutiat et al., 2018). Cysteine rich metallothionein proteins play an important role in immobilization of toxic heavy metals within the bacterial cell; thereby protecting their enzyme catalyzed metabolic processes (Choudhary, 2019). The thiol groups of cysteine residues enable MTs to bind essential and non-essential metals with high affinity (Li et al., 2015). Due to metal detoxification property bacteria possessing metallothioneins are considered an ideal tool for bioremediation of heavy metal contaminated environments (Choudhary, 2019). Moreover, MT has been used as a biomarker of metal exposure in several ecotoxicological investigations (Mikawska et al., 2018).

Being an industrial city, Guelma province (Northeast of Algeria) is facing pollution problems. Heavy metals discharged from industries and agricultural activities pose threat to human population, aquatic biodiversity as well as agricultural environment. There are multiple causes for the water contamination in the Seybouse River Basin, which has been identified as one of the polluted rivers in Guelma province (Guettaf et al., 2014; Talbi and Kachi, 2019). Currently, direct diversion of untreated waste water from municipal areas, industrial wastage and extensive agricultural practices are observed along the banks of the Seybouse River. Land degradation is becoming a serious problem in the area, and recent studies have shown that the waters of the Seybouse River contain a series of heavy metals (Belabed et al., 2017; Talbi and Kachi, 2019).

One of the best ways to remove heavy metals from the environment, which recently have attracted a lot of interest, is the use of microorganisms. The use of microorganisms not only low cost and safe for the environment, but also has a high yield and is readily available (Mohseni et al., 2014). So, the study of bacteria with different resistance mechanisms is urgent, in order to discover potential candidates for the bio-removal of contaminants of diverse origins from the environment (Giovannella et al., 2017).

In this context, the present study aims to evaluate the levels of contamination by copper and cadmium in the surface waters of Seybouse River Basin, to isolate copper-resistant and cadmium-resistant bacteria, to identify those bacteria and their ability to induce metallothionein as a fundamental research to ensure the basis of their resistance in order to use them for detoxification in further bioremediation studies.

Materials and Methods

Site description and sample collection

The study area is located in the Seybouse watershed (*Fig. 1*), which is situated in the extreme Northeast of Algeria with a surface of about 6,471 km² and has a population of 1.5 million. The river basin lies within the territories of Guelma province, El-Taref province (near Drea), and Annaba province. It is bordered in the north by the Mediterranean Sea, in the south by the Wilaya of Souk-Ahras, in the west by Edough Massif, Lake Fetzara, and in the east by Mafragh wadi (Louhi et al., 2012). Water of Seybouse River contributes in the irrigation of the plains of Guelma and Annaba provinces. The area is characterized by an annual average rainfall of 600 mm, a more or

less cool winter and a hot dry summer (Guettaf et al., 2014). Water samples were collected from four sites (S1, S2, S3, S4) in the middle of the Seybouse Basin (Guelma province) (Fig. 1). The characteristics of the sampling sites are shown in Table 1.

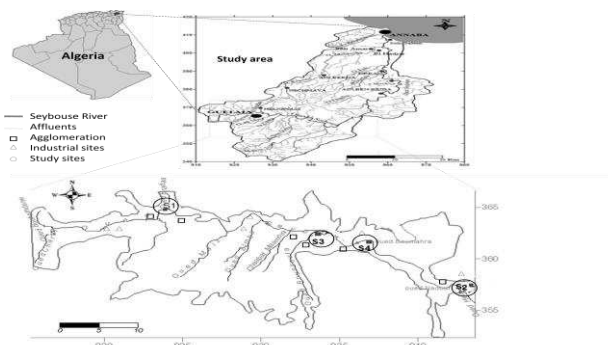


Figure 1. Map of the four selected sampling sites in Seybouse River. S1: Bradaa wadi, S2: Nadhor wadi, S3: Boussora wadi, S4: Boumahra wadi

Table 1. Characterization of sampling sites at Seybouse River (Source: author's data)

Sampling sites	Geographic coordinates	Pollution
Bradaa wadi (S1)	36.29376 N 7.26483 E	Agricultural activities
Nadhor wadi (S2)	36.25017 N 7.37485 E	Sewage effluents of canned tomato factory
Boussora wadi (S3)	36.28113 N 7.32064 E	Agricultural water discharges
Boumahra wadi (S4)	36.27427 N 7.31498 E	Sewage of marble factory

Twenty-four samples were collected from Seybouse River during two periods, March and April, 2019. At each sampling site, 500 mL water samples were collected for bacteriological analysis in sterile water sampling bottles (VWR, USA). Simultaneously, samples for trace metal elements (TME) were collected in 1.5 L decontaminated polyethylene bottles (VWR, USA). Water samples were acidified using 1% HNO₃ (REACH, Netherlands) to reach a pH lower than 2. Using a vacuum pump (MIDLAND, USA), 0.5% (v/v) was filtered with a membrane of 1.2 µm porosity (SARTORIUS, France) and then preserved at 0°C prior to TME analysis.

Environmental factor measurements

Water temperature (T), pH, salinity, dissolved oxygen (DO) and electrical conductivity (EC), were measured in situ at the time of sampling using a field multimeter (WTW Multi 340i, Germany). The concentrations of two trace metal elements (Cu and Cd) in the water were determined using an Inductively Coupled Plasma-Atomic Emission Spectroscopy (ICP-AES, Thermo Electron IRIS Intrepid II XSP, USA). The results were expressed in mg/L for water. All the measurements were performed in triplicate.

Screening and characterization of metal-resistant bacteria

Two metals (Cd²⁺ and Cu²⁺) were selected for metal resistance screening based on a wide range of expected toxicities and their presence in water samples. Bacteria from the water samples were isolated using the spread plate technique. During routine culture

and experimental procedures, bacterial cells were grown in liquid Luria Broth (LB) (pH 7.2–7.4) (KD Medical, Germany) in the presence of 100 µg/mL heavy metal and incubated at 37 °C with shaking at 150 rpm for 24 h (Xiaoyan et al., 2016). The metals were added as CdCl₂·2H₂O and CuSO₄·5H₂O (Merck, Germany). Control plates also prepared with LB media without including any heavy metal to make comparison. Individual distinct colonies were identified by their morphological and biochemical characteristics according to procedures described by Holt et al. (1994).

Minimum inhibitory concentration (MIC) and Minimal biocidal concentration (MBC)

The Minimal Inhibitory Concentration (MIC) for each metal-resistant bacterial isolate was determined using LB (KD Medical, Germany) containing different concentrations of one of the two heavy metals (Cd⁺², Cu⁺²): 12.5, 25, 50, 100, 200, 400, 800, 1600, 3200 µg/mL. Metal salts (CdCl₂ and CuSO₄ 5H₂O) were used to prepare 5 g/L stock solution. Each stock solution was filter-sterilized and used for preparation of the final concentrations. After standardization of the inoculums, 1 mL of the diluted inoculums was added to 1 mL of each metal concentration except for the sterility control, which contained only LB (Keevil, 2001). Subsequently, the tubes were incubated in an oven at 37 °C for 24 h. Microbial growth was considered as positive in the tubes that showed any increase in turbidity or growth at the bottom. The MIC was defined as the lowest dilution with negative growth. To determine the minimum bactericidal concentration (MBC), a 10 µL from those tubes, which did not show any visible growth in MIC assay, was cultured on LB agar (KD Medical, Germany) and incubated at 37 °C for 18 to 24 h. The lowest concentration of metal producing no growth was considered to be the minimum bactericidal concentration (MBC). When growth was observed with the highest concentration of the antibacterial, the MBC was considered as the highest dilution and was indicated by the sign "greater than (>)" (Keevil, 2001). Non-inoculated LB culture medium was used as the negative control and LB culture medium without the addition of metals as the positive control.

Extraction and estimation of metallothionein (MT)

Five best isolates (KZ2, KZ5, KZ8, KZ10 and KZ11) were selected based on degree of resistance to heavy metals. The metallothioneins (MTs) secreted by strains under heavy metal pressure were quantitatively assessed by the method of Murthy et al. (2011). The amounts of metallothionein in the samples were estimated using the GSH standard (Bio-tech, China), assuming that 1 mol of MT contains 20 mol of cysteine and were expressed in nmol/g bacterial biomass (Ana and Garcia-Vazquez, 2006). All experiments were performed in triplicate.

Data analysis

The data are expressed in mean values±standard deviation of the mean (SD). Statistical analysis of the data was performed using SPSS (Ver. 25.0, 2017), and the normal distribution was verified by applying the Kolmogorov–Smirnov, making it possible to choose parametric methods for the statistical analysis. Inter-site comparisons were performed using the analysis of variance (one-way ANOVA test). If significant difference between the mean values of the physicochemical parameters and TME concentrations in all studied sites was observed, Student-Newman-Keuls post hoc test

was used to determine differences between study sites. Student's t-test was conducted to identify the significant differences between the MT variations. The correlation between MT levels and metal concentrations are evaluated by the Pearson correlation coefficient (r) ($p < 0.05$).

Results

Environmental characterization

The variations of physicochemical parameters and TME (Cu, Cd) in water are given in *Table 2*. The thermal water revealed similar mean values in the four sites ($p = 0.765$). Regarding pH, the analytical data revealed that water in the four sites was alkaline. Salinity and conductivity results showed that the maximum mean values are registered at site S4 and the lowest mean values are recorded at site S1. The dissolved oxygen levels reveal different means between the four sites, the highest level were recorded at site S3. The concentrations of the heavy metals investigated were significantly different between the different sampling sites (ANOVA, Student-Newman-Keuls post hoc test). The maximum metal concentrations were observed at Bradaa wadi and Boumahra wadi for Cu and Cd, respectively. The concentrations of copper in water were within the respective international and national recommended limits for natural water. For Cd, the concentrations were above the limit of detection (*Table 2*).

Table 2. Variations of physicochemical parameters and TME concentrations in water samples analyzed at the four sampling sites of Seybouse River on March and April 2019 (Mean values \pm SD, $n = 3$)

Variable	S1	S2	S3	S4	F-ratio	Sig.
T (°C)	7.1 \pm 0.05	7.03 \pm 0.03	7.12 \pm 0.01	7.16 \pm 0.16	0.388	0.765
pH	8.0 \pm 0.04 ^b	8.03 \pm 0.02 ^b	7.83 \pm 0.01 ^a	8.65 \pm 0.01 ^c	159.11	0.000*
Salinity (PSU)	0.12 \pm 0.003 ^a	0.62 \pm 0.005 ^b	0.5 \pm 0.003 ^c	0.64 \pm 0.003 ^d	3431.28	0.000*
DO (mg/L)	6.52 \pm 0.1 ^b	7.24 \pm 0.01 ^c	7.82 \pm 0.01 ^d	6.21 \pm 0.01 ^a	6298.09	0.000*
EC (μ S/mg)	898.7 \pm 0.33 ^a	1532.3 \pm 0.9 ^c	1335 \pm 0.33 ^b	1552 \pm 1.15 ^d	157880.94	0.000*
Cu (mg/L)	0.185 \pm 0.00 ^d	0.147 \pm 0.00 ^a	0.165 \pm 0.00 ^b	0.177 \pm 0.00 ^c	1203.67	0.000*
Cd (mg/L)	0.123 \pm 0.00 ^b	0.117 \pm 0.00 ^a	0.131 \pm 0.00 ^c	0.145 \pm 0.00 ^d	1329.0	0.000*
International and national thresholds values for Cu concentrations in rivers	2 mg/L			Zaigham et al. (2012) OJAR (2014)		
International and national thresholds values for Cd concentrations in rivers	0.005 mg/L					

Sig: significance; * $p < 0.001$ (one-way ANOVA); a, b, c, d indicate significant differences by Student-Newman-Keuls post hoc test; S1: Bradaa wadi; S2: Nadhor wadi; S3: Boussora wadi; S4: Boumahra wadi. Limit of detection: Cu = 0.1 μ g/L; Cd = 0.01 μ g/L

Screening and characterization of metal-resistant bacteria

Twelve metal-resistant bacteria were isolated from surface water in middle of Seybouse basin using a spread plate procedure, and were designated KZ1 to KZ12. Physiological and biochemical characterization of the bacterial strains was shown in *Table 3*. All of the bacteria were Gram-negative bacilli, smooth, sticky, non spore-forming and formed opaque colonies. Strain KZ5 produced a blue-green pigment that could be seen clearly in the liquid LB medium. This blue-green pigment, formed in the medium without Cd, was not present in the medium containing Cd, demonstrating that addition of Cd inhibits pigment formation (*Fig. 2*).

Table 3. Physiological and biochemical characteristics of the heavy metal resistant bacterial strains

Site Strain N°	S1			S2			S3			S4		
	KZ1	KZ2	KZ3	KZ4	KZ5	KZ6	KZ7	KZ8	KZ9	KZ10	KZ11	KZ12
Glucose	+	+	-	+	+	+	+	+	+	+	+	+
Sucrose	+	+	-	+	-	+	-	+	+	+	+	-
Xylose	ND	-	-	+	+	ND	ND	+	-	-	ND	-
Mannitol	+	+	-	+	+	+	-	+	-	+	+	+
Maltose	-	+	-	+	+	+	-	+	-	+	+	-
Rhamnose	+	+	-	+	-	-	-	+	-	-	+	-
Lactose	+	+	-	-	-	-	-	+	-	-	-	-
Melibiose	+	+	-	+	-	+	+	+	-	-	+	+
Amygdalin	-	-	ND	+	ND	+	-	+	-	+	+	-
Esculoside	-	+	-	+	+	-	-	-	+	-	+	-
Arabinose	+	+	-	+	-	+	+	+	-	-	+	-
H ₂ S	-	+	-	-	-	-	-	-	-	+	+	-
Simmons citrate	-	+	-	+	+	+	+	+	-	-	+	-
Nitrate reduction	-	+	+	+	-	+	-	+	+	+	+	+
Uree	-	-	-	+	+	+	-	-	-	+	+	-
Indole	+	-	-	+	-	-	-	-	+	-	-	-
Gelatine liquefaction	-	+	+	-	+	+	-	-	-	+	+	-
Methyl red test	+	+	-	-	-	+	-	+	-	+	+	+
Ornithine decarboxylase	-	-	-	+	-	-	-	+	-	-	+	-
Lysine decarboxylase	+	-	-	+	-	+	-	+	-	-	+	-
Arginine decarboxylase	+	+	-	+	+	+	-	+	-	-	+	-
Catalase	+	+	+	+	+	+	+	+	+	+	+	+
Oxidase	-	-	+	-	-	-	-	-	+	-	-	-
VP test	-	-	-	+	-	-	+	-	-	-	-	-
β-galactosidase	+	+	+	+	+	+	-	+	-	-	-	-
42°C growth	+	+	ND	ND	+	ND	-	+	ND	+	+	-
Identification results	<i>Escherichia coli</i>	<i>Citrobacter freundii</i>	<i>Chryseobacterium indologenes</i>	<i>Raoultella ornithinolytica</i>	<i>Pseudomonas aeruginosa</i>	<i>Aeromonas hydrophila</i>	<i>Acinetobacter baumannii</i>	<i>Klebsiella oxytoca</i>	<i>Pasteurella trehalosi</i>	<i>Proteus vulgaris</i>	<i>Salmonella Typhimurium</i>	<i>Shigella</i> spp.

(+) indicates positive; (-) indicates negative; (ND) indicates not detected

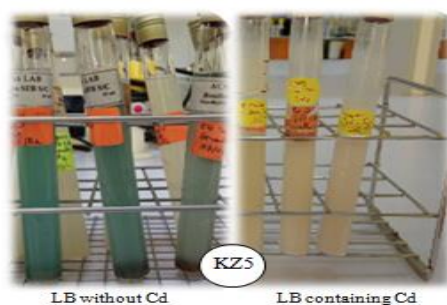


Figure 2. Inhibition of blue-green pigment production by the isolate KZ5 after exposure to cadmium

Minimum inhibitory concentration (MIC) and Minimal biocidal concentration (MBC)

The order of MICs and MBCs for the majority of bacterial isolates was found to be Cu > Cd (Table 4). More than 40% of the strains possessed maximum tolerable concentration equal or higher than 800 µg/mL metal (Fig. 3). KZ2, KZ5, KZ8, KZ10 and KZ11 are resistant against Cu and Cd with the highest MIC and MBC (3600 µg/mL and > 3600 µg/mL, respectively). Cadmium tolerance was higher for *Pseudomonas aeruginosa* (KZ5) (MBC > 3600 µg/mL). Besides, *Aeromonas hydrophila* (KZ6) shows highest sensitivity to Cd as well as their resistance capacity against Cu are also lower compared to other bacteria. Comparison between all isolates to the same concentration of metal showed that the *p* values were significantly different (*p* = 0.03).

Table 4. Minimum inhibitory concentration (MIC) and Minimal biocidal concentration (MBC) of copper and cadmium against bacteria isolated from surface water

Bacterial isolates	Copper		Cadmium	
	MIC (µg/mL)	MBC (µg/mL)	MIC (µg/mL)	MBC (µg/mL)
KZ1	400	800	200	400
KZ2	3600	>3600	3600	3600
KZ3	800	1600	400	800
KZ4	800	1600	200	400
KZ5	3600	>3600	3600	>3600
KZ6	200	800	50	100
KZ7	800	1600	100	400
KZ8	3600	>3600	3600	3600
KZ9	1600	3600	800	1600
KZ10	3600	>3600	3600	3600
KZ11	3600	>3600	3600	3600
KZ12	800	1600	200	400

Extraction and estimation of metallothionein (MT)

Figure 4 shows the estimation of MT concentrations in the five best isolates (KZ2, KZ5, KZ8, KZ10 and KZ11). The MT concentration in the control (without metals) was zero whereas the levels of MT dosed are usually high at 1600 µg/mL metal compared to other metal concentrations. The MT level increased significantly (*r* = 0.936, *p* = 0.006)

in a metal concentrations. Results of this part revealed that Cd was the better inducer for MT than copper by the five isolates. The application of the Student's t-test for comparing the MT variation reveal a significant difference between MT concentration in the bacteria strains exposed to copper and MT content after exposure to cadmium ($p = 0.005$).

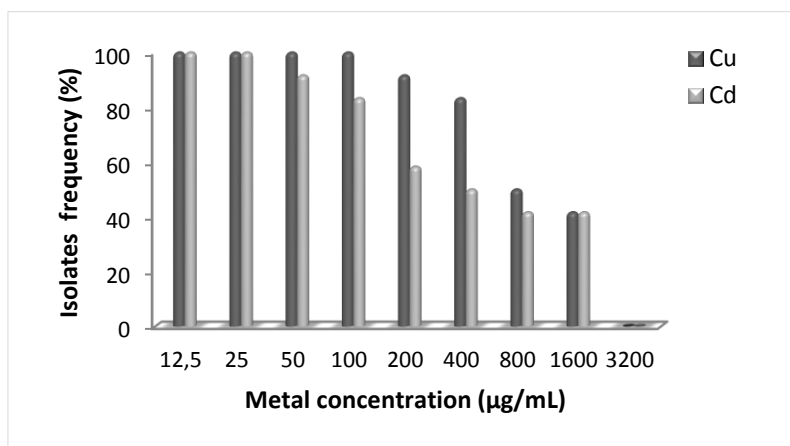


Figure 3. Percentage of metal-resistant bacteria in relation to concentrations of heavy metals

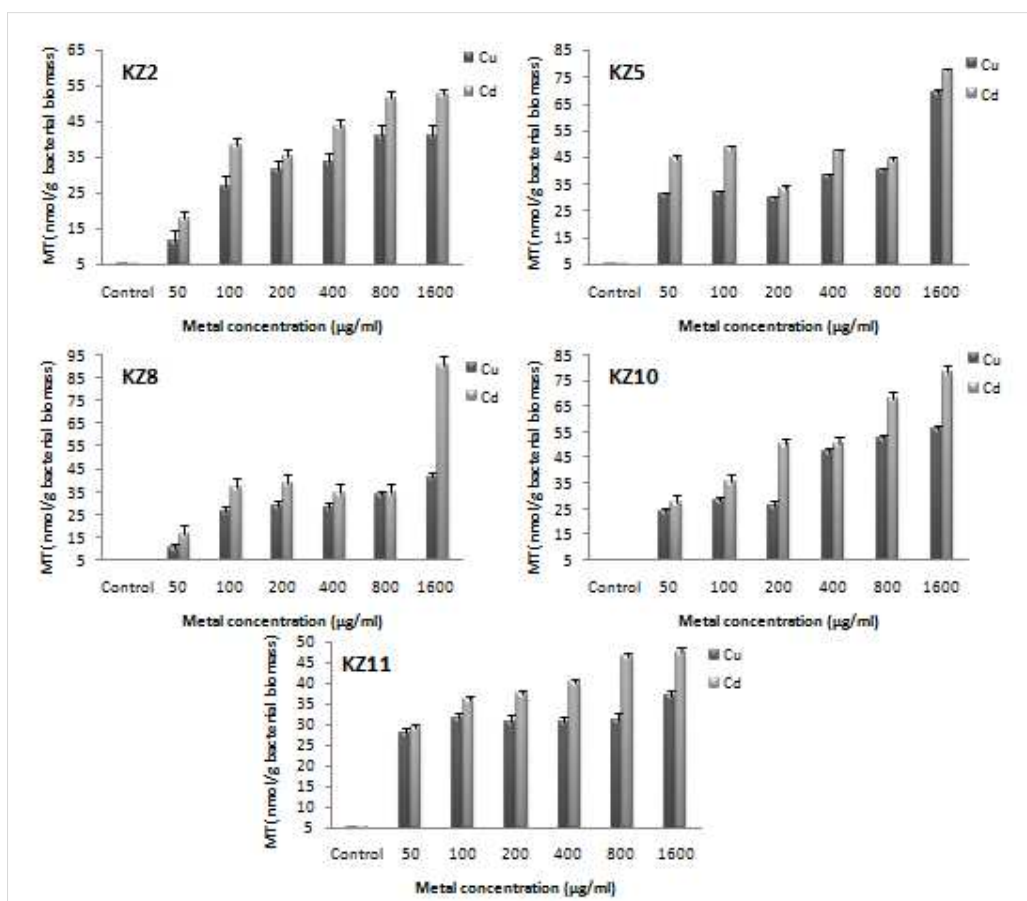


Figure 4. Metallothionein content in bacteria isolates treated with different concentrations of copper and cadmium

Discussion

Environmental characterization

The thermal water revealed similar mean values in the four sites and it depends clearly on climatic conditions (Benhalima et al., 2018). The recorded pH values demonstrated a slight water alkalinity and did not show a variation between the sites S1 and S2 (Student- Newman-Keuls test). The pH of most freshwater systems is dependent on the mineral content of the surrounding rocks, soils and contamination by agricultural, urban or industrial discharges, and often ranges from 6 to 8 (Aminot and K  rouel, 2004). Generally, the optimum pH for bacterial growth is between 6.5 and 7.5. Salinity values were slightly low in Bradaa wadi (S1) compared to the other sites; this would probably be related to the dilution phenomenon during wet periods. Ca  edo-Arg  uelles et al. (2019) indicate that urbanization and agriculture are the main drivers of river and stream salinization. The increase in conductivity at Nadhor wadi (S2), Boussora wadi (S3) and Boumahra wadi (S4) may be due to its proximity to the intense anthropogenic activities in this part of the basin. The dissolved oxygen levels reveal different means between the four sites, the highest level were recorded at site S3. Dissolved Oxygen is essential for the survival of the aerobic organisms present in the waterbody. In addition, microorganisms such as bacteria use the dissolved oxygen to decompose the organic material at the bottom of the water, which contributes to the recycling of nutrients (Eljaiek-Urzola et al., 2019). The high concentrations of dissolved oxygen during the study period can be explained by phytoplankton flares that can cause a temporary endogenous oxygen supply in aquatic environmental (Aminot and K  rouel, 2004). The results obtained of temperature, pH and the dissolved oxygen correspond with the work performed in the northeastern surface water of Algeria (Guettaf et al., 2014; Chaoui et al., 2015).

Heavy metal pollution is a worldwide predicament which disturbs the environmental equilibrium by gaining entry into the ecosystem due to their small size and bioaccumulation tendency (Manasi and Rajesh, 2016). The measured TME in the water of the four sampling sites revealed that the two elements (Cu and Cd) are present. Copper concentrations in surface waters of surveyed wadis are not homogeneous (Student-Newman-Keuls test) but they do not exceed the international and national threshold values 2 mg/L (Zaigham et al., 2012; OJAR, 2014). The main source of Cu is telluric and would be related to the soil geology of this part of the Seybouse basin. In the study area, the importance of agricultural practices, traffic activities and municipal wastewater discharge is likely to increase transfers of Cu to surface waters. Jiang et al. (2017) indicate that copper distribution depends on the local dominance of farming and animal husbandry. In addition, Belabed et al. (2013) and Diop (2014) indicate that deterioration of sulfates (especially chalcopyrite and galenite) can increase sulfates and acidity justifying the presence of copper which increase is mainly related to the mining activity inducing trace metal mobilization. Also, DIOP (2014) indicate that copper are associated to sandy facieses directly exposed to waste discharges.

Concerning Cd, its concentration was recorded above the international and national permissible limit 0.005 mg/L (Zaigham et al., 2012; OJAR, 2014) in all the water samples. Metals in higher concentrations displace the essential nutritional minerals in the living systems and prove deleterious to them by disrupting the functioning of vital organs making it a global environmental concern (Manasi and Rajesh, 2016). The high levels of cadmium in study sites may be explained by the leaching of agriculture lands

enriched with phosphate fertilizers and industrial liquid wastes. Huang et al. (2019) indicated that agricultural materials (including mineral fertilizers, organic fertilizers, pesticides, plastic films, etc.) have been highlighted as a major source of Cd. Results of this study are in agreement with the studies of Louhi et al. (2012), Khaled-Khodja et al. (2016), Belabed et al. (2017) and Talbi and Kachi (2019), who reported that the level of heavy metals increasing in the Seybouse rivers due to discharge of industrial effluents, the sewage discharged by the localities and the intensive use of chemical fertilizers and pesticides in agriculture.

Screening and characterization of metal-resistant bacteria

Results revealed a predominance of Gram-negative bacteria; the strains were predominantly glucose fermentative bacteria, which belonged to the *Enterobacteriaceae* family. There are obvious differences in the physiological and biochemical characteristics of the twelve bacteria. The strains were identified as *Escherichia coli*, *Citrobacter freundii*, *Chryseobacterium indologenes*, *Raoultella ornithinolytica*, *Pseudomonas aeruginosa*, *Aeromonas hydrophila*, *Acinetobacter baumannii*, *Klebsiella oxytoca*, *Pasteurella trehalosi*, *Proteus vulgaris*, *Salmonella Typhimurium* and *Shigella* spp.

Pseudomonas aeruginosa did not form a blue-green pigment after exposure to cadmium. Bacterial pigments are known to protect the cell against any photo oxidative damage caused due to the toxic metal ions. So, the lack of pigment production indicates a toxic concentration of Cd. It is already reported that at low metal concentrations, bacterial pigmentation is inhibited (Manasi and Rajesh, 2016).

Resistance in bacteria against these toxic metals reflects the threshold of environmental contamination and the direct or indirect exposure of these bacteria to the toxic compounds (Manasi and Rajesh, 2016). Bacteria have metal binding abilities and they are known to exhibit not only tolerance to metals but also their detoxification. There are many reports describing microbes, especially from enterobacteria and *Pseudomonas* genus, that are resistant to heavy metals. Niveshika et al. (2016) isolated Cd- and Cu-resistant strains of *Proteus vulgaris*, *Serratia* and *Pseudomonas* from water samples of Ganga River in India. Marzan et al. (2017) isolated Cd-resistant enterobacteria from tannery effluent in Chittagong city, Bangladesh. Türetken et al. (2019) isolated several metal-resistant bacterial strains from water samples collected from a Lake in Turkey.

Minimum inhibitory concentration (MIC) and minimal biocidal concentration (MBC)

The multi-metal resistance of the 12 bacterial strains of interest in liquid medium was tested by determining the minimal inhibitory concentrations (MIC) following a two-fold dilution technique approach. High MIC values indicate high tolerance of the bacterial isolate toward the metal and vice-versa. The results of growth pattern of bacterial isolates in presence of different of Cu and Cd concentration showed that all strains were multi-metal-resistant (Cu- and Cd-resistant). Several studies have shown the existence of multi-metal-resistant bacteria (Banerjee et al., 2015; Hoque and Fritscher, 2019; Türetken et al., 2019), and this is intimately related to the coresistance mechanism found in bacteria. Cai et al. (2019) demonstrated that flanked insert sequence elements on the heavy metal resistant genes suggested that horizontal gene transfer events may have resulted in multiple heavy metal resistance phenotypes and genotypes in bacterial strains.

Upon above experiments, the resistance level $Cu > Cd$ showed for all bacterial isolates. This result may be explained by the fact that the toxicity of Cu is lower than Cd. At lower concentration, copper is an essential trace element participating in many vital biological processes but at high concentrations, it exerts inhibitory action on bacteria by blocking essential functional groups or modifying. On the other hand, bacteria cells have evolved and now provide complex and efficient regulation mechanisms to neutralize toxic copper (Li et al., 2019). While, cadmium is highly toxic, it is non-essential heavy metal element for all organisms that can accumulate in cells, where it disturbs the function of some enzymes and directly attacks nuclear DNA in microorganisms (Abbas et al., 2017; Chellaiah, 2018).

The continued environmental heavy metal pollution enables bacteria to develop resistance against these substances (Türetken et al., 2019). To counteract copper intoxication, bacteria can express a wide range of efflux systems to maintain metal ion homeostasis. Other copper resistance systems found in Gram-negative bacteria, such as the periplasmic multi-copper oxidase (e.g., CueO from *E. coli*), that oxidizes Cu^{1+} to Cu^{2+} were detected (Alquethamy et al., 2019). For cadmium, three metal resistance mechanisms in bacteria have been revealed: Cd ions can be prevented from flowing into cells by the presence of polysaccharides, proteins and fats on their surfaces; Cd can be expelled through efflux pumps and it can be chelated by intracellular metallothionein (Qin et al., 2019). However, aside from these mechanisms Cd resistant genes are present in plasmid DNA of Enterobacteria (Vidhyaparkavi et al., 2017).

Among all cultures, cadmium tolerance was higher for *Pseudomonas aeruginosa*. *Pseudomonas aeruginosa* is ubiquitous in water ecosystems and showed high resistance to heavy metals (Chellaiah, 2018). Various studies have been published of different heavy metal resistant mechanisms found in the genus *Pseudomonas*, as well as reports of chromosome and plasmid-encoded genetic determinants for resistance to heavy metals (Wright et al., 2019). Many researchers have reported that *P. aeruginosa* as Cd- and Cu-resistant bacteria were isolated from different environment regions (Chen et al., 2016; Chellaiah, 2018; Karimpour et al., 2018; Wright et al., 2019).

High MIC values against two types of heavy metals recorded for *Citrobacter freundii*, *Klebsiella oxytoca*, *Proteus vulgaris* and *Salmonella Typhimurium* can be explained by the fact that *Enterobacteriaceae* species are able to resist toxic metals, which are widely spread in the natural environment. High levels of metal ions represent a stress factor for Enterobacteria, which then enlarge their plasmids under stress conditions. However, under appropriate conditions, plasmids shrink and disappear and can adapt to the environment. Furthermore, the resistance of the *Enterobacteriaceae* members to heavy metal salts is also related to metal pollution in the environment (Çardak and Altug, 2014). Heavy metal resistance of *Enterobacteriaceae* was showed by many studies (Rafiq et al., 2017; Kyaing et al., 2019; Bhardwaj et al., 2018). Altimera et al. (2012) showed that bacteria were tolerant to copper with MIC value ranging from 3.1 to 4.7 mM. In Addition, Mathivanan and Rajaram (2014) studied that some cadmium tolerant bacteria able to tolerance up to 400 mg/L of Cd^{2+} which were isolated from the polluted coastal. Irawati et al. (2017) identified indigenous heavy metal tolerant bacteria from Kemisan River and the highest copper tolerant bacteria showed MIC value of 10 mM showing those isolates were used for further study of copper contamination control.

The *Aeromonas hydrophila* strain (KZ6) was the isolate showing the lowest metal-resistant capacity compared to other bacteria, which could be related to the toxic effect

of metals on this bacterial cells. Moreover, microorganisms can interact with heavy metal via many mechanisms and different level of metal tolerant level might be due to different types of mechanisms such as bioaccumulation and biosorption processes within each isolates (Kyaing et al., 2019).

The reason why microbial populations differ so hugely in their ability to tolerate such deadly pollutants can be explain by the fact that such variable metal tolerance behavior occurring naturally among microbes towards various heavy metals could be due to (i) the differences in available macro and micro nutrient elements in growth media/water supporting bacterial growth (ii), variable genetic constituents of bacterial strains and (iii) the growth conditions/environmental variables affecting the bacterial growth (Rizvi et al., 2019).

Extraction and estimation of metallothionein (MT)

Considering the importance of MTs in metal detoxification, the five best isolates (KZ2, KZ5, KZ8, KZ10 and KZ11) were screened to see whether these strains were able to induce MTs production while growing in the presence of Cu and Cd. Indeed, the five strains exhibited greater production of MTs in the presence of both Cu and Cd, suggesting an obvious role of metals in MTs induction (*Fig. 2*). Maximum MT levels were recorded for *Pseudomonas aeruginosa* KZ5, *Proteus vulgaris* KZ10 and *Klebsiella oxytoca* KZ8 (77.13, 78.11 and 90.53 nmol MT/g bacterial biomass, respectively). The metallothioneins have been found in some limited *Procaryota*, including cyanobacteria, pseudomonads and mycobacteria (Genetyki et al., 2017). The first bacterial metallothionein SmtA was characterized in *Synechococcus* PCC 7942 function as sequester and detoxifies Cd²⁺ and Zn²⁺. Later SmtA also is found in the *Anabaena* PCC 7120, *P. aeruginosa* and *Pseudomonas putida* (Malekzadeh and Shahpiri, 2017). Subsequently, proteins similar to SmtA were found in other cyanobacteria and γ -*proteobacteria*, such as the genus *Pseudomonas*. All those bacterial proteins similar to SmtA were included in BmtA (bacterial MTs) family (Gutiérrez et al., 2019). Furthermore, Gram-negative bacterial species such as *E. coli*, *Serratia liquefaciens*, *Klebsiella pneumoniae* was recognized on production of intracellular cadmium-binding proteins (Kumar et al., 2019). The bacterial MTs differ in terms of primary structure, the number and type of metal ions they bind, as well as with regard to their physiological functions. The expression of bacterial MTs is regulated by metals via metalosensors (Genetyki et al., 2017). MTs from *Enterobacteriaceae* seem to be involved in zinc and copper homeostasis, while in *Pseudomonas* they are linked to cadmium detoxification.

Results revealed that the MT level increased significantly in a metal concentration ($r = 0.936$, $p = 0.006$). Generally, the MT expression level is dose-dependent on heavy metals (Walker et al., 2014). In bacteria strains, intracellular sequestration of metals is mostly based on the presence of metallothionein which is involved in many cellular functions, particularly in the transport, storage and detoxification of metals (Chudobova et al., 2015). Therefore, an increased concentration of metallothionein can be important for homeostasis and detoxification of metals to acquire resistance to heavy metal in the bacterial strains isolated from surface water. Accordingly, the ability of bacteria isolates express metallothionein due to the expose of heavy metals compared to control (without metal) was tested. Numerous reports have shown that MTs play crucial roles in maintaining metal homeostasis and protect against heavy metal toxicity through intracellular sequestration (Chudobova et al., 2015). Mikowska et al. (2018) and Xu et

al. (2018) revealed that MTs are implicated in homeostasis of essential heavy metals such as copper, detoxification of noxious metal cations such as cadmium. Also, Abbas et al. (2017) indicate that the cadmium-resistant bacteria have also adopted the strategy to bind the cadmium with intracellular binding proteins (bacterial metallothioneins).

According to the literature, MT is predominantly a Cu-binding protein, but results of this part revealed that Cd was however, found, to be a superior inducer of MTs compared to Cu ($p = 0.005$). The strength of MT defense depends on several factors connected with the metal characteristics and organism attributes (Mikawska et al., 2018). Therefore, an increase in MT levels may reflect an elevated demand to detoxify Cd. Wang et al. (2014) reviewed the recent advances of characteristics, functions and applications of metallothionein and they demonstrated that Cd was the most potential for MTs induction among three metals (i.e., Cd, Cu, and Zn). Xu et al. (2018) demonstrate that metallothionein-like protein type 3 (CsMTL3) can improve metal tolerance, especially for Cd²⁺ ions and suggest that the composition and arrangement of N-terminal Cys residues are associated with binding capacity and preference for different metal ions. Similar to our research, habjanic et al. (2018) showed that a Gram-negative bacteria has a histidine-rich Mt with a disordered tail displays higher binding capacity for cadmium than other metal.

Conclusion

The results of the present study showed that the waters of Seybouse River are under the influences of heavy metal pollution (especially Cd). Eleven metal-resistant bacterial strains were isolated and identified from surface water in Seybouse basin. All of the strains were showed the resistance level Cu > Cd. The isolates *Citrobacter freundii*, *Pseudomonas aeruginosa*, *Klebsiella oxytoca*, *Proteus vulgaris* and *Salmonella* Typhimurium showed the high MIC values against Cd and Cu. These five isolates presented metallothionein induction as its mechanisms of metal resistance. It has been shown that Cd was found, to be a superior inducer of MTs compared to Cu.

The results obtained in this study, therefore, clearly establish the fact that MTs so generated by bacterial communities in stressed environments could be useful in efficiently detoxifying metal contaminated environments. Hence, the use of bacteria possessing this property of secreting MTs could be explored as a cost effective approach in bioremediation strategies. Further study of the effects of different supplements and conditions in their growth is needed to identify their efficiency as bioremediation agents, where optimization of pH, temperature, and incubation time can influence metal resistance capacity.

Acknowledgements. The research was supported by the General Manager for Scientific Research and Technological Development (DGRSDT). The authors thank Brahmia S., Souadkia K., Soucha I., Benchikh S., Boumaza K., Chitour R., Souilah N., for their assistance in the manipulations.

Conflict of interests. The authors declare no conflict of interests.

REFERENCES

- [1] Abbas, S. Z., Rafatullah, M., Hossain, K., Ismail, N., Tajarudin, H. A., Abdulkhalil, H. P. S. (2017): A review on mechanism and future perspectives of cadmium-resistant bacteria. – *International Journal of Environmental Science and Technology* 15: 243-262.
- [2] Aljerf, L., Almasri, N. (2018): A gateway to metal resistance: Bacterial response to heavy metal toxicity in the biological environment. – *Annals of Advances in Chemistry* 2:32-44.
- [3] Alquethamy, S. F., Khorvash, M., Pederick, V. G., Whittall, J. J., Paton, J. C., Paulsen, I. T., Hassan, K. A., Mcdevitt, C. A., Eijkelkamp, B. A. (2019): The role of the CopA copper efflux system in *Acinetobacter baumannii* virulence. – *International Journal of Molecular Sciences* 20: 575.
- [4] Altimera, F., Yanez, C., Bravo, G. (2012): Characterization of copper resistant bacteria and bacterial communities from copper-polluted agricultural soils of central Chile. – *BMC Microbiology* 12: 1-12.
- [5] Aminot, A., K erouel, R. (2004): Major physicochemical characteristics. – In: Aminot, A., K erouel, R. (eds.) *Hydrobiology of marine ecosystems: parametres and analyzes*. 8th ed., Ifremer, Brest.
- [6] Ana, R. L., Garcia-Vazquez, E. (2006): A simple assay to quantify metallothionein helps to learn about bioindicators and environmental health. – *Biochemistry and Molecular Biology Education* 34(5): 360-363.
- [7] Banerjee, S., Goyalwal, R., Sahu, P. K., Sao, S. (2015): Microbial observation in bioaccumulation of heavy metals from the ash dyke of thermal power plants of Chhattisgarh, India. – *Advances in Bioscience and Biotechnology* 6: 131-138.
- [8] Belabed, B. E., Frossard, V., Dhib, A., Turki, S., Aleya, L. (2013): What factors determine trace metal contamination in Lake Tonga (Algeria)? – *Environment Monitoring and Assessment* 185: 9905-9915.
- [9] Belabed, B. E., Meddour, A., Samraoui, B., Chenchouni, H. (2017): Modeling seasonal and spatial contamination of surface waters and upper sediments with trace metal elements across industrialized urban areas of the Seybouse watershed in North Africa. – *Environment Monitoring and Assessment* 189: 265.
- [10] Benhalima, L., Kadri, S., Barour, C., Bensouilah M., Ouzrout, R. (2018): Water Quality Assessment of a Coastal Canal within a Protected Zone in Algeria using Principal Component Analysis. – *Indian Journal of Science and Technology* 11(32).
- [11] Bhardwaj, R., Gupta, A., Garg, J.K. (2018): Impact of heavy metals on inhibitory concentration of *Escherichia coli*- a case study of river Yamuna system, Delhi, India. – *Environment Monitoring and Assessment* 190: 674.
- [12] Cai, X., Zheng, X., Zhang, D., Iqbal, W., Liu, C., Yang, B., Zhao, X., Lu, X., Mao, Y. (2019): Microbial characterization of heavy metal resistant bacterial strains isolated from an electroplating wastewater treatment plant. – *Ecotoxicology and Environmental Safety* 181:472-480.
- [13] Ca nedo-Arg uelles, M., Kefford, B., Sch afer, R. (2019): Salt in freshwaters: causes, effects and prospects - introduction to the theme issue. – *Philosophical Transaction Royal Society B* 374: 20180002.
- [14]  ardak, M., Altug, G. (2014): Species distribution and heavy metal resistance of *Enterobacteriaceae* members isolated from Istanbul Strait. – *Fresenius Environmental Bulletin* 23(10a): 2620-2626.
- [15] Chaoui, W., Attoui, B., Benhamza, M., Bouchami, T., Alimi, L. (2015): Water quality of the plain of El-Hadjar wilaya of Annaba (Northeast Algeria). – *Energy Procedia* 74: 1174-1181.
- [16] Chellaiah, E. R. (2018): Cadmium (heavy metals) bioremediation by *Pseudomonas aeruginosa*: a minireview. – *Applied Water Science* 8: 154.
- [17] Chen, B., Stein, A. F., Castell, N., Gonzalez-Castanedo, Y., Sanchez De La Campa, A. M., De La Rosa, J. D. (2016): Modeling and evaluation of urban pollution events of

- atmospheric heavy metals from a large Cu-smelter. – *Science of the Total Environment* 539: 17-25.
- [18] Choudhary, S. (2019): In silico analysis of potential metallothioneins in *Pseudomonas*. – *Research Journal of life Sciences, Bioinformatics, Pharmaceutical and Chemical Sciences* 5(1): 101-115.
- [19] Chudobova, D., Dostalova, S., Ruttkay-Nedecky, B., Guran, R., Rodrigo, M. A. M., Tmejova, K., Krizkova, S., Zitka, O., Adam, V., Kizek, R. (2015): The effect of metal ions on *Staphylococcus aureus* revealed by biochemical and mass spectrometric analyses. – *Microbiological Research* 170: 147-156.
- [20] Diop, C. (2014): Study of the contamination, speciation and bioavailability of heavy metal traces in coastal and estuarine waters and sediments in Senegal: Evaluation of potential toxicity. – Ph.D. Thesis. Doctoral School Sciences of matter, radiation and the environment, University of Lille 1, France.
- [21] Eljaiek-Urzola, M., Romero-Sierra, N., Segrera-Cabarcas, L., Valdelamar-Martínez, D., Quiñones-Bolaños, É. (2019): Oil and grease as a water quality index parameter for the conservation of marine biota. – *Water* 11: 856.
- [22] Genetyki, Z., Biologii, W., Środowska, O. (2017): Bacterial metallothionein. – *Post Mikrobiology* 56(2): 171-179.
- [23] Giovanella, P., Cabral, L., Costa, A. P., De Oliveira Camargo, A. F., Gianello, C., Bento, F. M. (2017): Metal resistance mechanisms in Gram-negative bacteria and their potential to remove Hg in the presence of other metals. – *Ecotoxicology and Environmental Safety* 140: 162-169.
- [24] Guettaf, M., Maoui, A., Ihdene, Z. (2014): Assessment of water quality: a case study of the Seybouse River (North East of Algeria). – *Applied Water Science*. DOI 10.1007/s13201-014-0245-z.
- [25] Gupta, P., Diwan, B. (2017): Bacterial Exopolysaccharide mediated heavy metal removal: A Review on biosynthesis, mechanism and remediation strategies. – *Biotechnology Reports* 13: 58-71.
- [26] Gutiérrez, J. C., De Francisco, P., Amaro, F., Díaz, S., Martín-González, A. (2019): Structural and Functional Diversity of Microbial Metallothionein Genes. – *Microbial Diversity in the Genomic Era* 387-407.
- [27] Habjanic, J., Zerbe, O., Freisinger, E. (2018): A histidine-rich *Pseudomonas* metallothionein with a disordered tail displays higher binding capacity for cadmium than zinc. – *Metallomics* 10: 1415-1429.
- [28] Holt, J. G., Krieg, N. R., Sneath, P. H. A., Staley, J. T., Williams, S. T. (1994): *Bergey's Manual of Determinative Bacteriology* (9th ed.). – Williams and Wilkins Press, Baltimore.
- [29] Hoque, E., Fritscher, J. (2019): Multimetal bioremediation and biomining by a combination of new aquatic strains of *Mucor hiemalis*. – *Scientific Reports* 9: 10318.
- [30] Huang, J., Peng, S., Maoc, X., Lia, F., Guoa, S., Shia, L., Shia, Y., Yua, H., Zeng, G. (2019): Source apportionment and spatial and quantitative ecological risk assessment of heavy metals in soils from a typical Chinese agricultural county. – *Process Safety and Environmental Protection* 126: 339-347.
- [31] Irawati, W., Riak, S., Sopia, N., Sulistia, S. (2017): Heavy metal tolerance in indigenous bacteria isolated from the industrial sewage in Kemisan River, Tangerang, Banten, Indonesia. – *Biodiversitas* 18: 1481-1486.
- [32] Jaishankar, M., Tseten, T., Anbalagan, N., Mathew, B. B., Beeregowda, K. N. (2014): Toxicity: mechanism and health effects of some heavy metals. – *Interdisciplinary Toxicology* 7: 60-72.
- [33] Jiang, Y., Chao, S., Liu, J., Yang, Y., Chen, Y., Zhang, A., Cao, H. (2017): Source apportionment and health risk assessment of heavy metals in soil for a township in Jiangsu Province, China. – *Chemosphere* 168: 1658-1668.

- [34] Karimpour, M., Ashrafi, S. D., Taghavi, K., Mojtahedi, A., Roohbakhsh, E., Naghipour, D. (2018): Adsorption of cadmium and lead onto live and dead cell mass of *Pseudomonas aeruginosa*: a dataset. – Data Brief 18: 1185-1192.
- [35] Keevil, W. (2001): Antibacterial properties of copper and brass demonstrate potential to combat toxic *E. coli* O157 outbreaks in the food processing industry (Centre for Applied Microbiology and Research, UK). – In: Symposium on Copper and Health, held in CEPAL, Santiago, Chile. Available online: <https://www.copper.org> (accessed on 5 January 2019).
- [36] Khaled-Khodja, S., Samar, M. H., Durand, G. (2016): Metallic contamination of water and sediment of Boumahra wadi. – Synthèse: Revue des Sciences et de la Technologie 32:135-146.
- [37] Kumar, P., Gupta, S., Anurag, B., Soni, R. (2019): Bioremediation of cadmium by mixed indigenous isolates *Serratia liquefaciens* BSWC3 and *Klebsiella pneumoniae* RpSWC3 isolated from industrial and mining affected water samples. – Pollution 5(2): 351-360.
- [38] Kyaing, M. S., Khaing, M. T., Saing, K. M. (2019): Screening of heavy metal (Lead) and antibiotics resistant soil bacteria from Myanmar industrial sites. – International Journal of Current Microbiology and Applied Sciences 8(4): 1319-1325.
- [39] Li, Y., Yang, H., Liu, N., Luo, J., Wang, Q., Wang, L. (2015): Cadmium accumulation and metallothionein biosynthesis in cadmium-treated freshwater mussel *Anodonta woodiana*. – Plos One 10(2): e0117037.
- [40] Li, C., Li, Y., Ding, C. (2019): The role of copper homeostasis at the host-pathogen axis: From bacteria to fungi. – International Journal of Molecular Sciences 20: 175.
- [41] Louhi, A., Hammadi, A., Achouri, M. (2012): Determination of some heavy metal pollutants in sediments of the Seybouse River in Annaba, Algeria. – Air, Soil and Water Research 5: 91-101.
- [42] Malekzadeh, R., Shahpiri, A. (2017): Independent metal-thiolate cluster formation in C-terminal Cys-rich region of a rice type 1 metallothionein isoform. – International Journal of Biological Macromolecules 96: 436-441.
- [43] Manasi, N. R., Rajesh, V. (2016): Evaluation of the genetic basis of heavy metal resistance in an isolate from electronic industry effluent. – Journal of Genetic Engineering and Biotechnology 14: 177-180.
- [44] Marzan, L. W., Hossain, M., Mina, S. A., Akter, Y., Azad Chowdhury, A. M. M. (2017): Isolation and biochemical characterization of heavy-metal resistant bacteria from tannery effluent in Chittagong city, Bangladesh: Bioremediation viewpoint. – Egyptian Journal of Aquatic Research 43: 65-74.
- [45] Mathivanan, K., Rajaram, R. (2014): Isolation and characterization of cadmium resistant bacteria from an industrially polluted coastal ecosystem on the southeast coast of India. – Chemistry and Ecology 30(7): 622-635.
- [46] Mikawska, M., Dziublińska, B., Świergosz-Kowalewska, R. (2018): Variation of metallothionein I and II gene expression in the bank vole (*Clethrionomys glareolus*) under environmental zinc and cadmium exposure. – Archives of Environmental Contamination and Toxicology 75: 66-74.
- [47] Mohseni, M., Khosravi, F., Mohajerani, M., Chaichi, M. J. (2014): Bioremediation activity of Pb (II) resistance *Citrobacter* sp. MKH2 isolated from heavy metal contaminated sites in Iran. – Journal of Sciences, Islamic Republic of Iran 25(2): 105-110.
- [48] Murthy, S., Bali, G., Sarangi, S. K. (2011): Effect of lead on metallothionein concentration in lead resistant bacteria *Bacillus cereus* isolated from industrial effluent. – African Journal of Biotechnology 10(71): 15966-15972.
- [49] Mutiat, F. B. Y., Gbolahan, B., Olu, O. (2018): A comparative study of the wild and mutated heavy metal resistant *Klebsiella variicola* generated for cadmium bioremediation. – Bioremediation Journal 22(1-2): 28-42.

- [50] Niveshika, S. S., Verma, E., Mishra, A. K. (2016): Isolation, characterization and molecular phylogeny of multiple metal tolerant and antibiotics resistant bacterial isolates from river Ganga, Varanasi, India. – *Cogent Environmental Science* 2: 1273750.
- [51] Official Journal of Algerian Republic (OJAR). (2014): Executive decree n°14-96 March 04th 2014. – Setting the quality goals of superficial and ground waters intended for the water supply of the populations.
- [52] Qin, W., Zhao, J., Yu, X., Liu, X., Chu, X., Tian, J., Wu, N. (2019): Improving cadmium resistance in *Escherichia coli* through continuous genome evolution. – *Frontiers in Microbiology* 10: 278.
- [53] Rafiq, M., Hayat, M., Anesio, A. M., Jamil, S. U. U., Hassan, N., Shah, A. A. (2017): Recovery of metallo-tolerant and antibiotic resistant psychrophilic bacteria from Siachen glacier, Pakistan. – *PLoS ONE* 12(7): e0178180.
- [54] Rizvi, A., Ahmed, B., Zaidi, A., Khan, M. S. (2019): Heavy metal mediated phytotoxic impact on winter wheat: oxidative stress and microbial management of toxicity by *Bacillus subtilis* BM2. – *Royale Society of Chemistry Advances* 9: 6125-6142.
- [55] Talbi, H., Kachi, S. (2019): Evaluation of heavy metal contamination in sediments of the Seybouse River, Guelma – Annaba, Algeria. – *Journal of Water Land Development* 40(I-III): 81-86.
- [56] Türetken, P. S. Ç., Altuğ, G., Çardak, M., Güneş, K. (2019): Bacteriological quality, heavy metal and antibiotic resistance in Sapanca Lake, Turkey. – *Environment Monitoring and Assessment* 191: 469.
- [57] Vidhyaparkavi, A., Osborne, J., Babu, S. (2017): Analysis of *zntA* gene in environmental *Escherichia coli* and additional implications on its role in zinc translocation. – *3 Biotech* 7: 9.
- [58] Walker, C. J., Gelsleichter, J., Adams, D.H., Manire, C.A. (2014): Evaluation of the use of metallothionein as a biomarker for detecting physiological responses to mercury exposure in the bonnethead, *Sphyrna tiburo*. – *Fish Physiology and Biochemistry* 40(5): 1361.
- [59] Wang, W. C., Mao, H., Ma, D. D., Yang, W. X. (2014): Characteristics, functions, and applications of metallothionein in aquatic vertebrates. – *Frontiers in Marine Science* 1(34).
- [60] Wright, B. W., Kamath, K. S., Krisp, C., Molloy, M. P. (2019): Proteome profiling of *Pseudomonas aeruginosa* PAO1 identifies novel responders to copper stress. – *BMC Microbiology* 19: 69.
- [61] Xiaoyan, L., Mou, R., Cao, Z., Xu, P., Wu, X., Zhu, Z., Chen, M. (2016): Characterization of cadmium-resistant bacteria and their potential for reducing accumulation of cadmium in rice grains. – *Science of the Total Environment* 569: 97-104.
- [62] Xu, X., Duan, L., Yu, J., Su, C., Li, J., Chen, D., Zhang, X., Song, H., Pan, Y. (2018): Characterization analysis and heavy metal-binding properties of CsMTL3 in *Escherichia coli*. – *FEBS Open Bio* 8: 1820-1829.
- [63] Zaigham, H., Anwar, Z., Khattak, K. U., Islam, M., Ullah Khan, R., Khattak, J. Z. K. (2012): Civic pollution and its effect on water quality of River Toi at District Kohat, NWFP. – *Research Journal of Environmental and Earth Sciences* 334-339.

RELATIONSHIPS BETWEEN ALPHA PLANT SPECIES DIVERSITY AND ENVIRONMENTAL VARIABLES IN DEDEGÖL (YENİŞARBADEMLİ) MOUNTAIN AREA

NEGİZ, M. G.^{1*} – AYGÜL, E. Ö.²

¹*Applied Sciences University of Isparta, Sütçüler Prof. Dr. Hasan Gürbüz Vocational School, Forestry Department, Sütçüler / Isparta, Turkey
(phone: +90-555-694-5786; fax: +90-246-351-2901)*

²*Yozgat Bozok University, Boğazlıyan Vocational School, Forestry Department
Boğazlıyan / Yozgat, Turkey
(phone: +90-354-290-3002; fax: +90-354-290-3003)*

*Corresponding author

e-mail: mehmetnegiz@isparta.edu.tr; phone: +90-555-694-5786; fax: +90-246-351-2901

(Received 22nd Jul 2019; accepted 28th Nov 2019)

Abstract. This study was conducted to determine the relationships between woody plant species alpha diversity (α) and environmental factors in Dedegöl (Yenişarbademli) Mountain area. The research data obtained from 103 sampling plots after the land inventory study was used to calculate the diversity variables. The coverage area and habitat characteristics of woody plant species in each sampling plot were recorded during the field work. Clustering analysis (CLA) was used to group the sampling plots base on the vegetation data matrix. Correspondence Analysis (CA) and detrended correspondence analysis (DCA) from the ordination techniques were applied in the study to the vegetation matrix in order to determine the distribution degree of the sampling plots on the ordination axis. As a result of the CA applied, surface stoniness was found to be the environmental factor that had the highest correlation. In conclusion, surface stoniness was found to have an important impact on the vegetation distribution. Furthermore, canonical correspondence analysis (CCA) was applied at the final stage of the study. In conclusion, Shannon-Wiener was the most effective index to calculate the alpha species diversity while surface stoniness and elevation were the most explanatory variables for alpha species diversity in the study site.

Keywords: *biodiversity, forest ecosystems, habitat factors, Shannon-Wiener index, ordination methods*

Introduction

Biological diversity is the degree of variation in the living organisms in a specific ecosystem, biome or in the entire world, referring to the variability in the species, functions and structures among the living organisms. Forest ecosystems constitute the most important sources of biological diversity as they contain 2/3 of the world's ecosystems (Thompson et al., 2009).

Biological diversity is a very broad concept that covers genetic diversity, species diversity and ecosystem diversity (Hunter, 1996; Aertsens et al., 2010; Negiz, 2013).

Species diversity is one of the most important elements to determine the biological diversity in forest ecosystems. Studies on forest ecology mainly focus on plant species diversity (Özkan, 2006; Özkan and Süel, 2008; Negiz, 2013; Özkan, 2016; Negiz and Aygül, 2019).

Species diversity is divided into three categories of alpha diversity (α), beta diversity (β) and gamma (γ) diversity (Gülsoy and Özkan, 2008). Alpha diversity is determined for a specific area while beta diversity is the measure of diversity among areas. Gamma

diversity refers to the total diversity of the relevant ecosystem covering these areas (Whittaker, 1972; Zhao et al., 2005; Mareno et al., 2006; Hashemi, 2010).

High species diversity is very important for a forest ecosystem. Ecosystems, which have a rich species diversity, are more resilient against any kind of adverse impacts. In other words, it plays a key role in the sustainability of ecosystems (Negiz, 2013).

On the other hand, there are important relationships between species diversity and habitat characteristics in forest ecosystems. It is clear that the areas with high potential in terms of species diversity can be identified if such relationships are known (Linder, 2001; Özkan, 2006).

Our study site – Dedegöl Mountains – (Yenişarbademli) region has a very rich forest asset. However, the amount of forestlands, which were degraded by people, is close to that of the actual forestlands. Potential areas should be identified to establish new forests. Therefore, it is important to determine the biological diversity of the area. This study was conducted in order to determine the relationships between the alpha diversity of Dedegöl Mountain (Yenişarbademli) region having a very high plant species diversity in the Mediterranean region and the habitat characteristics.

Material and Methods

Study area

The study site is located in the Dedegöl (Yenişarbademli) Mountain areas in Turkey at 37°38'35" north and 31°21'17" east coordinates. The study site is situated in the Lakes Region of the Mediterranean Region, in the west of Beyşehir Lake, and the vast majority of the site is contained in Isparta- Yenişarbademli and Isparta-Konya provincial boundaries (Fig. 1). The elevation of the region varies from 820 m to 2992 m. The mean monthly temperature during many years is 10.7 degrees. The total mean annual precipitation is 727 mm.

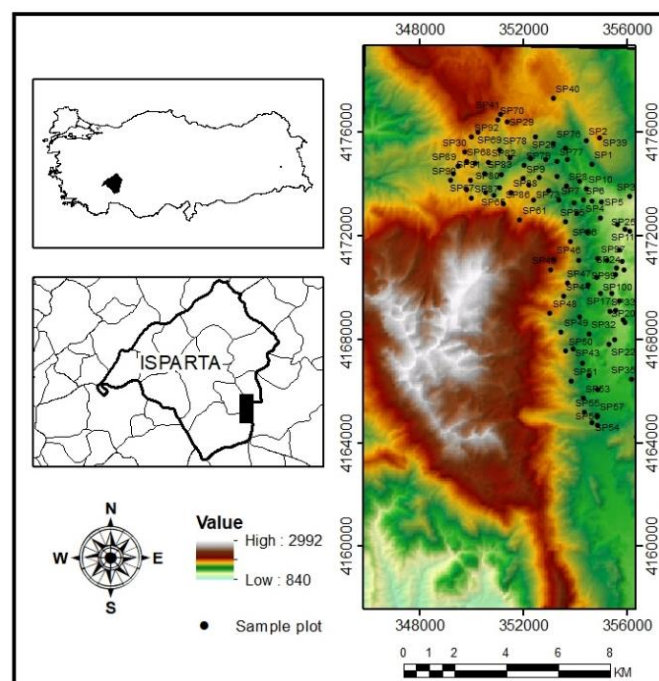


Figure 1. Location Map of Dedegöl Mountain Region

Sampling method

In this study, 103 sampling plots were used. Studies on sampling areas were carried out between April and September, which was the vegetation period in 2016-2017. The sampling plots were selected randomly at a size of 20 m x20 m. The woody plant species in the sampling plots were identified and recorded in the inventory cards according to the Braun-Blanquet method.

From the environmental variables; latitude, longitudes and elevation were determined with global position systems (GPS), while slope was determined with abney level and aspect was determined with a compass and slope position was determined in 5 classes (Valley Floor: 1, Lower: 2, Intermediate: 3, Upper: 4, Ridge: 5). Surface stoniness was calculated as the mean percentage (%) of 20 different points in the lower sampling plots with an iron bar and recorded to be associated with the alpha diversity inputs. Obtained environmental variables and the codes given to them for use in statistical analysis are given in *Table 1*.

Table 1. Environmental variables and their codes

Codes	Environmental variables
LATITU	Latitude
LONGTI	Longitude
ELEVATION	Elevation
ASPECT	Aspect
ALTITUDE	Altitude
SLOPOS	Slope Position
SURSTON	Surface Stoniness

Data analysis

First, the environmental variables were determined for alpha diversity. During the office work, firstly the coverage area of woody plant species was digitalized according to the method propose by Fontaine et al. (2007) and Özkan (2009) to calculate the alpha diversity ($r:0.01$, $+:0.02$, $1:0.04$, $2:0.15$, $3:0.375$, $4:0.625$, $5:0.875$).

The climate data was obtained from 19 different climate data downloaded from <http://www.worldclim.org> (*Table 2*). This data was downloaded at the world scale, and was then reduced to the scale of the study site and made available to be used in the study.

The environmental variables were obtained through the digital elevation model. First the slope and aspect maps were created with ArcGIS software, then the topographic position index (TPI), ruggedness index (EI), roughness index (PI) and shading index (GI) were created. Following these stages, different equations were used to calculate the values of the aspect compliance index (AC), temperature index (TI) and radiation index (RI).

The researchers have developed indexes to calculate the alpha species diversity such as Shannon- Wiener, Brillouin, Simpson, Margalef D and Berger- Parker (Shannon, 1948; Simpson, 1949; Berger and Parker, 1970; Clifford and Stephenson, 1975; Pielou, 1975; Özkan, 2016). Basic components analysis was applied with the help of SPSS software so as to decide which of these indexes should be used. In order to determine the relationships between the alpha values and environmental factors, spearman rank correlation analysis and regression analysis were applied with the help of SPSS software. Clustering analysis was performed according to the Ward's method through the Past program to divide the vegetation groups by using the woody plants identified in the sampling plots. The

relationship analysis among the qualities was performed via the SPSS software in order to determine the indicator species of the groups which were divided with the clustering analysis. Ordination methods (DCA; CCA; CA) were used with the help of PC-ORD for more clear interpretation of the relationships between the woody vegetation identified in the sampling plots and the environmental factors.

Table 2. Climate variables and their codes

Codes	Climate variables
BIO1	Annual Mean Temperature
BIO2	Mean Diurnal Range
BIO3	Isothermality
BIO4	Temperature Seasonality
BIO5	Max Temperature of Warmest Month
BIO6	Min Temperature of Coldest Month
BIO7	Temperature Annual Range
BIO8	Mean Temperature of Wettest Quarter
BIO9	Mean Temperature of Driest Quarter
BIO10	Mean Temperature of Warmest Quarter
BIO11	Mean Temperature of Coldest Quarter
BIO12	Annual Precipitation
BIO13	Precipitation of Wettest Month
BIO14	Precipitation of Driest Month
BIO15	Precipitation Seasonality
BIO16	Precipitation of Wettest Quarter
BIO17	Precipitation of Driest Quarter
BIO18	Precipitation of Warmest Quarter
BIO19	Precipitation of Coldest Quarter

Results and Discussion

The data obtained from 103 sampling plots were used. The species that had the highest presence in the study site were *Pinus nigra* (98.06%), *Cistus laurifolius* (57.28%), *Verbascum glomeratum* (57.28%).

As a result of the basic components analysis (BCA) performed to determine the representative diversity index out of the alpha diversity indexes; Taxa_S (0.937), Simpson_1-D (0.917), Shannon-Wiener index (0.950), Shannon-Wiener index were found to have the highest coefficient.

In many studies on biodiversity, usually Shannon-Wiener index was used to calculate the alpha diversity index while the results were consistent with that finding (Gorelick, 2006; Ohsawa and Nagaike, 2006; Liang et al., 2007; Gülsoy and Özkan, 2008; Negiz, 2013).

As a result of the basic components analysis (BCA) performed to reduce the climate variables or select the most suitable representative climate variables; two components with a variance greater than and variance contribution greater than 10% were found. The variance contribution of the first component was 83.3% while that of the second component was 12.7% and the rate of these two components in the total variance was 96%.

According to the Spearman rank correlation analysis that showed the relationships between the alpha species diversity and environmental factors; the alpha species diversity (Shannon_H) had a significantly positive correlation with BIO1 ($r_s=0.269$ and $p<0.01$), BIO2 ($r_s=0.278$ and $p<0.01$), BIO4 ($r_s=0.273$ and $p<0.01$) and BIO10 ($r_s=0.274$ and

$p < 0.01$); BIO11 ($r_s = 0.273$ and $p < 0.01$); ALTITUDE ($r_s = 0.292$ and $p < 0.01$) and SURSTON ($r_s = 0.359$ and $p < 0.01$) while it had a negative relationship with BIO12 ($r_s = -0.360$ and $p < 0.01$) and ELEVATION ($r_s = -0.220$ and $p < 0.05$).

The alpha diversity values had positive correlations with several climate variables selected as the representative climate variables whereas it had a negative relationship with only annual precipitation (BIO12). As mentioned above, heavy snow and snow thickness at especially higher elevations in the region can be suggested as the most important reason for that. Another important aspect of the Spearman rank correlation analysis results was that the alpha diversity variables had a positive correlation with SURSTON while it had a negative relationship with ELEVATION. The positive correlation with surface stoniness can be explained by the fact that the areas with high surface stoniness were located in the south-eastern parts of the study site and thus the sunshine duration was longer in those area compared to the others.

According to the results of the multiple regression analysis performed to model the alpha diversity; R^2 value of the best model was 0.272 and its standard error was 0.348. That is, the model explained 27.2% of the variance and it is significant at the level of $p < 0.01$. This model was constituted with SURSTON, ELEVATION, BIO5, TPI. The variance inflation factors of the model were lower than 5. Its tolerance values were closer to 1. The significance level of all variables including the model's constant was lower than 5%. Beta value indicates the significance of the variables in the model. In this context, ELEVATION was the most important variable.

The relationships with ELEVATION were negative as those in the Spearman rank correlation analysis. This shows that the alpha diversity was higher at lower elevations.

As a result of the clustering analysis performed according to the Ward's method; groups of 2 (T:-31.7211; A:0.05868; P:0), 3 (T:-29.3821; A:0.078724; P:0), 4 (T:-32.8804; A:0.107194; P:0) and 5 (T:-30.6251; A:0.68298; P:0) were used. In order to decide the most suitable group separation, MRPP analysis was conducted with PC-ORD program. According to the MRPP analysis; it was decided that the group of 4 had the most effective results in terms of T, A and P values.

A relationship analysis between qualities was performed to determine the indicator plant species of the groups. The analysis revealed that the most important indicator species in Group A were *Cistus laurifolius* and *Rosa canina*, while *Cistus laurifolius*, *Euphorbia* sp., *Juniperus excelsa*, *Laurus nobilis*, *Populus tremula* and *Thymus samius* were the most important indicator species in Group B. The most important indicator species of Group C were *Cistus laurifolius*, *Euphorbia* sp., *Juniperus oxycedrus* subsp. *oxycedrus*, *Rosa canina* and *Verbascum* sp. while *Sambucus ebulus* and *Abies cilicica* subsp. *isaurica* were the most important indicator species in Group D.

The results of the Spearman rank correlation analysis performed to investigate the relationships between the abovementioned groups and the alpha species diversity (Shannon_H). Group A (Correlation Coefficient: 0.358; Significance Level:0) and Group D (Correlation Coefficient: 0.281; Significance Level:0.004) had a positive relationship with the groups whereas Group C (Correlation Coefficient: -0.384; Significance Level:0) had a negative relationship with the groups.

In conclusion, the sampling plots in Group A were located at the intermediate elevations in the study site (1226-1694). *Rosa canina* and *Cistus laurifolius* that were the indicator species in Group A verify this finding. Group A had a higher alpha diversity than the other groups. This leads to the conclusion that the species diversity is higher at intermediate elevations in the study site. It was found that the species diversity decreased

as the elevation increased in the study site. This can be explained by the fact that there were some snow-covered locations at high elevations in the study site with heavy snow for a long time (approximately 6 months a year). Many plant species in the region preferred low elevations due to the snow cover (Özkan, 2006; Özkan and Negiz, 2011).

The ranking and association analysis were conducted according to the ordination methods. First, the location of the vegetation communities on the axis was determined according to different ordination methods. Furthermore, the groups identified according to the clustering analysis were transferred to the ordination axis at this point to demonstrate the relationship between the groups and the distribution of vegetation communities. Finally, the environmental variables included in the data as the second matrix were associated with the ordination axis so that the vegetation-environment relationships on the axis were interpreted.

Correspondence Analysis (CA) was the first ranking-association analysis to have been applied in the study. The vegetation data matrix was evaluated with the correspondence analysis. The location of the sampling plots was identified on the ordination axis. 3 axis were obtained with this analysis, while Axis 1 (0.339; 7.72), Axis 2 (0.261; 5.93), Axis 3 (0.238; 5.43) were identified according to the Eigenvalue coefficient and variance explanation power of the axis. This indicates that Axis 1 had the highest Eigenvalue coefficient and variance explanation power. Therefore, it was decided to include only the Axis 1 in the analysis. The location of the sampling plots on Axis 1-2 is shown in Fig. 2.

The correlation coefficients of the relationships between the Axis 1-2 and plant species in the vegetation data matrix were found to be *Cirsium arvense* subsp. *vestitum* (0.519), *Euphorbia* sp. (0.664), *Populus tremula* (-0.564) and *Thymus samius* (0.550) while the plant species had the highest correlation with Axis 1.

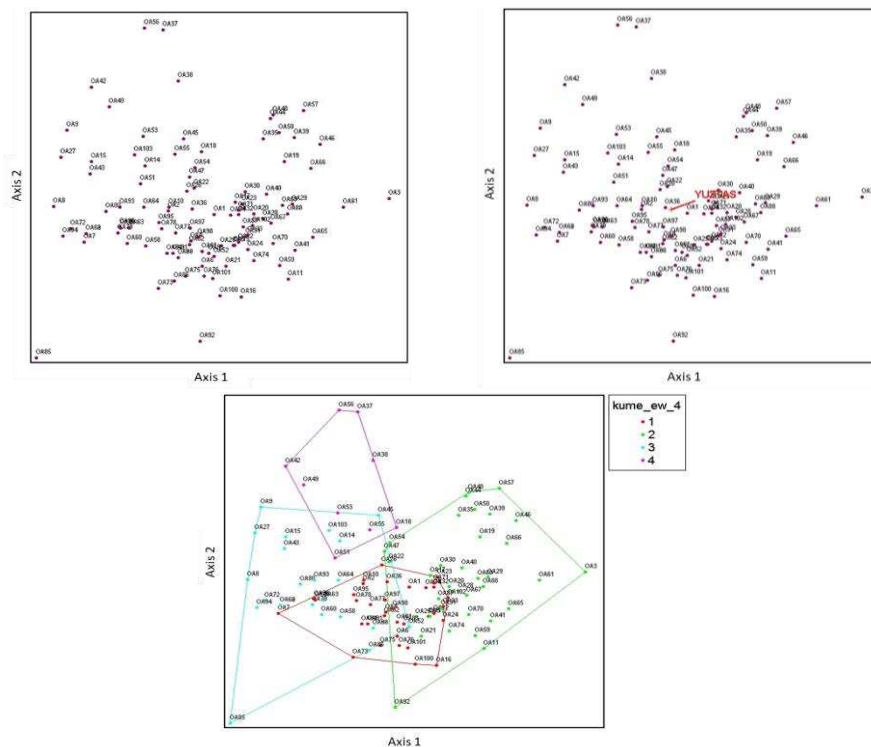


Figure 2. Location of sampling plots on Axis 1-2 according to the correspondence analysis, location of environmental variables and Euclidean-Ward's 4 groups according to the clustering analysis

As regards the correlation coefficients of the environmental variables according to the association between the axis and environmental data matrix; SURSTON (0.368) were found to be the environmental factor that had the highest correlation with the axis while it had a positive correlation with Axis 1. The location of the statistically significant environmental variables on the axis is shown in *Fig. 2*.

When the results relating to the vegetation data matrix and those of the environmental variables were interpreted together on Axis 1, it was understood to have a positive correlation with *Cirsium arvense* subsp. *vestitum*, *Euphorbia* sp., *Populus tremula*, *Thymus samius*.

At the next stage, the location of the groups identified at the Euclidean-Ward's 4 Groups separation stage in the clustering analysis according to the results of the grouping analyses was transferred to the Axis 1-2 identified in the correspondence analysis (*Fig. 2*).

The detrended correspondence analysis (DCA) was another ranking-association analysis applied in the study. With this analysis, 3 axis were identified, which were Axis 1 (0.339; 3.155), Axis 2 (0.234; 2.567) and Axis 3 (0.182; 2.193) according to their Eigenvalue coefficients and variance explanation power. Axis 2 had the highest Eigenvalue coefficient and variance explanation power. Therefore, it was decided to include only the Axis 1 in the analysis. The location of the sampling plots on Axis 1-2 is shown in *Fig. 3*.

The correlation coefficients of the relationships between Axis 1-2 and the plant species in the vegetation data matrix were found to be *Cirsium arvense* subsp. *vestitum* (0.531), *Euphorbia* sp. (0.678), *Juniperus excelsa* (0.508), *Populus tremula* (-0.562) and *Thymus samius* (0.552) while the plant species had the highest correlation with Axis 1.

As regards the correlation coefficients of the environmental variables according to the association between the axis and environmental data matrix; SURSTON (0.375) were found to be the environmental factor that had the highest correlation with the axis while it had a positive correlation with Axis 1. The location of the statistically significant environmental variables on the axis is shown in *Fig. 3*.

When the results relating to the vegetation data matrix and those of the environmental variables were interpreted together on Axis 1, it was understood that there was a positive correlation with *Cirsium arvense* subsp. *vestitum*, *Euphorbia* sp., *Juniperus excelsa*, *Populus tremula* and *Thymus samius*.

At the next stage, the location of the groups identified at the Euclidean-Ward's 4 Groups separation stage in the clustering analysis according to the results of the grouping analyses was transferred to the Axis 1-2 identified in the correspondence analysis (*Fig. 3*).

The canonical correspondence analysis (CCA) was another analysis applied in the study. With this analysis, 3 axes were identified, which were Axis 1 (0.179; 4.7), Axis 2 (0.151; 4), Axis 3 (0.118; 2.9) according to their Eigenvalue coefficients and variance explanation power. This indicates that Axis 1 had the highest Eigenvalue coefficient and variance explanation power. Therefore, it was decided to include only the Axis 1 in the analysis. The location of the sampling plots on Axis 1-2 is shown in *Fig. 4*.

The correlation coefficients of the relationships between Axis 1-2 and the plant species in the vegetation data matrix were found to be *Cistus laurifolius* (-0.557), *Cirsium arvense* subsp. *vestitum* (0.501), *Euphorbia* sp. (0.609), *Laurus nobilis* (0.540) and *Thymus samius* (0.549) while the plant species had the highest correlation with Axis 1.

As regards the correlation coefficients of the environmental variables according to the association between the axis and environmental data matrix; SURSTON (0.477) and BIO12 (0.393) were found to be the environmental factor that had the highest correlation

with the axis while they had a positive correlation with Axis 1. The location of the statistically significant environmental variables on the axis is shown in Fig. 4.

When the results relating to the vegetation data matrix and those of the environmental variables were interpreted together on Axis 1, it was understood that there was a positive correlation with *Cistus laurifolius*, *Cirsium arvense* subsp. *vestitum*, *Laurus nobilis*, *Thymus samius*, *Euphorbia* sp., SURSTON and BIO12.

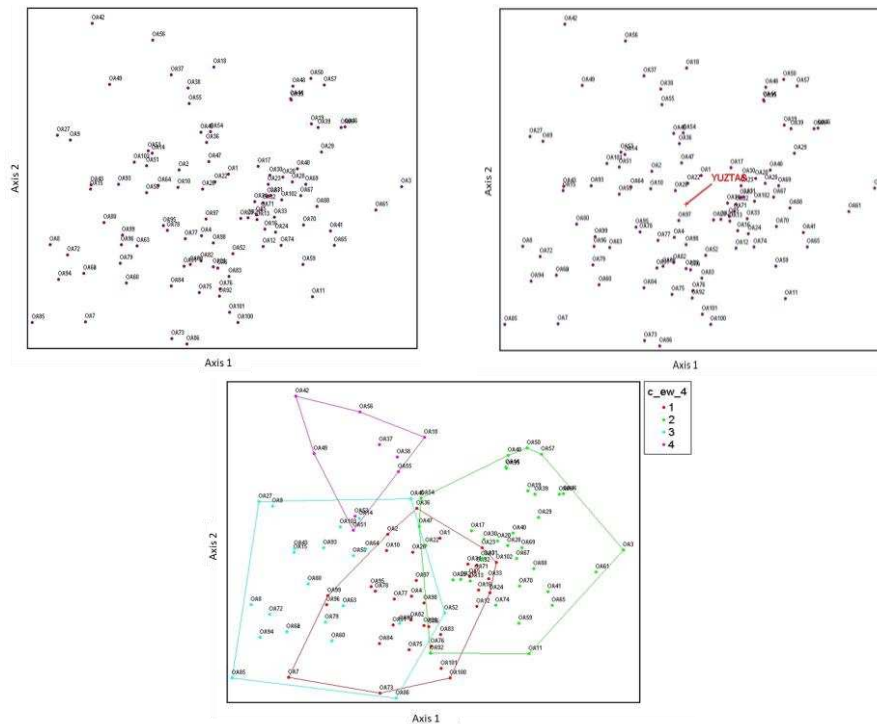


Figure 3. Location of sampling plots on Axis 1-2 according to the detrended correspondence analysis, location of environmental variables and Euclidean-Ward's 4 groups according to the clustering analysis

At the next stage, the location of the groups identified at the Euclidean-Ward's 4 Groups separation stage in the clustering analysis according to the results of the grouping analyses was transferred to the Axis 1-2 identified in the correspondence analysis (Fig. 4).

The relationships between the results of these analyses (ordination axis values of sampling plots) and habitat characteristics were tested with the Pearson correlation analysis. The results of the ordination analysis were similar concerning the statistical significance of the environmental variables. The structured groups were transferred to the graphical result of each ordination analysis and the conformity of the sampling plots with their respective groups was tested in their distribution in the ordination axis.

The results of DCA, one of the ordination methods applied, demonstrated that four groups identified in the clustering analysis were more clearly separated compared to the other ordination methods (CA, CCA) to explain the vegetation-environment relationships in Yenişarbademli.

DCA results also showed that SURSTON had the highest positive correlation with especially Axis 1 regarding the location of the sampling plots. Similarly, SURSTON was the environmental variable that had the strongest positive relationship also in RA and

CCA. Several studies conducted in the Mediterranean region found that elevation was the most important habitat factor that had an impact on the vegetation distribution (Fontaine et al., 2007; Özkan et al., 2009; Şentürk et al., 2013). The reason why SURSTON was found to be the most important variable in this study was that the areas with high surface stoniness were located in the southeast part of the study site as in the Spearman rank analysis and multiple regression analysis and thus the duration of sunlight in these areas was higher than the other locations.

As regards the CCA process, the relationships between the environmental variables demonstrate that SURSTON, BIO4, BIO12 had high relationships with one another. Therefore, the distribution of vegetation was denser especially in the southeast locations with high surface stoniness as the annual precipitation and seasonal temperature in the region increased.

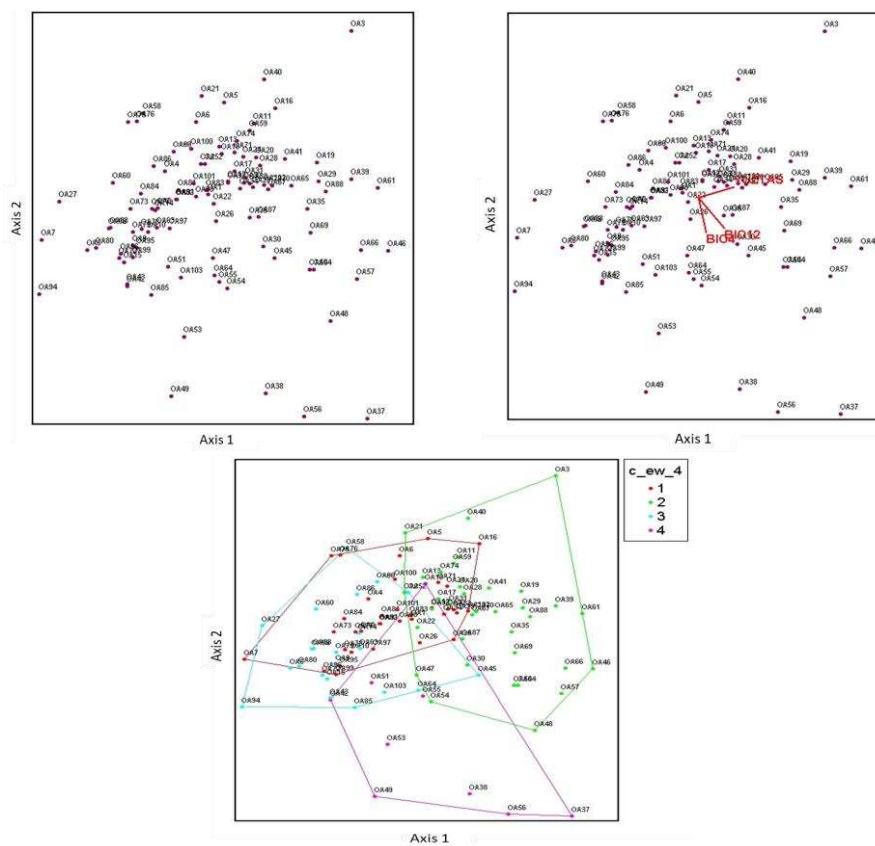


Figure 4. Location of sampling plots on Axis 1-2 according to the canonical correspondence analysis, location of environmental variables and Euclidean-Ward's 4 groups according to the clustering analysis

Conclusions

In summary, this study demonstrated that the sampling plots had a higher alpha diversity when the elevation variability was lower and surface stoniness variability was higher. It was also found that the distribution of vegetation was denser in areas where the seasonal temperature and annual precipitation were higher.

The study area was mountainous and carstic, which played a significant role in these findings. This information is also important to determine the areas with high potential for

the components of species diversity. The Lakes Region was one of the oldest settlements in Yenişarbademli while the ecosystem had been destroyed by people for a long time (Vanhaverbeke and Waelkens, 2003; Karaca, 2005; Özkan et al., 2010). Most of the forests have been degraded due to the destruction; therefore, it is important to understand/predict the potential of especially the destroyed areas with the help of the actual information.

Acknowledgements. We would like to thank Süleyman Demirel University, Head of Scientific Research Projects Management Unit for their support to our work with Project No: 4817-YL1-16.

REFERENCES

- [1] Aertsen, W., Kint, V., Van Orshoven, J., Özkan, K., Muys, B. (2010): Comparison and Ranking of Different Modelling Techniques For Prediction of Site Index in Mediterranean Mountain Forests. – *Ecological Modelling* 221: 1119-1130.
- [2] Berger, W. H., Parker, F. L. (1970): Diversity Of Planktonic Foraminifera in Deep-Sea Sediments. – *Science* 168: 1345-1347.
- [3] Clifford, H. T., Stephenson, W. (1975): An introduction to numerical classification. – Academic Press, New York.
- [4] Fontaine, M., Aerts, R., Özkan, K., Mert, A., Gülsoy, S., Süel, H., Waelkens, M., Muys, B. (2007): Elevation and Exposition Rather Than Soil Types Determine Communities and Site Suitability in Mediterranean Mountain Forests of Southern Anatolia, Turkey. – *Forest Ecology and Management* 247: 18-25.
- [5] Gorelick, R. (2006): Combining Richness and Abundance Into a Single Diversity Index Using Matrix Analogues of Shannon's and Simpson's Indices. – *Ecography* 29: 525-530.
- [6] Gülsoy, S., Özkan, K. (2008): Importance of biodiversity from the ecological standpoint and some diversity indexes. – *Turkish Journal of Forestry* 1: 168-178. (In Turkish).
- [7] Hashemi, S. A. (2010): Evaluating plant species diversity and physiographical factors in natural broad leaf forest. – *American Journal of Environmental Science* 6(1): 20-25.
- [8] Hunter Jr, M. (1996): Benchmarks for managing ecosystems: are human activities natural? – *Conservation Biology* 10(3): 695-697.
- [9] Karaca, V. (2005): Belgelerle Yenişar. – Kardelen Sanat Publishing, Isparta. (In Turkish).
- [10] Liang, J., Buongiorno, J., Monserud, R. A., Kruger, E. L., Zhou, M. (2007): Effects of Diversity of Tree Species And Size on Forest Basal Area Growth, Recruitment, And Mortality. – *Forest Ecology and Management* 243: 116-127.
- [11] Linder, H. P. (2001): Plant diversity and endemism in sub-saharan tropical africa. – *Journal of Biogeography* 28: 169-182.
- [12] Mareno, C., Zuria, I., García-Zentono, M., Sánchez-Rojas, G., Castellanos, I., Martínez-Morales, M., Rojas-Martínez, A. (2006): Trends in the measurement of alpha diversity in the last two decades. – *Interciencia* 31(1): 67-71.
- [13] Negiz, M. G. (2013): Relationships between woody plant diversity and environmental factors in the Gölhisar (Burdur) district. – Ph.D. Thesis, Graduate School of Applied and Natural Sciences, Suleyman Demirel University, Isparta. (In Turkish).
- [14] Negiz, M. G., Aygül, T. İ. (2019): Distribution of woody species richness in Kurucuova Region according to environmental factors. – *Turkish Journal of Forestry* 20(2): 123-132.
- [15] Ohsawa, M., Nagaike, T. (2006): Influence of Forest Types And Effects of Forestry Activities on Species Richness and Composition of Chrysomelidae in the Central Mountainous Region of Japan. – *Biodiversity and Conservation* 15(4): 1179-1191.
- [16] Özkan, K. (2006): Relationships between tree and scrub species diversity and physiographic site factors in Çarıksaraylar site section groups, Beyşehir watershed. – *Anadolu University Journal of Science and Technology* 7(1): 157-166. (In Turkish).

- [17] Özkan, K., Süel, H. (2008): Endemic plant species in a karstic canyon (mediterranean region, Turkey): relation to relief and vegetation diversity. – *Polish Journal of Ecology* 56(4): 709-715.
- [18] Özkan, K. (2009): Environmental Factors as Influencing Vegetation Communities in Acipayam District of Turkey. – *Journal Environmental Biology* 30(5): 741-746.
- [19] Özkan, K., Gülsoy, S., Mert, A., Öztürk, M., Muys, B. (2010): Plant Distribution-Altitude and Landform Relationships in Karstic Sinkholes of Mediterranean Region of Turkey. – *Journal of Environmental Biology* 31: 51-60.
- [20] Özkan, K., Negiz, M. G. (2011): Woody Vegetation Classification and Mapping by Using Hierarchical Methods in Isparta- Yukarıgökdere District. – *SDU Faculty of Forestry Journal* 12: 27-33. (In Turkish).
- [21] Özkan, K. (2016): Biyolojik Çeşitlilik Bileşenleri (α , β ve γ) Nasıl Ölçülür? – Süleyman Demirel Üniversitesi Orman Fakültesi Yayınları, Isparta. (In Turkish).
- [22] Pielou, E. C. (1975): *Ecological Diversity*. – Wiley InterScience 165p, New York.
- [23] Shannon, C. E. (1948): A Mathematical Theory of Communication. – *The Bell System Technical Journal* 27: 379-423.
- [24] Simpson, E. H. (1949): Measurement of diversity. – *Nature* 163: 688.
- [25] Şentürk, Ö., Uluşan, M. D., Eser, Y., Şenol, A., Özkan, K. (2013): Investigation of relationships between vegetation and environmental factors in the Cariksaraylar district of the sultan mountains. – *GeoMed 2013, The 3rd International Geography Symposium*: 597-607.
- [26] Thompson, I., Mackey, B., McNulty, S., Mosseler, A. (2009): Forest Resilience, Biodiversity, and Climate Change. A synthesis of the biodiversity/resilience/stability relationship in forest ecosystems. – Secretariat of the Convention on Biological Diversity, Montreal. Technical Series 43: 67.
- [27] Vanhaverbeke, H., Waelkens, M. (2003): *The chora of sagalassos. The Evolution of the Settlement Pattern From Prehistoric Until Recent Times*. – Brepols Publishers.
- [28] Whittaker, R. H. (1972): Evolution and Measurement of Species Diversity. – *Taxon* 21(2): 213-251.
- [29] Zhao, C. M., Chen, W. L., Tian, Z. Q., Xie, Z. Q. (2005): Altitudinal Pattern of Plant Species Diversity in Shennongjia Mountains, Central China. – *Journal of Integrative Plant Biology* 47(12): 1431-1449.

CHARACTERIZATION OF GENETIC DIVERSITY AND RELATIONSHIP IN ALMOND (*PRUNUS DULCIS* [MILL.] D.A. WEBB.) GENOTYPES BY RAPD AND ISSR MARKERS IN SULAIMANI GOVERNORATE

MAHOOD, A. M. R. * – HAMA-SALIH, F. M.

Horticulture Department, College of Agricultural engineering Sciences, University of Sulaimani Sulaimani-Kurdistan Region, Iraq

*Corresponding author

e-mail: anwar.rauf@univsul.edu.iq; phone: +96-4770-1532-547

(Received 13th Oct 2019; accepted 21st Jan 2020)

Abstract. Genetic diversity of 38 almond local genotypes was investigated using RADP and ISSR markers with the analysis of nut morphology. Samples were taken from five locations for this study, including Sharbazher, Mergapan, Qaradakh, Barznja, and Hawraman. Almond nuts width, length and thickness were studied and their mean values were observed to range between 16.18-27.21 mm, 24.18-41.07 mm and 11.49-16.81 mm, respectively. Polymorphic bands of mean values were 9.5 for random amplified polymorphic DNA (RAPD) and 8 for inter-simple sequence repeat (ISSR). The PIC values were recorded for RAPD primers to range between 0.77 to 0.97 and those for ISSR primers were also verified between 0.36 to 0.97. Based on Jaccard similarity coefficients, the genetic distances were recorded between 0.32 (B-G3 vs. B-G4) (M-G2 vs. M-G1) to 0.75 (H-G5 vs. Q-G1) and all genotypes were grouped into 3 major clusters (A, B and C) with a mean dissimilarity 0.535 for 20 RADP markers. In the case of the 15 ISSR markers, a genetic distance between 0.19 (H-G13 vs. H-G12) to 0.78 (H-G5 vs. B-G6) was also observed, with four clades (A, B, C and D) with a mean dissimilarity of 0.485. According to STRUCTURE analysis, all genotypes were divided into two groups. Analysis of molecular variance (AMOVA) demonstrated a high-level genetic differentiation within a population 88% for RAPD and 87% for ISSR.

Keywords: *morphological traits, genetic relationship, genetic structure, random amplified polymorphic DNA, inter-simple sequence repeat*

Introduction

Almond (*Prunus dulcis* (Mill.) D.A. Webb syn. *P. amygdalus* L. Batsch is a commercially important fruit plant, from the *Rosaceae* family (Zhu, 2014; Sakar et al., 2019). The place of wild almond is originated at the arid mountainous region of Central Asia and deserts of western China, Iran, Turkistan, Afghanistan, Kurdistan, and Southwest Asia with subsequent expansion into European and North African regions (Browicz and Zohary, 1996; Kester and Gradziel, 1996; Xu et al., 2004) and it is also grown commercially around the world. Global almond production for 2018/19 is an estimated 1.4 million metric tons (USDA, 2018). Botanists observed over 30 species, subspecies with ecotype (Grasselly, 1976; Ladizinsky, 1999). Genetically, Almond is diploid, the chromosome number is $2n = 2x = 16$ with a genome size approximately 246 Mb (Sánchez-Pérez et al., 2019).

Almond is one of the vital plants that can grow under the rain-fed condition in Iraq, particularly in the Kurdistan region. Therefore, it is important to know the adaptation of this tree that able to tolerate the biotic and abiotic stresses. Almond is a large-sized tree, with long generation time and also has a low level of variability in morphology traits (Casas et al., 1999; Sorkheh et al., 2007, 2009; Zeinalabedini et al., 2008; Bouhadida et al., 2009). To provide information about genetic relationships it is important to study the

differences at the level of agronomic, morphological and biochemical traits (Khan et al., 2016). Genetic diversity is an important tool that breeders can use to detect and identify with differentiation all genotypes and also it is a useful tool to improve the chances of the selection of better segregates for various characters (Dwevedi and Lal, 2009). Using morphological traits to the identification of almond plants is restricted, because of their environmental variations. However, morphological traits, including seed length and kernel size normally can be used.

In Kurdistan, Iraq, information about almond genotypes has been poorly recognized. Therefore, the modern molecular genetic tool can be applied to identify and characterize the relationships among them. However, several similar studies have been performed regarding genetically recognized cultivars and wild species of almond.

Molecular markers have shown the vital role in crop breeding, particularly in genetic diversity research and gene bank. PCR-based DNA marker systems are generally used, including Random amplified polymorphic DNA (RAPD), inter-simple sequence repeat (ISSR), amplified fragment length polymorphism (AFLP) and more recently simple sequence repeats (SSRs) or microsatellites (Gupta et al., 2000).

Since no molecular evidence was obtainable concerning the almond genotypes grown in Sulaimani region, therefore, the consciousness and conception of the genetic diversity in Sulaimani almond accessions are important for the implementation of degree addressed to their usages and preservations. The present study was aimed to estimate the genetic diversity with relatedness among the most important almond genotypes and for the first time their population structure in Sulaimani was developed for almond genotypes by using RAPD and ISSR markers.

Materials and Methods

Locations and plant material

Five locations (*Fig. 1, Table 1*) were selected for this study with thirty-eight almond local genotype trees distributed, including Sharbazher (9), Mergapan (3), Qaradakh (5), Barznja (7), and Hawraman (14).

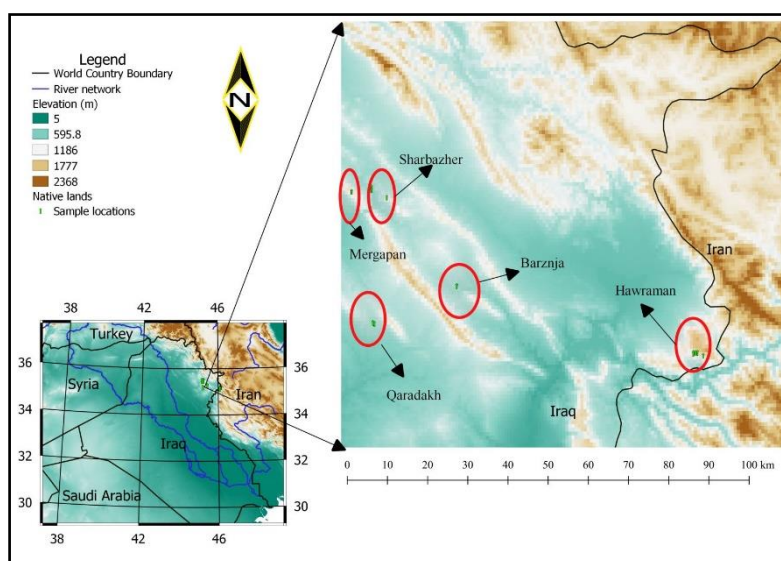


Figure 1. Distribution of collection sites of study plant materials in Sulaimani governorate

Table 1. Genotypes name, location, latitude and altitude

Genotypes name	Locations	Latitude		Altitude
		N°	W°	
SH-G1 to SH-G9	Sharbazher	35°49'30"	45°18'93"	997.6
M-G1 to M-G3	Mergapan	35°48'93"	45°13'47"	1148
Q-G1 to Q-G5	Qaradagh	35°19'29"	45°19'69"	925.8
B-G1 to B-G7	Barznja	35°27'69"	45°42'21"	1154
H-G1 to H-G14	Hawraman	35°12'38"	46°07'80"	1402

Morphological study of seeds

Almond nuts were collected from each genotype (*Fig. 2*) Impurities such as damaged or broken nut, dust and dirt have been eliminated. For each nut, weight and size dimensions (the three axial dimensions) including length, width, and thickness of the nuts were measured by using a digital calliper with an accuracy of 0.01mm. The nuts were cracked, then using a hammer and kernel weighted to calculate shelling percentage.

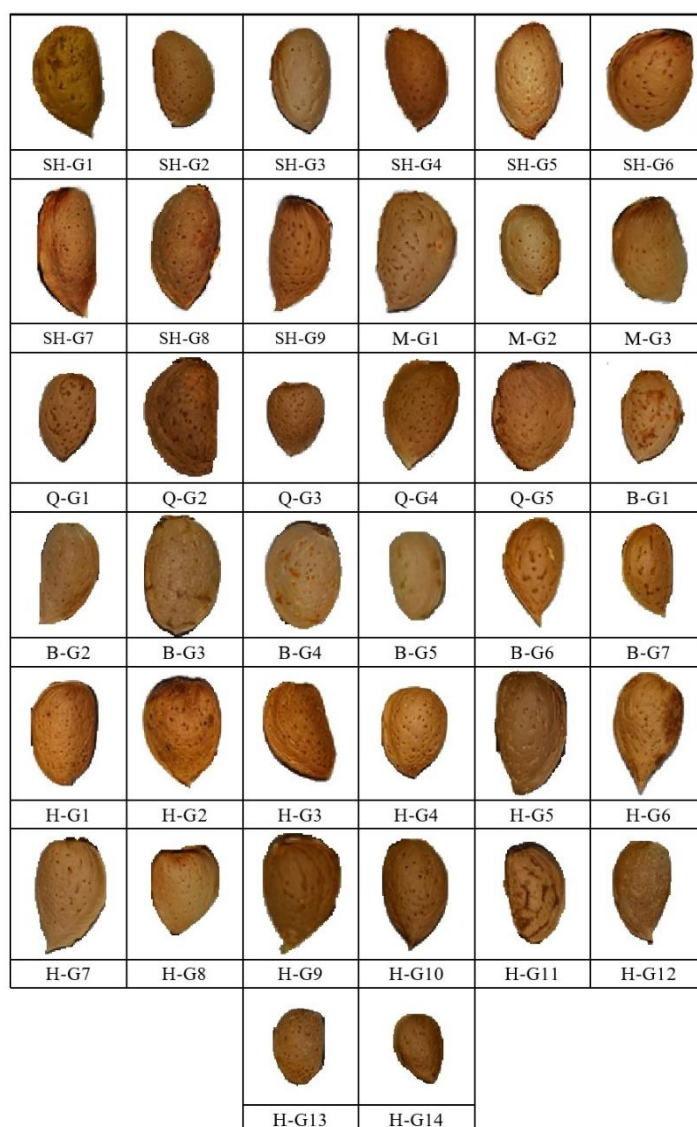


Figure 2. Shows the different morphological shapes of all almond genotypes nut, (Scale 1:1.75)

Genomic DNA extraction and purification

The CTAB DNA extraction protocol with some modifications was used to isolate genomic DNA, according to (Tahir and Hama Karim, 2011). Briefly, 1 gram of fresh leaves was ground and frozen in liquid nitrogen and then 2 ml of CTAB buffer was added and incubated at 60°C for 60 min. (1 M Tris HCl (pH 8.0), 5 M NaCl, 0.5 M EDTA and 2 g of CTAB (cetyltrimethyl ammonium bromide)), the DNA sample was precipitated with 0.08 volumes of ammonium acetate and 0.54 volumes of ice isopropanol, and then the DNA pellet was washed with 1 ml of ice-cold 70% ethanol and then the dried pellet was resuspended in 50-100 µl of deionized water. DNA was treated with RNase to remove RNA contamination. The DNA concentration was analyzed by electrophoresis using a 1.5% agarose gel.

RAPD analysis

Twenty primers were utilized in this work, (*Table 2*). The reaction mixture (20 µl) was prepared for 1 volume sample (1x) which is 10 µl of master mix buffer with (0.7 µl) primer (20 pmol/ µl), 4 µl genomic DNA (100 ng/ µl) and then the total volume was completed up to 20 µl by distilled water. Amplification was carried out in a thermo-cycler (Master cycler) for 36 cycles, each consisting of an initial denaturation step at 94°C for 10 minutes, denaturation at 94°C for 1 minute, annealing temperature at 36°C for 1 minute with extension step at 72°C for 2 minutes and then final synthesis step of 10 minutes at 72°C, Amplification products were separated on 1.5% agarose gel in 1X TAE (Tris base, acetic acid and EDTA) buffer. Gels were run at a constant voltage of 100V for 60 minutes, then imaged using a UV trans-illuminator. The image was captured by a digital imaging system.

ISSR analysis

Fifteen primers were utilized in this study, (*Table 2*). The reaction mixture (20 µl) was prepared for one volume sample (1x) which is 10 µl of master mix buffer with 0.7 µl primer 20 pmol/ µl, 4 µl genomic DNA (100 ng/ µl) and then the total volume was completed up to 20 µl by distilled water. Amplification was carried out in a thermo-cycler (Master cycler) for 36 cycles, each consisting of an initial denaturation step at 94°C for ten minutes, denaturation at 94°C for 1 minute, annealing temperature at 50°C for 1 minute with extension step at 72°C for 2 minutes and then final synthesis step of 10 minutes at 72°C, Amplification products were separated on 1.5% agarose gel in 1X TAE (Tris base, acetic acid and EDTA) buffer.

Design primers

Primers were designed regarding many papers including (Martins et al., 2003; Sharma et al., 2012; Pinar et al., 2015; Abodoma et al., 2017; Saleh et al., 2018).

Statistical analysis data and counting

ANOVA and comparison test among genotypes were performed by XLSTAT software. The scorable bands were coded manually as either present (1) or absent (0) (Tahir et al., 2019) and morphological data were converted to matrix data to create the PCA plot and dendrogram using Euclidean distance and Jaccard methods.

Table 2. Primer names, sequences and annealing temperature of RAPD and ISSR markers used in this study

Primer Number	Primer Name	Primer Sequences 5 → 3	Annealing Temperature (°C)	Molecular Weight of Bands (pb)
RAPD				
1	OPA-08	GTGACGTAGG	36	250-1500
2	OPA-10	GTGATCGCAG	36	500-2000
3	OPA-11	CAATCGCCGT	36	500-2000
4	OPA-16	AGCCAGCGAA	36	500-1750
5	OPB-11	GTAGACCCGT	36	260-2200
6	S075	ACGGATCCTG	36	240-2500
7	S084	CAGACAAGCC	36	270-2100
8	S085	CTCTGTTCCG	36	350-2600
9	S081	TCGCCAGCCA	36	250-1750
10	S093	CCACCGCCAG	36	360-1600
11	S078	GGCTGCAGAA	36	250-2100
12	S094	AGAGATGCC	36	260-1550
13	S087	GGTGCAGTCG	36	270-1600
14	S088	GGTCCACAGG	36	250-2500
15	S089	CAGTTCGAGG	36	260-1900
16	S090	TACCGACACC	36	265-1850
17	S091	TCGGAGTGGC	36	260-1950
18	S092	ACTCAGGAGC	36	350-2100
19	S095	CAGTTCTGGC	36	1750-380
20	S073	CCAGATGCAC	36	340-1900
ISSR				
1	807	AGAGAGAGAGAGAGAGT	50	400-1000
2	17898A	CACACACACACAAC	55	260-2200
3	HB04	GACAGACAGACAGACA	60	260-1500
4	HB 8	GAGAGAGAGAGAGG	50	270-1700
5	HB10	GAGAGAGAGAGACC	50	300-1700
6	HB11	GTGTGTGTGTGTCC	50	370-1650
7	HB12	CACCACCACGC	50	275-1850
8	HB15	GTGGTGGTGGC	50	250-1850
9	AG7YC	AGAGAGAGAGAGAGYC	55	450-1400
10	AGC6G	AGCAGCAGCAGCAGCAGCG	55	260-1450
11	IS06	GTGCGTGCCTGCCTGC	60	380-1100
12	IS16	DHBCGACGACGACGACGA	60	280-1500
13	IS17	BDBACAACAACAACAACA	57	300-1700
14	IS19	YHYGTGTGTGTGTG	57	270-1600
15	ISSR.08	ACACACACACACACACYA	52	250-2000

Results and Discussion

Morphological data analysis

Agro-morphological important traits in almond genotypes are nut phenotypic parameters including width, length, thickness, weight, shelling percentage for the economic and health sector. Therefore, identification of morphological traits can be discussed alongside with genetic diversity. To improve the gene pool, the physical traits are inappropriate because environmental factors have a direct influence on developmental stages of the plant with all traits consequently, they demonstrate the diversity among genotypes are just limited (Terzopoulos and Bebeli, 2008). (Table 3) shows the mean values of width, length, thickness, weight and shell to the kernel of nuts from thirty-eight almond genotypes, statistical differences were observed. Nut width of the almond genotypes ranged between 16.18 to 27.21 mm, length from 24.18 to 41.07 mm, thickness between 11.49 to 16.81 mm, nut weight from 2.13 to 7.52 g and shell to kernel percentage between 16.39 to 30.84%. It can be seen that our results nearly agree with Esfahlan

et al., 2012. The values of some almond nut parameters in 40 almond genotypes statistically varied. Nut weight ranged between 3.23 to 8.34 g, nut length from 30.5 to 43.6 mm, nut width from 18.3 to 29.4 mm, and nut thickness 15.00 to 22.33 mm. Kodad et al. (2014) recorded that physical nut traits in 45 almonds with Moroccan genotypes the minimum and maximum nut width were 15.90-27.19 mm, nut length 19.25 to 41.24 mm, nut thickness 11.48-19.61 mm, nut weight 1.15-7.34 g and shelling percentage 19.91-63.79%. In addition, differences in agronomical nut data might be due to the insentience characteristics of genotypes (Kumar and Ahmed, 2015). Furthermore, geographical locations with cross-pollination by insects could be another evidence of almond diversity. (Kester and Gradziel, 1996; Woolley et al., 2000).

Table 3. Effect of almond tree genotypes on some nut characteristics

Genotype	Nut Width (mm)		Nut Length (mm)		Nut Thickness (mm)		Nut Weight (g)		Shell to Kernel (%)	
SH-G1	23.41	c-e	38.62	a-d	14.88	c-g	4.94	c-e	19.09	j-m
SH-G2	20.18	h-l	33.35	f-m	14.81	c-g	4.03	e-l	17.93	l-n
SH-G3	19.20	j-o	32.13	j-n	13.87	e-l	4.61	c-h	21.33	e-j
SH-G4	20.61	h-k	34.42	e-l	15.03	c-g	4.98	c-e	19.80	h-l
SH-G5	20.79	g-j	36.82	b-f	15.22	b-e	4.60	c-h	21.21	f-j
SH-G6	20.78	g-j	36.58	c-g	15.61	a-d	4.08	e-l	22.08	e-h
SH-G7	20.39	h-k	39.65	a-c	14.37	c-j	5.00	c-e	22.56	d-f
SH-G8	22.52	d-g	38.54	a-d	15.70	a-c	4.25	e-k	21.90	e-i
SH-G9	17.64	n-q	36.40	c-h	12.98	k-n	3.75	h-m	24.57	cd
M-G1	22.76	d-f	40.39	ab	14.62	c-i	4.91	c-f	16.39	n
M-G2	21.92	e-h	32.86	g-n	15.06	c-g	4.35	c-j	16.49	n
M-G3	23.63	c-e	40.55	ab	14.82	c-g	6.31	b	16.97	mn
Q-G1	21.22	f-i	30.74	l-n	14.95	c-g	4.46	c-i	19.68	h-l
Q-G2	26.65	a	41.07	a	14.60	c-i	4.79	c-g	29.14	ab
Q-G3	20.91	g-j	25.75	o	16.37	ab	3.72	h-m	27.74	b
Q-G4	25.97	ab	35.52	d-k	16.81	a	7.52	a	16.41	n
Q-G5	27.21	a	35.68	d-j	14.57	c-i	6.40	b	17.08	mn
B-G1	19.34	j-n	29.73	mn	12.66	l-o	2.40	op	20.71	f-j
B-G2	19.15	j-o	31.78	k-n	12.28	m-o	3.44	j-n	25.29	c
B-G3	24.56	bc	38.05	a-e	14.61	c-i	5.24	cd	18.22	k-n
B-G4	24.04	cd	32.62	h-n	14.67	c-h	4.48	c-i	20.36	f-k
B-G5	17.49	o-q	28.97	n	12.91	k-n	3.50	i-n	20.36	f-k
B-G6	16.54	pq	32.44	i-n	11.87	no	2.13	p	19.80	h-l
B-G7	16.18	q	30.23	mn	13.38	h-m	2.17	p	30.84	a
H-G1	19.11	j-o	31.54	l-n	12.99	k-n	3.82	g-l	23.58	c-e
H-G2	22.78	d-f	33.02	g-m	15.30	b-d	2.80	m-p	20.57	f-k
H-G3	18.18	m-p	31.55	l-n	11.49	o	3.44	j-n	19.63	i-l
H-G4	22.84	c-f	29.80	mn	15.13	b-f	2.73	n-p	21.29	e-j
H-G5	22.55	d-g	37.19	b-e	13.16	j-n	5.31	c	19.16	j-m
H-G6	19.78	i-m	36.21	c-i	13.27	i-m	3.91	f-l	22.56	d-f
H-G7	24.28	cd	36.20	c-i	14.22	d-k	4.30	d-k	22.00	e-i
H-G8	22.96	c-f	30.42	mn	12.92	k-n	4.07	e-l	19.44	j-l
H-G9	21.50	f-i	39.10	a-d	13.77	f-l	4.06	e-l	20.77	f-j
H-G10	20.72	h-k	32.67	h-n	14.82	c-g	4.01	e-l	20.41	f-k
H-G11	18.56	l-o	31.59	l-n	13.44	h-m	3.42	j-n	25.67	c
H-G12	17.74	n-q	31.80	k-n	13.07	j-n	3.32	k-o	20.16	g-l
H-G13	18.96	k-o	24.88	o	13.74	g-l	3.13	l-o	24.76	c
H-G14	16.81	pq	24.18	o	12.24	m-o	2.48	op	22.45	d-g

Different letters in the same column indicate significant differences between means according to Duncan multiple range test at $P \leq 0.05$.

The principal component analyses (PCA) plot (Fig. 3) showed the distribution of all genotypes and morphological data on the plot. The plot demonstrated a negative relationship between shell to the kernel and nut weight. It displayed also, a positive linkage between nut width and nut thickness.

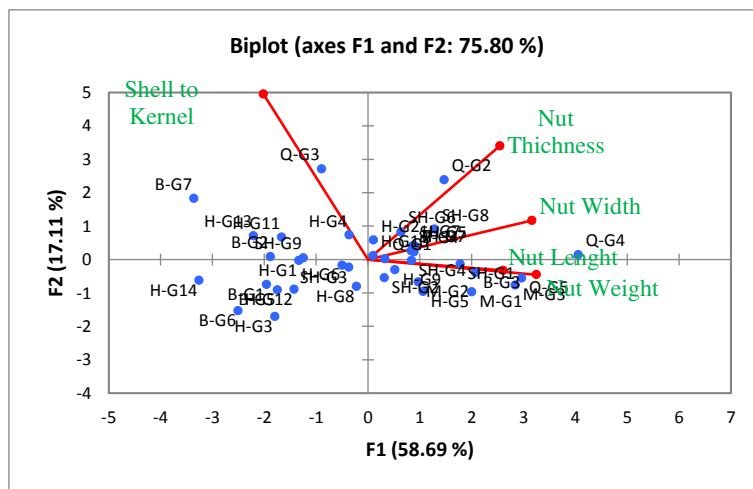


Figure 3. PCA plot among 38 genotype accessions based on 5 nut characteristics in different locations

Allelic variation in almond accessions using RAPD and ISSR markers

RAPD and ISSR markers were used to analyze the genetic diversity of almond genotypes. The assessment of genetic diversity and relationships among almond specimens has been more important to improve the chances of better selection segregates for various characters (Pinar et al., 2015). The valuation of genetic diversity is significant not only for plant development but also for efficient management and conservation of germplasm resources. Information about genetic relationships is important to represent the differences at the DNA level and molecular characteristics about all genotypes. It is also significant for the breeding program which detects drought-resistant traits which is a vital trait to improve economically important crops (Khan et al., 2016). In our results of the primers tested, 20 (out of 21) RAPD and 15 (out of 17) ISSR primers were confirmed as amplified fragments for their reproducibility and high polymorphism (Table 4). The maximum, minimum and mean values of polymorphic bands were 5, 15 and 9.5 for RAPD and 4, 12 and 8 for ISSR, respectively. The PIC values were recorded for RAPD primes that ranged between 0.77 to 0.97 and for ISSR primers it was also verified between 0.35 to 0.96. The PIC values discovered are nearly similar to those reported such as The PIC values for 16 RAPD primers exhibited by Sharma et al. (2012) ranging from 0.26 to 0.87. Mean value of PIC was reported 0.77 using 80 primers of RAPD to 29 almond cultivars (Sorkheh et al., 2009). Shiran et al., (2007) demonstrated that the PIC values were confirmed as ranged 0.47 to 0.97 using 42 RAPD randomly primer to apply 39 almond varieties. In addition, for ISSR markers, range of PIC was got from (0.59 to 0.69) by using 21 primers that applied to 29 *prunus* species (Sarhan et al., 2015). In another research 9 ISSR primers were used in the peach plant, PIC ranged between 0.71 to 0.88 was documented (Tian et al., 2015). Furthermore, PIC values ranging from 0.13 to 0.47 and 0.12 to 0.47 were verified after using (37 RAPD and 38 ISSR) random primers for

45 peach cultivars respectively (Sharma and Sharma, 2018). Regarding the polymorphic bands, El Hawary et al. (2014) demonstrated 2.8 mean value of the polymeric band for 10 primers, and also mean of the polymorphic band was recorded as 8.36 (Gouta et al., 2008). Abodoma et al. (2017) also reported that the polymorphic band for using nine ISSR primer was 13.2 and mean value of polymeric band was 5.53 using 13 primers (Cabrita et al., 2014) recorded polymorphic band was 4.23 for 13 RAPD primer (Pinar et al., 2015) but 5 was got for 4 ISSR primers. Moreover, the average allele polymorphism was 18.6 per primer using ISSR primers applied to 29 *prunus* species (Sarhan et al., 2015).

Table 4. Markers name, number of polymorphic bands, major allele frequency, gene diversity and PIC value of 20 RAPD and 15 ISSR

Marker	Number of polymorphic bands	Major Allele Frequency	Gene Diversity	PIC
RAPD				
OPA-08	5	0.18	0.89	0.88
OPA-10	11	0.13	0.96	0.96
OPA-11	11	0.05	0.97	0.97
OPA-16	7	0.13	0.94	0.94
OPB-11	12	0.21	0.92	0.92
S075	15	0.08	0.96	0.96
S084	10	0.13	0.94	0.94
S085	12	0.24	0.92	0.92
S081	8	0.32	0.87	0.86
S093	11	0.45	0.78	0.77
S078	12	0.21	0.91	0.91
S094	9	0.08	0.96	0.96
S087	8	0.24	0.87	0.86
S088	10	0.16	0.95	0.95
S089	8	0.08	0.96	0.95
S090	7	0.13	0.93	0.93
S091	7	0.24	0.89	0.88
S092	9	0.16	0.93	0.93
S095	10	0.16	0.93	0.93
S073	8	0.16	0.93	0.92
Mean	9.5	0.18	0.92	0.92
ISSR				
807	7	0.63	0.59	0.58
17898A	11	0.08	0.96	0.96
HB04	10	0.13	0.94	0.93
HB8	7	0.08	0.96	0.96
HB10	4	0.53	0.66	0.62
HB11	7	0.13	0.92	0.91
HB12	12	0.18	0.92	0.91
HB15	4	0.79	0.37	0.35
AG7YC	11	0.08	0.97	0.96
AGC6G	8	0.11	0.95	0.94
IS06	10	0.08	0.96	0.96
IS16	6	0.50	0.69	0.66
IS17	5	0.50	0.71	0.69
IS19	9	0.16	0.92	0.91
ISSR.08	9	0.34	0.86	0.85
Mean	8	0.29	0.82	0.81

Clustering and AMOVA analysis

Clustering analyses were performed for assessing the connection between Almond genotypes, based on the Jaccard similarity coefficients using the unweighted pair-group method (UPGMA). The dissimilarity coefficients were ranged between 0.32 (B-G3 vs. B-G4) (M-G2 vs. M-G1) to 0.75 (H-G5 vs. Q-G1), all 38 Almond genotypes were clustered into 3 groups (A, B and C) with a mean dissimilarity (0.54) for 20 RADP markers (Fig. 4), cluster A include H-G3, SH-G3, SH-G6, H-G4, H-G8, SH-G7, H-G11, H-G5, H-G9, H-G12, H-G7, H-G6, H-G2 and H-G10, only Q-G1 was observed in cluster B, the rest of the genotypes were found in cluster C. In addition, dissimilarity values were also observed between 0.19 (H-G13 vs. H-G12) to 0.78 (H-G5 vs. B-G6) by using 15 ISSR markers which clustered all genotypes into A, B, C and D with a mean dissimilarity of 0.49 (Fig. 5). Cluster A includes only H-G7, and group B is consist of all genotypes without cluster A, C, D) group C involves H-G1, SH-G6 and SH-G7, H-G3, H-G5, H-G4, H-G6 and H-G14 belong to cluster D. In addition, both RADP and ISSR markers, exhibited a dissimilarity between 0.32 (B-G3 vs. B-G4) to 0.72 (H-G1 vs. H-G9) and clustered all genotypes into 4 groups (A, B, C and D) with a mean dissimilarity of 0.52 (Fig. 6). Cluster A, include H-G7, group B involves H-G4, H-G6, H-G8, H-G5, H-G11, H-G10, H-G12, H-G13, H-G2 and H-G9, cluster C includes all genotypes that are not in cluster A, B, and D and cluster D includes H-G14, H-G3, SH-G3, SH-G6 and SH-G7. Many researchers registered regarding Almond genetic diversity and their relationships. Martins et al. (2003) studied the genetic diversity of Portuguese *Prunus dulcis* cultivars and their relationship using (RAPD) and (ISSR) markers, the UPGMA dendrogram also achieved a good degree of confidence between associations which was a cophenetic correlation higher than 0.80 for 124 amplified fragments. In addition, four main clusters included *P. dulcis* cultivars (cluster I); P5 (cluster II); *P. webbii* (cluster III); and *P. persica* (cluster IV), the outgroup. Pinar et al. (2015) demonstrated that dissimilarity coefficients were 0.90 and clusters and sub-clusters of the dendrogram had values of cophenetic correlation higher than 0.85 between genotypes by using the UPGMA method for the total number of amplified RAPD plus ISSR fragments with a dendrogram consisting of nine main clusters.

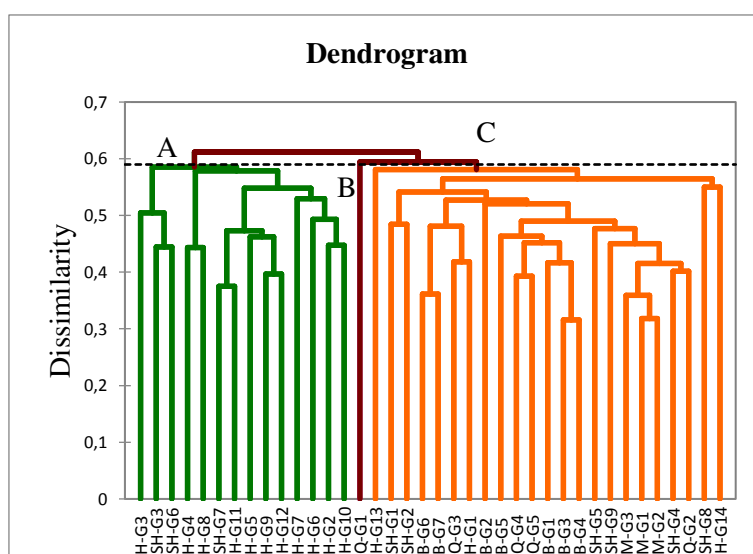


Figure 4. Cluster tree created by UPGMA method based on 20 RAPD markers among 38 almond genotypes

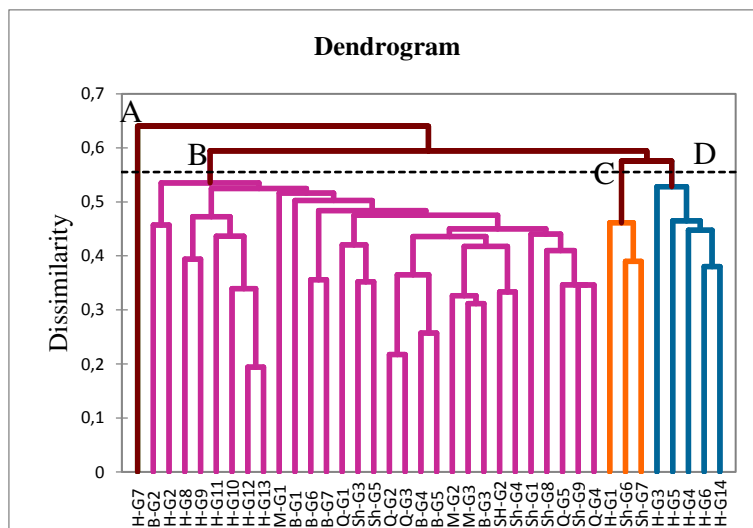


Figure 5. Cluster tree created by UPGMA method based on 15 ISSR markers among 38 almond genotypes

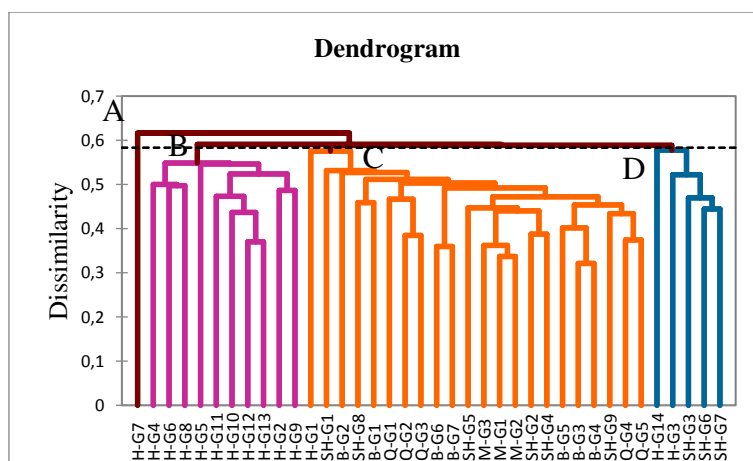


Figure 6. Cluster tree created by UPGMA method based on 20 RAPD with 15 ISSR markers among 38 almond genotypes

The genetic variety among the 86 almond cultivars and genotypes were assessed using 15 SSR marker and also UPGMA cluster analysis based on the similarity matrix coefficient was analyzed. Genetic similarities ranged from 0.03 (*P. tenella* and ‘Ne Plus Ultra’) to 1.00 (three accessions from Akdamar Island and Turkey) with an average of 0.29. Almond genotypes were clustered according to their pedigree and geographic origin. Based on the dendrogram of 86 almond cultivars genotypes, and wild species two groups of different size were formed, with *P. tenella* forming an outgroup and separated from the rest of the genotypes (Halász et al., 2019).

Analysis of molecular variance (AMOVA) of the 38 Almond genotypes in RAPD analysis demonstrated 88% of the total variation within the populations, and 12% was credited to differences between populations (Table 5). In addition, the ISSR marker revealed high variance in the intra-populations (87% of the total variation), and merely 13% could be qualified to differences between sub-populations. AMOVA analysis for 86

genotypes using 15 SSR markers revealed that considerable genetic variation occurred within populations (71.30%), and genetic variation among populations was 28.70% which is a significant reaching value (Halász et al., 2019). This level of variation among populations is much higher than the value estimated for *P. sibirica* (Wang et al., 2014) or *P. mahaleb* (Jordano and Godoy, 2000), and that shown by Fernández i Martí et al. (2015) in almond.

Table 5. Analysis of molecular variance (AMOVA) of the five populations for 38 Almond genotypes

Source	df	SS	MS	Est. Var.	%	P-Value
RAPD						
Among Pops	4	307.18	76.80	5.29	12%	0.001
Within Pops	33	1289.06	39.06	39.06	88%	0.001
Total	37	1596.24		44.35	100%	
ISSR						
Among Pops	4	188.16	47.04	3.391	13%	0.001
Within Pops	33	754.31	22.86	22.86	87%	0.001
Total	37	942.47		26.25	100%	

Genetic structure for all genotypes using RAPD and ISSR markers

STRUCTURE method was used to collect evidence about population structure for almond genotypes depending on allele frequencies (Evanno et al., 2005) therefore, in this work, according to Delta K, genotypes were divided into two groups or sub-populations, group 1 (green line) and group 2 (red line). For RAPD and ISSR (Fig. 7A and B) clusters were also represented by colour, the red line in RAPD and the green line in ISSR consisted of Hawraman location, but the green line in RAPD and the red line in ISSR conceited other locations including Sharbazher, Mergapan, Qaradakh and Barznja. In addition, a combination class of genotypes may refer to more than one background. For example, samples SH-G3 and Q-G1 in RAPD markers (Fig. 7A), and only sample Sh-G1 in ISSR marker (Fig. 7B) could possibly have a complicated history linking intercrossing or practicably resulting from the gene flow between taxa, in addition, the high variability between genotypes may be the consequences of the changing climates found within the locations. The true number of clusters (K) in a sample of individuals was observed and determined for 20 RAPD and 15 ISSR markers, that the real highest K value was K= 2 for each marker (Fig. 7C and D).

Allele frequencies using STRUCTURE analysis was investigated to determine the genetic constitution of different groups. The Evanno criterion gave a strong signal for K = 9 indicating nine genetically distinct subgroups resided within the studied genotypes (Halász et al., 2019). Our results are assessed depending on genetic diversity and relationships between different accessions in different locations of Sulaimani governorate, that had some morphological similarities within genotypes and molecular studies also have verified it. It can be said that this hypothesis may be conducted the self-incompatible nature of the almond plants. Janick (1990) demonstrated that the high heterosis of the cultivars is mostly due to cross-pollination among them and also it is recorded high genetic variability. In addition, growing almonds in different regions have also been isolated during the time period that has progressed of characteristic ecotypes.

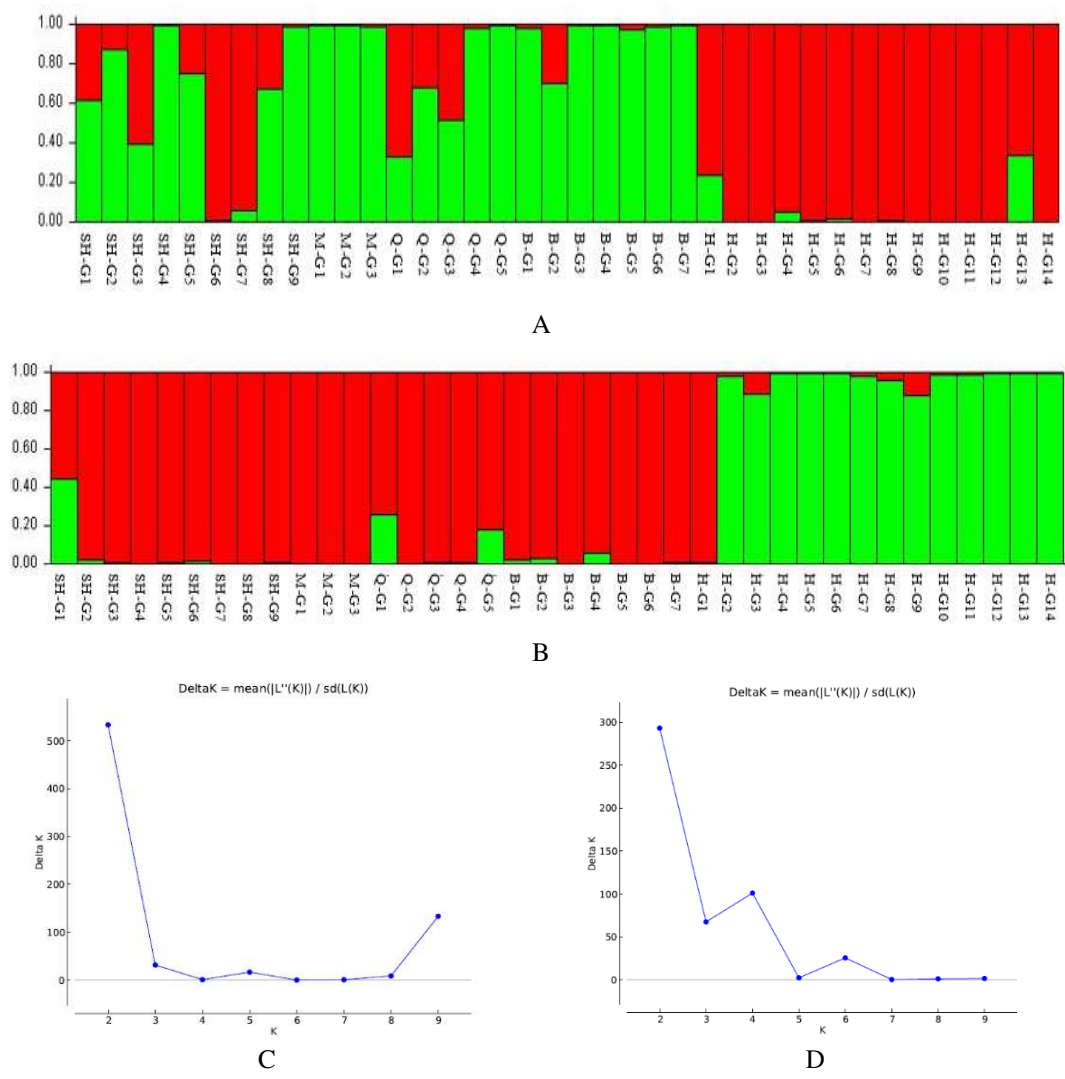


Figure 7. Thirty-eight almond genotypes clustered into different sub-populations by *STRUCTURE* software. (A) for RAPD and (B) ISSR. Accessions are coordinated as per estimated membership coefficients (q) in K= 2 clusters. (C) for RAPD and (D) for ISSR, Determining the optimal value of K by the (ΔK) procedure described by Evanno et al., 2005

Conclusions

This work aimed to assess the genetic diversity using RAPD and ISSR mark with nut agronomical traits to 38 almond accessions grown in Sulaimani Iraq region. According to our research, Agronomical nuts (width, length, thickness, weight and shell to kernel data) were studied for each genotype that mean values of those parameters were significantly documented. Genetically, the number of polymorphic bands, major allele frequency, gene diversity and the polymorphism information content (PIC), were demonstrated. The polymorphic bands of mean value were 9.5 for RAPD and 8 for ISSR. The PIC values were recorded for RAPD primers ranging between (0.77 to 0.97) and for ISSR primers it was also verified between 0.35 to 0.96. Jaccard similarity coefficients were achieved between 0.32 (B-G3 vs. B-G4) (M-G2 vs. M-G1) to 0.75 (H-G5 vs. Q-G1) and clustered into 3 clusters (A, B and C) with a mean similarity of 0.54 for 20 RADP markers. For 15

ISSR markers, 0.19 (H-G13 vs. H-G12) to 0.78 (H-G5 vs. B-G6) were also observed, and clustered into 4 clusters (A, B, C and D) with a mean similarity of 0.49. In addition, based on the analysis of STRUCTURE software, RAPD and ISSR were analyzed and were divided into two groups, analysis of molecular variance stated a low variation among groups (12%) for RAPD and (13%) for ISSR. Therefore, the consequence of the genetic diversity in Sulaimani Almond accessions is important for breeding as well as to the implementation of degree addressed to their usages and preservations.

Our recommendations for future researches will be conducting quantitative traits loci analysis and genome-wide associated to determine QTL that associated with drought tolerance in almond genotypes, and also to assist future conservation and breeding programs to use different locations and accessions of almonds with using various types of markers including SNIPs, SRAPs, ALFPs, and SSRs.

Acknowledgements. We are grateful and thankful to Prof. Dr. Nawroz Abdula-razzak Tahir for his help with the software analysis and statistical analysis and also to Dr. Jamal Mahmood Faraj for his helpful comments and advice on an earlier draft of the manuscript.

REFERENCES

- [1] Abodoma, A. F., Shehata, M. M., Elsherif, N. S., Amar, M. H., Khar, Kh. A. (2017): Biodiversity assessment for some almond genotypes cultivated in Libya using SRAP and ISSR. – Egyptian Journal of Genetics and Cytology 46(2): 13-41.
- [2] Bouhadida, M., Casas, A. M., Gonzalo, M. J., Arús, P., Moreno, M. A., Gogorcena, Y. (2009): Molecular characterization and genetic diversity of *Prunus* rootstocks. – Scientia horticulturae 120(2): 237-245.
- [3] Browicz, K., Zohary, D. (1996): The genus *Amygdalus* L. (Rosaceae): Species relationships, distribution and evolution under domestication. – Genetic Resources and Crop Evolution 43(3): 229-247.
- [4] Cabrita, L., Apostolova, E., Neves, A., Marreiros, A., Leitão, J. (2014): Genetic diversity assessment of the almond (*Prunus dulcis* (Mill.) DA Webb) traditional germplasm of Algarve, Portugal, using molecular markers. – Plant Genetic Resources 12(S1): S164-S167.
- [5] Casas, A. M., Igartua, E., Balaguer, G., Moreno, M. A. (1999): Genetic diversity of *Prunus* rootstocks analyzed by RAPD markers. – Euphytica 110(2): 139-149.
- [6] Dwevedi, K. K., Lal, G. M. (2009): Assessment of genetic diversity of cultivated chickpea (*Cicer arietinum* L.). – Asian Journal of Agricultural Sciences 1(1): 7-8.
- [7] El Hawary, S. S., Sokkar, N. M., El Halawany, A. M., Kandil, Z. A., Tawab, S. A., Mokbel, H. A. (2014): Phytochemical screening, botanical study and DNA fingerprinting of *Prunus amygdalus* batsch “UMM alfahm” cultivar cultivated in Egypt. – International Journal of Pharmacy and Pharmaceutical Sciences 6(11): 466-473.
- [8] Esfahlan, A. J., Esfahlan, R. J., Jamei, R., Esfahlan, A. J. (2012): Morphology and physicochemical properties of 40 genotypes of almond (*Amygdalus communis* L.) fruits. – European Journal of Experimental Biology 2(6): 2456-2464.
- [9] Evanno, G., Regnaut, S., Goudet, J. (2005): Detecting the number of clusters of individuals using the software STRUCTURE: a simulation study. – Molecular Ecology 14(8): 2611-2620.
- [10] Gouta, H., Ksia, E., Zoghlami, N., Zarrouk, M., Mliki, A. (2008): Genetic diversity and phylogenetic relationships among Tunisian almond cultivars revealed by RAPD markers. – The Journal of Horticultural Science and Biotechnology 83(6): 707-712.

- [11] Grasselly, C. (1976): Origine et evolution de l'amandier cultivate. – Options Méditerranéenne 32: 45-49.
- [12] Gupta, P. K., Varshney, R. K. (2000): The development and use of microsatellite markers for genetic analysis and plant breeding with emphasis on bread wheat. – Euphytica 113(3): 163-185.
- [13] Halász, J., Kodad, O., Galiba, G. M., Skola, I., Ercisli, S., Ledbetter, C. A., Hegedüs, A. (2019): Genetic variability is preserved among strongly differentiated and geographically diverse almond germplasm: an assessment by simple sequence repeat markers. – Tree Genetics & Genomes 15(1): 1-12.
- [14] i Martí, A. F., i Forcada, C. F., Kamali, K., Rubio-Cabetas, M. J., Wirthensohn, M., i Company, R. S. (2015): Molecular analyses of evolution and population structure in a worldwide almond [*Prunus dulcis* (Mill.) D.A. Webb syn. *P. amygdalus* Batsch] pool assessed by microsatellite markers. – Genetic Resources and Crop Evolution 62(2): 205-219.
- [15] Janick, J. (1990): Plant Breeding Reviews, Volume 8. – John Wiley & Sons, Inc.
- [16] Jordano, P., Godoy, J. A. (2000): RAPD variation and population genetic structure in *Prunus mahaleb* (Rosaceae), an animal-dispersed tree. – Molecular Ecology 9: 1293-1305.
- [17] Kester, D. E., Gradziel, T. M. (1996): Almonds (*Prunus*). – In: Moore, J. N, Janick, J. (ed.) Fruit Breeding. Wiley and Sons, New York.
- [18] Khan, A., Sovero, V., Gemenet, D. (2016): Genome-assisted breeding for drought resistance. – Current genomics 17(4): 330-342.
- [19] Kodad, O., Lebrighi, L., El-Amrani, L., i Company, R. S. (2014): Physical fruit traits in Moroccan almond seedlings: Quality aspects and post-harvest uses. – International Journal of Fruit Science 15(1): 36-53.
- [20] Kumar, D., Ahmed, N. (2015): Morphological and pomological evaluation of almond (*Prunus dulcis*) cultivars under North West Himalayan region of India. – International Journal of Horticulture 5(15): 1-6.
- [21] Ladizinsky, G. (1999): On the origin of almond. – Genetic Resources and Crop Evolution 46(2): 143-147.
- [22] Martins, M., Tenreiro, R., Oliveira, M. M. (2003): Genetic relatedness of Portuguese almond cultivars assessed by RAPD and ISSR markers. – Plant cell reports 22(1): 71-78.
- [23] Pinar, H., Ercisli, S., Unlu, M., Bircan, M., Uzun, A., Keles, D., Baysal, F., Atli, H. S., Yilmaz, K. U. (2015): Determination of genetic diversity among some almond accessions. – Genetika 47(1): 13-22.
- [24] Sakar, E. H., El Yamani, M., Rharrabti, Y. (2019): Geometrical traits in almond fruit as affected by genotypic and environmental variations in Northern Morocco. – Erwerbs-Obstbau 61(2): 103-112.
- [25] Saleh, S., Ehsan, N., Mohamed, S., Mohamed, T. (2018): Molecular genetic variability of some deciduous fruit rootstocks in Egypt. – Journal of Scientific Research in Science 35(1): 95-111.
- [26] Sánchez-Pérez, R., Pavan, S., Mazzeo, R., Moldovan, C., Cigliano, R. A., Del Cueto, J., Ricciardi, F., Lotti, C., Ricciardi, L., Dicenta, F., López-Marqués, R. L., Møller, B. L. (2019): Mutation of a bHLH transcription factor allowed almond domestication. – Science 364(6445): 1095-1098.
- [27] Sarhan, S., Hamed, F., Lawand, S., Al-Youssef, W. (2015): Relationships among Peach, almond, and related species as detected by SSR/ ISSR markers. – International Journal of ChemTech Research 8(1): 82-88.
- [28] Sharma, D., Kaur, R., Kumar, K., Bhardwaj, S. (2012): Genetic diversity among selected genotypes of almond *Prunus dulcis* Miller D.A. Webb assessed by random amplified polymorphic DNA (RAPD) markers. – African Journal of Biotechnology 11(83): 14877-14883.

- [29] Sharma, P., Sharma, R. (2018): DNA fingerprinting of peach (*Prunus persica*) germplasm in accessing genetic variation using arbitrary oligonucleotide markers system. – Indian Journal of Biotechnology 17(3): 484-491.
- [30] Shiran, B., Amirbakhtiar, N., Kiani, S., Mohammadi, S. H., Sayed-Tabatabaei, B. E., Moradi, H. (2007): Molecular characterization and genetic relationship among almond cultivars assessed by RAPD and SSR markers. – Scientia Horticulturae 111(3): 280-292.
- [31] Sorkheh, K., Shiran, B., Gradziel, T. M., Epperson, B. K., Martínez-Gómez, P., Asadi, E. (2007): Amplified fragment length polymorphism as a tool for molecular characterization of almond germplasm: genetic diversity among cultivated genotypes and related wild species of almond, and its relationships with agronomic traits. – Euphytica 156(3): 327-344.
- [32] Sorkheh, K., Shiran, B., Kiani, S., Amirbakhtiar, N., Mousavi, S., Rouhi, V., Mohammady, D. S., Gradziel, T. M., Malysheva-Otto, L. V., Martínez-Gómez, P. (2009): Discriminating ability of molecular markers and morphological characterization in the establishment of genetic relationships in cultivated genotypes of almond and related wild species. – Journal of Forestry Research 20(3): 183-194.
- [33] Tahir, N. A., Hama Karim, H. F. (2011): Determination of genetic relationship among some varieties of chickpea (*Cicer arietinum* L) in Sulaimani by RAPD and ISSR markers. – Jordan Journal of Biological Sciences 4(4): 77-86.
- [34] Tahir, N. A., Omer, D. A., Lateef, D. A., Ahmad, S. H., Salih, S. H., Hiwakhah, L. (2019): Diversity and population structure analysis of faba bean (*Vicia faba* L.) accessions using SSR markers. – Journal of Agricultural Science and Technology 21(2): 463-474.
- [35] Terzopoulos, P. J., Bebeli, P. J. (2008): Genetic diversity analysis of Mediterranean faba bean (*Vicia faba* L.) with ISSR markers. – Field Crops Research 108(1): 39-44.
- [36] Tian, Y., Xing, C., Cao, Y., Wang, C., Guan, F., Li, R., Meng, F. (2015): Evaluation of genetic diversity on *Prunus mira* Koehne by using ISSR and RAPD markers. – Biotechnology, Biotechnological Equipment 29(6): 1053-1061.
- [37] United States Department of Agriculture National Agricultural Statistics Service USDA (2018): California Almond Forecast. – https://www.nass.usda.gov/Statistics_by_State/California/Publications/Specialty_and_Other_Releases/Almond/Forecast/201805almpd.pdf.
- [38] Wang, Z., Kang, M., Liu, H., Gao, J., Zhang, Z., Li, Y., Wu, R., Pang, X. (2014): High-level genetic diversity and complex population structure of Siberian apricot (*Prunus sibirica* L.) in China as revealed by nuclear SSR markers. – PLoS One 9(2): e87381.
- [39] Woolley, F. M., Collins, G. G., Sedgley, M. (2000): Application of DNA fingerprinting for the classification of selected almond [*Prunus dulcis* (Mill.) D. A. Webb] cultivars. – Australian Journal of Experimental Agriculture 40(7): 995-1001.
- [40] Xu, Y., Ma, R. C., Xie, H., Liu, J. T., Cao, M. Q. (2004): Development of SSR markers for the phylogenetic analysis of almond trees from China and the Mediterranean region. – Genome 47(6): 1091-1104.
- [41] Zeinalabedini, M., Majourhat, K., Khayam-Nekoui, M., Grigorian, V., Torchi, M., Dicenta, F., Martínez-Gómez, P. (2008): Comparison of the use of morphological, protein and DNA markers in the genetic characterization of Iranian wild *Prunus* species. – Scientia Horticulturae 116(1): 80-88.
- [42] Zhu, Y. (2014): Almond (*Prunus dulcis* (Mill.) D.A. Webb) fatty acids and tocopherols under different conditions. – PhD Thesis, School of Agriculture, Food and Wine. University of Adelaide, Australia.

THE EFFECT OF DEFICIT IRRIGATION APPLIED IN DIFFERENT PHENOLOGICAL PERIODS ON SAFFLOWER YIELD AND QUALITY

KARAŞ, E.

*Osmangazi University, Department of Biosystem Engineering, Eskisehir, Turkey
(e-mail: ekaras@ogu.edu.tr)*

(Received 15th Oct 2019; accepted 23rd Jan 2020)

Abstract. A field study was carried out to investigate the effect of deficit irrigation applied in the different phenological periods of safflowers (*Carthamus tinctorius* L.) at the Central Anatolian region in Turkey between 2007 and 2009. A randomized split block design in fourteen subjects with three replications was used. According to the results, the highest yield was obtained from the issue when there was no water stress during the growing period. It was found that there was a decrease in yield from the subjects when periodic water deficit was applied at various rates. At the end of the research, the most effective periods for yield were determined as flowering, vegetation, and yield formation. The average seasonal water consumption was between 234 and 591 mm; the highest and the lowest grain yield was 5.10 t ha⁻¹ and 2.48 t ha⁻¹, respectively. Irrigation water usage efficiency (IWUE) ranged between 7.3 kg ha⁻¹ mm⁻¹ and 11 kg ha⁻¹ mm⁻¹. The amount of irrigation water applied had no effect on oil ratios ranging from 28.89% to 30.66%. The effect of irrigation water applied was observed only on stearic and linoleic fatty acids. The coefficient of determination (r²) of water-yield relationships during the experiment was obtained as 0.44, 0.71, and 0.68, respectively.

Keywords: *water use efficiency, evapotranspiration, water–yield relationship, fatty acids, oil content*

Introduction

The effects of global warming, which has increased markedly since 1980, are much more noticeable in arid and semi-arid climates (Pankova and Konyushkova, 2014; Cook et al., 2014). Due to the increasing temperatures, drought in agricultural areas makes the management of soil water in agricultural lands more and more important (Diogo, 2018; Shkolnik et al., 2019). Drought forecasts suggest that it will be more effective in the Mediterranean basin, including the Central Anatolia region (Hertig and Trambly, 2017; Lionello et al., 2017). The main effects of drought on agricultural areas are the decrease in rainfall, the increase in recurring periods of aridity, and the lowering of groundwater due to excessive irrigation and low penetration (Gouveia et al., 2017; Caloiero et al., 2018).

Management of soil moisture in the root area is vital for plants, determination of critical and water-sensitive periods and possible drought scenarios (Pan et al., 2018; Grecksch, 2019). The main objective of water management is to maximize yield by determining the periods during which the plant is most susceptible to water shortages and the levels of sensitivity during these periods. Thanks to the development of water management strategies in plant breeding, the main objective of productive agricultural management on a watershed basis are to irrigate more land with existing water and improve the efficiency of water use (Bacelar et al., 2013; Choudhury and Singh, 2016). The development of water-saving deficit irrigation programs is also a way of ensuring food safety (Ward and Pulido-Velazquez, 2008; Shammout et al., 2018).

In Turkey, production of oilseeds (sunflower, cotton, soybean, rapeseed and safflower seeds) ranges from 2.3 to 2.7 million tonnes annually. Oilseed production distribution in

Turkey consists of sunflower (46%), cottonseed (41%), soybean (6%), canola (5%), and safflower 2% (TUIK, 2018). Although safflower is a widely recommended plant in arid conditions such as exists in Central Anatolia, some preliminary studies have shown that the plant will produce very positive results from irrigable conditions. Many studies have been carried out on plant water consumption, water use efficiency, yield, and quality under limited irrigation conditions of the safflower in Turkey (İstanbulluoğlu, 2009; İstanbulluoğlu et al., 2009; Öztürk et al., 2009). However, the research on growing safflower in arid and semi-arid conditions as in Central Anatolia has not been sufficient. This study aims to investigate the yield, some physical characteristics (grain weight, fat ratio) and changes in the fatty acid composition at various irrigation levels during the phenological periods of safflower plants in an arid and semi-arid climate.

Material And Method

Site Description

The experimental area is located at the Soil and Water Resources Research Institute in the Alpu plain, east of Eskişehir province in Central Anatolia, Turkey. The trial site coordinates are 39° 46' north latitude and 30° 36' east longitude, and the elevation is 780 m above sea level.

Climate

The climate characteristics of the research area are continental and fall under the influence of the Central Western Anatolia climate. In general, summers are hot and dry, and winters are cold and snowy. The average annual temperature is 10.7°C, the first frost is on average October 18, the last frost is on average April 20, the lowest temperature is -26.7°C, the average annual rainfall is 343.2 mm, the evaporation value is 975.7 mm and the annual average relative humidity is 62% (SWRI, 2011). The monthly average temperature, rainfall and relative humidity values of the years when the trial period was carried out are given in *Table 1*.

Table 1. Some climatic values of the experimental area during the study

Month	Temperature, °C				Rainfall, mm				Relative Humidity, %			
	2007	2008	2009	Mean	2007	2008	2009	Mean*	2007	2008	2009	Mean*
I	0.0	-3.5	0.9	-0.2	42.2	13.1	66.3	36.1	74.1	72.2	71.2	74.8
II	1.5	0.0	3.1	1.3	14.2	2.7	74	26.7	68.1	59.4	66.6	70.3
III	5.4	8.4	4.6	5.0	24.0	29.9	39.8	35.6	63.0	56.1	60.5	63.5
IV	7.5	11.5	10.0	10.1	25.0	38.1	26.0	42.4	54.7	61.6	55.7	59.8
V	17.8	14.3	14.8	14.8	65.6	14.4	28.9	42.7	49.1	49.5	50.7	57.9
VI	20.8	20.2	20.4	18.6	58.6	2.8	7.9	31.2	47.9	40.9	41.0	54.6
VII	23.8	21.9	22.2	21.4	-	0.8	11.4	10.5	40.0	40.2	42.9	51.1
VIII	23.9	23.4	21.0	21.0	1.9	4.7	2.0	9.1	43.5	40.9	42.2	53.0
IX	17.7	17.0	16.5	16.9	-	30.9	7.2	13.4	44.9	54.7	52.8	54.8
X	12.6	11.7	14.5	11.7	19.1	8.1	18.3	25.6	57.7	59.0	52.1	61.1
XI	4.9	6.8	6.0	6.0	91.7	50.5	29.3	27.6	73.9	65.5	68.0	68.5
XII	0.6	1.5	4.6	2.1	46.1	34.7	69.7	42.3	73.3	68.5	69.7	75.7
Mean/Total	11.4	11.1	11.6	10.7	388.4	230.7	380.8	343.2	56.0	54.2	56.1	62.1

*Mean (1957–2011)

Soil

Soil analysis tests, including physical (structure, volume weight) and chemical (pH, total salt, lime, phosphorus, potassium, organic matter) as well as infiltration tests were performed on the soils taken up to a depth of 120 cm at the research area (Tüzüner, 1990). The soil of the test area has a clay structure, consisting of slightly alkaline alluvial soils with pH values ranging between 7.50 and 8.03, and salt values varying between 0.102% and 0.187%. Although heavily structured, it is generally classified as too calcic. The soil of the test sites is defined as having high phosphorus, sufficient potassium, and low organic matter.

Irrigation water quality

The pH value of the irrigation water samples taken from the deep well in the research area was 6.8, the EC value was 0.747, the SAR value was 1.10, and no boron problem was detected (Boyacı and Karas, 2011).

Safflower variety

The safflower plant variety, Dincer, which was used in the experiment, was registered in 1977 by the Eskişehir Anatolian Agricultural Research Institute. Plant height is around 90–110 cm, the flower color is orange, the grain color is white and the plant has a thorny structure. The plant usually lasts from 127–130 days in the growing season (Boyacı and Karas, 2011).

Experimental design and field work

The experiment was conducted with a randomized split block design with 14 subjects and 3 replications (see *Table 2*). Irrigation subjects were arranged considering three different phenological periods (vegetative [V], flowering [F], yield formation [Y]) during the growing period. The plot areas were mouldboard ploughed in the fall and cultivated twice in the spring.

Table 2. Trial subjects

Subjects	Application	Stage of development		
		Vegetative (V)	Flowering (F)	Yield formation (Y)
S ₁	VFY	I	I	I
S ₂	VFY ₀	I	I	0
S ₃	VF ₀ Y	I	0	I
S ₄	V ₀ FY	0	I	I
S ₅	VF ₀ Y ₀	I	0	0
S ₆	V ₀ FY ₀	0	I	0
S ₇	V ₀ F ₀ Y	0	0	I
S ₈	V ₆₀ FY	I ₁	I	I
S ₉	V ₄₀ FY	I ₂	I	I
S ₁₀	VF ₆₀ Y	I	I ₁	I
S ₁₁	VF ₄₀ Y	I	I ₂	I
S ₁₂	VFY ₆₀	I	I	I ₁
S ₁₃	VFY ₄₀	I	I	I ₂
S ₁₄	V ₀ F ₀ Y ₀	0	0	0

Description of symbols: S₁-Full irrigated, I₁-0.6×S₁, I₂- 0.40×S₁, 0- No irrigation

In the research, no water stress occurred in the subjects of irrigation (VFY) during the growing period of the plant. On the other hand, there was a certain amount of water stress in all other subjects and at least one period. For example, in VFY₀, no water stress occurred during vegetative and flowering periods and irrigation water was applied to meet plant water consumption needs during these periods; however, no irrigation was applied during the yield formation period. The index value in any period indicates the rate of application of irrigation water in that period. For example, the application of V₆₀FY, which is given as the subject of S₈ in *Table 2*, shows that 60% of plant water consumption is given in the vegetative period and full irrigation is performed during flowering and yield formation periods.

The plots were arranged in October (4.5 m x 6.0 m = 27 m²), planted at the beginning of April and harvested (3.9 m x 5.0 m = 19.5 m²) at the beginning of September. In the experiment, safflower was planted in 30 cm plant-row spacing and 10 cm plant-on-plant row. Fertilization was carried out according to soil analysis results. Base fertilization was applied to the soil by mixing before planting. All the phosphorus fertilizer and half of the nitrogen fertilizer were given up to planting depth of 4–6 cm with planting. During the second fertilization period, the remaining nitrogen was applied under the soil. The fertilizer requirement of the plant was realized according to the research results proposed by Yıldırım (2005); all parcels were based on 16 kg N, 8 kg P₂O₅ as a pure substance. 20-20-0 compound fertilizer with planting, Ammonium nitrate (33%) fertilizer was used as the top fertilizer.

Irrigation treatments, water use, and soil moisture measurements

In the experiment, the V, F and Y phenological periods were selected for the determination of irrigation periods in the experiment. Also taken into consideration were the principles specified by Doorenbos and Kassam (1979). Irrigation applications were carried out considering the effective root depth of 90 cm. Irrigation water was given to test plots utilizing a furrow method with plastic pipes and measured with a water meter. Soil moisture measurements were taken weekly from 0–30, 30–60 and 60–90 cm depths and determined by the gravimetric method.

Water budget equality was used to calculate plant water consumption.

$$ET_a = I + P - R - DP + CR \pm \Delta SF \pm \Delta SW \quad (\text{Eq.1})$$

where ET_a: Actual evapotranspiration (mm), I: irrigation water (mm), P: precipitation (mm), R: surface runoff (mm), DP: deep percolation (mm), CR: capillary rise, ΔSF: subsurface flow (mm), ΔSW: change in soil water content (mm).

In the experiment, rainfall and irrigation water are directly measured values. Since the amount of water given at the effective root depth is as much as the field capacity, it is assumed that there is no deep percolation.

The agricultural operations and observations including irrigation made during the trial years are given in *Table 3*.

Seed Oil Content

The seeds were dried in the oven for 4 hours at 40°C and then ground using a blender. 4 grams of dried safflower seeds were extracted with petroleum ether for 6 hours in a Soxhlet system according to the AOCS method (AOCS, 1993). The n-hexane and oil mixture obtained after extraction was filtered and separated under vacuum using a rotary

evaporator (Heidolph® brand Laborota 4000 Efficient) at 45°C. The crude oil ratio was calculated by weighing the obtained safflower oil weight.

Table 3. Agricultural operations and observations in the experimental years

Agricultural applications and observations	2007	2008	2009
Fallow	10/15	10/10	17/10
Tillage	04/08	03/28	04/02
Seeding	04/12	04/02	04/02
Germination	04/28	04/11	04/24
Emergence	05/02	04/20	04/30
Rosette	05/20	05/05	05/30
Fertilizing	05/30	06/02	05/25
First irrigation	06/12	06/05	06/10
Flowering (%5)	06/28	06/27	06/28
Second irrigation	07/04	07/02	07/02
Flowering (%100)	07/18	07/06	07/16
The beginning of maturity period	07/26	07/25	07/26
Third irrigation	07/28	08/01	08/01
Harvest	09/01	08/28	08/28

Fatty Acid Composition

The fatty acid composition of the safflower oils was analyzed by gas chromatography according to the AOCS standard method. The oil samples were diluted with hexane and converted into methyl esters by esterification. Fatty acid methyl esters were analyzed by Agilent 7890A model gas chromatography using a Supelco 2380 capillary column (60 m x 0.25 mm x 0.20 µm) and flame ionization detector (FID). Helium was used as carrier gas at a flow rate of 20 cm s⁻¹. Injection, furnace and detector temperatures are 250, 185 and 260°C, respectively. 1 µL of methyl ester sample was injected into the device with a split ratio of 1/100. Fatty acid methyl esters were determined by comparing retention times with reference standards. The amounts of fatty acid methyl esters were determined by using internal standard (Methyl nonadecanoate). The contents of palmitic (16:0), stearic (18:0), oleic (18:1), and linoleic (18:2) acids were determined using a computing integrator. The effects of the independent variables on oil content and palmitic, stearic, oleic, and linoleic acid concentrations of the oil were analyzed on a percentage basis.

Statistical Analysis

Statistical analysis of the data obtained from the research was carried out following the procedure proposed by Yurtsever (1984). All data were subjected to ANOVA based on general linear models for factorial arrangement of treatments in a completely randomised design using the Statview statistical package (SAS Institute, 1998). Multiple comparisons with Duncan were used to determine the effects of treatment.

Water Use Efficiency

Water Use Efficiency (WUE) is defined as the amount of carbon assimilated as biomass or grain (Yield, Y kg ha⁻¹) produced per unit (ET, mm) of water used by the crop (kg ha⁻¹mm⁻¹).

$$WUE = \frac{Y}{ET} \quad (\text{Eq.2})$$

Irrigation Water Use Efficiency (IWUE): It takes into account the amount of irrigation water (IW, mm) applied during the trial period ($\text{kg ha}^{-1}\text{mm}^{-1}$).

$$IWUE = \frac{Y}{IW} \quad (\text{Eq.3})$$

Water use–yield relationship

The data obtained from the study were used linear regression to obtain the relationship between seasonal ET and yield. Seasonal yield response factor (ky) for each year was determined using the Stewart model (Stewart et al., 1977).

$$\left(1 - \frac{Y_a}{Y_m}\right) = ky\left(1 - \frac{ET_a}{ET_m}\right) \quad (\text{Eq.4})$$

where, Y_a , actual yield (kg ha^{-1}); Y_m , maximum yield (kg ha^{-1}); ET_a , actual evapotranspiration (mm), ET_m , maximum evapotranspiration (mm); ky, yield response factor

The ET_a and ET_m values in the Stewart equation are the actual ET and maximum ET values during the study. The ET_a / ET_m value in the equation is considered to be 1.00 for the absence of plant water stress; It is calculated by comparing the ET_a value measured for other subjects where water stress occurs to the ET_a value measured for the subject without water stress. The meaning of the Ky value can be interpreted as follows considering the results obtained:

$Ky > 1$: crop response is very sensitive to water deficit with proportional larger yield reductions when water use is reduced because of stress.

$Ky < 1$: crop is more tolerant to water deficit, and recovers partially from stress, exhibiting less than proportional reductions in yield with reduced water use.

$Ky = 1$: yield reduction is directly proportional to reduced water use.

Results and Discussion

The effect of water stress on grain yield

The statistical results obtained during the study are given in *Table 4*, *Table 5* and *Figure 1*. Seed yield ranged between 2.48 and 5.10 t ha. The highest yield was obtained from full irrigation (S_1) application and the lowest yield was obtained from the non-irrigation (S_{14}) subject. Seed yield showed significant fluctuations between years according to water applications. In the second and third years of the experiment, higher yields were recorded in the parcels where full water was applied, whereas no significant differences were observed between the years in S_{10} application. In other applications, different reactions have occurred. This has led to significant interactions of the year x application. The combined analysis of the results have shown that seed yield was higher in the second year of the experiment compared to the other experimental years. While the highest seed yield was obtained from full irrigation application, the lowest yield was obtained from the rainfed conditions in the experiment. In general, decreasing irrigation water causes a reduction in seed yield. In the experiment, the flowering period was the most sensitive to yield loss, followed by the vegetation and yield-formation periods, respectively. The graph of the yield in the experiment carried out is given in *Figure 1-A*.

Table 4. The effect of irrigation treatment on trial subjects

Subjects	Treatment	Yield (t ha ⁻¹)	1000 Seed weight (g)	IWUE kg ha ⁻¹ mm ⁻¹	Oil rate (%)	Fatty Acid				
						Myristic (%)	Palmitic (%)	Stearic (%)	Oleic (%)	Linoleic (%)
S ₁	VFY	5.10 ^a	48.96 ^a	8.8 ^c	27.83	0.11	6.17	2.14 ^{abc}	11.67	75.52 ^a
S ₂	VFY ₀	4.14 ^b	47.67 ^{bc}	9.1 ^c	28.85	0.12	6.07	2.04 ^{bc}	11.53	71.62 ^c
S ₃	VF ₀ Y	3.56 ^{ef}	47.64 ^{bc}	8.1 ^d	27.88	0.11	6.11	2.10 ^{bc}	11.41	73.32 ^b
S ₄	V ₀ FY	3.84 ^{cd}	48.58 ^{ab}	8.0 ^d	28.77	0.13	6.37	2.10 ^{bc}	11.85	71.97 ^c
S ₅	VF ₀ Y ₀	3.24 ^g	48.22 ^{abc}	10.2 ^{ab}	28.95	0.12	6.24	2.15 ^{abc}	11.32	71.49 ^c
S ₆	V ₀ FY ₀	3.56 ^{ef}	48.58 ^{ab}	9.9 ^b	28.01	0.13	6.30	2.05 ^{bc}	11.35	73.28 ^b
S ₇	V ₀ F ₀ Y	3.52 ^{ef}	48.62 ^{ab}	10.6 ^a	28.34	0.12	6.13	2.05 ^{bc}	11.04	73.84 ^b
S ₈	V ₆₀ FY	4.25 ^b	47.96 ^{abc}	8.0 ^d	28.55	0.12	6.03	2.22 ^{ab}	11.37	73.77 ^b
S ₉	V ₄₀ FY	4.04 ^{bcd}	48.18 ^{abc}	7.9 ^d	28.46	0.12	6.09	2.10 ^{bc}	11.48	73.98 ^b
S ₁₀	VF ₆₀ Y	4.13 ^b	47.41 ^{cd}	7.7 ^d	28.55	0.11	6.03	2.06 ^{bc}	11.53	73.14 ^b
S ₁₁	VF ₄₀ Y	3.78 ^{de}	48.39 ^{abc}	7.9 ^d	28.08	0.11	6.02	2.06 ^{bc}	11.63	73.37 ^b
S ₁₂	VFY ₆₀	4.07 ^{bc}	46.59 ^d	7.8 ^d	28.12	0.12	6.13	2.05 ^{bc}	11.43	73.97 ^b
S ₁₃	VFY ₄₀	3.85 ^{cd}	48.09 ^{abc}	7.8 ^d	27.60	0.13	5.59	1.94 ^c	11.46	69.32 ^d
S ₁₄	V ₀ F ₀ Y ₀	2.48 ^h	48.26 ^{abc}	10.8 ^a	28.57	0.12	6.42	2.34 ^a	11.82	71.28 ^c
Mean		3.82	48.08	8.8	28.3	0.12	6.12	2.10	11.49	72.85
Year										
2007		3.65 ^b	47.46 ^b	6.9 ^c	26.79 ^c	0.13	6.32 ^a	2.27 ^a	13.17 ^a	73.34 ^a
2008		4.07 ^a	47.29 ^b	10.6 ^a	28.60 ^b	0.12	6.20 ^a	2.11 ^b	11.44 ^b	73.59 ^a
2009		3.73 ^b	49.50 ^a	8.8 ^b	29.51 ^a	0.11	5.84 ^b	1.92 ^c	9.87 ^c	71.62 ^b
Average		3.82	48.08	8.8	28.3	0.12	6.12	2.10	11.49	72.85
R		**	**	**	ns	ns	ns	**	ns	**
Y		**	**	**	**	ns	**	**	**	**
R X Y		**	**	**	ns	ns	ns	*	**	**

**Means within columns but not followed by the same letter are significantly different at the p<0.01 level by Duncan's multiple range test. ns: Not significant

Table 5. Evapotranspiration, irrigation, seasonal irrigation water quantities, saving, water use efficiencies and yield of safflower for the treatments

Subjects	Application	ET (mm)	Irrigation (mm)	Number of irrigation	Irrigation water saving (%)	WUE kg ha ⁻¹ mm ⁻¹	IWUE kg ha ⁻¹ mm ⁻¹
S ₁	VFY	591	428	3	-	8.8 ^c	11.92
S ₂	VFY ₀	459	266	2	37.9	9.1 ^c	15.58
S ₃	VF ₀ Y	451	272	2	36.4	8.1 ^d	13.10
S ₄	V ₀ FY	510	317	2	25.9	8.0 ^d	12.13
S ₅	VF ₀ Y ₀	322	111	1	74.1	10.2 ^{ab}	29.28
S ₆	V ₀ FY ₀	364	155	1	63.8	9.9 ^b	22.68
S ₇	V ₀ F ₀ Y	335	161	1	62.4	10.6 ^a	21.32
S ₈	V ₆₀ FY	553	383	3	10.5	8.0 ^d	11.11
S ₉	V ₄₀ FY	536	361	3	15.7	7.9 ^d	11.20
S ₁₀	VF ₆₀ Y	554	365	3	14.7	7.7 ^d	11.32
S ₁₁	VF ₄₀ Y	499	334	3	22.0	7.9 ^d	11.31
S ₁₂	VFY ₆₀	544	363	3	15.2	7.8 ^d	11.23
S ₁₃	VFY ₄₀	513	331	3	22.7	7.8 ^d	11.65
S ₁₄	V ₀ F ₀ Y ₀	234	0	0	100	10.8 ^a	-

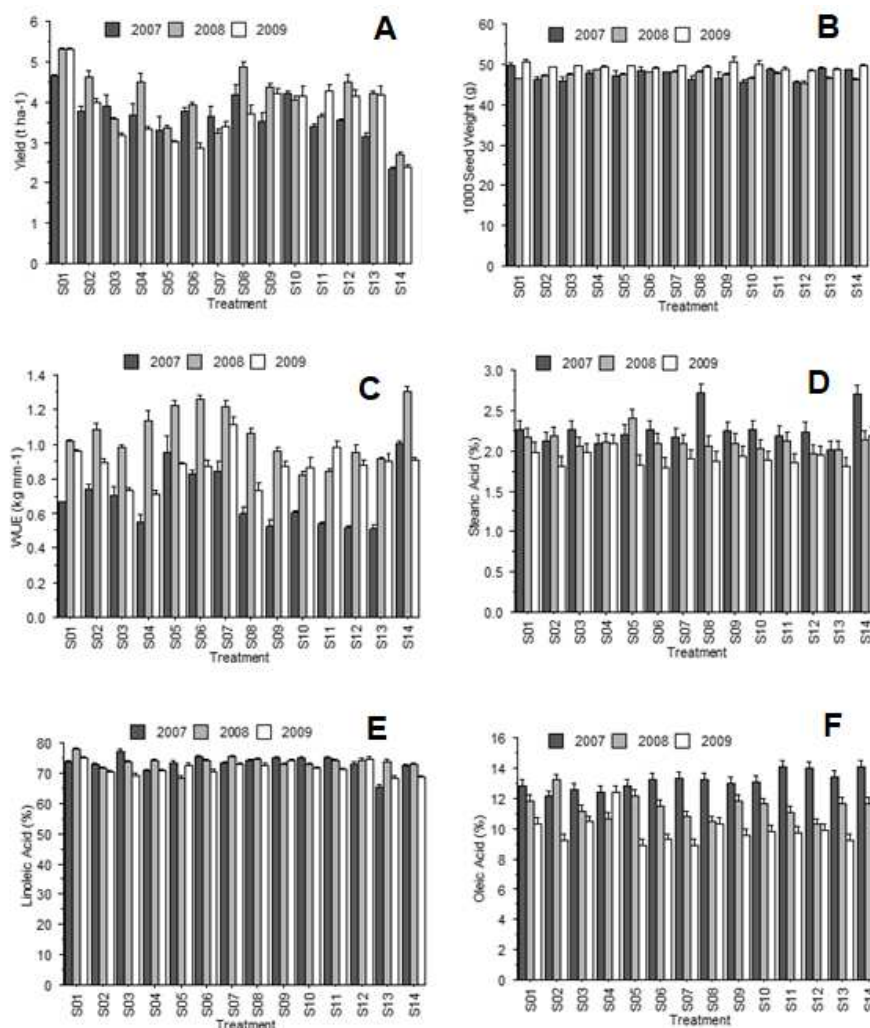


Figure 1. Duncan grouped data in the experiment. A, yield (t ha⁻¹); B, 1000 Seed weight (g); C, WUE, kg mm⁻¹; D, stearic acid (%); E, Linoleic acid (%); F, Oleic acid (%)

While Leonard and French (1968) obtained the highest yield as 3.68 t ha⁻¹ with irrigation until the end of flowering, the lowest yield was obtained as 0.8 t ha⁻¹ from irrigated subject applied until the beginning of flowering. Albel (1976) stated that the flowering period reached the maximum value of plant water consumption and that termination of irrigation during this period caused significant losses in yield. Hang and Evans (1985) indicated that water stress causes shortening in plant height, early flowering, early ripening and decrease in seed yield. Dashora and Sharma (2006) received the highest seed yield from the subject that was irrigated twice during flowering and yield formation periods. Nabipour et al. (2007) obtained the highest yield from the subject of full irrigation, whereas the lowest yield was obtained from the subject without irrigation during the flowering period. Istanbuluoglu et al. (2009) said that the effect of pre-flowering water deficit on winter safflower cultivation had more effect on the yield. Ghamarnia et al. (2010) mentioned that seed yield depends on the amount of water available in the soil. Sharrifmoghaddasi and Omidi (2010) point out that the effect on yield components of stopping irrigation after the flowering period is weak. Jabbari et al. (2010) reported that water limitation before flowering causes drastic effects. Omidi et al.

(2012) stated that drought stress before flowering importantly influenced seed yield per plant and the number of buds per plant. The reduction rate of grain yield of safflower changed from about 10% to 38%, considering the decrease of soil moisture level. Santos et al. (2018) specified that deficit irrigation in phenological stages remarkably impacted plant height, diameter, length, fresh weight, dry weight and number of stems. They pointed out the benefit of irrigation during the vegetation period but stated that irrigation during the flowering period was more effective.

Seed Weight

The highest 1000 seed weight is achieved in full irrigation, while there is a significant reduction in limited irrigation issues. The 1000 seed weights obtained in the third year of the experiment are higher than in the first two years. While the S₅, S₈, S₉, S₁₁, S₁₃ and S₁₄ subjects are in the same group statistically, the data of the S₄, S₆ and S₇ subjects are listed after the statistics of full irrigation. The effect of full watering during the vegetative period led to a higher seed weight of 1000 compared to the flowering and yield formation periods. The graph of the 1000 seed weight in the experiment carried out is given in *Figure 1-B*.

Irrigation Water Use Efficiency (IWUE)

The highest IWUE value was obtained from the S₁₄ subjects where no irrigation was applied and from the S₇ subjects where irrigation was performed only during the yield formation period. Full irrigation did not give the highest IWUE value. The lowest IWUE values were observed in S₃, S₄, S₈, S₉, S₁₀, S₁₁, S₁₂ and S₁₃, in which 40% and 60% of deficit water were applied in the vegetative, flowering and yield formation periods. Subject S₁ and subject S₂ were statistically in the same group. In the annual assessment, all trial years were in different groups, while in 2008 group A, which received the least rainfall during the irrigation period, in Group B in 2009 and in 2007, in which the highest rainfall occurred in the vegetative period were in the (c) group. The graph of the IWUE in the experiment is given in *Figure 1-C*.

Low irrigation water applications generally resulted in higher IWUE values. Our results are in agreement with Lovelli et al. (2007), Istanbuluoğlu (2009) and Singh et al. (2016). Conversely, Kar et al. (2007) indicated an increase in the water use of the additional irrigation number. As the irrigation number increased, the IWUE value increased. In a two-year study, the IWUE value was 1.23 kg ha⁻¹ mm⁻¹ with one irrigation and 2.11 kg ha⁻¹ mm⁻¹ with a 71% increase with two irrigations. The highest IWUE was achieved with the mean value being 2.96 kg ha⁻¹ mm⁻¹ with three supplemental irrigations. Abd El-Lattief (2013) obtained the highest IWUE value for irrigation when there was a 50% reduction in soil moisture levels with 20 plants per square meter.

Oil Rate and Fatty Acid Composition

The irrigation subjects applied did not have any effect on the oil ratio of the safflower. The results of this study are also confirmed by Albel (1976), Hang and Evans (1985), Hamrouni et al. (2007) and Omidı et al. (2012). Conversely, while Amini et al. (2013) determined an 8.8% reduction of the mean oil content due to water-deficit stress, Hasanvandi et al. (2014), observed an increase in oil content under irrigation conditions.

When the results of the fatty acid composition were taken into account, no effect of restricted irrigation practices on fatty acids other than stearic and linoleic acid could be

determined. In the stearic acid composition, where four different groups were formed, the subject S₁₄, where irrigation water was never applied, formed group (a). The graphs of the stearic, oleic and linoleic acid composition are given in *Figures 1-D, 1-E and 1-F*, respectively. Similar findings were found by Cosge et al. (2007). Hamrouni et al. (2007) indicated that excessive water stress led to a decrease in linoleic acid ratios, while moderate stress increased all the fatty acids proportionately. Ashrafi and Razmjo (2010) found that stearic, oleic and linoleic fatty acids in the safflower plant decreased by 5 to 14% depending on the degree of drought stress.

Irrigation water requirements and evapotranspiration

Table 5 summarizes the average evapotranspiration, irrigation water requirement, the number of irrigation treatments, conserved proportional irrigation water, WUE, IWUE and the yield values of applied irrigation water issues.

The amount of irrigation water applied to the experimental subjects and plant water consumption values differed due to variable climatic conditions and precipitation. The lowest ET value was naturally occurring at 234 mm from the subject S₁₄ where no water was given, and the highest ET value was 591 mm from the subject S₁ where full irrigation was performed. Although the ET values of S₂ and S₃ subjects, which did not irrigate only during the flowering and yield formation periods, showed significant differences during the year, the values were very close to each other on a three-year average. In spite of this proximity in terms of average value of water consumed, the average yield values obtained for 3 years led to the yields per hectare being statistically different in terms of S₂ and S₃ yields of 4.14 and 3.56 tons, respectively. In this case, it can be said that the flowering period is more sensitive to water constraints than the yield formation period. In the vegetative period, the average ET value for the S₄, where irrigation was not performed, was 510 mm and the average yield was 3.84 tons ha⁻¹. When these three periods are compared with each other, flowering, vegetative and yield formation can be listed in terms of sensitivity to water stress. In this case, when limited irrigation needs to be implemented due to lack of water in the irrigation network, the restriction should be applied in other periods, excluding the flowering period.

For the subjects S₅, S₆, and S₇ only one irrigation was carried out during the growing period. In terms of ET value, the highest plant water consumption was in the flowering period (S₆) with an average of 364 mm, followed by yield formation (S₇) with 335 mm and vegetative (S₅) with 322 mm. Although the ET values of the S₆ and S₇ periods showed a 42 mm consumption difference on average, they were in the same group in terms of average yield with 3.56 and 3.52 t ha⁻¹ yield, respectively. In this case, it can be said that there will not be any difference in the preference of one of the flowering or yield formation periods in irrigation networks where there is only one irrigation opportunity during the year.

The subjects S₈, S₁₀, and S₁₂, where 60% water is applied for a single period compared to full irrigation, represent subjects where irrigation is applied at 60% during the vegetation, flowering, and yield formation periods. This means that two of these three periods are fully irrigated and 60% of water is applied for the remaining period. The mean ET values of S₈ and S₁₀ were 553 and 554 mm, respectively, and the yield values were 4.25 and 4.13 t ha⁻¹, respectively. While the S₈ and S₁₀ issues are in the same group in terms of yield, their irrigation water needs are 383 and 365 mm, respectively. The ET value for S₁₂ was 544 mm, the yield was 4.07 t ha⁻¹ and the irrigation water requirement was 363 mm.

The subjects S₉, S₁₁, and S₁₃ represent subjects where 40% of total irrigation is provided during water application periods. These issues indicate that 40% of the full irrigation is given in the plant root zone and the other two periods are fully irrigated. The measured ET values for these subjects are 536 mm, 499 mm and 513 mm, respectively. The yield values obtained for these subjects, where irrigation water was applied three times, were 4.04, 3.78 and 3.85 tons per hectare, respectively, and each of them was statistically different. The water savings for the subjects were 15.7%, 22%, and 22.7%, respectively, whereas all three subjects were in the same group in terms of water application efficiency. The results of the yield–response factor are given in *Figure 2*.

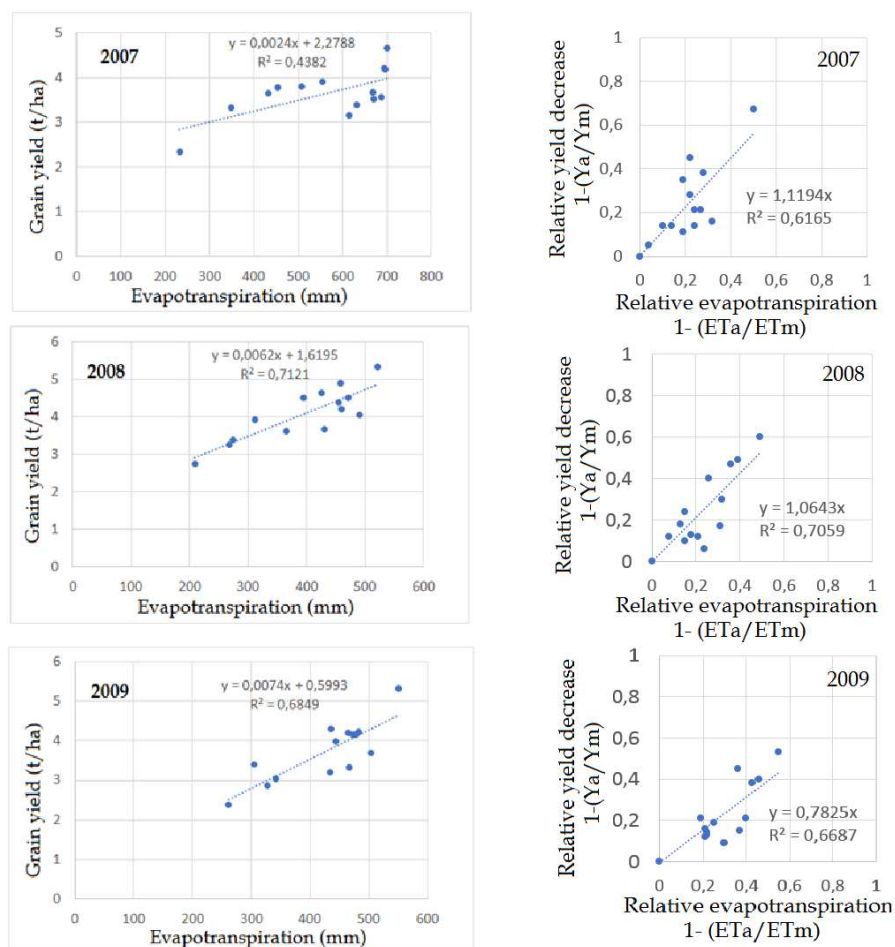


Figure 2. Relationship between grain yield and evapotranspiration (left side), Relationship between relative evapotranspiration deficit $1 - (ET_a/ET_m)$ and relative yield decrease $1 - (Y_a/Y_m)$ (confidence level $p < 0.01$) (right side)

Water–yield relationships and yield response factor (k_y)

Irrigation water and plant water consumption and yields of the subjects were evaluated mutually and water–yield relationships were obtained during the experiment. Since yields obtained from plant water consumption values vary from year to year, water–yield relationship graphs are given separately for the years in which the experiment is

conducted. Since the maximum amount of irrigation water applied does not exceed the field capacity, the water yield relation is indicated by a linear equation.

The k_y values for the experimental years of 2007, 2008 and 2009 were 0.77, 0.84 and 1.15, respectively (mean = 0.92). The obtained k_y values for the whole growth period in this study were very close to the value of 0.80 proposed by Doorenbos and Kassam (1979), 0.93 by Lovelli et al. (2007) and 0.97 by Istanbuluoglu et al. (2009). The yield response factor (k_y) for each specific growth period proved to be an important criterion to decide which stage was the most sensitive to water. According to Lovelli et al. (2007), the k_y value, which is under 1 for safflower, indicates that the decrease in production is very low. It means that there is not much change in yield and that the plant is more resistant to water stress. Pourghasemin and Zahedi (2009) indicated that the effects of the decrease in soil moisture levels on plant growth vary according to the percentage of flowering. The decrease in soil moisture, plant height, leaf area index, plant dry matter, the number of trays per plant, bud seed weight and seed number per harvest index were not reduced at 50% of flowering. On the other hand, the decrease in soil moisture in the period when flowering is 100% leads to a decrease in these characteristics.

Phenological periods were evaluated separately by taking into consideration the values obtained during the three years of the study. The mean values obtained for the vegetation, flowering, and yield formation periods were 1.03, 1.18 and 1.00, respectively. In this case, the flowering period takes the first place in terms of its effect on yield, followed by the vegetative and yield formation periods. According to Istanbuluoglu et al. (2009), the safflower plant is most susceptible to water stress during the vegetative period, whereas Omid et al. (2012) and Santos et al. (2018) stated that it was most susceptible during the flowering period.

Conclusions

The obtained results showed that for maximum yield in safflower cultivation, irrigation should be done without problems during all developmental stages of the plant. The flowering period is the most sensitive period for safflower productivity. Therefore, there is no compensation for the water deficit during the flowering period. The yield formation period was determined to be the second most sensitive period for soil moisture in terms of irrigation. Irrigation during this period increases the weight of 1000 grains, with especially the hectoliter weight being higher. When the k_y values obtained are evaluated together with the yield, the effect of water stress that may occur during the yield formation is seen. In this study, the effects of the safflower plant on the fat content and the fatty acid composition were investigated. The results showed that water deficit had no effect on the fat ratio, but it was found that water deficit did affect the stearic and linoleic acid ratios in the fatty acid compositions.

REFERENCES

- [1] Abd El-Lattief, E. A. (2013): Impact of integrated use of bio and mineral nitrogen fertilizers on productivity and profitability of wheat (*Triticum aestivum* L.) under Upper Egypt conditions. – International Journal of Agronomy and Agricultural Research 3(12): 67-73.
- [2] Albel, G. H. (1976): Effects of irrigation regimes, planting dates, nitrogen levels and row spacing on safflower cultivars. – Agronomy Journal 68(3): 448-451.
- [3] AOCS. (1993): Official methods and recommended practices of the American Oil

- Chemists' Society. – AOCs Press, Champaign, U.S.A.
- [4] Ashrafi, E., Razmjoo, K. (2010): Effect of Irrigation Regimes on Oil Content and Composition of Safflower (*Carthamus tinctorius* L.) Cultivars. – Journal of the American Oil Chemists' Society 87(5): 499-506.
- [5] Bacelar, E. L. V. A., Moutinho-Pereira, J. M., Berta, M. C., Gonçalves, C. V. Q., Gomes-Laranjo, B. J., Ferreira, H. M. F., Correia, C. M. (2013): Water use strategies of plants under drought conditions. – In: Aroca, R. (ed.) Plant Responses to Drought Stress. DOI: 10.1007/978-3-642-32653-0_6. Book ISBN: 978-3-642-32652-3.
- [6] Boyacı, H., Karas, E. (2011): Water-yield relationships of safflower plant in Eskişehir conditions. – II. National Soil and Water Resources Congress, Kızılcahamam-Ankara.
- [7] Caloiero, T., Simone Veltri, I. D., Caloiero, P., Frustaci, F. (2018): Drought Analysis in Europe and in the Mediterranean Basin Using the Standardized Precipitation Index. – Water 10: 1043. DOI:10.3390/w10081043.
- [8] Choudhury, B. U., Singh, A. K. (2016): Estimation of crop coefficient of irrigated transplanted puddled rice by field-scale water balance in the semi-arid Indo-Gangetic Plains, India. – Agricultural Water Management 176: 142-150. <https://doi.org/10.1016/j.agwat.2016.05.027>.
- [9] Cook, B. I., Smerdon, J. E., Seager, R., Coats, S. (2014): Global warming and 21-st century drying. – Climate Dynamics 43: 2607-2627. DOI 10.1007/s00382-014-2075-y.
- [10] Cosge, B., Gürbüz, B., Kıralan, M. (2007): Oil Content and Fatty Acid Composition of Some Safflower (*Carthamus tinctorus* L.) Varieties Sown In Spring and Winter. – International Journal Of Natural And Engineering Sciences 1(3): 11-16.
- [11] Dashora, P., Sharma, R. P. (2006): Effect of sowing date, irrigation and sulphur nutrition on yield attributes, yield and oil content of safflower. – Crop Research 31(1): 56-57.
- [12] Diogo, V. P. N. N. (2018): Agricultural land systems: explaining and simulating agricultural land-use patterns. – Ph.D. Thesis, Vrije Universiteit, p. 340, Amsterdam.
- [13] Doorenbos, J., Kassam, A. H. (1979): Yield response to water. – Irrigation and Drainage, pp 33. FAO, United Nations, Rome.
- [14] Ghamarnia, H., Khosravy, H., Sepehri, S. (2010): Yield and water use efficiency of (*Nigella sativa* L.) under different irrigation treatments in a semi arid region in the West of Iran. – Journal of Medicinal Plants Research 4(16): 1612-1616.
- [15] Gouveia, C. M., Trigo, R. M., Beguería, S., Vicente-Serrano, S. M. (2017): Drought impacts on vegetation activity in the Mediterranean region: An assessment using remote sensing data and multi-scale drought indicators. – Global and Planetary Change 151: 15-27. <https://doi.org/10.1016/j.gloplacha.2016.06.011>.
- [16] Grecksch, K. (2019): Scenarios for resilient drought and water scarcity management in England and Wales. – International Journal of River Basin Management 17(2): 219-227.
- [17] Hamrouni, I., Salah, H., Marzouli, B. (2007): Effects of Water- Dificit on Lipids of Safflower Aierial Parts. – Phytochemistry 58(2): 277-280. [https://doi.org/10.1016/S0031-9422\(01\)00210-2](https://doi.org/10.1016/S0031-9422(01)00210-2).
- [18] Hang, A. N., Evans, D. W. (1985): Deficit Sprinkler Irrigation of Sunflower and Safflower. – Agronomy Journal 77(4): 588-592.
- [19] Hertig, E., Trambly, Y. (2017): Regional downscaling of Mediterranean droughts under past and future climatic conditions. – Global and Planetary Change 151: 36-48. <https://doi.org/10.1016/j.gloplacha.2016.10.015>.
- [20] Howell, T. A., Tolk, J. A., Schneider, A. D., Evett, S. R. (1998): Evapotranspiration, Yield, and Water Use Efficiency of Corn Hybrids Differing in Maturity. – Agronomy journal 90(1). DOI:10.2134/agronj1998.00021962009000010002x.
- [21] Istanbuluoglu, A. (2009): Effects of irrigation regimes on yield and water productivity of safflower (*Carthamus tinctorius* L.) under Mediterranean climate conditions. – Agric. Water Management 96: 1792-1798.
- [22] Istanbuluoglu, A., Gocmen, E., Gezer, E., Pasa, C., Konukcu, F. (2009): Effects of water stress at different development stages on yield and water productivity of winter and summer

- safflower (*Carthamus tinctorius* L.). – Agricultural Water Management 96: 1429-1434.
- [23] Jabbari, M., Ebadi, A., Tobeh, A., Mostafaii, H. (2010): Effects of supplemental irrigation on yield and yield components of spring safflower genotypes. – Recent Res. Sci. Technol. 2: 23-28.
- [24] Kar, G., Kumar, A., Martha, M. (2007): Water use efficiency and crop coefficients of dry season oilseed crops. – Agricultural Water Management 87(1): 73-82.
DOI: 10.1016/j.agwat.2006.06.002.
- [25] Leonard, J., French, O. F. (1968): Growth yield and yield components of safflower as affected by irrigation regimes. – Agron. J. 61: 111-113.
DOI:10.2134/agronj1969.00021962006100010037x.
- [26] Lionello, P., Ozsoy, E., Planton, S., Zanchetta, G. (2017): Climate Variability and Change in the Mediterranean Region. – Global, and Planetary Change 151: 1-152.
- [27] Lovelli, S., Perniola, M., Ferrara, A., Tommaso, T. D. (2007): Yield response factor to water (ky) and water use efficiency of *Carthamus tinctorius* L. and *Solanum melongena* L. – Agricultural Water Management 92: 73-80.
- [28] Nabipour, M., Meskerbashee, M., Yousefpour, H. (2007): The effect of water deficit on yield and yield components of safflower (*Carthamus tinctorius* L.). – Pak J Biol Sci 10(3): 421-6.
- [29] Omid, A. H., Khazaei, H., Monneveux, P., Stoddard, F. (2012): Effect of cultivar and water regime on yield and yield components in safflower (*Carthamus tinctorius* L.). – Turkish Journal of Field Crops 17(1): 10-15.
- [30] Öztürk, Ö., Ada, R., Akinerdem, F. (2009): Determination of yield and yield components of some safflower cultivars in irrigated and dry conditions. – Selçuk University Journal of Agricultural and Food Sciences 23(50): 16-27. ISSN:1309-0550.
- [31] Pan, T., Chen, J., Liu, Y. (2018): Spatial and Temporal Pattern of Drought Hazard under Different RCP Scenarios for China in the 21st century. – <https://doi.org/10.5194/nhess-2018-242>.
- [32] Pankova, Ye. I., Konyushkova, M. V. (2014): Effect of Global Warming on Soil Salinity of the Arid Regions. – Russian Agricultural Sciences 39(5-6): 464-467. ISSN 10683674.
- [33] Pourghasemin, N., Zahedi, M. (2009): Effects of Planting Pattern and Level of Soil Moisture on Yield and Yield Components of Two Safflower Cultivars in Isfahan. – <http://www.doaj.org>.
- [34] Rahiz, M., New, M. K. (2012): 21st Century Drought Scenarios for the UK. – Water Resources Management 27(4): 1039-1061. DOI: 10.1007/s11269-012-0183-1.
- [35] Santos, R. F., Bassegio, D., Silva, M. A., Klar, A. E., Silva, A. A. F., Silva, T. R. B. (2018): Irrigated safflower at different phenological stages of Brazilian southeast dry season. – Irriga 23(3): 493.
- [36] SAS Institute. (1998): Statistical Analysis System Institute: StatView Reference Manual. – SAS Institute, Cary, NC.
- [37] Shammout, M. W., Qtaishat, T., Rawabdeh, H., Shatanawi, M. (2018): Improving Water Use Efficiency under Deficit Irrigation in the Jordan Valley. – Sustainability 10: 4317. DOI:10.3390/su10114317.
- [38] Sharrifmoghaddasi, M., Omid, A. H. (2010): Study of interrupting irrigation effects at different growth stages on grain and oil yields of new safflower varieties. – Advances in Environmental Biology 4(3): 387-391. ISSN 1995-0756.
- [39] Shkolnik, I. M., Pigol'tsina, G. B., Efimov, S. V. (2019): Agriculture in the Arid Regions of Eurasia and Global Warming: RCM Ensemble Projections for the Middle of the 21st Century. – Russian Meteorology and Hydrology 44(8): 540-547. ISSN 1068-3739.
- [40] Singh, S., Angadi, S. V., Grover, K., Begna, S., Auld, D. (2016): Drought response and yield formation of spring safflower under different water regimes in the semiarid Southern High Plains. – Agricultural Water Management 163: 354-362.
DOI: 10.1016/j.agwat.2015.10.010.
- [41] Stewart, J. I., Cuenca, R. H., Pruitt, W. O., Hagan, R. M., Tosso, J. (1977): Determination

- and utilization of water production functions for principal California crops. – W-67 California Contributory Project, University of California, California, USA.
- [42] SWRI. (2011): Climatological data of the Soil and Water Research Institute of Eskisehir (1957-2011). – Unpublished report, 12 p.
- [43] TÜİK. (2018): Turkish Statistical Institute. Agricultural Statistics. – <http://tuik.gov.tr/UstMenu.do?metod=temelist> [Accessed 28.09.2019].
- [44] Tüzüner, A. (1990): Soil and Water Analysis Laboratory Handbook. – Ministry of Agriculture, General Directorate of Rural Service, Ankara.
- [45] Ward, F. A., Pulido-Velazquez, M. (2008): Water conservation in irrigation can increase water use. – Proceedings of the National Academy of Sciences of the United States of America 105(47): 18215-18220. DOI:10.1073/pnas.0805554105.
- [46] Yurtsever, N. (1984): Experimental Methods in Statistics. – Ministry of Agriculture and Rural Affairs, Ankara, Turkey: 625-632.

DEVELOPMENT OF NEW VALUABLE INTROGRESSION LINES FROM THE INTERSPECIFIC CROSS IN EGGPLANT (*SOLANUM MELONGENA* L.)

BOYACI, H. F.

*Bati Akdeniz Agricultural Res. Inst., Dept. Of Vegetable Crops And Ornamentals
07100 Antalya, Turkey*

(e-mail: filiz_boyaci@yahoo.com; phone: +90-242-724-5292; fax: +90-242-724-5293)

(Received 16th Oct 2019; accepted 8th Jan 2020)

Abstract. Genetic diversity in eggplant cultivars has drastically decreased due to developed varieties having similar desirable characteristics. In recent years, the breeders have taken much effort to enrich eggplant (*Solanum melongena* L.) genome by utilizing local populations and wild relatives similarly to the case of other plant species. In addition, wild relatives make it possible to benefit from their resistance genes which provide tolerance to biotic and abiotic stress factors. In this study, preservation and maintenance of genetic diversity by utilizing wild eggplant species to alleviate the restrictions in eggplant breeding programs caused by the limited genetic background through creating interspecific crosses was established as the main goal. In total, nine species chosen among the wild relatives of eggplant were crossed with two inbred lines developed from *Solanum melongena* L. Hybrid seed was available only in five crosses. Just, 38 lines developed in F4 stage from *Solanum insanum*. These lines were examined morphologically by using 27 descriptors. The data was analyzed by NTSYSpC: Numerical Taxonomy and Multivariate Analysis System (Version 2.0) program for understanding their phylogenetic relationship. A high variance changing in between 27% and 97% was observed among them. This result showed that they have good potentials to be used in breeding programs.

Keywords: *ancestor, genetic diversity, phylogenetic relationship, relative*

Introduction

Eggplant is one of the most valuable vegetables highly consumed in populated countries like India, China, Indonesia, Japan, the Philippines, in Asian countries, also in European and African countries (Frery et al., 2007; Looney, 2016). It has rich contents of minerals, antioxidants, fiber and vitamins (Kalloo, 1993; Scorsatto et al., 2017), which makes it suitable for human nutrition. Its production quantity is increasing year by year in the world. A significant part of commercialized eggplant F1 hybrid varieties have black color fruits and they are quite similar to each other (Muñoz Falcón et al., 2009). The breeder's genetic resource capacities and variants have become decreased because the gene pools used in breeding programs have been focused to develop F1 varieties that are indistinguishable from one another. Furthermore, the wide-spreading use of these commercial varieties pose a risk to the extinct of genetic diversity in a long term period (Cericola et al., 2013). Another problem faced by the breeders is that these commercial varieties are susceptible to biotic and abiotic stress factors (Rotino et al., 2014; Kacjan Maršić et al., 2014). In recent years, several studies have been launched to overcome of these problems. Eggplant's wild relatives have given opportunity to provide the enrichment of genetic diversity, improve resistance to biotic and abiotic stress factors and develop nutritional quality (Rotino et al., 2014; Syfert et al., 2016).

The studies on genetic relationship of eggplant wild relatives in genomic levels demonstrated their potential breeding values. The genetic diversity were determined among the eggplants including the usage of SSR marker systems. The close genetic relationship

were revealed among *S. anguvi* and *S. aethiopicum*. Moreover *S. melongena* and *S. aethiopicum* showed high similarity. *S. macrocarpon* showed less genetic similarity. *S. linnaeanum* showed a close genetic relationship with *S. aethiopicum* compared with other species (Tümbilen et al., 2011). Constructed genetic map to found out phylogenetic relationship by using AFLPs markers has been revealed that Asian plants indicated one species *S. insanum* (*S. incanum*+*S. undatum*) as their ancestors. Another valuable wild relative of eggplant is *S. incanum* which is being used in eggplant breeding programmes for developing ILs against drought resistance. Also *S. linnaeanum* can be good resource for breeding programs regarding bacterial wilt resistance (Knapp et al., 2013). According to transcriptome analysis, the *S. aethiopicum* accession has highly intraspecific polymorphisms compared with *S. incanum*. But these African eggplants have limited potential for breeding programs in contrast to previous studies (Gramazio et al., 2016). An investigation result on gene divergence between wild and domesticated eggplants clearly showed that *S. aethiopicum* and *S. integrifolium* from section *Oliganthes* were placed in the same clade, but *S. sisymbriifolium* in the *Sisymbriifolium* clade was in the most distant clade from the cultivated eggplant on the generated phylogenetic tree (Wei et al., 2019).

Although eggplant has a large number and valuable of wild relatives, most of them has not been fully evaluated in breeding programs due to sexual barriers encountered during the interspecific crosses (Sihachakr et al., 1994). For example, it was declared that *S. melongena* were crossed with 19 well known relatives and fertile hybrids have been obtained only from four wild relatives' (*S. incanum*, *S. linneanum*, *S. macrocarpon*, and *S. aethiopicum*) crosses (Daunay and Lester, 1989). *S. aethiopicum* L. and *S. macrocarpon* L. have been the most remarkable species for the breeders (Daunay et al., 2019). Also, an inbred line successfully produced through interspecific hybridization from *S. linneanum* to ensure resistance against *Verticillium* wilt has been reported (Liu et al., 2015). BC and F2 progenies, having high phenolic content that are the health-beneficial compounds, obtained from hybridization of *S. melongena* and *S. incanum* have been evidence for genetic progress (Prohens et al., 2013). Despite all these successes obtained in interspecific hybridization of wild species and cultivar form of eggplant so far, the use of outputs is limited in the breeding program in practice. There is still no available commercial eggplant cultivar has been improved by using its wild relatives excepting rootstocks (Plazas et al., 2016). So there is still a need for further studies achieving gene pool having high genetic variability that can be useful for intense and public breeding programs from these precious resources.

The aim of this work is to develop more distant inbred lines in eggplant by taking advantage of its ancestors and contribute to increase genetic diversity which is the most important factor in increasing the success of breeding programs.

Materials and methods

Totally nine wild relatives and two inbred lines of *Solanum melongena* were used in the study. All the plant materials belonging to the wild relatives of eggplant were provided from INRA, in the Unit of Genetics and Breeding of Fruits and Vegetable, Avignon, France, by a senior researcher, Daunay, M. C. The inbred lines P45 and P5/2, having high General Combining Ability, were developed in a breeding program carried out Bati Akdeniz Agricultural Research Institute (BATEM) Antalya, Turkey. The detailed information about plant materials code, species name and origin used in the study were given in *Table 1*.

Table 1. The plant materials code, species name and origin used in the study

Code	Species name	Origin of materials
MM132	<i>S. macrocarpon</i> L.	INRA, France
MM195	<i>S. linnaeanum</i> Hepper & Jaeger	INRA, France
MM232	<i>S. aethiopicum</i> L. Group Gilo	INRA, France
MM497	<i>S. violaceum</i> Ort.	INRA, France
MM511	<i>S. virginianum</i> L.	INRA, France
MM684	<i>S. incanum</i> L. group C	INRA, France
MM1602	<i>S. viarum</i> Dunal	INRA, France
MM1689	<i>S. anguivi</i> Lam.	INRA, France
MM510	<i>S. insanum</i> (<i>S. melongena</i> L. group E)	INRA, France
P45	<i>S. melongena</i> L. (inbred line)	BATEM, Turkey
P5/2	<i>S. melongena</i> L. (inbred line)	BATEM, Turkey

The plants of study were grown under glasshouse conditions. Two inbred lines (P45 and P5/2) belonging to *S. melongena* used as females were crossed with nine wild relatives of eggplant. The fertile F1 hybrids obtained from interspecific cross were selfed to produce F2 plants. The most fertile F2 plants were selected to construct lines and F3 to F4 progenies were raised from initial P45 x *S. insanum* and P5/2 x *S. insanum* crosses. Totally 38 lines in F4 stage were generated. These lines morphology-based phylogenies were examined with 27 descriptors selected from UPOV (Union of Plant Variety), IPGRI (International Plant Genetic Research Institution) and experiences of breeder (Table 2).

Table 2. The traits, descriptors and score range used in observation for inbred lines generated from interspecific hybridization of *S. melongena* (P45) and *S. insanum*

Traits	Description and Score range
Plant habitat	1=Open, 3=Bushy
Plant height	1=Long, 3=Intermediate, 5=Short
Stem thickness	1=Thick, 3=Intermediate, 5=Thin
Stem hairiness	1=Dense, 3=Intermediate, 5=Tenuous
Stem color	1=Grayish-green, 3=Green, 5=Green-purple 7=Purple
Shoot tip color	1=Grayish-green, 3=Green, 5=Green-purple 7=Purple
Length of internodes	1=Long, 3=Intermediate, 5=Short
Leaf color	1=Green, 3= Light green, 5= Dark green
Leaf size	1=Large, 3=Intermediate, 5=Small
Leaf hairiness	1=Dense, 3=Intermediate, 5=Tenuous
Presence of spine on petiole	1=Many, 3=Intermediate, 5=Few, 7=Absent
Bud size	1=Large, 3=Intermediate, 5=Small
Bud hairiness	1=Dense, 3=Intermediate, 5=Tenuous, 7=Absent
Presence of spine on bud	1=Many, 3=Intermediate, 5=Few, 7=Absent
Flower color	1=Light purple, 3=Purple, 5=Dark purple, 7=White
Flower size	1=Large, 3=Intermediate, 5=Small
Fruit shape	1=Long, 3=Intermediate, 5=Short, 7=Ovoid, 9=Pear shaped
Fruit color	1=Light purple, 3=Purple, 5=Green
Fruit length (cm)	1=2-3, 3=4-5, 5=6-7, 7=8-9
Fruit diameter (cm)	1=5-7, 3=8-10, 5=11-13, 7=14-16
Average fruit weight (g)	1=9-34,3= 35-60, 5=61-86, 7=87-112, 9=113-138, 11=139-164
Fruit flesh color	1=Greenish-cream, 3=Green, 5=White
Fruit end shape	1= Round, 3=Pointed, 5=Flat
Fruit groove	1=Present, 3=Absent
Calyx size	1=Large, 3=Intermediate, 5=Small
Presence of seed in fruit	1=Absent, 3=One or two, 5=Few, 7=Intermediate, 9=Many
Seed mature	1=Absent, 3=Immature, 5=Mature, 7=Imbibed mature seeds

Descriptions and score range were modified from UPOV and IPGRI eggplant descriptors. The characteristics were scored according to and compared with recognized cultivar *S. melongena* cv. Long Purple. All observations determined by measurement or counting were made on 10 plants or parts taken from each of 10 plants. Numerical data regarding fruit characteristics for each line were collected from ten harvested fruits.

The relationship among inbred lines was investigated by the technique of UPGMA, the clustering procedure was carried out using NTSYS-PC version 2.2 (Rohlf, 1998). Through the utilization of clustering technique UPGMA via SHAN module, the dendrograms were created. The cophenetic correlation coefficient was determined with the Mantel technique so as to assess the clustering effectiveness.

Results and discussion

The F1 hybrids from some interspecific crosses between the inbred lines and wild species were produced to create novel diversity that is peculiar to wild species. Only five interspecific hybrids were attained from crosses between P45 which is a parental line and *S. macrocarpon*, *S. linnaeanum*, *S. aethiopicum*, *S. incanum* and *S. insanum* among the nine species were tested in the study. Also, P5/2 produced just four hybrids from *S. macrocarpon*, *S. linnaeanum*, *S. incanum* and *S. insanum* crosses. However, interspecific F1 hybrid of *S. aethiopicum* was unfertile. The interspecific hybridization between inbred lines and *S. violaceum*, *S. virginianum* and *S. anguvi* were unsuccessful (Table 3). Some hybrids and their parents obtained from *S. melongena* (P45) x *S. incanum*, *S. melongena* (P45) x *S. macrocarpon*, *S. melongena* (P45) x *S. insanum*, *S. melongena* (P5/2) x *S. insanum* crossing are shown in Fig. 1.

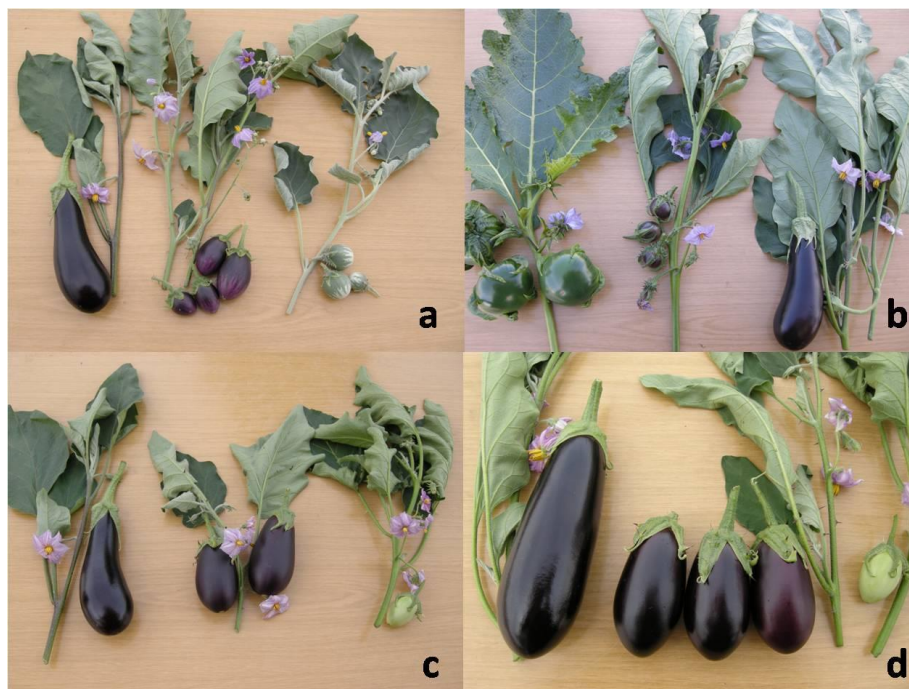


Figure 1. Some hybrids and their parents obtained from crosses of *S. melongena* (P45) x *S. incanum* (a), *S. melongena* (P45) x *S. macrocarpon* (b), *S. melongena* (P45) x *S. insanum* (c), *S. melongena* (P5/2) x *S. insanum* (d)

Table 3. The results of interspecific crosses between two inbred lines belonging to the *S. melongena* and nine wild relatives of eggplant

X	<i>S. macrocarpon</i>	<i>S. linnaeanum</i>	<i>S. aethiopicum</i>	<i>S. violaceum</i>	<i>S. insanum</i>	<i>S. virginianum</i>	<i>S. incanum</i>	<i>S. anguvi</i>	<i>S. melongena</i> (P45)	<i>S. melongena</i> (P5/2)
<i>S. macrocarpon</i>	+									
<i>S. linnaeanum</i>		+								
<i>S. aethiopicum</i>			+							
<i>S. violaceum</i>				+						
<i>S. insanum</i>					+					
<i>S. virginianum</i>						-				
<i>S. incanum</i>							+			
<i>S. anguvi</i>								-		
<i>S. melongena</i> (P45)	+	+	+	-	+	-	+	-	+	+
<i>S. melongena</i> (P5/2)	+	+	-**	-	+	-	+	-	+	+

*: Successful crosses, F1 hybrids were obtained (+), **: Unsuccessful crosses, F1 hybrid were not obtained because of sexual barriers (-)

The production of F2 generation plants were realized by hand pollination of F1 plants obtained from only three crosses performed among P45 and three wild relatives (*S. macrocarpon*, *S. incanum* and *S. insanum*) and P5/2 x *S. insanum*. Only, the progenies derived from inbred lines (P45 and P5/2) and *S. insanum* crosses were appropriated to sustain of F4 generations having desirable morphologic characters. 38 inbred lines in F4 stage were produced from YAB3-YAB15: P45 x *S. insanum*, YAB7-YAB16: P5/2 x *S. insanum* crosses. The other progenies generated from *S. macrocarpon* and *S. incanum* showed inconvenient characteristic specials sourced from recombination. And they were not sustainable for breeding studies. These findings were consistent with some results presented in previous studies, but not with the others. Schaff et al. (1982) reported that the fertile F1 and F2 plants have been produced from *S. melongena* x *S. macrocarpon* crosses where as the F1 hybrids could be obtained after embryo rescue from *S. melongena* x *S. aethiopicum* and *S. melongena* x *S. insanum*. *S. melongena* x *S. gilo* produced only sterile F1 hybrids. Also, the producing fertile hybrid from *S. macrocarpon* was notified by Kashyap (2002). In another study, Bletsos et al. (2004) obtained success from one cross among three crosses of *S. melongena* and *S. macrocarpon*. They stated that the female genotype plays a major effect on the success of interspecific cross. Similarly, we detected maternal effect in our study. For example, although P45 produced F1 hybrid in hybridization with *S. aethiopicum* but P5/2 did not show good performance in hybridization. This means that crossability of P45 with wild relatives can be sourced from its ancestor genes in the background. Additionally, F1 hybrids produced from crosses P5/2 and two wild relatives of eggplant (*S. macrocarpon*, *S. incanum*) had ungerminated seeds. In other study, Gowda et al. (1990) claimed contrarily that the interspecific cross of *S. macrocarpon* produce sterile hybrids due to the ovule abortion. It has been reported by Schaff et al. (1982) that the subsequent progenies were limited due to the recombination effect observed in the formation of F2 produced from *S. macrocarpon* hybrids. Taher et al. (2017) also mentioned translocation formation during meiosis in plants. Davidar et al. (2015) found out that the interspecific cross between *S. insanum* and eggplant cultivars by hand pollination had low fruit set. However, Prohens et al. (2013) informed that the highly valuable BC1P2 plants have been developed from *S. incanum* for phenolic compound improvement of functional quality. In another study, a new wild genepool constructed from interspecific cross of *S. melongena* and *S. elaeagnifolium*. This genepool carries to BC1 generation had intermediate attribute according to their parents and it is quite valuable for eggplant breeding, as it was reported by García-Forte et al. (2019). Furthermore, Kouassi et al. (2016) have made interspecific cross between six eggplant varieties and 10 accessions of wild relatives. They obtained 44 interspecific hybrids *S. insanum*, *S. anguivi*, *S. dasyphyllum*, *S. incanum*, *S. lichtensteinii*, and *S. tomentosum*. The first backcross generations from crosses with hybrids between *S. melongena* and *S. insanum* had been achieved. Identically, the most efficient wild relative of eggplant was *S. insanum* in our study.

Using morphologic descriptors, the phylogenetic relationships among 38 inbred lines were revealed. While 24 of the 27 criteria used revealed the morphological differences among the inbred lines, 3 criteria regarding stem, shoot tip and leaf color did not affect the separation of the lines. The eigenvalue was 92% for 5 determinants. Mantel t-test values were approximately $t = 6.5842$, $p = 1.0000$ for the 2-way technique of Mantel Test (Mantel, 1967). Matrix correlation (r) was 0.87 (as normalized Mantel Z-Statistic) and this value was in acceptable levels. The r value verified a significant relationship

between genetic distance matrices. The graph created from comparison of similarity matrices contains points indicating high correlation (Fig. 2).

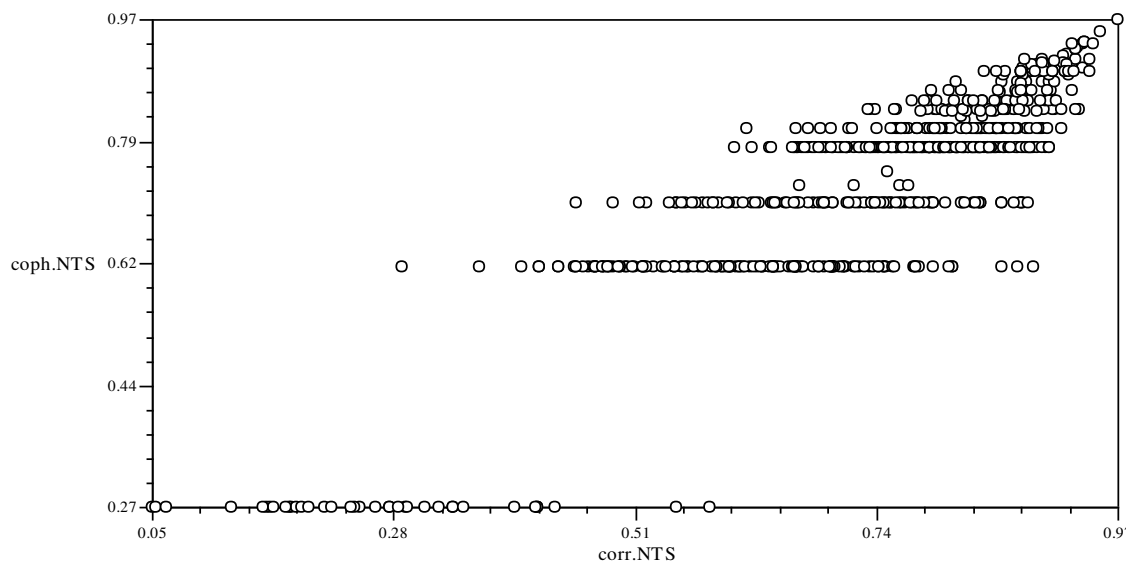


Figure 2. The correlation between the genetic distance matrices constructed from morphological data of F4 inbred lines improved from interspecific cross between *S. melongena* and *S. insanum* using Mantel tests

The dendrogram was formed with matrices of distance by following the unweighted pair group technique with arithmetic means (UPGMA) for phylogenetic examination (Fig. 3). The rates of similarity in accordance with inbred lines' coefficient similarity varied between 0.27 and 0.97. Following the UPGMA method, the lines in F4 stage generated from interspecific crosses were divided into 2 primary groups. One inbred line formed the first group (A). This line was considerably distinct compared to all other inbred line genotypes. 37 inbred lines as a majority formed the second group (B) and they were once again divided into 2 different subgroups. The first subgroup (C) consisted of four inbred lines that were developed from P45 x *S. insanum*. The greatest similarity was discovered in the 2nd subgroup (D). The inbred lines of YAB 16/9-3 and YAB 16/9-4 which belonged to the 2nd subgroup demonstrated high genetic similarity with 97% similarity rate. Although, YAB3/1-4 and YAB3/1-6 were developed from same the crosses, they had the furthest genetic distance (27% similarity rate). It was observed in the dendrogram that the lines developed from both sources were dispersed scatter inside each other. The lines which were developed from both sources did not show a significant distribution amongst themselves. The appearance regarding fruit characteristics of some lines in F4 stage are given in Figure 4.

Similarity rates in other studies related to intercrosses of eggplant wild relatives are as follows. Kaushik et al. (2018) evaluated 45 hybrids that were generated from inbred *S. melongena* and *S. insanum* intercrosses by using 14 morphological and agronomic descriptors. A broad range of genetic diversity among these genotypes was also founded by them. *S. melongena* consisting eighty-eight accessions, and four wild relatives (*S. insanum*, *S. incanum*, *S. integrifolium* and *S. sysimbriifolium*) have been examined to determine genetic similarity by using molecular markers. The lowest and highest similarity rate was found to be as 0.47 and 0.67, respectively (Behera et al., 2006).

Likewise, Karihaloo et al. detected in both molecular (1995a) and enzyme electrophoretic (1995b) studies that the similarity rate of *S. melongena* and *S. insanum* is more than 91%. In contrast, the similarity rate changed in between 0.27 and 0.97 in our findings and the genetic diversity had considerably high values.

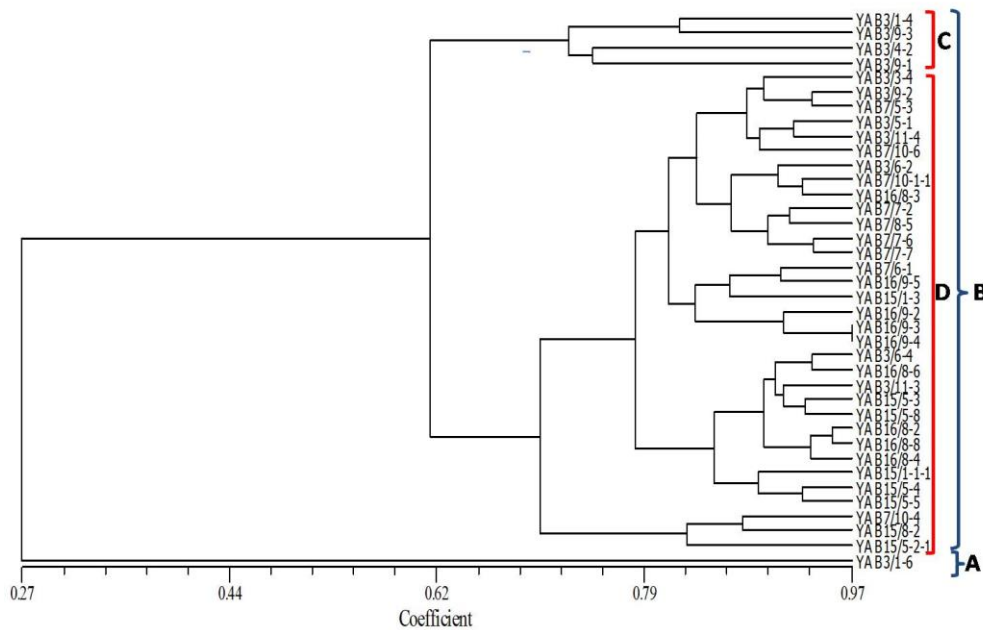


Figure 3. Dendrogram generated based morphological data of 38 inbred lines (YAB3-YAB15: P45 x *S. insanum*, YAB7-YAB16: P5/2 x *S. insanum*) using the Underweighted Pair-Group Method with Arithmetic Mean cluster analysis of DICE (1945) genetic similarity coefficients



Figure 4. The appearance regarding fruit characteristics of some lines (YAB3-YAB15: P45 x *S. insanum*, YAB7-YAB16: P5/2 x *S. insanum*) in F4 stage

It was specified by Kaushik (2019) that *S. insanum* which was used as a tester for observing specific combining ability (SCA) and general combining ability (GCA) components effects and heterosis rates was a better tester for important morphological features. Although *Solanum insanum* L., natural plant of Asia and Africa, carried great potential for breeding studies, it has not paid enough attention by the breeders. Because of having great potential to cross with eggplant cultivar forms, more effort is needed to use it in breeding programs (Ranil et al., 2017).

Conclusion

This study yielded a first report related on genetic diversity of inbred lines developed in interspecific hybridization. *Solanum insanum*, ancestor of *Solanum melongena*, was identified as a good source for emerging survival next generations of inbred lines. It was defined that these lines carried F4 stage had a wide diversity in point of morphologic characters, carried biotic/abiotic stress resistance and being a good source for improving new eggplant variety that shows multiple resistance against some important stress factors. Since the success of these interspecific hybridization programs are highly dependent upon the parents used, a serious effort should be required on new interspecific crosses by using different female parents.

In conclusion, eggplant successful hybridized with *S. insanum*. Integrossion of ancestor genes to the cultivar form provided increase of genetic diversity. The developed lines from the *S. insanum* can contribute to develop commercial variety because they have the desired features like purple-colored fruit, without prickles plants etc. Our results may be relevant for the breeders and contribute to the enhancement of eggplant gene pool.

Acknowledgements. This research was financially supported by grants from the General Directorate of Agricultural Research and Policy, Republic of Turkey Ministry of Agriculture and Forestry under TAGEM/BBAD/10/A09/P01/12 project number.

REFERENCES

- [1] Behera, T. K., Sharma, P., Singh, B. K., Kumar, G., Kumar, R., Mohapatra, T., Singh, N. K. (2006): Assessment of genetic diversity and species relationships in eggplant (*Solanum melongena* L.) using STMS markers. – *Scientia Horticulturae* 107(4): 352-357.
- [2] Bletsos, F., Roupakias, D., Tsaktsira, M., Scaltsoyannes, A. (2004): Production and characterization of interspecific hybrids between three eggplant (*Solanum melongena* L.) cultivars and *Solanum macrocarpon* L. – *Scientia Horticulturae* 101(1-2): 11-21.
- [3] Cericola, F., Portis, E., Toppino, L., Barchi, L., Acciarri, N., Ciriacci, T., Sala, T., Rotino, G. L., Lanteri, S. (2013): The population structure and diversity of eggplant from Asia and the Mediterranean Basin. – *PloS one* 8(9): e73702.
- [4] Daunay, M. C., Lester, R. N. (1989): The usefulness of taxonomy for Solanaceae breeders, with special reference to the genus *Solanum* and to *Solanum melongena* L. (eggplant). – *Capsicum Newslett* 7: 10.
- [5] Daunay, M.-C., Salinier, J., Aubriot, X. (2019): Crossability and Diversity of Eggplants and Their Wild Relatives. – In: Chapman, M. (ed.) *The Eggplant Genome*: 135-191.
- [6] Davidar, P., Snow, A. A., Rajkumar, M., Pasquet, R., Daunay, M. C., Mutegi, E. (2015): The potential for crop to wild hybridization in eggplant (*Solanum melongena*; Solanaceae) in southern India. – *American Journal of Botany* 102(1): 129-139.

- [7] Frary, A., Doganlar, S., Daunay, M. C. (2007): Eggplant. – In: Kole C. (ed.) Genome Mapping and Molecular Breeding in Plants, Vol. 5: Vegetables: 287-313. Berlin: Springer. doi: 10.1007/978-3-540-34536-7_9.
- [8] García-Forteza, E., Gramazio, P., Vilanova, S., Fita, A., Mangino, G., Villanueva, G., Arrones, A., Knapp, S., Prohens, J., Plazas, M. (2019): First successful backcrossing towards eggplant (*Solanum melongena*) of a New World species, the silverleaf nightshade (*S. elaeagnifolium*), and characterization of interspecific hybrids and backcrosses. – *Scientia Horticulturae* 246: 563-573.
- [9] Gowda, P. H. R., Shivashankar, K. T., Joshi, S. H. (1990): Interspecific hybridization between *Solanum melongena* and *Solanum macrocarpon*: study of the F1 hybrid plants. – *Euphytica* 48(1): 59-61.
- [10] Gramazio, P., Blanca, J., Ziarsolo, P., Herraiz, F. J., Plazas, M., Prohens, J., Vilanova, S. (2016): Transcriptome analysis and molecular marker discovery in *Solanum incanum* and *S. aethiopicum*, two close relatives of the common eggplant (*Solanum melongena*) with interest for breeding. – *BMC genomics* 17(1): 300.
- [11] Kacjan Maršič, N., Mikulič-Petkovšek, M., Štampar, F. (2014): Grafting influences phenolic profile and carpometric traits of fruits of greenhouse-grown eggplant (*Solanum melongena* L.). – *Journal of Agricultural and Food Chemistry* 62(43): 10504-10514.
- [12] Kalloo, G. (1993): Eggplant: *Solanum melongena* L. – In: Genetic improvement of vegetable crops: 587-604. Pergamon.
- [13] Karihaloo, J. L., Brauner, S., Gottlieb, L. D. (1995a): Random amplified polymorphic DNA variation in the eggplant, *Solanum melongena* L. (Solanaceae). – *Theoretical and Applied Genetics* 90(6): 767-770.
- [14] Karihaloo, J. L., Gottlieb, L. D. (1995b): Allozyme variation in the eggplant, *Solanum melongena* L. (Solanaceae). – *Theoretical and Applied Genetics* 90(3-4): 578-583.
- [15] Kashyap, V., Kumar, S. V., Collonnier, C., Fusari, F., Haicour, R., Rotino, G. L., Sihachakr, D., Rajam, M. V. (2003): Biotechnology of eggplant. – *Scientia Horticulturae* 97(1): 1-25.
- [16] Kaushik, P., Plazas, M., Prohens, J., Vilanova, S., Gramazio, P. (2018): Diallel genetic analysis for multiple traits in eggplant and assessment of genetic distances for predicting hybrids performance. – *PloS one* 13(6): e0199943.
- [17] Kaushik, P. (2019): Line× Tester Analysis for Morphological and Fruit Biochemical Traits in Eggplant (*Solanum melongena* L.) Using Wild Relatives as Testers. – *Agronomy* 9(4): 185.
- [18] Knapp, S., Vorontsova, M. S., Prohens, J. (2013): Wild relatives of the eggplant (*Solanum melongena* L.: Solanaceae): new understanding of species names in a complex group. – *PloS one* 8(2): e57039.
- [19] Kouassi, B., Prohens, J., Gramazio, P., Kouassi, A. B., Vilanova, S., Galán-Ávila, A., Herraiz, F. J., Kouassi, A., Seguí-Simarro, J. M., Plazas, M. (2016): Development of backcross generations and new interspecific hybrid combinations for introgression breeding in eggplant (*Solanum melongena*). – *Scientia Horticulturae* 213: 199-207.
- [20] Liu, J., Zheng, Z., Zhou, X., Feng, C., Zhuang, Y. (2015): Improving the resistance of eggplant (*Solanum melongena*) to Verticillium wilt using wild species *Solanum linnaeanum*. – *Euphytica* 201(3): 463-469.
- [21] Looney, N. E. (2016): Fruits, vegetables and tubers: bountiful resources for achieving and sustaining food and nutrition security. – In: Pritchard, B., Ortiz, R., Shekar, M. (eds.) *Routledge Handbook of Food and Nutrition Security*: 38-58. Routledge, New York.
- [22] Mantel, N. (1967): Assumption-free Estimators Using U Statistics and a Relationship to the Jackknife Method. – *Biometrics* 23(3): 567-571.
- [23] Muñoz Falcón, J. E., Prohens, J., Vilanova, S., Nuez, F. (2009): Diversity in commercial varieties and landraces of black eggplants and implications for broadening the breeders' gene pool. – *Annals of Applied Biology* 154(3): 453-465.

- [24] Plazas, M., Vilanova, S., Gramazio, P., Rodríguez-Burruezo, A., Fita, A., Herraiz, F. J., Ranil, R., Fonseka, R. M., Niran, L., Fonseka, H., Kouassi, B., Kouassi, A. B., Kouassi, A., Prohens, J. (2016): Interspecific hybridization between eggplant and wild relatives from different gene pools. – *Journal of the American Society for Horticultural Science* 141(1): 34-44.
- [25] Prohens, J., Whitaker, B. D., Plazas, M., Vilanova, S., Hurtado, M., Blasco, M., Gramazio, P., Stommel, J. R. (2013): Genetic diversity in morphological characters and phenolic acids content resulting from an interspecific cross between eggplant, *Solanum melongena*, and its wild ancestor (*S. incanum*). – *Annals of Applied Biology* 162(2): 242-257.
- [26] Ranil, R. H. G., Prohens, J., Aubriot, X., Niran, H. M. L., Plazas, M., Fonseka, R. M., Vilanova, S., Fonseka, H. H., Gramazio, P., Knapp, S. (2017): *Solanum insanum* L. (subgenus *Leptostemonum* Bitter, Solanaceae), the neglected wild progenitor of eggplant (*S. melongena* L.): a review of taxonomy, characteristics and uses aimed at its enhancement for improved eggplant breeding. – *Genetic resources and crop evolution* 64(7): 1707-1722.
- [27] Rohlf, F. J. (1998): NTSYS-PC: Numerical taxonomy and multivariate analysis system. Release 2.20j. – Exeter Software, Setauket, NY.
- [28] Rotino, G. L., Sala, T., Toppino, L. (2014): Eggplant. – In: Pratap, A., Kumar, J. (eds.) *Alien Gene Transfer in Crop Plants*, Vol. 2: 381-409. Springer, New York, NY.
- [29] Schaff, D. A., Jelenkovic, G., Boyer, C. D., Pollack, B. L. (1982): Hybridization and fertility of hybrid derivatives of *Solanum melongena* L. and *Solanum macrocarpon* L. – *Theoretical and Applied Genetics* 62(2): 149-153.
- [30] Scorsatto, M., Rosa, G., Raggio Luiz, R., da Rocha Pinheiro Mulder, A., Junger Teodoro, A., Moraes de Oliveira, G. M. (2019): Effect of Eggplant Flour (*Solanum melongena* L.) associated with hypoenergetic diet on antioxidant status in overweight women—a randomised clinical trial. – *International Journal of Food Science & Technology* 54(6): 2182-2189.
- [31] Sihachakr, D., Daunay, M. C., Serraf, I., Chaput, M. H., Mussio, I., Haicour, R., Rossignol, L., Ducreux, G. (1994): Somatic hybridization of eggplant (*Solanum melongena* L.) with its close and wild relatives. – In: Bajaj, Y. P. S. (ed.) *Biotechnology in Agriculture Forestry 27, Somatic Hybridization in Crop Improvement I*: 255-278. Springer, Berlin, Heidelberg.
- [32] Syfert, M. M., Castañeda-Álvarez, N. P., Khoury, C. K., Särkinen, T., Sosa, C. C., Achicanoy, H. A., Bernau, V., Prohens, J., Daunay, M. C., Knapp, S. (2016): Crop wild relatives of the brinjal eggplant (*Solanum melongena*): poorly represented in genebanks and many species at risk of extinction. – *American journal of botany* 103(4): 635-651.
- [33] Taher, D., Solberg, S. Ø., Prohens, J., Chou, Y. Y., Rakha, M., Wu, T. H. (2017): World Vegetable Center Eggplant Collection: Origin, Composition, Seed Dissemination and Utilization in Breeding. – *Frontiers in plant science* 8: 1484.
- [34] Tümbilen, Y., Frary, A., Daunay, M. C., Doğanlar, S. (2011): Application of EST-SSRs to examine genetic diversity in eggplant and its close relatives. – *Turkish Journal of Biology* 35(2): 125-136.
- [35] Wei, Q., Du, L., Wang, W., Hu, T., Hu, H., Wang, J., David, K., Bao, C. (2019): Comparative Transcriptome Analysis in Eggplant Reveals Selection Trends during Eggplant Domestication. – *International journal of genomics*, Vol. 2019.

SOIL WATER DYNAMICS OF CROPLANDS AND ORCHARDS AFTER LAND RECLAMATION IN THE WEIBEI AREA, NORTHWEST CHINA

ZHANG, L.^{1,2,3,4} – WANG, Y. Q.^{1,2,3,4*}

¹*Shaanxi Provincial Land Engineering Construction Group Co. Ltd., Xi'an 710075, China*

²*Shaanxi Key Laboratory of Land Consolidation, Xi'an 710064, China*

³*Institute of Land Engineering and Technology, Shaanxi Provincial Land Engineering Construction Group Co., Ltd., Xi'an 710021, China*

⁴*Key Laboratory of Degraded and Unused Land Consolidation Engineering, The Ministry of Natural Resources, Xi'an 710021, China*

**Corresponding author
e-mail: luluqiaofeng@.com*

(Received 18th Oct 2019; accepted 23rd Jan 2020)

Abstract. This study compared the soil water characteristics of croplands (wheat) and orchards (apple orchard) after the reclamation of hollow villages in the Weibei rainfed highland in Shaanxi Province, China. Soil water content in the 0–150 cm soil profile was monitored during apple tree growth from March to September in 2018. The results showed that the water content of different soil layers varied through time and space in both croplands and orchards. Soil water content was significantly higher in orchards than croplands, whereas soil water stress exhibited an inverse trend. A significant drought occurred in the 0–120 cm soil profile of croplands from mid-April to mid-July, especially before the rainy season (mid-May to mid-July). Water stress was most likely to occur at the 20–60 cm soil depth. There were 78 days of soil water stress in the 20–40 cm soil layer, and soil water content was below the permanent wilting coefficient for 42 days in the 40–60 cm soil layer. Therefore, orchards are more sustainable than croplands for agricultural production after the rehabilitation of hollow villages in the Weibei area, and the development of a tree-fruit industry here is reasonable.

Keywords: *soil water, wheat field, apple orchard, spatiotemporal dynamics, water stress*

Introduction

Hollow villages have long been a problem in China, which are the result of rural residents leaving their villages in search of employment in large cities (Cheng et al., 2001; Xu, 2004; Li and Li, 2008). In response to this phenomenon, the Chinese government implemented a series of land reclamation policies (Wang, 2019; Guo et al., 2005; Fan et al., 2011; Qian et al., 2011; Chen et al., 2014).

Previous research has investigated the spatial characteristics of hollow villages (Wang et al., 2005), their evolutionary features (Xue and Wu, 2001), causes of formation (Zhong, 2008), and potential effects (Lei, 2002; Feng and Chen, 2003). It was affirmed that the reclamation of hollow villages increased agricultural land use and improved the living environment of local residents (Zhu et al., 2010). However, not knowing how to use the land after reclamation has plagued people. Soil water status is one of the most important factors for determining the suitability of different land uses (Vachaud et al., 1985; Grayson and Western, 1998; Kim and Barros, 2002; Jacobs et al.,

2004; Vereecken et al., 2007; Famiglietti et al., 2008; Guber et al., 2008; Brocca et al., 2010; Wang et al., 2012).

The Weibei rainfed highland has experienced a transformation of agricultural production from crops to fruits. In this study, we determined the spatial and temporal variability of soil water by monitoring the soil water profile in croplands and orchards after the reclamation of hollow villages. Our results could be useful for the selection of appropriate land uses in the Weibei rainfed highland after the reclamation of hollow villages.

Materials and methods

Study area

The study area was located in Yuandi Town, Xunyi County, Shaanxi Province, China (E108°08' –108°52', N34°57'–35°33'). The hollow village had been under reclamation for 20 years in the northern boundary of Guanzhong Plain (*Fig. 1*). The terrain is relatively complex being mountainous in the northeast with lowlands in the southwest. The area is a typical loess plateau gully in terms of landform type, and it is cut into four north-south loess ridges by gullies. The ridges were wide and flat. The soil type is mainly black loess. The top-loose and bottom-compacted soil structure shows the features of “Mengjin (gold-covered)” soil profile configuration, with a high capability for water and fertility conservation (Dörner et al., 2015). The deep and loose geological conditions can meet the growth requirements of crops and fruit trees.

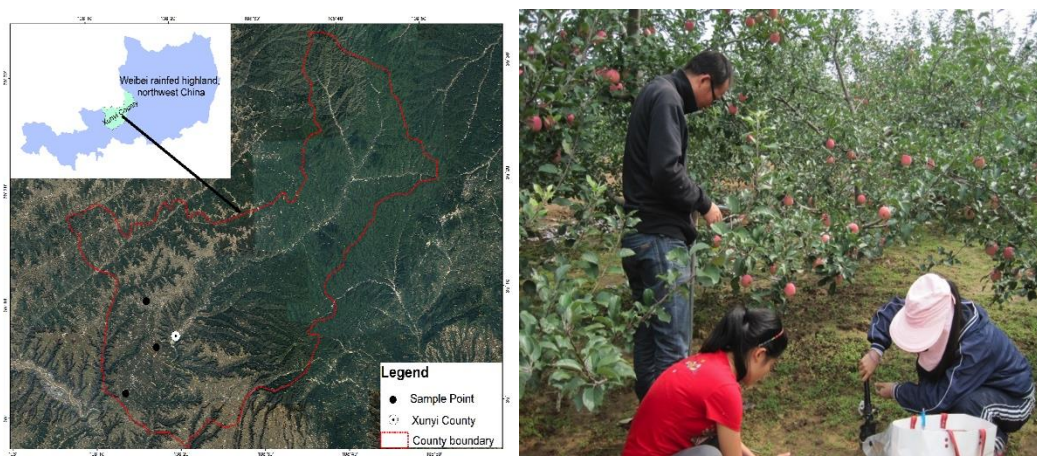


Figure 1. Sampling area chart

The Yuandi Town hollow village land reclamation project area included abandoned and vacant homesteads throughout the territory. The project mainly included leveling land, irrigation installation, field road construction, cropland shelterbelts, and other projects. One focus was the land leveling project, in which the old walls around the hollow villages were leveled, plowed, and reclaimed as agricultural land with a slope that could ensure the uniformity for irrigation. A balanced fertilization method was used to establish the tillage layer of cropland or orchard in the reclaimed land, in order to meet the growth requirements of crops or fruit trees. The topsoil of the reclaimed land

contained: organic matter, 9.7–11.7 g·kg⁻¹; total nitrogen, 0.4–1.0 g·kg⁻¹; total phosphorous, 1.5–1.6 g·kg⁻¹; and total potassium, 21.2–24.2 g·kg⁻¹.

Sample collection

To monitor soil water, three fields of winter wheat were selected after the reclamation of hollow villages in Yuandi Town. The winter wheat cultivar tested was *Triticum aestivum* L., whose growth period lasts from October to June of the following year. In addition, three young apple orchards (<10 years old) were selected in the same vicinity of the wheat fields. The apple variety tested was *Malus domestica* Borkh. 'Red Fuji', whose growth period lasts 184 days from mid-March to mid-September. Wheat fertilization was performed by a single application of all fertilizers as basal dressing during soil preparation, whereas apple tree fertilization was applied by ditching. There were no other plants or weeds covering the ground of croplands or orchards.

Soil samples were collected with a 6 cm-diameter soil drill once a month from March (leaf budding) through September (apple harvest) in 2018. For each treatment, three replicate plots (500 m × 400 m per plot) were sampled. In each plot, five points were randomly selected in a plum-blossom pattern (Fig. 2), and each sampling unit was smaller than 20 ha. The replicate samples from three plots were mixed and five replications per treatment were obtained. Three soil samples from the same soil layer were mixed to form a composite sample of the eight soil layers along the 0–150 cm profile (0–10 cm, 10–20 cm, 20–40 cm, 40–60 cm, 60–80 cm, 80–100 cm, 100–120 cm, and 120–150 cm).

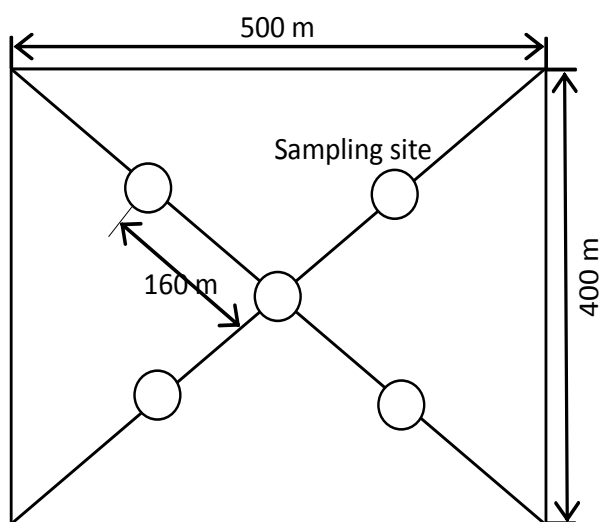


Figure 2. Distribution of soil sampling points in each plot

Test methods

The soil samples were transported to the laboratory within 2 h of collection and immediately weighed using an electronic balance (0.0001 g) upon arrival. Soil water content of each soil layer was determined by oven-drying at 105 °C for 24 h (Gardner, 1965). Then, the 60% field capacity in each soil layer was calculated (Table 1), which was equivalent to the soil water stress point, or the capillary fracture water content (Chen et al., 2008).

Table 1. The field capacity of each soil layer in Weibei rainfed highland (%v)

Soil layer (cm)		Field capacity	60% field capacity	Permanent wilting coefficient
Covering soil	0–10	25.56 ± 2.5319	15.34 ± 1.5624	11.12 ± 0.9542
	10–20	25.56 ± 1.0242	15.34 ± 1.2306	11.12 ± 1.1240
	20–40	25.56 ± 2.1648	15.34 ± 1.6417	10.80 ± 0.8256
Dark loessial	40–60	28.65 ± 2.8901	17.19 ± 1.2492	13.14 ± 0.9408
	60–80	28.65 ± 1.8726	17.19 ± 1.6741	13.04 ± 1.1506
Loess subsoil	80–100	27.41 ± 2.6034	16.45 ± 2.4825	11.20 ± 0.9402
	100–120	27.76 ± 2.2217	16.65 ± 1.0348	11.64 ± 1.1203
	120–150	27.76 ± 1.4563	16.65 ± 1.5607	11.66 ± 1.2056

Data are means ± standard deviation (n = 5)

Daily rainfall was measured in Xunyi for 2018 using a SDM6A stainless ombrometer (Fenghai, Tianjin, China). Monthly values were calculated from the daily values for January to November (Fig. 3). The year 2018 was a normal water year, in which the rainfall from July to September accounted for 60.4% of total annual rainfall. The total rainfall was 569.1 mm over the growth period of apple from growth initiation in March to fruit harvest in September 2018 (Xunyi County Chronicle Compilation Committee, 2018).

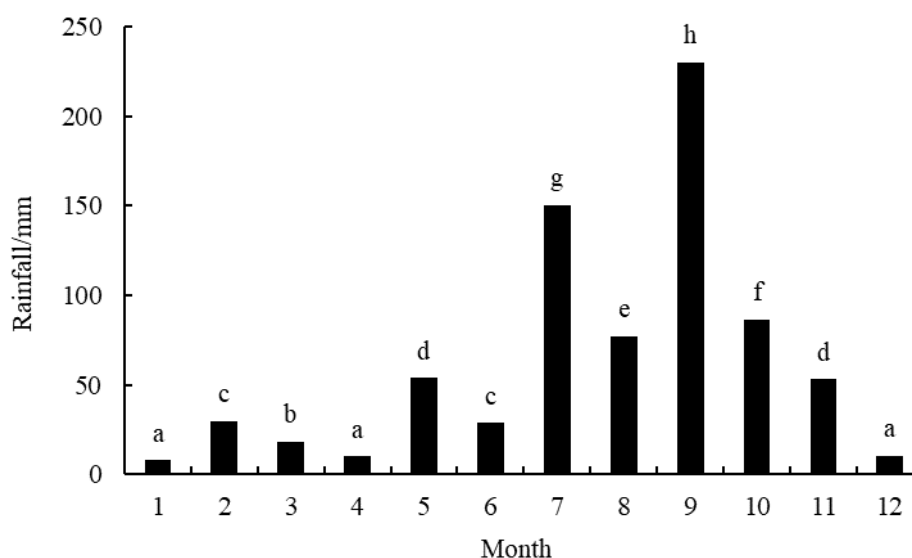


Figure 3. Monthly precipitation in Xunyi County, Shaanxi Province, China for 2018 (n = 3, based on daily rainfall measured using a stainless ombrometer from January to November)

Data analysis

To evaluate soil water changes during crop growth, soil water content and its changes were divided into four states using the field capacity, 60% field capacity, and permanent wilting coefficient as thresholds (Table 2). Then the percentage of days of each water state in apple growth period (184 days) was calculated for croplands and

orchards to quantitatively analyze the soil water status under different land use types. Mathematical modeling was carried out using Excel 2016 to simulate the process of changes of soil water content in each soil layer during apple tree growth.

Table 2. Water content and evaluation indexes

Soil water range	Evaluation of water status
Greater than field capacity	Water excess state (waterlogging)
Between the field capacity and 60% of field capacity	Easy to use state of water
Between 60% of field capacity and permanent wilting coefficient	Water stress state
Less than permanent wilting coefficient	Invalid state of water (drought to death)

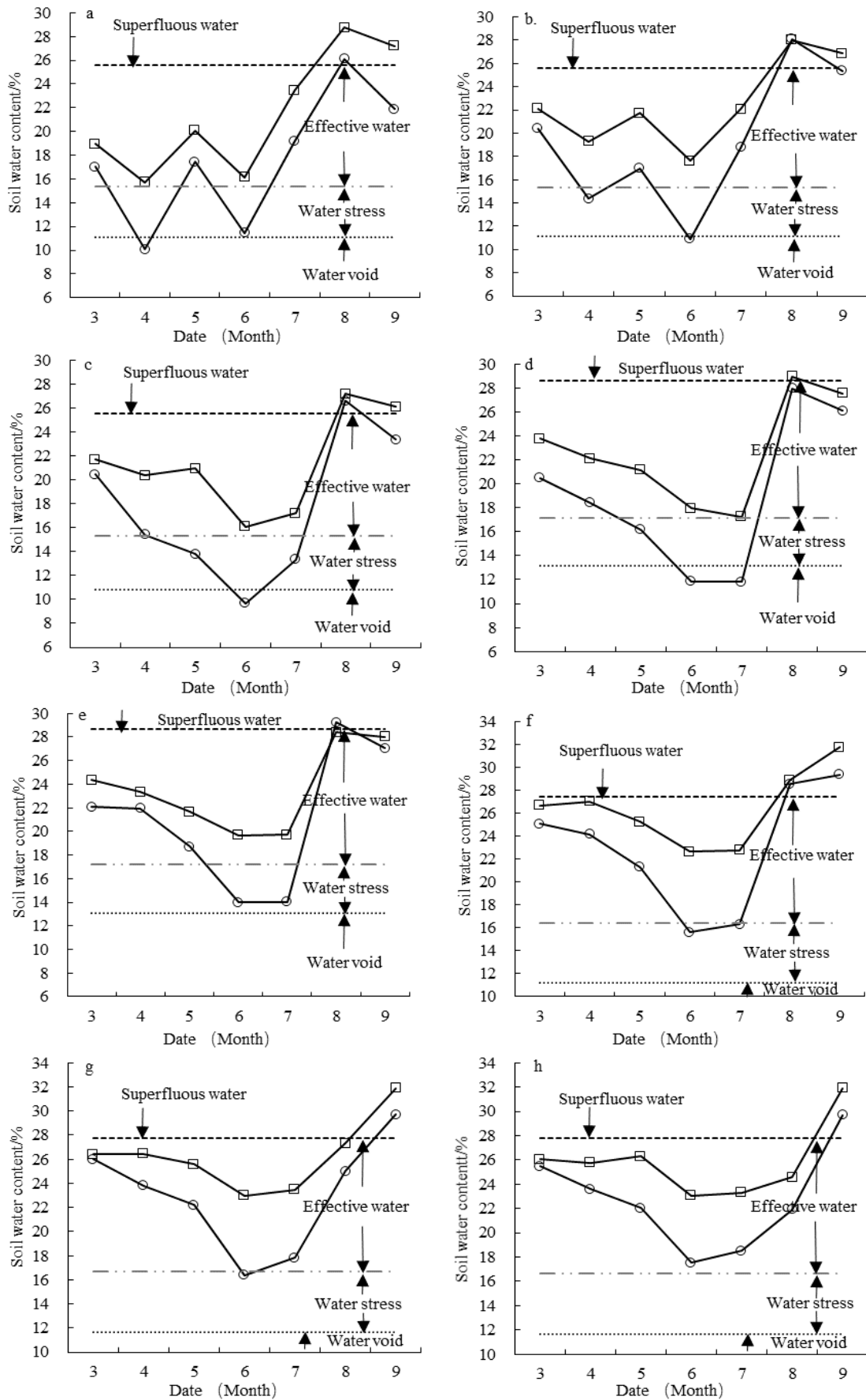
When the soil water content exceeded field capacity, the oxygen supply was limited and drainage was needed. The most preferable state of water supply was when the soil water content was between field capacity and capillary fracture water content (equivalent to 60% of field capacity). Water stress became greater as it got closer to the permanent wilting coefficient, which was considered the state of drought and death. If the duration of water stress was short, then some drought-tolerant crops may recover, but if water stress occurs too long than even rehydrated plants will not recover.

Data are means \pm standard deviation ($n = 5$). Statistical analysis was performed by t-test with SPSS Statistics 18.0 (SPSS Inc., Chicago, USA). A P value of less than 0.05 was considered to indicate statistical significance.

Results and discussion

Analysis of temporal and spatial changes in soil water content

Figure 4 illustrates the process of changes of soil water content through time and space for croplands and orchards during apple tree growth. After a long winter, in the spring stage, the soil water content of croplands in the 0–10 cm soil layer was 1.92% lower than that of the orchards (Fig. 4a). This result indicates that although the apple trees shed their leaves in winter, the dense trunks changed the wind speed and temperature near the ground, which could reduce the loss of soil water. During the whole growth period of apple trees, the water content of the 0–10 cm soil layer in orchards was always higher than that of croplands, and mostly in the most comfortable state of water. In croplands, the soil water content was in water stress or transient drought for 4 months, and the decline of soil water content was most obvious from March to April when soil water content fell below the permanent wilting coefficient. However, the drought was less serious in orchards. The maximal relative difference in soil water content between croplands and orchards occurred at the end of April when the sustained drought was most severe, and the soil water content of orchards was 56.04% higher than that of croplands. The minimal relative difference was found in August during the rainy season, with the soil water content of orchards being 10.03% higher than that of croplands. The difference in soil water content was generally large in the drought period, while it became smaller difference during the compensatory period of soil water.



Legend	-----	- . - . - . -
	Field capacity	60% Field capacity	Permanent wilting coefficient
	—○—	—■—	
	Croplands	Orchards	

Figure 4. Changes in soil water content with time in 0 to 150 cm profile (a) 0–10 cm soil layer, (b) 10–20 cm soil layer, (c) 20–40 cm soil layer, (d) 40–60 cm soil layer, (e) 60–80 cm soil layer, (f) 80–100 cm soil layer, (g) 100–120 cm soil layer, (h) 120–150 cm soil layer

In the 10–20 cm soil layer (*Fig. 4b*), the water content of the croplands was also consistently lower than that of orchards. The soil water content of orchards varied between field capacity and capillary water content, which was in a suitable state of water condition. However, the water content of 10–20 cm soil layer in croplands continued to decline from the beginning of spring and did not gradually recover until mid-June before the rainy season. The maximal relative difference in soil water content between croplands and orchards occurred in mid-June, when the soil water content of orchards was 61.40% higher than that of croplands. The minimal relative difference appeared in August, with the soil water content of orchards being 0.35% higher than that of croplands. The difference in soil water content diminished in the rainy season compared with the drought period. In the 20–40 cm soil layer (*Fig. 4c*), the temporal changes in soil water content of croplands and orchards were synchronous with the change in the upper soil layer (0–20 cm). However, the effect of weak rainfall on soil water content was negligible and did not have a significant trend like the 0–20 cm soil layer. In the 20–40 cm soil layer, the maximal relative difference in soil water content between croplands and orchards occurred in May, 7.15%, whereas the minimal difference appeared in August, 0.59%.

Compared with the upper and lower soil layers, the 40–60 cm soil layer showed the highest degree of desiccation during apple tree growth (*Fig. 4d*). The maximal relative difference in soil water content between croplands and orchards occurred in June, and a 51.68% increase was found in the soil water content of orchards relative to croplands. The minimal relative difference appeared in August, with the soil water content of orchards being 3.55% higher than that of croplands. The characteristics of water consumption and compensatory period of water change in the 60–80 cm soil layer were also obvious (*Fig. 4e*). The greatest difference of water content occurred in June (5.69%), and the minimal difference occurred in August (0.86%). The soil water content of croplands was lower than that of orchards, but the relative difference in soil water content between different land use types was reduced in this soil layer. The largest relative increase in soil water content of orchards relative to croplands was 40.64%.

The soil calcium layer and the loess parent layer occurred at deeper soil depths. During the growth period of apple trees, the deep soil water content of croplands and orchards changed in the most comfortable state between field capacity and capillary water content, and there was no problem of drought stress. The compensation period of deep soil water also lagged about 1 month behind soil layers above 40 cm (*Fig. 4f, g, h*). At the end of the rainy season, the soil water compensation amount had been significantly higher than the field capacity, which will inevitably move further into the deeper soil layer. The greatest difference in soil water content in the 60–80 cm soil layer between croplands and orchards occurred in June (7.01%), and the minimal difference

occurred in August (0.36%). The maximal relative increase in soil water content of orchards relative to croplands reached 44.83% in the 80–100 cm soil layer, 40.52% in the 100–120 cm soil layer, and 31.46% in the 120–150 cm soil layer.

Through the layer-by-layer analysis of the variation of soil water content over time in croplands and orchards after many years of reclamation in Weibei area, we found that the effect of vegetation on the water content of the soil profile can be reflected across the whole 0–150 cm gradient, but the difference decreased with increased soil depth. The cropland soil had a relatively heavy and long-term drought in the middle and deep soil layers, but this drought was temporary with the arrival of the rainy season. However, the soil water content of the orchard was always higher than that of croplands during the growth period, there was almost no obvious water stress, and no internal dry soil layer was found within the spatial scale of the study.

Mathematical simulation of soil water change process

In any case, soil water is a process of fluctuation. The effects of water stress or severe water deficiency on plant growth processes depend not only on the severity of stress and water scarcity, but more importantly on the duration of stress and scarcity. The greater the degree of stress and deficiencies, the greater the harm to plants, the longer the continuous stagnation, the more likely the plant to die in drought even if rehydrated. Thus, this paper took the soil water constant as the threshold and the duration of the soil water content (d) as the index to quantitatively analyze the soil water status of croplands and orchards after the reclamation of hollow villages.

To improve the reliability of the quantitative analysis results, it was first necessary to carry out mathematical simulations of the process of changing the soil water content of each soil layer during the growth period of apple trees (Fig. 4). The model was mainly to change the line graph of the soil water content change process in various soil layers of Figure 4 into curves to more accurately calculate the soil water change. The statistical results were shown in Table 3.

Table 3. The mathematical simulation of soil water change in different cover conditions in Weibei

Soil layer (cm)	Cropland		Orchard	
	Model	R^2	Model	R^2
0–10	$y = 17.84 + 5.90 \sin\left(\frac{2\pi x}{7.62} + 2.52\right)$	0.6836	$y = 22.17 + 5.88 \sin\left(\frac{2\pi x}{8.87} + 2.96\right)$	0.8299
10–20	$y = 19.57 + 7.00 \sin\left(\frac{2\pi x}{7.41} + 2.07\right)$	0.7891	$y = 23.28 + 4.44 \sin\left(\frac{2\pi x}{8.71} - 3.70\right)$	0.7579
20–40	$y = 17.20 + 7.10 \sin\left(\frac{2\pi x}{6.65} + 1.43\right)$	0.8169	$y = 20.35 + 4.55 \sin\left(\frac{2\pi x}{0.45} - 0.91\right)$	0.6370
40–60	$y = 19.50 + 7.27 \sin\left(\frac{2\pi x}{7.53} + 1.73\right)$	0.7023	$y = 21.58 + 4.81 \sin\left(\frac{2\pi x}{4.93} + 5.79\right)$	0.6624
60–80	$y = 19.41 + 7.04 \sin\left(\frac{2\pi x}{4.76} + 5.52\right)$	0.7635	$y = 24.35 + 4.5 \sin\left(\frac{2\pi x}{1.14} + 1.1\right)$	0.7455
80–100	$y = 21.41 + 6.68 \sin\left(\frac{2\pi x}{5} - 5.37\right)$	0.8525	$y = 25.61 + 3.84 \sin\left(\frac{2\pi x}{4.96} + 5.56\right)$	0.7746
100–120	$y = 21.93 + 5.55 \sin\left(\frac{2\pi x}{5.54} - 0.069\right)$	0.8857	$y = 12.54 + 12510 \sin\left(\frac{2\pi x}{629.2} + 4.68\right)$	0.8098
120–150	$y = 22 + 4.77 \sin\left(\frac{2\pi x}{0.014} + 0.15\right)$	0.8324	$y = 20.47 + 20450 \sin\left(\frac{2\pi x}{834.2} + 4.69\right)$	0.6345

In the model, y is the water content (%) in x th measured, x is the cumulative number of measured water content in the field

Using the soil water change model in *Table 3* and the proposed soil water state interval index in *Table 2*, we calculated the daily soil water state for croplands and orchards layer by layer, the results of which were shown in *Tables 4* and *5*.

Table 4. *The analysis of soil water status in 0 – 150 cm soil profile of Weibei croplands*

Soil layer (cm)	Water status and evaluation	Monthly water status (days)						Percentage of days in apple growth period (%)
		3/15–4/15	4/16–5/15	5/16–6/15	6/16–7/15	7/16–8/15	8/16–9/15	
0–10	Superfluous water	0	0	0	0	3	4	3.80
	Effective water	8	9	11	15	28	27	53.26
	Water stress	21	17	20	15	0	0	39.67
	Unavailable water	2	4	0	0	0	0	3.27
10–20	Superfluous water	0	0	0	0	8	29	20.10
	Effective water	26	19	8	7	23	2	46.20
	Water stress	5	11	22	22	0	0	32.61
	Unavailable water	0	0	1	1	0	0	1.09
20–40	Superfluous water	0	0	0	0	2	10	6.52
	Effective water	31	1	0	0	24	21	41.85
	Water stress	0	29	23	21	5	0	42.39
	Unavailable water	0	0	8	9	0	0	9.24
40–60	Superfluous water	0	0	0	0	0	0	0
	Effective water	31	16	0	0	21	31	53.80
	Water stress	0	14	22	0	7	0	23.37
	Unavailable water	0	0	9	30	3	0	22.83
60–80	Superfluous water	0	0	0	0	1	8	4.89
	Effective water	31	30	10	0	24	23	64.13
	Water stress	0	0	21	30	6	0	30.98
	Unavailable water	0	0	0	0	0	0	0
80–100	Superfluous water	0	0	0	0	3	31	18.48
	Effective water	31	30	27	5	28	0	65.76
	Water stress	0	0	4	25	0	0	15.76
	Unavailable water	0	0	0	0	0	0	0
100–120	Superfluous water	0	0	0	0	0	25	13.59
	Effective water	31	30	30	24	31	6	82.61
	Water stress	0	0	1	6	0	0	3.80
	Unavailable water	0	0	0	0	0	0	0
120–150	Superfluous water	0	0	0	0	0	8	4.35
	Effective water	31	30	31	30	31	23	95.65
	Water stress	0	0	0	0	0	0	0
	Unavailable water	0	0	0	0	0	0	0

Table 5. The analysis of soil water status in 0 – 150 cm soil profile of Weibei orchards

Soil layer (cm)	Water status and evaluation	Monthly water status (d)						Percentage of days in apple growth period (%)
		3/15–4/15	4/16–5/15	5/16–6/15	6/16–7/15	7/16–8/15	8/16–9/15	
0–10	Superfluous water	0	0	0	0	19	31	27.17
	Effective water	31	30	31	30	12	0	72.83
	Water stress	0	0	0	0	0	0	0
	Unavailable water	0	0	0	0	0	0	0
10–20	Superfluous water	0	0	0	0	4	31	19.02
	Effective water	31	30	31	30	27	0	80.98
	Water stress	0	0	0	0	0	0	0
	Unavailable water	0	0	0	0	0	0	0
20–40	Superfluous water	0	0	0	0	5	31	19.57
	Effective water	31	30	31	30	26	0	80.43
	Water stress	0	0	0	0	0	0	0
	Unavailable water	0	0	0	0	0	0	0
40–60	Superfluous water	0	0	0	0	1	7	4.35
	Effective water	31	30	31	30	30	24	95.65
	Water stress	0	0	0	0	0	0	0
	Unavailable water	0	0	0	0	0	0	0
60–80	Superfluous water	0	0	0	0	0	0	0
	Effective water	31	30	31	30	31	31	100
	Water stress	0	0	0	0	0	0	0
	Unavailable water	0	0	0	0	0	0	0
80–100	Superfluous water	0	0	0	0	8	31	21.20
	Effective water	31	30	31	30	23	0	78.8
	Water stress	0	0	0	0	0	0	0
	Unavailable water	0	0	0	0	0	0	0
100–120	Superfluous water	0	0	0	0	6	31	20.11
	Effective water	31	30	31	30	25	0	79.89
	Water stress	0	0	0	0	0	0	0
	Unavailable water	0	0	0	0	0	0	0
120–150	Superfluous water	0	0	0	0	0	17	9.24
	Effective water	31	30	31	30	31	14	90.76
	Water stress	0	0	0	0	0	0	0
	Unavailable water	0	0	0	0	0	0	0

Quantitative analysis of soil water status in cropland

As can be seen from *Table 4*, the soil water excess period was 7 days, the water susceptibility period was 98 days, the water stress period was 73 days, and the water

ineffective period was 6 days in 0–10 cm soil layer during the growth period of apple trees, which accounted for 3.80%, 53.26%, 39.67%, and 3.27% of the apple trees growth period, respectively. Soil water accumulation in the excess period, water susceptibility period, water stress period, and water ineffective period accounted for 20.10%, 46.20%, 32.61%, and 1.09% in the 10–20 cm soil layer. Compared to the 0–10 cm soil layer in the rainy season, the soil water of the 10–20 cm soil layer was retained and the number of days in water excess increased significantly, which may be directly related to the tightening of the subsurface soil of croplands after the land reclamation, the increase of soil bulk density, the use of chemical fertilizers, and the shallow rotary tillage over many years (Zhu, 2014; Wang et al., 2017). Compared to the 0–20 cm soil layer, the spring soil drought increased significantly in the 20–40 cm soil layer and there was also a long period of soil layer water retention and excess water similar to the 10–20 cm soil layer in the rainy season, which reflected the compaction of cropland soil.

Compared to the 0–40 cm soil layer, there was no excess water in the 40–60 cm soil layer. The soil drought in spring was more serious, and the water ineffective period had a longer duration, which indicated that crops were threatened by drought. There was no water ineffective period in the 60–80 cm soil layer during apple tree growth, where the drought had been relatively eased compared to the 20–60 cm soil layer.

In the 80–100 cm soil layer, there were 34 days of excess soil water, 121 days of water susceptibility, and 29 days of water stress during apple tree growth. In the 100–120 cm soil layer, there were 25 days of excess soil water, 152 days of water susceptibility, and 7 days of water stress, which accounted for 13.59%, 82.61%, and 3.81% of the apple tree growth period, respectively. There was no water ineffective period in the 80–120 cm soil layer. There were 8 days with excess soil water and 176 days of water susceptibility, which accounted for 4.35% and 95.65% of the apple tree growth period.

During the apple tree growth period, the cropland soil drought mainly occurred from the spring to the early summer. The drought was more serious in the 20–60 cm soil layer, especially in the 40–60 cm soil layer, and the soil water stress gradually decreased below 60 cm. The water retention period in the 10–40 cm soil layer was longer than that of the 0–10 cm surface layer, which indicated that compaction was a problem and water conduction was blocked. In the rainy season, there was a phenomenon of excessive water retention in the soil section to varying degrees, so the “internal dry soil layer” can be reclaimed during the rainy season.

Quantitative analysis of soil water status in orchard

As can be seen from *Table 5*, the soil water content was always accessible in the 0–10 cm soil surface from mid-March to mid-July. However, the days of effective soil water were reduced to 12 days from mid-July to mid-September. Due to the rainy season, the soil water in the 0–10 cm soil layer was in a surplus for up to 50 days, accounting for 27.17% of the total days of apple tree growth. There was no water stress period. Excessive water at the surface provided a prerequisite for replenishing water in deep soil. From mid-March to mid-July, the soil water content in the 10–20 cm soil layer had been in effective water state. From mid-July to mid-September, the days of effective water decreased in lieu of excess water, which occurred for 35 days in total and accounted for 19.02% of the total days of apple tree growth. The soil water susceptibility in the 20–40 cm soil layer accounted for 83.43% of the apple tree growth

period. From mid-July to mid-September, water surplus occurred for 36 days and accounted for 19.57% of the total days of apple tree growth.

The water content in the 40–60 cm soil layer was water-susceptible from mid-March to mid-July. Other than the water-susceptibility period, excess water occurred in 8 days from mid-July to mid-September, accounting for 4.35% of the apple tree growth period. The water content in the 60–80 cm soil layer had been in a state of water efficiency during apple tree growth period.

The 80–100 cm soil layer was effective water state from mid-March to mid-July. Excess water occurred in 39 days from mid-July to mid-September, accounting for 21.2% of the apple tree growth period. The soil water content in the 100–120 cm soil layer was mostly in a water-susceptible state during apple tree growth. Excess water occurred in 37 days, accounting for 20.11% of the apple tree growth period. In addition to the water-susceptible state, there was also a water surplus period of 17 days in the 120–150 cm soil layer, which accounted for 9.24% of the total days during apple tree growth.

The soil water status of orchards during the growth period of apple trees was not affected by water stress and there was deep movement of soil water during the rainy season after the reclamation of hollow villages in Weibei area.

Analysis of soil water stress in croplands and orchards

We also found that cropland soil water stress after hollow village reclamation was significantly stronger than that of orchards in Weibei rainfed highland. Adjusting the existing agricultural structure by converting large areas of cropland into orchards alleviated the sharp distinction between natural precipitation and soil water mitigation (Glaser et al., 2013). Further statistical analysis of *Tables 4* and *5* showed that orchard soil water content did not reach the level of water stress and water ineffectiveness in the 0–150 cm soil profile. However, cropland experienced soil water stress throughout the entire 120 cm soil profile. Some studies previously found that the total water requirement for growing apples in Weibei area was about 500 mm (Wang and Zhang, 2000). However, the average daily water requirement for wheat has been estimated to be about 5 mm (Wang et al., 2018).

The percentage of days of effective soil water in apple tree growth period tended to decrease in the top soil layers then increase with soil depth, which accorded with the polynomial variation law of $y = 1.54x^2 - 7.18x + 55.96$ (where y is the percentage of water equivalent days, %, x is the soil depth, cm, $R^2 = 0.9587$). The length of cropland water stress in the 20–40 cm soil layer was longer than the water susceptibility time, in which the existence of such long-term water stress made it extremely difficult to recover without precipitation or irrigation. The number of days of excess water in croplands was significantly less than that in orchards between mid-July to mid-September, which indicated that water stress in croplands was stronger than orchards and that recovery was more difficult. Trees canopies can suppress evaporation from the soil more so than croplands, which can greatly alleviate the problem of soil water stress caused by improper crop selection after reclamation. However, after the apple harvest, soil water consumption in orchards fall after fruit production and leaf drop. Thus, the excess water from the autumn rainy season may cause short-term waterlogging, which suggests that attention should be given to improving soil water permeability when planting apple trees (Nolz et al., 2014).

Conclusions

(1) After the reclamation of hollow villages, the soil water content of orchards was significantly higher than that of croplands due to the difference in the amount and timing of water demanded by these land use types.

(2) There was no soil drought stress in orchards during the growth period. More specifically, the soil water content throughout the 0–150 cm soil profile was stable between field capacity and capillary water content (stress point). On the contrary, the soil drought in croplands was severe in degree, length, and depth from spring to early summer. Soil water stress lasted for 78 days in the 20–40 cm soil layer. The soil water content was below the permanent wilting coefficient for 42 days in the 40–60 cm soil layer.

(3) There was a significant drought in the entire 0–120 cm soil profile from mid-April to mid-July, especially before the rainy season between mid-May and mid-July, and water stress was most likely to occur in the 20–60 cm soil layer.

Therefore, future study should focus on the development of soil water conservation technologies in the Weibei rainfed highland after the reclamation of hollow villages. In particular, the results obtained in this study indicate that vegetation coverage has a pronounced effect on soil water conditions in the reclaimed land. Therefore, it is necessary to strengthen the research regarding the selection and effect of “cover crops” based on water-saving technologies such as straw mulching and plastic mulching that have been applied extensively. An effective approach to inhibit water consumption via evaporation from land surface is to select suitable cover crops based on local climate conditions and minimize the exposure time of bare croplands as much as possible.

Acknowledgments. This work was financially supported by the Fundamental Research Funds for the Central Universities, CHD “Study on the plant cover influence on soil moisture in Weibei rainfed highland, northwest China”.

REFERENCES

- [1] Brocca, L., Melone, F., Moramarco, T., Morbidelli, R. (2010): Spatial-temporal variability of soil moisture and its estimation across scales. – *Water Resour. Res.* 46(2): W02516.
- [2] Chen, H. S., Shao, M. A., Li, Y. Y. (2008): Soil desiccation in the Loess Plateau of China. – *Geoderma* 143(1): 91-100.
- [3] Chen, Q., Liu, S. J., Bai, Y., Li, Y. X., Hao, C. H., Zhang, Q., Li, J. H. (2014): Screening and identification of phosphate-solubilizing bacteria from reclaimed soil in Shanxi mining area. – *Plant Nutr. Fert Sci.* 20(6): 1505-1516.
- [4] Cheng, L. S., Feng, W. Y., Jiang, L. H. (2001): The analysis of rural settlement hollowizing system of the southeast of Taiyuan basin. – *Acta Geogr. Sin.* 56(4): 437-446.
- [5] Dörner, J., Huertas, J., Cuevas, J. G., Leiva, C., Paulino, L., Arumí, J. L. (2015): Water content dynamics in a volcanic ash soil slope in southern Chile. – *J. Plant Nutr. Soil Sci.* 178: 693-702.
- [6] Famiglietti, J. S., Ryu, D., Berg, A. A., Rodell, M., Jackson, T. J. (2008): Field observations of soil moisture variability across scales. – *Water Resour. Res.* 44(1): 186-192.
- [7] Fan, W. H., Bai, Z. K., Li, H. F., Qiao, J. Y., Xu, J. W. (2011): Effects of different vegetation restoration patterns and reclamation years on microbes in reclaimed soil. – *Trans. Chin. Soc. Agric. Eng.* 27(2): 330-336.

- [8] Feng, W. Y., Chen, X. M. (2003): Analysis on the rural settlement expansion of the Jinzhong plain. – *Human Geogr.* 18(6): 93-96.
- [9] Gardner, W. H. (1965): Water Content. – In: Black, C. A. (ed.) *Methods of Soil Analysis. Monograph 9.* Am. Soc. Agron., Madison, WI, pp. 82-127.
- [10] Glaser, B., Jentsch, A., Kreyling, J., Beierkuhnlein, C. (2013): Soil–moisture change caused by experimental extreme summer drought is similar to natural inter–annual variation in a loamy sand in Central Europe. – *J. Plant Nutr. Soil Sci.* 176: 27-34.
- [11] Grayson, R. B., Western, A. W. (1998): Towards areal estimation of soil water content from point measurements: time and space stability of mean response. – *J. Hydrol.* 207(1-2): 68-82.
- [12] Guber, A. K., Gish, T. J., Pachepsky, Y. A., Genuchten, M. T. V., Daughtry, C. S. T., Nicholson, T. J. (2008): Temporal stability in soil water content patterns across agricultural fields. – *Catena.* 73(1): 125-133.
- [13] Guo, X. Y., Zhang, J. T., Gong, H. L., Zhang, G. L., Dong, Z. (2005): Analysis of changes of the species diversity in the process of vegetation restoration in Antaibao mining field, China. – *Acta Ecol. Sin.* 25(4): 763-770.
- [14] Jacobs, J. M., Mohanty, B. P., Hsu, E. C., Miller, D. (2004): Smex02: field scale variability, time stability and similarity of soil moisture. – *Remote Sens. Environ.* 92(4): 436-446.
- [15] Kim, G., Barros, A. P. (2002): Space–time characterization of soil moisture from passive microwave remotely sensed imagery and ancillary data. – *Remote Sens. Environ.* 81: 393-403.
- [16] Lei, Z. D. (2002): Ruual habitat empty-disusing concept and quantitative analysis model. – *J. Northwest Univ. (Nat. Sci. Ed.).* 32(4): 421-424.
- [17] Li, J., Li, X. J. (2008): The microscopic analysis on village-hollowing in medium income and hilly land region of Henan province. – *Chin. Popul. Resour. Environ.* 18(1): 170-175.
- [18] Nolz, R., Cepuder, P., Kammerer, G. (2014): Determining soil water-balance components using an irrigated grass lysimeter in NE Austria. – *J. Plant Nutr. Soil Sci.* 177: 237-244.
- [19] Qian, K. M., Wang, L. P., Li, J. (2011): Variation of microbial activity in reclaimed soil in mining area. – *J. Ecol. Rura. Environ.* 27(6): 59-63.
- [20] Vachaud, G., Silans, A. P. D., Balabanis, P., Vauclin, M. (1985): Temporal stability of spatially measured soil water probability density function. – *Soil Sci. Soc. Am. J.* 49(4): 822-828.
- [21] Vereecken, H., Kamaï, T., Harter, T., Kasteel, R., Hopmans, J., Vanderborght, J. (2007): Explaining soil moisture variability as a function of mean soil moisture: a stochastic unsaturated flow perspective. – *Geophys. Res. Lett.* 34(22): 315-324.
- [22] Wang, C. X., Yao, S. M., Chen, C. H. (2005): Empirical study on “village-hollowing” in China. – *Sci. Geogr. Sin.* 25(3): 257-262.
- [23] Wang, J. (2019): Short-term geochemical investigation and assessment of dissolved elements from simulated ash reclaimed soil into groundwater. – *Environ. Pollut.* 247: 302-311.
- [24] Wang, J. Q., Liu, X. Y., Cheng, K., X. H., Zhang, Li, L. Q., Pan, G. X. (2018): Winter wheat water requirement and utilization efficiency under simulated climate change conditions: a Penman-Monteith model evaluation. – *Agr. Water Manage.* 197: 100-109.
- [25] Wang, J. X., Zhang, X. P., Gao, B. S., He, X. X. (2000): Study on wayer requirement and limited irrigation effects of dwarfing red fuji apple tree on Weibei of Loess Plateau. – *Res. Soil Water Conserv.* 7(1): 69-72.
- [26] Wang, J. X., Wang, Y. Q., Li, X., Liang, H. W., Shi, H. P., Shi, Z. L. (2017): Evaluation of soil physical state in Guanzhogn cropland. – *Agric. Res. Arid Areas.* 35(3): 245-252.
- [27] Wang, Y. Q., Shao, M. A., Liu, Z. P. (2012): Spatial variability of soil moisture at a regional scale in the Loess Plateau. – *Advan. Water Sci.* 23(3): 310-316.
- [28] Xu, S. H. (2004): The integral regimes and countermeasure study on hollow-oriented houses in rural regions. – *Terri. Nat. Res.* 1: 11-12.

- [29] Xue, L., Wu, M. W. (2001): Spatial differentiation and countermeasures of rural people's environment construction in Jiangsu province. – *J. Urban Plan.* 1: 41-45.
- [30] Xunyi County Chronicle Compilation Committee (2018): *Xunyi County Annals.* – San Qin Press, Xi'an.
- [31] Zhong, Z. M. (2008): Analysis on the causes and treatment of rural homestead idle. – *Agricul. Econ.* 6: 57-58.
- [32] Zhu, F. H. (2014): The degradation features of cropland soil physical and its harmfulness in Guanzhong area. – Northwest A & F University, Yangling.
- [33] Zhu, X. H., Chen, Y. F., Liu, Y. S., Zhang, J., Li, Y. Y., Ding, J. J. (2010): Technique and method of rural land consolidation potential investigation and assessment. – *Acta Geogr. Sin.* 25(6): 736-744.

ASSESSING MACRO-NUTRIENT REMOVAL POTENTIAL OF NINE NATIVE PLANT SPECIES GROWN AT A SEWAGE SLUDGE DUMP SITE

ABDALLAH, S. M.^{1,2,3} – FARAHAT, E. A.⁴ – SHALTOUT, K. H.⁵ – EID, E. M.^{1,6*}

¹Biology Department, College of Science, King Khalid University, Abha 61321, P.O. Box 9004, Saudi Arabia

²Prince Sultan Bin Abdul-Aziz Center for Environment and Tourism Research and Studies, King Khalid University, Abha 61421, P.O. Box 960, Saudi Arabia

³Department of Soils and Water, Faculty of Agriculture, Ain Shams University, P.O. Box 68, Hadayek Shoubra, 11241 Cairo, Egypt

⁴Botany and Microbiology Department, Faculty of Science, Helwan University, Cairo, Egypt

⁵Botany Department, Faculty of Science, Tanta University, 31527 Tanta, Egypt

⁶Botany Department, Faculty of Science, Kafr El-Sheikh University, 33516 Kafr El-Sheikh, Egypt

*Corresponding author

e-mail: ebrahim.eid@sci.kfs.edu.eg, eeid@kku.edu.sa, ebrahim.eid@gmail.com; phone: +966-55-271-7026; fax: +966-17-241-8205

(Received 19th Oct 2019; accepted 8th Jan 2020)

Abstract. Searching for new plants that could phytoextract soil macro-nutrients is one of the main research interests nowadays. In the present study, nine native plant species were collected to determine their potential to uptake six macro-nutrients from the soil of a sewage sludge dump site (SS) in comparison with a reference site (RS). The results showed that the studied native plants can accumulate the macro-nutrients in their tissues regardless of their size or vegetative stages. The concentrations of all macro-nutrients (except K) in the tissues of the most studied plant species were positively correlated with those in the soil. The stoichiometric ratios vary among species and depend on many limiting factors. The values of bioaccumulation and translocation factors were > 1.0, indicating the high tendency of the plants to accumulate the macro-nutrients. *Portulaca oleracea* growing in the SS accumulated larger quantities of macro-nutrients compared to two perennials growing at the same place. *Phragmites australis*, *Rumex dentatus*, *Portulaca oleracea*, *Bassia indica*, *Amaranthus viridis* and *Pluchea dioscoridis* from the SS; and *Portulaca oleracea*, *Rumex dentatus*, *Pluchea dioscoridis* and *Solanum nigrum* from the control site showed the highest element accumulation indices, which could be recommended for the phytoextraction of macro-nutrients. We recommend using the studied species in mitigation of the eutrophic status of agricultural soil amended with sewage sludge.

Keywords: bioindicator, biosolids, Nile delta, nutrient elements, phytoextraction, wastewater treatment plants, wild plants

Introduction

Sewage sludge is defined as an organic byproduct of the treatment of municipal and/or industrial wastewater. It contains high amounts of macro-nutrients and heavy metals (Eid and Shaltout, 2016). It is used as fertilizers in many agricultural lands and it has significant positive influences on soil fertility and plant macro-nutrients (Aráujo et al., 2007). On the other hand, the presence of toxic levels of heavy metals in the sludge

due to the contribution of industrial effluents may have adverse effects on agriculture and food chain (Singh and Agrawal, 2007; Eid et al., 2018a). Moreover, availability of nitrogen and phosphorus from sludge-amended soils and their transfer in runoff may lead to eutrophication of soil and downstream surface water (Quilbé et al., 2005). The worldwide production of sewage sludge is increasing with the populations, as well as their use as soil amendments on agricultural lands (Moreno-Caselles et al., 1997; Eid et al., 2018a). Numerous studies on the use of sewage sludge as soil amendments have been conducted on agricultural crops, wood- and wetlands (e.g., Fuentes et al., 2007; Yu et al., 2014; Eid et al., 2017a, b, 2018b, 2019, 2020a, b, c). Few studies were conducted on wild native plants (e.g., Ho and Wong, 1994; Korboulewskya et al., 2002; Farahat and Linderholm, 2013; Eid and Shaltout, 2016).

Native plants are key species in the ecosystems and play important roles in degrading and removing macro-nutrients, heavy metals, and other pollutants from the environment (Eid and Shaltout, 2016). This green technology is called “Phytoremediation” (Peng et al., 2008). It includes many methods, one of them is phytostabilization, where plants are used to immobilize metals and store them in their below-ground tissues and/or soil. In addition, plants may play an important role in element removal (phytoextraction) through many ways, such as absorption and cation exchange (Chandra et al., 2017).

Many studies were conducted to investigate the influences of sewage sludge on the growth, yield and solute contents in crops and forest trees (e.g. Henry et al., 1994; Antolín et al., 2010; Singh and Agrawal, 2010). Some other studies tried to identify the health risks that could be associated with using sewage sludge and/or sewage wastewater in agriculture (e.g., Singh and Agrawal, 2007; Galal, 2016; Farahat et al., 2017; Eid et al., 2018a). Most of these studies were interested in evaluating the role of plants in phytoremediation of heavy metals, but not macro-nutrients. The soil pollution by macro-nutrients is unusual, but especially problematic when involves eutrophication. These levels of high concentrations of macro-nutrients in the soil will adversely affect the biodiversity of native species and it may introduce only the species that grow well on eutrophic soil (El-Sheikh et al., 2012; Shaltout et al., 2019). In addition, over-use of sewage sludge in agricultural practices may lead to over concentrations of macro-nutrients that lead to eutrophication of soil and downstream surface water (Quilbé et al., 2005). The application of sewage sludge in high quantities to the agricultural lands without prior knowledge to its chemical structure may lead to presence of high non-desirable concentrations of macro-nutrients (Quilbé et al., 2005). Presence of native species that able to uptake extra concentrations of macro-nutrients and reduce the macro-nutrient loads in soil will represent a good service to the ecosystem.

Wild plants play an important role in macro-nutrient cycling through uptake, sequestering and release of macro-nutrient elements (Eid et al., 2012a). Utilization of these wild plants as phytoremediators in eutrophic habitats requires emphasis on the effect of macro-nutrient loadings on these plants, but this effect has received little attention and is still not well understood (Eid et al., 2010; Zhao et al., 2013). According to the authors’ knowledge, so far no studies have been carried out in Egypt on the grown plant of native species at a sewage sludge dump site in comparison with the reference site in the context of their usefulness for macro-nutrients phytoremediation. Therefore, the wider objective of this study was to assess the removal efficiency of macro-nutrients by nine native plant species grown at a sewage sludge dump site (SS) in Egypt. The specific objectives of the present study were to: (1) to assess the ability of nine Tropical and Mediterranean native plant species grown on SS to accumulate

macro-nutrients in their tissues compared to a reference site (RS); and (2) to examine the roles of these nine species as potential bioindicators of macro-nutrients. The results of the present study could be useful when designing a phytoremediation system.

Materials and methods

Study area

The study area is the dump site of Kafr El-Sheikh Wastewater Treatment Plant in the northern Nile Delta, Egypt (Lat. 31° 05' 05.42" N, Long. 30° 57' 43.24" E), and the adjacent agricultural farms are the reference site (RS) (Lat. 31° 04' 53.46" N, Long. 30° 57' 31.60" E). The RS is located about 1 km away from the dump site and its soil type is clay. The climatic conditions are warm summers (20 to 30 °C) and mild winters (≥ 10 °C) (EMA, 1980).

Field sampling process

The sampling process was carried out at six locations, three of which represent each of the SS and RS (Fig. 1). Nine native plant species dominating the study area were chosen at each site (*Amaranthus viridis* L.: *Amaranthaceae*, slender amaranth, annual herb, often 60-80 cm tall; *Bassia indica* (Wight) A. J. Scott: *Amaranthaceae*, kochia, annual richly branched herb, often 2 m tall; *Conyza bonariensis* (L.) Cronquist: *Asteraceae*, flax-leaf fleabane, annual herb, often 75 cm tall; *Portulaca oleracea* L.: *Portulacaceae*, common purslane, glabrous fleshy herb, may reach 40 cm in height; *Rumex dentatus* L.: *Polygonaceae*, toothed dock, annual or biennial herb, erect stem up to 70-80 cm in height; *Solanum nigrum* L.: *Solanaceae*, black nightshade, herb or short-lived perennial shrub, often 30-120 cm tall; *Lycopersicon esculentum* Mill.: *Solanaceae*, tomato, perennial in native habitat, but cultivated as annual, grows up to 1-3 m in height. *Phragmites australis* (Cav.) Trin. ex Steud.: *Poaceae*, common reed, perennial robust reed, erect stem up to 5 m in height; and *Pluchea dioscoridis* (L.) DC.: *Asteraceae*, camphorweeds, richly branched hairy shrub, often 2-3 m high). For each plant species, three mature and healthy replicates were collected from each sampling location during May 2014. Plants were identified following Boulos (1999, 2002, 2005). In the laboratory, samples were carefully washed with tap water over a 4 mm mesh sieve to minimize material loss, separated into leaves, stems and roots, oven dried at 85 °C to a constant weight, and then ground using a metal-free plastic mill. Roots were collected by excavated carefully around the root system of each plant. At each sampling location, a composite soil sample was collected as a profile from three holes, each about 20 cm deep. The soil samples were air dried and passed through a 2 mm sieve to separate gravel and debris.

Chemical analysis

Soil samples were analyzed for organic matter (OM) content using loss-on-ignition method at 550 °C for 2 h (Wilke, 2005). Soil-water extracts at 1:5 were prepared for the determination of pH and electric conductivity (EC). Macro-nutrients (except N) in soil and plant samples were extracted from 0.5 to 1 g using a mixed-acid digestion method. EC and pH were measured using conductivity and pH meters, respectively. Calcium, Mg, Na and K were determined by atomic absorption, while total P was determined by spectrophotometer using the ammonium-molybdate method. Total N was determined in

plant and soil samples using a CHN Elemental Analyzer (Yanako CHN Corder MT-5, Japan). All these procedures are outlined in Allen (1989) and APHA (1998).



Figure 1. Location map of study area showing the sampling sites. SS: sewage sludge dump site, RS: reference site

Calculations

The bioaccumulation factor (BF) was calculated to determine the efficiency of the plant for accumulating a macro-nutrient from the soil (Xiao et al., 2011):

$$BF = \frac{\text{Concentration of a macronutrient in belowground tissues (mg/kg)}}{\text{Concentration of the same macronutrient in soil at the same site (mg/kg)}} \quad (\text{Eq.1})$$

The translocation factor (TF) was calculated to depict the ability of plants to translocate a macro-nutrient from below- to above-ground tissues (Gupta et al., 2008):

$$TF = \frac{\text{Concentration of a macronutrient in aboveground tissues (mg/kg)}}{\text{Concentration of a macronutrient in belowground tissues (mg/kg)}} \quad (\text{Eq.2})$$

The element accumulation index (EAI) was used to assess the overall performance of macro-nutrient accumulation in plants (Liu et al., 2007):

$$EAI = (1/N) \sum_{j=1}^N I_j; I_j = \frac{x}{\delta x} \quad (\text{Eq.3})$$

where N is the total number of the analyzed macro-nutrients and I_j is the sub-index for a macro-nutrient j , obtained by dividing the mean concentration of a macro-nutrient (x) by its standard deviation (δx).

Statistical analysis

Before performing an analysis of variance (ANOVA), the data were tested for their normality of distribution (Shapiro-Wilk's W test) and homogeneity of variance (Levene's

test), and when necessary, the data were log-transformed. Macro-nutrients data for nine plant species were subjected to a three-way ANOVA (the assumptions have been met) to identify the interactions in the independent variables (species, tissues, and sites). The significance of variation in the relative concentrations of the different macro-nutrients (considering whole plant), one species at a time at the two different sites (SS/RS) was assessed using a paired *t*-test, while one-way ANOVA was used to analyze the variation among species within the same site. The significant differences between means, among the nine plant species were identified using the Tukey HSD test at $P < 0.05$. The significance of variation in soil quality parameters between the SS and RS was assessed using a paired *t*-test. EAI data for nine plant species were subjected to a two-way analysis of variance (ANOVA-2) to test the differences between species and sites. Correlations between the concentrations of macro-nutrients in plant tissues and soil samples (the SS and RS) were evaluated using the Pearson's *r* coefficient. Statistical analyses were carried out using Statistica 7.1 (Statsoft, 2007). Stoichiometric ratios were calculated for some of the analyzed macro-nutrients. To identify statistically significant differences in the stoichiometric ratios among different sites, the paired *t*-test was performed.

Results

The soil of the SS was rich in OM, N, P, Ca and it was also slightly acidic, while EC, Mg, Na and K concentrations of the RS were significantly higher than those of the SS (Table 1). Macro-nutrient concentrations in the soil of the SS had the following sequence: $Ca > N > Mg > Na > K > P$; while in soil of the RS the sequence was: $Ca > Na > Mg > K > N > P$.

Table 1. Mean \pm standard error ($n = 3$) of soil physico-chemical characteristics for sewage sludge dump site and reference site, where the present study was carried out

Characteristics	Sewage sludge dump site	Reference site	<i>t</i> -value	<i>p</i>
EC (mS cm ⁻¹)	0.04 \pm 0.01	3.46 \pm 0.08	38.9	0.001
pH	6.40 \pm 0.08	7.76 \pm 0.03	14.8	0.000
OM (%)	51.50 \pm 0.23	6.74 \pm 0.07	148.6	0.000
N (mg g ⁻¹)	30.27 \pm 0.52	2.00 \pm 0.23	37.9	0.001
P (mg g ⁻¹)	2.36 \pm 0.09	0.89 \pm 0.02	14.9	0.000
Ca (mg g ⁻¹)	53.36 \pm 0.57	40.90 \pm 1.39	10.1	0.000
Mg (mg g ⁻¹)	6.34 \pm 0.18	8.29 \pm 0.29	6.3	0.000
Na (mg g ⁻¹)	6.22 \pm 0.26	8.50 \pm 0.20	15.5	0.000
K (mg g ⁻¹)	4.69 \pm 0.07	6.03 \pm 0.13	14.7	0.000

t-values represent the paired *t*-test, EC: electric conductivity, OM: organic matter content

Regarding the studied plant species, concentrations of N, P and Na were significantly affected by site; those of N, Ca, Mg and Na were significantly affected by plant species, while those of N, Ca, Mg and K were significantly affected by plant tissue (Table 2). N, P and K concentrations were significantly higher in the plant species of the SS as compared to the RS (Table 3; Appendix 1). In addition, concentrations of N, P, Ca, Mg and Na were higher in the leaf; but K was higher in the stem. The highest N, P and K concentrations (48.2, 3.2 and 80.2 mg g⁻¹, respectively) was observed in *P. oleracea*

grown at the SS, while the lowest (17.7, 0.3 and 17.7 mg g⁻¹, respectively) was observed in *P. dioscoridis*, *A. viridis*, *C. bonariensis* and *P. australis* grown at the RS (Table 3). The highest Ca and Mg concentrations (45.1 and 15.2 mg g⁻¹) were observed in *L. esculentum* and *P. oleracea* has grown at the RS, while the lowest (8.9 and 1.4 mg g⁻¹) were observed in *P. australis* has grown at the same site. The highest Na concentration (53.0 mg g⁻¹) was recorded in *B. indica* has grown at the SS, while the lowest (2.8 mg g⁻¹) was detected in *S. nigrum* has grown at the RS.

Table 2. Results of three-way ANOVA (*F*-values) of macro-nutrients concentrations of nine native plant species in north Nile Delta, Egypt

Effect	df	Dependent variables					
		N	P	Ca	Mg	Na	K
Site	1	55.4**	9.2*	0.1 ^{ns}	2.1 ^{ns}	9.3*	1.3 ^{ns}
Species	8	4.4*	0.7 ^{ns}	6.4**	5.5**	4.8**	2.2 ^{ns}
Tissue	3	63.1***	4.5 ^{ns}	16.7**	8.2**	2.6 ^{ns}	4.8*
Site × Species	8	1.3 ^{ns}	2.7*	4.3**	4.7**	1.9 ^{ns}	4.3**
Site × Tissue	3	0.8 ^{ns}	0.6 ^{ns}	0.2 ^{ns}	1.2 ^{ns}	1.2 ^{ns}	2.6 ^{ns}
Species × Tissue	16	2.0 ^{ns}	1.1 ^{ns}	1.9 ^{ns}	10.2***	4.9**	4.4**
Site × Species × Tissue	16	36.5***	20.9***	22.7***	16.3***	53.9***	18.9***

Site: Sewage sludge dump site/Reference site, Species: nine native plant species, Tissue: fruit/leaf/stem/root. *: p < 0.05, **: p < 0.01, ***: p < 0.001, ns: not significant (i.e., p > 0.05), df: degree of freedom

All the investigated species were characterized by a bioaccumulation factor (BF) > 1.0 for some macro-nutrients (Fig. 2). *A. viridis* showed the higher BF value for K (14.4), *P. oleracea* showed higher BF values for N (1.3), P (1.6) and Mg (1.5), *R. dentatus* showed the higher BF value for Na (3.3). At the RS, *B. indica* showed the higher BF value for Na (2.8), *P. oleracea* showed higher BF values for N (12.3) and Mg (0.9), *L. esculentum* showed higher BF values for P (3.6) and Ca (1.1), and *P. dioscoridis* showed the higher BF value for K (6.9).

In the present study, the translocation factor (TF) varied among the studied sites, plant species and among the macro-nutrients (Fig. 3). Regarding the SS, *A. viridis* had the highest TF for Mg (3.8), *B. indica* for Na (5.2), *P. oleracea* for K (1.6), *S. nigrum* for N (2.2), *L. esculentum* for P (2.0) and *P. dioscoridis* for Ca (2.3). At the RS, *B. indica* had the highest TF for P (98.0), *C. bonariensis* for Mg (3.12), *P. oleracea* for Ca (1.9) and Na (3.4), and *R. dentatus* for N (4.1) and K (2.0).

Element accumulation index (EAI) were significantly higher in all plant species at the SS as compared to the RS (except *C. bonariensis* and *P. dioscoridis*; Fig. 4). The species with the highest EAI at the SS were *P. oleracea* (41.6), followed by *P. australis* (30.6), *R. dentatus* (27.7), *P. dioscoridis* (27.4), *A. viridis* (26.9) and *B. indica* (26.7). In contrast, *C. bonariensis* showed the lowest EAI value (19.2). In addition, *P. oleracea* (31.0), followed by *P. dioscoridis* (29.5), *R. dentatus* (24.7) and *S. nigrum* (24.5) that had the highest EAI in the RS, while *P. australis* (16.3) had the lowest. Positive linear correlations were detected between N, P, Ca, Mg and Na concentrations in all tissues of *A. viridis* and the soil of both sites (Appendix 2); N, P, Ca and Na for *B. indica*; N and P for *C. bonariensis*; N, P, Ca and Na for *P. oleracea*; Ca for *R. dentatus*; N, P, Mg and Na for *S. nigrum*; N and Na for *L. esculentum*; N, P, Ca and Na for *P. australis*; N for *P. dioscoridis*.

Table 3. Mean macro-nutrients concentrations \pm standard errors in nine native plant species that grown at sewage sludge dump site (SS) and reference site (RS) in north Nile Delta, Egypt. (Detailed values for each tissue are present in Appendix 1)

Species	Site	Macro-nutrient (mg g ⁻¹)					
		N	P	Ca	Mg	Na	K
<i>A. viridis</i>	SS	40.9 \pm 4.5bc	2.0 \pm 0.2bc	40.8 \pm 3.0b	6.3 \pm 1.5b	3.3 \pm 0.2a	65.6 \pm 6.8bc
	RS	23.7 \pm 4.8a	0.3 \pm 0.1ab	29.0 \pm 1.9bc	11.5 \pm 1.5c	7.0 \pm 0.4a	49.9 \pm 5.7b
	t-value	22.2***	29.8***	9.3***	10.3***	7.4***	4.3**
<i>B. indica</i>	SS	33.4 \pm 4.4ab	2.8 \pm 0.1cd	16.9 \pm 1.5a	4.2 \pm 0.6ab	37.5 \pm 7.3d	44.3 \pm 3.5a
	RS	25.5 \pm 3.7a	0.7 \pm 0.2abc	11.0 \pm 0.8a	3.2 \pm 0.2ab	53.0 \pm 7.3c	46.5 \pm 2.2b
	t-value	9.1***	16.3***	5.7***	2.4*	6.6***	0.6^{ns}
<i>C. bonariensis</i>	SS	29.4 \pm 3.5ab	2.1 \pm 0.4bc	13.9 \pm 2.1a	2.8 \pm 0.5ab	14.2 \pm 1.3bc	39.0 \pm 2.3a
	RS	22.7 \pm 3.9a	0.3 \pm 0.1a	17.6 \pm 1.2ab	3.2 \pm 0.6ab	14.6 \pm 2.9ab	38.0 \pm 2.5b
	t-value	3.4**	5.2**	2.2^{ns}	0.9^{ns}	0.2^{ns}	0.3^{ns}
<i>L. esculentum</i>	SS	41.8 \pm 1.9c	0.5 \pm 0.2a	36.4 \pm 5.8b	5.8 \pm 0.7ab	9.6 \pm 1.2abc	46.3 \pm 2.5a
	RS	29.1 \pm 1.9a	1.5 \pm 0.3cd	45.1 \pm 8.2d	5.9 \pm 0.9ab	13.3 \pm 1.5ab	46.8 \pm 4.2b
	t-value	15.0***	2.8*	2.0^{ns}	0.2^{ns}	7.4***	0.2^{ns}
<i>P. australis</i>	SS	24.5 \pm 3.1a	1.6 \pm 0.3b	14.6 \pm 1.7a	2.1 \pm 0.4a	4.4 \pm 0.3ab	33.2 \pm 1.2a
	RS	18.9 \pm 2.7a	0.4 \pm 0.2ab	8.9 \pm 0.2a	1.4 \pm 0.3a	13.9 \pm 2.0ab	17.7 \pm 1.6a
	t-value	6.2***	2.7*	3.2**	1.0^{ns}	7.1***	7.2***
<i>P. dioscoridis</i>	SS	27.8 \pm 3.2ab	1.5 \pm 0.3b	18.0 \pm 3.9a	4.4 \pm 0.7ab	14.4 \pm 1.8bc	36.8 \pm 2.4a
	RS	17.7 \pm 3.9a	1.2 \pm 0.3abcd	19.9 \pm 2.3ab	3.7 \pm 0.6ab	13.4 \pm 2.3ab	48.6 \pm 2.0b
	t-value	7.0***	2.1^{ns}	1.2^{ns}	1.9^{ns}	1.1^{ns}	2.9*
<i>P. oleracea</i>	SS	48.2 \pm 2.9c	3.2 \pm 0.4d	27.5 \pm 4.7ab	13.8 \pm 1.9c	5.2 \pm 0.5ab	80.2 \pm 10.1c
	RS	30.6 \pm 2.4a	1.6 \pm 0.1d	17.5 \pm 2.8ab	15.2 \pm 2.5c	22.8 \pm 4.2b	51.8 \pm 6.5b
	t-value	4.4**	5.0**	5.3**	1.5^{ns}	4.8**	6.4***
<i>R. dentatus</i>	SS	24.6 \pm 2.5a	1.6 \pm 0.3b	20.0 \pm 0.7a	4.9 \pm 0.2ab	18.8 \pm 0.6c	37.2 \pm 1.2a
	RS	19.5 \pm 5.2a	1.3 \pm 0.3bcd	15.9 \pm 1.0ab	6.4 \pm 0.7b	26.3 \pm 4.2b	37.1 \pm 3.8b
	t-value	1.9^{ns}	0.7^{ns}	3.6**	2.8*	1.7^{ns}	0.1^{ns}
<i>S. nigrum</i>	SS	31.8 \pm 5.2ab	2.2 \pm 0.2bcd	22.4 \pm 0.6a	2.6 \pm 0.3ab	2.8 \pm 0.4a	50.3 \pm 3.0ab
	RS	22.5 \pm 4.8a	1.4 \pm 0.1cd	37.6 \pm 0.8cd	5.1 \pm 0.4ab	6.1 \pm 0.1a	51.4 \pm 3.3b
	t-value	6.0***	7.6***	19.3***	24.4***	10.3***	1.1^{ns}

t-values represent the paired t-test. Means in the same columns (for each site) followed by different letters are significantly different at $p < 0.05$ according to Tukey HSD test. *: $p < 0.05$, **: $p < 0.01$, ***: $p < 0.001$, ns: not significant (i.e., $p > 0.05$)

Regarding the stoichiometric ratios, both SS and RS were only significantly different in K/Na and P/K ratios at $p < 0.01$ (Table 4). For individual plant species, it was noticed that the following stoichiometric ratios were significantly different among sites: P/K in *B. indica*, N/P and K/Na in *A. viridis*, N/P in *C. bonariensis*, K/Na in *P. australis*. On the contrary, *S. nigrum*, *P. dioscoridis* and *L. esculentum* showed no significant differences in the estimated stoichiometric ratios among sites.

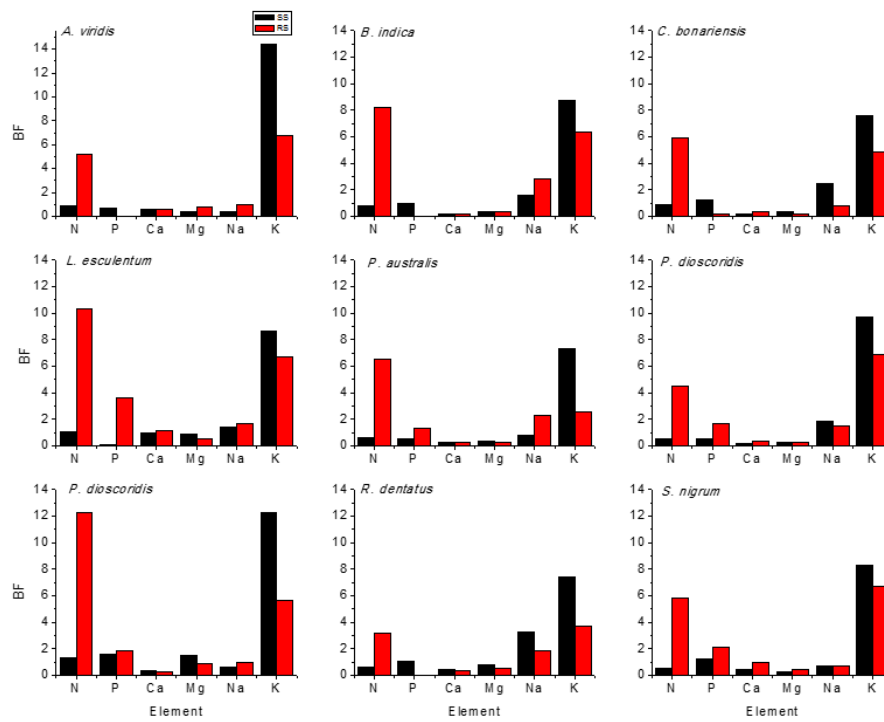


Figure 2. Mean ($n = 3$) of bioaccumulation factors (BFs) from soil to below-ground tissues of macro-nutrients in nine native plant species that grown at sewage sludge dump site (SS) and reference site (RS) in north Nile Delta, Egypt

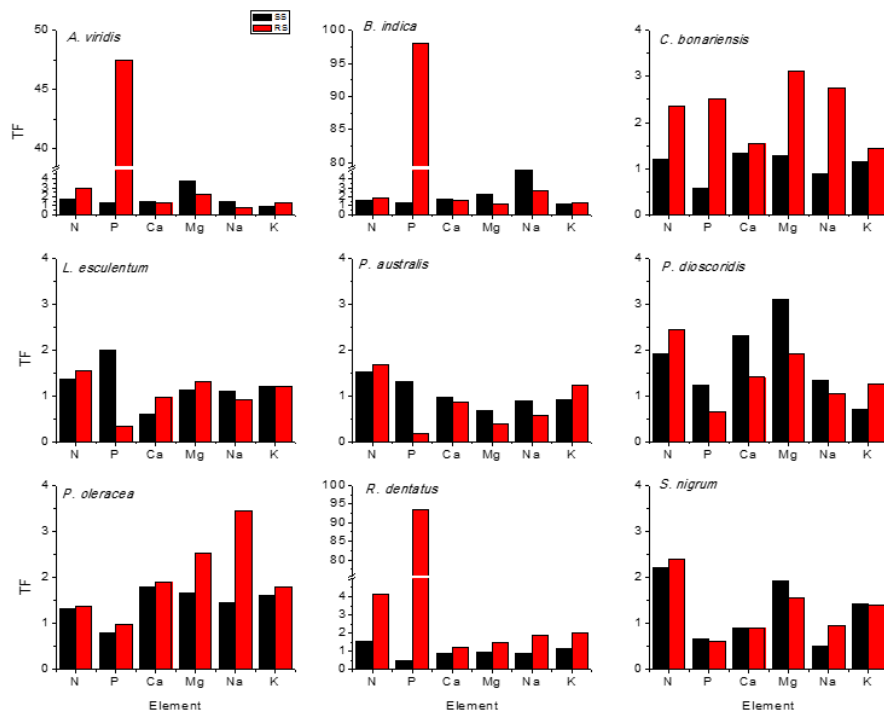


Figure 3. Mean ($n = 3$) of translocation factors (TFs) from below- to above-ground tissues of macro-nutrients in nine native plant species that grown at sewage sludge dump site (SS) and reference site (RS) in north Nile Delta, Egypt

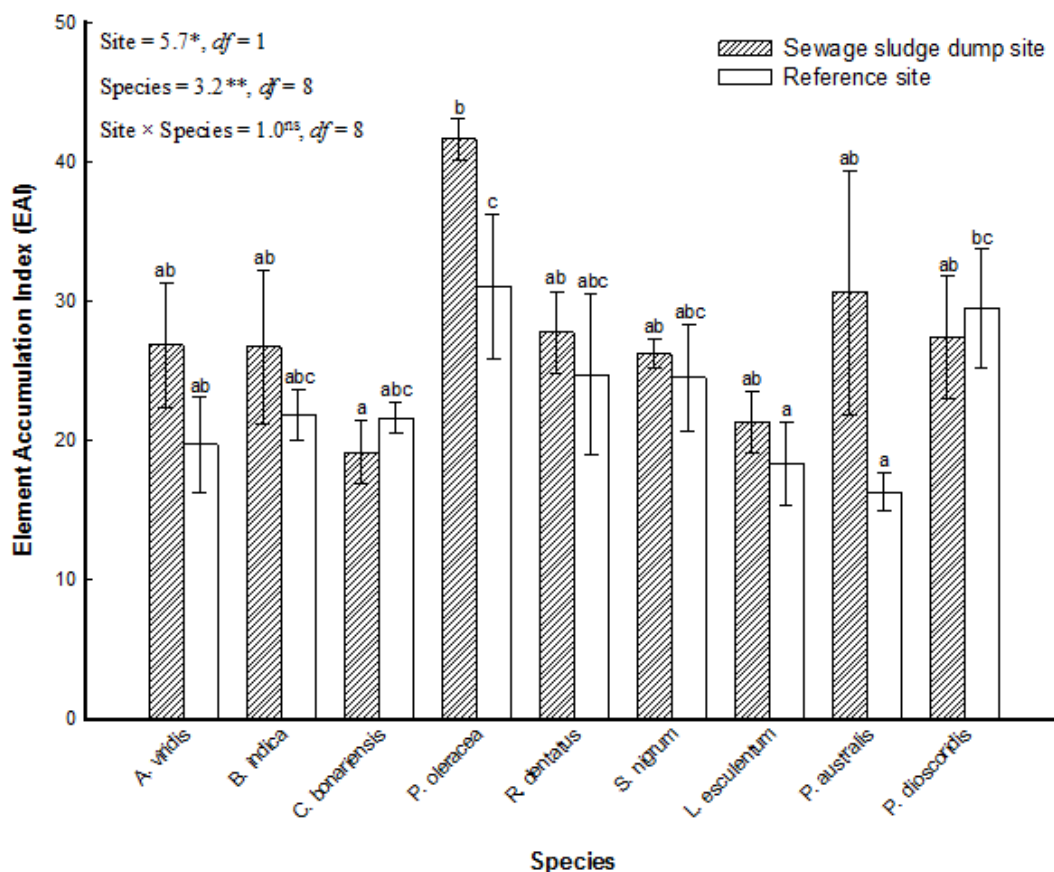


Figure 4. Element accumulation index (EAI) in nine native plant species that grown at sewage sludge dump site and reference site in north Nile Delta, Egypt. Site: Sewage sludge dump site/Reference site, Species: 9 native plant species, *: $p < 0.05$, **: $p < 0.01$, ns: not significant (i.e., $p > 0.05$), df: degree of freedom. Means followed by different letters are significantly different at $p < 0.05$ according to Tukey HSD test

Discussion

The collected soil from the SS was characterized by a higher N concentration than the RS, which could be ascribed to the high organic matter in its contents. The present study showed that the tissues of the studied plant species were characterized by high macro-nutrient concentrations at the SS more than at the soil of agricultural farms (control). This could be ascribed to the low pH value of the SS and its high concentrations of these elements. The results of some previous investigations indicated that the land application of sewage sludge increased soil N and P content (Bai et al., 2012), and plant uptake of N and P (Andres et al., 2010).

The uptake of macro-nutrients by plants varies among species and depends on the macro-nutrient demands of each species to apply their physiological and biochemical requirements. Plants differ both in their capacity to acquire macro-nutrients from the soil and in the amount of macro-nutrients they need per unit growth, the macro-nutrient concentrations in their tissue, and the time and extent to which they withdraw macro-nutrients during leaf senescence before leaf abscission (Kabata-Pendias, 2011). Lambers et al. (2008) reported that plants differ in the concentration of macro-nutrients in their

tissue, depending on environment, allocation to woody and herbaceous tissues, developmental stage, and species. Moreover, N, P, and K are the macro-nutrients that most frequently limit plant growth. However, N tends to limit plant productivity on young soils, whereas P becomes increasingly limiting as soils age. The presence of high concentrations of N, P, Ca and K in the sampled plants from the SS compared to control site because these elements are essential for the plant growth. However, the presence of a specific mineral in plant tissues does not imply that the plant needs this mineral for growth. For example, high Na concentrations are not required for growth (Lambers et al., 2008).

Table 4. Stoichiometric ratios (\pm standard deviations) of the studied nine plant species that grown at sewage sludge dump site (SS) and reference site (RS) in north Nile Delta, Egypt. Bold values of the ratios in each column are significantly different among sites at $p < 0.05$. F-values and significance level are shown for each column

Species	Site	Ca/Mg	N/P	K/Na	N/K	P/K
<i>A. viridus</i>	SS	9.1 \pm 5.0	20.5 \pm 3.1	20.4 \pm 7.6	0.7 \pm 0.6	0.04 \pm 0.02
	RS	2.8 \pm 0.9	73.1 \pm 28.8	7.2 \pm 2.4	0.6 \pm 0.5	0.01 \pm 0.01
<i>B. indica</i>	SS	4.3 \pm 0.7	12.1 \pm 4.4	2.0 \pm 1.9	0.8 \pm 0.6	0.1 \pm 0.02
	RS	3.6 \pm 1.2	41.2 \pm 6.7	1.0 \pm 0.5	0.5 \pm 0.2	0.01 \pm 0.0
<i>C. bonariensis</i>	SS	5.1 \pm 0.6	17.7 \pm 9.4	2.9 \pm 0.7	0.7 \pm 0.2	0.05 \pm 0.03
	RS	6.9 \pm 3.0	95.3 \pm 21.8	3.4 \pm 1.6	0.6 \pm 0.3	0.01 \pm 0.0
<i>L. esculentum</i>	SS	5.8 \pm 3.1	183.2 \pm 6.7	6.0 \pm 4.0	0.9 \pm 0.3	0.01 \pm 0.0
	RS	6.8 \pm 3.4	40.3 \pm 6.5	4.6 \pm 1.0	0.7 \pm 0.4	0.04 \pm 0.0
<i>P. australis</i>	SS	7.8 \pm 2.1	17.4 \pm 11.3	7.6 \pm 0.3	0.8 \pm 0.6	0.05 \pm 0.01
	RS	7.5 \pm 2.8	10.9 \pm 0.0	1.8 \pm 1.7	1.0 \pm 0.2	0.03 \pm 0.01
<i>P. dioscoridis</i>	SS	4.1 \pm 1.6	24.3 \pm 17.5	2.9 \pm 1.3	0.8 \pm 0.5	0.04 \pm 0.0
	RS	5.7 \pm 1.1	26.5 \pm 5.5	5.0 \pm 3.8	0.4 \pm 0.2	0.02 \pm 0.0
<i>P. oleracea</i>	SS	1.9 \pm 0.2	18.3 \pm 2.8	17.0 \pm 9.7	0.6 \pm 0.1	0.05 \pm 0.01
	RS	1.2 \pm 0.3	18.7 \pm 3.9	2.8 \pm 1.4	0.7 \pm 0.3	0.04 \pm 0.02
<i>R. dentatus</i>	SS	4.1 \pm 0.4	29.2 \pm 4.5	2.0 \pm 0.3	0.7 \pm 0.3	0.04 \pm 0.0
	RS	2.6 \pm 0.4	31.3 \pm 9.1	1.5 \pm 0.3	0.5 \pm 0.3	0.03 \pm 0.0
<i>S. nigrum</i>	SS	9.8 \pm 4.9	15.5 \pm 8.1	21.3 \pm 10.4	0.6 \pm 0.3	0.05 \pm 0.0
	RS	7.9 \pm 2.7	17.3 \pm 11.6	8.5 \pm 2.2	0.4 \pm 0.02	0.03 \pm 0.0
F-value		0.7	0.001	7.7	3.2	8.5
p		0.4	0.9	0.008	0.08	0.005

The presence of high macro-nutrients concentrations in leaves compared to the other tissues because leaves are the main sink for minerals in plants. Macro-nutrients associated with metabolism (e.g., N, P, and K) have their highest concentrations when a leaf or other tissue is first produced, then concentrations decline by dilution during cell wall formation and then by resorption of macro-nutrients during senescence, while the roots have intermediate concentrations. Species differ in the macro-nutrient requirement for growth but the physiological mechanisms for this are not always known (Woodward et al., 1984). The variations in macro-nutrient concentrations in various parts of plants have been ascribed to compartmentalization and translocation through the vascular

system (Kim et al., 2003). As stem plays the role of a transferring tissue, minimum concentrations of macro-nutrients were found in stem (Planquart et al., 1999).

The evaluation of the bioaccumulation factor (BF) represents a simple method to characterize quantitatively the transfer of available macro-nutrients from the soil to the plant (Branzini et al., 2012; Farahat et al., 2017), while its ability to translocate them from the roots to the shoots is measured using the translocation factor (TF). Both BF and TF can be used to estimate a plant's potential for phytoremediation purposes (Galal and Shehata, 2015). According to Zu et al. (2005), $BF > 1.0$ were found in macro-nutrient- and heavy metal-accumulating plants, whereas they were typically < 1.0 in macro-nutrient- and heavy metal-excluding plants. $TF > 1.0$ indicate that the plant is effective in the translocation of macro-nutrients from root to shoot tissue (Ma et al., 2001). In the present study, all studied species were characterized by BF values > 1.0 for some of the macro-nutrients, showing that they can accumulate macro-nutrients and are therefore more suitable for phytoextraction purposes. In the present study, the accumulation of macro-nutrients was done regardless of their stem size or life form of the species. For instance, *P. oleracea* as short (20-40 cm) annual herbaceous plant tend to accumulate high concentrations of N, P and K more than other perennial tall species e.g., *P. dioscoridis* and *P. australis*. The same observations were reported by Farahat and Linderholm (2013) for medicinal native plants that irrigated by sewage wastewater. Although the BF values for some macro-nutrients were > 1.0 , which means that our study species could accumulate these macro-nutrients, but none of them are hyper-accumulator (Kabata-Pendias, 2011).

The presence of TF values > 1.0 for N, P, Ca, Mg, and K mean that plants allocate the macro-nutrients in their vegetative parts because it is essential for growth. This behavior is opposite in many cases to the TF values for heavy metals that estimated in many aquatic and terrestrial plants (e.g., Galal and Farahat, 2015; Galal and Shehata, 2015; Eid et al., 2018a). This could be attributed to the fact that macro-nutrients are more essential for plant growth than heavy metals (Lambers et al., 2008). As a rule, when a plant has TF value > 1.0 for a certain mineral, this indicates the its suitability for the phytoextraction of this mineral, while TF value < 1.0 indicates its suitability for the phytostabilization of this mineral. For instance, *A. viridus* and *B. indica* are good phytoextractor for N, P, Ca, Mg and Na

Plant species accumulate different elements simultaneously, so the element accumulation index (EAI) was used to assess the overall performance of macro-nutrient accumulation in the studied plant species. Thus, in the present study, the highest EAI values of *P. oleracea*, *P. australis*, *R. dentatus*, *P. dioscoridis*, *A. viridis* and *B. indica* from the SS; and *P. oleracea*, *P. dioscoridis*, *R. dentatus* and *S. nigrum* from the cultivated field soil, indicates that these species are better able to accumulate macro-nutrients, and are therefore more suitable for phytoextraction purposes.

The stoichiometric ratios vary among species and depends on many limiting factors. For instance, N:P ratios are, on average, higher in graminoids than in forbs and higher in stress-tolerant species than in ruderals. This ratio declines with increasing growth rates (Lambers et al., 2008). The whole-plant biomass N:P ratios may vary up to 50-fold, due to differences in macro-nutrient uptake, biomass turnover, root allocation, and reproductive output (Aerts and Chapin, 2000). In the present study, there were few ratios that are significantly different among sites and species. In our opinion the availability of water and macro-nutrients in the studied sites interacts differently according to the species. This agrees with the findings of Lü et al. (2012) and Farahat

and Linderholm (2015). They reported that in rich N habitats, water availability can modulate the plant nutritional and stoichiometric responses to increased N and other macro-nutrients.

The present study proved that the concentrations of all macro-nutrients (except K) in the tissues of the most studied plant species were positively correlated with those in the soil. Such correlations indicate that these species reflect the cumulative effects of environmental pollution from the soil, and thereby suggesting their potential use in the biomonitoring of most macro-nutrients examined. This indication is supported by several studies according to which the total quantity of some macro-nutrients in a soil is correlated with the quantity of macro-nutrients absorbed by plants (Bonanno, 2011, 2013; Bonanno and Lo Giudice, 2010; Eid et al., 2012a, b; Eid and Shaltout, 2014). Moreover, plants with macro-nutrient concentrations strongly correlated with those in the soil have been considered potential indicators of macro-nutrient availability (Alyemeni and Almohisen, 2014).

Conclusion and recommendations

In this study, it was found that some plant species were more effective in absorbing certain macro-nutrients compared to other species that grown in the same soil. *L. esculentum* can bioaccumulate many of the macro-nutrients from sewage sludge without excessive quantities of macro-nutrients being translocated into the edible portions of the plant (fruits). In the present study, establishing a pattern of translocation of macro-nutrients from root to shoot of a plant can be very useful in biological monitoring of macro-nutrient contamination as well as a selection of macro-nutrient accumulator species. The highest EAI values of *P. oleracea*, *P. australis*, *R. dentatus*, *P. dioscoridis*, *A. viridis* and *B. indica* growing in the SS; and of *P. oleracea*, *P. dioscoridis*, *R. dentatus* and *S. nigrum* growing in the cultivated field soil, indicate that they are better able to accumulate macro-nutrients and are therefore more suitable for phytoextraction purposes.

Due to the noticeable high concentrations of macro-nutrients in the different tissues of the studied species, we recommend it in mitigation of the eutrophic status of SS when applied to the agricultural lands. This will be achieved through leaving these weeds grow prior to cultivation of the agricultural crops. This needs further investigation to determine the best density for each native species that helps efficiently in reducing the macro-nutrients load of sewage sludge on the cultivated plants.

Acknowledgements. This work was supported by the Deanship of Scientific Research at King Khalid University under Grant number R.G.P. 1/94/40.

REFERENCES

- [1] Aerts, R., Chapin, F. S. (2000): The mineral nutrition of wild plants revisited: a re-evaluation of processes and patterns. – *Advanced Ecological Research* 30: 1-67.
- [2] Allen, S. (1989): *Chemical Analysis of Ecological Materials*. – Blackwell Scientific Publications, London.
- [3] Alyemeni, M. N., Almohisen, I. A. A. (2014): Traffic and industrial activities around Riyadh cause the accumulation of heavy metals in legumes: a case study. – *Saudi Journal of Biological Science* 21: 167-172.

- [4] Andres, E. F., Tenorio, J. L., Walter, I. (2010): Biomass production and nutrient concentration of kenaf grown on sewage sludge-amended soil. – Spanish Journal of Agriculture Research 8: 472-480.
- [5] Antolín, C. M., Muro, I., Sánchez-Díaz, M. (2010): Application of sewage sludge improves growth, photosynthesis and antioxidant activities of nodulated alfalfa plants under drought conditions. – Environmental and Experimental Botany 68: 75-82.
- [6] APHA (1998): Standard Methods for the Examination of Water and Wastewater. – American Public Health Association, Washington, DC.
- [7] Araújo, A. S. F., Monteiro, R. T. R., Carvalho, E. M. S. (2007): Effects of composted textile nodulation and nitrogen fixation of soybean and cowpea. – Bioresource Technology 98: 1028-1032.
- [8] Bai, Y. C., Wang, L., Tao, T. Y., Chen, G. H., Qian, X. Q., Feng, K., Shan, Y. H. (2012): Study on the amendment of physicochemical properties of tidal flat soil by sewage sludge application. – Plant Nutrition and Fertilizer Science 18: 1019-1025.
- [9] Bonanno, G. (2011): Trace element accumulation and distribution in the organs of *Phragmites australis* (common reed) and biomonitoring applications. – Ecotoxicology and Environmental Safety 74: 1057-1064.
- [10] Bonanno, G. (2013): Comparative performance of trace element bioaccumulation and biomonitoring in the plant species *Typha domingensis*, *Phragmites australis* and *Arundo donax*. – Ecotoxicology and Environmental Safety 97: 124-130.
- [11] Bonanno, G., Lo Giudice, R. (2010): Heavy metal bioaccumulation by the organs of *Phragmites australis* (common reed) and their potential use as contamination indicators. – Ecological Indicators 10: 639-645.
- [12] Boulos, L. (1999): Flora of Egypt. Vol. 1 (*Azollaceae* - *Oxalidaceae*). – Al-Hadara Publishing, Cairo.
- [13] Boulos, L. (2002): Flora of Egypt. Vol. 3 (*Verbenaceae* - *Compositae*). – Al-Hadara Publishing, Cairo.
- [14] Boulos, L. (2005): Flora of Egypt. Vol. 4. Monocotyledons, (*Alismataceae* - *Orchidaceae*). – Al-Hadara Publishing, Cairo.
- [15] Branzini, A., González, R. S., Zubillaga, M. (2012): Absorption and translocation of copper, zinc and chromium by *Sesbania virgata*. – Journal of Environmental Management 102: 50-54.
- [16] Chandra, R., Yadav, S., Yadav, S. (2017): Phytoextraction potential of heavy metals by native wetland plants growing on chlorolignin containing sludge of pulp and paper industry. – Ecological Engineering 98: 134-145.
- [17] Eid, E. M., Alamri, S. A. M., Shaltout, K. H., Galal, T. M., Ahmed, M. T., Brima, E. I., Sewelam, N. (2020c): A sustainable food security approach: Controlled land application of sewage sludge recirculates nutrients to agricultural soils and enhances crop productivity. – Food and Energy Security (accepted).
- [18] Eid, E. M., Alrumman, S. A., El-Bebany, A. F., Fawy, K. F., Taher, M. A., Hesham, A., El-Shaboury, G. A., Ahmed, M. T. (2018b): The evaluation of sewage sludge application as a fertilizer for broad bean (*Faba sativa* Bernh.) crops. – Food and Energy Security 7: e00142.
- [19] Eid, E. M., Alrumman, S. A., El-Bebany, A. F., Fawy, K. F., Taher, M. A., Hesham, A., El-Shaboury, G. A., Ahmed, M. T. (2019): Evaluation of the potential of sewage sludge as a valuable fertilizer for wheat (*Triticum aestivum* L.) crops. – Environmental Science and Pollution Research 26: 392-401.
- [20] Eid, E. M., Alrumman, S. A., El-Bebany, A. F., Hesham, A., Taher, M. A., Fawy, K. F. (2017b): The effects of different sewage sludge amendment rates on the heavy metal bioaccumulation, growth and biomass of cucumbers (*Cucumis sativus* L.). – Environmental Science and Pollution Research 24: 16371-16382.
- [21] Eid, E. M., Alrumman, S. A., Farahat, E. A., El-Bebany, A. F. (2018a): Prediction models for evaluating the uptake of heavy metals by cucumbers (*Cucumis sativus* L.) grown in

- agricultural soils amended with sewage sludge. – Environmental Monitoring and Assessment 190: 501.
- [22] Eid, E. M., El-Bebany, A. F., Alrumman, S. A., Hesham, A., Taher, M. A., Fawy, K. F. (2017a): Effects of different sewage sludge applications on heavy metal accumulation, growth and yield of spinach (*Spinacia oleracea* L.). – International Journal of Phytoremediation 19: 340-347.
- [23] Eid, E. M., El-Bebany, A. F., Taher, M. A., Alrumman, S. A., Hussain, A. A., Galal, T. M., Shaltout, K. H., Sewelam, N. A., Ahmed, M. T., El-Shaboury, G. A. (2020b): Influences of sewage sludge-amended soil on heavy metal accumulation, growth and yield of rocket plant (*Eruca sativa*). – Applied Ecology and Environmental Research (accepted).
- [24] Eid, E. M., El-Sheikh, M. A., Alatar, A. A. (2012b): Uptake of Ag, Co and Ni by the organs of *Typha domingensis* (Pers.) Poir. ex Steud. in Lake Burullus and their potential use as contamination indicators. – Open Journal of Modern Hydrology 2: 21-27.
- [25] Eid, E. M., Hussain, A. A., Taher, M. A., Galal, T. M., Shaltout, K. H., Sewelam, N. (2020a): Sewage sludge application enhances the growth of *Corchorus olitorius* plants and provides a sustainable practice for nutrient recirculation in agricultural soils. – Journal of Soil Science and Plant Nutrition 20: 149-159.
- [26] Eid, E. M., Shaltout, K. H. (2014): Monthly variations of trace elements accumulation and distribution in above- and below-ground biomass of *Phragmites australis* (Cav.) Trin. ex Steudel in Lake Burullus (Egypt): a biomonitoring application. – Ecological Engineering 73: 17-25.
- [27] Eid, E. M., Shaltout, K. H. (2016): Bioaccumulation and translocation of heavy metals by nine native plant species grown at a sewage sludge dump site. – International Journal of Phytoremediation 18: 1075-1085.
- [28] Eid, E. M., Shaltout, K. H., Al-Sodany, Y. M., Jensen, K. (2010): Effects of abiotic conditions on *Phragmites australis* along geographic gradients in Lake Burullus, Egypt. – Aquatic Botany 92: 86-92.
- [29] Eid, E. M., Shaltout, K. H., El-Sheikh, M. A., Asaeda, T. (2012a): Seasonal courses of nutrients and heavy metals in water, sediment and above- and below-ground *Typha domingensis* biomass in Lake Burullus (Egypt): perspective for phytoremediation. – Flora 207: 783-794.
- [30] El-Sheikh, M. A., Al-Sodany, Y. M., Eid, E. M., Shaltout, K. H. (2012): Ten years primary succession on a newly created landfill at a lagoon of the Mediterranean Sea (Lake Burullus RAMSAR site). – Flora 207: 459-468.
- [31] EMA (1980): Climatic Normals for the Arab Republic of Egypt up to 1975. – Ministry of Civil Aviation, Egyptian Meteorological Authority, General Organization for Governmental Printing Offices, Cairo.
- [32] Farahat, E. A., Galal, T., Elawa, O., Hassan, L. M. (2017): Health risk assessment and growth characteristics of wheat and maize crops irrigated with contaminated wastewater. – Environmental Monitoring and Assessment 189: 535.
- [33] Farahat, E. A., Linderholm, H. W. (2013): Effects of treated wastewater irrigation on size-structure, biochemical products and mineral content of native medicinal shrubs. – Ecological Engineering 60: 235-241.
- [34] Farahat, E. A., Linderholm, H. W. (2015): Nutrient resorption efficiency and proficiency in economic wood trees irrigated by treated wastewater in desert planted forests. – Agriculture Water Management 155: 67-75.
- [35] Fuentes, D., Valdecantos, A., Cortina, J., Vallejo, V. R. (2007): Seedling performance in sewage sludge-amended degraded Mediterranean woodlands. – Ecological Engineering 31: 281-291.
- [36] Galal, T. M. (2016): Health hazards and heavy metals accumulation by summer squash (*Cucurbita pepo* L.) cultivated in contaminated soils. – Environmental Monitoring and Assessment 188: 434.

- [37] Galal, T. M., Farahat, E. (2015): The invasive macrophyte *Pistia stratiotes* L. as a bioindicator and a biomonitor for water pollution in Lake Mariut, Egypt. – Environmental Monitoring and Assessment 187: 701-711.
- [38] Galal, T. M., Shehata, H. S. (2015): Bioaccumulation and translocation of heavy metals by *Plantago major* L. grown in contaminated soils under the effect of traffic pollution. – Ecological Indicators 48: 244-251.
- [39] Gupta, S., Nayek, S., Saha, R. N., Satpati, S. (2008): Assessment of heavy metal accumulation in macrophyte, agricultural soil and crop plants adjacent to discharge zone of sponge iron factory. – Environmental Geology 55: 731-739.
- [40] Henry, C. L., Cole, D. W., Harrison, R. B. (1994): Use of municipal sludge to restore and improve site productivity in forestry: the pack forest sludge research program. – Forest Ecology and Management 66: 137-149.
- [41] Ho, Y. B., Wong, W. (1994): Growth and macronutrient removal of water hyacinth in a small secondary sewage treatment plant. – Resources, Conservation and Recycling 11: 161-178.
- [42] Kabata-Pendias, A. (2011): Trace Elements in Soils and Plants. – CRC Press, Boca Raton, FL.
- [43] Kim, I. S., Kang, H. K., Johnson-Green, P., Lee, E. J. (2003): Investigation of heavy metal accumulation in *Polygonum thunbergii* for phytoextraction. – Environmental Pollution 126: 235-243.
- [44] Korboulewskya, N., Bonina, G., Massiani, C. (2002): Biological and ecophysiological reactions of white wall rocket (*Diplotaxis erucooides* L.) grown on sewage sludge compost. – Environmental Pollution 117: 365-370.
- [45] Lambers, H., Stuart Chapin III, F., Pons, T. L. (2008): Plant Physiological Ecology. Second Ed. – Springer-Verlag, New York.
- [46] Liu, Y. J., Zhu, Y. G., Ding, H. (2007): Lead and cadmium in leaves of deciduous trees in Beijing, China: development of a metal accumulation index (MAI). – Environmental Pollution 145: 387-390.
- [47] Lü, X. T., Kong, D. L., Pan, Q. M., Simmons, M. E., Han, X. G. (2012): Nitrogen and water availability interact to affect leaf stoichiometry in a semi-arid grassland. – Oecologia 168: 301-310.
- [48] Ma, L. Q., Komar, K. M., Tu, C., Zhang, W., Cai, Y., Kennelley, E. D. (2001): A fern that hyperaccumulates arsenic. – Nature 409: 579.
- [49] Moreno-Caselles, J., Pérez-Murcia, M. D., Pérez-Espinosa, A., Moral, R. (1997): Heavy metal pollution in sewage sludges and agricultural impact. – Fresenius Environmental Bulletin 6: 519-524.
- [50] Peng, K., Luo, C., Lou, L., Li, X., Shen, Z. (2008): Bioaccumulation of heavy metals by the aquatic plants *Potamogeton pectinatus* L. and *Potamogeton malaianus* Miq. and their potential use for contamination indicators and in wastewater treatment. – Science of the Total Environment 392: 22-29.
- [51] Planquart, P., Bonin, G., Prone, A., Massiani, C. (1999): Distribution, movement and plant availability of trace metals in soils amended with sewage sludge compost: application to low metal loading. – Science of the Total Environment 241: 161-179.
- [52] Quilbé, R., Serreau, C., Wicherek, S., Bernard, C., Thomas, Y., Oudinet, J.-P. (2005): Nutrient transfer by runoff from sewage sludge amended soil under simulated rainfall. – Environmental Monitoring and Assessment 100: 177.
- [53] Shaltout, K. H., El-Hamdi, K. H., El-Masry, S. A., Eid, E. M. (2019): Bedouin farms in the Saint Katherine mountainous area (South Sinai, Egypt). – Journal of Mountain Science 16: 2232-2242.
- [54] Singh, R. P., Agrawal, M. (2007): Effects of sewage sludge amendment on heavy metal accumulation and consequent responses of *Beta vulgaris* plants. – Chemosphere 67: 2229-2240.

- [55] Singh, R. P., Agrawal, M. (2010): Variations in heavy metal accumulation, growth and yield of rice plants grown at different sewage sludge amendment rates. – *Ecotoxicology and Environmental Safety* 73: 632-641.
- [56] Statsoft (2007): Statistica Version 7.1. – Statsoft Inc: Tulsa, OK.
- [57] Wilke, B. M. (2005): Determination of Chemical and Physical Soil Properties. In: Margesin, R., Schinner, F. (eds.) *Manual for Soil Analysis - Monitoring and Assessing Soil Bioremediation*. – Springer-Verlag, Heidelberg, pp. 47-95.
- [58] Woodward, R. A., Harper, K. T., Tiedemann, A. R. (1984): An ecological consideration of the significance of cation exchange capacity of roots of some Utah range plants. – *Plant and Soil* 79: 169-180.
- [59] Xiao, R., Bai, J., Zhang, H., Gao, H., Liua, X., Wilkes, A. (2011): Changes of P, Ca, Al and Fe contents in fringe marshes along a pedogenic chronosequence in the Pearl River estuary, South China. – *Continental Shelf Research* 31: 739-747.
- [60] Yu, S., Chen, W., He, X., Liu, Z., Huang, Y. (2014): Biomass accumulation and nutrient uptake of 16 riparian woody plant species in Northeast China. – *Journal of Forestry Research* 25: 773-778.
- [61] Zhao, Y., Xia, X., Yang, Z. (2013): Growth and nutrient accumulation of *Phragmites australis* in relation to water level variation and nutrient loadings in a shallow lake. – *Journal of Environmental Sciences* 25: 16-25.
- [62] Zu, Y. Q., Li, Y., Chen, J. J., Chen, H. Y., Qin, L., Schwartz, C. (2005): Hyperaccumulation of Pb, Zn and Cd in herbaceous grown on lead-zinc mining area in Yunnan, China. – *Environment International* 31: 755-762.

APPENDIX

Appendix 1. Macro-nutrient concentrations \pm standard errors in nine native plant species grown at sewage sludge dump site (SS) and reference site (RS) in north Nile Delta, Egypt

Species	Site	Tissue	Macro-nutrient (mg g ⁻¹)					
			N	P	Ca	Mg	Na	K
<i>A. viridis</i>	SS	L (n = 3)	57.5 \pm 0.7	2.6 \pm 0.0	51.9 \pm 0.9	12.2 \pm 0.2	3.4 \pm 0.1	41.2 \pm 0.7
		S (n = 3)	38.1 \pm 0.7	1.7 \pm 0.0	39.1 \pm 0.8	4.5 \pm 0.1	4.0 \pm 0.1	88.0 \pm 2.3
		R (n = 3)	27.0 \pm 0.2	1.6 \pm 0.0	31.3 \pm 0.5	2.2 \pm 0.0	2.5 \pm 0.1	67.5 \pm 1.5
		M (n = 9)	40.9 \pm 4.5bc	2.0 \pm 0.2bc	40.8 \pm 3.0b	6.3 \pm 1.5b	3.3 \pm 0.2a	65.6 \pm 6.8bc
	RS	L (n = 3)	42.2 \pm 0.6	0.8 \pm 0.0	36.6 \pm 0.8	16.6 \pm 0.3	5.5 \pm 0.2	36.9 \pm 0.4
		S (n = 3)	18.7 \pm 0.3	0.2 \pm 0.0	26.0 \pm 0.6	11.6 \pm 0.2	7.4 \pm 0.2	72.2 \pm 3.3
		R (n = 3)	10.3 \pm 0.1	0.0 \pm 0.0	24.4 \pm 0.4	6.2 \pm 0.1	8.0 \pm 0.2	40.7 \pm 0.9
		M (n = 9)	23.7 \pm 4.8a	0.3 \pm 0.1ab	29.0 \pm 1.9bc	11.5 \pm 1.5c	7.0 \pm 0.4a	49.9 \pm 5.7b
t-value		22.2***	29.8***	9.3***	10.3***	7.4***	4.3**	
<i>B. indica</i>	SS	L (n = 3)	50.9 \pm 0.3	3.0 \pm 0.0	21.9 \pm 0.4	6.3 \pm 0.1	59.4 \pm 1.0	34.1 \pm 0.6
		S (n = 3)	24.9 \pm 0.5	2.9 \pm 0.0	17.5 \pm 0.4	4.0 \pm 0.1	43.3 \pm 1.5	57.6 \pm 1.5
		R (n = 3)	24.4 \pm 0.1	2.3 \pm 0.0	11.4 \pm 0.1	2.3 \pm 0.0	9.9 \pm 0.2	41.1 \pm 1.0
		M (n = 9)	33.4 \pm 4.4ab	2.8 \pm 0.1cd	16.9 \pm 1.5a	4.2 \pm 0.6ab	37.5 \pm 7.3d	44.3 \pm 3.5a
	RS	L (n = 3)	40.3 \pm 0.5	0.6 \pm 0.0	11.9 \pm 0.2	3.9 \pm 0.1	68.1 \pm 0.5	51.1 \pm 1.6
		S (n = 3)	19.8 \pm 0.2	1.3 \pm 0.0	13.2 \pm 0.1	2.7 \pm 0.0	66.5 \pm 4.4	50.2 \pm 1.1
		R (n = 3)	16.4 \pm 0.4	0.0 \pm 0.0	7.9 \pm 0.1	2.9 \pm 0.0	24.4 \pm 0.9	38.1 \pm 1.1
		M (n = 9)	25.5 \pm 3.7a	0.7 \pm 0.2abc	11.0 \pm 0.8a	3.2 \pm 0.2ab	53.0 \pm 7.3c	46.5 \pm 2.2b
t-value		9.1***	16.3***	5.7***	2.4*	6.6***	0.6^{ns}	
<i>C. bonariensis</i>	SS	L (n = 3)	43.0 \pm 0.2	2.6 \pm 0.2	22.2 \pm 0.4	4.7 \pm 0.1	17.8 \pm 0.4	48.0 \pm 1.3
		S (n = 3)	19.3 \pm 0.4	0.7 \pm 0.0	8.0 \pm 0.1	1.4 \pm 0.0	9.3 \pm 0.4	33.4 \pm 0.9
		R (n = 3)	25.8 \pm 0.3	2.9 \pm 0.2	11.3 \pm 0.1	2.4 \pm 0.1	15.5 \pm 0.3	35.7 \pm 0.9
		M (n = 9)	29.4 \pm 3.5ab	2.1 \pm 0.4bc	13.9 \pm 2.1a	2.8 \pm 0.5ab	14.2 \pm 1.3bc	39.0 \pm 2.3a
	RS	L (n = 3)	38.0 \pm 0.9	0.5 \pm 0.0	21.4 \pm 0.2	5.3 \pm 0.1	26.3 \pm 0.3	38.8 \pm 1.0
		S (n = 3)	18.2 \pm 0.1	0.2 \pm 0.0	18.5 \pm 0.2	2.8 \pm 0.1	10.7 \pm 0.2	45.8 \pm 1.4
		R (n = 3)	11.9 \pm 0.7	0.1 \pm 0.0	13.0 \pm 0.1	1.3 \pm 0.0	6.7 \pm 0.1	29.3 \pm 1.1
		M (n = 9)	22.7 \pm 3.9a	0.3 \pm 0.1a	17.6 \pm 1.2ab	3.2 \pm 0.6ab	14.6 \pm 2.9ab	38.0 \pm 2.5b
t-value		3.4**	5.2**	2.2^{ns}	0.9^{ns}	0.2^{ns}	0.3^{ns}	
<i>L. esculentum</i>	SS	F (n = 3)	43.1 \pm 0.2	0.0 \pm 0.0	5.0 \pm 0.0	2.1 \pm 0.0	4.1 \pm 0.1	49.4 \pm 2.2
		L (n = 3)	50.4 \pm 0.7	1.5 \pm 0.0	50.9 \pm 1.1	8.4 \pm 0.1	9.9 \pm 0.2	37.3 \pm 0.5
		S (n = 3)	40.6 \pm 0.9	0.1 \pm 0.0	37.0 \pm 0.5	7.4 \pm 0.1	15.6 \pm 0.3	58.1 \pm 1.2
		R (n = 3)	33.0 \pm 0.4	0.3 \pm 0.0	52.7 \pm 0.7	5.3 \pm 0.1	8.9 \pm 0.1	40.5 \pm 0.9
		M (n = 12)	41.8 \pm 1.9c	0.5 \pm 0.2a	36.4 \pm 5.8b	5.8 \pm 0.7ab	9.6 \pm 1.2abc	46.3 \pm 2.5a
	RS	F (n = 3)	27.5 \pm 2.3	0.3 \pm 0.0	4.7 \pm 0.0	1.8 \pm 0.0	5.8 \pm 0.1	62.2 \pm 2.4
		L (n = 3)	38.0 \pm 0.6	1.5 \pm 0.1	80.9 \pm 2.4	8.3 \pm 0.4	14.6 \pm 0.7	27.9 \pm 1.1
		S (n = 3)	30.3 \pm 0.1	0.8 \pm 0.0	49.0 \pm 1.1	8.8 \pm 0.2	18.7 \pm 1.2	56.5 \pm 3.9
R (n = 3)		20.6 \pm 0.4	3.2 \pm 0.0	45.8 \pm 0.6	4.8 \pm 0.1	14.0 \pm 0.5	40.7 \pm 1.5	
M (n = 12)		29.1 \pm 1.9a	1.5 \pm 0.3cd	45.1 \pm 8.2d	5.9 \pm 0.9ab	13.3 \pm 1.5ab	46.8 \pm 4.2b	
t-value		15.0***	2.8*	2.0^{ns}	0.2^{ns}	7.4***	0.2^{ns}	
<i>P. australis</i>	SS	L (n = 3)	42.0 \pm 0.2	1.4 \pm 0.0	16.6 \pm 0.3	2.2 \pm 0.0	3.5 \pm 0.0	27.5 \pm 0.7
		S (n = 3)	17.0 \pm 0.2	2.1 \pm 0.4	12.1 \pm 0.1	1.2 \pm 0.0	4.8 \pm 0.1	36.5 \pm 0.9
		R (n = 3)	19.6 \pm 0.8	1.4 \pm 0.5	14.8 \pm 3.4	2.5 \pm 0.8	4.7 \pm 0.5	34.4 \pm 1.0
		M (n = 9)	24.5 \pm 3.1a	1.6 \pm 0.3b	14.6 \pm 1.7a	2.1 \pm 0.4a	4.4 \pm 0.3ab	33.2 \pm 1.2a
	RS	L (n = 3)	29.5 \pm 0.6	0.0 \pm 0.0	8.7 \pm 0.1	1.0 \pm 0.0	6.2 \pm 0.1	23.8 \pm 1.1
		S (n = 3)	14.2 \pm 1.3	0.0 \pm 0.0	8.3 \pm 0.1	0.9 \pm 0.0	16.1 \pm 0.5	14.1 \pm 0.5
		R (n = 3)	13.1 \pm 0.5	1.2 \pm 0.0	9.8 \pm 0.2	2.4 \pm 0.1	19.5 \pm 0.9	15.3 \pm 0.6
		M (n = 9)	18.9 \pm 2.7a	0.4 \pm 0.2ab	8.9 \pm 0.2a	1.4 \pm 0.3a	13.9 \pm 2.0ab	17.7 \pm 1.6a

	<i>t</i> -value	6.2***	2.7*	3.2**	1.0^{ns}	7.1***	7.2***	
<i>P. dioscoridis</i>	SS	L (<i>n</i> = 3)	39.5 ± 0.5	2.6 ± 0.0	33.5 ± 0.8	6.7 ± 0.1	21.3 ± 0.4	30.3 ± 0.6
		S (<i>n</i> = 3)	26.7 ± 0.1	0.6 ± 0.0	10.8 ± 0.2	4.8 ± 0.1	10.0 ± 0.2	34.3 ± 0.9
		R (<i>n</i> = 3)	17.3 ± 0.3	1.3 ± 0.0	9.6 ± 0.2	1.9 ± 0.0	11.7 ± 0.3	45.7 ± 1.4
		M (<i>n</i> = 9)	27.8 ± 3.2ab	1.5 ± 0.3b	18.0 ± 3.9a	4.4 ± 0.7ab	14.4 ± 1.8bc	36.8 ± 2.4a
	RS	L (<i>n</i> = 3)	33.1 ± 0.2	1.8 ± 0.0	29.2 ± 0.5	6.2 ± 0.0	21.6 ± 1.0	51.5 ± 1.2
		S (<i>n</i> = 3)	11.0 ± 0.1	0.2 ± 0.0	14.8 ± 0.1	2.6 ± 0.0	5.6 ± 0.1	52.9 ± 2.0
		R (<i>n</i> = 3)	9.0 ± 0.1	1.5 ± 0.0	15.7 ± 0.2	2.3 ± 0.0	12.9 ± 0.2	41.4 ± 1.1
		M (<i>n</i> = 9)	17.7 ± 3.9a	1.2 ± 0.3abcd	19.9 ± 2.3ab	3.7 ± 0.6ab	13.4 ± 2.3ab	48.6 ± 2.0b
<i>t</i> -value	7.0***	2.1^{ns}	1.2^{ns}	1.9^{ns}	1.1^{ns}	2.9*		
<i>P. oleracea</i>	SS	L (<i>n</i> = 3)	45.3 ± 0.1	4.1 ± 0.1	46.1 ± 0.9	21.4 ± 0.5	7.2 ± 0.1	63.7 ± 2.4
		S (<i>n</i> = 3)	59.7 ± 0.2	1.8 ± 0.0	18.2 ± 0.2	10.4 ± 0.1	4.3 ± 0.1	119.7 ± 6.0
		R (<i>n</i> = 3)	39.7 ± 0.1	3.7 ± 0.0	18.1 ± 0.2	9.6 ± 0.2	4.0 ± 0.0	57.4 ± 1.4
		M (<i>n</i> = 9)	48.2 ± 2.9c	3.2 ± 0.4d	27.5 ± 4.7ab	13.8 ± 1.9c	5.2 ± 0.5ab	80.2 ± 10.1c
	RS	L (<i>n</i> = 3)	40.1 ± 1.1	1.8 ± 0.0	28.8 ± 0.5	24.4 ± 0.5	37.5 ± 0.7	44.8 ± 1.1
		S (<i>n</i> = 3)	27.1 ± 0.1	1.4 ± 0.0	12.8 ± 0.1	13.6 ± 0.1	22.3 ± 0.6	76.8 ± 3.6
		R (<i>n</i> = 3)	24.6 ± 0.1	1.7 ± 0.0	11.0 ± 0.4	7.5 ± 0.4	8.7 ± 0.3	33.8 ± 0.9
		M (<i>n</i> = 9)	30.6 ± 2.4a	1.6 ± 0.1d	17.5 ± 2.8ab	15.2 ± 2.5c	22.8 ± 4.2b	51.8 ± 6.5b
<i>t</i> -value	4.4**	5.0**	5.3**	1.5^{ns}	4.8**	6.4***		
<i>R. dentatus</i>	SS	L (<i>n</i> = 3)	34.5 ± 0.1	0.5 ± 0.0	20.2 ± 0.3	5.6 ± 0.1	17.5 ± 0.6	35.3 ± 0.8
		S (<i>n</i> = 3)	21.6 ± 0.1	1.9 ± 0.0	17.7 ± 0.6	4.1 ± 0.1	18.7 ± 0.8	41.6 ± 1.3
		R (<i>n</i> = 3)	17.9 ± 0.8	2.5 ± 0.0	22.1 ± 0.3	5.0 ± 0.1	20.3 ± 1.0	34.8 ± 0.8
		M (<i>n</i> = 9)	24.6 ± 2.5a	1.6 ± 0.3b	20.0 ± 0.7a	4.9 ± 0.2ab	18.8 ± 0.6c	37.2 ± 1.2a
	RS	L (<i>n</i> = 3)	40.1 ± 0.3	1.6 ± 0.0	19.9 ± 0.4	9.1 ± 0.1	42.7 ± 0.7	47.7 ± 1.1
		S (<i>n</i> = 3)	12.1 ± 0.3	2.1 ± 0.0	13.9 ± 0.0	5.3 ± 0.1	20.3 ± 0.3	41.4 ± 0.9
		R (<i>n</i> = 3)	6.3 ± 0.4	0.0 ± 0.0	14.0 ± 0.4	4.8 ± 0.1	15.9 ± 0.2	22.3 ± 0.5
		M (<i>n</i> = 9)	19.5 ± 5.2a	1.3 ± 0.3bcd	15.9 ± 1.0ab	6.4 ± 0.7b	26.3 ± 4.2b	37.1 ± 3.8b
<i>t</i> -value	1.9^{ns}	0.7^{ns}	3.6**	2.8*	1.7^{ns}	0.1^{ns}		
<i>S. nigrum</i>	SS	L (<i>n</i> = 3)	51.9 ± 0.7	2.4 ± 0.0	20.2 ± 0.4	3.7 ± 0.1	2.0 ± 0.1	53.4 ± 1.1
		S (<i>n</i> = 3)	25.9 ± 0.1	1.4 ± 0.2	22.8 ± 0.5	2.6 ± 0.0	2.1 ± 0.0	58.4 ± 1.5
		R (<i>n</i> = 3)	17.6 ± 0.2	2.8 ± 0.0	24.1 ± 0.5	1.6 ± 0.0	4.2 ± 0.1	39.0 ± 1.2
		M (<i>n</i> = 9)	31.8 ± 5.2ab	2.2 ± 0.2bcd	22.4 ± 0.6a	2.6 ± 0.3ab	2.8 ± 0.4a	50.3 ± 3.0ab
	RS	L (<i>n</i> = 3)	41.1 ± 4.4	1.4 ± 0.0	37.5 ± 0.3	6.4 ± 0.1	6.2 ± 0.2	50.8 ± 1.4
		S (<i>n</i> = 3)	14.8 ± 0.7	0.9 ± 0.0	35.0 ± 0.3	5.1 ± 0.1	5.8 ± 0.3	62.9 ± 1.9
		R (<i>n</i> = 3)	11.7 ± 0.1	1.9 ± 0.0	40.4 ± 0.4	3.7 ± 0.1	6.3 ± 0.0	40.5 ± 1.3
		M (<i>n</i> = 9)	22.5 ± 4.8a	1.4 ± 0.1cd	37.6 ± 0.8cd	5.1 ± 0.4ab	6.1 ± 0.1a	51.4 ± 3.3b
<i>t</i> -value	6.0***	7.6***	19.3***	24.4***	10.3***	1.1^{ns}		
<i>F</i> -value _{Sewage sludge dump site}	5.7***	9.6***	8.3***	14.9***	19.8***	12.4***		
<i>F</i> -value _{Reference site}	1.4^{ns}	5.9***	11.1***	16.5***	17.7***	7.5***		

t-values represent the paired *t*-test. Means in the same columns (for each site) followed by different letters are significantly different at *p* < 0.05 according to Tukey HSD test. F: fruit, L: leaf, S: stem, R: root, M: mean of tissues, *: *p* < 0.05, **: *p* < 0.01, ***: *p* < 0.001, ns: not significant (i.e., *p* > 0.05)

Appendix 2. Significant Pearson correlation coefficient ($p < 0.05$) between macro-nutrients concentrations in soil and nine native plant species in north Nile Delta, Egypt. Above diagonal represent the positive correlations and below diagonal represent the negative correlations

Species		Soil	Leaf	Stem	Root	
<i>A. viridis</i>	Soil	—	N, P, Ca, Mg, Na	N, P, Ca, Mg, Na	N, P, Ca, Mg, Na	
	Leaf	K	—	N, P, Ca, Mg, Na, K	N, P, Ca, Mg, Na, K	
	Stem	K		—	N, P, Ca, Mg, Na, K	
	Root	K			—	
<i>B. indica</i>	Soil	—	N, P, Ca, Na, K	N, P, Ca, Na	N, P, Ca, Mg, Na	
	Leaf	Mg	—	N, P, Ca, Mg, Na	N, P, Ca, Na	
	Stem	Mg, K	K	—	N, P, Ca, Na, K	
	Root	K	Mg, K	Mg	—	
<i>C. bonariensis</i>	Soil	—	N, P, Ca, Mg, Na	N, P, Mg, Na, K	N, P	
	Leaf	K	—	N, P, Mg, Na	N, P, K	
	Stem	Ca	Ca, K	—	N, P, Ca	
	Root	Ca, Mg, Na, K	Ca, Mg, Na	Mg, Na, K	—	
<i>P. australis</i>	Soil	—	N, P, Ca, Na	N, P, Ca, Na	N, P, Ca, Na	
	Leaf	Mg, K	—	N, P, Ca, Mg, Na, K	N, P, Ca, Mg, Na, K	
	Stem	Mg, K		—	N, P, Ca, Mg, Na, K	
	Root	K			—	
<i>P. dioscoridis</i>	Soil	—	N, P, Ca, Na, K	N, P, K	N, Mg, Na	
	Leaf	Mg	—	N, P, Mg, K	N, Na	
	Stem	Ca, Mg, Na	Ca	—	N, Ca	
	Root	P, Ca, K	P, Ca, Mg, K	P, Mg, Na, K	—	
<i>P. oleracea</i>	Soil	—	N, P, Ca, Mg, Na	N, P, Ca, Mg, Na	N, P, Ca, Na	
	Leaf	K	—	N, P, Ca, Mg, Na, K	N, P, Ca, Na, K	
	Stem	K		—	N, P, Ca, Na, K	
	Root	Mg, K	Mg	Mg	—	
<i>R. dentatus</i>	Soil	—	Ca, Mg, Na, K	N, Ca, Mg, Na	N, P, Ca	
	Leaf	N, P, Ca	—	P, Ca, Mg, Na	Ca	
	Stem	P	N	—	N, Ca	
	Root	Mg, Na, K	N, P, Mg, Na, K	P, Mg, Na	—	
<i>S. nigrum</i>	Soil	—	N, P, Mg, Na	N, P, Mg, Na, K	N, P, Mg, Na, K	
	Leaf	Ca, K	—	N, P, Ca, Mg, Na	N, P, Ca, Mg, Na, K	
	Stem	Ca		—	N, P, Ca, Mg, Na, K	
	Root	Ca			—	
<i>L. esculentum</i>		Soil	Fruit	Leaf	Stem	Root
	Soil	—	N, Ca, Na, K	N, Na	N, Mg, Na	N, Ca, Na, K
	Fruit	P, Mg	—	N, P, Na	N, P, Na	N, P, Ca, Mg, Na
	Leaf	P, Ca, K	Ca, K	—	N, P, Ca, Na, K	N, P, Na
	Stem	P, Ca, Mg	Ca, Mg, K		—	N, P, Na, K
Root	P		Ca	Ca, Mg	—	

FIELD TRIAL OF LIQUID PHEROMONE CAPSULE (GALLOPRO PINOWIT®) AGAINST BARK BEETLES IN İSTANBUL (TURKEY) FORESTS

HAKYEMEZ, A. * – CEBECİ, H. H.

Faculty of Forestry, Istanbul University-Cerrahpasa, Istanbul, Turkey

**Corresponding author
e-mail: hakyemez@istanbul.edu.tr*

(Received 21st Oct 2019; accepted 30th Jan 2020)

Abstract. This study has been done in the pine forests, located in Çamlık within Çatalca Forest Management's (Istanbul-Turkey) Silivri Forestry Department, in 2018. The purpose of the study was to investigate biological efficacy of GALLOPRO PINOWIT® commercial pheromone product against *Monochamus galloprovincialis* (Olivier), *Ips sexdentatus* (Boerner), *Orthotomicus erosus* (Wollaston) and *Hylurgus ligniperda* (Fabricius) insect pests on the field. In the study, Scandinavian three funnel traps were used and SMC-ORTIR, TRIPHERON-IPSEX and TRIPHERON-ORTERO pheromone preparations were used as comparison products. For the evaluation of collected insects count data, two-way ANOVA analysis has been used, variance between preparations-insect counts have been investigated using t test and activity of each preparation has been designated as %. According to the results obtained, it can be concluded that Gallopro Pinowit® preparation can be effectively used against pest insects *Ips sexdentatus*, *Orthotomicus erosus*, *Tomicus sp.* and *Monochamus galloprovincialis* which cause serious damage to coniferous trees.

Keywords: *pheromone, Scolytidae, pine forests, Çamlık, Silivri, biotechnical, Scandinavian type three-funnel trap*

Introduction

Insect pests are undoubtedly an important factor threatening sustainability of forests and forestry products. According to FAO's 2010 data, almost 35 million ha of forest area is being devastated by forest pests every year (Yalçın et al., 2016).

Bark beetles (*Scolytidae*) have an important place among forest pests. Many researchers, local and foreign (Defne, 1954; Can, 1964; Ekici, 1971; Sekendiz, 1974; Hakyemez et al., 2013; Serez, 1986, 1987; Öymen, 1989; Pfeffer, 1995; Selmi, 1998; Oğurlu, 2000; Faccoli, 2004; Kanat and Laz, 2005; Sarıkaya, 2008; Wong et al., 2017) carried out studies on bark beetles and provided information regarding status of bark beetles in Turkey's forests. During some years, those insects can even cause great economic loss by reproducing in mass under appropriate conditions.

Pheromones are a biotechnical method which is used effectively against bark beetles damaging and causing great losses in forests. Pheromone is a sort of odor, released by both male and female insects to find their mates. Each species has a pheromone to communicate with each other (Galko et al., 2016; Straw et al., 2013). The case of monogamous insects, females, and in polygamous insects, both sexes release these pheromones. The pheromone which is used to communicate among the same species is called "Allomone" while pheromone released by different species is called "Kairomone" (Serez, 1987).

In other terms, pheromones are released by an individual insect and have an effect on behavior of the same species (Coulson and Witter, 1984).

Pheromones are species-specific. This property brought forward the idea of collecting insects in mass and then exterminate them. They can be synthetically produced and can be used to capture insect pests with special traps (Baker, 2008).

Pheromones do not have any negative impact on beneficial life forms, such as parasites and predators, honey bees, vertebrates and humans. For that reason, its area of usage is expanding every year. Primary reason of emergence of pheromone traps is their ability neutralize pests without disturbing the natural equilibrium with ease (Küçükosmanoğlu and Arslangündoğdu, 2002).

Use of pheromones play an important role in controlling bark beetle population in recent years. Consequently, it is imperative to investigate efficacies of pheromones manufactured by various companies and that consumers then use those successful products in controlling insects.

In forests (Turkey), pheromone traps started to be used in 1982 and their usage increased exponentially since then. Considerable results have been obtained against bark beetles with this method (Serez, 1987).

Applications of this method are constantly increasing in the recent years. It has been stated that in the 40,000 pheromone traps set up by Ministry of Forestry of Turkey, an average of 100 million pest insects are captured every year. Those captured insects are both exterminated and used as feed for the predator insects grown specifically for biological combat (Yalçın et al., 2016).

Hundreds of pheromones have been discovered that are used to monitor the presence and abundance of insects and to protect plants and animals against insects. Pheromones are increasingly efficient at low population densities, they do not adversely affect natural enemies, and they can, therefore, bring about a long term reduction in insect populations that cannot be accomplished with conventional insecticides (Witzgall et al., 2010).

Insecticides do not achieve a long-term pest population decrease. In contrast, an observation shared by many working with pheromone-based control is that continuous long-term use does decrease population levels of target species (Ioriatti et al., 2008; Weddle et al., 2009).

This stud has been done to determine efficacy of Galopro Pinowit® pheromone which contains Ipsdienol (1.6%), Ipsenol (1.9%), Alphapinene (47.7%) and Ethanol (48.8%) and used against *Monochamus galloprovincialis*, *Ips sexdentatus*, *Orthotomicus erosus* and *Hylurgus ligniperda*, in the pests' target pine forest area between 04.05.2018 and 28.08.2018.

Galopro Pinowit is a newly produced pheromone. Therefore it has been the subject of our study.

Materials and methods

In order to determine the field for trials and evaluating presence of target pest population, appraisal tours have been done in the pine forest which is under Istanbul (Turkey) Regional Forestry Directorate's supervision, with the help and support of Department of Combatting Forests Pests. Previous years' reports have been considered and pine stands in Çamlık, Çatalca Forestry Department – Silivri Forest Department have been selected as the trial area (*Fig. 1*).

There are 20-25 years old *Pinus maritima* (Maritime Pine), *P. nigra* (Black pine) and *P. pinea* (Stone pine) trees (*Fig. 2*). The elevation of the study area ranges from 117 to 176 m above sea level (a.s.l.). In this study, 24 funnel type traps (*Fig. 1*), L shaped

wooden stakes to fix on the ground and pheromone preparations (GALLOPRO-PINOWIT, SMC-ORTIR, TRIPHERON-IPSEX, TRIPHERON-ORTERO) have been used (Table 1). Funnel type trap is preferred for most often used in Turkey (Fig. 3).

The location coordinates of the traps has been included in Table 1 data.

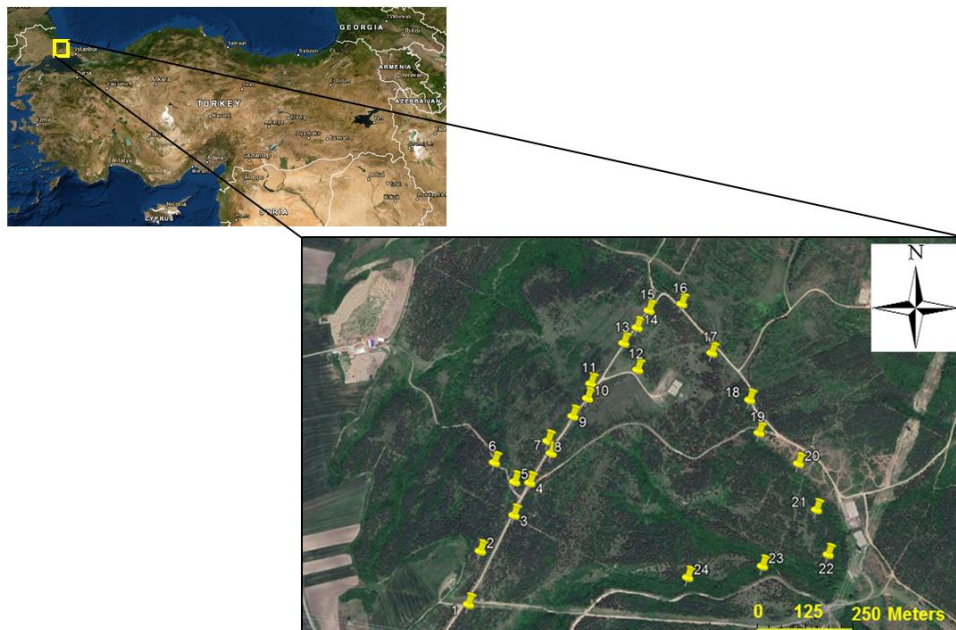


Figure 1. The locations where Funnel type traps were established



Figure 2. The view from the working area

GalloPro Pinowit® (Liquid)

Content:	Ipsdienol (1.6%), Ipsenol (1.9%), Alphapinene (47.7%) ve Ethanol (48.8%)
Production:	June -2017
Code:	86-292
Manufacturer:	Witasek PflanzenSchutz GmbH, Mozartsraße 1a, 9560 Feldkirchen, Austria

SMC ORTIR® (Liquid)

Content:	Ipsdienol (25 mg), 2-methyl-3-buten-2-ol (1500 mg), Cis-Verbenol (80 mg)
Registration:	5525/18.05.2006
Production:	Jan-2018
Lot No:	115-50-1
Manufacturer:	ChemTica Internacional S.A., P.O. Box 40301, Santo Domingo, Costa Rica

Tripheron IPSSEX® (Granule)

Content:	Ipsdienol (105 mg)
Registration:	1/14.12.2001
Production:	Feb-2018
Lot No:	540-621-1
Manufacturer:	Trifolio-M GmbH, Dr Hans Wilhelmi-Weg 1, 35633 Lahnau, Germany

Tripheron ORTERO® (Granule)

Content:	Ipsdienol (30 mg), Methyl-butanol (1500 mg), Cis-Verbenol (100 mg)
Registration:	3/14.12.2001
Production:	Feb-2018
Lot No:	540-624-1
Manufacturer:	Trifolio-M GmbH, Dr Hans Wilhelmi-Weg 1, 35633 Lahnau, Germany



Figure 3. Funnel type trap

One week after the traps were placed, captured insects were gathered from each trap, placed inside jars and brought to the lab and counted on petri dishes. For the evaluation of collected insects count data, two-way ANOVA analysis has been used, variance

between preparations-insect counts have been investigated using t test and activity of each preparation has been designated as %. Trial area's dense population of target insects (*I. sexdentatus*, *O. erosus*, *T. destruens*, *T. minor*, *T. piniperda*, *M. galloprovincialis*) and collected insect amounts were noted. Total number of *Tomicus* species has been included to the table data.

The months in the study were not considered as a factor. Because the working time does not include all months.

Table 1. Trap locations and their contents

Trap #	Preparation	Coordinates		Elevation
		N	E	M
1	Gallopro Pinowit	41°09'18"	28°03'00"	176
2	SMC ORTIR	41°09'28"	28°03'05"	176
3	Tripheron IPSSEX	41°09'27"	28°03'06"	176
4	Tripheron ORTERO	41°09'30"	28°03'08"	167
5	Gallopro Pinowit	41°09'30"	28°03'06"	176
6	Tripheron IPSSEX	41°09'32"	28°03'03"	159
7	Gallopro Pinowit	41°09'33"	28°03'11"	167
8	SMC ORTIR	41°09'33"	28°03'11"	167
9	Tripheron IPSSEX	41°09'37"	28°03'14"	167
10	Tripheron ORTERO	41°09'39"	28°03'16"	167
11	Gallopro Pinowit	41°09'42"	28°03'20"	176
12	Tripheron IPSSEX	41°09'42"	28°03'23"	176
13	SMC ORTIR	41°09'45"	28°03'21"	167
14	Gallopro Pinowit	41°09'46"	28°03'23"	167
15	Tripheron IPSSEX	41°09'46"	28°03'23"	167
16	Tripheron ORTERO	41°09'48"	28°03'30"	167
17	Gallopro Pinowit	41°09'45"	28°03'34"	159
18	Tripheron IPSSEX	41°09'42"	28°03'38"	159
19	Gallopro Pinowit	41°09'39"	28°03'40"	150
20	SMC ORTIR	41°09'39"	28°03'40"	150
21	Gallopro Pinowit	41°09'35"	28°03'43"	142
22	Tripheron IPSSEX	41°09'33"	28°03'48"	134
23	Tripheron ORTERO	41°09'29"	28°03'53"	117
24	Tripheron IPSSEX	41°09'25"	28°03'55"	117

During trials, except Gallopro Pinowit, all other preparations have been renewed on 29.06.2018. According to instruction guidelines, Gallopro Pinowit keeps its activity for 18-20 weeks, therefore during trials we have also tested its durability in field.

Results and discussion

Identified species on pheromone traps in the trial area were mostly; *Ips sexdentatus*, *Orthotomicus erosus*, *Tomicus destruens*, *Tomicus minor*, *Tomicus piniperda* and *Monochamus galloprovincialis*. Apart from those, many Coleoptera species (pest or predators) were found in the pheromone traps.

Galopro Pinowit® had the most captures. Additionally, during rainy days while other pheromone preparations had their performances decreased, however, Galopro Pinowit® preparation continued to work without being affected.

Counts during field application of pheromone preparations, statistical processes and evaluations after that has been shown in detail in *Tables 2, 3 and 4*.

No phyto-toxicological effects have been detected on trees of the site during field trials.

When preparations were compared, Galopro Pinowit's attractivity was found to be: *I. sexdentatus* 20.27%, *O. erosus* 2.52%, *Tomicus sp.* 88% and *M. galloprovincialis* 80%. SMC ORTIR's attractivity for the same species, respectively 21.43%, 56.34%, 3.77% and 10.31%; Tripheron IPSSEX's attractivity, respectively 39.87%, 4.74%, 4.55% and 7.85%; Tripheron ORTERO's attractivity, respectively 18.43%, 36.40%, 3.68% and 1.84%. The results indicate, unlike other dispensers which have been renewed (29.06.2018), Galopro Pinowit's performance still exhibited sufficient insect attractivity throughout trial period (which can also be seen from the ratios) as indicated on the usage instructions.

This assessment also conforms with the results of variance analysis and from dispensers' attractivity and count of insect species aspect, there is an important difference of $p = 0.001$ between. With regards to attracting pest insects, preparations had no difference of $p = 0.05$ meaning all dispensers have attracted more or less respectively.

Table 2. Captured insects throughout the trials

		Preparations				Totals
		Galopro Pinowit	SMC ORTIR	Tripheron IPSSEX	Tripheron ORTERO	
<i>Ips sexdentatus</i>	May	37	14	270	59	380
	June	174	145	85	109	513
	July	25	85	123	48	281
	August	7	13	0	5	25
<i>Orthotomicus erosus</i>	May	233	5091	423	3499	9246
	June	87	2043	176	981	3287
	July	23	380	67	506	976
	August	12	416	1	135	564
<i>Tomicus sp.</i>	May	1271	40	108	81	1500
	June	1180	60	47	43	1330
	July	311	29	32	20	392
	August	850	26	0	7	883
<i>Monoctonus galloprovincialis</i>	May	124	3	18	6	151
	June	426	76	4	5	511
	July	79	5	42	4	130
	August	23	0	0	0	23
Totals		4862	8426	1396	5508	20192

Table 3. Comparison results of insect species and dispensers with two-way ANOVA analysis

Source of variance (source)	Degree of freedom (df)	Sum of squares (SS)	Mean squares (MS)	F	P
Preparation	3	1561936.5	520645.5	1.55	P > 0.05
Insect	3	7191860.3	2397287.0	7.14	P < 0.002
Pheromone x insect	9	17158127.8	1906459.0	5.67	P < 0.001
Error	48	16126461.0	335967.9		
Total	63	42038386.0			

Table 4. In and in-between dispensers trap capture ratios (%) during trial period

		Gallopro Pinowit	SMC ORTIR	Triperon IPSSEX	Triperon ORTERO
<i>Ips sexdentatus</i>	In-between dispensers	20.27	21.43	39.87	18.43
	In dispensers	5	3.05	34.24	4.01
<i>Orthotomicus erosus</i>	In-between dispensers	2.52	56.34	4.74	36.4
	In dispensers	7.3	94.11	47.78	92.98
<i>Tomicus sp.</i>	In-between dispensers	88	3.77	4.55	3.68
	In dispensers	74.29	1.84	13.4	2.74
<i>Monochamus galloprovincialis</i>	In-between dispensers	80	10.31	7.85	1.84
	In dispensers	13.41	1	4.58	0.27

Conclusions

As a result, field trial and counts clearly show that pheromone preparation, commercially known as, Gallopro Pinowit® can be effectively used against *Ips sexdentatus*, *Orthotomicus erosus*, *Tomicus sp.* and *Monochamus galloprovincialis*, important pests of coniferous trees.

Pheromones are indeed elegant and safe tools for insect control. The fascination of being able to control insect populations through species-specific manipulation of sexual communication, without adversely affecting other, beneficial organisms, has been a driving force for research on insect pheromones during four decades.

The importance of pheromone-based methods is accentuated in view of increasing problems associated with the use of conventional insecticides. However, for a more widespread use of pheromones, application techniques must become more reliable and more economic. The key to further development is closer communication and

collaboration between academic research institutions, plant protection industry and extension services (Witzgall, 2001).

Use of pheromones for controlling pest population has significant advantages over chemical treatments to humans, to environment and to other life forms by not harming those. For that reason, beside taking preventive measures, greater success will be achieved when field-tested and proven biologically efficient pheromone preparations are used in controlling bark beetle population.

Acknowledgements. We would like to kindly thank to Ömer ÜLKÜ and Cengiz ÜLKÜ (Verim İnşaat ve Turizm Ltd. Company) who requested biological efficacy study of Galopro Pinowit® and provided their help in both logistics and preparing this research paper, to Mr. Ahmet Yasin ÇELEN (Pest Control Department Manager - Istanbul District Directorate of Forestry) and finally to Mrs. Gaye ERCAN (Head of Silivri Forestry Department) for providing their valuable contributions in the field studies.

REFERENCES

- [1] Baker, T. C. (2008): Use of Pheromones in IPM. – In: Radeliffe T., Hutchinson, B. (eds.) Integrated Pest Management. Cambridge University Press, Cambridge, pp. 273-285.
- [2] Can, E. (1964): Zur Kenntnis des *Orthotomicus tridentatus* Egg. (Zedern-borkenkäfer) einem Schädling der Zedern Wälder der Türkei. – Anzeiger für Schädlingskunde 37: 113-117.
- [3] Coulson, R. N., Witter, J. A. (1984): Forest Entomology. – John Wiley and Sons, NewYork.
- [4] Defne, M. (1954): *Ips sexdentatus* Boerner Kabuk böceğinin Çorum Ormanlarındaki Durumu ve Tevhit ettiği zararlar. – İstanbul Üniversitesi Orman Fakültesi Dergisi 4(2): 80-91 (in Turkish).
- [5] Ekici, M. (1971): Sedir (*Cedrus libani*) Zararlı Böceklerinin Biyolojisi ve Mücadelesi Ormancılık Araştırma Enstitüsü Yayınları. – Teknik bülten, Seri No: 45-56 (in Turkish).
- [6] Faccoli, M. (2004): Morphological illustrated key to European species of the genus *Ips* Degeer (Coleoptera, Scolytidae). – The Coleopterist 13(3): 103-119.
- [7] Galko, J., Nikolov, C., Kunca, A., Vakula, J. (2016): Effectiveness of pheromone traps for the European spruce bark beetle: a comparative study of four commercial products and two new models. – Forestry Journal 62: 207-215.
- [8] Hakyemez, A., Köse, M., Özcan, Y., Eker, N., Kaynar, D. (2013): Pheromone Trials Against *Orthotomicus erosus* (Woll.) in Istanbul Princess Islands, Turkey. – Journal of Animal and Veterinary Advances 2013: 1367-1371.
- [9] Ioriatti, C., Lucchi, A., Bagnoli, B. (2008): Grape Areawide Pest Management in Italy. – In: Cuperus, G. W., Koul, O. (eds.) Areawide Pest Management: Theory and Implementation CAB International, Wallingford, UK, , pp. 208-225.
- [10] Kanat, M., Laz, B. (2005): Kahramanmaraş Göknar Ormanlarında *Pityokteines curvidens* (Germ.) in Feromon Tuzaklarına Yakalanma Sonuçları. – KSÜ, Fen ve Mühendislik Dergisi Kahramanmaraş 8(2): 62-69. (in Turkish).
- [11] Küçükosmanoğlu, A., Arslangündoğdu, Z. (2002): İzmir Orman Bölge Müdürlüğü'nde Çam kese böceğine karşı feromon denemeleri. – Ülkemiz Ormanlarında Çam kese böceği Sorunu ve Önerileri Sempozyumu, 24-25 Nisan 2002, Kahramanmaraş (in Turkish).
- [12] Oğurlu, İ. (2000): Biyolojik Mücadele. – Süleyman Demirel Üniversitesi Yayın No: 8, Orman Fakültesi Yayın No:1. Isparta (in Turkish).
- [13] Öymen, T. (1989): Kabuk böceklerine karşı Alınabilecek Koruyucu Önlemler ve Savaş. – İstanbul Üniversitesi, Orman Fakültesi Dergisi, Seri B 39(2): 117-123 (in Turkish).
- [14] Pfeffer, A. (1995): Zentral and Westpalaarktische Borken und Kernkäfer. – Naturhistorisches Museum, Basel.

- [15] Sarıkaya, O. (2008): Batı Akdeniz Bölgesi İğne Yapraklı Ormanlarının Scolytidae (Coleoptera) faunası. – Doktora tezi, Orman Genel Müdürlüğü Yayını 111 + 225 (in Turkish).
- [16] Sekendiz, O. (1974): *Orthotomicus erosus* Wollaston (Coleoptera, Scolytidae)'nın Yayılışı ve Zararları Üzerinde Gözlemler. – İstanbul Üniversitesi Orman Fakültesi Dergisi, Seri A 24(2): 209-217 (in Turkish).
- [17] Selmi, E. (1989): Türkiye Kabuk Böcekleri ve Savaşı. – İstanbul Üniversitesi Yayın No: 4042, Fen Bilimleri Enstitüsü Yayın No: 11. İstanbul (in Turkish).
- [18] Serez, M. (1986): Kabuk böceklerine Karşı Feromon Tuzaklarıyla Orman Koruması. – Orman Böcek ve Hastalıkları ile Mücadele Semineri, 12-16 Nisan 1986, İzmir (in Turkish).
- [19] Serez, M. (1987): Bazı Önemli Kabuk Böcekleriyle Savaşta Feromonların Kullanılma Olanakları. – Karadeniz Teknik Üniversitesi, Orman Fakültesi Dergisi 1(1-2): 99-131 (in Turkish).
- [20] Straw, N., Williams, D., Tilbury, C. (2013): Monitoring the Oak Processionary Moth with Pheromone Traps. – Forest Commission Practice Note. FCPN020.HMSO, UK.
- [21] Weddle, P. W., Welter, S. C., Thomson, D. (2009): History of IPM in California pears-50 years of pesticide use and the transition to biologically intensive IPM. – Pest Manag. Sci. 65: 1287-1292.
- [22] Witzgall, P. (2001): Pheromones - future techniques for insect control? – Pheromones for Insect Control in Orchards and Vineyards. IOBC wprs Bulletin 24(2): 114-122.
- [23] Witzgall, P., Kirsch, P., Cork, A. (2010): Sex Pheromones and Their Impact on Pest Management. – Journal of Chemical Ecology 36(1): 80-100.
- [24] Wong, J. C. H., Meier, L. R., Zou, Y., Mongold-Diers, J. A., Hanks, L. M. (2017): Evaluation of methods used in testing attraction of cerambycid beetles to pheromone-baited traps. – J Econ Entomol 110: 2269-2274.
- [25] Yalçın, M., Yüksel, B., Akçay, Ç., Çil, M. (2016): Zararlı Böceklerin Toplanmasında Kullanılacak Entegre Feromon Tuzak Sistemi. – KSÜ. Doğa Bil. Derg. 19(4): 355-361. Kahramanmaraş (in Turkish).

GENERATION OF LAND QUALITY INDEX FOR AGRICULTURAL USAGE AT GÜVENÇ BASIN, TURKEY

DEDEOĞLU, M.

*Selçuk University, Agriculture Faculty, Department of Soil Science and Plant Nutrition
42100 Konya, Turkey
e-mail: mertdedeoglu@gmail.com; phone: +90-530-416-0006*

(Received 26th Oct 2019; accepted 30th Jan 2020)

Abstract. The aim of this study is to develop the land quality index (LQI) based on expert opinion and multi-criteria decision support approaches for agricultural lands. The study was conducted on 8 soil series and 20 land units belonging to the lands of Ankara-Güvenç Basin, Turkey which covers about 17.5 km², representing the ecological conditions of a semi-arid climate. In this research, 9 main indicators were chosen including depth, slope, stoniness, bulk density (BD), texture, electrical conductivity (EC), pH, organic matter (OM) and CaCO₃. Analytical Hierarchical Process (AHP) method was used a pairwise comparison of indicators. As a result of the LQI assessment, while 17.14% of the lands were classified as “High” and 37.41% Moderate, the agricultural quality class of 41.55% of the studies land was determined as “Low” and “Very Low” and mapped in GIS. In this study, it was determined that the final index value of the land was affected by depth (24.2%), slope (21.1%) and bulk density (16.6%) indicators with high weight coefficients. In addition, the values of the LQI were compared with Normalized Difference Vegetation Index (NDVI) values for testing and it has been determined that land quality assessment for agricultural usage has been performed with high accuracy for NDVI ($r^2 = 0.74\%$). Finally, the results of the study showed that the LQI was achieved for micro basin scale under semi-arid climate conditions.

Keywords: *analytic hierarchy process, GIS, land indicators, NDVI, semi-arid climate*

Introduction

Sustainable agricultural production is most important target of agricultural policies of developed or developing countries (Kumar and Jhariya, 2015). In the line with this target, these policies aim to balance the soil with the requests of the product to be grown and to ensure the long-term efficiency by optimizing the resource utilization (Joshua et al., 2013). To achieve these aim and objectives, the determination of land quality in the planning of sustainable agricultural practices has been one of the important ecological approaches in the World (Xue et al., 2019). Land quality is defined as the capacity of the functions resulting from the nature of the soil within a certain ecosystem and depending on its use under a certain management (Karlen et al., 2013). The determination of this capacity requires a multi-decision approach that requires the standardization and weighting of the effects of many factors that affect each other, such as physical, chemical, morphological, topographic and climatic soil characteristics, which are interrelated and differentiated (Mokarram and Mirsoleimani, 2018). Many methods have been developed for land quality assessment, from qualitative or semiquantitative visual approaches (Shepherd, 2009) to quantitative methods based on laboratory analysis and calculating land quality index using mathematic and statistical methods (Karlen et al., 1998; Imaz et al., 2010; Askari and Holden, 2014). The indexing methods are most commonly used (Rahmanipour et al., 2014), usually integrating several indicators associated with soil functions appropriate to the intended use into a quantitative factor that can be used for multi-criteria decision making (Karlen et al., 1998). Thus, AHP (Saaty, 1980), which is the Multiple Criteria Decision Analysis, is preferred in the evaluation of multiple -

heterogeneous factors (Ceballos and Lopez, 2003; Malczewski, 2006; Dengiz and Sarıoğlu, 2013; Akıncı et al., 2013; Askari and Holden, 2014; Xue et al., 2019; Özkan et al., 2019). AHP is a decision-supported method that divides complex multiple-factor problems into a hierarchical structure (Yang et al., 2008). At the same time, integration of analytical models with geographic information system (GIS) is reliably used by researchers in the production and interpretation of LQI maps (Malczewski, 2006; Yalew et al., 2016). The LQI is commonly developed using a four-step process: indicator selection, indicator standardization and scoring to sub criteria, weighting of indicators according to importance level, and calculation of scores into a model (Andrews et al., 2004; Askari and Holden, 2014; Xue et al., 2019). But there is no comprehensive LQI that can be used as a universal method across regions and scales (Zhang et al., 2004), and many LQI have been developed for specific purposes and index are usually valid under particular environmental conditions (Imaz et al., 2010; Askari and Holden, 2014). Thus, it can be unexpected that there is index that can determine the land and soil characteristics for all geographies, type of usage and plant species for land quality (Bydekerke et al., 1998; Store and Kangas, 2001). At the same time, it is not practically possible to develop a model that can represent all ecological variables and sociocultural habits, but in theory it is not economic in terms of time, labor and cost (Doran and Parkin, 1996). Therefore, similar studies should be conducted to determine the quality of agricultural lands under different management systems in Turkey (Dengiz et al., 2014). In this study, it was aimed to develop an agricultural land quality index which is genuine to the semi-arid terrestrial climate ecology of Central Anatolia and applicable in the similar geographies by using the expert opinion and AHP approaches. In addition to that, the land of the region was mapped in GIS environment by scoring quality of the basin lands. At the same time, the success of the developed index was tested by comparing the plant density values derived from Sentinel 2A satellite image. Finally, the quality map was produced in GIS environment to decision makers and agricultural policy producers to be a base for land management planning.

Materials and Methods

Field description and study

Güvenç Basin is located between 40° 08' 39" - 40° 06' 13" North latitudes, 32° 44' 39" - 32° 47' 59" East longitudes in the Ankara province of Central Anatolian, Turkey (Fig. 1). The total area of the basin is 17.5 km² and its altitude above sea level between 1040 m and 1440 m. The distribution of land use types for the basin consist 45% of wheat, 35% of pasture, 11.2% of heath and garden, 8.2% of no tillage and rocky, 0.6% of pond (Turan and Dengiz, 2015).

In the study, phase separations (depth, texture, slope, stoniness) and spatial distributions of the soil series mentioned in the detailed survey report and map of the basin were used (Dengiz and Baskan, 2005). Thus, land quality assessments were made at the level of mapping unit. The soils of study area were classified into 8 different series, Typic Xerofluvent, Mollic Xerofluvent and Aquic Xerofluvent in 20 mapping units (land units) and Lithic Xerorhent in subgroups according to soil taxonomy (Table 1) (Soil Survey Staff, 1999). In order to determine soil properties affecting land quality, eight disturbed and undisturbed soil samples which are representing the predefined soil series were taken from topsoil between 0-30 cm depth in year of 2018 according to Soil Science Division Staff (2017). Basin soils reflect the typical soil characteristics in different slope

groups formed from alluvial deposits of physiographic units and high calcareous, low-moderate organic matter content, high pH, stoniness and different depth classes developed under semi-arid climate conditions of Central Anatolia region. This situation indicates the presence of land in the basin which will represent different quality classes.

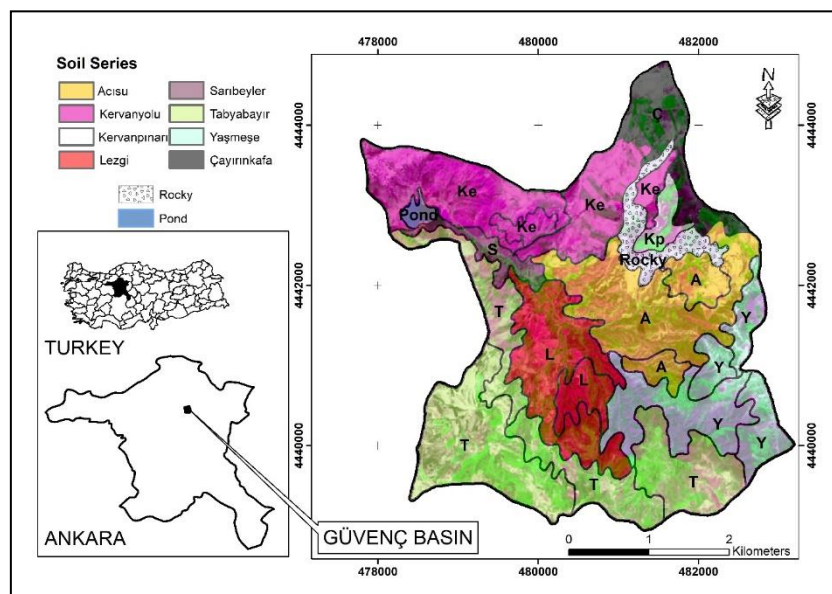


Figure 1. Soil series and location map of the study area

Table 1. Distribution of soil series in the basin according to Soil Taxonomy

	Soil Series	Subgroups	Area (ha)	Proportion (%)
GÜVENÇ BASIN	Acısu	Lithic Haploxerept	285.16	16.18
	Kervanyolu	Typic Xerorthent	312.23	5.58
	Kervanpınarı	Chromic Haploxerept	29.43	17.71
	Lezgi	Typic Haploxerept	218.02	1.67
	Sarıbeyler	Typic Xerofluvent	37.36	12.37
	Tabyabayır	Lithic Xerorthent	479.97	0.67
	Yaşmeşe	Typic Xerorthent	233.73	3.23
	Çayırınkafa	Vertic Haploxerept	98.33	2.12
	Rocky	-	56.96	27.23
	Pond	-	11.74	13.24
	Total	-	1762.92	100

Climate characteristics

Based on the climate values of the region for many years; it represents semi-arid climate characteristics of hot and dry summers and cold and rainy winters. The average annual rainfall and average temperature in the region for the last 20 years is 478.1 mm and 11.4°C, respectively. The hottest month is July with 24.0°C and the coldest month is January with an average of -3°C (Anonymous, 2017). According to soil climate regime of Newhall simulation model (Van Wambeke et al., 2000), the study area has Mesic soil temperature regime and Xeric (Dry Xeric in subgroup) moisture regime. Particularly, potential evapotranspiration is higher than precipitation between April and October. Soil needs irrigation particularly between May and July.

Indicator selection, sub-group scoring and weighting

Nine parameters affecting crop development in agricultural land quality index; depth, slope, stoniness, BD, texture, EC, pH, OM and CaCO₃ were selected as the evaluation parameters using many literature (Huddleston et al., 1987; McVay et al., 1989; Soil Survey Staff, 1999; Arshad and Martin, 2002; Hazelton and Murphy, 2007; De La Rosa and Van Diepen, 2009; Iojă et al., 2014; Mustafa et al., 2017; Aldababseh et al., 2018). In this study, land indicators were produced as digital layers in GIS environment from the study report and map of the regional soils. The values of other indicators were obtained from the results of laboratory analysis. The laboratory analyses conducted in the research are presented in *Table 2* and the descriptive statistics of the results are given in *Table 3*.

Table 2. Physicochemical analysis and methods performed in the study

Indicators	Units	Procedure	References
BD	g cm ⁻³	Undisturbed soil samples	Blake and Hartge, 1986
Depth	cm	Soil survey	Soil Science Division Staff, 2017
Slope	%	Soil survey	
Texture	%	Hydrometer method	Bouyoucos, 1951
OM	%	By Potassium dichromate (K ₂ Cr ₂ O ₇) Oxidation method (Walkley-Black)	Nelson and Sommers, 1982
pH	1:2.5	Soil-water suspension (w:v)	Soil Survey Staff, 2011
EC	dS m ⁻¹		
CaCO ₃	%	Scheibler calcimeter	

Table 3. Descriptive statistics of physical and chemical properties of soil series

Indicators	Min.	Max.	Mean	StDev.	SE Mean	Variance	CoefVar
BD, gr cm ⁻³	1.21	1.42	1.32	0.07	0.02	0.01	5.52
Sand, %	25.80	52.44	36.60	11.44	3.62	130.78	30.33
Silt, %	16.60	25.20	22.40	4.61	1.46	21.24	21.14
Clay, %	28.84	64.66	40.64	10.06	3.18	101.18	24.81
OM, %	0.82	3.64	2.11	0.82	0.26	0.68	38.10
pH, 1:2.5	7.00	7.85	7.60	0.21	0.07	0.04	2.74
EC, dS m ⁻¹	1.12	1.44	1.32	0.18	0.06	0.03	13.65
CaCO ₃ , %	5.20	32.29	14.12	8.00	2.53	63.95	57.21

The selection of indicators to determine the quality of the land is very important (Zhan et al., 2016). There are many characteristics that affect the quality of lands under different agricultural uses in varying amounts and it is not possible to use all of them (Karlen et al., 2013). In this regard, Doran and Parkin (1996), have suggested the use of as few parameters as possible in modeling approaches. Thus, it is known that there is a high correlation between some physical, chemical and biological properties, it is not practically possible to use all of them as indicators at the same time and it is stated that it is contrary to the basic principles of land evaluation measurement paradigm (Andrews et al., 2004). In another aspect, when numerous soil analysis is performed for model production, the application of the developed index becomes cumbersome (Askari and Holden, 2014). For this reason, the indicators used in the study were chosen according to an expert opinion and literature knowledge by taking into consideration the quality representation from one or more soil properties and their effectiveness is presented in *Table 4*, and sub-factor scoring of parameters is presented in *Table 5*. In addition, in the selection of land indicators, the phases specified in the detailed soil map and which are defined as limiting factor to plant growth were used.

Table 4. Selected parameters for land quality index and their effectiveness

Indicators	Effectiveness	Source
Depth	Root development, water storage capacity	Sarkar et al., 2014
Slope	runoff and losses	FAO, 1977
Stoniness	Crop emergence, soil tillage, water retention	Miller and Guthrie, 1984; Sauer et al., 2010
Texture	Infiltration rate, structure type, plant – water relationship	Ahmed et al., 2016
Bulk density	Soil compaction, aeration, infiltration	Şeker and Işıldar, 2000; Pagliai et al., 2004
EC	Osmotic potential, ion toxicity	Miransari and Smith, 2007
pH	Nutrient availability, microbial activities	Baridón and Casas, 2014
Organic Matter	Soil quality, biological activities	Riley et al., 2008; Guo et al., 2015; Kurzatkowski et al., 2004
CaCO ₃	Fixation of plant nutrients, aggregation	Erdal et al., 2000; Turgut et al., 2008

Table 5. The sub-score values of the parameters to be used in the land quality index determined using expert opinion and literature knowledge

Depth (cm)		Slope %		Stoniness %			
Sub-factor	Weight	Sub-factor	Weight	Sub-factor	Weight		
0-25	1	0-2	4	% 0-1	4		
25-50	2	2-6	3	% 2 – 5	3		
50-100	3	6-12	2	% 5 – 15	2		
100+	4	12-20	1	% 15 – 50	1		
Texture*			Bulk density g cm ⁻³				
Sub-factor		Weight	Sub-factor		Weight		
fS, LS, SL, cS and Si		1	< 1.50 - > 0.80		4		
			1.50 – 1.55		3		
			1.56 - 1.60		2		
			>1.60- < 0.80		1		
C->%45 -C, SC, SiC		2	< 1.25 - >0.80		4		
			1.25 -1.35		3		
C-<%45 - C, CL, SL, SC, SiCL		3	1.36-1.45		2		
			>1.45 - <0.80		1		
L, SiL and SCL		4	< 1.30 - > 0.80		4		
			1.30 – 1.35		3		
			1.36 – 1.50		2		
			> 1.50 - < 0.80		1		
pH		EC (dS m ⁻¹)		CaCO ₃ (%)		Organic matter %	
Sub-factor	Weight	Sub-factor	Weight	Sub-factor	Weight	Sub-factor	Weight
> 8.2 < 5.5	1	0-2	4	< 5	4	0-1	1
5.5 – 6.5	3	2-4	3	5-10	3	1-2	2
6.5-7.5	4	4-8	2	10-25	2	2-3	3
7.5-8.2	2	8-10	1	> 25	1	>3	4

*fS: Fine sand, LS: Loamy sand, SL: Sandy loam, S: Sand, C: Clay, Si: Silt, SiC: Silty clay, cS: Coarse sand, SC: Sandy clay, CL:Clay loam, SiCL: Silty clay loam, L: Loam, SiL: Silt loam, SCL: Sandy clay loam

In the study, score values between 1 and 4 were assigned for the parameters of each indicator. The criterion classes are given as 4 in case agricultural farming is allowed and take value of 1 if agricultural farming is not allowed. These two values were evaluated according to the limiting factor and degree. Analytical Hierarchical Process (AHP), which is a multi-criteria decision-making algorithm, was used in pairwise comparison of the indicators of the study (Saaty, 2008).

Calculation to land quality index values of mapping units

In order to determine the land quality scores of the study area, a parametric approach named Linear Combination Technique (LCT) was applied to 20 different mapping units prepared by ArcGIS 9.3 (ESRI, 2010), a geographic information system program. LCT is a practical and reliable mathematical equation used in several similar studies in the evaluation of sub-factor scores and weight ratios of the parameters together (Eastman and Jiang, 1996; Dengiz and Sarioğlu, 2013; Romano et al., 2015). The model for the LCT approach is presented in the following *Equation 1*.

$$LQI = \sum_{i=1}^n (W_i \cdot X_i) \quad (\text{Eq.1})$$

Here LQI, Land quality index; W_i , i weight value of parameters; X_i , sub-criteria score belonging to i parameters; n , the total number of parameters discussed. Land quality index class ranges calculated according to Jenks (1967), were determined using the basis of ArcGIS 9.3 software (*Table 6*). The index values calculated for all mapping units were categorized according to the ranges of natural diffraction from the histogram graph (Zhang et al., 2015). In this way, an index was developed according to the degree of effect of the region-specific parameters on the final score value.

Table 6. Agricultural land quality classes

Land Quality	Classes	Index Values
High	I	> 2.850
Moderate	II	2.554-2.849
Low	III	2.061-2.553
Very Low	IV	< 2.061

Land quality classes were categorized as a “High: I’ where there are no limiting factors for agricultural plant cultivation and development, “Moderate: II” where there are some slightly restrictive factors, “Low: III’ where there are factors affecting cultivation at a severe level and “Very Low: IV’ under conditions unfavorable for plant cultivation.

Determination of biomass density

Today remote sensing imaging is considered one of the main sources of information about the land vegetation (Campbell and Wynne, 2011; Singh et al., 2018). Vegetation index represent the most common remote sensing technique used for this purpose (Al-Doski et al., 2013; An, 2018), while NDVI is the most commonly used vegetation index (Tucker, 1979; DeFries et al., 1995; Garrigues et al., 2007; Tyagi and Bhosle, 2010; Olimb et al., 2018). For this purpose, Song et al. (2016), have stated that prediction coefficient with R^2 of 0.87 was found between NDVI values obtained from Landsat 8 OLI satellite images for winter wheat at different growth periods and the yield values in a farm-based study. NDVI is sensitive to active photosynthetic compounds and is, therefore, a popular method used to measure the biomass of vegetation or “greenness” in a defined area (Mezera et al., 2017). Thus, the fit between biomass of winter wheat from the field and the NDVI values obtained for the same locations were well and significantly ($P < 0.05$) correlated in the two regions, with coefficients of determination of 0.82 and

0.92 (Li et al., 2019). In this study, a multitemporal Sentinel–2A images in the year 2018, May were used to calculate NDVI values which were utilized for validation LQI classes with biomass density. NDVI values were calculated according to the *Equations 2*.

$$NDVI = (NIR - RED) / (NIR + RED) \quad (\text{Eq.2})$$

where,

NDVI= Normalized Difference Vegetation Index

NIR = Near infrared band

RED = Visible red band.

Sentinel–2A has (1) a temporal resolution lower than a week, (2) a spatial resolution of up to 10 m, and (3) narrow bands in the red and red-edge region, which makes it a highly reliable sensor for agricultural monitoring (Pasqualotto et al., 2019). The image was downloaded free of charge from the ESA server (<https://scihub.copernicus.eu/>) that provides Level–2A images that are geometrically and atmospherically corrected with top-of-canopy (TOC) reflectance as cloud-free (Pandžić et al., 2016). In addition, it was used Erdas Imagine 9 (ERDAS, 2009) to perform NDVI analysis, and ArcGis 9.3 (ESRI, 2010) software was used to store data and generate thematic maps.

Spatial statistical analysis and map production in GIS

The Spatial Analysis tool of the software ArcGIS version 9.3 (ESRI, 2010) was used to spatially compare the LQI classes and NDVI values of the land units. The LQI and mean NDVI values of the land units were extracted using the Zonal Statistics tool and imported into MS Excel. Thereafter, all the data were statistically compared and regression equations, graphs, and accuracy coefficients (r^2) were produced.

Results and Discussions

In the study, the weight values of 20 mapping units based on pairwise comparisons for selected indicators for the determination of agricultural land quality were presented in *Table 7*.

Consistency Ratio; CR = 0.09 (<0.10) was determined by pairwise comparisons and the method was found to be valid (Saaty, 2008). In the pairwise comparison of obtained indicators evaluated by AHP; (1) land conditions for plant cultivation, (2) the importance of indicators and parameters relative to each other, (3) the elimination of the restrictive effects of the parameters and (4) by considering the degree of change of the parameters in the regional soils, weight scores were determined. Thus, in the studies carried out at the regional scale, the weight value of the region-specific characteristics (such as pH and CaCO₃) is lower compared to other parameters, but high level scoring of non-economic (e.g. slope degree, effective soil depth) and continuous risk (stoniness) properties in the land improvement or modification is recommended (Patrono, 1998; Dengiz and Sarıoğlu, 2013; Ahmed et al., 2016). However, it is known that their presence in the environment is not necessary for crop production, but if it is found to influence soil quality (e.g. organic matter), it should also have a moderate weight ratio (Riley et al., 2008). Due to all these evaluations, as a result of the pairwise comparisons by taking into account the ecology of the region, the effect levels of the indicators considered in the agricultural land quality measurement of the basin soils were evaluated in 3 groups as high, moderate and low. The results of AHP applications indicated that depth (24.2%), slope (21.1%) and texture

(16.6%) indicators had a high-level weight coefficient. Although plants can grow in soils at different depths under favorable climatic conditions, usually optimum root development occurs in soils with high soil depth (Sarkar et al., 2014). It is can be explained by taking high weight coefficients of soil depth in the evaluation of land quality. In addition, the depth of the soil is very variable in the basin, which increases its impact on the assessment. Similarly, Slope degree is known to influence land quality for agricultural purpose and the assessment of land quality is important in determining soil-management practices (Paz-Kagan et al., 2016), and in recent studies, soil scientists have stated that the determination of land quality is particularly important to identify low-quality soils caused by high slopes (Vinhai-Freitas et al., 2017; Nabiollahi et al., 2018). Soil texture is another important factor used in the assessment of land quality (Aderonke and Gbadegesin, 2013), influencing the behavior of plant growth with infiltration rate, structure type and soil-water movement (Ahmed et al., 2016; Ennaji et al., 2018). In the light of past research, the effect levels of these indicators have high coefficients in the evaluation of the land quality in terms of plant cultivation.

Table 7. Pairwise comparison matrix and eigenvector of indicators in AHP

Pairwise Comparison Matrix									
Indicators	Depth	Slope	EC	Stoniness	Texture	OM	pH	CaCO ₃	BD
Depth	1.00	2.00	3.00	3.00	3.00	3.00	5.00	5.00	3.00
Slope	0.50	1.00	3.00	3.00	3.00	3.00	5.00	7.00	3.00
EC	0.33	0.33	1.00	0.33	0.33	3.00	2.00	2.00	0.33
Stoniness	0.33	0.33	3.00	1.00	0.33	3.00	3.00	3.00	2.00
Texture	0.33	0.33	3.00	3.00	1.00	5.00	3.00	5.00	4.00
OM	0.33	0.33	0.33	0.33	0.20	1.00	2.00	2.00	0.33
pH	0.20	0.20	0.50	0.33	0.33	0.50	1.00	3.00	1.00
CaCO ₃	0.20	0.14	0.50	0.33	0.20	0.50	0.33	1.00	0.33
BD	0.33	0.33	3.00	0.50	0.25	3.00	1.00	3.00	1.00
Total	1.00	2.00	3.00	3.00	3.00	3.00	5.00	5.00	3.00
Normalized Pairwise Comparison Matrix									
Indicators	Depth	Slope	EC	Stoniness	Texture	OM	pH	CaCO ₃	BD
Depth	0.28	0.40	0.17	0.25	0.35	0.14	0.22	0.16	0.20
Slope	0.14	0.20	0.17	0.25	0.35	0.14	0.22	0.23	0.20
EC	0.09	0.07	0.06	0.03	0.04	0.14	0.09	0.06	0.02
Stoniness	0.09	0.07	0.17	0.08	0.04	0.14	0.13	0.10	0.13
Texture	0.09	0.07	0.17	0.25	0.12	0.23	0.13	0.16	0.27
OM	0.09	0.07	0.02	0.03	0.02	0.05	0.09	0.06	0.02
pH	0.06	0.04	0.03	0.03	0.04	0.02	0.04	0.10	0.07
CaCO ₃	0.06	0.03	0.03	0.03	0.02	0.02	0.01	0.03	0.02
BD	0.09	0.07	0.17	0.04	0.03	0.14	0.04	0.10	0.07
Eigenvector									
Indicators	Normalized Sum of Rows		Normalized Average Rows		Eigenvector				
Depth	2.17		2.17/9		0.242				
Slope	1.90		1.90/9		0.211				
EC	0.60		0.60/9		0.066				
Stoniness	0.96		0.96/9		0.106				
Texture	1.49		1.49/9		0.166				
OM	0.45		0.45/9		0.050				
pH	0.42		0.42/9		0.047				
CaCO ₃	0.26		0.26/9		0.029				
BD	0.75		0.75/9		0.083				
$\lambda_{\max}=10.05$; $CI = 0.131$; $CR = 0.090$									

On the other hand, stoniness (10.6%), bulk density (8.3%), EC and organic matter (5%) had moderate level of weight values. This is also a finding of the fact that the rehabilitated land conditions and the physical properties that can be improved by organic matter increasing applications can positively change the land quality index class. Thus, it has been stated that the mechanization is facilitated by the removal of the stoniness problem and increased values of crop emergence and yield in the agricultural lands were indicated (Miller and Guthrie, 1984; Sauer et al., 2010). Similarly, the positive effects of organic matter on water retention, soil compaction, aeration and biological activity reduce the restrictive effect of bulk density and improve land quality (Kurzatkowski, 2004; Guo et al., 2015). In addition, salinity problems were not determined according to EC values. However, intensive fertilizer and irrigation practices based on agricultural activities in the study area, the evaluation of salinity potential as potential risk is required (Miransari and Smith, 2007). This was reflected in the indicator's weight values and the effect of reducing the quality classes was modeled in case of a dramatic increase in EC values. With the application of AHP, pH (4.7%) and CaCO_3 (2.9%) indicators established a function with low weight scores. Both factors indicate changes in the calcareous- high calcareous and slightly alkaline classes in the value ranges specific to the terrestrial climatic conditions of Central Anatolia. Although these indicators have high impacts on product-based land assessment studies (Andrews et al., 2004), due to the characteristic features in the determination of land quality at the regional scale, it has functioned at low impact levels. Thus, pH directly or indirectly affects many physical, chemical and biological events occurring in the soil (Baridón and Casas, 2014), it is known that phosphorus and trace elements decrease their movement ability in the soil at high pH values and plant uptake of toxic elements increases in acid reaction soils (Leonard et al., 1976). Similarly, it is stated that CaCO_3 content is a factor that should be prevented especially in the applications such as phosphorus fertilization (Erdal et al., 2000). Therefore, it is required to functionalize pH and CaCO_3 indicators in LQI for being taken into consideration in managerial planning. The LQI map generated for the Güvenç basin is presented in *Fig. 2* and the LQI classes and their spatial distributions of each mapping unit are presented in *Table 8*.

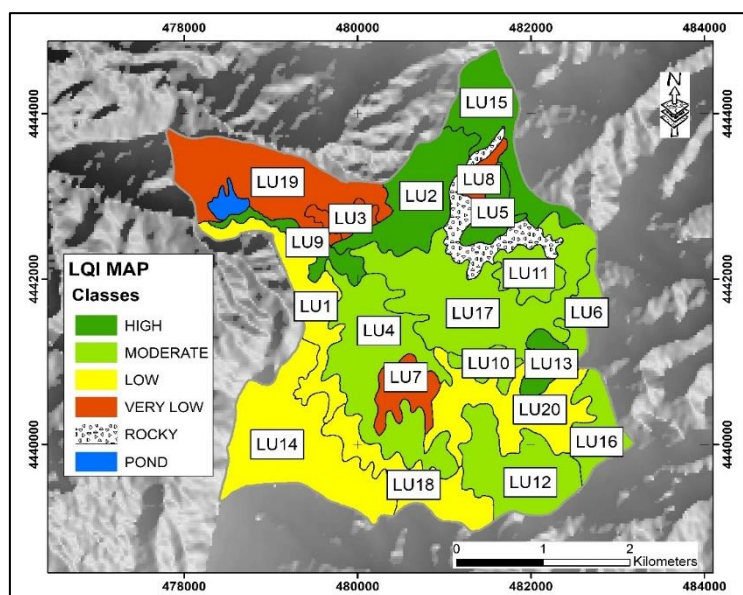


Figure 2. The map of LQI classes and distributions

Table 8. Class sizes determined by LQI result (except pond and rocky)

Land Units	LQI	Classes	Area (ha)	Land Units	LQI	Classes	Area (ha)
LU1	2.061	III	82.94	LU11	2.671	II	40.14
LU2	2.856	I	108.82	LU12	2.726	II	114.74
LU3	2.055	IV	21.63	LU13	3.07	I	28.19
LU4	2.781	II	177.05	LU14	2.183	III	197.98
LU5	3.205	I	29.43	LU15	3.18	I	98.33
LU6	2.828	II	33.51	LU16	2.828	II	49.07
LU7	1.874	IV	40.97	LU17	2.596	II	220.91
LU8	1.949	IV	19.08	LU18	2.061	III	84.32
LU9	3.433	I	37.36	LU19	1.843	IV	162.70
LU10	2.702	II	24.11	LU20	2.163	III	122.96

As a result of the study, the lands indicating distribution in all conformity classes were determined in Güvenç basin. According to the generated LQI map, 302.13 ha area (17.14%) was classified as Quality High in the study area. Although these areas have 0-1% stoniness and heavy structure together or separate effects, they are the most suitable agricultural areas within the basin. The 659.52 ha (37.41%) of the total study area was defined as 'Moderate'. These areas have soil depths of 50-100 cm and have lands found in different slope groups (1-6). However, heavy structure factor (Heavy Clay), high bulk density for clay structure, low organic matter content and stoniness problem varying between 2-15% reduce the LQI value. As a result of LQI assessment, 732.57 ha (41.55%) land was classified as low-very low due to soil depth of 0-50 cm and very steep slope (> 12%) in the study area. It was determined in the ground control that these areas were mostly used for pasture. Although this situation increased the organic matter content of soils, it did not have a class increasing effect on the final index value. In this study, it was determined that the effect of pH, EC, CaCO₃ and organic matter indicators on quality final index values of the regional land did not create significant differences and this situation was caused by the fact that the indicators had similar values both in the fields and in themselves. The most important soil problems seen in the basin are soil depth, slope and stoniness. However, although some lands have a flat slope, high organic material content and soil depth of 25-50 cm, 5-15% stoniness problem, heavy texture and high bulk density required these areas to be classified as Low Quality. Similarly, areas with 0-2% stoniness, high organic matter and 5-15% CaCO₃ content but soil depth of 0-25 cm and slope of 6-12% were also included in the very low-quality class. However, it is foreseen that if the necessary conservation measures are taken (ground leveling planning, deep tillage and cracking, addition of organic matter, stone collection), the low-quality regional lands can be classified as moderate or high quality.

Validation of the LQI

The final index values of the quality classes determined as a result of the LQI evaluation were compared with NDVI ratios derived from Sentinel-2A satellite image in 2018-May using linear regression analysis. The evaluation of the data, $r^2 = 0.74\%$ relationship was determined (Fig. 3).

The validation values obtained showed that the use of AHP-LCT in sub-factor weighting of selected criteria for LQI gave reliable results. At the same time, it was concluded that NDVI values can be used to test the index developed in cases where biomass data of vegetation are limited in local based studies. Similarly, a significant

correlation was observed between the NDVI values of plants for the month of May and biomass ($r^2 = 0.69$), using the SPOT 2 satellite images (Usul, 2010). Further, a strong correlation was reported between NDVI and biomass density (Salazar et al., 2007; Olimb et al., 2018; Li et al., 2019), and NDVI provided a more accurate estimation of biomass than the other vegetation index for the purpose of assessing land cover and soil quality by remote sensing technique (de Paul Obade and Lal, 2013; Lambert et al., 2018).

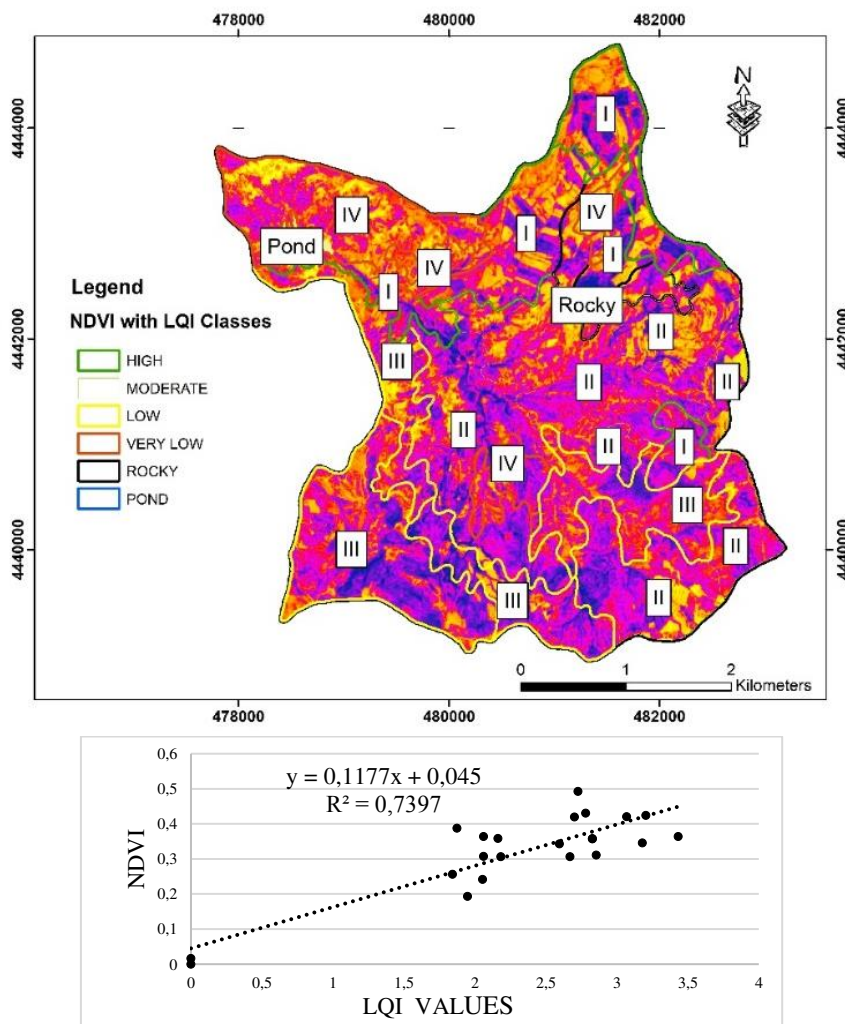


Figure 3. Distribution of LQI classes on NDVI map from Sentinel 2A and regression graph

Conclusion

In order to determine the quality index of agricultural land, which is compatible for semi-arid climate and integrated with GIS a practical LQI has been developed and found successful in Central Anatolia region due to showing a high relationship with canopy reflectance values. The most remarkable finding of the study is that the parameters selected for the LQI is the necessity to represent the study area, their topography, and the change in soil properties. In this way, region-specific evaluations can be made, and more reliable results are obtained. Thus, nine parameters used in the determination of land quality classes for Güvenç Basin reflect both the regional pedology and the effect of

climate characteristics. Another important point here is the weighting of the effect level of the selected parameters on each other and on the land quality. The AHP method used for pairwise comparison and weighting of parameters in the study presented a reliable index approach in the determination of land quality for agricultural purposes. While the relationship between each factor and AHP method is revealed, it is consistent to make common decision weights where the literature knowledge and expert opinion overlap (Expert System). Thus, the study showed similarity with the previous research findings that AHP has high capacity for integration of heterogeneous data. The obtained all findings showed that the development and use of region-specific index in the determination of the quality of agricultural land will enable the production of more accurate and reliable policies. In this way, climate, physiography and soil characteristics of different geographies can be evaluated within itself. Otherwise, evaluating our own lands with parametric approaches which are used in many studies but developed in different region ecologies causes wrong inferences. For instance, public institutions in Turkey for producing agricultural policy uses the Storie Index for land evaluation and classification. However, this approach scores the characteristics of the terrain indicated in the scoring of parameters to the same extent for different geographies. This reduced sensitivity in the assessment of land of different geography, such ecology particularly Turkey. At the same time, the indicator ratios specified in many parametric models are multiplied by each other and the effect level of each indicator is considered equal in terms of agriculture. In this case, even if a very important parameter such as effective soil depth in terms of agricultural land quality gets low score, high value of other parameters decreases the level effect of depth and improves the class of agricultural land quality. The most important advantage of regional-based index approaches is that, in addition to sub-categorizing the selected indicators at a regional scale, they weight the relevant indicators according to the regional characteristics. Thus, all factors can be evaluated according to the importance level of the specific region. However, since the different indicators (e.g. macro-micronutrients, heavy metals, biological factors) can be easily adapted to the index, it can be suggested that they can be reconstructed in areas indicating different soil properties. With all these evaluations and contributions, it will be ensured that the index fully represents the ecology of the region in which it is developed. The capabilities of satellite images of the basin were also utilized in the study. Our results have demonstrated the potential use of NDVI derived from high-resolution, multitemporal Sentinel-2A images for the comparison of biomass density with land quality scores in the basin. Similar studies have suggested that if there is limited data on vegetation, a different option of validation may be used. Moreover, the usability of vegetation indices for monitoring and estimation of land quality was evaluated with a different perspective and a window was opened for future research. In this way, changes in land quality determined by using parameters which were representing agricultural areas can be monitored by using vegetation indices in the following years compared with the past findings, and the cause of radical changes in biomass reflections could be determined by field studies. As a matter of fact, sustainable agricultural techniques suggest applications based on sustainability of land quality and productivity for agriculture areas in today and future. Consequently, land quality map for study area generated using AHP, GIS and LCT, can enhance the planning alternatives within an area with meaningful strategy in terms of location. Therefore, the present model will provide logical guidance for new land allocation of agricultural usage for decision makers.

REFERENCES

- [1] Aderonke, D. O., Gbadegesin, G. A. (2013): Spatial variability in soil properties of a continuously cultivated land. – *African Journal of Agricultural Research* 8(5): 475-483.
- [2] Ahmed, G. B., Shariff, A. R. M., Balasundram, S. K., bin Abdullah, A. F. (2016): Agriculture land suitability analysis evaluation based multi criteria and GIS approach. – In: *IOP Conference Series. Earth and Environmental Science* 37(1): 12-44.
- [3] Akıncı, H., Özalp, A. Y., Turgut, B. (2013): Agricultural land use suitability analysis using GIS and AHP technique. – *Computers and Electronics in Agriculture* 97(2013): 71-82.
- [4] Aldababseh, A., Temimi, M., Maghelal, P., Branch, O., Wulfmeyer, V. (2018): Multi-criteria evaluation of irrigated agriculture suitability to achieve food security in an arid environment. – *Sustainability* 10(3): 803.
- [5] Al-Doski, J., Mansor, S. B., Shafri, H. Z. M. (2013): NDVI differencing and postclassification to detect vegetation changes in Halabja city, Iraq. – *IOSR Journal of Applied Geology and Geophysics* 1(2): 01-10.
- [6] An, S. (2018): Research on Dynamic Change and Relationship Between Land Use/Cover and Evapotranspiration in Beijing-Tianjin-Hebei Region. – Hebei University of Science and Technology Publishing, China.
- [7] Andrews, S. S., Karlen, D. L., Cambardella, C. A. (2004): The soil management assessment framework: A quantitative soil quality evaluation method. – *Science Society of America* 68(6): 1945-1962.
- [8] Anonymous (2017): Turkish state meteorological service. – <https://mgm.gov.tr/eng/forecast-cities.aspx>.
- [9] Arshad, M. A., Martin, S. (2002): Identifying critical limits for soil quality indicators in agro-ecosystems. – *Ecosystems & Environment* 88(2002): 153-160.
- [10] Askari, M. S., Holden, N. M. (2014): Indices for quantitative evaluation of soil quality under grassland management. – *Geoderma* 230(2014): 131-142.
- [11] Baridón, J. E., Casas, R. R. (2014): Quality indicators in subtropical soils of formosa, Argentina: changes for agriculturization process. – *International Soil and Water Conservation Research* 2(4): 13-24.
- [12] Blake, G. R., Hartge, K. H. (1986): Bulk Density. – In: Klute, A. (ed.) *Methods of Soil Analysis, Physical and Mineralogical Methods*. Soil Science Society of America, Madison, pp. 363-376.
- [13] Bouyoucos, G. J. (1951): A recalibration of the hydrometer method for making mechanical analysis of soils. – *Agronomy Journal* 43(9): 434-438.
- [14] Bydekerke, L., Van Ranst, E., Vanmechelen, L., Groenemans, R. (1998): Land suitability assessment for Cherimoya in Southern Ecuador using expert knowledge and GIS. – *Agriculture, Ecosystems & Environment* 69(2): 89-98.
- [15] Campbell, J. B., Wynne, R. H. (2011): *Introduction to Remote Sensing*. – Guilford Press, New York.
- [16] Ceballos, S. A., López, B. J. (2003): Delineation of suitable areas for crops using a multi-criteria evaluation approach and land use/cover mapping: A case study in Central Mexico. – *Agricultural Systems* 77(2003): 117-136.
- [17] De la Rosa, D., Van Diepen, C. A. (2009): Qualitative and Quantitative Land Evaluations. – In: Verheye, W. H. (ed.) *Encyclopedia of Land Use, Land Cover and Soil Sciences Volume II*. Eolss Publishers, Oxford, United Kingdom.
- [18] de Paul Obade, V., Lal, R. (2013): Assessing land cover and soil quality by remote sensing and geographical information systems (GIS). – *Catena* 104(2013): 77-92.
- [19] DeFries, R., Hansen, M., Townshend, J. (1995): Global discrimination of land cover types from metrics derived from AVHRR pathfinder data. – *Remote Sensing of Environment* 54(3): 209-222.
- [20] Dengiz, O., Başkan, O. (2005): Basic properties and classification of Güvenç Basin soil, Ankara. – *Selcuk J Agr Food Sci.* 19(37): 27-36.

- [21] Dengiz, O., Sarıoğlu, F. E. (2013): Parametric approach with linear combination technique in land evaluation studies. – *Journal of Agricultural Sciences* 19(2): 101-112.
- [22] Dengiz, O., Şişman, A., Gülser, C., Şişman, Y. (2014): Alternative approach for land quality classification used for land consolidation. – *Soil and Water Journal* 3(1): 59-69.
- [23] Doran, J. W., Parkin, T. B. (1996): Quantitative Indicators of Soil Quality: a Minimum Data Set. – In: Doran, J. W., Jones, A. J. (eds.) *Methods for Assessing Soil Quality*. Soil Science Society of America Special Publication, Madison, pp. 25-37.
- [24] Eastman, J. R., Jiang, H. (1996): *Fuzzy Measures in Multi-Criteria Evaluation*. – United States Department of Agriculture Forest Service General Technical Report RM, 527-534.
- [25] Ennaji, W., Barakat, A., El Baghdadi, M., Oumenskou, H., Aadraoui, M., Karroum, L. A., Hilali, A. (2018): GIS-based multi-criteria land suitability analysis for sustainable agriculture in the northeast area of Tadla plain (Morocco). – *Journal of Earth System Science* 127(6): 79.
- [26] Erdal, İ., Bozkurt, M. A., Çimrin, K. M., Karaca, S., Sağlam, M. (2000): Effects of humic acid and phosphorus applications on growth and phosphorus uptake of corn plant (*Zea mays* L.) grown in a calcareous soil. – *Turkish Journal of Agriculture and Forestry* 24(2000): 663-668.
- [27] ERDAS (2009): *User's guide*. – <http://www.erdas.com>.
- [28] ESRI (2010): *User's guide*. – <http://www.esri.com>.
- [29] FAO (1977): *A Framework for Land Evaluation*. – International Institute for Land Reclamation and Improvement Published No.22, Wageningen.
- [30] Garrigues, S., Allard, D., Baret, F. (2007): Using first-and second-order variograms for characterizing landscape spatial structures from remote sensing imagery. – *IEEE Transactions on Geoscience and Remote Sensing* 45(6): 1823-1834.
- [31] Guo, L. J., Zhang, Z. S., Wang, D. D., Li, C. F., Cao, C. G. (2015): Effects of short-term conservation management practices on soil organic carbon fractions and microbial community composition under a rice-wheat rotation system. – *Biology and Fertility of Soils* 51(1): 65-75.
- [32] Hazelton, P., Murphy, B. (2007): *Interpreting Soil Test Results, What Do All the Numbers Mean*. – Commonwealth Scientific and Industrial Research Organization Publishing, Australia.
- [33] Huddleston, J. H., Pease, J. R., Forrest, W. G., Hickerson, H. J., Langridge, R. W. (1987): Use of agricultural land evaluation and site assessment in Linn County, Oregon, USA. – *Environmental Management* 11(3): 389-405.
- [34] Imaz, M. J., Virto, I., Bescansa, P., Enrique, A., Fernandez, A. O., Karlen, D. L. (2010): Soil quality indicator response to tillage and residue management on semi-arid Mediterranean cropland. – *Soil and Tillage Research* 107(1): 17-25.
- [35] Iojă, C. I., Niță, M. R., Vânău, G. O., Onose, D. A., Gavrilidis, A. A. (2014): Using multi-criteria analysis for the identification of spatial land-use conflicts in the Bucharest Metropolitan area. – *Ecological Indicators* 42(2014): 112-121.
- [36] Jenks, G. F. (1967): The data model concept in statistical mapping. – *International Yearbook of Cartography* 7(1967): 186-190.
- [37] Joshua, J. K., Anyanwu, N. C., Ahmed, A. J. (2013): Land suitability analysis for agricultural planning using GIS and multi criteria decision analysis approach in Greater Karu Urban Area, Nasarawa State, Nigeria. – *Afr J Agric Sci Technol* 1(1): 14-23.
- [38] Karlen, D. L., Gardner, J. C., Rosek, M. J. (1998): A soil quality framework for evaluating the impact of CRP. – *Journal of Production Agriculture* 11(1): 56-60.
- [39] Karlen, D. L., Cambardella, C. A., Kovar, J. L., Colvin, T. S. (2013): Soil quality response to long-term tillage and crop rotation practices. – *Soil and Tillage Research* 133(2013): 54-64.
- [40] Kumar, T., Jhariya, D. C. (2015): Land quality index assessment for agricultural purpose using multi-criteria decision analysis (MCDA). – *Geocarto International* 30(7): 822-841.

- [41] Kurzatkowski, D., Martius, C., Höfer, H., Garcia, M., Förster, B., Beck, L., Vlek, P. (2004): Litter decomposition, microbial biomass and activity of soil organisms in three agroforestry sites in Central Amazonia. – *Nutrient Cycling in Agroecosystems* 69(3): 257-267.
- [42] Lambert, M. J., Traoré, P. C. S., Blaes, X., Baret, P., Defourny, P. (2018): Estimating smallholder crops production at village level from Sentinel-2 time series in Mali's cotton belt. – *Remote Sensing of Environment* 216(2018): 647-657.
- [43] Leonard, W. H., Stamp, D. L., Martin, J. H. (1976): *Principles of Field Crop Production*. – Macmillan Publishing Company, New York.
- [44] Li, C., Li, H., Li, J., Lei, Y., Li, C., Manevski, K., Shen, Y. (2019): Using NDVI percentiles to monitor real-time crop growth. – *Computers and Electronics in Agriculture* 162(2019): 357-363.
- [45] Malczewski, J. (2006): Ordered weighted averaging with fuzzy quantifiers: GIS-based multicriteria evaluation for land-use suitability analysis. – *International Journal of Applied Earth Observation and Geoinformation* 8(4): 270-277.
- [46] McVay, K., Radcliffe, D., Hargrove, W. L. (1989): Winter legume effects on soil properties and nitrogen fertilizer requirements. – *Soil Science Society of America Journal* 53(6): 1856-1862.
- [47] Mezera, J., Lukas, V., Elbl, J. (2017): Evaluation of crop yield spatial variability in relation to variable rate application of fertilizers. – *MendelNet* 24(1).
- [48] Miller, F., Guthrie, R. L. (1984): *Classification and Distribution of Soils Containing Rock Fragments in the United States. Erosion and Productivity of Soils Containing Rock Fragments*. – Soil Science Society of America Publishing, Madison, pp. 1-6.
- [49] Miransari, M., Smith, D. L. (2007): Overcoming the stressful effects of salinity and acidity on soybean nodulation and yields using signal molecule genistein under field conditions. – *Journal of Plant Nutrition* 30(12): 1967-1992.
- [50] Mokarram, M., Mirsoleimani, A. (2018): Using Fuzzy-AHP and order weight average (OWA) methods for land suitability determination for citrus cultivation in ArcGIS (Case study: Fars province, Iran). – *Physica A: Statistical Mechanics and its Applications* 508(2018): 506-518.
- [51] Mustafa, S. M. T., Vanuytrecht, E., Huysmans, M. (2017): Combined deficit irrigation and soil fertility management on different soil textures to improve wheat yield in drought-prone Bangladesh. – *Agricultural Water Management* 191(2017): 124-137.
- [52] Nabiollahi, K., Golmohamadi, F., Taghizadeh-Mehrjardi, R., Kerry, R., Davari, M. (2018): Assessing the effects of slope gradient and land use change on soil quality degradation through digital mapping of soil quality indices and soil loss rate. – *Geoderma* 318(2018): 16-28.
- [53] Nelson, D. W., Sommers, L. (1982): Total Carbon, Organic Carbon, and Organic Matter. – In: Page, A. L. (ed.) *Methods of Soil Analysis, Part 2: Chemical and Microbiological Properties*. American Society of Agronomy, Inc., and Soil Science Society of America, Inc., Madison, pp. 539-579.
- [54] Olimb, S. K., Dixon, A. P., Dolfi, E., Engstrom, R., Anderson, K. (2018): Prairie or planted? Using time-series NDVI to determine grassland characteristics in Montana. – *GeoJournal* 83(4): 819-834.
- [55] Özkan, B., Dengiz, O., Demirağ, T. İ. (2019): Site suitability assessment and mapping for rice cultivation using multi-criteria decision analysis based on fuzzy-AHP and TOPSIS approaches under semihumid ecological condition in delta plain. – *Paddy and Water Environment* 2019: 1-12.
- [56] Pagliai, M., Vignozzi, N., Pellegrini, S. (2004): Soil structure and the effect of management practices. – *Soil and Tillage Research* 79(2): 131-143.
- [57] Pandžić, M., Mihajlović, D., Pandžić, J., Pfeifer, N. (2016): Assessment of the geometric quality of Sentinel-2 data. – *International Archives of the Photogrammetry, Remote Sensing & Spatial Information Sciences* 41: 489-494.

- [58] Pasqualotto, N., Delegido, J., Van Wittenberghe, S., Rinaldi, M., Moreno, J. (2019): Multi-crop green LAI estimation with a new simple Sentinel-2 LAI index (SeLI). – *Sensors* 19(4): 904.
- [59] Patrono, A. (1998): *Multi-Criteria Analysis and Geographic Information Systems: Analysis of Natural Areas and Ecological Distributions. Multicriteria Analysis for Land-Use Management.* – In: Beinat, E. (ed.) *Environment and Management.* Kluwer Academic Publishers, The Netherlands, pp. 271-292.
- [60] Paz-Kagan, T., Ohana-Levi, N., Herrmann, I., Zaady, E., Henkin, Z., Karnieli, A. (2016): Grazing intensity effects on soil quality: A spatial analysis of a Mediterranean grassland. – *Catena* 146(2016): 100-110.
- [61] Rahmanipour, F., Marzaioli, R., Bahrami, H. A., Fereidouni, Z., Bandarabadi, S. R. (2014): Assessment of soil quality indices in agricultural lands of Qazvin Province, Iran. – *Ecological Indicators* 40(2014): 19-26.
- [62] Riley, H., Pommeresche, R., Eltun, R., Hansen, S., Korsæth, A. (2008): Soil structure, organic matter and earthworm activity in a comparison of cropping systems with contrasting tillage, rotations, fertilizer levels and manure use agriculture. – *Ecosystems & Environment* 124(3-4): 275-284.
- [63] Romano, G., Dal Sasso, P., Trisorio Liuzzi, G., Gentile, F. (2015): Multi-criteria decision analysis for land suitability mapping in a rural area of Southern Italy. – *Land Use Policy* 48(2015): 131-143.
- [64] Saaty, T. L. (1980): *The Analytical Hierarchy Process, Planning, Priority.* – Resource Allocation: RWS Publications, USA.
- [65] Saaty, T. L. (2008): Decision making with the analytic hierarchy process. – *International Journal of Services Sciences* 1(1): 83-98.
- [66] Salazar, L., Kogan, F., Roytman, L. (2007): Use of remote sensing data for estimation of winter wheat yield in the United States. – *International Journal of Remote Sensing* 28(17): 3795-3811.
- [67] Sarkar, A., Ghosh, A., Banik, P. (2014): Multi-criteria land evaluation for suitability analysis of wheat: A case study of a watershed in eastern plateau region, India. – *Geo-Spatial Information Science* 17(2): 119-128.
- [68] Sauer, T., Havlík, P., Schneider, U. A., Schmid, E., Kindermann, G., Obersteiner, M. (2010): Agriculture and Resource availability in a changing world: The role of irrigation. – *Water Resources Research* 46(6): 1-12.
- [69] Shepherd, T. G. (2009): *Visual Soil Assessment: Field Guide for Pastoral Grazing and Cropping on Flat to Rolling Country.* – Horizons Regional Council, Palmerston North, New Zealand.
- [70] Singh, J., Devi, U., Hazra, J., Kalyanaraman, S. (2018): Crop-identification using Sentinel-1 and Sentinel-2 data for Indian region. – In: *IGARSS 2018, IEEE International Geoscience and Remote Sensing Symposium*, pp. 5312-5314.
- [71] Soil Science Division Staff. (2017): *Soil Survey Manual.* – USDA-NRCS. U.S. Gov. Print. Off, Washington, DC., Handbook No 18.
- [72] Soil Survey Staff. (1999): *Soil Taxonomy: A Basic System of Soil Classification for Making and Interpreting Soil Surveys.* – US Government Printing Office.
- [73] Soil Survey Staff. (2011): *Soil Survey Laboratory Methods Manual: Soil Survey Investigations Report.* – Lincoln, NE.
- [74] Song, R., Cheng, T., Yao, X., Tian, Y., Zhu, Y., Cao, W. (2016): Evaluation of Landsat 8 time series image stacks for predicting yield and yield components of winter wheat. – In: *IGARSS 2016, IEEE International Geoscience and Remote Sensing Symposium*, pp. 6300-6303.
- [75] Store, R., Kangas, J. (2001): Integrating spatial multi-criteria evaluation and expert knowledge for GIS-based habitat suitability modelling. – *Landscape and Urban Planning* 55(2): 79-93.

- [76] Şeker, C., Işıldar, A. (2000): Effects of wheel traffic porosity and compaction of soil profile. – *Turkish Journal of Agriculture and Forestry* 24(2000): 71-77.
- [77] Tucker, C. J. (1979): Red and photographic infrared linear combinations for monitoring vegetation. – *Remote Sensing of Environment* 8(2): 127-150.
- [78] Turan, İ. D., Dengiz, O. (2015): Erosion risk prediction using multi-criteria assessment in Ankara Güvenç Basin. – *Journal of Agricultural Sciences* 23(3): 285-297.
- [79] Turgut, B., Aksakal, E. L., Öztaş, T., Babagil, G. E. (2008): Defining partial effect coefficients of soil properties affecting on soil penetration resistance using multiple regression analysis. – *Atatürk University Journal of The Agricultural Faculty* 39(1): 115-121.
- [80] Tyagi, P., Bhosle, U. (2010): Image based atmospheric correction of remotely sensed images. – In: *Computer Applications and Industrial Electronics (ICCAIE) 2010 International Conference*, pp. 63-68.
- [81] Usul, M. (2010): Determination of Effects of Land Quality Parameters on Wheat Yield by using Remote Sensing and Geographic Information Systems, Case Study; Altinova State Farm. – Ankara University, PhD Thesis (published).
- [82] Van Wambeke, A. R. (2000): The Newhall Simulation Model for Estimating Soil Moisture & Temperature Regimes Preliminary Assumptions of the Newhall Model. – *Geogr. Rev.* 1-9.
- [83] Vinhal-Freitas, I. C., Corrêa, G. F., Wendling, B., Bobuľská, L., Ferreira, A. S. (2017): Soil textural class plays a major role in evaluating the effects of land use on soil quality indicators. – *Ecological Indicators* 74(2017): 182-190.
- [84] Xue, R., Wang, C., Liu, M., Zhang, D., Li, K., Li, N. (2019): A new method for soil health assessment based on analytic hierarchy process and meta-analysis. – *Science of The Total Environment* 650(2019): 2771-2777.
- [85] Yalew, S. G., van Griensven, A., Mul, M. L., van der Zaag, P. (2016): Land suitability analysis for agriculture in the Abbay basin using remote sensing, GIS and AHP techniques. – *Modeling Earth Systems and Environment* 2(101).
- [86] Yang, F., Zeng, G., Du, C., Tang, L., Zhou, J., Li, Z. (2008): Spatial analyzing system for urban land-use management based on GIS and multi-criteria assessment modeling. – *Progress in Natural Science* 18(2008): 1279-1284.
- [87] Zhan, A., Zou, C., Ye, Y., Liu, Z., Cui, Z., Chen, X. (2016): Estimating on-farm wheat yield response to potassium and potassium uptake requirement in China. – *Field Crops Research* 191(2016): 13-19.
- [88] Zhang, B., Zhang, Y., Chen, D., White, R. E., Li, Y. (2004): A quantitative evaluation system of soil productivity for intensive agriculture in China. – *Geoderma* 123(3-4): 319-331.
- [89] Zhang, J., Su, Y., Wu, J., Liang, H. (2015): GIS based land suitability assessment for tobacco production using ahp and fuzzy set in Shandong Province of China. – *Computers and Electronics in Agriculture* 114(2015): 202-211.

EFFECTS OF EMITTER SPACING AND IRRIGATION RATE ON THE YIELD, QUALITY AND ENERGY REQUIREMENTS OF DRIP-IRRIGATED TOMATOES (*SOLANUM LYCOPERSICUM* L.)

KARAŞ, E.

Department of Biosystem Engineering, Osmangazi University, Eskisehir, Turkey
(*e-mail: ekaras@ogu.edu.tr*)

(Received 29th Oct 2019; accepted 30th Jan 2020)

Abstract. An experiment with a randomised split plot design was performed to assess the yield, irrigation water use efficiency, energy requirements and quality of tomatoes (*Lycopersicon esculentum* cv. BT236 F₁) grown with drip irrigation on the Alpu Plain in north-western Central Anatolia, Turkey. During a trial period involving three replications from 2009 to 2011, a Class A pan was used to measure the daily evaporation values of treatments in split plots with different emitter spacing (25 cm and 50 cm) and irrigation rates (20%, 30%, 40% and 50% of the evaporation rate of the Class A pan). Among the results, annual evaporation during the trial period ranged from 550.9 mm to 721.4 mm, and whereas higher irrigation rates afforded higher yields, lower ones afforded higher irrigation water use efficiency (IWUE). The average weight, vitamin C content, total soluble solid (TSS) content and pH values for tomatoes, all used in the proposed irrigation ratio, were 149 g, 99.18 mg kg⁻¹, 6.21% and 4.17, respectively. The energy requirement of irrigation water for diesel and electric consumption changed from 42 to 105 L and 140.6 and 351.4 kWh/ha, on average, respectively.

Keywords: *drip irrigation, irrigation water use efficiency, energy consumption, tomato quality*

Introduction

Tomato cultivation in Turkey plays an important economic role and it constitutes almost 40% of the total vegetable production (Aksoy and Kaymak, 2016; Guvenc, 2019). Global tomato production is currently 130 million tons. China, the European Union, India, the USA, and Turkey are known to be the top five largest tomato producers. These five producers account for 70% of global production (Eurofresh, 2016). Tomato breeding in Turkey is displaying a rising trend, which enables the country to keep its position as one of the biggest tomato producing countries in the world.

There are three cases of irrigation, which can be classified as: inadequate, excessive and optimum. First, inadequate irrigation leads to the formation of stress conditions by limiting the uptake of plant nutrients and water consumption, resulting in some quality problems and reduced yield (Lisar et al., 2012). Second, excessive irrigation causes leaching of the plant nutrients together with water and thus reduces water and nitrogen utilization efficiency (Xu et al., 2013; Huang et al., 2018; Thapa and Scott, 2019). Application of excess water to the soil not only affects seed germination and aeration of the root zone but also leads to many environmental problems such as waterlogging and salinization, contamination of groundwater's by minerals (Malash et al., 2008; Greene et al., 2016; Biswas and Kalra, 2018), nitrogen loss through leaching (Oenema et al., 2015; Shrivastava and Kumar, 2015; Musyoka et al., 2019; Rotiroti et al., 2019) and increasing irrigation costs (Kuşçu et al., 2013). Third, optimum irrigation ensures maximum water and nitrogen usage with optimal plant growth by avoiding excess water and loss of plant nutrients. Excessive usage of water not only causes a reduction in the amount of irrigated area but also more energy

supply to carry the water into the area which is going to be irrigated. Therefore, proper management of water usage is of considerable significance for sustainable agriculture and energy conservation.

In the world's arid and semi-arid regions, water use efficiency (WUE) in general and IWUE in particular are persistent concerns as water becomes an increasingly limited resource. During the past half-century, water management has intensified in an effort to increase WUE (Medrano et al., 2015; Hatfield and Dold, 2019), which has been shown to relate closely to the method applied. Of available methods, drip irrigation, in use for nearly 50 years, has been accepted as the most efficient method of maintaining soil moisture in the root zone. Drip irrigation not only controls the amount of water used but also affords plants the efficient uptake of nutrients and pesticides (Shock, 2006). The Class A evaporation pan is one of the universally used and easy-to-control tools for water management. The results of various studies have shown that the low level of error in estimates makes Class A pan a favorable tool for the establishing of water consumption and irrigation scheduling for many plants (Ayas, 2015; Senyigit and Arslan, 2018). Numerous surveys have been conducted to assign the pan (k_p) and crop coefficients (k_c) of tomato in the drip irrigation method (Smajstrla and Locascio, 1990; Locascio and Smajstrla, 1996; Kirnak and Kaya, 2004; Harmanto et al., 2005; Ertek, 2011). In coarse-textured soils, the water requirements of tomatoes varied from 0.5 to 1.0 times the pan evaporation (Locascio and Smajstrla, 1989; Locascio et al., 1989), and in finer-textured soils, the results were highly similar: 0.75 times the pan evaporation for spring crops (Locascio et al., 1989) and 0.5 times the pan evaporation for fall ones (Olson and Rhoads, 1992).

Because sustainable agriculture involving the responsible use of water resources is necessary to meet the nutritional demands of expanding populations and to ensure the continuity of economic development, the study presented here was performed to assess the yield, IWUE, quality and energy requirements of drip-irrigated tomatoes using data gathered with a Class A evaporation pan.

Materials and methods

Experimental site and analysis

This research was conducted between the years 2009 and 2011 in Eskişehir-Alpu, Turkey, located at 39° 46' N, 30° 31' E, with a mean elevation of 780 m. The province is placed in a territory of a semi-arid climate with a mean temperature of 10.7 °C, the relative humidity of 62.1%, annual precipitation, and evaporation are 343.5 and 976 mm, respectively. Some of the climatological values throughout the research duration were given in *Table 1*.

Soils in the study area are almost homogenous and classified as Aridisol considering United States Department of Agriculture (USDA) Soil Taxonomy (Soil Survey Staff, 2014). Three soil samples from each plot were taken using an auger from three depths (0-30, 30-60, and 60-90 cm). General characteristics of the soil before the experiment were given in *Table 2*.

Soil particle size analysis was determined by using hydrometer method (Gee and Or, 2002), CaCO₃ content of the soil by Scheibler calcimeter (Loeppert and Suarez, 1996), soil organic matter by Smith-Weldon method (Nelson and Sommers, 1996), soil phosphorus content by sodium bicarbonate method (Kuo, 1996), pH value by using glass electrode pH meter (Thomas, 1996) and soil electrical conductivity (EC) value

using standard EC electrode (Rhoades, 1996), respectively. Field capacity (FC) and wilting point (WP) moisture contents were obtained in -0.033 MPa and -1.5 MPa pressures, respectively, using a membrane extractor (Cassel and Nielsen, 1986). Available water (AW) was measured from the difference between the moisture contents of FC and WP. Bulk densities were determined by using the core method (Grossman and Reinsch, 2002). The infiltration rate was determined by a double ring infiltrometer. The AW content of the soil was 53.8 mm for 30 cm depth. The characteristics of irrigation water were determined by the methods proposed by the AWWA (American Water Works Association; Greenberg et al., 1992; Table 3).

During the research, trial plots were installed in different parts of the land having the same soil characteristics.

Table 1. Some climatic parameters throughout the research period

Month	Climatic parameters											
	Temperature (°C)				Relative humidity (%)				Precipitation (mm)			
	2009	2010	2011	Mean ^a	2009	2010	2011	Mean ^a	2009	2010	2011	Mean ^a
January	1.0	2.3	1.0	-0.2	87.2	69.0	70.9	74.8	77.2	31.5	18.3	36.1
February	3.6	5.7	1.3	1.3	81.2	66.4	65.9	70.3	93.6	50.3	10.6	26.7
March	5.7	6.7	4.8	5.0	76.5	59.3	64.8	63.5	55.4	27.7	16.6	35.6
April	12.8	10.2	8.0	10.1	70.7	61.2	69.9	59.8	36.0	41.2	60.8	42.4
May	18.6	16.4	13.7	14.8	66.4	55.3	64.9	57.9	23.7	5.7	92.3	42.7
June	26.2	19.4	18.1	18.6	52.4	59.9	60.3	54.6	5.9	46.6	32.0	31.2
July	33.5	23.3	23.4	21.4	53.0	59.8	51.4	51.1	1.9	14.3	20.0	10.5
August	27.3	25.3	20.6	21.0	55.2	52.1	54.7	53.0	2.6	1.5	2.2	9.1
September	18.6	19.0	18.3	16.9	56.4	59.0	52.7	54.8	6.4	26.2	7.1	13.4
October	15.3	10.8	9.1	11.7	64.6	74.6	65.3	61.1	22.7	105.9	64.0	25.6
November	6.0	10.0	1.5	6.0	68.0	59.9	62.0	68.5	14.9	10.1	0.1	27.6
December	4.6	4.9	1.7	2.1	69.7	74.7	69.4	75.7	32.2	57.1	42.4	42.3

^a48 years mean (1957-2005)

Table 2. General physical and chemical properties of the research area

Depth (cm)	pH	EC (dS m ⁻¹)	CaCO ₃ (%)	P ₂ O ₅ (kg ha ⁻¹)	Org. mat. (%)	Texture (%)			Field cap. (m ³ m ⁻³)	Wilt. point (m ³ m ⁻³)	Bulk density (g cm ⁻³)	Infiltration rate (mm h ⁻¹)
						Sand	Silt	Clay				
0-30	7.9	0.7	29.6	27.2	0.78	36	24	40	0.34	0.21	1.38	11.0
30-60	8.0	0.7	28.1	49.0	1.42	35	25	41	0.33	0.22	1.34	
60-90	8.0	0.6	25.9	59.2	1.53	34	23	43	0.33	0.21	1.35	

Table 3. Characteristics of irrigation water used in the study

Cations (meq l ⁻¹)		Anions (meq l ⁻¹)		Other parameters	
Na ⁺	2.66	CO ₃ ²⁻	0.0	pH	
K ⁺	0.04	HCO ₃ ⁻	4.42	EC (dS m ⁻¹)	
Ca ⁺⁺	4.14	Cl ⁻	1.44	B (mg l ⁻¹)	
Mg ⁺⁺	4.89	SO ₄ ²⁻	5.87	SAR	
Total	11.73	Total	11.73		

Irrigation scheduling

Irrigation scheduling was prepared based on the water holding capacity (WHC) for top 0-30 cm depth. The net irrigation depth (d_{net}), which is accepted as 40% of field capacity, was about 25.0 mm for the experimental area. Amounts of waters to be applied were calculated by the multiplication of d_{net} with evaporation rates. Irrigation water was applied when the evaporated water from the Class A pan reached to the calculated d_{net} value of the soil. There was not a constant irrigation interval during the research period. The coefficient of Class A pan (k_p) was assumed as 1.00 for evaporation calculations. Wetting areas were determined by using the method suggested by Keller and Bliesner (1990). The maximum and minimum wetting areas were found as 30.7% and 18.5%, respectively.

The irrigation water (I , m^3) amount was calculated using the following equation:

$$I = A \times E_p \times k_p \times E_r \quad (\text{Eq.1})$$

where A is the plot area (m^2); E_p is the accumulated evaporation for irrigation interval (10^{-3} mm); k_p , pan coefficient (1.00); E_r is the evaporation rate (%).

Daily evaporation data were obtained from the weather station placed in the study area. Before the experiment, all plots were irrigated until they reach field capacity for the depth of 0-30 cm. Subsequent irrigations were carried out when the cumulative evaporation amount measured daily from the class A pan reached 25 mm.

In this study, the moisture changes in the soil were checked by three tensiometers measuring soil moisture to 0-90 cm depth (0-30, 30-60 and 60-90 cm). Soil moisture measurements were followed in only one replicate of the experimental subjects. Since the maximum amount of irrigation water applied in each irrigation was 25 mm, no pressure changes were observed in the tensiometers at depths below 30 cm. Thus, no deep percolation was detected under the depth of 30 cm in the measurements made during the trial.

Experimental design

The experiment was organized as a split-plot randomized block design with three replications in 24 plots, each measuring $31.2 m^2$ (6.0 m length \times 5.2 m width), with a separate strip of 2 m between them (Figs. 1 and 2).

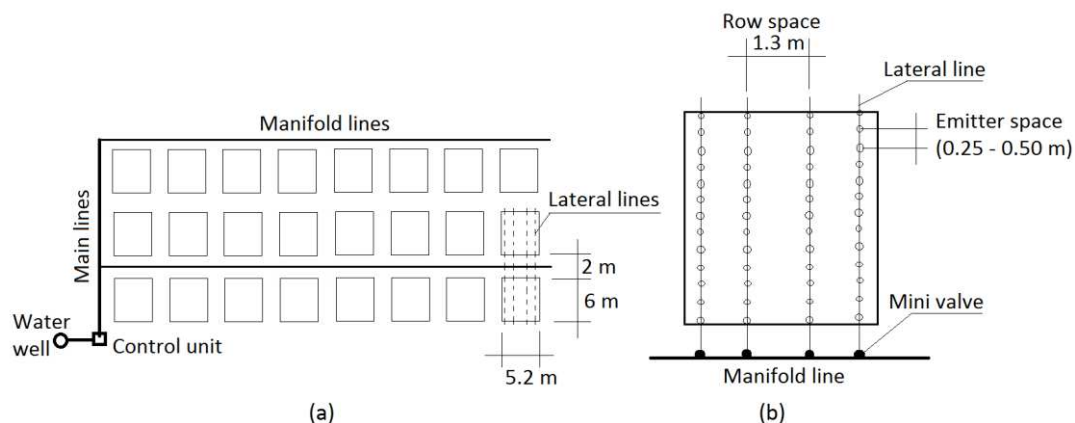


Figure 1. General view of the irrigation system in the research area (a), and lateral lines, row and emitter spaces (b)



Figure 2. General view of the parcels and plants in the trial area

The irrigation water, pumped from a deep well (15 m in depth), was conveyed to experimental plots with main and sub-main poly-etylen (PE) lines of 75 mm diameter. The control unit of the irrigation system had a hydro-cyclone filter, a sand filter, a screen filter, a mesh filter, pressure gauges, and a fertilizer tank with a dosage pump. Lateral lines with a diameter of 16 mm were laid down perpendicular along each tomato row at 1.3 m spacing. The flow rate of the drippers in the lateral lines was 4 L/h at a working pressure of 1 atmosphere. The evaporation rates of Class A pan (A: 20%, B: 30%, C: 40%, and D: 50%) and the emitter spaces (a: 25 cm, and b: 50 cm) were selected as main and subplot in the experiment, respectively. Two weeks old tomato seedlings were transplanted into the plots in the middle of May. The chemical fertilizing applications were carried out as suggested by Hartz (2006). There were four lateral lines in each plot. Row spaces between lateral lines were 1.3 m. There were 12 plants in each line and a total of 48 plants in each plot. IWUE values were calculated according to the method proposed by Howell (2001). The energy requirement for irrigation water is calculated considering diesel and electric systems. Statistical analyses were achieved with SPSS 17.0 (SPSS Inc, 2008). Data were tested by ANOVA with the factors years, evaporation rates, drip space, and yield and the possible interaction between both factors. Duncan's multiple comparison test was used to determine mean differences.

Tomato quality analysis

Samples for quality analysis were made in the first week of September to determine the fruit weight, pH, TSS and vitamin C values in tomato fruit in all trial years.

Fruit Weight: The average weights of tomato fruits randomly taken around 5 kg from the middle rows of the experimental plots were determined.

pH: Tomato juice was prepared by pouring the fruits into the blender for 10 min. Then, buffer solutions were prepared by pH meter, 10 mL of tomato juice was added into a 50 mL beaker. The pH of the obtained sample was measured using a pH meter (pH-Vision, model 6071, Taiwan).

Total soluble solids (TSS): The TSS was determined as a percentage (%) value at 20° using a digital refractometer (Atago Co. Ltd., Japan) in three replicates of 1 kg sample.

Vitamin C content: It was determined in tomato puree using the method determined by Riemschneider et al. (1976).

Energy requirements

In the Alpu plain where the experiment is conducted, irrigation water is commonly taken from deep (>6 m) wells using electric submersible pumps and from shallow wells (≤6 m) using diesel-consuming motor pumps. The aquifer formation in the Alpu plain is ground alluvial. Its thickness varies between 5-95 m. The depths of the drilling wells drilled in the plain are between 11-250 m and their yield is 10-50 L s⁻¹.

The average well flow rates of 50 m³ h⁻¹ are considered as two different sources, diesel and electric. In order to calculate the energy need, the energy consumption of the 17 hp diesel fuel consuming engine pump, which is widely used in the Alpu plain, is taken into consideration. The diesel fuel consuming pump is used to supply water from wells that are no deeper than 6 m and the hourly flow rate of 2/3 gas is 50 m³. The energy requirement of the electric submersible pump with an hourly capacity of 50 m³ from deep wells up to 50 m in the study area is taken into consideration.

Results and discussion

Yield and irrigation water use efficiency

The use of Class A pan is a common practice in the field trials for the calculation of plant water consumption and irrigation water amounts. Although the coefficient of Class A pan (k_p) was assumed as 1.00 for evaporation calculations in this study, many studies used different coefficients such as 0, 0.25, 0.50, 0.75, and 1.00 (Locascio and Samjstrla, 1996), 0.75 (Harmanto et al., 2005), and 0.80 (Kırnak and Kaya, 2004). These studies have shown that the highest yields were obtained by assuming a pan coefficient of 0.75 and 1.00.

The effects of deficit irrigation on yield, seasonal water application (IW), and IWUE are given in *Table 4* and *Figures 3* and *4*.

Table 4. Effects of deficit irrigation on yield, seasonal water application and IWUE

ER* (%)	Yield (t ha ⁻¹)				IW (m ³ ha ⁻¹)				IWUE (kg m ⁻³)			
	2009	2010	2011	Mean	2009	2010	2011	Mean	2009	2010	2011	Mean
20%	133.3 ^b	67.6 ^b	66.4 ^b	89.2 ^c	1440	1100	1230	1257	92.45 ^a	61.40 ^a	54.03 ^a	69.29 ^a
30%	129.9 ^b	88.3 ^a	84.3 ^a	102.1 ^b	2160	1660	1840	1867	60.03 ^b	55.62 ^a	45.85 ^b	53.83 ^b
40%	175.6 ^a	93.4 ^a	85.7 ^a	118.3 ^a	2890	2200	2450	2513	60.88 ^b	42.42 ^b	35.03 ^c	46.11 ^c
50%	161.6 ^a	107.0 ^a	91.7 ^a	120.1 ^a	3610	2760	3070	3147	44.82 ^c	38.85 ^b	29.85 ^d	37.84 ^d
Mean	150.2 ^a	90.0 ^b	82.1 ^c		2525	1930	2148		64.55 ^a	49.57 ^b	41.19 ^c	

*ER: Evaporation rate of Class A pan, IW: Seasonal water application (mm), IWUE: Irrigation water use efficiency (kg m⁻³)

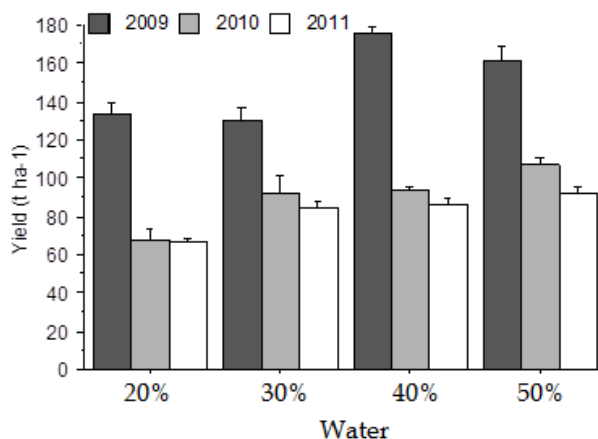


Figure 3. Effects of deficit irrigation (% of ER) on the yield of tomato (t/ha)

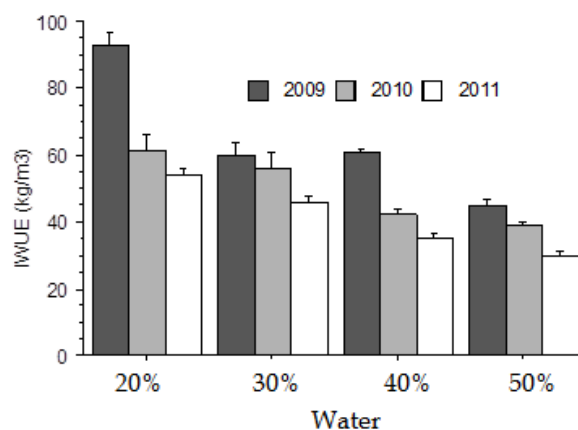


Figure 4. Effects of deficit irrigation (% of ER) on IWUE (kg/m³)

There were significant differences between the years studied. The yields obtained in the first year of the study (2009) were higher than that of the following two years (2010 and 2011). The reason for reduced yield in these years could be related to the negative effects of climatic conditions in the growing season (earlier frost occurring date) and disease (Early blight, Septoria leaf spot, Fusarium wilt, Verticillium wilt) development. In 2009, while the highest yield was obtained from the subject where 40% of evaporation was applied (40% of ER) as 175.6 t ha⁻¹, the yield of the highest seasonal water application (50% of ER) was found as 161.6 t ha⁻¹. The lowest yields were obtained from 20% and 30% of ER as 133.3 and 129.9 t ha⁻¹, respectively (Fig. 3). While the amount of seasonal water application is twice between the subjects 20% and 40% of ER, the amount of increase in yield is found just as 31.7%, in 2009. Except for 2009, the highest and the lowest yields were obtained from the subjects where the highest and the lowest irrigation waters were applied, respectively. The minimum and maximum yields per hectare were found as 67.6 and 107.0 tons for 20% and 50% of ER for 2010, respectively. The amount of seasonal water application was 1100 and 2760 m³ for these subjects. Although the amount of irrigation water applied in 2011 was relatively higher than that of 2010, the yields obtained were almost similar for the same subjects. The highest yield per hectare was obtained from 50% of ER as 91.7 tons, and

the lowest from 20% of ER as 66.4 tons. In general, the increase in the amount of water applied to the increased yield obtained. However, there was no clear trend between the amount of water applied and the extent of the response. While the amount of applied water between 50% of ER and 20% of ER was 2.5 folds, the amount of increase in yield was found as 21.2%, 58.3%, and 38.1% for years 2009, 2010, and 2011, respectively.

The values of IWUE calculated for various deficit irrigation practices in all experimental years are summarized in *Table 4* and *Figure 4*. The IWUE gradually decreased from 50% of ER to 20% of ER, providing that tomato uses the water more efficiently under stress conditions. As expected, the highest and the lowest IWUE values were obtained from 20% and 50% of ER, respectively. Irrigation time and frequency play an important role in tomato production and productivity, hence in IWUE. Chen et al. (2013), have found that full irrigation at the seedling stage did not affect tomato yield and fruit quality. On the other hand, tomato yield decreased significantly depending on the degree of water stress applied during flowering and fruit development periods. Marouelli et al. (2004), have stated that the highest WUE in tomato occurs between flowering and fruit formation stages. Therefore, it is necessary to plan irrigation considering the water content of the soil at different growth stages of the plant. Continuous monitoring of soil moisture content is of vital importance. Results of this study have shown that even under deficit irrigation conditions high yields can be achieved by continuous monitoring of soil moisture.

All crops take water from wherever it is most readily available within the root zone. Most of the studies conducted on tomato are focused on the effective root depth of 50-60 cm. However, it is well known that on average 40% of water uptake is assumed to be taken from the upper quarter of the rooting depth, and 30% from the second quarter. Therefore, 25-30 cm rooting depth is responsible for 70% of water uptake. This study demonstrated that, even under deficit irrigation conditions, 30 cm rooting depth can be considered as an effective rooting depth for tomato and performing irrigation when 40% of the available water holding capacity calculated for 30 cm soil depth is evaporated from the Class A pan can give fairly good results. Emitter spacing did not affect yield and IWUE.

Fruit quality

The results of the application subjects on fruit weight, pH, TSS, and vitamin C are given in *Figure 5*.

Fruit Weight: The effect of irrigation water on fruit weight was significant both in terms of annual and amount of irrigation water. The average fruit weights of 2009 and 2011 were in the same group with 159.25 and 156.25 grams respectively, while the results obtained in 2010 constituted another group with 138.58 grams. Differences between irrigation practices led to different fruit weights each year. The highest fruit weight was obtained from the highest irrigation application in three years. In 2009, evaporation ratio of 50% gave the highest fruit weight with statistical group a followed by 30%, 40% (ab) and 20% with group b. Similarly, evaporation ratio of 50% was the best application for fruit weight while the lowest value was observed in evaporation rate of 20% in 2010. In 2011, 50% was the first statistical group while the others followed with the same group.

The effect of deficit irrigation on tomato fruit quality has been investigated in many studies (Colla et al., 1999; Machade and Oliviera, 2005; Patane and Cosentino, 2010; Patane et al., 2011; Garnett et al., 2013; Cantore et al., 2016; Hashem et al., 2018). The

effect of limited irrigation on fruit quality is generally inversely related to fruit yield. The results show the effect of irrigation water applied, but their impact on quality is unstable. Fruit weight is a factor that is largely affected by the amount of irrigation water or applied water stress. Some studies indicate that fruit weight increases with irrigation water, whereas stress conditions decrease. In our study, fruit weights were affected by water stress in the other two years (2010 and 2011) except in the first year (2009). In general, the highest amount of irrigation water applied gave higher fruit weight values. According to the three-year average results of the study, it is understood that all the subjects except 50% ER, where the highest irrigation water is applied, give the same average fruit weight values statistically. Mitchell et al. (1991) reported the decrease in tomato fruit weights due to deficit water and salinity as 37% and 42%, respectively. Similar results are pointed out by Yurtseven et al. (2005), It was observed that raising salinity levels in irrigation water resulted in a dramatic decrease in fruit weight. Birhanu and Tilahun (2010) and Patane et al. (2011) observed that deficit irrigation reduces fruit weight due to water stress. In the study conducted by Helyes et al. (2012), fruit weights obtained by the cut off irrigation in the early period with full irrigation in tomato did not differ statistically. However, the average fruit weights obtained by cultivation under rainfed conditions were lower than full irrigation.

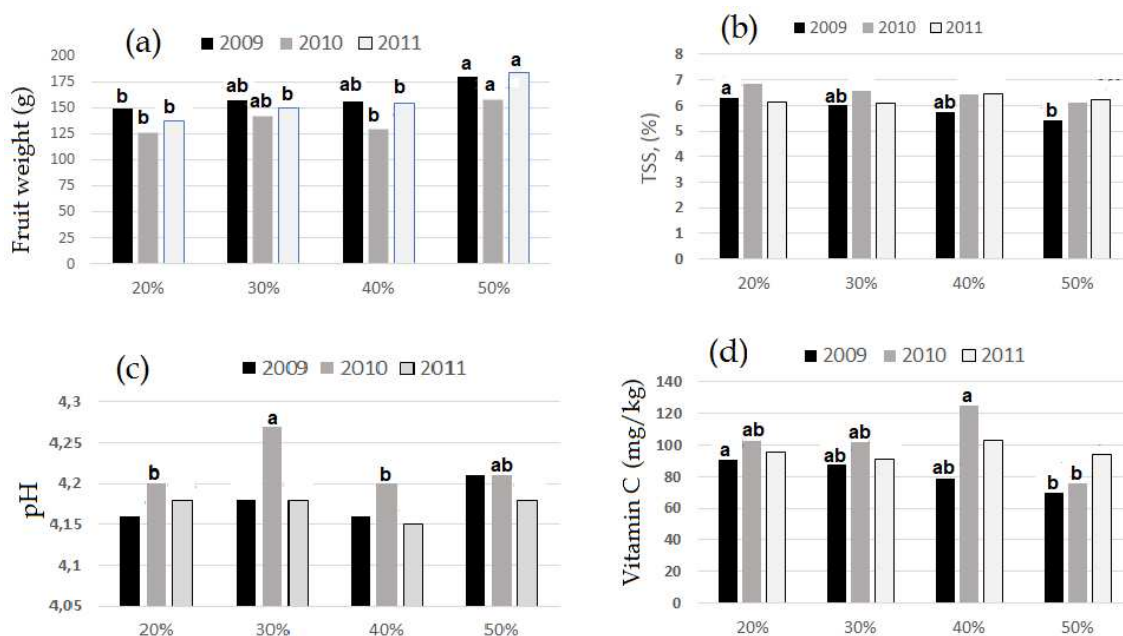


Figure 5. The effects of applied irrigation water on fruit weight (a), TSS (b), pH (c), and Vitamin C (d)

TSS: The TSS contents differed both in terms of year and amount of irrigation water. In general, the average values for 2010 and 2011 are in the same group and 2009 is in another group. In terms of average values of the issues, the highest TSS content was obtained as 6.43% on the lowest application rate (20% of ER). The results obtained in 2009 in terms of irrigation practices gave the same result as the general average. The data for this year gave the highest value of 6.31% for 20% of ER and 5.42% for 50% of ER. The impact of irrigation practices for 2010 and 2011 was statistically insignificant. The values obtained in terms of TSS followed a decreasing trend for the first two years

due to the decrease in the amount of irrigation water: $TSS = 6.6 - 0.291 ER$ ($r^2 = 0.996$) equation (TSS as Brix, and ER: Applied water as Evaporation Rate, %) for 2009 and $TSS = 7.085 - 0.243 ER$ ($r^2 = 0.983$) for 2010. No meaningful equality has occurred for 2011.

In Mohammed et al.'s (2018) study, considering the vegetative, flowering and fruit maturity stages during tomato cultivation, the lowest TSS values occurred in the control plants, which were not exposed to any water stress, whereas the highest occurred when deficit water was applied during fruit maturity. Other researchers, by contrast, have demonstrated the inverse relationship between deficit irrigation and TSS (Zegbe-Dominguez et al., 2003; Garcia and Barrett, 2006; Helyes et al., 2012; Kuşçu et al., 2014). Contrary to those results, Dumas et al. (2003) observed that the effect of deficit water on TSS content was negligible, and Yurtseven et al. (2005) found that TSS content in tomatoes increased by 100% when exposed to irrigation water with a salinity of 10 dS m^{-1} compared to controls. Expanding upon those results, Birhanu and Tilahun (2010), who observed that moderate drought stress caused significant increases in the TSS content of tomatoes, proposed that the increased TSS content of tomatoes grown in soil with a water deficit directly related to their decreased water content. Added to that, Banjaw et al. (2018) found that TSS content in tomatoes increased with stress and varied among cultivars, while their water content decreased. Last, Mitchell et al. (1991) noted that terminating irrigation 50 days before harvest prompted significant increases in the quality of tomatoes in terms of TSS content.

pH: While the difference in the amount of irrigation water applied for pH values was observed only in 2010, there was no difference between 2009 and 2011 data. When the general average results of the years are compared, 2010 constitutes group a, while 2009 and 2011 constitute 4.18 and 4.17, respectively. No effect of the mean values of irrigation water on pH was determined.

The pH of tomatoes is determined primarily by the acid content of the fruit. The acidity of the fruit is also important as a contributor to the flavor of the tomato products (Anton et al., 2010). The acidity values of vegetables and fruits vary according to species, varieties, growing period and maturity. According to the US Food and Drug Administration Food Safety and Applied Nutrition Center (CFSAN), the acidity value of fresh tomatoes ranges from 4.3-4.9, while the pH range for canned tomatoes and tomato paste is 3.5-4.7. The range for tomato juice is 4.1-4.6. The acidity of fresh tomatoes may be closely related to their maturity. As the tomato fruit ripens, its acidity decreases and the pH approaches 4.9 ends of the previously described range. Canned tomatoes are typically more acidic than fresh tomatoes due to the effect of canning, and Canned tomatoes have a pH of about 3.5 (Mohammed et al., 1999; CFSAN, 2019). According to Hernández-Suarez et al. (2008), tomato fruit with a pH below 4.5 is classified as acidic. pH is important due to acidity influences the thermal processing conditions required for producing safe products (Garcia and Barrett, 2006). Based on this information, it can be said that the pH value of tomato fruit juice obtained in our research is all acidic. Many research findings show that the amount of irrigation water applied is not effective on the pH of tomato fruit juice. These results are consistent with those reported by Nuruddin et al. (2003) and Amor and Amor (2007). In contrast, Wahb-Allah and Al-Oman (2012) mention the positive effect of deficit water on pH. Increased salinity levels in irrigation water caused by the production of smaller sized fruits, but this leads to a decrease in the pH of the fruit juice (Yurtseven et al., 2005).

Vitamin C: The rates of irrigation water applied were statistically different in both year and rate. Although the year 2010 data is the year in which the highest value is obtained, it is in the same group in 2011 as the general average. On the other hand, 81.80 in 2009 constituted the other group. According to 2009 data, the highest vitamin C value was obtained from the issue of 20% of ER with the lowest water application, the 40% of ER subject was in the (ab) group, and the 30% and 50% of ER subjects were in the (ab) group. The results in 2010 differed from the previous year; this time 40% ER constitutes group (a) an alone, 50% of ER group (ab) and 20% and 30% both group (b). The 2011 data showed no difference in terms of vitamin C values measured according to the applied irrigation water data. According to the 3-year average data, the differences in irrigation water issues on vitamin C were observed statistically. According to the results of the research, there is an inverse relationship between the amount of vitamin C and evaporation rates, depending on the water stress applied in general. As the amount of irrigation water applied in 2009 and 2010 increased, vitamin C values decreased. According to Dumas et al. (2003), vitamin C content in tomato depends on the growing season, favorable plant nutrients and environment. Studies are indicating that the change in the scope of vitamin C is an element of increasing plant water consumption and variety features (Mahajan and Singh, 2006; Mitchell et al. 1991). Lovelli et al. (2017) found that no significant effects were observed on the vitamin C content.

Energy requirements

Energy requirements for diesel fuel and electric powered pumps of the irrigation subjects are shown in *Figure 6*.

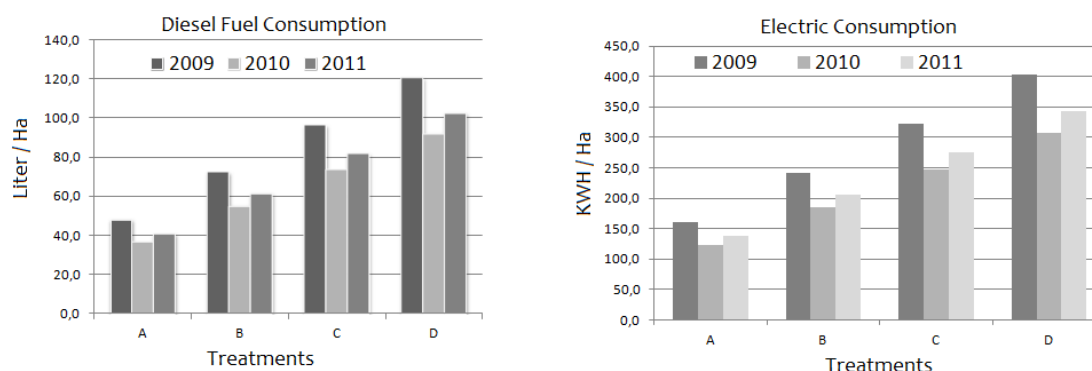


Figure 6. Energy requirements for diesel fuel and electric powered pumps of the treatments

While diesel fuel consumption for the irrigation subject is changing from 42 to 105 L, electric consumption ranged between 140.6 and 351.4 kWh/ha, averagely.

In the study, considering the distance between the lateral lines, the equality that can be used in the calculation of the amount of irrigation water that can be applied in heavy textured soils is found as follows:

$$Q = 8663.3 X^{-0.996} \quad (r^2 = 0.99) \quad (\text{Eq.2})$$

where Q: irrigation water per hectare as m³; X: lateral line spacing (X, cm).

Conclusion

Banjaw (2017) states that deficit irrigation is an optimization strategy implemented in a way that there is no decrease in yield during certain growth periods of the plant. Restricted irrigation provides storage of water in areas with water shortage and the use of water saved during long dry periods to ensure sustainable yield. Reducing irrigation water is an opportunity to save water by reducing production costs, as well as minimizing leachable nutrients such as nitrogen by deep infiltration.

The research that used the pan coefficient in tomato irrigation time planning has been carried out under various soil, climatic conditions. Application variations such as pan coefficient, lateral and emitter spacing, irrigation interval can give different results in a similar climate, even in the same climatic and soil conditions. Therefore, it is not possible to make generalizations and to say of the existence of a single truth. The results obtained with this can be evaluated by comparing the data within them.

The amount of evaporating water from the class A pan represents a saturated condition in which there is no water shortage in the soil. Although the plant's developmental status (i.e. root and leaf growth) varies, their response to water stress is also different. In many studies conducted using class A pan, a constant K_{pc} was used during the growing period. However, the results obtained from many studies showed that plants' reactions to periodic water constraints were not the same. Considering this situation, the use of different coefficients for each period can be one of the solutions that can be used for irrigation planning by using Class A pan for optimum water and nutrient management and saving water in the root zone. It may be possible to develop regional equities or use of coefficients, taking into account the climate and soil conditions.

An equation was developed to be used for different lateral spacing for heavy textured soils, taking into account the proposed evaporation rates obtained. In that process, lateral intervals and the amounts of irrigation water required for each lateral interval were analyzed together. When different lateral spacings are used, the volume of irrigation water per hectare can determine.

The root system of many plants in the vegetable group is shallow depth. Optimal irrigation programs can be developed on soils with different soil structures without causing deep penetration and therefore no leaching and stress on plants. For this reason, future research programs should be focused on improving IWUE and nutrient utilization efficiencies, especially by preventing water and nutrient losses. In this way, significant savings in irrigation energy can be achieved.

REFERENCES

- [1] Aksoy, A., Kaymak, H. Ç. (2016): Outlook on the Turkish tomato sector. – Iğdır Univ. J. Inst. Sci. Tech. 6(2): 121-129.
- [2] Amor, M. A., Amor, F. M. (2007): Response of tomato plants to deficit irrigation under surface or subsurface drip irrigation. – Journal of Applied Horticulture 9(2): 97-100.
- [3] Anthon, G. E., LeStrange, M., Barretta, D. M. (2011): Changes in pH, acids, sugars and other quality parameters during extended vine holding of ripe processing tomatoes. – J Sci Food Agric. DOI: 10.1002/jsfa.4312.
- [4] Ayas, S. (2015): The effects of different regimes on tomato (*Lycopersicon lycopersicum* L. var. Hazal) yield and quality characteristics under unheated greenhouse conditions. – Bulgarian Journal of Agricultural Science 21(6): 1235-1241.

- [5] Banjaw, D. T., Megersa, H. G., Lemma, D. T. (2017): Effect of water quality and deficit irrigation on tomatoes yield and quality: a review. – *Adv Crop Sci Tech* 5: 295. DOI: 10.4172/2329-8863.1000295.
- [6] Birhanu, K., Tilahun, K. (2010): Fruit yield and quality of drip-irrigated tomato under deficit irrigation. – *African Journal of Food, Agriculture, Nutrition and Development* 10(2).
- [7] Biswas, J. C., Kalra, N. (2018): Effect of waterlogging and submergence on crop physiology and growth of different crops and its remedies: Bangladesh perspectives. – *Saudi J. Eng. Technol.* 3(6): 315-329.
- [8] Cantore, V., Lechkar, O., Karabulut, E., Sellami, M. H., Albrizio, R., Boari, F., Stellacci, A. M., Todorovic, M. (2016): Combined effect of deficit irrigation and strobilurin application on yield, fruit quality and water use efficiency of “cherry” tomato (*Solanum Lycopersicum* L.). – *Agr. Water Manage.* 167: 53-61.
- [9] Cassel, D. K., Nielsen, D. R. (1986): Field Capacity and Available Water Capacity. – In: Klute, A. (ed.) *Methods of Soil Analysis. Part I. Physical and Mineralogical Methods*, Agronomy Monograph No. 9, Soil Science Society of America, Madison, WI, pp. 901-926.
- [10] CFSAN (2019): Can you tell me about the acidity in tomatoes. – <http://whfoods.org/genpage.php?pfriendly=1&tname=dailytip&dbid=383> (accessed on 24.10.2019).
- [11] Chen, J., Kang, S., Du, T., Qiu, R., Guo, P., Chen, R. (2013): Quantitative response of greenhouse tomato yield and quality to water deficit at different growth stages. – *Agricultural Water Management* 129(C): 152-162. DOI: 10.1016/j.agwat.2013.07.011.
- [12] Colla, G., Casa, R., Locascio, B., Saccardo, F., Temperini, O., Leoni, C. (1999): Responses of processing tomato to water regime and fertilization, in Central Italy. – *Acta Hort.* 487: 531-5.
- [13] Dumas, Y., Dadomo, A., Di Lucca, G., Grolier, P. (2003): Effects of environmental factors and agricultural techniques on the antioxidant content of tomatoes. – *J Sci Food Agric* 83: 369-382.
- [14] Ertek, A. (2011): Importance of pan evaporation for irrigation scheduling and proper use of crop-pan coefficient (Kcp), crop coefficient (Kc) and pan coefficient (Kp). – *African Journal of Agricultural Research* 6(32): 6706-6718.
- [15] Eurofresh (2016): Around the world: tomatoes. – <https://www.eurofresh-distribution.com/news/around-world-tomatoes>.
- [16] Garcia, E., Barrett, D. M. (2006): Peelability and yield of processing tomatoes by steam or lye. – *Journal of Food Processing and Preservation* 30(1): 3-14.
- [17] Garnett, T., Appleby, M. C., Balmford, A., Bateman, I. J., Benton, T. G., Bloomer, P., Burlingame, B., Dawkins, M., Dolan, L., Fraser, D., Herrero, M., Hoffmann, I., Smith, P., Thornton, P. K., Toulmin, C., Vermeulen, S. J., Godfray, H. C. (2013): Sustainable intensification in agriculture: premises and policies. – *Science* 341: 33-4.
- [18] Gee, G. W., Or, D. (2002): Particle Size Analysis. – In: Dane, J. H., Topp, G. C. (eds.) *Methods of Soil Analysis. Part 4: Physical Methods*. Soils Science Society of America, Book Series No. 5, Madison, WI, pp. 255-293.
- [19] Greenberg, A. E., Clesceri, L. S., Eaton, A. D. (1992): *Standard Methods for the Examination of Water and Wastewater*. 18th Ed. – Am. Public Health Assoc., Am. Water Works Assoc., and Water Environment Fed: Washington, DC.
- [20] Greene, R., Timms, W., Rengasamy, P., Arshad, M., Cresswell, R. (2016): Soil and Aquifer Salinization: Toward an Integrated Approach for Salinity Management of Groundwater. – In: Jakeman, A. J., Barreteau, O., Hunt, R. J., Rinaudo, J. D., Ross, A. (eds.) *Integrated Groundwater Management*. Springer, Cham. https://doi.org/10.1007/978-3-319-23576-9_15.

- [21] Grossman, R. B., Reinsch, T. G. (2002): Bulk Density and Linear Extensibility. – In: Dane, J. H., Topp, G. C. (eds.) *Methods of Soil Analysis: Physical Methods. Part 4.* Soil Science Society of America, Madison, WI, pp. 201-228.
- [22] Guvenc, İ. (2019): Tomato production in Turkey, foreign trade and competitiveness. – *KSU J. Agric Nat* 22(1): 57-61. DOI: 10.18016/ksutarimdog.vi.432316.
- [23] Harmanto, V. M., Salohke, V. M., Babel, M. S., Tantau H. J. (2005): Water requirement of drip- irrigated tomatoes grown in the greenhouse in tropical environment. – *Agricultural Water Management* 71(3): 225-242. DOI: 10.1016/j.agwat.2004.09.003.
- [24] Hartz, T. K., Miyao, E. M., Davis, R. M., Kochi, M. (2006): Influence of mustard cover crops on processing tomato production in the lower Sacramento Valley of California. – *Proceedings of the 9th ISHS Symposium on the Processing Tomato, Acta Horticulturae.*
- [25] Hashem, M. S., El-Abedin, T. Z., Al-Ghobari, H. M. (2018): Rational water use by applying regulated deficit and partial root-zone drying irrigation techniques in tomato under arid conditions. – *Chilean Journal of Agricultural Research* 79(1). DOI: 10.4067/S0718-58392019000100075.
- [26] Hatfield, J. L., Dold, C. (2019): Water-use efficiency: advances and challenges in a changing climate. – *Front. Plant Sci.* <https://doi.org/10.3389/fpls.2019.00103>.
- [27] Helyes, L., Lugasi, A., Pek, Z. (2012): Effect of irrigation on processing tomato yield and antioxidant components. – *Turkish Journal of Agricultural and Forestry* 36: 702-709. DOI: 10.3906/tar-1107-9.
- [28] Hernández-Suárez, M. H., Rodríguez, E. R., Romero, C. D. (2008): Chemical composition of tomato (*Lycopersicon esculentum*) from Tenerife, the Canary Islands. – *Food Chem* 106(3): 1046-1056. <http://dx.doi.org/10.1016/j.foodchem.2007.07.025>.
- [29] Howell, T. A. (2001): Enhancing water use efficiency in irrigated agriculture. – *Agron. J.* 93: 281-289.
- [30] Huang, S., Zhao, C., Zhang, Y., Wang, C. (2018): Nitrogen Use Efficiency in Rice. – In: Amaullah, Fahad, S. (eds.) *Nitrogen in Agriculture-Updates.* InTech, Christchurch, New Zealand.
- [31] Ismail, S., Ozawa, K., Khondaker, N. A. (2007): Effect of irrigation frequency and timing on tomato yield, soil water dynamics and water use efficiency under drip irrigation. – *Eleventh International Water Technology Conference, IWTC11 2007 Sharm El-Sheikh, Egypt.*
- [32] Keller, J., Bliesner, R. D. (1990): *Sprinkle and Trickle Irrigation.* – Van Nostrand Reinhold, New York.
- [33] Kırnak, H., Kaya, C. (2004): Determination of irrigation scheduling of tomato using pan-evaporation in Harran plain. *GOÜ. – Journal of Agricultural Engineering* 21(1): 43-50.
- [34] Kuo, S. (1996): Phosphorus. – In: Sparks, D. L. (ed.) *Methods of Soil Analysis. Part 3: Chemical Methods.* SSSA Book Ser. 5. SSSA and ASA, Madison, WI. pp. 869-919. DOI: 10.2136/sssabookser5.3.c32.
- [35] Kuşçu, H., Karasu, A., Öz, M., Demir, A. O., Turgut, İ. (2013): Effect of irrigation amounts applied with drip irrigation on maize evapotranspiration, yield, water use efficiency, and net return in a sub-humid climate. – *Turkish Journal of Field Crops* 18(1): 13-19.
- [36] Kuşçu, H., Turhan, A., Demir, A. O. (2014): The response of processing tomato to deficit irrigation at various phenological stages in a sub-humid environment. – *Journal of Agricultural Water Management* 133: 92-103.
- [37] Lisar, S. Y. S., Motafakkerazad, R., Hossain, M. M., Rahman, I. M. M. (2012): Water Stress in Plants: Causes, Effects and Responses. – In: Rahman, I. M. M., Hasegawa, H. (eds.) *Water Stress.* Chap. 1. InTech, Rijeka, pp. 1-14. DOI: 10.5772/39363.
- [38] Locascio, S. J., Smajstrla, A. G. (1996): Water application scheduling by pan evaporation for drip-irrigated tomato. – *JASHS* 121(1): 63-68.
- [39] Locascio, S. J., Olson, S. M., Rhoads, F. M. (1989): Water quantity and time of N and K application for trickle-irrigated tomatoes. – *J. Amer. Soc. Hort. Sci.* 114: 265-268.

- [40] Loeppert, R. H., Suarez, D. L. (1996): Carbonate. – In: Sparks, D. L., et al. (eds.) Methods of Soil Analysis. Part 3: Chemical Methods. ASA and SSSA, Madison, WI, pp. 437-474.
- [41] Machade, R., Oliviera, M. R. G. (2005): Tomato root distribution, yield and fruit quality under different subsurface drip irrigation regimes and depths. – Irrigation Science 24(1): 15-24. DOI: 10.1007/s00271-005-0002-z.
- [42] Mahajan, G., Singh, K. G. (2006): Response of greenhouse tomato to irrigation and fertigation. – Agricultural Water Management 84: 202-206.
- [43] Malash N. M., Flowers T. J., Ragab, R. (2008): Effect of irrigation methods, management and salinity of irrigation water on tomato yield, soil moisture and salinity distribution. – Irrigation Science 26(4): 313-323.
- [44] Marouelli, W. A., Silva, W. L. C., Moretti, C. L. (2004): Production, quality and water use efficiency of processing tomato as affected by the final irrigation timing. – Hort. Bras. 22(2). <http://dx.doi.org/10.1590/S0102-05362004000200013>.
- [45] Medrano, H., Tomas, M., Martorell, S., Flexas, J., Hernandez, E., Rosello, J., Escalona, J. M., Bota, J. (2015): From leaf to whole plant water efficiency (WUE) in complex canopies: limitations of leaf WUE as a selection target. – The Crop Journal 3(3): 220-228. <https://doi.org/10.1016/j.cj.2015.04.00>.
- [46] Mitchell, J. P., Shennan, C., Grattan, S. R., May, D. M. (1991): Tomato yields and quality under water deficit and salinity. – J. Amer. Soc. Hort. Sci. 116: 215-221.
- [47] Mohammed, H. N., Mahmud, T. M. M., Puteri Edaroyati, M. W. (2018): Deficit irrigation for improving the postharvest quality of lowland tomato fruits. – Pertanika J. Trop. Agric. Sci. 41(2): 741-758.
- [48] Mohammed, M., Wilson, L. A., Gomes, P. L. (1999): Postharvest sensory and physiochemical attributes of processing and non-processing tomato cultivar. – J. Food Qual. 22: 167-182. DOI: 10.1111/j.1745-4557.1999.tb00549.x.
- [49] Musyoka, M., Adamtey, N., Muriuki A. W., Bautze D., Karanje E., Mucheru-Muna M., Fiaboe K. K. M., Cadisch G. (2019): Nitrogen leaching losses and balances in conventional and organic farming systems in Kenya. – Nutrient Cycling in Agroecosystems. DOI: 10.1007/s10705-019-10002-7.
- [50] Nelson, D. W., Sommers, L. E. (1996): Total Carbon, Organic Carbon, and Organic Matter. – In Sparks, D. L. et al. (eds.) Methods of Soil Analysis. Part 3. SSSA Book Series, Madison, WI, pp. 961-1010.
- [51] Nuruddin, M. M., Madramootoo, C. A., Dodds, G. T. (2003): Effects of water stress at different growth stages on greenhouse tomato yield and quality. – Journal of Hort. Science 38(7): 1389-1393.
- [52] Oenema, O., Brentrup, F., Lammel, J., Bascou, P., Billen, G., Dobermann, A., Erisman, J. W., Garnett, T., Hammel, M., Hanjotis, T., Hillier, J., Hoxha, A., Jensen, L. S., Oleszek, W., Pallière, C., Powelson, D., Quemada, M., Schulman, M., Sutton, M. A., Van Grinsven, H. J. M., Winiwarer, W. (2015): EU Nitrogen Expert Panel, Nitrogen Use Efficiency (NUE) - An Indicator for the Utilization of Nitrogen in Agriculture and Food Systems. – Wageningen University, Wageningen.
- [53] Olson, S. M., Rhoads F. M. (1992): Effect of water quantity on fall tomato production in North Florida. – Proceedings of Florida State Horticultural Society 105: 334-336.
- [54] Patanè, C., Cosentino, S. L. (2010): Effects of soil water deficit on yield and quality of processing tomato under a Mediterranean climate. – Agr. Water Manage. 97: 131-8.
- [55] Patanè, C., Tringali, S., Sortino, O. (2011): Effects of deficit irrigation on biomass, yield, water productivity and fruit quality of processing tomato under semi-arid Mediterranean climate conditions. – Scientia Horticulturae 129(4): 590-596. <https://doi.org/10.1016/j.scienta.2011.04.030>.
- [56] Rhoades, J. D. (1996): Salinity: Electrical Conductivity and Total Dissolved Solids. – In: Sparks, R. L. (ed.) Methods for Soil Analysis. Part 3: Chemical Methods. Soil Science Society of America, Madison, WI, pp. 417-435.

- [57] Rotiroti, M., Bonomi, T., Sacchi, E., McArthur, J. M., Stefania, G. A., Zanotti, C., Taviani, S., Patelli, M., Nava, V., Soler, V., Fumagalli, L., Leoni, B. (2019): The effects of irrigation on groundwater quality and quantity in a human-modified hydro-system: the Oglio River basin, Po Plain, northern Italy. – *Science of the Total Environment* 672: 342-356.
- [58] Senyigit, U., Arslan, M. (2018): Effects of irrigation programs formed by different approaches on the yield and water consumption of black cumin (*Nigella sativa* L.) under transition zone in the West Anatolia conditions. – *Journal of Agricultural Sciences* 24: 22-32.
- [59] Shock, C. (2006): Drip Irrigation: An Introduction. – Oregon State University, Corvallis. <https://catalog.extension.oregonstate.edu/sites/catalog/files/project/pdf/em8782.pdf> (accessed on 13.07.2012).
- [60] Shrivastava, P., Kumar, R. (2015): Soil salinity: a serious environmental issue and plant growth promoting bacteria as one of the tools for its alleviation. – *Saudi Journal of Biological Sciences* 22(2): 123-131. DOI: 10.1016/j.sjbs.2014.12.001.
- [61] Smajstrla, A. G., Locascio S. J. (1989): Drip irrigated tomato as affected by water quantity by N and K application timing. – *Proceedings of Florida State Horticultural Society* 102: 307-309.
- [62] Smajstrla, A. G., Locascio S. J. (1990): Irrigation scheduling of drip irrigated tomato using tensiometers. – *Proc. Florida State Hort. Soc.* 103: 88-91.
- [63] Soil Survey Staff. (2014): Keys to Soil Taxonomy. 12th Ed. – USDA-Natural Resources Conservation Service, Washington, DC.
- [64] SPSS (2008): SPSS Statistics for Windows, Version 17.0. – SPSS Inc., Chicago.
- [65] Thapa, B., Scott, C. A. (2019): Institutional strategies for adaptation to water stress in farmer-managed irrigation systems of Nepal. – *International Journal of the Commons* 13(2): 892-908. DOI: <http://doi.org/10.5334/ijc.901>.
- [66] Thomas, G. W. (1996): Soil pH and Soil Acidity. – In Sparks, D. L. (ed.) *Methods of Soil Analysis. Part 3: Chemical Methods*. SSSA Book Ser. 5. SSSA, Madison, WI, pp. 475-490.
- [67] Xu, L., Niu H., Xu, J., Wang X. (2013): Nitrate-nitrogen leaching and modeling in intensive agriculture farmland in China. – *The Scientific World Journal*. <http://dx.doi.org/10.1155/2013/353086>.
- [68] Wahb-Allah, M. A., Al-Omran, A. M. (2012): Effect of water quality and deficit irrigation on tomato growth, yield and water use efficiency at different developmental stages. – *Journal of Agricultural & Environmental Sciences* 11(2): 80-109.
- [69] Yurtseven, E., Kesmez, G. D., Ünlükara, A. (2005): The effects of water salinity and potassium levels on yield, fruit quality and water consumption of a native central anatolian tomato species (*Lycopersicon esculentum*). – *Agricultural Water Management* 78: 128-135.
- [70] Zegbe-Dominguez, J. A., Behboudian, M. H., Lang, A., Clothier, B. E. (2003): Deficit irrigation and partial rootzone drying maintain fruit dry mass and enhance fruit quality in “Petopride” processing tomato (*Lycopersicon Esculentum*, Mill.). – *Journal of Scientia Horticulturae* 98(4): 505-510.

EFFICACY OF IPM, MASS TRAPPING AND CHEMICAL CONTROL IN THE SUPPRESSING OF MEDITERRANEAN FRUIT FLY, [*CERATITIS CAPITATA* (WIEDEMANN) (DIPTERA: TEPHRITIDAE)] IN CITRUS

ELEKCIÖĞLU, N. Z.

Cukurova University, Vocational School of Karaisalı, Department of Plant and Animal Production, 01170 Adana, Turkey
(e-mail: nelekcioglu@cu.edu.tr; phone: +90-322-551-2057; fax: +90-322-551-2255)

(Received 22nd Jul 2019; accepted 25th Nov 2019)

Abstract. The management of the Mediterranean fruit fly, *Ceratitis capitata* (Wiedemann) (Diptera: Tephritidae) in Turkey is mainly through chemical control. In this study, the effectiveness of the integrated pest management (IPM), mass trapping and chemical control were compared in an orange orchard in Tarsus (Mersin) during 2015 and 2016. The IPM program was based on the use of the synthetic food attractant lure Biolure, paired with sanitation of infected fruits and chemical control if necessary. In mass trapping plots the female targeted attractant lure Biolure and the male targeted sex attractant lure Trimedlure were used. Chemical control was based on bait treatments with Spinosad. The efficiency of the applications was evaluated according to the rate of infected fruits during harvest. The highest number of flies was detected in the Control plot as 404 flies/trap/week in 2015 and in Chemical Control plot as 429 flies/trap/week in 2016. No statistical difference was found between the applications regarding the number of male flies weekly captured and number of infected fruits. However, it was determined that the ratio of infected fruits in the IPM plot was lower than that of other plots (1.57% in 2015 and 0.89% in 2016) at harvest, followed by Biolure, Trimedlure and Spinosad, respectively. It was concluded that IPM, which included the application of several methods, was the most effective control practice for *C. capitata*.

Keywords: *Ceratitis capitata*, food attractant, IPM, lure, sanitation, spinosad

Introduction

The Mediterranean fruit fly, *Ceratitis capitata* (Wiedemann, 1824) (Diptera: Tephritidae) is a significant quarantine pest. It is spread out over a wide area around the world due to its high tolerance to climatic changes compared to many other fruit fly species. Worldwide, *C. capitata* has over 579 fruits and vegetables as hosts (Liquidó et al., 2017). It causes economic damage to many fruit species in Turkey, first and foremost to citrus fruits. The pest completes its generation on these hosts before the citrus fruits mature, therefore, pest population is higher on citrus. Yield loss can reach 100% if the necessary pest control measures are not taken (Thomas et al., 2001; Umeh et al., 2004). The economic consequences of its presence include not only direct losses in yield and increased control costs, but also indirect damage, which is usually higher, such as loss of export markets, severe restriction of exports of most commercial fruits as a result of quarantine laws, and the cost of maintaining facilities for fruit treatment and eradication (Radonjić, 2013). There are various control methods used for this pest, including chemical control (bait application, foliar application), biotechnological control (mass trapping) and the release of sterile insects, which is applied in some countries (Martinez-Ferrer et al., 2010; Anonymous, 2018; Gëzhilli et al., 2018). Bait application is recommended in Turkey as it allows the maintenance of natural balance, protects human and environmental health and enables the reduction of the number of insecticides used in chemical control. Due to the limits of chemical control, alternative solutions that do not

leave pesticide residues have been sought after and trials based on mass trapping have been conducted. In Turkey, the use of biotechnological control techniques has been continuous since the 1970s. The effect of different attractants or trap and attractant combinations on the pest has been studied (Zümreoğlu, 1990; Epsky et al., 1999; Başpınar et al., 2011). Various studies, in which male and female attractants were used, have been performed in *C. capitata* mass trapping (Heath et al., 2004; Navarro-Llopis et al., 2008; Satar and Tireng, 2016). Trimedlure has been reported as the most effective and the most used male-specific attractant for detection and suppressing *C. capitata* (Hill, 1987; Tan et al., 2014). Heath et al. (1997) developed a synthetic food lure system that attracts both females and males (Biolure, 3-component fruit fly attractant). This attractant has been commonly used in many studies in order to monitor and suppress the pest population (Epsky et al., 1999; Cohen and Yuval, 2000; Papadopoulos et al., 2001; Broughton and De Lima, 2002; McQuate et al., 2005; Navarro Llopis et al., 2008; Martinez-Ferrer et al., 2012). Although it has increased over the years, only a limited number of producers apply the mass trapping method for *C. capitata* control in Turkey. While some producers think this control method is not sufficient for suppressing the pest, others think the method is difficult to apply. For this reason, they prefer chemical control, which is easier and cheaper but requires repetition at certain intervals. However, problems such as labour and loss of time have also been reported in the application of this method, particularly in large orchards. The damage rate varies between 8-15% in mass trapping applications performed on citrus orchards (Satar and Tireng, 2016; Demirel and Akyol, 2017; Yayla and Satar, 2017). It has also been reported that successful results were obtained with the application of mass trapping in an integrated pest management program and that 0.5% damage rate was achieved as a result of cultural control and other methods together until harvest (Martinez-Ferrer et al., 2012). The objective of this study was to compare the effectiveness of male-targeted and female-targeted *C. capitata* attractants, IPM and also chemical control against *C. capitata*.

Materials and methods

Groves and trapping scheme

The trial was conducted on a citrus orchard located in the eastern Mediterranean region of Turkey (Tarsus/Mersin). The orchard (36°55'04.90" N, 34°56'06.12" E) was a 7,5 ha area, drip irrigated and 15 m above sea level. It was planted with orange trees (*Citrus sinensis* var. Washington navel) that were 20 years old. Up until the experiment began, Spinosad was applied as bait (1 L/10 L-with 10 day intervals) in the orchard against *C. capitata*. The orchard was surrounded by a mandarin orchard on the north, a factory on the east and an area of field crops on the west and south. It was divided into six plots, with each plot being 1 ha for different treatments. All plots were besides each other at one edge of the orchard whereas only the control plot was at the other edge. Two rows were kept between the plots as barriers. To evaluate the efficacy of the applications, a randomized block design with four replicates was used. The following treatments were compared: 1) Chemical control with Success 0.24 CB bait application (CC), 2) Mass trapping with male attractant Trimedlure (MMT), 3) Mass trapping with female attractant Biolure, (3 component female-biased attractant - ammonium acetate, trimethylamine and putrescine) (FMT), 4) Integrated pest management program (Mass trapping with female attractant Biolure + sanitation by eliminating the punctured dropped fruits weekly + bait application if necessary) (IPM), and 5) Untreated control (C) (*Table 1*).

The insecticide treatments on the chemical control plot were performed according to the bait application method (Anonymous, 2015). Spinosad (1 L/10 L) was applied as insecticide at 10-day intervals and 150 ml pesticide-water mixture was used per tree. The remaining trees in the orchard were also treated with Spinosad. In the first mass trapping plot (MMT), experiments were performed using Eostrap® invaginada traps (Sanidad Agricola Econex, Santomera, Murcia, Spain) baited with %95 Trimedlure (formulated in a polymeric plug-type dispenser) (Sanidad Agricola Econex, Santomera, Murcia, Spain) and 2,2- dichlorovinyl dimethyl phosphate (DDVP) tablet (Sanidad Agricola Econex, Santomera, Murcia, Spain) as insecticide. A trap density of 20 traps/ha was applied for capturing adult males in both years. In the second mass trapping plot (FMT), Tephri-traps baited with synthetic female-targeted food attractant lure marketed as BioLure®Unipak™ (AgriSense-BCS Ltd., Pontypridd, South Wales, UK) and the insecticide dichlorvos (DDVP strips) (AgriSense-BCS Ltd., Pontypridd, South Wales, UK) were used (Fig. 1). A trap density of 50 traps/ha was applied for capturing adult females and males in both years. The adults captured in the traps were counted and recorded separately as females and males. In IPM plot the program was designed identically to the FMT plot. All the infected fallen fruits from all trees on this plot were collected once a week and destroyed. In addition, Spinosad was treated as bait when it was necessary.

Table 1. Treatment regimes during the study period

No	Trials		Treatments
1	Chemical control	CC	Spinosad bait application - 1L/10L
2	Mass trapping	MMT	Trimedlure male attractant - 20 traps/ha
3	Mass trapping	FMT	Biolure female attractant - 50 traps/ha
4	Integrated pest management	IPM	Mass trapping with Biolure + sanitation by eliminating the punctured dropped fruits + bait application if necessary
5	Untreated control	C	-



Figure 1. Trapping devices used in the field trials: a, b: Tephti trap with Biolure, c, d: Eostrap with Trimedlure

Treatments and population monitoring

Ceratitis capitata population was monitored by counting the males captured in 10 Jackson traps with Trimedlure as the attractant, hung on each tree in the middle row of all the plots. The traps were checked once a week. In the plots with Biolure use, the number of females was determined by counting the females captured in 10 traps which were marked at the beginning of the study. In all plots, mass traps and monitoring traps were hung in 29 August 2015 and 30 August 2016. They were hung at a height of 1.5-2.0 m from the ground in a shaded part of the canopy facing the south-east and were homogeneously distributed throughout the plots. The pheromone dispensers in the Eostrap traps were changed once every 90 days, while the pheromone dispensers in the Biolure traps were changed once every 120 days. Furthermore, the pheromone dispensers in the monitoring traps were changed once every 6 weeks.

Fruit damage assessment

Ten trees were chosen randomly from the middle row of all plots. The fallen fruits from these trees were collected every week, recorded as healthy or infected and removed from the orchard. The main assessment was performed during harvest; 100 fruits were controlled randomly from all sides of these trees and recorded as healthy or infected. The damage ratios (%) were calculated from the results of both counts.

Statistical analysis

The effect of applications on the male captures and fruit damage was analysed using a one-way Anova, where the applications were used as independent variables and “number of males captured” and “total number of infected fruits” were used as dependent variables. Means were separated by Tukey’s honestly significant difference (HSD) test at $P < 0.05$. All analysis were performed using the Microsoft statistics program SPSS 25.0. Damage ratio (%) was determined from the number of infected fruits recorded weekly and during harvest. The impacts of the IPM, mass trapping and bait treatments on the pest population were measured according to the Abbot formula [Effectiveness % = (Infected fruit % in Control - Infected fruit % in Trials/ Infected fruit % in Control) x 100] by the infected fruit reduction between the plots (Abbott, 1925). Results were expressed as percentage of damaged fruits.

Meteorological data were obtained from ‘Tarsus Soil and Water Sources Research Center’ located 2 km away from the tested orchard.

Results

Ceratitis capitata flight activity

The number of *C. capitata* males captured in Jackson traps on the CC plot were low in number throughout September for all applications in 2015 and 2016. In 2015, pest population started to increase as of October and reached the highest number on the second half of the month (22.10.2015). Pest population was determined as 369 flies/trap/week averagely for this period, remained within similar levels from the end of October to the mid of November and showed a decreasing trend in the following counts until harvest. The average number of males was determined as 124.64 adults/trap for this plot throughout the season. The first Spinosad treatment in this plot was carried out on 28 September 2015. Treatments continued at 10-day intervals, and a total of 8 treatments

were performed until the harvest on 17 December 2015. In 2016, pest population peaked at the end of October (31.10.2016) with averagely 429 flies/trap/week. Throughout the season, the average number of males for this plot was 122.79 adults/trap (*Table 2*). The first insecticide was treated on 03 October 2016, and a total of 7 treatments were performed until harvest on 22 December 2016. In the MMT and FMT plots, the highest number of adults in 2015 were recorded at the end of October as averagely 325 and 256 flies/trap/week, respectively. Pest population showed a decreasing trend until harvest (*Fig. 2*). The average number of males on these plots throughout the season was determined as 120.14 and 104.14 adults/trap, respectively (*Table 2*). On the IPM plot, pest population started to increase after the second half of October, and the highest number of adults was counted as 383 flies/trap/week on average on 29 October 2015. In order to increase the efficiency of mass trapping, Spinosad bait was applied just after this date. The pest population immediately decreased after the application. The average number of males on this plot throughout the season was determined as 109.29 adults/trap. The number of males captured in the traps was highest in the Control plot. The highest number of adults was again determined at the end of October (29.10.2015) as averagely 404 flies/trap/week. The number of males on this plot throughout the season was averagely 141.71 adults/trap (*Table 2*).

Table 2. Average number of male *Ceratitis capitata* captured and infected fruits under different application regimes during 2015 and 2016

Trials	Mean male medflies captured/Trap±SE (Min. -Max.)		Infected fruit number±SE (Min. -Max.)	
	2015	2016	2015	2016
Chemical Control	124.64±28.15a* (25-369)	122.79±31.86a (34-429)	11.86±2.23A* (0-26)	9.14±2.11A (0-25)
Mass Trapping (Male)	120.14±25.12a (28-325)	110.14±31.07a (12-383)	8.36±1.71A (0-19)	7.07±1.64A (0-18)
Mass Trapping (Female)	104.14±21.39a (17-256)	114.79±34.52a (21-397)	4.21±0.90A (0-9)	3.71±1.00A (0-12)
Integrated Pest Management	109.29±3.83a (14-383)	111.86±23.33a (22-286)	3.29±0.58A (0-7)	3.07±0.70A (0-6)
Control	141.71±35.79a (33-404)	137.57±25.94a (31-356)	26.21±4.05B (0-43)	23.57±3.74B (0-44)

*Means followed by the same letter within a column are not significantly different by Tukey's multiple comparison test where $P < 0.05$

Considering all applications, pest population was determined to be high particularly from the second week of October until the mid of November. Although the highest number of adults was counted in the Control plot, no statistical difference was determined among the applications ($F=0.273$; $df=4, 65$; $P = 0.894$). In 2016, the highest number of adults was captured on 31 October 2016, with averagely 429, 383, 397, 286 flies/trap/week for the CC, MMT, FMT, IPM plots, respectively. In the Control plot, the highest number of adults was determined one week before the other plots on 24 October 2016 with an average of 356 flies/trap/week. Throughout the season, the average number of males were determined as 122.79, 110.14, 114.79, 111.87, and 137.57 adults/trap in the CC, MMT, FMT, IPM, and Control plots, respectively (*Table 2*).

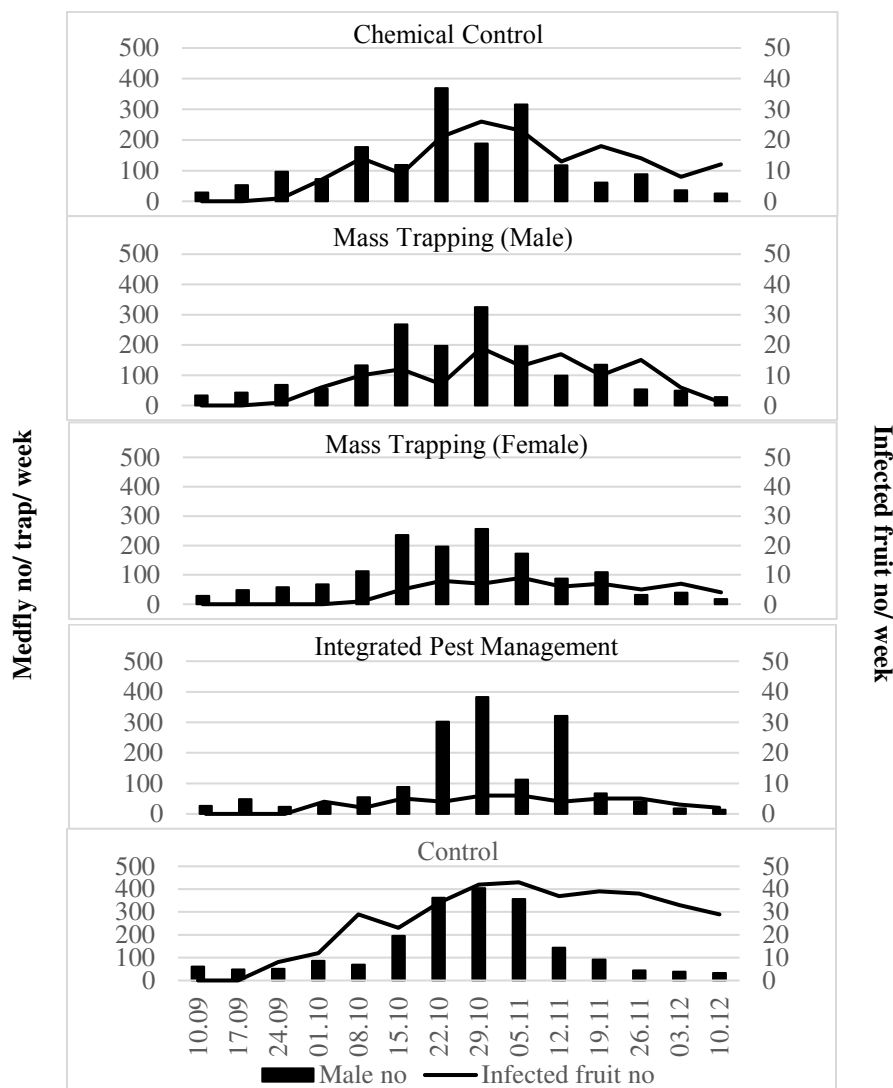


Figure 2. The number of males captured in the Jackson traps and the infected fruits in the plots comparing different methods against *Ceratitis capitata* in Tarsus (Mersin) in 2015

In 2016, until harvest, the adults continued to be captured in the traps on all the plots (Fig. 3). No insecticides were treated on the IPM plot this year. The highest number of males was determined in the Control plot, however, no statistical difference was determined among the applications this year ($F=0.138$; $df=4, 65$; $P=0.968$).

On the FMT plot, the number of females was higher than the males. In 2015, 4.312 and 4.925 females were captured from the FMT and IPM plots, respectively. Accordingly, the rate of males on the FMT plot was determined as 25,27%, while the rate of females was determined as 74,73%. In addition, the ♂:♀ ratio was 23,70% : 76,30% on the IPM plot. In 2016, the total number of females on the FMT plot was 5.039, and number of males was 1.607. The rate of females was determined as 75,82%, while the rate of males was 24,18%. A total of 6.857 adults were collected from the traps on the IPM plot in the second year of the study, and the ♂:♀ ratio was determined as 22,83% : 77,17%. It has been observed that the number of females captured in traps is three times higher than males.

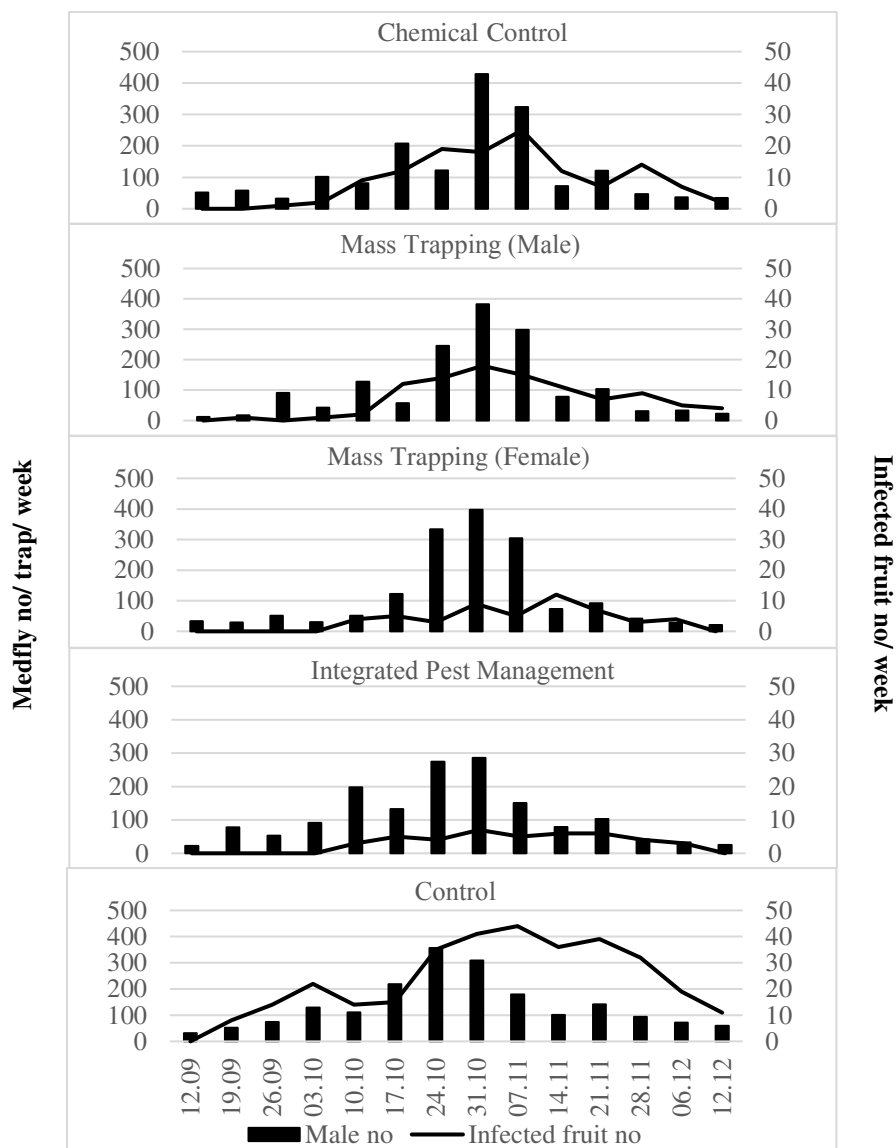


Figure 3. The number of males captured in the Jackson traps and the infected fruits in the plots comparing different methods against *Ceratitis capitata* in Tarsus (Mersin) in 2016

Fruit damage assessment

The average number of punctured fruits due to *C. capitata* infection in different applications is given in Table 2. In 2015, the first infected fruits were observed in the CC, MMT and Control plots on 24 September 2015, in the IPM plot on 01 October 2015 and on 08 October 2015 on the FMT plots (Fig. 2). Throughout the season, the highest number of infected fruits was observed in the Control plot (an average of 26.21 fruits). The maximum number of infected fruits (an average 43 fruits) on this plot was observed on 05 November 2015. This date corresponds to the week after the date when the highest number of adults were captured in the traps. The lowest number of infected fruits was observed on the IPM plot (an average of 3.29 fruits). Among the infected fruits throughout the season, it was observed that the difference between applications was statistically significant. CC, MMT, FMT and IPM plots were in the same group while the Control plot

was in different group ($F=16,919$; $df=4, 65$; $P<0.001$). Similar results were also obtained in 2016 (Fig. 3). The number of infected fruits observed in the CC, MMT, FMT, IPM and Control plots throughout the season were 9.14, 7.07, 3.71, 3.07 and 23.57, respectively. Following the *C. capitata* infection, the difference between the weekly number of the dropped fruits was determined as statistically significant among the applications. CC, MMT, FMT and IPM plots were in the same group, while Control was in another group ($F=15.388$; $df=4, 65$; $P<0.001$).

Since all the applications were performed on the same orchard, impacts of the climatic factors affected all plots. No rainfall that required the applications to be repeated was experienced throughout the study. Therefore, it was considered that there were no conditions among applications that were caused by climatic factors (Fig. 4). The average temperature in august was 27.1 and 29.9°C in 2015 and 2016, respectively. The temperature followed a decreasing trend until harvest, but until November it was over 21°C both years. The relative humidity was over 50% and no heavy rainfall that limited the pest population occurred during the study both years.

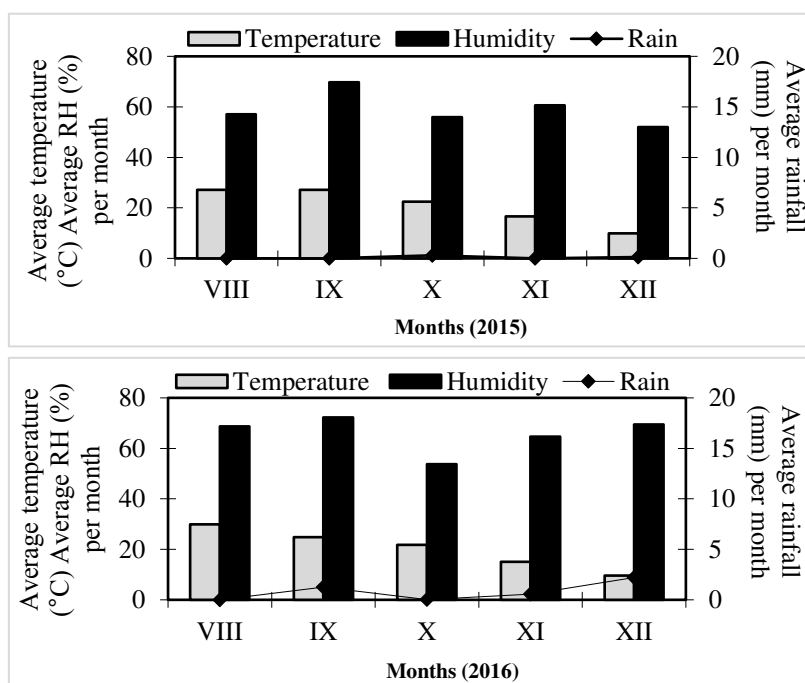


Figure 4. Climatic datas in Tarsus (Mersin) in 2015 and 2016

At the harvest, the efficiency of the CC, MMT, FMT and IPM applications against *C. capitata* in 2015 was 88.62%, 91.46%, 94.21% and 95.33%, respectively. The difference between the applications were statistically significant ($F=10.892$; $df=3, 36$; $P<0.001$). The CC, MMT, FMT and IPM applications showed average efficiency of 87.43%, 90.65%, 94.29% and 97.17%, respectively in 2016.

A statistical difference was determined between the applications ($F=17.188$; $df=3, 6$; $P<0.001$) and between the years ($F=20.456$; $df=3, 6$; $P<0.001$ in 2015, $F=12.148$; $df=3, 6$; $P<0.001$ in 2019). It was determined that the ratio of infected fruits in the IPM plot was lower than that of other plots (1.57% in 2015 and 0.89% in 2016) at harvest, followed by Biolure, Trimedlure and Spinosad, respectively (Table 3).

Table 3. Effect of the pest control techniques on the percentage of damaged fruits (mean±SE) at harvest in orange orchard in 2015 and 2016

Trials	% of infected fruits±SE	
	2015	2016
Chemical Control	3.75±1.12 a* A**	3.94±1.33 a A
Mass Trapping (Male)	2.81±1.05 ab A	2.90±1.29 ab AB
Mass Trapping (Female)	1.96±0.77 bc B	1.78±0.71 bc BC
Integrated Pest Management	1.57±0.60 c B	0.89±0.53 c C
	<i>F</i> = 10,892	<i>F</i> = 17,188
	<i>df</i> = 3, 36	<i>df</i> = 3, 36
	<i>P</i> = 0,001	<i>P</i> = 0,000
Control	33.93	31.76

*Values followed by the same letter within a column, **Values followed by the same letter within a line are not significantly different at $P < 0.05$

Discussion

Ceratitis capitata flight activity

Several mass trapping systems have been developed to control *C. capitata* worldwide. Depending on the strength of the attractant, this tactic targets females or males. In Turkey, there is very little mass trapping for the pest. Başpınar et al. (2011), Satar and Tireng (2016) and Demirel and Akyol (2017) reported that the mass trapping is being used successfully against *C. capitata*.

Results obtained from this study showed that considering all applications, pest population was determined to be high particularly from the second week of October until the mid of November in 2015 and 2016. The highest number of males was determined in the Control plot, however, no difference was determined among the applications both years. The fact that the number of males captured in the traps from different plots was not statistically different in both years has suggested that the pest showed homogeneous distribution among applications in the orchard. In 2015 and 2016, although the fruits had not reached infection maturity, the adults captured in the traps showed that the flies had flown to the study orchard from neighbouring orchards which had hosts of the pest. However, while pest population was low at the beginning of September, when the study started, the population increased when the fruits changed colour and the number of males captured in the traps was high in October and November. There are many studies in Turkey and in the world on the population dynamics of *C. capitata*. Katsoyannos et al. (1998) in their study performed in Chios (Greece) determined the highest number of adults captured in traps were in October and November. In addition, Martinez-Ferrer et al. (2010) determined similar results with mandarins in Spain and Boulahia-Kheder et al. (2012) with mandarins and oranges in Tunisia. Demirel and Akyol (2017) reported that pest population increased in October and November, in the mass trapping study performed with Eostrap invaginada traps in a satsuma mandarin orchard in Hatay (Turkey). Elekcioglu (2013) stated that *C. capitata* population peaked in June, between 2008-2010 in a Washington navel orchard in Adana, which had similar climatic conditions to the orchard in the present study. The reason for this population increase during this period, when the fruits haven't yet reached infection maturity, is that there were other hosts for the pest around the study

orchard and the fact that the pest reproduced. The pest population increased on these fruit trees and moved to citrus in the late summer or autumn. A high number of adults were captured from the mid of September until the mid of November in the study years and six to nine treatments were done per year on the citrus according to the weather conditions. The present study showed parallel results with the literature. It is considered that the high pest population and the fact that they reproduced in the citrus fruits during this period is due to the decrease in or non-existence of host plants, apart from the citrus species.

It has been observed that the number of females captured in traps is three times higher than males in the present study and in different studies from the literature that had different pest population, citrus type, traps, climatic conditions, etc. It is considered that capturing females is crucial for *C. capitata* control since the number of eggs laid decreases automatically. While males were captured primarily in the traps on MMT plot, females were also captured, even though the number of females was lower than males. Leza et al. (2008) determined that the rate of females varied between 70.10% : 78.70%, in which they used Biolure as a food lure and different insecticides. In their study performed on mandarins by using Tephri traps with attractants containing ammonium acetate, putrescine and trimethylamine as food, which is identical to the attractants used in the present study. Mediouni-Ben Jemâa et al. (2010) determined that the rate of females varied between 68.79% - 73.70% and 72.26% - 72.30% in a Washington navel orange orchard. Satar and Tireng (2016) determined the ♂:♀ rate as 27.00% : 73.00% and 31.00% : 69.00% in their mass trapping study, where they used ammonium acetate+chlorohydrate trimethylamine+diamineopentane as food for the pest control in an Okitsu wase mandarin orchard.

Fruit damage assessment

In all applications, the infected fruits were first observed at the end of September and the first half of October. After then, the number of infected fruits increased with the increasing pest population. The lowest number of infected fruits was observed in the IPM plot in both years. It is considered that the females were primarily attracted to the smell of the food and therefore directed to the traps with the yellow plates and did not infect the fruit in this plot. The bait application for suppressing the population in this plot during the high pest population contributed to reducing the population. The IPM plot was followed by FMT, MMT and CC plots, respectively.

The results show similarities with the study of Leza et al. (2008), who obtained the most successful result for *C. capitata* control when they used Biolure as attractant (50 Probodelt trap/ha) and one bait application of fenthion or Spinosad or lambda-cyhalothrin if required. The pest damage rate varies in the mass trapping studies in the literature on different citrus species. Boulahia-Kheder et al. (2010) reported more than 30% damage with only mass trapping in a Navel orange orchard in Tunisia. However, they determined a 5% damage rate on Navel orange at harvest with 4 foliar Spinosad treatments, sanitation and female mass trapping with Moskisan + Biolure as attractant (Boulahia-Kheder et al., 2015). In Spain, Martinez-Ferrer et al. (2012) detected <2% infected fruit rate with early maturing mandarin varieties (Loretina and Marisol) by using 50 Maxitrap (Probodelt®) traps/ha baited with Ferag CC D TM (SEDQ) + chemical treatments with Malathion or Spinosad. Nevertheless, it was determined that population decreased in midseason for Clemenules, and even in the case that the number of traps was reduced by half, the population still decreased, and less than 0.5% of infected fruit rate was detected. Demirel and Akyol (2017) determined 10.91% and 8.56% rate of infected fruits in 2011-2012, respectively, in a Satsuma mandarin orchard

in Hatay (Turkey) by using Eostrap traps (48 traps/0.7 ha and 23 traps/0.7 ha) baited with 95% Trimedlure. In their study, they also used Eostrap traps, as this study, and obtained similar results despite having a higher number of traps per hectare. Yayla and Satar (2017) determined this rate as 8.57% in 2015 and 15.03% in 2016, in which they used Lastfly *Ceratitis* (4 traps/ha) traps for an Okitsu wase mandarin variety in Adana (Turkey). Various mass trapping systems have been developed worldwide for the control of fruit flies. These systems target capturing males or females according to the effect of the attractant. Better results have been reported from many mass trapping studies that used female-targeted attractants (Leza et al., 2008; Navarro-Llopis et al., 2008; Médiouni-Ben Jemaa et al., 2010; Trabelsi and Boulahia-Kheder, 2011; Boulahia-Kheder et al., 2015; Vargas et al., 2018). Biolure, which contains 3 synthetic components and targets mostly females, has been determined as one of the most suitable attractant for *C. capitata* (Epsky et al., 1999). In various Mediterranean countries, significant decreases have been reported in damage for citrus fruits or different hosts in IPM programs using this attractant (Navarro-Llopis et al., 2008; Martinez-Ferrer et al., 2012). The type of attractant is highly important for capturing a high number of females. The use of trimethylamine, the most efficient attractant, with ammonium acetate and with or without putrescine gives outstanding results against the pest (Heath et al., 2004). Food attractants containing more ammonium acetate and trimethylamine are most successful for capturing insects (Navarro-Llopis et al., 2008; Başpınar et al., 2011). Katsoyannos et al. (1999 a,b) determined that traps using 3-component synthetic lures are more specific for *C. capitata* than other female-targeted traps, and attract less non-target insects than 2-component lures and hydrolysed proteins. Broughton and De Lima (2002) reported a significant decrease in pest population and the number of infected fruits in their study in Western Australia using Biolure as an attractant compared to bait application using Spinosad. Furthermore, a higher number of females was captured by using Biolure, independent of trap type, climate, host plant or pest population. Miranda et al. (2001) stated that synthetic food lures (putrescine, ammonium acetate, and trimethylamine) were highly efficient on both high and low populations in their mass trapping study that targeted capturing *C. capitata* females in Spain. Mass trapping has been reported as an increasing controlling method in Turkey and worldwide against *C. capitata* in larger sized orchards (Broumas et al., 2002; McQuate et al., 2005; Demirel and Akyol, 2017; Yayla and Satar, 2017). Cohen and Yuval (2000) expressed that more successful results were obtained with increasing orchard size, and that this was due to the fact that trap systems and attractants are improved over time. In this study, as stated by researcher, regular implementation of control methods (chemical or biotechnological) in neighboring orchards, and regular collection and destruction of fallen fruits throughout the orchard contribute in reducing the pest population in the application orchard beyond any doubt. Organic farming orchards achieved the most success in *C. capitata* control due to the consumption of the fallen fruits by chickens and ducks, resulting in the destruction of pest larvae and pupae, in addition to mass trapping (80 traps/ha) (Leza et al., 2008). A more holistic and successful pest control is achieved in cases where several or all control methods consisting of biological, biotechnological, chemical and cultural practices are applied (Rachid and Ahmed, 2018). It can be suggested that the reason for the decreased pest population in some plots, as observed in this study, may be due to the decrease in the pest population posed with two years of trap application. However, it is thought that this should not be considered as a result that is always valid. Despite the regular pest control in an orchard, if there is no efficient control in neighbouring orchards, adults from these orchards will always pose a threat for the application orchard. The fact that the neighbouring

orchards belong to the same producer, and that the producer applied control methods in these orchards contributed to the decrease in the population. The efficiency of pest control with mass trapping in wide areas has been observed better in this study.

Climate characteristics, besides food source, could influence the diversification of *C. capitata* activity, development and distribution (Cohen et al., 2008). *C. capitata* prefers hot and dry areas over wet and cold areas (Israely et al., 2005). Mersin Province which is in the Mediterranean region of Turkey has a Mediterranean climate: hot dry summer, wet mild winter. The optimum temperature for the development of this pest is between 21-26.7°C. The effect of rainfall on the medfly population has been related to a decrease in adult captures on rainy days and an increase a few days later, because flies are generally inactive during periods of moderate to heavy rainfall (Papadopoulos et al., 1996; Cohen et al., 2008). In the present study no heavy rainfall that limited the pest population occurred during the study both years. Moustafa et al. (2014) mentioned that *C. capitata* population is significantly affected by some weather factors especially temperature degrees. Relative humidity plays a minor role in the build-up of the pest population (Ghanim and Moustafa, 2009; Ghanim, 2017). The average temperature in august was 27.1 and 29.9°C in 2015 and 2016, respectively. The temperature followed a decreasing trend until harvest, but until November it was over 21°C both years. The relative humidity was between 52% and 72%. Kasap and Aslan (2016) specify that the pest is active at daily average humidity of 40-80%. No heavy rainfall that limited the pest population occurred during the study both years. According to Ghanim and Moustafa (2009) and Ghanim (2012, 2017), the activity of *C. capitata* is mainly correlated with the presence of fruit ripening of its host plants. It is unavoidable that global warming also will affect *C. capitata* population as other insects. *C. capitata* is likely to spread to other regions in Turkey in the near future (Kaya et al., 2017).

Conclusion

According to the results, the highest number of flies was detected in the Control plot (404 flies/trap/week) in 2015 and in Chemical Control plot (429 flies/trap/week) in 2016. Between the trials no statistical difference was found regarding the number of male flies weekly captured and number of infected fruits. The ratio of infected fruits in the IPM plot was lower than other plots (1.57% in 2015 and 0.89% in 2016) at harvest, followed by Biolure, Trimedlure and Spinosad, respectively. It was concluded that, the use of food lures to attract females, which are mainly responsible for the population growth of, was more ideal for mass trapping in the control of *C. capitata*, instead of traps using sex pheromones to attract males. IPM was the most effective control method for *C. capitata*. It is evident that the sanitation by eliminating the punctured fruits together with the bait application decreased the infected fruit number moreover the tolerance of the pest is 'zero' during export. Since citrus is an important export product for Turkey, a combination of several techniques as part of an integrated pest management approach can provide an inclusive, permanent and effective strategy, with a limited negative effect on the environment. It is unavoidable that global warming will affect *C. capitata* population. Therefore, the pest control may be necessary in winter months in the near future. Integrated control of *C. capitata*, if properly carried out, thought to be successful in minimizing the pest population. In order for the IPM programme for the pest to be successful, an organization must be established, cooperation between growers, extension agents and researchers encouraged and a national policy drawn up that supports the IPM programme for citrus.

REFERENCES

- [1] Abbott, W.S. (1925): A method of computing the effectiveness of an insecticide. – Journal of Economic Entomology 18: 265-267.
- [2] Anonymous. (2015): Plant Pests Standard Pesticide Trial Methods, Mediterranean Fruit Fly [*Ceratitis capitata* (Wied.) (Dip.: Tephritidae)] Standard Pesticide Trial Method. – <http://www.tagem.gov.tr>. (Date accessed: June 2015).
- [3] Anonymous. (2018): Trapping Guidelines for Area - Wide Fruit Fly Programmes. – FAO/IAEA Programme of Nuclear Techniques in Food and Agriculture, Second edition, Vienna, 66 pp.
- [4] Başpınar, H., Karsavuran, Y., Başpınar, N., Kaya Apak, F. (2011): The effect of some attractants in mass trapping in controlling of Medfly, *Ceratitis capitata* (Wiedemann) (Diptera: Tephritidae). – Proceedings of Turkish IV. Plant Protection Congress, 28-30 June, Kahramanmaraş, Turkey, 496 pp.
- [5] Boulahia-Kheder, S., Jerraya, S., Fezzani, M., Jrad, F. (2010): First results in Tunisia on the mass-trapping an alternative way to control the Mediterranean fruit fly *Ceratitis capitata* (Diptera: Tephritidae). – Annals INRAT. 82: 168-180.
- [6] Boulahia-Kheder, S., Trabelsi, I., Aouadi, N. (2012): From Chemicals to IPM Against the Mediterranean Fruit Fly *Ceratitis capitata*. – In: Soloneski, S. (ed.) Integrated Pest Management and Pest Control - Current and Future Tactic. InTech, Rijeka, Tunisia.
- [7] Boulahia-Kheder, S., Chaaabane-Boujnah, H., Bouratbine, M., Rezgui, S. (2015): IPM based on mass trapping systems: a control solution for *Ceratitis capitata* (Wiedemann, 1824) (Diptera: Tephritidae) in organic citrus orchard of Tunisia. – Research Journal of Agriculture and Environmental Management 4(10): 459-469.
- [8] Broughton, S., Francis De Lima, C. P. (2002): Field evaluation of female attractants for monitoring *Ceratitis capitata* (Diptera: Tephritidae) under a range of climatic conditions and population levels in Western Australia. – Journal of Economic Entomology 95: 507-512.
- [9] Broumas, T., Haniotakis, G., Liaropoulos, C., Tomazou, T., Ragoussis, N. (2002): The efficacy of improved form of the mass-trapping method for the control of the olive fruit fly, *Bactrocea oleae* (Gmelin) (Dipt., Tephritidae): pilot-scale feasibility studies. – Journal of Applied Entomology 126: 217-223.
- [10] Cohen, H., Yuval, B. (2000): Perimeter trapping strategy to reduce Mediterranean fruit fly (Diptera: Tephritidae) damage on different host species in Israel. – Journal of Economic Entomology 93(3): 721-725.
- [11] Cohen, Y., Cohen, A., Hetzroni, A., Alchanatis, V., Broday, D., Gazit, Y., Timar, D. (2008): Spatial decision support system for medfly control in citrus. – Computers and Electronics in Agriculture 62(2): 107-117.
- [12] Demirel, N., Akyol, E. (2017): Evaluation of mass trapping for control of Mediterranean fruit fly, *Ceratitis capitata* (Wiedemann) (Diptera: Tephritidae) in satsuma mandarin in Hatay province of Turkey. – International Journal of Environmental and Agriculture Research 3(12): 32-37.
- [13] Elekcioglu, N. Z. (2013): Current status of Mediterranean fruit fly, *Ceratitis capitata* (Wiedemann) (Diptera: Tephritidae), in Turkey. – IOBC/WPRS Bulletin 95: 15-22.
- [14] Epsky, N. D., Hendrichs, J., Katsoyannos, B. I., Vasquez, L. A., Ros, J. P., Zümreoğlu, A., Pereira, R., Bakri, A., Seewooruthun, S. I., Heath, R. R. (1999): Field evaluation of female-targeted trapping systems for *Ceratitis capitata* (Diptera: Tephritidae) in seven countries. – Journal of Economic Entomology 92: 156-164.
- [15] Gëzhilli, A., Velo, E., Bino, S., Kadriaj, P., Zaimaj, E., Haka Duraj, N. (2018): Integrated control of Mediterranean fruit fly *Ceratitis capitata* (Wiedemann) by mass trapping in Tirana, Albania. – International Research Journal of Advanced Engineering and Science 3(2): 70-71.

- [16] Ghanim, N. M., Moustafa, S. A. (2009): Flight activity of Mediterranean fruit fly, *Ceratitis capitata* Wiedemann in response to temperature degrees and relative humidity at Dakahlia governorate. – Bulletin of the Entomological Society of Egypt 86: 209-221.
- [17] Ghanim, N. M. (2012): Responses of *Ceratitis capitata* Wiedemann and *Bactrocera zonata* (Saunders) to some weather factors and fruit ripening in persimmon orchards. – Bulletin of the Entomological Society of Egypt 89: 201-214.
- [18] Ghanim, N. M. (2017): Population fluctuations of the Mediterranean fruit fly, *Ceratitis capitata* (Wiedemann) with respect to some ecological factors in peach orchards. – Journal of Plant Protection and Pathology 8(11): 555-559.
- [19] Heath, R. R., Epsky, N. D., Guzman, A., Rizzo, J., Dueben, B. D., Jeronimo, F. (1997): Adding methyl-substituted ammonia derivatives to a food-based synthetic attractant on capture of Mediterranean and Mexican fruit flies (Diptera: Tephritidae). – Journal of Economic Entomology 90: 1584-1589.
- [20] Heath, R. R., Epsky, N. D., Midgarden, D., Katsoyannos, B. I. (2004): Efficacy of 1,4-diaminobutane (Putrescine) in a food-based synthetic attractant for capture of Mediterranean and Mexican fruit flies (Diptera: Tephritidae). – Journal of Economic Entomology 97: 1126-1131.
- [21] Hill, A. R. (1987): Comparison between trimedlure and capilure attractants for male *Ceratitis capitata* (Wiedemann) (Diptera: Tephritidae). – Journal of the Australian Entomological Society 26: 35-36.
- [22] Israely, N., Ziv, Y., Calun, R. (2005): Metapopulation spatial-temporal distribution patterns of Mediterranean fruit fly (Diptera: Tephritidae) in a patchy environment. – Annals of the Entomological Society of America, BioOne 98(3): 302-308.
- [23] Kasap, A., Aslan, M. M. (2016): The monitoring the population and detection of the loss ratio of the Mediterranean fruit fly (*Ceratitis capitata* Wied.) (Diptera: Tephritidae) by pheromone traps in pomegranate and persimmon varieties. – KSU Journal of Natural Sciences 19(1): 43-50.
- [24] Katsoyannos, B. I., Kouloussis, N. A., Carey, J. R. (1998): Seasonal and annual occurrence of Mediterranean fruit flies (Diptera: Tephritidae) on Chios Island, Greece: Differences between two neighboring citrus orchards. – Annals of the Entomological Society of America 91(1): 43-51.
- [25] Katsoyannos, B. I., Heath, R. R., Papadopoulos, N. T., Epsky, N. D., Hendrichs, J. (1999a): Field evaluation of Mediterranean fruit fly (Diptera: Tephritidae) female selective attractants for use in monitoring programs. – Journal of Economic Entomology 92: 583-589.
- [26] Katsoyannos, B. I., Papadopoulos, N. T., Heath, R. R., Hendrichs, J., Kouloussis, N. A. (1999b): Evaluation of synthetic food-based attractants for female Mediterranean fruit flies (Dipt., Tephritidae) in McPhail type traps. – Journal of Applied Entomology 123: 607-612.
- [27] Kaya, T., Ada, E., İpekdal, K. (2017): Modeling the distribution of the Mediterranean fruit fly, *Ceratitis capitata* (Wiedemann, 1824) (Diptera, Tephritidae) in Turkey and its range expansion in Black Sea Region. – Turkish Journal of Entomology 41(1): 43-52.
- [28] Leza, M. M., Juan, A., Capllonch, M., Alemany, A. (2008): Female-biased mass trapping vs. bait application techniques against the Mediterranean fruit fly, *Ceratitis capitata* (Dipt., Tephritidae). – Journal of Economic Entomology 132: 753-761.
- [29] Liquido, N. J., McQuate, G. T., Hanlin, G. T., Suiter, K. A. (2017): Host plants of the Mediterranean fruit fly, *Ceratitis capitata* (Wiedemann). – Version 3.5. USDA CPHST Online Database. <https://coffhi.cphst.org/>. Date accessed: January 2019.
- [30] Martinez-Ferrer, M. T., Campos, J. M., Fibia, J. M. (2010): Mediterranean fruit fly *Ceratitis capitata* (Wiedemann) mass trapping on clementine groves in Spain. – Journal of Applied Entomology 136(3): 181-190.
- [31] Martinez-Ferrer, M. T., Campos, J. M., Fibla, J. M. (2012): Field efficacy of *Ceratitis capitata* (Diptera: Tephritidae) mass trapping technique on clementine groves in Spain. – Journal of Applied Entomology 136: 181-190.

- [32] McQuate, C. D., Sylva, C. D., Jang, E. B. (2005): Mediterranean fruit fly (Dipt., Tephritidae) suppression in persimmon through bait sprays in adjacent coffee plantings. – *Journal of Applied Entomology* 129: 110-117.
- [33] Mediouni-Ben Jemâa, J., Bachrouch, O., Allimi, E., Dhouibi, M. H. (2010): Field evaluation of Mediterranean fruit fly mass trapping with Tripack® as alternative to malathion bait-spraying in citrus orchards. – *Spanish Journal of Agricultural Research* 8: 400-408.
- [34] Miranda, M. A., Alonso, R., Alemany, A. (2001): Field evaluation of medfly (*Ceratitis capitata*, Dip. Tephritidae) female attractants in a Mediterranean agrosystem (Balearic Islands, Spain). – *Journal of Applied Entomology* 125: 333-339.
- [35] Moustafa, S. A., Ghanim, N. M., Shower, D. M. (2014): Presence of *Ceratitis capitata* Wiedemann and *Bactrocera zonata* (Saunders) in apple orchards at Dakahlia governorate. – *Bulletin of the Entomological Society of Egypt* 91: 149-161.
- [36] Navarro-Llopis, V., Alfaro, F., Dominguez, J., Sanchis, J., Primo, J. (2008): Evaluation of traps and lures for mass trapping of Mediterranean fruit fly in citrus groves. – *Journal of Economic Entomology* 101: 126-131.
- [37] Papadopoulos, N. T., Carey, J. R., Katsoyannos, B. I., Kouloussis, N. A. (1996): Overwintering of the Mediterranean fruit fly (Diptera: Tephritidae) in northern Greece. – *Annals of the Entomological Society of America* 89: 526-534.
- [38] Papadopoulos, N. T., Katsoyannos, B. I., Kouloussis, N. A., Hendrichs, J., Carey, J. R., Heath, R. R. (2001): Early detection and monitoring of *Ceratitis capitata* (Diptera: Tephritidae) in a mixed-fruit orchard in northern Greece. – *Journal of Economic Entomology* 94: 971-978.
- [39] Rachid, E., Ahmed, M. (2018): Current status and future prospects of *Ceratitis capitata* Wiedemann (Diptera: Tephritidae) control in Morocco. – *Journal of Entomology* 15(1): 47-55.
- [40] Radonjić, S. (2013): Dispersion of the Mediterranean fruit fly *Ceratitis capitata* Wied. (Diptera: Tephritidae) in mandarin orchards on Montenegrin seacoast. – *Pesticides and Phytomedicine* 28(1): 31-38.
- [41] Satar, S., Tireng, G. (2016): Determined of effectiveness of the use of traps against the *Ceratitis capitata* Wied. (Diptera: Tephritidae) in Okitsu wase mandarin and relationship between fruit pomological characteristics and infestation. – *Derim* 33(2): 221-236.
- [42] Tan, K. H., Nishida, R., Jang, E. B., Shelly, T. E. (2014): Pheromones, Male Lures, And Trapping Of Tephritid Fruit Flies. – In: Shelly, T., Epsky, N., Jang, E. B., Reyes-Flores, J., Vargas, R. (eds.) *Trapping and the Detection, Control, and Regulation of Tephritid Fruit Flies*. Springer, Dordrecht, The Netherlands.
- [43] Thomas, M. C., Heppner, J. B., Woodruff, R. E., Weems, H. V., Steck, G. J., Fasulo, T. R. (2001): *Mediterranean Fruit Fly, Ceratitis capitata* (Wiedemann) (Insecta: Diptera, Tephritidae). – University of Florida, IFAS Extension. EENY - 214.
- [44] Trabelsi, I., Boulahia-Kheder, S. (2011): The use of mass-trapping technique in an integrated pest management program against the mediterranean fruit fly *Ceratitis capitata* Wied. (Diptera: Tephritidae). – *IOBC/WPRS Bulletin* 62: 183-188.
- [45] Umeh, V. C., Olaniyan, A. A., Ker, J., Andir, J. (2004): Development of citrus fruit fly control strategies for small-holders in Nigeria. – *Fruits* 59(4): 265-274.
- [46] Vargas, R., Souder, S. K., Rendon, P., Mackey, B. (2018): Suppression of Mediterranean fruit fly (Diptera: Tephritidae) with trimedlure and biolure dispensers in *Coffea arabica* (Gentianales: Rubiaceae) in Hawaii. – *Journal of Economic Entomology* 111(1): 293-297.
- [47] Yayla, M., Satar, S. (2017): Efficacy of different methods to control Mediterranean fruit fly. – *Turkish Bulletin of Entomology* 7(4): 267-276.
- [48] Zümreoğlu, A. (1990): Standardization of trap systems for combine the sterile-male technique Mediterranean fruit fly, *Ceratitis capitata* Wied., two years studies on various trap systems in Aegean region. – *Turkish Journal of Plant Protection* 14(3): 155-166.

AN ASSESSMENT OF THE NET ECOSYSTEM METABOLISM AND RESPIRATION OF A TROPICAL CORAL REEF

PRAMNEECHOTE, P.^{1,2} – SINUTOK, S.^{2,3} – WONGKAMHAENG, K.⁴ – CHOTIKARN, P.^{1,2*}

¹*Marine and Coastal Resources Institute, Prince of Songkla University, Kho Hong, Hat Yai, Songkhla 90110, Thailand*

²*Coastal Oceanography and Climate Change Research Center, Prince of Songkla University, Kho Hong, Hat Yai, Songkhla 90110, Thailand*

³*Faculty of Environmental Management, Prince of Songkla University, Kho Hong, Hat Yai, Songkhla 90110, Thailand*

⁴*Department of Zoology, Faculty of Science, Kasetsart University, Bangkok 10900, Thailand*

*Corresponding author

e-mail: ponlachart.c@psu.ac.th; phone: +66-74-282-335; fax: +66-74-212-782

(Received 29th Oct 2019; accepted 30th Jan 2020)

Abstract. The article aimed to assess the net ecosystem metabolism (NEM), and photosynthesis performance of *Pocillopora acuta* coral on the reef flat and reef slope of the southeast fringing reef of Phuket, Thailand, from June 2017 to January 2018, using 30 x 45-cm benthic oxygen flux chambers and a Junior Pulse Amplitude Modulated fluorometer. The results showed the NEM at both sites was significantly higher in the dry season. The effective quantum yield of *P. acuta* on the reef slope was significantly higher than that of the reef flat in both seasons. The maximum quantum yield showed seasonal variation, which was significantly higher on the reef slope during the dry season than that in the wet season. This study demonstrated temporal and spatial variations in ecosystem metabolism and photosynthetic activity due to different physical characteristics, such as light intensity, which is the main driver of coral reef ecosystem and different biological characteristics, such as the percentage of live coral, the number of microalgae and the symbiont density. The results provide a better understanding of how *P. acuta* responds to changes in depth and season and why corals on reef slopes might be more susceptible to bleaching than corals on reef flats.

Keywords: coral metabolisms, oxygen evolution, benthic chamber, photosynthetic capacity, zooxanthellae

Introduction

Coral reefs are among the most productive and biologically diverse ecosystems in the world (Slavov et al., 2016), with a gross primary productivity of 1-15 g C m⁻² day⁻¹ (ca. 0.4-5.5 kg C m⁻² year⁻¹) (Douglas, 2010). Coral reefs cover 600,000 km² of the earth's surface or 0.1-0.5% of the ocean surface (Crossland et al., 1991; Moberg and Folke, 1999). Coral reef ecosystems are constructed by reef-building scleractinian corals (Buddemeier et al., 2004), coralline algae and other calcifying organisms (Smith et al., 2006), providing an important habitat for many marine organisms, such as microalgae, macroalgae, molluscs, crustaceans, and vertebrates, including fish and marine mammals (Harrison and Booth, 2007). Coral reefs support a huge number of people with goods and services in the form of food production, coastal protection and tourism, and provide ecosystem services with a value of 36,794 \$ ha⁻¹ yr⁻¹ to 2,129,122 \$ ha⁻¹ yr⁻¹ (Costanza et al., 2014). Scleractinian corals are major contributors to the productivity of coral reef ecosystems (Lesser, 2011). However, many coral reefs are suffering serious decline due

to global climate change and human activities, such as overfishing, agricultural run-off, deforestation that increases soil erosion and runoff then increases sediment load into coral reef, tourism, and industrialization (Moberg and Folke, 1999; Hughes, 2008).

Since the last century, an increase in global temperatures caused by the rising CO₂ concentration in the atmosphere has led to a 0.6°C increase in seawater temperature (Solomon et al., 2007). Elevated sea temperatures can result in a rise in sea level due to the changing of density and volume of water and the melting of the polar ice caps. Moreover, increases in temperature also increase precipitation and evaporation, which leads to more frequent and intense storms (Emanuel, 2005). Further, reductions in pH and CO₃²⁻ ions, which are essential for calcification (CaCO₃ deposition), affect a range of marine organisms including scleractinian corals. Many studies have shown that ocean warming causes coral bleaching, the expulsion of symbiotic dinoflagellates (zooxanthellae) from coral tissue, and influences the health and survivorship of scleractinian corals (Jokiel et al., 2008; Randall and Szmant, 2009). Other environmental stresses include forms of marine pollution, such as nutrient enrichment and sedimentation, have also been found to reduce growth, increase mortality, and cause bleaching in coral worldwide (Alva-Basurto and Arias-González, 2014).

The aquatic light environment plays a major role in the productivity, physiology and ecology of corals (Mass et al., 2010). Light intensity decreases and light quantity (spectrum) changes with increasing depth. Zooxanthellae are capable of photoacclimation to different light regimes (Mass et al., 2010). Photoacclimation includes changes in chlorophyll pigment concentrations, chloroplast volume, the number and length of thylakoids, and the light utilization efficiency of photosynthesis and respiration (Mass et al., 2010). Exposure to high irradiance also leads to photoinhibition, a down-regulation of the photosynthetic process (Li et al., 2018) and coral bleaching (Lesser, 2011). These processes could result in changes to the productivity of corals.

There are many types of coral response to seasonal and spatial variation which include changes in pigment, photosynthesis and metabolism. Fitt et al. (2000) and Warner et al. (2002) found a similar pattern of response with season in biomass, zooxanthellae density and photosynthetic rate, which are lowest during summer and highest during winter, whereas metabolism shows the opposite trend (Kayanne et al., 2005; Falter et al., 2012). Coral at different depths has also demonstrated spatial variation with the highest variation of maximum quantum yield (F_v/F_m) found in coral at 1-2 m depth, but coral at 3-4 and 14 m had higher values (Warner et al., 2002).

Mass coral bleaching has been a major issue in Thailand for decades and some threatened areas have not yet recovered (Yeemin et al., 2013). Many studies have shown that coral bleaching, the loss of endosymbiotic dinoflagellates associated with coral, is caused by thermal and light stress leading to photoinhibition, which damages chloroplasts and photosynthetic apparatus, resulting in oxidative stress (the production and accumulation of reduced oxygen species) (Lesser, 2011; Downs et al., 2013). Coral bleaching is different from seasonal variation in zooxanthellae density, and the number of functional photosystem II (PSII) reaction centers (Lesser, 2011). It has been suggested that the frequency and intensity of bleaching increases with anthropogenic climate change. The susceptibility of corals to bleaching varies greatly among coral genera and reef areas (Pratchett et al., 2013). It has been found that symbiont density is a function of environmental conditions (e.g., nutrient pollution, irradiance), whilst the

susceptibility to bleaching increases in corals with higher symbiont densities (Cunning and Baker, 2013).

A reduction in coral growth, increased mortality, and coral bleaching can lead to the degradation and loss of biological diversity of the reefs, which can affect the structure and functions of coral reef ecosystems. Therefore, it is important to identify which reef areas and coral species are most resilient to the effects of global climate change and other disturbances in order to support coral reef management (Cunning and Baker, 2013). Mass coral bleaching has been a major issue in Phuket but the ecophysiology of corals and zooxanthellae from this area has not often been investigated (Yeemin et al., 2013). The measurement of photosynthesis and ecosystem metabolism of coral is essential to understanding these threatened species. Understanding the ecophysiology of corals and zooxanthellae under different environmental conditions is important for predicting the potential for, severity, and consequences of coral bleaching.

The aim of this study was to investigate seasonal variation (wet and dry) in ecosystem metabolism and photosynthesis of corals at two depths. This study will provide a better understanding of how coral species respond to changes in depth and season and which corals are more susceptible to bleaching.

Materials and methods

Study site

Phuket Island is located in the southern part of Thailand, on the Andaman Sea coast. The island is partly fringed by reefs with a total area of about 6 square kilometers of reef. The study site is located on the southeastern tip of Phuket Island (*Fig. 1*) (Panwa Cape: 7°48'06.9"N, 98°24'24.4"E). The reef is characterized by extensive reef flats that extend up to 200 m from shore (Brown et al., 2002) with a depth that increases at the reef edge (5 m).

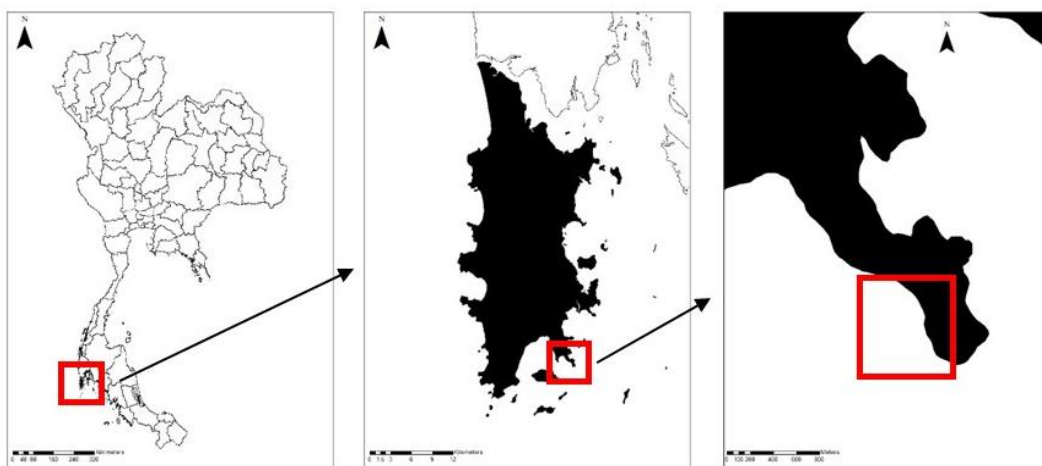


Figure 1. Panwa Cape, Phuket Province, Thailand

In this study, three photographic transects (Jokiel et al., 2015) were placed next to each other parallel to the shoreline in two areas (reef flat and reef slope) to determine the coral percentage cover and the number and types of substrate (e.g. coral, coral

rubble, sand, rocks, algae) at Panwa Cape, Phuket Province (*Fig. 1*) (Panwa Cape: 7°48'06.9"N, 98°24'24.4"E) in June 2017 using Coral Point Count with Excel extensions (CPCe) (Kohler and Gill, 2006). A digital camera with a wide-angle lens was used to obtain the images by positioning the camera above a 0.25 m² quadrat every 50 cm along the 30 m transect line without overlap. A total of 60 images per transect line were obtained covering a total of 45 m² per area (Jokiel et al., 2015).

The primary productivity and photosynthetic activity of *P. acuta* from two depths at the same sampling site (7°48'06.9"N, 98°24'24.4"E) were investigated from June 2017 to January 2018 using benthic oxygen flux chambers (three replicates/depth/month). The benthic oxygen flux chambers were modified from Olivé et al. (2016) and their design is described below and illustrated in *Fig. 2*. They were deployed for 3 h for incubation (Camp et al., 2015).



Figure 2. Dark (left) and light (right) benthic oxygen flux chamber ($n=3$)

Coral samples were collected at the same sampling site for photosynthetic measurements (four replicates/depth/time). Photosynthetic activity was investigated as chlorophyll fluorescence using a Junior Pulse Amplitude Modulated fluorometer (Junior-PAM: Walz GmbH, Effeltrich, Germany) *in situ* after which the coral samples were frozen and transported to the laboratory for analysis of their zooxanthellae density and pigment contents to support the photosynthesis data.

Physical and chemical parameters (e.g. light intensity, temperature, pH, dissolved oxygen, salinity) from two depths from each time of sampling were determined using a YSI Pro Plus multiparameter meter (YSI Inc. / Xylem Inc, USA) and a Hobo data logger (OneTemp Pty Ltd, Australia).

Productivity

The productivity of *P. acuta* was investigated by determining the dissolved oxygen evolution in benthic chambers over time under light (transparent chamber) and dark (non-transparent chamber) conditions to determine the ecosystem respiration (R_e), gross ecosystem metabolism (GEM) and net ecosystem metabolism (NEM). The benthic

oxygen flux chambers consisted of 30 x 45-cm polypropylene cylinders accommodating a 6 liter-volume of water (Fig. 2), which was sufficient to measure the ecosystem metabolism without hypoxia during light or anoxia during darkness within a 3 h incubation period (Camp et al., 2015). The chambers were flexible due to the nature of the plastic bags from which they were constructed and allowed the propagation of external turbulence to the interior of the chambers (Barrón and Duarte, 2009). The benthic chambers were placed above the coral colony *in situ* and secured with a valve for water collection using a syringe to measure the dissolved oxygen concentration hourly. The GEM, NEM and Re were calculated using the standard equations (Eq.1 and Eq.2) following Olivé et al. (2016).

$$\text{NEM} = \text{GEM} - \text{Re} \quad (\text{Eq.1})$$

$$\text{NEM or Re} = [(\text{O}_2)_{\text{final}} - (\text{O}_2)_{\text{initial}}]/[(\text{T})_{\text{final}} - (\text{T})_{\text{initial}}] \quad (\text{Eq.2})$$

Photosynthetic efficiency

The photosynthetic activity of the coral-zooxanthellae was determined through the measurement of chlorophyll (Chl) *a* fluorescence, zooxanthellae density and the photosynthetic pigment concentration. Photosynthetic performance was determined by performing rapid light curves (RLCs) using a junior-PAM fluorometer (Walz, Germany). RLCs with nine increasing actinic light intensities were applied with 0.8 s saturating pulses ($>4500 \mu\text{mol photons m}^{-2} \text{s}^{-1}$) between each actinic light intensity, every 10 s. The effective quantum yield of PSII ($\Delta F/F_m$; Schreiber, 2004), F_v/F_m , maximum relative electron transport rate ($r\text{ETR}_{\text{max}}$), minimum saturating irradiance (I_k) and initial slope (α) of the RLCs were calculated using curve fitting protocols following Ralph and Gademann (2005).

Symbiont density and pigment contents

The coral samples (nubbins) were airbrushed into 10 mL of 0.2- μm -filtered seawater to remove the tissue from the skeleton. The slurry was centrifuged at 4,000 rpm for 4 min to separate the symbiont cells from the animal tissue (Hill and Ralph, 2007). The supernatant containing animal tissue was discarded, and the symbiont pellet was resuspended in 10 mL of 0.2- μm -filtered seawater, then homogenized for 10 s at 15,000 rpm and centrifuged again. The pellet was resuspended in 1 mL filtered seawater for cell counts and chlorophyll analyses. For zooxanthellae density analysis, four replicate cell counts were performed using a haemocytometer under a light microscope. The cell density was determined per cm^2 following coral surface area calculations using the paraffin wax technique (Hill and Ralph, 2007). For the photosynthetic pigment concentration (chlorophyll (Chl) *a* and *c*₂) analysis, the algal pellets were resuspended in 90% acetone and stored in darkness overnight at 4°C. After centrifugation, the chlorophyll *a* and *c*₂ ($\mu\text{g cm}^{-2}$) were then determined using the standard spectrophotometric method of Ritchie (2006) (Eqs.3 and 4), with absorbance measured at 630, 664 and 750 nm (Winters et al., 2009).

$$\text{Chlorophyll } a = (-0.4574 \times A_{630 \text{ nm}}) + (11.4754 \times A_{664 \text{ nm}}) \quad (\text{Eq.3})$$

$$\text{Chlorophyll } c_2 = (23.3900 \times A_{630 \text{ nm}}) + (-3.5322 \times A_{664 \text{ nm}}) \quad (\text{Eq.4})$$

Water quality

Physical and chemical parameters such as temperature, salinity, dissolved oxygen and pH were measured with a YSI Pro Plus multiparameter meter (YSI Inc. / Xylem Inc, USA) in both sites (reef flat and slope) and inside the benthic oxygen flux chambers at the initial time.

Statistical analyses

Two-way ANOVA was used to test for significant differences among depths over time in chlorophyll fluorescence parameters, percentage cover, productivity (GEM, NEM, Re), zooxanthellae density and pigment contents. Tukey's Honestly Significant Difference post-hoc test was used to identify the statistically distinct groups. All tests were performed with a significance level of 95%. If the data did not meet the assumptions of normality (Kolmogorov-Smirnov test) and equal variance (Levene's test), the data was transformed using the square root or \log_{10} . If the transformed data did not meet the assumptions, non-parametric tests were used.

Results

Coral diversity

The results showed a total of 9 families and 17 genera on the reef flat and 12 families and 25 genera on the reef slope (*Appendix Table 1*). On the reef flat, the mean percentage cover of live corals, dead corals, sand and sponges were 43.93%, 51.64%, 4.36% and 0.06%, respectively (*Fig. 3*) and the dominant genus were *Porites* sp. (31.38%), followed by *Favites* sp. (4.80%) and *Goniastrea* sp. (3.35%) (*Fig. 4a*). On the reef slope, the mean percentage cover of live corals, dead corals, sand and sponges were 21.65%, 62.53%, 15.44% and 0.38%, respectively (*Fig. 3*) and the dominant genus were *Porites* sp. (5.05%), followed by *Acropora* sp. (2.84%) and *Goniastrea* sp. (2.49%) (*Fig. 4b*). Shannon's diversity indexes of reef flat and reef slope were 1.13 and 2.67, respectively.

The coral status of the reef flat and slope were categorized as fair (25-49.9%) and poor (0-24.9%), respectively following the standard criteria for assessing the health of coral reefs (Madduppa and Zamani, 2011).

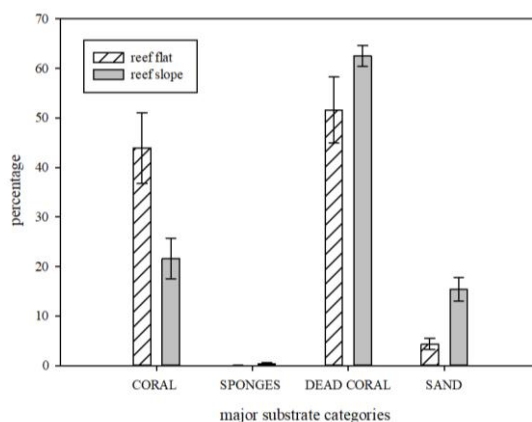


Figure 3. Major category of substrate from reef flat and reef slope. Data represents Mean \pm SE ($n=3$)

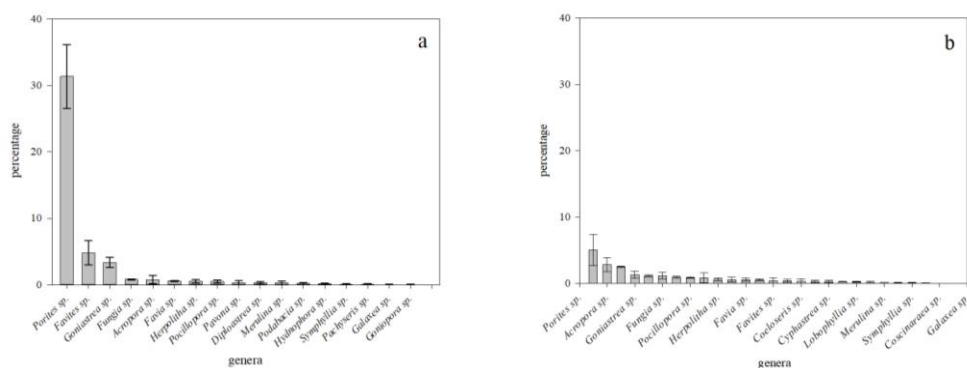


Figure 4. Percentage cover of coral genus from reef flat (a) and reef slope (b). Data represents Mean±SE (n=3)

Primary productivity

The GEM on the reef slope ranged from 281.44 (±63.95) to 994.47 (±167.33) mmol O₂ m⁻² d⁻¹ and 313.93 (±45.38) to 860.62 (±268.66) mmol O₂ m⁻² d⁻¹ for the reef flat (Fig. 5b). The results, however were not significantly different between sites or seasons (p>0.05). The NEM on the reef slope ranged from 184.07 (±71.02) to 867.41 (±206.84) mmol O₂ m⁻² d⁻¹ and 130.32 (±18.79) to 646.69 (±239.39) mmol O₂ m⁻² d⁻¹ for reef flat. On the reef slope, the NEM was significantly higher in the dry season (p=0.01) (Appendix Table 2). The Re on the reef slope ranged from -60.81 (±4.73) to -97.37 (±24.50) mmol O₂ m⁻² d⁻¹ and -112.76 (±17.09) to (-204.52 (±70.85) mmol O₂ m⁻² d⁻¹ for the reef flat. The results, however were not significantly different between either sites or seasons (p>0.05).

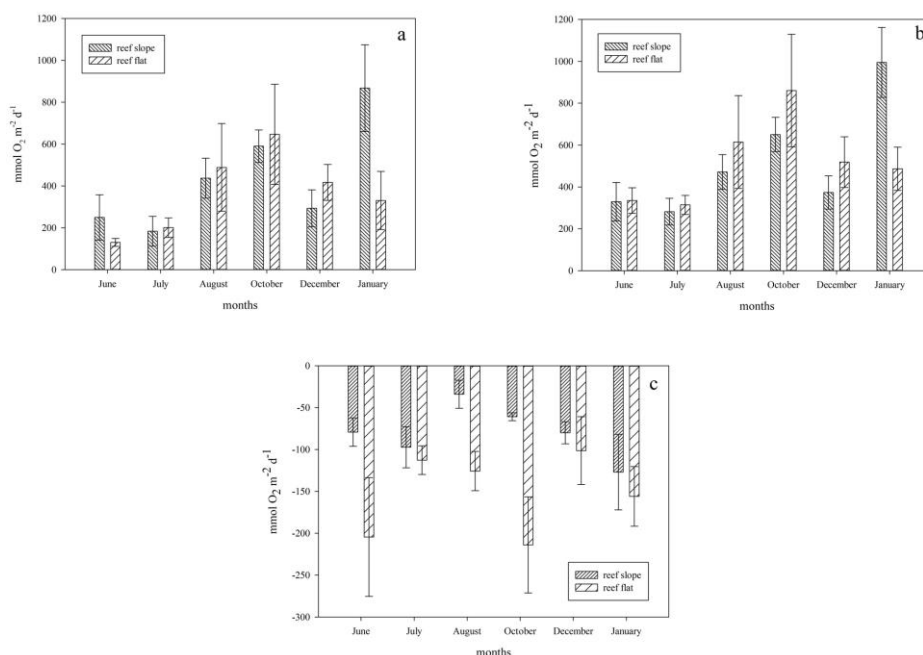


Figure 5. Net ecosystem metabolism (NEM) (a), Gross ecosystem metabolism (GEM) (b) and respiration (Re) (c) of *P. acuta* from reef flat and reef slope. Data represents Mean±SE (n=3)

Photosynthetic performance

The $\Delta F/F_m'$ on the reef slope ranged from 0.640 (± 0.010) to 0.661 (± 0.010) and 0.614 (± 0.017) to 0.661 (± 0.010) for reef flat (Fig. 6a). The $\Delta F/F_m'$ of coral on the reef slope was significantly higher than that on the flat in both seasons ($p=0.002$) (Appendix Table 2).

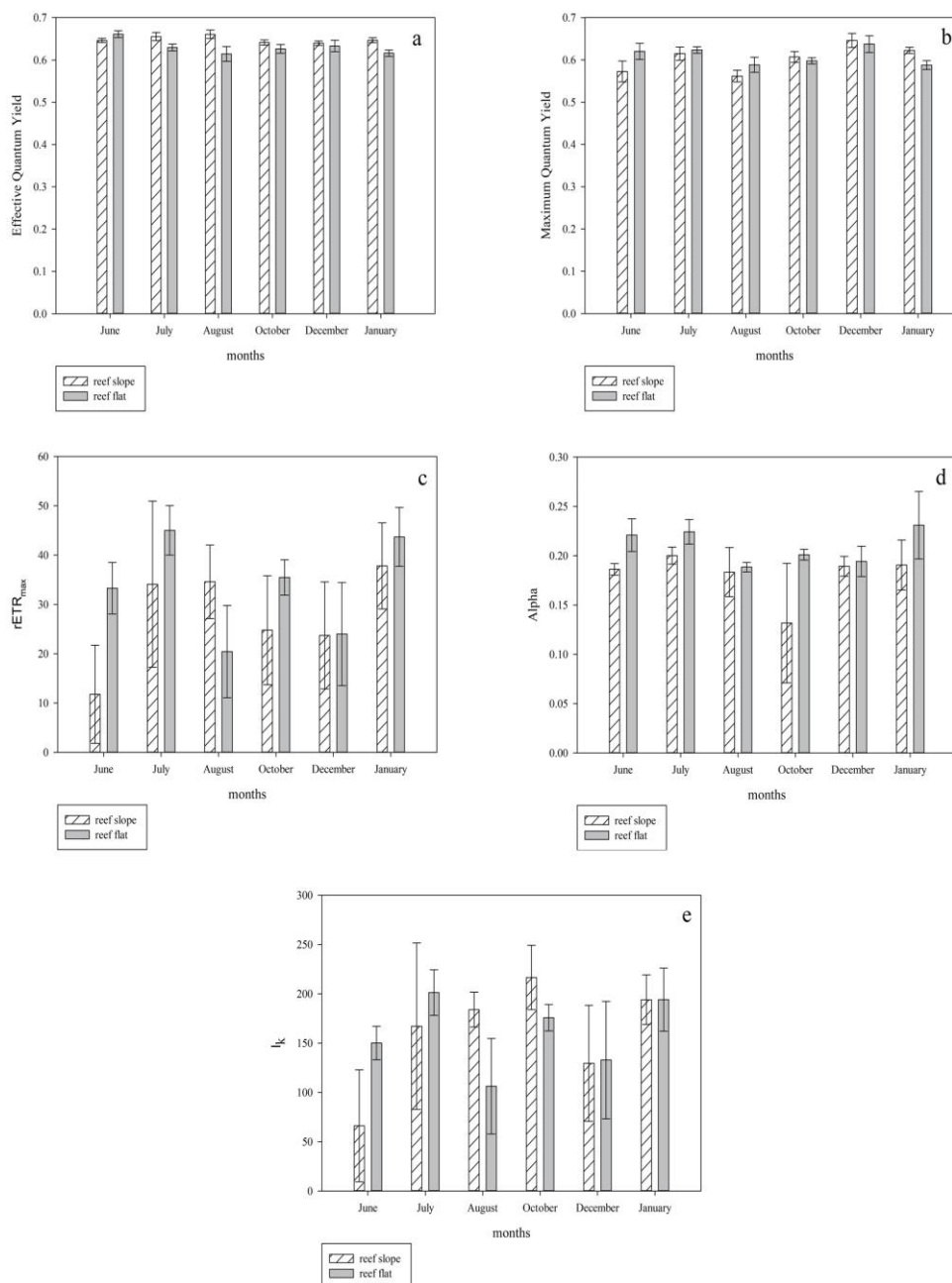


Figure 6. Photosynthetic performance (effective quantum yield of PSII ($\Delta F/F_m'$) (a), Maximum quantum yield of PSII (F_v/F_m) (b)), maximum relative electron transport rate ($rETR_{max}$) (c), initial slope (α) (d) and minimum saturating irradiance (I_k) (e) of *P. acuta* from reef flat and reef slope. Data represents Mean \pm SE ($n=4$)

While the F_v/F_m showed its maximum of the range at December (0.646 (± 0.017)) and 0.637 (± 0.020)), minimum of the range at August (0.562 (± 0.014)) and 0.588 (± 0.018)) for the reef slope and flat, respectively (Fig. 6b). The F_v/F_m of the corals on the reef flat was significantly lower than that for the reef slope in the dry season as well as being higher in the wet season ($p=0.034$) (Appendix Table 2).

The average $rETR_{max}$ (Fig. 6c) of the corals on the reef slope in both the wet and dry seasons tended to be higher than those on the reef flat but there was no significant difference between either sites or seasons ($p>0.05$). However, the Initial slope (α) of the corals on the reef flat was significantly higher than that on the slope ($p=0.037$) (Appendix Table 2).

The I_k ranged from 66.19 to 216.68 $\mu\text{mol photons m}^{-2} \text{ s}^{-1}$ for corals on the reef slope and 106.33 to 201.32 $\mu\text{mol photons m}^{-2} \text{ s}^{-1}$ for those on the reef flat (Fig. 6e). However, the results produced no significant differences between either sites or seasons ($p>0.05$).

Symbiont density

The cell density of corals on the reef slope and flat was in the range of 4.55×10^6 ($\pm 0.97 \times 10^6$) to 11.84×10^6 ($\pm 3.88 \times 10^6$) cells cm^{-2} and 2.96×10^6 ($\pm 0.83 \times 10^6$) to 6.84×10^6 ($\pm 0.69 \times 10^6$) cells cm^{-2} , respectively (Fig. 7). However, there were no significant differences between either sites or seasons ($p>0.05$).

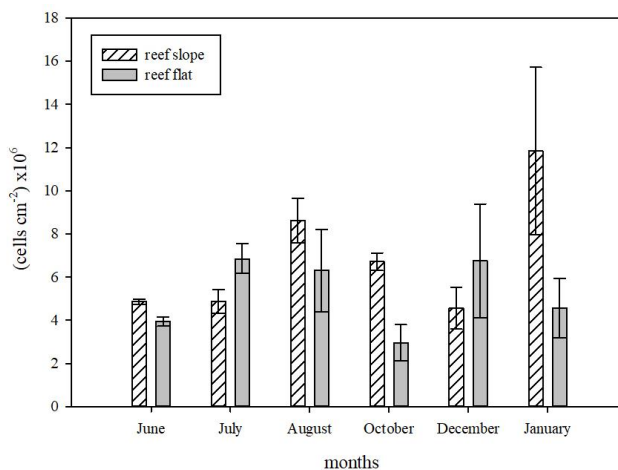


Figure 7. Symbiont density of *P. acuta* from reef flat and reef slope. Data represents Mean \pm SE ($n=4$)

Chlorophyll *a* and *c*₂

The chlorophyll *a* of *P. acuta* corals on the reef slope ranged from 0.016 (± 0.005) to 0.071 (± 0.013) $\mu\text{g mm}^{-2}$ and on the reef flat ranged from 0.023 (± 0.005) to 0.047 (± 0.017) $\mu\text{g mm}^{-2}$ (Fig. 8a). While the Chlorophyll *c*₂ of corals on the reef slope ranged from 0.006 (± 0.002) to 0.014 (± 0.002) $\mu\text{g mm}^{-2}$ and on the reef flat ranged from 0.005 (± 0.001) to 0.039 (± 0.031) $\mu\text{g mm}^{-2}$ (Fig. 8b). However, there were no significant differences between either sites or seasons ($p>0.05$).

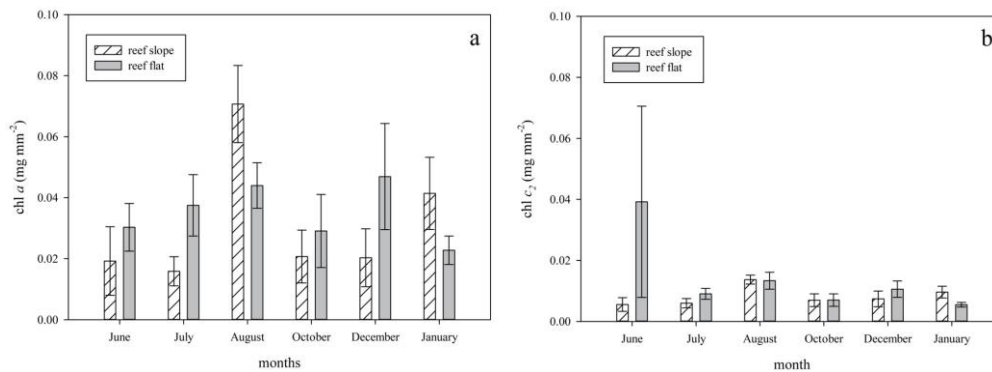


Figure 8. Chlorophyll *a* (a) and *c*₂ (b) concentration of *P. acuta* from reef flat and reef slope. Data represents Mean±SE (n=4)

Discussion

Coral diversity

This is the first study of the coral photosynthesis and reef ecosystem metabolism of the southeast fringing reef of Phuket Island. The results showed more percentage cover of live coral but less coral genera on the reef flat than the reef slope, which might be due to different levels of irradiance at different depths as suggested by Hughes et al. (2015), who found that light is the main factor affecting coral growth and zonation. In the present study the light intensity on the reef flat was noted to be double that on the reef slope. Higher Shannon's diversity indexes on the reef slope (2.67) suggested that there was more coral diversity there than on the reef flat. This is due to differences in physical parameters such as the sediment accumulation rate, light availability and depth, which are limiting factors for different coral species (Kahng et al., 2019) with different levels of resilience (Putnam et al., 2017). Slow growing massive corals, such as *Porites* sp. and *Goniastrea* sp. can survive in conditions of air exposure (Meixia et al., 2008) and demonstrate more tolerance to a changing environment (van Woesik et al., 2011). In contrast, fast growing, branching species, such as *Acropora* sp. and *Pocillopora* sp. (Al-Sofyani and Floos, 2013), prefer a limited range of temperatures (Williams et al., 2017), but have a greater ability to adapt to higher sediment accumulation rates because of their ability to self-clean (Duckworth et al., 2017). Consistent with Brown et al. (1999), the results of the present study show that massive coral species dominate the reefs because they are physiologically adapted to intertidal living. Moreover, Meixia et al. (2008) showed similar results, finding that *Porites lutea* was the dominant species with zonal characteristics with more coral species occurring on the reef slope than the reef flat.

Ecosystem metabolisms

Ecosystem metabolism is a biomass indicator which reflects energy storage in coral and the health of corals in each area, as well as how corals act as a carbon sink. The factors which affect ecosystem metabolism in the ocean are the light intensity, the time of day or year, the weather (Sathyendranath and Platt, 2001), adaptation of phytoplankton, the temperature and the available nutrients. The main factor is light intensity (Hughes et al., 2015) and that is usually correlated with depth.

The NEM showed seasonal variation with higher metabolism in the dry season (Appendix Table 2). When the light intensity data (measured with a HOBO data logger) was compared, it was found that the reef flat had twice the light intensity of the reef slope which led to a higher rate of metabolism. The lower light intensity on the reef slope is caused by greater water depth reducing the light intensity (Kahng et al., 2019). Irradiance is important for photosynthesis of symbiotic algae living with corals and coral reefs metabolisms (Iluz and Dubinsky, 2015) and affect dissolved oxygen which is an indicator of coral reef metabolism (Camp et al., 2015). Moreover, the sediment accumulation rate on the reef slope ($11.76 \text{ g m}^{-2} \text{ d}^{-1}$) was three times higher than that on the reef flat ($3.70 \text{ g m}^{-2} \text{ d}^{-1}$). A high sediment accumulation rate can reduce the light intensity which is the main factor in zooxanthellae's photosynthesis and ecosystem metabolism (Iluz and Dubinsky, 2015). Differences in sediment accumulation rates depend on seasonal variation and weather (Browne et al., 2019). Furthermore, biological characteristics such as the percentage of live coral cover, macroalgae and cyanobacteria also affect the NEM. This study revealed that the reef flat had a greater percentage of live coral cover, macroalgae and cyanobacteria than the reef slope which led to a higher NEM.

The results of the present study were also broadly similar in respect of oxygen evolution ($130.79\text{-}867.41 \text{ mmol O}_2 \text{ m}^{-2} \text{ d}^{-1}$) to those of Camp et al. (2015) who found that the ecosystem metabolic activity (P, R and G) of three coral species, *Mussismilia harttii*, *Siderastrea cf. stellata* and *Porites astreoides* were in the range of $43.2\text{-}158.4 \text{ mmol O}_2 \text{ m}^{-2} \text{ d}^{-1}$. Moreover, all the ratios of GEM to Re were higher than 1 indicating that this ecosystem is autotrophic and that *P. acuta* is an important species in high productivity coral reef ecosystems.

Photosynthesis efficiency

Seasonal or spatial variation in photosynthesis and the photosynthetic capacity of corals have been observed in previous studies (Levy et al., 2004; Kuffner, 2005; Ulstrup et al., 2011; Sawall et al., 2014). These variations occur due to changes in environmental factors such as light intensity (Iluz and Dubinsky, 2015), temperature (Levy et al., 2004; Caroselli et al., 2015), salinity (Sandoval-Gil et al., 2012), sediment accumulation rate (Rogers, 1990), water velocity (Lesser et al., 1994) and other chemical factors (Redfield, 1958).

Browne et al. (2015) estimated the coral health of four common inshore reef corals in response to seasonal and anthropogenic changes in water quality, and found that temperature has the greatest influence on branching coral (*P. damicornis*). Moreover, higher sedimentation rate and nutrient availability in the rainy season might affect coral health and physiology (Brown et al., 1999).

The $\Delta F/F_m'$ of *P. acuta* in this study showed spatial variation in both seasons suggesting that coral on the reef slope has higher photosynthesis efficiency than that of the reef flat since there is higher light intensity on the reef flat (*ca.* $600 \mu\text{mol photons m}^{-2} \text{ s}^{-1}$) and this value exceeded the I_k (Fig. 6e) at the same site leading to photoinhibition in the reef-flat coral. While the light intensity on the reef slope (*ca.* $300 \mu\text{mol photons m}^{-2} \text{ s}^{-1}$) was lower it was closer to the I_k than the light intensity on the reef flat, which means that although photoinhibition still occurs, it is of less effect. Therefore, the photosynthesis of symbionts on the reef slope is more efficient. Further, when comparing between seasons, the results showed higher photosynthesis efficiency for the coral on the reef slope in the wet season since the $\Delta F/F_m'$ and I_k values were

closer in the same season at each site. Moreover, diel variation of photosynthesis, which is down-regulated by intense light in the afternoon (Hill and Ralph, 2005) also reduced the $\Delta F/F_m'$ in this study.

On the other hand, no significant difference of $\Delta F/F_m'$ was noted on coral on the reef flat in different seasons since the shallow water condition meant that only highly tolerant corals can survive. This finding is consistent with that relating to F_v/F_m , which showed the same pattern. F_v/F_m representing the photosynthetic capacity of zooxanthellae and indicating coral stresses. When compared between seasons, the coral on the reef flat showed no significant differences in respect of F_v/F_m . On the other hand, the coral on the reef slope showed high variation between seasons with the F_v/F_m lower than that on the reef flat in the wet season but higher in the dry season. This might be due to the higher accumulation of sediment in the wet season. Sediment reduces the light available to coral and increases coral stress which is reflected in the F_v/F_m (Zhao and Yu, 2014). A similar trend was found for the symbiont density and pigment content but these indices are not as sensitive as the F_v/F_m .

The initial slope (α) showed some spatial variation with the reef-flat coral α being greater in both seasons. The results showed that the reef-flat coral had a greater ability to harvest light and a higher photosynthetic ability, and these adaptations led to the reef-flat corals higher photosynthesis efficiency. On the other hand, comparisons of symbiont density and pigment content did not show any significant differences between sites although the α values were different, indicating that the reef-slope corals were exposed to an unsuitable environment which did not allow them to adapt and led to photosynthetic stress.

The I_k is one of the main factors which can reveal the adaptation of coral (Zhao and Yu, 2014). The present study found no significant difference in I_k due to the high sediment accumulation rate on the reef slope ($76.11 \text{ g m}^{-2} \text{ d}^{-1}$) (Appendix Table 3) which was three times as great as that on the reef flat ($70.3 \text{ g m}^{-2} \text{ d}^{-1}$) (Appendix Table 4) and led to the corals being stressed. Sediment was one of many factors which reduced the photosynthesis efficiency of the reef-slope corals, while the lower sediment accumulation on the reef flat was more suitable and allowed the corals to adapt. The reef-flat corals with better α adaptation were able to reduce their pigments and zooxanthellae cells whereas the reef-slope corals did not do so and this resulted in the finding of no significant differences between either sites or seasons in the I_k and $rETR_{\max}$ indices.

The effect of sediment on zooxanthellae photosynthesis was demonstrated in Philipp and Fabricius (2003) who showed that the $\Delta F/F_m'$ and F_v/F_m respond to sediment ($79\text{-}234 \text{ mg cm}^{-2}$) and exposure time (0–36 hr) by being reduced. In addition, the photosynthesis and adaptation of zooxanthellae are affected by depth. Mass et al. (2007) revealed that the adaptation of *Stylophora pistillata* through a depth range of 5–65 m produced a lower R_e , P_{\max} , I_c and I_k as the depth increased. On the other hand, the α increased with depth.

There is a limitation in using the Junior PAM (Walz GmbH, Effeltrich, Germany) since it is not a submersible device. Therefore, photosynthetic measurements that are not derived *in situ* might be in error, and this would affect the $\Delta F/F_m'$ representing the sensitivity to light intensity flux. Including dark adapted measurements before fitting the RLCs which might lead to the opening of all the reaction centers which would affect the I_k and $rETR_{\max}$ values, which in this study showed no significant differences between either sites or seasons.

Symbionts density and chlorophyll concentration

The photosynthesis data, zooxanthellae cell density and chlorophyll concentration in the coral tissues were measured and the results produced no significant differences between either sites or seasons. This might be due to photo-acclimation of the zooxanthellae on the reef flat by reducing the numbers of cells and pigment (Cooper and Ulstrup, 2009) while the zooxanthellae on the reef slope did not, which might be due to the predominance of the *Symbiodinium* genotype (Hennige et al., 2009).

Cooper and Ulstrup (2009), who estimated the spatial variation in the photophysiology of the zooxanthellae of *P. damicornis*, found that photoacclimation occurred in both shallow and deep corals but via different mechanisms. Thus, to deal with changes in irradiance, changes in symbionts such as the size and the location of their zooxanthellae, the zooxanthellae density and the chlorophyll contents might have occurred (Zhao and Yu, 2014). In addition, Frade et al. (2007) found a correlation between the *Symbiodinium* genotype (clade) in the coral genus *Madracis* and the water depth, with clade B7 being a generalist while clades B13 and B15 were restricted to shallow and deepwater reef environments, respectively. There have also been found to be differences in terms of the photoacclimation response for each genotype (Hennige et al., 2009). Meanwhile, Philipp and Fabricius (2003) found that the cell density and pigment concentration of zooxanthellae per coral surface area decreased with increased amounts of sediment but the decrease was not as fast as those noted in the $\Delta F/F_m$ and F_v/F_m .

The optimal zooxanthellae densities found in the present study were lower than those found by Wooldridge (2016; $1-3 \times 10^6$ cells cm^{-2}) and this might be due to the study site being a marine attraction. Human activities, urban run off or wastewater could lead to high nutrient concentrations in the water, which can lead to an increase in cell density, pigment and maximum gross photosynthesis (Marubini and Davies, 1996). However, the $rETR_{max}$, I_k , symbiont density and pigment showed no significant differences between sites or between seasons and this might be due to the better adaptation of reef-flat coral demonstrated by the reduced number of cells and pigment (Cooper and Ulstrup, 2009). Nevertheless, the environment on the reef slope was not suitable to adaptation by corals.

The lack of any correlation between ecosystem metabolism and zooxanthellae photosynthesis might be due to the assessment of ecosystem metabolism representing all living things in the chamber that including coral, algae and plankton, whereas photosynthesis was assessed based only on zooxanthellae.

Chambers

The design of the benthic chambers by which oxygen flux was measured described above in *Materials and Methods* entailed the limitation that its chamber shape was more suited to be deployed to collect data from branching or sub-massive coral or from coral where the colony size was smaller than the chamber. On the other hand, the design of the chamber was cost effective. Camp et al. (2015) used a flexible chamber to measure the ecosystem metabolic activity (P, R and G) of three coral species, *Mussismilia harttii*, *Siderastrea cf. stellata* and *Porites astreoides*. The results of that study produced values which were broadly similar to those produced by the present study. Further, Olivé et al. (2016) estimated the ecosystem metabolism using chambers in a seagrass meadow and the results were also broadly in-line with those from the present study.

Conclusion

An assessment of GEM, NEM and Re was conducted in a tropical coral reef at the Southeast tip of Phuket Island, Thailand between June 2017 and January 2018. The findings of this study suggest that coral diversity is a result of a combination of light intensity, sediment accumulation, depth, other physical and chemical factors and ecosystem metabolism is mainly driven by the number of organisms, the light availability and depth.

Due to limitations of this chamber design, benthic oxygen flux chamber can estimate only in ecosystem scale and be deployed only on branching corals. The design of the chamber should be improved for measuring on various kinds of colony shape (e.g. plate, massive and branching). Real-time data collection on dissolved oxygen, irradiance and temperature inside the chamber could be developed.

This study provides a better understanding of how corals from different habitats respond to changes in season and are more susceptible to bleaching. The data from this study can be used for marine and coastal management and conservation.

Acknowledgements. This work is financially supported by the Coastal Oceanography and Climate Change Research Center, Prince of Songkla University, The Institute for the Promotion of Teaching Science and Technology (IPST; DPST Graduate with First Placement; Grant number: 006/2559), and National Research Council of Thailand (NRCT). We thank Assistant Professor Pattara Aiyarak and Professor Peter J. Ralph for support. We thank the Marine and Coastal Resources Institute, and the Faculty of Environmental Management, Prince of Songkla University, Associate Professor Raymond Ritchie and Phuket Marine Biological Center for research facilities.

REFERENCES

- [1] Al-Sofyani, A. A., Floos, Y. A. M. (2013): Effect of temperature on two reef-building corals *Pocillopora damicornis* and *P. verrucosa* in the Red Sea. – *Oceanologia* 55(4): 917-935.
- [2] Alva-Basurto, J. C., Arias-González, J. E. (2014): Modelling the effects of climate change on a Caribbean coral reef food web. – *Ecological Modelling* 289: 1-14.
- [3] Barrón, C., Duarte, C. (2009): Dissolved organic matter release in a *Posidonia oceanica* meadow. – *Marine Ecology Progress Series* 374: 75-84.
- [4] Brown, B., Dunne, R., Ambarsari, I., Le Tissier, M., Satapoomin, U. (1999): Seasonal fluctuations in environmental factors and variations in symbiotic algae and chlorophyll pigments in four Indo-Pacific coral species. – *Marine Ecology Progress Series* 191: 53-69.
- [5] Brown, B., Clarke, K., Warwick, R. (2002): Serial patterns of biodiversity change in corals across shallow reef flats in Ko Phuket, Thailand, due to the effects of local (sedimentation) and regional (climatic) perturbations. – *Marine Biology* 141(1): 21-29.
- [6] Browne, N. K., Tay, J., Todd, P. A. (2015): Recreating pulsed turbidity events to determine coral–sediment thresholds for active management. – *Journal of Experimental Marine Biology and Ecology* 466 (Supplement C): 98-109.
- [7] Browne, N., Braoun, C., McIlwain, J., Nagarajan, R., Zinke, J. (2019): Borneo coral reefs subject to high sediment loads show evidence of resilience to various environmental stressors. – *PeerJ* 7: e7382.
- [8] Buddemeier, R. W., Baker, A. C., Fautin, D. G., Jacobs, J. R. (2004): The Adaptive Hypothesis of Bleaching. – In: Rosenberg, E., Loya, Y. (eds.) *Coral Health and Disease*. Springer Berlin Heidelberg, Berlin.

- [9] Camp, E. F., Krause, S.-L., Santos, L. M. F., Naumann, M. S., Kikuchi, R. K. P., Smith, D. J., Wild, C., Suggett, D. J. (2015): The “Flexi-Chamber”: A Novel Cost-Effective *In Situ* Respirometry Chamber for Coral Physiological Measurements. – PLOS ONE 10(10): e0138800.
- [10] Caroselli, E., Falini, G., Goffredo, S., Dubinsky, Z., Levy, O. (2015): Negative response of photosynthesis to natural and projected high seawater temperatures estimated by pulse amplitude modulation fluorometry in a temperate coral. – *Frontiers in Physiology* 6: 317.
- [11] Cooper, T. F., Ulstrup, K. E. (2009): Mesoscale variation in the photophysiology of the reef building coral *Pocillopora damicornis* along an environmental gradient. – *Estuarine, Coastal and Shelf Science* 83(2): 186-196.
- [12] Costanza, R., de Groot, R., Sutton, P., van der Ploeg, S., Anderson, S. J., Kubiszewski, I., Farber, S., Turner, R. K. (2014): Changes in the global value of ecosystem services. – *Global Environmental Change* 26: 152-158.
- [13] Crossland, C. J., Hatcher, B. G., Smith, S. V. (1991): Role of coral reefs in global ocean production. – *Coral Reefs* 10(2): 55-64.
- [14] Cunning, R., Baker, A. C. (2013): Excess algal symbionts increase the susceptibility of reef corals to bleaching. – *Nature Climate Change* 3(3): 259-262.
- [15] Douglas, A. E. (2010): *The symbiotic habit*. – Princeton University Press, Princeton.
- [16] Downs, C. A., McDougall, K. E., Woodley, C. M., Fauth, J. E., Richmond, R. H., Kushmaro, A., Gibb, S. W., Loya, Y., Ostrander, G. K., Kramarsky-Winter, E. (2013): Heat-Stress and Light-Stress Induce Different Cellular Pathologies in the Symbiotic Dinoflagellate during Coral Bleaching. – PLOS ONE 8(12): e77173.
- [17] Duckworth, A., Giofre, N., Jones, R. (2017): Coral morphology and sedimentation. – *Marine Pollution Bulletin* 125(1-2): 289-300.
- [18] Emanuel, K. (2005): Increasing destructiveness of tropical cyclones over the past 30 years. – *Nature* 436: 686.
- [19] Falter, J. L., Lowe, R. J., Atkinson, M. J., Cuet, P. (2012): Seasonal coupling and decoupling of net calcification rates from coral reef metabolism and carbonate chemistry at Ningaloo Reef, Western Australia: coupling of reef calcification. – *Journal of Geophysical Research: Oceans* 117: C05003.
- [20] Fitt, W. K., McFarland, F. K., Warner, M. E., Chilcoat, G. C. (2000): Seasonal patterns of tissue biomass and densities of symbiotic dinoflagellates in reef corals and relation to coral bleaching. – *Limnology and Oceanography* 45(3): 677-685.
- [21] Frade, P. R., De Jongh, F., Vermeulen, F., Van Bleijswijk, J., Bak, R. P. M. (2007): Variation in symbiont distribution between closely related coral species over large depth ranges: coral symbiont distribution over large depths. – *Molecular Ecology* 17(2): 691-703.
- [22] Harrison, P. L., Booth, D. J. (2007): Coral reefs: naturally dynamic and increasingly disturbed ecosystems. – *Marine ecology* 2007(1): 316-377.
- [23] Hennige, S. J., Suggett, D. J., Warner, M. E., McDougall, K. E., Smith, D. J. (2009): Photobiology of *Symbiodinium* revisited: bio-physical and bio-optical signatures. – *Coral Reefs* 28(1): 179-195.
- [24] Hill, R., Ralph, P. J. (2005): Diel and seasonal changes in fluorescence rise kinetics of three scleractinian corals. – *Functional Plant Biology* 32(6): 549.
- [25] Hill, R., Ralph, P. (2007): Post-bleaching viability of expelled zooxanthellae from the scleractinian coral *Pocillopora damicornis*. – *Marine Ecology Progress Series* 352: 137-144.
- [26] Hughes, R., Hughes, D., Smith, I., Dale, A. (2015): *Oceanography and Marine Biology: An Annual Review*, Volume 53. – Crc press, Boca raton.
- [27] Iluz, D., Dubinsky, Z. (2015): Coral photobiology: new light on old views. – *Zoology* 118(2): 71-78.

- [28] Jokiel, P. L., Rodgers, K. S., Kuffner, I. B., Andersson, A. J., Cox, E. F., Mackenzie, F. T. (2008): Ocean acidification and calcifying reef organisms: a mesocosm investigation. – *Coral Reefs* 27(3): 473-483.
- [29] Jokiel, P. L., Rodgers, K. S., Brown, E. K., Kenyon, J. C., Aeby, G., Smith, W. R., Farrell, F. (2015): Comparison of methods used to estimate coral cover in the Hawaiian Islands. – *PeerJ* 3: e954.
- [30] Kahng, S. E., Akkaynak, D., Shlesinger, T., Hochberg, E. J., Wiedenmann, J., Tamir, R., Tchernov, D. (2019): Light, Temperature, Photosynthesis, Heterotrophy, and the Lower Depth Limits of Mesophotic Coral Ecosystems. – In: Loya, Y., Puglise, K. A., Bridge, T. C. L. (eds.) *Mesophotic Coral Ecosystems*. Springer International Publishing, Cham.
- [31] Kayanne, H., Hata, H., Kudo, S., Yamano, H., Watanabe, A., Ikeda, Y., Nozaki, K., Kato, K., Negishi, A., Saito, H. (2005): Seasonal and bleaching-induced changes in coral reef metabolism and CO₂ flux: coral reef metabolism and CO₂ flux. – *Global Biogeochemical Cycles* 19(3): GB3015.
- [32] Kohler, K. E., Gill, S. M. (2006): Coral Point Count with Excel extensions (CPCe): A Visual Basic program for the determination of coral and substrate coverage using random point count methodology. – *Computers & Geosciences* 32(9): 1259-1269.
- [33] Kuffner, I. B. (2005): Temporal Variation in Photosynthetic Pigments and UV-Absorbing Compounds in Shallow Populations of Two Hawaiian Reef Corals. – *Pacific Science* 59(4): 561-580.
- [34] Lesser, M. P., Weis, V. M., Patterson, M. R., Jokiel, P. L. (1994): Effects of morphology and water motion on carbon delivery and productivity in the reef coral, *Pocillopora damicornis* (Linnaeus): Diffusion barriers, inorganic carbon limitation, and biochemical plasticity. – *Journal of Experimental Marine Biology and Ecology* 178(2): 153-179.
- [35] Lesser, M. P. (2011): Coral Bleaching: Causes and Mechanisms. – In: Dubinsky, Z., Stambler, N. (eds.) *Coral Reefs: An Ecosystem in Transition*. Springer Netherlands, Dordrecht.
- [36] Levy, O., Dubinsky, Z., Schneider, K., Achituv, Y., Zakai, D., Gorbunov, M. (2004): Diurnal hysteresis in coral photosynthesis. – *Marine Ecology Progress Series* 268: 105-117.
- [37] Li, L., Aro, E.-M., Millar, A. H. (2018): Mechanisms of Photodamage and Protein Turnover in Photoinhibition. – *Trends in Plant Science* 23(8): 667-676.
- [38] Madduppa, H., Zamani, N. (2011): A Standard Criteria for Assessing the Health of Coral Reefs: Implication for Management and Conservation. – *Journal of Indonesia Coral Reefs* 1: 137-146.
- [39] Marubini, F., Davies, P. S. (1996): Nitrate increases zooxanthellae population density and reduces skeletogenesis in corals. – *Marine Biology* 127(2): 319-328.
- [40] Mass, T., Einbinder, S., Brokovich, E., Shashar, N., Vago, R., Erez, J., Dubinsky, Z. (2007): Photoacclimation of *Stylophora pistillata* to light extremes: metabolism and calcification. – *Marine Ecology Progress Series* 334: 93-102.
- [41] Mass, T., Kline, D. I., Roopin, M., Veal, C. J., Cohen, S., Iluz, D., Levy, O. (2010): The spectral quality of light is a key driver of photosynthesis and photoadaptation in *Stylophora pistillata* colonies from different depths in the Red Sea. – *Journal of Experimental Biology* 213(23): 4084-4091.
- [42] Meixia, Z., Kefu, Y., Qiaomin, Z., Qi, S. (2008): Spatial pattern of coral diversity in Luhuitou fringing reef, Sanya, China. – *Acta Ecologica Sinica* 28(4): 1419-1428.
- [43] Moberg, F., Folke, C. (1999): Ecological goods and services of coral reef ecosystems. – *Ecological Economics* 29(2): 215-233.
- [44] Olivé, I., Silva, J., Costa, M. M., Santos, R. (2016): Estimating Seagrass Community Metabolism Using Benthic Chambers: The Effect of Incubation Time. – *Estuaries and Coasts* 39(1): 138-144.

- [45] Philipp, E., Fabricius, K. (2003): Photophysiological stress in scleractinian corals in response to short-term sedimentation. – *Journal of Experimental Marine Biology and Ecology* 287(1): 57-78.
- [46] Pratchett, M. S., McCowan, D., Maynard, J. A., Heron, S. F. (2013): Changes in Bleaching Susceptibility among Corals Subject to Ocean Warming and Recurrent Bleaching in Moorea, French Polynesia. – *PLoS ONE* 8(7): e70443.
- [47] Putnam, H. M., Barott, K. L., Ainsworth, T. D., Gates, R. D. (2017): The Vulnerability and Resilience of Reef-Building Corals. – *Current Biology* 27(11): R528-R540.
- [48] Ralph, P. J., Gademann, R. (2005): Rapid light curves: A powerful tool to assess photosynthetic activity. – *Aquatic Botany* 82(3): 222-237.
- [49] Randall, C. J., Szmant, A. M. (2009): Elevated Temperature Affects Development, Survivorship, and Settlement of the Elkhorn Coral, *Acropora palmata* (Lamarck 1816). – *The Biological Bulletin* 217(3): 269-282.
- [50] Redfield, A. C. (1958): The biological control of chemical factors in the environment. – *American Scientist* 46(3): 230A-221.
- [51] Ritchie, R. J. (2006): Consistent Sets of Spectrophotometric Chlorophyll Equations for Acetone, Methanol and Ethanol Solvents. – *Photosynthesis Research* 89(1): 27-41.
- [52] Rogers, C. (1990): Responses of coral reefs and reef organisms to sedimentation. – *Marine Ecology Progress Series* 62: 185-202.
- [53] Sandoval-Gil, J. M., Marín-Guirao, L., Ruiz, J. M. (2012): The effect of salinity increase on the photosynthesis, growth and survival of the Mediterranean seagrass *Cymodocea nodosa*. – *Estuarine, Coastal and Shelf Science* 115: 260-271.
- [54] Sathyendranath, S., Platt, T. (2001): Primary Production Distribution. – In: Steele, J. H., Thorpe, S. A., Turekian, K. K. (eds.) *Encyclopedia of Ocean Sciences*. Elsevier. Dalhousie University, NS, Canada.
- [55] Sawall, Y., Al-Sofyani, A., Banguera-Hinestroza, E., Voolstra, C. R. (2014): Spatio-Temporal Analyses of *Symbiodinium* Physiology of the Coral *Pocillopora verrucosa* along Large-Scale Nutrient and Temperature Gradients in the Red Sea. – *PLOS ONE* 9(8): e103179.
- [56] Schreiber, U. (2004): Pulse-Amplitude-Modulation (PAM) Fluorometry and Saturation Pulse Method: An Overview. – In: Papageorgiou, G. C., Govindjee (eds.) *Chlorophyll a Fluorescence*. Springer Netherlands. Dordrecht.
- [57] Slavov, C., Schrammeyer, V., Reus, M., Ralph, P. J., Hill, R., Büchel, C., Larkum, A. W. D., Holzwarth, A. R. (2016): “Super-quenching” state protects *Symbiodinium* from thermal stress - Implications for coral bleaching. – *Biochimica et Biophysica Acta (BBA) - Bioenergetics* 1857(6): 840-847.
- [58] Solomon, S. (2007): *Climate change 2007: the physical science basis*. – Working group I contribution to the fourth assessment report of the Intergovernmental Panel on Climate Change. Cambridge university press. New York.
- [59] Smith, J. E., Shaw, M., Edwards, R. A., Obura, D., Pantos, O., Sala, E., Sandin, S. A., Smriga, S., Hatay, M., Rohwer, F. L. (2006): Indirect effects of algae on coral: algae-mediated, microbe-induced coral mortality. – *Ecology Letters* 9(7): 835-845.
- [60] Ulstrup, K., Kühl, M., van Oppen, M., Cooper, T., Ralph, P. (2011): Variation in photosynthesis and respiration in geographically distinct populations of two reef building coral species. – *Aquatic Biology* 12(3): 241-248.
- [61] van Woesik, R., Sakai, K., Ganase, A., Loya, Y. (2011): Revisiting the winners and the losers a decade after coral bleaching. – *Marine Ecology Progress Series* 434: 67-76.
- [62] Warner, M., Chilcoat, G., McFarland, F., Fitt, W. (2002): Seasonal fluctuations in the photosynthetic capacity of photosystem II in symbiotic dinoflagellates in the Caribbean reef-building coral *Montastraea*. – *Marine Biology* 141(1): 31-38.
- [63] Williams, D. E., Miller, M. W., Bright, A. J., Pausch, R. E., Valdivia, A. (2017): Thermal stress exposure, bleaching response, and mortality in the threatened coral *Acropora palmata*. – *Marine Pollution Bulletin* 124(1): 189-197.

- [64] Winters, G., Holzman, R., Blekhan, A., Beer, S., Loya, Y. (2009): Photographic assessment of coral chlorophyll contents: Implications for ecophysiological studies and coral monitoring. – *Journal of Experimental Marine Biology and Ecology* 380(1-2): 25-35.
- [65] Wooldridge, S. A. (2016): Excess seawater nutrients, enlarged algal symbiont densities and bleaching sensitive reef locations: 1. Identifying thresholds of concern for the Great Barrier Reef, Australia. – *Marine Pollution Bulletin* 114(1): 343-354.
- [66] Yeemin, T., Pengsakun, S., Yucharoen, M., Klinthong, W., Sangmanee, K., Sutthacheep, M. (2013): Long-term changes in coral communities under stress from sediment. – *Deep Sea Research Part II: Topical Studies in Oceanography* 96: 32-40.
- [67] Zhao, M., Yu, K. (2014): Application of chlorophyll fluorescence technique in the study of coral symbiotic zooxanthellae micro-ecology. – *Acta Ecologica Sinica* 34(3): 165-169.

APPENDIX

Table 1. Coral percentage cover at reef flat and reef slope for each genus. Data represents mean (\pm SE) ($n=3$)

families	genera	coral percentage cover \pm (SE)	
		reef flat	reef slope
Poritidae	<i>Porites</i> sp.	31.38 \pm (4.79)	5.05 \pm (2.34)
	<i>Goniopora</i> sp.	0.03 \pm (0.03)	0.03 \pm (0.03)
Faviidae	<i>Favites</i> sp.	4.80 \pm (1.81)	0.88 \pm (0.08)
	<i>Goniastrea</i> sp.	3.35 \pm (0.78)	2.49 \pm (0.13)
	<i>Favia</i> sp.	0.54 \pm (0.09)	0.91 \pm (0.14)
	<i>Diploastrea</i> sp.	0.29 \pm (0.20)	0.16 \pm (0.03)
	<i>Cyphastrea</i> sp.	x	0.63 \pm (0.22)
Fungiidae	<i>Fungia</i> sp.	0.77 \pm (0.11)	1.33 \pm (0.52)
	<i>Herpolitha</i> sp.	0.51 \pm (0.28)	1.17 \pm (0.50)
	<i>Podabacia</i> sp.	0.19 \pm (0.14)	0.25 \pm (0.03)
Acroporidae	<i>Acropora</i> sp.	0.76 \pm (0.62)	2.84 \pm (1.04)
Pocilloporiidae	<i>Pocillopora</i> sp.	0.48 \pm (0.22)	1.17 \pm (0.18)
Agariciidae	<i>Pavona</i> sp.	0.29 \pm (0.29)	0.22 \pm (0.08)
	<i>Pachyseris</i> sp.	0.06 \pm (0.06)	0.35 \pm (0.35)
	<i>Coeloseris</i> sp.	x	0.82 \pm (0.77)
	<i>Gardineroseris</i> sp.	x	0.09 \pm (0.09)
Merulinidae	<i>Merulina</i> sp.	0.26 \pm (0.26)	0.57 \pm (0.27)
	<i>Hydnophora</i> sp.	0.13 \pm (0.13)	0.28 \pm (0.16)
Mussidae	<i>Symphyllia</i> sp.	0.06 \pm (0.06)	0.54 \pm (0.18)
	<i>Lobophyllia</i> sp.	x	0.57 \pm (0.36)
Oculinidae	<i>Galaxea</i> sp.	0.03 \pm (0.03)	0.38 \pm (0.25)
Pectiniidae	<i>Pectinia</i> sp.	x	0.16 \pm (0.16)
	<i>Mycedium</i> sp.	x	0.28 \pm (0.20)
Dendrophylliidae	<i>Turbinaria</i> sp.	x	0.06 \pm (0.06)
Dendrophylliidae	<i>Turbinaria</i> sp.	x	0.06 \pm (0.06)
Siderastreidae	<i>Coscinaraea</i> sp.	x	0.41 \pm (0.41)

x = absent

Table 2. Statistical indices of all parameters (Two-way ANOVA)

Parameters	Site			Season			Site*Season		
	df	F	sig	df	F	sig	df	F	sig
GEM	1	0.005	0.943	1	0.878	0.356	1	0.111	0.742
NEM	1	0.589	0.448	1	7.502	0.010*	1	0.330	0.570
Re	1	0.066	0.799	1	0.026	0.874	1	0.014	0.907
F_v/F_m	1	0.664	0.417	1	4.587	0.034*	1	6.197	0.014*
ΔF/F_m	1	10.466	0.002*	1	3.539	0.062	1	0.025	0.874
rETR_{max}	1	1.072	0.308	1	0.091	0.765	1	0.002	0.968
I_k	1	0.000	0.986	1	1.135	0.295	1	0.243	0.625
Alpha	1	4.763	0.037*	1	0.621	0.436	1	0.382	0.541
Chl <i>a</i>	1	0.255	0.617	1	0.679	0.416	1	0.055	0.816
Chl <i>c</i>₂	1	1.266	0.269	1	1.595	0.216	1	1.396	0.246
cell density	1	2.433	0.129	1	0.090	0.766	1	1.361	0.252
Salinity	1	8.59	0.005*	1	62.427	<0.001*	1	9.069	0.004*
Temperature	1	0.025	0.876	1	1.209	0.275	1	4.521	0.037*
pH	1	0.001	0.976	1	23.016	<0.001*	1	0.054	0.817
DO (mg/l)	1	0.613	0.436	1	15.682	<0.001*	1	0.437	0.511
DO (%)	1	1.621	0.207	1	0.060	0.807	1	1.790	0.185

*significant different

Table 3. Environmental parameters on reef slope from June 2017 to January 2018. Data represents mean (\pm SE) (n=3)

Months	Salinity (PSU)	Temperature (°C)	pH	DO (mg/l)	DO (%)	Sediment accumulation rate (g m ⁻² d ⁻¹)
June	32.00 (\pm 0.00)	31.13 (\pm 0.14)	8.11 (\pm 0.01)	7.09 (\pm 0.09)	95.67 (\pm 1.12)	x
July	34.00 (\pm 0.00)	30.00 (\pm 0.00)	7.26 (\pm 0.00)	7.19 (\pm 0.14)	95.03 (\pm 2.00)	15.86 (\pm 8.16)
August	32.99 (\pm 0.03)	31.35 (\pm 0.02)	8.19 (\pm 0.02)	5.53 (\pm 0.03)	91.80 (\pm 0.66)	17.93 (\pm 16.68)
October	32.87 (\pm 0.05)	30.40 (\pm 0.00)	8.23 (\pm 0.01)	5.73 (\pm 0.23)	91.75 (\pm 3.59)	1.49 (\pm 0.39)
December	32.00 (\pm 0.04)	30.42 (\pm 0.08)	8.16 (\pm 0.01)	6.08 (\pm 0.18)	96.97 (\pm 2.85)	x
January	31.90 (\pm 0.03)	29.10 (\pm 0.03)	8.17 (\pm 0.00)	5.60 (\pm 0.17)	87.57 (\pm 2.59)	x

x = absent

Table 4. Environmental parameters on reef flat from June 2017 to January 2018. Data represents mean (\pm SE) (n=3)

Months	Salinity (PSU)	Temperature (°C)	pH	DO (mg/l)	DO (%)	Sediment accumulation rate (g m ⁻² d ⁻¹)
June	34.67 (\pm 0.21)	28.95 (\pm 0.10)	8.09 (\pm 0.03)	7.14 (\pm 0.30)	93.72 (\pm 4.08)	x
July	34.00 (\pm 0.00)	29.33 (\pm 0.22)	7.25 (\pm 0.00)	6.99 (\pm 0.31)	93.08 (\pm 4.14)	4.13 (\pm 1.38)
August	33.02 (\pm 0.03)	32.38 (\pm 0.71)	8.17 (\pm 0.01)	5.75 (\pm 0.12)	95.33 (\pm 1.93)	4.63 (\pm 1.54)
October	32.80 (\pm 0.04)	31.03 (\pm 0.19)	8.29 (\pm 0.09)	5.67 (\pm 0.17)	92.53 (\pm 2.72)	2.34 (\pm 0.78)
December	32.02 (\pm 0.04)	30.65 (\pm 0.03)	8.21 (\pm 0.01)	6.03 (\pm 0.22)	96.38 (\pm 3.46)	x
January	31.92 (\pm 0.03)	29.80 (\pm 0.20)	8.13 (\pm 0.02)	6.46 (\pm 0.37)	102.22 (\pm 5.97)	x

x = absent

CO-APPLICATION OF HUMIC ACID AND *BACILLUS* STRAINS ENHANCES SEED AND OIL YIELDS BY MEDIATING NUTRIENT ACQUISITION OF SAFFLOWER (*CARTHAMUS TINCTORIUS* L.) PLANTS IN A SEMI-ARID REGION

EKIN, Z.

*Faculty of Agriculture, Department of Field Crops, Van Yuzuncu Yil University, Van, Turkey
(e-mail: zehraekin@yyu.edu.tr; phone: +90-432-225-1056; fax: +90-432-225-1104)*

(Received 16th Nov 2019; accepted 30th Jan 2020)

Abstract. Faced with the deterioration of natural resources, current trends in agriculture are focused on seeking eco-friendly methods to improve plant growth promotion and crop productivity. Plant growth promoting rhizobacteria (PGPR) and humic substances can improve crop production in sustainable farming due to their various features. This study examined how humic acid (HA) and inoculation with PGPR (*Bacillus megatorium* and *Bacillus subtilis*) affect the agronomic performance of safflower (*Carthamus tinctorius* L.) in a semi-arid environment. In the field experiments, PGPR inoculated and non-inoculated safflower seeds were cultivated in soil treated with humic acid (0, 200, 300, and 400 kg ha⁻¹), alone or in combination. It was observed that PGPR and HA improved growth, yield parameters and seed mineral contents. Their plant growth responded positively to inoculation with *Bacillus* sp. strains owing to the N-fixing and P-solubilizing capabilities, whereas greatly positive response in the seed yield and quality was found when applied in combination with humic acids. The combined application of 300 and 400 kg ha⁻¹ HA with *Bacillus subtilis* inoculation enhanced seed and oil yields by an average of 162% and 221% relative to the control plants. This study confirms that integrated management strategies can ensure higher crop productivity of safflower in sustainable and semi-arid environments.

Keywords: *energy crop, humic substances, plant growth promoting rhizobacteria, seed yield, sustainable agriculture*

Introduction

Safflower (*Carthamus tinctorius* L.) is an annual oilseed and energy crop belonging to the *Asteraceae* family. The crop was once grown for colorful petals used in food coloring, fabric dyes, flavoring agent and medicinal use (Ekin, 2005). Nowadays, scientific interest in this species is mainly due to its high quality vegetable oil for nutritional and industrial applications. However, safflower has gained importance in recent years as a result of its vegetable oil for human consumption and biodiesel production in arid and semi-arid regions in the world. Safflower is also one of the most adapted oilseed crops to dryland cropping systems with good drought tolerance due to its deep taproot, but it's sensitive to dry soil condition in which kernel filling (flowering) are affected by water stress conditions (Dajue and Mündel, 2006).

To improve the plant productivity, it is of paramount importance to supply adequate water and nutrient acquisition in semi-arid regions typically characterized by variable and unpredictable rainfall, large diurnal ranges in temperature, frequent strong winds and poor moisture storing capacity of soils (Chavoushi et al., 2019). Moreover, this is crucial to producers in semi-arid regions of world and Turkey, including eastern Anatolia, south eastern Anatolia and central Anatolia. In particular, water resources need to be used efficiently because of the anticipated water scarcity in the face of global warming and the increasing competition between domestic, industrial, and agricultural water consumptions. Therefore, it is imperative to improve the drought tolerance of

crops as well as its salt tolerance, heavy metal stress tolerance and disease resistance, and to protect soil health and fertility under the changing circumstances. Currently, there are no economically viable technological means to facilitate crop production under various stress conditions. Towards a sustainable agricultural vision, the uses of plant growth promoting rhizobacteria and humic acid might also be a promising alternative eco-friendly approach, which helps in protecting the soil health, increasing the nutrient uptake capacity and water use efficiency and decreasing the effects of drought, salinity and heavy metal pollution etc.

Plant growth promoting rhizobacteria (PGPR) are bacteria colonizing rhizospheres of plant that, unlike fertilizers and pesticides, depend on various mechanisms like nitrogen fixation, solubilization of phosphate, production of different phytohormones like indole-3-acetic acid, gibberellic acid and cytokines for its success in promoting crop yield (Calvo et al., 2014). In this sense, plant growth promoting rhizobacteria can be used to enhance plant health and promote plant growth rate without environmental contamination. For decades, varieties of PGPR including the species *Pseudomonas*, *Bacillus*, *Enterobacter*, *Klebsiella*, *Azotobacter*, *Variovorax* *Azospirillum*, and *Serratia* have been well studied in various field crops as rhizosphere-colonizing microorganisms (Glick, 2012), such as wheat (Rosas et al., 2009; Hungria et al., 2010; Rana et al., 2012), sugar beet and barley (Cakmakci et al., 2001, 2006), sugarcane (Silva et al., 2017), sunflower (Shadid et al., 2012), rice (Lucas et al., 2009), bean (Hoyos-Carvajal et al., 2009), canola (El-Howeity and Asfour, 2012), maize (Thonar et al., 2017) and soybean (Cassán et al., 2009). However, only limited data are reported in the beneficial effects of PGPR on safflower growth promotion. The literature on PGPR regarding safflower included mostly *Pseudomonas*, *Azospirillum* and *Azotobacter* spp. inoculation which were used to improve nitrogen uptake (Mirzakhani et al., 2009; Soleymanifard and Sidat, 2011; Sharifi et al., 2017; Nosheen et al., 2018), root morphology (Nosheen et al., 2011) and protein quantity and quality of safflower seeds (Nosheen et al., 2016). The various studies also reported that inoculation of specific PGPR species like N₂-fixing *Bacillus subtilis* and phosphorus solubilizing *Bacillus megatorium* instead of synthetic chemicals may serve as an effective alternative and environmental friendly practice since they improve plant nutrition by increasing N and P uptake by plants (Cakmakci et al., 2001; Esitken et al., 2003). But, up till now no data are available with respect to the use of this genus in safflower plants.

Similarly, humic acid (HA) are naturally-available substance in the soil that are end products of microbial decomposition and chemical degradation of dead biota. Humic substances can promote plant growth through improvement in root architecture and morphology, enhancement of nutrient availability, uptake and translocation, promotion of plant physiology and development due to their hormone-like activities and promotion of soil biological activity (Puglisi et al., 2013; Canellas and Olivares, 2014; Ahmad et al., 2016). In the various experiments, direct effects of humic acid on plant growth were well described in cultivation of various crops, such as potato (Suh et al., 2014), tomato (Olivares et al., 2015), maize (Canellas et al., 2013), Hungarian vetch (Esringu et al., 2016) and blueberry (Schoebitz et al., 2016). However, basic mechanisms and benefits of the combined application of humic substances and plant growth promoting rhizobacteria have been recently demonstrated for several plant species grown under field conditions and have been attributed to an increase in the adaptation of seedlings to stress conditions, which result to cause an increase in the macro- and micro nutrient uptakes and root growth (Nardi et al., 2009; Dobbss et al., 2010; Busato et al., 2012;

Puglisi et al., 2013; Canellas and Olivares, 2014). Olivares et al. (2015) observed that co-application of humates isolated from vermicompost with diazotrophic endophytic *Herbaspirillum seropedicae* inoculation can increase significantly nitrate uptake, nitrate reductase activity, fruit biomass, leading to to increased tomato yield. The researchs previously reported that humic substances have potential as enhancer of plant growth promoting bacteria inoculation benefits (Canellas et al., 2013; Estringu et al., 2016; Schoebitz et al., 2016; Silva et al., 2017).

Keeping in view the characteristics of plant growth promoting rhizobacteria and humic acid as a helping way for crop plants to be grown in arid and semi-arid areas we hypothesized that they can enhance the agronomic performance of safflower through the activation of natural processes like nutrient release and uptake by various mechanisms described above. Extensive root system created by improved root growth and architecture by plant growth promoting rhizobacteria and humic acid can also enhance the seed quality by increasing the uptake of nutrients by exploring more and more soil volume. Stimulation of biological activity by humic acid can further enhance nutrient cycling through the action of microorganisms. In this regard, to evaluate the potential of plant growth promoting rhizobacteria and humic acid for agronomic performance of safflower we planned 2 years field experiment in a semi-arid environment. In this experiments we used *Bacillus megatorium* M3 (P-solubilizing), *Bacillus subtilis* OSU-142 (N₂-fixing) and humic acid (obtained from leonardite).

Materials and Methods

Study Site

Field experiments were carried out under rainfed conditions at a research farm located in Ahlat district (38° 46'N and 42°30'E with an altitude of 1722 m) in Eastern Anatolia region, Turkey during 2010 and 2011 (*Fig. 1*). The climate at this location is classified as continental with a total long-term average (1958-2017) precipitation of 562.6 mm mainly in winter. Annual mean air temperature is 9.3°C, with an average temperature of -2.5°C in January and 21.9°C in July. Annual mean relative humidity is 63.8%. The study site climate variables were collected from weather station and averaged for each month (*Table 1*). In 2010 and 2011, total precipitation during the crop season (from April to August) was 291.0 mm, and 269.4 mm, respectively, and the long-term average for the same period was 136.2 mm (*Table 1*). The mean air temperature was 16.5°C, 16.0°C in 2010, 2011, respectively, and long-term average was 16.1°C.

Table 1. Climate data: Monthly means of climate variables for the crop seasons of 2010, 2011 and long-term average (LTA: 1958-2017) in Ahlat, Turkey

Months	Temperature (°C)			Precipitation (mm)			Relative humidity (%)		
	2010	2011	LTA	2010	2011	LTA	2010	2011	LTA
April	7.3	6.9	6.9	154.4	159.0	87.1	71.0	71.0	69.4
May	11.4	11.2	13.1	106.2	90.0	70.2	65.8	69.1	65.0
June	18.3	17.6	18.9	28.0	15.6	28.7	50.4	52.1	55.6
July	22.8	22.3	21.5	1.8	3.2	8.3	37.3	41.3	49.4
August	22.5	22.0	22.8	0.6	1.6	5.7	35.6	40.4	47.7
Season(M/T)*	16.5	16.0	16.1	291.0	269.4	136.2	52.0	54.8	57.4
Yearly(M/T)	10.9	8.6	9.3	399.0	566.6	562.6	59.6	56.4	63.8

* M: Mean, T: Total

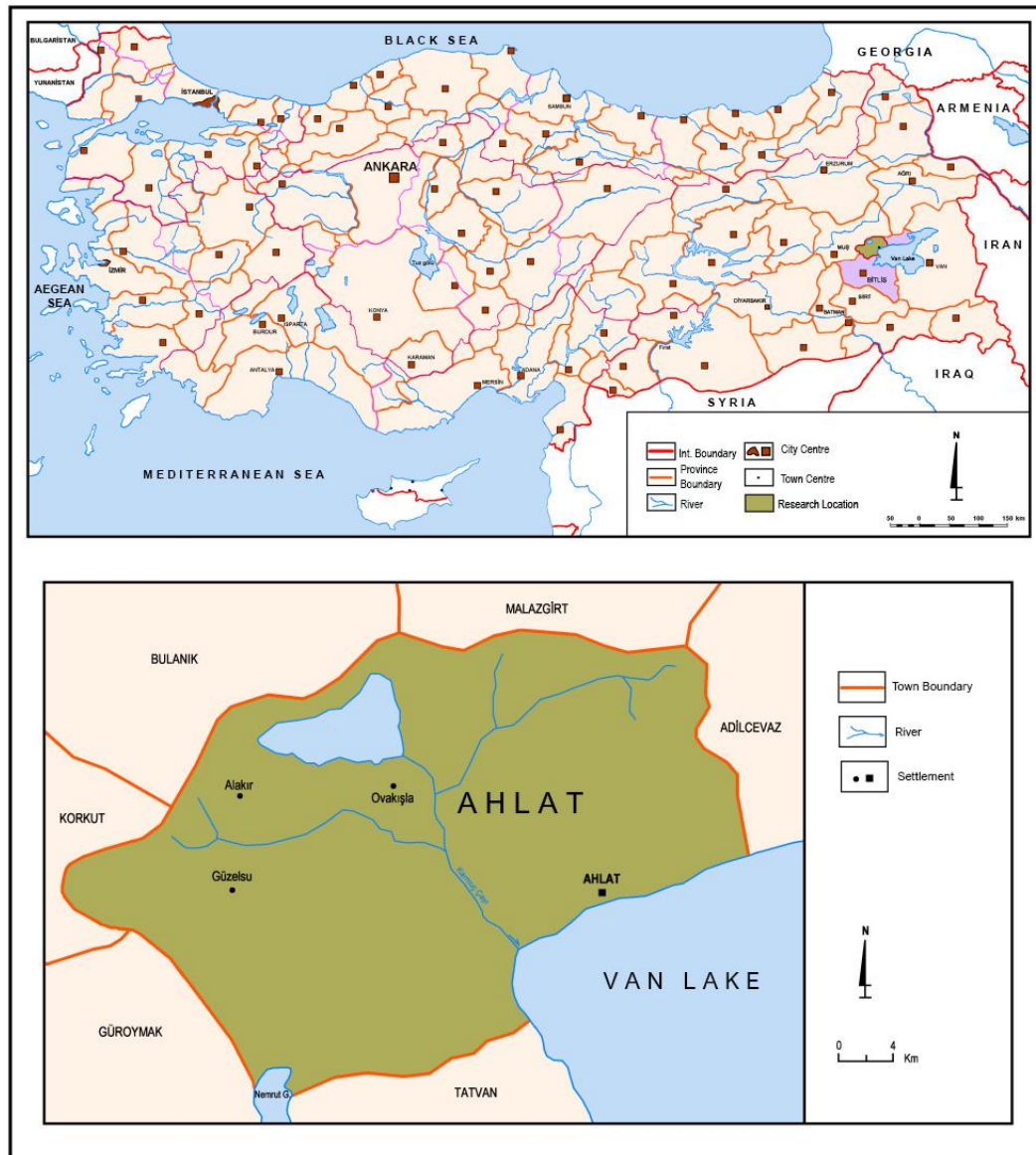


Figure 1. Map of study site

Prior to the experiments, soil samples were collected in the experiment site and analyzed for their physical and chemical properties using the methods described in Soil and Plant Analysis Laboratory Manual by Ryan et al. (2012). Soil samples were collected in the top 30 cm (<2 mm fraction) of soil at different locations of the experiment site. The experiment site soil was silt-clay-loam with a pH of 7.41, total nitrogen content of 0.15 g kg⁻¹, organic matter content of 1.60%, CaCO₃ content of 6.8%, electrical conductivity of 1.16 dS m⁻¹, available phosphorus content of 7.95 mg kg⁻¹, available potassium content of 196 mg kg⁻¹, available manganese content of 3.30 mg kg⁻¹, zinc content of 1.44 mg kg⁻¹, iron content of 5.85 mg kg⁻¹ and copper content of 0.59 mg kg⁻¹.

Plant Material and Experimental Design

Safflower (*Carthamus tinctorius* L.) var. Dincer, Turkey of origin, which exhibits early maturity, spineless, open-pollinated, yellow-orange flower color, white seed color,

28-32% oil content and high-linoleic oil type, was used as plant material. The field trials were set up a factorial design including the two following factors: four HA doses (0= without the addition of HA, 20= 200 kg ha⁻¹ HA, 30= 300 kg ha⁻¹ HA and 40= 400 kg ha⁻¹ HA) and three PGPR applications (B0= no bacterial inoculation, B1: *Bacillus subtilis* OSU-142 and B2: *Bacillus megatorium* M3) with three replications.

Humic Acid Characteristics, PGPR Culture Condition and Seed Inoculation

Agro-Lig, a commercial product, was produced through crude humic acids derived from leonardite and provided by Altintar Chemicals Company (Turkey). Agro-Lig contains total humic acid 85%, total organic matter 75%, pH 3.5-5.5, max moisture 22%, silicon 0.5%, iron 0.5%, magnesium 0.5%, calcium 3.0%, sodium 0.3%, manganese 0.02%, copper 0.0003%, potassium 0.07%, titanium 0.02%, barium 0.03%, boron 0.01%, cobalt 0.0002% dry matter basis. Three HA doses (200, 300 and 400 kg ha⁻¹) were prepared by Agro-Lig in granule form.

The two plant growth promoting rhizobacteria strains (*Bacillus subtilis* strain OSU-142 and *Bacillus megatorium* strain M3) tested were kindly procured at Atatürk University, Department of Plant Protection, Turkey. Currently, these strains are protected in culture collection unit in the Department of Genetic and Bioengineering, Faculty of Engineering at Yeditepe University, İstanbul, Turkey. The choice of these two bacteria is based on their published ability to act as potential biostimulants and biofertilizers. The gram-positive *Bacillus megatorium* M3 has demonstrated abilities to increase the solubilization of inorganic phosphates and to promote plant growth in various plant species (Cakmakci et al., 2001; Orhan et al., 2006). The gram-positive *Bacillus subtilis* OSU-142 is an efficient root colonizer and has been shown to N₂-fixing under field conditions (Cakmakci et al., 2001, 2006). Moreover, it has widely shown the potential to improve plant growth and nitrogen acquisition when inoculated to various plant species (Cakmakci et al., 2001, 2006; Esitken et al., 2003; Orhan et al., 2006; Elkoca et al., 2010; Acikgoz et al., 2016; Ekin, 2019). These strains are indigenous, and are kept in nutrient broth (NB) with 15% glycerol at -80°C for long-term storage, and grown on nutrient agar (NA) for routine use. Single colonies were transferred to 500 ml flasks that contained NB and incubated aerobically on a rotating shaker (150 rpm) overnight at 28°C (Cakmakci et al., 2001, 2006). The bacterial suspension was then diluted in sterilized water to final concentration at cell densities of 10⁹ colony forming units (CFU) ml⁻¹. Seeds were surface sterilized prior to bacterial inoculation with 95% ethanol then sterilized with 10% chlorox for 3 min and washed successively 3–4 times with distilled water. Seeds were inoculated with the liquid cultures of rhizobacteria (*Bacillus megatorium* M3 and *Bacillus subtilis* OSU-142) mixed with 10% sugar solution for 30 min, and were stored overnight to dry under room temperature.

Crop Husbandry and Data Recording

The tillage system was fall plow and spring cultivate. Different doses of humic acid (granule form) were applied to the soil in humic acid treated plots, according to the layout. Humic acid was applied once during planting and then mixed well with the soil. PGPR inoculated and non-inoculated seeds were sown in early April in each year. In the present study, plots were 1.5 m wide and 5 m long and consisted of five rows spaced 0.3 m apart. Plot stands were over sown and hand-thinned approximately at the first four-true leaf stage to 10 cm apart within a row. Throughout the growth season, the production system was

managed based on management practices recommended for the region, which included weed control by hand as required. The safflower plants were manually harvested at the stage of physiological maturity, when most of the leaves turn a brown color and very little green remains on the bracts of the latest flowering heads in late August in each year. Data collecting on the plant height (cm), stem diameter (mm), number of branches per plant, number of capitula per plant, number of seeds per capitulum and capitulum diameter (cm) were recorded for ten randomly selected safflower plants in the central three rows of each plot. The seed yield was expressed in $t\ ha^{-1}$. The seed oil and total nitrogen contents were determined by Soxhlet extraction and Kjeldahl methods. Then, total N content was also used for the calculation of the seed protein concentration by multiplication with a conversion factor of 6.25 (Ryan et al., 2012). For mineral content analysis (P, K, Ca, Mg, Fe, Zn, Cu, Mn), safflower seed was ground in a Wiley Mill to pass through an 840- μm screen and wet-digested in $HNO_3:HClO_4$ (6:2 v/v) with the Advanced Microwave Digestion System, Ethos Easy, then analyzed with the Inductively Coupled Plasma Optical Emission Spectrometry (iCAP 6000 SERIES, ICP Spectrometer).

Data Analysis

The data were tested for homogeneity and normality of residuals using the Kolmogorov–Smirnov and Bartlett tests, respectively. Afterwards, a combined analysis of variance (ANOVA) was used to compare the effects of humic acid doses and bacterial treatments by field experiment interactions for 2 years using PROC GLM of SAS 9. Mean comparisons were conducted using Fisher's least significant difference ($LSD_{0.05}$) test.

Results

Morphological and Yield Parameters

The results regarding morphological and yield parameters of safflower in relation to humic acid dose and plant growth promoting rhizobacteria inoculation are presented in *Table 2*. Highly significant increases were observed in safflower growth and yield parameters after inoculation with PGPR (*Bacillus* strains), and further improved after combined application with humic acid doses. When compared to plant growth promoting rhizobacteria treatments both with and without humic acids, it was observed that inoculation with *Bacillus subtilis* OSU-142 (B_1) was more effective when compared to *Bacillus megatorium* M3 (B_2). Furthermore, a significant interaction between the tested factors was observed in the case of stem diameter, number of branches and capitula per plant, number of seeds per capitulum, capitulum diameter and 1000 seed weight, whereas plant height was highly influenced by humic acid dose and plant growth promoting rhizobacteria inoculation with no significant HA x PGPR interaction (*Table 2*, *Fig. 2*). The tallest plant height values were recorded in both *Bacillus subtilis* OSU-142 inoculation and $400\ kg\ ha^{-1}$ HA dose, while the highest numbers of capitula per plant and seeds per capitulum, largest capitulum diameter and 1000 seed weight values were recorded in co-application of *Bacillus subtilis* OSU-142 with 300 and $400\ kg\ ha^{-1}$ HA doses ($HA_{30}+B_1$ and $HA_{40}+B_1$). Likewise, the application of $400\ kg\ ha^{-1}$ HA dose significantly increased numbers of branch per plant and seeds per capitulum at both B_1 and B_2 inoculation by 81.3% and 90.6% in branch numbers and 85.5% and 83.6% in seed numbers increases when compared to the untreated control plants, respectively (*Table 2*, *Fig. 2*).

Table 2. Mean of morphological and yield traits of safflower affected by plant growth promoting rhizobacteria and humic acid doses¹

Treatments	Plant height (cm)	Stem diameter (mm)	No. of branches per plant	No. of capitula per plant	No. of seeds per capitulum	Capitulum diameter (cm)	1000 seed weight (g)
Humic acid (HA)							
0	73.0 d	5.64 c	4.3 d	6.7 d	25.5 d	2.07 b	33.1 d
20	77.4 c	6.70 b	4.9 c	10.4 c	34.8 c	2.39 a	37.0 c
30	82.7 b	6.98 a	5.3 b	10.9 b	35.8 b	2.39 a	38.1 b
40	85.2 a	7.05 a	5.9 a	11.3 a	36.7 a	2.40 a	38.5 a
LSD _{0,05}	2.383	0.118	0.129	0.125	0.627	0.024	0.405
Significance	**	**	**	**	**	**	**
Plant growth promoting rhizobacteria (PGPR)							
B ₀	71.9 c	6.18 c	4.6 c	8.4 c	30.4 c	2.20 c	34.6 c
B ₁	87.6 a	6.91 a	5.6 a	11.3 a	35.6 a	2.41 a	38.5 a
B ₂	79.2 b	6.70 b	5.1 b	10.0 b	33.8 b	2.32 b	37.0 b
LSD _{0,05}	2.064	1.102	0.112	0.108	0.543	0.021	0.350
Significance	**	**	**	**	**	**	**
HA x PGPR							
HA ₀ +B ₀	66.6	4.56 g	3.2 e	4.9 j	20.7 g	1.90 f	29.2 g
HA ₀ +B ₁	79.9	6.40 e	4.9 c	8.6 h	29.0 e	2.20 d	36.0 e
HA ₀ +B ₂	71.8	5.78 f	4.5 d	6.3 i	26.2 f	2.09 e	33.7 f
HA ₂₀ +B ₀	69.7	6.40 e	4.3 d	8.9 g	32.3 d	2.31 c	35.5 e
HA ₂₀ +B ₁	85.3	6.80 d	5.4 b	11.5 b	37.1 ab	2.46 a	38.2 c
HA ₂₀ +B ₂	77.4	6.90 d	4.9 c	10.9 d	34.9 c	2.40 b	37.3 d
HA ₃₀ +B ₀	73.9	6.71 d	4.7 d	9.2 f	33.1d	2.29 c	36.1 e
HA ₃₀ +B ₁	92.9	7.11 b	6.1 a	12.5 a	38.2 a	2.51 a	40.0 a
HA ₃₀ +B ₂	81.4	7.11 b	5.0 c	11.1 c	36.3 b	2.36 b	38.1 c
HA ₄₀ +B ₀	76.5	6.78 d	5.8 a	10.3 e	34.1 c	2.28 c	36.8 d
HA ₄₀ +B ₁	92.5	7.33 a	6.1 a	12.6 a	38.4 a	2.48 a	39.8 a
HA ₄₀ +B ₂	86.6	7.03 c	5.8 a	11.7 b	38.0 a	2.41 b	39.0 b
Significance	ns	**	**	**	**	**	**
CV (%)	4.38	2.62	3.70	1.84	2.79	1.53	1.61

¹20, 30 and 40 treatments refer to safflower plants growing under field condition with 200, 300 and 400 kg ha⁻¹ of HA; B₀ treatment without any application of the bacteria, B₁ treatment with *Bacillus subtilis* OSU-142 inoculation; B₁+20, B₁+30, and B₁+40 with *Bacillus subtilis* OSU-142 and 200, 300 and 400 kg ha⁻¹ of HA, respectively; B₂ treatment with *Bacillus megatorium* M3 inoculation; B₂+20, B₂+30, and B₂+40 with *Bacillus megatorium* M3 and 200, 300 and 400 kg ha⁻¹ of HA, respectively. Means followed by different letters are different by LSD test. *: P < 0.05, **: P<0.01, ns: not significant; CV: coefficient of variations

Seed Yield and Quality Parameters

Seed, oil and protein yields and certain quality parameters of safflower were significantly affected by plant growth promoting rhizobacteria and humic acid treatments based on the two-year average data (Table 3). For most of the measured quality parameters, no significant interaction between plant growth promoting rhizobacteria and humic acid application was recorded, except for the seed yield and fertile and sterile seed ratio (Table 3, Fig. 3).

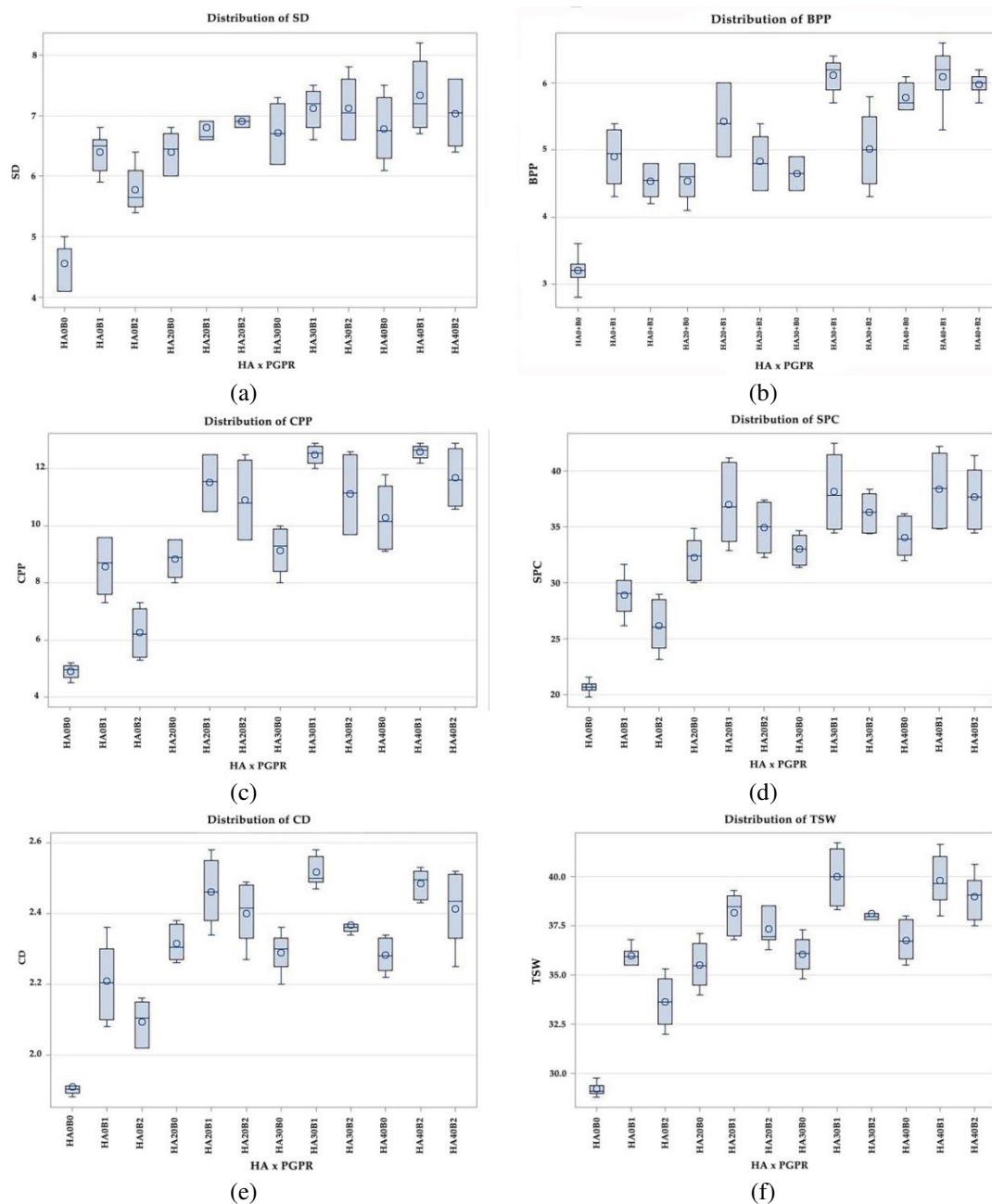


Figure 2. Stem diameter (mm) (a), number of branch per plant (b), number of capitula per plant (c), number of seeds per capitulum (d), capitulum diameter (cm) (e) and thousand seed weight (g) (f) of safflower affected by bacterial inoculation and humic acid. B₀: without bacteria; B₁: *B. subtilis* OSU-142; B₁+20, B₁+30, and B₁+40: *B. subtilis* OSU-142 with 200, 300 and 400 kg ha⁻¹ of HA, respectively; B₂: *B. megatorium* M3; B₂+20, B₂+30 and B₂+40: *B. megatorium* M3 with 200, 300 and 400 kg ha⁻¹ of HA, respectively

Fertile and sterile seed percentages, the most important quality characteristics for safflower, were significantly affected by both plant growth promoting rhizobacteria and humic acid treatments; however, its co-application significantly reduced sterile seed percentage, whereas an opposite trend was observed for the fertile seed percentage (Table 3). The highest fertile seed and lowest sterile seed percentages were recorded in co-application of

both PGPR strains with 300 kg ha⁻¹ humic acid dose (HA₃₀+B₁ and HA₃₀+B₂), whose values were higher by 9.0 and 8.6% and lower by 85.1% and 79.9%, respectively, compared to the untreated control. In the present study, a significant interaction between the tested factors was also observed for the seed yield (Table 3). Inoculation with *Bacillus subtilis* OSU-142 triggered ameliorative effects in terms of seed yield at both 300 and 400 kg ha⁻¹ humic acid doses and led to an increase in seed yield by 163.6% and 161.4%, respectively, when compared to the control (Table 3, Fig. 3). Furthermore, its effect was much more pronounced than that of inoculation with *Bacillus megatorium* M3. Among the humic acid doses, the highest seed yields were also recorded with the application of 300 and 400 kg ha⁻¹ humic acid doses which was statistically similar (Table 3).

Table 3. Mean of seed yield and certain quality traits of safflower affected by plant growth promoting rhizobacteria and humic acid doses¹

Treatments	Seed ratio (%)		Seed content (%)		Yield (t ha ⁻¹)		
	Fertile	Sterile	Oil	Protein	Seed	Oil	Protein
Humic acid (HA)							
0	92.72 d	7.27 a	27.1 c	13.9	1.22 c	0.33 c	0.16 b
20	94.90 c	4.17 c	29.0 bc	13.6	1.74 b	0.51 b	0.24 a
30	95.89 b	2.25 d	30.7 ab	13.2	1.95 a	0.59 a	0.25 a
40	97.75 a	5.10 b	31.3 a	12.8	2.01 a	0.62 a	0.26 a
LSD _{0,05}	0.745	0.751	2.186	1.438	0.149	0.022	0.051
Significance	**	**	**	ns	**	**	**
Plant growth promoting rhizobacteria (PGPR)							
B ₀	94.24 b	5.78 a	27.7 b	12.7	1.40 c	0.39 c	0.19 c
B ₁	95.62 a	4.38 b	30.5 a	13.8	2.06 a	0.63 a	0.28 a
B ₂	96.15 a	3.89 b	30.4 a	13.5	1.73 b	0.52 b	0.22 b
LSD _{0,05}	0.645	0.651	1.892	1.245	0.174	0.052	0.034
Significance	**	**	**	ns	**	**	**
HA x PGPR							
HA ₀ +B ₀	90.37 d	9.85 a	25.7	14.0	0.88 h	0.23	0.12
HA ₀ +B ₁	94.22 bc	5.77 bc	27.1	14.1	1.56 ef	0.42	0.22
HA ₀ +B ₂	93.17 c	6.82 b	28.3	13.5	1.15 g	0.33	0.15
HA ₂₀ +B ₀	93.98 c	6.02 b	26.8	13.9	1.41 f	0.37	0.19
HA ₂₀ +B ₁	95.77 b	4.22 c	30.6	14.0	2.05 b	0.62	0.29
HA ₂₀ +B ₂	97.92 a	2.25 cd	29.8	12.9	1.76 d	0.52	0.23
HA ₃₀ +B ₀	96.70 ab	3.29 c	28.3	13.3	1.60 e	0.45	0.21
HA ₃₀ +B ₁	98.52 a	1.47 d	32.4	13.8	2.32 a	0.75	0.31
HA ₃₀ +B ₂	98.03 a	1.98 d	31.4	12.5	1.93 c	0.59	0.25
HA ₄₀ +B ₀	95.25 b	4.74 c	29.9	13.1	16.4 e	0.48	0.21
HA ₄₀ +B ₁	93.95 c	6.04 b	31.5	13.2	2.30 a	0.73	0.31
HA ₄₀ +B ₂	95.50 b	4.50 c	32.4	11.9	2.06 b	0.66	0.24
Significance	**	**	ns	ns	*	ns	ns
CV (%)	1.15	13.64	5.84	4.80	7.32	4.84	7.50

¹20, 30 and 40 treatments refer to safflower plants growing under field condition with 200, 300 and 400 kg ha⁻¹ of HA; B₀ treatment without any application of the bacteria, B₁ treatment with *Bacillus subtilis* OSU-142 inoculation; B₁+20, B₁+30, and B₁+40 with *Bacillus subtilis* OSU-142 and 200, 300 and 400 kg ha⁻¹ of HA, respectively; B₂ treatment with *Bacillus megatorium* M3 inoculation; B₂+20, B₂+30, and B₂+40 with *Bacillus megatorium* M3 and 200, 300 and 400 kg ha⁻¹ of HA, respectively. Means followed by different letters are different by LSD test. *: P < 0.05, **: P<0.01, ns: not significant; CV: coefficient of variations

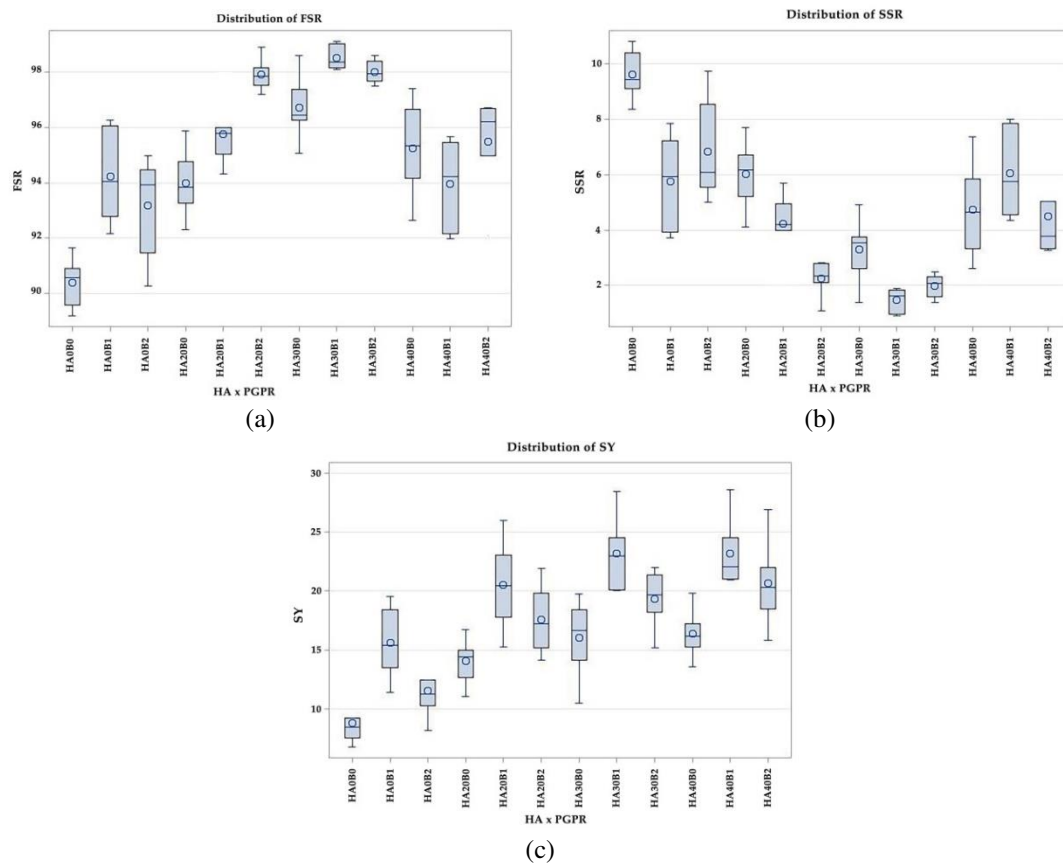


Figure 3. Fertile seed ratio (%) (a), Sterile seed ratio (%) (b) and seed yield ($t\ ha^{-1}$) (c) of safflower affected by bacterial inoculation and humic acid. B₀: without bacteria; B₁: *B. subtilis* OSU-142; B₁+20, B₁+30, and B₁+40: *B. subtilis* OSU-142 with 200, 300 and 400 kg ha⁻¹ of HA, respectively; B₂: *B. megatorium* M3; B₂+20, B₂+30 and B₂+40: *B. megatorium* M3 with 200, 300 and 400 kg ha⁻¹ of HA, respectively

Neither humic acid doses nor plant growth promoting rhizobacteria inoculation had a significant influence on protein content in seeds, whereas seed oil concentration, oil and protein yields were highly influenced by humic acid dose and PGPR application with no significant HA x PGPR interaction (Table 3, Fig. 2). The oil concentration in seeds was positively affected by increasing the humic acid doses with no significant effect for inoculation with B₁ and B₂ (30.5% and 30.4%, respectively), and the highest value by 31.3% was recorded with 400 kg ha⁻¹ humic acid application (Table 3). However, significant increases in oil and protein yields were obtained with separate 300 and 400 kg ha⁻¹ humic acid dose and *Bacillus subtilis* OSU-142 applications (Table 3).

Mineral Composition of Seeds

The two years long field trials demonstrated that safflower seed mineral composition was significantly affected by both plant growth promoting rhizobacteria and humic acid treatments, however, these integrated administrations significantly increased the mineral concentrations in seeds (except for Cu) when compared to single treatments (Table 4). The Cu concentration in seeds was only negatively affected by both increasing humic acid doses and inoculation with PGPR strains.

Table 4. Mean of mineral composition (mg kg^{-1}) of safflower seeds affected by plant growth promoting rhizobacteria and humic acid doses¹

Treatments	P	K	Ca	Mg	Fe	Zn	Cu	Mn
Humic acid (HA)								
0	3789.5 d	3687.7 d	2026.7 d	1235.1 d	49.21 d	30.81 c	15.59 a	11.09 b
20	4181.7 c	4128.3 c	2384.5 c	1391.9 c	54.14 c	34.66 b	15.42 ab	12.12 a
30	4394.9 b	4299.9 b	2519.5 b	1510.6 a	58.88 b	35.71 a	15.04 b	12.08 a
40	4506.2 a	4374.4 a	2710.3 a	1475.4 b	61.43 a	35.97 a	14.41 c	12.45 a
LSD _{0.05}	21.658	32.421	17.067	5.777	0.506	0.455	0.390	0.399
Significance	**	**	**	**	**	**	**	**
Plant growth promoting rhizobacteria (PGPR)								
B ₀	3456.8 c	3800.9 c	2215.0 c	1194.4 c	51.40 c	31.10 b	16.00 a	11.10 c
B ₁	4161.9 b	4356.6 a	2533.1 a	1593.0 a	60.20 a	35.69 a	14.41 c	12.82 a
B ₂	5042.1 a	4210.1 b	2482.5 b	1422.3 b	56.26 b	36.08 a	14.97 b	11.89 b
LSD _{0.05}	18.757	28.077	14.780	5.003	0.439	0.394	0.338	0.345
Significance	**	**	**	**	**	**	**	**
HA x PGPR								
HA ₀ +B ₀	2743.0 k	2883.3 g	1763.1 j	940.4 j	39.77 h	21.19 d	16.69	9.50 d
HA ₀ +B ₁	3959.1 g	4133.2 d	2094.7 i	1430.9 e	54.61 e	35.66 a	14.74	12.07 b
HA ₀ +B ₂	4693.2 d	4046.6 e	2222.1 g	1334.2 g	51.68 g	34.14 b	15.54	11.44 b
HA ₂₀ +B ₀	3527.7 j	3974.1 f	2166.4 h	1236.5 I	51.10 g	34.83 b	16.29	11.83 b
HA ₂₀ +B ₁	4083.3 f	4264.5 c	2557.8 d	1553.4 c	57.88 d	36.97 a	14.77	12.03 b
HA ₂₀ +B ₂	4933.8 c	4146.3 d	2429.0 f	1385.9 f	53.45 f	36.10 a	15.21	12.49 b
HA ₃₀ +B ₀	3701.5 i	4116.8 d	2441.7 f	1327.4g	54.82 e	34.05 b	15.92	10.98 c
HA ₃₀ +B ₁	4306.4 e	4530.5 a	2607.0 c	1685.4 b	63.14 b	36.38 a	14.40	13.49 a
HA ₃₀ +B ₂	5176.5 b	4252.4 c	2510.1 e	1519.0 d	58.69 d	36.69 a	14.78	11.77 b
HA ₄₀ +B ₀	3854.6 h	4229.5 c	2488.6 e	1273.4 h	57.95d	32.84 c	15.22	11.81 b
HA ₄₀ +B ₁	4298.9 e	4498.4 a	2873.2 a	1702.6 a	65.15 a	33.76 b	13.69	13.68 a
HA ₄₀ +B ₂	5364.8 a	4395.2 b	2769.1 b	1450.3 e	61.20 c	37.38 a	14.32	11.87 b
Significance	**	**	**	**	**	**	ns	**
CV (%)	1.76	2.16	2.07	1.60	2.32	2.94	3.78	4.89

¹20, 30 and 40 treatments refer to safflower plants growing under field condition with 200, 300 and 400 kg ha⁻¹ of HA; B₀ treatment without any application of the bacteria, B₁ treatment with *Bacillus subtilis* OSU-142 inoculation; B₁+20, B₁+30, and B₁+40 with *Bacillus subtilis* OSU-142 and 200, 300 and 400 kg ha⁻¹ of HA, respectively; B₂ treatment with *Bacillus megatorium* M3 inoculation; B₂+20, B₂+30, and B₂+40 with *Bacillus megatorium* M3 and 200, 300 and 400 kg ha⁻¹ of HA, respectively. Means followed by different letters are different by LSD test. *: P < 0.05, **: P<0.01, ns: not significant; CV: coefficient of variations

The study results indicated that increasing the humic acid dose from 200 kg ha⁻¹ to 400 kg ha⁻¹ was accompanied by a linear increase in important mineral contents such as the P, K, Ca and Fe (Table 4). Furthermore, plant growth promoting rhizobacteria inoculation significantly improved in these contents after combined application with humic acid dose. The highest P concentration was obtained with *Bacillus megatorium* M3 bacterial treatment in 400 kg ha⁻¹ humic acid dose by 95.6% increase when compared to control, while the highest K, Ca, Mg, Fe and Mn concentrations were recorded with the 400 kg ha⁻¹ humic acid dose with *Bacillus subtilis* OSU-142 bacterial inoculation (56.1%, 62.9%, 81.1%, 63.8% and 44.0% increases in K, Ca, Mg, Fe and Mn when compared to control, respectively). For Zn concentration, a significant interaction between the HA and PGPR factors was observed, where the inoculation with plant growth promoting rhizobacteria strains in all of humic acid doses significantly increased Zn accumulation in seed about 68.3% - 76.4 %, compared to untreated safflower plants (Table 4, Fig. 4).

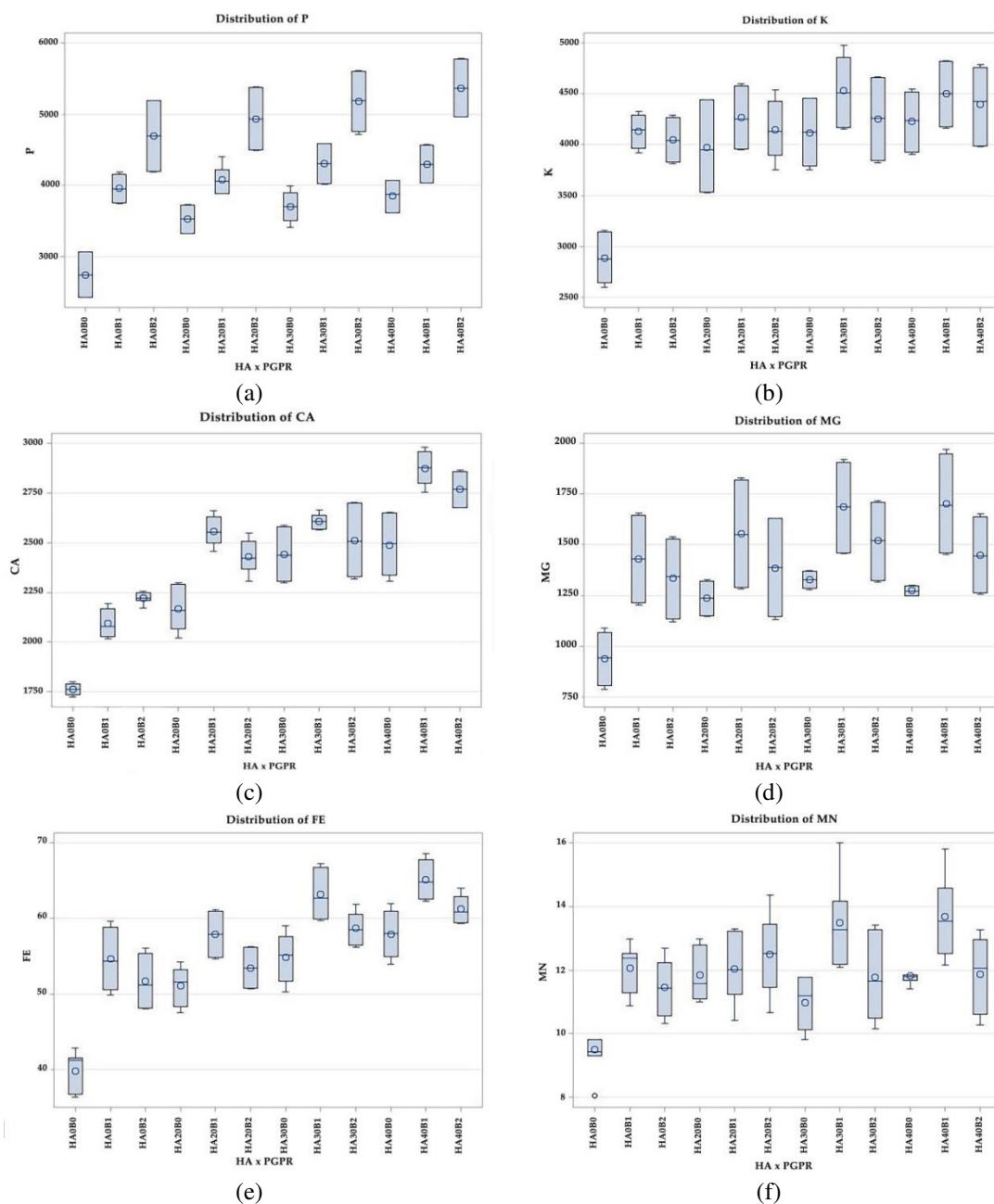


Figure 4. Phosphorus content (mg kg^{-1}) (a), potassium content (mg kg^{-1}) (b), calcium content (mg kg^{-1}) (c), magnesium content (mg kg^{-1}) (d), iron content (mg kg^{-1}) (e) and manganese content (mg kg^{-1}) (f) of safflower seeds affected by bacterial inoculation and humic acid. B₀: without bacteria; B₁: *B. subtilis* OSU-142; B₁+20, B₁+30, and B₁+40: *B. subtilis* OSU-142 with 200, 300 and 400 kg ha^{-1} of HA, respectively; B₂: *B. megatorium* M3; B₂+20, B₂+30 and B₂+40: *B. megatorium* M3 with 200, 300 and 400 kg ha^{-1} of HA, respectively

Discussion

In the present study, the plant growth-promoting rhizobacteria (*Bacillus megatorium* and *Bacillus subtilis*) and humic acids isolated from leonardite, individually or in combinations, was applied on safflower plants grown in the field trials under semi-arid conditions. Both plant growth promoting rhizobacteria inoculation and humic acid doses

significantly increased the growth parameters, seed yield and mineral concentrations in seeds (except for Cu) in comparison with control plants (grown in without PGPR and HA application), and further improved when applied in combination with humic acids. Inoculation of N₂-fixing *Bacillus subtilis* strain OSU-142 effectively improved plant growth when compared to P-solubilizing *Bacillus megatorium* strain M3 and control, and increased plant height by 21.8%, stem diameter by 11.8%, numbers of branch and capitula per plant by 22.1 and 34.5%, respectively, number of seeds per capitulum by 17.1, seed and oil yields by 47.1 and 61.5%, when compared to the untreated control plants. Inoculation of *Bacillus megatorium* M3 produced the highest P concentration in seed, while the highest K, Ca, Mg, Fe and Mn concentrations were recorded with *Bacillus subtilis* OSU-142 bacterial inoculation (56.1%, 62.9%, 81.1%, 63.8% and 44.0% increases in K, Ca, Mg, Fe and Mn when compared to control, respectively). The inoculation with PGPR strains in all of humic acid doses significantly increased Zn accumulation in seed about 68.3% - 76.4 %, compared to untreated safflower plants. Nitrogen and water requirements are the major limiting factors in safflower plant growth and productivity (Dajue and Mündel, 2006). Cakmakci et al. (2001) reported that inoculation of N₂-fixing *Bacillus subtilis* OSU-142 may satisfy nitrogen requirements of sugar beet and barley under field conditions in highland areas, and this bacteria inoculant significantly improved seed yields. Another field studies indicated that *Bacillus megatorium* might have phosphorus dissolving ability since it gave similar increases in growth and yield consistently to alone P application (Cakmakci et al., 2006; Orhan et al., 2006; Elkoca et al., 2010). Furthermore, the various studies with *Bacillus subtilis* and *Bacillus megatorium* reported remarkable growth and yield increases in potato (Ekin, 2019), common bean (Elkoca et al., 2010), sour cherry (Karakurt et al., 2011), raspberry (Orhan et al., 2006), apricot (Esitken et al., 2003) and some turfgrass species (Acikgoz et al., 2016). However, no data were reported on growth promotion with inoculation of this *Bacillus* genus in safflower plants. The literature on plant growth promoting rhizobacteria regarding safflower included mostly *Pseudomonas*, *Azospirillum* and *Azotobacter* spp. inoculation which were used to improve nitrogen uptake (Mirzakhani et al., 2009; Soleymanifard and Sidat, 2011; Sharifi et al., 2017; Nosheen et al., 2018), root morphology (Nosheen et al., 2011) and protein quantity and quality of safflower seeds (Nosheen et al., 2016). These researchers mainly observed marked changes in primary safflower metabolism in response to plant growth-promoting bacterial species; there were also strong effects of PGPR applied in improving root morphology and plant growth, and increasing endogenous hormonal levels (indole-3-acetic acid and gibberellic acid) in safflower leaves.

In the present study, humic acid treatment increased growth parameters and yields above values in controls (*Tables 2 and 3*). The increasing the humic acid dose from 200 kg ha⁻¹ to 400 kg ha⁻¹ generally was accompanied by a linear increase in growth parameters (except capitulum diameter and sterile seed percentage). Humic acid doses affected not significantly capitulum diameter only, while 200 kg ha⁻¹ humic acid dose significantly decreased the sterile seed percentage compared to the control (*Tables 2 and 3*). However, the highest seed yields recorded with the application of 300 and 400 kg ha⁻¹ humic acid doses which was statistically similar (*Table 3*). In different studies, safflower crops showed consistent increases with humic acid treatments at the different locations (Basalma, 2014; Mehraban and Miri, 2017). Enhanced plant growth and seed yield were also suggested to explain the beneficial effects of humic acid. Hajghani et al. (2016) similarly promoted the safflower growth and development as well as seed and oil

yields by humic substance application. Previous reports had shown that the beneficial effect of humic substances on plant growth may be related to increased fertilizer and water use efficiency, reducing soil compaction, enhancing total root area (especially lateral root emergence and root hairs) and plant biomass (Canellas and Olivares, 2014) and increasing soil microflora (Puglisi et al., 2013). In various field experiments, direct effects of humic acids on plant growth were well described in cultivation of various crops, such as potato (Suh et al., 2014), tomato (Olivares et al., 2015), maize (Canellas et al., 2013) and Hungarian vetch (Esringu et al., 2016). However, Canellas and Olivares (2014) recently reviewed the effects on plant metabolism of humic substance alone and in combination with plant growth promoting rhizobacteria, and their agronomical relevance.

Humic acid and plant growth promoting rhizobacteria application significantly affected plant growth development and production of safflower seed; however, their co-application further increased these agronomical parameters. Inoculation with *Bacillus subtilis* OSU-142 triggered ameliorative effects in terms of seed and oil yields at both 300 and 400 kg ha⁻¹ humic acid doses; these effects enhanced seed and oil production by average 162% and 221%, respectively, relative the control plants in semi-arid conditions (Table 3, Fig. 3). Previous reports had shown that integrated effects of plant growth promoting rhizobacteria and humic acid further increased plant growth, seed yield and quality in safflower (Mirzakhani et al., 2009; Sharifi et al., 2017), probably because of synergisms between improved nutritional status and plant stimulation factors; the net effects increased branch numbers, capitulum and stem diameters, 1000 seed weight, seed oil percentage, seed and oil yields and mineral compositions of seeds (Figs. 2, 3 and 4). Furthermore, humic substances are the most complex and biologically active organic matter compounds in the soil and stimulates both plants and microbial activities including plant growth promoting rhizobacteria through a number of mechanisms (e.g. through humic extracts of leonardite, compost or other organic fertilizer) (Nardi et al., 2009; Puglisi et al., 2013; Canellas and Olivares, 2014). PGPR enhancement of soil is largely attributable to biological N₂ fixation, phosphorus solubilization and increases in the availability of nutrients in the rhizosphere. Availability of nutrients increases in response to root surface area enhancement, which is one of several architectural and biochemical changes in the root system induced by humic substance (Nardi et al., 2009; Canellas and Olivares, 2014). Inoculation of humic acids with plant growth promoting rhizobacteria may be used for both plant growth stimulation (Dobbss et al., 2010; Busato et al., 2012; Schoebitz et al., 2016; Silva et al., 2017; Shah and Wu, 2019) and plant disease protection (Cakmakci et al., 2001). The studies with co-application of humates and different PGPR strains previously reported remarkable growth and yield increases in safflower (Sharifi et al., 2017; Nosheen et al., 2018).

Conclusions

Recently, interest in safflower production has been renewed as a result of drought tolerance and the suitability of its oil for nutritional, industrial or biofuel purposes. This study shows that safflower variety Dincer adapted well to semi-arid conditions of Turkey and is a viable alternative to other oilseed crops. In the study, alone application of safflower seeds with both humic acid and plant growth-promoting rhizobacteria (*Bacillus megatorium* and *Bacillus subtilis*) produced highly increases in terms of seed

and oil yields of safflower in semi-arid area. However combined application of plant growth promoting rhizobacteria and humic acid significantly improved growth and yield more than alone application of each partner under rainfed field condition. This increase was also supported by the enhancement of nutrient contents in the safflower seeds. Finally, the *Bacillus* inoculants should be assessed for their potential to increase crop yields and food production under real field environment and this integrated approach could become an effective method for safflower production under semi-arid conditions in sustainable agriculture systems.

Acknowledgements. The author appreciates the valuable contributions by Dr. M. Figen Dönmez (kindly provided the PGPR), Prof. Dr. Ismail Hakki Ekin (Department of Microbiology), Faruk Oguz (technical support) and Prof. Dr. Abdullah Yesilova (statistical analyses).

REFERENCES

- [1] Acikgoz, E., Bilgili, U., Sahin, F., Guillard, K. (2016): Effect of plant growth-promoting *Bacillus* sp. on color and clipping yield of three turfgrass species. – J. of Plant Nutr 39(10): 1404-1411. <https://doi.org/10.1080/01904167.2016.1143501>.
- [2] Ahmad, S., Daur, I., Al-Solaimani, S. G., Mahmood, S. (2016): Plant growth promoting rhizobacteria and humic acid improve growth and yield of organically grown canola. – Int. J. of Engineering Research & Techn 5(5): 424-428.
- [3] Basalma, D. (2014): Effects of humic acid on the emergence and seedling growth of safflower (*Carthamus tinctorius* L.). – Turkish J. of Agricultural and Natural Sci. Special Issue 2: 1402-1406. <https://dergipark.org.tr/download/article-file/142280>.
- [4] Busato, J. G., Silva, L. L., Aguiar, N. O., Canellas, L. P., Olivares, F. L. (2012): Changes in labile phosphorus forms during maturation of vermicompost enriched with phosphorus-solubilizing and diazotrophic bacteria. – Bioresour. Technol. 110: 390-395. <https://doi.org/10.1016/j.biortech.2012.01.126>.
- [5] Cakmakci, R., Kantar, F., Sahin, F. (2001): Effect of N₂-fixing bacterial inoculations on yield of sugar beet and barley. – J. Plant Nutr. Soil Sci. 164: 527-531. [https://doi.org/10.1002/1522624\(200110\)164:5<527::AID-JPLN527>3.0.CO;2-1](https://doi.org/10.1002/1522624(200110)164:5<527::AID-JPLN527>3.0.CO;2-1).
- [6] Cakmakci, R., Donmez, F., Aydın, A., Sahin, F. (2006): Growth promotion of plants by plant growth promoting rhizobacteria under greenhouse and two different field soil conditions. – Soil Biol. and Biochem. 38: 1482-1487. <https://doi.org/10.1016/j.soilbio.2005.09.019>.
- [7] Calvo, P., Nelson, L., Kloepper, J. W. (2014): Agricultural uses of plant biostimulants. – Plant Soil 383: 3-41. <https://doi.org/10.1007/s11104-014-2131-8>.
- [8] Canellas, L. P., Balmori, D. M., Médici, L. O., Aguiar, N. O., Campostrini, E., Rosa, R. C. C., Façanha, A. R., Olivares, F. L. (2013): A combination of humic substances and *Herbaspirillum seropedicae* inoculation enhances the growth of maize (*Zea mays* L.). – Plant Soil 366: 119-132.
- [9] Canellas, L. P., Olivares, F. L. (2014): Physiological responses to humic substances as plant growth promoter. – Chem Biol Technol Agric 4: 1-3. <https://doi.org/10.1186/2196-5641-1-3> <https://doi.org/10.1007/s11104-012-1382-5>.
- [10] Cassán, F., Perrig, D., Sgroj, V., Masciarelli, O., Penna, C., Luna, V. (2009): *Azospirillum brasilense* Az39 and *Bradyrhizobium japonicum* E109, inoculated singly or in combination, promote seed germination and early seedling growth in corn (*Zea mays* L.) and soybean (*Glycine max* L.). – Eur J Soil Biol 45: 28-35. <https://doi.org/10.1016/j.ejsobi.2008.08.005>.

- [11] Chavoushi, M., Najafi, F., Salimi, A., Angaji, S. A. (2019): Improvement in drought stress tolerance of safflower during vegetative growth by exogenous application of salicylic acid and sodium nitroprusside. – *Ind. Crops Prod.* 134: 168-176. <https://doi.org/10.22059/ijhst.2019.277800.283>.
- [12] Dajue, L., Mündel, H. H. (2006): Safflower. *Carthamus tinctorius* L. Promoting the conservation and use of under-utilized and neglected crops. – 7. Institute of Plant Genetics and Crop Plant Research, Gatersleben/International Plant Genetic Resources Institute, Rome, Italy, pp. 83.
- [13] Dobbss, L. B., Canellas, L. P., Olivares, F. L., Aguiar, N. O., Peres, L. E. P., Azevedo, M., Spaccini, R., Piccolo, A., Facanha, A. R. (2010): Bioactivity of chemically transformed humic matter from vermicompost on plant root growth. – *J. Agric. Food Chem.* 58: 3681-3688. <https://doi.org/10.1021/jf904385c>.
- [14] Ekin, Z. (2005): Resurgence of safflower (*Carthamus tinctorius* L.) utilization: A global view. – *Journal of Agronomy* 4(2): 83-87. <https://doi.org/10.3923/ja.2005.83.87>.
- [15] Ekin, Z. (2019): Integrated use of humic acid and plant growth promoting rhizobacteria to ensure higher potato productivity in sustainable agriculture. – *Sustainability* 11: 3417. <https://doi.org/10.3390/su11123417>.
- [16] El-Howeity, M. A., Asfour, M. M. (2012): Response of some varieties of canola plant (*Brassica napus* L.) cultivated in a newly reclaimed desert to plant growth promoting rhizobacteria and mineral nitrogen fertilizer. – *Annals of Agricultural Sciences* 57(2): 129-136. <https://doi.org/10.1016/j.aogas.2012.08.006>.
- [17] Elkoca, E., Turan, M., Donmez, M. F. (2010): Effects of single, dual and triple inoculations with *Bacillus subtilis*, *Bacillus megaterium* and *Rhizobium leguminosarum* Bv. *Phaseoli* on nodulation, nutrient uptake, yield and yield parameters of common bean (*Phaseolus vulgaris* L. Cv. 'Elkoca-05'). – *Journal of Plant Nutrition* 33(14): 2104-2119. <https://doi.org/10.1080/01904167.2010.519084>.
- [18] Esitken, A., Karlidag, H., Ercisli, S., Turan, M., Sahin, F. (2003): The effect of spraying a growth promoting bacterium on the yield, growth and nutrient element composition of leaves of apricot (*Prunus armeniaca* L. cv. Hacihaliloglu). – *Australian J. of Agric. Res.* 54: 377-380. <https://doi.org/10.1071/AR02098>.
- [19] Esringu, A., Kaynar, D., Turan, M., Ercisli, S. (2016): Ameliorative effect of humic acid and plant growth-promoting rhizobacteria (PGPR) on Hungarian vetch plants under salinity stress. – *Commun Soil Sci Plant Anal* 47: 602-18. <https://doi.org/10.1080/00103624.2016.1141922>.
- [20] Glick, B. R. (2012): *Plant Growth-Promoting Bacteria: Mechanisms and Applications*. – Hindawi Publishing Corporation, Scientifica: Waterloo, Canada.
- [21] Hajghani, M., Ghalavand, A., Modarres-Sanavy, S. A. M., Asadipour, A. (2016): The response of safflower seed quality characteristics to organic and chemical fertilization. – *Biological Agric. & Hort.* 32(2): 139-147. <https://doi.org/10.1080/01448765.2015.1094674>.
- [22] Hoyos-Carvajal, L., Orduz, S., Bissett, J. (2009): Growth stimulation in bean (*Phaseolus vulgaris* L.) by *Trichoderma*. – *Biol Control* 51: 409-416. <https://doi.org/10.1016/j.biocontrol.2009.07.018>.
- [23] Hungria, M., Campo, R. J., Souza, E. M., Pedrosa, F. O. (2010): Inoculation with selected strains of *Azospirillum brasilense* and *A. lipoferum* improves yields of maize and wheat in Brazil. – *Plant Soil* 331: 413-425. <https://doi.org/10.1007/s11104-009-0262-0>.
- [24] Karakurt, H., Kotan, R., Dadasoglu, F., Aslantas, R., Sahin, F. (2011): Effects of plant growth promoting rhizobacteria on fruit set, pomological and chemical characteristics, color values, and vegetative growth of sour cherry (*Prunus cerasus* cv. Kütahya). – *Turk J Biol* 35: 283-291. <https://doi.org/10.3906/biy-0908-35>.
- [25] Lucas, J. A., Ramos Solano, B., Montes, F., Ojeda, J., Megias, M., Gutierrez Mañero, F. J. (2009): Use of two PGPR strains in the integrated management of blast disease in rice (*Oryza sativa* L.) in Southern Spain. – *Field Crops Res* 114: 404-410.

- <https://doi.org/10.1016/j.fcr.2009.09.013>.
- [26] Mehraban, A., Miri, M. (2017): Influence of humic acid and mycorrhiza on some characteristics of safflower (*Carthamus tinctorius*). – Journal of Research in Ecology 5(1): 508-514. <http://jresearchbiology.com/documents/EC0275.pdf>.
- [27] Mirzakhani, M., Ardakani, M. R., Aeene Band, A., Rejali, F., Shirani Rad, A. H. (2009): Response of spring safflower to co-inoculation with *Azotobacter chroococum* and *Glomus intraradices* under different levels of nitrogen and phosphorus. – American J. of Agric. and Biol. Sci. 4: 255-261. <https://doi.org/10.3844/ajabssp.2009.255.261>.
- [28] Nardi, S., Carletti, P., Pizzeghello, D., Muscolo, A. (2009): Biological activities of humic substances. – In: Seni, N., Xing, B., Huang, P. M. (eds.) Biophysico-chemical Processes Involving Natural Nonliving Organic Matter in Environmental Systems. Wiley, New Jersey, pp. 305-340.
- [29] Nosheen, A., Bano, A., Ullah, F., Farooq, U., Yasmin, Y., Hussain, I. (2011): Effect of plant growth promoting rhizobacteria on root morphology of safflower (*Carthamus tinctorius* L.). – African J. of Biotech. 10(59): 12639-12649. <https://doi.org/10.5897/AJB11.1647>.
- [30] Nosheen, A., Bano, A., Yasmin, H., Keyani, R., Habib, R., Shah, S. T. A., Naz, R. (2016): Protein quantity and quality of safflower seed improved by NP fertilizer and Rhizobacteria (*Azospirillum* and *Azotobacter* spp.). – Front. Plant Sci. 7: 104. <https://doi.org/10.3389/fpls.2016.00104>.
- [31] Nosheen, A., Naz, R., Tahir, A. T., Yasmin, H., Keyani, R., Mitrevski, B., Bano, A., Chin, S. T., Marriott, P. J. (2018): Improvement of safflower oil quality for biodiesel production by integrated application of PGPR under reduced amount of NP fertilizers. – PLoS ONE 13: 8. <https://doi.org/10.1371/journal.pone.0187111>.
- [32] Olivares, F. L., Aguiar, N. O., Rosa, R. C. C., Canellas, L. P. (2015): Substrate biofortification in combination with foliar sprays of plant growth promoting bacteria and humic substances boosts production of organic tomatoes. – Sci. Hortic. 183: 100-108. <https://doi.org/10.1016/j.scienta.2014.11.012>.
- [33] Orhan, E., Esitken, A., Ercisli, S., Turan, M., Fikretin, S. (2006): Effects of plant growth promoting rhizobacteria (PGPR) on yield, growth and nutrient contents in organically growing raspberry. – Sci. Hort. 111: 38-43. <https://doi.org/10.1016/j.scienta.2006.09.002>.
- [34] Puglisi, E., Pascazio, S., Suci, N., Cattani, I., Fait, G., Spaccini, R., Crecchio, C., Piccolo, A., Trevisan, M. (2013): Rhizosphere microbial diversity as influenced by humic substance amendments and chemical composition of rhizodeposits. – J. Geochem. Explor. 129: 82-94.
- [35] Rana, A., Joshi, M., Prasanna, R., Shivay, Y. S., Nain, L. (2012): Biofortification of wheat through inoculation of plant growth promoting rhizobacteria and cyanobacteria. – European J Soil Biol 50: 118-26. <https://doi.org/10.1016/j.ejsobi.2012.01.005>.
- [36] Rosas, S. B., Avanzin, G., Carlier, E., Pasluosta, C., Pastor, N., Rovera, M. (2009): Root colonization and growth promotion of wheat and maize by *Pseudomonas aurantiaca* SR1. – Soil Biol Biochem 41: 1802-1806. <https://doi.org/10.1016/j.soilbio.2008.10.009>.
- [37] Ryan, J., Estefan, G., Rashid, A. (2012): Soil and Plant Analysis Laboratory Manual. – Sentific Publishers, 2nd Edition. ISBN-10: 8172337655, ISBN-13: 978-8172337650.
- [38] Schoebitz, M., López, M. D., Serrí, H., Martínez, O., Zagal, E. (2016): Combined application of microbial consortium and humic substances to improve the growth performance of blueberry seedlings. – J Soil Sci Plant Nutr. 16: 1010-1023. <http://dx.doi.org/10.4067/S0718-95162016005000074>.
- [39] Shah, F., Wu, W. (2019): Soil and crop management strategies to ensure higher crop productivity within sustainable environments. – Sustainability 11(5): 1485-1504. <https://doi.org/10.3390/su11051485>.
- [40] Shahid, M., Hameed, S., Imran, A., Ali, S., Elsas, J. D. (2012): Root colonization and growth promotion of sunflower (*Helianthus annuus* L.) by phosphate solubilizing

- Enterobacter* sp. Fs-11. – World J Microbiol Biotechnol 28: 2749-2758. <https://doi.org/10.1007/s11274-012-1086-2>.
- [41] Sharifi, R. S., Namvar, A., Sharifi, R. S. (2017): Grain filling and fatty acid composition of safflower fertilized with integrated nitrogen fertilizer and biofertilizers. – Pesq. agropec. bras. Brasília 52(4): 236-243. <http://dx.doi.org/10.1590/s0100-204x2017000400003>.
- [42] Silva, S. F., Olivares, F. L., Canellas, L. P. (2017): The biostimulant manufactured using diazotrophic endophytic bacteria and humates is effective to increase sugarcane yield. – Chem Biol Technol Agric 4: 24. <https://doi.org/10.1186/s40538-017-0106-8>.
- [43] Soleymanifard, A., Sidat, S. A. (2011): Effect of inoculation with bio-fertilizer in different nitrogen levels on yield and yields components of safflower under dry land conditions. – American Eurasian J. of Agric. and Envir. Sci. 11: 473-477. [https://www.idosi.org/aejaes/jaes11\(4\)11/3.pdf](https://www.idosi.org/aejaes/jaes11(4)11/3.pdf).
- [44] Suh, H. Y., Yoo, K. S., Suh, S. G. (2014): Tuber growth and quality of potato (*Solanum tuberosum* L.) as affected by foliar or soil application of fulvic and humic acids. – Hortic. Environ. Biotechnol. 55(3): 183-189. <https://doi.org/10.1007/s13580-014-0005-x>.
- [45] Thonar, C., Lekfeldt, J. D. S., Cozzolino, V., Kundel, D., Kulhánek, M., Mosimann, C., Neumann, G., Piccolo, A., Symanczik, S., Walder, F. (2017): Potential of three microbial bio-effectors to promote maize growth and nutrient acquisition from alternative phosphorous fertilizers in contrasting soils. – Chem Biol Technol Agric. 4: 7. <https://doi.org/10.1186/s40538-017-0088-6>.

COMPARATIVE ANALYSIS OF MASS-BALANCED MODELS FOR A TROPICAL RESERVOIR TO ASSESS THE IMPACT OF A MANAGEMENT PRACTICE

KHATUN, M. H.¹ – BARMAN, P. P.^{1,2} – LUPA, S. T.³ – ZAHANGIR, M. M.⁴ – ASHA, S. N.¹ – LIU, Q.^{1*}

¹College of Fisheries, Ocean University of China, Qingdao, 266003 Shandong, P.R. China

²Department of Coastal and Marine Fisheries, Sylhet Agricultural University, Sylhet,
Bangladesh

³Department of Fisheries Management, Bangladesh Agricultural University, Mymensingh 2202,
Bangladesh

⁴Department of Fish Biology and Biotechnology, Chittagong Veterinary and Animal Sciences
University, Chittagong 4225, Bangladesh

*Corresponding author
e-mail: qunliu@ouc.edu.cn

(Received 17th Nov 2019; accepted 30th Jan 2020)

Abstract. Mass-balanced models were constructed for pre and post fishing ban period to compare the possible impacts of the introduction of the fishing closure management practice on the reservoir resources through estimating the trophic status and energy flow. The decreased biomass of high value fishes (Carps, Sheatfishes, Tilapia, *Anabas testudineus* and Knife fishes) despite the implementation of fishing closure pinpoints the excessive fishing pressure on these target species. However, the increased biomass of minnows and clupeids may pose a serious threat to reservoir stability and sustainability altering the trophic structure. Mixed trophic impact indicates that functional groups at the lower trophic level had positive effect on most of the groups. The ratio of primary production/respiration was 13.154 and 1.969 during pre-ban and post-ban season respectively. The relative overhead increased (22.48%) while ascendancy was found to be lower (-0.43%) during the post-ban period. The reservoir was more vulnerable to disruptions before the implementation of fishing ban. Some ecosystem attributes such as TPP/TB, TB/TST, TPP/TR, TPP – TR reveal that the Kaptai reservoir gained higher resilience, stability, maturity and complexity in food web after discontinuing the unlimited fishing access but it still requires attention to overcome the stresses associated with human activities.

Keywords: Kaptai reservoir, ascendancy, food web, sustainable management, overfishing

Abbreviations: B: Biomass, BFDC: Bangladesh Fisheries Development Corporation, CI: Connectance Index, DC: Diet composition, EE-Ecotrophic efficiency, EwE: Ecopath with Ecosim, EX: export, *F* - fishing mortality, FCI: Finn's Cycling Index, FMPL: Finn's mean path length, M: Natural mortality, MTI: Mixed trophic impact, OI: Omnivory Index, P/B: Production/Biomass, P/Q: Production/Consumption, P/R: Production/Respiration, Q/B: consumption/biomass, SOI-System Omnivory Index, TB/TR: Total biomass/Total respiration, TB/TST: Total biomass/Total system throughput, TE: Transfer efficiency, TL: Trophic level, TPP/TB: Total primary production/Total biomass, TPP-TR: Total primary production – Total respiration, TST: Total system throughput, Y: Yield, Z: Total mortality

Introduction

The determination of ecosystem structure, flow of energy through trophic interaction and its functional integrity has been widely recognized to ensure a sustainable habitat for living resources (Christensen and Pauly, 1995). Information about ecosystem structure and functions measuring the transferred biomass within ecological groups and

trophic efficiency could help investigate the possible impacts of changes on different groups and ecosystem as well (Christian et al., 1996). The ecological attributes of an ecosystem delineated from fish population, components of the community, environmental status and flow of energy indicate the quality of an ecosystem. The Ecopath model incorporated different approaches of theoretical ecology (Odum, 1969; Ulanowicz, 1986) to analyze the energy flows between ecosystem components and to define the ecosystem maturity, resilience and stability. It predicts the health of an ecosystem, trophic functioning and its capacity to uphold the biological production. Furthermore, ecosystem properties help to investigate how fish population response to natural and human-made perturbations and thus support effective fisheries management. Moreau et al. (2001) stated that, the output of Ecopath model contributes in the management decision process where multi-species inhabit together.

The Kaptai reservoir is considered as one of the largest supports for freshwater capture fisheries in Bangladesh. It shows both lacustrine and riverine characteristics due to its construction damming a river and multiple other uses by surrounding community. However, due to the rapid economic development and natural perturbations since last few decades the reservoir has experienced ecological changes and severe stresses. Multi-disciplinary uses of reservoir, hydroelectric power generation, overfishing, and oil discharge from mechanized fishing and navigation boats have posed a serious threat to the reservoir fishery and ecology by degrading the water quality. In general, the multiple uses of reservoirs along with excessive fishing pressure, changes in diet make these systems as “unstable ecosystem”. The impact is evident by the remarkable decline in the productivity of high-value fishes in this reservoir (Khatun et al., 2019). This was due to high accessibility to this reservoir resource.

Therefore, the detailed study is warranted to get information of the developmental status of this ecosystem facilitating the thoughtful understanding on the structural and functional principles of the whole system, which will be helpful to know the impact of human perturbations. Unfortunately, no attempt has been carried out yet to know the structure, function, existing trophic interactions and energy flow among different functional groups of the Kaptai reservoir unifying the available information. A mass-balance ecosystem model summarizes the changes in the species and helps to compare the direct and indirect effects of one species on others and the overall functioning of the system as well. The ecosystem-based software Ecopath with Ecosim (EwE) allows the analysis of mass-balance trophic models of aquatic ecosystem (Christensen et al., 2005). Furthermore, it helps to compare between the models of two different periods of same ecosystem.

Since the 1980's, fishing has been banned for different period in the Kaptai reservoir depending on season, weather, production target etc. However, fishing closure from May 1st to July 31st has become a routine management practice from the year 2003 onwards in this reservoir. Considering this, we constructed two models of the Kaptai reservoir ecosystem for two different periods with different management approaches, the pre ban fishing, 2001 and post ban fishing, 2016. The study was conducted to assess the possible effect of fishing closure on whole ecosystem, to quantify the energy flows and biomass of different ecological groups, to compare the ecosystem structure, trophic interactions and trophic efficiencies of pre and post fishing closure. In doing so, this contribution will help to know the significance of seasonal fishing banning management on the ecological production, health and stability of the tropical reservoir system. Further remedial management measures also could be suggested identifying the existing bottlenecks and executing the wise use of this reservoir resource.

Materials and methods

Study site

The Kaptai reservoir (22°22' N and 23°18' N latitude, and 92°00' E and 92°26' E longitude), the largest synthetic freshwater reservoir of South-East Asia and first man-made reservoir of Bangladesh was constructed primarily for the purpose of hydro-electric power generation on the River Karnafuli in 1961 (*Fig. 1*). It encompasses an area of 688 km² with the average depth of 9 m and average annual temperature of 27 °C. It receives nutrient-enriched waters from rivers, which helps to increase biological productivity and sustain high value fisheries. About 73 species of fishes belonging to 47 genera and 25 families, 2 species of freshwater prawn and 1 species of dolphin have been described in this reservoir (Ahmed, 1999). Among these, 31 species contribute commercially. Artisanal fishing approaches are typically used here to exploit fishery. Unfortunately, indiscriminate use of multispecies gears without concerning about the proper mesh size and mechanization of fishing vessels are putting the signs of excessive fishing effort on the aquatic resources. Surprisingly, since 1999, clupeids have been dominating the reservoir as it breeds profusely in reservoir. In the early post-impoundment period carps used to be the predominant reservoir species contributing 81.4% of the total catch (Ahmed et al., 2006) but it steadily decreased to only 0.96% in 2016 (DoF, 2016). On the other hand, clupeids are increasing at a rate of 8.7% annually (Ahmed et al., 2006) while it contributed 59% of the total catch in 2016 (DoF, 2016).

Modelling approach

The preliminary Ecopath software was based on the approaches developed by Polovina (1984) to analyze flows of energy between ecological groups of an aquatic ecosystem. Later on, subsequent modifications took place (Christensen and Pauly, 1993; Pauly et al., 2000; Christensen et al., 2002) following Ulanowicz (1986). Moreover, Odum's theory of ecosystem development was also incorporated in Ecopath model. In this study, mass-balanced Ecopath models were constructed using 14 ecological components for pre fishing ban (2001) and post fishing ban (2016) periods integrating the available information on food intake, population dynamics, catch and biomass of same or similar system. We used a user-friendly Ecopath with Ecosim suite version 6.5 (Christensen et al., 2008) in our study to construct Ecopath models to compare the changes between the continuous fishing and self-imposed fishing ban. The assumption of EwE is based on the two following equations e.g. 1) production = Catch + Predation + Net migration + Biomass + Accumulation + Other mortality; and 2) Consumption = Production + Respiration + Unassimilated Food. This is expressed by the following equation (*Eq. 1*) proposed by Christensen et al. (2005):

$$Bi * \left(\frac{P}{B}\right) i * EEi = Yi + \sum(Bj) * \left(\frac{Q}{B}\right) j * DCij + EXi \quad (\text{Eq.1})$$

Here, B_i defines the biomass of prey group i ; P/B_i is the production/biomass ratio of group i ; EE_i represents the ecotrophic efficiency; Y_i is its yield (fishery catch); B_j defines the biomass of predator group j ; Q/B_j is the food consumption per unit biomass of j ; DC_{ji} is the fraction of i in the diet of j and EX_i is the export of (i).

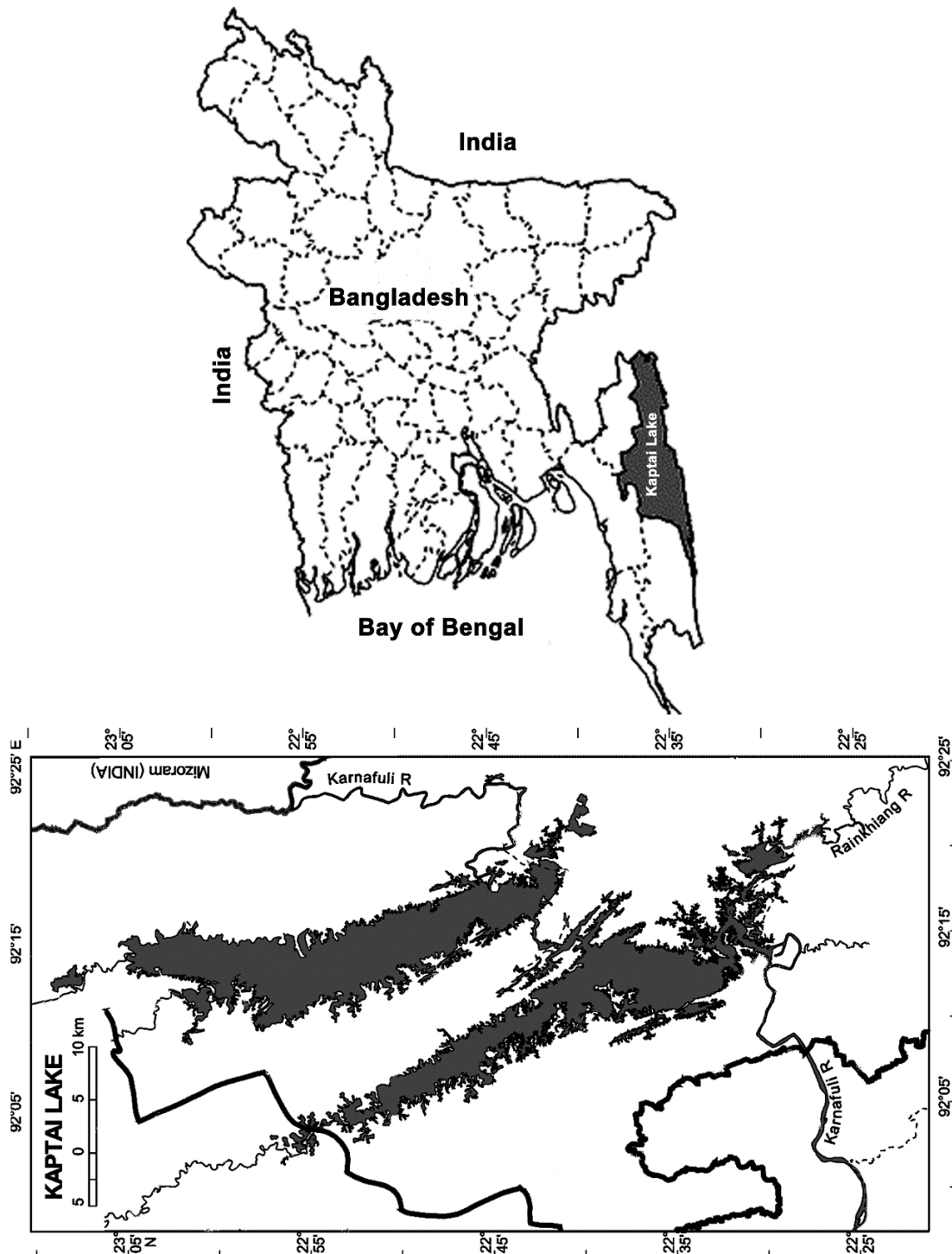


Figure 1. Geographical location of Kaptai reservoir

Model parameterization

The model input parameters include biomass B (t/km^2), production/biomass P/B (yr^{-1}), consumption/biomass Q/B (yr^{-1}), Ecotrophic efficiency (EE) and diet composition (must be entered as input). Inputting any three of the former parameters will estimate the fourth one. EE is the proportion of the production that is consumed or predated. EE

should be between 0 and 1. Since there is no empirical relationship to calculate EE , Ecopath model calculates it as output (Christensen et al., 2000). However, in absence of any other parameter EE could be set as 0.95 for highly exploited groups (Christensen and Pauly, 1992). The biomass of both phases was determined from the annual landing information provided by Bangladesh Fisheries Development Corporation (BFDC). We used $B = Y/F$ (here Y = annual average yield of a group, F = fishing mortality) equation proposed by Gulland (1971) to calculate the biomass. In absence of landing data of any group, we used EE as 0.95 (for minnows and prawns in 2001). The total fish biomass was found to be 5.256 t/km² and 6.245 t/km² during pre-ban and post-ban period respectively. EE was also set as 0.95 to balance the model where the diet adjustment was ineffective. Notably, EE cannot be greater than 1 in a balanced model. The biomass of unexploited groups such as insects and larvae, zooplankton and phytoplankton for both phases was either estimated by the model or obtained from other models. The input and output values of both models are presented in *Table 1*.

The ratio of production over biomass (P/B) is considered as equivalent to total mortality Z (Pauly et al., 2000). Total mortality Z (=Fishing mortality F + natural mortality M) was estimated following Beverton and Holt (1993) while natural mortality M was calculated using Pauly's empirical equation (Pauly, 1984). Consumption (Q) is the food intake by a group over a specific period. Consumption/biomass (Q/B) was calculated using the empirical equation developed by Palomares and Pauly (1998) along with the help of Fishbase database for every species of each group and the average value was taken as group Q/B value. P/B and Q/B for some functional groups were obtained from other studied models (*Table 1*).

The diet matrix (*Table A2* in the *Appendix*) of different groups was collected either from the available literatures (Khumar and Siddiqui, 1989; Mamun et al., 2004; Islam et al., 2006; Welianje and Amarasinghe, 2007; Azadi and Mamun, 2009; Sarkar and Deepak, 2009; Mondal and Kaviraj, 2010; Srivastava et al., 2012; Roy et al., 2013; Gupta, 2015; Sakhare and Jetithor, 2016) or from Fishbase (www.fishbase.org; Froese and Pauly, 2019). The model was balanced in a way so that for each group EE does not exceed 1, P/Q remains between 0.1 and 0.3 and P/R ratio (production/respiration) ranges from 0 to 1. The estimated pedigree values were observed 0.56 and 0.533 for the year 2001 and 2016 respectively, which agrees with the statement of Christensen et al. (2002).

Ecological groups

Ecological groups were classified depending on population parameters, food and feeding habits, preference of habitat, physiology, taxonomy, body size and distribution. About 14 functional groups for each year including nine fish groups and one group of prawn were selected as per their abundance and economic importance. The selection of other groups were based on their preference in fish diet. Despite of the role as grazing ground for carps we excluded macrophytes for their minor presence in diet matrix (Panikkar et al., 2015). We used information from available literatures (see *Table A1*) and FishBase (www.fishbase.org; Froese and Pauly, 2019) to bridge the gaps.

Carps

Carps are the most popular reservoir fishes. The most dominant carps include *Labeo rohita*, *Catla catla*, *Cirrhinus cirrhosis*, *Labeo calbasu*, *Labeo bata*, *Labeo gonius* and *Cyprinus carpio*. Stocking of carps is a routine management practice in Kaptai

reservoir, which is done to decrease the reduction of fish due to excessive fishing pressure. Despite of this stocking a clear declining trend has been noticed in carp production. These fishes feed on zooplankton, phytoplankton, detritus etc.

Table 1. Input features of the Ecopath models for pre-fishing ban (2001) and post-fishing ban period (2016) for Kaptai reservoir

Group no.	Functional group	Trophic level (TL)	Biomass (B) (t/km ²)	P/B (yr ⁻¹)	Q/B (yr ⁻¹)	Ecotrophic efficiency (EE)	P/Q	OI
(a) Pre fishing ban								
1	Carps	2.143	0.396	3.038	18	0.824	0.169	0.137
2	Catfishes	3.261	0.71	1.432	14.9	0.706	0.096	0.284
3	Sheatfishes	3.186	0.161	5.59	18.4	0.264	0.304	0.506
4	Tilapia	2.316	0.71	1.39	23.8	0.268	0.058	0.237
5	<i>Anabas testudineus</i>	2.971	0.056	2.85	10.9	0.331	0.261	0.305
6	Knife fishes	3.257	0.768	1.19	9.8	0.035	0.121	0.178
7	Snakehead	3.251	0.178	3.13	11.4	0.95	0.275	0.297
8	Minnnows	2.137	0.797	5.4	57.56	0.95	0.094	0.125
9	Clupeids	2.580	1.48	6.63	25.8	0.530	0.257	0.313
10	Prawns	2.512	2.580	3.16	12.64	0.950	0.250	0.329
11	Insects/Larvae	2.132	3.84	4	30	0.837	0.133	0.121
12	Zooplankton	2.053	12.85	35	140	0.310	0.250	0.0526
13	Phytoplankton	1.00	57	184	-	0.148	-	-
14	Detritus	1.00	0.35	-	-	0.036	-	0.115
(b) Post fishing ban								
1	Carps	2.143	0.212	3.038	18.00	0.950	0.169	0.137
2	Catfishes	3.266	1.375	0.900	5.250	0.982	0.171	0.296
3	Sheatfishes	3.187	0.141	2.795	18.40	0.950	0.152	0.508
4	Tilapia	2.316	0.394	1.390	23.80	0.753	0.058	0.237
5	<i>Anabas testudineus</i>	2.971	0.037	3.790	10.90	0.757	0.348	0.305
6	Knife fishes	3.257	0.384	1.190	9.800	0.282	0.121	0.178
7	Snakehead	3.362	0.242	3.130	11.40	0.950	0.275	0.206
8	Minnnows	2.137	1.430	2.915	56.05	0.950	0.052	0.125
9	Clupeids	2.580	2.03	7.570	46.30	0.744	0.163	0.313
10	Prawns	2.512	3.234	3.160	12.64	0.950	0.250	0.329
11	Insects/Larvae	2.132	4.125	4.000	30.00	0.950	0.133	0.121
12	Zooplankton	2.053	12.85	35.00	140.0	0.373	0.250	0.053
13	Phytoplankton	1.000	11.7	203.0	-	0.671	-	-
14	Detritus	1.00	1.00	-	-	0.243	-	-

*P/Q defines production/consumption, OI represents omnivory index

Catfishes

Mystus spp. formed this group. *M. aor* and *M. seenghala* are the dominant catfishes in this reservoir. Other catfish includes *M. cavasius*, *M. vittatus* and *M. tengara*. Catfishes are mainly caught by gill net, seine net and sometimes by hook and line. They

are voracious eater and carnivorous by nature. Their food consists of carps, minnows, clupeids, insects and larvae, etc. Cannibalism is also a common feature among catfishes.

Sheatfishes

Wallago attu and *Ompok pabda* are grouped as sheatfishes. A decreasing trend during the study periods suggests excess fishing pressure on these fishes. Minnows, Prawns and Detritus were found as their main food item.

Tilapia

Both species of Tilapia, *Oreochromis mossambicus* and *O. niloticus* are dominant in this reservoir and play an important role in the total reservoir production. They are well known as voracious feeder and feed on mainly on phytoplankton and zooplankton. Tilapia can survive in much stress conditions.

Anabas testudineus

Anabas testudineus, locally known as koi is a popular freshwater perch in Bangladesh. The decrease production of this fish even after banning fishing reveals excessive fishing pressure on it. They feed on zooplankton, minnows, clupeids, insects and larvae, etc.

Knife fishes

The production record states that the productivity of *Notopterus notopterus* and *N. chitala* has decreased two times recently than the unlimited fishing access period. Knife fishes feed on small fishes, prawns, insects and larvae and so on.

Snakehaed

Channa marulius, *C. striatus* and *C. punctatus* constitute this group. These air-breathing fishes are mainly piscivorous and feed on small fishes especially minnows, clupeids and prawns. The production of these voracious feeders declined despite of the fishing ban implementation.

Minnows

Puntius sarana and *Amblypharyngodon mola* are the most abundant minnows of Kaptai reservoir. The closure of fishing management helped this fishery to increase tremendously. These fishes are caught on any small mesh size nets, hooks and dragnets. They feed on phytoplankton, zooplankton and minor portion of detritus.

Clupeids

Corica soborna and *Gudusia chapra*, commonly known as “weed fishes” contribute the major portion in the reservoir fishery as the breed profusely there. According to the production history, their production increased at higher rate after the introduction of the fishing closure. Interestingly, they compete for their diet with carps providing a forage base for catfish development. Zooplankton, phytoplankton, detritus and aquatic insects mainly form their diet.

Prawns

The freshwater prawn *Macrobrachium lamarrei* is commonly available type of prawns in Kaptai reservoir. Since there is no information available for this species, we adopted the input data from Reyes (1993). Detritus forms their main diet besides insects and larvae, zooplankton and phytoplankton.

Insect/larvae

Aquatic insects and larvae play important role in the diet of carps, minnows and clupeids. This functional group consist of midges, mayflies, caddisflies, caddisworms, oligochaetes, insect larvae, bivalves and gastropods. We adopted the input value of this ecological group from Villanueva et al. (2006).

Zooplankton

The main constituting form of zooplankton refers to Copepods (*Diaptomus*, *Cyclops* and nauplii), cladocerans (*Daphnia*, *Cheriodaphnia*, *Moina*), and rotifers (*Keratella*, *Filinia*, *Brachionus*, *Asplanhna*). These are the main food item of major and minor carps, Tilapia and *A. testudineus*. Limited data encouraged us to adopt data from other models (Lauzanne, 1983; Moreau and Villanueva, 2002; Traore et al., 2008).

Phytoplankton

Chlorophyceae, Myxophyceae, Bacillariophyceae and Dinophyceae create the phytoplankton group. Among them Chlorophyceae (*Spirogyra*, *Volvox*, *Coelastrum* and so on), Myxophyceae notably *Microcystis*, Bacillariophyceae (*Navicula*, *Gyrosigma*, *Fragilaria* etc.) and Dinophyceae such as *Ceratium* and *Peridinium* are dominant here. Information of phytoplankton for pre-ban and post-ban phase were obtained from Traore et al. (2008) and Panikkar et al. (2015) respectively. Balancing the models was also the reason of this choice.

Detritus

We used the biomass of detritus as 0.35 t/km² for the year of 2001 (Panikkar et al., 2015) and 1 t/km² for the year of 2016 (Traore et al., 2008) from similar systems. The biomass of detritus adopted for both period was estimated using Pauly's equation of empirical relationship (Pauly et al., 1993).

Model analysis

Mixed trophic impact (MTI) routine developed by Ulanowicz and Puccia (1990) has been integrated in EwE to assess the relative impact biomass change of one group on another in an ecosystem trophically. Another routine incorporated with EwE that turns the complex food web into simpler one is defined as "Lindeman spine" (Lindeman, 1942). It aggregates the complex fractional trophic levels into discrete one and calculates the transferred energy flow and efficiency from one trophic level to the next. Ecopath can identify probable extinction prey group due to excessive predation by a large number of predator groups (Pauly et al., 2000). The impact of closure management practice on the basic pattern changes of reservoir system were determined comparing the trophic structure and transfer efficiency during both periods. This

comparison will help the managers to get some ideas of the reservoir at ecosystem level and may drag their concern for further management steps.

A number of ecosystem attributes have been included in EwE following Odum (1971) to assess the ecosystem maturity. The comparison of net primary production/biomass, biomass/total system throughput, net primary production/total respiration and net primary production - total respiration - these four ecosystem indices were done to know the basic difference about the resilience of the reservoir in both phases. Another three attributes such as ascendancy, overhead and developmental capacity developed by Ulanowicz (1986) were compared to know the overall ecosystem health and stability in both periods.

Results

Some of the parameters of resulted mass-balanced Ecopath models explain the quantitative trends of pre and post ban-fishing implementation for Kaptai reservoir. Our study focus was to compare some parameters for same reservoir for pre-fishing closure period (2001) and post-fishing closure period (2016).

Trophic relationship

The basic inputs of the balanced models and the estimates are shown in *Table 1*. Close observation shows that the biomass of high value fishes such as Carps, Sheatfishes, Tilapia, *Anabas testudineus* and Knife fishes decreased between 2001 and 2016 despite of fishing closure. This might be due to the excessive fishing pressure on these target species, poor implementation of fishing acts, hazardous environment etc. The biomass of the top predator Snakehead and Catfishes along with some other low value fishes from trophic level II for instances minnows, clupeids and prawns increased after stopping the unlimited fishing access throughout the year. Study states that, in spite of fishing ban enforcement, *EE* values of all commercially important fish groups were higher in 2016 compared to 2001 (*Table 1*). Important role of these groups in food web and huge predation pressure might be the reasons behind this. Lower *EE* values of primary producer and detritus in 2001 compared to post fishing-ban explains them as underexploited during this period. *EE* of phytoplankton in 2001 ($EE = 0.148$) indicates that most of the primary production died due to less predation pressure by plankton eater zooplankton. *EE* value for detritus was higher in post fishing-ban phase ($EE = 0.243$) compared to pre fishing-ban phase ($EE = 0.036$) indicating that the lower accumulation of biomass than consumption. It reveals the better utilization of detritus by some groups (snakehead, clupeids, and minnows) with greater biomass in post fishing closure period.

Trophic structure

The trophic structure of the Kaptai reservoir has three trophic levels (*Fig. 2*). In both seasons' catfishes, sheatfishes, snakehead and knife fishes are found to be the top predators of the system (*Table 1*). The trophic levels could be either fractional (Christensen and Pauly, 1992) or integers (Lindeman, 1942). The resulted energy flows are shown in *Figure 3* while the transfer efficiencies at each trophic level generated from the trophic aggregation routine are presented in *Table 2*. It shows that majorities of the biomasses and flows are concentrated in two lower trophic levels (I and II). Trophic

level II mainly involved the flow from zooplankton (primary herbivore). TLIII involved the flows from clupeids, tilapia, *Anabas testudineus* and prawns while catfishes, sheatfishes, snakehead and knife fishes dominate the flow from trophic level IV. The mean transfer efficiency for 2001 and 2016 were 6.718% and 9.752% respectively (Table 2). The trophic aggregation routine shows the presence of six trophic levels in both seasons.

Table 2. Transferred efficiency at different trophic levels for pre fishing ban (2001) and post fishing ban period (2016) for Kaptai reservoir

Phase/TL	II	III	IV	V	VI	Mean transfer efficiency (%)	Total flow proportion from detritus
Pre fishing ban	3.743	11.17	7.255	6.232	7.458	6.718	46%
Post fishing ban	5.378	12.55	13.74	13.83	16.18	9.752	32%

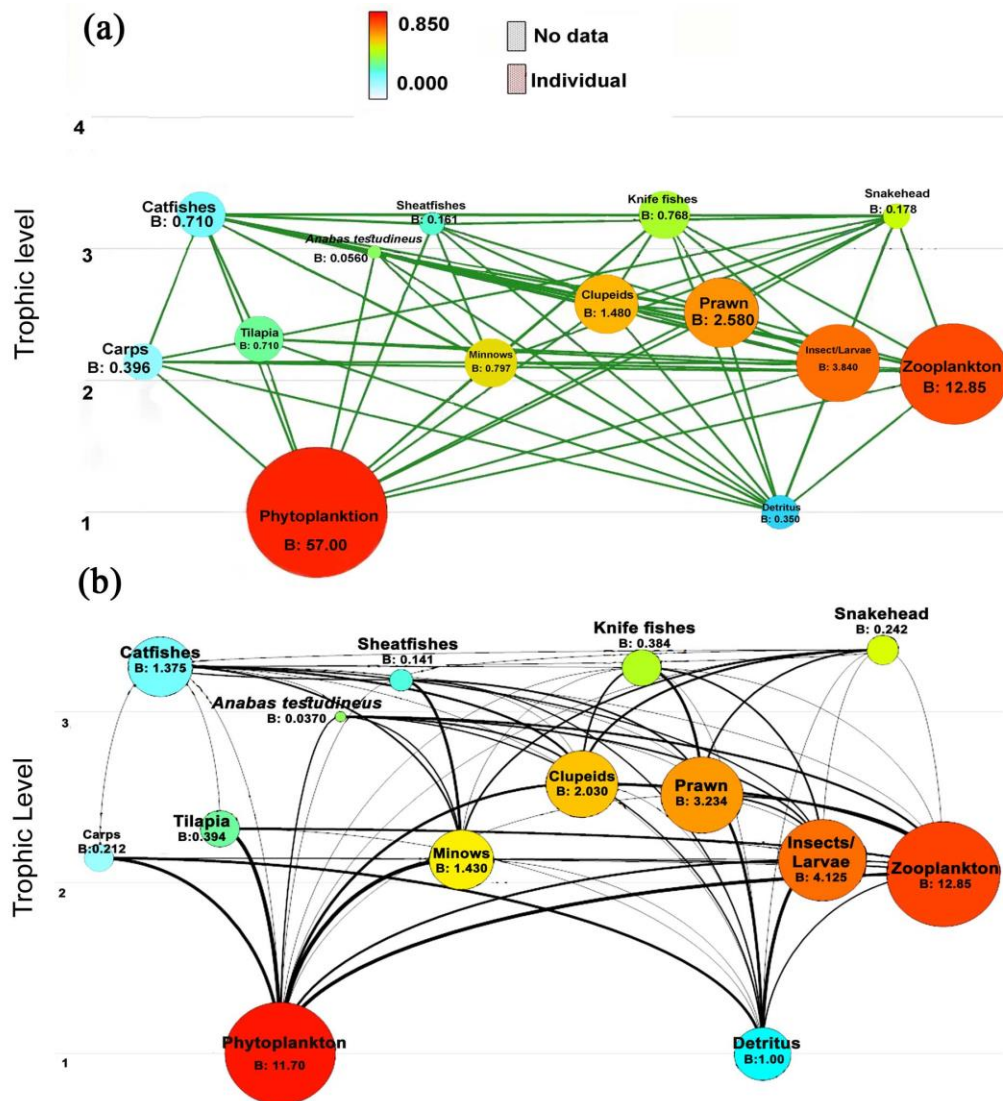


Figure 2. Food web structure of Kaptai reservoir with relative abundance, (a) Pre- ban phase (2001) and (b) post-ban phase (2016). B stands for biomass and 1, 2, 3, 4 represent the trophic levels

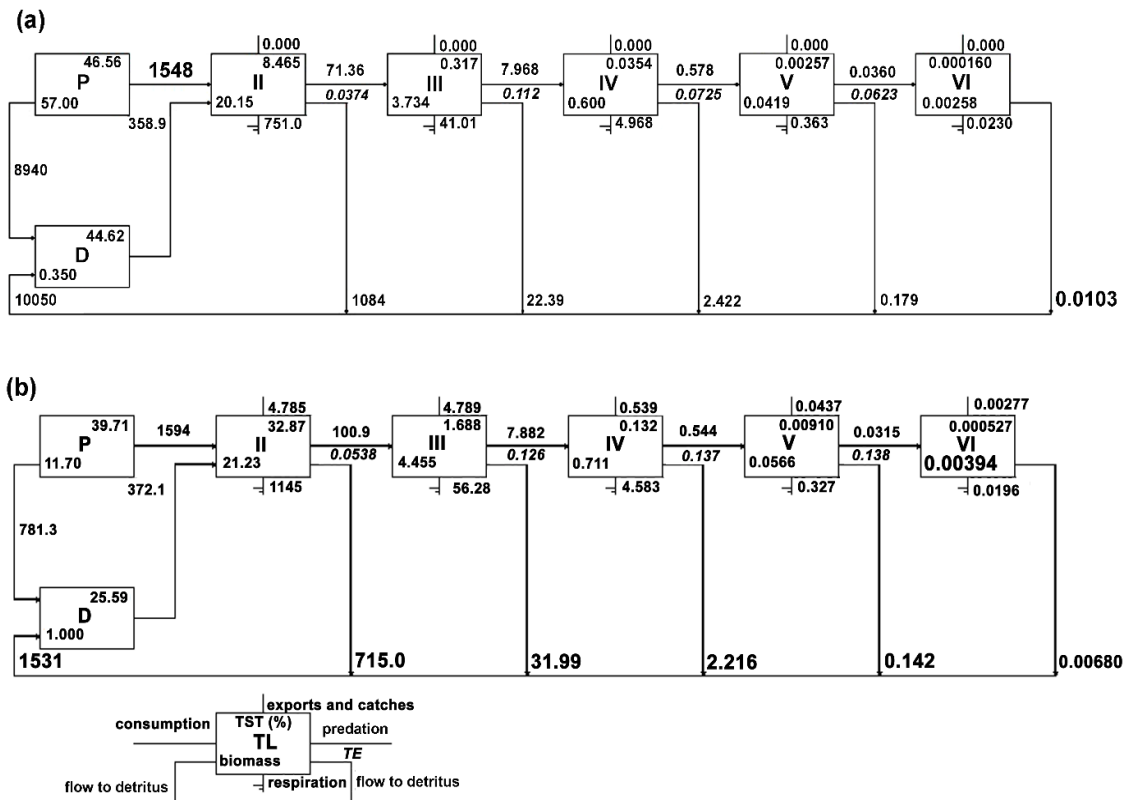


Figure 3. Trophic aggregation routine presenting transferred flows of Kaptai reservoir during (a) pre-ban phase, 2001 and (b) post-ban phase, 2016

Mixed trophic impact

The MTI routine on the Kaptai reservoir in two periods are illustrated in Fig. 4a and b. It assesses the relative impact (direct or indirect) of increase of one group on others in the system. Prey and predator have positive and negative impact on each other respectively. Almost all groups had negative impacts on themselves suggesting competition for same resources. The insignificant decline exhibited by some groups was due to presence of competition within groups for food and habitat. Tilapia and *Anabas testudineus* had almost no effect on other groups. Minor increase in predator depicts the reduction of prey biomass. Functional groups at the lower trophic level such as phytoplankton and detritus shows positive effect on most of the groups. Phytoplankton shows positive impact on its primary consumers such as zooplankton, minnows, clupeids, tilapia and carps.

In contrast, zooplankton showed most negative effect on phytoplankton. The increase in phytoplankton biomass had positive effect on some groups at higher TL but minor negative impact on prawns in both periods. Snakehead had greater negative effect on maximum groups in pre fishing-ban phase than post fishing-ban period. Interestingly, it shows positive impact on catfishes in both seasons. An increased biomass of catfishes shows the decreasing of several groups biomass in both terms while the impact was greater in pre-ban time. Both catfish and snakehead had positive effect on prawns in pre fishing closure course but no effect after fishing ban period. However, the subsequent increase in catfishes led to the decline in the abundance of carps.

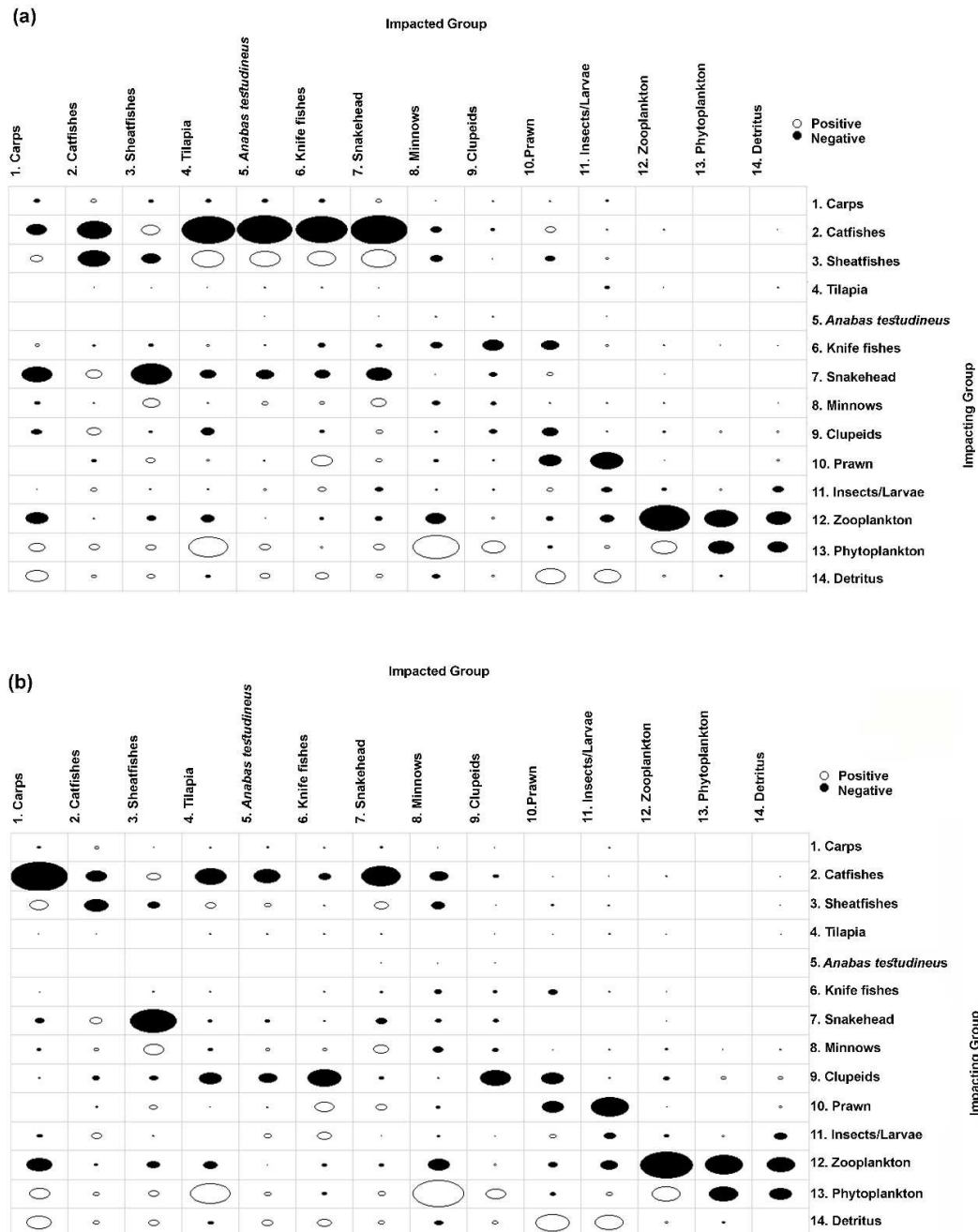


Figure 4. MTI of Kaptai reservoir, (a) pre fishing ban phase (2001) and (b) post fishing ban phase (2016). The circles (shaded black) indicate negative impacts and circles (without shade) indicate positive impacts. The size of the circles denotes relative response

Summary statistics

Ecopath computed some important indices of ecosystem maturity and stability supporting Odum's theory (Odum, 1969) and are shown in *Table 3*. A decrease of total system throughput, TST (-73.144%) from pre fishing closure stage to post closure period is evident. An increase of total biomass/total system throughput (50%) and a decrease of *TST* (-87.9%), *PP/B* (-51.61%) and *PP/R* (-11.185%) were observed indicating the post ban period more stable and mature. About 84.76% detritus

accumulation decreased from 10049.52 t/km²/year during pre-fishing closure to 6073.396 t/km²/year in post-ban period. The fish biomass of Kaptai reservoir was greater in post-ban phase (6.245 t/km²) than pre-ban phase (5.256 t/km²) which could be due to the presence of greater amount of small fishes in recent years.

Table 3. Summary attributes computed for pre-fishing ban (2001) and post-fishing ban period (2016) in Kaptai reservoir

Indices	Value pre-ban	Value post-ban	Unit	% difference Post ban - pre ban / pre ban*%
Sum of all consumption	2078.591	2167.709	t/km ² /year	
Sum of all exports	9690.649	1168.645	t/km ² /year	
Sum of all respiratory flows	797.351	1206.455	t/km ² /year	
Sum of all flows into detritus	10049.52	1530.586	t/km ² /year	-84.76
Total system throughput	22616.109	6073.396	t/km ² /year	-73.144
Sum of all production	10981.11	2875.284	t/km ² /year	
Calculated total net primary production	10488	2375.1	t/km ² /year	
Primary production required for catch		699.0	t/km ² /year	
Total primary production/total respiration	13.154	1.969		-11.185
Net system production	9690.649	1168.645	t/km ² /year	
Total primary production/total biomass	128.647	62.250		-51.61
Total biomass/total throughput	0.004	0.006	/year	50%
Net primary production-total respiration	9690.649	1168.645		-87.94
Total biomass (excluding detritus)	81.526	38.154	t/km ²	
Connectance index	0.423	0.417		
System omnivory index	0.196	0.198		
Ecopath pedigree index	0.56	0.533		
Measure of fit, t*	2.242	2.091		
Throughput cycled (including detritus)	310.5	348.1	t/km ² /year	
Ascendency	52.61	30.13	%	-0.43
Overhead	47.39	69.87	%	0.47
Predatory cycling index (% of throughput without detritus)	3.65	3.061		
Finn's cycling index	1.373	5.732	% of total throughput	
Finn's mean path length	2.156	2.557	-	

Different flows such as total consumption, total exports, total flows into detritus and the total system throughput as well were bigger in 2001 than 2016 (Table 3). Greater values of ecosystem indices suggest that the food web of pre fishing ban season was better than the post- fishing ban period (Table 3). Ascendency was found to be lower (-0.43%) in post-ban season while overhead was lower in pre-ban (47.39%) phase than post ban (69.87%). Connectance index (CI) reflects the proportion of total probable connections in an ecosystem. On the other hand, system omnivory index (SOI) refers the diversification in diet of different groups. SOI is alternative to CI. The model for 2001 had 0.423 and 0.196 connectance index and SOI respectively while it was 0.417 and 0.198 respectively for the model of 2016. Both models had similar values for CI and SOI.

Finn's cycling index (with detritus) increased at a considerable rate after stopping the unlimited fishing access. Higher Finn's cycling index (5.732) and mean path length (2.557) in post-ban time reveals the much more importance of detritus in the system.

The species with low biomass but structuring role in the ecosystem food web are defined as keystone species. They strongly influence the dynamics of the whole ecosystem and the abundance of other species maintaining their own low biomass (Libralato et al., 2006). The keystone-ness of different functional groups of Kaptai reservoir before and after banning fishing is shown in *Figure 5a* and *b*.

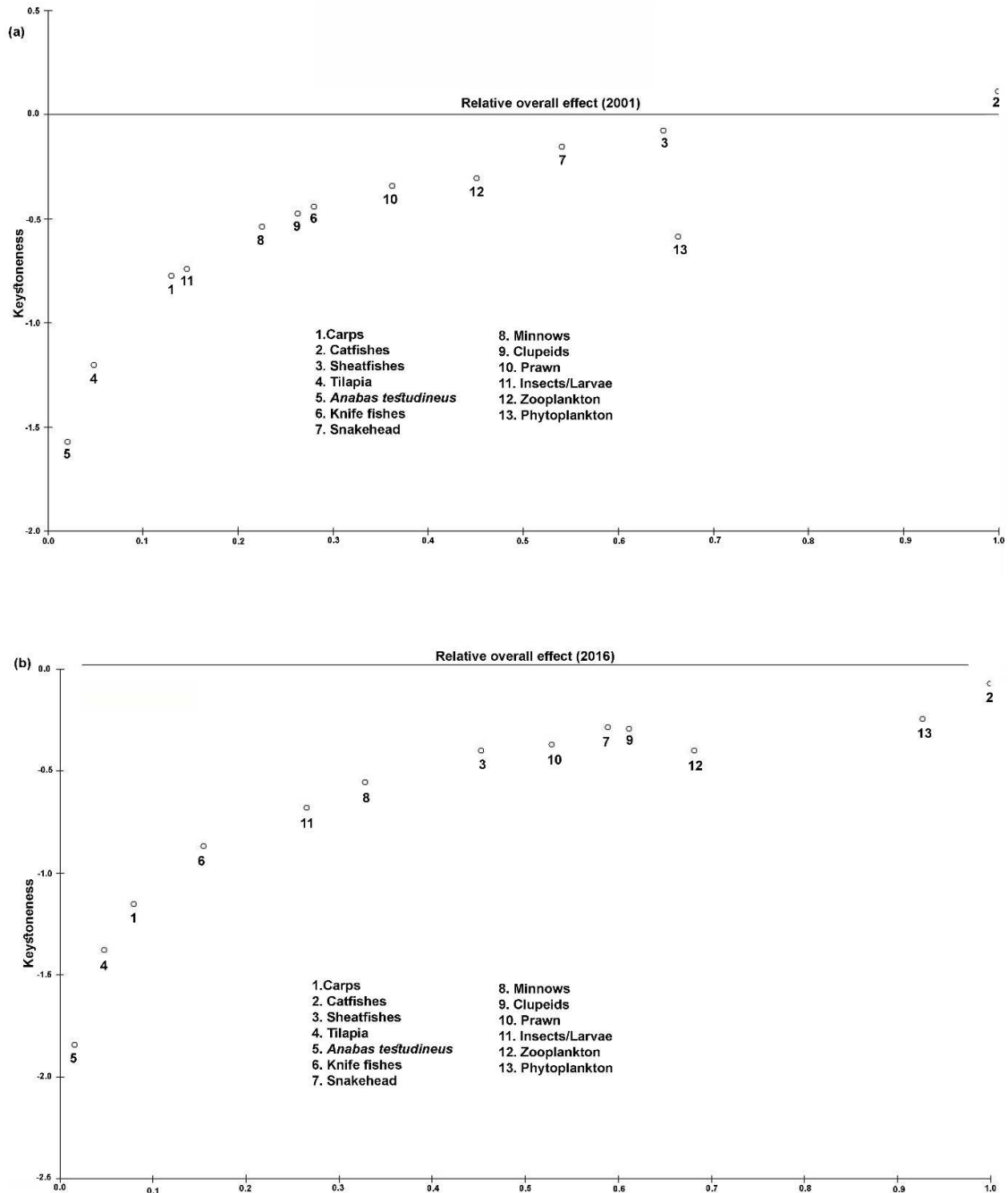


Figure 5. Keystone-ness index for different ecological groups of Kaptai reservoir during a) pre-ban (2001) and b) post-ban period (2016). Higher keystone index and higher relative overall effect denote the keystone species of this ecosystem

The species are considered as keystone when the proposed keystone index value gets close to or greater than value “zero”. Catfish, sheat fishes and snakehead were identified as keystone species in pre-ban period. In post-ban fishing time catfish stood as keystone species along with phytoplankton. In both terms, catfish had relatively higher effect and therefore it had an important role in the maintenance of the ecosystem structure.

Discussion

Sustainability of exploited resources and their effective management require ecosystem-based approach. We used Ecopath with Ecosim to balance the biomass and annual yield of the main interacting groups of pre stopping unlimited access for fishing (2001) and post fishing closure period (2016). Current work will visualize the existing reservoir ecosystem' complexity to the respective management bodies, which may help them to modify the present fishery regimes. The higher ecotrophic efficiency of some groups such as catfish, tilapia, sheatfishes, and *Anabas testudineus* in post-ban fishing period can be attributed either by increasing fishing predation or by predation pressure by other groups (Gamito and Erzini, 2005). The less abundant groups with higher EE (tilapia, sheatfishes, and *Anabas testudineus*) during post-fishing closure season indicates that they utilized the available biomass more efficiently. The flow to detritus of these groups were also lower compared to pre fishing ban period because of the higher competition of the consumers. This supports the finding for Lake Nakuru (Moreau et al., 2001). The increasing biomass with increasing EE (i.e. clupeids) might be due to the raise in predator biomass (e.g. catfish) in post-ban time. Low EE of phytoplankton (pre ban phase) granting the presence of Tilapia which mainly feed on phytoplankton might be due to grand biomass of phytoplankton or may have any other alternative food source (Fetahi and Mengistou, 2007). The exclusion of bacteria as a functional group might attributed to the lower EE of phytoplankton in 2001 (Fetahi and Mengistou, 2007). The decrease of some groups due to uncontrolled fishing effort and relatively higher predation rate may cause the ultimate increase of some other groups. For example, the biomass of minnows and clupeids increased as they had weaker competition for food with Carps or lower predation risk on them. This may lead alterations in trophic structure and could be a potential threat for reservoir stability and sustainability of the reservoir resources.

Theoretical ecology says, transfer efficiency decrease approaching toward the higher trophic levels (Odum, 1971) and this decreasing trend was observed in both phases in the Kaptai system. Comparatively low transfer efficiency was found in pre-ban phase (6.718%). It could be due to the lower utilization of primary producer during this phase. However, Moreau et al. (2001), Tomaczak et al. (2005), and Panikkar and Khan (2008) also documented a low value of transfer efficiency in their studies due to the same reason. The mean transfer efficiency this system after banning period (9.752%) was within the average range (8-15%) (Christensen and Pauly, 1993; Wolff, 1994). The post-ban transfer efficiency was higher than the observation of same phase from Wyra reservoir (7%) and lower than other studies (Bradford-Grieve et al., 1994; Mohamed et al., 2005). In addition, TE of TLV was lower than TLVI, which suggests that a smaller scale of production consumed within this trophic level. Furthermore, the greater TE at every TL after post-ban period indicates better energy flows within the system network. It suggests that, during post fishing ban period most of the groups were utilized at

higher level by either fishing predation or predation by other groups. In addition, detritus was found to be about 46% of total system throughput in pre ban phase and 32% in post-ban stage indicating its important role in the ecosystem. It implies the reservoir system as phytoplankton based while importance of detritus as food was also evident. The contribution of detritus in Kaptai reservoir supports the range of other tropical system (Christensen and Pauly, 1993).

Mixed trophic impact is known as an ordinary form of sensitivity analysis (Majkowski, 1982). It helps to predict the direct and indirect impact of one group on others in near future. Group competition for same resources was obvious in both phases as all groups had negative impact on themselves except detritus (Christensen et al., 2000). Detritus, as it is not a living group, had no effect on itself in Kaptai system like other studies (Christensen and Pauly, 1993; Moreau et al., 2001; Fetahi, 2005; Fetahi and Mengistou, 2007; Panikkar and Khan, 2008). The positive effect of detritus on most groups would have beneficial role for detritivorous fish groups, especially for prawns. This observation is supported by Gamito and Erzini (2005) and Panikkar and Khan (2008). Phytoplankton had positive impact on most groups but interestingly it had negative impact on itself, which might be due to the competition for nutrients (Moreau et al., 1997). No impact of *Tilapia* and *Anabas testudineus* might be attributed due to the presence of their very low biomass in the system or may be their main food item was not entered to the diet matrix due to limited information (Neira et al., 2004). Bangladesh Fisheries Development Corporation (BFDC) liberates 30 mt of carp fingerlings every year in the Kaptai reservoir. Nevertheless, a noticeable decline of carps due to the increase in catfish biomass was observed during this study. Catfishes exert predation pressure on stocked carps (see *Table A2*). Future works are suggested to investigate why the carp production does not increase in spite of huge fingerling liberation. Does the predation pressure by the catfishes solely influence their tremendous reduction or is there any other hidden reasons related to environmental changes?

Ecosystem undergoes through many developmental phases and acquires maturity by the orderly succession of community development (Odum, 1969). Ecopath computes some important ecosystem indices related to ecosystem maturity and stability (Christensen, 1995). The present comparative mass-balance models of before and after fishing closure shows the health development of the tropical Kaptai reservoir due to this management practice. TST in pre-ban phase was greater than post-ban phase as younger ecosystem has higher TST. The decrease of the flows throughout the system during post-ban period along with ascendancy supports the finding of Ulanowicz (1986), and Ulanowicz and Norden (1990). The ratio of total biomass on total system throughput (TB/TST) should increase over time and maturity. In mature system, it stores energy in system' components and conserve it (Ulanowicz, 1986). Again, total primary production/total biomass (TPP/TB) tends to be lower from developmental phase toward mature state due to high biomass or low production rate (Christensen, 1995). The ratio of total primary production/total respiration, TPP/TR tends to be "1" for mature system. Higher TPP/TR (13.154) in pre-ban phase compared to post-ban (1.969) interprets the later phase as more mature. It is obvious that the reservoir had enough strength to fight against human perturbations such as overfishing, pollution, water diversion etc. for acquiring this sort of maturity. TPP/TR values of both phases for Kaptai reservoir was higher than Wyra reservoir (Panikkar and Khan, 2008), Bakreswar reservoir (Banarjee et al., 2016). On the other hand, Ravishankar sagar reservoir (10.36) has greater TPP/TR than post-ban phase but lower compared to pre-ban phase of Kaptai reservoir

(Panikkar et al., 2015). Christensen (1995) did study to rank the ecosystem maturity indicators and concluded that disturbances reduce maturity. The present paper also examines some of the vital ecosystem attributes such as TPP/TB, TB/TST, TPP/TR, TPP – TR and reveals that the Kaptai reservoir got more resilience after stopping the unlimited fishing access throughout the year than pre-ban phase. Therefore, the post-ban phase shows more maturity and stability as well compared to pre-ban phase.

Ascendancy and overhead are related to ecosystem stability, maturity, eutrophication and human perturbations (Aoki 1995; Christensen 1995; Ulanowicz, 1997; Neilsen and Ulanowicz, 2000). Overhead represents the presence of strength in an ecosystem to overcome any disturbances. The impact of the introduction of fishing closure is evident as the relative overhead increased (22.48%) during the post-ban period. It also signifies more resilient trophic network in post-ban than pre-ban period supporting the findings of Althausen (2003). Nevertheless, about 10% changes in relative overhead was observed in marine upwelling system during pre and post stressed period (Heymans et al., 2004). The ascendancy and overhead values are comparable with the findings of Panikkar and Khan (2008) and Panikkar et al. (2015).

Connectance index (CI) and system omnivory index (SOI) denote the existing complexity in the food web structure and the diversity in diet matrix. These also describe the level of maturity of an ecosystem. CI and SOI values tend to be higher in mature ecosystem. The values of CI and SOI were found as (0.423, 0.196) in pre-ban phase and (0.417, 0.198) in post-ban phase respectively. The similar CI indicates the similar diet in both terms. CI and SOI of the Kaptai reservoir for both periods were comparatively greater than the Bakreswar reservoir (Banerjee et al., 2016), Ravishankar sagar reservoir (Panikkar et al., 2015) while it was similar to lake Ayame (Traore et al., 2008). Moreover, higher CI indicates the importance of detritus as alternative diet in the system, diversity in diet of some groups and some sort of maturity as well.

Finn's cycling index (FCI) has correlation with system maturity, stability and resilience. A higher FCI value represents more mature and stable ecosystem (Odum, 1969). Greater FCI in post-ban (5.732) phase than pre-ban (1.373) supports more maturity and resilience during post-ban phase. FCI values for the kaptai reservoir was lower than Bakreswar reservoir (Banarjee et al., 2016) while greater than Ravishankar sagar reservoir (Panikkar et al., 2015). Ecopath computed predatory cycling index (PCI) excluding detritus cycles. PCI was a bit higher in pre-ban period (3.65) than post-ban (3.06). FCI and PCI values also support the statement of being more mature, complex and detritus dependent ecosystem. Higher Finn's mean path length (FMPL) in post fishing closure period (2.557) compared to pre fishing closure era (2.156) also suggest post-ban period with more maturity and complexity. However, high FCI value indicates an ecosystem as mature one but a very high value describes the ecosystem at vulnerable condition (Christensen and Pauly, 1993). In that sense, the Kaptai reservoir seems to be a bit sensitive to disruptions.

A similar study was done to assess the impact of fishing ban management practice for a tropical Wyra reservoir, India (Panikkar and Khan, 2008). They found (-82.7%) decrease of total flows during post-ban period while it decreased (-73.144%) in Kaptai reservoir. Lower ascendancy (-0.14%) and higher overhead (0.05%) after the introduction of fishing closure supports our finding for Kaptai reservoir. TPP/TR for both reservoirs decreased after the implementation of management approach but it was closer to 1 for Wyra reservoir (1.053) compared to Kaptai reservoir (1.969) indicating Wyra more mature. In brief, the comparative mass-balanced models for pre-ban (2001)

and post-ban period (2016) support the improvement of “health” for Kaptai reservoir due to management interventions during this period. The similar observed improvement for Wyra reservoir encourages implementing this environmental management measure for the stability of the reservoir and its resources.

Moreover, overfishing, both in marine and freshwater sector is a matter of concern nowadays to meet the increasing food security throughout the world. It does not only influence the aquatic resources but also the ecosystem. These are the driving forces to do detailed study of the aquatic ecosystems to ensure efficient management for the sustainability of the aquatic resources and greater the stability of the reservoir ecosystem. Uncontrolled fishing pressure impact the trophic structure of an ecosystem significantly. It also accelerates the rapid reproduction and reduce the size of fishes (Travers et al., 2010). Thus, the decrease of top predators from higher trophic levels and the increase of smaller size fishes was termed as “fishing down the food web”. Overfishing accelerate the fish species to suffer from the reduction of genetic diversity within and among population for long time before extinction (Musick et al., 2000). Selective fishing intensifies the alteration of genetic diversity, heritable difference in yield and life history traits of any particular fish species (Reviewed by Kenchington, 2003). Calculating the effects of overfishing on the molecular genetic level and in understanding life history traits will be helpful to get prior idea about stock status and level of extinction of any particular species. Further studies are suggested to know the possible effects of overfishing on ecosystem and molecular level.

Conclusion

Ecosystem modelling are now widely used for stock assessment and for the development of fisheries management policies for tropical fisheries. This study explains how fishing closure management helped the reservoir to get more maturity, stability, resilience and more complexity in food web than previous period. Moreover, TPP/TR near to unity predicts the reservoir as a healthy ecosystem but still it seeks attention to overcome the stress due to exercising overfishing. Our study also reveals that the Kaptai reservoir was more vulnerable to disruptions before the introduction of fishing ban management practice. In spite of its remarkable contribution to the capture fisheries of Bangladesh due to natural and human perturbations especially for the high catching activities, the reservoir resources have collapsed. Although, the fishing closure management step along with other practices led this system to achieve more maturity than before but still the reservoir fishery has been experiencing excessive fishing effort. Therefore, we can conclude that further necessary ecosystem-based management actions will help to be a sustainable aquatic resource in Bangladesh fighting against any natural or anthropogenic perturbations. Notably, the most abundant but low economic fish in the reservoir such as *Corica soborn*, *Gudusia chapra* could be used as processed food or as fishmeal. This paper provides a framework of better understanding of the trophodynamics of the Kaptai reservoir and the effects of taking environmental-based fisheries management. However, the scarcity of relevant data and uncertainties in input parameters especially for lower trophic level could be some feasible limitations of this study. Despite of these uncertainties we regard that the constructed models provide reasonable presentation of the Kaptai ecosystem structure and dynamics. Therefore, future works for instances collecting data with intensive care for further study related to ecosystem dynamics, study of effects of climate changes and pollutants on reservoir

resources, detailed study of the present modelling using Ecosim are recommended to explore new fishery policies for the reservoir sustainability.

Acknowledgements. All authors show immense gratitude to the Chinese Scholarship Council and Ocean University of China for their support in this journey.

REFERENCES

- [1] Ahmed, K. K. (1999): Options for the management of major carp fishery in Kaptai reservoir, Bangladesh. – PhD Dissertation, School of Environment, Resources and Development, Asian Institute of Technology, Bangkok.
- [2] Ahmed, K. K., Rahman, S., Ahammed, S. U. (2006): Managing fisheries resources in Kaptai reservoir, Bangladesh. – *Outlook on Agriculture* 35(4): 281-289.
- [3] Ahmed, K. K. U., Amin, S. M. N., Haldar, G. C., Dewan, S. (2003): Population dynamics and stock assessment of *Oreochromis niloticus* (Linnaeus) in the Kaptai Reservoir, Bangladesh. – *Indian Journal of Fisheries* 50(1): 47-52.
- [4] Ahmed, K. K. U., Amin, S. M. N., Haldar, G. C., Dewan, S., Hossain, M. M. (2005): Population dynamics and stock assessment of *Labeo rohita* (Hamilton) in the Kaptai Reservoir, Bangladesh. – *Asian Journal of Fisheries Science* 18: 1-14.
- [5] Althausen, L. (2003): An Ecopath/Ecosim analysis of an estuarine food web: seasonal energy flow and response to river-flow related perturbations. – Thesis Submitted to the Graduate Faculty of the Louisiana State University and Agricultural and Mechanical College, The Development of Oceanography and Coastal Sciences.
- [6] Aoki, I. (1995): Flow-indices characterizing eutrophication in lake-ecosystems. – *Ecological Modelling* 126: 131-137.
- [7] Azadi, M. A., Mamun, A. (2009): Population dynamics of the cyprinid fish, *Amblypharyngodon mola* (Hamilton) from the Kaptai lake, Bangladesh. – *Chittagong University Journal of Biological Science* 2009: 141-151.
- [8] Azadi, M. A., Mustafa, M. G., Naser, A. (1996): Studies on some aspects of population dynamics of *Labeo bata* (Hamilton) from Kaptai Reservoir, Bangladesh. – *Chittagong University Studies, Part II: Science* 20: 13-18.
- [9] Banerjee, A., Banerjee, M., Mukharjee, J., Rakhit, N., Ray, S. (2016): Trophic relationships and ecosystem functioning of Bakreswar Reservoir, India. – *Ecological Informatics* 36: 50-60.
- [10] Beverton, R. J. H., Holt, S. J. (1993): *On the Dynamics of Exploited Fish Populations*. – Chapman and Hall, London (facsimile, reprinted).
- [11] Bradford-Grieve, L., Bull, M., Murdoch, R., Nodder, S. (1994): Summary of fisheries knowledge of the Tasman and Golden Bay Marine environment relevant to fisheries enhancement. – Report Prepared for Southern Scallops Fishery Advisory Committee MAF (Central) Tasman District Council.
- [12] Christensen, V. (1995): Ecosystem maturity - towards quantification. – *Ecological Modelling* 77: 3-32.
- [13] Christensen, V., Pauly, D. (1992): ECOPATH II—a software for balancing steady-state ecosystem models and calculating network characteristics. – *Ecological Modelling* 61(3-4): 169-185.
- [14] Christensen, V., Pauly, D. (1993): *Trophic Models of Aquatic Ecosystems*. – World Fish, ICLARM Conference Proceedings 26, Manila.
- [15] Christensen, V., Pauly, D. (1995): Fish production, catches and the carrying capacity of the world oceans. – *Naga, ICLARM Q* 18(3): 34-40.
- [16] Christensen, V., Walters, C. J., Pauly, D. (2000): *Ecopath with Ecosim: A User's Guide*. – University of British Columbia. Fisheries Centre, Vancouver.

- [17] Christensen, V., Walters, C. J., Pauly, D. (2002): Ecopath with Ecosim Version 5, Help System©. – University of British Columbia. Fisheries Centre, Vancouver, BC, Canada.
- [18] Christensen, V., Walter, C. J., Pauly, D. (2005): Ecopath with Ecosim: A User's Guide. – Fisheries Centre, University of British Columbia, Vancouver.
- [19] Christensen, V., Walters, C. J., Pauly, D., Forrest, R. (2008): Ecopath with Ecosim Version 6 User Guide. – Lenfest Ocean Futures Project.
- [20] Christian, R. R., Froese, E., Comin, F., Viaroli, P., Naldi, M., Ferrari, I. (1996): Nitrogen cycling networks of coastal waters: influence of trophic status and primary producer form. – *Ecological Modelling* 87(1-3): 111-129.
- [21] DoF (2016): Yearbook of Fisheries Statistics of Bangladesh, 2016-2017. – Director General Department of Fisheries, Bangladesh, Dhaka.
- [22] Fetahi, T. (2005): Trophic analysis of Lake Awassa using mass-balance Ecopath model. – A Thesis Presented to the School of Graduate Studies, Addis Ababa University, Department of Biology.
- [23] Fetahi, T., Mengistou, S. (2007): Trophic analysis of Lake Awassa (Ethiopia) using mass-balance Ecopath model. – *Ecological Modelling* 201(3-4): 398-408.
- [24] Froese, R., Pauly, D. (2019): FishBase. – World Wide Web Electronic Publication. www.fishbase.org.
- [25] Gamito, S., Erzini, K. (2005): Trophic food web and ecosystem attributes of a water reservoir of the Ria Formosa (south Portugal). – *Ecological Modelling* 181(4): 509-520.
- [26] Gulland, J. A. (1971): The Fish Resources of the Oceans West by Fleet. – Fishing News (Book) Ltd for FAO, Rome.
- [27] Gupta, B. K., Sarkar, U. K., Bharadwaj, S. K. (2015): Analysis of morphometric characters and population dynamics of *Ompok pabda* (Hamilton, 1822) from Gomti River in Northern India. – *Journal of Biological Science and Medicine* 1(1): 49-58.
- [28] Gupta, S. (2015): Review on *Sperata seenghala* (Sykes, 1839), a freshwater catfish of Indian subcontinent. – *Journal of Aquatic Research Development* 6: 290.
- [29] Haroon, A. Y., Razzaque, A., Dewan, S., Amin, S. N., Rahman, S. L. (2001): Population Dynamics and Stock Assessment of *Labeo rohita* (Ham.), *L. calbasu* (Ham.) and *L. gonius* (Ham.) From the Mymensingh Basin. – *Journal of Biological Science* 1: 671-675.
- [30] Heymans, J. J., Shanon, L. J., Jarre, A. (2004): Changes in the Northern Benguela Ecosystem over three decades: 1970s, 1980s, and 1990s. – *Ecological Modelling* 172: 175-195.
- [31] Islam, M. S., Rahman, M. M., Halder, G. C., Tanaka, M. (2006): Fish assemblage of a traditional fishery and the seasonal variations in diet of its most abundant species *Wallago attu* (Siluriformes: Siluridae) from a tropical floodplain. – *Aquatic Ecology* 40(2): 263-272.
- [32] Kenchington, E. L. (2003): The Effects of Fishing on Species and Genetic Diversity. – In: Sinclari, M. et al. (eds.) *Responsible Fisheries in the Marine Ecosystem*. Chap. 14. CAB International, Wallingford.
- [33] Khatun, M., Lupa, S., Rahman, M., Barman, P., Liu, Q. (2019): Evaluation of *Labeo calbasu* fishery status using surplus production models in Kaptai reservoir, Bangladesh. – *Applied Ecology and Environmental Research* 17(2): 2519-2532.
- [34] Khumar, F., Siddiqui, M. S. (1989): Food and feeding habits of the carp *Labeo calbasu* Ham. in north Indian waters. – *Acta Ichthyologica Et Piscatoria* 1(19).
- [35] Kumari, S., Sarkar, U. K., Mandhir, S. K., Lianthuamluaia, L., Panda, D., Chakraborty, S. K., Karnatak, G., Kumar, V., Puthiyottill, M. (2018): Studies on the growth and mortality of Indian River shad, *Gudusia chapra* (Hamilton, 1822) from Panchet reservoir, India. – *Environmental Science and Pollutant Research* 25: 33768-33772.
- [36] Lauzanne, L. (1983): Trophic Relations of Fishes in Lake Chad. – In: Carmouze, J. P., Durand, J. R., Leveque, C. (eds.) *Lake Chad: Ecology and Productivity of a Shallow Tropical Ecosystem*. Junk Publ., The Hague, pp. 489-518.

- [37] Libralato, S., Christensen, V., Pauly, D. (2006): A method for identifying keystone species in food web models. – *Ecological Modelling* 195: 153-171.
- [38] Lindeman, R. L. (1942): The trophic-dynamic aspect of ecology. – *Ecology* 23: 399-417.
- [39] Majkowski, J. (1982): Usefulness and Applicability of Sensitivity Analysis in a Multi-Species Approach to Fisheries Management. – In: Pauly, D., Murphy, G. I. (eds.) *Theory and Management of Tropical Fisheries*. ICLRM Conference Proceedings 9, pp.149-165.
- [40] Mamun, A., Tareq, K. M. A., Azadi, M. A. (2004): Food and feeding habits of *Amblypharyngodon mola* (Hamilton) from Kaptai reservoir, Bangladesh. – *Pakistani Journal of Biological Science* 7(4): 584-588.
- [41] Mohamed, K. S., Zacharia., Muthiah, C., Abdurahiman, K. P., Nayak, T. H. (2005): A trophic model of the Arabian Sea Ecosystem off Karnataka and Simulation of Fishery Yields for its Multigear Marine Fisheries. – *CMFRI Special Publication*, Kochi, pp. 1-55.
- [42] Mondal, D. K., Kaviraj, A. (2010): Feeding and reproductive biology of Indian shad *Gudusia chapra* in two floodplain lakes of India. – *Electronic Journal of Biology* 6(4): 98-102.
- [43] Moreau, J., Villanueva, M. C. (2002): Exploratory Analysis of Possible Management Strategies in Lake Victoria Fisheries (Kenyan Sector) Using the Recent Ecosim Software. – In: Pitcher, T., Cochrane, K. (eds.) *On the Use of Ecosystem Models to Investigate Multi-Species Management Strategies for Capture Fisheries*. Fisheries Center Research Report 10, pp.150-154. www.fisheries.ubc.ca.
- [44] Moreau, J. C., Gertrud, G., Ian, H., Kit, K., Nils, K., Martina, M., Cecil, M., Brian, M. (1997): Biomass Flows in Lake Kariba, towards an Ecosystem's Approach. – In: Moreau, J. (ed.) *Advances in the Ecology of Lake Kariba*. University of Zimbabwe Publication, pp. 219-230.
- [45] Moreau, J., Mavuti, K., Daufresne, T. (2001): A synoptic Ecopath model of biomass flows during two different static ecological situations in Lake Nakuru (Kenya). – *Hydrobiologia* 458(1-3): 63-74.
- [46] Musick, J. A., Harbin, M. M., Berkeley, S. A., Burgess, G. H., Eklund, A. M., Findley, L., Gilmore, R. G., Golden, J. T., Ha, D. S., Huntsman, G. R., McGovern, J. C., Sedberry, G. R., Parker, S. J., Poss, S. G., Sala, E., Schmidt, T. W., Weeks, H., Wright, S. G. (2000): Marine, estuarine and diadromous fish stocks at risk of extinction in North America (exclusive of Pacific salmonids). – *Fisheries* 25: 6-29.
- [47] Mustafa, M. G., De Graaf, G. (2008): Population parameters of important species in inland fisheries of Bangladesh. – *Asian Journal of Fisheries Science* 21(2): 147-158.
- [48] Mustafa, M. G., Singha, S., Islam, M. R., Mallick, N. (2014): Population dynamics of *Notopterus notopterus* (Pallas, 1769) from the Kaptai reservoir of Bangladesh. – *SAARC Journal of Agriculture* 12(2): 112-122.
- [49] Neira, S., Arancibia, H., Cubillos, L. (2004): Comparative analysis of trophic structure of commercial fishery species off Central Chile in 1992 and 1998. – *Ecological Modelling* 172(2-4): 233-248.
- [50] Niesen, S. N., Ulanowicz, R. E. (2000): On the consistency between thermodynamical and network approaches to ecosystems. – *Ecological Modelling* 132: 23-31.
- [51] Odum, E. P. (1969): The strategy of ecosystem development. – *Science* 104: 262-270.
- [52] Odum, E. P. (1971): *Fundamentals of Ecology*. – W. B. Saunders Co., Philadelphia.
- [53] Palaniswamy, R., Manoharan, S., Geethalakshmi, V. (2011): Assessment of population parameters of Indian major carps and common carp in a culture-based reservoir. – *Indian Journal of Fisheries* 58(2): 41-44.
- [54] Palomares, M. L. D., Pauly, D. (1998): Predicting food consumption of fish populations as functions of mortality, food type, morphometrics, temperature and salinity. – *Marine Freshwater Research* 49(5): 447-453.

- [55] Panikkar, P., Khan, M. F. (2008): Comparative mass-balanced trophic models to assess the impact of environmental management measures in a tropical reservoir ecosystem. – *Ecological Modelling* 212(3-4): 280-291.
- [56] Panikkar, P., Khan, M. F., Desai, V. R., Shrivastava, N. P., Sharma, A. P. (2015): Characterizing trophic interactions of a catfish dominated tropical reservoir ecosystem to assess the effects of management practices. – *Environmental Biology of Fishes* 98(1): 237-47.
- [57] Pauly, D. (1984): *Fish Population Dynamics in Tropical Waters: A Manual for Use with Programmable Calculators*. ICLARM Studies and Reviews 8. – International Center for Living Aquatic Resources Management, Manila.
- [58] Pauly, D., Palomares, M. L., Froese, R. (1993): Some prose on a database of indigenous knowledge on fish. – *Indigenous Knowledge and Development Monitor* 1(1): 26-7.
- [59] Pauly, D., Christensen, V., Walters, C. (2000): Ecopath, Ecosim, and Ecospace as tools for evaluating ecosystem impact of fisheries. – *ICES Journal of Marine Science* 57(3): 697-706.
- [60] Polovina, J. J. (1984): Models of coral reef ecosystems. I: the ECOPATH model and its application to French Frigate Shoal. – *Coral Reefs* 3: 1-11.
- [61] Reyes, M. D. (1993): Fishpen Culture and Its Impact on the Ecosystem of Laguna de Bay, Philippines. – In: Christensen, V., Pauly, D. (eds.) *Trophic Models of Aquatic Ecosystems*. ICLARM Conference Proceedings 26, Manila, pp 74-84.
- [62] Roy, D., Masud, A. A., Bhuiyan, N. A., Naser, M. N. (2013): Food and Feeding habits of Koi *Anabas testudineus* (Bloch) and indigenous catfish *Rita rita* (Hamilton). – *International Journal of Biological Research* 15(1): 1-6.
- [63] Sakhare, V. B., Jetithor, S. G. (2016): Food and feeding behaviour of Mozambique tilapia (*Oreochromis mossambicus* Peters) from Borna Reservoir of Maharashtra. – *Indian Journal of Fisheries* 4: 431-434.
- [64] Sarkar, U. K., Deepak, P. K. (2009): The diet of clown knife fish *Chitala chitala* (Hamilton–Buchanan) an endangered notopterid from different wild population (India). – *Electronic Journal of Ichthyology* 1: 11-20.
- [65] Srivastava, S. M., Singh, S. P., Pandey, A. K. (2012): Food and feeding habits of threatened *Notopterus notopterus* in Gomti river, Lucknow (India). – *Journal of Experimental Zoology, India* 15(2): 395-402.
- [66] Thella, R., Dahanukar, N., Eldho, P., Ali, A., Raghavan, R. (2018): Population dynamics of *Wallago attu* (Bloch and Schneider 1801) (Osteichthyes, Siluridae) in three small rivers of southern India. – *Asian Fisheries Science* 31: 172-178.
- [67] Tomaczack, M. T., Jarv, L., Martin, G., Minde, A., Muller-Karulis, B., Pollumae, A., Razinkovas, A., Strake, S. (2005): Trophic networks and Carbon flows in South Eastern Baltic coastal ecosystems. – *ICES CM 2005/M*: 01.
- [68] Traore, A., Ouattara, A., Doumbia, L., Tah, L., Moreau, J., Gourène, G. (2008): Trophic structure and interactions in Lake Ayamé (Côte d'Ivoire). – *Knowledge and Management of Aquatic Ecosystem* 388: 02. <https://doi.org/10.1051/kmae:2008002>.
- [69] Travers, M., Watermeyer, K., Shannon, L. J., Shin, Y. J. (2010): Change in food web structure under scenarios of overfishing in the Southern Benguela: comparison of the Ecosim and OSMOSE modelling approaches. – *Journal of Marine Systems* 79: 101-111.
- [70] Ulanowicz, R. E. (1986): *Growth and Development: Ecosystem Phenomenology*. – Springer-Verlag, New York.
- [71] Ulanowicz, R. E. (1997): *Ecology, the Ascendent Perspective*. – Columbia University Press, New York.
- [72] Ulanowicz, R. E., Norden, J. S. (1990): Symmetrical overhead in flow networks. – *International Journal of Systematic Science* 21: 429-437.
- [73] Ulanowicz, R. E., Puccia, C. J. (1990): Mixed trophic impacts in ecosystems. – *Coenoses* 5: 7-16.

- [74] Villanueva, M. C., Ouedraogo, M., Moreau, J. (2006): Trophic relationships in the recently impounded Bagré reservoir in Burkina Faso. – *Ecological Modelling* 191(2): 243-259.
- [75] Weliange, W. S., Amarasinghe, U. S. (2007): Relationship between body shape and food habits of fish from three reservoirs of Sri Lanka. – *Asian Fisheries Science* 20: 257-270.
- [76] Wolff, M. (1994): A trophic model for Tongoy Bay - a system exposed to suspended scallop culture (Northern Chile). – *Journal of Experimental Marine Biology and Ecology* 182: 149-168.

APPENDIX

Table A1. Population parameters of the representative species of different functional groups used for pre-fishing ban (2001) and post-fishing ban period (2016) in Kaptai reservoir system

Group/species	L_{∞}	K (yr ⁻¹)	M (yr ⁻¹)	F (yr ⁻¹)	Z (yr ⁻¹)	E	Reference
Carps							
<i>Labeo rohita</i>	93.28	0.920	1.220	1.310	2.53	0.500	Ahmed et al., 2005
<i>Catla catla</i>	94.30	0.959	0.629	2.600	3.23	0.805	Palaniswamy et al., 2011
<i>Cirrhinus cirrhosus</i>	71.00	0.845	0.627	1.470	2.1	0.701	Palaniswamy et al., 2011
<i>Labeo calbasu</i>	69.00	1.100	1.480	4.230	5.71	0.740	Haroon et al., 2001
<i>Labeo bata</i>	32.10	1.500	2.285	1.400	2.80	0.500	Azadi et al., 1996
<i>Labeo gonius</i>	53.00	0.890	1.390	1.390	2.78	0.500	Haroon et al., 2001
<i>Cyprinus carpio</i>	58.66	0.958	0.708	1.412	2.12	0.663	Palaniswamy et al., 2011
Catfishes	53.00	0.280	0.450	0.450	0.90	0.500	Villanueva et al., 2006
Sheatfishes							
<i>Wallago attu</i>	99.75	1.300	1.470	1.900	3.37	0.560	Thella et al., 2018
<i>Ompok pabda</i>	21.00	1.000	1.920	0.290	2.22	0.130	Gupta et al., 2015
Tilapia							
<i>Oreochromis niloticus</i>	55.59	0.390	0.800	0.590	1.39	0.420	Ahmed et al., 2003
<i>Anabas testudineus</i>	17.10	1.400	2.520	1.895	3.79	0.500	Mustafa and Graaf, 2008
Knife fishes							
<i>Notopterus notopterus</i>	34.91	0.380	0.910	0.280	1.19	0.240	Mustafa et al., 2014
Snakehead							
<i>Channa punctatus</i>	24.00	0.900	2.160	1.565	3.13	0.500	Mustafa and Graaf, 2008
Minnnows							
<i>Puntius sarana</i>	26.00	0.400	0.930	1.640	2.57	0.640	FishBase
<i>Amblypharyngodon mola</i>	10.46	0.950	1.220	2.040	3.26	0.630	Azadi and Mamun, 2009
Clupeids							
<i>Corica soborna</i>	5.700	2.620	5.110	3.400	8.51	0.400	FishBase
<i>Gudusia chapra</i>	19.40	1.230	2.450	4.180	6.63	0.630	Kumari et al., 2018

Table A2. Input diet matrix for different functional groups for pre-fishing ban (2001) and post-fishing ban period (2016) in Kaptai reservoir

Group no.	Prey/predator	1	2	3	4	5	6	7	8	9	10	11	12
1	Carp	-	0.065	-	-	-	-	- (0.150)	-	-	-	-	-
2	Catfishes	-	0.023	0.150	-	-	-	0.015	-	-	-	-	-
3	Sheatfishes	-	0.009	-	-	-	-	0.07	-	-	-	-	-
4	Tilapia	-	0.025	-	-	-	-	-	-	-	-	-	-
5	<i>Anabas testudineus</i>	-	0.005	-	-	-	-	-	-	-	-	-	-
6	Knife fishes	-	0.003	-	-	-	-	-	-	-	-	-	-
7	Snakehead	-	0.05	-	-	-	-	-	-	-	-	-	-
8	Minnows	-	0.17	0.340	-	0.110	0.100	0.228	-	-	-	-	-
9	Clupeids	-	0.25	0.100	-	0.200	0.200	0.310	-	-	-	-	-
10	Prawns	-	0.08	0.200	-	0.050	0.350	0.180 (0.05)	-	0.050	0.05	-	-
11	Insects/larvae	0.075	0.15	-	0.050	0.160	0.180	0.080 (0.004)	-	0.050	0.2	-	-
12	Zooplankton	0.055	0.07	-	0.246	0.260	0.090	0.060	0.130	0.425	0.2	0.125	0.05
13	Phytoplankton	0.520	0.05	0.080	0.700	0.110	0.050	0.025	0.850	0.375	0.1	0.305	0.8
14	Detritus	0.350	0.05	0.130	0.004	0.110	0.030	0.032 (0.088)	0.020	0.100	0.45	0.570	0.15

*The input value within bracket (bold) were used for modelling of pre-fishing ban period (2001)

SORPTION KINETICS AND ISOTHERM STUDIES OF CATIONIC DYES USING GROUNDNUT (*ARACHIS HYPOGAEA*) SHELL DERIVED BIOCHAR A LOW-COST ADSORBENT

JEGAN, J.¹ – PRAVEEN, S.^{2*} – BHAGAVATHI PUSHPA, T.¹ – GOKULAN, R.²

¹Department of Civil Engineering, University College of Engineering Ramanathapuram, Ramanathapuram 623513, Tamil Nadu, India

²Department of Civil Engineering, G. M. R Institute of Technology, Rajam 532127, Srikakulam District, Andhra Pradesh, India

*Corresponding author

e-mail: praveensarvan@gmail.com, praveen.s@gmrit.edu.in; phone: +91-90-4846-3402

(Received 12th Nov 2019; accepted 30th Jan 2020)

Abstract. The removal of a Basic Blue 41 (BB41) and Basic Red 09 (BR09) from an aqueous solution by biochar derived from *Arachis hypogaea* shell (Groundnut shell) was studied. The sorption of cationic dyes (BB41 and BR09) was studied by varying biochar dosage (1–10 g/L), solution pH (3–10), temperature (30 to 50 °C), contact time (0–360 min) and initial dye concentration (25–200 mg/L). At optimum biochar dosages of 2 g/L (BB41) and 1 g/L (BR09), solution pH (8), initial concentration of dye (50 mg/L), and equilibrium time (240 min), groundnut shell derived biochar recorded BB41 and BR09 uptakes of 22.322 and 40.655 mg/g. The kinetic research confirmed that the biosorption rate was quick for groundnut shell-based biochar, and the results were effectively modeled using the Pseudo's first-order and second-order kinetic models. The sorption isotherm studies exhibited that the Sips model provided better results with high correlation coefficients.

Keywords: biomass, pyrolysis, groundnut, water quality, treatment

Introduction

Dyes have been used as coloring agents in the textile industries for many years (Wu and Ng, 2008). Different types of dyes are used for diverse applications in the textile manufacturing process; among these, cationic dyes are used the most (Zolliger, 2003).

During the manufacturing of textiles, an enormous quantity of waste sludge and chemically contaminated water are generated. This chemically contaminated wastewater taints the water quality and soil fertility of the affected land cover. Compared to wastewaters released from other industrial applications, those from textile manufacturing are incredibly complex (Gokulan et al., 2019a).

The appearance of colors in the chemically contaminated sewage could be highly visible and harmful even at lower concentrations (Nigam et al., 2000). These polluted wastewaters not only damage the aesthetic nature of the aquatic ecosystem but also affect the photosynthetic activity of aquatic environments by reducing the level of light penetration through it (Kang et al., 2019). These polluted waters contain toxic and carcinogenic substances that must be treated before being discharged into the aquatic systems (Siddique et al., 2017). However, treatment technologies are often not sufficient to remedy these volumes of wastewater (Gokulan et al., 2019b). Since the removal of wastewater is considered as an environmental challenge and mandate of government legislations made in force of these industries to focus on effective treatment of wastewater techniques.

In order to arrest these environmental challenges, various treatment techniques have been used for the removal of dye from wastewater in textile processing units, as insisted by the legislative mandate of government. The most commonly used treatment techniques are Fenton process, photo-Fenton processes (Rosembergue et al., 2019), photoelectro-Fenton (Paz et al., 2020), photo-ferrioxalate (Sankar et al., 2015), reverse osmosis (Sahinkaya et al., 2019), electrochemical oxidation (Nidheesh, 2018), adsorption (Mu et al., 2019), chemical coagulation/flocculation (Beluci et al., 2019).

There are certain disadvantages and limitations of existing dye removal methods in real-time applications. For example, the operating cost of the process is expensive, and they would generate particular wastes that should be treated and disposed of in order to avoid collateral pollution of the environment (Hua et al., 2019). Biological-adsorption can be defined as the uptake of pollutants by inactive biomass through physiochemical treatments (Bhagavathi et al., 2019). Hence adsorption process is viable in dye removal for industrial applications due to its simplicity and sustainability of a broad variety of sorbents that can be used in water treatment (Gupta et al., 2009; Mironyuk et al., 2019).

For this purpose, adsorption by agricultural waste by-products have great potential for removal of different pollutants (Mohebbi et al., 2019) has proved to be an efficient remediation technique for removing various contaminants such as Dyes (Charola et al., 2018; Wakkal et al., 2019), COD (Mohammad-pajooch et al., 2018) Phenol (da Gama et al., 2018) and heavy metals (Mohammad-pajooch et al., 2018; Liu et al., 2019). In addition to that, agro wastes, by-products are low-cost, available in abundance around the world, renewable resources, eco-friendly, and easy to regenerate (Zhou et al., 2015).

Arachis hypogaea or Groundnut shells are the residual waste produced after the eradication of groundnut seed from its pod. This is a vast agricultural waste with a minor rate of degradation (Zheng et al., 2013). However, groundnut shells have diverse applications such as bioethanol production biodiesel production, carbon nano-sheet formation, and enzyme production. These shells are used as feedstock for biochar preparation, too (Duc et al., 2019). Biochar is a new and popular alternative for the treatment of dye-bearing effluents to selectively isolate dye molecules (Gokulan et al., 2019c). Since the biochar derived from the Groundnut Shell contains various bioactive and different functional compounds, it can be assessed as a feasible bio-sorbent for the adsorptive removal of cationic dyes.

Moreover, the use of groundnut shell derived biochar as a biosorbent in the adsorptive removal of cationic dyes (Basic Blue 41 and Basic red 09) has not been reported, so far. Therefore, in this study, the Groundnut shell derived biochar (GnSB) was examined for the adsorptive removal of Basic Blue 41 (BB41) and Basic Red 09 (BR09) as a model cationic dye and characterized in detail. The influencing parameters of adsorption, including biochar dose, solution pH, initial dye concentration, and temperature, were correlated with the sorption capacity of the biochar. The adsorptive performance of biochar for the removal of BB41 and BR09 was evaluated and modeled.

Materials and methods

Biomass and chemicals

Groundnut shell leftover after the removal of seeds from its pod in the oil mills was used. These shells were obtained from various agro oil processing units in and around Karumathampatti village of Coimbatore city in Tamil Nadu, India. The collected

groundnut shells were used as a feedstock for biochar preparation. These feedstocks were initially washed up with water to remove soil with dust and then exposed to natural sundry for 48 h. Further, the feedstocks were dried up to at 70 °C for 24 h and then pulverized to less than 100 mm for biochar production (Luo et al., 2015). BB41 and BR09 cationic dyes of analytical grade and all other analytical grade chemical agents were obtained from Sigma Aldrich, India. The dye solution was prepared by the dissolution of the required amount of BB41 and BR09 in deionized water. The solution pH of the dye was adjusted to the desired value using 0.1 M HCl or 0.1 M NaOH (Jegan et al., 2016). The chemical structure and characteristics of all the cationic dyes were illustrated in *Figure 1* and *Table 1*.

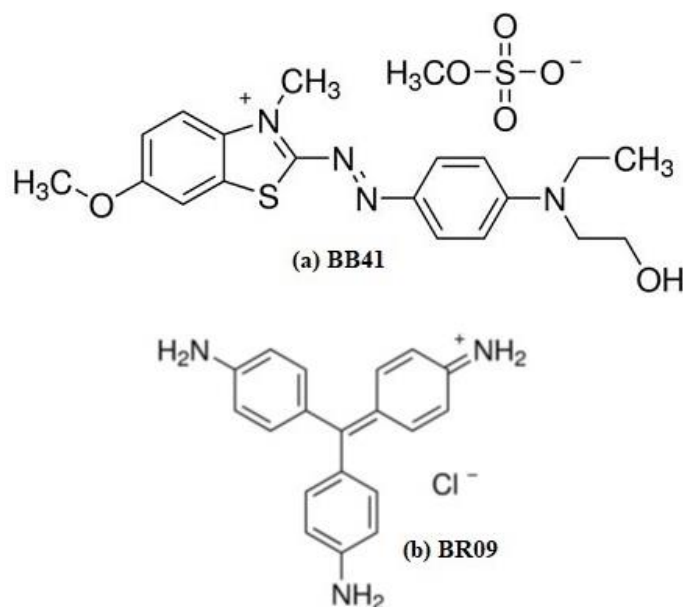


Figure 1. The structure of cationic dyes Basic Blue 41 (a) and Basic Red 09 (b)

Table 1. The characteristics of cationic dyes

Dyes	Empirical formula	Colour index	Molecular weight (g/mol)	λ max (nm)
Basic Blue 41	C ₂₀ H ₂₆ N ₄ O ₆ S ₂	11105	482.57	618
Basic Red 09	C ₁₉ H ₁₇ N ₃ HCl	42500	323.82	546

Pyrolysis of biomass

The biomass of 100 g was kept in a crucible covered with small holes of alumina foil and then flamed at a preferred temperature in a muffle furnace (Mahdi et al., 2017) and maintained it for 120 min in the existing operating conditions under O₂ limited environment (Luo et al., 2015). The heating rate was maintained at 5 °C/min in the pyrolysis, and the resultant biochar was further allowed to cool to room temperature overnight. This experiment was performed at different temperatures (300, 350, 400, 450, and 500 °C) with three trails at each condition to find out the optimum condition. The resultant biochar was moved to a desiccator and further used for various sorption studies.

Characterization of biochar

The Scanning Electron Microscope was used to determine the surface morphological conditions of the biochar using ZEISS- GeminiSEM. Before analysis, all dried biochar samples were coated with a thin layer of gold for electrical conduction. A Fourier Transform Infrared (FTIR) spectrophotometer (Thermo Scientific Ltd., USA & Nicolet 6700) has been used to study the availability of different surface functional groups on the sample. Before these analyses, these dried samples were assorted with KBr to form pellets (Zama et al., 2017).

Adsorption studies

By optimizing the operating parameters with a target to achieve the maximum sorption uptake, batch trial experiments were performed. The biochar dose was added to a 250 mL of Erlenmeyer flask consist of 100 mL of dye concentration, and it was mixed well using an incubated shaker at 200 rpm for 6 h. Then centrifuged for 10 min at 4000 rpm. Finally, the dye concentration was measured from the UV-Spectrophotometer using the supernatant. These adsorption trials were performed for different process conditions.

Isotherm and kinetic studies

In order to determine the maximum dye sorption capacity of the biosorbent, isotherm experiments were carried out by varying the concentrations from 25 to 200 mg/L. The experiment trials were performed at the desired pH, temperature, and adsorbent dosage. The amount of dye sorbed was determined by the differences observed between the amount of dye added to the biomass and the amount present in the supernatant using *Equation 1*:

$$\text{Biochar uptake: } Q = \frac{V(C_0 - C_e)}{W} \quad (\text{Eq.1})$$

The removal efficiency (%) was calculated by using *Equation 2*:

$$\text{Removal efficiency (\%)} = \frac{C_0 - C_e}{C_0} \times 100 \quad (\text{Eq.2})$$

where Q is the uptake of dye by sorbent mg/g, V is the dye solution volume (L), C₀ is the initial concentration of dye used (mg/L), C_e is the final (equilibrium) concentration of dye remained in the solution (mg/L), and W is the mass of biochar (g).

Four different equilibrium isotherm models were used to fit the experimental data of BB41 and BR09, biosorption onto Groundnut Shell Biochar as given in *Equations 3, 4, 5 and 6* (Ayawei et al., 2017).

Freundlich model:

$$Q = K_F C_e^{\frac{1}{n_F}} \quad (\text{Eq.3})$$

Langmuir model:

$$Q = \frac{Q_{max} b_L C_e}{1 + b_L C_e} \quad (\text{Eq.4})$$

Sips model:

$$Q = \frac{K_S C_e^{\beta_S}}{1 + a_S C_e^{\beta_S}} \quad (\text{Eq.5})$$

Toth model:

$$Q = \frac{Q_{max} b_T C_e}{[1 + (b_T C_e)^{n_T}]^{1/n_T}} \quad (\text{Eq.6})$$

where Q_{max} is the maximum uptake of dye by the sorbent (mg/g), n_F is the Freundlich exponent, K_F is the coefficient of the Freundlich model (mg/g) (L/mg)^{1/n_F}, b_L is the equilibrium coefficient of Langmuir model (L/mg), a_S is the coefficient of Sips model (L/mg), β_S is the exponent of Sips model, K_S is the isotherm coefficient of Sips model (L/g). b_T is the constant of Toth model (L/mg), and n_T is Toth model exponent.

The kinetic models have been utilized to describe the sorption kinetics as provided in the following equations (Eqs. 7 and 8):

Pseudo-first-order kinetic model:

$$Q_t = Q_e (1 - \exp(-k_1 t)) \quad (\text{Eq.7})$$

Pseudo-second-order kinetic model:

$$Q_t = \frac{Q_e^2 k_2 t}{1 + Q_e k_2 t} \quad (\text{Eq.8})$$

where Q_t is the dye uptake capacity at any time t (mg/g), Q_e is the equilibrium dye uptake capacity (mg/g), k_1 (1/min) and k_2 (g/mg.min) are the rate constants of the pseudo-first and pseudo-second-order models, respectively.

Results and discussion

Effect of pyrolysis on biomass

The yield of biochar was strongly influenced by the pyrolytic atmosphere. The biochar yield was defined as a weight percentage of the biochar recovered after pyrolysis (Ronsse et al. 2013). *Figure 2* illustrates the pyrolytic temperature influences on biochar yields for the feedstocks. It was evident that the surge in pyrolytic temperature results in decreases the yield of biochar. This was due to more decomposition of residues at higher temperatures. After a cautious assessment of the results presented in *Figure 2*, the maximum biochar yield was obtained at 350 °C was used for further studies.

Characterization of groundnutshell derived biochar

The surface morphological functionalities of the cationic dye bounded biochar derived from the groundnut shell were assessed by the scanning electron microscope, as shown in *Figure 3*. From this figure, it is evident that the groundnut shell surface was

observed to be smooth before pyrolysis, and it is found to be pore and rough after pyrolysis. The surface sites of the biochar after pyrolysis was enlarged and attained more binding action between the cationic dyes onto the biochar. The change in action on the surface of biochar revealed that ion exchange had happened between the adsorbent and adsorbate (Gokulan et al. 2019d) which in turns on adsorption, this adsorption of cationic dyes on the surface of biochar decreases its porosity, as reported (Ahmadi et al., 2012).

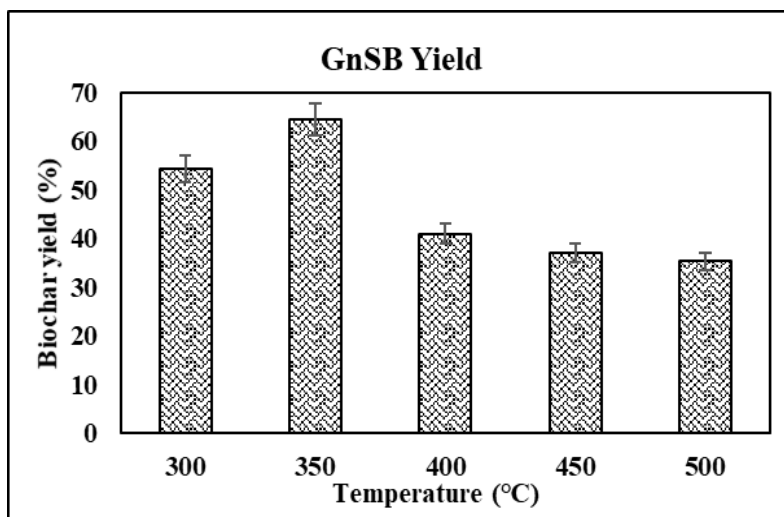


Figure 2. Effect of pyrolysis temperature on the biochar yield

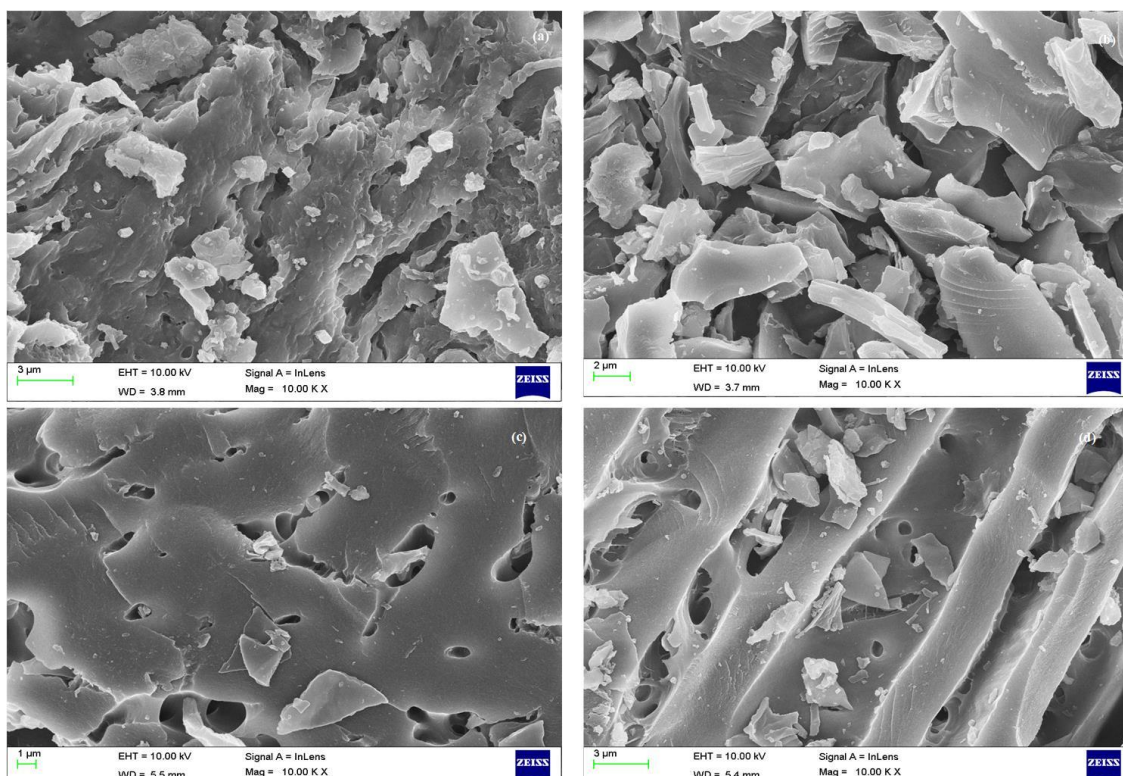


Figure 3. SEM images of Groundnut Shell (GnS) (a), GnS derived Biochar (GnSB) (b), BB41 bounded GnSB (c) and BR09 bounded GnSB (d)

In the Energy Dispersive Spectroscopy (EDS) analysis, strong peaks of C, N, O and S are obtained as depicted in *Figure 4*. The results demonstrated that carbon (67.00% to 69.53) and nitrogen (6.13% to 7.31%) content increases and whereas oxygen (26.78% to 23.01%) and sulphur (0.09% to 0.014%) content decreases after pyrolysis. This decrease is due to the decarboxylation and dehydration with subsequent loss of hydroxyl and aliphatic groups.

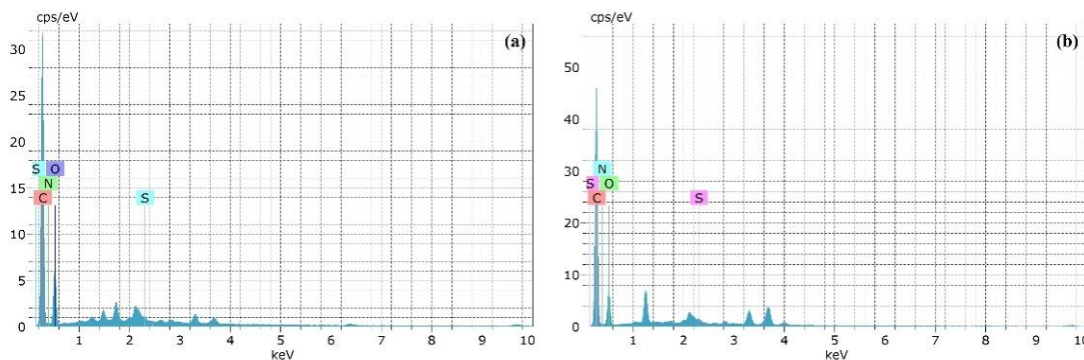


Figure 4. EDS spectrum of groundnut shell (a) and groundnut shell derived biochar (b)

The FT-IR spectrum of groundnut shell derived biochar, and cationic dyes bounded biochar are presented in *Figure 5*. The spectrum shows a number of peaks, which indicates the complex nature of the biochars.

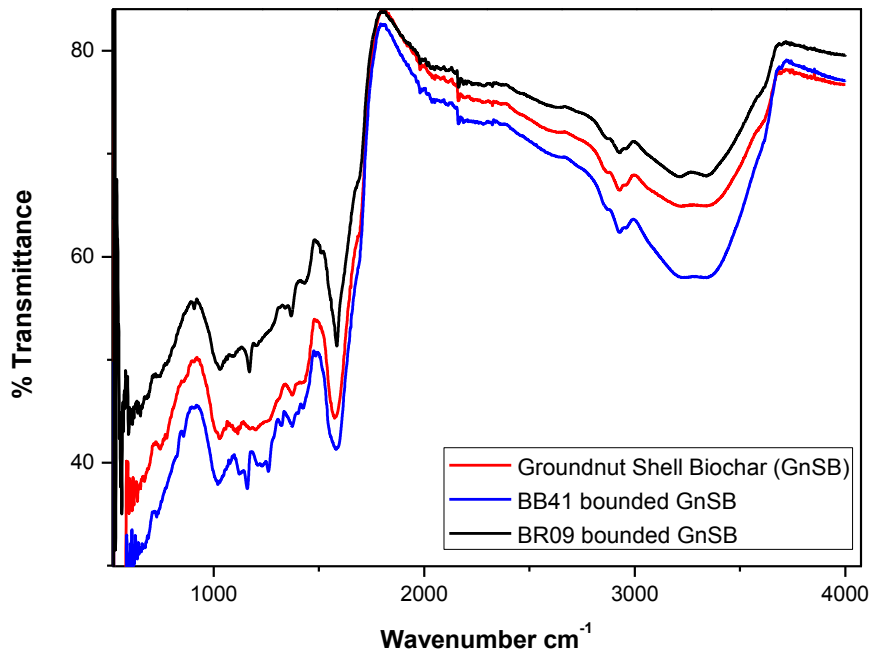


Figure 5. FT-IR spectra of groundnut shell biochar and basic dyes bounded biochar

The FT-IR spectrum of biochar barbed out the presence of strong bands at 613 cm^{-1} (C–H (alkynes) band), 744 cm^{-1} (C–H bend), 1114 cm^{-1} (C–O stretch (primary alcohols), 1574 cm^{-1} (C = C stretch, N–H bend) 2928 cm^{-1} (C–H stretch (Alkanes and Alkyls)) and

3339 cm^{-1} (O–H, N–H, stretch). After batch experiments, the biochar spectrum is insignificantly affected by a particular temperature. However, when the BB41 is adsorbed on the biochar surface, several adsorption peak bands are observed at 616, 732, 1160, 1583, 2926, and 3341 cm^{-1} . The peak at 732 cm^{-1} can be indorsed to aromatic compounds (Nasuha et al., 2010). When the BR09 is adsorbed, the peaks are observed at 595, 747, 1170, 1588, 2924, and 3349 cm^{-1} . From the FT-IR spectrum, it is clear that the biochar bounded with cationic dyes revealed the shifts in a functional group, and it is due to the transformation of various ions existent in the active sites of the surface of the adsorbent by dyes sorption. These changes indicate that functional groups on the biochar may be the potential adsorption sites for biosorption of cationic dyes.

Effect of biochar dosage

The influence of biochar dosage is shown in *Figure 6*. Biochar dose was varied from 1 to 10 g/L. From the study, it was evident that the percentage removal increases with an increase in biochar dose and a decrease in dye uptake capacity. For Instance, the removal efficiency of BB41 and BR09 increases from 83.82 to 95.71% and 92.59 to 97.84%, when the dosage increased from 1 to 10 g/L. The experimental rise in efficiency with the surge in biochar dosage could be due to the presence of diversified functional groups and surface sites of the biochar (Slimani et al., 2014). Furthermore, the dye uptake decreases on increasing the biochar dosage. For example, the sorption ability of BB41 and BR09 by groundnut shell derived biochar declined from 41.913 to 4.786 mg/g and 46.299 to 4.892 mg/g, when the biochar dosage increased from 1 to 10 g/L. At low and high sorbent dosages, the dye sorption uptake is greatly affected. Similar results were reported (Vijayaraghavan et al., 2015; Jegan et al., 2016). Comparing the % of removal and dye sorption uptake values, a dose of 2 g/L and 1 g/L, was selected as an optimal dose for BB41 and BR09 for further experiments.

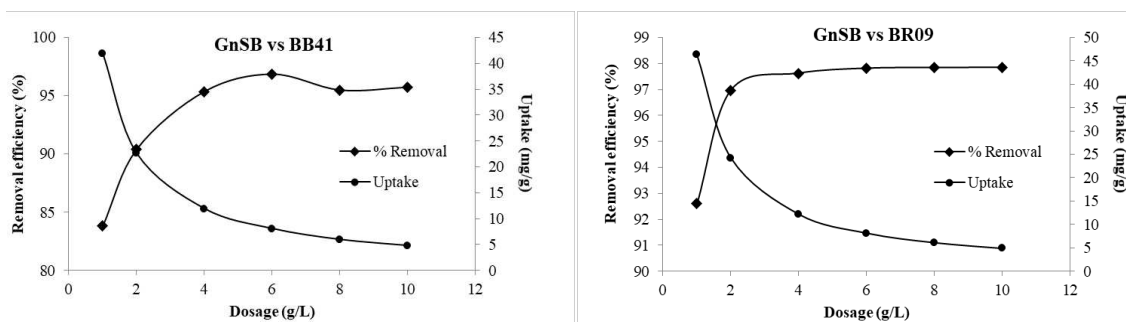


Figure 6. Effect of biochar dose on the BB41 & BR09 removal efficiency and sorption uptake capacity

Effect of pH

The pH is the vital parameter which regulates not only the sorption capacity but also the sorption efficiency. With due consideration, the experimental trials were conducted at an optimized biochar dose and desired initial dye concentration of 50 mg/L, the temperature of 35 °C by varying the pH (3-10). *Figure 7* illustrates the influence of pH on dye sorption capacity and the percentage of removal. While varying the pH from 3 to 8, the sorption uptake capacity of groundnut shell derived

biochar onto BB41 and BR09 are increased from 20.01 to 22.60 mg/g and 39.17 to 46.30. Similarly, the percentage of removal also increases from 80.06 to 90.39% and 78.34 to 92.59%, for BB41 and BR09. The initial pH value may influence to increase or decrease the uptake. The increase in the value of pH may decrease the concentration of active H⁺ ions, which simultaneously raises the negatively charged sites (Premkumar and Vijayaraghavan, 2015). Due to this negatively charged surface area, the sorption of cationic dye molecules gets increased through electrostatic forces of attraction (Santhi et al., 2016). Comparing the extent of removal and dye sorption capacity values of GnSB favored BR09 followed by BB41. However, the pH value of 8 was taken as optimal for peak performance.

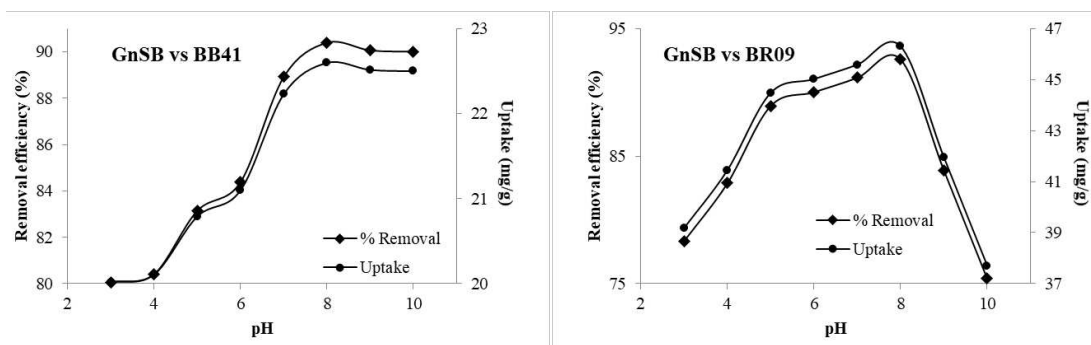


Figure 7. Effect of solution pH on the BB41 & BR09 removal efficiency and sorption uptake capacity

Effect of temperature

Figure 8 shows the effect of temperature on the removal efficiency of cationic dyes onto GnSB at different temperatures within the range of 30 to 50 °C at optimized biochar dose and pH with a fixed dye concentration of 50 mg/L were examined. The percentage of BB41 and BR09 removal by GnSB are varying from 90.40 to 80.96% and 92.60 to 77.96%. The surge in temperature accelerates the degree of diffusion of solute and thus strongly influences the uptake capacity of adsorbent towards solutes (Kankilic et al., 2016). While increasing the adsorption temperature of BB41 and BR09 adsorption indicates the fall in uptake capacity. Similar results were reported (Zeng et al., 2006). With this investigation, an ideal temperature of 35 °C has opted for the BB41 and BR09 sorption process.

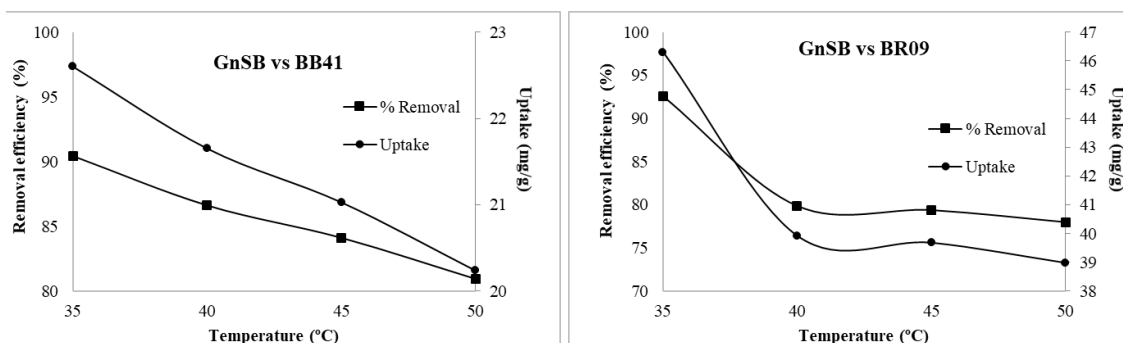


Figure 8. Effect of adsorption temperature on the BB41 & BR09 removal efficiency and sorption uptake capacity

Influence of initial dye concentration

The influence of initial dye concentration on the sorption of cationic dyes onto GnSB was experimentally carried out by varying the initial concentration from 25 to 200 mg/L for the optimized biochar dose and pH with ideal temperatures as shown in *Figure 9*. From the experiment data, it was evident that % removal of cationic dyes decreased with a surge in dye concentration. At higher concentrations, the available dye molecules in the solution do not interact with adsorbent binding sites due to the limited number of active sites that become saturated at a certain concentration (Saha et al., 2010). However, the dye sorption capacity at equilibrium condition was increased with a surge in dye concentration. This was due to the initial concentration of the cationic dye, which provides a significant driving force to overcome any mass transfer resistance of the dye between the aqueous and the solid phases (Pirbazari et al., 2014). With due consideration on all these above facts, 50 mg/L was selected as optimal for BB41 and BR09 concentration for GnSB.

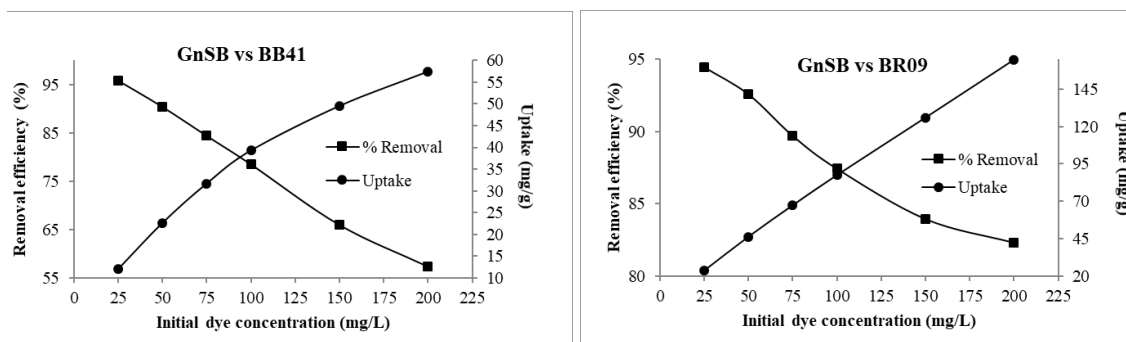


Figure 9. Effect of initial dye concentration on the BB41 & BR09 removal efficiency and sorption uptake capacity

Sorption isotherms

The analysis and design of the sorption process require the relevant adsorption equilibrium conditions, which is the most important set of information in understanding an adsorption process. Adsorption equilibrium provides fundamental physiochemical data for evaluating the applicability of the sorption process as a unit operation. By varying the initial concentration of cationic dyes of 25, 50, 75, 100, 150 200 mg/L at optimized pH value and temperature, the adsorption isotherm was determined. From the experiment data, it was seen that sorption potential improved with the increase in initial dye concentration.

To facilitate the adsorption capacities, the equilibrium adsorption models of Freundlich (1906), Langmuir (1916), Sips (1948), and Toth (1971) models were employed. Freundlich and Langmuir are the two-parameter isotherm models, and Sips and Toth are the three-parameter isotherm models used (*Table 2*). In two-parameter isotherms, the Freundlich model was found to be the best-fit isotherm data when compared to other with low correlation coefficient (<0.992) and high % error values, and it can be summarized that K_F and n_F of GnSB were in the following order: BR09 > BB41. The Sips isotherm model has shown a better prophecy of experiments with minimal error and a high correlation coefficient (>0.994) when compared to Toth

isotherm model. BR09 followed by BB41 are provided the maximum constant values for sips model when compared to others.

Sorption kinetics

The sorption kinetics of cationic dyes onto GnSB was carried out by varying the dye concentration from 25 to 200 mg/L at optimized operating parameters until the equilibrium condition attained. The experimental kinetic data indicated that the rate of dye sorption capacity was rapid during the initial hours of the contact, followed by slow attainments in equilibrium. This rapid sorption in the early hours is due to the accessibility of the free functional groups on the biochar surface and, thus, a high concentration gradient that inhibits the system (Zhu et al., 2018). In the same manner on varying initial concentrations of BB41 from 25 to 200 mg/L, equilibrium BB41 uptake capacity of groundnut shell derived biochar increased from 11.40 to 81.27 mg/g. By comparing the different cationic dyes, GnSB exhibited the highest uptake of 164 mg/g for BR09 at 200 mg/L, followed by BB41 (81.27 mg/g).

Table 2. Isotherm model parameters during adsorption of BB41 and BR09 onto groundnut shell derived biochar

Models		BB41	BR09
Langmuir	Q _{Max}	59.888	256.219
	b _L	0.110	0.045
	R ²	0.971	0.984
	% Error	0.380	0.365
Freundlich	K _F	13.838	20.019
	n _F	0.324	0.586
	R ²	0.993	0.998
	% Error	-0.054	0.021
Sips	K _S	13.168	20.251
	β _s	0.494	0.583
	a _s	0.119	0.022
	R ²	0.999	0.998
	% Error	-0.001	0.216
Toth	Q _{Max}	208.881	978.565
	b _T	1.504	0.034
	n _T	4.460	2.747
	R ²	0.996	0.953
	% Error	0.002	0.052

*Q_{max} in mg/g; b_L, b_T in L/mg; K_F in mg/g; (L/g)^{1/n_F}; K_S in (L/g)^{β_S}; a_S in (L/mg)^{β_S}

The experimental kinetics are fitted with the Pseudo first order and Pseudo second-order models. The kinetic constants, along with correlation coefficient values, are given in Table 3. The first-order model provided the best prediction with an over correlation coefficient of 0.990.

Table 3. Kinetic parameters of pseudo's model during sorption of cationic dyes onto groundnut shell derived biochar

Dye	C ₀ (mg/L)	First-order model				Second-order model			
		q _{eq} (mg/g)	K ₁ (1/min)	R ²	% error	q _{eq} (mg/g)	K ₂ (1/min)	R ²	% error
BB41	25	11.097	0.364	0.993	0.0031	11.403	0.0861	0.9951	0.001
	50	22.302	0.422	0.995	0.0044	22.873	0.0549	0.9979	0.0048
	75	30.514	0.153	0.996	0.0013	32.399	0.0079	0.9870	-0.070
	100	36.463	0.173	0.996	0.0017	38.474	0.0078	0.9907	-0.044
	150	49.626	0.288	0.996	0.0016	51.839	0.0119	0.9977	-0.066
	200	79.562	0.231	0.996	0.0037	84.368	0.0050	0.9975	-0.001
BR09	25	23.234	0.213	0.993	0.008	24.617	0.0154	0.9931	-0.002
	50	39.626	0.136	0.995	-0.008	42.802	0.0049	0.9873	-0.010
	75	67.388	0.045	0.997	0.014	76.766	0.0007	0.9922	-0.036
	100	82.582	0.104	0.994	0.028	89.996	0.0017	0.9892	-0.013
	150	125.95	0.320	0.994	0.005	129.70	0.0060	0.9958	-0.021
	200	161.11	0.261	0.998	0.005	167.17	0.0033	0.9958	-0.010

Conclusion

The following conclusions are derived from the present study:

- The biochar derived from groundnut shell biomass at 350 °C through slow pyrolysis was obtained to be the most operative biosorbent.
- The biosorption capacity of GnSB was sturdily dependent upon the biochar dosage. Experiment trials show that maximum dye sorption capacity was attained at 2 and 1 g/L of biochar dosage for BB41 and BR09 sorption.
- The solution pH sturdily influences the sorption capacity of GnSB with a pH value of 8 as an optimal condition for the efficient removal of cationic dyes.
- The SEM and FT-IR analyses exhibited the presence of various functional groups on the surfaces of GnSB.
- The sorption equilibrium was attained within 240 min, and the biosorption rate was fast. Application of BB41 and BR09 kinetics data disclosed that pseudo's first-order kinetics is better in prediction than the second-order model.
- According to the Langmuir model, the maximum biosorption capacity of BB41 and BR09 was identified as 59.888 and 256.219 mg/g for GnSB, respectively.
- From these results, it can be concluded that biochar derived from Ground Shells could be used as a practical bio-based sorbent for the removal of BB41 and BR09 molecules in wastewater.
- In the future the study may extend in the use of treated or modified biochar for wastewater treatment.

REFERENCES

- [1] Ahmadi, S., Chia, C. H., Zakaria, S., Saeedfar, K., Asim, N. (2012): Synthesis of Fe₃O₄ nanocrystals using hydrothermal approach. – Journal of Magnetism and Magnetic Materials 324: 4147-4150.

- [2] Ayawei, N., Ebelegi, A. N., Wankasi, D. (2017): Modelling and interpretation of adsorption isotherms. – *Journal of Chemistry* 2017: 1-11.
- [3] Bhagavathi Pushpa, T., Jegan, J., Praveen, S., Gokulan, R. (2019): Biodecolorization of Basic Blue 41 using EM based composts: isotherm and kinetics. – *Chemistry Select* 4(34): 10006-10012.
- [4] Charola, S., Yadav, R., Das, P., Maiti, S. (2018): Fixed-bed adsorption of Reactive Orange 84 dye onto activated carbon prepared from empty cotton flower agro-waste. – *Sustainable Environment Research* 28(6): 298-308.
- [5] De Camargo Lima Beluci, N., Mateus, G. A. P., Miyashiro, C. S., Homem, N. C., Gomes, R. G., Fagundes-Klen, M. R., Vieira, A. M. S. (2019): Hybrid treatment of coagulation/flocculation process followed by ultrafiltration in TiO₂-modified membranes to improve the removal of reactive black 5 dye. – *Science of The Total Environment* 664: 222-229.
- [6] Duc, P. A., Dharanipriya, P., Velmurugan, B. K., Shanmugavadivu, M. (2019): Groundnut shell - a beneficial bio-waste. – *Biocatalysis and Agricultural Biotechnology* 20: 101206.
- [7] Freundlich, H. M. F. (1906): Uber die Adsorption in Lösungen. – *Zeitschrift für Physikalische Chemie* 57: 385-470.
- [8] Gokulan, R., Prabhu, G. G., Jegan, J. (2019a): Remediation of complex remazol effluent using biochar derived from green seaweed biomass. – *International Journal of Phytoremediation* 21(12):1179-1189.
- [9] Gokulan, R., Raja, M. J., Jegan, J., Avinash, A. (2019b): Comparative desorption studies on remediation of remazol dyes using biochar (sorbent) derived from green marine seaweeds. – *Chemistry Select* 4(25): 7437-7445.
- [10] Gokulan, R., Ganesh, P. G., Jegan, J., Avinash, A. (2019c): A critical insight into biomass derived biosorbent for bioremediation of dyes. – *Chemistry Select* 4(33): 9762-9775.
- [11] Gokulan, R., Avinash, A., Ganesh, P. G., Jegan, J. (2019d): Remediation of remazol dyes by biochar derived from *Caulerpa scalpelliformis* - an eco-friendly approach. – *Journal of Environmental Chemical Engineering* 7(5): 103297.
- [12] Gonçalves, R. G. L., Lopes, P. A., Resende, J. A., Pinto, F. G., Tronto, J., Guerreiro, M. C., Neto, J. L. (2019): Performance of magnetite/layered double hydroxide composite for dye removal via adsorption, Fenton and photo-Fenton processes. – *Applied Clay Science* 179: 105152.
- [13] Gupta, V. K., Carrott, P. J. M., Ribeiro Carrott, Suhas, M. M. L. (2009): Low-cost adsorbents: growing approach to wastewater treatment review. – *Critical Reviews in Environmental Science and Technology* 39: 783-842.
- [14] Hua, P., Sellaoui, L., Franco, D., Netto, M. S., Luiz Dotto, G., Bajahzar, A., Li, Z. (2019): Adsorption of acid green and procion red on a magnetic geopolymer based adsorbent: experiments, characterization and theoretical treatment. – *Chemical Engineering Journal* 123113.
- [15] Jegan, J., Vijayaraghavan, J., Bhagavathi Pushpa, T., Sardhar Basha, S. J. (2016): Application of seaweeds for the removal of cationic dye from aqueous solution. – *Desalination and Water Treatment* 57(53): 25812-25821.
- [16] Kang, D., Kim, K. T., Heo, T. Y., Kwon, G., Lim, C., Park, J (2019): Inhibition of Photosynthetic Activity in Wastewater-Borne Microalgal-Bacterial Consortia under Various Light Conditions. – *Sustainability* 11: 2951.
- [17] Kankiliç, G. B., Metin, A. U., Tuzun, I. (2016): *Phragmites australis*: an alternative biosorbent for basic dye removal. – *Ecological Engineering* 86: 85-94.
- [18] Langmuir, I. (1916): The constitution and fundamental properties of solids and liquids. Part I. Solids. – *Journal of the American Chemical Society* 38(11): 2221-2295.
- [19] Liu, L., Huang, Y., Zhang, S., Gong, Y., Su, Y., Cao, J., Hu, H. (2019): Adsorption characteristics and mechanism of Pb (II) by agricultural waste-derived biochars produced from a pilot-scale pyrolysis system. – *Waste Management* 100: 287-295.

- [20] Luo, Z., Wang, E., Zheng, H., Baldock, J. A., Sun, O. J., Shao, Q. (2015): Convergent modelling of past soil organic carbon stocks but divergent projections. – *Biogeosciences* 12: 4373-4383.
- [21] Mahdi, Z., Hanandeh, A. E., Yu, Q. (2017): Date seed-derived biochar for Ni (II) removal from aqueous solutions. – *MATEC Web of Conferences* 120: 05005.
- [22] Mironyuk, I. F., Gun'ko, V. M., Vasylyeva, H. V., Goncharuk, O. V., Tatarchuk, T. R., Mandzyuk, V. I., Bezruka, N. A., Dmytrotso, T. V. (2019): Effects of enhanced clusterization of water at a surface of partially silylated nanosilica on adsorption of cations and anions from aqueous media. – *Microporous and Mesoporous Materials* 277: 95-104.
- [23] Mohammad-pajoo, E., Turcios, A. E., Cuff, G., Weichgrebe, D., Rosenwinkel, K.-H., Vedenyapina, M. D., Sharifullina, L. R. (2018): Removal of inert COD and trace metals from stabilized landfill leachate by granular activated carbon (GAC) adsorption. – *Journal of Environmental Management* 228: 189-196.
- [24] Mohebbali, S., Bastani, D., Shayesteh, H. (2019): Equilibrium, kinetic and thermodynamic studies of a low-cost biosorbent for the removal of Congo red dye: acid and CTAB acid modified celery (*Apium graveolens*). – *Journal of Molecular Structure* 1176: 181-193.
- [25] Mu, N., Alqadami, A. A., AlOthman, Z. A., Alsohaimi, I. H., Algamdi, M. S., Aldawsari, A. M. (2019): Adsorption kinetics, isotherm and reusability studies for the removal of cationic dye from aqueous medium using arginine modified activated carbon. – *Journal of Molecular Liquids* 293: 111442.
- [26] Nasuha, N., Hameed, B. H., Din, A. T. M. (2010): Rejected tea as a potential low-cost adsorbent for the removal of methylene blue. – *Journal of Hazardous Materials* 175: 126-132.
- [27] Nidheesh, P. V., Zhou, M., Oturan, M. A. (2018): An overview on the removal of synthetic dyes from water by electrochemical advanced oxidation processes. – *Chemosphere* 197: 210-227.
- [28] Nigam, P., Armour, G., Banat, I. M., Singh, D., Marchant, R. (2000): Physical removal of textile dyes and solid-state fermentation of dye adsorbed agricultural residues. – *Bioresource Technology* 72(3): 219-226.
- [29] Paz, E. C., Pinheiro, V. S., Sousa Joca, J. F., Sotana de Souza, R. A., Gentil, T. C., Lanza, M. R. V., de Oliveira, H. P. M., Pereira Neto, A. M., Gaubeur, I., Santos, M. C. (2020): Removal of Orange II (OII) dye by simulated solar photoelectro-Fenton and stability of WO_{2.72}/Vulcan XC72 gas diffusion electrode. – *Chemosphere* 239: 124670.
- [30] Pirbazari, A. E., Saberikhah, E., Badrouh, M., Emami, M. S. (2014): Alkali treated Foumanat tea waste as an efficient adsorbent for methylene blue adsorption from aqueous solution. – *Water Resources and Industry* 6: 64-80.
- [31] Premkumar, Y., Vijayaraghavan, K. (2015): Biosorption potential of coco-peat in the removal of methylene blue from aqueous solutions. – *Separation Science and Technology* 50: 1439-1446.
- [32] Ronsse, F., van Hecke, S., Dickinson, D., Prins, W. (2013): Production and characterization of slow pyrolysis biochar: influence of feedstock type and pyrolysis conditions. – *GCB Bioenergy* 5(2): 104-115.
- [33] Saha, P., Chowdhury, S., Gupta, S., Kumar, I. (2010): Insight into adsorption equilibrium, kinetics and thermodynamics of malachite green onto clayey soil of Indian origin. – *Chemical Engineering Journal* 165: 874-882.
- [34] Sahinkaya, E., Tuncman, S., Koc, I., Guner, A. R., Ciftci, S., Aygun, A., Sengul, S. (2019): Performance of a pilot-scale reverse osmosis process for water recovery from biologically-treated textile wastewater. – *Journal of Environmental Management* 249: 109382.
- [35] Sankar, C., Lokesh, D., Moholkar, V. S. (2015): Dye decolorization with hybrid advanced oxidation processes comprising sonolysis/Fenton-like/photo-ferrioxalate

- systems: a mechanistic investigation. – *Separation and Purification Technology* 156 (2): 596-607.
- [36] Santhi, T., Manonmani, S., Vasantha, V. S., Chang, Y. T. (2016): A new alternative adsorbent for the removal of cationic dyes from aqueous solution. – *Arabian Journal of Chemistry* 9(1): S466-S474.
- [37] Siddique, K., Rizwan, M., Shahid, M. J., Ali, S., Ahmad, R., Rizvi, H. (2017): Textile Wastewater Treatment Options: A Critical Review. – In: Anjum, N., Gill, S., Tuteja, N. (eds.) *Enhancing Cleanup of Environmental Pollutants* 2: 183-207.
- [38] Sips, R. (1948): On the structure of a catalyst surface. – *The Journal of Chemical Physics* 16: 490-495.
- [39] Slimani, R., Ouahabi, I. E., Abidi, F., Haddad, M. E., Regti, A., Laamari, M. R., Antri, S. E., Lazar, S. (2014): Calcined eggshells as a new biosorbent to remove basic dye from aqueous solutions: Thermodynamics, kinetics, isotherms and error analysis. – *Journal of Taiwan Institute of Chemical Engineers* 45:578-1587.
- [40] Toth, J. (1971): State equation of the solid gas interface layer. – *Acta Chimica (Academiae Scientiarum) Hungaricae* 6: 311-317.
- [41] Vijayaraghavan, J., Bhagavathi Pushpa, T., Sardhar Basha, S. J., Vijayaraghavan, K., Jegan, J. (2015): Evaluation of red marine alga *Kappaphycus alvarezii* as biosorbent for methylene blue: Isotherm, kinetic and mechanism studies. – *Separation Science and Technology* 50: 1-7.
- [42] Villar da Gama, B. M., do Nascimento, G. E., Silva Sales, D. C., Rodríguez-Díaz, M. M., de Menezes Barbosa, C. M. B., Bezerra Duarte, M. M. M. (2018): Mono and binary component adsorption of phenol and cadmium using adsorbent derived from peanut shells. – *Journal of Cleaner Production* 201: 219-228.
- [43] Wakkal, M., Khiari, B., Zagrouba, F. (2019): Textile wastewater treatment by agro-industrial waste: equilibrium modeling, thermodynamics and mass transfer mechanisms of cationic dyes adsorption onto low-cost lignocellulosic adsorbent. – *Journal of the Taiwan Institute of Chemical Engineers* 96: 439-452.
- [44] Wu, C. H., Ng, H. Y. (2008): Degradation of C. I. Reactive Red 2 (RR2) using ozone-based systems: comparisons of decolorization efficiency and power consumption. – *Journal of Hazardous Materials* 152: 120-127.
- [45] Zama, E. F., Zhu, Y. G., Reid, B. J., Sun, G. X. (2017): The role of biochar properties in influencing the sorption and desorption of Pb (II), Cd (II) and as (III) in aqueous solution. – *Journal of Cleaner Production* 148: 127-136.
- [46] Zeng, G., Zhang, C., Huang, G., Yu, J., Wang, Q., Li, J., Xi, B., Liu, H. (2006): Adsorption behavior of bisphenol A on sediments in Xiangjiang River, Central-south China. – *Chemosphere* 65: 1440-1499.
- [47] Zheng, W., Phoungthong, K., Lü, F., Shao, L. M., He, P. J. (2013): Evaluation of a classification method for biodegradable solid wastes using anaerobic degradation parameters. – *Waste Management* 33(12): 2632-2640.
- [48] Zhou, Y., Zhang, L., Cheng, Z. (2015): Removal of organic pollutants from aqueous solution using agricultural wastes: a review. – *Journal of Molecular Liquids* 212:739-762.
- [49] Zhu, Y., Yi, B., Yuan, Q., Wu, Y., Wang, M., Yan, S. (2018): Removal of methylene blue from aqueous solution by cattle manure-derived low-temperature biochar. – *RSC Advances* 8(36): 19917-19929.
- [50] Zolliger, H. (2003): *Color chemistry-syntheses, properties, and applications of organic dyes and pigments.* – Verlag Helvetica Chimica Acta, Wiley-VCH, Germany.

ARSENIC CONTENTS AND SPECIATION AT DIFFERENT GROWTH STAGES OF *SARGASSUM FUSIFORME* [HARV.] SETCHELL (HIJIKI), AN EDIBLE SEAWEED

HUANG, S. X.^{1,2} – JIANG, Q.² – DING, Y. F.² – WANG, F. J.² – ZHU, C.^{1,2*}

¹College of Life Sciences, Zhejiang University, Hangzhou 310058, China

²Key Laboratory of Marine Food Quality and Hazard Controlling Technology of Zhejiang Province, China Jiliang University, Hangzhou 310018, China

*Corresponding author
e-mail: pzhch@cjlu.edu.cn

(Received 19th Nov 2019; accepted 10th Feb 2020)

Abstract. *Sargassum fusiforme* (hijiki) is a popular edible seaweed in some Asian countries. However, it has been shown to have high concentrations of arsenic, mainly the more toxic inorganic arsenic. In this study, we determined the concentration, species, distribution, and absorption kinetics of arsenic (As), and the influence of different exogenous substances on its absorption. Arsenic content in the mature stage of *hijiki* reached up to 84.37 mg/kg dry weight. Inorganic arsenic (iAs) accounted for 68% of the total arsenic, while Arsenate (As (V)) accounted for more than 50% of total inorganic arsenic. The contents of arsenic in different *hijiki* organs decreased in the following order rhizoid > stem > leaf > airbag. Subcellular distribution of arsenic in untreated *hijiki* decreased in the order: cell walls > cell organelles > cytoplasm. In *hijiki*, arsenate had a higher absorption rate than arsenite (As (III)), with V_{max} and k_m about 2 times and 3 times those of As (III), respectively. The absorption of As (V) was inhibited by phosphorus, but was not affected by glycerol. The opposite was true in the case of As (III) adsorption. Sodium vanadate significantly increased the efflux of As (V), but had no effect on As (III). Carbonylcyanide-p-chlorophenyl hydrazone (CCCP) and glycerol inhibited the arsenite efflux, but had no influence on arsenate.

Keywords: arsenic speciation, arsenic distribution, arsenic absorption, influx, efflux

Introduction

Arsenic is a semi-metal or metalloid which is widely distributed in the environment and it is present in both terrestrial and aquatic systems (Wang et al., 2019). It is a known human carcinogen (Rosen, 2002; García Salgado et al., 2008; Carey et al., 2012). The Agency for Toxic Substances and Disease Registry (ATSDR) ranked arsenic at the top of the substance priority list (ATSDR, 2018). The toxicity of arsenic is especially associated with liver, bladder, lung, and skin cancer (Rose et al., 2007). This element occurs in various chemical forms with different toxicological characteristics in the environment and organisms (Kohlmeyer et al., 2003; Panuccio et al., 2012). Arsenic speciation in the environment is complex and includes both inorganic and organic forms. Inorganic arsenic comprises of arsenate and arsenite. Organic arsenicals include monomethylarsonic acid (MMA), dimethylarsinic acid (DMA), trimethylarsine (TMA), tetramethylarsonium ion (TMA), arsenobetaine (AsBet), arsenocholine (AsCho), and arsenosugars (Kohlmeyer et al., 2003; Quaghebeur et al., 2005). Moreover, inter-conversions between species regulated by both biotic and abiotic processes have been reported (Carey et al., 2012).

Generally speaking, inorganic arsenicals are more toxic than their organic counterparts (Nogueira et al., 2018), and arsenite is much more toxic, soluble, and

mobile than arsenate (Quaghebeur et al., 2005; Raab et al., 2007; Yang et al., 2016). Organic arsenicals such as DMA and MMA usually have lower toxicities. Therefore, determination of arsenic speciation is essential for understanding and evaluating the safety of edible organisms which accumulate arsenic.

Marine algae are usually thought of as “health food” and consumed directly as such. This is because of the nutritional and therapeutic benefits that they provide. *Sargassum fusiforme* (*hijiki*), a brown edible algae (*Phaeophyta*, *Sargassum*), is traditionally consumed by the Japanese as one of seaweed foodstuffs due to its richness in essential minerals, and dietary fibre content. The total fiber in *hijiki* was much higher compared with other seaweeds, such as *Laminaria japonica*, *Porphyra tenera*, which showed more benefits to human health especially to intestines. (Zheng et al., 2013) However, marine algae have a greater ability to accumulate arsenic and usually have higher arsenic contents than terrestrial organisms (Hanaoka et al., 2006). In terrestrial organisms, the arsenic content rarely exceeds 1 µg/g (dry weight), while it ranges from 1 to 100 µg/g in marine organisms (Ichikawa et al., 2006).

The concentration of arsenic varies in different organisms, as well as its species. In rice, the predominant inorganic arsenic is arsenite, whereas in marine algae, inorganic arsenic is present mostly as arsenate (Kohlmeyer et al., 2003). It has been reported that the arsenic species in marine organisms are usually organic arsenicals such as arsenobetaine and arsenosugars which are forms considered less toxic than the inorganic forms of arsenic (Ichikawa et al., 2010). However, there are exceptions. In *hijiki*, the concentration of iAs is up to 135 mg/kg of dry weight, while the content of inorganic arsenic may range from 50 to 80% of its total arsenic content (Almela et al., 2005; Yokoi et al., 2012). Thus, the high contents of inorganic arsenic in *hijiki* have raised serious toxicological concerns among consumers in the past decades (Wondimu et al., 2007). Indeed, the Food Inspection Agency of Canada (2001), the UK Food Standards Agency (2004), and similar institutions in other countries, have warned consumers not to eat *hijiki* (Wondimu et al., 2007; Yokoi et al., 2012).

In this study, we determined the concentration, species, distribution, and absorption kinetics of arsenic, and the influence of different exogenous substances on its absorption.

Materials and Methods

Sample preparation

The research was carried out in the year of 2016. The samples used in this research were cultivated, in Dongtou breeding base of Zhejiang Mariculture Research Institute (Dongtou County, Zhejiang Province, China), under natural conditions. In order to track the changes of arsenic content in *hijiki*, we took samples at monthly interval from January to May, that was cover the growth period of *hijiki* from seedling to maturity. There were two varieties of *hijiki* were sampled. Fresh weight of the native species (250 g of whole plant) was sampled monthly, whereas 250 g of each Korean sample (whole plant) was collected from January to March. Three separate samples were collected each time. The samples were washed in seawater, kept in plastic bags, and immediately transported to the laboratory. All samples were then washed with tap water, followed by washing three times in ultra-pure water. Thereafter, each sample was freeze-dried to a constant mass and ground to homogenous powder before use. For the

study of arsenic distribution, different organs (stem, leaf, air sac and rhizoid) were separated before freeze-drying, and then ground to homogenous powder.

Determination of total arsenic in hijiki (S. fusiforme) and different hijiki organs

Milled sample of *hijiki* (0.2 g) was added to 6 ml concentrated nitric acid. The mixture was left for 12 h, and then digested in a MARS 5 microwave oven. Each sample was digested in triplicate. The following conditions were used in the microwave digestion which was modified by Han et al. (2009): the temperature was increased to 120°C in 5 min, held for 5 min, then increased to 160°C in 5 min, kept constant for 20 min, and finally increased to 180°C for 20 min. After dilution and filtering, the digest was brought to a final volume of 25 ml with ultra-pure water. Then, total arsenic was measured using hydride generation-flame atomic absorption spectrometry (HVG-FAAS).

Determination of inorganic arsenic

The inorganic arsenic was extracted in accordance with the procedure of National Standards of China (National Food Safety standard, 2003).

Hijiki powder (1.00 g) was weighed into a 25 ml test tube, and 20 ml of 50% (v/v) hydrochloric acid was added. The mixture was kept in a water bath at 60°C for 18 h, during which time it was shaken several times in order to complete the extraction. On cooling to room temperature, the solution was filtered, and 1 ml potassium iodide (10% m/v) - thiocarbamide (5% m/v) was added to 4 ml of the filtrate. The volume of the solution was made up to 10 ml with ultra-pure water. Inorganic arsenic was determined using HVG-FAAS.

Determination of arsenic speciation

Arsenic speciation was determined using the method referred to in the manufacturer's manual of the SA-10 Atomic Fluorescence Speciation Analyzer. Each *hijiki* sample was weighed (0.5 g) and put in a test tube, 4 ml of 10% (v/v) HCl was added. Then, the sample was spun at 100 rpm in a water bath at 70°C for 1 h, and 4 ml of ultra-pure water was added. The mixture was warmed in a water bath at 70°C for 1 h, and centrifuged at 3000 rpm for 15 min. The supernatant (2 ml) was mixed with 2 ml 20% (v/v) hydrogen peroxide and put into a water bath at 70°C for 20 min. Thereafter, the mixture was filtered through a 0.45 µm filter membrane before injection into a chromatographic column. The speciation was analysed using SA-10 Atomic Fluorescence Speciation Analyzer (SA-10 AFSA). Triplicate analyses were performed for each sample.

Subcellular distribution of arsenic in hijiki

Fresh sample (0.5 g) and samples treated with 5 µmol/L and 50 µmol/L A sodium arsenate (As) for 24 h were used for subcellular distribution experiments. The samples were homogenized with precooled homogenate, and all homogenization and separation processes were carried out on ice. The total volume of homogenate and tissue was controlled at about 20 ml. The homogenate was transferred into a 50-ml centrifuge tube, and ultrasonic cell breaker was used for ultrasonic crushing. Thereafter, it was centrifuged in a high-speed freezing centrifuge for 30 sec at 300 g, and the precipitate (cell wall component) was collected. The supernatant was centrifuged in a high-speed

freezing centrifuge for 45 min at 20000 g. The bottom debris contained the cytosolic organelles, while the supernatant was the cytosolic portion containing macromolecular organic matter and inorganic ions in the cytoplasm and vacuole. Each of the portions from centrifugation was subjected to microwave digestion, and the content of arsenic was determined as described earlier.

Kinetics of arsenic uptake by hijiki

Fresh *hijiki* samples were cleaned with ultra-pure water and dried with absorbent paper. About 15-g samples of *hijiki* were weighed and put in 0.5 L artificial seawater with different concentrations of arsenate or arsenite (0, 10, 20, 40, 60 and 80 $\mu\text{mol/L}$), each of which was repeated 3 times. After 30 min of treatment, all samples were soaked in phosphate buffer solution (1 mmol/L K_2HPO_4 , 5 mmol/L MES, 0.5 mmol/L CaCl_2 , pH 6.0) for 10 min to wash off the As on the surface (Xu et al., 2007). Then, samples were washed with ultra-pure water, and the surface water was removed with absorbent paper, followed by drying. Finally, the arsenic content was determined as described earlier.

Arsenic influx and efflux in hijiki

This experiment was used to determine if arsenate and arsenite are taken up via the P and aquaporin transporters, respectively. The effect of P ($\text{K}_2\text{HPO}_4 \cdot 3\text{H}_2\text{O}$) and glycerol on arsenic influx were investigated. Shoots of the plant (about 15 g) were subjected to three treatments: control (50 $\mu\text{mol/L}$ sodium arsenate As (V) or sodium arsenite As (III) solution +100 $\mu\text{mol/L}$ P ($\text{K}_2\text{HPO}_4 \cdot 3\text{H}_2\text{O}$) or + 20 mmol/L glycerol. After treating for 1 h, the samples were immersed in 1 mmol/L K_2HPO_4 solution containing 5 mmol/L MES and 0.5 mmol/L CaCl_2 , pH 6.0, in ice bath for 10 min to wash off the surface As (Xue et al., 2012). Then, the samples were washed and dried to constant weight, and ground into powder. The arsenic content was determined after microwave digestion.

The metabolic inhibitor carbonyl cyanide m-chlorophenylhydrazone (CCCP), P-type ATPase inhibitor sodium vanadate, and glycerol were used to investigate whether the efflux of As by *hijiki* followed the same transport pathway as its influx. The samples of *hijiki* treated with 50 $\mu\text{mol/L}$ arsenate As (V) or arsenite As (III) for 24 h were soaked in 1 mmol/L K_2HPO_4 solution containing 5 mmol/L MES and 0.5 mmol/L CaCl_2 , pH 6.0, in ice bath for 10 min (Xue et al., 2012). Then the samples were cleaned and divided into 4 groups, and exposed to fresh artificial seawater with different treatments: control (artificial seawater), 1 $\mu\text{mol/L}$ CCCP, 200 $\mu\text{mol/L}$ sodium vanadate, or 10 mmol/L glycerol. After 2 hours of treatment, 25 ml water samples were taken from each group, and the arsenic content was determined after filtration with 0.45 $\mu\text{mol/L}$ microporous membrane.

Triplicate analyses were performed for each sample. The final results were expressed in mean \pm SD.

Results

Total and inorganic arsenic contents

The total and inorganic arsenic contents at different growth stages of the two *hijiki* varieties (Chinese and Korean) are shown in *Table 1*. The total arsenic concentration varied from 35.05 to 84.37 mg/kg (dry weight) at different growth stages from January

to May. With growth of the seaweed, the total arsenic concentration increased. The variation in the levels of inorganic arsenic was in accord with that of total arsenic concentration, varying from 24.21 to 58.00 mg/kg dry weight. Thus, the arsenic concentration in the two hijiki varieties increased with growth.

Table 1. Arsenic contents at different stages of growth of two *Sargassum fusiforme* varieties

Stage of growth	Native variety			Korean variety		
	t-As	i-As	% i- As	t-As	i-As	% i- As
Jan	48.72±7.98a	40.29±4.27f	82.69%	35.05±2.56d	24.21±1.89h	69.07%
Feb	56.98±7.97a	49.18±11.21fg	86.31%	38.31±4.72d	37.99±2.80fgi	99.16%
Mar	68.54±6.48b	51.30±4.55g	74.85%	56.97±3.67ae	45.44±1.14gj	79.76%
Apr	72.29±4.17b	54.08±2.21g	74.81%	ND	ND	ND
May	84.37±8.27c	58.00±0.91g	68.74%	ND	ND	ND

t-As: total arsenic. i-As: inorganic arsenic. percentage of i- As: percentage of inorganic arsenic. ND: not determined. Data are expressed in mg/kg dry weight, and are mean of triplicate assays. The final results were expressed in mean±SD

The percentage of inorganic arsenic varied from 68.74 to 86.31% in the native variety. In general, in native *hijiki*, the percentage of inorganic arsenic decreased with growth. This trend was close to those reported previously i.e. 69 to 72% (Rose et al., 2007).

Arsenic contents in different hijiki organs

The arsenic contents of different *hijiki* organs showed a lot of variation. The arsenic levels in the rhizoid, leaf, air sac and stem were 31.92, 27.23, 20.66 and 14.66 mg/kg dry weight, respectively. These results are shown in *Figure 1*.

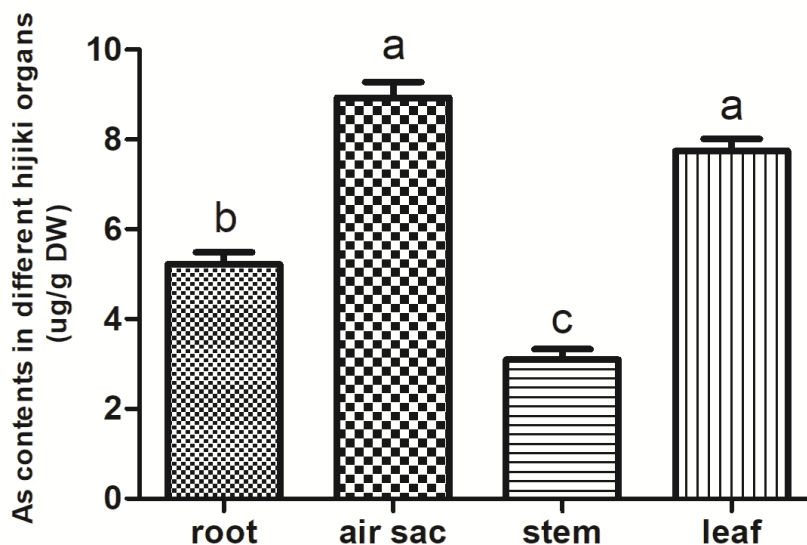


Figure 1. Arsenic contents in different organs of *Sargassum fusiforme*

Subcellular distribution of arsenic in hijiki

The subcellular distribution of arsenic in *hijiki* is shown in *Figure 2*. The results showed that the subcellular distribution and compartmentalization of arsenic in *hijiki* differed greatly. In the untreated *hijiki*, the content of arsenic decreased in the order: cell wall > organelle > cell fluid, accounting for 48, 33 and 19% of total arsenic, respectively. However, the arsenic content in each component of *hijiki* increased after 5 and 50 $\mu\text{mol/L}$ arsenic treatment. After 5 $\mu\text{mol/L}$ sodium arsenate treatment, the order of arsenic content was: cell wall > cell fluid > organelle, accounting for 53, 24 and 23% of the total, respectively. After 50 $\mu\text{mol/L}$ As treatment, the content of arsenic in each part was in the order of cell wall > cell fluid > organelle, accounting for 51, 11 and 38% of the total, respectively. The content of arsenic varied in the order of cell wall > cell fluid > organelle after treatment with 5 $\mu\text{mol/L}$ As and 50 $\mu\text{mol/L}$ As, with highest proportion of arsenic in cell wall. Moreover, the increment in arsenic level in cell wall was the largest after 5 $\mu\text{mol/L}$ As treatment, but the increment of arsenic in cell fluid was the largest after 50 $\mu\text{mol/L}$ As treatment. Thus, the increase in arsenic was mainly concentrated in the cell wall of *hijiki* under low concentration of arsenic, while the increase in arsenic was mainly concentrated in the cell fluid after treatment with high concentration of arsenic.

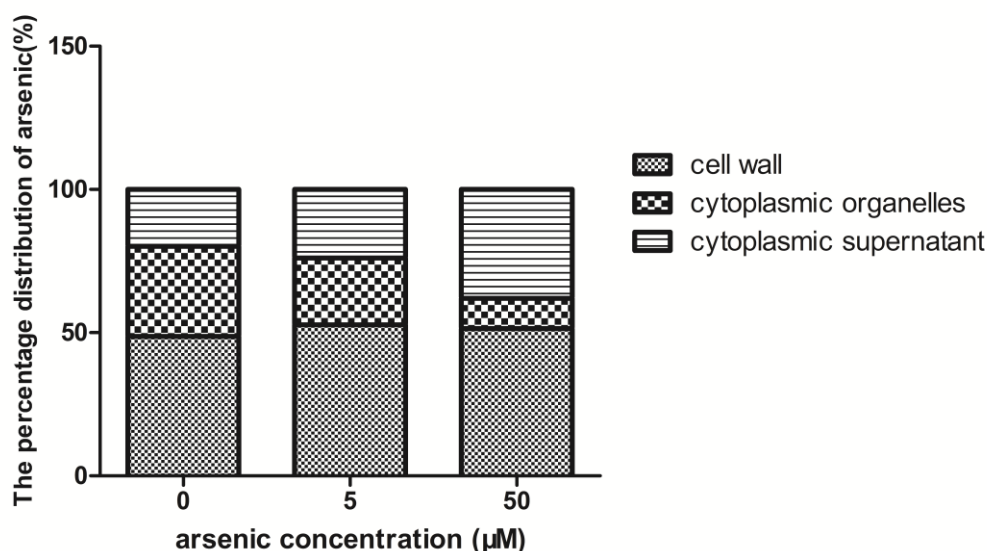


Figure 2. Subcellular distribution of arsenic in *Sargassum fusiforme*

Results of arsenic speciation analysis

The species of arsenic were determined with SA-10 Atomic Fluorescence Speciation Analyzer. The contents of arsenic species in each growth stage of the two *hijiki* are shown in *Table 2*. In this study, the extraction efficiency ranged from 75 to 90%. Irrespective of the growth stage, inorganic arsenic (especially arsenate) was always the main form of arsenic present, accounting for about 77 to 88% of the total arsenic.

The contents of four arsenic species decreased in the order: AsV > AsIII > DMA > MMA. The organic arsenic content was negligible: the DMA and MMA contents were 1 - 4% and 1 - 3% of the total arsenic, respectively.

Table 2. Contents of four arsenical species in different growth stages of the two *Sargassum fusiforme* varieties

Growth stage	t-As	As (V)	As (III)	DMA	MMA
Native					
Jan	48.72±7.98	30.06±2.10	6.21±1.32	0.68±0.05	0.22±0.01
Feb	56.98±17.97	34.23±6.59	7.2±0.48	1.24±0.12	0.34±0.07
Mar	68.54±16.48	42.46±10.13	7.78±1.09	0.49±0.10	0.21±0.08
Apr	72.29±22.17	56.92±10.52	6.25±0.74	0.92±0.09	0.26±0.09
May	84.37±8.27	67.63±8.43	7.18±1.22	1.18±0.14	1.02±0.02
Korean					
Jan	35.05±2.56	24.75±2.40	6.75±1.56	1.04±0.06	0.19±0.16
Feb	38.31±4.72	28.24±0.25	7.47±0.45	0.73±0.05	0.32±0.07
Mar	56.97±3.67	34.24±9.35	7.67±2.72	1.66±0.08	0.39±0.04

Native: native *hijiki* variety. Korean: Korean *hijiki* variety. t-As: total arsenic. As (V): arsenate. As (III): arsenite. DMA: dimethylarsinic acid. MMA: monomethylarsonic acid. Results expressed in mg/kg dry weight and as mean of triplicate assays

Kinetics of arsenic uptake

The results showed that with increase in As concentration, arsenic absorption increased gradually, and the trivalent arsenic tended to be stable when the arsenic concentration reached 20 $\mu\text{mol/L}$. The absorption of the pentavalent arsenic tended to be stable after the arsenic concentration reached 60 $\mu\text{mol/L}$ (Figure 3). The kinetics of arsenic and arsenate were in accord with the Michaelis–Menten equation, with R^2 values of 0.9744 and 0.9624 for arsenic and arsenate, respectively. The V_{max} for arsenate uptake (1202 ng/g DW min^{-1}) was about twice that of arsenic uptake (619 ng/DW min^{-1}). The K_m value of arsenate (12.91 $\mu\text{mol/L}$) was about three times that of arsenic (4.591 $\mu\text{mol/L}$).

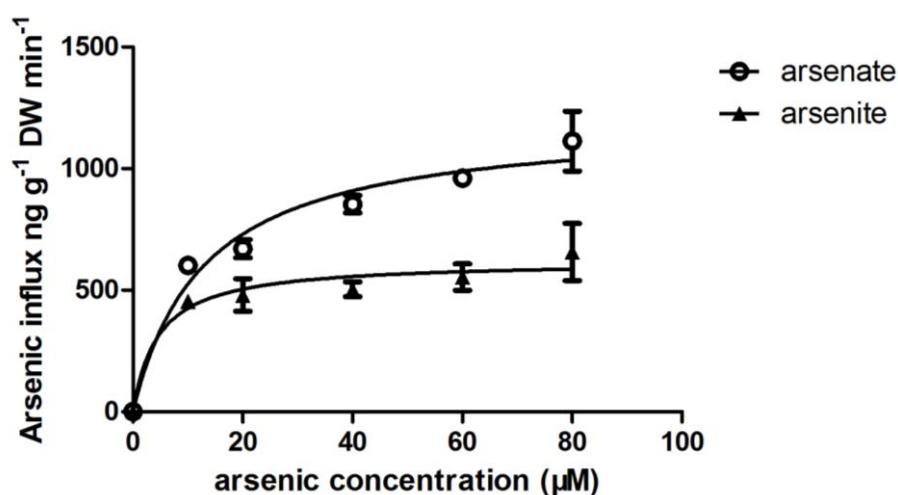


Figure 3. Concentration-dependent kinetics for arsenate (open circles) and arsenite (closed triangles) uptake in *Sargassum fusiforme*

Arsenic influx and efflux in hijiki

After treatment with 50 $\mu\text{mol/L}$ As for 1 h, the contents of arsenic and arsenate in *hijiki* were 61.8 and 39.9 $\mu\text{g/g}$ dry weight, respectively. The absorption of arsenic was significantly higher than that of arsenate, about 1.5 times higher. The absorption of arsenate was obviously inhibited by phosphorus, while arsenic was not inhibited by phosphorus. Although glycerol inhibited the absorption of arsenic, it had little effect on the absorption of arsenate (Figure 4). In the control group, the amount of arsenic in *hijiki* was slightly higher than that of arsenate. After CCCP, sodium vanadate and glycerol were added to the solution. Sodium vanadate significantly increased the efflux of arsenate, but it had no effect on the efflux of arsenic. Treatment with CCCP and glycerol inhibited the efflux of arsenic, but there was no significant difference between them, and they had little effect on the efflux of arsenate (Figure 5).

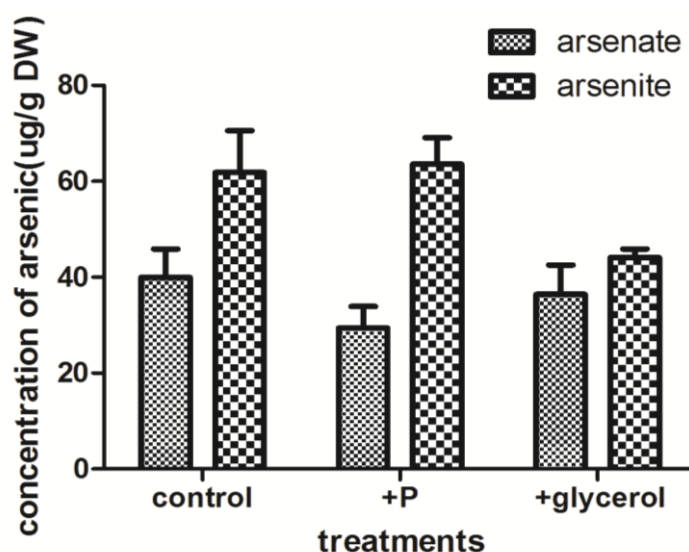


Figure 4. Influence of P (100 $\mu\text{mol/L}$) and glycerol (20 mmol/L) on the uptake of arsenate and arsenite

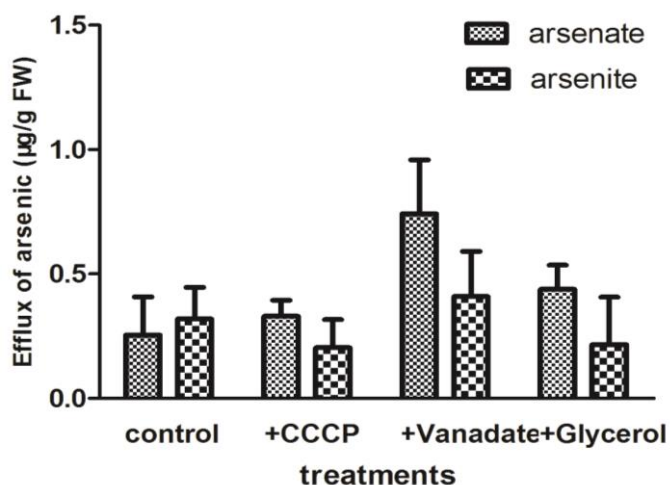


Figure 5. Effects of CCCP (1 $\mu\text{mol/L}$), sodium vanadate (200 $\mu\text{mol/L}$), and glycerol (10 mmol/L) on the efflux of arsenate and arsenite

Discussion

Several studies have reported total and inorganic arsenic contents in seaweeds. A study on a wide variety of seaweeds found that the concentrations of total arsenic varied from 2.2 to 149 mg/kg dry weight, and that the total arsenic content was related to the type of seaweed, decreasing in the order: brown seaweed > red seaweed > green seaweed (Almela et al., 2002). The arsenic contents of *hijiki* were especially high (68.3 to 149 mg/kg dry weight), as had been reported in the literature, which indicated that it could attain 179 mg/kg dry weight (Almela et al., 2002, 2006; Rose et al., 2007; Hamano-Nagaoka et al., 2008; Yokoi et al., 2012). Thus, the contents detected in the present study were high, but were still low, when compared to values reported in other studies. In the organs, the levels decreased in the order: rhizoid > leaf > air sac > stem. Since rhizoid is an inedible part of *hijiki*, this result suggests that *hijiki* with more stem and leaves than air sac should be selected.

In this research, the total arsenic content of the native *hijiki* was always higher than that of the Korean *hijiki*. These results differ from those of Ichikawa (2006), in which the ranges of total arsenic concentrations in *hijiki* gathered from the shores in Japan, South Korea, and China were 41.7- 46.7, 65.6 - 79.8, and 36.0 - 48.6 mg As/kg, respectively. Besides, arsenic concentrations in *hijiki* grown in gulfs were higher in than those in *hijiki* grown in coastline of open sea. This may have been influenced by lower pollutant concentrations and increased circulatory flow in the coastline of open sea. However, the arsenic concentrations in *hijiki* increased with growth. In this study, we also detected the arsenic content in the seawater from where the *hijiki* planted. The results showed that the content of arsenic in seawater is very low (1-7 ug/L). So we think that the arsenic contents in *hijiki* were not consistent with that in the seawater. The high content of arsenic in *hijiki* is not caused by the amount of arsenic in seawater. This may indicate that the accumulation of high arsenic content in *hijiki* was not caused by the arsenic content of seawater but by the high ability of arsenic absorption of *hijiki*.

Marine organisms have been examined extensively for arsenic species in recent decades. Marine animals contain mainly arsenobetaine, and nearly no MMA, DMA, TMA, AsCho, or TMAs (Kohlmeyer et al., 2003). Arsenosugars and arsenobetaine have been found in bivalves (Lai et al., 2001). In fish, there is hardly any inorganic arsenic or arsenosugars but trimethylarsoniopropionate has been detected in fish muscle (Francesconi et al., 2000). Many scholars have reported that the main arsenic species in *hijiki* is arsenate, and the level can reach approximately 65% of the total arsenic (Kohlmeyer et al., 2003; Raab et al., 2005; Hanaoka et al., 2006; Ichikawa et al., 2006; Hamano-Nagaoka et al., 2008). Park et al. (2019) also found that arsenate was the predominant arsenic species in *hijiki*, accounting for approximately 60% of the total arsenic content. These are similar to the results of this study, although the proportion of arsenate was greater (77 to 88%): the proportion of arsenite was between 10 to 20%. The concentration of organic arsenic was low, the DMA content being just 1 to 4% of the total arsenic present, and the MMA content was much smaller. These data are in agreement with the findings of Ichikawa et al. (2006).

In this study, after treatment with 50 $\mu\text{mol/L}$ arsenic and arsenate for 1 h, the content of arsenate in *hijiki* was higher than that of arsenic. Compared with arsenic, arsenate had higher V_{max} and smaller K_{m} value in *hijiki*, and the absorption of arsenate was higher than that of arsenic. Compared with other aquatic plants such as *Azolla caroliniana*, *Azolla filiculoides* and *Ceratophyllum demersum*, *hijiki* has higher degree of absorption and lower K_{m} value for arsenate (Xue et al., 2012). This also shows that *hijiki* has a

transport system with high affinity for arsenate. In the study of Xue et al. (2012), the V_{\max} values of arsenic and arsenate in *C. demersum* were 214 and 128 nmol/L/g DW min, respectively, which were lower than that in *hijiki*. The K_m values of arsenic and arsenate in *C. demersum* were 18 and 120 $\mu\text{mol/L}$, respectively, which were about 1.5 and 25 times, respectively higher than that of *hijiki*. Compared with *C. demersum*, *hijiki* had higher affinity for arsenic and arsenate.

Phosphorus and arsenic are homologous elements. The chemical properties of phosphate and arsenate are similar. Therefore, in higher plants, arsenate enters plants by sharing the same uptake and transport protein with phosphate (Asher and Reay, 1979). The absorption process is mainly completed by the coordinated transport of arsenate or phosphate ($\text{H}_2\text{PO}_4/\text{H}_2\text{AsO}_4^-$) and protons. The results of this study also showed that the absorption of arsenic in *hijiki* was inhibited by P in the environment, indicating that As and P share the same absorption channel in *hijiki*. Some plants can adjust the expression of phosphate transporters to reduce the absorption of arsenate, thereby adapting to the high concentration of arsenic pollution in soil (Meharg and Hartley Whitaker, 2002).

Unlike arsenate, the absorption of arsenic is not affected by phosphate. Arsenic has been shown to be able to enter the cell through water channel proteins in many plants (Meharg and Jardine, 2003; Zhao et al., 2009). Xue et al. (2012) found that the absorption of arsenate by *C. demersum* was significantly inhibited by P ($\text{K}_2\text{HPO}_4 \cdot 3\text{H}_2\text{O}$) in solution, but was not inhibited by glycerol and Sb ($\text{C}_4\text{H}_4\text{KO}_7\text{Sb} \cdot 1/2\text{H}_2\text{O}$) in solution, while the absorption of arsenic was the opposite. This also shows that the uptake of arsenate in *C. demersum* shares the same transport protein with phosphate, and arsenic can enter the cells of *C. demersum* through water channels. In this study, it was found that the absorption and efflux of arsenic in *hijiki* were inhibited by glycerol, which is consistent with the previous results for *Saccharomyces cerevisiae* and rice (Wysocki et al., 2001; Meharg and Jardine, 2003). It can also be concluded that, like other plants, arsenate is mainly transported in and out of cells by active transport, while arsenic is mainly transported in and out of cells by passive transport.

Conclusion

Overall, the results support the view that *hijiki* has a high concentration of inorganic arsenic. The dominant arsenic species in *hijiki* was found to be arsenate. To guarantee public food safety, besides warning people not to eat *hijiki*, future research into the selection of a *hijiki* variety which accumulates less arsenic, such as the Korean *hijiki* studied here, is recommended. Moreover, it is important to select a variety which has more leaves and stem instead of varieties with more air sacs. Harvesting *hijiki* a little earlier may also be a way of ensuring decreased accumulation of arsenic.

Research on the absorption and metabolism of arsenic can help in understanding of the mechanism of arsenic uptake and transport. This study lays the foundation for As control technology in *hijiki*, and is important for the safety of edible *hijiki*, and the development of *hijiki* industry. But what does the mechanism of arsenic absorption in *hijiki*? How to reduce the arsenic absorption of *hijiki*? These are all issues that need further study in the future.

Acknowledgements. This research was financially supported by the Natural Science Foundation of Zhejiang Province (LY15C020003), the 'Five-twelfth' National Science and Technology Support Program (No. 2012BAK17B03), and Natural Science Foundation of China (31101133).

REFERENCES

- [1] Agency for Toxic Substances and Disease Registry. (2018): Public health statement for arsenic.
- [2] Almela, C., Algora, S., Benito, V., Clemente, M. J., Devesa, V., Suñer, M. A., Vélez, D., Montoro, R. (2002): Heavy metals, total arsenic and inorganic arsenic contents of algae food products. – *Journal of Agricultural and Food Chemistry* 50(4): 918-923.
- [3] Almela, C., Laparra, J. M., Vélez, D., Barberá, R., Farré, R., Montoro, R. (2005): Arsenosugars in Raw and Cooked Edible Seaweed: Characterization and Bioaccessibility. – *Journal of Agricultural and Food Chemistry* 53(18): 7344-7351.
- [4] Almela, C., Clemente, M. J., Vélez, D., Montoro, R. (2006): Total arsenic, inorganic arsenic, lead and cadmium contents in edible seaweed sold in Spain. – *Food and Chemical Toxicology* 44(11): 1901-1908.
- [5] Asher, C. J., Reay, P. F. (1979): Arsenic uptake by barley seedlings. – *Functional Plant Biology* 6(4): 459-466.
- [6] Carey, A. M., Lombi, E., Donner, E., de Jonge, M. D., Punshon, T., Jackson, B. P., Guerinot, M. L., Price, A. H., Meharg, A. A. (2012): A review of recent developments in the speciation and location of arsenic and selenium in rice grain. – *Analytical and Bioanalytical Chemistry* 402(10): 3275-3286.
- [7] Francesconi, K. A., Khokiattiwong, S., Goessler, W., Pedersen, S. N., Pavkov, M. (2000): A new arsenobetaine from marine organisms identified by liquid chromatography-mass spectrometry. – *Chemical Communications* 12: 1083-1084.
- [8] García Salgado, S., Quijano Nieto, M. A., Bonilla Simón, M. M. (2008): Assessment of total arsenic and arsenic species stability in alga samples and their aqueous extracts. – *Talanta* 75: 897-903.
- [9] Hamano-Nagaoka, M., Hanaoka, K., Usui, M., Nishimura, T., Maitani, T. (2008): Nitric Acid-based Partial-digestion Method for Selective Determination of Inorganic Arsenic in Hijiki and Application to Soaked Hijiki. – *Journal of the Food Hygienic Society of Japan* 49(2): 88-94.
- [10] Han, C., Cao, X., Yu, J., Wang, X. R., Shen, Y. (2009): Determination of Trace Elements in *Sargassum Fusiforme* by Microwave Digestion with ICP-MS. – *Chinese Journal of Spectroscopy Laboratory* 26(3): 480-483.
- [11] Hanaoka, K., Yosida, K., Tamano, M., Kuroiwa, T., Kaise, T., Maeda, S. (2006): Arsenic in the prepared edible brown alga hijiki, *Hizikia fusiforme*. – *Applied Organometallic Chemistry* 15: 561-565.
- [12] Ichikawa, S., Kamoshida, M., Hanaoka, K., Hamano, M., Maitani, T., Kaise, T. (2006): Decrease of arsenic in edible brown algae *Hizikia fusiforme* by the cooking process. – *Applied Organometallic Chemistry* 20: 585-590.
- [13] Ichikawa, S., Nozawa, S., Hanaoka, K., Kaise, T. (2010): Ingestion and excretion of arsenic compounds present in edible brown algae, *Hizikia fusiforme*, by mice. – *Food and Chemical Toxicology* 48: 465-469.
- [14] Kohlmeyer, U., Jantzen, E., Kuballa, J., Jakubik, S. (2003): Benefits of high resolution IC-ICP-MS for the routine analysis of inorganic and organic arsenic species in food products of marine and terrestrial origin. – *Analytical and Bioanalytical Chemistry* 377: 6-13.
- [15] Lai, V. W. M., Cullen, W. R., Ray, S. (2001): Arsenic speciation in sea scallop gonads. – *Applied Organometallic Chemistry* 15(6): 533-538.

- [16] Meharg, A. A., Hartley-Whitaker, J. (2002): Arsenic uptake and metabolism in arsenic resistant and nonresistant plant species. – *New Phytologist* 154(1): 29-43.
- [17] Meharg, A. A., Jardine, L. (2003): Arsenite transport into paddy rice (*Oryza sativa*) roots. – *New Phytologist* 157: 39-44.
- [18] National Food Safety standard (2003): Determination of Total Arsenic and Abio-Arsenic In Foods. – GB/T 5009.11, 2003.
- [19] Nogueira, R., Melo, E. A., Figueiredo, J. L., Santosa, J. J., Nascimento Neto, A. P. (2018): Arsenic Speciation in Fish and Rice by HPLC-ICP-MS Using Salt Gradient Elution. – *Journal of Brazilian Chemical Society* 29(8): 1593-1600.
- [20] Panuccio, M. R., Logoteta, B., Beone, G. M., Cagnin, M., Cacco, G. (2012): Arsenic uptake and speciation and the effects of phosphate nutrition in hydroponically grown kikuyu grass (*Pennisetum clandestinum* Hochst). – *Environmental Science and Pollution Research* 19: 3046-3053.
- [21] Park, G. Y., Kang, D. E., Davaatseren, M. S. C., Kang, G. J., Chung, M. S. (2019): Reduction of total, organic, and inorganic arsenic content in *Hizikia fusiforme* (Hijiki). – *Food Science and Biotechnology* 28(2): 615-622.
- [22] Quaghebeur, M., Rengel, Z. (2005): Arsenic Speciation Governs Arsenic Uptake and Transport in Terrestrial Plants. – *Microchimica Acta* 151: 141-152.
- [23] Raab, A., Fecher, P., Feldmann, J. (2005): Determination of Arsenic in Algae- Results of an Interlaboratory Trial: Determination of Arsenic Species in the Water-Soluble Fraction. – *Microchimica Acta* 151: 153-166.
- [24] Raab, A., Paul, W., Meharg, A. A., Feldmann, J. (2007): Uptake and translocation of inorganic and methylated arsenic species by plants. – *Environmental Chemistry* 4(3): 197-203.
- [25] Rose, M., Lewis, J., Langford, N., Baxter, M., Origgi, S., Barber, M., Origgi, S., Barber, M., MacBain, H., Thomas, K. (2007): Arsenic in seaweed—Forms, concentration and dietary exposure. – *Food and Chemical Toxicology* 45(7): 1263-1267.
- [26] Rosen, B. P. (2002): Biochemistry of arsenic detoxification. – *FEBS Letters* 529: 86-92.
- [27] Wang, L., Gao, S., Yin, X., Yu, X., Luan, L. (2019): Arsenic accumulation, distribution and source analysis of rice in a typical growing area in north China. – *Ecotoxicology and Environmental Safety* 167: 429-434.
- [28] Wondimu, T., Ueno, A., Kanamaru, I., Yamaguchi, Y., McCrindle, R., Hanaoka, K. (2007): Temperature-dependent extraction of trace elements in edible brown alga hijiki, *Hizikia fusiforme*. – *Food Chemistry* 104: 542-550.
- [29] Wysocki, R., Chery, C. C., Wawrzycka, D., Van Hulle, M., Cornelis, R., Thevelein, J. M., Tamas, M. J. (2001): The glycerol channel Fps1p mediates the uptake of arsenite and antimonite in *Saccharomyces cerevisiae*. – *Molecular Microbiology* 40: 1391-1401.
- [30] Xu, X. Y., McGrath, S. P., Zhao, F. J. (2007): Rapid reduction of arsenate in the medium mediated by plant roots. – *New Phytol* 176: 590-599.
- [31] Xue, P., Yan, C., Sun, G., Luo, Z. (2012): Arsenic accumulation and speciation in the submerged macrophyte *Ceratophyllum demersum* L. – *Environmental Science and Pollution Research* 19: 3969-3976.
- [32] Yang, S. H., Park, J. S., Cho, M. J., Choi, H. (2016): Risk analysis of inorganic arsenic in foods. – *Journal of Food Hygiene Safety* 31(4): 227-249.
- [33] Yokoi, K., Konomi, A. (2012): Toxicity of so-called edible hijiki seaweed (*Sargassum fusiforme*) containing inorganic arsenic. – *Regulatory Toxicology and Pharmacology* 63: 291-297.
- [34] Zhao, F. J., Ma, J. F., Meharg, A. A., McGrath, S. P. (2009): Arsenic uptake and metabolism in plants. – *New Phytologist* 181: 777-794.
- [35] Zheng, T., Liu, C. C., Yang, J. Y., Liu, Q. G. (2013): Hijiki Seaweed (*Hizikia fusiformis*): Nutritional Value, Safety Concern and Arsenic Removal Method. – *Advanced Materials Research* 638(1): 1247-1252.

HIGH PREVALENCE OF *EHRlichIA CANIS* IN DOGS IN VAN, TURKEY

AYAN, A.^{1*} – ORUNC KİLİNC, O.² – ERDOĞAN, S.³ – AKYİLDİZ, G.⁴ – BİA, M. M.⁵ – LEE, D.⁵

¹*Department of Genetics, Faculty of Veterinary Medicine, Van Yuzuncu Yil University
65080 Van, Turkey*

²*Özalp Vocational School, Van Yuzuncu Yil University, 65100 Van, Turkey*

³*Department of Internal Medicine, Faculty of Veterinary Medicine, Aydın Adnan Menderes
University, 09100 Aydın, Turkey*

⁴*Genkord Health and Biotechnology Services Inc., 34212 Istanbul, Turkey*

⁵*Department of Parasitology, Parasite Research Center and Parasite Resource Bank, School of
Medicine, Chungbuk National University, Korea*

**Corresponding author*

e-mail: adnanayan@yyu.edu.tr; phone: +90-432-225-1128 / 21549

(Received 20th Nov 2019; accepted 30th Jan 2020)

Abstract. Tropical and subtropical regions have seen an alarming increase in vector-borne diseases especially tick-borne diseases. Ehrlichiosis is one of the most important vector-borne disease from a zoonotic perspective and it can be even more lethal in dogs and humans a compromised immune system. This study was conducted to determine the prevalence and molecular characterization of *E. canis* in Van province of Turkey. A total of 387 blood samples were collected from dogs in Van veterinary clinics in 2019. Extracted DNAs were run through Nested PCR using the appropriate primers. A total of 79 samples out of 387 were *E. canis* positive at 389 bp revealed by Nested PCR. Sanger method was used for DNA sequencing of two selected positive samples. Phylogenetic analysis revealed that relevant amplicon was 100% compatible with 16S RNA gene isolated from *E. canis* in many geographical regions.

Keywords: ehrlichiosis, molecular characterization, Nested PCR, phylogenetic analyses, prevalence, tick

Introduction

Tick-borne diseases in cats and dogs have seen an upward trend in recent years posing public health risks especially for those having close contact with their pets (Claerebout et al., 2013; Maia et al., 2014). Tick-borne bacterial and protozoal infections affect the dogs in many parts of the world depending on the distribution of vectors (Aktas et al., 2015). Ehrlichiosis is a zoonotic disease mentioned at the top of list and its pathogenicity becomes more lethal in immunocompromised dogs and humans (Perez et al., 2006). Ehrlichia sp. are obligate intracellular parasites infecting the blood cells. The etiologic agent of canine monocytic ehrlichiosis (CME) is *E. canis* should be resides in canine monocytes and macrophages. Depending on the immune status of the host, CME may be asymptomatic or symptomatic causing severe anemia, leukopenia, thrombocytopenia, fever, and even death especially in dogs with poor immunity (Kakoma et al., 1994; Mathew et al., 1996; Oliveira et al., 2019). Vector-borne diseases especially those involving ticks as vectors are highly prevalent in tropical and subtropical regions (Springer et al., 2019). To date, DNAs of *E. chaffeensis*, *E. ewingi*, and *E. muris* have been isolated from canine blood from South Central United States, Europe and Costa Rica

(Skotorczak, 2003; Little et al., 2010; Springer et al., 2019). In our previous study, *E. canis* was identified in the ticks collected from stray dogs in Van region of Turkey (Ayan et al., 2019). However, the prevalence and molecular characterization of *E. canis* in stray dogs were not carried out in Van province. Therefore, the present study was conducted to determine the prevalence and molecular characterization of *E. canis* in stray dogs in the Van province, Turkey so that proper strategies may be devised to control the infection.

Materials and Methods

Collection of samples

Blood samples were collected in EDTA vacutainers from 387 stray dogs presented at three veterinary clinics (Kent Veterinary Clinic (121 samples), Cetin Veterinary clinics (129 samples), and Tamara Pet Veterinary clinic (137 samples)) in central Van in 2019 as shown in *Figure 1*. Blood samples were transported to the laboratory in cold chain at -20°C for further analysis.



Figure 1. Map of Turkey showing the localities of the investigation area for collection *Ehrlichia canis* from dogs. In 2019, 387 specimens were collected from 3 veterinary clinics in Van centre in Van province of Turkey

DNA extraction

Extraction of DNA from each blood sample was carried out using Invitrogen PureLink™ Genomic DNA Mini Kit (USA, K182002) according to the procedure outlined in the kit protocol. Extracted DNAs were stored at -20°C until PCR amplification.

PCR amplification

The 16S rRNA gene region of *E. canis* was amplified using nested PCR. The first amplification primers: ECC (5' AGAACGAACGCTGGCGGCAAGC-3') and ECB (5' CGTATTACCGCGGCTGCTGGCA-3'). The second amplification primers: ECAN5 (5'- CAATTATTTATAGCCTCTGGCTATAGGA-3') and HE3 (5'- TATAGGTACCGTCATTATCTTCCCTAT-3') (Murphy et al., 1998; Alves et al., 2014;

Makino et al., 2016). For this purpose, each reaction contained 12.5 pmol forward primer, 12.5 pmol reverse primer, 0.625 U of HOT FIREPol DNA polymerase (Solis BioDyne, Tartu, Estonia), 1X PCR Buffer (Solis BioDyne, Tartu, Estonia), 1 mM MgCl₂ (Solis BioDyne, Tartu, Estonia), 120 μM dNTP (Solis BioDyne, Tartu, Estonia), extracted DNA samples (50-200 ng) and DNase/RNase Free Distilled Water (Gibco Thermo Fisher Scientific, Waltham, MA USA) were mixed to make a final volume of 25 μL. PCR was performed in Eppendorf Mastercycler® pro automatic thermal cycler. In the first stage of Nested PCR: 95°C for 15 min and 37 cycles of 95°C for 1 min and 30 seconds, annealing at 55°C for 1 min and 30 seconds and 72°C for 1 min and 30 seconds, followed by a final extension 72°C for 10 min. In the second stage of Nested PCR: 95°C for 15 min and 40 cycles of 95°C for 1 min, annealing at 65°C for 1 min and 72°C for 1 min, followed by a final extension 72°C for 10 min. The amplified products were separated on a 1.5% agarose gel and visualized by Safe-T stain (BioShop, Canada) staining under imaging system (Syngene Bio Imaging System).

DNA sequencing and phylogenetic analysis

Two positive samples, confirmed by PCR, were selected at random and DNA (forward and reverse) sequence was determined according to the Sanger sequencing method. Forward and reverse sequences of each sample were compared using the Bioedit Sequence Alignment Editor Program (Hall, 1999). Finally, the resulting DNA sequences were compared with the similar sequences in NCBI database using BLAST. The evolutionary history was inferred by using the Maximum Likelihood method based on the Kimura 2-parameter model (Kimura, 1980). The tree with the highest log likelihood (-951,11) is shown. The percentage of trees in which the associated taxa clustered together is shown next to the branches. Initial tree(s) for the heuristic search were obtained automatically by applying Neighbor-Join and BioNJ algorithms to a matrix of pairwise distances estimated using the Maximum Composite Likelihood (MCL) approach, and then selecting the topology with superior log likelihood value. A discrete Gamma distribution was used to model evolutionary rate differences among sites (5 categories (+G, parameter = 0,1908)). The tree is drawn to scale, with branch lengths measured in the number of substitutions per site. The analysis involved 15 nucleotide sequences. All positions containing gaps and missing data were eliminated. There were a total of 362 positions in the final dataset.

Evolutionary analyses were conducted in MEGA X (Kumar et al., 2018).

Ethical considerations

All the procedures involved in the study were approved by the local ethics committee of Van Yuzuncu Yil University, Van, Turkey vide letter no. VAN YUHADYEK/2019/10 dated 31 October 2019.

Results

In the first stage of nested PCR, *Ehrlichia* spp. specific bands of 458 bp were obtained. Nested PCR revealed that *E. canis* specific 389 bp bands were obtained in 79 of 387 samples. Agarose gel images for amplicons of each samples in the PCR shows in *Figure 2*.

The results showed that a 20.41% positivity of *E. canis* detected in Van province. Two of the 79 samples were randomly selected for sequence analysis. The DNA sequences

obtained from Sanger sequencing were 100% compatible with the *E. canis* specific 16S rRNA gene in NCBI database. The sequences of two positive samples obtained from Bioedit Sequence Allignment Editor program were 359 bp and 367 bp, respectively. The tree with the highest log likelihood (-943.20) is shown. The percentage of trees in which the associated taxa clustered together is shown next to the branches. Initial tree(s) for the heuristic search were obtained automatically by applying Neighbor-Join and BioNJ algorithms to a matrix of pairwise distances estimated using the Maximum Composite Likelihood (MCL) approach, and then selecting the topology with superior log likelihood value. The tree is drawn to scale, with branch lengths measured in the number of substitutions per site. The analysis involved 16 nucleotide sequences. All positions containing gaps and missing data were eliminated. There were a total of 357 positions in the final dataset. Phylogenetic analysis of *E. canis* in dogs from Van province of Tukey showed that there were no genetic differences between the two samples based on the relevant amplicons as shown in *Figure 3*.

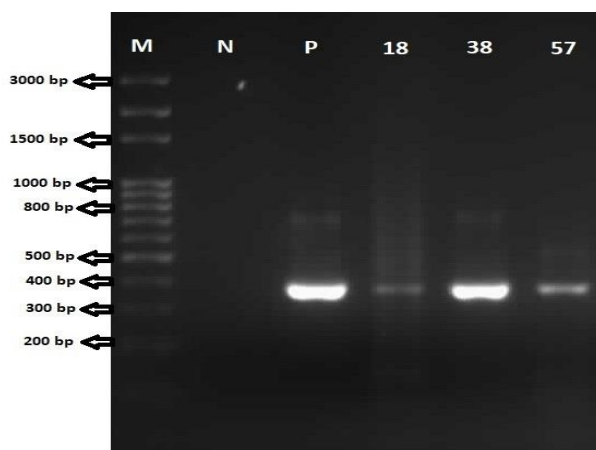


Figure 2. Agarose gel images for amplicons of each samples in the PCR. (M: Marker, P: Positive control, 18, 38, 57: Positive samples)

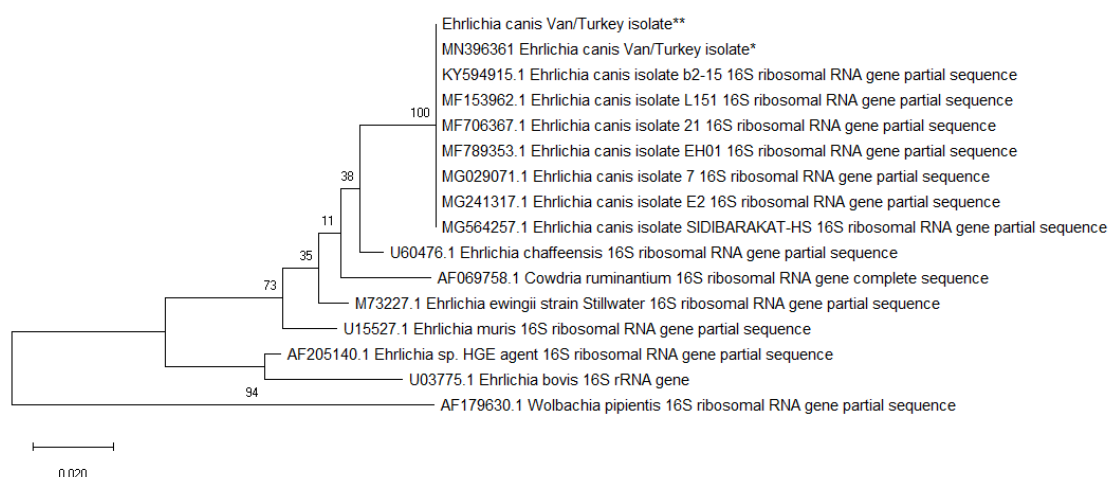


Figure 3. Molecular Phylogenetic analysis by Maximum Likelihood method of 16S rRNA gene of *E. canis*. Two samples (*: MN396361 *Ehrlichia canis* Van/Turkey isolate, **: *Ehrlichia canis* Van/Turkey isolate) in the same node as seen in the tree

Discussion

Tick-borne diseases, a cosmopolitan problem resulting in subclinical or severe infections in their hosts, are increasingly affecting the public and animal health around the globe (Hofmann-Lehmann et al., 2016). Zoonotic importance of canine tick-borne pathogens has increased in the recent years as dogs play a major role as reservoir host, Ehrlichiosis being one of those diseases (Ozubek et al., 2018). In the present study, the prevalence of *E. canis* in dogs in Van province was investigated on a molecular basis. At the end of the study, *E. canis* DNA was detected in 79 (20.41%) of 387 blood samples collected. This is the first report that describes the molecular detection of Ehrlichiosis in dog populations in Van, Turkey. Previous studies have reported the prevalence of *E. canis* in dogs in different parts of Turkey and the world alike, including some reports investigated the prevalence based on molecular studies. According to the molecular studies conducted in Turkey, the prevalence of *E. canis* 23 out of 219 blood samples in Diyarbakır was (10.5%) (Ozubek et al., 2018), *E. canis* was not detected in 133 samples from Konya (Guo et al., 2017), 58 out of 400 blood samples in Kayseri was (14.5%) (Duzlu et al., 2014), 37 out of 757 samples collected from different provinces (Elazığ, Diyarbakır, Erzurum, Ankara, Nevşehir, Adapazarı, İzmit, Mersin, Giresun, İzmir) was 4.9% (Aktas et al., 2015), 47 out of 400 blood samples in Thrace was 11.75% (Cetinkaya et al., 2016), 3 out of 12 dogs with clinical symptoms in Ankara (Unver et al., 2005). Similarly, Hofmann-Lehmann et al. (2016) reported that 14 out of 249 blood samples collected from Sicily (Italy) and Portugal were *Anaplasma platys* and *E. canis* positive whereas the DNA of *E. canis* was not detected in samples from Switzerland, Spain, and Terasa and Bologna regions of Italy. In addition, Cardoso et al. (2016) reported *E. canis* in 5.8% of 103 blood samples in Luanda region of Angola and Alho et al. (2017) found *E. canis* in 3.1% of 64 blood samples in Qatar. In contrast, *E. canis* DNA was not found in 97 blood samples collected from Iraq (Otranto et al., 2019). In this study, Ehrlichia infection in Van, Turkey was found to be 20.41% prevalent that is high. There may be different reasons underlying the high prevalence of related infections in the region. Inadequate external parasite spraying in dogs and the presence of *R. sanguineus* in the region can be considered as the main reasons for the high prevalence of Ehrlichiosis. The importance of this disease is increasing all over the world including Turkey. It is noteworthy that global warming, environmental and ecological changes, and the existence of appropriate habitats increase the impact of ticks that results in frequent emergence and re-emergence of tick-borne diseases of zoonotic importance (Inci et al., 2016).

Vector hemoparasites can be diagnosed by examining the clinical signs and blood staining methods, however, diagnostic may arise attributed to the similarities in symptoms and microscopic structures of the etiologic agents. Consequently, test based on serological and molecular techniques should be preferred in order to diagnose the hemoparasites. Nonetheless, it becomes difficult to extricate between current and previous exposure to pathogens that might result in false negative results in case of acute ehrlichiosis. Therefore, diagnosis based on molecular tests is the best option (Neer et al., 1998; Little et al., 2010; Aktas et al., 2015; Springer et al., 2019). The most common method used to diagnose ehrlichiosis is one-step PCR analysis to amplify the 16S rRNA gene region, however, its sensitivity is low. Therefore, diagnosis through Nested PCR increases the sensitivity and is more reliable (Bulla et al., 2004; Macieira et al., 2005; Nakaghi et al., 2008; Santos et al., 2009). However, non-specific amplification among the strains of Ehrlichia species due to highly conserved 16S rRNA gene and higher risk of DNA cross-contamination are inevitable in this method (Labruna et al., 2007).

Consequently, the sequencing and phylogenetic analyses are important so as to prove the accuracy of the results in addition to identify the molecular similarity among the species (Sumner et al., 2000).

E. canis, a proteobacter that causes ehrlichiosis, possess a 16S rRNA gene consisting of 1380 bp in size. In our study, we identified and amplified a gene of 390 bp in size that is repeatedly employed in the molecular diagnosis of *E. canis*. The DNA sequence analysis of the region revealed the identification of a subtype of *E. canis* that is distributed in different geographical regions. The DNA sequence analysis of our *E. canis* DNA samples showed 100% similarities with those of NCBI database isolated from *E. canis* in different geographies such as Elazığ/Turkey (Accession number: KY594915), Panama (Accession number: MF789353), Egypt (Accession number: MG564257), Romania (Accession number: MG241317), India (Accession number: MF706367), Mexico (Accession number: MG029071), and Brazil (Accession number: MF153962). All genomic analysis is possible using new generation sequencing technologies along with the identification of new or unknown subtypes of proteobacter *E. canis*.

Conclusion

In conclusion, this molecular study confirmed the presence and prevalence of *E. canis* in dogs in Van province of Turkey. This shows that Ehrlichiosis in dogs in this region may pose threats to public health especially in immunocompromised people. We believe that the density of dog population and lack of effective control of ticks especially in stray dogs are the possible predisposing factors for this high prevalence of ehrlichiosis in dogs in Van, Turkey. In order to determine the zoonotic potential of ehrlichiosis, it is necessary to compare the genetic factors and genetic proximity of ehrlichiosis in humans with that of dogs. As the tick-borne diseases are increasing around the globe, we believe that the control of ticks in domestic animal and effective treatment of animals infested with ticks will be key to preventing tick-borne diseases. Since the Van province shares its border with Iran, ticks and tick-borne diseases in this region have potential to create an international problem. In addition, changing climatic conditions and human migration have created variability especially in vectors of vector-borne diseases. Therefore, further studies in this area should not only focus *R. sanguineus*, but also other tick species by molecular methods. In addition, scientists in the countries sharing the border in the region should carry out joint and collaborative studies especially in terms of vector diseases and the molecular proximity of the agents should be demonstrated.

REFERENCES

- [1] Aktas, M., Özübek, S., Altay, K., Sayin Ipek, N. D., Balkaya, İ., Utuk, A. E., Kirbas, A., Şimsek, S., Dumanlı, N. (2015): Molecular detection of tick-borne rickettsial and protozoan pathogens in domestic dogs from Turkey. – *Parasites & Vectors* 8: 157.
- [2] Alho, A. M., Lima, C., Latrofa, M. S., Colella, V., Ravagnan, S., Capelli, G., Carvalho, L. M., Cardoso, L., Otranto, D. (2017): Molecular detection of vector-borne pathogens in dogs and cats from Qatar. – *Parasites & Vectors* 10: 298.
- [3] Alves, R. N., Rieck, S. E., Ueira-Vieira, C., Labruna, M. B., Beletti, M. E. (2014): Isolation, in vitro propagation, genetic analysis, and immunogenic characterization of an *Ehrlichia canis* strain from southeastern Brazil. – *Journal of Veterinary Science* 15(2): 241-8.

- [4] Ayan, A., Alic Ural, D., Erdogan, H., Orunc Kilinc, O., Gültekin, M., Ural, K. (2019): Prevalance and Molecular Characterization of *Giardia duodenalis* in Livestock in Van, Turkey. – International Journal of Ecosystems and Ecology Science 9(2): 289-296.
- [5] Bulla, C., Takahira, R. K., Araújo, J. P., Trinca, L. A., Lopes, R. S., Wiedmeyer, C. E. (2004): The relationship between the degree of thrombocytopenia and infection with *Ehrlichia canis* in an endemic area. – Veterinary Research 35(1): 141-146.
- [6] Cardoso, L., Oliveira, A. C., Granada, S., Nachum-Biala, Y., Gilad, M., Lopes, A. P., Sousa, S. R., Vilhena, H., Baneth, G., (2016): Molecular investigation of tick-borne pathogens in dogs from Luanda, Angola. – Parasites & Vectors 9: 252.
- [7] Cetinkaya, H., Matur, E., Akyazi, I., Ekiz, E. E., Aydin, L., Toparlak, M. (2016): Serological and molecular investigation of Ehrlichia spp. and Anaplasma spp. in ticks and blood of dogs, in the Thrace Region of Turkey. – Ticks and Tick-borne Diseases 7(5): 706-714.
- [8] Claerebout, E., Losson, B., Cochez, C., Casaert, S., Dalemans, A. C., De Cat, A., Madder, M., Saegerman, C., Heyman, P., Lempereur, L. (2013): Ticks and associated pathogens collected from dogs and cats in Belgium. – Parasites & Vectors 6: 183.
- [9] Duzlu, O., Inci, A., Yildirim, A., Onder, Z., Ciloglu, A. (2014): The investigation of some tick-borne protozoon and rickettsial infections in dogs by Real Time PCR and the molecular characterizations of the detected isolates. – Ankara Üniversitesi Veteriner Fakültesi Dergisi 61: 275-282.
- [10] Guo, H., Sevinc, F., Ceylan, O., Sevinc, M., Ince, E., Gao, Y., Moumouni, P. F. A., Liu, M., Efstratiou, A., Wang, G., Cao, S., Zhou, M., Jirapattharasate, C., Ringo, A. E., Zehng, W., Cao, S. (2017): A PCR survey of vector-borne pathogens in different dog populations from Turkey. – Acta Parasitologica 62(3): 533-540.
- [11] Hall, T. A. (1999): BioEdit: a user-friendly biological sequence alignment editor and analysis program for Windows 95/98/NT. – Nucleic Acids Symposium Series 41: 95-98.
- [12] Hofmann-Lehmann, R., Wagmann, N., Meli, M. L., Riond, B., Novacco, M., Joekel, D., Gentilini, F., Marsilio, F., Pennisi, M. G., Lloret, A., Carrapiço, T., Boretti, F. S. (2016): Detection of “*Candidatus Neoehrlichia mikurensis*” and other Anaplasmataceae and Rickettsiaceae in Canidae in Switzerland and Mediterranean countries. – Schweiz Arch Tierheilkd 158: 691-700.
- [13] Inci, A., Yildirim, A., Onder, O., Doganay, M., Aksoy, S. (2016): Tick-Borne Diseases in Turkey: A Review Based on One Health Perspective. – PLOS Neglected Tropical Diseases 10(12): e0005021.
- [14] Kakoma, I., Hansen, R. D., Anderson, B. E., Hanley, T. A., Sims, K. G., Liu, L., Bellamy, C., Long, M. T., Baek, B. K. (1994): Cultural, molecular and immunological characterization of the etiologic agent for atypical canine ehrlichiosis. – Journal of Clinical Microbiology 32: 170-175.
- [15] Kimura, M. (1980): A simple method for estimating evolutionary rate of base substitutions through comparative studies of nucleotide sequences. – Journal of Molecular Evolution 16: 111-120.
- [16] Kumar, S., Stecher, G., Li, M., Knyaz, C., Tamura, K. (2018): MEGA X: Molecular Evolutionary Genetics Analysis across computing platforms. – Molecular Biology and Evolution 35: 1547-1549.
- [17] Labruna, M. B., McBride, J. W., Camargo, L. M., Aguiar, D. M., Yabsley, M. J., Davidson, W. R., Stromdahl, E. Y., Williamson, P. C., Stich, R. W., Long, S. W., Camargo, E. P., Walker, D. H. (2007): A preliminary investigation of Ehrlichia species in ticks, humans, dogs, and capybaras from Brazil. – Veterinary Parasitology 143(2): 189-95.
- [18] Little, S. E., O’Connor, T. P., Hempstead, J., Saucier, J., Reichard, M. V., Meinkoth, K., Meinkoth, J. H., Andrews, B., Ullom, S., Ewing, S. A., Chandrashekar, R. (2010): *Ehrlichia ewingii* infection and exposure rates in dogs from the southcentral United States. – Veterinary Parasitology 172: 355-360.

- [19] Macieira, D. B., Messick, J. B., Cerqueira, A. M., Freire, I. M., Linhares, G. F., Almeida, N. K., Almosny, N. R. (2005): Prevalence of *Ehrlichia canis* infection in thrombocytopenic dogs from Rio de Janeiro, Brazil. – *Veterinary Clinical Pathology* 34(1): 44-48.
- [20] Maia, C., Ferreira, A., Nunes, M., Vieira, M. L., Campino, L., Cardoso, L. (2014): Molecular detection of bacterial and parasitic pathogens in hard ticks from Portugal. – *Ticks and Tick-borne Diseases* 5: 409-14.
- [21] Makino, H., Sousa, V. R. F., Fujimori, M., Rodrigues, J. Y., Dias, A. F. L. R., Dutra, V., Nakazato, L., de Almeida, A. B. P. F. (2016): *Ehrlichia canis* detection in dogs from Várzea Grande: a comparative analysis of blood and bone marrow samples. – *Ciência Rural* 46(2): 310-314.
- [22] Mathew, J. S., Ewing, S. A., Barker, R. W., Fox, J. C., Dawson, J. E., Warner, C. K., Murphy, G. L., Kocan, K. M. (1996): Attempted transmission of *Ehrlichia canis* by *Rhipicephalus sanguineus* after passage in cell culture. – *American Journal of Veterinary Research* 57: 1594-1598.
- [23] Murphy, G. L., Ewing, S. A., Whitworth, L. C., Fox, J. C., Kocan, A. A. (1998): A molecular and serologic survey of *Ehrlichia canis*, *Ehrlichia chaffeensis* and *E. ewingii* in dogs and ticks from Oklahoma. – *Veterinary Parasitology* 79(4): 325-339.
- [24] Nakaghi, A. C. H., Machado, R. Z., Costa, M. T., André, M. R., Baldani, C. D. (2008): Canine ehrlichiosis: Clinical, hematological, serological and molecular aspects. – *Ciencia Rural* 38(3): 766-770.
- [25] Neer, T. (1998): Canine Monocytic and Granulocytic Ehrlichiosis. – In: Greene, C. E. (ed.) *Infectious diseases of the dog and cat*. 2nd ed. Philadelphia, USA: WB Saunders; 1998. pp. 139-147.
- [26] Oliveira, B. C. M., Ferrari, E. D., Viol, M. A., André, M. R., Machado, R. Z., de Aquino, M. C. C., Inácio, S. V., Gomes, J. F., Guerrero, F. D., Bresciani, K. D. S. (2019): Prevalence of *Ehrlichia canis* (Rickettsiales: Ehrlichieae) DNA in Tissues From *Rhipicephalus sanguineus* (Acari: Ixodidae) Ticks in Areas Endemic for Canine Monocytic Ehrlichiosis in Brazil. – *Journal of Medical Entomology* 56(3): 828-831.
- [27] Otranto, D., Iatta, R., Baneth, G., Cavalera, A. M., Bianco, A., Parisi, A., Dantas-Torres, F., Colella, V., McMillan-Cole, A. C., Chomel, B. (2019): High prevalence of vector-borne pathogens in domestic and wild carnivores in Iraq. – *Acta Tropica* 197: 105058.
- [28] Ozubek, S., Ipek, D. N. S., Aktas, M. (2018): A molecular survey of rickettsias in shelter dogs and distribution of *Rhipicephalus sanguineus* (Acari: Ixodidae) sensu lato in Southeast Turkey. – *Journal of Medical Entomology* 55(2): 459-463.
- [29] Perez, M., Bodor, M., Zhang, C., Xiong, Q., Rikihisa, Y. (2006): Human infection with *Ehrlichia canis* accompanied by clinical signs in Venezuela. – *Annals of the New York Academy of Sciences* 1078: 110-117.
- [30] Santos, F., Coppede, J. S., Pereira, A. L. A., Oliveira, L. P., Roberto, P. G., Benedetti, R. B. R., Zucoloto, L. B., Lucas, F., Sobreira, L. (2009): Molecular evaluation of the incidence of *Ehrlichia canis*, *Anaplasma platys* and *Babesia* spp. in dogs from Ribeirão Preto, Brazil. – *The Veterinary Journal* 179(1): 145-148.
- [31] Skotorzak, B. (2003): Canine ehrlichiosis. – *Ann Agric Environ Med* 10: 137-141.
- [32] Springer, A., Montenegro, V. M., Schicht, S., Vrohvec, M. G., Pantchev, N., Balzer, J., Strube, C. (2019): Seroprevalence and Current Infections of Canine Vector-Borne Diseases in Costa Rica. – *Frontiers in Veterinary Science* 6: 164.
- [33] Sumner, J. W., Storch, G. A., Buller, R. S., Liddell, A. M., Stockham, S. L., Rikihisa, Y., Messenger, S., Paddock, C. D. (2000): PCR Amplification and Phylogenetic Analysis of groESL Operon Sequences from *Ehrlichia ewingii* and *Ehrlichia muris*. – *Journal of Clinical Microbiology* 38(7): 2746-2749.
- [34] Unver, A., Rikihisa, Y., Borku, K., Ozkanlar, Y., Hanedan, B. (2005): Molecular detection and characterization of *Ehrlichia canis* from dogs in Turkey. – *Berliner und Münchener tierärztliche Wochenschrift* 118(7-8): 300-304.

STOICHIOMETRIC CHARACTERISTICS AND DRIVING MECHANISMS OF PLANTS IN KARST AREAS OF ROCKY DESERTIFICATION OF SOUTHERN CHINA

ZHANG, Y. – XIONG, K. N.* – YU, Y. H. – YANG, S. – LIU, H. Y.

School of Karst Science, Guizhou Normal University/State Engineering Technology Institute for Karst Desertification Control, No. 116 Baoshan North Road, Yunyan District, Guiyang City, Guizhou Province 550001, China

**Corresponding author
e-mail: hxcandzy@163.com*

(Received 20th Nov 2019; accepted 12th Feb 2020)

Abstract. In this study, we selected karst areas of rocky desertification in southern China as a subject analyze the nutrient transport patterns of the plant–litter–soil continuum and the effect of soil environmental factors on plant stoichiometry in two areas: potential-mild and moderate-severe rocky desertification. The results show that (1) the carbon (C), nitrogen (N), and phosphorus (P) contents of plant leaves in karst areas are higher than those of litter or soil; (2) the plant leaves have a high C storage capacity, P sufficiency, and N deficiency; and (3) the Monte Carlo test of eight soil environmental factors showed that the influences of soil environmental factors on plant stoichiometry vary with the level of rocky desertification. In the area of potential-mild rocky desertification, soil pH, TP, C:P, and SOC were the main driving factors. In the area of moderate-severe rocky desertification, soil TP, TP, C:N, and SWC were the primary driving factors. The comprehensive analysis can provide a theoretical basis for nutrient transport and soil environmental factor regulation in areas with different levels of rocky desertification. It is necessary to target the primary factors for fertilization management and nutrient transport protection in future rock desertification control.

Keywords: *ecosystem, rocky desertification degree, nutrient cycling, environmental factor*

Introduction

The karst region in southern China, centered in Guizhou, is one of the three continuous karst distribution centers in the world and one of China's four ecologically fragile areas, making it the nation's key ecological development hinterland and poverty alleviation core area (LeGrand, 1973; Sheng et al., 2015; Wang et al., 2016a; Wang et al., 2016b). The karst rocky desertification ecosystem has low environmental capacity and poor anti-interference ability and is thus vulnerable to disruptions in ecological security and regional economic and social development (Xiong et al., 2016). Since the 1990s, a large number of vegetation restoration projects have been carried out in the region to promote the comprehensive management of rocky desertification, but the artificial vegetation ecosystem constructed is monotonous in structure and poor in stability, making it ill equipped to mitigate the ecological problems caused by the ecological environment with its shallow and noncontinuous soil layer and poor water conservation capacity (Zeng et al., 2015). Under intensive interference by human activities, natural secondary forests dominated by viny and thorny shrubs and scrub-grassland were formed (Zhong et al., 2018). Therefore, vegetation restoration and reconstruction are a necessary measure for the control of karst rock desertification.

Ecological stoichiometry is a discipline that studies the balance between important elements, such as carbon (C), nitrogen (N), and phosphorus (P), in ecosystem interactions (Zhao et al., 2019). Plant stoichiometric characteristics can characterize the plant's ability

to maintain internal stoichiometric stability while reflecting its adaptability to environmental changes (Sterner and Elser, 2002; Elser et al., 2010). In this way, they can provide the basis for the equilibriums of energy and chemical elements of the ecosystem as well as the structure and function of the ecosystem and soil nutritional diagnosis (Elser et al., 2000; Zhao et al., 2016). In the past, the characterization of stoichiometric characteristics has been focused on individual components of the ecosystem (e.g., soil, vegetation, or litter) or plant organs (plant leaves or fine roots, etc.) (Pena-Claros, 2003; Wu et al., 2010; Wang et al., 2011). Some other studies only examined the differences in stoichiometric characteristics and their intraspecies variation in different succession stages and during seasonal changes. These studies demonstrated that the stoichiometric characteristics of C, N, and P of plant leaves vary with vegetation type, functional group, and species (Sterner and Elser, 2002; Agren, 2004; Reich, 2003), but they rarely addressed the comprehensive situation of the community composed of trees, shrubs, and grasses and thus failed to integrate ecosystem components or comprehensively characterize the stoichiometric characteristics by taking into account environmental factors (Hu et al., 2014; Cao et al., 2015).

Soil is an important factor of terrestrial ecosystems (Gusewell, 2004). To examine the variation characteristics of nutrient elements, it is necessary to thoroughly investigate the conversions between the nutrient return from litter decomposition, soil nutrient supply, and plant nutrient demand in different environments (Xiang et al., 2015). Soil environmental factors not only provide plant nutrients but also catalyze and regulate the process of litter decomposition, thereby sensitively reflecting the direction and intensity of the driving mechanism of nutrients in different karst areas of rocky desertification. Currently, the nutrient element transfer and its regulation mechanism in karst areas with different levels of rocky desertification have rarely been addressed, and there has been no study on the soil environmental factors that drive the plant stoichiometry (including leaf stoichiometry and litter stoichiometry), making it difficult to systematically reveal the coupling mechanism between plants and the environment. Therefore, it is necessary to conduct an in-depth stoichiometric study that takes plants and soil as a whole (Du et al., 2016, 2017).

In this study, our aims were to: (1) examined vegetation, litter, and soil as a whole system and investigated the stoichiometric characteristics of karst areas. (2) Describe the elemental circulation and balance mechanism of the soil–litter–vegetation continuum in environments with different levels of rocky desertification. (3) Revealed the synergistic driving effect of soil environmental factors on the stoichiometric characteristics of plant leaves and litter. Our findings are conducive to strengthening the management and protection of the ecological environment in areas of rocky desertification and provide a theoretical basis for the management of vegetation restoration and reconstruction in karst areas of rocky desertification.

Materials and methods

Overview of the study area

The Salaxi Rocky Desertification Comprehensive Management Demonstration Area of Bijie and the Guanling-Zhenfenghuajiang Rocky Desertification Comprehensive Management Demonstration Area (*Fig. 1*) are the two most representative areas of rocky desertification in Guizhou Province of southwest China, with diverse rocky desertification levels and typical rocky desertification status. These were selected as the

study area. Both demonstration areas have been used as special study cases for the comprehensive control of rocky desertification of Guizhou Province from 1995 to 2019.

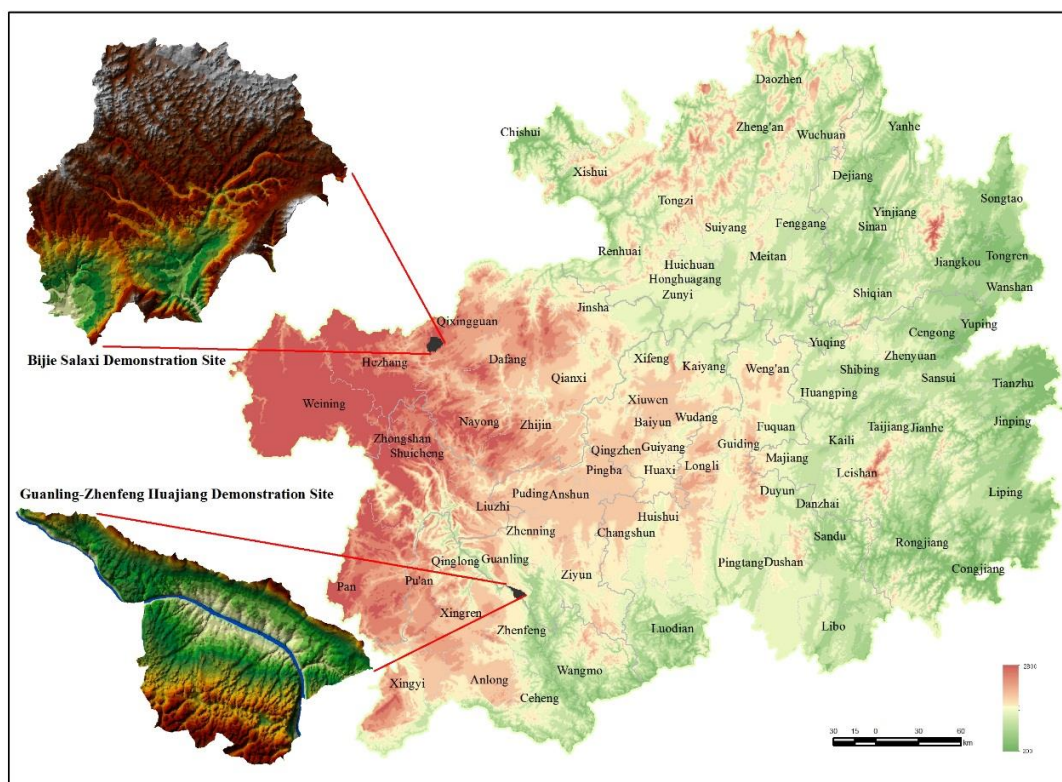


Figure 1. The location of the two demonstration areas in Guizhou Province

The Salaxi Rocky Desertification Comprehensive Management Demonstration Area of Bijie (Fig. 2), located in the northwest of Guizhou Province ($105^{\circ}01'10''$ - $105^{\circ}08'39''$ E, $27^{\circ}11'08''$ - $27^{\circ}17'30''$ N) and the southwest of Bijie city, is within the tributary area of the Liuchong River Basin. It has a north subtropical humid monsoon climate (annual average temperature: 12°C ; annual average precipitation: 984.40 mm) and an altitude of 1,495-2,200 m (relative height difference: 705 m). The total size of the demonstration area is 86.27 km^2 , of which the karst area accounts for 73.94%. The areas of potential, mild, moderate, and severe rock desertification account for 30.91%, 22.26%, 8.57%, and 3.09% of the karst area, respectively. The soil is dominated by zonal yellow soil, with a small proportion of yellow-brown soil and weathered calcareous soil. The native vegetation was mostly destroyed and is now dominated by secondary forests, in which *Pinus armandii*, *Pinus yunnanensis*, *Betula luminifera*, *Populus alba*, and *Quercus variabilis* dominate the arborous layer; *Pyracantha fortuneana*, *Rosa roxburghii*, *Cotoneaster franchetii*, *Hypericum chinense* L., *Rhododendron simsii*, and *Corylus heterophylla* var. *sutchuenensis* dominate the shrub layer; and *Trifolium repens*, *Lolium perenne*, *Dactylis glomerata* L., *Bromus catharticus*, and *Imperata cylindrica* dominate the grassland.

The Guanling-Zhenfenghuajiang Desertification Comprehensive Management Demonstration Zone of Bijie (Fig. 3) is in the southwestern part of Guizhou Province ($105^{\circ}36'30''$ - $105^{\circ}46'30''$ E, $25^{\circ}39'13''$ - $25^{\circ}41'00''$ N) and the river banks of the Huajiang Valley of the Beipan River, which is to the south of Guanling County and the north of Zhenfeng County. It has a north subtropical monsoon climate (annual average

temperature: 18.4 °C; annual average precipitation: 1,100 mm) and an altitude of 450-1,450 m (relative height difference: 1,000 m). The total area of the demonstration area is 51.62 km², of which the karst area accounts for 87.92%, and the areas of potential, mild, moderate, and severe rock desertification account for 24.54%, 40.48%, 17.93%, and 17.06% of the total karst area, respectively. The soil is dominated by yellow soil and yellow calcareous soil. The natural vegetation in the area includes *Cupressus funebris*, *Eucalyptus* spp., *Tectona grandis*, *Koelreuteria paniculata*, and *Cladrastis platycarpa* (Maxim.) Makino in the arborous layer; *Broussonetia papyrifera*, *Viburnum foetidum* var. *ceanothoides*, *Alchornea trewioides*, and *Rhus chinensis* Mill. in the shrub layer; and *Pennisetum hybridum*, *Lonicera japonica*, *Miscanthus sinensis*, *Arthraxon hispidus*, and *Imperata cylindrica* in the grassland.

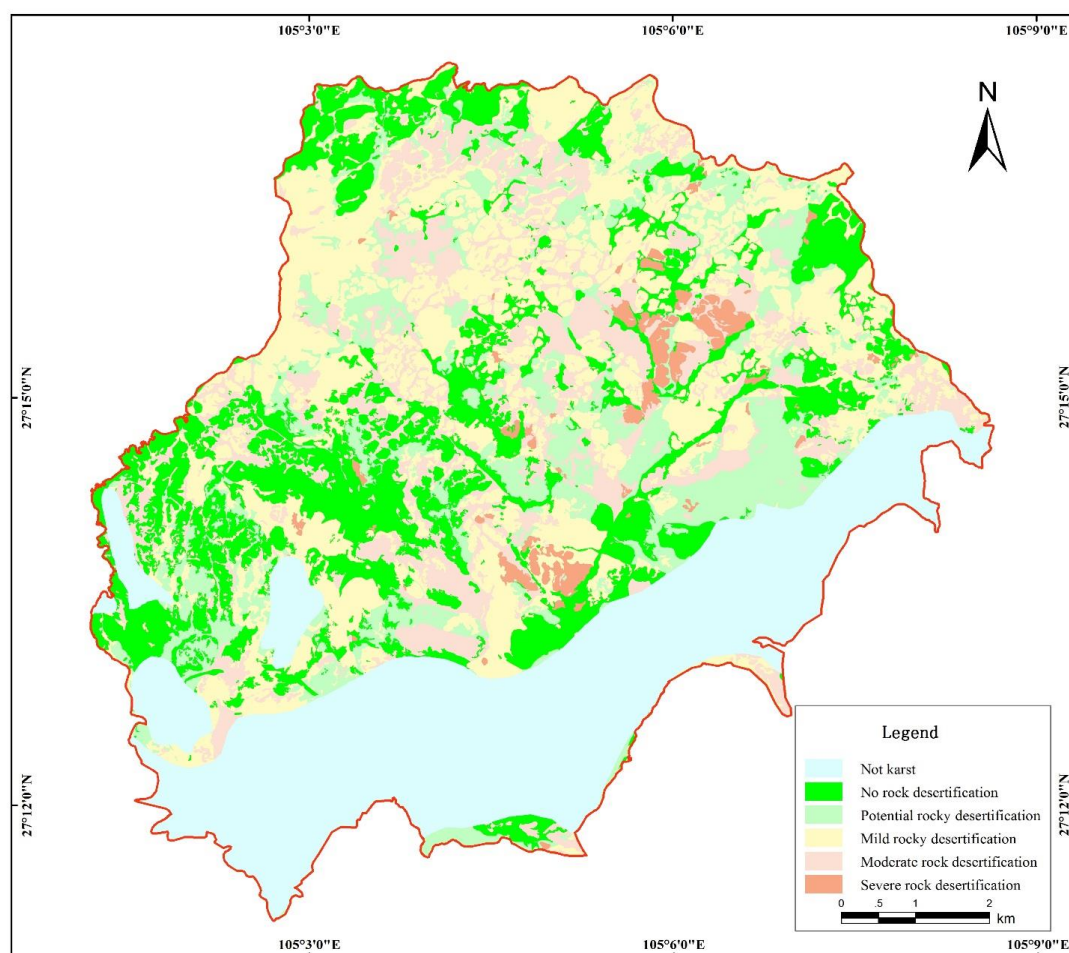


Figure 2. The Salaxi Rocky Desertification Comprehensive Management Demonstration Zone of Bijie

Sample collection

In the study area, the communities of trees, shrubs, and herbs with neat forests, uniform forest distribution, and similar average forest age were selected as subjects. In each demonstration area, 40 experimental plots were designed (80 in total in the two demonstration areas), including 27, 27, and 26 plots for trees, shrubs, and herbs,

respectively, in which typical quadrats of 20 m × 20 m were designed. The samples were collected in late August 2018, when plants were in the fast growth season. When collecting plant leaves, five to six healthy individual plants of the dominant species with similar vigor were randomly chosen from each quadrant, and healthy and mature leaves were collected from each of these plants facing four directions, i.e., east, west, south, and north, which were then mixed well and placed in a brown paper bag to be transferred to the laboratory. In each quadrant, approximately 350 g of each of dry, undecomposed, and semi-decomposed litter was collected from multiple spots. At each sampling site, soil samples were collected from the 0-20 cm soil depth (due to the shallow topsoil depth, in places with a topsoil depth shallower than 20 cm, the samples were collected from the actual soil depth) in 3-4 root zones in an S-shaped sampling line and mixed, from which 1 kg was taken using the quartering method and brought back to the laboratory. Plant leaves and litter were baked in an oven at 65 °C to constant weight and then pulverized to powder 0.1 mm in size. The soil samples were air-dried, removed of impurities such as animal and plant residues and gravels, and then ground using an agate mortar and sieved through a 100-mm sieve. The sieved soil sample was placed in a plastic bag for analysis of soil chemical properties.

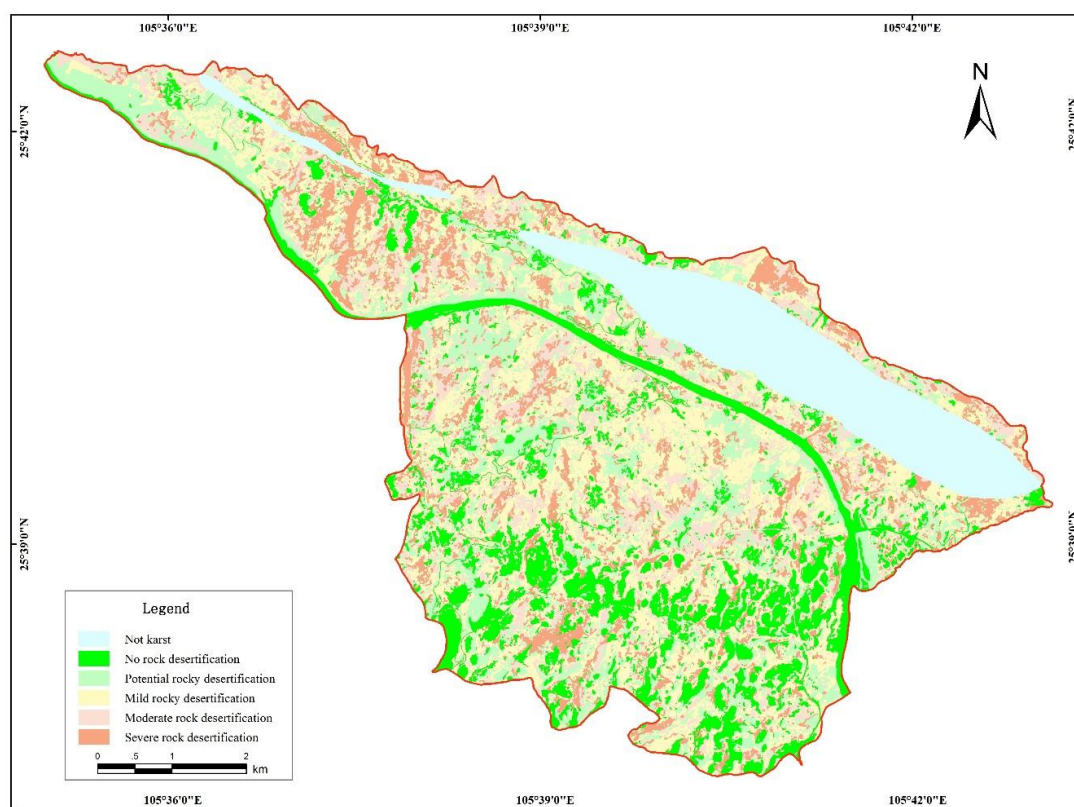


Figure 3. The Guanling-Zhenfenghuajiang Desertification Comprehensive Management Demonstration Zone

Sample analysis

The organic carbon (OC) contents of the leaf, litter, and soil were determined by oxidation with potassium dichromate under external heating, the total nitrogen (TN)

contents using the semi-micro Kjeldahl method after heating in perchloric acid-sulphate acid, and the total phosphorus (TP) contents using Mo-Sb colorimetry–UV spectrophotometry after heating in perchloric acid and sulfuric acid. Soil pH was determined using a potentiometer in the soil solution (water: soil ratio 2.5:1). Soil water content (SWC) was determined using the cutting ring method.

Data processing and statistical analysis

The nutrient content data of plant leaf, litter, and root-zone soil were performed with one-way analysis of variance and regression analysis. The result of a data distribution test showed that the contents of C, N, and P of plant leaf, litter, and soil samples mostly assumed nonnormal distributions but were normally distributed after logarithmic transformation, so their log-transformed values were described with geometric means. The significance test of multiple comparisons was performed using the least significant difference method, and $P < 0.05$ indicated that the difference was significant. The C:N:P comparison results were plotted using 3D Scatter software. The above-described statistical analyses of the data were performed within Origin 8.6 for Windows.

The soil C, N, and P contents of different sampling sites and their respective stoichiometric variation strengths were categorized into three levels (Eq. 1): low [coefficient of variation (CV) < 10%], moderate (10% < CV < 100%), and high (CV > 100%) (Zheng et al., 2004). According to the method of Xiong et al. (2011) (Table 1), the 80 experimental plots were categorized into two types: potential-mild rocky desertification and moderate-severe rocky desertification.

$$CV = \frac{SD}{MN} \times 100\% \quad (\text{Eq.1})$$

SD is the standard deviation; MN is the mean.

Table 1. Classification standard of karst rock desertification

Rocky desertification level	Rock exposure rate	Vegetation + soil coverage	Reference indicator
No rock desertification	< 20	> 80	Nonterraced dry hillside land with a slope of $\leq 15^\circ$, dikes, construction land, etc., with good ecological environment, densely populated trees and shrubs, with no or insignificant soil erosion; suitable for agricultural, forestry, or animal husbandry production
Potential rocky desertification	20–30	80–70	Nonterraced dry hillside land and grassland, etc. with a slope of $> 15^\circ$, with sparsely populated arbor, shrubby and herbaceous vegetation, and good soil-forming conditions but obvious soil erosion; showing a tendency of rock exposure
Mild rocky desertification	31–50	69–50	Rocks begin to be exposed, with obvious soil erosion, low vegetative patch structure, and dominance of sparse shrubs or artificial dry-land vegetation
Moderate rock desertification	51–70	49–30	Rocky desertification is intensifying, with severe soil erosion, shallow topsoil, dominance of rocky hillside land, and sparse shrub-grass zone
Severe rock desertification	> 70	< 30	Rocky desertification is severe, with essentially no soil erosion due to the absence of topsoil, and dominant with lands difficult to use that is about to lose agricultural value

The relationship between plant leaf and litter stoichiometry and soil environmental factors was analyzed using Canoco 4.5 for Windows. First, we performed detrended correspondence analysis on the indicators and found that when the maximum value of the gradient length was less than 3, the linear ranking method was suitable, so we adopted the redundancy analysis of the linear model as the ranking model to examine the relationship between the stoichiometry and the environmental factors. The importance of soil environmental factors was ranked through the Monte Carlo test, and the effect of individual environmental factors on plant stoichiometry was determined using the *t*-value biplot of Canoco 4.5. When interpreting the biplot, if the arrowed connection line of a certain plant stoichiometric indicator was completely within a circle, then it indicated that this indicator was significantly correlated with the soil environmental factor (in the red circle: significant positive correlation; in the blue circle: significant negative correlation; the percentage and length of the arrow that fall within the circle represent the strength of the correlation) (Leps and Smilauer, 2003).

Results and analysis

Stoichiometric characteristics of nutrients of Karst rocky desertification ecosystems

The contents of C, N, and P in plant leaves in karst rocky desertification ecosystems were higher than those in litter or soil, while the ratios of C:N, C:P, and N:P of litter were higher than those of plant leaves or soil. The CVs of stoichiometric values of different nutrients differed, and the variations were mostly moderate. Overall, the CV of stoichiometric values of soil was the highest, followed by that of litter and that of plant leaves. The CV of stoichiometric values of soil was significantly different from those of soil or litter ($P < 0.05$) (Table 2).

Table 2. *Stoichiometric characteristics of nutrients in karst areas of rocky desertification*

	C		N		P		C:N		C:P		N:P	
	Mean±SE	CV (%)	Mean±SE	CV (%)	Mean±SE	CV (%)	Mean±SE	CV (%)	Mean±SE	CV (%)	Mean±SE	CV (%)
Plant leaves	482.96±4.36a	8	12.39±0.6a	40	1.76±0.07a	35	43.77±1.57a	30	303.09±11.41a	32	7.06±0.16a	19
Litter	166.4±4.8a	22	10.55±0.31a	23	1.24±0.07b	44	46.95±1.68a	28	432.41±18.50b	34	9.61±0.46b	38
Soil	38.24±1.73b	40	2.62±0.15b	50	0.9±0.05c	43	18.84±1.40b	65	51.81±3.66c	65	3.02±0.14c	40

In the same column, the different lower-case letters represent statistically significant differences ($P < 0.05$); the data are presented as mean ± SE (standard error)

The stoichiometric characteristics of plant leaf, litter, and soil under different levels of rocky desertification

The stoichiometric characteristics differed significantly between the areas with different levels of rocky desertification (Fig. 4). The C:N:P ratios of plant leaves, litter, and soil in the area of potential-mild rocky desertification were 361:7:1, 498:12:1, and 69:3:1, respectively, and those in the area of moderate-severe rocky desertification were 224:7:1, 301:6:1, and 29:3:1, respectively. Compared with the area with a higher level of rocky desertification, the area with a lower level of rocky desertification had higher ratios of C:N and C:P in the soil and plant leaves and higher ratios of C:P and N:P in the

litter. The N:P ratio of plant leaves and litter were 7.25 and 12.58 in the area of potential-mild rocky desertification, respectively, and 6.91 and 6.64 in the area of moderate-severe rocky desertification. The results indicate that the C content and the N:P ratios of plant leaves and litter in the area of potential-mild rocky desertification are higher than in the area of moderate-severe rocky desertification.

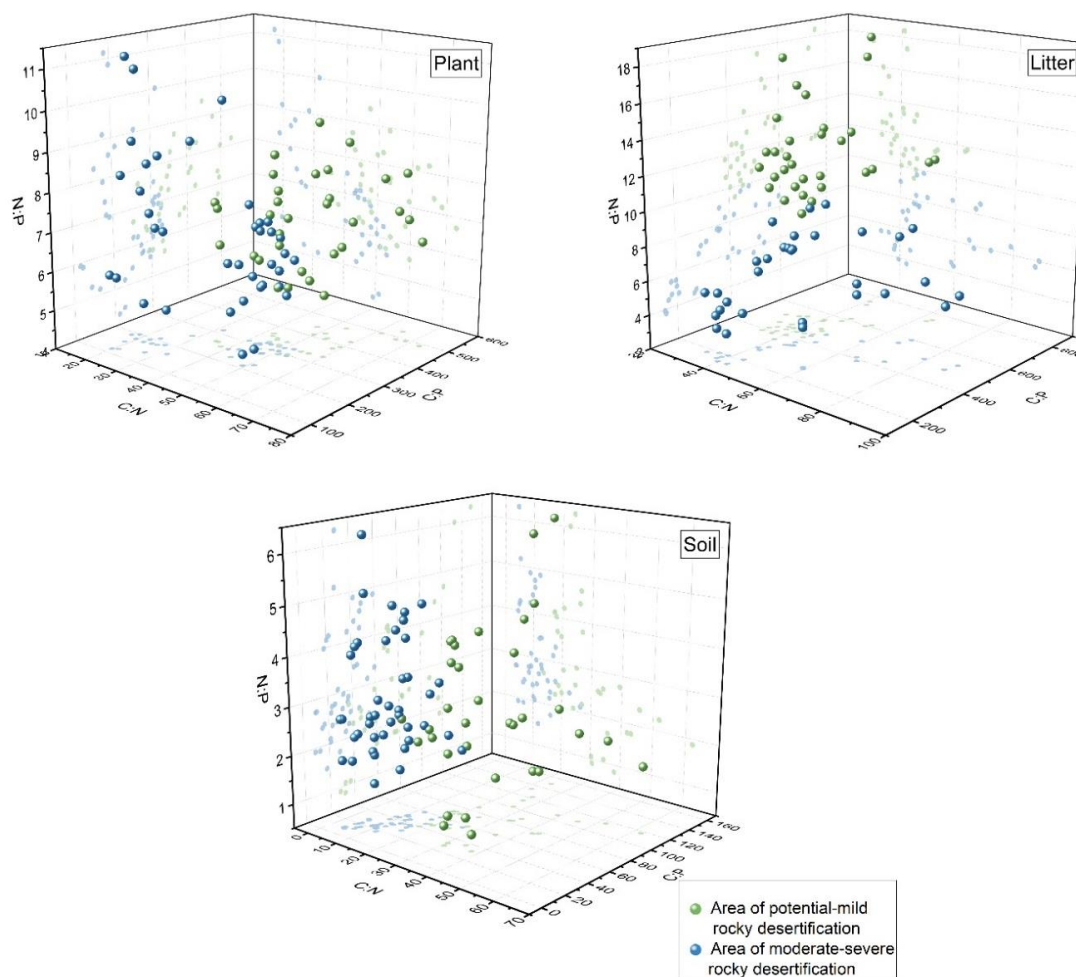


Figure 4. Stoichiometric characteristics of areas with different levels of rocky desertification

Relationship between stoichiometric characteristics of plant leaves, litter, and soil environmental factors in areas of rocky desertification

Stoichiometric characteristics of the areas of rocky desertification and RDA ordination of their respective interpretation powers

The stoichiometric characteristics and the RDA ordination of their respective interpretation powers (Table 3) showed that the cumulative interpretation power of the area of potential-mild rocky desertification and that of the area of moderate-severe rocky desertification on the first and second RDA ordination axes were 72.6% and 68.4%, respectively. The correlation between the stoichiometry of the first and second axes and the soil environmental factors of the area of potential-mild rocky desertification were 0.953 and 0.969, respectively, and the correlation between the

stoichiometry of the first and second axes and the soil environmental factors of the area of moderate-severe rocky desertification were 0.916 and 0.853, respectively. Therefore, the two ordination axes were essentially vertical, indicating that the ordination results were credible. The cumulative interpretation power on the relationship between the stoichiometry and the soil environmental factors was 80% and 90.9% for the area of potential-mild rocky desertification and the area of moderate-severe rocky desertification, respectively, accounting for 81.5% and 91.8% of the total interpretation power. These data indicate that the first and second axes can well reflect the relationship between the stoichiometry and soil environmental factors.

Table 3. The stoichiometric characteristics and their RDA ordination analysis on the interpretation power

	Ordination axis	Axis I	Axis II	Axis III	Axis IV
Potential-mild rock desertification	Interpretation power of stoichiometric characteristics, %	43.4	29.2	9.5	6
	Correlation between stoichiometric characteristics and the soil environmental factors	0.953	0.969	0.872	0.95
	Cumulative interpretation power of stoichiometric characteristics, %	43.4	72.6	82.1	88.1
	The cumulative interpretation power of stoichiometry-soil environmental factor relationship, %	48.3	80.0	91.4	98.1
	Canonical eigenvalue		89.9		
	Total eigenvalue		1.00		
Moderate-mild rocky desertification	Interpretation power of stoichiometric characteristics /%	53.3	15.1	4.4	1.7
	Correlation between stoichiometry and soil environmental factors	0.916	0.853	0.643	0.781
	Cumulative interpretation power of stoichiometric characteristics /%	53.3	68.4	72.7	74.5
	The cumulative interpretation power of stoichiometry-soil environmental factor relationship /%	70.8	90.9	96.7	99.0
	Canonical eigenvalue		0.752		
	Total eigenvalue		1.00		

The 2-D RDA ordination results show that the lengths of arrowed connection lines of the soil environmental factors pH, TP, C:P, and SOC were the longest in *Figure 5a* and that those of C:P, TP, C:N, and SWC were the longest in *Figure 5b*, indicating that these soil environmental factors had good interpretation power for the differences in the changes in plant leaves and litter, which are consistent with the importance ordination results shown in *Table 4*. *Figure 5a* also shows that the directions of the arrows between C:P and DC:P, between pH or SOC and DC, and between TP or SWC and DP were consistent; that the angles between the lines were small; and that the factors had a positive correlation, indicating that C:P, pH, SOC, TP, and SWC had a positive effect on some plant ecological stoichiometric characteristics and were important factors affecting plant ecological stoichiometric properties in the area of

potential-mild rocky desertification. *Figure 5b* shows that the directions of the arrows between C:P and ZC:P, between TP and ZP, between C:P and ZC:P, between SOC or N:P and DN:P, and between SWC and ZN were consistent; that the angles between the lines were small; and that the factors had a positive correlation. The results indicate that C:P, TP, C:N, SWC, C:P, and N:P had a positive effect on some plant ecological stoichiometric characteristics and were important factors affecting plant ecological stoichiometric properties in the area of moderate-severe rocky desertification.

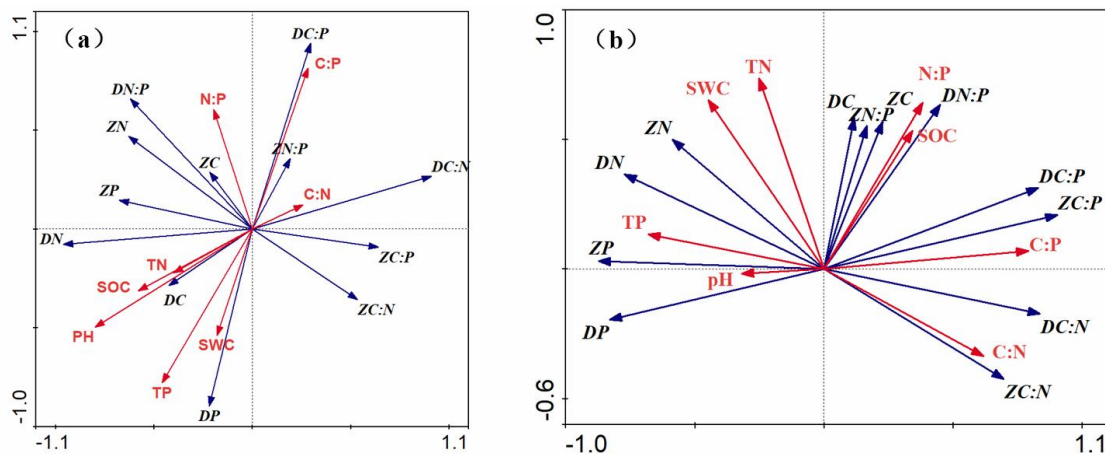


Figure 5. Redundancy analysis on plant stoichiometric characteristics and soil environmental factors. Note: pH, SOC, TN, TP, C:N, C:P, and N:P are the soil pH, soil organic carbon content, soil total nitrogen content, soil total phosphorus content, and their respective stoichiometric ratios, respectively; ZC, ZN, ZP, ZC:N, ZC:P, and ZN:P are the organic carbon content, total nitrogen content, and total phosphorus content in plant leaves and their respective stoichiometric ratios, respectively; DC, DN, DP, DC:N, DC:P, and DN:P are the organic carbon content in the litter, total nitrogen content in plant litter, total phosphorus content in plant litter, and their respective stoichiometric ratios, respectively. Part (a) shows the RDA results of plant stoichiometric characteristics and soil environmental factors in the area of potential-mild rocky desertification. Part (b) shows the RDA results of plant stoichiometric characteristics and soil environmental factors in the area of moderate-severe rocky desertification

Ranking the importance of soil environmental factors to plant stoichiometric characteristics

We performed the Monte Carlo test to rank the eight soil environmental factors (Table 4) and found that the effects of soil environmental factors on plant stoichiometric characteristics differed between areas with different levels of rocky desertification. The order of importance of the soil environmental factors in the area of potential-mild rocky desertification was pH > TP > C:P > SOC > N:P > TN > SWC > C:N. The effects of pH, TP, C:P, and SOC on plant stoichiometric characteristics were significant ($P < 0.05$). Compared with other soil environmental factors, pH could better represent the difference in plant stoichiometric characteristics. The order of importance of the soil environmental factors in the area of moderate-severe rocky desertification was C:P > TP > C:N > SWC > N:P > TN > SOC > pH. The effects of C:P, TP, C:N, and

SWC were significant ($P < 0.05$), and compared with the other soil environmental factors, C:P better represented the difference in plant stoichiometric characteristics.

Table 4. Monte Carlo test ranking of eight soil environmental factors

	Soil factor	Order of importance	Interpretation power (%)	Importance (F)	Significance (P)
Area of potential-mild rocky desertification	pH	1	35.6	6.625	0.002
	TP	2	27.8	4.625	0.006
	C:P	3	23.4	3.666	0.012
	SOC	4	19	2.809	0.036
	N:P	5	13.5	1.874	0.128
	TN	6	10.9	1.472	0.218
	SWC	7	10.0	1.336	0.264
	C:N	8	4.5	0.57	0.684
Area of moderate-severe rocky desertification	C:P	1	33.7	9.138	0.002
	TP	2	25.9	6.294	0.004
	C:N	3	22.6	5.252	0.004
	SWC	4	17.3	3.76	0.016
	N:P	5	14.7	3.106	0.066
	TN	6	12.3	2.525	0.076
	SOC	7	10.8	2.184	0.134
	pH	8	5.6	1.067	0.354

Effects of individual soil environmental factors on plant stoichiometry

We generated impact diagrams of individual soil environmental factors using the t-value biplots of the first four factors affecting plant stoichiometry in the area of potential-mild rocky desertification (Fig. 6). The Canoco biplot for pH (Fig. 6a) shows that the DP arrow falls within the red circle and that the DC:P arrow falls within the blue circle, indicating that pH had a significantly positive correlation with DP but a significantly negative correlation with DC:P. Figure 6b shows that soil TP had a significantly positive correlation with DN:P and DN and a positive correlation with plant C, N, and P. Figure 6c and d show that the plant stoichiometric indicators do not fall within the circle but mostly pass through the red circle or the blue circle, indicating that the plant stoichiometric characteristics were correlated ($P < 0.05$) with the soil environmental factors C:P and SOC, but not highly correlated ($P < 0.01$).

The t-value biplot of the area of moderate-severe rocky desertification is shown in Figure 7. Figure 7a shows that the DC:N and ZC:N arrows pass through the red circle and that the ZC:N arrow has more of its length within the red circle, indicating that C:P had a positive correlation with DC:N and ZC:N (with a stronger correlation for ZC:N). Figure 7b and c show that DC, ZC, ZN:P, DN:P, DC:P, and ZC:P pass through the blue circle and the red circle, respectively, indicating that these environmental factors were correlated negatively with TP but positively with C:N. Figure 7d shows the analysis result of SWC, indicating that SWC had a significantly positive correlation with ZP and DP, which fall into the red circle, but a significantly negative correlation with DN:P, DC:P, ZC:P, and DC:N, which fall into the blue circle.

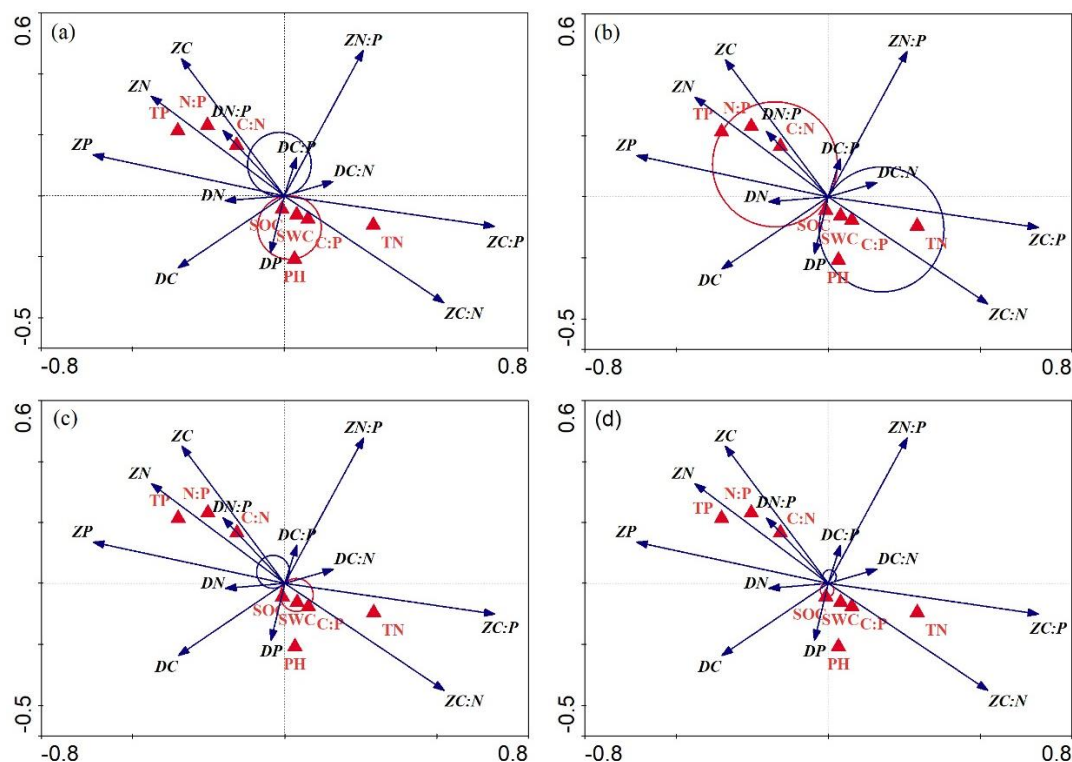


Figure 6. Effect of individual soil environmental factors on plant stoichiometry in the area of potential-mild rocky desertification. (a) pH; (b) TP; (c) C:P; (d) SOC

Discussion

Ecological stoichiometric characteristics of karst areas of rocky desertification

In this study, we examined the stoichiometric characteristics of plant leaves, litter, and soil of karst areas and found that the C, N, and P contents of plant leaves in karst areas of rocky desertification were higher than those of litter or soil. This was because the C, N, and P contents of plant leaves, an important nutrient storage organ, are much higher than in other plant organs (Minden and Kleyer, 2014). After fresh leaves fall, the organic components such as crude fat, tannins, and soluble sugars are decomposed, leading to significantly reduced C content in the litter (Yang et al., 2007). Litter had lower contents of N and P than leaves. This is because before leaves fall, the nutrients in the leaves are transferred to other components, absorbed, and utilized. The reduction in N may happen because the leaves utilizes nitrogen in photosynthesis, and high N use efficiency reduces the P content in litter (Zhao et al., 2016). Plants absorb N and P from the soil and further transfer some nutrients to plants through the nutrient reabsorption process, resulting in larger changes to the N and P contents in litter than in plant leaves, and thus the C:N and C:P contents are found in the order litter > plant > soil (Zeng et al., 2015). Soil nutrient content is an important indicator for evaluating organic matter composition and soil quality, and the soil nutrient variability in the same ecosystem is largely affected by environmental factors (Li et al., 2018). Soil nutrients in karst areas showed moderate variation but had significant fluctuations, which are caused by the changes in environmental factors derived from complicated landforms, high spatial heterogeneity, and the interference of human activities, which are consistent with the conclusions of Zhu et al. (2013) and Li et al. (2014).

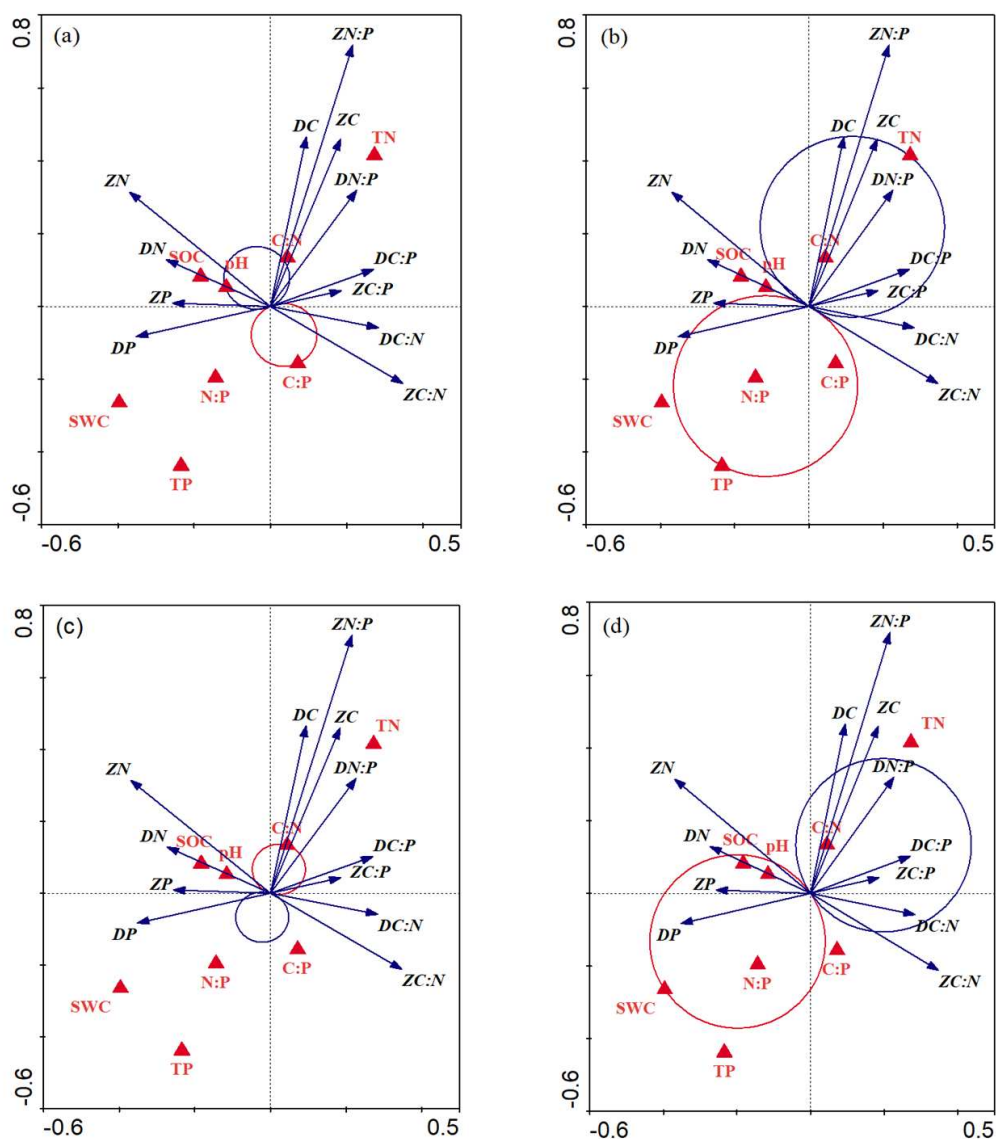


Figure 7. Effect of individual soil environmental factors on plant stoichiometry in the area of moderate-severe rocky desertification. (a) C:P; (b) TP; (c) C:N; (d) SWC

In this study, the soil P content of the areas of rocky desertification was $0.9 \text{ mg} \cdot \text{g}^{-1}$, which is lower than that of other ecosystems (Koerselma and Meuleman, 1996; Jiao et al., 2013). This was likely caused by the strong leaching effect derived from high precipitation in karst areas in southwestern China. However, compared with the average content of soil P in China (0.56 g/kg) (Tian et al., 2010), the P content of the karst areas is still higher, indicating that despite strong leaching effects in the rocky desertification environment, the P content of the karstification product from bare rocks can readily accumulate in the soil, showing a significant aggregation effect, which is consistent with the findings of Sheng et al. (2013). We also found that the average C content in plant leaves was $482.96 \text{ mg} \cdot \text{g}^{-1}$, which is higher than that ($464.00 \text{ mg} \cdot \text{g}^{-1}$) of 492 terrestrial plant species around the world reported by Elser et al. (2000) and that ($438.00 \text{ mg} \cdot \text{g}^{-1}$) of China's grassland ecosystem (He et al., 2006), indicating

that the karst area has strong C storage capacity and thus high accumulation of organic matter. The average N content in plant leaves was $12.39 \text{ mg}\cdot\text{g}^{-1}$, which is significantly lower than that ($20.09 \text{ mg}\cdot\text{g}^{-1}$) at the global scale (Reich and Oleksyn, 2004) and that of 753 species reported by Han et al. (2005), indicating N deficiency in the karst area, likely because the high precipitation in the region (over 980 mm annually) is prone to cause the leaching of available nitrogen, which has a high mobility.

Ecological stoichiometric characteristics of areas with different levels of rocky desertification

Due to differences in geographical conditions, the N and P contents and the stoichiometric characteristics of C:N:P of plant leaves in different habitats and different tree species vary profoundly (Reich and Oleksyn, 2004; Han et al., 2005). In this study, we found that the C content in plant leaves in the area of potential-mild rocky desertification was higher than that in the area of moderate-severe rocky desertification. Because the soil is a primary environmental factor in karst areas, its stoichiometric characteristics affect the plant community characteristics of areas with different levels of rocky desertification (Zhao et al., 2019). In the area of moderate-severe rocky desertification, the rock exposure rate was high, the vegetation coverage was low, and the biomass was low, leading to the reduced stock of soil organic carbon and the accelerated decomposition of organic matter and thus a lower C content than in the area with a lower level of rocky desertification. This finding is consistent with the findings of Yang (2000) and Long et al. (2002). They found that soil C:N is inversely proportional to the decomposition rate of organic matter and that the soil with a lower C:N ratio is faster at mineralization (Zhu et al., 2013). In this study, we found that the soil C:N ratio was 28.72 in the area of potential-mild rocky desertification and was 10.85 in the area of moderate-severe rocky desertification. The soil C:N ratio in the area of moderate-severe rocky desertification was lower than the global average (14.3) (Zhao et al. 2015), indicating higher rates of decomposition and mineralization of soil organic matter. The C:N and C:P ratios in plant leaves and soil in the area of potential-mild rocky desertification were higher than those in the area of moderate-severe rocky desertification because in the area of moderate-severe rocky desertification, topsoil was shallow and had high temperature and humidity, weak nutrient retention ability, and fast nutrient turnover, leading to low nutrient use efficiency and nutrient resorption rate in plants (Cui et al., 2015). The critical values for plant N:P are 14 and 16. When $\text{N:P} < 14$, the ecosystem is N-limited, and when $\text{N:P} > 16$, it is P-limited (Koerselman and Meuleman, 1996; Tessier and Raynal, 2003). In this study, we found that the N:P ratios of the area of potential-mild rocky desertification and the area of moderate-severe rocky desertification were 6.91 and 7.25, respectively, indicating that both areas were N-limited. In the shrub and grass vegetation of the karst areas, we found that N was deficient while P was sufficient, mainly because in these areas, the rock exposure rate was high, the vegetation coverage was low, nutrients were concentrated in the arborous layer, and the symbiotic nitrogen fixation system and the slightly weathered soil were scarce (Hedin, 2004). Thus, supplementation with N fertilizer during the control process can increase the N content of the vegetation. Our results indicate that the limiting factors inhibit vegetation recovery and development and that limiting factors should be effectively regulated in forest management strategies.

Driving mechanisms of the effect of soil environmental factors on plant stoichiometry

The chemical elements of vegetation are mainly derived from the soil, and their contents are closely related to their soil contents. C, N, and P are the basic constituent elements of plants that are converted in the plant–litter–soil continuum, manifesting the nutrient cycling and use efficiency (Zeng et al., 2015). Soil pH, TP, C:P, SOC, C:N, and SWC are the main driving factors affecting plant stoichiometry. The soil environmental factors TP and C:P significantly affected the stoichiometric characteristics of the vegetation in both areas of rocky desertification, indicating that the P level in plants is closely coupled with that in soil. Soil P level is positively correlated to C, N, and P levels in plant leaves, indicating that the soil P can facilitate the absorption of C, N, and P by plant leaves. The reason that P is an important factor is that the P in soil is directly produced by rock weathering and thus is a sedimentary element. In karst areas, soil and rock are in direct contact, which is prone to cause soil erosion and slides. Therefore, the fluctuation in the content of P exerts a greater influence on the ratios of elements than other fluctuations. In the future plant nutrient recycling and utilization processes, soil P should be optimized and adjusted to achieve nutrient balance.

The soil environmental factor TP was positively correlated with DN:P and DN (Fig. 6b) but negatively correlated with DC, ZC, ZN:P, DN:P, DC:P, and ZC:P (Fig. 7b), indicating that in environments with different levels of rocky desertification, the driving effect of soil environmental factors on plant nutrient absorption varies, which is consistent with the findings of Chen et al. (2018). The soil environmental factors TP (Fig. 7b) and SWC (Fig. 7d) in the moderate-severe rocky desertification demonstration area showed similar correlations in the analysis of the effects of individual environmental factors, indicating that the driving mechanisms of the two are identical. This is mainly because the high rainfall in the karst area accelerates TP leaching, which, coupled with ground runoff, leads to the simultaneous losses of soil TP and SWC and thus a certain correlation between TP and SWC. SWC showed a significantly positive correlation with ZP and DP and a significantly negative correlation with DN:P, DC:P, ZC:P, and DC:N (Fig. 7d), indicating that the increase in SWC significantly increases P contents in plant leaves and litter while decreasing the contents of C:N, C:P, and N:P of litter, indicating that SWC can effectively increase the nutrient transfer rate of plant leaves, resulting in reduced C:N, C:P, and N:P ratios in litter.

The changes to soil nutrient supply in the environment of karst rocky desertification can affect various plant physiological and biochemical reactions to some extent. After long evolutionary adaptation, plants form relatively stable elemental stoichiometries, which also reflects plants' adaptation strategy to extreme environments. The RDA on the area of potential-mild rocky desertification showed that soil pH played the most critical role in plant stoichiometry. Past studies have shown that soil pH directly affects the decomposition, mineralization, redox reaction, and enzyme reaction rates of soil organic matter, and species richness is positively correlated with pH value (Dick et al., 2000; Xu et al., 2006; Tian et al., 2019). The species richness and the pH-driving impact of the area of potential-mild rocky desertification was higher than those of the area of moderate-severe rocky desertification. Among the soil environmental factors in area of moderate-severe rocky desertification, soil C:P showed a more profound effect and a positive correlation with DC:N and ZC:N (Fig. 7a), indicating that the increase in soil C:P can promote the C:N in plant leaves, while the C:N in litter is fully in line with the characteristics of C:N in plant leaves, consistent with the conclusions on the stoichiometric characteristics of wetland plants and litter by Wang et al. (2011).

Conclusions

Nutrient cycling and transfer occur in the plant–litter–soil continuum in karst areas of rocky desertification, which is manifested in the C, N, and P contents in plant leaves being higher than those in litter or soil.

The leaves of plants in karst areas showed N deficiency, P sufficiency, and a strong C storage capacity. Supplementation with N fertilizer during the control process can increase the vegetation biomass yield.

The decomposition and mineralization rates of soil organic matter in the area of moderate-severe rocky desertification is higher than in the area of potential-mild rocky desertification. The order of importance of soil environmental factors in the area of potential-mild rocky desertification is $\text{pH} > \text{TP} > \text{C:P} > \text{SOC}$. The soil pH has the strongest driving effect on plant stoichiometry. The order of importance of soil environmental factors in the area of moderate-severe rocky desertification is $\text{C:P} > \text{TP} > \text{C:N} > \text{SWC}$. The soil C:P has the strongest driving effect on plant stoichiometry.

It is necessary to target the primary factors for fertilization management and nutrient transport protection in future rock desertification control. In the diagnosis of plant nutrient restriction, in addition to considering the role of soil environmental nutrient factors, it is also necessary to increase the mechanism of plant photosynthesis and respiration on the maintenance of plant nutrients, as well as the decomposition and interference of underforest microenvironment, soil animals and microbial activities on litter. In the future, we should increase the systematic research of multi-disciplinary, multi-angle and multi-thinking. At the same time, the environment and livelihood problems caused by stony desertification need to be paid more attention all over the world.

Acknowledgements. This research was funded by the Project of National Key Research and Development Program of China in the 13th Five-year Plan Period: Ecological Industry Model and Integrated Technology Demonstration of the Karst Plateau-Gorge Rocky Desertification Control (2016YFC0502607); The Key Project of Science and Technology Program of Guizhou Province: Model and Technology demonstration for from the karst desertification control (No.5411 2017 Qiankehe Pingtai Rencai).

REFERENCES

- [1] Agren, G. I. (2004): The C:N:P stoichiometry of autotrophs. Theory and observations. – *Ecology Letters* 7: 185-191.
- [2] Cao, G. Y., Cao, Y., Chen, Y. M. (2015): Characteristics of nitrogen and phosphorus stoichiometry across components of forest ecosystem in Shaanxi Province. – *Chinese Journal of Plant Ecology* 39(12): 1146-1155.
- [3] Chen, A. N., Wang, G. J., Chen, C., Li, S. Y., Li, W. J. (2018): Variation in the N and P stoichiometry of leaf-root-soil during stand development in a *Cunninghamia lanceolata* plantation in subtropical China. – *Acta Ecologica Sinica* 38(11): 4027-4036.
- [4] Cui, G. Y., Cao, Y., Chen, Y. M. (2015): Characteristics of nitrogen and phosphorus stoichiometry across components of forest ecosystem in Shaanxi Province. – *Chinese Journal of Plant Ecology* 39: 1146-1155.
- [5] Dick, W. A., Cheng, L., Wang, P. (2000): Soil acid and alkaline phosphatase activity as PH adjustment indicators. – *Soil Biology and Biochemistry* 32(13): 1915-1919.

- [6] Du, J. Y., Wang, L. J., Sheng, M. Y., Wen, P. C. (2017): Soil C, N and P stoichiometry of rocky desertification ecosystems in the Karst Plateau Canyon area. – *Journal of Sichuan Agricultural University* 35(1): 45-51.
- [7] Du, M. Y., Fan, S. H., Liu, G. L., Feng, H. Y., Guo, B. H., Tang, X. L. (2016): Stoichiometric characteristics of carbon, nitrogen and phosphorus in *Phyllostachys edulis* forests of China. – *Chinese Journal of Plant Ecology* 40(8): 760-774.
- [8] Elser, J. J., Fagan, W. F., Denno, R. F., Dobberfuhl, D. R., Folarin, A., Huberty, A., Interlandi, S., Kilham, S. S., McCauley, E., Schulz, K. L., Siemann, E. H., Sterner, R. W. (2000): Nutritional constraints in terrestrial and freshwater food webs. – *Nature* 408: 578-580.
- [9] Elser, J. J., Fagan, W. F., Kerkhoff, A. J., Swenson, N. G., Enquist, B. J. (2010): Biological stoichiometry of plant production: Metabolism, scaling and ecological response to global change. – *New Phytologist* 186: 593-608.
- [10] Gusewell, S. (2004): N:P ratios in terrestrial plants: variation and functional significance. – *New Phytologist* 164: 243-266.
- [11] Han, W. X., Fang, J. Y., Guo, D. L., Zhang, Y. (2005): Leaf nitrogen and phosphorus stoichiometry across 753 terrestrial plant species in Chinese. – *New Phytologist* 168: 377-385.
- [12] He, J. S., Fanf, J. Y., Wang, Z. H., Guo, D. L., Flynn, D. F. B., Geng, Z. (2006): Stoichiometry and large-scale patterns of leaf carbon and nitrogen in the grassland biomes of China. – *Oecologia* 149(1): 115-122.
- [13] Hedin, L. O. (2004): Global organization of terrestrial plant-nutrient interactions. – *Proceedings of the National Academy of Sciences of the United States of America* 101: 10849-10850.
- [14] Hu, Y. S., Me, X. Y., Liu, Y. H. (2014): N and P stoichiometric traits of plant and soil in different forest succession stages in Changbai Mountains. – *Chinese Journal of Applied Ecology* 25(3): 632-638.
- [15] Jiao, F., Wen, Z. M., An, S. S., Yuan, Z. (2013): Successional changes in soil stoichiometry after land abandonment in Loess Plateau, China. – *Ecological Engineering* 58: 249-254.
- [16] Koerselman, W., Meuleman, A. F. M. (1996): The vegetation N:P ratio: a new tool to detect the nature of nutrient limitation. – *Journal of Applied Ecology* 33(6): 1441-1450.
- [17] LeGrand, H. E. (1973): Hydrological and ecological problems of karst regions: hydrological actions on limestone regions cause distinctive ecological problems. – *Science* 179(4076): 859-864.
- [18] Leps, J., Smilauer, P. (2003): *Multivariate Analysis of Ecological Data Using CANOCO*. – Cambridge University Press, Cambridge, UK.
- [19] Li, C. J., Xu, X. W., Sun, Y. Q., Qiu, Y. Z., Li, S. Y., Gao, P., Zhong, X. B., Yan, J., Wang, G. F. (2014): Stoichiometric characteristics of C, N, P for three desert plants leaf and soil at different habitats. – *Arid Land Geography* 37(5): 996-1004.
- [20] Li, Y. Q., Huang, Y. Q., Xu, G. P., Sun, Y. J., Zhang, Z. F., He, C. X., Huang, K. C., He, W. (2018): Characteristics of soil nutrients and microbial activities of reed vegetation in the Huixian karst wetland, Guilin, China. – *Chinese Journal of Ecology* 37(1): 64-74.
- [21] Long, J., Huang, C. Y., Li, J. (2002): Effects of land use on soil quality in karst hilly area. – *Journal of Soil and Water Conservation* 16(1): 76-79.
- [22] Minden, V., Kleyer, M. (2014): Internal and external regulation of plant organ stoichiometry. – *Plant Biology* 16: 897-907.
- [23] Pena-Claros, M. (2003): Changes in forest structure and species composition during secondary forest succession in the Bolivian Amazon. – *Biotropica* 35: 450-461.
- [24] Reich, P. B. (2003): The evolution of plant functional variation: traits, spectra and strategies. – *International Journal of Plant Sciences* 164: 143-164.

- [25] Reich, P. B., Oleksyn, J. (2004): Global patterns of plant leaf N and P in relation to temperature and latitude. – *Proceedings of the National Academy of Sciences of the United States of America* 101: 11001-11006.
- [26] Sheng, M. Y., Liu, Y., Xiong, K. N. (2013): Response of soil physical-chemical properties to rocky desertification succession in South China Karst. – *Acta Ecologica Sinica* 33(19): 6303-6313.
- [27] Sheng, M. Y., Xiong, K. N., Cui, G. Y., Liu, Y. (2015): Plant diversity and soil physical-chemical properties in karst rocky desertification ecosystem of Guizhou, China. – *Acta Ecologica Sinica* 35(2): 434-448.
- [28] Sterner, R. W., Elser, J. J. (2002): *Ecological Stoichiometry: The Biology of Elements from Molecules to the Biosphere*. – Princeton University Press, Princeton.
- [29] Tessier, J. T., Raynal, D. J. (2003): Use of nitrogen to phosphorus ratios in plant tissue as an indicator of nutrient limitation and nitrogen saturation. – *Journal of Applied Ecology* 40: 523-534.
- [30] Tian, H. Q., Chen, G. S., Zhang, C., Melillo, J. M., Hall, C. A. S. (2010): Pattern and variation of C:N:P ratios in China's soils: a synthesis of observational data. – *Biogeochemistry* 98(1/3): 139-151.
- [31] Tian, J., Sheng, M. Y., Wang, P., Wen, P. C. (2019): Influence of land use change on litter and soil C, N, P stoichiometric characteristics and soil enzyme activity in karst ecosystem, Southwest China. – *Environmental Science* 40(9): 4278-4286.
- [32] Wang, J. Y., Wang, S. Q., Li, R. L., Yan, J. H., Sha, L. Q., Han, S. J. (2011): Leaf stoichiometry of trees in three forest types in Pearl River Delta, South China. – *Chinese Journal of Plant Ecology* 35(6): 587-595.
- [33] Wang, K. L., Yue, Y. M., Ma, Z. L., Lei, T. W., Li, D. J., Song, T. Q. (2016a): Research and demonstration on technologies for rocky desertification treatment and ecosystem service enhancement in karst peak-cluster depression regions. – *Acta Ecologica Sinica* 36(22): 7098-7102.
- [34] Wang, M. C., Zhang, X. C., Li, H. J., Zhou, H. Y., Wei, X. H., Guan, G. C. (2016b): An analysis of soil quality changes in the process of ecological restoration in karst rocky desertification area: a case study in karst ecological restoration and rehabilitation region of Guizhou Village. – *Ecology and Environmental Sciences* 25(6): 947-955.
- [35] Wang, W. Q., Xu, L. L., Zeng, C. S., Tong, C., Zhang, L. H. (2011): Carbon, nitrogen and phosphorus ecological stoichiometric ratios among live plant-litter-soil systems in estuarine wetland. – *Acta Ecologica Sinica* 31(23): 134-139.
- [36] Wu, T. G., Chen, B. F., Xiao, Y. H., Pan, Y. J., Chen, Y., Xiao, J. H. (2010): Leaf stoichiometry of trees in three forest types in Pearl River Delta, South China. – *Chinese Journal of Plant Ecology* 34(1): 58-63.
- [37] Xiang, Y., Cheng, M., An, S. S., Zeng, Q. C. (2015): Soil-plant-litter stoichiometry under different site conditions in Yanhe Catchment, China. – *Journal of Natural Resource* 30(10): 1642-1652.
- [38] Xiong, K. N., Chen, Y. B., Chen, H. (2011): *Gold Formation from Points of Stone. Technology and Model of Stone Desertification Control in Guizhou Province*. – Guizhou Science and Technology Publishing House, Guiyang, China.
- [39] Xiong, K. N., Zhu, D. Y., Peng, T., Yu, L. F., Xue, J. H., Li, P. (2016): Study on Ecological industry technology and demonstration for Karst rocky desertification control of the Karst Plateau-Gorge. – *Acta Ecologica Sinica* 36(22): 7109-7113.
- [40] Xu, Z. G., He, Y., Yan, B. X., Song, C. C. (2006): Effects of plant N/P and Soil pH on species richness of wetland plants. – *China Environmental Science* 3: 346-349.
- [41] Yang, C. J., Zeng, J., Xu, D. P., Li, S. J., Lu, J. (2007): The processes and dominant factors of forest litter decomposition: a review. – *Ecology and Environmental Sciences* 16(2): 649-654.
- [42] Yang, S. T., Zhu, Q. J. (2000): The rate of environmental degradation and natural rehabilitation in typical karst area of Guizhou. – *Acta Geographica Sinica* 55(4): 459-466.

- [43] Zeng, Z. X., Wang, K. L., Liu, X. L., Zeng, F. P., Song, T. Q., Peng, W. X., Zhang, H., Du, H. (2015): Stoichiometric characteristics of plants, litter and soils in karst plant communities of Northwest Guangxi. – *Chinese Journal of Plant Ecology* 39(7): 682-693.
- [44] Zhao, F. Z., Sun, J., Ren, C. J., Kang, D., Deng, J., Han, X. H., Yang, G. H., Feng, Y. Z., Ren, G. X. (2015): Land use change influences soil C, N, and P stoichiometry under ‘Grain-to-Green Program’ in China. – *Scientific Reports* 5: 10195.
- [45] Zhao, W. J., Liu, X. D., Jin, M., Zhang, X. L., Che, Z. S., Jing, W. M., Wang, S. L., Niu, Y., Qi, P., Li, J. W. (2016): Ecological stoichiometric characteristics of carbon, nitrogen and phosphorus in leaf-litter-soil system of picea crassifolia forest in the Qilian Mountains. – *Acta Pedologica Sinica* 53(2): 477-489.
- [46] Zhao, W. J., Li, Q., Cui, Y. C., Hou, Y. J., Yang, B., Ding, F. J., Wu, P. (2019): Effects on nutrient content and stoichiometric characteristics during rocky desertification control in karst region: a case study of Gangzhai small watershed of central Guizhou Province. – *Journal of Central South University of Forestry & Technology* 39(8): 76-86.
- [47] Zheng, J. Y., Shao, M. A., Zhang, X. C. (2004): Spatial variation of surface soil’s bulk density and saturated hydraulic conductivity on slope in loess region. – *Journal of Soil and Water Conservation* 18(3): 53-56.
- [48] Zhong, Q. L., Liu, L. B., Xu, X., Yang, Y., Guo, Y. M., Xu, H. Y., Cai, X. L., Ni, J. (2018): Variations of plant functional traits and adaptive strategy of woody species in a karst forest of central Guizhou Province, southwestern China. – *Chinese Journal of Plant Ecology* 42(5): 562-572.
- [49] Zhu, Q. L., Xing, X. Y., Zhang, H., An, S. S. (2013): Soil ecological stoichiometry under different vegetation area on loess hillygully region. – *Acta Ecologica Sinica* 33(15): 4674-4682.

PREDICTING WILDLIFE–VEHICLE COLLISIONS IN AN URBAN AREA BY THE EXAMPLE OF LUBLIN IN POLAND

TAJCHMAN, K.¹ – GAWRYLUK, A.^{2*} – FONSECA, C.³

¹*Department of Animal Ethology and Wildlife Management, Faculty of Animal Sciences and Bioeconomy, University of Life Sciences in Lublin, Lublin, Poland
(e-mail: katarzyna.tajchman@up.lublin.pl; phone: +48-81-445-6848)*

²*Department of Grassland and Landscape Shaping, Faculty of Agrobiotechnology, University of Life Sciences in Lublin, Lublin, Poland*

³*Department of Biology & CESAM, University of Aveiro, Campus de Santiago, 3810-193 Aveiro, Portugal
(e-mail: cfonseca@ua.pt; phone: +351-234-247-103)*

**Corresponding author
e-mail: adam.gawryluk@up.lublin.pl; phone: +48-81-445-6994*

(Received 20th Nov 2019; accepted 30th Jan 2020)

Abstract. The aim of the study was to develop a new model for the prediction of wildlife-vehicle collisions (WVC) in urban areas, more specifically in the city of Lublin (Poland) and its surroundings. Prediction new model probability of WVC will be a valuable tool for city planners and will increase road safety for drivers and animals. The number of WVC was compared with data on traffic intensity in the same period, land use forms and seasons of the year. The data were analyzed statistically and the values of the parameters were presented as the mean value and standard error or standard deviation. Almost half (42.7%) of the analyzed collisions took place on roads characterized by traffic that does not exceed 100 vehicles/day. The highest number of collisions with animals was reported in summer and spring, i.e. 91 and 78 events, respectively. There was also a highly significant positive correlation between the increase in the number of accidents with animals and the traffic intensity of 501-600 and 1101-1200 vehicles/day on the roads. The distances from river valleys, residential buildings, and industrial development turned out to be significant predictor variables for WVC.

Keywords: *wildlife-vehicle collisions, models probability of collisions, urban area, traffic intensity, wild animals*

Introduction

In the last decade, there has been a steady increase in the number of protected animal species (e.g. beaver by 76%) and medium wild game (e.g. hare by 40% or pheasant by 13%) in Poland, which is a positive phenomenon concerning the protection of biodiversity and genetic resources of populations of these species (GUS, 2010-2018). As shown by GUS data (2010-2018), the number of large game has increased (elk by 170%, red deer by 50%, roe deer by 12%, and fallow deer by 2.5%), which may have adverse consequences for both animals and humans. Animal overpopulation may lead to the reduction of the food base, which forces animals to migrate in search of better living areas and contributes to an increase in road events involving animals (Huijser et al., 2008; Tajchman et al., 2017A).

Wildlife-vehicle collisions (WVC) are one of the most widespread and persistent conflicts between humans and wildlife worldwide, especially since the increasing numbers of humans and animals inhabiting smaller areas (Huijser et al., 2009; Conover, 2010). In Poland and many other countries, it is very difficult to provide accurate data

on road events with animals and their number is often underestimated because many collisions are not reported (Huijser et al., 2008; Snow et al., 2015).

In the Lublin region based on documentation data from the years 2011-2013 1073 deer-vehicle collisions occurred (Tajchman et al., 2017a), while in the city of Lublin in the period of 2009-2012 the number of incidents with wild animals was recorded to be 930 (Tajchman et al., 2017b). WVC are associated with financial consequences. In Poland, the cost of one collision with an animal was estimated at ca. 2 144 USD; the cost of an accident resulting in human body injury is 7 621 USD, and an accident with human casualties reaches 2 692 405 USD. The mean cost of the accidents in 2001-2010 was 45 657 961 USD. In Utah, the USA, the total cost of wildlife-vehicle collisions for the period of 1992-2001 was estimated at 470 million dollars (Tyburski and Czerniak, 2013). On average of São Paulo reported 2 611 animal-vehicle crashes per year. The total annual cost to society was estimated at 25 144 794 USD. The average cost for an animal-vehicle crash, regardless of whether human injuries and fatalities occurred, was 9 629 USD. The Brazilian legal system overwhelmingly (91.7% of the cases) holds the road administrator liable for animal-vehicle collisions, both with wild and domestic species. On average, road administrators spent 1 005 051 USD per year compensating victims (Abra et al., 2019). Huijser et al. (2008) have shown that collisions with large animals, e.g. deer or elk, result in the highest number of injuries and fatalities in humans. It is estimated that property damages associated with collisions with ungulates reach 300 million USD per year in Canada and over 6 milliard USD per year in the USA (the average cost per event: 6 717 USD). It has also been demonstrated that 90% of road collisions with cervids result in fatalities, and trauma is reported in 56-65% of humans (Conover et al., 1995; Transport Canada, 2003; Huijser et al., 2009).

Attention should also be paid to other species of animals that fall victim to vehicle wheels as well. Such investigations are rarely conducted, as collisions with e.g. a fox or a mink do not usually cause large material loss, or the damage is invisible at first glance.

The presence of animals has been shown to be strongly correlated with the type and function of the habitat, proximity to resources (such as food or shelter), and the reason for the presence of the animal at the roadside (e.g. foraging or attempt to cross the road). The frequency of collisions is also correlated with the features of the road itself (width, curvature, and surface type), climatic conditions, road traffic intensity, and driver's condition (Ramp et al., 2006).

Currently, increasing numbers of animals move to cities or migrate through urban areas (Kalinowska, 2008). Despite the threats to biodiversity posed by living in the city, there are also many undeniable advantages (Wheater, 1999). An important factor ensuring favorable conditions of living in cities is the absence of hunting events or other forms elimination of species, especially large birds and mammals. In cities, which are inhabited by large numbers of people, there is always food available for animals, due to the presence of garbage containers, waste bins, or kitchen leftovers. More importantly, the food is available throughout the year. The city also provides regular access to water in park water reservoirs or decorative fountains. An advantage for many animal species living in urban areas is the milder winters (the average temperature in the city is higher by at least 1 °C) (Wheater, 1999; Reichholf, 2009). All these factors promote animal migration to cities. The greater number of wild animals living in urban habitats is associated with an increased risk of animal-vehicle collisions, although the permissible speed of vehicles in built-up areas is 50 km/h (Road Traffic Department in Poland).

Knowledge of the determinants of animal migration and identification of specific areas with a high risk of this type of accidents can improve drivers' safety on newly built road sections. Methods for mitigation of such conflicts (wildlife-human) are a current priority for both city authorities and handlers of wildlife (Found and Boyce, 2011).

Gunson et al. (2011) suggested a need for future research to be focused on modelling specific to each animal species and modelling the measurement of predictive power in specific areas so that the models can be used in similar landscapes. There are sparse investigations of wildlife-vehicle collisions in medium-sized cities. Therefore, the present study will fill the gap in data on such accidents in such agglomerations as Lublin. Road ecologists have analyzed the available georeferenced localizations of WVC to identify their distribution patterns along roads (Puglisi et al., 1974; Krisp and Durot, 2007; Ramp et al., 2005, 2006; Mountrakis and Gunson, 2009). These analyses have revealed that WVC along roads do not occur randomly but are spatially concentrated for specific vertebrate species, including ungulates (Puglisi et al., 1974; Hubbard et al., 2000; Joyce and Mahoney, 2001) and other species (Clevenger et al., 2003; Ramp et al., 2006). Therefore, an attempt was made to detect such areas in the city of Lublin and its surroundings.

Material and methods

Study area

Lublin is a city in the eastern part of Poland (22°34'E 51°14'N) with an area of approx. 147 km². Its area comprises 195.75 ha of parks and gardens, 1674.29 ha of forests (occupying 11.35% of the land), 5633 ha of agricultural land (38.2%), including 4745 ha of arable land, 153 ha of orchards, and 452 ha of meadows and pastures, rivers (45.1 km long), and public roads (317.4 km/100 km²). The city has 339 850 inhabitants and the population density is 2305 people/km² (Study of conditions..., 2019). The mean annual air temperature in the city is 7.3 °C. The lowest average monthly temperature is noted in February (-4.0 °C) and the highest value is recorded in July (18.2 °C). Negative temperatures are recorded from December to March, whereas hot days with air temperatures above 25 °C occur from April to September. The mean annual precipitation sum in the city is approx. 560 mm, with the highest values in July (77.0 mm) and the lowest in January (29.6 mm) (<https://www.lublin.eu/mieszkancy/srodowisko/srodowisko-przyrodnicze-lublina/klimat/>, Kłysik et al., 2008).

Collision data

The aim of the study was to carry out an analysis of wildlife-vehicle collisions in the area of Lublin city, Poland, between the beginning of December 2017 and the end of November 2018. Mutual correlations of the number of WVC with the traffic volume, land use, and seasons of the year were examined. Based on registered road events with wild animals, new models were developed to determine the risk of occurrence of collisions with wild animals in the city of Lublin. The animals were divided into large species (over 30 kg): fallow deer (*Dama dama*), wildboar (*Sus scrofa*), red deer (*Cervus elaphus*) (Fig. 1), and roe deer (*Capreolus capreolus*); medium animals: European badger (*Meles meles*), European beaver (*Castor fiber*), domestic ferret (*Mustela putoriusfuro*), raccoon dog (*Nyctereutes procyonoides*), stone marten (*Martes foina*)

(Fig. 2), red fox (*Vulpes vulpes*), European otter (*Lutra lutra*), brown hare (*Lepus europaeus*) and small: European hedgehog (*Erinaceus europaeus*), red squirrel (*Sciurus vulgaris*), etc., and other animal species.



Figure 1. WVC with large animal (*Cervus elaphus*)



Figure 2. WVC with small animal (*Martes foina*)

The data on wildlife-vehicle collisions in the city of Lublin they were collected from roads where there were no technical barriers. The information were reported to municipal services that arrive directly at the scene of the incident (to help injured animals and/or remove dead animals from the road). The collision sites were converted to GPS (Global Positioning System) coordinates with the use of a Hi-Target Qstar6 receiver with the accuracy of determination of a single point of 2.5 m. Next, using Arc GIS Pro 2.0 software, they were transferred as vectors onto digital maps of Lublin at an accuracy level corresponding to scale 1: 50000.

New landscape-based models and statistical analysis

The number of WVC was compared with data on traffic intensity (vehicle/day) in the same period, land use forms (residential buildings, industrial development, urban greenery, river valleys, agricultural areas, and forests), and seasons of the year. The data were analyzed statistically and the values of the parameters were presented as the mean value and standard error or standard deviation.

It was assumed in the study that the registered WVC sites might be located at a considerable distance from the actual place of the event, as large animals (e.g. red deer) are able to cover even another 800 m after the accident (Found and Boyce, 2011; Finder et al., 1999). Therefore, buffers with a radius of 800 m were established in the sites of collision with large animals. To create a result map showing the impact of land use on the probability of wildlife-vehicle collisions, Lublin was divided into six forms of land use mentioned above, which were considered important from the point of view of landscape ecology by Ng et al. (2008).

The impact of land use on the probability of wildlife-vehicle collisions was assessed by mounting the layers of collision maps onto a map showing the selected forms of land use. Then, in each site of collision, the distance (in a straight line) from the nearest land use forms was determined. Knowing the lengths of the sections connecting the collision sites with the forms of land use and using logistic regression, the following new models of the probability of collisions with animals were proposed (*Eq. 1*):

$$\ln\left(\frac{p_A}{1-p_A}\right) = \alpha_0 + \sum \alpha_i x_i \quad (\text{Eq.1})$$

where: \ln - natural logarithm function, p_A - probability of collision, x_i - predictor variables, α_0 , α_i - regression coefficients.

To develop new models for prediction of the risk of wildlife-vehicle collisions in the area of the city of Lublin and its surroundings, a random sample of points was determined for the location of roads (i.e. a land use form). The spatial data were processed in the ArcGIS for Desktop 10 environment. Next, to generate a grid of 300 objects, the Create Random Points tool, which is part of the data management tool set in the ArcToolbox application, was used. While generating the grid of objects, the minimum distance between two closest randomly designated points was assumed as ≥ 50 m. Subsequently, the data were verified manually. Based on estimation of the regression coefficients and with the use of logistic regression, models were generated for prediction of the risk of collision with medium and small (*Eq. 4*) (P_{AS}) and large animals (*Eq. 3*) (P_{AB}), as well as all animals regardless of their size (*Eq. 2*) (P_A). With the use of the ArcGIS tools, the model compliance with the actual data was 74.9%,

77.8%, and 73.5%, respectively. The predictor variables and the transforming function are presented in *Table 1*.

Table 1. Marks of predictor variables and transforming function

Prediction variable	Transformation	Designation
Distance from river valleys	$\log_{10}(x + 1)$	LR
Distance from forests	$\log_{10}(x + 1)$	LF
Distance from public greenery	$\log_{10}(x + 1)$	LG
Distance from agricultural land	-	A
Distance to housing	$\log_{10}(x + 1)$	LH
Distance from industrial buildings	$\log_{10}(x + 1)$	LI

LR- distance from river valleys, LF- distance from forests, LG- distance from public greenery, A- distance from agricultural land, LH- distance to housing, LI- distance from industrial buildings

Model of risk of collision with all animal species:

$$P_A = \frac{1}{1 + \exp(0.3474 \cdot LR + 1.0709 \cdot LH - 1.1671 \cdot LI)} \quad (\text{Eq.2})$$

Model of risk of collision with large animals:

$$P_{AB} = \frac{1}{1 + \exp(0.4688 \cdot LR + 1.2746 \cdot LH - 1.2928 \cdot LI + 0.00027 \cdot LF)} \quad (\text{Eq.3})$$

Model of risk of collision with medium and small animals:

$$P_{AS} = \frac{1}{1 + \exp(0.3797 \cdot LR + 1.1130 \cdot LH - 0.9798 \cdot LI)} \quad (\text{Eq.4})$$

where: LR- distance from river valleys, LH- distance to housing, LI- distance from industrial buildings, LF- distance from forests.

The statistical analyses of the probability of collision with medium and small animals were carried out at a significance level of $P = 0.05$ in the Statistical Analysis System (SAS, 2012). Distances from river valleys (LR), forests (LF), urban greenery (LG), agricultural land (LA), residential buildings (LH), and industrial development (LI) were regarded as dependent variables. With the exception of the distance from forests, the variables were transformed by the decimal logarithm to reduce the skewness of the distribution of the distances to the analyzed areas (Zar, 2010). Additionally, mutual correlations (CORR procedure) between the variables were analyzed to eliminate the highly correlated ones (Zar, 2010). The variables were then used as predictor variables in the logistic regression model with the maximum likelihood method (LOGISTIC procedure) for the resulting binary variable, specifying whether a collision had occurred at a given point (1 - collision, 0 - no collision at a random point) (SAS, 2012). To develop the final model, we used a full model with all potential predictor variables and different modes of choice of only relevant variables:

stepwise, forward, and backward elimination. The best model was selected using the Akaike information criterion, AIC (Akaike, 1974). To simplify the model, the interactions between the variables were disregarded. New models of the risk of wildlife-vehicle collisions were developed taking into account the division into large, medium, small, and all animal species.

Due to the large variability of the data in relation to the low number of collisions, a method used commonly in the case of concentration of events (hot spot analysis) had to be employed. It allows graphic representation of areas with high intensity of a given phenomenon (hot spot).

Results

The analyzed data showed that there were 291 collisions with animals in the city of Lublin and its surroundings during the study period, with almost half (42.7%) taking place on roads where the traffic intensity did not exceed 100 vehicles/day, and the collisions with medium and small animals accounted for 57.9%.

Areas especially susceptible to WVC (hot spots) in Lublin were identified where minimum two 800-meter buffers extending from the event sites overlapped (*Fig. 3*). The analyses demonstrated 105 hotspots in the area of Lublin, with more than half (58.1%) of the sites where only two buffers overlapped. Three buffers overlapped in 28.6% of the hot spots. In turn, 8.6% of the hot spots were located in sites with 4 overlapping buffers. Only 2.9% of and 1.9% the hot spots comprised 5 and 6 overlapping buffers, respectively (*Fig. 3*). The hot spots of collisions with large animals were located mainly in the areas of urban greenery (40.0%), agricultural land (20.0%), and forests (15.4%). In turn, the other collision hot spots were located near residential buildings (18.5%), industrial development (4.6%), and river valleys (1.5%). The vast majority (83.8%) of the hot spots of collisions with large animals were located on the outskirts of the city, along the main communication routes leading to the city center (*Fig. 3*).

The results of the analysis of the correlation between the traffic volume (vehicles/day) and the number of road collisions with wild animals revealed significant relationships between these factors (*Table 2*). There was no significant correlation between the increase in the number of wildlife-vehicle collisions and the increase in traffic intensity in any of the analyzed cases of events with large animals. An exception was the road sections with traffic intensity of 501-600 and 1101-1200 vehicles/day, where a highly significant positive correlation of the increase in the number of WVC with the increase in traffic intensity was demonstrated ($R = 0.4779$ and $R = 0.3589$, respectively). Similarly, in the case of collisions with medium and small animals, no significant positive correlations were found between the number of events and the increase in traffic intensity. However, there was a significant negative correlation ($R = -0.2774$) between the number of WVC and the increase in traffic volume on road sections exhibiting traffic intensity of 1101-1200 vehicles/day. This indicates that higher traffic intensity is correlated with a lower number of WVC (*Table 2*).

The analysis of the traffic intensity (vehicles/day) and the number of road collisions (regardless of the animal species) revealed a very strong negative correlation ($R = -0.3384$) between the number of WVC and the increase in traffic intensity on road sections with traffic intensity of 301-400 vehicles/day (*Table 2*).

This indicates a significant decline in the number of collisions with animals at a higher traffic volume. In turn, there was a significant positive correlation between the number of WVC and the increase in traffic in the case of roads with 501-600 vehicles/day ($R = 0.2675$). Compared to the former correlation, this relationship is weaker but justified by the considerably lower impact of traffic on the number of wildlife-vehicle collisions.

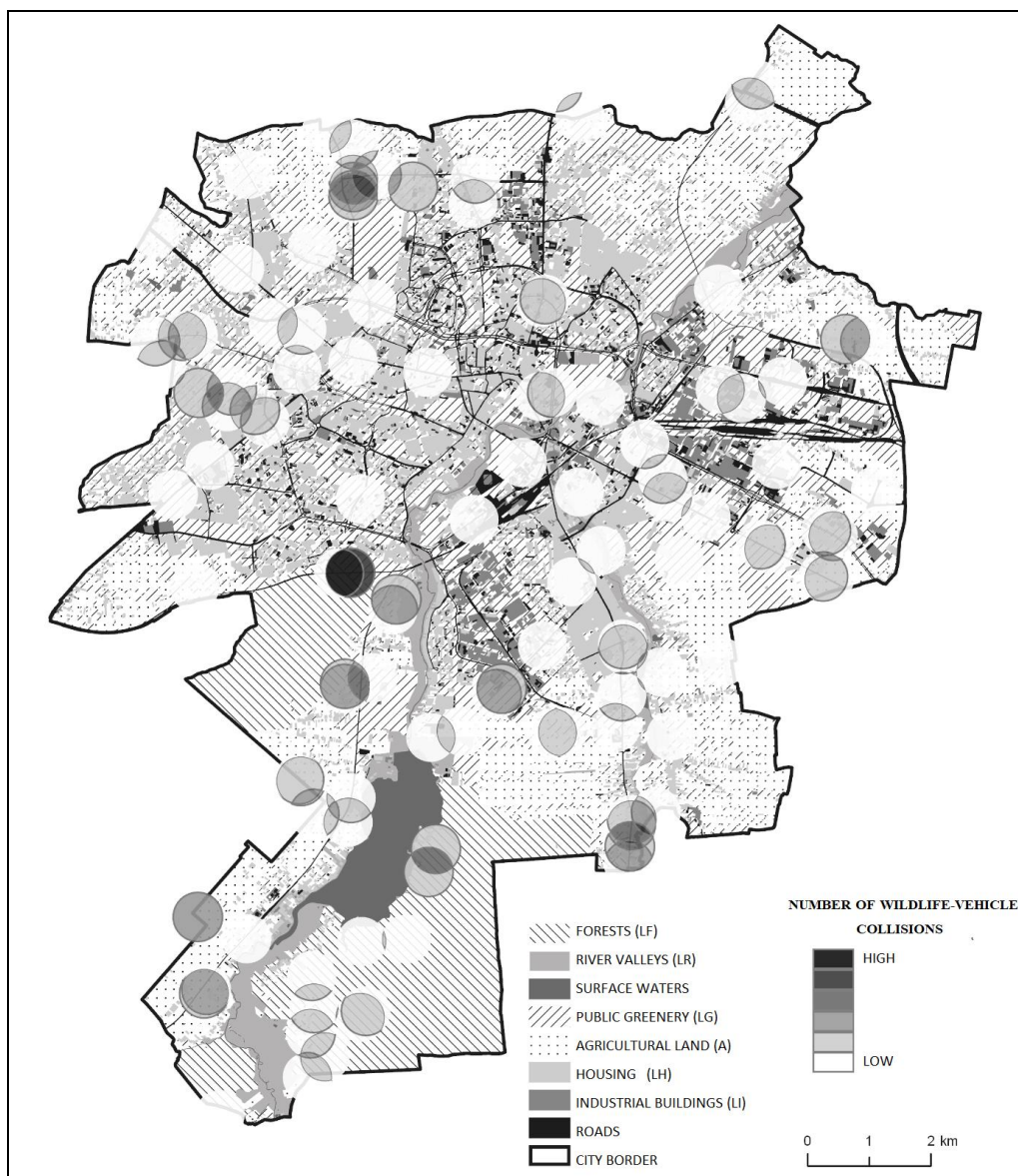


Figure 3. Location and number of collisions (hot spot) with large animals in the city of Lublin

No statistically significant correlation between the number of collisions and the season of the year was noted during the investigation period in the analysed area (Lublin). The highest number of WVC was recorded in summer and spring, i.e. 91 and 78 events with animals, respectively, which accounted for more than half (58.07%) of all recorded collisions (Table 3). The highest number of single collisions (79) and double collisions (two accidents in one place) was found for 12 city points in summer.

Also in spring, the vast majority of events were single collisions (68), double collisions took place in 8 city areas, and triple collisions were found in 2 city points; they constituted 87.18%, 10.26%, and 2.56%, respectively, of all collisions recorded at this time of the year (Table 3). In autumn, the vast majority of collisions (88.41%) were single collisions (68). Double collisions in autumn were recorded in 7 points of the city (10.14%). In the same season, 5 collisions were reported from 1 site in the city, which constituted 1.45% of all events recorded at this time of the year. The smallest number of wildlife-vehicle collisions, i.e. 53, which accounted for 18.21% of all collisions recorded in the investigation period, occurred in winter. As in the other seasons, the vast majority of collisions (96.23%) in this period were single events, while double events occurred only in two city locations (Table 3).

No significant correlations were found between the WVC and the forms of land use in any of the analyzed cases. The highest correlation was determined for forests and arable land ($R = 0.31$) and there was a negative correlation between arable land and industrial development ($R = -0.36$). In the case of large, medium, small, and all animals, models comprising only significant predictor variables were the best according to the AIC criterion. All methods for selection of the variables (stepwise, forward, backward) yielded the same models.

Regardless of the animal species, the distances from river valleys, residential buildings, and industrial development turned out to be significant predictor variables (Table 4). In the case of the first two variables, the risk of WVC increased with their decreasing value, while the risk of collision in the industrial development increased with the increasing distance from such areas.

Table 2. Relationship between wildlife-vehicle collisions (WVC) and intensity of traffic road (for $P > 0.05$)

Traffic intensity (vehicles/day)	WVC				Regardless of the species	SD
	Large animals	SD	Medium and small animals	SD		
< 100	0.2618	±0.45	0.0900	±0.28	0.0802	±0.24
100-200	-0.1995	±0.49	-0.01855	±0.35	-0.1827	±0.40
201-300	-0.0971	±1.15	0	±0.00	-0.1978	±0.79
301-400	0	±0.00	0	±0.49	-0.3384**	±0.43
401-500	0.0290	±0.36	-0.1676	±0.25	-0.812	±0.30
501-600	0.4779**	±0.25	0	±0.00	0.2675**	±0.21
601-700	-0.1526	±0.31	-0.2244	±0.68	-0.2131	±0.54
701-800	0	±0.00	0.0857	±0.40	0.0662	±0.31
801-900	0	±0.00	0.1162	±0.35	0.1037	±0.28
901-1000	0	±0.00	0	±0.00	0	±0.00
1001-1100	0	±0.00	0	±0.00	0	±0.00
1101-1200	0.3589**	±0.28	-0.2774*	±0.33	0.1816	±0.30
1201-1300	0	±0.00	0	±0.00	0	±0.00
1301-1400	0	±0.00	0	±0.00	0	±0.00
1501-2,000	0	±0.00	0	±0.00	0	±0.50
> 2000	0	±0.00	0	±0.46	0	±0.00

SD - standard deviation, *significant dependence, **very strong dependence

Table 3. Dependence of wildlife-vehicle collisions (WVC) quantity distributions from seasons (for $P > 0.05$)

Seasons	WVC depending on location and season	Number of WVC in a given place				Total
		1	2	3	5	
Autumn	WVC number	61	7	0	1	69
	Percent of WVC in a given place %	23.55	24.14	0	100.00	23.71
	Percentage of WVC in a given season %	88.41	10.14	0	1.45	
	WVC percent of the full year %	20.96	2.41	0	0.34	
Summer	WVC number	79	12	0	0	91
	Percent of WVC in a given place %	30.50	41.38	0	0	31.27
	Percentage WVC in a given season %	86.81	13.19	0	0	
	WVC percent of the full year %	27.15	4.12	0	0	
Spring	WVC number	68	8	2	0	78
	Percent of WVC in a given place %	26.25	27.59	100.00	0	26.80
	Percentage WVC in a given season %	87.18	10.26	2.56	0	
	WVC percent of the full year %	23.37	2.75	0.69	0	
Winter	WVC number	51	2	0	0	53
	Percent of WVC in a given place %	19.69	6.90	0	0	18.21
	Percentage WVC in a given season %	96.23	3.77	0	0	
	WVC percent of the full year %	17.53	0.69	0	0	
Total	WVC number	259	29	2	1	291
	WVC percent of the full year %	89.00	9.97	0.69	0.34	

Table 4. Estimators of regression coefficients and their statistical significance for all animals

Parameter	DF	Estimate	SE	Wald chi-square	P-value
All animals					
LR	1	-0.347	0.094	13.656	0.0002
LH	1	-1.071	0.134	64.348	< 0.0001
LI	1	1.167	0.142	67.361	< 0.0001
Large animals					
LF	1	-0.0003	0.0001	6.868	0.0090
LR	1	-0.4690	0.1480	9.999	0.0020
LH	1	-1.2750	0.1830	48.324	< 0.0001
LI	1	1.2930	0.1950	44.004	< 0.0001
Medium and small animals					
LR	1	-0.379	0.109	12.251	0.0005
LH	1	-1.113	0.153	52.669	< 0.0001
LI	1	0.979	0.164	35.930	< 0.0001

DF- degrees of freedom used in the Wald-chi-square test, SE- Standard prediction error of the estimator (regression coefficient), Wald Chi-Square - Wald Chi-Square test values, P-value - the assumed level of significance of the test. P-value less than 0.05 (assumed test significance level) specifies that the given parameter is significant in the model (significantly different from 0), LR- distance from river valleys, LH- distance to housing, LI- distance from industrial buildings, LF- distance from forests

In the analysis of collisions with large animals only, the variables indicated for all animals (distances from river valleys, residential buildings, and industrial development) and additionally the distance from forests (*Table 4*), for which it was found that the closer the distance to the forest the greater the risk of collision with large animals, turned out to be significant predictor variables. For the other predictor variables, the trend in the impact was similar to that in the case of all animals. While assessing the risk of collision with medium and small animals, the variables indicated for all animals, i.e. the distances from river valleys, residential buildings, and industrial development turned out to be significant predictor variables (*Table 4*). They had a similar effect to that noted in the analysis of all animals. The estimation of the probability of WVC shows the highest risk of such events in areas located on the outskirts of Lublin (Southern, South-eastern and north-western parts) (*Figs. 4–5*). A high risk of accidents with wild animals has also been identified for residential areas adjacent to the Bystrzyca and Czerniejówka river valleys in the central part of Lublin. The smallest risk of WVC was indicated near the industrial areas in the north and south of Lublin.

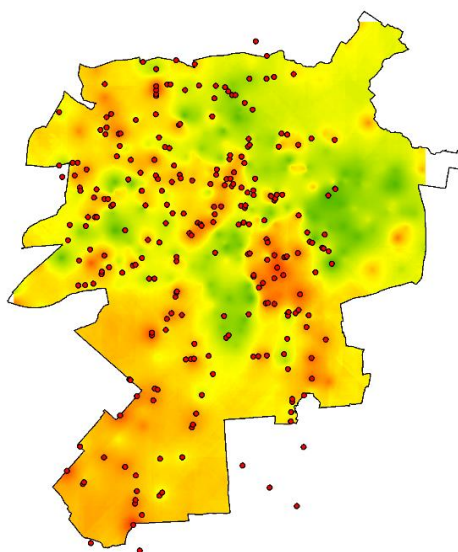


Figure 4. The probability of an accident with wild animals, regardless of the species, in Lublin (red color - high probability, green - low probability)

The analysis of the probability of collisions with animals indicates the greatest risk of collisions with large animals in an area located to the south-east from the center of Lublin (area adjacent to the Czerniejówka River valley) (*Fig. 5A*). It is a part of the city with compact single-family residential buildings with house gardens. A high risk of collisions with large animals has been noted in the southern part of Lublin, i.e. in the area of a large water reservoir (Zemborzycki Lake) surrounded by a forest complex, and in the central part - in a large city park (Ludowy Park) situated in the Bystrzyca River valley. As demonstrated by the analyses, areas located near the industrial development located in the northern, central, and southern parts of Lublin exhibit the lowest risk of collisions with large animals.

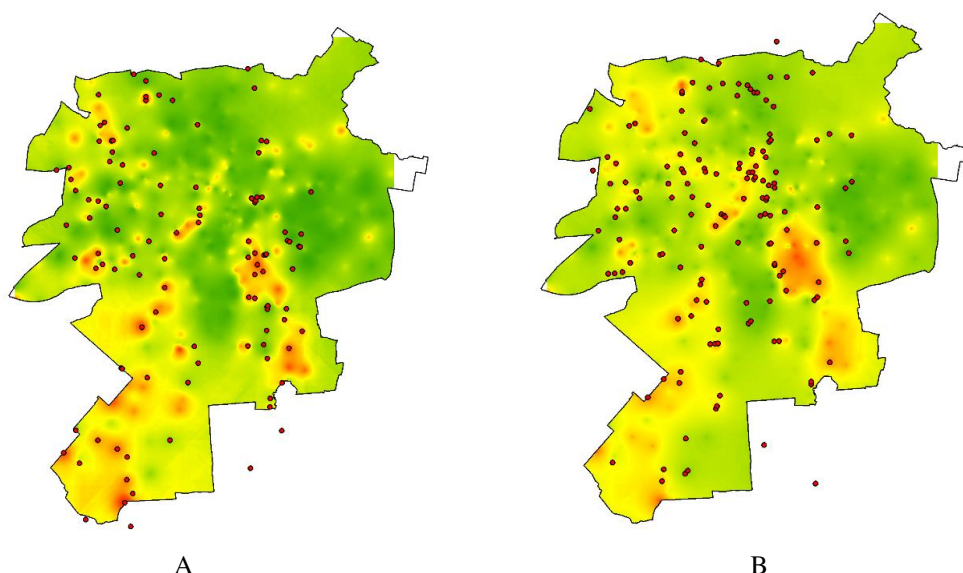


Figure 5. Maps of probability of collisions with animals in Lublin: A - with large animals, B - with medium and small animals (red color - high probability, green - low probability)

The highest probability of collisions with medium and small animals was shown for the south-eastern part of Lublin (Fig. 5B). This is probably related to the presence of residential buildings and the Czermiejówka River valley. Other areas with a high probability of collisions with medium and small animals are located in the central and north-western part of the city. The central part of the city comprises residential buildings located in the immediate vicinity of dry loess gorges serving as a city park. In turn, the area located in the north-western part of the city is the Czechówka River valley near a two-lane express road (Fig. 5B). As in the case of large animals, a high risk of collisions with medium and small animals was estimated for the southern part of Lublin around the water reservoir (Zemborzycki Lake) and for areas to the north and south of the lake located near the wetlands of the Bystrzyca River valley, which flows out of this water body. Areas with the lowest risk of collision with medium and small animals, as in the case of large animals, are located in industrial development areas in the northern, central, and southern parts of Lublin.

Discussion

The present investigations have demonstrated that the number of WVC decreases with the increase of traffic intensity. This is consistent with the results reported by Forman and Alexander (1998), who showed a road avoidance effect. Busy roads sometimes deter animals sufficiently to prevent them from crossing (Clevenger et al., 2003); thus, animal mortality declines. The exceptions were road sections with traffic intensity of 501-600 and 1101-1200 vehicles/day, where there was a highly significant positive correlation between the increase in the number of WVC and the increase in traffic volume. This may be associated with the substantially higher speed of driving on these roads, and traffic intensity and speed are the main factors WVC, as shown in many studies (Forman and Alexander, 1998; Hubbard et al., 2000; Jones, 2000; Trombulak and Frissell, 2000; Dique et al., 2003; Seiler, 2003).

In the analyzed data from in the city of Lublin and its surroundings during the study period, there were no high correlations between WVC and land use forms. The sites of concentration of collisions with large animals (hot spots) were located mostly in the areas of urban greenery, agricultural land, and forest. This was confirmed in studies conducted by other authors (Hubbard et al., 2000; Nielsen et al., 2003; Farrell and Tappe, 2007; Ng et al., 2008), who found that wooded and open areas were the most attractive foraging sites for deer. The vast majority of sites of concentration of hot spots were located on the outskirts of the city along major communication routes leading to the city center. As demonstrated by Premo and Rogers (2001), there was an increase in collisions with deer in suburban areas.

The present study also showed the highest positive correlation between forests and arable land and a negative correlation between arable land and industrial development. These results are in agreement with those reported by Stewart et al. (2007) as well as Farrell and Tappe (2007), who have shown that cervids choose clearings with adjacent wooded areas and completely forested areas. The presence of open land near forested areas together with higher vehicle speeds and higher traffic volumes has been correlated with higher frequencies of deer-vehicle collisions (Bashore et al., 1985; Nielsen et al., 2003; Ng et al., 2008; McShea et al., 2008).

The analysis carried out in the city of Lublin and its surroundings shows the highest number of WVC in summer and spring. This is probably associated with the duration of the day and the seasonal activity of the animals. For many species of animals, spring is a time of reproduction, establishment of home ranges, fights for females, search for breeding places, and migration over distances larger than usual. Spring and summer are seasons when roebucks show increased activity establishing and protecting their territory (Ignatavicius and Valskys, 2018). In medium animals, e.g. fox and marten, this is a period of development of offspring and increased activity of females questing for food for their young ones (Goszczyński, 1995; Goszczyński et al., 1994; Herr, 2008). Interestingly, many studies indicate that autumn is another period (besides spring) with the highest number of accidents (39%). This season is a time of migrations to wintering grounds and mating in some species (especially deer). In this period, males are particularly vulnerable to the risk of road collision, as they expand their territories in search and fight for females (Tajchman et al., 2017A). Researchers agree that, despite the increased frequency of road collisions with ungulates in Europe and the United States in recent years, the events are not associated with the threat of extinction of species involved. It is prevented by the high reproduction rate of these species and/or the high ability to re-colonise habitats where the population has gone extinct (Found and Boyce, 2011; Hubbard et al., 2000).

The investigations studies carried out in the city of Lublin and its surroundings demonstrate that most of WVC cases involve medium and small animals (57.9%), with the greatest number of the events recorded in spring and summer. This phenomenon is disturbing, as the group of small animals often comprises species with small population sizes. Surveys carried out in Poland and Sweden (Seiler, 2004; Seiler et al., 2004) have shown that the brown hare is characterized by the highest rate of fatalities on the roads. It has been estimated that 35% of the 200,000 population of hares in Sweden die in wildlife-vehicle collisions. The survival of populations of this species is also threatened in the Netherlands and Denmark, and mortality associated with collisions with motor vehicles may turn out to be an increasingly important factor limiting the population size of this species, which is endangered also in Poland. In the case of rare and endangered

species, each individual dying under car wheels is a big loss. Quick recognition of the problem and mitigation actions can improve the status of the population. Intensive work is carried out to reduce otter mortality on the roads in Denmark and the death rate of the badger, i.e. a species threatened with extinction and decimated in wildlife-vehicle collisions, in the Netherlands (Lankester et al., 1991). Special attention should therefore be paid to this group of animals. In the present study, the risk of collisions with medium and small animals increased with the proximity to open water bodies or wetlands adjacent to roads (Gunson et al., 2011). This is in agreement with the results reported by Kanda et al. (2006), who noted collisions with small and medium vertebrates at low altitudes, which most likely provide favorable habitats for these animal species. The opposite was found for areas with higher road and building density (Bashore et al., 1985; Nielsen et al., 2003; Ng et al., 2008; McShea et al., 2008), which was also confirmed by the analyses carried out in Lublin. Interestingly, the present study has shown an increase in the number of WVC farther away from industrial development. This may be related to the fact that such facilities are most often located on the outskirts of the city, i.e. in open areas where animals dwell eagerly and humans are present only during working hours.

In the research carried out by Found and Boyce (2011) in the city of Edmonton, modelling was performed only for road collisions with cervids. It was demonstrated that the density of vegetation was by 52% higher in the established hot spots than in cold spots; additionally, the percentage of habitats available for animals was by 21% higher. This was also confirmed in the investigations conducted in Lublin showing that a closer distance to the forest was associated with a greater the risk of collisions with large animals. It should be remembered that increasing density of high vegetation causes poorer visibility and thus raises the risk of WVC due to the shorter time between noticing the animal and driver's reaction, which also increases the risk of WVC (Found and Boyce, 2011). Malo et al. (2004) emphasized that vegetation should be mown regularly within 40-80 m roadside buffers, which could lower the attractiveness of roadsides to herbivores. However, other studies have demonstrated that enlargement of the road width and visibility in roadside corridors increases the rate of WVC, as drivers move at higher speeds in such conditions. Another effective solution is the use of barriers or protective fences (Gunson et al., 2011).

Conclusion

Reliable and effective methods for WVC prediction and mitigation have become a priority for various city planners and wildlife handlers (Farrell and Tappe, 2007). Hence, similar studies should be carried out in all European cities with focus on the causes of the increased rates of wildlife-vehicle collisions. The existing WVC probability models should be used for graphic design - city maps with accident locations - hot spots. In addition, WVC probability models with individual groups of animals with similar biology and behavior should be constructed. This should be preceded by a thorough analysis of the number of WVC with large, medium and small animals. In aim of quick recognition of the problem and introduce mitigation actions which can improve the status of the animal population.

The distances from river valleys, residential buildings, and industrial development turned out to be significant predictor variables for WVCs. In the analysis of collisions with large animals, the variables were found that the closer the distance to the forest the

greater the risk of collision increases. While assessing the risk of collision with small animals, the variables: the distances from river valleys, residential buildings, and industrial development turned out to be significant predictor variables. The highest number of WVC was recorded in summer and spring, which accounted for more than half (58.07%) of all recorded collisions. When planning the expansion of cities, pay special attention to the listed places, which depend on WVC, with particular regard to animal species or their groups using available minimizing solutions.

Moreover, migrating animals tend to take the easiest paths (Boone et al., 1996; Schippers et al., 1996; Larkin et al., 2004); hence, the risk of WVC increases when roads are situated at the ground level (Clevenger et al., 2003; Malo et al., 2004; Ramp et al., 2005). Such areas are found in most parts of Lublin. Roads run along embankments and are additionally fenced with acoustic screens preventing free migration of wild animals only in the northern part of Lublin. These are pilot studies, therefore in the future, it is worth investigating the number of WVC in correlation with the terrain level and the location of roads. In addition, human factors/behavior and weather conditions should also be taken into account.

REFERENCES

- [1] Abra, F. D., Granziera, B. M., Huijser, M. P., Ferraz, K. M., Haddad, C. M., Paolino, R. M. (2019): Pay or prevent? Human safety, costs to society and legal perspectives on animal-vehicle collisions in São Paulo state, Brazil. – *PLoS ONE* 14(4): e0215152.
- [2] Akaike, H. (1974): A new look at the statistical model identification – *IEEE Trans. Auto. Control.* 19: 716-723.
- [3] Bashore, T. L., Tzilkowski, W. M., Bellis, E. D. (1985): Analysis of deer-vehicle collision sites in Pennsylvania, USA – *Journal of Wildlife Management* 49: 770-774.
- [4] Boone, R. B., Hunter, M. L., Cook, I. J. (1996): Using diffusion models to simulate the effects of land use on grizzly bear dispersal in the Rocky Mountains – *Landscape Ecology* 11: 51-64.
- [5] Clevenger, A. P., Chruszcz, B., Gunson, K. E. (2003): Spatial patterns and factors influencing small vertebrate fauna road-kill aggregations – *Biology Conservation* 109: 15-26.
- [6] Conover, M. R. (2010): *Resolving Human-Wildlife Conflicts: The Science of Wildlife Damage Management.* – CRC Press, Boca Raton, FL.
- [7] Conover, M. R., Pitt, W. C., Kessler, K. K., DuBow, T. J., Sanborn, W. A. (1995): Review of human injuries, illnesses, and economic losses caused by wildlife in the United States – *Wildlife Society Bulletin* 23: 407-414.
- [8] Dique, D. S., Thompson, J., Preece, H. J., Penfold, G. C., de Villiers, D. L., Leslie, R. S. (2003): Koala mortality on roads in south-east Queensland: the koala speed-zone trial – *Wildlife Research* 30: 419-426.
- [9] Farrell, M. C., Tappe, P. A. (2007): County-level factors contributing to deer-vehicle collisions in Arkansas – *Journal of Wildlife Management* 71: 2727-2731.
- [10] Finder, R. A., Roseberry, J. L., Woolf, A. (1999): Site and landscape conditions at white-tailed deer/vehicle collision locations in Illinois – *Landscape and Urban Planning* 44: 77-85.
- [11] Forman, R. T. T., Alexander, L. E. (1998): Roads and their major ecological effects – *Annual Review of Ecology and Systematic* 29: 207-231.
- [12] Found, R., Boyce, M. S. (2011): Predicting deer-vehicle collisions in an urban area. – *Journal of Environmental Management* 92(2011): 2486-2493.

- [13] Goszczyński, J. (1995): Fox – Monograph Natural and Hunting. – Publishing House Oikos Sp. Z O. O., Warsaw (in Polish).
- [14] Goszczyński, J., Romanowski, J., Zalewski, A. (1994): Martens. – Publishing Editorial Publishing World, Warsaw (in Polish).
- [15] Gunson, K. E., Muntrakis, G., Quackenbush, L. J. (2011): Spatial wildlife-vehicle collision models: A review of current work and its application to transportation mitigation projects – *Journal of Environmental Management* 92: 1074-1082.
- [16] GUS 2001-2018 www.stat.gov.pl (access July 15, 2019).
- [17] Herr, J. (2008): Ecology and behaviour of urban stone martens (*Martes foina*) in Luxembourg. – University of Sussex, Brighton (PhD thesis).
- [18] <https://www.lublin.eu/mieszkanicy/srodowisko/srodowisko-przyrodnicze-lublina/klimat/> (access July 15, 2019).
- [19] Hubbard, M. W., Danielson, B. J., Schmitz, R. A. (2000): Factors influencing the location of deer-vehicle accidents in Iowa – *Journal of Wildlife Management* 64: 707-712.
- [20] Huijser, M. P., Duffield, J. W., Clevenger, A. P., Ament, R. J., McGowen, P. T. (2009): Cost benefit analyses of mitigation measures aimed at reducing collisions with large ungulates in the United States and Canada: a decision support tool – *Ecology and Society* 14(2): 15-22.
- [21] Huijser, M. P., McGowen, P. T., Fuller, J., Hardy, A., Kociolek, A. (2008): Wildlife-Vehicle Collision Reduction Study: Report to Congress. – U.S. Department of Transportation, Federal Highway Administration, Washington.
- [22] Ignatavicius, G., Valskys, V. (2018): The influence of time factors on the dynamics of road deer collisions with vehicles – *Landscape and Ecology Engineering* 14(2): 221-229.
- [23] Jones, M. E. (2000): Road upgrade, road mortality and remedial measures: impacts on a population of eastern quolls and Tasmanian devils – *Wildlife Research* 27: 289-296.
- [24] Joyce, T. L., Mahoney, S. P. (2001): Spatial and temporal distributions of moose-vehicle collisions in Newfoundland – *Wildlife Society Bulletin* 29: 281-291.
- [25] Kalinowska, A. (2008): Climate change - current and predictable impact on biodiversity in Poland and in the world. – In: *Climate Change and Nature Protection - VI Kampinos Meetings with Nature. Conference Materials April 16, 2008, Kampinos National Park. Foundation of the Ecological Education Center, Warsaw*, pp. 1-6.
- [26] Kanda, L. L., Fuller, T. K., Sievert, P. R. (2006): Landscape associations of road-killed virginia possums (*Diderphis virginiana*) in Central Massachusetts – *The American Midland Naturalist* 156: 128-134.
- [27] Kłysik, K., Wibig, J., Fortuniak, K. (2008): Climate and bioclimate of cities – University of Lodz Publishing, Łódź (in Polish).
- [28] Krisp, J. M., Durot, S. (2007): Segmentation of lines based on point densities-An optimization of wildlife warning sign placement in southern Finland – *Accident Analysis and Prevention* 39: 38-46.
- [29] Lankester, K., van Apeldoorn, R. C., Meelis, E. i Verboom, J. (1991): Management perspectives for populations of the Eurasian badger (*Meles meles*) in a fragmented landscape – *J. Applied Ecology* 28: 561-573.
- [30] Larkin, J. L., Maehr, D. S., Hootor, T. S., Orlando, M. A., Whitney, K. (2004): Landscape linkages and conservation planning for the black bear in west-central Florida – *Animal Conservation* 7: 23-34.
- [31] Malo, J. E., Suarez, F., Diez, A. (2004): Can we mitigate animal-vehicle accidents using predictive models? – *Journal of Applied Ecology* 41: 701-710.
- [32] McShea, W. J., Stewart, C. M., Kearns, L. J., Liccioli, S., Kocka, D. (2008): Factors affecting autumn deer-vehicle collisions in a rural Virginia county – *Human–Wildlife Interactions* 2: 110-121.
- [33] Mountrakis, G., Gunson, K. E. (2009): Multi-scale spatiotemporal analyses of moose vehicle collisions: a case study in northern Vermont – *International Journal of Geographical Information System* 23: 1389-1412.

- [34] Ng, J. W., Nielsen, C., St. Clair, C. C. (2008): Landscape and traffic factors influencing deer-vehicle collisions in an urban environment – *Humane Wildlife Conflicts* 2: 102-109.
- [35] Nielsen, C. K., Anderson, R. G., Grund, M. D. (2003): Landscape influences on deer-vehicle accident areas in an urban environment – *Journal of Wildlife Management* 67: 46-51.
- [36] Premo, D. B., Rogers, E. I. (2001): Creating and urban deer vehicle accident management plan using information from a town’s GIS project. – *Proceedings of the 2001 International Conference on Ecology and Transportation*, Raleigh, NC.
- [37] Puglisi, M. J., Lindzey, J. S., Bellis, E. D. (1974): Factors associated with highway mortality of white-tailed deer – *Journal of Wildlife Management* 38: 799-807.
- [38] Ramp, D., Wilson, V. K., Croft, D. B. (2006): Assessing the impacts of roads in peri-urban reserves: Road-based fatalities and road usage by wildlife in the Royal National Park, New South Wales, Australia – *Biology Conservation* 129: 348-359.
- [39] Ramp, D. J., Caldwell, J., Edwards, K. A., Warton, D., Croft, D. B. (2005): Modelling of wildlife fatality hotspots along the snowy mountain highway in New South Wales – Australia. *Biology Conservation* 126: 474-490.
- [40] Reichholf, J. H. (2009): *The Demise of Diversity. Loss and Extinction* – Haus Publishing, London.
- [41] SAS Institute Incorporated (SAS) (2012): *SAS/STAT®12.1 User’s Guide*, Electronic book 1. – SAS Institute Inc., Cary, NC.
- [42] Schippers, P., Verboom, J., Knappen, J. P., Apeldoorn, R. C. V. (1996): Dispersal and habitat connectivity in complex heterogeneous landscapes: an analysis with a GIS-based random walk model – *Ecography* 19(2): 97-106.
- [43] Seiler, A. (2003): *The toll of the automobile: wildlife and roads in Sweden*. – PhD Thesis. Swedish University of Agricultural Sciences, Uppsala, Sweden.
- [44] Seiler, A. (2004): Trends and spatial patterns in ungulate-vehicle collisions in Sweden – *Wildlife Biology* 10: 301-313.
- [45] Seiler, A., Helldin, J. O., Seiler Ch. (2004): Road mortality in Swedish mammals: results of a drivers’ questionnaire – *Wildlife Biology* 10: 225-233.
- [46] Snow, N. P., Porter, W. F., Williams, D. M. (2015): Underreporting of wildlife-vehicle collisions does not hinder predictive models for large ungulates – *Biology Conservation* 181: 44-53.
- [47] Stewart, C. M., McShea, W. J., Piccolo, B. P. (2007): The impact of white-tailed deer on agricultural landscapes in 3 national historical parks in Maryland – *Journal of Wildlife Management* 71(5): 1525-1530.
- [48] Study of conditions and directions of spatial development of the city of Lublin, Resolution No. 283 / VIII / 2019 of the Lublin City Council of 1 July 2019.
- [49] Tajchman, K., Gawryluk, A., Drozd, L., Czyżowski, P., Karpiński, M., Goleman, M. (2017a): Deer-vehicle collisions in Lubelskie region in Poland. Safety coefficients. – *Applied Ecology of Environmental Research* 15(3): 1485-1498.
- [50] Tajchman, K., Drozd, L., Karpiński, M., Czyżowski, P., Goleman, M., Chmielewski, S. (2017b): Wildlife-vehicle collisions in urban area in relations to the behaviour and density of mammals. – *Polish Journal of Natural Science* 32(1): 49-59.
- [51] Transport Canada (2003): *Overview of Technologies Aimed at Reducing and Preventing Large Animal Strikes*. – Standards Research and Development Branch, Ottawa, Ontario, Canada.
- [52] Trombulak, S. C., Frissell, C. A. (2000): Review of ecological effects of roads on terrestrial and aquatic communities – *Conservation Biology* 14(1): 18-30.
- [53] Tyburski, Ł., Czerniak, A. (2013): The costs of road accidents involving animals. – *Study Materials and CEPL in Rogow R.15. notebook* 36/3/2013 (in Polish).
- [54] Wheater, C. P. (1999): *Urban Habitats* – Routledge, London and New York.
- [55] Zar, J. H. (2010): *Biostatistical Analysis*. 5th Ed. – Prentice-Hall, Englewood Cliffs, NJ.

COMPARISON OF ROOTING SITUATIONS FOR SALAKHANI AND ZIVZIK POMEGRANATES UNDER DIFFERENT IBA DOSES

AL-JABBARI, K. H.¹ – PAKYÜREK, M.^{1*} – YAVIÇ, A.²

¹*Department of Horticulture, Faculty of Agriculture, Siirt University, 56100 Siirt, Turkey*

²*Department of Horticulture, Faculty of Agriculture, Yüzüncü Yıl University, 65080 Van, Turkey*

**Corresponding author*

e-mail: mine.pakyurek@siirt.edu.tr

(Received 28th Jul 2019; accepted 31st Oct 2019)

Abstract. Rooting performance of Salakhani, a local variety of Iraq and Zivzik (*Punica granatum* L.), a local pomegranate of Siirt, were compared in our study. For this purpose, the effect of different doses of indole butyric acid (IBA) (0.00, 1000, 2000, 4000, 6000 mg / L) on rooting was examined. Cuttings were kept in the rooting environment for five months and rooting rates, root number, root lengths, survival rates, shoot lengths, shoot and leaf number were determined. Salakhani were found to be the best cultivar only in terms of the root length, sprout length, shoot number and leaf number. Zivzik were found to be the best variety with regard to the other properties. IBA application of 4000 ppm was found to be the best all the shoot number, leaf number and root length. The hormone dose of 6000 ppm was found to be the most beneficial for survival and rooting rates. Application of 1000 ppm was found to be the best dose among the doses of hormone only on account of root number.

Keywords: *plant growth regulators, Punica granatum L., cutting production, vegetative growth, hormone effect*

Introduction

Pomegranate is one of the first five important fruits together with fig, date, olive and grape which are old known cultivated plants. The domestication of pomegranate started 3000-4000 BC in the North of Iran and Turkey (Usanmaz et al., 2014). It is a perennial plant grown in tropical and subtropical regions (Schubert et al., 1999). Iran and the Himalayas of Northern India are the central origin of pomegranate. This fruit grows well in semi-arid temperate and subtropical climate and it is naturally grown in any climate with cool winter and hot summer. Pomegranate is deciduous in the subtropics and is evergreen in the tropical regions.

It is a species found in temperate forests that requires high temperatures in summer in order to reach full maturity and achieve commercial production (Melgarejo and Martinez, 1989). For most species of pomegranate, the suitable temperature degrees are between 21°C and 27°C during day-time and 15°C of night-time temperatures (Hartmann et al., 1997). It is naturally grown and is well adapted to the regional climate in Afghanistan, China, Morocco, Palestine, India, Iraq, Iran, Israel, Italy, Cyprus, Egypt, Syria, Saudi Arabia, Thailand, Tunisia, Turkey. Iran, Spain, Tunisia and Turkey are the countries exporting pomegranates (Özgüven and Yılmaz, 2000). India is first in terms of pomegranate production and production area. When it comes productivity, Spain (18.5 t/ha) comes first, traced by USA (18.3 t/ha). On the other hand, Iran (60.000 t/year) is first in point of exports, chased by India (37.176 t/year) (Chandra et al., 2006, 2008; Chandra and Meshram, 2010; Silva et al., 2013).

Pomegranate cultivation is done in different soil types, such as sand, gravel, clay and heavy clay soils. Optimal development of pomegranate is observed in deep, permeable, alkali and sandy loam soils. In Turkey, pomegranate cultivation can be done in all regions, except for very cold regions. Furthermore, pomegranate can withstand the lowest temperature range from -10°C up to -15°C , while the temperature lower than -20°C causes the death of the plant. Period of vegetative growth ranges between 180-215 days. In addition, the flowering period ranges between 50-75 days, and the fruit growth and development period ranges between 120-160 days (Onur, 1983).

Its fruit is rich in vitamins, iron, folic acid, potassium and polyphenol antioxidants, which are used to treat different diseases and pomegranate extract is used as an alternative method for the treatment of especially different types of cancer, such as breast cancer and prostate cancer, skin cancer, colon cancer, and lung cancer. Pomegranate extract includes seed oil and pomegranate juice, pomegranate peel, and different parts of the plant roots, bark and flowers (Kavaklı et al., 2011). Several parts of pomegranate have the biological properties of extracts, which have been used in therapeutics, such as in the prevention of infection, inflammation, cancer, and in other applications (Miguel et al., 2010). Fruit juice is an excellent source of sugars, vitamins (B and C) and minerals, potassium, iron, antioxidants, polyphenols, and some parts of the pomegranate tree, such as leaves, immature fruits, fruit peel, flower buds are used in medicinal applications and also for the tanning of leather. Wild pomegranate has a very tart flavor and is of a little value, it is used only as a souring factor. The double-flowered pomegranate used for decorative purposes (non-fruitful) is grown in parks and ornamental gardens for its beautiful red flowers and for the beauty of its appearance (Raj and Kanwar, 2010). Recent studies suggest that pomegranate juice contains anticancer, antimicrobial, and antiviral components (Reddy et al., 2007; Kotwal, 2007; Schwartz et al., 2009).

The propagation of pomegranate is performed either sexually by seeds or by using the vegetative method (asexual) with cuttings and less frequently it is performed using layers, suckers or graftings (Hartmann et al., 1997; Melgarejo et al., 2008; Polat and Çalışkan, 2009). The propagation from cutting (cloning) is an easy, quick and economical method which produces a plant of the same characteristics as the mother plant and which is uniform in sprouting, comes into bearing and fruiting earlier than the seedling and does not need any new techniques in grafting, budding and layering. The success of this process depends on some factors such as the condition of the mother plant, the age of the plant, planting time, temperature, and rooting media (Frey et al., 2006). Cutting is the simple and successful method of pomegranate propagation with 15-20 cm in length and of the pencil size or bigger in diameter and the use of semi-hardwood or hardwood rooting hormone is possible in this method (Melgarejo et al., 2008; Saroj et al., 2008; Polat and Çalışkan, 2009). The cuttings collected at the end of February have a higher rooting potential than those collected at the beginning of October (Polat and Çalışkan, 2009). Grafting is one of the propagation methods which is used for varieties to be propagated of which there are barely specimens from which cutting can be obtained; this process should be conducted at specific times, in May or in July, although it can also be done at the end of the summer (with dormant buds) (Melgarejo and Martinez, 1992). Tissue culture (micropropagation), which is another method of vegetative reproduction of fruit crops, helps in overcoming problems of sexual propagation, producing new plants of the same characteristics with their parents, quick, and mass production of planting materials (El-Agamy et al., 2009).

Aim of this study is to compare effects of the application of IBA growth hormone on sprouting and rooting situations of two local pomegranate varieties, Salakhani, in Halabja province in North of Iraq and Zivzik, in South East of Turkey. There is no experiment about either Salakhani or Zivzik varieties on rooting with cuttings until now. Therefore this study is unique and important to guide subsequent studies.

Literature Research

Melgarejo et al. (2008) reported that the application of exogenous auxins to pomegranate cuttings resulted in the increase of rooting percentages up to three folds. Owais (2010) stated that the application of rooting hormones can increase the rooting percentage of pomegranate cuttings at the rate of 49-73%. Rooting is significantly increased by the addition of synthetic auxins (Hartman and Kester, 1983). Polat and Çalışkan (2009) revealed that some factors, such as the physiological conditions of the parent plant, cutting types, the dates of their taking and medium type, affect the rooting of pomegranate cuttings. They suggested that the cuttings collected at the end of February had a higher rooting potential than those taken at the beginning of October.

In other investigation accomplished under mist chamber by Singh (2014) it was shown that different concentrations of IBA had a significant effect on some growth characteristics of hardwood cuttings in *Punica granatum* L. It was noted that the maximum rooted percentage, root length, sprouted length and leaf number percutting were obtained at the 5000 ppm dose of IBA, while the minimum value was reached in the control group. Alikhani et al. (2011) conducted an experiment to determine the effects of the kind of medium and the kind of pomegranate cuttings on the rooting ability and growth of cuttings under greenhouse conditions. In this experiment, two different medium cultures (sand/peat and sand) and three kinds of pomegranate cuttings (one bud, three buds, more than three buds) were used. At the end of the study, it was revealed that the effect of cutting type on leaf number was significant ($p < 0.05$). However, it was found out that the effects of medium and interaction between cutting type and medium type on leaf number were not so significant, additionally, the type of the cutting had an influence on leaf number. It was noted that the cutting type had a significant effect on shoot number. On the contrary, the effect of medium and interaction between cutting type and medium type on shoot number was not significant. In terms of raised bud numbers, the effect of medium and cutting type was not significant. However, the effect of cutting type on raised bud number and the effect of interaction between medium type and cutting type on raised bud number were significant. Eventually, the effect of medium and cutting types and the effect of interaction between them on root length were significant.

Abu-Zahra et al. (2013) examined in their study the application of exogenous auxins to ornamental plants such Rosemary, Hedera, Syngonium and Gardenia (all of them are difficult to root without using a rooting hormone) in six different concentrations of NAA (0, 1000, 2000, 3000, 4000 and 5000 ppm NAA). Result of their study showed that the highest rooting percentages as the number of roots, the best length, in comparison to the control treatment, were obtained with 3000 ppm NAA in Rosemary and Hedera cuttings, while the best results were obtained with 4000 and 1000 ppm NAA in Gardenia and Syngonium cuttings, respectively. Adekola and Akpan (2012) realized an experiment to assess the effect of the application of two growth hormones, NAA and IBA, on sprouting and rooting behaviours of Nigerian (*Jatropha*). The growth regulator was applied by adopting the slow dip method (for 24 h). In addition, the

untreated replication was accepted as a control group. The results showed that there were no significant treatment differences in the survival percentage and sprouting behaviour of *J. curcas*. A slight selective response to the application of growth hormones was observed in terms of rooting behaviour, as IBA treated cuttings rooted better than the NAA-treated cuttings. However, the untreated cuttings gave the best performance for all the parameters assessed on the sprouting and rooting ability of *J. curcas*. Hence, the untreated cuttings can be used for the mass production of *Jatropha* since they are good propagating materials.

Sharma et al. (2009) executed an experiment to improve the rooting and reduce the mortality of rooted cuttings under field conditions. The results clearly indicated that the treatment of IBA 500 ppm with Borax 1% produced the greatest root number and root length in semi-hardwood and hardwood cuttings of pomegranate. Consequently, the semi-hardwood and hardwood cuttings of pomegranate cultivars. Ganesh treated with IBA 500 ppm + Boron 1%, IBA 300 ppm + Borax 2% and IBA 5000 ppm gave 100% survival of the rooted cuttings under field conditions. Babaie et al. (2014) investigated the effect of different IBA concentrations (control, 2000, 4000 and 6000 ppm) and the time of taking acutting (late June and early September) on the rooting growth and survival of *F. Binnendijkii* 'Amstel Queen' cuttings. Detected that at 6000 ppm and 4000 ppm of IBA and the time of cutting in early September, the highest percentage of rooting ranging from 100% to 96.66%, respectively, the longest root length (16.61 cm) and the greatest number of roots were recorded (15.69 and 14.27, respectively). Whereas the greatest length of new shoots was obtained in the IBA concentration of 2000 ppm and 4000 ppm in late June, the maximum number of new leaves was obtained in the IBA concentration of 2000 ppm and 4000 ppm, with the cutting taken in late June.

Ansari (2013) noticed in his testing that different media and pomegranate cutting separation dates had highly significant effects on rooting characteristics. If suitable media are used, a better cutting separation takes place at the end of they are in terms of a higher rooting percent and increasing root number (Singh, 2009; Janner, 2012; Young, 2012). Furthermore, among different media, vermiculite and its mix with sand were the best for a higher rooting percent and root number. A research actualized on five pomegranate varieties by Owais (2010) was determined all of them had root ability higher than 80% at 9000 ppm IBA treatment, and although the ability of generating roots was enhanced by IBA treatment, it seemed to be that much variability was related to the variety. Hardwood cuttings of pomegranate varieties seem to have a clearly higher root ability than those of semi-hardwood cuttings at different IBA levels for different pomegranate varieties.

Singh et al. (2011) carried out a search to study the effect of planting time and IBA (Indole Butyric Acid) on rooting and vegetative growth of pomegranate cuttings (Ganesh) with different concentrations of IBA 50, 100 and 200 ppm (s.d) for 24 h and IBA 1000, 1500, and 2000 ppm (q.d) for 15 s, on December 15 and January 15, respectively. The results showed that there were significant differences between the time of plantation, IBA treatment concentrations and their interaction with regard to sprouting and last survival percentage of cuttings and statistically significant differences were observed between the dates of plantation and IBA concentrations applied with regard to the number of roots, length of the longest root and root weight characteristics, as well as significant variations between the time of plantation and growth regulator concentrations were observed with regard to the plant height.

In another study succeeded in July, December and January by Kahlon (2007) it was shown that season and shoot part had a significant effect on the sprouting percentage and growth of pomegranate. Also, in that experiment was noted that the greatest sprouting was observed in January and the least one in July plantings and a much higher one was observed in January plantings. Furthermore, the sprouting percentage was the highest in the middle part when compared to the basal and sub-apical types of cuttings. Melgarejo et al. (2000) worked on the effect of 2000, 4000, 8000 and 12.000 ppm indole butyric acid (IBA) concentrations and wounding at the cutting base in pomegranate. Results showed that IBA markedly increased the percentage of rooting (although not at all concentrations), with a high concentration of 12.000 ppm producing the best results in the clones studied. Moreover, wounding carried out at the base of the cutting further increased the percentage of rooting in most of the clones studied.

Mehraj et al. (2013) achieved a trial to study the influence of IBA on the sprouting and rooting potential of (*Bougainville spectabilis*) stem cutting during the period from May to August, with different concentrations of Indole Butyric Acid (control, IBA in dust form, 500 ppm, 1000 ppm, 2000 ppm). The cuttings were soaked in IBA solution for (24 h) and the IBA dust was attached to the cutting just before the establishment in soil. They found out that IBA at 1000 ppm resulted in most sprouting, rooting and a higher survival percentage of rooted cuttings along with a higher number of roots, sprout buds, maximum root length and diameter. Singh et al. (2015) conducted one another experiment under valley condition to study the effect of different growing conditions (two different conditions, namely, shade house and mist chamber) and various concentrations (control, 1000, 1500, and 2000 ppm) of IBA on the rooting and shooting of hardwood cutting of phalas (*Grewia asetica* L.) in the month of September. Result of the study showed the greatest success of hardwood cuttings in the mist chamber growing condition, while IBA 2000 ppm gave the highest success rate of cuttings in all aspects, such as rooting percentage, the length of shoot, the length of root, thickening of root and leaf sprouting in the shoot.

Singh et al. (2014), performed a search in the mist house to study the effect of different concentrations (control, 1000, 2000, 3000, 4000, 5000 ppm) of IBA on inducing rooting in stem cutting (softwood cutting) of *Duranta erecta* var. golden. Softwood cuttings of *Duranta erecta* var. golden were obtained from 2 to 4-year-old plants and 15 cm long cuttings with the apical part. They found out that IBA at 4000 ppm resulted in the maximum percentage of rooted cuttings, followed by 5000 ppm concentration of IBA and the minimum percentage of rooted cuttings was observed under control. Fouda and Schmidt (1995) informed the effect of different concentrations (500, 1000, and 2000 ppm) of IBA on root development in *Rosa canica* and *Rosa rugosa* leafy cuttings. They found out that IBA increased rooting percentage in *Rosa canica*, the maximum rooting percentage was achieved with the cuttings collected at the beginning of June and treated with 1000 ppm IBA.

Ghosh et al. (1988) declared the effect of NAA and IBA on adventitious root formation in the stem cutting of pomegranate (*Punica granatum* L.) under intermittent mist. They found that IBA was more effective than NAA in inducing rooting of hardwood, semi-hardwood and softwood cutting. IBA at 5000 ppm resulted in the maximum rooting success (83.33%), but at higher concentration (10.000 ppm), a greater number of roots and increased root length were recorded. The greatest rooting success was obtained with hardwood cutting. Hedge and Sulikeri (1989) studied the effect of indole butyric acid (IBA) on the rooting in the air layers of pomegranate. In the trials

with cv. Jyothi, mature shoots were treated with IBA at 250-1500 ppm and air layered between June and August. Rooting increased with IBA concentration from 84.38% at 250 ppm to 93.75% at 1500 ppm and 68.75% in the control.

Hansen (1986) carried out a research under the controlled greenhouse condition for 13 weeks to study the effects of cutting position and stem length in *Schefflera arboricola* and to develop propagation technique to obtain a fast and uniform root formation. Eight cuttings from the sub-apical to basal regions were excised from each stock plant. The stem length above the node was the same for all cuttings, whereas the stem length below the node was cut to different lengths, ranging from 0.5 to 3.0 cm. He found that cuttings from sub-apical positions rooted more slowly, produced fewer roots and had a lower rooting percentage than cuttings from the more basal regions, furthermore, the number of roots and rooting percentage increased with the length of the stem below the node.

Materials and Methods

Plant Material

This study was carried out in 2015-2016, at 25°C room conditions in the Physiology Laboratory of the Department of Horticulture, Faculty of Agriculture, Siirt University in Turkey. In this experiment, a private orchard of pomegranate Salakhani and Zivzik were selected, and the plant age ranged between 20-25 years for Salakhani and 20-25 years for Zivzik and trees were selected on the basis of their uniformity in appearance, growth habits and vigour. Salakhani variety is a local pomegranate genotype grown naturally, specifically in Halabja province, Northern of Iraq, and Zivzik variety is considered to be one of the local varieties available in Siirt province in the Southeast of Turkey. Cuttings of Salakhani variety were collected from their natural area in Halabja and cuttings of Zivzik variety were collected from Zivzik Village in Şirvan district of Siirt at the beginning of the Spring.

Preparation of Experiment

Our experiment was conducted to study effect of different concentrations of (IBA) Indole Butyric Acid on rooting percentage, survival percentage, branches number, sprout length, root number, root length and leaves number of pomegranate cuttings of Salakhani cultivars and Zivzik cultivars, during the period from May to August. Five treatments (control, 1000 ppm, 2000 ppm, 4000 ppm and 6000 ppm) were applied in the experiment with three replications. 25 cm in length cuttings were obtained from 1 m in length cuttings. 10 cuttings were used per treatment in a pot with three replications. Therefore, there were 30 cuttings in each treatment and 300 cuttings in total were used in the experiment for both cultivars (Salakhani and Zivzik variety). The data on the root and shoot characteristics were collected five months after planting. Perlite and peatmoss were used as rooting media. A mix of peatmoss and perlite at a ratio 1-1 was used for both varieties.

Hormone solutions were prepared by dissolving 0.1, 0.2, 0.4 and 0.6 g, respectively, of IBA pure powder and diluting with 50% alcohol (ethanol), and adding 50% pure water to make 100 ml of each concentration. Pure water and alcohol were used as control treatment. Preparation process of cuttings was conducted in the laboratory of the Department of Horticulture, Agriculture Faculty, Siirt University. Vigorous shoots from

the previous year of grown and healthy pomegranate trees were used for obtaining the cuttings, and the cuttings of a standard size were washed with tap water. Subsequently, a sharp knife was used in the preparation of cuttings for the experiment to avoid the injury of the cutting. The cuttings of uniform lengths, approximately 15 cm in length, were taken in the month of February when the plants are dormant with wounding by making two opposite longitudinal incisions at the base of each cutting. At least three nodes were included in each cutting. The bottom of the cuttings was treated with hormone of Indole Butyric Acid (IBA) at different concentrations. Basal 1-1.5 cm portion of the cutting was dipped in the growth regulator solution of IBA for 10 seconds (q.d) and immediately inserted in the media at a slight angle to the vertical, to a depth of 10-11 cm (as shown in *Figure 1*).



Figure 1. Preparing of the cuttings

Experimental Procedures and Statistical Calculations

Parameters obtained from our experiment were measured in the laboratory of the Department of Horticulture, Siirt University. These traits included the rooting percentage, number of roots per cutting, survival cutting rate, number of shoots per cutting, root length (mm), sprout length (mm) and the number of leaves per cutting, which were recorded at the termination of the experiment (*Figure 2*) after five months, at harvesting early in August. The roots were examined by lifting cuttings carefully from the rooting media and washing them with tap water. The measurement process was conducted by a tape-measure. The data were collected from all of the cuttings and then the mean value was calculated. Experimental design used which was factorial design in randomised plots. The treatment in each experiment had three replicates and each pot (container) consisted of 10 cuttings. The results of the experiment were statistically analysed and the means were compared using Duncan's Multiple Range Test at the level of 0.05. All analyses were performed by JMP Version 5.0.1 statistical software and letterings were shown in graphs (*Figures 3 and 4*) and *Table 1*.

Results and Discussions

The following findings were obtained in our rooting study. When the data on rooting percentage were examined, there was found 1% statistical significance in terms of varieties and hormone doses. While 5% significance level in terms of IBA type hormone interactions.



Figure 2. A view of the experiment

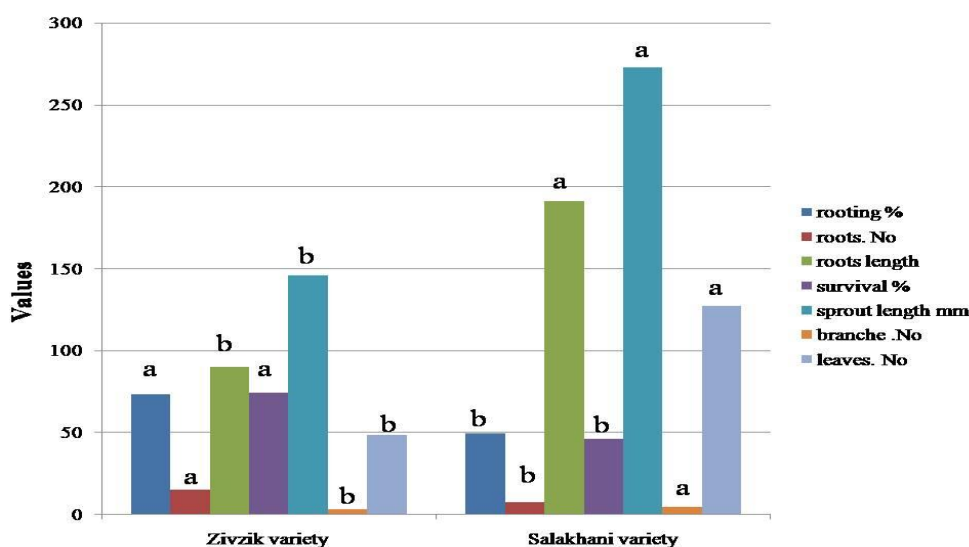


*Figure 3. Effect of different IBA treatments on rooting forms of Zivzik and Salakhani varieties. *Letterings were obtained from statistical data: $P < 0.001$; 0.05% level of probability using LSD*

Rooting Findings

Rooting Percentage (%)

Highest percentage of rooting (73%) was observed in Zivzik variety, Siirt native. While, Salakhani variety was the second and last one with the rooting percentage of 49%, respectively (Figure 3). Among the hormone doses used, the highest percentage (72%) of the hormone dose was a demonstrated at 6000 ppm, while, the control group was the second one with 67% rooting percentage (Figure 4). The hormone dose group

with the lowest percentage of rooting (43%) was the 4000 ppm dose group. The highest (93%) rooting percentage in the variant IBA hormone interactions was found to be related to the 6000 ppm dose applied to Zivzik variety, while the lowest value (23%) was obtained in the case of Salakhani variety with the 4000 ppm dose of IBA (Table 1). Hormone use is more effective in clones, especially in rooting fractions (Melgarejo et al., 2000). However, that the untreated stem cuttings had the best performance in terms of rooting of (*Punica granatum* L.) Salakhani variety could be due to the fact that growth hormones may not be the essential major factor influencing root induction in that variety. The rooting of cuttings may be influenced more by other factors such as the physiological age of cuttings and the status of rooting media in terms of aeration and drainage properties as stated by Narin and Watna (1983). In this experiment, the highest hormone concentration was the most positive effective dose in terms of the rooting percentage. This result is in conformity with the findings of Melgarejo et al. (2000) and Singh et al. (2015) who reported that the highest percentage of rooting was observed due to the increased hormone concentration. Similar results were also reported by Mehraj et al. (2013), Fouda and Schmidt (1995). Owais (2010) indicated that IBA had a significant effect on the rooting. Abu-Zahra et al. (2013) found different results, so it is thought that the hormones used are derived from different types.

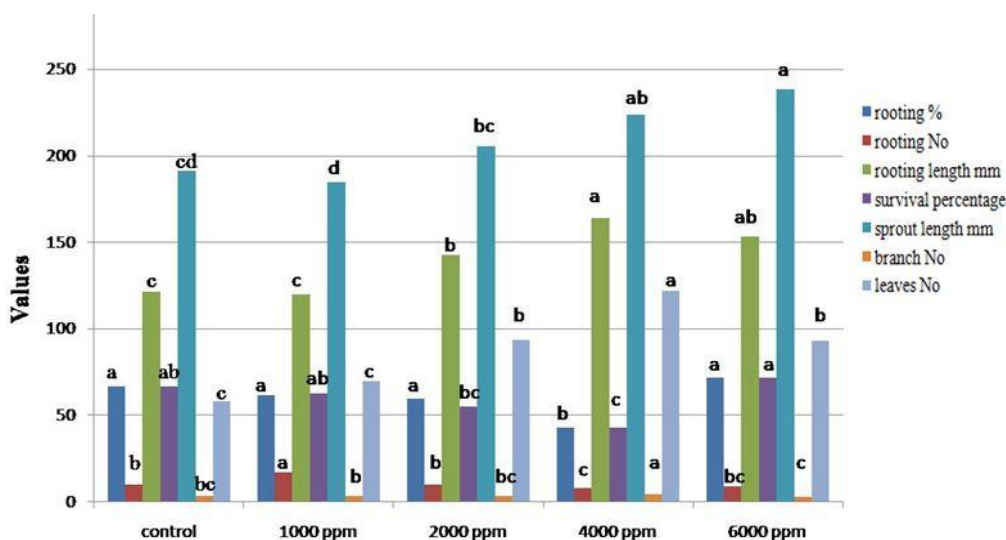


Figure 4. Effect of IBA concentrations on survival performance and growth of the cuttings.
 *Letterings were obtained from statistical data: $P < 0.001$; 0.05% level of probability using LSD

Number of Root

When the measurements of rooted number were examined for Zivzik and Salakhani pomegranate, it was observed that Zivzik variety increased the number of roots up to two folds compared to Salakhani variety, whereas, the values obtained for both cultivars in the root number percentage were as follows: 14.7 for Zivzik variety and 7.03 for Salakhani variety (Figure 3). Considering the root characteristics such as the number of roots per cutting for both varieties (Salakhani and Zivzik cultivars), it was determined that Zivzik cultivars produced the maximum root number and that the IBA treatment at 1000 ppm produced the highest root number (17.06) and the lowest number of roots (7.93) was determined with IBA at 4000 ppm (Figure 4). When the table is examined

according to the IBA type hormone interactions in terms of the number of rooted seedlings, it is seen that the number of seedlings rooted at the highest level (27.08) is in Zivzik variety at 1000 ppm. In contrast, the lowest number (5.44) of seedlings rooted is in Salakhani variety, with 4000 ppm of IBA (q.d) treatment (*Table 1*). From the present study, it is revealed that soaking the cutting in IBA solution increases the number of roots on cuttings due to the rooting ability of IBA. Hartmann et al. (1997) stated that the concentration of auxins substantially higher than that normally found in plant tissues may play an inhibitory role for the growth and root formation. Ramdayal et al. (2001) and Gupta et al. (2002) also found the maximum number of roots at 1000 ppm IBA. The findings related to the number of rooted seedlings were found to be parallel with the findings of Ghosh et al. (1988) who applied doses of 5000-10.000 ppm, Hegde and Sulikeri (1989) who applied 250-1500 ppm IBA and Mehraj et al. (2013) who used doses of 500-1000 and 2000 ppm. The difference in regard to the findings of Abu-Zahra et al. (2013) could be attributed to the difference of hormones used.

Table 1. Effect of the interaction among IBA doses and vegetative growth of the cuttings

Cultivars	hormone doses	rooting rate (%)	roots number	roots length (mm)	survival rate (%)	shoot length (mm)	shoot number	leaves number
Zivzik	0	0.67 BC	13.59 B	89.08 D	0.67 BC	110.47 G	3.13 CD	23.03 G
	1000	0.73 B	27.08 A	84.79 D	0.77 AB	128.69 FG	3.17 CD	39.37 FG
	2000	0.67 BC	12.74 BC	98.91 D	0.70 B	148.51 EF	2.58 D	49.76 EFG
	4000	0.63 BC	10.42 CD	100.31 D	0.63 BC	162.83 DE	3.17 CD	71.73 DE
	6000	0.93 A	9.68 D	76.50 D	0.93 A	177.48 D	2.70 D	56.38 EF
Salakhani	0	0.67 BC	7.05 EF	153.98 C	0.67 BC	273.01 AB	3.68 BC	93.94 D
	1000	0.50 C	7.03 EF	155.84 C	0.50 CD	241.50 C	4.31 B	100.96 CD
	2000	0.53 C	7.16 EF	186.98 B	0.40 DE	262.62 BC	4.28 B	137.70 B
	4000	0.23 D	5.44 F	227.69 A	0.23 E	285.55 AB	5.44 A	177.44 A
	6000	0.50 C	8.47 DE	230.76 A	0.50 CD	300.23 A	3.65 C	130.19 B

Length of Root (mm)

While the highest root length (191.05 mm) was determined in the seedlings belongs to Salakhani variety, Zivzik seedlings were the lowest one with the length of 89.92 mm (*Figure 3*). When the effects of hormone doses on root length were examined, it was found out that the longest roots (164 mm) were obtained at dose of 4000 ppm, whereas the lowest one (120.32 mm) was obtained at dose of 1000 ppm (*Figure 4*). At the same time, the control group without hormone treatment had longer lengths (121.53 mm) than the 1000 ppm dose group (*Figure 4*). Based on the analysis of variance of the effect of IBA type hormone interactions on root lengths, the highest root length values (230.76 mm) compared to other subjects were obtained in Salakhani variety with 6000 ppm IBA hormone (q.d) treatment, while the lowest root length values were obtained in Zivzik variety with 6000 ppm hormone dose (*Table 1*). Statistical significance at the 1% significance level was found in all subjects. The findings of Abu-Zahra et al. (2013)

were different, which was due to the differences in the hormones used. The findings of Hartman and Kester (1983) who indicated that rooted seedlings increased significantly; Owais (2010) and Sharma et al. (2009) who found that the longest roots were derived from hormone-containing plants; Singh et al. (2011) and Ghosh et al. (1988) who identified the statistical differences between practices are similar to the findings in this study.

Survival Cutting Rates

The highest value (74%) in terms of the survival rate was obtained from Zivzik variety. Whereas, the survival rate value measured in Salakhani variety used in the experiment was determined to be 46% as shown in *Figure 3*. Parallel results between the rooting rates and survival cutting rates were determined. When the effects of the hormones used in different doses on survival rates were examined, it was found that 6000 ppm of hormone application provided the highest survival rates with 72%, the control group (T0) was the second with 67% survival rates value while 4000 ppm hormone dose application was the last (*Figure 4*). When the values of the IBA type hormone interaction were examined in terms of the survival rates, it was determined that the highest value (93%) belonged to Zivzik variety with IBA at 6000 ppm. The interaction of Salakhani variety control group was better than other interactions. It is observed that Salakhani variety and 4000 ppm hormone dose interaction was in the last place with the value of 0.23% survival rates (*Table 1*).

Length of Sprout (mm)

The highest value of sprout length (272.58 mm) was found in Salakhani variety and the lowest value (145.59 mm) was found to belong to Zivzik variety (*Figure 3*). When the effects of hormone doses on sprout length were examined in Zivzik and Salakhani varieties, it was found that among the hormone doses applied 6000 ppm dose gave the highest (238.85 mm) sprout length and IBA at 1000 ppm hormone dose gave the lowest (185.09 mm) sprout length (*Figure 4*). Among the IBA type hormone interaction, the highest sprout length (300.23 mm) was determined in Salakhani variety with IBA at 6000 ppm and the lowest sprout length value (110.47 mm) was determined in Zivzik variety without hormone treatment (control group) as shown in *Table 1*.

Number of Shoot

It was determined that the average number of shoot in Salakhani variety (4.27) was higher than in Zivzik variety with 2.95 (*Figure 3*). According to the effects of hormone doses on shoots number, it was found out that the value belonging to 4000 ppm hormone dose application (4.31) was higher than the values of other hormone doses. The lowest shoots number (3.18) was found in 6000 ppm application (*Figure 4*). The shoots number of Salakhani variety observed in the hormone and variety interactions is superior to Zivzik variety. When the interactions were examined, the highest average value of shoots number (5.44) was obtained in Salakhani variety with the 4000 ppm IBA hormone dose and the lowest value of shoot number (2.58) was obtained in Zivzik variety with 2000 ppm (*Table 1*). Especially, the number of shoots and survival rates increased with the use of hormones in parallel with the findings of Janick (1972) and Hartmann and Kester (1983) who determined that the use of natural hormones increases the survival percentage as well as all vegetative developments in seedlings.

Number of Leaves

When the varieties and hormone doses were examined in terms of the number of leaves, it was determined that the highest leaf number average value (127.05) was obtained from Salakhani variety and the lowest leaf number average value (48.05) was obtained from Zivzik variety (*Figure 3*). It was noted that the hormone dose of 4000 ppm had the highest mean leaf number value (122.09) and the control value was the lowest value of the mean leaf number (58.48) (*Figure 4*). It has been determined that the leaf number is influenced by the variety and hormone interaction but not statistically significant. However, the highest leaf number average value (177.44 mm) was obtained from the interaction of Salakhani variety with IBA at 4000 ppm (q.d) treatment and the lowest value (23.03 mm) was obtained from Zivzik variety without hormone treatment (control treatment) (*Table 1*). Babaie et al. (2014) who performed similar studies and used IBA as a hormone reported that the largest number of leaves was available at doses of 2000 and 4000 ppm. Mehraj et al. (2013) found that the maximum vegetative growth was achieved with 1000 ppm of IBA.

Furthermore, more adventitious roots were observed on the pomegranate seedlings belonging to Zivzik variety. Meanwhile, strong and thick roots were observed on the pomegranate seedling of Salakhani variety which was more when compared to Zivzik cultivars. Moreover, the period required for the first sprouting of Salakhani variety ranged between 10-11 days. Whereas, the period required for the first sprouting of Zivzik variety reached 12-13 days. The above-mentioned period was considered to be the period between the days of planting the cutting to the day of sprouting the first bud on the cutting.

Conclusion

Upon examining sprouting and rooting behaviour in stem cuttings, highly contrasting responses to IBA addition were indicated among various concentrations of IBA, each variety had superiority to the other one in different aspects. Zivzik variety had a higher value of rooting number, rooting percentage and survival percentage than Salakhani variety. Salakhani variety had a higher value of root length, sprout length, shoots number and the number of leaves than Zivzik variety pomegranate. The highest dose of hormone (6000 ppm) was found to be the most effective on rooting percentage, survival percentage and sprout length, while 4000 ppm was found to be the most effective on root length, shoots number and the number of leaves. The 1000 ppm dose was determined to significantly increase the root number compared to other doses. Regarding to the interaction effect of IBA doses, it was shown that the best performance in terms of rooting percentage, survival percentage, root length and sprout length was observed at the 6000 ppm dose of IBA, whereas 4000 ppm was found to be the most effective on shoots number and leaves number. The 1000 ppm dose was determined to significantly increase root number compared to other doses. Hence, it can be concluded from the present experiment that the higher concentrations of IBA (6000 ppm) and (4000 ppm) positively affect the sprouting and rooting ability in the stem cuttings of pomegranate cv. Zivzik and Salakhani. In contrast, the optimum IBA concentration for the number of roots per cutting was found to be 1000 ppm (Shoots and roots of the cuttings rooted in different hormone doses are given in *Figure 5* and *Figure 6*). Based on the findings of current investigation, the results have proved that Zivzik variety gives better results than Salakhani variety in terms of rooting percentage, survival percentage

and roots number in Turkey environmental conditions. From the results obtained in the present experiment and discussion, from the economic point of view, it can be concluded soaking the cut stem on 1000 ppm IBA solution for 10 second (q.d) before the establishment of the stem cuttings show maximum result in terms of root number was obtained at the 1000 ppm dose of IBA and we recommend using 1000 ppm of IBA, which will provide a significant increase in root number compared to other doses. In conclusion, pomegranate cuttings with different doses of IBA were successfully rooted in our study. As it is known, pomegranate is produced without vaccination. Therefore, it is important that pomegranate seedlings can be reproduced quickly and rapidly with cuttings. Because of this reason, further studies also can be done using different hormones and their doses to obtain the best sprouting and rooting results for cuttings of both Salakhani and Zivzik variety.



Figure 5. Root and shoot views of the cuttings (Control & 1000 ppm IBA dose).



Figure 6. Root and shoot views of the cuttings (2000&4000&6000 ppm IBA doses)

Acknowledgements. This article is a part of Master Thesis belonging to Khabbat H. AL-JABBARI.

REFERENCES

- [1] Abu-Zahra, T. R., Al-Shadaideh, A. N., Abubaker, S. M., Qrunfleh, I. M. (2013): Influence of auxin concentrations on different ornamental plants rooting. – *International Journal of Botany* 9(2): 96-99.
- [2] Adekola, O. F., Akpan, I. G. (2012): Effects of growth hormones on sprouting and rooting of *Jatropha Curcas* L. Stem Cuttings. – *J. Appl. Sci. Environ.* 16(1): 165-168.
- [3] Alikhani, L., Ansari, K., Jamnezhad, M., Tabatabaie, Z. (2011): The effect of different mediums and cuttings on growth and rooting of pomegranate cuttings. – *Iranian Journal of Plant Physiology* 1(3): 199-203.
- [4] Ansari, K. (2013): Effects of different collecting time and different medium on rooting of pomegranate Malas Torsh Cv. cuttings. – *Bull. Env. Pharmacol. Life Sci* 2(12): 164-168.
- [5] Babaie, H., Zarel, K., Nikde, K., Firoozjai, M. N. (2014): Effect of different concentrations of IBA and time of taking cutting on rooting, growth and survival of. – *Notulae Scientia Biologicae* 6(2): 163-166.
- [6] Chandra, R., Marathe, R. A., Kumar, P. (2006): Present status of pomegranate and its scope for crop diversification in arid and semi-arid region of Maharashtra. – In: *Proceedings of the National Symposium on Agro-forestry for Livelihood Security Environment Protection and Biofuel Production*, Jhansi, India, pp. 77-78 (Abstract).
- [7] Chandra, R., Marathe, R. A., Jadhav, V. T., Sharma, K. K., Dhinesh Babu, K. (2008): Appraisal of constraints of pomegranate cultivation in Karnataka (*Punica granatum* L.). – In: *Proceedings of the 3rd Indian Horticulture Congress: New R&D Initiatives in Horticulture for Accelerated Growth and Prosperity*, Orissa, India, p. 252 (Abstract).
- [8] Chandra, R., Meshram, D. T. (2010): Pomegranate culture in Deccan plateau of India. – In: Chandra, R. (ed.) *Pomegranate. Fruit Veg. Cereal Sci. Biotechnol.* 4, Special Issue 2: 113-119.
- [9] El-Agamy, S. Z., Mostafa, R. A. A., Shaaban, M. M., El-Mahdy, M. T. (2009): *In vitro* propagation of manfalouty and nab elgamel pomegranate cultivars research. – *J. Agric. Biol. Sci.* 5(6): 1169-1175.
- [10] Fouda, R. A., Schmidt, G. (1995): Histological changes in the stems of some rosa species propagated by leafy cuttings as affected by IBA treatments. – *I. Acta Agronomica Hungarica* (43): 265-276.
- [11] Frey, B., Hagedorn, F., Gludici, F. (2006): Effect of girdling on soil respiration and root composition in sweet chestnut forest. – *For. Ecol. Manage.* 225(1-3): 271-277.
- [12] Ghosh, D., Bamdyopadhyay, A., Sen, S. K. (1988): Effect of NAA and IBA on adventitious root formation in stem cuttings of pomegranate (*Punica granatum* L.) under intermittent mist. – *Indian Agriculturist* 32(4): 239-243.
- [13] Gupta, V. N., Banerj, B. K., Datta, S. K. (2002): Effect of auxin on rooting and sprouting behaviour of stem cuttings of Bougainvillea under mist. – *Haryana J. Hort. Sci.* (31): 42-44.
- [14] Hansen, J. (1986): Influence of cutting position and stem length on rooting of leaf-bud cuttings of Schefflera arboricola. – *Scientia horticulturae* 28(1): 177-186.
- [15] Hartmann, H. T., Kester, D. F. (1983): *Plant propagation principles and practices*. – 4th ed., Prentice hall, inc. Engle wood cliffs. New Jersey: 256-303, 676-678 and 727.
- [16] Hartmann, H. T., Kester, D. E., Davies, F. T. Jr., Geneve, R. L. (1997): *Plant propagation: principles and practices*. – 6th ed., Prentice hall of India Private Ltd., New Delhi, India.
- [17] Hedge, N. K., Sulikeri, G. S. (1989): Effect of indole butyric acid (IBA) on the rooting of air layers of pomegranate. – *Curr. Res. Univ. Agric. Sci., Bangalore* 18(11): 161-162.
- [18] Janick, J. (1972): *Horticultural Science* (2nd ed.). – W. H. Freeman and Co., San Francisco, USA. 586 p.

- [19] Janner, R. Y. (2012): Pomegranate (1st Ed.) – Clemson University Press. USA.
- [20] Kahlon, P. S. (2007): Studies on the propagation of pomegranate as influenced by season and shoot portion. – Asian Journal of Horticulture 2(1): 6-8.
- [21] Kavaklı, Ş., Zainal, A. A., Hepaksoy, S. (2011): Shield against cancer: pomegranate. – The abstract book of the Turkish VI. national horticulture congress. 4-8 October 2011. Şanlıurfa, pp 807-811.
- [22] Kotwal, G. J. (2007): Genetic diversity-independent neutralization of pandemic viruses (e.g. HIV), potentially pandemic (e.g. H5N1 strain of influenza) and carcinogenic (e.g. HBV and HCV) viruses and possible agents of bioterrorism (variola) by enveloped virus neutralizing compounds (EVNCs). – Vaccine 26: 3055-3058.
- [23] Mehraj, H., Shiam, I. H., Taufique, T., Shahrin, S., Uddin, A. J. (2013): Influence of Indole-3-Butyric Acid (IBA) on sprouting and rooting potential of Bougainvilleaspectabilis cuttings. – Bangladesh Research Publications Journal 9(1): 44-49.
- [24] Melgarejo, P., Martinez, R. (1989): Pomegranate. – Official College of Agricultural Engineering Press. Valencia, Spain. 111p (In Spanish).
- [25] Melgarejo, P., Martinez, R. (1992): Pomegranate. – Mundi Press. Madrid, Spain. 163p (In Spanish).
- [26] Melgarejo, P., Martinez, J., Amoros, A., Martinez, R. (2000): Study of the rooting capacity of ten pomegranate clones (*Punica granatum* L.). – Adv. Res. Tech. 1: 253-259.
- [27] Melgarejo, P., Martinez, J., Martine, J. J., Sanchez, M. (2008): Preliminary Survival Experiments in Transplanting Pomegranate. – In: Production, Processing and Marketing of Pomegranate in the Mediterranean Region: - Advances in Research and Technology. Europe: CIHEAM Publication: 163-167.
- [28] Miguel, M., Neves, G., Antunes, M. D. (2010): Pomegranate (*Punica granatum* L.): A medicinal plant with myriad biological properties-A short review. – J Med Plants Res (4): 2836-2847.
- [29] Narin, S., Watna, S. (1983): Effect of IBA on root formation of stem cuttings of purging nut, *Jatropha curcas* (in Thailand). – Faculty of agriculture, Department of Horticulture, Kasetsart University of Bangkok, Thailand: 1-19.
- [30] Onur, C. (1983): Selection of mediterranean region pomegranate (PhD Thesis). – Alata Horticulture Research and Training Center. Publication No: 46, Mersin.
- [31] Owais, S. J. (2010): Rooting response of five pomegranate varieties to Indole butyric acid concentration and cuttings age. – Pakistan journal of biological sciences 13(2): 51-58.
- [32] Özgüven, A. I., Yılmaz, C. (2000): Pomegranate growing in Turkey. – I. Int. Symp. on pomegranate, 15-17 October, Orihuela (Alicante) Spain: 41-48.
- [33] Polat, A. A., Çalışkan, O. (2009): Effect of indol butyric acid (IBA) on the rooting cutting in various pomegranate genotypes. – Acta. Hort. (ISHS) 818: 187-192.
- [34] Raj, D., Kanwar, K. (2010): *In vitro* regeneration of (*Punica granatum* L.). Plants from different juvenile explants. – J. Fruit Ornamental Plant Res. 18(1): 5-22.
- [35] Ramdayal, P., Gupta, A. K., Saini, R. S., Sharma, J. R. (2001): Effect of auxin on the rooting of cutting in *Bougainvilleavar* Mary Palmer. – Haryana J. Hort. Sci. 30: 215-216.
- [36] Reddy, M. K., Gupta, S. K., Jacob, M. R., Khan, S. I., Ferreira, D. (2007): Antioxidant, mantimalarial and antimicrobial activities of tannin-rich fractions, elagitannins and phenolic acids from *Punica granatum* L. – Planta Medica 73: 461-467.
- [37] Saroj, P. L., Awasthi, O. P., Bhargava, R., Singh, U. V. (2008): Standardization of Pomegranate propagation by cutting under mist system in hot arid region. – Indian J. Horti. 65(1): 25-30.
- [38] Schubert, S. Y., Lansky, E. P., Neeman, I. (1999): Antioxidant and eicosanoid enzyme inhibition properties of pomegranate seed oil and fermented juice flavonoids. – Journal of Ethnopharmacology 66: 11-17.

- [39] Schwartz, E., Glazer, I., Bar-Yaakov, I., Matityaha, I., Bar-Ilan, I., Holland, D., Amir, R. (2009): Changes in chemical constituents during the maturation and ripening of two commercially important pomegranate accessions. – *Food Chemistry* 115: 965-973.
- [40] Sharma, A., Chandraker, S., Patel, V. K., Ramteke, P. (2009): Anti bacterial activity of medicinal plants against pathogens causing complicate durinary tract infections. – *Indian J. Pharm. Sci.* 71: 136-139.
- [41] Silva, J. A. T., Rana, T. S., Narzary, D., Verma, N., Meshram, D. T., Ranade, S. A. (2013): Pomegranate biology and biotechnology: A review. – *Scientia Horticulturae* 160: 85-107.
- [42] Singh, B. (2009): Influence of planting time and IBA on rooting and growth of pomegranate “Ganesh” Cuttings. – Second international symposium on pomegranate and minor fruit.
- [43] Singh, B., Singh, S., Singh, G. (2011): Influence of planting time and IBA on rooting and growth of pomegranate (*Punica granatum* L.) 'Ganesh'Cuttings. – *Acta horticulturae* 890: 183.
- [44] Singh, K. K. (2014): Effect of IBA concentrations on the rooting of pomegranate (*Punica granatum* L.) cv. Ganesh hardwood cuttings under mist house condition. – *Plant Archives* 14(2): 1111-1114.
- [45] Singh, K. K., Choudhary, T., Kumar, P., Rawat, J. M. S. (2014): Effect of IBA for inducing rooting in stem cuttings of *Duranta golden*. – *HortFlora Res. Spectrum* 3(1): 77-80.
- [46] Singh, K. K., Chauhan, J. S., Rawat, J. M. S., Rana, D. K. (2015): Effect of different growing conditions and various concentrations of IBA on the rooting and shooting of hardwood cutting of phalsa (*Grewiaaetical*.) under valley condition of Garhwal Himalayas. – *Plant Archives* 15(1): 131-136.
- [47] Usanmaz, S., Kahramanoğlu, I., Yılmaz, N. (2014): Yield and pomological characteristics of three pomegranate (*Punica granatum* L.) cultivars: wonderful, Acco and Herskovitz. – *Am J Agric For* (2): 61-65.
- [48] Young, J. (2012): The best time to plant pomegranate cutting. – eHow.com.

ANTIBIOFILM POTENCY OF GINGER (*ZINGIBER OFFICINALE*) AND QUERCETIN AGAINST *STAPHYLOCOCCUS AUREUS* ISOLATED FROM URINARY TRACT CATHETERIZED PATIENTS

HAMASALIH, R. M.* – ABDULRAHMAN, Z. F. A.

Department of Biology, Salahaddin University-Erbil, Erbil, Iraq

**Corresponding author*

e-mail: rebwar.hamasalih@su.edu.krd; phone: +964-751-268-6561

(Received 28th Jul 2019; accepted 28th Nov 2019)

Abstract. *Staphylococcus aureus* is a common cause of urinary tract infections associated with catheters. Biofilm is a community of microbial cells attached to a surface and is embedded in the extracellular polymeric substances. Catheters were collected from 157 patients; *S. aureus* was identified by molecular and conventional microbiological methods. *S. aureus* isolates showed a higher level of biofilm production, and all isolates showed biofilm production using Microtiter plate assay, while 89% of the isolates produced using Congo red agar method. All biofilm-producing isolates were positive for *icaC*, *icaD*, and *cna* genes, except isolate SA88, indicating the vital role of *ica* genes as markers of virulence in *S. aureus* infections. The difference in the inhibition of biofilm formation between the culture containing *Z. officinale* extract and the control was recorded. The high percentage of biofilm inhibition was 61.4 against SA04 at a concentration of 16%, whereas there is no effect on the formation of biofilm at concentrations 4, 2, 1, and 0.5% against each of SA36, SA48, and SA62. Quercetin lowers the formation of biofilm against SA36 of *S. aureus* at 32 µg/mL compared to a positive control ($p=0.0041$), and the percentage of inhibition power reached to 92. At a concentration 32 µg/mL, the highest antibiofilm potential of ascorbic acid was 62 percent against SA86 strain, while at a concentration of 4 µg/mL, the minimum potency was recorded toward SA62 isolate.

Keywords: *bacterial isolates, catheters, biofilm-related genes, PCR*

Introduction

Staphylococcus aureus is responsible for causing a variety of human-acquired community and hospital-acquired infections worldwide. A significant number of *S. aureus* clinical isolates have evolved to be resistant to commonly used antibiotics (Jeong et al., 2019). The importance of nosocomial diseases caused by *S. aureus*, especially by methicillin resistant *S. aureus* (MRSA), is well known for its frequency, morbidity, mortality, and principally for its difficulty to treat (Shin et al., 2010; Saraiva et al., 2012). Resistance has also been reported against both newly introduced and last-resort drugs such as vancomycin, daptomycin, and linezolid used for the treatment of *S. aureus* infection. Therefore, new therapies against this series human pathogens need to be developed urgently (Nair et al., 2016). *S. aureus*, including antibiotic-resistant strains, are highly biofilm-producing bacteria and are dangerous causes of common infectious diseases in humans (Phuong et al., 2017; Wang et al., 2017). Due to genetic and metabolic adaptations of cells in films, the bacteria in biofilms are highly tolerant to antimicrobials. Biofilms consist of both the cells and the extracellular matrix produced by the cells (Shahmoradi et al., 2019), bacterial cell communities in a self-produced polymer matrix, and adhere to an inert or living surface (Onsare and Arora, 2015; Singh et al., 2015).

S. aureus is known to form biofilms, and it has been shown that reside in biofilms are highly resistant to antibiotics (Rodrigues et al., 2017), and also is a leading cause of skin

structure infections and it is particularly associated with urinary tract catheters (Bayer et al., 2016; Trübe et al., 2019). *S. aureus* produces several virulence factors that enable it to colonize, adhere to surfaces and form biofilms, invade or escape the immune system, develop resistance to multiple antibiotics and cause host toxicity (Fey et al., 2003; Cheung et al., 2004). *S. aureus* is commonly observed, colonizing several parts of the body in healthy individuals (Kiedrowski and Horswill, 2011) and causing associated biofilm infections (Balamurugan et al., 2017). The ability of *S. aureus* to form an extracellular slime and constitutive a biofilm assists this organism to endure the host immune response, thus impairing clinical treatment since biofilm formation defends bacteria from antimicrobial agents (Foster, 2005). *Zingiber officinale* has been used for thousands of years as a culinary and medicinal herb. A recent study has shown that *Z. officinale* has antibacterial activity against *S. aureus*, and that is higher than the antibiotics on the market (Kim and Park, 2013). The rhizome is rich in secondary metabolites such as phenolic compounds (gingerol, paradol, and shogunal), volatile sesquiterpenes (zingiberene and bisabolene) and monoterpenoids (curcumin and citral). Among herbal extracts, the inhibitory effect of *Z. officinale* extract on microorganisms has been well documented (Ali et al., 2008). Previous studies have demonstrated that isolated compounds from *Z. officinale* possess potent antioxidant, antibacterial, antifungal, anticancer, and anti-inflammatory effects (Habib et al., 2008), as well as the impact of this extract on biofilm formation (Stoilova et al., 2007).

Quercetin, the most commonly studied flavonoid, has a wide range of biological activities, including antimicrobial activities (Hirai et al., 2010). Quercetin also influences quorum sensing, hence acts as an antibiofilm compound against *S. aureus*. It inhibits alginate production in a concentration-dependent manner, resulting in declination in the adherence during biofilm formation. It also reduces exopolysaccharide (EPS) production required for the initial attachment of bacteria. Some other reports also suggested that usinic acid show inhibitory effect on the *S. aureus* biofilm, and this has been hypothesized that this may be due to any interference in quorum sensing, but the exact mechanism of action is still indistinct (Roy et al., 2018). Based on quantification of the biofilm extracellular polymeric substances content and cell viability, quantitative proteome analyses and genome-scale metabolic modeling point to a vitamin C-dependent inhibition of the synthesis of polysaccharides that form the biofilm matrix. This proceeds *via* inhibition of the quorum sensing and other regulatory mechanisms, leading to repression of specific biosynthetic operons. Once the EPS content is reduced beyond a critical point, bacterial cells become exposed and more susceptible to killing by any external factors (Pandit et al., 2017).

Ascorbic acid has been shown to be an effective antioxidant, acting both directly through aqueous peroxy radical's reaction and indirectly through the restoration of the antioxidant properties of fat-soluble vitamin E. Interestingly, ascorbic acid has been reported to increase the effectiveness of antibiotics *vs.* a wide range of bacteria through a synergistic effect, but this synergy's mechanism remains unclear (Helgadóttir et al., 2017).

The main objective of this study was using *S. aureus*, a model biofilm-forming microorganism, also investigated the effects of *Z. officinale* extract, quercetin, and ascorbic acid on biofilm formation using a static biofilm assay. The distinction in the inhibition of biofilm between the culture containing *Z. officinale* extract and the control.

Materials and method

Clinical isolate repository

In the period from July 2016 to March 2017, 157 samples taken from catheter patients received from the Rizgary Urinary Unit and Artificial Kidney Hospitals were investigated in Erbil City, Erbil, Iraq after cutting catheter (inside parts of the body) into 2 cm pieces and then incubating in brain heart infusion broth for 24–48 hrs. with shaking at 250 rpm, after that, the positive growth was cultured on Nutrient, Blood agar (BA), MacConkey and Mannitol Salt Agar (MSA) (Oxoid, UK).

Culture and identification

Primarily, isolates were cultured on MSA and BA (Oxoid, UK) and incubated at 37°C for 24 hrs. The assumed colonies of *S. aureus* were identified by using conventional methods; include gram staining, biochemical tests which comprise: catalase, oxidase, urease, coagulase using tube coagulase test (TCT) (Karasu and Rathish, 2014), gelatin liquefaction, hemolysis, staphyloxanthin and protease, tellurite reduction, lipase and lecithinase production, dextrose reduction, carbohydrate fermentation and tellurite reduction, and DNase with methyl green, followed by VITEK II Compact System (bioMérieux, Inc., France). Finally, identity of the isolates was confirmed *via* polymerase chain reaction (PCR) (Alpha PCRmax, UK) based on identifying *16S* rRNA and *nuc* genes. The sequences of both genes and PCR setup can be found in *Table 1*.

Table 1. Sequences of oligonucleotide primers used for PCR amplification of biofilm-associated genes with *16S* rRNA, *nuc* and *mecA* genes used in this study

Gene name	Primers detail			References
	Primer Sequence (5' – 3') (Oligonucleotide)	Amplicon size (bp)	Cycling program	
<i>16S</i> rRNA	CAC CTT CCG ATA CCG CTA CC GTT GAC TGC CGG TGA CAA AC	372	95°C–30 s; 59°C–45 s; 72°C– 1 min; 35 cycles	In this study
<i>nuc</i>	GCG ATT GAT GGT GAT ACG GTT AGC CAA GCC TTG ACG AAC TAA AGC	279	95°C–30 s; 53°C–45 s; 72°C– 40 s; 40 cycles	(Blaiotta et al., 2004)
<i>mecA</i>	ATG TCT GCA GTA CCG GAG CTT T AAA AT CGA TGG TAA AGG TTG GC	533	94°C–30 s; 55°C–45 s; 72°C– 1 min; 40 cycles	(Alli et al., 2015)
<i>icaA</i>	ACA CTT GCT GGC GCA GTC AA TCT GGA ACC AAC ATC CAA CA	188	94°C–30 s; 56°C–60 s; 72°C– 45 s; 30 cycles	(Kouidhi et al., 2010)
<i>icaB</i>	CCC AAC GCT AAA ATC ATC GC ATT GGA GTT CGG AGT GAC TGC	1080	95°C–30 s; 58°C–30 s; 72°C– 45 s; 40 cycles	(Gowrishankar et al., 2016)
<i>icaC</i>	CTT GGG TAT TTG CAC GCA TT GCA ATA TCA TGC CGA CAC CT	209	95°C–30 s; 55°C–40 s; 72°C– 45 s; 40 cycles	(Nourbakhsh and Namvar, 2016)
<i>icaD</i>	ATG GTC AAG CCC AGA CAG AG CGT GTT TTC AAC ATT TAA TGC AA	198	94°C–30 s; 55°C–40 s; 72°C– 45 s; 30 cycles	(Kouidhi et al., 2010)
<i>cna</i>	CGA TAA CAT CTG GGA ATA AA ATA GTC TCC ACT AGG CAA CG	716	95°C–30 s; 54°C–40 s; 72°C– 45 s; 35 cycles	(Tang et al., 2011)
<i>atl</i>	GCC TGT TGC AAA GTC AAC AA CAC CGA CAC CCC AAG ATA AG	600	95°C–30 s; 56°C–30 s; 72°C– 45 s; 40 cycles	In this study
<i>fmbA</i>	GAT ACA AAC CCA GGT GGT GG TGT GCT TGA CCA TGC TCT TC	191	95°C–30 s; 57°C–1 min; 72°C–1 min; 35 cycles	(Kouidhi et al., 2010)
<i>fmbB</i>	GAC CTG CTT CGC TAT CCA CA AGT CGT AAT GGC GAC AGG TG	980	95°C–30 s; 57°C–30 s; 72°C– 1 min; 40 cycles	In this study

Antimicrobial susceptibility screening

According to the references of the Clinical and Laboratory Standards Institute (CLSI) (CLSI, 2017), antimicrobial sensitivity testing was carried out against the following antimicrobials using disk diffusion method; Amikacin AK 30 µg, Azithromycin AZM

15 µg, Ciprofloxacin CIP 5 µg, Clindamycin CD 2 µg, Erythromycin E 15 µg, Gentamicin G 10 µg, Levofloxacin LEV 5 µg, Netilmicin NET 30 µg, Nitrofurantoin NIT 300 µg, Norfloxacin NOR 10 µg, Oxacillin OX 1 µg, Penicillin P 10 U, Tetracycline TE 30 µg, Tobramycin TOB 10 µg, Trimethoprim+Sulfamethoxazole SXT 1.25+23.75 µg, and Vancomycin VA 30 µg (Bioanalyse, Turkey). A lawn of test *S. aureus* was prepared by evenly spreading 100 µL inoculums (1.5×10^8 CFU/ml) according to 0.5 McFarland (1907) standard solution with the sterilized swab on top of the entire surface of Mueller Hinton Agar plate (Oxoid, UK). The disks were resolutely applied onto the agar plates surface within 15 minutes of inoculation (Bimanand et al., 2018).

Assessment of biofilm synthesis by *S. aureus*

Congo red agar method

Phenotypical biofilm production in all *S. aureus* isolates was evaluated through culturing CRA plates and explained by (Szczyka et al., 2013; Khoramrooz et al., 2016). First of all, they prepared CRA plates by adding 0.8 g of Congo red (Merck, Germany) and 36 g of sucrose (Sigma, USA) to one liter of brain heart infusion agar (BHI) (Merck, Germany). The plates have been incubated for 24 hours at 37°C. The morphology of colonies was then interpreted based on colony color as Bordeaux pink (red), almost black, black, and strong black. Strains with red colonies were classified as strains that are unable to produce biofilm, while nearly black color indicated a weak activity in biofilm production. Whereas, colonies that were very black and black were considered strong strains of biofilm producers.

Polystyrene microtiter plate assay

Biofilm production was quantitatively determined through an MTP method as defined by Yousefi et al. (2016). In short, bacterial isolates were grown with 0.5 percent glucose in trypticase soy broth (TSB) (Merck, Germany) and incubated at 37°C overnight. Cultures with 0.5 percent glucose with 1:40 in fresh TSB were diluted (Sigma, USA). Two hundred µL of the diluted solution was added to Microtiter plate wells and incubated at 37°C for 48 hrs. The negative control wells contained only 200 µL of TSB–0.5% glucose without bacterial suspension. Wells were gently washed with phosphate buffer saline (PBS) (pH 7.2) three times and fixed with methanol for 20 minutes, dried at room temperature, then stained with crystal violet 0.1 percent. The dye attached to the adhering cells was dissolved with 1 mL of 95% ethanol per well. Finally, optical density (OD) was obtained at 570 nm (A_{570}) for each well using ELISA reader (BioTek ELx800, USA). The average OD of negative control + 3 standard deviation (SD) of negative control was calculated for the optical density cut-off (ODc). Based on the absorbance of crystal violet stain linked to the adhered cells, biofilms formed by various strains have been analyzed and categorized (Table 2).

Table 2. Classification of biofilm formation abilities by Microtiter plate method

Cut-off value calculation	Mean of OD ₅₇₀ values results	Biofilm formation abilities
OD > 4×ODc	OD > 0.557	Strong
2×ODc < OD ≤ 4×ODc	0.278 < OD ≤ 0.557	Moderate
ODc < OD ≤ 2×ODc	0.139 < OD ≤ 0.278	Weak
OD ≤ 0.139	OD ≤ 0.139	None

Genomic DNA extraction

According to the manufacturer's instructions, genomic DNA was extracted from pure cultures through the Presto™ Mini gDNA Bacteria Kit (Geneaid, Taiwan); extract was eluted with an elution buffer of 100 µL. Before running PCR, extracts were stored at -20°C. The NanoDrop 1000 spectrophotometer (ThermoFisher Scientific, USA) was used to evaluate DNA concentration and purity in which one µL of the genome DNA was used to define DNA concentration and purity.

PCR screening of biofilm genetic determinants

In our research, detection in *S. aureus* isolates for biofilm-related genes was carried out using the PCR technique. The final volume of the PCR reaction was 25 µL using 12.5 µL of 2x HotStart Taq Master Mix, one µL of the DNA template, one µL of each primer (20 pmol) and 9.5 µL of ddH₂O. DNA amplification was done in a thermocycler PCR. Primers and amplification conditions for PCR programs are mentioned in *Table 1*. Amplified products were subjected to electrophoresis using 1.2% agarose (GeNet Bio, Korea) gel containing 1x GelRed DNA stain.

Ferric Reducing Antioxidant Power (FRAP) assay

To be able to measure the ferric reduction activity of our samples, the test was performed based on Benzie and Strain (1996). The FRAP solution was freshly prepared by combination of acetate buffer (0.3 Mol/L) (pH= 3.6), 2, 4, 6-tripyridyltriazine (TPTZ) (0.01 Mol/L in HCl (0.04 Mol/L) and FeCl₃ (0.02 Mol/L) (10:1:1) by volume, respectively. The test was performed by placing 100 µL of the tested chemicals in a test tube (Conc. 1 mg / mL) and 2 mL of the FRAP reagent, the samples were continuously shaken and leave in the dark place for 30 min. Then the absorbance at 593 nm was recorded. The standard ascorbic acid curve was prepared for comparison using various concentrations, as shown in *Fig. 1*. The FRAP value calculated by *Equation 1* for each compound. In this study, the test solution's yellow color reduces ferric complex with TPTZ (less color) to ferrous complex with TPTZ (violet color) changes to different shades of violet depending on each compound's reduced power. The higher reduction potential was determined by higher absorbance of the reaction mixture.

$$FRAP \text{ value of sample } (\mu\text{M}) = Abs. (sample) \times \frac{FRAP \text{ value of standard } (\mu\text{M})}{Abs. of standard} \quad (\text{Eq.1})$$

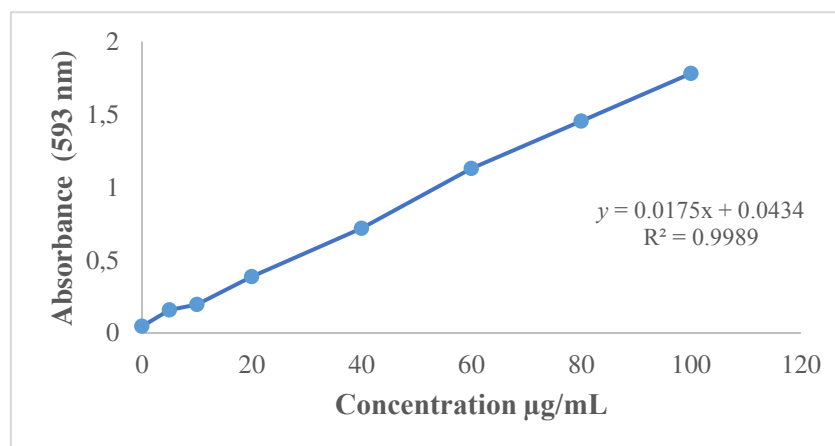


Figure 1. The standard curve of ascorbic acid

Biofilm formation inhibition test

Preparation of *Z. officinale* extract

Z. officinale extract was prepared under the protocol described by Kim and Park (2013). In short, 150 g of shredded rhizome of *Z. officinale* was mixed with 300 mL toluene. The debris was allowed to settle at room temperature for 24 hrs. A Whatman No. 1 filter paper (pore size = 11 µm) had been used for filtration of the supernatant. Then the mixture was stirred for 24 hrs. at room temperature using a magnetic stirrer. Then the mixture was left to form phases of water and toluene. Using a pipette, the water phase was collected and filtered through a 0.22 µm microfilter. The filtrate (100% *Z. officinale* extract) was used to test if *Z. officinale* extract inhibits the formation of biofilms.

Antimicrobial activity of quercetin

The antimicrobial activity of quercetin was performed by the microdilution method, already described previously, according to the CLSI. The range of concentration of quercetin used in this study was 2 to 256 µg/ml (Sérgio et al., 2018). The experiment was performed in triplicate.

Preparation and dilution of ascorbic acid

One milligram of ascorbic acid was dissolved in 1 ml of TSB medium to get a stock solution of 1000 µg/ml. Final concentrations of 2, 4, 8, 16, 32, 64, 128, and 256 µg/ml were obtained through serial dilutions to explore the antibiofilm activity against *S. aureus*. Ascorbic acid was mixed for two minutes with TSB medium and vortex. It was covered with aluminum foil to prevent light. At the time of their use, all solutions were prepared.

Static biofilm formation assay

To test the effect of plant extract on biofilm formation, a modified crystal violet assay was used. In sterile 96 well plates containing 50 µL of nutrient broth per well, two-fold serial dilutions of compounds were made. The concentration range of the compounds tested is 2 to 256 µg/mL in separate wells. Each well was supplemented with a 50 µL fresh bacterial suspension (0.5 McFarland) with growth control (*cells + broth*). The biofilm biomass was tested using the crystal violet staining assay after incubation at 37°C for 48 h (Kim and Park, 2013). The biofilm inhibition percentage was calculated using Equation 2.

$$\text{Biofilm inhibition\%} = \frac{OD \text{ growth control} - OD \text{ sample}}{OD \text{ growth control}} \times 100 \quad (\text{Eq.2})$$

Data analysis

For statistical analysis, the Social Science Statistical Package (SPSS 24.0) software (SPSS Inc., USA) was used. The statistical significance was assessed through *Turkey's multiple comparisons*; the test was used to analyze the association between phenotypic biofilm formation methods and biofilm-related genes, and also the significant difference in biofilm inhibition percentage between active, positive-controlled biofilm producers and *p*-value < 0.05 was considered statistically significant.

Results

Isolation and characterization of S. aureus

Based on biochemical tests, isolates from one hundred catheter specimens (63.69%) were identified as *S. aureus* (Table 3). The strains were from samples belonging to 67 male patients (67%), and 33 female patients (33%). To support the identification of *S. aureus* isolates by a conventional method, VITEK II Compact System was performed, and all strains of *S. aureus* were reidentified by this system, some results contradicted the traditional tests and identified a different staphylococcal species than *S. aureus*. The present findings of the VITEK II system show that 83 isolates were identified as *S. aureus* among 100 isolates that were identified in the conventional method, and the remaining strains identified were *xylosus* ($n=6$), *sciuri* ($n=6$), *vitulinus* ($n=1$), *warneri* ($n=1$), *lentus* ($n=1$), *hemolyticus* ($n=1$), and *gallinarum* ($n=1$). To further confirm the identity of the isolates, all *S. aureus* were examined for the presence of the *16S* rRNA and *nuc* genes to characterize and validate the *S. aureus*. All of the strains were confirmed as *S. aureus* by the occurrence of *16S* rRNA, and *nuc* genes (Fig. 2). About two-thirds of catheter-isolated bacteria were identified as *S. aureus*.

Table 3. The morphological, cultural, biochemical, and molecular tests for the identification of *S. aureus* isolates

Biochemical tests	Positive <i>S. aureus</i>		Positive% among catheter specimens ($n=157$)
	Positive <i>n.</i> (%)	Negative <i>n.</i> (%)	
Mannitol fermentation	100 (100)	0 (0)	63.69
Coagulase HP	91 (91)	9 (9)	57.95
Coagulase RP	96 (96)	4 (4)	61.14
Catalase	100 (100)	0 (0)	63.69
Oxidase	0 (0)	100 (100)	0
Urease	54 (54)	46 (46)	34.39
Gelatinase	100 (100)	0 (0)	63.69
β Hemolysis	71 (71)	45.21
α Hemolysis	2 (2)	1.27
γ Hemolysis	27 (27)	17.19
DNase	100 (100)	0 (0)	63.69
Staphyloxanthin	85 (85)	15 (15)	54.13
Caseinase	82 (82)	18 (18)	52.22
Tellurite reduction	100 (100)	0 (0)	63.69
Shiny colonies	100 (100)	0 (0)	63.69
Lipase activities	64 (64)	36 (36)	40.76
Lecithinase production	62 (62)	38 (38)	39.48
VITEK II System	83 (83)	17 (17)	52.86
<i>16S</i> rRNA gene	100 (100)	0 (0)	63.69
<i>nuc</i> gene	100 (100)	0 (0)	63.69

Susceptibility patterns of S. aureus against different antimicrobials

The results of the antimicrobial sensitivity test for all *S. aureus* isolates against 16 antimicrobials demonstrated various sensitivity patterns (Table 4). The highest resistant percentage recorded was against oxacillin (99%), followed by penicillin (97%). However, the lowest resistant 1% recorded was against each of gentamycin, nitrofurantoin, and trimethoprim-sulfamethoxazole.

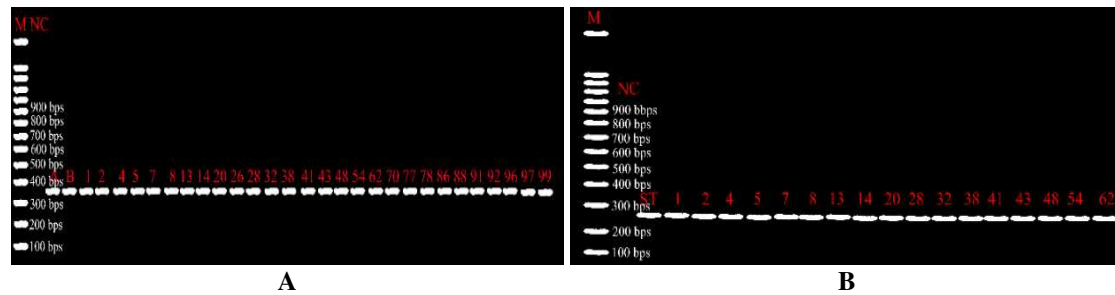


Figure 2. Agarose gel electrophoresis of PCR amplification products of *S. aureus*. **A:** 16S rRNA gene, M: The DNA marker (100 bp ladder), lane A and B: *S. aureus* ATCC 23925, lanes (1–99) positive amplification of 372 bp for 16S rRNA gene. **B:** nuc gene, M: The DNA marker (100 bp ladder), lane NC: *S. epidermidis* ATCC 22922, lane ST: *S. aureus* ATCC 23925, lanes (1–62) positive amplification of 279 bp for nuc gene

Table 4. Susceptibility patterns of *S. aureus* isolate toward antimicrobials

Antimicrobials	Resistance	Intermediate	Sensitivity
	n. (%)	n. (%)	n. (%)
AK*	1 (1)	1 (1)	98 (98)
AZM	47 (47)	4 (4)	49 (49)
CIP	11 (11)	1 (1)	88 (88)
CD	30 (30)	19 (19)	51 (51)
E	53 (53)	6 (6)	41 (41)
G	1 (1)	4 (4)	95 (95)
LEV	9 (9)	0 (0)	91 (91)
NET	1 (1)	3 (3)	96 (96)
NIT	21 (21)	1 (1)	78 (78)
NOR	18 (18)	34 (34)	58 (58)
OX	99 (99)	0 (0)	1 (1)
P	97 (97)	0 (0)	3 (3)
TE	23 (23)	3 (3)	74 (74)
TOB	19 (19)	3 (3)	78 (78)
SXT	1 (1)	8 (8)	91 (91)
VA	38 (38)	25 (25)	47 (47)

*: AK: Amikacin, AZM: Azithromycin, CIP: Ciprofloxacin, CD: Clindamycin, E: Erythromycin, G: Gentamicin, LEV: Levofloxacin, NET: Netilmicin, NIT: Nitrofurantoin, NOR: Norfloxacin, OX: Oxacillin, P: Penicillin, TE: Tetracycline, TOB: Tobramycin, SXT: Trimethoprim+Sulfamethoxazole, and VA: Vancomycin

Biofilm formation through microtiter plate test

The ability to form a biofilm was evaluated using the MTP described elsewhere (Yousefi et al., 2016). In this study, OD₅₇₀ mean of microplate readings after crystal violet staining ranged from 0.216 to 0.827. The mean of negative control was 0.054. An ODC₅₇₀ of biofilm formation was defined as 0.139. The strains were divided into four groups: non-biofilm producer (–), OD₅₇₀ ≤ 0.139; weak biofilm producer (+), 0.139 < OD₅₇₀ ≤ 0.278; moderate biofilm producer (++), 0.278 < OD₅₇₀ ≤ 0.557; strong biofilm producer (+++), 0.557 ≤ OD₅₇₀. Our data shows that 100% of *S. aureus* isolates were positive for biofilms, 21% of which were recorded as a strong producer of biofilms (n=21), 71% as a moderate producer of biofilms (n=71) and 8% as a weak producer of biofilms (n=8).

Biofilm formation determination by Congo red agar test

In vitro biofilm formation by the CRA method differs from MTP assay. Results show that 49% of the isolates ($n=49$) demonstrated strong biofilm formation (strong black), 15% were moderate biofilm producer, 25% weak biofilm producer, and 11% of the isolates were classified as non-biofilm producer. Statistically, there is not a significant difference ($p= 0.8997$) between the total percent formation in both MTP assay, and CRA methods for the detection of phenotypic biofilm formation among isolates of *S. aureus* was observed (Table 5). While there are highly significant differences among biofilm formation status when compared between both MTA assay and CRA method (Fig. 3).

Table 5. Screening of *S. aureus* isolates from biofilm production by CRA and MPM assay

Biofilm formation status	Screening method		P-value
	CRA n. (%)	MTP n. (%)	
Strong	49 (49%)	21 (21%)	=0.8997
Moderate	15 (15%)	71 (71%)	
Weak	25 (25%)	8 (8%)	
None	11 (11%)	0 (0%)	
Total	89 (89%)	100 (100%)	

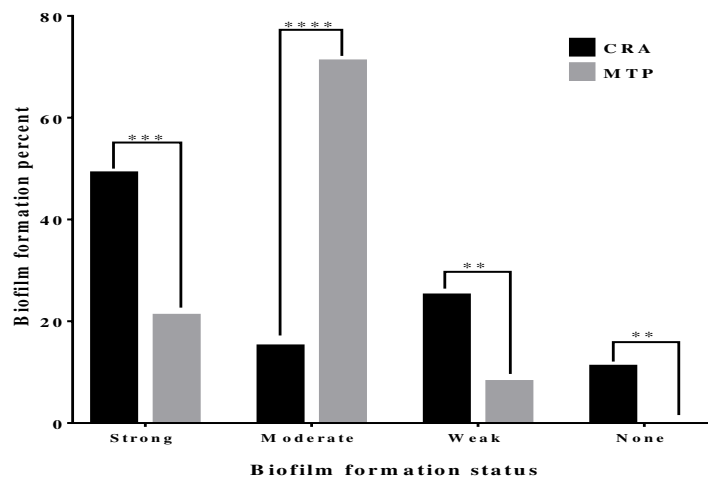


Figure 3. Comparison of biofilm formation status

Detection of genes involved in biofilm formation

PCR assay was used to detect *icaA*, *icaB*, *icaC*, *icaD*, *cna*, *atl*, *fnbA*, and *fnbB* genes among the primary intention of this study are the genotypically characterization of biofilm responsible genes. Ninety-six percent of *S. aureus* isolates have been selected for this purpose. We evaluated the relationship between the formation of biofilm and the eight genes associated with biofilm. The distribution of these genes in *S. aureus* isolates is illustrated in Table 6. All of the eight genes were detected among isolates with different frequencies. As can be seen, the majority of *S. aureus* isolates (96% [$n=24$]) were found to be positive for the *icaC* and *cna* gene (Fig. 4). The prevalence rates of the *icaA*, *icaB*, *icaD*, *atl*, *fnbA*, and *fnbB* genes were unswervingly found to be 76%, 68%, 88%, 92%, 84%, and 80%, respectively. Nine of the isolates (36%) ($n=9$) that were biofilm producers were shown to possess all of the eight genes aimed to detect in the current study. A

significant association was only observed between the presence of *icaB* gene ($p= 0.028$) and phenotypic biofilm formation in *S. aureus* isolates, while non-significant association was noticed for each of *icaA* ($p = 0.2085$), *icaC* ($p=0.9894$), *icaD* ($p= 0.7238$), *cna* ($p= 0.9894$), *atl* ($p= 0.9004$), *fnbA* ($p= 0.5207$) and *fnbB* ($p= 0.3421$) and phenotypic biofilm formation features.

Table 6. Relationships between biofilm-related genes and biofilm formation detection (MTP assay and CRA method) in *S. aureus* isolates

Isolates	In vitro Adherence (MTP) Assay		CRA method		Presence of biofilm-related genes							
	Adherence A ₅₇₀ nm Mean	Adherence Ability	Biofilm phenotype	Biofilm producer	<i>icaA</i>	<i>icaB</i>	<i>icaC</i>	<i>icaD</i>	<i>cna</i>	<i>atl</i>	<i>fnbA</i>	<i>fnbB</i>
SA01	0.236	+	Black**	Producer	+	+	+	+	+	+	—	+
SA02	0.488	++	Strong Black	Producer	+	—	+	—	+	+	+	+
SA04	0.608	+++	Strong Black	Producer	+	—	+	+	+	+	—	+
SA05	0.379	++	Strong Black	Producer	+	+	+	+	+	+	+	+
SA07	0.578	+++	Black	Producer	—	+	+	+	+	+	+	+
SA08	0.402	++	Black	Producer	+	+	+	+	+	+	+	—
SA13	0.491	++	Almost Black	Producer	—	—	+	+	+	+	+	+
SA14	0.586	+++	Almost Black	Producer	+	+	+	—	+	+	+	—
SA20	0.216	+	Bordeaux pink	Nonproducer	+	+	+	+	+	+	+	+
SA26	0.552	++	Almost Black	Producer	+	+	+	+	+	+	—	+
SA28	0.297	++	Almost Black	Producer	+	+	+	+	+	+	+	+
SA32	0.36	++	Strong Black	Producer	—	+	+	+	+	+	+	+
SA38	0.318	++	Bordeaux pink	Nonproducer	—	—	+	+	+	+	+	+
SA41	0.379	++	Strong Black	Producer	+	+	+	+	+	+	+	+
SA43	0.317	++	Strong Black	Producer	+	+	+	+	+	+	+	+
SA48	0.667	+++	Strong Black	Producer	+	+	+	+	+	—	+	—
SA49	0.376	++	Bordeaux pink	Nonproducer	—	—	—	—	—	—	+	—
SA54	0.26	+	Black	Producer	+	—	+	+	+	+	—	+
SA62	0.458	++	Strong Black	Producer	+	+	+	+	+	+	+	+
SA70	0.349	++	Strong Black	Producer	+	+	+	+	+	+	+	+
SA77	0.36	++	Strong Black	Producer	+	—	+	+	+	+	+	+
SA78	0.383	++	Almost Black	Producer	+	+	+	+	+	+	+	+
SA86	0.425	++	Strong Black	Producer	+	+	+	+	+	+	+	—
SA88	0.352	++	Strong Black	Producer	—	—	+	+	+	+	+	+
SA93	0.284	++	Strong Black	Producer	+	+	+	+	+	+	+	+
Total positive	25		22		19	17	24	22	24	23	21	20
Percent	100		88		76	68	96	88	96	92	84	80
P-value			0.8997		0.2085	0.028	0.9894	0.7238	0.9894	0.9004	0.5207	0.3421

*: indicates the varied adhering ability of *S. aureus* isolates, where strong black colonies; strong biofilm producer, black colonies; moderate biofilm producer, almost black colonies; weak biofilm producer, Bordeaux pink colonies; non – biofilm producer, also +: weak biofilm producer. ++: moderate biofilm producer. +++: strong biofilm producer. †: ODC: mean + 3 standard deviation of negative control in microplate. ODC=0.139, 2ODC=0.278, 4ODC=0.556

FRAP reducing power

The antioxidant activity of the *Z. officinale*, quercetin, and ascorbic acid was measured by FRAP assay and has been presented in Table 7. It shows that electron-donating groups enhanced reducing power. Quercetin indicates that they are most effective electron donor and can reduce the oxidized intermediates highly reactive molecules like free radicals and reactive oxygen species of peroxidation processes and the FRAP value 10406.4 $\mu\text{M/g}$ while the *Z. officinale* extract has low antioxidant activity (FRAP value = 5420.8 $\mu\text{M/g}$) when compared with both quercetin and ascorbic acid. Ascorbic acid usually used as a standard for preparing the standard curve and has high antioxidant activity (FRAP value = 8379.5 $\mu\text{M/g}$).

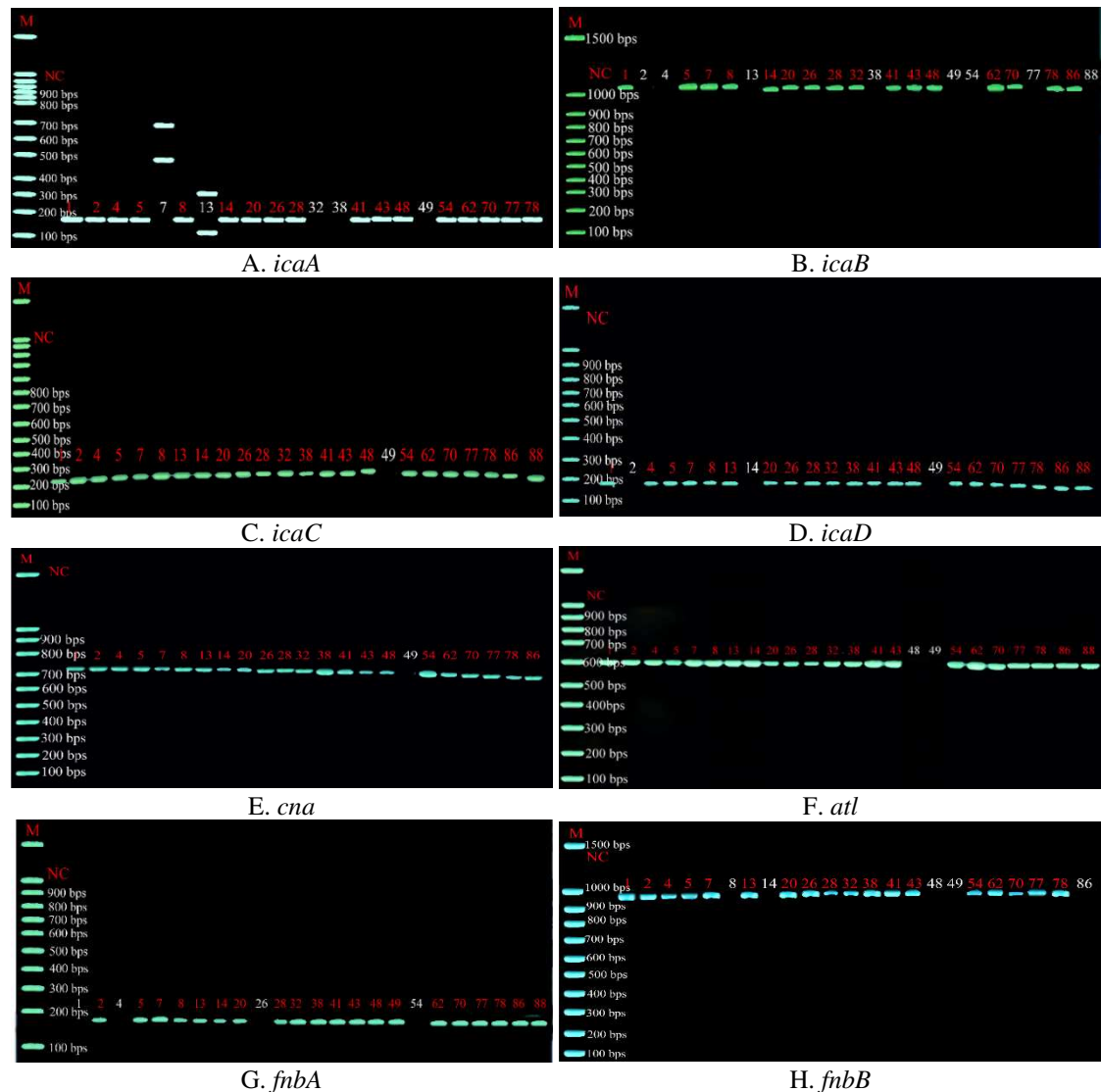


Figure 4. Agarose gel electrophoresis graphic of PCR amplification for biofilm-related genes in *S. aureus* isolates

Table 7. Anti-oxidant activity of the *Z. officinale*, quercetin and ascorbic acid measured by FRAP assay

Compounds	Absorbance	FERAP value		
		μM	$\mu\text{M}/\text{mg}$	$\mu\text{M}/\text{g}$
<i>Z. officinale</i>	1.507	54.208	542.08	5420.8
Quercetin	2.893	104.064	1040.64	10406.4
Ascorbic acid	2.327	83.705	837.05	8370.5

Effect of *Z. officinale* extract on biofilm formation

A static biofilm quantification assay was performed to evaluate the effect of *Z. officinale* extract on five strong biofilm isolates of *S. aureus*. Table 8 shows the difference in biofilm inhibition between the culture containing *Z. officinale* extract and the control (i.e., no *Z. officinale* extract addition). The high biofilm inhibition percent

were 61.4 at concentration 16% against SA04 while there is no any effect on biofilm formation at concentrations 4, 2, 1, and 0.5% against each of SA36, and SA62 isolates. Significantly, there were differences in biofilm reduction for *Z. officinale* extract at concentration 32, 16, and 8% ($p = 0.0458$, $p = 0.0391$, and $p = 0.0247$, respectively). In spite of decreasing of biofilm formation, there were no observed significant at concentrations 64, 4, 2, 1, and 0.5% ($p = 0.1015$, $p = 0.1676$, $p = 0.8017$, $p = 0.8811$, and $p = 0.5925$, respectively). The inhibition of *Z. officinale* extract to biofilm formation was not due to minor toluene contamination or something extracted from the glassware during the preparation of *Z. officinale* extract, which was confirmed by an experiment using mock extraction.

Table 8. Antibiofilm potency of *Z. officinale*, quercetin and ascorbic acid

Isolates	% of Biofilm Inhibitors of <i>Z. officinale</i> (%)								Growth Control (OD)
	64	32	16	8	4	2	1	0.5	
SA04	54	59	61.4	57	41	41	47	9.7	0.131
SA36	14	28	36.4	36	0	0	0	0	0.109
SA48	36	47	43.1	45	30	0	17	43	0.108
SA62	47	46	45	45	46	0	0	0	0.143
SA86	47	45	47.4	46	46	30	0.9	40	0.157
<i>P value</i>	0.1015	0.0458	0.0391	0.0247	0.1676	0.8017	0.8811	0.5925	
Isolates	% of Biofilm Inhibitors of Quercetin (µg/mL)								Growth Control (OD)
	256	128	64	32	16	8	4	2	
SA04	18	76	79.4	58	56	48	43	40	0.139
SA36	25	31	0	92	20	43	43	45	0.134
SA48	23	16	0	52	34	41	41	38	0.155
SA62	34	38	20.3	57	55	41	41	36	0.137
SA86	24	48	28.7	59	59	61	61	62	0.15
<i>P value</i>	0.0221	0.1426	0.6646	0.0041	0.0855	0.0221	0.0246	0.0369	
Isolates	% of Biofilm Inhibitors of Vitamin C (µg/mL)								Growth Control (OD)
	256	128	64	32	16	8	4	2	
SA04	57	57	59	55	57	55	49	50	0.145
SA36	51	52	53	59	57	56	48	56	0.088
SA48	58	59	61.9	60	59	57	50	60	0.109
SA62	53	58	59.1	55	55	50	15	49	0.111
SA86	56	61	60	62	61	59	55	51	0.114
<i>P value</i>	0.0003	0.0062	0.071	0.0079	0.0271	0.240	0.840	0.406	

Antibiofilm activities of quercetin

Concerning the action of quercetin as antibiofilm, this molecule reduces biofilm formation against SA36 isolate of *S. aureus* at 32 µg/mL, and the inhibition potency percent reached to 92, and have a significant difference when compared to a positive control ($p = 0.0041$). Quercetin reduced biofilm formation at all concentrations against all five isolates except concentrations of 64 µg/mL against both SA36 and SA48 isolates. In particular, the lowest inhibited biofilm formation was 16%, and the highest was 92% (Table 8). Significant differences was recorded at concentrations 256, 8, 4, and 2 µg/mL when compared with positive control ($p = 0.0221$, $p = 0.02$, $p = 0.0246$, $p = 0.0369$) respectively.

Biofilm inhibitory activity of ascorbic acid

Once the antibiofilm efficacy of ascorbic acid has been determined, we analyze their potential action against *S. aureus* biofilm formation. MTP assessed this ability, and these results showed complete inhibition of biofilm formation by ascorbate when compared to

growth control (*Table 8*). The highest antibiofilm potency of ascorbic acid was 62% against SA86 isolate at concentration 32 µg/mL, while the minimum power was recorded at concentration four µg/ml a toward SA62 isolate. In spite of the low inhibition percent of biofilm formation, while there are a significant differences in the decreasing of biofilm formation at concentrations 256, 128, 32, and 16 µg/mL ($p = 0.0003$, $p = 0.0062$, $p = 0.0079$, and $p = 0.0271$) respectively when compared with OD of growth control.

Discussion

All 100 *S. aureus* isolates were branded as Gram-positive; further cultural characteristics and biochemical test results were stated in *Table 3*. Out of these isolates, 91 isolates were coagulase-positive *S. aureus*, and nine were recorded as coagulase-negative. Results obtained from the conventional biochemical tests and PCR method match with a statistical confidence of 91% (The remaining 9% non—reluctant possibly due to analysis conditions and sample preparation) between the methods. This probably will be due to the concealing of the clumping factor by the capsular polysaccharides or due to misidentification of particular clumping factor producing CoNS; by this means, lessening its efficiency, reliability, and sensitivity (Subramanian et al., 2017). An additional test used *S. aureus* identification is the DNase test. All isolates of *S. aureus* have been positive for DNase activity in the present study. Parallel results have been reported previously with a lack of clarification; thus, additional tests are required for confirmation purposes.

In our study, 78 *S. aureus* isolates showed the ability to hydrolyze gelatin, thus confirming the presence of the gelatinase enzyme. However, 81, 51, and 48 strains of *S. aureus* secrete protease, lipase enzymes, and nonwhite pigmented colonies, respectively. Among the 100 strains of *S. aureus* showed β -hemolytic, γ -hemolytic and α -hemolytic properties, 71 strains of *S. aureus* showed the ability of β -hemolysin and only two isolates expressed α -hemolysin, and 27 isolates demonstrated the γ -hemolytic activity. Likewise, hemolytic activity among 57 different clinical sources of *S. aureus* exhibited vigorous hemolytic activities and five clinical strains that had no ability of blood hydrolysis on blood agar (Tang et al., 2013). All isolates of *S. aureus* were undergone PCR assay using universally conserved *16S* rRNA and *nuc* genes, specifically designed primers were used for discrimination of *S. aureus* isolates (*Table 1*), and all of the strains were positive for both genes (*Fig. 3*). Antimicrobial susceptibility carried out for 16 antimicrobials through disc diffusion methods, and the results are presented in *Table 6*. The highly resistant percentage was seen against oxacillin (99%) followed by penicillin (97%), and the lowest resistant 1% recorded was against each of gentamycin, nitrofurantoin, and trimethoprim–sulfamethoxazole. Based on the antimicrobial susceptibility reports by Boada et al. (2018), among the 765 assessed *S. aureus* isolates, the maximum resistance rates were observed to a penicillin (87.1%), followed by azithromycin (11.6%), erythromycin (11.2%) and clindamycin (9.7%). Oxacillin and methicillin resistance mechanism is by gaining a gene that encodes a PBP2 homolog called PBP2a that is not susceptible to drug deed, and this is due to the serine residue that is not reachable by β -lactams at the active site of the TP of PBP2a (Foster, 2017).

Different results in both methods used for β -lactamase detection in all *S. aureus* isolates, the positive result in an iodometric method was 91%, while 73 isolates could produce β -lactamase through Cefinase disk. Most strains of *S. aureus* were resistant to penicillin; nearly 20% of *S. aureus* remained susceptible to penicillin (Parija, 2014).

Clinical *S. aureus* isolates were examined for biofilm formation *via* phenotypic and molecular assays, and any possible association between biofilm formation and bacterial genetic lineage was investigated. *S. aureus* remains the most recurrently encountered bacterial pathogen and is responsible for a variety of mild to life-threatening infections (El-Huneidi et al., 2006). The ability of *S. aureus* to adhere and form biofilm makes them more resistant against antibiotics. Bacterial virulence factors such as adhesion play a vital role in catheter-related infections. Staphylococcus' ability to settle in artificial material is linked to two main mechanisms; polysaccharide slime production and host matrix protein adsorption on the biomaterial surface. When the biofilm is produced, it would be easy to run away from immune systems and to cause chronic infections. While PIA is essential for the formation of biofilm by *S. aureus*, in this study, we found in these isolates more than one gene of *ica* operon, i.e. *icaADBC*, *cna*, *atl*, *fnbA* and *fnbB* genes are associated with the production of biofilm in these isolates.

Although many genes and conditions are responsible for biofilm production, our results demonstrated that *icaA*, *icaB*, *icaC*, *icaD*, *cna*, *atl*, *fnbA*, and *fnbB* genes have a critical role in the production of biofilms. In this work we found that 89 out of 100 strains were biofilm producers developing almost black ($n=25$), black ($n=15$) or strong black colonies ($n=49$) on CRA plate, while in MTP assay, all isolates produce biofilm with ranging from weak ($n=8$), moderate ($n=71$) and strong biofilm production ($n=21$). Comparatively, similar results have been achieved elsewhere, stating that 50% of clinical *S. aureus* isolates to form a biofilm (Kouidhi et al., 2010). Out of 100 bacterial isolates, the formation of biofilm was recorded in 60% of isolates by CRA method, while PCR detection of biofilm-related genes, *icaA*, and *icaD*, revealed that both genes were present in 78% of the isolates (Salehzadeh et al., 2016). Discrepancies have been reported between phenotypic and genotypic methods for the detection of *S. aureus* producing biofilms (Yazdani et al., 2006). Statistical analysis revealed there is no significant difference between the biofilm formation using the MTP assay and the CRA method ($p = 0.8997$). Numerous studies have confirmed that some *S. aureus* strains need *icaADBC* to form biofilms (Johnson et al., 2008). On the other hand, adhesion to host cells requires genes such as *fnbA*, *fnbB*, and *cna* that encode microbial surface constituents known as adhesive matrix molecules that are different from those involved in the adhesion on abiotic surfaces (Arciola et al., 2005).

In the present study, the prevalence of the *icaC*, *icaD*, and *cna* (96%) and *icaA*, *icaB*, *atl*, *fnbA*, and genes were found to be 80%, 72%, 80% and 86%, respectively. This result may reflect the role of these genes in the pathogenicity of *S. aureus* isolates. However, *fnbB* was found in a lower percentage (60%). The prevalence of twelve genes involved in biofilm production explains that numerous factors may be useful in various stages of biofilm formation due to the ability of all the strains identified to form biofilm at different levels, but the gene incidence was different. Further research to clarify the expression of these genes in *S. aureus* strains should be considered (Nourbakhsh and Namvar, 2016), and they stated that the prevalence of the genes involved in biofilm production was: *icaA* (34.2%), *icaB* (29.7%), *icaC* (69.3%), *icaD* (54.8%), *fnbA* (38.1%), *fnbB* (46.6%), and *can* (18.3%). Similar to our study, several other researchers have shown that the formation of slime and biofilm in *S. aureus* is associated with the presence of *icaA* and *icaD* genes (Cramton et al., 1999; Arciola et al., 2001; Vasudevan et al., 2003). Production of intercellular adhesion molecules, e.g., by *icaABCD* and other genes, plays an essential role in staphylococcal biofilm. Biofilm production may be the fundamental reason for the increasing antibiotic resistance of *S. aureus* strains. A

significant association was observed between the presence of genes such as *icaA*, *icaB*, *icaC*, *icaD*, *can*, *atl*, *fnbA* and *fnbB*, and biofilm formation. Although not all of the genes were found simultaneously in all the isolates of the biofilm producers, at least one of the related genes was detected in the entire isolates of the biofilm producers (except one strain). The ability to form biofilm in negative strains for one or more genes may be associated with some other genes associated with biofilm.

In the present study, the prevalence of the *icaC*, *icaD*, and *cna* (96%) and *icaA*, *icaB*, *atl*, *fnbA*, and genes were found to be 80%, 72%, 80% and 86%, respectively. This result may reflect the role of these genes in the pathogenicity of *S. aureus* isolates. However, *fnbB* was found in a lower percentage (60%). The prevalence of twelve genes involved in production of biofilm explains that numerous factors may be useful in different steps of biofilm formation because all of the strains identified could form biofilm at various levels, but the incidence of genes was different. Further research should be considered to elucidate the expression of these genes in *S. aureus* strains. We investigated the effects of *Z. officinale* extract, quercetin, and ascorbic acid on biofilm formation using a static biofilm assay and using *S. aureus* as a model biofilm-forming microorganism, and found that quercetin inhibits the formation of biofilm when compared with *Z. officinale* extract and Ascorbic acid through the percentage of biofilm inhibition.

Conclusion

In the current study, a significant association between the presence of *icaA*, *icaB*, *icaC*, *icaD*, *can*, *atl*, *fnbA*, and *fnbB* genes and biofilm formation were observed. Although all of the genes were not found in all of the biofilm producer isolates, however, in the entire biofilm producer isolates (except one isolate) at least one of the related genes was detected. The ability of biofilm formation in isolates negative for one or more genes might be related to some other biofilm-associated genes. The most critical future suggestions are to use all active components which present in the *Z. officinale* against biofilm formation in different bacterial species and genera.

Acknowledgments. This work supported by Salahaddin University-Erbil, Erbil, Iraq, as the Ph.D. program (No. 15738 on December 12, 2015). The authors would like to thank and grateful to *Prof. Dr. Jawher F. Saeed* for his support and technical assistance and *Dr. Abdullah M.A. Qassab* for his scientific evaluating.

REFERENCES

- [1] Ali, B. H., Blunden, G., Tanira, M. O., Nemmar, A. (2008): Some phytochemical, pharmacological and toxicological properties of ginger (*Zingiber officinale* Roscoe): a review of recent research. – *Food and Chemical Toxicology* 46: 409-420.
- [2] Alli, O. A., Ogbolu, D. O., Shittu, A. O., Okorie, A. N., Akinola, J. O., Daniel, J. B. (2015): Association of virulence genes with *mecA* gene in *Staphylococcus aureus* isolates from Tertiary Hospitals in Nigeria. – *Indian Journal of Pathology and Microbiology* 58: 464-71.
- [3] Arciola, C. R., Baldassarri, L., Montanaro, L. (2001): Presence of *icaA* and *icaD* genes and slime production in a collection of Staphylococcal strains from catheter-associated infections. – *Journal of clinical microbiology* 39: 2151-2156.
- [4] Arciola, C. R., Campoccia, D., Gamberini, S., Baldassarri, L., Montanaro, L. (2005): Prevalence of *cna*, *fnbA* and *fnbB* adhesin genes among *Staphylococcus aureus* isolates

- from orthopedic infections associated to different types of implant. – FEMS Microbiol Lett. 246: 81-6.
- [5] Balamurugan, P., Praveen Krishna, V., Bharath, D., Lavanya, R., Vairaprakash, P., Adline Princy, S. (2017): *Staphylococcus aureus* quorum regulator *SarA* targeted compound, 2-[(Methylamino) methyl] phenol inhibits biofilm and down-regulates virulence genes. – Frontiers in Microbiology 8: 1290.
- [6] Bayer, A. S., Abdelhady, W., Li, L., Gonzales, R., Xiong, Y. Q. (2016): Comparative efficacies of tedizolid phosphate, linezolid, and vancomycin in a murine model of subcutaneous catheter-related biofilm infection due to methicillin-susceptible and-resistant *Staphylococcus aureus*. – Antimicrobial agents and chemotherapy 60: 5092-5096.
- [7] Benzie, I. F. F., Strain, J. J. (1996): The Ferric Reducing Ability of Plasma (FRAP) as a Measure of “Antioxidant Power”: The FRAP Assay. – Analytical Biochemistry 239: 70-76.
- [8] Bimanand, L., Taherikalani, M., Jalilian, F. A., Sadeghifard, N., Ghafourian, S., Mahdavi, Z., Mohamadi, S., Sayehmiri, K., Hematian, A., Pakzad, I. (2018): Association between biofilm production, adhesion genes and drugs resistance in different *SCCmec* types of methicillin-resistant *Staphylococcus aureus* strains isolated from several major hospitals of Iran. – Iran J Bas Med Sci 21: 400.
- [9] Blaiotta, G., Ercolini, D., Pennacchia, C., Fusco, V., Casaburi, A., Pepe, O., Villani, F. (2004): PCR detection of staphylococcal enterotoxin genes in *Staphylococcus* spp. strains isolated from meat and dairy products. Evidence for new variants of *seG* and *seI* in *Staphylococcus aureus* AB-8802. – J Appl Microbiol 97: 719-730.
- [10] Boada, A., Pons-Vigués, M., Real, J., Grezner, E., Bolívar, B., Llor, C. (2018): Previous antibiotic exposure and antibiotic resistance of commensal *Staphylococcus aureus* in Spanish primary care. – European Journal of General Practice 24: 125-130.
- [11] Cheung, A. L., Bayer, A. S., Zhang, G., Gresham, H., Xiong, Y.-Q. (2004): Regulation of virulence determinants *in vitro* and *in vivo* in *Staphylococcus aureus*. – FEMS Immunology & Medical Microbiology 40: 1-9.
- [12] CLSI (2017). Performance Standards for Antimicrobial Susceptibility Testing. – Clinical and Laboratory Standards Institute, M100.
- [13] Cramton, S. E., Gerke, C., Schnell, N. F., Nichols, W. W., Götz, F. (1999): The intercellular adhesion (*ica*) locus is present in *Staphylococcus aureus* and is required for biofilm formation. – Infection and Immunity 67: 5427-5433.
- [14] El-Huneidi, W., Bdour, S., Mahasneh, A. (2006): Detection of enterotoxin genes *seg*, *seh*, *sei*, and *sej* and of a novel *aroA* genotype in Jordanian clinical isolates of *Staphylococcus aureus*. – Diagn Microbiol Infect Dis 56: 127-132.
- [15] Fey, P., Said-Salim, B., Rupp, M., Hinrichs, S., Boxrud, D., Davis, C., Kreiswirth, B., Schlievert, P. (2003): Comparative molecular analysis of community-or hospital-acquired methicillin-resistant *Staphylococcus aureus*. – Antimicrobial agents and chemotherapy 47: 196-203.
- [16] Foster, T. J. (2005): Immune evasion by staphylococci. – Nature reviews microbiology 3: 948.
- [17] Foster, T. J. (2017): Antibiotic resistance in *Staphylococcus aureus*: Current status and future prospects. – Fems microbiology reviews 41: 430-449.
- [18] Gowrishankar, S., Kamaladevi, A., Balamurugan, K., Pandian, S. K. (2016): *In vitro* and *in vivo* biofilm characterization of methicillin-resistant *Staphylococcus aureus* from patients associated with pharyngitis infection. – BioMed research international 16: 1-16.
- [19] Habib, S. H. M., Makpol, S., Hamid, N. A. A., Das, S., Ngah, W. Z. W., Yusof, Y. A. M. (2008): Ginger extract (*Zingiber officinale*) has anti-cancer and anti-inflammatory effects on ethionine-induced hepatoma rats. – Clinics 63: 807-813.
- [20] Helgadóttir, S., Pandit, S., Mokkaapati, V. R., Westerlund, F., Apell, P., Mijakovic, I. (2017): Vitamin C pretreatment enhances the antibacterial effect of cold atmospheric plasma. – Frontiers in cellular and infection microbiology 7: 43.

- [21] Hirai, I., Okuno, M., Katsuma, R., Arita, N., Tachibana, M., Yamamoto, Y. (2010): Characterisation of anti-*Staphylococcus aureus* activity of quercetin. – International Journal of Food Science and Technology 45: 1250-1254.
- [22] Jeong, S., Kim, H. J., Ha, N.-C., Kwon, A.-R. (2019): Crystal Structure of SAV0927 and Its Functional Implications. – Journal of microbiology and biotechnology 29: 500-505.
- [23] Johnson, M., Cockayne, A., Morrissey, J. A. (2008): Iron-regulated biofilm formation in *Staphylococcus aureus* Newman requires ica and the secreted protein Emp. – Infect Immun 76: 1756-1765.
- [24] Karasu, S. T., Rathish, K. C. (2014): Evaluation of Direct Tube Coagulase Test in Diagnosing Staphylococcal Bacteremia. – Journal of Clinical and Diagnostic Research 8: DC19-DC21.
- [25] Khoramrooz, S. S., Mansouri, F., Marashifard, M., Malek Hosseini, S. A., Akbarian, C. F., Ganavehei, B., Gharibpour, F., Shahbazi, A., Mirzaii, M., Darban-Sarokhalil, D. (2016): Detection of biofilm related genes, classical enterotoxin genes and agr typing among *Staphylococcus aureus* isolated from bovine with subclinical mastitis in southwest of Iran. – Microb Pathog 97: 45-51.
- [26] Kiedrowski, M. R., Horswill, A. R. (2011): New approaches for treating staphylococcal biofilm infections. – Annals of the New York Academy of Sciences 1241: 104-121.
- [27] Kim, H.-S., Park, H.-D. (2013): Ginger extract inhibits biofilm formation by *Pseudomonas aeruginosa* PA14. – PloS one 8: e76106.
- [28] Kouidhi, B., Zmantar, T., Hentati, H., Bakhrouf, A. (2010): Cell surface hydrophobicity, biofilm formation, adhesives properties and molecular detection of adhesins genes in *Staphylococcus aureus* associated to dental caries. – Microbial pathogenesis 49: 14-22.
- [29] Mcfarland, J. (1907): Nephelometer: an instrument for media used for estimating the number of bacteria in suspensions used for calculating the opsonic index and for vaccines. – Journal of American Medical Association 14: 1176-1178.
- [30] Nair, S., Desai, S., Poonacha, N., Vipra, A., Sharma, U. (2016): Antibiofilm Activity and Synergistic Inhibition of *Staphylococcus aureus* Biofilms by Bactericidal Protein P128 in Combination with Antibiotics. – Antimicrob Agents Chemother 60: 7280-7289.
- [31] Nourbakhsh, F., Namvar, A. E. (2016): Detection of genes involved in biofilm formation in *Staphylococcus aureus* isolates. – GMS hygiene and infection control 11: 1-11.
- [32] Onsare, J. G., Arora, D. S. (2015): Antibiofilm potential of flavonoids extracted from *Moringa oleifera* seed coat against *Staphylococcus aureus*, *Pseudomonas aeruginosa* and *Candida albicans*. – J Appl Microbiol 118: 313-25.
- [33] Pandit, S., Ravikumar, V., Abdel-Haleem, A. M., Derouiche, A., Mokkaapati, V. R. S. S., Sihlbom, C., Mineta, K., Gojobori, T., Gao, X., Westerlund, F., Mijakovic, I. (2017): Low Concentrations of Vitamin C Reduce the Synthesis of Extracellular Polymers and Destabilize Bacterial Biofilms. – Frontiers in Microbiology 8.
- [34] Parija, S. C. (2014): Textbook of Microbiology and Immunology. – India, Elsevier Health Sciences.
- [35] Phuong, N. T. M., Van Quang, N., Mai, T. T., Anh, N. V., Kuhakarn, C., Reutrakul, V., Bolhuis, A. (2017): Antibiofilm activity of alpha-mangostin extracted from *Garcinia mangostana* L. against *Staphylococcus aureus*. – Asian Pac J Trop Med 10: 1154-1160.
- [36] Rodrigues, A., Gomes, A., Marcal, P. H., Dias-Souza, M. V. (2017): Dexamethasone abrogates the antimicrobial and antibiofilm activities of different drugs against clinical isolates of *Staphylococcus aureus* and *Pseudomonas aeruginosa*. – J Adv Res 8: 55-61.
- [37] Roy, R., Tiwari, M., Donelli, G., Tiwari, V. (2018): Strategies for combating bacterial biofilms: A focus on anti-biofilm agents and their mechanisms of action. – Virulence 9: 522-554.
- [38] Salehzadeh, A., Zamani, H., Langeroudi, M. K., Mirzaie, A. (2016): Molecular typing of nosocomial *Staphylococcus aureus* strains associated to biofilm based on the coagulase and protein A gene polymorphisms. – Iranian journal of basic medical sciences 19: 1325.

- [39] Saraiva, A. M., Saraiva, C. L., Gonçalves, A. M., Soares, R. R., Mendes, F. D. O., Cordeiro, R. P., Xavier, H. S., Pisciotano, M. N. C. (2012): Antimicrobial activity and bioautographic study of antistaphylococcal components from *Caesalpinia pyramidalis* Tull. – Brazilian Journal of Pharmaceutical Sciences 48: 147-154.
- [40] Sérgio, D. D. C. J., João, V. D. O. S., Luís, A. D., Almeida, C., Marcela, A. P., Nereide, S. S. M., Cavalcanti, I. M. F. (2018): Antibacterial and antibiofilm activities of quercetin against clinical isolates of *Staphylococcus aureus* and *Staphylococcus saprophyticus* with resistance profile. – International Journal of Environment, Agriculture and Biotechnology 3: 1948-1958.
- [41] Shahmoradi, M., Faridifar, P., Shapouri, R., Mousavi, S. F., Ezzedin, M., Mirzaei, B. (2019): Determining the Biofilm Forming Gene Profile of *Staphylococcus aureus* Clinical Isolates via Multiplex Colony PCR Method. – Reports of Biochemistry and Molecular Biology 7: 181.
- [42] Shin, H. J., Lee, H.-S., Lee, D.-S. (2010): The synergistic antibacterial activity of 1-acetyl-beta-carboline and beta-lactams against methicillin-resistant *Staphylococcus aureus* (MRSA). – Journal of microbiology and biotechnology 20: 501-505.
- [43] Singh, A., Ahmed, A., Prasad, K. N., Khanduja, S., Singh, S. K., Srivastava, J. K., Gajbhiye, N. S. (2015): Antibiofilm and membrane-damaging potential of cuprous oxide nanoparticles against *Staphylococcus aureus* with reduced susceptibility to vancomycin. – Antimicrob Agents Chemother 59: 6882-90.
- [44] Stoilova, I., Krastanov, A., Stoyanova, A., Denev, P., Gargova, S. (2007): Antioxidant activity of a ginger extract *Zingiber officinale*. – Food chemistry 102: 764-770.
- [45] Subramanian, A., Chitalia, V. K., Bangera, K., Vaidya, S. P., Warke, R., Chowdhary, A., Deshmukh, R. A. (2017): Evaluation of Hiaureus™ Coagulase Confirmation Kit in Identification of *Staphylococcus aureus*. – Journal of clinical and diagnostic research 11: DC08-DC13.
- [46] Szczuka, E., Urbańska, K., Pietryka, M., Kaznowski, A. (2013): Biofilm density and detection of biofilm-producing genes in methicillin-resistant *Staphylococcus aureus* strains. – Folia microbiologica 58: 47-52.
- [47] Tang, J., Tang, C., Chen, J., Du, Y., Yang, X. N., Wang, C., Zhang, H., Yue, H. (2011): Phenotypic characterization and prevalence of enterotoxin genes in *Staphylococcus aureus* isolates from outbreaks of illness in Chengdu City. – Foodborne Pathogenic Diseases 8: 1317-20.
- [48] Tang, J., Chen, J., Li, H., Zeng, P., Li, J. (2013): Characterization of adhesin genes, staphylococcal nuclease, hemolysis, and biofilm formation among *Staphylococcus aureus* strains isolated from different sources. – Foodborne pathogens and disease 10: 757-763.
- [49] Trübe, P., Hertlein, T., Mrochen, D. M., Schulz, D., Jorde, I., Krause, B., Zeun, J., Fischer, S., Wolf, S. A., Walther, B. (2019): Bringing together what belongs together: Optimizing murine infection models by using mouse-adapted *Staphylococcus aureus* strains. – International Journal of Medical Microbiology 309: 26-38.
- [50] Vasudevan, P., Nair, M. K. M., Annamalai, T., Venkitanarayanan, K. S. (2003): Phenotypic and genotypic characterization of bovine mastitis isolates of *Staphylococcus aureus* for biofilm formation. – Veterinary microbiology 92: 179-185.
- [51] Wang, J., Nong, X.-H., Zhang, X.-Y., Xu, X.-Y., Amin, M., Qi, S.-H. (2017): Screening of anti-biofilm compounds from marine-derived fungi and the effects of secalonic acid D on *Staphylococcus aureus* biofilm. – Journal of Microbiology and Biotechnology 27: 1078-1089.
- [52] Yazdani, R., Oshaghi, M., Havayi, A., Pishva, E., Salehi, R., Sadeghizadeh, M., Foroohesh, H. (2006): Detection of *icaAD* gene and biofilm formation in *Staphylococcus aureus* isolates from wound infections. – Iran J Publ Health 35(2): 25-28.
- [53] Yousefi, M., Pourmand, M. R., Fallah, F., Hashemi, A., Mashhadi, R., Nazari-Alam, A. (2016): Characterization of *Staphylococcus aureus* biofilm formation in urinary tract infection. – Iranian journal of public health 45(4): 485-493.

BIOREMEDIATION OF AGRICULTURAL SOIL CONTAMINATED BY A CRUDE OIL SPILL

ALI, W. A.^{1*} – FARID, W. A.¹ – AL-SALMAN, A. N. K.²

¹*Department of Community Health Technology, College of Health and Medical Technology in Basrah, Southern Technical University, Basrah, Iraq
(e-mail: wisam710@yahoo.com; phone: +964-77-0310-6873)*

²*Department of Pathology and Poultry, Veterinary College, University of Basrah, Basrah, Iraq
(e-mail: aseelnk1979@gmail.com; phone: +964-77-3011-1274)*

**Corresponding author
e-mail: wasen336@yahoo.com; phone: +964-77-1493-9973*

(Received 29th Jul 2019; accepted 25th Nov 2019)

Abstract. A local oil spill is the main cause of hydrocarbon soil pollution. Biological treatment of oil polluted soil may be possible due to the presence of oil-utilizing microorganisms at the site. Several factors affecting soil oil degradation include hydrocarbons solubility, soil texture, ventilation, oil toxicity, availability of nutrients, etc. Many techniques are used in the bioremediation of oil polluted soil. In this study, the compost system was used to increase the oxygen transmission with the addition of nutrients (NPK), hay (bulking agent) and biosurfactants producing bacteria (*B. cereus* WR146) to enhance the hydrocarbons degradation in agricultural soil. After 3 months of biological treatment, crude oil content decreased to 3.73-2.42% from the initial 4.20%. The percentage of crude oil degradation ranged from 20.1-44.5 depending on the treatment method used. Carbon dioxide development rates ranged from 30.6-55.0 $\mu\text{g g}^{-1} \text{day}^{-1}$, indicating a significant crude oil degradation due to aerobic microorganisms. There is no clear picture of whether nutrients and bulking agent increase the crude oil degradation rates in the current study. The results indicate that the bioremediation of soil polluted with crude oil is more efficient when using compost system, good ventilation, nutrients, and biosurfactants producing bacteria.

Keywords: biodegradation, oil pollution, agricultural soil, biosurfactants, bacteria

Introduction

Oils are the main source of energy in most industries and modern life. Leakages and accidental spills of oil and its products occur throughout production, export, refining, transport and storage. The quantity of leaking crude oil is estimated at 600,000 metric tons per year at the rate of 200,000 metric tons annually (Prathyusha et al., 2016). The introduction of hydrocarbons into the environment is one of the main causes of water and soil pollution. Hydrocarbons reach soils (including agricultural soils) from a variety of natural and anthropogenic sources. Technological hydrocarbons penetrate the soil after the soil surface is contaminated with crude oil and its products and hydrocarbon-containing materials. One of the most common anthropogenic sources is the leakage of underground storage tanks. Other major sources include spillage during refueling and lubrication. Sites where transportation and handling of crude oil are potential places for oil pollution. Shale oil retorting plants provide another source of hydrocarbon pollution (Boitsov et al., 2011; Pinedo et al., 2014; Ivshina et al., 2015). Although most of the hydrocarbons in the soil environment are of an anthropogenic nature, there are some natural sources of these substances. These may include the hydrocarbons resulting from the biogeochemical processes in the soil and those that migrate from the deep, oil-bearing ground layers. It also includes hydrocarbons released from the biodegradation

of organic matter. There is also accumulated evidences that some organisms, especially higher plants, are capable of synthesizing certain hydrocarbons that may also find their way into the soil. However, the natural sources are fairly simple and are unlikely to cause significant hydrocarbon pollution of the soil (Biache et al., 2014; Gennadiev et al., 2015). Soil contamination with petroleum hydrocarbons adversely affects human and animal health and plant production as most substances are toxic to living organisms. This contamination can also have long-term implications for soil quality and function and food quality (Agarry and Ogunleye, 2012; Tang et al., 2012; Ng et al., 2017). Most methods used to treat soil pollution include mechanical techniques, burial, vaporization, dispersal and washing. However, these methods are costly and can lead to the imperfect degradation of pollutants (Chee and Shih, 2019).

Bioremediation is defined as the employ of microorganisms to remove environmental contaminants for their various metabolic capacities, a satisfactory and acceptable technique for the removal and degradation of many pollutants, including oil and its products (Adams et al., 2015). Bioremediation technology is thought to be relatively inexpensive and effective (Nwankwegu et al., 2016). Biodegradation by natural microbiological communities is one of the main mechanisms by which oil contaminants can be removed from the environment and are cheaper than other treatment methods (Ron and Rosenberg, 2014).

The prosperity of the oil bioremediation depends on the provision and maintenance of favorable environmental conditions to improve oil degradation. Several researchers have reported several factors affecting the biodegradation rate of oil (Jahangeer and Kumar, 2013; Varjani and Upasani, 2017; Ali, 2019). An important need for bioremediation is the existence of microorganisms with suitable metabolic capacity. If microorganisms are found, optimum growth rates and microbial degradation of hydrocarbons can then be maintained by assuring sufficient nutrient and oxygen concentrations and a pH (6-9). The physiochemical properties of the oil and area of oil surface are also significant factors for the successful of bioremediation (Eze et al., 2014). The two techniques taken for the bioremediation of oil pollutants are the addition of microorganisms (eligible to degrade hydrocarbons) and surfactants [bioaugmentation], and the modification of the environment by adding fertilizers (N and P) or other cosubstrates limit the growth of microbes and aerating the contaminated site (composting and bulking) [biostimulation] (Ikuesan, 2017). The success of bioremediation attempts to clean up the crude oil spill from the Exxon Valdez tanker in Prince William Sound and the Alaska Gulf in 1989 generated considerable interest in the technology of microbial degradation and remediation (Atlas and Hazen, 2011).

Large numbers of hydrocarbons in crude oil are readily degraded, but others are more stable compounds, which include the hydrocarbons with a large number of methyl substitutes or intensive aromatic rings (Polycyclic Aromatic Hydrocarbon-PAHs) that have low solubility (Šolevic et al., 2011). so as to full degradation of such hydrocarbons must be available for microorganisms and their enzymes.

Surfactants were utilized to elevate the unsolvable organic matter bioavailability (ex. during desorption from solid materials). Surfactants (artificial and natural) were examined with different grades of hit (Biria et al., 2010; Rufino et al., 2014). Persistent organic pollutants can oxidize chemically, but this process seems to be expensive. The incorporation of chemical oxidation and biological remediation should be cost effective, where the primary chemical operation transforms contaminants into low toxic substances and compounds that can be biodegraded (Rufino et al., 2014).

The compost system with the presence or absence of bulking agents are used to promote oxygen input and improve aerobic biological degradation. In addition, the introduction of microbial nutrients and microorganisms with them can lead to significant degradation of petroleum hydrocarbons (Lukic, 2016; Sari et al., 2019) Most soil systems comprise oil-utilizing bacteria and fungi (Ikuesan, 2017; Ali, 2019), but their counts and metabolic characteristic could not be important. The bioaugmentation permits the addition of microbes with suitable metabolic capacity and an increase in the microbial community that can accelerate the process of bioremediation.

Most of the current studies have focused on assessing the factors that influence bioremediation or experimenting of appropriate products or procedures via the laboratory researches (Das and Chandran, 2011). Only a finite number of field experiences have been given persuasive proof of this technique. In this study, compost systems were examined with the addition of nutrients and microorganisms for the biological treatment of polluted agricultural soil by the leakage of crude oil in southern Iraq.

Materials and methods

Ten experimental fields were designed in contaminated agricultural soil with an accidental spill of crude oil in the Abu-Al-Khaseeb region (30°27'00" N, 47°59'27" E) of Basrah province in southern Iraq (Fig. 1), during the Spring of 2018. The oil spill covered about 500 m² of agricultural soil and reached a depth of 50 cm. The measurement of each designed field was 4 m length, 4 m width, and 50 m depth. The soil of fields was manually drilled using a hoe and shovel at a depth of 50 cm and turned to mixing crude oil with soil components. The fields were then processed in different increments as shown in Table 1. Some fields were fertilized by NPK (0.015 kg N 1 m⁻², 0.015 kg P₂O₂ 1 m⁻² and 0.015 kg K₂O 1 m⁻²) to outdo the restriction of inorganic nutrients. Bermuda grass (*Cynodon dactylon* L.) hay (chopped to 4.5 cm size, ρ_b of 0.019 g cm⁻³) was added to some fields at a 1:2 hay:soil volume ratio, as a absorbent agent for crude oil and a bulking agent to promote oxygen transport. The strain, *Bacillus cereus* WR146 (biosurfactant-producing bacteria), previously isolated from the same site, has been added to fields (25 ml kg⁻¹ soil of bacterial suspension at 1×10^{-6} density were sprayed on the field surface) for the production of biosurfactant compounds. The strain was identified using standard biochemical and sugar fermentation test. The species level identification was done using 16S rRNA sequencing. *B. cereus* WR146 is a gram positive, motile, facultative and spore forming bacterium that can produce biosurfactant in 40 °C and salinities 25%. These capabilities make it a useful candidate to serve in microbial enhanced oil recovery processes. The purpose of installing of some plastic drainage pipes vertically in some fields was to enhance the transfer of oxygen by forming an air flow in the field based on variations in temperature between the inside of the field and the external atmosphere. Table 2 shows the monthly range and annual average of some environmental factors affecting the soil of the study area, and hence bioremediation.

Three samples were collected from the soil under study prior to the design of the experimental fields to determine the soil properties, assess the level of crude oil pollution and estimate the content of bacteria. The first sample (I) was a soil with little oil pollution. The second (II) was a soil heavily polluted with crude oil. The third (III) was a soil unpolluted with oil located near the spill area. While two soil samples were taken from all experimental fields that were designed to determine the temporal difference in

populations of bacteria. One of the samples (IV) was from the surface of the field and the other (V) was 50 cm deep. The IV and V soil samples were taken for each field to take account of evaporation of hydrocarbon and to monitor the bioremediation process at both sites. Each soil sample consisted of five randomly collected samples (1 kg), each carefully mixed, and 100 g of each was taken and thoroughly mixed together. Some characteristics of the agricultural soil are given in *Table 3*.

For the five different samples, 1 g of soil was used to count heterotrophic bacteria (HB) and oil-utilizing bacteria (OUB) by the standard dilution plate method. The soil was suspended in 99 mL sterile water, shaken, 120 rpm for 30 min, this stock was used to prepare dilution series, 10^{-1} - 10^{-10} . The HB were counted on nutrient agar medium. The OUB were counted on a solid mineral medium containing as sole sources of carbon and energy, 2 mL of sterile crude oil into a filter paper lining every Petri-dish cover, and tightly sealing the dish. The mineral medium (MM) was composed of $0.68 \text{ g L}^{-1} \text{ KH}_2\text{PO}_4$, $1.79 \text{ g L}^{-1} \text{ HPO}_4$, $0.35 \text{ g L}^{-1} \text{ MgSO}_4$, $1 \text{ g L}^{-1} \text{ NO}_3\text{NH}_4$, $0.4 \text{ mg L}^{-1} \text{ CaCl}_2$, $0.4 \text{ mg L}^{-1} \text{ FeSO}_4$, and 0.1 mL of solution containing 100 mg L^{-1} of H_3BO_4 , MnSO_4 , ZnSO_4 , CuSO_4 , and CoCl_2 , and 20 g L^{-1} of agar. For each of the above soil dilutions, five replicate plates were inoculated with 0.25 mL each, and the plates were incubated at $30 \text{ }^\circ\text{C}$ for 48 h of HB and at $30 \text{ }^\circ\text{C}$ for 21 day of OUB. The bacterial colony numbers were counted, the mean values were obtained and taking the dilution factor into consideration, the total numbers of colony forming units (CFU) per gram dry soil were calculated.

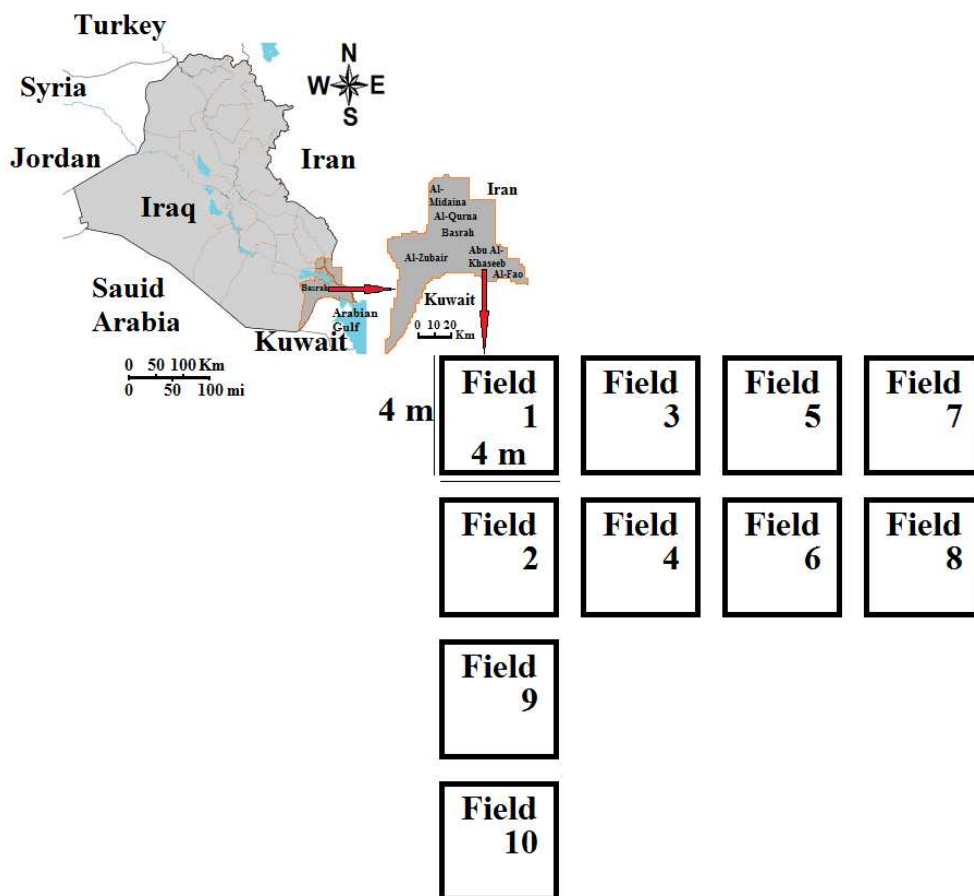


Figure 1. Map of study area and schematic representation of the layout of the accomplished site

Table 1. The designed experimental fields and their additions

Fields	Addition
1	Without addition
2	Fertilizer (NPK)
3	Hay (<i>Cynodon dactylon</i> L.)
4	Plastic pipes
5	Bacteria (<i>Bacillus cereus</i> WR146)
6	Fertilizer (NPK) + Plastic pipes
7	Hay (<i>Cynodon dactylon</i> L.) + Plastic pipes
8	Fertilizer (NPK) + Hay (<i>Cynodon dactylon</i> L.) + Plastic pipes
9	Hay (<i>Cynodon dactylon</i> L.) + Plastic pipes + Bacteria (<i>Bacillus cereus</i> WR146)
10	Fertilizer (NPK) + Hay (<i>Cynodon dactylon</i> L.) + Plastic pipes + Bacteria (<i>Bacillus cereus</i> WR146)

Table 2. Some environmental climatic factors for the current study area

Factor	Monthly range	Annual average
Solar radiation	7.37 (January) - 13.16 (June)	10.14
Temperature (°C)	18.2 (January) - 46.9 (August)	33.75
Precipitation (mm)	0-26.4 (January)	11.34
Evaporation (mm)	277.3 (December) - 3006.5 (July)	1702.93
Relative humidity (%)	20.52 (June) - 67.7 (January)	40.35
Wind speed (m/s)	3 (October) - 5.6 (June)	3.73

Table 3. Characteristics of the agricultural soil

Property	Polluted	Unpolluted
PH	7.30	7.10
Silt %	32.5	32.5
Clay %	72.4	72.4
Sand %	3.50	3.50
Texture	Clay	Clay
Total Ca %	0.40	0.43
TOC %	9.60	7.20
P ₂ O ₅ %	0.08	0.10
K ₂ O %	0.18	0.12
Total N %	0.009	1.00
Particle density (Mg m ⁻³)	---	1.5
Bulk density (Mg m ⁻³)	---	2.5
Porosity %	---	40.5
Water Infiltration rate (cm h ⁻¹)	---	1.4
Saturation hydraulic Conductivity (m day ⁻¹)	---	0.43
Electrical conductivity (ds m ⁻¹)	---	7.60
Temperature (°C)	---	40
Moisture:		
-Field capacity %	---	27.9
-Permanent wilting point %	---	17.5
-Available water %	---	10.5

Crude oil content in soil was determined by the method of Villalobos et al. (2008), a sample of 50 g was sieved through a 62 μm stainless steel sieve, which was dried for 12 h at 105 °C and mechanically homogenized. Exactly 10 g of soil was placed in a dried and weighed round flask. Anhydrous sodium sulphate (10 g) was then added to the flask and 35 mL of n-hexane were utilized for extraction process in a ultrasound bath. The extract was filtered over a column filled with 0.6 g of glass wool, 5 g of silica gel, and 1 g of celite respectively, and washed with 25 mL of n-hexane. The n-hexane was evaporated in a rotary evaporator and the residue of crude oil was then weighed. This execution was reiterated 3 time for each sample of soil to extract the most quantity of crude oil.

Soil microbial activity was estimated by measuring the concentration of carbon dioxide formed 10 days after incubation of samples of soil in glass-tight vessels in 20 °C. Water was append to the soils by 50-60% of water holding capacity. Concentration of carbon dioxide in the head space was analyzed by a Shimadzu (GC-14, Japan) gas chromatography provided with a Thermal Conductivity Detector (TCD) in 60 °C. The samples of gas were analyzed in 40 °C using of column (2 m) packed with Porapak Q with He as a carrier gas flowing at 40 mL min⁻¹ rate. The gas analyses was achieved in triplicate. The values were expressed in $\mu\text{g CO}_2 \text{ g}^{-1} \text{ soil day}^{-1}$. The difference in carbon dioxide formation between unpolluted soil and crude oil polluted one was utilized to estimate the degradation of crude oil.

Effect of fertilizers on biodegradation was laboratory assessed, 0.66 mg g⁻¹ of urea (nitrogen source), 0.31 mg g⁻¹ of superphosphate (phosphorus source), and oleophilic fertilizer S200 (developed by IEP Europe, Madrid, Spain) in dosage as described by IEP Europe, were added to soil samples and tested. The S200 containing nitrogen (7.9%) and phosphorus (0.6%), consisted of a microemulsion of a saturated solution of urea as a nitrogen source in oleic acid as a carrier, an oleophilic phosphate ester as a phosphorus source and surfactant, and a viscosity reducer. The critical micelle dilution (CMD) of S200 was estimated and the critical micelle concentration (CMC) was measured by the surface tension method. The surface tension measurements were done by duNouy ring method using a KSV Sigma 701 model tensiometer and platinum ring at 20 °C (Lima et al., 2017). The CMC was then determined by plotting surface tension as a function of the S200 concentrations. A range of concentrations under CMC were used to evaluate the impact of S200 on biodegradation.

Biosurfactant role created by *B. cereus* WR146 in the elimination of crude oil sorbed on the soil surface has been investigated. The isolate was grown on 50 mL of MM supplemented with crude oil (1%, v/v) in a Erlenmeyer flask (250 ml) and was incubated at 37 °C for 4 days in an incubator shaker at 185 rpm. The bacterial cells were then harvested by centrifugation at 10,000 $\times g$ for 10 min. The resulting supernatant was examined for production of biosurfactant by oil spreading method and drop collapse test according to the method described by Barin et al. (2014) and Janaki et al. (2016) respectively. Surface tension measurement of biosurfactant positive sample was determined in a KSV Sigma 701 model tensiometer using the duNouy ring method at 23 °C (Lima et al., 2017). Emulsification ability of the sample was estimated by calculating E₂₄ index (Hamzah et al., 2013). All the assays were performed in triplicate with distilled water as the control. The biosurfactant was purified by the centrifugation of culture broth at 12,000 $\times g$ for 20 min and extracted twice with chloroform and methanol (2:1, v/v). The solvents were evaporated by a rotary evaporator and the residue was purified in a silica gel (60-120 mesh) column. The sample was then eluted

with chloroform and methanol (20:1 to 2:1 v/v). The fractions were collected and the solvents were removed by evaporation, the resulting residue was dialysed with distilled water and lyophilized. The crude biosurfactant was expressed in g L^{-1} . The isolated biosurfactant was then characterized by estimation of the protein concentration (by total protein test kit from Supplimed International, India) (Rufino et al., 2014), the total carbohydrate content (by the phenol-sulphuric acid method) (Lobna and Ahmed, 2013), the fatty acids content (by gas chromatography) (Rufino et al., 2014), and the peptide groups (by Lowry test) (Lowry et al., 1951).

Fifty gram of washed sand was mixed with crude oil (1 g) in flasks (250 mL) and 100 mL of water was added. Different concentrations of crude biosurfactant extract (0.001, 0.01, 0.1, 0.15, 1, 1.5, 3, 6, and 10 g L^{-1}) were prepared and then added to sand contaminated with crude oil in the flasks. The mixtures were shaken (75 rpm) for 2 days at room temperature. Controls treatment without biosurfactant extract were achieved.

Statistical analysis of the data was done by ANOVA, with differences by the least significant differences method being determined at 5% ($P < 0.05$). Statistical analysis was performed using SPSS 16.0 for Windows (IBM, Armonk, New York, USA).

Results

Table 4 shows the counts of HB and OUB in the I, II and III samples. The II sample generally contained the highest counts of HB and OUB. While the samples I and III contained a lower counts of HB and OUB respectively (Table 5). Figure 2 exhibits the temporal variation in the counts of HB and OUB in IV and V soil samples of the fields 1 and 10. The results indicated that the counts of HB did not show clear tendencies in fields 1 and 10. Nutrient supplementation and aeration were not necessary to increase bacterial counts. While the counts of OUB increases in field 10, but after a period of time, their counts are similar to the counts of bacteria in field 1 (Table 6).

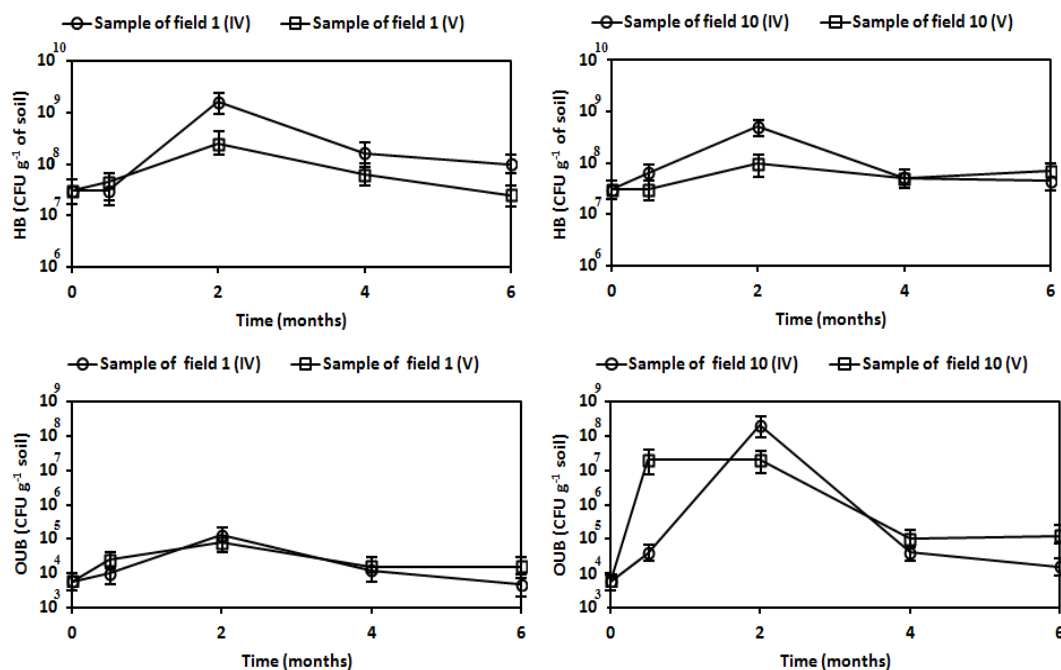


Figure 2. Temporal variations in the counts of HB and OUB in experimental fields. Error bars represent standard deviation (95% confidence interval, C.I.)

Table 4. Initial count of bacteria (CFU g⁻¹) in the soil samples of the study area

Soil sample	HB	OUB
I	4×10 ⁸	7×10 ⁶
II	5×10 ⁹	4×10 ⁷
III	2×10 ⁷	5×10 ⁴

Table 5. Mean count of bacteria (HB and OUB) (CFU g⁻¹) in the soil samples (I, II and III) of the study area and RLSD_{0.05} value

Soil sample			Bacteria	
I	II	III	HB	OUB
6.1×10 ⁷	4.7×10 ⁸	5.1×10 ⁶	4.9×10 ⁷	6.0×10 ⁶
RLSD _{0.05} 1.9×10 ⁶			RLSD _{0.05} 1.4×10 ⁵	

Table 6. Mean count of bacteria (HB and OUB) (CFU g⁻¹) in the soil samples (IV and V) of experimental fields (1 and 10) over the time (month) and RLSD_{0.05} value

Soil sample (HB)	1 (IV)	8.6×10 ⁷	RLSD _{0.05} 2.3×10 ⁶
	1 (V)	8.2×10 ⁷	
	10 (IV)	8.3×10 ⁷	
	10 (V)	8.5×10 ⁷	
Time (HB)	0	7.7×10 ⁷	RLSD _{0.05} 2.7×10 ⁶
	0.5	7.9×10 ⁷	
	2	7.8×10 ⁷	
	4	8.0×10 ⁷	
	6	8.1×10 ⁷	
Soil sample (OUB)	1 (IV)	5.3×10 ³	RLSD _{0.05} 2.2×10 ⁴
	1 (V)	4.8×10 ⁴	
	10 (IV)	5.7×10 ⁵	
	10 (V)	6.1×10 ⁶	
Time (OUB)	0	5.3×10 ³	RLSD _{0.05} 2.3×10 ³
	0.5	5.3×10 ⁵	
	2	6.7×10 ⁶	
	4	5.4×10 ⁴	
	6	4.6×10 ⁴	
Bacteria	HB	8.3×10 ⁷	RLSD _{0.05} 1.5×10 ⁵
	OUB	4.4×10 ⁵	

Crude oil content was measured in the soil samples obtained prior to the design of the experimental fields to gain an image of the average and highest grades of crude oil contamination in the study area. After the design of the fields, soil samples were collected from each field to acquire a zero-time determine of the crude oil concentration in the each field. There are apparent differences in the content of crude oil in the

remediation fields because of their asymmetrical nature. Nevertheless, there is a obvious decline in crude oil content over time (Fig. 3). The results of the fields 1 and 10 indicated a reduce in crude oil content, with similarities in the rudimentary crude oil removal rates in both fields, which may be due to the elimination of volatile light compounds from the soil. After 3 months ago, crude oil was removed more in field 10 than field 1. No statistically significant differences were found in the elimination of crude oil from soil surface of fields 1 and 10 to illustrate the importance of bioaugmentation (Table 7). Low microbial effectiveness, estimated from the development of carbon dioxide in vitro was found in samples of surface soil. Figure 4 and Table 8 show variations in the development of carbon dioxide in V soil sample of all fields. Field 10 exhibited the highest degradation capability.

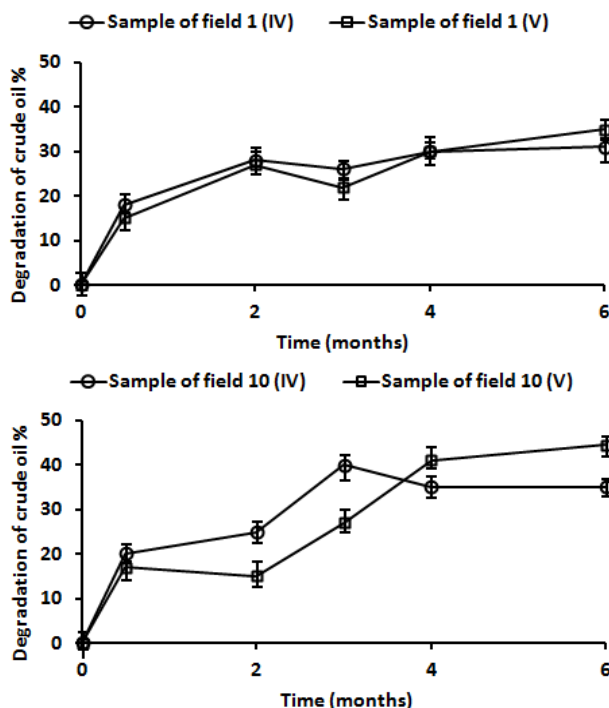


Figure 3. Percentage of crude oil degradation in experimental fields. Error bars represent standard deviation (95% C.I.)

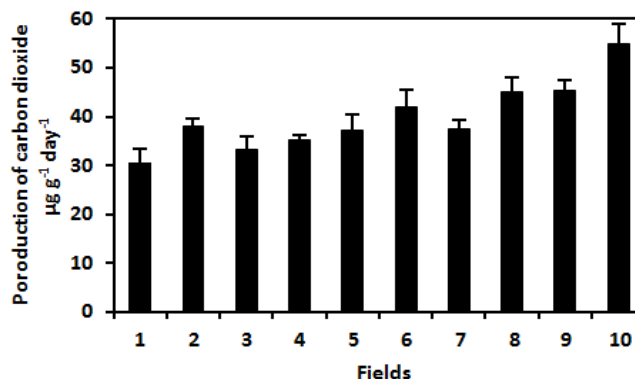


Figure 4. Carbon dioxide produced by microbial activity in the soil samples (V) of experimental fields. Error bars represent standard deviation (95% C.I.)

Table 7. Mean of crude oil degradation percentage in the soil samples (IV and V) of experimental fields (1 and 10) over the time (month) and RLSD_{0.05} value

Soil sample				Time					
1 (IV)	1 (V)	10 (IV)	10 (V)	0	0.5	2	3	4	6
20.6	21.5	24.8	23.7	0	16.9	23.8	29.2	33.8	37.2
RLSD _{0.05} 3.12				RLSD _{0.05} 4.05					

Table 8. Mean of carbon dioxide ($\mu\text{g g}^{-1} \text{day}^{-1}$) produced by microbial activity in the soil samples (V) of experimental fields (1-10) and RLSD_{0.05} value

Field									
1	2	3	4	5	6	7	8	8	10
29.8	36.2	33.5	34.1	35.4	41.9	36.5	45.6	46.0	54.2
RLSD _{0.05} 5.77									

Table 9 exhibits the mean of alterations in crude oil content after three months of biological treatment in surface soil samples for all experimental fields. The proportion of crude oil content alterations in the soil has been transformed to daily rates of degradation of crude oil and carbon. The degradation was estimated depending on that content of carbon in crude oil ranges from 80-88% (Eschrich, 1980). The theoretical carbon dioxide rates based on carbon degradation were higher than those obtained from laboratory experiments (Fig. 4), which may be due to the loss of crude oil in the fields by evaporation. The laboratory average rates of carbon dioxide development in crude oil polluted and unpolluted soils fertilized with nitrogen and phosphorus were 30.6-55.0 $\mu\text{g g}^{-1} \text{day}^{-1}$. The laboratory temperature was 22 °C while the temperature of the fields ranged from 34-37 °C. The results of carbon dioxide development at soil samples, IV and V indicate that the lowest microbial effectiveness was in the unpolluted soil and active degradation was found in the polluted one.

Table 9. Average changes in oil content over a three-month period of biological treatment in soil samples (IV) of experimental fields (2-10) and the rates of theoretical degradation

	Time (months)			
	0	1	2	3
Content of oil (%)	4.20	3.73	3.02	2.42
Degradation of oil ($\mu\text{g g}^{-1} \text{day}^{-1}$)	---	---	---	43
Degradation of carbon ($\mu\text{g g}^{-1} \text{day}^{-1}$)	---	126.2	190.1	31.8
Production of carbon dioxide ($\mu\text{g g}^{-1} \text{day}^{-1}$)	---	534.1	700.2	116.4

Adding S200 fertilizer to crude oil polluted soil with a less concentration than CMC improves the crude oil degradation process, while the addition of nitrogen and phosphorus only leads to higher degradation of crude oil. S200 fertilizer contains surfactant compound, an oleophile phosphate ester. The utilize of biosurfactant to liberation hydrocarbons sorbed on solid soil materials was less toxic than synthetic

surfactants. The current study demonstrated that the biosurfactants produced by *B. cereus* WR146 had a high capacity to desorption of crude oil from the sand up to 100% at a concentration of 6 and 10 g L⁻¹ of the biosurfactants (Fig. 5; Table 10). The use of synthetic surfactants would logically improve the production of biosurfactant in oil-utilizing microbes, which are added or naturally found in the soil.

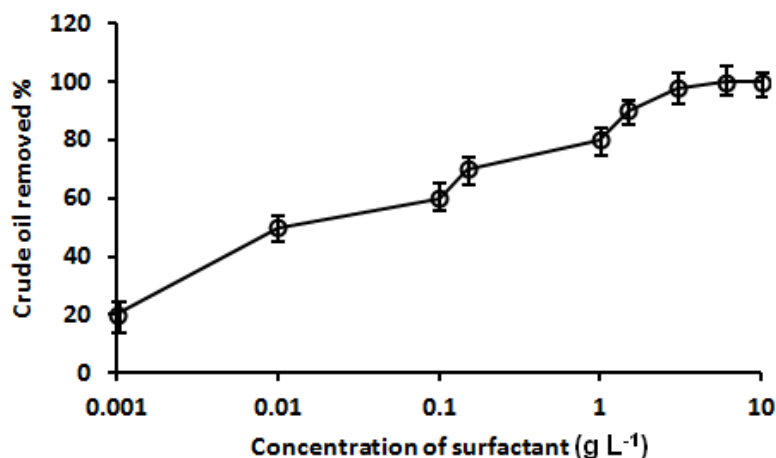


Figure 5. Effect of surfactant produced by *B. cereus* WR146 on the removal of crude oil from sand. Error bars represent standard deviation (95% C.I.)

Table 10. Mean of percentage of crude oil removal from sand by different concentrations (g L⁻¹) of surfactant produced by *B. cereus* WR146 and RLSD_{0.05} value

Concentration								
0.001	0.01	0.01	0.15	1	1.5	3	6	10
21.3	49.7	61.9	74.9	81.6	89.3	97.5	99.8	100
RLSD _{0.05} 7.04								

Discussion

Many large oil spill accidents in the marine environment have acquired considerable popularity in the media. While, smaller and more recurrent spills are often the most damaging to the ecosystem. Crude oil is not only directly toxic to organisms, but also has a suffocating impact (Buskey et al., 2016).

Bioremediation works, as documented in the literatures, may be confounding, especially when applied commercially. Where, there are predominately no endeavor to differentiate between the factors attributed to the success or fiasco of the process. Absolutely, each site has a unique case. All environmental factors such as weather, fertility of soil, pH, type of soil, etc. have an important impact on bioremediation. Climate is particularly important in Iraq, which can be considered a bit extremist continental in most of its regions. In the summer, when the effectiveness of bioremediation process is at its top, is long, sweltering, arid, and clear, resulting to water drop in experimental fields. While, the Winter is cool, dry, and mostly clear. The site under study is an area of the crude oil spill incident, which covered about 500 m² of agricultural land. The harmful impact of crude oil was on trees and other field crops,

which were killed due to crude oil concentrations through their root area. Agricultural soil was polluted with crude oil almost at a depth of 50 cm. The first solution to this trouble was to cover the crude oil polluted site with a surface layer of unpolluted soil.

In the present investigation, the compost system was used in bioremediation of crude oil in soil. This system has been works to improve rates of crude oil removal by biophysical methods. Where, a considerable removal of crude oil from polluted soil was observed after three months and reached 50% relying on the type of compost system. The carbon dioxide development rates in the laboratory (*Fig. 4*) were lower than the theoretical rates of carbon dioxide estimated (*Table 9*), suggesting that a large amount of crude oil was disposed by ventilation process. The rates of lab for carbon dioxide development indicate the need for 6 years or more for the degradation of crude oil. This is in the case that 2.81% of the crude oil components in the soil can be degraded. Customary, the presence of many volatile fractions in the crude oil will decrease the time of biological treatment, however, the bioremediation of crude oil in the soil will remain very long without any treatment.

The primary degradation is quickly for certain hydrocarbons in the manipulating system. Analysis by gas chromatography of soil contaminated with crude oil exhibited the effective disposal of low molecular weight hydrocarbons over time. While some compounds such as polycyclic aromatic hydrocarbons (PAHs) need longer degradation time when suitable oil-utilizing microorganisms are exist. The degradation of these compounds may also want desorption from solid surfaces. The utilize of surfactant compounds for desorb hydrocarbon contaminants and impact on their microbial degradation has been exceedingly investigated. Non-ionic surfactants can increase the degradation of many PAHs in the watery phase (Zhu and Aitken, 2010; Zhentian et al., 2015; Yu et al., 2014). While, Alden et al. (2016) reported that non-ionic surfactants at a higher concentration than the CMC prevented degradation of PAHs. It has been shown that the capability of eight artificial surfactants to solubilize PAHs is varied. The most hydrophobic surfactants were more likely to solubilize PAHs. Whilst conflicting outcomes were gained from studying the biodegradation potential of PAHs solubilized by artificial surfactants (Adrion et al., 2016). The most hydrophobic surfactants were less endured by bacteria (Zheng et al., 2015). Barrios et al. (2005) and Zhu and Aitken (2010) demonstrated that Brij 30 degraded with naphthalene, while the Triton X-100 was not degraded. However, the addendum of the surfactants did not impact the degradation rate of naphthalene or the final quantity degraded, in spite of ameliorated bioavailability.

The S-200 fertilizer has been utilized in the biological treatment of heavy fuel oil spilled from the oil tanker Prestige in November 2002 along the Atlantic coast of Galicia (Spain). Our experiments with soil (non-existent results) exhibited that the crude oil biodegradation rates with S200 fertilizer are low compared to the use of urea and phosphorus only. Fertilizer, S200 is a microemulsion made up of an artificial surfactant that is probable to be an inhibitor in the concentrations applied. The value of half maximal effective concentration (EC_{50}) of S200 fertilizer (Microtox bioassay) was 0.3 mg L^{-1} , which is more toxic than the EC_{50} value of biosurfactants produced by bacteria, *Bacillus cereus* WR146 (540 mg L^{-1}). Although the S200 fertilizer shows a inhibitory effect, it has the feature that the S200 in this oleophilic substrate does not wash readily from the soil.

Undoubtedly, the biosurfactants are lower toxic and more susceptible to microbial degradation than synthetic surfactants and are preferred in biological treatment. The production and employ of biosurfactants as raw extracts of microbial cultures or as purified materials is very costly. The biosurfactants can also be created from

monosaccharides or sugar alcohols and fatty acids through esterification of enzyme-catalysed in organic solvents (Satpute et al., 2010; Gumel et al., 2011). The growth of microorganisms that produce biosurfactants at the site would logically promote the desorption of hydrocarbon compounds. The present study exhibits that biosurfactants eliminate a large proportion of crude oil polluted to soil (non-existent results). The addition of biosurfactants-producing bacteria (*B. cereus* WR146) increases the removal of crude oil from the soil. This is reflected in soil samples taken from a depth of 50 cm from field 10, which displays the highest rates of carbon dioxide development (Fig. 5). It is necessary to evolve methods to increase the production of biosurfactants in the environment or introduce oil-utilizing microorganisms to the soil.

There are many factors that restrict the process of bioremediation in the term microbiology. The transfer of the organic contaminates mass from the soil particles to the liquid phase may be a restricting factor as previously explained, so synthetic and biosurfactants are used. Also, many enzymes embroiled in the bioremediation process require molecular oxygen. Therefore, the transfer of oxygen mass to the soil may be a critical factor in many cases. In the current bioremediation process, locally obtainable accessories have been utilized to attempt to help oxygen transfer.

An important aspect of bioremediation, which has acquired only a small amount of attentiveness, is that the microbiological restriction is likely to be due to the catabolite repression. When a assortment of carbon substrates are present, the bacterium will logically select the substrates that can be easily used. However, such substrates may be plentiful and the requisite bacteria are present, but the biodegradation of contaminants may not forward. There is some clue to suggest that *Bacillus* lack the catabolite repression of other bacteria. Actually, the presence of glucose may promote the microbial degradation of hydrocarbon pollutants (Xu et al., 2018). If this is the case, *Bacillus* will have a great characteristic over others, so the bacteria will be the ideal option in the bioaugmentation.

This study is destined to identify the effects of some commonly used methods to optimize treatment and stratify them more generally to other areas polluted with crude oil.

Conclusions

Based on the results of this research, it was concluded that a better outcome could be achieved for the biological treatment of crude oil polluted agricultural soil using the composting systems, good ventilation, nutrients and biosurfactants producing bacteria. The research also showed that a noticeable degradation of crude oil occurred after 3 months of bioremediation up to 50%. Further studies to determine the effectiveness of bioremediation in oils polluted soil are needed.

Acknowledgements. The authors would like to thank the Marine Science Center and the College of Agriculture, University of Basrah and the College of Science, University of Baghdad for providing the laboratory facilities.

REFERENCES

- [1] Adams, G. O., Fufeyin, P. T., Okoro, S. E., Ehinomen, I. (2015): Bioremediation, biostimulation and bioaugmentation: a review. – International Journal of Environmental Bioremediation & Biodegradation 3(1): 28-39.

- [2] Adrion, A. C., Nakamura, J., Shea, D., Aitken, M. D. (2016): Screening nonionic surfactants for enhanced biodegradation of polycyclic aromatic hydrocarbons remaining in soil after conventional biological treatment. – *Environmental Science & Technology* 50(7): 3838-3845.
- [3] Agarry, S. E., Ogunleye, O. (2012): Factorial designs application to study enhanced bioremediation of soil artificially contaminated with weathered Bonny light crude oil through biostimulation and bioaugmentation strategy. – *Journal of Environmental Protection* 3: 748-759.
- [4] Alden, C. A., David, R. S., Jun, N., Damian, S., Michael, D. A. (2016): Improving polycyclic aromatic hydrocarbon biodegradation in contaminated soil through low-level surfactant addition after conventional bioremediation. – *Environmental Engineering Science* 33(9): 659-670.
- [5] Ali, W. A. (2019): Biodegradation and phytotoxicity of crude oil hydrocarbons in an agricultural soil. – *Chilean Journal of Agricultural Research* 79(2): 266-277.
- [6] Atlas, R. M., Hazen, T. C. (2011): Oil biodegradation and bioremediation: a tale of the two worst spills in U.S. history. – *Environmental Science Technology* 45: 6709-6715.
- [7] Barin, R., Talebi, M., Biria, D., Beheshti, M. (2014): Fast bioremediation of petroleum-contaminated soils by a consortium of biosurfactant/bioemulsifier producing bacteria. – *International Journal of Environmental Science and Technology* 11: 1701-1710.
- [8] Barrios, N., Sivov, P., D'Andrea, D., Nunez, O. (2005): Conditions for Selective Photocatalytic Degradation of Naphthalene in TritonX-100 Water Solutions. – *International Journal of Chemical Kinetic* 37(7): 414-419.
- [9] Biache, C., Mansuy-Huault, L., Faure, P. (2014): Impact of oxidation and biodegradation on the most commonly used polycyclic aromatic hydrocarbon (PAH) diagnostic ratios: implications for the source identifications. – *Journal of Hazardous Materials* 267: 31-39.
- [10] Biria, D., Maghsoudi, E., Roostaazad, R., Dadafarin, H., Lotfi, A. S., Amoozegar, M. A. (2010): Purification and characterization of a novel biosurfactant produced by *Bacillus licheniformis* MS3. – *World Journal of Microbiology & Biotechnology* 26: 871-878.
- [11] Boitsov, S., Petrova, V., Jensen, H. K. B., Kursheva, A., Litvinenko, I., Chen, Y., Klungsoyr, J. (2011): Petroleum related hydrocarbons in deep and subsurface sediments from South-Western Barents Sea. – *Marine Environmental Research* 71(5): 357-368.
- [12] Buskey, E. J., White, H. K., Esbaugh, A. J. (2016): Impact of oil spills on marine life in the Gulf of Mexico: effects on plankton, nekton, and deep-sea benthos. – *Oceanography* 29(3): 174-181.
- [13] Chee, K. Y., Shih, H. T. P. (2019): Cleaning contaminated soils by using microbial remediation: a review and challenges to the weaknesses. – *American Journal of Biomedical Science & Research* 2(3): 126-128.
- [14] Das, N., Chandran, P. (2011): Microbial degradation of petroleum hydrocarbon contaminants: an overview. – *Biotechnology Research International* 2011: 1-13.
- [15] Eschrich, H. (1980): Properties and long term behavior of bitumen and radioactive waste bitumen mixtures. – Swedish Nuclear Fuel and waste Management Company (SKB) Technical Report TR 80-14.
- [16] Eze, V. C., Onwuakor, C. E., Orok, F. E. (2014): Microbiological and physicochemical characteristics of soil contaminated with used petroleum products in Umuahia, Abia State, Nigeria. – *Journal of Applied & Environmental Microbiology* 2(6): 281-286.
- [17] Gennadiev, A. N., Pikovskii, Y. I., Tsi bart, A. S., Smirnova, M. A. (2015): Hydrocarbons in soils: origin, composition, and behavior (review). – *Eurasian Soil Science* 48(10): 1076-1089.
- [18] Gumel, A. M., Annuar, M. S. M., Heidelberg, T., Chisti, Y. (2011): Lipase mediated synthesis of sugar fatty acid esters. – *Process Biochemistry* 46: 2079-2090.
- [19] Hamzah, A., Sabturani, N., Radiman, S. (2013): Screening and optimization of biosurfactant production by the hydrocarbon-degrading bacteria. – *Sains Malaysiana* 42(5): 615-623.

- [20] Ikuesan, F. A. (2017): Evaluation of crude oil biodegradation potentials of some indigenous soil microorganisms. – *Journal of Scientific Research and Reports* 13: 1-9.
- [21] Ivshina, I. B., Kuyukina, M. S., Krivoruchko, A. V., Elkin, A. A., Makarov, S. O., Cunningham, C. J., Peshkur, T. A., Atlas, R. M., Philp, J. C. (2015): Oil spill problems and sustainable response strategies through new technologies. – *Environmental Science Processes & Impacts* 17: 1201-1219.
- [22] Jahangeer, Kumar, V. (2013): An overview on microbial degradation of petroleum hydrocarbon contaminants. – *International Journal of Engineering and Technical Research* 1: 34-37.
- [23] Lima, R. A., Andrade, R. F. S., Rodríguez, D. M., Araújo, H. W. C., Santos, V. P., Campos-Takaki, G. M. (2017): Production and characterization of biosurfactant isolated from *Candida glabrata* using renewable substrates. – *African Journal of Microbiology Research* 11(6): 237-244.
- [24] Lobna, A. M. and Ahmed, Z. A. (2013): Identification and characterization of biosurfactants produced by *Rhodococcus Equi* and *Bacillus Methyotrophicus*. – *Journal of Biological Chemistry and Environmental Sciences* 8(2): 341-358.
- [25] Lowry, O. H., Rosebrough, N. J., Farr, A. L., Randall, R. J. (1951): Protein measurement with the folin phenol reagent. – *Journal of Biological Chemistry* 193: 265-275.
- [26] Lukic, B. (2016): Composting of organic waste for enhanced bioremediation of PAHs contaminated soils. – *Materials, Université Paris-Est, English NNT2016PESC1134*: 1-174.
- [27] Ng, W., Malone, B. P., Minasny, B. (2017): Rapid assessment of petroleum-contaminated soils with infrared spectroscopy. – *Geoderma* 289: 150-160.
- [28] Nwankwegu, A. S., Orji, M. U., Onwosi, C. O. (2016): Studies on organic and in-organic biostimulants in bioremediation of diesel-contaminated arable soil. – *Chemosphere* 162: 148-156.
- [29] Pinedo, J., Ibanez, R., Primo, O., Gomez, P., Irabien, A., (2014): Preliminary assessment of soil contamination by hydrocarbon storage activities: main site investigation selection. – *Journal of Geochemical Exploration B* 147: 283-290.
- [30] Prathyusha, K., Jagan Mohan, Y. S. Y. V., Sridevi, S., Sandeep, B. V. (2016): Isolation and characterization of petroleum hydrocarbon degrading indigenous bacteria from contaminated sites of Visakhapatnam. – *International Journal of Advanced Research* 4(3): 357-362.
- [31] Ron, E. Z., Rosenberg, E. (2014): Enhanced bioremediation of oil spills in the sea. – *Current Opinion in Biotechnology* 27: 191-194.
- [32] Rufino, R. D., de Luna, J. M., de Campos Takaki, G. M., Sarubbo, L. A. (2014): Characterization and properties of the biosurfactant produced by *Candida lipolytica* UCP 0988. – *Electronic Journal of Biotechnology* 17: 34-38.
- [33] Sari, G. L., Trihadiningrum, Y., Ni'matuzahroh (2019): Bioremediation of petroleum hydrocarbons in crude oil contaminated soil from Wonocolo public oilfields using aerobic composting with yard waste and rumen residue amendments. – *Journal of Sustainable Development of Energy, Water and Environment systems* 7(3): 482-492.
- [34] Satpute, S. K., Banpurkar, A. G., Dhakephalkar, P. K., Banat, I. M., Chopade, B. A. (2010): Methods for investigating biosurfactants and bioemulsifiers: a review. – *Critical Reviews in Biotechnology* 30(2): 127-44.
- [35] Šolevic, T., Novaković, M., Ilić, M., Antić, M., Vrvic, M. M., Jovančićević, B. (2011): Investigation of the bioremediation potential of aerobic zymogenous microorganisms in soil for crude oil biodegradation. – *Journal of Serbian Chemical Society* 76(3): 425-438.
- [36] Tang, J., Lu, X., Sun, Q., Zhu, W. (2012): Aging effect of petroleum hydrocarbons in soil under different attenuation conditions. – *Agriculture, Ecosystems and Environment* 149: 109-117.

- [37] Varjani, S. J., Upasani, V. N. (2017): A new look on factors affecting microbial degradation of petroleum hydrocarbons pollutants. – *International Biodeterioration and Biodegradation* 120: 71-83.
- [38] Villalobos, M., Avila-Forcada, A. P., Gutierrez-Ruiz, M. E. (2008): An improved gravimetric method to determine total petroleum hydrocarbons in contaminated soils. – *Water, Air, & Soil Pollution* 194: 151-161.
- [39] Xu, X., Liu, W., Tian, S., Wang, W., Qi, Q., Jiang, P., Gao, X., Li, F., Li, H., Yu, H., (2018): Petroleum hydrocarbon-degrading bacteria for the remediation of oil pollution under aerobic conditions: a perspective analysis. – *Frontiers Microbiology* 9: 2885.
- [40] Yu, H., Xiao, H., Wang, D. (2014): Effects of soil properties and biosurfactant on the behavior of PAHs in soil-water systems. – *Environmental Systems Research* 3: 6.
- [41] Zheng, Y., Li, L., Shi, X., Huang, Z., Jianmin, Y., Guo, Y. (2018): Nonionic surfactants and their effects on asymmetric reduction of 2-octanone with *Saccharomyces cerevisiae*. – *AMB Express* 8: 111.
- [42] Zhentian, S., Jiajun, C., Xue, Y. (2013): Effect of anionic–nonionic-mixed surfactant micelles on solubilization of PAHs. – *Journal of the Air & Waste Management Association* 63(6): 694-701.
- [43] Zhu, H., Aitken, M. D. (2010): Surfactant-enhanced desorption and biodegradation of polycyclic aromatic hydrocarbons in contaminated soil. – *Environmental Science & Technology* 44(19): 7260-7265.

SEASONAL CHANGES OF SOME MICROBIOLOGICAL PROPERTIES OF SOILS IN A FIELD OF HAZELNUT (*CORYLUS AVELLANA* L.) GROWING

IRMAK YILMAZ, F.

Department of Soil Science and Plant Nutrition, Faculty of Agriculture, Ordu University, Ordu, Turkey

(e-mail: fundairmak@hotmail.com; phone: +90-452-234-5010; fax: +90-452-226-5269)

(Received 30th Jul 2019; accepted 25th Nov 2019)

Abstract. The aim of this study is to identify the effects of the compost obtained from hazelnut husks by using biological techniques, on soil quality at different sampling times. The composted hazelnut husk was used at 6 application doses and with 3 replications in order to increase the organic material content of the soils at doses of 0, 0.5%, 1%, 2%, 3% and 4%. The hazelnut husk compost was applied at the Akçatepe/Ordu/Turkey experiment area on the 23rd of November 2012 by using the mattock planting method. The soil samples were collected from the field at 4 different sampling seasons and consequently, various chemical and biological soil characteristics were detected. The results shows; certain doses and different sampling seasons have a significant effect on the beta-glucosidase, urease and acid phosphatase enzyme activities in soils; the most effective doses were 4% and 3%; the 1st and 4th seasons provided the best results. As for other biological characteristics the highest values were as follows: CO₂ production at 1% dose, microbial biomass-C value at 2% dose. The application of hazelnut husk compost, which has a rich organic matter content and is an organic material itself, to soils, promotes an increase in soil organic materials.

Keywords: *hazelnut husk, compost, soil enzymes, organic material, microbial biomass-C*

Introduction

The use of wastes, which have an important place in agricultural production, as an organic matter source for soils, has recently become a common practice. The utilization of wastes is also a solution for environmental pollution. Especially following the hazelnut (*Corylus avellana* L.) harvest season, its husk is either used as fuel, as cushions for animals or left aside as idle wastes. Especially in Turkey's Black Sea region, hazelnut is an important product. It is known that approximately 550.000 tons of shelled hazelnut is produced annually in this region. After the harvest, from 1 kg of fresh hazelnut, remains around 1/3 and from shelled hazelnut 1/5 (200 gr) of dry husk shell (Çalışkan et al., 1996; Bender Özenç, 2008; Amiri et al., 2017).

Turkey is the world's leading hazelnut producer, accounting for about 75% of world hazelnut supply. According to FAO data, Turkey is the first world hazelnut producer and exporter that covers approximately 70% and 82% of the world's production and export respectively. It is followed by Italy with nearly 20% in production and 15% in export. That is why the Turkey is at the focus of the international academic studies about hazelnut, hazelnut husk compost etc. and references about these issues (FAO, 2019). Solely 10% of the hazelnut consumption is accounted in-shell, the rest of this ratio is shelled and evaluated for industrial objectives (Tous, 2001; Stévigny et al., 2007).

Especially in Giresun, Ordu, Trabzon and Samsun in the Black Sea Region and Sakarya in the Marmara Region, hazelnut cultivation is the main source of living. The Black Sea Region's ecological structure is suitable for hazelnut production. Thus

hazelnut is an essential product in Turkey's economy. Most densely in the Black Sea Region, hazelnut is produced in 39 provinces of Turkey. Hazelnut production is mainly run as family-owned businesses. According to Republic of Turkey Ministry of Agriculture and Forestry, around 395 thousand families are economically focused on hazelnut production with a total area of 700 thousand hectares (GTB, 2013). The increase in world's population, accelerates the agricultural activities on soils. The excessive and unconscious use of fertilizers and chemicals common in traditional agricultural system, generates both environmental and soil issues. Most of soil issues arise from the wrong or misuse of it, which ends up with the soil impairment. The soil is a natural and living substance, which together with air and water contains millions of microorganisms and provides an environment for human beings, plants and animals to live. Even the smallest piece of land needs thousands of years to form; hence, our soils are invaluable within the ecosystem. Especially the benefits provided by the environment that soils render for plant production, show how crucial it is for human being's life. A healthy soil means a healthy plant production environment, which eventually connotes that plants grown on such lands will be healthier. In order to ensure healthier plants, to protect their quality features, fertility and sustainability, it is necessary to protect the soil idiosyncrasy. All these features are related to the quality of soils, the sustainability or developability of some characteristics, which appear in the soil quality (Aygün, 2015).

Microbial biomass carbon, CO₂ production (soil respiration) and dehydrogenase activity are commonly used parameters to identify the biological effects of organic and inorganic matters penetrated into the soils (Meli et al., 2002).

The application of hazelnut husk compost into the soils, provides an increase by means of organic matter, ensuring as a consequence many of its physical, chemical and biological features to improve. This application radically improved the microbial activities in the soil, by means of soil buffer capacity (thus chemical soil properties like pH, electrical conductivity, the amount of exchangeable cations, organic matter and total amount of nitrogen content; by means of physical properties: aggregate stability, bulk density, field capacity and wilting point; by means of biological properties: soil respiration and biomass-C content increased (Bırol and Bender Özenç, 2011; Aygün, 2015; İslam, 2016).

The application of clinoptilolite, leonardite, organic commercial fertilizer (biofarm) and two different types of hazelnut husk (fresh and composted), which is a regional waste, as soil regulators in a certified organic hazelnut garden revealed positive postharvest developments by means of soil enzymes (dehydrogenase, urease, phosphatase and sulfatase) and the amount of microbial biomass (Özyazıcı et al., 2011).

Soil enzymes are basically produced by soil microorganisms, which are able to show the microbial activities observed in the soil environment and play a crucial role during the decomposition of organic matters and transformation of plant available nutrition elements (Xiu-Mei et al., 2008).

The aim of this study; is to examine the relationship between the effects of the application of the compost, at varying doses, obtained from hazelnut husk by using biotechnological techniques and the effects of sampling seasons on various biological and chemical properties of the soil.

Materials and methods

The experiment was carried out in the high tunnel greenhouse established in Ordu University experiment area. The study area is located in Ordu province, Altınordu district, Eastern Black Sea Region, Turkey in 2016. The province of Ordu is located between the northern latitudes of 37T 4534765, with eastern longitudes of 411638 (Fig. 1).

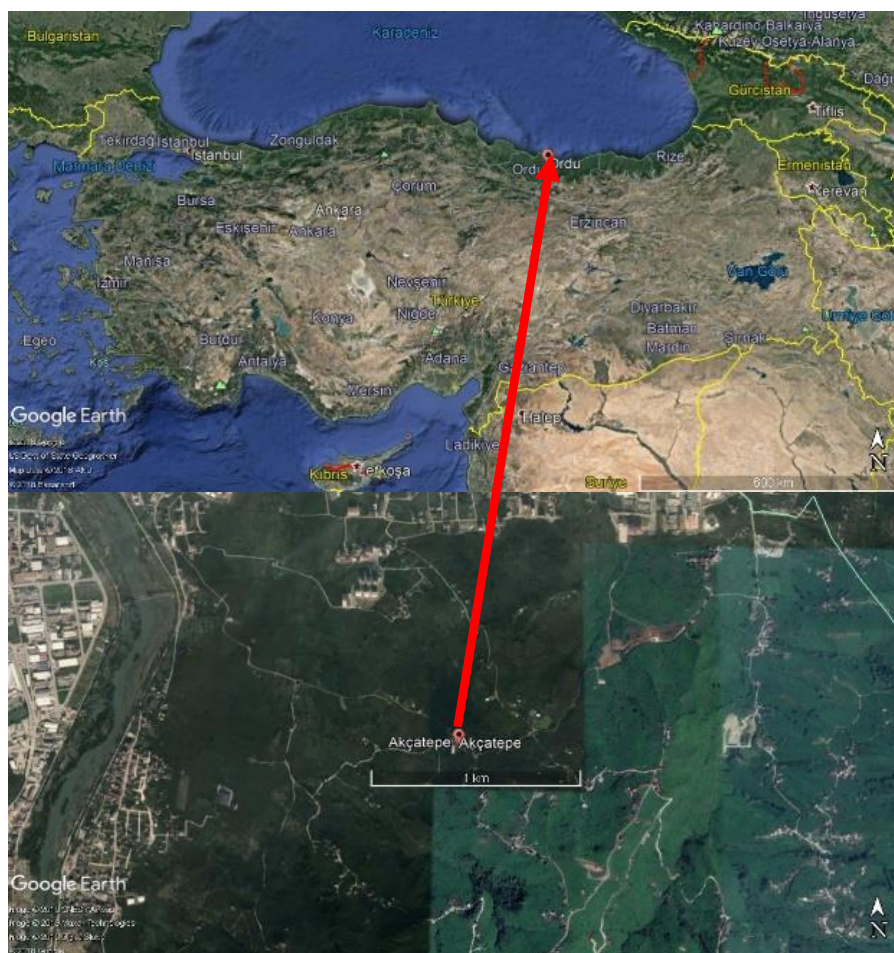


Figure 1. Map shows the location of Akçatepe district experiment area in the Ordu Province, Turkey

In this study, the compost of hazelnut husk, which was obtained by using microbial biotechnological methods, has been used as material. The field test (Akçatepe District) was conducted on the 23rd of November 2012; varying application doses of hazelnut husk compost were applied in order to increase the soils organic material content as of 0 (control), 0.5% (0.125 kg ha⁻¹), 1% (0.25 kg ha⁻¹), 2% (0.50 kg ha⁻¹), 3% (0.75 kg ha⁻¹) and 4% (1 kg ha⁻¹); the compost was applied uniformly to a 50-60 cm diameter circle around the hazelnut plots by mattocking and mixing with soil to a 10-15 cm depth. The sampling was realized in four sampling seasons: autumn (I, 25 November 2016), winter (II, 23 February 2017), spring (III; 24 May 2017) and summer (IV, 22 August 2017). The tests were carried out according to randomized blocks trial design with three replications (Aygün, 2015). Hazelnut husk (C/N ratio 55.71; pH 5.81; EC25 °C

1.93 dS m⁻¹; 0.97% N) was collected from the hazelnut orchard, inoculated with carbon and the microorganisms used as energy sources were composted by windrow method and eventually used as a material in experiments using a windrow machine in the Research Facility of Soil Science and Plant Nutrition Department at Ondokuz Mayıs University, Samsun, Turkey. HHC properties are as follows: pH is 6.76, EC₂₅ °C is 3.56 dS m⁻¹, organic matter (OM) content is 94.75%, total N content is 2.48% and C/N ratio is 22.16 (Kızılkaya et al., 2015a,b).

The loamy soil of the experiment land in Akçatepe shows a neutral ground reaction and a saline electrical conductivity (*Table 1*). The lime (CaCO₃), organic matter content, total nitrogen and available phosphorus contents in Akçatepe soil were adequate (Aygün, 2015).

Table 1. The soils physico-chemical properties (Aygün, 2015)

Analyses	Akçatepe Dist. (Ordu Province)
% sand	33.55
Texture % silt	27.86
% clay	38.59
Textural class	Loamy soil (CL)
Soil reaction-pH (1/2.5)	6.69
Electrical conductivity (dS m ⁻¹) (1/2.5)	1.43
Lime content (CaCO ₃), %	5.23
Organic matter, %	2.58
Total N, %	0.196
Available P, mg kg ⁻¹	15.39
Exchangeable Na, cmol(+) kg ⁻¹	0.326
Exchangeable K, cmol(+) kg ⁻¹	0.444
Exchangeable Ca, cmol(+) kg ⁻¹	39.90
Exchangeable Mg, cmol(+) kg ⁻¹	1.26

Soil physico-chemical analyses

Soil samples, grated to 2 millimeters were kept waiting and prepared for the analyses in + 4 °C refrigerator immediately after, and biological analyses were initiated. To identify the properties of the sample soil, the texture was examined by hydrometer method as told by Bouyoucos (1962), soil reaction (pH) and saltiness (EC) by U.S. Salinity Laboratory Staff (1954), organic material by Nelson and Sommers (1982), total nitrogen by Bremner (1965), extractable potassium by Knudsen et al. (1982) as told by Müftüoğlu et al. (2012).

Soil biological analyses

For the biological analyses of the soil; CO₂ production was identified using the method told by Isermeyer (1952); microbial biomass-C by Anderson and Domsch (1978), β-Glucosidase Enzyme activity Eivazı and Tabatabai (1988), urease enzyme activity by Kandeler and Gerber (1988), acid phosphatase enzyme activity by Tabatabai and Bremner (1969) as told by Schinner et al. (1996).

Statistical analysis

At the end of the study, the variance analysis of the obtained data was performed using the JMP package program and the important results were evaluated according to the LSD test.

Results and discussion

The effects of the beta-glucosidase enzyme activity ($p < 0.01$), urease enzyme activity ($p < 0.01$) and acid phosphatase enzyme activity ($p < 0.01$) were relevant to application and season interactions effect revealed statistically significant results (Table 2). When the application doses of hazelnut husk compost and sampling seasons are taken into consideration, the highest β - glucosidase enzyme activity occurred at 0.1 kg ha⁻¹ compost dose on the 4th season (summer), this value has been followed by the 2nd season (winter) application with a compost dose of 0.25 kg ha⁻¹ and the lowest control was detected on the 1st season (autumn). As both the hazelnut husk compost application doses on the 4th season (summer) and sampling seasons multiplied, the beta- glucosidase enzyme activity of soils increased accordingly. It has been stated that the soil organic matter absorbs the beta-glucosidase enzyme and therefore induces the activity in the soil to continue (Wang et al., 2006). The β -Glucosidase enzyme activity is one of the essential soil enzymes, which is responsible for the C cycle (Nannipieri et al., 2002; Kayıkçioğlu and Okur, 2011).

The urease enzyme activity's peak (73.55) occurred on the 1st season (winter) at a dose of 0.75 kg ha⁻¹, this was followed by the 0.125 kg ha⁻¹ dose and these two doses were identified as the most effective ones. The lowest urease enzyme activity dose was 0.50 kg ha⁻¹ and it was identified on the 4th season (summer). The applications of hazelnut husk increased the soils urease enzyme activity; however, during the summer season the increasing temperature accelerated the decomposition of organic materials, resulting in the 4th sampling season (summer) to reveal the lowest urease enzyme activity values.

Table 2. The effects of application seasons of the hazelnut husk compost on the β -glucosidase, urease and acid phosphatase enzyme activities

Beta glucosidase enzyme activity (mg p-nitrophenol gr dry soil h ⁻¹)					Urease enzyme activity ($\mu\text{g N gr dry. soil}^{-1} 2 \text{ h}^{-1}$)					Acid phosphatase enzyme activity ($\mu\text{g P- N gr dry. soil}^{-1}$)				
Doses (kg ha ⁻¹)	1.P	2.P	3.P	4.P	Doses (kg ha ⁻¹)	1.P	2.P	3.P	4.P	Doses (kg ha ⁻¹)	1.P	2.P	3.P	4.P
0	1.98fg	7.03efg	8.91efg	1.76g	0	12.58e-g	16.97e-g	9.96e-g	5.26fg	0	6.01c-f	5.32c-f	8.25c-f	1.76f
0.125	2.15fg	13.42c-g	12.13c-g	8.28e-g	0.125	67.93a	22.74c-g	18.61d-g	5.66fg	0.125	6.61c-f	4.70d-f	11.23cd	8.28c-f
0.25	4.75efg	28.83ab	15.11c-f	10.47d-g	0.25	63.26ab	29.70c-e	13.44e-g	5.45fg	0.25	12.34c	7.45d-f	30.34ab	10.47cd
0.5	3.52fg	15.1c-f	17.81b-e	4.14fg	0.5	43.40bc	24.67c-g	19.52d-g	4.14g	0.5	9.20c-e	4.90d-f	23.04b	4.13d-f
0.75	2.78fg	25.07abc	22.35a-d	2.5fg	0.75	73.55a	20.95d-g	22.15d-g	5.25fg	0.75	8.40c-f	6.09c-f	27.16ab	2.50ef
1	3.23fg	10.61d-g	13.28c-g	32.15a	1	30.20c-e	37.87cd	25.21c-f	5.78fg	1	6.57c-f	5.57c-f	30.14ab	32.15a
LSD ($p < 0.01$) = 6.55826					LSD ($p < 0.01$) = 10.329					LSD ($p < 0.01$) = 3.68094				

As the strongest acid phosphatase enzyme activity occurs in the beta-glucosidase enzyme activity, a 1 kg ha⁻¹ dose application of the hazelnut husk compost on the 4th sampling season (summer) revealed the highest values (32.15 $\mu\text{g P- N g.d.s}^{-1}$), whereas the lowest acid phosphatase enzyme activity value was identified during an application of a 1.25 kg ha⁻¹ dose and on the 2nd (winter) sampling season (4.70 $\mu\text{g P- N g.d.s}^{-1}$). In

previous studies, the effects of vegetable substances like wheat and corn stalk and as animal products, the effects of horse, hog and cow manure on soils were investigated, ultimately it was determined that all these applications boost the urease, phosphatase and interphase activities, revealing the lowest rate of increase in the interphase activity and the highest in urease and phosphatase activities (Guan, 1989; Aygün, 2015).

Among the application doses of the hazelnut husk compost, the highest soil respiration (0.60 mg CO₂/24 h/g) was detected at the 0.25 kg ha⁻¹ application dose and the lowest (0.42 mg CO₂/24 h/g) at the compost's control application. The difference between these values was statistically highly significant (p < 0.01). Furthermore, through the application of this dose, the CO₂ production value revealed a 1.4 times increase comparing to the control application (Table 3).

Considering the sampling seasons, the highest CO₂ production value was identified on the 1st and 4th seasons (autumn and summer) (0.30 mg CO₂/24 h/g), whereas the lowest value was identified on the 3rd season (spring) (0.21 mg CO₂/24 h/g). The difference between these seasonal values was statistically highly significant (p < 0.01). The CO₂ production on the loamy soil of the experiment area, decreased gradually from the 1st sampling season (spring) to the 3rd (winter) and increased again on the 4th season (summer). The CO₂ formation in agricultural soils usually varies between 3.5 and 35 mg CO₂-C 100 g.d.s⁻¹ values (Alexander, 1961; Kayıkçıoğlu and Okur, 2013). It has been stated that the CO₂ amount in organic farms is higher than in conventional agriculture farms (Melero, 2006; Tuomisto et al., 2012).

Table 3. The effects of application doses of the hazelnut husk compost on the sampling seasons, CO₂ production (mg CO₂/100 g⁻¹ day⁻¹) based on doses, microbial biomass -C (MBC mg biomass-C 100 g.d.s⁻¹) and other soil properties (organic matter OM:%, total N %, K: mg kg⁻¹, Mg and Ca: cmol₍₊₎kg⁻¹)

	Doses						Season			
	0	1.25	2.5	5	7.5	10	1	2	3	4
CO ₂	0.42b	0.58a	0.60a	0.58a	0.54a	0.52a	1.30a	0.28c	0.21c	1.30a
MBC	42.60b	68.83a	67.50a	74.85a	70.13a	69.16a	24.82c	52.05b	14.20c	170.98a
OM	1.60	1.71	1.65	1.41	1.38	1.61	1.43b	1.93a	1.35b	1.53ab
Total N	0.13	0.14	0.13	0.12	0.13	0.13	0.10c	0.50a	0.13bc	0.14ab
K	162b	176b	185b	199b	202b	266a	204	207	205	178
Mg	5.09c	6.12bc	6.72ab	5.97bc	7.70a	6.90ab	8.40a	5.60b	6.04b	5.60b
Ca	26.82a	24.41ab	24.28abc	22.17bc	20.71cd	17.36d	18.22c	26.47a	23.84ab	22.00b
pH	6.70a	6.36ab	6.23b	6.20b	6.10b	6.03b	6.52a	6.16b	6.32ab	6.08b

When the application doses of hazelnut husk are taken into consideration, the microbial biomass -C (MBC) value was between 42.60 -74.85 mg biomass-C 100 g.d.s⁻¹ and the difference between the hazelnut husk doses were statistically insignificant (p < 0.01). The doses have increased the MBC values comparing to the control and the highest value was identified at a dose of 0.5 kg ha⁻¹.

When the sampling season is considered, the MBC value showed a regular increase from the 1st (autumn) season to the 4th (summer) season (except the 3rd- spring season); the highest value arose on the 4th season (summer) and the difference between seasons was statistically significant (p < 0.01).

In respect to hazelnut husk doses, organic matter (OM) content increased and this increment showed seasonal changes. The effects of doses were statistically insignificant, however the highest value has been observed at a dose of 0.125 kg ha⁻¹. When taking the sampling seasons into account, the highest organic material value was detected on the 2nd season (winter). The loamy soils own high surface areas and a high cation exchange capacity, thus showing protective features against the fragmentation of organic substances (Giller et al., 1997; Aygün, 2015). It was reported that organic waste applications radically improve the chemical features of loamy sand soils like the content of organic matter and exchangeable cations and enhance the soil quality (Candemir and Gülser, 2011). There are also other studies, which explain that hazelnut husk may be utilized as an organic material and nutritional source, which enhances the physical properties of the soils (Zeytin and Baran, 2003; Bender Özenç et al., 2019).

Garcia et al. (2004) investigated the effects of various plants on pH, EC, total organic carbon and carbon fractions, microbial biomass carbon, soil respiration, dehydrogenase, phosphatase, β -glycosidase and urease characteristics for 6 years. At the end of the researches they reported that; the aggregate stability, soil respiration, dehydrogenase, urease and phosphatase activities occur more strongly in plant growing soils; pH (7.5-8.0) and EC levels are lower compared to control; the total organic carbon and microbial biomass carbon available in the rhizosphere zone are higher compared to control application.

In consequence of statistical evaluations, the effects of hazelnut husk applications on total N were found insignificant, remaining within an interval of % 0.12-0.14 and showing the highest results at a dose of 0.25 kg ha⁻¹. However the sampling season was statistically significant ($p < 0.01$). When sampling seasons are considered, it was determined that the 2nd season (winter) revealed the highest total N content (0.50%), while the 1st season (autumn) demonstrated the lowest total N content (0.10%). Shenbagavalli and Mahimairaja (2012) on the other hand reported that as the incubation season extends, the mineral N values radically reduce. Besides, as an expected result, when the microorganisms decompose the organic materials in the soil in order to create a source of nitrogen, the nitrogen content of the soil decreases (Bender Özenç et al., 2019).

The effects of hazelnut husk compost doses on extractable K were significant ($p < 0.01$). The application of the hazelnut husk compost in different doses, increased the extractable K content of the soil. The highest K value was detected at a dose of 1 kg ha⁻¹ (266 mg kg⁻¹) and increased 1.65 times compared to control.

In terms of the exchangeable Mg and Ca values, doses and sampling seasons were statistically significant ($p < 0.01$). According to doses, the exchangeable Mg value was between 7.70-5.09 cmol₍₊₎kg⁻¹ and the highest dose was 0.75 kg ha⁻¹, the exchangeable Ca value on the other hand was between 17.36-26.82 cmol₍₊₎kg⁻¹, showing the highest value at the control dose. The exchangeable Mg and Ca values were statistically significant in consideration of sampling seasons. The exchangeable Mg highest value (8.40 cmol₍₊₎kg⁻¹) was identified on the 1st sampling season (autumn), while it was the lowest (5.6 cmol₍₊₎kg⁻¹) during the 2nd (winter) and 4th (summer) sampling seasons. The exchangeable Ca value was between 18.22-26.47 cmol₍₊₎kg⁻¹ (2nd-winter and 1st-autumn season).

When the soil reaction is analyzed, the effects of the hazelnut husk compost on doses and sampling times revealed statistically significant results ($p < 0.01$). The highest pH value was identified at the control application (6.70), the lowest pH value on the other

hand was determined at a compost application dose of 1 kg ha⁻¹ (6.03). And when the sampling seasons are examined, the highest value was observed at the 1st (autumn) (6.52) and the lowest at the 4th (summer) season (6.08).

Conclusion

Within the scope of this study, where the effects of different application doses and sampling seasons of hazelnut husk compost, obtained through microbial biotechnological methods, on the soil various biological features were examined, the biological soil properties showed improvements and positive developments. While the beta-glucosidase and acid phosphatase enzyme activities were the highest at a dose of 1 kg ha⁻¹, the most effective sampling season was the 4th (summer) one. Urease enzyme activity on the other hand was more effective during the 1st (autumn) season and the 0.75 kg ha⁻¹ dose was sufficient. For the production of CO₂ the 0.25 kg ha⁻¹ dose, for MBC the 0.5 kg ha⁻¹ dose, for total N and organic matter content the 0.125 kg ha⁻¹ dose were sufficient. To blend the hazelnut husk compost, which is an organic material containing a large amount of organic matter, with the soil, provided the soil organic matter content to increase, which ultimately was an intended result. Increased doses of hazelnut husk compost to the soil, although there is an increase in the amount of organic matter due to dose increase. The optimum level of the compost to be applied must be decided, the initial organic matter content of the soil is recommended.

REFERENCES

- [1] Alexander, M. (1961): Introduction to Soil Microbiology. – John Wiley and Sons, Inc., New York.
- [2] Amiri, H., Ismaili, A., Hosseinzadeh, S. R. (2017): Influence of vermicompost fertilizer and water deficit stress on morpho-physiological features of chickpea (*Cicer arietinum* L. cv. Karaj). – Compost Science & Utilization 25(3): 152-165.
- [3] Anderson, T. H., Domsch. K. H. (1978): A physiological method for the quantitative measurement of microbial biomass in soils. – Soil Biology and Chemistry 10: 215-221.
- [4] Aygün, S. (2015): The effect of adding of hazelnut husk compost on soil quality, Fındık zurufu kompostunun toprak kalitesi üzerine etkisi. – MSC Thesis University of Ordu, Institute for Graduate Studies in Science and Technology Department of Soil Science and Plant Nutrition, Ordu, Turkey.
- [5] Birol Y., Bender Özenç D (2011): Fındık zuruf kompostunun sıkıştırılmış killi tınlı bir toprağın fiziksel özellikleri üzerine etkisi. – Prof. Dr. Nuri Munsuz Ulusal Toprak ve Su Sempozyumu, Ankara, pp. 77-85.
- [6] Bouyoucos, G. J. (1962): Hydrometer method improved for making particle size analysis of soil. – Agronomy Journal 54: 434-438.
- [7] Bremner, J. M. (1965): Total Nitrogen 1. – In: Page, A. L. (ed.) Methods of Soil Analysis. Part 2. Chemical and Microbiological Properties. ASA, Madison, WI, pp. 1149-1178.
- [8] Çalışkan N., Koç N., Kaya A., Şenses T. (1996): Obtaining the Hazelnut Husk Compost (Fındık Zurufundan Kompost Elde Edilmesi). – Fındık Araştırma Enstitüsü Müdürlüğü Sonuç Raporu, Giresun.
- [9] Candemir, F., and Gülser, C. (2011): Effects of different agricultural wastes on some soil quality indexes in clay and loamy sand fields. – Communications in Soil Science and Plant Analysis 42(1): 13-28.

- [10] Eivazi F., Tabatabai M. A. (1988): Glucosidases and galactosidases in soils. – *Soil Biology and Biochemistry* 20(5): 601-606.
- [11] FAO (2019): Hazelnut production. – <http://www.fao.org/3/x4484e/x4484e03.htm#TopOfPage> (access: 30.10.2019).
- [12] Garcia, C., Roldan, A., Hernandez, T. (2004): Ability of different plant species to promote microbiological processes in semiarid soil. – *Geoderma* 124: 193-202.
- [13] Giller, K. E., Cadish, G., Ehaliotis, C., Adams, E., Sakala, W., Mafongoya, P. (1997): Building Soil Nitrogen Capital in Africa. – In: Buresh, R. J., Sanchez, P. A., Calhoun, F. (eds.) *Replenishing Soil Fertility in Africa*. SSSA Special Publication No. 51, Madison, WI, pp. 151-192.
- [14] GTB (2013): Gümrük ve Ticaret Bakanlığı 2013 Yılı Fındık Raporu. – <http://koop.gtb.gov.tr/data/5342b62e487c8ea5e4b4d9bc/2013%20F%C4%B1nd%C4%B1k%20Raporu.pdf> (date of access: 03.04.2015).
- [15] Guan, S. Y. (1989): Studies on the factors influencing soil enzyme activities: I. Effects of organic manures on soil enzyme activities and N and P transformations. – *Acta Pedologica Sinica* 26: 72-78.
- [16] İslam, E. (2016): The Effect of Hazelnut Husk Compost on Soil Mechanical Properties (Fındık Zurufu Kompostunun Toprak Mekaniksel Özellikleri Üzerine Etkisi). – Ordu Üniversitesi Fen Bilimleri Enstitüsü, Toprak Bilimi ve Bitki Besleme Anabilim Dalı, Yüksek Lisans Tezi.
- [17] Kandeler, E., Gerber, H. (1988): Short-term assay of soil urease activity using colorimetric determination of ammonium. – *Biology and Fertility of Soils* 6(1): 68-72.
- [18] Kayıkçıoğlu, H. H., Okur, N. (2011): Evolution of enzyme activities during composting of tobacco waste. – *Waste Management & Research* 29(11): 1124-1133.
- [19] Kayıkçıoğlu, H. H., Okur, N. (2013): Seasonal changes of microbial biomass-C, N and P in soils under different plant covers. – *Ege Üniversitesi Ziraat Fakültesi Dergisi* 50(1): 57-65.
- [20] Kızılkaya, R., Sahin, N., Askin, T., Sushkova, S. (2015a): Isolation, characterization and genetic identification of natural fungal strains from decomposing hazelnut husk. – 50th Croatian & 10th International Symposium on Agriculture. February 16-20, 2015, Opatija, Croatia.
- [21] Kızılkaya, R., Sahin, N., Tatar, D., Veyisoglu, A., Askin, T., Sushkova, S. N., Minkina, T. (2015b): Isolation and identification of bacterial strains from decomposing hazelnut husk. – *Compost Science & Utilization* 23(3): 173-184.
- [22] Knudsen, D., Peterson, G. A., Pratt, P. F. (1982): Lithium, Sodium, and Potassium. – In: Page, A. L. (ed.) *Methods of Soil Analysis. Part 2. Chemical and Microbiological Properties*. ASA, Madison, WI, pp. 225-246.
- [23] Melero, S., Porras, J. C. R., Herencia, J. F., Madejon, E. (2006): Chemical and biochemical properties in a silty loam soil under conventional and organic management. – *Soil & Tillage Research* 90: 162-170.
- [24] Meli, S., Porto M., Belligno, A., Bufo, S. A., Mazzatura, A., Scapa, A. (2002): Influence of irrigation with lagooned urban wastewater on chemical and microbiological soil parameters in a citrus orchard under Mediterranean condition. – *Sci. Total Environ.* 285: 69-77.
- [25] Müftüoğlu, N. M., Türkmen, C., Çıkkılı, Y. (2012): Soil and Plant Fertility Analysis (Toprak ve Bitkide Verimlilik Analizleri, Kriter Yayınevi). – Nobel, Ankara.
- [26] Nannipieri, P., Kandeler, E., Ruggiero, P. (2002): Enzyme Activities and Microbiological and Biochemical Processes in Soil. – In: Burns, R. G., Dick, R. P. (eds.) *Enzymes in the Environment*. Marcel Dekker, New York, pp. 1-33.
- [27] Nelson, D. W., Sommers, L. E. (1982): Total Carbon, Organic Carbon and Soil Organic Matter. – In: Page, A. L. et al. (eds.) *Methods of Soil Analysis. Part 2: Chemical and Microbiological Properties*. ASA-SSSA, Madison, WI, pp. 539-579.

- [28] Özenç, D. B. (2008): Growth and transpiration of tomato seedlings grown in Hazelnut Husk compost under water-deficit stress. – *Compost Science & Utilization* 16(2): 125-131.
- [29] Özenç, D. B., Yılmaz, F. I., Tarakçıoğlu, C., Aygün, S. (2019): Fındıktan üretilen atıkların toprağın fiziko-kimyasal ve biyolojik özelliklerine etkileri. Effects of hazelnut produced wastes on physico-chemical and biological properties of soil. – *Mediterranean Agricultural Sciences* 32: 7-13.
- [30] Ozyazıcı, G., Ozdemir, O., Ozyazıcı, M. A., Ustun, G. Y. (2011): The effects of organic materials and soil regulators in organic hazelnut production on yield and some soil properties (Bazı organik materyallerin ve toprak düzenleyicilerin organik fındık yetiştiriciliğinde verim ve toprak özellikleri üzerine etkileri). – Poster at Türkiye IV. Organik Tarım Sempozyumu, Erzurum, 28 Haziran-1 Temmuz 2010.
- [31] Schinner, F., Öhlinger, R., Kandeler, E., Margesin, R. (eds.) (1996): *Methods in Soil Biology*. – Springer-Verlag, Berlin.
- [32] Sermeyer, H. (1952): Eine einfache Methode zur Bestimmung der Karbonate im Boden. – *Zeitschrift für Pflanzenernährung, Düngung, Bodenkunde* 561(3): 26-38.
- [33] Shenbagavalli, S., Mahimairaja, S. (2012). Characterization and effect of biochar on nitrogen and carbon dynamics in soil. – *International Journal of Advanced Biological Research* 2(2): 249-255.
- [34] Stévigny, C., Rolle, L., Valentini, N., Zeppa, G. (2007). Optimization of extraction of phenolic content from hazelnut shell using response surface methodology. – *Journal of the Science of Food and Agriculture* 87(15): 2817-2822.
- [35] Tabatabai, M. A., Bremner, J. M. (1969): Use of p-nitrophenyl phosphate for assay of soil phosphatase activity. – *Soil Biology and Biochemistry* 1(4): 301-307.
- [36] Tous, M. J. (2001): Hazelnut technology for warm climates. – *Proceedings of the Ninth Australasian Conference on Trees and Nut Crops*, Perth, Western Australia.
- [37] Tuomisto, H. L., Hodge, I. D., Riordan, P., Macdonald, D. W. (2012). Does organic farming reduce environmental impacts? A meta-analysis of European research. – *Journal of Environmental Management* 112: 309-320.
- [38] U.S. Salinity Laboratory Staff (1954): *Diagnosis and Improvement of Saline and Alkali Soils*. – Handbook No. 60. U.S. Salinity Laboratory, Riverside, CA.
- [39] Wang, L., Zhang, Y., Gao, P., Shi, D., Liu, H., Gao, H. (2006). Changes in the structural properties and rate of hydrolysis of cotton fibers during extended enzymatic hydrolysis. – *Biotechnology and Bioengineering* 93(3): 443-456.
- [40] Xiao-Chang, W. A. N. G., Qin, L. (2006): Beta-glucosidase activity in paddy soils of the Taihu Lake region, China. – *Pedosphere* 16(1): 118-124.
- [41] Xiu-Mei, L. I. U., Qi, L. I., Liang, W. J., Jiang, Y. (2008): Distribution of soil enzyme activities and microbial biomass along a latitudinal gradient in farmlands of Songliao Plain, Northeast China. – *Pedosphere* 18(4): 431-440.
- [42] Zeytin, S., Baran, A. (2003): Influences of composted hazelnut husk on some physical properties of soils. – *Bioresource Technology* 88(3): 241-244.

THE IMPACT OF DIFFERENT TYPES OF FOLIAR FEEDING ON THE ARCHITECTURE ELEMENTS OF A WINTER RAPE (*BRASSICA NAPUS* L.) FIELD

SIKORSKA, A.¹ – GUGAŁA, M.^{2*} – ZARZECKA, K.²

¹*Department of Agriculture, Vocational State School of Ignacy Mościcki in Ciechanów,
ul. Narutowicza 9, 06-400 Ciechanów, Poland
(e-mail: anna.sikorska@puzim.edu.pl)*

²*Faculty of Agrobioengineering and Animal Husbandry, University of Natural Sciences and
Humanities in Siedlce, ul. Prusa 14, 08-110 Siedlce, Poland
ul. Prusa 14, 08-110 Siedlce, Poland
(e-mail: gugala@uph.edu.pl; kzarzecka@uph.edu.pl)*

**Corresponding author
e-mail: gugala@uph.edu.pl*

(Received 1st Aug 2019; accepted 14th Nov 2019)

Abstract. The field experiment was carried out in 2016-2019 at the Agricultural Experimental Station Zawady (52°03'N and 22°33'E) belonging to the University of Natural Sciences and Humanities in Siedlce, Poland. The experiment was established in a random layout (split - plot) with triplicates. The examined factors were I - three varieties of winter rape: Monolit, PX115, PT248. II - four types of foliar feeding: 1. control object, 2. biostimulator Aminoplant, 3. Foliar fertilizer Siarkomag + foliar fertilizer Bormax, 4. Foliar fertilizer Siarkomag + foliar fertilizer Bormax + biostimulator Aminoplant. The aim of the study was to determine the effect of foliar fertilizers containing amino acids, sulphur and boron on planting before harvest, plant height before harvest, root thickness, height to the first productive branching, deflection of three varieties of winter rape. The use of the Aminoplant biostimulator in combination with foliar fertilizers containing sulphur and boron significantly increased the planting density, the stem thickness at the root, the height to the first productive branching, compared to the control treatment. Foliar application of amino acids, boron, sulphur did not significantly increase the height of plants before harvesting and did not affect the deflection of the field.

Keywords: *plant density, plant height, stem thickness, height to the first productive branching, plant morphology before harvest, field deflection*

Introduction

Currently, one of the basic elements of agrotechnics of many crops is foliar feeding. This treatment entails the introduction of deficient nutrients to aboveground parts of plants (Szewczuk and Sugier, 2009). Singh et al. (2013) state that this is an alternative way to provide plants with missing macro and micronutrients consisting of sprinkling leaves with a dilute solution of mineral salts, chelates with the addition of a surface tension reducing agent. According to many authors (Fageria et al., 2009; Singh et al., 2013), foliar nutrition affects the correction of poor nutritional status of plants.

Kinaci and Gulmezoglu (2007) and Babaeian et al. (2011) believe that foliar spraying is very beneficial when the roots cannot provide the necessary nutrients to the plants, due to improper soil pH (pH), drying time, and heavy texture. Similarly, Kocoń (2009) emphasizes that it is much more beneficial to apply foliar spray instead of direct soil application.

According to Kaur et al. (2019), foliar feeding plays a significant role in areas with changing climatic conditions. Stress caused by drought reduces both uptake of nutrients

through the roots and transport from roots to shoots, due to limited transpiration and weakened active transport (Yuncaï and Schmidhalter, 2005). Well-nourished plants with essential nutrients are more resistant to abiotic stresses.

The reaction of plants to foliar nutrition varies greatly between plant species, growth stages, the concentration of the added nutrient solution and the relative water content in plant parts (Noreen et al., 2018).

The paper assumes a research hypothesis that biostimulators combined with foliar feeding can have a beneficial effect on the architectural elements of winter rape fields.

The aim of the study was to determine the effect of foliar fertilizers containing amino acids, sulphur, boron on planting before harvest, plant height before harvest, root thickness, height to the first productive branching, deflection of three varieties of winter rape (Monolit, PX115, PT248).

Materials and methods

Experimental and agronomic management

The field experiment was carried out in 2016-2019 at the Agricultural Experimental Station Zawady (52°03'N and 22°33'E) belonging to the University of Natural Sciences and Humanities in Siedlce, Poland. The experiment was established in a random layout (split - plot) in triplicate. The surface of each plot was 21 m². *Table 1* presents the agrotechnical factors included in the experiment.

Table 1. Agrotechnical factors included in the experiment (RSD Zawady)

Agrotechnical factors	
Three morphotypes	<ul style="list-style-type: none"> • Population morphotype (Monolit variety) • Restored morphotype with the traditional growth type (PT248) • Restored morphotype with semi-dwarf growth type (PX115 variety)
Four types of foliar feeding	<ul style="list-style-type: none"> • Control object – without using foliar feeding and amino acids • Biostimulator Aminoplant: I term – in autumn in the phase of 4-6 leaves (BBCH 14-16), II term – in spring after the beginning of vegetation (BBCH 28-30), III term – in the phase of development of flower buds (budding) – beginning of flowering (BBCH 50-61), at doses of 1.0 dm³·ha⁻¹ • Foliar fertilizer Siarkomag + foliar fertilizer Bormax: I term – in autumn in the phase of 4-6 leaves (BBCH 14-16), II term – in spring after the beginning of vegetation (BBCH 28-30), III term – in the phase of development of flower buds (budding) – beginning of flowering (BBCH 50-61), at doses of 2.0 dm³·ha⁻¹ + 0.5 dm³·ha⁻¹ • Foliar fertilizer Siarkomag + foliar fertilizer Bormax + biostimulator Aminoplant: I term – in autumn in the phase of 4-6 leaves (BBCH 14-16), II term – in spring after the beginning of vegetation (BBCH 28-30), III term – in the phase of development of flower buds (budding) – beginning of flowering (BBCH 50-61), at doses of 2.0 dm³·ha⁻¹ + 0.5 dm³·ha⁻¹ + 1.0 dm³·ha⁻¹

In the 2016-2017 growing season, the forecrop for winter rape was spring wheat, in the second and final year of research – winter triticale. The experiment was carried out on soil classified according to the World reference base for soil resources (2014) to the Haplic Luvisol group, sated, belonging to the very good rye soil complex, Iva valuation class. During the research years, the soil pH (pH in 1N KCl) was slightly acidic and

ranged from 5.68 to 5.75. The soil was characterised by a low total nitrogen content (average from 0.80 to 0.90 g·kg⁻¹), phosphorous content (average from 0.33 to 0.55 g·kg⁻¹), potassium content (average from 0.61 to 0.67 g·kg⁻¹) and calcium content (average from 0.82 to 0.85 g·kg⁻¹) and the average magnesium content (from 0.38 to 0.46 g·kg⁻¹) and sulphur content (from 0.11 to 0.15 g·kg⁻¹).

The soil was characterized by low abundance in available forms of phosphorus and average bioavailability in potassium and magnesium (Table 2).

Table 2. Characteristics of soil conditions - Zawady Meteorological Station, Poland (2016-2019)

Vegetation seasons	pH (1 mol·dm ⁻³ KCl)	The content of available forms of elements (mg·kg ⁻¹)		
		P	K	Mg
2016-2017	5.70	81.0	200.0	63.0
2017-2018	5.68	75.0	199.0	60.0
2018-2019	5.75	79.0	202.0	59.0

After forecrop harvest, a set of post-harvest procedures was carried out using the ploughing aggregate + open cage roller, and then two weeks after the first procedure, pre-sow ploughing at the depth of 20.0 cm was carried out, using a ring roller at the same time. To prepare the soil for sowing and to mix fertilizers, a complex soil tillage unit was used. Before sowing, phosphorus-potassium fertilization was applied at the dose of 40 kg P·ha⁻¹ and 110 kg K·ha⁻¹ and the first dose of 40 kg N·ha⁻¹. Fertilization was applied in the form of Lubofos at the dose of 600 kg. Fertilizing doses were supplemented with 55.9 kg·ha⁻¹ of ammonium nitrate (19 kg N·ha⁻¹), 29.6 kg·ha⁻¹ triple superphosphate (13.6 kg P·ha⁻¹) and 29 kg·ha⁻¹ potassium salt (17.9 kg K·ha⁻¹). The second dose of nitrogen in the amount of 100 kg·ha⁻¹ was applied in spring, before vegetation started (BBCH 28-30) applying ammonium nitrate at the dose of 255.5 kg·ha⁻¹ (86.9 kg N·ha⁻¹) and ammonium sulphate at the dose of 62.5 kg·ha⁻¹. The third dose of ammonium 60 kg·ha⁻¹ was applied at the inflorescence emergence (BBCH 50). by applying ammonium nitrate at the dose of 176.5 kg·ha⁻¹ (60 kg N·ha⁻¹).

Winter rapeseed sowing was made at spacing between rows of 22.5 cm, assuming a case of 60 pcs·m⁻². Sowing was made at the optimal time recommended for this region (in 2016 – on August 12, in 2017 – on August 14, and in 2018 – on August 13).

Chemical protection against weeds, diseases and pests was applied in accordance with the recommendations of good agricultural practice. Directly after sowing, herbicide Command 480 EC at the dose of 0.25 dm³·ha⁻¹ was applied to carefully cultivated soil. Next, at the stage of BBCH 13-14, Fusilade Forte 150 EG at the dose of 2.0 dm³·ha⁻¹ was applied. At the 4-8 leaves unfolded stage (BBCH 14-18) fungicide Horizon 250 EW was applied (0.75 dm³·ha⁻¹). At the stem elongation stage (BBCH 30), flower bud emergence stage (BBCH 50-58), flowering (BBCH 60-69) – Proteus 110 OD insecticide was applied at the dose of 0.6 dm³·ha⁻¹. At the beginning of flowering (BBCH 61) – Propulse 250 SE fungicide was applied at the dose of 1.0 dm³·ha⁻¹. At the stage of first petals falling – Mondatak 450 EC was applied at the dose of 1.0 dm³·ha⁻¹.

Rape was harvested in two stages in the first and second decade of July.

Immediately prior to harvest (BBCH 86-87) the case per 1 m⁻² was marked and elements of field architecture were determined for a sample of 20 plants from each plot, such as:

- Plant height before harvest (cm)

- Stem thickness at the base (mm)
- Height of seating of the first productive branch (cm)
- Field deflection (%)

Weather conditions in vegetation period

During the years of conducting the experiment, varied weather conditions prevailed (Table 3). In the first *vegetation period*, the annual precipitation totalled 389.2 mm and was 8.9% lower compared to the multi-annual average (427.5 mm), while the average air temperature was similar and amounted to 7.9 °C. Based on the calculated Sielianinov hydrothermal coefficient, it was found that the years 2016-2017 and 2017-2018 were optimal. In the second year of research, the largest annual precipitation was recorded (414.5 mm), 13 mm lower than the average for 1996-2010, while the average air temperature was higher by 1 °C and amounted to 9.3 °C. The last year of research was the most dry and warm. The annual amount of rainfall was lower by 174.6 mm, while the temperature was higher than the long-term average by 1.6 °C.

Table 3. Characteristics of weather conditions in the years 2016-2019 (Zawady Meteorological Station, Poland)

Years	Months												VIII-VII	
	VIII	IX	X	XI	XII	I	II	III	IV	V	VI	VII		
Rainfalls (mm)													Sum	
2016-2017	31.7	13.6	69.8	19.5	22.5	0.4	15.9	25.1	59.7	49.5	57.9	23.6	389.2	
2017-2018	54.7	80.6	53.0	21.3	15.8	10.1	3.2	15.4	34.5	27.3	31.5	67.1	414.5	
2018-2019	24.5	27.4	23.3	9.8	9.0	7.9	4.7	15.0	5.9	59.8	35.9	29.7	252.9	
Multiyear sum (1996-2010)	59.9	42.3	24.2	20.2	18.6	19.0	16.0	18.3	33.6	58.3	59.6	57.5	427.5	
Air temperature (°C)													Mean	
2016-2017	18.0	14.9	7.0	2.4	0.0	-6.6	-1.3	5.5	6.9	13.9	17.8	16.9	7.9	
2017-2018	18.4	13.9	9.0	4.1	2.7	-0.7	-4.0	-0.3	13.1	17.0	18.3	20.4	9.3	
2018-2019	20.6	15.9	9.6	7.9	0.3	-3.0	2.2	4.8	9.8	13.3	17.9	18.5	9.8	
Multiyear mean (1996-2010)	18.5	13.5	7.9	4.0	-0.1	-3.2	-2.3	2.4	8.0	13.5	17.0	19.7	8.2	
Sielianinovs hydrothermic coefficients*														
	VIII	IX	X	III	IV	V	VI	VII						Mean
2016-2017	0.61	0.28	3.02	1.79	3.19	1.52	1.06	0.47						1.49
2017-2018	1.00	1.92	2.36	2.97	0.99	0.59	0.61	1.12						1.44
2018-2019	0.40	0.71	0.94	1.16	0.20	1.37	0.63	0.56						0.75

*Index value (Skowera, 2014): Extremely dry $k \leq 0.4$. Very dry $0.4 < k \leq 0.7$. Dry $0.7 < k \leq 1.0$. Rather dry $1.0 < k \leq 1.3$. Optimal $1.3 < k \leq 1.6$. Rather humid $1.6 < k \leq 2.0$. Humid $2.0 < k \leq 2.5$. very humid $2.5 < k \leq 3.0$. Extremely humid $k > 3.0$

Statistical analysis

The results of the study were statistically analysed with the use of the analysis of variance. The significance of variation sources was tested with the “F” Fischer-Snedecor test and the assessment of significance at the significance level of $p = 0.05$ between compared means - with Tukey’s range test.

Results and discussion

Based on our own studies, it was found that the types of foliar nutrition significantly increased the number of plants determined before harvesting (*Table 4*). The largest plant density was recorded after the use of the Siarkomag foliar fertilizer with the Bormax foliar fertilizer and the Aminoplant biostimulator (object 4). After using the bioregulator with an amino acid, the plant density was only an average higher by one item compared to the control object. Jarecki et al. (2019) obtained a significant increase in the number of plants compared to the object without feeding after the application of the Insol5 foliar preparation in autumn, autumn and spring, autumn and twice in spring, while the value of this feature on the objects was the same. Different results were obtained by Czarnik et al. (2015) and Chwil (2016). Similarly, Jankowski et al. (2016a, b) under the influence of foliar application of boron did not find a significant effect of the factor on the value of this feature, as well as Szczepanek and Brach (2019) after the application of the Phostrade® BMo foliar preparation.

The genetic factor significantly influenced the planting before harvest (*Table 4*). The highest value of this feature was demonstrated in the PX115 semi-dwarf hybrid. The population variety Monolit had, on average, from 2 to 3 plants less per unit area compared to restored hybrids. Different results were obtained by Czarnik et al. (2015), who did not find significant differences between the Arot population variety and the Primus hybrid variety.

Preparations containing amino acids, sulphur and boron increased the height of plants before harvest on average from 2.3 to 5.5 cm, but the differences between the examined objects were statistically insignificant (*Table 4*). Similar results were obtained by Jarecki and Bobrecka-Jamro (2008) after the application of foliar fertilizers Basfoliar 36 Extra, Basfoliar 12-4-6 + S, Solubor DF, Adob Mn and mixtures of Basfoliar 36 Extra with Solubor DF, Basfoliar 12-4-6 + S with Solubor DF. Przybysz et al. (2008), Sikorska et al. (2018) after using the Asahi SL biostimulator obtained a significant increase in the plant height. Similarly, Rabiee et al. (2013), Riki et al. (2014) and Cheema et al. (2012) obtained a significant increase of this feature under the influence of foliar nutrition. Habbasha and Salam (2009) emphasized that the dual application of foliar fertilization in the rosette and budding phase has a more favourable effect on the plant height compared to the single dose used in autumn.

In own studies, the height of a hybrid with a traditional type of growth and a population variant was the same (*Table 4*). A similar tendency was noted by Sikorska et al. (2018), while Jarecki and Bobrecka-Jamro (2008) did not find significant differences in the amount of plants of the evaluated varieties (Lirajet, Marita, Lisek).

The application of foliar fertilization influenced the increase of stem thickness at the base from 0.42 to 10.4 mm. The highest value of this feature was noted on object 4 after the application of Siarkomag foliar fertilizer with Bormax and Aminoplant biostimulator (*Table 4*).

From the compared morphotypes, the largest stem thickness at the base was distinguished among the Monolit population variety, while the smallest among the restored hybrid with a traditional growth type (*Table 4*). Different results were obtained by Sikorska et al. (2018). The authors recorded the largest thickness of the stem at the base of restored hybrids (PT205 and PR44D06), and significantly smaller in the Monolit population variety.

Table 4. Plant number before harvest (pcs.), plant height before harvest (cm), stem thickness at the base (mm) depending on factors of experience

Types of foliar feeding	Cultivars			Mean
	Monolit	PT 248	PX 115	
Plant number before harvest (pcs.)				
1. Control variant	50.7	53.1	54.4	52.7^a
2. Biostimulator Aminoplant	51.7	54.0	55.6	53.7^b
3. Foliar fertilizer Siarkomag + foliar fertilizer Bormax	52.9	55.1	56.1	54.7^c
4. Foliar fertilizer Siarkomag + foliar fertilizer Bormax + biostimulator Aminoplant	53.6	55.6	56.6	55.2^d
Mean	52.2^a	54.4^b	55.7^c	-
LSD_{0.05} for:				
Cultivars				0.45
Types of foliar feeding				0.57
Interaction: cultivars x types of foliar feeding				n.s.
Plant height before harvest (cm)				
1. Control variant	129.9	126.2	110.2	122.1
2. Biostimulator Aminoplant	131.1	128.9	113.2	124.4
3. Foliar fertilizer Siarkomag + foliar fertilizer Bormax	134.2	130.5	103.9	122.9
4. Foliar fertilizer Siarkomag + foliar fertilizer Bormax + biostimulator Aminoplant	134.8	132.1	116.1	127.6
Mean	132.5^a	129.4^a	110.8^b	-
LSD_{0.05} for:				
Cultivars				6.24
Types of foliar feeding				n.s.
Interaction: cultivars x types of foliar feeding				n.s.
Stem thickness at the base (mm)				
1. Control variant	14.23 ^a	14.06 ^{ac}	14.28 ^a	14.19^a
2. Biostimulator Aminoplant	15.06 ^{bc}	14.43 ^{ad}	14.36 ^a	14.61^b
3. Foliar fertilizer Siarkomag + foliar fertilizer Bormax	15.26 ^{bg}	14.48 ^{df}	14.77 ^{edf}	14.83^c
4. Foliar fertilizer Siarkomag + foliar fertilizer Bormax + biostimulator Aminoplant	15.48 ^g	14.89 ^h	15.32 ^b	15.23^d
Mean	15.01^a	14.46^b	14.68^c	-
LSD_{0.05} for:				
Cultivars				0.23
Types of foliar feeding				0.24
Interaction: cultivars x types of foliar feeding				0.37

Values marked with the same letter do not differ significantly at $P \leq 0.05$. n.s. - non significant differences

The effect of foliar feeding on the thickness of the stem at the base depended on the genetic factor (*Table 4*). The studies have shown that on the control object the differences between the tested varieties were statistically insignificant. The use of the Aminoplant biostimulator (object 2) in restored hybrids PT248 and PX115 did not significantly affect the increase of the thickness of the stem at the base when

compared to the object on which no foliar nutrition was applied. The largest significant increase was found in the population variety after the application of the Aminoplant biostimulator with sulphur fertilizers (object 3) and sulphur and boron (object 4), while the differences between variants 3 and 4 were statistically insignificant, and in the case of restored hybrids only after the application of the Aminoplant biostimulator in connection with foliar fertilizers containing sulphur and boron.

In own studies it was found that the height to the first productive branching on control objects and the biostimulator containing amino acids was the same. The highest value of this feature was noted after the use of preparations containing sulphur (object 3) and sulphur and boron (object 4) (Table 5). Sikorska et al. (2018) after using the biostimulator Asahi SL obtained an increase in the value of this feature by an average of 4.6 cm. While Jarecki and Bobrecka-Jamro (2008) did not find a significant influence of this factor.

The studied varieties were distinguished by varying height to the first productive branching. The highest first productive branching was noted in the population variety, significantly lower in the re-cultivated hybrid with the traditional type of growth (Table 5).

Table 5. First productive branch placement (cm), canopy lodging (%) depending on factors of experience

Types of foliar feeding	Cultivars			Mean
	Monolit	PT 248	PX 115	
First productive branch placement (cm)				
1. Control variant	46.14	37.82	36.70	40.22^a
2. Biostimulator Aminoplant	47.77	39.14	38.66	41.86^{ab}
3. Foliar fertilizer Siarkomag + foliar fertilizer Bormax	48.74	40.18	38.99	42.64^c
4. Foliar fertilizer Siarkomag + foliar fertilizer Bormax + biostimulator Aminoplant	48.68	40.53	39.78	43.00^c
Mean	47.83^a	39.42^b	38.53^c	-
LSD_{0.05} for:				
Cultivars				0.42
Types of foliar feeding				0.63
Interaction: cultivars x types of foliar feeding				n.s.
Canopy lodging (%)				
1. Control variant	10.8	6.8	5.1	7.6
2. Biostimulator Aminoplant	10.9	7.1	6.6	8.2
3. Foliar fertilizer Siarkomag + foliar fertilizer Bormax	11.8	7.3	5.7	8.3
4. Foliar fertilizer Siarkomag + foliar fertilizer Bormax + biostimulator Aminoplant	9.2	7.3	6.9	7.8
Mean	10.7^a	7.1^b	6.1^b	-
LSD_{0.05} for:				
Cultivars				1.33
Types of foliar feeding				n.s.
Interaction: cultivars x types of foliar feeding				n.s.

Values marked with the same letter do not differ significantly at $P \leq 0.05$. n.s. - non significant differences

The types of foliar nutrition did not affect the field deflection of the studied varieties of winter rape. Among the studied varieties, the greatest deflection of the field was recorded in the population variety, while the differences between the restored hybrids were statistically insignificant (*Table 5*).

Weather conditions influenced a significant diversity of morphological characteristics marked before harvest (*Tables 6-7*). The sum of rainfall significantly higher than the average for many years in the period from March to April in the first year of research caused that the plants grew higher, had a greater thickness of the stem at the root, developed the first productive branching higher. The smallest values of these features were noted in the last *vegetation period*, in which the sum of precipitation in April was lower by 82.5% compared to the average for many years, and the average air temperature higher by 1.8 °C. The largest number of plants before harvest was noted in a warm and dry *vegetation period*, which was characterized by a higher average air temperature from November to April and a lower amount of rainfall in this period compared to the average for many years, while the smallest cast was demonstrated in 2017-2018, characterized by lower average air temperature in the period from February to March.

Table 6. Plant number before harvest (pcs), plant height before harvest (cm), stem thickness at the base (mm) depending on cultivars and years

Years	Cultivars			Mean
	Monolit	PT 248	PX 115	
Plant number before harvest (pcs.)				
2016-2017	50.2 ^a	54.3 ^b	56.1 ^c	53.5^a
2017-2018	49.6 ^a	51.3 ^e	52.9 ^g	51.3^b
2018-2019	56.8 ^d	57.8 ^f	58.0 ^f	57.5^c
Mean	52.2	54.4	55.7	-
LSD_{0.05} for:				
Cultivars				0.45
Years				0.45
Interaction: cultivars x years				0.77
Plant height before harvest (cm)				
2016-2017	141.8	139.3	120.2	133.7^a
2017-2018	132.4	129.5	105.5	122.5^b
2018-2019	123.3	119.5	106.8	116.5^b
Mean	132.5	129.4	110.8	-
LSD_{0.05} for:				
Cultivars				6.24
Years				6.24
Interaction: cultivars x years				n.s.
Stem thickness at the base (mm)				
2016-2017	15.43	15.04	15.02	15.16^a
2017-2018	14.99	14.33	14.59	14.64^b
2018-2019	14.60	14.03	14.43	14.35^c
Mean	15.01	14.46	14.68	-
LSD_{0.05} for:				
Cultivars				0.23
Years				0.23
Interaction: cultivars x years				n.s.

Values marked with the same letter do not differ significantly at $P \leq 0.05$. n.s. - non significant differences

Table 7. First productive branch placement (cm), canopy lodging (%) depending on cultivars and years

Years	Cultivars			Mean
	Monolit	PT 248	PX 115	
First productive branch placement (cm)				
2016-2017	54.03 ^a	40.23 ^d	39.26 ^e	44.51^a
2017-2018	45.58 ^b	39.10 ^e	39.03 ^e	41.24^b
2018-2019	43.89 ^c	38.93 ^e	37.30 ^f	40.04^c
Mean	47.83	39.42	38.53	
LSD_{0.05} for:				
Cultivars				0.42
Years				0.42
Interaction: cultivars x years				0.72
Canopy lodging (%)				
2016-2017	13.3 ^a	11.0 ^b	8.8 ^c	11.0^a
2017-2018	10.6 ^b	7.0 ^c	4.7 ^d	7.4^b
2018-2019	8.2 ^c	3.3 ^d	4.8 ^d	5.4^c
Mean	10.7	7.1	6.1	-
LSD_{0.05} for:				
Cultivars				1.33
Years				1.33
Interaction: cultivars x years				2.3

Values marked with the same letter do not differ significantly at $P \leq 0.05$. n.s. - non significant differences

Interactions of varieties and years of research have been found in relations to planting before harvesting, heights to the first productive branching, sowing of the field, which indicates the individual reactions of the studied varieties to climatic conditions prevailing in particular years of research (Tables 6-7). It was observed that all varieties were distinguished by the largest planting diversity in the driest and warmest year of research. The population variety had the same number of plants in the first and second growing season, while in the restored hybrids, the differences in the value of this feature in the last year of the research were statistically insignificant. The studied morphotypes were distinguished by the highest height to the first productive branching in the first year of study, the value of which was the same in the PT248 variety in the last two years of research, and in the semi-dwarf morphotype in 2016-2017 and 2017-2018.

Conclusions

1. The use of the Aminoplant biostimulator in combination with foliar fertilizers containing sulphur and boron significantly increased the planting density (on average by 4.7%), the stem thickness at the root (on average by 7.3%), the height to the first productive branching (on average by 6.9%), compared to the control object.
2. Foliar application of amino acids, boron, sulphur did not significantly increase the height of plants before harvesting and did not affect the deflection of the field.

3. The morphotype determined the morphological characteristics of the plants before harvesting. The largest plant density was found in the semi-dwarf hybrids, while the population variety was distinguished by the largest thickness of the stem at the base, the height to the first productive branching. The plant height was the same in the population morphotype and the restored hybrid with a traditional growth type.
4. The climatic conditions in the *vegetation period* the experiment significantly influenced the examined elements of the field architecture.
5. Foliar fertilization should be used as a permanent element of winter rapeseed cultivation technology, therefore further research is needed to evaluate the performance of these preparations on various soil types.

Acknowledgements. The research was carried out under the research project No. 363/S/13, financed from a science grant by the Ministry of Science and Higher Education.

REFERENCES

- [1] Babaeian, M., Tavassoli, A., Ghanbari, A., Esmailian, Y., Fahimifard, M. (2011): Effects of foliar micronutrient application on osmotic adjustments, grain yield and yield components in sunflower (Alstar cultivar) under water stress at three stages. – Afr. J. Agric. Res. 6(5): 1204-1208.
- [2] Cheema, M. A., Sattar, A. Rasul, F., Saleem, M. F. (2012): Influence of different levels of potassium on growth, yield and quality of canola (*Brassica napus* L.) cultivars. – Pak. J. Agr. Sci. 49: 163-168.
- [3] Chwil, S. (2016): The effect of foliar feeding under different soil fertilization conditions on the yield structure and quality of winter oilseed rape (*Brassica napus* L.). – EJPAU 19, #02.
- [4] Czarnik, M., Jarecki, W., Bobrecka-Jamro, D., Jarecka, A. (2015): The effects of sowing density and foliar feeding on yielding of winter oilseed rape cultivars. – Rośliny Oleiste - Oilseed Crops 36(1): 60-68 (in Polish).
- [5] El Habbasha, E. F., El Salam, M. (2009): Response of two canola varieties (*Brassica napus* L.) to nitrogen fertilizer levels and zinc foliar application. – Department of Plant Sciences, UC, Davis. <https://escholarship.org/uc/item/68f0h22d>.
- [6] Fageria, N. K., Filho, B. M. P., Moreira, A., Guimarães, C. M. (2009): Foliar fertilization of crop plants. – J. Plant Nutrition 32: 1044-1064.
- [7] Kinaci, E., Gulmezoglu, N. (2007): Grain yield and yield components of triticale upon application of different foliar fertilizers. – Interciencia 32(9): 624-628.
- [8] Jankowski, K. J., Hulanicki, P. S., Krzbiec, S., Żarczyński, P., Hulanicki, P., Sokólski, M. (2016a): Yield and quality of winter oilseed rape in response to different systems of foliar fertilization. – J. Elem. 21(4): 1017-1027. DOI: 10.5601/jelem.2016.21.1.1108.
- [9] Jankowski, K. J., Sokólski, M., Dubis, B., Krzbiec, S., Żarczyński, P., Hulanicki, P. S., Hulanicki (2016b): Yield and quality of winter oilseed rape (*Brassica napus* L.) seeds in response to foliar application of boron. – Agricultural and Food Science 25: 164-176.
- [10] Jarecki, W., Bobrecka-Jamro, D. (2008): Reaction of winter rape to the extra feeding of its leaves. – Annales Universitatis Mariae Curie-Skłodowska Lublin – Polonia LXIII(2)E: 86-96.
- [11] Jarecki, W., Buczek, J., Bobrecka-Jamro, D. (2019): The response of winter oilseed rape to diverse foliar fertilization. – Plant Soil Environ. 65: 125-130.

- [12] Kaur, M., Kumar, S., Kaur, A. (2019): Effect of foliar application of nitrogen, phosphorus and sulphur on growth and yield of Gobhi Sarson (*Brassica napus* L.) in central Punjab. – Journal of Oilseed Brassica 10(1): 47-50.
- [13] Kinaci, E., Gulmezoglu, N. (2007): Grain yield and yield components of triticale upon application of different foliar fertilizers. – Interciencia 32(9): 624-628. doi.org/10.1016/S0308-521X(01)00023-3.
- [14] Kocoń, A. (2009): Effectiveness of foliar feeding of wheat and winter rape with selected fertilizers under conditions of optimal fertilization and soil moisture. – Annales Universitatis Mariae Curie-Skłodowska Sectio E, Agricultura 64(2): 23-28 (in Polish).
- [15] Noreen, S., Fatima, Z., Ahmad, S., Athar, H. R., Ashraf, M. (2018): Foliar Application of Micronutrients in Mitigating Abiotic Stress in Crop Plants. – In: Hasanuzzaman, M., Fujita, M., Oku, H., Nahar, K., Hawrylak-Nowak, B. (eds.) Plant Nutrients and Abiotic Stress Tolerance. Springer, Singapore.
- [16] Przybysz, A., Małecka-Przybysz, M., Słowiński, A., Gawrońska, H. (2008): The Effect of Asahi SL on Growth, Efficiency of Photosynthetic Apparatus and Yield of Field Grown Oilseed Rape. – In: Dąbrowski, Z. T. (ed.) Monographs Series: Biostimulators in Modern Agriculture: Field Crops, Editorial House Wieś Jutra, Warsaw, pp. 7-17.
- [17] Rabiee, M., Kavosi, M., Vahed, H. S., Kehal, P. T. (2013): Effect of concentration and time of foliar spraying of nitrogen fertilizer on grain yield and important traits of rapeseed (*Brassica napus* L.) cv. Hyola 401. – Journal of Science and Technology of Agriculture and Natural Resources 17(64): 43-53 ref.19.
- [18] Riki, G., Mobasser, H. R., Ganjali, H. R. (2014): Effect of iron and manganese foliar spraying on some quantitative characteristics of canola. – International Journal of Biosciences 5(1): 61-68.
- [19] Sikorska, A., Gugala, M., Zarzecka, K. (2018): Response of winter rapeseed to biostimulator application and sowing method. Part I. Field architecture elements. – Acta Sci. Pol. Agricultura 17(4): 205-214.
- [20] Singh, J., Singh, M., Jain, A., Bhardwaj, S., Singh, A., Singh, D. K., Bhushan, B., Dubey, S. K. (2013): An introduction of Plant Nutrients and Foliar Fertilization: A Review. In: Precision farming: a new approach. – Daya Publishing Company, New Delhi, pp. 252-320.
- [21] Skowera, B. (2014): Changes of hydrothermal conditions in the Polish area (1971–2010). Fragm. Agron. 31(2): 74-87 (in Polish).
- [22] Szczepanek, M., Bech, A. (2019): Technology of winter oilseed rape with foliar fertilization. – Acta Sci. Pol. Agricultura 18(1): 39-47.
- [23] Szewczuk, Cz., Sugier, D. (2009): General characteristics and types of foliar fertilizers offered on the Polish market. – Annales UMCS. s. E. LXIV(1): 29-36 (in Polish).
- [24] World Reference Base for Soil Resources (2014): International Soil Classification System for Naming Soils and Creating Legends for Soil. Field Experiment. – FAO, WorldSoil Resources Reports, 106, Rome. <http://www.fao.org>.
- [25] Yuncai, H., Schmidhalter, U. (2005): Drought and salinity: A comparison of the effects of drought and salinity. – J. Plant Nutr. Soil Sci. 168: 541-549.

DEVELOPMENT AND METHODS OF VALIDATION FOR MEASUREMENT OF PESTICIDES IN MUSCLE TISSUE USING GAS CHROMATOGRAPHY BASED MODIFIED ANALYTICAL QUECHERS APPROACH

AHMAD, Y. H.^{1*} – KHULOD, I. H.²

¹*Department of Microbiology, College of Veterinary Medicine, University of Sulaimani, New Sulaimani, Street 27, P.C 46001, Sulaymaniyah, Northern Iraq*

²*Department of Food Science and Human Nutrition, College of Agricultural Sciences, University of Sulaimani, Street 27, P.C 46001, Sulaymaniyah, Northern Iraq
(phone: +964-771-948-1949)*

**Corresponding author*

e-mail: ahmad.hamadamin@univsul.edu.iq; phone: +964-771-666-2829

(Received 5th Aug 2019; accepted 25th Nov 2019)

Abstract. A multi residue detection method for the quantification of six wide spectrum non-polar pesticides in the muscle of cattle, sheep, and goats was developed in this study. The method was based on a modified QuEChERS procedure adapted to gas chromatography coupled with mass spectrometry (GC–MS). About 150 meat samples were analyzed to detect and quantify pyrethroids (PYRs) including cypermethrin (CMT), deltamethrin (DMT), organochlorines (OCs) including hexachlorobenzene (HCB), α -hexachlorocyclohexane (α -HCH) and organophosphates (OPs), such as chlorpyrifos (CPS) and fenitrothion (FTN). Subsequently, the effects of boiling (100 °C, 30 min) and broiling (176 °C, 20 min) on the level of pesticides in the meat were tested. Acceptable responses of analytes were obtained at validation levels of 0.01 to 0.1 mg/kg. The linear coefficients (r^2) were ≥ 0.9997 , and limits of detection (LOD) and limit of quantification (LOQ) values ranged from 0.004 to 0.014 and 0.012 to 0.043 mg/kg respectively. Satisfactory recovery (79.2 to 104.3%) was obtained for all spiked levels with acceptable relative standard deviation (RSD) ($\leq 14.6\%$). The dominant compound found in cattle muscle was hexachlorobenzene (HCB), while deltamethrin (DMT) was the most dominant pesticide in sheep and goats samples. Boiling technique reduced meat pesticides significantly ($P < 0.05$), whereas the effects of broiling were questionable. The validation results confirmed that the proposed method can be utilized as a dependable screening apparatus and analytical procedure for quantitative determination of studied pesticides in animal tissues.

Keywords: *pyrethroids, organochlorines, organophosphoruses, boiling, broiling*

Abbreviations: GC: Gas Chromatography; MS: Mass spectrometry; QuEChERS: Quick, Easy, Cheap, Effective, Rugged, and Safe; PYRs: Pyrethroids; OCs: Organochlorines; OPs: Organophosphoruses; DMT: Deltamethrin; CMT: Cypermethrin; HCB: Hexachlorobenzene; α -HCH: α -hexachlorocyclohexane; CPS: Chlorpyrifos; FTN: Fenitrothion; LOD: Limit of detection; LOQ: Limit of quantification; RSD: Relative standard deviation; r^2 : linear coefficients; SPE: Solid phase extraction; SPA: Primary Secondary amines; C18: Octadecylsilane; ACN: Acetonitrile; $MgSO_4$: Magnesium sulphate; NaCl: Sodium chloride; d-SPE: Dispersive solid phase extraction; MS/MS: Tandem mass spectrometry; ECD: Electron capture detection; n: number of samples; mm: millimeter; μ m: Micromillipore; cm: centimeter; WSS: Working standard solution; MMC: Matrix-matched calibration; ANOVA: Analysis of Variance; LLE: Liquid-liquid extraction; LLP: Liquid-liquid partitioning; MRLs: Maximum residue limits

Introduction

The innovation of pesticides has played a vital role in the development of agriculture and veterinary science, and they have been irreplaceable until now. In veterinary

medicine, pesticides are used for the treatment of external parasites, while in agriculture, they are used intensively for prevention and treatment of crops pre and post-harvests (Lainsbury, 2019). Their extensive use of pesticides has resulted in their widespread distribution and transfer to animals (MacBean, 2015). These contamination routes can lead to bioaccumulation of pesticides in food products of animal origin such as meat, fat, and milk, finally leading to pesticides being transferred to humans via the food chain (Castillo et al., 2012).

Pyrethroids (PYRs), organochlorines (OCs), and organophosphorus (OPs) pesticides are effective against variety of pests, have been widely used around the world (Castillo et al., 2012). Their extreme stability, low volatility, and probable indiscriminate use in the past have led to their high persistence in the environment and in organisms after exposure (Lainsbury, 2019). Among these groups of pesticides, non-polar pesticides are more hazardous than polar pesticides because they have a strong tendency to be stored in body tissues and only small amounts are excreted through kidneys (MacBean, 2015). Ingestion of tiny doses of pesticides daily or weekly may cause life-long illnesses, neurological problems, cancers, anemia, and cardiovascular illnesses in humans (MacBean, 2015).

Several methods have been used to quantify of pesticide residues in animal derived foods, but the key technique is: firstly, how several pesticides residues can be efficiently extracted from the complex matrixes; secondly, how cleaning up is performed to minimise matters co-extracts; thirdly, what analytical method should be proposed for accurate quantification.

QuEChERS (quick, easy, cheap, effective, rugged and safe) extraction technique is the most popular extraction method (Anastassiades et al., 2003). The method is based on acetonitrile extraction followed by a cleanup, using dispersive solid phase extraction (d-SPE) with a primary secondary amine (PSA), octadecylsilane (C18). At first, the method was simply used for determination of specified groups of pesticide in fruit and vegetables. Later, it was validated for a variety of pesticide groups in high fat content foods, such as meat and internal organs (Meligy et al., 2019), chicken eggs (Nardelli et al., 2018) and fish (Sahu and Nelapati, 2018).

Among chromatographic techniques, GC is the most frequently used technique (Vitha, 2016). The GC has been used for detection of multi-residues in liquid matrices (Schettgen et al., 2016), and complex tissue matrices (Letta and Attah, 2013). Variety of detectors have been used with GC, such as tandem MS (MS/MS) (Arioli et al., 2019), mass spectrometry (MS) (Meligy et al., 2019) electron capture detection (ECD) (Dimitrova et al., 2018). The most preferred by laboratories is GC, due to its high sensitivity suitability for halogen and non-halogen containing compounds (Grimalt and Dehouck, 2016). MS suffers more from sample matrix interferences than other detection methods (Meligy et al., 2019); this has made it difficult to optimize a method which reliably screens several groups of pesticides in a complex tissue.

Moreover, risk assessments of residues in meat are based on the level of residues in uncooked meat, even though a large proportion of consumed meat is either cooked or processed before consumption. In order to thoroughly assess the risks to consumers of pesticide residues, the effects of heat treatment on the residues should be considered (Kiranmayi et al., 2016; Yun-Sang et al., 2016). Studies have shown that heat treatment can cause considerable reduction of pesticide residues in food commodities (Witczak, 2009; Muthukumar et al., 2010). The presence of residues above the permissible levels is a major barrier in the approval of meats, as well as posing domestic public health

issue. Therefore, to confirm the safety of meats, the levels of pesticides in meat should be determined professionally before and after heat treatments.

To date, no enough study performed to assess the effect of boiling at 100 °C for 30 min and broiling at 176 °C for 20 min on studied pesticides in meat tissues which are the most commonly used temperature (Goldwyn and Blonder, 2016).

The aim of this study was to optimize GC–MS and to adapt a modified QuEChERS method for detection and quantification of six pesticides belonging to three classes, by optimising experimental conditions in both sample preparation and chromatography using an acceptable validation procedure. With this technique the levels of the six pesticide residues in tissues and effects of boiling (100 °C, 30 min) and broiling (176 °C, 20 min) on the pesticides residual levels were measured.

Material and methods

Sample collection

Meat samples (n = 150) were randomly collected from adult cattle (n = 50), sheep (n = 50), and goat (n = 50) carcasses at the Sulaimaniyah slaughterhouse. Each sample was sliced into three equivalent portions of 50 g (150 × 3). The first portion (n = 150) was straightforwardly prepared for extraction and analysis. The second (n = 150) and third (n = 150) portions were boiled (100 °C, 30 min) and broiled (176 °C, 20 min) respectively. Blank meat samples were acquired from animals free from all pesticides obtained formally from the Brazilian Agricultural Research Cooperation Center. Samples collection and the study performed in Sulaimaniyah city/Kurdistan region of Iraq.

The blank samples were tested to confirm that they were free from the studied pesticides. Then aliquot of samples for selectivity study, the rest portion spiked and used for recovery, matrix matched standards calibration, and sensitivity studies.

Chemical and apparatus

All solvents were of pesticide-residue grade. Pesticides standards of cypermethrin (CMT)(94%), deltamethrin (DMT)(99%), hexachlorobenzene (HCB)(98%), α -hexachlorocyclohexane (α -HCH)(98%), chlorpyrifos (CPS)(96%) and fenitrothion (FTN)(95.5%) were obtained from Dr. Ehrenerstorfer TM (Augsberg, Germany). Acetonitrile (ACN) (99.5%), acetic acid (99.9%) primary secondary amine (PSA) 40 μ m particle size, octadecylsilane (C18, 50 μ m), sodium chloride (NaCl), and anhydrous magnesium sulphate (MgSO₄) were obtained from Merck Ltd. Syringe filters (0.45 μ m), and capillary columns, 30 m DB-5, with an internal diameter of 0.25 mm and thickness of 0.1 μ m were purchased from Supelco Analytical Co., UK.

GC–MS system

The pesticides' concentrations were detected by gas chromatography, along with mass spectrometry. This was performed using a QP GC–MS gas chromatograph from Shimadzu (Kyoto, Japan), equipped with a mass-selective detector and capillary column of a 30 m DB-5, with 0.25 mm internal diameter and 0.1 μ m film thicknesses. The injector, interface, and ion source temperatures were 250 °C, and splitless injection (1.0 min) was performed using helium as the carrier gas with a flow rate of 0.75 mL/min. The oven temperature was set to increase at a pace of 4 °C /min from

120 °C to 190 °C. Next, the temperature was increased from 32 °C/min to 270 °C, and held for 4 min. The mass spectrometer was operated with scan mode, put between m/z 45 and m/z 475 Daltons, which can detect analytes in a solvent to a limit of 1.0 mg/kg. The injection volume was 50 μ L with a splitless injection mode.

Heat treatment

Samples were made into small patties of about 1.5 cm thickness. About 150 samples were placed separately into low-density water-impermeable polyethylene bags and cooked in boiling water (100 °C, 30 min) using a water bath (Memmert W200, Germany). Similarly, the other 150 samples were put in a glass bowl and broiled in a preheated air oven (Memmert 93/42 EEC, Germany), at 176 °C for 20 min, being turned over every 5 min. During the experiment, the water bath and oven temperature were monitored with a thermometer and oven thermometer gauge respectively.

Method of validation

Validation method for this study was carried out according to the internationally accepted SANTE/11813/2017 criteria, i.e., selectivity, recovery percentages, precision, linearity, and sensitivity. Method selectivity was tested by injection of 10 independent meat sample extracts into GC–MS. The absence of interfering peaks above a signal-to-noise ratio of 3 at the retention time window of interest was checked for each analyte. The target retention times of the analytes were identified by separately injecting analytical standards (10 mg/L) into the GC–MS apparatus. Multi-standard solutions were injected in to the GC–MS to check maximum retention time tolerance range (± 0.2 min), and improve analytical validation. Recovery was determined by comparing the obtained concentrations with the same concentrations of the pesticides prepared in the dissolvent. The inter-day precisions (3 replicates in 3 successive days) were determined by analyzing all spiked levels through the injection of multi-standard solutions, containing six analytes, at concentrations of 0.010, 0.025, 0.050, and 0.100 mg/kg for control matrices. Since a different maximum residue limit (MRL) has been established for each analyte in meat, 0.01 – 0.1 mg/kg of standard solutions were spiked into blank matrices to obtain the highest method reliability during screening. The linearity test in meat was carried out by injecting six matrix-matched standards for calibration studies. Limits of detection (LOD) and quantitation (LOQ) were determined based on a signal-to-noise ratio, and concentrations showing peak intensity of signal-to-noise ratio of 3 and 10 were designated as LOD and LOQ, respectively.

Matrix-matched calibration (MMC)

According to SANTE/11813/2017 criteria, matrix constituents negatively influence the quantitation of target analyses in GC–MS analyses and may increase or decrease the analytical signals. Hence, matrix-matching (standards added to blank extracts) is performed mainly to minimize matrix effects. For the preparation of analytical MMC curves, individual stock solutions of HCB, α -HCH, FTN, CPS, CMT, and DMT were prepared in acetonitrile in Pyrex glass vials at a concentration of 100 mg/L and stored at -20 °C in dark amber bottles. Working standard solutions (WSS) was prepared at a concentration of 50 mg/L by diluting stock solution in acetonitrile. Matrix-matched calibration standards was prepared just before injection by diluting the working solutions and spiked into extracted blank samples to obtain concentrations of 0.010,

0.025, 0.050, 0.100, 0.200 and 0.500 mg/kg. The MMC curves for each compound were built, and coefficients (r^2) of calibration curves were used to assess linearity.

Preparation of meat samples

The extraction and cleanup procedures performed based on original QuEChERS method (Anastassiades et al., 2003) and (Lehotay et al., 2005) with few modifications. Meat samples were thawed at 4 °C overnight prior to use. Blank meat samples (2 g) were homogenised and fortified with 20 µL of each 10, 5, 2.5 and 1 mg/L of multi-standards solution (including the six pesticides) to prepare samples of 0.1, 0.05, 0.025 and 0.01 mg/kg. These were mixed with the matrix for 2 min and left to interact for 30 min. The blended meat samples were transferred to a 50 mL Falcon tube. Next, 4 mL of ACN (containing 1% acetic acid), 1.6 g of anhydrous MgSO₄, and 0.4 g of NaCl were added and the mixture was agitated in a vortex mixer for 1 min. The mixture was centrifuged at 3000 rpm for 3 min to separate the phases (liquid-liquid partition). The supernatant, corresponding to the organic solvent ACN, was transferred to a tube containing 70 mg of C18, 70 mg of the adsorbent PSA and 150 mg of MgSO₄. The tube was shaken by hand for half a minute, and centrifuged at 4000 rpm for 1 min. The supernatant was filtered by syringe filter (0.45 µm) to remove the excess of colouring materials. The filtered supernatant was subjected to evaporation under a stream of nitrogen (Hopkinton, LabX, USA) at 45 °C and stored at 4 °C. The solutions were transferred to an autosampler vial and injected into the GC-MS under optimum conditions.

Data processing and statistical analysis

Matrix-matched standards data were subjected to the computer programs of Excel (Analysis ToolPak, Regression) for sensitivity and F test. The obtained real samples data (concentration data for each pesticide and animal species, heat treatment data) subjected to the Analysis of Variance (One-way ANOVA, Post Hoc = Duncan, using SPSS software (Version 18.0), multiple ranges used to significantly compare means ($p < 0.05$).

Results and discussion

Development of QuEChERS method

Traditionally, non-polar pesticides have been extracted by liquid-liquid extraction (LLE) and solid-phase extraction (SPE). These extraction procedures are not recommended as they are time-consuming, multi-step procedures and need large amounts of organic solvents (Kang et al., 2011). By contrast, the use of the QuEChERS technique has significantly reduced the demerits of traditional extraction procedures because of its small scale LLE and d-SPE (Lehotay et al., 2005). Hence, in the present study, the original QuEChERS method was considered, which was proposed by Anastassiades et al. (2003) and Lehotay et al. (2005). In the first step of the test, the method of (Anastassiades et al., 2003) was applied, in which 10 g of the meat sample and 10 mL of ACN, 4 g of MgSO₄, and 1 g of NaCl were used for liquid-liquid partitioning (LLP). For the second step (d-SPE), the method of Lehotay et al. (2005) was used, in which 50 mg of C18, 50 mg of PSA and 150 mg of MgSO₄ were added to the mixture. The method of Anastassiades et al. (2003) was used in the first step of the

procedure because this method does not require buffers for the extraction of analytes. For the second step, the method of Lehotay et al. (2005) was used, because it provides better cleanup due to the use of a larger mass of PSA and the addition of C18. Unexpectedly, the obtained recovery values varied from 60 to 74%, with high RSD values (>20%). Hence, additional tests were carried out. In the second test, the QuEChERS method was modified. Meat samples (2 g), 4 mL of ACN, 1.6 g of MgSO₄, and 0.4 g of NaCl were used, as well as for the d-SPE, 70 mg of PSA, 70 mg of C18, and 150 mg of MgSO₄. The obtained recovery and RSD rates were satisfactory according to SANTE/11813/2017 (Table 1). Many parameters can influence the extraction efficiency, including the type of solvent, polarity, and cleanup sorbents including C18 and PSA (Okimashi et al., 2007). Hence, the second test, the ratio of ACN to sample weight was changed from 1:1 to 1:2, and PSA and C18 were increased to 70 mg, and the quantity of MgSO₄ held constant with additional one filtration step.

The extraction of pesticide residues depends on the polarity of pesticides and type of matrix contained pesticides (Peng et al., 2016). In this test, ACN was selected for extraction of pesticides because of its effectiveness in the extraction of polar and non-polar pesticides from the diverse range of matrices. The cleanup step also improved by increasing PSA and C18 from 50 to 70 mg. The PSA could effectively eliminate polar matrix components, such as organic acids, certain polar pigments, and sugars. The C18 also thoroughly removed fatty acids, which are considered the main co-extract of the non-polar pesticides in meat, among other components (Paramasivam et al., 2011). MgSO₄ could also bind with organic acids, polar material and/or glucosides. The salt combination (NaCl, MgSO₄) produced heat and forced the majority of co-extracts into the acetonitrile layer. The filtration step finally could totally remove the coloring materials in the solution, prompted cleanup and prepared the solution for injection.

In this study, cleaning up step was mostly considered to optimise and adapt the QuEChERS technique; firstly, to obtain acceptable recovery and, RSD, and to maximize extraction efficiency, and peak resolution; secondly, insufficient cleaning up of samples from the co-extractives in the extract causes deterioration of the GC system and precludes reliable results (Peng et al., 2016). Optimization of the chromatographic conditions was carried out to obtain a good compromise between low chromatographic times and suitable peak resolutions. Under the optimized chromatographic conditions, a satisfying separation was achieved with symmetrical and narrow peaks in the retention times between 2.93 and 9.75 min (Fig. 1A).

The extraction efficiency of the proposed method was assessed by spiking meat samples with multi pesticides at four concentrations level (0.01, 0.025, 0.050 and 0.1 mg/kg). Good methodology efficiency was obtained in all concentrations regarding recovery percentages. To assess the possible existence of matrix effects, meat samples were extracted and spiked, and then they were compared with analytical standards at same concentrations. The calculations were performed using the peak areas and concluded that there were no significant differences between signal responses (ANOVA, $p > 0.05$).

Precision and recovery

Recovery percentages were evaluated by comparing the concentrations of spiked samples, with the nominal fortification level. The recovery of each analyte was verified by calculating their average and put in compliance with the recovery range reported in SANTE/11813/2017.

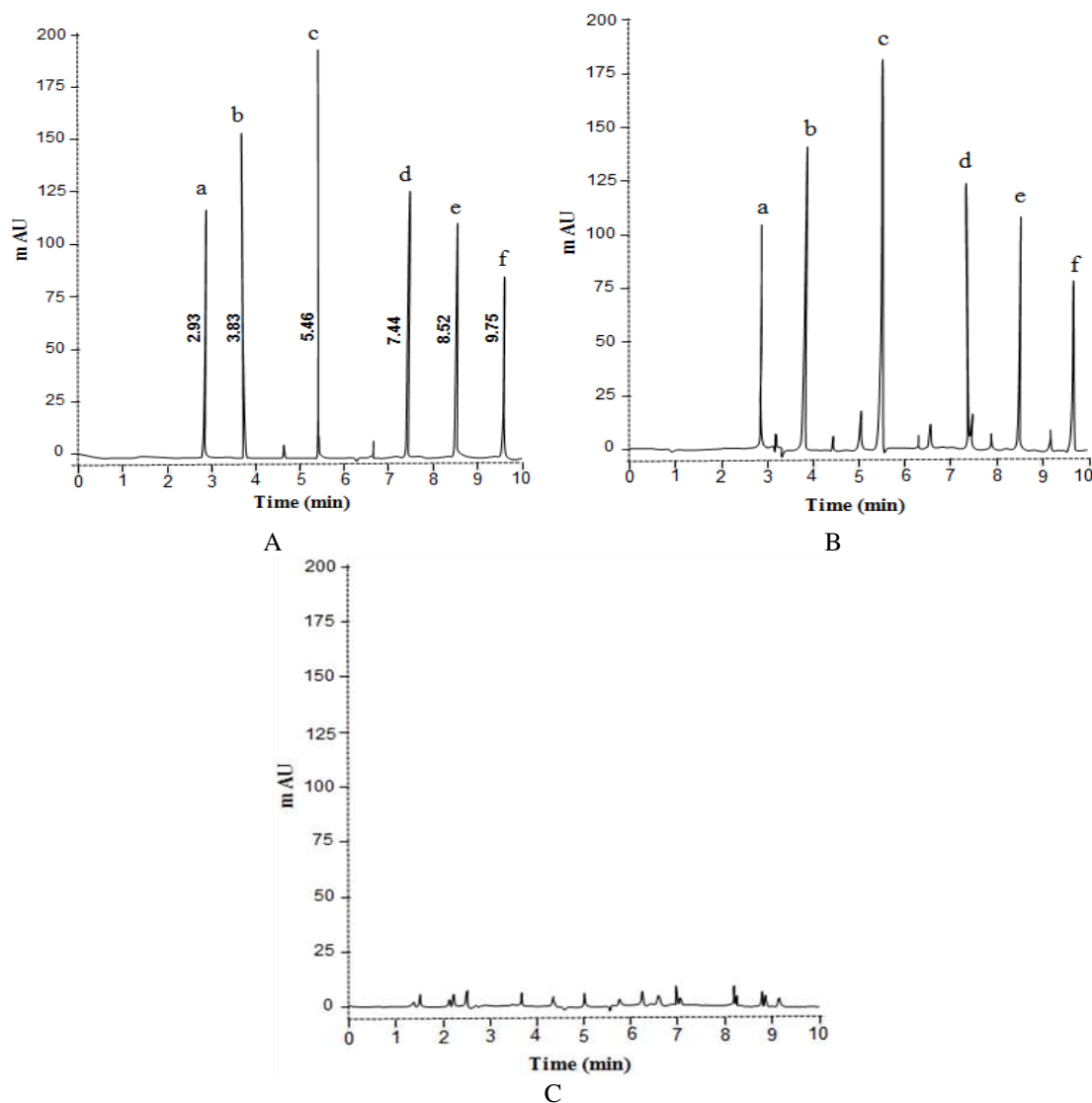


Figure 1. GC chromatograms of QuEChERS method. A: A multi-standard solutions (10 mg/L). B: Spiked blank samples after extraction (0.1 mg/kg). C: Blank meat samples. a. Hexachlorobenzene; b. Hexachlorocyclohexane; c. Fenitrothion; d. Chlorpyrifos; e. Cypermethrin; f. Deltamethrin

The recovery values and RSDs were obtained using meat samples spiked with four different concentrations (0.01, 0.025, 0.05 and 0.1 mg/kg). Acceptable recoveries (79.2 to 104.3%) were obtained for all spiked levels, demonstrating that the matrix of meat samples was not affected by the extraction of the analytes (Table 1). The precision of the method was determined in two stages: repeatability (intra-day) and intermediate precision (inter-day). The intermediate precision was expressed by the RSD of the results of nine analyses performed on three different days (n = 3), three analyses/day, by the same instrument. The obtained RSD in this work was 0.32-14.6% for different spiked concentrations, which meets the recommendation of the SANTE/11813/2017 guidelines (RSD \leq 20%) (Table 1). These results demonstrate that the method possesses good accuracy and can be considered to be a useful tool for the screening of the six analytes in meat. Some of the tested compounds showed lower recovery than others.

This might be due to some kind of interaction which could not be corrected with matrix matching, or the samples might have been decomposed in the processes of extraction, cleanup, or evaporation (Okihashi et al., 2007). High RDS in some analytes might be due to a high level of co-extracts that interfered in the GC system. By contrast, some showed low RDS, which could be due to ion speculation (Okihashi et al., 2007). The main analytical problem in chromatographic analysis has been reported to be the complexity of the matrix together with interfering co-extractive substances. These factors may deteriorate the chromatographic column (Frenich et al., 2006). Therefore, the analysis of three groups of pesticides in meat samples is recommended that samples should be cleaned up thoroughly prior extraction process.

Table 1. Recovery and relative standard deviations (RSD %) in different spiked concentrations ($n = 3$)

Spiked matrix Conc. (mg/kg)	Recovery \pm RDS (%)					
	CMT	DMT	HCB	α -HCH	CPS	FTN
0.01	79.2 \pm 7.4	85.8 \pm 1.7	85.8 \pm 13.09	82.7 \pm 3.8	88.3 \pm 13.3	97.6 \pm 6.3
0.025	82.7 \pm 7	88.9 \pm 1.8	86.1 \pm 10.2	104.3 \pm 4.6	91.4 \pm 8.6	96.28 \pm 3.1
0.05	86.8 \pm 4.1	93.5 \pm 1.3	88.6 \pm 14.6	98.7 \pm 5.1	92.1 \pm 9	96.3 \pm 4.8
0.10	97.3 \pm 0.9	98.1 \pm 0.32	98.07 \pm 1.5	97.5 \pm 3.1	98.6 \pm 1.5	99.6 \pm 0.6

RSD: Relative standard deviation, CMT: Cypermethrin, DMT: Deltamethrin, HCB: Hexachlorobenzene, α -HCH: alpha-Hexachlorocyclohexane, CPS: Chlorpyrifos, FTN: Fenitrothion

Linearity and limits of detection and quantification

While, linearity can be tested using standard working solutions, in this study the spiked blank sample after extraction was used to correct matrix effects. The linearity was evaluated by constructing regression graphs at concentrations of 0.010, 0.025, 0.050, 0.100, 0.200 and 0.500 mg/kg. The acceptability of the regression model was also confirmed by using all the calibration datasets (six calibration points with three replicates at each calibration point). The regression was statistically analysed by the determination coefficients (r^2), and the homoscedasticity assumption was evaluated by plotting residue versus concentration. The coefficients (r^2) were ≥ 0.9997 , and the residual plot showed that the errors were randomly distributed around the concentration axis. The F -test, performed according to the recommendation of the Analytical Methods Committee criteria reported by Johnson et al. (2010), and validated the linearity of a model for significance level of 0.05 (Analysis ToolPak, Regression). According to Kaonga et al. (2015), the response of the detector to any analysed pesticide by GC was found to be dependent on the studied matrix properties. Therefore; the achieved slope (r^2) values for the analytes were close to each other due to the similarity in the composition of the matrices.

Test sensitivity or matrix effects and fluctuation in baseline noise have a strong impact on LOD and LOQ values. For this reason, their validation under these conditions is mandatory. In this work, the LOD and LOQ values ranged from 0.004 to 0.014 and 0.012 to 0.043 mg/kg respectively (Table 2). The LOD and LOQ for all the studied compounds were lower than the maximum residue limits (MRLs) established by EU 396/2005 and EU No 149/2008. This suggests that the method can detect the studied pesticides at an adequately low level, which confirms its validity. The method described

here provides higher sensitivity than methods used by other researchers for quantifying pesticides in meat such as, GC–MS (Meligy et al., 2019), GC–MS-MS (Meligy et al., 2019), and GC–ECD (Dimitrova et al., 2018). This aspect is the key-factor for evaluating analytical methods, because the lower the LOD values, the lower the probability of false negative results (Stefanelli et al., 2009).

Table 2. Linearity range, regression equation, coefficients, limits of detection and limit of quantification

Pesticides	Linearity range	Regression equation	r ²	LOD (mg/kg)	LOQ (mg/kg)
CMT	0.01-0.5	y = 1102 x + 2010.9	0.9998	0.014	0.043
DMT	0.01-0.5	y = 820.48x + 835.28	0.9999	0.009	0.027
HCB	0.01-0.5	y = 1120.2x + 1060.5	0.9999	0.006	0.019
α-HCH	0.01-0.5	y = 1442.3x + 846.02	0.9999	0.006	0.020
CPS	0.01-0.5	y = 1195.5x + 502.26	0.9997	0.014	0.043
FTN	0.01-0.5	y = 1900.6x + 679.8	0.9999	0.004	0.012

r²: coefficient, LOD: limit of detection, LOQ: limit of quantification

Real samples analysis

In this work, the level of DMT in sheep samples was the highest (0.210 ± 0.010 mg/kg), followed by HCB in cattle samples (0.204 ± 0.008 mg/kg). The concentration of FTN presented the lowest residual in all the meat samples from cattle (0.040 ± 0.002 mg/kg), sheep (0.059 ± 0.003 mg/kg) and goats (0.019 ± 0.002 mg/kg) (Table 3).

The level of DMT and CMT detected in sheep and goat meat were high and exceeded than the acceptable limits of DMT (0.03 mg/kg) and CMT (0.05 mg/kg) set by EU R No.396/2005. These results agreed with other studies that also detected a high level of DMT from sheep and goats' meat near Sulaimaniyah (Abdulrahman, 2016) and with another study (Khashan, 2016) that found high DMT levels in cattle meat in Baghdad. High levels of HCB and α-HCH were also detected in cattle samples which exceed than the acceptable limits of HCB and α-HCH (0.02 mg/kg) set by EU R No.149/2008. The same result found in another research (Kiranmayi et al., 2016), which showed that the result is due to extreme use of these pesticides in agriculture.

The higher incidence of DMT, CMT, HCB and α-HCH might be due to the extensive use of these pesticides in livestock and agriculture due to their wide spectrum of biological activity and high stability in the environment (MacBean, 2015). These pesticides are mostly used in Kurdistan and northern Iraq because they are legally allowed to use DMT and CMT to control ticks, flies, fleas, lice, and mites in animal, and to treat seasonal crops with HCB and α-HCH for controlling fungal disease and mosquito and as an antifouling agent. The reason of finding high level of PYRs, OCS pesticide residues could be due to their rapid effects and low cost compared to OPs pesticides.

The OPs pesticides detected in meat samples in this study are CPS and FTN, which presented lower concentration residues than PYRs and OCPs in cattle, sheep and goat samples. The concentration of CPS residues found in cattle (0.124 mg/kg), sheep (0.110 mg/kg), and goat (0.071 mg/kg) samples were higher than acceptable limits (0.05 mg/kg) set by EU R No 396/2005. Moreover, the FTN residues in cattle (0.04 mg/kg) and goat (0.019) samples were less than the acceptable limit (0.05 mg/kg)

set by EU R No 396/2005 except sheep samples (0.059 mg/kg) which were almost about over the acceptable level. Low CPS levels also found by Muhammad et al. (2010) and FTN have been found in buffalo and cattle grazing outdoor (Park et al., 2006). The low incidence of CPS and FTN could be due to low stability of the compounds in the environment and lower use by farmers due to their costs.

Statistically, there was a significant difference between animal species in terms of residual levels among all pesticides (ANOVA, $p < 0.05$) except α -HCH and CPS between cattle and sheep samples. In cattle samples, there was no significant difference between the CMT and DMT (ANOVA, $p > 0.05$), the rest pesticides residual levels were different statistically (ANOVA, $p < 0.05$). In sheep samples significant difference was noticed between all pesticides residual levels (ANOVA, $p < 0.05$) except CMT and CPS. While, in goat samples no difference was presented between DMT, HCB and α -HCH (ANOVA, $p > 0.05$), and no difference was also noticed between CMT and CPS.

Table 3. Mean residual levels of the studied pesticides in meat tissues

Pesticides	Fresh (cattle) samples (mg/kg \pm RSE)	Fresh (sheep) samples (mg/kg \pm RSE)	Fresh (goats) samples (mg/kg \pm RSE)
CMT	0.060 ^{Ab} \pm 0.004	0.102 ^{Cb} \pm 0.004	0.076 ^{Bb} \pm 0.003
DMT	0.057 ^{Ab} \pm 0.005	0.210 ^{Cc} \pm 0.010	0.100 ^{Bc} \pm 0.005
HCB	0.204 ^{Cc} \pm 0.008	0.131 ^{Bc} \pm 0.005	0.091 ^{Ac} \pm 0.004
α -HCH	0.152 ^{Bd} \pm 0.009	0.151 ^{Bd} \pm 0.006	0.090 ^{Ac} \pm 0.005
CPS	0.124 ^{Bc} \pm 0.007	0.110 ^{Bb} \pm 0.004	0.071 ^{Ab} \pm 0.005
FTN	0.040 ^{Ba} \pm 0.002	0.059 ^{Ca} \pm 0.003	0.019 ^{Aa} \pm 0.002

Values in the “Fresh samples” column are presented as a mean of 50 samples \pm SEM (standard error of mean), statistical analysis by one-way ANOVA, post hoc = Duncan

A, B, C Different superscript letters denote significant differences within row ($p \leq 0.05$)

a, b, c, d, e Different superscript letters denote significant differences within column ($p \leq 0.05$)

Heat treatment

As shown in Table 4, boiling at 100 °C for 30 min reduced the concentrations of the pesticides significantly (ANOVA, $p < 0.05$) in cattle, sheep, and goat muscle tissues. On the other hand, the reduction in concentration of the studied pesticides after broiling at 176 °C for 20 min was questionable. The significant reduction of the six pesticides during boiling could be attributed to the volatility of these compounds and the elimination of these compounds due to fat rendering induced by exposure to high temperature for a long time, which does not happen in open heating treatments (Khan and Rahman, 2017).

In the boiling and broiling process, the most reduced pesticide group in cattle, sheep and goat samples was the PYRs including CMT and DMT (Table 4). Followed by OCs (HCB and α -HCH), and the least reduction of pesticides were OP pesticides including CPS and FTN (Table 4).

The dissipation percentages in both methods were higher for PYR and OC pesticides, when compared to OPs pesticides (Table 4). This might be due to the chemical and physical properties of these pesticides and variation in susceptibility to heat among the different chemical compounds in pesticides affected by boiling and broiling (Muthukumar et al., 2010). The reduction in level was almost similar between PYRs and OCs, whereas the reduction of OPs differed noticeably. However, there is no strong

correlation between the physiochemical properties of PYRs and OCs. Since various parameters involving molecular weight, volatility (vapour pressure), hydrolysis rate, and water solubility affect the reduction rate, no conclusive statement can be made about the degree to each parameter to the loss of pesticides during boiling or broiling.

However, boiling at high temperatures is more advisable; it dissolves and washes away water-soluble vitamins and 60 to 70% of minerals (Yun-Sang et al., 2016). Although, effects of broiling process were less than boiling, it is still preferred to obtain the maximum nutritional values without sacrificing flavor by consumers. Hence, it is recommended that consumers might consume heat treated meat by boiling to avoid pesticide health issues, which could be better than tasty broiled meat contained higher pesticides residues.

Table 4. Effects of cooking methods on the concentration of pesticides (mg/kg ± RSE)

Pesticides	Species	Raw meat	Boiling at 100 °C for 30 min	Broiling at 176 °C for 20 min
CMT	Cattle	0.060 ^{Bb} ± 0.004	0.038 ^{Aa} ± 0.003	0.051 ^{Bb} ± 0.003
	Sheep	0.102 ^{Cb} ± 0.004	0.059 ^{Ab} ± 0.002	0.086 ^{Bb} ± 0.003
	Goat	0.076 ^{Cb} ± 0.003	0.048 ^{Ab} ± 0.003	0.065 ^{Bb} ± 0.002
DMT	Cattle	0.057 ^{Bb} ± 0.005	0.036 ^{Aa} ± 0.003	0.048 ^{Bb} ± 0.004
	Sheep	0.210 ^{Cc} ± 0.011	0.134 ^{Ac} ± 0.007	0.172 ^{Be} ± 0.009
	Goat	0.100 ^{Cc} ± 0.005	0.065 ^{Ad} ± 0.004	0.086 ^{Bc} ± 0.005
HCB	Cattle	0.204 ^{Cc} ± 0.008	0.139 ^{Ad} ± 0.005	0.177 ^{Be} ± 0.007
	Sheep	0.131 ^{Cc} ± 0.005	0.088 ^{Ax} ± 0.003	0.114 ^{Bc} ± 0.004
	Goat	0.091 ^{Cc} ± 0.004	0.057 ^{Ac} ± 0.002	0.082 ^{Bc} ± 0.003
α-HCH	Cattle	0.152 ^{Bd} ± 0.009	0.099 ^{Ac} ± 0.006	0.135 ^{Bd} ± 0.008
	Sheep	0.151 ^{Cd} ± 0.006	0.098 ^{Ad} ± 0.004	0.130 ^{Bd} ± 0.006
	Goat	0.090 ^{Bc} ± 0.005	0.058 ^{Ac} ± 0.003	0.080 ^{Bc} ± 0.004
CPS	Cattle	0.124 ^{Bc} ± 0.007	0.087 ^{Ab} ± 0.005	0.110 ^{Ac} ± 0.006
	Sheep	0.110 ^{Cb} ± 0.004	0.082 ^{Ac} ± 0.003	0.099 ^{Bb} ± 0.004
	Goat	0.071 ^{Bb} ± 0.005	0.054 ^{Ac} ± 0.003	0.064 ^{ABb} ± 0.004
FTN	Cattle	0.040 ^{Ba} ± 0.002	0.031 ^{Aa} ± 0.002	0.036 ^{ABa} ± 0.002
	Sheep	0.059 ^{Ba} ± 0.003	0.044 ^{Aa} ± 0.002	0.054 ^{Ba} ± 0.003
	Goat	0.019 ^{av} ± 0.002	0.015 ^{av} ± 0.002	0.017 ^{av} ± 0.001

A, B, C Different superscript letters denote significant differences within a row ($p \leq 0.05$)

a, b, c, d, e Different superscript letters denote significant differences within each species, between each pesticide ($p < 0.05$)

Conclusion

The goal of this study to develop a simple, accurate, and inexpensive method for the extraction and analysis of six pesticides from three different groups has been achieved. The method developed here can detect of pesticides residues in meat above the level of 0.01 mg/kg. The optimization of chromatographic conditions in this work involved the use of few organic solvents, suitable sample preparation, proper clean up and ensuring good extraction efficiency and response sensitivity. Hence, GC–MS adapted to solid phase extraction, and QuEChERS preparation were successfully employed for the quantification of pesticides residues in animal tissues. All six commonly used pesticides

were found in cattle, sheep and goat samples, and only FTN in cattle and goat samples was lower than MRLs. The process of boiling at 100 °C for 30 min destroyed pesticides significantly, but it cannot reduce the concentration to safe level or below the MRLs, if the residuals begin at high level. Therefore, it is suggested that farmers should use pesticides in recommended amount and butchers should also avoid slaughtering animals directly after treatment with insecticides. Finally, consumers might consume boiled meat and meat products instead of broiled.

Further research could be applied on a wide range of PYRs, OCs and OPs pesticides to strongly find the effects of heat treatment on pesticides regarding their properties such as molecular weight, volatility (vapor pressure), hydrolysis rate and solubility behavior. The use of modified QuEChERS method in this study, for extraction of destroyed pesticides and byproducts after heating and detection by GC could be another part of the next research.

Acknowledgments. The authors would like to thank Food Hygiene laboratory at the College of Veterinary Medicine/University of Sulaimani, for the opportunity to use their specific equipment.

REFERENCES

- [1] Abdulrahman, P. (2016): Determination of a pyrethroid insecticide deltamethrin residues in sheep's and goat's meat in Sulaimaniya Province. – *International Journal of Advanced Biological Research Sciences* 3: 48-53.
- [2] Anastassiades, M., Lehotay, S. J., Štajnbaher, D., Schenck, F. J. (2003): Fast and easy multiresidue method employing acetonitrile extraction/partitioning and “dispersive solid-phase extraction” for the determination of pesticide residues in produce. – *Journal of AOAC International* 86: 412-431.
- [3] Arioli, F., Ceriani, F., Nobile, M., Vigano, R., Besozzi, M., Panseri, S., Chiesa, L. M. (2019): Presence of organic halogenated compounds, organophosphorus insecticides and polycyclic aromatic hydrocarbons in meat of different game animal species from an Italian subalpine area. – *Food Additives & Contaminants: Part A* 36: 1244-1252.
- [4] Castillo, M., Carbonell, E., González, C., Miralles-Marco, A. (2012): Pesticide Residue Analysis in Animal Origin Food. – IntechOpen, London.
- [5] Dimitrova, R. T., Stoykova, I. I., Yankovska-Stefanova, T. T., Yaneva, S. A., Stoyanchev, T. T. (2018): Development of analytical method for determination of organochlorine pesticides residues in meat by GC-ECD. – *Revue Méd. Vét.* 169: 77-86.
- [6] Frenich, A. G., Vidal, J. M., Sicilia, A. C., Rodríguez, M. G., Bolanos, P. P. (2006): Multiresidue analysis of organochlorine and organophosphorus pesticides in muscle of chicken, pork and lamb by gas chromatography–triple quadrupole mass spectrometry. – *Analytica Chimica Acta* 558: 42-52.
- [7] Goldwyn, M., Blonder, G. (2016): *Meathead: The Science of Great Barbecue and Grilling*. – Houghton Mifflin Harcourt, New York.
- [8] Grimalt, S. and Dehouck, P. (2016): Review of analytical methods for the determination of pesticide residues in grapes. – *Journal of Chromatography A* 1433: 1-23.
- [9] Johnson, D., Lorenz, G., Studebaker, G., Hopkins, D. (2010): Ticks on Beef Cattle. *Pest Management News*. – University of Arkansas, University of Arkansas, USDA, and County Governments Cooperating, Carolina.
- [10] Kang, S., Chang, N., Zhao, Y., Pan, C. (2011): Development of a method for the simultaneous determination of six sulfonylurea herbicides in wheat, rice, and corn by liquid chromatography–tandem mass spectrometry. – *Journal of Agricultural and Food Chemistry* 59: 9776-9781.

- [11] Kaonga, C. C., Takeda, K., Sakugawa, H. (2015): Diuron, Irgarol 1051 and Fenitrothion contamination for a river passing through an agricultural and urban area in Higashi Hiroshima City, Japan. – *Sci Total Environ* 15: 450-458.
- [12] Khan, M. S., Rahman, M. S. (2017): *Pesticide Residue in Foods: Sources, Management, and Control*. – Springer International Publishing, Steinhausen.
- [13] Khashan, H. T. (2016): Determination of pyrethroid insecticide deltamethrin residues in cattle meat in Baghdad Province/Al-Rusafa. – *International Journal of Advance Research of Biological Sciences* 3: 193-199.
- [14] Kiranmayi, C. B., Krishnaiah, N., Kumar, M. M., Kumar, M. S., Subhashini, N., Rao, T. M. (2016): Multiresidue analysis of pesticides in beef and mutton samples and study on effect of cooking on residual levels of aldrin and dieldrin. – *International Journal of Environmental Technology* 5: 195-203.
- [15] Lainsbury, M. (2019): *The UK Pesticide Guide 2018*. – British Crop Production Council, Hampshire.
- [16] Lehotay, S. J., Maštovská, K., Yun, S. J. (2005): Evaluation of two fast and easy methods for pesticide residue analysis in fatty food matrixes. – *Journal of AOAC International* 88: 630-638.
- [17] Letta, B. D., Attah, L. E. (2013): Residue levels of organochlorine pesticides in cattle meat and organs slaughtered in selected towns in West Shoa Zone, Ethiopia. – *Journal of Environmental Science and Health, Part B* 48: 23-32.
- [18] MacBean, C. (2015): *The Pesticide Manual*. 15th Ed. – British Crop Protection Council, London.
- [19] Meligy, A., Al-taher, A., Ismail, M., Al-naeem, A., El-bahr, S., El-ghareeb, W. (2019): Pesticides and toxic metals residues in muscle and liver tissues of sheep, cattle and dromedary camel in Saudi Arabia. – *Slov Vet Res* 56: 157-166.
- [20] Muhammad, F., Akhtar, M., Rahman, Z., Farooq, H., Khaliq, T., Anwar, M. (2010): Multi-residue determination of pesticides in the meat of cattle in Faisalabad-Pakistan. – *Egyptian Academic Journal of Biological Sciences* 2: 19-28.
- [21] Muthukumar, M., Reddy, K. S., Reddy, C. N., Reddy, K. K., Reddy, A. G., Reddy, D. J., Kondaiah, N. (2010): Detection of cyclodiene pesticide residues in buffalo meat and effect of cooking on residual level of endosulfan. – *Journal of Food Science and Technology* 47: 325-329.
- [22] Nardelli, V., Casamassima, F., Gesualdo, G., Li, D., Marchesiello, W. M., Nardiello, D., Quinto, M. (2018): Sensitive screening method for determination of pyrethroids in chicken eggs and various meat samples by gas chromatography and electron capture detection. – *Journal of Agricultural and Food Chemistry* 66: 10267-10273.
- [23] Okihashi, M., Kitagawa, Y., Obana, H., Tanaka, Y., Yamagishi, Y., Sugitate, K., Saito, K., Kubota, M., Kanai, M., Ueda, T. (2007): Rapid multiresidue method for the determination of more than 300 pesticide residues in food. – *Food* 1: 101-110.
- [24] Paramasivam, M., Naik, R. H., Chandrasekaran, S. (2011): QuEChERS method for determination of some chlorinated hydrocarbon and synthetic pyrethroid residues in sheep meat by gas chromatography-electron capture detector. – *Madras Agricultural Journal* 98: 282-285.
- [25] Park, J.-W., El-Aty, A. A., Lee, M.-H., Song, S.-O., Shim, J.-H. (2006): Residue analysis of organophosphorus and organochlorine pesticides in fatty matrices by gas chromatography coupled with electron-capture detection. – *Zeitschrift für Naturforschung C* 61: 341-346.
- [26] Peng, G., He, Q., Lu, Y., Mmereki, D., Zhong, Z. (2016): Determination of organophosphorus pesticides and their major degradation product residues in food samples by HPLC-UV. – *Environmental Science and Pollution Research* 23: 19409-19416.
- [27] Sahu, R. K., Nelapati, K. (2018): Method validation for analysis of pesticide residues in *Labeo rohita* fish through GC-MS/MS. – *Int J Chem Std* 6: 1448-1452.

- [28] Schettgen, T., Dewes, P., Kraus, T. (2016): A method for the simultaneous quantification of eight metabolites of synthetic pyrethroids in urine of the general population using gas chromatography-tandem mass spectrometry. – *Analytical and Bioanalytical Chemistry* 408: 5467-5478.
- [29] Stefanelli, P., Santilio, A., Cataldi, L., Dommarco, R. (2009): Multiresidue analysis of organochlorine and pyrethroid pesticides in ground beef meat by gas chromatography-mass spectrometry. – *Journal of Environmental Science and Health Part B* 44: 350-356.
- [30] Vitha, M. F. (2016): *Chromatography: Principles and Instrumentation*. – John Wiley & Sons, Washington.
- [31] Witczak, A. (2009): Effect of heat treatment on organochlorine pesticide residues in selected fish species. – *Polish Journal of Food and Nutrition Sciences* 59: 231-235.
- [32] Yun-Sang, C., Hwang, K. E., Jeong, T. J., Kim, Y. B., Jeon, K. H., Kim, E. M., Sung, J. M., Kim, H. W., Kim, C. J. (2016): Comparative study on the effects of boiling, steaming, grilling, microwaving and superheated steaming on quality characteristics of marinated chicken steak. – *Korean Journal for Food Science of Animal Resources* 36: 1-7.

EFFECTS OF COLCHICINE APPLICATION AND PLOIDY LEVEL ON FRUIT SECONDARY METABOLITE PROFILES OF GOLDENBERRY (*PHYSALIS PERUVIANA* L.)

ÇÖMLEKÇİOĞLU, N.^{1*} – ÖZDEN, M.²

¹*Department of Horticulture, Faculty of Agriculture, Eskişehir Osmangazi University, Eskişehir, Turkey*

²*Faculty of Agricultural Sciences and Technologies, Niğde Ömer Halisdemir University, Niğde, Turkey*

**Corresponding author*

e-mail: ncomlekcioglu@ogu.edu.tr; phone: +90-222-239-3750 fax: +90-222-324-2990

(Received 7th Aug 2019; accepted 28th Nov 2019)

Abstract. The aim of this study was to investigate changes of phenolic accumulation and antioxidant potential of goldenberry fruits collected from diploid plants, under colchicine treatments of different doses and exposure time, including colchicine induced synthetic tetraploid plants. Three colchicine application methods were utilized; i) immersion of seeds in colchicine solution at concentrations of 0.0, 0.6, 0.9% for 24 h and 36 h; ii) keeping germinated seeds (with 2-3 mm long roots) in a colchicine solution with concentrations of 0.6% and 0.9% for 24 h iii) incubation of seeds on semi solid nutrient medium containing 0.6% and 0.9% colchicine for 14 and 21 days. Total antioxidant activity of fruits varied according to the dose and exposure time of colchicine applications. The most important change was observed in the fruits of plants that turned tetraploid as a result of colchicine applications. Tetraploid fruits generally produced higher amounts of secondary compounds compared to diploid progenitors and their antioxidant capacity was also higher. However, the results show that polyploidization is important but cannot be generalized as a strategy to increase secondary metabolite production. It was determined that the relationship between total anthocyanin and total phenolic content with antioxidant capacity of fruits was significant and parallel. We suggest the use of the lowest colchicine concentration tested. 0.6% colchicine to enhance metabolite production cannot be generalized.

Keywords: *tetraploid, anthocyanin, phenolic, flavonoid, antioxidant*

Introduction

Goldenberry (*Physalis peruviana* L.) is a small fruit, belonging to the Solanaceae family. Recently it has gained much attention in our country and in the world, because of its nutritional, medicinal and industrial properties. Goldenberry is most important fruits that is recommended to be consumed as functional drinks and fruit due to high rates of water and oil soluble bioactive substances, vitamins and minerals (Ramadan Hassanien, 2011). Valdenegro et al. (2012) reported that goldenberry is a fruit rich in vitamin C, carotenoids and phenolic compounds. In phytochemical studies, flavonoids, saponins and phenols which are the main compounds in goldenberry fruit extracts, were also determined (Arun and Asha, 2006). It has been reported that goldenberry has a high antioxidant capacity and synergistic effects of different antioxidants. In addition, high levels of phenolic compounds in fruit have been reported (Ramadan and Mörsel, 2003; Ramadan Hassanien, 2011). Phenolic compounds are important in terms of human health as well as their contribution to color, taste and aroma of fruits (Valdenegro, et al., 2012). It is desirable some chemicals in plants to have protective, preventive and therapeutic effects from various diseases in humans.

Recently interest of researchers, in nutrient richness of fruits, vegetables and contain high levels of bioactive compounds that act as antioxidants, have been increasing. Plant breeders are trying to develop polyploid plants in order to increase the yield and certain useful fruit quality properties of the fruit. Polyploids have superior agronomic properties compared to diploids. An increase in the number of chromosomes could improve basic secondary metabolites and concentrations of preservatives (Gao et al., 1996; Głowacka et al., 2010; Hannweg et al., 2016; Nori et al., 2017). It has been reported that enzyme activity (Dhawan and Lavania, 1996; Lavania, 2005), secondary metabolites that are important for taste and flavor and biochemical profiles (Gao et al., 1996; Predieri, 2001; Urwin et al., 2007; Zhang et al., 2010; Caruso et al., 2011; te Beest et al., 2012) in plants improved by polyploidy.

Numerous factors (abiotic and biotic) are directly effective on the biochemical pathways in plants and affect the metabolism of secondary metabolite products (Alkhsabah et al., 2018). Aina et al. (2019) stated that the levels of bioactive compounds and antioxidant activities of tomato fruits cultivated on different soil amendments showed strong relationship between the level of macronutrients in the soil and the level phenolics, flavonoids, beta-carotene and lycopene contents in tomato. Shafiq et al. (2019) reported that selenium content in garlic increased by sodium selenate application. A significant increase in total phenolic content, total flavonoid content and total antioxidant capacity was also observed in the garlic. It has been noted that gibberellic acid had a negative effect on the content of extract, flavonoids and ascorbic acid, while it had no effect on the anthocyanin level. The antioxidant activity determined by the DPPH assay depended on dose and the number of treatments was shown to decrease significantly with increasing application number. Gibberellic acid application had a significantly increased DPPH level compared to the control. The GA3 treatments were shown to have a significant influence on phenolic acid content (Kaplan et al., 2019).

In order to improve the quality of important medicinal compounds, the plants' natural secondary metabolite production potentials, aromatics can be artificially promoted and increased by experimental arrangements. These crops can hold a market value as functional food. The enhance nutrients in food crops is powerful strategy to overcome micronutrient deficiency.

The main purpose of this study were to determine the changes of total anthocyanin, phenolic, flavonoid contents, free radical scavenging capacity and total antioxidant activity of goldenberry fruits by colchicines ($C_{22}H_{25}NO_6$) application to the plants.

Materials and methods

This study was conducted in the University of Eskisehir Osmangazi (Eskisehir, TURKEY) laboratories and greenhouse. *Physalis peruviana* cv. Golden Berry (average fruit diameter is 1-2 inch. Pulp is very flavorful and sweet) was used as plant material in this study. The treated seeds were sown into peat containing plastic seedling tray in the 1st week of March. 45 days old (at 4-5 true leaf stage) seedlings (*Fig. 1*) were transplanted to peat containing pots (15 L) at the end of May in plastic greenhouse.

All plants were irrigated with drip irrigation system (*Fig. 2*) and fertilized with 13 g of 15: 8: 25: 3.5 nitrogen: phosphorus: potassium: magnesium oxide per plant. During the growing season, the average temperature of greenhouse varied between 14-18 °C at night and 22-30 °C at daytime.



Figure 1. Seedling at planting stage



Figure 2. Plants grown in pots and irrigated by drip irrigation system

Colchicine at different doses and exposure times were applied to goldenberry seeds by different methods. Diploid plants that were not treated were evaluated as control. As a result of the applications, chromosomes of some plants were doubled (tetraploid; chromosomes were determined by flowcytometry, Comlekcioglu and Ozden, 2019). Fruits of plants in different application groups were used as material in this study.

Colchicine applications; i) keeping the seeds in colchicine solution (*Fig. 3A*) at 0.0 (T11), 0.6, 0.9% concentration for 24 h and 36 h (T1, T2, T3 and T4); ii) keeping germinated seeds (*Fig. 3B*) with 2-3 mm long roots in colchicine solution at 0.6% (T9) and 0.9% (T10) concentrations for 24 h; and iii) incubation of seeds on semi solid Murashige and Skoog (MS, 1962) medium (*Fig. 3C*) supplemented with colchicine at 0.6% and 0.9% concentrations for 14 and 21 days (T5, T6, T7 and T8).

Twenty seeds for each treatment, with three replications were used. Untreated diploid plants grown from untreated seeds were used as control. Ten plants (*Fig. 4*) with tree replication had been examined within a treatment for the evaluation of phenolic accumulation and antioxidant potential of fruits.

Fruits of plants in different application groups were harvested at full maturity (*Fig. 5*) and fruit weights were determined.

The doses and duration of colchicine applications and application methods are presented in *Table 1*.

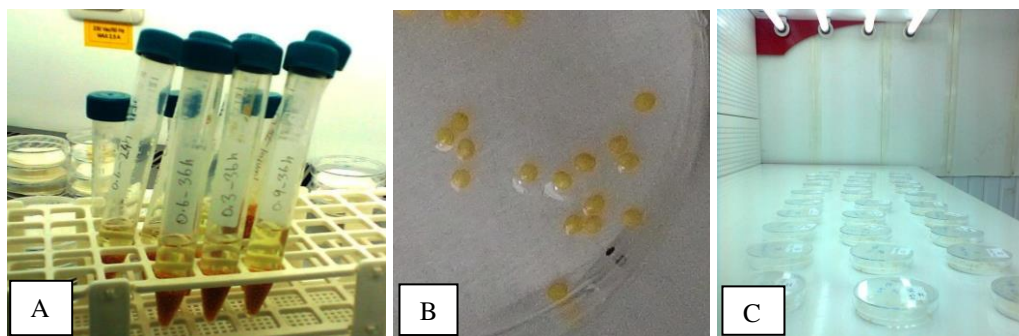


Figure 3. Colchicine application at different doses and exposure time to seeds by different methods. A; keeping the seeds in colchicine solution, B; keeping germinated seeds in colchicine solution C) incubation of seeds on colchicines contained semi solid MS medium



Figure 4. An appearance of growing plants in the greenhouse



Figure 5. Mature fruits used for evaluations phenolic accumulation and antioxidant potential

Table 1. Colchicine application doses, exposure times and application methods

Treatments	Doses %	Exposure times	Application methods
T1	0.6	24 h	Seed
T2	0.6	36 h	Seed
T3	0.9	24 h	Seed
T4	0.9	36 h	Seed
T5	0.6	14 d	MS medium
T6	0.6	21 d	MS medium
T7	0.9	14 d	MS medium
T8	0.9	21 d	MS medium
T9	0.6	24 h	Germinated seed
T10	0.9	24 h	Germinated seed
T11	Control - Diploid control plants		
T12	Tetraploid plants - Colchicine induced		

Extraction of fruit samples

For extraction of the samples, the fruits were mashed in a cold blender. The 25 g homogenate was macerated in darkness for 24 h in 100 ml of ethanol containing 0.1% HCl. The extracts were then filtered through Whatman No.1 filter paper under vacuum and extraction was continued with the same solvent until the pulp was colorless. 50 ml of the extract was separated and used to determine the total amount of anthocyanin. The other 50 ml of the extraction was concentrated on a rotary evaporator by evaporating ethanol at 50 °C and used to determine total phenolic compounds and total flavonoids.

Determination of total anthocyanins (TA)

TA contents of the extracts were determined by pH-differential method (Giusti and Wrolstad, 2001). According to this method, fruit extracts were incubated in 0.025 M KCl buffer (pH 1.0) and 0.4 M CH₃COONa buffer (pH 4.5) for 15 min at room temperature. Absorbance was measured at 520 and 700 nm and the absorbance values were found by Equation 1:

$$A = (A_{\lambda 520} - A_{\lambda 700})_{\text{pH 1.0}} - (A_{\lambda 520} - A_{\lambda 700})_{\text{pH 4.5}} \quad (\text{Eq.1})$$

According to Wrolstad (1976), the total amount of anthocyanin was calculated as follows:

$$\text{TA (mg kg}^{-1}\text{)} = A \times \text{MA} \times \text{DF} \times 1000 / \varepsilon \times 1$$

A: absorbance, MA: Molecular weight of Malvidin-3-O-glucoside; 493.5 g mol⁻¹, DF: Dilution factor, ε, molar absorption coefficient (28,000).

Determination of total phenolic compounds (TP)

TP contents of goldenberry fruit extracts were determined by modification of Slinkard and Singleton (1977) method. 2.37 ml H₂O and 0.15 ml Folin-Ciocalteu's reagent were added to fruit extract (0.03 ml) respectively. After about 8 min, Na₂CO₃

(0.45 ml) was added and the contents were mixed thoroughly. After the mixtures were allowed to stand at room temperature for 30 min, the absorbance measured at 750 nm with spectrophotometer. The concentrations of the total phenolic compounds in the fruit extracts were expressed as mg of gallic acid equivalent (GAE) per kg of fresh weight (FW).

Determination of total flavonoids (TF)

Total flavonoids contents of the samples were determined by aluminum chloride colorimetric method applied by Zhishen et al. (1999). 4 ml H₂O, 5 ml 0.3% NaNO₂ were added to 1 ml of fruit extract or standard catechin solution (20, 40, 60, 80, 100 mg l⁻¹). After 5 min, 0.3 ml of 10% AlCl₃ was added to the mixture. Then at 6 min, 2 ml of 1 M NaOH was added to the mixture and the total volume was completed to 10 ml with H₂O. The solution was mixed thoroughly. The absorbance measured at 510 nm with spectrophotometer. Total flavonide contents of the samples were given in µg catechin equivalent (CE) per g of FW.

Determination of total antioxidant activity (AA)

Antioxidant capacities of ethanolic extracts were determined by the 1,1-diphenyl-2-picrylhydrazyl (DPPH) free radical scavenging, Ferric Reducing Antioxidant Power (FRAP), and Phosphomolybdenum (Mo) methods.

The free radical scavenging capacity of the samples were measured by the 1,1-diphenyl-2-picrylhydrazyl (DPPH) method according to Blois (1958). 2.9 ml of DPPH (0.1 mM) was added to fruit extracts of various concentrations obtained by dilution with ethanol. After 15 min, the absorbance of the mixture was measured at 517 nm. The capacity of each application to reduce free radicals of the sample is determined in% by Equation 2:

$$\text{DPPH Inhibition (\%)} = [(Ac - As) / Ac \times 100] \quad (\text{Eq.2})$$

Ac; control absorbance, As; absorbance of samples.

The determination of total antioxidant capacities of the samples was done by Phosphomolybdenum (MO) and Ferric Reducing Antioxidant Power (FRAP) methods. As described by Prieto et al. (1999) 0.3 ml (20 µg/ml) sample extract was mixed with 1 ml reagent solution (0.6 M sulfuric acid, 28 mM sodium phosphate, 4 mM ammonium molybdate) and incubated for 90 min at 95 °C. After the samples were quickly cooled in crushed ice to room temperature the absorbance at 695 nm was measured. The obtained values were expressed as µg ascorbic acid equivalent (AE) per ml extract by using the ascorbic acid standard curve prepared at different concentrations (20-250 mg ml⁻¹) of ascorbic acid used as positive control.

Ferric Reducing Antioxidant Power (FRAP) were determined according to Oyaizu (1986). 1 ml ethanolic fruit extracts (20 µg ml⁻¹), 2.5 ml phosphate buffer solution (0.2 M pH: 6.6) and 2.5 ml 1% potassium ferricyanate ([K₃Fe (CN)₆] solution were mixed. The mixture was incubated for 20 min at 50 °C and then cooled rapidly in crushed ice. Then, 2.5 ml of 10% trichloroacetic acid (TCA) was added to the mixtures and centrifuged at 2000 rpm for 15 min. The upper layer of the supernatant (2.5 ml) was diluted with distilled water and 0.5 ml of 0.1% FeCl₃ was added. Then the absorbance was read spectrophotometrically at 700 nm against water blank. Using the calibration curve of

Butylhydroxytoluene (BHT) (20-250 mg/ml) at different concentrations used as positive control, the antioxidant activity of the samples was expressed as μg BHT per ml extract.

In the study, all analyzes were measured with three replications. The data presented here are the mean of three replications with \pm SEM. The significance of the mean differences was determined by the least significant differences (LSD) test using the general linear model (GLM) at $P < 0.05$.

Results and discussion

The main objective of this study was to determine the effects of different doses and exposure times colchicine applications, resulted with or without chromosome doubling, on secondary metabolite profiles in goldenberry fruits.

The fruits of plants from different colchicine treatment groups were harvested at commercial maturity stage and 100 fruit weights were determined (*Fig. 6*).

In the study, 100 of the control group fruits were weighed as 356.58 g, followed by the fruits of T6 application group (367.65 g). The heaviest fruits were obtained from tetraploid plants in the T12 treatment group (411.25 g), while the fruit from all other colchicine treatment groups remained low in weight relative to the control (*Fig. 6*).

Total anthocyanin (TA), total phenolic compounds (TP) and total flavonoid content (TF) of the fruits of the plants treated with different colchicine showed significant differences.

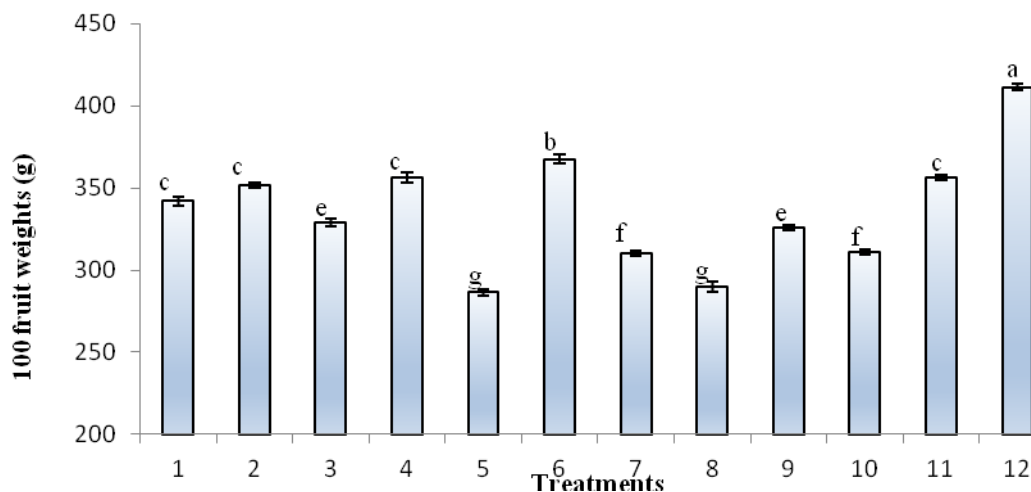


Figure 6. Average weights of 100 fruit measured from different colchicine treatment groups. Different letters on the columns are expressed statistical difference at $P \leq 0.05$ determined by the LSD test

TA content of ethanolic extracts of the goldenberry fruit is given in *Figure 7*. According to the analysis results, the highest (559.60 mg malvidin-3-glucoside kg^{-1} FW) was measured in tetraploid plant fruits, followed by the amount of anthocyanin (539.32 mg kg^{-1}) in T9 fruits. The anthocyanin contents of the tetraploid samples were found to be significantly higher than the control group. Except for the T9 application, the effect of all applications on the anthocyanin contents of the fruits was measured less than the control. TA value of tetraploid fruits increased by 9.1% compared to diploid.

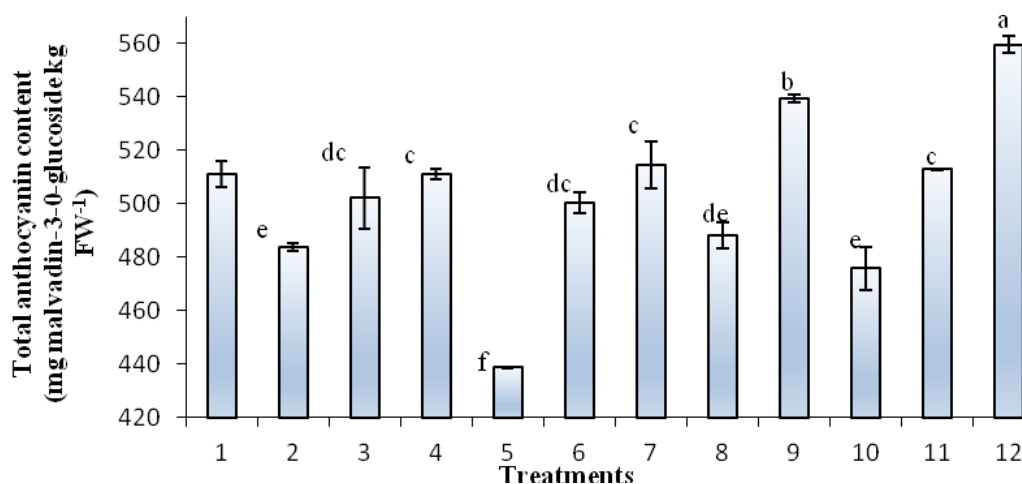


Figure 7. Total anthocyanin content (mg malvidin-3-0-glucoside kg⁻¹ FW) of goldenberry fruits from different colchicine treatment groups. Different letters on the columns are expressed statistical difference at $P \leq 0.05$ determined by the LSD test

TP contents of fruit extracts were expressed as mg GAE kg fresh weight using the gallic acid standard curve (Fig. 8). According to the results of the analysis carried out in the goldenberry fruits under the effect of different colchicine applications, the highest TP content was measured in the fruits of tetraploid plants (1128 mg GAE kg⁻¹ FW). The tetraploid fruits were follow by T1 (1079.0 mg GAE kg⁻¹ FW) T11 and T9 applications (Fig. 8).

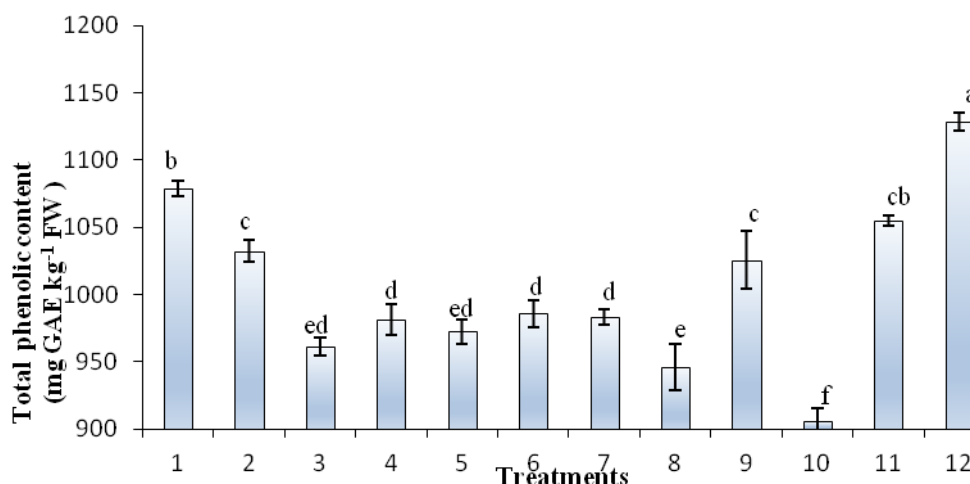


Figure 8. Total phenolic content (mg GAE kg⁻¹ FW) of goldenberry fruits from different colchicine treatment groups. Different letters on the columns are expressed statistical difference at $P \leq 0.05$ determined by the LSD test

In the study, tetraploid fruits phenolic compounds were also found to be richer than control group as in the anthocyanin content. Except for T1 and T12 applications, the effects of other colchicine applications on the TP content of the fruits were limited compared to the control group.

According to the analysis results, TF contents of fruits ranged from 579.38 $\mu\text{g CE g}^{-1}$ FW (T10) to 1282.02 $\mu\text{g CE g}^{-1}$ FW (T2). Unlike TA and TP, the increase in TF was found to be independent of chromosome doubling. The highest value was obtained from T2 application. This value was followed by flavonoid contents measured in T9 (961.84 $\mu\text{g CE g}^{-1}$ FW) and T5 (906.57 $\mu\text{g CE g}^{-1}$ FW) fruits. Fruits from T2 and T12 (tetraploid fruits) treatments had 88.7% and 21.95% respectively higher TF content than diploid progenitor control group. Tetraploid fruits showed an increasing tendency compared to diploids. Except for T3 and T10 treatments, the effects of colchicine applications on the TF contents of fruits were found to be significant compared to the control (*Fig. 9*).

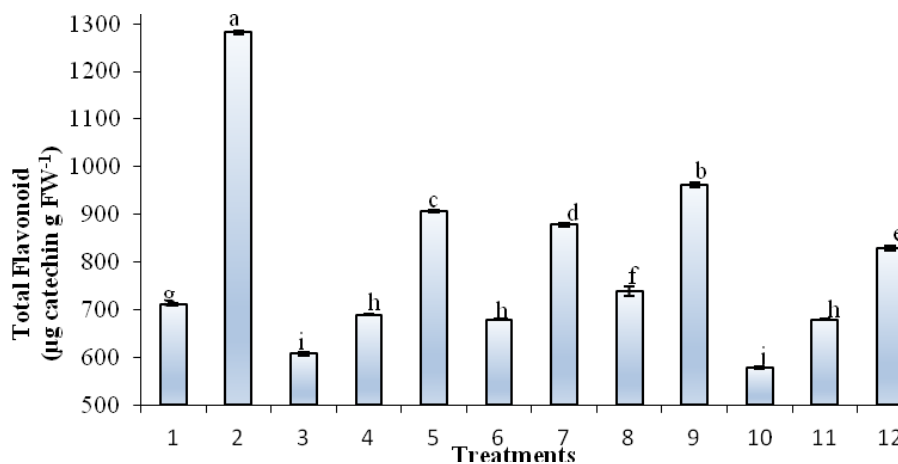


Figure 9. Total flavonoid content ($\mu\text{g CE g}^{-1}$ FW) of goldenberry fruits from different colchicine treatment groups. Different letters on the columns are expressed statistical difference at $P \leq 0.05$ determined by the LSD test

The free radical scavenging capacity of fruit samples was determined by using a synthetic, stable free radical molecule of 1,1-diphenyl-2-picrylhydrazyl (DPPH) (Blois, 1958).

The ethanolic extracts of the fruits of the plants with different colchicine treatment groups were found to have different free radical scavenging capacity, and the highest inhibition capacity was determined in fruit of tetraploid plants.

When DPPH free radical scavenging capacity was compared between the application groups, the highest value (65.96%) compared to the control (50.82%) was measured in tetraploid fruits (*Fig. 10*).

The increase rate of free radical scavenging capacity in tetraploid fruits was 29.79% compared to diploid progenitors. These results show that antioxidant capacity (DPPH inhibition) in fruit was increased rather associated with chromosome doubling, as well as increasing TA and TP values. The effectiveness of other treatments was limited compared to the control and was found to be statistically insignificant. Results of total antioxidant activity of the samples determined by phosphomolybdenum method are given in *Figure 11*. The highest antioxidant capacity of fruit samples (130.03 $\mu\text{g AE ml}^{-1}$ extract) was determined in tetraploid (T12) fruit samples.

As in the DPPH results, T12 was followed by T8 (116.57 $\mu\text{g GAE ml}^{-1}$ extract) and T1 (114.926 $\mu\text{g GAE ml}^{-1}$ extract). The effectiveness of other applications was considered to be limited or statistically insignificant compared to the control.

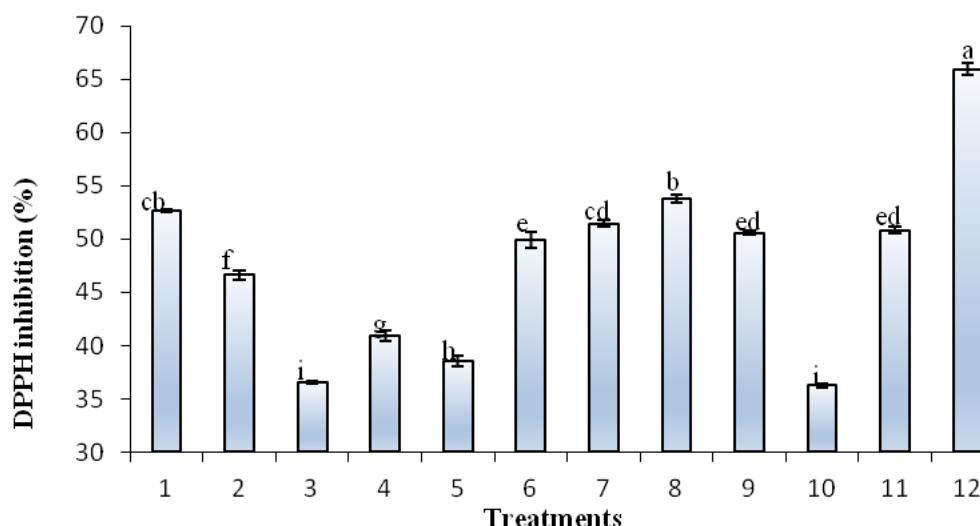


Figure 10. DPPH free radical scavenging activity (%) of goldenberry fruit extracts from different colchicine treatment groups. Different letters on the columns are expressed statistical difference at $P \leq 0.05$ determined by the LSD test

The total antioxidant capacity of the fruits determined by the MO method was similar to the values determined by the DPPH method. Although different colchicine applications cause increasing or decreasing effects compared to control fruits, it was determined that the most important increase was obtained due to polyploidy (Fig. 11).

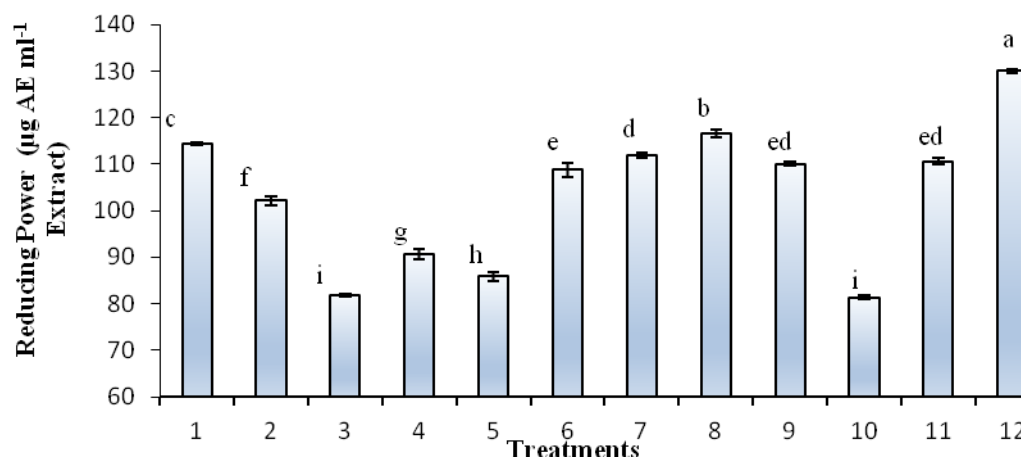


Figure 11. Antioxidant activity ($\mu\text{g AE ml}^{-1}$ extract) of goldenberry fruit extracts from different colchicine treatment groups determined by phosphomolybdenum method (reduction of Mo-VI to Mo-V). Different letters on the columns are expressed statistical difference at $P \leq 0.05$ determined by the LSD test

When the antioxidant capacity of ethanolic fruit extracts from different colchisin applications were evaluated, the highest value was determined as 218.85 ($\mu\text{g BHT ml}^{-1}$ extract) in T2 application fruit samples. This was followed by T1 (107.35 $\mu\text{g BHT ml}^{-1}$ extract), and fruit extracts from T9 treatment (83.21 $\mu\text{g BHT ml}^{-1}$ extract) (Fig. 12).

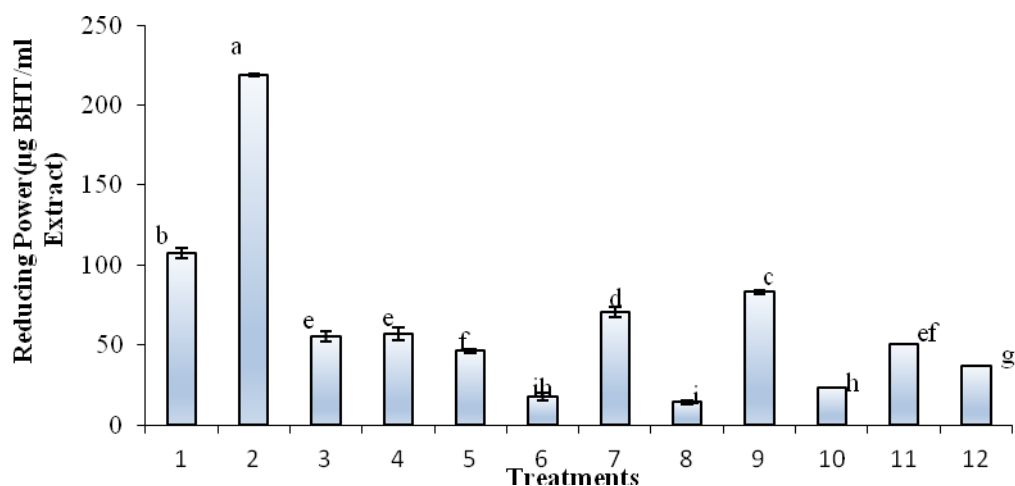


Figure 12. Ferric Reducing Antioxidant Power (FRAP) ($\mu\text{g BHT ml}^{-1}$ extract) of goldenberry ethanolic fruit extracts from different colchicine treatment groups. Different letters on the columns indicate the difference at $P \leq 0.05$ level determined by the LSD test

According to the data obtained from the research, the secondary metabolite contents of diploid, colchicine treated and tetraploid plants showed significant differences. The amount of anthocyanin and phenolic compounds of tetraploid fruits was higher than diploid and colchicine treated fruits.

Different colchicine applications significantly affected the TA content of fruits ($P \leq 0.05$).

Among colchicine applications that could not induce chromosomes doubling, TA increases were determined in T9 compared to control. However, the greatest increase in TA content was determined by the increase in ploidy level. The highest TA ($559.59 \text{ mg kg}^{-1}$) was reached in the tetraploid fruits (Fig. 7). TA value of tetraploid fruits increased by 9.1% compared to diploid. As a result of colchicine applications, the change in total phenolic content of fruits was found to be significant. Total phenolic contents ranged from $905.77 \text{ mg GAE kg}^{-1}$ fresh weight to $1128.00 \text{ mg GAE kg}^{-1}$ fresh weight (Fig. 8). As in TA content, the highest value was also determined in tetraploid fruits. It was determined that the effects of different colchicines applications on the total flavonoid content of the fruits were significant. Total flavonoids of the fruits ranged from $579.38 \mu\text{g KE g}^{-1}$ fresh weight (T10) to $1282.02 \mu\text{g KE g}^{-1}$ fresh weight (T2) (Fig. 9). Tetraploids showed an increasing tendency compared to diploid fruits. Colchicine application also caused an increase in TF compared to control, except T3 and T10 treatments. Among applications T2 fruits showed 88.7%, and T12 (tetraploid) fruits 21.95% higher TF contents than control (diploid progenitor) (Fig. 8).

The antioxidant capacities of the samples, expressed as DPPH scavenging (%) extract concentrations, were strongly influenced by colchicine applications. Increases and decreases were determined in different treatments compared to the control and tetraploid fruits (T12) had higher DPPH sweeping capacity than all other treatments (Fig. 10). The increasing rate in tetraploid fruits was 29.79% compared to diploid progenitor (Fig. 10). These results show that antioxidant capacity (DPPH inhibition) in fruit is increased in association with chromosome doubling, as in the increase in TA and TP values. In this study, total antioxidant capacity of the fruits determined by FRAP

method decreased in contrast to increasing ploidy level. FRAP values were the highest in T2 (218.85 µg BHT ml⁻¹ extract) and T1 (107.35 µg BHT ml⁻¹ extract).

As a result of this research, total phenolic and flavonoid content of fruits of plants with different colchicine application and different ploidy level the samples swept the DPPH free radical and the Mo (VI) (*Fig. 11*) ions were reduced. The results presented in this study clearly indicate that the antioxidant activity was correlated with the phenolic content of fruits own.

In addition T3, T4, T7 and T9 treatments showed significantly higher antioxidant capacity than both diploid and tetraploid fruits with FRAP method (*Fig. 12*). Consistent with the results of this research, according to Özden and Özden (2014) research on 14 different fruit varieties, it is stated that antioxidant properties of fruits are related to total phenolic content of fruits.

Conclusions

Oxidation, a side effect of numerous physiological and biochemical processes in the human body, is an important and natural process. In many ways it is good, but it has the potential to be bad. In case of high oxidation, the body's aging and rusting rate increases. Damage caused by free radicals can be prevented by free radicals bounding to an antioxidant and swept from the body without damaging other cells. Therefore, high antioxidant content of foods slows down the aging process. The quantity of important medicinal compounds, aromatics, natural secondary metabolite production and antioxidant potentials of the plants can be artificially enhanced by experimental arrangements. Caruso et al. (2013) reported that tetraploid genotypes of *Solanum bulbocastanum* exhibited either a similar or a lower phenylpropanoids, tryptophan, tyrosine and chaconine content compared to the diploid parent.

Although fruits of tetraploid plants generally produce higher amounts of secondary compounds than diploid progenitors and have higher antioxidant capacities, our results show that polyploidization is important as a strategy to increase secondary metabolite production, but it cannot be generalized. It was determined that the relationship between total anthocyanin and total phenolic contents and antioxidant capacity of fruits was significant and parallel. Finally, colchicine can be used for polyploidization as strategy and we suggest the use of the lowest colchicine concentration tested, 0.6% colchicine to enhance metabolite production cannot be generalized.

Acknowledgement. This article is a part of research project No. 2013-191 supported by the Scientific Research Projects Commission of Eskisehir Osmangazi University.

REFERENCES

- [1] Alkhsabah, I. A., Alsharafa, K. Y., Kalaji, H. M. (2018): Effects of abiotic factors on internal homeostasis of *Mentha spicata* leaves. – Applied Ecology and Environmental Research 16(3): 2537-2564.
- [2] Aina, O. E., Amoo, S. O., Mugivhisa, L. L., Olowoyo, J. O. (2019): Effect of organic and inorganic sources of nutrients on the bioactive compounds and antioxidant activity of tomato. – Applied Ecology and Environmental Research 17(2): 3681-3694.

- [3] Arun, M., Asha, V. V. (2006): Preliminary studies on antihepatotoxic effect of *Physalis peruviana* Linn. (Solanaceae) against carbon tetrachloride induced acute liver injury in rats. – *Journal of Ethnopharmacology* 111: 110-114.
- [4] Blois, M. S. (1958): Antioxidant determinations by the use of a stable free radical. – *Nature* 181: 1199-1200.
- [5] Caruso, I., Lepore, L., De Tommasi, N., Dal Piaz, F., Aversano, R., Garramone, R., Carputo, D. (2011): Secondary metabolite profile in induced tetraploids of wild *Solanum commersonii* Dun. – *Chemistry & Biodiversity* 8: 2226-2237.
- [6] Caruso, I., Dal Piaz, F., Malafrente, N., De Tommasi, N., Aversano, R., Zottele, C. W., Scarano, M. T., Carputo, D. (2013): Impact of ploidy change on secondary metabolites and photochemical efficiency in *Solanum bulbocastanum*. – *Natural Product Communications* 8: 1387-1392.
- [7] Comlekcioglu, N., Ozden, M. (2019): Polyploid induction by colchicine treatment in goldenberry (*Physalis peruviana*), and effects of polyploidy on certain traits. – *The J. Anim. Plant Sci.* 29(5): 1336-1343.
- [8] Dhawan, O. E., Lavania, U. C. (1996): Enhancing the productivity of secondary metabolites via induced polyploidy: a review. – *Euphytica* 87: 81-89.
- [9] Gao, S. L., Zhu, D. N., Caiz, H., Xu, D. R. (1996): Autotetraploid plants from colchicine-treated bud culture of *Salvia miltiorrhiza* Bge. – *Plant Cell, Tissue and Organ Culture* 47: 73-77.
- [10] Głowacka, K., Jezowski, S., Kaczmarek, Z. (2010): In vitro induction of polyploidy by colchicine treatment of shoots and preliminary characterisation of induced polyploids in two *Miscanthus* species. – *Ind Crops Prod* 32: 88-96.
- [11] Giusti, M. M., Wrolstad, R. E. (2001): Characterization and Measurement of Anthocyanins by UV-Visible Spectroscopy. – In: Wrolstad, R. E. (ed.) *Current Protocols in Food Analytical Chemistry*. John Wiley & Sons, New York.
- [12] Hannweg, K., Visser, G. de Jager, K., Bertling, I. (2016): In vitro-induced polyploidy and its effect on horticultural characteristics, essential oil composition and bioactivity of *Tetradenia riparia*. – *S Afr J Bot* 106: 186-191.
- [13] Kaplan, M., Najda, A., Klimek, K., Borowy, A. (2019): Effect of gibberellic acid (GA3) inflorescence application on content of bioactive compounds and antioxidant potential of grape (*Vitis* L.) ‘Einset seedless’ berries. – *S. Afr. J. Enol. Vitic.* 40(1). DOI: <http://dx.doi.org/10.21548/40-1-3004>.
- [14] Lavania, U. C. (2005): Genomic and ploidy manipulation for enhanced production of phyto-pharmaceuticals. – *Plant Genetic Resources* 3(2): 170-177.
- [15] Murashige, T., Skoog, F. (1962): A revised medium for rapid growth and bioassay with tobacco tissue cultures. – *Physiol. Plant.* 15: 473-497.
- [16] Noori, S. A. S., Norouzi, M., Karimzadeh, G., Shirkoob, K., Niazi, M. (2017): Effect of colchicine-induced polyploidy on morphological characteristics and essential oil composition of ajowan (*Trachyspermum ammi* L.). – *Plant Cell Tiss Organ Cult.* 130: 543-551.
- [17] Oyaizu, M. (1986): Studies on product of browning reaction prepared from glucose amine. – *Japanese Journal of Nutrition* 44: 307-315.
- [18] Özden, M., Özden, A. N. (2014): Comparison of different coloured fruits in terms of total anthocyanins total phenolics and total antioxidant capacity. – *Electronic Journal of Food Technologies* 9(2): 1-12.
- [19] Predieri, S. (2001): Mutation induction and tissue culture in improving fruits. – *Plant Cell, Tissue and Organ Culture* 64: 185-210.
- [20] Prieto, P., Pineda, M., Aguilar, M. (1999): Spectrophotometric quantitation of antioxidant capacity through the formation of a phosphomolybdenum complex: specific application to the determination of vitamin E. – *Analytical Biochemistry* 269(2): 337-341.

- [21] Ramadan Hassanien, M. F. (2011): *Physalis peruviana*: a rich source of bioactive phytochemicals for functional foods and pharmaceuticals. – *Food Reviews International* 27: 259-273.
- [22] Ramadan, M. F., Mörsel, J. T. (2007): Oil goldenberry (*Physalis peruviana* L.). – *Journal of Agricultural Food Chemistry* 51: 969-974.
- [23] Shafiq, M., Qadir, A., Ahmad, S. R. (2019): Biofortification: a sustainable agronomic strategy to increase selenium content and antioxidant activity in garlic. – *Applied Ecology and Environmental Research* 17(2): 1685-1704.
- [24] Slinkard, K., Singleton, V. L. (1977): Total phenol analysis: automation and comparison with manual methods. – *American Journal of Enology and Viticulture* 28: 49-55.
- [25] te Beest, M., Le Roux, J. J., Richardson, D. M., Brysting, A. K., Suda, J., Kubesova, M., Pysek, P. (2012): The more the better? The role of polyploidy in facilitating plant invasions. – *Ann Bot* 109: 19-45.
- [26] Urwin, N. A. R., Horsnell, J., Moon, T. (2007): Generation and characterisation of colchicine-induced autotetraploid *Lavandula angustifolia*. – *Euphytica* 156: 257-266.
- [27] Valdenegro, M., Fuentes, L., Herrera, R., Moya-León, M. A. (2012): Changes in antioxidant capacity during development and ripening of goldenberry (*Physalis peruviana* L.) fruit and in response to 1-methylcyclopropene treatment. – *Postharvest Biology and Technology* 67: 110-117.
- [28] Zhang, X. Y., Hu, C. G., Yao, J. L. (2010): Tetraploidization of diploid dioscorea results in activation of the antioxidant defense system and increased heat tolerance. – *Journal of Plant Physiology* 167(2): 88-94.
- [29] Zhishen, J., Mengcheng, T., Jianming, W. (1999): Determination of flavonoid contents in mulberry and their scavenging effects on superoxide radicals. – *Food Chemistry* 64: 555-559.

RESIDUAL EFFECT OF ORGANIC MANURE AND RECOMMENDED NPK FERTILIZER ON YIELD AND BULB PERFORMANCE OF ONION (*ALLIUM CEPA* L.) AS SECOND CROP UNDER GREENHOUSE CONDITIONS

YOLDAS, F.^{1*} – CEYLAN, S.¹ – MORDOGAN, N.²

¹Department of Organic Production, Ödemiş Vocational Training High School, Ege University
35750 İzmir, Turkey

²Department of Soil Science and Plant Nutrition, Faculty of Agriculture, Ege University
35100 İzmir, Turkey

*Corresponding author

e-mail: funda.yoldas@ege.edu.tr; phone: +90-542-322-5385; fax: +90-232-544-4356

(Received 28th Aug 2019; accepted 25th Nov 2019)

Abstract. This study was conducted to determine the residual effects of chicken manure on the yield and yield performance of eight onion varieties as second crops after lettuce under greenhouse condition. 14-16, Burgaz, Karbeyazı, Naz, NWG, Perwana, Seyhan, Şampiyon varieties and also four different doses of chicken manure at the rates of 0, 20, 40, 60 t ha⁻¹ with the recommended dose of NPK were used. A non-fertilized parcel was used as control. The experiment was laid out in split plot design and replicated three times. Yield and yield components were investigated. According to the results residual effect of chicken manure and onion varieties as second crop significantly affected the yield and bulb production in the greenhouse condition. The application of chicken manure significantly improved yield, bulb weight, bulb height, number of shoot tip, number of dried leaf compared to control. Highest yields (72.99 t ha⁻¹) were obtained in the parcels where the chicken manure was applied at a rate of 20 t ha⁻¹. The onion cultivar Burgaz was more responsive to the chicken manure compared to other onion cultivars. The best yield was shown of Burgaz cultivar and the 20 t ha⁻¹ chicken manure treatments by the interaction. As a result, this method is the most suitable for onion production.

Keywords: residual effect, organic manure, NPK, second crop, greenhouse, onion growth characters, macro-micro elements

Introduction

Onions are members of the *Allium* genus of flowering plants that also includes garlic, shallots, leeks and chives. Onion is rich in several phytonutrients that are recognized as important elements of the Mediterranean diet but it has received attention also for its biological properties and potential application in the treatment and prevention of a number of diseases (Lim, 2015; Marrelli et al., 2019). Onion (*Allium cepa* L.) is also a vegetable that is widely consumed due to its flavoring and health-promoting properties. Onions have many possible health benefits including reducing the risk of obesity, heart disease, and cancer. Onion bulb is a rich source of minerals like phosphorus, calcium, magnesium, iron, manganese and carbohydrates. It also contains protein, Vitamin C, Vitamin B6 and antioxidants and is rich in sulphur amino acids (Ware, 2017). Moreover, a variety of secondary metabolites have been identified in this species, such as flavonoids (particularly flavonols and anthocyanin), phytosterols and saponins (Griffiths et al., 2002; Marrelli et al., 2019).

According to the statistics, Turkey's bulb onion production is 1 930 695 tons over a 53 000-hectare area (Anonymous, 2018).

Healthy life and environmental consciousness are important today. In this case it caused to increase on naturel feeding. With the development and perfection of market economy, agriculture and rural economy is coming to a new stage and the lives of people working in this sector, since there is now a demand for production of safe and high quality agricultural products (Liu et al., 2011). The reasonable use of organic manure can improve soil fertility and microbial content, decrease soil nitrogen accumulation and leaching loss, increase yield and quality, and improve human ecological environment (Yi et al., 2004; Gao et al., 2005; Liu et al., 2011).

Pollution with chemical fertilizers arose as an aim of health care, thus attempts were made for solving problems of chemical fertilization, and the organic farming technique represents a move towards an alternative system of agriculture (Abd-Allah et al., 2001; Yassen and Khalid, 2009). Organic material, such as sheep and chicken manure, improves soil physical properties (structure and aggregation) and soil chemical properties (decrease soil pH, increase cation exchange capacity and enhance most nutrients) that are important for plant growth (Snyman et al., 1998; Yassen and Khalid, 2009). Using of chemical matter was decreased and naturel productions get importance. But soil fertility is important in this case. Organic matter improves soil's physical, chemical, biological properties and is also effect the availability of nutrient. But high level organic material in soils especially in dry conditions may be caused unable effects and also it can create organo-mineral complex and it reduced the availability of some mineral (Sezen, 1995). Animal fertilizers are major source of organic matter for soil.

Organic fertilizer has been widely used as alternative fertilizers for organically grown fields (Jongtae, 2010). Organic manures can serve as alternative to mineral fertilizers as reported by Naeem et al. (2006) for improving soil structure (Dauda et al., 2008) and microbial biomass (Suresh et al., 2004).

Organic material, such as farmyard manure improves soil physico-chemical properties that are important for plant growth (Snyman et al., 1998). Decomposition of materials would provide additional nutrients to the growing medium which may lead to higher uptake of nutrient by the crop and subsequently high yield. Besides, organic manures have positive effect on root growth by improving the root rhizosphere conditions (structure, humidity, etc.) and also plant growth is encouraged by increasing the population of microorganisms (Shaheen et al., 2007; Kidanu, 2017).

Comparisons of conventional and organic farms matched by soil type indicated that organic practices improved soil fertility (Liebig and Doran, 1999). This included a 22% increase in organic matter, 20% more total N, lower bulk density and higher water holding capacity.

Organic farming provides several benefits to the growers. It reduces production cost and it is an environmentally friendly method of cultivation. Addition of organic fertilizers improves soil structure and enhances activities of useful soil organisms (Snyman et al., 1998; Ramesh et al., 2005). Agricultural commodities resulted from organic cultivation are good for human health. however, organic manures alone cannot provide sufficient quantities of required nutrients and are unable to give economic yield and hence, it is vital to find appropriate combinations of inorganic and organic manure to obtain financially viable yield of crops. Jayathilake et al. (2006) reported that integrated use of bio-fertilizer, organic manure and chemical fertilizers resulted in onion yield increase in comparison with the exclusive application of chemical fertilizers (Kidanu, 2017).

Organic manure increases the nutrient status of a soil which leads to increase in onion yield (Akoun, 2004; Kidanu, 2017).

Boyhan and Hill (2008) found that fertilizer requirements were higher with organic fertilizer sources compared with conventional fertilizers presumably because nutrients were less available in organic compounds due to slow mineralization rates.

Work has been done to predict the availability of plant nutrients from organic sources over time. Whitmore (2007), for example, found that 40% of the total N from composted chicken manure was available in the first year, with the remainder available in subsequent years at a rate of 6% to 12% per year.

A number of studies have been conducted evaluating the organic production of onions (Piazza et al., 2003; Sharma et al., 2004; Gonçalves and Sousa e Silva, 2004; Beek, 2005; Russo, 2005; Boyhan et al., 2006; Boyhan and Hill, 2008). These studies have evaluated fertility, insect control, weed control, transplant production, various cropping systems, and varieties (George et al., 2010; Ewais et al., 2010). Many researchers reported that soil application of chicken manure increased yield and yield criteria of onion (Shaheen et al., 2007; Dina et al., 2010; El-Shatanofy and Manar, 2011; Yoldas et al., 2011; Ali et al., 2018).

Onion shows significant response to organic and inorganic fertilizers (Nasreen and Hossain, 2000; Soleymani and Shahrajabian, 2012; Kidanu, 2017). Therefore, the usage of organic manures as alternative source of nitrogen would give better result in its growth and yield.

The objective of this study was to evaluate residual effect of organic manure and recommended NPK fertilizer on yield and bulb performance of onion (*Allium cepa* L.) as second crop under greenhouse condition.

Materials and Methods

The study was carried out in experimental area of the Ödemiş Vocational School, at the Ege University, in İzmir (38°16'N, 27°59'E), Turkey during the 2017 year. The experimental designs were split plot with three replications. Before sowing of lettuce, the chicken manure was applied to soil at the rates of 0 – 20 – 40 – 60 t ha⁻¹ and also recommended dose of NPK (150:100:150 kg ha⁻¹). Mineral fertilizers have applied as NH₄NO₃ and K₂SO₄ formulated product. Five different treatments with control and three replications were conducted in 15 plots. In the control treatment neither organic nor mineral fertilization had been done. Lolla Rossa lettuce variety was sown and harvested at the end of vegetation. After harvesting the lettuce plant, onion varieties were sown in order to determine the residual effect of chicken manure and chemical fertilizer in greenhouse conditions. No nutrient addition was made for onion. In this study, during the growth period, weeds were removed by hand hoeing and irrigation was done on a regular basis. The spraying procedures and plant protection were regularly applied throughout the production.

Eight onion varieties called 14-16, Burgaz, Karbeyazı, Naz, NWG, Pewana, Seyhan, Şampiyon were used. They are long day / storage. Their fruits are a round, brown-shelled, widely known and kept Variety on the market due to its uniform nature. Due to their very strong root structure. Resistant to pink root rot and Fusarium. *Allium cepa* L. was planted in each plot with 30 cm between rows and 15 cm within the rows. Total plot length is 11.5 m and plot width is 6.2 m.

The composition of chicken manure that residual effect investigated was analyzed according to Kacar (1995) and is presented in *Table 1*.

Soil samples (0-20 cm) were collected from the individual experimental plots (15 samples) at the beginning of onion vegetation. The soil sample was air dried, ground, and passed through 2 mm sieve for the determination of chemical parameters. pH (Jackson, 1967), total soluble salt (Anonymous, 1951), CaCO₃ (Kacar, 1995), organic matter content (Reuterberg and Kremkurs, 1951) were determined in the soil. Total N was also analyzed according to Bremner (1965), the available K⁺, was determined after extracting with 1 N NH₄OAc by flame photometer (Atalay et al., 1986) and available P was measured by colorimeter (Olsen et al., 1954).

Table 1. Some properties of chicken manure

pH	8.55	C/N	12.1
Total Salt (ms/cm)	2.47	P (%)	0.70
Ash 550 °C (%)	79	K (%)	1.02
Organic Matter (%)	19.8	Ca (%)	1.37
Organic Carbon (%)	11.51	Mg (ppm)	3729
Total N (%)	0.95	Na (ppm)	1248

At the end of the vegetation, onions were harvested. Average bulb head weight, bulb height, bulb width and flesh thickness, number of storage leaf, number of shoot tip, and number of dried leaf were determined as growth and yield parameters.

Ten randomly selected plants were harvested from each plot (avoiding side effect) to record the data on data set for all characters. Bulb length and diameter refers to the height of the bulb and the average width at the widest point in the middle portion of the mature bulb measured using vernier caliper. Average bulb weight computed by weighing ten bulbs together and calculating the average. Total bulb yield was computed based on the weight of matured bulbs yield per plot and converted in to hectare base and expressed in tones. Marketable bulb yield was determined after discarding bulbs smaller than 3 cm in diameter, splitted, thick necked, rotten and discolored. Split bulbs percentage was determined by counting the number of split bulbs per plot and expressed in percentage in reference to total number of normal bulbs per plot.

The collected data on various parameters were statistically analyzed. Analysis of variance was computed and LSD was used to compare means. Trial statistical evaluation result of data was done using software package TARIST (Açikgöz et al., 1993).

Results and Discussion

Soil properties

Some chemical properties and macro-micro nutrient contents of greenhouse trial soil before onion sowing are presented in *Tables 2 and 3*. pH, organic matter, lime, P, K, Ca, Mg, Na, Fe, Zn, Mn, Cu values in the soil did not show any statistical difference between applications at the beginning of vegetation. On the contrary, total N content of the soil was significantly affected by the applications. The highest values (0.084%) were analyzed in the parcels which the chicken manure was applied as 40 t ha⁻¹.

Before onion sowing, greenhouse soil properties are neutral (6.6-7.3) except the parcels which the chicken manure was applied as 20 t ha⁻¹. However, in this application, soils showed slightly alkaline properties (7.4-7.8). Low humus (1.33-1.61%) and lime (0-2.5%) poor. When the productivity status of the soil is investigated, N is moderate

(0.05-0.1%); K (< 150 ppm), Ca (715-1430 ppm) poor; rich in P (3.26 ppm); Mg (> 114 ppm) is good; Fe (> 4.5 ppm), Zn (> 1 ppm), Mn (> 1 ppm) and Cu (> 0.2 ppm) is determined to be sufficient according to Güneş et al. (2000).

Table 2. Some chemical properties of greenhouse trial soils at the beginning of onion vegetation

Treatment	pH	O.M. (%)	CaCO ₃ (%)
0	7.24	1.57	0.92
NPK	7.25	1.47	0.43
20 t ha ⁻¹	7.44	1.61	0.86
40 t ha ⁻¹	7.29	1.33	0.42
60 t ha ⁻¹	7.15	1.47	0.36
LSD	n.s.	n.s.	n.s.

**: p<0.01; *: p<0.05; n.s.: not significant

Table 3. Macro-micro nutrient contents of greenhouse trial soils at the beginning of vegetation

Treatment	Total N	P	K	Ca	Mg
	(%)	(mg kg ⁻¹)	(mg kg ⁻¹)	(mg kg ⁻¹)	(mg kg ⁻¹)
0	0.056 c	51.30	104.4	1386	323
NPK	0.078 ab	56.35	133.5	1023	305
20 t ha ⁻¹	0.067 bc	60.51	133.4	1254	303
40 t ha ⁻¹	0.084 a	63.45	136.4	1188	318
60 t ha ⁻¹	0.081 ab	62.05	146.5	1221	308
LSD	0.015**	n.s.	n.s.	n.s.	n.s.

Treatment	Na	Fe	Zn	Mn	Cu
	(mg kg ⁻¹)	(mg kg ⁻¹)	(mg kg ⁻¹)	(mg kg ⁻¹)	(mg kg ⁻¹)
0	35.3	29.49	5.30	14.57	2.92
NPK	26.0	23.16	4.40	12.93	2.73
20 t ha ⁻¹	25.8	23.51	4.71	13.45	2.65
40 t ha ⁻¹	32.0	27.13	4.72	13.91	2.78
60 t ha ⁻¹	57.7	23.58	5.33	14.31	2.83
LSD	n.s.	n.s.	n.s.	n.s.	n.s.

**: p<0.01; *: p<0.05; n.s.: not significant

Onion yield and yield characteristics

Residue effect of chicken manure on yield and some quality criteria of onion as second crop after the lettuce production are given in *Table 4*.

Yield

In the greenhouse condition, the results showed significant differences in yield amongst treatments (p< 0.01) (*Table 4*). Highest yields (72.99 t ha⁻¹) were obtained in the parcels which the chicken manure was applied as 20 t ha⁻¹. This application increased yield by 8% compared to the control plots. But there is no statistically significant difference in yield between mineral fertilizer and 20 t ha⁻¹ of chicken manure application. Similarly, Rumpel (1998), Sharma et al. (2003), Yoldas et al. (2011), Indira and Singh (2014) and Zewde et al. (2018) found that animal manure applications increased onion yield.

Many researchers also reported similar results that soil application of chicken manure increased yield and yield criteria of onion (Shaheen et al., 2007; Dina et al., 2010; El-Shatanofy and Manar, 2011; Yoldas et al., 2011; Ali et al., 2018).

Organic manures activate many species of living organisms which release phytohormones and may stimulate the plant growth and absorption of nutrients (Arisha et al., 2003). Organic manures improved the water holding capacity of soil and provide nutrients for a long duration due to less leaching of nutrients and increase efficiency (Carol et al., 1999). Mahala et al. (2018) reported that the increased yield and yield parameters with poultry manure might be because of rapid availability and utilization of nitrogen for various internal plant processes for carbohydrates production. Later on these carbohydrates may undergo hydrolysis and get converted into reproductive sugars which ultimately helped in increasing yield.

Table 4. Residue effect of chicken manure on yield and some quality criteria of onion as second crop in the greenhouse condition

Treatment	Yield	Bulb weight	Bulb width	Bulb height	Number of stored leaf	Number of shoot tip	Number of dried leaf
	(t ha ⁻¹)	(g no ⁻¹)	(cm)	(cm)	(no)	(no)	(no)
0	67.54 bc	202.641 bc	7.265 ab	7.491 a	2.188 c	1.569 b	6.830 c
NPK	71.87 ab	215.638 ab	7.377 ab	7.513 a	2.278 b	1.722 a	7.111 b
20 t ha ⁻¹	72.99 a	219.006 a	7.494 a	7.329 b	2.313 b	1.730 a	7.395 a
40 t ha ⁻¹	66.02 c	198.068 c	7.188 b	7.368 b	2.430 a	1.666 a	6.757 c
60 t ha ⁻¹	66.91 c	200.735 c	7.396 ab	7.054 c	2.097 d	1.694 a	6.742 c
LSD	4.418**	13.255**	0.267**	0.097**	0.081**	0.077**	0.196**

** : p<0.01; * : p<0.05; n.s.: not significant

Similar results were found by Jongtae (2010). In that research, no significant yield difference was found between chemical fertilization and organic fertilization with mulch.

Velmurugan and Swarnam (2017) explained similar to the results that rice grain yield was significantly affected by the residual effect of manures and inorganic fertilizer to okra.

Different our results, Abdelrezzag (2002) reported that chicken manure tended to reduce onion yield for all levels in cooperation with fertilizer and control. The usage of organic manures as alternative source of nitrogen would give better result in its growth and yield (Nasreen and Hossain, 2000; Kidanu, 2017).

In the study, the highest yield was observed Burgaz variety (p< 0.01) (Table 5). Highest yield after Burgaz obtained with Şampiyon variety. The differences in yield among varieties can be caused by differences in genetic characteristics of varieties (Khan et al., 2011; Abou-El-Hassan et al., 2018).

Bulb weight

Treatments, variety and the interaction between onion cultivars and treatment affected bulb weight of onion significantly (p< 0.01). Highest values (219.006 g) were obtained in the parcels which the chicken manure was applied as 20 t ha⁻¹ in the greenhouse (Table 4). This application increased weight of onion by 8% compared to the control plots. But there was no statistically significant difference in bulb weight between mineral fertilizer and 20 t ha⁻¹ of chicken manure application. Similarly, Yohannes et al. (2013)

reported that farmyard manure and nitrogen fertilizer increased bulb weight. Organic fertilizers provide nutrients to the plants by decomposing and increase growth and yield. Manures improved the soil structure, fertile and availability of nutrient to the plant. Better nutrition of the plant; increase the cell division of plant tissues and the rate of photosynthesis. This is reflected in product growth and the bulb weight (Ewais et al., 2010).

Bulb weights of Burgaz variety (316.283 g) were higher than the others onion variety significantly (Table 5).

The interaction between onion cultivars and treatment for bulb weight was found statistically significant. The highest bulb weights was obtained in Burgaz variety with 20 t ha⁻¹ as 339.267 g in greenhouse condition.

Table 5. Effect of variety on yield and same quality criteria of onion as second crop depending on residue effect of chicken manure in greenhouse condition

Variety	Yield	Bulb weight	Bulb width	Bulb height	Number of storage leaf	Number of shoot tip	Number of dried leaf
	(t ha ⁻¹)	(g no ⁻¹)	(cm)	(cm)	(no)	(no)	(no)
14-16	60.23 d	180.697 d	7.115 cd	7.089 d	2.189 d	1.911 b	6.167 d
Burgaz	105.40 a	316.283 a	8.745 a	8.648 a	3.101 a	2.611 a	8.289 b
Kar Beyazi	67.69 c	203.087 c	7.163 cd	8.029 b	2.599 c	1.611 c	8.971 a
Naz	60.25 d	180.761 d	7.334 c	6.667 e	1.521 e	1.489 d	5.456 f
NWG	61.43 d	184.309 d	6.589 e	7.527 c	1.545 e	1.577 c	6.389 c
Perwana	50.73 e	152.195 e	6.995 de	5.752 g	2.199 d	1.600 c	5.567 f
Seyhan	49.51 e	148.535 e	6.382 f	6.276 f	2.156 d	1.611 c	5.911 e
Şampiyon	97.30 b	291.919 b	8.160 b	8.820 a	2.778 b	1.000 e	8.989 a
LSD	4.28**	12.841**	0.228**	0.245**	0.094**	0.070**	0.189**

** : p<0.01; * : p<0.05; n.s.: not significant

Bulb width

The residual effect of chicken manure and mineral NPK applications on onion bulb width was found significant (Table 4). Contrarily, Yohannes et al. (2013) and Mekonnen et al. (2017) reported that farmyard manure did not affect bulb width of onion in their work.

The highest bulb width (8.745 cm) was observed Burgaz variety (p< 0.01) followed by the bulb width (8.160 cm) in Şampiyon variety (Table 5). The interaction between onion cultivars and treatment for bulb width was statistically important. Maximum bulb width was obtained in Burgaz variety with 20 t ha⁻¹ as 8.897 cm.

Bulb height

Onion bulb height was significantly (p< 0.01) affected by the residual effect of chicken manure and mineral NPK applications (Table 4). The highest value (7.513 cm) was determined in mineral NPK application and followed bulb height (6.49 cm) by the application of control. There is contrast with Yohannes et al. (2013) who reported that application of FYM at a rate of 45 ton ha⁻¹ gave the highest mean bulb diameter (5.99 cm). Consistent with their results Metwally and Bary (1999) suggested that the poultry manure improve the bulb growth by enhancing the soil properties and overcome the leaching of

nutrients from the root zone. As different Mekonnen et al. (2017) reported that organic manure did not significantly influence bulb length.

In the study, bulb height of Şampiyon variety (8.820 cm) was reported higher than other varieties ($p < 0.01$) (Table 5). The interaction between onion cultivars and treatment for bulb height was also found significant. Maximum bulb height was obtained in Şampiyon variety with the mineral fertilizer NPK as 9.857 cm.

The differences in the responses to the applications of onion varieties may be genetic variation and also depending on the adoptability of variety in specific environment (Shah et al., 2012; Ali et al., 2018).

Number of storage leaf

According to statistical analyzes, number of storage leaf was affected from the treatments. But these characteristics have changed significantly in relation to the varieties (Tables 4 and 5). Highest value was obtained in Burgaz variety (3.101) followed by Şampiyon variety (2.778) (Table 5). There was statistically significant difference between Burgaz and Şampiyon variety. The interaction between onion cultivars and treatment had a significant effect on the number of storage leaf ($p < 0.01$). The number of storage leaf was highest in the application of 40 t ha⁻¹ and Burgaz variety.

Number of shoot tip

The results presented in Tables 4 and 5 showed that treatment and onion variety had significantly affected number of shoot tip of onion, where the interaction had also significantly affected. The highest number of shoot tip (1.730) was observed with the application of chicken manure at the rate of 20 t ha⁻¹ (Table 4). While the lowest numbers of shoot tip (1.569) was observed in control application. Among the onion variety highest number of shoot tip was recorded in variety Burgaz (2.611).

Maximum number of shoot tip was obtained in Burgaz variety with the 40 t ha⁻¹ of chicken manure application.

Number of dried leaf

Treatments, variety and the interaction between onion cultivars and treatment affected number of dried leaf of onion significantly ($p < 0.01$) (Tables 4 and 5). Highest value (7.395) was obtained in the parcels which the chicken manure was applied as 20 t ha⁻¹ in the field. Number of dried leaf of Şampiyon variety (8.989) were higher than the others onion variety significantly (Table 5). The highest number of dried leaf was obtained in Karbeyazı variety with 20 t ha⁻¹ as 10.220.

Conclusion

As a conclusion it was found that residual effect of chicken manures recommended NPK fertilizer and onion varieties as second crop significantly affected the yield and bulb production in the greenhouse condition. Residual of chicken manure increased yield, bulb weight, bulb height, number of dry shell, number of shoots of onion varieties. The highest results were obtained especially with 20 t ha⁻¹ of chicken manure application in the greenhouse condition. The onion varieties Burgaz gave more response to the organic manure as compare with other onion varieties in yield, bulb weight, bulb height, bulb width, number of storage leaf. The lowest amount of animal manure improved many

examined parameters significantly but increasing the rate of using the chicken manure had negative effects.

In today's world, where healthy life and environmental consciousness is gaining importance, it should be aimed to increase the conscious use of natural organic fertilizers.

Acknowledgement. This research is a work supported by Scientific Research Project Commission of Ege University; Contact no: 2017/OMYO/001.

REFERENCES

- [1] Abd-Allah, A. M., Adam, S. M., Abou-Hadid, A. F. (2001): Productivity of green cowpea in sandy soil as influenced by different organic manure rates and sources. – Egypt. J. Hort.Sci. 28(3): 331-340.
- [2] Abdelrazzag, A. (2002): Effect of chicken manure, sheep manure and inorganic fertilizer on yield and nutrients uptake by onion. – Pakistan J. Biol. Sci. 5(3): 266-268.
- [3] Abou-El-Hassan, S., Elmehrat, H. G., Ragab, A. A., Abo-Dahab, A. M. M. A. (2018): Growth, yield, bulb quality and storability of some onion cultivars response to compost, vermicompost and plant growth promoting Rhizobacteria. – Middle East J. Agric. Res. 7(2): 292-306.
- [4] Açıkgöz, N., Akka, M. E., Maghaddam, A., Özcan, K. (1993): Database dependent. – Congress of International Practice of Computer, p: 133.
- [5] Akoun, J. (2004): Effect of plant density and manure on the yield and yield components of the common onion (*Allium cepa* L.) variety nsukka red. – Nigerian Journal of Horticultural Science 9: 43-48.
- [6] Ali, M., Khan, N., Khan, A., Ullah, R., Naeem, A., Khan, M. W., Khan, K., Farooq, S., Rauf, K. (2018): Organic manures effect on the bulb production of onion cultivars under semiarid condition. – Pure Appl. Biol. 7(3): 1161-1170.
- [7] Anonymous. (1951): U.S. soil survey staff, soil survey manual. – U.S. Dept. Agr. Handbook 18, U.S. Govt. Printing Office, Washington DC, USA.
- [8] Anonymous. (2018): Plant Production Statistics. – www.tuik.gov.tr.
- [9] Arisha, H. M. E., Gad, A. A., Younes, S. E. (2003): Response of some pepper cultivars to organic and mineral nitrogen fertilizer under sandy soil conditions. – Zagazig J. Agr. Res. 30: 1875-1899.
- [10] Atalay, I. Z., Kılınç, R., Anaç, D., Yokaş, İ. (1986): Gediz havzası rendzina topraklarının potasyum durumu ve bu topraklarda alınabilir potasyum miktarlarının tayininde kullanılacak yöntemler. – Bilgehan Matbaası, İzmir, s.25.
- [11] Beek, M. A. (2005): Perspectives of organic onion production: The Dutch experience as an example for an emerging market economy as China. – Acta Hort. 688: 339-346.
- [12] Boyhan, G. E., Hicks, R., Hill, C. R. (2006): Natural mulches are not very effective for weed control in onions. – HortTechnology 16: 523-526.
- [13] Boyhan, G. E., Hill, C. R. (2008): Organic fertility sources for the production of short-day organic onion transplants. – Hort. Technology 18: 227-231.
- [14] Boyhan, G. E., Hicks, R. J., Torrance, R. L., Riner, C. M., Hill, C. R. (2010): Evaluation of Poultry Litter and Organic Fertilizer Rate and Source for Production of Organic Short-day Onions. – Horttechnology 20(2): 304-307.
- [15] Bremner, J. M. (1965): Total Nitrogen. – In: Black, C. A., Evans, D. D., White, J. L., Ensminger, L. E., Clark, F. E., Dinauer, R. C. (eds.) Methods of soil analysis. Part 2: Chemical and microbiological properties. Am. Soc. of Agron., Madison, Wisc. Agron Ser. 9: 1149-1237.

- [16] Carol, M., Tanya, C., Tamera, F. (1999): A manure resource guide for farmers and gardeners in Western Washington. – King Conservation District 935 Powell Ave SW Renton. WA 98055. pp 206.
- [17] Dauda, S. N., Ajayi, F. A., Ndor, E. (2008): Growth and yield of water melon (*Citrulluslanatus*) as affected by poultry manure application. – Journal of Agriculture and Social Science 4: 121-124.
- [18] Dina, M. S., Shafeek, M. R., Abdallah, M. M. F. (2010): Effect of different nitrogen sources and soil solarization on green onion productivity for exportation. – Annals of Agric. Sci., Cairo Univ. 55(1): 97-106.
- [19] El-Shatanofy, Manar, M. E. (2011): Influence of organic manure and inorganic fertilizers on growth, yield and chemical contents of onion (*Allium cepa*, L.). – M.Sc. Thesis, Fac. of Agric. Alex. Univ.
- [20] Ewais, M. A., Mahmoud, A. A., Khalil, A. A. (2010): Effect of nitrogen fertigation in comparison with soil application on onion production in sandy soils. – Alex J Agric Res 55(3): 75-83.
- [21] Gao, X., Zhang, Z., Guo, S. (2005): Effects of combined top application of inorganic nitrogen and potassium on the yield and quality of overwintering tomato in greenhouse. – Plant Nutrition and Fertilizer Science 11(3): 375-378.
- [22] Gonçalves, P. A., de Souza, C. R., Sousa, E. S. (2004): Mineral and organic fertilization and onion thrips, Thripstabaci Lind. (Thysanoptera: Thripidae) population density. – Ciencia Rural 34: 1255-1257.
- [23] Griffiths, G., Trueman, L., Crowther, T., Thomas, B., Smith, B. (2002): Onions—A global benefit to health. – Phytother. Res. 16: 603-615. doi: 10.1002/ptr.1222.
- [24] Guneş, A., Alpaslan Inal, M. (2000): Bitki besleme ve gübreleme. – Ankara Üniversitesi Ziraat Fak. Yayın No: 1514, s: 199.
- [25] Indira, S., Singh, S. J. (2014): Effect of vermicompost and bio fertilizer on yield and quality of rabi onion (*Allium cepa* L) cv. puna red. – Agric. Sci. Digest. 34(2): 144-146.
- [26] Jackson, M. L. (1967): Soil chemical analysis. – Prentice-Hall of India Pvt. Ltd., New Delhi.
- [27] Jayathilake, P. K. S., Reddy, I. P., Srihari, D., Reddy, K. R. (2006): Productivity and soil fertility status as influenced integrated use of N-fixing Bio fertilizers, organic manures and inorganic fertilizers in onion. – Journal of Agricultural Sciences 2(1): 46-58.
- [28] Jongtae, L. (2010): Effect of application methods of organic fertilizer on growth, soil chemical properties and microbial densities in organic bulb onion production. – Scientia Horticulturæ 124: 299-305.
- [29] Kacar, B. (1995): Toprak analizleri: Bitki ve toprağın kimyasal analizleri III. – Ankara Üni., Zir. Fak., Eğitim Araş. ve Geliştirme Vakfı Yayınları: 81-86.
- [30] Khan, I. M., Hassan, G., Khan, I., Marwat, K. B. (2011): Testing of herbicides at various doses on the growth stages of wild onion grown in pots. – Sarhad J Agric 27(1): 85-91.
- [31] Kidanu, Y. G. (2017): Effect of Integrated Nutrient Management on Growth, Bulb Yield and Storability of Onion (*Allium Cepa* L.) Under Irrigation at Selekleka, Northern Ethiopia. – M.Sc. Thesis, 111 Pages. February 2017, Haramaya University, Haramaya.
- [32] Liebig, M. A., Doran, J. W. (1999): Impact of organic production practices on soil quality indicators. – J. Environ. Qual. 28: 1601-1609.
- [33] Lim, T. K. (2015): Edible Medicinal and Non-Medicinal Plants. – Volume 9. Springer; Dordrecht, the Netherlands: 2015. Modified Stems, Roots, Bulbs; pp. 124-203.
- [34] Liu, X., Guangxi, R., Yan, S. (2011): The effect of organic manure and chemical fertilizer on growth and development of *Stevia rebaudiana* Bertoni. – Energy Procedia 5: 1200-1204.
- [35] Mahala, P., Chaudhary, M. R., Garhwal, O. P. (2018): Yield and quality of rabi onion (*allium cepa* l.) influenced by integrated nutrient management. – Int. J. Curr. Microbiol. App. Sci. 7(5): 3313-3321.

- [36] Marrelli, M., Amodeo, V., Statti, G., Conforti, F. (2019): Biological Properties and Bioactive Components of *Allium cepa* L.: Focus on Potential Benefits in the Treatment of Obesity and Related Comorbidities. – *Molecules* 24(1): 119.
- [37] Mekonnen, D. A., Mihretu, F. G., Woldetsadi, K. (2017): Farmyard manure and intra-row spacing on yield and yield components of adama red onion (*Allium cepa* L.) cultivar under irrigation in gewane district, Afar Region, Ethiopia. – *J. Hortic. For.* 9(5): 40-48.
- [38] Metwally, S. M., Abdel-Bary, E. A. (1999): Assessment of application of amendments to sandy soils using a computer model. – *Zagazig J Agric Res* 2: 947-962.
- [39] Naeem, M., Iqbal, J., Bakhsh, M. A. A. (2006): Comparative study of inorganic fertilizers and organic manures on yield and yield components of mung bean (*Vignaradiate* L.). – *Journal of Agriculture and Social Science* 2: 227-229.
- [40] Nasreen, S., Haque, M. M., Hossain, M. A., Farid, A. T. M. (2007): Nutrient uptake and yield of onion as influenced by nitrogen and Sulphur fertilization. – *Bangladesh Journal of Agricultural Research* 32(3): 413-420.
- [41] Olsen, S. R., Cole, C. V., Watanbe, F. S., Dean, L. A. (1954): Estimation of available phosphorus in soils by extraction with sodium bicarbonate. – *USDA Cir. No.* 939.
- [42] Piazza, C., Reggiani, R., Cera, M. C. (2003): Varietal experiments on organically grown onions. – *Sementi Elette* 49: 39-41.
- [43] Ramesh, P., Singh, M., Rao, S. A. (2005): Organic Farming: It's Relevance to the Indian Context. – *Current Science* 88(4): 561-568.
- [44] Reuterberg, E., Kremkus, F. (1951): Bestimmung von gesamthumus und alkalischen humusstoffen im boden, z. pflanzenernaehr. Düng. und Bodenkd. – *Verlag Chemie GmbH, Weinheim.*
- [45] Rumpel, J. (1998): Effect of long-term organic, mineral, and combined organic-mineral fertilization on yield of onions (*Allium cepa* L.) grown from seeds. – *Biuletyn Warzywniczy* 48: 5-15.
- [46] Russo, V. M. (2005): Organic vegetable transplant production. – *HortScience* 40: 623-628.
- [47] Sezen, Y. (1995): Soil chemistry Edition of Atatürk University No: 790. – *Atatürk Univ. Faculty of Agriculture. No: 322. Series of Lesson Book. 71. Erzurum.*
- [48] Shah, S. T., Sajid, M., Alam, R., Rab, A., Mateen, A., Jan, I., Ali, A., Wahid, F. (2012): Comparative study of onion cultivars at Mardan, Khyber Pakhtunkhwa - Pakistan. – *Sarhad J Agric* 28(3): 399-402.
- [49] Shaheen, A., Fatma, M., Rizk, A., Singer, S. M. (2007): Growing onion plants without chemical fertilization. – *Res. J. Agr. Biol. Sci.* 3(2): 95-104.
- [50] Sharma, R. P., Datt, N., Sharma, P. K. (2003): Combined application of nitrogen, phosphorus, potassium and farmyard manure in onion under high hills, Dry temperate conditions of North-Western Himalayas. – *Indian J. Agr. Sci.* 73(4): 225-227.
- [51] Sharma, R. P., Pathak, S. K., Haque, M., Raman, K. R. (2004): Diversification of traditional rice (*Oryza sativa*)-based cropping system for sustainable production in South Bihar alluvial plains. – *Indian J. Agron.* 49: 218-222.
- [52] Snyman, H. G., Jong, D. E., Aveling, T. A. S. (1998): The stabilization of sewage sludge applied to agricultural land and the effects on maize seedlings. – *Water Sci. Technol.* 38(2): 87-95.
- [53] Soleymani, A., Shahrajabian, M. H. (2012): Effects of different levels of nitrogen on yield and nitrate content of four spring onion genotypes. – *Inter. J. of Agric. and Crop Sci.* 4(4): 179-182.
- [54] Suresh, K. D., Sneha, G., Krishn, K. K., Mool, C. M. (2004): Microbial biomass carbon and microbial activities of soils receiving chemical fertilizers and organic amendments. – *Archives Agronomy Soil Science* 50: 641-647.
- [55] Velmurugan, A., Swarnam, P. (2017): Nutrient uptake and residual effect of organic treatments applied to vegetable-rice system in an acid soil. – *Journal of Plant Nutrition* 40(12): 1755-1772.
- [56] Ware, M. (2017): <https://www.medicalnewstoday.com/articles/276714.php>. (2019).

- [57] Whitmore, A. P. (2007): Determination of the mineralization of nitrogen from composted chicken manure as affected by temperature. – *Nutr. Cycl. Agroecosyst.* 77: 225-232.
- [58] Yassen, A. A., Khalid, Kh. A. (2009): Influence of organic fertilizers on the yield, essential oil and mineral content of onion. – *Int. Agrophysics* 23(2): 183-188.
- [59] Yi, D., Cao, W., Xiao, G. (2004): Effect of Balanced Fertilization to Potato in High Altitude Areas of Guizhou Province. – *Chinese Journal of Soil Science* 35(1): 48-51.
- [60] Yohannes, K. W., Belew, D., Debela, A. (2013): Effect of farmyard manure and nitrogen fertilizer rates on growth, yield and yield components of onion (*Allium cepa* L.) at Jimma, Southwest Ethiopia. – *Asian Journal of Plant Sciences* 12(6-8): 228-234.
- [61] Yoldas, F., Ceylan, S., Mordogan, N., Esetlili, B. C. (2011): Effect of organic and inorganic fertilizers on yield and mineral content of onion (*Allium cepa* L.). – *African J. of Biotech.* 10(55): 11488-11492.
- [62] Zewde, A., Mulatu, A., Astatkie, T. (2018): Inorganic and organic liquid fertilizer effects on growth and yield of onion. – *International Journal of Vegetable Science* 24(6): 567-573.

STUDY ON THE CD (II) ADSORPTION CHARACTERISTICS OF DIFFERENT SALINE-ALKALINE SOILS IN WESTERN JILIN PROVINCE, CHINA

MA, X. L.[#] – ZHANG, J.[#] – YAN, T. Y.[#] – SUN, J. – WANG, J. H. – FENG, J. – WANG, H. B.*

College of Resources and Environment, Jilin Agricultural University, Changchun 130118, China

[#]These authors contributed equally to this work

**Corresponding author*

e-mail: 814634273@qq.com; phone: +86-130-3901-0128

(Received 29th Aug 2019; accepted 25th Nov 2019)

Abstract. In order to effectively control the environmental behavior of cadmium in saline-alkaline soil, it is imperative to understand its adsorption capacity. In this study, the kinetics, adsorption isotherm and two environmental parameters (pH and addition of biochar) of the adsorption behavior of Cd (II) in three saline-alkaline soil samples from western Jilin province, China were investigated. This study was an optimal fit for the pseudo-second-order kinetics model, as well as Langmuir adsorption isotherm model. The adsorption effect was the strongest at a pH of 7, the addition of biochar could increase Cd (II) adsorption of the soil. The adsorption of Cd (II) by saline-alkaline soil was a spontaneous, disordered and heat-absorbing reaction. Compared with mildly and moderately saline-alkaline soil, the adsorption of Cd (II) by severely saline-alkaline soil was the highest, and the adsorption was the best when the pH was neutral. Moreover, the addition of biochar could increase the organic matter in the soil and improve the adsorption capacity of Cd (II).

Keywords: *heavy metal, saline-alkali soil, properties, pH, biochar*

Introduction

Saline-alkaline soil is a common soil type on Earth, accounting for about 7% of the total soil area of the world. It is widely distributed in arid and semi-arid regions of Asia, Australia, Africa and South America (Yang et al., 2018; Saifullah et al., 2018). China ranks third in the world in terms of saline-alkaline soil area, mainly distributed in the northeast, north China, northwest inland and coastal areas along the Yangtze River. In the western region of Jilin province, there are 3.2 million hm² of saline-alkali soil, which is one of the three most concentrated saline-alkali areas in the world (Shi et al., 2018), which has brought serious harm to the development of agriculture and animal husbandry in Songnen plain (Zhao et al., 2018; He et al., 2008).

With the rapid development of industrial and agricultural production, the sources of heavy metals in soil, including the use of pesticides, excessive application of chemical fertilizers, industrial wastewater, bio-fats and so on (Ashraf et al., 2019), especially phosphate fertilizer containing relatively high concentrations of cadmium, which is different deposits varies greatly, and the overall average concentration of cadmium in sediments is 21 mg/kg, ranging from 1 to 150 mg/kg (Roberts, 2014). Soil cadmium pollution is a serious problem in China and is the main cause of cadmium contaminated rice (Wu et al., 2018). According to 2014 National Soil Pollution Survey data, 16.1% of the soil pollution sites (including agriculture and industry) exceeded the allowable limit of the second-level soil environmental quality standards, among which heavy metal pollution sites accounted for 82.8%. Among them, cadmium exceeded the standard by

7.0% (He et al., 2019), and heavy metal pollution events such as “cadmium rice”, “blood lead” and “arsenic toxin” occurred frequently, which arouse people’s great attention to it (Zhai et al., 2019; Hwang et al., 2019; Jain and Chandramani, 2018). Cadmium is a non-essential element for plant and human growth and one of the most toxic heavy metal elements (Sun et al., 2018).

Into the soil of the Cd (II) in a dynamic balance of adsorption and desorption, because of the heterogeneity of soil surface, there are different adsorption sites, including the binding energy of the high level and the low level. When the lower initial concentration of exogenous Cd (II), Cd (II) was first adsorbed on the binding energy of high level, giving priority to with obligate adsorption, adsorption speed faster, with the increase of initial concentration of Cd (II), obligate adsorption points gradually reduced, Cd (II) from predominantly obligate adsorption to give priority to with non-obligate adsorption, adsorption speed slower (Naiya et al., 2009). In general, temperature, soil type, organic matter, and clay minerals content type and amount, iron, manganese oxide, and calcium carbonate content are different, all can lead to different adsorption quantity of Cd (II) in soil, which greatly influenced by the pH (Liao, 2006; Sprynskyy et al., 2011). The adsorption capacity of heavy metal increases with the increase of pH value. Wang (Wang, 2012) investigated 18 kinds of typical soil in China, the study found the temperature rising in different soil types on Cd (II) adsorption capacity increased, but instead of desorption quantity was reduced, soil showed that under the condition of high temperature on Cd (II) stronger adsorption ability, and difficult to desorption. A study conducted by Yuan et al. (2019) claimed that the addition of organic matter can effectively immobilize soil Cd (II) at an appropriate concentration in the environment by stimulating the reduction of primary oxidation components of soil by microorganisms. Li et al. (2007) studied Cd (II) in the black soil, yellow-brown soil, yellow soil, red soil of different graded composition of cadmium adsorption effect, four kinds of soil adsorption Cd (II) capacities were in the form of clay > silt > fine sand > coarse sand.

For adsorption of soil heavy metal and saline-alkaline soil restoration work have been reported more. In this study, we objected of the adsorption characteristics of Cd (II) in Jilin province three different saline-alkaline soil samples and the influence of adding biochar adsorption behavior for Cd (II), starting from the physical and chemical properties of saline-alkaline soil itself directly, to study the adsorption of Cd (II) in soil potential, in order to fully understand the degree of saline-alkaline of soil Cd (II) adsorption ability. Moreover, we studied the different pH values and the addition of biochar to saline-alkaline soil adsorption of Cd (II), to seek effective measures to control soil Cd (II) environment behavior, as well as to provide a theoretical basis for Cd (II) saline-alkaline soil restoration.

Materials and methods

Test samples

Sampling sites were located in Da ‘an Lesheng township west 10 km shop in Jilin province, China (45°33’4” N, 123°45’58” E). Because of terrain elevation difference and different slope direction, this place formed a natural depression “Disk depressions”, which subtle differences in the terrain height caused soil surface salinity distribution unevenly, formed a different saline-alkaline degree of soil in the micro-region (Wang et al., 2009; Martin et al., 2019). The sampling terrain was shown in *Figure 1*. In the “Disc

depression” in the micro-region, sampling sites were taken the surface soil in 0-20 cm arranged according to different contour lines and removed off the sundries such as gravel, root plants and straw from the soil samples, then air-dried through a 100-mesh sieve, and stored in self-sealing bags for later use.

With the increase of terrain height in different micro-regions, pH value of soil, conductivity and total salt content gradually increased. Three test samples were determined in three separate contour lines, which were respectively: mildly saline-alkaline soil, moderately saline-alkaline soil, and severely saline-alkaline soil. The basic physical and chemical properties of the soil were given in *Table 1* and the water-soluble salt content in *Table 2*.

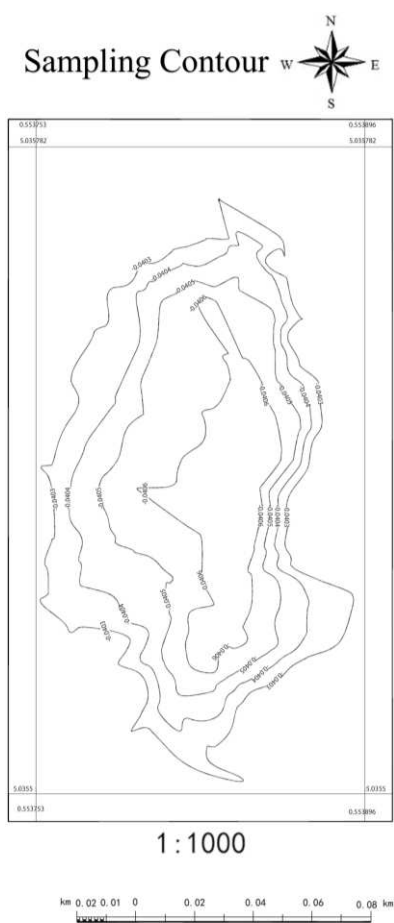


Figure 1. Sampling point topographic map

Table 1. Basic physical and chemical properties of the tested soil

Soil type	pH	Exchangeable Na (mol·kg ⁻¹)	Conductivity (S/m)	Organic matters (g·kg ⁻¹)	CEC (mol·kg ⁻¹)	Cd (II) concentration (mg·kg ⁻¹)	Composition (%)		
							Clay	Silt	Sand
Mildly saline-alkaline soil	8.68	0.34	17.8	1.05	14.2	0.07	29.1	21.3	49.6
Moderately saline-alkaline soil	9.42	0.57	19.6	1.34	18.6	0.08	29.7	32.1	38.2
Severely saline-alkaline soil	11.08	0.75	25.3	1.91	21.5	0.08	34.8	39.7	25.5

Table 2. Water soluble salt content in the tested soil (g/kg)

Soil type	Na ⁺	K ⁺	Ca ²⁺	Mg ²⁺	CO ₃ ²⁻	HCO ₃ ⁻	Cl ⁻	SO ₄ ²⁻
Mildly saline-alkaline soil	5.7	1.17	0.09	0.15	3.57	0.32	0.09	0.29
Moderately saline-alkaline soil	7.01	2.23	0.21	0.21	8.72	1.21	0.73	0.31
Severely saline-alkaline soil	15.02	3.18	0.36	0.51	7.34	1.63	1.04	0.36

Test design

Different saline-alkaline soil of Cd (II) adsorption kinetics test

Took the sample (0.5000 ± 0.0005) g in a centrifuge tube, added 25 mL Cd (II) solution with concentration of 20 mg·L⁻¹ in the background solution of 0.01 mol·L⁻¹ NaNO₃(Analytical purity), oscillated the sample for 1, 5, 10, 20, 30, 60, 120, 240, 360, 480, 600, 1440 min, centrifuged for 10 min in a high-speed tabletop centrifuge of 10000 r·min⁻¹ (TDL-40B from Agilent Company in America), and then filtered. The concentration of Cd (II) in the supernatant was determined by the atomic absorption spectrophotometer (TAS-990 from Pursee Company in Beijing, China).

Different saline-alkaline soil of Cd (II) adsorption isothermal test

The sample (0.5000 ± 0.0005) g was placed in a centrifuge tube, and 25 mL Cd (II) solution with a concentration gradient of 10, 20, 30, 50, 100, 150, 200 and 300 mg·L⁻¹ solutions were added with 0.01 mol·L⁻¹ NaNO₃ as the background solution. The adsorption isotherm was determined by oscillating for 24 h at a constant temperature of 25 °C (adsorption kinetics test confirmed that adsorption saturation had been reached for 24 h). Repeat isothermal adsorption experiments were performed at temperatures of 15 °C, 25 °C and 35 °C, to study the effect of different temperatures on adsorption.

Different pH and added biochar in saline-alkaline soil of Cd (II) absorption test

The pH of the background solution was adjusted to 3.0, 5.0, 7.0, 9.0 and 11.0 with 1 mol·L⁻¹ HCl (Analytical purity) and NaOH (Analytical purity) solution. Added 0.00%, 0.5%, 1%, 3%, 5% and 10% biochar [The tested biochar is made from corn stalks that have passed through a 20 mesh sieve. Pyrolyzed in a muffle furnace (Jiangsu Zhengfei Electric Furnace Factory) at 500 °C for 3 h, after the end of pyrolysis, cooled to room temperature, passed through a 100 mesh sieve)]. Kept constant temperature and shocked for 24 h at 25 °C, and determined the concentration of Cd (II) in the supernatant.

Data processing and calculation

All experiments were repeated three times. The obtained data were calculated and plotted by Excel 2010 and Origin 8.5.

The adsorption capacity of the solution

Equation 1 was used to measure the adsorption capacity of the solution.

$$q_t = \frac{(c_0 - c_t)V}{m} \quad (\text{Eq.1})$$

where q_t is the adsorption amount of Cd (II) ($\text{mg}\cdot\text{kg}^{-1}$); C_0 is the initial concentration of Cd (II) ($\text{mg}\cdot\text{L}^{-1}$). C_t is used to measure the concentration of Cd (II) in the supernatant ($\text{mg}\cdot\text{L}^{-1}$). V is the volume of Cd (II) solution (mL); m is the mass of soil or soil plus biochar (g).

Kinetic model

Pseudo-first-order kinetic model:

$$q_t = Q_{e,1}(1 - e^{-k_1 t}) \quad (\text{Eq.2})$$

Pseudo-second-order kinetics model:

$$q_t = \frac{Q_{e,2}^2 k_2 t}{1 + Q_{e,2} k_2 t} \quad (\text{Nonlinear form}) \quad (\text{Eq.3})$$

Elovich model:

$$q_t = a + b \ln t \quad (\text{Eq.4})$$

where q_t is the adsorption amount of Cd (II) at time t ($\text{mg}\cdot\text{g}^{-1}$); In *Equation 2*, $Q_{e,1}$ and k_1 represent the adsorption equilibrium quantity ($\text{mg}\cdot\text{g}^{-1}$) and the adsorption rate constant ($\text{g}\cdot\text{mg}^{-1}\cdot\text{min}^{-1}$) of Cd (II) respectively. In *Equation 3*, $Q_{e,2}$ and k_2 represent the adsorption equilibrium quantity ($\text{mg}\cdot\text{g}^{-1}$) and adsorption rate constant ($\text{g}\cdot\text{mg}^{-1}\cdot\text{min}^{-1}$) of Cd (II) respectively. In *Equation 4*, a is the adsorption constant related to the maximum adsorption capacity, and b is the adsorption rate coefficient, which is a measure of how fast the reaction rate decreases with the extension of time.

Isotherm model

Langmuir model:

$$q_e = \frac{K_L q_m C_t}{1 + K_L C_t} \quad (\text{Nonlinear form}) \quad (\text{Eq.5})$$

Freundlich model:

$$q_e = K_F C_t^{1/n} \quad (\text{Nonlinear form}) \quad (\text{Eq.6})$$

where q_e is the equilibrium adsorption amount of Cd (II) ($\text{mg}\cdot\text{g}^{-1}$); q_m and K_L is Langmuir model parameters, representing the maximum adsorption capacity ($\text{mg}\cdot\text{g}^{-1}$) and adsorption energy ($\text{L}\cdot\text{mg}^{-1}$) of Cd (II), respectively. K_F and n are Freundlich model parameters, representing Cd (II) adsorption capacity ($\text{mg}\cdot\text{g}^{-1}$) and adsorption strength, respectively.

The thermodynamic model parameter calculation

$$K_d = \frac{(C_0 - C_t)V}{C_t m} \quad (\text{Eq.7})$$

$$\ln K_d = \frac{\Delta S^\circ}{R} - \frac{\Delta H^\circ}{RT} \quad (\text{Eq.8})$$

$$\Delta G^\circ = \Delta H^\circ - T\Delta S^\circ \quad (\text{Eq.9})$$

where ΔG° is the standard free energy change ($\text{kJ}\cdot\text{mol}^{-1}$), ΔH° is the standard enthalpy change ($\text{kJ}\cdot\text{mol}^{-1}$) and ΔS° is the standard entropy change ($\text{kJ}\cdot\text{mol}^{-1}$), K_d is the thermodynamic equilibrium constant ($\text{mL}\cdot\text{g}^{-1}$), R is the ideal gas constant R ($8.314 \text{ J}\cdot\text{mol}^{-1}\cdot\text{K}^{-1}$), T is the temperature (K), the value of ΔH° and ΔS° are the slope and intercept of $\ln K_d\text{-}T^{-1}$ diagram, respectively.

Correlation coefficient significance test

Find the correlation coefficient significance test table, and then determine the degree of freedom ($n-2$), where n represents the number of samples; find the value corresponding to $a0.001$, $a0.005$, $a0.01$ in the test table, and the fit will be obtained. The correlation coefficient r value is compared with a to determine the level of significance. For example, if $r > a$, it is extremely significant.

Results and discussion

Study on adsorption kinetics of Cd (II) in different saline-alkaline soils

The initial concentration of Cd (II) was $20 \text{ mg}\cdot\text{L}^{-1}$, and the adsorption capacity of Cd (II) in mildly, moderately and severely saline-alkaline soil changed with time, as shown in *Figure 2*.

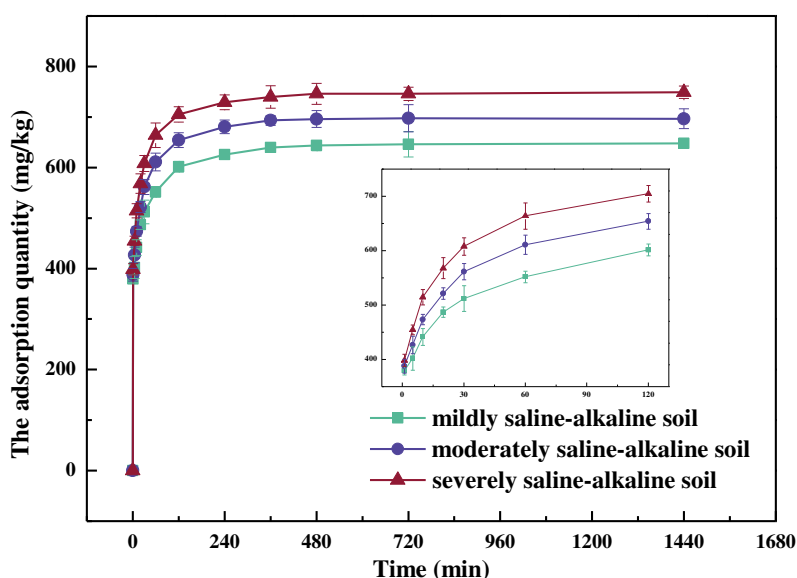


Figure 2. Adsorption kinetics of Cd (II) in sample soil with three different saline-alkaline stresses

The adsorption process of Cd (II) in the three tested soil samples can be divided into three stages: fast adsorption, slow adsorption, and equilibrium adsorption (*Figure 2*). Within 0~120 min was the rapid adsorption stage, the adsorption capacity of mildly,

moderately and severely saline-alkaline soil accounted for 92.840%, 93.941% and 94.126% of the total adsorption capacity, respectively. The adsorption rate of Cd (II) in the three tested samples was: severely saline-alkaline soil > moderately saline-alkaline soil > mildly saline-alkaline soil. At the initial stage of adsorption, there were many adsorption sites on the soil surface, and the adsorption rate was fast.

When the adsorption sites on the soil surface reached saturation, Cd (II) was adsorbed to the internal sites of the soil, and the adsorption rate slowed down up to a threshold (Tsang et al., 2007; Arias et al., 2005). These interactions including different interactions: first, surface complexation reactions which are basically inner-sphere surface complexes of the Cd (II) and the respective surface functional groups; second, electrostatic interactions where the Cd (II) form outer-sphere, complexes at a certain distance from the surface; third, hydrophobic expulsion of metal complexes containing highly nonpolar organic solutes, and fourth, surfactant adsorption of metal-polyelectrolyte complexes due to reduced surface tension (Bradl, 2004).

The pseudo-first-order kinetic model is a single adsorption process, while the pseudo-second-order kinetic model usually describes the chemical adsorption process, including electron sharing and transfer (covalent bond and ion exchange) between adsorbents and adsorbents (Ho, 2006). Elovich tends to describe a series of reaction mechanisms such as solute diffusion at the solid-liquid interface. The adsorption kinetics of Cd (II) in mildly, moderately and severely saline-alkaline soils were fitted by the pseudo-first-order kinetic model, pseudo-second-order kinetic model, and Elovich model. The fitting results were given in *Table 3*.

Table 3. Adsorption kinetics fitting parameters of Cd (II) in soils with three different saline-alkaline stresses

Soil type	Pseudo-first-order kinetic model			Pseudo-second-order kinetic model			Elovich model		
	$Q_{e.1}$	k_1	r	$Q_{e.2}$	K_2	r	a	b	r
Mildly saline-alkaline soil	548.225	103.094	0.828**	594.169	0.001	0.931**	360.163	44.615	0.993**
Moderately saline-alkaline soil	591.688	111.385	0.815**	649.824	0.001	0.938**	379.229	50.402	0.992**
Severely saline-alkaline soil	635.225	119.060	0.810**	702.594	0.001	0.948**	403.729	54.919	0.991**

**Highly significant correlation ($n = 12$, $r_{0.05} = 0.576$, $r_{0.01} = 0.708$)

It can be seen from *Table 3* that the fitting effect of pseudo-first-order dynamic model was the worst, and the correlation coefficient r value was the minimum of 0.810-0.828. The Elovich model had the largest correlation coefficient r value, which was 0.931, 0.938 and 0.948, respectively. However, according to the fitting model, the equilibrium adsorption capacity of mildly, moderately and severely saline-alkaline soil to Cd (II) was 360.163, 379.229 and 403.729 $\text{mg}\cdot\text{kg}^{-1}$, respectively, which were significantly different from the experimental values of 648.000, 696.500 and 749.000 $\text{mg}\cdot\text{kg}^{-1}$, respectively. The pseudo-second-order kinetic model could better describe the Cd (II) adsorption characteristics of the three sample soil, and the r values of the correlation coefficients are 0.931, 0.938 and 0.948, respectively. The fitted equilibrium adsorption capacities of 594.169, 649.824 and 702.594 $\text{mg}\cdot\text{kg}^{-1}$ were closed

to the experimental values. The pseudo-second-order kinetic model was usually used to describe the chemical adsorption process, and it was concluded that the adsorption of Cd (II) in the three kinds of soil was dominated by chemical adsorption (Rao et al., 2010).

Adsorption isotherms of Cd (II) in different saline-alkaline soils

The Cd (II) solutions of 0, 20, 30, 50, 100, 150, 200, and 300 mg·L⁻¹ were added to the mildly, moderately, and severely saline-alkaline soil, and were oscillated for 24 h at a constant temperature of 25 °C to determine the adsorption capacity of Cd (II), as shown in *Figure 3*.

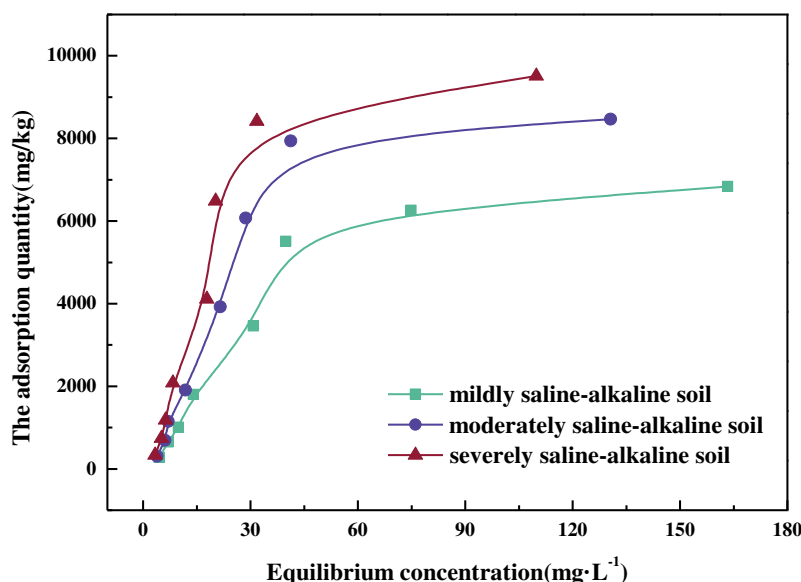
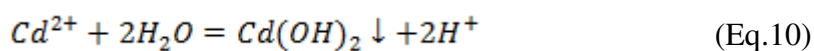


Figure 3. Adsorption isotherms of Cd (II) in sample soil with three different saline-alkaline stresses

It can be seen from *Figure 3*, with the increasing of Cd (II) concentration, three kinds of soil on Cd (II) adsorption quantity also promoted, *Table 1* showed that three of the pH value of the soil samples were 8.68, 9.42, 11.08, respectively, all belong to saline-alkaline soil. Due to Cd (II) hydroxide insoluble in water, after the Cd (II) into the soil and water mixture, Cd (II) with OH⁻ formed hydrated metal ions in the solution or hydroxide precipitation, the model was as follows:



With the increasing concentration of Cd (II) ions, Eq.10 reaction continued to the right, and the hydroxide precipitation of Cd (II) continues to be generated (Wang et al., 2019), which showed that the adsorption capacity of soil to Cd (II) gradually increased. At the same concentration of Cd (II), the adsorption capacity of Cd (II) in the three tested soil was: severely saline-alkaline soil > moderately saline-alkaline soil > mildly saline-alkaline soil. When the concentration of Cd (II) in the equilibrium solution was 0-50 mg·L⁻¹, the slope of the adsorption isotherm was large, that meaning the adsorbed amount of Cd (II) in the three soils increased rapidly with the increasing of Cd (II) concentration.

When the equilibrium concentration of Cd (II) was greater than $50 \text{ mg}\cdot\text{L}^{-1}$, the slope of the adsorption isothermal curve gradually decreased, and the maximum adsorption capacity of the three kinds of soil reached 1798.803, 1909.739 and $2083.779 \text{ mg}\cdot\text{kg}^{-1}$, respectively. That was, the change range of the adsorption capacity of Cd (II) reduced until it finally reached adsorption saturation. Since obligate adsorption was dominant in the region with low adsorption capacity, most Cd (II) may be adsorbed at high energy sites, and the adsorption speed was fast. After reaching a certain saturation, obligate adsorption sites gradually decreased, and Cd (II) changed from obligate adsorption to non-obligate adsorption, with a slower adsorption speed (Hu et al., 2010).

The adsorption isotherms of mildly, moderately and severely saline-alkaline soil to Cd (II) was fitted by Langmuir and Freundlich models, and the fitting parameters were shown in *Table 4*.

Table 4. Adsorption isotherm parameters of Cd (II) on three different soils with saline-alkaline stress

Soil type	Langmuir parameter			Freundlich parameter		
	q_m	K_L	r	n	K_F	r
Mildly saline-alkaline soil	9573.048	0.021	0.963**	553.913	1.924	0.907**
Moderately saline-alkaline soil	12046.321	0.026	0.941**	787.720	1.940	0.907**
Severely saline-alkaline soil	13248.917	0.032	0.938**	958.990	1.947	0.867**

**Highly significant correlation ($n = 8$, $r_{0.05} = 0.707$, $r_{0.01} = 0.834$)

As can be seen from *Table 4*, Langmuir model was used to better fit the adsorption process of Cd (II) of the three soil samples, and the correlation coefficient r values were 0.963, 0.941 and 0.938 respectively. The K_L value in the Langmuir model represents the adsorption affinity constant (Xie et al., 2019), and the larger K_L was, the better the adsorption effect. In the adsorption process of Cd (II) in the three soils, K_L values were 0.021, 0.026 and 0.032, respectively, all of which were greater than zero, indicating that the adsorption reaction could be spontaneous at room temperature. The K_F value in the Freundlich model represents the adsorption capacity of Cd (II). The higher the K_F value is, the stronger the adsorption capacity is. The K_F values in the three kinds of saline-alkaline soil were 553.913, 787.702 and 958.990, respectively, which were consistent with the conclusion obtained in the Langmuir model that was: severely saline-alkaline soil > moderately saline-alkaline soil > mildly saline-alkaline soil. The n value in the Freundlich model can represent the adsorption strength, and the larger n value is, the stronger the adsorption strength will be (Ma et al., 2015). The n values of the three kinds of soils were 553.913, 787.720 and 958.990, respectively, indicating that the severely saline-alkaline soil had more and more complex energy adsorption sites.

Study on adsorption thermodynamics of Cd (II) in different saline-alkaline soil

Within the test temperature range (15, 25, 35 °C), thermodynamic fitting parameters of Cd (II) adsorption in mildly, moderately and severely saline-alkaline soil was shown in *Table 5*.

It can be seen from *Table 5* that, with the increasing of temperature, the adsorption capacity of three kinds of soil to Cd (II) gradually increased, and the adsorption capacity of severely saline-alkaline soil was the largest. The Langmuir model had the best fitting

effect on Cd (II) adsorption in the three soil, and the correlation coefficient r was greater than 0.915. The higher the temperature was, the more favorable it was for Cd (II) adsorbed on the soil surface to diffuse into the particles, for the transformation of the outer complex to inner complex, and for the transformation of thermodynamically unstable combination to stable combination (Xie et al., 2019). According to the different temperature adsorption capacity, can calculate the 3 different saline-alkaline soil adsorption thermodynamic parameters of ΔH° , ΔG° and ΔS° , ΔG° on behalf of the reaction is a spontaneous or spontaneous reaction, ΔH° on behalf of the reaction is an endothermic or exothermic reaction, ΔS° representative is an orderly or disorderly reaction, the thermodynamic parameters as shown in *Table 6*.

Table 5. Thermodynamic models for adsorption of Cd (II) at different temperatures

Soil type	Temperature T (°C)	Langmuir parameter			Freundlich parameter		
		q_m	K_L	r	n	K_F	r
Mildly saline-alkaline soil	15	9427.858	0.018	0.960**	475.065	1.860	0.909**
	25	9573.048	0.021	0.963**	553.913	1.924	0.907**
	35	13820.899	0.018	0.915**	594.036	1.711	0.863**
Moderately saline-alkaline soil	15	10195.745	0.023	0.955**	647.129	1.963	0.894**
	25	12046.321	0.026	0.941**	787.720	1.940	0.870**
	35	14591.058	0.023	0.970**	743.431	1.752	1.323**
Severely saline-alkaline soil	15	10568.180	0.029	0.956**	802.741	2.054	0.887**
	25	13248.917	0.032	0.938**	958.990	1.947	0.867**
	35	14799.801	0.032	0.937**	978.863	1.846	0.874**

**Highly significant correlation ($n = 8$, $r_{0.05} = 0.707$, $r_{0.01} = 0.834$)

Table 6. Thermodynamic parameters of Cd (II) in three sample soil

Soil type	Temperature T (°C)	ΔG (kJ·mol ⁻¹)	ΔH (kJ·mol ⁻¹)	ΔS (J·mol ⁻¹ ·K ⁻¹)
Mildly saline-alkaline soil	15	-21.773	9.554	0.109
	25	-23.404		
	35	-25.036		
Moderately saline-alkaline soil	15	-22.084	9.080	0.108
	25	-23.707		
	35	-25.330		
Severely saline-alkaline soil	15	-22.223	8.588	0.107
	25	-23.828		
	35	-25.433		

It can be seen from *Table 6*, experimental design temperature 15 °C, 25 °C and 35 °C range, three kinds of soil ΔG° values are less than zero, the adsorption process is spontaneous, and with the increasing of temperature, ΔG° gradually became smaller, the higher the temperature of three kinds of soil Cd (II) adsorption spontaneous stronger; Three kinds of soil reaction enthalpy changing ΔH° were positive, suggests that Cd (II) in three kinds of soil adsorption process was endothermic reaction; ΔS° greater than zero, which indicated that adsorption process was disorderly.

Effect of pH on Cd (II) adsorption in soil

pH is one of the most important factors affecting soil adsorption and desorption of Cd (II) (Li et al., 2013). In the pH range of the test (3.0~11.0), the adsorption of Cd (II) by mildly, moderately and severely saline-alkaline soil was shown in *Figure 4*.

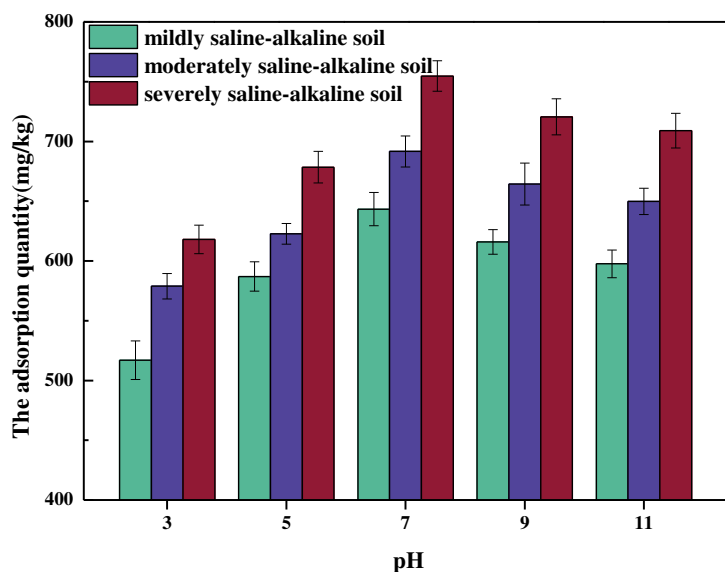


Figure 4. Effect of different pH values on adsorption of Cd (II) in three sample soil

It can be seen from *Figure 4* that, with the initial pH of the background adsorption solution increasing, the adsorption capacity of the three tested soil to Cd (II) first increased and then decreased. When the pH of the background solution was 7.0, the adsorption capacity of Cd (II) was the largest, and the adsorption capacity of mildly, moderately and severely saline-alkaline soil to Cd (II) was $643.344 \text{ mg}\cdot\text{kg}^{-1}$, $691.604 \text{ mg}\cdot\text{kg}^{-1}$ and $754.728 \text{ mg}\cdot\text{kg}^{-1}$, respectively. According to different adsorption mechanisms, pH may mainly affect Cd (II) adsorption by affecting the hydrolysis of Cd (II), the exchange between Cd (II) and H^+ , the type of adsorption surface, the adsorption surface charge, and the distribution coefficient of Cd (II) in the competitive system. There was a close relationship between pH and Cd (II) adsorption (Adhikari et al., 2003). When pH was low ($\text{pH} < 7$), Cd (II) was subject to competitive adsorption of H^+ , with a small amount of adsorption (Xie et al., 2019). With the increase of initial pH, OH^- increased, while the competitive adsorption of H^+ decreased and the adsorption of Cd (II) increased. At a high pH ($\text{pH} > 7.0$), there were a large number of surface functional groups such as sialons, inorganic hydroxyl groups and organic functional groups in the soil, which had negative charges with $\cdot\text{OH}$ functional groups that broke the bond with the side and adsorbed with Cd (II) to form inner ring compounds, increasing the adsorption capacity of Cd (II) (Bradl, 2004).

Effect of adding biochar on Cd (II) adsorption

Biochar is a kind of porous, stable, carbonaceous and highly aromatic solid material obtained by pyrolysis of biomass under hypoxic or anaerobic conditions (Bashir et al., 2018), which has abundant functional groups. The effects of different biochar additions on Cd (II) adsorption capacity were shown in *Figure 5*.

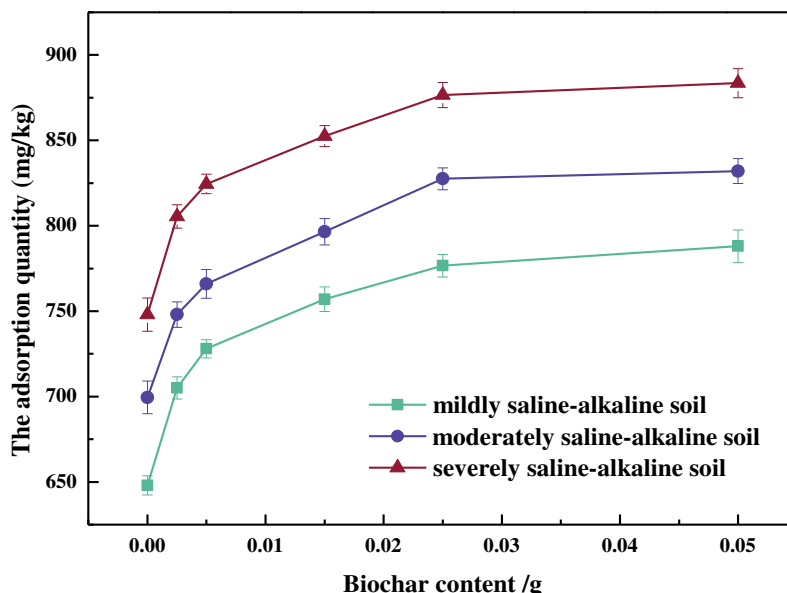


Figure 5. Relationship between the addition of biochar and pH on adsorption of Cd (II) in three sample soil

It can be seen from *Figure 5* that, with the increasing of biochar quantity, the adsorption capacity of mildly, moderately and severely saline-alkaline soil to Cd (II) gradually promoted. Due to the high content of organic matter in biochar, organic matter will react with Cd (II) to form stable complexes (Van Poucke et al., 2018). Surface complexation (inner- and outer-sphere) forms multiatom structures with unique metal-functional groups interactions, playing a predominant role in adsorption of heavy metals onto biochar. For example, heavy metals can be effectively bound by complexation with the carboxyl, phenolic and lactonic functional groups in biochar (Yang, 2019). The addition of biochar will increase the content of organic matter in the three kinds of soil, thus increasing the adsorption capacity of Cd (II). Among them, mildly saline-alkaline soil organic matter content was the lowest, so the increase of adsorption to Cd (II) was the largest, increasing by 21.605%. The three soil tends to be saturated when the biochar content reaches a certain level.

Conclusion

This study examined the kinetics, adsorption isotherm of three different saline-alkaline soil and two environmental parameters (pH and addition of biochar) on Cd (II). Our results indicated the following: (1) The adsorption process of Cd (II) in three different saline-alkaline soil showed a trend of first fast and then slow. The pseudo-second-order kinetic model had a better fitting effect on adsorption kinetics. (2) The adsorption capacity of Cd (II) was: severely saline-alkaline soil > moderately saline-alkaline soil > mildly saline-alkaline soil and the adsorption capacity gradually increased with the increase of Cd (II) concentration. The Langmuir model fitted the adsorption isotherm well. (3) The adsorption of Cd (II) by saline-alkaline soil was a spontaneous, disordered and heat-absorbing reaction under the test temperature 15 °C, 25 °C, and 35 °C. (4) Cd (II) adsorption effect of three soil was the best when pH was 7.0 between 3.0 and 11.0. (5) With the addition of biochar, the adsorption of Cd (II) in

sample soil was increased, and which in mildly saline-alkaline soil promoted most significantly.

Our research demonstrated the importance of temperature, pH and organic matter in controlling the environmental behavior of cadmium in saline-alkaline soil. For example, Cd content in the same area saline-alkaline soil in summer will be lower than the same year winter, especially severely saline-alkaline soil areas, considering adding the biochar to increase soil organic matter content, reducing the content of Cd in soil, or adopting dripping irrigation technology to decrease the soil pH around the crop root, reducing Cd in the soil solution and thus reducing crop uptake Cd. As a result, the investigation of saline-alkaline soil's characteristics will improve the saline-alkaline soil restoration technology which is a benefit to the environment and human health. Hence, there have two methods to recover saline-alkaline soil: one of it is to adjust pH in soil to neutral to remove heavy metal. In addition, its perspective to research environmental-friendly adsorbents like biochar with more active sites, lower energy cost and could recycle wastes as stalks.

Acknowledgements. This work was supported by The National Key Research and Development Support Project (2016YFC0501201), Major Science and Technology Project of Jilin Province (20170204002SF), Natural Science Foundation of Jilin Province (20180101086JC), and Grant of National Natural Science Foundation (41877027).

REFERENCES

- [1] Adhikari, T., Singh, M. V. (2003): Sorption characteristics of lead and cadmium in some soils of India. – *Geoderma* 114(1-2): 81-92.
- [2] Arias, M., Perez-Novo, C., Osorio, F., López, E., Soto, B. (2005): Adsorption and desorption of copper and zinc in the surface layer of acid soils. – *Journal of Colloid and Interface Science* 288(1): 21-29.
- [3] Ashraf, S., Ali, Q., Zahir, Z. A., Ashraf, S., Asghar, H. N. (2019): Phytoremediation: Environmentally sustainable way for reclamation of heavy metal polluted soils. – *Ecotoxicology and Environmental Safety* 174: 714-727.
- [4] Bashir, S., Zhu, J., Fu, Q. L., Hu, H. Q. (2018): Cadmium mobility, uptake and antioxidative response of water spinach (*Ipomoea aquatic*) under rice straw biochar, zeolite and rock phosphate as amendments. – *Chemosphere* 194: 579-587.
- [5] Bradl, H. B. (2004): Adsorption of heavy metal ions on soils and soils constituents. – *Journal of Colloid & Interface Science* 277(1): 1-18.
- [6] He, H. S., Wang, W. J., Zhu, H., Zu, Y. G., Zhang, Z. H., Guan, Y., Xu, H. N., Yu, X. Y. (2008): Influences of addition of different krillium in saline-sodic soil on the seed germination and growth of cabbage. – *ActaEcologica Sinica* 28(11): 5338-5346.
- [7] He, L. Z., Zhong, H., Liu, G. X., Dai, Z. M., Brookes, P. C., Xu, J. M. (2019): Remediation of heavy metal contaminated soils by biochar: mechanisms, potential risks and applications in China. – *Environmental Pollution* 252: 846-855.
- [8] Ho, Y. S. (2006): Review of second-order models for adsorption systems. – *Journal of Hazardous Materials* 3(136): 681-689.
- [9] Hu, N. J., Luo, Y. M., Zhong, S. J. (2010): Adsorption of cadmium on typical soils in the Yangtze river delta and its relationship with organic matter, pH and temperature. – *Actasodiae sinica* 44(2): 437-443.
- [10] Hwang, Y. H., Hsiao, C. K., Lin, P. W. (2019): Globally temporal transitions of blood lead levels of preschool children across countries of different categories of Human Development Index. – *Science of the Total Environment* 659: 1395-1402.

- [11] Jain, N., Chandramani, S. (2018): Arsenic poisoning. An overview. – *Indian Journal of Medical Specialities* 9(3): 143-145.
- [12] Li, C. L., Zhou, L. X. (2007): Study on the effects of different grain size components on cadmium adsorption behavior in several typical soils in China. – *Journal of Agro-Environmental Science* 26(2): 516-520.
- [13] Li, Y. M., Kang, C. L., Chen, W. W., Ming, L., Zhang, S., Guo, P. (2013): Thermodynamic characteristics and mechanisms of heavy metals adsorbed onto urban soil. – *Chemical Research in Chinese Universities* 29(1): 42-47.
- [14] Liao, M. (2006): Effects of organic acids on adsorption of cadmium onto kaolinite, goethite and bayerite. – *Pedosphere* 16(2): 185-191.
- [15] Ma, W., Zhang, M. M., Wang, R. Q., Xin, B. P., Guo, W., Dai, J. L. (2015): Mercury (II) Adsorption on three contrasting Chinese soils treated with two sources of dissolved organic matter: II. Spectroscopic characterization. – *Soil and Sediment Contamination* 24(6): 719-730.
- [16] Martin, I., Matthias, W., Armin, K., Michael, M., Mark, R., Katy, M., Katharina, K., Emmanuel, F., Wolfgang, W., Moritz, B. (2019): Towards an understanding of the Cd (II) isotope fractionation during transfer from the soil to the cereal grain. – *Environmental Pollution* 244: 834-844.
- [17] Naiya, T. K., Bhattacharya, A. K., Das, S. K. (2009): Adsorption of Cd (II) and Pb (II) from aqueous solutions on activated alumina. – *Journal of Colloid and Interface Science* 333(1): 14-26.
- [18] Rao, K. S., Anand, S., Venkateswarlu, P. (2010): Adsorption of cadmium (II) ions from aqueous solution by *Tectonagrandis* L. F. (teak leaves powder). – *Bio Resources* 5(1): 438-454.
- [19] Roberts, T. L. (2014): Cadmium and phosphorous fertilizers: the issues and the science. – *Procedia Engineering* 83: 52-59.
- [20] Saifullah, Dahlawi, S., Naeem, A., Rengel, Z., Naidu, R. (2018): Biochar application for the remediation of salt-affected soils: challenges and opportunities. – *Science of the Total Environment* 625: 320-335.
- [21] Shi, S. H., Tian, L., Nasir, F., Bahadur, A., Batool, A., Luo, S. S., Yang, F., Wang, Z. C., Tian, C. J. (2018): The response of microbial communities and enzyme activities to amendments in saline-alkaline soils. – *Applied Soil Ecology* 135: 16-24.
- [22] Sprynskyy, M., Kowalkowski, T., Tutu, H., Cozmuta, L. M., Cukrowska, E. A., Buszewski, B. (2011): The adsorption properties of agricultural and forest soils towards heavy metal ions (Ni, Cu, Zn, and Cd (II)). – *Journal of Soil Contamination* 20(1): 12-29.
- [23] Sun, X. B., Zhu, J. F., Gu, Q. Y., You, Y. H. (2018): Surface-modified chitin by TEMPO-mediated oxidation and adsorption of Cd (II). – *Colloids and Surfaces A* 555: 103-110.
- [24] Tsang, D. C. W., Zhang, W. H., Lo Irene, M. C. (2007): Modeling cadmium transport in soils using sequential extraction, batch, and miscible displacement experiments. – *Soil Science Society of America Journal* 71(3): 674-681.
- [25] Van Poucke, R., Ainsworth, J., Maesele, M., Ok, Y. S., Meers, E., Tack, F. M. G. (2018): Chemical stabilization of Cd (II)-contaminated soil using biochar. – *Applied Geochemistry* 88: 122-130.
- [26] Wang, J. G. (2012): Study on the adsorption and desorption characteristics of heavy metal cadmium in typical farmland soil in China. – Dissertation for doctor degree, Northwest Agricultural and Forestry University, Yangling, Shaanxi, China.
- [27] Wang, L., Seki, K., Miyazaki, T., Ishihama, Y. (2009): The causes of soil alkalization in the Songnen Plain of Northeast China. – *Paddy and Water Environment* 7(3): 259-270.
- [28] Wang, L. L., Shi, Y., Yao, D. K., Pan, H., Hou, H. J., Chen, J., Crittenden, J. C. (2019): Cd (II) complexation with mercapto-functionalized attapulgite (MATP): adsorption and DFT study. – *Chemical Engineering Journal* 366: 569-576.

- [29] Wu, B., Guo, S. H., Zhang, L. Y., Li, F. M. (2018): Risk forewarning model for rice grain Cd (II) pollution based on Bayes theory. – *Science of the Total Environment* 618: 1343-1349.
- [30] Xie, X. L., Gao, H. L., Luo, X., Su, T. M., Zhang, Y. Q., Qin, Z. Z. (2019): Polyethyleneimine modified activated carbon for adsorption of Cd (II) in aqueous solution. – *Journal of Environmental Chemical Engineering* 7(3): 103183.
- [31] Yang, W. Z., Yang, M. D., Wen, H. Y., Jiao, Y. (2018): Global warming potential of CH₄ uptake and N₂O emissions in saline-alkaline soils. – *Atmospheric Environment* 191: 172-180.
- [32] Yang, X. D., Wan, Y. S., Zheng, Y. L., He, F., Yu, Z. B., Huang, J., Wang, H. L., O, Y. S., Jiang, Y. S., Gao, B.(2019): Surface functional groups of carbon-based adsorbents and their roles in the removal of heavy metals from aqueous solutions: a critical review. – *Chemical Engineering Journal* 366: 608-621.
- [33] Yuan, C. L., Li, F. B., Cao, W. H., Yang, Z., Hu, M., Sun, W. M. (2019): Cadmium solubility in paddy soil amended with organic matter, sulfate, and iron oxide in alternative watering conditions. – *Journal of Hazardous Materials* 378: 120672.
- [34] Zhai, Q. X., Guo, Y., Tang, X. S., Tian, F. W., Zhao, J. X., Zhang, H., Chen, W. (2019): Removal of cadmium from rice by *Lactobacillus plantarum* fermentation. – *Food Control* 96: 357-364.
- [35] Zhao, Y. G., Wang, S. J., Li, Y., Liu, J., Zhuo, Y. Q., Chen, H. X., Wang, J., Xu, L. Z., Sun, Z. T. (2018): Extensive reclamation of saline-sodic soils with flue gas desulfurization gypsum on the Songnen Plain, Northeast China. – *Geoderma* 321(1): 52-60.

EARLY WARNING OF INSTABILITY DURING MESOPHILIC ANAEROBIC DIGESTION OF CHICKEN MANURE

CHEN, L.^{1,3} – ZHENG, T.^{1,2*} – CAO, Q.³ – ZHOU, Y.⁴ – LIU, X.³ – LI, D.^{3*}

¹*Institute of Urban and Rural Mining, Changzhou University, Changzhou 213164, China*

²*Guangzhou Institute of Energy Conversion, Chinese Academy of Sciences, Guangzhou 510640, China*

³*Key Laboratory of Environmental and Applied Microbiology, Environmental Microbiology Key Laboratory of Sichuan Province, Chengdu Institute of Biology, Chinese Academy of Sciences, Chengdu 610041, China*

⁴*Chengdu Zhongke Energy & Environmental Protection Co. Ltd, Chengdu 610041, China*

**Corresponding author*

e-mail: zhengtao@ms.giec.ac.cn

(Received 29th Aug 2019; accepted 14th Nov 2019)

Abstract. Anaerobic digestion (AD) of chicken manure (CM) is easily inhibited by excessive ammonia. To determine early warning indicators of this process, mesophilic AD of CM was conducted by organic loading rate (OLR) from 1.0 to 7.0 g volatile solids (VS)/(L·d). Process parameters were monitored every day. At the maximum stable OLR of 5.0 g VS/(L·d), the volumetric methane production rate reached the maximum value of 1.13 L/(L·d), and the yield of methane was 178 ml/g VS. Meanwhile, the total and free ammonia nitrogen increases to 3900 and 300 mg/L (the maximum value), respectively. Bicarbonate alkalinity (BA) and volatile fatty acid (VFA) values were 12200~17400 mg/L and 1000~2200 mg/L, respectively. This process was severely inhibited by high ammonia concentration when the OLR reached 6-7 g VS/(L·d). According to our study, the most useful early warning indicators are CH₄/CO₂, VFA/BA, and individual VFAs for AD of CM.

Keywords: *chicken manure, anaerobic digestion, organic loading rate, early warning indicators, ammonia inhibition*

Abbreviations: AD: anaerobic digestion; CM: chicken manure; OLR: organic loading rate; VFA: volatile fatty acid; BA: bicarbonate alkalinity; TAN: total ammonia nitrogen; FA: free ammonia; CSTR: continuous stirred tank reactor; TS: total solid; VS: volatile solid; HRT: hydraulic retention time; FID: flame ionization detector; PA: partial alkalinity; IA: intermediate alkalinity; TA: total alkalinity; VMPR: volumetric methane production rate; MY: methane yield; ORP: redox potential

Introduction

Anaerobic digestion (AD) is an effective approach to minimizing organic waste and recovering valuable energy (Cioabla et al., 2013). AD is a multi-stage biochemical process (MBP) in which complex organic materials undergo the reaction series of hydrolysis, acidogenesis, acetogenesis, and methanogenesis. Each metabolic stage is controlled by various types of microorganisms, which differ in their habitat requirements, nutritional needs, ability, and growth kinetics to tolerate environment stresses.

Chicken manure (CM) has higher nitrogen contents than other substrates, such as cow manure, pig manure, waste active sludge, and food waste (Qiao et al., 2011). This nitrogen is translated to amino acids, which can be used to synthesize substrate for cell utilization. However, excess nitrogen is further decomposed to ammonia, which exerts a

toxic inhibitory effect on microorganism metabolism, and causes failure of AD under high organic loading rates (OLR) (Angeladaki et al., 2003; Malollari et al., 2016). Several previous studies have reported AD inhibition at 1.5 to 4.0 g N/L of ammonia concentrations for different strains and culture conditions (Hashimoto, 1986; Hendriksen et al., 1991), and severe inhibition at higher ammonia concentrations. Ahring (1995) reported that AD of livestock was inhibited when ammonia nitrogen (AN) concentrations were 3000~4000 mg/L. Hashimoto (1986) and Zeeman (1985) reported that AD process was imbalanced at 2500 mg/L and 1700 mg/L of total ammonia nitrogen (TAN), respectively. Furthermore, methanogens are severely inhibited, and more than 80% of methane production is suppressed, at TAN values of 8000 mg/L (Krylova et al., 1997).

However, the non-ionized form of ammonia nitrogen: free ammonia (FA), also influences AD inhibition. Studies have shown that it is FA rather than TAN that inhibits methanogenesis. For example, AD inhibition in livestock waste and swine manure occurred at FA concentrations of 700~1100 mg/L (Kayhanian, 1994).

Hence, to maintain steady operation, most large-scale AD are usually operated at low OLR, resulting in a less efficient, low biogas production, and less economic process (Tampio et al., 2014). Ensuring stable AD under high OLR is an urgent problem that should be solved. Previous research has involved monitoring and controlling the process to improve stability and efficiency (Li et al., 2014), using a number of parameters including pH, alkalinity, volatile fatty acids (VFAs), AN, methane contents, biogas production, coupling indicators, and alkalinity ratios. However, the early warning indicators of AD inhibition differed in each study.

Review of literature

Fischer et al. (1984) found that propionic acid rises prior to the failure of digesters for treating swine waste. Nakakubo (2008) concluded that butyrate, valerate, and isobutyrate could be used as the warning indicators in continuous stirred tank reactors (CSTR) for pig manure treatment, whereas acetate and propionate were not suitable. Li (2014) performed AD of food waste by a CSTR, and concluded that several coupled indicators, such as alkalinity ratios (IA/BA, BA/TA), VFA ratio, and alkalinity (VFA/BA) could be used for reflecting the metabolism of AD system to generate rapid and effective early warnings. Furthermore, Martín-González (2013) recommended an IA/PA ratio < 0.3 for maintaining stable operation in mesophilic AD process of sorted organic fractions from municipal solid waste.

However, there are few studies evaluating the instability of chicken manure anaerobic digestion. Therefore, early warning indicators applicable to indicate instability during the CM AD process were determined in this study. Instability mechanisms of high-nitrogen substrate AD were analyzed. Controlled measures were recommended to ensure stable mesophilic AD of CM.

Materials and methods

Substrate and inoculum

Five batches of CM were collected from a chicken farm (Chengdu, China), then, the CM was stored at 4 °C after removing visible bristles. CM characteristics, such as the

total solid (TS), volatile solid (VS), total carbonate (C %TS), total nitrogen (N %TS), and the ratio of C and N (C/N) were analyzed and listed in *Table 1*.

Table 1. *Composition of chicken manure*

Characteristics	Batch 1	Batch 2	Batch 3	Batch 4	Batch 5
TS (g/kg)	207.1	174.4	155.8	215.3	262.3
VS (g/kg)	119.0	122.0	119.0	125.0	146.0
Carbon (%TS)	29.6	29.8	30.1	30.5	29.0
Nitrogen (%TS)	3.1	3.2	3.2	3.3	2.3
C/N	9.5	9.4	9.4	9.3	12.9
Ammonia nitrogen (mg/L)	2800	3000	2820	2900	2750

The inoculum was the digested residue taken from an AD for pig waste treatment. The inoculum was acclimated for 25 d in the CSTR system under mesophilic conditions (35 °C) fed CM as a substrate until the methane contents were > 60%. The pH in the acclimated inoculum was 7.5.

AD

A bench-scale CSTR with a working volume of 55 L was operated at mesophilic conditions (35 ± 2 °C) as shown in *Figure 1*. The reactor was designed by laboratory, which was heated by the electric heating layer and mixed with a motor. An gas flow-meter and online biogas analyzer were used to measure the biogas production and contents of methane (CH₄) and carbon dioxide (CO₂), respectively. Other indicators, such as temperature, pH, and redox potential, were monitored using the online liquid monitoring system. The substrate tank was stirred 8 times per day at 40 rpm for 30 min to maintain the material in a constant state.

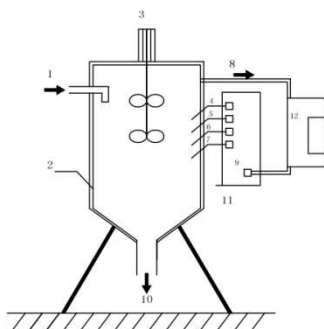


Figure 1. *Schematic diagram of the CM AD in CSTR. (1. Feed inlet, 2. Heating layer, 3. Rabbler, 4. pH probe, 5. Oxidation reduction probe, 6. Electrical conductivity probe, 7. Temperature probe, 8. Air outlet, 9. Gas flow indicator, 10. Discharge outlet, 11. Instrument cabinet, 12. Automatic monitoring instrument for methane analysis)*

The mesophilic AD of CM was carried out at OLRs of 1.0, 2.0, 3.0, 4.0, 5.0, 6.0, and 7.0 g VS/(L·d). After successful start-up, AD was operated in semi-continuous mode. The substrate was added once per day after sampling. By restricting the total feed to

2.75 kg, the hydraulic retention time (HRT) was set at 20 d. The daily feedstock amount and discharge is for different OLRs listed in *Table 2*.

Table 2. Operating conditions for the mesophilic AD of CM

Period	Running time (d)	OLR (g VS/(L·d))	HRT (d)	Daily feedstock (g)		Daily discharge (g)
				CM	Water	
Starting stage	1-30	1.0	20	463	2287	2750
	31-60	2.0	20	926	1824	2750
Steady stage	61-90	3.0	20	1352	1398	2750
	91-120	4.0	20	1848	902	2750
	121-150	5.0	20	2310	439	2750
Inhibition stage	151-180	6.0	20	2640	110	2750
	181-200	7.0	20	2636	114	2750

Analytical methods of samples

TS and VS were measured by standard methods (Walter et al., 1998). C and N were monitored by a Vario EL element analyzer (Elementar Analysensysteme GmbH, Germany). Daily gas production and cumulative gas production were analyzed online by the gas flowmeter manufactured by Beijing Sevenstar Electronics Co., Ltd in China. Biogas composition analyses were performed online by an automatic biogas analyzer made in Wuhan Cubic Optoelectronics Co., Ltd, China. Individual VFA were measured by a gas chromatographer (GC, Agilent-6890N) equipped with a flame ionization detector (FID) (Li et al., 2010). Partial alkalinity (PA), total alkalinity (TA), intermediate alkalinity (IA), and bicarbonate alkalinity (BA) were monitored by a ZDJ-4B Automatic Potentiometric Titrator (Shanghai Precision & Scientific Instrument Co., Ltd, China), in accordance with the methods of Anderson and Yang (1992). The alkalinity was titrated to a PA of pH 5.75, and an IA of pH 5.75 to 4.30 (Ripley et al., 1986). The pH end-point for TA was 4.00. BA was calculated from *Equation 1* (Jenkins et al., 1983).

$$BA = 1.25 PA \quad (\text{Eq.1})$$

where BA is bicarbonate alkalinity (mg/L) and PA is partial alkalinity (mg/L). TAN was determined by Nessler's reagent spectrophotometry according to Chinese Standard (GB 7479-87). The FA was calculated by *Equation 2* (Kayhanian, 1999).

$$FA = \frac{TAN \times K_a}{K_a + [H]} \quad (\text{Eq.2})$$

where FA is represented by FA concentration (mg/L), TAN is represented by TAN concentration (mg/L), K_a is represented by temperature dependent dissociation constant (25 °C: 0.564×10^{-9} , 35 °C: 1.097×10^{-9} , 55 °C: 3.77×10^{-9}), and [H] is represented by hydrogen ion concentration ($10^{-\text{pH}}$).

Results and discussion

Volumetric methane production rate (VMPR) and methane yield (MY)

Methane generation is an important parameter for the stability of AD. VMPR and MY were used to describe the biogas production process. The HRT was 20 days and OLR was maintained at a steady-state in the latter 10 days. *Figure 2a* and *b* presents the VMPR and MY of seven OLRs 1.0–7.0 g VS/(L·d).

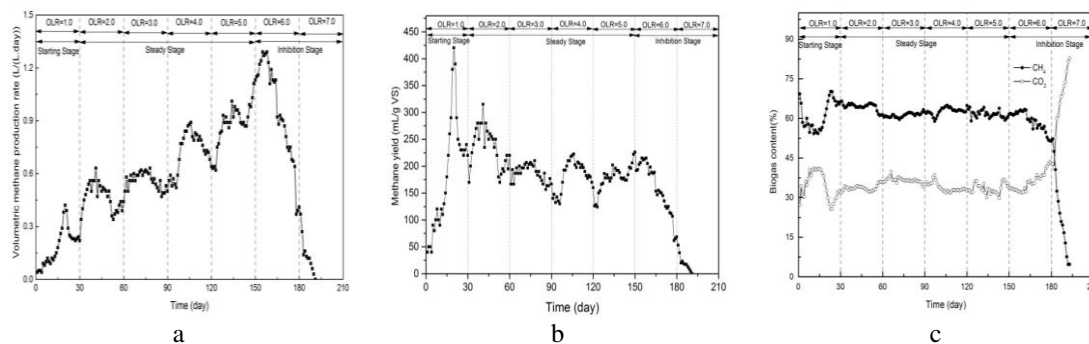


Figure 2. Evaluation of (a) volumetric biogas production rate, (b) material yield, and (c) biogas content

During the starting stage, VMPR was low (0.22–0.39 L/(L·d)). Subsequently, AD reached a steady stage, where VMPR increased continually with the increase in OLR. The VMPR was achieved at 0.44, 0.57, 0.81, and 1.13 L/(L·d) at OLR of 2.0, 3.0, 4.0, and 5.0 g VS/(L·d), respectively. As AD reached the inhibition stage (6.0–7.0 g VS/(L·d)), VMPR began to decline until methane production ceased on day 191.

MY reflects the biotransformation of substrate by AD microorganisms, which illustrates the metabolic process of microorganisms. In the starting stage, MY was in the range of 220–390 mL/g VS. With OLR increase, the MY of AD displayed a narrower range between 155 and 225 mL/g VS. During the inhibition stage, MY decreased sharply to zero.

Biogas contents

CH₄ is the terminal metabolite of anaerobic digestion, and it can directly reflect the metabolic activity of methanogens (Charles et al., 2011). As shown in *Figure 2c*, in the initial 20 days of the starting stage, CH₄ content was less than 60% and CO₂ content was approximately 40%. During the steady stage, the CH₄ and CO₂ contents were maintained at 60%–65% and 30%–35%, respectively. As OLR increases to 6.0–7.0 g VS/(L·d), the CH₄ contents decrease to < 60% on the 165th day. Then, CH₄ contents drop rapidly to < 50% on 180th day, while CO₂ contents increase.

VFAs

VFAs are the important intermediate metabolite of AD, which are mainly generated from hydrolysis and acidogenesis. All VFAs must first be degraded to acetate then degraded to methane. The conversion rate of different individual VFAs varies in the following order: acetate > n-butyrate > propionic acid (Ren et al., 2003). Propionic acid value was suggested as early warning indicators for the AD failure of pig manure

treatment (Pullammanappallil et al., 2011). Hill (1988) showed that *iso*-acid value would be a better indicator, while Ahring (1991) recommended that the concentration of butyrate acid and its isoforms could be indicated early AD instability.

In this study, individual VFAs, including acetate, propionate, *n*-butyrate, *iso*-butyrate, *n*-Valerate, and *iso*-Valerate, were detected each day, as shown in *Figure 3*. It was clear that each individual VFA increased with OLR, especially during the inhibition stage. Individual VFAs fluctuated slightly as the OLR to 1.0 g VS/(L·d), owing to the microorganism community adapting to the new material. During the steady stage, VFA levels maintained a stable range. As the OLR lower than 4.0 g VS/(L·d), acetate and propionate concentration remained below 1000 and 100 mg/L, respectively. Values of *n*-butyrate, *iso*-butyrate, *n*-Valerate, and *iso*-Valerate were below 60, 50, 10, and 80 mg/L, respectively. With the OLR increase from 4.0 to 5.0 g VS/(L·d), the concentration of acetate and propionate reached more than 1500 and 250 mg/L, respectively.

As OLR higher than 5.0 g VS/(L·d), individual VFAs increased dramatically. Among these, acetate and propionate increased by more than 4 and 9 times during the inhibition stage to 14387 mg/L and 2818 mg/L, respectively. The other VFAs, such as *n*-butyrate, *iso*-butyrate, *n*-Valerate, and *iso*-Valerate, increased by approximately 40, 26, 32, and 19 times during the instability period, respectively. This could lead to the irreversible acidification of AD, adversely affecting the methanogenesis process and even terminating gas production. The detailed VFA changes are listed in *Table 3*.

Table 3. Significant changes in indicator level during inhibition stage

Indicators	Sudden change	Days of sudden change (d)	Threshold of inhibition	Warning time (d)
CH ₄ (%)	56→54	175	< 55	16
CO ₂ (%)	38→41	175	> 40	16
pH	No	/	/	/
ORP (mV)	-535→-524	169	> -530	22
Acetate (mg/L)	1600→2044	167	> 2000	24
Propionate (mg/L)	320→441	169	> 400	22
<i>n</i> -Butyrate (mg/L)	45→75	167	> 50	24
<i>i</i> -Butyrate (mg/L)	51→99	167	> 50	24
<i>n</i> -Valerate (mg/L)	8→18	167	> 10	24
<i>i</i> -Valerate (mg/L)	88→126	168	> 100	23
TA (mg/L)	No	/	/	/
BA (mg/L)	No	/	/	/
IA (mg/L)	2926→3284	174	> 3000	24
TAN (mg/L)	No	/	/	/
FA (mg/L)	No	/	/	/
VFA/TA	0.19→0.23	174	> 0.2	24
VFA/BA	0.17→0.22	174	> 0.2	24
IA/BA	0.13→0.15	180	> 0.15	18
BA/TA	0.81→0.76	187	< 0.80	4
VFA/FA	9.6→12.2	181	> 12.0	10
CH ₄ /CO ₂	1.5→1.1	169	< 1.5	22

Total ammonia nitrogen (TAN) and free ammonia (FA)

Ammonia is produced from nitrogenous compounds, which contain protein, phospholipids, nucleic acids, and other nitrogenous lipids (Kayhanian, 1999). Theoretically, all organic nitrogen material in the feedstock can be converted to ammonia (NH_3 and NH_4^+). Relationship between the ionized and non-ionized forms of ammonia nitrogen is shown in Equation 3. NH_3 is suggested as the main factor of AD inhibition due to its freely membrane permeable (Kroeker et al., 1979).



In this study, the ammonia nitrogen content of substrate was 4000 mg/L. TAN increased slowly from 1040 mg/L to 3700 mg/L at day 1 to day 150 (1.0–5.0 g VS/(L·d)) shown in Figure 4a. The methane content was over 60% during these stages. FA increased from 46 to 224 mg/L with pH increasing. The level of TAN and FA was low; approximately 3000 and 200 mg/L, respectively, and no inhibition occurred. This contrasts with the conclusion of Velsen (1979), that is TAN concentration above 3000 mg/L exerts an inhibiting effect on the reactor. With OLR increased to 6.0 g VS/(L·d), TAN and FA increased dramatically. On day 167, TAN concentration was higher than 5000 mg/L, FA exceeded 500 mg/L, and the methane content decreased slightly to < 60%, which was consistent with VFAs increase. Methane contents remained at 55%–60%, but volumetric methane generation rate decreased sharply, from 0.91 to 0.43 L/(L·d), during days 167–180. Therefore, the reactor was severely inhibited.

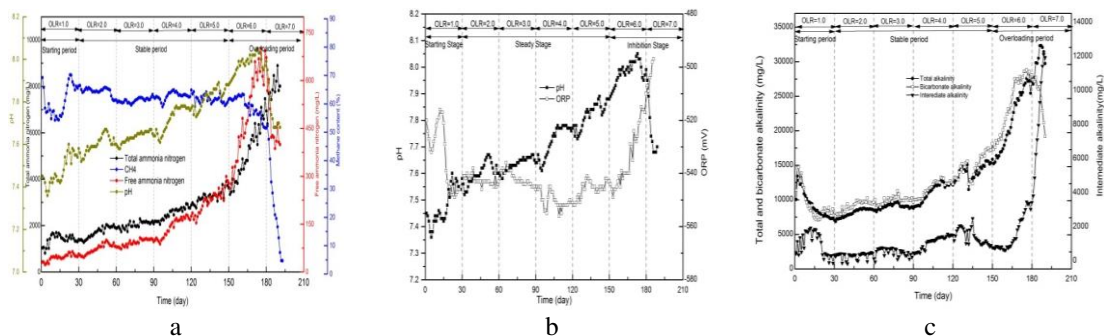


Figure 3. Evaluation of (a) total ammonia nitrogen and free ammonia nitrogen, (b) pH and redox potential (ORP), and (c) alkalinity

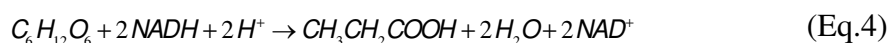
After 180 days, TAN increased continuously to above 8000 mg/L, pH decreased from 7.99 to 7.68, respectively, leading to a slight decrease in FA, with the average value being 456 mg/L. When the VFA levels were higher than 6600 mg/L, volumetric methane production rate decreased < 0.4 L/(L·d). When biogas production ceased, TAN, VFA, and FA levels reached 8009 mg/L, 20945 mg/L, and 400 mg/L, respectively. TAN increased steadily, with no sudden changes. FA concentration showed a positive correlation to pH value (correlation coefficient: 0.846). Therefore, TAN and FA values on their own were proved unsuitable for indicating AD instability. It is essential to combine them with other indicators to decide threshold of TAN and FA that inhibits the process of AD.

pH

pH is a crucial parameter related to growth and metabolism of microorganism. Accumulation of VFAs could cause pH to rapidly decrease in the low buffering capacity digester. However, in the high buffering capacity digester (Anderson et al., 1992), especially during fermentation of high ammonia nitrogen material, pH levels gradually increase until failure. In this study, as shown in *Figure 4b*, pH value increased from 7.48 to 7.98 during the first 173 days. Although the pH level declined after day 174, it remained in the normal range, with pH at an average of 7.74. The pH value was in the optimal range for fermentation during inhibition stage; however, biogas production and methane content were low. Synergistic action between NH₃, VFAs, and pH lead to a special state called the “inhibited steady state” (Li et al., 2008). Therefore, pH is not regarded as an early warning indicator in high ammonia nitrogen systems.

Redox potential (ORP)

The redox potential (ORP) reflects the redox situation in the microbial cell. It is related to the level of NADH/NAD⁺, which affects the growth and metabolism of microorganisms (Graef et al., 1999). Some studies suggested a good correlation between the accumulation of VFAs and ORP (Switzenbaum et al., 1990). As shown in *Figure 4b*, ORP fluctuated from -530 mV to -510 mV in the first 17 days of the starting stage. Despite the increase of OLR, ORP remained lower than -530 mV until day 167. The sharp increase in ORP may be due to microorganisms oxidizing NADH to NAD⁺ by producing propionic acid and hydrogen (*Eqs. 4-5*). Hydrogen was not detected in the gas phase during AD in this study. That is because hydrogen was consumed by homoacetogenic bacteria or hydrotrophic methanogens (*Eqs. 6-7*). However, the variation of ORP should be based on the NADH and NAD⁺ concentration. In future, it is necessary to quantitatively determine concentrations of NAD⁺ and other related enzymes.



Alkalinity

During AD, buffering capacities are typically evaluated using alkalinity levels, including TA, BA, PA, and IA. Before sudden change of pH, alkalinity is sensitive to accumulation of VFAs. In the anaerobic digester, TA was proved to be insensitive as the result of the combination of VFA and bicarbonate (Björnsson et al., 2001). BA has an empirical correlation with VFA accumulation (Hawkes et al., 1994); thus, BA is used to neutralize VFA instead of TA (Moosbrugger et al., 1993). However, as the ammonia adds alkalinity to the system in the high ammonia system, the relationship is not observed in response to ammonia overload.

As shown in *Figure 4c*, alkalinity level showed a constant increasing trend, while the TAN level in the digester increased continuously. During the steady stage, that is 2.0–5.0 g VS/(L·d), the TA, BA, and IA were at the range of 9000–15000 mg/L, 10000–17000 mg/L, and 900–2500 mg/L, respectively. For an OLR of 6.0 g VS/(L·d), TA and BA increased obviously from 15000 to 27000 mg/L, 17000 to 28000 mg/L, respectively. IA levels exceeded 3000 mg/L on day 174. After 180 days, BA decreased from 28000 to 19000 mg/L until biogas production ceased, owing to the IA level increasing dramatically to 12576 mg/L, the maximum value. In high ammonia system, the main buffers in AD are bicarbonate (HCO_3^-) and NH_3 , with a pKa of 6.3 and 9.3, respectively (Moosbrugger et al., 1993) The accumulation of VFA did not lead to a decline in pH or BA because the ammonia reacts with the accumulated VFA before BA due to the higher pKa. The accumulated VFAs consume BA, producing equivalent IA. Therefore, TA and BA are unsuitable warning indicators due to their insensitivity to the high ammonia system. IA does response to the overloading, so it is thought to be an effective indicator during AD of CM.

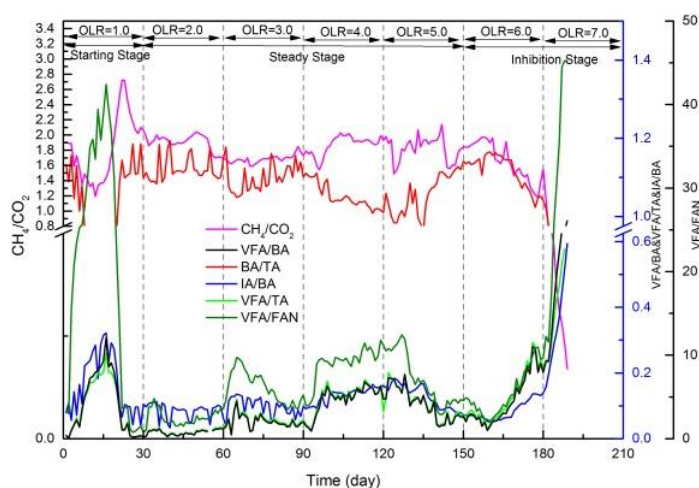


Figure 4. Development of coupling indicators

Screening for early warning indicators

Gas production rates are potential indicators in the metabolic status of the digester. Lowering gas production rate, compared with influent rate of organic matter, provides a warning of soluble acid product accumulation in the liquid phase. Unfortunately, that is the result of an imbalance rather than a warning of an imbalance. Changes in the biogas production rate depend on HRT, OLR, and feed composition. Moreover, gas production rate is low sensitive to overload compared to other process indicators. Therefore, it is not a significant early warning indicator. Warning time was defined as the day on which the biogas production ceased minus the day of sudden change in this study. Biogas production ceased on day 191.

Several studies defined alkalinity ratio as monitoring parameter to indicate AD instability. Actually, diverse stability limit values have been proposed in many studies dealing with various substrate and experimental conditions (Rincón et al., 2008). In the mesophilic lab-scale upflow anaerobic sludge blanket (UASB) which is rearing potato-starch wastewater, the IP/PA ratio of 0.4 was suggested to ensure reactor stable, and

IA/PA below 0.3 was proposed to maintain operation stable in the AD of municipal solid waste. In this study, combined parameters, including the ratio of CH_4/CO_2 , VFA/TA, VFA/BA, VFA/FAN, IA/BA, and BA/TA were calculated, as shown in *Figure 4*, and evaluated as potential indicators of AD instability.

During the starting and stable stages, all ratios became relatively stable after 20 days. However, during the inhibition stage, the ratios increased or decreased by varying degrees. The VFA/BA and VFA/TA curves almost overlapped. Before 150 days, the ratios of VFA/TA and VFA/BA were below 0.2. After 174 days, the ratios increased sharply to 0.98 and 0.66, respectively, until gas production ceased. However, there were no crucial sudden changes in the ratios of IA/BA and BA/TA. Before 182 days, the range of IA/BA was 0.05–0.15 whereas BA/TA was 0.8–1.2 prior to 187 days. The sharp curve of the VFA/FA ratio was similar to that of VFA/TA and VFA/BA. Before 181 days, the ratio of VFA/FA was below 12. Early warning days and sudden changes in each indicator are listed in *Table 3*.

According to the early warning times of VFAs indicators, propionate is later than all other individual VFAs, which is including acetate, n-butyrate, i-butyrate, n-valerate, and i-valerate. In theory, individual VFAs are the most sensitive early warning indicators. Meanwhile, among the combined indicators, the early warning order was $\text{VFA/BA} = \text{VFA/TA} > \text{CH}_4/\text{CO}_2 > \text{IA/BA} > \text{VFA/FA} > \text{BA/TA}$. The VFA/TA, VFA/BA, and IA/BA indicators represent acid-base balance in the system., VFA/TA and VFA/BA were dominant indicators for comprehensively reflecting process status in the high ammonia nitrogen system. The warning time of CH_4 was the same as CO_2 ; however, the ratio of CH_4/CO_2 showed an earlier warning time than individual biogas contents. Therefore, individual VFAs, as well as the combined indicators, including CH_4/CO_2 and VFA/BA, can be selected as early warning indicators for AD of CM instability under mesophilic conditions. The thresholds of each indicator are shown in *Table 3*.

In our experiments, the biogas content was determined online by an automatic biogas analyzer. CH_4/CO_2 was more sensitive to AD instability owing to the superposition effect. Individual VFAs can be detected online by gas chromatography or near-infrared spectroscopy. It is more convenient for indicators to be monitored online to control AD instability. Therefore, the ratio of CH_4/CO_2 and individual VFAs can be monitored online in real time, enabling effective warnings of AD instability during CM engineering applications.

Inhibitory conduction process

High ammonia concentration of substrate and increasing OLR led to ammonia nitrogen accumulation in the system., The difference in intracellular pH caused transformation between NH_4^+ and NH_3 due to ammonia molecules diffusing into the cells of methanogens. Accumulated NH_4^+ may inhibit the methane-synthesizing enzyme, NH_3 could break the imbalance of protons and result in a potassium deficiency (Kayhanian, 1999). High concentrations of NH_3 mainly inhibit the metabolism of methanogens, particularly aceticlastic methanogens, as well as severely affecting the growth rates of hydrogen-utilizing methanogens (Björnsson et al., 2001). H_2 and CO_2 is used by homoacetogenic bacteria to produce acetate. These factors caused the increase of acetate concentration during the inhibition stage. Subsequently, the accumulation of propionate, n-butyrate, iso-butyrate, n-valerate, and iso-valerate was observed owing to the inhibition of syntrophic VFA-oxidizing bacteria. With ammonia nitrogen

concentration increasing, the pH of the system increased continuously. The NH_3 reacted with CO_2 induced during to form bicarbonate. The buffering capacity increases during AD owing to the reaction. Therefore, BA and TA increased during the stable stage. Due to the accumulation of VFA, on day 180, BA was consumed, producing IA, and releasing the gas phase as CO_2 . Therefore, BA decreased and IA increased. At the same time, CO_2 content increased and CH_4 content declined sharply. Finally, acetotrophic methanogens and hydrotrophic methanogens were completely inhibited, causing biogas production to cease.

Conclusions

For AD of CM with high ammonia nitrogen concentration, increasing the OLR led to ammonia accumulation, and high pH values led to the release of free ammonia. This effected the growth and metabolism of methanogens, causing VFA accumulation and termination of biogas production. For the early warning of AD instability, CH_4/CO_2 , VFA/BA ratios, as well as individual VFAs, are regarded as effective indicators. To measure AD stable operation at a high OLR, it is critically to take suitable measures, including dilution, bioaugmentation, and other efficient methods. In this study, the high-ammonia nitrogen materials were selected for AD, and the instability early warning indicators were obtained, which provides a theoretical basis for the stable operation of high ammonia nitrogen materials under high loading rate. Furthermore, in the future study, it is necessary to research the microbial community structure in order to analyze the mechanism of the instability deeply.

Acknowledgements. The authors would like to gratefully acknowledge research grants from Science and Technology Project of Guangdong Province, PR China (No. 2016A010105017) and (No. 2017B040404009), the National Natural Science Foundation of China (21476222), Youth Innovation Promotion Association CAS (2017423), Program of Strategic Resource Service Network CAS (ZSYS-009), Chengdu science and technology Huimin project (2016-HM02-00092-SF), the Key Laboratory of Environmental and Applied Microbiology, and Chengdu Institute of Biology CAS (KLCAS-2016-10).

REFERENCES

- [1] Ahring, B. K., Sandberg, M., Angelidaki, I. (1995): Volatile fatty-acids as indicators of process imbalance in anaerobic digesters. – *Appl Microbiol Biotechnol.* 43(3):559-565.
- [2] Anderson, G. K., Yang, G. (1992): Determination of bicarbonate and total volatile acid concentration in anaerobic digesters using a simple titration. – *Water Environ Res.* 64(1): 53-59.
- [3] Angelidaki, I., Ellegaard, L. (2003): Codigestion of manure and organic wastes in centralized biogas plants. – *Applied Biochemistry & Biotechnology* 109(1-3): 95-105.
- [4] Björnsson, L., Murto, M., Jantsch, T. G., Mattiasson, B. (2001): Evaluation of new methods for the monitoring of alkalinity, dissolved hydrogen and the microbial community in anaerobic digestion. – *Water Research* 35(12): 2833-2840.
- [5] Charles, W., Carnaje, N. P., Cordruwisch, R. (2011): Methane conversion efficiency as a simple control parameter for an anaerobic digester at high loading rates. – *Water Science & Technology* 64(2): 534-539.
- [6] Cioabla, A. E., Ionel, I., Trif, G., -tordai, Irimescu, A., Vetres, I. (2013): Study on the Quality of Biogas Obtained from Agricultural Residues during Anaerobic Fermentation. – *J Environ Prot. Ecol.* 14(1): 247-255.

- [7] Fischer, J. R., Iannotti, E. L., Porter, J. H. (1984): Anaerobic digestion of swine manure at various influent solids concentrations. – *Agricultural Wastes* 11(3): 157-166.
- [8] Graef, M. d., Alexeeva, S., Snoep, J., Teixeira, M. (1999): The steady-state internal redox state (NADH/NAD) reflects the external redox state and is correlated with catabolic adaptation in *Escherichia coli*. – *Journal of Bacteriology* 181(8): 2351-2357.
- [9] Hashimoto, A. G. (1986): Ammonia inhibition of the methanogenesis from cattle waste. – *Agricultural Wastes* 17: 241-261.
- [10] Hawkes, F. L., Guwy, A. J., Hawkes, D. L., Rozzi, A. G. (1994): On-line monitoring of anaerobic digestion: Application of a device for continuous measurement of bicarbonate alkalinity. – *Water Science & Technology* 30(12): 1-10.
- [11] Hendriksen, H. V., Ahring, B. K. (1991): Effects of ammonia on growth and morphology of thermophilic hydrogen-oxidizing methanogenic bacteria. – *Fems Microbiology Ecology* 85(3): 241-246.
- [12] Hill, D. T., Holmberg, R. D. (1988): Long chain volatile fatty acid relationships in anaerobic digestion of swine waste. – *Biological Wastes* 23(3): 195-214.
- [13] Jenkins, S. R., Morgan, J. M., Sawyer, C. L. (1983): Measuring anaerobic sludge digestion and growth by a simple alkalimetric titration. – *Water Pollution Control Federation* 55(5): 448-453.
- [14] Kayhania, M. (1994): Performance of a high-solids anaerobic-digestion process under various ammonia concentrations. – *Journal of Chemical Technology and Biotechnology* 59(4): 349-352.
- [15] Kayhanian, M. (1999): Ammonia inhibition in high-solids biogasification: an overview and practical solutions. – *Environmental Technology* 20(4): 355-365.
- [16] Kroeker, E. J., Schulte, D. D., Sparling, A. B., Lapp, H. M. (1979): Anaerobic treatment process stability. – *Water Environment Research* 51(4): 718-727.
- [17] Krylova, N. I., Khabiboulline, R. E., Naumova, R. P., Nagel, M. A. (1997): The influence of ammonium and methods for removal during the anaerobic treatment of poultry manure. – *Journal of Chemical Technology and Biotechnology* 70(1): 99-105.
- [18] Li, D., Yuan, Z., Zhang, Y., Sun, Y., Kong, X., Li, L. (2008): Anaerobic biochemical methane potential of organic fraction of municipal solid waste. – *Acta Scientiae Circumstantiae* 28(11): 2284-2290.
- [19] Li, D., Yuan, Z., Sun, Y., Ma, L. (2010): Evaluation of pretreatment methods on harvesting hydrogen producing seeds from anaerobic digested organic fraction of municipal solid waste (OFMSW). – *International Journal of Hydrogen Energy* 35(15): 8234-8240.
- [20] Li, L., He, Q., Wei, Y., He, Q., Peng, X. (2014): Early warning indicators for monitoring the process failure of anaerobic digestion system of food waste. – *Bioresource Technology* 171: 491-494.
- [21] Malollari, I., Kotori, P., Hoxha, P., Lici, L., Lajqi, V., Baruti, B., Cani, X. H., Buzo, R. (2016): Anaerobic codigestion of organic substrate for energetic biogas obtaining and review. – *J Environ Prot. Ecol.* 17(1):323-330.
- [22] Moosbrugger, R. E., Wentzel, M. C., Ekama, G. A., Marais, G. V. R. (1993): A 5 pH point titration method for determining the carbonate and SCFA weak acid/bases in anaerobic systems. – *Water Research & Technology*.28(2): 237-245.
- [23] Nakakubo, R., Møller, H. B., Nielsen, A. M., Matsuda, J. (2008): Ammonia inhibition of methanogenesis and identification of process indicators during anaerobic digestion. – *Environmental Engineering Science* 25(10): 1487-1496.
- [24] Pullammanappallil, P. C., Chynoweth, D. P., Lyberatos, G., Svoronos, S. A. (2001): Stable performance of anaerobic digestion in the presence of a high concentration of propionic acid. – *Bioresource Technology* 78(2): 165-169.
- [25] Qiao, W., Yan, X., Ye, J., Sun, Y., Wang, W., Zhang, Z. (2011): Evaluation of biogas production from different biomass wastes with/without hydrothermal pretreatment. – *Renewable Energy* 36(12):3313-3318.

- [26] Ren, N., Liu, M., Wang, A., Ding, J., Li, H. (2003): Organic acids conversion in methanogenic-phase reactor of the two-phase anaerobic process. – *Chinese Journal of Environmental Science* 24(4): 89.
- [27] Rincón, B., Borja, R., González, J. M., Portillo, M. C., Sáiz-Jiménez, C. (2008): Influence of organic loading rate and hydraulic retention time on the performance, stability and microbial communities of one-stage anaerobic digestion of two-phase olive mill solid residue. – *Biochemical Engineering Journal* 40(2): 253-261.
- [28] Ripley, L. E., Boyle, W. C., Converse, J. C. (1986): Improved alkalimetric monitoring for anaerobic digestion of high-strength wastes. – *Water Environment Research* 58(5): 406-411.
- [29] Switzenbaum, M. S., Giraldogomez, E., Hickey, R. F. (1990): Monitoring of the anaerobic methane fermentation process. – *Enzyme & Microbial Technology* 12(10): 722-730.
- [30] Tampio, E., Ervasti, S., Paavola, T., Heaven, S., Banks, C., Rintala, J. (2014): Anaerobic digestion of autoclaved and untreated food waste. – *Waste Management* 34(2): 370-377.
- [31] Walter, W. G. (1998): Standard methods for the examination of water and wastewater. – American Public Health Association, Washington, DC.
- [32] Zeeman, G., Wiegant, W. M., Koster-Treffers, M. E., Lettinga, G. (1985): The influence of the total ammonia concentration on the thermophilic digestion of cow manure. – *Agricultural Wastes* 14:19-35.

COMPARISON OF SYMPTOM TYPE DIFFERENCES IN ENVIRONMENTAL PRICKLYASH RUST AND POPULATION GENETIC STRUCTURE OF COLEOSPORIUM

PU, S.^{1#} – QI, G.^{1#} – YANG, J.^{1#} – WANG, N.² – GUO, J.³ – ZHANG, P.⁴ – YANG, X.⁵ – LIU, L.^{1,2*} – LI, C.^{1*}

¹State Key Laboratory for Conservation and Utilization of Bio-resources in Yunnan; Yunnan Agricultural University, Kunming, China

²College of Tobacco Science, Yunnan Agricultural University, Kunming, China

³Key Laboratory of Higher Quality and Efficient Cultivation and Security Control of Crops for Yunnan Province, Honghe University, Honghe, China

⁴Dehong Plant Protection and Inspection Station, Mangshi, China

⁵Wenshan University, Wenshan, China

[#]These authors contributed equally to this paper

*Corresponding authors

e-mail: Liulin6032@163.com, Li.chengyun@163.com

(Received 29th Aug 2019; accepted 14th Nov 2019)

Abstract. Pricklyash has important economic, medicinal and ecological value. Pricklyash rust is one of the main diseases of the plant, it often causes discoloration, necrosis and abscission of Pricklyash leaves. When the disease is serious, it can cause entire leaves of pricklyash to fall off and infect repeatedly, which can lead to the weakening of pricklyash, even death, and seriously affects its yield and quality. The spore morphology of pricklyash rust with different symptoms was observed and ITS sequence was analyzed and compared, the results showed that 60 samples of pricklyash rust collected from wild pricklyash, Qujing pricklyash, red pricklyash and green pricklyash belong to Basidio-mycotina, Teliomycetes, Uredinales, Coleosporaceae, *Coleosporium*, *Coleosporium zanthoxyli*. By comparing and analyzing the results of previous studies on *Dendrobium* rust with of pricklyash rust, it was found that *Dendrobium* rust and pricklyash rust were clustered in two populations and the genetic similarity coefficient of ISSR was 0.67. The genetic diversity of *Dendrobium* rust was richer than of pricklyash rust.
Keywords: pricklyash rust, coleosporium, population genetic structure, molecular marker

Introduction

Pricklyash (*Zanthoxylum* spp.) belongs to deciduous small trees or shrubs of Rutaceae, *Zanthoxylum* spp. There are about 250 species of pricklyash in the world, widely distributed in tropical and subtropical regions of Asia, Africa, America and Oceania (Huang, 1997). China is the first country to produce pricklyash and also one of its main cultivating countries in Asia (Li, 2014). There are about 39 species and 14 varieties of pricklyash in China, ranging from Liaodong Peninsula in the Hainan Island in the south, Taiwan in the southeast, and Southeast Tibet in the west (Huang, 1997). Artificially cultivated varieties have green (green pricklyash) and red (red pricklyash) fruits after ripening (Li, 2014).

Pricklyash is not only an important seasoning, but also a key traditional Chinese medicine (Gu, 2015). Pricklyash has a strong aromatic odor, which can mask other smells, disperse cold in the warm, cool down body temperature and relieve pain, thus

can be used to treat many diseases. With the continuous understanding and analysis of chemical constituents of pricklyash, it has been found that pricklyash contains a variety of chemical constituents which are beneficial to human health and disease treatment. Its rich α -linolenic acid, palmitic acid, linoleic acid and polyunsaturated fatty acid have anti-cancer, anti-inflammatory, anti-oxidation, bacteriostasis, insecticidal and antiseptic effects (Chen, 2016; Chang, 1997; Lee, 2012; Li, 2009; Liu, 2007; Mi, 2014; Paik, 2005). In addition, pricklyash has a strong root system which grows rapidly and has many advantages, such as water and soil conservation, good growth in arid and barren areas, and thus can be used to improve the ecological environment (Gu, 2015). With important economic, medicinal and ecological values, pricklyash has attracted the attention of governments at all levels and enterprises. By 2014, the planting area of pricklyash in China was 1.67×10^6 hm² while that in Yunnan Province was 3.03×10^5 hm², which accounts for more than 10% of the total planting area of pricklyash in China. Yunnan Province is one of the important production bases of pricklyash in China (Gu, 2015).

Pricklyash rust (*Coleosporium zanthoxyli*) is a common leaf disease in the cultivation area of pricklyash which is less harmful to fruits and infects both seedlings and grown plants of pricklyash (Cao, 1989, 1994; Zhang, 2006). It often causes discoloration, necrosis and abscission of pricklyash leaves. When the disease is serious, it can cause the whole leaves of pricklyash to fall off and infect repeatedly, which can lead to the weakening of pricklyash, even death, and seriously affects the yield and quality of pricklyash. In recent years, pricklyash rust has occurred in large areas in Shandong, Shaanxi and other major pricklyash production areas, causing great losses to pricklyash production (Cao, 1989, 1994; Chen, 2007).

Coleosporium zanthoxyli which causes pricklyash rust, belongs to Basidiomycetes, Uredinales, Melampsoraceae, *Coleosporium* fungus. The process of the study of Chinese prickly ash rust, *Coleosporium* fungus can be observed from rust spores of summer and winter spore on the pricklyash, the other rust spore type has not been observed, and its life cycle was unclear. At present, there are few studies on the morphology of *Coleosporium zanthoxyli* and the population genetic structure of *Coleosporium zanthoxyli* on different types of pricklyash. Therefore, on the basis of previous investigation, rust samples from red, green and wild pricklyash in Qujing, Yunnan Province were collected in 2018 and were observed carefully. The population genetic structure of *Coleosporium* on different *Coleosporium zanthoxyli* was analyzed by ISSR molecular markers, and was compared with those on Dendrobium rust. The comparative analysis was carried out in order to provide theoretical basis for the prevention and control of pricklyash rust and the related research fields of *Coleosporium*.

Materials and methods

Materials

Collection of pricklyash rust samples

In this study, rust samples from red, green, wild and local pricklyash were collected from Qujing (N26°53'49", E103°34'42"), Yunnan Province. When collecting rust samples, the collected rust samples were packed independently with absorbent paper, recorded and then air-dried or stored in a refrigerator at – 80 °C for reserve. Details of the samples are shown in *Table 1*.

Table 1. Collection information of pricklyash rust samples

Pricklyash type	No. of samples	Sampling time	Sample number
Red pricklyash	15	2018.10	HHJ
Wild pricklyash	15	2018.10	YHJ
Qujing pricklyash	15	2018.10	QJHJ
Green pricklyash	15	2018.10	LHJ
Total	60		

Primer ISSR

The molecular markers used in this study were fungal ribosomal rDNA-ITS primers (forward primers: TCCGTAGGTGAACCTGCGG; reverse primers: TCCTCCGCTTATTGATATGC) (Chen, 2007), and six ISSR primers designed and developed by our team. All the primers were synthesized by Shanghai Invitrogen Company. Detailed information is shown in Table 2.

Table 2. The primers used in genetic analysis

Primer name	Primer sequence	Tm/°C
ISSR1	AGAGAGAGAGAGAGTC	50
ISSR2	AGAGAGAGAGAGAGKG	48
ISSR3	ACACACACACACTG	50
ISSR4	ACACACACACACACWC	52
ISSR5	ACACACACACACACYA	50
ISSR6	AGAGAGAGAGAGAGTC	50

Instruments used

The main instruments used in this experiment are: ultra clean workbench, autoclave, drying box, electronic balance, HH-4 digital constant temperature water bath pot, Microfuge18 centrifuge, Blue Shield 522 visible light gel electrophoresis transmission meter, ABI-9700 PCR, 78HW-1 constant temperature heating magnetic stirrer, GeneQuant Pro protein nucleic acid analyzer, Imagequant-300 gel imaging system, ABI-3730XL genetic analytical system, Lycra fluorescence microscope and stereomicroscope.

Methods

Morphology identification of *Coleosporium*

The symptoms of rust samples collected were carefully observed, and both sides of the susceptible parts of rust plants' leaves were recorded by camera. The morphology of pathogens in the susceptible parts was observed by stereomicroscope, the symptoms were recorded, the spores of rust were picked up for observation, and the infected tissues were cut into water slides to observe the structure of sporulation tissues. The spore morphology, color and size were recorded.

Extraction of *Coleosporium* DNA

The genomic DNA of plant rust was extracted by Chelex-100 method (Liu, 2015). The details are as follows: 150 uL Chelex-100 (concentration percentage is 20%, 1/3

chelex should be absorbed) solution is absorbed by a pipette into a 1.5 mL centrifugal tube, 5 uL supernatant of Chelex-100 is absorbed by a 10 uL pipette to the lesion with rust spores, and the rust spores on the lesion are washed repeatedly so as to elute the spores off the lesion as far as possible, and the washed spores are sucked into a 1.5 mL centrifugal tube containing 150 uL Chelex-100 solution by a 10 uL pipette. The centrifugal tube was placed in boiling water for 2 min, oscillated on vortex oscillator for 20 s, centrifuged for 10 s, then water bath for 5 min, oscillated for 20 s and centrifuged for 30 s. The obtained supernatant is the extracted DNA, which is stored in the refrigerator at -20 °C for reserve.

Molecular identification of Coleosporium

The total volume of PCR reaction was 50 uL according to ITS sequence analysis of common primers of fungi ITS sequence, among which: 2×phanta max ×Buffer 25 uL (the final concentration of Mg²⁺ is 2 mM), dNTP Mix 0.2 mM, Phanta Max Super-Fidelity DNA Polymerase 1U, primers ITS1 and ITS4 0.5 mM, template DNA 25 ng/uL. A negative control group of ddH₂O was established for each reaction. Amplification was performed by ABI-PCR. The reaction procedures were as follows: pre-denaturation for 3 min at 95 °C, denaturation for 15 s at 95 °C, annealing for 15 s at 57 °C, extension for 30 s at 72 °C, running for 35 cycles; extension of 5 min at 72 °C, preservation at 4 °C; after the end of PCR, 5 uL PCR fidelity product was mixed with 2 uL loading-buffer which contains anthocyanin (1 mL Loading buffer + 10 uL Anthocyanin), conducted electrophoresis with 1.5% agarose gel for 45 min under 120 V, and then photographed with gel imaging system so as to analyze PCR product initially. The PCR product with identical fragment size was recycled with gel, and then cloned to test its sequences; sequence comparative analysis of the tested ITS sequences was conducted on NCBI website, and the ITS sequences of different plant *Coleosporium* were clustered by the neighbor-joining method using the software of molecular evolutionary genetics analysis (MAGE 5.1) (Saitou, 1987).

Population genetic structure analysis

The total volume of ISSR-PCR reaction for population genetic structure analysis of various plant rust was 30 uL, including: 10×Easy Buffer (containing Mg²⁺) 3.0 uL, 2.5 mM dNTPs 2.4 uL, ISSR primer 1.2 uL, TaqE 0.3 uL, template DNA (25 ng/uL) 1 uL, ddH₂O 22.1uL. *Coleosporium* was used as positive control group and ddH₂O as negative control group each time. The reaction procedures were as follows: pre-denaturation for 2 min 30 s at 95 °C; denaturation for 30 s at 94 °C, annealing for 1 min at 50 °C (the specific annealing temperature of each primer was shown in *Table 2*), extension for 1 min at 72 °C, running for 35 cycles; extension for 10 min at 72 °C, preservation at 4 °C; after the end of PCR, 5 uL PCR product was mixed with 2 uL Loading-buffer which contains anthocyanin (10 uL/mL anthocyanin), conducted electrophoresis with 1.5% agarose gel for 45 min under 120 V, and then photographed with gel imaging system so as to analyze PCR product initially. Samples with PCR products were sent to Kunming Shuo Qing Biological Co., Ltd. for further analysis with ABI-3730XL genetic analysis system.

ISSR-PCR amplified fragments were analyzed by genetic analysis system. The size of ISSR-PCR amplified fragments ranged from 100 bp to 700 bp (internal standard ABI-LIZ1200). The fragments of PCR products obtained by genetic analysis system

were transformed into 01 matrix. The PCR products were packed in a box with a width of 10 bp. The population structure was analyzed by unweighted pair group method of with arithmetical averages (UGPMA) cluster analysis NTSY spc 2.1 soft (Rohlf, 2000).

Results and analysis

Observation of pricklyash rust symptoms

By observing the rust samples collected from wild pricklyash, Qujing pricklyash, green pricklyash and red pricklyash, it was found that there are various types of symptoms of rust infection (*Fig. 1*). In the early stage of pricklyash rust, pricklyash leaves produced one or more spots of varying sizes. With the deepening of infection, yellow to orange naked summer spore piles appeared on the back of pricklyash leaves. The size of summer spore piles was 0.1-0.7 mm, and the size of winter spore piles was 0.2-1.0 mm at the corresponding parts of late summer spore piles. Some of the lesions of pricklyash rust are irregularly distributed, forming a lesion (wild pricklyash rust) by a single summer spore pile; some are centered on one point with others forming a circle (Qujing pricklyash rust and green pricklyash rust); others are centered on one point, surrounded by two circles, and at the later stage of infection, the outer circle turns red-brown (red pricklyash rust).



Figure 1. Symptoms of different types of pricklyash rust

The pathogenic morphology of pricklyash rust was observed under a microscope. It was found that the color of summer spores of pricklyash rust varied from light yellow to yellow. Most of the summer spores were oval, elliptical, rough and warty. The size of summer spores was 30-60 $\mu\text{m} \times 18-25 \mu\text{m}$ (*Fig. 2*). There are 3-4 cells in the winter spores, the top 3 cells are yellow and the base cell is colorless, and the spore size is 55-91 $\mu\text{m} \times 18-29 \mu\text{m}$ (*Fig. 3*). The winter spore often germinates from the top cells and grows germ tubes.

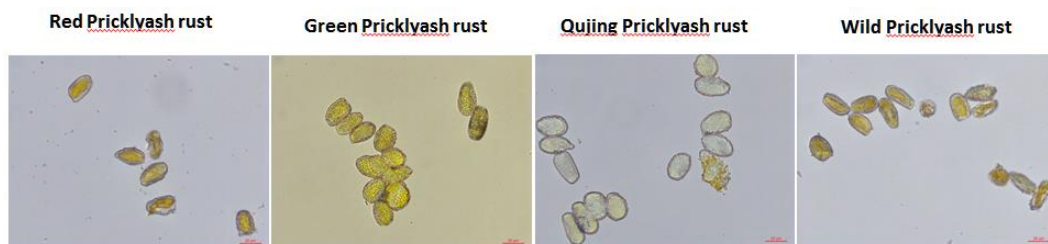


Figure 2. Urediospore morphology of pricklyash rust fungus with different symptoms



Figure 3. Teleutospore morphology of pricklyash rust fungus (germinated teleutospore)

ITS sequence analysis of pricklyash rust

In this paper, the ITS sequences amplified by fungal ITS universal primers were compared and analyzed on NCBI website. It was found that the rust collected from red pricklyash, green pricklyash, Qujing pricklyash and wild pricklyash belongs to Basidiomycotina, Teliomycetes, Uredinales, Coleosporaceae, *Coleosporium*, *Coleosporium zanthoxyli* (Table 3). The genetic relationship of the rust samples collected from different types of pricklyash was analyzed by MAGE 5.1. The results showed that except for YHJ-2 having 96% coverage rate and 97.83% similarity rate with *Coleosporium zanthoxyli* of registration number MH465095.1 published on NCBI website, ITS sequences of other samples have 99% or above coverage rate and 99% and above similarity rate with *Coleosporium zanthoxyli* of registration number MH465095.1, especially the 7 samples of QJHJ-1, QJHJ-2, YHJ-3, HHJ-1, HHJ-3, LHJ-1, HHJ-2, which have 99% coverage rate and 100% similarity rate.

Table 3. Comparison of ITS sequences of pricklyash rust fungus with different symptom types

Sample name	Query cover%	E-value	Ident %	Homologous species	Accession	Host
QJHJ-1	99	0.0	100.00	<i>Coleosporium zanthoxyli</i>	MH465095.1	Qujing pricklyash
QJHJ-2	99	0.0	100.00	<i>Coleosporium zanthoxyli</i>	MH465095.1	Qujing pricklyash
QJ-HJ-3	99	0.0	99.87	<i>Coleosporium zanthoxyli</i>	MH465095.1	Qujing pricklyash
YHJ-1	100	0.0	99.85	<i>Coleosporium zanthoxyli</i>	MH465095.1	Wild pricklyash
YHJ-2	96	0.0	97.83	<i>Coleosporium zanthoxyli</i>	MH465095.1	Wild pricklyash
YHJ-3	99	0.0	100.00	<i>Coleosporium zanthoxyli</i>	MH465095.1	Wild pricklyash
HHJ-1	99	0.0	100.00	<i>Coleosporium zanthoxyli</i>	MH465095.1	Red pricklyash
HHJ-2	99	0.0	99.73	<i>Coleosporium zanthoxyli</i>	MH465095.1	Red pricklyash
HHJ-3	99	0.0	100.00	<i>Coleosporium zanthoxyli</i>	MH465095.1	Red pricklyash
LHJ-1	99	0.0	100.00	<i>Coleosporium zanthoxyli</i>	MH465095.1	Green pricklyash
LHJ-2	99	0.0	100.00	<i>Coleosporium zanthoxyli</i>	MH465095.1	Green pricklyash

In this paper, the genetic relationships between the obtained ITS sequences of pricklyash rust, the ITS sequences of *Dendrobium Coleosporium* in our previous studies and the ITS sequences of *Coleosporium zanthoxyli* of registration number MH465095.1

published on NCBI website were analyzed by MEGA5.10 software. It was found that *Dendrobium Coleosporium* could be clustered into categories I, II and III, and all of *Coleosporium zanthoxyli* were clustered in category I except from TP-SH-3 and TP-SH-4, which were clustered in category III. The rust collected from other *Dendrobium* species were clustered in category II.

Genetic diversity analysis of different pricklyash rust

Popgene 1.32 software was used to analyze the genetic diversity of four different types of pricklyash rust. The results (Table 4) showed that the population level, Nei's gene diversity index (H), Shannon's information index and percentage of polymorphic loci of wild pricklyash rust were the largest, indicating that the genetic diversity of wild pricklyash rust was the richest, followed by Qujing pricklyash rust, while red pricklyash and green pricklyash have similar genetic diversity. Generally speaking, the genetic diversity of the four types of pricklyash rust is not much different. At the same species level, the percentage of polymorphic loci was 82.72%, the number of observed alleles (Na) was 1.8272, the number of effective alleles (Ne) was 1.2383, the genetic diversity index (H) and information index (I) were 0.1551 and 0.2560, respectively. The number of polymorphic loci was 268, and the percentage of polymorphic loci was 82.72%, indicating the rich genetic diversity of pricklyash rust population (Fig. 4).

Table 4. Genetic diversity of rust fungi populations on different pricklyash

Population code	Alleles (Na)	Effective allele (Ne)	Nei gene diversity index (H)	Shannon's (I) Shannon information index	Number of polymorphic loci	Percentage of polymorphic loci
HHJ	1.5556	1.1976	0.1277	0.2068	180	55.56
LHJ	1.537	1.2041	0.1292	0.2069	174	53.70
YHJ	1.6296	1.2465	0.1577	0.2519	204	62.96
QJHJ	1.5031	1.2368	0.1424	0.2199	163	50.31
Average	1.5563	1.2213	0.1393	0.2214	180	55.63
Total of species	1.8272	1.2383	0.1551	0.2560	268	82.72

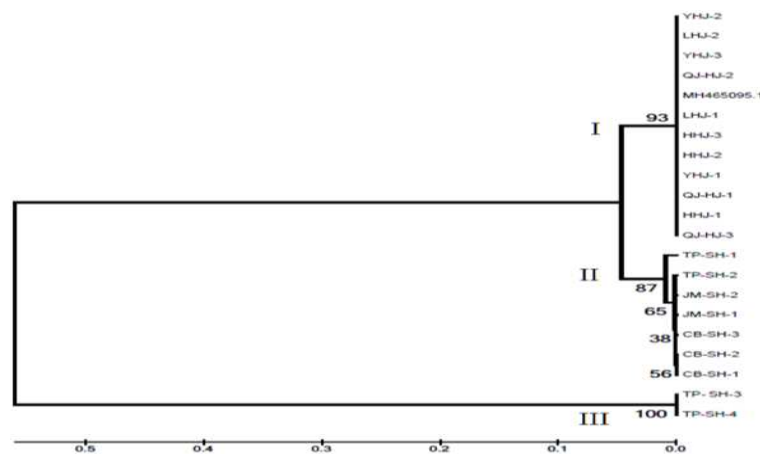


Figure 4. ITS sequence comparison dendrogram of different pricklyash and *Dendrobium* rust.
Note: MH465095.1 is: ITS sequence of *Zanthoxylum bungeanum* with login number MH465095.1 published by NCBI website; ITS sequences of TP-SH-1, TP-SH-2, TP-SH-3, TP-SH-4, JM-SH-1, JM-SH-2, CB-SH-2, CB-SH-3 are the experimental data of this group (Pu, 2019)

NTsis software was used to analyze the population genetic structure of different types of pricklyash rust. The results (Fig. 5) showed that the similarity of four pricklyash rust populations was above 0.74, which was relatively high, and the genetic structure was more complex, and the classification was not very obvious. Especially for wild pricklyash rust and Qujing pricklyash rust, the clustering was dispersed.

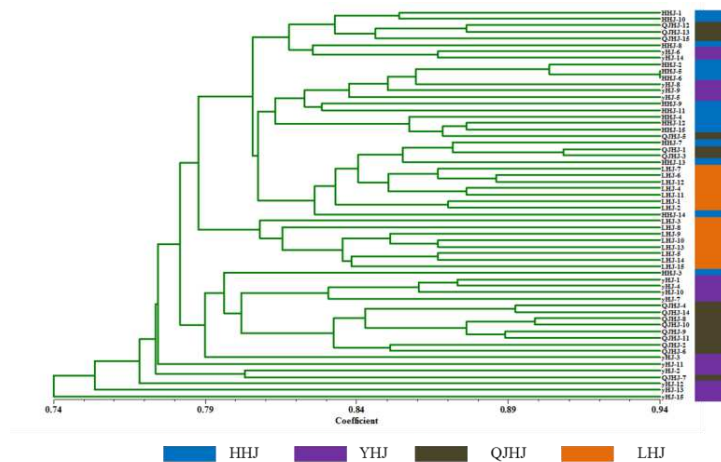


Figure 5. Population genetic structure of rust on different pricklyash

Population structural genetic analysis of *Coleosporium*

The ISSR molecular markers designed by the team were used to analyze the population genetic structure of rusts collected from different varieties of pricklyash and *Dendrobium*. NTsis software analysis results (Fig. 6) showed that rusts on pricklyash and on *Dendrobium* were clustered in two groups, namely, rusts on *Dendrobium* clustered in category I while rusts on pricklyash clustered in category II with a similarity coefficient of 0.67, which means that the population differentiation between the rusts on pricklyash and the rusts on *Dendrobium* was obvious.

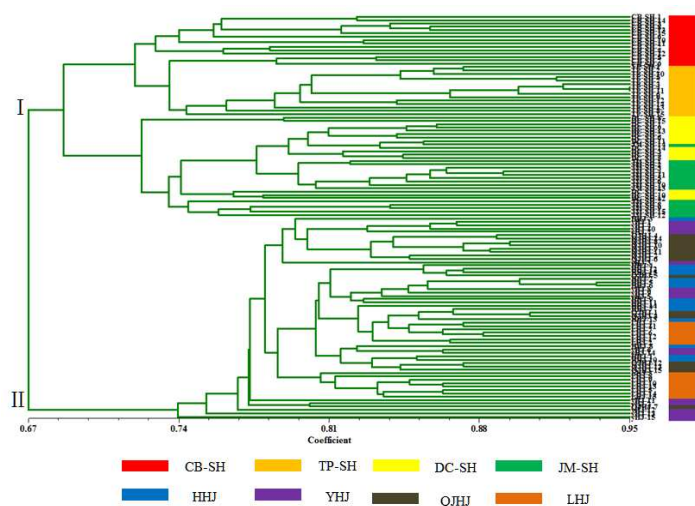


Figure 6. Population genetic structure of *Coleosporium* on different pricklyash and *Dendrobium*. Note: CB-SH, TP-SH, DC-SH and JM-SH are the experimental data of our group (Pu, 2019)

Discussion

Pricklyash (*Zanthoxylum* spp.) has many species. There are about 250 species of *Zanthoxylum* spp. plants in the world. There are about 50 species, 13 varieties and 2 variants of *Zanthoxylum* in China. Artificially cultivated varieties have green (green pricklyash) and red (red pricklyash) fruits after ripening. Pricklyash rust is one of the common diseases on pricklyash, it often causes discoloration, necrosis and abscission of pricklyash leaves, which seriously affects the yield and quality of pricklyash.

The symptoms and spore morphology of 60 samples of rust collected from red pricklyash, green pricklyash, Qujing pricklyash and wild pricklyash were observed in this study. It was found that the symptoms of rust were varied and the size of summer spores of rust varied greatly. ITS sequence analysis showed that these pricklyash rusts with different symptoms and collected from different types of pricklyash were caused by *Coleosporium*. Scholars have reported that *Coleosporium zanthoxyli* is hosted by 9 species of *Zanthoxylum* plants, such as pricklyash and wild pricklyash, as well as *Dendrobium candidum*, *Dendrobium globosa*, etc. (Xi, 2018). Moreover, the ITS sequences of pricklyash and *Dendrobium* rusts were compared and analyzed to find that most of them had a high similarity of 0.96 (Fig. 4), but the population genetic structure of *Coleosporium* derived from pricklyash and *Dendrobium* was quite different. Therefore, for the highly host-specific *Coleosporium* rust, whether pricklyash rust and *Dendrobium* rust can be infected by each other requires further research and study.

After analysis, it was found that the population genetic structure of rust on pricklyash was rich. From the ISSR population genetic structure map, we can see that rust on wild pricklyash are distributed in all large populations, which indicates that some rust on wild pricklyash may have close genetic relationship with rust samples on Qujing pricklyash, red pricklyash and green pricklyash. It is speculated that rust on wild pricklyash may be transmitted to each other. Figure 5 shows that the population differentiation of rust on *Dendrobium* and rust on pricklyash is obvious. The population genetic similarity coefficient of ISSR is 0.67. The rust on *Dendrobium* and rust on pricklyash are clustered in two populations respectively. Moreover, *Dendrobium* rust is closely related to the host varieties of *Dendrobium*, but pricklyash does not show this pattern. This may be mainly due to the fact that the collected samples of *Dendrobium* rust come from greenhouse cultivation, and the possibility of its transmission in the air is relatively small, while pricklyash rust is collected from the field, and its rust spores can be transmitted with the airflow. It can be seen from this paper that while preventing and treating pricklyash rust on different varieties of pricklyash, control of rust on wild pricklyash needs to be further strengthened.

Conclusions

(1) The spore morphology of pricklyash with different symptoms of pricklyash rust was observed, and ITS sequence was analyzed and compared to show that the symptoms of rust on wild pricklyash, Qujing pricklyash, red pricklyash and green pricklyash were various. The pathogens causing different symptoms of pricklyash rust belong to Basidio-mycotina, Teliomycetes, Uredinales, Coleosporaceae, *Coleosporium*, *Coleosporium zanthoxyli*.

(2) By comparing and analyzing the results with previous studies on *Dendrobium* rust, we found that rust on *Dendrobium* and rust on pricklyash were clustered in two populations, and the genetic similarity coefficient of ISSR was 0.67.

(3) The genetic structure of *Coleosporium* on wild pricklyash was rich. The *Coleosporium* on wild pricklyash can be clustered into *Coleosporium* on other varieties of pricklyash, which means that *Coleosporium* on wild pricklyash may be the source of infection of other types of pricklyash rust.

Acknowledgments. Many thanks to the National Natural Science Foundation of China (31560046), the State Key R & D Program (2018YFD0200500), Key research & development of Yunnan science & technology department (2018BB016) and State Key Laboratory for Conservation and Utilization of Bio-Resources in Yunnan (2016-001) that has granted this experiment.

REFERENCES

- [1] Cao, Z., Tian, C., Liang, Y. (1989): A preliminary study pricklyash rust. – Shaanxi Forest Science and Technology 4: 63-65.
- [2] Cao, Z., Tian, C., Liang, Y. (1994): An investigation of pricklyash diseases in Shaanxi and Gansu Provinces. – Journal of Northwest Forestry College 9(2): 39-43.
- [3] Chang, C. T., Dong, S. L., Tsai, I. L. (1997): Coumarins and anti-HBV constituents from *Zanthoxylum schinifolium*. – Phytochemistry 45: 1419-1422.
- [4] Chen, J., Zheng, F. (2007): Application of ITS sequences in fungi classification and identification. – Journal of Anhui Agriculture 35(13): 3785-3786.
- [5] Chen, L., Zhang, F., Sun, D., Zhang, W. (2016): Research progress of biological activity and mechanism in *Zanthoxylum schinifolium* Sieb. et Zucc. – Chinese Wild Plant Resources 35(4): 43-47.
- [6] Gu, L., Wang, X., Zhang, F., Duan, Z., Zhou, B., Guo, Y. (2015): The current situation and development strategy of *Zanthoxylum bungeanum* industry in Yunnan. – Journal of West China Forestry Science 44(5): 142-147.
- [7] Huang, C. (1997): Flora Reipublicae Popularis Sinicae. 43 Vol., 2 Fascicule. – Science Press, Beijing.
- [8] Lee, Y. J., Yoon, J. J., Lee, S. M., et al. (2012): Inhibitory effect of *Zanthoxylum schinifolium* on vascular smooth muscle proliferation. – Immunopharmacology 34(2): 354-361.
- [9] Li, H., Xue, T. (2014): Research progress of Pericarpium *Zanthoxyli* peel. – China Condiment 39(1): 124-128,135.
- [10] Li, H., Lee, Y. J., Kang, D. G., et al. (2009): Effect of *Zanthoxylum schinifolium* on TNF-alpha induced vascular inflammation in human umbilical vein endothelial cells. – Vascular Pharmacology 50(5-6): 200-207.
- [11] Liu, L., Wang, C., Peng, W., Yang, J., Lan, M., Li, J., Zhu, Y., Li, C. (2015): Direct DNA extraction method of obligate parasitic fungus from infected plant tissue. – Genetics and Molecular Research 14(4): 18546-18551.
- [12] Liu, S., He, Y., Zhao, Y., Qin, Q., Zheng, H. (2007): Bioactivity of extracts from *Zanthoxylum bungeanum* against *Plutella xylostella*. – Chinese Agricultural Science Bulletin (9): 427-430.
- [13] Mi, O., Chung, M. S. (2014): Effects of oils and essential oils from seeds of *Zanthoxylum schinifolium* against foodborne viral surrogates. – Evidence-based Complementary and Alternative Medicine 135797-135797.
- [14] Paik, S. Y., Koh, K. H., Beak, S. M., et al. (2005): The essential oils from *Zanthoxylum schinifolium* pericarp induce apoptosis of HepG2 human hepatoma cells through

- increased production of reactive oxygen species. – *Biological & Pharmaceutical Bulletin* 28(5): 802-807.
- [15] Pu, S., Yu, H., Li, G., Yang, J., Li, Z., Bai, Y., Zhang, C., Wang, N., Li, C., Liu, L. (2019): Methods of dendrobium rust detection and analysis on the genetic structure of dendrobium rust populations. – *International Journal of Agriculture & Biology* 21: 885-890.
- [16] Rohlf, F. J. (2000): NTSY Spc, Numerical Taxonomy and Multivariate Analysis System, Version 2.1. – Exeter Publication Ltd, Setauket, NY.
- [17] Saitou, N., Nei, M. (1987): The neighbor-joining method: a new method for reconstructing phylogenetic trees. – *Mol Biol Evol* 4(4): 406-425.
- [18] Xi, G., Zhao, N., Zhao, J., Zhao, G. (2018): Identification of new diseases of *Coleosporium zanthoxyli* in *Dendrobium officinale*. – *Journal of Southwest Forestry University* 38(2): 202-205.
- [19] Zhang, Z. (2006): Study on the pathogenesis and prevention of prickly ash rust. – *Shandong Forestry Science and Technology* 4: 6-8.

ENVIRONMENTAL ANALYSIS OF COMMON IONS IN THE DOMINANT PLANTS OF THE MINQIN DESERT AREA OF GANSU PROVINCE, CHINA

CHEN, Y.¹ – CHANG, G.¹ – GAO, T.^{1,2} – YUE, B.¹ – YIN, Z.^{1*}

¹College of Geography and Environmental Engineering, Lanzhou City University, 730070 Gansu, China

²The Engineering Research Center of Mining Pollution Treatment and Ecological Restoration of Gansu Province, 730070 Gansu, China

*Corresponding author
e-mail: yinzhx13@163.com

(Received 29th Aug 2019; accepted 14th Nov 2019)

Abstract. Diurnal changes of K⁺, Ca²⁺, Na⁺ and Mg²⁺ contents in *Nitraria tangutorum*, *Lycium ruthenicum*, *Peganum harmala* L and *Reaumuria soongorica* were measured to investigate the variation in singular characteristics in dominant plants from Minqin Desert. Sequence of ions contents excluding *Reaumuria soongorica* in an ascending order were Na⁺ > K⁺ > Mg²⁺ > Ca²⁺, while in *Reaumuria soongorica* it was Na⁺ > Mg²⁺ > K⁺ > Ca²⁺. Diurnal changes of Ca²⁺ contents in *Nitraria tangutorum* and *Reaumuria soongorica* were not obvious, while, that of Mg²⁺ and K⁺ contents had similar U-curve trends in *Nitraria tangutorum*. Na⁺ contents varied greatly, content of Mg²⁺ was negatively correlated with light intensity, and positively correlated with K⁺ content. Diurnal changes of Ca²⁺ content in *Lycium ruthenicum* were bimodal, while Mg²⁺ content had a U-curve and was negatively correlated with Na⁺ content. Diurnal changes of K⁺ and Ca²⁺ content in *Peganum harmala* L were not significant, while those of Mg²⁺ content showing U-curve positively correlated with Na⁺ content, which had similar trends in *Peganum harmala* L and *Lycium ruthenicum*. Diurnal changes of K⁺ and Na⁺ contents presented U-curves in *Reaumuria soongorica*, while Mg²⁺ content showed a inverted U-curve. There were no significant correlations between ions, total ions sequence was *Peganum harmala* L > *Lycium ruthenicum* > *Reaumuria soongorica* > *Nitraria tangutorum*.

Keywords: desert plants, dominant species, illumination intensity, ions contents, correlation

Introduction

Desertification was the land degradation process in arid area, semiarid area and semi humid region caused by multiple factors including natural factors and human factors. It often caused decreasing in terrestrial ecosystem stability, the reducing in biodiversity and ecological carrying capacity, the degradation in physical and chemical properties of soil, which resulted in ecological environment fragmentation and loss of land productivity (Chen, 2014). Desertification was one of the major ecological environmental problems around the world, while China was one of the countries seriously affected by desertification in the world, and the economic loss caused by desertification had become billions of Yuan (Qi, 2011). Gansu Province was one of the provinces threaten heavily by desertification, especially in Minqin Country. It has become one of the most drought-ridden and desertification hazards regions in China even the world, and it also one of the four birthplaces of sandstorms in Northern China (Yao, 2014; Zhou, 2005). Minqin Country of Gansu Province located in the northeastern of Hexi Corridor, the lower Shiyang River. It was a narrow oasis area between the Tengger Desert and Badan-Jilin Desert. It was an important green barrier to stop two big dessert joining which play an important role in ecological security (Dai,

2008). At the moment, the oasis in Minqin Country was facing the ecological and environmental crisis (Wei, 2015). So it had great significance in combating desertification of Minqin Country, protecting ecological environment in oasis, and constructing ecological safety barrier of China.

The growth and health status of vegetation determined the recession and expansion of oasis, and the growth of vegetation need nutrient elements. Potassium, calcium, sodium, magnesium was the essential nutrients elements for plants growth and development. Potassium could affect the procedure of plants growth, development and physiological metabolism. Investigating results from Chen et al. (2017) showed the lacking of potassium could restrain the growth of plant roots, and decreased the root-shoot ratio; blocked the synthesis of photosynthetic products at the same time, and declined biomass in the end. Calcium was effective in plant yield increasing and disease prevention, it also played an important role in maintaining the structure stability of cell membrane and cell wall, participating in regulating growth, development and intracellular homeostasis. Calcium was also widely involved in signal transduction in response to various abiotic and biological stresses as a second messenger in plants (Liu, 2014). Deficiency of sodium could cause chlorosis in plants, while high sodium content in soil could cause soil salinization which was a threat to plant growth. Wang et al. (2012) investigated the response from seed germination and seedling growth of *Lycium ruthenicum* to stress, and found that with the increasing concentration of sodium salt, the seed germination rate decreased, and inhibition of seedling growth appeared. Magnesium had important nutritional and physiological functions on plants. It was the central ion of chlorophyll, and activator for many kinds of enzymes which took part in energy metabolism (Wang, 2016). The plants lacking of magnesium could seriously affects the normal growth of plants by the suppression of chlorophyll synthesis and various enzymes activation (Li, 2017), so the investigation on the content and characteristics of these elements could help us for the further understanding of growth characteristics, drought resistance, and stress resistance mechanism of plants.

The investigations of physiological and ecological adaptability for desert plants at present mostly focused on the photosynthesis, transpiration, water use efficiency, and the relationship with the arid environment of desert plants (Zhou, 2005; Su, 2013), while there were only research in the fields of ionization and ion absorption equilibrium for different desert plants (Bai, 2010). Our investigation mainly analyzed the change characteristics of contents of four ions (K^+ , Ca^{2+} , Na^+ , Mg^{2+}) in desert dominant plants, and the correlation of ion contents with light intensity, which could help people to explore the characteristics of resistances and mineral substances absorption of plants under desert and arid conditions.

Materials and methods

General situation of research area

The research area located in Minqin county of Gansu Corridor in Gansu Province, China (101°49'-104°12' E, 38°3'-39°27' N), Tenggeli Desert was in its northeastern, Badanjilin Desert in the northwestern, and oasis zone was in the central.

It was one of the typical Desert oasis in China whose mean altitude was 1400 m, and it was constituted of three kinds of basic landform such as desert, plain, low mountains and hills. The weather in Minqin Country was cold in winter, hot in summer, small amount of rainfalls and droughts, abundant sunlight, strong evaporation, which was

typical temperate territoriality monsoon climate, annual average precipitation was 113.8 mm, average annual evaporation capacity was as high as 2604.3 mm, the annual average temperature was 7.8 °C, the annual average sunshine hours were 3073.5 h, and frostless season was 162 d. Vegetation in research was desert vegetation, which was mainly consisted of herb, shrub and subshrub, included *Reaumuria soongorica*, *Peganum harmala* L, *Lycium ruthenicum*, *Nitraria tangutorum*, *Artemisia desertorum*, and *Ephedra przewalskii* (Chang, 2008).

Experimental methods

We choose the representative community plots near the Qingtu Lake in Minqin County (102° 51 9 E, 38°34 3 N) in August2017, and set up three quadrats 10 m × 10 m, then statistic the kinds, density, height, coverage of plants in quadrats. We calculated the dominance of every plants (Wang, 2016), and selected four kinds of plants with greater superiority, *Nitraria tangutorum*, *Lycium ruthenicum*, *Peganum harmala* L and *Reaumuria soongorica*. Samples were picked up from overground part of plants every 2 h from 7:00 a.m. for 7 times. Plants samples were prepared by drying , grinding and sieving, the contents of ions such as K⁺, Ca²⁺, Na⁺ and Mg²⁺ were measured by Atomic Absorption Method (LBA600,2015.China), determination of local luminous intensity was from Portable Photosynthesis Measurer LI-6400 (LI-COR,1995.USA). The software program SPSS 19.0 was used for statistical analysis of data, program Origin 9.0 for making graphs, respectively.

Statistical methods

Calculation method of coverage

Coverage was the percentage of summation of canopy projection area of all individuals with same kind in quadrats, because the canopy projection was oval, so the calculation formula was:

$$\text{Canopy Projection Area} = \text{Long Crown} \times \text{Short Crown} \times \pi / 4 \quad (\text{Eq.1})$$

Calculation methods of density radio, coverage radio and height radio

$$\text{Density Radio} = \text{Relative Density} / \text{Maximal Relative Density in Quadrat} \quad (\text{Eq.2})$$

$$\text{Coverage Radio} = \text{Relative Coverage} / \text{Maximal Relative Coverage in Quadrat} \quad (\text{Eq.3})$$

$$\text{Height Radio} = \text{Relative Height} / \text{Maximal Relative Height in Quadrat} \quad (\text{Eq.4})$$

Calculation method of dominance

$$\text{Dominance} = (\text{Density Radio} + \text{Coverage Radio} + \text{Height Radio}) / 3 \quad (\text{Eq.5})$$

Results

Diurnal changes of four kinds of ion contents in *Nitraria tangutorum*

Diurnal changes of contents of K⁺, Ca²⁺, Na⁺ and Mg²⁺ in *Nitraria tangutorum* were shown in *Figure 1*. Diurnal variation of K⁺ content in *Nitraria tangutorum* presented U-shaped curve, K⁺ content was 31.38 g·kg⁻¹ at 7:00 a.m., then it declined over time and

reached minimum value of 15.83 g·kg⁻¹ at 13:00 p.m., which rose again to 30.28 g·kg⁻¹ at 19:00 pm. Diurnal change of Ca²⁺ content was not obvious with time passed, which mainly in range of 1.36 g·kg⁻¹ – 2.55 g·kg⁻¹. While there is large variation in content of Na⁺ which was unchanged from 07:00 – 11:00 a.m.; after 11:00 a.m., Na⁺ content decreased significantly and reached minimum value of 24.60 g·kg⁻¹, then it recovering gradually after 13:00 a.m. and achieved 46.71 g·kg⁻¹. Diurnal changes tendency of Mg²⁺ content was also U-type curve. Mg²⁺ content was 8.49 g·kg⁻¹ at 7:00 a.m., decreased gradually and reached minimum value of 5.03 g·kg⁻¹ at 15:00 p.m., then it recovering gradually to 8.95 g·kg⁻¹ at 19:00 p.m. Content change of K⁺ and Na⁺ has the greatest change than other ions in *Nitraria tangutorum*. The range from maximum to minimum value of K⁺ contents was 15.50 g·kg⁻¹, which was 30.37 g·kg⁻¹ of Na⁺ content.

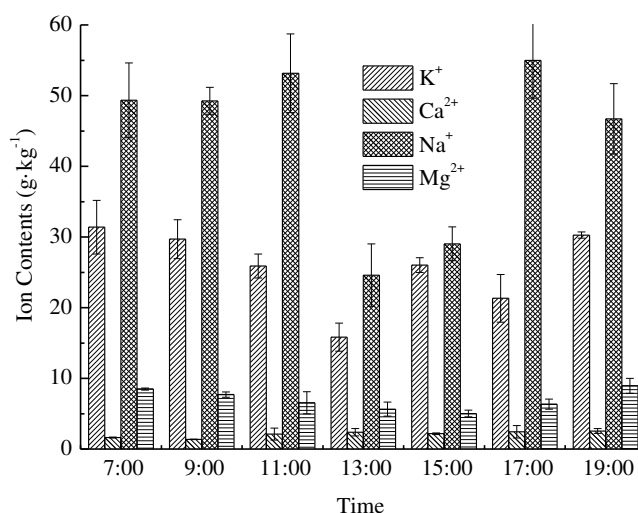


Figure 1. Diurnal changes of four kinds of ion contents in *Nitraria tangutorum*

Diurnal changes of four kinds of ion contents in *Lycium ruthenicum*

Diurnal changes for contents of K⁺, Ca²⁺, Na⁺ and Mg²⁺ in *Lycium ruthenicum* were shown in Figure 2. Diurnal variation tendency of K⁺ content in *Lycium ruthenicum* was W-curve. Content of K⁺ in *Lycium ruthenicum* was 47.55 g·kg⁻¹ at 7:00 a.m., then it decreased to minimum value of 19.73 g·kg⁻¹ at 09:00 a.m., recovering to 44.62 g·kg⁻¹ at 11:00 a.m., and decreased gradually to lower value of 31.51 g·kg⁻¹ at 17:00 p.m. It increased to 35.86 g·kg⁻¹ at 19:00 p.m. in the end. Diurnal change of K⁺ content was always lower than Na⁺ content in *Lycium ruthenicum* except at 07:00 a.m. Diurnal variation tendency of Ca²⁺ content appeared double-peak type, and reached peaks of 4.14 g·kg⁻¹ / 3.65 g·kg⁻¹ at 11:00 a.m. and 17:00 p.m., respectively. Content of Na⁺ increased gradually from 07:00 a.m. to 13:00 p.m, and reached 57.91 g·kg⁻¹ at 13:00 p.m., then it decreased and shown a lower value of 45.24 g·kg⁻¹ at 15:00 p.m, and which increased to a maximum value of 66.10 g·kg⁻¹ at 17:00 p.m. Diurnal change tendency of Mg²⁺ content was U-shape curve, which declined gradually during 07:00 a.m. to 15:00 p.m. and reached minimum value of 9.73 g·kg⁻¹ at 15:00 p.m., then it recovering to 12.03 g·kg⁻¹ at 19:00 p.m. Great change of ion contents in *Lycium ruthenicum* was the K⁺ content (whose difference between the maximum and minimum value was 27.82 g·kg⁻¹) and Na⁺ content (whose difference between the maximum and minimum value was 40.72 g·kg⁻¹).

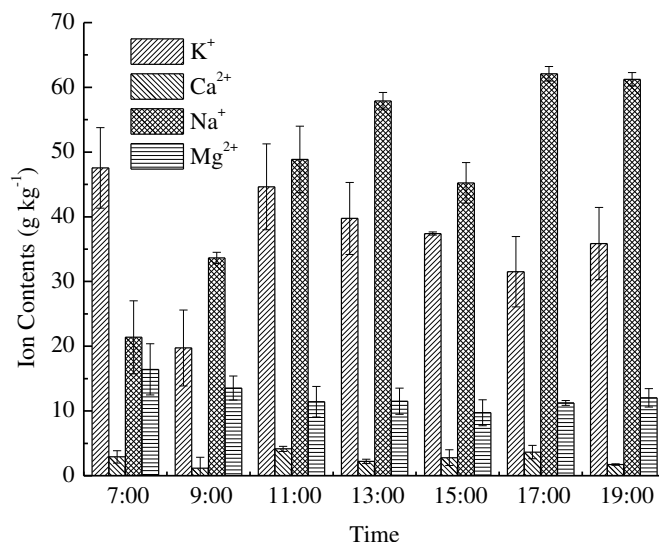


Figure 2. Diurnal changes of four kinds of ion contents in *Lycium ruthenicum*

Diurnal changes of four kinds of ion contents in *Peganum harmala* L

Diurnal variation in contents of K^+ , Ca^{2+} , Na^+ and Mg^{2+} in *Peganum harmala* L were shown in *Figure 3*. Potassium content in *Peganum harmala* L decreased gradually within 07:00 a.m. – 11:00 a.m., and reveal a minimum value of $19.36 \text{ g}\cdot\text{kg}^{-1}$, then it increased and reached a maximum value of $26.22 \text{ g}\cdot\text{kg}^{-1}$ at 13:00, and becoming decreased to $23.20 \text{ g}\cdot\text{kg}^{-1}$ at 19:00 p.m. Diurnal change of calcium content was not obvious the value kept stable at $1.33 \text{ g}\cdot\text{kg}^{-1}$. Sodium content increased gradually with 07:00 a.m. – 13:00 p.m., and reached $92.51 \text{ g}\cdot\text{kg}^{-1}$ at 13:00 p.m., then it decreased to the minimum value at $48.18 \text{ g}\cdot\text{kg}^{-1}$ at 15:00 p.m., and increased to $96.77 \text{ g}\cdot\text{kg}^{-1}$ at 19:00 p.m. Diurnal change curve of magnesium content was double-peak curve, content of Mg^{2+} increasing gradually from 07:00 a.m. to 11:00 a.m. and reached peak value of $11.42 \text{ g}\cdot\text{kg}^{-1}$ at 11:00 a.m., then it decreasing gradually and reached a lower value of $8.35 \text{ g}\cdot\text{kg}^{-1}$ at 15:00 p.m. Content of Mg^{2+} increased to the maximum value of $13.44 \text{ g}\cdot\text{kg}^{-1}$ at 19:00 p.m. Greatest change of ion contents in *Peganum harmala* L was sodium content, whose difference of maximum and minimum value was $48.59 \text{ g}\cdot\text{kg}^{-1}$.

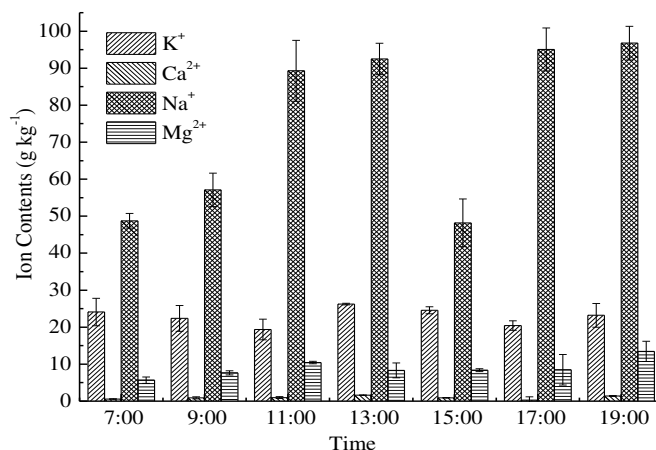


Figure 3. Diurnal changes of four kinds of ion contents in *Peganum harmala* L

Diurnal changes of four kinds of ions in *Reaumuria soongorica*

Diurnal variation in contents of K^+ , Ca^{2+} , Na^+ and Mg^{2+} in *Reaumuria soongorica* were shown in Figure 4. Diurnal change tendency of potassium content in *Reaumuria soongorica* was a U-shape curve. Content of K^+ decreasing gradually during 07:00 a.m. – 13:00 p.m. and appeared a minimum value of $11.03 \text{ g}\cdot\text{kg}^{-1}$ at 13:00 p.m., then recovering to $14.79 \text{ g}\cdot\text{kg}^{-1}$ at 19:00 p.m. Calcium content changed little over time. It decreasing gradually during 07:00 a.m. – 13:00 p.m. and appeared a lower value of $2.74 \text{ g}\cdot\text{kg}^{-1}$ at 13:00 a.m.; then it increasing and reached $3.71 \text{ g}\cdot\text{kg}^{-1}$ at 15:00 p.m. Later it decreasing and reached a minimum value of $2.45 \text{ g}\cdot\text{kg}^{-1}$ at 17:00 p.m., afterwards it increasing and reached a maximum value of $3.86 \text{ g}\cdot\text{kg}^{-1}$ at 19:00 p.m. Sodium content increasing during 07:00 a.m. – 09:00 a.m. and reached a maximum value of $49.62 \text{ g}\cdot\text{kg}^{-1}$ at 09:00 a.m. Afterwards, the change tendency of sodium content was U-shaped curve, Na^+ content decreasing during 09:00 a.m. – 15:00 p.m. and the minimum value of $38.87 \text{ g}\cdot\text{kg}^{-1}$ appeared at 15:00 p.m., then sodium content increasing to $43.19 \text{ g}\cdot\text{kg}^{-1}$ at 19:00 p.m. Magnesium content increasing gradually during 07:00 a.m. – 11:00 a.m. and reached a maximum value of $25.26 \text{ g}\cdot\text{kg}^{-1}$ at 11:00 a.m., then it became decreasing, a minimum value of $17.38 \text{ g}\cdot\text{kg}^{-1}$ appeared at 17:00 p.m., afterwards it increasing to $23.42 \text{ g}\cdot\text{kg}^{-1}$ at 19:00 p.m. Contents of sodium and magnesium in *Reaumuria soongorica* changed a lot. The difference between maximum and minimum value of Na^+ content and Mg^{2+} were $10.75 \text{ g}\cdot\text{kg}^{-1}$ and $7.88 \text{ g}\cdot\text{kg}^{-1}$, respectively.

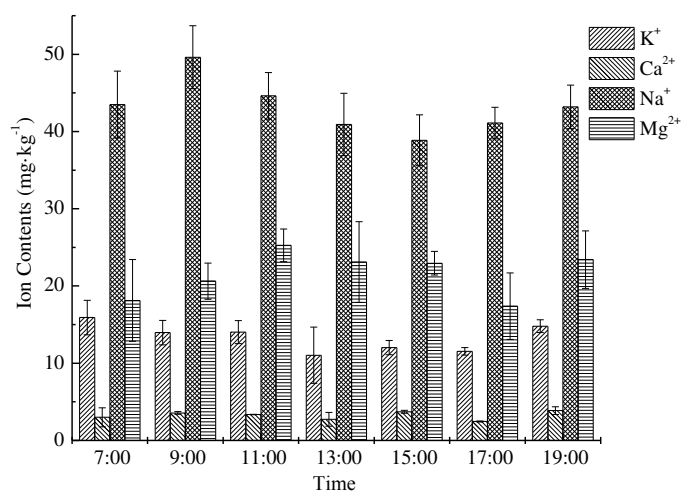


Figure 4. Diurnal changes of four kinds of ions in *Reaumuria soongorica*

The average content of four ions and their total amount in four plants

Average contents of the elements investigated and total ions of four plants were shown in Figure 5. Elements contents sequences of K^+ , Ca^{2+} , Na^+ and Mg^{2+} in *Nitraria tangutorum*, *Lycium ruthenicum* and *Peganum harmala* L were all $Na^+ > K^+ > Mg^{2+} > Ca^{2+}$. The sequence of four element contents in *Reaumuria soongorica* was $Na^+ > Mg^{2+} > K^+ > Ca^{2+}$. For the four plants investigated, the average content of Ca^{2+} was the least, average content of Na^+ was the most. The ascending sequence of average Ca^{2+} content in plants was *Reaumuria soongorica* ($3.24 \text{ g}\cdot\text{kg}^{-1}$) $>$ *Lycium ruthenicum* ($2.66 \text{ g}\cdot\text{kg}^{-1}$) $>$ *Nitraria tangutorum* ($2.09 \text{ g}\cdot\text{kg}^{-1}$) $>$ *Peganum harmala* L ($0.94 \text{ g}\cdot\text{kg}^{-1}$), which for Na^+ average content in plants was *Peganum harmala*

L ($75.39 \text{ g}\cdot\text{kg}^{-1}$) > *Lycium ruthenicum* ($47.77 \text{ g}\cdot\text{kg}^{-1}$) > *Nitraria tangutorum* ($43.87 \text{ g}\cdot\text{kg}^{-1}$) > *Reaumuria soongorica* ($43.11 \text{ g}\cdot\text{kg}^{-1}$). Sequence for total amount of ions in four plants was *Peganum harmala* L > *Lycium ruthenicum* > *Reaumuria soongorica* > *Nitraria tangutorum*. Total amount of four ions in *Peganum harmala* L was twice of it for *Lycium ruthenicum*, four time of it in *Reaumuria soongorica*, 8 times of it in *Nitraria tangutorum*.

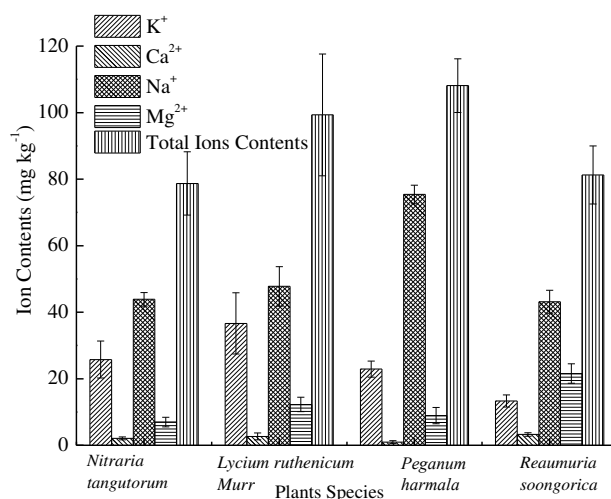


Figure 5. Average content of four ions and their total amount in the four plants

The correlation between ion content and light intensity in plants

Pearson correlation analysis between total amount of ions and light intensity in four plants was shown in *Figure 1*. Magnesium content in *Nitraria tangutorum* was significantly negatively correlated with light intensity at the 0.01 level (-0.896), while the Mg²⁺ contents in *Lycium ruthenicum* and *Reaumuria soongorica* had little correlations with light intensity, and Mg²⁺ content in *Peganum harmala* L had no correlations with light intensity. The correlations between the contents of K⁺ and Na⁺ with light intensity was not significant, while the contents of K⁺ and Na⁺ in *Lycium ruthenicum* and *Peganum harmala* L cannot be correlated with light intensity, content of K⁺ in *Reaumuria soongorica* was negatively correlated with light intensity at the 0.05 level (-0.700). Content of Na⁺ had no correlation with light intensity, while contents of Ca²⁺ in *Nitraria tangutorum*, *Lycium ruthenicum* and *Rsa* also cannot be correlated with light intensity, and Ca²⁺ content in *Peganum harmala* L had little correlation with light intensity. Contents of Mg²⁺ and K⁺ in *Nitraria tangutorum* had significant positive correlation (0.731) at the 0.05 level, while in *Lycium ruthenicum* Mg²⁺ content was significantly negatively correlated (-0.738) with Na⁺ content at the level of 0.05, in *Peganum harmala* L Mg²⁺ content was significantly positively correlated (0.670) with Na⁺ content at the level of 0.05; and there had weak correlations between the ions content in *Reaumuria soongorica* (*Table 1*).

Discussion

The plants of *Nitraria tangutorum*, *Lycium ruthenicum*, *Peganum harmala* L and *Reaumuria soongorica* had the effect of desert soil improvement and ecological balance

maintenance, they had good adaptability to grow in desert environment in Minqin Country. *Nitraria tangutorum* was a kind of plant in *Zygophyllaceae*, *Nitraria tangutorum*, whose appearance was xeric shrubs, xerophytic, or undershrub. It has the characteristics to resist drought, wind erosion, sand burial and saline alkali tolerance. *Nitraria tangutorum* was high branched structure, and tufted creep in sandy land, semi-flow or mobile dune. It could produce adventitious root or new branch easily if it was buried by sand (Zhou, 2005). *Lycium ruthenicum* belonged to plants of *Solanaceae* wolfberry with many branch and characteristics of wind, sand, drought, and high-temperature resistance, and its fruits were abundance of anthocyanin and trace elements (Chen, 2011; Gu, 2014) which had highly economic and medicinal value. So it was one of the minority plants in arid area which could not only fixate sand and resist drought, but also can generate economic benefits. *Peganum harmala* L was a kind of perennial plant belongs to *zygophyllaceae*, it was widely spread in arid and semi-arid area with developed root system with drought resistance and saline alkali tolerance (Liu, 2011). *Reaumuria soongorica* belongs to subshrub or shrub, it was the major constructive species in dessert and grassland in China, and widely spread in the arid hungeriness regions of our country. It has strong ability of saline alkali tolerance and sand fixation (Liu, 2011).

Table 1. Correlation between ion content and light intensity in plants

Plants		Light intensity	K ⁺	Ca ²⁺	Na ⁺	Mg ²⁺
<i>Nitraria tangutorum</i>	Light intensity	1				
	K ⁺	-0.656	1			
	Ca ²⁺	0.133	-0.535	1		
	Na ⁺	-0.627	0.509	-0.245	1	
	Mg ²⁺	-0.896**	0.731*	-0.287	0.580	1
<i>Lycium ruthenicum</i>	Light intensity	1				
	K ⁺	0.041	1			
	Ca ²⁺	0.216	0.591	1		
	Na ⁺	0.192	-0.131	0.167	1	
	Mg ²⁺	-0.650	0.157	-0.212	-0.738*	1
<i>Peganum harmala</i>	Light intensity	1				
	K ⁺	0.150	1			
	Ca ²⁺	0.336	0.526	1		
	Na ⁺	0.010	-0.313	0.327	1	
	Mg ²⁺	-0.111	-0.260	0.495	0.670*	1
<i>Reaumuria soongorica</i>	Light intensity	1				
	K ⁺	-0.700*	1			
	Ca ²⁺	-0.067	0.439	1		
	Na ⁺	-0.294	0.541	0.265	1	
	Mg ²⁺	0.537	-0.063	0.578	-0.041	1

*Data were significant correlation under the P value degree of 0.05 level. **Data were significant correlation under the P value degree of 0.01 level

Potassium ion plays an important role in promoting plant growth, protein synthesis, carbohydrates formation and transportation. It also has close relationship with drought resistance of plants, and could also increase the adversity resistance, decrease the water potential of the leaves under the condition of drought to rise the relative water content

(Wang, 2016). The photosynthesis, photorespiration, growth and development were all effected, by the content of K^+ (Gattward, 2012), the differences of K^+ sorption, conversion and transportation in various kinds of plants were controlled by genetic gene (Wang, 2009). The highest contents of potassium ion in the plants of our research field was *Lycium ruthenicum*, the decreasing sequence was *Nitraria tangutorum*, *Peganum harmala* L, the *Reaumuria soongorica* was in the end. The results may indicate that the *Lycium ruthenicum* has stronger adaptability under drought stress than other plants. There are great variation in K^+ absorption contents of 4 plants, which may be resulted from the differences in plant species and genetic gene. Zhao et al. (2005) investigated the diurnal photosynthesis changes in *Nitraria tangutorum*, the results showed that with the increase of light intensity and temperature, the net photosynthetic rate and stomatal conductance of *Nitraria tangutorum* decreased, and the stomatal closure induced midday-depression of photosynthesis; when temperature decreased, the stomatal conductance increased. The research of *Nitraria tangutorum* and *Sarcozygium xanthoxylon* from *Ulanbuh Desert* (Huang, 2016) compared their characteristics diurnal photosynthesis changes in autumn, the results also showed their midday-depression of photosynthesis was caused by stomatal factor. The diurnal changes tendency of K^+ contents in *Nitraria tangutorum* and *Reaumuria soongorica* were similar to the characteristic of diurnal photosynthesis changes, the K^+ contents was lowest at noon. Luminous intensity was correlated with K^+ content of *Reaumuria soongorica*, which did not have obvious correlation with K^+ content of *Reaumuria soongorica*. The results may be attributed to the reasons that the K^+ contents in *Nitraria tangutorum* and *Reaumuria soongorica* dominated their changes of stomatal conductance and photosynthetic rate, while the K^+ contents in *Lycium ruthenicum* and *Peganum harmala* L did not have obvious relationship with their stomatal conductance and photosynthetic rate. Perhaps there are other ions took part in the procedure, so we need further research.

Calcium was a component of plants structure, which increased the growth of cells and roots (Li, 2017). The content of Ca^{2+} will change will change with the kinds, organs and growth conditions of plants, the extra Ca^{2+} content will be used as the nutrition for the growth of new organs, satisfied the stability of cell membrane, maintained the structural function of cell walls, increased the stress-chilling and chilling-chilling of plants, also it could regulate the responses of stress, the growth and development of plants as well (Wang, 2016). Investigations from Larkindale (2002) showed that high temperature damage maybe resulted in oxidative damage of plant cell membrane, while the contents of Ca^{2+} in plants have significant effect on recovering the oxidative plant damage from high temperature. Calcium contents of *Nitraria tangutorum*, *Lycium ruthenicum* and *Reaumuria soongorica* differs little (about $1.0 \text{ g}\cdot\text{kg}^{-1}$) in this research, which had no correlation with luminous intensity. However, content of calcium in *Peganum harmala* L was least in four plants, which was weakly dependent with luminous intensity. The results may demonstrated that *Nitraria tangutorum*, *Lycium ruthenicum* and *Reaumuria soongorica* had stronger drought-resistance than *Peganum harmala* L under drought-stress.

Contents of Na^+ in plants related its salt-tolerance, the absorption, transportation and storage determined weather plants could live under salt-stress. Different plants had different way for salt-tolerance, some kinds of plants remained their internal and external environment stable by osmotic adjustment, some kinds could make active choice whether to absorb Na^+ , or activated the functions of potassium-absorption and sodium-excretion to control ions-balance and increase salt-tolerance (Garthwaite, 2005).

Sodium contents of four plants investigated in this paper were relatively high. Content of sodium was highest in *Peganum harmala* L, which was lower in *Lycium ruthenicum*; sodium contents in *Nitraria tangutorum* and *Reaumuria soongorica* nearly equal. Total ionic content was highest in *Peganum harmala* L of four plants, which refer to that *Peganum harmala* L had strong absorptive capacity for ions in soil, it was easily existence in soil with high salinity, strong salt-tolerance. Sodium contents in four plants had acute diurnal changes, in 13:00-15:00 p.m., sodium contents in four plants were all decreased, which may refer to the reason that Luminous intensity was too strong in this period which could affect the permeability of plants, decrease transportation of Na^+ , and then reduce the content of Na^+ .

Magnesium ion could be the activator of many kinds of enzymes, it took part in synthesis of fat, protein, carbohydrate and nucleic acid, which also regulated content of Mg^{2+} in their stable metabolic library (Liao, 2003). Magnesium was the center atom of chlorophyll in photosynthesis, which played important role by directly involving in photosynthesis, promoting carbon assimilation, adjusting the distribution of Excitation energy of chloroplast and so on. There were antagonistic relationship between potassium and magnesium. Ohno and Grunes (1985) considered antagonistic action happened in transport process of Mg^{2+} from root to overground part of plants. Huang et al. (1992) also thought that there was negative correlations between the transportation of Mg^{2+} and concentration of K^+ . The increase of Mg^{2+} content and decrease of K^+ content showed that the existence of K^+ restrained absorption of Mg^{2+} in plants. The increasing Mg^{2+} content and decreasing contents of Na^+ and K^+ demonstrated that the existence of Na^+ and K^+ restrained Mg^{2+} absorption in plants. The increase of Mg^{2+} content and increase of Ca^{2+} content showed perhaps there were antagonism between Mg^{2+} and Ca^{2+} , the existence of Ca^{2+} suppressed absorption of Mg^{2+} . There were research showed absorption contents of Mg^{2+} decreased with the increasing luminous intensity. For the four plants in this research, the Mg^{2+} contents were lower at noon, this may be resulted from the Mg^{2+} absorption suppression by the intense illumination at noon.

Conclusions

The ability for ion absorption of K^+ , Ca^{2+} , Na^+ , Mg^{2+} in different plants were various. The amount of Na^+ in four plants were highest while the amount of Ca^{2+} was lowest compared with amount of four ions. The increasing sequences of four ions in plants of *Nitraria tangutorum*, *Lycium ruthenicum* and *Peganum harmala* L was $\text{Na}^+ > \text{K}^+ > \text{Mg}^{2+} > \text{Ca}^{2+}$, while the order of ions contents in *Reaumuria soongorica* was different that the content sequence of ions was $\text{Na}^+ > \text{Mg}^{2+} > \text{K}^+ > \text{Ca}^{2+}$. Diurnal variations of Ca^{2+} contents in *Nitraria tangutorum*, *Reaumuria soongorica* and *Peganum harmala* L was slight, while the diurnal variation of Ca^{2+} content in *Lycium ruthenicum* was bimodal, and the two peak values were $4.14 \text{ g}\cdot\text{kg}^{-1}$ and $3.65 \text{ g}\cdot\text{kg}^{-1}$, respectively. The diurnal variations of Mg^{2+} contents presented U-shaped curves in *Nitraria tangutorum*, *Lycium ruthenicum* and *Peganum harmala* L, which followed by an inverted U-curve in *Reaumuria soongorica*. Diurnal variations of K^+ contents in *Nitraria tangutorum* and *Reaumuria soongorica* was U-curves, which was strong in *Lycium ruthenicum* and slight in *Peganum harmala* L. Diurnal variation of K^+ contents in *Nitraria tangutorum* was strong, while it in *Lycium ruthenicum* increased in the morning, and kept stable in the afternoon, and its tendency were also U-shaped curve in *Peganum harmala* L and *Reaumuria soongorica*. Mg^{2+} content was positively

correlated with K^+ content in *Nitraria tangutorum*, while Mg^{2+} content was negatively correlated with Na^+ content in *Lycium ruthenicum*. Mg^{2+} content was positively correlated with Na^+ content in *Peganum harmala* L, but Mg^{2+} content and Na^+ content in *Reaumuria soongorica* didn't have significant correlations. Sequence of total ion contents in four plants was *Peganum harmala* L > *Lycium ruthenicum* > *Reaumuria soongorica* > *Nitraria tangutorum*. Mg^{2+} content was negatively correlated with illumination intensity in *Nitraria tangutorum* under the *P* value degree of 0.01 level and in *Reaumuria soongorica* under *P* value degree of 0.05 with correlation coefficient equal to -0.700.

Acknowledgments. This research was funded by the National Natural Science Foundation of China (Grant No. 31860176), Doctoral Research Initiation Fund of Lanzhou City University (LZCU-BS2015-07) and the Research Project of Universities in Gansu (2019B-169).

REFERENCES

- [1] Bai, X., Zhu, J., Wang, Z., Bian, D., Liu, L. (2010): Ion uptake and distribution in relation to the adaptability of several desert species. – Acta Ecologica Sinica 12: 3247-3253.
- [2] Chang, Z., Zhao, M., Han, F., Zhong, S., Li, F. (2008): Phenological characteristics of desert plant in Minqin Desert area. – Scientia Silvae Sinicae 5: 58-64.
- [3] Chen, C., Wen, H., Zhao, X., Shao, Y., Tao, Y., Mei, L. (2011): Determination of oligomeric proantho cyanidins in *Lycium Ruthenicum* Murr. pigment. – Chinese Journal of Spectroscopy Laboratory 4: 1767-1769.
- [4] Chen, G., Gao, Z., Xu, G. (2017): Adaption of plants to potassium deficiency and strategies to improve potassium use efficiency. – Bulletin of Botany 1: 89-101.
- [5] Chen, X., Gao, B., Wang, X., Zhang, C. (2014): Change and status of desertification land in Minqin, Gansu, China. – Journal of Desert Research 4: 970-974.
- [6] Dai, S., Qiu, G., Zhao, M. (2008): Study on land desertification and its prevention and control measures in the Minqin Oasis in Gansu Province. – Arid Zone Research 3: 319-324.
- [7] Garthwaite, A. J., Bothmer, R. V., Colmer, T. D. (2005): Salt tolerance in wild hordeum species is associated with restricted entry of Na^+ and Cl^- in the shoots. – Journal of Experimental Botany 419: 2365-2378.
- [8] Gattward, J. N., Almeida, A. A., Souza, J. O. J., Gomes, F. P., Kronzucker, H. J. (2012): Sodium-potassium synergism in *Theobroma cacao*: stimulation of photosynthesis, water-use efficiency and mineral nutrition. – Physiol Plantarum 1: 350-362.
- [9] Gu, X., Zhang, X., Song, X., Zang, Y., Li, Y., Ma, C., Zhao, B., Liu, C. (2014): A new herbs traceability method based on DNA barcoding-origin-morphology analysis-an example from an adulterant of *Lycium Ruthenicum* Murr. – China Journal of Chinese Materia Medica 24: 4759-4762.
- [10] Huang, J. W., Shaff, J. E., Grunes, D. L., Kochian, L. V. (1992): Aluminum effects on calcium fluxes at the root apex of aluminum-tolerant and aluminum-sensitive wheat cultivars. – Physiol Plantarum 1: 230-237.
- [11] Huang, Y., Liu, F., Ma, Y., Al., E. (2016): A comparison of diurnal variations of photosynthetic characteristics of *Nitraria tangutorum* and *Sarcogygium xanthoxylon* in autumn in ulanbuh desert. – Journal of Gansu Agricultural University 4: 78-83.
- [12] Larkindale, J., Knight, M. R. (2002): Protection against heat stress-induced oxidative damage in arabidopsis involves calcium, abscisic acid, ethylene, and salicylic acid. – Plant Physiology 2: 682-695.

- [13] Li, Y., Tu, J., Zhang, D., Wang, L., Tian, C., Wu, G., Zhang, F., Zhao, Z., Zhang, K. (2017): Ion content and distribution in *Suaeda physophora*. – Arid Land Geography 2: 365-372.
- [14] Liao, H., Yan, X. (2003): Advanced Plant Nutrition. – Science Press, Beijing.
- [15] Liu, X., Li, X., Qian, B., Tang, Y. (2014): Ca²⁺ signal transduction and its regulation role under drought stress in plant. – Acta Botanica Boreali-Occidentalia Sinica 9: 1927-1936.
- [16] Liu, Y., Zhou, H., Zhao, X., Al., E. (2011): Preliminary study on dormancy mechanism of several desert plants under drought stress. – Journal of Desert Research 1: 76-81.
- [17] Ohno, T., Grunes, D. L. (1985): Potassium-agnesium interactions affecting nutrient uptake by wheat forage. – Soil Science Society of America Journal 1: 685-690.
- [18] Qi, Y., Chang, Q., Liu, M., Liu, J., Chen, T. (2011): Characteristics of desertified soil in desertification reversing process by artificial vegetation. – Agricultural Research in The Arid Areas 3: 180-185.
- [19] Su, P., Zhou, Z., Zhang, H., Li, S., Xie, T. (2013): Canopy photosynthesis and soil respiration of desert plant *Calligonum Potanini*. – Journal of Beijing Forestry University 3: 56-64.
- [20] Wang, J., Chen, W. (2012): Responses of seed germination and seedling growth of *Lycium ruthenicum* to salt stress. – Chinese Journal of Ecology 4: 804-810.
- [21] Wang, X., Luo, N., Shan, H., Wang, X. (2016): Responses characteristics of 4 desert shrubs in Minqin under drought stress. – Arid Land Geography 2: 1025-1035.
- [22] Wang, Y., Wu, W. (2009): Molecular genetic mechanism of high efficient potassium uptake in plants. – Bulletin of Botany 1: 27-36.
- [23] Wei, X., Zhou, L., Ma, Y., Huang, S., Lu, H., Chen, Y. (2015): Ecological and economic impacts of water conservancy construction in Minqin Oasis of more than 50 years. – Arid Land Geography 5: 1014-1021.
- [24] Yao, A., Che, T., Jiang, L., Feng, Y. (2014): Unused land RS classification study of desertification region in Minqin County, Gansu Province. – Forest Research 2: 195-200.
- [25] Zhao, C., Wei, X., Yu, Q., Al., E. (2005): Photosynthetic characteristics of *Nitraria tangutorum* and *Haloxylon ammodendron* in the ecotone between oasis and desert in Minqin, region, country. – Acta Ecologica Sinica 8: 1908-1913.
- [26] Zhou, Z., Xu, X., Yang, L. (2005): Physiological response and high-temperature resistance of three species of psammophytes under high-temperature stress. – Arid Land Geography 6: 824-830.

SPECIES COMPOSITION OF COCCINELLIDAE (COLEOPTERA) AND THEIR PREYS IN ADANA (TURKEY) WITH OBSERVATIONS ON POTENTIAL HOST MEDICINAL AND AROMATIC PLANTS

ELEKCIÖĞLU, N. Z.

*Cukurova University, Vocational School of Karaisalı, Department of Plant and Animal
Production, 01170 Adana, Turkey*
(e-mail: nelekcioğlu@cu.edu.tr; phone: +90 322 5512057; fax: +90-322-551-2255)

(Received 29th Aug 2019; accepted 25th Nov 2019)

Abstract. This study was carried out to determine the Coccinellidae (Coleoptera) species and their preys in Adana Province of Turkey. The samples were collected from medicinal and aromatic plants in 2016-2018. Coccinellidae species were sampled by using sweep-net, handheld aspirator or by handpicking. Total of 1470 individuals were collected and 28 species belonging to 20 genera were identified. The common species according to their frequency were; *Coccinella septempunctata* (Linnaeus) (24.56%), *Hippodamia (Adonia) variegata* (Goeze) (15.92%), *Scymnus pallipediformis* Günther (11.29%), *Chilocorus bipustulatus* (L.) (5.65%), *Scymnus levaillanti* M. (5.51%). Coccinellid species were found widely distributed in both localities studied, whereas, Sarıçam locality represented higher diversity indices of Shannon-Weiner's (2.810) and Simpson's (0.076). Similarity index was observed as 0.727. A total of 42 pest species were observed. Twenty predator species were recorded to be primarily feeding on aphids. For almost all coccinellid species, population was highest in spring and in the early summer. Beetles were collected from 54 medicinal and aromatic plants with 18 species from the Lamiceae and 12 species from the Asteraceae families.

Keywords: medicinal and aromatic plant, Coccinellidae, *Coccinella septempunctata*, aphid, Lamiaceae, diversity

Introduction

In Turkey, 30% of the plant species in the natural flora are medicinal and aromatic plants (MAPs) (Faydaoğlu and Sürücüoğlu, 2011). These plants are becoming increasingly important in terms of being potentially integrated into alternative cropping systems, a raw material supply for the food industry, used as a complementary environment in alternative wards, and as organic pesticides in controlling pests at different habitats, which have become more widespread in recent years. The essential oils of MAPs are generally used in drugs, cosmetics, perfumes, aroma therapy and other industrial branches. In order to competently evaluate the sustainable production and market potential of medical and aromatic plants, they must be of the required quantity and quality (Bayram et al., 2010). The use of MAPs is increasing throughout Turkey and the world nowadays as control of pest insect species that restrict the production is gaining importance. Chemical control is the main control method against pest species in protecting agricultural products. Using pesticides against pests in MAPs, which are used mainly for therapy, is known to negatively affect human health. Consequently, control methods that do not disrupt natural balance, and cause resistance problem are appropriate for ecological and sustainable agriculture are needed. In line with these points, biological-based techniques are being proposed for the management of pest. Biological control is one of these methods. In this context, researches on the determination of the pest species and natural enemy fauna of medicinal and aromatic

plants in Turkey will be helpful. Coccinellidae family (ladybirds), which most of them are predators, is one of the natural enemies that feeds on aphids, scale insects, whiteflies, mites and small arthropods. Due to the predatory nature of most of the coccinellids, they have an important role in biological control-based pest management in agricultural production (Khan et al., 2007; Uygun and Karabüyük, 2013). 6000 Coccinellidae species from 360 genera have been reported worldwide (Tomaszewka and Szawaryn, 2016). In Turkey 104 species from 39 genus and 6 subfamilies have been recorded (Uygun and Karabüyük, 2013). Many studies have been done on the determination of coccinellid species on various plant species in almost all regions of Turkey (Uygun, 1981; Ölmez, 2000; Tezcan et al., 2003; Aslan and Uygun, 2005; Özgen and Karsavuran, 2005a; Bolu et al., 2007; Efil et al., 2010; Portakaldalı and Satar, 2010; Özsisili, 2011; Gözüaçık et al., 2012; Şahin and Işık, 2014; Kaplan et al., 2019). However, the studies on the determination of coccinellid species on medicinal and aromatic plants in Turkey is very limited. Few studies have been conducted in the Aegean region of Turkey. Investigation of coccinellidae species at geographically different habitats and on different plants are important and crucial at revealing biological diversity and the potential of biological control and organic agriculture.

The objective of this study is to explore and identify ladybird species associated with medicinal and aromatic plants, and their prey species in Adana Province of Turkey. The results will be helpful in solving entomological problems on MAPs.

Materials and Methods

Study site

This study was conducted during 2016-2018 in Sarıçam and Karaisalı district of Adana. Coccinellid specimens were collected from CU Ali Nihat Gökyiğit Botanical Garden (Balcalı/Sarıçam) and CU Karaisalı Vocational School Campus (Karaisalı) from MAP plots (Fig. 1).

Both districts are located in southern Turkey (Balcalı: 37° 3' 2.53"N; 35° 21' 15.49"E - 23 meters above sea level, Karaisalı: 37° 15' 12.96"N; 35° 4' 7.28"E - 235 meter above sea level) and represent typical Mediterranean climate: hot dry summers and wet mild winters.

Sampling and laboratory processing of specimens

In Sarıçam 200 and in Karaisalı 30 MAPs were investigated. Collection of coccinellid beetles was carried out once per week during March-December and biweekly during the other months. All the plant parts from randomly chosen 10 plants were examined from each MAP plots. Collection of both beetles and pest species differed according to plant and pest species; by shaking and knocking branches into a standard sweeping net for 10 seconds, by a handheld aspirator or by handpicking. Coccinellid individuals on short plants were captured by using sweepnet and then they were sucked by an aspirator. All plants from each medicinal and aromatic plant (herbaceous, trees and shrubs etc.) plots were examined visually and the coccinellid individuals were picked by hand or handheld aspirator. Insects were then transferred to the killing bottles and brought to the laboratory for pinning and labeling. Coccinellid specimens were tagged with information about host plants, locality and date for identification (Uygun, 1981). Pest and plant species on which larvae and adult beetles

were found feeding constantly on were considered to be potential host pest and plants. To increase our confidence in the determination of true pest associations, obvious damage levels on the vegetation and number of adult beetles feeding observed were also taken into consideration. High population density of feeding beetles was accepted as the main factor in related host plant determination. Beetles on plants without a pest were ignored and controlled the following weeks. The predator larvae were also collected with the preys to obtain adults in the laboratory. Specimens of aphids, mites and thrips were directly taken from the plants with fine brush and then placed separately in Eppendorf tubes containing 70% elthy alcohol (Hille Ris Lambers, 1950; Atakan and Uygur, 2005). Each plant sample infected by scale insects and whiteflies was cut and put into first a paper bag and then a plastic bag. Separately labelled samples were taken away to the laboratory. Scale insects and whiteflies on plants were put into Eppendorf tubes with 70% elthy alcohol for further examination (Kosztarab and Kozár, 1988) The identification of the specimens were performed by specialized experts. All of coccinellid specimens were deposited in the laboratory of Department of Plant and Animal Production, Karaisalı Vocational School, Cukurova University, Turkey.

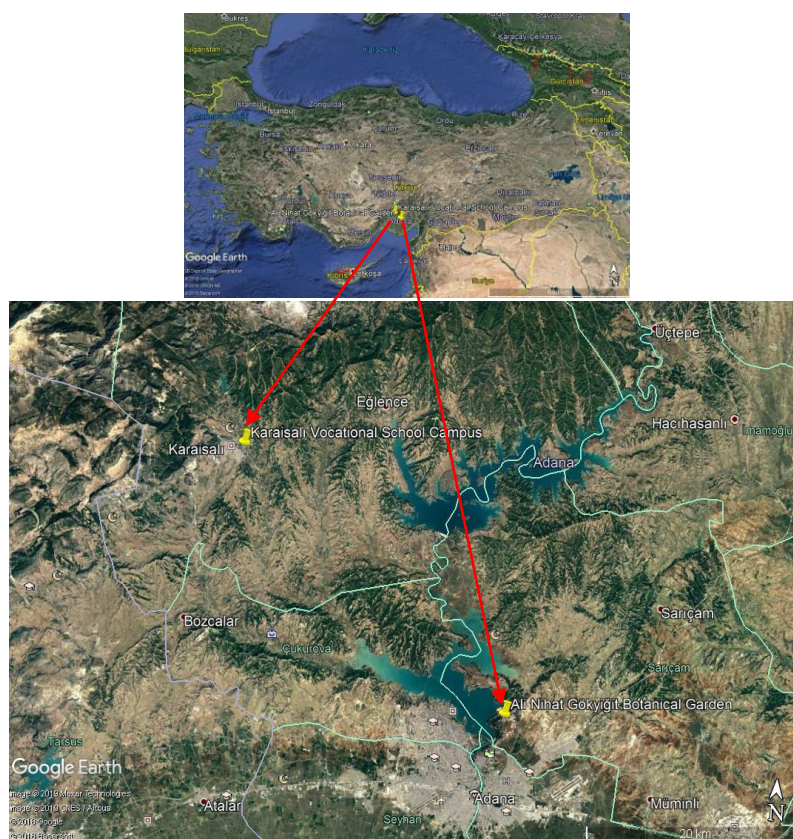


Figure 1. Location of study areas (Sarıçam and Karaisalı Districts of Adana/Turkey)

Statistical analysis

Collected data were employed for statistical analyses to calculate species diversity and similarity in different localities by applying Shannon-Wiener and Simpson's diversity indexes and Sorenson similarity index (Magurran, 1988; Southwood and Henderson, 2000).

Shannon-Wiener diversity index (H'):

$$H' = - \sum p_i \ln(p_i) \quad (\text{Eq.1})$$

where, p_i : proportion of i^{th} species to others, \ln : Natural logarithm.

The index values are among 0.0 and 5.0. In the majority of cases the calculated values range from 1.5 to 2.5. The values above 2.5 indicate that the habitat is stable and has high diversity, whereas all values below 1.5 indicate a degraded habitat or low diversity.

Simpson diversity index (S):

$$S = 1 - \sum n_i(n_i-1) / N(N-1) \quad (\text{Eq.2})$$

where, i : Number of species, n_i : Individual number in a species, N : Total number of individuals in all species in a community.

The value of S ranges from 0 to 1. With this index, 0 represents infinite diversity and 1 no diversity. That is, the bigger the value the lower the diversity.

Species similarity between two communities was calculated by Sorenson's index (SQ):

$$SQ = 2J / a+b \quad (\text{Eq.3})$$

where, J = number of similar species in both communities, a = total number of species in community A, b = total number of species in community B.

The value of SQ ranges from 0 to 1. With this index, 0 represents no similarity and 1 complete similarity. That is, the bigger the value the higher the similarity.

Meteorological data were obtained from HOBO data logger placed in the botanical garden in Sariçam and 'Ministry of Food, Agriculture and Livestock, Karaisalı District Directorate of Agriculture and Forestry' in Karaisalı located one km away from the tested orchard.

Results

Ladybirds were collected from totally 54 species of MAPs from Sariçam and Karaisalı districts of Adana (Turkey); 50 of the MAP species were in Sariçam and 20 of the MAP species were in Karaisalı (*Fig. 2*).

A total of 1470 coccinellid specimens representing 5 subfamilies, 20 genera and 28 species were collected in both provinces during 2016-2018 (*Table 1*). Species are listed in *Table 1* with habitat information, sampling year and abundance data. The number of individuals collected in 2018 (647 individuals belonging to 25 species) were higher than those collected in 2017 (579 individuals belonging to 25 species) and in 2016 (244 individuals belonging to 13 species).

The species were from the subfamilies Chilocorinae, Coccidulinae, Coccinellinae, Scymninae and Sticholotidinae. Subfamily Chilocorinae represented four species, Coccinellinae 10 species, Scymninae 12 species, and Coccidulinae and Sticholotidinae represented one species each. Scymninae was determined as the richest species subfamily in the area comprising 12 out of 28 species collected (*Fig. 3*). The most frequently collected coccinellid species of the study were; *Coccinella septempunctata* (Linnaeus) (24.56%), *Hippodamia* (Adonia) *variegata* (Goeze) (15.92%),

Scymnus pallipediformis Günther (11.29%), *Chilocorus bipustulatus* (L.) (5.65%), *Scymnus levaillanti* M. (5.51%). *Psyllobora vigintiduopunctata* (L.) had the least relative abundance (0.07%) with only one specimen found (Table 2).



Figure 2. Adult and larval coccinellid individuals on *Mentha piperita* (a), *Salvia officinalis* (b), *Coriandrum sativum* (c), *Matricaria chamomilla* (d). *Coccinella septempunctata* L. adult and larvae (a,b, c), *Scymnus* larvae (d)

The prey preferences of Coccinellidae family species determined in this study showed differences between the species. Twenty seven of these species are predators while one of them is phytophagous, *P. vigintiduopunctata*. Twenty species were determined to be aphidophagus. *Cheliomenes propinqua*, *Brumus (Exochomus) quadripustulatus*, *E. nigromaculatus*, *Nephus (Sidis) hiekei*, *N. nigricans*, *N. includens*, *Pharoscyrnus pharoides* were recorded feeding on primarily the mealybugs. *C. bipustulatus*, *Brumus (Exochomus) quadripustulatus*, *Rhyzobius lophanthae*, *Rodolia cardinalis*, *Scymnus rubromaculatus*, *S. pallipediformis*, *S. (Pullus) subvillosus* were recorded feeding on the scale insects and coccids. One species (*S. gilvifrons*) was only feeding on mites while another species (*S. pallipediformis*) fed on aphids, scale insects and cicadellids. *Clitestetus arcuatus* were determined to be primarily feeding on whiteflies and on aphids. *P. vigintiduopunctata* fed both on fungi and aphids. *C. septempunctata* primarily fed on aphids and also on thrips. It was determined that *P. pharoides* and *S. leveillantii* were also fed on red spiders. The primary host of the most encountered coccinellid species were aphids; *C. septempunctata* was determined to feed on 8 aphid species on 10 MAPs, *H. variegata* on 12 aphid species on 15 MAPs, and *S. pallipediformis* on 5 aphid species on 6 MAP species. Coccinellid species were determined to feed on totally 42 pest species; 19 aphid, 8 coccid and pseudococcid, 5 diaspidid, 4 aleyrodid, 3 spidermite, 2 cicadellid and 1 thysanopter species. The MAPs found on, prey, location, capture months and adult number of each coccinellid species are given in Table 2.

According to data obtained from sampled Coccinellid species and specimens number; species richness was 27 and 17 in Sariçam and Karaisalı agroecosystems, respectively (Table 3). Specimens number was parallel to species number (953 in Sariçam and 531 in Karaisalı). Among the districts, Sariçam had higher biological

diversity than Karaisalı with Shannon-Wiener diversity index value of 2,810 and Simpson diversity index value of 0.076.

Sorenson similarity index value was 0,727. According to index value Sariçam and Karaisalı agroecosystems are similar in the ratio of 72.7% in terms of coccinellid species.

Table 1. List of recorded coccinellid species of Sariçam and Karaisalı Districts during 2016-2018, with the number of individuals

Coccinellid species	S*			K			Total
	2016	2017	2018	2016	2017	2018	
<i>Adalia bipunctata</i> (Linneaus)		6			2	2	10
<i>Adalia decempunctata</i> (Linneaus)		15	3				18
<i>Adalia fasciatopunctata revelierei</i> Mulsant	3	3	3				9
<i>Cheliomenes propinqua</i> Mulsant	8	13			3	6	30
<i>Chilocorus bipustulatus</i> (Linneaus)	30	16		26	11		83
<i>Clitostethus arcuatus</i> (Rossi)		6	8		3	5	22
<i>Coccinella septempunctata</i> Linnaeus	32	71	98	35	71	54	361
<i>Brumus (Exochomus) quadripustulatus</i> (Linneaus)		14	24		3	5	46
<i>Exochomus nigromaculatus</i> (Goeze)		28	36				64
<i>Hippodamia (Adonia) variegata</i> (Goeze)	26	68	86	11	14	29	234
<i>Hyperaspis quadrimaculata</i> Redtenbacher		3					3
<i>Myrrha octodecimguttata</i> (Linneaus)	1	1					2
<i>Nephus (Sidis) hiekei</i> (Fürsch)		2	4				6
<i>Nephus nigricans</i> Weise		14	10		4	8	36
<i>Nephus includens</i> Kirsch			2			3	5
<i>Oenopia (Synharmonia) conglobata</i> (Linneaus)	6	8	16		2	4	36
<i>Pharoscymnus pharoides</i> Marseul		3	4				7
<i>Platynaspis luteorubra</i> (Goeze)			3				3
<i>Propylaea quatuordecimpunctata</i> (Linneaus)		2	4			2	8
<i>Psyllobora vigintiduopunctata</i> (Linneaus)			1				1
<i>Rhyzobius lophanthae</i> Blaisdell		8	9				17
<i>Rodolia cardinalis</i> (Mulsant)				2	9	18	29
<i>Scymnus (Pullus) flagellisiphonatus</i> (Fürsch)		1	3				4
<i>Scymnus rubromaculatus</i> (Goeze)	5	4	7	2	8	6	32
<i>Scymnus pallipediformis</i> Günther,	5	20	41	25	34	41	166
<i>Scymnus (Pullus) subvillosus</i> (Goeze)	6	20	34	1	6	10	77
<i>Scymnus levaillantii</i> Mulsant	4	11	15	10	25	16	81
<i>Stethorus gilvifrons</i> Mulsant	3	42	20	3	5	7	80
TOTAL	129	379	431	115	200	216	1470

*S: Sariçam, K: Karaisalı

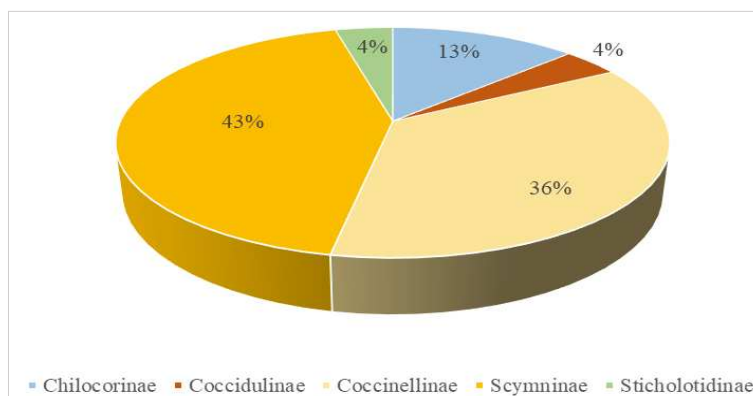


Figure 3. Percentage of ladybird subfamilies in terms of species number collected from the study areas

Table 2. Coccinellid species, their preys, distribution, relative abundance according to medicinal and aromatic plants determined in Adana province in 2016-2018

Species	MAP	Prey	Collection months	Locality		n	% in total individuals
				S	K		
<i>Adalia bipunctata</i> (Linneaus, 1758)	<i>Artemisia dracunculus</i> L. (Asteraceae)	<i>Macrosiphoniella abrotani</i> (Walker) (Hemiptera: Aphididae)	IV, XI	+		5	0.68
	<i>Foeniculum vulgare</i> Mill. (Apiaceae)	<i>Aphis fabae</i> Scopoli (Hemiptera: Aphididae)	II, III, IV	+	+	5	
<i>Adalia decempunctata</i> (Linneaus, 1758)	<i>Matricaria chamomilla</i> L. (Asteraceae)	<i>Brachycaudus helichrysi</i> (Kaltenbach) (Hemiptera: Aphididae)	IV, VIII	+		11	1.22
	<i>Teucrium chamaedrys</i> L. (Lamiaceae)	<i>Aphis fabae</i> Scopoli (Hemiptera: Aphididae)	I, IV, XII	+		7	
<i>Adalia fasciatopunctata revelierei</i> Mulsant, 1866	<i>Silybum marianum</i> (L.) Gaertner (Asteraceae)	<i>Aphis fabae</i> Scopoli	IV, XII	+		5	0.61
	<i>Alcea rosea</i> L. (Malvaceae)	"	V	+		4	
<i>Cheliomenes propinqua</i> Mulsant, 1850	<i>Artemisia annua</i> L. (Asteraceae)	<i>Kaltenbachiella pallida</i> (Haliday) (Hemiptera: Aphididae)	V, IX	+		3	2.04
	<i>Hypericum perforatum</i> L. (Hypericaceae)	<i>Myzus (Nectarosiphon) persicae</i> (Sulzer) (Hemiptera: Aphididae)	VI	+		5	
	<i>Brassica rapa subsp. nipposinica</i> (Brassicaceae)	<i>Brevicoryne brassicae</i> (Linnaeus) (Hemiptera: Aphididae)	IV	+		2	
	<i>Capsicum annum</i> L. (Solanaceae)	<i>Phenacoccus solenopsis</i> Tinsley (Hemiptera: Pseudococcidae)	IX		+	2	
	<i>Ocimum bacilicum</i> L. (Lamiaceae)	"	VII, VIII		+	9	
	<i>Pelargonium graveolens</i> L. (Geraniaceae)	"	VII, VIII	+		5	
<i>Chilocorus bipustulatus</i> (Linneaus, 1758)	<i>Malva sylvestris</i> L. (Malvaceae)	"	IX	+		4	5.65
	<i>Laurus nobilis</i> L. (Lauraceae)	<i>Aonidia lauri</i> (Bouche) (Hemiptera: Diaspididae)	VI, VII, VIII, IX	+		17	
	"	<i>Coccus</i> sp. (Coccidae: Hemiptera)	VI, VII	+		7	
	<i>Rosa</i> sp. (Rosaceae)	<i>Aonidiella auranti</i> Maskell (Hemiptera: Diaspididae)	IX, X, XI		+	15	
	<i>Cerantonis siliqua</i> L. (Fabaceae)	<i>Aspidiotus nerii</i> Bouche (Hemiptera: Diaspididae)	VI	+		5	
	<i>Nerium oleander</i> L. (Apocynaceae)	"	VI, VII	+		10	
	<i>Rhododendron</i> sp. (Ericaceae)	"	III		+	4	
	<i>Pistacia terebinthus</i> L. (Anacardiaceae)	<i>Melonaspsis inopinata</i> (Leonardi) (Hemiptera: Diaspididae)	V, VI		+	4	
	"	<i>Parlatoria oleae</i> (Colvée) (Hemiptera: Diaspididae)	V, VII		+	2	
	<i>Artemisia dracunculus</i> L.	<i>Ceroplastes floridensis</i> Comstock (Hemiptera: Coccidae)	IX	+		1	
	<i>Laurus nobilis</i> L.	"	VI, VII, VIII	+		11	
<i>Myrtus communis</i> L. (Myrtaceae)	"	VII, VIII, IX	+	+	5		
<i>Lycium barbarum</i> (Solanaceae)	<i>Parthenolecanium corni</i> Bouche (Hemiptera: Coccidae)	IX	+		2		

Species	MAP	Prey	Collection months	Locality		n	% in total individuals
				S	K		
<i>Clitostethus arcuatus</i> (Rossi, 1794)	<i>Melissa officinalis</i> L. (Lamiaceae)	<i>Bemisia tabaci</i> (Gennadius) (Hemiptera: Aleyrodidae)	X	+		2	1.50
	<i>Salvia sclarea</i> L. (Lamiaceae)	"	X	+		1	
	<i>Rosa x damascena</i> (Rosaceae)	"	X	+		1	
	<i>Cerantonía siliqua</i> L.	<i>Bemisia afer</i> Priesner & Hosny (Hemiptera: Aleyrodidae)	IX		+	6	
	<i>Ocimum basilicum</i> L.	<i>Bemisia argentifolii</i> Bellowa and Perring (Hemiptera: Aleyrodidae)	X	+		2	
	<i>Melissa officinalis</i> L.	"	IX	+		4	
	<i>Salvia officinalis</i> L. (Lamiaceae)	<i>Trialeurodes vaporariorum</i> (Westwood) (Hemiptera: Aleyrodidae)	X		+	2	
	<i>Mentha spicata</i> L. (Lamiaceae)	<i>Aphis affinis</i> deI Guercio (Hemiptera: Aphididae)	IV		+	4	
<i>Coccinella septempunctata</i> Linnaeus, 1758	<i>Salvia officinalis</i> L.	<i>Aphis affinis</i> deI Guercio	IV, V		+	20	24.56
	"	<i>Eucarazzia elegans</i> (Ferrari) (Hemiptera: Aphididae)	IV, V	+		29	
	<i>S. fruticosa</i> Mill. (Lamiaceae)	"	III, V	+	+	27	
	<i>Cynara scolymus</i> L. (Asteraceae)	<i>Brachycaudus (Acaudus) cardui</i>	III, IV, V	+	+	47	
	<i>Coriandrum sativum</i> L. (Apiaceae)	<i>Hyadaphis coriandri</i> (B. Das) (Hemiptera: Aphididae)	IV, V		+	33	
	<i>Silybum marianum</i> (L.) Gaertn.	<i>Aphis fabae</i> Scopoli	IV, XI	+		26	
	<i>Foeniculum vulgare</i> Mill.	"	V, VI		+	24	
	<i>Artemisia annua</i> L.	<i>Kaltenbachella pallida</i> (Haliday)	V	+		38	
	<i>Mentha piperita</i> L. (Lamiaceae)	<i>Aphis affinis</i> deI Guercio	IV, V	+	+	36	
	<i>Origanum onites</i> L. (Lamiaceae)	<i>Aulacorthum solani</i> (Kaltenbach) (Hemiptera: Aphididae)	IV, V	+	+	38	
	<i>Rosmarinus officinalis</i> L. (Lamiaceae)	<i>Myzus (Nectarosiphon) persicae</i> (Sulzer)	IV	+	+	39	
	<i>Euryops pectinatus</i> L. (Asteraceae)	<i>Frankliniella occidentalis</i> (Pergande) (Thysanoptera: Thripidae)	VII		+	4	
<i>Brumus (Exochomus) quadripustulatus</i> (Linnaeus, 1758)	<i>Stevia rebaudiana</i> Bertoni (Asteraceae)	<i>Myzus (Nectarosiphon) persicae</i> (Sulzer)	VIII	+		13	3.13
	<i>Hypericum perforatum</i> L. (Hypericaceae)	"	VIII	+		8	
	<i>Pelargonium graveolens</i> L.	<i>Phenacoccus solenopsis</i> Tinsley (Hemiptera: Pseudococcidae)	VI, VII	+		7	
	<i>Cerantonía siliqua</i> L.	<i>Aspidiotus nerii</i> Bouche (Hemiptera: Diaspididae)	VI, VII, VIII		+	18	
<i>Exochomus nigromaculatus</i> (Goeze, 1777)	<i>Stevia rebaudiana</i> Bertoni	<i>Phenacoccus madeirensis</i> Green (Hemiptera: Pseudococcidae)	VI	+		17	4.35
	<i>Stevia rebaudiana</i> Bertoni	<i>Myzus (Nectarosiphon) persicae</i> (Sulzer)	I, II	+		37	
	<i>Coriandrum sativum</i> L.	<i>Hyadaphis coriandri</i> (B. Das) (Hemiptera: Aphididae)	VI	+		10	
<i>Hippodamia (Adonia) variegata</i> (Goeze, 1777)	<i>Silybum marianum</i> (L.) Gaertn.	<i>Aphis fabae</i> Scopoli	IV, V	+		35	15.92
	<i>Artemisia dracunculus</i> L.	<i>Macrosiphoniella abrotani</i> (Walker)	IV	+		20	

Species	MAP	Prey	Collection months	Locality		n	% in total individuals
				S	K		
		(Hemiptera: Aphididae)					
	<i>Melissa officinalis</i> L.	<i>Cryptomyzus ribis</i> (Linnaeus)	IV, V, VI	+		32	
	<i>Brassica rapa</i> subsp. <i>nipposinica</i> (L.H. Bailey)	<i>Brevicoryne brassicae</i> (Linnaeus)	IV	+		33	
	<i>Cynara scolymus</i> L.	<i>Brachycaudus (Acaudus) cardui</i> (Linnaeus)	III, IV, V, XI	+	+	22	
	<i>Coriandrum sativum</i> L.	<i>Cavariella theobaldi</i> (Gillette & Bragg) (Hemiptera: Aphididae)	IV, V		+	12	
	<i>Matricaria chamomilla</i> L.	<i>Brachycaudus helichrysi</i> (Kaltenbach)	IV, VIII	+		15	
	<i>Thymus vulgaris</i> L. (Lamiaceae)	<i>Ovatus mentharius</i> (van der Goot)	IV	+		3	
	<i>Artemisia annua</i> L.	<i>Kaltenbachiella pallida</i> (Haliday)	IV, V, VII	+		8	
	<i>Stevia rebaudiana</i> Bertoni	<i>Myzus (Nectarosiphon) persicae</i> (Sulzer)	IV, V, VI	+		24	
	<i>Carthamus tinctorius</i> L. (Asteraceae)	<i>Brachycaudus helichrysi</i> (Kaltenbach)	VII	+		5	
	<i>Artemisia annua</i> L.	<i>Macrosiphoniella abrotani</i> (Walker)	IV	+		4	
	<i>Urtica dioica</i> L. (Urticaceae)	<i>Microlophium carnosum</i> (Buckton)	IV	+		2	
	<i>Teucrium chamaedrys</i> L.	<i>Aphis fabae</i> Scopoli	XI	+		4	
	<i>Origanum majorana</i> L. (Lamiaceae)	<i>Aulacorthum solani</i> (Kaltenbach)	II, IV, V	+		7	
	<i>Origanum vulgare</i> L. (Lamiaceae)	"	IV, V	+	+	8	
<i>Hyperaspis quadrimaculata</i> Redtenbacher, 1843	<i>Calendula officinalis</i> L. (Asteraceae)	<i>Macrosiphum euphorbiae</i> (Thomas)	V	+		3	0.20
<i>Myrrha octodecimguttata</i> (Linnaeus, 1758)	<i>Hypericum perforatum</i> L.	<i>Myzus (Nectarosiphon) persicae</i> (Sulzer)	IV, V	+		2	0.14
<i>Nephus (Sidis) hiekei</i> (Fursch, 1965)	<i>Stevia rebaudiana</i> Bertoni	<i>Phenacoccus madeirensis</i> Green	VI	+		6	0.41
<i>Nephus nigricans</i> Weise, 1879	<i>Rosmarinus officinalis</i> L.	<i>Myzus (Nectarosiphon) persicae</i> (Sulzer)	III		+	3	
	<i>Mentha spicata</i> L. (Lamiaceae)	<i>Aphis affinis</i> deI Guercio	IV, V	+		9	
	<i>Origanum majorana</i> L.	<i>Aphis gossypii</i> Glover	IV, V, VII	+		10	
	<i>Artemisia annua</i> L.	"	IV, V	+		6	
	<i>Salvia fruticosa</i> Mill.	"	V		+	1	
	<i>Euryops pectinatus</i> (L.)	<i>Aphis fabae</i> Scopoli	V	+		1	
	<i>Pelargonium graveolens</i> L.	<i>Phenacoccus solenopsis</i> Tinsley	VII	+		2	
	<i>Stevia rebaudiana</i> Bertoni	<i>Phenacoccus madeirensis</i> Green	V, VI	+		4	2.45
<i>Nephus includens</i> Kirsch, 1870	<i>Capsicum annuum</i> L.	<i>Phenacoccus solenopsis</i> Tinsley	IX		+	2	
	<i>Cerantonis siliqua</i> L.	<i>Planococcus citri</i> Risso (Hemiptera: Pseudococcidae)	VI	+		3	0.34
<i>Oenopia (Synharmonia) conglobata</i> (Linnaeus, 1758)	<i>Salvia officinalis</i> L.	<i>Eucarazzia elegans</i> (Ferrari)	IV, V	+		8	
	<i>Mentha piperita</i> L.	<i>Aphis affinis</i> deI Guercio	VI	+	+	6	
	<i>Matricaria chamomilla</i> L.	"	IV, V, VII	+		15	
	<i>Carthamus tinctorius</i> L.	<i>Brachycaudus helichrysi</i>	IV	+		3	2.45

Species	MAP	Prey	Collection months	Locality		n	% in total individuals
				S	K		
	<i>Hypericum perforatum</i> L.	(Kaltenbach) <i>Myzus (Nectarosiphon) persicae</i> (Sulzer)	VIII	+		4	
<i>Pharoscyrmus pharoides</i> Marseul, 1868	<i>Leonurus cardiaca</i> L. (Lamiaceae)	<i>Tetranychus cinnabarinus</i> (Boisd.) (Acari: Tetranychidae)	V	+		4	0.48
	<i>Brassica rapa subsp. nipposinica</i> (L.H. Bailey)	<i>Phenacoccus solenopsis</i> Tinsley	IV	+		3	
<i>Platynaspis luteorubra</i> (Goeze, 1777)	<i>Sedum album</i> L. (Crassulaceae)	<i>Aphis fabae</i> Scopoli	V	+		3	0.20
<i>Propylaea quatuordecimpunctata</i> (Linnaeus, 1758)	<i>Trigonella foenum-graecum</i> L. (Fabaceae)	<i>Aphis craccivora</i> Koch (Hemiptera: Aphididae)	V	+		4	0.54
	<i>Artemisia annua</i> L.	<i>Kaltenbachiella pallida</i> (Haliday)	V	+		2	
	<i>Salvia officinalis</i> L.	<i>Eucarazzia elegans</i> (Ferrari)	VII		+	2	
<i>Psyllobora vigintiduopunctata</i> (Linnaeus, 1758)	<i>Hypericum perforatum</i> L.	<i>Myzus (Nectarosiphon) persicae</i> (Sulzer)	IV	+		1	0.07
<i>Rhyzobius lophanthae</i> Blaisdell, 1892	<i>Hyssopus officinalis</i> L. (Lamiaceae)	<i>Coccus hesperidum</i> Linnaeus (Hemiptera: Coccidae)	VI, VII, IX	+		9	1.16
	<i>Nerium oleander</i> L. (Apocynaceae)	<i>Aspidiotus nerii</i> Bouche	VI, VII, VIII	+		8	
<i>Rodolia cardinalis</i> (Mulsant, 1850)	<i>Rosmarinus officinalis</i> L.	<i>Icerya purchasi</i> Maskell (Hemiptera: Monophellidae)	V, VI		+	7	1.97
	<i>Rosa</i> sp.	"	X		+	9	
	<i>Lavandula angustifolia</i> Mill. (Lamiaceae)	"	VIII, IX		+	5	
	<i>Origanum onites</i> Mill.	"	VIII, IX		+	8	
<i>Scymnus (Pullus) flagellisiphonatus</i> (Fürsch, 1969)	<i>Melissa officinalis</i> L.	<i>Cryptomyzus ribis</i> (Linnaeus) (Aphididae: Hemiptera)	V	+		4	0.27
<i>Scymnus rubromaculatus</i> (Goeze, 1778)	<i>Salvia officinalis</i> L.	<i>Eucarazzia elegans</i> (Ferrari)	VII		+	10	2.18
	<i>S. fruticosa</i> L.	"	VII		+	9	
	<i>Hypericum perforatum</i> L.	<i>Myzus (Nectarosiphon) persicae</i> (Sulzer)	VIII	+		7	
	<i>Myrtus communis</i> L.	<i>Ceroplastes floridensis</i> Comstok (Hemiptera: Coccidae)	IX	+	+	3	
	<i>Cerantonia siliqua</i> L.	<i>Aonidiella aurantii</i> Mask.	IX	+		3	
<i>Scymnus pallipediformis</i> Günther, 1958	<i>Achillea millefolium</i> L. (Asteraceae)	<i>Brachycaudus helichrysi</i> (Kaltenbach)	V, VI	+		24	11.29
	<i>Matricaria chamomilla</i> L.	"	VI, VIII	+		12	
	<i>Salvia officinalis</i> L.	<i>Eucarazzia elegans</i> (Ferrari)	VII		+	22	
	<i>Mentha arvensis</i> L. (Lamiaceae)	<i>Aphis affinis</i> deI Guercio	III, IV		+	28	
	<i>Artemisia annua</i> L.	<i>Kaltenbachiella pallida</i> (Haliday)	VI, IX	+		13	
	<i>Rosmarinus officinalis</i> L.	<i>Myzus (Nectarosiphon) persicae</i> (Sulzer)	III, IV, V		+	21	
	<i>Rhododendron</i> sp. (Ericaceae)	<i>Aspidiotus nerii</i> Bouche	III, IV, V		+	19	
	<i>Salvia officinalis</i> L.	<i>Empoasca decipiens</i> Paoli (Cicadellidae: Hemiptera)	IV, V		+	3	
	<i>Rosmarinus officinalis</i> L.	"	V, VI, VII		+	8	
	<i>Origanum onites</i> Mill.	<i>Eupteryx</i> sp. (Hemiptera: Cicadellidae)	IV, V	+	+	9	
<i>Salvia officinalis</i> L.	"	IV, V		+	7		

Species	MAP	Prey	Collection months	Locality		n	% in total individuals
				S	K		
<i>Scymnus (Pullus) subvillosus</i> (Goeze, 1777)	<i>Origanum syriacum</i> var. <i>bevanii</i> L. (Lamiaceae)	<i>Aulacorthum solani</i> (Kaltenbach)	VI	+		11	5.24
	<i>Capsicum annuum</i> L.	<i>Myzus (Nectarosiphon) persicae</i> (Sulzer)	VI	+	+	19	
	<i>Achillea asplenifolia</i> Vent. (Asteraceae)	<i>Brachycaudus helichrysi</i> (Kaltenbach)	VI	+		14	
	<i>Artemisia annua</i> L.	<i>Kaltenbachiella pallida</i> (Haliday)	V, IX	+		11	
	<i>Laurus nobilis</i> L.	<i>Aonidia lauri</i> Bouche	VI, VII, VIII	+		22	
<i>Scymnus levaillantii</i> Mulsant, 1850	<i>Mentha piperita</i> L.	<i>Tetranychus urticae</i> Koch (Acari: Tetranychidae)	VI, X, XII		+	7	5.51
	<i>Coriandrum sativum</i> L.	"	IV		+	9	
	<i>Ocimum basilicum</i> L.	"	V		+	11	
	<i>Hypericum perforatum</i> L.	<i>Myzus (Nectarosiphon) persicae</i> (Sulzer)	IV	+		8	
	<i>Teucrium chamaedrys</i> L.	<i>Aphis fabae</i> Scopoli	IV, XI	+		11	
	<i>Mentha spicata</i> L.	<i>Aphis affinis</i> deI Guercio	IV		+	13	
	<i>M. piperita</i> L.	"	VII	+		22	
<i>Stethorus gilvifrons</i> Mulsant, 1850	<i>Ricinus communis</i> L. (Euphorbiaceae)	<i>Tetranychus cinnabarinus</i> (Boisd.) (Acari: Tetranychidae)	IV, V, VI	+		14	5.44
	<i>Carthamus tinctorius</i> L.	"	IV, V	+		5	
	<i>Achillea millefolium</i> L.	"	VI	+		3	
	<i>Leonurus cardiaca</i> L.	"	V	+		4	
	<i>Stevia rebaudiana</i> Bertoni	"	VI	+		2	
	<i>Althaea officinalis</i> L. (Malvaceae)	"	IV	+		3	
	<i>Aloysia citrodora</i> Palau (Verbenaceae)	"	IV	+		3	
	<i>Coriandrum sativum</i> L.	"	IV		+	7	
	<i>Tagetes patula</i> L. (Asteraceae)	<i>Tetranychus urticae</i> Koch	IV, V	+		17	
	<i>Cymbopogon citratus</i> Stapf. (DC) (Poaceae)	"	IV	+		6	
	<i>Capsicum annuum</i> L.	<i>Polyphagotarsonemus latus</i> (Banks) (Acari: Tarsonemidae)	IV		+	9	
	<i>Mentha arvensis</i> L.	"	IV		+	7	
TOTAL						1470	100

S: Sarıçam, K: Karaisalı, n: Total Abundance of Species

Climatic data of the study years of Sarıçam and Karaisalı were given in *Figure 4*. The family Coccinellidae was found to be fluctuating throughout the sampling period. Seasonal abundance peaked in spring (including April-May). In April the highest population (530 adults) was recorded. Thereafter gradually decreased and continued until the end of the year (*Fig. 5*). For almost all subfamilies, dominance and species richness values were maximum in spring and in the early summer (*Table 2*).

Ladybirds were collected from totally 54 species of MAPs belonging to 20 families from both provinces. Eighteen MAP species were from the Lamiaceae, 12 from Asteraceae, and 3 from Malvaceae families, and 1 or 2 species from the others (*Fig. 6*).

Table 3. Biological diversity values of coccinellid species in medicinal and aromatic plants in Sariçam and Karaisalı Districts

	Sariçam	Karaisalı
Species number	27	17
Specimens number	939	531
Diversity indexes		
Shannon-Wiener [H']	2,810	2,530
Simpson diversity [S]	0,076	0,100

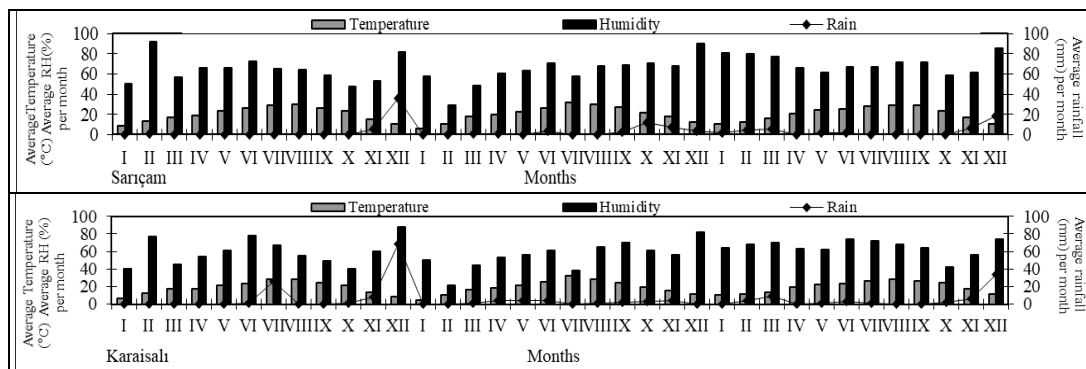


Figure 4. Climatic datas in Sariçam and Karaisalı (Adana) in 2016-2018

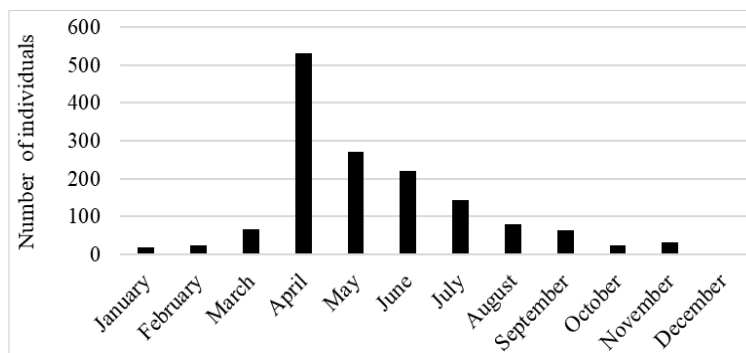


Figure 5. Seasonal abundance of ladybirds in 2016-2018

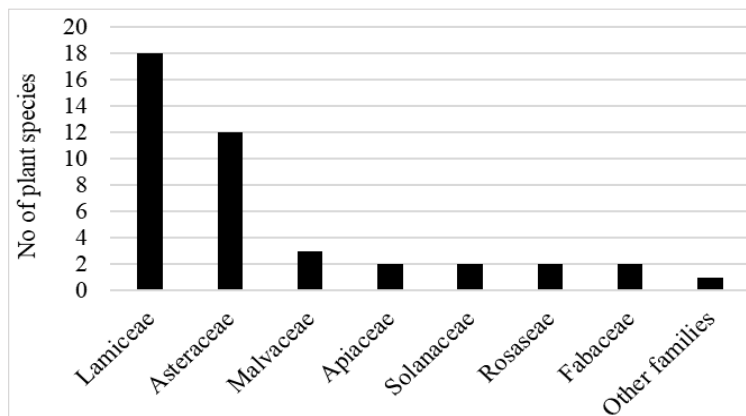


Figure 6. Number of host plant species per family on which the coccinellids were collected

Discussion

Coccinellids are predators primarily of Hemipteran pests such as aphids, mealybugs and scale insects. The majority members of the family have received considerable research attention because of their potential to act as biocontrol agents (Kılınçer et al., 2010). Prey preferences of Coccinellidae species showed differences between the species in this study. Most of the species primarily preferred aphids. Nearly 68% (in Middle Europe) and 35% (worldwide) of the coccinellids are aphidophag, whereas 20% (in Middle Europe) and 36% (worldwide) are reported to be coccidophag. It is concluded that the distribution of the coccinellids are related to their preys distribution (Klausnitzer and Klausnitzer, 1972). Hodek and Honek (1996) reported that the species from Scymnini tribus feed on scale insects in ratio of 62% and 23% for aphids. Eighty-five percent species from Coccinellini tribus feed on aphids, psyllids and Chrysomelidae family. Uygun and Karabüyük (2013) states that Coccinellids, which has a large amount of predators, feed on spider mites, cicadellids, whiteflies, aphids, scale insects, mealybugs, coccids and larvae of Lepidoptera, Coleoptera and Hymenoptera.

The most abundant coccinellid species, *C. septempunctata* which constituted 24.56% of the specimens has been reported to have a wide variety of host species from the family Aphididae. It can be found in all type of habitats and agro-ecosystems on different crops worldwide feeding voraciously on aphids (Horion, 1961; Uygun, 1981; Aslan and Uygun, 2005; Zare et al., 2013), mealybugs and psyllids (Ullah et al., 2012), scale insects (Uygun, 1981; Zare et al., 2013) and thrips (Sanjta and Chauhan, 2018). In this study it was collected from various medicinal and aromatic plants infested with aphids and thrips (Table 2). *C. septempunctata* has been reported to on with pest species from the families Aphididae, Callaphididae, Chaitophoridae, Cicadellidae, Coccidae, Diaspididae, Lachnidae, Pemphigidae, Psyllidae, Tingidae (Hemiptera) in Turkey (Erler, 2002; Bolu et al., 2007).

Hippodamia (Adonia) variegata was the second dominant species (15.92%). Primarily, it prefers Aphididae species, although it has other host species such as psyllids and scale insects (Uygun, 1981; Ives et al., 1993; Ullah et al., 2012). *H. variegata* was found on more MAP species than *C. septempunctata*. Tezcan and Uygun (2003) determined this species as one of the most encountered species collected from *Origanum* spp. fields in Manisa province of Turkey. Göven and Özgür (1990) and Yumruktepe and Uygun (1994) reported that *H. variegata* feeds on aphids and thrips. Aslan and Uygun (2005) collected this species from *M. arvensis* infested with *Aphis affinis* del Guercio and *Ovatus mentharius* (van der Goot), and from *Achillea millefolium* infested with *Brachycaudus helichrysi* (Kalt.) in Kahramanmaraş. It has a wide variety of prey species from the families Aphididae, Aleyrodidae, Chaitophoridae, Coccidae, Diaspididae, Psyllidae (Hemiptera) (Özgen and Karsavuran, 2005a,b; Bolu et al., 2007).

Scymnus pallipediformis was the other dominant species in this study (11.29%). It mainly preys on aphids and to a lesser extent on scale insects and cicadellids (Aslan and Uygun, 2005; Bolu et al., 2007). In this study it was also found feeding on aphids, scale insects and cicadellids. Furthermore, it is reported to feed on species from Chaitophoridae, Coccidae and Psyllidae families in Turkey (Ölmez, 2000; Aslan and Uygun, 2005).

Chilocorus bipustulatus is a common predator of many scale insect, mealybug and waxscale species of Coccoidea family (Uygun, 1981). This armored-scale lady beetle

was the most abundant and important predator species collected from diaspidids and coccids. It also feeds on whiteflies and aphids (Karaat and Göven, 1986; Telli and Yiğit, 2007). Bolu et al. (2007) reported that both adults and larvae of this ladybeetle feed on Coccoid species, especially on the nymphs and the eggs of *Planococcus citri* Risso (Hemiptera: Pseudococcidae).

Stethorus gilvifrons is specialized to spider mites (Uygun, 1981; Uygun and Karabüyük, 2013) and is the most abundant species feeding on smites (*T. cinnabarinus*, *T. urticae* and *P. tarsenomuslatus*) in this study. It also feeds on aphids, scale insects, coccids and psyllids (Erler, 2002; Aslan and Uygun, 2005; Bolu et al., 2007). Aslan and Uygun (2005) collected this species from *M. arvensis* feeding on *A. affinis* Del Guercio in Kahramanmaraş.

Clitostethus arcuatus is primarily a whitefly predator (Uygun and Karabüyük, 2013) and in this study it is the only predator species primarily feeding on whiteflies. Most of them were collected in autumn months from mainly whitefly infested medicinal and aromatic plants (Table 2). Besides whiteflies, it also feeds on aphids and mites (Ulusoy and Ülgentürk, 2003; Kaya Başar and Yaşar, 2011).

Rodolia cardinalis is the main natural enemy of *Icerya purchasi*, used in the biological control of this pest in citrus worldwide successfully (Kılınçer et al., 2010; Anonymous, 2019). *I. purchasi* is a polyphag pest on ornamental plants in Turkey (Kaydan et al., 2013) and the presence of it on lavender, rosemary and thyme was reported for the first time in Turkey (Elekcioglu, 2018). Because of the many uses of these plants, a reduction of its productivity would have a significant economic impact for Turkey. So the presence of this ladybeetle on these plants is thought to be very important.

Psyllobora vigintiduopunctata was the only phytophagous species feeding on fungi from Erysiphaceae family (Horion, 1961; Cruz et al., 1990; Yiğit and Soylu, 2002). It was also observed feeding on aphids as Düzgüneş et al. (1982) mentioned. In this study it was reported on *Hypericum perforatum* feeding on aphids and on *Rosa x damascena* and *H. perforatum* on fungi.

In Turkey, a limited number of survey studies have been reported on the pest species and natural enemy fauna on MAPs which well matches the results of this study. Zarkani and Turanlı (2019) collected *C. septempunctata*, *H. variegata*, *Adalia bipunctata* (L.), *Scymnus frontalis* (Fabricius), *Exochomus nigromaculatus* (Goeze), *Cryptolaemus montrouzieri* Mulsant from *Salvia officinalis* fields in İzmir province (Turkey). They observed *A. bipunctata*, *C. septempunctata* L., *E. nigromaculatus*, *H. variegata*, *C. montrouzieri* Mulsant and *S. frontalis* (Fabricius) feeding on *Aphis passeriniana* (Del Guercio) (Hemiptera: Aphididae) and *Eucarazzia elegans* (Ferrari). Tezcan et al. (2003) detected 9 coccinellid species from thyme fields (*Origanum* spp.) in Manisa Province (Salihli and Turgutlu districts) of Turkey: *S. frontalis*, *S. inderihensis* Mulsant, *S. quadriguttatus* Fürsch, *S. rubromaculatus* (Goeze), *Nephus nigricans* Weise, *E. nigromaculatus* (Goeze), *H. variegata*, *Coccinula quatuordecimpustulata* (Linnaeus) and *C. septempunctata*. *S. frontalis*, *S. rubromaculatus* and *H. variegata* were the most abundant species. *C. septempunctata* was the most encountered species among coccinellid species at thyme fields in Denizli and Manisa. Its population was higher during May-June (Şahin and Işık, 2014). Their results are in conformity with data collected in this study. In order to determine the predator and parasitoid insect species in the oil-bearing rose fields in Isparta province, Demirözer and Karaca (2014) determined 8 coccinellid species. The most abundant

species were: *A. bipunctata*, *A. fasciatopunctata revelierei* Mulstant, *C. bipustulatus* (Linnaeus), *C. septempunctata*, *E. quadripustulatus*, *H. variegata*, *Oenopia oncina* (Olivier) (Coleoptera: Coccinellidae). Metin (2017) detected *C. septempunctata* as a predator insect species in lavender fields (*Lavandula angustifolia* and *Lavandula x intermedia*) in Isparta Province.

Spring and early summer were found more favorable for the family Coccinellidae. The most important reason for this is that aphids are more intense in this period. In addition, mites were also seen in this period. Pest species belonging to Diaspididae, Coccidae, Pseudococcidae and Monophellidae families were also seen apart from spring and so their predators were collected in other months. In spring period the vegetative growth of the plants are intensive and most of them are at flowering period. It is known that plant chemistry is the main factor influencing the feeding behaviour and host selection of phytophagous insects. Secondary metabolites work as important feeding stimulants in the selection of host plants (Matsuda, 1988; Jolivet, 1992). Plants secrete essential oils or protective chemical oils when they are attacked by pests (Rhoades, 1985). The nectar and pollens of flowers and their chemical contents and chemicals secreted by vegetative parts and roots are attractive to pest species in turn of the natural enemies (Knudsen et al., 1993; Riudavets, 1995; Atakan and Pehlivan, 2018). However, some of the medicinal and aromatic plants are repellent, prohibitive and toxic to some insects pests because of the chemical ingredients they have (Bakkali et al., 2008; Zoubiri and Baaliouamer, 2014; Bayram and Tonga, 2017). Scalera (2006) states that *Ocimum basilicum* L. (Lamiaceae) is an attractive plant to natural enemies and mainly flowers are the attractive plant parts. According to the author, to attract many other species of beneficial insects to an area, plants with essential nectar and pollen that bloom at different periods throughout the year must be provided. Yarrow, tarragon, fennel and marigold are plants attractive to ladybirds. *Foeniculum vulgare* Mill. (Apiaceae) is a promising nectar or pollen source and can be considered as an attractive source for ladybirds (Kopta et al., 2012).

The number of coccinellid species were found to be more on the MAPs from the Lamiaceae and Asteraceae families. It is thought that it is either influenced by MAP species or the pest species feeding on them. Plant volatiles can act as chemical signals that influence the behavior and distribution of both herbivores and natural enemies (Rhoades, 1985; Dicke and Grostal, 2001; Thöming et al., 2014). There are complex trophic relationships between plants, herbivores and natural enemies. The compounds released as a result of the feeding herbivores in plants are chemical signals to find the hosts and prey of the natural enemies of the herbivores (Tunca et al., 2011). Some volatile compounds and secondary compounds are reported to be attractive or abductive for many parasitoid and predators (Song et al., 2011; Tang et al., 2013; Wan et al., 2015; Togni et al., 2016). Aromatic plants can affect arthropod community composition and reduce herbivore populations by attracting beneficial insects such as generalist predators. Aromatic plants, *Tagetes patula* L. (Asteraceae) and *Nepeta cataria* L. (Lamiaceae) increase the resistance of apple trees to *Aphis citricola* van der Goot (Hemiptera: Aphididae) both directly, by reducing the population of *A. citricola* through chemical repulsion, and indirectly, by increasing the *Harmonia axyridis* (Pallas) (Coleoptera: Coccinellidae) population through chemical attraction in the field and the laboratory (Song et al., 2017). Informations about the mechanisms governing host and prey search behavior in natural enemies is crucial for the success of the control program.

The complexity of the food chain between living organisms in any ecosystem increases the resistance of that ecosystem to external environmental pressures. In other words, the strong relationships between the living organisms in the ecosystem will prevent the excessive increase in the population density of the species, thus preventing the domination at the habitat. The results of the biodiversity parameters of the present study, shows that both of the study sites have high species diversity which means they have stable agroecosystems. Predator species belonging to the Coccinellidae family play an important role in the formation of agroecosystems having natural balance. The increase of the specimens number as of the years in both localities shows that there is a natural balance between the pest species and coccinellid species. Generally, coccinellids are density-dependent predators, i.e. their number rises as the prey number increases (Dixon, 2000). The predaceous role of coccinellids benefits from the maintenance of field diversity, which supports the population of prey such as aphids, thrips and mites (Iperti, 1999). Ladybirds migrate between various crop fields throughout the season depending upon the availability of prey and habitat disturbance (Maredia et al., 1992). Dixon (2000) reports that the number of species largely depends on the number of preys. For example, in spring (April) most of pests yield great populations, thus the amount of feeding for coccinellids increases too, in the present study.

The results of this study is thought to be helpful in the production of medicinal and plants, especially for the pest management. Distribution and existing periods of the predators would help farmers in choosing the control methods. The results would be used in biological control studies within integrated pest management programs against the pest species in larger fields. Since the use and production of medicinal and aromatic plants are increasing in Turkey, the Ministry of Agriculture and Livestock of Turkey should consider granting support to farmers in MAP production. It is thought that this study will contribute to the determination of insect biodiversity of medicinal and aromatic plant fields in Turkey.

Conclusion

The coccinellid beetles are considered economically very important in agroecosystem as they have been successfully employed in the biological control of many injurious insects. The present study aimed at explore and identify the coccinellid fauna of the medicinal and aromatic plants in Sarıçam and Karaisalı Districts of Adana (Turkey). A total of 28 species belonging to 20 genera were identified and 5 subfamilies. Diversity indexes were high in both localities studied. This study is a preliminary step in the description of the insect and natural enemy fauna (Coccinellidae) of medicinal and aromatic plants and can be used as a reference study for similar faunistic studies in the future. These findings will finally lead to the development of a conservation-based biological control strategy for indigenous plant protection programs. There are no registered pesticides against pests that can be used in medicinal and aromatic plant fields in Turkey. In order to prevent pest species from becoming a potential pest, care must be taken to protect the beneficial species and increase their effectiveness. Therefore, unnecessary spraying should be avoided and appropriate specific pesticides should be used if necessary.

Acknowledgments. The author is grateful to Dr. Nedim UYGUN (Cukurova University Agricultural Faculty, Department of Plant Protection) for determining coccinellid species, Dr. Ekrem ATAKAN,

(Cukurova University Agricultural Faculty, Department of Plant Protection) for determining thrips species, Dr. Işıl ÖZDEMİR (Ministry of Agriculture and Forestry, Directorate of Plant Protection Central Research Institute) for determining aphid species, Dr. Bora KAYDAN (Cukurova University Vocational School of Imamoğlu) for determining Coccoidea species.

REFERENCES

- [1] Anonymous. (2019): *Icerya purchasi* (cottony cushion scale); Invasive species compendium. – <https://www.cabi.org/isc/datasheet/>. Data accessed: August 2019.
- [2] Aslan, M. M., Uygun, N. (2005): The aphidophagous Coccinellid (Coleoptera: Coccinellidae) species in Kahramanmaraş, Turkey. – Turkish Journal of Zoology 29: 1-8.
- [3] Atakan, E., Uygur, S. (2005): Winter and spring abundance of *Frankliniella* spp. and *Thrips tabaci* Lindeman (Thysan., Thripidae) on weed host plants in Turkey. – Journal of Applied Entomology 129: 17-26.
- [4] Atakan, E., Pehlivan, S. (2018): Predatory insect species associated with thrips (Thysanoptera) species on some medicinal and aromatic plants. – Derim 35(1): 37-44.
- [5] Bakkali, F., Averbeck, S., Averbeck, D., Idaomar, M. (2008): Biological effects of essential oils – a review. – Food and Chemical Toxicology 46(2): 466-475.
- [6] Bayram, E., Kırıcı, S., Tansı, S., Yılmaz, G., Arabacı, O., Kızıl, S., Telci, İ. (2010): Possibilities to increase the production of medicinal and aromatic plants. – VII. Technical Congress of Turkey Agricultural Engineering, Ankara: 437-457. (In Turkish).
- [7] Bayram, A., Tonga, A. (2017): Methyl Jasmonate affects population densities of phytophagous and entomophagous insects in wheat. – Applied Ecology And Environmental Research 16(1): 181-198.
- [8] Bolu, H., Özgen, İ., Bayram, A., Çınar, M. (2007): Coccinellidae species, distribution areas and their preys in pistachio, almond and cherry orchards in Southeastern and Eastern Anatolian regions. – Journal of Agricultural Faculty of Harran University 11(1-2): 39-47.
- [9] Cruz, B., Chiang-Lok, M. L., Castaneda-Ruiz, R. F. (1990): *Psyllobora nana* (Coleoptera: Coccinellidae), biological control agent. – Ciencias de la Agricultura 40: 168.
- [10] Demirözer, O., Karaca, İ. (2014): Predator and parasitoid species associated with oil-bearing rose (*Rosa damascena* Miller) production areas in Isparta province with distributional remarks. – Turkish Bulletin of Entomology 4(3): 171-184.
- [11] Dicke, M., Grostal, P. (2001): Chemical detection of natural enemies by arthropods: an ecological perspective. – Annual Review of Ecology, Evolution, and Systematics 32: 1-23. doi:10.1146/annurev.ecolsys.32.081501.113951.
- [12] Dixon, A. F. G. (2000): Insect Predator-prey Dynamics Lady Bird Beetles and Biological Control. – University Press, New York, 257 pp.
- [13] Düzgüneş, Z., Toros, S., Kılınçer, N., Kovancı, B. (1982): Detection of Parasitoid and Predators of Aphidoidea Species in Ankara. – Ministry of Agriculture and Forestry General Directorate of Plant Protection and Agricultural Quarantine, Ankara 251 pp.
- [14] Efil, L., Bayram, A., Ayaz, T., Şenal, D. (2010): Coccinellidae species and their population changes in alfalfa field of Akçakale country of Şanlıurfa province and a new record, *Exochomus pubescens* Küster for Turkey. – Plant Protection Bulletin 50(3): 101-109.
- [15] Elekcioğlu, N. Z. (2018): New host plant species of the Cottony cushion scale, *Icerya purchasi* Maskell, 1878 (Hemiptera: Monophlebidae) in Turkey. – Turkey 7. Plant Protection Congress with International Participation, 14-17 November 2018, Muğla, p: 200.
- [16] Erler, F. (2002): Predators associated with *Cacopsylla pyri* (L.) (Homoptera: Psyllidae) and their population fluctuations in sprayed and non-sprayed pear orchards in Antalya

- Province. – Proceedings of the 5. Turkish National Congress of Biological Control, 4-7 September 2002, Erzurum, 117-126.
- [17] Faydaoğlu, E., Sürücüoğlu, M. S. (2011). History of the use of medical and aromatic plants and their economic importance. – Kastamonu Univ., Journal of Forestry Faculty 11(1): 52-67.
- [18] Göven, M. A., Özgür, A. F. (1990): L'influence des ennemis naturels sur la population the *Thrips tabaci* Lind. sur les cultures du cotonnier dans la Region de Sud-Esr Anatolie. – Proceedings of the 2. Turkish National Congress of Biological Control, 26-29 September 1990, Ankara, 155-164.
- [19] Gözüaçık, C., Yiğit, A., Uygun, N. (2012): Coccinellidae (Coleoptera) species in different habitats at Southeastern Anatolia Region of Turkey. – Turkish Journal of Biological Control 3(1): 69-88.
- [20] Hille Ris Lambers, D. (1950): On mounting aphids and other soft skinned insects. – Entomologische Berichten, XIII: 55-58.
- [21] Hodek, I., Honek, A. (1996): Ecology of Coccinellidae. – Kluwer Academic Publ., Dordrecht / Boston / London 464 pp.
- [22] Horion, A. (1961): Faunistik der mitteleuropischen käfer. – Eigenverlag, Cornell University.
- [23] Iperti, G. (1999): Biodiversity of predaceous coccinellidae in relation to bioindication and economic importance. – Agriculture, Ecosystems and Environment 74: 323-342.
- [24] Ives, A. R., Kareiva, P., Perry, R. (1993): Response of a predator to variation in prey density at three hierarchical scales lady beetles feeding on aphids. – Ecology 74: 1929-1938. <https://doi.org/10.2307/1940836>.
- [25] Jolivet, P. (1992): Insects and plants parallel evolution and adaptations. – Flora and Fauna Handbook No. 2. Sandhill Crane Press, Inc. Gainesville, Florida, 190.
- [26] Kaplan, E., Mart, A., Şenal, D. (2019): A study on the family of Coccinellidae (Coleoptera) in Bingöl and Muş provinces. – Plant Protection Bulletin 59(1): 43-52.
- [27] Karaat, Ş., Göven, M. A. (1986): General status of natural enemies in tobacco areas in southeastern Anatolia. – Proceedings of the 1. Turkish National Congress of Biological Control, 12-14 February 1986, Adana, 162-172.
- [28] Kaya Başar, M., Yaşar, B. (2011): Determination of Ladybird species (Coleoptera: Coccinellidae) on fruit trees in Isparta, Turkey. – Turkish Journal of Entomology 35(3): 519-534.
- [29] Kaydan, M. B., Ülgentürk, S., Erkılıç, L. (2013): Checklist of Turkish Coccoidea (Hemiptera: Sternorrhyncha) species. – Turkish Bulletin of Entomology 3(4): 157-182.
- [30] Khan, I., Din, S., Khalil, S. K., Rafi, M. A. (2007): Survey of predatory Coccinellids (Coleoptera: Coccinellidae) in the Chitral district, Pakistan. – Journal of Insect Science 7(7): 1-6.
- [31] Kılınçer, N., Yiğit, A., Kazak, C., Er, M. K., Kurtuluş, A., Uygun, N. (2010): Biological control of pests from theory to practice. – Turkish Journal of Biological Control 1(1): 15-59.
- [32] Klausnitzer, B., Klausnitzer, H. (1972): Marienkaefer (Coccinellidae). A. ziemsen Verlag. – Wittenberg Lutherstadt, 88 pp.
- [33] Knudsen, J. T., Tollsten, L., Bergstrom, L. G. (1993): Floral scents a checklist of volatile compounds isolated by head-space techniques. – Phytochemistry 33: 253-280.
- [34] Kopta, T., Pokluda, R., Psota, V. (2012): Attractiveness of flowering plants for natural enemies. – Horticultural Science 39(2): 89-96.
- [35] Kosztab, M., Kozár, F. (1988): Scale Insects of Central Europe. – Akademiai Kiadó, Budapest, Hungary, 456 pp.
- [36] Magurran, A. E. (1988): Ecological Diversity and Its Measurement. – Princeton University Press, 179 pp.

- [37] Maredia, K. M., Gage, S. H., Landis, D. A., Scriber, J. M. (1992): Habitat use patterns by the seven spotted lady beetle (Coleoptera: Coccinellidae) in a diverse agricultural landscape. – *Biological Control* 2: 159-165.
- [38] Matsuda, K. (1988): Feeding stimulants of leaf beetles. – In: Jolivet, P., Petitpierre, E., Hsiao, T. H. (eds.) *Biology of Chrysomelidae*. Kluwer Academic Publishers, Dordrecht, The Netherlands, 41-56.
- [39] Metin, F. (2017): Insect Species Found In The Lavender Plantations In The Isparta. – Süleyman Demirel University Graduate School of Natural and Applied Sciences, MSc. Thesis, Isparta, 56 pp. (In Turkish).
- [40] Ölmez, S. (2000): Determination of Aphidoidea (Homoptera) Species and Their Parasitoid and Predators in Diyarbakır Province. – Çukurova University Graduate School of Natural and Applied Sciences, MSc. Thesis, Adana, 109 pp. (In Turkish).
- [41] Özgen, İ., Karsavuran, Y. (2005a): Research on Coccinellidae (Col.) species, densities and preys in the pistachio (*Pistacia vera*) agroecosystem in Siirt Province. – *Proceedings of the GAP IV. Agriculture Congress*, 21-23 September 2005, Şanlıurfa 2: p: 1393. (In Turkish).
- [42] Özgen, İ., Karsavuran, Y. (2005b): Investigations on the determination of the natural enemies of *Lepidosaphes pistaciae* (Archangelskaya) (Homoptera: Diaspididae) on pistachio trees. – *Turkish Journal of Entomology* 29(4): 309-316.
- [43] Özsüslü, T. (2011): Coccinellidae (Coleoptera) species of vegetable plants from Kahramanmaraş, Turkey. – *Turkish Bulletin of Entomology* 1(1): 23-26.
- [44] Portakaldalı, M., Satar, S. (2010): Research on Coccinellidae (Coleoptera) fauna in Artvin and Rize province. – *Plant Protection Bulletin* 50(3): 89-99.
- [45] Rhoades, D. F. (1985): Offensive-defensive interactions between herbivores and plants. Their relevance in herbivore population dynamics and ecological theory. – *The American Naturalist* 125: 205-238.
- [46] Riudavets, J. (1995): Predators of *Frankliniella occidentalis* (Perg.) and *Thrips tabaci* Lind.: a review. – In: Loomans, A. J. M., Van Lenteren, J. C., Tommasini, M. G., Maini, S., Riudavets, J. (eds.) *Biological Control of Thrips Pests*. Wageningen Agricultural University Papers, 95. I, Wageningen, the Netherlands, pp. 49-87. <http://library.wur.nl/WebQuery/wurpubs/fulltext/282973>.
- [47] Sanjta, S., Chauhan, U. (2018): Incidence and diversity of thrips and its associated natural enemies in medicinal plants. – *Journal of Medicinal Plants Studies* 6(1): 01-02.
- [48] Scalera, S. (2006): Plants that attract beneficial insects. – Fact Sheet, FS 6050 HORT, University of Florida IFAS Extension.
- [49] Song, B. Z., Zhang, J., Hu, J. H., Wu, H. Y., Kong, Y., Yao, Y. C. (2011): Temporal dynamics of arthropod community in pear orchards intercropping with aromatic plants. – *Pest Management Science* 67: 1107-1114.
- [50] Song, B., Liang, Y., Liu, S., Zhang, L., Tang, G., Ma, T., Yao, Y. (2017): Behavioral responses of *Aphis citricola* (Hemiptera: Aphididae) and its natural enemy *Harmonia axyridis* (Coleoptera: Coccinellidae) to non-host plant volatiles. – *Florida Entomologist* 100(2): 411-421.
- [51] Southwood, T. R. E., Henderson, P. A. (2000): *Ecological Methods*. – Third edition, Blackwell Sciences Oxford 592 pp.
- [52] Şahin, Ç., Işık, F. (2014): A study on beneficial species found in oregano fields. – II. Medicinal and Aromatic Plants Symposium, 23-25 September 2014, Yalova, p: 705. (In Turkish).
- [53] Tang, G. B., Song, B. Z., Zhao, L. L., Sang, X. S., Wan, H. H., Zhang, J., Yao, Y. C. (2013): Repellent and attractive effects of herbs on insects in pear orchards intercropped with aromatic plants. – *Agroforestry Systems* 87: 273-285.
- [54] Telli, O., Yiğit, A. (2007): Natural enemies of Citrus woolly whitefly, *Aleurothrixus floccosus* (Maskell) and Nesting whitefly, *Paraleyrodes minei* Iaccarino (Hemiptera:

- Aleyrodidae) in Hatay Province, Turkey. – Turkish Journal of Entomology 36(1): 147-154.
- [55] Tezcan, S., Beyaz, G., Uygun, N. (2003): Studies on the Determination of Coccinellidae Fauna on *Origanum* spp. (Lamiaceae) of Manisa Province, Turkey. – Alatarım 2(2): 30-33.
- [56] Thöming, G., Norli, H., Saucke, H., Knudsen, G. (2014): Pea plant volatiles guide host location behaviour in the pea moth. – Arthropod Plant Interact 8: 109-122. doi:10.1007/s11829-014-9292-5.
- [57] Togni, P. H. B., Venzon, M., Muniz, C. A., Martins, E. F., Pallini, A., Sujii, E. R. (2016): Mechanisms underlying the innate attraction of an aphidophagous coccinellid to coriander plants: Implications for conservation biological control. – Biological Control 92: 77-84.
- [58] Tomaszewska, W., Szawaryn, K. (2016): Epilachnini (Coleoptera: Coccinellidae). A Revision of the World Genera. – Journal of Insect Science 16(1): 101.
- [59] Tunca, H., Kılınçer, N., Özkan, C. (2011): Trophic interactions among plants, herbivores and natural enemies. – Ankara University Journal of Environmental Sciences 3(29): 37-45.
- [60] Ullah, R., Haq, F., Ahmad, H., Inayatullah, M., Saeed, K., Khan, S. (2012): Morphological characteristics of ladybird beetles collected from District Dir Lower, Pakistan. – African Journal of Biotechnology 11: 9149-9155.
- [61] Ulusoy, M. R., Ülgentürk, S. (2003): The natural enemies of whiteflies (Hemiptera: Aleyrodidae) in southern Anatolia. – Zoology in the Middle East 28: 119-124.
- [62] Uygun, N. (1981): Taxonomic research on Coccinellidae (Coleoptera) fauna of Turkey. – Çukurova University, Faculty of Agriculture, Publications No: 157, Adana, Turkey 48: 110.
- [63] Uygun, N., Karabüyük, F. (2013): Coccinellidae (Gelin Böcekleri). – <http://www.biyolojikmucadele.org.tr/uploads/Coccinellidae.pdf>. Data accessed: August 2019.
- [64] Wan, H. H., Song, B. Z., Tang, G. B., Zhang, J., Yao, Y. C. (2015): What are the effects of aromatic plants and meteorological factor on *Pseudococcus comstocki* and its predators in pear orchards. – Agroforestry Systems 89(3): 537-547.
- [65] Yiğit, A., Soyulu, S. (2002): Feeding of ladybird, *Psyllobora bisoctonotata* (Muls.) (Coleoptera, Coccinellidae) on causal agent of powdery mildew. – Proceedings of the 5. Turkish National Congress of Biological Control, 4-7 September 2002, Erzurum, 353-358. (In Turkish).
- [66] Yumruktepe, R., Uygun, N. (1994): Determination of aphid species (Homoptera: Aphididae) and their natural enemies in citrus orchards in Eastern Mediterranean region. – Proceedings of the 3. Turkish National Congress of Biological Control, 25-28 January 1994, İzmir, 481-492. (In Turkish).
- [67] Zare, K. M., Biranvand, A., Shakarami, J. (2013): The faunistic survey of lady beetles (Coleoptera, Coccinellidae) in the Mehriz region (Yazd province), Iran. – Bulletin of the Iraq Natural History Museum 12: 43-51.
- [68] Zarkani, A., Turanlı, F. (2019): Insect pests complex of common sage (*Salvia officinalis* L.) (Lamiaceae) and their natural enemies. – Yüzüncü Yıl University Journal of Agricultural Sciences 29(1): 34-42.
- [69] Zoubiri, S., Baaliouamer, A. (2014): Potentiality of plants as source of insecticide principles. – Journal of Saudi Chemistry Society 18(6): 925-938.

ZINC RESISTANCE OF SIX DARK SEPTATE ENDOPHYTIC FUNGI AND THE GROWTH RESPONSE OF TOMATO

LIN, L. C.

*Department of Forestry and Natural Resources, National Chiayi University
Chiayi, Taiwan 60004, Republic of China
(e-mail: linerml@mail.ncyu.edu.tw; phone: +886-5-271-7474; fax: + 86-5-271-7467)*

(Received 3rd Sep 2019; accepted 15th Nov 2019)

Abstract. Dark septate endophytic fungi (DSEF) can promote the growth response of host plants and can increase their resistance to heavy metals. In this study, six isolated DSEFs were proven to be able to form microsclerotia with plants. The objective of this study was to investigate the promoting and inoculation effects of these six DSEFs. Molecular analysis showed that the DSEFs may be new additions to the fungal flora of Taiwan and may be new species in the world. Screening and selection of Zn-resistant DSEFs showed that only two strains, CkDB5 and RrtHH10, were Zn-resistant. Evaluation of the Zn resistance range of CkDB5 and RrtHH10 revealed that the former presented lower EM₅₀ values than the latter, and that both strains showed the same minimum inhibitory concentration values. As the Zn concentration increased, twisting and looping of the mycelial morphology of the strains was observed. Resynthesis experiments proved that CkDB5 and RrtHH10 could promote the growth response of tomato. The biomasses of CkDB5-inoculated plants was up to four times higher than that of the controls. This study showed that, of the six DSEFs, only CkDB5 and RrtHH10 showed Zn-resistance. CkDB5 is a fungus with particularly high Zn resistance, and it could facilitate tomato growth.

Keywords: *dark septate endophytic fungi, growth response, half maximal effective, resynthesis, Zn-resistant*

Introduction

Heavy metals are some of the most toxic inorganic substances known to mankind, and they can contaminate the environment (Upadhyaya et al., 2010). Phytoremediation removes heavy metals through synthesis with plants and microorganisms; to date, it remains the best strategy for heavy-metal recovery with the least harmful effects to the environment (Diagne et al., 2015; Helmisaari et al., 2007). Mycorrhizae promote the growth (Azcón-Aguilar and Barea, 1997; Schmid et al., 1995) and tolerance (Gibson and Mitchell, 2005; Lin et al., 2011) of host plants. Mycorrhizal associations have also been shown to enhance the tolerance of host plants to Zn and Cu (Bradley et al., 1981). Some fungi can alleviate toxic metal stress under certain circumstances (Smith and Read, 1997).

Dark septate endophytic fungi (DSEFs), which are commonly found in the roots of healthy plants, present dark pigmentation and septate hyphae (Mathew and Malathy, 2008) and are often sterile in culture (Newsham, 1999; Piercey et al., 2004). DSEFs refer to miscellaneous groups of anamorphic ascomycetous fungi that can colonize the intracellular or intercellular tissues of roots, and maintain an important functional relationship with host plants. DSEFs can enhance the growth and mineral nutrition of hosts (Fernando and Currah, 1996; Jumpponen et al., 1998; Lin, 2016; Shivanna et al., 1994). Several studies have indicated that some endophytes could promote the growth of host plants in soils that have been contaminated by heavy metals (Monnet et al., 2001; Sun et al., 2011; Xu et al., 2015; Zhang et al., 2010).

Li et al. (2012) suggested that fungal endophyte colonization in Pb- Zn contaminated plants is moderately abundant and that some isolates adapt remarkably well to Pb²⁺ and

Zn²⁺. These findings indicate a potential application in phytoremediation. Diao et al. (2013) indicated that Zn is an essential micronutrient required by a wide variety of cellular processes. However, excessive Zn can be toxic to organisms (Jaekel et al., 2005). Zn is also proposed in the 13-metal contamination list published by the US Environmental Protection Agency (Ramos et al., 2002). In the laboratory, many researchers have demonstrated that DSEF isolates could facilitate the growth of host plants. However, the Zn resistance of these DSEFs to various metal concentrations remains unknown. The purpose of this study is to examine the response of six DSEFs to Zn.

Material and methods

Strains

Six DSEFs were used in this study. Strains CkDB2 and CkDB5 were previously isolated from the roots of *Cinnamomum kanehirae* (120°47'37.33" E, 23°28'16.12" N) from a plantation located in Dabang Township, Chiayi County, Taiwan (Hong et al., 2014). Strain CoLG3 was previously isolated from the roots of *C. osmophloeum* (120°47'15" E, 23°43'47" N) in a plantation located in Lugu Township, Nantou County, Taiwan. Strain MoAL5 was previously isolated from the roots of *Mahonia oiwakensis* (120°48'45" E, 23°30'46" N) in a plantation located in Alishan Township, Chiayi County, Taiwan (Tan et al., 2016). Strain RhYM6 was previously isolated from the roots of *Rhododendron hyperythrum* (121°33'40" E, 25°09'20" N) in a plantation located in Beitou District, Taipei City, Taiwan. Finally, strain RrtHH10 was previously isolated from the roots of *R. rubropilosum* var. *taiwanalpinum* (121°17'21" E, 24°09'58" N) in a plantation located in Renai Township, Nantou County, Taiwan. These six strains were deposited at the Tree Mycorrhiza Laboratory of National Chiayi University.

Seeds

The seeds of ARIA tomatoes (*Solanum lycopersicum* L.) used in this experiment, were kindly provided by the Known-You Seed Co., Ltd.

DNA extraction, sequencing and phylogenetic analysis

The methods described by Phosri et al. (2007) were followed. Mycelia for deoxyribonucleic acid (DNA) extraction, amplification, and sequencing were scraped from the surfaces of PDA cultures. Genomic DNA was extracted using Puregene Proteinase K. Total fungal DNA was used as the template for amplification with primers ITS1-F and ITS4 (Gardes and Bruns, 1993). Polymerase chain reaction (PCR) products were sequenced by Genomics BioSci and Tech Company. Sequences were assembled and related sequences were analyzed using the basic local alignment search tool (BLAST) searches. The phylogenetic relationships were analyzed by Molecular Evolutionary Genetics Analysis software (Tamura et al., 2011). Bootstrapping was performed using neighbor-joining (Saitou and Nei, 1987).

Screening and selection of Zn-resistant DSEFs

Screening and selection of Zn-resistant DSEFs was performed using the methods of Ban et al. (2012) and Zeng et al. (2008) with modifications. The Zn-resistance of the six DSEFs was determined by placing two 0.5 mm³ plugs of the mycelium from each DSEF

into an Erlenmeyer flask (125 mL) containing 25 mL of modified Melin-Norkrans liquid medium (MMN) (Marx, 1969). Each DSEF was placed in 6 flasks, 3 with Zn (ZnCl_2 , 1 mg/mL) and another 3 without. After 14 days of cultivation, the flasks were autoclaved (liquid cycle at 121 °C for 20 min), harvested by filtration (filter paper, AdvanTec No. 1), dried to a constant mass at 70 °C, and weighed.

Evaluation of metal tolerance range

Strains that survived cultivation in Zn medium were evaluated for their Zn tolerance range using the method of Ban et al. (2012) with modifications. The sensitivity of select DSEFs to Zn was evaluated by measuring their minimum inhibitory concentration (MIC) and the effective concentration inhibiting 50% of mycelial growth (EC_{50}). Petri dishes with MMN medium (Marx, 1969) were used to cultivate the selected DSEFs for 14 days. Each DSEF was exposed to six Zn concentrations (0, 0.4, 0.8, 1.2, 1.6, and 2.0 mg/mL) in three replicates. Two 0.5-cm diameter plugs were removed from the edge of 14-day-old colonies and placed in flasks. All treated samples were harvested after incubation in the dark for 14 days, after which the flasks with medium were autoclaved (liquid cycle at 121 °C for 20 min), filtered (filter paper, AdvanTec No. 1), dried to a constant mass at 70 °C, and weighed.

Observation of mycelial morphology under different concentrations of Zn

All mycelium treatments were observed. After 14 days of cultivation in different concentrations of Zn, several mycelia were obtained and carefully placed onto slides. Lactophenol cotton blue (BD BBL™) was applied to stain hyphae, and morphological observations were made using a light microscope; photos were taken for recording purposes (Hutton et al., 1994; Piercey et al., 2002; Sigler and Flis, 1998).

Evaluation of the growth responses of tomato inoculated with DSEFs

After the desired DSEFs were screened, they were applied to the roots of ARIA tomatoes under different environments with or without Zn. Pure resynthesis was done through the method proposed by Dalpé (1986). After surface cleaning, tomato seeds were sterilized with 10% sodium hypochlorite solution for 15 min, rinsed 3 times with sterilized distilled water, and then incubated in glass jars containing 1% agar for germination. Germinated seedlings were transplanted to 100 g of peat substrate (containing 100 mL MMN medium with or without Zn (ZnCl_2 , 1 or 0 mg/mL)) in a glass jar ($95 \times 73 \text{ mm}^2$). Five aseptic tomato seedlings were inoculated with each DSEF. Growth was then allowed to proceed for 42 days in a growth chamber (22 °C, 65% RH, and 16 h of light with a maximum illumination of 5,000 lx). To determine the growth responses of the plants, the seedlings were carefully removed from the jar after incubation.

Evaluation of Zn concentrations in tomato

Evaluation of Zn concentrations in the seedlings was performed following the method described by Yang et al. (2015). Each plant sample was washed thoroughly with tap water and rinsed five times with deionized water to remove surface dust and soil. The cleaned samples were then dried at 80 °C in an oven for 48 h until a constant

weight was achieved. Afterward, the samples were crushed using a microphyte disintegrator.

The concentrations of Zn in the plant samples were determined using the method described by Allen (1989). Samples were completely digested in concentrated HNO₃ (16 mol/L) and HClO₄ (12 mol/L) at a ratio of 4:1 (v/v). The digestion tubes were removed from the digestion block to cool. After the solution had cleared, it was filtered through AdvanTec No. 1 filter paper and transferred quantitatively into a 10-mL volumetric flask by addition of distilled water. Metal concentrations were determined by flame atomic absorption spectrometry (FAAS).

Statistical analyses

Statistical Package for the Social Sciences (version 12.0) (Illinois, USA) for Windows was used for statistical analysis. Means of 3 or 5 separate experiments \pm standard deviations ($n = 3$ or 5) were calculated from the collected data. Tukey's multiple range test at the $p \leq 0.05$ significance level was used to analyze differences between treatments.

Results

Molecular identification of six DSEFs

The data matrix used to construct the neighbor-joining tree was comprised of 18 taxa and 704 aligned characters (including gaps/missing data) (Fig. 1). Based on the results of the phylogenetic analysis, the internal transcribed spacer (ITS) sequences of RrtHH10 clustered with those of *Phialocephala*, forming a cluster with 100% bootstrap support. RrtHH10 shared the closest sequence identity with *Phialocephala fortinii* (GQ302683). The ITS sequences of CoLG3 were similar to those of CkDB2 and clustered with those of *Wiesneriomyces laurinus* (KR822217; KP057801), forming a cluster with 100% bootstrap support. The ITS sequences of RhYM6 were clustered with those of Herpotrichiellaceae sp. (KJ471529) and Eurotiomycetes sp. (KM520020), forming a cluster with 98% bootstrap support. The ITS sequences of MoAL5 were clustered with those of *Cladophialophora*, forming a cluster with 95% bootstrap support. MoAL5 shared the closest sequence identity with *Cladophialophora chaetospira* (EU035406). The ITS sequences of CkDB5 were clustered with those of *Scolecobasidium*, forming a cluster with 99% bootstrap support. CkDB5 shared the closest sequence identity with *Scolecobasidium humicola* (AY265334).

Screening of Zn-resistant DSEFs

After 14 days of incubation, the samples were harvested and dried at 70 °C until a constant weight was achieved (Table 1). In treatments without Zn, all six DSEFs survived; in contrast, only strains CkDB5 and RrtHH10 survived in treatments with Zn.

In treatments without Zn (Table 1), strain CkDB2 showed the highest dry weight of 74.0 ± 6.4 mg. By comparison, the dry weights of MoAL5, RrtHH10, RhYM6, CoLG3, and CkDB5 were 65.4 ± 5.7 , 59.8 ± 6.3 , 57.7 ± 4.9 , 44.7 ± 1.9 , and 39.2 ± 3.2 mg, respectively.

In treatments with Zn (Table 1), only strains CkDB5 and RrtHH10 survived; the dry weights of these strains were 28.8 ± 2.8 and 29.5 ± 1.2 mg, respectively.

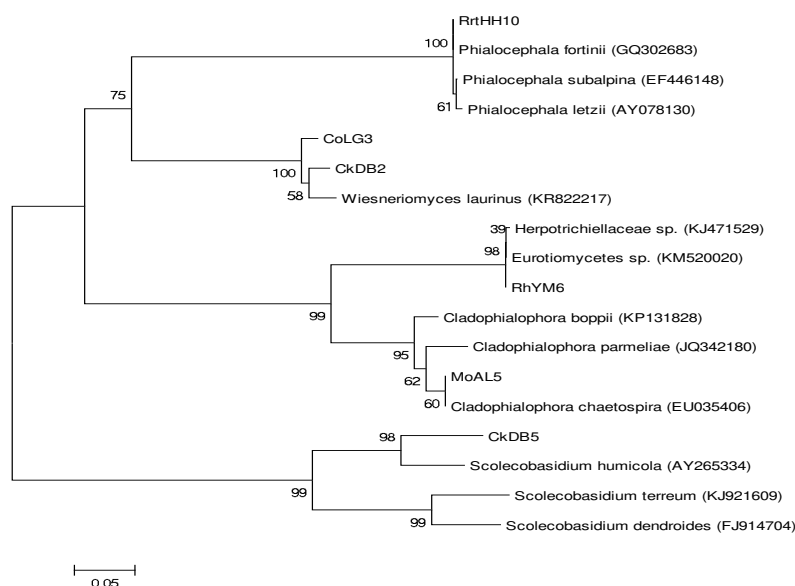


Figure 1. The neighbor-joining phylogenetic tree of the six strains of interest. The tree was obtained using the maximum composite likelihood model for pairwise distance measurements based on ITS sequences. Numbers on branches indicate values generated from 1,000 bootstrap replica

Table 1. Dry weights of six DSEFs in MMN medium with and without Zn

Treatment (strain)	Dry weight (mg)	
	Zn-free	Zn
CoLG3	44.7 ± 1.9 ^b	-
CkDB2	74.0 ± 6.4 ^a	-
CkDB5	39.2 ± 3.2 ^b	28.8 ± 2.8 ^a
MoAL5	65.4 ± 5.7 ^{ab}	-
RhYM6	57.7 ± 4.9 ^{ab}	-
RrtHH10	59.8 ± 6.3 ^{ab}	29.5 ± 1.2 ^a

All values represent the means ± standard deviations of three replicate cultures. Values in the same column with different letters indicate a difference at the 5% significance level

Evaluation of Zn tolerance range

Strains CkDB5 and RrtHH10 produced varying dry weights in media with different Zn concentrations after 14 days of incubation (Table 2).

Strain CkDB5 showed significantly different dry weights under different Zn concentrations (Table 2). The highest dry weight value in 0 mg/mL is 28.4 ± 1.8 mg, compared to 0.4 mg/mL (22.1 ± 4.2 mg), 0.8 mg/mL (19.1 ± 3.9 mg), 1.2 mg/mL (16.9 ± 1.9 mg), 1.6 mg/mL (16.0 ± 2.5 mg), 2.0 mg/mL (4.9 ± 0.6 mg) and 2.4 mg/mL (0 mg).

Strain RrtHH10 also showed significantly different dry weights under different Zn concentrations (Table 2). The highest dry weight value in 0 mg/mL is 53.4 ± 8.1 mg, compared to 0.4 mg/mL (42.4 ± 16.0 mg), 0.8 mg/mL (34.9 ± 6.2 mg), 1.2 mg/mL (11.5 ± 1.7 mg), 1.6 mg/mL (7.7 ± 1.9 mg), 2.0 mg/mL (5.9 ± 2.3 mg) and 2.4 mg/mL (0 mg).

Table 2. Dry weights of strains *CkDB5* and *RrtHH10* in MMN medium with different Zn concentrations

Zn concentrations (mg/mL)	Dry weight (mg)	
	<i>CkDB5</i>	<i>RrtHH10</i>
0	28.4 ± 1.8 ^a	53.4 ± 8.1 ^a
0.4	22.1 ± 4.2 ^{ab}	42.4 ± 16.0 ^a
0.8	19.1 ± 3.9 ^b	34.9 ± 6.2 ^a
1.2	16.9 ± 1.9 ^b	11.5 ± 1.7 ^b
1.6	16.0 ± 2.5 ^b	7.7 ± 1.9 ^b
2.0	4.9 ± 0.6 ^c	5.9 ± 2.3 ^b
2.4	0 ^d	0 ^c

All values represent the means ± standard deviations of three replicate cultures. Values in the same column with different letters indicate a difference at the 5% significance level

Morphological changes of the DSEFs under different Zn concentrations

The mycelial morphology of strains *CkDB5* and *RrtHH10* were observed under a light microscope after cultivation in MMN medium with different Zn concentrations for 14 days. Strains *CkDB5* (Fig. 2A–C) and *RrtHH10* (Fig. 2D–F) showed notable morphological changes in the presence of different Zn concentrations.

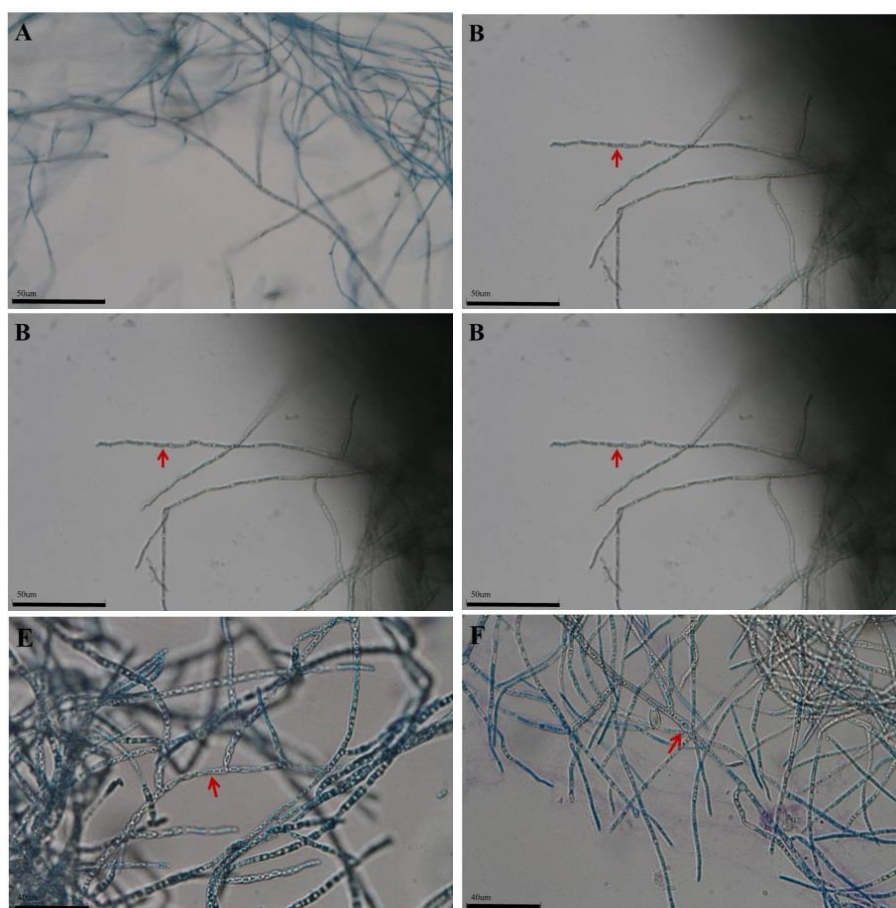


Figure 2. Mycelial morphology of strains *CkDB5* and *RrtHH10* in different Zn concentrations. A–C. Strain *CkDB5*. D–F. *RrtHH10*. A and D, 0 mg/mL. B and E, 0.8 mg/mL. C and F, 1.6 mg/mL

Growth response

After 42 days of incubation, all treated tomato seedlings (with/without Zn) had survived (*Fig. 3*), and the fresh weights of all treatments showed significant differences ($p < 0.05$) (*Table 3*).

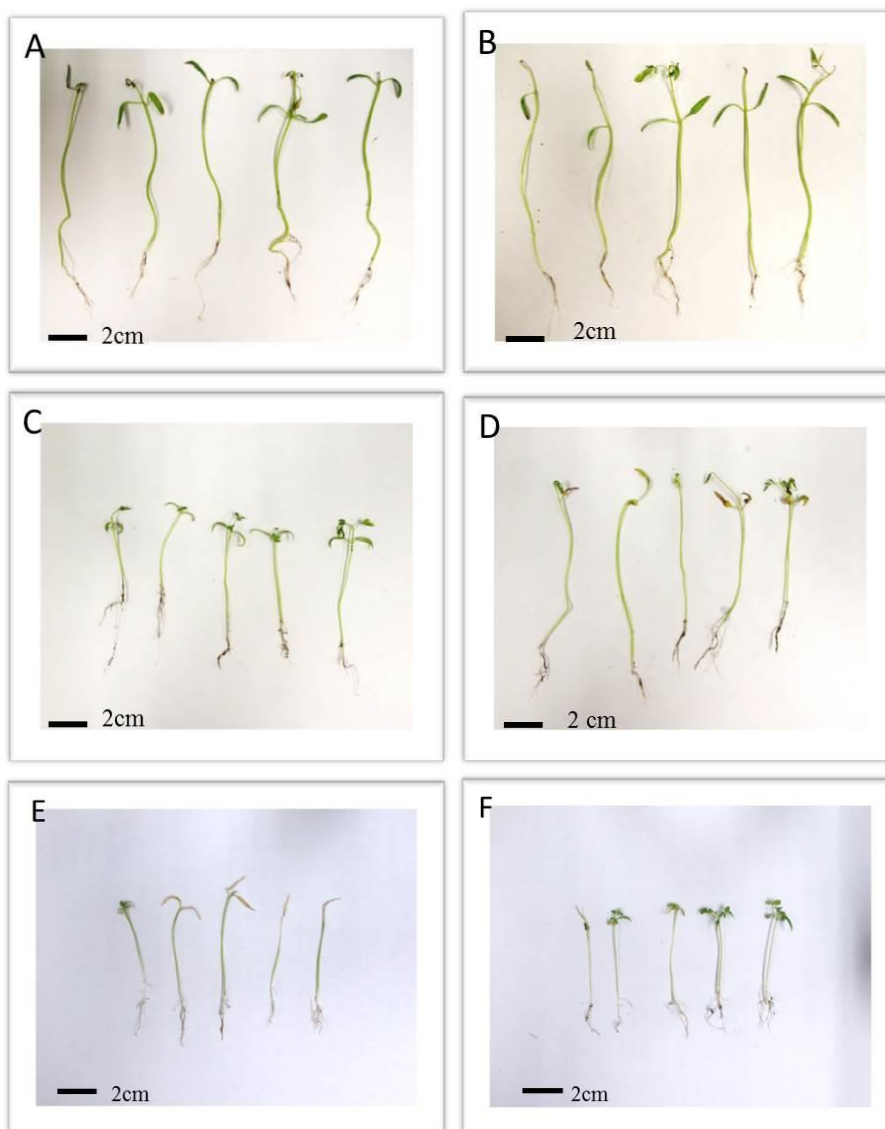


Figure 3. Morphology of tomato seedlings after incubation for 42 days. A. Plants inoculated with CkDB5 without Zn. B. Plants inoculated with CkDB5 with Zn. C. Plants inoculated with RrtHH10 without Zn. D. Plants inoculated with RrtHH10 with Zn. E. Controls without Zn. F. Controls with Zn

In treatments without Zn (*Table 3*), plants inoculated with CkDB5 generated the highest fresh weights of 229.2 ± 5.1 mg compared to plants inoculated with RrtHH10 (81.5 ± 3.3 mg) and the control (54.7 ± 3.4 mg).

In treatments with Zn (*Table 3*), plants inoculated with CkDB5 also showed the highest fresh weights, 174.4 ± 11.4 mg, compared to plants inoculated with RrtHH10 (104.3 ± 11.2 mg) and the control (49.7 ± 4.0 mg).

Table 3. Biomasses of tomato seedlings grown for 42 days in different treatments

Treatment (mg mL ⁻¹)	Fresh weight (mg)		
	CkDB5-inoculation	RrtHH10-inoculation	Control
0	229.2 ± 5.1 ^{aA}	81.5 ± 3.3 ^{bB}	54.7 ± 3.4 ^{aC}
1	174.4 ± 11.4 ^{bA}	104.3 ± 11.2 ^{aB}	49.7 ± 4.0 ^{aC}

All values represent the means ± standard deviations of five replicate cultures. Values in the same row with different lowercase letters are significantly different at 5% significant level. Values in the same column with different capital letters are significantly different at 5% significant level

Evaluation of Zn concentrations in tomato

At harvest, the Zn concentrations of all treatments were determined by FAAS. The Zn concentrations of all treatments with Zn showed significant differences compared to all treatments without Zn ($p < 0.05$) (Table 4).

In treatments without Zn (Table 4), plants inoculated with CkDB5 showed the highest Zn concentration ($92.99 \pm 0.5 \mu\text{g/g}$) compared to the control ($56.4 \pm 4.5 \mu\text{g/g}$) and plants inoculated with RrtHH10 ($0 \mu\text{g/g}$).

In treatments with Zn (Table 4), plants inoculated with RrtHH10 demonstrated the highest Zn concentration ($1,083.03 \pm 13.0 \mu\text{g/g}$) compared to plants inoculated with CkDB5 ($912.83 \pm 6.2 \mu\text{g/g}$) and the control ($279.09 \pm 6.3 \mu\text{g/g}$).

Table 4. Zn concentrations of tomato seedlings grown for 42 days in different treatments

Treatment (mg mL ⁻¹)	Zn concentration ($\mu\text{g/g}$)		
	CkDB5-inoculation	RrtHH10-inoculation	Control
0	$92.99 \pm 0.5^{\text{bA}}$	0^{bC}	$56.4 \pm 4.5^{\text{bB}}$
1	$912.83 \pm 6.2^{\text{aB}}$	$1083.03 \pm 13.0^{\text{aA}}$	$279.09 \pm 6.3^{\text{aC}}$

All values represent the means ± standard deviations of five replicate cultures. Values in the same row with different lowercase letters are significantly different at 5% significant level. Values in the same column with different capital letters are significantly different at 5% significant level

Discussion

In our laboratory, six isolates were shown to be DSEFs, which are known to facilitate the growth of host plants. The six isolates belonged to five taxa (Fig. 1); CoLG3 and CkDB2 belonged to *W. laurinus*, RrtHH10 belonged to *P. fortinii*, CkDB5 belonged to *S. humicola*, RhYM6 belonged to Herpotrichiellaceae, and MoAL5 belonged to *C. chaetospora*.

All six DSEFs that were cultivated in treatments without Zn survived after incubation for 14 days, but only strains CkDB5 and RrtHH10 survived in treatments with Zn (Table 1). Although strains CkDB5 and RrtHH10 did not show significant growth in MMN medium without Zn, they unexpectedly survived in MMN medium with Zn. Therefore, strains CkDB5 and RrtHH10 were selected for further study (Table 1).

The sensitivity of strains CkDB5 and RrtHH10 to Zn was determined based on MIC and EC₅₀. Following the different Zn concentrations in MMN medium for evaluation of Zn tolerance range (Table 2), strain CkDB5 had shown significant differences at a lower Zn concentration (0.8 mg/mL), while strain RrtHH10 showed significant differences at a higher Zn concentration (1.2 mg/mL). The MIC of CkDB5 was over 2.0 mg/mL, and its ME₅₀ was over 1.6 mg/ml. The MIC of RrtHH10 was over 2.0 mg/mL, and its ME₅₀

was over 0.8 mg/mL. Strain CkDB5 showed the same Zn resistance as the fungal endophyte H93 (EU797525) ($ME_{50} = 1.5$ mg/mL) (Zhang et al., 2008). Therefore, strain CkDB5 could belong to a group of highly tolerant fungi based on the studies by Wainwright and Gadd (1997) and Zhang et al. (2008). The mycelial morphology of the strains was twisted and looped with increasing Zn concentrations (Fig. 2). Ban et al. (2012) and Zhang et al. (2008) reported similar results.

Although all treated tomato seedlings (with/without Zn) survived 42 days of incubation (Fig. 3; Table 3), the fresh weights of plants inoculated with CkDB5 and RrtHH10 were significantly higher than those of the control. The fresh weight of plants inoculated with CkDB5 without Zn (229.2 ± 5.1 mg) was significantly higher than that of plants inoculated with CkDB5 with Zn (174.4 ± 11.4 mg). Compared to the fresh weight of the control (54.7 ± 3.4 mg), the fresh weight of plants inoculated with CkDB5 without Zn was 4 times higher (229.2 ± 5.1 mg). Compared to the fresh weight of the control (54.7 ± 3.4 mg), the fresh weight of plants inoculated with RrtHH10 without Zn was only 1.6 times higher (81.5 ± 3.3 mg). DSEFs can enhance the growth of their host plant (Fernando and Currah, 1996; Jumpponen et al., 1998; Shivanna et al., 1994). While strain CkDB5 could increase the biomass of *C. kanehirae* cuttings by 200% (Lin, 2016), the same strain increased the biomass of inoculated tomatoes by up to 400% in this study (Table 3).

Of the six treatments (Table 4) studied, the Zn concentration of plants inoculated with RrtHH10 with Zn was 1,000 times higher than that of plants without Zn. The Zn concentration of plants inoculated with CkDB5 with Zn was 10 times higher than that of plants without Zn. The Zn concentration of the control with Zn was 5 times higher than that of plants without Zn.

Based on our results, only strains CkDB5 and RrtHH10 were Zn-resistant. While CkDB5 and RrtHH10 presented identical MIC values (Table 2), the former indicated higher ME_{50} values than the latter (Table 2). With or without Zn, CkDB5 could promote the growth response of tomato (Table 3). Ban et al. (2012) indicated that DSEFs are typical root endophytes, and they believed that potential effects of DSEFs on host plants should be considered. DSEFs can affect the heavy-metal uptake of their host plants and enhance the tolerance of these plants to heavy metal stress. DSEFs have also been shown to promote the growth response of their host plants (Gadd, 2007; Lin, 2016; Selosse et al., 2004). These fungi have been observed to transport absorbed nutrients to host plants to support their growth in harsh habitats (Deram et al., 2008; Likar and Regvar, 2009; Zhang et al., 2013).

Conclusion

Molecular analysis revealed that the six DSEFs studied in this work could be divided into five clusters; strain CoLG3 and CkDB2 were classified as *W. laurinus*, while strain RrtHH10 was classified as *P. fortinii*. Strain MoAL5 was classified as *C. chaetospora*, while strain RhYM6 was classified as Herpotrichiellaceae or Eurotiomycetes. Finally, strain CkDB5 was classified as *S. humicola*. These strains may be new species in the world or new species in the fungal flora of Taiwan. Of these six DSEFs, only strains CkDB5 and RrtHH10 were Zn-resistant and could promote the growth response of *S. lycopersicum*. Of the two endophytes, strain CkDB5 was more tolerant to Zn and showed better growth responses. CkDB5 is not only Zn-resistant, but it is also a promoter of tomato growth.

Acknowledgements. The author appreciates the assistance of all members of Tree Mycorrhiza Laboratory in National Chiayi University.

REFERENCES

- [1] Allen, S. E. (1989): Chemical Analysis of Ecological Materials. 2nd Ed. – Blackwell Scientific Publications, Oxford.
- [2] Azcón-Aguilar, C., Barea, J. M. (1997): Applying mycorrhiza biotechnology to horticulture: significance and potentials. – *Scientia Horticulturae* 68(1): 1-24.
- [3] Ban, Y., Tang, M., Chen, H., Xu, Z., Zhang, H., Yang, Y. (2012): The response of dark septate endophytes (DSE) to heavy metals in pure culture. – *PloS One* 7: e47968.
- [4] Bradley, R., Burt, A. J., Read, D. J. (1981): Mycorrhizal infection and resistance to heavy metal toxicity in *Calluna vulgaris*. – *Nature* 292: 335-337.
- [5] Dalpé, Y. (1986): Axenic synthesis of ericoid mycorrhiza in *Vaccinium angustifolium* Ait. by *Oidiiodendron* species. – *New Phytologist* 103: 391-396.
- [6] Deram, A., Languereau-Leman, F., Howsam, M., Petit, D., Van Haluwyn, C. (2008): Seasonal patterns of cadmium accumulation in *Arrhenatherum elatius* (Poaceae): influence of mycorrhizal and endophytic fungal colonisation. – *Soil Biology and Biochemistry* 40: 845-848.
- [7] Diagne, N., Ngom, M., Djighaly, P. I., Ngom, D., Ndour, B., Cissokho, M., Faye, M. N., Sarr, A., Sy, M. O., Laplaze, L., Champion, A. (2015): Remediation of Heavy Metal-Contaminated Soils and Enhancement of Their Fertility with Actinorhizal Plants. – In Sherameti, I., Varma, A. (eds.) *Heavy Metal Contamination of Soils*. Springer, Switzerland, pp. 355-366.
- [8] Diao, Y. H., Li, T., Zhao, Z. W. (2013): Zinc accumulation characteristics of two *Exophiala* strains and their antioxidant response to Zn²⁺ stress. – *Journal of Environmental Protection* 4: 12-19.
- [9] Fernando, A. A., Currah, R. S. (1996): A comparative study of the effects of the root endophytes *Leptodontidium orchidicola* and *Phialocephala fortinii* (Fungi imperfecti) on the growth of some subalpine plants in culture. – *Canadian Journal of Botany* 74: 1071-1078.
- [10] Gadd, G. M. (2007): Geomycology: biogeochemical transformations of rocks, minerals, metals and radionuclides by fungi, bioweathering and bioremediation. – *Mycological Research* 111: 3-49.
- [11] Gardes, M., Bruns, T. D. (1993): ITS primers with enhanced specificity for basidiomycetes - applications to the identification of mycorrhizae and rusts. – *Molecular Ecology* 1: 113-118.
- [12] Gibson, B. R., Mitchell, D. T. (2005): Influence of pH on copper and zinc sensitivity of ericoid mycobionts in vitro. – *Mycorrhiza* 15: 231-234.
- [13] Helmisaari, H. S., Salemaa, M., Derome, J., Kiikkilä, O., Uhlig, C., Nieminen, T. M. (2007): Remediation of heavy metal contaminated forest soil using recycled organic matter and native woody plants. – *Journal of Environmental Quality* 36: 1145-1153.
- [14] Hong, S. L., Lin, T. C., Lin, L. C. (2014): Preliminary study on morphology of root-fungus association of *Cinnamomum kanehirai* at Dabang area. – *Quarterly Journal of Chinese Forestry* 47: 393-398 (in Chinese).
- [15] Hutton, B. J., Dixon, K. W., Sivasithamparam, K. (1994): Ericoid endophytes of western Australian heaths (Epacridaceae). – *New Phytologist* 127: 557-566.
- [16] Jaeckel, P., Krauss, G. J., Krauss, G. (2005): Cadmium and zinc response of the fungi *Heliscus lugdunensis* and *Verticillium* cf. *alboatrum* isolated from highly polluted water. – *Science of the Total Environment* 346: 274-279.

- [17] Jumpponen, A., Mattson, K. G., Trappe, J. M. (1998): Mycorrhizal functioning of *Phialocephala fortinii* with *Pinus contorta* on glacier forefront soil: interactions with soil nitrogen and organic matter. – *Mycorrhiza* 7: 261-265.
- [18] Li, H. Y., Li, D. W., He, C. M., Zhou, Z. P., Mei, T., Xu, H. M. (2012): Diversity and heavy metal tolerance of endophytic fungi from six dominant plant species in a Pb-Zn mine wasteland in China. – *Fungal Ecology* 5: 309-315.
- [19] Likar, M., Regvar, M. (2009): Application of temporal temperature gradient gel electrophoresis for characterisation of fungal endophyte communities of *Salix caprea* L. in a heavy metal polluted soil. – *Science of the Total Environment* 407: 6179-6187.
- [20] Lin, L. C. (2016): Growth effect of *Cinnamomum kanehirae* cuttings associated with its dark septate endophytes. – *Pakistan Journal of Biological Sciences* 19: 299-305.
- [21] Lin, L. C., Lee, M. J., Chen, J. L. (2011): Decomposition of organic matter by the ericoid mycorrhizal endophytes of Formosan rhododendron (*Rhododendron formosanum* Hemsl.). – *Mycorrhiza* 21: 331-339.
- [22] Marx, D. H. (1969): The influence of ectotrophic mycorrhizal fungi on the resistance of pine roots to pathogenic infections. I. Antagonism of mycorrhizal fungi to root pathogenic fungi and soil bacteria. – *Phytopathology* 59: 153-163.
- [23] Mathew, A., Malathy, R. M. (2008): The evidence of mycorrhizal fungi and dark septate endophytes in roots of *Chlorophytum borivillianum*. – *Acta Botanica Croatica* 67(1): 91-96.
- [24] Monnet, F., Vaillant, N., Hitmi, A., Coudret, A., Sallanon, H. (2001): Endophytic *Neotyphodium lolii* induced tolerance to Zn stress in *Lolium perenne*. – *Physiologia Plantarum* 113: 557-563.
- [25] Newsham, K. K. (1999): *Phialophora graminicola*, a dark septate fungus, is a beneficial associate of the grass *Vulpia ciliata* ssp. *ambigua*. – *New Phytologist* 144: 517-524.
- [26] Phosri, C., Martin, M. P., Sihanonth, P., Whalley, A. J. S., Watling, R. (2007): Molecular study of the genus *Astraeus*. – *Mycological Research* 3: 275-286.
- [27] Piercey, M. M., Thormann, M. N., Currah, R. S. (2002): Saprobic characteristics of three fungal taxa from ericalean roots and their association with the roots of *Rhododendron groenlandicum* and *Picea mariana* in culture. – *Mycorrhiza* 12: 175-180.
- [28] Piercey, M. M., Graham, S. W., Currah, R. S. (2004): Patterns of genetic variation in *Phialocephala fortinii* across a broad latitudinal transect in Canada. – *Mycological Research* 108(8): 955-964.
- [29] Ramos, R. L. L., Jacome, A. B., Barron, J. M., Rubio, L. F., Coronado, R. G. (2002): Adsorption of zinc (II) from an aqueous solution onto activated carbon. – *Journal of Hazardous Materials* 90: 27-38.
- [30] Saitou, N., Nei, M. (1987): The neighbor-joining method: a new method for reconstructing phylogenetic trees. – *Molecular Biology and Evolution* 4: 406-425.
- [31] Schmid, E., Obnerwikler, F., Gomez, L. D. (1995): Light and electron microscopy of a host-fungus interaction in the roots of some epiphytic ferns from Costa Rica. – *Canadian Journal of Botany* 73: 991-996.
- [32] Selosse, M. A., Baudoin, E., Vandenkoornhuyse, P. (2004): Symbiotic microorganisms, a key for ecological success and protection of plants. – *Comptes Rendus Biologies* 327: 639-648.
- [33] Shivanna, M. B., Meera, M. S., Hyakumachi, M. (1994): Sterile fungi from zoysiagrass rhizosphere as plant-growth promoters in spring wheat. – *Canadian Journal of Microbiology* 40(8): 637-644.
- [34] Sigler, L., Flis, A. L. (1998): Catalogue of the University of Alberta Microfungus Collection and Herbarium. 3rd Ed. – University of Alberta, Edmonton.
- [35] Smith, S. E., Read, D. J. (1997): *Mycorrhizal Symbiosis*. 2nd Ed. – Academic Press, London.
- [36] Sun, X., Guo, L. D., Hyde, K. D. (2011): Community composition of endophytic fungi in *Acer truncatum* and their role in decomposition. – *Fungal Diversity* 47: 85-95.

- [37] Tamura, K., Peterson, D., Peterson, N., Stecher, G., Nei, M., Kumar, S. (2011): MEGA5: Molecular evolutionary genetics analysis using maximum likelihood, evolutionary distance, and maximum parsimony methods. – *Molecular Biology and Evolution* 28(10): 2731-273.
- [38] Tan, Y. L., Chang, T. P., Chen, J. L., Ku, K. L., Lin, L. C. (2016): Morphology of root-fungus association of *Mahonia oiwakensis* and its endophytes. – *Quarterly Journal of Chinese Forestry* 49: 1-12 (in Chinese).
- [39] Upadhyaya, H., Panda, S. K., Bhattacharjee, M. K., Dutta, S. (2010): Role of arbuscular mycorrhiza in heavy metal tolerance in plants: prospects for phytoremediation. – *Journal of Phytology* 2: 16-27.
- [40] Wainwright, M., Gadd, G. M. (1997): Fungi and Industrial Pollutants. – In: Wicklow, D. T., Söderström, B. (eds.) *The Mycota IV. Environmental and Microbial Relationships*. Springer, Berlin.
- [41] Xu, R., Li, T., Cui, H., Wang, J., Yu, X., Ding, Y., Wang, C., Yang, Z., Zhao, Z. (2015): Diversity and characterization of Cd-tolerant dark septate endophytes (DSEs) associated with the roots of Nepal alder (*Alnus nepalensis*) in a metal mine tailing of southwest China. – *Applied Soil Ecology* 93: 11-18.
- [42] Yang, Y., Liang, Y., Ghosh, A., Song, Y., Chen, H., Tang, M. (2015): Assessment of arbuscular mycorrhizal fungi status and heavy metal accumulation characteristics of tree species in a lead-zinc mine area: potential applications for phytoremediation. – *Environmental Science and Pollution Research* 22: 13179-13193.
- [43] Zeng, M., Liao, B. H., Lei, M., Zhang, Y., Zeng, Q., Ouyang, B. (2008): Arsenic removal from contaminated soil using phosphoric acid and phosphate. – *Journal of Environmental Sciences* 20: 75-79.
- [44] Zhang, X., Li, C., Nan, Z. (2010): Effects of cadmium stress on growth and anti-oxidative systems in *Achnatherum inebrians* symbiotic with *Neotyphodium gansuense*. – *Journal of Hazardous Materials* 175: 703-709.
- [45] Zhang, Y., Zhang, Y., Liu, M., Shi, X., Zhao, Z. (2008): Dark septate endophyte (DSE) fungi isolated from metal polluted soils: Their taxonomic position, tolerance, and accumulation of heavy metals *in vitro*. – *Journal of Microbiology* 46: 624-632.
- [46] Zhang, Y., Li, T., Zhao, Z. (2013): Colonization characteristics and composition of dark septate endophytes (DSE) in a lead and zinc slag heap in southwest China. – *Soil and Sediment Contamination: An International Journal* 22: 532-545.

DETERMINATION OF BOTANICAL COMPOSITION, HAY YIELD AND FORAGE QUALITY OF SOME NATURAL RANGELANDS IN KYRGYZSTAN'S CHUY REGION

CINAR, S.^{1,2*} – ABDULLAYEV, A.¹ – ESENOV, N.¹ – KARADAG, Y.³

¹*Department of Horticulture and Field Crops, Faculty of Agriculture, Kyrgyz-Turkish Manas University, Bishkek, Kyrgyzstan*

²*Department of Plant and Animal Production, Technical Vocational School, Kilis 7 Aralik University, Kilis, Turkey*

³*Faculty of Applied Sciences, Mus Alparslan University, Mus, Turkey*

*Corresponding author

e-mail: scinar01@hotmail.com ; selahattin.cinar@manas.edu.kg

(Received 4th Sep 2019; accepted 4th Dec 2019)

Abstract. This research was carried out in 2018 in order to determine the hay yields, forage qualities botanical compositions and range conditions of 5 different natural rangelands located at different altitudes the Chuy Region, Kyrgyzstan. In the rangelands, the ratio of plant coverage was 96.0-98.0%, the ratio of grasses, legumes, other plant families in the plant covered area was 24.5–48.1%, 4.7–24.0%, 36.2–63.8%, respectively. In the rangelands, the rate of decreaser, increaser and invader species was 37.0%, 7.3% and 55.7%, respectively. The average dry matter yield (DMY) of all five ranges was 2904.6 kg ha⁻¹, crude protein (CP) was 10.6%, acid detergent fiber (ADF) and neutral detergent fiber (NDF) compositions were 39.1%, 57.1%, respectively. The crude protein yield (CPY) was 307.8 kg ha⁻¹, digestible dry matter yield (DDMY) was 1699.1 kg ha⁻¹, and relative feed value (RFV) was 95.3. The rangeland yield increased with altitude. One of the rangelands was in the moderate condition and the others were in poor range condition. According to research results, extensive research targeting appropriate range improvement strategies for each individual rangeland with unique soil and topographic conditions is recommended in order to select among the top seeding, seeding or natural seeding, weed control, grazing methods alone or combined with other range improvement strategies.

Keywords: *Central Asia, range, yield, quality, range condition*

Introduction

Rangelands are one of the cheapest sources of roughage for animals. In addition to providing the basis for sustainable animal production, rangelands form a functional environment by maintaining the soil.

Plant communities in rangelands are formed as a result of lengthy processes with the combined effects of soil, topography, and climatic factors. Therefore, the vegetation of each rangeland is unique. All plant communities, regardless of their location, evolve over time due to changes in environmental conditions. This process is called plant succession and the change may be in the number of species that make up the vegetation, the ratio of each species in the botanical composition or the rate of vegetation covering the soil. The direction of this change could either be in a more desirable and productive direction or in an undesirable and less productive direction (Blanchet et al., 2003). Plant communities, like other living communities, are in a continuous dynamism.

The rangelands in the Central Asian countries such as Kyrgyzstan, Kazakhstan, Tajikistan, Turkmenistan, and Uzbekistan are the land where the world's largest nomadic

stockbreeding is carried out. Rangelands account for 65% of the total surface area of these 5 Central Asian countries. These rangelands are the most important feed source for people with low income nomadic livestock (Blench and Sommer, 1999).

Kyrgyzstan is a mountainous country and people live on agriculture and animal husbandry. 86% of the total agricultural area consists of mountain rangelands and animal husbandry is based on rangelands. About 6.8 million hectares of Kyrgyzstan rangelands were reported to be in the process of deterioration, 3.0 million hectares have been under the weed occupation, and 1.7 million hectares has been reported to be degraded by overgrazing (Nishanov, 2015). Large degradation in Kyrgyzstan rangelands in the past 25 years due to overgrazing, inadequate research on this subject, the need for determination of conditions of the rangelands, and the need for developing sustainable improvement strategies of rangelands were expressed. According to the results of research carried out in the rangelands in different regions of Narin, presence of a number of taxa including *Artemisia dracunculus*, *Lappula sp.*, *Galium verum*, *Dracocephalum integrifolium*, *Ranunculus sp.*, *Onopordum acanthium*, *Draba nemorosa* were reported (Eddy, 2016). Rosales and Livinets (2017) stated that the rangelands were over-grazed by nomads in Kyrgyzstan during the independence period, grass yield and quality in rangelands is reduced, there is a serious lack of management in rangelands, there is not enough statistical information about the degradation of rangelands, overgrazing causes degradation in rangelands, the degradation of rangelands should be determined and improved, and there is lack of enough statistical information about the state of rangelands.

About 9.3 million hectares of the Kyrgyzstan territory is composed of grass prairies and due to the mismanagement of the rangelands, vegetation, yield potential and quality have decreased. This situation adversely affects the livestock and economy of the country and causes the destruction of land and water resources (Mirzabaev et al., 2016). In order to solve these problems, rangelands which have a decreased yield and quality should be rehabilitated, and high-quality feed producing potential should be reinstated. However, in order to be successful in rangeland improvement, the knowledge of the vegetation structure of the rangeland is a prerequisite. Rangeland research conducted in different parts of Turkey revealed that the area covered with plants in rangelands vary greatly. Plant cover percentages of the rangelands were reported as 53.0%-66.0% by Erkun (1971), as 34.0% by Erkun (1972), as 14.0-37.0% by Ozmen (1977), as 17.0% by Gokkus (1984), as 78.5% by Cinar (2001), as 82.0% by Uslu (2005), as 71.9%-95.0% by Sen (2010), as 68.9-95.9% by Inal et al. (2011), as 84.4-99.0% by Cinar et al. (2014), as 83.3% by Ispirli et al. (2016), as 93.6% by Uzun et al. (2016). A great majority of the plants that are present and produce biomass of rangelands could not benefit animals as they are thorny species and weeds (Cinar et al., 2015).

This research was carried out to investigate the vegetation characteristics of natural rangelands in 5 different altitudes in the Chuy region, where 1/10 of Kyrgyzstan's rangelands is located, and to obtain information that can be used as a basis for improving rangelands in similar eco-geographic regions.

Materials and Methods

Materials

The vegetation studies were carried out between 1 June - 8 August 2018 in Tokbay (42°47'N, 74°25'E, elevation 810-945 m.), Kaskasu (42°40'N, 74°31'E, elevation 1540-1648 m.), Alaarca (42°35'N, 74°28'E, elevation 1750-1930 m.), Tamir (42°39'N,

74°39'E, elevation 1910-1950 m) and Chungurchak (42°38'N, 74°36'E, elevation 2090-2210 m) rangelands in different altitudes in Kyrgyzstan's Chuy region (Figure 1, Figure 2).

Table 1 shows the aspect, slope, distance to settlement, altitude and grazing intensity values of the rangelands whose vegetation were studied.

The closest meteorological station to the rangeland areas where the survey was conducted was in Bishkek. In Bishkek, total rainfall is 427 mm, average temperature is 10.4°C and the highest temperatures are recorded in July and the lowest temperatures are documented in January (Anonymous, 2019).



Figure 1. The map of study area

Methods

A modified wheel point method with loop for the vegetation survey was applied (Anonymous, 1962; Koc and Cakal, 2004) (Figure 2). Loop measurements were carried out in 3 different sections (in blocks) which were very homogeneous in terms of vegetation and soil in each range. The measurements were taken from four lines of 20 m extending in 4 directions in each block from a point considered as central. A total of 1200 loops were measured in each range, 100 in each 20 m line and 400 in each block. The ratio of plant covered area (%), botanical composition based on the percentage in the plant covered area (%) of the rangelands examined were determined according to the methods described by Gokkus et al. (2000).

Decreaser, increaser, and invader species expressing the responses of plant species to grazing were determined according to Anonymous (2008).

The quality scores of the species found in the rangelands were determined according to Bakır (1987) and degree of quality for each rangelands was estimated with the help of the following equation by Gokkus et al. (2000) (Eq.1) where the ratio of plant species in the botanical composition according to the coverage area and quality scores were used.

$$PQD: (\sum R \times QS) / 100 \quad (\text{Eq.1})$$

where:

PQD: Range quality degree,

R: The rate of the species in the botanical composition,

QS: Quality score of the species.



Figure 2. Point wheel method used in vegetation study and vegetation surveyed rangeland

Table 1. Aspect, altitude, slope, area, longitude and latitude values for the rangelands whose vegetation were studied

Range	Aspect	Slope (°)	Distance to Settlement (km)	Altitude (m.)	Grazing Intensity
Tokbay	Base	0-5	0-1	810-945	Heavy
Kaskasu	West	5-15	0-1	1540-1648	Moderate
Alaarca	South-North	30-40	10-15	1750-1930	Light
Tatir	West	15-25	3	1910-1950	Moderate
Chungurchak	East-West	0-30	10	2090-2210	Moderate

Plant identification in vegetation studies were conducted according to Edgecombe (1964), Garms et al. (1968), Davis (1970), Polunin and Huxley (1974), Huxley and Taylor (1977), Weymer (1981), Demiri (1983), Oztan and Okatan (1985) and Anonymous (2005, 2008, 2015). Life spans, families, and respons to grazing were determined according to Anonymous (2008, 2019).

The vegetation in the 70x70 cm dimension quadrats from the 5th, 10th, 15th m of each loop of the three plots were cut with scissors from soil level. The plant species that were

harvested from each quadrat were divided into groups as grasses, legumes and other plant families. Plant samples of each group were dried for 24 hours in a drier at 65°C until the samples reach a constant weight. Then, each of the three plant groups were separately weighed and the sum of the dry weights was recorded as dry matter yield. After the average of dry matter yield values were determined for 12 quadrats taken from each plot and were converted to dry matter yield per hectare.

After drying and weighing the plant samples, nitrogen content was determined by Kjeldahl method by combining the samples belonging to 12 quadrats of each group. The determined nitrogen content was multiplied by 6.25 conversion coefficient and crude protein % values were estimated in each plant sample of the plant groups (Anonymous, 1995). The average crude protein contents of the plant specimens were determined by summing the figures obtained by increasing the ratios of the plant groups in the botanical composition in each plot by the crude protein ratio values.

NDF and ADF contents of the dried hay samples were analyzed using ANKOM 220 Fiber Analyzer and according to the methods described by Ankom (2009). In the calculation of CP, ADF and NDF contents of plant samples in each plot, the ratios of plant groups in botanical composition based on the weight in each plot were multiplied with the CP, ADF and NDF and the sum of the obtained values were recorded as CP, ADF and NDF ratio of plant samples from the plot.

CPY, DDMY, dry matter intake (DMI), digestible dry matter (DDM) and RFV were estimated according to the following equations (Eq.2, Eq.3, Eq.4) adapted from Sheaffer et al. (1995):

$$\text{DMI} = 120/(\text{NDF}\%) \text{ dry matter basis} \quad (\text{Eq.2})$$

$$\text{DDM} = 88.9 - (0.779 \times \text{ADF}\% \text{ dry matter basis}) \quad (\text{Eq.3})$$

$$\text{RFV} = (\text{DDM}\% \times \text{DMI})/1.29 \quad (\text{Eq.4})$$

$$\text{CPY} = \text{CP}\% \times \text{DMY} \quad (\text{Eq.5})$$

Statistical Analyses

Considering the data gathered in a randomized complete block design, ANOVA analyses were performed for plant-covered area, botanical composition, DMY, CP, ADF, NDF, CPY, DDMY, RFV variables using MSTAT-C statistical package program (Steel and Torrie, 1960). Angle transformation was applied to data on the plant cover percentage and percentages of plant groups in the botanical composition before conducting analyses of variance (Tekindal, 1998). Duncan multiple comparison test was used for mean separations (Yurtsever, 1984).

Results and Discussion

Botanical Composition

The species, their families, life spans, types of response to grazing, coverage rates, percentages in botanical composition and some other vegetation characteristics of the five natural rangelands examined in the research are given in *Table 2* and *Table 3*.

Table 2. Life spans, families, response to grazing and plant coverage rates, botanical composition of the species determined in the investigated rangelands

Tokbay					
Family	Species	Life Span	Response to Grazing	Plant Coverage Rates (%)	Percentage in Botanical Composition (%)
Poaceae	<i>Bromus tomentellus</i>	Perennial	Decreaser	13.7	14.1
Poaceae	<i>Bromus japonicus</i>	Annual	Invader	13.7	14.1
Poaceae	<i>Cynodon dactylon</i>	Perennial	Increaser	1.0	1.0
Poaceae	<i>Hordeum bulbosum</i>	Perennial	Decreaser	0.3	0.3
Poaceae	<i>Nardus stricta</i>	Perennial	Invader	1.3	1.4
Poaceae	<i>Poa annua</i>	Annual	Invader	1.0	1.0
Poaceae	<i>T. caput medusa</i>	Annual	Invader	9.0	9.3
Fabaceae	<i>Alhagi pseudalhagi</i>	Perennial	Invader	0.7	0.7
Fabaceae	<i>Medicago minima</i>	Annual	Invader	20.3	20.9
Fabaceae	<i>Vicia tenuifolia</i>	Perennial	Decreaser	0.3	0.3
Asteraceae	<i>Achillea filipendula</i>	Perennial	Invader	2.3	2.4
Asteraceae	<i>Achillea wilhelmsi</i>	Perennial	Invader	7.3	7.6
Asteraceae	<i>Artemisia caucasica</i>	Perennial	Invader	10.3	10.7
Asteraceae	<i>Cichorium inybus</i>	Perennial	Invader	0.7	0.7
Asteraceae	<i>Picnomon acarna</i>	Annual	Invader	1.3	1.4
Asteraceae	<i>Gundelia tournofertii</i>	Perennial	Invader	9.0	9.3
Brassicaceae	<i>C.bursa pastoris</i>	Annual	Invader	0.5	0.3
Brassicaceae	<i>Lepidium perfoliatum</i>	Annual	Invader	0.7	0.7
Geraniaceae	<i>Geranium cicutarium</i>	Perennial	Invader	0.3	0.3
Papaveraceae	<i>Papaver orientale</i>	Perennial	Invader	0.3	0.3
Primulaceae	<i>Anagallis arvensis</i>	Annual	Invader	0.7	0.7
Rosaceae	<i>Potentilla bifurca</i>	Perennial	Invader	1.0	1.0
Rubiaceae	<i>Galium aparine</i>	Annual	Invader	1.0	1.0
Scrophulariaceae	<i>Verbascum songoricum</i>	Perennial	Invader	0.3	0.3
Total				97.0	100.0
Kaskasu					
Family	Species	Life Span	Response to Grazing	Plant Coverage Rates (%)	Percentage in Botanical Composition (%)
Poaceae	<i>Dactylis glomerata</i>	Perennial	Decreaser	0.3	0.3
Poaceae	<i>Festuca ovina</i>	Perennial	Increaser	11.0	11.5
Poaceae	<i>Lolium perenne</i>	Perennial	Decreaser	15.7	16.2
Poaceae	<i>Stipa lessingiana</i>	Perennial	Increaser	2.3	2.5
Fabaceae	<i>Medicago falcata</i>	Perennial	Decreaser	7.3	7.7
Fabaceae	<i>Onobrychis arenaria</i>	Perennial	Decreaser	6.7	7.0
Fabaceae	<i>Trifolium pratense</i>	Perennial	Decreaser	6.0	6.2
Fabaceae	<i>Trifolium repens</i>	Perennial	Decreaser	3.0	3.1
Asteraceae	<i>Achillea millefolium</i>	Perennial	Invader	9.0	9.4
Asteraceae	<i>Artemisia dracunculus</i>	Perennial	Invader	0.3	0.4
Asteraceae	<i>Conyza canadiensis</i>	Annual	Invader	0.3	0.3
Asteraceae	<i>Īnula oculus-christi</i>	Perennial	Invader	0.3	0.3
Asteraceae	<i>Taraxacum officinalis</i>	Perennial	Invader	0.3	0.3
Convolvulaceae	<i>Convolvulus arvensis</i>	Perennial	Invader	2.0	2.1
Hypericaceae	<i>Hypericum perforatum</i>	Perennial	Invader	3.3	3.5
Lamiaceae	<i>Origanum vulgare</i>	Perennial	Invader	3.0	3.1
Lamiaceae	<i>Phlomis oreophila</i>	Perennial	Invader	1.0	1.1
Lamiaceae	<i>Salvia verticillata</i>	Perennial	Invader	12.3	12.8
Plantaginaceae	<i>Plantago lanceolata</i>	Perennial	Increaser	1.7	1.7
Rosaceae	<i>Potentilla recta</i>	Perennial	Invader	9.0	9.4
Rubiaceae	<i>Galium verum</i>	Perennial	Invader	1.0	1.0
Total				96.0	100

Alaarca					
Family	Species	Life Span	Response to Grazing	Plant Coverage Rates (%)	Percentage in Botanical Composition (%)
Poaceae	<i>Dactylis glomerata</i>	Perennial	Decreaser	16.7	17.3
Poaceae	<i>Lolium rigidum</i>	Annual	Invader	3.3	3.4
Poaceae	<i>Poa bulbosa</i>	Perennial	Decreaser	3.7	3.8
Fabaceae	<i>Trifolium pratense</i>	Perennial	Decreaser	4.0	4.1
Fabaceae	<i>Trifolium repens</i>	Perennial	Decreaser	7.3	7.6
Asteraceae	<i>Achillea millefolium</i>	Perennial	Invader	7.7	7.9
Asteraceae	<i>Achillea wilhelmsi</i>	Perennial	Invader	5.3	5.5
Asteraceae	<i>Taraxacum officinalis</i>	Perennial	Invader	7.3	7.6
Geraniaceae	<i>Geranium molle</i>	Annual	Invader	9.0	9.3
Hypericaceae	<i>Hypericum perforatum</i>	Perennial	Invader	4.7	4.8
Lamiaceae	<i>Mentha longifolia</i>	Perennial	Invader	3.7	3.8
Lamiaceae	<i>Marrubium parviflorum</i>	Perennial	Invader	3.0	3.1
Lamiaceae	<i>Teucrium polium</i>	Perennial	Increaser	2.0	2.1
Lilliaceae	<i>Allium schoenoprosom</i>	Perennial	Invader	2.3	2.4
Plantaginaceae	<i>Plantago lanceolata</i>	Perennial	Invader	4.7	4.8
Polygonaceae	<i>Polygonum aviculare</i>	Perennial	Invader	1.7	1.7
Rosaceae	<i>Potentilla recta</i>	Perennial	Invader	5.7	5.9
Rubiaceae	<i>Galium verum</i>	Perennial	Invader	4.7	4.8
Total				96.7	100
Tamir					
Family	Species	Life Span	Response to Grazing	Plant Coverage Rates (%)	Percentage in Botanical Composition (%)
Poaceae	<i>Cynodon dactylon</i>	Perennial	Increaser	6.0	6.1
Poaceae	<i>Dactylis glomerata</i>	Perennial	Decreaser	23.7	24.2
Poaceae	<i>Poa bulbosa</i>	Perennial	Decreaser	3.0	3.1
Fabaceae	<i>Medicago falcata</i>	Perennial	Decreaser	0.7	0.7
Fabaceae	<i>Trifolium pratense</i>	Perennial	Decreaser	0.7	0.7
Fabaceae	<i>Trifolium repens</i>	Perennial	Decreaser	3.3	3.4
Apiaceae	<i>Carum carvi</i>	Perennial	Invader	4.7	4.7
Asteraceae	<i>Achillea millefolium</i>	Perennial	Invader	10.0	10.2
Asteraceae	<i>Artemisia dracunculus</i>	Perennial	Invader	0.3	0.3
Asteraceae	<i>Īnula oculus-christi</i>	Perennial	Invader	0.3	0.3
Asteraceae	<i>Taraxacum officinale</i>	Perennial	Invader	0.7	0.7
Boraginaceae	<i>B.incrassata</i>	Annual	Invader	0.3	0.3
Brassicaceae	<i>C.bursa-pastoris</i>	Annual	Invader	2.0	2.0
Caryophyllaceae	<i>Silene vulgaris</i>	Perennial	Invader	1.0	1.0
Geraniaceae	<i>Geranium collinum</i>	Perennial	Invader	11.0	11.3
Hypericaceae	<i>Hypericum perforatum</i>	Perennial	Invader	0.7	0.7
Lamiaceae	<i>Origanum vulgare</i>	Perennial	Invader	14.0	14.4
Lamiaceae	<i>Phlomis oreophila</i>	Perennial	Invader	2.7	2.7
Lamiaceae	<i>Stachys cretica</i>	Perennial	Invader	1.3	1.4
Polygonaceae	<i>Rumex crispus</i>	Perennial	Invader	0.3	0.3
Ranunculaceae	<i>Aconitum exelsum</i>	Perennial	Invader	3.3	3.4
Ranunculaceae	<i>Ranunculus kotschyi</i>	Perennial	Invader	1.0	1.0
Rosaceae	<i>Potentilla orientalis</i>	Perennial	Invader	7.0	7.1
Total				97.3	100.0
Chungurchak					
Family	Species	Life Span	Response to Grazing	Plant Coverage Rates (%)	Percentage in Botanical Composition (%)
Poaceae	<i>Agropyron intermedium</i>	Perennial	Decreaser	1.3	1.3
Poaceae	<i>Cynodon dactylon</i>	Perennial	Increaser	10.7	11.1
Poaceae	<i>Dactylis glomerata</i>	Perennial	Decreaser	18.0	18.3
Poaceae	<i>Poa bulbosa</i>	Perennial	Decreaser	17.0	17.4

Fabaceae	<i>Astragalus onobrychis</i>	Perennial	Decreaser	1.3	1.4
Fabaceae	<i>Trifolium repens</i>	Perennial	Decreaser	12.3	12.6
Fabaceae	<i>Trifolium pratense</i>	Perennial	Decreaser	1.7	1.7
Asteraceae	<i>Achillea millefolium</i>	Perennial	Invader	8.7	8.9
Asteraceae	<i>Artemisia dracunculus</i>	Perennial	Invader	0.3	0.3
Asteraceae	<i>Înula oculus-christi</i>	Perennial	Invader	0.3	0.3
Asteraceae	<i>Taraxacum officinale</i>	Perennial	Invader	7.3	7.6
Geraniaceae	<i>Geranium collinum</i>	Perennial	Invader	13.3	13.9
Geraniaceae	<i>Geranium verum</i>	Perennial	Invader	0.3	0.3
Lamiaceae	<i>Phlomis oreophila</i>	Perennial	Invader	1.7	1.7
Plantaginaceae	<i>Plantago lanceolata</i>	Perennial	Increaser	1.0	1.0
Polygonaceae	<i>Polygonum aviculare</i>	Perennial	Invader	0.3	0.3
Ranunculaceae	<i>Aconitum exelsum</i>	Perennial	Invader	1.0	1.0
Rosaceae	<i>Potentilla orientalis</i>	Perennial	Invader	0.3	0.3
Rosaceae	<i>Rosa dumalis</i>	Perennial	Invader	0.3	0.3
Total				98.0	100.0

24 species belonging to 22 genera of 10 families in Tokbay rangeland, 18 species belonging to 16 genera in 11 families in Alaarca rangeland, 21 species belonging to 20 genera of 9 families in Kaskasu rangeland, 19 species belonging to 17 genera of 9 families in Chungurchak rangeland, 23 species belonging to 22 genera of 13 families in Tatr rangeland were identified (Table 2, Table 3). It was determined that the number of species varied in the range of 19-24, while the highest number of species was in the Tokbay rangeland, and the lowest was in the Alaarca rangeland. The most common species in the rangelands were from the grasses (Poaceae) followed by legumes (Fabaceae) and chamomile (Asteraceae) (Table 2).

Table 3. Vegetation Characteristics of Rangelands Examined

Range	Number of Families	Number of Genera	Number of Species	Coverage rate (%)	Botanical Composition		
					Grasses (%)	Legumes (%)	Other Families (%)
Tokbay	10	22	24	97.0	41.2 b*	22.0 a	36.8 c
Kaskasu	9	20	21	96.0	30.5 c	24.0 a	45.5 b
Alaarca	11	16	18	96.7	24.5 d	11.7 c	63.8 a
Tatr	13	22	23	98.0	33.3 c	4.7 d	62.0 a
Chungurchak	9	17	19	97.3	48.1 a	15.7 b	36.2 c
Mean	10.4	19.4	21.0	97.0	35.5	15.6	48.9

* The mean values indicated by different letters in the same column are significantly different ($P \leq 0.05$) based on Duncan test

According to the life cycle, 15 species of Tokbay range were perennial and 9 of them were annual, 20 of species of Kaskasu range were perennial and one of them were annual, 16 species of Alaarca range were perennial and 2 of them were annual, all of 19 of species in Chungurchak range were perennial, and 21 of the species in the Tamir range were perennial and 2 were identified as annual species.

Depending on their responses to grazing, 3 of the species identified in Tokbay rangeland were decreaser, 1 was increaser, and 20 were invader. Among the species identified in Kaskasu rangeland 6 were decreaser, 3 were increaser, and 12 were invader. In Alaarca rangeland, 4 of the identified species were decreaser, one was increaser, and

13 were invader. In Chungurchak rangeland, 6 of the species were decreaser, 2 were increaser, and 11 were invader. In Tatr rangeland, 5 were decreaser, 1 was increaser, and 17 were found to be invader species.

Medicago minima (20.3%) in Tokbay rangeland, *Dactylis glomerata* (16.7%) in Alaarca rangeland, *Lolium perenne* (15.7%) in Kaskasu rangeland, *Dactylis glomerata* (23.7) in Tatr rangeland, and *Dactylis glomerata* (18.0%) in Chungurchak rangeland were the species with high coverage rates (Table 2).

The number of species in similar studies conducted in natural rangelands was reported by Bakır (1970) as 82, by Erkun (1972) as 121, by Koc and Gokkus (1994) as 152, by Cinar (2001) as 77, by Sen (2010) as 111, by Inal et al. (2011) as 37, by Cinar et al. (2014) as 41, by Gur and Altin (2015) as 149-177, and by Cinar et al. (2019) reported as 8-22. The differences in the number of species among the reports can be explained by differences in grazing pressure (Bakır, 1970; Altin et al., 2011).

The ratio of plant-covered area for the rangelands investigated here were similar to the ones reported by Cinar et al. (2014) in Hatay Kirikhan and by Inal et al. (2011) Çukurova lowland rangelands. Nonetheless, the values determined in this research are much higher than the ratio of plant coverage reported by Erkun (1971), Ozmen (1977), Tukul (1981), and Buyukburc (1983) in Central Anatolian rangelands, by Gokkus (1984), Koc and Gokkus (1994) in the Eastern Anatolian rangelands, and those reported by Seydosoglu et al. (2019) in Batman Kozluk. The discrepancy among results can be attributed to the difference between the vegetation measurement methods, as well as the difference between the soil, climate, precipitation, grazing pressure and grazing animals.

As seen in Table 3, the highest and lowest number of species were determined in Tokbay and Alaarca rangelands, respectively. Coverage ratios of the plants ranged from 96.0% to 98.0% in the rangelands examined and this variation among rangelands was not significant.

In the rangelands examined, the ratio of grasses in the plant covered area ranged between 24.5% and 48.1% and this difference was significant. It was determined that range with the highest rate of grasses (48.1%) was Chungurchak and the lowest rate of grasses (24.5%) was Alaarca. The rate of legumes ranged between 4.7-24.0% and this variation was also significant. The rangeland with the highest legume composition (24.0%) was Kaskasu and the lowest one (4.7%) was the rangeland in Tatr. The ratio of other family species in the plant covered area ranged between 36.2-63.8% and was significantly different among rangelands. The rangeland with the highest percentage (63.8%) of other family group was one in Alaarca. The finding that Poaceae were more abundant in the Chungurchak rangeland in comparison to the others may be explained by that it is farther away from settlement areas in comparison to the other rangelands and moderate grazed (Table 1, Table 3).

Total percentage of *Geranium molle*, *Achillea millefolium*, *Taraxacum officinalis* species in the botanical composition of the rangeland in Alaarca was calculated as 24.8% while the total percentage of *Origanum vulgare*, *Geranium collinum*, *Achillea millefolium* in botanical composition of the rangeland in Tatr was 35.9%. Since the 3 species found in both rangelands were from other plant families, it can be concluded that the ratios of other plant families in Alaarca and Tamir were higher in the botanical composition compared to the covering area of other plant families. However, the reason for the high number of species in other plant families in these rangelands is the early and heavy grazing.

In similar studies conducted in natural rangelands, the rate of grasses in the area covered with plants was determined by Erkun (1972) as 56.0%, by Gokkus (1984) as 57.0%, by Cinar et al. (2014) as 54.0%, by Cinar et al. (2019) as 54.0%, and by Seydosoglu et al. (2019) as 25.4%. The rate of grasses determined in this research is lower than that of reported by Seydosoglu et al. (2019). This may be due to the different ecological conditions and grazing pressures of the rangelands.

In the previous research carried out in the rangelands, the rate of legumes in botanical composition was determined by Erkun (1972) as 8.0%, by Gokkus (1984) as 7.8%, by Uslu (2005) as 17.8%, by Sen (2010) as 15.0%, by Cinar et al. (2014) as 15.5%, by Cinar et al. (2019) as 22.0%, and by Seydosoglu et al. (2019) as 36.8%. The composition of legume in this research was similar to the one in Sen (2010), Cinar et al. (2014), Cinar et al. (2019) but deviated from other studies. The differences among the rangelands could be attributed to the climate and grazing pressure differences.

The average rate of other family plants in botanical composition in the rangelands examined in the research is consistent with the findings of Erkun (1972) and Sen (2010), and deviates from the composition reported in Cinar (2001), Uslu (2005) and Cinar et al. (2014). It can be concluded that the differences in ecological conditions and grazing pressure between the rangelands contributed to the observed difference in botanical composition.

It was determined that the majority of the species found in the rangelands with the exception of the rangeland in the Tokbay range were perennial (87.3-100.0%), the number of annual species in the Tokbay rangeland and their percentage in the botanic composition are 9 and 49.4%, respectively (*Table 4*).

Table 4. Number and percentage (%) of species in each range based on the life span

Range	Annual		Perennial	
	Number of Species	Botanical Composition Ratio (%)	Number of Species	Botanical Composition Ratio(%)
Tokbay	9	49.4	15	50.6
Kaskasu	1	0.3	20	99.7
Alaarca	2	12.7	16	87.3
Tatır	2	2.3	21	97.7
Chungurchak	-	-	19	100.0

While the range of Tokbay is located immediately adjacent to a settlement, the distance of the rangelands other than the rangeland. The high number of annual species in Tokbay rangeland can be explained as heavy and uncontrolled grazing due to its close proximity to the settlement (*Table 1*).

Plant species in rangelands are classified according to their response to grazing as decreaser, increaser, and invader (Altin et al., 2011). The most sensitive to grazing and high-quality species are decreaser species and their rates in the rangelands examined were 29.4-51.0%, having a lower quality compared to the decreaser species, the proportion of increaser species ranged from 1.0% to 15.7%. With the withdrawing of decreaser and increaser species increases the proportion of the invader species, and they had a rate of 37.3- 69.6% (*Table 5*). As the average of the five rangelands examined, the proportion of the decreaser species was 37.0%, the proportion of increaser species was 7.3% and that of invader species was 55.7%. The high amount of decreaser species in the Chungurchak rangeland where these were the most abundant may be explained by the it is grazed

moderately due to its distance to settlement areas, while the low amount of these species in the Tokbay rangeland where these were the least abundant may be explained by that it is grazed heavily due to its proximity to settlement areas (*Table 1*). With heavy grazing, the decreaser species decrease and increaser species increase in a rangeland in time, and in the case of continuation of heavy grazing, the increaser species also decrease, but invader species increase (Bakir, 1987; Altin et al., 2011).

The high rate of invader species in the plant-covered area indicates that rangelands were grazed early, heavily, and over the capacity for many years, and were not utilized in accordance with proper grazing management (Altin et al., 2011).

Table 5. Botanical compositions of the rangelands based on the plant groups with different responses to grazing according to the degree of effect in the examined rangelands

Range	Decreaser	Increaser	Invader
Tokbay	29.4	1.0	69.6
Kaskasu	40.5	15.7	43.8
Alaarca	32.7	2.0	65.3
Tatır	31.4	6.1	62.5
Chungurchak	51.0	11.7	37.3
Mean	37.0	7.3	55.7

The average coverage proportions of the decreaser and increaser species determined in the present research were higher than the proportions reported by Cinar et al. (2014) in the Kirikhan rangelands of Hatay, and those reported by Cinar et al. (2019) in the high plateaus of Adana; however, the proportions were lower than those reported by Gur and Altin (2015) in Tekirdag and by Seydosoglu et al. (2019) in Batman. Proportion of invader species were lower than those reported by Seydosoglu et al. (2019), and higher than those reported by Cinar et al. (2019) and Gur and Altin (2015). This difference might be due to the difference in the climate and grazing pressure (Gokkus, 1991).

The excess of invasive species is an indication that rangelands are not managed in accordance with the appropriate range utilization techniques (Holecek et al., 2004). Decreaser species are the most delicious species preferred by animals in the first place. As a result of early and heavy grazing in the rangelands, initially decreaser species disappear from the rangelands, and if the grazing pressure continues, the increaser species withdraw from the environment and invader species occupy the rangeland vegetation area (Gokkus, 1991; Altin et al., 2011). In terms of animal nutrition, low quality annual grasses and legumes are classified as invader species (Gokkus, 1991). 58.1% of the rangeland areas examined were covered with invasive species. This is an indication of early and heavy grazing (Cinar et al., 2019).

Hay Yield and Forage Quality

The data related to herbage yield and herbage quality in the rangelands examined in the current research are listed in *Table 6*.

As shown in *Table 6*, DMY varied between 2053.0 and 3690.0 kg ha⁻¹, CPY between 221.7 and 417.0 kg ha⁻¹, DDMY between 118.7 and 216.2 kg ha⁻¹, RFV between 94.5 and 96.7. Differences among rangelands in DMY and DDMY were statistically significant. The highest DMY, CPY and DDMY were found in Chungurchak rangeland, the lowest DMY, CPY, and DDMY were determined in Tokbay rangeland.

The highest yield in the Chungurcak rangeland is the distance of this its to the settlement, grazing density, and the decreasing species are higher than other pastures. In Tokbay pasture, it can be explained as low yield, close to settlement, heavy grazing and very low rate of reducing species (*Table 1, Table 5*). DDMY was generally calculated as high in pastures with high yields. This is an expected result.

Among the various studies carried out in rangelands, Sen (2010) reported DMY of 850-1720 kg ha⁻¹, the proportion of CP of 17.2%, CPY of 230 kg ha⁻¹. Cinar et al. (2015) reported DMY of 830 kg ha⁻¹, CP of 11.0%, of CPY of 90 kg ha⁻¹, ADF composition of 33.4%, NDF composition of 49.4%, and DDMY of 630 kg ha⁻¹. DMY was reported by Cacan and Basbag (2016) as 1440 kg ha⁻¹ and by Seydosoglu et al. (2019) as 2980 kg ha⁻¹. Ozaslan Parlak et al. (2015) reported DMY as 900-3330 kg ha⁻¹, the proportion of CP as 11.0%, ADF composition as 30.2%, and NDF composition as 47.5%. Polat et al. (2018) noted the DMY as 1840 kg ha⁻¹, CP content as 7.5%, CPY as 130 kg ha⁻¹. Surmen and Kara (2018) estimated the DMY as 1630, CP content as 6.1%, CPY as 150 kg ha⁻¹, ADF composition as 39.5%, NDF composition as 60.3%, and the RFV as 91.4. According to the results obtained from the current research, DMY was similar to the value reported by Ozaslan Parlak et al. (2015), the rate of CP was closer to Cinar et al. (2015), and ADF and NDF composition values were in agreement with Surmen and Kara (2018). Ozaslan Parlak et al. (2015) stated that CP content above 7.5% is acceptable for livestock. In general, it can be concluded that DMY, CPY, and DDMY increased as the altitude increased. There was no coherence with the aforementioned studies in terms of other investigated variables. The reason for this may be the difference in the ratio of species found in the botanical composition in rangelands, climatic conditions, soil variables, precipitation patterns, and grazing pressures.

Table 6. DMY, CP, ADF, NDF, CPY, DDMY and RFV in investigated rangelands

Range	DMY (kg ha ⁻¹)	CP (%)	ADF (%)	NDF (%)	CPY (kg ha ⁻¹)	DDMY (kg ha ⁻¹)	RFV
Tokbay	2053.0 c*	10.8	39.9	56.3	221.7 c	1187.0 d	95.5
Kaskasu	2354.0 c	10.4	39.4	56.4	244.8 c	1370.0 c	96.7
Alaarca	2995.0 b	10.2	38.9	57.7	305.5 b	1755.5 b	94.5
Tatir	3431.0 ab	10.2	38.5	57.9	350.0 a	2021.0 a	94.6
Chungurchak	3690.0 a	11.3	38.9	57.2	417.0 a	2162.0 a	95.3
Mean	2904.6	10.6	39.1	57.1	307.8	1699.1	95.3

* The mean values indicated by different letters in the same column are significantly different ($P \leq 0.05$) based on Duncan test

Range Condition

The range quality scores calculated using botanical composition ratios and quality scores of plant species found in each rangeland ranged from 3.6 to 5.1. Chungurchak rangeland was found to be moderate and other rangelands were classified as poor. quality scores and range condition of the five rangelands examined are shown in *Table 7*.

The low range quality in the examined rangelands might can be attributed to disappearance of high-quality species due to uncontrolled, early, and heavy grazing for many years that have led spread of lower quality species (Koc, 1995; Cinar et al., 2014). Similarly, range statue ranged between very poor and poor were reported in Kilis rangelands (Sen, 2010), in the Kırıkhan rangelands of Hatay (Cinar et al., 2014), and in the higher parts of Adana (Cinar et al., 2019).

Table 7. Quality scores and range condition of the five rangelands examined

Range	Range Quality Score	Range Status
Tokbay	3.6	Poor
Kaskasu	4.6	Poor
Alaarca	4.5	Poor
Tatır	4.0	Poor
Chungurchak	5.1	Moderate

Conclusions

This research was carried out in order to determine the hay yield, forage quality, botanical composition and range condition in different natural rangelands (Tokbay, Kaskasu, Alaarca, Tatır, Chungurchak) located in different altitudes in Chuy Region, Kyrgyzstan. In the vegetation research, average of 21 species belonging to 19.4 genera from 10.4 families were identified. In these rangelands, the ratio of plant coverage was 96.0-98.0%, the ratio of grasses in the plant covered area was 24.5–48.1%, the proportion of legumes was 4.7–22.0%, and the proportion of other family plants ranged from 36.2-63.8%. In the rangelands, the rate of decreaser species was 37.0%, the rate of increaser species was 7.3% and the rate of invader species was 55.7%. The average dry matter yield of range was 2904.6 kg ha⁻¹, crude protein was 10.6%, ADF and NDF compositions were 39.1%, 57.1%, respectively. The crude protein yield was 307.8 kg ha⁻¹, digestible dry matter yield was 1699.1 kg ha⁻¹, and relative feed value was 95.3.

We can say that rangelands are different in aspect, slope, distance to settlement and grazing pressure.

It has been determined that approximately half of the rangelands are other family species, more than half are perennial species, and more than half are invasive species. We can say that the grazing pressure decreases as the pastures move away from the settlement area, the yield increases as the altitude rises, and grazing without control. One of the rangelands was in the moderate condition and the others were in poor range condition.

In the rangelands investigation and in similar ecological conditions, it is necessary that increase hay yield and forage quality to regulate grazing, minimize invasive species and weed rate and increase the decreasing species.

For this purpose, investigated rangelands and with similar ecological conditions is recommended to make and implement new projects for pasture control, fertilization, over-seeding and grazing.

Acknowledgements. The research is part of the project BAP-2018.FBE.07 supported by Kyrgyz-Turk Manas University. We thank Kyrgyz-Turk Manas University for supporting the project.

REFERENCES

- [1] Altın, M., Gökkuş, A., Koc, A. (2011): Meadow Range Management, 2nd volume. – Ministry of Agriculture and Rural Affairs TUGEM Publications, Ankara-Turkey.
- [2] ANKOM (2009): Method for determining acid detergent fiber and neutral detergent fiber. – Ankom Technology, www.ankom.com, Access on 15 August 2009.
- [3] Anonymous (1962): Range Research: Basic problems and techniques. – National Academy of Science. National Research Council Pub. .

- [4] Anonymous (1995): The Determination Of Nitrogen According To Kjeldahl Using Block Digestion And Steam Distillation. – Tecator Application Note An 300, Tecator Ab Sweden: 1-11.
- [5] Anonymous (2005): Guide to Range Crops. – Ministry of Agriculture and Rural Affairs General Directorate of Agricultural Production and Development, Ankara-Turkey.
- [6] Anonymous (2008): Guide to Range Crops. – Ministry of Agriculture and Rural Affairs General Directorate of Agricultural Production and Development, Ankara-Turkey.
- [7] Anonymous (2015): Kyrgyzstan Pasture Plants Catalog, Flermoneca.
- [8] Anonymous (2019): <https://tr.climate-data.org/asya/k%C4%B1rg%C4%B1zistan/chui-province/biskek-484/#climate-graph> (02.05.2019).
- [9] Bakır, O. (1970): A Pasture Study on the Land of Middle East Technical University. – AU Faculty of Agriculture Publications: 232, Ankara-Turkey.
- [10] Bakır, O. (1987): Meadow-Range Management. – Ankara University Faculty of Agriculture Publications: 992, Ankara-Turkey.
- [11] Blanchet, K., Moechnig, H., DeJong-Hughes, J. (2003): Grazing systems planning guide. – University of Minnesota Extension Service, BU-07606-S, <http://www.extension.umn.edu/agriculture/beef/components/docs/grazingsystemsplanning.guide.pdf> (01.11.2018).
- [12] Blench, R., Sommer, F. (1999): Understanding Rangeland Biodiversity. – In: Working Paper 121. Overseas Development Institute. London: Chameleon Press, 51.
- [13] Buyukburc, U. (1983): A Research on the Possibilities of Breeding the Pastures of Yavrucak Village in Ankara by Fertilizing and Resting. – Meadow-Range-Animal Science Research Institute Publications No: 79, Ankara.
- [14] Cacan, E., Basbag, M. (2016): Change of Botanic Composition and Herb Yields in Pasture Sections of Yelesen-Dikme Villages in Bingöl Province in Different Directories and Elevations. – Journal of Ege Univ. Faculty of Agriculture 53(1): 1-9.
- [15] Cinar, S. (2001): A Research on Determination of Yield and Botanical Composition in Hanyeri Village Pasture in Tufanbeyli District of Adana Province. – C.U. Graduate School of Natural and Applied Sciences, Field Crops Department Master Thesis, 70 p. Adana.
- [16] Cinar, S., Hatipoglu, R., Avci, M., Yucel, C., Inal, I., Avag, A. (2014): Hatay Province Kırkhan District a Research on Vegetation Structure of Base Pastures. – Gaziosmanpasa U. Journal of Faculty of Agriculture JAFAG 31(2): 52-60.
- [17] Cinar, S., Hatipoglu, R., Avci, M. (2015): Effects of Some Weed Control Methods on Herb Yield, Botanical Composition and Weed Quality in the Pastures of Mediterranean Region. – Journal of Agricultural Sciences 21(1): 39-49.
- [18] Cinar, S., Hatipoğlu, R., Avci, M., Yucel, C., Inal, I. (2019): A Research on Vegetation Structure of Pastures in Tufanbeyli District of Adana Province. – KSU J. Agric Nat 22(1): 143-152.
- [19] Davis, P. H. (1970): Flora of Turkey and the East Aegean Islands. – University of Edinburgh Press, Volume 1-3, Edinburgh.
- [20] Demiri, M. (1983): Flora Ekskursionistee Shqiperise T, Shtepia Botuese Librit Shkollor Tirane.
- [21] Eddy, I. (2016): Land degradation in Central Asia. – The Faculty of Graduate and Postdoctoral Studies Master of Science, The University of British Columbia.
- [22] Edgecombe, W. (1964): Weeds of Lebanon. – Faculty of Agriculture Sciences, American University of Beirut, Lebanon, Publication No: 24.
- [23] Erkun, V. (1971): Pasture Surveys in Hakkari and Van Provinces. – Ministry of Agriculture General Directorate of Agriculture Affairs Publications, G.13, Ankara. (In Turkish).
- [24] Erkun, V. (1972): Research on Pastures of Bala District. – Ministry of Agriculture Livestock Development Publications, Ankara.
- [25] Garms, H., Eigener, W., Melderis, A., Pope, T., Durrell, G. (1968): The Natural History of Europe. – Paol Hamilyn Limited, London.

- [26] Gokkus, A. (1984): Investigation on Herbal and Crude Protein Yields and Botanical Composition of Erzurum Natural Pastures Applied to Different Breeding Methods. – A.Ü Institute of Science and Technology, Doctorate Thesis, Field Crops Department, 145p. Erzurum.
- [27] Gokkus, A. (1991): Training Seminar on Meadow Pasture and Forage Crops and Livestock Development Project in Eastern and Southeastern Anatolia Regions. – February 20-22, 1991, Erzurum.
- [28] Gokkus, A., Koc, A., Comakli, B. (2000): Meadow Pasture Application Guide. Extended 3rd Edition. – Atatürk University Faculty of Agriculture Publications No: 142. (In Turkish).
- [29] Gur, M., Altin, M. (2015): Some properties of floristic compositions of pastures with different usage history in Trakya region. – Journal of Anatolian Agricultural Sciences 30: 60-67.
- [30] Holecek, J. L., Pieper, R. D., Herbel, C. H. (2004): Range management: Principles and practices. – Prentice Hall, New Jersey 607p.
- [31] Huxley, A., Taylor, W. (1977): Flowers of Greece and the Aegean. – Chatto and Windus Ltd. Printed Great Britain by Richard Clay Ltd Bunges, Suffolk.
- [32] Inal, I., Avci, M., Cinar, S., Yucel, C., Hatipoglu, R. (2011): A Research on Vegetation Structure of Coast Pastures. – IX. Field Crops Congress Presentation 3: 1664-1667. September 12-15 Bursa.
- [33] Koc, A., Gokkus, A. (1994): Determination of the optimum stubble height to be left by the botanical composition and soil covering area of the pasture vegetation in Güzelyurt. – Turkish Journal of Agriculture and Forestry 18(6): 498-500.
- [34] Koc, A. (1995): Topography and soil moisture and temperature effects on some properties of pasture vegetation. – Atatürk Univ. Graduate School of Natural and Applied Sciences, Field Crops Department, 177p. Erzurum.
- [35] Koc, A., Cakal, S. (2004): Comparison of some rangeland canopy coverage methods. – Int. Soil Cong. On Natural Resource Manage, for Sust. Develop., June 7-10, 2004, Erzurum, Turkey, D7, pp. 41-45.
- [36] Mirzabaev, A., Ahmed, M., Werner, J., Pender, J., Louhaichi, M. (2016): Rangelands of Central Asia: Challenges and Opportunities. – J. Arid Land 8(1): 93-108.
- [37] Nishanov, N. (2015): Sustainable livestock management under changing climate in Central Asia. – https://www.iamo.de/fileadmin/user_upload/Bilder_und_Dokumente/06-veranstaltungen/recca/C1_2_Nariman_Nishanov.pdf (16.01.2018).
- [38] Ozaslan Parlak, A., Parlak, M., Gokkus, A., Demiray, H. C. (2015): Herb Yield and Quality, Botanical Composition and Some Soil Properties of Mediterranean Pastures. – COMU J. Agric. Fac. 2(1): 99-108.
- [39] Ozmen, T. (1977): Research on the vegetation of the pastures of Konya. – Ankara Univ. Graduate School of Natural and Applied Sciences Field Crops Department, Ph.D. 126p. Ankara.
- [40] Oztan, Y., Okatan, A. (1985): Introduction to pasture legumes and forage crops. Volume II. – K.Ü. Faculty of Forestry. Karadeniz University Press Publication No: 95, Faculty Publication No: 8, Trabzon.
- [41] Polat, T., Buyukhatipoglu, S., Akkaya, G. (2018): Determination of Plant Composition, Herb Yield and Quality of Pastures in Different Directories in the Individual Mountains of Sanliurfa. – Harran Journal of Agriculture and Food 22(2): 248-254.
- [42] Polunin, O., Huxley, A. (1974): Flowers of the Mediterranean. – Chatto and Windus, London.
- [43] Rosales, M., Livinets, S. (2017): Grazing and Land Degradation in C1s Countries and Mongolia. – http://www.fao.org/fileadmin/templates/lead/pdf/e-conf_05-06_background.pdf (18.01.2018).
- [44] Sen, C. (2010): A Research on the Vegetation Structure in Pastures in Some Villages of Kilis Province. – Master Thesis. Cukurova University Graduate School of Natural and Applied Sciences Field Crops, Adana. (In Turkish).

- [45] Seydosoglu, S., Cacan, E., Sevilmis, U. (2019): Determination of Botanical composition, yield and range quality ratings of intertile rangelands in Kozluk district of Batman province of Turkey. – *Fresenius Environmental Bulletin* 28(4A): 3388-3394.
- [46] Sheaffer, C. C., Peterson, M. A., Mccalin, M., Volene, J. J., Cherney, J. H., Johnson, K. D., Woodward, W. T., Viands, D. R. (1995): Acid detergent fiber, neutral detergent fiber concentration and relative feed value. – North American Alfalfa Improvement Conference, Minneapolis.
- [47] Steel, R. G. D., Torrie, J. H. (1960): Principles and Procedures of Statistics with Special Reference to the Biological Sciences. – Mc Graw-Hill Book Co., Inc., London.
- [48] Surmen, M., Kara, E. (2018): Yield and Quality Characteristics of Pasture Vegetations on Different Slopes in Aydin Province Ecological Conditions. – *Derim* 35(1): 67-72.
- [49] Tekindal, B. (1998): Prerequisites and Analysis of Variance Analysis. – A.Ü Ziraat Fak. Graduate School of Natural and Applied Sciences, Department of Animal Science PhD thesis, 70p.
- [50] Tukul, T. (1981): Investigations on Determination of Vegetation and Yield Strengths of Meadows that are Common to a Typical Steppe Mountain Preserved in Ulukisla. – Associate Professor Thesis. Cukurova University Faculty of Agriculture, Adana. (In Turkish).
- [51] Uslu, O. S. (2005): Research on the Determination of Botanic Composition in Yeniyapan Pasture in Araplar Village of Turkoglu District of Kahramanmaras Province and Effects of Different Fertilizer Applications on Yield and Botanic Composition of Pasture. – Ç.Ü. Graduate School of Natural and Applied Sciences Field Crops Ph.D. Thesis, 162p., Adana.
- [52] Uzun, F., Alay, F., Ispirli, K. (2016): Some characteristics of the pastures of Bartın province. – *Turkey Agricultural Research Journal* 3(2): 174-183.
- [53] Weymer, H. (1981): *Lernt Pflanze Kennen*. – Ferdinand Enke Verlag, Stuttgart.
- [54] Yurtsever, N. (1984): *Experimental Statistical Methods*. – General Directorate of Rural Services Publications No: 121, Ankara.

EFFECTS OF NITROGEN FERTILIZATION RATES ON FORAGE YIELD AND QUALITY OF ANNUAL RYEGRASS (*LOLIUM MULTIFLORUM* L.) IN CENTRAL BLACK SEA CLIMATIC ZONE IN TURKEY

CINAR, S.^{1,2*} – OZKURT, M.³ – CETIN, R.⁴

¹Department of Plant and Animal Production, Technical Vocational School, Kilis 7 Aralik University, Kilis, Turkey

²Department of Horticulture and Field Crops, Faculty of Agriculture, Kyrgyz-Turkish Manas University, Bishkek, Kyrgyzstan

³Mus Alparslan University, Faculty of Applied Sciences, Mus, Turkey

⁴Gaziosmanpasa University, Graduate School of Natural and Applied Sciences, Tokat, Turkey

*Corresponding author

e-mail: scinar01@hotmail.com; selahattin.cinar@manas.edu.kg

(Received 6th Sep 2019; accepted 4th Dec 2019)

Abstract. In this research, we aimed to determine the effects of nitrogen fertilization on forage yield and forage quality of annual ryegrass (*Lolium multiflorum* L.) in Kazova, Tokat/Turkey conditions (the Central Black Sea Climate Zone) in 2014/2015 and 2015/2016 growing years. The experiment consisted of four replications in randomized complete block design to test effect of seven nitrogen rates (0, 50, 100, 150, 200, 250, 300 kg ha⁻¹) on plant height (PH), fresh forage yield (FFY), dry matter yield (DMY), crude protein ratio (CP), crude protein yield (CPY), Acid Detergent Fiber (ADF) ratio, Neutral Detergent Fiber (NDF) ratio, digestible dry matter ratio (DDM), digestible dry matter yield (DDMY), and relative feed value (RFV). The results revealed that the highest plant height (86.7 cm) was at the 200 kg ha⁻¹ of nitrogen rate, highest fresh forage yield (48360 kg ha⁻¹), dry matter yield (13325 kg ha⁻¹), crude protein yield (1870 kg ha⁻¹) and digestible dry matter yield (8340 kg ha⁻¹) was obtained at the 250 kg ha⁻¹ of nitrogen rate, and the highest digestible dry matter rate (62.72%) was determined at the 150 kg ha⁻¹ nitrogen rate. Thus, 250 kg ha⁻¹ nitrogen rate was the optimal dose for high forage yield and increasing nitrogen doses did not affect the ADF and NDF rates. Nevertheless, application of 300 kg ha⁻¹ of nitrogen decreased yield but increased crude protein yield. Therefore, a nitrogen fertilization rate of 250 kg ha⁻¹ is recommended for high forage yield of annual ryegrass (*Lolium multiflorum* L.) in the Central Black Sea Climate Zone or similar climatic conditions.

Keywords: ADF, NDF, DMY, DDMY, RFV

Introduction

Cost of animal derived food and food products are high in Turkey. One of the most important reasons for this is the insufficient production of high quality roughage. In order to meet the high quality roughage requirement in Turkey, it is necessary to improve the meadow pastures, increase the forage crop production areas, introduce other cheap and alternative roughage resources to animal production systems, and transfer the quality roughage production techniques to the producers (Serin and Tan, 2001).

Forage crop cultivation is one of the strategies to meet the high quality roughage need of the country's livestock. Forage legumes are the source of protein and forage grasses are the source of carbohydrates in animal diet. The annual forage grass *Lolium*

multiflorum L. is one of the grasses with highest forage production potential and fertilizer use efficiency (Acıkgöz, 2001). The annual ryegrass is also known as annual ryegrass since it was initially cultivated in Italy as a annual forage crop.

Annual ryegrass, which is a grassy forage plant of Southern Europe origin, is a one-year species cultivated in the genera *Lolium* (Gençkan, 1983). It is an important alternative source of roughage in cool and temperate climates, in areas where barley and oats from winter cool climate cereals are grown for feed production. Under normal conditions, green yields varying from 15000 to 25000 kg ha⁻¹ per hectare and hay yields of 5000-8000 kg ha⁻¹ can be obtained. In areas where water is sufficient, it is harvested 2-3 times, 40000-60000 kg ha⁻¹ green, 7500-15000 kg ha⁻¹ dry grass can be taken (Baytekin et al. 2009).

In general, the crop is harvested and fed to livestock freshly; however, it can also be utilized as hay or silage. Annual forage grass production in Turkey has increased in recent years owing to the government subsidies for forage crops. The cultivation area of 4.832 da and green grass production of 17.023 tons in 2014 has increased to a cultivation area 103.410 da and green grass production of 448.086 tons in 2019 (TUIK, 2019).

In order to achieve the expected yield and quality of forage crops, the plants should be fertilized with the appropriate combination and rate in the required period. In addition to yield, forage quality is also of great importance for animal health. Nitrogen, which is the most important nutrient for plants, constitutes the majority of dry matter. In addition, nitrogen is incorporated to proteins, chlorophyll, enzymes, and vitamins in plants. Nitrogen is the most commonly used nutrient in grasses. Appropriate amounts of nitrogenous fertilizers increase the protein content in grasses, but the use of excess nitrogen in plants also leads to the accumulation of nitrate and alkaloids. A positive response was reported in annual ryegrass with the application of nitrogen fertilizers (Colak, 2015; Ozdemir et al., 2019).

Different results have been obtained in studies on fertilizer use on annual ryegrass. Celen (1991) reported that the highest yields were achieved at 100 and 150 kg ha⁻¹ nitrogen (N) application in Bornova, İzmir/Turkey conditions. Seker (1992) realized highest dry matter and crude protein yields 200 kg ha⁻¹ N and the highest crude protein ratio at the rate of 250 kg ha⁻¹ N application rate in trials in Erzurum/Turkey. Parlak et al. (2007) indicated the highest fresh forage yield (11630 kg ha⁻¹), dry matter (3840 kg ha⁻¹) and crude protein yield (800 kg ha⁻¹) at 200 kg ha⁻¹ N application in Ankara/Turkey. In a study carried out in Serbia, Simic et al. (2009) reported that the highest dry matter yield varied between years and achieved in N application rates of 50-150 kg ha⁻¹. Kesiktas (2010) reported the highest dry matter yield at the application of 100 to 150 kg ha⁻¹ of N and the highest crude protein ratio at the 150 kg ha⁻¹ N applications in Karaman/Turkey conditions. Pavinato et al. (2014) reported that the increase in the N rate increased dry matter and crude protein yield and the best results were attained from the dose of 120 kg ha⁻¹ of N in Brazil. Colak (2015) declared 80 kg ha⁻¹ of N being sufficient to achieve high yield in Ankara and Ozdemir et al. (2019) reported that 500 kg ha⁻¹ of N was suitable for high yield and high quality product of annual forage grass in a study conducted in Bursa/Turkey.

Annual ryegrass, high growth rate and nitrogen absorption in fertilization due to the ability to (Ozkul et al., 2012) is an alternative forage crops can be obtained high yield. Turkey and Turkey's Central Black Sea region is a plant that has the potential to close the fodder deficit in the region.

The purpose of the study, Turkey's Central Black Sea Region in the efficiency and high level of quality forage in closing the deficit will be an alternative forage crops in one annual ryegrass (*Lolium multiflorum* L.) to determine the appropriate nitrogen levels.

Materials and Method

Materials

The experimental trial was established in the Research and Application Center of Faculty of Agriculture located at Tasliciftlik Campus of Gaziosmanpasa University in Tokat Turkey for two years, 2014-2015 and 2015-2016 growing seasons. Trial area was 598 m above the sea level, at the 40°19'58.17 North latitude and 36°28'05 East longitude (*Figure 1*).



Figure 1. Geographic location of the field trial

Long term average rainfall, temperature, and relative humidity records of the research place was gathered compared to the temperature (°C), monthly total rainfall (mm) and monthly average relative humidity (%) of the breeding periods in which the experiment was conducted. The average temperatures of breeding periods (2014-2015, 2015-2016) (13.6, 12.0°C) in which the experiment was carried out were higher than the average long-term temperature (11.7°C), and total rainfall in the first breeding period (419.4 mm) is lower than the long year average (428.5 mm) and higher in the second breeding period (463.4 mm) than long year average. In addition, the relative humidity in the in the first breeding period (57.0%) is lower than the long year average (59.6%) and higher in the second breeding period (63.7%) than long year average (Anonymous, 2017). According to this, it can be concluded that the years in which the experiment was conducted were hotter and rainfall and humidity also different than the long-term averages (*Table 1*).

Chemical analyses of soil samples taken from 0-20 and 20-40 cm depths in the research area were carried out in Gaziosmanpasa University, Faculty of Agriculture, Department of Soil Science. According to the analysis results, the soil of the trial area was found to be poor in terms of organic matter, potassium, and lime, and it was clayey alkaline (Kacar, 2016).

In the research, Caramba cultivar (*Lolium multiflorum* cv. Caramba) was used and seven doses of nitrogen (0, 50, 100, 150, 200, 250, 300 kg ha⁻¹) were evaluated.

Table 1. Climate data for breeding periods (2014-2015, 2015-2016) and long year average of the region where the research was conducted

Aylar	Temperature (°C)			Precipitation (mm)			Relative Humidity (%)		
	2014-2015	2015-2016	LYA	2014-2015	2015-2016	LYA	2014-2015	2015-2016	LYA
September	20.2	22.9	18.8	39.0	0.2	18.5	54.2	49.6	56.2
October	14.1	15.1	13.7	51.6	55.6	38.8	68.5	69.2	58.6
November	7.1	8.6	7.9	63.1	15.8	44.1	73.1	65.6	52.2
December	7.0	1.0	3.8	39.4	35.5	46.6	75.6	81.6	70.1
January	4.1	2.4	1.9	38.4	104.6	41.4	68.6	69.0	74.8
February	8.0	5.2	3.5	25.8	42.6	34.0	49.6	62.5	65.0
March	11.1	8.1	7.4	57.0	49.4	40.7	50.7	65.6	54.8
April	16.2	10.0	12.5	34.5	23.4	55.4	43.0	58.3	47.8
May	17.5	16.9	16.5	34.8	89.5	58.5	57.4	57.1	62.4
June	20.3	19.9	19.9	35.6	33.1	38.3	57.0	63.7	59.6
July	24.2	22.1	22.3	0.2	13.7	12.2	49.4	55.0	55.4
Average/Total	13.6	12.0	11.7	419.4	463.4	428.5	58.8	63.3	59.7

LYA: Long Year Average

Method

The experiment consisted of four replications in randomized complete block design (RCBD) with seven plots in each replication. Each plot consisted of 6 rows with 5 m length and 20 cm row spacing. Plants were seeded at 2-3 cm planting depth in 1st year on 16 October 2014 and 2nd year on 12 October 2015. In the experiment, the plot sizes were determined as 1.2x5 m = 6 m² (Avcioglu and Geren, 1996).

Sowing was based on 30 kg ha⁻¹ seed amount (Acikgoz, 2001). Seeds weighed for each row were planted by hand in rows opened by marker. About ¼ of the predetermined nitrogen rate was applied after planting, another ¼ was applied during the tillering, ¼ was applied after the first harvest, and last ¼ was applied after the second harvest (Kesiktas, 2010). TSP (Triple Super Phosphate) was used as phosphorus fertilizer and urea was used as nitrogen fertilizer in the experiment. Pure 50 kg ha⁻¹ phosphorus was applied to each parcel in planting (Kusvuran and Tansi, 2005). In both years, plots were harvested three times and irrigation was performed after the harvests.

The general view of the trial parcels is shown in *Figure 2*.



Figure 2. General views from trial parcels in different periods

The height of the 10 plants randomly selected from each plot were measured from the soil surface to the highest point of the plant and the plot based plant height was determined by taking the mean of the measured plants. The plots were harvested during

the beginning of heading (10% heading). One row from the edges of each plot, top and bottom 0.5 m was mowed and removed, the remaining area was harvested. The fresh biomass obtained from each plot was weighed and converted to the fresh forage yield per ha (Anonymous, 2001). A randomly selected 500 g fresh forage sample was dried to a constant weight at 60°C and dry weights ratios were determined based on dried samples (Sleugh et al., 2000). Samples of 5 g from the dried herbage were dried further for 24 hours in the oven set at 105°C, cooled in a desiccator, and subsequently weighed on sensitive a balance to determine the dry matter ratios. Dry matter yields were calculated based on the obtained dry matter ratio. Some of the samples dried at 60°C were ground and nitrogen was determined in the grass samples by Kjeldahl method. Determined nitrogen values were multiplied by 6.25 conversion coefficient to determine crude protein contents (%) of the of samples (Tan, 1995). In the experiment, ADF (Acid Detergent Fiber) and NDF (Neutral Detergent Fiber) analyses were performed, according to Van Soest et al. (1991) using the ANKOM 200/220 device.

Digestible dry matter ratio, ADF composition, relative feed value (RFV), dry matter consumption values were calculated using formulas (Eq.1, Eq.2, Eq.3) provided by Sheaffer et al. (1995).

$$\text{Digestible Dry Matter (DDM)} = 88.9 - (0.779 \times \% \text{ ADF}) \quad (\text{Eq.1})$$

$$\text{Dry Matter Intake (DMI)} = 120 / (\% \text{ NDF}) \quad (\text{Eq.2})$$

$$\text{Relative Feed Value} = (\% \text{ DDM} \times \% \text{ DMI}) / 1.29 \quad (\text{Eq.3})$$

The digestible dry matter yield was obtained by multiplying the dry matter yield with the digestible dry matter ratio and the crude protein yield was obtained by multiplying the crude protein ratios and the dry matter yield.

The variance analysis (ANOVA) of the data was performed in the first year, second year and combined randomized block experiment design in MSTATC statistical program. Mean separations of significant traits were conducted using Duncan's multiple comparison test (Duzgunes et al., 1987).

Results and Discussion

The table of the variance analysis of the combined data is as follows (Table 2).

Table 2. Results of analysis of variance and mean squares of the traits determined

	DF	PH	FFY	DMY	CP	CPY	ADF	NDF	DDM	DDMY	RFV
Year (Y)	1	45.2	1998788.8	352126.9*	0.03	6393.3*	4.7*	9.8	2.9*	153911.4*	90.6
Error 1	6	8.8	640803.8	30728.0	0.70	844.7	0.7	5.7	0.4	12838.03	34.9
Nitrogen (N)	6	39.3**	1342460.5**	102591.8**	6.32**	3626.2**	2.2*	10.2*	1.3*	40573.4**	65.8**
NxY	6	5.5	92145.4	7161.7	0.20	153.21	1.0	3.5	0.6	2486.7	14.7
Error 2	36	11.8	1980817.8	9564.9	0.38	265.7	0.9	3.4	0.6	3458.7	18.5
CV		4.1	10.2	8.5	4.5	10.4	2.8	3.4	1.2	8.2	4.0

DF: Degree of freedom; * P<0.05 and ** P<0.01

According to the variance analysis, combined data of two years made a significant statistical difference in nitrogen applications, plant height, fresh forage yield, dry matter

yield, crude protein yield, ADF, NDF, DDM, crude protein yield, DDMY and RFV. Nitrogen applications were found to be statistically significant in dry matter yield, crude protein yield, ADF, DDM, DDMY between years. Nitrogen x year interaction was not statistically significant in any parameter.

Plant Height (cm)

According to the ANOVA results, the nitrogen rate has a significant effect on plant height values of the first year and two-year average. However, nitrogen rates did not affect plant height of annual ryegrass in the second year. The average plant height values determined in the plots with different nitrogen rates are shown in *Table 3*.

Although the average plant height in the second year was higher than the first year, it was found that year effect was not statistically significant. In the first year and two-year averages, plant height was significantly higher in the plots where nitrogen was applied compare to the control group. Nitrogen dose applied to annual ryegrass increased the plant height (*Table 3*). This increase can be attributed to the vegetative growth stimulating effect of nitrogen fertilizers in plants (Kun, 1994; Gokmen et al., 2001).

Table 3. Average plant height values (cm) of annual ryegrass based on nitrogen fertilizer rates

Nitrogen (kg ha ⁻¹)	Years		
	2015	2016	Mean
0	76.9 b**	82.1	79.5 b
50	83.2 a	84.3	83.7 a
100	83.0 a	85.3	84.1 a
150	83.8 a	85.7	84.8 a
200	86.6 a	86.8	86.7 a
250	84.8 a	85.5	85.2 a
300	83.0 a	84.4	83.7 a
Mean	83.1	84.9	

** Values within the same columns followed by different letters are significantly different based on Duncan's test at $P < 0.01$

The average plant height of annual ryegrass was reported to be 60-90 cm by Erkun (1954), 65.7-68.6 cm by Kusvuran and Tansi (2005), 48.4 cm by Demiroglu et al. (2007), 64.5 cm by Kesiktas (2010), 88.4 cm by Cinar et al. (2011), 50.1-68.3 cm by Colak and Sancak (2017). The plant height measurement in the present study was closer to the values reported in the study of Cinar et al. (2011) and deviated from the other studies. This may be due to the variations in ecological conditions, cultivation techniques and the cultivars tested.

Fresh Forage Yield (kg ha⁻¹)

Difference in the nitrogen rate had a significant effect on fresh forage yield of annual ryegrass in both years and in the mean of the two years. The average fresh forage yield values based on the nitrogen rates are given in *Table 4*.

As shown in *Table 4*, fresh forage yield ranged from 32330 kg ha⁻¹ to 46150 kg ha⁻¹ in the first year, from 40420 kg ha⁻¹ to 50570 kg ha⁻¹ in the second year, and from 36375 kg ha⁻¹ to 48360 kg ha⁻¹ in the two-year average depending on the fertilizer rate applied. In the first year, second year and two-year average, the highest fresh forage yield was obtained from the application of nitrogen rate of 250 kg ha⁻¹. However, fresh

forage yield obtained from the nitrogen rates between 50-200 kg ha⁻¹ in the first year, from the nitrogen rates of 150-200 kg ha⁻¹ in the second year, and from the nitrogen rates between 150-200 kg ha⁻¹ at the two-year averages were not significantly different from that of the nitrogen rate of 250 kg ha⁻¹. In both years separately and on a two-year average, the nitrogen rate of 300 kg ha⁻¹ decreased fresh forage weight.

Table 4. Fresh forage yield values (kg ha⁻¹) of annual ryegrass based on nitrogen fertilizer rates

Nitrogen (kg ha ⁻¹)	Years		
	2015	2016	Mean
0	32330 b**	40420 d	36375 d
50	41150 a	44520 bcd	42835 bc
100	38510 ab	42670 bcd	40590 cd
150	43790 a	45790 abc	44790 abc
200	45930 a	47760 ab	46845 ab
250	46150 a	50570 a	48360 a
300	39660 ab	42230 cd	40945 cd
Mean	41074	44851	

** Values within the same columns followed by different small letters are significantly different based on Duncan's test at $P < 0.01$

The fresh forage yield of the annual ryegrass was reported to be 5500 kg ha⁻¹ with the application of 150 kg ha⁻¹ nitrogen (Alvim and Moojen, 1984), 13500.0 kg ha⁻¹ with 55 kg ha⁻¹ nitrogen application (Kallenbach et al., 2003), 11630 kg ha⁻¹ with 200 kg ha⁻¹ nitrogen application (Bright et al., 2006), 15430 kg ha⁻¹ with 65 kg ha⁻¹ nitrogen application (Piskin, 2007), 32450 kg ha⁻¹ with 200 kg ha⁻¹ nitrogen application (Kusvuran and Tansi, 2005), 19270, 19320, 19320 kg ha⁻¹ with 40, 80, 120 kg ha⁻¹ of nitrogen dose applications, respectively (Colak and Sancak, 2017).

When compared with the abovementioned previous research, it is evident that both fresh forage yield values and nitrogen rates vary greatly. This discrepancy may be due to differences in the nature of the studies, ecology, nitrogen rate, and the cultivar tested.

Dry Matter Yield (kg ha⁻¹)

According to the ANOVA results for dry matter yield values, different nitrogen fertilizer rates had a significant effect on dry matter yield in the first year, second year, and two-year average. Average dry matter yield values in respect to nitrogen rates are given in Table 5.

Depending on the fertilizer rates applied, dry matter yield ranged from 8590 kg ha⁻¹ to 12410 kg ha⁻¹ in the first year, 11340 kg ha⁻¹ to 14240 kg ha⁻¹ in the second year, and 9965 kg ha⁻¹ to 13325 kg ha⁻¹ when means were averaged over two years. The highest dry matter yield in the first year, second year and two-year average was obtained from the application of 250 kg ha⁻¹ nitrogen rate. Dry matter yield decreased at 300 kg ha⁻¹ nitrogen rate for each of the two years and on average. Dry matter yield in the second year was significantly higher than that in the first year (Table 4). The reason for the higher average dry matter yield in the second year is higher rainfall in the second year (Table 1).

In general, dry matter yield results were parallel to fresh forage yield (Table 4) as expected. The earlier research revealed that dry matter yield of annual ryegrass was 9600 kg ha⁻¹ when 350 kg ha⁻¹ nitrogen fertilizer is applied (Corainville et al., 1973),

was 8760 kg ha⁻¹ with 90 kg ha⁻¹ nitrogen application (Bartholomew and Williams, 1978), was 2020 kg ha⁻¹ with 55 kg ha⁻¹ nitrogen application (Piskin, 2007). In the research reported here, the highest dry matter yield was obtained with the application of 250 kg ha⁻¹ pure nitrogen. There is a discrepancy between our results and the previous results listed above. Different ecological conditions, variation in the rate of fertilizer, management differences and the difference in cultivar may have led the discrepancy among reported results.

Table 5. Average dry matter yield values (kg ha⁻¹) of annual ryegrass based on nitrogen fertilizer rates

Nitrogen (kg ha ⁻¹)	Years		
	2015	2016	Mean
0	8590 d**	11340 c	9965 e
50	10510 bc	12070 bc	11290 cd
100	9830 cd	11400 c	10615 de
150	11190 abc	12550 bc	11870 bc
200	11870 ab	12980 ab	12425 ab
250	12410 a	14240 a	13325 a
300	10620 bc	11540 bc	11080 cd
Mean	10717 B ⁺	12303 A	

** Values within the same columns followed by different letters are significantly different based on Duncan's test at P < 0.01.

+ Values within the same row followed by different capital letters are significantly different based on Duncan's test at P < 0.05

Crude Protein Ratio (%)

ANOVA results for crude protein ratio based on different nitrogen rates revealed that nitrogen rates had a significant effect on the crude protein ratio in the first year, second year and on the two-year averages. Average crude protein ratios determined according to nitrogen rates are provided in *Table 6*.

The ratio of crude protein, one of the most important forage quality parameter, increased in parallel to the increase in the nitrogen rate in annual ryegrass. The highest crude protein content was obtained from 300 kg ha⁻¹ nitrogen rate in both trial years and in two-year average. It has been stated by many researchers that nitrogen increases the crude protein content of annual grasses (Colak, 2015).

In the previous research, the highest crude protein ratio was reported at 200 and 250 kg ha⁻¹ nitrogen application in Kusvuran and Tansi (2005), at 150 kg ha⁻¹ nitrogen application in Simic et al. (2009) and Kesiktas (2010), at 470 kg ha⁻¹ nitrogen application in Kusvuran (2011), and at 200 kg ha⁻¹ nitrogen application in Colak (2015). When the results obtained here are compared with the abovementioned studies, no concordance is observed. Different ecological conditions, variation in the rate of fertilizer, management differences along with the difference in tested cultivars may have led this difference.

Crude Protein Yield (kg ha⁻¹)

One way ANOVA results discerned that the crude protein yield significantly differ with the various fertilizer rates in the first year, second year, and two-year average. Average crude protein yields determined according to nitrogen rates are listed in *Table 7*.

Table 6. Determination of the crude protein ratio (%) of annual ryegrass based on nitrogen fertilizer rates

Nitrogen (kg ha ⁻¹)	Years		
	2015	2016	Mean
0	11.91 b**	12.37 d	12.14 d
50	12.70 b	12.99 cd	12.85 c
100	13.93 a	13.61 bc	13.77 b
150	14.12 a	14.15 ab	14.13 b
200	13.83 a	13.43 bc	13.63 b
250	13.96 a	14.02 b	13.99 b
300	14.75 a	14.96 a	14.86 a
Mean	13.60	13.65	

** Values within the same columns followed by different small letters are significantly different based on Duncan's test at P < 0.01

Table 7. Average crude protein yield values (kg ha⁻¹) of annual ryegrass based on nitrogen fertilizer rates

Nitrogen (kg ha ⁻¹)	Years		
	2015	2016	Mean
0	1030 c**	1400 c	1220 d
50	1340 b	1570 bc	1460 c
100	1370 b	1550 bc	1460 c
150	1580 ab	1780 ab	1680 b
200	1650 a	1750 b	1700 b
250	1730 a	2000 a	1870 a
300	1570 ab	1730 b	1650 b
Mean	1467 B ⁺	1682 A	

** Values within the same columns followed by different small letters are significantly different based on Duncan's test at P < 0.01.

+ Values within the same row followed by different capital letters are significantly different based on Duncan's test at P < 0.05

The crude protein yield was calculated by multiplying the crude protein ratio and dry matter yield and the highest crude protein yield was obtained at the nitrogen rate of 250 kg ha⁻¹ in the first year, in the second year and in two-year average. In general, the crude protein yields of the plots with high crude protein content and dry matter yield were high as expected (Table 5).

Crude protein yield of annual ryegrass was reported as 1200 kg ha⁻¹ by Alvim and Moojen (1984), as 1290 kg ha⁻¹ by Basbug (1990), as 470 kg ha⁻¹ by Karakurt and Ekiz (1991), as 1150 kg ha⁻¹ by Kusvuran and Tansi (2005), as 800 kg ha⁻¹ by Bright et al. (2007), as 920 kg ha⁻¹ by Kesiktas (2010), as 820 kg ha⁻¹ by Kusvuran et al. (2014), and as 680 kg ha⁻¹ by Colak and Sancak (2017). The results obtained in this study do not comply with the results listed above. It can be concluded that the difference in crude protein yields is not surprised as the trials were carried out in regions with different ecological characteristics, distinctive applications were performed, and different cultivars were tested.

ADF Concentration (%)

According to the one way ANOVA results, ADF concentration was not affected by the nitrogen fertilizer rate in the first year and in the second year. Nonetheless, nitrogen fertilizer application rates had a significant effect on two-year average ADF

concentration values. The average ADF concentration values determined according to the nitrogen rates are given in *Table 8*.

According to the two-year averages, the ADF content was significantly higher at nitrogen rates of 50 kg ha⁻¹ and 100 kg ha⁻¹ compared to 150 kg ha⁻¹ nitrogen application rate. However, the ADF concentrations at 0, 200, 250, and 300 kg ha⁻¹ nitrogen rates were not different from both higher or lower concentrations of 50, 100 or 150 kg ha⁻¹ doses. The mean ADF concentration in the first year was significantly higher than in the second year (*Table 8*). This may be due to the fact that the second falling rainfall and relative humidity are higher than the first year (*Table 1*).

Table 8. Average ADF concentration (%) values of annual ryegrass based on nitrogen fertilizer rates

Nitrogen (kg ha ⁻¹)	Years		
	2015	2016	Mean
0	33.64	33.65	33.64 ab*
50	34.72	34.66	34.69 a
100	34.62	34.81	34.71 a
150	33.86	33.33	33.59 b
200	35.95	33.72	34.65 ab
250	34.36	33.31	33.83 ab
300	34.15	33.40	33.78 ab
Mean	34.42 A+	33.84 B	

* Values within the same columns followed by different small letters are significantly different based on Duncan's test at P < 0.05.

+ Values within the same row followed by different capital letters are significantly different based on Duncan's test at P < 0.05

ADF concentrations of the annual ryegrass reported by Caddel and Allen (1997) were 31.0-35.0%, by Meeske et al. (2009) were 31.4%-32.3, by Kusvuran et al. (2014) was 37.4%, by Colak and Sancak (2017) were 31.1-32.1%, and by Ozdemir et al. (2019) were 30.5-34.2. The results obtained in this study are in agreement with Caddel and Allen (1997) and Ozdemir et al. (2019) but not with other studies. The difference can be attributed to the change in the cellulose and lignin contents of the cultivars along with the different ecological conditions and harvest regimen.

NDF Concentration (%)

According to the ANOVA results of NDF concentrations based on different nitrogen rates, the first year and the second year nitrogen rates did not affect the NDF concentrations. Nevertheless, nitrogen rates had a significant effect on the two-year average NDF concentrations in annual ryegrass (*Table 9*).

According to the two-year averages, the NDF composition of the herbage at 200 kg ha⁻¹ nitrogen rate was significantly higher than that of the control and 250 to 300 kg ha⁻¹ nitrogen rates (*Table 9*).

Van Soest (1985) stated that in order to ensure optimum milk yield in dairy cattle, NDF composition should be 36%. Yavuz (2005) affirmed that the amount of feed digested by the animal decreased with the increase in NDF ratio and the increase in NDF ratio in roughage caused a decrease of 1-2% of milk yield. Thus, it can be concluded that due to the high NDF composition, annual ryegrass alone is not suitable for feeding dairy cattle.

NDF composition in annual ryegrass was reported to be in the range of 47.7-54.7% by Viviani Rossi et al. (1994), was in the range of 40-46% according to Caddel and Allen (1997), was in the range of 42.2-50.6% in Teutsch and Smith (2001), was 47% in Meeske (2009), was 58.7% in Kusvuran and Tansi (2005), was 59.6% in Simsek (2015), and was in the range of 56.01-54.14% in Colak (2015). The results obtained in the current research did not show compliance with Caddel and Allen (1997), Meeske (2009), Kusvuran et al. (2014), Simsek (2015): however, they were in agreement with the Viviani Rossi et al. (1994), Teutsch and Smith (2001) and Colak (2015). It can be concluded that the differences in NDF composition can be attributed to the fact that the trials were carried out in regions with different ecological characteristics, with distinctive applications, and different cultivars.

Table 9. Average NDF concentrations (%) of annual ryegrass based on nitrogen fertilizer rates

Nitrogen (kg ha ⁻¹)	Years		
	2015	2016	Mean
0	54.85	51.35	53.10 b*
50	55.23	55.02	55.12 ab
100	55.40	54.34	54.87 ab
150	55.43	54.47	54.95 ab
200	56.38	56.45	56.42 a
250	54.23	53.39	53.81 b
300	53.28	53.90	53.59 b
Mean	54.97	54.13	

* Values within the same columns followed by different small letters are significantly different based on Duncan's test at $P < 0.05$

Digestible Dry Matter Ratio (%)

One way ANOVA analyses targeting the effect of nitrogen rate on digestible dry matter ratio revealed that different nitrogen rate did not lead a significant difference in the digestible dry matter ratios in the first and in the second years whereas a significant difference was observed among the nitrogen rates for the analysis of values averaged over two years (Table 10).

As indicated in Table 10, the average digestible dry matter ratio varied between 61.85% and 62.72% for the two-year averages depending on the nitrogen rates applied. The highest DDM ratio was found at 150 kg ha⁻¹ nitrogen dose and the lowest was at 100 kg ha⁻¹ nitrogen dose. The mean DDM ratio in the second year was significantly higher than the one in the first year. As expected, the rate of digestible dry matter, which was negatively correlated with the ADF composition of the herbage, was higher in the nitrogen dose with low ADF and higher in the year with the low ADF composition (Table 8).

Digestible Dry Matter Yield (kg ha⁻¹)

Nitrogen rate significantly affected digestible dry matter yield in the first year, in the second year, in average over the two years (Table 11).

The digestible dry matter yield increased in annual ryegrass in parallel to nitrogen application rate. In the first year, the digestible dry matter yield at 250 kg ha⁻¹ nitrogen rate was significantly higher than the those of rates other than 150 and 200 kg ha⁻¹. In the second year, the digestible dry matter yield at 250 kg ha⁻¹ nitrogen rate was

significantly higher than those in rates other than 200 kg ha⁻¹. In the two-year average values, the digestible dry matter yield at 250 kg ha⁻¹ nitrogen rate was significantly higher than in all other nitrogen rates (*Table 11*).

Digestible dry matter yield is a variable that depends on digestible dry matter content and dry matter yield. Therefore, digestible dry matter yield was high when both digestible dry matter ratio and dry matter yield were high (*Table 5, Table 10*).

Table 10. Digestible dry matter ratios (%) of annual ryegrass based on nitrogen fertilizer rates

Nitrogen (kg ha ⁻¹)	Years		
	2015	2016	Mean
0	62.69	62.68	62.68 ab*
50	61.85	61.89	61.87 b
100	61.92	61.78	61.85 b
150	62.51	62.93	62.72 a
200	61.16	62.63	61.90 ab
250	62.13	62.95	62.54 ab
300	62.29	62.87	62.58 ab
Mean	62.08 B ⁺	62.53 A	

* Values within the same columns followed by different small letters are significantly different based on Duncan's test at P < 0.05.

+ Values within the same row followed by different capital letters are significantly different based on Duncan's test at P < 0.05

Table 11. Average digestible dry matter yield values (kg ha⁻¹) of annual ryegrass based on nitrogen fertilizer rates

Nitrogen (kg ha ⁻¹)	Years		
	2015	2016	Mean
0	5370 d**	7110 c	6240 e
50	6500 bc	7470 bc	6985 cd
100	6080 cd	7040 c	6560 de
150	7000 abc	7900 bc	7450 bc
200	7260 ab	8130 ab	7695 b
250	7710 a	8970 a	8340 a
300	6620 bc	7260 bc	6940 cd
Mean	6648 B ⁺	7697 A	

** Values within the same columns followed by different small letters are significantly different based on Duncan's test at P < 0.01.

+ Values within the same row followed by different capital letters are significantly different based on Duncan's test at P < 0.05

Relative Feed Value (RFV)

According to the ANOVA results, nitrogen rates did not significantly affect the relative feed value in the first year. Nonetheless, relative feed values of the second year and two-year averages indicated that nitrogen rates had a significant effect on relative feed values in annual ryegrass (*Table 12*).

In the second year of the study and at the two-year averages, the lowest RFV was obtained from 200 kg ha⁻¹ nitrogen application. The relative feed value is calculated using the ADF and NDF ratios and has a negative correlation with the ADF and NDF ratios. Therefore, a high relative feed value is expected at low ADF and NDF composition values.

Colak and Sancak (2017) reported RFV of 111.2 in annual ryegrass at 240 kg ha⁻¹ nitrogen rate in a study conducted in Ankara. Kusvuran et al. (2014) reported RFV of 94.0 in annual ryegrass. RFV obtained from the present study is lower than the values reported in Colak and Sancak (2017) and higher than those reported in Kusvuran et al. (2014).

Caddel and Allen (1997) reported the relative feed value of completely headed wheat as lower than 77. Schroeder (2004) stated that the relative feed value decreases as the harvest time delayed, and Linn and Martin (1999) argued that the relative feed value of forage for high-milk yield dairy cows should be at least 124. The RFV obtained from the current study is below the stated value. RFV is a value obtained from ADF and NDF values. It is inversely proportional to ADF and NDF, and low RFV is obtained from high ADF and NDF values.

Table 12. The average RFV of annual ryegrass based on nitrogen fertilizer rates

Nitrogen (kg ha ⁻¹)	Years		
	2015	2016	Mean
0	106.4	114.5 a*	110.4 a**
50	104.2	104.6 b	104.4 bc
100	104.0	105.8 b	104.9 bc
150	105.0	107.5 ab	106.2 abc
200	100.9	103.3 b	102.1 c
250	106.5	109.6 ab	108.1 ab
300	108.9	108.5 ab	108.7 ab
Mean	105.1	107.6	

** Values within the same columns followed by different small letters are significantly different based on Duncan's test at P < 0.01

Conclusions

Forage crops produced in Turkey are not enough for animals. Therefore, meat and milk production is low. Annual ryegrass is a high yield and high quality alternative fodder plant due to its high growth rate and ability to absorb nitrogen. Annual ryegrass, fertilizer is a forage plant with high yield. The production of forage crops may increase with the determination of suitable fertilizer feeds. Meat and milk production can be increased by increasing forage crop production.

In this research, we aimed to determine the optimum rate of nitrogen fertilization to achieve high yield and high quality forage from annual ryegrass (*Lolium multiflorum* L.) in the Central Black Sea Climate Zone in Turkey. According to the results of the research, we conclude that (i) it is possible to obtain high yield and high forage quality with nitrogen fertilization under the conditions of Central Black Sea Climate Zone, (ii) application of 250 kg ha⁻¹ nitrogen rate is appropriate for high yield, (iii) increasing nitrogen doses do not affect the ADF and NDF rates, and (iv) yield decreases with 300 kg ha⁻¹ nitrogen application rate but the crude protein yield increases. For the annual ryegrass, 250 kg ha⁻¹ nitrogen rate is recommended to achieve high yield in the Central Black Sea Climate Zone in Turkey and possibly in similar ecological conditions.

REFERENCES

- [1] Acikgoz, E. (2001): Forage Crops. – Uludag University Empowerment Foundation Publication No: 182, VIPAS Publication No: 58, Bursa, 180-187p.
- [2] Alvim, M. J., Moojen, E. L. (1984): Effects of sources and rates of nitrogen and management practices on production and quality of ryegrass forages. – *Herbage Abst* 56: 387.
- [3] Anonymous (2001): Ministry of Agriculture and Forestry, TTSM Technical Instructions. – <https://www.tarimorman.gov.tr/BUGEM/TTSM/Sayfalar/Detay.aspx?SayfaId=62> (Last access:30.05.2019).
- [4] Anonymous (2017): Meteorology Provincial Directorate records, Tokat.
- [5] Avcioglu, R., Geren, H. (1996): Forage plants. – Harvest Publishing, İzmir.
- [6] Bartholomew, P. W., Willams, R. J. (1978): Nitrogen Requirement for Direct Drilled Ryegrass. – Joint Agricultural Research & Development Project, University College of North Wales, Bangor, UK and Ministry of Agriculture & Water, Saudi Arabia. Publication No.: 129.
- [7] Basbug, S. (1990): Research on the yield and quality of some perennial and one-year grasses forage crops in Bursa conditions. – Master Thesis, Uludag University Institute of Science and Technology, Bursa.
- [8] Baytekin, H., Kızılsimsek, M., Demiroglu, G. (2009): Grass and Discrete Types. – In: Avcioglu, R., Hatipoğlu, R., Karadağ, Y. (eds.) Forage Crops General Chapter Volume III. Ministry of Agriculture and Rural Affairs General Directorate of Agricultural Production and Development, İzmir, p. 561-572.
- [9] Bright, J., Desikan, R., Hancock, J. T., Weir, I. S., Neill, S. J. (2006): ABA-induced NO generation and stomatal closure in Arabidopsis are dependent on H₂O₂ synthesis. – *The Plant Journal* 45: 113-122.
- [10] Caddel, J., Allen, E. (1997): Forage Quality Interpretations. – <http://virtual.chapingo.mx/dona/paginaCBasicos/f-2117.pdf>. (Last Access: 14.03.2016).
- [11] Celen, A. E. (1991): Possibilities to benefit from one-year grass (*Lolium multiflorum* var. *Westerwoldicum*) in Aegean Region conditions. – Turkey 2. Grassland and Forage Crops Congress, 28-31 May 1991, EU Printing, İzmir, 424-4 29 p.
- [12] Cinar, S., Avci, M., Hatipoglu, R., Kizil Aydemir, E. S. (2011): A Research on Hay Yields of Some One - Year Grass Varieties. – 9. Field Crops Congress, Bursa 3: 1864-1867.
- [13] Colak, E. (2015): Effect of nitrogen fertilizer doses on grass yield, quality and some agricultural properties of grass (*Lolium italicum* L.) varieties. – Ankara University, Institute of Science and Technology, Field Crops Department, Ph.D. Thesis, 62 p Ankara.
- [14] Colak, E., Sancak, C. (2017): Effect of nitrogen fertilizer doses on grass quality of grass (*Lolium italicum* L.) varieties. – *Mediterranean Agri. Sci.* 30(3): 245-251.
- [15] Corainville, R. C. D., Mauet, A., Plancquaert, P. (1973): The intensive use of fertilizer for Ryegrass in the west. – *Bulletin Technique d'information* 281: 499-504.
- [16] Demiroglu, G., Avcioglu, R., Kir, B., Geren, H., Budak, B., Kavut, Y. T. (2007): A study on the performance of some grass forage crops in Mediterranean climate conditions. – Turkey VII. Field Crops Congress, 25-27 June 2007, Erzurum.
- [17] Duzgunes, O., Kesici, T., Kavuncu, O., Gürbüz, F. (1987): Research and Experimental Methods. – Ankara University, Faculty of Agriculture, Textbook Publication No. 1021, p. 381, Ankara.
- [18] Erkun, V. (1954): Seed Production Methods of Meadow and Rangeland Plants. – Central Research Institute of Animal Husbandry, Ankara.
- [19] Genckan, M. S. (1983): Forage Crops Agriculture. – Ege University Faculty of Agriculture, p. 520, İzmir.
- [20] Gokmen, S., Sencar, Ö., Sakin, M. A. (2001): Response of Popcorn (*Zea mays evarta*) to Nitrogen Rates and Plant Densities. – *Türk J. Agric. For.* 25: 15-23.

- [21] Kacar, B. (2016): Plant, Soil and Fertilizer Analysis. – Nobel Publications, Publication No.: 1524, Ankara.
- [22] Kallenbach, R., Massie, M., Crawford, R. (2003): Nitrogen fertilization strategies for annual ryegrass pastures. – University of Missouri Extension.
- [23] Karakurt, E., Ekiz, H. (1991): The effect of mixture of Alexandria trifolium (*Trifolium alexandrinum* L.) and grass (*Lolium multiflorum* Lam.) on herbage yield. – Ankara University, Faculty of Agriculture 1999(44): 97-104.
- [24] Kesiktas, M. (2010): The effects of different sowing times and nitrogen fertilizer dose applications on the yield of grass (*Lolium multiflorum westervoldicum* Caramba) in Karaman. – Cukurova University, Institute of Science and Technology, Field Crops Department, Master Thesis, 59 p., Adana.
- [25] Kun, E. (1994): Cereals II (Warm season Cereals). – Ankara University Faculty of Agriculture Publications, 1452, Ankara.
- [26] Kusvuran, A., Tansi, V. (2005): Determination of the effect of different form number and nitrogen dose on one-year grass (*Lolium multiflorum* cv. Caramba) grass and seed yield in Cukurova conditions. – Turkey VI. Field Crops Congress, 5-9 September 2005, Antalya, Research Presentation II: 797-802.
- [27] Kusvuran, A. (2011): The effects of different nitrogen doses on herbage and seed yields of annual ryegrass (*Lolium multiflorum* cv. Caramba). – African Journal of Biotechnology 10(60): 12916-12924.
- [28] Kusvuran, A., Kaplan, M., Nazlı, R. İ. (2014): Effects of ratio and row spacing in hungarian vetch (*Vicia pannonica* Crantz.) and annual ryegrass (*Lolium multiflorum* Lam.) intercropping system on yield and quality under semi arid climate conditions. – Turkish Journal of Field Crops 19(1): 118-128.
- [29] Linn, J. G., Martin, N. P. (1999): Forage Quality Tests and Interpretations. – In: Kallenbach, R., Massie, M., Crawford, R. (eds.) Nitrogen fertilization strategies for annual ryegrass pasture. University of Missouri Extension, USA.
- [30] Meeske, R., Botha, P. R., Van Der Merwe, G. D., Greyling, J. F., Hopkins, C., Marais, J. P. (2009): Milk production potential of two ryegrass cultivars with different total non-structural carbohydrate contents. – South African Journal of Animal Science 39(1).
- [31] Ozdemir, S., Budaklı, Carpici, E., Asik, B. B. (2019): Effects of Different Nitrogen Doses on Herb Yield and Quality of Grass. – KSU J.Agric. Nat 22(1): 131-137.
- [32] Ozkul, H., Kirkpınar, F., Tan, K. (2012): The use of Caramba (*Lolium multiflorum* cv. Caramba) grass in ruminant feeding. – Animal Production 53(1): 21-26.
- [33] Parlak, A. O., Akgul, F., Gokkus, A. (2007): The effects of sowing and nitrogen fertilization on one year grass (*Lolium multiflorum* Lam.) Grass yield and quality under different row spacing in Ankara conditions. – Turkey VII. Field Crops Congress, 25-27 June 2007, Erzurum, Presentation with Presentation: 139-142 p.
- [34] Pavinato, P. S., Restelatto, R., Sartor, L. R., Paris, W. (2014): Production and nutritive value of ryegrass (cv. Barjumbo) under nitrogen fertilization. – Revista Ciência Agronômica 45(2): 230-237.
- [35] Piskin, M. (2007): Effects of different seed amounts on yield and some yield components of perennial grass (*Lolium multiflorum* Lam). – Master Thesis. Selcuk University. Graduate School of Natural and Applied Sciences, Konya, 46 p.
- [36] Schroeder, J. W. (2004): Forage Nutrition for Ruminants, AS-1250. – www.ag.ndsu.edu.tr. (Last access: 24.01.2012).
- [37] Seker, H. (1992): Effects of different nitrogen doses and seed amounts on the yield and some chemical properties of the grass in Multimo cultivar (*Lolium multiflorum* Lam.). – Atatürk University, Institute of Science and Technology, Field Crops Department, Master Thesis, 52 p., Erzurum.
- [38] Serin, Y., Tan, M. (2001): Introduction to Forage Crop Culture. – Atatürk University Faculty of Agriculture Publications, No: 206, 217 p., Erzurum.

- [39] Sheaffer, C. C., Peterson, M. A., Mc Caslin, M., Volenec, J. J., Cherney, J. H., Johnson, K. D., Woodward, W. T., Viands, D. R. (1995): Acid detergent fiber, neutral detergent fiber concentration and relative feed value. – Available from URL: <https://www.umvotiagri.co.za/linked/adf%20ndf%20in%20silage.pdf>. (Last access 23.12.2014).
- [40] Simic, A., Vucković, S., Kresović, M., Vrbničanin, S., Božić, D. (2009): Changes of crude protein content in ryegrass influenced by spring nitrogen application. – *Biotechnology in Animal Husbandry* 25(5-6): 1171-1179.
- [41] Simsek, S. (2015): A study on the effects of different Hungarian vetch (*Vicia pannonica* Crantz) and one-year turf (*Lolium multiflorum* Lam.) Mixture ratios on yield and quality in Kırşehir conditions. – Ahi Evran University, Institute of Science and Technology, Field Crops Departmen, Kırşehir.
- [42] Sleugh, B., Moore, K. J., George, J. R., Brummer, E. C. (2000): Binary legume – grass mixtures improve forage yield, quality, and seasonal distribution. – *Agronomy Journal* 92: 24-29.
- [43] TAN (1995): The determination of nitrogen according to kjeldahl using block digestion and steam distillation. – Tecator Application Note AN 300, Tecator AB Sweden: 1-11.
- [44] Teutsch, C., Smith, R. (2001): Does annual ryegrass fit into Virginia's pasture systems? – *Crop and soil environmental news*, September, USA.
- [45] Van Soest, P. J., Robertson, J. B., Lewis, B. A. (1991): Methods for Dietary Fiber, Neutral Detergent Fiber, and Nonstarch Polysaccharides in Relation to Animal Nutrition. – *J. Dairy Sci.* 74: 3583-3597.
- [46] Viviani Rossi, E. M., Gutierrez, L. M., Moreno, E., Mazzanti, A. (1994): Nitrogen fertilizer effects upon silage composition and quality of *Lolium multiflorum* L. – CC 276 (7620) Argentina.
- [47] Yavuz, M. (2005): Detergent Fiber System. – *Journal of Gaziosmanpasa University, Faculty of Agriculture* 22(1): 93-96.

YIELD RESPONSE OF WINTER WHEAT (*TRITICUM AESTIVUM* L.) TO WATER STRESS IN NORTHERN CHINA: A META-ANALYSIS

JING, B. H. – WANG, C. – KHAN, S. – YUAN, Y. C. – YANG, W. D.* – FENG, M. C.*

*College of Agriculture, Shanxi Agricultural University, Taigu, China
(phone: +86-1580-3431-035)*

**Corresponding authors*

e-mail: sxauywd@126.com; phone: +86-1383-4835-129 (Yang, W. D.)

e-mail: fmc101@163.com; phone: +86-1383-4838-834 (Feng, M. C.)

(Received 7th Sep 2019; accepted 14th Nov 2019)

Abstract. Water deficit is one of the main environmental constraints affecting the yield of winter wheat. We quantified the effect of water stress on the grain yield of winter wheat in northern China, by using meta-analysis method. Database was obtained through 1921 experimental observations derived from 53 research articles of the 2000 to 2017 period. The results showed that the grain yield was significantly affected by the water and latitude. Grain yield and number of spikes (ha^{-1}) increased with the total water from $1001 \text{ m}^3 \text{ ha}^{-1}$ to $4000 \text{ m}^3 \text{ ha}^{-1}$. However, grain yield and number of spikes did not increase further at higher rates ($>4000 \text{ m}^3 \text{ ha}^{-1}$). The grain yield, number of spikes and thousand grain weight were higher at a total water of $1\text{-}1000 \text{ m}^3 \text{ ha}^{-1}$, than those at $1001\text{-}2000 \text{ m}^3 \text{ ha}^{-1}$. Water stress had no significant effect on grain number per ear. The grain yield first increased with the latitude to a maximum of $36\text{-}37^\circ$ and then decreased with increasing latitude ($>37^\circ$). In conclusion, the maximum yield of winter wheat was attained at $36\text{-}37^\circ$ latitude and $3001\text{-}4000 \text{ m}^3 \text{ ha}^{-1}$ total water.

Keywords: *crop, drought stress, yield components, latitude, integrated analysis*

Introduction

Water is essential for ensuring agricultural productivity. As a result of global warming, water shortages are becoming a major problem affecting the sustainable production of global crops (Sauer et al., 2010; Cai et al., 2011). Studies have shown that the frequency and intensity of droughts will be increased in future, which may lead to severe declines in future crop yield (Dai, 2012; Daryanto et al., 2016). The wheat (*Triticum aestivum* L.) which is the second largest cereal crop in the world is very susceptible to water stress (Reyer et al., 2013). Under water stress, plants tend to close leaf stomata to reduce transpiration loss, which adversely affects its physiological processes and nutrient uptake finally leading to the decreased yield (Rossini et al., 2013; Zhang et al., 2017a). The yield components (spike number, grain number, and grain weight) directly affect the formation of wheat yield. Moderate drought can affect grain weight, and severe water shortage will lead to an obvious decrease in the spikelets and grain numbers (Giunta et al., 1993). Moderate water stress occurred at a certain stage of wheat, after re-watering could make a positive effect on the growth and developments of wheat and its yield compensation. Therefore, it is not always necessary to maintain sufficient water throughout the growing period of wheat, which may cause excessive vegetative growth and lower the economic coefficient. Moreover, due to the uneven distribution of water resources in region and time in China, and the traditional irrigation rate is always excessive which is 1~1.5 times than the demand of crops, the problem of low water efficiency seriously restricts China's agricultural development (Du et al.,

2010; Wei et al., 2018). Therefore, how to scientifically use water, how to improve water use efficiency, and how to formulate effective water-saving agricultural practices are major issues that needs to be urgently solved in current years.

The degree of water stress of wheat in different regions is different, and the influence of temperature on it can't be ignored. Temperature is critical for controlling winter wheat growth and yield (Asseng et al., 2011; Farhangfar et al., 2015). Water stress is expected to increase in the future, and water stress may reduce crop yields in many parts of the world (Qin et al., 2018). Increased temperature shortens the duration of the wheat growing season, resulting in a decline in yield, and Temperature differences in different regions also indicate differences in latitude. Latitude is an important geographic factor that significantly affects temperature, sunshine hours and crop growth (Liu et al., 2013b). However, under different degrees of water stress, the variation of wheat yield with latitude remains to be studied. Therefore, this paper studied the variation of wheat yield under different degrees of water stress, and hoped that the results could improve our quantitative understanding of the impact of water stress on wheat yield in China.

Meta-analysis can quantitatively synthesize existing test data, systematically analyze the combined effects and influencing factors of specific measures, and determine the general trends in many independent experiments (Hedges et al., 1999). At present, most of the experiments on wheat water stress focus on the scale of individual test sites, and the results are not consistent due to differences in factors such as climate, soil and planting system. Therefore, present study was designed to study the effect of water stress and latitude on the yield and yield components of winter wheat in northern China based on the meta-analysis method.

Materials and methods

Data collection and classification

Various English (Web of Science, Google Scholar, Science Direct, Wiley online library, Springer) and Chinese (CNKI) databases were searched by using keywords: wheat, yield, water stress, water deficiency, China and their combinations. The articles related with water stress on winter wheat in China from 2000-2017 were collected and screened on the basis of the following criteria: (1) area was located in northern China and year and latitude and longitude of the test site was clearly mentioned; (2) the test plot was a field whereas pot experiments were not included; (3) the experimental study had a water stress treatment and also a well-watered control; (4) only the water stress as treatment along with control, and yield data were collected in the multi-factor study, whereas, other treatments were routinely processed in the local field. As a result of screening, 53 research articles containing 486 sets of data and 1921 test observations were obtained (*Fig. 1*). The distribution of study site was shown in (*Fig. 2*).

The sum of the irrigation rate and rainfall during the growth period of wheat (if test areas have no canopy to protect from rainfall) was taken as the total water, in order to investigate the effect of different the total water on winter wheat yield the collected data were classified into 5 irrigation ranges (*Table 1*). The treatment with no external irrigation and rainfall was taken as the control in study (total water is 0). Latitude of each test site was divided into four categories as: 34-35°, 35-36°, 36-37°, >37°, and 34-35° was taken as the control. Moreover, as only one experimental site having latitude <34° was obtained, which is not enough for meta-analysis, so this latitude was excluded (Red sites in *Fig. 2*).

Study site

The study site is located at 34°-39° north latitude and 103°-121° east longitude, in the Loess Plateau and the North China Plain (Fig. 2). It is dry in winter and has four distinct seasons and the coldest is in January, the precipitation is 400-800 mm and is concentrated in July and August and it belongs to monsoon climate of medium latitudes and temperate continental climate. The soil is mainly cinnamon soil and loessial soil. The cinnamon soil has a neutral to slightly alkaline reaction, the middle and lower parts have the accumulation of clay particle and calcium. The loessial soil is soft soil and organic matter content is low, has strong calcareous reaction and good water permeability and cultivability.

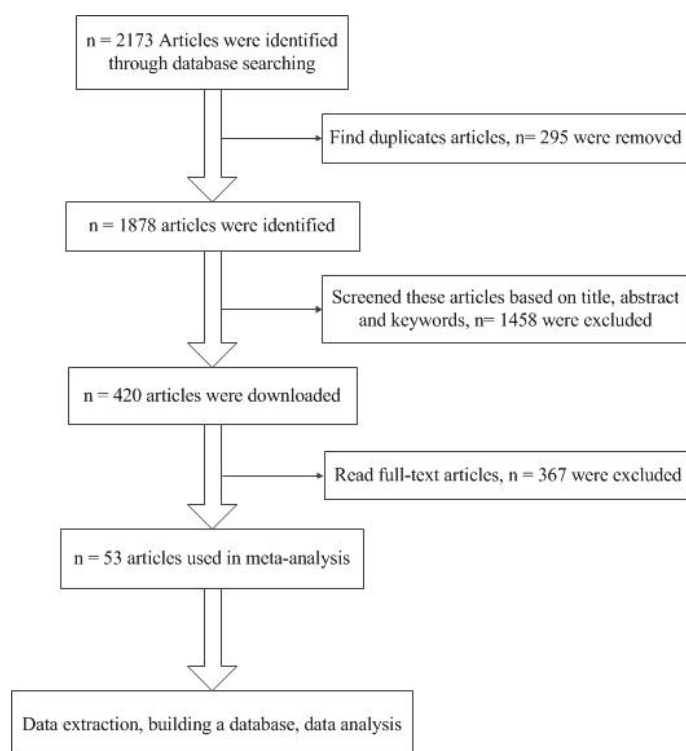


Figure 1. Flowchart of the process of building the database and meta-analysis

Data processing

Data analysis was performed using the integrated analysis method described by Hedges and Olkin (Hedges and Olkin, 1985). The effect size of water stress on GY, SN, GN and GW was evaluated by standardized mean difference (SMD), which is the relative value of the overlap between the two sets of data, and reflects the difference and representativeness between each other:

$$g = \frac{(\bar{X}_E - \bar{X}_C)}{S_{\text{within}}} \left(1 - \frac{3}{4(N_C + N_E - 2) - 1}\right) \quad (\text{Eq.1})$$

$$S_{\text{within}} = \sqrt{\frac{(N_E - 1)(S_E)^2 + (N_C - 1)(S_C)^2}{N_E + N_C - 2}} \quad (\text{Eq.2})$$

$$V_g = \left(\frac{N_C + N_E}{N_C N_E} + \frac{d^2}{2(N_C + N_E)} \right) \left(1 - \frac{3}{4(N_C + N_E - 2) - 1} \right)^2 \quad (\text{Eq.3})$$

where \bar{X}_E and \bar{X}_C are the average values of the treatment and the control group, g is standardized mean difference; N_E and N_C are the number of samples for the treatment and control groups; V_g is the variance of the independence study; S_E and S_C were the standard deviations of all comparisons between treatment and control, respectively, and S_{within} was the composite standard deviation within each study group. When studies do not report standard deviation, the missing standard deviation values were estimated by calculating the average coefficient of variation between each data set.

The combined effects and confidence intervals were calculated as follows:

$$W = \frac{1}{V_g} \quad (\text{Eq.4})$$

$$M = \frac{\sum_{i=1}^k W_i g_i}{\sum_{i=1}^k W_i} \quad (\text{Eq.5})$$

$$V_M = \frac{1}{\sum_{i=1}^k W_i} \quad (\text{Eq.6})$$

$$SE_M = \sqrt{V_M} \quad (\text{Eq.7})$$

$$LL_M = M - 1.96 * SE_M, \quad UL_M = M + 1.96 * SE_M \quad (\text{Eq.8})$$

In the equation, W is the weight of each independent study; M is the weighted mean; VM is the variance of the combined effect; SE_M is the standard error of the combined effect; LL_M and UL_M are the upper and lower limits of the 95% confidence interval.

The relevant indicators in study were continuous variables, and the standardized mean difference after the integrated analysis represented the effect of different total water on wheat yield under water stress. Variables GY, SN, TGW and GN under different total water were calculated by the fixed- or random-effects model using software Revman (version 5.3, The Cochrane Collaboration, 2014). In this study, the inverse variance and the standardized mean difference were used as the effect size of the statistical measures and the meta-analysis, respectively. Random-effect model was used for moderate to high heterogeneity ($I^2 > 50\%$ and a chi-square P -value < 0.05) (Smithers et al., 2008). The heterogeneity test of the data in this paper reached a significant level ($P_Q < 0.05$), so a random effects model was used. The difference between total water and the control was measured by the number of samples and the standard deviation. Confidence interval was finally generated by the effect size. If the 95% confidence interval size for a variable didn't cover 0, it indicated that irrigation treatment had a significant effect on yield compared to control. Engauge digitizer was used to extract data such as histograms in paper.

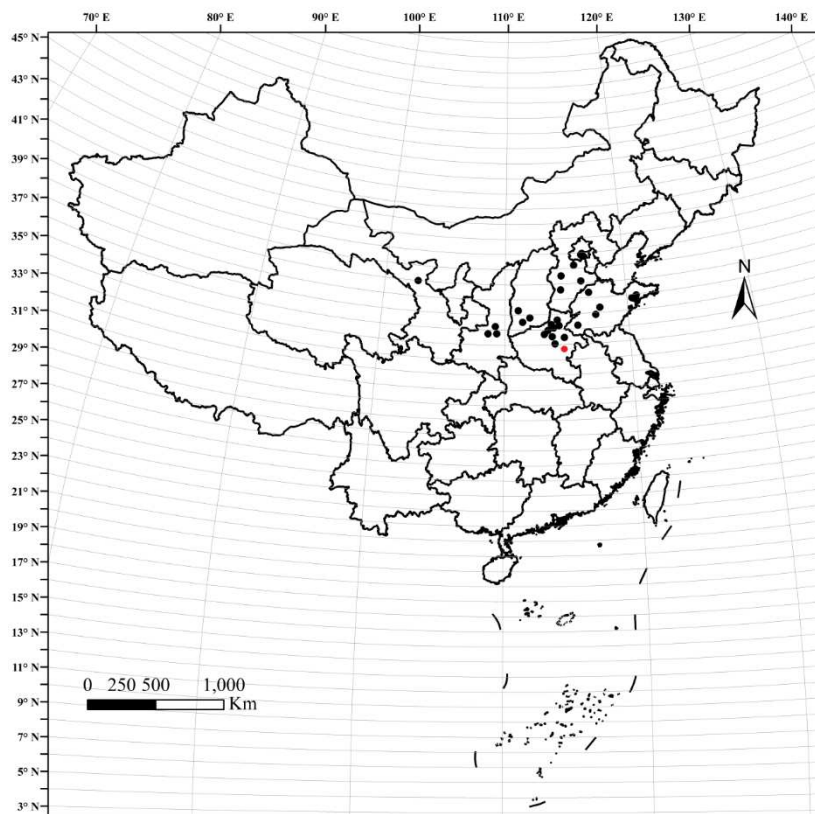


Figure 2. Distribution of selected experimental sites studied in this meta-analysis in northern China

Table 1. Variables included in the meta-analysis

Category	Variables	Abbreviations
Yield	Grain yield	GY
	Spike number	SN
	Grain number	GN
	Thousand grain weight	TGW
Total water (m ³ ha ⁻¹)	1-1000	W1
	1001-2000	W2
	2001-3000	W3
	3001-4000	W4
	>4000	W5

Results

Heterogeneity test analysis

The obtained data was analyzed by heterogeneity test and the results are shown in (Table 2). Results showed that the P-values of the meta-analysis of GY, SN and TGW were all less than 0.05, which indicated the data were statistically significant and can be used for further meta-analysis. However, the meta-analysis P-value for GN was greater than 0.05, which mean it was not statistically significant. All P-value of heterogeneity test were greater than 0.05 and I^2 was less than 50%, indicating that there was no significant heterogeneity in each group of data.

Table 2. Heterogeneity analysis of yield and yield components of winter wheat under different total water

Variables		No. of samples	Meta-analysis (<i>P</i> -value)	Heterogeneity	
				I ² (%)	Chi-square test (<i>P</i> -value)
GY(kg ha ⁻¹)	W1	51	<0.0005	4	0.21
	W2	117	<0.00001	0	0.33
	W3	189	<0.00001	17	0.46
	W4	103	<0.00001	21	0.27
	W5	72	<0.0001	18	0.32
SN (10 ⁴ × ha ⁻¹)	W1	33	0.03	0	0.83
	W2	89	0.005	0	0.70
	W3	125	<0.0001	1	0.66
	W4	73	<0.0001	12	0.40
	W5	56	0.008	4	0.44
TGW(g)	W1	32	0.01	8	0.13
	W2	101	<0.0001	5	0.18
	W3	138	<0.00001	33	0.06
	W4	71	0.002	23	0.09
	W5	49	0.03	12	0.20
GN	W1	45	0.12	0	0.84
	W2	103	0.08	0	0.91
	W3	135	0.06	0	0.81
	W4	89	0.06	0	0.77
	W5	70	0.1	0	0.88

GY: grain yield; SN: spike number per hectare; TGW: thousand grain weight; GN: grain number per ear; W1, W2, W3, W4 and W5 were total water

Response of wheat yield to water stress

A meta-analysis of winter wheat yield in northern China showed that GY was affected by different total water (Fig. 3). The 95% confidence interval of GY effect size did not overlap with 0 indicating that the total water had a significant positive effect on GY. GY increased gradually with increasing the total water from W2 to W4. The GY reached the maximum at W4 and was decreased at W5. The GY at W1 was slightly higher than W2. The average increase of GY at W4 was 148% relative to control.

Response of wheat yield components to water stress

The results indicated the SN and TGW were significantly affected by total water (Fig. 4). The SN and TGW at W1 were higher than W2, and SN was increased by increasing total water from W2 to W4. The SN at W4 was 39.7% higher than control. The TGW was highest at W3, which was 79.7% higher than control. The 95% confidence interval of GN effect size contains 0, which indicate that different total water have no significant effect on GN.

Effect of latitude on winter wheat yield

It can be seen that winter wheat yield under different total water responded differently at different latitudes (Fig. 5). The GY at total water of W0, W2, W3 and W4 was significantly positive effect by increasing the latitudes (35-36°, 36-37°, and >37) as

compared to 34-35° (control). At W0, W2, W3 and W4, the grain yield was first increased with increasing the latitude and then decreased with the highest GY was recorded at 36-37° latitude. However, at latitudes of 35-36° and > 37°, the GY of W5 (total water >4000 m³ ha⁻¹) has a negative impact, as compared to 34-35° (control). The effect of latitude 36-37° was non-significant on GY at W5.

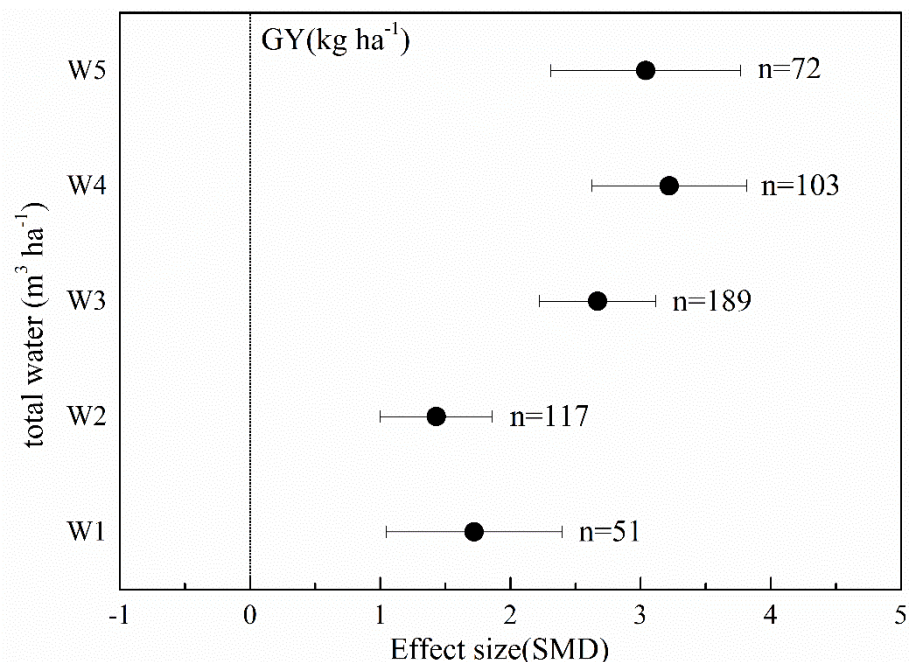


Figure 3. The relative effect size of grain yield of winter wheat under different total water, error bars represent 95% confidence interval, and n values represent the corresponding number of observations. SMD: standardized mean difference; GY: grain yield

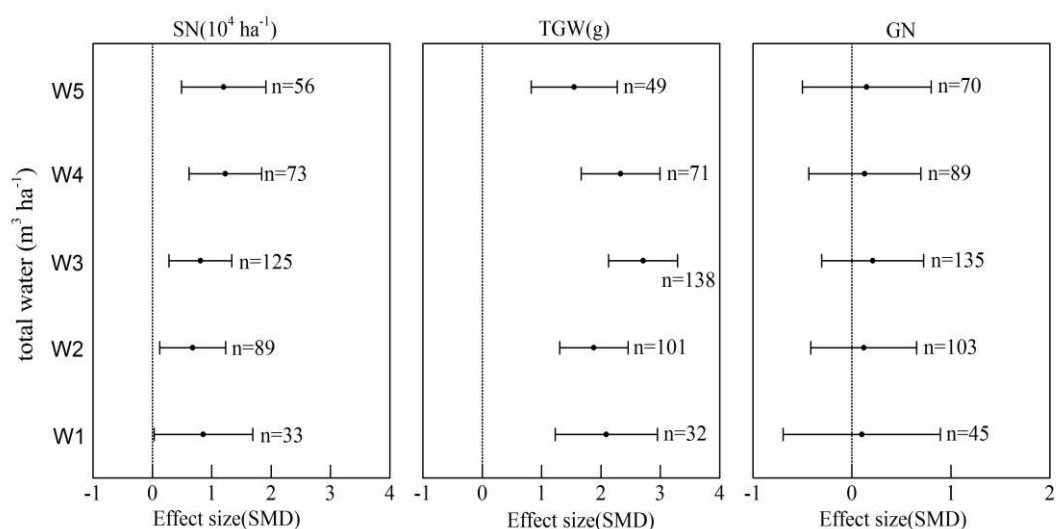


Figure 4. The relative effect size of SN, TGW and GN of winter wheat at different total water, error bars represent 95% confidence interval, n values represent the corresponding number of observations. SMD: standardized mean difference; SN: spike number per hectare; TGW: thousand grain weight; GN: grain number per ear

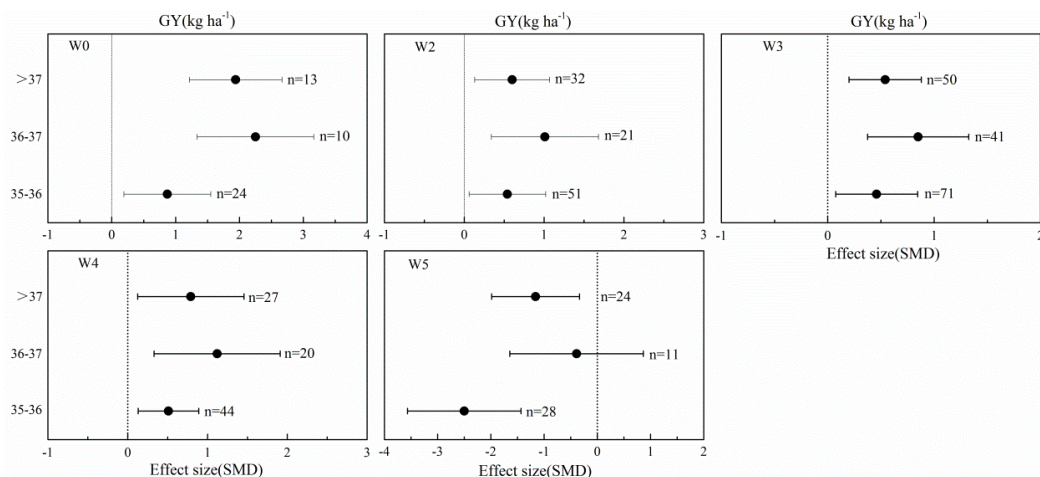


Figure 5. The effect of different latitudes on the grain yield of wheat under different total water, error bars represent 95% confidence interval, and n values represent the corresponding number of observations. W0: total water 0-1000 m³ ha⁻¹; W2: total water 1001-2000 m³ ha⁻¹; W3: total water 2001-3000 m³ ha⁻¹; W4: total water 3001-4000 m³ ha⁻¹; W5: total water >4000 m³ ha⁻¹

Discussion

Water plays a pivotal role in nutrient availability and other physiological processes, and a major determinant of crop yield (Adu et al., 2018). It is well known that differences in water stress can lead to differences in yield. In this study, the grain yield, spikelet numbers and thousand grains weight of winter wheat were decreased with the decrease of the total water. Previous reports have shown that wheat yield decreased with increasing the degree of water stress (Zhang et al., 2016; Jin et al., 2018). Plants responds to water stress by closing the stomatal pores in order to reduce transpiration losses, resulting in insufficient photosynthesis, reduction in crop growth, biomass accumulation and yield (Guerfel et al., 2009; Mäkinen et al., 2018). Studies have shown that spikelet numbers, grain number and thousand grains weight were directly related to wheat yield and reduced under drought stress (Shamsuddin, 1987; Kiliç and Yağbasanlar, 2010). Moderate drought affects post-anthesis biomass production and transport of photosynthetic products to kernels, thereby affecting grain weight and reducing grain yield (Liu et al., 2016). Therefore, the yield was decreased with decreasing the total water from W4 (3001-4000 m³ ha⁻¹) to W2 (1001-2000 m³ ha⁻¹). However, the effect values of grain yield, spikelet numbers and thousand grains weight at W1 (1-1000 m³ ha⁻¹, severe water stress) were greater than W2 (1001-2000 m³ ha⁻¹). It may be due to the reason that drought triggers the antioxidant activity in plants and up-regulated the function of photosynthesis organs, improve leaf chlorophyll and Rubisco content through improved leaf water potential and improved photoprotection (Crafts-Brandner and Law, 2000; Abid et al., 2016). The increase in yield under W1 as compared to W2 may be related to the amount of nitrogen applied and the efficiency of nitrogen use. Proper nitrogen supply can increase cell number and volume, increase leaf photosynthetic rate and WUE, and mitigate the effects of drought stress. At low tissue water potential, nitrogen reduced the effects of drought stress on grain yield by maintaining metabolic activity, increasing leaf water potential, membrane stability index, and antioxidant activity (Zhang et al., 2007; Abid et al., 2016). Nitrogen use efficiency is generally increased in crops under water stress and higher nitrogen

application rates increases crop drought resistance (Zhang et al., 2017b). Therefore, suitable application of water and nitrogen could enhance material accumulation, improve photosynthetic capacity, and promote grain formation. Although the data of normal nitrogen application in each experiment were extracted from this study, however, it is still impossible to rule out the effect of different nitrogen application rates on the results.

In addition, root distribution (> 0.8 m) of wheat in deep soils is critical for nutrient and water uptake, affecting wheat growth and grain yield (Dai et al., 2014; Xu et al., 2016). On the one hand, the response of wheat root system to water shortage is reduced redundancy of top root growth and increased growth of deeper roots (Song et al., 2009; White and Kirkegaard, 2010), thereby enhancing the ability of roots to absorb nutrients and water (Kaisermann et al., 2017). Some microbial groups can increase plant drought tolerance by increasing root biomass and depth to absorb water and nitrogen from deep soils to maintain growth and maintain yield (Azarbad et al., 2018; Liu et al., 2018). Under the condition of water shortage, the water evapotranspiration was decreased in the aboveground part, and more photosynthetic products were stored in the root system to improve water use efficiency. Under drought stress, nitrogen deficiency leads to increased vertical root permeability, reduced top root length density, and increased roots in deeper soil, thereby affecting grain yield (Wang et al., 2014; Xu et al., 2016). Therefore, when the total water is W1, the wheat yield will increase slightly, which may be the result of the wheat itself coping with stress, enhancing photosynthesis, increasing water and nitrogen use efficiency, and increasing the growth of deep roots.

It is well known that wheat production increased with increasing irrigation rate within a certain range, but as irrigation reached a certain level, WUE and yield were decreased (Trout and Dejonge, 2017; Jin et al., 2018). This study showed that the grain yield, spikelet numbers and grain weight of winter wheat were decreased by increasing total water from W4 to W5. Studies have shown that excessive irrigation reduced wheat yield mainly because of leaching of root nitrate due to excessive irrigation, resulting in insufficient nitrogen supply, causing premature root senescence and inhibiting photosynthesis, thereby reducing water and nitrogen use efficiency (Agami et al., 2018). Similarly, in loamy silty soil, excessive water tends to cause hypoxia in the root zone of the crop, thereby damaging the roots and reducing yield (Mäkinen et al., 2018). In addition, excessive irrigation of wheat can easily lead to lodging, leaf rust or mildew, affecting normal wheat growth (Bennett, 1984; Roelfs et al., 1992).

Previous studies showed that drought stress significantly reduced spikelet numbers, grain numbers and grain weight of wheat, and reduction in grain numbers had the greatest direct impact on grain yield (Simane et al., 1993). However, in the present study, water stress had no significant effect on grain numbers. Wheat grain yield formation and grain number are genetically controlled but also affected by the environment (Wang et al., 2014). The drought resistance and yield potential of different varieties were different in the 53 collected studies. For example, water stress was applied during wheat microspore stage, and drought resistant wheat variety SYN604 was having more number of grains than Sundor which is drought resistant variety (Ji et al., 2010). In addition, the stage of differentiation of young spikes before flowering is the key period for the formation of GN, this period determines the number of fertile flowers in wheat spikelets, which determines GN. Studies have shown that during meiosis of pollen development in wheat, water stress blocks the relationship between pollen grains and tapetal layer during microspore stage, degenerates the filaments, and

the pollen grains cannot accumulate starch, resulting in nutrient deficiency and affecting pollen development, leads to a decrease in GN (Saini et al., 1984; Cattivelli et al., 2008). Moreover, under severe water stress, the use of male sterile materials to study the effects of wheat microspores stage on GN found that GN were decreased by 16.4% (Ji et al., 2010), even under mild water stress, starch accumulation and sucrose transport in the ovary are also severely affected. It indicated that the development of ovary under water stress had a certain effect on GN. Some studies have shown that under water stress, the cell wall invertase viability of sucrose transport in wheat anthers is related to pollen sterility, which is characterized by decreased cell wall invertase viability, blocked sucrose transport, and a large accumulation of sucrose in anthers, causes changes in the metabolism of other soluble sugars leading to infertility (Dorion et al., 1996; Koonjul et al., 2005; Ji et al., 2010). It can be seen that the reason that the water stress has no significant effect on GN may be due to the combined effects of variety and water in this study.

Latitude is an important geographic factor which affects temperature and solar radiation, thus affecting the duration of crop growth and yield (Liu et al., 2010, 2013b). This study showed that under different irrigation rate (except $>4000 \text{ m}^3 \text{ ha}^{-1}$), with the increase of latitude, the yield was first increased and then decreased. The maximum yield was attained at $36\text{-}37^\circ$. Similarly, Li (2010) indicated that with the increase of latitude in Henan Province, the yield of different wheat varieties was increased first and then decreased. Due to the large latitude span of China's wheat growing areas, the temperature difference is large, and the effect of temperature changes on wheat yield is not negligible (Asseng et al., 2011). In this study, the yield at latitude $35\text{-}36^\circ$ (except for $>4000 \text{ m}^3 \text{ ha}^{-1}$) was lower than $36\text{-}37^\circ$, which might be due attributed to the high temperature at low latitude and increasing temperature resulting in decrease of yield. There are significant changes in climatic variables at different altitudes, which in turn affect the development and yield of winter wheat (Xiao et al., 2008). Dryland wheat yield is highest at medium elevations with sufficient precipitation and mild temperatures. At high elevations, temperatures are too low to allow the crops to mature with fewer yields.

Higher temperatures shorten the wheat growing season, which leads to a shortening of the grain filling period and a decrease in wheat yield (Dias and Lidon, 2010; Xiao et al., 2010; Asseng et al., 2011). The decline in wheat yield with increasing temperature is mainly due to less spikelet numbers (Asseng et al., 2015). Elevated temperatures also increase evapotranspiration (Trnka et al., 2012; Liu et al., 2013a), reducing soil water content, increasing water stress, and thereby reducing wheat yield (Qin et al., 2018; Li et al., 2019). At high altitude, the wheat yield might be affected by various other interacting factors such as region, climate, variety, soil texture (Tapley et al., 2013; Daryanto et al., 2016; Zhang et al., 2017b).

Conclusion

The results from meta-analysis method showed that the grain yield, spikelet number and grain weight of winter wheat were significantly affected by the total water, whereas, effect of total water was not significant on grain number. Yield and yield components were not increased by increasing total water from W1 ($1\text{-}1000 \text{ m}^3 \text{ ha}^{-1}$) to W2 ($1001\text{-}2000 \text{ m}^3 \text{ ha}^{-1}$). Grain yield and spike numbers were increased by further increasing total water with maximum at W4 ($3001\text{-}4000 \text{ m}^3 \text{ ha}^{-1}$). At W4, grain yield

and spike numbers were 148.5% and 39.7% higher as compared to control, indicating that W4 was optimal total water. Thousand grain weight was highest at W3 (2001-3000 m³ ha⁻¹) with 79.7% increase as compared to control (total water is 0). Under different total water, grain yield was increased with increasing latitude from 35-36° to 36-37° and then decreases at latitude > 37°, and the specific reasons for decline in yield at high latitude remain to be further studied.

Acknowledgements. This work was supported by National Natural Science Foundation of China (31871571, 31371572), Outstanding Doctor Funding Award of Shanxi Province (SXYBKY2018040), Key Technologies R&D Program of Shanxi Province (201603D221037-3) and China Postdoctoral Science Foundation (2017M621105).

REFERENCES

- [1] Abid, M., Tian, Z. W., Ata-Ul-Karim, S. T., Liu, Y., Cui, Y. K., Zahoor, R. (2016): Improved tolerance to post-anthesis drought stress by pre-drought priming at vegetative stages in drought-tolerant and -sensitive wheat cultivars. – *Plant Physiology and Biochemistry* 106: 218-227.
- [2] Adu, M. O., Yawson, D. O., Armah, F. A., Asare, P. A., Frimpong, K. A. (2018): Meta-analysis of crop yields of full, deficit, and partial root-zone drying irrigation. – *Agricultural Water Management* 197: 79-90.
- [3] Agami, R. A., Alamri, S. A. M., El-Mageed, T. A. A., Abousekken, M. S. M., Hashem M. (2018): Role of exogenous nitrogen supply in alleviating the deficit irrigation stress in wheat plants. – *Agricultural Water Management* 210: 261-270.
- [4] Asseng, S., Foster, I., Turner, N. C. (2011): The impact of temperature variability on wheat yields. – *Global Change Biology* 17(2): 997-1012.
- [5] Asseng, S., Ewert, F., Martre, P., Rötter, R. P., Lobell, D. B., Cammarano, D., Kimball, B. A., Ottman, M. J., Wall, G. W., White, J. W., Reynolds, M. P., Alderman, P. D., Prasad, P. V. V., Aggarwal, P. K., Anothai, J., Basso, B., Biernath, C., Challinor, A. J., De Sanctis, G., Doltra, J., Fereres, E., Garcia-Vila, M., Gayler, S., Hoogenboom, G., Hunt, L. A., Izaurralde, R. C., Jabloun, M., Jones, C. D., Kersebaum, K. C., Koehler, A.-K., Müller, C., Naresh Kumar, S., Nendel, C., O’Leary, G., Olesen, J. E., Palosuo, T., Priesack, E., Eyshi Rezaei, E., Ruane, A. C., Semenov, M. A., Shcherbak, I., Stöckle, C., Stratonovitch, P., Streck, T., Supit, I., Tao, F., Thorburn, P. J., Waha, K., Wang, E., Wallach, D., Wolf, J., Zhao, Z., Zhu, Y. (2015): Rising temperatures reduce global wheat production. – *Nature Climate Change* 5: 143-147.
- [6] Azarbad, H., Constant, P., Giard-Laliberté, C., Bainard, L. D., Yergeau, E. (2018): Water stress history and wheat genotype modulate rhizosphere microbial response to drought. – *Soil Biology & Biochemistry* 126: 228-236.
- [7] Bennett, F. G. A. (1984): Resistance to powdery mildew in wheat: a review of its use in agriculture and breeding programmes. – *Plant Pathology* 33: 279-300.
- [8] Cai, X. L., Molden, D., Mainuddin, M., Sharma, B., Ahmad, M. D., Karimi, P. (2011): Producing more food with less water in a changing world: assessment of water productivity in 10 major river basins. – *Water International* 36(1): 42-62.
- [9] Cattivelli, L., Rizza, F., Badeck, F. W., Mazzucotelli, E., Mastrangelo, A. M., Francia, E., Marè, C., Tondelli, A., Stanca, A. M. (2008): Drought tolerance improvement in crop plants: An integrated view from breeding to genomics. – *Field Crops Research* 105(1-2): 1-14.
- [10] Crafts-Brandner, S. J., Law, R. D. (2000): Effect of heat stress on the inhibition and recovery of the ribulose-1, 5-bisphosphate carboxylase/oxygenase activation state. – *Planta* 212(1): 67-74.

- [11] Dai, A. (2012): Increasing drought under global warming in observations and models. – *Nature Climate Change* 3: 52-58.
- [12] Dai, X. L., Xiao, L. L., Jia, D. Y., Kong, H. B., Wang, Y. C., Li, C. X., Zhang, Y., He, M. R. (2014): Increased plant density of winter wheat can enhance nitrogen-uptake from deep soil. – *Plant and Soil* 384(1-2): 141-152.
- [13] Daryanto, S., Wang, L. X., Jacinthe, P. (2016): Global synthesis of drought effects on cereal, legume, tuber and root crops production: A review. – *Agricultural Water Management* 179(1): 18-33.
- [14] Dias, A. S., Lidon, F. C. (2010): Evaluation of grain filling rate and duration in bread and durum wheat, under heat stress after anthesis. – *Journal of Agronomy and Crop Science* 195(2): 137-147.
- [15] Dorion, S., Lalonde, S., Saini, H. S. (1996): Induction of male sterility in wheat by meiotic-stage water deficit is preceded by a decline in invertase activity and changes in carbohydrate metabolism in anthers. – *Plant Physiology* 111(1): 137-145.
- [16] Du, T. S., Kang, S. Z., Sun, J. S., Zhang, X. Y., Zhang, J. H. (2010): An improved water use efficiency of cereals under temporal and spatial deficit irrigation in north China. – *Agricultural Water Management* 97(1): 66-74.
- [17] Farhangfar, S., Bannayan, M., Khazaei, H. R., Baygi, M. M. (2015): Vulnerability assessment of wheat and maize production affected by drought and climate change. – *International Journal of Disaster Risk Reduction* 13: 37-51.
- [18] Giunta, F., Motzo, R., Deidda, M. (1993): Effect of drought on yield and yield components of durum wheat and triticale in a mediterranean environment. – *Field Crops Research* 33(4): 399-409.
- [19] Guerfel, M., Beis, A., Zotos, T., Boujnah, D., Zarrouk, M., Patakas, A. (2009): Differences in abscisic acid concentration in roots and leaves of two young olive (*Olea europaea* L.) cultivars in response to water deficit. – *Acta Physiologiae Plantarum* 31(4): 825-831.
- [20] Hedges, L. V., Olkin, I. (1985): *Statistical methods for meta-analysis*. – Academic Press, New York.
- [21] Hedges, L. V., Gurevitch, J., Curtis, P. S. (1999): The meta-analysis of response ratios in experimental ecology. – *Ecology* 80(4): 1150-1156.
- [22] Ji, X. M., Shiran, B., Wan, J. L., Lewis, D. C., Jenkins, C. L. D., Condon, A. G., Richards, R. A., Dolferus, R. (2010): Importance of pre-anthesis anther sink strength for maintenance of grain number during reproductive stage water stress in wheat. – *Plant, & Cell Environment* 33(6): 926-942.
- [23] Jin, N., Ren, W., Tao, B., He, L., Ren, Q. F., Li, S. Q., Yu, Q. (2018): Effects of water stress on water use efficiency of irrigated and rainfed wheat in the loess plateau, China. – *Science of The Total Environment* 642: 1-11.
- [24] Kaisermann, A., Vries, F. T., Griffiths, R. I., Bardgett, R. D. (2017): Legacy effects of drought on plant-soil feedbacks and plant-plant interactions. – *New Phytologist* 215(4): 1413-1424.
- [25] Kiliç, H., Yağbasanlar, T. (2010): The effect of drought stress on grain yield, yield components and some quality traits of durum wheat (*triticum turgidum* ssp. durum) cultivars. – *Notulae Botanicae Horti Agrobotanici Cluj-Napoca* 38(1): 164-170.
- [26] Koonjul, P. K., Minhas, J. S., Nunes, C., Sheoran, I. S., Saini, H. S. (2005): Selective transcriptional down-regulation of anther invertases precedes the failure of pollen development in water-stressed wheat. – *Journal of Experimental Botany* 56(409): 179-190.
- [27] Li, L. (2010): *The Analysis of Changes and Utilization Of Climatic Resources and Wheat Potential Productive In Different Latitudes Of Henan Province*. – Henan Agricultural University.

- [28] Li, J. Z., Dong, W. X., Oenema, O., Chen, T., Hu, C. S., Yuan, H. J., Zhao, L. Y. (2019): Irrigation reduces the negative effect of global warming on winter wheat yield and greenhouse gas intensity. – *Science of the Total Environment* 646: 290-299.
- [29] Liu, Y., Wang, E. L., Yang, X. G., Wang, J. (2010): Contributions of climatic and crop varietal changes to crop production in the north china plain, since 1980s. – *Global Change Biology* 16(8): 2287-2299.
- [30] Liu, L. T., Hu, C. S., Olesen, J. E., Ju, Z. Q., Yang, P. P., Zhang, Y. M. (2013a): Warming and nitrogen fertilization effects on winter wheat yields in northern china varied between four years. – *Field Crops Research* 151: 56-64.
- [31] Liu, Y. E., Xie, R. Z., Hou, P., Li, S. K., Zhang, H. B., Ming, B., Long, H. L., Liang, S. M. (2013b): Phenological responses of maize to changes in environment when grown at different latitudes in China. – *Field Crops Research* 144: 192-199.
- [32] Liu, E. K., Mei, X. R., Yan, C. R., Gong, D. Z., Zhang, Y. Q. (2016): Effects of water stress on photosynthetic characteristics, dry matter translocation and wue in two winter wheat genotypes. – *Agricultural Water Management* 167: 75-85.
- [33] Liu, W., Ma, G., Wang, C., Wang, J., Lu, H., Li, S., Feng, W., Xie, Y., Ma, D., Kang, G. (2018): Irrigation and Nitrogen Regimes Promote the Use of Soil Water and Nitrate Nitrogen from Deep Soil Layers by Regulating Root Growth in Wheat. – *Frontiers in Plant Science* 9: 32.
- [34] Mäkinen, H., Kaseva, J., Trnka, M., Balek, J., Kersebaum, K. C., Nendel, C., Gobin, A., Olesen, J. E., Bindi, M., Ferrise, R., Moriondo, M., Rodríguez, A., Ruiz-Ramos, M., Takáč, J., Bezák, P., Ventrella, D., Ruget, F., Capellades, G., Kahiluoto, H. (2018): Sensitivity of European wheat to extreme weather. – *Field Crops Research* 222: 209-217.
- [35] Qin, X. B., Wang, H., He, Y., Li, Y. E., Li, Z. G., Gao, Q. Z., Wan, Y. F., Qian, B. D., McConkey, B., DePauw, R., Lemke, R., Parton, W. J. (2018): Simulated adaptation strategies for spring wheat to climate change in a northern high latitude environment by DAYCENT model. – *European Journal of Agronomy* 95: 45-56.
- [36] Reyer, C. P. O., Leuzinger, S., Rammig, A., Wolf, A., Bartholomeus, R. P., Bonfante, A., de Lorenzi, F., Dury, M., Gloning, P., Jaoudé, R. A., Klein, T., Kuster, T. M., Martins, M., Niedrist, G., Riccardi, M., Wohlfahrt, G., de Angelis, P., de Dato, G., François, L., Menzel, A., Pereira, M. (2013): A plant's perspective of extremes: terrestrial plant responses to changing climatic variability. – *Global Change Biology* 19(1): 75-89.
- [37] Roelfs, A. P. (1992): *Rust diseases of wheat: concepts and methods of disease management*. – CIMMYT Publishing, Mexico.
- [38] Rossini, M., Fava, F., Cogliati, S., Meroni, M., Marchesi, A., Panigada, C., Giardino, C., Busetto, L., Migliavacca, M., Amaducci, S., Colombo, R. (2013): Assessing canopy PRI from airborne imagery to map water stress in maize. – *ISPRS Journal of Photogrammetry and Remote Sensing* 86: 168-177.
- [39] Saini, H. S., Sedgley, M., Aspinall, D. (1984): Development anatomy in wheat of male sterility induced by heat stress, water deficit or abscisic acid. – *Functional Plant Biology* 11(4): 243-253.
- [40] Sauer, T., Havlík, P., Schneider, U. A., Schmid, E., Kindermann, G., Obersteiner, M. (2010): Agriculture and resource availability in a changing world: The role of irrigation. – *Water Resources Research* 46(6): 666-669.
- [41] Shamsuddin, A. K. M. (1987): Path analysis in bread-wheat. – *Indian Journal of Agricultural Sciences* 57(1): 47-49.
- [42] Simane, B., Struik, P. C., Nachit, M. M., Peacock, J. M. (1993): Ontogenetic analysis of yield components and yield stability of durum wheat in water-limited environments. – *Euphytica* 71(3): 211-219.
- [43] Smithers, L. G., Gibson, R. A., Mcphee, A. J., Makrides, M. (2008): Effect of long-chain polyunsaturated fatty acid supplementation of preterm infants on disease risk and neurodevelopment: a systematic review of randomized controlled trials. – *American Journal of Clinical Nutrition* 87(4): 912-920.

- [44] Song, L., Li, F. M., Fan, X. W., Xiong, Y. C., Wang, W. Q., Wu, X. B., Turner, N. C. (2009): Soil water availability and plant competition affect the yield of spring wheat. – *European Journal of Agronomy* 31(1): 51-60.
- [45] Tapley, M., Ortiz, B. V., Santen, E. V., Balkcom, K. S., Mask, P., Weaver, D. B. (2013): Location, seeding date, and variety interactions on winter wheat yield in southeastern United States. – *Agronomy Journal* 105: 509-518.
- [46] Trnka, M., Brázdil, R., Olesen, J. E., Eitzinger, J., Zahradníček, P., Kocmánková, E., Dobrovolný, P., Štěpánek, P., Možný, M., Bartošová, L., Hlavinka, P., Semerádová, D., Valášek, H., Havlíček, M., Horáková, V., Fischer, M., Žalud, Z. (2012): Could the changes in regional crop yields be a pointer of climatic change. – *Agricultural and Forest Meteorology* 166-167: 62-71.
- [47] Trout, T. J., DeJonge, K. C. (2017): Water productivity of maize in the US high plains. – *Irrigation Science* 35(3): 251-266.
- [48] Wang, C. Y., Liu, W. X., Li, Q. X., Ma, D. Y., Lu, H. F., Feng, W., Xie, Y., Zhu, Y., Guo, T. C. (2014): Effects of different irrigation and nitrogen regimes on root growth and its correlation with above-ground plant parts in high-yielding wheat under field conditions. – *Field Crops Research* 165: 138-149.
- [49] Wei, T., Dong, Z. Y., Zhang, C., Ali, S., Chen, X. L., Han, Q. F., Zhang, F. C., Jia, Z., Zhang, P., Ren, X. (2018): Effects of rainwater harvesting planting combined with deficiency irrigation on soil water use efficiency and winter wheat (*Triticum aestivum* L.) yield in a semiarid area. – *Field Crops Research* 218: 231-242.
- [50] White, R. G., Kirkegaard, J. A. (2010): The distribution and abundance of wheat roots in a dense, structured subsoil—implications for water uptake. – *Plant, Cell & Environment* 33(2): 133-148.
- [51] Xiao, G. J., Zhang, Q., Yao, Y. B., Zhao, H., Wang, R. Y., Bai, H. Z., Zhang, F. J. (2008): Impact of recent climatic change on the yield of winter wheat at low and high altitudes in semi-arid northwestern China. – *Agriculture, Ecosystems & Environment* 127(1-2): 37-42.
- [52] Xiao, G. J., Zhang, Q., Li, Y., Wang, R. Y., Yao, Y. B., Zhao, H., Bai, H. Z. (2010): Impact of temperature increase on the yield of winter wheat at low and high altitudes in semiarid northwestern China. – *Agricultural Water Management* 97(9): 1360-1364.
- [53] Xu, C. L., Tao, H. B., Tian, B. J., Gao, Y. B., Ren, J. H., Wang, P. (2016): Limited-irrigation improves water use efficiency and soil reservoir capacity through regulating root and canopy growth of winter wheat. – *Field Crops Research* 196: 268-275.
- [54] Zhang, L. X., Li, S. X., Zhang, H., Liang, Z. S. (2007): Nitrogen rates and water stress effects on production, lipid peroxidation and antioxidative enzyme activities in two maize (*Zea mays* L.) genotypes. – *Journal of Agronomy and Crop Science* 193(6): 387-397.
- [55] Zhang, K., Chen, N. L., Gu, Q. Y. (2016): Trade-offs among light, water and nitrogen use efficiencies of wheat cultivars under different water and nitrogen application levels. – *Chinese Journal of Applied Ecology* 27(7): 2273-2282.
- [56] Zhang, H. H., Han, M., Chávez, J. L., Lan, Y. B. (2017a): Improvement in estimation of soil water deficit by integrating airborne imagery data into a soil water balance model. – *International Journal of Agricultural and Biological Engineering* 10(3): 37-46.
- [57] Zhang, X. Y., Qin, W. L., Chen, S. Y., Shao, L. W., Sun, H. Y. (2017b): Responses of yield and WUE of winter wheat to water stress during the past three decades—a case study in the north China plain. – *Agricultural Water Management* 179: 47-54.

EVALUATION OF THE FOREST STRUCTURE, DIVERSITY AND BIOMASS CARBON POTENTIAL IN THE SOUTHWEST REGION OF GUANGXI, CHINA

BADSHAH, M. T.¹ – AHMAD, A.¹ – MUNEER, M. A.² – REHMAN, A. U.¹ – WANG, J.¹ – KHAN, M. A.¹ – MUHAMMAD, B.¹ – AMIR, M.⁴ – MENG, J.^{1*}

¹Research Center of Forest Management Engineering of National Forestry and Grassland Administration, Beijing Forestry University, Beijing 100083, China

²College of Grassland Science, Beijing Forestry University, Beijing 100083, China

³Key Laboratory for Silviculture and Conservation of Ministry of Education, Beijing Forestry University, Beijing 100083, China

⁴Institute of Geographic Sciences and Natural Resources Research, University of Chinese Academy of Sciences, Beijing 100049, China

*Corresponding author
e-mail: jmeng@bjfu.edu.cn

(Received 7th Sep 2019; accepted 14th Nov 2019)

Abstract. Evaluation and monitoring of forest structure, diversity, and biomass carbon dynamics are essential for effective forest biodiversity and carbon conservation. Using inventory data of 174 field plots with a size of 400 m², this study estimated the forest structure, species diversity, growing stock characteristics and biomass carbon of the South West Region of Guangxi Zhuang Autonomous Region of China. Our results showed that a total of 198 species belonging to 51 families, and 128 genera were found. The results of different diversity indices showed a greater species variation across the forest. Furthermore, different tree attributes were recorded for forest structure. In this regard, the mean tree height was 10.3 m, while the mean basal area was 5.94 m² ha⁻¹. The mean growing stock volume was 104.14 m³ ha⁻¹, and the average biomass carbon was 110.36 Mg ha⁻¹. Among the dominant species, the maximum importance value index (14.81%) and basal area (17.3 ± 3.03 m² ha⁻¹) were recorded for *Pinus massoniana*. While the maximum growing stock volume (116.4 ± 20.2 m³ ha⁻¹) and biomass carbon (114 ± 18.3 Mg ha⁻¹) were found in the *Styrax subniveus*. Our results also highlighted that the basal area is a strong predictor of growing stock volume and biomass carbon compared to diameter and height. Moreover, the correlation between biomass carbon and diversity indices indicated a weak positive correlation, which provided the insight that high-value carbon- diversity forest can be achieved.

Keywords: forest structure, biomass carbon, Tree diversity and density, carbon sequestration, carbon-diversity relation, Guangxi region

Introduction

Forests are the largest contributors to territorial ecosystems on Earth and play a significant role in providing economic benefits as well as ecological services (Eckert, 2012; Meng et al., 2014). Forests are integral components of the global carbon cycle that take up and release a substantial amount of carbon (Wang et al., 2018). The regulation of atmospheric carbon concentration through forest carbon stock has been identified as a major political target to mitigate global climate change (Grassi et al., 2017). Forest ecosystems play an important role in the global carbon cycle (Li et al., 2017). While the estimation of carbon from forests brings an important understanding of global warming (Sierra et al., 2007). Globally, forests particularly tropical and sub-tropical forests are the center of biodiversity and carbon storage (Sullivan et al., 2017). About 60% of terrestrial

photosynthesis takes place in the tropical forest (Field et al., 1998; Liu et al., 2015). This region has been recognized as a significant hotspot for global carbon source and sink and biodiversity (Bazzaz, 1998).

Over the past two decades, there has been a strong emphasis on the role of biodiversity in ecosystem properties, processes, and services to enhance carbon sequestration and storage (Naeem et al., 2009). Climate change and habitat loss are the two major components for the loss of global biodiversity (Thomas et al., 2013). Similarly, changes in the land use of forests are leading to emission sources of carbon (Matthews et al., 2014). Therefore, different incentives such as United Nation (UN) REDD + have emerged for the protection and conservation of high carbon and diversity areas (Robbins, 2016). The protection of forests for carbon and biodiversity depends on the relationship between biomass carbon and tree diversity. The positive relationship between biomass carbon and tree diversity would indicate synergies whereas a negative relationship would indicate difficult tradeoffs (Meng et al., 2014). However, in case of the absence of any relationship, the optimal solutions are required towards an understanding of the distribution of biomass carbon and biodiversity (Thomas et al., 2013).

The forest structure determines the functions of a forest; therefore, forest structure provides the fundamental bases for the formulation of forest management regime aimed at specific objectives (Warfield, 2006). Forests structural attributes such as stem density, growing stock volume, stand basal area, diameter, and tree height are the important variables for the management of forests (Meng et al., 2016). In addition, forest structural diversity, i.e., species diversity, tree size diversity, and position diversity, is more important to inform forest management (Corona, 2016). A notable example is structured-based forest management. Additionally, many authors documented the positive relationship between carbon sequestration and structural diversity (Noumi et al., 2018). Therefore, quick acquisition of forest structural variables, structural diversity indices, and forest carbon stocking is urgent for sustainable forest management.

The methods used to derive forest attributes include the conventional method and remote sensing method. National or regional forest field inventories data are also used for the measurement of different forest stand variables. In China, there are three major types of forest inventories including the national forest inventory, the forest management planning inventory, and the forest design operational inventory, which are used to derive such precedent forest attributes (Lei et al., 2009). However, regardless of the type of forest inventories, it is labour-cost, time-consuming and expensive.

In China, the researchers mainly focused on the measurement of carbon stock in different forest types (Dixon et al., 1994; Fang et al., 2007; Zhang et al., 2013). Similarly, forest structure and structural diversity have been documented by various authors (Meng et al., 2016). However, there is a lack of integrated information regarding the forest structure, species composition and diversity, and carbon dynamics. Therefore, the objective of our study is first to derive the forest attributes, including forest variables and forest structural diversity indices based on conventional forest inventory plots, mainly focused to answer the following questions: (1) what is the forest structure and the species diversity?; (2) how the carbon is distributed among the different diameter classes, among the tree height, mean diameter and basal area, and which attribute shaped the biomass carbon strongly; (4) what is the relationship of species diversity and biomass carbon?; (5) what is the status of structural attributes and biomass carbon potential of dominant tree species?

Materials and methods

Study area

The field statistics were obtained from the Experimental Center for Subtropical Forestry of the Chinese Academy of Forestry of Southwest of the Guangxi Zhuang Autonomous Region of China. The study site is the tropical research center situated in Pingxiang City (Píngxiáng Shì). The latitude and longitude extend from 21°57' N to the 22°16' N, 106°41' E to 109°59' E, respectively (*Fig. 1*). The area lies in the southern subtropical warm and semi-humid monsoon climate that is characterized by dry and wet season with a total mean annual precipitation ranging from 1200 to 1500 mm and annual evaporation is 1261-1388 mm. The relative humidity is 80-84%, with an average annual air temperature of about 20.5-21.7 °C, and ranges from minimum to maximum about 13 to 28 °C. The landscape is characterized by low mountain elevation ranging from 250-800 m and a slope range from 25 to 30%. The dominant parent rocks are granite, purple sand shale, and sandstone. The soil for the forest is developed by granite bricks and mostly red and purple in color (Kang et al., 2006; Meng et al., 2014; Ming et al., 2014). The natural vegetation includes the subtropical forest with a mixture of evergreen and deciduous species (Bruelheide et al., 2011). This region is rich in species diversity and the area is generally mixed but the dominant species of the forest vegetation are *Cunninghamia lanceolata*, *Magnoliaceae glanca*, *Illicium verum*, *Pinus massoniana*, *Betula alnoides*, *Castanopsis hystrix*, and *Quercus griffithii*, *Erythrophleum fordii*, *Castanopsis hystrix*, which are hardwood and have high economic value for timber (Lu et al., 1999; Bruelheide et al., 2011; Tang et al., 2012; Zhu et al., 2013).

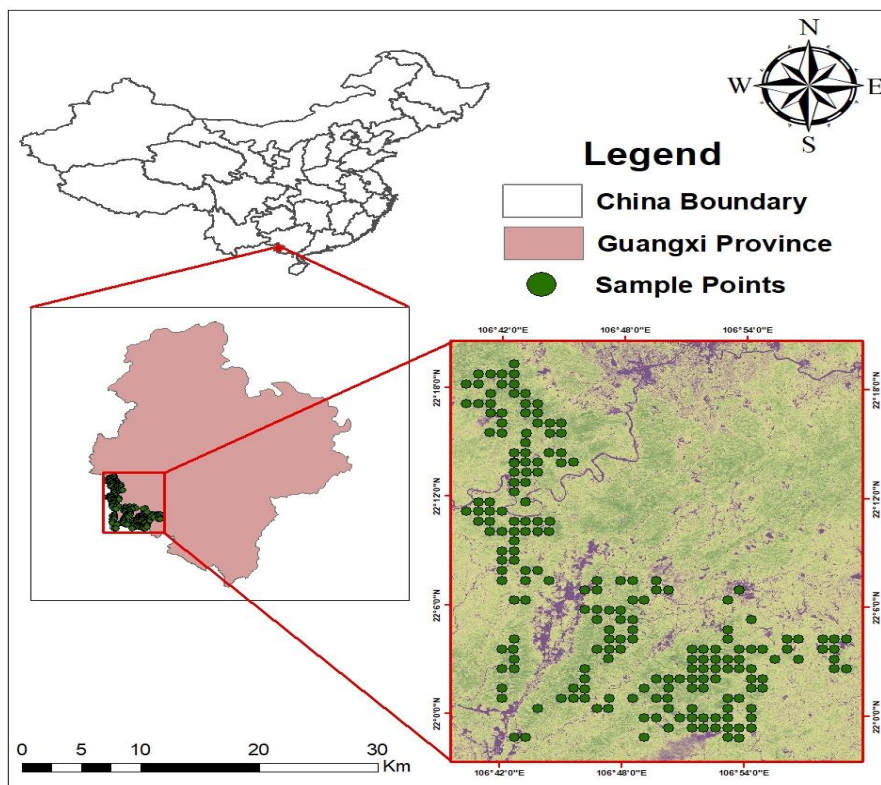


Figure 1. Overview of the study area, the RapidEye satellite image in which the green circles represent the forest plots

Research design and field inventory

For data collection, overall 174 sample plots were laid out in the forest. The size of each sample plot was 400 m². In each sample plot, the distance and bearing of each sample plot center were measured with each stem that was located within the radius of the circular plot, and each species was counted. The plant species were identified and their diameter at breast height (1.3 m from the above-ground) was recorded. On the basis of the size of the diameter, the classification was made. The values of stem density and relative stem density, basal area, and relative basal area and importance value index (IVI) were calculated for dominant plant species. The species diversity indices and height of the trees at the plot level were measured. From the height (m) and diameter (cm), the volume (m³ ha⁻¹) of the tree was measured. The volume was converted into biomass (Mg ha⁻¹). From the biomass value, the carbon content was estimated using the Intergovernmental Panel on Climate Change IPCC (2007) (Change, 2007; Keenan et al., 2015) guidelines. Biomass was then summed across all the plots to obtain carbon stock (Mg ha⁻¹).

Data analysis

Based on the collected information at the plot level, the data was analyzed for the various structural attributes such as diameter, basal area, and density. The relative stem density, basal area, relative basal area, and the importance value index (IVI) were assessed using *Equations 1-3*.

$$\text{Relative density (RD)} = \frac{\text{Number of particular species}}{\text{Number of all species}} \times 100 \quad (\text{Eq.1})$$

$$\text{Relative basal area (RB)} = \frac{\text{Basal area of a particular species}}{\text{Basal area of all species}} \times 100 \quad (\text{Eq.2})$$

$$\text{Importance value index (IVI)} = \frac{\text{RD} + \text{RB}}{2} \times 100 \quad (\text{Eq.3})$$

In order to compute the data for the description of the diversity, different community indices such as Shannon Wiener Diversity Index (SHI), Pielou Diversity Index (PI), and Simpson Diversity Index (SII) were used through *Equations 4-7*. (Magurran, 2013; Naidu and Kumar, 2016).

$$\text{SHI} = - \sum_{i=1}^n p_i \cdot \ln(p_i) \quad (\text{Eq.4})$$

$$\text{PI} = \frac{\text{SHI}}{\ln(S)} \quad (\text{Eq.5})$$

where SHI is the Shannon Wiener Diversity Index and S is the total number of species across all samples in a dataset.

$$SII = 1 - \sum_{i=1}^n p_i^2 \quad (\text{Eq.6})$$

Statistical Gini coefficient (GC) is one of the components of forest structure used for the distribution of tree diameter in a forest by the indicator of tree size variation (McElhinny et al., 2005). This was measured using *Equation 7*:

$$GC = \frac{\sum_{t=1}^n (2t - n - 1)ba_t}{\sum_{t=1}^n ba_t(n - 1)} \quad (\text{Eq.7})$$

where *ba* is a basal area for the tree in rink *t* ($\text{m}^2 \text{ha}^{-1}$), *t* is the rink from 1 to *n* number. Gini coefficient ranged from 0 to 1.

For biomass carbon estimation, we first calculated the volume of the tree (*Eq. 8*) then the volume was converted into biomass using the available regression models to estimate plant biomass (*Table 1*) (Wang et al., 2015; Du et al., 2015) The biomass was converted into carbon stock in the upper story vegetation using a conversion factor of 0.5 which indicates 50% of total plant biomass is equal to carbon stock (*Eq. 9*), this conversion factor has been used worldwide (Ahmad et al., 2019; Brown and Lugo, 1982; Xiao et al., 2003; Ahmad and Nizami, 2015).

$$\text{Volume of tree} = A \times H \times FF \quad (\text{Eq.8})$$

$$\text{Biomass carbon} = \text{Total biomass} * 0.5 \quad (\text{Eq.9})$$

Table 1. Allometric regression models used to estimate biomass

S. No	Species	Model
1	Eucalyptus	$W_T = 0.138D^{2.436}$
2	Quercus	$W_T = 0.174D^{2.39}$
3	Hardwood	$W_T = 0.186D^{2.377}$
4	Softwood	$W_T = 0.104D^{2.53}$

W is the dry weight of different components while T shows the total dry weight of leaf, stem, branches, and roots

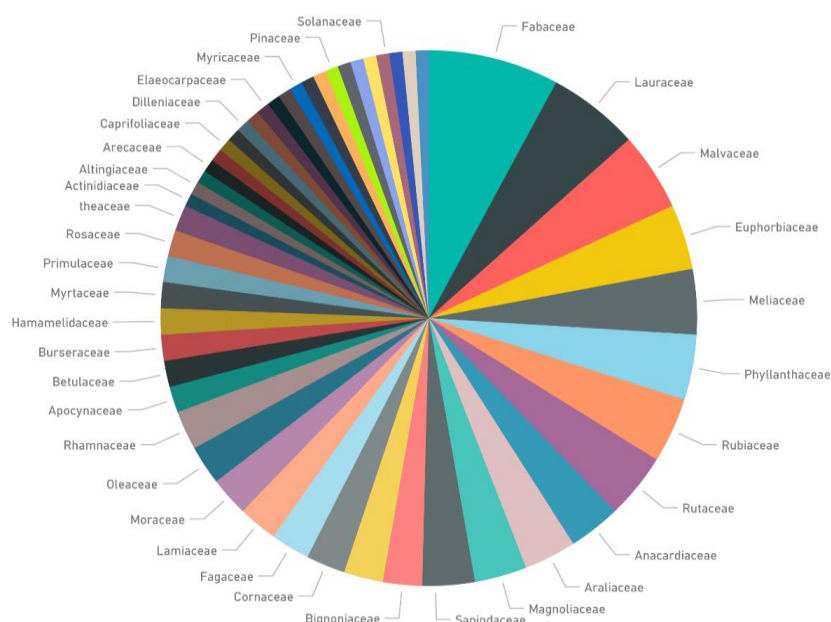
Statistical analysis

R package *vegan* was used for the calculation of the diversity indices (Team, 2013; Muneer et al., 2019) The variation in tree diameter, tree height, stem density, basal area, and biomass and carbon stock in the respective diameter classes (class-1 (5-11 cm), class-2 (12-16 cm), class-3 (17-28)) were determined by analysis of variance (ANOVA) using Statistix 8, version 8.1). Regression models were developed to study the relationship of tree height, diameter, and basal area with volume and biomass carbon by using Origin 2018. The correlation between respective diversity indices and biomass carbon was carried out using different correlation analyses such as the linear regression, Pearson correlation, and Spearman rank correlation.

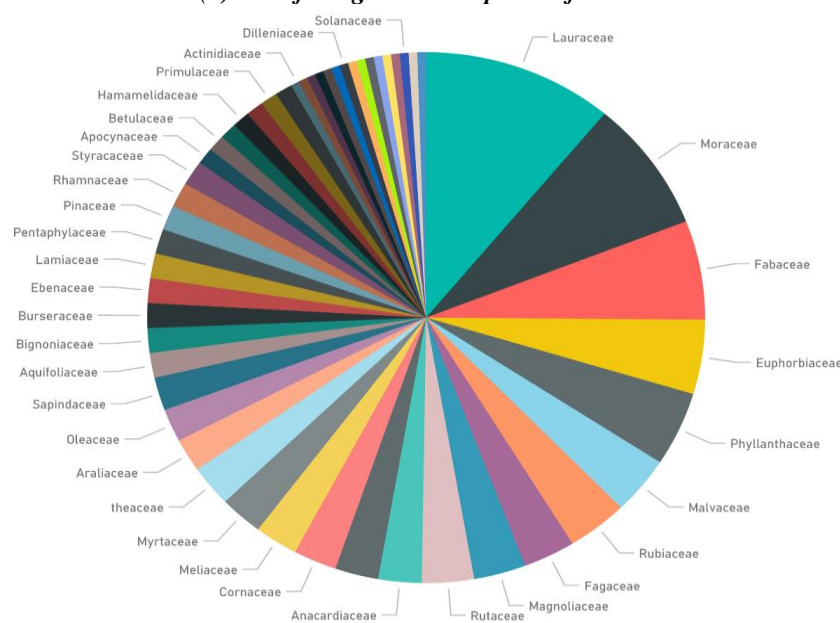
Results

Forest structure and species diversity

The results of the present study revealed that in this region 128 genera (*Fig. 2a*) and 198 species (*Fig. 2b*) belonging to 51 families were found. Among the 51 plant families, the highest number of genera i.e., 10, 7, 6, and 5 were found in *Fabaceae*, *Lauraceae*, *Malvaceae*, and *Rubiaceae* respectively. While the highest number of species were found in family Lauraceae, Moraceae and Fabaceae about 22, 16, and 12 respectively. Family *Phyllanthaceae* and *Euphorbiaceae* each consisting of 5 genera and 9 species. In contrast, 16 families consisting of single genus and species.



(a) No. of the genus in respective families



(b) No. of species in respective families

Figure 2. The relative contribution of the number of genera (a); and number of species (b) belonging to their respective families

Regarding the species diversity at the plot level, it showed that SHI varied between 0 to 2.67 with a mean value of 1.034, while the SII varied between 0 and 1 with a mean value of 0.478. The PI value was found at the range of 0 and 1 with a mean value of 0.582 and the GC was in the range of 0 and 1 with a mean of 0.384 (Fig. 3). For more detail see Appendix (Table A1).

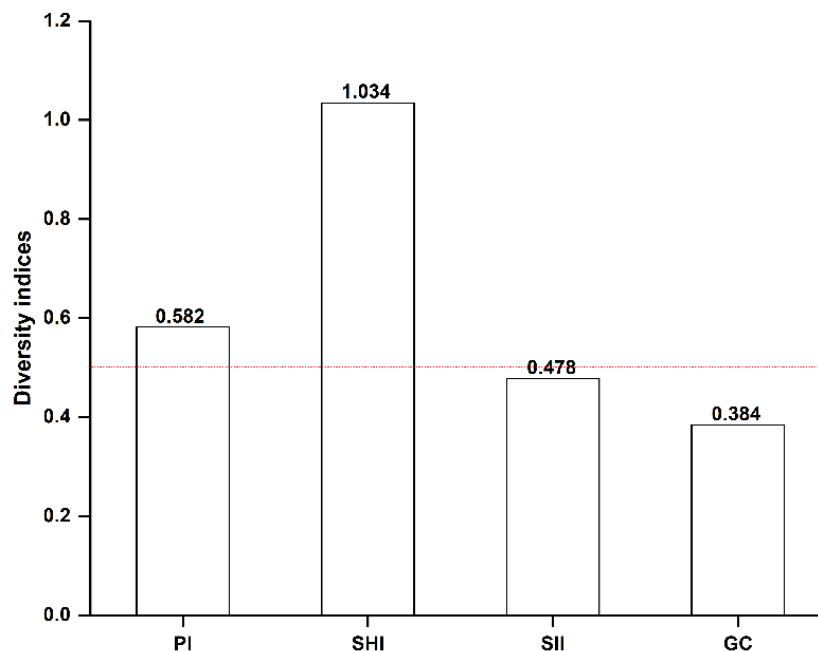


Figure 3. Diversity indices for all sampling plots

Growing stock characteristic and biomass carbon

This study revealed that in the tropical forest of Pingxing city, the average diameter varied significantly between the different diameter classes. The highest mean diameter was recorded in class-3, while the lowest was found in class-1. The significant higher value for the height was found for class-3 and the lowest was recorded in class-1. The average mean height was 10.3 ± 3.0 m. Mean density varied between 592.13 ± 280.24 to 955.70 ± 538.66 (trees ha^{-1}). A statistically lower stem density was recorded in the diameter class-1 compared to class-2 and class-3. While, the value of the basal area, stem volume, total tree biomass, and biomass carbon were recorded significantly higher in the class-3, while these were significantly lower in class-1 (Table 2).

Table 2. Growing stock characteristics and biomass carbon of the forest in different diameter classes

Diameter class (cm)	Mean diameter (cm)	Height (m)	Density (ha^{-1})	Basal area ($\text{m}^2 \text{ha}^{-1}$)	Volume ($\text{m}^3 \text{ha}^{-1}$)	Biomass (Mg ha^{-1})	Carbon stock (Mg ha^{-1})
Class-1	9.63±0.21c	7.77±0.22c	592±280.2b	8.84±0.75c	43.55±3.90c	51.54±4.50c	25.77±2.27c
Class-2	14.30±0.17b	10.35±0.22b	888.7±378.6a	17.81±0.96b	114.21±7.39b	119.27±7.24b	59.63±3.62b
Class-3	19.95±0.40a	13.06±0.40a	955.7±538.6a	21.19±1.37a	154.68±11.71a	160.27±12a	80.13±6a
Mean	14.62±2.98	10.3±1.52	812.17±111.75	15.94±3.68	104.14±32.47	110.36±31.70	55.17±15.84

The regression relationship of the basal area, diameter, and height with the volume and biomass carbon is presented in *Table 3* and *Figure 4*. The results of the analysis revealed that the basal area had a highly positive correlation with volume and biomass carbon. In contrast, a weak correlation was observed for diameter with volume and biomass carbon. Furthermore, the correlation of height with volume and biomass carbon was also found weak. These findings clearly explained that the basal area is the best predictor of growing stock and biomass carbon compared to stem diameter and tree height.

The relationship between diversity indices and biomass carbon is given in *Table 4*. It showed the positive but very weak correlation for all indices i.e., Pearson correlation, linear regression, and Spearman rank correlation.

Table 3. Regression analysis between the basal area with volume and biomass carbon, diameter with volume, and biomass carbon and height with volume and biomass carbon

	Relationship type	Equation	R ²	y0	A	P
Basal area vs volume	$f = y_0 + a \cdot x$	$V = y_0 + a \cdot x$	0.92	-91.91	7.75	< 0.0001
Basal area vs biomass carbon	$f = y_0 + a \cdot x$	$BMC = y_0 + a \cdot x$	0.91	-6.88	3.87b	< 0.0001
Diameter vs volume	$f = y_0 + a \cdot x$	$BMC = y_0 + a \cdot x$	0.40	-48.06	10.45	< 0.0001
Diameter vs biomass carbon	$f = y_0 + a \cdot x$	$V = y_0 + a \cdot x$	0.38	-40.49	10.35	< 0.0001
Height vs volume	$f = y_0 + a \cdot x$	$V = y_0 + a \cdot x$	0.50	-48.06	10.45	< 0.0001
Height vs biomass carbon	$f = y_0 + a \cdot x$	$BMC = y_0 + a \cdot x$	0.36	-40.49	10.35	< 0.0001

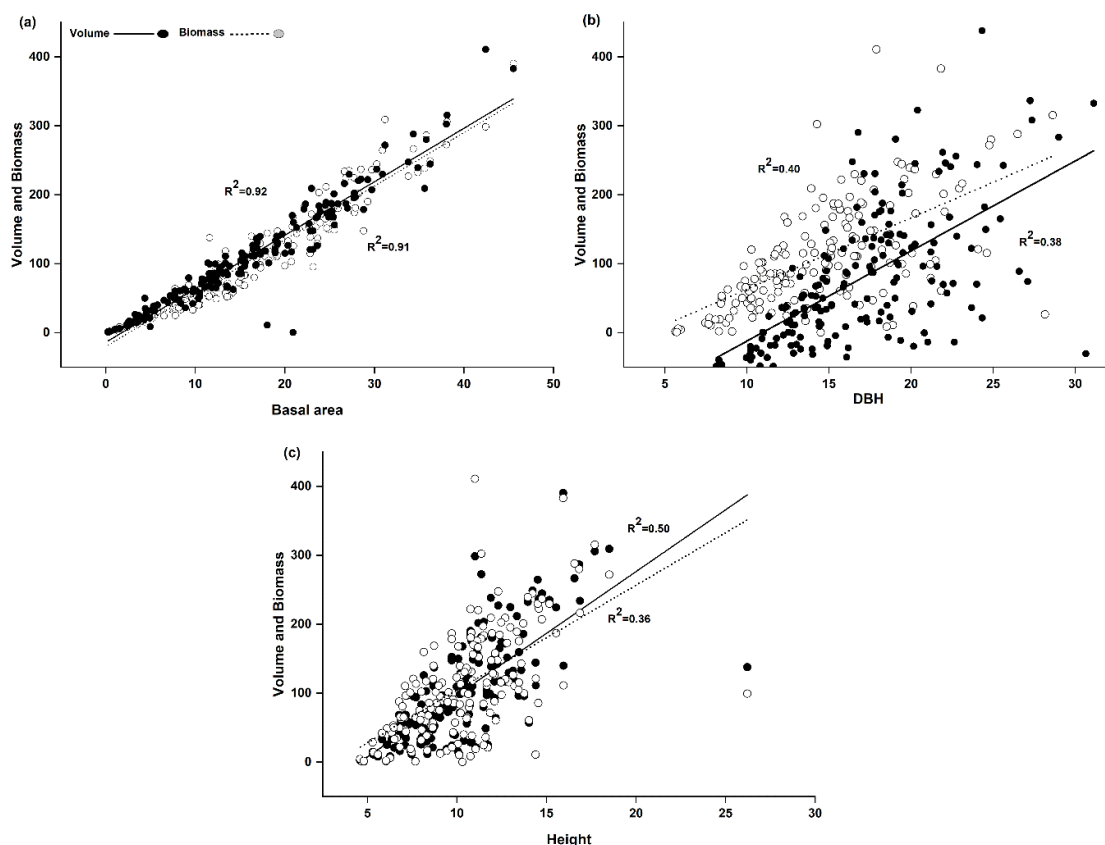


Figure 4. Forest attributes showing the correlation between; (a) volume and biomass with basal area; (b) volume and biomass with DBH; (c) volume and biomass with height

Table 4. Relationship between diversity indices and biomass carbon

Diversity indices	Pearson correlation		Linear regression (R ²)		Spearman rank correlation	
	PV	P	R ²	P	SRV	P
SII	0.14	0.0624	0.020	0.062	0.136	0.073
SHI	0.15	0.039	0.024	0.039	0.191	0.011
PI	0.102	0.0179	0.01	0.0150	-0.001	0.011
GC	0.29	0.000	0.088	0.000	0.299	0.000
MDI	0.17	0.0242	0.029	0.0242	0.163	0.0316

SII (Simpson Diversity Index), SHI (Shannon Wiener Diversity Index), PI (Pielou Diversity Index), GC (Gini coefficient)

Structural attributes, growing stock and biomass carbon of the dominant species

The results of various structural attributes, like stem density, basal area, relative stem density, relative basal area and importance value index (IVI) for individual dominant tree species (12) are given in Table 5. The results revealed that among the different dominant species, the highest stem density, basal area, relative stem density, relative basal area, and importance value index (IVI) were recorded for *Pinus massoniana*. Regarding growing stock characteristics, its maximum mean diameter was found for *Illicium verum* followed by *Styrax subniveus*, while the mean height was found the highest for *Styrax subniveus*, *Illicium verum*. The maximum growing stock volume and biomass carbon was observed for *Pinus massoniana* followed by *Manglietia hainanensis* (Table 6).

The results of the percentage distribution of different growing stock characteristics that include diameter, height, density, basal area, volume, and biomass carbon are given in Table 7. The results depicted that *Illicium verum* share a maximum percentage for diameter, while the highest percentage value for height was recorded for *Styrax subniveus*, for stem density, basal area, and biomass shared highest percentage value by *Pinus massoniana*, similarly, for volume the maximum percentage value was recorded for *Styrax subniveus*.

Table 5. Structural attributes of the dominant species

Species	Stem density ha ⁻¹	Basal area m ² ha ⁻¹	Relative stem density	Relative basal area	IVI %
<i>Illicium verum</i>	266.25 ± 35.69	6.2 ± 1.09	8.82	5.36	7.09
<i>Pinus massoniana</i>	442.37 ± 31.9	17.3 ± 3.03	14.66	14.95	14.81
<i>Cunninghamia lanceolata</i>	291.39 ± 58.4	7.13 ± 1.67	9.66	6.16	7.91
<i>Saurauia tristyla</i>	265.6 ± 63.9	6.8 ± 0.87	8.80	5.94	7.37
<i>Manglietia hainanensis</i>	262.5 ± 151.5	11.8 ± 8.4	8.70	10.23	9.47
<i>Styrax subniveus</i>	233.3 ± 10.5	13.6 ± 1.8	7.73	11.82	9.77
<i>Liquidambar formosana</i>	129 ± 12.9	5.2 ± 0.77	4.27	4.51	4.39
<i>Acacia confusa</i>	253.57 ± 89.7	11.5 ± 5.7	8.40	9.03	8.71
<i>Castanopsis hisystris</i>	277.2 ± 49.7	7.7 ± 1.88	9.19	6.66	7.92
<i>Cyclobalanopsis myrsinifolia</i>	216.66 ± 30	10.77 ± 5.47	7.18	9.29	8.24
<i>Quercus griffithii</i>	205 ± 40.62	8 ± 3.93	6.79	6.96	6.88
<i>Schima superba</i>	175 ± 42	10.53 ± 3.9	5.80	9.09	7.44

Table 6. Growing stock characteristics and biomass carbon of dominant tree species

Species	Mean diameter (cm)	Height (m)	Volume (m ³ ha ⁻¹)	Biomass (Mg ha ⁻¹)	Carbon stock (Mg ha ⁻¹)
<i>Illicium verum</i>	31.85 ± 15	16.9 ± 8.2	31.3 ± 6.3	47 ± 8.8	23.5 ± 4.4
<i>Pinus massoniana</i>	21.7 ± 0.6	13.5 ± 0.9	99.6 ± 7	106.5 ± 6.8	53.2 ± 3.4
<i>Cunninghamia lanceolata</i>	13.21 ± 0.92	9.6 ± 0.53	50.2 ± 12.6	52.4 ± 13.3	26.2 ± 11.6
<i>Saurauia tristyla</i>	18.2 ± 2.15	10.4 ± 1.37	44 ± 7.5	53.4 ± 8	26.7 ± 4
<i>Manglietia hainanensis</i>	17.19 ± 4.7	12.36 ± 2.8	96 ± 36.1	96 ± 80.3	48 ± 40.1
<i>Styrax subniveus</i>	25.34 ± 2	17.1 ± 1.5	116.4 ± 20.2	114 ± 18.3	57 ± 9.1
<i>Liquidambar formosana</i>	20.9 ± 1.6	12.1 ± 0.5	35.8 ± 5.8	43.2 ± 7.3	21.6 ± 0.7
<i>Acacia confusa</i>	17.8 ± 2.34	11.8 ± 0.8	77.5 ± 38.6	69.8 ± 13.6	34.9 ± 6.8
<i>Castanopsis hystrix</i>	17.4 ± 0.98	12.8 ± 0.6	55.9 ± 14.4	56.4 ± 14.1	28.2 ± 7
<i>Cyclobalanopsis myrsinifolia</i>	22.11 ± 4.73	14.80 ± 2.24	86.53 ± 48.11	87.47 ± 48.45	43.73 ± 24.22
<i>Quercus griffithii</i>	18.63 ± 3.11	12 ± 1.76	60.13 ± 34.24	63.66 ± 33.49	31.83 ± 16.74
<i>Schima superba</i>	23.75 ± 2.03	14 ± 1.4	78.1 ± 26.5	94.9 ± 41.2	47.4 ± 20.6

Table 7. Percentage contribution in growing stock characteristics and biomass carbon of the dominant tree species

Species	DBH	Height	Density	Basal area	Volume	Biomass	Carbon stock
<i>Illicium verum</i>	12.80	10.71	8.82	5.36	3.80	5.31	5.31
<i>Pinus massoniana</i>	8.73	8.56	14.66	14.95	12.08	12.03	12.03
<i>Cunninghamia lanceolata</i>	5.31	6.12	9.66	6.16	6.09	5.92	5.92
<i>Saurauia tristyla</i>	7.32	6.63	8.80	5.94	5.34	6.04	6.04
<i>Manglietia hainanensis</i>	6.91	7.81	8.70	10.23	11.63	10.86	10.86
<i>Styrax subniveus</i>	10.19	10.82	7.73	11.82	14.11	12.88	12.88
<i>Liquidambar formosana</i>	8.41	7.70	4.27	4.51	4.35	4.88	4.88
<i>Acacia confusa</i>	7.39	7.65	8.40	9.03	8.56	7.89	7.89
<i>Castanopsis hystrix</i>	7.01	8.13	9.19	6.66	6.79	6.38	6.38
<i>Cyclobalanopsis myrsinifolia</i>	8.89	9.36	7.18	9.29	10.48	9.88	9.88
<i>Quercus griffithii</i>	7.49	7.62	6.79	6.96	7.29	7.19	7.19
<i>Schima superba</i>	9.55	8.90	5.80	9.09	9.47	10.73	10.73

Discussion

The tropical forest that covers only 7-10% of the earth's land surface, is the hotspot for carbon storage and biodiversity (Bonan, 2008). and stores a significant part of global carbon and biodiversity (Poorter et al., 2015) In this study, we examined different structural attributes, species diversity and biomass carbon of the tropical forest in Guangxi Zhuang Autonomous Region of China. Our results reported a total of 198 species belonging to 51 families. Among the different families, family *Lauraceae* was the richest family with respect to the number of species followed by family *Moraceae* and *Phyllanthaceae*. The mean values of different diversity indices (Fig. 2) showed a greater variation in species across the forest. Similarly, at the plot level, the variation in the values of diversity indices pinpoints the diverse nature of the forest. The results of a number of species in this study are consistent with the results of the Dinghushan

tropical forests of China (Ostertag et al., 2014). In comparison, our results fall in the acceptable range of species numbers (192-240) and families (46-50) reported from the tropical forest in different regions of Colombia, Sri Lanka and Thailand. However, our results represent a higher number of species and families with respect to the tropical forest of different region of Taiwan, Puerto Rico, Brazil, India, and USA, while a lower species and family numbers with respect to the tropical forest in different regions of Malaysia, Ecuador, Thailand, Cameroon, and the Republic of Congo (Ostertag et al., 2014). The average stem density in this study area varies from 50 to 2525 with a mean value of 812.17 ± 111.75 , this value of stem density is greater from the reported value of the tropical forest of Mudumalai, India, but lower from the reported values across the tropical forest. The mean basal area ($15.94 \text{ m}^2 \text{ ha}^{-1}$) and biomass carbon (110.36 ± 31.70) of this study fall in the range of mean basal area and biomass carbon across the regions as reported in the previous study (Ostertag et al., 2014).

Stock is a key parameter for forest management as well in measuring biomass carbon of forest (Ahmad et al., 2019; Somogyi et al., 2008). Globally, national forestry inventories data are used for assessing forest growth. The FAO used national forest inventory data for global forestry statistics (FAO, 2010). In measuring forest growing stock and biomass carbon, tree height and diameter are the key components. Most of the volume tables are based on the height and diameter of a tree (Ahmad et al., 2019). But these tables represent the individual tree measurement. However, individual tree measurement is a time-consuming process that needs more financial and physical efforts. Therefore, there is a need for direct measurement of growing stock volume and biomass carbon. In this study, we test the scope of the tree height, diameter and basal area for the direct measurement of a tree growing stock volume and biomass carbon. The results that whether tree height, tree diameter, and basal area are in the best predictor of growing stock volume (GSV) and biomass carbon are presented in *Table 3*. The results in the table showed a strong positive correlation with the growing stock volume and biomass carbon with a coefficient of determination (R^2) value of 92 and 91, respectively. In the case of diameter, growing stock and biomass carbon relationship, there is a positive correlation, but the value of R^2 (0.40 and 0.38) represents a weak relationship compared to the basal area (*Fig. 3*) Similarly, height based growing stock volume and biomass carbon relationship also revealed a positive correlation, but not as strong as basal area based. These results clearly suggest that the basal area is the best predictor of growing stock volume and biomass carbon. Basal area is widely used in assessing forest growing stock and biomass carbon in the tropical wet and dry forest (Balderas Torres and Lovett, 2012).

Globally conservation measurements are emerging for forest biodiversity conservation with carbon management. The UN REED + policy helping in the establishment of safeguard areas with a high carbon stock and storage potential (Robbins, 2016). The potential of these safeguards areas for biodiversity and carbon conservation depends on the relationships between carbon and species diversity (Robbins, 2016). A positive correlation of species diversity indicates a potential interaction, while a negative would indicate "difficult trade-offs" (Gardner et al., 2012). Furthermore, the absence of any relationship would suggest different solutions for the establishment of safeguards areas (Thomas et al., 2013). Our present findings contrast with the reported positive diversity-biomass relationship (Cavanaugh et al., 2014). That tropical forests are positively but weakly correlated with species diversity in Asia. This presence of a weakly positive relationship indicates the driving mechanisms of

diversity-carbon relationships are scale-dependent or could be due to the environmental variations acting at a larger scale (Chisholm et al., 2013).

Conclusion

Assessing forest structural attributes, species diversity, growing stock characteristics, and biomass carbon is fundamental for effective forest carbon and biodiversity management. The results of the analysis of 174 field plots showed that the forest in the Guangxi region of China showed great variation in species diversity. The finding indicates that the forest vegetation had a large carbon mitigation potential. The basal area based growing stock and biomass carbon relationships highlighted that basal area is the best predictor for growing stock volume and biomass carbon compared to tree height and diameter. Thus, we suggest the use of the basal area for direct measurement of growing stock volume and biomass carbon to reduce both the financial and physical efforts. The positive but weak relationship of diversity indicates that a high carbon and biodiversity conservation forest can be achieved, that needs a further small scale and large-scale research. Our findings concluded that the forest of the Guangxi region, South China has not only a greater diversity but also has greater carbon mitigation potential.

Acknowledgments. This research was funded by National Key R&D Program of China, grant number 2016YFD060020501. We are thankful to Alamgir Khan, Sher Shah, Abdul Manan, Rohul Amin, and Muhammad Amir for their valuable suggestions to improve the article.

Data availability. The data used to support the findings of this study are available from the corresponding author upon request.

Conflict of interests. The authors declare that they have no conflict of interests.

REFERENCES

- [1] Ahmad, A., Nizami, S. M. (2015): Carbon stocks of different land uses in the Kumrat valley, Hindu Kush Region of Pakistan. – *Journal of forestry research* 26: 57-64.
- [2] Ahmad, A., Liu Q-J., Marwat, K. B., et al. (2019): Tree distribution pattern, growing stock characteristics and carbon mitigation potential of different forests ecosystems in Kumrat, Hindukush region of northern Pakistan. – *Pak. J. Bot* 51: 6.
- [3] Balderas Torres, A., Lovett, J. C. (2012): Using basal area to estimate aboveground carbon stocks in forests: La Primavera Biosphere's Reserve, Mexico. – *Forestry* 86: 267-281.
- [4] Bazzaz, F. (1998): Tropical Forests in a future Climate: Changes in Biological Diversity and Impact on the Global Carbon Cycle. – In: Markham, A. (ed.) *Potential Impacts of Climate Change on Tropical Forest Ecosystems*. Springer, Dordrecht, pp. 177-196.
- [5] Bonan, G. B. (2008): Forests and climate change: forcings, feedbacks, and the climate benefits of forests. – *Science* 320: 1444-1449.
- [6] Brown, S., Lugo, A. E. (1982): The storage and production of organic matter in tropical forests and their role in the global carbon cycle. – *Biotropica* 14: 161-187.
- [7] Bruelheide, H., Böhnke, M., Both, S., et al. (2011): Community assembly during secondary forest succession in a Chinese subtropical forest. – *Ecological Monographs* 81: 25-41.

- [8] Cavanaugh, K. C., Gosnell, J. S., Davis, S. L., et al. (2014): Carbon storage in tropical forests correlates with taxonomic diversity and functional dominance on a global scale. – *Global Ecology and Biogeography* 23: 563-573.
- [9] Change, I. C. (2007): Synthesis Report. – In: Pachauri, R. K., Reisinger, A. (eds.) *Contribution of Working Groups, I, II and III to the Fourth Assessment Report of the Intergovernmental Panel on Climate Change*. IPCC, Geneva, pp. 36-41.
- [10] Chisholm, R. A., Muller-Landau, H. C., Abdul Rahman, K., et al. (2013): Scale-dependent relationships between tree species richness and ecosystem function in forests. – *Journal of Ecology* 101: 1214-1224.
- [11] Corona, P. (2016): Consolidating new paradigms in large-scale monitoring and assessment of forest ecosystems. – *Environmental Research* 144: 8-14.
- [12] Dixon, R. K., Solomon, A., Brown, S., et al. (1994): Carbon pools and flux of global forest ecosystems. – *Science* 263: 185-190.
- [13] Du, H., Zeng, F., Peng, W., et al. (2015): Carbon storage in a Eucalyptus plantation chronosequence in Southern China. – *Forests* 6: 1763-1778.
- [14] Eckert, S. (2012): Improved forest biomass and carbon estimations using texture measures from WorldView-2 satellite data. – *Remote Sensing* 4: 810-829.
- [15] Fang, J., Guo, Z., Piao, S., et al. (2007): Terrestrial vegetation carbon sinks in China, 1981–2000. – *Science in China Series D: Earth Sciences* 50: 1341-1350.
- [16] Field, C. B., Behrenfeld, M. J., Randerson, J. T., et al. (1998): Primary production of the biosphere: integrating terrestrial and oceanic components. – *Science* 281: 237-240.
- [17] Gardner, T. A., Burgess, N. D., Aguilar-Amuchastegui, N., et al. (2012): A framework for integrating biodiversity concerns into national REDD + programmes. – *Biological Conservation* 154: 61-71.
- [18] Grassi, G., House, J., Dentener, F., et al. (2017): The key role of forests in meeting climate targets requires science for credible mitigation. – *Nature Climate Change* 7: 220.
- [19] Kang, B., Liu, S., Zhang, G., et al. (2006): Carbon accumulation and distribution in *Pinus massoniana* and *Cunninghamia lanceolata* mixed forest ecosystem in Daqingshan, Guangxi, China. – *Acta Ecologica Sinica* 26: 1320-1327.
- [20] Keenan, R. J., Reams, G. A., Achard, F., et al. (2015): Dynamics of global forest area: results from the FAO Global Forest Resources Assessment 2015. – *Forest Ecology and Management* 352: 9-20.
- [21] Lei, X., Tang, M., Lu, Y., et al. (2009): Forest inventory in China: status and challenges. – *International Forestry Review* 11: 52-63.
- [22] Li, X., Mao, F., Du, H., et al. (2017): Assimilating leaf area index of three typical types of subtropical forest in China from MODIS time series data based on the integrated ensemble Kalman filter and PROSAIL model. – *ISPRS Journal of Photogrammetry and Remote Sensing* 126: 68-78.
- [23] Liu, Y. Y., Van Dijk, A. I., De Jeu, R. A., et al. (2015): Recent reversal in loss of global terrestrial biomass. – *Nature Climate Change* 5: 470.
- [24] Lu, L., Wang, B., He, R. (1999): The effect of site and cultivation model on growth of *Castanopsis hystrix*. – *Forest Research* 12: 519-523.
- [25] Magurran, A. E. (2013): *Measuring Biological Diversity*. – John Wiley & Sons, New York.
- [26] Matthews, H. D., Graham, T. L., Keverian, S., et al. (2014): National contributions to observed global warming. – *Environmental Research Letters* 9: 014010.
- [27] McElhinny, C., Gibbons, P., Brack, C., et al. (2005): Forest and woodland stand structural complexity: its definition and measurement. – *Forest Ecology and Management* 218: 1-24.
- [28] Meng, J., Lu, Y., Zeng, J. (2014): Transformation of a degraded *Pinus massoniana* plantation into a mixed-species irregular forest: Impacts on stand structure and growth in southern China. – *Forests* 5: 3199-3221.

- [29] Meng, J., Li, S., Wang, W., et al. (2016): Estimation of forest structural diversity using the spectral and textural information derived from SPOT-5 satellite images. – *Remote Sensing* 8: 125.
- [30] Ming, A., Jia, H., Zhao, J., et al. (2014): Above-and below-ground carbon stocks in an indigenous tree (*Mytilaria laosensis*) plantation chronosequence in subtropical China. – *PloS One* 9: e109730.
- [31] Muneer, M.A., Wang, M., Jing, Z., et al. (2019): Low host specificity of arbuscular mycorrhizal fungi associated with dominant steppe plants in Inner Mongolia. – *Applied Ecology and Environmental Research* 17: 12073-12089.
- [32] Naeem, S., Bunker, D. E., Hector, A., et al. (2009): *Biodiversity, Ecosystem Functioning, and Human Wellbeing: An Ecological and Economic Perspective*. – Oxford University Press, Oxford.
- [33] Naidu, M. T., Kumar, O. A. (2016): Tree diversity, stand structure, and community composition of tropical forests in Eastern Ghats of Andhra Pradesh, India. – *Journal of Asia-Pacific Biodiversity* 9: 328-334.
- [34] Noumi, V. N., Djongmo, V. A., Nyeck, B., et al. (2018): Vegetation structure, carbon sequestration potential and species conservation in four agroforestry systems in Cameroon (Tropical Africa). – *Acta Botanica Brasilica*. DOI: 10.1590/0102-33062017abb0279.
- [35] Ostertag, R., Inman-Narahari, F., Cordell, S., et al. (2014): Forest structure in low-diversity tropical forests: a study of Hawaiian wet and dry forests. – *PloS One* 9: e103268.
- [36] Poorter, L., Van Der Sande, M., Thompson, J., et al. (2015): Diversity enhances carbon storage in tropical forests. – *Global Ecology and Biogeography* 24: 1314-1328.
- [37] Robbins, A. (2016): How to understand the results of the climate change summit: Conference of Parties21 (COP21) Paris 2015. – *Journal of Public Health Policy*. <https://doi.org/10.1057/jphp.2015.47>.
- [38] Sierra, C. A., del Valle, J. I., Orrego, S. A., et al. (2007): Total carbon stocks in a tropical forest landscape of the Porc region, Colombia. – *Forest Ecology and Management* 243: 299-309.
- [39] Somogyi, Z., Teobaldelli, M., Federici, S., et al. (2008): Allometric biomass and carbon factors database. – *Iforest-Biogeosciences and Forestry* 1: 107.
- [40] Sullivan, M. J., Talbot, J., Lewis, S. L., et al. (2017): Diversity and carbon storage across the tropical forest biome. – *Scientific Reports* 7: 39102.
- [41] Tang, J.-X., Bai, L.-H., Guo, W.-F., et al. (2012): Preliminary study on growth regularity of *Castanopsis hystrix* plantation. – *Journal of Central South University of Forestry & Technology* 2012(4).
- [42] Team, R. C. (2013): *R: A Language and Environment for Statistical Computing*. – R Core Team, Vienna.
- [43] Thomas, C. D., Anderson, B. J., Moilanen, A., et al. (2013): Reconciling biodiversity and carbon conservation. – *Ecology Letters* 16: 39-47.
- [44] Wang, L., Xue, C., Pan, X., et al. (2018): Application of controlled-release urea enhances grain yield and nitrogen use efficiency in irrigated rice in the Yangtze River Basin, China. – *Frontiers in Plant Science* 9. DOI: 10.3389/fpls.2018.00999.
- [45] Wang, Z., Du, H., Song, T., et al. (2015): Allometric models of major tree species and forest biomass in Guangxi. – *Acta Ecol. Sin* 35: 4462-4472.
- [46] Warfield, J. N. (2006): *An Introduction to Systems Science*. – World Scientific, River Edge, NJ.
- [47] Xiao C-W., Yuste, J. C., Janssens, I., et al. (2003): Above-and belowground biomass and net primary production in a 73-year-old Scots pine forest. – *Tree Physiology* 23: 505-516.
- [48] Zhang, C., Ju, W., Chen, J. M., et al. (2013): China's forest biomass carbon sink based on seven inventories from 1973 to 2008. – *Climatic Change* 118: 933-948.

- [49] Zhu, P., Wang, Z., Ye, W., et al. (2013): Preliminary studies on pollination and mating system of rare and endangered plant *Erythrophleum fordii* Oliv. – *Journal of Tropical and Subtropical Botany* 21: 38-44.

APPENDIX

Table A1. Diversity indices data for all plots

Plot No	Pielou's evenness	Shannon DI	Simpson	GINI Coefficient
1	0.576217	0.63304	0.349030471	0.366572
2	0.476463	0.766838	0.3488	0.28923
3	0.776771	1.076833	0.581446311	0.535711
4	0.287086	0.315396	0.139917695	0.277387
5	0.841636	1.93794	0.812071331	0.609881
6	0	0	0	0
7	0	0	0	0
8	0.748555	1.86009	0.75308642	0.533193
9	0.292665	0.524385	0.215251487	0.320634
11	0.968632	1.884871	0.840236686	0.622295
12	0.946395	1.039721	0.625	0.595755
13	0.906895	2.326139	0.880941603	0.529475
14	0.830451	1.726875	0.773175542	0.731258
15	0.468996	0.325083	0.18	0.25371
16	0.738021	1.436122	0.680272109	0.583156
17	0.668946	1.469825	0.664940828	0.442352
19	0.626512	1.219137	0.535147392	0.410751
20	0.827407	1.33166	0.6875	0.566102
21	0.431854	0.695042	0.396431722	0.304012
22	0.936304	2.245159	0.88	0.454053
24	0.452351	0.728032	0.36294896	0.311519
25	0.825631	1.814098	0.772727273	0.536075
27	0.521172	0.722498	0.37037037	0.283177
28	0.745657	1.033701	0.578125	0.293181
29	0.511688	0.709351	0.382271468	0.425373
30	0.69625	1.120571	0.545	0.473322
31	0.83875	2.151352	0.831020408	0.616176
34	0.777132	1.789411	0.77318641	0.659339
36	0.804497	1.76766	0.786703601	0.547489
37	0.872494	2.362757	0.867346939	0.640003
39	0.760738	2.109213	0.804664723	0.600097
40	0.867726	2.156218	0.853177502	0.606399
42	0.900092	2.495584	0.896333182	0.548714
44	0.344913	0.478151	0.217687075	0.428515
46	0.647978	1.347433	0.59833795	0.480582
47	0.733691	0.806042	0.527089073	0.580547
48	0.725226	1.593484	0.687277051	0.525282

49	0.786988	1.636496	0.71	0.47807
51	0	0	0	0
54	0.454262	0.813927	0.357659435	0.307899
56	0.723376	1.164229	0.6176	0.590368
58	0.372013	0.408698	0.196428571	0.226294
60	0.889231	2.280832	0.879501385	0.654842
61	0.276195	0.191444	0.090702948	0.15473
63	0.795854	2.041325	0.810657596	0.481883
65	0.832941	2.136452	0.843621399	0.572395
66	0.798255	1.43028	0.693333333	0.378562
67	0.766563	1.765076	0.737777778	0.413766
69	0.735509	0.509816	0.328180737	0.228401
70	0.864974	0.950271	0.56	0.137444
72	0.787629	1.813583	0.765868887	0.566309
73	0.371232	0.257319	0.132653061	0.084405
74	0.507101	1.054487	0.543905325	0.543927
75	0.73553	1.431275	0.674556213	0.567012
76	0	0	0	0
78	0.733595	1.180676	0.618923611	0.442309
80	0.860361	1.78907	0.806922661	0.674427
81	0.907208	2.570314	0.90877915	0.475267
83	0.811527	2.01657	0.796398892	0.586654
85	0.587947	1.222602	0.555785124	0.340998
86	0.266765	0.184907	0.08677686	0.385625
89	0.617059	0.677909	0.380622837	0.611744
90	0.941735	1.034601	0.62244898	0.38662
91	0.700221	1.362566	0.615702479	0.504637
94	0.272253	0.438174	0.181061394	0.396852
95	0.920325	1.649	0.780023781	0.526034
96	0.832378	1.339661	0.702947846	0.654079
97	0.873002	1.698783	0.763888889	0.572947
98	0.730985	1.520041	0.682926829	0.540197
99	0	0	0	0
100	0.802405	0.881532	0.5546875	0.596741
102	0	0	0	0
104	0.806027	2.002903	0.810249307	0.608665
106	0.381982	0.41965	0.207346939	0.468058
107	0.624889	1.119651	0.577609519	0.479489
110	0.681422	1.693271	0.725525098	0.512811
111	0.852664	1.963331	0.8096	0.640489
112	0.511614	0.995554	0.457593688	0.517096
115	0.650624	0.714783	0.453217956	0.285847
117	0.943511	2.673167	0.92	0.345099
119	0.593279	0.822459	0.422476587	0.401978
122	0.864737	1.39174	0.71875	0.247757
123	0.773601	1.608657	0.703703704	0.495338

124	0	0	0	0
125	0.543564	0.37677	0.21875	0.316422
127	0.908304	0.997874	0.6016	0.629252
128	0	0	0	0
129	0	0	0	0
130	0.567163	1.103647	0.497781065	0.385753
132	0.422001	0.292508	0.156734694	0.22161
134	0.620731	1.112201	0.524005487	0.497316
135	0.548065	1.066486	0.482103725	0.500377
136	0	0	0	0
137	0.717905	1.783926	0.697530864	0.484719
138	0.349642	0.626474	0.25462963	0.221132
139	0.556331	0.89538	0.42	0.434019
141	0.33729	0.233792	0.1171875	0.422432
142	0.608003	1.18312	0.549886621	0.341771
143	0	0	0	0
144	0.31969	0.514521	0.218490305	0.269218
145	0.824467	1.898405	0.806692773	0.329984
146	0.716323	1.890418	0.758494031	0.312573
147	0.782252	1.084432	0.594104308	0.456489
149	0.925863	1.017164	0.609418283	0.288092
151	0.882344	2.192543	0.865051903	0.588248
152	0.595906	0.65467	0.364197531	0.393768
153	0.858567	1.976923	0.8128	0.517908
154	0	0	0	0
155	0	0	0	0
157	0.421596	0.46317	0.229968311	0.210259
159	0.709446	0.983501	0.566162571	0.503001
161	0	0	0	0
162	0	0	0	0
164	0.559809	1.164091	0.594674556	0.536746
165	0	0	0	0
166	0.81752	0.898137	0.556213018	0.136753
167	0	0	0	0
168	0.383255	0.531304	0.242222222	0.561176
169	0.663489	1.188813	0.587890625	0.466275
170	0	0	0	0
171	0.952522	2.193262	0.879904875	0.608873
173	0.758818	1.577917	0.72543618	0.499811
174	0.905713	0.995027	0.592592593	0.441657
175	0.824044	1.975971	0.821037253	0.406082
176	0.607773	0.978173	0.467120181	0.464165
177	0.92062	1.011404	0.611111111	0.505057
178	0.447075	0.491162	0.257785467	0.445699
179	0.718373	0.789213	0.519395135	0.408087
180	0.735509	0.509816	0.328180737	0.261715

181	0.392378	0.431071	0.210059172	0.30596
182	0.685776	1.426031	0.637777778	0.478157
185	0.304221	0.334221	0.1504	0.240211
186	0.921628	2.122127	0.861602497	0.514186
187	0.921185	1.277034	0.693877551	0.699302
189	0.856326	1.78068	0.798353909	0.56952
191	0.515273	0.566086	0.291666667	0.324354
192	0	0	0	0
193	0.670877	1.079735	0.524691358	0.340699
194	0.233584	0.323816	0.130165289	0.280499
195	0.910864	1.63205	0.786703601	0.465055
196	0.717438	1.840192	0.783068783	0.666519
197	0.371232	0.257319	0.132653061	0.235044
198	0.304221	0.334221	0.1504	0.407337
200	0.845351	0.585953	0.396694215	0.693085
204	0	0	0	0
205	0.68567	0.753286	0.492438563	0.39043
206	0.704575	1.262429	0.611570248	0.44649
207	0	0	0	0
208	0.258019	0.178845	0.083175803	0.184031
209	0.818289	1.88418	0.7936	0.442242
211	0.303375	0.210283	0.102264427	0.236289
212	0.447814	0.620802	0.322845805	0.26649
213	0.795886	1.103332	0.597505669	0.492705
214	0.871049	1.56071	0.75	0.562479
215	0.782992	0.542729	0.357290298	0.283409
216	0.751085	1.729436	0.73	0.522164
218	0.568724	1.106685	0.51808021	0.146053
219	0.48689	0.534903	0.289704142	0.394593
220	0.767199	1.595346	0.72702332	0.301114
221	0.643968	1.153835	0.61257687	0.657433
222	0	0	0	0
224	0.918296	0.636514	0.444444444	0.357069
225	0.23494	0.420956	0.158333333	0.302133
226	0.315914	0.347067	0.16	0.384589
227	0.319337	0.221348	0.109220752	0.295215
229	0.646823	1.34503	0.60375	0.272159
230	0	0	0	0
231	0.736734	1.32005	0.655749377	0.084467
232	0.850594	1.655179	0.756944444	0.335953
233	0.854071	2.367989	0.862140775	0.583625
234	0.51972	0.836456	0.428571429	0.557649
235	0.594604	0.956979	0.464285714	0.34051
236	0.222285	0.154076	0.068877551	0.393967
237	0.558449	1.161261	0.51041047	0.302074

Table A2. Forest structure with respect to family, genera and species

	Family	Genera	Species
1	Actinidiaceae	Saurauia	<i>Saurauia tristyla</i>
2	Altingiaceae	Liquidambar	<i>Liquidambar formosana</i>
3	Anacardiaceae	Choerospondias, Pistacia, Rhus, Toxicodendron	<i>Choerospondias axillaris</i> , <i>Pistacia chinensis</i> , <i>Rush chinensis</i> , <i>Toxicodendron vernicifluum</i> , <i>Toxicodendron succedaneum</i>
4	Apocynaceae	Stropanthus, Rauvolfia	<i>Stropanthus divaricatus</i> , <i>Rauvolfia verticillata</i>
5	Aquifoliaceae	Ilex	<i>Ilex godajam</i> , <i>Ilex hainanensis</i> , <i>Ilex chinensis</i>
6	Araliaceae	Tetrapanax, Schefflera, Heteropanax, Aralia	<i>Tetrapanax papyrifer</i> , <i>Schefflera octophylla</i> , <i>Heteropanax fragrans</i> , <i>Aralia chinensis</i>
7	Arecaceae	Caryota	<i>Caryota ochlandra</i>
8	Betulaceae	Ostrya	<i>Ostrya japonica</i>
9	Bignoniaceae	Oroxylum, Redermachera, Dolichandrone	<i>Oroxylum indicum</i> , <i>Redermachera sinica</i> , <i>Dolichandrone sinica</i>
10	Boraginaceae	Cordia	<i>Cordia dichotoma</i>
11	Burseraceae	Garuga, Canarium	<i>Garuga floribunda</i> , <i>Canarium pimela</i> , <i>Canarium album</i>
12	Cannabaceae	Trema	<i>Trema dielsiana</i> , <i>Trema cannabina</i> , <i>Trema tomentosa</i>
13	Caprifoliaceae	Lonicera	<i>Lonicera chrysantha</i>
14	Cornaceae	Cornus, Aphanamixis, Alangium	<i>Cornus capitata</i> , <i>Aphanamixis grandifolia</i> , <i>Alangium feberi</i> , <i>Alangium kurzi</i>
15	Cupressaceae	Cunninghamia	<i>Cunninghamia lanceolata</i>
16	Dilleniaceae	Dillenia	<i>Dillenia indica</i>
17	Ebenaceae	Diospyros	<i>Diospyros kaki</i> , <i>Diospyros saxatilis</i> , <i>Diospyros morrisian</i>
18	Elaeocarpaceae	Elaeocarpus	<i>Elaeocarpus sylvestri</i>
19	Euphorbiaceae	Aleurites, Vernicia, Glochidion, Macaranga, Mallotus	<i>Aleurites montana</i> , <i>Vernicia fordii</i> , <i>Vernicia montana</i> , <i>Glochidion hirsutum</i> , <i>Macaranga denticulata</i> , <i>Mallotus barbatus</i> , <i>Mallotus japonicus</i> , <i>Mallotus paniculatus</i> , <i>Mallotus philippensis</i>
20	Euphorbioideae	Sapium	<i>Sapium sebiferum</i> , <i>Sapium discolor</i>
21	Fabaceae	Acacia, Adenantha, Albizia, Calliandra, Dalbergia, Erythrophleum, Leucaena, Millettia, Mimosa, Pithecellobium	<i>Acacia confusa</i> , <i>Adenantha pavonina</i> , <i>Albizia julibrissin</i> , <i>Albizia odoratissima</i> , <i>Calliandra brevipes</i> , <i>Dalbergia odorifera</i> , <i>Erythrophleum fordii</i> , <i>Leucaena leucocephala</i> , <i>Millettia speciosa</i> , <i>Mimosa sepiaria</i> , <i>Pithecellobium clypearia</i> , <i>Pithecellobium lucidum</i>
22	Fagaceae	Castanea, Castanopsis, Quercus	<i>Castanea mollissima</i> , <i>Castanopsis fargesii</i> , <i>Castanopsis hystrix</i> , <i>Quercus griffithii</i> , <i>Quercus linn</i>
23	Hamamelidaceae	Mytilaria, Rhodoleia	<i>Mytilaria laosensis</i> , <i>Rhodoleia championii</i>
24	Hypericaceae	Cratoxylum	<i>Cratoxylum cochinchinense</i>
25	Lamiaceae	Gmelina, Tectona, Clerodendrum	<i>Gmelina chinensis</i> , <i>Tectona grandis</i> , <i>Clerodendrum ervatamioides</i>

26	Lauraceae	Actinodaphne, Phoebe, Neolitsea, Machilus, Litsea, Lindera, Cinnamomum	<i>Actinodaphne pilosa, Actinodaphne angustifolia, Phoebe zhennan, Phoebe bournei, Neolitsea sericea, Machilus chinensis, Machilus pauhoi, Machilus pingii, Machilus velutina, Litsea cubeba, Litsea glutinosa, Litsea monopetala, Litsea elongata, Litsea forrestii, Litsea panamonja, Litsea pungens, Litsea yunnanensis, Lindera glauca, Cinnamomum bodinieri</i>
			<i>Cinnamomum camphora, Cinnamomum cassia,</i>
			<i>Cinnamomum Tonkinense</i>
27	Magnoliaceae	Tsoongiodendron, Manglietia, Michelia, Liriodendron	<i>Tsoongiodendron odorum, Manglietia glanca,</i>
			<i>Manglietia hainanensis, Michelia alba, Michelia macclurei, Liriodendron chinense</i>
28	Malvaceae	Microcos, Sterculia, Helicteres, Hibiscus, Excentrodendron, Bombax	<i>Microcos paniculata, Sterculia lanceolata, Sterculia nobilis, Helicteres angustifolia, Hibiscus mutabilis, Excentrodendron hsienmu, Bombax malabaricum</i>
29	Meliaceae	Chukrasia, Cipadessa, Melia, Khaya, Aphanamixis	<i>Chukrasia tabularis, Cipadessa cinerascens, Melia azedarach, Khaya senegalensis, Aphanamixis polystachya</i>
30	Moraceae	Artocarpus, Broussonetia, Ficus	<i>Artocarpus hypargyreus, Broussonetia kaempferi, Broussonetia papyrifera, Ficus altissima, Ficus auriculata, Ficus esquiroliana, Ficus hispida, Ficus oligdon, Ficus ruyuanensis, Ficus hirta, Ficus irisana, Ficus microcarpa, Ficus orthoneura, Ficus racemosa, Ficus tinctoria</i>
31	Myricaceae	Myrica	<i>Myrica rubra</i>
32	Myrtaceae	Eucalyptus, Syzygium	<i>Eucalyptus robusta, Eucalyptus urophylla, Eucalyptus fordii, Syzygium cumini, Syzygium hainanense</i>
33	Oleaceae	Olea, Ligustrum, Fraxinus	<i>Olea europaea, Ligustrum compactum, Ligustrum quihoui, Fraxinus chinensis</i>
34	Paeoniaceae	Paeonia	<i>Paeonia suffruticosa, Paeonia delavayi</i>
35	Pentaphylaceae	Eurya	<i>Eurya groffii, Eurya ciliata, Eurya japonica</i>
36	Phyllanthaceae	Antidesma, Phyllanthus, Bischofia, Bridelia, Glochidion	<i>Antidesma bunius, Antidesma celebicum, Antidesma fordii, Phyllanthus emblica, Bischofia javanica, Bischofia polycarpa, Bridelia tomentosa, Bridelia stipularis, Glochidion puberum</i>
37	Pinaceae	Pinus	<i>Pinus massoniana, Pinus elliotii, Pinus caribaea,</i>
38	Poaceae	Bambusa	<i>Bambusa rutila</i>
39	Primulaceae	Ardisia, Maesa	<i>Ardisia japonica, Maesa japonica</i>
40	Rhamnaceae	Ziziphus, Sageretia, Hovenia	<i>Ziziphus jujuba, Sageretia theezans, Hovenia acerba</i>
41	Rosaceae	Crataegus, Pyrus	<i>Crataegus pinnatifida, Pyrus calleryana</i>
42	Rubiaceae	Canthium, Catunaregam, Wendlandia, Psychotria, Pavetta	<i>Canthium horridum, Catunaregam spinosa, Wendlandia tinctoria, Wendlandia uvariifolia, Psychotria rubra, Pavetta arenosa, Pavetta hongkongensis</i>
43	Rutaceae	Citrus, Clausena, Zanthoxylum, Tetradium, Evodia	<i>Citrus reticulata, Clausena excavata, Zanthoxylum avicennae, Tetradium glabrifolium, Evodia lapa, Evodia trichotoma</i>
44	Sapindaceae	Acer, Sapindus, Litchi, Dimocarpus	<i>Acer momo, Sapindus mukorossi, Litchi chinensis, Dimocarpus longan</i>

45	Schisandraceae	Illicium	<i>Illicium verum</i>
46	Simaroubaceae	Brucea	<i>Brucea javanica</i>
47	Solanaceae	Solanum	<i>Solanum erianthum</i>
48	Staphyleaceae	Staphylea	<i>Staphylea forrestii</i>
49	Styracaceae	Styrax	<i>Styrax subniveus</i> , <i>Styrax tonkinensis</i> , <i>Styrax officinalis</i>
50	Symplocaceae	Symplocos	<i>Symplocos cochinchinensis</i>
51	Theaceae	Schima, Camellia	<i>Schima argenticornis</i> , <i>Schima superba</i> , <i>Schima wallichii</i> , <i>Camellia japonica</i> , <i>Camellia oleifera</i>

DROUGHT STRESS INTENSITY, DURATION AND ITS RESISTANCE IMPACT ON RICE (*ORYZA SATIVA* L.) SEEDLING

CHEN, Z. K.^{1#} – XU, W. W.^{1#} – NIE, J.¹ – KHAN, A.¹ – CAO, C. G.^{1,2} – LI, P.^{1*}

¹College of Plant Science and Technology, Huazhong Agricultural University, Wuhan, Hubei 430070, China

²Hubei Collaborative Innovation Center for Grain Industry, Yangtze University, Jingzhou, Hubei 434025, China

[#]These authors equally contributed to this work

*Corresponding author

e-mail: sleep1022@mail.hzau.edu.cn

(Received 7th Sep 2019; accepted 15th Nov 2019)

Abstract. Rice seedlings have a different response to drought stress intensity and duration, which reduces rice seedling growth and grain yield. In the year 2015, a greenhouse experiment was conducted to ascertain the effect of the relationship between drought stress intensity, duration, and drought resistance on rice seedling. Yangliangyou 6 (“super” rice variety) and Hanyou 113 (drought-resistance rice variety) were subjected to polyethylene glycol (PEG6000)-induced water stress. Drought stress intensities i.e. 10%, 15%, 20% and 25% PEG6000 with 4 d, 8 d or 12 d after emergence at 21 days was imposed, respectively. Control (0% PEG6000) was used for comparison. Drought dehydration factor (DDF) and root induction factor (RIF) increased with drought duration. In each drought stress duration, RIF, drought tolerance factor (DTF) and DDF were raised under moderate drought stress intensity (10-15% PEG6000), the advantage of DDF and DTF was shown at 12 d drought duration under severe drought stress intensity (20-25% PEG6000). Thus, drought stress intensity significantly negatively affected rice seedling growth compared with drought stress duration. Improvement in DDF and RIF enhanced rice seedling growth under moderate drought stress conditions, while severe drought stress positively stimulated DDF and DTF which resulted in improved rice seedling growth.

Keywords: polyethylene glycol, drought tolerance, drought dehydration, root induction, dry mass

Abbreviations: ARI: adversity resistance index; CDRF: comprehensive drought resistant factor; CK: control treatment (0% polyethylene glycol 6000 solution); Co: conductivity; DDF: drought dehydration factor; DM: dry mass; DTF: drought tolerance factor; HY113: Hanyou 113; LA: leaf area; LRL: longest root length; MLL: mean leaf length; MLW: mean leaf width; PEG: polyethylene glycol; Pro: proline; RDM: root dry matter; RIF: root induction factor; RN: root number; RV: root volume; RWC: relative water content; SDM: shoot dry matter; SH: seedling height; SS: soluble sugar; TDM: total dry matter; YLY6: Yangliangyou 6

Introduction

Rice (*Oryza sativa* L.) is the most important staple food crop for about 33% of people worldwide (Ye et al., 2013). Rice is grown under traditional flooding irrigation (Yang et al., 2008; Ye et al., 2013), but the shortage of water resources coupled with seasonal drought spell has limited rice production. Thus, stimulated the development of upland rice planting (Sun et al., 2012; Ye et al., 2013). Upland rice planting area has increased to 20 million ha worldwide and the planting area accounted for 12.7% of total rice planting area (Technology and Information Center of China Rice Research Institute, 2016). In China, due to limitations of hilly area, water shortage, suitable planting areas for upland rice were 5.3 million to 6.7 million ha (Technology and Information Center of China Rice Research

Institute, 2016). But rice dry cultivation is still facing some challenges such as, variety selection, soil moisture conditions required for sowing and maintaining seedling growth. To overcome these challenges, it is important to improve planting technologies of upland rice to achieve optimistic resource utilization.

In current agricultural production systems, super rice variety (rice yield potential was about 10.5-12.0 t ha⁻¹ and increased by 8-15% compared with ordinary hybrid and inbred varieties. This increment in yield was associated with more number per unit land area and large panicle size (Huang et al., 2011). Drought tolerance rice variety (the yield potential and good quality could be maintained under water-limited environments, as well as the capacity of water-saving or drought resistance (Luo et al., 2010)) were used in upland rice system to increase economic benefits. Upland rice is directly seeded by less water application which improved germination and emergence of rice seeds, and followed by no water application leading to seedling damage or death and consequently yields loss (Xu et al., 2017). Hence, it is necessary to define what modes of drought stress (different drought stress intensity and duration) had less effect on rice seedling during seedling stage. Also to identify drought tolerance of rice seedling growth in upland rice system. Rice dry cultivation mainly caused drought stress which impacted on rice seedling growth. Drought stress can induce various changes in morphological, metabolic and/or physiological functions and severely restrict both elongation and expansion of rice seedling (Kusaka et al., 2005). Drought stress also produced the reactive oxygen species (ROS), which could damage plant by lipid peroxidation, protein degradation, DNA fragmentation and ultimately cell death (Zhang et al., 2015). With increasing drought stress, shoot growth, root expansion and physiological function of rice seedling decreased (Pirdashti et al., 2003; Zheng et al., 2016). Increasing drought stress duration can restrain shoot growth of rice seedling and reducing yield and yield components (Asai et al., 2009; Duan et al., 2017). This indicated that drought stress intensity and duration had a negative effect on rice seedling growth. However, the effect of drought stress intensity coupled with duration on the rice seedling growth during seedling stage (after reviving stage) is lacking. Plants can avoid drought stress through two major mechanisms including drought dehydration and drought tolerance under drought stress conditions (Liu et al., 2003; Yue et al., 2006). Drought dehydration via using morphological plasticity of crops raised the water content of plant; drought tolerance indicated that crops could tolerate water loss and maintain certain metabolic or physiological processes such as, osmotic adjustment and antioxidant ability (Bandurska et al., 2003; Nazarli et al., 2014). Drought dehydration plays a crucial role in long-term drought duration, while drought tolerance had an obvious response to drought stress intensity (Yue et al., 2006; Farooq et al., 2009; Li et al., 2012). However, the relationship among the drought dehydration, tolerance, drought stress intensity and duration impact on rice seedling growth are poorly known.

Polyethylene glycol (PEG) is composed of a large molecular size and nontoxic in nature, therefore categorized as osmopriming reagents, which lowers the water potential without penetrating into seeds upon soaking (Chen and Arora, 2011; Zheng et al., 2016). Osmotic stress with PEG has been proposed to improve seed germination, early seedling vigor, antioxidant enzymes activity and eventually leading to increase stress tolerance in many crop plants (Chen and Arora, 2011). Seedlings death occurred at 8-12 d with water break after emergence under severe drought stress (Chen and Arora, 2011). Thus, in this study PEG was used to simulate drought stress in 12 d at water break after emergence (1) to investigate the morphology of shoot and root, anti-active substance

and the accumulation in rice seedling under different drought stress intensity and duration; (2) to examine the relationship between drought stress intensity and duration as well as drought resistance impacted on rice seedling growth.

Materials and methods

Experiment site and design

A greenhouse experiment was conducted at Huazhong Agricultural University, Hubei Province, China (E114°29', N30°29') in the 2017 growing season. Two rice varieties were used, Hanyou 113 (HY113), having the ability of drought resistance and water-saving. It was bred by Shanghai Agricultural Biological Gene Center (Shanghai province, China); Yangliangyou 6 (YLY6, “super” hybrid rice), indica and two-line hybrid rice, which was bred by Lixiahe Regional Research of Agricultural Science (Jiangsu province, China). It is widely cultivated in the middle and lower reaches of Yangtze River. The initial seed moisture contents of HY113 and YLY6 were 10.8% and 11.0%, respectively. Rice seeds were sterilized with 25% prochloraz for 10 min. The seeds of YLY6 and HY113 were sown in culture solution (pH 5.0) at room temperature. The culture solution was a modified rice nutrient solution (nutrient solution scheme was provided by Internal Rice Research Institute) with the compositions (*Table 1*). The nutrient solution was renewed after 4 days. Three-week-old seedlings were transplanted to plastic buckets containing (250 mL, diameter 10 cm, height 15 cm) the same nutrient solution and renewed time. The room temperature and humidity were 25-30 °C and 80%, respectively. The natural light was used during the whole experiment.

Table 1. Conventional nutrient solution

Chemical compound	Formula weight	Concentration (g/L)
NH ₄ NO ₃	80.04	22.8578
NaH ₂ PO ₄ ·2H ₂ O	156.01	10.072
K ₂ SO ₄	174.26	17.8284
CaCl ₂	110.99	22.1558
MgCl ₂ ·6H ₂ O	203.30	66.9182
Na ₂ SiO ₃ ·9H ₂ O	284.20	9.52
MnSO ₄ ·H ₂ O	169.01	0.769
Na ₂ MoO ₄ ·2H ₂ O	241.95	0.0605
H ₃ BO ₃	61.83	0.572
ZnSO ₄ ·7H ₂ O	287.56	0.0288
CuSO ₄ ·5H ₂ O	249.68	0.02
C ₆ H ₇ O ₈ ·H ₂ O	210.14	14.875
FeSO ₄ ·7H ₂ O	278.02	4.9766
EDTA-Na ₂ ·2H ₂ O	372.24	6.665

PEG-6000 solution was used to induce osmotic stress on rice seedling (Chen and Arora, 2011; Zheng et al., 2016). Thirty treatments in each of eight replications (eight pots per replication and each pot comprised of one rice seedling) were used as follows: two varieties Yangliangyou 6 (YLY 6) and Hanyou 113 (HY113); five PEG-6000 solutions, i.e. 0%, 10%, 15%, 20% or 25% PEG-6000 (kg kg⁻¹ (water)), the osmotic

potential in each solution respectively was maintained at 0 kPa, -10 kPa, -15 kPa, -20 kPa and -25 kPa, among these 0% PEG 6000 solution was used as control (CK); three drought duration with each PEG-6000 solutions to rice seedling were 4 d, 8 d and 12 d. In addition, 10%, 15% and 20-25% PEG-6000 concentration were regarded as mild, moderate and severe drought stress, respectively; and drought duration with 4 d, 8 d and 12 d were respectively referred to short-term, medium-term and long-term drought stress. Rice seedlings were watered with 0%, 10%, 15%, 20% or 25% PEG-6000 concentration at 5th days after seedlings transplanted to the plot.

Measurements

At 4 d, 8 d and 12 d after drought stress with two repetitions each treatment, seedlings were uprooted, washed, and placed into an insulated box to prevent deterioration. Rice seedlings, relative water content (RWC), soluble sugar (SS), proline content (Pro) and conductivity (Co) were assessed according to Basu et al. (2010).

Seedling morphological characteristics, dry mass and relative water content

Shoot length (SH), longest root length (LRL), mean leaf length (MLL) and mean leaf width (MLW) were measured with a ruler; leaf area (LA) were measured by LI-3100C (LI-COR Inc., Lincoln, NE, USA). Seedlings were dissected into roots and shoots to assess the fresh weight (FW), respectively.

The roots of each seedling were spread in a plastic tray contained deionized water and scanned using a flatbed scanner (300 dpi). Root images were analyzed using WinRhizo image analysis software (Regent Instruments, Quebec, Canada). The software was configured to measure root volume (RV, cm³) and root number (RN).

After scanning the roots, the root and shoot of rice seedling were oven-dried at 80°C for 48 h, and shoot dry mass (SDM) and root dry mass (RDM) was weighed to obtain dry mass (DM). Adversity resistance index (ARI) was calculated by the formula (Wang et al., 2007):

$$ARI = \left(\frac{DM_{(T)}}{DM_{(CK)}} \right) \times DM_{(A)} \quad (\text{Eq.1})$$

where $DM_{(T)}$ was the dry mass of each treatment except CK, $DM_{(CK)}$ was the dry mass in CK, $DM_{(A)}$ was the average value of dry mass in all treatments including CK.

RWC was calculated using the formula (Basu et al., 2010):

$$RWC = \frac{FW - DW}{FW} \quad (\text{Eq.2})$$

where FW and DM respectively indicated the fresh weight and the dry mass of organs in rice seedling.

Soluble sugar, proline content and conductivity

Soluble sugar (SS) content was determined by Anthrone colorimetry (Zhang and Qu, 2003). A 1.0 ml aliquot of the supernatant of tissue extract (root or shoot) was added 1.5 mL distilled water, which was mixed with 1 ml of 9% phenol method, then

homogenized in 5 mL of concentrated sulfuric acid. The mixture was at 25°C for 30 min. The absorption of chromophore was determined at 485 nm (Tecan-infinite M200, Switzerland).

Free proline content (Pro) of rice shoot and root were assayed according to the method (Bates et al., 1973). The samples were homogenized in 5 mL of 3% sulfo-salicylic acid and centrifuged at 6000 rpm for 10 min. The supernatant of 2 mL was heated with 2 mL of ninhydrin and 2 mL glacial acetic acid at 100°C for 1 h. The reaction was further extracted with 4 mL of toluene by vigorously vortexed for 30 s. The absorption of chromophore was determined at 520 nm.

To determine conductivity (Co), shoot or root materials (0.5 g) were washed with deionized water and placed in 20 ml deionized water tubes. The electrical conductivity of the solution was measured after 1 h of shaking at room temperature. Then samples were heated for 20 min and Co was measured. The Co measurements were performed (Li et al., 2013).

Statistical analysis

Analysis of variance (ANOVA), principal components analysis, correlation analysis and path analysis were performed using SPSS version 16.0 (SPSS Inc., Chicago, IL, USA) software. Differences between treatments were considered significant at $P < 0.01$ and $P < 0.05$ according to least significant difference (LSD) tests. Grey relational analysis was performed using DPS 7.5 (Zhejiang University, Hangzhou, China) software, gray correlation coefficient and grey incidence degrees were determined by the software. The value of the resolution ratio was 0.5. The figures were plotted using Sigma Plot software version 10.0 (Systat Software Inc., San Jose, CA, USA). Data represent means \pm SD.

Results

The change of rice seedling morphological and physiological traits under drought stress intensity

The value of the SH and RN had significant ($P < 0.01$) difference in drought stress intensity (Table 2), and reducing with the increasing PEG concentration, ARI raised and decreased later with increasing PEG concentration (Table 3). The high value ($P < 0.05$) of ARI for YLY6 were resulted in 15% PEG concentration level, AIR for HY113 in 10% PEG concentration level was significantly ($P < 0.05$) higher compared with others PEG concentrations. Both varieties had lower ($P < 0.05$) SH, MLL and MLW value when exposed to 20-25% PEG concentration. And SH, MLL and MLW showed no significant differences among 0%, 10% and 15% PEG concentration. While the RN and RV were resulted in higher values at 10% PEG concentration, while produced significantly lower values in 20-25% PEG concentration compared with 0%, 10% and 15% PEG levels. For both varieties, SS and Pro had higher value when subjected to 20-25% PEG concentration than other PEG concentration.

The vary of rice seedling morphological and physiological traits under drought stress processing duration

The SH, MLL, MLW, RN and RV were obviously influenced by drought stress duration (Table 2). Under both varieties, these parameters raised with the increase of

drought duration and greater ($P < 0.05$) value were resulted at 12 d drought duration compared with other drought duration (Table 4). While SH, RV and RN at 12 d maintained the maximum value ($P < 0.05$) compared to 4 d and 8 d drought duration. Pro content was significantly reduced during the 8-12 d drought duration; while SS at 12 d lowered ($P < 0.05$) than that in 4 d and 8 d drought duration.

The change of dry matter, leaf area, longest root length, conductivity and relative water content

Drought stress intensity and duration had significantly ($P < 0.01$) individual and interactive effects on the shoot and root dry mass and total dry mass (Table 2). For both varieties, the greater TDM (95.9-97.7) was exhibited at 12 d drought duration at 10% and 15% PEG concentration (Fig. 1); 15% PEG concentration induced greater SDM (70.1-77.3) during 12 d drought duration. A higher RDM (27.5-28.7) was formed during 10% PEG concentration at 12 d drought duration. A lower TDM, SDM and RDM (11.0-11.4) were produced under 20-25% PEG concentration during each drought duration.

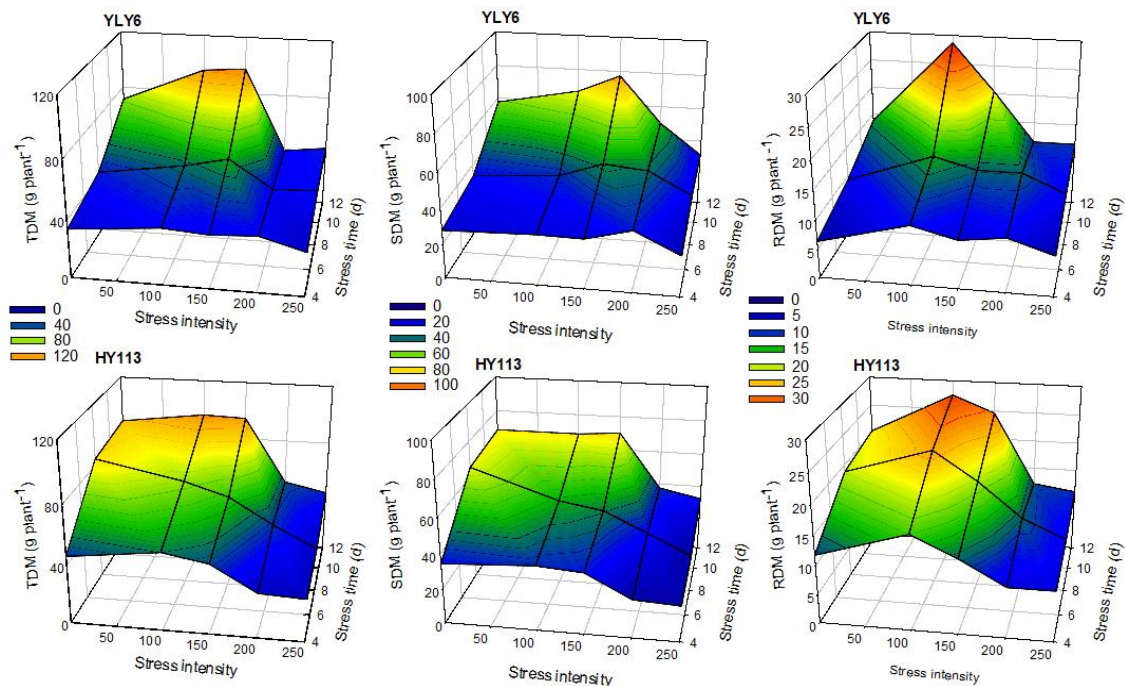


Figure 1. The total dry matter (TDM, $g\ plant^{-1}$), shoot dry matter (SDM, $g\ plant^{-1}$), root dry matter (RDM, $g\ plant^{-1}$) in the coupling of drought stress intensity and stress duration under Yangliangyou 6 (YLY6) and Hanyou 113 (HY113)

The individual and interactive effects of drought stress intensity and duration significantly ($P < 0.05$) changed the LA and LRL. The greatest LA (1.3-1.6) was observed for both varieties, respectively, at 12 d drought duration under 15% PEG level (Fig. 2). Both varieties had the greatest (10.7-13.1) LRL at 12 d processing duration with the 10% PEG concentration, while lowest (5.1-8.2) value resulted from 20% and 25% PEG concentration.

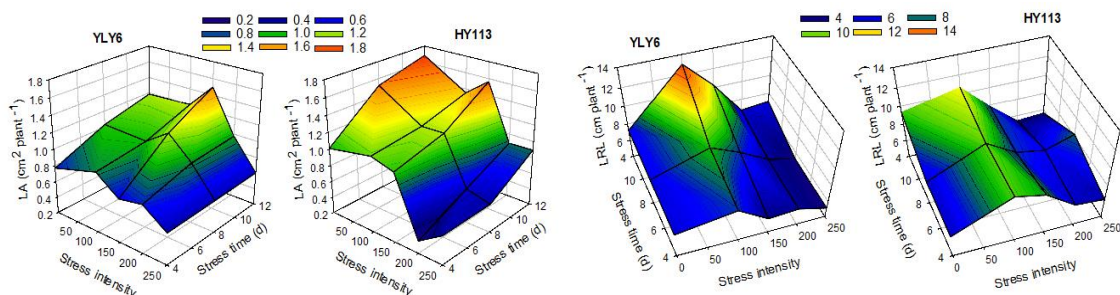


Figure 2. The leaf area (LA, $\text{cm}^2 \text{ plant}^{-1}$) and longest root length (LRL, cm plant^{-1}) in the coupling of drought stress intensity and stress duration under Yangliangyou 6 (YLY6) and Hanyou 113 (HY113)

Drought stress intensity and duration had significant ($P < 0.05$) interactive effects on Co and RWC (Table 2). The Co showed peak (472.3) value at 8 d drought duration with 25% PEG concentration (Fig. 3), while the valley (17.5-72.9) appeared at 12 d drought duration within 0-15% PEG concentration. A lower value of RWC (0.71-0.78) resulted at 20% and 25% PEG concentration during each processing duration compared with other PEG concentrations.

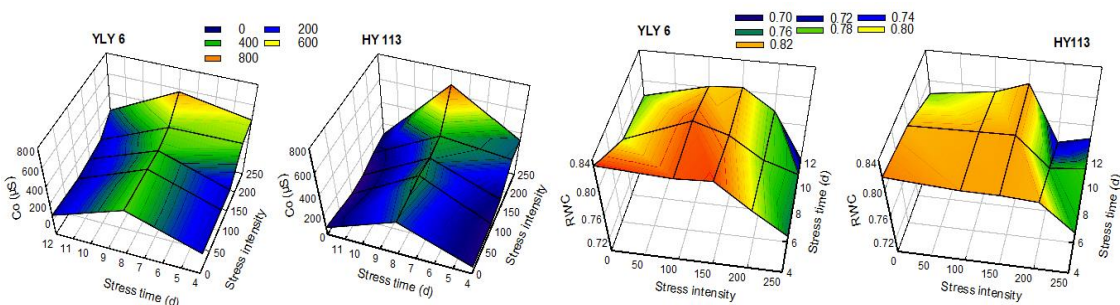


Figure 3. The conductivity (Co, μS) and conductivity (Co, μS) in the coupling of drought stress intensity and stress duration under Yangliangyou 6 (YLY6) and Hanyou 113 (HY113)

Table 2. The shoot dry matter (SDM, g plant^{-1}), root dry matter (RDM, g plant^{-1}), adversity resistance index (ARI), relative water content (RWC), seedling height (SH, cm plant^{-1}), mean leaf length (MLL, cm plant^{-1}), mean leaf width (MLW, cm plant^{-1}), leaf area (LA, $\text{cm}^2 \text{ plant}^{-1}$), longest root length (LRL, cm plant^{-1}), root number (RN, plant^{-1}), root volume (RV, $\text{cm}^3 \text{ plant}^{-1}$), conductivity (Co, μS), soluble sugar (SS, %), proline (Pro, $\mu\text{g g}^{-1}$) and total dry matter (g plant^{-1}) of drought stress intensity and stress duration under Yangliangyou 6 (YLY6) and Hanyou 113 (HY113)

	SDM	RDM	ARI	RWC	SH	MLL	MLW	LA	LRL	RN	RV	Co	SS	Pro	TDM
SI	**	**	**	**	**	**	**	**	**	**	**	**	**	**	**
SD	**	**	ns	**	**	**	**	**	**	**	**	**	**	**	**
V	ns	**	**	ns	**	**	**	**	**	**	**	ns	**	ns	**
SI×SD	**	**	ns	ns	**	**	**	**	**	*	**	**	**	**	**
SI×V	**	**	*	ns	**	**	**	**	**	ns	**	ns	**	ns	**
SD×V	ns	ns	ns	ns	ns	**	*	ns	**	**	**	**	ns	**	ns
SI×SD×V	*	ns	ns	ns	*	ns	*	ns	**	**	**	**	**	**	ns

“SI” means drought stress intensity, “SD” denotes drought stress duration, and “V” indicates varieties. “ns” indicates non-significant. “*” and “**” mean significantly different at $P = 0.05$ and $P = 0.01$ according to Duncan’s range test. The same below

Table 3. The shoot dry matter (SDM, g plant⁻¹), root dry matter (RDM, g plant⁻¹), adversity resistance index (ARI), relative water content (RWC), seedling height (SH, cm plant⁻¹), mean leaf length (MLL, cm plant⁻¹), mean leaf width (MLW, cm plant⁻¹), leaf area (LA, cm² plant⁻¹), longest root length (LRL, cm plant⁻¹), root number (RN, plant⁻¹), root volume (RV, cm³ plant⁻¹), conductivity (Co, µS), soluble sugar (SS, %), proline (Pro, µg g⁻¹) and total dry matter (g plant⁻¹) of drought stress intensity under Yangliangyou 6 (YLY6) and Hanyou 113 (HY113)

Varieties	YLY6					HY113				
	0	10	15	20	25	0	10	15	20	25
SDM (g plant ⁻¹)	39.51 ± 1.70c	44.33 ± 1.81b	50.59 ± 2.15a	42.84 ± 1.81b	28.32 ± 0.79d	56.01 ± 2.04a	51.45 ± 1.60a	50.00 ± 1.68a	30.86 ± 1.36b	24.75 ± 0.84b
RDM (g plant ⁻¹)	9.82 ± 0.49b	17.84 ± 0.86a	13.79 ± 0.59ab	11.13 ± 0.86b	9.27 ± 0.36b	16.96 ± 0.46b	22.37 ± 0.71a	18.66 ± 0.59b	11.12 ± 0.44c	9.66 ± 0.32c
ARI	0.92 ± 0.02b	1.49 ± 0.07a	1.41 ± 0.16a	1.26 ± 0.14b	0.62 ± 0.07c	1.25 ± 0.06a	1.23 ± 0.06a	1.08 ± 0.08b	0.38 ± 0.01c	0.40 ± 0.10c
RWC	0.80 ± 0.00a	0.82 ± 0.01a	0.81 ± 0.00a	0.78 ± 0.00a	0.74 ± 0.01b	0.80 ± 0.01a	0.80 ± 0.00a	0.81 ± 0.01a	0.77 ± 0.01a	0.76 ± 0.01a
SH (cm plant ⁻¹)	21.45 ± 0.32a	20.30 ± 0.27ab	20.83 ± 0.37ab	19.39 ± 0.27ab	18.21 ± 0.08b	22.21 ± 0.37a	20.00 ± 0.26b	19.62 ± 0.16b	15.71 ± 0.22c	16.08 ± 0.14c
MLL (cm plant ⁻¹)	9.70 ± 0.18a	10.04 ± 0.02a	10.37 ± 0.08a	10.53 ± 0.02a	8.63 ± 0.09b	11.18 ± 0.18a	10.33 ± 0.07a	10.27 ± 0.10a	7.34 ± 0.08b	7.93 ± 0.02b
MLW (cm plant ⁻¹)	0.32 ± 0.01a	0.33 ± 0.01a	0.32 ± 0.01a	0.27 ± 0.01b	0.21 ± 0.01c	0.39 ± 0.01a	0.37 ± 0.00a	0.38 ± 0.01a	0.26 ± 0.01b	0.26 ± 0.01b
LA (cm ² plant ⁻¹)	0.99 ± 0.03a	1.05 ± 0.02a	1.07 ± 0.03a	0.90 ± 0.02a	0.59 ± 0.01b	1.40 ± 0.03a	1.22 ± 0.02a	1.26 ± 0.03a	0.62 ± 0.03b	0.66 ± 0.03b
LRL (cm plant ⁻¹)	7.03 ± 0.08c	10.00 ± 0.26a	7.92 ± 0.23b	6.24 ± 0.26d	5.80 ± 0.14d	7.56 ± 0.22c	9.93 ± 0.19a	8.11 ± 0.17b	6.37 ± 0.17c	8.37 ± 0.33b
RN (plant ⁻¹)	17.33 ± 0.17a	15.72 ± 0.40ab	14.00 ± 0.34b	14.44 ± 0.4ab	13.00 ± 0.31b	19.33 ± 0.70a	16.78 ± 0.24b	16.78 ± 0.33b	14.56 ± 0.53c	13.22 ± 0.27c
RV (cm ³ plant ⁻¹)	0.09 ± 0.01c	0.15 ± 0.01a	0.13 ± 0.01b	0.09 ± 0.01c	0.07 ± 0.00d	0.12 ± 0.00a	0.15 ± 0.01a	0.14 ± 0.01a	0.06 ± 0.00b	0.07 ± 0.00b
Co (µS)	168.3 ± 14.41c	150.6 ± 15.01c	152.0 ± 13.82c	280.0 ± 15.01b	376.8 ± 13.42a	159.1 ± 13.07c	154.7 ± 16.71c	167.9 ± 15.17c	262.5 ± 15.80b	369.8 ± 26.44a
SS (%)	1.10 ± 0.03b	1.33 ± 0.04b	1.26 ± 0.03b	1.47 ± 0.04b	1.86 ± 0.06a	1.01 ± 0.02b	1.28 ± 0.03b	1.33 ± 0.04b	1.74 ± 0.04a	1.94 ± 0.05a
Pro (µg g ⁻¹)	2.23 ± 0.12c	2.85 ± 0.15c	2.68 ± 0.13c	4.61 ± 0.15b	5.83 ± 0.29a	2.40 ± 0.11c	2.61 ± 0.14c	2.68 ± 0.12c	4.19 ± 0.20b	5.50 ± 0.38a
TDM (g plant ⁻¹)	49.33 ± 2.14b	62.18 ± 2.66a	64.38 ± 2.71a	53.97 ± 2.66b	37.59 ± 1.12c	72.97 ± 2.41a	73.82 ± 2.26a	68.66 ± 2.21a	41.98 ± 1.78b	34.40 ± 1.14b

Bars indicate SD (n = 3). Different letters indicate a significant difference (p < 0.05) between the stress intensity

Table 4. The shoot dry matter (SDM, g plant⁻¹), root dry matter (RDM, g plant⁻¹), adversity resistance index (ARI), relative water content (RWC), seedling height (SH, cm plant⁻¹), mean leaf length (MLL, cm plant⁻¹), mean leaf width (MLW, cm plant⁻¹), leaf area (LA, cm² plant⁻¹), longest root length (LRL, cm plant⁻¹), root number (RN, plant⁻¹), root volume (RV, cm³ plant⁻¹), conductivity (Co, μS), soluble sugar (SS, %), proline (Pro, μg g⁻¹) and total dry matter (g plant⁻¹) of drought stress duration under Yangliangyou 6 (YLY6) and Hanyou 113 (HY113)

Varieties	YLY6			HY113		
	4	8	12	4	8	12
SDM (g plant ⁻¹)	28.87 ± 4.74b	39.24 ± 10.27b	54.24 ± 19.85a	29.85 ± 8.50c	42.69 ± 19.67b	55.30 ± 19.44a
RDM (g plant ⁻¹)	8.29 ± 2.05b	12.15 ± 3.38b	16.39 ± 7.89a	11.64 ± 3.57b	16.52 ± 6.65a	19.09 ± 7.86a
ARI	1.12 ± 0.36a	1.19 ± 0.33a	1.12 ± 0.57a	1.02 ± 0.36a	0.91 ± 0.45a	1.03 ± 0.48a
RWC	0.81 ± 0.04a	0.80 ± 0.04a	0.77 ± 0.05a	0.80 ± 0.05a	0.79 ± 0.06a	0.77 ± 0.05a
SH (cm plant ⁻¹)	18.77 ± 1.56b	19.04 ± 1.30b	22.09 ± 3.31a	17.38 ± 2.09b	18.44 ± 3.29b	20.35 ± 4.10a
MLL (cm plant ⁻¹)	9.66 ± 1.07a	9.91 ± 1.26a	9.98 ± 1.28a	8.68 ± 1.41b	9.50 ± 1.69b	10.05 ± 2.11a
MLW (cm plant ⁻¹)	0.24 ± 0.04b	0.31 ± 0.06a	0.31 ± 0.08a	0.28 ± 0.10b	0.32 ± 0.08b	0.39 ± 0.07a
LA (cm ² plant ⁻¹)	0.76 ± 0.15b	0.99 ± 0.23a	1.02 ± 0.34a	0.81 ± 0.37b	1.01 ± 0.39ab	1.28 ± 0.40a
LRL (cm plant ⁻¹)	6.32 ± 1.30b	7.09 ± 1.73b	8.68 ± 2.68a	8.77 ± 3.07a	7.87 ± 1.70a	7.56 ± 2.32a
RN (plant ⁻¹)	13.07 ± 3.63a	15.14 ± 2.98ab	16.41 ± 2.09a	12.40 ± 3.00b	16.93 ± 3.84a	19.07 ± 4.83a
RV (cm ³ plant ⁻¹)	0.08 ± 0.01b	0.09 ± 0.02b	0.14 ± 0.07a	0.07 ± 0.01c	0.11 ± 0.04b	0.15 ± 0.08a
Co (μS)	217.7 ± 17.01b	371.5 ± 53.70a	105.2 ± 12.72c	186.2 ± 14.92b	426.1 ± 134.1a	56.09 ± 40.04c
SS (%)	1.45 ± 0.54a	1.68 ± 0.33a	1.12 ± 0.33b	1.51 ± 0.32a	1.79 ± 0.51a	1.08 ± 0.31b
Pro (μg g ⁻¹)	5.72 ± 2.56a	2.48 ± 1.49b	2.71 ± 0.81b	5.78 ± 2.81a	1.86 ± 0.49b	2.78 ± 0.9b
TDM (g plant ⁻¹)	37.17 ± 5.83c	51.39 ± 12.54b	70.63 ± 26.44a	41.5 ± 11.55b	59.21 ± 25.09a	74.39 ± 26.76a

Bars indicate SD (n = 3). Different letters indicate a significant difference ($P < 0.05$) between the stress durations.

The principal component analysis of rice seedling morphological and physiological traits

The principal component analysis showed that RDM, SDM, SH, MLL, MLW, LA, RN and RV contributed to the first principal component (dehydration avoidance factor, DAF) (Table 5), while the LA was the major to the first principal component. ARI and RWC were summed up as the second principal component (comprehensive drought resistant factor, CDRF), RWC obviously supported on the factor. Co, SS and Pro were classified as the third principal component (drought tolerance factor, DTF), Co was leading component to the factor. In addition, RLR was called as fourth principal component (root induction factor, RIF).

Table 5. The principal component analysis of the root dry matter (RDM, g plant⁻¹), shoot dry matter (SDM, g plant⁻¹), adversity resistance index (ARI), relative water content (RWC), seedling height (SH, cm plant⁻¹), mean leaf length (MLL, cm plant⁻¹), mean leaf width (MLW, cm plant⁻¹), leaf area (LA, cm² plant⁻¹), longest root length (LRL, cm plant⁻¹), root number (RN, plant⁻¹), root volume (RV, cm³ plant⁻¹), conductivity (Co, μS), soluble sugar (SS, %), proline (Pro, μg g⁻¹) and total dry matter (g plant⁻¹) of drought stress intensity and stress duration under Yangliangyou 6 (YLY6) and Hanyou 113 (HY113)

Principal factors	RDM (g plant ⁻¹)	SDM (g plant ⁻¹)	ARI	RWC	SH (cm plant ⁻¹)	MLL (cm plant ⁻¹)	MLW (cm plant ⁻¹)	LA (cm ² plant ⁻¹)	LRL (cm plant ⁻¹)	RN (plant ⁻¹)	RV (cm ³ plant ⁻¹)	Co (μS)	SS (%)	Pro (μg g ⁻¹)
1	0.846	0.936	0.516	0.354	0.886	0.839	0.883	0.947	0.51	0.751	0.856	-0.576	-0.55	-0.62
2	-0.066	-0.105	0.711	0.743	0.048	0.176	-0.221	-0.096	0.293	-0.435	0.047	0.024	0.05	0.308
3	0.358	0.072	-0.028	-0.035	-0.113	-0.067	0.014	0.007	0.457	0.125	0.249	0.647	0.598	-0.623
4	-0.252	-0.045	0.174	0.24	0.058	0.322	0.045	0.142	-0.517	0.169	-0.247	0.431	0.128	-0.45

The relation and path analysis of principal component factors and dry matter accumulation

Correlation analysis explored that (Fig. 4), the TDM significantly ($P < 0.01$) positively related to LA, RWC, Co and LRL. The LA also significantly ($P < 0.01$) negatively correlated with Co, which indicated that dehydration avoidance factor, comprehensive drought resistant factor and drought tolerance factor related closely with biomass accumulation in rice seedling.

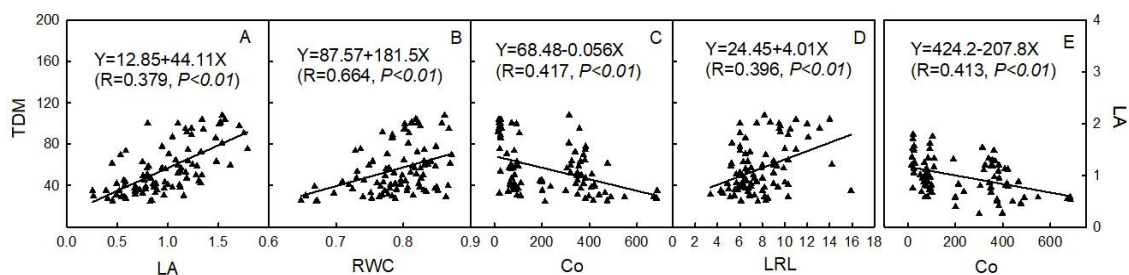


Figure 4. Relationship ($n = 90$) for total dry matter (TDM, g plant⁻¹) with leaf area (LA, cm² plant⁻¹), total dry matter (TDM, g plant⁻¹) with relative water content (RWC), total dry matter (TDM, g plant⁻¹) with conductivity (Co, μS), total dry matter (TDM, g plant⁻¹) with longest root length (LRL, cm plant⁻¹) and leaf area (LA, cm² plant⁻¹) with conductivity (Co, μS) of stress intensity and stress duration under Yangliangyou 6 (YLY6) and Hanyou 113 (HY113)

Path analysis (Table 6) showed that LA, RWC, Co and LRL had greater direct effect on TDM in rice seedling, respectively, and Co had good indirect effect on TDM through LA. It showed that drought dehydration factor, comprehensive drought resistant factor and drought tolerance factor had great separate effect on rice seedling growth.

Table 6. The path analysis ($n = 90$) for the direct or indirect effect on total dry matter (TDM, g plant⁻¹) by leaf area (LA, cm² plant⁻¹), relative water content (RWC), conductivity (Co, μ S) and longest root length (LRL, cm plant⁻¹) of drought stress intensity and duration under Yangliangyou 6 (YLY6) and Hanyou 113 (HY113)

	TDM (Y)			
	X1→Y	X2→Y	X3→Y	X4→Y
LA (X1)	0.53	0.06	0.03	0.05
Co (X2)	-0.22	-0.14	-0.02	-0.04
RWC (X3)	0.05	0.01	0.28	0.03
LRL (X4)	0.13	0.03	0.05	0.19

The association analysis of principal component factors and dry matter accumulation

In two varieties, under 0%-4 d (stress intensity (SI)-stress duration (SD), 15%-4 d, 10%-4 d and 20%-4 d condition (Table 7), RWC as the key enabling factor on TDM, followed by LA significantly contributed to TDM under 0%-8 d, 10%-8 d, 10%-12 d, 20%-12 d and 25%-12 d condition. Co mainly supported TDM in 0%-8 d, 10%-8 d, 20%-8 d, 20%-12 d and 25%-8 d; Co lowered contribution to rice seedling in 10%-4 d, 15%-4 d, 20%-4 d and 25%-4 d. LRL was the main factor for TDM in 10%-4 d and 15%-8 d condition.

Table 7. The association analysis of the leaf area (LA, cm² plant⁻¹), relative water content (RWC), conductivity (Co, μ S) and longest root length (LRL, cm plant⁻¹) with total dry matter (TDM, g plant⁻¹) of stress intensity (SI) and stress duration (ST) under Yangliangyou 6 (YLY6) and Hanyou 113 (HY113)

Stress intensity (%)	Stress duration (d)	YLY6				HY113			
		LA	RWC	SS	LRL	LA	RWC	SS	LRL
0	4	0.46	1.00	0.58	0.48	0.67	0.87	0.81	0.54
	8	0.99	0.65	0.68	0.51	0.68	0.58	0.67	0.46
	12	0.58	0.59	0.62	0.47	0.50	0.51	0.64	0.46
10	4	0.50	0.56	0.53	0.61	0.89	0.98	0.64	0.61
	8	0.60	0.52	0.62	0.58	0.53	0.90	0.68	0.48
	12	0.88	0.91	0.63	0.98	0.56	0.57	0.68	0.55
15	4	0.50	0.72	0.48	0.65	0.49	0.93	0.62	0.54
	8	0.46	0.96	0.68	0.56	0.46	0.54	0.66	0.66
	12	0.47	0.94	0.64	0.48	0.50	0.46	0.64	0.45
20	4	0.68	0.95	0.51	0.46	0.56	0.87	0.46	0.50
	8	0.46	0.45	0.68	0.46	0.50	0.46	0.68	0.52
	12	0.71	0.24	0.35	0.70	0.46	0.51	0.68	0.45
25	4	0.58	0.93	0.49	0.54	0.53	0.67	0.63	0.95
	8	0.52	0.64	0.62	0.52	0.46	0.47	0.67	0.48
	12	0.68	0.61	0.67	0.58	0.57	0.52	0.60	0.55

It is suggested that comprehensive drought resistant factor primarily supported seedling growth at 8-12 d stress duration at 10-15% PEG solution; under the coupling of the 20-25% PEG concentration and 12 d stress duration condition, drought dehydration factor mainly supported the seedling growth. Drought tolerance factor had an imperative role in seedling growth at 8-12 d stress duration under 15-20% PEG solution. The root induction factor was the major factor relating to seedling growth under 4 d drought stress duration with 10-15% PEG solution.

Discussion

Drought stress intensity had a great contribution to rice seedling growth compared with drought processing duration

Drought stress intensity and duration significantly alters rice seedling growth. In the present study, rice seedling growth showed a reducing trend in prolonged drought stress duration, while mild and moderate drought stress intensity (10-15% PEG concentration) enhanced rice seedling growth for all drought duration. In addition, shoot and root growth of rice seedling were more sensitive to drought stress intensity compared with drought duration, and root growth of rice seedling had a lower tolerance to drought stress intensity compared with the shoot of rice seedling.

Crop seedling growth slightly reduced with extending drought duration compared with control (Asai et al., 2009; Duan et al., 2017). As drought stress intensity increases, the root growth of seedling was decreased. Conversely, increases root physiological activity (root vigor and protective enzyme) (Sharma and Dubey, 2005; Ding et al., 2016). Rice shoot growth (biomass accumulation) was obviously reduced by lower leaf productivity (changed leaf morphology and gas exchange) under severe drought stress condition (Lu and Neumann, 1999). While moderate drought stress supported rice seedling growth because which motivated the compensatory capacity of the seedling (Sharma and Dubey, 2005; Yu et al., 2016). These data found that root and shoot of crop seedling were sensitive to drought stress while moderate drought stress had a positive effect on rice seedling growth.

In the present research, drought duration had less threaten to rice seedling growth compared to drought stress intensity, because rice seedling during long-term drought stress could counteract the adverse impact of moderate drought stress on rice seedling growth, or the compensatory capacity of rice seedling could be stimulated by long-term drought duration. Compared with the aerial part of rice seedling, root had a lower tolerance capacity to drought stress due to more sensitive to drought stress during rice seedling and was a source of drought stress signal. Thus, long-term drought duration or mild or moderate drought stress intensity had less effect on rice seedling growth. And to maintain root vigor was more benefit for rice seedling growth.

Drought stress intensity and processing duration could impact on drought dehydration factor, comprehensive drought resistant factor, drought tolerance factor, root induction factor and the relationship among them

The impact of drought stress on rice seedling growth and development was not only related to the drought stress intensity and processing duration, but also corrected to drought resistance (drought dehydration and drought tolerance) of crops (Liu et al., 2003; Özdemir et al., 2004; Farooq et al., 2009). In the present research, drought

dehydration, drought tolerance, comprehensive drought resistant and root induction factor increased when the plants were exposed to extending drought duration; moreover, drought dehydration, drought tolerance and comprehensive drought factor had greater value at moderate drought stress (15% PEG concentration) intensity within long term drought duration, while optimal root induction factor appeared at mild drought stress (10% PEG concentration) during medium and long term drought duration. And drought dehydration, comprehensive drought resistant, drought tolerance and root induction factors within each drought stress intensity, duration or their combination had a great independent effect.

Crops simultaneously had drought dehydration and tolerance ability (Liu et al., 2003; Chaves et al., 2003; Chang, 2008; Farooq et al., 2009). Drought tolerance or dehydration in crops showed a different size when crops faced a different drought stress intensity (Yu et al., 2016; Duan et al., 2017). Drought dehydration and drought tolerate ability had different ways to maintain the crops growth and avoid the much number water lose: short-term drought stress duration inspired the drought tolerance ability, while long-term drought stress duration easily induced the drought resistance (Yue et al., 2006; Farooq et al., 2009; Li et al., 2012). And these factors were respectively, controlled by a set of independent genetic characteristics, such as, root distribution (the longest root length) in the soil layer and leaf area was adjusted by related gene (Zhang et al., 2001; Yue et al., 2006; Du et al., 2018). In addition, under the assist of the compensation ability, mild and moderate drought stress intensity stimulated the formation of protection mechanisms in tissue cells to avoid the injury of tissue cells (Asai et al., 2009; Duan et al., 2017). With the raising stress duration, the generation of new cells replaced or eliminated which destroyed tissue cells or other matter in cells (Ming and Wang, 2002; Kottapalli et al., 2012). And the great activity or function of the new tissue cells raised the drought resistance ability supporting the rice seedling growth. Thus, drought dehydration played a crucial role in drought stress duration, while drought tolerance had an obvious response to drought stress intensity to support rice seedling growth. In addition, less alteration of seedling morphological traits, when seedling accumulated higher Pro and SS content, and rice seedling had low assimilate productivity during seedling stage. This indicated that the accumulated assimilates in seedling provided energy for the formation of the proteins and enzymes related to drought tolerance, while reducing the energy to support the morphogenesis of rice seedling, so that drought dehydration factor and drought tolerance factor showed an independent effect on rice seedling growth. And these factors had different acting time during drought stress.

Drought stress intensity and duration impacted on drought dehydration factor, comprehensive drought resistant factor, drought tolerance factor and root induction factor to adjust the rice seedling growth

In the present study, the rice seedling maintained the growth during drought stress, mainly supported by greater root induction, drought tolerance and drought dehydration factor at short-term, medium-term or long-term duration under mild drought stress intensity, respectively. The comprehensive drought resistant factor among all drought duration in moderate drought stress intensity, drought dehydration factor and drought tolerance factor at long-term processing time in severe stress intensity respectively played a crucial role in rice seedling growth.

The contribution of drought tolerance factor on rice seedling growth was mainly great physiological activity (polyphenols, flavonoids and antioxidant activity) under severe drought stress (Hussain et al., 2016, 2017). However, the formation of protective enzyme or cell activity was induced by environmental stress and reducing with increasing drought stress intensity (Manivannan et al., 2007; Samota et al., 2017). While Drought dehydration played a crucial role in long-term drought stress (Farooq et al., 2009; Li et al., 2012; Hussain et al., 2017). About RWC (comprehensive drought resistant factor) was considered to evaluate the response-ability of plant to drought stress (Farooq et al., 2009; Anjum et al., 2011), and the comprehensive drought resistant factor was supported by root or shoot physiological activity, decreasing water loss and enhancing physiological water use efficiency in rice seedling (Kaydan et al., 2008), but the comprehensive drought resistant factor also reduced with raising drought intensity (Nayyar et al., 2006; Anjum et al., 2011). Root induction factor including root distribution and the growth rate of root, rice root distribution in deep soil layer significantly related with drought stress and root growth rate was used to evaluate adaptability to stress environment, root growth and physiological activity (synthesis of protein) were stimulated by mild and moderate drought stress to increase water absorption (Farooq et al., 2009; Pérez et al., 2010). We concluded that drought tolerance factor and the comprehensive drought resistant factor reduced within severe drought stress, while root induction factor raised in mild and moderate drought stress, drought dehydration played a crucial role in long term drought stress. A greater drought tolerance showed under short-term drought stress; moreover, drought tolerance factor mainly improving drought resistance ability, the comprehensive drought resistant factor mainly raising the water use ability and root induction factor mainly promoting water absorption which all supported drought resistance ability during drought stress.

In the present study, the root is the first organ to contact with drought stress and is more sensitive to drought stress. This showed that root had an obvious change within a short time to face drought stress intensity. This improved root water absorption to support rice seedling growth in the short-term stress. Drought tolerance factor plays a key role in stress environment and mild drought stress had less effect on seedling growth. While mid drought stress coupled with medium-term drought duration could stimulate the drought tolerance factor by improving compensation ability to promote the drought tolerance ability of rice seedling. Under moderate drought stress, comprehensive drought resistant factor did not show a declining trend, it could be caused by great effect of the protection mechanism and drought dehydration factor, in each drought duration, respectively. This further directly supported rice seedling growth.

The drought dehydration factor and drought tolerance factor of rice seedling respectively including shoot or root morphological and physiologic traits. Drought dehydration factor and drought tolerance factor could take advantage during long term drought duration with severe drought stress, because the accumulation of carbohydrates, soluble proteins, some osmotic substances and the protective enzyme during a relatively long time improved water absorption or storage avoiding the destruction of free radicals to cells supporting rice seedling growth during severe drought stress. In addition, drought dehydration factor was supported by morphology of rice seedlings, such as root and leaf, which was the foundation of matter and energy to response or relieve drought stress of rice seedling. Hence, drought dehydration factor had a great contribution to rice seedling growth during a long-term drought stress condition.

Conclusion

Rice seedling growth in different drought stress intensity and duration was associated with their different stress resistant mode, including drought dehydration avoidance factor, comprehensive drought resistant factor, drought tolerance factor and root induction factor. Moreover, these factors have strong independent effect on seedling growth during different drought stress intensity and duration. The improved rice seedling growth was mainly associated with greater root induction factor, drought tolerance and drought dehydration factor at short, medium or long-term duration under mild drought stress intensity, respectively. While drought dehydration and drought tolerance factor at long-term processing duration under severe stress intensity played a crucial role to support the rice seedling growth. Thus, to focus on drought resistant traits under different drought environment are important way to evaluate rice seedling growth in rice dry cultivation systems.

At present, the breeding of drought-resistance rice variety uses the genetic advantage of rice varieties. In the future, genome, transcriptome, proteome, or metabolomics can be applied to study the interaction mechanism between the drought resistance ability (drought resistance, drought avoidance, drought dehydration and drought tolerance) and the environment (drought stress). It is of great significance to the future development of rice dry cultivation (reduce energy-saving production).

Acknowledgements. This study was funded by the National Natural Science Foundation of China (31801291) and State Key Special Program (2017YFD0301400).

Conflict of interests. There is no conflict of interests to declare.

REFERENCES

- [1] Anjum, S. A., Xie, X. Y., Wang, L. C., Saleem, M. F., Man, C., Lei, W. (2011): Morphological, physiological and biochemical responses of plants to drought stress. – African Journal of Agricultural Research 6: 2026-2032.
- [2] Asai, H., Samson, B. K., Stephan, H. M., Songyikhangsuthor, K., Homma, K., Kiyono, Y. (2009): Biochar amendment techniques for upland rice production in northern Laos: 1. soil physical properties, leaf spad and grain yield. – Field Crops Research 111: 81-84.
- [3] Bandurska, H., Stroiński, A., Kubiś, J. (2003): The effect of jasmonic acid on the accumulation of aba, proline and spermidine and its influence on membrane injury under water deficit in two barley genotypes. – Acta Physiologiae Plantarum 25: 279-285.
- [4] Basu, S., Roychoudhury, A., Saha, P. P., Sengupta, D. N. (2010): Differential antioxidative responses of indica rice cultivars to drought stress. – Plant Growth Regulation 60: 51-59.
- [5] Bates, L. S., Waldren, R. P., Teare, I. D. (1973): Rapid determination of free proline for water stress studies. – Plant and Soil 39: 205-207.
- [6] Chang, X. (2008): Study advances on the physiological adaptation mechanism to drought stress by plant. – Journal of Anhui Agricultural Science 36: 7549-7551.
- [7] Chaves, M. M., Maroco, J. P., Pereira, J. S. (2003): Understanding plant responses to drought - from genes to the whole plant. – Functional Plant Biology 30: 239-264.
- [8] Chen, K., Arora, R. (2011): Dynamics of the antioxidant system during seed osmopriming, post-priming germination, and seedling establishment in spinach (*Spinacia oleracea* L.). – Plant Science 180: 212-20.

- [9] Ding, L., Li, Y., Wang, Y., Gao, L., Wang, M., Chaumont, F., Shen, Q., Guo, S. (2016): Root ABA accumulation enhances rice seedling drought tolerance under ammonium supply: Interaction with aquaporins. – *Frontier in Plant Science* 7: 1206.
- [10] Du, H., Huang, F., Wu, N., Li, X., Hu, H., Xiong, L. (2018): Integrative regulation of drought escape through ABA dependent and independent pathways in rice. – *Molecular Plant*. DOI: 10.1016/j.molp.2018.01.004.
- [11] Duan, S., Yang, A., Huang, Y. (2017): Effects of water stress on growth and physiological features and yield of rice. – *China Rice* 23: 36-42.
- [12] Farooq, M., Wahid, A., Kobayashi, N. (2009): Plant drought stress: effects, mechanisms and management. – *Agronomy for Sustainable Development* 29: 185-212.
- [13] Huang, M., Zou, Y. B., Jiang, P. (2011): Relationship between grain yield and yield components in super hybrid rice. – *Agricultural Sciences in China* 10: 1537-1544.
- [14] Hussain, M., Farooq, M., Lee, D. J. (2017): Evaluating the role of seed priming in improving drought tolerance of pigmented and non-pigmented rice. – *Crop Science* 203: 269-276.
- [15] Hussain, S., Khan, F., Hussain, H. A., Nie, L. (2016): Physiological and biochemical mechanisms of seed priming-induced chilling tolerance in rice cultivars. – *Frontier in Plant Science* 7: 116.
- [16] Kaydan, D., Yagmur, M. (2008): Germination, seedling growth and relative water content of shoot in different seed sizes of triticale under osmotic stress of water and NaCl. – *African Journal of Biotechnology* 7: 2862-2868.
- [17] Kottapalli, K. R., Kottapalli, P., Payton, P. (2012): Peanut Seed Development: Molecular Mechanisms of Storage Reserve Mobilization and Effect of Water Deficit Stress on Seed Metabolism. – In: Agrawal, G. K., Rakwal, R. (eds.) *Seed Development: OMICS Technologies Toward Improvement of Seed Quality and Crop Yield*. – Springer, Netherlands, pp: 143-169.
- [18] Kusaka, M., Ohta, M., Fujimura, T. (2005): Contribution of inorganic components to osmotic adjustment and leaf folding for drought tolerance in pearl millet. – *Physiology Plantarum* 125: 474-489.
- [19] Li, H. S. (2012): *Modern Plant Physiology*. – Higher Education Press, Beijing, pp: 352-357.
- [20] Li, J., Besseau, S., Törönen, P., Sipari, N., Kollist, H., Holm, L. (2013): Defense-related transcription factors wrky70 and wrky54 modulate osmotic stress tolerance by regulating stomatal aperture in arabidopsis. – *New Phytologist* 200: 457-72.
- [21] Liu, C. L., Chen, H. P., Liu, E. E., Peng, X. X., Lu, S. Y., Guo, Z. F. (2003): Multiple tolerance of rice to abiotic stresses and its relationship with aba accumulation. – *Acta Agronomica Sinica* 29: 725-729.
- [22] Lu, Z., Neumann, P. M. (1999): Water stress inhibits hydraulic conductance and leaf growth in rice seedlings but not the transport of water via mercury-sensitive water channels in the root. – *Plant Physiology* 120: 143-152.
- [23] Luo, L. J. (2010): Breeding for water-saving and drought-resistance rice (WDR) in China. – *Journal of Experimental Botany* 61: 3509.
- [24] Manivannan, P., Abdul, J. C., Kishorekumar, A., Sankar, B., Somasundaram, R., Sridharan, R. (2007): Changes in antioxidant metabolism of *Vigna unguiculata*, (L.) walp. by propiconazole under water deficit stress. – *Colloids and Surfaces B Biointerfaces* 57: 69-74.
- [25] Ming, L., Wang, G. (2002): Effect of drought stress on activities of cell defense enzymes and lipid peroxidation in glycyrrhiza uralensis seedlings. – *Acta Ecologica Sinica* 22: 503-507.
- [26] Nayyar, H., Gupta, D. (2006): Differential sensitivity of C₃, and C₄, plants to water deficit stress: association with oxidative stress and antioxidants. – *Environmental and Experimental Botany* 58: 106-113.

- [27] Nazarli, H., Ahmadi, A., Hadian, J. (2014): Salicylic acid and methyl jasmonate enhance drought tolerance in chamomile plants. – *Journal of HerbMed Pharmacology* 3: 87-92.
- [28] Özdemir, F., Bor, M., Demiral, T. (2004): Effects of 24-epibrassinolide on seed germination, seedling growth, lipid peroxidation, proline content and antioxidative system of rice (*Oryza sativa* L.) under salinity stress. – *Plant Growth Regulation* 42: 203-211.
- [29] Pérez, M. B. E., Gidekel, M., Segura, N. M., Herrera, E. L., Ochoa, A. N. (2010): Effects of water stress on plant growth and root proteins in three cultivars of rice (*Oryza sativa* L.) with different level of drought tolerance. – *Physiology Plantarum* 96: 284-290.
- [30] Pirdashti, H., Sarvestani, Z. T., Nematzadeh, G., Ismail, A. (2003): Effect of water stress on seed germination and seedling growth of rice (*Oryza sativa* L.) genotypes. – *Journal of Agronomy* 6: 217-222.
- [31] Samota, M. K., Sasi, M., Awana, M., Yadav, O. P., Mithra, S. V. A., Tyagi, A. (2017): Elicitor-induced biochemical and molecular manifestations to improve drought tolerance in rice (*Oryza sativa* L.) through seed-priming. – *Frontier in Plant Science* 8: 934.
- [32] Sharma, P., Dubey, R. S. (2005): Drought induces oxidative stress and enhances the activities of antioxidant enzymes in growing rice seedlings. – *Plant Growth Regulation* 46: 209-221.
- [33] Sun, Y., Ma, J., Sun, Y., Xu, H., Yang, Z., Liu, S. (2012): The effects of different water and nitrogen managements on yield and nitrogen use efficiency in hybrid rice of China. – *Field Crops Research* 127: 85-98.
- [34] Technology and Information Center of China Rice Research Institute, National Rice Data Center (2016): *Technology Wikipedia Encyclopedia of Upland Rice*. – www.ricedata.cn/Baike/2016, 3-10.
- [35] Wang, S., Hu, Y., She, K. (2007): Gray relational grade analysis of agronomical and physi-biochemical traits related to drought tolerance in wheat. – *Scientia Agricultura Sinica* 40: 2452-2459.
- [36] Xu, Y. Z., Wu, W. G., Chen, G., Ding, G. L. (2017): Study and integration of key techniques for high-yielding and water-saving cultivation of upland hybrid rice. – *China Rice* 23: 39-43.
- [37] Yang, J. C., Yong, D. U., Liu, H. (2008): Cultivation approaches and techniques for annual super-high-yielding of rice and wheat in the lower reaches of Yangzi River. – *Scientia Agricultura Sinica* 41: 1611-1621.
- [38] Ye, Y., Liang, X., Chen, Y., Liu, J., Gu, J., Guo, R., Li, L. (2013): Alternate wetting and drying irrigation and controlled-release nitrogen fertilizer in late-season rice. Effects on dry matter accumulation, yield, water and nitrogen use. – *Field Crops Research* 144: 212-224.
- [39] Yu, X., James, A. T., Yang, A., Jones, A. (2016): A comparative proteomic study of drought-tolerant and drought-sensitive soybean seedlings under drought stress. – *Crop Pasture Science* 67: 528-540.
- [40] Yue, B., Xue, W., Xiong, L., Yu, X., Luo, L., Cui, K. (2006): Genetic basis of drought resistance at reproductive stage in rice: separation of drought tolerance from drought avoidance. – *Genetics* 172: 1213.
- [41] Zhang, J., Zheng, H. G., Aarti, A., Pantuwan, G., Nguyen, T. T., Tripathy, J. N. (2001): Locating genomic regions associated with components of drought resistance in rice: comparative mapping within and across species. – *Theoretical and Applied Genetics* 103: 19-29.
- [42] Zhang, M., Jin, Z. Q., Zhao, J., Zhang, G., Wu, F. (2015): Physiological and biochemical responses to drought stress in cultivated and Tibetan wild barley. – *Plant Growth Regulation* 75: 567-574.
- [43] Zhang, Z., Qu, W. (2003): *Guidance of plant Physiology Experiments*. 3rd Ed. – Higher Education Press, Beijing, pp. 127-132.

- [44] Zheng, M., Ye, T., Hussain, S., Jiang, Q., Peng, S., Huang, J. (2016): Seed priming in dry direct-seeded rice: consequences for emergence, seedling growth and associated metabolic events under drought stress. – *Plant Growth Regulation* 78: 167-178.

CAN SHELTERWOOD LOGGING MAINTAIN HERB LAYER DIVERSITY IN A BEECH FOREST IN TURKEY?

YILMAZ, O. Y.^{1*} – YILMAZ, H.²

¹*Department of Surveying and Cadastre, Faculty of Forestry, Istanbul University-Cerrahpaşa, Istanbul 34473, Turkey*

²*Ornamental Plant Cultivation Program, Vocational School of Forestry, Istanbul University-Cerrahpaşa, Istanbul 34473, Turkey
(phone: +90-212-338-2400; fax: +90-212-338-2428)*

**Corresponding author*

e-mail: yilmazy@istanbul.edu.tr; phone: +90-212-338-2400; fax: +90-212-226-1113

(Received 9th Sep 2019; accepted 15th Nov 2019)

Abstract. The abundance and diversity of forest understory vegetation can be significantly impacted by forest management. Besides having a wide geographical distribution in Turkey, the Oriental beech (*Fagus orientalis* Lipsky) is also one of the economically important timber species of the country. The aim of this study is to compare the understory herb layer communities of mature and young beech stands which regenerated as a result of the shelterwood method. We studied understory plant species diversity and composition in 16 plots in old and young beech stands in Belgrad Forest near İstanbul, Turkey. We found no significant differences between the two stand types in understory plant diversity but understory species compositions in two stand types were found to be different. Our finding can be useful for forest management planning; by focusing on stand scale to achieve forest management conserving understory plant diversity in a forest.

Keywords: *Belgrad Forest, understory composition, indicator species, pure beech stands, stand age*

Introduction

Herb layer vegetation is an important component for biodiversity conservation efforts because it contains the majority of vascular plant species diversity and plays a significant role in forest ecosystem functioning (Augusto et al., 2003; Lorenz et al., 2006; Gilliam, 2007; Ellum, 2009). Maintenance of biological diversity during timber harvesting and successful regeneration of forest tree species has gained importance as an issue for sustainable forest management. Investigating the potential effects of silvicultural treatments on the future plant species diversity in forests is crucial for the improvement of effective management strategies to achieve sustainable forest ecosystems (Roberts and Gilliam, 1995; Lindenmayer and Franklin, 2002; Ellum, 2009; Yılmaz et al., 2018). Past and present human activities and natural disturbances are a major factor affecting the composition and diversity of plant species in a forest (Elliott et al., 1997; Stefańska-Krzaczek et al., 2019). Forest management practices lead to changes in species composition, age structure, and vertical stratification of tree layer and also indirectly affect understory microclimate, light availability, litter and soil properties in a forest. These forest understory conditions can also impact the diversity and composition of the herb layer (Paillet et al., 2011). Different forest management operations are applied throughout the life of the forest from regeneration to harvesting. Therefore, it is necessary to ascertain the impact of different silvicultural practices on understory plant composition and diversity (Hunter, 1999; Barbier et al., 2008; Durak, 2012).

Oriental beech is one of the major broadleaved forest trees in Turkey. Oriental beech forests cover 1 899 929 hectares and comprise about 8.5% of the forestland in Turkey (OGM, 2015). The oriental beech is commonly distributed in the northern region of Turkey and it is also scattered in western and southern parts of the country. This species can form pure stands; however, more frequently it mixes with broadleaved and conifer trees such as oak (*Quercus* sp.), hornbeam (*Carpinus betulus* L.), chestnut (*Castanea sativa* Mill.), fir (*Abies* sp.), Anatolian blackpine (*Pinus nigra* Arnold), Scots pine (*P. sylvestris* L.), oriental spruce (*Picea orientalis* (L.) Link.) between (30) 700-1300 (2000) m in Turkey (Yaltırık, 1982; Yılmaz, 2014).

The present study examined effects of shelterwood silvicultural method practices on herb layer composition and diversity in beech forests. Our main purpose was to investigate patterns in herb layer plant species diversity in response to two levels of stand age and structure. We compared mature and naturally regenerated young oriental beech stands with regards to stand structural features, understory richness and composition in Belgrad Forest to understand how the stand age and stand structure influences understory plant diversity.

Materials and methods

Study area

The study was conducted in the Belgrad Forest of İstanbul, 28°54'25" - 28°56'37" E, 41°13'00" - 41°14'13" N in Turkey (Fig. 1), a region with humid, mesothermal and maritime climate. Annual mean precipitation is about 1091 mm and annual mean temperature is about 12.8 °C (Özhan et al., 2010). Soils in the region are loamy clay and are developed mainly from carboniferous clay schists and neogene deposits (Balci et al., 1986). The forest covers 5900 ha, elevation ranges from about 45 to 230 m a.s.l.

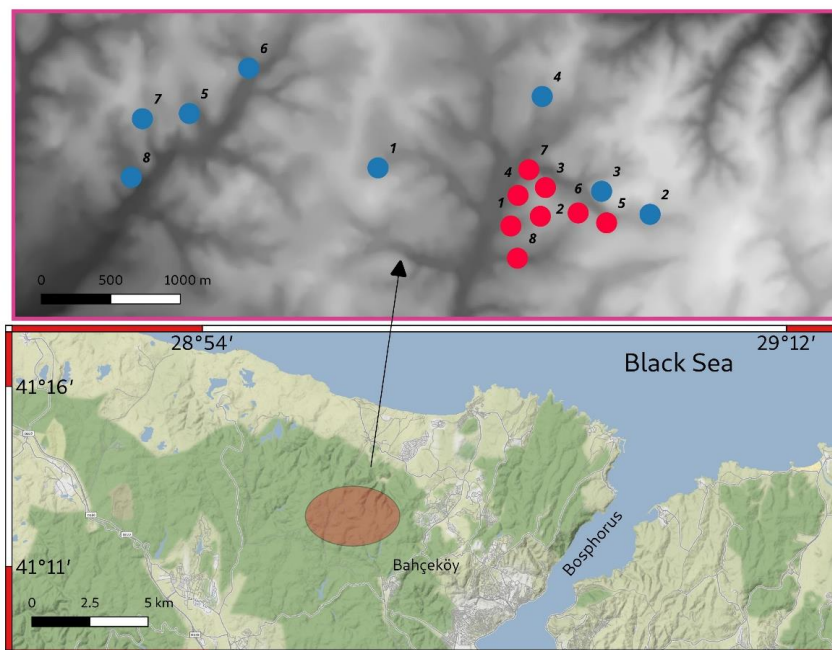


Figure 1. The study area within the Belgrad Forest, İstanbul (bottom). The sampling plots of beech stands are represented by circles (top) which are color coded based on the stand's development stage (blue: mature beech stands, red: young beech stands)

The Belgrad Forest is an old preserved mixed deciduous forest ecosystem. The natural forest is composed of oak species (*Quercus petraea* (Mattushka) Liebl., *Quercus frainetto* Ten., *Q. cerris* L.), oriental beech (*Fagus orientalis*), chestnut (*Castanea sativa*) and European hornbeam (*Carpinus betulus*) with minor occurrence of aspen (*Populus tremula* L.), common alder (*Alnus glutinosa* L.), field maple (*Acer campestre* L.) and field elm (*Ulmus minor* Mill.) (Yaltrık, 1966).

Pure oriental beech stands occupy the northwest and western slopes with an inclination of 10-40%, and are spread over the sandy loamy and loamy soils, the pH values of which vary from 4.4 to 5.8 in Belgrad Forest (Yaltrık et al., 1983). The beech stands in Belgrad Forest have been managed under the uniform shelterwood silvicultural method since 1959 (Saatçioğlu, 1970). Uniform shelterwood method used to regenerate an even age stand with multiple cuts to help shelter new establishment. Existing partial canopy which serves to modify understory conditions, create a favorable environment for reproduction, and provide a seed.

Vegetation data

A total of sixteen 20 m x 20 m permanent sample plots, 8 in naturally regenerated young beech stands (YB) and 8 mature beech stands (MB), were established in pure even aged beech forests in comparable site conditions in 2017. The sample plots were laid out in a homogenous and representative area located in each stand minimum 250 m far away each other to overcome spatial autocorrelation. Trees with a diameter at breast height (dbh) \geq 8 cm, taken in two perpendicular directions, were measured. Tree density and basal area were estimated for each quadrat (Table 1).

Table 1. Stand structural variables for the 16 plot in beech stands (dbh = 1.3 m, YB = young beech stands, MB = mature beech stands)

	Mean dbh (cm)	St. dev. dbh (cm)	Number of stem (ha ⁻¹)	Basal area (m ² ha ⁻¹)
MB				
MB1	57.66	24.18	175	57.66
MB2	35.42	19.68	350	44.38
MB3	37.00	11.23	425	49.65
MB4	44.85	13.19	225	38.28
MB5	34.09	19.85	275	32.84
MB6	28.79	16.79	400	34.34
MB7	46.00	25.41	250	52.95
MB8	42.15	16.36	350	55.67
Average	40.75	18.34	306.25	45.09
YB				
YB1	19.35	4.00	950	29.10
YB2	18.28	3.92	1025	28.12
YB3	16.23	4.56	900	20.06
YB4	16.09	4.11	975	21.08
YB5	16.10	4.81	1125	24.90
YB6	18.21	3.79	1000	27.13
YB7	14.00	5.27	950	16.64
YB8	13.85	3.68	1275	20.54
Average	16.51	4.27	1025	23.45

Four 1 m × 1 m subplots were established at the corners of each plot to sample the herb layer. Vegetation surveys in each subplot were carried out during the main growing season (May-June) to avoid vegetation bias. All herb layer species were identified in whole plot area and cover of each species was estimated separately in four subplots with the ordinal scale of Braun Blanquet (1964). All herbaceous plants, ferns, seedling and saplings with a height of less than 50 cm were considered as herb layer. The nomenclature of vascular plants follows the Flora of Turkey (Davis, 1965-1980).

Statistical analysis

To investigate the interactions between stand development stage and herb layer, the data set was prepared and organized before performing statistical analysis. Community tables were created in two different data sets. Presence/absence data set (hereafter PADS) is the presence/absence of species in the 4 subplots (1 m × 1 m), and species identified in the each 20-m x 20-m permanent plot. Abundance data set (hereafter ADS) is the average abundance of species in the 4 subplots. A table indicating the development stage of the stands was produced as the environmental data set (hereafter EDS).

Diversity indices (richness, abundance, Shannon, Simpson) were calculated using the two data sets which were previously prepared and organized. The species richness was expressed as the number of herb-layer species for the PADS and was compared between successional stages of beech stands using species accumulation curves. The rank-abundance curves of ten most abundant plants was created from the ADS. Permutational multivariate analysis of variance (PERMANOVA) was used to compare the similarity of these two stand types (MB and YB). ‘vegan’ (Oksanen et al., 2019) and ‘BiodiversityR’ (Kind and Joe, 2005) packages of the R 3.0.1 (R Development Core Team, 2017) were used for the analysis.

As a measure of species diversity and dominance/abundance, accumulation curves (Kindt and Coe, 2005) were constructed. An indicator species analysis was executed to reveal the relationship between the herb layer species and the overstory composition (Dufrêne and Legendre, 1997) using the R package “indicspecies” (De Cáceres and Jansen, 2013).

Results and discussion

In this study, we were interested in comparing understory species composition and richness of two different succession stages of beech stands. Predicting the response of forest understory plants to disturbances caused by timber harvest or other silvicultural interventions is important to implement silvicultural practices focusing on the conservation of all components of forest ecosystems (Ellum, 2009). Results of the study clearly indicated that overstory structure and age shaped understory species composition in young and old even-aged beech forests.

Stand characteristics

Mean diameter at breast height and basal area of mature beech stands were 40.75 cm and 45.09 m²/ha⁻¹ while in young beech stands, they were 16.51 cm and 23.45 m²/ha⁻¹, respectively (*Table 1*). The average number of trees was 306 in mature beech stands and 1025 in young beech stands. While the mean diameter of the breast height and the basal

area of mature beech stands are about twice as large as those of young beech stands, the number of trees in young stands is three times the amount in mature stands. According to these mean diameter values, the stands are in pole and mature development stage.

Diversity and abundance of understory herb layer

64 vascular plant species were identified in the understory of beech stands. 45 species occurred in young beech stands and 49 species were also found in mature stands (Table 2). All the species recorded were native in old beech stands but one non-native species was found in young beech stands (Table A1 in the Appendix). Of the species recorded, while 19 species are unique to mature beech stands, 15 species are unique to young stands. Mean species richness was found same within the two stand types as 20.25. *Epimedium pubigerum* (DC.) C. Morren & Decne. was the most abundant species in all quadrats of young and mature beech stands (Fig. 3). İster and Gökbülak (2009) compared the species diversity of the herbaceous plants in the beech and oak stands in the same study area, and they identified 12 herbaceous plant species in 3 beech stands using transect sampling method.

Table 2. Diversity indices of the mature and young beech stands (YB = young beech stands, MB = mature beech stands, PADS = 4 subplots plus whole plot area data, ADS = the average of 4 subplots data)

		Richness (abundance)	Mean richness	St. dev. of richness	Shannon index	Simpson index
PADS	MB	49	20.25	4.30	3.66	0.969
	YB	45	20.25	3.33	3.51	0.964
ADS	MB	24 (339.83)	42.47	5.47	2.94	0.94
	YB	21 (343.50)	42.94	8.94	2.77	0.93

Kelemen et al. (2012) reported that in European beech forests species composition changed over time within the gaps but all species found before cutting were still present in the area after 8 years. Similarly, fir-beech forest in Slovenia Kutnar et al. (2015) detected a significant increase in species richness two years after logging. In our study, according to Simpson and Shannon-Wiener index, mature stands are more diverse than young stands in the two data sets (Table 2).

Accumulation curves of the understory species

The species richness of the understory plants of mature beech stands are higher than young ones (Fig. 2). The rarefaction curves revealed very consistent patterns across the two stand types. This suggested that herb layer richness became similar after 30-40 years of regeneration. The species richness was not affected significantly by shelterwood logging (Nagaike et al., 1999).

Rank abundance of the understory

When the 10 most common species on the herbaceous layer of young and mature stands are examined, it can be seen that 8 species are common in both stand types, but their rankings are different (Fig. 3). *Epimedium pubigerum* was the most common species in both stand types. *Smilax excelsa* L., *Ruscus hypoglossum* L. occurred in

young beech stand in the top 10 species but did not occur in mature beech stands. On the other hand, *Ornithogalum wiedemannii* Boiss. and *Carex sylvatica* Huds. were found in the top 10 species in the mature beech stands while they were not found in young beech stands (Fig. 3).

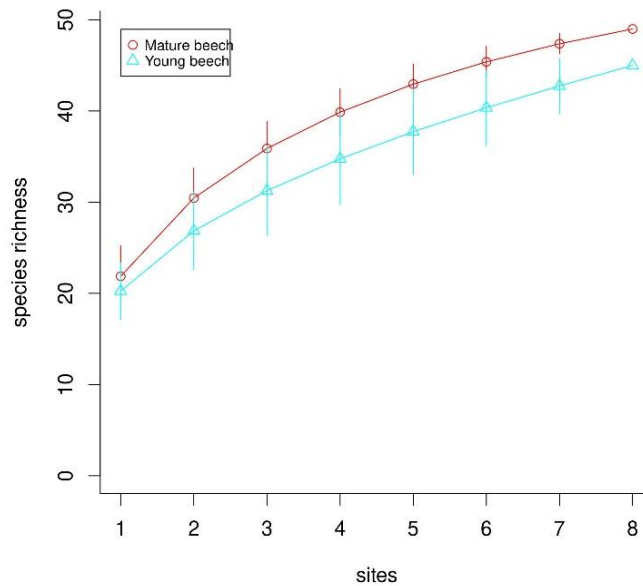


Figure 2. Species accumulation of the herb layer of beech stands in the young and mature beech stands. Rarefaction curves present the relationship between number of samples and understory species richness in beech forest stands. The whiskers show standard deviation of species richness

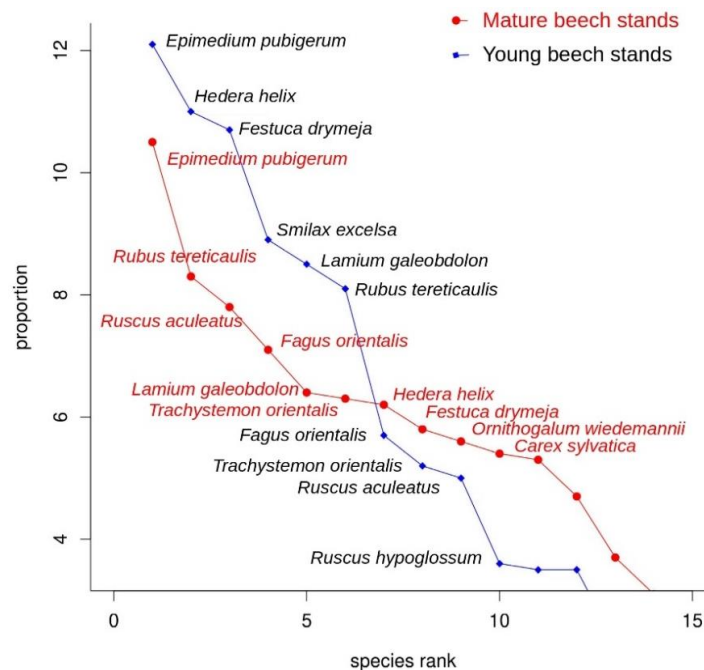


Figure 3. The herb layer species ranked in order of decreasing fidelity with respect to the two beech stand types. The proportional abundances of the species were calculated for two stand type separately

When we look at the diversity index values (Table A2) and accumulation curves graph of the two beech stand types (Fig. 2), the values of the old stands were determined to be higher.

Indicator species analysis

Only one indicator species was determined for each stand types by the multi-level pattern analysis (Table 3). This indicates that most of typical beech forest species were found in the herbaceous layer of both young and mature beech stands. The change in species composition during the successional stages is illustrated by the results of indicator species analysis. According to indicator species analysis, young beech stands were characterized by a shade plant species *Polystichum setiferum* (Forssk.) Moore ex Wyon. *Ornithogalum wiedemannii*, which is very seldom present in successional younger stands, was detected as an indicator of old beech stands. These results indicate that young beech stands seem to reach stable light condition and close canopy. According to Peet and Christensen (1988), however plant species and diversity decrease through substitution of natural succession in a forest but increase in steady-state phases of forest stand development.

Table 3. The indicator herbaceous species of the beech stands

Stand type	Indicator species	A	B	IndVal	p value
Mature beech	<i>Ornithogalum wiedemannii</i>	1.00	0.75	0.866	0.008**
Young beech	<i>Polystichum setiferum</i>	1.00	0.625	0.791	0.031*

The specificity (A), sensitivity (B), indicator value (IndVal) and significance (p value) are given. 'A' is the probability that the surveyed site belongs to the target site group, given that the species has been found. 'B' is the probability of finding the species in sites belonging to the site group. Significance codes: 0 '***' 0.001 '**' 0.01 '*' 0.05 '.' 0.1 ' ' 1

Similarity of herb layer composition in mature and young stands

According to the dissimilarity matrices, the community composition of the young and mature beech stands' herb layer was significantly different in terms of the compositional similarity (Bray-Curtis, $R^2_{\text{ADONIS}} = 0.16$, $P = 0.01$).

What causes the differences in composition and richness between these pure beech stands of two different successional stages? Since these areas are very close to each other, it is thought that there is not significant effect of climate and altitude factor. Previous studies have indicated the herb layer of beech stands various depending on the light conditions (Lysik, 2008). In a forest, understory light is closely dependent on the canopy structure and it is also considered the main limiting factor of understory plant richness and composition (Hill, 1979). Although understory plant species in a forest have different optimal light requirements, in beech forests, herb layer species are well adapted to low understory light conditions, or complete their life cycles before trees are completely foliated and therefore light would be less important for such species (Härdtle et al., 2003). The understory plant diversity in forests varies over time depending on stand structure. Namely, plant diversity increases rapidly in the years following the logging, then decreases when canopy closure occurs and increases slowly again depend on overstory tree density decreasing in overtime (Roberts and Gilliam, 1995; Ujházy et al., 2017).

The results of present study showed that successional stage was the main driver of understory herbaceous species composition in even aged beech forest and Aavik et al. (2009) reported similar results in boreonemoral forests. Herbaceous plants are less sensitive to shelterwood forestry than the other species groups in a forest (Brunet et al., 2010), and therefore the shelterwood system can be suggested as a suitable method for sustainable management of plant species diversity and composition of beech stands (Poorbabei and Poor-rostam, 2009).

Conclusions

Species composition of understory vegetation in oriental beech stands was related to management intensity. At the same time, our results indicate that natural regeneration in oriental beech forests using shelterwood systems did not cause significant differences in species richness but species composition may show differences over time in these forests. Forest managers should consider the actual and potential effects of their silvicultural practices on understory vegetation diversity and composition. Although there is a small difference in diversity index and rank abundance values, there is a significant difference between the community matrices of the two stand types and it shows that two stand types are different in understory plant species and compositions.

The results showed that species richness and coverage of vascular plants were related to overstory successional stage. The results suggest that stand age influences the herb layer composition in beech stands but 16 study plots do not allow broad generalization of our results. Therefore, further studies would be necessary to acquire more knowledge about change in species composition and diversity with stand development.

Acknowledgments. This study was supported by the Scientific Research Projects Coordination Unit of Istanbul University (Project Number FBA-2016-20319).

REFERENCES

- [1] Aavik, T., Püssa, K., Roosalu, E., Moora, M. (2009): Vegetation change in boreonemoral forest during succession - trends in species composition, richness and differentiation diversity. – *Annales Botanici Fennici* 46: 326-335.
- [2] Augusto, L., Dupouey, J. L., Ranger, J. (2003): Effects of tree species on understory vegetation and environmental conditions in temperate forests. – *Annals of Forest Science* 60: 823-831.
- [3] Balcı, A. N., Özyüvaci, N., Özhan, S. (1986): Sediment and nutrient discharge through stream water from two experimental watersheds in mature oak-beech forest ecosystems near Istanbul, Turkey. – *Journal of Hydrology* 85: 31-47.
- [4] Barbier, S., Gosselin, F., Balandier, P. (2008): Influence of tree species on understory vegetation diversity and mechanisms involved—a critical review for temperate and boreal forests. – *Forest Ecology Management* 254: 1-15.
- [5] Braun-Blanquet, J. (1964): *Pflanzensoziologie. Grundzüge der Vegetationskunde*. – Springer, Berlin.
- [6] Brunet, J., Fritz, Ö., Richnau, G. (2010): Biodiversity in European beech forests - a review with recommendations for sustainable forest management. – *Ecological Bulletin* 53: 77-94.
- [7] Davis, P. H. 1965-1985. *Flora of Turkey and the East Aegean Islands*. Vols. I-IX. – Edinburg University Press, UK.

- [8] De Cáceres, M., Jansen, F. (2013): Package 'indicspecies' version 1.6.7. – <http://cran.r-project.org/web/packages/indicspecies/index.html> (accessed on 24 Nov 2018).
- [9] Dufrêne, M., Legendre, P. (1997): Species assemblages and indicator species: the need for a flexible asymmetrical approach. – *Ecological Monographs* 67: 345-366.
- [10] Durak, T. (2012): Changes in diversity of the mountain beech forest herb layer as a function of the forest management method. – *Forest Ecology and Management* 276: 154-164.
- [11] Elliott, K. J., Boring, L. R., Swank, W. T., Haines, B. R. (1997): Successional changes in diversity and composition in a clearcut watershed in Coweeta Basin, North Carolina. – *Forest Ecology and Management* 92: 67-85.
- [12] Ellum, D. S. (2009): Floristic diversity in managed forests: demography and physiology of understory plants following disturbance in southern New England forests. – *Journal of Sustainable Forestry* 28: 132-151.
- [13] Gilliam, F. S. (2007): The ecological significance of the herbaceous layer in temperate forest ecosystems. – *Bioscience* 57: 845-858.
- [14] Härdtle, W., von Oheimb, G., Westphal, C. (2003): The effects of light and soil conditions on the species richness of the ground vegetation of deciduous forests in northern Germany (Schleswig-Holstein). – *Forest Ecology and Management* 182: 327-338.
- [15] Hill, M. O. (1979): The Development of a Flora in Even-Aged Plantations. – In: Ford, E. D., Malcolm, D. C., Atterson, J. (eds.) *The Ecology of Even-aged Forest Plantations*. Institute of Terrestrial Ecology, Cambridge.
- [16] Hunter, M. L. Jr. (1999): *Maintaining Biodiversity in Forest Ecosystems*. – Cambridge University Press, Cambridge.
- [17] İster, S. I., Gökbulak, F. (2009): Effect of stand types on understory vegetation. – *J. Environ. Biol.* 30: 595-600.
- [18] Kelemen, K., Mihók, B., Gálhidy, G., Standovár, T. (2012): Dynamic response of herbaceous vegetation to gap opening in a central European beech stand. – *Silva Fennica* 46: 53-65.
- [19] Kindt, R., Coe, R. (2005): *Tree Diversity Analysis: A Manual and Software for Common Statistical Methods for Ecological and Biodiversity Studies*. – World Agroforestry Centre, Nairobi.
- [20] Kutnar, L., Eler, K., Marinšek, A. (2015): Effects of different silvicultural measures on plant diversity—the case of the Illyrian *Fagus sylvatica* habitat type (Natura 2000). – *iForest – Biogeosciences and Forestry* 9: 318-324.
- [21] Lysik, M. (2008): Ten years of change in ground-layer vegetation of European beech forest in the protected area (Ojców National Park, South Poland). – *Polish Journal of Ecology* 56: 17-31.
- [22] Lorenz, M., Fischer, R., Becher, G., Mues, V., Seidling, W., Kraft, P., Nagel, H. D. (2006): *Forest Condition in Europe. Technical Report of ICP Forests*. – Institute for World Forestry, Hamburg. <http://icp-forests.net/> (accessed on 15 December 2018).
- [23] Lindenmayer, D. B., Franklin, J. F. (2002): *Conserving Forest Biodiversity: A Comprehensive Multiscaled Approach*. – Island Press, Washington.
- [24] Nagaike, T., Kamitani, T., Nakashizuk, T. (1999): The effect of shelterwood logging on the diversity of plant species in a beech (*Fagus crenata*) forest in Japan. – *Forest Ecology and Management* 118: 161-171.
- [25] OGM (General Directorate of Forestry) (2015): *Forests of Turkey*. – Turkey General Directorate of Forest Publications, Ankara.
- [26] Oksanen, J., Guillaume Blanchet, F., Friendly, M., Kindt, R., Legendre, P.; McGlinn, D.; Peter, Minchin, R.; O'Hara, R. B.; Simpson, G. L.; Solymos, P.; Stevens, M. H. H.; Szoecs, E.; Wagner, H. (2019): *vegan: Community Ecology Package*. R package version 2.5-5. – <https://CRAN.R-project.org/package=vegan> (accessed on 10 Nov 2018).

- [27] Özhan, S., Gökbülak, F., Serengil, Y., Özcan, M. (2010): Evapotranspiration form a mixed deciduous forest ecosystem. – *Water Resources Management* 24: 2353-2363.
- [28] Paillet, L., Bergès, L., Hjältén, J., Ódor, P., Avon, C., Bernhardt-Romermann, M., Bijlsma, R. J., De Bruyn, L., Fuhr, M., Grandin, U., Kanka, R., Lundin, L., Luque, S., Magura, T., Matesanz, S., Meszaros, I., Sebastia, M. T., Schmidt, W., Standovar, T., Tothmeresz, B., Uotila, A., Valladares, F., Vellak, K., Virtanen, R. (2011): Biodiversity differences between managed and unmanaged forests: meta-analysis of species richness in Europe. – *Conservation Biology* 24: 101-112.
- [29] Peet, R. K., Christensen, N. L. (1988): Changes in Species Diversity during Secondary Forest Succession on the North Carolina Piedmont. – In: During, H. J., Werger, M. J. (eds.) *Diversity and Pattern in Plant Communities*. SPB Academic Publishing, The Hague.
- [30] Poorbabaei, H., Poor-rostam, A. (2009): The effect of shelterwood silvicultural method on the plant species diversity in a beech (*Fagus orientalis* Lipsky) forest in the north of Iran. – *Journal of Forest Science* 55(8): 387-394.
- [31] R Development Core Team (2017): A Language and Environment for Statistical Computing. – R Foundation for Statistical Computing, Vienna. <http://www.R-project.org> (accessed on 10 October 2018).
- [32] Roberts, M. R., Gilliam, F. S. (1995): Patterns and mechanisms of plant diversity in forested ecosystems: implications for forest management. – *Ecological Applications* 5: 969-977.
- [33] Saatçioğlu, F. (1970): Ten year results of natural regeneration of oriental beech (*Fagus orientalis* Lipsky.) by using uniform shelterwood methods in Belgrad Forests in Turkey. – *Journal of the Faculty of Forestry Istanbul University* 20(2): 1-54.
- [34] Stefańska-Krzaczek, E., Staniaszek-Kik, M., Szczepańska, K., Szymura, T. H. (2019) Species diversity patterns in managed Scots pine stands in ancient forest sites. – *PLoS One* 14(7): e0219620. <https://doi.org/10.1371/journal.pone.0219620>.
- [35] Ujházy, K., Hederová, L., Máliš, F., Ujházyová, M., Bosela, M., Ciliak, M. (2017): Overstorey dynamics controls plant diversity in age-class temperate forests. – *Forest Ecology and Management* 391: 96-105.
- [36] Yaltrık, F. (1966): *Floristic Analysis of Belgrad Forest and Main Stand Composition*. – OGM Publications, Ankara.
- [37] Yaltrık, F. (1982): *Fagus L.* – In: Davis, P. H. (ed.) *Flora of Turkey and the East Aegean Islands*. Edinburgh University Press, Edinburgh.
- [38] Yaltrık, F., Akman, Y., Ketenoglu, O. (1983): A phytosociological research in the Belgrad Forest. – *Communications Faculty of Sciences University of Ankara* (1): 1-9.
- [39] Yılmaz, H. (2014): *Fagus L.* – In: Akkemik, Ü. (ed.) *Trees and Shrubs of Turkey I*. OGM Publications, Ankara (in Turkish).
- [40] Yılmaz, O. Y., Yılmaz, H., Akyüz, F. (2018): Effects of the overstorey on the diversity of the herb and shrub layers of Anatolian black pine forests. – *European Journal of Forest Research* 137: 433-445.

APPENDIX

Table A1. Presence/absence of plants in the herb layer of 16 plots

	Young beech stands								Mature beech stands							
	1	2	3	4	5	6	7	8	1	2	3	4	5	6	7	8
<i>Ajuga reptans</i> L.									1			1				
<i>Arum italicum</i> Mill.	1			1	1				1		1					1
<i>Arum maculatum</i> L.														1		
<i>Asparagus acutifolius</i> L.								1								

<i>Stellaria holostea</i> L.										1							
<i>Symphytum tuberosum</i> L.	1	1	1	1		1	1	1	1		1	1	1	1	1	1	1
<i>Tilia tomentosa</i> Moench										1							
<i>Trachystemon orientalis</i> (L.) D.Don	1	1	1	1	1	1	1	1	1		1	1			1	1	
<i>Veronica chamaedrys</i> L.									1								
<i>Viola odorata</i> L.	1	1	1	1	1	1	1	1	1		1	1	1	1	1	1	
<i>Viola sieheana</i> W.Becker									1			1	1				

Table A2. Diversity indices of the 16 beech stands (ADS = the average of 4 subplots data)

	Richness	Shannon index	Abundance (ADS)	Simpson index
Mature beech stands				
1	26	3.26	39.50	0.96
2	21	3.05	39.17	0.95
3	19	2.94	36.92	0.95
4	25	3.22	42.83	0.96
5	25	3.22	43.25	0.96
6	24	3.18	44.83	0.96
7	18	2.89	54.33	0.94
8	17	2.83	39.00	0.94
Young beech stands				
1	20	3.00	37.00	0.95
2	16	2.77	51.25	0.94
3	18	2.89	34.17	0.94
4	20	3.00	37.08	0.95
5	21	3.05	47.67	0.95
6	22	3.09	46.83	0.96
7	18	2.89	32.50	0.94
8	27	3.30	57.00	0.96

CHANGES IN GROWTH PARAMETERS, OIL YIELD, FATTY ACID COMPOSITION AND MINERAL CONTENT OF TWO SAFFLOWER (*CARTHAMUS TINCTORIUS* L.) GENOTYPES IN RESPONSE TO WATER STRESS

OZKAN, A.

*Department of Gastronomy and Culinary Arts Faculty of Fine Arts, Gaziantep University,
27000 Gaziantep, Turkey
(e-mail: aozkan27@gmail.com)*

(Received 9th Sep 2019; accepted 15th Nov 2019)

Abstract. The present study was designed to investigate the effects of water stress on growth and development parameters, oil yield coupled with their fatty acid composition as well as mineral content of two safflower genotypes including Remzibey-05 and Gokturk. Accordingly, significant differences regarding plant length, branch number per plant, capsule number per plant, capsule seed number, 1000-seed weight and seed yield per pot were assessed. However, first branch length did not exhibit significant differences between genotypes in response to the treatments. Furthermore, Oil yield was not significantly affected by severe water stress for Remzibey-05 even a 1.60% increase was observed under severe water stress but the yield was significantly increased by 2.37% in Gokturk. In terms of oil composition unsaturation degree, UFA/SFA significantly increased with stress for both genotypes. Concerning mineral content; Remzibey -05 genotype had the highest value of K and Na whereas Gokturk genotype had the highest values of Mg, Fe, Cu and Zn. Finally, the experimental groups were discriminated and identified using PCA and heatmap visualization.

Keywords: *fatty acid unsaturation degree, drought, Remzibey-05, Gokturk, water stress*

Introduction

Water stress resistance of crops is one of the great challenges for the world's agricultural systems. Water stress-induced loss in crop yield probably exceeds losses caused by other severe environmental constraints. Thereby, numerous researches in plants responses to water scarcity has been important interest for scientists for many years in order to develop, improve or explore drought-tolerant plant species or cultivars, genotypes within the same species for a sustainable agricultural production (Hamrouni et al., 2001; Turk et al., 2004; Al-Barrak, 2006; Bettaieb et al., 2009; Ozkan and Kulak, 2013; Zandalinas et al., 2018; Fahad et al., 2017; Shi et al., 2017; Ahmed et al., 2016; Ozkan, 2018; Rubin et al., 2017; Vurukonda et al., 2016; Pouri et al., 2019; Cetinkaya et al., 2016).

Water stress alters the biochemical synthesis pathways and subsequently production of primary and secondary metabolites is influenced. It is worthy to remark that industrially, medicinally or economically important metabolites may be accumulated beyond the decline in the growth and productivity of crops (Ozkan and Kulak, 2013; Hamrouni et al., 2001; Laribi et al., 2009). Of those, the variations in lipid content and its composition have been reported under varying irrigation degrees (Laribi et al., 2009; Bettaieb et al., 2010; Laribi et al., 2011; Ozkan and Kulak, 2013).

Safflower (*Carthamus tinctorius*) belonging to Asteraceae family is of the oldest cultivated oilseed crop but not common and not very popular when compared to other oil crops such as soybean, sunflower and peanut (Canavar et al., 2014; Bortolheiro and Silva, 2017). Of the oilseed crops, safflower has been well-documented to possess

ability in moderate tolerance of environmental constraints but changes in oil yield and subsequently fatty acid composition have been reported, indicating that water constraints water deficient condition might cause increase protein and decrease oil contents of safflower (Nabipour et al., 2007; Amini et al., 2014; El Sabagh et al., 2019). Seed oil of safflower is well characterized with a large amount of saturated (palmitic and stearic) and unsaturated (oleic, linoleic and linolenic) fatty acids and composition. However, the percentage and content of the compounds and oil yield are particularly affected by water stress (Bortolheiro and Silva, 2017; Nabipour et al., 2007; Ashrafi and Razmjoo, 2010; Eslam, 2011; Amini et al., 2014; Ozkan and Kulak, 2013; Nazari et al., 2017). Since each species of the plants have been comprised of genotypes, cultivars, varieties, populations and chemotypes, many studies can be performed on the different genotypes of the same species. As well-known and documented that, plants have been adapted to environmental conditions through not only based their genetic inheritance and but also the primary and secondary metabolites inside. Through profiling the metabolite content, plants have been sorted as tolerant or sensitive. Along with the present study, two different safflower genotypes were used in order to determine their oil yield combined with fatty acid compositional profiling in response to water stress conditions. In addition to the oil and its composition, mineral content or accumulation of seed samples belonging to both genotypes were determined. Furthermore, growth and developmental parameters of genotypes were compared after subjection water stress and normal life span under irrigated conditions (control).

Materials and methods

Plant material and water deficit treatment

Experiments were performed under greenhouse conditions with pots including 2 kg soil mixture of 3:1:1 (soil-peat-perlite) at Gaziantep, Turkey. The experiments were carried out with three replicates corresponding 10 plants for each replicate. Each pot included one plant seedling. The effects of severe water stress (SWD) on safflower genotypes (Remzibey-05 and Gokturk) were investigated. The safflower genotypes are of the significant oil crops. The materials used herein are of the developed in Turkey. Herewith, the studies regarding adaptation of the genotypes in arid and semi-arid regions corresponding to the limited water sources are required. In this context, the genotypes were screened for their low water content tolerance corresponding to the oil yield coupled with their fatty acid composition in addition to basic agricultural parameters.

For the experimental processes, similar methods with Bettaieb et al. (2009) were followed. In brief, during the first 35 days of the study, plants were irrigated with tap water, and subsequently exposed to different water regimes: 100% (control group: C; 600 ml) 25% (severe water deficit group: SWD; 150 ml) of field capacity (FC). The properties of experimental soils were as follows: Potassium (297.75 ppm), organic matter (1.16%), salt (0.059) at a set pH (8.0). Experiments were conducted in a greenhouse with a 14-h photoperiod and performed between October 13, 2018 and July 26, 2019. Mean temperature was kept at 25 ± 2 °C during daytime and 14 ± 2 °C at nighttime, respectively, with a relative humidity of 70%. After harvest, seeds were airdried and stored at 4 °C until use for further analysis.

Growth and yield parameter measurements

For each treatment, measurement of plant length, seed number per capsule, capsule number, 1000-seed weight, total weight per pot, and single plant yield were evaluated by harvest of six randomly selected plants from each experimental replicate (Ozkan and Kulak, 2013; Ozkan, 2018).

Oil extraction and fatty acid composition analysis

Oil extraction and then fatty acids of oil were determined according to our previous methods applied (Ozkan and Kulak, 2013; Ozkan, 2018). Briefly, oils were extracted from safflower seeds (each 2 g sample) with n-hexane for 4 h using a Soxhlet extraction apparatus. Subsequently, the solvent was evaporated under reduced pressure and temperature using a Rotary evaporator (Heidolph). 0.1 g of safflower oil was added to 2 ml n-heptanes into a screw-capped tube for esterification. The fatty acid analyses were conducted according to the official method COI/T.20/Doc.no.24 2001. 0.1 g of safflower oil was taken into screw-capped tube. 2 ml n-heptane was added and shaken. After 0.2 ml methanolic potassium hydroxide was added for esterification, tubes were vigorously shaken for 30 s after the vials were closed. The supernatant of the solution was taken followed after 1 h of incubation at room temperature. Then, the supernatant was put in 2 ml vials for injection.

Fatty acid composition profile determination

GC-FID analyses of fatty acids methyl esters were carried out on a Shimadzu gas chromatography (GC2010 series) equipped with a Supelco SP 2380 fused silica capillary column (100 m, 0.25 mm i.d., 0.2 µm film thickness). Helium was used as carrier gas, at a flow rate of 3 mL/min. The injection and detector temperature were 140 °C and 240 °C, respectively. The oven temperature was held isothermal at 140 °C for 5 min, then raised to 240 °C at 4 °C/min and held isothermal at 240 °C for 15 min. Injection volume of Diluted samples [1/100 (v/v) in n-heptanes] of 1.0 µL were injected automatically in the split mode (1/100). The identification of the constituents was based on comparison of the GC-retention times with those of available analytical standards (Larodan Fine chemicals, mixture of 37 components of fatty acids methyl esters). Peak area was used to obtain the percentage of individual fatty acid.

Sample preparation and measurement for mineral content

The harvested seed samples were cleaned, washed by de-ionized water, and dried. Pre-dried samples were de-moisturized at 70 °C for 48 h in an oven and ground for chemical analysis. 0.2 g of ground powdered seed samples were immediately placed into burning cup with 5 ml HNO₃ 65% and 2 ml H₂O₂ 30%. After the incineration process, the solution was cooled at room temperature for 45 min. The extracts were passed through a Whatman 42 filter paper. These filtrates were collected by de-ionized water in a 20 ml-polyethylene bottles and kept at 4 °C in laboratory for ICP-OES analysis. Each sample was analyzed in triplicate.

Statistical analysis

SPSS statistical program was used to determine statistical significance levels by employing the independent one-way ANOVA followed by Duncan multiple range test

and the differences between individual means were considered to be statistically important at $p < 0.05$. Moreover, specifically for each genotype, control and stress group of plants were compared using independent t-test in order to determine to clarify their behaviour against stress. Also, the discrimination for experimental groups was done with the principal component analysis using SPSS software. Finally, heatmap was 209 constructed using ClustVis (<https://biit.cs.ut.ee/clustvis/>).

Results and discussion

Effect of water stress on plant growth and development parameters

Based on independent t-test, there were significant differences between plant length ($t = 2.274$; $p < 0.05$), capsule seed number ($t = 3.688$; $p < 0.01$), 1000-seed weight ($t = 2.333$; $p < 0.05$), seed yield per pot ($t = 5.231$; $p < 0.01$) for Remzibey-05 genotype in response to water stress. However, first branch length, branch number per plant and capsule number per plant did not exhibit significant differences between treatments ($p > 0.05$) (Table 1).

Table 1. t-test analysis of growth and yield parameters of Remzibey-05 genotype exposed to water stress

Growth and yield parameters	Control	SWD	t-statistic	p value
Plant length (cm)	37.50±6.02	29.33±6.41	2.274	0.046*
First branch length (cm)	18.50±6.29	17.33±5.57	0.340	0.741
Branch number per plant	4.83±1.33	3.83±1.17	1.384	0.197
Capsule number per plant	5.83±2.23	3.83±1.17	1.947	0.080~
Capsule seed number	30.17±9.70	15.34±1.70	3.688	0.004**
1000-seed weight (g)	51.66±14.09	35.20±10.01	2.333	0.042*
Seed yield per pot (g)	5.99±1.44	2.40±0.87	5.231	0.000**

** $p < 0.01$; * $p < 0.05$; ~ $p < 0.10$; SWD: severe water deficit

Severe water stress significantly affected plant length ($t = 3.353$; $p < 0.01$), branch number per plant ($t = 3.835$; $p < 0.01$), capsule number per plant ($t = 4.715$; $p < 0.01$), capsule seed number (3.664; $p < 0.01$), seed yield per plant ($t = 8.871$; $p < 0.01$) in Gokturk genotype. However, first branch length ($t = 0.902$; $p > 0.05$) and 1000-seed weight ($t = 1.987$; $p > 0.05$) did not differ in Gokturk genotype in response to severe water stress (Table 2).

Table 2. t-test analysis of growth and yield parameters of Gokturk genotype exposed to water stress

Growth and yield parameters	Control	SWD	t-statistic	p value
Plant length (cm)	34.00±5.514	22.83±6.014	3.353	0.007**
First branch length (cm)	18.17±6.113	14.83±6.68	0.902	0.388
Branch number per plant	4.83±.41	3.17±.98	3.835	0.003**
Capsule number per plant	6.00±1.10	3.17±.98	4.715	0.001**
Capsule seed number	23.67±7.71	11.74±2.03	3.664	0.004**
1000-seed weight (g)	49.85±7.21	40.91±8.34	1.987	0.075~
Seed yield per pot (g)	5.29±.82	1.54±.64	8.871	0.000**

** $p < 0.01$; ~ $p < 0.10$; SWD: severe water deficit

Furthermore, independent t-test was performed in order to determine the differences between control and stress groups of genotypes. No differences were observed for the parameters of both genotypes in control groups (*Table 3*). Also, there were no significant differences-except capsule seed number between genotypes under severe stress conditions (*Table 4*).

Table 3. *t*-test analysis of growth and yield parameters of both genotypes under irrigated conditions (control)

Growth and yield parameters	Remzibey-05 control	Gokturk control	t-statistic	p value
Plant length (cm)	37.50±6.03	34.00±5.52	1.050	0.319
First branch length (cm)	18.50±6.29	18.17±6.11	0.093	0.928
Branch number per plant	4.83±1.33	4.83±0.41	0.000	1.000
Capsule number per plant	5.83±2.23	6.00±1.10	-0.164	0.873
Capsule seed number	30.17±9.71	23.67±7.71	1.285	0.228
1000-seed weight (g)	51.66±14.1	49.85±7.21	0.281	0.785
Seed yield per pot (g)	5.99±1.44	5.3±.82	1.045	0.320

Table 4. *t*-test analysis of growth and yield parameters of both genotypes under severe water stress

Growth and yield parameters	Remzibey-05 SWD	Gokturk SWD	t-statistic	p value
Plant length (cm)	29.33±6.41	22.83±6.02	1.812	0.100
First branch length (cm)	17.33±5.57	14.83±6.68	.704	0.497
Branch number per plant	3.83±1.17	3.17±0.98	1.069	0.310
Capsule number per plant	3.83±1.17	3.17±0.98	1.069	0.310
Capsule seed number	15.34±1.70	11.75±2.03	3.327	0.008**
1000-seed weight (g)	35.20±10.00	40.90±8.34	-1.073	0.308
Seed yield per pot (g)	2.40±0.875	1.54±0.64	1.959	0.079~

**p < 0.01 ~p < 0.10; SWD: severe water deficit

One-way variance analysis reveals significant differences in terms of plant length ($F = 6.708$; $p < 0.01$), branch number per plant ($F = 3.750$; $p < 0.05$), capsule number per plant ($F = 5.719$; $p < 0.01$), capsule seed number ($F = 10.289$; $p < 0.01$), 1000-seed weight ($F = 3.413$; $p < 0.05$) and seed yield per pot ($F = 28.921$; $p < 0.01$). However, first branch length did not exhibit significant differences between genotypes in response to the treatments (*Table 5*).

In many and various studies regarding water stress and agronomical yield attributes interaction, stress conditions have been reported to exhibit inhibitory impacts on stem growth and plant height due to shrinkage in output changes in cellular water status of the plant. The effects of the water stress on the plant parts are variable for the examined parameters. The effects can be observed at certain developmental stages of the plant, a trait of the plant or genotypes of the same plant species (Prasad and Staggenborg, 2008).

Table 5. One-way variance analysis of growth and yield parameters of genotypes in response to treatments

Growth and yield parameters	Remzibey-05 control	Remzibey-05 SWD	Gokturk control	Gokturk SWD	ANOVA F-statistic
Plant length (cm)	37.50±6.02a	29.33±6.40bc	34.00±5.51ab	22.83±6.01c	6.708**
First branch length (cm)	18.50±6.29	17.33±5.57	18.17±6.11	14.83±6.68	.432
Branch number per plant	4.83±1.33 a	3.83±1.17 ab	4.83±.401 a	3.17±.98 b	3.750*
Capsule number per plant	5.83±2.229 a	3.83±1.169 b	6.00±1.095 a	3.17±.983 b	5.719**
Capsule seed number	30.17±9.70 a	15.34±1.70 b	23.67±7.71 a	11.74±2.03 b	10.289**
1000-seed weight (g)	51.66±14.09 a	35.20±10.01 b	49.85±7.21 a	40.90±8.34 ab	3.413*
Seed yield per pot (g)	5.99±1.44 a	2.40±0.88 b	5.30±0.82 a	1.54±0.64 b	28.921**

Means±SD in the same row by the same letter are not significantly different to the test of Duncan ($\alpha = 0.05$). ** $p < 0.01$ * $p < 0.05$; SWD: severe water deficit

Correlation analysis of growth and yield parameters of safflower

Table 6 presents the correlation analysis of plant length, first branch length, number of branches, capsule number, seed number, 1000-seed weight and seed yield in *Carthamus tinctorius* genotypes. Significant and positive relation was observed by 64.2% between plant height and first branch length ($r = 0.642$; $p < 0.01$). Also, 69.9% ratio between plant length and branch number was found to be significant with positive correlation ($r = 0.699$; $p < 0.01$). Plant length was also positively correlated with capsule number per plant by 80.4% ($r = 0.804$; $p < 0.01$). Plant length was furthermore positively correlated with seed yield per pot ($r = 0.782$; $p < 0.01$). moreover, significant and positive correlation coefficients between first branch length and capsule number per plant ($r = 0.417$; $p < 0.05$), first branch length and seed yield per pot ($r = 0.465$; $p < 0.05$), branch number per plant and capsule number per plant ($r = 0.900$; $p < 0.01$), branch number per plant and seed yield per pot ($r = 0.742$; $p < 0.01$), capsule seed number and seed yield per pot ($r = 0.790$; $p < 0.01$), capsule seed number and seed yield per pot ($r = 0.727$; $p < 0.01$) as well as 1000-seed weight and seed yield per pot ($r = 0.508$; $p < 0.05$) were observed. The remained coefficients were all positive but not significant. No negative correlations were found between investigated parameters (Table 6).

Table 6. Correlation analysis of growth and yield parameters of safflower

	Plant length	First branch length	Branch number per plant	Capsule number per plant	Capsule seed number	1000-seed weight	Seed yield per pot
Plant length	1						
First branch length	.642**	1					
Branch number per plant	.699**	0.39	1				
Capsule number per plant	.804**	.417*	.900**	1			
Capsule seed number	0.395	0.228	0.322	0.294	1		
1000-seed weight	0.336	0.219	0.288	0.279	0.26	1	
Seed yield per pot	.782**	.465*	.742**	.790**	.727**	.508*	1

** $p < 0.01$, * $p < 0.05$

Effects of water stress on oil yield and fatty acid composition

Oil yield was not significantly affected with severe water stress in Remzibey-05 even a 1.60% increase was observed under severe water stress but the yield was significantly augmented by 2.37% in Gokturk. The non-significant changes in oil percentage could be attributed to stress timing at vegetation of the plant. In the current study, severe water stress was applied at the flowering. Nazari et al. (2017) also reported that drought stress at the flowering stage of some safflower did not influence seed oil percentages. In the studies performed on different genotypes of safflower, six different safflower lines were exposed to water stress and subsequently followed by rehydration. The oil yield increased from 24.18 ± 5.01 to 26.61 ± 6.21 (Bortolheiro and Silva, 2017). However, oil yield significantly decreased under water stress (Nabipour et al., 2007; Ashrafi and Razmjoo, 2010; Ensiye and Khorshid, 2010; Eslam, 2011; Amini et al., 2014). Ozkan and Kulak (2013) reported a non-significant slight increase in oil content of seeds of sesame seedlings exposed to severe water stress. Furthermore, drought stress did not cause significant changes in percentage of seed oil content of safflower species (Nazari et al., 2017).

After oil esterification, the fatty acid compounds in oil were identified using gas chromatography. Of the fatty acid compounds identified for both genotypes, oleic acid, linoleic acid, palmitic acid, stearic acid and behenic acid were of compounds with percentage over 1% (Table 7).

Their total percentage for treatments were 98.62% for Remzibey-05 control, 99.02% for Remzibey-05 SWD, 98.80% Gokturk control and 99.12% Gokturk SWD. The yield and percentage can change but the composition of the oil was not affected by severe water stress.

Of the compounds, palmitic acid percentage significantly decreased with severe water stress by 28.30% for Remzibey-05 and 15.61% in Gokturk genotype. No differences regarding percentage of the palmitic acid in control and SWD groups of both genotypes, respectively were found. The decline in palmitic acid under water stress was also reported (Ashrafi and Razmjoo, 2010; Petcu et al., 2001). However, Nazari et al. (2017) reported slight increases in palmitic percentages of for safflower species.

Stearic acid also exhibited similar manner with palmitic acid in both genotypes in response to severe water stress. Stearic acid decreased by 45.36% in Remzibey-05 and 26.66% in Gokturk genotypes. The decreases in percentage of stearic acid were documented (Ashrafi and Razmjoo, 2010). However, Laribi et al. (2009) noted an increase in palmitic acid (110%) and stearic acid (269%) and a decline in petroselinic acid (18.47%) in *Carum carvi* under severe water stress.

Oleic acid percentage significantly increased by 7.85% with severe water stress in Remzibey-05 but the percentage did not significantly vary with severe water stress in Gokturk genotype. Ashrafi and Razmjoo (2010) reported a decline in oleic acid percentage in different safflower genotypes but an increase was documented by Gao et al. (2009). In the study by Ozkan and Kulak (2013), two sesame genotypes were exposed to moderate and severe water stress, documenting that no significant changes in percentage of oleic acid in Cumhuriyet genotype were found while there was a slight but significant change Özberk genotype under severe water stress.

Linoleic acid percentage was not affected by severe water stress in Remzibey-05 genotype but increased by 1.80% in Gokturk under severe stress conditions. Linoleic acid percentage did not significantly vary in sesame (Cumhuriyet genotype) but increased with stress in sesame (Özberk genotype) (Ozkan and Kulak, 2013). Ashrafi

and Razmjoo (2010) also reported a decline in percentage of linoleic acid in safflower genotypes.

Oleic acid and linoleic acid ratio increased in Remzibey-05 under severe water stress (ratio: 0.511 and 0.545 for control and SWD, respectively) but it decreased in Gokturk (0.554 and 0.545 for control and SWD, respectively). Laribi et al. (2009) reported decreases in oleic acid and linoleic acid ratio under severe water stress but an increased ratio of oleic acid/linoleic acid was reported (Talha and Osman, 1975).

Percentage of behenic acid increased by 10.64% and 17.19% in both genotypes in response to water stress Remzibey-05 and Gokturk, respectively. Behenic acid did not change in sesame seeds in response to water stress (Ozkan and Kulak, 2013; Ozkan, 2018).

Table 7. Effects of water stress on oil yield and fatty acid composition of both safflower genotypes

Fatty acid compounds	Remzibey-05 control	Remzibey-05 SWD	Change (%)	Gokturk control	Gokturk SWD	Change (%)
Myristic acid	.0762a	.0201b	-73.62%	.0460	.0314	-31.74%
Palmitic acid	6.3492a	4.5521b	-28.30%	4.4915a	3.7903b	-15.61%
Palmitoleic acid	.0665b	.0918a	38.05%	.0759	.0932	22.79%
Heptadecanoic acid	.0316	.0256	-18.99%	.0244	.0163	-33.20%
Cis-10Heptadecanoic	.0674	.0757	12.31%	.0750b	.0825a	10.00%
Stearic acid	2.1725a	1.1871b	-45.36%	1.2532a	.9191b	-26.66%
Oleic acid	29.8967b	32.2424a	7.85%	32.7382	32.8169	0.24%
Linoleic acid	58.4864	59.1422	1.12%	59.0845b	60.1460a	1.80%
Arachidic acid	.2454a	.1163b	-52.61%	.1557	.1136	-27.04%
Cis11Eicosenoic acid	.0688	.0762	10.76%	.0727	.0762	4.81%
Linolenic acid	.1985b	.2755a	38.79%	.2591	.2748	6.06%
Heneicosanoic acid	.1916a	.0724b	-62.21%	.0484	.0331	-31.61%
Behenic acid	1.7107b	1.8928a	10.64%	1.2362	1.4487	17.19%
Lignoceric acid	.0970	.0985	1.55%	.1034	.1055	2.03%
Oilyield (%)	27.89	29.49	1.60	25.48b	27.85a	2.37%

SWD: Severe water deficit; Means for same genotypes with different superscripts (a-b) are significantly different according to Student t test ($\alpha = 0.05$)

Fatty acid unsaturation degree

Based on our experimental data (Table 8), lipids extracted from safflower seeds are dominated by C16 and C18 fatty acids which are common in higher plants (Rebey et al., 2017). Analysis of fatty acid composition indicated that safflower seeds in control plants of Remzibey-05 genotype were characterized by a high proportion of polyunsaturated fatty acids (PUFA) (58.68%) versus 30.10% of monounsaturated fatty acids (MUFA) and 10.87% of saturated fatty acids. SWD significantly decreased saturated fatty acids (SFA) whereas significantly increased MUFA, UFA and UFA/SFA. However, SWD did not elicit any significant changes in PUFA in Remzibey-05 genotype.

In control groups, safflower seeds in control plants of Gokturk genotype were characterized by a high proportion of polyunsaturated fatty acids (PUFA) (59.34%)

versus 32.96% of monounsaturated fatty acids (MUFA) and 7.36% of saturated fatty acids. SWD significantly decreased saturated fatty acids (SFA) whereas significantly increased PUFA, UFA and UFA/SFA. However, SWD did not elicit any significant changes in MUFA in Gokturk genotype.

Fatty acid unsaturation degree has been considered important in maintenance of membrane fluidity and providing optimal environment for proper membrane functions (Xu and Beardall, 1997; Rebey et al., 2017). In safflower seeds, under control and SWD, the unsaturated fatty acid (UFA) to saturated fatty acid (SFA) ratio was 8.17 and 11.54, respectively for genotype Remzibey-05. UFA/SFA was 12.55 (control) and 14.48 (SWD) for Gokturk genotype. Both genotypes exhibited similar manner regarding fatty acid unsaturation degree.

Table 8. Fatty acid unsaturation degree of genotypes in response to water stress

Fatty acid unsaturation degree	Genotype: Remzibey-05			Genotype: Gokturk		
	Control	SWD	Change (%)	Control	SWD	Change (%)
SFA	10.87a	7.96b	-26.77%	7.36a	6.46b	-12.23%
MUFA	30.10b	32.49a	7.94%	32.96	33.07	0.33%
PUFA	58.68	59.42	1.26%	59.34b	60.42a	1.82%
UFA	88.78b	91.90a	3.51%	92.31b	93.49a	1.28%
UFA/SFA	8.17b	11.54a	41.25%	12.55b	14.48a	15.38%

SWD: Severe water deficit; Means for same genotypes with different superscripts (a-b) are significantly different according to Student t test ($\alpha = 0.05$)

However, UFA/SFA was significantly decreased with rising water deficit levels, indicating that severe water stress causes a decline in the passive membrane permeability (Rebey et al., 2017) and coupling with an increase of cellular membrane rigidity (Monteiro de Paula et al., 1993). Herewith, plant might protect itself against possible accumulation oxidative stressors through modifying or re-structuring the membranes with less unsaturated fatty acids.

Correlations between major fatty acids and oil yield

Along with the present study, two correlation analyses for fatty acids were done (Tables 9-10). In the first correlation analysis (Table 9), all data obtained from both genotypes were pooled- not considering the experimental groups- and then correlated. According to the correlation coefficients, palmitic acid was positively correlated with stearic acid ($r = .955$; $p < 0.01$), oleic acid ($r = .882$; $p < 0.01$) but negatively correlated with behenic acid ($r = -.680$; $p < 0.05$). Stearic acid was positively correlated with oleic acid ($r = .938$; $p < 0.01$) but negatively correlated with linoleic acid ($r = -.917$; $p < 0.01$) and behenic acid ($r = -.650$; $p < 0.05$). Oleic acid was negatively correlated with linoleic acid ($r = -.0996$; $p < 0.01$).

According to the second correlation analysis done in order to determine whether correlation coefficients vary depending control and stress groups (Table 10), in control group, palmitic acid was positively and significantly correlated with linoleic acid ($r = .850$; $p < 0.05$) but in stress group, palmitic acid was again positively correlated but not significant. Also, palmitic acid was negatively and significantly correlated with

behenic acid ($r = -0.831$; $p < 0.05$) but in stress groups, the coefficient was .060 and not significant. Oleic acid was positively and significantly correlated with behenic acid ($r = 0.980$; $p < 0.01$) in control group. However, the coefficient strongly shifted towards negative correlation from .980 to -.494. As expected, opposite changes were observed between linoleic acid and behenic acid from -.993 to .537 (Table 10).

Table 9. Correlations between major fatty acids and oil yield in safflower seeds ($n = 12$)

	Palmitic acid	Stearic acid	Oleic acid	Linoleic acid	Behenic acid	Oil yield
Palmitic acid	1					
Stearic acid	.955**	1				
Oleic acid	.882**	.938**	1			
Linoleic acid	-.917**	-.961**	-.996**	1		
Behenic acid	-.680*	-.650*	-.376	.442	1	
Oil yield	-.332	-.296	-.181	.217	.302	1

* $p < 0.05$ ** $p < 0.01$

Table 10. Correlations between major fatty acids in control and SWD respectively ($n = 6$)

	Palmitic acid	Stearic acid	Oleic acid	Linoleic acid	Behenic acid	Oil yield
Palmitic acid	1					
Stearic acid control SWD	.185 -.730	1				
Oleic acid control SWD	-.882* -.820*	-.426 .317	1			
Linoleic Acid control SWD	.850* .639	.418 -.189	-.990** -.924**	1		
Behenic acid control SWD	-.831* .060	-.335 .603	.980** -.494	-.993** .537	1	
Oil yield control SWD	-.175 -.399	-.437 .241	.276 .481	-.267 -.246	.201 .056	1

* $p < 0.05$; ** $p < 0.01$; SWD: severe water deficit

Effects of water stress on seed mineral content of safflower

The changes mineral contents in both genotypes with respect to the water stress treatments were statistically significant (Table 11). For Remzibey-05 genotype, K and Mg content significantly increased and as expectedly Na content significantly decreased. However, micro elements did not significantly differ as a response to severe water stress. For Gokturk genotype, K content significantly increased with severe stress. In similar to the Remzibey-05 genotype, there were decreases in Na content and increase in Mg content in Gokturk genotype. However, those changes were not statistically significant. Mg content diminished with drought (Grabová and Martinková, 2001). Of the micro elements, Cu content significantly decreased with stress. The changes in content of micro elements were significant.

Any external stimuli-mediated internal changes in plant metabolism cause perturbations and pose impairments in mineral uptake and their translocation in the plants. Hu and Schmidhalter (2005) highlighted that the water stress induced- nutrient reductions might be attributed to the low transpiration ratio, decreased active transport and disrupted membrane permeability. In the former reports, K content decreased under drought conditions (Mahouachi, 2007). However, Ozkan and Kulak (2013) examined the K content in seeds of two genotypes of sesame, genotypes exhibited opposite behaviour of K accumulation in response to severe water stress. Arjenaki et al. (2012) reported the changes mineral elements of two wheat varieties contrasting drought stress, documenting that tolerant varieties had the highest value of K while sensitive variety had the highest value of Na. Along with the study, Remzibey-05 had the highest values of both K and Na in comparison with Gokturk. Furthermore, when evaluated the growth and yield, all parameters except 1000-seed weight favoured for Remzibey-05 genotype, which seems to be more tolerant against severe water stress.

Overall, it must be highlighted that the mineral uptake and sequential accumulation or partitioning of the minerals thought out the complex plant system are dependent many factors including species, genotypes, cultivars, age of the plant and then stress type and duration of the stress, timing of the stress (pre-flowering, flowering and post-flowering vegetative stage). Up to best knowledge and survey of the literature, the studies regarding with interaction of mineral uptake and following processes in response to water stress are scarce even though there are many studies focusing only the last accumulation and content of the status. Forthcoming studies are required to focus on the whole plant system response in terms of minerals and their fate after subjection to the water stress.

Table 11. Water stress treatments on the mineral content of safflower seed (mg kg^{-1})

	Remzibey-05		Gokturk		F values
	Control	SWD	Control	SWD	
K	6872.00±128.01b	7510.67±173.50a	6405.00±213.58c	7004.67±121.78b	36.162**
Na	831.00±10.13 a	660.19±60.67b	347.80±7.700c	318.83±23.99c	167.464**
Mg	624.90±10.55c	685.37±15.84b	890.63±34.40a	928.40±14.70a	152.702**
Fe	40.62±3.49b	42.30±6.14b	50.61±4.02a	51.28±3.36a	4.754*
Cu	4.63±0.26 c	4.52±0.28c	14.66±0.81a	12.33±1.67b	91.204**
Zn	32.24±2.99b	36.96±5.16b	47.28±2.45a	50.15±4.05a	14.796**

SWD: severe water deficit. Means \pm SD in the same row by the same letter are not significantly different to the test of Duncan ($\alpha = 0.05$). ** $p < 0.01$; * $p < 0.05$

Principal components analysis (PCA) of genotypes

PCA is of the powerful statistical tools in discrimination of the samples based on identified components. Along with the study, two genotypes under two experimental groups with their fatty acid profiles were submitted to Principal Component Analysis. Accordingly, components extracted (Table 12), total variance explained (Table 13) and 2-D visualization of the experimental groups (Fig. 1) were obtained. Herewith, the first component (factor) explained 76.476% of total variances. The second and third components explained 18.965% and 45.596% of total variances respectively. Experimental groups were well-discriminated, clarified and identified using PCA,

documenting that any external deviation from regular irrigation of the plants would cause changes in fatty acid metabolites with their percentage. Herein, genotype Remzibey-05 grown under control groups was quite differentiated from other groups (Fig. 1).

Table 12. Components extracted based on fatty acid compounds corresponding to the their loadings

Components	PC 1	PC 2	PC 3
Myristic acid	-0.26061	-0.2416	0.2832
Palmitic acid	-0.294	0.049671	0.045667
Palmitoleic acid	0.26381	0.25974	0.11928
Heptadecanoic acid	-0.27315	0.10474	-0.40634
Cis-10Heptadecanoic	0.28756	-0.024918	0.2695
Stearic acid	-0.29412	0.0032959	0.10548
Oleic acid	0.28051	-0.10805	-0.3063
Linoleic acid	0.26744	-0.042402	0.50497
Arachidic acid	-0.28525	-0.1282	0.17041
Cis11Eicosenoic acid	0.27601	0.2089	-0.053246
Linolenic acid	0.28407	0.087706	-0.27679
Heneicosanoic acid	-0.28516	0.10642	0.22612
Behenic acid	-0.089875	0.56431	0.046164
Lignoceric acid	0.23315	-0.34263	0.24914
Oilyield (%)	0.0057603	0.57592	0.28634

Table 13. Total variance explained

PC	Eigenvalue	% variance
1	114.714	76.476
2	28.447	18.965
3	0.683934	45.596

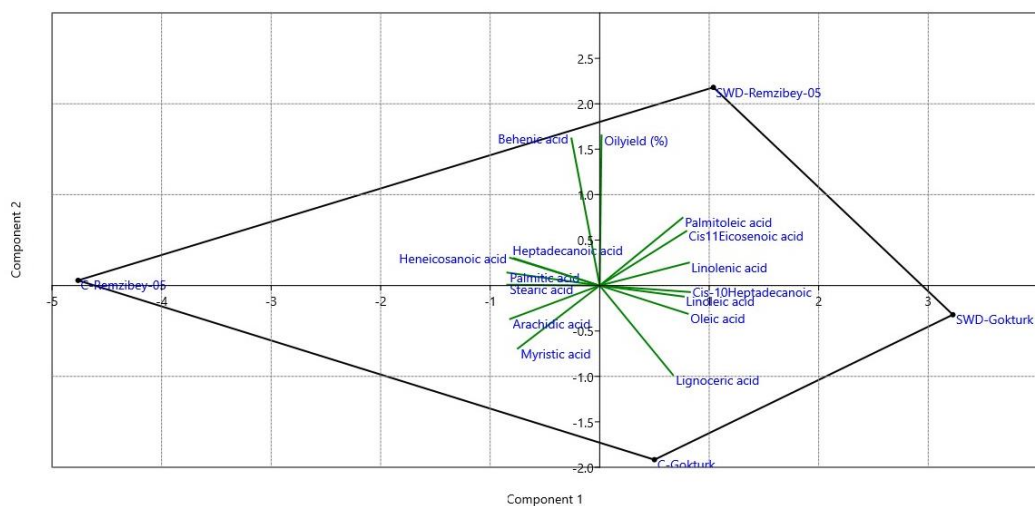


Figure 1. Principal component analysis of genotypes corresponding to the control and severe water stress

Heatmap construction for genotypes for their fatty acid profile corresponding to control and stress conditions

According to the heatmap (Fig. 2), arachidic acid, myristic acid, stearic acid, palmitic acid and heneicosanoic acid were more pronounced under control conditions but SWD suppressed their content. SWD increased behenic acid, linoleic acid, cis-11-eicosanoic acid and palmitoleic acid in Remzibey-05 genotype.

SWD topped the percentage of linoleic acid, cis-10-heptadecanoic acid, lignoceric acid, linoleic acid, oleic acid, cis-11-eicasenoic acid and palmitoleic acid in comparison with the control group of Gokturk.

As seen in Figure 2, control and SWD experimental groups exhibited clear different behaviour corresponding to the fatty acid profiles, which were also coupled and supported with principal component analysis (Fig. 1).

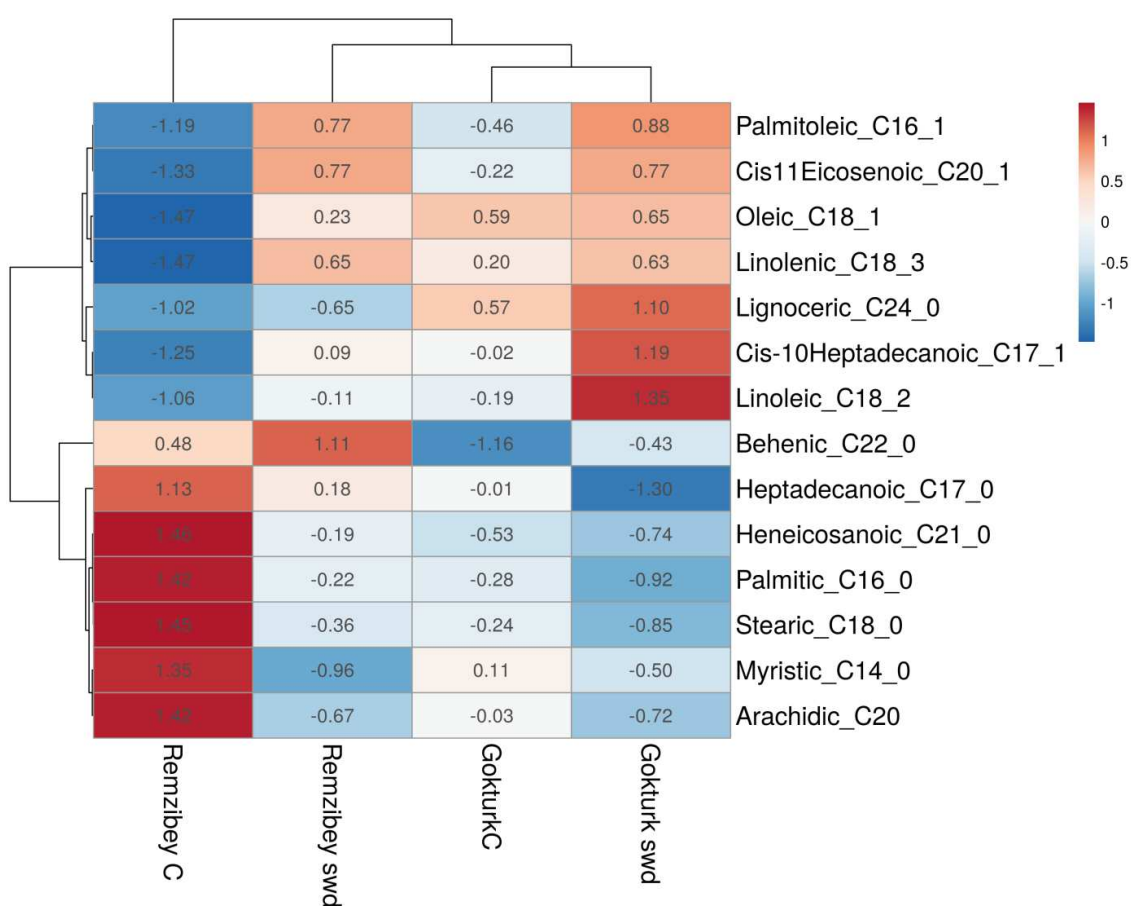


Figure 2. Heatmap constructed for both genotypes concerned with fatty acid profile corresponding to control and stress groups

Conclusion

The present study was designed to investigate the effects water stress on oil yield combined with their fatty acid profile and mineral contents of seeds of two safflower genotypes. The most important conclusions of this study are:

- Regarding growth and yield parameters under stress, Remzibey-05 genotype had higher values except 1000-seed weight but the values were not significant.

- Capsule number differences were reported to be significant under stress.
- Oil yield increased under stress conditions for both genotypes.
- UFA/SFA was significantly increased with stress for both genotypes.
- For Remzibey-05 genotype, K and Mg content significantly increased and as expected Na content significantly decreased. However, micro elements did not significantly differ as a response to severe water stress. For Gokturk genotype, K content significantly increased with severe stress.

Finally, genotypes exhibited similar behaviour regarding unsaturation degree of the oil, also increments in their oil yield.

For the forthcoming studies, field experiments regarding those genotypes should be performed since the present study was carried under controlled green house conditions. The study can be deemed as preliminary study to ascertain some basic properties of the two safflower genotypes under limited water sources. Moreover, more genotypes of the safflower can be screened for their performance and then a selection concerning high tolerant against low water content of soils for genotypes can be made.

REFERENCES

- [1] Ahmed, N., Chowdhry, M. A., Khaliq, I., Maekawa, M. (2016): The inheritance of yield and yield components of five wheat hybrid populations under drought conditions. – Indonesian Journal of Agricultural Science 8(2): 53-59.
- [2] Al-Barrak, K. M. (2006): Irrigation interval and nitrogen level effects on growth and yield of canola (*Brassica napus* L.). – Scientific Journal of King Faisal University (Basic and Applied Sciences) 7(1): 87-103.
- [3] Amini, H., Arzani, A., Karami, M. (2014): Effect of water deficiency on seed quality and physiological traits of different safflower genotypes. – Turkish Journal of Biology 38(2): 271-282.
- [4] Arjenaki, F. G., Jabbari, R., Morshedi, A. (2012): Evaluation of drought stress on relative water content, chlorophyll content and mineral elements of wheat (*Triticum aestivum* L.) varieties. – International Journal of Agriculture and Crop Sciences 4(11): 726-729.
- [5] Ashrafi, E., Razmjoo, K. (2010): Effect of irrigation regimes on oil content and composition of safflower (*Carthamus tinctorius* L.) cultivars. – Journal of the American OilChemist' Society 87(5): 499-506.
- [6] Bettaieb, I., Zakhama, N., Wannas, W. A., Marzouk, B. (2009): Water deficit effects on *Salvia officinalis*. Fatty acid and essential oils composition. – Scientia Horticulturae 120: 271-275.
- [7] Bortolheiro, F. P., Silva, M. A. (2017): Physiological response and productivity of safflower lines under water deficit and rehydration. – Anais da Academia Brasileira de Ciências 89(4): 3051-3066.
- [8] Canavar, Ö., Götz, K. P., Koca, Y. O., Ellmer, F. (2014): Relationship between water use efficiency and δ^{13} isotope discrimination of safflower (*Carthamus tinctorius* L.) under drought Stress. – Turkish Journal of Field Crops 19(2): 203-211.
- [9] Cetinkaya, H., Koc, M., Kulak, M. (2016): Monitoring of mineral and polyphenol content in olive leaves under drought conditions: Application chemometric techniques. – Industrial Crops and Products 88: 78-84.
- [10] El Sabagh, A., Hossain, A., Barutcular, C., Gormus, O., Ahmad, Z., Hussain, S., Akdeniz, A. (2019): Effects of drought stress on the quality of major oilseed crops: implications and possible mitigation strategies. A Review. – Applied Ecology and Environmental Research 17(2): 4019-4043.

- [11] Ensiye, A., Razmjoo, K. (2010): Effect of irrigation regimes on oil content and composition of safflower (*Carthamus tinctorius* L.) cultivars. – Journal of American Oil and Chemical Society 87: 499-506.
- [12] Eslam, B. P. (2011): Evaluation of physiological indices for improving water deficit tolerance in spring safflower. – Journal of Agricultural Sciences Technology 13: 327-338.
- [13] Fahad, S., Bajwa, A. A., Nazir, U., Anjum, S. A., Farooq, A., Zohaib, A., Sadia, S., Nasim, W., Adkins, S., Said, S., Ihsan, M. Z., Alharby, H., Wu, C., Wang, D., Huang, J. (2017): Crop production under drought and heat stress: plant responses and management options. – Frontiers in Plant Science 8: 1147. DOI: 10.3389/fpls.2017.01147.
- [14] Gao, J., Hao, X., Thelen, K. D., Robertson, G. P. (2009): Agronomic management system and precipitation effects on soybean oil and fatty acid profiles. – Crop Science 49: 10491057.
- [15] Grabaová, S., Martinková, M. (2001): Changes in mineral nutrition of Norway spruce (*Picea abies* [L.] Karst.) under the impact of drought. – Ekologia Bratislava 20: 46-60.
- [16] Hamrouni, I., Salah, H. B., Marzouk, B. (2001): Effects of water-deficit on lipids of sunflower aerial parts. – Phytochemistry 58: 227-280.
- [17] Hu, Y., Schmidhalter, U. (2005): Drought and salinity: a comparison of their effects on mineral nutrition of plants. – Journal of Plant Nutrition and Soil Science 168(4): 541-549. DOI: 10.1002/jpln.200420516.
- [18] Laribi, B., Bettaieb, I., Kouki, K., Sahli, A., Mougou, A., Marzouk, B. (2009): Water deficit effects on caraway (*Carum carvi* L.) growth, essential oil and fatty acid composition. – Industrial Crops and Products 30(3): 372-379.
- [19] Laribi, B., Kouki, K., Sahli, A., Mougou, A., Marzouk, B. (2011): Essential oil and fatty acid composition of a Tunisian caraway (*Carum carvi* L.) seed ecotype cultivated under water deficit. – Advances in Environmental Biology 257-265.
- [20] Mahouachi, J. (2007): Growth and mineral nutrient content of developing fruit on banana plants (*Musa acuminata* AAA, 'Grand Nain') subjected to water stress and recovery. – Journal of Horticultural Science and Biotechnology 82: 839-844.
- [21] Monteiro de Paula, F., Thi, A. T. P., Zuily-Fodil, Y., Ferrari-Iliou, R., Vieira da Silva, J., Mazliak, P. (1993): Effects of water stress on the biosynthesis and degradation of polyunsaturated lipid molecular species in leaves of *Vigna unguiculata*. – Plant Physiology and Biochemistry 31(5): 707-715.
- [22] Nabipour, M., Meskarbashee, M., Yousefpour, H. (2007): The effect of water deficit on yield and yield components of safflower (*Carthamus tinctorius* L.). – Pakistan Journal of Biological Sciences 10(3): 421-426.
- [23] Nazari, M., Mirlohi, A., Majidi, M. M. (2017): Effects of drought stress on oil characteristics of *Carthamus* species. – Journal of American Oil and Chemistry Society 94: 247-256.
- [24] Ozkan, A. (2018): Effect of water deficit on biochemical and growth of sesame in the Middle East Euphrates Valley. – KSÜ Doğa Bilimleri Dergisi 21(1): 91-99.
- [25] Ozkan, A., Kulak, M. (2013): Effects of water stress on growth, oil yield, fatty acid composition and mineral content of *Sesamum indicum*. – Journal of Animal Plant Sciences 23(6): 1686-90.
- [26] Petcu, E., Adrian, A., Danil, S. (2001): The effect of drought stress on fatty acid composition in some Romanian sunflower hybrids. – Romanian Agric Res 15: 39-42.
- [27] Pouri, K., Mardeh, A. S. S., Sohrabi, Y., Soltani, A. (2019): Crop phenotyping for wheat yield and yield components against drought stress. – Cereal Research Communications 47(2): 383-393.
- [28] Prasad, P. V. V., Staggenborg, S. A. (2008): Impacts of Drought and/or Heat Stress on Physiological, Developmental, Growth, and Yield Processes of Crop Plants. – In: Ahuja, L. R. et al. (eds.) Response of Crops to Limited Water: Understanding and Modeling Water Stress Effects on Plant Growth Processes. (Advances in Agricultural Systems Modeling, Series 1.) American Society of Agronomy, Madison, WI.

- [29] Rebey, I. B., Bourgou, S., Rahali, F. Z., Msaada, K., Ksouri, R., Marzouk, B. (2017): Relation between salt tolerance and biochemical changes in cumin (*Cuminum cyminum* L.) seeds. – *Journal of Food and Drug Analysis* 25(2): 391-402.
- [30] Rubin, R. L., van Groenigen, K. J., Hungate, B. A. (2017): Plant growth promoting rhizobacteria are more effective under drought: a meta-analysis. – *Plant and Soil* 416(1-2): 309-323.
- [31] Shi, J., Gao, H., Wang, H., Lafitte, H. R., Archibald, R. L., Yang, M., Hakimi, S. M., Mo, H., Habben, J. E. (2017): ARGOS8 variants generated by CRISPR-Cas9 improve maize grain yield under field drought stress conditions. – *Plant Biotechnology Journal* 15(2): 207-216.
- [32] Talha, M., Osman, F. (1975): Effect of soil water stress on water economy and oil composition in sunflower (*Helianthus annuus* L.). – *The Journal of Agricultural Science* 84(1): 49-56.
- [33] Turk, M. A., Tawaha, A. R. M., Lee, K. D. (2004): Seed germination and seedling growth of three lentil cultivars under moisture stress. – *Asian Journal of Plant Sciences* 3: 394-397.
- [34] Vurukonda, S. S. K. P., Vardharajula, S., Shrivastava, M., SkZ, A. (2016): Enhancement of drought stress tolerance in crops by plant growth promoting rhizobacteria. – *Microbiological Research* 184: 13-24.
- [35] Xu, X. Q., Beardall, J. (1997): Effect of salinity on fatty acid composition of a green microalga from an Antarctic hypersaline lake. – *Phytochemistry* 45(4): 655-658.
- [36] Zandalinas, S. I., Mittler, R., Balfagón, D., Arbona, V., Gómez-Cadenas, A. (2018): Plant adaptations to the combination of drought and high temperatures. – *Physiologia Plantarum* 162(1): 2-12.

IMMOBILIZATION OF COLD-RESISTANT MIXED BACTERIA AND ITS APPLICATION IN SEQUENCING BATCH REACTOR WASTEWATER TREATMENT

YANG, Y. W.¹ – DUAN, X. Y.² – JIANG, J.¹ – XU, X. Y.¹ – TANG, M. Z.^{1*}

¹Key Laboratory of Nasihu Lake Wetland Ecosystem & Environment Protection, Qufu Normal University, Qufu, Shandong, China

(e-mail: yangyuwei@163.com (Yang, Y. W.), naruto4869@163.com (Jiang, J.), Xuxiaoyan32112@163.com (Xu, X. Y.); phone: +86-136-7547-8229)

²Nankai University, Tianjin, China

(e-mail: 479828612@qq.com; phone: +86-185-2632-9818)

*Corresponding author

e-mail: qsd_tmzh@qfnu.edu.cn

(Received 28th Sep 2019; accepted 4th Dec 2019)

Abstract. Immobilized microbial degradation technology has the advantages of simple solid-liquid separation, strong toxicity resistance, and low sludge yield. This study creatively added biochar to the immobilized microbial activated pellets and optimized the immobilization conditions for these pellets. This experiment also studied the removal efficiency of chemical oxygen demand (COD), total phosphorus (TP), ammonia nitrogen (NH₃-N) and total nitrogen (TN) for immobilized microbial pellets in the SBR (Sequencing Batch Reactor) with different dosages and hydraulic retention time (HRT). Results showed that the optimal conditions were reached when: the mass fraction of SA (sodium alginate) was 2%, the amount of PVA (polyvinyl alcohol) was 4%, and cross-linking time 24 h, the best biochar added was RS700. Mixed bacteria under the condition of the optimization system for immobilized pellets were added to the continuously running of SBR process, 20 mL bacteria suspension of immobilized pellets could be used to test the best dosage through the experiment monitoring. In a comprehensive consideration, the optimal HRT was 4 d, and the removal efficiency of COD, TP, NH₃-N and TN under the best dosage was reached at 76.79%, 56.50%, 67.60 % and 54.92% at 4 days, respectively. In the SBR process, the degradation efficiency of immobilized pellets for each pollutant COD, TP, NH₃-N and TN in the SBR conforms to the first-order kinetic model.

Keywords: immobilized microbial pellets, SBR, first-order kinetic model, biochar, sewage treatment

Introduction

The research on cold-resistant bacteria in China is relatively new, which has attracted extensive attention. It wasn't until the 1990s that people had a systematic understanding of the cold-resistant bacteria in the past century. The rate of contaminant biodegradation by cold-resistant bacteria at low temperature was also explored at that time (Tang et al., 2018). Psychrotolerant or psychrophilic microorganisms are extremophilic organisms, which can grow and reproduce at the temperatures ranging from -15°C to +20°C. The cold-resistant microorganisms can grow from 0°C to 40°C, and the optimal temperature is between 20°C and 40°C. However, the psychrophilic microorganisms can grow from 0°C to 20°C and the optimal temperature is below 15°C. The environments they inhabit are ubiquitous on earth, as a large fraction of our planetary surface experiences temperatures below 15°C. Most psychrophiles are bacteria or archaea. They belong to *Arthrobacter sp.*, *Psychrobacter sp.*, members of the genera *Halomonas*, *Pseudomonas*, *Hyphomonas*, and *Sphingomonas* (Mei et al., 2016). Generally speaking, mixed bacteria refer to the

mixed bacteria whose dominant strains are combined by measuring the functions of two or more microbial strains. It can be composed of different types of bacteria, such as fungi. It can also be a combination of different types of bacteria, such as bacteria and fungi. Also, it was found that the mixing of strains had better synergistic effect than that of a single strain.

Immobilized microbial degradation technology has been favored for its high density of bacteria, low yield of sludge, strong resistance to toxicity and continuous operation. Through immobilization, microorganisms are fixed on the carrier to maintain a highly dense and bioactive function and to proliferate to adsorb and degrade organic compounds in water under appropriate conditions (Rao and Viraraghavan, 2002; Hachicha et al., 2009). Immobilized microbial degradation technology also has the advantages of keeping the dominant bacteria of high processing efficiency, large amount of biomass, stable operation, easy solid–liquid separation, and low price, etc., which is of great research value in organic wastewater treatment. At present, immobilization technology has been widely used in the practical production of sewage treatment in all walks of life. For example, Liu et al. (2013) have studied the treatment of heavy oil wastewater from the Liaohe oil field of China by using the upper flow anaerobic sludge bed and the fixed biological aeration filter combined biological process. Zhao et al. (2010) used immobilized microorganism technology to treat red water through an aerobic biofilter, and the 2,4,6-nitrotoluene (TNT) was ultimately degraded. For an ideal immobilized microorganism technology, the selection of immobilized carrier is the most important in addition to establishing a highly efficient immobilized reactor and highly efficient and intensive microorganisms with strong resistance. It is of significant importance to find immobilized carriers with stable performance, good mass transfer, high intensity, long life span, and low price (Vázquez et al., 2006). The common carriers for immobilization include natural materials and synthesized materials. There is no doubt that the former has the advantages of lower cost, easy to obtain, and no complicated experimental preparation at earlier stage, which can be widely used in production (Shen and Duvnjak, 2005). In recent years, some agricultural byproducts, such as rice husk, pine bark, peanut shell, sawdust and cork biomass have been used in different kinds of wastewater treatment (He et al., 2019). Straw is the biomass material rich in cellulose, lignin, and other natural polymers (Marshall and Johns, 1996; Gundogdu et al., 2009). Its molecular chains is distributed with a large number of active groups such as hydroxyl and carboxyl groups, which has good complexation, adsorption, and flocculation effects on contaminants in water. At the same time, carboxyl, sulfonic acid group, amino, imino, acylamino, and other groups are good for cell adhesion and proliferation (Van Wyk, 1997; Argun et al., 2009).

Compared with traditional or conventional treatments Sequencing Batch Reactor (SBR) is an easily obtainable, on timescale, highly operational, flexible technology for newer and varied pollutants (Kulkarni, 2013; Dutta and Sarkar, 2015; Popple et al., 2016). The SBR systems have many advantages of lower operational cost, less bulking and higher flexibility to combine nitrification and denitrification phases into one reactor (Lim et al., 2011) with good removal efficiency for nitrogen, phosphorus and chemical oxygen demand (Ding et al., 2011; Popple et al., 2016; Khan et al., 2019; Showkat and Najar, 2019). Microbial degradation plays a dominant role in the removal of soluble/colloidal biodegradable organics in wastewater (Nguyen, 2000; Chen et al., 2017). However, the sewage treatment efficiency of SBR in northern China is rather

low in winter. This is because microbial activity is decreases as the water temperature decreases, and the biological activity of SBR might decrease under winter conditions. Thereby the pollutant removal efficiency and, more importantly, the efficacy of this contaminant removal technique might be affected by seasonal changes (Tang et al., 2018).

In this study, it creatively added rice straw biochar to the sodium alginate and agar, and finally formed immobilized microbial pellets concluded mixed bacteria. The removal efficiencies of chemical oxygen demand (COD), total phosphorus (TP), ammonianitrogen (NH₃-N) and total nitrogen (TN) were measured to test the biotreatment performance of immobilized microbial pellets in the SBR system. The objectives of this study were to: i) prepare and introduce immobilized microbial pellets and optimize the immobilization conditions for immobilized pellets. ii) determine the removal efficiencies of chemical oxygen demand (COD), total phosphorus (TP), ammonianitrogen (NH₃-N) and total nitrogen (TN) with immobilized microbial pellets in the SBR. iii) evaluate the effects of different dosages and hydraulic retention time (HRT) with immobilized microbial pellets in the SBR. iii) provide a modelling tool to simulate and evaluate the pollutant removal efficiency of the immobilized microbial pellets. The results of this study provide a theoretical foundation and scientific support for the use of SBR in wastewater treatment, and may have great significance in solving the increasingly severe water pollution problem in China.

Materials and methods

Enrichment culture, separation, screening, and identification of the mixed Psychrotrophic bacteria species

The strains including three types of bacteria, used in the experiment, were isolated from the soil samples collected from the constructed wetlands in the Nansihu Lake in Shandong Province, China. Under cold-temperature conditions (6(±2)°C), Strain 1 was composed of a Gram-positive translucent circular ivory colony, with a moist surface, and regular edge. Strain 4 was a Gram-negative opaque round milky colony with a moist surface, and irregular edge. Strain 5 was a Gram-positive translucent yellow colony with a moist surface and irregular edges. Strains 1, 4 and 5 were all spherical with no flagella. After the strains 1, 4, and 5 were cultured, total DNA was extracted and used as a template. Using Primers 8f (5'AGAGTTTGATCCTGGCTCAG3') 20bp and 1492r (5'GGTTACCTTGTTACGACT-T3') and after cloning and purification, the PCR product was then carried out by Shanghai Biological Engineering Co, Ltd. The 16S rDNA specific sequence of strain 1 was 1498bp (GenBank acceptance number: KR083014), the 16S rDNA specific sequence of strain 4 was 1489bp (GenBank acceptance number: KR083015), and the rDNA specific sequence of strain 5 was 1469bp (GenBank acceptance number: KR083016), after the three strain sequences were analyzed, strain 1 was named Psychrobacter TM-1, strain 4 was named Sphingobacterium TM-2, and strain 5 was named Pseudomonas TM-3. Tang et al. (2018) had produced the phylogenetic tree in our previous research.

The process was repeated three times so that the remaining nutrients could be removed. Finally, the absorbance of the solution was adjusted to 1.2 using normal saline. The bacterial solutions were then mixed together at a volume ratio of 1:1:1 and were placed at 6°C for later use.

Biochar preparation

The rice straw was collected from Nanquan Village, Qufu Country, Jining City, Shandong Province, China. 20 g of crushed feedstocks were covered with a fitted lid and pyrolyzed under oxygen-limited conditions in a muffle furnace. The pyrolysis temperature was heated from room temperature to different temperatures (300, 500 and 700°C) for 3 h, naturally cooled to room temperature, sealed and bottled for use. After treatment with 300 ml of 1 mol/L hydrochloric acid for 4 h, the ash substances such as calcium carbonate were removed, and then filtered, washed with distilled water until the washing liquid was neutral, and oven dried at 80°C for 24 h. The entire carbonized product was ground and sieved through a 60-mesh screen, transferred into a plastic bag. The biochar were denoted as RS300, RS500, RS700 (RS stands for rice straw, the number represents carbonization temperature), respectively.

Pellets with immobilized microbials

Biochar powder, sodium alginate, microbial liquid and polyvinyl alcohol (PVA) was used to prepare the immobilized microbial activated pellets. The preparation process for pellets is presented in *Figure 1*.

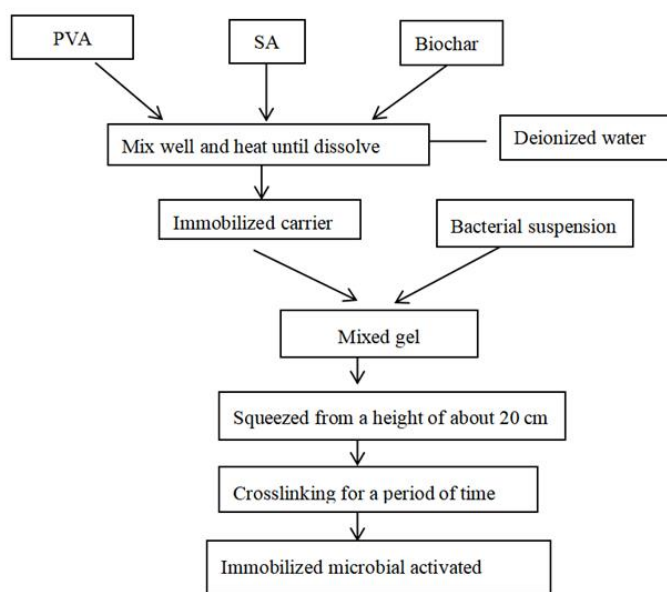


Figure 1. The preparation process of immobilized pellets

Add 4 g polyvinyl alcohol (PVA) to 100 mL deionized water in a beaker, heat it in water bath at 50-60°C until it is evenly dissolved. Then add 2 g alginic acid sodium (SA) and 0.4 g biochar as gelling agent after stirring and cooling to room temperature, 20 mL of the previously treated bacterial suspension was added and mixed well. The crosslinking agents were made by boronic acid, anhydrous calcium chloride and water at pH 6.5. The mixed gel was dripped to the crosslinking agent by a syringe and squeezed slightly from a height of about 20 cm. And the shape of pellets was naturally spherical, smooth and elastic. To obtain immobilized microbial activated pellets whose particle size 5.0 mm, it was placed at 6-8°C in the freezer for the cross-linking for 0, 8, 16, 24, 36, and 48 h, respectively (Fu et al., 2018).

The optimization conditions are set as follows using one-variable-at-a-time approach, various immobilization parameters were optimized by maintaining all factors at a constant level, except the variable under study. To determine the optimum addition amount of PVA, various concentrations of 0%, 2%, 3%, 4% and 5% (w/v) were added to prepare the pellets, respectively, when the amount of SA is fixed at 2%. Similarly, the addition amount of SA was 0%, 0.5%, 1%, 2%, 3%, and 4% (w/v), respectively, when the PVA was 4%. The cross-linking time was set to 0 h, 8 h, 16 h, 24 h and 36 h under the remaining conditions have not changed. For the effect of biochars at different temperature in the study, add RS300, RS500, RS700 0.4 g to the system, and the rest of the conditions were unchanged, immobilized pellets without biochar were added as blank controls at the same time, and triplicate for each experiment (Bisht et al., 2013).

Sequencing Batch Reactor (SBR)

The reactor is made of plexiglass and has a cylindrical shape with a bottom diameter of 15 cm, a column height of 25 cm, a volume of about 3 L, and an effective volume of 2 L. The experimental device was operated by mechanical agitation, and an aerator was placed at the bottom for aeration to control the DO concentration in the reactor during the aeration phase. The schematic diagram of the SBR is shown in *Figure 2*, and the operating cycle is shown in *Table 1*.

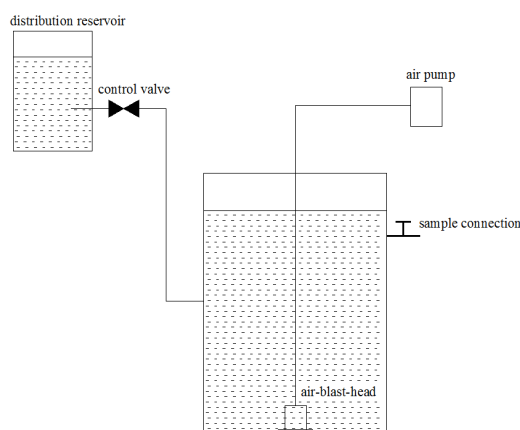


Figure 2. The test installation diagram of SBR (Sequencing Batch Reactor, SBR)

Table 1. Experimental device operating cycle of SBR (Sequencing Batch Reactor, SBR)

Number	Inflow (min)	Stirring (h)	Aeration (h)	Still standing (min)	Effluent (min)
1	2	0	0	55	3
2	2	1	2	55	3
3	2	1	4	55	3
4	2	1	6	55	3
5	2	1	8	55	3

In the simulated wastewater, glucose is used as carbon source, ammonium chloride as nitrogen source, and sodium dihydrogen phosphate as phosphorus source, and appropriate amount of trace elements are added to make C: N: P = 100:5:1. The initial values of COD, total nitrogen, total phosphorus and ammonia nitrogen are about 1000, 50, 10, 15 mg·ml⁻¹ and pH =7.0, respectively.

Batch experiment

The pellets with immobilized microbials were introduced into SBR to verify the contaminants removing ability in engineering application, while exploring the ability to remove contaminants in different conditions and the effects of dose-up and HRT on the ability to remove contaminants. Each reactor was filled with 2.0 L wastewater and added different dosages and types of pellets with immobilized microbial under different conditions. As a control, the other reactor was not added pellets. Then, placed the two reactions in $6\pm 2^{\circ}\text{C}$ constant temperature incubator for five days. Samples were taken from the reactor to determine the concentration of COD, TP, $\text{NH}_3\text{-N}$ and TN in the influent and effluent per 6 h. Triplicate of each set of experiments.

Analytical method and statistical analysis

The removal efficiencies of COD, TP, $\text{NH}_3\text{-N}$ and TN were measured to test the biotreatment performance of immobilized microbial pellets in the SBR system. COD was determined by potassium dichromate oxidation method, TP was determined by ammonium molybdate spectrophotometry, $\text{NH}_3\text{-N}$ was determined by phenol disulfonic acid spectrophotometry, and TN was determined by Peroxide of potassium sulfate - ultraviolet spectro- photometry. The specific operation steps for the determination of each index are detailed in Water and Wastewater monitoring analysis method. 4th Edition. Beijing: China Environmental Science Press, 2002, in Chinese. Optical density of bacteria suspension was measured at 600 nm using a double beam spectrophotometer (UV-T9, Puxi, Beijing), pH was measured with a pH meter (ZD-2, Leici). The data were processed with the excel software and plotted with Origin 8.6.

Discussion and results

Optimization of immobilization conditions

PVA with resistance to microbial decomposition characteristics such as good mechanical strength, which makes it suitable as immobilized microorganism carrier. *Figure 3a* represents the effect of immobilized pellets with different PVA addition on COD, TP, $\text{NH}_3\text{-N}$ and TN removal. Immobilized pellets after joining PVA mold faster, and with the increase of the amount of PVA, the pellets present ascendant trend on the COD and $\text{NH}_3\text{-N}$ removal efficiency, but the removal efficiency of TP and TN decreased first, then increased slightly and then decreased. As shown in *Figure 4*, although the removal efficiency of TP reached the maximum without adding PVA (PVA(w/v) = 0%), considering that the mechanical strength of the pellets was too low at this time and had a certain viscosity, and the mechanical strength and molding speed were improved after adding PVA. When the PVA content was 4%, the removal efficiency of COD TP, $\text{NH}_3\text{-N}$ and TN reached 50.57%, 58.41%, 48.95%, and 46.43%, respectively. The above conclusions indicated that the immobilized pellet with 4% PVA concentration was the most appropriate.

Calcium salt of SA is often used for embedding and fixation of microbial cells, and SA has a great impact on mechanical strength and mass transfer effect of immobilized pellets. The immobilized pellets without SA are difficult to form due to insufficient mechanical strength. After the addition of SA, the molding became easier, but when the SA concentration reached 3%, the molding became difficult due to the increased viscosity. As can be seen from *Figure 3b*, it can be seen that 2% SA concentration is the

best choice for the preparation of immobilized microbial pellets, and the removal efficiency of COD, TP, NH₃-N and TN reaches 47.25%, 46.06%, 47.68% and 40.94%, respectively.

The results of the best concentration of PVA and SV in immobilized microorganism carrier were similar to Ali et al.'s research (2015), which was use 6% (w/v) PVA and 2% (w/v) SA as the most appropriate mixture gel concentration in anammox biomass for meeting the criterion of rapid and successful start-up of anammox process.

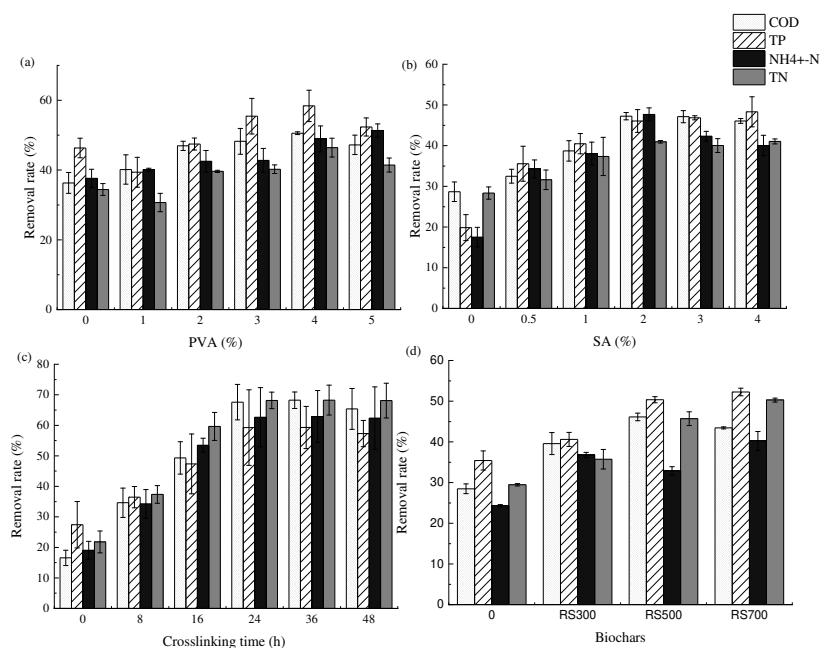


Figure 3. The removal efficiency of COD (chemical oxygen demand, COD), TP (total phosphorus, TP), NH₃-N (ammonianitrogen, NH₃-N) and TN (total nitrogen, TN) for different immobilized pellets, as (a), (b), (c) and (d) shows the effect of PVA (polyvinyl alcohol, PVA), SA (alginic acid sodium, SA), crosslinking time and biochars type on the SBR (Sequencing Batch Reactor, SBR)

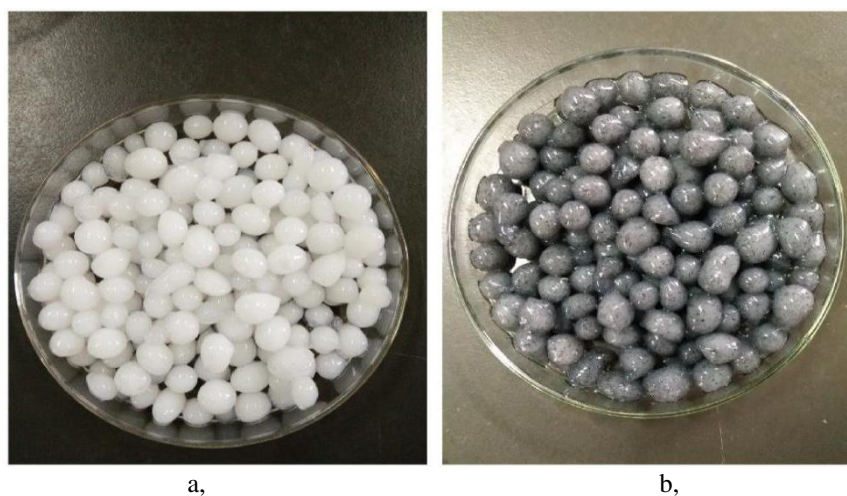


Figure 4. The picture of immobilized pellets ((a) shows pellets without biochar, (b) shows pellets added RS700)

In order to explore the effect of immobilized microbial pellets prepared with different immobilization time, COD, TP, NH₃-N and TN concentrations in simulated wastewater were monitored. It can be seen that with the increase of crosslinking time, the removal efficiency of COD, TP, NH₃-N and TN of microbial immobilized pellets gradually increased. As can be seen from *Figure 3c*, the removal efficiency of COD, TP, and NH₃-N reaches the maximum at 24 h (91.41%, 79.08%, 47.68% and 84.51%, respectively). The removal rate of TN is relatively high, which reached 96.03%. Thus the optimal immobilization time for microbial immobilized pellets is 24 h, which was faster than Zhu et al.'s study (2009). In that research, the nitrite concentrations almost did not change from 39 hours to 49 hours at PVA-SA immobilized gel beads system because the ammonium was almost completely removed before 39 hours. As is shown in *Figure 3c*, the removal efficiency of NH₃-N was lower than Zhu et al.'s study (2009), which may be because of the reaction temperature and initial concentration.

To explore the removal rate of COD, TP, NH₃-N and TN effects of immobilized pellets added biochar with different temperature, immobilized microbes pellets were added rice straw biochar 300°C (RS300), 500°C (RS500), 700°C (RS700) 0.4 g, respectively, at the same time immobilized pellet without biochar was used as a control. It can be seen from *Figure 3d* that the removal efficiency of COD, TP, NH₃-N and TN were significantly improved after the addition of biochar RS700, which were achieved 99.42%, 98.24%, 94.23% and 99.01%, respectively. The mechanical strength was relatively stable. Meanwhile, the experimental data showed that the removal efficiency of COD, TP, NH₃-N and TN were RS700 > RS500 > RS300 > 0. Removing of COD, TP, NH₃-N and TN from water onto biochar occurs due to its high surface area and microporosity (Lou et al., 2011). The differences of removal efficiency results between RS700, RS500, RS300 were due to that biochars produced at > 400°C are more effective for organic contaminant sorption because of their high surface area and micropore development (Ahmad et al., 2012, 2014).

Effect of different dosages and HRT on Sequencing Batch Reactor (SBR)

To explore the effect of different dosages of immobilized microbe pellets on sewage treatment, the SBR reactor runs continuously for 5 days. The results showed an excellent sewage treatment efficiency of immobilized pellets added RS700. As shown in *Figure 5*, the removal efficiency of COD, TP, NH₃-N and TN increased with the dose (0-30 mL).

Actually, when the dosage of mixed bacterial solutions was increased from 0 mL to 10 mL, the removal efficiency of sewage in SBR was significantly improved. When the dosage was increased from 10 mL to 30 mL, the purification efficiency was improved; but, the improvement was not significant. Apparently, each sewage index has the best removal efficiency when the bacteria dosage is 30 mL, but the cost was too high to make it feasible. As can be seen from *Figure 5*, when the mixed bacterial liquid additive amount was 20 mL, within hydraulic retention time 5 d and water temperature 6 to 8°C, the removal efficiency of each index in SBR was gradually increased, eventually the removal rate of COD, TP, NH₃-N and TN reached 80.89%, 59.80%, 77.60% and 58.28%, respectively. From the perspective of operation cost and the efficaciousness of sewage treatment, 20 ml should be selected as the best dosage of the mixed bacterial solutions for the SBR.

HRT usually plays a key role in the removal of pollutants in water, and explores the best HRT is one of the steps necessary to conduct an SBR experiment (Hamjinda et al.,

2017). In order to evaluate the effect of immobilized pellets with different HRT on sewage treatment, the SBR system was kept at 6 to 8°C when the dosage was 20 mL. It can be seen in *Figure 6* that the removal efficiency of each index changes with HRT. As the HRT increased from 0 to 3 day, the removal efficiencies of COD, TP, NH₃-N and TN improved significantly. When HRT is increased from 3 days to 5 days, purification efficiency was improved. However, the improvement was not obvious. Considering the operating costs and experimental operation, 4 days should be selected as the best HRT for the SBR. When the HRT was 4 days, the removal rate of COD, TP, NH₃-N and TN for the pellets reached 79.32%, 59.31%, 72.35%, and 87.14%, respectively.

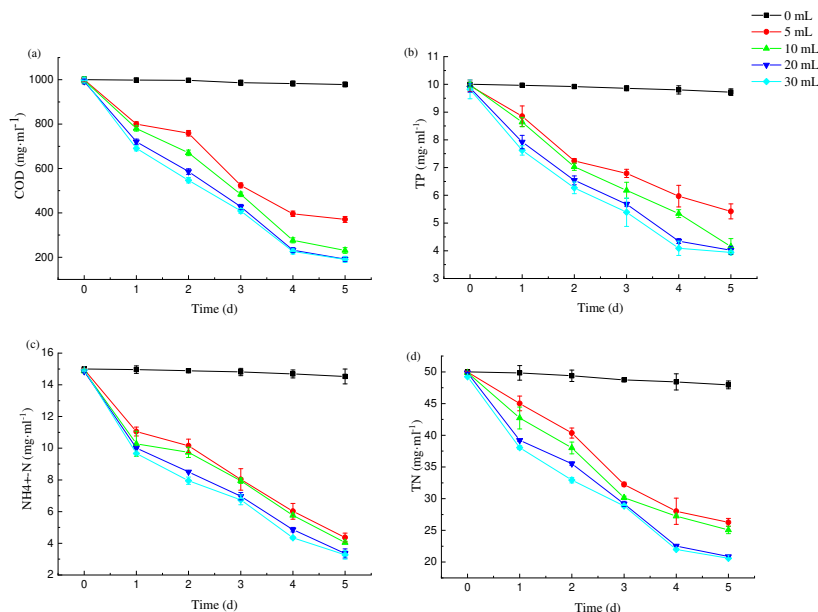


Figure 5. The concentration of COD (chemical oxygen demand, COD), TP (total phosphorus, TP), NH₃-N (ammonianitrogen, NH₃-N) and TN (total nitrogen, TN) changes with dosages in the SBR(as figure (a), (b), (c) and (d) shows the change of removal rate of COD, TP, NH₃-N and TN with the increase of dosage)

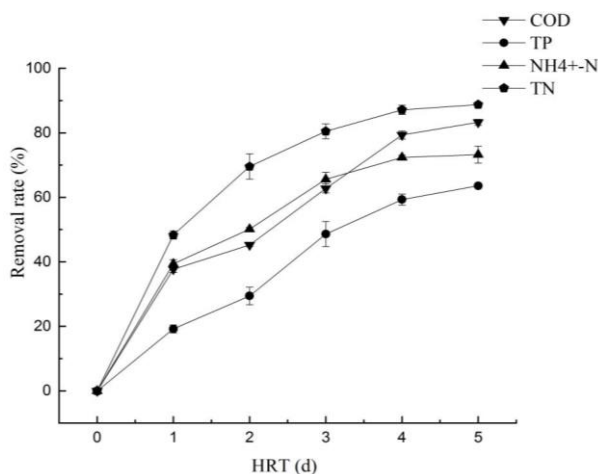


Figure 6. The concentration of COD (chemical oxygen demand, COD), TP (total phosphorus, TP), NH₃-N (ammonianitrogen, NH₃-N) and TN (total nitrogen, TN) changes with hydraulic retention time (HRT) in the SBR (Sequencing Batch Reactor, SBR)

Wastewater treatment dynamics equation

Kinetic research could optimize the technology and methods of biochemical processes. In fact, the patterns of microbial degradation could be predicted by modeling kinetic degradation models and modern techniques to simulate degradation (Jou et al., 2008). Kinetic model was used to describe an aerobic granular sludge reactor, fed with a defined influent, capable of simultaneously removing COD, nitrogen and phosphate in one sequencing batch reactor (SBR). The model could describe the experimental data from the SBR sufficiently. Thus, the effect of process parameters on the nutrient removal rates could be reliably evaluated (Chung and Rittmann, 2007). In the SBR system, the degradation efficiency of immobilized microbial pellets to pollutants in sewage can be simulated by first-order kinetic equation:

$$\ln \frac{C_e}{C_0} = -k_v t \quad (\text{Eq.1})$$

$$k_v = \frac{-1}{t} \ln \left(\frac{C_0}{C_e} \right) \quad (\text{Eq.2})$$

where k_v is the contaminant volume removal rate constant, d^{-1} ; C_e and C_0 are the influent and effluent concentration, $\text{mg} \cdot \text{mL}^{-1}$; t is the hydraulic retention time, d .

According to the above kinetic model, the average effluent concentration of each contaminant in the SBR system was denoted as C_e , and the average influent concentration was denoted as C_0 . $\ln(C_0 / C_e)$ was taken as the ordinate, and t (time) as the abscissa. The $\ln(C_0 / C_e)$ of different dosage of bacteria and different hydraulic retention time (dosage of bacteria is 20 mL) are taken as ordinate in the *Figure 7*, *Figure 8*, respectively.

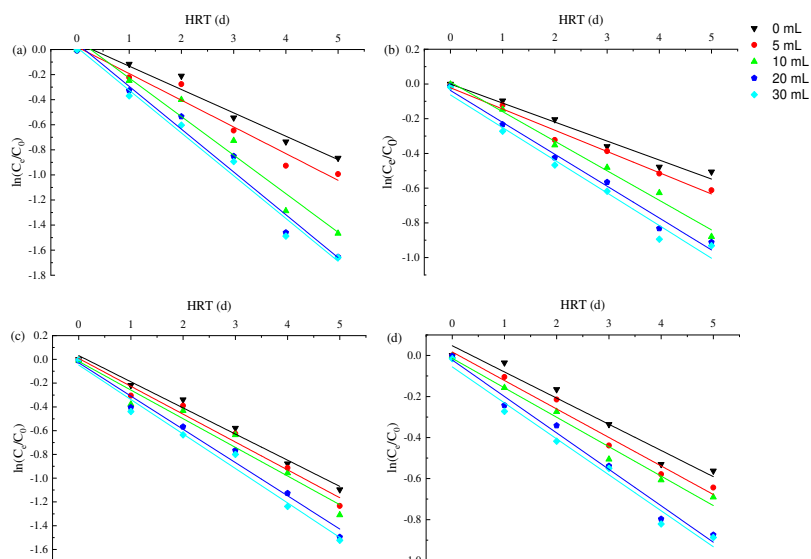


Figure 7. First-order degradation of organic matter with different dosage of immobilized pellets added RS700 in the SBR (Sequencing Batch Reactor, SBR) units operated under $6 \sim 8^\circ\text{C}$, and (a), (b), (c), (d) represent the time curves of COD (chemical oxygen demand, COD), TP (total phosphorus, TP), $\text{NH}_3\text{-N}$ (ammonianitrogen, $\text{NH}_3\text{-N}$) and TN (total nitrogen, TN)

The first-order kinetic model and R^2 value of each contaminant with different dosage of immobilized pellets added RS700 in the SBR are shown in *Table 2*. And, the first-order kinetic model of organic matter with immobilized pellets added RS700 at different hydraulic retention time in the SBR are shown in *Table 3*. The measurement results of COD, TP, $\text{NH}_3\text{-N}$ and TN were substituted into equation (*Eq.2*) at HRT of 4 days, and k_v was calculated as shown in *Table 4*.

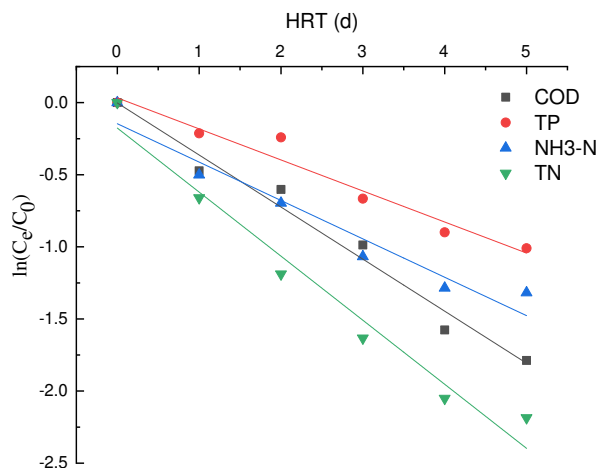


Figure 8. First-order degradation of organic matter with immobilized pellets added RS700 at different hydraulic retention time in the SBR (Sequencing Batch Reactor, SBR) units operated under 6 ~8 °C

Table 2. First-order kinetics model and the R^2 value of removal with different dosage of immobilized pellets added RS700 in the SBR

Pollution parameter	Dosage (mL)	First-order kinetics model	R^2 value	Pollution parameter	Dosage (mL)	First-order kinetics model	R^2 value
COD	0	$y = -0.18632x + 0.05374$	0.9629	$\text{NH}_3\text{-N}$	0	$y = -0.22013x + 0.03185$	0.9841
	5	$y = -0.21281x + 0.02113$	0.9535		5	$y = -0.23455x + 0.00806$	0.9729
	10	$y = -0.30757x + 0.08038$	0.9579		10	$y = -0.24126x - 0.0168$	0.9548
	20	$y = -0.34145x + 0.04786$	0.9697		20	$y = -0.27993x - 0.02865$	0.9772
	30	$y = -0.34099x + 0.01643$	0.9761		30	$y = -0.29023x - 0.04761$	0.9770
TP	0	$y = -0.10939x - 6.00345E-4$	0.9727	TN	0	$y = -0.12763x + 0.04747$	0.9521
	5	$y = -0.12236x - 0.0217$	0.9793		5	$y = -0.1389x + 0.01707$	0.9745
	10	$y = -0.17028x + 0.01092$	0.9889		10	$y = -0.14349x - 0.0141$	0.9771
	20	$y = -0.18371x - 0.03745$	0.9848		20	$y = -0.17757x - 0.02229$	0.9795
	30	$y = -0.18812x - 0.06308$	0.9711		30	$y = -0.17531x - 0.05582$	0.9756

By monitoring the SBR operation system, the degradation efficiency of pollutants was improved under conditions of different amount of bacteria and different hydraulic residence time. As *Figure 7* and *Figure 8* showed that the removal kinetics of contaminants in the SBR conforms to the first-order kinetic model. The volume degradation rate k_v represents the treatment efficiency of the contaminants. Mixed Psychotropic bacterial flora had a noticeably high disposal rate for pollutants at a HRT of 4 days. Furthermore, the degradation rates of COD, TP, $\text{NH}_3\text{-N}$ and TN significantly increased as the dosage of bacteria was increased. The R^2 of each k_v reached 0.78, 0.95, 0.98, 0.91. Similarly, Tang et al. (2018) added a mixed of *Psychrotrophic* bacteria

strains in an integrated vertical-flow constructed wetland at a temperature of $(6 \pm 1)^\circ\text{C}$, which had a high disposal rate for pollutants at a HRT of 5 days and the degradation rates of COD, $\text{NH}_3\text{-N}$, $\text{NO}_2^- \text{-N}$, $\text{NO}_3^- \text{-N}$, TN and TP significantly increased as the dosage of bacteria was increased.

Table 3. First-order kinetics model and the R^2 value of removal with different dosage of immobilized pellets added RS700 in the SBR

Pollution parameter	First-order kinetics model	R^2 value
COD	$y=-0.36096x-0.00205$	0.9712
TP	$y=-0.21519x+0.0331$	0.9475
$\text{NH}_3\text{-N}$	$y=-0.26618x-0.14604$	0.9283
TN	$y=-0.44416x-0.17614$	0.9587

Table 4. k_v in the pseudo-first order reaction of pollutants removal at HRT of 4 days in the SBR

Dosage of immobilized pellets/mL	K_v/d^{-1}			
	COD	TP	$\text{NH}_3\text{-N}$	TN
0	0.184	0.120	0.220	0.133
5	0.232	0.129	0.228	0.145
10	0.322	0.157	0.239	0.152
20	0.365	0.208	0.282	0.199
30	0.372	0.224	0.309	0.205
R2	0.78	0.95	0.98	0.91

Conclusions

1) For immobilized microbe pellets, the optimal optimization conditions were reached when: the mass fraction of SA was 2%, the amount of PVA was 4%, and cross-linking time 24 h, the best biochar added was RS700. The results of the immobilization experiment provide a methodological support for improving the sewage treatment effect under low temperature conditions.

2) Mixed bacteria under the condition of optimization system for immobilized pellets was added to the continuous running of SBR process, 20 mL bacteria suspension of immobilized pellets could use to test the best dosage through the experiment monitoring. Under the optimal addition condition, the longer the HRT in the SBR process, the better the treatment effect would be. In a comprehensive consideration, the optimal HRT was 4 d, and the removal efficiency of COD, TP, $\text{NH}_3\text{-N}$ and TN under the best dosage was reached at 76.79%, 56.50%, 67.60% and 54.92% at 4 days, respectively.

3) In the SBR process, the degradation efficiency of immobilized pellets for each pollutant COD, TP, $\text{NH}_3\text{-N}$ and TN in the SBR conforms to the first-order kinetic model.

4) The results of this study provide a theoretical foundation and scientific support for the use of SBR in wastewater treatment, and may have great significance in solving the increasingly severe water pollution problem in China. In future research, the selection of microbial species and the optimization of immobilization conditions should be carried out for different types of sewage. At the same time, new materials should be considered as additives to promote the study of microbial activity.

Acknowledgements. The authors gratefully thank the financial support provided by the National Natural Science Foundation of China (No. 31700433; No. 31672314).

REFERENCES

- [1] Ahmad, M., Lee, S. S., Dou, X. M., Mohan, D., Sung, J-K., Yang, J. E., Ok, Y. S. (2012): Effects of pyrolysis temperature on soybean stover- and peanut shell-derived biochar properties and TCE adsorption in water. – *Bioresource Technology* 118: 536-544. doi: 10.1016/j.biortech.2012.05.042.
- [2] Ahmad, M., Rajapaksha, A. U., Lim, J. E., Zhang, M., Bolan, N., Mohan, D., Vithanage, M., Lee, S. S., Ok, Y. S. (2014): Biochar as a sorbent for contaminant management in soil and water: A review. – *Chemosphere* 99: 19-33. doi: 10.1016/j.chemosphere.2013.10.071.
- [3] Ali, M., Oshiki, M., Rathnayake, L., Ishii, S., Satoh, H., Okabe, S. (2015): Rapid and successful start-up of anammox process by immobilizing the minimal quantity of biomass in PVA-SA gel beads. – *Water Research* 79: 147-157. doi: 10.1016/j.watres.2015.04.024.
- [4] Argun, M. E., Dursun, S., Karatas, M. (2009): Removal of Cd(II), Pb(II), Cu(II) and Ni(II) from water using modified pine bark. – *Desalination* 249(2): 519-527. doi: 10.1016/j.desal.2009.01.020.
- [5] Bisht, D., Yadav, S. K., Darmwal, N. S. (2013): Optimization of immobilization conditions by conventional and statistical strategies for alkaline lipase production by *Pseudomonas aeruginosa* mutant cells: Scale-up at bench-scale bioreactor level. – *Turkish Journal of Biology* 37(4): 392-404. doi: 10.3906/biy-1209-19.
- [6] Chen, J., Hu, Y., Zhang, L., Huang, W., Sun, J. (2017): Bacterial community shift and improved performance induced by in situ preparing dual graphene modified bioelectrode in microbial fuel cell. – *Bioresource Technology* 238: 273-280. doi: 10.1016/j.biortech.2017.04.044.
- [7] Chung, J., Rittmann, B. E. (2007): Trichloroethane and Chloroform Using a Hydrogen-Based Membrane Biofilm Reactor. – *Biotechnology* 97(1): 52-60. doi: 10.1002/bit.
- [8] Ding, D., Feng, C. P., Jin, Y. X., Hao, C. B., Zhao, Y. X., Suemura, T. (2011): Domestic sewage treatment in a sequencing batch biofilm reactor (SBBR) with an intelligent controlling system. – *Desalination* 276(1-3): 260-265. doi: 10.1016/j.desal.2011.03.059.
- [9] Dutta, A., Sarkar, S. (2015): Sequencing Batch Reactor for Wastewater Treatment: Recent Advances. – *Current Pollution Reports* 1(3): 177-190. doi: 10.1007/s40726-015-0016-y.
- [10] Fu, D., Singh, R. P., Yang, X., Ojha, C. S. P., Surampalli, R. Y., Kumar, A. J. (2018): Sediment in-situ bioremediation by immobilized microbial activated beads: Pilot-scale study. – *Journal of Environmental Management* 226(July): 62-69. doi: 10.1016/j.jenvman.2018.08.021.
- [11] Gundogdu, A., Ozdes, D., Duran, C., Bulut, V. N., Soylak, M., Senturk, H. B. (2009): Biosorption of Pb(II) ions from aqueous solution by pine bark (*Pinus brutia* Ten.). – *Chemical Engineering Journal* 153(1-3): 62-69. doi: 10.1016/j.cej.2009.06.017.
- [12] Hachicha, S., Cegarra, J., Sellami, F., Hachicha, R., Drira, N., Medhioub, K., Ammar, E. (2009): Elimination of polyphenols toxicity from olive mill wastewater sludge by its co-composting with sesame bark. – *Journal of Hazardous Materials* 161(2-3): 1131-1139. doi: 10.1016/j.jhazmat.2008.04.066.
- [13] Hamjinda, N. S., Chiemchaisri, W., Chiemchaisri, C. (2017): Upgrading two-stage membrane bioreactor by bioaugmentation of *Pseudomonas putida* entrapment in PVA/SA gel beads in treatment of ciprofloxacin. – *International Biodeterioration and Biodegradation* 119: 595-604. doi: 10.1016/j.ibiod.2016.10.020.

- [14] He, J., Zhang, W., Ren, X. H., Xing, L. F., Chen, S., Wang, C. (2019): Preparation of Different Activated Sludge Immobilized Carriers and Their Organic Wastewater Treatment Performance by Microbial Community. – *Environmental Engineering Science* 36(5): 604-613. doi: 10.1089/ees.2018.0295.
- [15] Jou, C. J., Chen, S. W., Kao, C. M., Lee, C. L. (2008): Assessing the efficiency of a constructed wetland using a first-order biokinetic model. – *Wetlands* 28(1): 215-219. doi: 10.1672/07-60.1.
- [16] Khan, N. A., Ahmed, S., Islamia, J. M. (2019): Review on SBR Technology of Industrial Wastewater treatment.
- [17] Kulkarni, P. (2013): Nitrophenol removal by simultaneous nitrification denitrification (SND) using *T. pantotropha* in sequencing batch reactors (SBR). – *Bioresource Technology* 128: 273-280. doi: 10.1016/j.biortech.2012.10.054.
- [18] Lim, J. W., Seng, C. E., Lim, P. E., Ng, S. L., Ahmad Sujari, A. N. (2011): Nitrogen removal in moving bed sequencing batch reactor using polyurethane foam cubes of various sizes as carrier materials. – *Bioresource Technology* 102(21): 9876-9883. doi: 10.1016/j.biortech.2011.08.014.
- [19] Liu, G. H., Ye, Z. F., Tong, K., Zhang, Y. H. (2013): Biotreatment of heavy oil wastewater by combined upflow anaerobic sludge blanket and immobilized biological aerated filter in a pilot-scale test. – *Biochemical Engineering Journal* 72: 48-53. doi: 10.1016/j.bej.2012.12.017.
- [20] Lou, L., Wu, B., Wang, L., Luo, L., Xu, X., Hou, J., Xun, B., Hu, B., Chen, Y. (2011): Sorption and ecotoxicity of pentachlorophenol polluted sediment amended with rice-straw derived biochar. – *Bioresource Technology* 102(5): 4036-4041. doi: 10.1016/j.biortech.2010.12.010.
- [21] Marshall, W. E., Johns, M. M. (1996): Agricultural by-products as metal adsorbents: Sorption properties and resistance to mechanical abrasion. – *Journal of Chemical Technology and Biotechnology* 66(2): 192-198. doi:10.1002/(SICI)1097-4660(199606)66:2<192::AID-JCTB489>3.0.CO;2-C.
- [22] Mei, Y. Z., Huang, P. W., Liu, Y., He, W., Fang, W. W. (2016): Cold stress promoting a psychrotolerant bacterium *Pseudomonas fragi* P121 producing trehalase. – *World Journal of Microbiology and Biotechnology* 32(8): 1-9. doi: 10.1007/s11274-016-2097-1.
- [23] Nguyen, L. M. (2000): Organic matter composition, microbial biomass and microbial activity in gravel-bed constructed wetlands treating farm dairy wastewaters. – *Ecological Engineering* 16(2): 199-221. doi: 10.1016/S0925-8574(00)00044-6.
- [24] Popple, T., Williams, J. B., May, E., Mills, G. A., Oliver, R. (2016): Evaluation of a sequencing batch reactor sewage treatment rig for investigating the fate of radioactively labelled pharmaceuticals: Case study of propranolol. – *Water Research* 88: 83-92. doi: 10.1016/j.watres.2015.09.033.
- [25] Rao, J. R., Viraraghavan, T. (2002): Biosorption of phenol from an aqueous solution by *Aspergillus niger* biomass. – *Bioresource Technology* 85(2): 165-171. doi: 10.1016/S0960-8524(02)00079-2.
- [26] Shen, J., Duvnjak, Z. (2005): Adsorption isotherms for cupric and cadmium ions on corncob particles. – *Separation Science and Technology* 40(7): 1461-1481. doi: 10.1081/SS-200053319.
- [27] Showkat, U., Najar, I. A. (2019): Study on the efficiency of sequential batch reactor (SBR)-based sewage treatment plant. – *Applied Water Science* 9:2. doi: 10.1007/s13201-018-0882-8.
- [28] Tang, M., Li, Z., Yang, Y., Chen, J., Jiang, J. (2018): Effects of the inclusion of a mixed Psychrotrophic bacteria strain for sewage treatment in constructed wetland in winter seasons. – *Royal Society Open Science* 5(4). doi: 10.1098/rsos.172360.
- [29] Van Wyk, J. P. H. (1997): Cellulose hydrolysis and cellulase adsorption after pretreatment of cellulose materials. – *Biotechnology Techniques* 11(6): 443-445. doi: 10.1023/A:1018485226767.

- [30] Vázquez, G., Alonso, R., Freire, S., González-Álvarez, J., Antorrena, G. (2006): Uptake of phenol from aqueous solutions by adsorption in a Pinus pinaster bark packed bed. – *Journal of Hazardous Materials* 133(1-3): 61-67. doi: 10.1016/j.jhazmat.2004.12.041.
- [31] Zhao, Q., Ye, Z., Zhang, M. (2010): Treatment of 2,4,6-trinitrotoluene (TNT) red water by vacuum distillation. – *Chemosphere* 80(8): 947-950. doi:10.1016/j.chemosphere.2010.05.004.
- [32] Zhu, G. L., Hu, Y. Y., Wang, Q. R. (2009): Nitrogen removal performance of anaerobic ammonia oxidation co-culture immobilized in different gel carriers. – *Water Science and Technology* 59(12): 2379-2386. doi: 10.2166/wst.2009.293.

REDUCTION OF WATER CONTAMINATION, GAS EMISSION AND PRODUCTION OF ENERGY FROM THE WASTE OF DHAKA CITY, BANGLADESH

ASADUZZAMAN, M.^{1*} – TSUTSUMI, J. G.¹ – NAKAMATSU, R.¹ – SIDDIQUEA, L. A.² – MOKHLAS, A.³

¹*Department of Civil Engineering, University of the Ryukyus, Okinawa 903-0129, Japan*

²*Chorbashi Government School, Government Republic of Bangladesh, Tangail 1900, Bangladesh*

³*Faculty of Agriculture, University of the Ryukyus, Okinawa 903-0213, Japan*

**Corresponding author*

e-mail: jamannoor@gmail.com; phone: +81-804-312-8793

(Received 7th Jun 2019; accepted 9th Sep 2019)

Abstract. The current condition of waste management in Dhaka is a clear manifestation of poor sanitation in less developed nations. The city has been experiencing waste dumping on a daily basis. The aim of this research is to minimize waste, eliminate water contamination as well as greenhouse gas (GHG) emission by producing electricity from waste. An experiment was performed on a collection of wastewater samples and it was found that high level of water contamination is brought by extensive waste water contamination. The study found that wastewater from Dhaka city contained a diverse array of chemicals including toxic and non-toxic heavy metals, nitrates, phosphates, sodium (Na⁺), potassium (K⁺), sodium sulphate (SO₄²⁻), Calcium (Ca²⁺), chloride (Cl⁻) and harmful polyaromatic hydrocarbons. A multivariate analysis was applied and the level of contamination was detected to exceed the World Health Organization (WHO) permissible limit in all areas. Software simulation was also used in data analysis. The study found that 90% waste collection rate and High tech solid waste incinerator plan could produce 262.125 MW electricity per day and potentially reduce 2.375 million tons GHG emission in total per year.

Keywords: *water quality, green energy, water contamination, organic waste, and wastewater evacuation*

Introduction and literature

Dhaka is the capital of Bangladesh. The city is surrounded by four main rivers along with their many small canals. Apart from these water masses there are several inland lakes and lowland inside the city. The source of water for these water masses is rain and seasonal rivers. The city population is estimated to be around 19 million hence the city is considered as one of the most highly populated towns on Earth. Moreover, the city is known to produce tremendous amount of solid wastes on a daily basis. Rising waste volumes together with the increasing complexity of waste treatment have become not only a major and growing public health but also environmental concerns. Due to the population growth, changing lifestyle and spending sequence of individuals, the amount of waste production is ever growing. The eminence as well as the composition of wastes are varying radically. Water pollution is not only impacting water organisms alone but also damages the natural biodiversity.

From the map (*Fig. 1*) we can see rivers around Dhaka City. These water-bodies are highly polluted and have reached alarming levels of pollution that is both economic and health concerns to inhabitants, mainly to the less endowed in the city. Generally, consumption of water originated from several of sources such as rivers, lakes and ponds and ground water. These waters are contaminated with arsenic (As), a toxic metalloid.

Arsenic exists in inorganic form (As^{3+} and As^{5+}) in aquatic system and poses a large public health threat when combined with methyl and dimethyl arsenic composites from natural systems including, anthropogenic as well as ecological sources (Chatterji, Arlosoroff and Guha, 2017; Cordonet et al., 2018; Cui et al., 2018; Ijumulana et al., 2016). Comparative studies have shown that arsenic in water causes health risks such as generating non cancer effects, hypertension, cardiovascular diseases and diabetes (Tripathee et al., 2016; Khuhawar et al., 2019; Kumar et al., 2015; Song et al., 2016; Ijumulana et al., 2016). Inorganic arsenicals which fall in group I carcinogens create a high health risk which claims about 60–100 million people in India and Bangladesh after being found in drinking water as major contaminant from river, canal and lake (Huang et al., 2016; Antoniadis et al., 2017; Bettoschi et al., 2018). UNICEF has reported high awareness in Arsenic contamination in various parts in the country (Mehrotra et al., 2016; Ur Rehman et al., 2018).

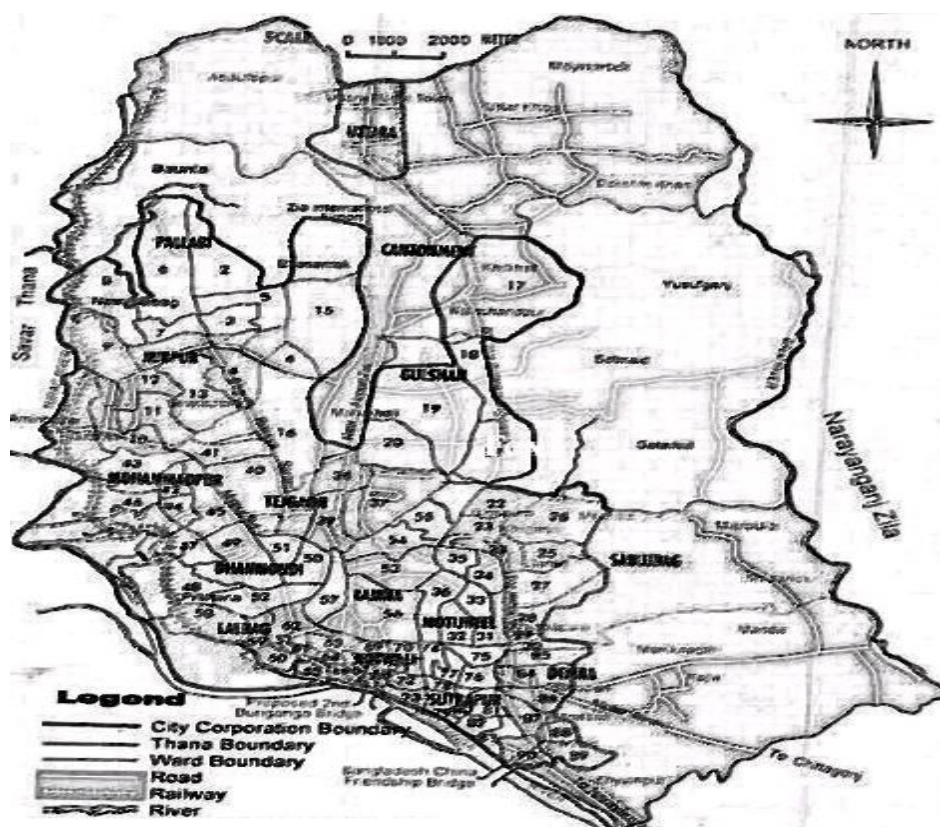


Figure 1. Dhaka City location map

This arsenic contamination happened due to household solid wastes, wastes from small industries and tannery effluents with multifarious features. The wastes are also linked with high level of organic pollutants mainly made up of chemicals as well as significant amounts of inorganic components which are toxic together which cause inhibitory effects on biological system (Ouyang et al., 2018 and Mohammadi et al., 2015). The water sources are polluted with more than 138 different pollutants. In addition, inhabitants are also throwing wastes directly and indirectly into the rivers. The biggest sources are Hazaribagh tannery wastes; water containing COD and the toxic stench wafting throughout the whole area is almost suffocating. Based on the current

statistics lack of waste management in the city is turning out to be the main cause of water pollution. During the rainy season wastes and wastewater production is 100% higher than in the dry season.

The main supply of water in the city is (83%) ground water and surface water (17%). The peripheral rivers have undergone major pollution due to indiscriminate discharge of domestic and industrial wastes (Figs. 2–5). As a result, surface and ground waters are highly contaminated by different types of chemicals and microbes. Some other identified contaminants are residual chlorine, coliform and faecal coliform. According to Dhaka Water Supply and Sewerage Authority (DWASA, 2013), the city experiences high concentrations of *E. coli* in the ground water in the downtown area while water supply is also contaminated.



Figure 2. Waste mixing with rain water at primary collection area



Figure 3. Bank of the river final dumping site

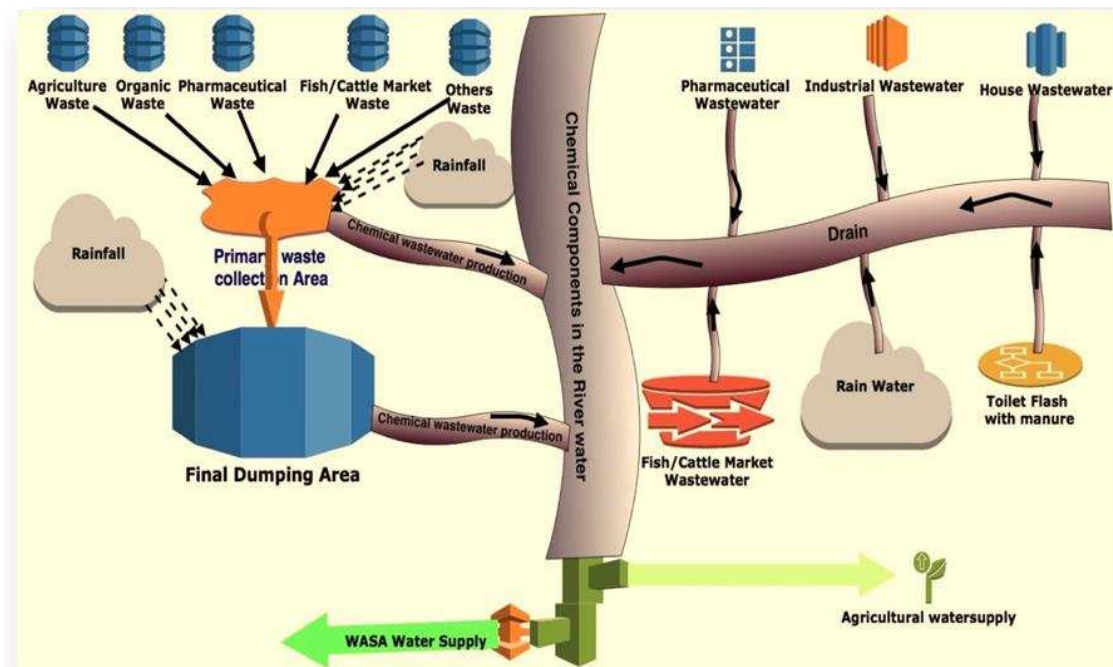


Figure 4. Waste water generation process

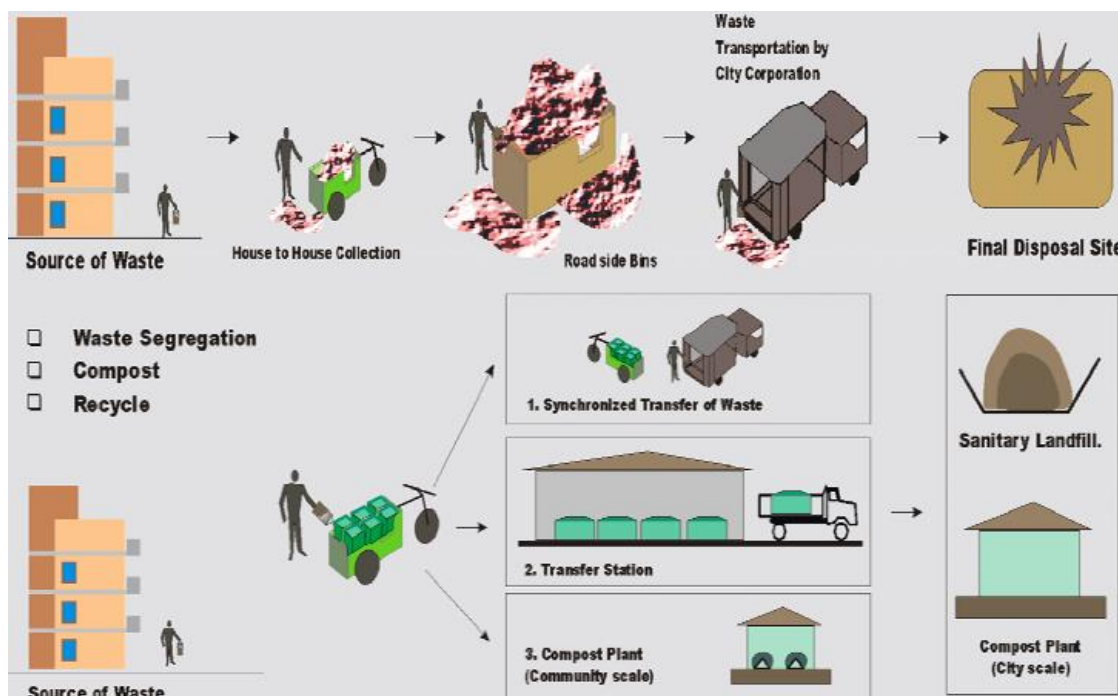


Figure 5. Traditional waste management system in Dhaka City

The fact that untreated industrial wastes are playing a critical role in the degradation of the environment, it is yet to receive international recognition. The poor in the city are highly affected by the pollution based on the current report. The city watershed has reduced by more than 30% over the past decade (Ana and Nandini, 2009). Ground water level is rapidly declining 3 m/yr (DWASA, 2013) due to a large-scale abstraction.

Therefore, ground water is no longer a viable option for water supply and the surface water will be the only option for water sources within the next half-century. To address the tremendous water pollution problem, specialists ought to independently collect as well as treat wastes in order to save the surface and the ground waters.

Currently there is no government agency which has carried out research concerning this on-going environmental issue. There is a great need for arsenic assessment study in the area to establish the level of waste and water pollution in the city of Dhaka (Bangladesh) as well as to assess the level of pollution and the main cause of pollution. The paper also sought to determine water quality parameter such as temperature, pH as well as other parameters in the water sources. In this outline, the objectives of the study were the followings: to show how wastes are converted to wastewater and mix with the water body (*Figure 4*); to use a high tech advance waste management system in Dhaka City and to show GHG emission load reduction in order to save the valuable water resources.

Materials and methods

Study area

The study was conducted in Dhaka City. Dhaka is situated at 23°42'58"N 90°23'46"E on the eastern bank of the Buriganga River as shown in *Figure 1*.

Water sampling and analysis

Primary data was collected through sampling method and later on analysed independently based on the water sample origin. Water samples were collected from Buriganga River, Balu River, Turag River and in Tongi Canal around Dhaka City. Wastewater from tannery examined in the study was sourced from various sites such as Hazaribagh. Over 200 larger tanneries as well as other small ones collectively made up the largest fraction of wastewaters in the city. Grab samples collected from different drain tanneries were assessed to determine the conventional characterization of the raw tannery wastewater in the area. The recommended analyses were carried out in pair in accordance with required standard methods (Clessceri et al., 1998). More than 256 water samples from various sources were taken independently and from separate sampling points within Buriganga River, Balu River, Turag River and in Tongi Canal at Dhaka City. Of all collected water samples more than 153 were taken from > 15 m depth while the same number were taken from surface water. Van Dorn plastic bottles were used to gather samples. The collected water samples were stored in plastic bottles that were previously soaked in 10% nitric acid. During the study period, the researcher assessed water temperature, its pH as well as the concentration of dissolved solids using various instruments such as thermometer, pH meter respectively. The samples which were previously collected were then stored in an ice box, and transported to the lab in the same day to avoid delay.

A dilution of 1000 mg recommended standard solutions were sourced from internationally certified lab to be used as a control in the study of the various metals. In order to prevent contamination of the samples, all the glassware and plastic containers were treated with 5M HNO₃ and rinsed with distilled water and completely with ultrapure water. The physicochemical levels were established using recommended techniques (Tamasi and Cini, 2004; APHA, 1998). Moreover, methyl-orange was used to assess the level of alkalinity in the sample waters. EDTA was used to measure Calcium concentration in the

samples using of complexometric titration (Eaton et al., 1995). In respect to analysis of arsenic as well as other metals water samples were pre-concentrated different zones (Arain et al., 2007; AOAC, 1995). Saturation indices were measured using speciation-modeling to determine the equilibrium condition of the minerals in the samples (USGS, 2007).

Filtered samples of aliquot were measured by evaporation method to estimate the amount of dissolved solid in the water samples. Both Sodium (Na) and Potassium (K) were determined using flame-photometer while Calcium (Ca) and Magnesium (Mg) were examined by complexometric titration technique using Na₂ EDTA as titrant. Other cations such as Fe²⁺, Fe³⁺, Mn²⁺, Cu²⁺, Zn²⁺, B³⁻, together with anions such as Cl⁻, NO₃⁻-N, SO₄²⁻-S, HCO₃⁻, and CO₃²⁻ were examined based on recommended procedures. Qualitative test was done to detect the presence or absence of Arsenic (As). Irrigated water quality parameters viz. SAR, SSP, and H_T were used to classify the suitability of waters, along with pH, EC, and TDS.

For both quality assurance and control (QA/QC), data were examined based on the recommended method (Zacheus and Martikainen, 1997). Flame atomic absorption spectrophotometer technique was used to examine sodium, iron, and potassium within given limits of 0.02 g LOD. Consequently, sulphate concentration together with chloride, as well as nitrate concentrations were assessed using LOD 1.2, 1.4, 1.5 and 2.7 g, in that order. For the purpose of validation of ions, the researcher carried out ionic balance test (Lopez et al., 1999) as

$$\text{Ion balance percent} = \left\{ \frac{\sum_{\text{cations}} - \sum_{\text{anions}}}{\sum_{\text{cations}} + \sum_{\text{anions}}} \right\} \times 100 \quad (\text{Eq.1})$$

On average the ion balance was around 1.18% with two outliers of around 1.8% and -3.1% were determined, the mean of the ion balance was around 0.6% (Table 1). The parameters of SAR, SSP, and H_T were measured from the analyzed data using the following formula:

$$\text{SAR} = \frac{[\text{Na}^+]}{\left\{ \frac{([\text{Ca}^{2+}] + [\text{Mg}^{2+}])}{2} \right\}^{\frac{1}{2}}} \quad (\text{Eq.2})$$

$$\text{SSP} = \frac{\text{Soluble Na concentration (meL}^{-1}\text{)}}{\text{Total cation concentration (meL}^{-1}\text{)}} \times 100 \quad (\text{Eq.3})$$

$$\text{H}_T (\text{mgL}^{-1}) = 2.5 \times \text{Ca}^{2+} + 4.1 \times \text{Mg}^{2+} \quad (\text{Eq.4})$$

Correlation coefficient analysis was done for all possible combinations within the quality parameter.

Waste sample analysis

Primary and secondary data were used for this study purpose. Secondary data was collected through various books, reports, journals and articles, such as JAICA, Ministry of Environment and Forest (MOEF), Dhaka City Corporation (DCC) reports and different waste management plants in Japan. Data collection methods included document/literature review, semi-structured interviews, checklists and observation.

Table 1a. The mean values of physico-chemical parameters and arsenic concentration in ground water from Dhaka District, Bangladesh

Sample ID	T (°C)	pH	EC (mS cm ⁻¹)	As (µg)	TDS (mg)	Ca ²⁺ (mg)	Mg ²⁺ (mg)	Na ⁺ (mg)	K ⁺ (mg)	HCO ₃ ²⁻ (mg)	Cl ⁻ (mg)	NO ₂ ⁻ (mg)	NO ₃ ⁻ (mg)	SO ₄ ²⁻ (mg)	Fe (mg)
PS1	29.2	8.3	2.39	83.01	1148	219	49.3	755	43	1360	233	2.43	25	1017	4.01
PS2	27.3	7.1	1.7	14.01	783	168	26.3	653	9.1	967	267	1.39	12.3	709	0.26
PS3	28.5	8.9	4.15	108.0	1951	299	99.6	801	18.8	355	646	4.23	47.9	1519	4.29
PS4	26.1	7.1	3.93	15.31	1846	79.1	35.1	526	55.9	219	419	2.35	41.3	723	0.21
PS5	28.5	9.0	2.99	55.13	1396	102	63.8	946	52.7	537	718	1.58	27.5	1050	0.10
PS6	29.3	8.3	1.97	26.3	911	87.7	42.3	532	17.5	221	347	0.56	13.1	830	1.11
PS7	26.4	7.8	0.88	31.2	490	34.5	40.3	368	14.4	270	236	3.47	6.1	467	0.53
PS8	26.1	7.7	1.65	57.1	720	37.7	11.6	239	6.9	178	179	1.03	13.2	248	0.09
PS9	27.2	7.9	2.41	4.03	897	38.4	26.7	201	4.3	271	198	0.97	1.3	110	0.10
PS10	31.0	7.1	4.56	20.2	298	110.5	57.2	737	10.1	521	523	0.94	26.5	907	0.63
PS11	30.3	7.6	1.11	54.3	881	50	21.3	749	8.3	311	521	7.55	12.4	782	0.21
PS12	30.1	7.9	1.09	27.1	2227	89.1	27.9	561	17.3	337	293	1.22	12.3	881	0.60
PS13	29.4	8.0	1.01	55.2	523	55.5	18.1	598	13.1	287	278	0.93	9.7	411	0.20
PS14	28.5	8.1	2.53	45.1	497	38.7	68.3	297	17.9	279	203	2.53	12.9	333	0.20
PS15	27.4	7.6	0.49	43.13	433	231.2	23.3	321	14.0	513	513	2.23	11.9	1107	0.59
PS16	28.3	7.2	2.79	57.9	1253	243.5	25.3	633	4.0	304	464	2.71	25.6	1122	0.42
PS17	27.1	7.9	0.49	29.1	205	124.3	21.9	541	10.5	287	232	0.49	6.0	978	0.43
PS18	29.3	8.1	0.75	13.3	271	43.7	2.9	501	9.1	451	163	0.67	24.9	317	0.59
PS19	31.4	8	1.11	20.1	521	78.5	17	489	11.1	449	232	0.49	7.1	563	0.32
DTS1	32.3	7.9	1.13	37.2	347	71.3	82.5	339	8.2	320	193	0.99	6.1	452	0.14
DTS2	35.9	8.0	1.09	45.9	489	52.1	27.1	417	7.2	330	227	1.65	6.2	367	0.32
DTS3	28.1	7.6	1.13	66.1	543	59.5	21.7	397	7.9	220	143	0.97	0.9	723	0.23
DTS4	32.4	7.8	1.19	36.2	649	41.3	28.9	247	6.1	320	291	0.20	12.5	477	0.21
DTS5	25.1	8.1	1.16	44.9	621	61.1	21.1	241	7.1	230	130	0.30	0.8	366	0.50
DTS6	32.2	7.9	1.11	36.1	679	42.1	28	397	5.2	209	197	1.67	12.9	631	0.33

PS: pump sample, DTS: deep tube well sample

Table 1b. The mean values of physico-chemical parameters and arsenic concentration in surface water from Dhaka District, Bangladesh

Sample ID	T (°C)	pH	EC (mS cm ⁻¹)	As (µg)	TDS (mg)	Ca ²⁺ (mg)	Mg ²⁺ (mg)	Na ⁺ (mg)	K ⁺ (mg)	HCO ₃ ²⁻ (mg)	Cl ⁻ (mg)	NO ₂ ⁻ (mg)	NO ₃ ⁻ (mg)	SO ₄ ²⁻ (mg)	Fe (mg)
RS1	21.2	7.3	0.42	3.01	189	25.9	13.3	223	4.2	180	163	0.43	6.5	247	0.09
RS2	22.3	7.1	0.40	4.01	183	8.3	8.3	215	2.9	287	117	0.49	6.3	109	0.12
RS3	23.5	7.9	2.67	38.0	251	86.1	39.6	709	18.9	345	156	1.03	17.9	1239	0.39
MS1	22.1	7.1	0.43	5.31	186	40.1	15.1	239	5.9	249	179	0.53	6.3	196	0.21
MS2	21.5	7.0	0.40	5.13	256	13.2	8.1	183	6.7	271	68	1.58	5.9	117	0.10
MS3	22.3	8.3	1.84	16.3	211	51.7	21.1	465	17.9	231	272	0.56	16.1	613	0.11
MS4	22.4	7.0	0.47	6.31	190	16.5	5.5	243	7.6	210	186	1.13	6.1	187	0.13
MS5	23.1	7.6	1.69	50.1	220	224.7	36.9	483	15.9	278	359	0.53	13.1	988	0.09
MS6	25.2	7.1	0.46	4.03	197	12.4	9.5	211	5.3	201	178	0.97	6.9	130	0.10
MS7	22.5	7.9	3.62	5.91	198	25.5	12.3	227	12.1	191	173	0.54	16.5	207	0.03
MS8	23.3	7.2	0.41	5.01	211	6.3	23.6	271	35.1	201	333	0.55	6.4	162	0.11
MS9	24.1	7.1	0.49	4.33	207	23.1	17.9	239	7.3	197	223	0.62	14.3	181	0.15
MS10	22.4	7.0	0.50	11.02	230	17.5	18.1	213	15.1	187	208	0.73	4.9	241	0.13
MS11	23.5	7.1	0.53	7.91	197	18.7	11.3	357	43.1	479	243	2.83	73.9	263	0.29
MS12	23.4	7.5	0.40	17.13	233	11.2	33.3	401	15.1	173	283	1.53	11.9	597	0.11
MS13	22.3	7.2	0.49	6.09	253	33.5	3.3	333	45.7	164	244	1.11	0.8	352	0.12
MS14	22.1	7.1	3.71	6.11	215	22.3	11.9	241	14.5	157	282	0.59	0.4	207	0.03
MS15	23.3	7.5	0.55	5.23	171	82.1	2.9	251	10.1	151	243	3.17	48.9	217	0.29
MS16	22.4	7.8	3.49	11.21	121	22.5	45.5	539	7.2	149	235	1.29	13.1	893	0.02
MS17	23.3	7.6	1.44	11.2	247	81.3	25.5	439	25.1	123	196	1.59	14.1	622	0.14
MS18	24.9	8.0	3.27	7.99	169	32.1	7.1	327	14.2	134	317	1.50	3.2	207	0.12
MS19	22.1	8.6	0.91	8.2	243	15.5	10.7	139	9.1	118	63	0.87	33.1	243	0.13
MS20	23.4	7.5	0.34	6.09	149	42.3	8.9	297	6.1	119	231	0.50	12.5	227	0.11

A semi-structured interview refers to a gathering in which the interviewer asks open-ended questions and allows for a discussion with the interviewee. There is no formalized process which is used while asking or answering the questions. In most cases, the interviewer asks the general questions which lead to further short questions within the discussion.

A checklist structures an individual's evaluation or observation of performance or even an artifact. They use simple criteria which can be labelled as present or absent and provide space for the observer to comment. Checklist can also be used to evaluate a database or structure out a peer observation and guide well while collecting data from a sample of the population.

The measure of combined dissolved solids in waters were determined by evaporating the filtrate of filtered samples. Sodium and Potassium levels were obtained by flame-photometer where else Calcium and Magnesium were obtained through complexometric titration using Na₂EDTA as reference sample titrant. Cations like Cu²⁺, Zn²⁺, and anions like Cl⁻, NO₃⁻-N, SO₄²⁻-S, HCO₃⁻, and CO₃²⁻ were measured through photometry. The presence or absence of Arsenic (As) metal was determined using qualitative test.

The cation levels were obtained by atomic spectrophotometry by mechanism of flame absorption for potassium, sodium and iron while for the other cations hydride generation was used in their spectrophotometry. Anion concentrations were obtained through ion chromatography (Metrohm 838) and validated then calculated using *Equation 1*.

Lastly, observation involved direct or indirect viewing of object whether aware or unaware if it is being observed. In observation, the researcher may choose to collect data through a set of time periods or progressive observation throughout the project.

To properly investigate on waste generation (*Fig. 4*) and disposal system (*Fig. 2,3 & 5*), some areas were selected as sampling areas, such as Hazaribagh located at 23.734722°N, 90.369444°E with a total area of around 3.58 km²; Gabtoli situated at 24°53'N 89° 27'E; Uttara on the other hand is situated at 23° 52'N 90°24.3'E; Dholpur (23.71674°N 90.4323178°E) and Mirpur located at 23.809309°N 90.360928°E. Stratified random sampling technique was used for public opinion survey on some attributes, such as waste generation (*Fig. 4*), waste dumping (*Fig. 2,&3*), and waste safety. The analysis was done using Urban Co-benefits Evaluation Tools and statistical tools, like Microsoft Excel used to perform calculation, visualization and analysis of data and information. It aids researchers to structure and process data through utilization of rows, columns and a combination of different formulas.

The method was to determine whether the current waste management process (*Fig. 5*) was being done as per legislation, the frequency in which environmental harm occurs and its significance. These measures were put in place to verify environmental damages (*Fig. 3*) and the optimal usage of water, energy and natural resources. In the project we have done the software simulation by classifying the wastes where combustible and non-combustible items are separated from the beginning. Step by step waste generation (*Fig. 4*), collection separation processes were done. Only the combustible wastes are simulated by the software. Hopefully, some medical wastes were also included in this system because in Dhaka City all

wastes are dumped in the open pit and one dumping site. The aim was to answer the questions of this study which were: (1) how wastes convert to a wastewater stream, (2) chemical pollutants confirmation, (3) greenhouse gases production by conventional waste management procedure, and (4) a solution for saving surface water and GHG reduction

Total energy in MSW

Total energy in MSW was determined by its composition and moisture content. The MSW was reported to produce 95 m³ of methane gas per tonne with an efficiency of 80% and energy production of 12.98·10⁵ KWh/year (Kumar et al., 2009). The energy content of waste was measured by bomb calorimeter which entailed total combustion of the sample and then gauging the heat rise in surrounding water bath (Masters and Ela, 2013). This temperature value obtained is mainly higher in industries which manufacture products such as paper, metal and plastics. Khan et al. (1919) formulated formulas that determine temperature in food and paper industries. This formula was expressed in the equation below:

$$\text{HHV} \left(\frac{\text{kJ}}{\text{kg}} \right) = 53.5(f + 3.6cp) + 372plr \quad (\text{Eq.5})$$

where f is food, cp is paper and cardboard, and plr is plastic. However, some amount of HHV energy is lost through vaporization of the moisture.

Results

The results for the study were as follows:

Test results (water sample)

The tests were carried out in water samples in two depths; groundwater water and surface water. The ground water samples were classified depending on the mode they are found. Pump samples (PS, $n = 113$) were obtained at a depth range of 15.85 to 33.5 m and deep-tube well samples (DTS, $n = 40$) were obtained at a depth variation up to 120 m depth as shown in *Table 1a*. Surface water samples were classified into two categories, namely river samples (RS, $n = 33$) and municipal samples (MS, $n = 120$), depending on the place the samples were obtained from. Physical and chemical analysis of all samples were done.

The pH and EC of all samples were measured and their range obtained. The pH range for PS was 7.1-9.0 while for DTS was 7.9-8.1. The EC range for groundwater samples were 0.49–4.56 mS cm⁻¹ for PS and 1.09–1.10 mS cm⁻¹ for DTS. Alkalinity ranged from 178–1360 mg for both groundwater samples. The pH range for RS was 7.1-7.9 while that of MS was 7.0-8.6 where else the EC values ranged from 0.40–2.67 mS cm⁻¹ and 0.40–3.71 mS cm⁻¹, respectively. Alkalinity in both samples of surface water ranged from 118–479 mg. The composition of major ion was almost similar in both categories of surface water.

Groundwater had significant Fe concentration ranging from 0.1 to 4.01 mg while surface water the level ranged much below the WHO recommendable range except at sampling point RS3. Arsenic concentration was more in the groundwater

compared to surface water with ground water registering the highest level of 108 g compared to 50.1 g for surface water.

Simulation results

The simulation result is shown in *Figures 6–8*. *Figure 6* shows almost 49% for landfill and open burning is almost 12%. *Figures 7* and *8* show that greenhouse gas emission is extremely high level in conventional approach.

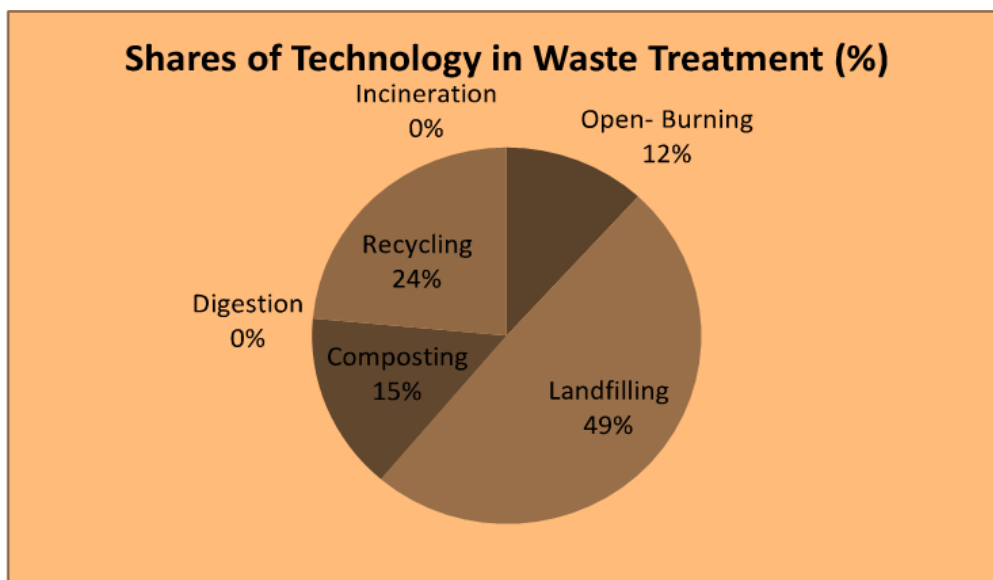


Figure 6. Current waste dumping

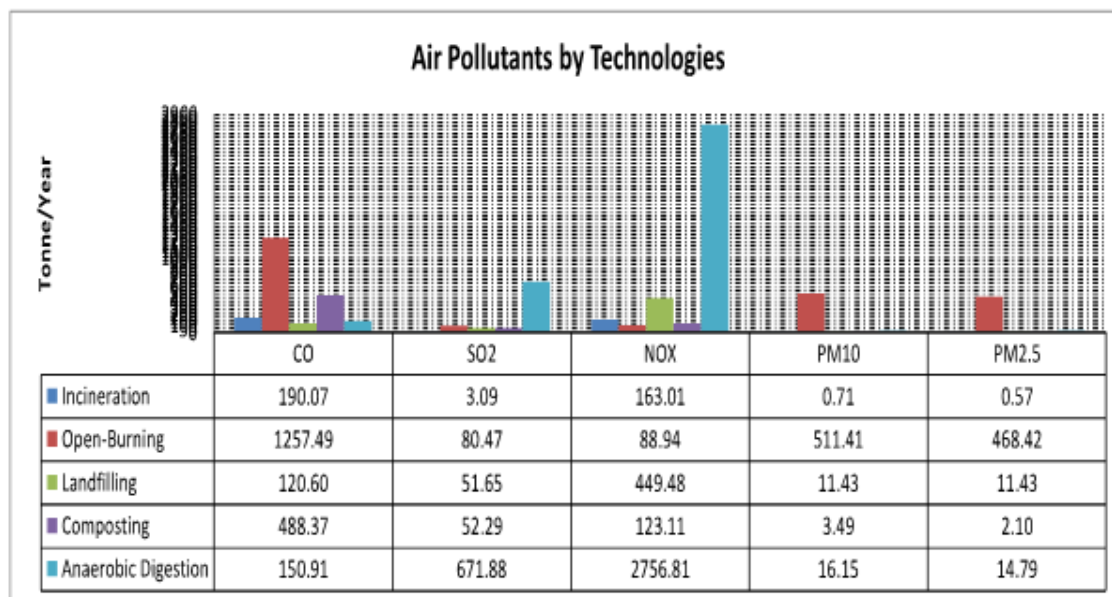


Figure 7. Current GHG emission

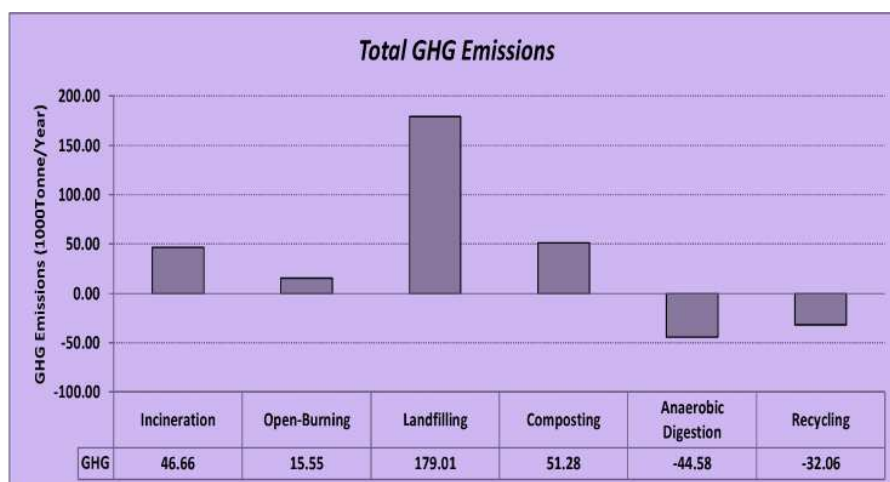


Figure 8. Current air pollution

Discussion

The pH of all samples was nearly above the acceptable level of World Health Organization (WHO) with high level of EC and alkalinity in samples which were obtained at deep points ($p > 0.05$). This variation in the levels of pH and alkalinity in groundwater samples compared to surface water samples was due to excess dissolution of organic and inorganic compounds which sediment at the ground of the water as thousands of tonnes of wastes are produced during the wet season (Fig. 2). Due to lack of proper treatment, wastes are terminated to the final dumping areas (Fig. 3) or open pits in main streets or close to the city emitting GHG gases which are dissolved in water by rainwater or seasonal water creating more anions in the surface of the water (Fig. 2), and finally the wastewaters are flowing into the rivers (Fig. 3). In the study the large concentration of cations and anions were due to more solubility of GHG gases emitted upon the burning of large quantities of waste production within the city. There was similar concentration of major ion in both municipal treated water samples and river surface water due to even distribution of ions in the water at a similar depth. There was a relative range in levels of different cations and anions. Sulphate (SO_4^{2-}) ions ranged from 109–1519 mg, chloride Cl^- ions ranging from 63 to 718 mg, while Sodium ions (Na^+) ranged from 139 to 946 mg. Calcium ions ranged from 6.3 to 299 mg. The levels of concentration of different cations and anions depended on the nature of waste being dumped openly in the pit and their solubility levels in water (Fig. 3).

This 3R approach in stimulant results is very good (Fig. 5). However, this approach has its limitation, it can cover only small amount of wastes per day. To tackle huge amount of wastes (12-15 thousand tons/day) that produced in Dhaka City, it is not an ideal approach. In this situation, we are proposing an advanced technology for waste management system that could cover all the wastes in Dhaka City.

Proposed technology

Waste life cycle

After reviewing the waste disposal system and 3R approach (Fig. 5) in Dhaka City, we propose a design for waste life cycle to achieve our final goal. Figure 9 shows the

proposed life cycle for solid wastes where waste-classification is started at sources (Burnable, non-burnable, recyclable, organic particularly kitchen wastes) and each of the waste will be treated accordingly.

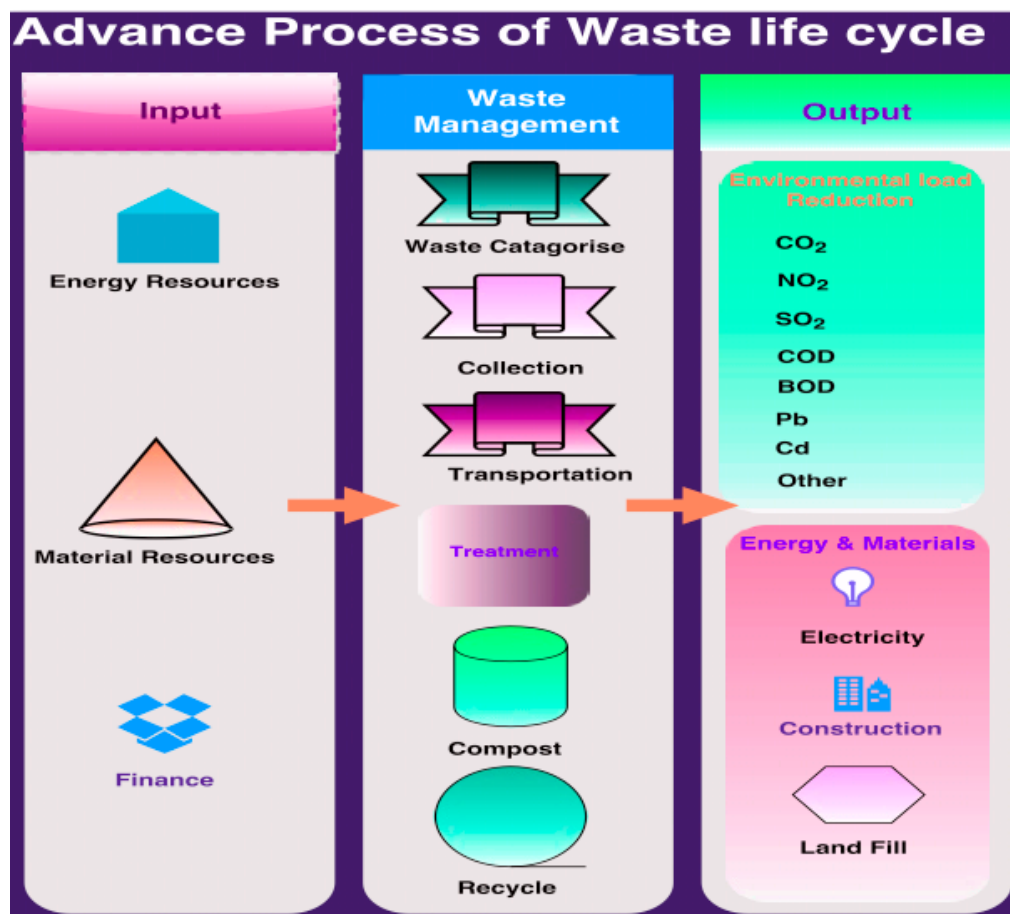


Figure 9. Proposed system

Proposed treatment plant

Figure 10 depicts incineration structure where burnable wastes are burned at 500 to 600 °C to keep valuable aluminium and un-oxidised ferrous metal that can be recovered by recycling. Non-combustible materials and sand are discharged from the bottom of the furnace through the non-combustible discharge conveyor. There are two types of separators here. If there are any ferrous metals contained in the non-combustible these are recovered with a magnetic separator, and the aluminium is recovered with an aluminium separator. The sand is stored in the sand storage tank.

Second stage is ash melting. The ash melting furnace has higher temperature because the gas is combusted while being circulated at the relatively high temperature at 1300 to 1400 °C (Kurahama Sanitary Facilities Association, Japan). This high temperature melts the ash contained in the gas, turning it into the slag, while greatly decreasing the amount of generated dioxins. The bottom of the ash-melting furnace is a discharge system for slag. Slag scraper conveyor is keeping and cooling slag by circulating cool water. This water is cooled by the water cooler and recycled for slag cooling system. Finally, slag is crushed by the slag crusher and stored in the slag storage yard.

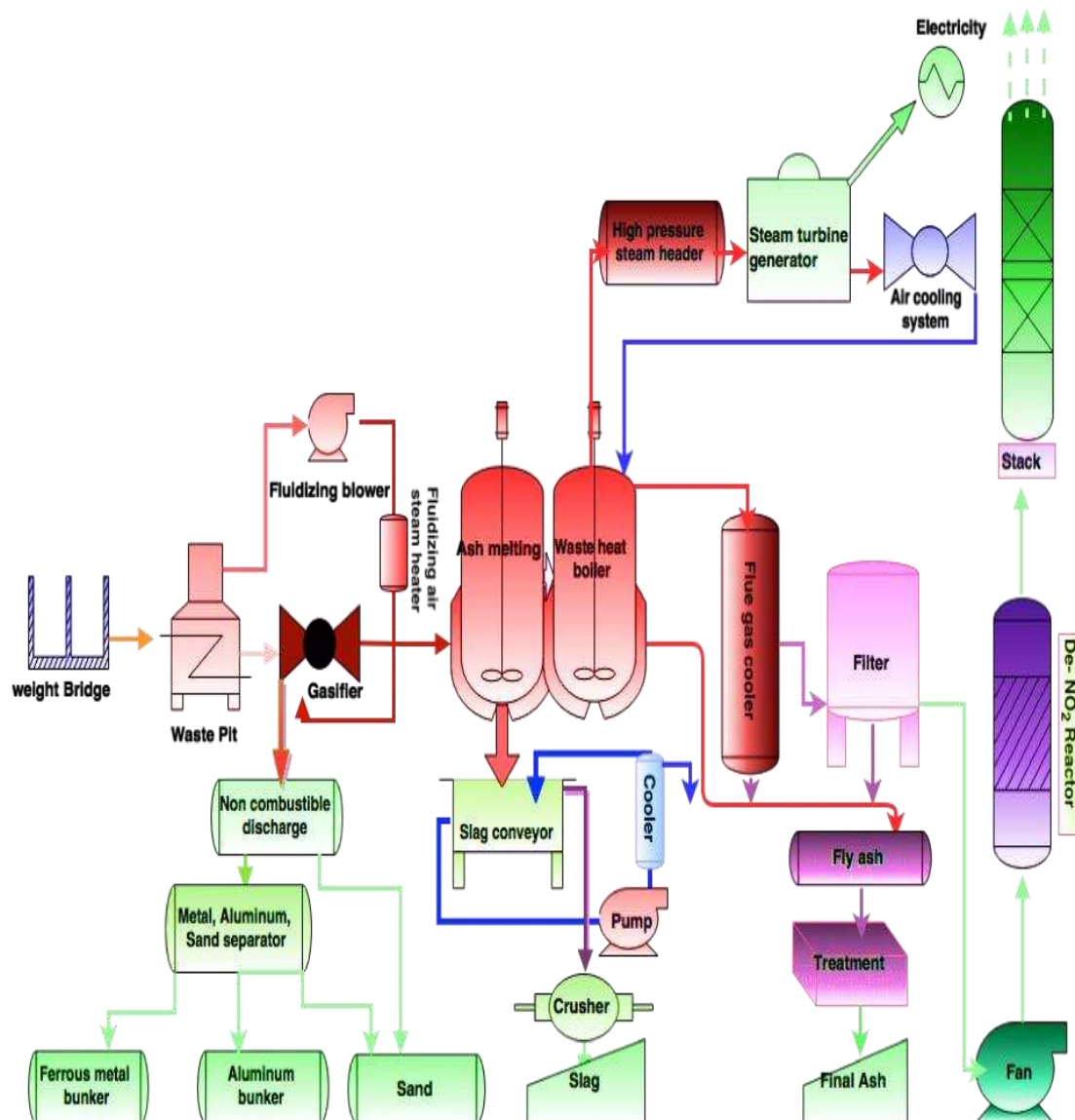


Figure 10. Advance waste treatment plant

The ash melting furnace and the waste heat boiler are directly connected to a heat boiler which has a high-pressure steam header that uses steam to generate power. The power generated is used to power the facilities and surplus sold. The steam is also used to provide hot water. The heat boiler discharges fly ash with flue gas at the bottom where the gas is taken back to the cooler while the ash is moved to a fly ash silo. This fly ash silo is also receiving ash from bag filter. Finally, fly ashes are treated by the treatment facility and sent to the hopper.

The gas is then cooled in water and filtered through filter bags made of fabrics to remove dust then reheated and passed through De-NO₂ reactor which removes nitrogen oxides contained in the gas as they react with ammonia through a catalytic reaction. Finally, it will discharge to the atmosphere by the stack. If we can implement this plant, our simulation result showed that GHG emission would be the same as of Kuraham waste management plant (Kurahama Sanitary Facilities Association, Japan). Thus, we can control environmental standard.

Proposed treatment plant's simulation result

Compared to the conventional waste treatment process, the High Tech system reduced the production of pollutants; particularly GHG is a million tonnes lower (180 to 0.03 thousand tonnes) as shown in *Figure 11* and *Table 2*.

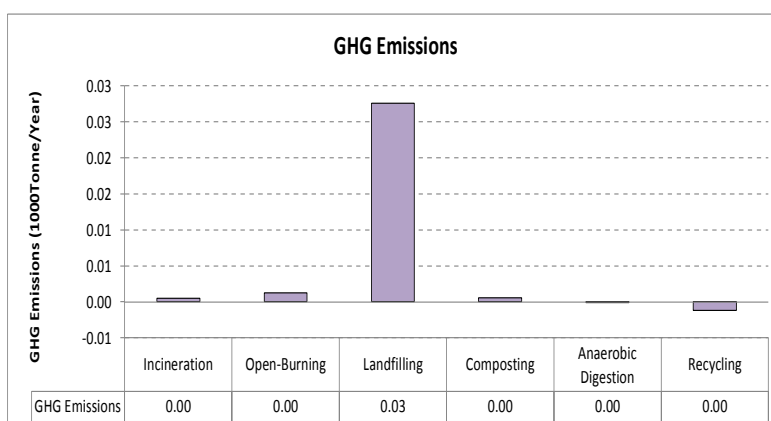


Figure 11. Advance waste treatment plant gas emission

Table 2. Ranges of analytical data of the ground and surface water sample in Dhaka District, Bangladesh

Parameter	Recommended values (WHO, 2004)	Water type											
		Ground water						Surface water					
		Pump water n = 113 ^a			Deep tube well water n = 40 ^a			River water n = 33 ^a			MS water n = 120 ^a		
		Min	Max	Mean	Min	Max	Mean	Min	Max	Mean	Min	Max	Mean
T (°C)	-	26.1	31.4	27.1	25.1	35.9	31	21.2	23.5	22.3	21.5	25.2	22.9
pH	6.5-8.5	7.1	8.3	7.87	7.6	8.1	7.88	7.1	7.9	7.43	7	8.6	7.46
EC (mS cm ⁻¹)	0.40	0.49	4.56	2.0	1.09	1.19	1.14	0.4	2.67	1.16	0.34	3.71	1.27
TDS (mg)	1000	271	1951	907.95	347	679	554.67	183	251	207.67	121	256	205.2
Ca ²⁺ (mg)	100	37.7	299	112.13	42.1	71.3	54.57	8.3	86.1	40.1	6.3	224.7	39.63
Mg ²⁺ (mg)	50	2.9	99.6	35.69	21.1	82.5	34.88	8.3	39.6	20.4	2.9	45.5	16.43
Na ⁺ (mg)	200	201	946	549.89	241	417	339.67	215	709	382.33	139	539	304.9
K ⁺ (mg)	12	4	55.9	17.79	5.2	8.2	6.95	2.9	18.9	8.67	6.1	45.7	15.96
HCO ₃ ²⁻ (mg)	-	178	1360	427.21	209	330	271.5	180	345	270.67	118	479	199.15
Cl ⁻ (mg)	250	163	718	350.79	130	291	196.83	117	163	145.33	63	359	225.8
NO ₂ ⁻ (mg)	3	0.49	7.55	1.99	0.2	1.67	0.96	0.43	1.03	0.65	0.5	3.17	1.14
NO ₃ ⁻ (mg)	50	1.3	47.9	17.74	0.8	12.9	6.57	6.3	17.9	10.23	0.4	73.9	15.42
SO ₄ ²⁻ (mg)	250	110	1519	740.74	366	631	502.67	109	1239	531.67	117	988	342.5
As (µg)	10	13.3	108	39.97	36.1	66.1	44.4	3.01	38	15.00	4.03	50.1	10.03
Fe (mg)	0.3	0.1	4.01	0.78	0.14	2.1	0.60	0.09	0.39	0.2	0.02	0.29	0.13

Conclusion

The research concluded that the level of arsenic in different samples was higher than the acceptable level expected by WHO. The higher levels were mainly found in the ground water compared to the surface water were mainly due to waste dumping factors including the nature of waste, solubility that influence pH level, and concentration of different cations and anions. This High Tech waste treatment plant can potentially

reduce totally 2.4 million tons GHG per year. The plant can also produce 256.125 MW electricity daily. Thus, the system is self-sustainable and environmental friendly. It will reduce polluted wastewater effluents from flowing into the water bodies and GHG emission in the environment significantly. Further research is required to identify how electricity can be generated. Moreover, the study was conducted in a developing country. To enable generalization of the findings, the study suggests a similar research to be conducted concerning under-developed and developed nations.

REFERENCES

- [1] Ana, M., Nandini, D. (2009): Industrial water pollution in Dhaka, Bangladesh: strategies and incentives for pollution control in small and medium enterprises. – *The International Journal of Interdisciplinary Social Sciences* 3(11): 97-108.
- [2] Anawar, H. M., Akai, J., Komaki, K., Terao, H., Yoshioka, T., Ishizuka, T., Safiullah, S., Kato, K. (2003): Geochemical occurrence of arsenic in groundwater of Bangladesh: sources and mobilization processes. – *J. Geochem. Explor.* 77: 109-131.
- [3] Antoniadis, V., Golia, E. E., Shaheen, S. M., Rinklebe, J. (2017): Bioavailability and health risk assessment of potentially toxic elements in Thriasio Plain, near Athens, Greece. – *Environmental Geochemistry and Health* 39(2): 319-330.
- [4] AOAC, Association of Official Analytical Chemists (1995): *Official Methods of Analysis*. 16th Ed. – AOAC International, Gaithersburg, MD (March 1998 revision).
- [5] APHA (American Public Health Association) (1998): *Standard Methods for the Examination of Water and Wastewater*. 20th Ed. – APHA, American Water Works Association, and Water Pollution Control Federation, Washington, DC.
- [6] Arain, M. B., Kazi, T. G., Jamali, M. K., Jalbani, N., Afridi, H. I., Shah, A. (2007): Total dissolved and bioavailable elements in water and sediment samples and their accumulation in *Oreochromis mossambicus* of polluted Manchar Lake. – *Chemosphere* 70: 1845-1856.
- [7] Bettoschi, A., Marrucci, A., Marras, B., Atzori, M., Schintu, M. (2018): Arsenic speciation in marine sediments: a comparison between two sequential extraction procedures. – *Soil and Sediment Contamination: An International Journal* 27(8): 723-735.
- [8] Chandan, C., Mazaharul, H. M., Sobur, A., Taslima, T., Miah, R. M. (2013): Analysis of the causes and impacts of water pollution of Buriganga River: a critical study. – *International Journal of Scientific & Technology Research* 2: 245-252.
- [9] Chappell, W. R., Abernathy, C. O., Calderon, R. L. (eds.) (2001): *Arsenic Exposure and Health Effects*. Vol. 24. – Elsevier, New York, pp. 27-52.
- [10] Chatterji, M., Arlosoroff, S., Guha, G. (2017): *Conflict Management of Water Resources*. – Routledge, London.
- [11] Clesceri, L. S., Greenberg, A. E., Eaton, A. D. (eds.) (1998): *Standard Methods for the Examination of Water and Wastewater*. 20th Ed. – American Public Health Association, Washington, DC, USA.
- [12] Cordon, G., Iriel, A., Cirelli, A. F., Lagorio, M. G. (2018): Arsenic effects on some photophysical parameters of *Cichorium intybus* under different radiation and water irrigation regimes. – *Chemosphere* 204: 398-404.
- [13] Cui, J. L., Zhao, Y. P., Li, J. S., Beiyuan, J. Z., Tsang, D. C., Poon, C. S., ... Li, X. D. (2018): Speciation, mobilization, and bioaccessibility of arsenic in geogenic soil profile from Hong Kong. – *Environmental Pollution* 232: 375-384.
- [14] Eaton, D. A., Clesceri, L. S. (1995): *Greenberg, Standard Methods*. 19th Ed. for the Examination of Water and Wastewater. – American Public Health Association, Washington, DC.

- [15] Elci, L., Divrikli, U., Soylak, M. (2008): Inorganic arsenic speciation in various waters amples with GF-AAS using coprecipitation. – *Int. J. Environ. Anal. Chem.* 88: 711-723.
- [16] Huang, X., Betha, R., Tan, L. Y., Balasubramanian, R. (2016): Risk assessment of bioaccessible trace elements in smoke haze aerosols versus urban aerosols using simulated lung fluids. – *Atmospheric Environment* 125: 505-511.
- [17] Ijumulana, J., Mtaló, F., Bhattacharya, P., Bundschuh, J. (2016): Arsenic Occurrence in Groundwater Sources of Lake Victoria Basin in Tanzania. – In: *Arsenic Research and Global Sustainability: Proceedings of the Sixth International Congress on Arsenic in the Environment (As2016)*, June 19-23, 2016, Stockholm, Sweden. CRC Press, Boca Raton, FL.
- [18] Khuhawar, M. Y., Ursani, H., Khuahwar, T. M. J., Lanjwani, M. F., Mahessar, A. A. (2019): Assessment of Water Quality of Groundwater of Thar Desert, Sindh. Pakistan. *J Hydrogeol Hydrol Eng* 7(2): 2.
- [19] Kumar, A., Kumar, R., Rahman, M. S., Iqbal, M. A., Anand, G., Niraj, P. K., Ali, M. (2015): Phytoremedial effect of *Withania somnifera* against arsenic-induced testicular toxicity in Charles Foster rats. – *Avicenna Journal of Phytomedicine* 5(4): 355.
- [20] Kumar, S., Bhattacharyya, J., Vaidya, A., Chakrabati, T., Devotta, S. and Akolkar, A. (2009): Assesment of the status of municipal solid waste management in metro cities, state capitals, class I cities, and class II towns in India: An insight. – *Waste Management* 29: 883-395.
- [21] Lopez, P. L., Auque, L. F., Garces, I., Chong, W. (1999): Geochemical characteristics and patterns of evolution of Salmueras superficiales del Salar de Llamara, Chile Brines surface of Salar Llamara, Chile. – *Geol. Mag. Chile* 26: 89-108.
- [22] Man-Hong H., Yong-mei, L., Guo-wei, G. (2010): Chemical composition of organic matter in domestic wastewater. – *Desalination* 262: 36-42.
- [23] Mehrotra, A., Mishra, A., Tripathi, R. M., Shukla, N. (2016): Mapping of arsenic contamination severity in Bahraich district of Ghagra basin, Uttar Pradesh, India. – *Geomatics, Natural Hazards and Risk* 7(1): 101-112.
- [24] Milton, A. H., Hasan, Z., Shahidullah, S. M., Sharmin, S., Jakariya, M. D., Rahman, M., Keithdear, and Smith, W. (2004): Association between nutritional status and arsenicosis due to chronic arsenic exposure in Bangladesh. – *Int. J. Environ. Health Res.* 14: 99-108.
- [25] Mohammadi, S., Kargari, A., Sanaeepur, H., Abbassian, K., Najafi, A., Mofarrah, E. (2015): Phenol removal from industrial wastewaters: a short review. – *Desalination and Water Treatment* 53(8): 2215-2234.
- [26] Ouyang, Y., Peng, Y., Li, J., Holmgren, A., Lu, J. (2018): Modulation of thiol-dependent redox system by metal ions via thioredoxin and glutaredoxin systems. – *Metallomics* 10(2): 218-228.
- [27] Pariatamby, A., Tanaka, M. (eds.) (2014): *Municipal Solid Waste Management in Asia and Pacific Island: Challenges and Strategic Solutions*. – Springer, Singapore.
- [28] Rehman, S., Hussain, Z., Zafar, S., Ullah, H., Badshah, S., Ahmad, S. S., Saleem, J. (2018): Assessment of ground water quality of Dera Ismail Khan, Pakistan, using multivariate statistical approach. – *Science* 37(4): 173-183.
- [29] Shaikha, B. A., Zubayed, B. R. (2013): Generation and quality analysis of greywater at Dhaka City. – *Environmental Research, Engineering and Management* 2(64): 29-41.
- [30] Song, L., Mao, K., Zhou, X., Hu, J. (2016): A novel biosensor based on Au@ Ag core-shell nanoparticles for SERS detection of arsenic (III). – *Talanta* 146: 285-290.
- [31] Tamasi, G., Cini, R. (2004): Heavy metals in drinking waters from Mount Amiata (Tuscany, Italy) Possible risks from arsenic for public health in the Province of Siena. – *Sci. Total. Environ.* 327: 41-51.
- [32] Tripathee, L., Kang, S., Rupakheti, D., Zhang, Q., Bajracharya, R. M., Sharma, C. M., ... Sillanpää, M. (2016): Spatial distribution, sources and risk assessment of potentially toxic trace elements and rare earth elements in soils of the Langtang Himalaya, Nepal. – *Environmental Earth Sciences* 75(19): 1332.

- [33] U.S. Environmental Protection Agency (1984): Characterization of Hazardous Waste Sites. A Methods Manual: Volume II. Available Sampling Methods. Second Ed. – EPA/600/4-84-076, EPA, Washington, DC.
- [34] WHO (1996): Guidelines for Drinking Water Quality, Vol. 2. Health Criteria and Other Supporting Information. 2nd Ed. – World Health Organization, Geneva.
- [35] Zacheus, O. M., Martikainen, P. J. (1997): Physicochemical quality of drinking and hot waters in Finnish buildings originated from groundwater or surface water plants. – Sci. Total. Environ. 204: 1-10.

MISTLETOE (*VISCUM ALBUM* L.) DAMAGE AND ITS ECONOMIC EFFECTS IN SCOTS PINE (*PINUS SYLVESTRIS* L.) NATURAL REGENERATION AND AFFORESTATION AREAS

ERTUĞRUL, M. H.¹ – KOMUT, O.^{2*}

¹Department of Forestry, Kürtün Vocational High School, Gümüşhane University, 29000 Gümüşhane, Turkey

²Department of Forestry, Gümüşhane Vocational High School, Gümüşhane University, 29000 Gümüşhane, Turkey

*Corresponding author

e-mail: osmankomut@gumushane.edu.tr; phone: +90-456-233-1060; fax: +90-456-233-1067

(Received 14th Sep 2019; accepted 15th Nov 2019)

Abstract. This study discusses the development of mistletoe (*Viscum album* L.) and its economic impacts on natural afforestation and regeneration areas. In this context, a total of 16 sample areas were determined in Scots pine natural regeneration and afforestation areas with resembling habitat characteristics. The occurrence status of mistletoe in Scots pine (*Pinus sylvestris* L.) individuals in these areas was determined according to stem, branch and corolla parts and morphological age determination was also conducted for the plants. Additionally, the relationship between diameter and length increase of healthy individuals, and ones affected by mistletoe were modelled with simple linear regression analysis. Besides, the tree asset values of the stands were calculated by estimating maintenance and afforestation costs at the working sites, and economic loss potential was determined through the targeted forest product revenue. Study results have revealed that natural regeneration sites are less exposed to mistletoe damage than afforestation sites. While the mistletoe exposure was found to be 27% in the study areas, it was determined that there was a potential revenue loss of 21% concerning the target economic revenue as well as additional labour and afforestation costs.

Keywords: forest cultivation, mistletoe, revenue loss, parasitic plant

Introduction

Mistletoe is an evergreen hemiparasite plant which has chlorophyll to be able to make photosynthesis and can live in the branches and trunks of trees (Yüksel et al., 2005). There are 36 genus and 1400 species of mistletoe which have been identified throughout the world. Mistletoes spread generally in temperate and tropical zones. The parasitism characteristic of mistletoe was revealed first in 305 BC. and was described for the first time by the Greek botanist Theophrastus (Janssen, 2001; Zuber, 2004). Mistletoe is part of the Santatales order of Viscaceae (Loranthaceae) family. It has three subspecies as *V. album* ssp. *album*: observed in all trees, *V. album* ssp. *austriacum*: frequently in pine species, *V. album* ssp. *abietis* in firs (Bilgili et al., 2014). Mistletoes are observed in almost all Scots pine forests spreading in Turkey (Eroğlu and Başkaya, 1995; Zuber, 2004).

Mistletoe seeds are consumed fondly by the nectar birds. The mistletoe seeds stick firmly to the branches thanks to their adhesive covering and fibres on their outer surfaces (Frochot and Salle, 1980). Often the first contamination is observed in old trees and large branches. The reason for this is explained by that birds arrive at the top of tall trees (Yüksel et al., 2005). Mistletoe seeds which sprout on individuals express themselves through the bark with the radicles. Absorbent aerial roots growing from the

radicles penetrate into the cortex and advance to the cambium of the host individual. Lateral roots advancing down and up occur from roots which reached cambium (Glatzel, 1983; Tennakoon and Pate, 1996; Anonymous, 1998). These radicles form 1-2 radicles each year, but they do not exhibit an active grow into the wood. However, they show growth as each annual ring thickness and passively enter into the wood (Yüksel et al., 2005). The mistletoe disturbs the normal growth by using the host plant's mineral nutrients via their absorbent roots, thus weakening the host plant and often it results in the loss of vital functions. Besides, they create swelling in the branches they occupy and prevent the use of these parts (Popp and Richter, 1998; Zuber, 2004; Yüksel et al., 2005). It has been reported that the anatomic parameter values of individuals with mistletoe contamination vary between 19-82% (Göl et al., 2018). It is known that the volume and quality of timber to be obtained from logs are also affected by natural and ecological conditions (Mutanen and Toppinen, 2007; Malinen et al., 2015; Merganič et al., 2016; Gejdoš et al., 2019). It is also reported that biotic and abiotic pests have important effects on this issue (Fidan et al., 2016; Yaşar et al., 2016).

It is recommended that cleansing the mistletoe contaminated trunk parts by scraping and preventing any contact of these parts with sunlight and air are among recommended precautions. In the case that the mistletoe is observed on the branches, it is recommended that these branches are cut and removed (Yüksel et al., 2005). It is found that mistletoe affects the industrial use of the tree as well as economic losses because of the maintenance works which would be conducted. In addition, anomalies in the wood-based products introduced to the market adversely affect the demand of consumers (Öztürk, 2010).

In this study, it is aimed to determine the effect of mistletoe on the increase and growth, thus to determine the economic loss it causes by investigating Scots pine afforestation and natural regeneration areas in terms of mistletoe exposure.

Materials and methods

Materials

Research was conducted in Gumushane province of Turkey. Natural rejuvenation and afforestation areas within the borders of Gümüşhane Forest Management Directorate were selected as the study area. The working area is between 40° 32' and 40° 14' northern latitudes and 39° 56' and 40° 20' east longitudes (*Fig. 1*). In this context, the attention has been paid to work in areas where there are no significant elevation differences, slope and habitat differences in order to better deliver the differences between natural regeneration areas and afforestation areas. The average elevation of the study area has been measured as 1690 m in natural regeneration areas and as 1710 m in afforestation areas.

Sampling areas were determined as a result of the investigations for natural regeneration areas and afforestation areas which do not have slope, elevation and serious elevation differences under the same habitat conditions, by using the current stand map (*Fig. 2*).

Eight sample areas have been determined in the 162 numbered natural regeneration area which is 16.9 ha, 8 sample areas have been determined in the 207 numbered afforestation area which is 26.8 ha, and in total 16 sample areas have been determined. These areas have been determined as 100 m² in Çsa natural regeneration areas which are in "a" age and as 200 m² in Çsab afforestation areas, which are in "ab" age, as stated in

the management plans. The difference of the sample size of the selected area was due to the different size of the area of natural regeneration and afforestation. The stands of the selected sample areas have been transformed into Google Earth image by digitizing the existing stand maps with the help of Netcad program. Field works were carried out in April and May 2018.

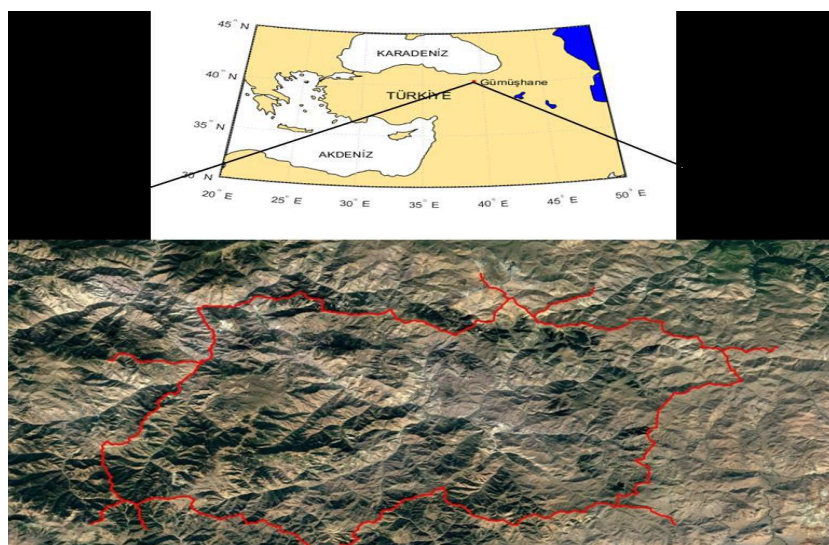


Figure 1. General location of the research area

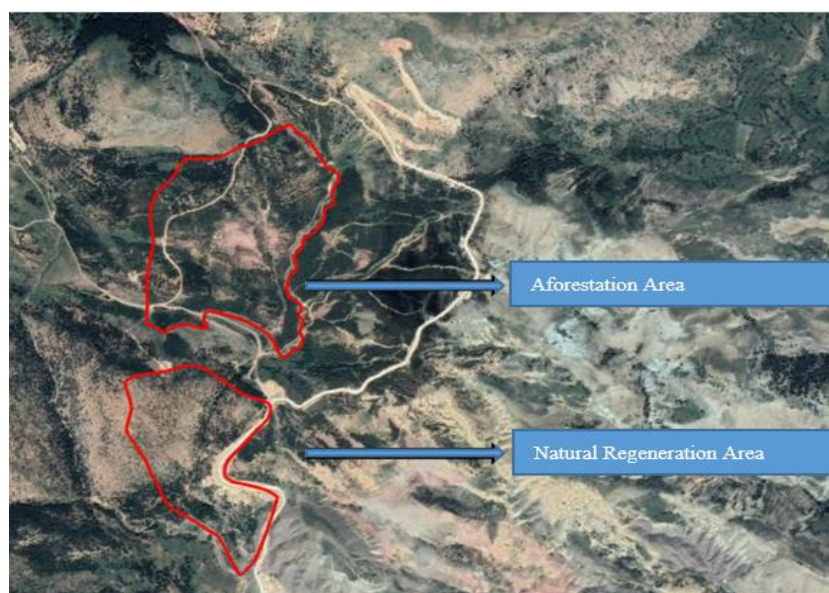


Figure 2. Sample areas of the research area

Methods

Diameter and length measurements were conducted for each tree in the sampling areas. On the other hand, the mistletoe age was determined with the morphological age determination method for individuals in the sampling areas. The diameter of the trees

was measured as d_{130} diameter by using a calliper. The length of the trees was measured with the help of SILVA CM 10152025 LA DP slope and length measuring compass. In this study, each tree has been divided into three parts as trunk, branch and canopy and mistletoe contamination conditions were determined in all trees that were analyzed. In this study, the power of mistletoe infection was evaluated on the basis of contamination on the top, branch and trunk of the tree, the age of exposure of the trees to the infection and the age of the mistletoe detected. The parameters of the infected and non-infected trees were evaluated together in order to analyze the effects of mistletoe on the development of individuals.

In order to determine the relationship of mistletoe contamination in the sampling areas with the diameter and length, t-test application was carried out with the help of the SPSS program. T-test, which is used to determine the differences between the variances of 2 independent variables, was utilized in order to identify whether or not there is a difference between the determined natural regeneration areas and afforestation areas for mistletoe contamination. In addition, one-way variance analysis and Tukey HSD Post-Hoc test were applied for identification of the difference in the sample areas in terms of contamination status.

Simple linear regression analysis was conducted to form the growth models of healthy individuals and individuals where mistletoe was observed. The tree assets cost value of the research area was determined primarily, in order to determine the economic value losses that might arise because of the mistletoe observed in natural regeneration and afforestation areas (Türker, 2013). In this context, afforestation costs, land value, annual administration costs, interest rates and economic revenue obtained as a result of the previous maintenance interference were determined. On the other hand, the economic damage of Forestry Managements (FM) from 1 m³ Scots pine wood product has been determined by assuming that mistletoe spread has stopped. While calculating this loss, the product classes which Gümüşhane FM can obtain in the future and today have been taken into consideration.

Tree assets cost value (TACV) was calculated with *Equation 1* (Türker, 2013).

$$ASMD = (c + B + V) * 1.0P^m - (B + V) - (D_a * 1.0P^{m-a} + \dots) \quad (\text{Eq.1})$$

c: cost of afforestation, B: land value, V: annual administration costs, P^m: interest rate, P^{m-a}: the revenue received with the inference maintenance conducted before.

Results and discussion

In the natural regeneration and afforestation areas, 330 Scots pine individuals were examined in the 16 sample areas.

It was determined that 19 of 203 individuals were determined to be exposed to mistletoe in the natural regeneration area and 60 of 127 individuals were determined in the afforestation area (*Table 1*).

Afforestation areas were identified to be exposed to more mistletoe damage than natural regeneration areas. On the other hand, the mistletoe was found out to be the most effective on the trunks of the individuals, the least damage occurred on the top parts (*Fig. 3*). Age measurement was neglected due to the evaluation that the ages of the individuals in the sample areas where the study was conducted were approximately the same.

Table 1. The main findings concerning the study area

Sample field attribute	Sample field	Number of trees in sample area	d ₁₃₀ diameter average (cm)	Length average (cm)	Number of trees infected with mistletoe
Natural regeneration	1	9	9.44	460	4
	2	14	5.21	290	2
	3	61	3.06	200	4
	4	7	11.5	650	4
	5	13	6.15	300	1
	6	50	3.77	240	3
	7	16	1.43	84	1
	8	33	9.75	598	0
	Total	203	-	-	19
Average	25.38	6.29	352.75	2.38	
Afforestation	1	22	11.52	518	2
	2	17	13.16	494	8
	3	7	15.25	487	2
	4	9	15.83	622	4
	5	13	12.05	437	7
	6	17	10.97	491	8
	7	18	9.03	450	10
	8	24	10.65	439	19
	Total	127	-	-	60
Average	15.88	12.31	492.25	7.5	
Total	16	330	-	-	79
Average	-	20.63	9.30	422.50	4.94

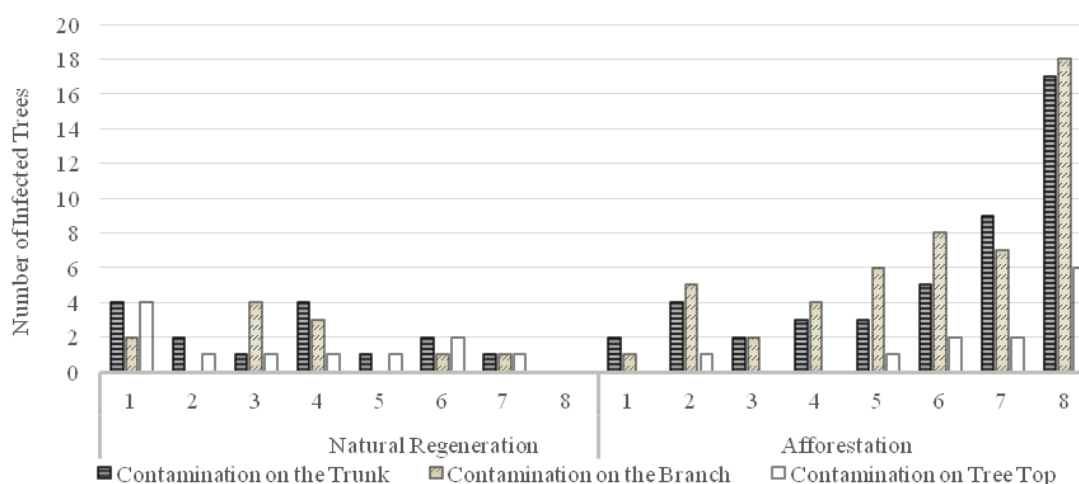


Figure 3. Contamination status of mistletoe damage to trunk parts

In the evaluations conducted, it is determined that the mistletoe occurs especially in the trunk parts, which is valid for both natural regeneration and afforestation areas. On the other hand, it was found out that the contamination to the top of the individuals in

the natural regeneration areas has occurred earlier and close to the time of the occurrence in the trunk. In afforestation areas, it was found that the contamination to the top of the trees occurred approximately 3 years after the contamination to the trunk (Fig. 4). As a result of the morphological age measurement, the average mistletoe age detected in the trunks was detected as 6 in the natural regeneration area, the average mistletoe age was detected as 4 in the branches and the average mistletoe age was detected as 4 in the canopy. In the afforestation areas, the mistletoe age was observed as 7 in the trunk, the mistletoe age was observed as 6 in the branch and the mistletoe age was observed as 3 in the canopy. As a result of the field study conducted, mistletoe contamination was detected in 15 sampling areas and no mistletoe was observed in only 1 area.

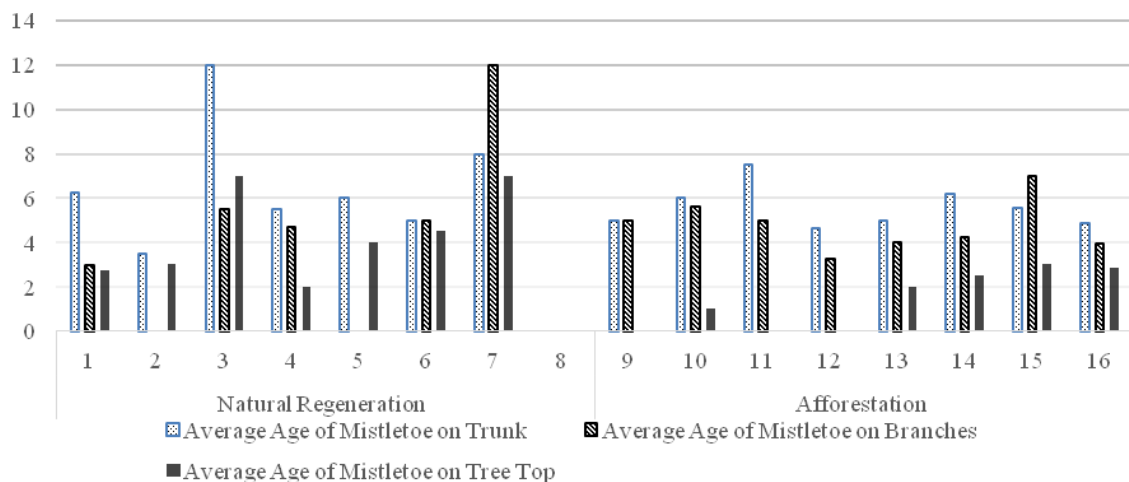


Figure 4. Mistletoe age status in the sample areas

As a result of the Single Sample T-Test we carried, it was found that the mistletoe exposure has increased as the d_{130} diameter and length of the individuals increased in the study areas. It can be said that the difference in question arose from the fact that mistletoe can receive more water and mineral nutrients from individuals with good diameter increase and thus show better development. Eroğlu and Başkaya (1995) have proved that mistletoe leads to an increase in the loss with 16-55% in the Scots pine individuals. It has been revealed in previous studies that mistletoe gets completely deteriorated of its closure as a result of fire, grazing and irregular exploitation and that it has affected negatively the stand increase by 8.5-16.5% in Sürmene-Çamburnu Scots pine forests (Sönmez, 2014). Sekendiz (1984) states that the annual increase loss of individuals will be 20% in the situations where the mistletoe is dense. Therefore, the processing of low diameter logs from these trees will decrease productivity and increase processing costs (Rast, 1974; Luppold and Bumgardner, 2019).

Conducted analyses showed that mistletoe exposure has occurred at a higher level in long individuals (Fig. 5). This difference can be said to be due to the fact that mistletoe can get more water and mineral nutrients from individuals with good length increase and thus enable better development. In a previous study, mistletoe was found to negatively affect the development of scots pine by 47% (Sönmez, 2014). Çatal and Carus (2011) found in a different study they carried out that the adverse impact of mistletoe is in the range of 26-63%. Similarly, Kanat et al. (2010) reported that

mistletoe negatively affected 22% increase in diameter in larch. Besides, Eroğlu (1993) has shown that the chemical structure of wood is deteriorated in scots pine individuals, where mistletoe contamination is observed, and therefore its usage properties are affected by this situation. According to Eroğlu and Başkaya (1995), while the rate of trees that dried in these forests was 1-2% per year ten years ago, it increased to 3.5% in recent years.

On the other hand, it is determined that mistletoe spread occurs more densely in afforestation areas than natural regeneration areas. All together statistically significant ($p < 0.05$) differences were identified between these areas in terms of mistletoe contamination (Fig. 5). The reason for this situation can be said to be that the afforestation areas are close to the old stands where mistletoe spread is observed, and the maintenance works conducted in these areas decrease the closeness. On the other hand, the presence of dense mistletoe which is detected especially in seed trees in natural regeneration areas has been observed to affect the young scots pine individuals living nearby.

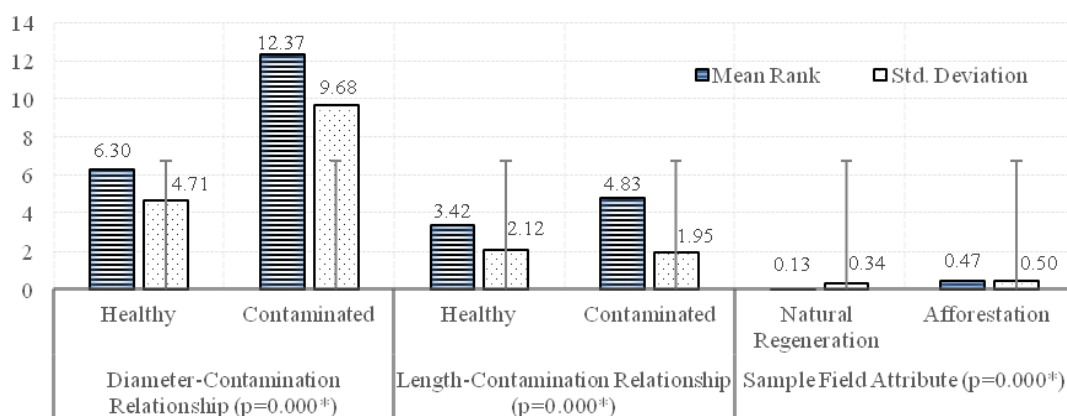


Figure 5. Statistical comparisons concerning mistletoe contamination

The results of the statistically significant differences between the sampling areas are given in Table 2 in terms of mistletoe exposure. According to this, only difference were found between the sample areas 4 and 8 in natural regeneration sample areas. In the afforestation sample areas, the differences were identified between field 9, field 15 and 16. On the other hand, the differences were determined between all-natural regeneration and afforestation sample areas except for areas 1 and 4. Table 2 shows the differences between the natural rejuvenation sample sites with (○), the differences between the afforestation sample sites with (●) and the differences between the two sites with (◐).

The findings concerning simple linear regression analysis conducted on healthy and mistletoe contaminated individuals in natural regeneration areas and afforestation areas are given in Table 3. In the study conducted on healthy and mistletoe contaminated individuals, the length was chosen as a variable depending on diameter and growth model equation, which reveals length values of individuals with respect to diameter, was developed (Table 3; Eqs. 2 and 3).

The obtained growth model revealed that mistletoe has an ever-increasing negative effect on the development of individuals. It has been emphasized in previous studies that the scots pine individuals in natural regeneration and afforestation areas lose their vital functions because of the mistletoe pest (Yüksel et al., 2005).

Table 2. Differences between sample areas according to the Tukey HSD post-hoc test

Sample areas		Natural regeneration								Afforestation							
		1	2	3	4	5	6	7	8	9	10	11	12	13	14	15	16
Natural regeneration	1																
	2																●
	3										●		●	●	●	●	●
	4							○									
	5															●	●
	6																●
	7															●	●
	8										●			●	●	●	●
Afforestation	9														●	●	
	10			●					●								
	11																
	12																
	13			●					●								
	14			●					●								
	15			●				●	●	●							
	16		●	●		●	●	●	●	●							

Table 3. Simple linear regression analysis results for length variable according to diameter

Variables		B	Std. error	Beta	t	p
Infected individuals	Constant	3.912	0.318	0.369	12.301	0.000*
	Diameter	0.074	0.020		3.663	0.000*
Healthy individuals	Constant	0.999	0.121	0.867	8.231	0.000*
	Diameter	0.386	0.015		24.953	0.000*

P < 0.05

The length equation in individuals where mistletoe is observed:

$$Length = 3.912 + 0.074 * d_{1,30} \quad (Eq.2)$$

Length equation in healthy individuals:

$$Length = 0.999 + 0.386 * d_{1,30} \quad (Eq.3)$$

The regression analysis trend graph to determine the relationship between diameter and height in the measured individuals is given in *Figure 6a* for healthy individuals and *Figure 6b* for infected individuals.

It is thought that the maintenance interferences which the Scots pines exposed to mistletoe undergo until they lose their vital functions may cause a serious cost burden to the FMs. It was calculated that the annual maintenance cost covering the parameters such as identification and marking of the future trees, determination of the individuals to be cut off from the field and removal of these individuals from the field, labour costs and transportation expenses have been estimated as 78.81 \$/ha. It has been determined that the land value is 78.81 \$/ha and the annual land expenses are 12.26 \$/ha from the records of Gümüşhane Forest Management Directorate.

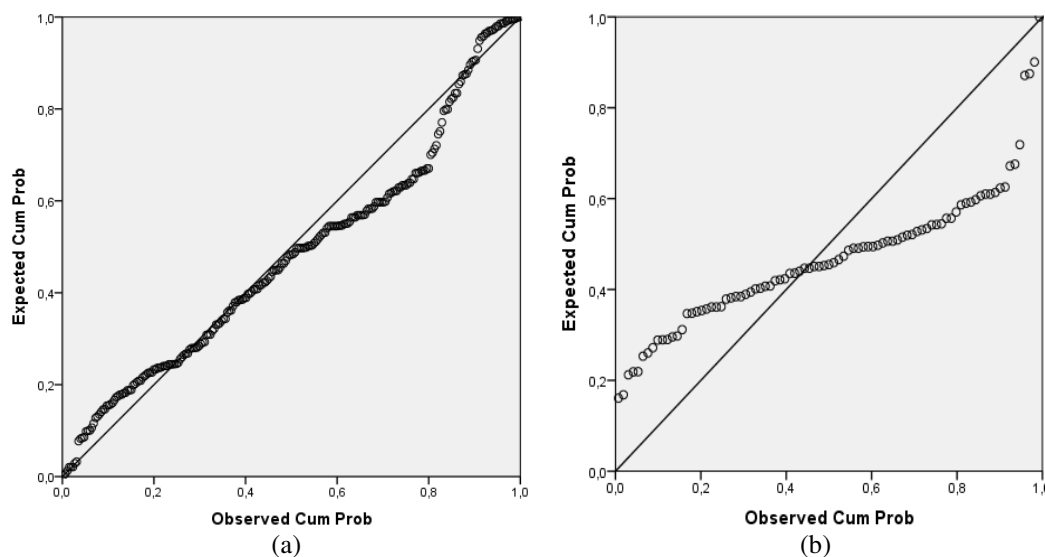


Figure 6. Statistical comparisons concerning mistletoe contamination

The products occurred in the maintenance of healthy individuals with d_{130} chest diameters of more than 8 cm are offered for sale in forest depots or ramps at a cost value. The products formed during the maintenance processes of the individuals with mistletoe contamination are put upon to the market as firewood regardless of the product class. The absence of any enterprises producing paper, fibre and particle boards in the region can be said to increase the revenue loss of FMs in the products where mistletoe contamination is observed.

It is understood that the afforestation and natural regeneration areas will lose the economic value of the individuals in the areas to a great extent before reaching the targeted administration period due to the mistletoe damage. Therefore, the necessity of reforestation of these areas emerges. Gümüşhane Forest Management Directorate, the unit responsible for the study area of this research, reported that the cost of reforestation in these areas is 874.29 \$/ha and the cost of regeneration is 524.58 \$/ha.

In the tree assets cost estimations we conducted (TACV), it was determined that 10 years ago 338.38 \$ product was obtained from the area and that the stands were at the end of the 1st year class, meaning 20 years old, by making use of the management plans. As a result of the analysis, the TACV was identified to be approximately 1224.86 \$. Besides, it was found that mistletoe caused approximately 21% loss from each targeted 1 m³ forest product revenue in the study areas where the average contamination was found as 27% (Table 4). In the determination of this damage, the cost of firewood was taken into consideration for all targeted forest product varieties.

Table 4. The damage detected in the target forest products

Product type	Price (\$/m ³)	Economic damage (\$/m ³)	Economic damage rate (%)
Log	27.32	5.85	21
Mine pole	23.06	4.79	21
Pole	20.22	3.64	18
Paper firewood	18.80	4.08	22
Average	22.35	4.59	21

Conclusions

The results of this study have proved that mistletoe can be effective in both natural regeneration and afforestation areas. The average contamination rate was determined as 27%. On the other hand, it is understood that mistletoe has an average revenue loss potential of 21% for the target forest products for the research areas. However, in the case that a decrease in revenue loss and forest products in the desired quality are wanted, additional costs must be endured.

According to the results of the study, mistletoe is more effective in afforestation areas when compared with natural regeneration areas in terms of distribution. Seed trees where mistletoe has occurred in the natural regeneration areas have an important effect on the increase of mistletoe spread in these areas.

At the same time, mistletoe occurrence negatively affects length and diameter growth in individuals. Therefore, it is seen that mistletoe causes quality and quantity loss in terms of forest products in natural regeneration and afforestation areas.

In future research, it will be useful to consider the effect of mistletoe on natural rejuvenation and afforestation sites on the basis of different tree species.

Acknowledgements. This study is a part of a master thesis entitled “The Increment-Growth Relationships and Economic Conditions of Scots Pine Natural Regeneration and Afforestation Areas: Gümüşhane Case” prepared by Murat Han ERTUĞRUL under the supervision of Assistant Professor Osman KOMUT in Gümüşhane University. This research was supported by Gümüşhane University Scientific Research Projects Coordinator (Project No: 18.B0122.07.01).

REFERENCES

- [1] Anonymous (1998): <http://www.parasiticplants.siu.edu/Viscaceae/index.html>.
- [2] Bilgili, E., Eroğlu, M., Yavuz, H., Yılmaz, M. (2014): Determination of the spread of mistletoe (*Viscum album* L.) on Scotch pine (*Pinus sylvestris* L.) stands in Eastern Black Sea Region and modeling of its effect on diameter increase. – TUBITAK Project, Project No: 1120258, Trabzon.
- [3] Çatal, Y., Carus, S. (2011): Effect of pine mistletoe on radial growth of Crimean pine (*Pinus nigra*) in Turkey. – J. Environ. Biol. 32: 263-270.
- [4] Eroğlu, M. (1993): Mistletoe (*Viscum album* L.) in Scots Pine forests. – Journal of Forest Engineering 7: 6-10.
- [5] Eroğlu, M., Başkaya, Ş. (1995): Causes and consequences of severe damage of mistletoe (*Viscum album* L.). – Journal of Forest Engineering 4(32): 25-31.
- [6] Fidan, M. S., Yaşar, Ş. Ş., Yaşar, M., Atar, M., Alkan, E. (2016): Combustion characteristics of impregnated and surface treated chestnut *Castanea sativa* Mill wood left outdoors for one year. – BioResources 11(1): 2083-2095.

- [7] Frochot, H., Salle, G. (1980): Methods of dispersal and implantation of mistletoe. – *Revue-Forestiere-Francaise* 32(6): 505-519.
- [8] Gejdoš, M., Lieskovský, M., Giertliová, B., Němec, M., Danihelová, Z. (2019): Prices of raw-wood assortments in selected markets of central Europe and their development in the future. – *BioRes.* 14(2): 2995-3011.
- [9] Glatzel, G. (1983): Mineral nutrition and water relations of hemiparasitic mistletoes a question of partitioning experiments with *Loranthus europaeus* on *Quercus petraea* and *Quercus robur*. – *Oecologia* 56(2-3): 193-201.
- [10] Göl, Ç., Serdar, B., Öztürk, M., Kadir, A., Bilgili, E. (2018): *Viscum album* L. subsp. *austriacum* (Wiesb.) Vollman (Pine mistletoe) effect of *Pinus sylvestris* L. (Scots Pine) on wood elements. – *Duzce University Journal of Science and Technology* 6: 1354-1363.
- [11] Janssen, T. (2001): Zur gemeinen Mistel (*Viscum album* L.). – *Forst und Holz* 56: 215-219.
- [12] Kanat, M., Alma, M. H., Sivrikaya, F. (2010): The effect of *Viscum album* L. on annual diameter increment of *Pinus nigra* Arn. – *African Journal of Agricultural Research* 5(2): 166-171.
- [13] Luppold, W. G., Bumgardner, M. S. (2019): Changes in the quality of the Northern U.S. hardwood timber resource from 2008 to 2017. – *BioRes.* 14(3): 6304-6315.
- [14] Malinen, J., Haring, M., Kilpeläinen, H., Verkasalo, E. (2015): Comparison of alternative roundwood pricing systems - a simulation approach. – *Silva Fenn.* 49(3): 1293.
- [15] Merganič, J., Merganičová, K., Marušák, R., Tipmann, L., Šálek, L., Dragoun, L., Stolariková, R. (2016): Relation between forest stand diversity and anticipated log quality in managed Central European forests. – *International Journal of Biodiversity Science, Ecosystem Services & Management* 12(1-2): 128-138.
- [16] Mutanen, A., Toppinen, A. (2007): Price dynamics in the Russian–Finnish roundwood trade. – *Scand. J. Forest Res.* 22: 71-80.
- [17] Öztürk, A. (2010): Artvin Forest Regional Directorate participating in auction sales determination of customers' demands and expectations. – *Artvin Çoruh University Faculty of Forestry Journal* 11(2): 61-73.
- [18] Popp, M., Richter, A. (1998): Ecophysiology of Xylem-Tapping Mistletoes. – In: Behnke, H.-D. et al. (eds.) *Progress in Botany: Genetics Cell Biology and Physiology Ecology and Vegetation Science*. Springer, Berlin, pp. 659-674.
- [19] Rast, E. D. (1974): *Log and Tree Sawing Times for Hardwood Mills*. – Research Paper NE-304. U.S. Department of Agriculture, Forest Service, Northeastern Forest Experiment Station, Upper Darby, PA.
- [20] Sekendiz, O. A. (1984): Important insects in our forests can be seen bark beetles. – *Scolytidae (Apidae) Family Species, Protection and Control Methods*, 16-24 April 1984, Antalya-İncekum Forest Insect and Diseases Seminar.
- [21] Sönmez, T. (2014): The effect of mistletoe on the development of Scots Pine (*Pinus sylvestris* L.). – *Artvin Coruh University Journal of Forestry Faculty* 15(1): 64-72.
- [22] Tennakoon, K. U., Pate, J. S. (1996): Effects of parasitism by a mistletoe on the structure and functioning of branches of its host. – *Plant Cell and Environment* 19(5): 517-528.
- [23] Türker, M. F. (2013): *Forestry Business Economics. Updated and Expanded 2nd Ed.* – Foundation for the Protection of Forestry and Nature Publication No. 5.
- [24] Yaşar, Ş. Ş., Fidan, M. S., Yaşar, M., Atar, M., Alkan, E. (2016). Determining the effect of seasonal variation in spruce *Picea orientalis* L. wood treated with various impregnations on combustion resistance. – *BioResources* 11(4): 9467-9479.
- [25] Yüksel, B., Akbulut, S., Keten, A. (2005): Damage, biology and control of Pine Mistletoe (*Viscum album* ssp. *austriacum* (Wiesb.) Vollman). – *Süleyman Demirel University Journal of the Faculty of Forestry* 2: 111-124.
- [26] Zuber, D. (2004): *Biological Flora of Central Europe: Viscum album* L. – Geobotanisches Institut ETH, Zürich.

EFFECT OF SILICON ON PHYTOCHEMICAL AND MEDICINAL PROPERTIES OF *ALOE VERA* UNDER COLD STRESS

AZARFAM, S. P.^{1*} – NADIAN, H.² – MOEZZI, A.³ – GHOLAMI, A.¹

¹*Department of Agriculture, Islamic Azad University, Ahvaz, Iran
(phone: +98-91-3326-7562; fax: +98-21-7751-7398)*

²*University of Agricultural Sciences and Natural Resources of Ramin, Ahvaz, Iran
(phone: +98-91-6113-3710; fax: +98-21-7751-7398)*

³*University of Shahid Chamran, Ahvaz, Iran
(phone: +98-91-6313-9813; fax: +98-21-7751-7398)*

**Corresponding author*

P.azarfam2018@gmail.com; phone +98-91-2135-0769; fax +98-21-7751-7398

(Received 11th Aug 2018; accepted 2nd Jan 2019)

Abstract. Plants use the enzymatic and non-enzymatic antioxidant defense mechanisms to avoid and/or tolerate environmental stresses. As a useful element in plants, silicon plays an important role in activating these defense systems and thus in improving plant resistance to environmental stresses. The present research studied the effect of silicon on important antioxidants including Super Oxide Dismutase (SOD) and Catalase (CAT) and also on glucomannan, mannose, and aloin in *Aloe vera*. 60 *Aloe vera* plant of *Aloe barbadensis* Mill variety were taken. After applying the fertilizer treatments during cold stress treatment, 30 pots were placed at 25 °C (control) and 30 pots at 4 °C (stress), and then fertilizer side-treatments were applied. During their growth, the plants were treated with various silicon concentrations (500, 1000, 1500, and 2000 mg/l). Ninety days after they were planted, 30 of the plants were separated and exposed to cold stress at 4 °C for seven days. After applying the cold stress treatment, leaf samples were taken and analyzed simultaneously from treated and untreated plants. Results of ANOVA showed that cold stress and silicon treatments had significant effects on SOD, CAT, glucomannan, mannose, and aloin. Application of cold stress increased SOD and CAT activities and reduced glucomannan, mannose, and aloin concentrations. Increases in silicon concentration improved both enzymatic antioxidant activity and concentrations of soluble sugars and of aloin in *Aloe vera*. These results indicate that silicon plays a key role in enhancing plant defense systems against cold stress. Therefore, application of silicon fertilizers is of great importance in reducing losses caused by climatic stresses and in achieving the goals of sustainable agriculture.

Keywords: *antioxidant, aloe vera, silicon, plant resistance, sustainable agriculture*

Introduction

Among the various biotic stresses, cold stress or low temperature (LT) is one of the common important climatic factors that limit plant growth and yield (Adam and Murthy, 2014). It has been estimated that more than 15 percent of global agricultural products are lost annually due to frost damage (Zou et al., 2007). This type of stress also occurs repeatedly in Iran every year and inflicts heavy losses on farmers and orchard owners (Talebi, 2013). Considering the ever-growing human population and the purpose of developing sustainable agriculture and food security, enhancement of plant resistance to environmental stresses becomes important (Liang et al., 2015).

Plants continuously respond to changes in their surrounding environment and develop various efficient mechanisms to adapt themselves in the best possible way to various stresses in order to survive. Use of enzymatic and non-enzymatic antioxidant

systems is among the important strategies that plants employ to avoid and/or tolerate environmental stresses (Jung, 2004). In recent years, many advances have been made in understanding the mechanisms and processes involved in defensive adaptation to abiotic stresses in various plant species (Adam and Murthy, 2014). When faced with stresses, reactive oxygen species (ROS_s) such as superoxide anions (O²⁻), hydroxyl radicals (OH), and hydrogen peroxide (H₂O₂) are excessively produced in plants. This increases cellular antioxidant potential that causes oxidative damages in plants (Ali and Alqurainy, 2006). Production of ROSs at times of stress is a natural metabolic process that happens in cells of all aerobic organisms (Alsher et al., 1997) and plays a very important role in activating the defensive system against biotic and abiotic stresses (Bafana et al., 2011). Due to the limitations in the quantities of NADP⁺, one of the sites where ROSs may form is in the electron transfer chain. Induction of ROSs starts the processes of Lipid Per Oxidation (LPO) and also degradation of protein, pigments, and other cellular compounds (Allen, 1995; Balakhnina et al., 2010; Halliwell, 1984). Therefore, plants have efficient antioxidant defense systems to detoxify these ROSs and reduce damages that they cause (Gill and Tuteja, 2010). These defense systems consist of molecular antioxidants and antioxidant enzymes that degrade ROSs (Larson, 1988). The enzymatic antioxidant system includes several efficient enzymes such as SOD and CAT, guaiacol peroxidase, ascorbate peroxidase, and glutathione reductase (Asada, 2006; Gunes et al., 2007b). The first enzyme to detoxify these reactive oxygen species in plants is SOD that converts superoxide into H₂O₂ and O₂ and protects cells against the oxidative stress resulting from superoxide. Nevertheless, H₂O₂ is also toxic to cells and is detoxified into water and oxygen by CAT (Zhu et al., 2010). Plant's ability to activate its defense mechanism against oxidative degradation is a key link in its mechanism of tolerance to unfavorable environmental conditions. Any change in the activity level of one or more antioxidant enzymes influences plant resistance to stressful factors (Bennicelli et al., 2005).

In addition to using the enzymatic antioxidant defense system, plants react to stress by accumulating compatible solutes such as proline (Gzik, 1997), glycinebetaine (Mansour, 1998), carbohydrates (Balibrea et al., 1997), and polyol (Kumar and Bandhu, 2005). One of the common features of compatible solutes is that they can accumulate to high levels without interfering with natural biochemical reactions (Zhang et al., 2004). In fact, they are hydrophilic and can replace water on the surface of proteins, protein complexes or membranes without disrupting their structure and function (Bohnert and Shen, 1999). These compounds can reduce the inhibitory effects of high concentrations of ions on the activities of the enzymes through fixation of proteins, protein complexes, or membranes under environmental stresses (Bohnert and Shen, 1999; Ashraf and Foolad, 2007). Moreover, compatible solutes may act as absorbers of reactive oxygen species (Seckin et al., 2009; An and Liang, 2013). As a non-toxic and protective osmolyte in higher plants, proline is usually involved in tolerance to salinity (Flowers et al., 1986).

***Aloe vera* and its derivatives**

Aloe vera is a succulent plant species of the genus *Aloe*. An evergreen perennial, it is a stemless or very short-stemmed plant. The leaves are thick and fleshy. The margin of the leaf is serrated and has small white teeth. It has a variety species. *A. vera* is considered to be native to Africa. Different species of *Aloe vera* spread widely in North Africa as well as hot mountains in Africa, Madagascar, and Jordan. Some African native *Aloe vera* species are very similar to the tree (Royal Botanical Garden, 2014).

As a medicinal plant, *Aloe vera* plant is widely used in the medicinal, cosmetics and health sectors. *Aloe vera* plant contains chemical compounds and strong complexes, vitamins, enzymes, minerals, sugars, lignin, saponin, amino acids, and fats. Due to its many properties in the treatment of various diseases, *Aloe vera* has a worldwide reputation as a magic or multi-use plant. Some properties of *Aloe vera* plant include: gastric and duodenal ulcer treatment, ileus treatment, laxative, glucose and cholesterol regulator, kidney stones treatment, improving liver function, hemorrhoid treatment, reducing anemia, treatment of migraines, weight loss, reducing heartburn and brash, anti-stress, providing essential amino acids for the body, eczema treatment, fungicide, fast antipyretic, hair tonic, arthritis treatment, etc (Shelton, 1991).

Aloe vera requires high temperatures, light soil, and intense sunlight for growth and reproduction. Excessive accumulation of water around the root is a limiting factor in the growth of *Aloe vera*, which can result in root rot and attack of pathogenic fungi to the root of the plant (Royal Botanical Garden, 2014). The low temperature, especially the temperature that causes the plant's gel to freeze, can disrupt all the meristem activities of the plant, and thereby prevent it from survival. High salinity is another limiting factor in plant growth.

In the green leaf area of the *Aloe vera*, 20 species of anthraquinone, which is a phenolic compound, are found. Aloin and emodin are two well-known anthraquinones in *Aloe vera*. In addition to being known as a strong antibacterial and antiviral, these two compounds can prolong cell life and prevent live cell death. These two compounds contribute to destroy cancer cells, heal wounds, and strengthen the immune system. Two types of aloin, i.e. barbaloin and nataloin, with nitric acid under thermal condition and with fumingic acid under cold condition, produce oxalic acid, aloetic acid, and chismatic acid.

Considering the importance and great properties of the *Aloe vera* plant and its cultivation at a very broad level, it is obvious that in order to have a healthy plant containing large quantities of white chemicals, the plant should provide with proper nutrition through supplying all nutrients and water needs as well as suitable temperature conditions. According to the plant nutrition science, it can be achieved the maximum plant growth as well as the best possible quality of the elements by providing maximum nutrients with appropriate concentrations, adjusting the pH of the food solution, the proper ratio of minerals to organic elements in the plant nutrition. With a proper nutrition, it can maximize the concentrations of the resulted elements from the plant, which will result in cost savings and increased yield per unit area. Maximum production quality and plant growth can be achieved by using chemical and organic codes.

References review

Many studies have shown that not only does silicon improve plant growth and yield (Ahmed et al., 2011; Balakhnina et al., 2012; Gunset al., 2007a; Ma et al., 2004; Savant et al., 1997; Hattori et al., 2005) but it also plays a key role in activating the enzymatic and non-enzymatic defense mechanisms of plants against biotic and abiotic stresses (Richmond and Sussman, 2003; Ma and Yamaji, 2006; Liang et al., 2007; Kim et al., 2011; Van Bockhaven et al., 2013). Molecular and biochemical mechanisms of silicon in relation to increases in plant resistance to stress are not well-known and require further research (Sivanesan and Park, 2014). Therefore, the present research intended to study the effect of silicon on some of the important antioxidant enzymes and phytochemical compounds in *Aloe vera*.

Murillo-Amador et al. (2014) investigated the effect of salinity on minerals and various chemicals found in *Aloe vera*. They investigated the effect of various concentrations of sodium chloride on proline concentration, phosphor-phenyl carboxylate enzyme in parenchyma and chlorophyll. They concluded that when salinity increased, the concentrations of proline and pepase enzyme increased in both parenchyma and chlorophyll. However, with increasing salinity, total protein concentration increased in parenchyma but decreased in chlorophyll.

Materials and methods

The greenhouse location

The experiment was carried out in No. 256, the greenhouse townhouse, in the Hashtgerd region located West of Alborz province in the Iran. Hashtgerd is located in the central part of Savojbolagh.

Hydroponic greenhouse

The greenhouse is of Dutch type with two layer coating of UV and anti-fog, and has a gas-fired heating system, fan cooling system, and side and ceiling valves. The greenhouse is equipped with an automatic temperature and humidity control system. The moisture and temperature data are measured by sensors and thermometers and instantaneously transmitted to the central processing system of the greenhouse. If the greenhouse humidity exceeds the limit, the processing center will immediately order the automatic opening of the side and ceiling valves, with the help of control switches. When the moisture content reaches the optimum level, the valves closing command is again given. In the case of insufficient moisture, the fog system automatically adjusts the moisture content. In the case of temperature sensors, if the temperature exceeds the programmed limit, the fan and pad system start until the desired temperature reaches. If the greenhouse temperature is lower than the desired temperature, the greenhouse processing unit will order turning on the heating system (gas-fired heaters). All information sent to the processing center is evaluated and, given the temperature and humidity requirements, the operating instructions are executed by the micro-switches. The irrigation system consists of two 5000-L reservoir tanks, a pumping system including pump and its related connections, as well as transmission lines and a nutritional solution collection system that is spaced 50 cm from each other. The whole greenhouse floor is concreted, sloped, and drained. The hydroponic greenhouse is of closed type, and nutritional solution is collected into the reservoir after watering the pots and restored to the system.

At first, 60 pots were placed in greenhouses 1 and 2 (30 pots per greenhouse). It should be noted that the greenhouses were divided into two equal parts of five 500 m by polyethylene coating.

A completely randomized factorial design including 2 temperature treatments, 2 silica fertilizer treatments, 5 silica surface treatments, each with three replications, and a total of 60 plots, were designed and implemented.

Aloe vera cultivation

60 *Aloe vera* plant of *Aloe barbadensis* Mill variety were taken. After applying the fertilizer treatments during cold stress treatment, 30 pots were placed at 25 °C (control) and 30 pots at 4 °C (stress), and then fertilizer side-treatments were applied.

Irrigation time

Each pot is irrigated for half an hour with two drippers with a flow rate of 4 L/h. Three irrigation were determined along with two hydroponic nutritional solutions at 10 am and 17 pm.

Sampling

Step 1: Before the temperature was reduced, sampling from the second leaves was performed in order to investigate and compare the effect of temperatures of 25 °C and 4 °C in greenhouse No. 2. According to standard condition, the samples were sent to the Standard Reference Laboratory of Iran to perform measurement tests of SOD, CAT, glucomannan, mannose, and aloin.

Step 2, after applying cold stress: According to the previous research (Liang et al., 2008), the activity of SOD and catalase increased and reached the maximum level in rape and wheat after 7 and 4 days of cold stress, respectively. Nayyar and Walia (2003) studied the 14-day seedlings under cold stress. They observed that reducing temperature to 4 °C increased the ion permeation, while adaptation to a low temperature of 10 °C for 6 days reduced the production of hydrogen peroxide LTS.

In order to compare the effect of reducing temperature in the greenhouse No. 2 after 7 days, sampling was carried out and the samples were sent to the Laboratory of National Genetic Bank Center (Standard Reference Laboratory, Iran), according to standard conditions. The comparison of fertilizer treatments means as well as the fertilizer treatment and temperature interaction are specified in *Table 3*. Temperatures of 25 °C and 4 °C correspond to before and after applying the cold stress, respectively (Control = 25 °C, cold stress = 4 °C). The zero concentration of silica (ppm = 0) is related to the control treatment, where no fertilizer treatment was applied.

Nutritional solution

At the first of the season, the temperatures of the both greenhouses were set at 25 °C. Then the pots were irrigated with water containing nutritional solution. Irrigation with water containing nutritional solution was performed daily, at 10 am and 17 pm, for 30 min. The nutritional solution used for the plant growth was modified Hoagland hormone in a hydroponic culture system (*Table 1*).

Table 1. The morning and evening nutritional solution

Morning nutritional solution	Evening nutritional solution
N (235 ppm)	Ca (14 ppm)
P (73 ppm)	K (65 ppm)
K (110 ppm)	Fe (1.8 ppm)
Mg (22 ppm)	
Zn (1.36 ppm)	
B (1.1 ppm)	
Mn (2.4 ppm)	

One month after planting *Aloe vera* in pots and using nutritional solutions in morning and evening, fertilizer treatments were applied to the pots every Monday. To this end,

after morning irrigation, some fertilizer was mixed with 20 ml of distilled water and added to the pots by hand. The numbering of the pots is done in a complete random manner. The zero concentration of silica was considered as control treatment. One month after treatments were applied, the temperature of greenhouse No. 2 was set at 4 °C, and this greenhouse was exposed to cold stress. After reducing temperature, fertilizer treatments were applied to the both greenhouses.

Planting Aloe vera and applying silicon fertilizer treatments

An experiment was conducted in the greenhouse town of Hashtgerd in Karaj on 60 (*Aloe barbadensis* Miller) plants with the average height of 15 cm and each with at least three leaves. They were planted in 18*14.7 cm polyethylene pots filled with a perlite and coco peat mix in a hydroponic system. The pots were automatically irrigated and fed with a standard nutrient solution once in the morning and another time in the afternoon. In addition, they were treated once a week with various levels of silicon (0 [in the control], and 500, 1000, 1500, and 2000 ppm) using potassium silicate and silicic acid.

Applying cold stress

The average temperature of the greenhouse was first set at 25 °C. After the plants were grown under normal conditions for three months, 30 of the pots were exposed to cold stress at 4 °C for seven days. 3. Sampling and measuring phytochemical and medicinal properties of *Aloe vera*

Following the cold stress, the second leaf of every plant was simultaneously removed and the samples were transferred to the lab in ice bags. The leaves were washed with distilled water, their surfaces were dried, and activities of the antioxidant enzymes (including SOD and CAT) and of the compatible solutes (including mannose, glucomannan, as well as aloin [as a medicinal compound]) were evaluated as follows.

Measuring activities of the antioxidant enzymes

To prepare enzymatic extracts (Sairamet al., 2002), 0.5 g of the frozen leaf sample was turned in to a homogeneous powder in a mortar with 10 ml of cold 0.1 M phosphate buffer (pH = 7.8) containing 0.5 mmol EDTA. The homogenized powder was transferred to centrifuge tubes and then centrifuged at 13000 rpm for 30 min at 4 °C. Using a spectrophotometer at 25 °C, enzymatic measurement of the supernatant was carried out with three replications.

SOD activity was measured based on the ability to prevent photo reduction of Nitro BlueTetrazolium (NBT) chloride using the method introduced by Giannopolitis and Ries (1977). Three mL of reaction solution containing 13 mmol of methionine, 75 µmol of NBT chloride, 2 µmol of riboflavin, 50 mmol phosphate buffer, and 50 µl of the extracted enzyme was exposed to two 15-Watt fluorescent light bulbs (with light intensity of 1000 lux) for 10 min at a distance of 20 cm. The reaction began when light was turned on and ended when it was turned off. The reaction solution was then covered with a black cloth until absorbance was measured. Absorbance was read at 560 nm using a model BT 600 spectrophotometer. One unit of SOD activity was considered to be the amount of the enzyme that could prevent photo reduction of NBT (p-nitro blue tetrazolium chloride) by 50 percent (Liang et al., 2008).

CAT activity was determined according to Chance and Maehly (1955). The CAT reaction solution containing 15 mmol of H₂O₂, 50 mmol of phosphate buffer, and 100 µl of the extracted enzyme were used. The reaction began by adding the enzyme and, after 1 min, reduction in H₂O₂ absorbance at 240 nm in 1 min was recorded. In this method, one unit of CAT activity was considered to be the amount of the enzyme that could oxidize one mmol of H₂O₂ in 1 min.

Measuring compatible solutes

The method introduced by Dubois et al. (1956), which is based on acidic hydrolysis of soluble sugars and production of furfural that generates a colored complex with phenol, was used to measure mannose. The leaf sample (0.2 g) was ground and homogenized in 4 ml of 25 mM sodium phosphate buffer (pH = 6.8). The reaction solution was prepared by pouring 0.5 ml of the extracted sugar solution, 0.5 ml of 5% phenol, and 2.5 ml of pure sulfuric acid in a test tube. The reaction began with the addition of the sulfuric acid. It was an exothermic reaction and produced an orange color. After the solution cooled, absorbance was read at 490 nm using the spectrophotometer. The standard curve was drawn using various concentrations of mannose from 0 to 20 µg/ml.

To measure glucomannan, the method introduced by Eberendu et al. (2005) was used. This method is based on measuring changes in the Congo red indicator made by the presence of glucomannan in the reaction. The leaf sample (40 mg) was transferred to each conical polypropylene tube, 20 ml of distilled water was added to the tube and it was shaken at 200 rpm for 4 h. Forty ml of the Congo red indicator (sodium 4,4'-diphenyl-2,2'-diazo-bis-1-naphthylamino-4-sulfonate) was then poured into the tube, the tube was left at room temperature for 20 minutes, and absorbance was read at 540 nm. Standard solutions containing *Aloe vera* polysaccharides were prepared using the Waller et al. (1978) method. After the standard curve was drawn, glucomannan content was read in mg/L.

Measuring aloin

To measure aloin concentration in the green skin of *Aloe vera* leaves, the spectrophotometric method was used (Ellaithy et al., 1984). One gram of the green leaf tissue was ground and homogenized by liquid nitrogen in a crucible, 10 ml of methanol extraction solvent was added, and the solution was kept in a refrigerator at 4 °C for 24 h. The solution containing aloin was then centrifuged at 10,000 rpm for 10 min. The supernatant was passed through 0.45 µm filter paper, 2 mL of the magnesium acetate was added, and light absorption intensity was read at 262 nm.

Statistical analysis of the data

The factorial experiment with two factors (silicon at five concentration levels and temperature at the two levels of normal and low temperature) was carried out using a completely randomized design with three replications and the data was analyzed employing SAS. Before performing ANOVA, normality of the data was tested using the Kolmogorov-Smirnov (K-S) test.

Results

Results of ANOVA indicate that the effects of silicon and cold stress on levels of enzyme activity and on phytochemicals including SOD, CAT, glucomannan, mannose, and aloin, were significant at the 0.01 level ($P < 0.01$). The mutual effects of silicon and cold stress were also significant at the 0.01 level (*Table 2*).

Table 2. Results of ANOVA related to biochemical properties

Source of variance	df	SOD (Umg ⁻¹ of protein)	CAT (Umg ⁻¹ of protein)	Glucomannan (mg L ⁻¹)	Mannose (mg L ⁻¹)	Aloin (%)
The Si treatment	4	82.680**	0.5597**	0.000654**	0.0429**	0.441*
Temperature	1	17.168**	0.4359**	0.3824**	21.780**	695.641ns
The Si*temperature treatment	4	57.187**	0.230**	0.000381**	0.02532**	0.0941**
Error	20					
CV (%)	-	0.867	1.183	2.27	1.162	0.584

The symbols *, **, and ns mean significance at $P < 0.05$ and $P < 0.01$ levels and not significant, respectively, and the numbers in the table are means of squares of the effects

The highest level of SOD activity (34.86 $\mu\text{mol}/\text{min}$) belonged to the 2000 ppm silicon concentration and the lowest (27.68 $\mu\text{mol}/\text{min}$) to the control (no silicon concentration). SOD activity at silicon concentrations of 500, 1000, 1500, and 2000 ppm increased by 17.3, 20.5, 23.4, and 25.9 percent, respectively, compared to the control (*Table 3*). The higher level of CAT activity was also observed in the treatments with high silicon concentrations (1500 and 2000 ppm) and the lowest in the control. CAT activity at silicon concentration of 2000 ppm (2.37 $\mu\text{mol}/\text{min}$) was about 37% higher than that of the control (1.72 $\mu\text{mol}/\text{min}$).

Table 3. Comparison of the means of the main effects on antioxidant activities

Source of variation	Treatment	SOD (Umg ⁻¹ of protein)	CAT (Umg ⁻¹ of protein)	Glucomannan (mg L ⁻¹)	Mannose (mg L ⁻¹)	Aloin (%)
Temperature	Control (25 °C)	27.81 b	1.97 b	0.35 a	0.75b	11.10 a
	Cold Stress (4 °C)	37.22 a	2.14 a	0.31 b	1.95a	4.29b
Concentration	0 ppm	27.68 b	1.72 b	0.31 c	1.28 c	7.44b
	500 ppm	32.49 a	1.99 ab	0.33 b	1.32 bc	7.58 bc
	1000 ppm	33.38 a	2.07 ab	0.33 ab	1.33 b	7.70 b
	1500 ppm	32.18 a	2.36 a	0.33 ab	1.36 b	7.83 ab
	2000 ppm	34.86 a	2.37 a	0.34 a	1.45 a	7.97 a

Means with similar Latin letters are not significantly different

Comparison of the means of the phytochemicals including glucomannan and mannose in *Aloe vera* indicated that cold stress was an influential factor on them so that their mean concentration in samples exposed to cold stress was significantly lower. These results suggest stoppage or reduction of plant metabolic processes. The average contents of glucomannan and mannose in plants not treated with cold stress were about 13 and 15 percent greater, respectively, compared to those that were exposed to cold stress. The aloin content in plants not exposed to cold stress was higher, compared to

plants that were treated with cold stress; however, the difference was not statistically significant.

Investigating the interaction between temperature and concentration of silicon on the activities of antioxidants (*Table 4*) indicates that at 25 °C or control temperature, increasing the concentration of silicon results in the increase in the activities of CAT and SOD enzymes as well as the concentrations of glucomannan, mannose, and aloin, and there is an ascending trend. This suggests that silicon has increased the activities of antioxidant enzymes in the plant by improving the nutritional value of *Aloe vera* plant under normal condition. Under stress temperature or at 4 °C, the activities of SOD and CAT enzymes increased with the different levels of silicon fertilizer treatments, and there was a significant difference when compared with control group. The highest and lowest values of SOD activity was related to 2000 ppm and 1000 pp, respectively. There were no significant differences between 500 ppm and 1000 ppm silicon treatments. That is, both have the same effect on SOD enzyme activity. The highest increase of CAT enzyme activity was due to 2000 ppm fertilizer treatment, which has a significant difference with the control group. Under cold stress or at 4 °C, the SOD enzyme activity increased by about 37%, using 2000 ppm silicon fertilizer treatment, compared with fertilizer treatment at 25 °C, indicating the effect of the temperature of 4 °C on the sudden increase of SOD activity at this temperature (the interaction between Si and stress temperature).

Investigating the interaction between control temperature and silicon concentration as well as stress temperature or 4 °C and silicon concentration on the CAT enzyme activity indicates that CAT activity increased under the stress temperature by 11% more than control temperature. This indicates the effect of the stress temperature and the concentration of silicon on the increase of activity of CAT antioxidant enzyme, which in turn shows the effect of Si on this enzyme. These two suggest the stimulation of the defense system and the increase in the activity of antioxidant enzymes. Investigating the interactions between temperature and concentration of silicon on the concentration of aloin indicates that temperature has a significant effect on the concentration of aloin. As the temperature decreases, the aloin concentration decreases, and when the temperature increases, the aloin concentration increases under the influence of the concentration of silicon.

Table 4. Comparison of the interaction effects on antioxidant activities

Temperature	Si Concentration	CAT (Umg ⁻¹ of protein)	SOD (Umg ⁻¹ of protein)	Aloin (%)	Mannose (%)	Glucomannan (%)
Control	0 ppm	25.51d *	1.84c	0.38 c	1.71c	10.73 b
	500 ppm	27.19cd	1.91b	0.39 b	0.75c	10.95 b
	1000 ppm	27.89cd	1.92b	0.41ab	0.74c	11.1ab
	1500 ppm	28.18c	1.96b	0.41ab	0.76c	11.28 a
	2000 ppm	29.31c	2.24ab	0.43 a	0.78c	11.55 a
Cold Stress	0 ppm	28.86c	1.59c	0.24 d	0.85b	4.16 c
	500 ppm	37.79b	2.06b	0.24 d	0.89b	4.21 c
	1000 ppm	38.87b	2.22ab	0.25 d	0.92ab	4.31 c
	1500 ppm	40.18a	2.35ab	0.25 d	0.96a	4.38 c
	2000 ppm	40.41a	2.50a	0.25 d	2.13 a	4.40 c

Investigating the interactions between temperature and concentration of silicon on mannose indicates that the concentration of mannose has increased due to temperature reduction and increase in the concentration of silicon fertilizer. Investigating the trends of glucomannan changes suggests that the temperature reduction has resulted in the decrease of glucomannan concentration. That is, the concentration of glucomannan decreased under stress condition. At 25 °C, the concentration of glucomannan is increasing due to the increase in silicon concentration. At 4 °C, the increase in consumed level of silicon leads no significant difference in glucomannan concentration. Perhaps one of the reasons is that glucomannan is converted into simpler sugars to be consumed and moderating the cold stress at 4 °C.

Discussion

In order to investigate the effect of stress temperature (4 °C) on CAT, SOD, mannose, glucomannan, and aloin components as phytochemical and medicinal parameters of *Aloe vera* plant, as well as comparing it with optimum growth or control temperature (25 °C), and also studying the effect of type of the fertilizer, two type of silica fertilizer, i.e. salicylic acid and potassium silicate, with five levels of fertilizer treatments including 0, 500, 1000, 1500, and 2000 ppm for 60 potted *Aloe vera* plants under hydroponics cultivation were used. The temperatures of 4 °C and 25 °C were selected as stress and control or optimal conditions for plant growth, respectively. Different concentrations or treatment levels were tested for both plants exposed to 4 °C and 25 °C. Therefore, the interaction between temperature and silica treatment levels can be investigated. The results show that the concentrations of CAT and SOD increased due to cold stress and silica fertilizer treatment, when compared to 25 °C. Increasing SOD activity at 4 °C directly related to increase in silica concentration. That is, at 4 °C, with increasing silica concentration, the activity of SOD increased, and its most activity was in the concentration of 2000 ppm, which was 34.86 Vmg⁻¹ of protein.

At 25 °C, application of fertilizer treatment could increase the SOD concentration in the plant, which has an activity of 27.81 Vmg⁻¹ of protein. The examination of these two values indicates that the stress temperature (4 °C) triggered the plant's defense system and could increase the SOD concentration by about 6.99 units, when compared to 25 °C. This increase is about 25.13%.

Comparison of the means showed that the highest SOD and CAT activities were those of the cold stress treatment. Many studies have indicated that there is a direct relationship between antioxidant enzyme activity and plant resistance to cold stress (Javadian et al., 2010; Luo et al., 2011; Radyuk et al., 2009). Mean SOD activity in samples exposed to cold stress was 33.8 percent higher than that of the samples not exposed to cold stress. CAT was also influenced by cold stress, and its mean activity in samples exposed to cold stress was about 8.6% higher than that of the samples not treated with cold stress. These results indicated plant defense mechanism against cold stress.

Comparison of the means of various silicon concentrations revealed that there were significant differences between the control and the treatments. However, the differences between the various levels of silicon concentrations were not significant. This suggests that presence of silicon, even at low amounts, plays a significant role in improving and activating plant antioxidant defense system.

The results show the positive effect of silicon in the process of antioxidant synthesis. Comparison of the means of glucomannan, mannose, and aloin contents at various silicon concentrations showed that there was a direct relationship between silicon concentration and the contents of the phytochemicals so that their lowest contents were observed in the control treatment and the highest at silicon concentration of 2000 ppm.

As shown in the ANOVA table, the application of the 7-day cold treatment significantly affected antioxidant activity levels probably because of the positive effects that silicon had in the mechanism of inducing resistance in plants against the cold stress (Ma and Yamaji, 2006; Kim et al., 2011). Interaction effects of temperature and silicon concentration showed that the highest levels of antioxidant enzyme activity were observed at silicon concentrations of 1500 and 2000 ppm and the lowest in the control (no silicon application). In a similar study, Zhu et al. (2006) stated that silicon increased plant resistance against cold and frost.

The greater SOD and CAT contents were observed at high silicon concentrations, which indicated the role silicon played in the activities of these antioxidants. In a similar study, Gunes et al. (2008) reported that, depending on plant type and variety, silicon influenced the levels of antioxidant enzyme activity, especially those of SOD and CAT. They stated that plants increased their antioxidant activities under stress conditions to be able to neutralize or minimize the stress. They noticed that applying the silicon treatment enhanced plant defense system through increasing antioxidant synthesis and, hence, modified the destructive effects resulting from the stress. Liang et al. (2008) reported that silicon application under cold stress down to -5 °C increased SOD activity in wheat. They demonstrated that SOD activity increased and reached its highest level following cold storage treatment for four days. Fahimirad et al. (2013) noticed that SOD activity reached its highest level after applying cold stress for 7 days in colza.

Plants usually respond by accumulating compatible solutes such as soluble sugars, carbohydrates, and polyol. Study of the trend of changes in the phytochemicals glucomannan, mannose, and aloin caused by cold stress and by concentrations of applied silicon shows that they had their highest concentrations when silicon was applied at 2000 ppm. These results are consistent with those of other studies. For example, Duan et al. (2013) reported that silicon improved *Dendrobium moniliforme* resistance against cold stress by increasing free proline, soluble sugars, and soluble protein contents and by decreasing Malonaldehyde (MDA) content.

Yin et al. (2013) also reported that applying silicon to sorghum under salt stress could considerably increase the levels of soluble sugars such as sucrose and fructose. Other researchers reported the contradictory results that silicon application decreased the contents of compatible solutes such as proline in various plants (Soylemezoglu et al., 2009; Lee et al., 2010; Tuna et al., 2008; Gunes et al., 2007a). Some researchers consider proline accumulation in plant organs a sign of damages inflicted by stresses and, therefore, reduction in proline content resulting from silicon application can be attributed to the reduction in the damage caused by stresses. Kumar et al. (2010) noticed that pea cultivars resistant to cold had greater contents of proline and ascorbic acid and higher levels of SOD and CAT activities. In general, silicon can enhance the conditions for production of antioxidants and other plant materials, and protect plants against wilting caused by cold stress, through influencing their qualitative and quantitative characteristics including photosynthesis and respiration.

Moreover, the protective role of silicon in plants may also be due to accumulation of polysilicic acids inside cells. There are reports that show silicon can enhance plant

defense mechanisms through other processes such as accumulation of lignin, phenol compounds and phytoalexins (Epstein, 1999). Results of the present research indicate that increases in anthraquinone and aloin concentrations may be due to accumulation of lignin and phenolic compounds when silicon is applied. At the temperature of 255 °C, suitable photosynthetic conditions were prepared for the plants to produce higher quantities of aloin phenolic materials. Silicon influenced aloin concentration by affecting photosynthetic performance of *Aloe vera* and through inducing deposition of materials inside cells. At the temperature of 45 °C, silicon was able to increase the aloin content of plants compared to the control through stimulating the defense system of the plants and by increasing their photosynthetic ability.

Conclusions

Cold stress increased antioxidant enzymes and reduced metabolic activities of *Aloevera*. As an agent activating enzymatic and non-enzymatic defense system, silicon plays a key role in inducing plant resistance against cold stress. Applying silicon fertilizer augmented activities of SOD and CAT, enhanced contents of compatible solutes such as glucomannan and mannose, and also increased aloin concentration in *Aloevera*. The findings of the present research show the importance of applying silicon fertilizers in increasing plant resistance, in reducing damages caused by cold stress, and consequently, in achieving sustainable agricultural production.

Considering the effect of Si on the induction of plant defense system against the environmental stress, it is suggested that the effects of elements such as cobalt (K) on the activity of oxidative enzymes under cold and saline stresses would be tested. The effect of Si as spraying on the growth factors and antioxidant components of the plant in order to accelerate the absorption of the element and to reduce the stress of cold and drought stresses under sudden stresses can also be investigated.

Acknowledgements. This work was financially supported by the Zarafshan manufacturer of fertilizer and pesticide, Iran. The authors are grateful to Dr. Mehdi Tehrani of Institute of Soil and Water Research and Dr. Babak Motesharezadeh of Tehran University, Iran. Also, this research received no specific grant from any funding agency in the public, commercial or not-for-profit sectors.

REFERENCES

- [1] Adam, S., Murthy, S. (2014): Effect of Cold Stress on Photosynthesis of Plants and Possible Protection Mechanisms. – In: Gaur, P. S. (ed.) Approaches to Plant Stress and their Management. Springer, New Delhi.
- [2] Ahmed, M., Hassen, F. U., Qadeer, U., Aslam, M. A. (2011): Silicon application and drought tolerance mechanism of sorghum. – Africa Journal Agriculture Research 6: 594-607.
- [3] Ali, A. A., Alqurainy, F. (2006): Activities of Antioxidants in Plants under Environmental Stress. – In: Motohashi, N. (ed.) The Lutein-Prevention and Treatment for Diseases. Transworld Research Network Press, Trivandrum, India.
- [4] Allen, R. D. (1995): Dissection of oxidative stress tolerance using transgenic plants. – Plant Physiol 107: 1049-1054.
- [5] Alsher, R. G., Donahue, J. L., Cramer, C. L. (1997): Reactive oxygen species and antioxidants: relationship in green cells. – Physiol Plant 100: 224-233.

- [6] An, Y. Y., Liang, Z. S. (2013): Drought tolerance of *Periploca sepium* during seed germination: antioxidant defense and compatible solutes accumulation. – *Acta Physiologiae Plantarum* 35: 959-967.
- [7] Asada, K. (2006): Production and scavenging of reactive oxygen species in chloroplasts and their functions. – *Plant Physiology* 141: 391-396.
- [8] Ashraf, M., Foolad, M. R. (2007): Roles of glycine betaine and proline in improving plant abiotic stress resistance. – *Environ Exp Bot* 59: 206-216.
- [9] Bafana, A., Dutt, S., Kumar, A., Kumar, S., Ahuja, P. S. (2011): The basic and applied aspects of superoxide dismutase. – *J Mol Catal B Enzym* 68(2): 129-138.
- [10] Balakhnina, T. I., Bennicelli, R. P., Stępniewska, Z., Stępniewski, W., Fomina, I. R. (2010): Oxidative damage and antioxidant defense system in leaves of *Vicia faba* major L. cv. Bartom during soil flooding and subsequent drainage. – *Plant Soil* 327: 293-301.
- [11] Balakhnina, T. I., Matichenkov, V. V., Włodarczyk, T. M., Borkowska, A., Nosalewicz, M., Fomina, I. R. (2012): Effects of silicon on growth processes and adaptive potential of barley plants under optimal soil watering and flooding. – *Plant Growth Reg.* DOI: 10.1007/s10725-012-9658-6.
- [12] Balibrea, M. E., Rus-Alvarez, A. M., Bolarfn, M. C., Pérez-Alfocea, F. (1997): Fast changes in soluble carbohydrates and proline contents in tomato seedlings in response to ionic and non-ionic iso-osmotic stresses. – *J Plant Physiology* 151: 221-226.
- [13] Bennicelli, R. P., Balakhnina, T. I., Szajnocha, K., Banach, A. (2005): Aerobic conditions and antioxidative system of *Azolla caroliniana* Willd in the presence of Hg in water solution. – *Int Agrophysic* 19: 27-30.
- [14] Bohnert, H. J., Shen, B. (1999): Transformation and compatible solutes. – *Sci Hortic* 78: 237-260.
- [15] Chance, B., Maehly, A. (1955): Assay of catalase and peroxidase. – *Methods in Enzymology* 2: 764-817.
- [16] Duan, X., Tang, M., Wang, W. (2013): Effects of silicon on physiology and biochemistry of dendrobium moniliforme plantlets under cold stress. – *Agric Biotechnol* 2: 18-21.
- [17] Dubois, M., Gilles, K. A., Hamilton, J. K., Rebes, P. A., Smith, P. A. (1956): Colorimetric Method for Determination of Sugars and Related Substrates, *Anal. Chem.* 28: 350-356.
- [18] Eberendu, A. R., Luta, G., Edwards, J. A., McAnalley, B. H., Davis, B. (2005): Quantitative colorimetric analysis of aloe polysaccharides as a measure of *Aloe vera* quality in commercial products. – *AOAC International* 88: 684-691.
- [19] Ellaithy, M. M., Sayed, L., Bebawy, L. (1984): Spectrophotometric determination of barbaloin. – *An International Journal for Rapid Communication* 17(11): 743-750.
- [20] Epstein, E. (1999): Silicon. – *Annual Review of Plant Physiology* 50: 641-664.
- [21] Fahimirad, S., Karimzadeh, G., Ghanati, F. (2013): Cold-induced changes of antioxidant enzymes activity and lipid per oxidation in two canola (*Brassica napus* L.) cultivars. – *Journal of Plant Physiology and Breeding* 3(1): 1-11.
- [22] Flowers, T. J., Hajibagueri, M. A., Clipson, N. C. W. (1986): Halophytes. – *Q Rev Biol* 61: 313-337.
- [23] Giannopolitis, C. N., Ries, S. K. (1977): Superoxide dismutase I, occurrence in higher plants. – *Plant Physiology* 59: 309-314.
- [24] Gill, S. S., Tuteja, N. (2010): Reactive oxygen species and antioxidant machinery in abiotic stress tolerance in crop plants. – *Plant Physiology Biochem* 48: 909-930.
- [25] Gunes, A., Ali, I., Bagci, E. G., Pilbeam, D. J. (2007a): Silicon-mediated changes of some physiological and enzymatic parameters symptomatic for oxidative stress in spinach and tomato grown in sodic B toxic soil. – *Plant Soil* 290: 103-114.
- [26] Gunes, A., Inal, A., Bagci, E. G., Coban, S. (2007b): Silicon-mediated changes on some physiological and enzymatic parameters symptomatic of oxidative stress in barley grown in sodic-B toxic soil. – *J Plant Physiology* 164: 807-811.

- [27] Gunes, A., Pilbeam, D. J., Inal, A., Coban, S. (2008): Influence of silicon on sunflower cultivars under drought stress. I: Growth, antioxidant mechanisms and lipid per oxidation. – *Common Soil Sci Plant Anal* 39: 1885-1903.
- [28] Gzik, A. (1997): Accumulation of proline and pattern of α -amino acids in sugar beet plants in response to osmotic, water and salt stress. – *Environ Exp Bot* 36: 29-38.
- [29] Halliwell, B. (1984): Oxidative damage, lipid per oxidation and antioxidant protection in chloroplasts. – *Chem Phys Lipids* 44: 327-340.
- [30] Hattori, T., Inanaga, S., Araki, H., An, P., Morita, S., Luxova, M., Lux, A. (2005): Application of silicon enhanced drought tolerance in *Sorghum bicolor*. – *Physiol Plant* 123: 454-466.
- [31] Javadian, N., Karimzadeh, G., Mahfoozi, S., Ghanati, F. (2010): Cold-induced changes of enzymes, proline, carbohydrates and chlorophyll in wheat. – *Russ J Plant Physiol* 57: 540-547.
- [32] Jung, S. (2004): Variation in antioxidant metabolism of young and mature leaves of *Arabidopsis thaliana* subjected to drought. – *Plant Science* 166: 459-466.
- [33] Kim, Y. H., Khan, A. L., Hamayun, M., Kang, S. M., Beom, Y. J., Lee, I. J. (2011): Influence of short-term silicon application on endogenous phytohormonal levels of *Oryza sativa* L. under wounding stress. – *Biol Trace Elem Res* 144: 1175-1185.
- [34] Kumar, A. P., Bandhu, A. D. (2005): Salt tolerance and salinity effects on plants: a review. – *Ecotoxicol Environ Saf* 60: 324-349.
- [35] Kumar, S., Malik, J., Thakur, P., Kaistha, S., Sharma, K. D., Upadhyaya, H. D., Berger, J. D., Nayyar, H. (2010): Growth and metabolic responses of contrasting chickpea (*Cicerari entinum* L.) genotypes to chilling stress at reproductive phase. – *Acta Physiol Plant* 33(3): 779-787.
- [36] Larson, R. A. (1988): The antioxidants of higher plants. – *Phytochem* 27: 969-978.
- [37] Lee, S. K., Sohn, E. Y., Hamayun, M., Yoon, J. Y., Lee, I. J. (2010): Effect of silicon on growth and salinity stress of soybean plant grown under hydroponic system. – *Agro for Syst* 80: 333-340.
- [38] Liang, Y. C., Sun, W. C., Zhu, Y. G., Christie, P. (2007): Mechanisms of silicon-mediated alleviation of abiotic stresses in higher plants: a review. – *Environ Pollut* 147: 422-428.
- [39] Liang, Y. C., Zhu, J., Li, Z., Chu, G., Ding, Y., Zhang, J., Sun, W. (2008): Role of silicon in enhancing resistance to freezing stress in two contrasting winter wheat cultivars. – *Environment and Experimental Botany* 64: 286-294.
- [40] Liang, Y., Nikolic, M., Bélanger, R., Gong, H., Song, A. (2015): *Silicon in Agriculture*. – Springer, Dordrecht.
- [41] Luo, H., Li, H., Zhang, X., Fu, J. (2011): Antioxidant responses and gene expression in perennial ryegrass (*Lolium perenne* L.) under cadmium stress. – *Ecotoxicology* 20: 770-778.
- [42] Ma, J. F., Yamaji, N. (2006): Silicon uptake and accumulation in lower plants. – *Trends Plant Sci* 11(8): 392-397.
- [43] Ma, J. F., Mitani, N., Nagao, S., Konishi, S., Tamai, K., Iwashita, T., Yano, M. (2004): Characterization of the silicon uptake system and molecular mapping of the silicon transporter gene in rice. – *Plant Physiology* 136: 3284-3289.
- [44] Mansour, M. M. F. (1998): Protection of plasma membrane of onion epidermal cells by glycine betaine and proline against NaCl stress. – *Plant Physiol Biochem* 36: 767-772.
- [45] Murillo-Amador, B., Córdoba-Matson, M. V., Villegas-Espinoza, J. A., Hernández-Montiel, L. G., Troyo-Diéguez, E., García-Hernández, J. L. (2014): Mineral content and biochemical variables of *Aloe vera* L. under salt stress. – *PLoS One* 9(4): e94870. DOI: 10.1371/journal.pone.0094870.
- [46] Nayyar, H., Walia, D. P. (2003): Water stress induced proline accumulation in contrasting wheat genotypes as affected by calcium and abscisic acid. – *Biol Plant* 46: 275-279.

- [47] Radyuk, M. S., Domanskaya, I. N., Shcherbakov, R. A., Shalygo, N. V. (2009): Effect of low above zero temperature on the content of low molecular antioxidants and activities of antioxidant enzymes in green barley leaves. – Russ J Plant Physiol 56(2): 175-180.
- [48] Richmond, K. E., Sussman, M. (2003): Got silicon? The non-essential beneficial plant nutrient. – Curr Opin Plant Biol 6: 268-272.
- [49] Royal Botanic Gardens (2014): Royal Botanic Gardens and Domain Trust Annual Report. – Royal Botanic Gardens, Sydney.
- [50] Sairam, R. K., Rao, K. V., Srivastava, G. C. (2002): Differential response of wheat genotypes to long-term salinity stress in relation to oxidative stress, antioxidant activity and osmolyte concentration. – Plant Sci 163: 1037-1046.
- [51] Savant, N. K., Snyder, G. H., Datnoff, L. E. (1997): Silicon management and sustainable rice production. – Adv Agron 58: 151-199.
- [52] Seckin, B., Sekmen, A. H., Türkan, İ. (2009): An enhancing effect of exogenous mannitol on the antioxidant enzyme activities in roots of wheat under salt stress. – J Plant Growth Regul 28: 12-20.
- [53] Shelton, R. M. (1991): *Aloe vera*: its chemical and therapeutic properties. – Int J Dermatol 30: 679-83.
- [54] Sivanesan, I., Park, W. (2014): The role of silicon in plant tissue culture. – Front. Plant Sci 5: 571.
- [55] Soylemezoglu, G., Demir, K., Inal, A., Gunes, A. (2009): Effect of silicon on antioxidant and stomata response of two grapevine (*Vitis vinifera* L.) rootstocks grown in boron toxic, saline and boron toxic-saline soil. – Sci Hortic Amst 123: 240-246.
- [56] Talebi, M. (2013): Bank Keshavarzi's experience in compensating for losses suffered by Iranian farmers as a result of natural disasters. – 4th World Congress on Agricultural and Rural Finance, 26-28 September 2013, Paris.
- [57] Tuna, A. L., Kaya, C., Higgs, D., Murillo-Amador, B., Aydemir, S., Girgin, A. R (2008): Silicon improves salinity tolerance in wheat plants. – Environ Exp Bot 62: 10-16.
- [58] Van Bockhaven, J., De Vleeschauwer, D., Höfte, M. (2013): towards establishing broad-spectrum disease resistance in plants: silicon leads the way. – J Exp Bot 64: 1281-1293.
- [59] Waller, G. R., Mangiafico, S., Ritchey, C. R. (1978): A chemical investigation of *Aloe barbadensis*. – Proceedings of the Oklahoma Academy of Science 58: 69-76.
- [60] Yin, L. N., Wang, S. W., Li, J. Y., Tanaka, K., Oka, M. (2013): Application of silicon improves salt tolerance through ameliorating osmotic and ionic stresses in the seedling of *Sorghum bicolor*. – Acta Physiol Plant 35(11): 3099-3107.
- [61] Zhang, F., Liang, Y. C., He, W. L., Zhao, X., Zhang, L. X. (2004): Effects of salinity on growth and compatible solutes of callus induced from *Populus euphratica*. – In Vitro Cell Dev Pl 40: 491-494.
- [62] Zhu, J., Liang, Y. C., Ding, Y. F., Li, Z. J. (2006): Effect of silicon on photosynthesis and its related physiological parameters in two winter wheat cultivars under cold stress. – Science Agriculture Sinica 39: 1780-1788.
- [63] Zhu, X., Song, F., Xu, H (2010): Influence of arbuscular mycorrhiza on lipid peroxidation and antioxidant enzyme activity of maize plants under temperature stress. – Mycorrhiza 20: 325-332.
- [64] Zou, W., Chen, Y., Lu, C. (2007): Differences in biochemical responses to cold stress in two contrasting varieties of rape seed (*Brassica napus* L.). – For Stud China 9(2): 142-146.

DETERMINATION OF LETHAL AND SUB-LETHAL CONCENTRATIONS OF ARSENIC IN *CYPRINUS CARPIO*

MALIK, R.* – NAEEM, M.*

Institute of Pure and Applied Biology, Bahauddin Zakariya University, Multan, Pakistan

**Corresponding authors*

e-mail: rozinasattar04@gmail.com; drnaeem@bzu.edu.pk

(Received 16th Sep 2018; accepted 21st Jan 2020)

Abstract. The experiment was conducted to determine the lethal and sub-lethal concentrations of arsenic (As) in European carp (*Cyprinus carpio* L.) at College of Veterinary Sciences, BZU, Bahadur sub Campus Layyah Pakistan. The experimental fish were kept in aquarium and exposed to 5, 10, 15, 20, 25, 30 and 35 mg/L concentrations of As in laboratory. One group was considered to be the control where fish were not exposed to As. In each concentration, 10 fish were kept for a 96-h exposure period. There were five replications in each group. Dead fish were removed regularly from each test aquarium. Collected data of mortality were analyzed by using the Probit analysis in order to determine the 96-h LC₅₀ of As on *Cyprinus carpio* with $P \leq 0.05$ probability level. Hepatosomatic index (HSI), gonadosomatic index (GSI) and intestinalsomatic index (ISI) were calculated based on weight of the body and weight of the respective organ of *Cyprinus carpio* fish. Results indicated that 96-h LC₅₀ value of As in *Cyprinus carpio* was 25 mg L⁻¹. Sub lethal concentrations were 5.0, 2.5, 1.65 and 1.25 mg L⁻¹ that were determined by taking 1/5th, 1/10th, 1/15th and 1/20th of LC₅₀. Likewise, increasing concentration of As significantly enhanced the value of HSI and reduced the value of GSI and ISI of *Cyprinus carpio* species. This study concluded that 25 mg L⁻¹ As was found to be 50% lethal concentration for *Cyprinus carpio* species.

Keywords: acute toxicity, hepatosomatic, gonadosomatic, intestinalsomatic, LC₅₀

Introduction

Heavy metals are serious environmental pollutants effecting human beings differential injuriousness and aquatic organisms due to their high toxicity (Yang et al., 2014; Javed, 2015). To perform various physiological functions vital metals are required by the living organisms but beyond definite concentrations they may become hazardous to the organisms due to generation of free radicals leading to oxidative stress (Merciai et al., 2014). The important factors influencing the differential injuriousness of metallic ions are metal specific, including the mode of action and the solubility of the metal along with the physicochemical properties of the test medium (Naz and Javed, 2012; Gupta and Karthikeyan, 2016).

In different region of the world many types of contaminants are spread such as arsenic (As) (Flora et al., 2005; Shrivastava et al., 2015). Naturally As is present in the water in different chemical species and different oxidation states. The As known as a toxic trace element. The arsenite (AsO₃³⁻) or arsenate (AsO₄³⁻) are inorganic forms of this heavy metal and commonly its abundant forms are inorganic in the nature (Akter et al., 2005; Pedlar et al., 2002). The effect of As is more prominent when it interfere in accumulation, concentration, excretion and the gastrointestinal tract, skin, kidney and liver. As disturbs the biochemical, haematological and most important ion-regulatory factors of organisms and mainly fish present in the aquatic media, and variations of previous factors can be beneficial in environmental bio-monitoring from the contamination of As (Lavanya et al., 2011). For evaluating the effects of environmental pollution on aquatic ecosystems fish are choice of an organism (Gaim et al., 2015). As-

contaminated food by a fish intake through their gills, skin, and they are continuously exposed to it. Fishes are good indicators of As toxicity, they have long sentinels and used for biomonitoring of aquatic life and contaminants that is present in the water (Tisler and Zagorc-Koncan, 2002). Lethal toxicity of toxicant can be tested through the determination of LC₅₀ value which is the most reliable for assessing the adverse effect on fish (Kumari et al., 2017). To make or establish the biomarkers of exposure fishes have good power of models as to study the toxicogenomics fishes are perfect organisms to work (Das et al., 2012). To reduce the hazardous forms of As in aquatic life fishes are best as they have different mechanisms for biotransformation (Bears et al., 2006). When the concentration of As increases in an aquatic ecosystem, than it affects various physiological systems like growth, reproduction, immune function, gene expression, histopathology and enzyme activities in the body of fish (Datta et al., 2009). It will be negative for the health of humans if As-contaminated fish intake by the humans (Kar et al., 2011). The As involved in a series of molecular events like iron homeostasis, oxidative stress, carcinogenesis and lipid metabolism disorder (Xu et al., 2013). The As contamination is linked with the formation of Reactive oxygen species (ROS) causes severe injury and damage to the biological systems of organisms that is result of the As contamination (Patlolla and Tchounwou, 2005). The bioindicator of contaminant exposure is basically known as hepatosomatic index (HSI) (Sadekarpawar and Parikh, 2013). The changing in size of liver hypertrophy (an increase in size) and hyperplasia (an increase in number) is the result of detoxification of As contamination (Solé et al., 2010). The Study evaluate the relative liver size of fishes from contaminated places and disturbed locations also utilize the HSI, that expresses liver size in the form of percentage of the total body weight (Sadekarpawar and Parikh, 2013). Structural information and more functional like health and gonadal maturation status is supply by gonadosomatic index (GSI) which is also a bioindicator. The majority of the species go through the reproductive cycle and, commonly, difference in the gonadal size is observed in the cycle (Sadekarpawar and Parikh, 2013). The gonadal weight of the body in percentage used for defining the reproductive maturity and replies of environmental dynamics (e.g., seasonal changes) similarly, the exogenous stress also (e.g., exposition to contaminants). The gonad alterations like reduction of GSI and morphological changes are caused by the result of several environmental pollutants it is significant evidence (Sakamoto et al., 2003). Keeping in view the present issues connecting to freshwater fisheries in Pakistan the current research work was carried out to determine the lethal and sub lethal concentration of As to *C. carpio* that will help in the expansion of proper strategies for sustainable conservation of the fish.

Materials and methods

European carp (*Cyprinus carpio* L.) 400 fish (10 ± 0.5 cm length and 60 ± 5 g weight) were collected from fish nursery Karor Lali Ehsan Layyah Pakistan, acclimatized in aquaria for 15 days under laboratory conditions at College of Veterinary Sciences, BZU, Bahadur sub Campus Layyah Pakistan. The aquaria were continuously aerated through stone diffusers connected to a mechanical air compressor. Water temperature was 25 ± 2 °C and pH was maintained between 6.6 and 7.5. The fish were fed twice daily alternately with egg, goat liver and raw brine shrimp pellets. The experimental fish were exposed to different concentrations of arsenic *viz*: 5, 10, 15, 20, 25, 30 and 35 mg/L. One group was considered as a control where fish were not exposed to As. The 10 fish for

each concentration of As test were used. In the experimental aquaria water was replaced daily with fresh treatment of As. Five replicates for each concentration of arsenic were arranged under Complete Randomized Design (CRD). The experimental treatments were 0 (control), 5.0, 10.0, 15.0, 20.0, 25.0, 30.0 and 35.0 mg/L arsenic. Following parameters were studied during the course of study.

Determination of LC₅₀ arsenic concentration

Ten fish samples were transferred to each aquarium and exposed to different concentrations of As (5, 10, 15, 20, 25, 30 and 35 mg/L) from sodium arsenite (NaAsO₂) was used as arsenic source. In all cases, control groups of fish were maintained. This trial was carried out for a period of 96 h LC₅₀. The mortality of the fish was recorded at 96 h of exposure. The effect of each concentration was tested at least in duplicate to verify reproducibility. The data were obtained in course of the investigation was analyzed statistically to see whether there is any influence of different treatments concentrations on the mortality of fish.

Sub-lethal concentration of arsenic

The concentrations of arsenic viz: 5, 10, 15, 20, 25, 30 and 35 mg/L were maintained in each treatment. Control group of fish was maintained without application of As. Sub lethal concentrations were determined by taking 1/5th, 1/10th, 1/15th and 1/20th of LC₅₀ (Abdel-Hameid, 2009).

Length and weight

Samples of fish were removed from the aquaria of respective treatments. All samples were washed with distilled water, and transferred to the laboratory. Length of the fish was measured with the help of measuring tap and weight was noted with electronic balance (Digital Bench Scale - QM7264, Electric Burst Australia Pty Ltd).

Somatic indices

After the period of exposure fishes were removed and washed with freshwater. Control as well as treated groups were anesthetized by immersion in 50 mg/L tricaine methane sulphonate solution for 5–10 min before they were killed by decapitation and weighed; blood was allowed to drain and dissected to take out organs. Hence the liver, gonads and intestines weight was taken for the Hepatosomatic index (HSI), Gonadosomatic index (GSI) and Intestinal somatic index (ISI). The indices were calculated according to the following formula Parmeswaran (1974):

$$\text{HSI} = (\text{Liver weight (g)} / \text{Fish weight (g)}) \times 100 \quad (\text{Eq.1})$$

$$\text{GSI} = (\text{Gonad weight (g)} / \text{Fish weight (g)}) \times 100 \quad (\text{Eq.2})$$

$$\text{ISI} = (\text{Intestines weight (g)} / \text{Fish weight (g)}) \times 100 \quad (\text{Eq.3})$$

Statistical analysis

The statistical analysis of this work was done using STATISTIX 8.1. The data of this work was presented as means \pm standard deviation. Pair wise comparison was done

between control and experimental groups by employing Duncan multiple variance test to resolve the statistical significance of the difference between the groups (Pipkin, 1984).

Results

Analyzed data reveal that mortality of *C. carpio* was increased by increasing the concentration of As. The 50% mortality was recorded at 25 mg L⁻¹ As concentration while it caused 60% and 80% mortality at 30 and 35 mg L⁻¹ respectively (Table 1). Whereas; other As concentrations 5, 10, 15 and 20 mg L⁻¹ caused the 10, 30 and 40% mortality in *C. carpio* (Table 1). These lethal concentrations of As to tested fish species was determined by the mean value of 96 h LC₅₀ and with 95% confidence interval significant $P < 0.05$. The other concentrations of As were observed below the concentration of 25 mg L⁻¹. The upper and lower 95% confidence limits. Thus, As rated as highly toxic to *C. carpio*. Non-significant mortality was observed in control and 5 mg L⁻¹ during the experimental periods (Table 1).

Table 1. Effect of different concentration of arsenic on mortality of *Cyprinus carpio*

Arsenic conc. (mg L ⁻¹)	Log conc.	Number of fish alive out of fifty	Mortality %	Probit kill
0.0 (control)	--	50	0	--
5.0	0.70	50	0	--
10.0	1.00	45	10	3.73
15.0	1.18	35	30	4.48
20.0	1.30	35	30	4.48
25.0	1.40	25	50	5.00
30.0	1.40	20	60	5.25
35.0	1.48	10	80	5.84

The various concentrations of As showed significant difference in mean length and weight of *C. carpio*. Significantly higher mean length and weight was gained in control group and that differences were not statistically significant where As was applied at the rate 5 and 10 mg L⁻¹ respectively (Fig. 1). After that there was gradual decrease in mean length and weight with increasing the concentration of As (Figs. 1 and 2). Results indicated that value of HSI decreased significantly with increasing the level of As concentrations. Highest value of HSI was recorded in control treatment where As was not applied which was not statistically significant with lowest concentration (5 mg L⁻¹) of As (Fig. 3). It was found that there is gradual decrease in the value of HSI. Whereas; lowest value of HSI was measured at the highest concentration of As (Fig. 3). The GSI value showed significant difference among all As concentration. Significantly higher value of GSI was recorded in the control treatment that there were not statistically significant at 5 and 10 mg L⁻¹ respectively (Fig. 4). After that there was gradual decrease in the value of GSI with increasing the concentration of As. In addition, lowest value of GSI was observed in the group where As was applied 35 mg L⁻¹ while differences were not statistically significant to the group 7th where As was applied 30 mg L⁻¹ (Fig. 4). The value of ISI significantly decreased in fish subjected to As levels. Higher value of ISI was determined in the fish in control group that there were no significant differences where

fish was exposed to As level of 5 and 10 mg L⁻¹ respectively. After that there was gradual decrease in the value of ISI with increasing the concentration of As (Fig. 5). In addition, lowest value of ISI was observed at 35.0 mg L⁻¹ As concentration which was not statistically different to 30 mg L⁻¹ As concentration (Fig. 5).

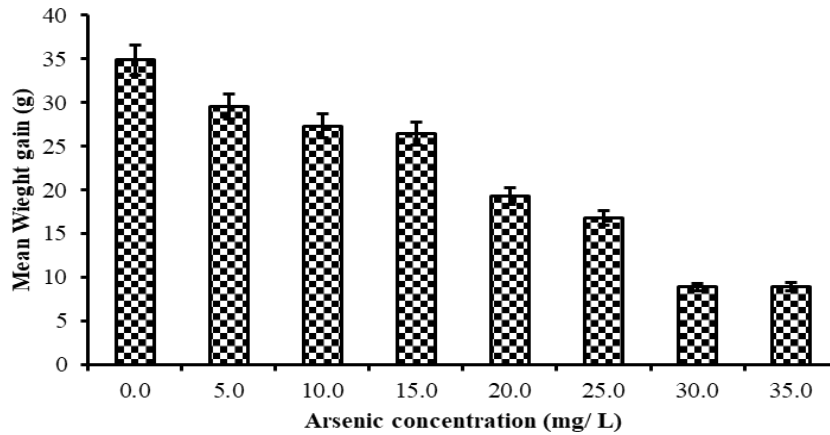


Figure 1. Effect of different concentration of arsenic on mean weight gain of *Cyprinus carpio*

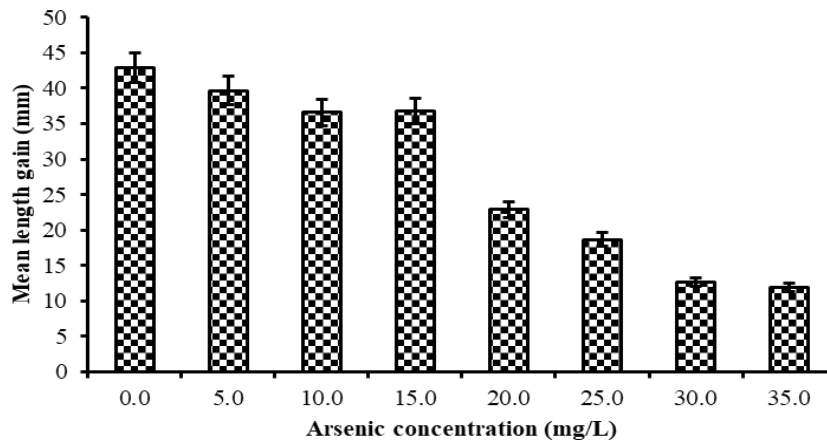


Figure 2. Effect of different concentration of arsenic on mean length gain of *Cyprinus carpio*

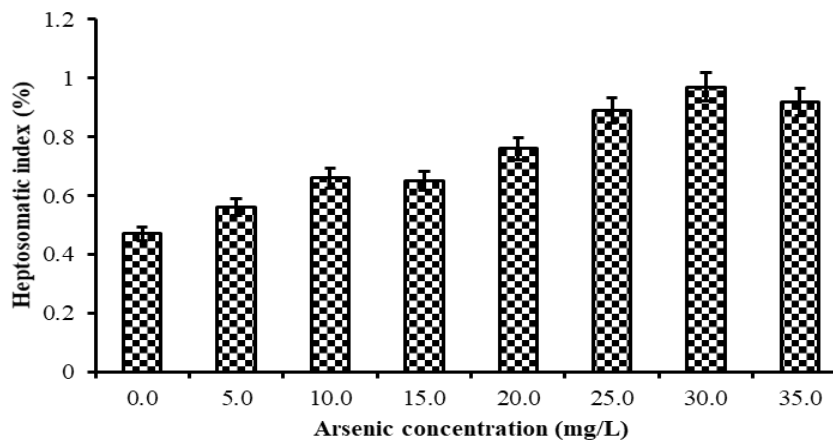


Figure 3. Effect of different concentration of arsenic on heptosomatic index of *Cyprinus carpio*

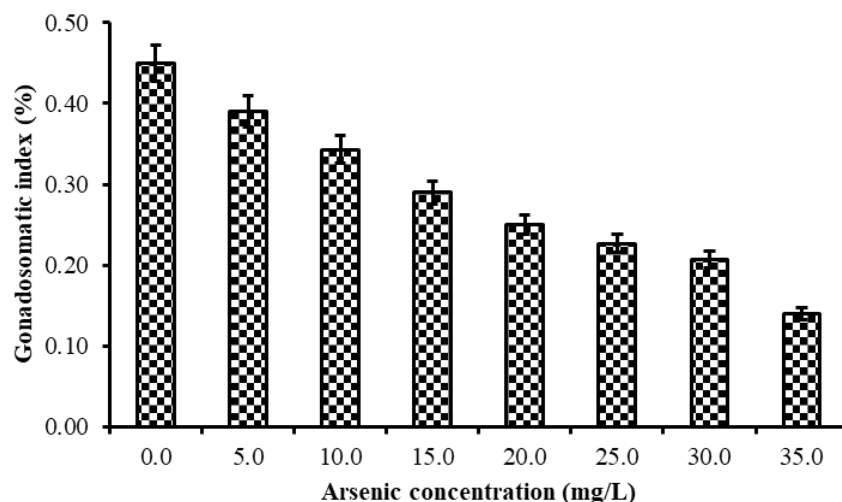


Figure 4. Effect of different concentration of arsenic on gonadosomatic index of *Cyprinus carpio*

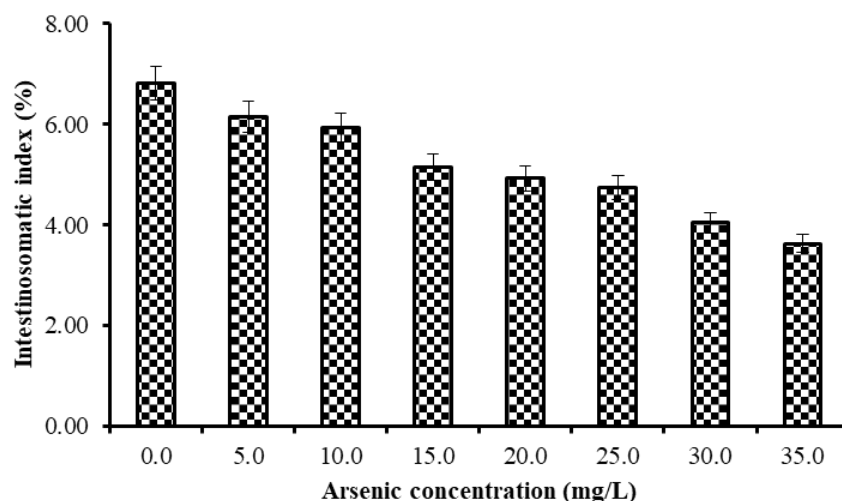


Figure 5. Effect of different concentration of arsenic on intestinosomatic index of *Cyprinus carpio*

Discussion

Instant and delayed toxic effects that occur in fish are the results of lethal toxicity. This delayed effect results in discoloration of skin and death of fish occurs ultimately (Abdullah and Javed, 2006). For 96-h LC₅₀ determination, species-specific factor like fish sensitivity towards particular metals is important. In current study, the mortality of *Cyprinus carpio* increased gradually with increasing the level of As (Fig. 6). Pandey et al. (2005) reported the acute toxicity caused by arsenic in *Dicentrarchus labrax* based on dosage. Morcillo et al. (2015) reported mercuric chloride and malathion toxicity at 96-h time dependent dose in *Channa puctatus*. The results of our experiment showed that 25 mg L⁻¹ was found to be 96-h LC₅₀ and lethal concentrations of As for *C. carpio*. This indicates the mortality rate which increased with the increase in concentration for a particular time with regular mode of toxicant action at dangerous level due to As

accumulation ultimately leading to fish death (Reddy et al., 2016). Over the gills fish, a mucus film formed when oxygen culminates hence damage occurs by respiratory epithelium causing mortality. (Das and Sahu, 2005) because gills tissues are main target organ of the fish imposed to As. As exposure to fish cause clogging of gills resulting in breathing anxiety because As damages directly the blood vessels and collapse them in gills (Mondal and Samanta, 2015). Kovendan et al. (2013) determined the 32 mg L⁻¹ Arsenic tri-oxide to the adults' fish *C. carpio*. In another study, 24.5 mg L⁻¹ was found to be 96-h LC₅₀ and above that are lethal concentrations of As to *Ctenopharyngodonidella* (Kousar and Javed, 2014).

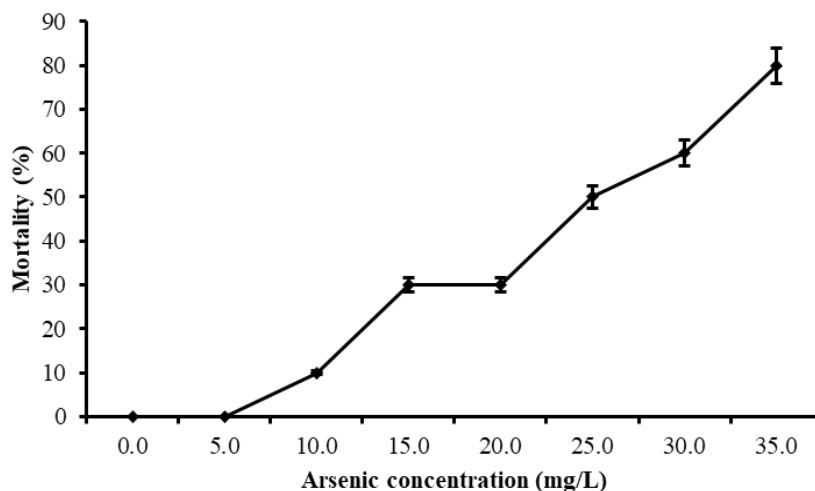


Figure 6. Graphical estimation of 96-h LC₅₀ of arsenic against the *Cyprinus carpio*

The decreased in mean length and weight due to As exposure in fish can be explained by direct metabolic impacts study or by food chain destitution, both of these actions decreases the fish growth (Eastwood and Couture, 2002). Moreover; higher concentrations of As can change muscle fiber size that ultimately reduced the weight and length of fish (D'Amico et al., 2014). In another study, Begum et al. (2013) exposed fish with As from dose of 7 and 20 mg/L in *H. fossilis* and concluded that muscles bundles started to degenerate when As is exposed.

Current study indicated that value of hepato-somatic indices increased significantly with increasing the level of As concentrations. Changes in HSI may be considered as a good indicator generally of the tested population of fish (Bolger and Connolly, 1989). HIS increases with the increase in arsenic concentration due to hepatocytes or hyperplasia (Crunkhorn et al., 2004). These researches not only favours previous findings about arsenic toxicity but also leads to the suggestion about changes in the liver of *C. batrachus* by sub lethal toxicity of As. (Lu et al., 2001; Chen et al., 2004). Hepatomegaly, reported earlier about fishes by many pollutants (Pait and Nelson, 2003; Barseet al., 2006; Abdel-Hameid, 2007; Datta et al., 2007). In our current study, the value of GSI decreased with increasing concentration of arsenic for *Cyprinus carpio*. These results are in line with the findings of Yamaguchi et al. (2007) about catfish (*Pangasianodon hypophthalmus*) exposed to metal water contamination. They reported that As when exposed to the fish, spermatogonia necrosis and sertoli cells vacillation occurs. This study records the ISI value reduction when As exposed. This result is

almost same who worked to check effects by other pollutants (Abdel-Hameid, 2007; Abdel-Tawwab et al., 2007). It may result in appetite loss and body weight reduction. Many research findings use ISI values as indicator to check physiological responses and changes by less feeding (Abdel-Tawwab et al., 2006, 2007; Abdel-Hameid, 2007).

Conclusion

Exposure of *Cyprinus carpio* to various concentration of As induced the harmful effect. Results indicated that 96-h LC₅₀ values of As for *Cyprinus carpio* was 25 mg L⁻¹. Sub lethal concentrations were determined by taking 1/5th, 1/10th, 1/15th and 1/20th of LC₅₀ that were found to be 5.0, 2.5, 1.65 and 1.25 mg L⁻¹. Likewise, increasing concentration of As significantly enhanced the value of HSI and reduced the value of GSI and ISI of *Cyprinus carpio* species.

REFERENCES

- [1] Abdel-Hameid, N. A. H. (2007): Physiological and histological changes induced by phenol exposure in *Oreochromis aureus* juveniles. – Turk. J. Fish. Aquat. Sci. 7: 131-138.
- [2] Abdel-Hameid, N. A. H. (2009): A protective effect of calcium carbonate against arsenic toxicity of the Nile catfish, *Claria sgariepinus*. – Turk. J. Fish. Aquat. Sci. 9: 191-200.
- [3] Abdel-Tawwab, M., Khattab, Y. A. E., Ahmad, M. H., Shalaby, A. M. E. (2006): Compensatory growth, feed utilization, whole-body composition and hematological changes in starved juvenile Nile tilapia, *Oreochromis niloticus* (L.). – J. World Aquat. Soc. 18: 234-239.
- [4] Abdel-Tawwab, M., Mousa, M. A. A., Ahmad, M. H., Sakr, S. F. (2007): The use of calcium pre-exposure as a protective agent against environmental copper toxicity for juvenile Nile tilapia, *Oreochromis niloticus* (L.). – Aqua 264: 236-246.
- [5] Abdullah, S., Muhammad, J. (2006): Studies on acute toxicity of metals to the fish, *Catlacatla*. – Pak. J. Biol. Sci. 9: 1807-1811.
- [6] Akter, K. F., Owens, G., Davey, D. E., Naidu, R. (2005): Arsenic speciation and toxicity in biological systems. – Rev. Environ. Contam. Toxicol. 184: 97-149.
- [7] Barse, A. V., Chakrabarti, T., Ghosh, T. K., Pal, A. K., Jadhao, S. B. (2006): One-tenth dose of LC₅₀ of 4-tert-butylphenol causes endocrine disruption and metabolic changes in *Cyprinus carpio*. – Pestic. Biochem. Physiol. 86: 172-179.
- [8] Bears, H., Richards, J. G. Schulte, P. M. (2006): Arsenic exposure alters hepatic arsenic species composition and stress-mediated gene expression in the common killifish (*Fundulus heteroclitus*). – Aquat. Toxicol. 77: 257-266.
- [9] Begum, A., Mustafa, A. I., Amin, M. N., Banu, N., Chowdhury, T. R. (2013): Accumulation and histopathological effects of arsenic in tissues of shingi fish (Stinging Catfish) *Heteropneustes fossilis*. – J. Asiat. Soc. Bangladesh Sci. 39: 221-230.
- [10] Bolger, T., Connolly, P. L. (1989): The selection of suitable indices for the measurement and analysis of fish condition. – J. Fish Biol. 34: 171-182.
- [11] Chen, H., Li, S. F., Liu, J., Diwan, B. A., Barrett, J. C. Waalkes, M. P. (2004): Chronic inorganic arsenic exposure induces hepatic global and individual gene hypomethylation: implications for arsenic hepatocarcinogenesis. – Carcinogenesis 25: 1779-1786.
- [12] Crunkhorn, S. E., Plant, K. E., Gibson, G. G., Kramer, K., Lyon, J., Lord, P. G. Plant, N. J. (2004): Gene expression changes in rat liver following exposure to liver growth agents: role of Kupffer cells in xenobiotic-mediated liver growth. – Biochem. Pharmacol. 67: 107-118.

- [13] D'Amico, A. R., Gibson, A. W., Bain, L. J. (2014): Embryonic arsenic exposure reduces the number of muscle fibers in killifish (*Fundulus heteroclitus*). – *Aquat. Toxicol.* 146: 196-204.
- [14] Das, S., Sahu, B. (2005): Interaction of pH with mercuric chloride toxicity to penaeid prawns from a tropical estuary, East Coast of India: enhanced toxicity at low pH. – *Chemosphere* 58: 1241-8.
- [15] Das, S., Unni, B., Bhattacharjee, M., Wann, S. B., Rao, P. G. (2012): Toxicological effects of arsenic exposure in a freshwater teleost fish, *Channa punctatus*. *Afr. – J. Biotechnol.* 11: 4447-4454.
- [16] Datta, S., Saha, D. R., Gosh, D., Majumdar, T., Bhattacharya, S., Mazumder, S. (2007): Sub-lethal concentration of arsenic interferes with the proliferation of hepatocytes and induces in vivo apoptosis in *Clarias batrachus* L. *Comp. – Biochem. Physiol.* 145: 339-349.
- [17] Datta, S., Ghosh, D., Saha, D. R., Bhattacharaya, S., Mazumder, S. (2009): Chronic exposure to low concentration of arsenic is immuno-toxic to fish: role of head kidney macrophages arsenic biomarkers of arsenic toxicity to *Clarias batrachus*. – *Aquat. Toxicol.* 92: 86-94.
- [18] Eastwood, S., Couture, P. (2002): Seasonal variations in condition and liver metal concentrations of yellow perch (*Perca flavescens*) from a metal-contaminated environment. – *Aquat. Toxicol.* 58: 43-56.
- [19] Flora, S. J., Bhadauria, S. C., Pant, R. K. (2005): Induced blood and brain oxidative stress and its responses to some thiol chelators in rats. – *Life Sci.* 77: 2324-2337.
- [20] Gaim, K., Gebru, G., Abba, S. (2015): The effect of arsenic on liver tissue of experimental animals (Fishes and Mice). A review article. – *Int. J. Sci. Res. Publ.* 5: 1-9.
- [21] Gernhofer, M., Pawert, M., Schramm, M., Müller, E., Triebkorn, R. (2001): Ultra structural biomarkers as tools to characterize the health status of fish in contaminated streams. – *J. Aquat. Ecosyst. Stress Recovery* 8: 241-260.
- [22] Gupta, A. D., Karthikeyan, S. (2016): Individual and combined toxic effect of nickel and chromium on biochemical constituents in *E. coli* using FTIR spectroscopy and Principle component analysis. – *Ecotoxicol. Environ. Saf.* 130: 289-94.
- [23] Javed, M. (2015): Chronic dual exposure (waterborne plus dietary) effects of cadmium, zinc and copper on growth and their bioaccumulation in *Cirrhina mrigala*. – *Pak. Veter. J.* 35: 143-146.
- [24] Kar, S., Maity, J. P., Jean, J. S., Liu, C. C., Liu, C. W., Bundschuh, J., Lu, H. Y. (2011): Health risks for human intake of aquacultural fish: arsenic bioaccumulation and contamination. – *J. Environ. Sci. Health* 46: 1266-1273.
- [25] Kousar, S., Javed, M. (2014): Heavy metals toxicity and bioaccumulation patterns in the body organs of four fresh water fish species. – *Pak. Veter. J.* 34: 161-164.
- [26] Kovendan, K., Vincent, S., Janarthanan, S., Saravanan, M. (2013): Expression of metallothionein in liver and kidney of freshwater fish *Cyprinus carpio* var. *communis* (Linn) exposed to arsenic trioxide. – *Am. J. Sci. Ind. Res.* 4: 1-10.
- [27] Kumari, B., Vikas, K., Amit, K. S., Jawaid, A., Ghosh, A. K., Hanping, W., DeBoeck, G. (2017): Toxicology of arsenic in fish and aquatic systems. – *Environ. Chem. Lett.* 15: 43-64.
- [28] Lavanya, S., Ramesh, M., Kavitha, C., Malarvizhi., A. (2011): Hematological, biochemical and ionoregulatory responses of Indian major carp *Catla catla* during chronic sublethal exposure to inorganic arsenic. – *Chemosphere* 82: 977-985.
- [29] Lu, T., Liu, J., LeCluyse, E. L., Zhou, Y. S., Cheng, M. L., Waalkes, M. P. (2001): Application of cDNA microarray to the study of arsenic-induced liver diseases in the population of Guizhou, China. – *J. Toxicol. Sci.* 59: 185-192.
- [30] Mondal, K., Samanta, S. (2015): A review on arsenic contamination in fresh water fishes of West Bengal. – *J. Global Biosci.* 4: 2369-2374.

- [31] Morcillo, P., Cordero, H., Meseguer, J., Esteban, M. A., Cuesta, A. (2015): In vitro immunotoxicological effects of heavy metals on European sea bass *Dicentrarchus labrax* L. head kidney leucocytes. – *Fish Shellfish Immunol.* 47: 245-254.
- [32] Naz, S., Javed, M. (2012): Acute toxicity of metals mixtures for fish, *Catla catla*, *Labeo rohita* and *Cirrhina mrigala*. – *Pak. J. Agric. Sci.* 49: 387-391.
- [33] Pait, A. S., Nelson, J. O. (2003): Vitellogenesis in male *Fundulus heteroclitus* (Killifish) induced by selected estrogenic compounds. – *Aquat. Toxicol.* 64: 331-342.
- [34] Pandey, S., Parvez, S., Sayeed, I., Haque, R., Bin-Hafeez, B., Raisuddin, S. (2005): Biomarkers of oxidative stress: a comparative study of river Yamuna fish *Wallago attu* (Bl. & Schn.). – *Sci. Total Environ.* 309: 105-115.
- [35] Parameswaran, S., Selvaraj, C., Radhakrishnan, S. (1974): Observation on the biology of *Labeo gonius* (Ham.). – *Indian J. Fish.* 21: 54-75.
- [36] Patlolla, A. K., Tchounwou, P. B. (2005): Serum acetyl cholinesterase arsenic a biomarker of arsenic-induced neurotoxicity in Sprague–Dawley rats. – *Int. J. Environ. Res. Public Health* 2: 80-83.
- [37] Pedlar, R. M., Ptashynski, M. D., Evans, R., Klaverkamp, J. F. (2002): Toxicological effects of dietary arsenic exposure in lake whitefish (*Coregonus clupeaformis*). – *Aquat. Toxicol.* 57: 167-189.
- [38] Pipkin, F. B. (1964): *Medical Statistics Made Easy*. – Churchill Livingstone, Edinburgh.
- [39] Reddy, P. P., Jagadeshwarlu, R., Sunitha, G., Devi. (2016): Determination of lethal concentration (LC50) of copper to *Sarotherodon mossambica*. – *Int. J. Fish. Aquat. Stud.* 4(1): 172-175.
- [40] Sadekarpawar, S., Parikh, P. (2013): Gonadosomatic and Hepatosomatic indices of freshwater fish world. – *J. Zool.* 8: 110-118.
- [41] Sakamoto, K. Q., Nakai, K., Aoto, T., Yokoyama, A., Ushikoshi, R., Hirose, H., Ishizuka, M., Kazusaka, A., Fujita, S. (2003): Cytochrome P450 induction and gonadal status alteration in common carp (*Cyprinus carpio*) associated with the discharge of dioxin contaminated effluent to the Hikiji River, Kanagawa Prefecture, Japan. – *Chemosphere* 51: 491-500.
- [42] Shrivastava, A., Ghosh, D., Dash, A., Bose, S. (2015): Arsenic contamination in soil and sediment in India: sources, effects, and remediation. – *Curr. Pollut. Rep.* 1(1): 35-46.
- [43] Solé, M., Antó, M., Baena, M., Carrasson, M., Cartes J. E., Maynou, F. (2010): Hepatic biomarkers of xenobiotic metabolism in eighteen marine fish from NW Mediterranean shelf and slope waters in relation to some of their biological and ecological variables. – *Mar. Environ. Res.* 70: 181-188.
- [44] Tisler, T., Zagorc-Koncan, J. (2002): Acute and chronic toxicity of arsenic to some aquatic organisms. – *Bull. Environ. Contam. Toxicol.* 69: 4210-29.
- [45] Xu, H., Lam, S. H., Shen, Y., Gong, Z. (2013): Genome-wide identification of molecular pathways and biomarkers in response to arsenic exposure in zebrafish liver. – *PLoS One* 8: 68737.
- [46] Yamaguchi, S., Miura, C., Ito, A., Agusa, T., Iwata, H., Tanabe, S., Tuyen, B. C., Miura, T. (2007): Effects of lead, molybdenum, rubidium, arsenic and organochlorines on spermatogenesis in fish: monitoring at Mekong Delta area and in vitro experiment. – *Aquat. Toxicol.* 83: 43-51.
- [47] Yang, J., Chen, L., Liu, L., Shi, W., Meng, X. (2014): Comprehensive risk assessment of heavy metals in lake sediment from public parks in Shanghai. – *Ecotoxicol. Environ. Saf.* 102: 129-135.

EFFECTS OF SINGLE AND MIXED SOWING OF PERENNIAL GRASS (*LOLIUM PERENNE* L.) WITH COOL SEASON SPECIES ON GRASS PERFORMANCE

BIRER, S.^{1*} – GÖKKUŞ, A.²

¹Bayramiç Vocational College, Çanakkale Onsekiz Mart University, 17100 Çanakkale, Turkey

²Field Crops Department, Agricultural Faculty, Çanakkale Onsekiz Mart University, 17100 Çanakkale, Turkey

*Corresponding author
e-mail: selcukbirer@comu.edu.tr

(Received 16th Nov 2018; accepted 11th Jan 2019)

Abstract. This study has been conducted in Bayramiç District of Çanakkale Province in 2017 aiming to determine the seasonal performance of single and mixed sowing of perennial grass with some cool seasoned Gramineae species. Integra of *Lolium perenne*, Rebel XLR of *Festuca arundinacea*, Dumas1 of *F. ovina*, J-5 of *F. rubra commutata*, Redskin of *F. rubra rubra*, Samantha of *F. rubra trichophylla* and Miracle of *Poa pratensis* were used as the experimental subjects of this study. Total biomass production and grass quality attributes were investigated based on the number of species in mixtures and seasons. Fresh and dry biomass values significantly varied correlating to the seasons. The highest biomass productions were observed in spring and autumn. The highest values for grass quality, color, width, and coverage were observed in autumn. Single-sown *L. perenne* plots had superior attributes as compared to the mixed-sown plots. But grass color had darker green tones with the increasing number of species in mixtures. Present findings revealed that single-sowings yielded better grasslands than that of mixed-sowings and better structures were observed in autumn and spring as compared in summer. To establish quality grasslands in similar ecologies, *L. perenne* should be preferred and 2-3 species should be incorporated into the mixtures.

Keywords: *L. perenne*, mixed sowing, cool season, grass performance, grass color

Introduction

Just depending on increasing world population and developing industries, majority of the population is concentrated at city centers. People are in need of parks and recreation spots to meet their yearnings and devotion to nature (Avcıoğlu, 1997; Oral and Açıkgöz, 2002). Increasing urbanization in Turkey also increased people's interest in green zones. Lawns constitute the highest green zones of urban life. These zones are commonly established with the aid of architectural techniques as green covers for visual and esthetic purposes. They appeal to the eye and offer mental comfort, thus constitute a resting place for people (Avcıoğlu, 1997). Besides, lawns are natural oxygen depots of the cities, thus they purify city air and regulate precipitation regimes (Oral and Açıkgöz, 2002). Such green zones are also significant in mitigation the impact of climate change through absorbing sunrays and in reduction of pollution through absorbing environmental dust particles (Avcıoğlu, 1997). Maintenance of football pitches over which various sport activities are performed is a quite troublesome and difficult job requiring expertise. To establish high-quality long-lasting grasslands with attractive color, well cover ratio and rate, fast regeneration rates, resistant to pests, diseases and negative conditions and requiring less maintenance and mowing, the grass species to be used, their characteristics and adaptation capacities to the places they used should

thoroughly be investigated and appropriate ones should be selected meticulously (Avcioğlu, 1997). Grasslands are green spots composed of plant species covering the entire ground surface with a uniform appearance and able to be continuously mowed. According to data of the World Health Organization (WHO), the amount of green spots per capita should be at least 9 m². While such an area is around 8-12 m² in EU countries, it is only 2 m² in Turkey. The amount of green spots open to public in metropolitan cities of New York, Paris, London, Rio de Janeiro and İstanbul was respectively reported as 14%, 9.4%, 38.4%, 29% and 1.5% (Sözen et al., 1991; Önder and Polat, 2012).

In this study, the plant species of *Lolium*, *Festuca* and *Poa*, *Lolium perenne*, *F. ovina*, *F. rubra commutata*, *F. rubra rubra*, *F. rubra trichophylla* and *Poa pratensis* plant species of the genus *Lolium*, *Festuca* and *Poa* have been used in the studies that was carried out in order to create grass areas in the ecology of Mediterranean countries. It was aimed to determine the performance and quality characteristics of different grass using single as well as mix-cropping systems.

Materials and methods

Experiments were conducted in Bayramiç town of Çanakkale province in the year 2017 (Fig. 1; see also photos in the Appendix). While the long-term annual precipitation of the experimental site was 647.5 mm, the annual precipitation of the experimental year was 656.5 mm. While the months November, December and January had the highest precipitation, the months July, August and September had the least precipitation. The average monthly temperature has been recorded as 16.2 °C until the study was conducted and the average monthly temperature decreased to 16.1 °C in 2017. While the months June, July and August were the hottest months, the months December, January and February were the coldest months. Experimental soils were clay-loam in texture. Soils were non-saline (EC 0.85 mS/cm), slightly alkaline (pH 7.85), slightly limey (0.8%), poor in organic matter (0.78%), sufficient in available phosphorus (10.81 mg kg⁻¹) and potassium (329.75 mg kg⁻¹).



Figure 1. Study area situated in Bayramiç District of Çanakkale Province

In the research; double, triple, quartet, fivefold, sixfold and septet mixtures of *Lolium perenne* Integra (LP) single and *Festuca arundinacea* Rebel XLR (FA), *F. ovina* Dumas1 (FO), *F. rubra commutata* J-5 (FRC), *F. rubra rubra* Redskin (FRR), *F. rubra trichophylla* Samantha (FRT) and *Poa pratensis*'s Miracle (PP) varieties have been applied (*Table 1*).

Table 1. Applied mixing ratios and plants used in the experiment

Number	Groups of plant	Mixture ratios (%)						
1	LP	100	-	-	-	-	-	-
2	FA+LP	60	40	-	-	-	-	-
3	LP+FO	60	40	-	-	-	-	-
4	LP+FRC	60	40	-	-	-	-	-
5	LP+FRR	60	40	-	-	-	-	-
6	LP+FRT	60	40	-	-	-	-	-
7	LP+PP	60	40	-	-	-	-	-
8	FA+LP+FO	40	40	20	-	-	-	-
9	FA+LP+FRC	40	40	20	-	-	-	-
10	FA+LP+FRR	40	40	20	-	-	-	-
11	FA+LP+FRT	40	40	20	-	-	-	-
12	FA+LP+PP	40	40	20	-	-	-	-
13	FA+LP+FO+FRC	30	30	20	20	-	-	-
14	FA+LP+FO+FRR	30	30	20	20	-	-	-
15	FA+LP+FO+FRT	30	30	20	20	-	-	-
16	FA+LP+FO+PP	30	30	20	20	-	-	-
17	FA+LP+FRC+FRR	30	30	20	20	-	-	-
18	FA+LP+FRC+FRT	30	30	20	20	-	-	-
19	FA+LP+FRC+PP	30	30	20	20	-	-	-
20	FA+LP+FRR+FRT	30	30	20	20	-	-	-
21	FA+LP+FRR+PP	30	30	20	20	-	-	-
22	FA+LP+FRT+PP	30	30	20	20	-	-	-
23	FA+LP+FO+FRC+FRR	25	25	20	15	15	-	-
24	FA+LP+FO+FRC+FRT	25	25	20	15	15	-	-
25	FA+LP+FO+FRR+FRT	25	25	20	15	15	-	-
26	FA+LP+FRC+FRR+FRT	25	25	20	15	15	-	-
27	FA+LP+FO+FRC+PP	25	25	20	15	15	-	-
28	FA+LP+FO+FRR+PP	25	25	20	15	15	-	-
29	FA+LP+FRC+FRR+PP	25	25	20	15	15	-	-
30	FA+LP+FO+FRT+PP	25	25	20	15	15	-	-
31	FA+LP+FRC+FRT+PP	25	25	20	15	15	-	-
32	FA+LP+FRR+FRT+PP	25	25	20	15	15	-	-
33	FA+LP+FO+FRC+FRR+FRT	30	30	10	10	10	10	-
34	FA+LP+FO+FRC+FRR+PP	30	30	10	10	10	10	-
35	FA+LP+FO+FRC+FRT+PP	30	30	10	10	10	10	-
36	FA+LP+FO+FRR+FRT+PP	30	30	10	10	10	10	-
37	FA+LP+FRC+FRR+FRT+PP	30	30	10	10	10	10	-
38	FA+LP+FO+FRC+FRR+FRT+PP	25	25	10	10	10	10	10

Experiments were conducted over 114 plots (1 m x 2 m = 2 m²) in randomized blocks design with 3 replications. Sowing norm in the shape of seed/m². Plots were 20 cm apart and blocks were 40 cm apart from each other. Before sowing, nitrogen (N), phosphorus (P₂O₅) and potassium (K₂O) were applied to soils as composed fertilizer (15.15.15) as to have 10 g/m² on 19.10.2015. Ammonium sulphate was also applied to each plot on 02.05.2016 and 17.10.2016 as to have 5 g/m² N. Green and dry biomass along with grass quality according to Sills and Carrow (1983), Mehall et al., (1983) and Avcioglu (1997), grass color, width and coating ratios have been determined according to Spangenberg et al. (1986), Wenher et al. (1988), Goatley et al. (1994) and Avcioglu (1997). Resultant data were subjected to statistical analyses in accordance with randomized blocks split plots experimental design. Means were compared with Duncan's multiple comparison test (Düzgüneş et al., 1987).

Results

Fresh and dry biomass

While fresh biomass of grasslands significantly varied with the seasons, effects of number of species in mixtures and number of species x season interactions did not have significant effects on fresh biomass values. The highest fresh biomass (459.0 g/m²) was obtained from spring and the least fresh biomass (314.9 g/m²) was obtained from summer season. Based on the number of species in mixtures, fresh biomass values varied between 347.4–427.9 g/m². Despite the insignificant differences between them, single-sown and senary mixtures of *L. perenne* had slightly greater fresh biomass quantities (Table 2).

Table 2. Number of species in the mixture and green mass amounts of grass area according to season (g/m²)

Number of species	Spring	Summer	Autumn	Mean
1	504.7	318.8	450.8	424.7
2	424.7	341.4	371.7	379.3
3	442.5	311.6	366.4	371.5
4	440.2	295.6	364.6	366.8
5	460.7	311.9	412.9	395.1
6	517.7	321.4	444.6	427.9
7	422.7	303.3	316.3	347.4
Mean	459.0 a	314.9 c	388.8 b	-
Significance	P _{number of species} = 0.1795, P _{season} = 0.0001, P _{number of species*season} = 0.9586			

While the dry biomass of single-sown and mixtures of *L. perenne* did not significantly vary relative to the number subject of species in mixtures, but significant differences were observed between the dry biomass values of the seasons. Based on number of species in mixtures, dry biomass values varied between 97.3–110.9 g/m². On the other hand, while the highest dry biomass values were observed in spring (112.6 g/m²) and autumn (111.9 g/m²), plants had less dry biomass in summer (87.0 g/m²) (Table 3).

Table 3. Number of species in the mixture and dry mass of grass area according to the season (g/m²)

Number of species	Spring	Summer	Autumn	Mean
1	121.4	86.8	124.3	110.9
2	107.2	94.4	111.7	104.4
3	107.4	83.6	105.7	98.9
4	109.3	82.9	107.7	100.0
5	112.9	86.4	115.9	105.0
6	122.1	86.0	122.1	110.0
7	107.9	88.6	95.6	97.3
Mean	112.6 a	87.0 b	111.9 a	-
Significance	P _{number of species} = 0.2220 P _{season} = 0.0001, P _{number of species*season} = 0.8270			

Grass quality

In order to determine the quality values of pre-harvest quality in each plot that applied by Sills and Carrow (1983) and Mehall et al. (1983), and the quality values were also determined according to the scale of 1-9 (1: worst, 9: best) with regard to the uniformity, frequency and cleanliness of the grass that described by Avcioğlu (1997). While number of species in *L. perenne* mixtures and seasons had significant effects on grass quality, the effects of interactions were not found to be significant. The best quality (with a score of 9.0 points) was achieved in autumn and the poorest quality (with a score of 7.4 points) was observed in spring. Slight decreases were observed in quality scores with the increasing number of species in mixtures (Table 4).

Table 4. Grass quality based on number of species in mixtures and seasons

Number of species	Spring	Summer	Autumn	Mean
1	7.7	8.3	9.0	8.3 a
2	7.5	8.1	9.0	8.2 ab
3	7.5	8.1	8.9	8.2 ab
4	7.2	8.1	9.0	8.1 b
5	7.2	7.1	9.0	8.1 b
6	7.4	8.2	8.8	8.1 b
7	7.0	8.1	9.0	8.0 b
Mean	7.4 c	8.1 b	9.0 a	-
Significance	P _{number of species} = 0.0310, P _{season} = 0.0001, P _{number of species*season} = 0.0705			

Grass color

In each plot, the color of the grass was determined in the period in which the harvesting was not done in order to determine the color of the plot periodically applied by Spangenberg et al. (1986); Wenher et al. (1988) and Goatley et al. (1994), and the color of the grass has also been determined according to the harvesting scale of 1-9 (1: yellow, 9: dark green) as indicated by Avcioğlu (1997). Grass color

significantly varied with number of species in mixtures, seasons and their interactions. The best grass color (7.34) was observed in autumn and it was followed by summer (6.30) and spring (3.68). Increasing number of species in mixtures improved grass color (Table 5).

Table 5. Grass color based on number of species in mixtures and seasons

Number of species	Spring	Summer	Autumn	Mean
1	3.70 g	6.53 e	7.00 d	5.74 BC
2	3.67 g	6.13 f	7.13 cd	5.64 C
3	3.70 g	6.23 f	7.30 bc	5.74 BC
4	3.67 g	6.17 f	7.30 bc	5.71 BC
5	3.63 g	6.37 ef	7.37 bc	5.79 B
6	3.70 g	6.37 ef	7.40 b	5.82 B
7	3.70 g	6.30 ef	7.90 a	5.97 A
Mean	3.68 C	6.30 B	7.34 A	-
Significance	P _{number of species} = 0.0021, P _{season} = 0.0001, P _{number of species*season} = 0.0001			

Grass width

While number of species had significant effects on grass width, the effects of seasons and interactions were not found to be significant. Grass widths decreased with increasing number of species in mixtures. The highest grass width (3.98 mm) was obtained from single-sown *L. perenne* plots. Based on seasons, grass widths varied between 3.34-3.90 mm (Table 6).

Table 6. Grass width based on number of species in mixtures and seasons (mm)

Number of species	Spring	Summer	Autumn	Mean
1	3.97	3.97	4.00	3.98 A
2	3.73	3.83	3.87	3.81 B
3	3.30	3.37	3.40	3.36 C
4	3.17	3.27	3.27	3.23 CD
5	3.13	3.13	3.20	3.16 D
6	3.13	3.13	3.17	3.14 D
7	3.93	3.03	3.03	3.00 E
Mean	3.34	3.90	3.42	-
Significance	P _{number of species} = 0.0001, P _{season} = 0.1744, P _{number of species*season} = 0.9999			

Grass coverage

Grass coverage was significantly greater in autumn (8.96) than in the other seasons. The lowest coverage (8.29) was observed in summer. Number of species in mixtures did not yield significant variations in grass coverage and the values varied between 8.46–8.68 (Table 7).

Table 7. Grass coverage based on number of species in mixtures and seasons

Number of species	Spring	Summer	Autumn	Mean
1	8.10 b	8.30 b	9.00 a	8.46
2	8.10 b	8.30 b	9.00 a	8.46
3	8.77 a	8.27 b	8.83 a	8.62
4	8.73 a	8.30 b	9.00 a	8.67
5	8.77 a	8.30 b	9.00 a	8.68
6	8.77 a	8.27 b	8.90 a	8.64
7	8.77 a	8.30 b	9.00 a	8.68
Mean	8.57 B	8.29 C	8.96 A	-
Significance	P _{number of species} = 0.0484, P _{season} = 0.0001, P _{number of species*season} = 0.0033			

Discussion

The species used in formation of grasslands are cool season species. Cool season species exhibit their best growth and development in spring (Miller, 1984). Plants then exhibit regrowth in autumn with cooling weathers (Altın et al., 2011). Since hot weathers of summer put plants into stress, expected growth is not achieved even with evaporative cooling and fertilizations (Gökkuş, 1989). Therefore, in grasslands established with cool season species, the greatest biomass is observed in spring and autumn.

The best quality of single-sown *L. perenne* plots was attributed to genetic characteristics and this plant being well-adapted to grasslands. Since cool season species exhibit their best growth and development in spring and autumn, they are expected to have greater quality scores in these seasons. But, cold weather of winter and spring of the experimental year recessed plant growth and development. Such a case then yielded greater quality scores in summer instead of spring. Regrowth in autumn again increased the quality scores of grasslands.

Color is the primary quality attribute for grasslands. It is an indicator of agronomic and physiological characteristics and also plays a great role in visually (Kroon and Knops, 1991; Williems et al., 1993). Grassland color is directly related to chlorophyll content of gramineae species (Açıkgöz, 1994; Avcıoğlu, 1997). Besides chloroplasts, color is also dependent on plant nitrogen, iron, and manganese uptake from the soil and plant water content. Therefore, each gramineae species has its specific color tone (Beard, 1973; Açıkgöz, 1994; Avcıoğlu, 1997). Seasonal changes in color characteristics of grasslands continuously increased from spring to autumn. This is because single-sown and mixture grasses exhibited slow growth and development in spring, spent the summer in dormant nature and exhibited the most significant portion of growth and development in autumn. Therefore, the highest color scores were achieved in autumn (Açıkgöz, 1994).

The highest grass width of single-sown plots was attributed to less competition of single-sown plots for water and nutrients than the mixed-sown plots. Single-sown plants had greater plant widths as compared to plant heights. In competitive environments, plants generally have longer, but weaker stems.

Heat requirements of the plants were effective in coverage levels. Since experimented grass species were cool season species, coverage levels were also greater

in cool seasons (autumn and spring). These plants generally get into dormant season in summers (Altın et al., 2011), thus they have low coverage levels in summers.

Conclusions

In this study, carried out in Çanakkale province, seasonal (spring, summer and autumn) performance of single-sown *Lolium perenne* and mixtures with *Festuca arundinacea*, *F. ovina*, *F. rubra commutata*, *F. rubra rubra*, *F. rubra trichophylla* and *Poa pratensis* have been investigated. Present findings revealed increasing fresh and dry biomass in spring and autumn and decreasing values in summer. Grass quality was ordered as autumn > summer > spring and the highest values were observed in single-sown plots. Grass colors increased with increasing number of species in mixtures. Grass quality did not change significantly with the seasons. The darkest grass color was observed in autumn. While grass widths did not change significantly with the seasons, but decreased with increasing number of species in mixtures. The highest grass coverage was attained in autumn. It was concluded based on present findings that single-sown *L. perenne* plots yielded the highest biomass values and quality attributes.

Acknowledgements. This paper is a part of the doctorate dissertation of Mr. Selçuk Birer's entitled, "The Effects of Chewing in Different Grass Mixtures on Plant Growth and Grass Quality."

REFERENCES

- [1] Açıkgöz, E. (1994): Çim Alanlar Yapım ve Bakım Tekniği. – Uludağ Üniversitesi Ziraat Fakültesi, Bursa.
- [2] Altın, M., Gökkuş, A., Koç, A. (2011): Çayır ve Mera Yönetimi (2. Cilt). – Tarım ve Köyişleri Bakanlığı, Tarımsal Üretim ve Geliştirme Genel Müdürlüğü, Ankara.
- [3] Avcıoğlu, R. (1997): *Çim Tekniği, Yeşil Alanların Ekimi, Dikimi ve Bakımı*. – Ege Üniversitesi Ziraat Fakültesi, Tarla Bitkileri Anabilim Dalı, Bornova-İzmir.
- [4] Beard, J. B. (1973): Turfgrass Science and Culture. – Prentice Hall, Englewood Cliffs, NJ.
- [5] Düzgüneş, O., Kesici, T., Kavuncu, O., Gürbüz, F. (1987): Araştırma ve Deneme Metotları (İstatistik Metotları-II). – A. Ü. Zir. Fak. Yayınları, 1021/295.
- [6] Goatley, J. M., Maddox, V. L., Watkins, R. M. (1996): Growth regulation of bahiagrass (*Paspalum notatum* Fluegge) with imazaquin and AC 263,222. – HortScience 31(3): 396-399.
- [7] Gökkuş, A. (1989): Gübreleme, sulama ve otlatma uygulamalarının Erzurum ovasındaki çayırların kuru ot ve ham protein verimlerine etkileri. – DOĞA Tu. Tar. ve Orm. Dergisi 13(3b): 1002-1020.
- [8] Kroon, H. D., Knops, J. (1991): Habitat exploration through morphological plasticity in two chalk grassland perennials. – Herbage Abst. 61: 8.
- [9] Mehall, B. J., Hull, R. J., Skogley, C. R. (1983): Cultivar variation in Kentucky bluegrass: P and K nutritional facts. – Argon. J. 75: 767-772.
- [10] Miller, D. A. (1984): Forage Crops. – McGraw Hill Book Co., New York.
- [11] Oral, N., Açıkgöz, E. (2002): Çim Alanlar için Tohum Karışımları. – TMMOB Ziraat Mühendisleri Odası Bursa Şubesi Başkanlığı Yayınları, 1.
- [12] Önder, S., Polat, A. (2012): Kentsel açık-yeşil alanların kent yaşamındaki yeri ve önemi. – Kentsel Peyzaj Alanlarının Oluşumu ve Bakım Esasları Semineri, Konya, pp. 73-96.

- [13] Sills, M. J., Carrow, R. N. (1983): Turfgrass growth, N use and water use under soil compaction and N fertilization. – *Argon. J.* 75: 488-492.
- [14] Sözen, N., Halepoğlu, N., Şahin, Ş. (1991): Ülkemizde süs fidancılığının durumu ve pazar açısından karşılaşılan sorunlar. – *Türkiye I. Fidancılık Sempozyumu*, pp. 411-419.
- [15] Spangenberg, B. G., Fermanian, T. W., Wehner, D. V. (1986): Valuation of liquid-applied nitrogen fertilizers on Kentucky bluegrass turf. – *Argon. J.* 78: 1002-1006.
- [16] Wehner, D. J., Haley, J. E., Martin, D. L. (1988): Late fall fertilization of Kentucky bluegrass. – *Argon. J.* 80: 466-471.
- [17] Williems, J. H., Peet, K. R., Bık, L. (1993): Changes in chalk grassland structure and species richness resulting from selective nutrient additions. – *Herb. Abstract* 63(7).

APPENDIX

Photos of the study area





EFFECT OF LONG-TERM POTASSIUM FERTILIZER LEVELS ON THE YIELD OF RAINFED CORN IN NORTHEAST CHINA

WANG, Y. – ZHANG, T. – LI, B. – FENG, G. – YAN, L.* – GAO, Q.*

Key Laboratory of Groundwater Resources and Environment, Ministry of Education, Jilin University, Changchun 130021, China

College of Resource and Environment, Jilin Agricultural University, Changchun 130118, China

**Corresponding authors*

e-mail/phone: yanlijau@163.com/+86-155-2686-6351; gaoqinglunwen@163.com/+86-131-3445-7702

(Received 3rd Apr 2019; accepted 12th Dec 2019)

Abstract. The excessive application of potassium (K) fertilizer over the last 30 years has resulted in considerable resource waste and environmental risk. In order to economize and protect the environment, China launched a soil testing and fertilizer recommendation project from 2005 to 2015. A total of 1370 on-farm experiments were conducted concerning maize fields in Jilin Province Northeast China, also called the golden maize (*Zea mays* L.) belt, over the past ten years to evaluate the effects of the implemented project and to provide farmers with an improved fertilizer recommendation system. The results showed that the average yield of maize with K0 treatment was 9000 kg ha⁻¹. Its maximum yield (Max.yield) and increased yield (IY k) after application of K fertilizer averaged at 10200 kg ha⁻¹ and 1100 kg ha⁻¹, respectively. Significant variability was evident in K0 yield and Max.yield over the years. Maize hybrids and different soil types had significant differences in IY yield. Meanwhile, IY k can either increase or decrease depending on K0 yield, which suggest that a suitable K fertilizer can improve the yield, whereas excessive fertilizing would have no obvious effect on the yield. In addition, the yield was found to be affected by environment, maize hybrids, soil types, and K fertilizer rate.

Keywords: *increasing yield, soil fertility, hybrids, soil types, fertilizer use efficiency*

Introduction

Alongside developing modern hybrids and improving agronomic management, fertilizer use is recognized in China as one of the key methods for increasing yield. Indeed, the effects of nitrogen (N) and phosphorus (P) fertilizers on corn production have been extensively studied; however, the effect of potassium (K) fertilizer has not been given much attention. As one of the three major plant macronutrients, potassium has multiple functions in the activation of cellular enzymes; the synthesis of proteins, starch, cellulose, and vitamins; the development of resistance to abiotic and biotic stresses; the improvement of N and P fertilizer use efficiency; and the enhancement of productivity and quality of agricultural produce (Ogundijo et al., 2017; Chen et al., 2012a; Epstein and Bloom, 2005). Neglect of the importance of potassium coupled with high input of inorganic N and P fertilizers to meet the continually increasing demand for food has resulted in their low use efficiency, as well as N:P:K imbalance in plant and soil systems leading to severe eutrophication (Tian et al., 2017; Zhang et al., 2011). Potassium deficiency is a nationwide phenomenon, with approximately 43% of soils requiring additional potassium (Zoerb et al., 2013). However, excessive application of potassium fertilizer, which could persist in the soil for years after application, is also a documented occurrence (Xie, 2000; Tenkorang and Lowenberg-DeBoer, 2009).

Therefore, determining the appropriate potassium input is crucial to the achievement of high yield and high efficiency.

China produced 155 Mt of maize (*Zea mays* L.) in 2007 (National Bureau of Statistics of China, 2007; Wang et al., 2007), which made the country the second largest producer of maize worldwide (Zhang et al., 2011). In 2017, the yield of maize increased to 259 Mt (National Bureau of Statistics of China, 2011). The increase of yield was apparent in Northeast China, particularly in Jilin Province, which increased from 18 Mt in 2007 to 32.5 Mt in 2017 (National Bureau of Statistics of China, 2017). The recent long-term application of K fertilizer may be one of the reasons for this improvement.

Several studies have demonstrated that long-term potassium fertilizer application can maintain crop productivity and soil quality (Wang et al., 2007), and that K efficiency and partial balance condition can affect crop yield (Zhang et al., 2011). However, studies on the relationship between corn yield and the long-term application of potassium fertilizer in Northeast China are scarce. In 2005, China launched a nationwide soil testing and fertilizer recommendation project to mitigate excessive and unbalanced fertilizer application. Hereby, we just chose the data in Jilin Province as analysis sample due to large amount of data in whole project, the objective of this study was to examine the ten-year experiment of “soil testing and fertilizer recommendation” in Northeast China from 2005 to 2015 and to determine (1) the relationship between corn yield and potassium fertilizer in K deficient and K excessive conditions, and (2) whether the amount of recommended K rate (RKR) was optimized by the K fertilizer to satisfy the K requirement of corn.

Materials and methods

The study area was located in Jilin province in Northeast China with between 40° and 47° N latitude and between 121° and 131° E longitude in the east of Eurasian continent in the middle latitude, which is not only one of the three black soil regions in the world, but also one of three golden corn belts in the world. The climate in the study area is warm-temperate, sub-humid, continental monsoon with cold winters and hot summers. Annual precipitation ranges from 500 mm to 800 mm, with 60 to 70% of the rainfall occurring in the summer. No irrigation was supplied during the corn-growing season. There are more than 30 counties in nine cities in Jilin province with 187400 km². The soil types primarily included Haplic Luvisol, Albic Luvisol, Haplic Phaeozem, Cambisol, Haplic Kastanozem, Calcaric Arenosol, Haplic Chernozeme, and Luvic Phaeozem (http://en.wikipedia.org/wiki/FAO_soil_classification; Gong et al., 1999).

Experimental design

A total of 1370 on-farm experiments on corn production were chose from 2005 to 2015 in 55 counties of Jilin Province (*Fig. 1*). All experimental fields received four K treatments without replication: No K control (K0), RKR, 50% RKR, and 150% RKR. RKR was determined according to the recommendations of an agronomist based on the estimated soil fertility and the target yield (1.1 times the average yield for the past five years, which varied by field). RKR values in different farm fields were different because of diverse soil condition and environmental variables.

The experiments were conducted on a continuous corn system, and new experimental sites were selected every year. Generally, one-third of N and the total K and P fertilizers

were applied at pre-sowing, and the remaining two-thirds of N fertilizer was applied as top-dressing at around the six-leaf stage.

The plot size was approximately 40 m² (4 m × 10 m). Based on soil N and P levels, all plots received sufficient amounts of urea (185 kg to 250 kg N ha⁻¹) and triple superphosphate (60 kg to 120 kg P₂O₅ ha⁻¹) at pre-sowing. No organic manure was applied. All experiments were managed according to the same practices of each individual producer except for implementing the treatments and obtaining crop and soil samples, which were conducted by the researchers. A total of 71 maize hybrids were used in the experimental sites, which belong to four typical variety series in Jilin province, such as Zhengdan, Jidan, Xianyu, and Nongda, and these were individually selected by the farmers. Moreover, all hybrids had high yield potential. The corn was planted in the beginning of May and was harvested by the end of September. Weeds were controlled with herbicide after seedling, and no obvious water or pest stress was observed during the corn-growing seasons (the data in disaster such as flood, pest disaster, extreme drought in some trial sites and incomplete data have been eliminated). The plant population was about 55000 with 60 cm row spacing, which is typical in Jilin Province.

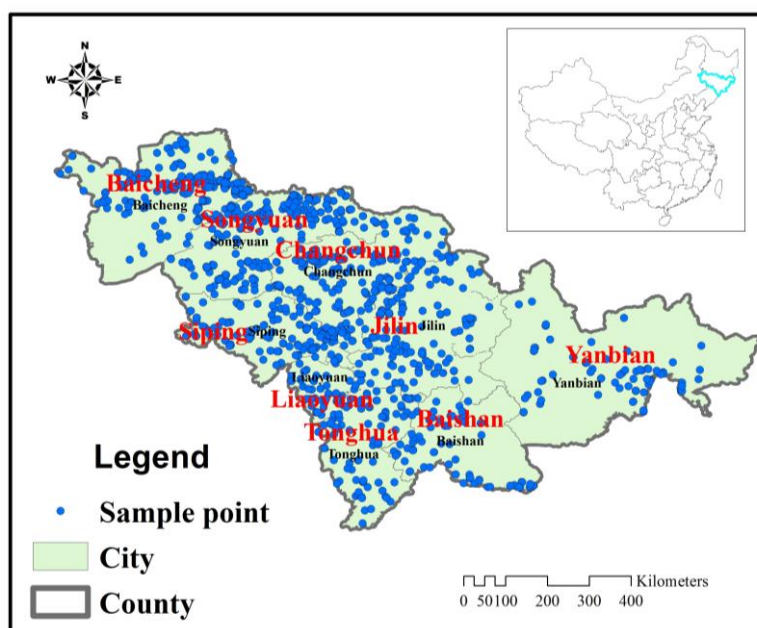


Figure 1. Sample point information map

Sampling and laboratory procedures

At least three samples of 20 cm soil layer were obtained from each field for all of the plots. The samples were air-dried, sieved, and used to measure the exchanged-K (Van Reeuwijk, 1992). For each experiment, gain yield at maturity was assessed by hand on a 2.5 m × 8 m section of each plot, and the value was adjusted to 14% moisture.

Data analysis

All experimental data were analyzed with correlation analysis method by using software SAS. Single factor analysis was employed to compare the mean yields of K

treatments based on the least significant difference (LSD) at a 0.05 level of probability. Given the data complication, data on four common soil types (Albic soils, Chernozem, Aeolian sand, and Phaeozem) in Northeast China and four typical hybrids (Zhengdan, Jidan, Xianyu, and Nongda) in farmer fields across all treatments in the 1370 fields were selected and analyzed. The product of the dimension model and the years degrees of freedom ($df = 10$), hybrids ($df = 3$), and soil type ($df = 3$) was used to assess the overall variability of the increased yield (IY k), the yield with N0 treatment, and the maximum yield (Max.yield).

Maximum grain yield was defined as the highest mean yield of all K treatments for each field. Increased yield for applied K fertilizer (IY k) was defined as the difference between Max.yield and the yield of the K0 treatment for each experiment. The agronomic K efficiency (AEK) and K partial factor productivity (PFPK) were calculated based on *Equations 1* and *2* (Ladha et al., 2005). AEK is the yield increase per unit of K applied, and PFPK is the most significant index for farmers because it integrates the usage efficiency of both indigenous and applied K resources.

$$AEK = (YK - Y0) / K \quad (\text{Eq.1})$$

$$PFPK = YK / K \quad (\text{Eq.2})$$

where YK and Y0 represent the grain yield in K application plots and K0 plots, respectively, and K is K from the applied fertilizer.

Results

Yield, increasing yield, AEK and PFPK with different K treatments

In this study, soil organic matter, TN, TP, and PH in the top 20 cm soil profile averaged at $17.4 \pm 19.6 \text{ g kg}^{-1}$, $1.4 \pm 1.3 \text{ g kg}^{-1}$, $0.8 \pm 0.4 \text{ g kg}^{-1}$, and 6.7 ± 1.0 , respectively. These values are typical for rainfed corn production in Northeast China. The grain yield for the K0 treatment across all of the 1370 experiment fields averaged at 9.0 Mg ha^{-1} and varied from 2.1 Mg ha^{-1} to 17.9 Mg ha^{-1} (*Table 1*). Increasing yield rate resulting from K fertilizer input was 5.6%, 10.0%, and 8.9% for 50% RKR, RKR and 150% RKR, respectively. So it can be seen that the K fertilizer is one of important factors to increase yield. Reasonable K fertilizer rate can reach the best effect of increasing yield comparing to less or excessive K fertilizer application. The RKR across 1370 experiment fields was $72 \pm 7.5 \text{ K}_2\text{O kg ha}^{-1}$ and varied from $19.5 \text{ K}_2\text{O kg ha}^{-1}$ to $180 \text{ K}_2\text{O kg ha}^{-1}$. The grain yield of RKR averaged at 9.9 Mg ha^{-1} and varied from 2.1 to 17.0 Mg ha^{-1} . AEK and PFPK for RKR averaged at 12.2 and 138.9 kg kg^{-1} , respectively (*Table 2*). Compared with RKR, the addition of more K beyond RKR (+50%) did not increase yields, but reduced AEK and PFPK. Treatments below RNR (-50%) resulted in a 0.4 Mg ha^{-1} yield loss. Therefore, RKR is a reasonable range to attain maximum grain yield.

Effect of years, hybrids and soil types on K fertilizer and yield

Year factor significantly affected the variation in Max.yield and K0 yield resulting from environmental factors such as rainfall, temperature, and insect pests (*Table 1*; $P = 0.01$). Max.yield among different years varied from 8.9 Mg ha^{-1} to 10.6 Mg ha^{-1} . The mean Max.yield in 2008 was 10.4 Mg ha^{-1} , which was caused by suitable rainfall

and sunlight. The yield decreased in 2007 and 2009 because of drought. In addition, the yield decreased in 2010 because of the flood in certain parts of Jilin Province.

Table 1. Mean grain yield with different K treatments, maximum yield (Max.yield), and increased yield to K fertilizer (IYK), optimum K fertilizer rate (OKR) with different sites, and their variation among 1370 experiment fields

K treatment	Mean	25%Q +	Median	75%Q +
Grain yield (t/ha)				
Yield at N0	9.0 ± 1.8	7.9	9.1	10.1
Yield at 50%RKR	9.5 ± 1.8	8.5	9.5	10.6
Yield at RKR	9.9 ± 1.8	8.8	10	11.2
Yield at 150%RKR	9.8 ± 1.8	8.7	9.9	11
Max.yield	10.2 ± 1.8	9.1	10.3	11.4
IYK	1.1 ± 0.7	0.7	1.1	1.6
Source of variation for yield at K0 treatment, Max.yield, IYK and OKR				
Source	K0 yield	Max.yield	IYk	OKR
Hybrids (3)	**	**	**	
Soil type (3)	**	**	ns	**
Year (10)	**	**		**

Q: quartile; ns: nonsignificant at 0.05 probability levels. *p = 0.05; **p = 0.01

Table 2. Mean agronomic K efficiency (AEK) and partial factor productivity (PFPK) and its variation with different K treatments among 1370 experimental fields

Item	K treatment	Mean	25%Q	Median	75%Q
AE _K (kg kg ⁻¹)	50%RKR	12.7	1.2	11.5	23.7
	RKR	12.2	4.4	11.8	19.4
	150%RKR	7.1	1.9	7.2	11.6
PFP _k (kg kg ⁻¹)	50%RKR	266	232.1	267.6	300
	RKR	138.9	120.6	140.7	156.6
	150%RKR	91.5	80.2	92.8	102.5

Q: quantile

Moreover, the different hybrids had extremely significant differences in Max.yield, K0 yield, and IY. Among the four typical maize (*Zea mays* L.) hybrids in Jilin Province, the Zhengdan hybrid has the highest K0 yield, which displayed higher tolerant ability of poor soil. However, the Xianyu hybrid has the highest Max.yield and IY, which indicate stronger sensitivity to potassium nutrition. The AE of the hybrid can be reflected by the following order: Xianyu > Jidan > Nongda > Zhengdan. The Xianyu hybrid exhibits high increased yield regardless of the environment. For example, in 2008 and 2007, the Xianyu hybrid had absolutely high IY, which exhibited better increasing potential (data did not show).

The yield from four typical soil types in Jilin Province had extremely significant differences in K0 treatment and Max.yield. The yield from Aeolian sand was the lowest,

whereas that from Phaeozem soils was the highest (Fig. 2). No difference in IY was observed. Optimum fertilizer rate was calculated via linear-regression analysis using SAS software. Results showed that the optimum fertilizer rate in Albic soils and Chernozem soils was generally higher than that in Aeolian sands. In an ideal environment, optimum K fertilizer rate in Albic soils, Phaeozem, Chernozem, and Aeolian sand soils was 63.2, 82.2, 58, and 51.6 kg/ha, respectively. The optimum yield calculated by SAS software was similar to the average yield, which indicated that RKR was a rational range.

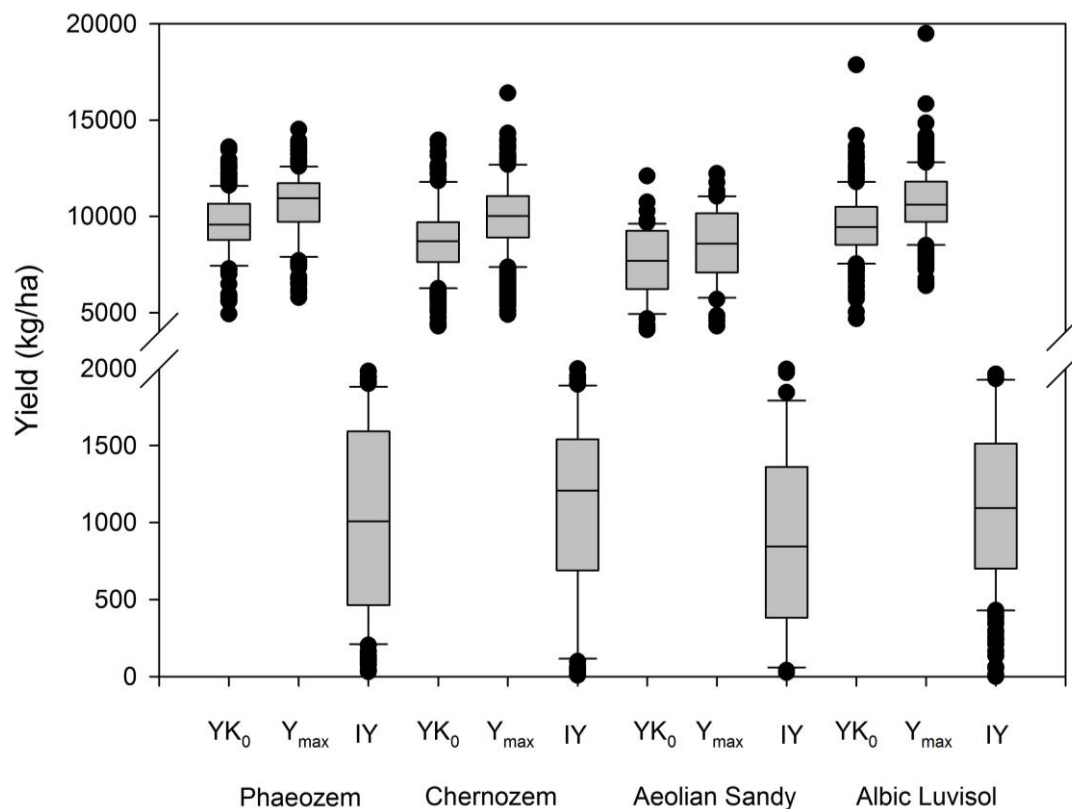


Figure 2. Averaged yield per hectare of 4 kinds of soil types in 2005-2010 in test fields. YK_0 means yield with K0 treatment; Y_{max} means the maximum yield with K treatment; IY means increasing yield. The upper and lower limits of each box represent 25% and 75% values, the horizontal solid lines inside the box indicate mean values, respectively

The relationships among Max yield, increasing yield and K0 yield

A close relationship was found between Max.yield and yield of K0 treatment across all fields ($R^2 = 0.87$; Fig. 3A). The maximum grain yield increased as the yield of K0 treatment was increased. According to statistics, the rate of corn yield of RKR with respect to Max.yield is 52%. The rate of corn yield of 150% RKR with respect to Max.yield is 42% in all fields. These results indicated that a sufficient amount of K fertilizer was applied, which resulted in high yield. However, compared with the RKR yield, the average yield of RKR was higher than the yield of 150% RKR, and agronomic efficiency of RKR was significantly higher than that of 150% RKR, which indicated that RKR was the suitable amount of fertilizer that must be applied in Northeast China.

IY k has correlation with increasing yield of K0 treatment ($R^2 = 0.1$; Fig. 3B). When the grain yield of K0 treatment is smaller than 8.0 Mg ha^{-1} , IY k increases with the yield of K0 treatment. However, when the grain yield of K0 treatment is greater than 8.0 Mg ha^{-1} , IY k decreases with the yield of K0 treatment. This phenomenon shows that a suitable amount of K fertilizer can improve the grain yield in the soil with K deficiency. However, the increase in yield caused by the application of K fertilizer in soils of middle and high yield is not significant. Moreover, when the corn grain yield is extremely high (greater than 12.0 Mg ha^{-1}), certain IY k were still higher (Fig. 3B). This finding partly indicated that the soils of certain plots were more fertile, which resulted in high yield, and the addition of K fertilizer input improved the soil fertility balance, which resulted in higher yield.

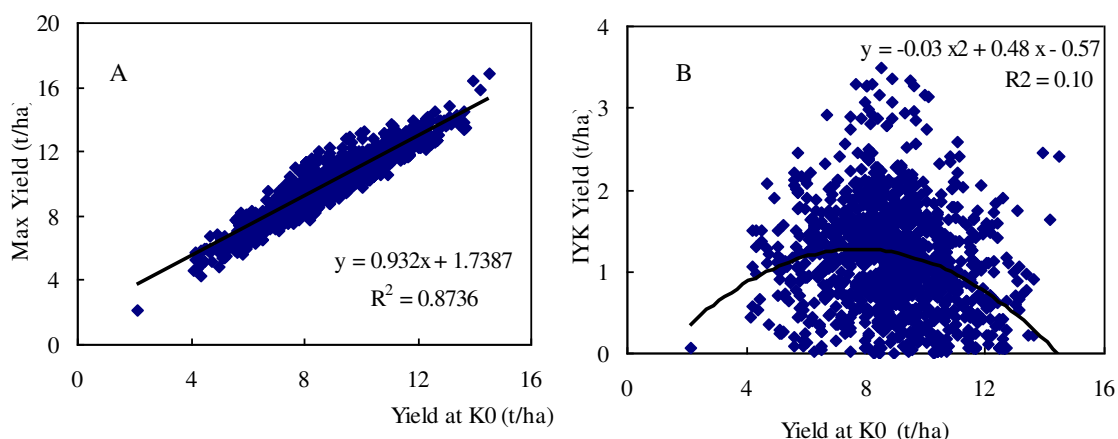


Figure 3. *A* Relationship between maximum yield (Max.yield) and grain yield at K0 treatments across all 1370 fields. *B* Relationship between increase yield (IYk) to applied K fertilizer and grain yield at K0 treatments across all 1370 fields

The percentage of IYk (Fig. 4) in maximum yield (IY k/Max.yield) decreased with increasing yield for K0 treatments, which suggested a conflict between improving usage efficiency and further increasing the yields (Gao et al., 2012).

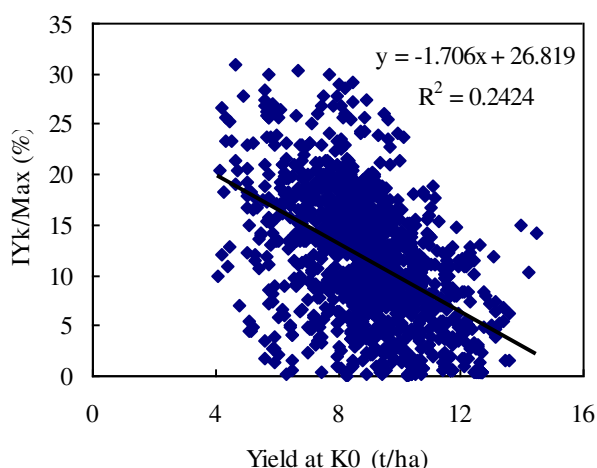


Figure 4. Relationship between the percentage of IYk in maximum yield (IY k/Max.yield) and grain yield at K0 treatments across all 1370 fields

Discussion

Yield, increasing yield, AEK and PFPK

Jilin Province in Northeast China is one of the three gold corn belts of the world. The province is the most significant maize-producing regions in China. As the population continues to grow, the amount of farmland has decreased in recent years. Therefore, adding yield per unit to increase maize production has been the focus of several studies in China. From the Chinese Revolution until today, maize yield per hectare has gone through several stages of rapid development with the emergence of maize hybrid varieties, fertilizer application, and management technology improvement (Ren et al., 2010). From 2005 to the 2011, the averaged yield per hectare is from 3.2 Mg ha⁻¹ to 7.5 Mg ha⁻¹ because of the implementation of the soil testing and fertilizer recommendation project and the high-yield, high-efficiency management in Jilin Province (National Bureau of Statistics of China 2007; National Bureau of Statistics of China 2011), however the averaged K fertilization rate applied (K₂O) is from 38.4 kg ha⁻¹ to 42.1 kg ha⁻¹ due to decreased maize planting areas and increased potassium fertilizer emphasis, which is obviously lower than national maize averaged 82kg ha⁻¹ (Li et al., 2010). Averaged agronomical efficiency (AE) and partial factor productivity from applied fertilizer (PFP) of potassium in 2005-2015 in Jilin province is 17.3 kg kg⁻¹ and 32.7 kg kg⁻¹ which is obviously higher than average level in China (Li et al., 2010). Compared with averaged yield per hectare in USA in 2005 9.3 Mg ha⁻¹ and higher potassium use efficiency (Zhang et al., 2008), yield and fertilizer use efficiency in China were still lower mainly by three factors. First is farmer experience unconscious fertilization, farmers yet applied old notion of more input, then more output. Second is ignorant of mix application of organic and inorganic fertilizer, and of macro element and microelement fertilizer. Last is low level of mechanization.

Effect of year, hybrids and soil types on K fertilizer and yield

According to above historical data, three factors affect the yield per unit of maize and potassium fertilizer rate. First is environmental condition such as temperature, sunlight, and rainfall. The suitable climate for maize growth consists of four distinct seasons, with abundant sunshine and rain at the same time (Li et al., 2001; Zheng and Dong, 2000), temperature and rainfall have significant correlation with maize yield (Peng et al., 2008; Drury and Tan, 1995). Moreover, moisture content in soil has obvious interaction with potassium fertilizer efficiency. Potassium in soil transport mainly by diffusion, and the water in soil was strongly affected diffusion condition. So it should be pay attention to apply potassium fertilizer in dry years, and decrease potassium fertilizer rate in higher rainfall years (Ortas, 2018; Shen et al., 2008).

Second, the development of hybrids affected yield and potassium fertilizer rate. China popularized breeding and corn hybridization during the 1960s, and yield per unit was increased by 2.5 times (Sun, 2010). The yields of different maize hybrids had obvious differences under the same conditions (Chen et al., 2012b). Dissimilar tolerance of such hybrids to drought or herbicide resulted in significant yield variability (Weber and Golebiowska, 2010; Vasal, 2000). The assessment of yield stability is a significant issue for maize cultivar evaluation and recommendation (Liu et al., 2011). Therefore, summarizing the requirements of selected maize hybrids is necessary in selecting high-yield and stable-yield hybrids based on local climate conditions observed in previous years. And the characteristics of absorb potassium of different hybrids existed

significant changed. The abilities of absorb potassium of different hybrids in soils and in fertilizer had difference, the divergence of potassium content in each stage can reach 0.9-1.6 times, so the hybrids of long-term and large quantities of absorbing potassium should apply base potassium fertilizer and top-dressing fertilizer (Wang et al., 2004).

Finally, soil types are crucial to improve yield and potassium use efficiency. Crop yield response was controlled by a complex interaction that varied annually with soil textural characteristics (Tolk et al., 1999). Soil textural affects water supply, ventilation, fertilizer supply, heat preservation and basic fertility of soil, also influenced soil physics, mechanics of machinery and a series of other characteristics. The yield per unit affected by climate and soils is close to real yield potential in the agreeable hybrids and management technology. Different soil types have different rational potassium rate and fertilization styles due to high spatial variability in soil K content, the forms and availability to plants of soil K, i.e. potential K-supplying capacity, were related to mineralogy in different soil types (Darunsontaya et al., 2012). In Jilin province available potassium contents of Phaeozem Soils and Chernozem Soils are higher and slow-available potassium contents are relatively richer, the potential of potassium supply are huge; available potassium of Albic Soils is middle, the potential of potassium supply is limited, so it should be replenish proper potassium fertilizer; and available potassium and potential of potassium supply of Aeolian Sand Soils are lower, so it is necessary to increase potassium fertilizer and split application (Wang, 1998).

The relationships among Max yield, increasing yield and K0 yield

Soil fertility determined Max yield, increasing yield and K0 yield of maize. The higher the soil fertility is, the higher K0 yield and Max yield are and the lower the potential of increasing yield is. Increasing yield has significant negative correlation with the available potassium content of soil (Wang et al., 2004). So identifying and quantifying soil fertility variation and subsequently determining the optimal fertilization levels associated with different management styles are necessary to implement nutrient management (Tabu et al., 2006). Rational fertilization improved fertilizer use efficiency, protected the environment, and maintained soil fertility for creating suitable soils. Therefore, modeling and calculating the optimal fertilization in different soils and different climate conditions based on experimental data analysis from previous years can guide farmers in the process of scientific fertilization.

Conclusion

The challenge of meeting food demand with less pollution on the environment in China in the next 50 years can be overcome by increasing usage efficiency simultaneously (Gao et al., 2012). The effect of “soil testing and fertilizer recommendation” project in China from 2005 to 2015 was remarkable. The results from Jilin province with 1370 field trials showed that the average yield of maize with K0 treatment was 9000 kg ha⁻¹. Its maximum yield (Max.yield) and increased yield (IY k) after application of K fertilizer averaged at 10200 kg ha⁻¹ and 1100 kg ha⁻¹, respectively. Significant variability was evident in K0 yield and Max.yield over the years. Maize hybrids and different soil types had significant differences in IY yield. Meanwhile, IY can either increase or decrease depending on K0 yield, which suggest that a suitable K fertilizer can improve the yield, whereas excessive K fertilizing would have no obvious effect on the yield. In addition, the yield was found to be affected by environment,

maize hybrids, soil types, and K fertilizer rate. Therefore, the research of precision K fertilizer application on different soils type and different maize hybrids in different climate condition should be carried out in the future, which will be of epoch-making significance for high-yield and high-efficiency of spring maize in Jilin province, in Northeast China.

Acknowledgements. The authors would like to acknowledge the National Key R&D Program of China (2017YFD0201804, 2018YFD0800101); Natural Science Foundation of Jilin province, China (20170101004JC); and the National Natural Science Foundation of China (Grant No. 31471945) for their financial support.

REFERENCES

- [1] Chen, G., Zhang, Z. D., Wang, P., Tao, H. B. (2012a): Comprehensive analysis on Ear characters and yield of the different maize varieties in dryland area. – *Journal Crops* 5: 100-104 (in Chinese).
- [2] Chen, N. X., Lv, C. H., Liu, Y. M. (2012b): Effect of 3414 formula fertilization on maize yield and nutrient content (in Chinese.). – *Journal Barley and Cereal Sciences* 4: 26-28.
- [3] Darunsontaya, T., Suddhiprakarn, A., Kheoruenromne, I., Prakongkep, N., Gilkes, R. (2012): The forms and availability to plants of soil potassium as related to mineralogy for upland Oxisols and Ultisols from Thailand. – *Geoderma* 170: 11-24.
- [4] Drury, C. F., Tan, C. S. (1995): Long-term (35years) effects of fertilization, rotation and weather on corn yield. – *Canadian Plant Science* 75: 355-362.
- [5] Epstein, E., Bloom, A. J. (2005): *Mineral Nutrition of Plants: Principles and Perspectives*. 2nd Ed. – Sinauer Associates, Inc., Sunderland, MA.
- [6] Gao, Q., Li, C. L., Feng, G. Z., Wang, J. F., Cui, Z. L., Chen, X. P., Zhang, F. S. (2012): Understanding yield response to nitrogen to achieve high yield and high nitrogen use efficiency in rainfed corn. – *Agronomy Journal* 104: 165-168.
- [7] Gong, Z. T., Chen, Z. C., Luo, G. B., Zhang, G. L., Zhao, W. J. (1999): Reference to Chinese soil taxonomy. – *Journal Soils* 2: 57-63 (in Chinese).
- [8] Ladha, J. K., Pathak, H., Krumpnik, T. J., Six, J., Kessel, C. V. (2005): Efficiency of fertilizer nitrogen in cereal production: retrospects and prospects. – *Advances in Agronomy* 87: 85-156.
- [9] Li, H. L., Zhang, W. F., Zhang, F. S., Du, F., Li, L. K. (2010): Chemical fertilizer use and efficiency change of main grain crops in China. – *Journal Plant Nutrition and Fertilizer Science* 16: 1136-1143 (in Chinese).
- [10] Li, Y. Z., Liu, G. L., Zhang, H. Y. (2001): The relationship of light and temperature factor and yield maize. – *Journal Acta Agriculture Boreali-Occidentalis Sinica* 10: 67-70 (in Chinese).
- [11] Liu, Y. J., Wei, B., Hu, E. L., Wu, Y. Q., Huang, Y. B. (2011): Yield stability of maize hybrids evaluated in national maize cultivar regional trials in southwestern China using parametric methods. – *Agricultural Sciences in China* 10: 1323-1335.
- [12] National Bureau of Statistics of China (2007): *China Statistical Yearbook*. – China Statistics Press, Beijing (in Chinese).
- [13] National Bureau of Statistics of China (2011): *China Statistical Yearbook*. – China Statistics Press, Beijing (in Chinese).
- [14] Ogundijo, S., Adetunji, M. T., Azeez, J. O., Arowolo, T. A. (2017): Integrated fertilizer management: influence on soil nitrogen, available phosphorus, potassium, nutrient uptake and maize yield. – *Communications in Soil Science and Plant Analysis* 48: 943-954.

- [15] Ortas, I. (2018): Influence of potassium and magnesium fertilizer application on the yield and nutrient accumulation of maize genotypes under field conditions. – *Journal of Plant Nutrition* 41(3): 330-339.
- [16] Peng, C., Gao, H. J., Niu, H. H., Yue, Y. L., Zhu, P. (2008): Long-term effects of fertilization and weather on corn yields in a clay loam soil in Northeast China – *Journal of Maize Sciences* 16: 179-183 (in Chinese).
- [17] Ren, H., Li, Y. Y., Han, C. W., Zhou, P. (2010): Potential analysis of maize increasing yield in Jilin Province – *Journal Maize Science* 18: 148-152 (in Chinese).
- [18] Shen, Q. R., Tan, J. F., Qian, X. Q. (2008): *The Theory of Soil and Fertilizer Science*. 11st Ed. – Beijing, China (in Chinese).
- [19] Sun, S. X. (2010): Popularization and effect of corn hybrid in China. – *Journal Crops* 3: 121-124 (in Chinese).
- [20] Tabu, I. M., Obura, R. M., Bationo, A., Mumera, L. (2006): Effect of soil fertility management and nitrogen fertilizer rate on maize yield in small holder farmers fields. – *Journal of Agronomy* 5: 191-195.
- [21] Tenkorang, F., Lowenberg-DeBoer, J. (2009): Forecasting long-term global fertilizer demand. – *Nutrition Cycling Agroecosystems* 83: 233-247.
- [22] Tian, X.; Li, C.; Zhang, M.; Lu, Y.; Guo, Y.; Liu, L. (2017): Effects of controlled-release potassium fertilizer on available potassium, photosynthetic performance, and yield of cotton. – *Journal Plant Nutrition Soil Science* 180: 505-515.
- [23] Tolck, J. A., Howell, T. A., Evett, S. R. (1999): Effect of mulch, irrigation and soil type on water use and yield of maize. – *Soil & Tillage Research* 50: 137-147.
- [24] Van Reewijk, L. P. (1992): *Procedures for Soil Analysis*. 3rd Ed. – ISRIC, Wageningen, the Netherlands.
- [25] Vasal, S. K. (2000): The quality protein maize story. – *Food and Nutrition Bulletin* 21. <https://doi.org/10.1177/156482650002100420>.
- [26] Wang, L. (1998): *Jilin Soil*. – Chinese Agricultural Press, Beijing (in Chinese).
- [27] Wang, X. B., Hoogmoed, W. B., Cai, D. X., Perdok, U. D., Oenema, O. (2007): Crop residue, manure and fertilizer in dryland maize under reduced tillage in northern China: II Nutrient balances and soil fertility. – *Nutrition Cycling Agroecosystems* 79: 17-34.
- [28] Wang, X. F., Zhang, K., Wang, L. C., Zhang, G. G., Xie, J. G. (2004): The main factors of effect of Spring maize on increasing yield and use efficiency with potassium fertilizer. – *Presiding for the 5th Cross Straits Soil Fertilizer International Conference*, pp. 192-198 (in Chinese).
- [29] Weber, R., Golebiowska, H. (2010): Discriminatory analysis of the yield variability of maize hybrids depending on the doses and time of herbicide application. – *Acta Scientiarum Polonorum Agricultura* 9: 69-76.
- [30] Xie, J. C. (2000): *Potassium in China Agriculture*. – Hohai University Press, Nanjing (in Chinese).
- [31] Zhang, F. S., Wang, J. Q., Zhang, W. F., Cui, Z. L., Ma, W. Q., Chen, X. P., Jiang, R. F. (2008): Nutrient use efficiencies of major cereal crops in China and measures for improvement. – *Journal Acta Pedologica Sinica* 45: 915-924 (in Chinese).
- [32] Zhang, H. M., Yang, X. Y., He, X. H., Xu, M. G., Huang, S. M., Liu, H., Wang, B. R. (2011): Effect of long-term potassium fertilization on crop yield and potassium efficiency and balance under wheat-maize rotation in China. – *Pedosphere* 21: 154-163.
- [33] Zheng, H. J., Dong, Z. T. (2000): Relationships between ecological factors and maize yield. – *Journal of Shandong Agricultural University (Natural Science)* 31: 315-319 (in Chinese).
- [34] Zoerb, C., Senbayram, M., Peiter, E. (2014): Potassium in agriculture—status and perspectives. – *Journal of Plant Physiology* 171: 656-669.

CONVERGENCE OF CHINA'S AGRICULTURAL GREENHOUSE GASES

LI, N.* – LI, Y. M. – MU, H. L. – ZHANG, P. P. – JIANG, Y. Q.

Key Laboratory of Ocean Energy Utilization and Energy Conservation of the Ministry of Education, Dalian University of Technology, Dalian, Liaoning 116024, China

**Corresponding author
e-mail: nanliln@yeah.net*

(Received 23rd Apr 2019; accepted 11th Jul 2019)

Abstract. Agriculture has become an important source of greenhouse gas emissions. This paper calculates the agricultural GHGs emissions of 30 provinces in China from 1997 to 2016, and analyzes the emission intensity of GDP of carbon dioxide, methane and nitrous oxide by club convergence. After using the DEA CCR model to divide the club, the absolute β -convergence analysis method is used to verify the emission trends of various greenhouse gases. The results showed that the carbon dioxide emission intensity showed obvious absolute β convergence in all three clubs. Methane and nitrous oxide only have absolute β convergence in one of the clubs, respectively, and there is divergence in other clubs. Since the emission trends of the three greenhouse gases in the clubs are different, the formulation of reasonable reduction target allocation plan should be more detailed and targeted, and more stringent emission reduction targets should be set for provinces with high GHGs intensity of GDP in order to reduce it rapidly.

Keywords: *greenhouse gases, agriculture, convergence carbon dioxide, methane, nitrous oxide, emission reduction, climate policy*

Introduction

China is a large agricultural country and the earliest origin of crop and farming culture. Since the 1980s, the annual growth rate of Chinese agriculture has been at the forefront of the world. In 1978-2008, agricultural growth increased by an average annual growth rate of 4.6%. At the same time, agriculture has become a significant source of greenhouse gases. SAIN (China-UK Sustainable Agriculture Innovation Network, www.sainonline.org) reported that Chinese agriculture-related GHGs emissions accounted for 17%-20% of the total GHGs in the atmosphere, a ratio above the world average. In order to realize China's emission reduction commitments at the World Climate Conference in Paris, agricultural GHGs emission reduction has become the direction and inevitable trend of agricultural development in the future.

Carbon dioxide, methane and nitrous oxide are the most GHGs emitted in agricultural activities, and they are hot spots of research. Agricultural CO₂ flux is mainly derived from the combustion of fossil fuels, the respiration of plant roots and decomposition of organic matter. Agriculture is the source and sink of CO₂ (Zhang and Liang, 2011). Lal (2004) pointed out that global agricultural carbon sinks were down to 50% to 66% in history. Norse (2012) put forward that in the process of agricultural production of CO₂ mainly by agricultural, agricultural machinery, agricultural irrigation and agricultural straw burning. Lelieveld et al. (1998) showed that biological processes produce about 70% of agricultural CH₄. Yang et al. (2003) advised that the main sources of agricultural CH₄ were rice fields, wetlands, sediments, intestinal fermentation, and animal manure treatment. Li et al. (2009) used GAINS model to predict the N₂O emissions of Chinese

agriculture. The results showed that the emissions would reach about 2 million t in 2030, an increase of 31% compared with 2000. Agricultural N₂O emission mainly comes from agricultural land, fertilizer application and animal manure management.

It can be seen that agricultural GHGs has been a hot issue in research, and its emissions should not be underestimated. So it has far-reaching significance for the accounting of China's agricultural GHGs emissions and emission intensity.

Regional convergence was proposed in the middle of the 20th century, and the empirical research was based on the Solow growth model. The results of the study within the neoclassical framework show that backward areas present a "catch-up effect" relative to advanced areas. In 1986, Baumol (1986) first proposed the hypothesis of regional convergence. Barro and Salaimartin (Barro and Salaimartin, 1992; Barro and Mankiw, 1995; Salaimartin, 1996) put forward the theory of σ convergence and β convergence.

Since regional convergence theory can give policy implications, some scholars have used this theory to study greenhouse gas emissions, but most of the research does not involve agricultural greenhouse gas emissions. Huang (2013) used the spatio-temporal dynamic convergence model to analyze the per capita carbon dioxide emissions of Chinese cities from 1985 to 2008. Hao (2015) studied the carbon dioxide emission intensity of 29 provinces in China from 1995 to 2011, and proved that there was absolute β convergence. Yang (2016) estimates total factor productivity from the perspective of whether there are environmental constraints, and examines the impact of carbon dioxide emissions on economic convergence in China's provinces. Robalino-Lopez (2016) studied the per capita carbon dioxide emissions of 10 South American countries from 1980 to 2010, and analyzed the convergence process of the per capita carbon dioxide emissions of these countries. Zang (2018) analyzed the per capita carbon dioxide emission convergence of 201 countries from 2003 to 2015, and calculated that the global per capita carbon emission convergence rate was less than 1% per year. Kouretas (2018) studied the convergence of energy consumption and carbon dioxide emission intensity in 23 European countries from 1970 to 2010 with the method of distribution dynamics, and the results showed that there was no convergence. Yu (2018) conducted a convergent analysis on the carbon intensity of China's industrial sector from 1995 to 2015, showing the existence of the condition convergent. The club convergence has also been used to study the issue of greenhouse gas emissions. The study of Jobert (2010) confirmed the convergence of European per capita carbon dioxide emissions. Based on China's provincial carbon intensity data from 1995 to 2011, Wang (2014) found that there was a significant divergence in carbon intensity at the national level by using logt test. Burnet (2016) studies the convergence of carbon dioxide emissions related to energy consumption across U.S. states between 1960 and 2010, forming a convergence club and two divergence groups. Apergis (2017) analyzed the carbon dioxide emissions of various states, and found empirically that there was no overall convergence of carbon dioxide emissions per capita in the United States. Liu (2018) studied the per capita emissions of industrial pollutants in 285 prefecture-level cities in China from 2003 to 2015, aiming to reveal the impact of industrial transfer on the formation of convergence clubs.

In this paper, the accounting of agricultural GHGs emissions and emission intensity is to understand the current situation of agricultural GHGs emissions in China more clearly. Because each club has a steady-state value of its emission intensity, the emission reduction share can be divided according to the decline rate of emission intensity. Therefore, the convergence analysis of agricultural GHGs emission intensity aims to

provide a reference for the Chinese government to define the reduction target allocation plan.

Methods

China's agricultural greenhouse gas emissions accounting

China's agricultural GHGs accounting method refers to the means recommended by IPCC (www.ipcc.ch), Min (2012) research results and the Provincial GHGs Inventory Compilation Guide. Carbon dioxide is calculated mainly from the use of fossil fuels in agricultural production. Methane comes from rice paddies, ruminant intestinal fermentation and animal waste treatment. Nitrous oxide emissions calculated in this paper also mainly come from three parts, namely, crop soil background, fertilizer application and animal manure management. Then, this paper uses the GWP value recommended by IPCC to derive the agricultural GHGs emissions in China.

Club convergence analysis

Convergence is not a black or white issue; it presents a trend of narrowing the gap. In this paper, the intensity of agricultural greenhouse gas emissions in China is mainly verified by club convergence.

According to the energy value theory, for CCR model, the input factors include chemical energy, mechanical power energy, thermal energy and bio-energy input in agricultural production. The output factor is greenhouse gas emissions. The rate of intra-club convergence is calculated according to the absolute β convergence regression equation.

$$\frac{1}{t-t_0} \ln \frac{x_{t,i}}{x_{0,i}} = \alpha - \frac{1-e^{-\beta(t-t_0)}}{t-t_0} \ln x_{0,i} + \varepsilon_{t,i} \quad (\text{Eq.1})$$

where $x_{t,i}$ and $x_{0,i}$ represent the intensity of agricultural GHGs emissions in the initial and final stages of the i -th province, t represents the t -year, t_0 represents the initial, β represents the convergence rate, α represents the intercept term, and $\varepsilon_{i,t}$ represents the error term. When there is a positive β value, it indicates that there is absolute β convergence in the intensity of agricultural greenhouse gas emissions in the club; conversely.

Data

The basic agricultural data are collected from the Statistical Yearbook of China, Husbandry/Energy/Agriculture Statistical Yearbook of China. The specific data are shown in *Table 1*.

Results and discussion

Results of agricultural GHGs flux accounting in China

The agricultural greenhouse gas emissions in China from 1997 to 2016 are shown in *Figure 1a*. GHGs emissions of CO₂ equivalent are on the rise. In 1997, the flux was

952.7404 Tg CO₂ e, and in 2016, it was 1031.5290 Tg CO₂ e, with an average annual growth rate of 0.42%.

Table 1. Data sources

The relevant data	Source
Acreage of crops; the number of various animals; China's agricultural GDP	Statistical Yearbook of China
The number of livestock service number	Husbandry Statistical Yearbook of China
Agricultural employment data	Statistical Yearbooks of various provinces in China
The physical quantity of energy used in agricultural production	Energy Statistical Yearbook of China
Nitrogen fertilizer, phosphate fertilizer, potash fertilizer, compound fertilizer, pesticide, plastic film data	Agriculture Statistical Yearbook of China

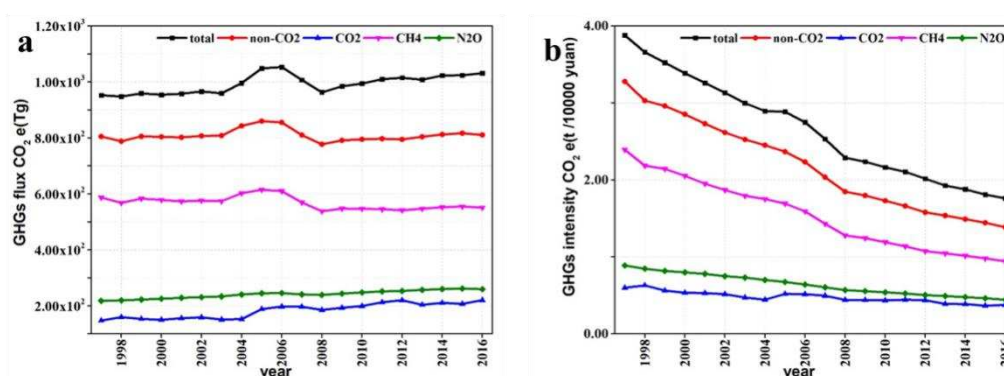


Figure 1. The agricultural GHGs flux in China from 1997 to 2016

Although agricultural GHGs flux in China shows an upward trend, the intensity of GDP declines obviously, almost linear (*Fig. 1b*). In 1997, the intensity was 3.8801 t/10,000 yuan (about 2.6744 kg/dollar), in 2016, 1.7621 t/10,000 yuan (about 1.2146 kg/dollar), the average annual decline rate was 4.24%.

Club convergence of agricultural GHGs intensity of GDP in China

According to the CCR model of DEA, the total factor energy efficiency of each province from 1997 to 2016 is calculated, and the average value is counted, and the club is divided according to the average value of total factor energy efficiency. Because the object of the study is 30 provinces, in order to ensure that the number of data substituted into the convergence model and the number of club members are relatively average, the corresponding critical value is taken to divide the clubs. Since the output in the CCR model (agricultural GHGs flux of CO₂ equivalent) is an undesired output, the lower efficiency value indicates that the situation of the region is more optimistic.

Club convergence of CO₂ intensity of GDP in China

Agricultural carbon dioxide flux and emission intensity distribution are shown in *Figure 2*. Agricultural carbon dioxide flux show a certain geographical difference, the

north is higher than the south, the middle and east are higher than the west. In particular, the provinces that gather in the Inner Mongolia-Guangdong axis have the largest flux. The distribution of CO₂ intensity of GDP is also geographically different. The provinces with high intensity are concentrated in the northwest, and the intensity decreases from northwest to southeast.

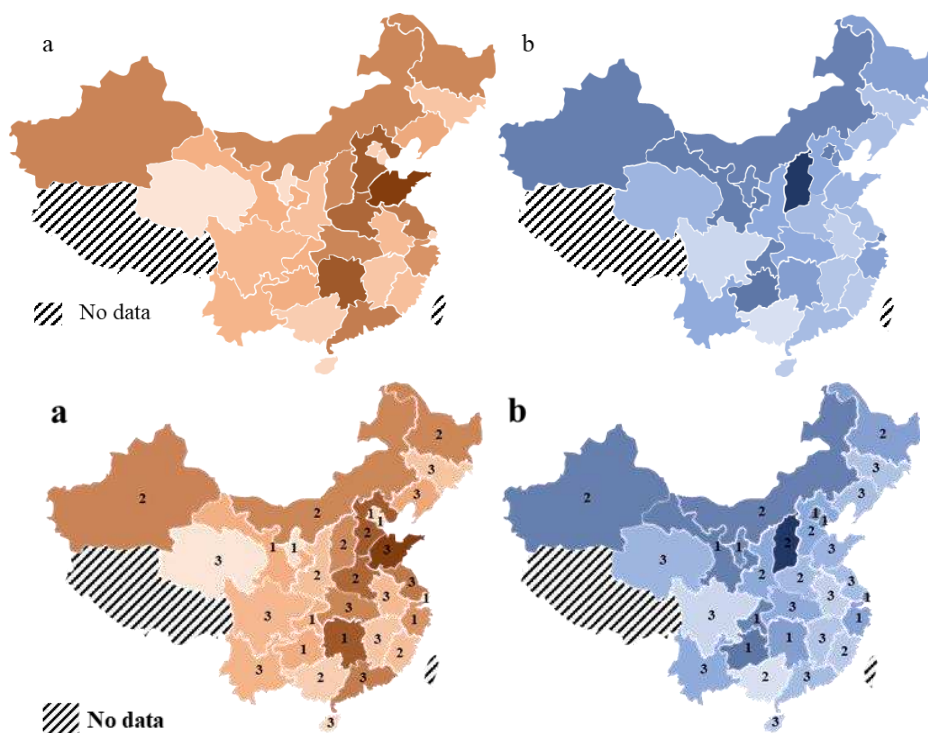


Figure 2. *a* Annual average flux of agricultural CO₂ from 1997 to 2016. *b* Annual average CO₂ intensity of GDP from 1997 to 2016. (Note: The color of each patch represents the size of its flux/intensity, where the darker the color, the greater the flux/intensity. The numbers 1, 2, and 3 indicate which club the area belongs to)

For the total factor energy efficiency of agricultural CO₂ emission, a threshold of 0.78 and 0.90 will be set for each of the three national clubs (as shown in Fig. 3).

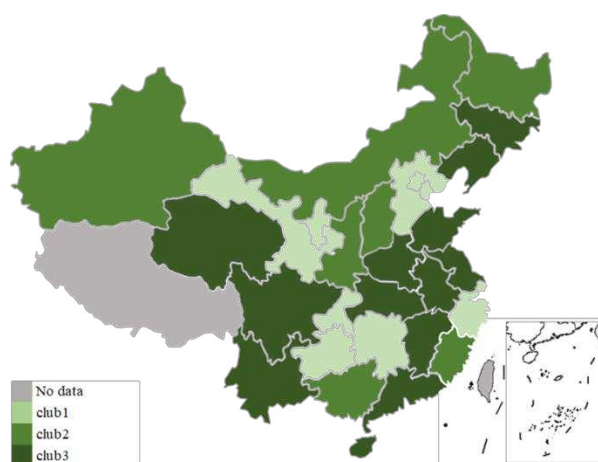


Figure 3. Club distribution of agricultural carbon dioxide intensity of GDP

In the past 20 years, agricultural carbon dioxide flux of club 1 accounted for about 24.26% of the national agricultural carbon dioxide flux, and the proportion is decreasing year by year (Fig. 4a). The agricultural CO₂ intensity of GDP was higher than other clubs, but the intensity declined at a higher rate, especially in Chongqing. As shown in Figure 4b, the strength of club 1 shows a downward trend, which also provides the possibility of verification of convergence. According to Equation 1, the calculation can obtain a positive β value, that is, within club 1, there is a significant absolute β convergence of agricultural CO₂ intensity, and the convergence rate is 15.55%. The existence of this convergence phenomenon indicates that the difference in the emission intensity of the club members will gradually disappear, and the intensity will eventually reach the same stable value. In order to achieve the development of low carbon in agriculture quickly, the club 1 should follow the pattern of the convergence of members' CO₂ intensity when designing reasonable reduction target allocation plan. Chongqing, Guizhou and Ningxia, where the emission intensity declines rapidly, should undertake heavier burden.

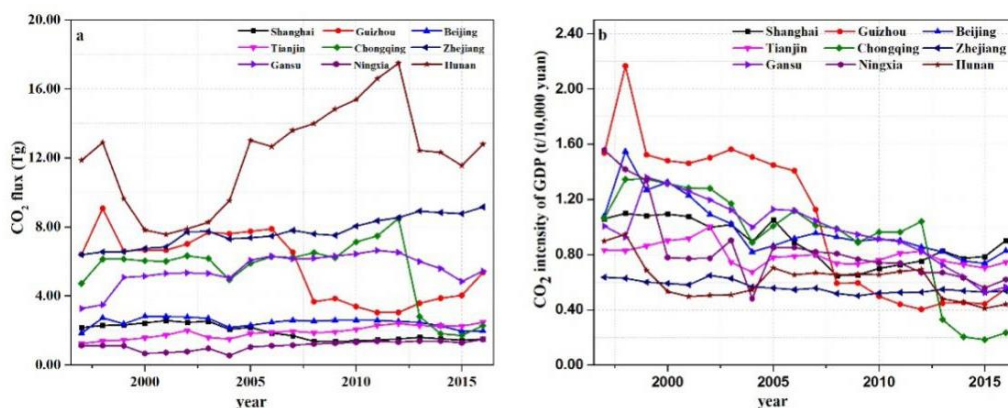


Figure 4. a Agricultural CO₂ flux in club 1. b Agricultural CO₂ intensity of GDP in club 1

From 1997 to 2016, the agricultural carbon dioxide flux of club 2 increased almost linearly (Fig. 5a). For the intensity of carbon dioxide, the reductions in Shanxi, Shaanxi and Henan are more obvious, and the intensity in Guangxi and Inner Mongolia is on the rise (Fig. 5b).

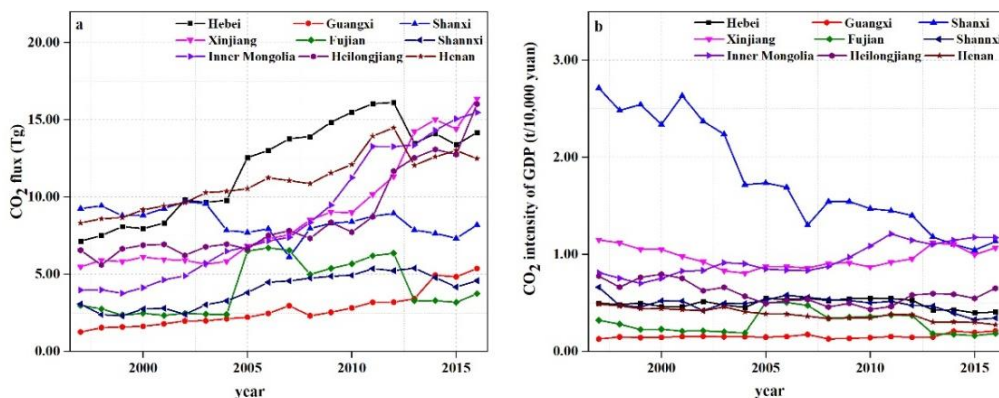


Figure 5. a Agricultural CO₂ flux in club 2. b Agricultural CO₂ intensity of GDP in club 2

The absolute β convergence rate of CO₂ intensity of club 2 is 1.69%. Members of club 2 are mostly energy-rich provinces. However, good resource endowments have made these places a rough way of using energy. At the same time, the economic development model of “energy dominates the economy” does not meet the requirements of sustainable development. Due to the special geographical and climatic conditions, Fujian and Guangxi have created distinctive subtropical agricultural farming methods, but the penetration rate of modern agricultural production methods is still low. Because of the absolute β convergence, reduction allocation plan of club 2 should abide by the convergence model. Considering the rate of decline in emission intensity, Shaanxi and Shanxi should bear more emission reduction tasks. At the present stage, it is impossible to completely abandon coal, and the clean and intensive use of coal is a strategic choice.

The CO₂ emission of club 3 is shown in the *Figure 6*. Club 3 is the group with the lowest carbon dioxide emission efficiency of agriculture. Its agricultural carbon dioxide flux accounts for 39.02% of the nation, and the ratio is decreasing. After calculation, the CO₂ intensity of GDP of club 3 satisfies the absolute β convergence condition, and the convergence rate is 5.08%. Except for Qinghai, Sichuan, Yunnan and Hubei, members of club 3 are mostly in the eastern coastal or offshore areas. At the same time, Guangdong and Jiangxi have the largest decline in emission intensity, so they should take more responsibility for cutting CO₂ emissions. As the members of this club are at the forefront of low-carbon development, it is a big problem to break the efficiency bottleneck.

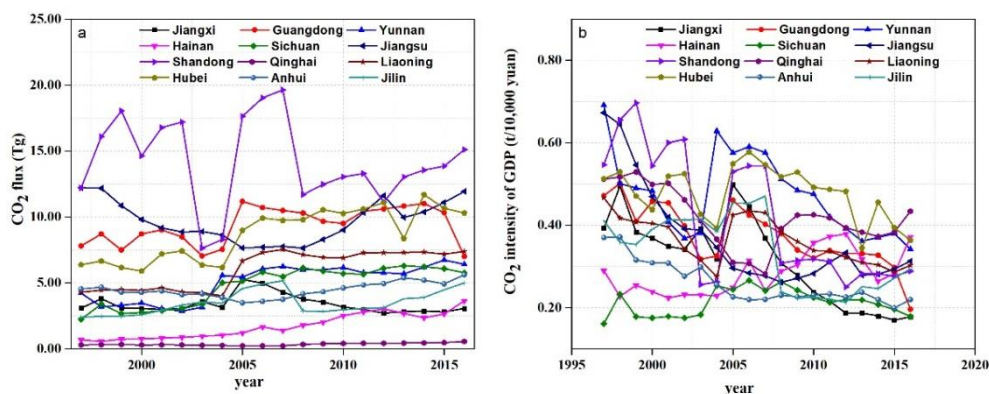


Figure 6. a Agricultural CO₂ flux in club 3. b Agricultural CO₂ intensity of GDP in club 3

The club convergence test results of agricultural CO₂ intensity is shown in *Table 2*. The decline of China's agricultural CO₂ emission intensity shows the increase of agricultural energy efficiency. However, according to the efficiency value calculated by DEA, it shows that each region has certain emission reduction potential. In other words, from club1 to club3, the potential to reduce emissions is decreasing in turn. The key to CO₂ emission reduction in China's agriculture is to adjust the structure of agricultural energy utilization and realize the clean utilization of coal.

Club convergence of CH₄ intensity of GDP in China

The flux of methane from agricultural production is diverging from the two provinces of Shaanxi and Shanxi, and the flux is increasing (*Fig. 7a*). This is mainly because the animal husbandry and planting industry in Shaanxi and Shanxi provinces

are not developed. The CH₄ intensity of GDP in the Bohai Rim region is the lowest. The intensity in the north and south of the region is increasing (Fig. 7b).

Table 2. Club convergence test results of agricultural carbon dioxide intensity

Test parameters	Club 1	Club 2	Club 3
α	-0.0301	-0.0201	-0.0503
t-Statistic	-3.9575	-2.2753	-4.9670
Prob.	0.0055	0.0570	0.0006
β	0.1555	0.0169	0.0508
t-Statistic	-1.7534	-1.5281	-2.9682
Prob.	0.1230*	0.1703	0.0141***
R2	0.3052	0.2501	0.4684

***, **, * mean accepting the convergence hypothesis at 5%, 10% and 15% significance level

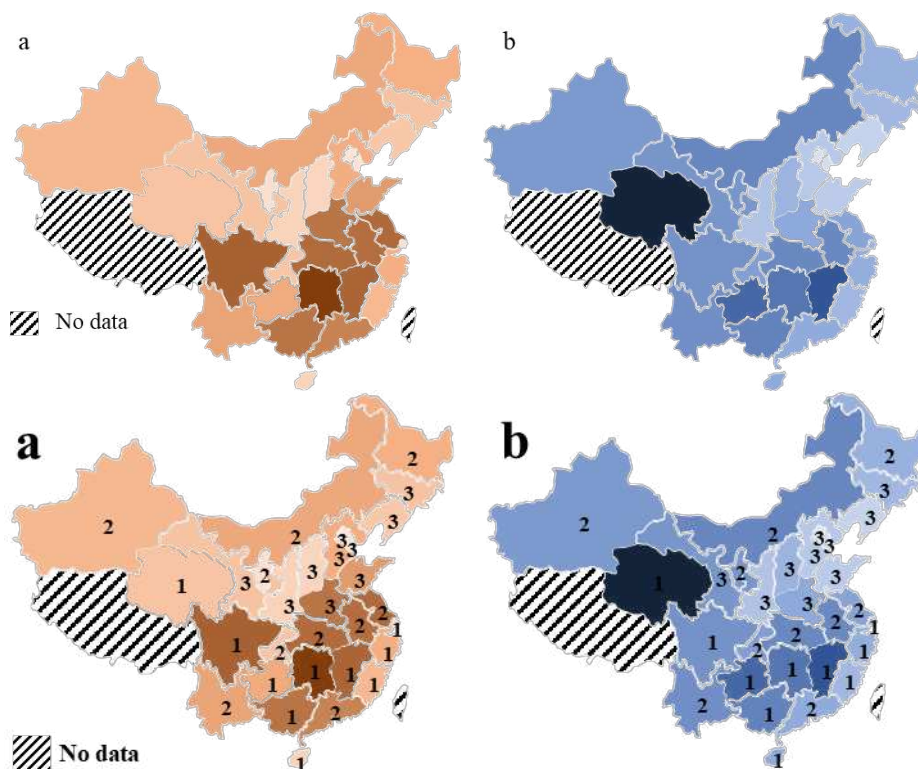


Figure 7. *a* Annual average flux of agricultural CH₄ from 1997 to 2016. *b* Annual average CH₄ intensity of GDP from 1997 to 2016. The numbers 1, 2, and 3 indicate which club the area belongs to

The average energy efficiency value calculated based on CCR model, with threshold values of 0.25 and 0.45, the state is divided into three clubs. The distribution map is shown in Figure 8.

For club 1, please see Figure 9. In club 1, CH₄ emission intensity shows a downward trend, but there is no obvious convergence effect. Using Equation 1, a negative β value is calculated. This is caused by large differences in the agricultural industrial structure

of each member. Therefore, the formulation of reduction plan should fully consider the imbalance of the emission intensity of club members. As the prime rice producing area in China, club 1 plays a significant role in China's food security. For large rice planting provinces, the focus of emission reduction should be on the rice planting season. Qinghai and Hainan should increase agricultural input, improve agricultural technology and develop leisure agriculture. As for Shanghai, with its current urban orientation, the development of primary industry has a low cost performance, and it should focus on the development of other high-tech industries.

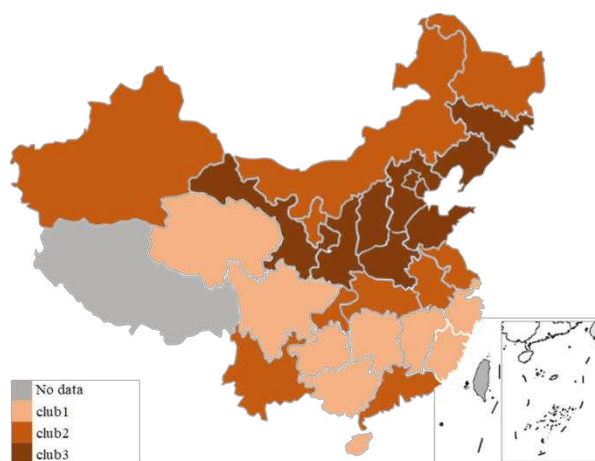


Figure 8. Club distribution of agricultural methane intensity of GDP

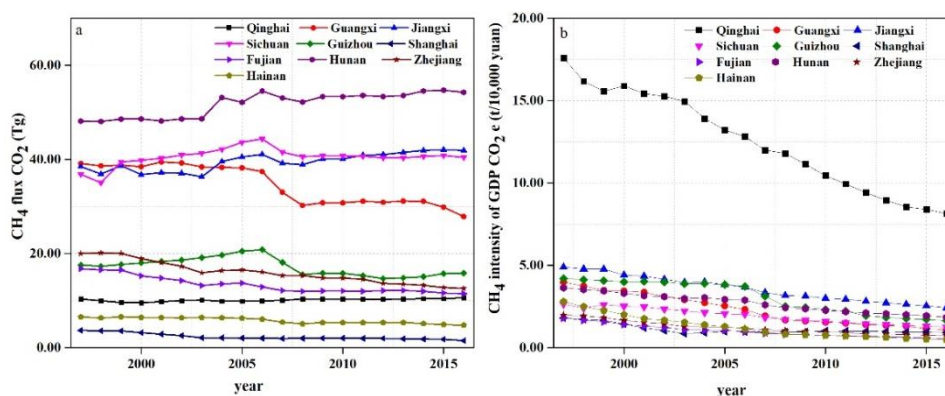


Figure 9. a Agricultural CH_4 flux in club 1. b Agricultural CH_4 intensity of GDP in club 1

Club 2 consists of seven major rice-growing provinces and three major livestock provinces. The club's agricultural CH_4 flux is slightly less than club 1 (Fig. 10a), accounting for 39.00% of the total, mainly from rice fields and animal husbandry. The intensity of members in the club showed a downward trend (Fig. 10b), and the gap between the maximum and minimum emission intensity in 2016 is less than the difference in 1997. However, the narrowing of the two extremes does not indicate the overall convergence of emission intensity. After calculation, a negative β value is obtained, that is, there is no absolute β convergence. The formulation of the target allocation project of club 2 should focus on two points, namely, animal husbandry and

rice field. Only by considering these two points can we create the optimal emission reduction effect.

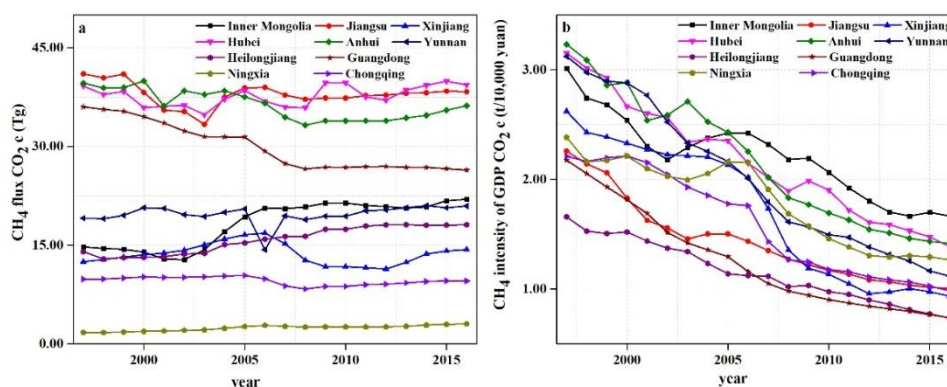


Figure 10. *a* Agricultural CH_4 flux in club 2. *b* Agricultural CH_4 intensity of GDP in club 2

Club 3 is the group with the lowest CH_4 emission efficiency in agriculture, and with the lowest methane emissions, the lowest methane intensity. It can be seen from *Figure 11b* that there is a clear downward trend of methane emission intensity. This is also verified on the model. After calculation, a positive β value is obtained, indicating that the rate of absolute β convergence is 2.19%. Similar agricultural bases and development patterns are the dominant factors of the convergence. Shanxi, Henan, Gansu, and Shaanxi, which have the highest rate of decline in emission intensity, should be allocated a larger share of CH_4 reduction. These regions have greater reduction potential than those with lower reduction rates such as Beijing and Liaoning.

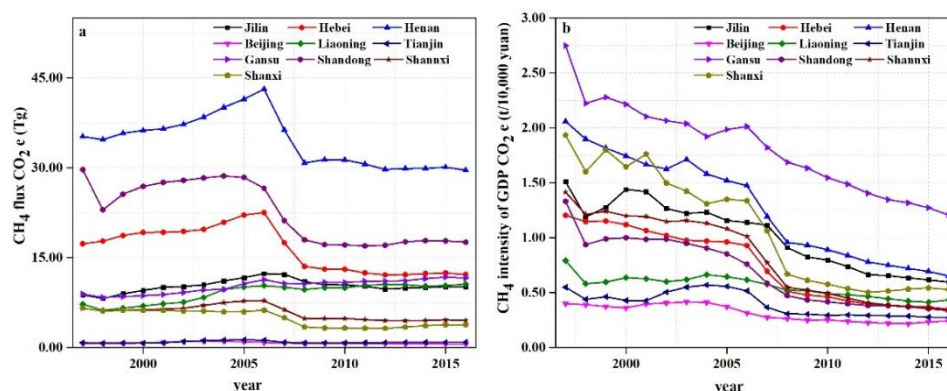


Figure 11. *a* Agricultural CH_4 flux in club 3. *b* Agricultural CH_4 intensity of GDP in club 3

CH_4 clubs are classified similarly to CO_2 , with the most efficient club 1 having the greatest potential to reduce emissions. The main source of CH_4 is agriculture. CH_4 emission reduction mainly lies in paddy fields and animal husbandry, so emission reduction policy formulation should pay attention to the mid-term sunning of paddy fields and fertilizer management. At the same time, the management of pastoral areas is particularly important. The number of grassland should be used to determine the number of livestock breeding, so as to avoid the ecological dead cycle of vulnerable

areas like Qinghai. In addition, the club convergence test results of agricultural CH₄ intensity is given in *Table 3*.

Table 3. Club convergence test results of agricultural methane intensity

Test parameters	Club 1	Club 2	Club 3
α	-0.0580	-0.0456	-0.0494
t-Statistic	-4.4246	-3.4347	-10.0059
Prob.	0.0022	0.0089	0.0000
β	-0.0053	-0.0012	0.0219
t-Statistic	0.6002	0.0900	-2.1846
Prob.	0.5650	0.9305	0.0604**
R ²	0.0431	0.0010	0.3737

***, **, * mean accepting the convergence hypothesis at 5%, 10% and 15% significance level

Club convergence of N₂O intensity of GDP in China

Agricultural nitrous oxide flux is mainly concentrated in the developed provinces of the planting industry, and the overall emissions in the east are greater than those in the west (*Fig. 12a*). The nitrous oxide intensity of GDP shows a different distribution pattern. The emission intensity in the west is greater than that in the east, showing a decreasing law from west to east, which is mainly caused by the fact that the agricultural output value in the east is much higher than that in the west (*Fig. 12b*).

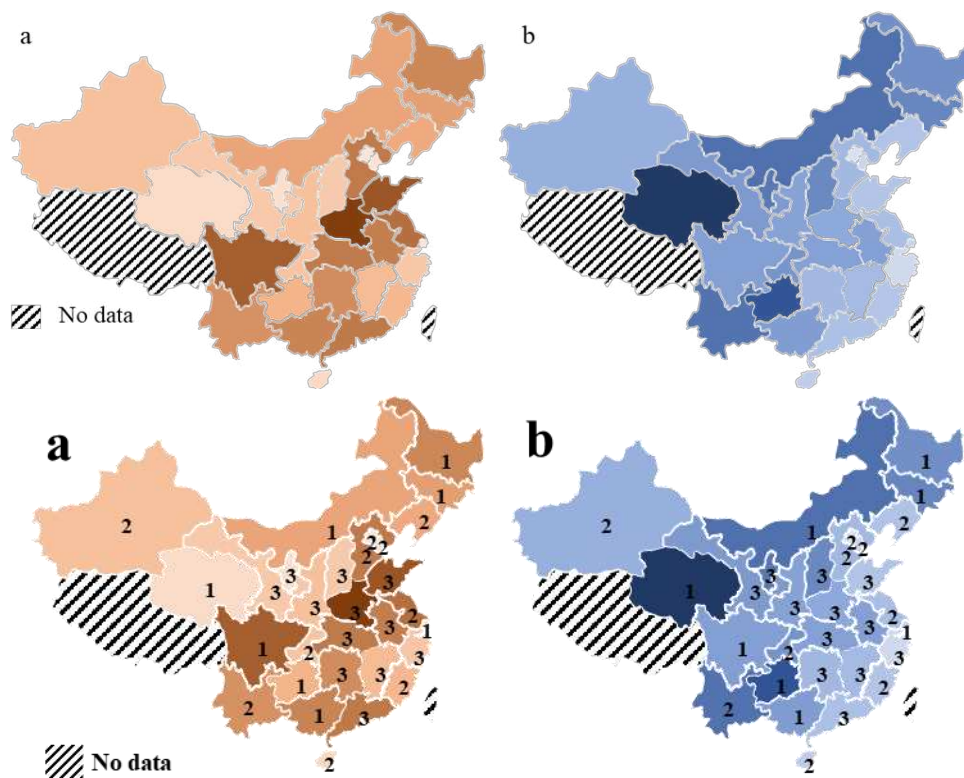


Figure 12. *a* Annual average flux of agricultural N₂O from 1997 to 2016. *b* Annual average N₂O intensity of GDP from 1997 to 2016. The numbers 1, 2, and 3 indicate which club the area belongs to

For nitrous oxide, the club is divided in the same way. The energy efficiency values are divided into three intervals with 0.70 and 0.90 as the two critical values. This resulted in 3 clubs as shown in *Figure 13*.

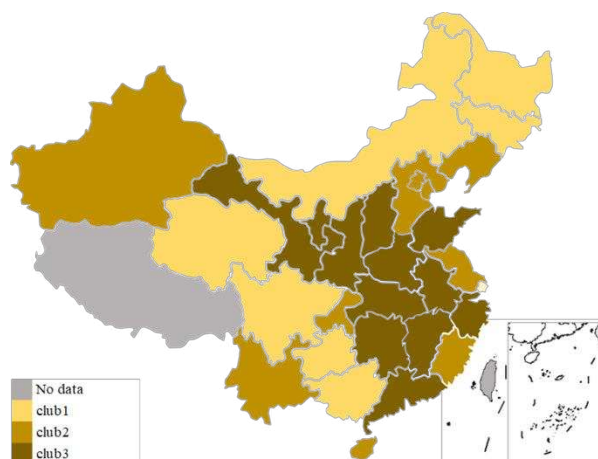


Figure 13. Club distribution of agricultural nitrous oxide intensity of GDP

The contradiction between people and land in the southwestern provinces of club 1 has intensified. In club 1, except for Shanghai, the agricultural N₂O flux of all members shows an increasing trend (*Fig. 14a*). According to *Equation 1*, a positive β value is calculated, which indicates that the absolute β convergence rate of the first club is 1.02%, that corresponds to *Figure 14b*. Agricultural N₂O reduction policy of the club should be formulated in accordance with the convergence model. Qinghai should undertake more emission reduction tasks and should reduce Shanghai's emission reduction pressure.

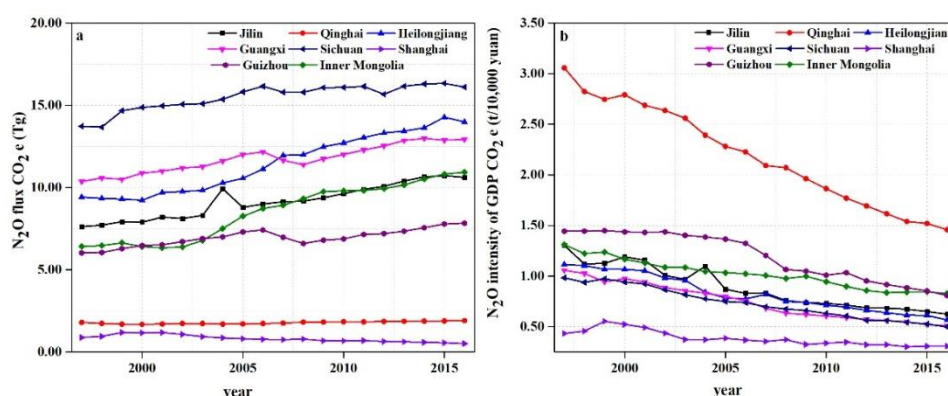


Figure 14. *a* Agricultural N₂O flux in club 1. *b* Agricultural N₂O intensity of GDP in club 1

The agricultural production of nitrous oxide flux is similar to club 1, but its emission intensity is only half of club 1 (*Fig. 15b*), which is mainly due to the fact that agricultural GDP of club 2 is much higher than club 1. There is no absolute β convergence in club 2, which indicates that the N₂O intensity of the members of the club will gradually increase, and its reduction target should be formulated according to

the divergent model. That is, each member's emission reduction policy has different emphasis.

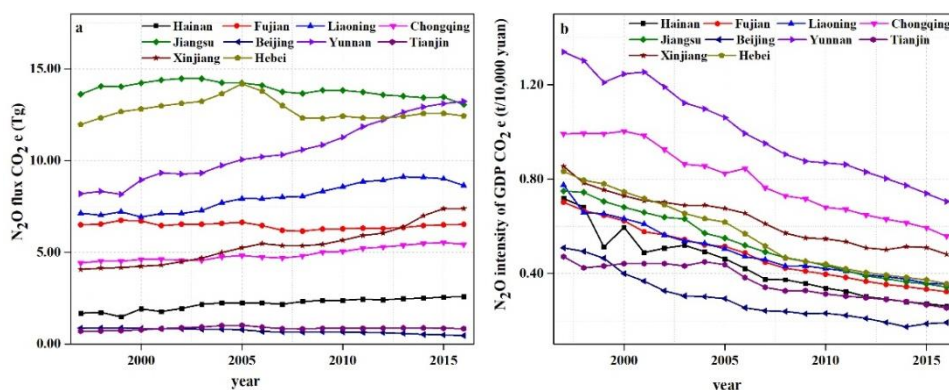


Figure 15. *a* Agricultural N₂O flux in club 2. *b* Agricultural N₂O intensity of GDP in club 2

Club 3 has the maximum number of members and the largest N₂O flux (Fig. 16a). Although flux has declined in 2005-2008, the overall trend is increasing. The intensity of N₂O of GDP within the club has decreased year by year and the gap has gradually constricted (Fig. 16b). A positive β value is calculated, and the β value is 0.17%, but the value of R² is only 0.0083, that is, the credibility of absolute β convergence is low. However, from Figure 16b, the narrowing of the difference in emission intensity seems to confirm the existence of the catch-up effect in the club.

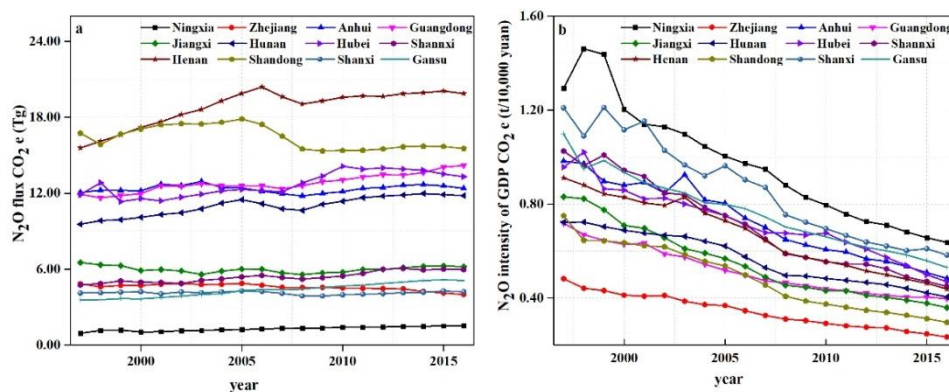


Figure 16. *a* Agricultural N₂O flux in club 3. *b* Agricultural N₂O intensity of GDP in club 3

Club 3 includes some crucial food production provinces, such as Shandong, Henan, Hunan, etc. The club plays an important role in ensuring Chinese food security. The SAIN another report pointed out that the excessive use of nitrogen fertilizer in cultivated wheat in Shaanxi reached 100%, and the excessive application of nitrogen fertilizer in the land where tomatoes were grown in Shandong reached 80-200%. According to the results of this study, club 3 has a huge potential for N₂O emission reduction in fertilizer. Club 3 has many plains and abundant labor force, so it is necessary to deepen the agricultural industrial chain and promote the urbanization process.

The club convergence test results of agricultural N₂O intensity is listed in *Table 4*. Agricultural N₂O mainly comes from planting industry. Based on the fact that China is a country with a large population, in order to feed more people on limited land, the agricultural input will be greatly increased, which will lead to the increase of N₂O emissions. However, the increase of economic benefits brought by the increase of input is limited. Therefore, this agricultural economy dominated by large input is not the optimal agricultural development path and is not conducive to emission reduction. In order to reduce the emission of N₂O, it is necessary to control the amount of nitrogen fertilizer and plant nitrogen-fixing crops with high economic benefits.

Table 4. Club convergence test results of agricultural nitrous oxide intensity

Test parameters	Club 1	Club 2	Club 3
α	-0.0376	-0.0370	-0.0388
t-Statistic	-9.3643	-10.5791	-23.0593
Prob.	0.0001	0.0000	0.0000
β	0.0102	-0.0096	0.0017
t-Statistic	1.0587	1.1839	-0.2896
Prob.	0.3305	0.2704	0.7780
R ²	0.1574	0.1491	0.0083

***, **, * mean accepting the convergence hypothesis at 5%, 10% and 15% significance level

Conclusion

GHGs reduction can bring co-benefits for air quality and human health (West et al., 2013), and has become the mainstream trend of economic development in various countries. The exploration of agricultural low-carbon development is a key area for scholars from all over the world.

The results of the club analysis show that the intensity of carbon dioxide in agriculture is in club convergence, and the absolute β convergence rate of club 1 is 15.55%, club 2 is 1.69%, and club 3 is 5.08%. Therefore, the emission reduction policy of carbon dioxide should be formulated according to the convergence model within the club. The two greenhouse gases, methane and nitrous oxide, only have convergence in one club. The methane emission intensity only converges at club 3, and the absolute β convergence rate is 2.19%. The nitrous oxide emission intensity only converges in club 1, and the absolute β convergence rate is 1.02%. Therefore, the emission reduction mode of these two gases should not only consider the convergence characteristics in the club, but also follow the divergence mode in the other two clubs.

The treatment of agricultural waste of resources, low level of mechanization of agriculture, agricultural pollution, and agricultural product safety are all issues that need to be addressed in the development of low-carbon agriculture (Peng and Liang, 2016). In view of the characteristics of China's agriculture, in order to achieve the development of low-carbon agriculture, it is necessary to improve the utilization efficiency of fossil fuels, explore more adaptable rice varieties and planting patterns, and promote more scientific animal farming techniques and nitrogen fertilizer application models. In particular, reducing the excessive use of nitrogen fertilizer will bring additional benefits, such as improving water quality, reducing soil acidification, enhancing air quality, increasing farmers' income, and improving the purchasing power

of the rural economy (Zhang et al., 2013). At the same time, agriculture as an important carbon sink, its role in greenhouse gas emission reduction can not be ignored, which will be gradually advanced in future research.

Acknowledgements. The authors gratefully acknowledge the financial support from the National Natural Science Foundation of China (71603039). This research has also been supported by Fundamental Research Funds for the Central Universities (DUT18JC12).

REFERENCES

- [1] Apergis, N., Payne, J. E. (2017): Per capita carbon dioxide emissions across US states by sector and fossil fuel source: evidence from club convergence tests. – *Energ Econ* 63: 365-372.
- [2] Barro, R. J., Salaimartin, X. (1992): Regional growth and migration - a Japan-United-States comparison. – *J Jpn Int Econ* 6: 312-346.
- [3] Barro, R. J., Mankiw, N. G., Salaimartin, X. (1995): Capital mobility in neoclassical models of growth. – *American Economic Review* 85: 103-115.
- [4] Baumol, W. J. (1986): Productivity growth, convergence, and welfare - what the long-run data show. – *Am Econ Rev* 76: 1072-1085.
- [5] Burnett, J. W. (2016): Club convergence and clustering of US energy-related CO₂ emissions. – *Resour Energy Econ* 46: 62-84.
- [6] Hao, Y., Liao, H., Wei, Y. (2015): Is China's carbon reduction target allocation reasonable? An analysis based on carbon intensity convergence. – *Appl Energ* 142: 229-239.
- [7] Huang, B., Meng, L. (2013): Convergence of per capita carbon dioxide emissions in urban China: a spatio-temporal perspective. – *Appl Geogr* 40: 21-29.
- [8] Jobert, T., Karanfil, F., Tykhonenko, A. (2010): Convergence of per capita carbon dioxide emissions in the EU: legend or reality? – *Energ Econ* 32: 1364-1373.
- [9] Kounetas, K. E. (2018): Energy consumption and CO₂ emissions convergence in European Union member countries. A tonneau des Danaïdes? – *Energ Econ* 69: 111-127.
- [10] Lal, R. (2004): Soil carbon sequestration impacts on global climate change and food security. – *Science* 304: 1623-1627.
- [11] Lelieveld, J., Crutzen, P. J., Dentener, F. J. (1998): Changing concentration, lifetime and climate forcing of atmospheric methane. – *Tellus Series B-Chemical and Physical Meteorology* 50: 128-150.
- [12] Li, Y., Lin, E., Xiong, W. (2009): Modeling N₂O emissions from agriculture in China. – *Progress in Geography* 28: 636-642 (in Chinese).
- [13] Liu, C., Hong, T., Li, H., Wang, L. (2018): From club convergence of per capita industrial pollutant emissions to industrial transfer effects: an empirical study across 285 cities in China. – *Energ Policy* 121: 300-313.
- [14] Min, J., Hu, H. (2012): Calculation of greenhouse gases emission from agricultural production in china. – *China Population, Resources and Environment* 22: 21-27 (in Chinese).
- [15] Norse, D. (2012): Low carbon agriculture: objectives and policy pathways. – *Environmental Development* 1: 25-39.
- [16] Peng, L., Liang, Y. H. (2016): Study on the Way to the Development of Low Carbon Agriculture in Henan Province. – In: Liu, X., Xu, G. (eds.) *Advances in Social Science Education and Humanities Research*. Atlantis Press, Paris.
- [17] Robalino-Lopez, A., Garcia-Ramos, J. E., Golpe, A. A., Mena-Nieto, A. (2016): CO₂ emissions convergence among 10 South American countries. A study of Kaya components (1980-2010). – *Carbon Manag* 7: 1-12.

- [18] Salaimartin, X. X. (1996): Regional cohesion: evidence and theories of regional growth and convergence. – *Eur Econ Rev* 40: 1325-1352.
- [19] Wang, Y., Zhang, P., Huang, D., Cai, C. (2014): Convergence behavior of carbon dioxide emissions in China. – *Econ Model* 43: 75-80.
- [20] West, J. J., Smith, S. J., Silva, R. A., Naik, V., Zhang, Y., Adelman, Z., Fry, M. M., Anenberg, S., Horowitz, L. W., Lamarque, J. (2013): Co-benefits of mitigating global greenhouse gas emissions for future air quality and human health. – *Nat Clim Change* 3: 885-889.
- [21] Yang, J., Zhang, T., Sheng, P., Shackman, J. D. (2016): Carbon dioxide emissions and interregional economic convergence in China. – *Econ Model* 52: 672-680.
- [22] Yang, S., Liu, C., Lai, C., et al. (2003): Estimation of methane and nitrous oxide emission from paddy fields and uplands during 1990-2000 in Taiwan. – *Chemosphere* 52: 1295-1305.
- [23] Yu, S., Hu, X., Fan, J., Cheng, J. (2018): Convergence of carbon emissions intensity across Chinese industrial sectors. – *J Clean Prod* 194: 179-192.
- [24] Zang, Z., Zou, X., Song, Q., Wang, T., Fu, G. (2018): Analysis of the global carbon dioxide emissions from 2003 to 2015: convergence trends and regional contributions. – *Carbon Manag* 9: 45-55.
- [25] Zhang, W., Dou, Z., He, P., Ju, X., Powlson, D., Chadwick, D., Norse, D., Lu, Y., Zhang, Y., Wu, L., Chen, X., Cassman, K. G., Zhang, F. (2013): New technologies reduce greenhouse gas emissions from nitrogenous fertilizer in China. – *P Natl Acad Sci USA* 110: 8375-8380.
- [26] Zhang, Y., Hu, C., Zhang, J. (2011): Research advances on source/sink intensities and greenhouse effects of CO₂, CH₄ and N₂O in agricultural soils. – *Chinese Journal of Eco-Agriculture* 19: 966-975 (in Chinese).

GEO-STATISTICAL ASSESSMENT OF GROUND WATER QUALITY IN DHAMAR BASIN, YEMEN

ALLAM, M.^{1,2} – MENG, Q. Y.^{1*} – AL-AIZARI, H.^{3,4*} – ELHAG, M.⁵ – YANG, J.⁶ – SAKR, M.⁷ –
WANG, Z.¹

¹*Aerospace Information Research Institute, Chinese Academy of Sciences, Beijing 100094, China*

²*Environment & Climate Change Research Institute, National Water Research Center, Cairo, Egypt*

³*Department of Chemistry, Faculty of Education, Thamar University, Yemen*

⁴*Laboratory of Biotechnology, Environment and Quality - UFR of process engineering, Faculty of Sciences, Ibn Tofail University, BP 133, Kenitra, 14000, Morocco*

⁵*Department of Hydrology and Water Resources Management, Faculty of Meteorology, Environment & Arid Land Agriculture, King Abdulaziz University, Jeddah 21589, Saudi Arabia*

⁶*Sanya Institute of Remote Sensing, Sanya 572029, China*

⁷*GIS and RS at King Mariout high Institute, Cairo, Egypt*

**Corresponding authors*

e-mail: mengqy@radi.ac.cn (Meng, Q. Y.); Alazari2@gmail.com (Al-Aizari, H.)

(Received 29th Apr 2019; accepted 31st Oct 2019)

Abstract. Groundwater quality in the Basin of Dhamar (Yemen) has been studied using geographic information system (GIS), principal component analysis (PCA) and correlation technique. A geographic information system is a tool for mapping and analyzing spatial data and is also used to retrieve groundwater quality information. For this study 26 wells were selected, for each well thirteen physicochemical parameters were analyzed including electrical conductivity, Calcium (Ca²⁺), Magnesium (Mg²⁺), Sodium (Na⁺), potassium (K⁺), bicarbonate (HCO₃⁻), Chloride (Cl⁻), Sulphate (SO₄²⁻), Nitrate (NO₃⁻), Iron (Fe²⁺), Fluoride (F⁻) and Total Hardness (TH). The collected groundwater was evaluated for its suitability for both drinking and irrigation purposes. Correlation and PCA have been utilized to analyze the parameters. Cartographic maps of the study area have been generated using multivariate statistical tools and GIS approach Inverse Distance Weighting (IDW) for all the above parameters. The created maps can be used to visualize, analyze, and understand the relationship among all locations. Most of the wells are found to be within the permissible limit except one well and this is due to the anthropogenic pollution received by human activities. Correlation and principal component analysis can help in selecting the most significant parameters to determine the status of water quality. The tools available in the GIS environment supported the study in the integration of data with very different data structures, i.e. point, 2D and 3D, towards spatial modeling of processes relevant to the assessment of groundwater resources.

Keywords: *ground water quality, PCA, IDW, piper diagram, Yemen*

Introduction

Water is a source of life for life. This substance must be preserved from all influences: modern civilization, industrialization, urbanization, and an increase of the population (Kot et al., 2000; Rafiullah et al., 2012). The groundwater contamination in an urban environment is due to the infiltration of domestic untreated wastewater into the natural receiving environment, accentuated by favorable hydrogeological conditions (Ayad and Kahoul, 2016). Around the world, pressure on water resources and particularly on groundwater resources is on the rise, mainly due to increasing demand.

The captured water may contain elements that may have adverse health effects, such as pathogenic microorganisms, unwanted substances or even toxic substances (Hartemann, 2000; Patil et al., 2012). Determining the quality of groundwater is important in deciding whether water is safe to drink, agriculture or industry. Water quality is a concept that refers to the chemical, biological and physical characteristics of water. The quality of the water required is determined by the purpose for which the water is to be used (domestic, urban, agricultural or industrial). Evaluation of water for uses is based on the characteristics of the water in relation to the quality required. In relation to drinking water, the required quality is defined by "standards" which define concentrations of constituents so that they have no adverse effect on the health of the consumer during the lifetime of consumption (Bakraji and Karajo, 1999).

Yemen is one of the countries most threatened by lack of water, it is already facing a serious water crisis: the annual consumption per individual is mediocre (135 m^3) compared to that recorded in the Middle East and North Africa (1250 m^3). Many cities face a serious water shortage, the prospect of sustainability of water resources, the main source of concern is the ever-increasing demand for water in water supply and irrigated groundwater agriculture in the same well field area (Glass, 2010; Whiting et al., 2011).

The aims of this study are to evaluate the groundwater quality of the Dhamar basin and its purposes for drinking and irrigation using GIS, correlation, and PCA, the second is to understand the variations in water quality in this reservoir.

Materials and Method

Study area

The governorate of Dhamar is situated in the middle of central highlands of Yemen with an area of 7.586 km^2 and 2700 m above sea level, it is divided into 12 administrative districts and 314 sub-districts (Figure 1). Dhamar has located 100 km to the south of Sana'a and north of Ibb city and west of Al-Beidha. Dhamar city is the capital of the governorate and it is situated on the main road that connects Sana'a with several other governorates. Dhamar basin is one of the largest water basins in Yemeni governorates and the most depletion one with over 6000 wells lastly reported in 2009 (Al-Aizari et al., 2017).

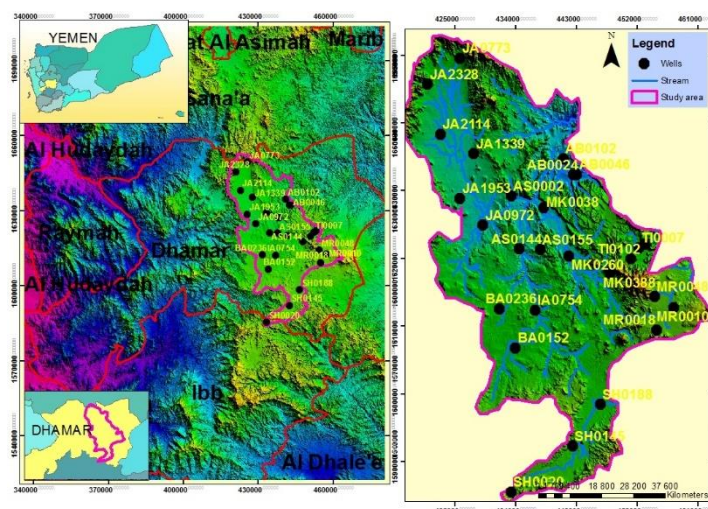


Figure 1. Study area and samples location

The climate of the study area is semi-arid. The annual rainfall is 407.8 mm, the maximum rainfall was 148.2 mm in June and the minimum was 88.2 mm in January during the period from 1999-2016. While the average monthly temperature varied from 21.4°C in December -27.7°C in June for the same period (Al-Aizari et al., 2017). The geology of the study area comprises Quaternary alluvium, Tertiary, Quaternary volcanic formations. Rhyolites, tuffs and ignimbrite ash-flow with occasional granite intrusions. The available hydrology data show that the main aquifers in Dhamar are Tertiary, Volcanic and Quaternary deposits. Groundwater subtraction through pumping wells in Quaternary deposits is more than Tertiary Volcanic. The outputs of this research are identifying the productive aquifers and dominant fissure in the north-northeast of the study region (Geukens, 1966; Chiesa, 1983; Overstreet et al., 1985; Al-Kohlani, 2009).

Data sampling

A total of 27 well representing the Dhamar basin were selected in our study *Table 1*, 14 groundwater samples were collected from each well in May 2009. These data have not been published earlier. The survey was carried out as part of a national program to monitor groundwater resources at a large number of locations nationwide. Since 2009 similar surveys have been carried out at other locations, which are not relevant for this study since samples were taken in different aquifers. It is not a common practice of this Government Department to publish the data they collect in response to governmental regulations. The samples were collected after pumping for 10 minutes, clean and dry polyethylene bottles are used for sample collection. The samples are tagged and stored in a refrigerator before the analysis (Girard, 1975). All samples were transported at temperature 4°C in portable coolers to the general agricultural research laboratory at Dahmer where the analyzes are carried out. Physio-chemical parameters were carried out EC, (Ca²⁺), (Mg²⁺), (Na⁺), (K⁺), (HCO₃⁻), (Cl⁻), (SO₄²⁻), (NO₂⁻), (Fe₂⁺), (F⁻) and (TH) and then compared with the guidelines admitted by the World Health Organization (WHO, 2003; Al-Asbahi, 2005).

Table 1. The site and the name of the studied well

No.	Well ID	Site name	No.	Well ID	Site name
1	AB0102	Abisiyah	15	JA1339	Jahran
2	AB0024	Abisiyah	16	JA1953	Jahran
3	AB0046	Abisiyah	17	JA2114	Jahran
4	AS0144	Aswad	18	JA2328	Jahran
5	AS0155	Aswad	19	MK0260	Makhderah
6	AS0002	Aswad	20	MK0038	Makhderah
7	BA0236	Balasan	21	MK0388	Makhderah
8	IA0754	Intervening	22	TI0102	Tinnan
9	MR0010	Maram	23	TI0049	Tinnan
10	MR0018	Maram	24	TI0007	Tinnan
11	MR0048	Maram	25	SH0020	Sherah
12	BA0152	Balasan	26	SH0188	Sherah
13	JA0773	Jahran	27	SH0145	Sherah
14	JA0972	Jahran			

Chemical analysis

EC is measured in the field using conductivity meter (Medium Conductivity Session CEL/850 (HACH)). PH is measured by pH-422. Ca^{2+} and Mg^{2+} are estimated titrimetrically using 0.02 N EDTA. HCO_3^- and Cl^- are estimated by H_2SO_4 and AgNO_3 titration (0.02 N), respectively. Na^+ and K^+ are measured by using a Flame photometer (PFP 7). F^- , Fe^{2+} , and NO_2^- are measured by the portable data logging spectrophotometer HACH DR/2400. This standard method is suggested by the American Public Health Association (WHO, 2003; APHA, 2005) (Table 2).

Table 2. Average physiochemical analyses for the grounds water and compared with YEMEN standards, WHO and Irrigation

Variable	Unit	Minimum	Maximum	Mean	STDEV	Yemen Standard	WHO Guideline
EC	$\mu\text{s}/\text{cm}$	312.7	1915.8	524	323.6	750-2000	1000-1500
pH	-	5.8	9.2	7.248	0.86	6.5-9	6.9-9.2
Ca^{2+}	mg/l	8	200	48.94	37.88	75-200	200
Mg^{2+}	mg/l	2.4	43.6	7.7	7.71	30-150	150
Na^+	mg/l	14.6	190	87.28	51.88	200-400	200
K^+	mg/l	0.8	10.7	4.27	2.597	8-12	8-20
HCO_3^-	mg/l	97.6	463.6	227.7	83.1	150-500	
Cl^-	mg/l	29	335	70.9	65.7	200-600	250
SO_4^{2-}	mg/l	20	320	58.5	64.5	200-400	250
NO_3^-	mg/l	1.50	49.70	15.64	14.68	0 -50	0-50
Fe^{2+}	mg/l	0	1.07	0.2122	0.2409	0.3-1	0.3
F^-	mg/l	0	0.09	0.01556	0.0268	0.5-1.5	1.5
TH	mg/l	40	680	149.6	122.1	100-500	500

Geo-statistical analysis

Statistical analysis was carried out using statistical package for social sciences (Minitab17). The physicochemical analysis for all the samples was analyzed by Pearson's correlation coefficient and principal component analysis. The PCA adopted in this paper is based on normalized and standardized data and exploits the correlation matrix between groundwater quality parameters rather than the covariance matrix (Sabnavis and Patangay, 1998; Van den Brink and Ter Braak, 1999; Singh et al., 2004; Joshi et al., 2009; Khatoon et al., 2013; Chaubey and Patil, 2015).

Interpolation methods fall into two categories, namely: the deterministic method and geostatistical method (Chen and Liu, 2012). Deterministic interpolation methods create surfaces from measured points, based on either the extent of similarity or the degree of smoothing. For instance, Inverse Distance Weighting (IDW), radial basis functions and splines function. The geostatistical interpolation methods such as Kriging method (Davis and Ierapetritou, 2007; Elhag and Bahrawi, 2017) can describe spatial patterns and interpolate the value of a primary variable at unmeasured locations, and quantify the uncertainty or error of estimated surface (Elhag, 2016a).

IDW assumes that the attribute value of unmeasured points is the weighted average of known values of the neighborhood. IDW will use the measured values surrounding the unmeasured locations to predict the values of the unmeasured ones. Those measured values closest to the prediction location will have more influence on the predicted value than those farther away. Thus, IDW assumes that each measured point has a local influence that diminishes with distance. It weights the points closer to the prediction location greater than

those far away. Maps layout are generated used ARCGIS 13 and AquaChem 2014 (Elhag, 2016a,b; Elhag and Bahrawi, 2016).

Sodium Adsorption Ratio

Sodium adsorption ratio (SAR) a formula used to evaluate salinity hazard and whether the water quality of the Groundwater Suitable or not acceptability for irrigation uses Lesch and Suarez (2009) (Table 3). SAR is calculated from the Na^+ , Ca^{++} , and Mg^+ using the following equation.

$$\text{SAR} = \text{Na} / [(\text{Ca} + \text{Mg})/2]^{1/2} \quad (\text{Eq.1})$$

where Na^+ , Ca^{++} , and Mg^{++} are the concentrations expressed in milli-equivalents per litre (meq/L).

Table 3. Irrigational Water Classification

SAR (epm)	Classification
<10	Excellent
10-18	good
18-26	Permissible
>26	Unsuitable

It depend on the distribution of SAR as described in Table 3 and Figure 2 indicating that all wells suitable for irrigation. In relation to the hazardous effects of sodium adsorption ratio, the irrigation water quality rating is given in Table 3.

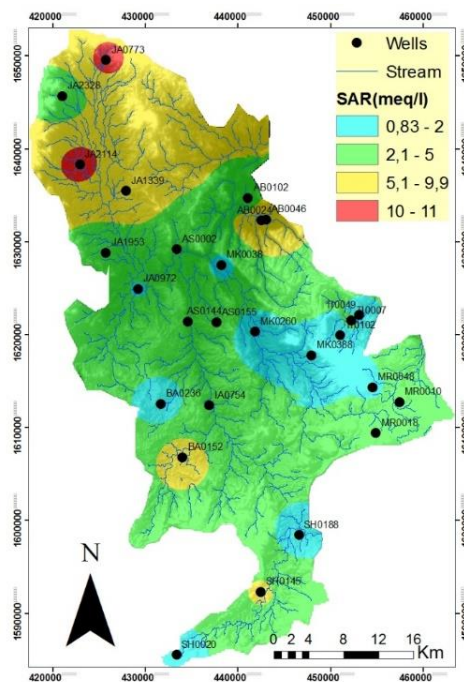


Figure 2. Distribution of SAR

Result and Discussions

The physicochemical analysis of 27 well and evaluating suitability for drinking water and irrigation purposes are summarized in *Table 2*.

The tested physiochemical parameters of the designated water wells in accordance with Yemen Maximum Allowable Unit (MAU) and compared to the World Health Organization (WHO) are cross-referenced in *Table 2*. The range of variation in Yemen standards is quite wide which makes it more difficult to have a fair judge. Generally, on one hand, the tested variables are within or slightly above the MAU. On the other hand, the tested variables are poorly recorded according to WHO.

EC in the collected samples is ranged from 312.7 to 1915.8 $\mu\text{s}/\text{cm}$ with an average value of 524 ± 323.6 . The map shows that the values of EC are within the permissible level except for some areas, mainly (well no. IA0754), in which the EC recorded 1915.8 $\mu\text{s}/\text{cm}$. Therefore, it exceeds the WHO permissible level but it still within the level of Yemen standard as in *Table 2*. The high value of EC in that location is due to contamination from the effluent of wastewater treatment plans (WWTP) as this well located in Mawaheb village. The cartographic map showing the distribution of EC is given in *Figure 3*. The EC showed strong correlation with Cl^- and SO_4^{2-} ($r = 0.94, 0.93$, respectively) and good correlation between with Ca^{2+} , Mg^{2+} , Na^+ and TH ($r = 0.76, 0.8, 0.52$ and 0.84 , respectively).

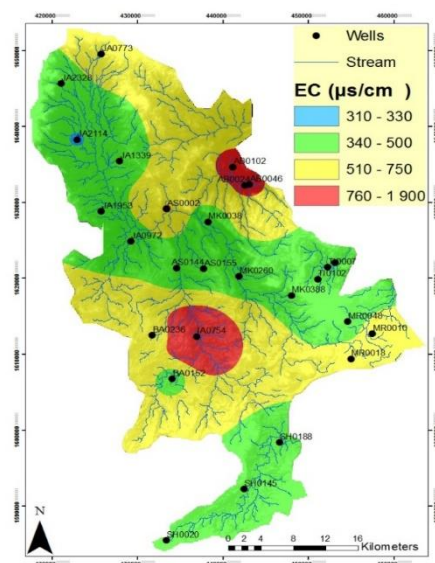


Figure 3. Distribution of EC

pH is considered as an important ecological factor that provides information on the types of geochemical equilibrium and solubility. From the thematic map (*Figure 4*), the pH is ranged from 5.8 to 9.2 so it is within the slandered of Yemen and WHO. The results show that three wells are basic and three well are acidic. The basic wells are Abisiyah (well no. ABS46, pH = 9.2), Balasan (well no. BB56, pH = 9.2) and Jahran (well no. QJB511, pH = 8.9). The three acidic wells are 6.3, 5.8 and 6.1 for the intervening area (well no. IA0754 pH = 6.3), Maram (well no. MR0018, pH = 5.8) and Jahran (well no. JA1953, pH = 6.1). pH showed negative correlation with all of parameters except Na^+ , Cl^- and Fe^{2+} ($r = 0.020, 00$ and 0.34 , respectively).

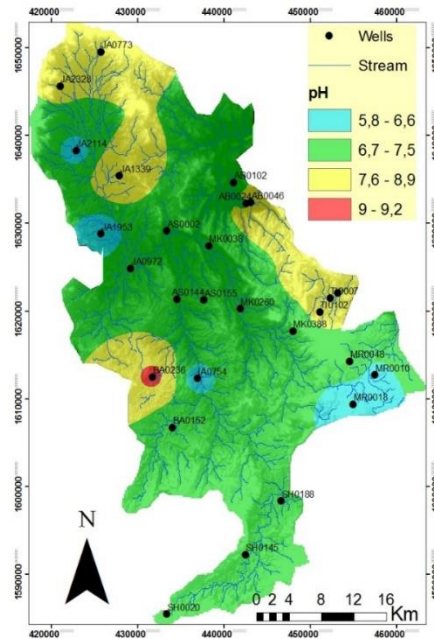


Figure 4. Distribution of pH

Na^+ varies from 14.6 to 190 mg/l with an average value of 87.28 ± 51.88 . The high concentration of sodium in water makes it unsatisfactory for use in irrigation purposes. The concentration of sodium in all samples are found to be within the permissible level of WHO and Yemen Standards *Table 2*. However, in well no AB0046, the concentration of sodium found to be near to the permissible level which is 190 mg/l. Na^+ has good correlation with Cl^- and SO_4^{2-} ($r = 0.60, 0.53$), demonstrated in *Figure 5*.

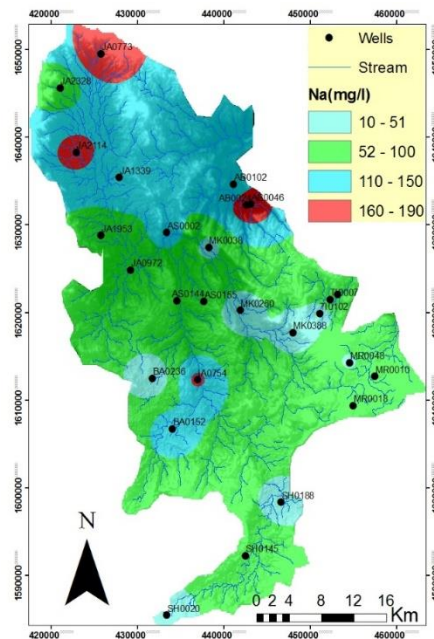


Figure 5. Distribution of Na

The concentration of K^+ varies from 0.8 to 10.7 mg/l with an average value of 4.27 ± 2.59 . The concentration of potassium in all samples is found to be within the permissible level (Table 2). K^+ has good correlation with F^- , ($r = 0.53$), demonstrated in Figure 6.

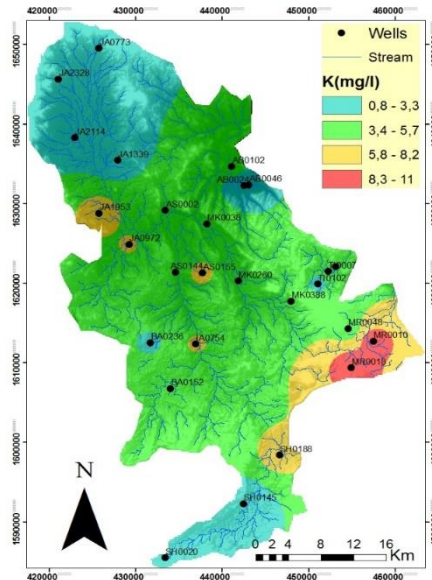


Figure 6. Distribution of K

The Mg^{2+} values range from 2.4 to 43.6 mg/l with an average value of 7.7 ± 7.71 , the presence of Mg^{2+} in water generally does not have any health hazards to humans. The concentrations of Mg^{2+} in all samples are found to be within the permissible level in Table 2 and Figure 7. Mg^{2+} is strong correlated with TH ($r = 0.98$) and with Ca^{2+} with Mg^{2+} , Cl^- and SO_4^{2-} ($r = 0.81, 0.59$ and 0.64), while it is good correlated with Cl^- and SO_4^{2-} ($r = 0.78, 0.76$) respectively.

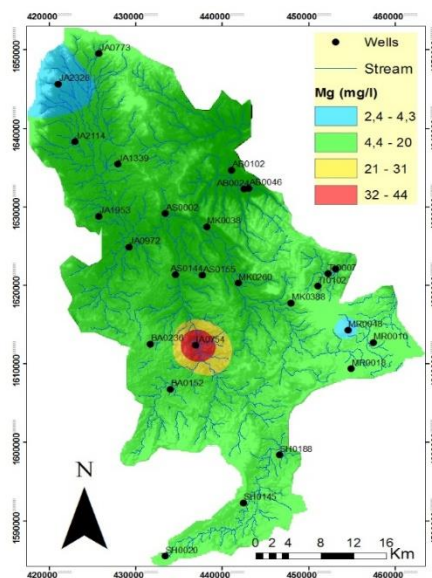


Figure 7. Distribution of Mg

Ca^{2+} ranges from 8 to 200 mg/l with an average value of 48.94 ± 37.88 . the presence of Ca^{2+} in water does not have health hazards to humans. Ca^{2+} values are within the permissible level in all samples except in the intervening area (well no. IA0754). This may be attributed to pollution by wastewater (Figure 8). Ca^{2+} shows strong correlation with TH, ($r = 0.98$) and good correlation with Mg^{2+} , Cl^- and SO_4^{2-} ($r = 0.81, 0.59$ and 0.64) respectively.

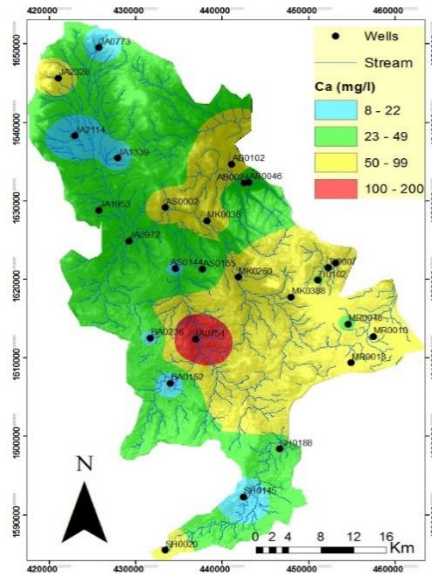


Figure 8. Distribution of Ca

SO_4^{2-} values various from 20-320 mg/l with an average value of 58.5 ± 64.5 . The concentration of sulfate in all locations are within the permissible limit except the intervening area (well no. IA0754) where the sulfate value 320 mg/l. The SO_4^{2-} was has a good correlation between SO_4^{2-} with TH ($r = 0.98$) as is illustrated in Figure 9.

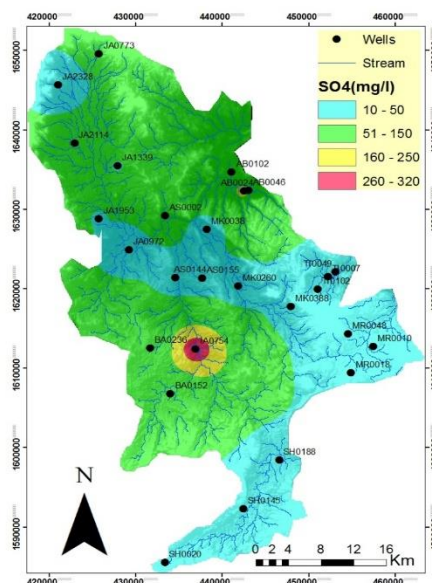


Figure 9. Distribution of SO_4^{2-}

The HCO_3^- varies from 97.6 to 463.6 mg/l with an average value of 227.7 ± 83.1 . The concentration of bicarbonate in all samples are found to be within the permissible limit (*Figure 10*). The HCO_3^- has strong correlation with SO_4^{2-} ($r = 0.98$).

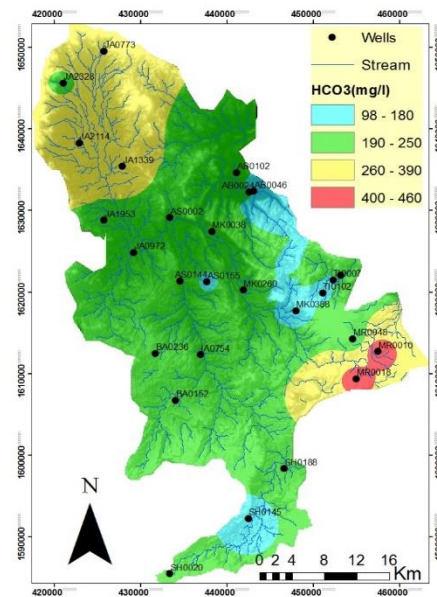


Figure 10. Distribution of HCO_3^-

WHO reported that atmosphere, legumes, plant debris, and animal excreta are the main source of water nitrate, alongside with the domestic water, sewage, septic tanks. Anionic and solubility of NO_3^- can also affect the concentration of NO_3^- in groundwater. In Yamen NO_3^- varies from 0.01 to 0.453 mg/l with an average value of 227.7 ± 83.1 . The concentrations of nitrates in all samples are found to be within the permissible limit (*Table 2*), and its distribution in *Figure 11*.

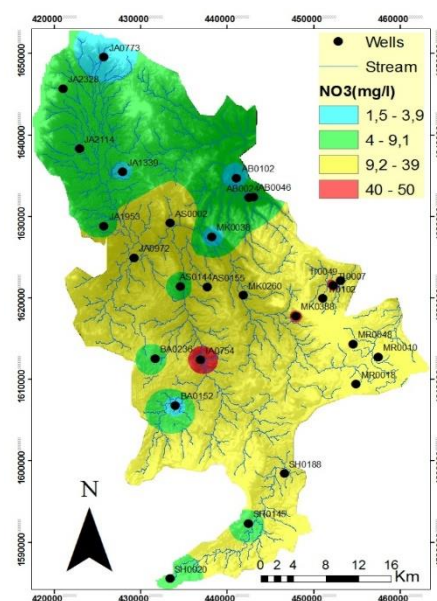


Figure 11. Distribution of NO_3^-

The F^- values various from 0 to 0.09 mg/l with an average value of 0.01556 ± 0.0268 . Fluoride concentration is within the permissible level in all locations. Fluoride above permissible level may cause mottled enamel of teeth and skeleton deformity. The cartographic map of F^- is given in *Table 2* and demonstrated in *Figure 12*.

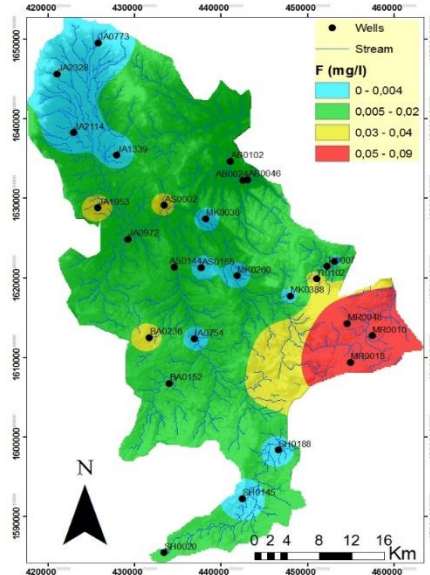


Figure 12. Distribution of F^-

Fe^{2+} concentration are varied from 0 to 1.07 mg/l with an average value of 0.2122 ± 0.2409 . From the cartographic map (*Figure 13*), iron exceeded the permissible level in some wells Tinnan (TI0102), Tinnan (TI0007), Sherah (SH0188), and Jahran (JA1339). In the case of Tinnan (TI0102) and Jahran (JA1339) this may be attributed to strains of oxides and hydroxides on laundry, sanitary and plumbing textures. At concentration above 0.5 mg/l, iron cause an unpleasant taste (*Table 2*).

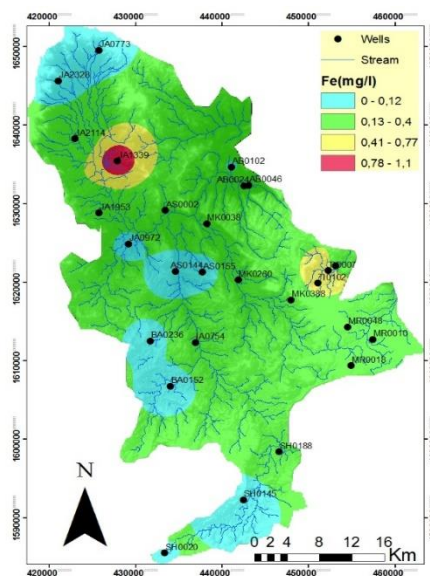


Figure 13. Distribution of Fe^{2+}

The TH values range from 40 to 680 mg/l with an average value of 149.6 ± 122.1 (Figure 14). All samples are within the permissible values as in Table 1 except well no. IA0754 has a comparatively high TH value of 680 mg/l.

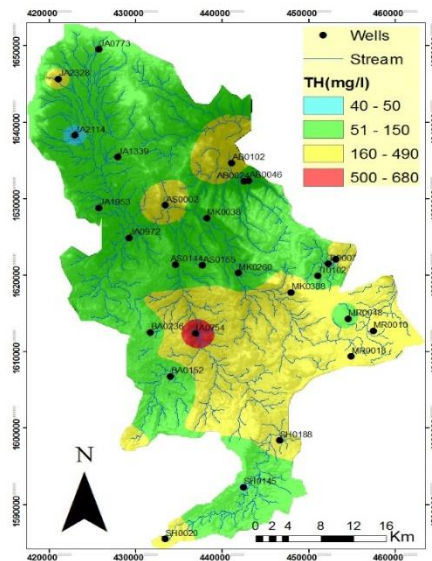


Figure 14. Distribution of TH

Cl^- is an important indicator of the contamination of groundwater by wastewater. The Cl^- values range from 29 to 335 mg/l with an average value of 70.9 ± 65.7 . The permissible limit of Cl^- in drinking water for WHO guideline is 250 mg/l, while it is 600 mg/l for Yemeni Standards. The concentrations of Cl^- are within the permissible limit in all locations, except the intervening area (well no. IA0754) where the chloride value is 335 mg/l. The reason for high chloride in that well is due to the contamination of groundwater from effluent as discussed earlier. The cartographic map of Ca^{2+} is given in Figure 15. The Cl^- has a strong correlation with SO_4^{2-} ($r = 0.98$).

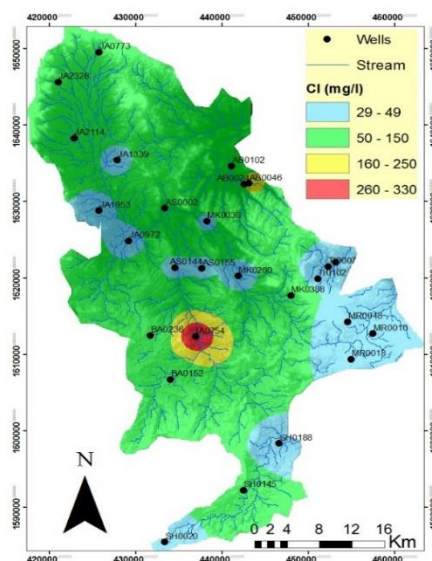


Figure 15. Distribution of Cl^-

Correlation analysis a widely used between variable, the correlation between two variables is the simple correlation that indicates the sufficiency of one variable to predict the other one (Sedgwick, 2012). This coefficient is used to determine the correlation between variables when the dependent (x) is only influenced by the independent (y) and vice versa (Benesty et al., 2009). *Table 4* displayed the values of the correlation coefficients between the parameters. Strong correlations $r > 0.9$ and good $r = 0.5-0.9$.

Table 4. Correlation matrix of all studied parameters

	EC	pH	Ca ²⁺	Mg ²⁺	Na ⁺	K ⁺	HCO ₃ ⁻	Cl ⁻	SO ₄ ²⁻	NO ₃ ⁻	Fe ²⁺	F	TH
Ec	1.00												
pH	-0.16	1.00											
Ca²⁺	0.76	-0.45	1.00										
Mg²⁺	0.88	-0.35	0.81	1.00									
Na⁺	0.52	0.02	0.01	0.29	1.00								
K⁺	0.14	-0.56	0.44	0.33	-0.27	1.00							
HCO₃⁻	0.10	-0.32	0.14	0.15	0.28	0.42	1.00						
Cl⁻	0.94	0.00	0.59	0.78	0.60	-0.10	-0.13	1.00					
SO₄²⁻	0.93	-0.09	0.64	0.76	0.53	-0.06	-0.06	0.91	1.00				
NO₃⁻	0.29	-0.16	0.58	0.43	-0.24	0.38	-0.13	0.21	0.17	1.00			
Fe²⁺	-0.07	0.34	0.04	-0.04	0.01	-0.12	0.07	-0.12	-0.04	0.27	1.00		
F	-0.01	-0.25	0.13	-0.02	-0.09	0.53	0.48	-0.18	-0.19	0.20	-0.02	1.00	
TH	0.84	-0.43	0.98	0.91	0.12	0.43	0.17	0.67	0.71	0.55	0.02	0.12	1.00

Principal Component Analysis

The principal component analysis is a multidimensional statistical method that can be used in the interpretation of a data matrix. This method, by looking for the reference directions of elongation of a multidimensional point cloud (eigenvalues), summarizes the information by projecting the point cloud on its preferential directions (factorial axes). Factors are linear combinations of the starting variables. Each variable contributing to the factor intervenes with a coefficient called "eigenvector" (Sabnavis and Patangay, 1998; Bahrawi et al., 2016; Elhag, 2016b).

Principal component analysis (PCA) for the groundwater allows determining its chemical characteristics, and their overall variations (factors). We select only the first two factors as they express 63.473% of the total variance. The analysis of the variables shows in *Tables 5, 6* and *Figures 16, 17*. The Factor 1 expresses 42.748% of the total factors and wells that correlated with the variables, these variables are conductivity, sodium, nitrates, chloride, calcium, sulfate, magnesium and Total hardens. While factor 2 expresses 20.725% of the total factors, these variables include bicarbonates, iron, fluoride, and potassium (*Figures 18 and 19*).

Table 5. Total variation explained by all parameter

	F1	F2	F3	F4	F5	F6	F7	F8	F9	F10	F11	F12	F13
Eigenvalue	5.557	2.6943	1.62	1.2571	0.654	0.4182	0.3071	0.2483	0.129	0.0832	0.023	0.008	0.0033
Proportion	0.427	0.207	0.12	0.097	0.05	0.032	0.024	0.019	0.01	0.006	0.002	0.001	0
Cumulative	0.427	0.635	0.76	0.856	0.906	0.938	0.962	0.981	0.991	0.997	0.999	1	1

Table 6. Coefficient of centered variables reduced in the linear equation of the principal axes

Variable	PC1	PC2
EC	0.404	0.144
pH	-0.158	0.357
TH	0.403	-0.116
HCO ₃ ⁻	0.064	-0.292
Cl	0.356	0.296
F	0.027	-0.417
NO ₃ ⁻	0.198	-0.215
SO ₄ ²⁻	0.361	0.263
Ca ²⁺	0.379	-0.155
Mg ²⁺	0.4	-0.004
Na ⁺	0.155	0.311
K ⁺	0.14	-0.504
Fe ²⁺	-0.02	0.027

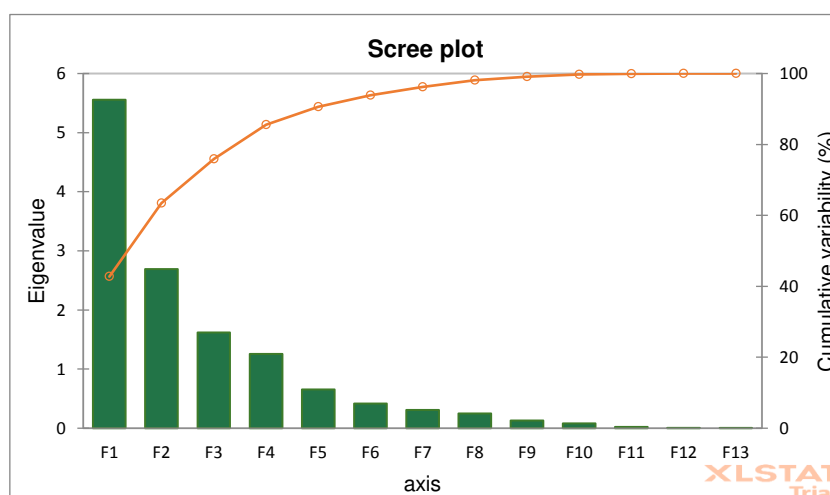


Figure 16. Scree plot for all samples

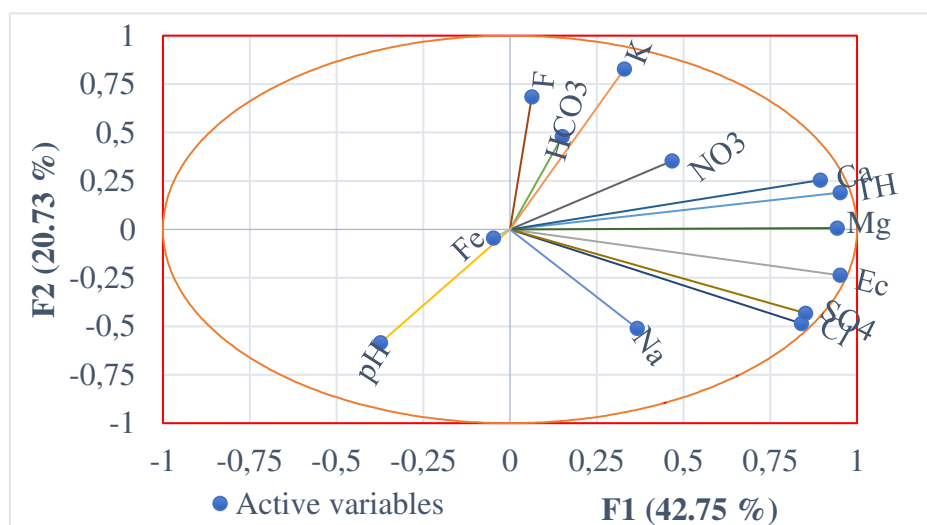


Figure 17. PCA Variables (axes F1 and F2: 63.47%)

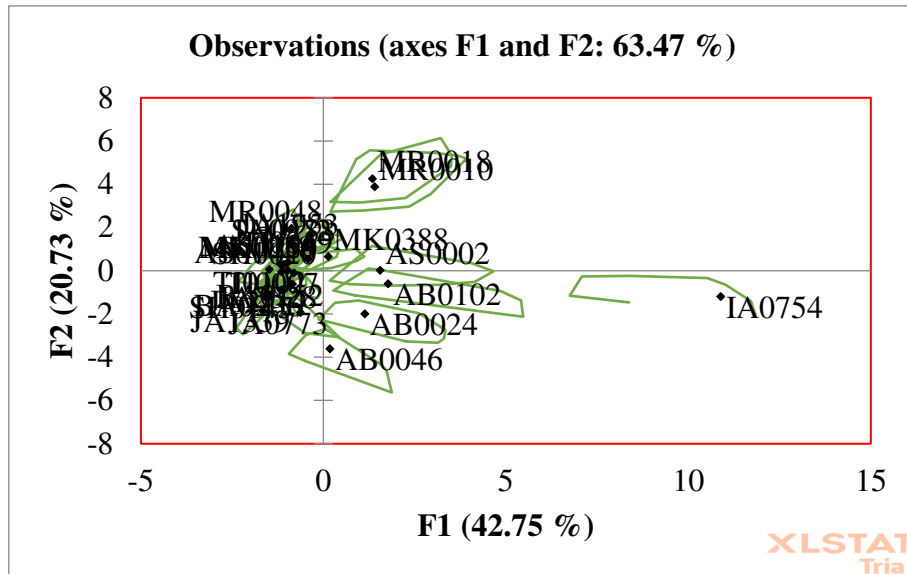


Figure 18. Projection of wells on the F1-F2 factorial plane

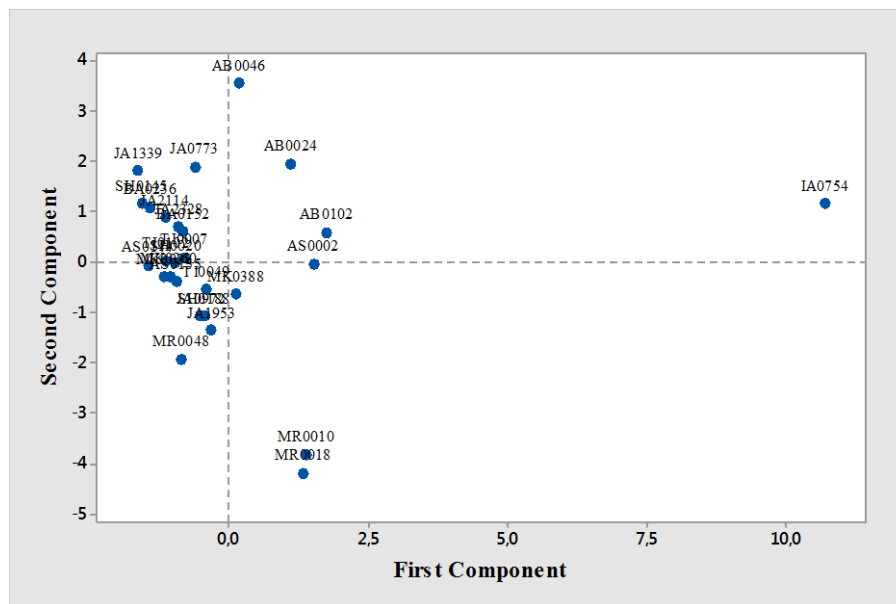


Figure 19. A score of all the samples on the plan

A piper diagram is a graphical representation of the chemistry of water samples. The cations and anions are shown by separate ternary plots. The apexes of the cation plot are calcium, magnesium, and sodium plus potassium cations. The piper diagram was preferred because of its accuracy in the identification of the water samples and the dominant component in the water chemistry (Piper, 1944; Elhag et al., 2019). Generally, the samples are showing different constituents of water as shown in *Table 7* and *Figure 20*. This indicates that the source's groundwater of these wells is different. The differences in compositions of the water are attributed to that the geology of the Dhamar area is generally volcanic and basaltic rock. However, some areas such as Jahran are having alluvial deposits.

Table 7. Chemical composition of water samples in various locations

No.	Well ID	Site name	Chemical Composition
1	AB0102	Abisiyah	Na-Ca-HCO3-Cl
2	AB0024	Abisiyah	Na-Ca-SO4-HCO3
3	AB0046	Abisiyah	Na-Cl-SO4
4	AS0144	Aswad	Na-HCO3-Cl
5	AS0155	Aswad	Na-Ca-HCO3-Cl
6	AS0002	Aswad	Na-Ca-HCO3-Cl
7	BA0236	Balasan	HCO3-Cl-SO4
8	IA0754	Intervening	Ca-Na-Cl-SO4
9	MR0010	Maram	Ca-Na-HCO3
10	MR0018	Maram	Ca-Na-HCO3
11	MR0048	Maram	Ca-Na-HCO3
12	BA0152	Balasan	Na-HCO3-Cl-SO4
13	JA0773	Jahran	Mg-Na-HCO3
14	JA0972	Jahran	Ca-Na-HCO3
15	JA1339	Jahran	Na-HCO3
16	JA1953	Jahran	Na-Ca-HCO3
17	JA2114	Jahran	Na-HCO3-Cl
18	JA2328	Jahran	Na-Ca-HCO3-Cl
19	MK0260	Makhderah	Ca-Na-HCO3
20	MK0038	Makhderah	Ca-Na-HCO3-Cl
21	MK0388	Makhderah	Ca-Na-HCO3-Cl
22	TI0102	Tinnan	Ca-Na-HCO3-Cl
23	TI0049	Tinnan	Ca-Na-HCO3-Cl
24	TI0007	Tinnan	Na-Ca-HCO3-Cl
25	SH0020	Sherah	Ca-Na-HCO3-Cl
26	SH0188	Sherah	Ca-Na-HCO3
27	SH0145	Sherah	Na-HCO3-Cl

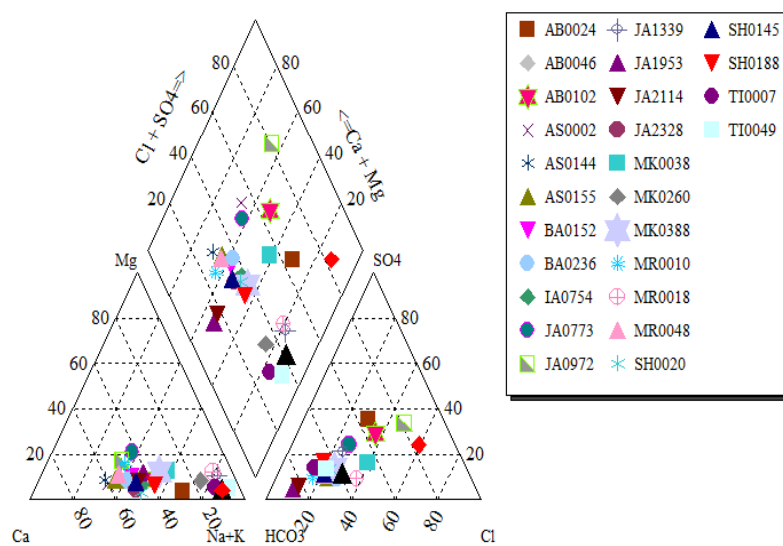


Figure 20. Piper diagram of all samples

Groundwater in different wells of Abisiyah is a mixture of Na^+ , Ca^{2+} , Cl^- , SO_4^{2-} and HCO_3^- . The geological nature of this area is basaltic rocks. Generally, the groundwater aquifers of basaltic rocks have Na^+ Ca^{2+} HCO_3^- composition and any change of this water are due to contamination from human activities or heavy exploitation. The high concentration of Cl and SO_4 without any natural sources indicate human contamination. However, the concentrations of Cl and SO_4 are within the permissible limit of WHO and standard Yemen illustrated in Figure 21.

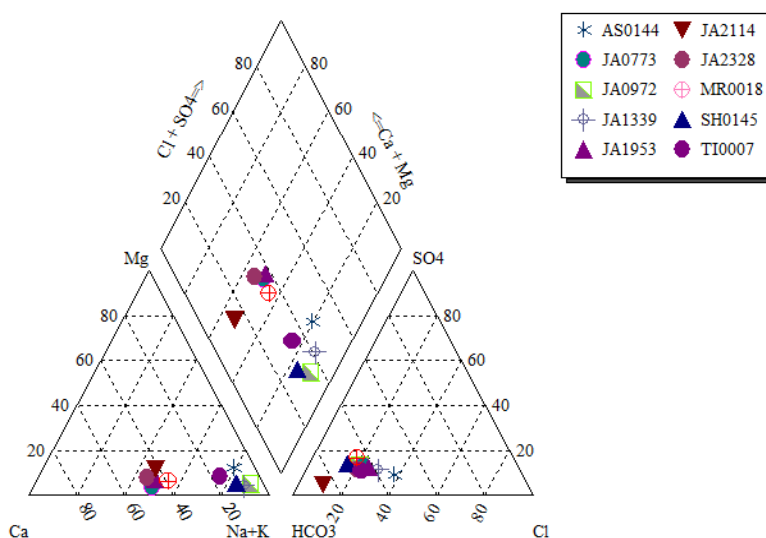


Figure 21. Piper diagram of volcanic aquifer

Predominantly, the water quality parameters used in the current research are varied based on the utilized sample in each rationing. Therefore, the categorization of different quality parameters using principal component analysis will help to examine the indices discrepancies (Yilmaz et al., 2018).

The dynamicity of the water quality monitoring process added further complications to designating mineral-affected wells in a systematic uniform perspective. The use of different quality parameters based on implementing different combinations and/or water samples in the form of water quality parameters evidenced to be more efficient to overcome wells' dynamicity problems (Elhag, 2016b; Bahrawi and Elhag, 2019; Elhag et al., 2019).

Earth is a forceful system that has been affected by natural and anthropological influences. One of the most substantial anthropogenic consequences on the earth are Land Use/Land Cover changes of (LULC) which take place over the earth surface. (Elhag, 2016c, Allam et al., 2019).

The water resources of the coastal region of the Gharb are susceptible to the pollution caused by the emergent industry and urbanization expansion. Certainly, the global economy growth, population density, and infrastructure developments stressed water quality and quantity (Elhag and Bahrawi 2014, Aremu, M. O. et al., 2017, Darwesh et al., 2019).

Conclusion

Geographic Information System (GIS), correlation and Principal Component Analysis have been found to be a highly useful technique towards water quality management. The results of this study provide some information that can be useful with respect to groundwater studies. Salinity values are an acceptable level, in spite of the strong water abstraction from the wells in Dhamar plain except for the well no IA0754 that its salinity recorded 1900 $\mu\text{S}/\text{cm}$ that is due to contamination from the effluent of wastewater treatment plants (WWTP) as this well located in Mawaheb village. The average salinity values are 524 $\mu\text{S}/\text{cm}$ at 25°C. About 99% of the wells are classified as suitable for drinking water, and only 1% of total wells exceed the Yemeni standard for drinking water with respect to the Iron element. All wells are suitable for irrigation purposes. The low TDS was found in the groundwater of the Dhamar area because groundwater drains in igneous rocks (acidic rock), which release a low concentration of major elements. The lower concentrations of Cl^- and SO_4^{2-} are due to an artificial source of pollution by human activities. Generally, groundwater quality is good in Dhamar plain. The presence of nitrates shows that the pollutant penetrates freely from the surface and that because of the hydrodynamic characteristics of the aquifers. The results of the good analysis of Dhamar plain indicates that the type of groundwater is Na-Ca- $\text{Cl}/\text{SO}_4^{2-}\text{HCO}_3^-$ and $\text{Ca}\cdot\text{Na}\cdot\text{HCO}_3\cdot\text{Cl}$, to mixed nature. The study recommended that modeling of groundwater quality in response to growing exploitation, particularly for irrigation. Irrigation leads to the percolation of water with higher salinity, thus potentially harmful for the long term sustainability of groundwater resources. Monitoring should be done more frequently and continuously to ensure timely detection of anomalies.

Acknowledgments. The authors are thankful to National Key Research and Development Program (China's 13th Five Year Plan) "Spatial information service and application demonstration of comprehensive monitoring of urban and rural ecological environment" (2017YFB0503900, 2017YFB0503905), and to the Science and technology cooperation project of Sanya Municipal Institute: Non-Point Source Pollution Risk Identification and Quantitative Assessment for Surface Water Source Using Remote Sensing, (2018YD10) and Hainan Province Natural Science Foundation: Urban Impervious Surface Remote Sensing Extraction and Study on the Characteristics of Multi Temporal and Spatial Evolution, (417218). The authors are also thankful to Renewable Natural Resources Research Center (RNRRC), Dhamar, Yemen, for helping in analyzing the ground water.

REFERENCES

- [1] Al-Aizari, H., Lebkiri, A., Fadli, M., Albaseer, S. S. (2017): Quality assessment of ground water in Dhamar City, Yemen. – International Journal of Environment 6(4): 56-71.
- [2] Al-Asbahi, Q. Y. A. M. (2005): Water resources information in Yemen. – United Nations Intersecretariat Working Group on Environment Statistics (IWG-ENV), International Work Session on Water Statistics, Vienna (June 20-22), available at: http://unstats.un.org/unsd/environment/envpdf/pap_wasess3a3yemen.
- [3] Al-Kohlani, T. A. M. (2009): Geochemistry of thermal waters from Al-Lisi-Isbil geothermal field, Dhamar governorate, Yemen. – Proceedings World Geothermal Congress, Bali, Indonesia.

- [4] Allam, M., Bakr, N., Elbably W., (2019): Multi-temporal assessment of land use/land cover change in arid region based on landsat satellite imagery: Case study in Fayoum Region, Egypt. *Remote Sensing Applications: Society and Environment* 14: 8–19.
- [5] APHA (2005): Standard methods for the examination of water and wastewater. – American Public Health Association: Washington, DC, USA.
- [6] Aremu, M.O., .Oko O.J., Andrew, C. (2017): Ground water and river quality assessment for some heavy metals and physicochemical parameters in Wukari town, Taraba state, Nigeria. *International Journal of sciences*. 6 (05): 37-80.
- [7] Ayad, W., Kahoul, M. (2016): Evaluation de la qualité physicochimique et bactériologique des eaux de puits dans la région d'El-Harrouch (NE-Algérie) [Assessment of physico-chemical and bacteriological quality of Well water in the region of El-Harrouch (NE-Algeria)]. – *Journal of Materials and Environmental Science* 7: 1288-1297.
- [8] Bahrawi, J. A., Elhag, M., Aldhebiani, A. Y., Galal, H. K., Hegazy, A. K., Alghailani, E. (2016): Soil Erosion Estimation Using Remote Sensing Techniques in Wadi Yalamlam Basin, Saudi Arabia. – *Advances in Materials Science and Engineering* Vol. 2016: 9585962.
- [9] Bahrawi, J., Elhag, M. (2019): Consideration of seasonal variations of water radiometric indices for the estimation of soil moisture content in erid environment in Saudi Arabia. – *Applied Ecology and Environmental Research* 17(1): 285-303.
- [10] Bakraji, E., Karajo, J. (1999): Determination of heavy metals in Damascus drinking water using total reflection X-ray fluorescence. – Atomic Energy Commission, Technical Report.
- [11] Benesty, J., Chen, J., Huang, Y., Cohen, I. (2009): Pearson correlation coefficient. – Noise reduction in speech processing. Springer Topics in Signal Processing, Vol. 2.
- [12] Chaubey, S., Patil, M. K. (2015): Correlation study and regression analysis of water quality assessment of Nagpur City, India. – *International Journal of Scientific and Research Publications* 5(11).
- [13] Chen, F.-W., Liu, C.-W. (2012): Estimation of the spatial rainfall distribution using inverse distance weighting (IDW) in the middle of Taiwan. – *Paddy and Water Environment* 10(3): 209-222.
- [14] Chiesa, S. (1983): Geology of the Dhamar-Rada' volcanic field, Yemen. – Arab Republic.
- [15] Darwesh, N., Allam, M., Meng, Q., Halfdhallah, A., Ramzy S. M, N., El Kharrin, K., Al Malik, A. Belghyti, D. (2019): Using Piper trilinear diagrams and principal component analysis to determine variation in hydrochemical faces and understand the evolution of groundwater in Sidi Slimane Region, Morocco. *Egyptian Journal of Aquatic Biology & Fisheries Zoology Department, Faculty of Science, Ain Shams University, Cairo, Egypt* 23(5): 17 – 30.
- [16] Davis, E., Ierapetritou, M. (2007): A kriging method for the solution of nonlinear programs with black-box functions. – *AIChE Journal* 53(8): 2001-2012.
- [17] Elhag, M. (2016a): Inconsistencies of SEBS Model Output Based on the Model Inputs: Global Sensitivity Contemplations. – *Journal of the Indian Society of Remote Sensing* 44(3): 435-442.
- [18] Elhag, M. (2016b): Evaluation of different soil salinity mapping using remote sensing techniques in arid ecosystems, Saudi Arabia. – *Journal of Sensors* Vol. 2016: 7596175.
- [19] Elhag, M. (2016c). Detection of Temporal Changes of Eastern Coast of Saudi Arabia for Better Natural Resources Management. *Indian Journal of Geo-Marine Sciences* 45(1): 29-37.
- [20] Elhag, M., Bahrawi, J. A. (2014). Potential rainwater harvesting improvement using advanced remote sensing applications. *The Scientific World Journal* 2014: p. 806959.
- [21] Elhag, M., Bahrawi, J. A. (2016): Consideration of geo-statistical analysis in soil pollution assessment caused by leachate breakout in the municipality of Thermi, Greece. – *Desalination and Water Treatment* 57(57): 27879-27889.

- [22] Elhag, M., Bahrawi, J. A. (2017): Spatial assessment of landfill sites based on remote sensing and GIS techniques in Tagarades, Greece. *Desalination and Water Treatment* 91: 395-401.
- [23] Elhag, M., Gitas, I., Othman, A., Bahrawi, J., Gikas, P. (2019): Assessment of Water Quality Parameters Using Temporal Remote Sensing Spectral Reflectance in Arid Environments, Saudi Arabia. – *Water* 11(3): 556.
- [24] Geukens, F. (1966): *Geology of the Arabian peninsula*. – Translated from French by SD Bowers, Professional paper.
- [25] Girard, M. (1975): Prélèvements d'échantillons en grotte et station de terrain sec en vue de l'analyse pollinique. – *Bulletin de la Société préhistorique française* 72(5): 158-160.
- [26] Glass, N. (2010): The water crisis in Yemen: causes, consequences and solutions. – *Global Majority E-Journal* 1(1): 17-30.
- [27] Hartemann, P. (2000): L'eau et la sante. – *Concours Medical* 122(26): 1761-1761.
- [28] Joshi, D. M., Bhandari, N. S., Kumar, A., Agrawal, N. (2009): Statistical analysis of physicochemical parameters of water of River Ganga in Haridwar district. – *Rasayan Journal of Chemistry* 2(3): 579-587.
- [29] Khatoon, N., Khan, A. H., Rehman, M., Pathak, V. (2013): Correlation study for the assessment of water quality and its parameters of Ganga River, Kanpur, Uttar Pradesh, India. – *IOSR Journal of Applied Chemistry* 5(3): 80-90.
- [30] Kot, B., Baranowski, R., Rybak, A. (2000): Analysis of mine waters using X-ray fluorescence spectrometry. – *Polish journal of environmental studies* 9(5): 429-432.
- [31] Lesch, S., Suarez, D. (2009): A short note on calculating the adjusted SAR index. – *Transactions of the ASABE* 52(2): 493-496.
- [32] Overstreet, W., Kiilsgaard, T., Grolier, M., Schmidt, D., Domenico, J., Donato, M., Botinelly, T., Harms, T. (1985): *Contributions to the geochemistry, economic geology, and geochronology of the Yemen Arab Republic*. – US Geological Survey.
- [33] Patil, P., Sawant, D., Deshmukh, R. (2012): Physico-chemical parameters for testing of water-A review. – *International Journal of Environmental Sciences* 3(3): 1194-1207.
- [34] Piper, A. M. (1944): A graphic procedure in the geochemical interpretation of water-analyses. – *Eos, Transactions American Geophysical Union* 25(6): 914-928.
- [35] Rafiullah, M., Milind, J., Ustad, I. (2012): Physico chemical analysis of Triveni lake water of Amravati district in (MS) India. – *Bioscience discovery* 3(1): 64-66.
- [36] Sabnavis, M., Patangay, N. S. (1998): *Principles and applications of groundwater geophysics*. – Association of Exploration Geophysicists.
- [37] Sedgwick, P. (2012): Pearson's correlation coefficient. – *BMJ* 345: e4483.
- [38] Singh, K. P., Malik, A., Mohan, D., Sinha, S. (2004): Multivariate statistical techniques for the evaluation of spatial and temporal variations in water quality of Gomti River (India)-a case study. – *Water research* 38(18): 3980-3992.
- [39] Van den Brink, P. J., Ter Braak, C. J. F. (1999): Principal response curves: Analysis of time-dependent multivariate responses of biological community to stress. – *Environmental Toxicology and Chemistry* 18(2): 138-148.
- [40] Whiting, D. R., Guariguata, L., Weil, C., Shaw, J. (2011): IDF diabetes atlas: global estimates of the prevalence of diabetes for 2011 and 2030. – *Diabetes research and clinical practice* 94(3): 311-321.
- [41] WHO (2003): *Selenium in drinking-water: Background document for development of WHO guidelines for drinking-water quality*. – World Health Organization.
- [42] Yilmaz, N., Yardimci, C., Elhag, M., Dumitrache, C. (2018): Phytoplankton Composition and Water Quality of Kamil Abduş Lagoon (Tuzla Lake), Istanbul-Turkey. – *Water* 10(5): 603.

THE THERMAL POWER PLANTS WITH THE VIEWPOINT OF FARMERS: THE CASE OF AMASYA PROVINCE

ERDAL, H.¹ – ERDAL, G.² – AYYILDIZ, B.³ – AYYILDIZ, M.³

¹*Department of Management and Organization, Social Sciences Vocational School, Tokat Gaziosmanpasa University, Tokat, Turkey*

²*Department of Agricultural Economics, Faculty of Agriculture, Tokat Gaziosmanpasa University, Tokat, Turkey*

³*Department of Agricultural Economics, Faculty of Agriculture, Yozgat Bozok University, Yozgat, Turkey*

**Corresponding author
e-mail: glerdal2@yahoo.com*

(Received 13th May 2019; accepted 30th Jan 2020)

Abstract. Thermal power plants are facilities that convert the chemical energy of solid, liquid and gas fuels respectively into thermal, mechanical and electric energy. The presumption of establishing a fossil fuel plant on this fertile area is putting the security of the agricultural products of the area at risk. A face to face survey was carried out with the 90 of the farmers living close to the planned area for the establishment of the fossil fuel plant in Suluova county of Amasya province. According to the survey results 43% of the farmers stated that fossil fuel plant is a necessity but it should be established far away from the agricultural estates whereas 30% of them think that these kind of fuel plants should not be established on any account and 27% of them expressed no opinion about the issue. A total of 60% of the farmers think that the agricultural consequences of the planned fossil fuel plant are not considered adequately; and 73% of the farmers think that a presumed fossil fuel plant in the area will negatively affect the yield and the quality of the agricultural products and 56% say that the agricultural estates will be negatively affected by it. Majority of the farmers stated that they would try to prevent the establishment of the plant even if they knew they would not succeed.

Keywords: *farmer, agriculture, thermal power plant, Amasya, pollution*

Introduction

Thermal power plants are the plants that convert the thermal energy of solid, liquid and gaseous fossil fuels into electrical energy. In this context, there are coal power plants, fuel-oil power plants and natural gas power plants. On the other hand, the plants that produce electricity from biomass are considered as thermal power plants (Chamber of Mechanical Engineers, 2017). It is stated that thermal power plants are preferred to produce electricity because of their advantages like being established with low costs and rapid feasibility and making use of the low-quality coal (Karaca et al., 2005).

As of late 2016, electricity production was 273,387 GWh, and 184,889 GWh of it was produced by thermal power plants in Turkey, 67,268 GWh was produced from hydroelectric plants, and 21,230 GWh from other renewable energy sources. In the same period, the rate of the electricity that was produced by thermal power plants to total electricity generation was 67.6%. Coal-originated power plants ranked the first in this rate with a share of 33.74%, followed by natural gas + LNG-based power plants with a rate of 32.1%, and followed by hydraulic power plants with 24.6%. As of the end

of 2016, it was of great importance that the share of electricity produced in wind power plants increased in total production from 3.4% to 5.7% (Table 1).

Table 1. Distribution of electricity production of Turkey according to energy sources (GWh) (Ministry of Energy and Natural Sources, 2018)

Primary energy source		2014		2015		2016	
		Production (GWh)	Share (%)	Production (GWh)	Share (%)	Production (GWh)	Share (%)
Coal	Mineral coal + imported coal + asphaltite	39,647	15.7	44,830	17.12	53,778	19.67
	Lignite	36,615	14.5	31,336	11.97	38,460	14.07
Liquid fuels	Fuel oil	1,663	0.66	980	0.37	1,103	0.40
	Diesel oil	482	0.19	1,244	0.48	1,548	0.57
	LPG		0.00		0.00		0.00
	Naphtha		0.00		0.00	2	0.00
Natural gas + Lng		120,576	47.9	99,219	37.9	87,820	32.1
Renewable + wastes		1,433	0.57	1,758	0.67	2,179	0.80
Thermal		200,417	79.5	179,366	68.52	184,889	67.63
Hydraulic		40,645	16.1	67,146	25.6	67,268	24.6
Wind		8,520	3.4	11,652	4.45	15,492	5.67
Geothermal		2,364	0.9	3,424	1.31	4,767	1.74
Solar		17	0.01	194	0.07	972	0.36
General sum		251,963	100.00	261,783	100.00	273,387	100.00

According to the data provided by Energy Market Regulatory Authority (EMRA), the domestic coal-fired power plants that are in operation in Turkey with production license are 34 in number; and one of them works on asphaltite, one on hard coal and the other is a lignite-fired power plant. There are also 6 power plants that are still under construction. The total installed capacity of the domestic coal, lignite and asphaltite-fired power plants was 9,842 MW at the end of 2016. A total of 38,460,314,490 kWh electricity was produced in lignite-fired power plants in 2016 in terms of capacity in production (Table 2).

The number of the plants in operation that have production license in Turkey with imported Coal is 10. There are also 7 other plants that are still under construction. The total established power of thermal power plants that run on imported coal is 7,571.4 MWe. A total of 53,777,704,022 kWh electricity was produced in 2016 in imported coal and hard coal-fired power plants. Although the number of natural gas-fired power plants that have production license is 326 in Turkey, those that are active are 252 in number. A total of 104 of these have over 10 MW capacity. The total established capacity of natural gas-fired thermal power plants was 22,156 MW as of the end of 2016. The total production of natural gas-fired power plants was 87,797,441,063 kWh in 2016 (EMRA, 2018).

The very fine ash particles, which are drawn upwards by the gases in chimneys because of the combustion in thermal power plants are considered to be important waste materials. It was reported that millions of ash, cinder and particles produced as waste by coal that is burnt in the power plants are stored at a certain height over a land of thousands of hectares and cause intense ash emission on forests, marquis, agricultural areas and residential areas (Pacyna, 1987).

Table 2. Coal-fired thermal power plants that have production licenses and 400 MWe and above capacity in Turkey (EPDK, 2018)

Fuel type	Name of the plant	City-county of plant	Established power (MWe)	Capacity in production (MWe)
Imported coal	Çatalağzı Thermal Power Plant	Zonguldak-Merkez	2,790.00	2,790.00
Domestic coal	Afşin - Elbistan B	Kahramanmaraş-Afşin	1,440.00	1,440.00
Domestic coal	Afşin - Elbistan A	Kahramanmaraş-Afşin	1,355.00	1,355.00
Imported coal	İskenderun Thermal Power Plant	Adana-Yumurtalık	1,210.00	1,210.00
Imported coal	İÇTAŞ Elektrik Enerjisi Üretim ve Yatırım Inc.	Çanakkale-Biga	1,200.00	1,200.00
Imported coal	Atlas Thermal Power Plant	Hatay- İskenderun	1,200.00	1,200.00
Domestic coal	Soma B Thermal Power Plant	Manisa -Soma	990.00	990.00
Coal	Kemerköy Thermal Power Plant	Muğla- Milas	630.00	630.00
Coal	Yatağan Thermal Power Plant	Muğla- Yatağan	630.00	630.00
Domestic coal	Çayırhan Thermal Power Plant	Ankara-Nallıhan	620.00	620.00
Domestic coal	Seyitömer Thermal Power Plant	Kütahya- Merkez	600.00	600.00
Domestic coal	Kangal Thermal Power Plant	Sivas- Kangal	457.00	457.00
Domestic coal	Tufanbeyli Thermal Power Plant	Adana -Tufanbeyli	450.00	450.00
Domestic coal	Yeniköy Thermal Power Plant	Muğla -Milas	420.00	420.00
Domestic asphaltite	Silopi Thermal Power Plant	Şırnak-Silopi	405.00	405.00

Numerous studies were carried out in the literature on thermal power plants. The importance of thermal power plants, environmental effects and their effects on the chemical properties of soil and microbial activity have been focused on in these studies (Adriano et al., 1980; Bunzl et al., 1983; Mejsrik and Suacha, 1988; Karaca, 1997; Onacak, 1999; Baba et al., 2003; Karaca et al., 2005; Deniz, 2010; Özcan et al., 2014).

In the present study, the awareness levels, judgments and attitudes of the farmers that continue agricultural activities in Suluova County in Amasya province where a thermal power is intended to be built were examined. Suluova County is a green plain that has fertile soils. The county is one of the locomotive regions of the city in terms of economic production with the factory that processes sugar beet, with four mine quarries, with onion and wheat cultivation, and with animal husbandry because the area is also suitable for agricultural production. Gürmin Enerji Madencilik Sanayi ve Tic. Inc. intends to build a thermal power plant within the boundaries of Merzifon and Suluova in the region with a total established capacity of 450 MW. The company made the application for the project in 2013, and EMRA approved the project. However, the objections on the power plant that would be established in the region where there was agricultural production, and the lack of the viewpoints of relevant institutions which failed to submit their investigation results at the 2nd Examining and Evaluation Commission meeting caused that the Environmental Impact Assessment (EIA) process were ceased on August 25, 2016. During the 13 months as of this date, the Ministry of Environment and Urbanization decided to terminate the EIA process when there were no revised reports and when the company did not present any data. This result was not revealed at the questionnaire stage of our study (April, 2016).

Materials and methods

The main material of the present study consisted of the data that were obtained with face-to-face interviews that were conducted with the farmers who lived in the villages of Suluova County of Amasya Province. In addition, the data that were provided by Energy Market Regulatory Authority and the Ministry of Energy and Natural Sources were also made use of. The study was conducted in 4 villages. In selecting the villages, the reactions to the thermal power plant that was intended to be established in the region were taken into consideration, and the farmers were selected with the Purposeful Sampling Method to represent the region. A total of 90 questionnaires were conducted with the farmers who lived in these 4 villages. The questionnaire was carried out in March and April 2016.

The findings that were obtained in the study are presented in the study in tables after calculating the percentages. The 5-Point Likert Scale was employed in designing the questions on the judgments of the farmers, and the average scores were calculated.

Results and discussion

Information on the enterprises and farmers who participated in the questionnaire are given in *Table 3*.

Table 3. *Some information on the farmers and enterprises that were included in the study*

Average age	46
Average income (\$)	1,020.21
Number of individuals of the enterprise family (persons)	6
Educational status	
Literate	2.22
Primary School	12.22
Secondary School	31.11
High School	48.89
College, faculty	5.56
Income sources of the enterprise (%)	
Agriculture	76.67
Free	20.00
Paid public employee	2.22
Pension	1.11
Distribution of agricultural fields according to possession status (da)	
Property field	87.62
Partnership	12.22
Rented	84.99
Crops cultivated (%)	
Dry onion	31.11
Sugar Beet	26.67
Wheat	16.67
Corn	10.00
Potatoes	10.00
Barley	5.56

The average age of the farmers who participated in the study was 46. It was observed that farmers were mostly secondary graduates (31.11%), and high school graduates (48.89%). The income level of the farmers was determined to be 1020,21 \$. A total of 77% of the income sources of the enterprises that were included in the study came from agriculture, and 20% from free trade; and 88% of the farmers had property lands. In addition, they were also tenants at a rate of 85%. When the products that were grown in the enterprises were examined, it was seen that dry onion was grown at the highest rate with a rate of 31.11%, followed by sugar beet (26.67%) and wheat (16.67%).

The farmers were asked if they had heard the name “thermal power plant” before. It was determined that approximately 96% of the farmers knew thermal power plants (Table 4). Especially in recent years, they had intense discussions about thermal power plants. Despite this, 4% of the farmers stated that they did not hear the name “thermal power plant” before.

Table 4. Had the farmers heard of the name “thermal power plant” before?

	Rate (%)
Yes	95.56
No	4.44
Total	100.00

The farmers who had heard the name “thermal power plant” and who were considered to have information on thermal power plants were asked about the establishment of the thermal power plants in their region. The results on this are given in Table 5. A total of 42.53% of the farmers had the same idea, which argued that thermal power plants must be established in our country; however, the place selection must be done very well. The rate of the farmers who thought that the energy that had to be produced with other means was 30%. The rate of those who had no clear idea on this subject was 24%.

Table 5. Opinions of the farmers on establishing thermal power plants in our country

	Rate (%)
Establishing thermal power plants is compulsory, they must definitely be established	3.45
They must definitely be established, but place selection must be made more accurately	42.53
They must definitely not be established; other ways must be found to produce energy	29.89
I do not have a clear idea about this	24.14
Total	100.00

On the other hand, more than half of the farmers who participated in the questionnaire (51.72%) claimed that it was completely wrong to establish Thermal Power Plant in the region that was close to their living area where they performed their agricultural activities. The rate of the farmers who thought that the establishment of the power plant in the region was the right decision remained as 1%. The rate of the farmers who did not have any ideas on this subject was 24.14% (Table 6).

The farmers thought that the agricultural effects of the thermal power plant that would be established in the Suluova region were not considered fully, and the necessary

sensitivity was not considered (*Table 7*). As a matter of fact, the EIA process was terminated due to objections and the lack of the opinions of the relevant institutions.

Table 6. *Opinions of the farmers on the thermal power plant that was intended to be established in Suluova*

	Rate (%)
The establishment of the power plant in the region is suitable, this is a righteous decision	1.15
This could not have been established in this region, but this is not a very wrong decision	22.99
The power plant must definitely not be established in this region, this is a completely wrong decision	51.72
I have no idea	24.14
Total	100.00

Table 7. *The opinions of the farmers on the sensitivity in place selection of the thermal power plant that was intended to be established in Suluova*

	Rate (%)
Yes, the place selection was very sensitive	3.45
No, the place selection was not very sensitive at all	59.77
I do not have any idea	36.78
Total	100.00

The opinions of the farmers on the negative impacts of the thermal power plant were examined and scored with a 5-point Likert scale. The farmers were asked to respond to the questions on the negative impacts as “very high-5”; “high-4”; “moderate-3”; “very low-2”; “none-1”. The average scores were calculated by considering the answers of each farmer according to the score next to each answer. In this way, the common decisions of all the farmers who participated in the questionnaire were determined. The findings on this subject are given in *Table 8*.

Table 8. *The opinions of the farmers on negative effects of the thermal power plant on their villages (%)*

Negative effects on...	Very high (5)	High (4)	Moderate (3)	Very low (2)	None (1)	Ave. score
the human health	45.35	44.19	6.98	3.49	0.00	4.31
the natural vegetation	27.91	47.67	19.77	3.49	1.16	3.98
the other creatures living in the region	36.05	44.19	15.12	3.49	1.16	4.10
the fertility of agricultural products	36.05	48.84	11.63	3.49	0.00	4.17
the quality of agricultural products	38.37	47.67	11.63	2.33	0.00	4.22
the image of the agricultural products	11.63	53.49	19.77	9.30	5.81	3.56
the air of the village	13.95	43.02	19.77	10.47	12.79	3.35
the environmental beauty of the village	17.44	44.19	24.42	11.63	2.33	3.63
the agricultural soils	32.56	48.84	13.95	2.33	2.33	4.07

As it may be seen in *Table 8*, the farmers thought that the thermal power plant will have negative impacts on human health, natural vegetation, the fertility of the agricultural

products, the quality and appearance of the agricultural products, the air and environmental beauty of the village and on agricultural lands at a high rate. As a matter of fact, in many previous studies, it was stated that the environmental pollution elements that stemmed from the thermal power plant were air, soil and water pollution (Goncaoglu et al., 2000). In one of the studies conducted on Afşin-Elbistan Thermal Power Plant, the effects of the ash caused by the power plant on the agricultural fields were examined, and it was determined that this caused the accumulation of heavy metals in the plants (Kahraman, 2011). It was determined that toxic dusts that contained CO₂, NO and SO₂ in the composition of the emissions coming from Afsin-Elbistan Thermal Power Plant chimneys caused burns in the leaves of the plants, and in this way, the leaves dried and eventually the trees dried (Özcan et al., 2014). Again, many researchers found that the emissions coming from thermal power plants had high heavy metal contents in the dominant wind directions, and that pollutant gases like Sulfur Dioxide (SO₂), Carbon Dioxide (CO₂) and Nitrogen Oxide (NO_x) had negative impacts on some tree species (Aydemir, 2008; Karaca et al., 2007; Deniz, 2010).

In the present study, the judgments of the farmers were determined with more detailed questions depending on the features and negative effects of thermal power plants. The findings on this subject are given in *Table 9*.

Table 9. *Judgments of the farmers on the characteristics of the thermal power plants (%)*

Thermal power plants	I definitely agree (5)	I agree (4)	I do not have any idea (3)	I do not agree (2)	I definitely do not agree (1)	Ave. score
...may cause various diseases depending on the fuel types used in them	55.81	40.70	0.00	2.33	1.16	4.48
...may cause acid rains	26.74	40.70	26.74	4.65	1.16	3.87
The air pollution caused by thermal power plants damage the living that inhale this air	47.67	46.51	2.33	2.33	1.16	4.37
...damage forests	27.91	59.30	8.14	3.49	1.16	4.09
...the gasses produced slows down the development of the vegetation	29.07	51.16	16.28	3.49	0.00	4.06
...damages the agricultural fields	39.53	50.00	8.14	2.33	0.00	4.27
...causes soil pollution	47.67	41.86	8.14	2.33	0.00	4.35
...causes desertification	47.67	41.86	8.14	2.33	0.00	4.35
...causes drops in the yield of agricultural production	53.49	36.05	6.98	3.49	0.00	4.40
...causes disruptions in the quality of the agricultural products	47.67	40.70	8.14	3.49	0.00	4.33
...the water used for cooling and cleaning threatens the existence of the water presence in the region	36.05	53.49	8.14	1.16	1.16	4.22
...pollutes the waters	26.74	48.84	15.12	6.98	2.33	3.91
...the damages are exaggerated	3.49	8.14	33.72	32.56	22.09	2.38
...the information on negative effects are malevolent	0.00	4.65	34.88	34.88	25.58	2.19
...these plants are necessary and beneficial for our country no matter where they are established	0.00	9.30	32.56	23.26	34.88	2.16
...they do not affect agricultural production very negatively in the region	0.00	6.98	26.74	20.93	45.35	1.95

The judgment to which the farmers highly agreed at a high rate (56%) was that various diseases emerged in humans depending on the fuels used in thermal power plants. In actual fact, the concern of the farmers on this subject was not unreasonable. Because in previous studies conducted in Turkey, it was determined that 20% of the health problems that could be attributed to exposure to particulate matter were caused by the burning of the coal in the thermal power plants (Gacal, 2017). The presence of gases SO₂, CO₂, NO_x in the waste gas that was released from coal thermal power plants may be taken in either by inhalation, directly or indirectly, through nutrients and water. It was stated that when people were exposed to an intense amount of these gases, the nervous system was affected, lung and respiratory problems were experienced, and cognitive development was affected negatively in children (Peden, 1997; Rusnak et al., 1997; Gacal, 2017). Secondly, the judgment to which the farmers highly agreed at a high rate (53%) was that the reason that these power plants caused loss of fertility in the products that were grown in the regions where thermal power plants were located. This was followed by the judgment that these plants caused soil pollution, soil desertification and product quality disorders with a participation rate of 47.67%. The farmers also approved “other” thermal power plant responses (average score: 1.95) that their thermal power plant would not have negative effects on agricultural production. In brief, the judgments of the farmers on the features of thermal power plants generally concentrated on damaging the soil, plants and human health. In many studies that were conducted on this subject support the judgments of farmers (Goncaoglu et al., 2000; Aydemir, 2008; Karaca et al., 2007; Deniz, 2010; Kahraman, 2011; Özcan et al., 2014).

Conclusion and recommendations

It was shown in many previous studies that thermal power plants caused air pollution, water pollution and soil pollution and these impurities had negative effects on the living and agricultural products. Of course, the fuel used in thermal power plants was considered to be mostly coal, and the resulting damage caused by the gases that were produced in this process.

In the present study, how the thermal power plants were perceived by farmers was investigated with the sample case of the Suluova Region where the power plant was planned to be established. In the study, the majority of the farmers stated that it was important to establish thermal power plants to meet the energy needs of the country; however, the place of the establishment for these thermal power plants must be selected better. On the other hand, the farmers were also very concerned about the negative impacts of the thermal power plants on human health, agricultural lands and products, the vegetation cover, and all other living things. For this reason, the farmers who participated in the study wanted to stop the establishment of the thermal power plant in question. As a matter of fact, following the questionnaire stage of our study, the EIA process of the thermal power plant, which was planned to be established in the region by Gürmin Enerji Madencilik Sanayi ve Tic. Inc., was terminated with the justification that there were several shortcomings. Although it changes every year, the share of the thermal power plants in electricity production of Turkey is about 70%. It seems that the dominance of the thermal power plants in producing electricity with domestic sources will continue for a long time in Turkey which is dependent to external sources in terms of energy raw material. In this sense, the benefits of the thermal power plants must also be brought to the forefront. Especially the benefits like using domestic coal, the fact that

coal may be transported to all areas for installation, the resulting steam and water allowing low-cost electricity production may be considered. In this sense, increasing the efficiency of the existing thermal power plants, minimizing the damage that is given to the environment, providing maximum occupational health and work safety, prioritizing the use of domestic coal and biomass instead of the imported ones, and ensuring the establishment of thermal power plants with environmentally-friendly technologies are important.

REFERENCES

- [1] Adriano, D. C., Page, A. L., Elseewi, A. A., Chang, A. C., Straugham, I. (1980): Utilization and disposal of fly ash and other coal residues in terrestrial ecosystems. A review. – *Journal of Environment Quality* 9: 333-444.
- [2] Aydemir, G. (2008): The determination of the effects of Afşin-Elbistan Power Plant emissions on regional soils. – Master Thesis, Ankara University.
- [3] Baba, A., Kaya, A., Birsoy, Y. K. (2003): The effect of Yatağan Thermal Power Plant (Muğla Turkey) on the quality of surface and ground waters. – *Water, Air, and Soil Pollution* 149: 93-111.
- [4] Bunzl, K., Rosner, G., Schmindt, W. (1983): Distribution of lead, cobalt and nickel in the soil around a coal fired power plant. – *Z. Pflanzenernaehr. Bodenk* 146: 705-713.
- [5] Deniz, M. (2010): Effect of thermal power plant pollution on mineral nutrition and antioxidative defence mechanism on eucalyptus and Morus species. – PhD thesis, Çukurova University Graduate School of Naturel and Applied Sciences, Adana.
- [6] Gacal, F. (2017): The effects of coal power plants on human health, health and environment association (HEAL). – [http://www.komuruzer.com/\(2017\):08/komurlu-termik-santrallerin-insan.html](http://www.komuruzer.com/(2017):08/komurlu-termik-santrallerin-insan.html).
- [7] Goncaloğlu, B. İ., Ertürk, F., Ekdal, A. (2000): Comparison of thermal power plants and nuclear power plants in terms of environmental impact assessment. – *Ecology Environmental Journal* 9(34): 9-14.
- [8] Kahraman, Y. (2011): Possibility of using Afsin-Elbistan Coal Power Plant Ashes in Agriculture. – Kahramanmaraş Sutcu Imam University Institute for Graduate Studies in Science and Technology Department of Soil Science and Plant Nutrition, Kahramanmaraş.
- [9] Karaca, A. (1997): Effects of Afsin-Elbistan Thermal Power Plant emissions on physical, chemical and biological properties of environmental soils. – Ph. D. Thesis, Ankara University Institute of Science and Technology, Ankara.
- [10] Karaca, A., Türkmen, C., Arcak, S., Haktanır, K., Topçuoğlu, B., Yıldız, H. (2005): The determination of the effect of Cayirhan coal-fired power plant emission on heavy metals and sulphur contents of regional soils. – *Ankara University Journal of Environmental Sciences* 1(1): 17-25.
- [11] Karaca, A., Turgay, O. C., Karaca, S., Sağlam, M., Türkmen, F., Deviren, S., Türkmen, N. (2007): Effects of Seyitömer Thermal Power Plant Emissions on Environmental Soils. – Unpublished Project, Ankara University.
- [12] Mejsrik, V., Suacha, J. (1988): Concentration of Co, Cr, Cd, Ni and Zn in crop plants cultivated in the vicinity of coal fired power plant. – *The Science of the Total Environment* 72: 57-67.
- [13] Ministry of Energy and Natural Resources (2018): World and Turkey's Energy and Natural Resources View. – http://www.enerji.gov.tr/File/?path=ROOT%2f1%2fDocuments%2fEnerji%20ve%20Tabii%20Kaynaklar%20G%20c%3%b6r%20c%3%bcn%20c%3%bcm%20c%3%bc%2fSayi_15.pdf
enerji.gov.tr.

- [14] MMO (Chamber of Mechanical Engineers) (2017): Thermal power plants in Turkey, 2017. – [https://www.mmo.org.tr/kitaplar/turkiyede-termik-santraller-\(2017\):oda-raporu](https://www.mmo.org.tr/kitaplar/turkiyede-termik-santraller-(2017):oda-raporu).
- [15] Onacak, T. (1999): Environmental impacts of coal thermal power plants fed and solid waste combustion resulting in Turkey. – Ph. D. Thesis, Hacettepe University Institute of Science, Ankara.
- [16] Özcan, İ., Bahadıroğlu, C., Bozdoğan, H. (2014): A research on the causes drying of seedlings planted in the areas of Afşin-Elbistan Thermal Power Plant environmental excavation casting standing. – *Nevşehir Journal of Science and Technology* 3(1) 8-16.
- [17] Pacyna, J. M. (1987): Atmospheric Emissions of As, Cd, Pd, and Hg from High Temperature Processes in Power Generation and Industry. – In: Hutchinson, T. C., Meema, K. M. (eds.) *Lead, Mercury, Cadmium and Arsenic in the Environment*. John Wiley & Sons Ltd, Chichester, UK.
- [18] Peden, D. B. (1997): Mechanisms of pollution-induced airway disease: in vivo studies. – *Allergy* 38: 37-44.
- [19] Rusznak, C., Bayram, H., Devalia, J. L., Davies, R. J. (1997): Impact of the environment on allergic lung diseases. – *Clin Exp Allergy* 27: 26-35.

ANTIOXIDANT AND QUALITY ASSESSMENT OF NUGGETS PREPARED FROM BROILER BREAST MEAT REARED ON NATURAL ANTIOXIDANT FROM CITRUS WASTE

FAIZ, F.^{1*} – WALI, A.¹ – HUSSAIN, A.¹ – RAZZAQ, A.² – ARSHAD, M.¹ – MANZOOR, H. M. I.¹ –
KHAN, S. S.¹

¹*Department of Agriculture and Food Technology, Karakoram International University, Gilgit,
Pakistan*

²*Department of Biological Sciences, Karakoram International University, Gilgit, Pakistan*

**Corresponding author
e-mail: dr.asifwali@kiu.edu.pk*

(Received 22nd May 2019; accepted 25th Oct 2019)

Abstract. Citrus is an important fruit produced in the Pakistan. The peel and waste of citrus after juice extraction is mostly wasted which contain important antioxidants and polyphenols. In current study citrus waste after juice extraction was utilized in the production of broiler meat as a feed ingredient, which have positive effects on antioxidant level of the meat. Chicken breast nuggets were prepared from that meat resulting in positive effect on Thiobarbituric acid reactive substances (TBARS) and 2,2-diphenyl-1-picrylhydrazyl (DDPH) activity of the nuggets. The pH of the nuggets reduced as the citrus waste supplementation in the feed of the broilers increased, color L* and b* values of the nuggets were reduced, and color a* value was increased as the citrus waste supplementation in the feed of the broilers increased. Texture and water holding capacity of the nuggets have significant effect due to interaction effect of storage and treatments.

Keywords: *color, meat, nuggets, nutrition, storage, texture, water activity*

Introduction

Chicken meat and its products are used worldwide due to many nutritionally important components which are good for human health i.e., low lipid contents and higher amount of polyunsaturated fatty acids, which are higher than that in any red meat (Jittrepotch et al., 2006). The major cause of deterioration of chicken meat and meat product is oxidation, especially autoxidation because of higher amount of polyunsaturated fatty acids in the meat of chicken which caused in the quality deterioration and off flavor, which can lead to serious health problems (Mohamed et al., 2008). Lipid oxidation in the meat causes undesirable changes by oxidizing fats enzymatically and non-enzymatically. Autoxidation is a chain reaction and causes the meat to deteriorate (Cheng, 2016). The control or minimizing the effect of oxidation is of greater interest for food industry. Oxidation of fats in the meat can be controlled by many strategies including animal dietary supplementation, processing, special packaging and use of antioxidants (Amaral et al., 2018). Because of oxidation problems in meat and meat products the trend of using synthetic antioxidants in broiler meat and meat products is increasing and possibility of toxicity of synthetic antioxidants is a concern for consumers using these products (Prasetyo et al., 2008).

The antioxidant potential of broiler meat and its meat products can be enhanced by feeding broilers with natural antioxidants in feed like alpha-tocopheryl acetate and alphalipoic acid (Sohaib et al., 2012). Alpha tocopherol acetate is effective antioxidant in

breaking of chain reactions of the oxidation of fats in foods (Miller et al., 2005). Arshad et al. (2011) working on vitamin E supplementation in feed of broiler meat observed that vitamin E as a source of natural antioxidant is effective in reducing oxidation of meat and meat products more than the control treatments. Kumar and Tanwar (2010) added ground mustard in the chicken meat nuggets and found that the treatments having mustard have greater potential of antioxidants and TBARS value of the treatments, with ground mustard have enhanced antioxidant potential as compared to treatment which were made without ground mustard. Citrus waste as a feed for different animals have studied and proven effective in enhancing antioxidant levels of animals and cost of production also reduced as citrus waste substituted the costly ingredients of feed.

Agricultural wastes including fruit wastes i.e. banana peel, citrus rind etc. are biodegradable and polluting agents for environment if not recycled and reused. But research has explored the importance of this waste material as source of nutrients for plants, animals and birds. Hence, fruit wastes are processed and utilized not only as supplements in food commodities but also as source of nutrients for plants (Arshad et al., 2018).

In the current study the broiler meat was produced using citrus waste supplementation as a feed ingredient. Meat produced from the citrus supplemented waste was incorporated in nuggets and observed for antioxidant and quality profile with objectives to enhance antioxidant profile of chicken meat products and to observe effect of natural antioxidants from broiler meat on storage properties of the nuggets.

Material and methods

The broiler birds of genus *Gallus Domesticus* were reared with experimental feed in the Research Farm of Institute of Animal Nutrition in University of Agriculture Faisalabad, Pakistan. Total of 225 birds were used in the study with 15 birds in each treatment. There were three replications of each treatment. The feed of broiler was made with the addition of citrus waste at five different proportions of citrus waste i.e., 0%, 2.5%, 5%, 7.5% and 10% using substitutional method and are indicated as MN₀, MN_{2.5}, MN₅, MN_{7.5}, and MN₁₀, respectively. The birds were reared for 42 days with standard conditions of food, water, and other environmental conditions. The temperature at the farm was maintained as 25-30°C with regular supply of water. Lightning was provided for at least 12 hours a day. After 42 days, birds were slaughtered and the breast meat of the broiler of different treatments was used for the preparation of meat nuggets.

Formulation for broiler meat nuggets

Five treatments of nuggets made with different chicken meat were fed on citrus supplemented feed having citrus waste level as 0%, 2.5%, 5%, 7.5% and 10%. The ingredients for preparation of nuggets were weighed and mixed according to the recipe (Table 1). The meat was washed with tap water, deboned manually and minced using electric mincer (MG 100). The broiler meat and onions were mixed in a meat mixer for five minutes, and then all other ingredients were added according to recipe and mixed using meat mixer to provide a uniform blend. The mixture was extended in a thin layer (10 mm thickness) and shaped into discs of 30 mm diameter (50±1 g/piece) to form a nugget. The nuggets were dipped in plain flour and bread crumbs separately and baked at 180°C till attaining the desire color and texture. The nuggets were also stored at -20°C for further analysis for different parameters at 0, 15 and 30 days of the storage.

Table 1. Recipe of the nuggets prepared from the broiler's breast meat fed on the feed with addition of citrus waste

Sr. No	Name of the ingredient	Quantity used
1	Chicken boneless	500g
2	Egg	01
3	Black pepper	12g
4	Garlic paste	15g
5	Onion	150g
6	Plain flour	120g
7	Bread crumbs	70g
8	Salt	15g

Quality analysis of nuggets

Color of the Nuggets was determined with the method described by El-Gasim and Al-Wesali (2000) using hunter lab color measurement device in AARI Faisalabad. The pH of the nuggets prepared with chicken meat was determined as described by Sallam et al. (2004). Water activity of meat nuggets was measured following the method of El-Gasim and Al-Wesali (2000) using combination of a ventilated humidity and temperature probe. The humidity and temperature probe automatically showed the water activity value when it was placed on the meat samples. Water holding capacity of broiler meat nuggets was determined according to the method of Qiao et al. (2001). The nuggets samples were placed in 11 cm diameter filter paper between Plexiglas plates and pressed at 2000 psi pressure for 1 minute. The water holding capacity was measured using formula as indicated in Eq. 1.

$$\text{Water Holding capacity} = \frac{100 \times (\text{total juice area} - \text{meat film area}) \times \text{water/squire inch filter paper}}{\text{Total moisture (mg) of original sample (sample weight in (mg) } \times \text{ \%moisture)}} \text{ (Eq.1)}$$

Thiobarbituric acid reactive substances (TBARS) assay was measured following the method of Asghar et al. (1989). The per-oxidative reaction was initiated by adding ferrous sulphate and hydrogen peroxide to the nuggets samples held in a water bath at 37°C. One mL sample prepared in buffer solution (0.1 M KCl; 0.05 M NaOH; 0.13 M Lactic acid) with pH 5.3–5.4 was withdrawn at 30 min intervals for a period of 120 min and mixed to a same volume of solution of Thiobarbituric acid (0.4%), trichloroacetic acid (10%), and hydrochloric acid (0.25 N). The mixture was heated in a boiling water bath for 15 min and then cooled. After centrifugation, absorbance of supernatant was measured at 532 nm. The extent of samples lipid peroxidation was calculated using the formula as indicated in Eq. 2.

$$n - \text{Moles of Malondialdehydes} = \frac{(\text{sample absorbance} - \text{blank}) \times \text{Total sample volume}}{0.00156 \times 1000 \text{ (per mL)}} \text{ (Eq.2)}$$

The DPPH radical scavenging activity of broiler meat nuggets was determined following the method of Jung et al. (2010). The antioxidant activity of meat muscles fractions estimated by measuring scavenging abilities to DPPH stable radicals. A sample of 125 µL was mixed with 0.0012 M DPPH solution followed by the addition of 95% MeOH up to final volume of 4 mL. The absorbance of the resulting solution and the blank was recorded after 30 min at room temperature. The disappearance of DPPH was noted

using spectrophotometer (CESIL CE7200, England) at 515 nm. Inhibition of free radicals by DPPH in percent (%) was calculated using formula as presented in Eq. 3.

$$\text{Inhibition (\%)} = [100 \times (A \text{ blank} - A \text{ sample}) \div A \text{ blank}] \quad (\text{Eq.3})$$

Statistical analysis

The data obtained from treatments and replications were subjected to statistical analysis using statistical program SAS version 9.0 to determine the level of significance by two-way factorial ANOVA and Least Significant Different test as described by Steel et al. (1997).

Result and discussion

TBRAS of the nuggets

TBARS is the standard to evaluate oxidation of meat and meat products. The higher value of TBARS shows that product is towards the oxidation. *Figure 1a* shows that the TBARS of chicken meat nuggets was significantly influence due to interaction effect of effect of treatment and storage. TBARS value of the nuggets reduced in the treatments (MN₁₀) of the nuggets which was prepared from the meat of the broilers that were fed on the feed with the higher levels of citrus supplemented feed and higher values of the TBARS were observed in the control treatment (MN₀) at storage of 30 days. However, the TBARS value of the nuggets increased with the storage time but this increase was minimum in the treatment which was made from the chicken meat which have higher antioxidants from the citrus waste. Sohaib et al. (2013) observed the quality of the nuggets which was made from the chicken meat that were fed on the feed with alpha lipoic acid and alpha tocopherol was higher as compared to the control treatment. He observed that the TBARS value of the nuggets was high in the control treatment and low on the treatment which were prepared from the meat which have higher level of alpha lipoic acid and alpha tocopherol. Divya and Singh (2013) investigated addition of bitter melon extract as a source of natural antioxidant in the chicken meat nuggets. It was observed that addition of bitter melon in the chicken nuggets at 1% level improved the antioxidant properties via TBARS of the nuggets and the nugget controlled more lipid oxidation with bitter guard as a source of antioxidant. Mishra et al. (2015) observed increased in the TBARS value of the dehydrated chicken meat balls stored at ambient temperature for 45 days and also decrease in the TBARS value was observed when treated meat with rice flour was used.

DPPH activity

The data for DPPH activity of the nuggets prepared with the broiler breast meat fed on the natural antioxidants from the citrus waste is presented in the *Figure 1b* and *Figure 1c*, that shows nuggets have significant effects for DPPH activity due to treatments and storage life.

The mean values showed that maximum DPPH activity of nuggets was observed in MN₁₀, which was prepared from meat of broilers that were fed on 10% citrus supplemented feed while minimum DPPH activity value was observed in MN₀, the meat of that treatment was taken from the broilers group which were fed on control feed. This

difference in the DPPH activity of different treatment is correlated with the amount of citrus waste used in the feed of broiler, as citrus waste is a rich source of phenolic substances like flavonoids which possess antioxidant activity and the natural antioxidants in the meat of the broilers raised DPPH activity. The DPPH activity of nuggets reduced during storage because of the loss in the polyphenolic contents of the meat.

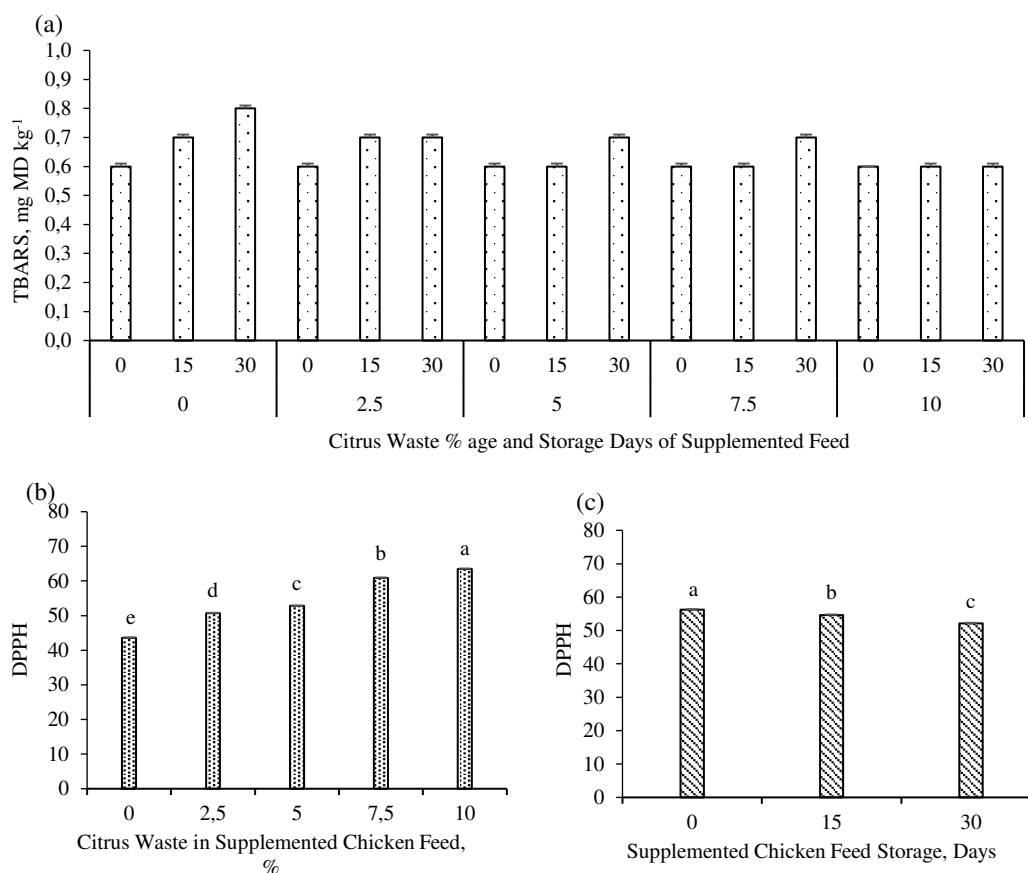


Figure 1. Interaction effect of citrus waste supplementation and storage on TBARS (a) and individual effect of citrus waste supplementation (b) and storage (b) on chicken meat nuggets

O’Sullivan et al. (2004) added different level of tocopherol acetate (vitamin E), rosemary (0.10%), sage (0.10%) and tea catechins (0.01%) in the feed of the broilers and concluded that nuggets made from the breast meat of broilers fed on the vitamin E alone have better antioxidant activities as measured by DPPH activity. Maliluan et al. (2013) added rice bran instead of wheat flour by substitution method in the formulation of the chicken nuggets and observed that antioxidant activity of the nuggets enhanced when rice bran was added in the nuggets however the sensory qualities of the nuggets decreased by adding rice bran.

pH of nuggets

The data for pH of the nuggets prepared with the broiler breast meat fed on the natural antioxidants from the citrus waste is presented in the Figure 2, that shows that the nuggets have significant effects for treatments and storage life. pH value of the nuggets showed

that maximum value of the pH was observed in the treatment which was made from the broiler meat which were fed on the control feed. Increased in the concentration of citrus waste in the feed of broiler decreased the pH of nuggets made from the broiler meat. pH value of nuggets increases as the storage period proceeded. Banerjee et al. (2012) prepared goat meat nuggets with broccoli powder extract as an antioxidant and observed decline in the pH of the nuggets when broccoli powder extract was used at the concentration of 2%. Yadav and Sanyal (1999) reported that pH of the nuggets was increased when antioxidants were added in the nuggets and pH also increased with storage.

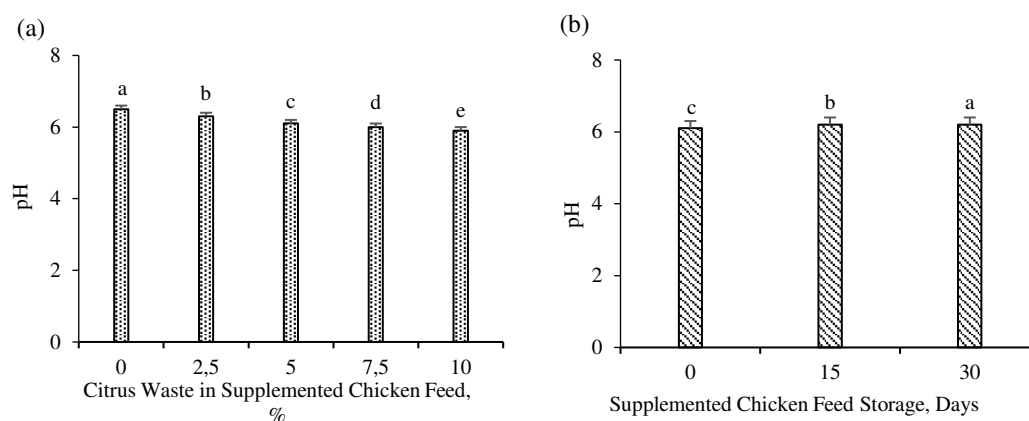


Figure 2. Effect of citrus waste supplementation (a) and storage (b) on pH of chicken meat nuggets

Color of nuggets

Color L* value of nuggets

The data for the color L* value of the nuggets is presented in the *Figure 3a*, which shows that the significant effects for the color L* value of the nuggets for treatments and storage was observed. The highest mean value (67.24) for color L* of nuggets was observed for treatment prepared with the meat of broilers fed on treatment plan MN₀ (control) which reduced significantly and lowest value of the color L* value of the nuggets was observed for the treatments of nugget prepared from meat of broilers fed on 10% citrus waste supplemented feed (MN₁₀). It is evident from the results that increase in level of citrus waste supplementation in feed increase the natural compound deposition in meat leading to a reduced of color L* value of nuggets. Decreasing trend for color L* value of the broiler meat nugget from zero-day interval to 30 days' interval was observed.

Bosale et al. (2011) evaluated functional chicken nuggets for quality and sensory parameters. They also observed decrease in the color value of the nuggets when ground carrot and mashed sweet potatoes were used as a functional ingredient in the chicken nuggets, which support current investigations. Naveena et al. (2008) observed decline in color for broiler nuggets when they were stored at freezing temperature and color of the nuggets changed from red to brown which was due to the formation of metmyoglobin in broiler meat. O'Sullivan et al. (2004) found increase in the color L* value of the chicken nuggets during storage when the meat of the broiler was used which was fed on Rosemary (0.10%) as a natural antioxidant in the feed.

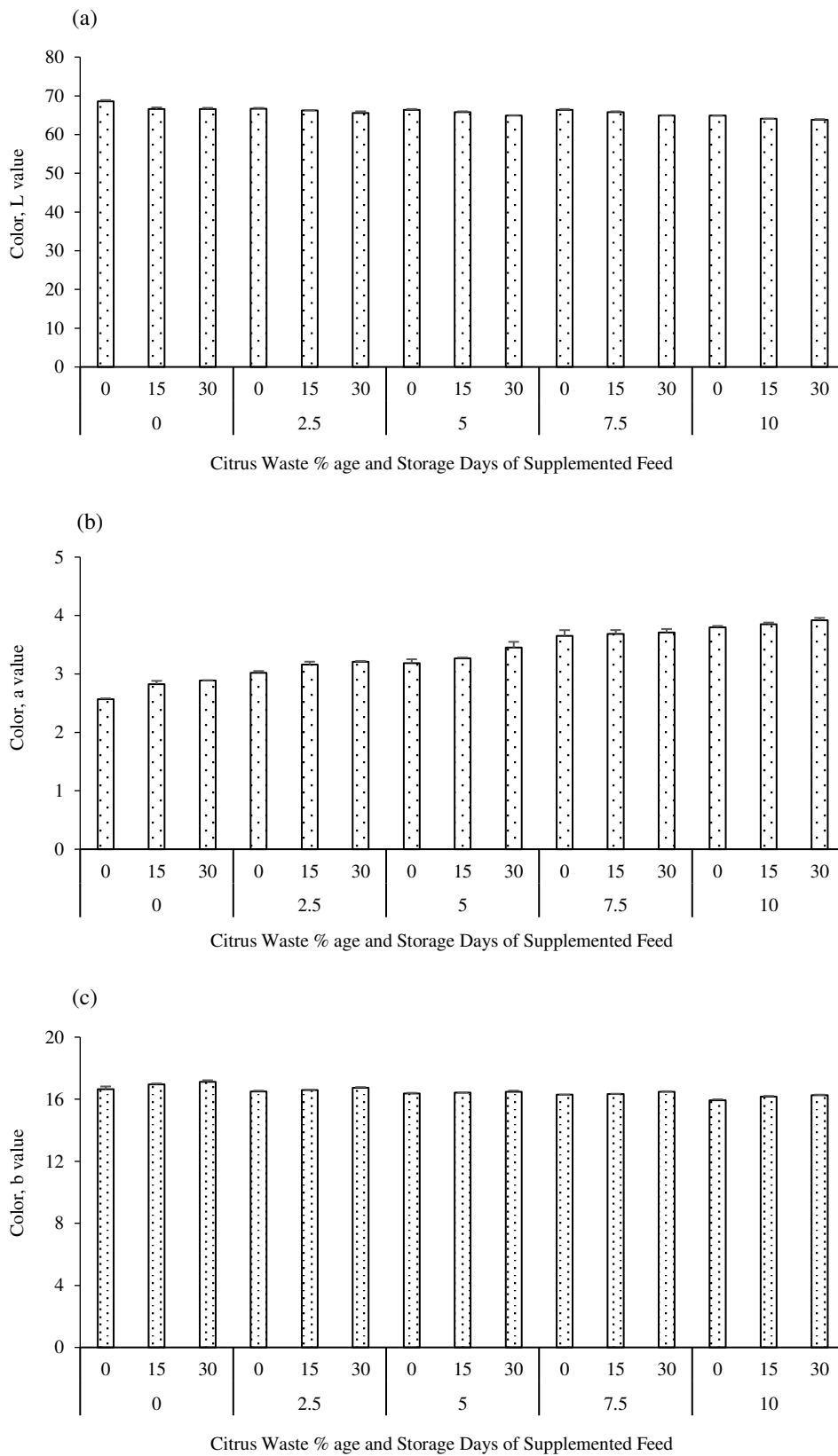


Figure 3. Interaction effect of citrus waste supplementation and storage on Color L value(a), a value (b) and b value (c) of chicken meat nuggets

Color a value (redness) of nuggets*

The data for the color a* value of the nuggets is presented in the *Figure 3b*, which shows significant effects for treatments and storage of the nuggets prepared from the broiler breast meat fed on the citrus waste supplemented feed. Maximum mean value for color a* of nuggets was observed for MN₁₀ which was prepared with the meat of the broilers which were fed on maximum citrus waste contents (10%) whereas minimum mean value for color a* values of nuggets was observed for MN₀ which was prepared with the meat of the broilers which were fed on control feed (0% citrus waste). Similarly, potential variation was observed when the nuggets were stored for 30 days under freezing conditions. Hunter a* values of chicken nuggets containing natural antioxidants in the feed of the broiler was also found increase by O'Sullivan et al. (2004) in their studies, which support findings of the current studies. Verma et al. (2013) in their studies observed increase in the color a* value of the sheep meat nuggets when they added guava powder in the nuggets.

Color b value (yellowness) of color of nuggets*

The data for the color b* value of the nuggets is presented in the *Figure 3c*, which shows significant effects for treatments and storage of the nuggets prepared from the broiler breast meat fed on the citrus waste supplemented feed. Maximum mean value for color b* of nuggets was observed for MN₀, the meat of which treatments was used from broilers that were reared on control feed (0% citrus waste in feed), whereas minimum value for b* values of color of nuggets was observed under MN₁₀, the meat of which treatments was used from birds that were reared on feed with maximum citrus waste contents (10% citrus waste in feed). The color b* value of the nuggets also increased as the storage period proceeded from 0 day to 30 days. Chandrlekha et al. (2012) reported that chicken meat balls incorporated with pomegranate rind powder extract as a source of natural antioxidant, secured significantly higher color value than all other treatments but the color value decreased during storage. Similar results have been reported by Kala et al. (2007) in refrigerated chicken patties who observed increased in the color b* value.

Texture (shear force) and water holding capacity of the nuggets

The data for texture of the nuggets prepared with the broiler breast meat fed on the natural antioxidants from the citrus waste is presented in the *Figure 4a and 4b*, which shows that the nuggets have significant effects for treatments and storage life. Maximum value for texture of the nuggets was observed after 30th days of storage whereas minimum value for texture of nuggets was observed after 0 days' interval. Texture values for nuggets increased from 0 day to 30 days of the storage. The results of current investigations are in line with the studies of Ruiz-Ramirez et al. (2005) who concluded that texture become harder as the storage period of the nuggets proceeded. Moran et al. (2012) reported lower values for shear force in groups of the nuggets in which antioxidant was used as compared to the control groups.

The data for the water holding capacity of nuggets is presented in the *Figure 4c*, which shows significant interaction effect of treatments and storage on water holding capacity of nuggets prepared from the broiler breast meat fed on the citrus waste supplemented feed. The highest value of water holding capacity of nuggets was observed in MN₁₀ (nuggets prepared from the breast meat of the broilers which were fed on 10% citrus waste supplemented feed) at 10 days of storage period while lowest was observed for MN₀

(nuggets prepared from the breast meat of the broilers which were fed on control feed) at 0 days of storage. Water holding capacity of the nuggets increased as the storage time proceeded from 0 day to 30 days. Kikki et al. (2014) reported similar results in their studies, they worked on development of functional chicken nuggets with the addition of fermented bamboo shoots, beet root and cabbage. They observed that nuggets with the cabbage incorporation possesses higher score for water holding capacity. Golsuch and Alvarado (2010) observed increased in the water holding capacity of the broiler normal and pale breast fillet, when used different marinating techniques. However, Arun et al. (2008) working on the effects of full fat soy paste and textural soy protein on the quality and shelf life of the goat meat nuggets on freeze storage observed non-significant effects on the water holding capacity of the nuggets.

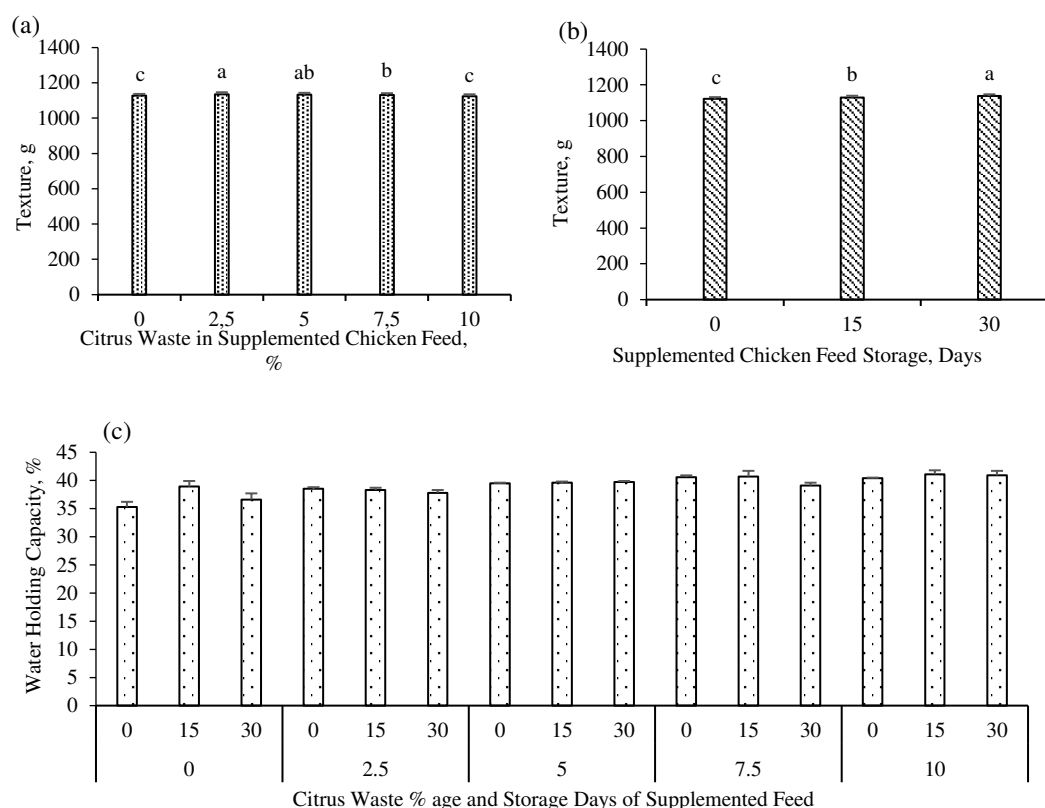


Figure 4. Individual effect of citrus waste treatment (a) and storage (b) on texture and interaction effect of treatment and storage on water holding capacity (c) of chicken meat nuggets

Conclusion

In the current findings citrus waste after juice extraction is used in the broiler meat production, the meat was further utilized in the nuggets preparation. The results showed positive effects on quality and the antioxidant profile of the nuggets. The citrus waste is normally wasted and in this study it is utilized for meat production. The study may be effective for the industry of food processing. Further studies might be conducted to increase utilization of citrus waste for different food products under different environmental conditions where different varieties of both citrus and the broiler chicken

can be tried for manufacturing of meat, eggs, and meat products. In this way the citrus waste may be properly utilized for the benefits of human being as it is good source of natural antioxidants that is usually wasted after juice extraction.

Acknowledgement. The principal investigator of the project is grateful to Higher Education Commission of Pakistan for financial support for completion of this project.

REFERENCES

- [1] Amaral, A. B., Marcondas, V. D., Suzana, C. D. S. L. (2018): Lipid oxidation in meat: mechanism and protective factors- A review. – Food Science and Technology Journal. DOI: <http://doi.org.10.1590/fst32518>.
- [2] Arshad, M. S., Anjum, F. M., Asghar, A., Khan, M. I., Yasin, M., Shahid, M., El-Ghorab, A. H. (2011): Lipid stability and antioxidant profile of microsomal fraction of broiler meat enriched with alpha-lipoic acid and alpha-tocopherol acetate. – Journal of Agricultural and Food Chemistry 59: 7346-7352.
- [3] Arshad, M., Nawaz, R., Ahmad, S., Qayyum, M. M. N., Ali, Z., Faiz, F., Manzoor, H. M. I. (2018): Morpho-nutritional response of lettuce (*Lactuca sativa* L.) to organic waste extracts grown under hydroponic condition. – Applied Ecology and Environmental Research 16(3): 3637-3648.
- [4] Arun, K. D., Anjaneyulu, A. S. R., Gadekar, Y. P., Singh, R. P., Pragati, H. (2008): Effect of full-fat soy paste and textured soy granules on quality and shelf-life of goat meat nuggets in frozen storage. – Meat Science 80: 607-614.
- [5] Asghar, A., Lin, C. F., Gray, G. I., Buckley, D. G., Booren, A. M., Flagel, C. J. (1989): Effect of dietary oil and alpha- tocopherol supplementation on membrane lipid stability of broiler meat. – Journal of Food Science 54(6).
- [6] Banerjee, R., Verma, A. K., Das, A. K., Rajkumar, V., Shewalkar, A. A., Narkhede, H. P. (2012): Antioxidant effects of broccoli powder extract in goat meat nuggets. – Meat Science 91(2): 179-184.
- [7] Bhosale, H. J., Sukalkar, S. R., Uzma, S. M. Z., Kadam, T. A. (2011): Production of xylanase by *Streptomyces rameus* grown on agricultural wastes. – Biotechnology 1(4): 505-512.
- [8] Chandralekha, S., Babu, A. J., Moorthy, P. R. S., Karthikeyan, B. (2012): Studies on the effect of pomegranate rind powder extract as natural antioxidant in chicken meat balls during refrigerated storage. – Journal of Advanced Veterinary Research 2(2): 107-112.
- [9] Cheng, J. H. (2016): Lipid oxidation in the meat. – Journal of Nutrition and Food Sciences 6(3).
- [10] Divya, Singh, R. P. (2013): Effect of bitter melon as antioxidant in chicken nuggets. – Indian Journal of Poultry Science 48(1): 63-67.
- [11] El-Gasim, E. A., Al-Wesali, M. S. (2000): Water activity and Hunter color values of beef patties extended with Samh flour. – Food Chemistry 69(2): 181-185.
- [12] Gorsuch, V., Alvarado, C. Z. (2010): Postrigor tumble marination strategies for improving color and water-holding capacity in normal and pale broiler breast fillets. – Poultry Science 89(5): 1002-1008.
- [13] Jittrepotch, N., Ushio, H., Ohshima, T. (2006): Effects of EDTA and a combined use of nitrite and ascorbate on lipid oxidation in cooked Japanese sardine (*Sardinops melanostictus*) during refrigerated storage. – Food Chemistry 99(1): 70-82.
- [14] Jung, S., Jun, H. C., Kim, B., Yun, H., Kruk, A. Z., Jo, C. (2010): Effect of dietary mixture of garlic acid and linoleic acid on antioxidative potential and quality of breast meat from broilers. – Meat Science 86(2): 520-526.

- [15] Kala, R. K., Kondaiah, N., Anjaneyulu, A. S. R., Thomas, R. (2007): Evaluation of quality of chicken emulsions stored at refrigeration for chicken patties. – *International Journal of Food Science & Technology* 42(7): 842-857.
- [16] Kikki, K., Diley, S., Sachdev, A. K., Biswas, A. K., Tyagi, P. K., Sen, A., Nath, A., Singh, M. (2014): Development of functional chicken nuggets incorporating functional bamboo shoots, beet roots and cabbage. – *Indian Journal of Poultry Science* 48(2): 257-260.
- [17] Kumar, D., Tanwar, V. K. (2010): Effects of incorporation of ground mustard on quality attributes of chicken nuggets. – *Journal of Food Science & Technology* 48(6): 759-762.
- [18] Maliluan, C., Pramono, Y. B., Dwiloka, B. (2013): Chemical and the acceptability of chicken nuggets as functional food with utilization rice bran to substitute wheat flour. – *Jurnal Gizidan Pangan* 4(1): 13-19.
- [19] Miller, E. R., Pastor-Barriuso, R., Dalal, D., Riemersma, R. A., Appel, L. J. (2005): Meta-analysis: high-dosage vitamin E supplementation may increase all-cause mortality. – *Annals of Internal Medicine* 42(1): 37-46.
- [20] Mishra, B. P., Geeta, G., Sanjod, K. M., Prasana, K. R., Renuka, N. (2015): Storage stability of aerobically packaged extended dehydrated chicken meat rings at ambient temperature. – *Turkish Journal of Veterinary and Animal Sciences* 39(4): 493-500.
- [21] Mohamed, A., Jamilah, B., Abbas, K. A., Rahman, A. R. (2008): A review on lipid oxidation of meat in active and modified atmosphere packaging and usage of some stabilizers. – *Journal of Food, Agriculture and Environment* 6(3): 76-81.
- [22] Moron, L., Andres, S., Bodas, R., Prieto, N., Giraldez, F. J. (2012): Meat Texture and Antioxidant Status Are Improved When Carnosic Acid Is Included in the Diet of Fattening Lambs. – *Meat Sci.* 9: 430-434.
- [23] Naveena, B. M., Sen, A. R., Vaithyanathan, S., Babji, Y., Kondaiah, N. (2008): Chicken patties. – *Meat Science* 80(4): 1304-1308.
- [24] O'sullivan, C. M., Lynch, A. M., Lynch, P. B., Buckley, D. J., Kerry, J. P. (2004): Use of antioxidants in chicken nuggets manufactured with and without the use of salt and/or Sodium Tripolyphosphate: Effects on product quality and shelf-life stability. – *International Journal of Poultry Science* 3(5): 345-353.
- [25] Prasetyo, M., Chia, M., Hughey, C., Were, L. M. (2008): Utilization of electron beam irradiated almond skin powder as a natural antioxidant in ground top round beef. – *Journal of Food Science* 73(1): 1-6.
- [26] Qiao, M., Fletcher, D. L., Smith, D. P., Northcutt, J. K. (2001): The Effect of Broiler Breast Meat Color on pH, Moisture, Water-Holding Capacity, and Emulsification Capacity. – *Poultry Science* 80(5): 676-680.
- [27] Ruiz-Ramirez, J., Serra, X., Arnau, J., Gou, P. (2005): Profiles of water content, water activity and texture in crusted dry-cured loin and in non-crusted dry-cured loin. – *Meat Science* 69(3): 519-525.
- [28] Sallam, K. I., Ishioroshib, M., Samejima, K. (2004): Antioxidant and antimicrobial effects of garlic in chicken sausage. – *Lebensmittel-Wissenschaft & Technologie* 37(8): 849-855.
- [29] Sohaib, M., Anjum, F. M., Khan, M. I., Arshad, M. S., Yasin, M., Shahid, M. (2013): Effect of α -Lipoic Acid and α -Tocopherol Acetate Enriched Broiler Diet on Oxidative Stability and Quality of Broiler Leg Meat and Meat Products. – *Journal of Food Processing and Technology* 4(7): 1-7.
- [30] Steel, R. G. D., Torrieand, J. H., Dicky, D. A. (1997): Principles and procedures of statistics. A biometrical approach. – 3rd ed. McGraw Hill Book Co. Incorporations, New York.
- [31] Verma, A. K., Rajkumar, V., Banargee, R., Biswas, S., Das, A. K. (2013): Guava (*Psidiumguajava* L) powder as dietary antioxidant in the sheep meat nuggets. – *Asian-Australasian Journal of Animal Sciences* 26(6): 886-895.
- [32] Yadav, P. L., Sanyal, M. K. (1999): Development of livestock products by combination preservation technique. – In: Proceedings of National Seminar on Food Preservation by Hurdle Technology and Related Areas, DFRL, Mysore, India: 104-109.

THE ENVIRONMENTAL CONDITIONS OF A LOCATION MAY INFLUENCE THE TREATMENT OF INDUSTRIAL SOLID WASTE

MORÁN-PALACIOS, H. * – MESA-FERNÁNDEZ, J. M. – ÁLVAREZ-CABAL, J. V. – MARTÍNEZ-HUERTA, G. M.

Project Engineering Department, University of Oviedo, Oviedo 33004, Spain

**Corresponding author*

e-mail: henar.moran@api.uniovi.es; phone: +34-985-104-272; fax: +34-985-104-256

(Received 29th May 2019; accepted 25th Nov 2019)

Abstract. The management of industrial solid waste demands the establishment of suitable management systems. Such systems must take into consideration multiple factors that allow selecting the most adequate treatment techniques among the ones available. The selection of these techniques is a complex process that not only depends on factors inherent to the treatment or the waste itself, but also on other factors. For this reason, this study analyses the influence of location on the management of an industrial solid waste such as LD sludge. Firstly, we used a methodology developed in a previous part of this study, that can identify six treatment solutions, then, a set of environmental, regulatory and socioeconomic indicators are chosen. Going a step further in this investigation, proves through the application of the methodology in five different locations, that environmental characteristics influence the final treatment solution for the same waste. According to this, two sets of groups can be identified for the best treatment solution: one in which the highest score is 1 A Ceramization and another in which the final result is 1 B Vitrification.

Keywords: *sludge, analytical hierarchy process, management methodology, system of indicators, industrial facilities*

Introduction

Over the course of history, and as the population has grown, the needs and level of comfort for individuals have increased exponentially, resulting in an excessive generation of waste parallel to the generation of goods. This lack of social conscience that until recently was undeniable, dumping this waste in an uncontrolled manner and causing serious economic, social and environmental problems, has been giving way to the emergence of a new social conscience.

The problem of environmental pollution has its origin in the fast urbanization and industrialization produced in the last few decades. Although the amount of waste produced in cities is worrying, the generation of waste at the industrial level is even more so. In spite of being more varied and numerous, they are more dangerous and, as a consequence, more difficult to control, causing serious problems in the operations of their use and subsequent disposal. This, in combination with greater social awareness, makes the need to develop new management methods and procedures becoming more and more evident. However, just as important as their development is the way they are applied and adapted to the constantly changing technological and social environment. One-way to go a step further and make the most of these management systems, is to incorporate specific tools that allow the influence of certain external agents to be measured.

Therefore, the industrial solid waste management (ISWM) is a complex issue that industrial companies around the world must tackle on a daily basis. All of them must try

to use the best techniques available to treat the waste material and establish the most suitable management and treatment systems.

In many cases, the selection of the most suitable treatment or set of treatments is a complex issue, due to the need to bear in mind a considerable amount of factors (technical, economic, social...). Obviously, the special characteristics of the industrial waste are often crucial, though the environmental conditions of the area where the waste is generated are also decisive.

In the managing of industrial solid waste (ISW) or any type of waste, not only should be taken into account, to study which treatment is the best according to the characteristics of the waste, if not that the process is much more complex. In addition, the performance produced should be analysed according to the environmental characteristics of the site or location where it is to be managed. Based on the measurement of this performance, it could be decided which environment is best to treat the waste.

Based on this hypothesis, it might appear that the research currently being carried out on this particular subject could be countless, but this is not the case. Since many of the existing works only study the optimal location of the industrial facilities to reduce its impact from the beginning using decision support systems (Arán et al., 2008) or multi-criteria decision making techniques (Çebi and Otay, 2015) including Analytic Hierarchy Processes (Kauko, 2006; Dey and Ramcharan, 2008; Srdjevic et al., 2007; Akıncı et al., 2013). Other researches use bi-level programming models (Wu and Yang, 2018) or analyse (Chen et al., 2014) or compare (Glatte, 2015) different models.

Some authors study the optimal location of the treatment plants using multi-criteria approaches, taking into account technical, economic and environmental aspects (Önüt and Soner, 2008; Wibowo and Grandhi, 2017; Wójcik et al., 2014; Kyriakis et al., 2017; Samah et al., 2017; Ulubeyli et al., 2017). For this purpose, different techniques and methodologies are used, including Analytic Hierarchy Processes (Önüt and Soner, 2008; Milutinović et al., 2014; Samah et al., 2017), programming models (Vaillancourt and Waub, 2002; Haastrup et al., 1998; Paul et al., 2018), or fuzzy systems (Carniel and Schneider, 2017; Abdulhasan et al., 2019). Other select the most appropriate treatments for waste at a given location (Achillas et al., 2010; Xu et al., 2014; Nouri et al., 2018) or a comparison between two locations (Milutinović et al., 2016; Inglezakis et al., 2018).

Thus, the work here presented pursues two goals:

- Check that the environmental conditions of a location can modify the most suitable treatment for a specific industrial waste.
- Verify that the previously developed methodology by the authors (Fernández et al., 2014) is capable of providing the best solution in several geographical locations with different physical, environmental and social conditions where the waste material is generated.

Materials and methods

Methodology for the ISWM

As described above, the methodology for the selection of the most suitable solution for the waste material that has been used, is the one defended by Fernández et al. (2014)

This methodology has a series of characteristics that makes it the most suitable for the study of the treatment of industrial solid waste:

- First, its adaptability to any type of waste, either solid or semisolid.
- It can be applied to any type of environment by adjusting the location conditions of the installation where the management process is taken place (climate, soil, closeness to populated areas or green areas, etc.).
- It is a flexible methodology that can consider different criteria or environmental indicators.
- It is user-friendly, since the decision process guides and helps users through the different options.
- It is easy to update, by including new treatment methods, changes derived from evolution in technology or social and economic conditions.

All these characteristics allow the methodology to continue evolution and thus be able to comply with the future lines contemplated in the first part of the study developed in Spain (Fernández et al., 2014). For its application, the methodology is structured in four stages, defined in *Figure 1*.

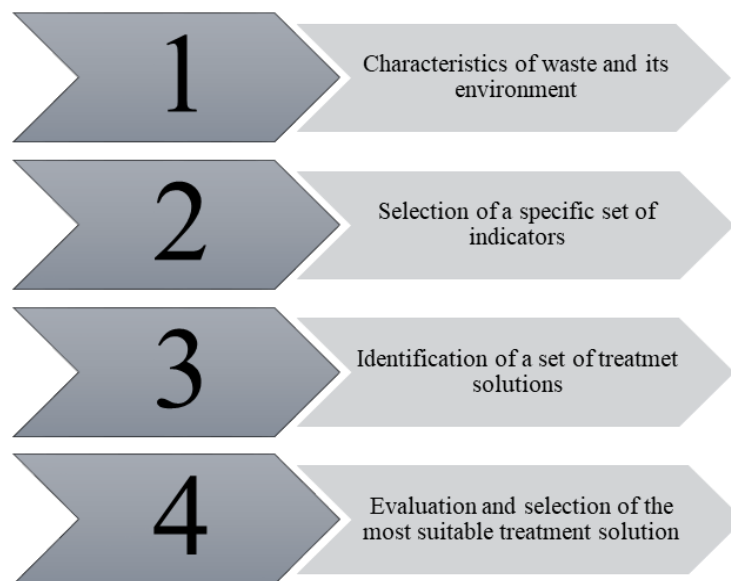


Figure 1. Methodology development diagram

The first thing to learn is the characteristics of the waste to be treated and the environment where the treatment will be developed. All this information is then collected in files or sheets, one with the characteristics of the waste material and the other with those of the environment, the first classifies the waste material according to information related to its identification, and the second collects information on the location where the treatment system will be set and its conditions.

The second stage involves the selection of a specific set of indicators for each case of application, the result of particularizing a system of general indicators.

For this purpose, the general Environmental Indicator System (EIS) for any area of the company, will be specific to waste management by configuring a System of Environmental Indicators for Solid Waste Management (SEISWAM) that will be the

means of subsequent evaluation of the possible treatment solutions applicable to this waste. The characteristics of the indicators are described in the “Indicator sheet”.

In the third stage, the treatment solutions are identified thanks to an “alternative selection chart” (Fernández et al., 2014), which presents the necessary process for the treatment of a solid waste from its generation to its disposal, elimination or reuse, and functions as a decision aid system. This identification is carried out taking into account the characteristics of the waste “Waste sheet” and the set of available techniques, “Process sheet”, which collects the main data of interest of each technique and waste to which is applicable. Each of these solutions can consist of more than one treatment process.

The last stage of the methodology presents the results of the study and allows us to select the most suitable solution among all the possible solutions previously identified in the previous stage. For this purpose, the selected set of indicators is available, which evaluates each of the available solutions. This evaluation is performed through the application of the Analytical Hierarchy Process (AHP), developed by Tomas Saaty in 1980 (Saaty, 1980).

Case study

Next, the application of this methodology to a particular case is described, where the goal is to search the optimal treatment solution for the same industrial waste in different locations worldwide.

Waste product studied

LD converter sludge is the waste material resulting from the wet processing of gas in the steel-making process in the Basic Oxygen Furnace (BOF) converter or LD converter, named after the Austrian towns Linz and Donawitz where this system was first developed. This waste material involves a serious concern due to the vast amount generated, around 27 kg of LD sludge per ton of hot metal. Its physical and chemical components allow different alternatives or possibilities of treatment. On the other hand, it has a percentage of recoverable material, its metal part, which makes it a reusable product both for the steelmaking and other types of industries (*Table 1*).

Selection of locations

In order to develop this study, 5 populations close to steel mills have been selected, where the LD slag is obtained and which have different physical, environmental and social environment conditions.

Among the possible locations, areas with different climate conditions have been selected, according to the climate classification developed by Köppen. This procedure is based on empirical observations (Köppen, 1900) to establish a climate classification system that uses monthly temperatures and rainfalls to define the limits of the different types of climate worldwide. This classification was revised and updated afterwards (Köppen and Geiger, 1930, 1936; Stern et al., 2000; Peel et al., 2007) and it is widely used worldwide by meteorologists and geologists (Chen and Chen, 2013; Feng et al., 2014), apart from being the base of multiple scientific studies (Pražnikar, 2017; Almorox and Quej, 2015; Yoo and Rohli, 2016).

According to these premises, the populations of Avilés (Spain), Lázaro Cárdenas (Mexico), Tubarao (Brazil), Newcastle (South Africa) and Beijing (China) were

selected for the study. The climatological conditions of these locations are displayed in *Table 2*. In the case of Spain, the data have been obtained from the State Meteorological Agency (AEMET, 2017) and the data of the rest of the locations have been collected from the WMO repository, World Meteorological Organization (WMO, 2017), from the official website of the NOAA, National Oceanic and Atmospheric Administration, which belongs to the USA Government.

Table 1. Waste characterization

Chemical description				
Component	Density (g/cm³)	Magnetic properties	Percentage (weight)	CASRN¹
Fe total	7.87	Ferromagnetic	64.12	7439-89-6
FeO	5.74	Paramagnetic	79.58	7439-89-6
CaO	3.30	Magnetic	8.9	1305-78-8
Fe ₂ O ₃ (magnetite)	5.24	Magnetic	2.79	1309-37-1
MgO (periclase)	3.79	No magnetic	0.38	1309-48-4
SiO ₂	2.64	No magnetic	0.71	7631-86-9
Al ₂ O ₃ (alumina)	3.96	Diamagnetic	0.32	1344-28-1
P	1.82	Anti-ferromagnetic	0.10	7723-14-0
MnO	5.10	Anti-ferromagnetic	0.10	1344-43-0
Zn	7.13	Diamagnetic	0.20-4.10	7440-66-6
Pb	11.30	Diamagnetic	0.04-0.14	7439-92-1
S	2.07	No Magnetic	0.03-0.35	7704-34-9
C	2.26	No Magnetic	0.70-4.60	7440-44-0
Physical and chemical properties				
Moisture	35-40%			
Physical condition	Semisolid			
Granulometry	Mostly from 38 µm			
% Weight of organic matter	4%			
% Inorganic matter weight	96%			
Appearance	liquefied, oily			
Colour	Dark grey/black			

¹Chemical Abstract Service Register Number (American Chemical Society)

The town of Avilés is located in the North East coast of Spain, with mild temperatures in all seasons, with an average temperature of 13.5 °C, high relative humidity (78%) and frequent rain. On the contrary, Newcastle (South Africa) has a drier climate, with lower relative humidity (59%) but higher average temperatures (21.9 °C) and less rainfall. On the other hand, Lázaro Cárdenas, a town located near the Pacific Coast of Mexico, has a tropical rainforest climate, where winters are cold but the average annual rainfall is still high all year around. The average rainfall level is 1278 mm and temperatures are high, with an average temperature of 27 °C and a high relative humidity. The humidity of the Brazilian city of Tubarao (61%) is lower than the case of Mexico, while the temperatures are also high (26.4 °C), with a lower rainfall level than in the previous case (1,003 mm), although relatively similar to the town of Avilés.

In Beijing, the weather conditions are quite similar to those of the city of Newcastle in South Africa, although it is colder, (11.8 °C) and drier (47%), and the level of rainfall is a bit higher (577 mm) than that of the Chinese capital.

Table 2. Climate characteristics according to location

	BOF	BOF	BOF	BOF	BOF
Steel mill	Avilés (Spain)	Lázaro Cárdenas (Mexico)	Tubarao (Brazil)	Newcastle (South Africa)	Beijing (China)
Measure location	Avilés	Acapulco	Sao Goncalo	Johannesburg	Beijing
Site	Industrial	Rural-town	Rural	Industrial	Industrial
WMO number station	NA	76805	82689	68368	54511
Period (years)	1981-2010	1961-1990	1961-1990	1961-1990	1961-1990
Type of climate according to Köppen	(Cfb) warm/very wet/warm summer	(Aw) tropical rainforest climate/dry winter	(Cfa) warm/very wet/hot summer	(Cwb) warm/dry winter/warm summer	(Cwa) warm/dry winter/hot summer
Distance (km)	0	300	510	289	0
Annual average temperature (°C)	13.50	27.50	26.4	21.90	11.80
Annual average humidity (%)	78	75.80	61	59.20	47
Annual rainfall total (mm)	1,062	1,278	1,003.30	543	577
Annual average wind speed (m/s)	3.50	2.20	2.82	2.78	2.50
Data source	AEMET	WMO	WMO	WMO	WMO

When selecting these populations, apart from the different climate characteristics, the type of location has also been taken into account, that is, if it is an industrial or rural area and if it is near or not to population centres or natural reserves. In this sense, Avilés, Newcastle and Beijing are considered as populations located in industrial areas, against Tubarao and Lázaro Cárdenas, which are closer to rural areas with small population centres and close to areas considered as natural heritage.

Selection of a specific set of indicators

The indicators system has been established as one of the most useful tools for monitoring the process information flows, which provide us with techniques to evaluate their efficiency.

The so-called SEISWAM was developed at the same time as the methodology used in this paper (Fernández et al., 2014) and it is based on the following two former systems:

- The first one is based on a system of indicators in which the principles of ISO 14031 standard are specified (ISO International Organization for Standardization), the European eco-management and audit scheme contained in the EMAS Regulation (Comision Europea, 2003; DOUE, 2009), extended with

the present classification in the report issued by the Public Society of Environmental Management of Basque Government IHOBE (IHOBE, 1999).

- The second one is the GRI system (Global Reporting Initiative), which is the main international standard for the drafting of Sustainability and Corporate Social Responsibility Reports (CSR) (GRI, 2005).

The indicators system is specialized in the management of industrial solid waste by using a selection chart to define the methodology of waste management. This gives a more complex system called SEISWAM, which is comprised of hundreds of indicators.

Among these indicators, the most representative ones in terms of measuring the impacts of inputs and outputs processes were selected resulting eleven (*Table 3*). These indicators collect globally the different environmental impacts (environmental indicators), socioeconomic impacts (financial behaviour indicators) and those affecting the management process according to the set of treatments that waste endures (environment indicators).

Table 3. *Indicators considered*

Number	Indicator name
1	Specific energy consumption
2	Specific water consumption
3	Specific consumption of chemical agents
4	Volume of liquid effluents
5	Volume of gas emissions
6	Total share of profitable solid
7	Operational costs of environmental protection
8	Average rainfall of the area where the installation is located
9	Wind speed in relation to the average in the area where the installation is located
10	Proportion of natural heritage affected
11	Proximity to local populations

Of these eleven indicators, the first seven are dependent on the characteristics of the waste material and measure the environmental, social, economic impacts of the waste management process. Essentially, it has been decided to select those that directly and easily quantify the inputs and outputs in the flowchart, to compare the results obtained with those of the first part of the study carried out by Fernández et al. (2014). For instance, the indicator ‘Specific water consumption’ has been selected over other possible ones like ‘Rate of type of water’, because the latter does not evaluate all the water in the whole process, but only of those processes that work with a certain type of water. The same happens with indicators concerning chemical agents, effluents and gas emissions.

The selection of the indicator ‘Operating costs of environmental protection’ incorporates the economic impact from the viewpoint of environmental protection related to the operations performed in the waste management facility. This is not the case in other possible suitable indicators such as ‘Environmental aid granted by the Government’ in which, besides taking into account mainly economic factors, there is no reference whatsoever to the management process.

Regarding the quantification of the system outputs, in the case of the indicator ‘Total share of profitable solid’, this more global indicator has been chosen rather than ‘Total amount of profitable solid with respect to energy consumption’, in which the usable solids are quantified, but only taking into account the input of energy to the process.

Regarding the indicators corresponding to the environmental conditions that affect the treatment processes, it has been selected the ones referring to the climate characteristics of the area most liable to affect the waste treatment system, such as rainfall and speed. Regarding the living conditions, the most representative indicators of this level have been chosen, such as the ‘natural heritage affected’ and the ‘Proximity to local populations’ without going into details about the classification or type of soil (rural or urban).

Set of treatment solutions

By the ‘alternative selection chart’ (Fernández et al., 2014) the different treatment solutions are identified, obtaining six possible treatment alternatives:

- Alternative 1 A. Ceramization
- Alternative 1 B. Vitrification
- Alternative 2.1 A. External manager of hazardous solids
- Alternative 2.2 A. Phytoremediation
- Alternative 2.2 B. Bioremediation
- Alternative 2.2 C. On site vitrification

Each of these alternatives is comprised of a set of treatments that start when the waste enters the facility and ends when the final product is obtained. To summarize, they are identified only with the name of the last valorization treatment applied to the waste. The treatments that constitute each alternative are described below.

In the alternative selection chart, the waste material goes through a series of initial considerations such as its categorization as a non-radioactive, hazardous and valuable slag, according to its initial classification. Afterwards, the sludge is dried to be submitted to a magnetic separation process. As a result, the solid magnetic fraction is usable while the non-magnetic part goes back into the decision process. This non-magnetic solid could be recovered (alternative 1) or not (alternative 2). If the recovery of such fraction is chosen, it would be possible to apply the treatments of ceramization (Alternative 1 A. Ceramization) or vitrification (Alternative 1 B. Vitrification). In the case of not choosing to recover the waste material (alternative 2), it must be determined if it is legally disposable or not. In this particular case, it would not be disposable, since, according to the legislation and the initial characterization, this waste material contains a series of toxic components that surpass the legal thresholds. Therefore, at this point, there are two options. The first one would be not treating the waste internally but carrying it instead to an External manager of hazardous solids (Alternative 2.1 A). The second one would be treating the waste internally, with these different treatment possibilities: Phytoremediation (Alternative 2.2 A. Phytoremediation), Bioremediation (Alternative 2.2 B. Bioremediation) or onsite vitrification (Alternative 2.2 C. On site vitrification).

Results

The five proposed locations are assessed using the eleven selected indicators that constitute the decision criteria of the AHP method (Fernández et al., 2014), which corresponds to the last stage of the methodology, *Evaluation of alternatives*, giving the results of the study. This way, the influence of weather conditions is opposed to the proximity to population areas, industrial zones, rural areas, nature reserves, etc. in the treatment processes. In this stage, the environmental impacts are taken into account when assessing the indicators. Therefore, each management solution will have a different score.

In the calculation of the judgment matrix by paired comparison of the treatment alternatives for each of the criteria or indicators related to the environment, the weights of each of these criteria vary depending on each location. For instance:

- In damp and rainy locations, landfill treatments produce more leachates than in drier climates. As a consequence, in Avilés or Lázaro Cárdenas, a higher quantity of liquid effluents and alternatives such as 2.2 A Phytoremediation and 2.2 B Bioremediation would be generated and, therefore, they receive a worse assessment than others such as 1A Ceramization. On the contrary, Newcastle and Beijing have a lower amount of effluents and the alternatives 2.2 Phytoremediation and 2.2 B Bioremediation obtain a better assessment.
- In locations with high wind speed, gas pollution moves to other nearby areas such as population centres or natural parks. In these cases, the criteria or indicators ‘Affected natural heritage’ or ‘Operational costs of environmental protection’, become negative factors or criteria when assessing certain treatments. This would be the case of towns such as Avilés or Tubarao, where the scores of valorization processes such as ceramization or vitrification are lower than those corresponding to landfill or shipping to an external manager of hazardous solids.

Taking into account this calculation and the weights of indicators according to the area where the treatment facility is located, the following scores are obtained in *Table 4*.

Table 4. Hierarchical analysis method solutions in different locations

Alternatives	Alternative priority vector				
	Avilés Industrial	Lázaro Cárdenas Rural	Tubarao Rural	Newcastle Industrial	Beijing Industrial
1 A Ceramization	0.2635	0.2705	0.2602	0.1857	0.1857
1 B Vitrification	0.2429	0.2516	0.2459	0.1923	0.1937
2.1 External manager of hazardous solids	0.2386	0.2381	0.2371	0.1801	0.1788
2.2 A Phytoremediation	0.0794	0.0882	0.0803	0.1776	0.1853
2.2 B Bioremediation	0.0692	0.0702	0.0703	0.1378	0.1393
2.2 C On site vitrification	0.1063	0.0814	0.1062	0.1265	0.1173

It can be noticed that the best-valued treatment alternative in each location, that is, the one with the highest value or score, vary in the different sites. The alternative 1A. Ceramization is the preferred option in the first three locations (Avilés, Lázaro Cárdenas and Tubarao) while in the other two (Newcastle and Beijing) the highest score is for alternative 1B Vitrification.

In all cases, a better assessment is given to the alternatives that end with the waste valorization (ceramization and vitrification) compared to those of final treatment (landfill, - phytoremediation and bioremediation - and external manager).

Discussion

According to the solution proposed by the methodology as the most suitable one, two sets of groups can be identified: one in which the highest score is 1 A Ceramization and another in which the final result is 1 B Vitrification.

In order to describe in a better way what is observed in *Table 4*, the distribution of two localities is shown in *Figure 2*, Lázaro Cárdenas belonging to the first site and Beijing belonging to the second, in the first case, the scores appear more concentrated in the treatment processes and external manager, while in the second the scores are similar.

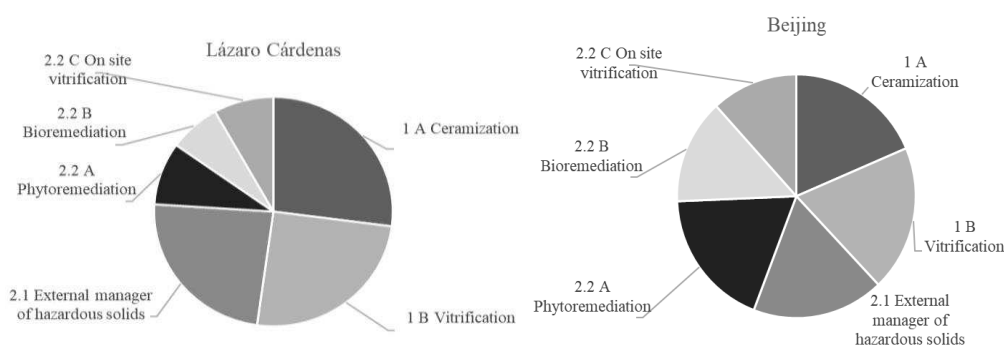


Figure 2. Priorities of treatment alternatives according to location

The scores given by the experts to the different treatment alternatives in the comparative analysis, depending on the selected criteria or indicators, vary due to the following causes:

1. Leachates can appear in damp and rainy climates so, as a consequence, the landfill treatment alternatives (phytoremediation and bioremediation) have poorer scores. This is what occurs in the first three locations (Avilés, Lázaro y Tubarao), for having more rainfall than the other two (Newcastle and Beijing).
2. On the other hand, the landfill treatment alternatives obtain higher scores for the good results obtained by these techniques in climates with less rainfall, as in the case of Newcastle. According to different studies (Sharma and Pandey, 2014; Liphadzi et al., 2005) the plants and microorganisms used in these areas (Yadav and Hassanizadeh, 2011; Hejazi et al., 2003) develop their activity effectively by clearing the soil of heavy metals due to favorable weather conditions.
3. Gas emissions occurring near rural areas where the natural habitat is more diverse, such as Lázaro Cárdenas and Tubarao, generate more environmental impact than in industrial areas, which favours the scoring of alternatives that include landfilling, such as 2.2 A Phytoremediation, 2.2 B Bioremediation, diminishing the scoring of the alternatives that do not include it, such as 1 B Vitrification and 2.1 A External manager. These impacts also occur in Aviles,

but since it has an industrial environment, the natural and rural heritage is less affected, so landfill scores do not rise as much as in rural locations.

4. Wind speed is similar in all studied locations, although the highest wind speed corresponds to Avilés. In this area, emissions in the form of leaks that can break into the atmosphere are more likely to be dragged to further area, thus extending the range of pollution. This makes the valorization processes more expensive than those of landfilling or manager dispatching. On the contrary, the opposite case occurs in the rest of the locations where the wind speeds are softer.

In the first analysis, the operability of the methodology was proved (Fernández et al., 2014), a locality with specific environmental conditions was chosen and the scores of the treatment alternatives were calculated, being the highest alternative 1A ceramization.

In this research, in which the type of waste and the evaluation criteria are the same, besides demonstrating the characteristics of the methodology described in the materials and methods section; adaptability, applicability, flexibility, user-friendly, easy to update; the treatment solutions obtained in each of the five locations have been compared, it can be observed that the changes in the environmental conditions of the site established at the beginning of the analysis differ significantly, therefore the evaluation of the indicators changes and, consequently, the results vary.

Conclusions

This study has implemented the methodology by Fernández et al. (2014) in order to select the most suitable treatment alternative to the same waste in five different locations. The results obtained show that the best solution may vary when environmental conditions are significantly changed.

In the case studied, the treatment of LD sludge, when analyzing the influence of the climatic and environmental conditions of the location in the different treatment processes, the following results were obtained:

A high-level rainfall constrains the suitability of the landfill treatments, since in this context there is a higher-level generation of leachates.

- The gas emissions produced at the output of some treatments (vitrification or ceramization), combined with the wind conditions may have a negative impact in rural locations or other places, as for instance natural reserves or protected areas. This makes these treatments less suitable. On the contrary, if these conditions are in industrial areas or its proximity, it has a less negative impact.
- In the case of the developed methodological process, a series of inherent characteristics of the methodology are reviewed and checked:
- Its applicability and flexibility, allow the use of the most suitable criteria or environmental indicators in each case, more or less according to the number of criteria of study required for each case.
- Its simple upgrading. This makes it easier to add new waste treatment techniques to the valorization decisions or treatment requirements included in the alternative selection chart.

Within the future lines of research in this study, the analysis developed can be perfectly extended to other similar facilities located in other cities under different climatic and environmental conditions, being able to obtain a different solution in a changing environment.

The same methodology can be applied in other industrial sectors (glass, textiles, mining, etc.) that generate other types of waste (liquid effluents, wastewater and gaseous emissions) and as a result with different treatments to those described above, allowing to personalize the system of general indicators and develop an alternative selection diagram similar to that exposed.

In the same way, another series of criteria can be incorporated into the study, either parameters related to the social or economic conditions of the environment, or other factors that could have a critical role in the security of the waste storage and other outputs, using the extensive system of indicators that includes the methodology or incorporating new indicators if necessary.

Finally, a software could be developed to support this methodology, allowing for each of the treatment alternatives, the quantitative determination of effluent outputs, energy consumption, chemical agents, etc.

Acknowledgements. This work has been subsidized through the Plan of Science, Technology and Innovation of the Principality of Asturias (Ref: FC-GRUPIN-IDI/2018/000225). We would also like to thank to Miss Marina Diaz Piloñeta for her accurate critical evaluations and contribution with their ideas to the present research.

REFERENCES

- [1] Abdulhasan, M. J., Anafiah, M. M., Satchet, M. S., Abdulaali, H. S., Toriman, M. E., Al-Raad, A. A. (2019): Combining Gis, fuzzy logic, and AHP models for solid waste disposal site selection in Nasiriyah, Iraq. – *Applied Ecology and Environmental Research* 13(3): 6701-6722.
- [2] Achillas, C., Vlachokostas, C., Moussiopoulos, N., Baniass, G. (2010): Decision support system for the optimal location of electrical and electronic waste treatment plants: a case study in Greece. – *Waste Management* 30(5): 870-879.
- [3] AEMET (2017): Valores climatológicos normales: Asturias Aeropuerto - Agencia Estatal de Meteorología - AEMET. Gobierno de España. – <http://www.aemet.es/es/serviciosclimaticos/datosclimatologicos/valoresclimatologicos> (accessed: March 17, 2017).
- [4] Akinci, H., Özalp, A. Y., Turgut, B. (2013): Agricultural land use suitability analysis using GIS and AHP technique. – *Computers and Electronics in Agriculture* 97: 71-82.
- [5] Almorox, J., Quej, V. H. (2015): Global performance ranking of temperature-based approaches for evapotranspiration estimation considering Köppen climate classes. – *Journal of Hydrology* 528: 514-522.
- [6] Arán, J., Espín, A., Aznar, F., Zamorano, M., Rodríguez, M., Ramos, A. (2008): Environmental decision-support systems for evaluating the carrying capacity of land areas: optimal site selection for grid-connected photovoltaic power plants. – *Renewable and Sustainable Energy Reviews* 12(9): 2358-2380.
- [7] Carniel, A. C., Schneider, M. (2017): Fuzzy inference on fuzzy spatial objects (FIFUS) for spatial decision support systems. – 2017 IEEE International Conference on Fuzzy Systems (FUZZ-IEEE), pp. 1-6.

- [8] Çebi, F., Otay, İ. (2015): Multi-criteria and multi-stage facility location selection under interval type-2 fuzzy environment: a case study for a cement factory. – *International Journal of Computational Intelligence Systems* 8(2): 330-344.
- [9] Chen, D., Chen, H. W. (2013): Using the Köppen classification to quantify climate variation and change: an example for 1901-2010. – *Environmental Development* 6: 69-79.
- [10] Chen, L., Olhager, J., Tang, O. (2014): Manufacturing facility location and sustainability: a literature review and research agenda. – *International Journal of Production Economics* 149: 154-163.
- [11] Comisión Europea (2003): CELEX1, Recomendación de la Comisión sobre las orientaciones para la aplicación del Reglamento (CE) n° 761/2001 del Parlamento Europeo y del Consejo. – Comisión Europea, Brussels.
- [12] Dey, P. K., Ramcharan, E. K. (2008): Analytic hierarchy process helps select site for limestone quarry expansion in Barbados. – *Journal of Environmental Management* 88(4): 1384-1395.
- [13] DOUE (2009): RE (CE) N° 1221/2009. REGLAMENTO (CE) N°1221/2009 del Parlamento Europeo y del Consejo de 25 de noviembre de 2009 relativo a la participación voluntaria de organizaciones en un sistema comunitario de gestión y auditoría medioambientales (EMAS), y por el que se derogan el Reglamento (CE) n° 761/2001 y las Decisiones 2001/681/CE y 2006/193/CE de la Comisión. – *Diario Oficial de la Unión Europea*.
- [14] Feng, S., Hu, Q., Huang, W., Ho, C.-H., Li, R., Tang, Z. (2014): Projected climate regime shift under future global warming from multi-model, multi-scenario CMIP5 simulations. – *Global and Planetary Change* 112: 41-52.
- [15] Fernández, M., Palacios, H. M., Cabal, J. V. A., Huerta, G. M. M. (2014): Methodology for industrial solid waste management: implementation to sludge management in Asturias (Spain). – *Waste Management & Research: The Journal of the International Solid Wastes and Public Cleansing Association, ISWA* 32(11): 1103-1112.
- [16] Glatte, T. (2015): Location strategies: methods and their methodological limitations. – *Journal for Engineering, Design and Technology* 13(3): 435-46.
- [17] GRI (2005): Suplemento GRI del sector Minería y Metales. – Global Reporting Initiative, Amsterdam.
- [18] Haastrup, P., Maniezzo, V., Mattarelli, M., Mazzeo Rinaldi, F., Mendes, I., Paruccini, M. (1998): A decision support system for urban waste management. – *European Journal of Operational Research* 109(2): 330-341.
- [19] Hejazi, R. F., Husain, T., Khan, F. I. (2003): Landfarming operation of oily sludge in arid region—human health risk assessment. – *Journal of Hazardous Materials* 99(3): 287-302.
- [20] IHOBE (1999): Guía de Indicadores Medioambientales para la Empresa. – IHOBE, Sociedad Pública Gestión Ambiental; Ministerio Federal de Medio Ambiente, Bonn; Agencia Federal Medioambiental, Berlin.
- [21] Inglezakis, V. J., Moustakas, K., Khamitova, G., Tokmurzin, D., Sarbassov, Y., Rakhmatulina, R., Serik, B., Abikak, Y., Pouloupoulos, S. G. (2018): Current municipal solid waste management in the cities of Astana and Almaty of Kazakhstan and evaluation of alternative management scenarios. – *Clean Technologies and Environmental Policy* 20(3): 503-516.
- [22] Kauko, T. (2006): What makes a location attractive for the housing consumer? Preliminary findings from metropolitan Helsinki and Randstad Holland using the analytical hierarchy process. – *Journal of Housing and the Built Environment* 21(2): 159-176.
- [23] Köppen, W. (1900): Versuch einer Klassifikation der Klimate, vorzugsweise nach ihren Beziehungen zur Pflanzenwelt. – *Geographische Zeitschrift* 6: 657-679.
- [24] Köppen, W., Geiger, R. (1930): *Handbuch der Klimatologie*. – Gebrueder Borntraeger, Berlin.

- [25] Kyriakis, E., Psomopoulos, C., Kokkotis, P., Bourtsalas, A., Themelis, N. (2017): A step by step selection method for the location and the size of a waste-to-energy facility targeting the maximum output energy and minimization of gate fee. – *Environmental Science and Pollution Research International* 25(27): 26715-26724.
- [26] Liphadzi, M. S., Kirkham, M. B., Musil, C. F. (2005): Phytoremediation of soil contaminated with heavy metals: a technology for rehabilitation of the environment. – *South African Journal of Botany* 71(1): 24-37.
- [27] Milutinović, B., Stefanović, G., Dassisti, M., Marković, D., Vučković, G. (2014): Multi-criteria analysis as a tool for sustainability assessment of a waste management model. – *Energy* 74: 190-201.
- [28] Milutinović, B., Stefanović, G., Kyoseva, V., Yordanova, D., Dombalov, I. (2016): Sustainability assessment and comparison of waste management systems: the cities of Sofia and Niš case studies. – *Waste Management & Research: The Journal of the International Solid Wastes and Public Cleansing Association, ISWA* 34(9): 896-904.
- [29] Nouri, D., Sabour, M. R., GhanbarzadehLak, M. (2018): Industrial solid waste management through the application of multi-criteria decision-making analysis: a case study of Shamsabad industrial complexes. – *Journal of Material Cycles and Waste Management* 20(1): 43-58.
- [30] Önüt, S., Soner, S. (2008): Transshipment site selection using the AHP and TOPSIS approaches under fuzzy environment. – *Waste Management* 28(9): 1552-1559.
- [31] Paul, K., Chattopadhyay, S., Dutta, A., Krishna, A. P., Ray, S. (2018): A comprehensive optimization model for integrated solid waste management system: a case study. – *Environmental Engineering Research* 24(2): 220-237.
- [32] Peel, M. C., Finlayson, B. L., McMahon, T. A. (2007): Updated world map of the Köppen-Geiger climate classification. – *Hydrol. Earth Syst. Sci* 11(5): 1633-1644.
- [33] Pražnikar, J. (2017): Particulate matter time-series and Köppen-Geiger climate classes in North America and Europe. – *Atmospheric Environment* 150: 136-145.
- [34] Saaty, T. L. (1980): *The Analytic Hierarchy Process*. – McGraw-Hill, New York.
- [35] Samah, M. A. A., Manaf, L. A., Aris, A. Z., Nor, W. (2017): Solid waste management: analytical hierarchy process (AHP): application of selecting treatment technology in Sepang Municipal Council, Malaysia. – *Current World Environment* 6(1).
- [36] Sharma, P., Pandey, S. (2014): Status of phytoremediation in world scenario. – *International Journal of Environmental Bioremediation & Biodegradation* 2(4): 178-191.
- [37] Srdjevic, Z., Kolarov, V., Srdjevic, B. (2007): Finding the best location for pumping stations in the Galovica drainage area of Serbia: the AHP approach for sustainable development. – *Business Strategy and the Environment* 16(7): 502-511.
- [38] Stern, H., de Hoedt, G., Ernst, J. (2000): Objective classification of Australian climates. – *Australian Meteorological Magazine* 49: 87-96.
- [39] Ulubeyli, S., Kazaz, A., Arslan, V. (2017): Construction and demolition waste recycling plants revisited: management issues. – *Procedia Engineering* 172: 1190-1197.
- [40] Vaillancourt, K., Waaub, J.-P. (2002): Environmental site evaluation of waste management facilities embedded into EUGÈNE model: a multicriteria approach. – *European Journal of Operational Research* 139(2): 436-448.
- [41] Köppen, W., Geiger, R. (1936): *Das geographische System der Klimate*. – Gebrüder Bornträger, Berlin.
- [42] Wibowo, S., Grandhi, S. (2017): A Multicriteria Approach for Selecting the Optimal Location of Waste Electrical and Electronic Treatment Plants. – In: *Computer and Information Science. Studies in Computational Intelligence. International Conference on Computer and Information Science*. Springer, Cham, pp. 139-147.
- [43] WMO (2017): *Global Climate Normals (1961-1990)*. National Centers for Environmental Information (NCEI). – <https://www.ncdc.noaa.gov/wdcmnet/data-access-search-viewer-tools/global-climate-normals-1961-1990> (accessed: March 17, 2017).

- [44] Wójcik, G., Jacyno, M., Korkosz-Gebska, J., Krasuska, E., Oniszk-Popławska, A., Trebaczf, D. (2014): Location selection analysis for biological treatment plants for municipal waste. – *Journal of Power Technologies* 94 (1): 1-19.
- [45] Wu, S., Yang, Z. (2018): Optimizing location of manufacturing industries in the context of economic globalization: a bi-level model based approach. – *Physica A: Statistical Mechanics and Its Applications* 501: 327-337.
- [46] Xu, Y., Wu, S., Zang, H., Hou, G. (2014): An interval joint-probabilistic programming method for solid waste management: a case study for the city of Tianjin, China. – *Frontiers of Environmental Science & Engineering* 8(2): 239-255.
- [47] Yadav, B. K., Hassanizadeh, S. M. (2011): An overview of biodegradation of LNAPLs in coastal (semi)-arid environment. – *Water, Air, and Soil Pollution* 220(1-4): 225-239.
- [48] Yoo, J., Rohli, R. V. (2016): Global distribution of Köppen–Geiger climate types during the Last Glacial Maximum, Mid-Holocene, and present. – *Palaeogeography, Palaeoclimatology, Palaeoecology* 446: 326-337.

SPECIES-SPECIFIC SEED VIGOR TEST OF AGING CHIVE FOR RESTORATION AND REGIONAL ADAPTATION UNDER CLIMATE CHANGE

NA, C. S.[#] – BAEK, S. G.[#] – YANG, S. Y. – PARK, C. Y. – KIM, J. H. – LEE, M. H. – PARK, Y. S.*

Seed Conservation Research Division, Baekdudaegan National Arboretum, Bonghwa 36209, Republic of Korea

[#]*These authors contributed equally to this work*

^{*}*Corresponding author*

e-mail: yspark1219@bdna.or.kr; phone: +82-54-679-0621; fax: +82-54-679-0626

(Received 30th May 2019; accepted 16th Oct 2019)

Abstract. This study aimed to develop a vigor test method that can be applied in the seed storage and ecological restoration of Aging chive (*Allium senescens* L). The impact weight of each temperature on germination was described with a sine curve equation. The closer the temperature was to 18.9 °C, the faster the germination was, and temperatures below 8.0 °C and above 29.7 °C negated the temperature accumulation effect. A verification and validation test confirmed the ‘impact weight on germination’ to be reasonable because it exhibited a hump-shaped relationship with the time to reach 85% germination among the temperature treatments. Furthermore, the time to reach 25, 50 and 75% germination and the change in germination with time did not differ between the actual and predicted values. The hourly accumulated value of ‘impact weight on germination’ was taken as the temperature score (TS), and the temperature requirement for vigorous germination was 294TS. The temperature requirement was applied to hourly temperature data from Geumsan, Korea, from 1999-2018, and the average date of vigorous seed germination was May 3. Increasing temperature elevation advanced the predicted germination date. Based on the earliest predicted date, germination will advance rapidly. If the temperature is elevated by 2.5 °C, the germination date will advance markedly to November 23.

Keywords: *Allium senescens* L., German garlic, germination, seed vault, wild plant

Introduction

The Baekdudaegan Global Seed Vault (BGSV) of the National Baekdudaegan Arboretum was established to preserve and safely store seeds of wild plants collected worldwide. A seed vault is a center for permanent storage, in contrast to a seed bank, which allows seeds to be deposited and removed easily. The permanent storage of seeds conserves biodiversity and allows restoration to prevent extinction, which could occur in response to climate change and natural disasters, among other events. Because seeds are the core of ecological restoration (Broadhurst et al., 2015), the BGSV could serve as a potential material supplier for a wide range of species restoration and ecosystem reconstruction activities as it includes seeds from wild plant species.

Seed viability is one of the most important factors for the permanent storage of seeds and ecological restoration (Marcos-Filho, 2015). Storing seeds confirmed to have high vitality by a vigor test not only increases their storability but also affects the efficiency of the seed vault. Moreover, a vigor test provides information that can be used to restore the germination of seeds stabilized for storage, which is a key factor in the restoration of natural habitats (van der Valk et al., 1999).

To achieve ecological restoration using seeds, information on germination characteristics and the environment of the target site should be taken into account. Since the selection of species for restoration gives priority to native species, vigor test results for the species and environmental information at the target site are especially important for determining the success or failure of the restoration.

The species used in this study, Aging chive (*Allium senescens* L.), is a perennial herb of the *Liliaceae* family with thicker leaves than other members of this family (Oh et al., 2012). Because of its very strong scent, its aromatic components and chemical composition have been studied (Chung and Lee, 2001; Chung, 2010). For example, methanol extracts of this species were found to suppress reactive oxygen species (ROS) production and lipid accumulation and consequently inhibit adipogenesis (Choi and Kim, 2014). Despite the studies on this species, it is classified as a rare plant in Korea and is in danger of extinction (Korea National Arboretum, 1997).

Thus, this study aimed to develop a vigor test method for *A. senescens*, an endangered species, that can be flexibly applied during seed storage and ecological restoration. Furthermore, germination timing was inferred using temporal temperature data from seed collection sites, and the variability of this trait in response to climate change was predicted. We intend to incorporate these results into the BGSV database (DB) of wild species seeds.

Materials and methods

Seed information and experimental conditions

Seeds of *A. senescens* collected from the Chungcheongnam-do Forest Environment Research Institute, Korea, in 2018 were used in this study (N36.4336, E127.3721). The collected seeds were stored at -20 °C before the experiment started. Nonempty and healthy seeds were selected for experiments using a soft X-ray test (EMT-F70, Softex Co., Ltd, Japan). The seed germination rate was measured using a thermal gradient plate (TGP, ONSOL Corp., Suwon, Korea). The TGP consisted of 60 compartments with individually controlled day and night temperature conditions. The day and night lengths were both fixed at 12 h. The day and night temperatures included 10- and 6-step gradational conditions with 3 °C intervals from 7 to 34 °C and 6 °C intervals from 5 to 35 °C, respectively. In total, 60 temperature combinations were implemented. The germination rate was observed until 22 days after sowing (DAS) (3 weeks). Over 40 seeds and 4 repeats were allocated per temperature condition, including temperatures below the experimental conditions for verification and validation.

Species-specific seed vigor test

Temperature data measured every hour were used in this study. Therefore, the day and night temperatures of each temperature condition were accumulated for 12 h per day. In the first step of the species-specific seed vigor test (SSVT), the effect of day and night temperatures on seed germination was evaluated by two-way analysis of variance (ANOVA). In the second step, the relationships between temperature and the germination rate were analyzed. Temperatures affecting or not affecting germination were distinguished by correlation analysis between the germination rate and cumulative hours at each temperature, and the directions of their effects, i.e., whether they were positive or negative, were investigated. In addition, to examine the effects of temperature on germination, the

standardized regression coefficient of each temperature condition was obtained by multiple linear regression analysis. In the third step of the SSVT, the cumulative score was calculated for each temperature. The largest standardized regression coefficient obtained in the previous step was set to 1, and the remaining values were converted into the ratios of the largest value. Therefore, the standardized regression coefficients, namely, the relative weights of the cumulative temperature effects on germination, were converted to a range with a maximum of 1. Nonlinear regression analysis was performed with the converted values, and the simplest equation, specifically, the one with statistical significance and an R^2 value greater than 0.9, was selected. The simplest form was selected for addition to the DB of seed vaults and seed banks. In the last (fourth) step, the temperature requirement for vigorous germination of *A. senescens* seeds was evaluated as the cumulative temperature score (TS) defined by the selected equation when the germination rate reached 85%. A germination rate of 85% is the standard rate used to evaluate seed vitality, as suggested by the Royal Botanic Gardens, Kew (Newton et al., 2009).

Verification and validation of the SSVT

For verification and validation of the SSVT, we simplified the temperature conditions irrespective of day or night. All compartments of the TGP were set at 20 °C until the first three DAS. Then, 7 gradational temperatures separated by 5 °C intervals from 5 to 35 °C were applied in accordance with each treatment. After 9 DAS, the temperature of all treatments was reset at 20 °C. Therefore, the temperature sets supplied to each treatment until 3 DAS, during 3-9 DAS and after 9 DAS were 20-5-20, 20-10-20, 20-15-20, 20-20-20, 20-25-20, 20-30-20 and 20-35-20 °C. These temperature sets were used to test the canceling effects of temperature accumulation and impact weight ratios on germination.

Verification and validation were performed from two main viewpoints. The first viewpoint was the property of ‘impact weight on germination’ being given to each temperature. To this end, the time it took to reach an 85% germination rate was compared with the ‘impact weight on germination’. The second was the accuracy of this property in predicting the temperature requirement of *A. senescens*. To this end, differences between the actual and predicted times required to reach germination rates of 25, 50 and 75% were evaluated. In addition, the predicted germination rates were compared with the actual values according to the elapsed time.

Regional temperature data and simulation of climate change

Hourly temperature data of the sampling area were collected. According to the Korea Biodiversity Information System (Korea National Arboretum, 2019), seeds of *A. senescens* are generally sown in late October and germinate in the spring of the following year. Thus, in this study, it was assumed that the seeds were sown in late October, and the temperature accumulation started on November 1. The temperature accumulation pattern was investigated by applying the equation developed as part of the SSVT to the hourly temperature data from 1999 to 2018 in Geumsan, Korea (N36.1056, E127.4817; Altitude 173 m). In addition, the time required to achieve vigorous seed germination was considered the time when the temperature requirement of *A. senescens* was fulfilled. To simulate climate change, the elevated temperature method applied by Park et al. (2018) was used. Temperature increases of 0.5 to 6.0 °C with a 0.5 °C interval were applied to the temperature data from 1999 to 2018.

Statistical analysis

For statistical analyses, SPSS 21 (SPSS Inc., Chicago, IL, USA) and the 'fRegression' package of the R program were used.

Results

Species-specific seed vigor test

In the first step of the SSVT, the effects of day and night temperatures on the germination rate were investigated by two-way ANOVA (*Table 1*). The germination rates were not influenced by day temperature, night temperature or their combination until 3 DAS because they remained at 0% during that period. In contrast, day temperature, night temperature and their combination began to elicit changes in germination rates 6 DAS. Thus, since the supplied temperatures affected the germination rate, regardless of whether they were supplied during day or night, the following steps of the SSVT focused on temperature itself without the separation of day and night.

Table 1. The *p*-values obtained from two-way ANOVA of the effects of day and night temperatures on the germination rate. The durations of both day and night were 12 h

Days after sowing	Temperature			N
	Day	Night	Day * Night	
3	-	-	-	480
6	0.000	0.000	0.000	480
9	0.000	0.000	0.000	480
12	0.000	0.000	0.000	480
15	0.000	0.000	0.000	480
19	0.000	0.000	0.000	480
22	0.000	0.000	0.000	480

In the second step, the relationship between the germination rate and temperature was investigated. In the correlation analysis results (*Table 2*), 29 °C was not related to the germination rate, but the remaining temperatures had an effect on the germination rate. Temperatures in the range of 10-28 °C increased the germination rate, but the low and high temperatures of 5, 7, 31, 34, and 35 °C reduced the germination rate by increasing the cumulative hours under those conditions. In the next step, the relative effect weights of temperatures except 29 °C on the germination rate were investigated by multiple regression analysis (*Table 2*). The standardized regression coefficient of each temperature indicates the relative weight of its effect on the germination rate. Based on the results, 19 °C had the largest effect weight, and the farther away the temperature was from 19 °C, the smaller the effect weight became. Additionally, the standardized coefficient of each temperature was converted to a ratio relative to 19 °C and combined with the effect direction, i.e., whether the effect on the germination rate was positive or negative, which was derived by correlation analysis.

Table 2. Correlation and multiple regression analyses between germination rates and the cumulative hours within the supplied temperatures. Correlation analysis was performed for all supplied temperatures. Temperatures confirmed to be not significant in the correlation analysis were not included in the multiple regression analysis. ‘Impact weight ratio’ was converted based on the largest absolute value of the standardized regression coefficients, specifically, that of 19 °C

Temperature (°C)	Correlation analysis	Multiple regression analysis	
	Correlation coefficient	Absolute value of the standardized regression coefficient	Impact weight ratio
5	-0.106**	0.092**	-0.22
7	-0.038**	0.116**	-0.27
10	0.043**	0.190**	0.45
11	0.107**	0.094**	0.22
13	0.103**	0.245**	0.58
16	0.194**	0.331**	0.78
17	0.473**	0.416**	0.99
19	0.293**	0.421**	1.00
22	0.258**	0.390**	0.92
23	0.420**	0.369**	0.88
25	0.124**	0.265**	0.63
28	0.080**	0.225**	0.53
29	-0.001 ^{ns}	-	0.00
31	-0.053**	0.101**	-0.24
34	-0.079**	0.077**	-0.18
35	-0.156**	0.137**	-0.32

Nonlinear regression analysis of these converted values was performed to estimate the effect of temperature, including the non-supplied temperature, on the germination rate (Fig. 1). When the temperatures with a 0.1 °C interval were substituted into the derived equation, the impact weight on germination was the highest for 18.9 °C and declined gradually for increasingly distant temperatures. The impact weights of 8.0 and 29.7 °C on germination were both 0.00, which indicated that those temperatures had no influence on the germination rate, and their contiguous temperatures also had little influence. In addition, temperatures below 8.0 °C and above 29.7 °C negated the temperature accumulation for germination because they were given a negative germination impact weight. These relationships between temperature and germination were consistent with the results of the analysis of the actual supplied temperatures (shown in Table 2).

Temperature requirement for vigorous germination based on the SSVT

The temperature requirement for vigorous seed germination of *A. senescens* was calculated by linear regression analysis between the germination rate and TS (Fig. 2). The TS was the hourly accumulated ‘impact weight on germination’. The temperature requirement of *A. senescens* was 294TS because the germination rate was above 85% when the TS was higher than 294.

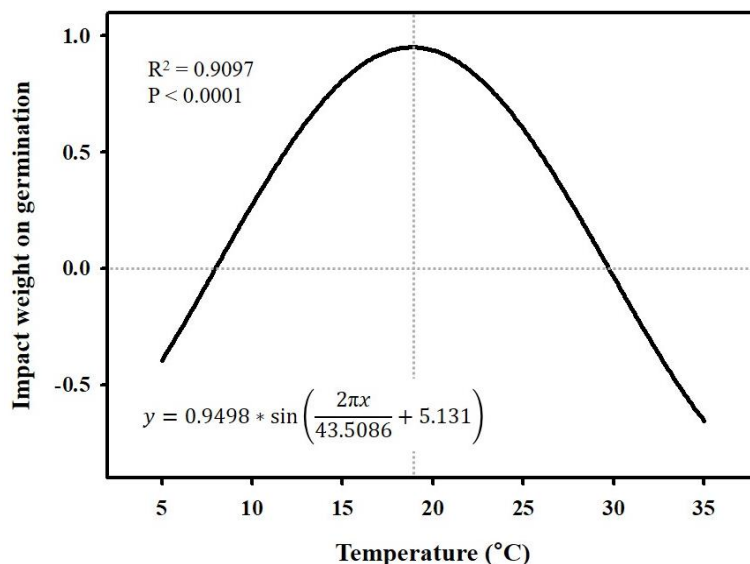


Figure 1. Regression curve of the impact weight on germination according to temperature. The curve was derived from the standardized regression coefficient ratios

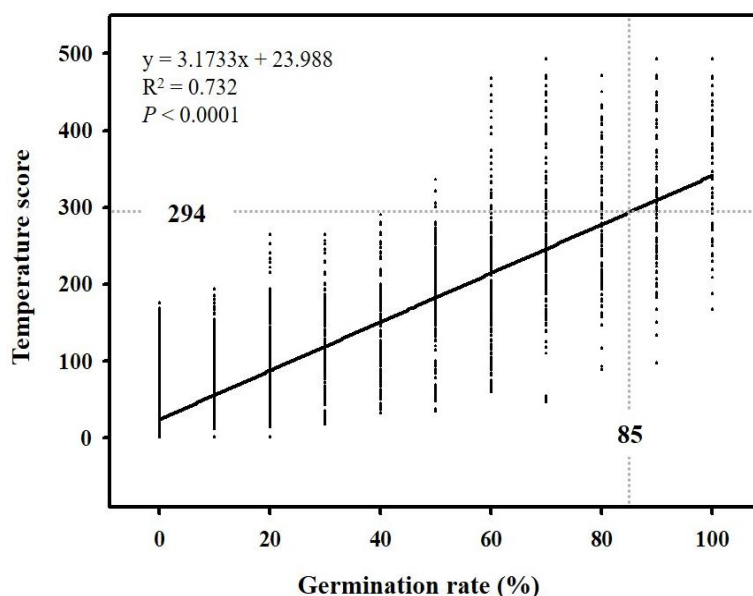


Figure 2. Linear regression analysis between the temperature score (TS) and germination rate. The TS is the accumulated value of the hourly temperature data according to the equation in Figure 1. A germination rate of 85% was the criterion used to evaluate seed vitality, as suggested by the Royal Botanic Gardens, Kew (Newton et al., 2009)

Verification and validation of the SSVT

A new germination test was performed to assess the validity of ‘impact weight on germination’ and the SSVT equation. To this end, the time required to reach an 85% germination rate in each temperature treatment was investigated (Fig. 3A). Since a higher ‘impact weight on germination’ induced earlier fulfillment of the temperature requirement, the time to reach 85% germination exhibited a hump-shaped relationship

with ‘impact weight on germination’. Germination in the 20 °C treatment, which was given the highest ‘impact weight on germination’, reached 85% at the earliest time, 15 DAS. The farther the temperature was from 20 °C, the more delayed the time to reach 85% germination became (in inverse proportion to the ‘impact weight on germination’). This pattern was especially pronounced in the 5, 30 and 35 °C treatments, which had negative ‘impact weight on germination’ values: the times to reach 85% germination were over 20 DAS and noticeably delayed compared to those of the other treatments. Thus, the ‘impact weight on germination’ metric and the equation established as part of the SSVT for comparing temperature treatments were effective.

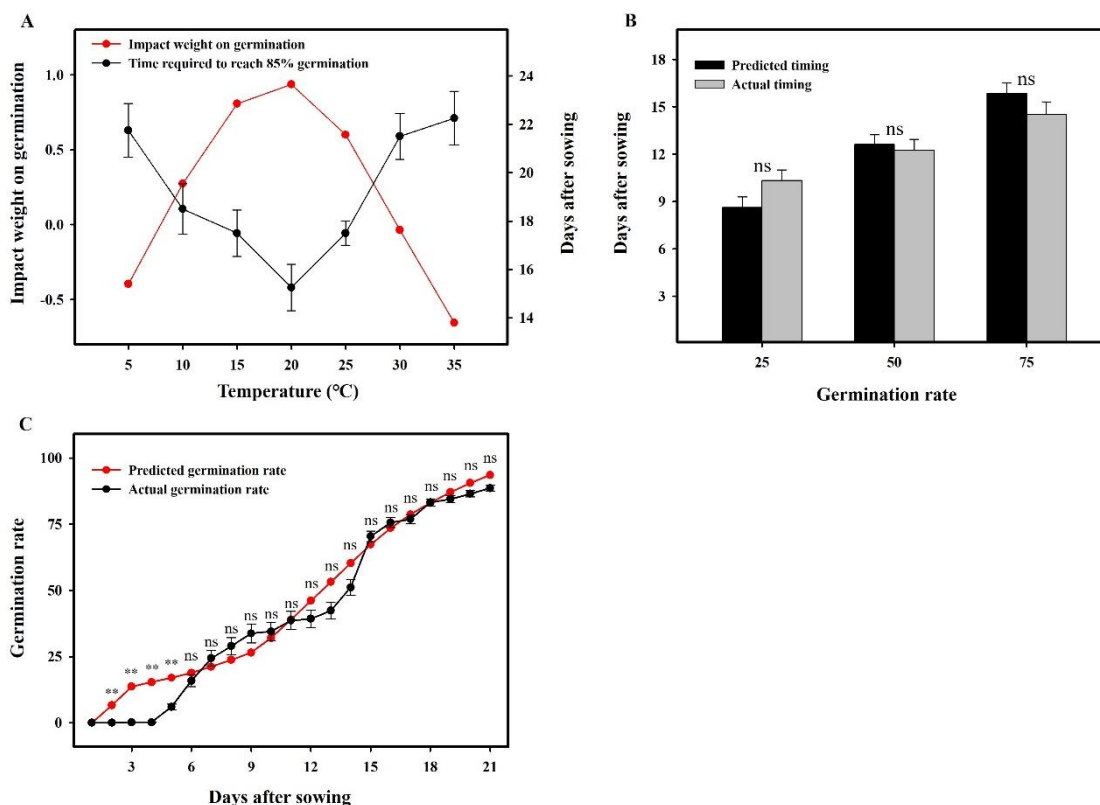


Figure 3. Verification and validation of the species-specific seed vigor test. (A) Impact weight on germination and the time required to reach 85% germination by temperature. In the germination test used for verification, temperatures on the X-axis were supplied to each treatment 3-9 days after sowing (DAS), and 20 °C was supplied before 3 and after 9 DAS. (B) The predicted and actual times required to reach 25, 50 and 75% germination. (C) The predicted and actual germination rates with increasing DAS

The adequacy of these methods for predicting the germination rate was also tested, which included validation of whether the temperature requirement of *A. senescens* for vigorous seed germination was correctly calculated. The predicted times to reach 25, 50 and 75% germination calculated by the regression between the TS and germination rate were compared to the actual measured times (Fig. 3B). The actual and predicted times to reach 25% germination were 10.3 and 8.6 DAS, respectively, differing by approximately 2 days. Discrepancies between the predicted and actual times were lowest at a 50% germination rate (0.4 days) and 75% germination rate (approximately

1 day). Consequently, the actual and predicted times to reach 25, 50 and 75% germination rates exhibited no significant differences, even though the largest discrepancy between them was approximately 2 days.

The predicted and actual changes in the germination rate with the elapse of DAS were also compared (Fig. 3C). The predicted germination rates until 5 DAS were higher than the actual values because the predicted germination rates estimated by linear regression increased from the beginning, while actual germination did not start until 3-4 DAS. Overall, the predicted and actual germination rate changes over time did not differ, except during the period before 5 DAS, even though the actual values fluctuated compared to the stable predicted line. The mean value of the difference between the predicted and actual values over the whole period was 5.4%, and the mean error after 6 DAS decreased to 4.2%. Thus, prediction of the germination rate by the SSVT equation and the temperature requirement of *A. senescens* was reliable with no significant error.

Regional adaptation under climate change

The temperature requirement and SSVT equation of *A. senescens* were applied to hourly temperature data from Geumsan, Chungcheongnam-do, in the 2017-2018 season (Fig. 4). Seeds sown in late October 2017 did not receive sufficient temperature accumulation for germination, namely, a TS, until March 10 of the following year (a period of more than 4 months). Since the mean temperature during the period was -0.3 °C, the nonaccumulation of the TS was likely due to the negating effect of the low-temperature part of the SSVT equation. As a result, seeds sown in late October 2017 began to undergo temperature accumulation on March 10 of the following year. On April 30, 2018, the accumulated TS reached 294TS, which indicated the time of vigorous seed germination. These results supported the ‘sowing in October and germination in spring of the following year’ specification in the Korea Biodiversity Information System (Korea National Arboretum, 2019).

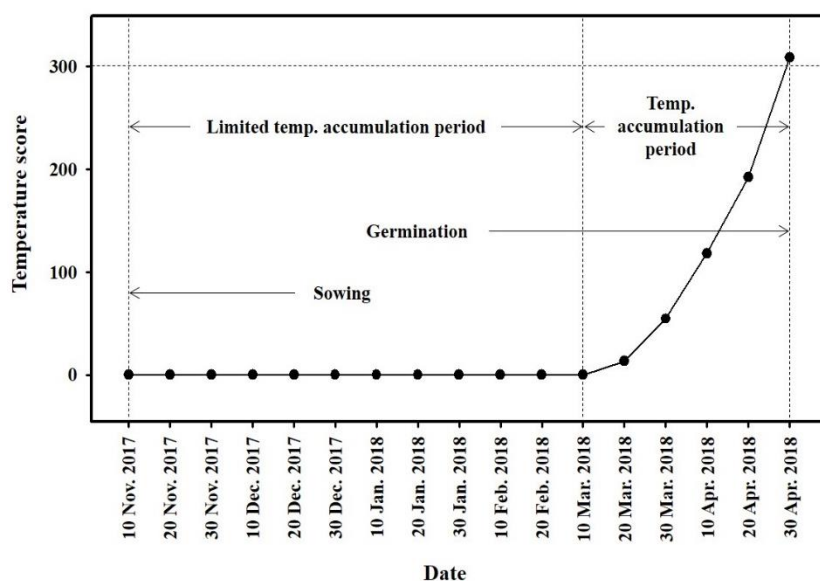


Figure 4. Temperature score accumulation patterns of *Allium senescens* L. seeds during the 2017-2018 season in Geumsan, Korea. It was assumed that seeds were sown in late October based on the Korea Biodiversity Information System (Korea National Arboretum, 2019)

The effect of climate change was estimated by hourly temperature data collected from 1999-2018 (Table 3). The mean date of germination in 1999-2018 was May 3, and the earliest date was April 23. The more elevated the temperature was, the more the predicted date of germination advanced. If the temperature was elevated by 6.0 °C, the germination date was predicted to be more than one and a half months earlier than at present. Based on the predicted earliest date, that germination date would move forward much more rapidly. The germination date, which is April 23 at present, gradually advanced with elevated temperature until the temperature was elevated by 2.0 °C. If the temperature was elevated by 2.5 °C, the germination date was predicted to be markedly advanced to November 23. These results indicate that seeds sown in October would germinate within one month in the same year without going through winter if the temperature was elevated by 2.5 °C or more.

Table 3. Predicted germination date of *Allium senescens* L. according to temperature elevation. The temperature elevations were applied to the hourly temperature data from Geumsan, Korea, collected in 1999-2018 by the method of Park et al. (2018)

Temperature elevation (°C)	Predicted germination date	
	Mean date	Earliest date
0.0	3 May ± 1.4	23 Apr.
0.5	1 May ± 1.5	21 Apr.
1.0	29 Apr. ± 1.5	18 Apr.
1.5	27 Apr. ± 1.5	16 Apr.
2.0	24 Apr. ± 1.5	14 Apr.
2.5	14 Apr. ± 8.1	23 Nov.
3.0	12 Apr. ± 8.0	21 Nov.
3.5	1 Apr. ± 10.9	19 Nov.
4.0	30 Mar. ± 10.7	19 Nov.
4.5	28 Mar. ± 10.6	18 Nov.
5.0	26 Mar. ± 10.5	18 Nov.
5.5	17 Mar. ± 12.0	17 Nov.
6.0	15 Mar. ± 11.8	17 Nov.

Discussion

Temperature is a dominant factor among the diverse environmental factors that affect the rate and velocity of germination (Bellairs and Bell, 1990; Cony and Trione, 1996). Since the rate and velocity of germination vary among not only species but also genotypes of the same species, many studies investigating the effect of temperature on germination have been performed on individual species or genotypes (Acharya et al., 1983). For example, in rapeseed (*Brassica napus* L.), cold-resistant varieties maintained high germination rates under low-temperature conditions, but the germination rates of cold-sensitive varieties were markedly reduced (Luo et al., 2018).

Base temperature (T_b) is an important factor in the relationship between seed germination and temperature. T_b is the lowest temperature threshold affecting seed germination, and the process of germination is controlled by the accumulation of temperature above T_b (Batlla and Benech-Arnold, 2015). Various models have been developed to investigate T_b (Dahal et al., 1990; Steinmaus et al., 2000; Tan et al., 2017),

and T_b can be set differently because calculation methods differ among models (Luo et al., 2018). These results suggest that the selection of a suitable model is required and that model fitting for the target species must be performed. The process examined in this study might be another useful method for investigating T_b . In the present study, the temperature corresponding to T_b was 8.0 °C, and germination was accelerated by the accumulation of temperature above 8.0 °C. In contrast, temperatures above 30 °C did not accelerate germination, which suggested that another T_b , representing the highest temperature threshold, was also required. The investigation of the upper and lower limits of T_b would enable the selection of effective temperatures for germination, which could be set to 8-30 °C.

The investigation of temperatures below T_b is also important. Seed germination is an essential stage that affects the maintenance of populations and regional adaptation for ecological restoration (Qiu et al., 2010). In actual field conditions, temperatures below T_b are common, in contrast to the constant or stable temperatures above T_b that are supplied in growth chambers. If T_b is applied at a lower threshold, then the temperatures below T_b are meaningless. In this study, in contrast, temperatures below T_b negated the effect of temperature accumulation on germination. These negating effects on temperature accumulation could be utilized during seed storage. When the accumulation of effective temperature leads to germination activation, the negating effect on temperature accumulation could be used to reverse the activated state back to the stable state. Many studies have reported that low temperatures limit the metabolic processes required for germination by controlling lipid and protein mobilization and enzyme activities (Nykiforuk and Johnson-Flanagan, 1994; Hoppe and Theimer, 1997).

In addition, the existence of optimal conditions for the acceleration of germination suggested that changes in the germination rate and velocity vary among temperature levels, even in the effective range (Luo et al., 2018). This variability in germination behavior among temperatures suggests that the timing of sowing must be flexible to accommodate the thermal conditions of the target area (King et al., 1986; Russo et al., 2010). In other words, the effect of ecological restoration could be maximized by sowing seeds at the optimal time, thereby minimizing the number of days to germination. The tool predicting germination in this study was ‘temperature requirement’, which was expressed as the TS. The TS represented the influence of a temperature regime on germination, and the ‘temperature requirement’ was the hourly accumulated value of the TS to a specific criterion. In this study, the TS accumulation criterion was 85%, which was chosen to add vigorous germination information to the seed storage DB. However, the germination rate criterion can be adjusted to calculate the temperature requirement. The objectives of this study were somewhat contradictory: to determine how to stabilize seeds for long-term storage and how to activate germination for restoration when needed.

Seed vigor information is only a small part of the seed storage DB, which includes diverse information, such as the weight and size of seeds, collection site and timing, and donating country or institution. Thus, we tried to input information that was simple but useful and diverse into the seed storage DB. The ‘impact weight on germination’ equation and ‘temperature requirement’ derived by the SSVT were entered into only two boxes in a small section of the seed storage DB. However, these conditions provide various types of information, such as the optimal and effective temperature ranges accelerating germination, the conditions that negate effective temperature accumulation and the time required to reach the ideal germination rate. Furthermore, this

formularization and quantification of the relationship between germination and temperature can be utilized in various ways. The estimation of the climate change effect performed in this study is only one example. Preferentially, ecosystem destruction and extinction should no longer occur. We anticipate that the results of this study on germination temperature and climate change effect estimation will be utilized as fundamental information in the preparation of stored seeds for restoration.

Conclusion

In this study, the effective or positive temperature range for germination of *A. senescens* was set, and the impact weight on germination by temperature levels was evaluated. Furthermore, the temperatures that negated the temperature accumulation for germination were verified. Since the SSVT equation was compared to the actual temperature data in the field, it was possible to predict the changes in germination timing. In general, temperate plants need to accumulate low-temperature effects to break their dormancy, and germination would begin only under this condition. Concretely, it was reported that seeds of *A. senescens* need a chilling period longer than 427 h at temperatures below 5 °C (Suh et al., 2005). Thus, it could be regarded that the changes in germination timing resulting from increased temperatures would occur for only the stored seeds in the low temperature range, as observed in this study. Self-sown seeds in the field may be more seriously affected by climate change than the seeds stored at low temperatures during certain periods. The period for vernalization by low-temperature accumulation required for dormancy release would be shortened due to the elevated temperature. If the chilling requirements of *A. senescens* are not fulfilled, the germination of seeds would become virtually impossible. These facts suggest that both temperature conditions for vernalization and germination must be considered together to more precisely predict the effects of climate change. In fact, the results of studies that examined both the chilling required for dormancy release and the temperature accumulation to germination are being reported on not only the seeds but also the buds of temperate plants (Park and Park, 2019).

Meanwhile, this study had modeling limitations that were aimed at seed storage and ecological restoration at the same time. If seed storage is then aim, further studies on actual storage conditions below 5 °C, which were examined in this study, should be performed. In contrast, if the final objective is ecological restoration, detailed habitat conditions such as soil characteristics and incline direction should also be considered.

Acknowledgements. We are very grateful to the Chungcheongnam-do Forest Environment Research Institute for providing seeds. This work was supported by a National Research Foundation of Korea (NRF) grant funded by the Korean government (MSIT) (No. NRF-2017R1D1A1B03034615).

REFERENCES

- [1] Acharya, S. N., Dueck, J., Downey, R. K. (1983): Selection and heritability studies on canola/rapeseed for low temperature germination. – Canadian Journal of Plant Science 63(2): 377-84.
- [2] Batlla, D., Benech-Arnold, R. L. (2015): A framework for the interpretation of temperature effects on dormancy and germination in seed populations showing dormancy. – Seed Science Research 25(2): 147-158.

- [3] Bellairs, S., Bell, D. T. (1990): Temperature effects on the seed-germination of 10 Kwongan species from Eneabba, Western-Australia. – Australian Journal of Botany 38(5): 451-458.
- [4] Broadhurst, L. M., Jones, T. A., Smith, F. S., North, T., Guja, L. (2015): Maximizing seed resources for restoration in an uncertain future. – BioScience 66(1): 73-79.
- [5] Choi, H.-Y., Kim, G.-H. (2014): Inhibitory effects of *Allium senescens* L. methanol extracts on reactive oxygen species production and lipid accumulation during differentiation in 3T3-L1 cells. – Korean Journal of Food Science and Technology 46(4): 498-504.
- [6] Chung, M.-S. (2010): Volatile compounds of the cultivated dumebuchu (*Allium senescens* L. var. *senescens*). – Food Science and Biotechnology 19(6): 1679-1682.
- [7] Chung, M. S., Lee, M. S. (2001): Chemical composition and texture of *Allium senescens*. – Journal of the Korean Society of Food Science 17: 60-64.
- [8] Cony, M., Trione, S. O. (1996): Germination with respect to temperature of two *Argentinian Prosopis* species. – Journal of Arid Environments 33: 225-236.
- [9] Dahal, P., Bradford, K. J., Jones, R. A. (1990): Effects of priming and endosperm integrity on seed germination rates of tomato genotypes: I. Germination at suboptimal temperature. – Journal of Experimental Botany 41(11): 1431-1439.
- [10] Hoppe, A., Theimer, R. R. (1997): Degradation of oil bodies isolated from cotyledons during germination of rapeseed seedlings. – Journal of Plant Physiology 151(4): 471-478.
- [11] King, J. R., Kondra, Z. P., Thiagarajah, M. R. (1986): Selection for fast germination in rapeseed (*Brassica napus* L. and *B. campestris* L.). – Euphytica 35(3): 835-842.
- [12] Korea National Arboretum (1997): Illustrated Rare and Endangered Species in Korea. – Korea National Arboretum, Seoul, Korea.
- [13] Korea National Arboretum (2019): Korea Biodiversity Information System. – <http://www.nature.go.kr/kbi/plant/pilbk/selectPlantPilbkDtl.do>.
- [14] Luo, T., Xian, M., Khan, M. N., Hu, L., Xu, Z. (2018): Estimation of base temperature for germination of rapeseed (*Brassica napus*) using different models. – International Journal of Agriculture and Biology 20(03): 524-530.
- [15] Marcos-Filho, J. (2015): Seed vigor testing: an overview of the past, present and future perspective. – Scientia Agricola 72: 363-374.
- [16] Newton, R., Hay, F., Probert, R. (2009): Protocol for Comparative Seed Longevity Testing. Technical Information Sheet 01. – Royal Botanic Gardens, Kew, London.
- [17] Nykiforuk, C. L., Johnson-Flanagan, A. M. (1994): Germination and early seedling development under low temperature in Canola. – Crop Science 34(4): 1047-1054.
- [18] Oh, M., Bae, S.-Y., Chung, M.-S. (2012): Volatile compounds of essential oils from *Allium senescens* L. var. *senescens*. – Korean Journal of Food and Cookery Science 28(2): 143-148.
- [19] Park, Y., Park, H.-S. (2019): Heat unit model for classifying the environmentally controlled period during ecodormancy. – Scientia Horticulturae 25: 6108536.
- [20] Park, Y., Lee, B., Park, H.-S. (2018): Predicted effects of climate change on winter chill accumulation by temperate trees in South Korea. – The Horticulture Journal 87(2): 166-173.
- [21] Qiu, J., Bai, Y., Fu, Y.-B., Wilmshurst, J. F. (2010): Spatial variation in temperature thresholds during seed germination of remnant *Festuca hallii* populations across the Canadian prairie. – Environmental and Experimental Botany 67(3): 479-486.
- [22] Russo, V. M., Bruton, B. D., Sams, C. E. (2010): Classification of temperature response in germination of *Brassicacae*. – Industrial Crops and Products 31(1): 48-51.
- [23] Steinmaus, S. J., Prather, T. S., Holt, J. S. (2000): Estimation of base temperatures for nine weed species. – Journal of Experimental Botany 51(343): 275-286.
- [24] Suh, J.-T., Hong, S.-Y., Yoo, D.-L., Ryu, S.-Y., Song, J.-S. (2005): Low temperature requirement hour for dormancy breaking of wild flowers in Highland, *Allium senescens*

- Lychnis cognata* and *Sedum kamtschaticum*. – Journal of the Korean Institute of Interior Landscape Architecture 7(1): 95-103.
- [25] Tan, M., Liao, F., Hou, L., Wang, J., Wei, L., Jian, H., Xu, X., Li, J., Liu, L. (2017): Genome-wide association analysis of seed germination percentage and germination index in *Brassica napus* L. under salt and drought stresses. – Euphytica 21: 340.
- [26] van der Valk, A. G., Bremholm, T. L., Gordon, E. (1999): The restoration of sedge meadows: seed viability, seed germination requirements, and seedling growth of *Carex* species. – Wetlands 19(4): 756-764.

URBANISATION PROCESSES IN PUSZCZA ZIELONKA LANDSCAPE PARK IN POLAND - AND ITS BUFFER ZONE IN THE CONTEXT OF PROTECTION OF NATURAL STRUCTURES

WILKANIEC, A.^{1*} – GAŁECKA-DROZDA, A.¹ – RASZEJA, E.² – SZCZEPAŃSKA, M.³

¹*Department of Landscape Architecture, Poznań University of Life Sciences
Dąbrowskiego 159, 60-594 Poznań, Poland
(e-mail: agnieszka.wilkaniec@up.poznan.pl; anna.galecka@up.poznan.pl)*

²*Department of Architecture and Urban Planning, Faculty of Architecture and Design,
University of the Arts in Poznań, 29 Aleje Marcinkowskiego, 60-967 Poznań, Poland
(e-mail: elzbieta.raszeja@uap.edu.pl)*

³*Faculty of Socio-Economic Geography and Spatial Management, Adam Mickiewicz
University in Poznań, Krygowskiego 10, 61-680 Poznań, Poland
(e-mail: szmagda@amu.edu.pl)*

**Corresponding author*

e-mail: agnieszka.wilkaniec@up.poznan.pl; phone: +48-618-487-990; fax: +48-618-487-959

(Received 12th Jun 2019; accepted 11th Oct 2019)

Abstract. Puszcza Zielonka Landscape Park (PZLP), located in western Poland is an area under the constant pressure of urbanization processes occurring in the zone of influence of the Poznań urban agglomeration. The park was established in 1993. The protected area is surrounded by built-up areas, which interrupt the continuity of wildlife corridors. The park and its buffer zone are located in six communes, which have their own spatial policies. The aim of the article was to determine changes in the trends, scale and rate of investments in the park and its buffer zone, expressed by changes in the land cover and use, which have taken place since the establishment of the park. These changes were considered important factors affecting the state of protected natural values and defining the effectiveness of protective instruments. The study included an analysis of the spatial policy of the communes expressed in Study of the Conditions and Directions of the Spatial Management (SCDSM) and its compliance with the Park protection trends indicated in the Protection Plan. The analyses were carried out with GIS tools. The results showed conflicts between the intended changes in land development expressed by local governments and the park protection objectives.

Keywords: *nature conservation, land use, cohesion policy, spatial planning, ecological network*

Introduction

According to the Nature Conservation Act (2004), a landscape park is a largescale form of nature conservation created for natural, historical, cultural and scenic values so as to preserve and popularise them with respect to sustainable development. 131 landscape parks have been established in Poland. They occupy a total area of about 2.61 million ha, i.e. 8.3% of the area of Poland and 2% of the protected area system. So far 13 landscape parks have been established in Greater Poland (Wielkopolska). They occupy a total area of 179,870.60 ha. A landscape park is a form of protection of natural and scenic values which does not involve restrictive protective provisions. Business activities are allowed in landscape parks and their buffer zones. They are only partly limited by specific regulations. This is in line with the concept of active protection, but simultaneously, it may cause different conflicts and threats. The continuous loss of

biodiversity and unfavourable changes in the natural environment, which are globally observed, are mostly caused by human activities such as intensive agricultural production, urbanization and infrastructure development, which lead to overexploitation of natural resources and degradation of the environment. These problems also affect particularly valuable areas, including protected areas. The need to combine the objectives of nature conservation and environment protection with the objectives resulting from the need for socioeconomic development and the needs of local communities is a significant challenge all over the world (Dimitrakopoulos et al., 2010; Bicknell et al., 2017; Lopez-Bao et al., 2017; Weaver and Lawton, 2017; Atmis, 2018).

Urbanization is thought to be the second (after agricultural production) most unfavourable factor exerting pressure on natural ecosystems, but it has the most degrading and the longest-lasting effects (Treby and Castley, 2016). It may cause the loss, fragmentation or isolation of valuable ecosystems (including forests) (Bradshaw, 2012) and the declining ecological stability (Muchová and Tárniková, 2018) the loss of open spaces (including agricultural areas) as well as increased environmental pollution, especially water (Maheshwari and Bristow, 2016), air and soil (Zhang, 2016). It may also limit biodiversity, threatening numerous species of plants and animals (Hamer and McDonnell, 2008; Border et al., 2017). The dynamic development of cities increases the urbanisation pressure exerted on protected areas (McDonald et al., 2009).

Changes induced by urbanization and manifested by the development of buildings in Puszcza Zielonka Landscape Park, located in Greater Poland (Wielkopolska) near the city of Poznań and, above all, in its buffer zone were the subject of research presented in this article. These changes are considered a significant factor affecting the state of protected natural values and determining the effectiveness of protective instruments, especially those related with spatial planning. The aim of the original research was to determine changes in the trends, scale and rate of investments in the park and its buffer zone, expressed by changes in the land cover and use, which have taken place since the establishment of the park. The study included an analysis of the spatial policy of the communes expressed in Study of the Conditions and Directions of the Spatial Management of a Commune (hereinafter SCDSM) and its compliance with the Park protection trends indicated in the Protection Plan.

Study area and methods

Puszcza Zielonka Landscape Park, established in 1993, hereinafter referred to as PZLP, is located about 30 km northeast of the city of Poznań (*Fig. 1*). There is about 120.4 km² of protected area, which is mostly covered by forests. There are a few villages and hamlets located within the boundaries of PZLP (Kamińsko, Pławno, Tuczno, Zielonka, Głębozec, Łopuchówko, Gać, Dzwonowo, Dąbrówka Kościelna). Apart from buildings, there are some small meadows, wastelands and cultivated lands in these places. The terrain also includes numerous ribbon lakes, which make the park particularly attractive to tourists. There are often recreational buildings near the lakes. They are mostly concentrated on Lake Kołatkowskie and Lake Tuczno in the village of Tuczno, and on Lake Miejskie in the village of Kamińsko.

The park is surrounded by a buffer zone, which occupies an area of about 97.8 km². The buffer zone terrain mostly includes arable lands, enclosures and suburban single-family buildings. The biggest settlements located in the PZLP buffer zone are: Kicin, Owińska, Bolechówko, Rakownia and Boduszewo.

The park area is located in the communes of Czerwonak, Skoki, Murowana Goślina, Kiszkowo, and Pobiedziska (part of the buffer zone is also located in the commune of Swarzędz) and in the counties of Poznań, Wągrowiec and Gniezno. The largest part of PZLP is located in the commune of Murowana Goślina and occupies an area of nearly 6,200 ha. The smallest part of the park is located in the commune of Kiszkowo, with about 360 ha of protected areas. More than a half of the buffer zone area is located in the communes of Czerwonak and Pobiedziska (2,870 ha and 2,500 ha, respectively). The smallest part of the buffer zone area is in the commune of Skoki – 870 ha (the author's calculation).

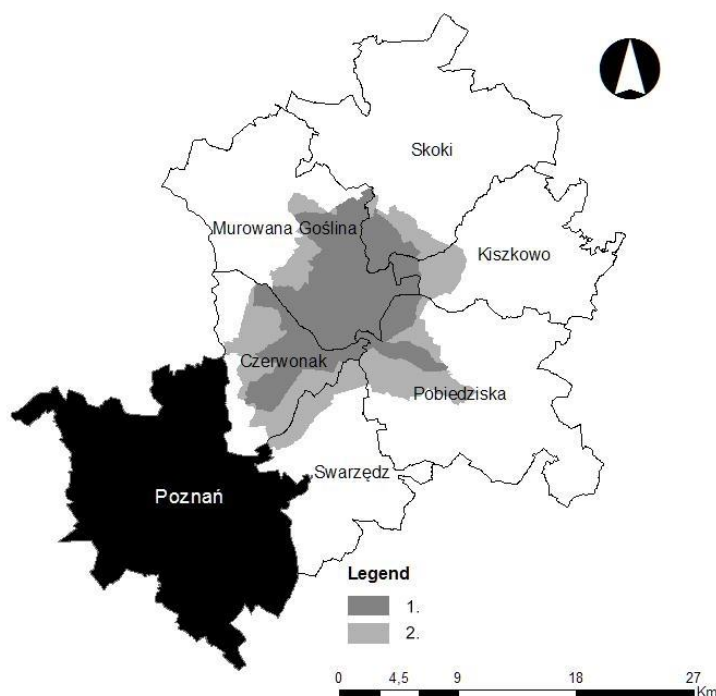


Figure 1. The administrative location of Puszcza Zielonka Landscape Park with its buffer zone: 1. Puszcza Zielonka Landscape Park, 2. The buffer zone of Puszcza Zielonka Landscape Park

The ArcGIS 10.5.1 version was used to investigate changes in the terrain occupied by the park and buffer zone. The rate and scale of transformations was observed at three chosen moments: first – in the past (1989); second – the current state (2017) and third – in the future, showing the changes predicted on the basis of planning documents. The first interval refers to the period before 1993, when the park was established. Data for this period were obtained by the digitalization of archival topographic maps scaled 1:25,000, which were imported by the WMS service. The maps were made between 1962 and 1989. Presented maps and data show distribution of the different land use types. We assumed a small scale of changes that took place at that time due to investment limitations before the transformation of the political system in Poland in 1989. The second time interval covers the changes which have taken place since the park was established and which were registered on the basis of current (2017) orthophoto maps (geoportal.gov.pl). Presented data and maps show distribution of the different land use types in about 2017 year. Next, the Study of the Conditions and

Directions of the Spatial Management of individual communes located in the Park and its buffer zone were studied to make a forecast of possible changes in the land cover and use. Local Spatial Management Plans were not taken into account due to the fact that these documents covered only a small part of the area under study.

As there were different thematic layers in the SCDSM of individual communes, it was necessary to simplify the provisions in them and adapt them to the terrain typology assumed in this article so as to identify and make a synthetic record of changes. The following 9 types of land cover were distinguished: (1) forests, (2) trees (mid-field afforestations, wastelands overgrown with trees, lanes of trees along watercourses), (3) surface waters, (4) meadows and pastures, (5) arable land, (6) permanent crops, (7) residential, recreational and service buildings, (8) storage and industrial areas, (9) roads. Then, the area was measured according to the aforementioned typology, allowing for the assumed research periods. The rate of dynamics of variation in the land cover was calculated according to the following formula developed by the authors (Gałęcka-Drozda et al., 2019), where the data for 1989 were assumed as the starting point (Eq. 1).

$$R_{dvlc} = \left(\frac{Ca \text{ or } Fa}{Ia} * 100\% \right) - 100\% \quad (\text{Eq.1})$$

where:

Rdvlc – the rate of dynamics of variation in the land cover [%];

Ca – the current area [ha] (data from 2017);

Fa – the forecast area [ha] (based on Studies of Conditions and Directions of the Spatial Management);

Ia – the input area [ha] (areas used as reference for other periods under analysis, data from 1989).

The results of investigations made at the three time intervals were presented in a standardised graphic form, which enabled a comparison of changes in the land cover and use during the entire research period. Changes in the park and its buffer zone were analysed separately. The research also included a comparative analysis of the spatial policies in individual communes based on the provisions included in SCDSM. Next, the provisions were compared with the recommendations included in the PZLP Protection Plan.

Content of Puszcza Zielonka Landscape Park Protection Plan

Following Art. 19 Para. 6 of the Nature Conservation Act of 16 April 2004 and in order to stop unfavourable processes occurring in PZLP the Park authorities prepared the Park Protection Plan (Puszcza Zielonka Landscape Park Protection Plan, 2005). 8 functional and landscape zones were identified in PZLP and its buffer zone. Orders and prohibitions regarding the conservation of resources were formulated for 5 zones, located within the Park. Recommendations concerning the economic use and space management were made for 3 zones located in the buffer zone.

Tasks, orders and prohibitions were formulated within the zones. Their aim was to conserve nature and protect landscape, allowing for sustainable development, without complete exclusion of business activity from the PZLP area. Recommendations related to the functioning of the zones should be transferred to the planning documents of municipalities in the Park. The protection plan included 37 arrangements concerning the elimination or limitation of external threats, which were included in the study of the

conditions and directions of the spatial management in communes, local spatial management plans and the voivodeship spatial development plan. Most provisions in the Park Protection Plan concern the limitation of urbanization pressure in PZLP and its buffer zone, for example by leaving undeveloped strips of land along the forest border and lake shores, by avoiding the scattering of buildings and locating them in areas without the infrastructure, by not separating new building plots in particularly valuable areas, including river valleys.

Results

Analysis of spatial policy of communes based on Study of the Conditions and Directions of the Spatial Management

The SCDSM of the communes located in PZLP and its buffer zone include declarations to protect the values due to which the park was established. However, the main goals of the spatial policy of communes are not always consistent with the objectives of PZLP protection, although all the SCDSM that were made after the Park Protection Plan refer to these documents. The functional and spatial zones and recommendations for them were transferred directly from the Park Protection Plan to the SCDSM of Murowana Goślina, Skoki and Swarzędz. The plans also include provisions which are beneficial to the Park protection. These provisions recommend the concentration rather than dispersion of buildings (Study of the Conditions and Directions of the Spatial Management of the Commune of Pobiedziska, 2011; Study of the Conditions and Directions of the Spatial Management of the Commune of Kiszkowo, 2012; Study of the Conditions and Directions of the Spatial Management of the Commune of Murowana Goślina, 2012), their location in places with adequate infrastructure (Study of the Conditions and Directions of the Spatial Management of the Commune of Pobiedziska, 2011), the will to inhibit space and environment degradation caused by uncontrolled development of holiday and residential buildings (Study of the Conditions and Directions of the Spatial Management of the Commune of Murowana Goślina, 2012). However, this did not prevent the provisions which allowed enlargement of built-up areas in the Park and the buffer zone. These areas became larger in all of the aforementioned communes, but to a different extent. In some communes the enlargement of built-up areas written in the SCDSM was moderate in relation to the areas belonging to the Park, whereas intensive building development was planned in areas of lower natural and scenic value, e.g. in the communes of Skoki, Swarzędz, and Czerwonak (including the repealed SCDSM of the Spatial Management (2010)).

During the period under study the commune of Czerwonak used the SCDSM adopted in 2000 and 2010 (Study of the Conditions and Directions of the Spatial Management of the Commune of Czerwonak, 2000, 2010). However, the sentence passed by the Provincial Administrative Court in Poznań in 2014 annulled the resolution concerning the newer variant of the document with more beneficial provisions referring to the protection of natural values in PZLP (Study of the Conditions and Directions of the Spatial Management of the Commune of Czerwonak, 2000, 2010).

Analysis of changes in land cover in Park and its buffer zone

At present more than 85% of the Puszcza Zielonka Landscape Park area is covered by forests (*Table 1*).

Table 1. Variation of the land cover structure in the area of Puszcza Zielonka Landscape Park and its buffer zone

Type of land cover	1989 [ha]*	Share [%]	2017 [ha]	Share [%]	Indicator of dynamics of changes in land cover 1989-2017 [%]	Forecast based on Studies of the Conditions and Directions of the Spatial Management [ha]	Share [%]	Indicator of dynamics of predicted changes in land cover [%]
PZLP								
Forests	10,103.09	83.94	10,316.08	85.71	2.11	10,332.79	85.85	2.27
Areas with trees	7.38	0.06	7.38	0.06	0.00	6.79	0.06	-7.99
Surface waters	356.07	2.96	356.07	2.96	0.00	356.07	2.96	0.00
Meadows and pastures	673.98	5.60	540.33	4.49	-19.83	443.88	3.69	-34.14
Arable land	769.8	6.40	618.6	5.14	-19.64	479.83	3.99	-37.67
Areas with permanent crops	23.37	0.19	26.9	0.22	15.10	24.63	0.20	5.39
Areas with residential buildings and services	94.89	0.79	162.45	1.35	71.20	383.82	3.19	304.49
Storage and industrial areas	4.07	0.03	4.84	0.04	18.92	4.84	0.04	18.92
Roads	3.56	0.03%	3.56	0.03	0.00	3.56	0.03	0.00
Total	12036.21	100.00	12,036.21	100.00	-	12,036.21	100.00	-
Buffer zone								
Forests	2,140.07	21.87	2,397.43	24.50	12.03	2427.9	24.79	13.45
Areas with trees	67.06	0.69	71.18	0.73	6.14	100.59	1.03	50.00
Surface waters	137.43	1.40	137.43	1.40	0.00	136.43	1.39	-0.73
Meadows and pastures	922.34	9.43	1711.44	17.49	85.55	873.12	8.91	-5.34
Arable land	6,230.84	63.68	4,937.32	50.46	-20.76	3678.83	37.56	-40.96
Areas with permanent crops	43.79	0.45	46.9	0.48	7.10	19.65	0.20	-55.13
Areas with residential buildings and services	198.36	2.03	428.5	4.38	116.02	2454.73	25.06	1137.51
Storage and industrial areas	18.69	0.19	28.38	0.29	51.85	77.24	0.79	313.27
Roads	25.54	0.26	25.54	0.26	0.00	25.54	0.26	0.00
Total	9,784.12	100.00	9,784.12	100.00	-	9,794.03	100.00	-

* initial state – areas used as reference for other periods under analysis

Meadows, pastures and arable lands cover about 5% of the Park area. The share of built-up areas is small – 1.35% of the Park area, i.e. 162.5 ha. The comparison of the current state with the state before 1989 revealed slight changes. The forest area

increased by over 200 ha (less than 2% of the total PZLP area), whereas the farmland area decreased (the area of meadows and pastures decreased by about 130 ha, whereas the area of plantations decreased by about 150 ha). At the same time, the built-up area increased by 68 ha (from 0.8% to 1.35% of the total area of the Park).

As results from the SCDSM of the communes belonging to the Park, the forest area will increase slightly, i.e. by about 16 ha, whereas the total farmland area may decrease by about 240 ha. The built-up area will increase by 221.4 ha (from 1.35% to 3.19% of the total PZLP area). The area of new buildings will significantly exceed the area that is currently occupied by buildings (*Fig. 2*). The areas of new investments are concentrated in Dąbrówka Kościelna (the commune of Kiszkowo) and in Tucznio (the commune of Pobiedziska). The areas of other building investments are scattered around the existing villages and hamlets in the Park.

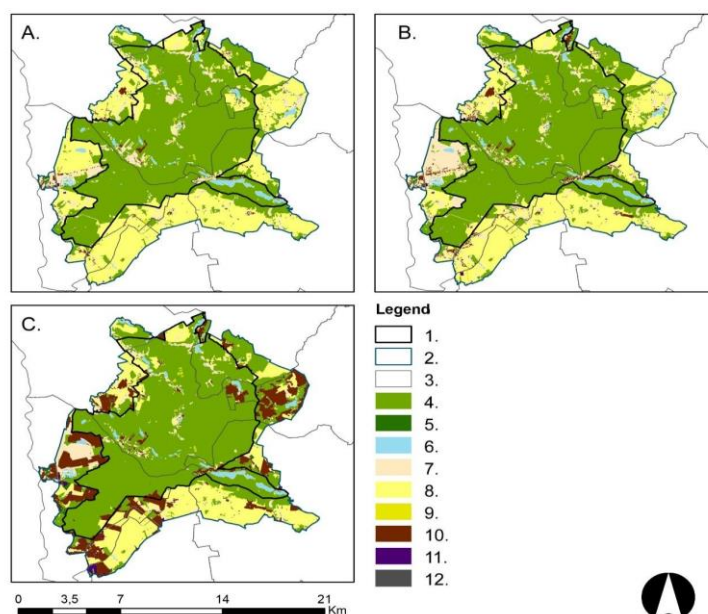


Figure 2. Changes in the land cover of Puszcza Zielonka Landscape Park and its buffer zone (A. Before 1989, B. Current state 2017; C. Forecast based on the Study of the Conditions and Directions of the Spatial Management; 1. Puszcza Zielonka Landscape Park, 2. Puszcza Zielonka Landscape Park buffer zone, 3. Commune boundaries, 4. Forests, 5. Trees, 6. Surface waters, 7. Meadows and pastures, 8. Arable land, 9. Permanent crops, 10. Residential, recreational and service buildings, 11. Storage and industrial areas, 12. roads)

At present the Park buffer zone is agricultural, as plantations, meadows and pastures occupy almost 70% of the area. The share of forests amounts to 25%. Built-up areas occupy about 430 ha, i.e. about 4.4% of the land cover. Since the end of the 1980s the area of arable land has decreased by almost 1,300 ha. It was mostly transformed into meadows and pastures, the area of which has increased by almost 790 ha. These changes resulted from the progressive fallowing of arable land, which is a common phenomenon in areas under high investment pressure. The forest cover in the buffer zone has increased by nearly 260 ha (from about 22% to 25% of the total area). The share of built-up areas has increased by more than two times (by 230 ha, from 2% to 4.4% of the total area). According to the SCDSM, the area occupied by residential, recreational and service buildings may increase. It may ultimately cover 25% of the

buffer zone, having increased by almost six times (by 2,026.23 ha). New building investments are planned in farmlands. The share of farmlands may decrease from 50.5% to 37.5% of the total buffer zone area, whereas the share of meadows and pastures may decrease from 17.5% to 9%.

Residential, recreational and service development was the main focus of the analysis of changes in the use of space in the Park and its buffer zone in individual communes (Table 2). The greatest changes were observed or forecasted in these types of land cover. Differences in the farmland area were also significant, but they were closely related to changes in built-up areas, so they were not described in detail.

Table 2. Changes in the area of residential, recreational and service developments in PZLP and its buffer zone in individual communes

Commune	PZLP area in commune [ha]	1989 [ha]*	Share [%]	2017 [ha]	Share [%]	Indicator of dynamics of changes in land cover 1989-2017 [%]	Forecast based on Study of the Conditions and Directions of the Spatial Management [ha]	Share [%]	Indicator of dynamics of predicted changes in land cover [%]
Czerwonak	2849.65	5.07	0.18	13.16	0.46	159.57	82.67	2.90	1530.57
Murowana Goślina	6199.33	59.43	0.96	89.51	1.44	50.61	111.25	1.79	87.20
Pobiedziska	1527.72	21.80	1.43	48.35	3.16	121.79	69.91	4.58	220.69
Swarzędz	-	-	-	-	-	-	-	-	-
Skoki	1098.01	3.55	0.32	3.55	0.32	0.00	12.14	1.11	241.97
Kiszkowo	361.49	5.04	1.39	7.87	2.18	56.15	107.85	29.83	2039.88
Commune	PZLP buffer zone area in commune [ha]	1989 [ha]*	Share [%]	2017 [ha]	Share [%]	Indicator of dynamics of changes in land cover 1989-2017 [%]	Forecast based on Study of the Conditions and Directions of the Spatial Management [ha]	Share [%]	Indicator of dynamics of predicted changes in land cover [%]
Czerwonak	2869.96	84.24	2.94	192.01	6.69	127.93	1169.13	40.74	1287.86
Murowana Goślina	1172.54	47.33	4.04	90.17	7.69	90.51	232.24	19.81	390.68
Pobiedziska	2488.35	29.43	1.18	69.64	2.80	136.63	232.80	9.36	691.03
Swarzędz	1358.12	8.85	0.65	11.79	0.87	33.22	171.90	12.66	1842.37
Skoki	873.31	12.46	1.43	38.55	4.41	209.39	104.00	11.91	734.67
Kiszkowo	1062.64	16.03	1.51	26.34	2.48	64.32	544.66	51.26	3297.75

* initial state – areas used as reference for other periods under analysis

The distribution of changes in the land cover (mostly the enlargement of developed areas) in individual communes in PZLP and its buffer zone was uneven. Since the late 1980s the most buildings have appeared in the communes of Poznań County: Murowana Goślina (increase by 30 ha), Pobiedziska (increase by 26.5 ha) and Czerwonak (increase by 8 ha). The analysis of changes in relation to the area of communes located in the Park shows that they were the least favourable in Pobiedziska, where 1.74% of the commune area belonging to the park was occupied by new buildings. In the communes of Murowana Goślina and Czerwonak the areas belonging to the park and occupied by new buildings amounted to 0.49% and 0.28%, respectively.

In the commune of Kiszkowo the areas with investments increased only by 3 ha. There was no change in the commune of Skoki. The increase in built-up areas in particular communes was correlated with their location in relation to Poznań. The changes were the smallest in the communes which were the most distant from the city limits.

According to the SCDSM, the biggest changes in built-up areas located in the Park can be expected in the commune of Kiszkowo, where the area of new investments may increase by nearly 100 ha, i.e. by about 45% of all newly built-up areas in PZLP. It is a very high increase because the area occupied by the Park in this commune is the smallest (almost a third of this area may be developed). According to the SCDSM of the Commune of Kiszkowo, large areas will be used for housing development and some areas will be used for tourist and recreational development. The development area in the commune of Czerwonak may increase by almost 70 ha (in comparison with Kiszkowo it is a slight increase, i.e. a fortieth of the commune area located in the Park). Also, according to the SCDSM of this commune, large areas were allocated for the development of 'tourist services' (understood as tourist and recreational services), but only some of them can be used for building development, including recreational buildings. The potential increase in the area of investments in the Park located in the communes of Murowana Goślina and Pobiedziska is very similar, i.e. over 21 ha. However, as far as the area of communes located in PZLP is concerned, the situation is much better in the commune of Murowana Goślina, where new developments may occupy 1/285 of the commune area belonging to the Park, whereas in the commune of Pobiedziska it will be a 1/17 of the Park area. The smallest increase in the area of new developments can be expected in the commune of Skoki, i.e. about 8.5 ha, which is 1/127 of the Park area. (Fig. 2).

The distribution of changes in individual communes in the Park buffer zone was different than in PZLP. Between 1989 and 2017 the largest amount of new developments was observed in the commune of Czerwonak (more than 100 ha), which was under the greatest influence of Poznań, and in the commune of Murowana Goślina (about 43 ha). In both communes it was an increase of about 3.7% of the area located in the buffer zone. In the commune of Skoki the increase amounted to about 3% (the area of new developments increased by 26 ha). Surprisingly, during the period under analysis the smallest amount of building developments in the Park buffer zone was observed in the commune of Swarzędz (only 3 ha), which is also strongly influenced by Poznań. The analysis of SCDSM of the commune showed that the potential areas of building developments were planned at other locations.

The greatest changes in the area of building developments in the Park buffer zone are forecasted in the commune of Czerwonak, where according to the SCDSM, almost 1,000 ha of new investments can be expected, which amounts to more than 48% of all new development areas in PZLP and nearly a third of the commune area in the Park buffer zone. In view of the Park protection aims, the provisions of the SCDSM of the Commune of Kiszkowo are the least favourable, where the increase in the area of new buildings concerns almost half of this area (about 540 ha). The potential increase in building development areas in the communes of Murowana Goślina, Pobiedziska and Swarzędz is very similar and amounts to 142, 163 and 160 ha, respectively. The Park buffer zone located in the communes of Murowana Goślina and Swarzędz occupies about a seventh of their areas, whereas in the commune of Pobiedziska it is a fifteenth of the area. The increase in development areas was the smallest in the buffer zone

located in the commune of Skoki (similar to that for the PZLP area) and amounted to 65 ha, i.e. about a thirteenth of the commune area being the buffer zone of the Park.

Discussion

The rapid global urban development decreases the distance between urban and protected areas. McDonald et al. (2009) proved that in many regions it was shorter than 50 km, so urban areas may significantly affect protected areas. Intensified urbanization is also noticeable in PZLP and the Park buffer zone, which are located closest to the city limits of Poznań. Agricultural landscape still prevails in the northeast of the Park buffer zone. On the other hand, urbanization is the strongest in the southern and western parts of the Park buffer zone, where it is manifested by progressive increase in built-up areas, as compared with the time when the Park was established, and its further development, as provided in the SCDSM.

The administrative conditions of the Park and its buffer zone do not favour the protection of natural and scenic values. This space is managed by six communes which implement their own spatial policies with different assumptions. Although they undertake many joint activities in the fields of tourism and water and wastewater management and they cooperate within the Puszcza Zielonka Intercommunal Union, but the planning activities of individual communes are not coordinated. In practice, the declared intentions to protect natural values turn out to be in opposition to specific provisions of SCDSM of these communes. In consequence, it may increase urbanization in the Park and its buffer zone, even in the zones that were designated in the Park Protection Plan for protection against urbanization pressure. From the point of view of the goals of PZLP protection, the commune of Murowana Goślina as well as the communes of Skoki, Pobiedziska and Czerwonak have the most favourable spatial policies concerning construction areas. The scale of the growth of new buildings in the commune of Kiszkowo is incomparable with other communes and it is inconsistent with the assumptions of PZLP protection.

On the other hand, the most favourable spatial policy of protection of the Park buffer zone is led by the communes of Pobiedziska, Skoki, Swarzędz and Murowana Goślina. According to the SCDSM, the largest increase in new building developments can be expected in the communes of Kiszkowo and Czerwonak. Geldmann et al. (2015) stressed the importance of monitoring the management of protected areas. The assessment of the effectiveness of protective activities enables evaluation of the strengths and weaknesses of this process and helps to improve it. It also applies to conservation activities implemented at the lowest communal level of spatial planning in Poland.

The creation of buffer zones is a commonly used method to protect valuable natural areas. Studies conducted by Lima and Ranieri (2018) in Brazil showed that protection plans usually set recommendations rather than detailed rules for the use of buffer zone resources. Apart from that, individual SCDSM were inconsistent as regards spatial development in buffer zones around protected areas. The results of this study indicate that the use of a buffer zone as an effective strategy of management of protected areas requires detailed arrangements between the managements of protected areas and local governments responsible for land use planning. Otherwise, the establishment of a buffer zone can only be a symbolic action, without any practical influence on the preservation of values and the functioning of the protected area.

The author's original research led to the conclusion that the presence of the PZLP buffer zone did not always isolate the Park from unfavourable spatial phenomena because the spatial policies of individual communes located in PZLP and its buffer zone were not always consistent with the Park protection goals. It is particularly worrying that according to the SCDSM, the commune governments have allocated such a large area of protected land for building developments. Different approaches of the communes to the spatial policy concerning valuable natural areas might indicate that not all local governments are aware of the significance of the existing values and the consequences of their loss. It is beneficial for the Park protection that according to the Studies of the Conditions and Directions of the Spatial Management (e.g. of Czerwonak (2010), Swarzędz (2011), Skoki (2010)), the local governments have allocated urbanized zones or strips for building developments outside the protected area and its buffer zone, in other parts of the communes. A similar solution was used in SCDSM of the commune of Pobiedziska (2011). However, a significant increase in housing and recreational investments in the Park and its buffer zone shows that the commune authorities have not been consistent in the implementation of this goal. Urbanization pressure is a commonly observed phenomenon also in other protected area in Poland (Wycichowska, 2008; Warczewska and Mastalarska-Cetera, 2011; Krajewski, 2014). Grochowska (2015) noted in Walbrzych Sudets Landscape Park the dispersion of buildings beyond shaped settlement systems and investment pressure directed at the most attractive landscapes and the expansion of summer construction, which is a result of improperly conducted municipal spatial policy.

As results from the SCDSM of Czerwonak, the situation is not good for the Park protection. In 2010, the authorities attempted to adopt a new Study. However, the sentence passed by the Provincial Administrative Court in Poznań in 2014 annulled the resolution of the Commune Council. In the new version of the document, the area of building developments was smaller than in the previous version, especially in the 'Forest Strip' and 'Open Landscape Strip', which covered the area of PZLP and its buffer zone. In contrast to the previous version of the SCDSM, according to the new version, one of the landowners was deprived of the right to build up plots in the village of Annowo, so he decided to go to court. The aforementioned areas were found to have natural and scenic values and were to be protected as the Annowo Meadows Protected Landscape Area. The sentence passed by the Provincial Administrative Court in Poznań in 2013 annulled also the resolution of the Commune Council in the matter of Annowo Meadows Protected Landscape Area creation, passed in 2008 (Environmental Protection Plan, 2013).

It is important not only to protect the Park area, but also to develop its connections with neighbouring valuable natural and protected areas such as: Promno Landscape Park, Natura 2000 areas (the Mała Wełna River Valley near Kiszkowo PLB300006, Biedrusko PLH300001, Kiszkowo Ponds PLH30_27, Biedrusko PLH300001), Biedrusko Protected Landscape Area, Lednica Landscape Park. The development of an ecological network combining valuable habitats into a system and preventing their fragmentation is considered to be one of the essential and most effective ways to protect biodiversity and preserve the stability of ecosystems (Closset-Kopp et al., 2016; Gonzalez et al., 2017; Fardila et al., 2017; Yang et al., 2017; Fletcher et al., 2018). One of the trends in nature conservation is to develop large-scale spatial systems consisting of protected areas, which are supplemented and connected by surrounding areas (Shwartz et al., 2017). The isolation of protected areas from their surroundings by

building developments, which may destroy the existing links with neighbouring valuable natural areas and prevent the creation of such links in the future, is a negative effect of the urbanization of the areas surrounding PZLP (Fig. 3).

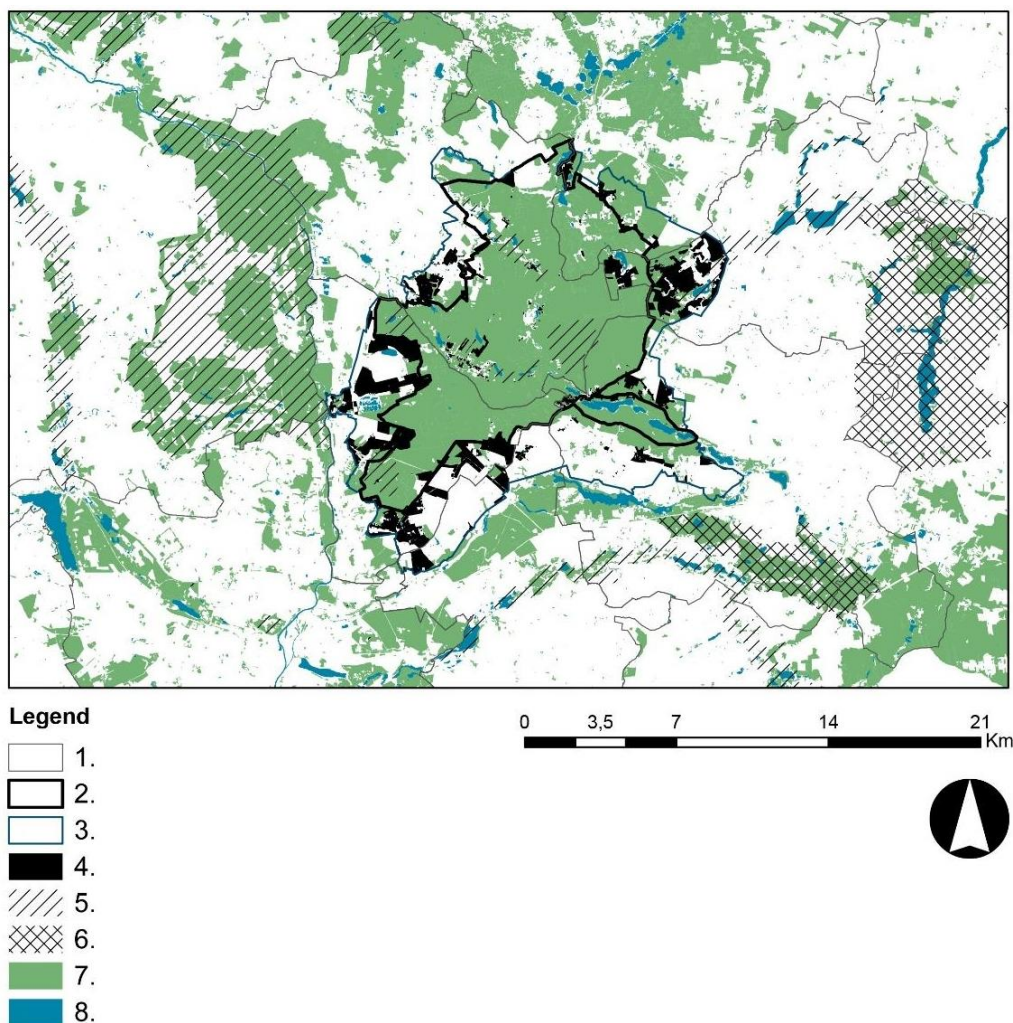


Figure 3. Areas for building developments in the Study of the Conditions and Directions of the Spatial Management of the communes vs. natural and protected areas in the surroundings of Puszcza Zielonka Landscape Park and its buffer zone (1. Commune boundaries, 2. Puszcza Zielonka Landscape Park, 3. Buffer zone, 4. Building development areas in the Park and its buffer zone according to the Study of the Conditions and Directions of the Spatial Management of the communes, 5. Natura 2000 areas, 6. Landscape parks, 7. Forests, 8. Open waters)

The problem particularly concerns the Park buffer zone, because it is subject to stronger urbanization pressure. As Xun et al. (2017) indicated, there is also an urgent need to protect or restore natural habitats located beyond directly protected areas so as to maintain the functional connection of habitat networks. In the past researchers indicated the problem of destruction of natural connections in PZLP by building developments, which enclosed forests with a ring (Raszka, 2010). Spatial planning tools give a possibility to create ecological networks (Szulczewska, 2004). However, as results from the research, not all communes are able and willing to use these tools. The

problem of destruction of the continuity of valuable natural areas by building developments is most likely to affect the southwestern part of the Park buffer zone, which has links with the Warta River valley and the protected area on the other riverbank within the Biedrusko range. It is also likely to affect the eastern part, where Promno Landscape Park and Natura 2000 areas in the Welna River valley are located near the Park buffer zone (*Fig. 3*).

Conclusions

Since the 1990s there have been changes in the land cover in Puszcza Zielonka Landscape Park. The forest area has increased slightly, the farmland area has decreased, and the share of built-up areas has increased. At the same time, there have been changes in the PZLP buffer zone. The area of arable land has decreased, the area of meadows, pastures and forests has increased whereas there has been a significant, more than a double increase in built-up areas. The observed changes show that this area is under the pressure of urbanization.

In the last twenty years there have been irregular changes in the land cover caused by the separation of new construction sites in individual communes located in PZLP and its buffer zone. Since the late 1990s the most buildings have appeared in the communes located in Poznań County due to the influence of the big city on the scale and rate of urbanization processes.

The analysis of the Studies of the Conditions and Directions of the Spatial Management of the communes located in the Park and its buffer zone showed the continuation of current spatial development trends, i.e. a slight increase in the forest area and an intensive growth of built-up areas at the expense of farmland. These changes are irregularly distributed around the area of six communes located in the Park and its buffer zone. It shows that individual local governments have different approaches to natural and spatial resources in their spatial policies.

The so-far collected materials suggest that further investigation into the pressure of urbanisation processes on protected areas is needed. Therefore, extending the research to other protected areas is recommended. Another prospect for further research is also to investigate the influence of local planning documents over landscape protection. Monitoring changes in the use of protected areas is also an important task for the future. Following existing trends in spatial development gives the opportunity to correct municipal spatial policy before it leads to irreversible losses of environmental and landscape resources. It would also be useful to follow trends in spatial development of the larger number of protected areas.

REFERENCES

- [1] Atmis, E. (2018): A critical review of the (potentially) negative impacts of current protected area policies on the nature conservation of forests in Turkey. – *Land Use Policy* 70: 675-684.
- [2] Bicknell, J. E., Collins, M. B., Pickles, R. S., McCann, N. P., Bernard, C. R., Fernandes, D. J., Davies, Z. G. (2017): Designing protected area networks that translate international conservation commitments into national action. – *Biological Conservation* 214: 168-175.

- [3] Border, J. A., Newson, S. E., White, D. C., Gillings, S. (2017): Predicting the likely impact of urbanisation on bat populations using citizen science data, a case study for Norfolk, UK. – *Landscape and Urban Planning* 162: 44-55.
- [4] Bradshaw, C. J. (2012): Little left to lose: deforestation and forest degradation in Australia since European colonization. – *Journal of Plant Ecology* 5(1): 109-120.
- [5] Closset-Kopp, P. D., Wasof, S., Decocq, G. (2016): Using process-based indicator species to evaluate ecological corridors in fragmented landscapes. – *Biological Conservation* 201: 152-159.
- [6] Dimitrakopoulos, P. G., Jones, N., Iosifides, T., Florokapi, I., Lasda, O., Paliouras, F., Evangelinos, K. I. (2010): Local attitudes on protected areas: Evidence from three Natura 2000 wetland sites in Greece. – *Journal of Environmental Management* 91(9): 1847-1854.
- [7] Environmental Protection Plan for the Commune of Czerwonak 2013-2016 with Possible Extension until 2020 (update). (2013). [In Polish].
- [8] Fardila, D., Kelly, L. T., Moore, J. L., McCarthy, M. A. (2017): A systematic review reveals changes in where and how we have studied habitat loss and fragmentation over 20 years. – *Biological Conservation* 212: 130-138.
- [9] Fletcher, R. J., Didham, R. K., Banks-Leite, C., Barlow, J., Ewers, R. M., Rosindell, J., Melo, F. P. (2018): Is habitat fragmentation good for biodiversity? – *Biological Conservation* 226: 9-15s.
- [10] Gałęcka-Drozda, A., Raszeja, E., Szczepańska, M., Wilkaniec, A. (2019): An analysis of Land Use Changes in Natura 2000 Areas Located in Suburban Zones – Planning Problems in the Context of Environmental Protection. – *Polish Journal of Environmental Studies* 28(2): 587-595.
- [11] Geldmann, J., Coad L., Barnes, M., Craigie, I. D., Hockings, M., Knights, K., Leverington, F., Cuadros, I. C., Zamora, C., Woodley, S., Burgess, N. D. (2015): Changes in protected area management effectiveness over time: a global analysis. – *Biological Conservation* 191: 692-699.
- [12] Gonzalez, A., Thompson, P., Loreau, M. (2017): Spatial ecological networks: planning for sustainability in the long-term. – *Current opinion in environmental sustainability* 29: 187-197.
- [13] Grochowska, A. (2015): Zagrożenia i konflikty w zakresie zagospodarowania przestrzennego na terenie Parku Krajobrazowego Sudetów Wałbrzyskich. – *Prace Naukowe Uniwersytetu Ekonomicznego we Wrocławiu* 391: 147-155.
- [14] Hamer, A. J., McDonnell, M. J. (2008): Amphibian ecology and conservation in the urbanising world: a review. – *Biological conservation* 141(10): 2432-2449.
- [15] Krajewski, P. (2014): Problemy planistyczne na terenach parków krajobrazowych w sąsiedztwie Wrocławia na przykładzie Ślęzańskiego Parku Krajobrazowego. – *Prace Naukowe Uniwersytetu Ekonomicznego we Wrocławiu* 367: 147-154.
- [16] Lima, E. A. C. F., Ranieri, V. E. L. (2018): Land use planning around protected areas: Case studies in four state parks in the Atlantic forest region of southeastern Brazil. – *Land Use Policy* 71: 453-458.
- [17] Lopez-Bao, J. V., Chapron, G., Treves, A. (2017): The Achilles heel of participatory conservation. – *Biological Conservation* 212: 139-143.
- [18] Maheshwari, B., Bristow, K. L. (2016): Peri-urban water, agriculture and urbanisation. – *Agricultural Water Management* 176: 263-265.
- [19] McDonald, R. I., Forman, R. T., Kareiva, P., Neugarten, R., Salzer, D., Fisher, R. J. (2009): Urban effects, distance, and protected areas in an urbanizing world. – *Landscape and Urban Planning* 93(1): 63-75.
- [20] Muchová, Z., Tárníková, M. (2018): Land cover change and its influence on the assessment of the ecological stability. – *Applied Ecology and Environmental Research* 16: 2169-2182.
- [21] Nature Conservation Act of 16 April 2004 (2004): Official Journal No. 92 Pos. 880 with amendments. [In Polish].

- [22] Puszcza Zielonka Landscape Park Protection Plan. (2005): Regulation of the Voivode of Greater Poland. – Voivodeship No. 4/05 of 4 April 2005. [In Polish].
- [23] Raszka, B. (2010): Identyfikacja konfliktów przestrzennych w parku krajobrazowym Puszcza Zielonka pod Poznaniem. – Zeszyty Naukowe Południowo-Wschodniego Oddziału Polskiego Towarzystwa Inżynierii Ekologicznej z siedzibą w Rzeszowie 12: 101-106.
- [24] Shwartz, A., Davies, Z. G., MacGregor, N. A., Crick, H. Q., Clarke, D., Eigenbrod, F., Gonner, C., Hill, C. T., Knight, A. T., Metcalfe, K., Osborne, P. E., Phalan, B., Smith, R. J. (2017): Scaling up from protected areas in England: The value of establishing large conservation areas. – *Biological conservation* 212: 279-287.
- [25] Study of the Conditions and Directions of the Spatial Management of the Commune of Czerwonak (2000): Commune Council Resolution No. 173/XXVIII/2000 of 14 June 2000 [Commune of Czerwonak planning document – manuscript in Polish] <http://pbip.czerwonak.pl/indexf3e.html?id=100502>.
- [26] Study of the Conditions and Directions of the Spatial Management of the Commune of Czerwonak (with amendments) (2010): Commune Council Resolution No. 406/LVII/2010 of 16 September 2010 [Commune of Czerwonak planning document – manuscript in Polish] <http://pbip.czerwonak.pl/index3e6c.html?id=94332>.
- [27] Study of the Conditions and Directions of the Spatial Management of the Commune of Kiszkowo (2012): Volume I Conditions. Volume II Trends. Commune Council Resolution No. XXI/167/12 of 6 November 2012 [Commune of Kiszkowo planning document – in Polish] <http://kiskowo.nowoczesnagmina.pl/?c=871>.
- [28] Study of the Conditions and Directions of the Spatial Management of the Commune of Murowana Goślina (with amendments) (2012): Volume I Conditions. Volume II Trends. Commune Council Resolution No. XX/196/2012 of 25 September 2012 [Commune of Murowana Goślina planning document – manuscript in Polish] http://bip.murowana-goslina.pl/wiadomosci/9836/wiadomosc/343161/studium_uwarunkowan_i_kierunkow_zagospodarowania_przestrzennego_.
- [29] Study of the Conditions and Directions of the Spatial Management of the Commune of Pobiedziska (2011): Commune Council Resolution No. V/40/2011 of 24 February 2011 [Commune of Pobiedziska planning document. – in Polish] http://www.bip.pobiedziska.pl/asp/pl_start.asp?podmiot=&strona=14&typ=podmenu&menu=161&id=164&str=1&m1=161&m2=164&m3=.
- [30] Study of the Conditions and Directions of the Spatial Management of the Commune of Skoki (2010): Volume I Conditions. Volume II Trends. Commune Council Resolution No. XLVI/279/10 of 24 June 2010 [Commune of Skoki planning document – manuscript in Polish] <http://skoki.nowoczesnagmina.pl/?c=923>.
- [31] Study of the Conditions and Directions of the Spatial Management of the Commune of Swarzędz (2011): Volume I Conditions. Volume II Trends. Commune Council Resolution No. 2011/51 of 22 November 2011 [Commune of Swarzędz planning document – manuscript in Polish] <http://bip.swarzedz.eu/index.php?id=198>.
- [32] Szulczewska, B. (2004): Planowanie przestrzenne jako instrument realizacji sieci ekologicznych: między teorią a praktyką. – *Problemy Ekologii Krajobrazu* 14(14): 54-62.
- [33] Treby, D. L., Castley, J. G. (2016): The impacts of historical land-use and landscape variables on hollow-bearing trees along an urbanisation gradient. – *Urban forestry & urban greening* 15: 190-199.
- [34] Warczewska, B., Mastalska-Cetera, B. (2011): Realizacja celów zrównoważonego rozwoju a konflikty w gospodarce przestrzennej (przykład Parku Krajobrazowego „Dolina Baryczy”) Implementation of Purposes of Sustainable Development against Clashes in Physical Planning on the Example of the Natural Landscape Park “Dolina Baryczy”. – *Studia KPZK* 142: 196-205.
- [35] Weaver, D. B., Lawton, L. J. (2017): A new visitation paradigm for protected areas. – *Tourism Management* 60: 140-146.

- [36] Wycichowska, B. (2008): Zawłaszczanie chronionego krajobrazu kulturowego przez samorządy gminne. Bilans strat na przykładzie Parku Krajobrazowego Wzniesień Łódzkich. – *Prace Komisji Krajobrazu Kulturowego PTG* 10: 368-376.
- [37] Xun, B., Yu, D., Wang, X. (2017): Prioritizing habitat conservation outside protected areas in rapidly urbanizing landscapes: A patch network approach. – *Landscape and Urban Planning* 157: 532-541.
- [38] Yang, H., Chen, W., Chen, X. (2017): Regional Ecological Network Planning for Biodiversity Conservation: A Case Study of China's Poyang Lake Eco-Economic Region. – *Polish Journal of Environmental Studies* 26(4): 1825-1833.
- [39] Zhang, X. Q. (2016): The trends, promises and challenges of urbanisation in the world. – *Habitat International* 54: 241-252.

COMPARATIVE EFFICACY OF SOME BOTANICAL EXTRACTS AND COMMERCIAL COATING MATERIALS FOR IMPROVING THE STORAGE LIFE AND MAINTAIN QUALITY OF KINNOW MANDARIN (*CITRUS RETICULATA* L.)

RASHID, M. Z.^{1*} – AHMAD, S.¹ – KHAN, A. S.¹ – ALI, B.²

¹*Institute of Horticultural Sciences, University of Agriculture, Faisalabad, Pakistan*

²*Department of Agronomy, University of Agriculture, Faisalabad, Pakistan*

*Corresponding author
e-mail: uafzahid@gmail.com

(Received 16th Jun 2019; accepted 16th Oct 2019)

Abstract. Citrus is one of the most promising fruit crops of Pakistan owing to its delicious taste and excellent aroma. Kinnow being a promising variety has a significant importance in the global market. Pakistan is facing a drastic reduction in Kinnow mandarin quality due to improper postharvest management and hence severe losses regarding quality and shelf life which might be up to 40%. The aim of this study was to find some alternative botanical product against chemical (fomesa) wax and fungicide to extend the shelf life of Kinnow mandarin. Fruits were treated with fomesa wax, 30% coconut oil, 60% aloe vera extract and Thiabendazole (TBZ) with standardized doses and stored at 5°C for 90 days. It was observed that 30% coconut oil performed almost at par to commercial wax and better than all other treatments. The fruits treated with 30% coconut oil showed minimum weight loss (11.70%), fruit rot (5.83%), maximum juice weight (42 g), biochemical parameters such as total soluble solids (10.90°Brix), titratable acidity (1.09%), ascorbic acid contents (40 mg 100 g⁻¹), total sugars (16%), maximum total antioxidants (70% inhibition) and maximum enzymatic activity [catalase (18.10U mg⁻¹ protein), peroxidase (0.79U mg⁻¹ protein) and superoxide dismutase (133.93 U mg⁻¹ protein)] of Kinnow fruits which were stored up to 90 days. It was concluded from the present study that pre storage treatment of 30% coconut oil was the most effective to reduce decay losses and maintain the fruit quality during 90 days storage.

Keywords: wax & fungicide, postharvest losses, coconut oil

Introduction

Citrus is ranked first among fruit crops, consisting almost 40% of fruits being grown in Pakistan, and enlists the country amongst top 15 producers of the world. The Kinnow is the extensively cultivated variety of citrus fruit and a common name of mandarin (*Citrus reticulata* L.) in Pakistan. The Kinnow grown in this region is a result of cross between King *Citrus nobilis* and *Citrus deliciosa* of Riverside California and is the principal citrus commercial cultivar. In Pakistan, Kinnow mandarin occupies imperative position among fruits (Siddique and Garnevska, 2018). In Pakistan, Kinnow export increased tremendously 2017-18 and touched a record of 370,000 tons compared to the previous year (Trade Development Authority of Pakistan, 2018).

Main Kinnow growing areas of Pakistan are Sargodha, Faisalabad, Bhalwal, Toba Tek Singh, Mandi Bahauddin and Sahiwal. Sargodha share 95% from total production of citrus in country (GOP, 2015). Kinnow is a good source of vitamin C, carbohydrates (fructose, glucose and sucrose), also having significant magnesium and calcium quantity. Similarly, Citrus fruits also have significant amount of

phytochemicals (monoterpenes, limonoids and flavonoids, carotenoids) which help to reduce the chance of cardiovascular diseases, cancer and cataracts (Arowora et al., 2013; Singh et al., 2018).

In Pakistan, Kinnow export increased tremendously 2017-18 and touched a record of 370,000 tons compared to the previous year (Trade Development Authority of Pakistan, 2018).

Postharvest losses ranges from 23-38% and sometimes up to 40% while 5-10% in developed countries containing Brazil, Australia, Spain, USA, Israel and Italy (FAOSTAT, 2017). These losses caused due to absence of suitable pre and post-harvest management practices, restricted cold chain services, inadequate packing houses and usually sluggish marketing system consequently low return to processor, farmer and trader (FAO, 2006). Kinnow need the proper management system to retain its good quality because there is a risk of deterioration of Kinnow after its harvesting in case of inappropriate management.

Among the various approaches applied to enhance the shelf life substitute of efficient cost technology, utilization of edible coating (wax, oil, extracts) to fruit has attained a considerable attention worldwide in these days (Tietel et al., 2010). For the formulation of comestible films and coatings, different kinds of materials are practiced having very indispensable features (Sindhu and Singhrot, 2016).

Effects of different treatments including commercial wax, herbal extracts (Fan et al., 2009; Romanazzi, 2010) essential oils, edible oils, Chitosan (Xu et al., 2007; Obenland et al., 2008; Paolo and Marisol, 2008) and fungicide has been studied to sustain quality of the fruit covering and increase shelf-life of citrus (Kinnow) fruits. Bisen et al. (2008) illustrated that increased kagzi lime's firmness and decreased fruit weight losses could be ensured with the optimum application of mustard oil. Though, short studies have been done regarding use of different edible oil base coatings to increase the storage life of the Kinnow fruit. In recent times, aloe vera gel based edible coating trend has been increasing for the preservation of different fruits and vegetables (Valverde et al., 2005; Chauhan et al., 2014; Hassanpour, 2015). This tasteless natural product eco-friendly substitute to artificial preservative and delays, respiration rate and reduce proliferation of microorganisms in fruits (Castillo et al., 2010; Garcia et al., 2013; Sogvar et al., 2016). Application of coconut oil, castor oil and sesame oil as postharvest covering of fruits cause reduction in moisture and weight loss of fruits (Creel et al., 2006; Ali et al., 2010).

A number of plants have recognized and classified by Grainge et al. (1984) which possess fungicidal and growth regulating properties, as well as some plants such as neem, lantana and melia. Moreover, neem leaves, fruits and bark have enormous pharmacological properties like anti-ulcer, anti-fungal, anti-bacterial, and pesticide (Biswas et al., 2002).

Aloe vera is a natural product having no taste which is safe and also environment friendly as the alternate for the synthetic preservative. It is used in numerous cases as prevention tool to manage fruit decay as its gel based edible coatings used to avert the respiration rate, delay oxidative browning, moisture loss and firmness. Owing to presence of numerous complex ingredients (enzymes, amino acid, phenolic compounds, salicylic acid, and glycoproteins) it is considered as a beneficial plant (Serrano et al., 2006). These ingredients possess the antifungal properties (Nidiray et al., 2011). Hence *Aloe vera* reduces the proliferation of various insects, pests and microorganisms in fruits (Castillo et al., 2010).

In Pakistan the use of fungicide is very common to control postharvest diseases but unfortunately, the application of non-chemical techniques is being ignored which can prevent the harmful consequences for human health. The use of chemicals has been discouraged to control the losses of fruits worldwide as there is emergence of concepts regarding food safety in the postharvest supply chain. The import of food commodities with chemical residues has been banned by numerous countries (Khalid et al., 2012).

The National standards fixed maximum residual limit (MRL) on fruits' exports which exceeds this limit would be rejected by importers (Pesticide Action Network, 2012). Industry is facing the challenge to maintain the quality of fruit with minimum chemical residues. The plant extract and organic nature mineral oil is the best alternate to control the pre and postharvest disease for the fruits across the world.

Commercial waxes are usually expensive which are being used in food industry so, there is need to introduce low-cost and effective eco-friendly bio product like oil and plant extracts which are edible and have no residual effect on human health. In view of contemporary scenario high priced wax, fungicide and to reduce postharvest losses, this current investigation was planned with this objective to ascertain the best local plant extract and oil to sustain the quality and storage life of Kinnow fruits.

Materials and methods

The current study was planned to assess the effectiveness of different coatings like oil, plant extracts, commercial wax and fungicide to increase the consumption period of Kinnow and all the experimentations were carried out at Postgraduate Pomology Laboratory (PPL) in University of Agriculture Faisalabad (UAF) Pakistan during 2015-2016. Physiologically matured Kinnow fruits were picked from Experimental Fruit Orchard, located in UAF. The fruits were brought to PPL and were graded to get rid of unhealthy or bruised ones. The fruits were cleaned up in tap water and dried under fan. All treatments (coating materials and storage day intervals) were evaluated under factorial CRD (Completely randomized design).

Plant extracts, oil were compared with commercial wax and fungicide. T₀: Control T₁: Fomesa wax, T₂: 30% Coconut oil, T₃: 60% Aloe vera extract (Best dose) and T₄: Thiabendazole (TBZ) Commercial Fungicide. 20 fruits of Kinnow were used and each treatment was replicated four time. These plant extract were simply treated by dipping method. Treated Kinnow fruits were placed in cold storage at 5°C and 85% RH for the time period of 90 days and quality parameters were studied up to 3 months (by keeping equal intervals of 15 days).

Physical and physiological characteristics

Fruits samples were weighed before storage and consecutive intervals of 15 days until the end of whole storage. The fruit parameters were calculated by using following formulas.

$$\text{Fruit rot (\%)} = \frac{\text{Spoiled fruits} \times 100}{\text{Total fruits}} \quad (\text{Eq.1})$$

$$\text{Weight loss (\%)} = \frac{\text{Initial weight of fruit} - \text{final weight of fruit} \times 100}{\text{Initial weight of fruit}} \quad (\text{Eq.2})$$

Peel weight (g)

The peel weight was measured using digital weight balance after peeling off fruit. Peel weight was denoted as in g.

$$\text{Juice contents (\%)} = \frac{\text{Average juice weight} \times 100}{\text{Average fruit weight}} \quad (\text{Eq.3})$$

Physiochemical characteristics

Total soluble solids (°Brix)

Total Soluble solid was measured by a digital device named refractometer (RX 5000, Atago, Japan).

Titrateable acidity (%)

$$\text{TA (\%)} = \frac{0.1 \text{ N NaOH} \times 0.0064 \times 100 \text{ ml juice used}}{\text{ml juice used}} \quad (\text{Eq.4})$$

Ascorbic acid

Juice contents regarding ascorbic acid were found following the procedure as described by AOAC (2000). A known quantity of juice (10 ml) was poured into 100 ml volumetric flask and final volume was prepared by adding 0.4% oxalic acid solution. 5 ml filtrated aliquot was taken from the volume, and titrated against 2, 6-dichlorophenolindophenol until the end point (light pink color).

$$\text{Ascorbic acid (mg } 100 \text{ g}^{-1}) = \frac{1 \times R1 \times V \times 100}{R \times W \times V1} \quad (\text{Eq.5})$$

Total phenolic and total antioxidants

The results regarding total Phenolic (mg GAE 100g⁻¹) were recorded using spectrophotometer at wavelength of 765 nm and 517 nm, respectively (Ainsworth and Gillespie, 2007).

Enzymes assay

Frozen juice was used to estimate the enzymatic activities of POD, CAT an SOD after homogenization using phosphate buffer. The enzyme extracts were prepared and readings were recorded at spectrophotometer at specific wavelengths. The activity of enzyme was demonstrated as **U mg⁻¹ protein** (Liu et al., 2011).

Statistical analysis

The recorded data were subjected to statistical analysis of variance using two way ANOVA to examine the overall significant data, whereas the (LSD) least significant difference test ($P \leq 0.05$) was performed for the comparison of means (treatments and storage periods) (Steel et al., 1997).

Results

Physical and physiological characteristics

Weight loss (%)

The weight of Kinnow fruit was gradually decreased during cold storage. The statistically evaluated data indicated significant results. The Kinnow fruits stored without any treatment indicated the highest weight loss than fomesa wax and 30% coconut oil treated fruits which showed 2.99 and 2.90-fold lower weight losses respectively. The interactive effects of different coatings and storage period showed higher weight loss (31.80%) in control treatment followed by fruit treated with TBZ, 60% aloe vera extract, 30% coconut oil and fomesa wax where weight losses were 13.10%, 12.55%, 11.70%, and 11.40%, respectively. The interaction suggested that during 15-90 days interval control treatments had a continuous reduction in fruit weight, but treated fruits showed less decrease during first 60 days and during 75-90 days fast reduction occurred in fruit weight. Among all treatments Kinnow fruits treated with 30% coconut oil extract exhibited lower weight loss up to 90 days (*Figure 1*).

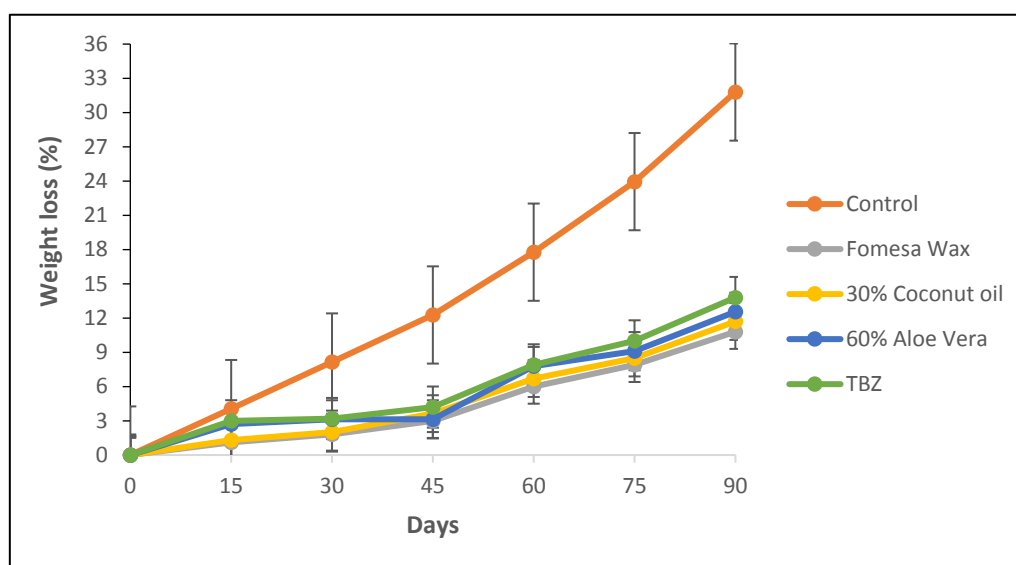


Figure 1. Effects of different coating treatments on weight loss (%) of 'Kinnow' fruit stored at 5°C. LSD value ($p \leq 0.05$) for treatments = 0.21, storage days = 0.25 and interaction = 0.56

Fruit rot (%)

Fruit rot of Kinnow mandarin fruit was progressively increased during storage period. The data depicted that Interactive effect of all treatments and storage days have significant impact on treatment means. The prestorage treatment of TBZ and 60% aloe vera showed lowest fruit rot (0.93% and 1.16%) than untreated fruit respectively over 90 days storage period. The Kinnow treated with TBZ and 60% aloe vera extract showed minor fruit rot which was statistically at par. The fruit rot was minimum (0.79%) when Kinnow were examined after 15 days of storage where fruit rot percentage was the highest i.e. (9.09%) when Kinnow were tested after 90 days. The interactive effects showed substantial results, the fruit rot (29.20%) was maximum in control treatment when assessed after 90 days storage followed by fruit treated with

30% coconut oil and fomesa wax, where fruit rot were 5.83%, 5.23%, 2.83% and 2.35%, respectively. Control treatments had swift increase in fruit rot (%) after 45 days while TBZ and 60% aloe vera extract coating treatment which were at par showed minimum decay even during 75-90 days. It was interesting to analyze that TBZ and 60% aloe vera extract treated fruit showed almost 0% decay during initial 30 days while untreated fruits had 6.25% fruit rot during the same period (*Figure 2*).

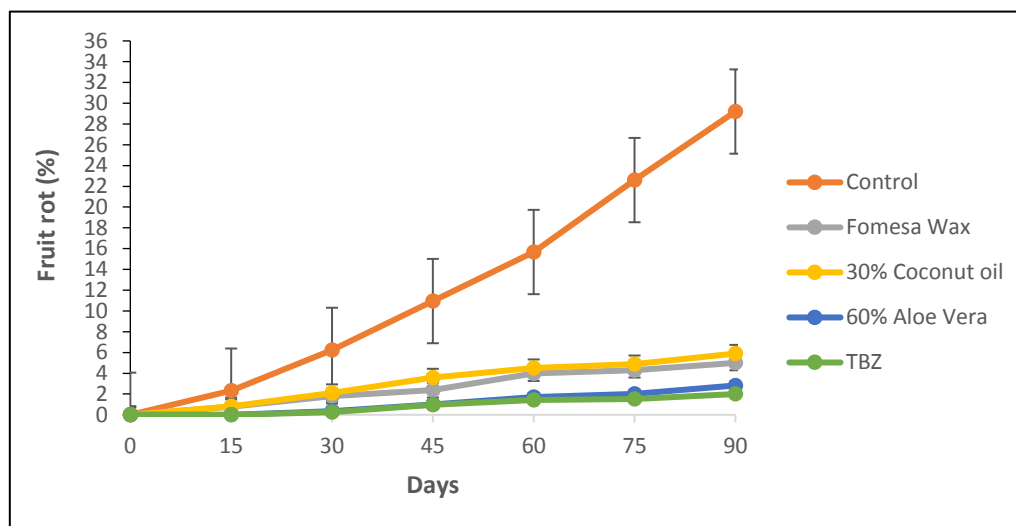


Figure 2. Effects of different coating treatments on fruit rot (%) of 'Kinnow' fruit stored at 5°C. LSD value ($p \leq 0.05$) for treatments = 0.44, storage days = 0.52 and interaction = 1.17

Peel weight (g)

Peel weight of Kinnow fruit was reduced due to loss of moisture, in this experimental study. The highest peel weight was maintained about 1.18 and 1.17-fold by fomesa wax and 30% coconut oil treated fruit than control respectively during prolonged storage. The peel weights were 1.18, 1.32 and 1.53-fold higher over 45, 60 and 90 days storage period, respectively. A reverse relation in weight of peel and storage time was noted as the storage progressed. Kinnow fruits treated with fomesa wax held higher peel weight from 0-45 days while fomesa wax and 30% coconut oil showed parallel results to limit weight reduction from peel of fruits. (*Figure 3*).

Juice contents (%)

It was noted that due to increased metabolic activities juice weight of Kinnow was steadily decreased in current study. The statistically investigated data depicted highly significant results among treatments, storage days and their interactions. Among different treatments Kinnow fruits treated with fomesa wax and 30% coconut oil revealed significantly 1.17 and 1.17-fold higher juice weight respectively after 90 days of cold storage. The application of coconut oil was effective to maintain the juice weight during storage period. A positive linear trend was observed for juice weight up to 0-45 days of storage when fruits were treated with 30% coconut oil and fomesa wax. However, an application 30% coconut oil and fomesa wax proved to be at par with each other, similarly a severe negative linear trend was observed in untreated Kinnow fruits for peel weight when observed during 15-90 days. The interactive effects showed highly

significant results, during storage period of 30, 45, 60 and 90 days, juice weights were 1.09, 1.15, 1.22 and 1.51-fold higher in fruits treated with 30% coconut oil than control fruit respectively (Figure 4).

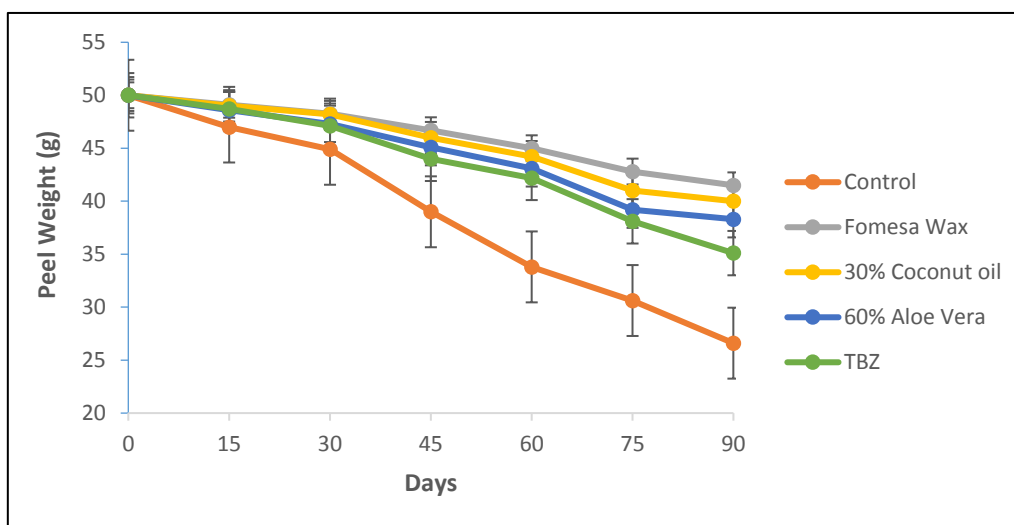


Figure 3. Effects of different coating treatments on peel weight (g) of 'Kinnow' fruit stored at 5°C. LSD value ($p \leq 0.05$) for treatments = 0.23, storage days = 0.28 and interaction = 0.62

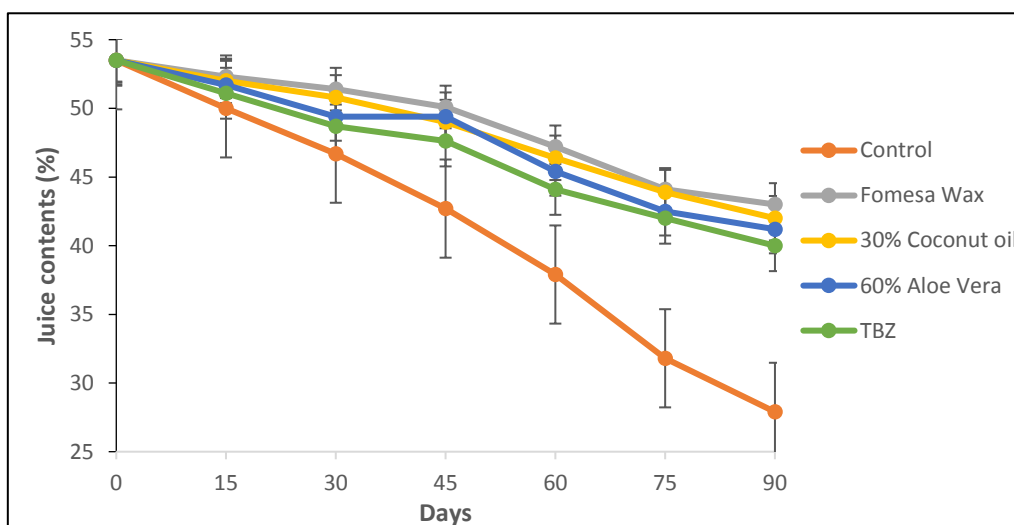


Figure 4. Effects of different coating treatments on juice contents (%) of Kinnow mandarin stored at 5°C. LSD value ($p \leq 0.05$) for treatments = 0.27, storage days = 0.32 and interaction = 0.73

Bio-chemical characteristics

Total soluble solids (°Brix)

The rapid increase in total soluble solid was found in control treatment than treated fruit. The Kinnow mandarin fruits treated with fomesa wax and 30% coconut oil exhibited the lower total soluble solid contents (1.12 and 1.11-fold) as matched to the untreated fruits respectively during whole storage time. The soluble solid contents were

minimum (9.25°Brix) when Kinnow were tested after 15 days of storage where soluble solid contents were highest i.e. 11.44°Brix when Kinnow were analyzed after 90 days of storage. The results showed that coconut oil has positive impact on the TSS of fruits. No sever turn in total soluble solid was observed up to 45 days of storage, however, a blunt increase in TSS during 60-90 days was recorded. Furthermore, commercial wax performed at par to 30% coconut oil and helpful to maintain the soluble solid contents. After 30 and 90 days cold storage, total soluble solid contents were 1.06 and 1.11-fold in 30% coconut oil treated fruit than control respectively (*Figure 5*).

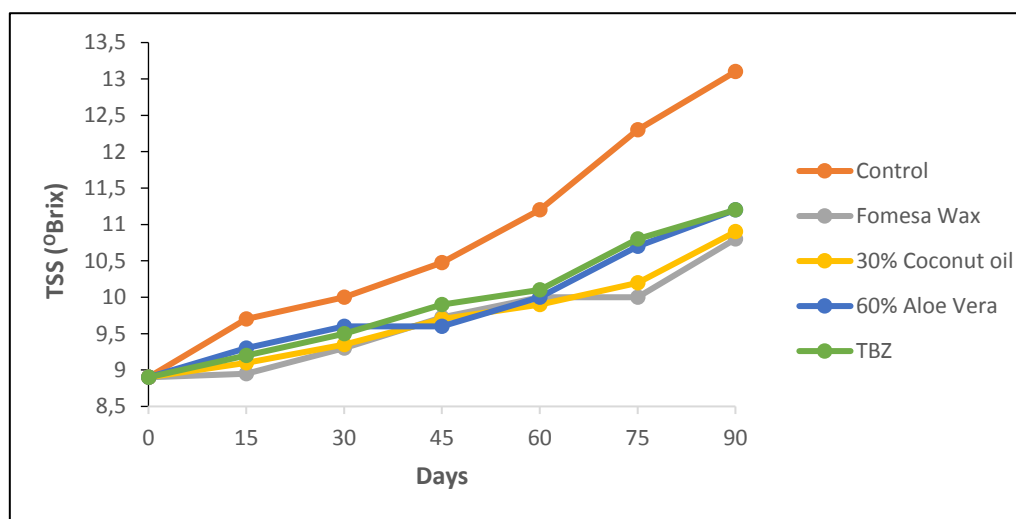


Figure 5. Effects of different coating treatments on TSS (°Brix) of Kinnow fruit stored at 5°C. LSD value ($p \leq 0.05$) for treatments = 0.17, storage days = 0.20 and interaction = 0.45

Titrateable acidity (%)

Among the treatments, fomesa wax and 30% coconut oil treated fruit resulted in 1.21-fold higher titrateable acidity than control during 90 days storage. Interactive effects exhibited that control treatments had an instant drop in TA after 45 days of storage, while, application of 30% coconut oil proved to be mandatory for sustaining the TA up to 60-90 days of storage. The interaction exhibited highest TA was observed in the treatments with fomesa wax (1.10) followed by the treatments of 30% coconut oil (1.09), 60% aloe vera extract (1.01), TBZ (0.98) and control treatment (0.68) respectively after 90 days of storage. 30% coconut oil treated fruit exhibited higher (1.17, 1.24, 1.32 and 1.60-fold) titrateable acidity in Kinnow fruits during storage (30, 45, 60 and 90 days) period respectively, than untreated fruit. It was found that titrateable acidity of fruits was inversely proportional with prolong storage period (*Figure 6*).

Vitamin C ($mg\ 100\ g^{-1}$)

The statistically investigated data showed highly significant results among treatments, storage days and their relation. The prestorage application of fomesa wax and 30% coconut oil indicated around 1.22 and 1.21-fold higher ascorbic acid contents in Kinnow fruit than untreated fruit respectively. However, a gradual decreasing trend was noted after 15 days in control treatment while commercial wax and 30% coconut oil treated fruit had greater drop during 75-90 days. It was noted that highest vitamin C

contents were observed in fruits treated with fomesa wax (40.60 mg 100 g⁻¹) followed by the treatments of 30% coconut oil (40.13 mg 100 g⁻¹), 60% aloe vera extract (38.70 mg 100 g⁻¹), TBZ (38.15 mg 100 g⁻¹) and control treatment (21.38 mg 100 g⁻¹) after 90 days of respectively. During storage period of 30, 60 and 90 days 30% coconut oil treated fruit exhibited 1.02, 1.33 and 1.87-fold higher than control fruit respectively (Table 1).

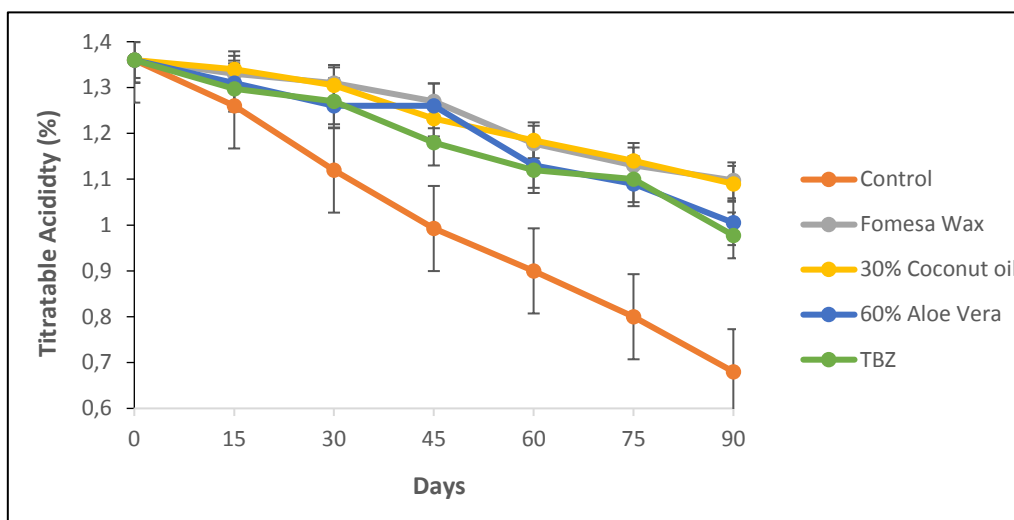


Figure 6. Effects of different coating treatments on titratable acidity (%) of Kinnow fruit stored at 5°C. LSD ($p \leq 0.05$): treatments = 0.02, storage days = 0.03 and interaction = 0.06

Table 1. Effects of different coating treatments on Vitamin C (mg 100 g⁻¹) of Kinnow fruit stored at 5°C

Treatments	Storage duration (days)							Mean
	0	15	30	45	60	75	90	
Control	45.00a	44.00bc	42.83ef	35.33 o	31.85 p	27.60 q	21.38 r	35.43C
Fomesa Wax	45.00a	45.15 a	44.00bc	43.45cde	43.00def	41.55 h	40.60ijk	43.25A
30% Coconut oil	45.00a	44.83ab	43.90bcd	43.10cdef	42.50fg	41.13 hi	40.13jkl	42.94A
60% Aloe Vera	45.00a	44.53ab	42.80ef	41.70gh	40.90hij	39.83kl	38.70mn	41.92B
TBZ	45.00a	44.60ab	42.85ef	41.58gh	40.20ijkl	39.60lm	38.15 n	41.71B
Mean	45.0A	44.6A	43.28B	41.03C	39.69D	37.94E	35.79F	

LSD value ($p \leq 0.05$) for treatments = 0.35, storage days = 0.42 and interaction = 0.94

Total phenolic contents (mg GAE 100 g⁻¹)

The statistically examined data indicated highly significant results in treatments, storage days and their relation. Increase in TPC activity was more distinct in coconut and oil and fomesa wax than control fruits. After 90 days mean total phenolic contents value was 1.11-fold higher in fruits treated with 30% coconut oil than untreated fruits. The interactive effects of treatments and storage days untreated fruits showed a continuous decrease in TPC from 30-90. Results revealed that fomesa wax treated fruits

showed maximum (214.35) total phenolic contents after 45 day storage period followed by fruit treated with 30% coconut oil (214.20), aloe vera extract 60% (213.9), TBZ (213.8) while minimum (200.70) was observed in untreated fruits. After 45 days and 90 days of storage period 30% coconut oil treated fruit 1.07 and 1.40-fold higher as compared to control fruit (Table 2).

Table 2. Effects of different coating treatments on TPC (mg GAE 100 g⁻¹) of 'Kinnow' fruit stored at 5°C

Treatments	Storage duration (days)							Mean
	0	15	30	45	60	75	90	
Control	213.50 def	211.93 ghi	206.90 l	200.70 m	189.35 n	171.55 o	150.18p	192.01C
Fomesa Wax	213.50 def	214.90 abc	215.83 a	214.35 bcd	212.80 efg	211.60 hi	210.20J	213.31A
30% Coconut oil	213.50 def	214.18 bcd	215.00 ab	214.20 bcd	212.50 fgh	211.28 ij	210.30J	212.99A
60% Aloe Vera	213.50 def	213.83 cde	214.35 bcd	213.90 bcde	211.20 ij	210.23 j	208.70k	212.24B
TBZ	213.50 def	213.60 def	214.00 bcd	213.80 cde	211.00 ij	210.40 J	207.90 kl	212.03B
Mean	213.50A	213.69A	213.22A	211.39B	207.37C	203.01D	197.46E	

LSD (p ≤ 0.05) treatment = 0.43, storage days = 0.51 and interaction = 1.14

Total antioxidants (%)

The statistically analyzed data indicated highly significant results. Postharvest application fomesa wax and 30% coconut oil enhanced (1.20 and 1.19-fold) higher antioxidant activity in contrast to untreated fruits respectively with entire storage period (Table 3).

Table 3. Effects of different coating treatments on total antioxidants (%) of Kinnow fruit stored at 5°C

Treatments	Storage duration (days)							Mean
	0	15	30	45	60	75	90	
Control	77.60bc	75.50def	71.63jk	65.67 o	60.70 p	50.64 q	39.75 r	63.07C
Fomesa Wax	77.60bc	78.50 ab	79.50 a	75.90def	74.55fgh	71.63jk	70.92klm	75.51A
30% coconut oil	77.60bc	78.24 ab	79.00ab	76.50 cd	73.50 hi	71.58jkl	70.00 m	75.20A
60% aloe vera extract	77.60bc	78.11 ab	77.91bc	75.18defg	74.00ghi	70.18lm	68.25 n	74.46B
TBZ	77.60bc	76.00 de	77.85bc	75.00efg	73.20 hi	72.78ij	67.55 n	74.28B
Mean	77.60A	77.27A	77.18A	73.65B	71.19C	67.36D	63.29E	

LSD value (p ≤ 0.05) for treatments = 0.54, storage days = 0.64 and interaction = 1.43

30% coconut oil treated fruits showed 1.10, 1.21 and 1.76-fold higher after 30, 45 and 90 days of cold storage than untreated fruits. Interaction showed that highest antioxidant activity (70.92) was observed in fomesa wax followed by the treatment of 30% coconut oil (70.0), 60% aloe vera extract (68.25%), TBZ (67.55) and control

treatment (39.75%) respectively after 90 day storage period. 30% coconut oil and commercial wax showed parallel results in stored fruits. The interactive effects revealed that antioxidant potential of fruit increased up to 0-30 days but reduced gradually up to 90 days. Moreover; 30% coconut oil was more useful to maintain antioxidant activities for long time period (Table 3).

Catalase ($U\ mg^{-1}\ protein$)

The data pertaining to CAT enzyme activity of Kinnow fruits illustrated statistically significant outcomes in treatments, storage days and their interactions. The control treatment exhibited the lowest catalase activity as compared to the Kinnow fruit treated with fomesa wax and 30% coconut oil having highest (1.31 and 1.30-fold) catalase activity respectively during storage. Interaction of treatment and storage time revealed falling trend in catalase enzyme activity with prolonged storage but also reduced after 30-60 days depending on treatments. Maximum catalase activity (18.70) was observed in fomesa wax treated fruits followed by treatments of 30% coconut oil (18.10), aloe vera extract 60% (17.23), TBZ (17.0) and control treatment (9.03) respectively after 90 days of storage period. Kinnow fruits treated with fomesa wax showed increase up to 45 days however 30% coconut oil also performed at par to maintain catalase activity on the other hand control treatment initially start decline (Figure 7).

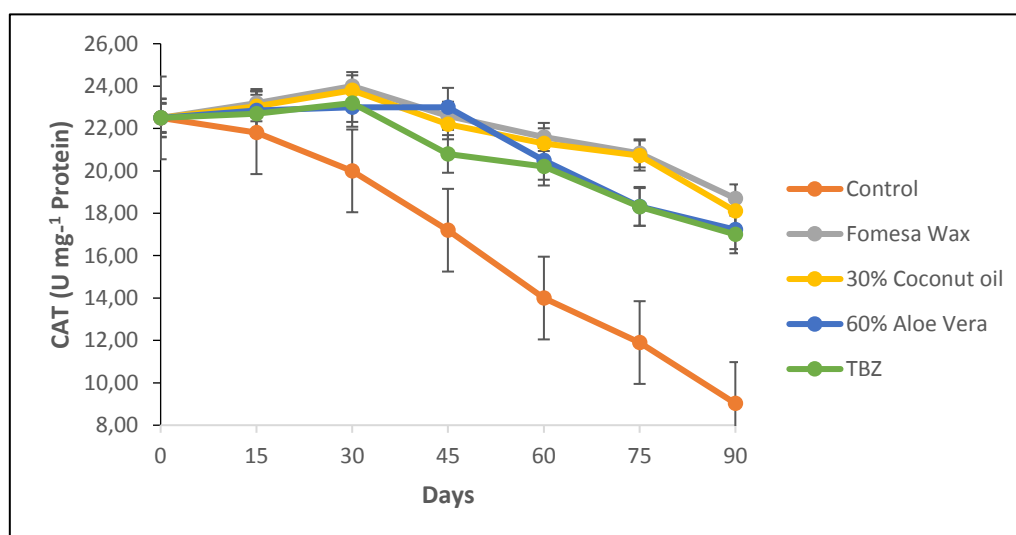


Figure 7. Effects of different coating treatments on catalase ($U\ mg^{-1}\ protein$) of Kinnow fruit stored at $5^{\circ}C$. LSD value ($p \leq 0.05$) for treatments = 0.27, storage days = 0.31 and interaction = 0.71

Peroxidase ($U\ mg^{-1}\ protein$)

The data regarding to POD enzyme activity of Kinnow fruits illustrated statistically non-significant results but their interactions for treatments and storage days was significant. The highest peroxidase enzyme activity (1.16-fold) was observed and Kinnow treated with fomesa wax and 30% coconut oil having highest (21.92) peroxidase enzyme activity followed by fruit treated with 30% coconut oil as compared to untreated fruit during storage. 30% coconut oil treated fruit showed 1.18, 1.23 and 1.46-fold higher POD enzyme activity after 45, 60 and 90 days of storage than control fruits (Figure 8).

Superoxide dismutase ($U\ mg^{-1}\ protein$)

The data related to SOD enzyme activity of Kinnow fruits demonstrated significant outcomes in treatments, storage time and their relation. The activity of SOD enzyme was increased to its peak when fruit treated with coconut oil than control fruit during entire storage. The Kinnow fruits dipped in fomesa wax and 30% coconut oil exhibited 1.08 and 1.07-fold higher SOD activity than untreated fruit during cold storage. It was noted that higher SOD enzyme activity was observed in fomesa wax treated fruits (1.15-fold) and 30% coconut oil (1.14-fold) as compared to untreated fruit after 90 days. High value of SOD activity (117.50) was observed in fomesa wax treated fruits after 15 days of storage period. 30% coconut oil and fomesa wax indicated almost at par to maintain SOD activity during storage (Figure 9).

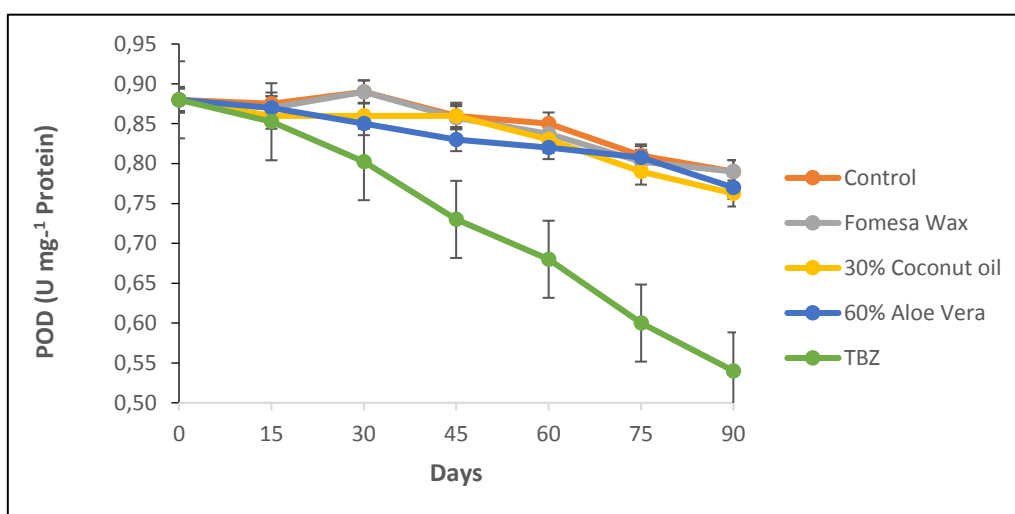


Figure 8. Effects of different coating treatments on peroxidase ($U\ mg^{-1}\ protein$) of Kinnow stored at $5^{\circ}C$. LSD value ($p \leq 0.05$) for treatments = 0.01, storage days = 0.02 and interaction = 0.04

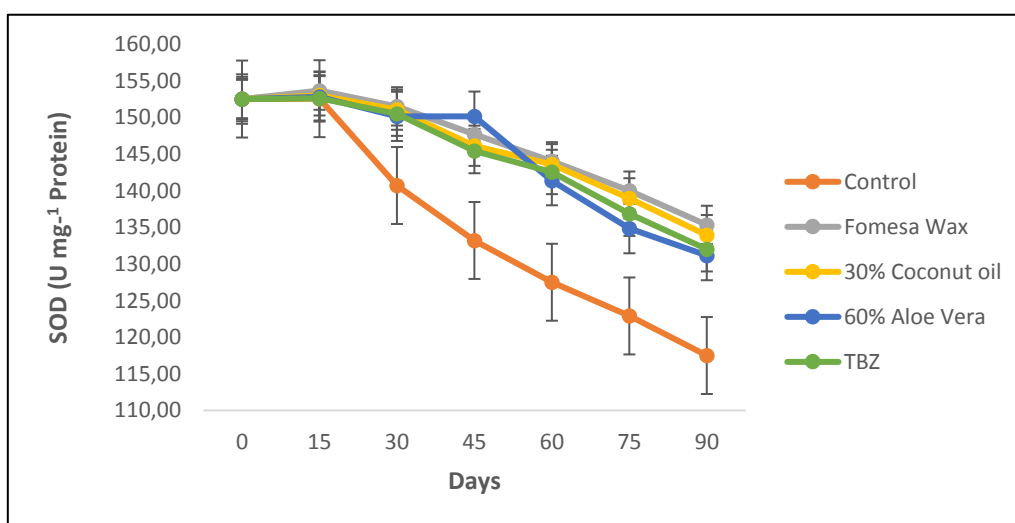


Figure 9. Effects of different coating treatments on superoxide dismutase ($U\ mg^{-1}\ protein$) of Kinnow fruit stored at $5^{\circ}C$. LSD value ($p \leq 0.05$) for treatments = 0.64, storage days = 0.75 and interaction = 1.68

Discussion

It is quite obvious from the results of the study that among all the treatment applied to Kinnow mandarin for the extension of storage life 30% coconut oil proved to be the best during 90 days of the storage. This is clear as fruit is living entity after the harvest and various physiological processes especially the respiration and transpiration are going on which utilizes the substrate present in the fruit so the fruit losses its weight because of these processes. Similar results of increasing physiological loss in weight during storage has also been reported in Grapes (Shiri et al., 2011), Jujube fruits (Xing et al., 2015; Shahi et al., 2015), and Mango (Carrillo et al., 2000; Gill et al., 2015). The results of current study for weight loss was in similar with the findings of Albanese et al. (2007) who explained that coating treatment slow down the weight loss. The coated fruits showed a positive action of prestorage treatment which slow down transpiration, because these coatings create a layer on citrus fruit surface that inhibit the evaporation. Likewise, in another study conducted by Krasniewska et al. (2014) it was found that the coatings of pullulan on apple and pepper decreased the weight loss in these fruits.

Coatings of fomesa wax and 30% coconut oil inhibited the agents of moisture particularly and due to this minimum decay loss happened. Yadav et al. (2010) described the reason of decay loss which was due to wax coating's interaction effect as moisture inhibitor as well as microbial inhibitor in their point of view. Similar results were found in Asian pear when observed by Mahajan et al. (2013). On the other hand, Gautam et al. (2003) reported the same results in mango, Ahmad et al. (2005) and Yadav et al. (2010) in Kinnow mandarin reported minimum decay loss during the period of storage by applying wax on these fruits.

Results concerning about TSS in this research showed that fruits treated with 30% coconut oil had lower total soluble solids as comparing them to control treatment. Increased TSS in control was due to solute accumulated in vacuoles of cells and starch gets hydrolyzed in to sugars. The increase in TSS up to 15 days may be attributed due to the hydrolysis of acid and deposition of polysaccharide as reported earlier by Omayma et al. (2010). Probable reason in reduction of TSS in 30% coconut oil treated fruit was due to the conversion of polysaccharides in to disaccharides and monosaccharaides means less hydrolysis of starch into sugars.

The higher titratable acidity in the commercial wax (fomesa wax) and 30% coconut oil treated Kinnow fruits could be because of least consumption of acids in the process of respiration during storage. The decrease in acidity in control treatment was probably due to the utilization of citric acid by the microbes as a source of carbon and O₂ collected inside caused acidosis after dissolving and developing carbonic acid (Carrillo et al., 1995). The coatings facilitated in better maintenance of titratable acidity than control fruits, which could be because of the positive role of coatings in delaying the process of ripening in fruits (El-Anany et al., 2009). Patriaca et al. (2005) indicated that coatings were effective in retention the titratable acidity of Kinnow.

Generally, vitamin C contents of fruits decreasing during storage. However, the 30% coconut oil and fomesa wax treated fruits showed higher contents of vitamin C as compared to control after 90 days storage. During the period of storage, the ascorbic acid was degraded which decreased the vitamin C. Similarly, Lee and Kader (2000) proposed that leaching in thermal breakdown and surrounding water became the reason of vitamin C loss. There were similar results shown by Sonkar et al. (2009) in Kinnow, Ahmad et al. (2005) in Kinnow, Deka et al. (2006) in mandarin. These studies indicated that there were maximum contents of Vitamin C in the fruits which were coated with

wax. Dehydro ascorbic acid is formulated as a result of moderate oxidation of vitamin C, as it is a fact that vitamin C is quite vulnerable to oxidative deterioration.

Shahid and Abbasi (2011) reported that there was maximum vitamin C in fresh fruit before ripening and after that due to the ascorbic acid oxidase action it was decreased. Generally, a major part of ascorbic acid transformed into juice and oxidized. The present study indicated that fruits treated with 30% coconut oil showed similar results as commercial wax had higher total phenolic contents of the Kinnow fruits in contrast to untreated fruits.

Paolo and Marisol (2008) in their research revealed that during storage, the total phenolic contents increased and vitamin C reduced. Consequently, phenolic compounds synthesis becomes the reason of increase in antioxidant activity during the period of storage of Kinnow fruit. They reported the reduction in phenol content of control and Kinnow coated with herbal extract, essential oil and commercial wax during the period of storage, these findings are a sequence of the results of Lim et al. (2006) who conducted research on fruit of citrus. During the period of storage, polyphenol oxidase enzymes' oxidative activity is related with the decrease in total phenols contents which makes the phenol to quinones compound. During the initial days, a sudden increase in the phenolic contents was observed it is due to the fact that due to reduction in temperature activation and generation of certain phenolic contents happened, as a result of above phenomenon dehydration of Kinnow occurred which further increased the juice phenolics (Silva et al., 2013). After a definite time period the phenolics decreased because antioxidant activity decrease which is sign of minimum resistance of fruits against the attack of pathogen.

The increase in activity of antioxidant enzymatic at early stages may because of environmental stress which increases the ROS level at protein, which finally modifies the cellular homeostasis (Suzuki and Mittler, 2006). Antioxidant activity's foresaid results demonstrated that Kinnow fruit which was coated with the wax and coconut oil with 30% encourage the scavenging capacity. Fruits of coated Kinnow which were stored at temperature of 4°C showed reduction in antioxidant activity after 90 days because of rigorous reduction in phenolics and ascorbic acid through biosynthesis. Hassanpour et al. (2015) reported the dependency of antioxidant activity upon flavonoids, anthocyanins, total phenols and ascorbic acid. They also supported the current results on antioxidant activity.

Conclusion

It was concluded that 30% coconut oil performed best among all the treatments. The fruits treated with 30% coconut oil showed minimum weight loss, fruit rot, maximum juice weight, biochemical parameters like total soluble solids, titratable acidity, ascorbic acid contents, total sugar, maximum total antioxidants and maximum enzymatic activity (CAT, POD and SOD) of Kinnow mandarin fruits which were stored up to 90 days. It was also evaluated that 60% aloe vera extract proved valuable for long term storage of Kinnow mandarin and to control the storage rot because it performed almost at par to commercial fungicide. Hence botanical extracts can improve the storage life of Kinnow mandarin so it can be recommended to overcome the storage issues of Kinnow fruits. Finally, it was obvious from experiment that prestorage treatment of 30% coconut oil was most effective to reduce decay losses and maintain the fruit quality during 90 days storage.

Future recommendations

There is a need to explore the penetration level of these treatments molecular level studies are also required to check the efficacy and accuracy. Effects of these prestorage applications on bio profile of phenolics and antioxidants, flavonoids should be checked to find a best treatment in terms of international standards.

REFERENCES

- [1] Ahmad, M. S., Thakur, K. S., Kaushal, B. B. L. (2005): Post-Harvest Treatments to Reduce Postharvest Losses in Kinnow Mandarin. – Indian J. Hortic. 62: 63-67.
- [2] Ainsworth, E. A., Gillespie, K. M. (2007): Estimation of total phenolic contents and other oxidation substances in plant tissue using Folin-Ciocalteu reagent. – Nature Protocols 2: 875-877.
- [3] Albanese, D., Cinquanta, L., Di Matteo, M. (2007): Effects of an innovative dipping treatment on the cold storage of minimally processed Annurca apples. – Food Chem. 105: 1054-1060.
- [4] AOAC. (2000): Official methods of analysis of Association of Official Analytical Chemists, 16th ed. – Association of Official Analytical Chemists, Arlington, VA.
- [5] Arowora, K. A., Williams, J. O., Adetunji, C. O., Fawole, O. B., Afolayan, S. S., Olaleye, O. O., Adetunji, J. B., Ogundele, B. A. (2013): Effects of Aloe vera Coatings on Quality Characteristics of Oranges Stored under Cold Storage. – Greener J. Agric. Sci. 3(1): 39-47.
- [6] Bisen, A., Pandey, S. K. (2008): Effect of postharvest treatments on biochemical and organoleptic constituents of Kazgi lime fruits during storage. – J. Hort. Sci. 3: 53-56.
- [7] Biswas, K. I., Chattopadhyay, I., Benerjee, R. K., Bandyopadhyay, U. (2002): Biological activities and medical properties of neem (*Azadirachta indica*). – Current Sci. 82: 701-711.
- [8] Carrillo, L. A., Ramirez-Bustamante, M. F., Valdez-Torres, J. B., Rojas-Villegas, R., Yahia, E. M (2000): Ripening and quality changes in Mango fruit as affected by coating with an edible film. – J. Food Qual. 23: 479-486.
- [9] Castillo, S., Navarro, D., Zapata, P. J., Guillen, F., Valero, D., Serrano, M., Martinez, R. D. (2010): Antifungal decay of Aloe vera in vitro and its use as a preharvest treatment to maintain postharvest table grape quality. – J. Postharvest Bio. Tech. 57: 183-188.
- [10] Chauhan, S. H., Gupta, K. C., Agrawal, M. (2014): Application of biodegradable *Aloe vera* gel to control postharvest decay and longer the shelf life of grapes. – Int. J. Current Microbiol. Appl. Sci. 3: 632-642.
- [11] Creel, R. E. (2006): Effect of acacia gum on postharvest quality of cut flowers. – Master of Science Thesis. Auburn, Alabama University. Pp.70.
- [12] Deka, B. C., Sharma, S., Borah, S. C. (2006): Postharvest management practices for shelf life extension of khasi mandarin. – Indian J. Horti. 63: 251-255.
- [13] El-Anany, A. M., Hasssan, G. F. A., Ali, F. M. R. (2009): Effects of edible coatings on the shelf life and quality of apple during cold storage. – J. Food Technol. 7: 5-11.
- [14] Fan, Y., Xu, Y., Wang, D., Zhang, L., Sun, J., Sun, L. (2009): Effect of alginate coating combined with yeast antagonist on strawberry (*Fragaria×ananassa*) preservation quality. – Postharvest Biol. Technol. 53: 84-90.
- [15] FAO. (2006): The impact of postharvest handling losses, sugar and beverage group raw materials, tropical and horticulture products service commodities and trade division. – Food Agri. Org. United Nations.
- [16] FAOSTAT. (2017): Food and Agricultural Organization of United Nations. – Available online with updates at <http://www.faostat.fao.org/site/342/default.aspx>.

- [17] Garcia, M. A., Marisabel, V., Diaz, R., Falco, S., Asariego, A. C. (2013): Effects of *Aloe vera* coating on postharvest quality of tomato Fruits. – J. Food Sci. 69: 117-126.
- [18] Gautam, B., Sarkar, S. K. Reddy, Y. N. (2003): Effect of post-harvest treatments on shelf life and quality of Banganapalli Mango. – Ind. J. Hortic. 60: 135-139.
- [19] Gill, P. P. S., Jawandha, S. K., Kaur, N., Singh, N., Sangwan, A. (2015): Effect of LDPE packaging on post-harvest quality of Mango fruits during low temperature storage. – The Bioscan. 10: 177-180.
- [20] GOP, Government of Pakistan. (2015): Pakistan Statistical Year Book. – Federal Bureau of Statistics, Statistic Division of Pakistan.
- [21] Grainge, M. S., Ahmed, W. C., Mitchel, L., Hysten, W. (1984): Plant species reportedly possessing pest control properties, an EWC/UN data base. – Resource system institute EWC Honoly College of Tropical Agriculture and Human Resource, UWV of Hawaii.
- [22] Hassanpour, H. (2015): Effect of *Aloe vera* gel coating on antioxidant capacity, antioxidant enzyme activities and decay in raspberry fruit. – J. Food Sci. Technol. 60: 495-501.
- [23] Khalid, M. S., Malik, A. U., Sleem, B. A., Khan, A. S., Javed, N. (2012): Horticultural mineral oil application and tree canopy management improve cosmetic fruit quality of Kinnow mandarin. – African J. Agri. Res. 7: 3464-3472.
- [24] Krasniewska, K., Gniewosz, M., Synowiec, A., Przybyl, J. L., Baczek, K., Weglarz, Z. (2014): The use of pullulan coating enriched with plant extracts from *Satureja hortensis* L. to maintain pepper and apple quality and safety. – Postharvest Biol. Technol. 90: 63-72.
- [25] Lim, Y. Y., Lim, T. T., Tee, J. J. (2006): Antioxidant properties of Guava fruit; comparison with some local fruit. – Suway. Acad. J. 3: 9-20.
- [26] Mahajan, B. V. C., Dhillon, W. S., Kumar, M. (2013): Effect of surface coatings on the shelf life and quality of Kinnow fruits during storage. – J. Postharvest Technol. 1: 8-15.
- [27] Nidiry, E., Ganeshan, G., Loksha, A. (2011): Antifungal activity of some extractives and constituents of aloe vera. – Res. J. of Medicinal Plant. 5: 196-200.
- [28] Obenland, D., Collin, S., Sievert, J., Fjeld, K., Doctor, J., Arpaia, M. L. (2008): Commercial packing and storage of navel oranges alters aroma volatiles and reduces flavor quality. – Postharvest Biol. Technol. 47: 159-167.
- [29] Omayma, M. I., Eman, A. A. E., Abd-Allah, A. S. E., El-Naggar, M. A. A. (2010): Influence of some post-harvest treatments on guava fruits. – Agric. Biol. J. N. Am. 1: 1309-1318.
- [30] Paolo, R., Marisol, L. B. (2008): Effect of cold storage on vitamin C, phenolic and antioxidant activity of five orange genotypes (*Citrus sinensis* (L.) Osbeck). – Postharvest Biol. Technol. 49: 348-354.
- [31] Patriaca, S., Palmu, T., Grosso, C. R. F. (2005): Effect of edible wheat gluten based films and coatings on refrigerated strawberry quality. – Postharvest Biol. Technol. 36: 199-208.
- [32] Pesticide Action Network. (2012): Pesticide residues in food. Pest management notes No. 8. – Available at: <http://www.pan-uk.org/archive/Internet/IPMinDC/pmn8.pdf>. Date of Retrieval: 06 August, 2012.
- [33] Romanazzi, G. (2010): Chitosan treatment for the control of postharvest decay of table grapes, strawberries and sweet cherries. – Global science Books 10: 111-114.
- [34] Serrano, M., Castillo, S., Valverde, J., Martiane-Romero, D., Guillean, F., Valero, D. (2006): Use of *Aloe vera* gel coating preserves the functional properties of table grapes. – J. Agri. Food Chem. 54: 3882-3886.
- [35] Shahi, M., Rastegar, S., Khankahdani, H. H. (2015): Effects of essential oil and calcium chloride on quantitative and qualitative features *Ziziphus mauritiana* during storage. – Int. J. Plant. Ani. Sci. 5: 25-31.
- [36] Shiri, M. A., Ghasemnezha, D., Bakhshi, D., Dadi, M. (2011): Changes in phenolic compounds and antioxidant capacity of fresh-cut table grape (*Vitis vinifera*) cultivar

- ‘Shahaneh’ as influence by fruit preparation methods and packagings. – Aus. J. Crop Sci. 5: 1515-1520.
- [37] Siddique, M. I., Garnevska, E. (2018): Citrus Value Chain (s). – A Survey of Pakistan Citrus Industry.
- [38] Sindhu, S. S., Singhrot, R. S. (2016): Effect of oil emulsion and chemicals on shelf life of baramasi lemon. – Haryana J. Hort. 25: 67-73.
- [39] Singh, D., Thakur, R. K., Singh, D. (2018): Effect of pre harvest sprays of fungicides and calcium nitrate on post-harvest rot of Kinnow in low storage. – Plant Dis. Res. 18: 9-11.
- [40] Sogvar, O. M., Saba, M. K., Emamifar, A. (2016): *Aloe vera* and ascorbic acid coatings maintain postharvest quality and reduce microbial load of strawberry fruit. – Postharvest Biol. Technol. 114: 29-35.
- [41] Sonkar, R. K., Sarnaik, D. A., Dikshit, S. N., Saxena, R. R. (2009): Individual Stretch Film Wrapped Kinnow Mandarin under Ambient Storage. – Ind. J. Hort. 66: 22-27.
- [42] Steel, R. G. D., Torrie, J. H., Dicky, D. A. (1997): Principles and Procedures of Statistics: A Biological Approach. 3rd ed. – McGraw Hill Book Co. Inc., New York, USA.
- [43] Suzuki, N., Mittler, R. (2006): Reactive oxygen species and temperature stresses: A delicate balance between signaling and destruction. – Physiol. Plant. 126: 45-51.
- [44] TDAP. (2018): Exports from Pakistan July-December, 2017-18 (Provisional). – Available online with Updates on <http://www.tdap.gov.pk/tdap-statistics.php>.
- [45] Tietel, Z., Bar, E., Lewinsohn, E., Feldmesser, E., Fallik, E., Porat, R. (2010): Effects of wax coatings and postharvest storage on sensory quality and aroma volatile composition of ‘Mor’ mandarins. – J. Sci. Food Agric. 90: 995-1007.
- [46] Valverde, J., Valero, D., Martinez-Romero, D., Guillen, F., Castillo, S., Serrano, M. (2005): Novel edible coating based of *Aloe vera* gel to maintain table grape quality and safety. – Agric Food Chem 53(20): 7807-13.
- [47] Xing, Y., Lin, H., Cao, D., Xu, Q., Han, W., Wang, R., Che, Z., Li, X. (2015): Effect of chitosan coating with cinnamon oil on the quality and physiological attributes of China jujube fruits. – Biomed. Res. Int. 15: 1-10.
- [48] Xu, W. T., Huang, K. L., Guo, F., Qu, W., Yang, J. J. (2007): Postharvest grapefruit seed extract and chitosan treatment of table grapes to control *Botrytis cinerea*. – Postharvest Biol. Technol. 46: 86-94.
- [49] Yadav, M., Kumar, N., Singh, D. B., Singh, G. K. (2010): Effect of postharvest treatments on shelf life and quality of Kinnow mandarin. – Ind. J. Hort. 67: 243-248.

DECOMPOSITION OF WETLAND MACROPHYTES AFFECTS THE RELEASE OF HEAVY METALS FROM SEDIMENTS TO THE OVERLYING WATER

FENG, Q.¹ – HAN, L.² – LOU, Q.² – FU, S. S.^{2*} – LIU, J. T.² – ZHANG, L. T.²

¹*Nanchang Institute of Technology, Nanchang 330099, People's Republic of China*

²*Jiangxi Institute of Water Sciences, Nanchang 330029, People's Republic of China*

**Corresponding author*

e-mail: fushasha1981@163.com

(Received 17th Jun 2019; accepted 25th Oct 2019)

Abstract. The study aimed to examine the effect of the decomposition of macrophyte materials on the release potential of heavy metals (Zn, Cu, Pb and Cd) from the lake sediment to the overlying water. A laboratory experiment was carried out with a common macrophyte species (*Carex cinerascens* Kukenth) to examine the effects of macrophyte decomposition on the release of heavy metals (Cu, Zn, Cd, Pb) from the sediment. Fresh aboveground parts of the macrophyte were added to the sediment and the treated sediment was subsequently subjected to a permanent flood condition. Dissolved organic carbon (DOC), pH and heavy metal concentrations of the overlying water were measured during the 135-day experiment. In most cases, the rate at which heavy metals were released from the sediments was reduced after the addition of macrophyte biomass. The greater the amount of the macrophyte amendment, the greater the decrease in heavy metals released from the sediment. There is no significant correlation between the DOC concentration in the overlying water and the four heavy metals released from sediments. The addition of macrophyte biomass can reduce the heavy metals release from sediments.

Keywords: *dissolved organic carbon, Carex cinerascens Kukenth, metal mobility*

Introduction

By acting as a sink of organic matter, wetland sediments generally play a fundamental role in determining the concentration of nutrients in waters (Yuan et al., 2011; Dittrich et al., 2013). However, sediments usually suffer severe levels of heavy metal pollution – up to hundreds of parts per million (Yin, 2011). There are several reports that wetland sediments are heavily contaminated with heavy metals (Kouba et al., 2010; Yuan et al., 2011; Schaller et al., 2013). This results in an enhanced environmental risk for associated ecosystems and organisms, especially as the heavy metals may be at concentrations that are toxic to many species (Nriagu and Pacyna, 1988).

Sediment can become remobilized and release metals into the water column; therefore, sediments are a potential source of contamination in wetland environments (Hafeznezami et al., 2012). Some studies have demonstrated that sediments can be a significant source of metal emissions (Chon et al., 2012; Schaller et al., 2013). The sediments most significant for binding metals are thought to be organic matter and Fe and Mn oxyhydroxides. Recent studies have demonstrated that organic matter in lake sediments can interact with heavy metals to form organometal complexes, and thus can significantly affect various aspects of heavy metals such as form, distribution, biotoxicity, migration and transformation (Yamashita and Jaffe, 2008; Guo et al., 2012).

In freshwater environments, organic matter is a ubiquitous, naturally occurring, heterogeneous mixture of organic compounds formed from the degradation of lignin-rich plant materials and the decay of dead organic biomass. Based on filtration, the organic matter fraction that passes through a 0.45- μm membrane is known as the dissolved organic matter (DOM), of which $\geq 50\%$ by mass is carbon. The concentration of DOM is widely variable in freshwater and commonly reported in mg C L^{-1} , as dissolved organic carbon (DOC) (Al-Reasi et al., 2013).

Organic matter in sediments is highly influenced by the primary production in lake ecosystems (Noges et al., 1999). After decaying, the detritus from macrophytes and algal biomass settles into sediments and will eventually be decomposed by the microbial community (Han et al., 2015). Microbial decay of organic matter in sediments is accompanied by the release of DOC into the water (Schaller et al., 2008). DOC is known to complex heavy metals and remains mobile (Sachs et al., 2007; Zhao et al., 2009). Ashworth and Alloway (2008) showed that the solubility of the heavy metals copper (Cu), nickel (Ni), and lead (Pb) in soil have a strong positive relationship to the solubility of organic matter. Soil DOM may increase aqueous heavy metal concentrations by forming metal-DOM aqueous complexes, as demonstrated by Wang and Mulligan (2009). However, Ranville et al. (2007) showed that high DOC levels had no effect on uranium remobilization when the pH was above 7. Moreover, there are observations that vegetated water bodies and related organic sediments have a higher capacity to immobilize the mobile metals (Dienemann et al., 2006; Ross and Dudel, 2008). Plant litter can provide a metal sink if, during decomposition, metals are bound to the litter by passive sorption on the organic surfaces or by accumulation by microbial colonizers of the litter (Du Laing et al., 2006, 2007; Guo et al., 2006). Accordingly, strong positive correlations have been found between metal concentrations in the sediment and organic matter concentrations in the upper sediment layer of the Scheldt marshes (Du Laing et al., 2007). As a result, the DOC produced during plant decomposition could enhance the mobility of heavy metals in the sediment or soil, but the plant materials could also provide a metal sink. It is unclear which process is dominant.

Therefore, a laboratory experiment was conducted to examine the effect of the decomposition of macrophyte materials (*Carex cinerascens* Kukenth) on the release potential of heavy metals (Zn, Cu, Pb and Cd) from the lake sediment to the overlying water.

Material and methods

The wetland plant selection and collection

Carex cinerascens is a good forage grass, and is distributed in Northeast, Northwest, North, East, Central and southwest alpine area of China. It grows on the lake, riverside or marshland.

On April 5th, 2016, the aboveground biomass of *C. cinerascens* was sampled from Xicha Lake located in Gongqingcheng city of Jiangxi province in China. The aboveground parts were harvested and thoroughly washed with deionized water. After allowing most of the water to drip off, the fresh macrophytes were chopped into approximate one-centimetre sections. Chopped plant parts were mixed in order to equalize any differences in the composition of various plant organs, the variability in their decomposition rates, and the resultant activity of microbial decomposers.

The wetland sediment collection and treatment

Surface sediment samples (0-10 cm) were collected from Xicha Lake located in Gongqingcheng city in December 2014 during the dry season. Upon return to the laboratory, the sediment was air dried and sieved through a 2-mm mesh nylon sieve. Heavy metals were added to the sediment in the form of $\text{CuSO}_4 \cdot 5\text{H}_2\text{O}$, ZnCl_2 , $\text{CdSO}_4 \cdot 8/3\text{H}_2\text{O}$ and $\text{Pb}(\text{NO}_3)_2$. The sediment was increased artificially to reach final values of $394 \text{ mg} \cdot \text{kg}^{-1}$ of Cu, $775 \text{ mg} \cdot \text{kg}^{-1}$ of Zn, $7 \text{ mg} \cdot \text{kg}^{-1}$ of Cd and $352 \text{ mg} \cdot \text{kg}^{-1}$ of Pb for the low levels of heavy metal contamination (LS), and $691 \text{ mg} \cdot \text{kg}^{-1}$ of Cu, $1445 \text{ mg} \cdot \text{kg}^{-1}$ of Zn, $12 \text{ mg} \cdot \text{kg}^{-1}$ of Cd and $596 \text{ mg} \cdot \text{kg}^{-1}$ of Pb for the high levels of heavy metal contamination (HS). The sediment was then placed in a plastic bucket and watered well. After 16 months, the sediment was sieved through a 2 mm mesh nylon sieve and was subjected to laboratory-scale incubation experiments. *Table 1* reports selected characteristics of the sediment used in the experiment.

Table 1. Physical and chemical properties of the two levels of heavy metal contamination

Parameters	Cu	Zn	Cd	Pb	Ca	Mg	TC	pH
	mg kg ⁻¹						%	
LS	394	775	7	352	4911	4269	0.46	5.50
HS	691	1445	12	596	5186	4597	0.48	5.54

LS and HS represent the low and high levels of heavy metal contamination in the sediment, respectively

The overlying water used in the experiment

On April 5th, 2016, water was collected from Xicha Lake located in Gongqingcheng city, where the water quality is relatively good. After being transported to the laboratory, the collected lake water was filtered immediately through a 0.45- μm membrane and stored at 4°C for the experiment. The pH of the lake water was 6.94. The concentrations of Cu, Zn, Cd, Pb, Ca and Mg in the lake water were $0.656 \mu\text{gL}^{-1}$, $4.980 \mu\text{gL}^{-1}$, $0.533 \mu\text{gL}^{-1}$, $0.385 \mu\text{gL}^{-1}$, $27461 \mu\text{gL}^{-1}$ and $3038 \mu\text{gL}^{-1}$, respectively.

Experimental conditions and design

To investigate the effects of the decomposition of the aboveground parts of *C. cinerascens* in flooding season on the release of heavy metals from the sediment, two levels of macrophyte biomass additions were used in the experiment. One level is 17 g of fresh weight, which represents the macrophyte biomass in the spring in the field, and the other is 7 g fresh weight. For the experiment with sediments, there were six treatments: LS+water, LS+7 g macrophyte+water, LS+17 g macrophyte+water, HS+water, HS+7 g macrophyte+water, and HS+17 g macrophyte+water. In addition, two treatments without sediments were included: 7 g macrophyte+water and, 17 g macrophyte+water. In total, eight treatments were conducted with each treatment performed in triplicate. The sediment+water and sediment+macrophyte+water treatments were used to test the effect of plant decomposition on the release of heavy metals from the sediments. The macrophyte+water treatment was used to determine the amount of heavy metal release from the plant itself to the overlying water.

The release experiments were performed in 2.0-L glass beakers 13.3 cm in diameter and 19.3 cm in height, and the beakers were side-wrapped in black plastic to avoid light exposure. First, 300 g of air-dried sediment were put into the bottom of the vessel, and mixed with increasing amounts of chopped fresh plant weight. Finally, 1.5 L of filtered lake water was added into each beaker. All experiments were conducted at the laboratory with no temperature control from April 5th to August 18th, 2016, and the incubation lasted 135 days. During the experimental period, water samples were taken (after 1, 4, 11, 18, 32, 90 and 135 days) from each vessel with a pipette at a depth of 5 cm above the sediment-water interface for the heavy metal and DOC analysis, and then the pH of the overlying water was determined. Before the first day of the sampling, the evaporated water was added and after the sampling, 20 ml of deionized water was added to supplement the sampling water. For heavy metal analysis, the 10-ml sample was centrifuged immediately after sampling and acidified with HNO₃. For the determination of dissolved organic carbon (DOC), 10 ml of water was sampled using PE (polyethylene) vessels, filtered using 0.45-μm cellulose-acetate filters and immediately measured.

Analytical methods

The element concentrations were analysed at the analytical laboratory of the Beijing Research Institute of Uranium Geology, which is registered to the China National Accreditation Service for Conformity Assessment and the China Metrology Accreditation system, using an inductively coupled plasma mass spectrometer (Perkin-Elmer Elan DRC-e, American). The DOC of the water samples was determined using a TOC analyser (Tekmar Torch, American). Carbon content in the sediment samples was measured with an element analyser (ElementarVario Macro Cube, Germany). The pH of the overlying water was determined using a pH meter (Leici PHSJ-3F, Shanghai) and the pH of the sediment was also determined by a pH meter according to the Standard of the Ministry of Agriculture of the People's Republic of China (NY/T 1377-2007).

Statistical analysis

The percent decrease of the concentration of metal *X* in overlying water at time *t* after addition of macrophytes (*PD_t*) was calculated according to the following formula:

$$PD_t(\%) = \frac{X_{t0}(mgL^{-1}) - X_{tp}(mgL^{-1})}{X_{t0}(mgL^{-1})} \times 100 \quad (\text{Eq.1})$$

where *PD_t* is the decreased percentage of metal *X* concentration in the overlying water after the addition of the macrophyte; *X_{t0}* is the metal *X* concentration in the overlying water with no addition of the macrophyte at time *t*; and *X_{tp}* is the metal *X* concentration in the overlying water after addition of the macrophyte at time *t*. *PD_t*<0 indicates a net increase of metal 'X' released from the sediment by the decaying plant, while *PD_t*>0 indicates a net decrease of metal 'X' released by the decaying plant.

For each heavy metal pollution level, differences in the measured parameters among three treatments were tested by a one-way analysis of variance (ANOVA) followed by Tukey's post hoc analysis when appropriate. A correlation analysis (Pearson's correlation coefficients) was used to test the relationships between DOC and heavy metal concentration during the 135-day period. Differences in the percentage decrease of the heavy metal concentration in overlying water after the macrophyte biomass

addition, between the earlier stage of the experiment (treatments for 1 day, 4 days and 11 days) and the later stage (treatments for 18 days, 32 days, 90 days and 135 days), were tested with a paired samples test. All statistical analyses were performed using the SPSS 11.5 software package.

Results

Dynamic changes in pH and DOC concentration in overlying water

The pH of the overlying water was significantly decreased by the macrophyte addition on the first day and then increased by the macrophyte addition (*Fig. 1*). However, there were no significant differences in pH between the sediment+water+7 g macrophyte treatment and the sediment+water+17 g macrophyte treatments ($p>0.05$). And there were no significant differences in pH between the two treatments with low and high concentrations of heavy metals in sediments ($p>0.05$) and the pH values shown in *Fig. 1* were the average of the treatments with low and high concentrations of heavy metal in sediments.

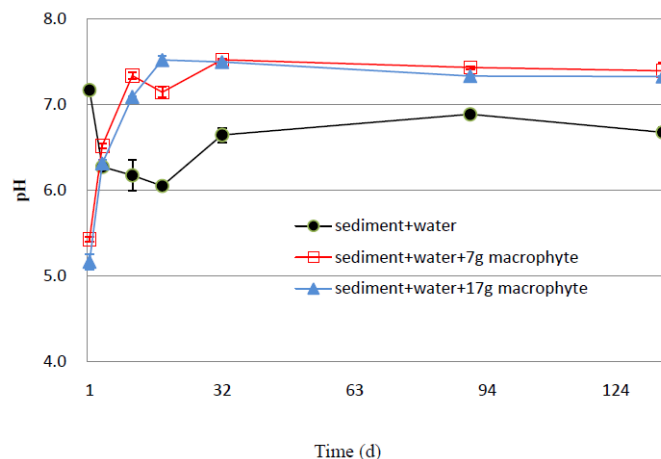


Figure 1. Change in pH value of overlying water during the *C. cinerascens* amendment. The pH values shown in the figure were the average of the treatments with low and high concentrations of heavy metal in sediments

The DOC concentrations of the overlying water in the treatments with macrophyte biomass amendments increased remarkably, and showed similar variation during the 135-day decomposition process (*Fig. 2*). For the treatments with low and high levels of heavy metal contamination in sediments, the DOC concentrations in treatments with the macrophyte addition increased with time and peaked around day 4 and day 11, and then decreased or remained relatively stable. In addition, the mean DOC concentrations followed the order: sediment+water+17 g macrophyte > sediment+water+7 g macrophyte > sediment+water (*Fig. 2a,b*). Within the treatments with the same amount of macrophyte biomass addition, there were no significant differences in DOC concentrations between the two treatments with low and high concentrations of heavy metal in sediments ($p>0.05$). DOC concentrations ranged from 0.47-5.05 mgL⁻¹ in the sediment treatments, 1.5-21.27 mgL⁻¹ in the sediment+water+7 g macrophyte treatment and 0.65-50.82 mgL⁻¹ in the sediment+water+17 g macrophyte treatments.

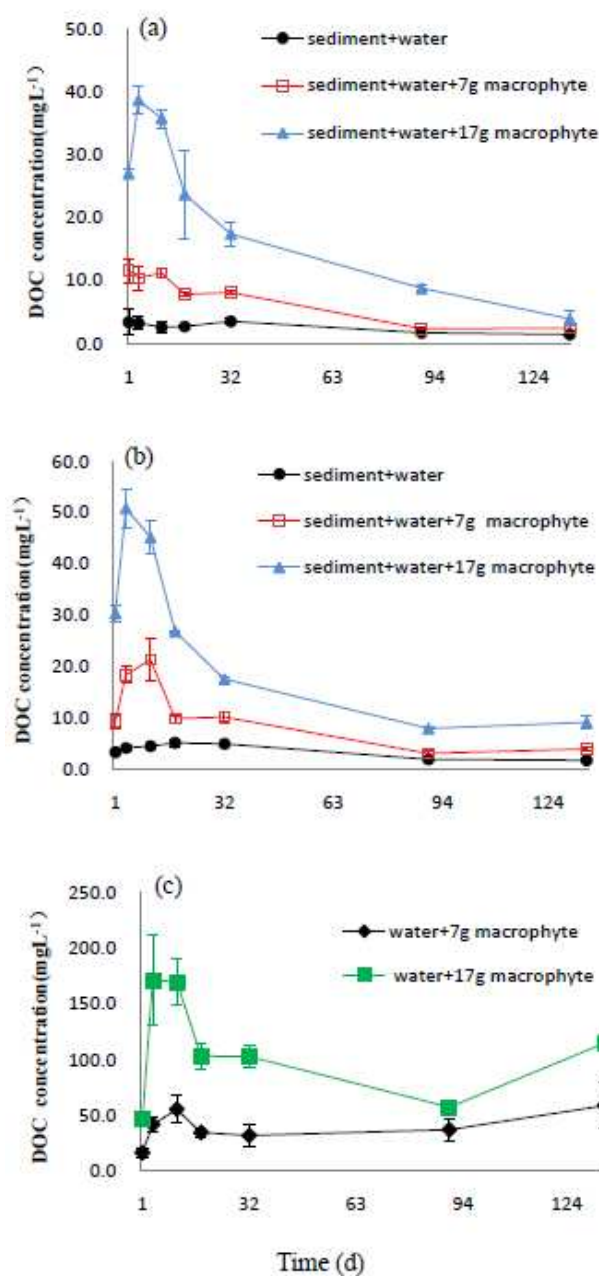


Figure 2. Change in DOC concentrations in overlying water during the *C. cinerascens* amendment. (a) The treatments with low concentrations of heavy metal in sediments; (b) the treatments with high concentrations of heavy metal in sediments; (c) the treatments without sediments, as a function of time after flooding. Error bars indicate standard deviations

However, DOC concentrations in the water+macrophyte treatment were significantly higher than in the sediment+water+macrophyte treatments with the same amount of macrophyte biomass added ($p < 0.05$). DOC concentrations in the water+7 g macrophyte treatments ranged from 15.93-58.49 mg L⁻¹ and from 45.83-171.75 mg L⁻¹ in the water+17 g macrophyte treatment. However, for the water+macrophyte treatments, DOC concentrations increased during the first few days, then declined, and increased at a later stage.

The effect of macrophyte addition on the release of heavy metals from sediments

Dynamic changes in heavy metal concentration of the overlying water

For the water+macrophyte treatments, the concentrations of four heavy metals in the water body were very low, at several parts per billion. Thus, the effect of heavy metals released by the macrophyte itself into the overlying water is negligible in the sediment+water+macrophyte treatment (Fig. 3c, Fig. 4c, Fig. 5c, and Fig. 6c).

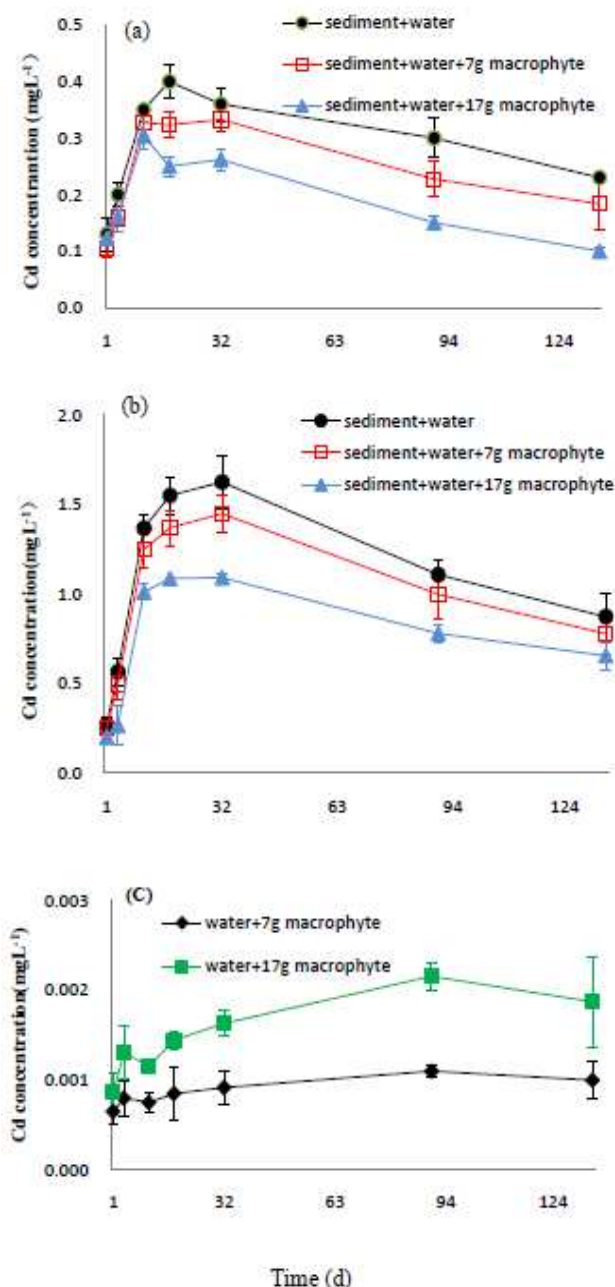


Figure 3. Changes in Cd concentrations in overlying water during the *C. cinerascens* amendment. (a) The treatments with low concentrations of heavy metal in sediments; (b) the treatments with high concentrations of heavy metal in sediments; (c) the treatments without sediments, as a function of time after flooding. Error bars indicate standard deviations

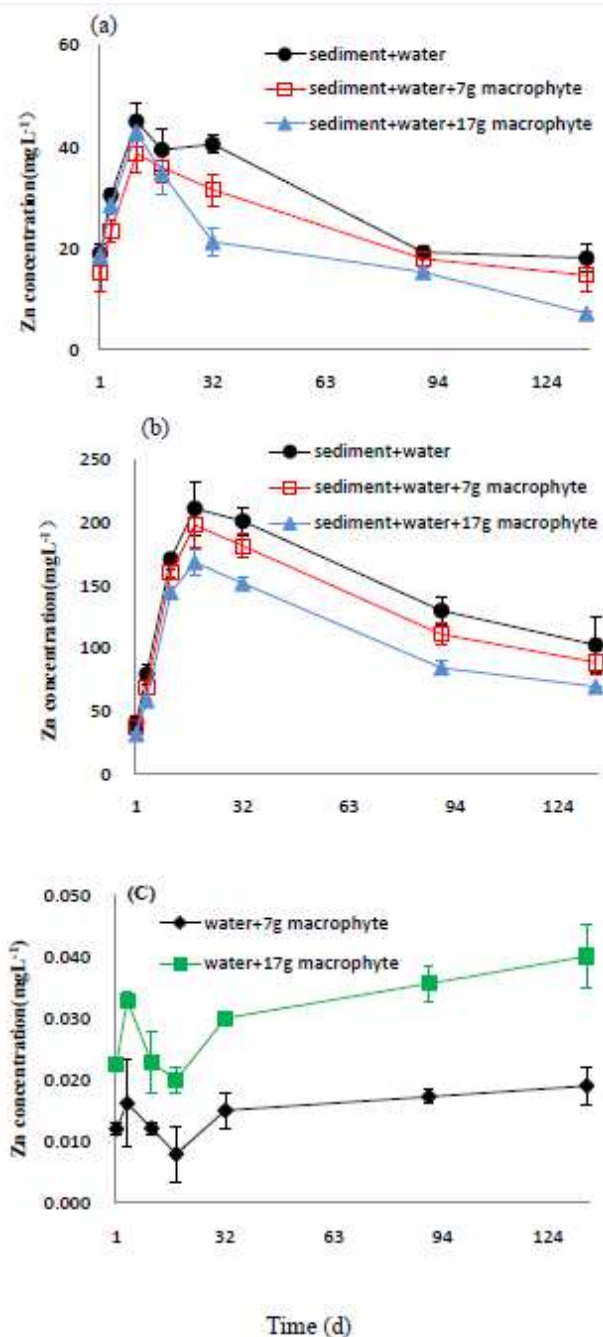


Figure 4. Changes in Zn concentrations in overlying water during the *C. cinerascens* amendment. (a) The treatments with low concentrations of heavy metal in sediments; (b) the treatments with high concentrations of heavy metal in sediments; (c) the treatments without sediments, as a function of time after flooding. Error bars indicate standard deviations

The release of four kinds of heavy metals in the sediments was not the same, as a function of time after flooding. However, in general, in the later stage of the experiment, the mean concentrations of Cd, Zn, Cu and Pb in the overlying water followed the order: sediment+water > sediment+water+7 g macrophyte > sediment+water+17 g macrophyte.

For both levels of heavy metal contamination in the sediment, Cd and Zn concentrations in the overlying water first increased with time and then decreased. In general, the effect of

the macrophyte addition on the release of heavy metals from sediment was not obvious in the early stage of the experiment, but in the later stage, the macrophyte addition could significantly reduce the release of heavy metals from sediment to the overlying water ($p < 0.05$). In general, the mean Cd and Zn concentrations in the overlying water followed the order: sediment+water > sediment+water+7 g macrophyte > sediment+water+17 g macrophyte (Fig. 3a,b and Fig. 4a,b).

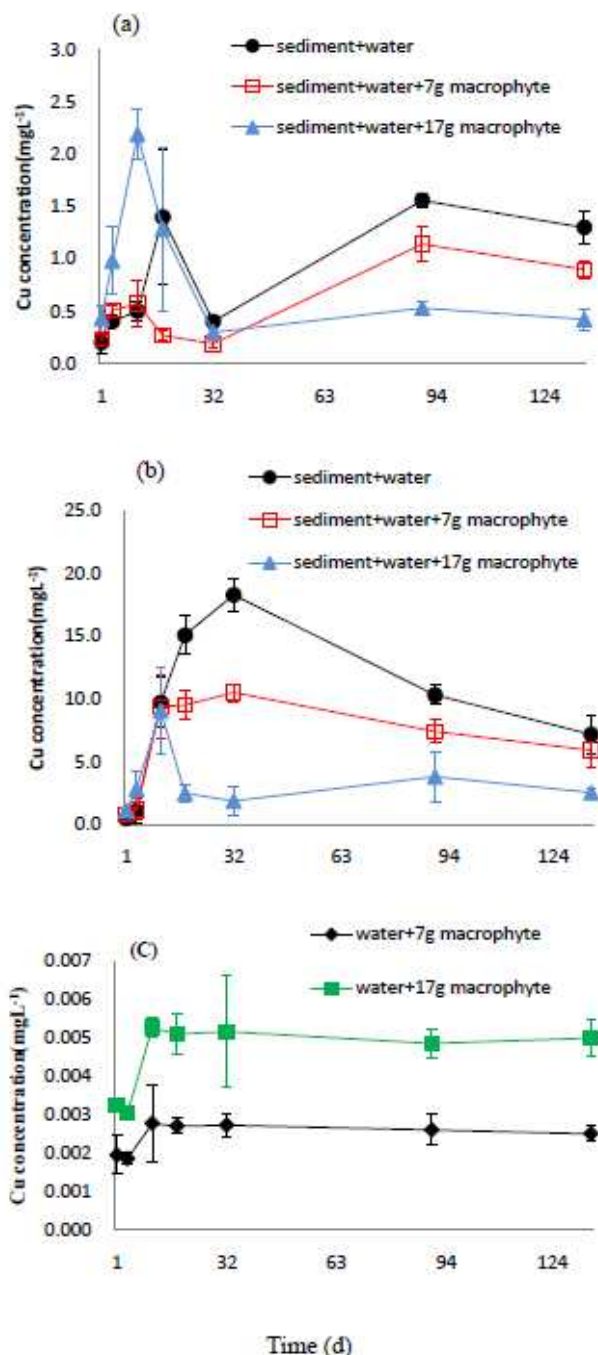


Figure 5. Changes in Cu concentrations in overlying water during the *C. cinerascens* amendment. (a) The treatments with low concentrations of heavy metal in sediments; (b) the treatments with high concentrations of heavy metal in sediments; (c) the treatments without sediments, as a function of time after flooding. Error bars indicate standard deviations

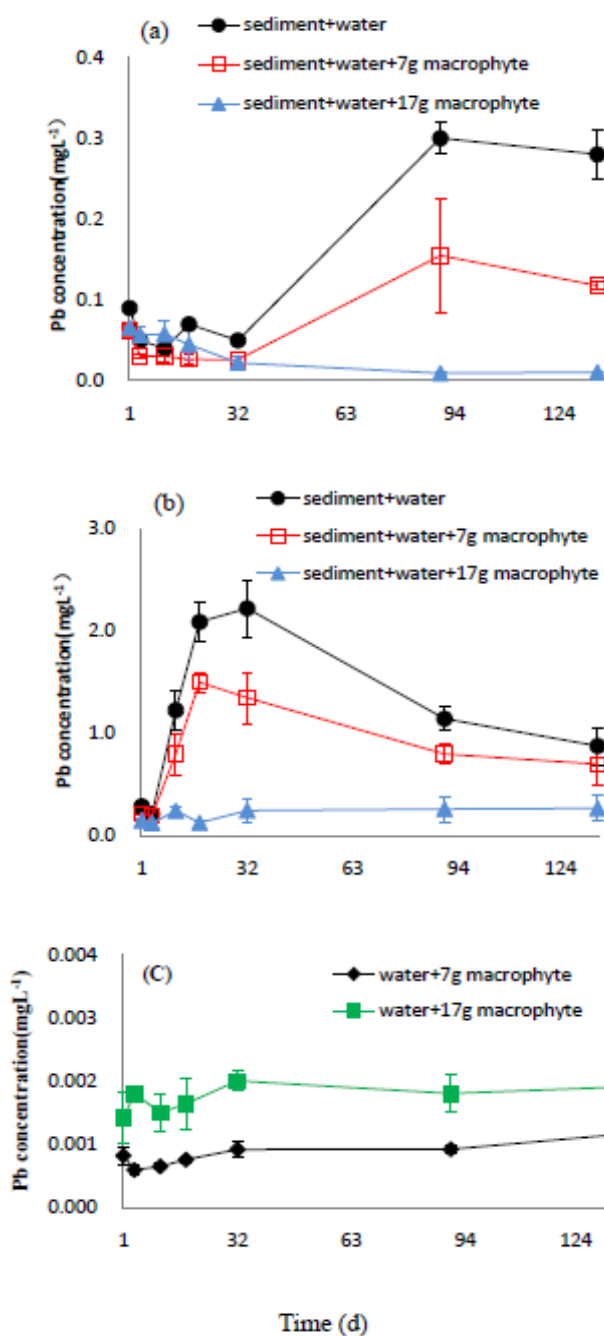


Figure 6. Changes in Pb concentrations in overlying water during the *C. cinerascens* amendment. (a) The treatments with low concentrations of heavy metal in sediments; (b) the treatments with high concentrations of heavy metal in sediments; (c) the treatments without sediments, as a function of time after flooding. Error bars indicate standard deviations

The release of Cu and Pb were slightly different from Cd and Zn, as a function of time after flooding. At low levels of heavy metal sediment contamination, both the Cu and Pb concentrations in the overlying water began to increase after 32 days, and the macrophyte addition significantly reduced the metal concentrations in the overlying water ($p < 0.05$). At high levels of heavy metal contamination, the Cu and Pb

concentrations in the overlying water first increased, then decreased and tended to be stable. At the two levels of heavy metal sediment contamination, the mean Cu and Pb concentrations in the later stage of the experiment followed the order: sediment+water> sediment+water+7 g macrophyte > sediment+water+17 g macrophyte (Fig. 5a,b and Fig. 6a,b). Moreover, the heavy metal concentration in the overlying water was significantly lower in the treatments with 17 g macrophyte addition than without macrophyte addition ($p<0.05$).

The decreased heavy metal concentrations in overlying water after the plant biomass addition to the sediment

To investigate the effect of the macrophyte biomass addition on the release of heavy metals from the sediments, $PD_i(\%)$ was calculated according to Eq. (1), and the results are shown in Table 2. It was found that the $PD_i(\%)$ values of Cd and Zn were all greater than zero. With low levels of heavy metal contamination in sediments, the Cd and Zn concentrations in the overlying water were decreased 6%-20% and 7%-23%, respectively, with the 7 g macrophyte biomass addition, and 6%-57% and 2-60%, respectively, with the 17 g macrophyte biomass addition.

Table 2. The decreased percentage of heavy metal concentration in overlying water after addition of plant biomass

Treatment	1d	4d	11d	18d	32d	90d	135d
Cd							
LS+water+7g macrophyte	19	21	6	19	8	24	20
LS+water+17g macrophyte	6	20	13	38	27	50	57
HS+water+7g macrophyte	8	12	9	12	11	10	11
HS+water+7g macrophyte	26	53	26	30	33	30	25
Zn							
LS+water+7g macrophyte	20	23	14	9	22	7	19
LS+water+17g macrophyte	2	7	5	12	48	20	60
HS+water+7g macrophyte	10	13	6	6	10	14	13
HS+water+7g macrophyte	23	26	15	20	25	35	32
Cu							
LS+water+7g macrophyte	-18	-28	-14	81	53	27	31
LS+water+17g macrophyte	-115	-145	-338	8	26	66	68
HS+water+7g macrophyte	-65	-12	3	37	43	28	18
HS+water+7g macrophyte	-128	-163	7	84	90	63	65
Pb							
LS+water+7g macrophyte	31	39	24	62	48	48	58
LS+water+17g macrophyte	27	-13	-45	36	55	97	96
HS+water+7g macrophyte	24	6	35	28	39	30	20
HS+water+7g macrophyte	48	42	80	94	89	77	69

With high levels of heavy metal contamination in sediments, the Cd and Zn concentrations in the overlying water were decreased 8%-12% and 6%-14%, respectively, with the 7 g macrophyte biomass addition, and 26%-53% and 15%-35%, respectively, with the 17 g macrophyte biomass addition. The $PD_i(\%)$ values of Cu and

Pb were all greater than zero in the late stage of the experiment. At low levels of heavy metal contamination in sediments, the Cu and Pb concentrations in the overlying water were decreased 27%-81% and 7%-23%, respectively, with the 7 g macrophyte biomass addition, and 6%-57% and 2%-60%, respectively, with the 17 g macrophyte biomass addition. The $PD_t(\%)$ values of Cu were less than 0 in the early stage, indicating that the addition of the macrophyte biomass promoted Cu release, but in the later stage of the experiment, the macrophyte biomass addition significantly reduced the release of Cu, reaching a maximum of 90%. For Pb, the addition of the macrophyte biomass reduced the release of Pb by up to 97%. The macrophyte additions have greater decreasing effects on the release of Pb and Cu than on the release of Cd and Zn.

There were no significant differences in the percentage of Cd and Zn concentrations in the overlying water in the macrophyte biomass addition treatments between the earlier stage and the later stage of the experiment ($p>0.05$). The decreased concentrations of Cu and Pb in the overlying water of the macrophyte biomass addition treatment in the later stages of the experiment were significantly higher than in the earlier stages of the experiment ($p<0.01$ and $p<0.05$, respectively).

Correlation between DOC and heavy metal release to the overlying water

The DOC concentration in the overlying water was tested for correlations with heavy metal concentrations in order to determine the share of metals bound directly to the DOC. With low levels of heavy metal contamination in sediments, DOC had a significantly negative correlation with Pb concentration ($R^2=-0.284$, $p<0.01$). No correlations between DOC concentration and Cd, Zn and Cu concentrations were observed. With high levels of heavy metal contamination in sediments, DOC had a significantly negative correlation with the Cd and Pb concentrations ($R^2=-0.266$ and -0.443 , respectively, $p<0.01$). No correlation between the DOC concentration and the Zn and Cu concentrations was observed.

Discussion

DOC is released during plant litter decomposition, when soluble polymeric organic substances are released into the water in the form of dissolved carbon (Bonanomi et al., 2014). The ability of DOC to bind metals during transport through water or soil and to form stable, aqueous complexes with copper, nickel, zinc and other ions has been shown in numerous works (Li and Shuman, 1997; Refaey et al., 2017). However, in this study, there were no significant positive correlations between the DOC concentration in the overlying water and the four heavy metals released from sediments. Some results also report that total dissolved metal concentrations (Cd, Zn, Cu, Pb, Co, Mn, Ni) generally did not show any significant or systematic correlation with DOC concentrations in river waters of Texas, and concluded that natural organic matter complexation was generally not a major process controlling trace metal concentrations (Jiann et al., 2013). Our results are also in accordance with other studies revealing an impact of invertebrate shredders on metal (calcium, manganese, iron, copper, zinc, arsenic, lead) fixation/remobilization with no influence on the DOC level (Schaller et al., 2010, 2013).

The releases of Cd, Zn, Cu and Pb from sediments were not identically affected by the fresh macrophyte biomass amendments. In most cases, the greater the amount of the plant biomass amendment, the greater the decrease in heavy metals released from

sediment to the overlying water. It was demonstrated that in the process of plant litters decomposition, metals are combined with litters through passive adsorption on organic surfaces or accumulated by microbial colonizers of the litter. And then plant litters can be places for metal sink (Du Laing et al., 2006, 2007; Guo et al., 2006). Therefore, studies have shown a strong positive correlation between the concentration of metal in the sediment and the concentration of organic matter in the upper sediment layer of the Scheldt marshes (Du Laing et al., 2007). The negative correlation and lack of correlation between the formation of DOC and the release of heavy metals in this study may be attributed to the fact that heavy metals were strongly bound to solid biomass and other colloids fixed on larger fractions but neither attached nor adsorbed the DOC (Schaller et al., 2010).

Conclusion

This study aimed to investigate the effects of the decomposition of macrophyte materials on heavy metals released from the lake sediment to the overlying water. In conclusion, wetland macrophytes could reduce the release of heavy metals from sediments to the overlying water. The release of heavy metals was not affected by DOC and the plant material may act as a metal sink.

The control of plant harvest or the stimulation of plant biomass production could be considered as management techniques to reduce the mobility of heavy metals in wetland ecosystems. Nevertheless, it is important to note that besides DOC and pH, the effects of decomposing plant materials on environmental conditions, such as electrolytic conductivity, dissolved oxygen and decomposition rate, are not considered in this study. Moreover, more investigations are necessary to understand the mechanisms and the fate of immobilized heavy metals after further decomposition.

Acknowledgements. This work was supported by the Natural Science Foundation of China (Nos.51409133, 51369011), the science and technology projects of the Jiangxi Provincial Department of Water Resources (KT201302, KT201510, KT201605, KT201712, 201820YBKT09) and the open fund of the Poyang Lake Water Resources, Water Ecology and Environment Research Center, MWR (KFJJ201404, ZXKT201701).

REFERENCES

- [1] Al-Reasi, H. A., Wood, C. M., Smith, D. S. (2013): Characterization of freshwater natural dissolved organic matter (DOM): Mechanistic explanations for protective effects against metal toxicity and direct effects on organisms. – *Environ Int* 59: 201-207.
- [2] Ashworth, D. J., Alloway, B. J. (2008): Influence of dissolved organic matter on the solubility of heavy metals in sewage-sludge-amended soils. – *Commun Soil Sci Plant Anal* 39: 538-550.
- [3] Bonanomi, G., Senatore, M., Migliozi, A., Marcob, A. D., Pintimallic, A., Lanzottia, V., Mazzolenia, S. (2014): Decomposition of submerged plant litter in a Mediterranean reservoir: A microcosm study. – *Aquat Bot* 120: 169-177.
- [4] Chon, H., Ohandja, D., Voulvoulis, N. (2012): The role of sediments as a source of metals in river catchments. – *Chemosphere* 88: 1250-1256.
- [5] Dienemann, H., Dienemann, C., Dudel, E. G. (2006): Influence of allochthonous plant litter on fixation of uranium in sediments. – In: Merkel, B., Hasche-Berger, A. (eds.) *Uranium in the Environment*. Springer, Berlin, pp. 149-157.

- [6] Dittrich, M., Chesnyuk, A., Gudimov, A., McCulloch, J., Quazi, S., Young, J., Winter, J., Stainsby, E., Arhonditsis, G. (2013): Phosphorus retention in a mesotrophic lake under transient loading conditions: insights from a sediment phosphorus binding form study. – *Water Resour* 47: 1433-1447.
- [7] Du Laing, G. (2006): Dynamics of heavy metals in reedbeds along the banks of the river Scheldt. – PhD thesis, Ghent University.
- [8] Du Laing, G., De Grauwe, P., Moors, W., Vandecasteele, B., Lesage, E., Meers, E., Tack, F. M. G., Verloo, M. G. (2007): Factors affecting metal concentrations in the upper sediment layer of intertidal reedbeds along the river Scheldt. – *Journal of Environ Monit* 9: 449-455.
- [9] Gessner, M. O. (2000): Breakdown and nutrient dynamics of submerged *Phragmites* shoots in the littoral zone of a temperate hardwater lake. – *Aquat Bot* 66: 9-20.
- [10] Guo, X. Y., Zhang, S. Z., Shan, X. Q., Luo, L., Pei, Z. G., Zhu, Y. G., Liu, T., Xie, Y. N., Gault, A. (2006): Characterization of Pb, Cu, and Cd adsorption on particulate organic matter in soil. – *Environ Toxicol Chem* 25: 2366-2373.
- [11] Guo, X. J., Yuan, D. H., Li, Q., Jiang, J. Y., Chen, F. X., Zhang, H. (2012): Spectroscopic techniques for quantitative characterization of Cu (II) and Hg (II) complexation by dissolved organic matter from lake sediment in arid and semiarid region. – *Ecotoxicol Environ Saf* 85: 144-150.
- [12] Hafeznezami, S., Kim, J. L., Redman, J. (2012): Evaluating removal efficiency of heavy metals in constructed wetlands. – *J Environ Eng* 138(4): 475-482.
- [13] Han, Z., Cui, B. S., Zhang, Y. T. (2015): Decomposition of *Phragmites australis* rhizomes in artificial land-water transitional zones (ALWTZs) and management implications. – *Frontiers of Earth Science* 9(3): 555-566.
- [14] Jiann, K., Santschi, P. H., Presley, B. J. (2013): Relationships between geochemical parameters (pH, DOC, SPM, EDTA concentrations) and trace metal (Cd, Co, Cu, Fe, Mn, Ni, Pb, Zn) concentrations in river waters of Texas (USA). – *Aquat Geochem* 19: 173-193.
- [15] Kouba, A., Buric, M., Kozak, P. (2010): Bioaccumulation and effects of heavy metals in crayfish: a review. – *Water Air Soil Pollut* 211: 5-16.
- [16] Li, Z., Shuman, L. M. (1997): Mobility of Zn, Cd and Pb in soils as affected by poultry litter extract I. Leaching in soil columns. – *Environ Pollut* 95: 219-226.
- [17] Noges, P., Tuvikene, L., Noges, T., Kisand, A. (1999): Primary production, sedimentation and resuspension in large shallow Lake Vortsjarv. – *Aquat Sci* 61: 168-182.
- [18] Nriagu, J. O., Pacyna, J. M. (1988): Quantitative assessment of worldwide contamination of air, water and soils by trace-metals. – *Nature* 333: 134-139.
- [19] Ranville, J. F., Hendry, M. J., Reszat, T. N., Xie, Q. L., Honeyman, B. D. (2007): Quantifying uranium complexation by groundwater dissolved organic carbon using asymmetrical flow field-flow fractionation. – *JContamHydrol* 91: 233-246.
- [20] Refaey, Y., Jansen, B., Parsons, J. R., de Voogt, P., Bagnis, S., Markus, A., El-Shater, A.-H., El-Haddad, A.-A., Kalbitz, K. (2017): Effects of clay minerals, hydroxides, and timing of dissolved organic matter addition on the competitive sorption of copper, nickel, and zinc: A column experiment. – *Journal of Environmental Management* 187: 273-285.
- [21] Ross, J. H., Dudel, E. G. (2008): Uranium loads and accumulation in a mine water contaminated wetland. – In: Rapantova, N., Hrkal, Z. (eds.) *Mine Water and the Environment*. Technical University of Ostrava, Ostrava, pp. 225-228.
- [22] Sachs, S., Brendler, V., Geipel, G. (2007): Uranium (VI) complexation by humic acid under neutral pH conditions studied by laser-induced fluorescence spectroscopy. – *Radiochim Acta* 95: 103-110.
- [23] Schaller, J., Weiske, A., Mkandawire, M., Dudel, E. G. (2008): Enrichment of uranium in particulate matter during litter decomposition affected by *Gammarus pulex* L. – *Environ Sci Technol* 42: 8721-8726.

- [24] Schaller, J., Mkandawire, M., Dudel, E. (2010): Heavy metals and arsenic fixation into fresh water organic matter under *Gammarus pulex* L. influence. – Environ Pollut 158: 2454-2458.
- [25] Schaller, J., Vymazal, J., Brackhage, C. (2013): Retention of resources (metals, metalloids and rare earth elements) by autochthonously/allochthonously dominated wetlands: A review. – Ecol Eng 53: 106-114.
- [26] Wang, S., Mulligan, C. (2009): Enhanced mobilization of arsenic and heavy metals from mine tailings by humic acid. – Chemosphere 74: 274-279.
- [27] Yamashita, Y., Jaffe, R. (2008): Characterizing the interactions between trace metals and dissolved organic matter using excitation-emission matrix and parallel factor analysis. – Environ Sci Technol 42: 7374-7379.
- [28] Yin, H. B., Gao, Y. N., Fan, C. X. (2011): Distribution, sources and ecological risk assessment of heavy metals in surface sediments from Lake Taihu, China. – Environ Res Lett 6: 044-012.
- [29] Yuan, G., Liu, C., Chen, L., Yang, Z. (2011): Inputting history of heavy metals into the inland lake recorded in sediment profiles: Poyang Lake in China. – J Hazard Mater 185: 336-345.
- [30] Zhao, L. Y. L., Schulin, R., Nowack, B. (2009): Cu and Zn mobilization in soil column spercolated by different irrigation solutions. – Environ Pollut 157: 823-833.

COMPARISON OF METHANOGENESIS BETWEEN SUNFLOWER AND CORN STALKS MIXED WITH PIG MANURE AT DIFFERENT TEMPERATURES

FENG, L.¹ – YU, Q.¹ – ZHEN, X. F.^{2*} – DONG, H. Y.² – ZHENG, J.³ – WANG, Y.³

¹*Liaoning Province Clean Energy Key Laboratory, Shenyang Aerospace University
Shenyang Daoyi Street 37, Shenyang 110136, China
(phone: +86-1804-0038-889)*

²*School of New Energy and Power Engineering, Lanzhou Jiaotong University
No. 88, Anning West Road, Anning District, Lanzhou 730070, China
(phone: +86-1391-9302-012)*

³*School of Energy and Power Engineering, Lanzhou University of Technology
No. 287, Langongping Road, Qilihe District, Lanzhou 730050, China
(phone: +86-1391-9257-393)*

**Corresponding author*

e-mail: farming478@outlook.com; phone: +86-1391-9302-012

(Received 21st Jun 2019; accepted 16th Oct 2019)

Abstract. The gas production effect of two kinds of straws mixed with pig manure via anaerobic fermentation under two sets of temperatures 32°C and 52°C has been studied in this experiment. In the process, sunflower and corn straw were used as raw materials with activated sludge as inoculum in a batch anaerobic fermentation reactor. The results showed that the average methane content of sunflower straw reached 62.55% at 37°C, which was 20.41% higher than that of sunflower straw at 52°C. The cumulative methanogenic yield of corn stalks was higher than that of sunflower stalks at different temperatures. The cumulative methane production of corn stalks was the highest at 52°C, and 67.99 L of methane was produced in 54 days. The cumulative methane production of sunflower stalks was the lowest at 52°C, and the methane production was 34.09 L in 53 days. The results showed that corn stalks produce more methane than sunflower stalks and are more suitable for high temperature anaerobic fermentation. On the other hand, sunflower stalks were found suitable for medium temperature fermentation.

Keywords: *anaerobic fermentation, biomass, resource utilization, livestock manure, biogas*

Introduction

The People's Republic of China as a large agricultural country has abundant straw resources. In 2017, the country's collectible straw production from the main crops reached 900 million tons (Liu et al., 2018). This production included the straw from corn (*Zea mays* L., Fam.: Poaceae) and sunflower (*Helianthes annuus* L., Fam.: Asteraceae). The amount was nearly more than 1/3 of the total straw production of China. In China, reasonable conversion of straw to available energy is crucial field of research (Du et al., 2015). At present, a large amount of straw in China is not being effectively utilized, resulting in wastage of resources and pollution to the environment due to indiscriminate burning (Fan et al., 2018). The anaerobic fermentation technology is an effective means to ensure the utilization of straw resources and the technology can sufficiently solve the problem of straw waste management and generate renewable energy such as methane gas to alleviate the energy shortage in China (Duan et al., 2016). The effort will promote

the sustainable development of the society and improve the economy and ecological condition of the environment (Wan et al., 2010; Jha et al., 2011; Sun, 2016).

Studies related to the methane production by straw is affected by a number of factors. Among which temperature is an important factor affecting anaerobic fermentation (Brown et al., 2012; Huang et al., 2018). It plays an important role in microbial growth rate, enzyme activity, biochemical reaction rate, etc. Generally, the anaerobic fermentation temperature is divided into three gradients: low temperature, medium temperature and high temperature (Liu et al., 2008; Yin et al., 2014). Juan et al. (2018) found that the methane production efficiency of corn straw increased with increasing temperature. During anaerobic fermentation at high temperature like 55°C, the total organic load (TS) was 100 g/L. The yield of TS in the corn straw unit was 44.68% higher than that under the anaerobic digestion at 45°C, which was 64.08% higher than 35°C. Studies by Pang et al. (2018) and others showed that the cumulative methane production of anaerobic fermentation of cow manure and straw at 35°C was 91.84 L, which was 20% higher than that at 25°C and 30°C. Contreras et al. (2012) explored the potential for methane production in rice straw and rice at 37°C and 55°C. It was found that the biogas production at high temperature was 0.43 m³·kg/vs, which was 0.09 m³·kg/vs higher than that under medium temperature. It was confirmed that the high-temperature fermentation of rice straw was better.

In the present research, studies on the effects of temperature on anaerobic fermentation of different types of straw have been reported (Gu et al., 2016). Some previous studies have shown different types of gas production by using different compositions of straw. However, there exists very few studies on the effect of temperature and on the potentiality of anaerobic fermentation of sunflower straw and its anaerobicity. In order to fill up the gap between theoretical research and the application of the technology in practice, the concept of present research has been developed. In this research, using batch anaerobic fermentation reactor, the effect of gas production changes by sunflower and corn straw at 37°C and 52°C has been compared during the research, the changes of various parameters while the anaerobic fermentation of two straws were in operation have also been studied. So, the aim of the present research is to maximize the utilization of straw anaerobic fermentation, improve the resource utilization of sunflower straw and corn straw and to provide data support for straw anaerobic fermentation technology.

Materials and Methods

Experiments

The corn straw for the present study was collected from the Shenbei New District of Shenyang City, Liaoning Province, China. The whole corn was harvested and after separating the grains of the cobs, the straws were air dried and crushed. The crushed biomass of the straw was passed through a 20-mesh sieve. The source and treatment of sunflower straw were the same as those applied for the corn straw. Fresh pig manure was collected from Shenbei New District, Shenyang City, Liaoning Province. The inoculum used for the experiment was the biogas slurry collected after carrying out in vitro anaerobic fermentation. Fresh pig manure (mass ratio 1:10) was added before the experiment which was carried out at medium (37°C) and high temperature (52°C) for 15

days. The characteristic parameters of the raw materials used in the anaerobic digestion processes have been presented in *Table 1*.

Table 1. Presenting the characteristic parameters of anaerobic digestion feedstock

Raw material	TS/% Total solids	VS/% volatile solids	C/N
Corn straw	89.78±0.01	71.68±0.01	ND
Sunflower straw	94.44±0.01	88.64±0.01	ND
Pig manure	29.28±0.02	19.8±0.01	24±0.03
Biogas slurry inoculum	2.09±0.01	0.885±0.001	ND

Data shown were the average and standard deviation based on triplicate runs; ND meant not determined

Main devices

A controllable constant temperature fermentation unit was used for carrying out the tests involved in the present investigation. The experimental protocol has been presented in *Fig. 1*.

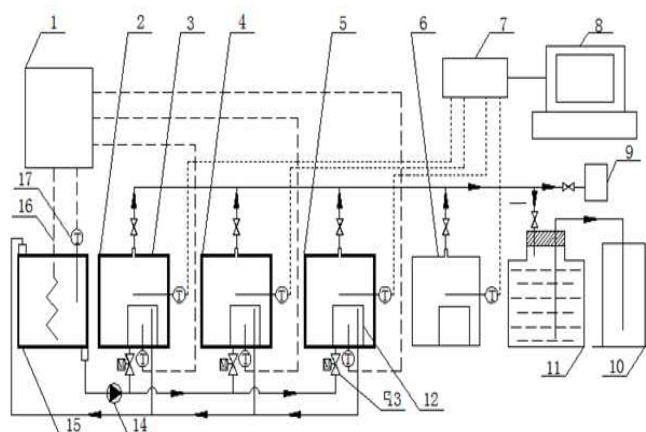


Figure 1. Schematic diagram of controllable constant-temperature fermenting equipment
 1. Temperature controller 2. Insulation layer 3. Fermentation cylinder 4. Fermentation cylinder
 5. Fermentation cylinder 6. Fermentation cylinder 7. Data collecting instrument 8. Computer 9.
 Biogas analyzer 10. Water storage tank 11. Gas storage tank 12. Internal water tank 13.
 Solenoid valve 14. Hot water pump 15. Constant temperature water tank 16. Heating wire 17.
 Temperature sensor

The device is mainly composed of a heating water tank, a temperature controller, a cylindrical 304 stainless steel fermenter with an effective volume of 10 L (with a height to diameter ratio of 1:1) and a gas collecting device. The fermenter of the device is insulated from the environment and the temperature of the fermenter is adjusted. The flow rate of the circulating heating water tank is precisely controlled, and the temperature is measured with a Pt100 platinum resistance temperature detecting device with an accuracy of $\pm 0.1^\circ\text{C}$.

Other instruments used for determining various other experimental parameters were: TDL-5-A centrifuge (Shanghai Anting Scientific Instrument Factory); GZX-9240MBE digital display blast drying oven (Shanghai Boxun Industrial Co., Ltd.); UV-9200 UV-visible spectrophotometer (Beijing Ruili Analytical Instruments Co., Ltd.); Biogas check

biogas analyzer (Geotech, UK); JSM5600LV scanning electron microscope (JEOL, Japan) and D/MAX-2004 powder X-ray diffractometer (Nippon Science).

Anaerobic digestion test design

The mass ratio of corn and sunflower stalk and pig manure was 1:2 and the amount of biogas slurry inoculation was 30% of the mass. The corn straw group contained: straw, pig manure, acclimated biogas slurry at the rate of 0.30 kg, 0.59 kg and 1.70 kg, respectively. On the other hand, sunflower straw group contained: 0.30 kg, 0.58 kg and 1.69 kg as straw, pig manure and acclimated biogas slurry, respectively after feeding, 6.0 kg distilled water was added.

The fermenter has a volume of about 6 L, and the temperature is controlled at $52 \pm 1^\circ\text{C}$ and $37 \pm 1^\circ\text{C}$, respectively. The reaction tank is shaken 3 times per day, and the digestion process is continued until no gas is produced. The test run cycle was fixed for 54 d. The pH value, gas composition and gas production of the fermentation broth were measured every 5 days, and indicators like the chemical oxygen demand (COD), volatile fatty acids (VFAs) and ammonia nitrogen ($\text{NH}_4^+\text{-N}$) of the fermentation broth were measured at intervals of 4 days. After the fermentation, the corn straw residue is separated, and the weight after drying was taken and recorded.

Analysis methods

The total solids (TS) and volatile solids (VS) of corn straw, sunflower straw, pig manure and biogas slurry inoculum samples were measured according to the standard methods (APHA, 1998). The biogas components were measured using a Biogas Check. The pH value was measured using an Oriol PHS3C portable pH meter. VFAs and COD determination is based on Liu et al. (2013), using spectrophotometry and potassium dichromate method respectively. While phenol sodium hypochlorite colorimetry method was used to determine $\text{NH}_4^+\text{-N}$ concentration. The measurement of alkalinity was carried out using an acid-base indicator titration method.

Neutral detergent fiber (NDF), acid detergent fiber (ADF) and acid detergent lignin (ADL) measurements were done via Paradigm analysis. Cellulose (CL) and hemicellulose (HC) quality scores were done after ADF-ADL and NDF-ADF. The structural analysis were carried out using scanning electron microscope (SEM) as well as X-ray diffraction (XRD).

Results and Discussion

Gas production changes of corn straw and sunflower straw under anaerobic fermentation at different temperatures

It can be seen from *Figs. 2-3* that the gas production amount is significantly different depending upon the temperature and straw varieties. During the 54 d fermentation period, the gas yield of corn straw reached the peak at 11.72 L/d on the 42nd day at 52°C . At this temperature, the sunflower straw reached the highest daily gas production at 4.94 L/d on the 44th day. At 37°C , the gas yield of corn straw reached the peak at 4.83 L/d on the 51st day, while the peak gas yield of sunflower straw appeared at 47 d, which was 5.92 L/d. In contrast, the peak gas production time during high temperature fermentation at 52°C was earlier than that at 37°C . In addition, the cumulative gas production of corn straw at 52°C was 140.31 L while the cumulative gas production of sunflower straw was 80.68 L.

On the other hand, the cumulative gas production of corn straw at 37°C was 92.46 L and the peak gas yield of sunflower straw was 67.55 L. Cumulative total biogas production in the present investigation followed an order: 52°C corn straw > 37°C corn straw > 52°C sunflower straw > 37°C sunflower straw. The cumulative gas production of corn straw and sunflower straw at 52°C is higher than the cumulative gas production at 37°C, indicating that the bioactivity of the bacteria is stronger under high temperature. During which, the decomposition efficiency of cellulose, hemicellulose and other substances is higher and the metabolic rate of microbial cells is accelerated. The anaerobic fermentation efficiency is improved. In addition, the cumulative gas production of corn straw was higher than that of sunflower straw. The daily gas production of sunflower straw during the late stage decreased to the initial stage of the reaction, indicating that the content of cellulose and other substances in sunflower straw was lower than that of corn straw. Insufficient accumulation leads to a decrease in gas production efficiency and a decrease in gas production during the later stages of methanogen production.

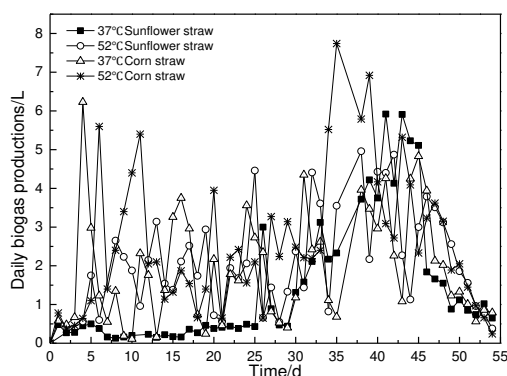


Figure 2. Daily biogas production trends of corn straw and sunflower straw at different temperatures

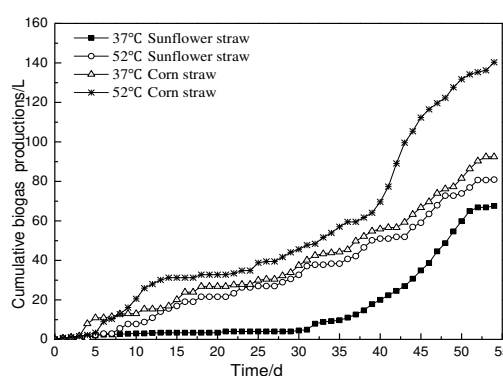


Figure 3. Cumulative biogas production trends of corn straw and sunflower straw at different temperatures

Anaerobic fermentation pH and fatty acid changes of corn straw and sunflower straw at different temperatures

Because, acid-producing bacteria have a wide range of pH adaptation and methane producing bacteria are sensitive to pH changes, pH plays a great role in the anaerobic digestion processes.

During the 54-day fermentation period, the pH of each group can be roughly divided into three stages: “stable-decline-fast rise”. The overall pH of the fermentation was between 6.5 and 7.9, indicating that the self-regulating pH inside the fermentation can maintain a stable fluctuation range (Zhou et al., 2014). Since the added activated sludge itself is weakly alkaline, the pH gradually rises during the initial stage of the reaction. During the period of 18 d-30 d, the pH value may decrease. It may be that the hydrolysis and acidification of the acetogenic bacteria decomposes the available materials in the straw and converts them into volatile fatty acids. At this time, the ammonia nitrogen content of the alkalinity in the fermentation system is insufficient, and the methanogens are still insufficiently adapted to the environment. A large amount of fatty acids accumulate, leading to a drop in pH (Fang et al., 2017). From 35 d to 47 d in the later stage of the experiment, as the reaction continued, the methanogens gradually adapted to

the environment. As a result the activity of the strains increased and began to reproduce, consuming large amounts of fatty acids and producing ammonia nitrogen. The pH level rose again. As seen from figures (Fig. 4 and Fig.5) there is an opposite trend of change of pH and VFAs in anaerobic fermentation. During the mid-stage pH drop, the fatty acid concentration was at a higher value; while the pH value increased at the late stage of fermentation, the concentration of volatile fatty acids began to decrease rapidly.

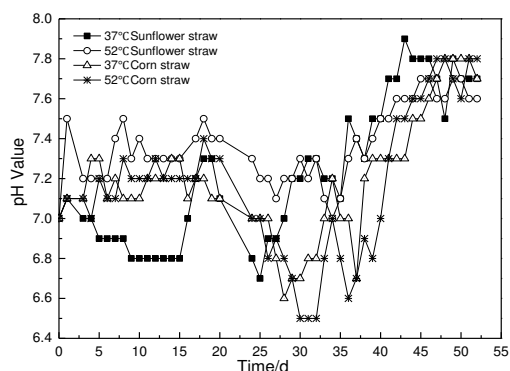


Figure 4. Change trend of pH value of corn straw and sunflower straw under different temperatures

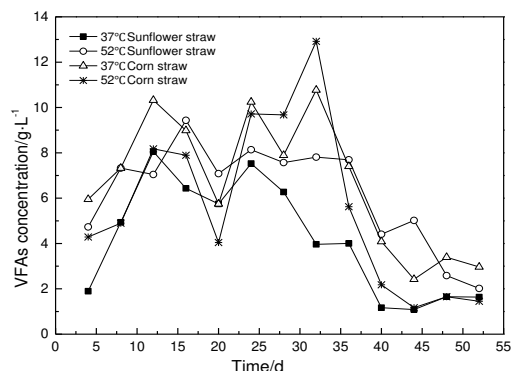


Figure 5. Change trend of volatile fatty acids concentration of corn straw and sunflower straw under different temperatures

Volatile fatty acids are important intermediary compounds for reflecting microbial metabolism during anaerobic fermentation of straw (Xu et al., 2016).

At 37°C, sunflower straw reaches almost in the acidification and gas-free stage within 30 days before the middle temperature anaerobic digestion. However, the average concentration of VFAs was the lowest at this stage, and the theoretical inhibition intensity was the lowest, but the cumulative gas production was the lowest. The analysis showed that the sunflower stalks were under medium temperature conditions. The volatile acid produced had the highest propionic acid content, while propionic acid had the most obvious inhibitory effect on methanogens, which led to the inhibition of gas production in the first and middle stages. The average concentration of VFAs in corn straw at 37°C was higher than 52°C. Although, the average content of methane in corn straw at 52°C and 37°C was not much different, only 2.8% higher, but the cumulative yield of corn straw methane at 52°C was much higher than that of sunflower straw. The results showed that different temperatures had different effects on the methanogenesis of sunflower straw and corn straw. At 37°C, the methane production increased rapidly and the average methane content was the highest. The analysis showed that the methanogens used acetic acid, the acetic acid content decreased, and the acetic acid was resistant to propionic acid. Oxygen digestion has the strongest inhibitory effect. The decrease in acetic acid content leads to an increase in the degradation ability of propionic acid, and the gas production efficiency of methanogens increases. The content of VFAs decreased at the beginning of 52°C corn straw for 30 days. At the same time, the methane production grew rapidly and the average methane content was higher than 37°C, indicating that corn straw was more suitable for 52°C high temperature anaerobic fermentation.

Ammonia nitrogen concentration changes in corn straw and sunflower straw under anaerobic fermentation at different temperatures

The change of ammonia nitrogen concentration is an important parameter for the stability of the reaction fermentation system. It can be seen from *Fig. 6* that the average ammonia nitrogen value of sunflower straw is 1.19 g/L at 37°C and 1.87 g/L at 52°C and the average ammonia nitrogen value of corn straw at 37°C is 1.85 g/L and at 52°C, it is 1.98 g/L. At 37°C, the ammonia nitrogen concentration and pH of the sunflower straw fermentation were lower than other groups. It may be that at 37°C sunflower straw has higher activity of acid-producing bacteria at this stage, while the methanogen has not adapted to the environment, resulting in low ammonia nitrogen concentration. On the 40th day of fermentation, the daily methane production of sunflower straw increased significantly at 37°C. It is known from *Figure 4* that the pH increased rapidly. At this stage, the ammonia nitrogen concentration decreased rapidly and the volatile fatty acid reached the lowest value (Lin et al., 2011). It indicated that low concentration of ammonia nitrogen can promote the proliferation and division of methanogens and increase the yield of methane, which is consistent with the experimental study of Shun et al. (2018).

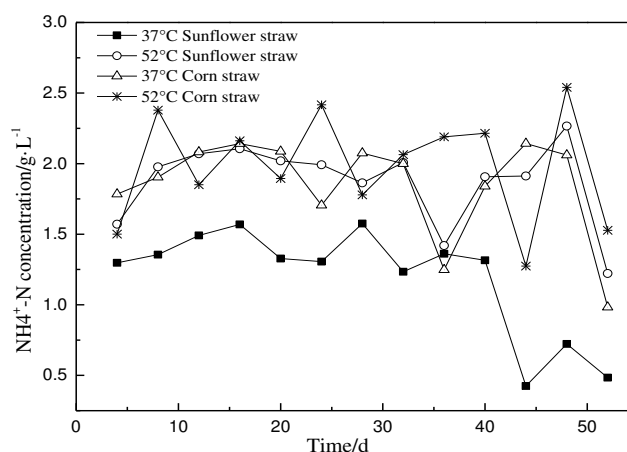


Figure 6. Change trend of ammonia nitrogen concentration of corn straw and sunflower straw under different temperatures

The average concentration of ammonia nitrogen in high temperature anaerobic fermentation of corn straw and sunflower straw was higher than that of medium temperature anaerobic fermentation. In the appropriate temperature range, as the temperature increases, the activity of the strain gradually increases resulting an increasing rate of ammonia nitrogen.

Anaerobic methanogenesis of corn straw and sunflower straw at different temperatures

It can be seen from *Figs. 7-8* that the methane production in the middle and early days before the reaction is low, and in the late, rate rises rapidly, The peak value appears between 42 d and 51 d, and the gas production fluctuates greatly, indicating that the experimental fermentation factors are excessive. At the temperature of 52°C, the methanogenic rate of corn stalks increased rapidly from 40 d to 44 d. It was found that a large amount of methanogenic precursors such as acetic acid, formic acid, ethanol and CO₂ were formed in the middle and early stages of corn stalks at the same temperature. Methanogens can be utilized, and gas production increases, leading to peak values. The peak daily methane production of sunflower straw at 37°C and sunflower straw at 52°C

was 47 d and 44 d, respectively. The peaks of daily methane production at 37°C and 52°C of corn straw were 51 d and 42 d, respectively. It can be seen that as the temperature increases, the peak value of the daily methane gas conversion is advanced. However, there is no such rule in methane production. From *Table 2*, the highest content of methane in corn stalks at 52°C is 73.7%, while the highest methane content in corn stalks at 37°C is 70.9%. However, sunflower straw and corn stalks showed an opposite trend. The maximum content of methane from sunflower straw at 37°C was 78.37%, while the same at 52°C was only 58.70%. It can be speculated that the cumulative methane production of corn stalks increases with increasing temperature within a certain temperature range. The accumulated methane production of sunflower straw at 37°C was higher than 52°C. The result showed that 37°C was closer to the optimum temperature of sunflower straw anaerobic fermentation. While the activity of methanogen was inhibited at 52°C, and the methane production decreased.

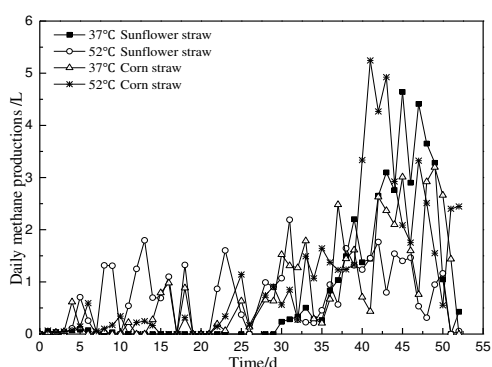


Figure 7. Daily methane production of corn straw and sunflower straw under different temperatures

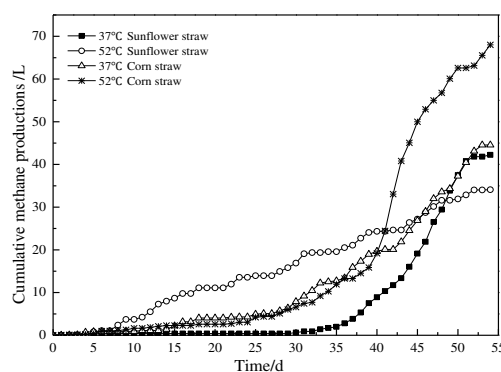


Figure 8. Cumulative methane production of corn straw and sunflower straw under different temperatures

Table 2. Biogas production and methane production changes

Grouping	Sunflower straw at 37°C	Sunflower straw at 52°C	Corn straw at 37°C	Corn straw at 52°C
Daily biogas productions/L	1.25	1.49	1.71	2.59
TS biogas productions/L·kg ⁻¹ TS	141.35	169.27	193.53	293.69
VS biogas productions/L·kg ⁻¹ VS	175.06	209.64	266.59	404.55
TS methane productions/L·kg ⁻¹ TS	88.41	71.33	93.28	142.32
VS methane productions/L·kg ⁻¹ VS	109.45	88.34	128.49	196.05
Average methane content%	62.55	42.14	48.20	48.46
Maximum methane content%	78.37	58.70	70.90	73.70

Conclusions

From the present investigation, experiments show that temperature has a significant effect on the gas production characteristics of combined sunflower straw and corn straw anaerobic fermentation.

In the 100-day fermentation test, the cumulative methane production of corn stalk at 52°C was 77.99 L, which was 128.77% higher than that of anaerobic fermentation of sunflower straw at the same temperature. When the fermentation temperature was

maintained at 37°C, the cumulative production of methane from sunflower straw The lowest amount, only 34.09 L. However, the average content of methane in sunflower straw at the fermentation temperature of 37°C was 62.55%, which was higher than the average content of corn stalks at 37 degrees Celsius and sunflower stalks at 52 degrees Celsius by 14.35% and 20.41%. In general, in order to improve the methane yield of anaerobic fermentation of straw, corn straw is more suitable for anaerobic fermentation at high temperature (52°C). Unlike corn straw, sunflower straw is more suitable for anaerobic fermentation at medium temperature (37°C).

The methane production characteristics of straw and pig manure under medium and high temperature anaerobic fermentation conditions were studied. It was proved that corn stalk and pig manure could effectively improve the C/N ratio of materials and improve anaerobic digestion efficiency, and synergistically in anaerobic fermentation.

There is no research on low temperature (<15°C). The winter temperature in northern China is low, and the anaerobic mixing of straw and pig manure at low temperature is studied. Fermentation has high value for the utilization of biomass resources.

Acknowledgements. This work was funded by the National Natural Science Foundation project (51509122), and Gansu Provincial Higher Education Science and Technology Achievements Transformation Project (2018D-04), Gansu Natural Science Foundation (18JR3RA154), 2018 Yangling Demonstration Zone Collaborative Innovation Major Project (2018CXY-14).

REFERENCES

- [1] APHA (1998): Standard Methods for the Examination of Water and Wastewater. – 18th ed., American Public Health Association, DC, US.
- [2] Brown, D., Shi, J., Li, Y. (2012): Comparison of solid-state to liquid anaerobic digestion of lignocellulosic feedstocks for biogas production. – *Bioresource Technology* 124(11): 379-386.
- [3] Chen, G., Du, J., Chang, Z., Ye, X., Xu, Y., Zhang, J. (2014): Characteristics of biogas producing by anaerobic co-digestion of agricultural straw and swine wastewater based on improved straw-bed bioreactor. – *Transactions of the Chinese Society of Agricultural Engineering* 30(20): 244-251.
- [4] Contreras, L. M., Schelle, H., Sebrango, C. R., Pereda, I. (2012): Methane potential and biodegradability of rice straw, rice husk and rice residues from the drying process. – *Water Science & Technology, A Journal of the International Association on Water Pollution Research* 65(6): 1142-9.
- [5] Du, J., Chen, G.-Y., Ye, X.-M., Fu, G.-Q. (2015): Effects of contact ratio of straw and free fermentation liquid on characteristics of anaerobic fermentation. – *China Environmental Science* 35(03): 811-816.
- [6] Duan, X., Wang, X., Xie, J., Feng, L., Yan, Y., Zhou, Q. (2016): Effect of nonylphenol on volatile fatty acids accumulation during anaerobic fermentation of waste activated sludge. – *Water Research* 105: 209-217.
- [7] Fan, X. S., Liu, C. R., Li, Y. C. et al. (2018): Influence of Fe₂(SO₄)₃ on the biogas production in the anaerobic fermentation system with rice straw and pig manure. – *Journal of Safety and Environment* 18(03): 1159-1165.
- [8] Fang, W., Ye, J., Zhang, P., Zhu, X., Zhou, S. (2017): Solid-state anaerobic fermentation of spent mushroom compost for volatile fatty acids production by pH regulation. – *International Journal of Hydrogen Energy* 42(27): 18295-18300.

- [9] Fleming, R. A., Barclay, H. J., Candau, J. N. (2002): Scaling-up an autoregressive time-series model (of spruce budworm population dynamics) changes its qualitative behaviour. – *Ecological Modelling* 149(1-2): 127-142.
- [10] Gu, Q., Chang, S. X., Wang, Z.-P., Feng, J.-C., Chen, Q.-S., Han, X.-G. (2016): Microbial versus non-microbial methane releases from fresh soils at different temperatures. – *Geoderma* 284: 178-184.
- [11] He, S., Xian, P., Li, Z., Tan, S., Xiong, H., Deng, Q., Liu, Q., Li, T., Huang, Y. (2018): Anaerobic fermentation characteristics of sludge mixed with banana straw. – *Chinese Journal of Environmental Engineering* 12(9): 2658-2663.
- [12] Huang, J. H., Wang, H. J., Huang, T. et al. (2018): Effects of temperature, salt content and oil content on combined anaerobic fermentation of kitchen waste and sludge. – *Chemical Industry Management* 483(12): 21-23.
- [13] Jha, A. K., Li, J. Z., Nies, L., Zhang, L. G. (2011): Research advances in dry anaerobic digestion process of solid organic wastes. – *African Journal of Biotechnology* 10(65): 14242-14253.
- [14] Li, J., Pang, Y. Z., Yuan, H. R. et al. (2018): Enhancing Methane Production from Corn Stalk by Mesophilic and Thermophilic Anaerobic Digestion. – *China Biogas* 36(01): 76-80.
- [15] Lin, C., Wang, Y., Hou, J., Hou, Y. (2011): Effects of bacterial protein and urea addition on straw anaerobic fermentation. – *Transactions of the Chinese Society of Agricultural Engineering* 27(1): 74-78.
- [16] Liu, C. F., Yuan, X. Z., Zeng, G. M., Li, W. W., Li, J. (2008): Prediction of methane yield at optimum pH for anaerobic digestion of organic fraction of municipal solid waste. – *Bioresource Technology* 99(4): 882-888.
- [17] Liu, S. Q., Zhang, W. D., Yin, F. (2013): *Biogas fermentation experiment tutorial*. – Chemical Industry Press.
- [18] Liu, Y., Zhao, L. X., Shen, Y. J. et al. (2018): Carbon and Nitrogen Changes in the Whole Process of Agricultural Waste Anaerobic Fermentation and Its residue Utilization as Fertilizer. – *China Biogas* 36(01): 65-70.
- [19] Pang, Z. P., Li, Y. P., Zhu, J. N., et al. (2018): Effects of Different Temperatures on Biogas Production from Anaerobic Fermentation of Cow Manure and Tomato Straw. – *Journal of Shan xi Agricultural Sciences* 46(08): 1338-1343.
- [20] Sun, Z., Zhang, J., Liu, Y., Wu, Y., Liu, D., Ma, W. (2016): Biochemical methane potential and kinetics of anaerobic digestion of cattle manure compared with corn straw. – *Chinese Journal of Environmental Engineering* 10(03): 1468-1474.
- [21] Wan, C. Y., Huang, F. F., Liu, R., Li, W., Deng, Q. (2010): Effect on increasing biogas production using rape straw by microbiological pretreatment. – *Transactions of the CSAE* 26(6): 267-271.
- [22] Xu, X. J. (2018): Analysis of Silage Technology of Corn Straw Feed. – *Chinese Journal of Animal Husbandry and Veterinary Medicine* 5: 232-232.
- [23] Zhou, Q., Liu, Y., Zou, D., Zhu, B., Yuan, H., Li, X. (2014): Methane Production Performance of Anaerobic Co-digestion of Food Waste and Corn Stalk. – *China Biogas* 32(01): 27-31, 48.

STABLE CARBON ISOTOPE COMPOSITION OF MOLLUSC TISSUES: EVIDENCE OF FOOD SOURCES

YAN, H.^{1*} – YU, X. X.¹ – YUAN, S. Y.¹ – SHEN, N. J.¹ – XIAO, J.²

¹*College of Urban-rural Planning and Landscape Architecture, Xuchang University
Xuchang 461000, China*

²*State Key Laboratory of Loess and Quaternary Geology, Institute of Earth Environment, CAS,
Xi'an 710075, China*

**Corresponding author
e-mail: yanhuichj08@163.com*

(Received 30th Jun 2019; accepted 11th Oct 2019)

Abstracts. Carbon isotope composition of the tissue of several mollusc species gathered from the Huaxi river, in China, a typical karst river, was analysed to determine their potential food sources. The results showed that $\delta^{13}\text{C}_{\text{tissues}}$ values of gastropod species *Cipangopaludina chinensis* are about 3‰ heavier than the values of bivalve species *Corbicula fluminea* and *Anodonta woodiana*, which indicates the different food and nutrition sources between species. According to the $\delta^{13}\text{C}$ values of mollusc's tissues and the potential food, bivalve species *C. fluminea* and *A. woodiana* mainly assimilate phytoplankton and terrestrial plant detritus as food, while gastropod species *C. chinensis* also utilize sediment organic matter as a food source excluding the phytoplankton and terrestrial plant detritus. Moreover, the preferential food selection behavior and varied metabolic intensity between different ages and individuals may lead to some variation of $\delta^{13}\text{C}_{\text{tissues}}$ values of *C. fluminea*. This study will be helpful in defining the role of molluscs in the energy flow of the karst river ecosystem, and to protect and manage those molluscs' resources.

Keywords: *nutrition, Corbicula fluminea, Anodonta woodiana, phytoplankton, terrestrial plant detritus*

Introduction

Molluscs, such as bivalves, and gastropods are important large benthic animals in river ecosystems, and they usually play an important role in the ecosystem through feeding and nutrient excretion activities as they often dominate the macrobenthic community (Boltovskoy et al., 1995; Nichols and Garling, 2000; Xu and Yang, 2007; Atkinson et al., 2010). Meanwhile, molluscs usually are important economic fishery resources. It is therefore essential to study the diet of those animals for better understanding the role of molluscs in carbon and nitrogen cycling in the freshwater ecosystems, and for the better management of molluscs resources (Paulet et al., 2006; Fukumoria et al., 2008).

There are several ways to better understand the diet of organisms, including direct observation of feeding behavior, gut contents analysis, and stable isotopes analysis of the soft tissues of organisms and the potential food sources (Raikow and Hamilton, 2001). Direct observation of the feeding behavior of bivalves are very complicated and

involved the measurement of filtering rates or examination of filtering morphology (Kryger and Riisgard, 1988; Ward et al., 1993; Silverman et al., 1997). Gut content analyses may be misleading because the method cannot distinguish ingested material that is not assimilated (Miura and Yamashiro, 1990; Raikow and Hamilton, 2001). In contrast to these conventional methods, stable isotope analysis has been used successfully in many studies of spatial and temporal variations in potential diets of invertebrates (DeNiro and Epstein, 1978; Stephenson and Lyon, 1982; Fry and Sherr, 1984; Zanden and Rasmussen, 1990; Kang et al., 1999; Cai et al., 2001; Kasai et al., 2006; Paulet et al., 2006; Fukumoria et al., 2008; Schlacher and Connolly, 2014; Graniero et al., 2016; Ishikawa et al., 2017; Zhao et al., 2019). The stable isotope techniques are based on the assumption that the isotopic composition of an organism is linked to its diet, such as it is generally accepted that the $\delta^{13}\text{C}$ value of an organism reflects the $\delta^{13}\text{C}$ value of its diet, with little ($\sim 1\%$) or no change (DeNiro and Epstein, 1978; Fry and Sherr, 1984).

In this study we analyzed the stable carbon isotope composition of several mollusc tissues in the Huaxi river, China, which is a typical karst river, to determine what carbon sources were being used by those molluscs and to define the role of molluscs in the energy flow of the karst river ecosystem, which will be very helpful to protect and better manage the molluscs resources.

Materials and Methods

On August 10, 2007, a number of animals, bivalve species *Corbicula fluminea*, *Anodonta woodiana* and gastropod species *Cipangopaludina chinensis* were collected from Huaxi river, Guiyang city, China, which is a typical karst region (Fig. 1). The animals were brought back to the laboratory and the shell height was accurately measured using a caliper, the tissue is quickly removed with a scalpel. According to the size of shell height, *C. fluminea* tissue samples were divided into 6 groups (Table 1), and there were two kind of tissue samples in each group, one included individual tissue samples, and the other was a mixture of several animal tissue samples with the similar shell height (about 10 to 15 animals mixed together). Three individual tissue samples both of *A. woodiana* and *C. chinensis* were selected to determine the composition of organic carbon isotopes.

Tissues were dried in an oven at 60°C for 24 hours, 5 drops of 2% hydrochloric acid was added to remove the inorganic carbonate (some *C. fluminea* mixed samples were not treated with hydrochloric acid) (Table 1). After acid treatment, *C. fluminea*, *A. woodiana* and *C. chinensis* tissue samples were dried again in an oven, and then ground into powder with a mortar and pestle, about 0.1 mg samples were placed in the tin cup, then wrapped the tin cup into cubes and no samples leakage was ensured. $\delta^{13}\text{C}_{\text{tissues}}$ are determined using EA-IRMS (Euro EA-3000) at the state key laboratory of

environmental geochemistry, CAS, China, IAEA C-3 cellulose (-24.91‰, PDB) was used for calibration, and the determination accuracy was 0.05‰.

Descriptive statistics and correlation analysis were used for data statistics, and SPSS13.0 software was used for data analysis.

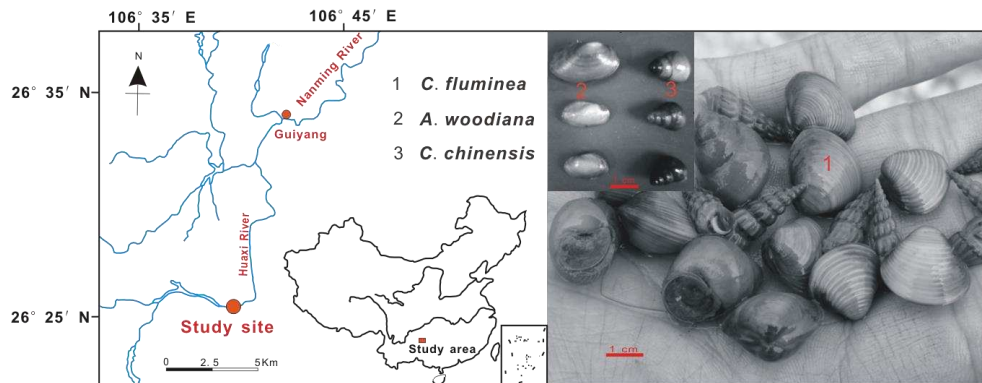


Figure 1. Sampling locations and images of *C. fluminea*, *A. woodiana* and *C. chinensis*

Table 1. Different group of *C. fluminea* tissue samples

Group	Shell height (mm)	Individual sample	Mixed sample	
1	4.0~ 5.9	1-1	1-2	-
2	6.0~ 7.9	2-1	2-2	-
3	12.0~13.9	3-1	3-2	3-3*
4	15.0~16.9	4-1	4-2	4-3*
5	17.0~19.9	5-1	5-2	5-3*
6	20.0~22.9	6-1	6-2	6-3*

*the samples were not treated with hydrochloric acid

Results

$\delta^{13}\text{C}_{\text{tissues}}$ values of *C. fluminea*

From group 1 to group 6, $\delta^{13}\text{C}_{\text{tissues}}$ values of *C. fluminea* individual samples were -28.49‰, -28.67‰, -28.96‰, -29.00‰, -29.02‰ and -28.42‰, respectively, while $\delta^{13}\text{C}_{\text{tissues}}$ values of mixed samples were -28.31‰, -28.60‰, -28.89‰, -28.93‰, -28.95‰ and -28.33‰, respectively. The results showed that there is no significant difference of $\delta^{13}\text{C}_{\text{tissues}}$ values between the individual samples and mixed samples in the same group ($R^2= 0.98$, $n=6$) (Fig. 2), which may indicate that animals with similar shell height (similar age) assimilate similar food and nutrition. However, in the different groups (different ages), $\delta^{13}\text{C}_{\text{tissues}}$ values of *C. fluminea* showed some variation, the biggest amplitudes of variation are 0.60‰ and 0.65‰ for individual samples and mixed

samples, respectively, this variation may indicate that *C. fluminea* has certain changes of food resources or different preferable choices of food and nutrition during the growth process.

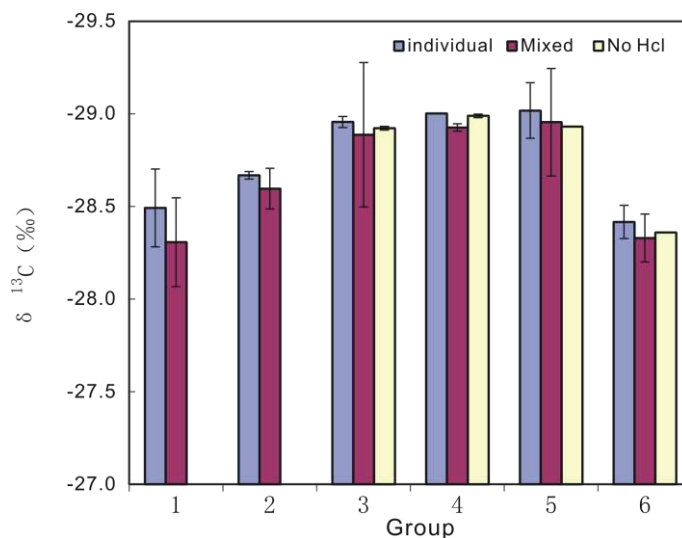


Figure 2. $\delta^{13}\text{C}_{\text{tissues}}$ values of *C. fluminea* samples (The vertical line is the standard deviation)

Effect of sample treatment on $\delta^{13}\text{C}_{\text{tissues}}$ values of *C. fluminea*

From Fig. 2, $\delta^{13}\text{C}_{\text{tissues}}$ values of *C. fluminea* did not show significant differences between samples that were treated by hydrochloric acid and those with no-hydrochloric acid treatment, this result may indicate that inorganic carbonate in *C. fluminea* tissue samples are very low, and have little impact on the analysis of $\delta^{13}\text{C}_{\text{tissues}}$ values, so it seems unnecessary to treat *C. fluminea* tissues with hydrochloric acid before isotope analysis. While some studies found that the acid treatments can change both $\delta^{13}\text{C}_{\text{tissues}}$ and $\delta^{15}\text{N}_{\text{tissues}}$ values, specially the $\delta^{13}\text{C}_{\text{tissues}}$ because of the removal of the isotopically heavier inorganic carbonate (Schlacher and Connolly, 2014). Zhao et al. (2019) also reported that the acid-treated mussel's periostracum showed lower $\delta^{13}\text{C}$ values compared to those in untreated specimens, the offsets ranging from 0.35 to 5.13‰, which show a statistically significant difference in $\delta^{13}\text{C}$ values. Since it is impossible to determine the amount of inorganic carbonate in advance, and mechanical removal is unfeasible, acid treatment is needed in carbonate-rich sample.

$\delta^{13}\text{C}_{\text{tissues}}$ values between different species

$\delta^{13}\text{C}_{\text{tissues}}$ values of three *A. woodiana* samples were -28.92‰, -29.00‰ and -29.04‰, respectively (Fig. 3a), which are highly consistent with the $\delta^{13}\text{C}_{\text{tissues}}$ values of *Anodonta spp* (-28.7±0.8‰) in Congjiang county, Guizhou province (Zhang et al., 2010). Considering that Congjiang county is very close to Huaxi river area, and are both belong to typical southwest karst regions of China, and have the same geological

bedrock, vegetation types and soil types, this being consistent of $\delta^{13}\text{C}_{\text{tissues}}$ indicate that the carbon isotopes of molluscs tissues can really record the host environmental information.

$\delta^{13}\text{C}_{\text{tissues}}$ values of three *C. chinensis* samples were -26.27‰, -26.05‰ and -26.34‰, respectively (Fig. 3a). Comparison to *C. fluminea* and *A. woodiana* is also shown in Fig. 3a. $\delta^{13}\text{C}$ tissue values of *C. fluminea* and *A. woodiana* are very close to each other, while *C. chinensis* are about 3‰ heavier than bivalve species, this may indicate that both bivalve species *C. fluminea* and *A. woodiana* are relatively consistent in their food and nutrition sources, and are significantly different from gastropod species *C. chinensis*. This is also consistent with the previous study result, which found that $\delta^{13}\text{C}_{\text{tissues}}$ values of gastropod species are usually more positive than those of bivalves (Fig. 3b) (Cai et al., 2001).

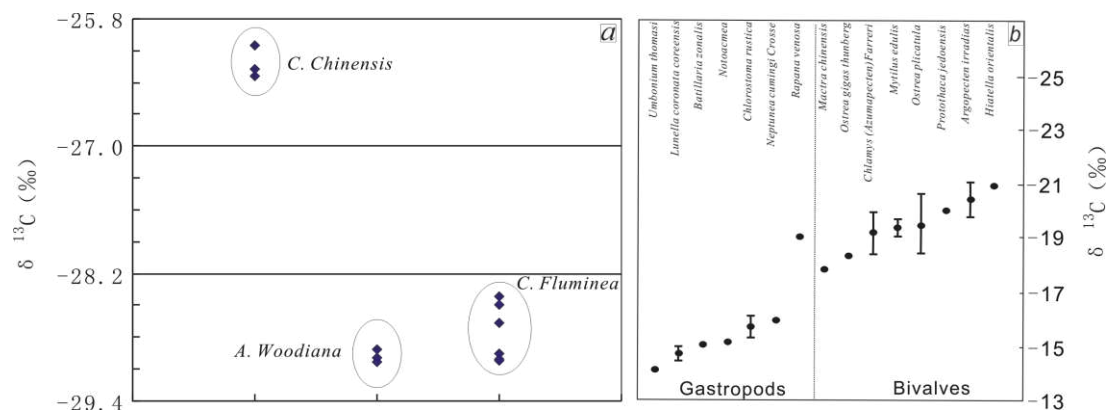


Figure 3. $\delta^{13}\text{C}_{\text{tissues}}$ values of molluscs (a: $\delta^{13}\text{C}_{\text{tissues}}$ values of *C. fluminea*, *A. woodiana* and *C. chinensis* in this study; b: $\delta^{13}\text{C}_{\text{tissues}}$ values of several gastropods and bivalves species from Cai et al., 2001)

Discussion

$\delta^{13}\text{C}_{\text{tissues}}$ values of *C. fluminea* between different groups

In the different groups (different ages), $\delta^{13}\text{C}_{\text{tissues}}$ values of *C. fluminea* show some variation both in individual samples and mixed samples, and the biggest amplitude of variation are 0.60‰ and 0.65‰ for individual samples and mixed samples, respectively. This variation of $\delta^{13}\text{C}_{\text{tissues}}$ values between different groups may indicate that *C. fluminea* has certain changes of food or different preferable choices of food during the growth process.

Studies have proved that bivalves have selective feeding characteristics at different ages, such as preferring different kinds of food or different sizes of particles in the same food (Ward and Shumway, 2004). They believed that filtering mollusc has two feeding mechanisms: (1) those that utilize mucous nets or strings (external to or within the

mantle cavity) to collect material, which known as hydrodynamic effect or passive feeding, and (2) those that rely on ciliated structures (proboscides, ctenidia) for particle collection, transport and processing, also known as mucilage ciliation effect or active feeding. There are also a few bivalves that rely on both of these mechanisms for particle collection (Ward and Shumway, 2004).

Ward and Shumway (2004) also found that the small size mollusc prefers to let the food flows through the main gill filaments directly into the back of the ventricle, along the back cilia swing into the lip, which known as hydrodynamic effect or passive feeding. The larger size of mollusc has strong active feeding ability, let the food flows enters the ventral edge of the gill under the action of the whole gill system, and enters the labial valve along the abdominal food delivery groove, also known as mucilage ciliation. Different ways of eating lead to absorb different or different sizes of food and nutrients, which can lead to differences in $\delta^{13}\text{C}_{\text{tissues}}$ values. Shumway et al. (1990) also found that the bivalve feeding behavior was related to the size of the food particles, and even related to the mucus action and chemical receptors of mollusc, which vary among individuals. Moreover, study on the scallop *Pecten maximus* in the field showed that tissue carbon isotopic composition can be also influenced by metabolic activity of the organism (Lorrain et al., 2002). Paulet et al. (2006) found that difference of $\delta^{13}\text{C}_{\text{tissues}}$ values between scallops and oysters could be due to differences in tissue growth rates between species. So the variation of $\delta^{13}\text{C}_{\text{tissues}}$ values of *C. fluminea* between different groups in this study may be caused by several reasons, such as the selective feeding characteristics and varied metabolic intensity at different ages.

$\delta^{13}\text{C}_{\text{tissues}}$ values between different species: a tool to determine the food sources

Gastropods are usually thought to be deposit-feeding, and food sources are mainly fluvial suspended material and sediment organic matter, while bivalves are defined as filter-feeding (Graney et al., 1984; Lorrain et al., 2002; Gillikin et al., 2006) and obtains suspended particles, such as plankton from the water through filtration by holding its inhalant siphon above the sediment surface (Britton and Morton, 1982; Kasai and Nakata, 2005; Kasai et al., 2006). While some studies found that filter-feeding alone cannot balance bivalve's energy budgets, the deposit feeding is also a significant source of nutrition for bivalve, especially in food-limiting situations (Aldridge and McMahon, 1978; Boltovskoy et al., 1995). For example, Hakenkamp and Palmer (1999) found that although *C. fluminea* is already known to be an important filterer of phytoplankton and seston from the water column, it has also been shown that it collects food within the stream through pedal-feeding, using cilia on the foot to collect subsurface organic matter. Moreover, Raikow and Hamilton (2001) found that potential food sources for bivalves also included epipsammon (detritus and possibly algae mixed with sand). An energy budget for the fingernail clam *Sphaerium striatinum* was reported by Hornbach et al. (1984), who estimated that 35% of its energy was derived from suspension feeding and the rest possibly from deposit feeding.

Determining the exact sources of food used by mollusc species can be difficult because of the heterogeneity of materials in suspension at any given time (Atkinson et al., 2010) and the co-existence of filter-feeding and deposit-feeding (McMahon and Bogan, 2001). However, from all the previous studies, we can still conclude that the main food sources of molluscs are POM (particle organic matter) and SOM (sediment organic matter). Both the POM and SOM pool are a mixture of different sources of carbon, each with an often distinct $\delta^{13}\text{C}$ value, the POM pool are mainly including phytoplankton, terrestrial plant detritus and soil organic carbon, the SOM pool are mainly including benthic algae, bacteria and sediment organic matter (Langdon and Newell, 1990; Cranford and Grant, 1990; Kang et al., 1999; Nichols and Garling, 2000).

$\delta^{13}\text{C}$ of phytoplankton

Although it is well established that the carbon isotope fractionation between phytoplankton and DIC is variable (Rau et al., 1992; Hinga et al., 1994), a value between 18‰ and 22‰ is often used as an estimate (Cai et al., 1988; Hellings et al., 1999). Therefore, similar to Fry (2002) and Gillkin et al. (2006), an average value of 20‰ is used in this study ($\delta^{13}\text{C}_{\text{DIC}-20}$) to represent $\delta^{13}\text{C}$ of phytoplankton. $\delta^{13}\text{C}_{\text{DIC}}$ of Huaxi river range from -9.58‰ to -3.60‰, with an average of -7.15‰ (Yan et al., 2009), so $\delta^{13}\text{C}_{\text{DIC}-20}$ range from -29.58‰ ~ -23.60‰, with an average of -27.15‰. $\delta^{13}\text{C}_{\text{DIC}-20}$ of Huaxi river are consistent to the typical values of freshwater phytoplankton, which is between -24‰ and -42‰ (Zanden and Rasmussen, 1999), and also consistent to $\delta^{13}\text{C}$ of Guizhou freshwater phytoplankton, which ranges from -35.03‰ to -22.97‰ (Li, 2009).

$\delta^{13}\text{C}$ of terrestrial plant detritus

Du et al. (2014) measured the $\delta^{13}\text{C}$ of common local plant species grown in Wangjiazhai catchments, a typical karst desertification area in Qingzhen City, which is very close to Huaxi river, $\delta^{13}\text{C}$ of plants ranged from -30.7‰ ~ -26.5‰, with an average value of -28.1‰. Since the $\delta^{13}\text{C}$ value remains the same when a plant dies and becomes detritus (Smith and Epstein, 1971; Haines, 1977), so -30.7‰ ~ -26.5‰, with an average value of -28.1‰ was used to represent the $\delta^{13}\text{C}$ of terrestrial plant detritus in this study.

$\delta^{13}\text{C}$ of sediment organic matter

Zhao et al. (2012) studied the geochemical characteristics in sediments in a small watershed of central Guizhou province, the results demonstrated that fluvial sediment are mainly derived from chemical weathering and soil physical erosion in the basin. The main soil types in Guizhou province were calcareous soil and yellow soil, and studies showed that the $\delta^{13}\text{C}$ values of calcareous soil and yellow soil were between -22.9‰ ~ -21.5‰ and -25.6‰ ~ -22.4‰ respectively (Li et al., 2012). The main soil type in Huaxi river area is yellow soil, so -25.6‰ ~ -22.4‰ was used in this study.

Fig. 4 shows the $\delta^{13}\text{C}_{\text{tissue}}$ values of mollusks that were analyzed in this study and their potential main food sources. According to the Fig. 4, we can conclude that bivalve species *C. fluminea* and *A. woodiana* main food sources are phytoplankton and terrestrial plant detritus. Phytoplankton as a main food source for bivalves was proved by many studies (Ogilvie et al., 2000; Gillikin et al., 2006), while some research studies also found that terrestrial plant detritus contribution in bivalve diet is important during the periods when abundance of phytoplankton is too low to satisfy bivalve energy needs (Cranford and Grant, 1990; Langdon and Newell, 1990). Kasai et al. (2005) also found that the contribution of terrestrial organic matter is significantly important for the corbicula diet, although the contribution gradually changes among sampling sites. However, it's more complicated for gastropod species, according to the $\delta^{13}\text{C}_{\text{tissues}}$ values, besides of the phytoplankton and terrestrial plant detritus, *C. chinensis* must also assimilate sediment organic matter as food sources, which have a significantly heavier carbon isotope composition.

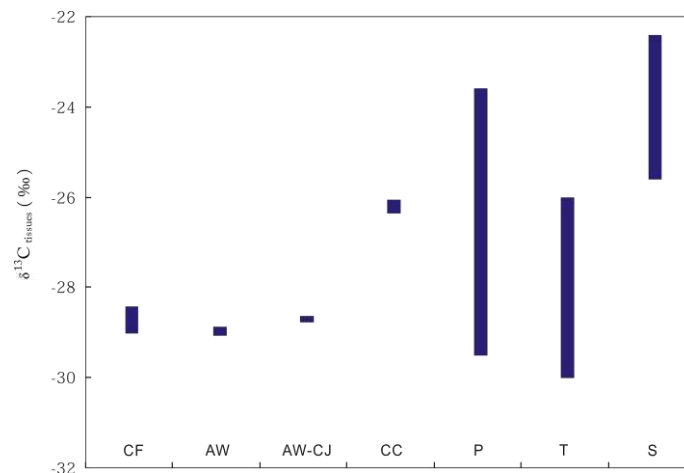


Figure 4. $\delta^{13}\text{C}$ values of molluscs and potential food sources (CF is *C. fluminea*; AW is *A. woodiana*; CC is *C. chinensis*; AW-CJ is *Anodonta* spp from Congjiang county; P, T, S are phytoplankton, terrestrial plant detritus and sediment organic matter, respectively)

The relative abundance of multiple food sources in the diet of organisms can be quantified using a classical isotope mixing model, which is related to the $\delta^{13}\text{C}$ values of each food resource (Gannes et al., 1997; Raikow and Hamilton, 2001). As we did not have stable isotope values of some molluscs potential food sources in the Huaxi river, such as benthic algae, bacteria, we cannot quantitatively evaluate the mollusks' diet. However, this study still further illustrates the values of stable carbon isotope of mollusk's tissues as a tool in tracing organic carbon flow and recycle through a typical karst river ecosystem.

Conclusion

$\delta^{13}\text{C}_{\text{tissues}}$ values of bivalve species *C. fluminea* and *A. woodiana* are very close to each other, while *C. chinensis* are about 3‰ heavier than bivalve species, which indicate the different food and nutrition sources between species.

Comparing the $\delta^{13}\text{C}$ values of molluscs tissues and the potential food, bivalve species, *C. fluminea* and *A. woodiana* mainly assimilate phytoplankton and terrestrial plant detritus as food, while gastropod species *C. chinensis* also use sediment organic matter as a food source besides the phytoplankton and terrestrial plant detritus.

$\delta^{13}\text{C}_{\text{tissues}}$ values of *C. fluminea* between different sizes showed some variation, which may be caused by several reasons, such as the selective feeding characteristics and variational metabolic intensity at different ages.

Acknowledgements. We express our gratitude to Dr Zhu Zhengjie for laboratory assistance and isotope measurement. This work was funded by the National Natural Science Foundation of China (Number 40403010), Henan Science and Technology Department project (1621023105000) and the Chinese Scholarship Council Scholarship (201708410459). We thank anonymous reviewers and technical Editors for their insightful comments and suggest on this manuscript.

REFERENCES

- [1] Aldridge, D. W., McMahon, R. F. (1978): Growth, fecundity, and bioenergetics in a natural population of the freshwater clam, *Corbicula fluminea* Philippi, from north central Texas. – *Journal of Molluscan Studies* 44: 49-70.
- [2] Atkinson, C. L., Opsahl, S. P., Covich, A. P., Golladay, S. W., Conner, L. M. (2010): Stable isotopic signatures, tissue stoichiometry, and nutrient cycling (C and N) of native and invasive freshwater bivalves. – *Journal of the North American Benthological Society* 29(2): 496-505.
- [3] Boltovskoy, D., Izaguirrel, I., Correa, N. (1995): Feeding selectivity of *Corbicula fluminea* (Bivalvia) on natural phytoplankton. – *Hydrobiologia* 312: 171-182.
- [4] Britton, J. C., Morton, B. (1982): A dissection guide, field and laboratory manual for the introduced bivalve *Corbicula fluminea*. – *Malacological Review* 3(suppl): 1-82.
- [5] Cai, D. L., Tan, F. C., Edmond, J. M. (1988): Sources and transport of particulate organic carbon in the Amazon River and estuary. – *Estuarine, Coastal and Shelf Science* 26: 1-14.
- [6] Cai, D. L., Hong, X. G., Mao, X. X., Zhang, S. F., Han, Y. B., Gao, S. L. (2001): Preliminary studies on trophic structure of tidal zone in the Laoshan Bay by using carbon stable isotopes. – *Acta Oceanologica Sinica* 23(4): 41-47.
- [7] Cranford, P. J., Grant, J. (1990): Particle clearance and absorption of phytoplankton and detritus by the sea scallop *Placopecten magellanicus* (Gmelin). – *Journal of Experimental Marine Biology and Ecology* 137: 105-121.
- [8] DeNiro, M., Epstein, S. (1978): Influence of diet on the distribution of carbon isotopes in animals. – *Geochim Cosmochim Acta* 42: 495-506.
- [9] Du, X. L., Wang, S. J., Luo, X. Q. (2014): Effects of different soil types on the foliar $\delta^{13}\text{C}$ values of common local plant species in karst rocky desertification area in central Guizhou Province. – *Environmental Science* 35(9): 3587-3594. (in Chinese).
- [10] Fry, B., Sherr, E. B. (1984): $\delta^{13}\text{C}$ measurements as indicators of carbon flow in marine and freshwater ecosystems. – *Contribution to Marine Science* 27: 13-47.

- [11] Fry, B. (2002): Conservative mixing of stable isotopes across estuarine salinity gradients: a conceptual framework for monitoring watershed influences on downstream fisheries production. – *Estuaries* 25: 264-271.
- [12] Fukumoria, K., Oi, M., Doi, H., Takahashi, D., Okuda, N., Miller, T. W. (2008): Bivalve tissue as a carbon and nitrogen isotope baseline indicator in coastal ecosystems. – *Estuarine, Coastal and Shelf Science* 79: 45-50.
- [13] Gannes, L. Z., O'Brien, D. M., Del Rio, C. M. (1997): Stable isotopes in animal ecology: Assumptions, caveats, and a call for more laboratory experiments. – *Ecology* 78: 1271-1276.
- [14] Gillikina, D. P., Lorrain, A., Bouillon, S., Willenz, P., Dehairs, F. (2006): Stable carbon isotopic composition of *Mytilus edulis* shells: relation to metabolism, salinity, $\delta^{13}\text{C}_{\text{DIC}}$ and phytoplankton. – *Organic Geochemistry* 37: 1371-1382.
- [15] Graney, Jr. R. L., Cherry, D. S., Cairns, Jr. J. (1984): The influence of substrate, pH, diet and temperature upon cadmium accumulation in the asiatic clam (*Corbicula fluminea*). – *Water Research* 18(7): 833-842.
- [16] Graniero, L. E., Grossman, E. L., O'Dea, A. (2016): Stable isotopes in bivalves as indicators of nutrient source in coastal waters in the Bocas del Toro Archipelago, Panama. – *PeerJ* 4: e2278. DOI 10.7717/peerj.2278.
- [17] Haines, E. B. (1977): The origins of detritus in Georgia salt marsh estuaries. – *Oikos* 29: 254-260.
- [18] Hakenkamp, C. C., Palmer, M. A. (1999): Introduced bivalves in freshwater ecosystems: the impact of *Corbicula* on organic matter dynamics in a sandy stream. – *Oecologia* 119: 445-451.
- [19] Hellings, L., Dehairs, F., Tackx, M., Keppens, E., Baeyens, W. (1999): Origin and fate of organic carbon in the freshwater part of the Scheldt Estuary as traced by stable carbon isotopic composition. – *Biogeochemistry* 47: 167-186.
- [20] Hinga, K. R., Arthur, M. A., Pilson, M. E. Q., Whitaker, D. (1994): Carbon isotope fractionation by marine phytoplankton in culture: the effects of CO_2 concentration, pH, temperature, and species. – *Global Biogeochemical Cycles* 8: 91-102.
- [21] Hornbach, D. J., Wissing, T. E., Burky, A. J. (1984): Energy budget for a stream population of the freshwater clam, *Sphaerium striatinum* Lamarck (Bivalvia: Psidiidae). – *Canadian Journal of Zoology* 62: 2410-2417.
- [22] Ishikawa, M., Ogawa, N. O., Ohkouchi, N., Husana, D. E. M., Kase, T. (2017): Stable carbon isotope compositions of foot tissue, conchiolin opercula, and organic matrix within the shells of two marine gastropods from a seagrass meadow in the philippines. – *Geochemical Journal* 51(3): 241-250.
- [23] Kang, C. K., Sauriau, P. G., Richard, P., Blanchard, G. F. (1999): Food sources of the infaunal suspension-feeding bivalve *Cerastoderma edule* in a muddy sand flat of Marennes–Oleron Bay, as determined by analyses of carbon and nitrogen stable isotopes. – *Marine Ecology Progress Series* 187: 147-158.
- [24] Kasai, A., Nakata, A. (2005): Utilization of terrestrial organic matter by the bivalve *Corbicula japonica* estimated from stable isotope analysis. – *Fisheries Science* 71: 151-158.
- [25] Kasai, A., Toyohare, H., Nakata, A., Miura, T., Azuma, N. (2006): Food sources for the bivalve *Corbicula japonica* in the foremost fishing lakes estimated from stable isotope analysis. – *Fisheries Science* 72: 105-114.
- [26] Kryger, J., Riisgard, H. U. (1988): Filtration capacities in 6 species of European freshwater bivalves. – *Oecologia* 77: 34-38.
- [27] Langdon, C. J., Newell, R. I. E. (1990): Utilization of detritus and bacteria as food sources by two bivalve suspension-feeders, the oyster *Crassostrea virginica* and the mussel *Geukensia demissa*. – *Marine Ecology Progress Series* 58: 299-310.

- [28] Li, G. R. (2009): Cascade damming of the river and its phytoplankton evolution carbon isotope compositions—A case study of Maitiao river drainage area in Guizhou province. – Guizhou Normal University: Guiyang, China.
- [29] Li, L. B., Liu, T. Z., Li, X. D., Liu, W. J., Liu, C. Q. (2012): Vertical distribution patterns of organic carbon and its isotopic composition in typical soil types in Guizhou karst areas of Southwest China. – *Chinese Journal of Ecology* 31(2): 241-247. (in Chinese).
- [30] Lorrain, A., Paulet, Y. M., Chauvaud, L., Savoye, N., Donval, A., Saout, C. (2002): Differential $\delta^{13}\text{C}$ and $\delta^{15}\text{N}$ signatures among scallop tissues: implications for ecology and physiology. – *Journal of Experimental Marine Biology and Ecology* 275: 47-61.
- [31] McMahon, R. F., Bogan, A. E. (2001): Mollusca: Bivalvia. – In: Thorp, J. H., Covich, A. P. (eds.) *Ecology and classification of North American freshwater invertebrates*. Academic Press, San Diego, California.
- [32] Miura, T., Yamashiro, T. (1990): Size selectivity of *Anodonta calipygos*, a phytoplanktivorous freshwater bivalve and viability of egested algae. – *Japanese Journal of Limnology* 51: 73-78.
- [33] Nichols, S. J., Garling, D. (2000): Food webs dynamics and trophic level interactions in a multispecies community of freshwater unionids. – *Canadian Journal of Zoology* 78: 871-882.
- [34] Ogilvie, S. C., Ross, A. H., James, M. R., Schiel, D. R. (2000): Phytoplankton biomass associated with mussel farms in Beatrix Bay, New Zealand. – *Aquaculture* 181: 71-80.
- [35] Paulet, Y. M., Lorrain, A., Richard, J., Pouvreau, S. (2006): Experimental shift in diet $\delta^{13}\text{C}$: A potential tool for ecophysiological studies in marine bivalves. – *Organic Geochemistry* 37: 1359-1370.
- [36] Raikow, D. F., Hamilton, S. K. (2001): Bivalve diets in a midwestern U.S. stream: A stable isotope enrichment study. *Limnol. – Oceanography* 46(3): 514-522.
- [37] Rau, G. H., Takahashi, T., Des Marais, D. J., Repeta, K. J., Martin, J. H. (1992): The relationship between $\delta^{13}\text{C}$ of organic matter and $[\text{CO}_2(\text{aq})]$ in ocean surface water: data from a JGOFS site in the northeast Atlantic Ocean and a model. – *Geochimica et Cosmochimica Acta* 56: 1413-1419.
- [38] Schlacher, T. A., Connolly, R. M. (2014): Effects of acid treatment on carbon and nitrogen stable isotope ratios in ecological samples: a review and synthesis. – *Methods in Ecology and Evolution* 5: 541-550.
- [39] Shumway, S. E., Newell, R. C., Crisp, D. J., Cucci, T. L. (1990): Particle selection in filter-feeding bivalve molluscs: a new technique on an old theme. – In: Morton, B. (ed.) *The Bivalvia. Proceedings of a Memorial Symposium in Honour of Sir Charles Maurice Yonge*, Edinburgh. Hong Kong Univ. Press, Hong Kong.
- [40] Silverman, H., Nichols, S. J., Cherry, J. S., Achberger, E., Lynn, J. W., Dietz, T. H. (1997): Clearance of laboratory-cultured bacteria by freshwater bivalves: Differences between lentic and lotic unionids. – *Canadian Journal of Zoology* 75: 1857-1866.
- [41] Smith, B. N., Epstein, S. (1971): Two categories of $^{13}\text{C}/^{12}\text{C}$ ratios for higher plants. – *Plant Physiology* 47: 380-384.
- [42] Stephenson, R. L., Lyon, G. L. (1982): Carbon-13 depletion in an estuarine bivalve: detection of marine and terrestrial food sources. – *Oecologia* 55: 110-113.
- [43] Ward, J. E., Macdonalds, B. A., Thompson, R. J. (1993): Mechanisms of suspension feeding in bivalves: Resolution of current controversies by means of endoscopy. – *Limnology & Oceanography* 38: 265-272.
- [44] Ward, J. E., Shumway, S. E. (2004): Separating the grain from the chaff: particle selection in suspension- and deposit-feeding bivalves. – *Journal of Experimental Marine Biology and Ecology* 300(1-2): 83-130.

- [45] Xu, Q., Yang, H. (2007): Food sources of three bivalves living in two habitats of Jiaozhou Bay (Qingdao, China): Indicated by lipid biomarkers and stable isotope analysis. – *Journal of Shellfish Research* 26(2): 1-7.
- [46] Yan, H., Lee, X. Q., Zhou, H., Cheng, H. G., Peng, Y., Zhou, Z. H. (2009): Stable isotope composition of the modern freshwater bivalve *Corbicula fluminea*. – *Geochemical Journal* 23: 379-387.
- [47] Zanden, M. J. V., Rasmussen, J. B. (1999): Primary consumer $\delta^{13}\text{C}$ and $\delta^{15}\text{N}$ and the trophic position of aquatic consumers. – *Ecology* 80(4): 1395-1404.
- [48] Zhang, D., Min, Q. W., Cheng, S. K., Wang, Y. Y., Yang, H. L., He, L. (2010): Ecological studies on the food web structures and trophic relationships of multiple species coexistence in paddy fields using stable carbon and nitrogen isotopes. – *Acta Ecologica Sinica* 30(24): 6734-6742.
- [49] Zhao, X. Y., Ji, H. B., Zhu, X. F., Cao, W. J., Gao, Y. X. (2012): Geochemical characteristics of trace elements in suspended matters and sediments in a small watershed of the central Guizhou Province and their provenance implications. – *Geochimica* 41(3): 250-265. (in Chinese).
- [50] Zhao, L. Q., Shirai, K., Sugihara, N. M., Higuchi, T., Takano, K. (2019): Mussel periostracum as a high-resolution archive of soft tissue $\delta^{13}\text{C}$ records in coastal ecosystems. – *Geochimica et Cosmochimica Acta*. DOI: 10.1016/j.gca. 2019.06.038.

THE EFFECT OF EXOGENOUS PHOSPHOROUS APPLICATION ON GROWTH, YIELD, QUALITY AND NET RETURNS OF UPLAND COTTON (*GOSSIPIUM HIRSUTUM* L.)

ALI, H. – AHMAD, A. – HUSSAIN, S.*

Department of Agronomy, Faculty of Agricultural Sciences and Technology, Bahauddin Zakariya University, Multan, Pakistan

**Corresponding author
e-mail: shabirhussain@bzu.edu.pk*

(Received 2nd Jul 2019; accepted 25th Oct 2019)

Abstract. Cotton crop is grown in China, Brazil, Pakistan, India and in the USA. It is a major global resource in textile production. Phosphorus has major role in the growth and yield of plants facilitating higher crop production. Phosphorous is involved in plant growth and opening of flower bud while low nitrogen and magnesium absorption inhibits plant growth. Higher input cost of fertilizers and numerous other yield limiting factors are major problems for farmers. To mitigate the problem, present study was carried out at the Central Cotton Research Institute (CCRI), Multan, Pakistan. The experimental treatments comprised of three cultivars viz. V₁ = MNH - 886, V₂ = CIM - 616 and V₃ = FH-LALAZAR and seven levels of Phosphorous viz. To = Zero kg ha⁻¹, T₁ = 50 kg ha⁻¹, T₂ = 50 kg ha⁻¹ + foliar (2% TSP solution), T₃ = 75 kg ha⁻¹, T₄ = 75 kg ha⁻¹ + foliar (2% solution of Triple super phosphate), T₅ = 100 kg ha⁻¹ + seed application (5% solution of triple super phosphate), T₆ = 100 kg ha⁻¹ phosphorous (with seed application of a 5% solution of triple super phosphate, and foliar application of a 2% solution). Different genotypes significantly differed in various growth, yield and quality attributes. In this regard, the cultivar FH- Lalazar produced the highest plant height (152.50 cm), lint yield (50.58 kg ha⁻¹), seed cotton harvest (27%), ginning out turn (0.02%), crop growth rate (4.79 kg ha⁻¹), fiber uniformity (45.50), fiber strength (30.16 tpsi) and micronair (4.72 µg/inch). CIM-616 showed the maximum number of bolls/plant (28.91), leaf area index (0.65 kg ha⁻¹), boll weight (2.98 g), and staple length (20.19 mm). In conclusion, cultivar FH-LZ using 100 kg ha⁻¹ phosphorous (with seed application of a 5% solution of triple super phosphate, and foliar application of a 2% solution) produced higher yield, ginning out turn, seed cotton harvest, crop growth rate and fiber uniformity with lower input cost and attained the maximum output with higher crop production.

Keywords: *yields, transgenic cotton, fiber quality, foliar application, phosphorous concentration*

Introduction

Cotton is a commercial crop for its excellent quality as fiber and oil so it is grown in whole regions of the world (Zhang et al., 2012). Lately, cotton has been grown in a region of 2907 thousand hectares while the ranks of production is 13.2 million bales (Govt. of Pakistan, 2018). During flowering and boll opening stage the continuous rain may possibly cause the reduction of pollination phenomenon and ultimately minimize fiber quality. Therefore, heavy rainfall causes flower buds and young bolls to fall during flowering (Gaikwad, 2018).

Nutritional quality of crops can be enhanced and may vary depending upon the soil conditions as well as genetic make-up of genotypes (Zhang et al., 2012; Ahmad et al., 2019). However, optimum dose of macro-nutrients as well as micronutrients and their proper application maximized crop production (Vance et al., 2003). Reduction of phosphorous availability resulted in minimizing the cotton plant growth. Reduction of phosphorus causes the minimization of different traits i.e. reduced flowering, imbalanced pollination, boll weight and boll size. Moreover, low phosphorus in cotton crop inhibits

dark green leaves and flower bud necrosis. Lower phosphorous availability in cotton crop also affects the development of flower buds and also minimized the absorption of nitrogen resulting in inhibited cell growth and their expansion (Dohary et al., 2004).

Phosphorous is taken up by the roots. So among all of this many factors which affect the cotton response to phosphorous the most is the type of soil. The acute amount of phosphorous is a main issue of actual concentration of phosphorous, which is provided at the time of cotton growth (Crozier et al., 2004). Numerous traits i.e. early phosphorous accumulation and lint yield positively respond to phosphorous in calcareous soils (Bronson et al., 2003). However, the reduction of phosphorous may possibly minimize the nitrogen level. Due to the indeterminate type of growth and deep-growing root system of cotton crop phosphorous concentration availability is low (Zhou et al., 2011).

Several nutrients were applied through foliar spray to leaves that may prevent their senescence and decline in photosynthesis allowing photosynthesis and carbon fixation to be prolonged thus increasing the yield of cotton (Bronson et al., 2001). Those resistant cultivars were selected that had greater capability to tolerate unfavorable conditions including nutritional stress which results in higher yield of crop (Zambrosi et al., 2012). The efficiency of phosphorus cultivars having the ability to grow well and produce the maximum yield in soil with the minimum phosphorous (Fageria et al., 2010). Thus, efficient application of phosphorus was recorded in several agronomic crops. (Zambrosi et al., 2012; Fageria and Moraes, 2013).

Foliar application and seed treatments are successfully used in application of several nutrients especially phosphorus. Among all the nutrient application methods, foliar application is considered as one of the most suitable method and it is also helpful for proper use of nutrients in plants (Girma et al., 2007). Furthermore, combination of foliar application and seed treatment results in efficient use of phosphorus to plants and ultimately enhanced cotton production. Application of phosphorus to all other agronomic crops is very common; however, its use in cotton is very limited. Therefore, current study is more helpful for cotton growers to enhance production through foliar application of phosphorus (Verma et al., 2018). The optimum dose of phosphorus and its timely application drastically enhance cotton crop production all over the globe (Araújo et al., 2012). So, the purpose of this current study was to demonstrate the optimum application of phosphorus for various cotton cultivars.

Materials and methods

Experimental details

Current study was conducted in the research farm of Central Cotton Research Institute (CCRI) Multan, Pakistan to mitigate various cultivars of cotton with various foliar application of phosphorus during 2015-2016. The soil at the Research Farm was silt loam and its organic content was 0.86%, Nitrogen concentration was 0.09%, Phosphorous concentration was 12.5 ppm, Sand was 16%, Silt was 57%, Clay was 27%. Experimental treatments comprised of three cotton cultivars viz. V₁ = MNH - 886, V₂ = CIM - 616 and V₃ = FH-LALAZAR and seven phosphorus levels viz. T₀ = Zero, T₁ = 50 kg ha⁻¹, T₂ = 50 kg ha⁻¹ + foliar (2% TSP solution), T₃ = 75 kg ha⁻¹, T₄ = 75 kg ha⁻¹ + application of foliar (2% solution of triple super phosphate), T₅ = 100 kg ha⁻¹ + seed application (5% solution of triple super phosphate), T₆ = 100 kg ha⁻¹ phosphorous (with seed application of a 5% solution of triple super phosphate, and foliar application of a 2% solution). One meter area was marked from the center of the plot from where sampling for various parameters

was done. CCRI lies at a latitude of 30°, and at a longitude of 71°, the altitude is 125 in the cotton belt of Punjab. After the preparation of seed bed the sowing was carried out with cotton Rabi drill on the 28th May, 2015 and on the 31st May, 2016 respectively. Net plot size was 6.1 m × 9.0 m = 54.9 m² with a sowing rate of 110 g/plot. Randomized Complete Block Design (RCBD) was applied along three replications. Urea fertilizers (36 kg ha⁻¹) were applied as per standard rule according to crop requirement, and seven phosphorous levels were used and TSP as a source were also applied. Whole of phosphorous according to treatments done on sowing time and application of nitrogen done on three intervals as per standard roles at both years. Pendimethaline (herbicide) was applied at the rate of 82.5 g ha⁻¹ to control weeds. For the chewing and sucking insect pest different products such as Nitenpyren, Diafenthoran, Triazophos were applied and Leuforan Irrigation was performed as crop needed. Harvesting was done from 05-11-2015 and 13-11-2016 and picking interval was two weeks.

Observations

Agronomic traits

Five plants were randomly chosen from every plot and the height of the plant was observed with a measuring tape in between about the base of the plant to the terminal bud. Same plants were used to measure no. of bolls/plant. One hundred fully opened bolls were selected for picking to get a hundred boll weight. Yield of cotton was calculated after picking by same plot, after this the bolls were weighed to get the yield (kg ha⁻¹). Ginning out turn (%) was calculated by the following formula: mass of cotton lint/mass of seed cotton × 100 (Baloch et al., 2014).

Allometry traits

Leaf area of each plant was measured with a leaf area meter (CI-203, LCI Bio Scientific, USA). Leaf area index (LAI) was calculated according to the method of Hunt (1978) using the following formula: LAI = Leaf Area/Ground Area Leaf. Area duration was recorded simultaneously by LAI₁ and LAI₂ with leaf area indices at times T₁ and T₂ and LAD (days) = (LAI₁ + LAI₂) × (T₂-T₁)/2 (Hassan et al., 2016). Crop growth rate was measured by collecting weighed samples of 10, 30, 60 g of green leaves, stalks and bolls collected by same treatment at various stages of plant growth, which then were dried in the oven at 80 °C. Crop growth rate was calculated by using the formula of Hunt (1978).

Quality traits

Quality traits, cotton seed were ginned in an electrically powered ginning machine to separate lint from seed followed by cleaning of those samples. Each sample was acclimatized at an optimum temperature of 20 °C with 65 % relative humidity level in an air conditioned chamber. The level of humidity was measured by a humidifier (HIV-900) at the humidity level of 8.5% Tisarum et al. (2019). Fiber strength is calculated by breaking the fibers held between clamp jaws. It is mentioned as g/tex, which is the force used to break bundle (Apel and Hirt2004)

Data analysis

Data was analyzed by using Statistix 8.1 (Tallahassee Florida, USA) on computer. The means of treatment were separately analyzed by LSD @ 5% level of probability.

Pearson's correlation was constructed through software XLSTAT, 2017 (Anjum et al., 2018; Ahmad and Anjum, 2018). Whereas economic analysis was performed as determined by Ahmad et al. (2016). Climatic data of experimental site was evaluated as described (Pakistan Metrological Department, 2016).

Results

Different cotton cultivars and yield related traits were significantly differed in the current study. Significantly higher plant height (60.03 inch) was recorded from Cultivar FH-Lalazar and the lowest height of plant (57.74 inch) was measured from MNH-886. The treatment 100 kg ha⁻¹ + seed application (5% solution of triple super phosphate) (61.02 inch), under 100 kg ha⁻¹ phosphorous (with seed application of a 5% solution of triple super phosphate, and foliar application of a 2% solution) resulted in a significantly higher plant height (61.93 inch), while the minimum plant height was calculated from control (56.38 inch). Cultivars and phosphorus levels interaction showing significantly higher plant height (61.81 inch) was recorded from FH-LZ with 75 kg ha⁻¹ + foliar (2% TSP solution), followed by the plant height (63.38) from FH-LZ with 100 kg ha⁻¹ + seed treatment (5% TSP solution), followed by the plant height (64.17 inch) from FH-LZ under 100 kg ha⁻¹ phosphorous (with seed application of a 5% solution of triple super phosphate, and foliar application of a 2% solution), while the minimum (55.24 inch) was recorded from MNH-886 with Zero kg ha⁻¹ (Table 1). The higher the no. of bolls/plant (28.91) recorded from CIM-616, the lower the no. of bolls/plant (24.50) occurred from cultivar MNH-886. From treatment 100 kg ha⁻¹ + seed solution (5% solution of triple super phosphate) (29.11) under 100 kg ha⁻¹ phosphorous (with seed application of a 5% solution of triple super phosphate, and foliar application of a 2% solution) higher no. of bolls/plant were found (29.65), the minimum in no. of bolls/plant was found in control (23.77). Regarding the level of phosphorous and cultivars interaction the highest no. of bolls/plant (35.33) occurred from CIM-612 under 100 kg ha⁻¹ phosphorous (with seed application of a 5% solution of triple super phosphate, and foliar application of a 2% solution), followed by (33.33) from CIM-612 with 100 kg ha⁻¹ + seed treatment (5% TSP solution). So the minimum no. of bolls/plant (22.00) was present in MNH-886 with control (Table 1).

The maximum boll weight (2.98 g) was measured from CIM-616, the lowest (1.21 g) from MNH-886. Concerning the phosphorus applications, the treatment 75 kg ha⁻¹ (2.26 g), 75 kg ha⁻¹ + foliar (2% TSP solution), (2.27 g), 100 kg ha⁻¹ + application of seed treatment (5% TSP solution) (2.29 g) under 100 kg ha⁻¹ phosphorous (with seed application of a 5% solution of triple super phosphate, and foliar application of a 2% solution) (2.45 g) increased boll weight, and a decrease of boll weight was measured from control (1.60 g). Regarding the levels of phosphorous and cultivars maximum weight of boll (3.20 g) was calculated from CIM-616 by 50 kg ha⁻¹, followed by (3.22 g) from CIM-616 with 50 kg ha⁻¹ + foliar (2% TSP solution), followed by (3.30 g) from CIM-616 with 75 kg ha⁻¹, followed by (3.32 g) from CIM-616 with 75 kg ha⁻¹ + foliar (2% TSP solution), followed by (3.30 g) from CIM-616 with 100 kg ha⁻¹ + seed treatment (5% TSP solution) and (3.32 g) from CIM-616 under 100 kg ha⁻¹ phosphorous (with seed application of a 5% solution of triple super phosphate, and foliar application of a 2% solution) (Table 1). The highest cotton yield was found from FH-Lalazar (2809.3 kg ha⁻¹), while the lowest was (1905.6 kg ha⁻¹) from MNH-886. Level of application 75 kg ha⁻¹ (2638.00 kg ha⁻¹), 75 kg ha⁻¹ + foliar (2% TSP solution), (2651.00 kg ha⁻¹), 100 kg ha⁻¹ + seed treatment (5% TSP solution) (2763.9 kg ha⁻¹), under 100 kg ha⁻¹ phosphorous (with seed application of a 5% solution of triple super

phosphate, and foliar application of a 2% solution) (2769.9 kg ha⁻¹) showed statistically higher yield of cotton, the minimum cotton yield (1941.1 kg ha⁻¹) was determined from control, and 50 kg ha⁻¹ (2002.3 kg ha⁻¹) and 50 kg ha⁻¹ + foliar (2% TSP solution) (2004.3 kg ha⁻¹). Cultivars with levels of phosphorus interaction gave the highest cotton yield (3776.3 kg ha⁻¹) measured from FH-Lalazar with 75 kg ha⁻¹, (3976.3 kg ha⁻¹) from cultivar FH-LZ with 75 kg ha⁻¹ + foliar (2% TSP solution), followed by (3844.00 kg ha⁻¹) from cultivar FH-Lalazar with 100 kg ha⁻¹ + seed treatment (5% TSP solution) and (4044.0 kg ha⁻¹) from FH-LZ under 100 kg ha⁻¹ phosphorous (with seed application of a 5% solution of triple super phosphate, and foliar application of a 2% solution); while lower cotton yield (1561.7 kg ha⁻¹) was measured from FH-LZ with Zero kg ha⁻¹ (Table 1).

Table 1. Influence of phosphorous application methods on plant height, number of bolls/plant, boll weight, seed cotton yield of cotton cultivars

Variables	Cultivars	Control	50 kg ha ⁻¹	50 + foliar	75 kg ha ⁻¹	75+foliar	100+seed treat	100+s+fol	Means
Plant height (inch)	MNH-886	55.24 f	58.53 d	58.53 d	58.53 d	59.84bc	60.23bc	60.62bc	57.74 c
	CIM-616	56.95 e	58.66 d	58.66 d	59.05 d	59.44 cd	59.44 cd	60.23 cd	58.53 b
	FH-LZ	56.95 e	58.79 d	58.79 d	61.02 b	62.99 a	63.38 a	63.77 a	60.03 a
	Means	56.38 d	58.13 c	58.62 c	59.53 b	60.07 b	61.02 a	61.93 a	-
LSD (P ≤ 0.05)	CULTIVAR (C) = 1.23		phosphorus level (P) = 1.57			C × P = 3.57			
Number of bolls/plant	MNH-886	22.00 f	23.66 ef	25.66 ef	25.66 cde	27.66 cde	27.00 bc	29.00 bc	24.50 c
	CIM-616	25.33 cde	27.66 bc	29.66 bc	29.33 b	31.33 b	33.33 a	35.33 a	28.91 a
	FH-LZ	24.00 def	25.66 cde	25.66 cde	26.66bcde	28.66 bcde	27.00 bc	29.00 bc	25.83 b
	Means	23.77 d	25.66 c	25.67 c	27.11 b	28.98 b	29.11 a	29.65 a	-
LSD (P ≤ 0.05)	CULTIVAR (C) = 1.04		phosphorus level (P) = 1.33			C × P = 3.02			
Boll weight (g)	MNH-886	1.03 e	1.16 e	1.18 e	1.33 de	1.35 de	1.33 de	1.35 de	1.21 c
	CIM-616	2.13 b	3.20 a	3.22 a	3.30 a	3.32 a	3.30 a	3.32 a	2.98 a
	FH-LZ	1.63 cd	1.93 bc	1.95 bc	2.26 b	2.28 b	2.23 b	2.25 b	1.99 b
	Means	1.60 c	2.10 b	2.13 b	2.26 a	2.27 a	2.29 a	2.45 a	-
LSD (P ≤ 0.05)	CULTIVAR (C) = 0.11		phosphorus level (P) = 0.15			C × P = 0.33			
Seed cotton yield %	MNH-886	1776.3 fg	1844.0efg	2044.0 efg	1932.7def	2132.7 def	2069.3 def	2269.3 def	1905.6 c
	CIM-616	2485.3 b	2108.0cde	2308 cde	2208.0cde	2408.0 cde	2378.3 bc	2578.3 bc	2294.9 b
	FH-LZ	1561.7g	2055.0def	2255.0 def	3776.3 a	3976.3 a	3844.0 a	4044.0 a	2809.3 a
	Means	1941.1 b	2002.3 b	2004.3 b	2638.0 a	2651.0 a	2763.9 a	2769.9 a	-
LSD (P ≤ 0.05)	CULTIVAR (C) = 104.88		phosphorus level (P) = 133.77			C × P = 302.71			

Mean values sharing similar letters are statistically significant at $p = 0.05$

Cultivar FH-Lalazar (50.58 kg ha⁻¹) gave the highest lint yield, the lowest yield of lint was measured (37.33 kg ha⁻¹) from cultivar MNH-886. The treatment 50 kg ha⁻¹ (44.00), 50 kg ha⁻¹ + foliar (2% TSP solution) (2004.3 kg ha⁻¹). (44.55), 75 kg ha⁻¹ (44.88), 75 kg ha⁻¹ + foliar (2% TSP solution) (45.00), 100 kg ha⁻¹ + seed application (5% solution of triple super phosphate) (45.55) under 100 kg ha⁻¹ phosphorous (with seed application of a 5% solution of triple super phosphate, and foliar application of a 2% solution) (45.89 kg ha⁻¹) resulted in statistically higher lint yield, the minimum lint yield was (40.00 kg ha⁻¹) obtained from control (Table 2). FH-Lalazar (0.76 kg ha⁻¹) showed statistically higher biological yield, the lowest biological yield was determined from two cultivars MNH-886 (0.69 kg ha⁻¹) and CIM-616 (0.67 kg ha⁻¹). Treatment 100 kg ha⁻¹ + seed treatment (5% TSP solution) (0.83 kg ha⁻¹) under 100 kg ha⁻¹ phosphorous (with seed application of a 5% solution of triple super phosphate, and foliar application of a 2% solution) (0.92 kg ha⁻¹) showed statistically higher biological

yield, the minimum biological yield (0.57 kg ha^{-1}) was obtained from control (Table 2). Higher seed cotton harvest (27%) was calculated from FH-LZ, while the minimum seed cotton harvest (19.00%) from MNH-886. The treatment 75 kg ha^{-1} (26.00%), 75 kg ha^{-1} + foliar (2% TSP solution) (27.00%), 100 kg ha^{-1} + seed application (5% solution of triple super phosphate) (27.00%) under 100 kg ha^{-1} phosphorous (with seed application of a 5% solution of triple super phosphate, and foliar application of a 2% solution). (27.00%) yielded statistically higher seed cotton harvest, the lowest seed cotton harvest was measured from control Zero kg ha^{-1} (19.00%), 50 kg ha^{-1} (20.00%), 50 kg ha^{-1} + foliar (2% TSP solution) (20.00%) (Table 2). FH-Lalazar (0.02%) showed statistically maximum ginning out turn, the lowest ginning out turn was found in two cultivars MNH-886 (0.019%) and CIM-616 (0.018%). Regarding the treatment under 100 kg ha^{-1} phosphorous (with seed application of a 5% solution of triple super phosphate, and foliar application of a 2% solution). (0.019%) higher ginning out turn was measured, lower ginning out turn was found from control Zero kg ha^{-1} (0.011%), 50 kg ha^{-1} (0.012%). Concerning cultivars and phosphorus levels interaction the highest ginning out turn (0.028 %) was recorded from FH-Lalazar with Zero kg ha^{-1} , the lowest got (0.016%) was found from CIM-616 with Zero kg ha^{-1} (Table 2).

Table 2. Influence of phosphorous application methods on biological yield, seed cotton harvest, lint yield and ginning out turn of cotton cultivars

Variables	Cultivars	Control	50 kg ha ⁻¹	50 + foliar	75 kg ha ⁻¹	75+foliar	100+seed treat	100+s+fol	Means
Biological yield (kg ha ⁻¹)	MNH-886	0.56 fg	0.69 bcd	0.71 bcd	0.73 bcd	0.75 bcd	0.79 ab	0.81 ab	0.69 b
	CIM-616	0.54 g	0.66 def	0.68 def	0.67 cde	0.69 cde	0.79 ab	0.81 ab	0.67 b
	FH-LZ	0.62 efg	0.76 bcd	0.78 bcd	0.75 bcd	0.77 bcd	0.90 a	0.92 a	0.76 a
	Means	0.57 c	0.70 b	0.71 b	0.71 b	0.80 b	0.83 a	0.92 a	-
LSD (P ≤ 0.05)	CULTIVAR (C) = 0.04		phosphorus level (P) = 0.05			C × P = 0.11			
Seed cotton harvest (%)	MNH-886	17 fg	18 efg	20 efg	19 def	21 def	20de	20 de	19 c
	CIM-616	24 b	21cde	23 cde	22 bcd	24 bcd	23 bc	25 bc	22 b
	FH-LZ	15 g	19df	21 de	37 a	39 a	38 a	40 a	27a
	Means	19 b	19 b	22 b	26 a	27 a	27 a	27 a	-
LSD (P ≤ 0.05)	CULTIVAR (C) = 104.88		phosphorus level (P) = 133.77			C × P = 302.7			
Lint yield (kg ha ⁻¹)	MNH-886	34.00 e	37.00 de	39.00 de	39.33 d	41.33 d	39.33 d	41.33 d	37.33 c
	CIM-616	40.66 cd	46.00 b	48.00 b	44.66 cd	46.66 cd	40.66 cd	44.66 cd	42.16 b
	FH-LZ	44.66 cd	48.33 b	50.33 b	54.00 a	56.00 a	55.33 a	57.33 a	50.58 a
	Means	39.77 b	43.77 a	43.98 a	44.88 a	44.78 a	45.00 a	45.90 a	-
LSD (P ≤ 0.05)	CULTIVAR (C) = 1.40		phosphorus level (P) = 1.78			C × P = 4.04			
Ginning out turn (%)	MNH-886	0.019 cd	0.020 bcd	0.050 bcd	0.022 bc	0.024 bc	0.018 cd	0.020 cd	0.019 ab
	CIM-616	0.016 d	0.022 bc	0.024 bc	0.018 cd	0.020 cd	0.018cde	0.020 cd	0.018 b
	FH-LZ	0.028 a	0.023 b	0.025 b	0.018 def	0.020 def	0.016 d	0.020 cd	0.020 a
	Means	0.011 c	0.012 c	0.015 b	0.017 b	0.017 b	0.018 b	0.019 a	-
LSD (P ≤ 0.05)	CULTIVAR (C) = 1.41		phosphorus level = 1.80			C × P = 4.07			

Mean values sharing similar letters are statistically significant at $p = 0.05$

Higher leaf area index ($0.65 \text{ m}^2/\text{m}^2$) was found from CIM-616, lower leaf area index ($0.49 \text{ m}^2/\text{m}^2$) was measured from MNH-886. Treatment under 100 kg ha^{-1} phosphorous (with seed application of a 5% solution of triple super phosphate, and foliar application of a 2% solution) (0.67 kg h^{-1}) resulted the statistically maximum leaf area index, the lowest ($0.51 \text{ m}^2/\text{m}^2$) was determined from control (Table 3). Cultivar FH-Lalazar ($4.79 \text{ g m}^{-2} \text{ day}^{-1}$) gave maximum crop growth rate, the minimum was found from cultivar MNH-

886 (4.15 g m⁻² day⁻¹). Concerning cultivars and phosphorus levels interaction higher crop growth rate (5.12 g m⁻² day⁻¹) was measured from FH-Lalazar under 100 kg ha⁻¹ phosphorous (with seed application of a 5% solution of triple super phosphate, and foliar application of a 2% solution). While the minimum (4.03 g m⁻² day⁻¹) was calculated from cultivar MNH-886 with Zero g m⁻² day⁻¹ (Table 3). Maximum leaf area duration was calculated from FH-Lalazar (659.7), while the lowest was in MNH-886 (381.9) (Table 3). The highest phosphorus concentration was recorded in 100 + seed treatment (591.2) and 100 + seed + foliar (597.2). The highest phosphorus concentration was in two cultivars i.e. MNH-886 (40.08%) and FH-LZ (45.50%). Further detail regarding the phosphorus concentration is shown (Table 3).

Table 3. Influence of Phosphorous application methods on ginning out turn, leaf area index, crop growth rate, leaf area duration and phosphorus concentration of cotton cultivars

Variables	Cultivars	Control	50 kg ha ⁻¹	50 + foliar	75 kg ha ⁻¹	75+foliar	100+seed treat	100+s+fol	Means
Leaf area index (m ² /m ²)	MNH-886	0.45 e	0.47 e	0.49 e	0.51 d	0.53 d	0.52 d	0.54 d	0.49 c
	CIM-616	0.56 c	0.65 b	0.67 b	0.67 b	0.69 b	0.72 a	0.74 a	0.65 a
	FH-LZ	0.52 d	0.56 c	0.58 c	0.65 b	0.67 b	0.67 b	0.69 b	0.60 b
	Means	0.51 d	0.56 c	0.60 b	0.61 b	0.63 b	0.64 b	0.67 a	-
LSD (P ≤ 0.05)	CULTIVAR (C) = 0.01		phosphorus level (P) = 0.02			C × P 0.03			
Crop growth rate (g m ⁻² day ⁻¹)	MNH-886	4.03 g	4.13 fg	4.15 fg	4.20 efg	4.22 efg	4.23 def	4.25 def	4.15 c
	CIM-616	4.36 cde	4.23 def	4.25 def	4.56 bcd	4.58 bcd	4.76 abc	4.78 abc	4.48 b
	FH-LZ	4.46 cde	4.63 bcd	4.65 bcd	4.96 ab	4.98 ab	5.10 a	5.12 a	4.79 a
	Means	4.28 b	4.33 b	4.47 a	4.57 a	4.57a	4.70a	4.78 a	-
LSD (P ≤ 0.05)	CULTIVAR (C) = 0.015		phosphorus level (P) = 0.019			C × P = 0.04			
Leaf area duration (days)	MNH-886	335.6 g	373.6 fg	375.6 fg	403.0 ef	405.0 ef	415.3 ef	417.3 ef	381.9 c
	CIM-616	428.3 e	494.3 d	496.3 d	509.0 d	511.0 d	588.0 c	590.0 c	504.9 b
	FH-LZ	594.6 c	618.3 bc	620.3 bc	655.6 b	657.6 b	770.3 a	772.3 a	659.7 a
	Means	452.8 d	452.8 d	500.0 c	522.5 b	532.5 b	591.2 a	597.2 a	-
LSD (P ≤ 0.05)	CULTIVAR (C) = 1.03		phosphorus level (P) = 1.32			C × P = 0.07			
Phosphorous concentration %	MNH-886	38.66 e	39.33 de	42.66 de	40.33 cde	42.33 cde	43.00 bcd	44.00 bcd	40.08 a
	CIM-616	45.33 abc	43.00 bcd	45.00 bcd	43.33 a	47.33 a	40.33 a	42.33 a	37.00 b
	FH-LZ	41.66 cde	43.33 bcd	45.33 bcd	47.66 ab	49.66 ab	49.33 a	49.33 a	45.50 a
	Means	41.55 b	41.88 b	43.78 b	45.77 a	45.99 a	47.55 a	48.34 a	-
LSD (P ≤ 0.05)	CULTIVAR (C) = 0.011		phosphorus level (P) = 0.014			C × P = 0.03			

Mean values sharing similar letters are statistically significant at $p = 0.05$

So due to all of this, cultivar CIM-616 (47.00), FH-Lalazar (45.50) showed statistically higher fiber uniformity. Treatment 75 kg ha⁻¹ (45.77), 75 kg ha⁻¹ + foliar (2% TSP solution) (45.99), 100 kg ha⁻¹ + seed application (5% solution of triple super phosphate) (47.55) under 100 kg ha⁻¹ phosphorous (with seed application of a 5% solution of triple super phosphate, and foliar application of a 2% solution) (48.34) resulted the statistically maximum fiber uniformity, the minimum fiber uniformity was determined from control (Table 4). Cultivar CIM-616 (20.19 mm) showed maximum staple length, and cultivar MNH-886 (14.83 mm) the minimum. So, the application of level of phosphorus, treatment 75 kg ha⁻¹ + foliar (2% TSP solution) (91.88 mm) 100 kg ha⁻¹ + application of seed treatment (5% TSP solution)(20.44 mm) under 100 kg ha⁻¹ phosphorous (with seed application of a 5% solution of triple super phosphate, and foliar application of a 2% solution).(21.00 mm) gave maximum staple length, so minimum staple length was calculated from control (15.22 mm) and 50 kg ha⁻¹ (16.33 mm) (Table 4). FH-LZ

exhibited the highest fiber strength (30.16 tpsi) while the minimum fiber strength was determined (23.08 tpsi) from MNH-886. The treatment under 100 kg ha⁻¹ phosphorous (with seed application of a 5% solution of triple super phosphate, and foliar application of a 2% solution) (28.00 tpsi) showed statistically higher fiber strength, lower fiber strength (24.33 tpsi) was recorded from control (*Table 4*). Cultivar FH-LZ showed the highest micronair (4.72 µg/inch), the minimum was found from cultivar MNH-886 (4.14). Application of treatment 100 kg ha⁻¹ + seed treatment (5% TSP solution) (4.68 µg/inch) under 100 kg ha⁻¹ phosphorous (with seed application of a 5% solution of triple super phosphate, and foliar application of a 2% solution): (4.75 µg/inch), 75 kg ha⁻¹ (4.45 µg/inch), 75 kg ha⁻¹ + foliar (2%TSPsolution) (4.51 µg/inch) resulted statistically higher micronair, lower was recorded from control (4.27 µg/inch), 50 kg ha⁻¹ (4.34 µg/inch), 50 kg ha⁻¹ + 5%foliar (2%TSPsolution) (4.40 µg/inch). Regarding phosphorus levels and cultivars interaction the highest micronair was measured from FH-Lalazar with 100 kg ha⁻¹ + seed treatment (5% TSP solution) (5.06) from cultivar CIM-616 under 100 kg ha⁻¹ phosphorous (with seed application of a 5% solution of triple super phosphate, and foliar application of a 2% solution)(5.08 µg/inch) (*Table 4*).

Table 4. Influence of phosphorous application methods on fiber uniformity, staple length, fiber strength and micronair of cotton cultivars

Variables	Cultivars	Control	50 kg ha ⁻¹	50 + foliar	75 kg ha ⁻¹	75+foliar	100+seed treat	100+s+fol	Means
Fiber uniformity	MNH-886	37.66 e	39.33 de	41.66 de	40.33 cde	42.33 cde	43.00 bcd	45.00 bcd	40.08 b
	CIM-616	45.33 abc	43.00 bcd	45.00 bcd	49.33 a	49.33 a	50.33 a	52.33 a	47.00 a
	FH-LZ	41.66 cde	43.33 bcd	45.33 bcd	47.66 ab	49.66 ab	49.33 a	49.33 a	45.50 a
	Means	41.55 b	41.88 b	43.78 b	45.77 a	45.99 a	47.55 a	48.34 a	-
LSD (P ≤ 0.05)	CULTIVAR (C) = 1.52		phosphorus level (P) = 1.93			C × P = 4.38			
Staple length (mm)	MNH-886	13.33 e	14.33 de	16.33 de	14.33 de	16.33 de	17.33 cd	19.33 cd	14.83 c
	CIM-616	19.00 bc	20.33 abc	22.33 abc	21.33 ab	23.33 ab	23.00 a	25.00 a	20.91 a
	FH-LZ	13.33 e	14.33 de	16.33 de	20.00 abc	22.00 abc	21.00 abc	23.00 abc	17.16 b
	Means	15.22 c	16.33 c	17.23 b	18.55 b	19.88 a	20.44 a	21.00 a	-
LSD (P ≤ 0.05)	CULTIVAR (C) = 1.30		phosphorus level (P) = 1.66			C × P = 3.76			
Fiber strength (tpsi)	MNH-886	22.33 e	23.33 de	25.33 de	23.33 de	25.33 de	23.66 de	25.66 de	23.16 c
	CIM-616	24.66 de	25.00 cde	27.00 cde	26.33 bcd	28.33 bcd	27.00 cb	29.00 bc	25.75 b
	FH-LZ	26.33bcd	28.68 b	30.68 b	32.33 a	34.33 a	33.33 a	35.33 a	30.16 a
	Means	24.44 b	25.66 b	26.00 b	27.33 a	27.83 a	28.00 a	28.90 a	-
LSD (P ≤ 0.05)	CULTIVAR (C) = 1.15		phosphorus level (P) = 1.47			C × P = 3.32			
Micronair (µg/inch)	MNH-886	4.03 g	4.13 fg	4.15 fg	4.20 efg	4.22 efg	4.23 def	4.25 def	4.15 c
	CIM-616	4.36 cde	4.23 def	4.25 def	4.56 bcd	4.58 bcd	4.76 abc	4.78 abc	4.48 b
	FH-LZ	4.46 cde	4.63 bcd	4.65 bcd	4.96 ab	4.98 ab	5.10 a	5.12 a	4.79 a
	Means	4.28 b	4.33 b	4.47 a	4.57 a	4.57 a	4.70 a	4.78 a	-
LSD (P ≤ 0.05)	CULTIVAR (C) = 0.13		phosphorus level (P) = 0.17			C × P = 0.40			

Mean values sharing similar letters are statistically significant at $p = 0.05$

Pearson's correlation of various cotton traits cultivars showed that plant height shared a direct significant correlation with all other studied traits i.e. no. of bolls/plant, boll weight, yield of cotton, lint yield, biological yield, seed cotton harvest, got, LAI, CGR, LAD, phosphorus concentration, fiber uniformity, staple length, fiber strength and micronair. Moreover, it has been studied that seed cotton harvest trait gave non-significant correlation with lint yield. Similarly, leaf area duration gave non-significant correlation with lint yield among all the studied traits (*Table 5*). Correlation matrix is an

important tool for the evaluation of trait association with each other (Anjum et al., 2018). Economic analysis of cost benefit ratio presented that maximum output can be attained with low input cost. And the highest benefit cost ratio was found 1.73 while the lowest was 1.27 during 2015, therefore in 2016 the highest was 1.81 and the lowest was 1.34 (Table 6). Eco-metrological data had long term effects on benefit cost ratio and net returns, therefore all these parameters must be calculated (Table 7).

Table 5. Pearson's correlation of different attributes of cotton cultivars

Variables	Plant height	No. of bolls/plant	Boll weight	Seed cotton yield	Lint yield	Biological yield	Seed cotton harvest	Ginning out turn	Leaf area index	Crop growth rate	Leaf area duration	Phosphorus concentration	Fiber uniformity	Staple length	Fiber strength	Micronair
Plant height	1															
No. of bolls/plant	0.97	1														
Boll weight	0.93	0.89	1													
Seed cotton yield	0.92	0.93	0.79	1												
Lint yield	0.91	0.86	0.99	0.75	1											
Biological yield	0.95	0.95	0.91	0.81	0.88	1										
Seed cotton harvest	0.90	0.92	0.81	0.96	0.78	0.81	1									
Ginning out turn	0.92	0.95	0.80	0.98	0.76	0.861	0.98	1								
Leaf area index	0.96	0.95	0.95	0.86	0.93	0.95	0.91	0.91	1							
Crop growth rate	0.96	0.93	0.86	0.91	0.83	0.92	0.93	0.95	0.96	1						
Leaf area duration	0.94	0.92	0.79	0.90	0.75	0.90	0.91	0.93	0.92	0.99	1					
Phosphorus concentration	0.96	0.94	0.84	0.95	0.81	0.90	0.96	0.97	0.95	0.99	0.98	1				
Fiber uniformity	0.96	0.94	0.84	0.95	0.81	0.90	0.96	0.97	0.95	0.99	0.98	0.99	1			
Staple length	0.97	0.99	0.88	0.94	0.84	0.94	0.95	0.97	0.96	0.97	0.96	0.98	0.98	1		
Fiber strength	0.97	0.98	0.92	0.94	0.89	0.95	0.94	0.97	0.97	0.97	0.93	0.97	0.97	0.90	1	
Micronair	0.96	0.93	0.86	0.91	0.83	0.92	0.93	0.95	0.96	0.99	0.98	0.99	0.99	0.97	0.97	1

Values in bold are different from 0 with a significance level $\alpha = 0.05$

Discussion

Different parameters such as structure of plants, production of total dry mater and economic yield become used to evaluate useful doses of fertilizer. When the main node stem was enhanced then it would be mainly obligate for height of plant, no. of bolls/plant and boll weight. Cultivar MNH-147 gave the highest height of plant and no. of bolls/plant in comparison to CIM-240. The reason was due to the growth habit of cultivar MNH-147 because it is more indeterminate as compared to CIM-240 (Malik et al., 2006). The

performance of cultivars may varied under different concentrations of phosphorus (Ramya and Hebsur, 2018). Phosphorous is an essential nutrient, the effect was stagnant to cotton crop, enhancing no. of flowers (Russell, 2001). Yield of cotton and lint significant were enhanced through application of phosphorus which is excellent trait for higher production. It has been noted that phosphorus affects photosynthesis so as essential commodities, while these commodities are the main factors affecting the yield of cotton. Phosphorous fertilizer is the main component to give power for plant growth and enhance weight of boll in cotton. Biological yield is equivalent to the above ground biomass. It is cumulative concerning both plant weight and root weight. Biological yield plays an imperative role in the increase of cotton production. Biological yield affected different parameters viz, environment, soil, and other plant factors. Results of the current experiment demonstrated the highest biological yield (Ramya and Hebsur, 2018). Biological yield was found highest when the spacing of plants was increased (Al-Dalain et al., 2012). Leaf area index is a main parameter for crop growth. It also describes raw materials produced by total radiation to plant for the initiation of leaf. There would be different ranges of leaf area index in young cotton plant. The cotton plant has ability to capture all of solar radiation when leaf area index reached the range of 3 (Zhou et al., 2011). Crop growth rate would be measured on different strategies such as that maximum calculated from NIAB-846 lower doses of nitrogen (50 kg ha⁻¹), the best crop growth rate on next cultivars, CIM-496, NIAB-824, demonstrated with increase of nitrogen doses of 100, 150 kg nitrogen per hectare simultaneously. While the reduction of CGR was observed with high stress treatments such as moisture stress and stages of vegetative growth (Hassan et al., 2016). Dry matter production of a crop is dependent on leaf area duration. Alkaline soils gave the highest yield when different relationship occurred between leaf area duration, yield and biomass. When there was no competition of weed, it was observed that leaf area duration gave the highest (136.85 days) in plots after transplantation so the reduction occurred due to the increase of competition. Reductions of LAD was observed in plots with competition of barnyard grass throughout the crop growth season. (Chen et al., 2018; Verma et al., 2018).

Table 6. Influence of phosphorus foliar application on benefit cost ratio (BCR) of cotton

Treatments (foliar applications) 2015	Yield (kg ha ⁻¹)	Value (\$ ha ⁻¹)	Stick value (\$ ha ⁻¹)	Gross value (\$ ha ⁻¹)	Total cost (\$ ha ⁻¹)	Net return (\$ ha ⁻¹)	BCR
P ₀ = Control	1941.1	908.8763	53.51171	962.388	754.1806	208.2074	1.27
P ₁ = 50 kg/ha	1982.3	928.1672	53.51171	981.6789	755.5184	226.1605	1.29
P ₂ = 50 +	2297.2	1075.612	53.51171	1129.124	778.9298	350.194	1.44
P ₃ = 75 kg/ha	2639.0	1235.652	66.88963	1302.542	785.9532	516.5886	1.65
P ₄ = 75 +	2798	1310.1	66.88963	1376.99	794.3144	582.6756	1.73
P ₅ = 100 kg/ha	2798	1310.1	66.88963	1376.99	794.3144	582.6756	1.73
P ₆ = 100 +	2763	1293.712	66.88963	1360.602	794.6488	565.9532	1.71
Treatments (foliar applications) 2016	Yield (\$ ha ⁻¹)	Value (\$ ha ⁻¹)	Stick value (\$ ha ⁻¹)	Gross value (\$ ha ⁻¹)	Total cost (\$ ha ⁻¹)	Net return (\$ ha ⁻¹)	BCR
P ₀ = Control	1941.1	973.796	53.51171	1027.308	762.2074	265.1003	1.34
P ₁ = 50 kg/ha	2002.3	1004.498	53.51171	1058.01	781.9398	276.0702	1.35
P ₂ = 50 +	2004.3	1005.502	53.51171	1059.013	782.2742	276.7391	1.35
P ₃ = 75 kg/ha	2638.0	1323.411	66.88963	1390.301	792.9766	597.3244	1.75
P ₄ = 75 +	2651.0	1329.933	66.88963	1396.823	793.311	603.5117	1.76
P ₅ = 100 kg/ha	2763.9	1386.572	66.88963	1453.462	802.3411	651.1204	1.81
P ₆ = 100 +	2769.9	1389.582	66.88963	1456.472	802.6756	653.796	1.81

Table 7. Eco-meteorological data of Multan, Punjab (Pakistan)

Months	Temperature (C)				Relative humidity (%)				Wind speed (km h ⁻¹)		Sunshine hours (h)		Rainfall (mm)	
	Max.	Min.	Max.	Min.	8 AM	5 PM	8 AM	5 PM	2015	2016	2015	2016	2015	2016
	2015		2016		2015		2016							
June	38.7	29.1	39.8	30.4	71.4	64.1	62.1	42.4	7.9	7.7	7.7	7.5	50.6	1.3
July	38.0	29.7	36.7	29.3	71.7	57.1	70.6	51.5	6.7	7.3	7.8	6.5	40.0	51.5
August	35.1	27.8	35.6	28.3	77.0	67.2	80.9	61.5	5.4	6.6	7.0	8.7	74.2	16.5
September	35.1	25.3	34.0	25.5	79.4	63.7	85.4	65.5	4.9	4.1	8.6	7.3	0.0	4.2
October	35.1	24.3	31.4	20.4	77.8	64.6	83.1	63.3	3.3	2.6	7.7	6.0	3.2	17.6
November	26.8	13.0	26.2	11.9	84.0	74.5	86.0	68.0	2.5	2.0	5.6	5.0	0.0	0.0
December	20.3	9.2	17.7	6.8	89.6	75.0	93.6	74.9	3.0	2.5	4.8	3.7	0.0	0.0

Many researcher papers demonstrated that phosphorous gave response to cotton crop such as that (Magare et al., 2018; Rosace et al., 2018). Khan et al., (2014) demonstrated FU gave a positive response for Ginning out turn and value of micronair. Positive response of fiber uniformity was found on yield of cotton for fiber strength whereas negative response demonstrated for mean length and upper half mean length. Fiber uniformity, staple length, fiber strength and micronair are excellent traits to enhance the potential of textile industry. All these traits were probably enhanced with phosphorus application.

Cotton growers have many difficulties due to enhanced commodities. So, increase of inputs cost resulting in decrease of output/ profit.. Improper fertilizer is a main source to increase the production cost. Most of all growers of cotton use nitrogen fertilizer; while 85% of growers use phosphorous fertilizer for higher rate of production (Miao et al., 2018). Fertilizer cost is a major problem and has the 2nd largest commodity value and accounts for 22% of total cost production (Makhdum et al., 2001). Phosphorous is a main nutrient but overall in cotton crop the efficiency of phosphorous is low because farmer could not facilitate phosphorous fertilizer in all soil type. Due to all of this various research studies on cotton which responds to phosphorus positively and economically were conducted (Miao et al., 2018). Results demonstrated that phosphorus is a main nutrient for cotton crop for the highest yield of cotton compared to nitrogen. So, phosphorus provides positive response for better production of cotton in Punjab.

Conclusion

It is concluded that decreased amount of phosphorus demonstrated in decreased yield of cotton along with its related traits. However, cultivar FH-LZ along with phosphorous level under 100 kg ha⁻¹ phosphorous (with seed application of a 5% solution of triple super phosphate, and foliar application of a 2% solution) demonstrated the highest values and excellent performance for many yield traits.

Therefore, it is recommended that farmers and researchers of the vicinity may use exogenous phosphorus to get the highest yield and excellent quality of fiber of cotton crop.

REFERENCES

- [1] Ahmad, D., Chani, M. I., Rauf, A., Afzal, M. (2016): Economic analysis of cotton cultivation under agro-climatic conditions of district Muzaffargarh. – American Journal of Agric. & Environ. Sci 16(8): 1498-1503.
- [2] Ahmad, R., Anjum, M. A. (2018): Applications of molecular markers to assess genetic diversity in vegetable and ornamental crops. – A Review. J. Hort. Sci. Technol. 1: 1-7.
- [3] Ahmad, R., Malik, W., Anjum, M. A. (2019): Genetic Diversity and Selection of Suitable Molecular Markers for Characterization of Indigenous *Zizyphus* Germplasm. – Erwerbs-Obstbau 6: 1-9.
- [4] Al-dalain, S. A., Abdel-ghani, A. H., Dala'een, A. (2012): Effect of planting date and spacing on growth and yield of fennel (*Foeniculum vulgare mill.*) under irrigated conditions. – Pak. J. Bio. Sci. 15: 1126-1132.
- [5] Anjum, M. A., Rauf, A., Bashir, M. A., Ahmad, R. (2018): The evaluation of biodiversity in some indigenous Indian jujube (*Zizyphusmauritiana*) germplasm through physico-chemical analysis. – Acta Scient. Polo-Hortorum Cultus 17(4): 39-52.
- [6] Apel, K., Hirt, H. (2004): Reactive oxygen Species: metabolism, oxidative stress, and signal transduction. – Annu. Rev. Plant Biol. 55: 373-399.
- [7] Araújo, E. O., Santos, G. Q., Oliveira, M. A., Camacho, Dresch, D. M. (2012): Nutritional efficiency of cowpea varieties in the absorption of phosphorus. – Agronomía Colombiana 30: 419-424.
- [8] Baloch, M. J., Khan, N. U., Rajput, M. A., Jatoi, W. A., Gul, S., Rind, I. H., Veesar, N. F. (2014): Yield related morphological measures of short duration cotton genotypes. – J. Anim. Plant Sci. 24(4): 1198-211.
- [9] Bronson, K. F., Keeling, J. W., Booker, J. D., Chua, T. T., Wheeler, T. A., Boman, R. K., Lascano, R. J. (2003): Influence of landscape position, soil series and phosphorus fertilizer on cotton lint yield. – Agron. J. 95: 949-957.
- [10] Bronson, K. F., Onken, A. B., Booker, J. D., Lascano, R. J., Provin, T. L., Torbert, H. A. (2001): Irrigated cotton yields as affected by phosphorus fertilizer and landscape position. – Commun. Soil Sci. Plant Anal. 32: 1959-1967.
- [11] Chen, J., Liu, L., Wang, Z., Sun, H., Zhang, Y., Lu, Z., Li, C. (2018): Determining the effects of nitrogen rate on cotton root growth and distribution with soil cores and mini rhizotrons. – PloS One 13(5): e0197284.
- [12] Crozier, C. R., Walls, B., Hardy, D. H., Barnes, J. S. (2004): Response of cotton to P and K soil fertility gradients in North Carolina. – J. Cotton. Sci. 8: 130-141.
- [13] Dohary, C. G., Rochester, I. J., Blair, G. J. (2004): Response of field grown cotton (*Gossypium hirsutum* L.) to phosphorus fertilization on alkaline soils in eastern Australia. – Aust. J. Soil Res. 42: 913-920.
- [14] Fageria, N. K., Moraes, M. F. (2013): Phosphorus nutrition of lowland rice in tropical lowland soil. – Communications in Soil Science and Plant Analysis 44: 2932-2940.
- [15] Fageria, N. K., Baligar, V. C., Moreira, A., Portes, T. A. (2010): Dry bean genotypes evaluation for growth, yield components and phosphorus use efficiency. – J. Plant Nut. 33: 2167-2181.
- [16] Gaikwad, J. L. (2018): Studies on weather indices in hirsutum cotton under varied condition. – Doctoral dissertation, Vasant Rao Naik Marathwada Krishi Vidyapeeth, Parbhani.
- [17] Girma, K., Roger, W., Freeman, K., Randal, K., Boman, W., Raun, R. (2007): Cotton Lint Yield and Quality As Affected by Applications of N, P and K Fertilizers Kefyalew. – The J. Cotton Sci. 11: 12-19.
- [18] G. O. P. (2018): Economic survey of Pakistan 2017-2018. – Ministry of Food and Agriculture, Finance Division, Economic Advisor Wing, Islamabad, Pakistan.

- [19] Hassan, M., Maqsood, M., Wajid, S. A., Ranjha, A. M. (2016): Impact of moisture stress and nitrogen on crop growth rate, nitrogen use efficiency, and harvest index of cotton (*Gossypium hirsutum* L.) – Pak. J. Agri. Sci. 53: 171-180.
- [20] Hunt, K. H. (1978): Kinematic Geometry of Mechanisms. – Oxford University Press, Oxford.
- [21] Khan, M. I., Dasti, M. A., Mahmood, Z. (2014): Effects of fiber traits on seed cotton yield of cotton (*Gossypium hirsutum* L.) – J. Agric. Res. 2: 52-56.
- [22] Magare, P. N., Jadhao, S. D., Farkade, B. K., Mali, D. V. (2018): Effect of levels of potassium on yield, nutrient uptake, fertility status and economics of cotton grown in vertisol. – Int. J. Curr. Microbiol. App. Sci. 7: 1292-1300.
- [23] Makhdum, M. I., Malik, M. N. A., Chaudhry, F. I., Shabab-Ud-Din, C. (2001): Effect of gypsum as a sulphur fertilizer in cotton production. – Int. J. Agric. Biol. Sci. 3: 298-300.
- [24] Malik, M. N. A., Chaudhry, F. I., Makhdum, M. I. (2006): Investigation on phosphorus availability and seed cotton yield in silt loam soils. – J. An. Plant Sci. 6: 21-23.
- [25] Miao, S., Pengcheng, L., Cangsong, Z., Shuai, L., Aizhong, L., Huimin, H., Jingran, L., Helin, D. (2018): Effects of low phosphorus stress on root morphology and physiological characteristics of different cotton genotypes at the seedling stage. – Cotton Sci. 30: 45-52.
- [26] Pakistan Meteorological Department (2015-2016): Government of Pakistan. – <http://www.pmd.gov.pk/>.
- [27] Ramya, S. H., Hebsur, N. S. (2018): Dry matter production and yield of BT cotton as influenced by available phosphorus in Vertisols. – Asian J. Soil Sci. 13: 63-69.
- [28] Rosace, G., Castellano, A., Trovato, V., Iacono, G., Malucelli, G. (2018): Thermal and flame retardant behaviour of cotton fabrics treated with a novel nitrogen-containing carboxyl-functionalized organophosphorus system. – Carbohydr. Poly. 196: 348-358.
- [29] Russell, E. W. (2001): Soil Condition and Plant Growth. – The English Language Book Society and Longman, London, pp. 56-87.
- [30] Tisarum, R., Theerawitaya, C., Samphumphung, T., Takabe, T., Cha-um, S. (2019): Exogenous foliar application of glycine betaine to alleviate water deficit tolerance in two indica rice genotypes under greenhouse conditions. – Agronomy 9(3): 138.
- [31] Vance, C. P., Stone, U. C., Allan D. L. (2003): Phosphorus acquisition and use critical adaptations by plants for securing a nonrenewable resource. – New Phytologist 157: 423-447.
- [32] Verma, N., Chaudhary, S., Goyal, S. (2018): Long term effects of inorganic fertilizers and organic amendments on ammonification and nitrification activity of soils under cotton wheat cropping system. – Int. J. Curr. Microbiol. App. Sci 7: 718-724.
- [33] Zambrosi, F. C., Junior, D. M., Furlani, R., Quaggio, J. A., Boaretto, R. M. (2012): Efficiency of phosphorus uptake and utilization in citrus rootstocks. - Revista Brasileira de Ciência do Solo. 36: 486-496.
- [34] Zhang, M., Alva, A. K., Li, Y. C., Calvert, D. V. (2012): Aluminum and iron fractions affecting phosphorus solubility and reactions in selected sandy soils. – Soil Sci. 166: 940-948.
- [35] Zhou, X. B., Chen, Y. H., Ouyang, Z. (2011b): Row spacing effect on leaf area development, light interception, crop growth and grain yield of summer soybean crops in Northern China. – Afr. J. Agri. Res. 6: 1430-1437.

ASSESSMENT OF SENTINEL-2-DERIVED VEGETATION INDICES FOR THE ESTIMATION OF ABOVE-GROUND BIOMASS/CARBON STOCK, TEMPORAL DEFORESTATION AND CARBON EMISSIONS ESTIMATION IN THE MOIST TEMPERATE FORESTS OF PAKISTAN

KHAN, K.^{1*} – IQBAL, J.¹ – ALI, A.² – KHAN, S. N.¹

¹*Institute of Geographical Information Systems, School of Civil and Environmental Engineering, National University of Sciences and Technology (NUST), Islamabad, Pakistan (phone: +92-51-9085-4473)*

²*Pakistan Forest Institute, Peshawar, Pakistan (phone: +92-91-9221-226)*

**Corresponding author
e-mail: kkhan.ms16igis@igis.nust.edu.pk*

(Received 3rd Jul 2019; accepted 14th Nov 2019)

Abstract. In developing countries like Pakistan, leading CO₂ emission source is deforestation of temperate forests, which must be estimated precisely for resilient climate policy. This research evaluates temporal deforestation, above and below ground carbon stock, biomass estimation potential of vegetation indices derived from Sentinel-2 imagery, carbon emission from deforestation and carbon sequestration potential. Forest inventory data was collected and used in allometric equations, to calculate aboveground biomass and carbon stock. The temporal deforestation rate was estimated using LANDSAT 7 & 8 (2000-2015) data. Biomass was predicted using the most optimal VI by developing linear regression model. The carbon emission from deforestation was estimated using activity data and emission factor. Above ground biomass and carbon stock estimated for the study area were 148.79 t/ha and 69.93 t/ha with mean CO₂ equivalent value of 322.5 t/ha. The estimated forest cover change using Landsat satellite data (2000-2015) was about 16.88% with 2.51% annual deforestation rate. Relationship between red-edge VIs and AGB were the best and reduced saturation problem. Carbon loss in fifteen years were about 6.96 Mt CO₂ e. The carbon sequestration capacity for the study area was 82.07 t/ha ± 13 t/ha. This research methodology is cost effective, helps in sustainable forest management and reduces carbon losses.

Keywords: *activity data, carbon losses, climate change, GIS, REDD+, remote sensing, sequestration potential*

Introduction

In sequestration of carbon forests play a significant role and act as a natural carbon sink to mitigate climate change. There is about 33% area of the world covered with forests which accounts for 80% aggregate over ground earthbound carbon and 40% below canopy carbon (Noble et al., 2000). The rate of carbon storage in the world's forests is estimated to be about 4.1 GtCyr⁻¹ from 2000 to 2007 (Stinson et al., 2011). The significant contribution of greenhouse gas emission is due to forest fire, degradation, fossil fuel burning, and deforestation. The Greenhouse gas emission can be reduced through sustainable management, conservation, restoring forest and increment in forest trees (Noble et al., 2000). While conservation of forest not only act to be the source of carbon but also gives a more extensive scope of services and products to people, and it also has natural, financial, social, ecological and environmental benefits. The carbon density in the forest is higher than in other type of environments and hence has a role in

decreasing atmospheric carbon emissions (Stinson et al., 2011). According to IPCC, outflow of carbon dioxide from a change in land use is about 10% of the outflows that are from human-made activities. As deforestation, degradation and erosion occur it leads to an increase in carbon emission and a decrease in sequestration (Dube et al., 2012). About 50.8% of coniferous wood comprises of carbon and herbs, woody plants in forest act as essential storage of carbon (Thomas and Martin, 2012). There is a significant role of forest in global climate change as about 17.4% of yearly CO₂ discharge are due to degradation and deforestation of forests (Egenhofer, 2007). Forests located at high-latitude in the northern hemisphere act as major sinks of carbon and play a leading part in reducing emissions of carbon in the global carbon cycle (Schimel et al., 2000; Valentini et al., 2000). Therefore, countries having more risk of deforestation and degradation should increase the protected areas as an effort for the conservation of their forest environmental services (Jackson and Baker, 2010; Lippke et al., 2003). Of the 3984 million ha worldwide forest area it is estimated that about 13.25% of the areas are protected forests (Keenan et al., 2015).

According to IPCC, a baseline must be created for the assessment of carbon stock, and it needs a mapping of vegetation biomass arrangement from local to worldwide scale (Dobbs et al., 2014; Pan et al., 2011). To counterbalance carbon release at less expense and obtain sustainable forest management REDD+ has promoted interest at international level (Caparros et al., 2011; Neilson et al., 2006). The primary aim of REDD+ is to make motivators for decreasing discharges from degradation and deforestation and enhancement of carbon stock through improvement, sustainable forest management and conservation in the developing countries (Balderas Torres and Skutsch, 2012). According to the strategy of UNFCCC on REDD+ release of carbon from the forests will be ascertained and the compensation will be given to developing countries in favor of a decrease in carbon emission. In order to receive the compensation, they should indicate that in the forest they increased carbon storage rate and due to degradation and deforestation national carbon release rate are decreased (increasing carbon sequestration) (Le Toan et al., 2011; Sessa and Dolman, 2008). Then an arrangement of “national forest reference emission level/reference levels (REL/RL) (or sub-national REL/RLs as an interval measure) and safeguards” should be set up and then by those results financing should be given (Brown, 2002; Lu, 2006).

Pakistan has a forest cover of 4.55 million hectares (5.1%). Most of the forest in the country is located in the northern part which is generally natural and coniferous. These forests can be categorized as moist temperate, dry temperate, sub-tropical chir pine and sub-alpine forests. These types comprise about 54% of the area of forests. Forest/tree cover stretches out over a region of 1.51 million ha (except alpine pasture), which makes about 20.3% of total land area of Khyber Pakhtunkhwa province. In Khyber Pakhtunkhwa, the natural forests comprise of sub-tropical chir pine forests having *Pinus roxburghii* (Chir pine), and *Quercus* spp. The dry and moist temperate forests have dominant species of *Pinus wallichiana* (Blue pine), *Picea smithiana* (Spruce) and *Cedrus deodara* (Deodar) as well as several broad-leaved species such as *Acer caesium* (Maple), *Aesculus indica* (Horse chestnut), *Juglans regia* (Walnut) and *Prunus padus* (Bird cherry).

It is estimated that over 1 million hectares of forests are lost in Pakistan between 1990 and 2015 (FAO, 2014), which is about 25% of its natural forests with the average deforestation rate of 42,200 ha per year. The above ground and below ground biomass are reduced due to deforestation at an annual rate of 2.2%, totaling over 100 million tons CO₂

e; from 330 million tons of CO₂ in 1990 to 213 million tons of CO₂ in 2010 (WorldBank, 2015). Deforestation is mainly driven by increasing demand of forest product such as fuelwood, fodder, and timber, outstripping the supply of these products, population expansion, grazing, land use change and illegal harvesting (FCPF, 2013). Coniferous forest area has been rapidly declining due to the high value of conifer timber. Government forests have been transferred to the non-forestry and commercial purpose such as infrastructure development, agriculture, defense, and tourism in recent decades (WorldBank, 2015). In Pakistan coniferous forests are considered to be the most important species for preservation due to their high carbon stock, the presence of peatlands, and longer maturity age (Karki et al., 2014). Deforestation and land-use change are identified as major sources of emissions. Forestry and land use change contribute approximately 3% to Pakistan's total GHG emissions (around 9 MtCO₂ e in 2008) (Aslam et al., 2011). Net emissions are forecast to rise from 10,000 GgCO₂ e in 2011 to 13,000 GgCO₂ e in 2020 and 15,000 GgCO₂ e in 2030 (PAEC-ASAD: Athar, 2009).

Pakistan commenced REDD+ activities in 2010 and it is a UN-REDD partner country. In 2012 REDD+ Preparedness Phase (R-PP) for Pakistan was initiated by the Worldwide Fund for Nature Pakistan (WWF-Pakistan), the International Center for Integrated Mountain Development (ICIMOD), and the Climate Change Ministry. For REDD+ guidance has been recommended by the United Nation Framework Convention on Climate Change using RS and ground-based carbon measurement for carbon, biomass estimation, GHG emissions and change in forest area due to deforestation and degradation. Subsequently, there is an absence of data for the appraisals of reasonable REDD+ action regions. Furthermore, tools have been developed since the 1990s to identify which zones are the most vulnerable to deforestation and ultimately releasing carbon (Päivinen et al., 2001; Piao et al., 2005). However, less data availability can be a barrier in their use in developing countries (Angelsen, 2009; Siteo et al., 2014). The decrease in carbon emission must be surveyed in order to create installments for REDD+ activity at the national or sub-national level. This incorporates the evaluation of the two factors, i.e., activity data (a change which occurred in a particular period in a forest area) and emission factor (change occurred in carbon stock of forest). Both of these factors must be assessed through the nations taking part in REDD+ through the usage of authentic MRV systems (Plugge et al., 2013). Field data and RS gives us a proficient answer to observe the condition and changes of forest carbon stock (Melville et al., 2015; Tomppo et al., 2008).

The conventional field inventory methods of forest carbon stock inventory are considered more accurate. The field technique can be further divided into two methods, i.e., destructive and non-destructive methods. The destructive method is also called harvest method (Gibbs et al., 2007). In this method the trees in a study area are all felled in the destructive method then their parts like a tree trunk, leaves, and branches are weighed and then after oven drying the weight of these components are recorded again. When biomass estimation is done without tree felling then it is called the non-destructive method, and it can be used for threatened and protected species (Montes et al., 2000), the above-ground biomass can also be evaluated from volume tables using DBH (Diameter at breast height) and trees height as a reference variable. These two parameters, i.e., height and DBH can be easily obtained and then using the allometric model tree biomass can be determined (Picard et al., 2012). However, it presents various challenges including limited to small scale survey, expensive, and time-consuming methods.

To estimate above ground biomass studies have been conducted using optical satellite images of medium-resolution (Fernández-Manso et al., 2014; Gizachew et al., 2016; Lu et al., 2002; Muukkonen and Heiskanen, 2005). For estimation of biomass VIs were derived in these studies from optical images (Landsat, ASTER) because there is correlation between AGB assessed from field data and VIs. Major problems in estimation of above ground biomass is low spatial resolution and saturation problem in the satellite imageries (Lu, 2005). Sentinel-2 satellite which is recently launched have high spatial, spectral and temporal resolution and also have new red-edge spectral band for vegetation monitoring which will further increase the accuracy of AGB estimation (Delegido et al., 2011).

Two components restrict carbon sequestration potential, i.e., carbon cannot be retained by the forests forever, and as growth occurs in the forest, a saturated state will be attained which is called as the carbon carrying capacity (CCC) (Keith et al., 2009). It means that carbon sequestration of forests has a maximum point of confinement (Odum) known as carbon sequestration potential (CSP) (Keith et al., 2009). On the other hand, degradation and deforestation conservation of all the forests is not possible. Hence for reciprocation between fulfilling forest products demands of humans and saving carbon sink capacity of forests attention should be given to those forests having high Carbon Carrying Capacity (CCC) and Carbon Sequestration Potential (CSP). Carbon density is decided by two variables which are the age of the forest (Pregitzer and Euskirchen, 2004) and climate (precipitation, temperature, etc.). Forests having old growth contain higher biomass and can represent the carbon carrying capacity of biomes (Keith et al., 2009). Assessment of Carbon Sequestration Potential (CSP) is challenging as old-growth forest data is not available (Cramer et al., 2001).

Geographic information systems (GIS) and Remote sensing (RS) techniques can effectively evaluate and analyze forest carbon stock at a regional and global scale. However, RS cannot directly measure carbon stock and need ground-based traditional field survey techniques. The RS techniques have been reported to be more accurate and useful where forest carbon densities are low, i.e., in temperate forest condition and young stand. However, the RS techniques are not very accurate in the tropical forest which are the most carbon-rich due to saturation of the remote sensing signals (Rosenqvist et al., 2003). Furthermore, since most of the remote sensing sensors are optical (visible and near-infrared bands) in nature; therefore, their use is limited due to higher cloud cover. To overcome this issue active remote sensing techniques like LIDAR are now becoming a prominent approach (Asner, 2001).

Currently, Very High-Resolution Satellite (VHRS) optical imagery, i.e., Quick bird, Geo-eye, are being used for the extraction of forest inventory parameters (Baral, 2011). Phua et al. (2014) found a strong positive correlation between forest inventory data such as DBH and Height and Satellite-based crown area data. SPOT, Landsat and ASTER imagery have been used for the estimation of AGB through the extraction of Vegetation Indices (VIs) from imagery and then through statistical techniques their relationship assessment with AGB. According to Silleos et al. (2006), optical satellite imagery sun-view angle, atmospheric effects, and soil-back ground can be reduced by VIs. Few studies (Fernández-Manso et al., 2014; Gizachew et al., 2016; Lu et al., 2002; Muukkonen and Heiskanen, 2005) reported on relationship between forest biomass and VIs derived from Sentinel-2 imagery. Hence, more research is needed on abilities of VIs which are obtained from optical satellite images of medium-resolution for forest biomass evaluation, specifically in Sentinel-2 satellite image which is recently launched.

Most of the studies discussed have assessed forest biomass/carbon stock using remote sensing techniques. This study estimates above and below ground carbon stock, temporal deforestation, potential of several type of vegetation indices from sentinel-2 imagery in estimation of biomass, carbon emission from deforestation and carbon sequestration potential using forest inventory and remote sensing data for sustainable management of forests.

Major objectives of the study were:

- Generating land cover maps for the assessment of temporal deforestation.
- Estimating above and below ground biomass/carbon stock from forest inventory data.
- Potential of Several type of vegetation indices from sentinel-2 imagery in the estimation of biomass.
- Producing and validating biomass maps by developing regression model between forest inventory and remotely sensed data.
- Quantifying carbon losses from land use change using forest inventory and remote sensing data.
- To assess the carbon sequestration potential of study area.

Materials and methods

Study area

Battagram (latitude 34.41 N and longitude 73.1 E), a district of Khyber-Pakhtunkhwa (KP) province of Pakistan was selected as a study area (*Fig. 1*). Its total area is about 1507 km². The district terrain is mountainous in nature with an altitude above 4000 m covered with thick forest. There are four ranges in Battagram district namely Hillan, Battagram, Allai, and Pashto range. It includes forests, rangeland, alpine pasture, and agriculture. The average temperature of the district is 18.5 °C with an average annual precipitation of 1218 mm during winter, snowfall used to be heavy on the northern part at higher altitudes of the mountainous regions.

The Battagram forests can be characterized as Himalayan moist temperate forest and Sub-alpine temperate regions. The legal status of most of the forest found is Guzara forest (community-owned forests).

The underlying rock in the area consists of gneissose – schist, gneiss, granitoid-schist and mica-schist. Shales occur in chir zone. Metamorphic and plutonic igneous rocks are also found. Low grade metamorphic rocks like (i) Graphite Schist, (ii) Recrys-talline limestone, (iii) Amphibole Schist (iv) Quart-mica Schist (v) Green Schist are exposed in the southern and the south-western part of the area.

Methods

Sample plots were laid out using stratified cluster sampling technique in the study area for the collection of forest inventory data. The forest inventory data was collected in June 2016 on tree diameter and height parameters and used in the allometric equations for the estimation of biomass. About 11 different vegetation indices (VIs) were derived from Sentinel-2 imagery to establish a relationship between VIs, and above ground biomass (AGB). For linear regression model development best VI was used in order to predict biomass. To assess the land use/landcover satellites Landsat-7 and Landsat-8 imagery data were used. Carbon emissions were estimated by

multiplying the emission factor with activity data. Activity data and emission factor were calculated from remotely sensed images and forest inventory data respectively. Finally, carbon sequestration potential was assessed from carbon carrying capacity (CCC) and carbon density. The complete methodology flow chart is given in *Figure 2*.

Data collection/field procedure

A total of fifty-five (55) plots were sampled using a stratified cluster sampling technique in the study area. Circular plots of radius 17.84 m were taken with a plot to plot distance of 200 m. Before final data processing field measurements errors were corrected (McRoberts et al., 2010) as accuracy and results of inventory is affected by these errors (Molto et al., 2013). Sample plots shape and size were taken according to UNFCCC guidelines. For carbon inventory trees having $DBH \geq 5$ cm were measured (Nizami, 2012). Plot measurement includes information about GPS coordinates, aspect, elevation, forest type, species, diameter at breast height (DBH), crown cover and tree height. The DBH was measured at 1.3 meters above the ground from collar point of trees on the uphill side and according to field measurement standard while tree height was measured by Haga Altimeter. The plot to plot navigation was done by Sunnto Compass, and within plot distance and plot to plot, the distance was measured using measuring tape (Nizami, 2012). Defected trees such as a buttressed tree, forked trees, and trees having butt log damaged by fire were also measured. All the field data was recorded in departmental field inventory forms and further transferred to Microsoft Excel sheets for the calculation of biomass and carbon stocks.

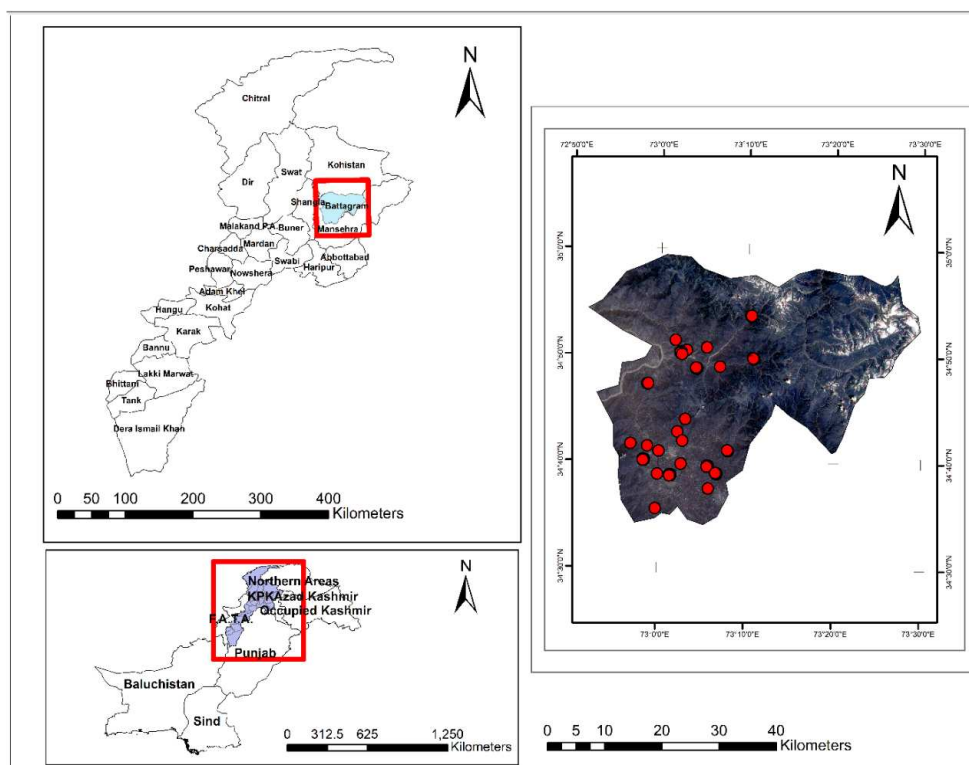


Figure 1. Study area map is showing its location, sentinel-2 imagery of study area and forest inventory sample plots analyzed in the study area using stratified cluster sampling according to national forest inventory and field surveying manual and UNFCCC guidelines with a plot to plot distance of 200 m

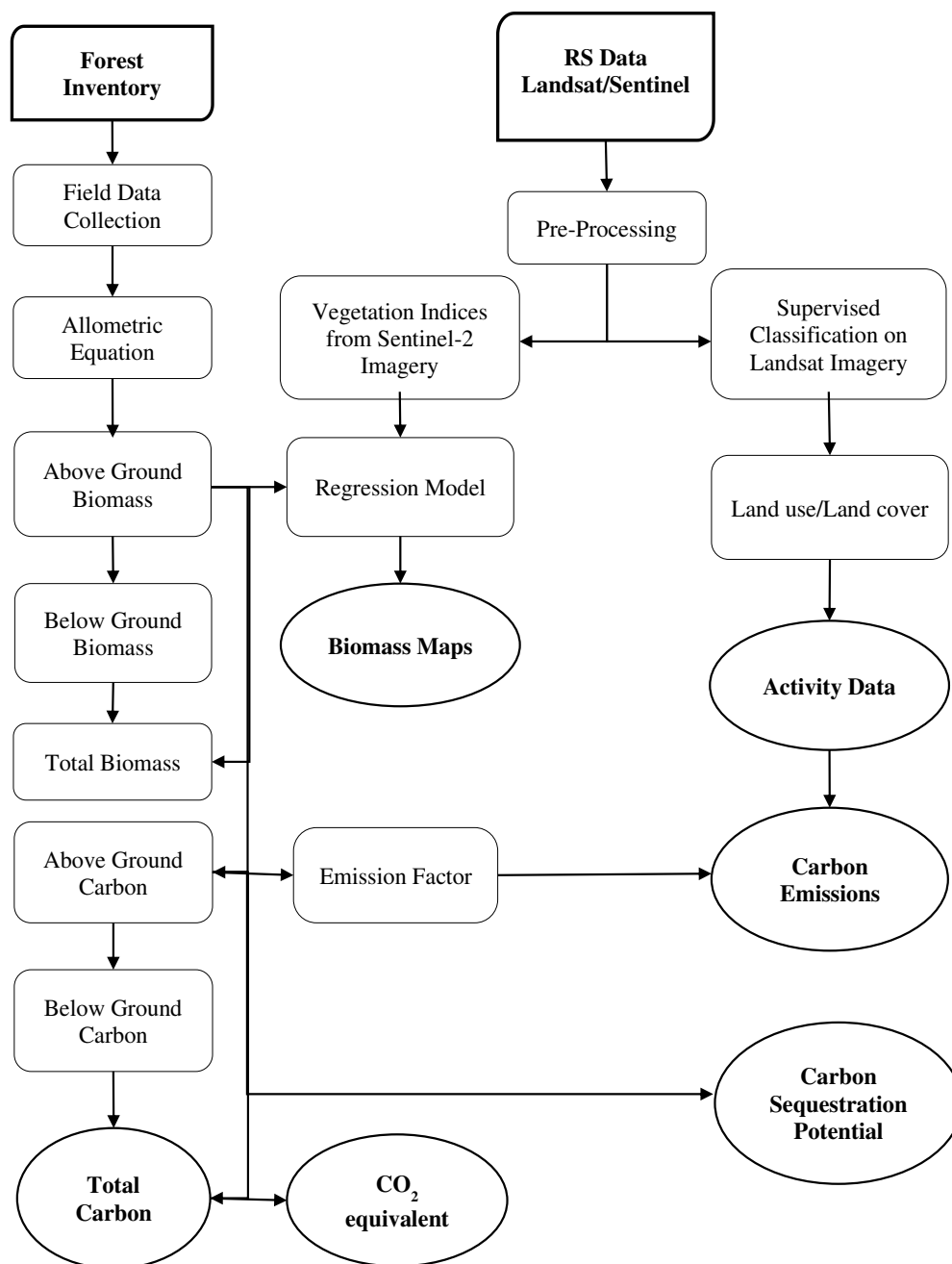


Figure 2. Workflow of the research method and data types used

Calculation of above/below ground biomass and carbon stock

The AGB can be computed by two methods: (i) Biomass expansion method and (ii) use of Allometric equations. In Biomass expansion factor method first volume is calculated with field measurements such as height, DBH, and Form factors and then the volume is multiplied with wood density and BEF (Biomass Expansion Factor) in order to get final biomass (Nizami, 2012). It is multiplied with wood density because there is a relationship between biomass and density of wood, i.e. the higher the density, the higher the biomass. While it is multiplied with BEF because we have calculated the volume of stem only while the biomass is also stored in branches so we cannot measure

the volume of each branch of tree, therefore, we multiply it with a fixed value of BEF for each species. For calculation of AGB allometric equations were used by using forest stands parameters such as trees height and Diameter at breast height (DBH). Allometric equations are the regression equations between forest attributes used for the estimation of tree height, biomass or other growth attributes (Chave et al., 2005; Gao et al., 2016; Shi and Liu, 2017). Hence with the use of field measurements such as diameter and height, we can assess biomass (Gao et al., 2015). The height represents primary growth while the secondary growth is represented by the diameter of trees. The allometric equations (*Table A1* in the *Appendix*) which were used in this research were formulated by Ali (Ali, 2015). These allometric equations are different for different species; it means that these are species specific. These allometric equations are acceptable for all bioclimatic conditions and forest types. The above ground biomass (AGB) in kgs per plot was then converted into per hectare by multiplying AGB of the plot with 10 as the size of our plot was one-tenth of a hectare. Then divided with 1000 in order to obtain AGB in tons. Finally, in order to obtain AGC (Above Ground Carbon stock), the biomass in tons was multiplied with 0.47, a conversion factor formulated by IPCC (*Eq. 1*; IPCC, 2006). According to the conversion factor, about one half of total dry biomass is carbon stock for given species. For assessment of BGB (below ground biomass) and BGC (below ground carbon stocks) the AGB (above ground biomass) and AGC (above ground carbon) were multiplied with a conversion factor of 0.26 (Ali et al., 2018; IPCC, 2006; Ravindranath and Ostwald, 2008). For the estimation of total carbon stocks above ground carbon and below ground carbon were added and converted into CO₂ equivalent by multiplying total carbon stocks with a 3.66 factor. While 3.66 is a ratio of molecular mass to the atomic mass of carbon.

$$C=AGB\times CF \quad (\text{Eq.1})$$

where C is Carbon stock, AGB is above ground biomass and CF is Conversion factor (0.47).

Satellite data

To generate biomass map the cloud-free ($\leq 10\%$) Sentinel-2 image data (orthorectified imagery with projection system of UTM/WGS84), of July 2016 was downloaded (<http://www.earthexplorer.usgs.gov>). Because of high spatial resolution (10 m) of imagery as compare to other open source satellite products it was considered acceptable for research. The Spectral resolution of Sentinel-2 imagery is high with Red, Blue, Green, and NIR bands; hence it is considered suitable for vegetation studies. For monitoring vegetation, it additionally accompanies three red-edge spectral bands.

Using ENVI software Sentinel-2 optical imagery was preprocessed for radiometric correction in order to improve image quality. The radiometric correction primary purpose was to reduce sun angle and atmospheric effects (Baillarin et al., 2012). In QGIS software semi-automatic classification plugin was used for the transformation of imagery from radiance to surface reflectance through the application of Dark Object Subtraction (DOS). The DOS method works by removing in every band the darkest pixel which will be affected by scattering in the atmosphere (Chavez Jr, 1988). This method does not need ground truth data as it is image based and is easy to apply (Chavez, 1996). The shortwave infrared band and red-edge band with a spatial resolution of 20 m were resampled into a 10 m spatial resolution using resampling tool in ArcMap.

Computation of VIs was done through various spectral bands combination having 10 m and 20 m spatial resolution hence to make all bands of same spatial resolution (10 m) resampling was performed. The imagery was clipped using the study area shapefile.

Deriving vegetation indices

Several vegetation indices have been reported in the literature for the derivation of biomass. In this study, three categories of vegetation indices were considered for the derivation of biomass, which includes: Broadband VIs, Canopy Water Content Indices, and Narrow Red Edge band VIs (*Table A2*). In broadband category, the sensitivity of vegetation indices is very high to canopy leaf area. The vegetation indices in the broadband category are sensitive to the canopy leaf area.

The Canopy Water Content Indices use the near-infrared spectral band and shortwave infrared (SWIR) spectral band. To study water content in the vegetation it is used. Through this VIs health of vegetation can be assessed as healthier vegetation have more carbon storage capacity as compared to trees having water stress. The Narrow Red Edge band vegetation indices use the near infra band. However, it does not utilize the red band rather it uses red-edge spectral band (690-740 nm). To study biophysical characters of vegetation these are mainly used (Mutanga and Skidmore, 2004b). These VIs show the vegetation photosynthesis in more detail than broadband indices. It overcomes the signal saturation issue of broadband indices which is due to high canopy density.

In this study twenty-five (25) different vegetation indices selected from the three broad categories were derived from high spectral and spatial resolution Sentinel-2 image of July 2016. Out of twenty-five indices, only eleven (11) vegetation indices were selected on the basis of their performance, i.e. having significant R-square value between the forty-five (45) field surveyed plots biomass and derived vegetation indices. However, only one vegetation index was selected on the basis of lowest root mean square error (RMSE) with the lowest p-value and high significant R-square value. A linear regression model was developed between the selected vegetation index and field surveyed biomass of the forty-five plots. The linear regression model was used in the ArcGIS software raster calculator to generate biomass map for the entire study area.

Validation of biomass map

The biomass map was validated using the remaining ten (10) plot data. Since out of fifty-five plot data only forty-five plots data were used to generate the linear regression model the rest of ten plot data was kept for validation of the biomass map. The biomass values were extracted from the thematic biomass maps for the 10 sites and compared with the field surveyed generated biomass data using the correlation coefficient, P-value and RMSE statistics. Model accuracy was assessed by the following formula (*Eq. 2*):

$$RMSE = \sqrt{\frac{\sum_{i=1}^n (y_i - \hat{y})^2}{n}} \quad (\text{Eq.2})$$

where “ Y_i ” is Measured value of biomass, “ \hat{Y} ” is Estimated value of biomass and “ n ” is Number of samples.

Activity data

Activity data (forest change/deforestation) was assessed in the study area from the year 2000 to 2015 using the Landsat-7 and Landsat-8 satellite Data (<http://www.earthexplorer.usgs.gov>). The temporal satellite data was preprocessed in ERDAS IMAGINE software and supervised classification algorithm was applied for the assessment of land cover classes and to find the change in forest cover which had occurred in the last fifteen years. A thematic map was obtained of seven major land use classes, i.e. forest, glacier and snow, water, barren land, settlement, shrub and grassland, and agriculture. The forest in the study area was extracted, and forest change thematic map was derived by subtracting forest area of the thematic map of 2015 from the forest area of the thematic map of 2000 and finally the deforested areas were obtained. *Equation 3* (Sader and Joyce, 1988) was used to assess the average annual deforestation rate in the study area.

$$\text{Annual Rate (\% per year)} = \left(\frac{(Y_1 - Y_2) \times 100}{(Y_1 \times N)} \right) \quad (\text{Eq.3})$$

where “Y₁” is the total area of forest on the initial date, i.e. 2000, “Y₂” is the total area of the forest on the final date, i.e. 2015 and “N” is the number of years in a particular period, i.e. 15 years.

Carbon emission estimation

To estimate carbon emission the activity data and emission factor were multiplied (*Eq. 4*; Plugge et al., 2013).

$$\text{CE} = \text{AD} \times \text{EF} \quad (\text{Eq.4})$$

where “CE” is Carbon Emissions, “AD” is Activity Data (Change in forest cover) and “EF” is Emission Factor which can be calculated using *Equation 5* (REDD+, 2006).

$$\text{EF} = [(\text{AGC2000} - \text{AGC2015}) \times 3.66] \quad (\text{Eq.5})$$

where “EF” is Emission Factor, “AGC2000” is Above ground carbon for the year 2000, and “AGC2015”. The Above ground carbon for the year 2015 while “3.66” or “44/12” is a conversion factor. This conversion factor is the ratio of molecular mass to the atomic mass of carbon.

Carbon sequestration potential

The storage capacity of carbon increases rapidly as the forest is in the developmental stage and hence forest act as a carbon sink. While the old forest (80-100 years age) carbon stock increases very slowly and exchange of carbon among the atmosphere and the forests reaches to a balanced state therefore forests reach to a stage of carbon neutrality (Zhou et al., 2002) and this old-growth forest could be taken as Carbon Carrying Capacity (CCC) reference of those forests having climatic condition similar to these old-growth forests. Assessment of Carbon Sequestration Potential (CSP) is challenging as old-growth forest data is not available (Cramer et al., 2001).

Carbon Sequestration Potential of a particular forest type can be evaluated through the difference between carbon density of the current forest and old-growth forest as shown in *Equation 6* (Hudiburg et al., 2009; Liu et al., 2011; Smithwick et al., 2002).

$$\text{CSP} = \text{CCC} - \text{CD} \quad (\text{Eq.6})$$

where CSP is Carbon Sequestration Potential, CCC is Carbon Carrying Capacity, and CD is Carbon Density.

Results

Landuse landcover change detection

The Landsat temporal (year 2000 and 2015) satellite data was classified into seven major classes (Glacier and snow, Water, Barren land, Settlement, Shrub and Grassland, Agriculture and Forest) (*Fig. 3*). Landsat-7 (ETM+) and Landsat-8 (OLI) data were used for generating LULC maps for the year 2000 and 2015. Over the fifteen years even though there was no significant change was found in the settlement (0.3%), but a major decreasing change was observed in the forest (-16.9%) and barren land (-7.7%) while an increasing change was recorded in the agriculture (12.2%). The data suggest that, since there was no significant change was found in the settlement most of the forest land was used for agricultural purposes while the major cause of deforestation could be illegal logging.

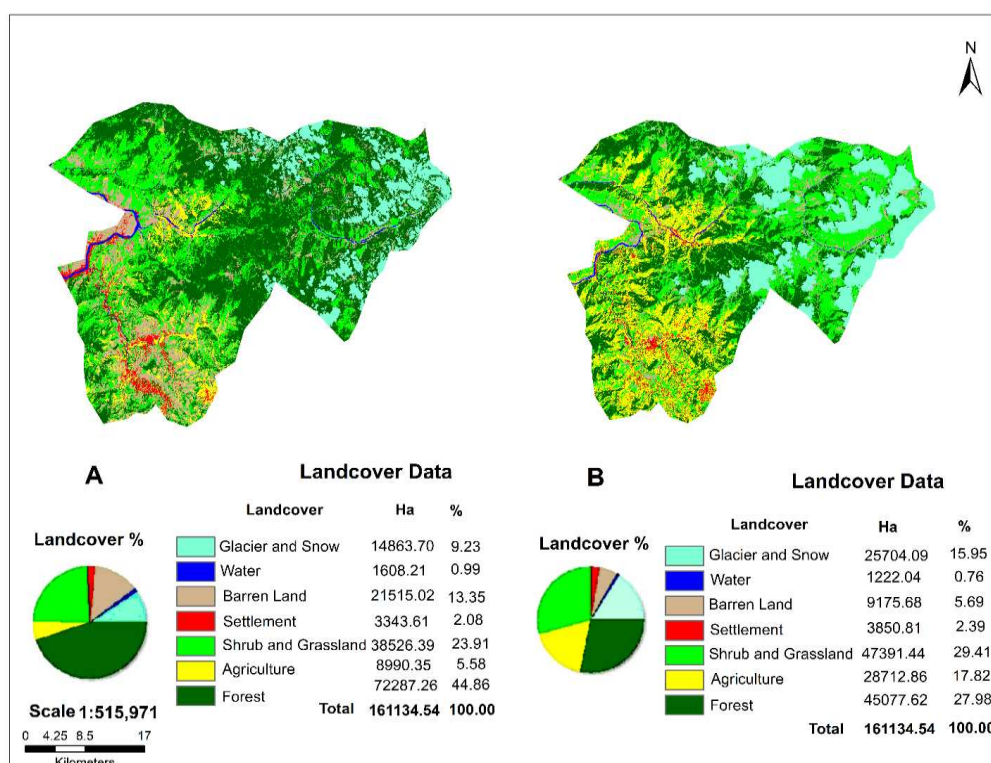


Figure 3. Study area Land cover/use map for the year 2000 (A) derived from Landsat-7 (ETM+) and Study area Land cover/use map for the year 2015 (B) derived from Landsat-8 (OLI/TIRS) using supervised classification and maximum likelihood algorithm in ERDAS Imagine 2015

Figure 4 shows the extracted forest land cover area from the land cover/land use map. In 2000 forest area was 72287.26 ha (44.86% of the total study area), which decreased to 45077.62 ha (27.98% of the study area) in 2015. It indicates a 27209.64 ha (-16.88%) loss with an annual deforestation rate of 2.51%, i.e. 1814.41 ha deforestation per year which is quite alarming. In order to decrease carbon emissions, forest conservation and sustainable forest management practices are required as the deforestation rate is very high in the study area. For agricultural purpose, natural forests are cleared hence disturbing the ecology of the area. Factors like illegal logging, wood harvesting for construction and fuel wood are the major reasons for deforestation. Moreover, the legal status of the forests in our study area is guzara forest which means it has community rights and all acts in guzara forests are allowed until and unless prohibited by the government, therefore, it is not protected or conserved like reserved forests.

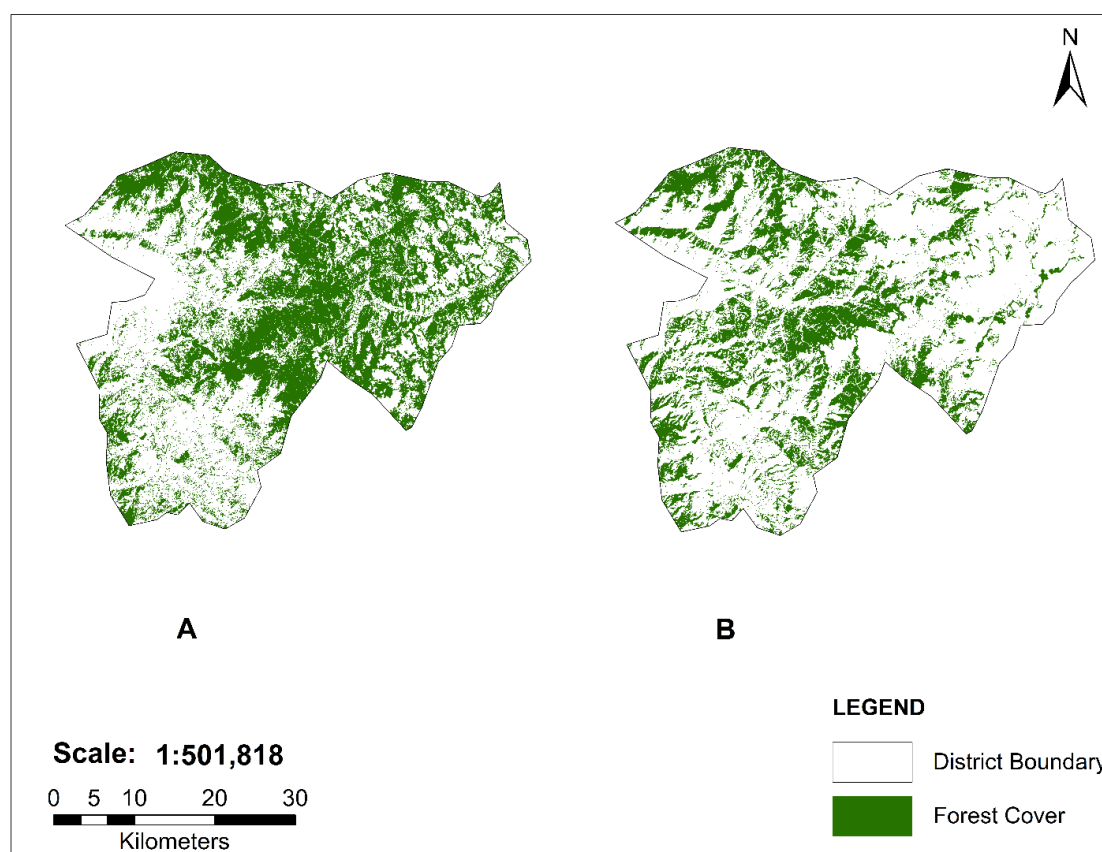


Figure 4. Study area forest cover map for the year 2000 (A) extracted from land use/cover map of 2000 and study area forest cover map for the year 2015 (B) extracted from land use/cover map of 2015 using conversion tool from raster to polygon and then dissolve tool in ArcMap 10.5.1

Validation of land use land cover map

LULC maps were validated using user's accuracy, producer's accuracy, kappa statistics and overall classification accuracy. 49 points were distributed randomly on each year imagery having seven classes. For each class there were seven points. Reference

points and results of classification were compared from which error matrices created and with the help of these error matrices producer's users and overall accuracy of the classification was assessed. Overall classification accuracy ranges from 80.44% -86.24 while overall kappa statistics ranges from 0.7621-0.8422. Accuracy results for each class can be seen in *Table 1* which are in acceptable range. Accuracy of the year 2000 imagery is less because of the less spatial resolution imagery availability at Google Earth on our study area so it was difficult to discriminate between various classes.

Table 1. Accuracy assessment results of LULC map

Years	Accuracy/classes	Glacier/snow	Water	Barren land	Settlement	Shrub and grassland	Agriculture	Forest
2000	Producer's accuracy (%)	71.54	90.54	68.77	65.31	89.23	74.19	86.79
	User's accuracy (%)	69.14	95.13	73.15	71.73	88.71	75.97	89.25
	Overall classification accuracy (%)	80.44				Overall kappa statistics = 0.7621		
2015	Producer's accuracy (%)	89.35	91.95	78.26	83.47	67.59	87.50	89.97
	User's accuracy (%)	87.73	97.79	81.35	85.71	79.53	77.59	93.97
	Overall classification accuracy (%)	86.24				Overall kappa statistics = 0.8422		

Biomass and carbon stock

The major forest tree species found in the study area were *Pinus wallichiana* (Kail), *Pinus roxburghii* (Chir pine), *Picea smithiana* (Spruce), *Abies pindrow* (Fir), *Cedrus deodara* (Deodar) as well as some broadleaved species. *Table 2* shows descriptive statistics of biomass, carbon stock and CO₂ e (carbon dioxide equivalent) calculated from the field survey data collected from the 55 plots in the study area while *Table A3* shows Biomass, Carbon Stock and CO₂ e estimated per plot in the study area. The above ground biomass (AGB) ranged from 279.59 t/ha to 46.45 t/ha with a mean of 148.79 t/ha (± 40.77). The above ground carbon (AGC) ranged from 131.41 t/ha to 21.83 t/ha with a mean of 69.93 t/ha (± 19.16). The denser the forest, the higher the value of biomass and carbon stock were. The CO₂ e ranged from 606 t/ha to 100 t/ha with a mean of 322 t/ha (± 88.36). Total AGB in the study area was 6.7 Mt, and total BGB (below ground biomass) was 1.74 Mt while the total Biomass (AGB + BGB) was 8.45 Mt. Similarly, the total AGC in the study area was 3.15 Mt and total BGC (below ground carbon) was 0.82 Mt while the total Carbon (AGC + BGC) was 3.97 Mt. Finally, the total CO₂ e in the study area was 14.53 Mt. According to Ahmad et al. (2014), the mean AGB and AGC in coniferous forests of Dir were found to be 258.98 t/ha and 129.49 t/ha, respectively. According to IPCC the range of AGB in the temperate forest is about 220 to 295 t/ha (IPCC, 2006). While according to Gairola et al. (2011), in the moist temperate forest of India the AGB ranges from 215.5-468.2 t/ha and AGC from 107.8-234.1 t/ha (Gairola et al., 2011). Similarly, Whittaker and Niering estimated AGB value in fir temperate forest which was 360-440 t/ha (Whittaker and Niering, 1975). The forest in our study area falls in the category of "Guzara Forest," and in guzara forest all the act are allowed until and unless prohibited by the government. Hence these are not reserved forests, the human interference and social pressure are more in these forests as compared to the reserved forest, as these have community rights. Therefore, more disturbance has been observed in these forests.

Table 2. Descriptive summary statistics of biomass, carbon stock, and CO₂ e

Statistics	AGB (t/ha)	BGB (t/ha)	Total biomass (t/ha)	AGC (t/ha)	BGC (t/ha)	Total carbon (t/ha)	CO ₂ e (t/ha)
Sum	8183.82	2127.79	10311.61	3846.39	1000.06	4846.46	17738.05
Mean	148.79	38.69	187.48	69.93	18.18	88.12	322.51
St. Dev	40.77	10.59	51.37	19.16	4.98	24.14	88.36
St. Err	5.49	1.43	6.93	2.58	0.67	3.25	11.92
Min	46.45	12.07	58.53	21.83	5.68	27.51	100.69
Max	279.59	72.69	352.29	131.41	34.16	165.58	606.02
Range	233.14	60.61	293.76	109.57	28.49	138.07	505.33
Skewness	0.72	0.72	0.72	0.72	0.72	0.72	0.72

AGB = Above Ground Biomass, BGB = Below Ground Biomass, AGC = Above Ground Carbon, BGC = Below Ground Carbon, CO₂ e = carbon dioxide equivalent

Relationship between biomass and vegetation indices

Evaluating several vegetation indices is helpful when vegetation canopies are not uniform in terms of species which leads to complexity and variation in groundcover. Factors such as topography, background soil reflectance and variation in internal canopy signal scattering could interfere with final vegetation signal since in different ranges of biomass and groundcover different indices are more sensitive (Huete, 1988). In this regard twenty-five (25) vegetation indices were calculated and tested concerning its relationship with the biomass. *Figure 5* shows eleven (11) vegetation indices which had a significant ($p \leq 0.01$) correlation with biomass. In comparison, narrowband red-edge vegetation indices performed better than the other types of indices. In the narrowband vegetation indices, RERVI had the highest R-square ($r^2 = 0.68$; $p \leq 0.01$) while the NDII which is canopy water content VI had the lowest R-square ($r^2 = 0.16$; $p \leq 0.005$).

Correlation between broadband vegetation indices and biomass

Figure B1 (see *Appendix*) shows scatter plot graphs depicting relationships between biomass and various broadband vegetation indices. The R-square values of EVI, GNDVI, NDVI, SAVI, SQSR, and TSAVI were 0.29, 0.33, 0.28, 0.28, 0.21, and 0.29, respectively. The coefficients of the linear models between biomass and broadband vegetation indices were significant ($p \leq 0.01$). Since most of these indices (broadband VIs) use NIR and Red bands, therefore, sensor saturation issues were encountered especially in areas where there was dense and mature vegetation (Lu et al., 2012; Wang et al., 2016).

Relationship between biomass and canopy water vegetation indices

Figure B2 shows relationships between biomass and two canopy water indices, i.e. Normalized Difference Infrared Index (NDII) and Normalized Difference Water Index (NDWI). Significant relationships were found between biomass vs. NDII ($R^2 = 0.16$, $p \leq 0.01$) and NDWI ($R^2 = 0.21$, $p \leq 0.01$). However, there R-square values were mostly lower comparatively than the broadband vegetation indices since these indices use mostly the shortwave infrared bands of the sentinel sensor i.e. band 12 ($\lambda = 1610$ nm) and band 13 ($\lambda = 2190$ nm) which are more sensitive to water in the green vegetation than to the chlorophyll content.

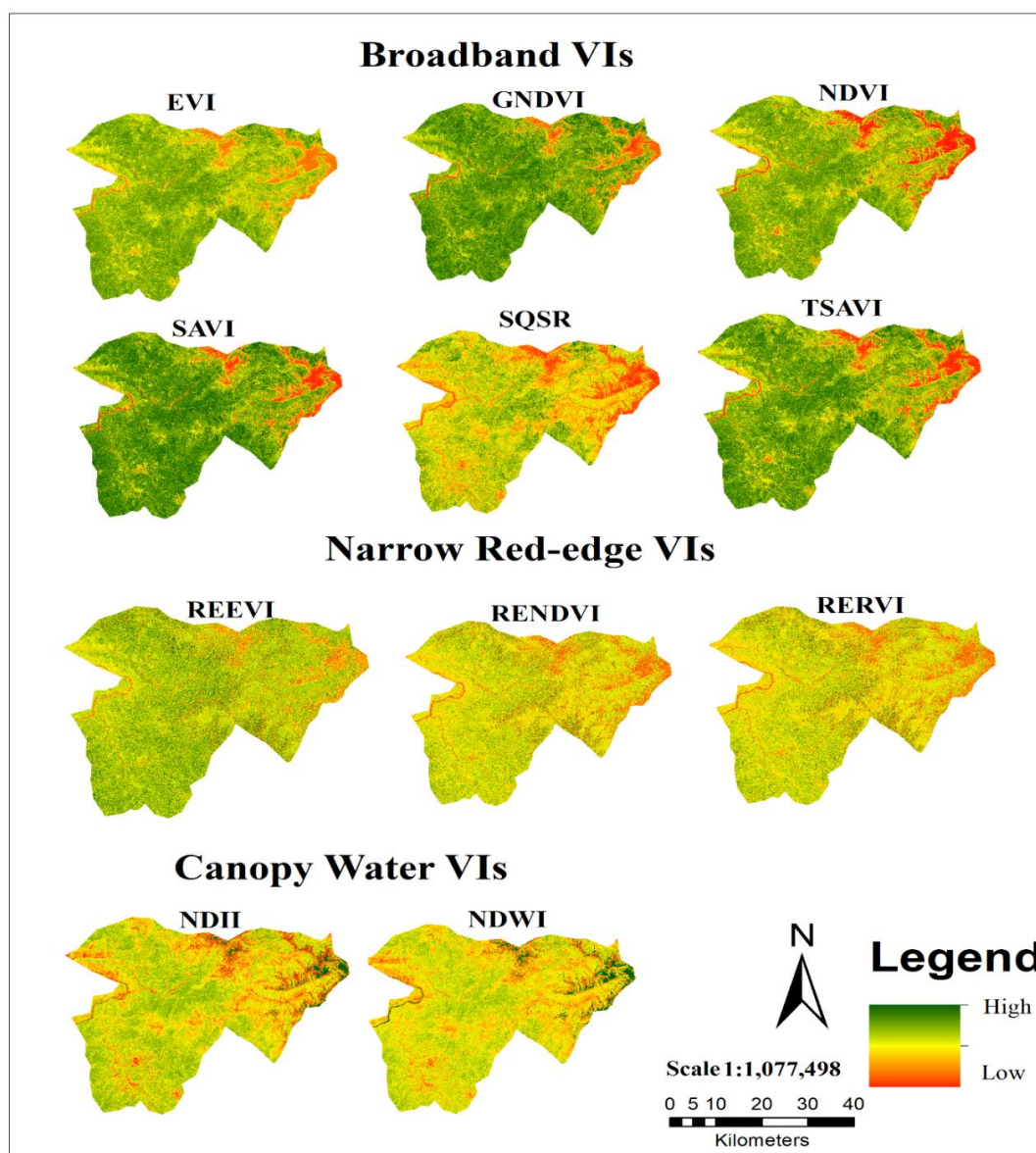


Figure 5. Broadband vegetation indices, narrow red-edge and canopy water vegetation indices derived from Sentinel-2 satellite imagery using their equations and distinct bands combination in ArcMap

Relationship between biomass and narrow red-edge indices

Using red-edge spectral bands VIs were calculated and saturation effects is decreased. Comparatively the red band ($\lambda = 665$ nm) is known to have high absorptivity/sensitivity compared to the red-edge band ($\lambda = 740$ nm). However, the red-edge band remains to be sensitive to chlorophyll but to a moderate extent which reduces the saturation effects (Gitelson et al., 1996). *Figure B3* shows relationships between biomass and red-edge vegetation indices, i.e. Red-edge Normalized Difference Vegetation Index (RENDVI), Red-edge Enhanced Vegetation Index (RE-EVI), and Red-edge Ratio Vegetation Index (RERVI). Due to narrow red-edge band, VIs saturation effect is reduced and the relationship of these indices with biomass was

highly significant, and yielded higher R-square values. Higher relationships of biomass were found with RE-EVI, RE-NDVI and RERVI ($R^2 = 0.67$, $p \leq 0.01$).

It can be deduced from the results of this study that red-edge bands are very useful in dense and mature forests where saturation has been reported to be a regular issue when using the red band in calculating the indices.

Mapping spatial distribution of biomass

Figure 6 shows spatial variability of predicted biomass using the forty-five (45) field surveyed data out of the fifty-five (55) total plot data. The remaining ten (10) biomass data was used for validation of the final biomass map. The best vegetation index was selected from the various indices which had the highest correlation coefficient and the lowest RMSE with field survey biomass data. A linear regression model was developed between RERVI and field surveyed 45 biomass data. The regression model was used in ArcMap's raster calculator tool to generate the final study area biomass map.

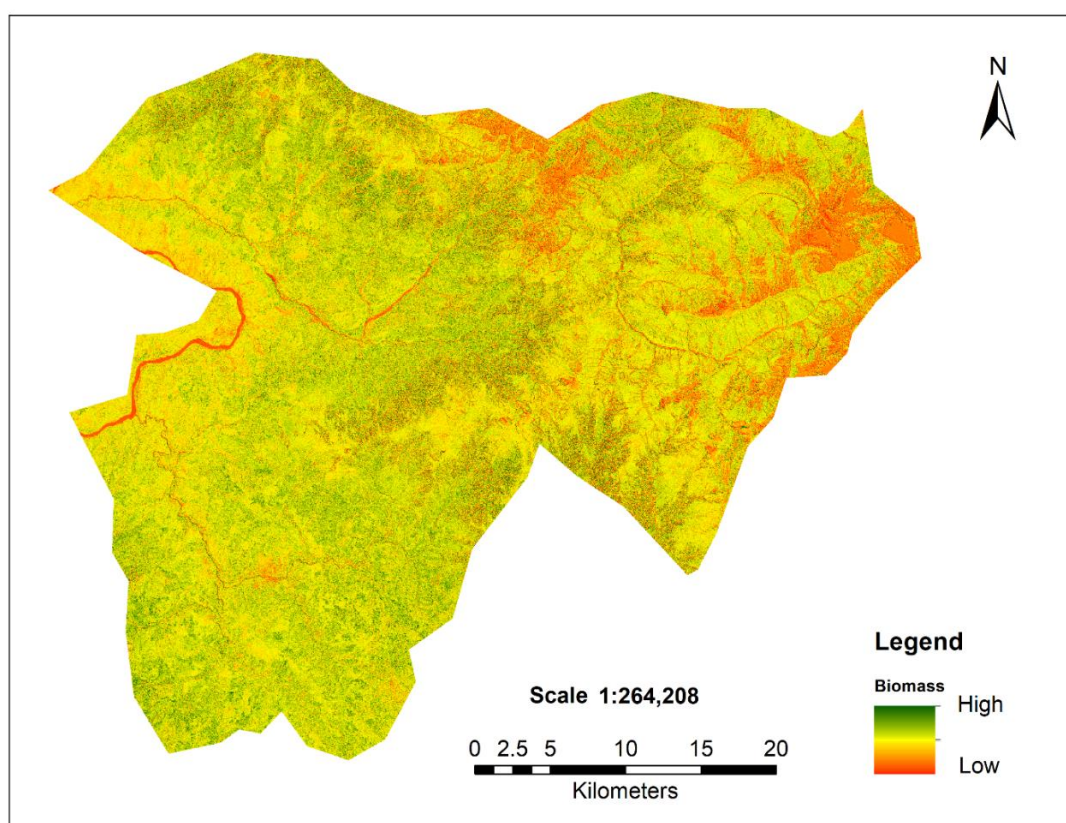


Figure 6. Study area biomass map derived from Sentinel-2 imagery best vegetation index (having high R-square, Low RMSE, and P-value less than 0.01) using its regression equation in ArcMap raster calculator from the best vegetation index (Red-edge Ratio Vegetation Index (RERVI))

Accuracy of biomass map

To evaluate how well the predicted biomass corresponds to the actual on-ground biomass, the remaining ten (10) ground surveyed data points were overlaid on the

predicted biomass map and data was extracted for statistical comparison. A significant ($p \leq 0.01$) R-square = 0.67 with an RMSE = 35.23 t/ha was found between the observed and predicted biomass which validates the final biomass map.

Calculation of carbon emissions

Emission factor determined was equal to 255.94 tCO₂ e/ha, and in fifteen years carbon emissions were about 6.96 Mt CO₂ e.

$$\text{Emission Factor} = 69.93 \times 3.66$$

$$\text{Emission Factor} = 255.94 \text{ tCO}_2 \text{ e/ha}$$

Activity data means a change in forest cover as we have already calculated the change in forest cover from 2000-2015 through remote sensing.

$$\text{Activity data} = 27209.64 \text{ ha}$$

By putting these values in the equation we get:

$$\text{CE} = \text{AD} \times \text{EF}$$

$$\text{CE} = 27209.64 \times 255.94$$

$$\text{CE} = 6964138.66 \text{ t CO}_2 \text{ e}$$

$$\text{CE} = 6.96 \text{ Mt CO}_2 \text{ e}$$

Carbon sequestration potential

For our study area, which is a temperate forest, the C sequestration potential was calculated using the following formula:

$$\text{Carbon Sequestration Potential (CSP)} = \text{Carbon Carrying Capacity (CCC)} - \text{Carbon Density (CD)}$$

$$\text{CSP} = (152 \pm 13)^* - (69.93) = 82.07 \pm 13 \text{ t/ha}$$

(Divide this value by the age of forest)

$$\text{CSP} = 82.07 \pm 13 \text{ t/ha} \div 100 \text{ years} = 0.82 \pm 0.13 \text{ t/ha/year}$$

(When forest age is assumed to be 100 years at maturity)

*This is a generic value of carbon carrying capacity (CCC) for the moist temperate forests (Yingchun et al., 2012).

The carbon sequestration potential estimated for the study area was 82.07 t/ha \pm 13 t/ha. Hence the temperate forest possesses carbon sequestration potential up to 82.07 t/ha \pm 13 t/ha. If we assume the rotation age of the forest to be hundred (100) years then the carbon sequestration potential will be 0.82 \pm 0.13 t/ha/year. It means that the forest can sequester about 0.82 \pm 0.13 tons of carbon per hectare in a year.

Discussion

Our study finding suggests that during the last fifteen-year deforestation had occurred at an alarming rate. The forested area has been mainly converted into agricultural land for food production. Subsequently, the CO₂ e emission rate is comparatively very high during the reporting period. Since the study area falls within the “Guzara forest” (forest with community rights) which mandate the resident’s rights to the forest wood for fuel and construction purpose. The deforestation rate could be reduced to a sustainable level and carbon sequestration potential can be enhanced by providing residents with alternative sources of energy and building construction material as well as through sustainable forest management practices. The REDD+ incentive should be extended to locals for carbon crediting and reforestation of the deforested area. Furthermore, our finding suggests that the narrowband red-edge vegetation indices (RE-EVI, RENDVI and RERVI) performed better in the estimation of forest biomass as compared to broadband vegetation indices (EVI, GNDVI, NDVI, SAVI, QSR and TSAVI) and canopy water vegetation indices (NDII and NDWI). Among the narrowband red-edge vegetation indices, RERVI performed the best in biomass estimation. Image of vegetation indices shows us less saturation in narrow band red-edge indices as compared to canopy water content and broad band VIs.

Landuse landcover change detection

Activity data means change occurred in the forest area. For land use change the Landsat-7 and Landsat-8 data was used. Data was downloaded from USGS earthexplorer website (Earthexplorer.usgs.gov) of June month for the year 2000 and for the month of September for 2015. These months images were downloaded because the vegetation is mostly visible having less cloud and snow cover. In erdas imagine 2015 supervised classification algorithm was applied for the assessment of land cover classes and to find change in the forest cover which had occurred in the last fifteen years. Landsat had a coarse resolution so it is difficult to correctly classify various land cover classes so for this purpose we connected the erdas imagine with google earth pro so when we go to the particular area on satellite imagery the google earth automatically goes to that place on that particular date and hence it is easy to classify various land features then. Spectral signatures were taken for particular classes and more than five hundred signatures were taken for single class using maximum likelihood algorithm, supervised classification was applied and thematic map of seven major classes was obtained (Glacier and Snow, Water, Barren Land, Settlement, Shrub and Grassland, Agriculture, Forest). After classification manual correction were done using recode option in Erdas imagine then mean filter was applied and finally accuracy assessment was done. Major decreasing change was observed in the forest (-16.9%) and barren land (-7.7%) while agricultural area was increased (12.2%). There was no significant change in settlement (0.3%) so the major cause of deforestation could be illegal logging. The annual deforestation rate was 2.51%.

Above ground biomass/carbon stock estimation

Above ground biomass was estimated in field through forest inventory (DBH and Height) and using allometric equations. Mean AGB of 148.79 t/ha was obtained which was then converted to carbon stock through a conversion factor and the mean value of

above ground carbon stock obtained was 69.93 t/ha. From sentinel-2 imagery several type of VIs indices were calculated and finally to assess the relationship between AGB and vegetation indices linear regression model was developed. Thus, the forest biomass was calculated by both methods (field inventory and remote sensing) and biomass map was validated from the field data.

Correlation between AGB and VIs

Relationship between AGB and VIs was assessed using linear regression model. In this study three categories of vegetation indices; broad band, canopy water content and narrow red-edge band VIs were used. These categories of indices were assessed in our study area as these have effect on assessment of above ground biomass performance and accuracy. Four different types of bands were used in the computation of these vegetation indices consisting of Red, Near Infrared (NIR), Short Wave Infrared (SWIR) and Red-edge bands.

Correlation between AGB and broadband VIs

Broadband VIs and AGB had weak relationship. The VIs includes EVI, GNDVI, NDVI, SAVI, SQSR and TSAVI. Our results of broadband VIs are similar to that of Mcmorrow et al. (Foody et al., 2001), according to which relationship between biomass and NDVI is poor. Using Landsat TM derived NDVI AGB was estimated by Mgaraganza and Lyaruu (2015) in Mgaraganza and Kitwe forest areas of Tanzania. From the results we see in both areas r^2 of 0.22 and 0.23. Nugroho (2006) assessed the relationship between VIs and AGB, r^2 value was 0.21 for EVI and 0.14 for NDVI. The main reason of less accuracy was saturation problem.

There are two main reasons of saturation, one is crops maturity (Mutanga and Skidmore, 2004a; Wang et al., 2016) while the other is due to complex forest structure (Lu et al., 2016; Sinha et al., 2016). Due to saturation VIs cannot sense increase in biomass and it occurs when the area is covered fully by leaves or vegetation fully covers the land. So the indices values do not change while the biomass continues to increase. According to Wang (Wang et al., 2016) saturation occurs due to the reason that Vegetation indices are computed using NIR and red spectral band (680nm). So electromagnetic spectrum radiations are absorbed by the red band and it does not increase continuously with increase in canopy cover due to the reason that when canopy closure is at 100% the amount of red energy absorbed reaches to peak. Besides this, due to multiple scattering the reflectance of NIR increases when canopy reaches 100% (Thenkabail et al., 2000). Therefore, in broad band indices ratio (EVI, SAVI, NDVI) an inequality is being caused because of increase in NIR band and decrease in red absorption band hence results are poor in the assessment of biomass (Mutanga and Skidmore, 2004a).

Correlation between AGB and canopy water content VIs

Relationship of AGB and canopy water content index was very weak with an r^2 of 0.16 for NDII and 0.22 for NDWI. Using SWIR bands canopy water content VIs computation was done (Lu et al., 2016). As canopy cover increases the water content also increases in leaf. Less research has been conducted on biomass estimation from canopy water content VIs.

Correlation between AGB and narrow red-edge VIs

Using band 6 of Sentinel-2 image which is a red-edge band of 740 nm wavelength and NIR band narrow red-edge VIs were calculated. Relationship between AGB and red edge VIs is the highest. The r^2 0.68 of RERVI was the highest. Narrow red-edge Vegetation Indices outperform the other two categories. Because the red-edge spectral band is between NIR and red region which is a high chlorophyll absorption and reflectance area. Therefore, the variations in leaf properties and chlorophyll highly affect the red-edge spectral bands (Slonecker et al., 2009). The red-edge and NIR (700 nm to 1300 nm) part of reflectance is higher (about 60%) while red region (500 to 700 nm) reflects less than 30% (Gitelson and Merzlyak, 1997). Several studies (Chen et al., 2007b; Zhao et al., 2007) were conducted to compare the performance of VIs (NDVI, EVI, SR) using NIR and red bands with red-edge bands. From the results we can see that relationship of red-edge indices were better as it improves the r^2 significantly than that of red band. Relationship between VIs derived from World-View 2 was assessed by Winmore (2012) for carbon stock estimation in the forests of south Africa. In this study mutual comparison of standard vegetation indices (NDVI, SAVI, SR) and red-edge indices (NDVI-RE, SAVI-RE and SR-RE) was conducted through simple linear regression. From the results it was concluded that using red-edge band the r^2 increased which concludes that carbon stock estimation accuracy was improved by red-edge band. According Mutanga et al. (2012) RENDVI performed better having an r^2 of 0.67 in comparison with standard NDVI having r^2 of 0.39. In these studies, the Standard NDVI performance were a bit high than those of our results because of medium spatial resolution (10 m) of sentinel-2 imagery than that of World-View-2 images (2 m) as we know from previous studies that on performance of VIs spatial resolution have an influence on the estimation of biomass (Gara et al., 2017). Besides this saturation problem is less in simple forest structure than that of complex forest structure.

Mapping spatial distribution of biomass

The biomass map shows a denser forest biomass in the northwestern and low in the northeastern quadrant of the study area so more dissimilarities are observed in the northeastern side of the study area due to less forest cover resulting in significant variation in the biomass (Chi et al., 2015). The lowest biomass could be due to the highest altitude of the study area as above 3500 m elevation there are subalpine and alpine pastures, so the biomass was found to be the lowest. Using remotely sensed optical data for biomass mapping have specific limitation such as if we use it in open tree canopy cover and near snow then it underestimates the biomass in both cases (Karlson et al., 2015). Also in the assessment of vegetation cover from optical data, there are more chances of neglecting little trees (Karlson et al., 2014). The openness in the forest maybe due to high anthropogenic activities related to illegal logging etc.

The overall spatial variability in the biomass could be due to different species occurrence, i.e. *Pinus roxburghii* (chir pine), *Pinus wallichiana* (Kail), *Pinus gerardiana* (Chilgoza), *Abies pindrow* (Fir), *Picea smithiana* (Spruce), *Cedrus deodara* (Deodar) and *Quercus* spp (Oak) in the study area. This could result in the variation of the final biomass while the biomass in coniferous species will be higher than that of broadleaved species because of its high wood density, volume, and age. Biomass also depends on the age of tree species; therefore, the younger trees have lower biomass while the mature trees have higher biomass. Northern aspect is cool and has more moisture and

vegetation cover; therefore, biomass could also be high on the northern aspect while the southern aspect is warmer having less moisture and vegetation cover, therefore, resulting in low biomass. The denser the vegetation and crown cover are the higher the biomass will be (Du et al., 2014).

Calculation of carbon emission

The historical forest inventory data was not available with the local forest department. Therefore, we assumed the year 2000 carbon stock data to be the same as carbon stock of 2015 (69.93) to calculate the carbon emission.

In our case, the forest acts as a source of carbon not sink. Forests are not protected according to forests policy, and forest law enforcement is also very weak due to which illegal logging and wood harvesting occur. Emissions of CO₂ results increased due to land-use change because of deforestation which is a major cause of climate change. According to Houghton (2003), on a global scale, the deforestation contributes about 156 Pg of carbon emitted to the atmosphere from 1850 to 2005 and 12% to 15% of total emissions of GHG. Our results suggest 6.96 MtCO₂ e contributed to the atmosphere from our study area during the 15 years (2000-2015). Since due to deforestation carbon is not only lost to the atmosphere but the mechanism of CO₂ absorption by trees is also eliminated (Rokityanskiy et al., 2007). Degradation and deforestation may be due to disease, flood, fire, and storm, (natural causes) while it may also be due to illegal wood harvesting, expansion of agriculture, government policies, development of infrastructure, poverty, as well as the cultural attitude that changed towards the forest (Keenan et al., 2015).

Carbon sequestration potential

To mitigate the atmospheric CO₂ effectively, one has to quantify the C sequestration potential of all C pools including a forest in order to best estimate its contribution. For example, when the forest is in the developmental stage, then the C storage capacity could be manifold, and it will act as a sink of C while the old forest (80-100 years age) stores carbon very slowly. So for reducing carbon emission, we should attain carbon carrying capacity and decrease human disturbance in our forests. The forest sequestration potential can be enhanced through afforestation, reforestation activities, reducing the anthropogenic activities as well using sustainable forest management practices.

Remote sensing applicability for REDD+ implementation

In third world countries where check and balance systems of monitoring are not adhered to fulfill the requirements of the international obligations, the RS techniques can play a critical and decisive role in successful forest activities monitoring and implementation of the REDD+ system at local and national spatial scales. The remote sensing technique for monitoring and implementation seems to be the best, cost-effective and accurate method for the assessment of carbon stock, biomass, and carbon emission. From our results, the VIs derived from Sentinel-2 are implicit for the assessment of carbon stock and the biomass as well. Besides this, the Sentinel-2 imagery is multi-spectral having 13-bands consisting of SWIR and Red-edge spectral bands and is freely available. As compared to other medium resolution satellite imageries it has 10 m spatial resolution which is high. The availability of Red-edge

band reduces the saturation problem. The method adopted in this study is feasible and could be applied on a larger spatial scale, i.e. at the regional and national level. For the assessment of forest cover change and carbon emission estimation Landsat open source and historic data increase its importance. Hence this study will serve REDD+ in its objective of sustainable forest management and reducing CO₂ emissions.

Study limitation and recommendation for future research

In Sentinel-2 satellite imagery, not all the spectral bands are of the same resolution, i.e. some of the bands are of 10 m resolution while others are of 20 m. In order to make all the bands of the same resolution (10 m), we had to resample the data due to which the accuracy of estimation of biomass from VIs might have been affected as some of the spectral information might be lost due to resampling. Use of high-resolution optical data both for the assessment of deforestation, degradation as well as biomass and carbon stock can further increase the accuracy of the results.

In the future, research is required on the integration of optical and RADAR data since optical data do not take into account the below canopy vegetation which could result in an underestimation of above ground biomass. This issue can be resolved by incorporating the RADAR data that could also reduce sensor saturation in optical-sensor images. Launching of additional advanced satellite sensors are required which are specifically designed for terrestrial carbon stock monitoring and particularly that of spaceborne LiDAR sensor. Hence LiDAR data use can further increase the accuracy.

Use of historical ground data can improve our understanding of carbon emission estimation. For a better insight of variation in carbon stock of forest ecosystem and carbon emissions, spatiotemporal analysis of carbon fluxes studies needs to be carried out. Furthermore, carbon sequestration potential can be assessed with better accuracy, if climatic variables (precipitation, temperature) and old-growth forest data are available (Cramer et al., 2001).

Farm forestry, agroforestry practices and technologies of clean energy should help in the reduction of carbon emissions. For sustainable forest management and climate change, clean development mechanism as well as UN REDD+ program could be helpful.

Conclusions

From this study, we conclude that forest land is decreased at an alarming rate because of increase in agricultural land, shrub/grassland and urban areas and about 16.88% of forest area is lost in fifteen years. The annual deforestation rate is 2.51% and due to deforestation carbon emissions were about 6.96 Mt CO₂ e in fifteen years. Natural forests are cleared for agricultural purpose due to which the ecology of the region is disturbed. To decrease carbon emissions, the deforestation and degradation must be lessened through conservation of forest and sustainable management of the forest. AGB and carbon stock in the study area were 148.79 t/ha and 69.93 t/ha. VIs derived from sentinel-2 imagery have the potential in the estimation of biomass. Saturation problem leads to poor estimation of AGB in canopy water content and broadband Vis. However, red-edge band reduces the saturation problem and thus it is more appropriate. Therefore, in future red-edge VIs should be used for biomass estimation instead of broadband VIs. Spatial distribution of biomass was mapped from

the best VI and validated with the ground data which is much important in order to know management, disturbance and carbon fluxes in the forest. Carbon sequestration potential was $82.07 \text{ t/ha} \pm 13 \text{ t/ha}$.

For better forest management, remote sensing and GIS should also be applied with ground forestry operations and in the estimation of biomass, carbon stock and carbon emissions the use of remotely sensed data such as Vegetation Indices. This can decrease labor force. The ground data can be applied on a large scale, i.e. at regional and national level through remote sensing. From the study, we can see that biomass and carbon stock can be estimated with better accuracy from vegetation indices derived from sentinel-2 imagery as compared to other sensors because of its high spatial resolution (10 m) as well as spectral bands for vegetation study.

The areas which are inaccessible and ground survey is difficult to be performed so this method is more suitable for biomass and carbon stock estimation. Hence this method seems to be the most cost-effective, best and most accurate for the assessment of biomass, carbon stock, change in forest cover and carbon emissions. This study will serve REDD+ in its objective of sustainable forest management and lessening emission of CO₂ in the atmosphere.

Acknowledgments. The authors acknowledge the financial support of National University of Sciences and Technology (NUST) for publishing this work. The authors are also very grateful to Pakistan Forest Institute (PFI), Peshawar for providing support and help in field data collection.

Funding. This research received no external funding.

Conflict of interests. The authors declare no conflict of interests.

REFERENCES

- [1] Abdel-Rahman, E. M., Landmann, T., Kyalo, R., Ong'amo, G., Mwalusepo, S., Sulieman, S., Le Ru, B. (2017): Predicting stem borer density in maize using RapidEye data and generalized linear models. – *International Journal of Applied Earth Observation and Geoinformation* 57: 61-74.
- [2] Ahmad, A., Mirza, S. N., Nizami, S. (2014): Assessment of biomass and carbon stocks in coniferous forest of Dir Kohistan, KPK. – *Pakistan Journal of Agricultural Sciences* 51: 35-350.
- [3] Ali, A. (2015): Biomass and Carbon Tables for Major Tree Species of Gilgit Baltistan, Pakistan. – *Gilgit-Baltistan Forests, Wildlife and Environment Department, Gilgit*.
- [4] Ali, A., Ullah, S., Bushra, S., Ahmad, N., Ali, A., Khan, M. A. (2018): Quantifying forest carbon stocks by integrating satellite images and forest inventory data. (Quantifizierung der Kohlenstoffvorräte in Wäldern durch die Integration von Satellitenbildern und Waldinventurdaten.) – *Austrian Journal of Forest Science* 2018(2): 93-17
- [5] Angelsen, A. (2009): Realising REDD+: National Strategy and Policy Options. – CIFOR, Bogor Barat, Indonesia.
- [6] Aslam, A., Amir, P., Ramay, S., Munawar, Z., Ahmad, V. (2011): National Economic and Environmental Development Study (NEEDS). – UNFCCC.
- [7] Asner, G. P. (2001): Cloud cover in Landsat observations of the Brazilian Amazon. – *International Journal of Remote Sensing* 22: 3855-3862.
- [8] Baillarin, S., Meygret, A., Dechoz, C., Petrucci, B., Lacherade, S., Tremas, T., Isola, C., Martimort, P., Spoto, F. (2012): Sentinel-2 level 1 products and image processing performances. *Geoscience and Remote Sensing Symposium (IGARSS)*. – *IEEE International 2012: 7003-7006*.

- [9] Balderas Torres, A., Skutsch, M. (2012): Splitting the difference: a proposal for benefit sharing in reduced emissions from deforestation and forest degradation (REDD+). – *Forests* 3: 137-154.
- [10] Baral, S. (2011): Mapping carbon stock using high resolution satellite images in sub-tropical forest of Nepal. – Unpublished, University of Twente (ITC), Enschede. http://www.itc.nl/library/papers_2011/msc/nrm/baral.pdf.
- [11] Baret, F., Guyot, G. (1991): Potentials and limits of vegetation indices for LAI and APAR assessment. – *Remote sensing of environment* 35: 161-173.
- [12] Brown, S. (2002): Measuring carbon in forests: current status and future challenges. – *Environmental pollution* 116: 363-372.
- [13] Cao, Q., Miao, Y., Shen, J., Yu, W., Yuan, F., Cheng, S., Huang, S., Wang, H., Yang, W., Liu, F. (2016): Improving in-season estimation of rice yield potential and responsiveness to topdressing nitrogen application with Crop Circle active crop canopy sensor. – *Precision agriculture* 17: 136-154.
- [14] Caparros, A., Ovando, P., Oviedo, J. L., Campos, P. (2011): Accounting for carbon in avoided degradation and reforestation programmes in Mediterranean forests. – *Environment and Development Economics* 16: 405-428.
- [15] Chave, J. R., Andalo, C., Brown, S., Cairns, M. A., Chambers, J., Eamus, D., Fölster, H., Fromard, F., Higuchi, N., Kira, T. (2005): Tree allometry and improved estimation of carbon stocks and balance in tropical forests. – *Oecologia* 145: 87-99.
- [16] Chavez Jr, P. S. (1988): An improved dark-object subtraction technique for atmospheric scattering correction of multispectral data. – *Remote sensing of environment* 24: 459-479.
- [17] Chavez, P. S. (1996): Image-based atmospheric corrections-revisited and improved. – *Photogrammetric Engineering and Remote Sensing* 62: 1025-1035.
- [18] Chen, J.-C., Yang, C.-M., Wu, S.-T., Chung, Y.-L., Charles, A. L., Chen, C.-T. (2007a): Leaf chlorophyll content and surface spectral reflectance of tree species along a terrain gradient in Taiwan's Kenting National Park. – *Bot Stud* 48: 71-77.
- [19] Chen, J.-C., Yang, C.-M., Wu, S.-T., Chung, Y.-L., Charles, A. L., Chen, C.-T. (2007b): Leaf chlorophyll content and surface spectral reflectance of tree species along a terrain gradient in Taiwan's Kenting National Park. – *Stud* 48: 71-77.
- [20] Chi, H., Sun, G., Huang, J., Guo, Z., Ni, W., Fu, A. (2015): National forest aboveground biomass mapping from ICESat/GLAS data and MODIS imagery in China. – *Remote Sensing* 7: 5534-5564.
- [21] Cramer, W., Bondeau, A., Woodward, F. I., Prentice, I. C., Betts, R. A., Brovkin, V., Cox, P. M., Fisher, V., Foley, J. A., Friend, A. D. (2001): Global response of terrestrial ecosystem structure and function to CO₂ and climate change: results from six dynamic global vegetation models. – *Global Change Biology* 7: 357-373.
- [22] Delegido, J., Verrelst, J., Alonso, L., Moreno, J. (2011): Evaluation of sentinel-2 red-edge bands for empirical estimation of green LAI and chlorophyll content. – *Sensors* 11: 7063-7081.
- [23] Dobbs, C., Kendal, D., Nitschke, C. R. (2014): Multiple ecosystem services and disservices of the urban forest establishing their connections with landscape structure and sociodemographics. – *Ecological Indicators* 43: 44-55.
- [24] Du, L., Zhou, T., Zou, Z., Zhao, X., Huang, K., Wu, H. (2014): Mapping forest biomass using remote sensing and national forest inventory in China. – *Forests* 5: 1267-1283.
- [25] Dube, F., Espinosa, M., Stolpe, N. B., Zagal, E., Thevathasan, N. V., Gordon, A. M. (2012): Productivity and carbon storage in silvopastoral systems with *Pinus ponderosa* and *Trifolium* spp., plantations and pasture on an Andisol in Patagonia, Chile. – *Agroforestry systems* 86: 113-128.
- [26] Egenhofer, C. (2007): The Making of the EU Emissions Trading Scheme: Status, Prospects and Implications for Business. – *European Management Journal* 25: 453-463.
- [27] FAO (2014): 2015 Forest Resource Assessment for Pakistan. Country Report Pakistan. – FAO, Rome.

- [28] FCPF (Forest Carbon Partnership Facility) (2013): Readiness Preparation Proposal (R-PP) for Country: Pakistan. Country Submission. – The UN Collaborative Programme on Reducing Emissions from Deforestation and Forest Degradation in Developing Countries (UN-REDD).
- [29] Fernández-Manso, O., Fernández-Manso, A., Quintano, C. (2014): Estimation of aboveground biomass in Mediterranean forests by statistical modelling of ASTER fraction images. – *International Journal of Applied Earth Observation and Geoinformation* 31: 45-56.
- [30] Foody, G. M., Cutler, M. E., Mcmorrow, J., Pelz, D., Tangki, H., Boyd, D. S., Douglas, I. (2001): Mapping the biomass of Bornean tropical rain forest from remotely sensed data. – *Global Ecology and Biogeography* 10: 379-387.
- [31] Gairola, S., Sharma, C., Ghildiyal, S., Suyal, S. (2011): Live tree biomass and carbon variation along an altitudinal gradient in moist temperate valley slopes of the Garhwal Himalaya (India). – *Current Science* 1862-1870.
- [32] Gao, B.-C. (1996): NDWI—A normalized difference water index for remote sensing of vegetation liquid water from space. – *Remote Sensing of Environment* 58: 257-266.
- [33] Gao, X., Jiang, Z., Guo, Q., Zhang, Y., Yin, H., He, F., Qi, L., Shi, L. (2015): Allometry and biomass production of *phyllostachys edulis* across the whole lifespan. – *Polish Journal of Environmental Studies* 24(2): 511-517.
- [34] Gao, X., Li, Z., Yu, H., Jiang, Z., Wang, C., Zhang, Y., Qi, L., Shi, L. (2016): Modeling of the height–diameter relationship using an allometric equation model: a case study of stands of *Phyllostachys edulis*. – *Journal of Forestry Research* 27: 339-347.
- [35] Gara, T. W., Murwira, A., Dube, T., Sibanda, M., Rwasoka, D. T., Ndaimani, H., Chivhenge, E., Hatendi, C. M. (2017): Estimating forest carbon stocks in tropical dry forests of Zimbabwe: exploring the performance of high and medium spatial-resolution multispectral sensors. – *Southern Forests: a Journal of Forest Science* 79: 31-40.
- [36] Gibbs, H. K., Brown, S., Niles, J. O., Foley, J. A. (2007): Monitoring and estimating tropical forest carbon stocks: making REDD a reality. – *Environmental Research Letters* 2: 045023.
- [37] Gitelson, A. A., Merzlyak, M. N. (1997): Remote estimation of chlorophyll content in higher plant leaves. – *International Journal of Remote Sensing* 18: 2691-2697.
- [38] Gitelson, A. A., Kaufman, Y. J., Merzlyak, M. N. (1996): Use of a green channel in remote sensing of global vegetation from EOS-MODIS. – *Remote sensing of Environment* 58: 289-298.
- [39] Gizachew, B., Solberg, S., Næsset, E., Gobakken, T., Bollandsås, O. M., Breidenbach, J., Zahabu, E., Mauya, E. W. (2016): Mapping and estimating the total living biomass and carbon in low-biomass woodlands using Landsat 8 CDR data. – *Carbon Balance and Management* 11: 13. <https://doi.org/10.1186/s13021-016-0055-8>.
- [40] Houghton, R. A. (2003): Revised estimates of the annual net flux of carbon to the atmosphere from changes in land use and land management 1850–2000. – *Tellus B* 55: 378-390.
- [41] Hudiburg, T., Law, B., Turner, D. P., Campbell, J., Donato, D., Duane, M. (2009): Carbon dynamics of Oregon and Northern California forests and potential land-based carbon storage. – *Ecological applications* 19: 163-180.
- [42] Huete, A. R. (1988): A soil-adjusted vegetation index (SAVI). – *Remote Sensing of Environment* 25: 295-309.
- [43] Hunt, E. R., Wang, L., Qu, J. J., Hao, X. (2012): Remote sensing of fuel moisture content from canopy water indices and normalized dry matter index. – *Journal of Applied Remote Sensing* 6: 061705.
- [44] Intergovernmental Panel on Climate Change (IPCC) (2006): IPCC Guidelines for National Greenhouse Gas Inventories. Vol. 5. Waste. – Prepared by the National Greenhouse Gas Inventories Programme, IGES, Japan.

- [45] Itkonen, P. (2012): Estimating leaf area index and aboveground biomass by empirical modeling using Spot HRVIR satellite imagery in the Taita Hills, SE Kenya. – Thesis, University of Helsinki, Faculty of Mathematics and Science, Department of Geosciences and Geography.
- [46] Jackson, R. B., Baker, J. S. (2010): Opportunities and constraints for forest climate mitigation. – *BioScience* 60: 698-707.
- [47] Jiang, Z., Huete, A. R., Didan, K., Miura, T. (2008): Development of a two-band enhanced vegetation index without a blue band. – *Remote Sensing of Environment* 112: 3833-3845.
- [48] Karki, S., Joshi, L., Karki, B. (2014): Learning on reducing emissions from deforestation and forest degradation. Regional Workshop, Kathmandu, Nepal, 24-27 July 2012. – International Centre for Integrated Mountain Development (ICIMOD), Lalitpur, Nepal.
- [49] Karlson, M., Reese, H., Ostwald, M. (2014): Tree crown mapping in managed woodlands (parklands) of semi-arid West Africa using WorldView-2 imagery and geographic object based image analysis. – *Sensors* 14: 22643-22669.
- [50] Karlson, M., Ostwald, M., Reese, H., Sanou, J., Tankoano, B., Mattsson, E. (2015): Mapping tree canopy cover and aboveground biomass in Sudano-Sahelian woodlands using Landsat 8 and random forest. – *Remote Sensing* 7: 10017-10041.
- [51] Keenan, R. J., Reams, G. A., Achard, F., De Freitas, J. V., Grainger, A., Lindquist, E. (2015): Dynamics of global forest area: results from the FAO Global Forest Resources Assessment 2015. – *Forest Ecology and Management* 352: 9-20.
- [52] Keith, H., Mackey, B. G., Lindenmayer, D. B. (2009): Re-evaluation of forest biomass carbon stocks and lessons from the world's most carbon-dense forests. – *Proceedings of the National Academy of Sciences* 106: 11635-11640.
- [53] Le Toan, T., Quegan, S., Davidson, M., Balzter, H., Paillou, P., Papathanassiou, K., Plummer, S., Rocca, F., Saatchi, S., Shugart, H. (2011): The BIOMASS mission: mapping global forest biomass to better understand the terrestrial carbon cycle. – *Remote sensing of environment* 115: 2850-2860.
- [54] Lippke, B., Perez-Garcia, J., Manriquez, C. (2003): Executive Summary: The Impact of Forests and Forest Management on Carbon Storage. – Rural Technological Initiative, College of Forest Resources, University of Washington, Seattle.
- [55] Liu, Y., Wang, Q., Yu, G., Zhu, X., Zhan, X., Guo, Q., Yang, H., Li, S., Hu, Z. (2011): Ecosystems carbon storage and carbon sequestration potential of two main tree species for the Grain for Green Project on China's hilly Loess Plateau. – *Shengtai Xuebao/Acta Ecologica Sinica* 31: 4277-4286.
- [56] Lu, D. (2005): Aboveground biomass estimation using Landsat TM data in the Brazilian Amazon. – *International Journal of Remote Sensing* 26: 2509-2525.
- [57] Lu, D. (2006): The potential and challenge of remote sensing-based biomass estimation. – *International Journal of Remote Sensing* 27: 1297-1328.
- [58] Lu, D., Mausel, P., Brondizio, E., Moran, E. (2002): Above-Ground Biomass Estimation of Successional and Mature Forests Using TM Images in the Amazon Basin. – In: Richardson, D. E., van Oosterom P. (eds.) *Advances in Spatial Data Handling*. Springer, Berlin.
- [59] Lu, D., Chen, Q., Wang, G., Moran, E., Batistella, M., Zhang, M., Vaglio Laurin, G., Saah, D. (2012): Aboveground forest biomass estimation with Landsat and LiDAR data and uncertainty analysis of the estimates. – *International Journal of Forestry Research* 2012.
- [60] Lu, D., Chen, Q., Wang, G., Liu, L., Li, G., Moran, E. (2016): A survey of remote sensing-based aboveground biomass estimation methods in forest ecosystems. – *International Journal of Digital Earth* 9: 63-105.
- [61] Mcroberts, R. E., Tomppo, E. O., Næsset, E. (2010): Advances and emerging issues in national forest inventories. – *Scandinavian Journal of Forest Research* 25: 368-381.

- [62] Melville, G., Stone, C., Turner, R. (2015): Application of LiDAR data to maximise the efficiency of inventory plots in softwood plantations. – *New Zealand Journal of Forestry Science* 45: 9.
- [63] Mganga, N., Lyaruu, H. (2015): Applicability of satellite remote sensing in accounting above-ground carbon in Miombo Woodlands. – *International Journal of Advanced Remote Sensing and GIS* 4: 1334-1343.
- [64] Molto, Q., Rossi, V., Blanc, L. (2013): Error propagation in biomass estimation in tropical forests. – *Methods in Ecology and Evolution* 4: 175-183.
- [65] Montes, N., Gauquelin, T., Badri, W., Bertaudiere, V., Zaoui, E. H. (2000): A non-destructive method for estimating above-ground forest biomass in threatened woodlands. – *Forest Ecology and Management* 130: 37-46.
- [66] Mutanga, O., Adam, E., Cho, M. A. (2012): High density biomass estimation for wetland vegetation using WorldView-2 imagery and random forest regression algorithm. – *International Journal of Applied Earth Observation and Geoinformation* 18: 399-406.
- [67] Mutanga, O., Skidmore, A. K. (2004a): Hyperspectral band depth analysis for a better estimation of grass biomass (*Cenchrus ciliaris*) measured under controlled laboratory conditions. – *International Journal of Applied Earth Observation and Geoinformation* 5: 87-96.
- [68] Mutanga, O., Skidmore, A. K. (2004b): Narrow band vegetation indices overcome the saturation problem in biomass estimation. – *International Journal of Remote Sensing* 25: 3999-4014.
- [69] Muukkonen, P., Heiskanen, J. (2005): Estimating biomass for boreal forests using ASTER satellite data combined with standwise forest inventory data. – *Remote Sensing of Environment* 99: 434-447.
- [70] Neilson, E., Maclean, D., Arp, P., Meng, F.-R., Bourque, C. P., Bhatti, J. (2006): Modeling carbon sequestration with CO2Fix and a timber supply model for use in forest management planning. – *Canadian Journal of Soil Science* 86: 219-233.
- [71] Nizami, S. M. (2012): The inventory of the carbon stocks in subtropical forests of Pakistan for reporting under Kyoto Protocol. – *Journal of Forestry Research* 23: 377-384.
- [72] Noble, I., Bolin, B., Ravindranath, N., Verardo, D., Dokken, D. (2000): *Land Use, Land Use Change, and Forestry*. – Cambridge University Press, Cambridge.
- [73] Nugroho, N. (2006): Estimating carbon sequestration in tropical rainforest using integrated remote sensing and ecosystem productivity modelling: a case study in Labanan Concession Area, East Kalimantan, Indonesia. – Master Thesis, ITC, International Institute for Geo-information Science and Earth Observation, Enschede.
- [74] PAEC-ASAD: Athar, G. R., Aijaz, A., Mumtaz, A. (2009): *Greenhouse Gas Emission Inventory of Pakistan for the year 2007-08*. – PAEC, Islamabad.
- [75] Päivinen, R., Lehikoinen, M., Schuck, A., Häme, T., Väätäinen, S., Kennedy, P., Folving, S. (2001): *Combining Earth Observation Data and Forest Statistics*. – European Forest Institute, Joensuu.
- [76] Pan, Y., Birdsey, R. A., Fang, J., Houghton, R., Kauppi, P. E., Kurz, W. A., Phillips, O. L., Shvidenko, A., Lewis, S. L., Canadell, J. G. (2011): A large and persistent carbon sink in the world's forests. – *Science*. DOI: 10.1126/science.1201609.
- [77] Phua, M.-H., Ling, Z.-Y., Wong, W., Korom, A., Ahmad, B., Besar, N. A., Tsuyuki, S., Ioki, K., Hoshimoto, K., Hirata, Y. (2014): Estimation of above-ground biomass of a tropical forest in Northern Borneo using high-resolution satellite image. – *Journal of Forest and Environmental Science* 30: 233-242.
- [78] Piao, S., Fang, J., Zhu, B., Tan, K. (2005): Forest biomass carbon stocks in China over the past 2 decades: estimation based on integrated inventory and satellite data. – *Journal of Geophysical Research: Biogeosciences* 110. <https://doi.org/10.1029/2005JG000014>.

- [79] Picard, N., Saint-André, L., Henry, M. (2012): Manual for Building Tree Volume and Biomass Allometric Equations: from Field Measurement to Prediction. – FAO, Rome.
- [80] Plugge, D., Baldauf, T., Köhl, M. (2013): The global climate change mitigation strategy REDD: monitoring costs and uncertainties jeopardize economic benefits. – *Climatic Change* 119: 247-259.
- [81] Pregitzer, K. S., Euskirchen, E. S. (2004): Carbon cycling and storage in world forests: biome patterns related to forest age. – *Global Change Biology* 10: 2052-2077.
- [82] Ravindranath, N., Ostwald, M. (2008): Carbon Inventory Methods for National Greenhouse Gas Inventory, Carbon Mitigation and Roundwood Production Projects. – Springer, Dordrecht, pp. 217-235.
- [83] REDD+, L. (2006): Leaf Technical Guidance Series for the Development of a National or Subnational Forest Monitoring System for REDD+ (Module EF-D: Emission Factor for Deforestation). – Winrock International, Washington, DC.
- [84] Rokityanskiy, D., Benítez, P. C., Kraxner, F., Mccallum, I., Obersteiner, M., Rametsteiner, E., Yamagata, Y. (2007): Geographically explicit global modeling of land-use change, carbon sequestration, and biomass supply. – *Technological Forecasting and Social Change* 74: 1057-1082.
- [85] Rosenqvist, A., Shimada, M., Igarashi, T., Watanabe, M., Tadono, T., Yamamoto, H. (2003): Support to multi-national environmental conventions and terrestrial carbon cycle science by ALOS and ADEOS-II-the Kyoto & Carbon Initiative. – IGARSS 2003 IEEE International Geoscience and Remote Sensing Symposium. Proceedings (IEEE Cat. No. 03CH37477) 2003, pp. 1471-1476.
- [86] Rouse Jr, J. W., Haas, R., Schell, J., Deering, D. (1974): Monitoring Vegetation Systems in the Great Plains with ERTS. – NASA, Washington, DC.
- [87] Sader, S. A., Joyce, A. T. (1988): Deforestation rates and trends in Costa Rica 1940 to 1983. – *Biotropica* 11-19.
- [88] Schimel, D., Melillo, J., Tian, H., Mcguire, A. D., Kicklighter, D., Kittel, T., Rosenbloom, N., Running, S., Thornton, P., Ojima, D. (2000): Contribution of increasing CO₂ and climate to carbon storage by ecosystems in the United States. – *Science* 287: 2004-2006.
- [89] Sessa, R., Dolman, H. (2008): Terrestrial Essential Climate Variables for Climate Change Assessment, Mitigation and Adaptation (GTOS 52). – FAO, Rome.
- [90] Shi, L., Liu, S. (2017): Methods of Estimating Forest Biomass: A Review. – In: Tumuluru, J. S. (ed.) Biomass Volume Estimation and Valorization for Energy. InTech, Rijeka.
- [91] Silleos, N. G., Alexandridis, T. K., Gitas, I. Z., Perakis, K. (2006): Vegetation indices: advances made in biomass estimation and vegetation monitoring in the last 30 years. – *Geocarto International* 21: 21-28.
- [92] Sinha, S., Jeganathan, C., Sharma, L., Nathawat, M., Das, A. K., Mohan, S. (2016): Developing synergy regression models with space-borne ALOS PALSAR and Landsat TM sensors for retrieving tropical forest biomass. – *Journal of Earth System Science* 125: 725-735.
- [93] Siteo, A. A., Mandlate, L. J. C., Guedes, B. S. (2014): Biomass and carbon stocks of Sofala bay mangrove forests. – *Forests* 5: 1967-1981.
- [94] Slonecker, T., Haack, B., Price, S. (2009): Spectroscopic analysis of arsenic uptake in Pteris ferns. – *Remote Sensing* 1: 644-675.
- [95] Smithwick, E. A., Harmon, M. E., Remillard, S. M., Acker, S. A., Franklin, J. F. (2002): Potential upper bounds of carbon stores in forests of the Pacific Northwest. – *Ecological Applications* 12: 1303-1317.
- [96] Stinson, G., Kurz, W., Smyth, C., Neilson, E., Dymond, C., Metsaranta, J., Boisvenue, C., Rampley, G., Li, Q., White, T. (2011): An inventory-based analysis of Canada's managed forest carbon dynamics, 1990 to 2008. – *Global Change Biology* 17: 2227-2244.

- [97] Thenkabail, P. S., Smith, R. B., De Pauw, E. 2000. Hyperspectral vegetation indices and their relationships with agricultural crop characteristics. – Remote Sensing of Environment 71: 158-182.
- [98] Thomas, S. C., Martin, A. R. (2012): Carbon content of tree tissues: a synthesis. – Forests 3: 332-352.
- [99] Tomppo, E., Olsson, H., Ståhl, G., Nilsson, M., Hagner, O., Katila, M. (2008): Combining national forest inventory field plots and remote sensing data for forest databases. – Remote Sensing of Environment 112: 1982-1999.
- [100] Valentini, R., Matteucci, G., Dolman, A., Schulze, E.-D., Rebmann, C., Moors, E., Granier, A., Gross, P., Jensen, N., Pilegaard, K. (2000): Respiration as the main determinant of carbon balance in European forests. – Nature 404: 861.
- [101] Wang, C., Feng, M.-C., Yang, W.-D., Ding, G.-W., Sun, H., Liang, Z.-Y., Xie, Y.-K., Qiao, X.-X. (2016): Impact of spectral saturation on leaf area index and aboveground biomass estimation of winter wheat. – Spectroscopy Letters 49: 241-248.
- [102] Whittaker, R. H., Niering, W. A. (1975): Vegetation of the Santa Catalina Mountains, Arizona. V. Biomass, production, and diversity along the elevation gradient. – Ecology 56: 771-790.
- [103] Winmore, G. T. (2012): Modelling spatial variations in wood volume and forest carbon stocks in dry forests of Southern Africa using remotely sensed data. – Msc. Thesis. University of Zimbabwe.
- [104] Worldbank (2015): Readiness Preparation Proposal Assessment Note on a Proposed {loan/credit} in the Amount {loan/credit} to the Islamic Republic of Pakistan. For REDD+ Readiness Preparation Support (p152465). – Worldbank, Washington, DC.
- [105] Yingchun, L., Guirui, Y., Qiufeng, W., Yangjian, Z. (2012): Huge carbon sequestration potential in global forests. – Journal of Resources and Ecology 3: 193-201.
- [106] Zhao, D., Huang, L., Li, J., Qi, J. (2007): A comparative analysis of broadband and narrowband derived vegetation indices in predicting LAI and CCD of a cotton canopy. – ISPRS Journal of Photogrammetry and Remote Sensing 62: 25-33.
- [107] Zhou, G., Wang, Y., Jiang, Y., Yang, Z. (2002): Estimating biomass and net primary production from forest inventory data: a case study of China's Larix forests. – Forest Ecology and Management 169: 149-157.

APPENDIX A

Table A1. List of allometric equations for major species

Species	Model	Allometric equation
General (coniferous)	$M=a(\rho \times D^2 \times H)^b$	$AGB=0.1645 \times (\rho \times D^2 \times H)^{0.8586}$
<i>Pinus roxberghii</i> (chir pine)	$M=a(D^2 \times H)^b$	$AGB=0.0224 \times (D^2 \times H)^{0.9767}$
<i>Cedrus deodara</i> (Deodar)	$M=a(D^2 \times H)^b$	$AGB=0.1779 \times (D^2 \times H)^{0.8103}$
<i>Pinus Wallichiana</i> (Kail)	$M=a(D^2 \times H)^b$	$AGB=0.0631 \times (D^2 \times H)^{0.8798}$
<i>Pinus gerardiana</i> (Chilghoza)	$M=a \times D^b$	$AGB=0.0253 \times D^{2.6077}$
<i>Abies Pindrow</i> (Fir)	$M=a(D^2 \times H)^b$	$AGB=0.0954 \times (D^2 \times H)^{0.8114}$
<i>Picea smithiana</i> (Spruce)	$M=a(D^2 \times H)^b$	$AGB=0.0843 \times (D^2 \times H)^{0.8472}$
<i>Quercus ilex</i> (Oak)	$M=a(D^2 \times H)^b$	$AGB=0.8277 \times (D^2 \times H)^{0.6655}$

Table A2. Description and formula of the categories of various vegetation indices

Vegetation index	Formula	Sentinel-2 bands	Reference
Broadband VIs			
EVI – Enhanced VI	$EVI = 2.5 \times \frac{NIR - Red}{NIR + 2.4Red + 1}$	Whereas NIR is spectral band 8, while the red is spectral band 4	Jiang et al., 2008
GNDVI – Green Normalized Difference VI	$GNDVI = \frac{NIR - Green}{NIR + Green}$	Where NIR is spectral band 8 while Green is spectral band 3	Gitelson et al., 1996
NDVI – Normalized Difference VI	$NDVI = \frac{NIR - Red}{NIR + Red}$	Where NIR is spectral band 8, while the red is spectral band 4	Rouse Jr et al., 1974
SAVI – Soil Adjusted VI	$SAVI = \frac{NIR - Red}{NIR + Red + L} \times (1 + L)$	Whereas NIR is spectral band 8 and Red is Spectral band 4	Huete, 1988
SQSR – Square Root Simple Ratio	$SQSR = \sqrt{\frac{NIR}{Red}}$	Whereas NIR is spectral band 8 and RED is spectral band 4	Itkonen, 2012
TSAVI – Transformed Soil Adjusted VI	$TSAVI = \frac{a(NIR - aR - b)}{[a(NIR - b) + 0.08(1 + a^2)]}$	Where NIR spectral band 8 and Red is Spectral band 4	Baret and Guyot, 1991
Canopy Water Content Indices			
NDII – Normalized Difference Infrared Index	$NDII = \frac{NIR - SWIR}{NIR + SWIR}$	Where: NIR is spectral band 8, while the shortwave infrared (SWIR) is spectral band 13	Hunt et al., 2012
NDWI – Normalized Difference Water Index	$NDWI = \frac{NIR - SWIR}{NIR + SWIR}$	Where: NIR is spectral band 8, while shortwave infrared (SWIR) is spectral band 12	Gao, 1996
Narrow Red Edge Band VIs			
RE-EVI – Re-Edge Enhanced VI	$RE_{EVI} = 2.5 \times \frac{NIR - RE}{NIR + 2.4RE + 1}$	Where: NIR is spectral band 8, While the red-edge is spectral band 6	Abdel-Rahman et al., 2017
RENDVI – Red-Edge Normalized Difference VI	$RENDVI = \frac{NIR - red}{NIR + red}$	Where: NIR is spectral band 8, while the red-edge spectral band 6	Chen et al., 2007a
RERVI – Red Edge Ratio Vegetation Index	$RERVI = \frac{NIR}{RE}$	Where: NIR is spectral band 8, while the red-edge is spectral band 6	Cao et al., 2016

Table A3. Biomass, carbon stock and CO₂ e estimated per plot in study area

Plot No.	Aspect	Elevation (m)	Slope	Forest type	Crown cover	AGB (t/ha)	BGB (t/ha)	Total B (t/ha)	AGC (t/ha)	BGC (t/ha)	Total C (t/ha)	CO ₂ e
1	Northern	1942	55	Moist Temperate	80	203.83	52.99	256.83	95.80	24.90	120.71	441.79
2	Northern	1927	55	Moist Temperate	70	116.40	30.26	146.67	54.71	14.22	68.93	252.29
3	Eastern	1884	90	Moist Temperate	100	171.53	44.59	216.13	80.62	20.96	101.58	371.79
4	Northern	1913	31	Moist Temperate	80	112.99	29.38	142.38	53.11	13.81	66.92	244.92
5	Eastern	1798	60	Moist Temperate	70	149.75	38.94	188.69	70.39	18.30	88.69	324.59
6	Eastern	1759	0	Moist Temperate	100	198.11	51.51	249.62	93.11	24.21	117.33	429.40
7	Northern	1753	70	Moist Temperate	65	105.94	27.55	133.49	49.79	12.95	62.74	229.63
8	Eastern	1786	60	Moist Temperate	70	193.58	50.33	243.92	90.98	23.66	114.64	419.58
9	Northern	1823	55	Moist Temperate	40	125.27	32.57	157.84	58.88	15.31	74.19	271.52
10	Northern	1305	45	Moist Temperate	60	194.13	50.47	244.60	91.24	23.72	114.96	420.76
11	Northern	1361	58	Moist Temperate	55	187.60	48.77	236.38	88.17	22.93	111.09	406.62
12	Northern	1325	50	Moist Temperate	65	144.99	37.69	182.69	68.15	17.72	85.86	314.26
13	Northern	1420	68	Moist Temperate	95	170.91	44.44	215.35	80.33	20.89	101.22	370.45
14	Western	1403	60	Moist Temperate	95	110.40	28.70	139.11	51.89	13.49	65.38	239.29
15	Southern	1431	50	Moist Temperate	5	115.76	30.09	145.86	54.41	14.15	68.55	250.90
16	Northern	1416	75	Moist Temperate	50	46.45	12.07	58.53	21.83	5.68	27.51	100.69
17	Northern	1441	65	Moist Temperate	95	124.48	32.37	156.85	58.51	15.21	73.72	269.81
18	Eastern	1470	53	Moist Temperate	90	113.31	29.46	142.77	53.26	13.85	67.10	245.59
19	Northern	1468	0	Moist Temperate	50	108.45	28.19	136.66	50.97	13.25	64.23	235.07
20	Western	1820	52	Moist Temperate	75	135.36	35.19	170.56	63.62	16.54	80.16	293.40
21	Northern	1605	75	Moist Temperate	80	165.24	42.96	208.20	77.66	20.19	97.86	358.15
22	Northern	1667	73	Moist Temperate	90	173.27	45.05	218.32	81.44	21.17	102.61	375.55
23	Northern	1667	80	Moist Temperate	80	151.05	39.27	190.32	70.99	18.46	89.45	327.39
24	Western	1680	50	Moist Temperate	90	146.90	38.19	185.09	69.04	17.95	86.99	318.40
25	Northern	1419	87	Moist Temperate	50	119.86	31.16	151.02	56.33	14.65	70.98	259.79
26	Northern	1388	88	Moist Temperate	45	114.85	29.86	144.70	53.98	14.03	68.01	248.92
27	Northern	1324	73	Moist Temperate	15	118.53	30.82	149.35	55.71	14.48	70.19	256.90
28	Northern	1500	67	Moist Temperate	40	151.36	39.35	190.71	71.14	18.49	89.64	328.06
29	Western	1930	90	Moist Temperate	85	134.91	35.08	169.99	63.41	16.49	79.89	292.41
30	Western	2132	95	Moist Temperate	90	170.06	44.21	214.27	79.93	20.78	100.71	368.59
31	Southern	2080	110	Moist Temperate	80	177.00	46.02	223.02	83.19	21.63	104.82	383.65
32	Northern	1677	60	Moist Temperate	80	173.36	45.07	218.43	81.48	21.18	102.66	375.75
33	Northern	1711	50	Moist Temperate	95	153.59	39.94	193.53	72.19	18.77	90.96	332.92
34	Western	1548	70	Chir Pine Forest	20	132.67	34.49	167.17	62.36	16.21	78.57	287.57
35	Northern	1150	60	Chir Pine Forest	75	174.88	45.46	220.35	82.19	21.37	103.57	379.05
36	Southern	1512	70	Chir Pine Forest	80	164.23	42.70	206.94	77.19	20.07	97.26	355.97
37	Northern	1522	75	Chir Pine Forest	80	279.59	72.69	352.29	131.41	34.17	165.58	606.01
38	Northern	1008	75	Chir Pine Forest	60	86.19	22.41	108.60	40.51	10.53	51.04	186.82
39	Western	1543	55	Chir Pine Forest	65	118.10	30.70	148.81	55.51	14.43	69.94	255.98
40	Southern	1525	75	Chir Pine Forest	65	179.58	46.69	226.28	84.41	21.95	106.35	389.25
41	Southern	1392	50	Chir Pine Forest	25	141.17	36.70	177.87	66.35	17.25	83.59	305.98
42	Southern	1353	60	Chir Pine Forest	10	145.65	37.87	183.52	68.46	17.79	86.25	315.69
43	Eastern	1017	25	Chir Pine Forest	30	136.51	35.49	172.01	64.16	16.68	80.84	295.89
44	Western	1300	45	Chir Pine Forest	35	111.33	28.95	140.28	52.33	13.60	65.93	241.31
45	Northern	1043	75	Chir Pine Forest	65	161.75	42.06	203.80	76.02	19.77	95.79	350.59
46	Northern	1029	60	Chir Pine Forest	60	136.09	35.38	171.48	63.96	16.63	80.59	294.97
47	Eastern	998	40	Chir Pine Forest	20	105.31	27.38	132.69	49.49	12.87	62.37	228.26
48	Southern	2319	72	Chir Pine Forest	90	115.00	29.90	144.91	54.05	14.05	68.12	249.27
49	Southern	2365	80	Moist Temperate	70	256.76	66.76	323.51	120.68	31.37	152.05	556.51
50	Southern	2402	90	Moist Temperate	100	220.00	57.20	277.21	103.40	26.89	130.29	476.86
51	Northern	1547	73	Moist Temperate	70	137.15	35.66	172.81	64.46	16.76	81.22	297.26
52	Northern	1612	0	Moist Temperate	60	161.82	42.07	203.89	76.06	19.77	95.83	350.74
53	Northern	1662	70	Moist Temperate	55	105.23	27.36	132.59	49.46	12.86	62.32	228.08
54	Eastern	1681	0	Moist Temperate	55	196.88	51.19	248.07	92.53	24.06	116.59	426.72
55	Eastern	1121	40	Moist Temperate	70	138.57	36.03	174.61	65.13	16.93	82.06	300.36

AGB = Above Ground Biomass, BGB = Below Ground Biomass, AGC = Above Ground Carbon, BGC = Below Ground Carbon and CO₂ e = carbon di oxide equivalent

APPENDIX B

Relationship between above ground biomass (AGB), several vegetation indices was assessed using regression analysis which can be seen below.

Figure B1. Scatter plot (a, b, c, d, e, f) derived using SigmaPlot 14.0 showing the relationship, regression equation and R-square value between broadband vegetation indices and above ground biomass

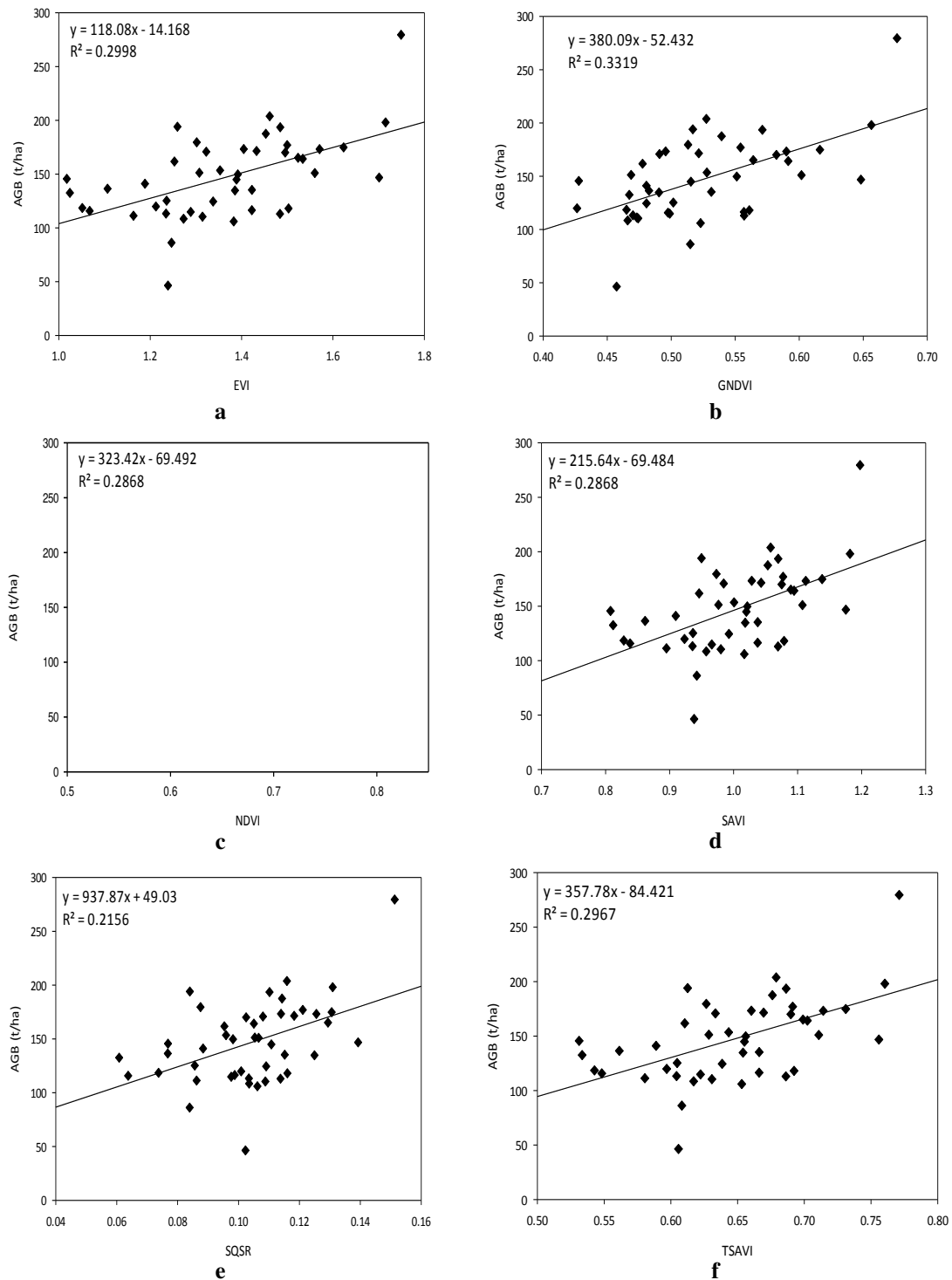


Figure B2. Scatter plot a and b derived using SigmaPlot 14.0 showing regression equation, R-square value and relationship between canopy water vegetation indices and above ground biomass

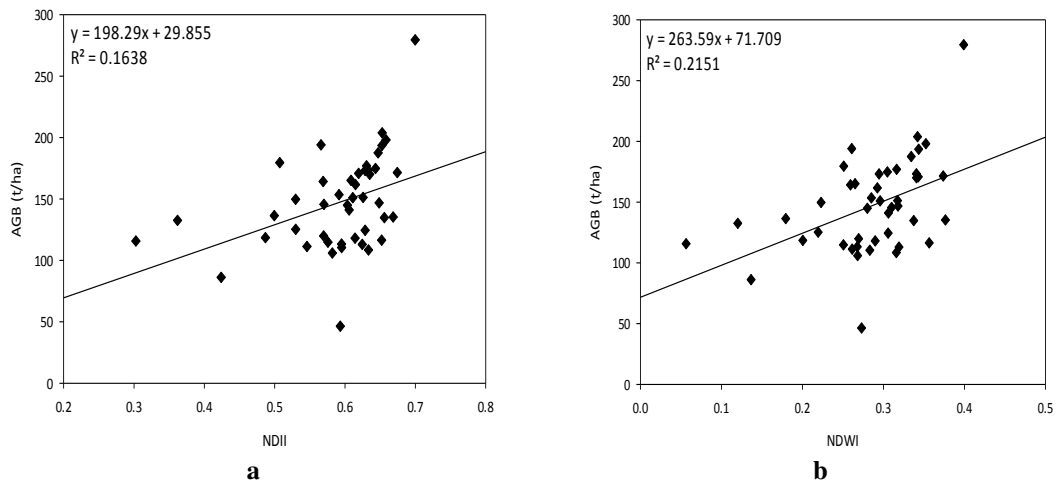
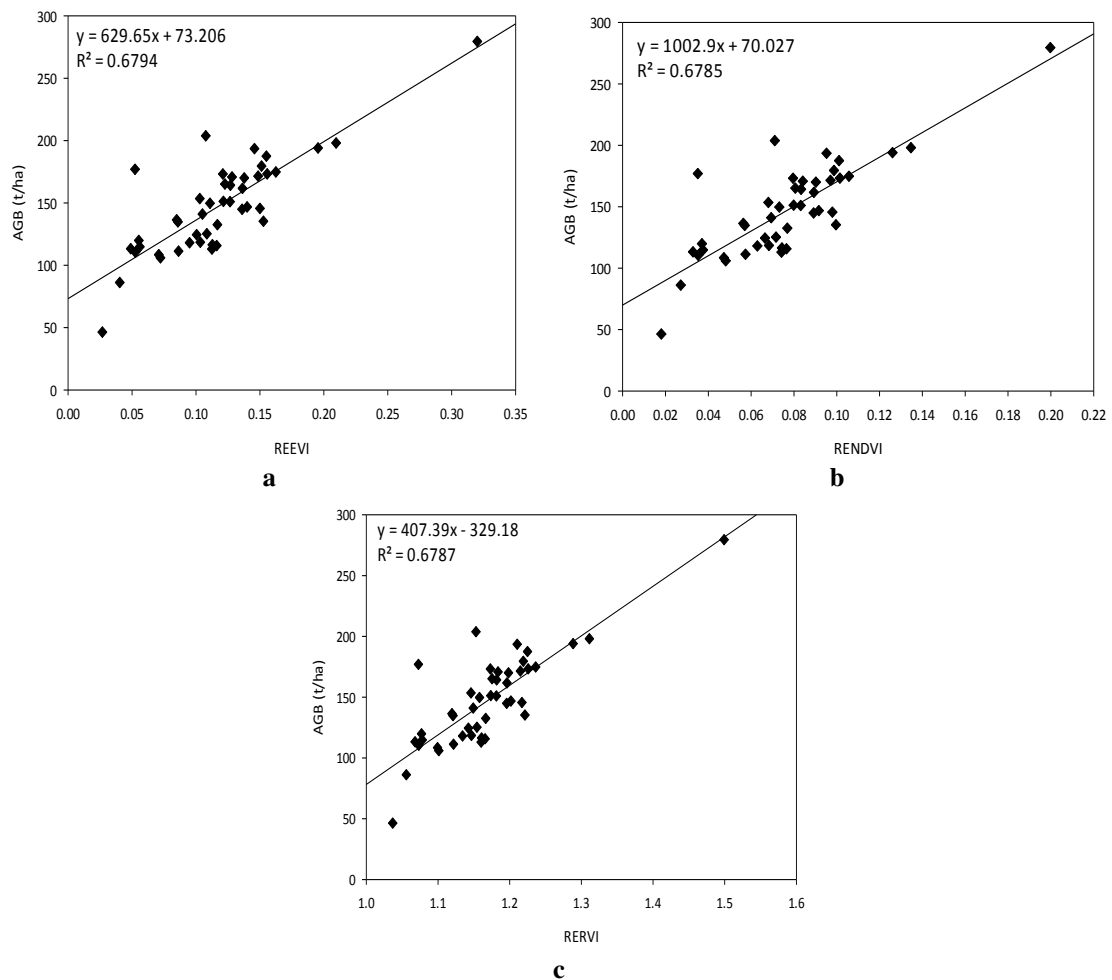


Figure B3. Scatter plot (a, b, c) derived using SigmaPlot 14.0 showing the relationship, regression equation and R-square value between narrow red-edge band vegetation indices and above ground biomass



DYNAMIC CHARACTERISTICS OF COMMUNITY STRUCTURE AND SEASONAL VARIATION OF FISHERY SPECIES IN THE BOHAI SEA, CHINA

FORRUQ RAHMAN, M.^{1,3} – SHAN, X. J.^{2,3} – LIN, Q.³ – CHEN, Y. L.³ – MAMUN, A. A.⁴ –
BARMAN, P. P.¹ – YANAN, H.¹ – LIU, Q.^{1*}

¹*College of Fisheries, Department of Marine Fisheries, Ocean University of China
Qingdao 266003, People's Republic of China*

²*Function Laboratory for Marine Fisheries Science and Food Production Processes, Pilot
National Laboratory for Marine Science and Technology (Qingdao)
Qingdao 266237, People's Republic of China*

³*Provincial Key Laboratory of Fishery Resources and Ecological Environment, Yellow Sea
Fisheries Research Institute, Chinese Academy of Fishery Sciences
Qingdao 266071, People's Republic of China*

⁴*College of Marine Life Science, Department of Marine Ecology, Ocean University of China
Qingdao 266003, People's Republic of China*

**Corresponding author*

e-mail: qunliu@mail.ouc.edu.cn; phone: +86-532-8203-1715

(Received 9th Jul 2019; accepted 15th Nov 2019)

Abstract. The structural patterns and the seasonal dynamics of fishery species were studied in the Bohai Sea, based on fishery-independent data surveyed in each season sampling stations. A total of 88 fishery species belonging to 64 families were recorded, in detail 43 fishes, 29 crustaceans, 12 molluscas, three echinoderms and one species of scyphozoan. Among them, 21 species commonly found throughout the study period defined as 'common' species, and eight species those were the highest contributors defined as 'dominant' species (based on SIMPER analysis, their cumulative contribution was more than 70%). Maximum abundance was recorded in the summer season while species number was higher in both summer and autumn season. Among the community parameters, species richness (3.79), diversity (2.31) and Simpson indices (0.88) peaked in the autumn season whereas species evenness (0.95) was in the winter. However, species diversity, evenness, and Simpson indices were lower in the summer season (0.57, 0.18 and 0.18, respectively) while species richness was in the winter (1.65). Multivariate PCoA analysis revealed that there was a significant seasonal variation in fisheries assemblages. Furthermore, ANOSIM (Global $R = 0.467$, $P = 0.01$) indicated a distinct community structure of fishery species between the four seasons. Thus, this result suggests that fisheries assemblages might be influenced by the seasonal dynamics of the ecological condition of the Bohai Sea.

Keywords: *fisheries assemblages, multivariate analyses, community parameters, seasonal patterns, trawl survey data*

Introduction

The Bohai Sea, a semi-enclosed inland sea is a unique waterbody that houses rich marine and coastal biological resources (i.e., fishes/shellfishes; oil, gas, and minerals; estuaries; tidal flats; seagrass beds) as well as a great potentiality for mariculture and tourism purpose in the northeastern China (Zhang et al., 2002; Song and Duan, 2018). However, the rapid human

settlement and industrial development that was triggered from 1985 along the coast of Bohai Sea accelerated the degradation in estuarine and marine ecosystems by altering hydro-pedological properties (i.e., water and sediments qualities) over the decades (Liu et al., 2011; Gao et al., 2014; Li et al., 2016). Besides, the changing climate variabilities such as temperature (T), salinity (S), and biogenic elements altered the Bohai Sea ecosystems which significantly influenced the living biotic communities (Lin et al., 2001; Yu et al., 2009). The variations of species in the communities are closely interrelated with the ecological conditions of water masses. Over the recent decades, anthropogenic activities mainly linked to urbanization and industrialization have a notable effect on the species diversity of the primary producers and benthos communities which may have triggered off the declining trend of fishery populations in the Bohai Sea (Hu et al., 2011; Liu et al., 2011).

Several studies have been focused on the characteristics of fish and fishery dynamics of the Bohai Sea (Chen et al., 1997; Tang et al., 2003; Jin, 2004; Shan et al., 2012, 2016; Zhang et al., 2012). Investigations have been reported that fishery stock status in the Bohai Sea experienced declining trends (Liu et al., 1990; Zhang et al., 2006; Zhou et al., 2013). Moreover, the Bohai Sea has been considered one of the most exploited fishing ground in the world (Wu et al., 2017; Liu et al., 2017). As a result, species abundance, diversity, and trophic structure had significantly shrunk in this ecosystem (Deng and Jin, 2001; Jin, 2004; Zhang and Tang, 2004; Shan et al., 2012). Spatio-temporal shifts of dominant species from large-size of high economic value to short-lived, low-trophic-level, low economic value and changes of ecosystem structure and functioning on the decadal-scale have been documented (Shan et al., 2013, 2016; Rahman et al., 2019).

The present study accounts the Bohai Sea as a major fishery center in China in view, and evaluated a one-year fishery-independent data (i.e., a pair of trawlers) to analyze the community patterns and dynamics of the fishery species. The specific aims of the research were (a) to document the taxonomic composition and species distribution patterns of fishery species, and (b) to illustrate the community patterns and the seasonal dynamics of fishery species during the study period.

Materials and methods

Study area

The Bohai Sea ($37^{\circ}07' \sim 41^{\circ}N$ and $117^{\circ}35' \sim 121^{\circ}10'E$) is a semi-enclosed marginal sea of the northwestern Pacific Ocean on the northern coast of China. It extends for about 450 km from north to south and about 350 km from east to west, where the Bohai Strait is used as a junction to the Yellow Sea between Shandong and Liaodong Peninsulas (*Fig. 1*). It has an area of 77,000 km², which includes Bohai, Laizhou, and Liaodong Bays. The water depth varies at 10-20 m in the continental shelf where maximal water depth of 70 m is recorded in the northern part of Bohai Strait. The hydrographic conditions have greatly influenced by many factors such as river discharges, wind-tide-thermohaline circulation, stratification during summer, and vertical and horizontal mixing of nutrients in winter that support higher primary productivity (Ning et al., 2010).

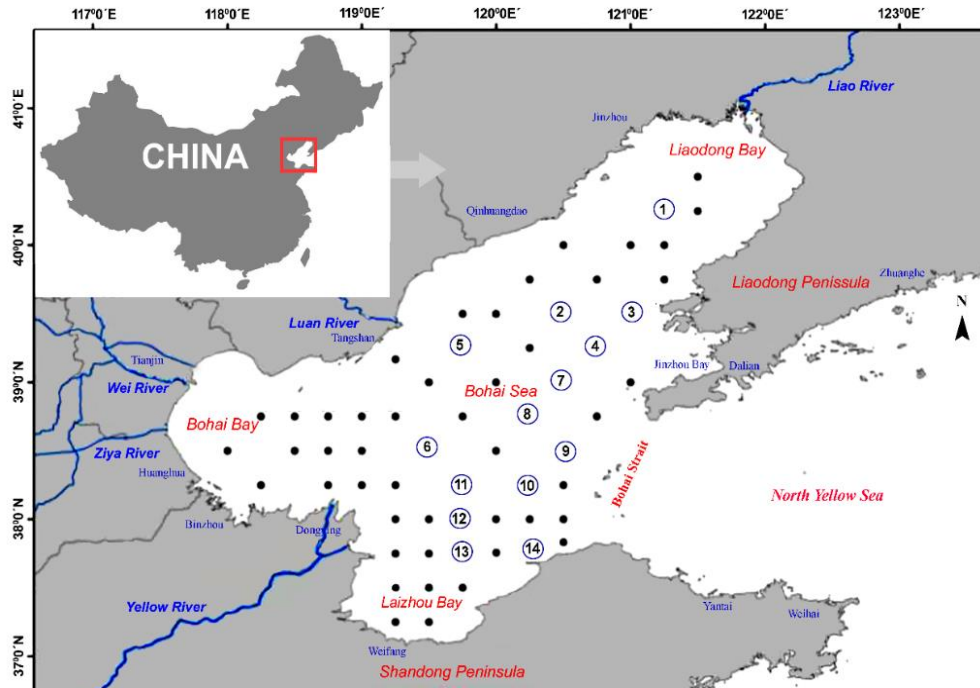


Figure 1. Geographical locations of sampling points in the Bohai Sea, China

Data source

Data were collected from a pair trawler (i.e., the capability was 200 horsepower; the distance between wings was 22.6 m, headline height was between 5 m and 6 m, cod mesh size was 2 cm, and circumference was 30.6 m.) survey carried out by the Yellow Sea Fisheries Research Institute. The surveyed sampling stations were designed on a fixed station grid of $0.5^{\circ}\text{N} \times 0.5^{\circ}\text{E}$. The hauls were lowered for sampling during the daytime, the duration at least 15 minutes to 60 minutes and an average hauling speed of 5.09 km/h. The average sampling depth was 23.18 meters (Table 1). All data were then standardized to a one-hour trawl duration for consistency. The survey period divided into four seasons namely as winter (January), spring (May), summer (August), and autumn (November) season. Samples were collected from the fixed 70 sampling stations. Among them, 14 stations were surveyed in each season. We selected these common sampling stations for analysis among the seasons.

Collected fishery specimens at each station were sorted firstly family and order level, then to species level, or the lowest possible taxon level. Subsequently, total abundance/individual abundance and species composition were recorded. The abundance of the species was expressed as the number of individual species catch per haul (ind./haul), and the composition of the species was expressed as a percentage of the total number of species recorded (%).

Table 1. Position and characteristics (latitude, longitude, sampling site, aver. depth and aver. haul speed) of the sampling stations during the pair-trawl survey in the Bohai Sea

Station SL No.	Net placement		Sampling site	Average depth (m)	Average haul speed (km/h)
	Latitude	Longitude			
1	40°25' N	121°25' E	Liaodong Bay	23.6	5.19
2	39°50' N	120°50' E	Liaodong Bay	25.9	5.06
3	39°50' N	121°00' E	Liaodong Bay	25.2	4.39
4	39°25' N	120°75' E	Liaodong Bay	25.73	4.87
5	39°25' N	119°75' E	Central Bohai	25.8	5.24
6	38°50' N	119°50' E	Central Bohai	25.83	5.0
7	39°00' N	120°50' E	Central Bohai	24.57	5.56
8	38°75' N	120°25' E	Central Bohai	25.83	5.13
9	38°50' N	120°50' E	Central Bohai	28.43	5.43
10	38°25' N	120°25' E	Central Bohai	23.93	4.95
11	38°25' N	119°75' E	Laizhou Bay	22.67	4.82
12	38°00' N	119°75' E	Laizhou Bay	16.73	5.69
13	37°75' N	119°75' E	Laizhou Bay	15.33	5.13
14	37°75' N	120°25' E	Laizhou Bay	14.93	4.82

Data analysis

Diversity patterns of fishery species were summarized by frequently used diversity measuring indices such as Shannon-Wiener Index (H') (Shannon & Weaver) (Eq. 1), species evenness (J') (Pielou) (Eq. 2), species richness (d) (Margalef) (Eq. 3) and Simpson index ($1-\lambda'$) (Simpson) (Eq. 4), these four indices were measured using the following formulas:

$$H' = \sum_{i=1}^s P_i(\ln P_i) \quad (\text{Eq.1})$$

$$J' = H' / \ln S \quad (\text{Eq.2})$$

$$d = (S - 1) / \ln N \quad (\text{Eq.3})$$

$$1 - \lambda' = 1 - \text{SUM} (N_i * (N_i - 1)) / (N * (N - 1)) \quad (\text{Eq.4})$$

where, H' = observed diversity index; P_i = proportion of the total count arising from the i th species; S = total number of species; and N = the total number of individuals.

Both multivariate and univariate analyses were conducted for summarizing seasonal variation in fishery dynamics and their seasonal patterns of community structure using PRIMER v7.0.13 and IBMSPSS v.22. The patterns of species distribution between the four seasons were analyzed by shade plotting analysis from average standardized species abundance data. The species whose presence was available in all four seasons were defined as 'common species' in the community. The contribution of each species to the average Bray-Curtis similarity among the 14 trawls stations was calculated using SIMPER (similarity percentage analysis) program. Based on the SIMPER analysis, those

species have a cumulative contribution of more than 70% in the total communities were defined as 'dominant species'. Both the dominant and common species identified as an important species in the fishery communities (Zhu and Tang, 2002; Shan et al., 2016). The significant differences of the fisheries community structure among the seasons were tested using ANOSIM (analysis of similarity) (Anderson et al., 2008; Clarke and Gorley, 2015). The seasonal variations in fishery assemblages were analyzed by coordination of the submodule of PCoA (Principal coordinates analysis) of PREMANOVA + of Bray–Curtis similarities from square root transformed species abundance data (Anderson et al., 2008; Clarke and Gorley, 2015).

A simple Pearson correlation matrix was performed to identify an existing correlation among the dominant species of fishery communities using IBMSPSS v.22, and data were log-transformed before analysis.

Results

Taxonomic composition and species distribution

A total of 88 species belonging to 64 families were identified. These fishery samples included 43 fish species belonging to 28 families, 29 crustacean species belonging to 21 families, 12 mollusca species belonging to 11 families, three echinoderm species belonging to three families and one species of scyphozoan. The list of identified fishery species including their seasonal distribution, average abundance, frequency of occurrence was summarized in *Table 2*. Among the species, 21 species were reported common in terms of their presence in all four seasons, and eight species were found to be dominant with their higher contribution in the communities.

Based on the species distribution patterns, 19 species were present in three seasons, 18 species were present in two seasons, and 30 species were distributed only in one season (*Fig. 2*).

In terms of dominance (result from SIMPER analysis >70%), six species belonged to crustaceans (*Alpheus japonicas*, 15.34%; *Oratosquilla oratoria*, 11.57%; *Palaemon gravieri*, 10.57%; *Crangon affinis*, 8.85%; *Acetes chinensis*, 7.53%; *Leptochela gracilis*, 7.19%) and others were one fish species (*Engraulis japonicas*, 6.30%) and one cephalopod species (*Loligo japonica*, 8.51%) (*Table 2* and *Fig. 2*).

In terms of species belonging to family, the maximum number of species were recorded under the family of Gobiidae with seven species (*Amblychaeturichthys hexanema*, *Chaeturichthys stigmatias*, *Cryptocentrus filifer*, *Favonigobius gymnauchen*, *Ctenotrypauchen chinensis*, *Synechogobius hasta*, and *Odontamblyopus rubicundus*), followed by the family of Engraulidae with five species (*Coilia mystus*, *Engraulis japonicas*, *Setipinna taty*, *Thrissa kammalensis*, and *Thrissa mystax*) and the Penaeidae with four species (*Fenneropenaeus chinensis*, *Marsupenaeus japonicas*, *Metapenaeopsis dalei* and *Trachypenaeus curvirostris*) (*Table 2*).

Table 2. List of fishery species recorded in the Bohai Sea during a one-year cycle including their seasonal distribution, average abundance, frequency of occurrence and dominant species based on SIMPER analysis

	Family	Species name	Dist.	Winter		Spring		Summer		Autumn	
				N	%	N	%	N	%	N	%
Fish	Ammodytidae	<i>Ammodytes personatus</i> (Girard, 1856)	---+	-	0	-	100	-	0	-	0
	Apogonidae	<i>Apogonichthys lineatus</i> ((Temminck & Schlegel, 1842)	---+	-	0	-	0	+	97.92	-	2.08
	Arcidae	<i>Scapharca broughtonii</i> (Schrenck, 1867)	+--	-	0	-	100	-	0	-	0
	Callionymidae	<i>Callionymus beniteguri</i> (Jordan & Snyder, 1900	++++	+	14.63	-	3.84	+	63.85	+	17.68
	Clupeidae	<i>Konosirus punctatus</i> ((Temminck & Schlegel, 1846)	--+	-	0	-	0	+	100	-	0
		<i>Sardinella zunasi</i> (Bleeker, 1854)	--+	-	0	-	0	+	100	-	0
	Cynoglossidae	<i>Cynoglossus lighti</i> (Norman, 1925)	++++	+	20.85	+	24.24	+	18.43	+	36.48
		<i>Cynoglossus semilaevis</i> (Günther, 1873)	+--	-	46.67	-	0	-	53.33	-	0
	Engraulidae	<i>Coilia mystus</i> ((Linnaeus, 1758)	---+	-	0	-	100	-	0	-	0
		<i>Engraulis japonicus</i> (Temminck & Schlegel, 1846)	---+	-	0	+	1.32	+++++	93.25	+++	5.43
		<i>Thrissa kammalensis</i> (Bleeker, 1849)	+--	-	0	+	0	+	0	+	100
		<i>Thrissa mystax</i> (Bloch & Schneider, 1801)	---+	-	0	-	9.62	-	82.52	-	7.86
		<i>Setipinna taty</i> ((Valenciennes, 1848)	+--	-	1.61	+	81.92	+++	15.38	++	1.08
	Gobiidae	<i>Amblychaeturichthys hexanema</i> ((Bleeker, 1853)	++++	-	0.01	+	0.32	+++++	68.74	++++	30.93
		<i>Chaeturichthys stigmatias</i> (Richardson, 1844)	++++	+	6.91	-	0.18	++	57.36	++	35.55
		<i>Cryptocentrus filifer</i> ((Valenciennes, 1837)	++++	-	4.98	+	56.93	-	12.77	-	25.32
		<i>Ctenotrypauchen chinensis</i> (Steindachner, 1867)	+--	-	0	+	11.95	+	60.51	+	27.54
		<i>Odontamblyopus rubicundus</i> (Hamilton, 1822)	---+	-	0	-	10.99	-	80.63	-	8.36
		<i>Favonigobius gymnauchen</i> (Bleeker, 1860)	--+	-	0	-	0	-	100	-	0
		<i>Synechogobius hasta</i> (Temminck & Schlegel, 1845)	+--+	+	0	-	5.89	-	69.43	-	24.69
Hexagrammidae	<i>Hexagrammos otakii</i> (Jordan & Starks, 1895)	---+	-	0	+	82.61	-	8.70	-	8.70	
Hemiramphidae	<i>Hyporhamphus sajori</i> ((Temminck & Schlegel, 1846)	+--	-	100	-	0	-	0	-	0	
Liparidae	<i>Liparis tanakae</i> ((Gilbert & Burke, 1912)	+--+	-	0.06	+++	99.87	-	0	-	0.07	
Lophiidae	<i>Lophius litulon</i> ((Jordan, 1902)	+--	-	0	-	3.86	+	65.27	+	30.87	

	Family	Species name	Dist.	Winter		Spring		Summer		Autumn	
				N	%	N	%	N	%	N	%
	Monacanthidae	<i>Navodon septentrionalis</i> (Günther, 1874)	----	-	0	-	6.92	-	25.68	-	66.59
	Mugilidae	<i>Liza haematocheila</i> ((Temminck & Schlegel, 1845)	+---	-	100	-	0	-	0	-	0
	Paralichthyidae	<i>Paralichthys olivaceus</i> ((Temminck & Schlegel, 1846)	--+	-	0	-	99.97	-	0	-	0.03
	Pholidae	<i>Enedrias fangi</i> (Wang & Wang, 1935)	+++	-	0.38	+++	97.92	+	1.71	-	0
	Platycephalidae	<i>Platycephalus indicus</i> (Linnaeus, 1758)	+--	-	0	-	2.30	+	56.21	-	41.49
	Pleuronectidae	<i>Pseudopleuronectes yokohamae</i> (Günther, 1877)	----	-	0	-	0	-	100	-	0
	Rajidae	<i>Raja porosa</i> (Günther, 1874)	--+	-	0	-	77.89	-	22.11	-	0
	Salangidae	<i>Protosalanx chinensis</i> (Osbeck, 1765)	++++	+	50.13	-	100	+	0	+	0
	Sciaenidae	<i>Argyrosomus argentatus</i> (Houttuyn, 1782)	--+	-	0	-	0	+	100	-	0
		<i>Johnius belangerii</i> (Cuvier, 1830)	+--	-	0	-	35.48	-	64.52	-	0
		<i>Larimichthys polyactis</i> ((Bleeker, 1877)	--+	-	0	-	0	+	99.51	-	0.49
	Scombridae	<i>Scomber japonicus</i> (Houttuyn, 1782)	--+	-	0	-	0	+	100	-	0
		<i>Scomberomorus niphonius</i> (Cuvier, 1832)	--+	-	0	-	0	+	100	-	0
	Sebastidae	<i>Sebastes schlegeli</i> (Hilgendorf, 1880)	++++	-	0.67	+	6.16	+	92.78	-	0.39
	Stromateidae	<i>Pampus argenteus</i> (Euphrasen, 1788)	--+	-	0	-	100	-	0	-	0
	Syngnathidae	<i>Syngnathus acus</i> (Linnaeus, 1758)	----	-	65.32	-	0	-	5.99	-	28.69
	Tetraodontidae	<i>Takifugu vermicularis</i> (Temminck & Schlegel, 1850)	---+	-	0	-	0	-	90	-	10
	Trichiuridae	<i>Eupleurogrammus muticus</i> (Gray, 1831)	+--	-	0	-	13.90	+	56.95	+	29.15
	Zoarcidae	<i>Zoarcis elongates</i> (Kner, 1868)	----	-	0	-	100	-	0	-	0
Crustacean	Alpheidae	<i>Alpheus distinguendus</i> (de Man, 1909)	--+	-	0	-	0	+	6.16	+	93.84
		<i>Alpheus heterocarpus</i> (Yu, 1935)	+++	-	7.99	+	92.01	-	0	-	0
		<i>Alpheus japonicus</i> (Miers, 1879)	++++	+++	32.62	+	3.89	++	16.83	+++	46.65
	Cancridae	<i>Cancer gibbosulus</i> (De Haan, 1833)	+--	-	0	+	75.51	-	24.49	-	0
	Crangonidae	<i>Crangon affinis</i> (De Haan, 1849)	++++	+	6.04	++++	85.18	+	0.36	+	8.43
	Dorippidae	<i>Dorippe japonica</i> (von Seibold, 1824)	+++	-	0.62	-	2.13	+	97.25	-	0
	Euryplacidae	<i>Eucrate crenata</i> (De Haan, 1835)	--+	-	0	-	0	+	99.11	-	0.89
	Euphausiidae	<i>Euphausia pacifica</i> (Hansen, 1911)	----	-	0	-	0	-	0	-	0

	Family	Species name	Dist.	Winter		Spring		Summer		Autumn	
				N	%	N	%	N	%	N	%
	Goneplacidae	<i>Carcinoplax vestita</i> (De Haan, 1835)	++++	+	42.07	+	12.38	+	31.32	+	14.22
	Hemiramphidae	<i>Hyporhamphus limbatus</i> (Valenciennes, 1847)	+---	-	100	-	0	-	0	-	0
	Hippolytidae	<i>Latreutes anoplonyx</i> (Kemp, 1914)	+++--	+	71.79	+	28.21	-	0	-	0
		<i>Latreutes planirostris</i> (De Haan, 1844)	+++	-	0.42	-	0	+	92.29	+	7.28
	Paguridae	<i>Paguridae</i> (Latreille, 1802)	+++	-	0	+	21.23	+	5.89	-	26.84
	Leucosiidae	<i>Arcania heptacantha</i> (De Man, 1907)	--+	-	0	-	0	-	100	-	0
	Palaemonidae	<i>Palaemon gravieri</i> ((Yu, 1930)	++++	++	46.06	+	0	+	62.12	+	37.88
	Pasiphaeidae	<i>Leptochela gracilis</i> (Stimpson, 1860)	+++	-	0	+	13.10	+	0.35	++++	86.55
	Portunidae	<i>Charybdis bimaculata</i> (Miers, 1886)	++++	-	1.32	-	10.52	+	23.85	+	64.32
		<i>Charybdis japonica</i> (A. Milne-Edwards, 1861)	++++	-	0.40	-	4.62	+	94.51	-	0.46
		<i>Portunus trituberculatus</i> (Miers, 1876)	+++	-	0	-	4.23	+	22.07	+	23.57
	Penaeidae	<i>Fenneropenaeus chinensis</i> (Osbeck, 1765)	--+	-	0	-	0	+	100	-	0
		<i>Marsupenaeus japonicus</i> (Spence Bate, 1888)	--+	-	0	-	0	-	100	-	0
		<i>Metapenaeopsis dalei</i> ((Rathbun, 1902)	+++	-	0	-	9.27	-	0	+	90.73
		<i>Trachypenaeus curvirostris</i> (Balss, 1933)	+++	-	0	-	0	+	0	+	100
	Pinnotheridae	<i>Pinnotheridae</i> (De Haan, 1833)	+++	-	0	-	10.43	-	89.57	+	0
	Macrophthalmidae	<i>Tritodynamia rathbunae</i> (Shen, 1932)	+++	-	0	-	0.75	+	7.55	-	91.70
	Matutidae	<i>Matuta planipes</i> (Fabricius, 1798)	--+	-	0	-	0	+	100	-	0
	Sergestidae	<i>Acetes chinensis</i> (Hansen, 199)	++++	+++	62.64	+	7.28	+	15.73	+	14.35
	Squillidae	<i>Oratosquilla oratoria</i> (De Haan, 1844)	++++	-	0.03	+++	60.08	+++++	39.92	++	0
	Upogebiidae	<i>Austinogebia edulis</i> (Ngoc-Ho & Chan, 1992)	----	-	0	-	0.54	-	0.54	+	98.92
Mollusca	Hiatellidae	<i>Panopea abrupta</i> ((Conrad, 1849) †	+---	-	0	-	21.69	-	42.15	-	36.16
	Loliginidae	<i>Loligo japonica</i> (Hoyle, 1885)	++++	-	0.17	+	6.40	++++	76.82	++	16.61
	Muricidae	<i>Rapana venosa</i> ((Valenciennes, 1846)	+---	-	0	+	0	-	100	-	0
	Mytilidae	<i>Mytilus edulis</i> (Linnaeus, 1758)	+++	-	0	-	0	-	100	-	0
	Nassariidae	<i>Nassariidae</i> (Iredale, 1916 (1835))	--+	-	0	-	100	-	0	-	0
	Naticidae	<i>Glossaulax didyma</i> ((Röding, 1798)	++++	-	5.74	+	88.52	-	4.92	-	0.82

	Family	Species name	Dist.	Winter		Spring		Summer		Autumn	
				N	%	N	%	N	%	N	%
	Nautilidae	<i>Nautiloidea</i> sp.	-+-	-	0	-	0	-	50	-	50
	Octopodidae	<i>Octopus ocellatus</i> (Gray, 1849)	++++	-	0.81	+	45.61	+	34.20	+	15.20
		<i>Octopus variabilis</i> ((Sasaki, 1929)	++++	-	4.99	-	0	-	100	-	0
	Philinidae	<i>Philine kinglipini</i> (Tchang, 1934)	-++	-	0	++++	100	-	0	-	0
	Pinnidae	<i>Pinna rudis</i> (Linnaeus, 1758)	--+	-	0	-	0	-	0	-	100
	Sepiolidae	<i>Sepiola birostrata</i> (Sasaki, 1918)	++++	-	0	+	0	+	0	-	0
Echinod.	Asteriidae	<i>Asierias rollestoni</i> (Bell, 1881)	-+++	-	0	+	44.06	-	11.59	+	44.35
	Luidiidae	<i>Luidia yesoensis</i> (Goto, 1914)	+++	+	18.25	+	68.45	-	0	+	13.30
	Strongylocentrotidae	<i>Hemicentrotus pulcherrimus</i> (A. Agassiz, 1864)	-+-	+	25.37	+	6.06	-	0.38	+	68.19
	Scyphozoa (Class)	<i>Scyphozoa</i> sp.	++++	+	98	-	0	-	2	-	0

Text bold, dominant species; Dist., distribution: +, present; -, absent; N, average abundance: > 500, "+++++", > 200, "++++", > 100, "+++", > 50, "++", > 1, "+", "-"; %, frequency of occurrence

According to the frequency of occurrence of the dominant species, *Acetes chinensis*, *Palaemon gravieri*, and *Alpheus japonicus* were accounting for 62.64%, 46.06%, and 32.62%, respectively in the winter season (January) while *Crangon affinis* and *Oratosquilla oratoria* were accounting for 85.18% and 60.08%, respectively in the spring season (May). In the summer season (August) *Engraulis japonicus*, *Loligo japonica*, *Palaemon gravieri*, and *Oratosquilla oratoria* were accounting for 93.25%, 76.82%, 62.12%, and 39.92%, respectively whereas *Alpheus japonicus*, *Leptochela gracilis* and *Palaemon gravieri* were accounting for 46.65%, 86.55%, 37.88%, respectively in the autumn season (November) (Table 2 and Fig. 2).

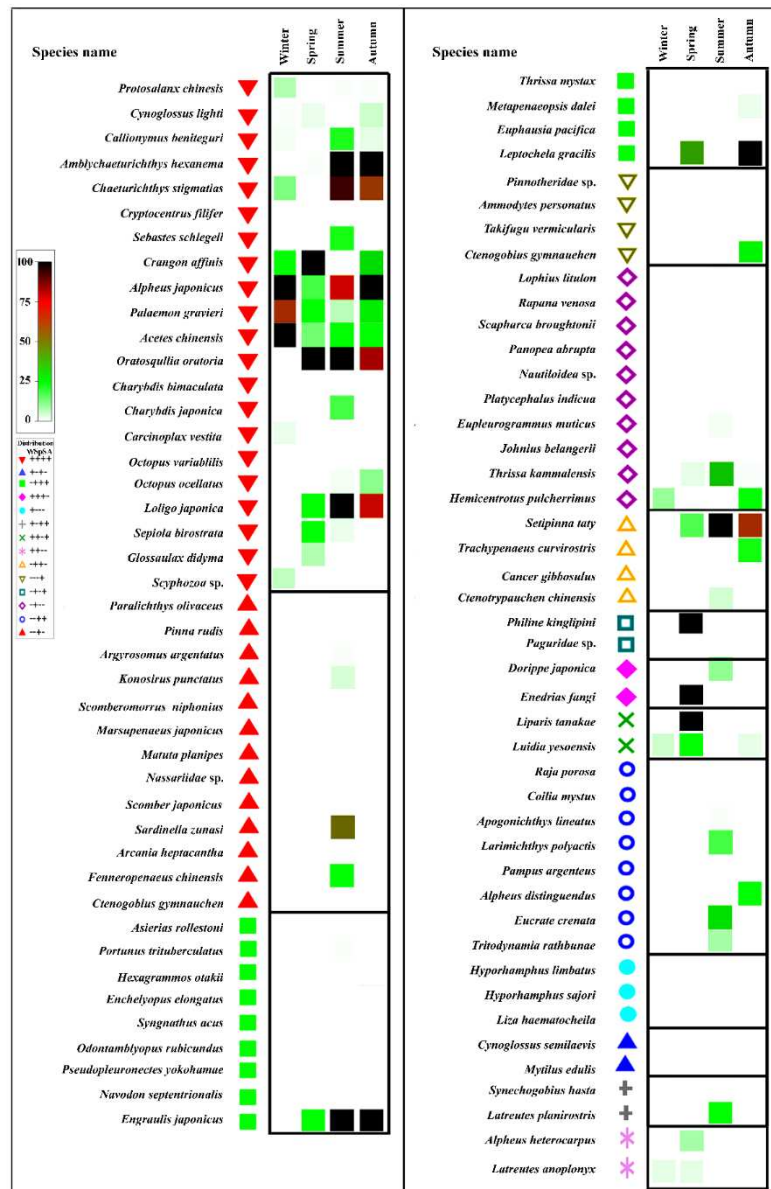


Figure 2. Shade plot showing the seasonal distribution pattern of fishery species in terms of their relative abundance during the study period in the Bohai Sea

Seasonal variation in fishery dynamics

In terms of abundance of dominant species per haul, the individual abundance found to be higher in the summer and lower in the winter (Fig. 3a). As to relative abundance, three species of crustaceans were predominant in the winter (*Alpheus japonicus*, *Acetes chinensis* and *Palaemon gravieri*); two species in the spring (*Crangos affinis* and *Oratosquilla oratoria*); two species in the summer (*Engraulis japonicus* and *Oratosquilla oratoria*); and two species in the autumn season (*Leptochela gracilis* and *Alpheus japonicus*) (Fig. 3b).

Based on species occurrence, the maximum species occurred in summer and autumn, whereas the minimum was in winter (Fig. 4a). For example, of these 88 species, 24 were occurred in summer and autumn, while only seven species were in winter. In terms of total abundance, the highest abundance recorded in summer, while the lowest was in winter (Fig. 4b).

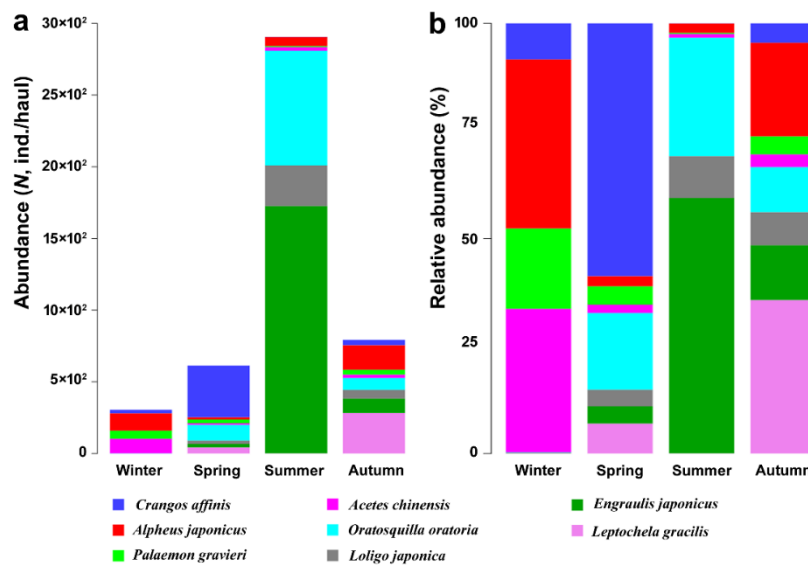


Figure 3. Variation in abundance and relative abundance of dominant species of fishery species during the study period in the Bohai Sea

The analysis of similarity (ANOSIM) revealed that there was a significant difference in fishery community structure between the four seasons (Global, $R = 0.467$, $P < 0.001$). Based on SIMPER analysis, seven typical species (*Crangon affinis*, *Enedrias fangi*, *Oratosquilla oratoria*, *Acetes chinensis*, *Alpheus japonicus*, *Liparis tanakae* and *Philine kinglipini*) driven 93.34% average dissimilarities between winter and spring seasons. Similarly, six species (*Engraulis japonicus*, *Oratosquilla oratoria*, *Loligo japonica*, *Alpheus japonicus*, *Acetes chinensis* and *Chaeturichthys stigmatias*) in winter and spring seasons (97.33%); eight species (*Leptochela gracilis*, *Alpheus japonicus*, *Acetes chinensis*, *Amblychaeturichthys hexanema*, *Engraulis japonicus*, *Setipinna taty*, *Palaemon gravieri*, and *Crangon affinis*) in winter and autumn seasons (90.37%); seven species (*Engraulis japonicus*, *Oratosquilla oratoria*, *Loligo japonica*, *Crangon affinis*, *Amblychaeturichthys hexanema*, *Setipinna taty* and *Enedrias fangi*) in spring and summer seasons (95.07); nine species (*Leptochela gracilis*, *Crangon affinis*,

Enedrias fangi, *Amblychaeturichthys hexanema*, *Oratosquilla oratoria*, *Liparis tanakae*, *Philine kinglipini*, *Alpheus japonicas* and *Engraulis japonicus*) in spring and autumn seasons (89.81%); and six species (*Engraulis japonicus*, *Oratosquilla oratoria*, *Loligo japonica*, *Amblychaeturichthys hexanema*, *Leptochela gracilis*, and *Setipinna taty*) in summer and autumn seasons (92.29%) (Table 3).

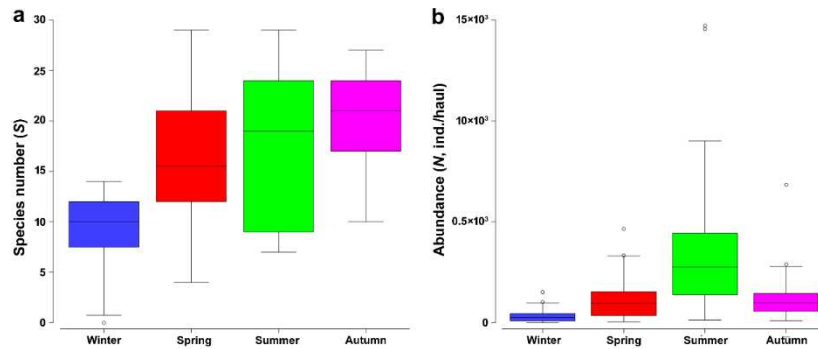


Figure 4. Seasonal variation in species number (a) and total abundance (b) in the fishery species during the study period in the Bohai Sea

Seasonal variation in diversity pattern of fishery species

Among the community parameters, the species richness showed increasing trend from winter to autumn season, with a higher value in the autumn and lower in winter while species evenness showed opposite that decreased from winter to summer, then again increased in autumn season with a value higher in winter and lower in summer season (Fig. 5a,b). The species diversity (H') and Simpson index ($1-\lambda'$) showed similar seasonal patterns and both indices values were higher in autumn and lower in the summer season (Fig. 5c,d).

In terms of fishery diversity status, there was a clear temporal variation revealed in the Bohai Sea during the study period (Fig. 5). For example, the highest value of species richness (3.79) was found in the autumn season whereas it was the lowest (1.65) in the winter with an average of 2.80 ± 0.59 . The species evenness was found to be maximum (0.95) in the winter season and minimum (0.18) in the summer season with an average of 0.63 ± 0.17 . The maximum species diversity index was (2.31) recorded in autumn season and minimum (0.57) was in summer season with an average of 1.82 ± 0.44 while Simpson index was found to be similar with diversity that was the highest (0.88) in autumn season and the lowest (0.18) in summer season with an average of 0.73 ± 0.18 (Fig. 5).

Patterns of community structural of fishery species

Principal analysis of coordinates (PCoA) summarized the seasonal structural variations in the fishery species. The first canonical axis (PCoA1) separated the samples in winter and spring (on the left) from those in summer and autumn (on the right), while the second canonical axis (PCoA2) discriminated the samples in winter and summer (upper) from those at the others two seasons spring and autumn (lower) (Fig. 6a).

Table 3. Results of the one-way analysis of similarity (ANOSIM) showing the significant differences and SIMPER results of the typical species driven the seasonal variation in the fishery species during the study period in the Bohai Sea

Global R=0.467, P=0.001	ANOSIM		Dissimilarity index from SIMPER		Cont. (%)
	R	P	Ave. Diss. (%)	Typical species	
Winter vs Spring	0.531	0.1	93.34	<i>Crangon affinis</i> <i>Enedrias fangi</i> <i>Oratosquilla oratoria</i> <i>Acetes chinensis</i> <i>Alpheus japonicas</i> <i>Liparis tanakae</i> <i>Philine kinglipini</i>	17.28 10.02 9.95 9.57 8.98 8.57 6.07
Winter vs Summer	0.593	0.1	97.33	<i>Engraulis japonicas</i> <i>Oratosquilla oratoria</i> <i>Loligo japonica</i> <i>Alpheus japonicas</i> <i>Acetes chinensis</i> <i>Chaeturichthys stigmatias</i>	27.82 18.46 12.25 5.17 5.09 5.04
Winter vs Autumn	0.485	0.1	90.37	<i>Leptochela gracilis</i> <i>Alpheus japonicas</i> <i>Acetes chinensis</i> <i>Amblychaeturichthys hexanema</i> <i>Engraulis japonicas</i> <i>Setipinna taty</i> <i>Palaemon gravieri</i> <i>Crangon affinis</i>	19.71 11.31 9.00 8.55 6.30 5.78 5.45 4.81
Spring vs Summer	0.449	0.1	95.07	<i>Engraulis japonicas</i> <i>Oratosquilla oratoria</i> <i>Loligo japonica</i> <i>Crangon affinis</i> <i>Amblychaeturichthys hexanema</i> <i>Setipinna taty</i> <i>Enedrias fangi</i>	23.82 17.22 9.56 8.22 4.84 4.69 4.65
Spring vs Autumn	0.369	0.1	89.81	<i>Leptochela gracilis</i> <i>Crangon affinis</i> <i>Enedrias fangi</i> <i>Amblychaeturichthys hexanema</i> <i>Oratosquilla oratoria</i> <i>Liparis tanakae</i> <i>Philine kinglipini</i> <i>Alpheus japonicas</i> <i>Engraulis japonicus</i>	15.11 13.55 7.47 7.01 6.87 5.84 5.46 5.41 5.23
Summer vs Autumn	0.359	0.1	92.29	<i>Engraulis japonicas</i> <i>Oratosquilla oratoria</i> <i>Loligo japonica</i> <i>Amblychaeturichthys hexanema</i> <i>Leptochela gracilis</i> <i>Setipinna taty</i>	24.26 16.48 9.74 9.52 9.02 6.27

Ave. Diss., average dissimilarity; Cont., contribution

Vector overlay of Pearson correlations of eight dominant species revealed that vectors of four species (*Engraulis japonicas*, *Oratosquilla oratoria*, *Loligo japonica* and *Leptochela gracilis*) pointed towards the sample clouds in summer season (upper right), three species (*Alpheus japonicas*, *Acetes chinensis* and *Palaemon gravieri*) of crustacean towards that in winter season (upper left), and one species (*Crangos affinis*) toward in spring season (lower left) (Fig. 6b).

A simple Pearson correlation among the eight dominant species was summarized in *Table 4* showed a significant correlation during the study period. Among these eight species, only four species showed significant correlations. For example, *Palaemon gravieri* showed a positively significant correlation with *Alpheus japonicus* ($r=0.427^{**}$, $P<0.01$) whereas *Loligo japonica* correlated with *Oratosquilla oratoria* ($r=0.517^{**}$, $P<0.01$) (*Table 4*).

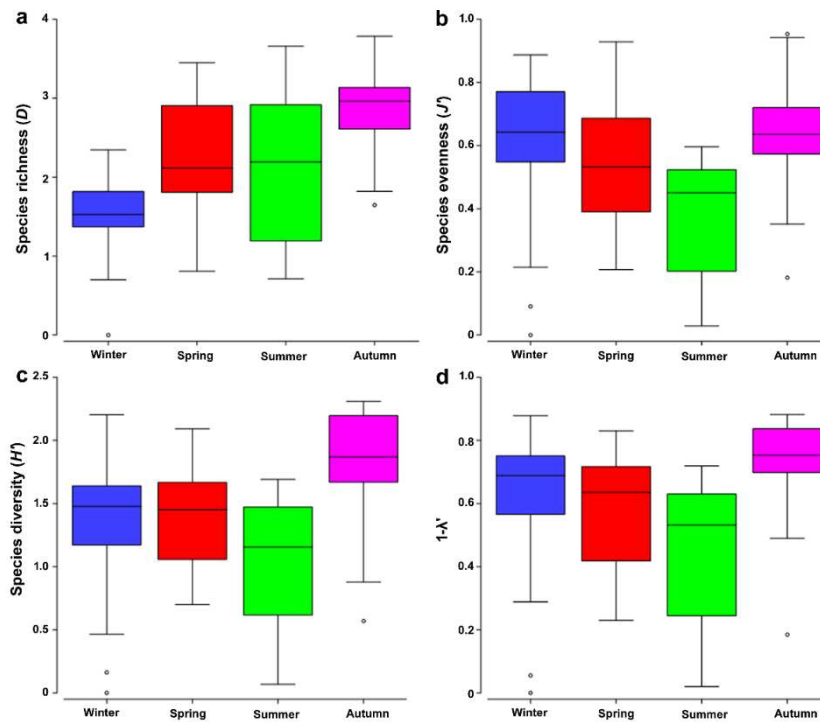


Figure 5. Variation in species richness (a), evenness (b), diversity (c) and Simpson index (d) during the study period in the Bohai Sea [Whiskers, minimum and maximum; boxes, $\pm 25\%$; lines, medians]

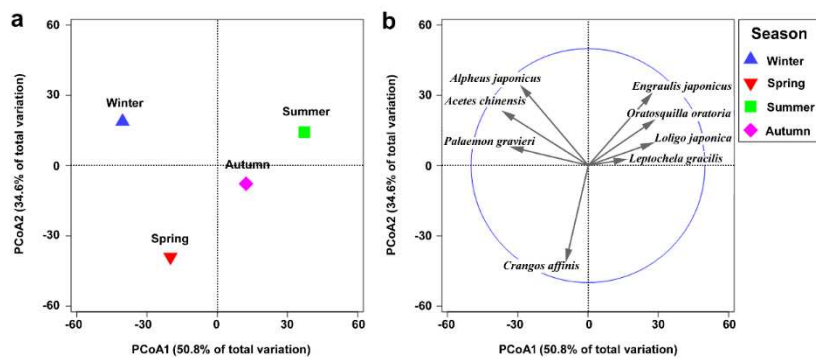


Figure 6. Principle coordinate analysis (PCoA) on Bray-Curtis similarities from square root transformed species abundance data (a); with vector correlation of eight dominant species with the PCoA axis (b), showing their seasonal variation in community structure of fishery species

Table 4. Pearson correlation coefficients among the eight dominant species during the study period in the Bohai Sea

	<i>Crangos affinis</i>	<i>Alpheus japonicus</i>	<i>Palaemon gravieri</i>	<i>Acetes chinensis</i>	<i>Oratosquilla oratoria</i>	<i>Loligo japonica</i>	<i>Engraulis japonicus</i>	<i>Leptochela gracilis</i>
<i>Crangos affinis</i>	1	-.090	.050	-.066	-.053	-.115	-.056	.005
<i>Alpheus japonicus</i>		1	.427**	-.073	.117	.142	-.064	-.065
<i>Palaemon gravieri</i>			1	-.040	-.110	-.149	-.119	.058
<i>Acetes chinensis</i>				1	-.031	-.040	-.067	-.058
<i>Oratosquilla oratoria</i>					1	.517**	-.075	-.110
<i>Loligo japonica</i>						1	-.061	-.129
<i>Engraulis japonicus</i>							1	-.068
<i>Leptochela gracilis</i>								1

Text bold, significant values; **, significant level at 0.05 ($P < 0.01$)

Discussion

The Bohai Sea is considered as an important fishery ground (i.e., spawning, nursing, and fishing) in northern China and the fishery resources have a dynamic nature (Chen et al., 1997; Deng and Jin, 2001). For instance, this shallow water mass used as an important migratory route for many marine species from the Yellow Sea (Liu, 1990). However, the increasing pressure of anthropogenic activities and climate variabilities have already altered the Bohai Sea ecosystem (Lin et al., 2001; Ning et al., 2010; Guo et al., 2013; Liu and Zhang, 2013; Pelling et al., 2013). Investigations have documented that change in climatic conditions and overfishing are the main drivers for fast-paced structural change in the marine ecosystem (Planque et al., 2010; Aschan et al., 2013; Rocha et al., 2015). In this study, we evaluated the characteristics of community structure and dynamics of fishery species in the Bohai Sea.

The Bohai Sea ecosystem is mainly composed of warm water and warm-temperate species. Previous research based on the ecotypes features (i.e., warm-water, warm-temperate, and cold-temperate species), a total of 97 fish species were reported over six decades where a rapid shifting of dominant species occurred (Shan et al., 2016). After 1982, both in the spring and summer season, the species of that ecotype decreased. In an earlier study in the Yellow River estuary of Laizhou Bay in the Bohai Sea, reported that 77 fish species were accounted for where eight pelagic fishes catch contributed more than 10% in every sampling year (Shan et al., 2013). The species composition changed during the survey periods in the Yellow River estuary. Another survey results in the Yellow and

Bohai Seas, reported a total of 126 species comprising 102 fishes, 17 crustaceans, five cephalopods and two medusas where *Acetes chinensis* was the most dominant in terms of biomass (Chen et al., 1997). Thirty-two crustacean species were enlisted, among them only single species *Crangon affinis* was the dominant species both in Yellow and Bohai Seas during the spring season (Wu et al., 2012). In our study results, *Crangon affinis* was found to be the dominant species which is consisted of previous research results. In addition, our present study found that major dominant species were belonging to crustacean group (*Alpheus japonicas*, 15.34%; *Oratosquilla oratoria*, 11.57%; *Palaemon gravieri*, 10.57%; *Crangon affinis*, 8.85%; *Acetes chinensis*, 7.53%; *Leptochela gracilis*, 7.19%) which clearly indicated the dominant fishery species shift in this ecosystem. The small-sized, pelagic fishes (*Engraulis japonicas*, 6.30%), and crustaceans' species prevailed in the Bohai Sea ecosystem were also reported (Xu and Jin, 2005; Wang et al., 2010; Li et al., 2013).

Based on species richness and total abundance, the maximum was recorded in the summer season. In addition, abundance of eight dominant species also showed similar community variation, thus might be due to variation in ecological conditions among the seasons. Several studies have stated that environmental factors (e.g., temperature, transparency, salinity, dissolved oxygen, nutrients, and water pH) can significantly influence the ecological condition of water in both temporal and spatial scales. Therefore, this ecological condition may shape the fishery species in the Bohai Sea ecosystem (Lin et al., 2001; Jin et al., 2013; Shan et al., 2016). The present study found that there was a significant seasonal shift of dominant fishery species which might be due to fluctuation of water parameters (e.g., temperature) over the decades (Jin 2004; Shan et al., 2016). Many studies showed that recent climate-change-induced variabilities negatively affected the pelagic fishery productivity (Jin et al., 2003; Stige et al., 2006; Perry et al., 2010). The changes in variabilities impede the supply of primary productivity and breakdown the interaction of the trophic levels. So the resultant of this lower food supply can affect the fishery recruitment patterns and dynamics by limiting species migration and shifting keystone species (Zhu and Tang, 2002; Ning et al., 2010) (Table 5).

Diversity indices are widely used in the representation of the homogeneity and heterogeneity of ecosystem status, such as existing fishery status on species levels (Shan et al., 2010a, 2011, 2013; Chen et al., 2018). Generally, higher indices values indicate a better environment/ecological quality status and represent a stable ecosystem condition (Chen et al., 1997; Shan et al., 2010b). In the present study we found, species richness, Simpson indices, and diversity were higher in the autumn season which indicated that the ecological condition of water was relatively favorable for fishery species in this season compared to the other three seasons. This variation might be occurred due to the fluctuation of water temperature in the Bohai Sea (Xia and Xiong, 2013). Besides, several anthropogenic stresses (e.g., both municipal/land-based pollution, beerier of natural water flow, coastal reclamation activities) have significant negative effects on fishery species composition and distribution (Zhao and Kong, 2000; Cui et al., 2005; Shan et al., 2013; Yan et al., 2013). In addition, changing of the ecological condition due to algal blooms in winter have a significant negative impact on fishery species was reported in elsewhere

which is consistent with the present study findings that fishery stock turns over in autumn season just after winter season (Wang et al., 2006; Tang et al., 2010). Thus, the findings of the present study suggest that the community patterns and dynamics structure of fishery species have closed interactions with climate and water ecological conditions in the Bohai Sea.

Multivariate analysis is a more useful tool than univariate analysis for summarizing the interaction of biotic communities with abiotic factors (Anderson et al., 2008; Clark and Gorley, 2015; Chen et al., 2018). Based on these strategies in the present study, PCoA (principal coordinates analysis) and ANOSIM (analysis of similarity) demonstrated that there was an apparent significant seasonal variation in community patterns and dynamics of fishery species in the Bohai Sea ecosystem. This variation is mainly driven by eight dominant species and their mutual interactions (*Table 4*) with typical species (*Table 3*).

Table 5. Fishery species composition in different studies in the Northwest Pacific Ocean

Location	Fishes	Crustaceans	Molluscs	Echinod.	Scyphozoan	References
Bohai Sea	43	29	12	3	1	Present study
Bohai Sea	97	-	-	-	-	Shan et al., 2016
Bohai Sea	75	10	6	-	-	Jin, 2004
Yellow River estuary ecosystem in the southern Bohai Sea	77	-	-	-	-	Shan et al., 2013
Yellow and Bohai Sea	102	17	5	-	2	Chen et al., 1997
Yellow Sea	214 (in 1959), 351 (in 1985)	-	-	-	-	Jin and Tang 1996
Middle Yellow Sea of Korea	40	22	17	2	-	Lee et al., 2010
East China Sea and southern Yellow Sea	149 (in autumn), 177 (in spring)	-	-	-	-	Jin et al., 2003
Middle continental shelf of the East China Sea	186	-	-	-	-	Shan et al., 2011

Conclusion

The shallow Bohai Sea ecosystem is used as a unique ground for spawning, feeding, and nursery for many commercial as well as ecological fishery species. The structural patterns and community dynamics of the fishery species in the Bohai Sea are complex and have complicated linked with multiple factors (e.g., pollution, overfishing, climate change, and water ecology). In our present study used a pair trawl survey data to observe the seasonal variation in community patterns and structural dynamics fishery species especially, their abundance, composition, distribution and dominant shift in the Bohai Sea. The community parameters mainly, species richness, diversity, and Simpson indices were higher in the autumn. Multivariate analyses revealed a significant seasonal variation in the fishery community structure patterns and structural dynamics. Our results suggest that ecological conditions may shape the community structure of fishery species in the Bohai

Sea. Although this study didn't include environmental and climate data, however, such results are important for fisheries assessment and maintaining sustainable fisheries management initiative. Moreover, further studies on the fishery community patterns based on climate and environmental observations are needed to verify this outcome.

Acknowledgments. The first author would like to express appreciation to the Chinese Scholarship Council (CSC) for sponsorship during his doctoral degree (CSC No. 2016GXY026). This work supported by the National Basic Research Program of China (No. 2015CB453303). The first author is very thankful and indebted to lab mates from both the Yellow Sea Fisheries Research Institute, Chinese Academy of Fishery Sciences and Laboratory of Fish Population Dynamics, Ocean University of China.

REFERENCES

- [1] Anderson, M. J., Gorley, R. N., Clarke, K. R. (2008): *PREMANOVA+ for PRIMER: Guide to software and statistical methods.* – PRIMER-E, Plymouth, UK: 1-214.
- [2] Aschan, M., Fossheim, M., Greenacre, M., Primicerio, R. (2013): Change in fish community structure in the Barents Sea. – *PLoS ONE* 8(4): e62748.
- [3] Chen, D., Liu, Q., Zeng, X., Su, Z. (1997): Catch composition and seasonal variation of setnet fisheries in the Yellow and Bohai Seas. – *Fisheries Research* 32: 61-68.
- [4] Chen, Y. L., Shan, X., Jin, X., Johannessen, A., Yang, T., Dai, F. (2018): Change in fish diversity and community in the central and southern Yellow Sea from 2003 to 2015. – *Chinese Journal of Oceanology and Limnology* 36(3): 805-817.
- [5] Clarke, R. K., Gorley, R. N. (2015): *PRIMER 7; User Manual/Tutorial.* – PRIMER-E Ltd, Plymouth, UK.
- [6] Cui, Y., Chen, B., Chen, J. (2005): Evaluation on self-pollution of marine culture in the Yellow Sea and Bohai Sea. – *Chinese Journal of Applied Ecology* 16: 180-185. (In Chinese).
- [7] Deng, J., Jin, X. (2001): Dynamic characteristics of abundance and community structure of fishery species in the overwintering ground of the Bohai Sea. – *Journal of Nature Resource* 16: 42-46.
- [8] Gao, X., Zhou, F., Chen, C. (2014): Pollution status of the Bohai Sea: An overview of the environmental quality assessment related trace metals. – *Environment International* 62: 12-30.
- [9] Guo, J., Liu, X., Xie, Q. (2013): Characteristics of the Bohai Sea oil spill and its impact on the Bohai Sea ecosystem. – *Chinese Science Bulletin* 58(19): 2276-2281.
- [10] Hu, L. M., Guo, Z. G., Shi, X. F., Qin, Y. W., Lei, K., Zhang, G. (2011): Temporal trends of aliphatic and polyaromatic hydrocarbons in the Bohai Sea, China: Evidence from the sedimentary record. – *Organic Geochemistry* 42: 1181-1193.
- [11] Jin, X., Xu, B., Tang, Q. (2003): Fish assemblage structure in the East China Sea and southern Yellow Sea during autumn and spring. – *Journal of Fish Biology* 62: 1194-1205.
- [12] Jin, X. S. (2004): Long-term changes in fish community structure in the Bohai Sea, China. – *Estuarine Coastal and Shelf Science* 59: 163-171.
- [13] Jin, X. S., Shan, X. J., Li, X. S., Wang, J., Cui, Y., Zuo, T. (2013): Long-term changes of fishery ecosystem in the Laizhou Bay. *Science in China.* – *Earth Science* 56: 366-374.
- [14] Lee, J.B., Lee, J.H., Shin, Y.J., Zhang, C.I., Cha, H.K. (2010): Seasonal variation of fisheries resources composition in the coastal ecosystem of the middle Yellow Sea of Korea. – *Journal of the Korean Society of Fisheries and Ocean Technology* 46 (2):126-138 (In Korean).

- [15] Li, X. S., Yu, Z. H., Sun, S., Jin, X. S. (2013): Ecological niche breadth and niche overlap of dominant species of fish assemblage in Yangtze River estuary and its adjacent waters. – *Chinese Journal of Applied Ecology* 24: 2353-2359.
- [16] Li, L., Cui, J., Liu, J., Gao, J., Bai, Y., Shi, X. (2016): Extensive study of potential harmful elements (Ag, As, Hg, Sb, and Se) in surface sediments of the Bohai Sea, China: Sources and environmental risks. – *Environmental Pollution* 219: 432-439.
- [17] Lin, C., Su, J., Xu, B., Tang, Q. (2001): Long-term variations of temperature and salinity of the Bohai Sea and their influence on its ecosystem. – *Progress in Oceanography* 49(1): 7-19.
- [18] Liu, X. (1990): Investigations and divisions of fishery resources in the Yellow Sea and Bohai Sea. – Ocean Press, Beijing, 295 pp. (In Chinese).
- [19] Liu, X., Wu, J., Han, G. (eds.) (1990): The fisheries resources investigation and division of Yellow and Bohai Seas. – Ocean Press, Beijing, 295 pp.
- [20] Liu, S., Lou, S., Kuang, C., Huang, W., Chen, W., Zhang, J. (2011): Water quality assessment by pollution-index method in the coastal waters of Hebei Province in western Bohai Sea, China. – *Marine Pollution Bulletin* 62(10): 2220-2229.
- [21] Liu, Q., Zhang, Q. (2013): Analysis on long-term change of sea surface temperature in the China seas. – *Journal of Ocean University of China (Oceanic and Coastal Sea Research)* 12(2): 295-300.
- [22] Liu, Y. Z., Shen, Y. L., Lv, X. Q., Liu, Q. (2017): Numeric modelling and risk assessment of pollutions in the Chinese Bohai Sea. – *Science China Earth Sciences* 60(8): 1546-1557.
- [23] Ning, X., Lin, C., Su, J., Liu, C., Hao, Q., Le, F., Tang, Q. (2010): Long-term environmental changes and the responses of the ecosystems in the Bohai Sea during 1960-1996. – *Deep-Sea Research Part II Topical Studies in Oceanography* 57: 1079-1091.
- [24] Pelling, H. E., Uehara, K., Green, J. A. M. (2013): The impact of rapid coastline changes and sea level rise on the tides in the Bohai Sea. – *Journal of Geophysical Research: Oceans* 118(7): 3462-3472.
- [25] Perry, R. I., Cury, P., Brander, K., Jennings, S., Mollmann, C., Planque, B. (2010): Sensitivity of marine systems to climate and fishing: Concepts, issues and management responses. – *Journal of Marine Systems* 79: 427-435.
- [26] Planque, B., Fromentin, J. M., Cury, P., Drinkwater, K. F., Jennings, S., Perry, R. I., Kifani, S. (2010): How does fishing alter marine populations and ecosystem sensitivity to climate? – *Journal of Marine Systems* 79(3-4): 403-417.
- [27] Rahman, M. F., Lin, Q., Shan, X. J., Chen, Y. L., Ding, X. S., Qun, L. (2019): Temporal changes of structure and functioning of the Bohai Sea ecosystem: Insights from Ecopath models. – *Thalassas: An International Journal of Marine Sciences* 35(2): 625-641.
- [28] Rocha, J., Yletyinen, J., Biggs, R., Blenckner, T., Peterson, G. (2015): Marine regime shifts: drivers and impacts on ecosystems services. – *Philosophical Transactions Royal Society B* 370: 20130273.
- [29] Shan, X. J., Jin, X., Wei, Y. (2010a): Taxonomic diversity of fish assemblages in the Changjiang Estuary and its adjacent waters. – *Acta Oceanologica Sinica* 29(2): 70-80.
- [30] Shan, X. J., Jin, X., Wei, Y. (2010b): Fish assemblage structure in the hypoxic zone in the Changjian (Yangtze River) estuary and its adjacent waters. – *Chinese Journal of Oceanology and Limnology* 28(3): 459-469.
- [31] Shan, X. J., Jin, X., Zhou, Z., Dai, F. (2011): Fish community diversity in the middle continental shelf of the East China Sea. – *Chinese Journal of Oceanology and Limnology* 29(6): 1199-1208.
- [32] Shan, X. J., Jin, X., Li, Z., Chen, Y., Dai, F. (2012): Fish community structure and stock dynamics of main releasing fish species in the Bohai Sea. – *Progress in Fishery Sciences* 33: 1-9.

- [33] Shan, X. J., Sun, P., Jin, X., Li, X., Dai, F. (2013): Long-term changes in fish assemblage structure in the Yellow River ecosystem, China. – *Marine and Coastal Fisheries: Dynamics, Management, and Ecosystem Science* 5: 65-78.
- [34] Shan, X. J., Jin, X., Dai, F., Chen, Y., Yang, T., Yao, J. (2016): Population dynamics of fish species in a marine ecosystem: A case study in the Bohai Sea, China. – *Marine and Coastal Fisheries: Dynamics, Management, and Ecosystem Science* 8: 100-117.
- [35] Song, J., Duan, L. (2018): The Bohai Sea. – In: Sheppard, C. (ed.) *World Seas: An Environmental Evaluation. Volume II: The Indian Ocean to the Pacific. Chapter 17, 2nd Edition, 5th September, 932 pp.*
- [36] Stige, L. C., Ottersen, G., Brander, K., Chan, K. S., Stenseth, N. C. (2006): Cod and climate: effect of the North Atlantic oscillation on recruitment in the North Atlantic. – *Marine Ecology Progress Series* 325: 227-241.
- [37] Tang, Q., Jin, X., Wang, J., Zhuang, Z., Cui, Y., Meng, T. (2003): Decadal scale variations of ecosystem productivity and control mechanisms in the Bohai Sea. – *Fisheries Oceanography* 12: 223-233.
- [38] Tang, Q., Su, J., Zhang, J. (2010): China GLOBEC II: a case study of the Yellow Sea and East China Sea ecosystem dynamics. – *Deep-Sea Research, Part II* 57: 993-995.
- [39] Wang, H., Yang, Z., Saito, Y., Liu, J., Sun, X. (2006): Interannual and seasonal variation of the Huanghe (Yellow River) water discharge over the past 50 years: connections to impacts from ENSO events and dams. – *Global and Planetary Change* 50: 212-225.
- [40] Wang, A. Y., Wan, R. J., Jin, X. S. (2010): Decadal variations of ichthyoplankton biodiversity in spring in Laizhou Bay of the Bohai Sea. – *Progress in Fishery Science* 31: 19-24.
- [41] Wu, Q., Wang, J., Li, Z., Chen, R., Sun, J., Jin, X. (2012): Spatial variation of crustacean community structure in Yellow Sea and Bohai Sea in Spring. – *Journal of Fisheries of China* 36(11): 1685.
- [42] Wu, J. Y., Xue, Y., Liu, X. X., Ren, Y. P., Wan, R. (2017): Long-term trends in the mean trophic level of marine fisheries in the Yellow Sea and Bohai Sea. – *Periodical of Ocean University of China* 47(11): 53-60. (In Chinese).
- [43] Xia, J., Xiong, X. J. (2013): Distributions and Seasonal Changes of Water Temperature in the Bohai Sea, Yellow Sea and East China Sea. – *Advances in Marine Science* 31(1): 55-68.
- [44] Xu, B., Jin, X. S. (2005): Variations in fish community structure during winter in the southern Yellow Sea over the period 1985–2002. – *Fisheries Research* 71: 79-91.
- [45] Yan, H. K., Wang, N., Yu, T. L., Fu, Q., Liang, C. (2013): Comparing effects of land reclamation techniques on water pollution and fishery loss for a large-scale offshore airport island in Jinzhou Bay, Bohai Sea, China. – *Marine Pollution Bulletin* 71(1-2): 29-40.
- [46] Yu, H. M., Bao, X. W., Lu, C. L., Chen, X., Kuang, L. (2009): Analyses of the long-term salinity variability in the Bohai Sea and the northern Huanghai (Yellow) Sea. – *Acta Oceanologica Sinica* 28(5): 1-8.
- [47] Zhang, Y. G., Guan, W., Li, C. P., Dong, L. J. (2002): A study on the exploitation and the sustainable utilization of marine resources in the Bohai Sea. – *Journal of Natural Resources* 17(6): 768-775. (In Chinese).
- [48] Zhang, B., Tang, Q. (2004): Study on trophic level of important resource species at high trophic levels in the Bohai Sea, Yellow Sea, and East China Sea. – *Advances in Marine Sciences* 22: 393-404.
- [49] Zhang, Z., Zhu, M., Wang, Z., Wang, J. (2006): Monitoring and managing pollution load in Bohai Sea PR China. – *Ocean & Coastal Management* 49(9-10): 706-716.
- [50] Zhang, B., Li, Z., Jin, X. (2012): Functional groups of fish assemblages and their major species in the Bohai Sea. – *Journal of Fisheries of China* 36: 64-72.

- [51] Zhao, Z., Kong, L. (2000): Environmental status quo and protection countermeasures in Bohai marine areas. – *Research of Marine Science* 13(2): 23-27.
- [52] Zhou, M., Yu, R., Meryl, W. (2013): Coastal eutrophication and its associated ecological and environmental problems. – In: *Ecosystem issues and policy options addressing the sustainable development of China's ocean and coasts*. China Council for International Cooperation on Environment and Development. China Environmental Press, Beijing. 47-61 pp.
- [53] Zhu, X. H., Tang, Q. S. (2002): Structuring dominant components within fish community in Bohai Sea ecosystem. – *Studia Marina Sinica* 44: 159-168.

PLUVIO-THERMAL CONDITIONS PERTAINING TO VEGETATION OF KEY CROPS IN SOUTHEASTERN POLAND 1901-2010

ZIERNICKA-WOJTASZEK, A.

*Department of Ecology, Climatology and Air Protection, Faculty of Environmental Engineering
and Land Surveying, University of Agriculture in Kraków
Al. Mickiewicza 24/28, 30-059 Kraków, Poland
(e-mail: a.ziernicka-wojtaszek@ar.krakow.pl)*

(Received 9th Jul 2019; accepted 16th Oct 2019)

Abstract. The aim of this article is to analyze the variability of current climate changes, as well as favorable and unfavorable trends in weather conditions for key crops in south-eastern Poland in the April-October period (1901-2010). The climate variability was analyzed for four time slices (climate normals): 1901-1930, 1931-1960, 1961-1990, and 1981-2010. The aforementioned slices include natural dry and wet cycles as well as cool and warm periods. Numerous weather bulletins and written accounts were used in this study, as well as mean area temperature values and precipitation totals. The data, especially from the last 30 years, implies that key crops will be less susceptible to heat related stress during spring months whilst becoming more susceptible to the precipitation deficit stress in the summer months (due to increased evaporation and the lack of a clear precipitation trend). The article also proves that climate analyses based on mean values recorded over an extended period of time are useful for characterizing current climate conditions in a historical context, but can neither be applied for forecasting purposes nor put to practical use.

Keywords: *the Subcarpathian voivodeship, plant vegetation, climate change, pluvio-thermal conditions, global warming*

Introduction

Due to natural climate variability, the characteristics that apply to resources, qualities and climatic hazards in a given region are assessed usually over a period of 30 years (climate normal recommended by the World Meteorological Organization). The World Meteorological Organization and its predecessor (the International Meteorological Organization) have initiated and coordinated the establishment of climate normals for its member states. This process started with the period 1901-1930 and continues today, with updates being made every 30 years such as 1931-1960, 1961-1990 (Arguez and Vose, 2011). This principle is not contradicted by long-term analyses of climate data as well as analyses of individual cases of extreme weather events that occur worldwide.

Owing to the clearly visible warming trend that has been observed in recent years and the intensifying process of global warming (Solomon et al., 2007; Milly et al., 2008) the idea to characterize current or future climate conditions by means of 30 year normals, is being questioned more and more often (Livezey et al., 2007). In the existing situation, in order to make the climate statistics more accurate, it becomes necessary to update climate normals not every 30 years, but every 10 years. For instance, instead of making 1991-2020 the next normal, the 1971-2000, and recently even 1981-2010 are being used. In order to obtain a broader temporal perspective, emission scenarios are elaborated by the IPCC (i.e. 2000 scenario), which are subsequently used by climate modelling centers as an integral component for predicting Earth's climate variability.

Natural climate variability and contemporary climate change affect certain aspects of the environment and human economic activity. In agriculture they lead to fluctuations of meteorological conditions during the vegetation period, which result in crop variability (Křen, 1995; Motha and Baier, 2005). In the past, variable weather conditions which often led to extreme events caused numerous crop failures. Long time ago scholars drew up chronicles of natural hazards that affected the Polish nation. The work of Bujak (1976) which analyzes periods: 1450 to 1700 and 1772-1848 for the Polish region of Galicia is worth mentioning at this point. A successful continuation of this trend in research, from the point of view of economic history, is presented in the study entitled *The History of the Climate of Galicia in the years 1848-1913* (Wnęk, 1999). The subtitle of this study is: *The Impact of Meteorological Phenomena on the Socio-economic Development of Galicia*. The author's decision to put meteorological phenomena first, indicates that such phenomena are far more destructive than other types of natural hazards. What is important, is that this study is based on instrumental data and emphasizes the climate's role in the nineteenth century society. It also shows the impact of the climate on plant production, price variations, and the mortality rate in Galicia.

The continuation of this trend in research is presented in the work of Zawora, who devised a calendar of meteorological conditions of the vegetation of crops in southeastern Poland in the years 1901-1990 (Zawora, 1993). The author of this study assigned intervals which are favorable or unfavorable in terms of excessive or insufficient precipitation, too high or too low temperatures and a combination of such elements, to each month of the vegetation period. This was possible thanks to the accounts provided by agricultural correspondents, who described the state of crops for each month of the vegetation period. The author treated this particular study as material for further climatic and agroclimatic studies. He did not carry out a periodization in the entire 90-year period either in terms of climatic or meteorological conditions of the vegetation of key crops. The presented study constitutes not only a continuation of studies by a 20-year extension period, (1991-2010) which is characterized by clear warming, but also provides a new viewpoint on climate conditions in this particular period and its impact on the meteorological conditions of vegetation. More recent research by other authors aim at being studies on the adaptation to climate extremes of some crop plant varieties, European varieties of wheat in particular (Mäkinen et al., 2018a,b; Kahiluoto et al., 2019). The forecasted climate, and environmental changes emphasise the need for plant breeding strategies which ensure both: a significant increase in crop potentials, and a resistance to extreme weather phenomena, such as heatwaves, late occurring frosts, and droughts (Stratonovitch and Semenov, 2015). It is noteworthy, that moderate climate areas with adequate conditions for vine cultivation are increasing (Machar et al., 2017).

The aim of this article, which simultaneously provides a new viewpoint on the studied period (110 years), is to present the frequency of both favorable and unfavorable meteorological conditions for key crops in the productive cycle in southeastern Poland. This analysis takes into account three different aspects: climate variability in selected time slices (1901-1930, 1931-1960, 1961-1990, 1971-2000 and 1981-2010), periods of wet-dry and warm-cool cycles, and, finally, an emphasis on the last 30 years, which are marked by a clearly increasing temperature trend (Kožuchowski and Żmudzka, 2001; IPCC, 2007; Żmudzka, 2009).

The authors propose two scientific hypotheses which can be phrased as follows: 1. The practical usability of climate studies, which are primarily based on standard values, can be limited by the periodicity of meteorological phenomena. 2. The progressing global warming, during its initial phase, leads to the improvement of the meteorological conditions of vegetation, whilst in the next stage (especially recent years), leads to the increasing frequency of dry periods despite the lack of clear trends regarding precipitation totals.

Materials and methods

The principle materials used in this study featured agriculture correspondent bulletins about the state of cultivation (qualifying levels 1-5), as well as other reports pertaining to the meteorological conditions of the vegetation of key crops. It should be noted that the crops have not been divided into cultivated plants' categories such as: winter crops, spring crops, root crops and productive grassland. The majority of the above-mentioned bulletins and reports were drawn up at the end of each month, and were successively published over a longer period of time in a wide variety of statistical, agrometeorological, and agricultural journals (Biuletyn Agrometeorologiczny, Biuletyn Państwowej Służby Hydrologiczno-Meteorologicznej, Doświadczalnictwo Rolnicze, Gazeta Rolnicza, Kwartalnik Statystyczny, Miesięcznik Statystyczny, Miesięczny Przegląd Agrometeorologiczny, Rolnik, System Monitoringu Suszy Rolniczej w Polsce (SMSR), Tygodnik Rolniczy, Wiadomości Korespondenta Rolnego GUS, Wiadomości Meteorologiczne PIM). In their original form, they focused on the four main plant groups: winter crops, spring crops, root crops and productive grassland, which clearly differed in terms of both thermal and pluvial requirements. The relationships between the aforementioned groups of plants were standardized having in mind the methodological rule, which can be expressed in the following way: climate variability during individual vegetation periods is superior to the requirements of specific cultivate plants.

The climate data were gathered throughout a 110-year period (1901-2010) which was analyzed during the vegetation period only i.e. April-October. Accounts pertaining to the state of crops were assembled at the end of each month, hence every year 7 reports were drawn up. The bulletins always pertained to administrative units. However, it should be noted that administrative divisions were changed 6 times during the studied period. Therefore, the authors of this article tried to modify the reports about cultivation state so that they fit into the current area of the Subcarpathian voivodeship which was implemented on January 1, 1999. The studied area can be assigned to temperate-transient climate type, which is influenced by oceanic air masses and an increasing continental impact (Obrębska-Starkłowa, 1977; Cebulak, 1992). In terms of the lie of the land, this area includes lowlands (the Sandomierz Basin), foothills and mountains (the Central and Eastern Beskid). The geographic coordinates of the extreme points are: 50°49' – 49°00'N, and 21°09' – 23°33'E (Fig. 1).

According to correspondents' accounts which pertain to the state of the crops at the end of each month, the pluvio-thermal conditions were labeled either as favorable or unfavorable. Among the unfavourable conditions, there are: too low temperature, very low precipitation, excessive precipitation, too low temperature combined with excessive precipitation, very low temperature and precipitation, and finally very high temperature combined with insufficient precipitation. The classification of favorable and

unfavorable pluvio-thermal conditions was based exclusively on the correspondents' accounts rather than on temperature or precipitation values (Zawora, 1993).

Apart from the calendar pertaining to meteorological conditions of vegetation of key crops, the authors also devised a pluvio-thermal calendar for the studied period (1901-2010), valid for vegetation period (April-October). They were mean area values for the studied area coming from 7 weather stations with long time observation stretches, taking into account the appropriate corrections resulting from the differences in the values of the meteorological elements, between the values from several weather stations, and from several dozens weather stations evenly distributed throughout the area. The homogeneity of the data was verified on the basis of two methods: difference stability (for temperature) and quotient stability (for precipitation).

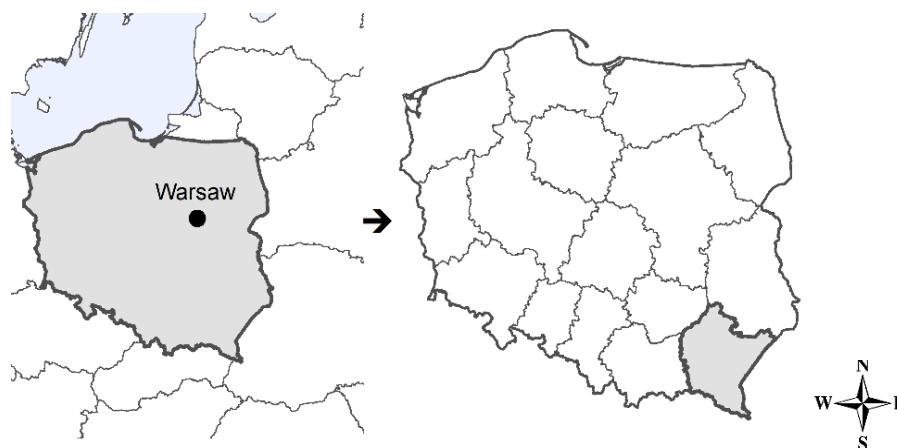


Figure 1. Area of investigations

The principle research method featured the comparison of the frequency of favorable and unfavorable pluvio-thermal conditions which pertain to the vegetation of key crops during the following climate normals: 1901-1930, 1931-1960, 1961-1990 and 1981-2010. The authors also carried out a comparison of the meteorological conditions and their changes over a longer period of time (such as 1901-1941 and 1942-1964). A detailed analysis of these changes and trends was included with reference to the last three decades (1981-2010), which is simultaneously the current climate normal, and a period of an intensified air temperature increase worldwide.

Results

In the period 1901-1930 favorable meteorological conditions for vegetation occurred with a 46% frequency. In the beginning of the vegetation period (April) such conditions were observed every three years. The primary limiting factors were very cold temperatures (20%), frequently combined with excessive precipitation (20%). Meteorological conditions during the vegetation period improved in the subsequent months, however they deteriorated again in September and October. In May, an important limiting factor were the dry conditions (23%), while in July - excessive precipitation (17%) often combined with very cold temperatures. In the remaining months one of the most unfavorable factors for the vegetation of plants was excessive precipitation (*Table 1*).

The characteristics of the 1901-1930 period reveal that it was cold and wet compared to the subsequent 1931-1960 period. The temperature mean during the vegetation period was 12.7°C and the precipitation total equaled 532 mm (1901-1930). The subsequent 30-year period was warmer and dryer. The vegetation period temperature mean reached 13.3°C and the precipitation total dropped to 496 mm. This gradually improved the vegetation of key crops. Also the frequency of months with favorable pluvio-thermal conditions increased from 46 to 53%. The percentage of very cold temperatures during April and May decreased by nearly half in the second 30-year period. In the month of June very cold temperatures were not observed during the 1931-1960 period. In general, the frequency of occurrence of dry months increased during the vegetation period from 15 to 20%. In contrast, the frequency of excessive precipitation decreased from 16 to 12%, and cases of excessive precipitation combined with too low temperature decreased by half (12 to 6%, *Tables 1 and 2*).

Table 1. The frequency of occurrence of favorable and unfavorable pluvio-thermal conditions for the vegetation of key crops in southeastern Poland in the period 1901-1930 (%)

Meteorological conditions of vegetation	Month							
	IV	V	VI	VII	VIII	IX	X	IV-X
Favorable thermal and pluvial conditions	33	50	47	50	63	43	33	46
Too low temperature	20	7	10	-	-	-	-	5
Insufficient precipitation	7	23	10	13	7	27	20	15
Excessive precipitation	7	-	3	17	23	27	37	16
Too low temperatures and excessive precipitation	20	13	13	17	7	3	7	12
Too low temperatures and insufficient precipitation	7	7	10	-	-	-	-	3
Too high temperatures and insufficient precipitation	6	-	7	3	-	-	3	3

Table 2. The frequency of occurrence of favorable and unfavorable pluvio-thermal conditions for the vegetation of key crops in southeastern Poland in the period 1931-1960 (%)

Meteorological conditions of vegetation	Month							
	IV	V	VI	VII	VIII	IX	X	IV-X
Favorable thermal and pluvial conditions	53	37	74	60	44	64	40	53
Too low temperature	10	3	-	-	-	-	-	2
Insufficient precipitation	7	17	17	23	30	23	23	20
Excessive precipitation	-	-	3	10	23	7	37	12
Too low temperatures and excessive precipitation	17	17	3	-	3	3	-	6
Too low temperatures and insufficient precipitation	3	10	3	-	-	-	-	2
Too high temperatures and insufficient precipitation	10	16	-	7	-	3	-	5

The period 1961-1990 with a mean temperature of 13.0°C is ranked between the first and second period. The precipitation total during the 1961-1990 period was 509 mm and was only 13 mm higher than during the previous period and 23 mm lower than during the 1901-1930 period. It should be noted, that the 1971-1980 decade was quite cold and wet. The meteorological conditions of vegetation deteriorated slightly compared with the previous 30-year period. Favorable meteorological conditions were

observed during 50% of the time from April to October. In general, the frequency of occurrence of unfavorable conditions during the 1961-1990 period was intermediate compared to the cold and wet 1901-1930 period, and, the warm and dryer 1931-1960 period. Only the frequency of occurrence of cold months was similar to the 1901-1930 period. Specifically, April was not as cool as during the 1901-1930 period, whilst the frequency of very cold temperatures was observed from April until July. One of the features of this period is the lowest occurrence of very dry and extremely hot months compared to individual decades in the years 1901-1960 (*Tables 1-3*).

Table 3. *The frequency of occurrence of favorable and unfavorable pluvio-thermal conditions for the vegetation of key crops in southeastern Poland in the period 1961-1990 (%)*

Meteorological conditions of vegetation	Month							
	IV	V	VI	VII	VIII	IX	X	IV-X
Favorable thermal and pluvial conditions	38	53	54	56	57	50	43	50
Too low temperature	13	7	7	7	-	-	-	5
Insufficient precipitation	10	13	13	10	17	20	37	17
Excessive precipitation	13	3	-	10	20	30	20	14
Too low temperatures and excessive precipitation	13	17	20	17	3	-	-	10
Too low temperatures and insufficient precipitation	10	7	3	-	3	-	-	3
Too high temperatures and insufficient precipitation	3	-	3	-	-	-	-	1

As noted at the beginning of this article, after 1961-1990, climate normals are changed every 10 years so they include for example periods: 1971-2000 and 1981-2010. The climate normal 1971-2000 should be omitted since it includes 20 years that overlap with each of the two above-mentioned periods. On the other hand, we should thoroughly analyze the recent 1981-2010 normal, since the last three decades were marked by an increasing warming occurring worldwide. In this particular period, the vegetation period temperature mean was highest 13.7°C, whilst precipitation totals were identical as in the 1961-1990 period (509 mm). A further improvement of meteorological conditions was observed during the vegetation period, and this fact was confirmed by a 57% monthly increase in favorable conditions. This of course is the highest frequency among all the analyzed 30-year periods. On the other hand, the frequency of cold months decreased, especially in April and May. The frequency of occurrence of relatively dry months increased, especially in the case of dry months combined with extremely high temperatures. It should be emphasized, that the frequency of dry months with very high temperatures increased dramatically. During the previous 30-year periods, such months occurred sporadically, whilst in the 1981-2010 period they occurred in every month of the vegetation period. They occurred with most intensity during the summer months (10% frequency, *Table 4*).

A very interesting aspect can be seen when we examine the evolution of meteorological conditions of vegetation in the period 1981-2010. As a rule, the closer we get to the end of the vegetation period, the more it turns out that the frequency of favorable meteorological conditions gradually decreases in the subsequent 30-year periods (57, 55, 53%, respectively). This is caused by the increasing frequency of dry periods, especially ones that are due to the increasing number of dry periods and, especially, to the occurrence of extreme temperature events (*Table 5*).

Table 4. The frequency of occurrence of favorable and unfavorable pluvio-thermal conditions for the vegetation of key crops in southeastern Poland in the period 1981-2010 (%)

Meteorological conditions of vegetation	Month							
	IV	V	VI	VII	VIII	IX	X	IV-X
Favorable thermal and pluvial conditions	67	67	59	51	53	50	50	57
Too low temperature	7	3	7	-	-	-	-	3
Insufficient precipitation	10	13	13	13	24	17	23	16
Excessive precipitation	3	7	7	23	13	27	13	13
Too low temperatures and excessive precipitation	3	7	7	3	-	3	7	4
Too low temperatures and insufficient precipitation	7	-	-	-	-	-	-	1
Too high temperatures and insufficient precipitation	3	3	7	10	10	3	7	6

Table 5. A comparison of the frequency of occurrence of favorable and unfavorable pluvio-thermal conditions during the vegetation of key crops in southeastern Poland in the periods: 1981-2010, 1991-2010 and 2001-2010 (%)

Meteorological conditions of vegetation	Period		
	1981-2010	1991-2010	2001-2010
Favorable thermal and pluvial conditions	57	55	53
Too low temperature	3	2	1
Insufficient precipitation	16	14	14
Excessive precipitation	13	17	19
Too low temperatures and excessive precipitation	4	3	-
Too low temperatures and insufficient precipitation	1	-	-
Too high temperatures and insufficient precipitation	6	9	13

The comparison of the frequency of occurrence of favorable and unfavorable pluvio-thermal conditions of vegetation of key crops in the period 1901-1980 (before rapid warming) and 1981-2010 (rapid warming phase), indicates that the frequency varies at the significance level $\alpha = 0,1\%$ in the months April, May and July and at the significance level 1% in August. In June and September, the differences are not statistically significant.

Discussion

The analysis of the frequency of occurrence of favorable pluvio-thermal conditions enables us to calculate mean optimal temperature values and precipitation totals for the relevant months, as well as to designate optimal value intervals. The difference between mean values of meteorological components and their optimal values constitutes both deficits and surpluses in terms of precipitation totals and temperature. The second problem that can be solved here, (in other words: the second methodological approach) is the calculation of the aforementioned deficits and surpluses by employing natural climate cycles (occurrence of dry-wet or warm-cool conditions). The idea behind such type of analysis can be explained by the example mentioned below.

During the post-war period a study was published, commissioned by the Main Spatial Planning Office, concerning the deficits and surpluses of atmospheric precipitation in individual Polish voivodeships (Hohendorf, 1948). The study period was 40 years long (1890-1930). Precipitation surpluses during the vegetation period in the former Rzeszów voivodeship equaled: for grains (103 mm), for beetroot (65 mm), for potatoes (93 mm), whilst for grassland there was a deficit equaled to 52 mm. If we assume an equal area for all of the aforementioned crops, this gives us an average surplus of 52 mm. Based on the analysis of data presented in the above-mentioned publication, the authors of this article suggest that the mean precipitation deficit for all studied crops in the period 1901-1941 (with optimal precipitation equal to 538 mm and 488 mm) could be estimated at about 50 mm. Therefore, this is the same order of magnitude as in Hohendorf's work, which, by the way, was conducted in a similar time period and in an area of about the same size.

If Hohendorf's research results had been used as indications for the planned irrigation projects, then the practical usage of this study comprised the post war years, which were marked by increasing levels of agrotechnics. In addition, this period was clearly marked by dry conditions (1941-1964). The precipitation total in the Rzeszów voivodeship equaled 455 mm, but the optimal precipitation increased due to the increasing temperature and the increasing level of agrotechnics (507 mm). As a result, the precipitation deficit during the vegetation period dropped to 52 mm. It should be noted, that during this period irrigation should have been employed instead of dehydration.

In this particular case, we are dealing with an adequate study assessment from a *post factum* perspective. This is due to the fact that a natural climate variability occurred after the study period, and we can expect possible consequences of these changes. Natural climate fluctuations also do not appear in elaborations that consist of data collected over long periods of time, as in the case of the aforementioned calendar of the meteorological conditions of key crops in southeastern Poland (Zawora, 1993). At present, when the anthropogenic factor of global warming is extensively mentioned in scientific studies, an assumption is made, that the analyses which pertain to present climate conditions need to be supplemented by basic climate forecasts (Górski, 2007; Górski and Kozyra, 2011).

There exist numerous scientific studies which present future visions of climate and selected causes of changes based on different climate change scenarios (IPCC, 2012, 2014a,b, 2018). The construction of such concepts is associated with a large degree of uncertainty, because each climate scenario is based on the fact that greenhouse gas emissions will increase depending on three factors: demographic development, implemented technology and assumed world economic development. At the same time, there is a large number of climate characteristics available, such as climate atlases that are based on past data, which are frequently out of date. This article attempts to eliminate such flaws, as well as present a description of contemporary agroclimate with reference to changes that have taken place since the beginnings of the twentieth century.

This study comprises simplifications, generalizations and shortcomings that can be supplemented in subsequent phases of this project. We can mention here such future suggestions as: the inclusion of the winter season, a variability analysis pertaining to yields of individual crop types (taking into account changing level of agrotechnics), the inclusion of meteorological conditions during field works, soil diversity, regional diversity of a given phenomenon. Conversely, a similar study or research could be carried out for individual physiographic regions or administrative units throughout Poland.

Conclusions

1. Large natural climate variability, periodicity and climatic fluctuations enable us to claim that 30-year climate normals are not always a relevant period for climate characteristics in terms of performed and projected climate irrigation projects as well as adaptation activities in terms of unfavorable meteorological conditions and future climate change. Better results are obtained when we include natural periods of temperature and precipitation variability.

2. Progressing global warming has generally improved meteorological conditions of vegetation of major crops. The frequency of occurrence of favorable months has increased from 46% (1901-1930) to 57% in 1981-2010. The amelioration of meteorological conditions is mainly due to a decrease in the frequency of cool months and cool and wet months in the beginning of the vegetation period.

3. The last 30-year period (1981-2010), which is simultaneously the new obligatory climate normal as well as a period with a clear increase in temperature (with lack of precipitation trend) is marked by a gradual decrease in favorable conditions for vegetation and a simultaneous increase in unfavorable conditions caused by the increased frequency of excessive precipitation and dry periods (caused mainly by occurrence of extremely high temperatures).

Acknowledgements. The research was carried out under Project No. DS-3337/KEKiOP/2018 financed from a research grant allocated by the Ministry of Science and Higher Education.

REFERENCES

- [1] Arguez, A., Vose, R. S. (2011): The Definition of the Standard WMO Climate Normal: The Key to Deriving Alternative Climate Normals. – *Bulletin of the American Meteorological Society* 92: 699-704.
- [2] Bujak, F. (1976): Selection of Articles. – Madurowicz-Urbańska, H. (ed.) Warszawa. (in Polish).
- [3] Cebulak, E. (1992): Maximum Daily Precipitation Totals in the Upper Vistula River Basin. – *Zeszyty Naukowe UJ, Prace Geograficzne* 90: 79-96. (in Polish).
- [4] Górski, T. (2007): Changes in Poland's Agroclimatic Conditions Over the Last Century. – *Papers on Global Change IG BP PAS* 14: 55-67.
- [5] Górski, T., Kozyra, J. (2011): Agroclimatic Normal of Air Temperature Mean in Poland in the Years 2011-2020. – *Polish Journal of Agronomy* 5: 21-28. (in Polish).
- [6] Hohendorf, E. (1948): Precipitation Surpluses and Deficits in Poland. – *Gospodarka Wodna* 10: 276-287. (in Polish).
- [7] IPCC. (2000): Emissions Scenarios. – A Special Report of IPCC Working Group III. Summary for Policymakers. Intergovernmental Panel on Climate Change.
- [8] IPCC. (2007): Climate Change 2007. The Physical Science Basis. – Summary for Policymakers. Contribution of Working Group I to the Fourth Assessment Report of the Intergovernmental Panel on Climate Change.
- [9] IPCC. (2012): Managing the Risks of Extreme Events and Disasters to Advance Climate Change Adaptation. – Field, C. B., Barros, V., Stocker, T. F., Dahe, Q. (eds.) <https://doi.org/10.1017/CBO9781139177245>.
- [10] IPCC. (2014a): Climate Change 2014 Synthesis Report. – Retrieved from <https://www.ipcc.ch/report/ar5/syr/>.

- [11] IPCC. (2014b): Impacts, Adaptation, and Vulnerability. – Summary for Policymakers. Contribution of Working Group II to the Fifth Assessment Report of the Intergovernmental Panel on Climate Change. IPCC.
- [12] IPCC. (2018): Global Warming of 1.5°C. – Summary for Policymakers. An IPCC Special Report on the Impacts of Global Warming of 1.5°C Above Pre-industrial Levels and Related Global Greenhouse Gas Emission Pathways, in the Context of Strengthening the Global Response to the Threat of Climate Change. Retrieved from <http://www.ipcc.ch/report/sr15/>.
- [13] Kahiluoto, H., Kaseva, J., Balek, J., Olesen, J. E., Ruiz-Ramos, M., Gobin, A., Kersebaum, K. C., Takáč, J., Ruget, F., Ferrise, R., Bezak, P., Capellades, G., Dibari, C., Mäkinen, H., Nendel, C., Ventrella, D., Rodríguez, A., Bindi, M., Trnka, M. (2019): Decline in Climate Resilience of European Wheat. – *Proceeding of the National Academy of Science of the United States of America* 116(1): 123-128.
- [14] Kożuchowski, K., Żmudzka, E. (2001): Climate Warming in Poland: the Range and Seasonality of the Changes in Air Temperature in the Second Half of the 20th Century. – *Przegląd Geofizyczny* 46(1-2): 81-90. (in Polish).
- [15] Křen, J. (1995): Production and Demand Trends of Small Grain Cereals in the Czech Republic. – *Fragmenta Agronomica* 2(46): 20-25.
- [16] Livezey, R. E., Vinnikov, K. Y., Timofeyeva, M. M., Tinker, R., van den Dool, H. M. (2007): Estimation and Extrapolation of Climate Normals and Climatic Trends. – *Journal of Applied Meteorology and Climatology* 46: 1759-1776.
- [17] Machar, I., Vlčková, V., Buček, A., Vrublová, K., Filippovová, J., Brus, J. (2017): Environmental Modelling of Climate Change Impact on Grapevines: Case Study from the Czech Republic. – *Polish Journal of Environmental Studies* 26(4): 1927-1934.
- [18] Mäkinen, H., Kaseva, J., Trnka, M., Balek, J., Kersebaum, K. C., Nendel, C., Gobin, A., Olesen, J. E., Bindi, M., Ferrise, R., Moriondo, M., Rodríguez, A., Ruiz-Ramos, M., Takáč, J., Bezák, P., Ventrella, D., Ruget, F., Capellades, G., Kahiluoto, H. (2018a): Sensitivity of European Wheat to Extreme Weather. – *Field Crops Research* 222: 209-217.
- [19] Mäkinen, H., Kaseva, J., Virkajärvi, P., Kahiluoto, H. (2018b): Gaps in the Capacity of Modern Forage Crops to Adapt to the Changing Climate in Northern Europe. – *Mitigation and Adaptation Strategies for Global Change* 23(1): 81-100.
- [20] Milly, P. C. D., Betancourt, J., Falkenmark, M., Hirsch, R. M., Kundzewicz, Z. W., Lettenmaier, D. P., Stouffer, R. J. (2008): Stationarity is Dead: Whither Water Management? – *Science* 319: 573-574.
- [21] Motha, R. P., Baier, W. (2005): Impact of Present and Future Climate Change and Climate Variability on Agriculture in the Temperate Regions: North America. – *Climatic Change* 70: 137-164.
- [22] Obrębska-Starkłowa, B. (1977): Feno-climatic Regionalization and Typology Based on the Upper Vistula River Basin Example. – *Rozprawy habilitacyjne UJ*, 11. (in Polish).
- [23] Solomon, S., Qin, D., Manning, M., Chen, Z., Marquis, M., Averyt, K. B., Tignor, M., Miller, H. L. (eds.) (2007): *Climate Change 2007: The Physical Science Basis*. – Cambridge University Press, 996 pp.
- [24] Stratonovitch, P., Semenov, M. A. (2015): Heat Tolerance Around Flowering in Wheat Identified as a Key Trait for Increased Yield Potential in Europe Under Climate Change. – *Journal of Experimental Botany* 66(12): 3599-3609.
- [25] Wnęk, K. (1999): *History of the Climate of Galicia in the Period 1848-1913: The Impact of Meteorological Phenomena on the Socio-economic Development of Galicia*. – *Historia Jagiellonica*, Kraków. (in Polish).
- [26] Zawora, T. (1993): *Calendar of Meteorological Conditions Affecting Vegetation of the Cultivated Plants in Southeastern Poland Over 1901-1990*. – *Zeszyty Naukowe UJ, Prace Geograficzne* 95: 223-227. (in Polish).
- [27] Żmudzka, E. (2009): Contemporary Changes of Climate of Poland. – *Acta Agrophysica* 13(2): 555-568. (in Polish).

EFFECT OF SEED PRIMING TREATMENT ON THE PHYSIOLOGICAL QUALITY OF NATURALLY AGED ONION (*ALLIUM CEPA* L.) SEEDS

BRAR, N. S.¹ – KAUSHIK, P.^{2,3*} – DUDI, B. S.⁴

¹*Department of Vegetable Science, Punjab Agricultural University, Ludhiana 141 004, India*

²*Instituto de Conservación y Mejora de la Agrodiversidad Valenciana, Universitat Politècnica de València, Valencia 46022, Spain*

³*Nagano University, 1088 Komaki, Ueda, Nagano 386-0031, Japan*

⁴*Department of Vegetable Science, CCS Haryana Agricultural University, Hisar 125001, India*

**Corresponding author*

e-mail: prakau@doctor.upv.es, prashantumri@gmail.com; phone: +34-96-387-7000

(Received 10th Jul 2019; accepted 11th Dec 2019)

Abstract. The experiment was conducted to investigate the effect of priming treatments on the physiological parameters of naturally aged onion (*Allium cepa* L.) seed, six seed priming treatments viz., Control, Hydro priming followed by dry dressing with Thiram (2 g/kg), Hydration with GA₃ (50 ppm), Hydration with KNO₃ (0.5% solution), Hydration with KH₂PO₄ (0.5% solution), and Biofertilizer (*Azotobacter*) were analyzed to identify the most suitable priming treatment. The standard seed germination, seedling length, seedling dry weight, seed vigour index-I & II and viability test (Tz test), decreased significantly, while electrical conductivity increased with the advancement of the ageing period. The field parameters viz., seedling emergence index and seedling establishment also decreased significantly with the natural ageing of seeds. The seed quality improvement through seed priming was noticed more in marginal seed lot, i.e., one-year-old seed lot. Among various priming treatments, hydration with GA₃ @ 50 PPM followed by biofertilizer, (*Azotobacter*) performed best in enhancing all seed vigour and viability characteristics and lowering the electrical conductivity of naturally aged onion seeds. In conclusion, the present study revealed that onion seed loses its viability rapidly under ambient storage conditions. Therefore, seed priming with GA₃ @ 50 ppm and biofertilizer, (*Azotobacter*) can be used effectively to enhance its vigour and viability. These priming treatments can aid to improve the quality of seed stored for one year, thus ensuring good plant stands from the stored seed of a poor storer crop.

Keywords: *onion, GA₃, Azotobacter, germination, viability, seedling emergence index*

Introduction

Onion (*Allium cepa* L.) is a bulb crop of worldwide importance. India ranks first in the cultivated area with 1.31 million ha but ranks second in terms of total production (22.42 million tons) after China (FAO, 2017). Most crucial input for improving the yield is the use of good quality seeds. However, onion seeds exhibit some poor attributes like inferior longevity and storability, which ultimately result in rapid loss of viability (Khan et al., 2004). Furthermore, low-quality seeds result in low and asynchronous germination and high numbers of abnormal seedlings under stress conditions in early spring planting (Borowski and Michalek, 2006). Ultimately, quality of onion seed is dependent on several factors, some of which are surrounding environment during plant growth and seed development, location of seeds on plant, time of seed harvest, seed harvesting techniques, storage conditions and seed treatment before sowing. In the case of onions, where seed size is small, and seed establishment is

poor, seed priming is the most promising method to improve seed establishment. Seed priming is a pre-sowing, controlled hydration treatment where physiological and biochemical activities are stimulated in the seed, but radicle protrusion is prevented (Khan, 1992). Bosland and Votara (2000) were of the view that priming leads to enhanced and uniform germination. Moreover, primed onion and leek seeds maintained viability after one year when stored at 10 °C (Drew et al., 1997). Similar results have been reported in the case of tomato, asparagus and canola (Argerich et al., 1989; Owen and Pill, 1994; Basra et al., 2003). Many researchers have studied effect of seed priming on enhancement of germination, morphological characters, yield, etc. (Thejeshwini et al., 2019; Muruli et al., 2016; Saranya, 2017; Patil and Manjare, 2013; Arin et al., 2011; Selvarani and Umarani, 2011; Nego et al., 2015).

Seed priming (pre-sowing hydration treatments of seeds) is widely used for enabling better crop establishment (Taylor et al., 1998). Priming is a process in which seeds are imbibed in either water or osmotic solution or a combination of solid matrix carrier and water in specific proportions followed by drying before radicle emergence. In several studies, an increase in the nuclear DNA contents of radicle meristem cells from the G1 to the S or G2 phases of the cell cycle was noticed. The recorded effects of priming treatments on the storability of seeds are contradictory. The advancement of the germination process during priming continuously consumes stored substances and consequently may shorten seed longevity. However, the repair of DNA damage will increase longevity (Osborne, 1983). The results obtained so far are few, limited, contrasting because of the variability of the response to treatments of cultivars and even seed lots (Bradford, 1986) which require a careful choice of the compounds to proper standardization of the seed priming method and methodology for individual crops is the most critical determinant of success of the seed priming treatment.

In storage, the viability and vigour of the seeds not only vary from genera to genera and variety to variety, but is also regulated by many physicochemical factors like moisture content, atmospheric relative humidity, temperature, initial seed quality, physical and chemical composition of seed, gaseous exchange, storage structure, packaging materials etc. (Doijode, 1988). It will be of immense use to seed industry and farming community that how best the seeds can be stored by treating the seeds with chemicals and inert matter at relatively low cost under ambient storage and refrigerated conditions, with minimum quantitative and qualitative losses. As the quality, seed plays an important role in obtaining higher returns, as it is expected to perform well under any given environmental conditions.

Keeping in view the above facts, the present study was conducted with the objective of determining the most appropriate seed priming treatment and its physiological effects in differentially aged onion seeds.

Materials and methods

Experimental layout

The freshly harvested seed of three onion cultivars viz., Hisar-2 (V1), Hisar Onion-3 (V2) and Hisar Onion-4 (V3) were brought to the laboratory and stored in cloth bags under room temperature conditions (27 ± 1 °C, relative humidity (RH) $54 \pm 3\%$) with seed moisture 7-8%. The seed lots of each of the three varieties were stored under ambient conditions in the laboratory of Seed Science and Technology, Haryana Agricultural University), Hisar, India This seed was used for further studies according

to different years of natural seed ageing. These varieties were selected based on their extensive cultivation and popularity among Haryana farmers. Details of the experimental material are provided in *Table 1*.

Table 1. Differentially aged seedlot during the two years of study

Year of study	Lots	Year of production	Age of seed lot/seed age
2013	A	2013	Fresh
	B	2012	1 years old
	C	2011	2 years old
2014	A	2014	Fresh
	B	2013	1 year old
	C	2012	2 years old
	D	2011	3 years old

Treatments

Six seed priming treatments were compared with untreated control. The treatments are detailed in *Table 2*.

Table 2. Details of priming treatments under study

Hydro-priming followed by dry dressing with Thiram (2 g/kg)	Hydration with distilled water and followed by dry dressing of seeds by thiram fungicides (2 g/kg seed)
Hydration with GA ₃ (50 ppm)	50 mg of gibberellic acid (GA ₃) was dissolved in 2 L of water to make solution of concentration of 50 ppm. One to three drops of acetone were also added as GA ₃ cannot dissolve in distilled water
Hydration with KNO ₃ (0.5% solution)	5 g of potassium nitrate (KNO ₃) was dissolved in 1 L of distilled water
Hydration with KH ₂ PO ₄ (0.5% solution)	5 g of potassium dihydrogen phosphate (KH ₂ PO ₄) was dissolved in 1 L of distilled water
Biofertilizer (<i>Azotobacter</i>)	Seeds were first treated with 2% jaggary solution and then with <i>Azotobacter</i> strain HT-57. The strain was taken from the biofertilizers unit of CCS HAU, Hisar

The seed of each lot was soaked in a sufficient amount of solution for 16 h in each treatment. Then the seed was dried in the shade at 20 °C to attain the initial seed weight to maintain original or near to safe moisture content.

Observations

Germination and seed viability determination

Germination assays were determined according to the procedure described by International rules for seed testing (ISTA, 2015) by placing seeds in Petri plates for germination at 20-22 °C and 90 ± 2% RH (100 sterilized seeds per Petri plate in four replicates) in a germination chamber. Germination (%) was scored at radicle growth of 2 mm, or more and counting of normal and abnormal seedlings was started on the 5th day

and continued up to the 20th day (final count) followed by calculation of germination percentage. After the germination test, seedling length, dry seedling weight and seed vigour index were measured and calculated as per the standard procedure. Seedling length (cm) was measured from 20 randomly selected healthy seedlings at the time of final count of germination. These selected seedlings were then kept in a hot air oven at 60 °C for 48 h for the recording of seedling dry weight (mg). Based on the seed germination, seedling length and seedling dry weight data, seed vigour index-I (SV-I) and seed vigour index-II (SVI-II) were calculated (Abdul Baki and Anderson, 1972). To evaluate the viability, 25 seeds were soaked in 50 ml water and kept in the incubator at 30 ± 1 °C (in three replicates) for 24 h. After incubation, seeds were cut longitudinally and maintained in 1% staining solution of 2,3,5-triphenyl tetrazolium chloride (TTC) for 4 h at 38 ± 1 °C under dark conditions (Moore, 1973). During the staining period, only viable part of the seed is converted into red colour due to the formation of triphenyl formazon from TTC solution.

Electrical conductivity test (EC)

The electrical conductivity of seed leachates was measured for seeds of different age. Fifty seeds were soaked in 75 ml deionised water and incubated at 25 °C for 24 h. Seed leachates were collected, and conductivity (dS/cm/seed) was recorded by using digital conductivity meter (Model 304, Systronics, Ahmedabad, India) along with deionised water as a control (Dadlani and Aggarwal, 1987).

Field parameters

Seedling emergence index (SEI)

The number of seedlings emerged under field conditions were counted daily from 1st day to 20th day, and the seedling emergence index was calculated as described by (Maguire, 1962).

$$SEI = \frac{\text{No. of seedlings emerged on the first day}}{\text{Day of the first count (1st)}} + \dots + \frac{\text{No. of seedlings emerged on last day}}{\text{Day of the last count (20th)}}$$

Seedling establishment (%)

Seedling establishment was estimated under field conditions by including the total number of seedlings after emergence or when there was no further addition to the total emergence.

Statistical analyses

The statistical analysis was carried out for each observed character under the study using MS-Excel and SPSS Statistics 20. The means of the treatments were compared using Duncan's Multiple Range Test (DMRT). Besides, the linear regressions were determined with the help of data analysis tool pack in MS Excel.

Experimental results

Results of the study showed that the effect of priming, seed age and their interaction were significant at $p < 0.05$ for all the seed quality parameters studied. Therefore, the seed lots of different ages were analysed separately for all the parameters. The

laboratory parameters study was laid in completely randomized design CRD (Table 3), and field parameters were laid in randomized block design RBD (Table 4). During the second year of study, an additional seed lot of three-year-old seed was also studied.

Table 3. Analysis of variance for seed quality characteristics of onion seed as affected by different priming treatments

Source of variation	df	Germination	SL	SDW	SVI-I	SVI-II	Viability	EC
Seed lot (L)	2	20,143.92*	432.81*	37.97*	16,315,106.15*	859,446.45*	20,447.85*	6.42*
Priming (P)	5	259.64*	126.96*	0.27*	846,361.19*	8,555.79*	111.45*	0.21*
L*P	10	13.03*	10.66*	0.02**	99,516.17*	747.50*	3.51*	0.16*
Error	108	1.99	0.69	0.01	6,374.95	139.23	1.40	0.002

*Significant at 1% level of significance; **Significant at 5% level of significance; SL- seedling length; SDW- seedling dry weight; SVI-I- Seed vigour index-I; SVI-II- seed vigour index-II; EC- electrical conductivity

Table 4. Analysis of variance for field parameters of onion seed as affected by different priming treatments

Source of variation	df	SEI	SE
Seed age (L)	2	267.71*	18,413.84*
Priming (P)	5	6.05*	101.54*
L*P	10	0.20**	17.57*
Error	105	0.13	0.79

*Significant at 1% level of significance; **Significant at 5% level of significance; SEI- seedling emergence index; SE- seedling establishment

Seed priming has significant influence ($p < 0.05$) on the different traits of onion seed. Among the different seed priming treatments, hydration with GA₃ (50 ppm) was most effective in enhancing different traits followed by treatment with biofertilizer *Azotobacter*. Other treatments in declining order of seed quality are, hydro priming followed by dry dressing with Thiram (2 g/kg), hydration with KH₂PO₄ (0.5%) and hydration with KNO₃ (0.5%). Priming of seeds with various treatments was found competent to improve the quality in fresh and marginal seed lots. Out of the differentially aged seed lots, fresh seed performed the best, and the seed quality tends to decline with the ageing of the seed. Fresh seed lot was characterized by a high number of germinating seeds, exceeding 80% even in unprimed seed (Table 5). GA₃ emerged as the most effective priming treatment as it registered 11.23% increase in germination over control. After a year of storage, germination under different priming treatments dropped by 12.45 (*Azotobacter*), 13.11 (GA₃), 17.55 (Thiram), 20.1 (KH₂PO₄) and 20.45% (KNO₃), while unprimed seed recorded a reduction of 21.45%. A decline in germination in all the treatments was above 40% after three years of storage when compared with germination after two years of storage. The decrease in germination after three years of storage was below 10%. A similar trend was observed in the case of seed viability, where there was a steep decline after one year of storage (Table 5).

Table 5. Germination (%) and viability (%) of differentially aged onion seed lots under different priming treatments

Priming treatment	Germination (%)				Viability (%)			
	Lot1	Lot2	Lot3	Lot4	Lot1	Lot2	Lot3	Lot4
Thiram	88.43b	70.88c	27.20a	20.11a	88.41a	67.43b	22.26b	19.44b
GA ₃	91.32a	78.21a	27.16a	20.67a	89.41a	70.71a	24.98a	22.89a
KNO ₃	84.88c	64.44d	21.73b	13.33b	84.26c	63.05c	18.37c	14.78c
KH ₂ PO ₄	85.43c	65.33d	22.05b	14.33b	83.26c	64.16c	19.01c	15.67c
<i>Azotobacter</i>	88.88b	76.43b	26.10a	18.89a	86.21b	68.18b	24.76a	21.89ab
Control	82.10d	60.53e	17.47c	8.56c	83.02c	61.33d	17.89c	14.11c

Means under same parameter sharing letters are not significantly different at $\alpha = 0.05$; Lot1: Fresh seed; Lot2: One-year old seed; Lot3: Two-year old seed; Lot4: Three-year-old seed

Seed priming with GA₃ in fresh seed was the best combination followed by priming with Thiram. More than 70.71% GA₃ primed seed was viable in the one-year-old seed lot. Viability of seed was below 25% in the primed and non-primed seed of two and three-year-old seed lot. A gradual decline in seedling length (cm) and seedling dry weight (mg) was observed in all the priming treatments with the progression of storage period (Table 6). In all of the aged seed lots, priming with GA₃ improved both seedling characteristics over other priming treatments in differentially aged seed lots. Seed vigour index- I (SVI-I) was highest in GA₃ primed seed in case of fresh, one year old and three-year-old seed lots (Table 7). While SVI-I was highest in Thiram primed seed that has been stored for two years.

Table 6. Seedling length (cm) and dry weight (mg) of differentially aged onion seed lots under different priming treatments

Priming treatment	Seedling length (cm)				Seedling dry weight (mg)			
	Lot1	Lot2	Lot3	Lot4	Lot1	Lot2	Lot3	Lot4
Thiram	16.45c	14.16b	12.47b	10.98b	3.57bc	2.76ab	1.77bc	0.95ab
GA ₃	18.98a	16.70a	14.53a	13.18a	3.75a	2.79a	1.94a	1.12a
KNO ₃	14.34d	10.82d	8.75d	6.46cd	3.49bc	2.49c	1.71c	0.98ab
KH ₂ PO ₄	16.12c	11.61c	10.01c	8.08c	3.49bc	2.71b	1.72c	0.90c
<i>Azotobacter</i>	17.63b	9.94e	8.34d	11.19b	3.62ab	2.73ab	1.86ab	1.00ab
Control	13.78d	9.26f	8.17d	5.91d	3.43c	2.53c	1.70c	0.89c

Means under same parameter sharing letters are not significantly different at $\alpha = 0.05$; Lot1: Fresh seed; Lot2: One-year-old seed; Lot3: Two-year-old seed; Lot4: Three-year-old seed

On the other hand, seed vigour index- II (SVI-II) was highest in *Azotobacter* primed two-year-old seed (Table 7). GA₃ priming recorded highest SVI-II in other aged seed lots. Electrical conductivity (EC) of GA₃ primed seed was lowest among the all priming treatments in the four seed lots studied (Table 8). This was followed by priming treatments of *Azotobacter* and Thiram, while the oldest aged seed had the highest EC values. The field parameters, i.e., seedling emergence index (SEI) and seedling establishment (SE) were also high in the fresh and one-year-old seed lot and followed a

steep decline in two and three-year-old seed lot (Table 9). GA₃ primed seed also performed best in case of the field parameters followed by treatment with *Azotobacter*.

Table 7. Seed vigour index-I (SVI-I) and seed vigour index- II (SVI-II) of differentially aged onion seed lots under different priming treatments

Priming treatment	Seed vigour index- I				Seed vigour index- II			
	Lot1	Lot2	Lot3	Lot4	Lot1	Lot2	Lot3	Lot4
Thiram	1459.38bc	1001.14b	342.31b	224.47b	316.54bc	196.07c	48.47a	19.51b
GA ₃	1738.16a	1302.87a	398.71a	276.76a	343.33a	219.09a	53.01a	23.25a
KNO ₃	1219.68d	694.64d	191.20c	86.40d	296.96cd	160.93e	36.94b	13.03c
KH ₂ PO ₄	1380.20c	756.47c	222.86c	118.62c	298.60cd	177.32d	38.29b	13.12c
<i>Azotobacter</i>	1570.35b	743.70cd	203.20c	214.69b	322.21b	209.04b	48.78a	19.06b
Control	1132.59d	59.96e	146.28d	52.28e	281.77d	153.52f	29.84c	7.95d

Means under same parameter sharing letters are not significantly different at $\alpha = 0.05$; Lot1: Fresh seed; Lot2: One-year old seed; Lot3: Two-year-old seed; Lot4: Three-year-old seed

Table 8. Electrical conductivity (dS/cm/seed) of differentially aged onion seed lots under different priming treatments

Priming treatment	Electrical conductivity (dS/cm/seed)			
	Lot1	Lot2	Lot3	Lot4
Thiram	0.256bc	0.721cd	0.830c	1.34bc
GA ₃	0.246c	0.714d	0.798c	1.29c
KNO ₃	0.276a	0.732bc	0.865c	1.39bc
KH ₂ PO ₄	0.265ab	0.739b	1.08b	1.60b
<i>Azotobacter</i>	0.256bc	0.714d	0.862c	1.35bc
Control	0.278a	0.757a	1.47a	2.02a

Means under same parameter sharing letters are not significantly different at $\alpha = 0.05$; Lot1: Fresh seed; Lot2: One-year-old seed; Lot3: Two-year-old seed; Lot4: Three-year-old seed

Table 9. Seedling emergence index and seedling establishment (%) of differentially aged onion seed lots under different priming treatments

Priming treatment	Seedling emergence index				Seedling establishment (%)			
	Lot1	Lot2	Lot3	Lot4	Lot1	Lot2	Lot3	Lot4
Thiram	6.89abc	5.66c	2.39c	1.98c	68.39bc	63.16b	11.61bc	5.94ab
GA ₃	7.39a	6.31a	3.14a	2.75a	71.28a	65.93a	12.78a	6.39a
KNO ₃	6.64bc	5.61c	2.10d	1.71cd	66.50cd	58.49d	10.01d	4.28c
KH ₂ PO ₄	6.66bc	5.66c	1.91e	1.46d	65.61d	60.38c	10.97c	5.28b
<i>Azotobacter</i>	7.12ab	5.88b	2.74b	2.34b	69.06b	65.49a	12.04b	5.94ab
Control	6.27c	4.75d	1.38f	0.95e	64.50d	49.05e	9.38d	3.72c

Means under same parameter sharing letters are not significantly different at $\alpha = 0.05$; Lot1: Fresh seed; Lot2: One-year-old seed; Lot3: Two-year-old seed; Lot4: Three-year-old seed

Based on the effectiveness for enhancement of germination, vigour and storage potential, the best priming treatment is GA₃ @ 50 ppm followed by Biofertilizer *Azotobacter*. While the least effective treatment was KNO₃. Priming of the seeds with various treatments was found competent to improve the seed quality in fresh as well as marginal (one-year-old) and sub-marginal (two-year-old) seed age. No doubt performance of fresh seed was found better over all the other lots but, the improvement was comparatively more in marginal seed age, i.e., one-year-old seed lot (Lot1) because in this lot seed germination achieved up to 70% as per Indian minimum seed certification standards (IMSCS) standards.

Linear regression analysis revealed that germination and SE exhibited significant positive relationship ($p < 0.05$) in one-year-old seed lot, where germination explained 81% variation in SE (Fig. 1). Successful SE depends on several factors and ability of seeds to germinate is one of them. Present studies reveal that higher germination capacity under laboratory conditions is quite apparent through better establishment of seedlings under field conditions. These two parameters had a high positive correlation ($r = 0.90$), which indicates that priming in the one-year-old seed can result in good performance in field conditions. Similarly, both the vigour indices, i.e., SVI-I ($p < 0.01$) and SVI-II ($p < 0.05$) also had a positive association with SEI in one-year-old seed lot. SVI-I and SVI-II explained 89 and 73% variation in SEI, respectively (Fig. 2). Correlation of SVI-I and SVI-II with SEI had high positive values of 0.94 and 0.85, respectively. Vigour indices are based on germination, seedling length and seedling dry weight, and high values of these indices indicate fast-growing seedlings with good quality characteristics which are ultimately reflected in SEI. Fast-growing and healthy seedlings (which are a basis for vigour indices) lead to the higher values of SEI. Overall, it could be said that priming of onion seed stored for one year has good performance under heterogeneous field conditions leading to a good plant stand.

Discussion

Seed priming was identified to improve the germination and seedling establishment in some of the critical field crops like soybean, wheat, maize, sunflower and sugarbeet (Singh, 1995; Khajeh-Hosseini et al., 2003; Sdeghian and Yavari, 2004). The improved performance and quality of seed after is due to several processes like DNA repair, activation of enzymes and endosperm weakening in primed seeds (Osborne, 1983; Dell'Aquila et al., 1998; Moosavi et al., 2009). Also, priming enhances antioxidant activity in the seeds, which results in reduced lipid peroxidation, improves seed quality (Hsu et al., 2003; Chiu et al., 2006). Davison and Bray (1991) have observed some changes in the protein pattern in the primed seeds. Vigorous crops grown from primed seeds were able to capture more nitrogen than plants grown from non-primed seeds, thus utilising nitrogen before leaching or volatilization losses (Byrum and Copland, 1995). Ramadevi and Gopalkrishan (2001) are of the view that enhanced hydration of all seed parts leading to reduced damage to the embryonic axis could be the reason behind the increased speed of emergence and seedling establishment. Toxic effect of potassium salts on the germinating seeds is the reason behind KNO₃ being the least effective treatment. Toxic effect of KCL has been reported by some workers where it has a negative effect on germinating embryos which leads to a reduction in germination and seedling death (Giri and Schillinger, 2003; Yari et al., 2011).

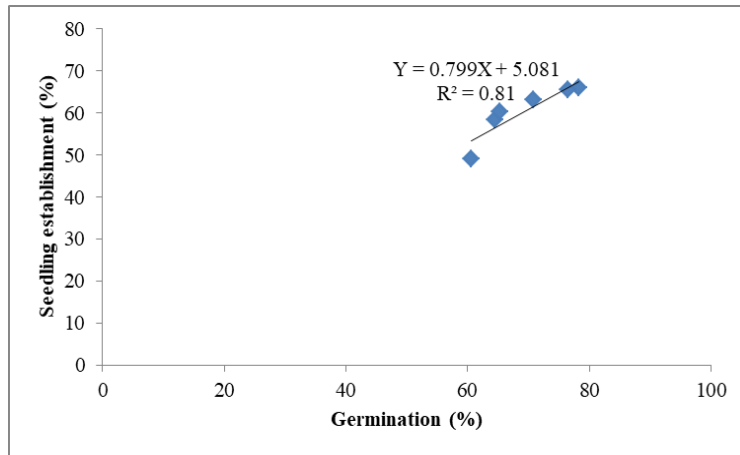


Figure 1. Relationship between seedling establishment (%) and germination (%) in one-year-old seed

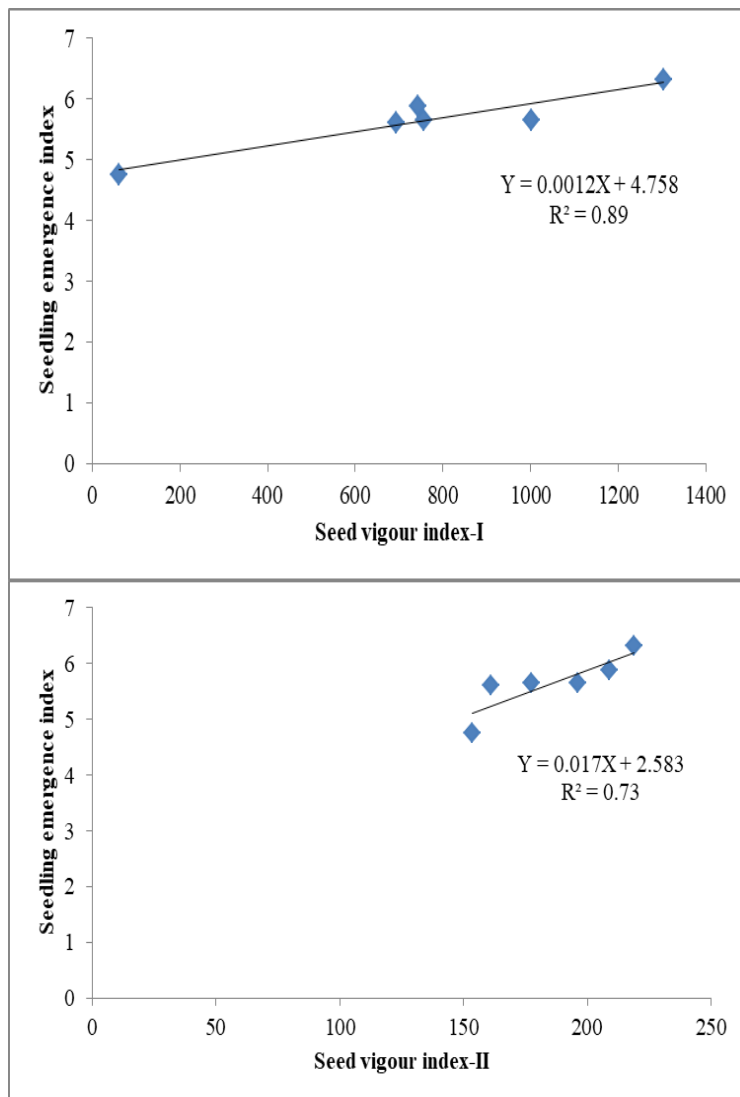


Figure 2. Relationship between seedling emergence index (SEI) and seed vigour index-I (SVI-I) and seed vigour index-II (SVI-II) in one-year-old seed

Gibberellic Acid (GA₃) is an essential growth regulator, which aids in breaking seed dormancy, promoting germination, internodal length, growth of hypocotyl and cell division in the cambial zone and enlargement of leaf size. GA₃ degrades cells surrounding the radicle by stimulating hydrolytic enzymes, which ultimately speeds germination (Rood et al., 1990). GA₃ also plays a vital role in the mobilization of endosperm reserves during germination of seeds (Weiss and Ori, 2007). During the germination process, GA₃ is released from an embryo, which activates genes responsible for alpha-amylase mRNA transcription (Taiz and Zeiger, 1991). Exogenous application of GA₃ might lead to activation of such genes in seeds, thus improving germination. Increased vigour characteristics elevated peroxide scavenging enzymes activities and decline in lipid peroxidation some of the possible reasons behind enhanced seed germination. Higher metabolic activity in primed seeds causes efficient food mobilization during early hours of germination, which leads to increased shoot and root lengths (Brar et al., 2019).

Consequently, it results in higher seedling dry weight (Bailly et al., 2002; Jett et al., 1996). Priming of fresh and aged onion seed with GA₃ (50 ppm) resulted in favourable impact on the germination ability and seed vigour. Also the aged seed was more responsive to priming as compared to the fresh seed (Muruli et al., 2016). Yarnia et al. (2012) determined the effect of hormonal treatments i.e., IAA, GA₃ and kinetin on germination and seedling growth of onion. Of these priming treatments GA₃ and IAA led to improved attributes such as germination, seedling length, root length, seedling dry weight etc. Helaly et al. (2016) also reported highest germination, seed yield and weight of thousand seeds in GA₃ (1000 ppm) primed onion seeds. In case of shallots also GA₃ priming significantly enhances the germination, speed of germination, seedling vigour and rate of seedling emergence (Agung and Diara, 2017).

GA₃ priming was followed by bio-priming with *Azotobacter*, which is known to promote plant growth through indole-3-acetic acid (IAA) production and nitrogen fixation (Hafeez et al., 2004). *Azotobacter* inoculations are known to produce GA₃, IAA and cytokinins (Barea and Brown, 1974), which enhances seedling development and plant growth (Brown, 1982). Bacteria produce plant growth regulators which alter morphology and metabolism of the plant, yields more extended root systems and improves absorption of water and minerals (Bashan et al., 2004; Lai et al., 2008; Fibach-Paldi et al., 2012). *Azotobacter* enhances germination in rice and cotton by the synthesis of growth promoters and antifungal antibiotic production, which ensure seed safety during germination (Shende et al., 1977). Inoculation with *Azotobacter* increases shoot, and root length in maize and sorghum and pre-soaking of seed improves germination and seedling establishment (Ahmed et al., 1998). Bio-agents are also more effective as compared to synthetic chemicals as they improve seed quality characteristics while providing tolerance to other toxic agents. Brar et al. (2015) reported improved seed quality characteristics in tomato with the supply of biofertilizers like *Azotobacter*. Treatment with biofertilizers also enhanced the seed yield and improved the fertility status of the soil by nitrogen fixation.

Lower EC for primed seed may be due to improved plasma membrane structure as a result of slow hydration in the priming treatments (McDonald, 1980). Kumar (2004) reported that onion seeds treated with GA₃ recorded the maximum decline in seed leachates in comparison to control. Improvement of germination at high levels of ageing was not achieved through priming as the irreversible damage could not be repaired (Butler et al., 2009). During the programmed cell death (PCD), catalase rate and

sensitivity reduce, which indicates that the ageing causes PCD and subsequent the reduction of seed viability.

Conclusion

It is concluded that the standard germination, vigour indices and EC tests could be used as reliable predictors of seed quality because of easiness, quickness and accuracy in their execution. Further, various seed priming treatments can be used for enhancing seed quality of marginal seed lot. GA₃ (50 ppm) was found to be best priming treatment for improving the seed quality followed by biofertilizer (*Azotobacter*), hydro priming and dry dressing with Thiram (2 g/kg), KH 2 PO 4 (0.5%) and KNO 3 (0.5%), respectively. Overall, the priming technology was found useful and beneficial for enhancing the physiological, biochemical and storage potential of onion seed. Indeed, in the case of these onion varieties, we recommend the priming treatment for getting a bumper harvest.

REFERENCES

- [1] Abdul-Baki, A. A., Anderson, J. D. (1972): Physiological and Biochemical Deterioration of Seeds. – In: Kozłowski, T. T. (ed.). Seed Biology. Academic Press, New York, pp. 283-315.
- [2] Agung, I. G. A. M. S., Diara, I. W. (2017): Pre-sowing treatment enhanced germination and vigour of true shallot (*Allium cepa* var. *aggregatum*) seeds. – International Journal of Environment Agriculture and Biotechnology 2: 3262-67.
- [3] Ahmed, S., Anwar, M., Ullah, H. (1998): Wheat seed presoaking for germination. – Journal of Agronomy and Crop Science 181: 125-27.
- [4] Argerich, C. A., Bradford, K. J., Tarquis, A. M. (1989): The effects of priming and ageing on resistance to deterioration of tomato seeds. – Journal of Experimental Botany 40: 593-98.
- [5] Arin, L., Polat, S., Devcci, M., Salk, A. (2011): Effect of different osmotic solutions on onion seed emergence. – African Journal of Agriculture Research 6: 986-91.
- [6] Bailly, C., Bogatek-Leszczynska, R., Côme, D., Corbineau, F. (2002): Changes in activities of antioxidant enzymes and lipoxygenase during growth of sunflower seedlings from seeds of different vigour. – Seed Science Research 12: 47-55.
- [7] Barea, J. M., Brown, M. E. (1974): Effect on plant growth produced by *A. paspali* related to the synthesis of plant growth regulating substance. – Journal of Applied Bacteriology 37: 583-93.
- [8] Bashan, Y., Holguin, K., de-Bashan, L. E. (2004): *Azospirillum*-plant relationships: physiological, molecular, agricultural and environmental advances. – Canadian Journal of Microbiology 50: 521-77.
- [9] Basra, S. M. A., Ullah, E., Warraich, E. A., Cheema, M. A., Afzal, I. (2003): Effect of storage on growth and yield of primed canola (*Brassica napus*) seeds. – International Journal of Agriculture and Biology 5: 117-20.
- [10] Borowski, E., Michałek, S. (2006): The effect of seed conditioning on the emergence and early growth of onion and carrot seedlings. – Annales Universitatis Mariae Curie-Skłodowska Setio EEE 16: 119-29.
- [11] Bosland, P. W., Votara, E. J. (2000): Peppers: Vegetable and Spice Capsicums. – CABI Publishing, New York.
- [12] Bradford, K. J. (1986): Manipulation of seed water relations via osmotic priming to improve germination under stress conditions. – Horticultural Science 21: 1105-12.

- [13] Brar, N. S., Thakur, K. S., Kumar, R., Mehta, D. K. (2015): Yield and quality of tomato seed and soil fertility as affected by organic manures and biofertilizers. – Green Farming 6: 1068-70.
- [14] Brar, N. S., Kaushik, P., Dudi, B. S. (2019): Assessment of natural ageing related physio-biochemical changes in onion seed. – Agriculture 9: 163.
- [15] Brown, M. E. (1982): Nitrogen Fixation by Free-Living Bacteria Associated with Plants—Fact or Fiction? – In: Rhodes-Roberts, M., Skinner, F. A. (eds.) Bacteria and Plants. Academic Press, London. pp 255-42.
- [16] Butler, L. H., Hay, F. R., Ellis, R. H., Smith, R. D., Murray, T. B. (2009): Priming and re-drying improve the survival of mature seeds of *Digitalis purpurea* during storage. – Annals of Botany 103: 1261-70.
- [17] Byrum, J. R., Copeland, L. O. (1995): Variability in vigour testing of maize (*Zea mays* L.) seed. – Seed Science and Technology 23: 543-49.
- [18] Chiu, K. Y., Chuang, S. J., Sung, J. M. (2006): Both anti-oxidation and lipid carbohydrate conversion enhancements are involved in priming improved emergence of *Echinacea purpurea* seeds that differ in size. – Scientia Horticulture 108: 220-26.
- [19] Dadlani, M., Agrawal, P. K. (1987): Techniques in Seed Science and Technology. – South Asian Publishers, New Delhi, pp. 103-104.
- [20] Davison, P. A., Bray, C. M. (1991): Protein synthesis during osmopriming of leek (*Allium porrum* L.) seeds. – Seed Science Research 1: 29-35.
- [21] Dell'Aquila, A., Corona, M. G., Turi, M. D. (1998): Heat-shock proteins in monitoring aging and heat-induced tolerance in germinating wheat and barley embryos. – Seed Science Research 8: 91-98.
- [22] Doijode, S. D. (1988): Comparison of storage of French bean seeds under ambient conditions. – Seed Research 16: 245-47.
- [23] Drew, R. L. K., Hands, L. J., Gray, D. (1997): Relating the effects of priming to germination of unprimed seeds. – Seed Science and Technology 25: 537-48.
- [24] FAO (2017): <http://www.fao.org/faostat/en/#data/QC>. – FAO, Rome.
- [25] Fibach-Paldi, S., Burdman, S., Okon, Y. (2012): Key physiological properties contributing to rhizosphere adaptation and plant growth promotion abilities of *Azospirillum brasilense*. – Microbiology Letters 326: 99-108.
- [26] Giri, G. S., Schillinger, W. F. (2003): Seed priming winter wheat for germination, emergence and yield. – Crop Science 43: 2135-41.
- [27] Hafeez, F. Y., Safdar, M. E., Chaudhry, A. U., Malik, K. A. (2004): Rhizobial inoculation improves seedling emergence, nutrient uptake and growth of cotton. – Australian Journal of Experimental Agriculture 44: 617-22.
- [28] Helaly, A. A., Abdelghafar, M. S., Al-Abd, M. T., Alkharpotly, A. A. (2016): Effect of soaked *Allium cepa* L. bulbs in growth regulators on their growth and seed production. – Advances in Plants and Agricultural Research 4: 283-88.
- [29] Hsu, C. C., Chen, C. L., Chen, J. J., Sung, J. M. (2003): Accelerated ageing enhanced lipid peroxidation in the bitter melon seeds and effects of priming and hot water soaking treatments. – Scientia Horticulture 98: 201-12.
- [30] ISTA (2015): International Rules for Seed Testing. – International Seed Testing Association, Bassersdorf, Switzerland.
- [31] Jett, L. W., Welbaum, G. E., Morse, R. D. (1996): Effect of matrix and osmotic priming treatments on Broccoli seed germination. – Journal of American Society for Horticultural Science 121: 423-29.
- [32] Khajeh-Hosseini, M., Powell, A. A., Bingham, I. J. (2003): The interaction between salinity stress and seed vigour during germination of soyabean seeds. – Seed Science and Technology 31: 715-25.
- [33] Khan, A. A. (1992): Preplant physiological seed conditioning. – Horticulture Review 13: 131-81.

- [34] Khan, M., Javed Iqbal, M., Abbas, M., Raza, H., Waseem, R., Arshad, A. (2004): Loss of vigour and viability in aged onion (*Allium cepa* L.) seeds. – International Journal of Agriculture and Biology 6: 708-71.
- [35] Kumar, R., Nagarajan, S., Rana, S. C. (2004): Effect of natural ageing under controlled storage on seed quality and yield performance of field pea cv. DMR-7. – Seed Research 32: 96-97.
- [36] Lai, W. A., Rekha, P. D., Arun, A. B., Young, C. C. (2008): Effect of mineral fertilizer, pig manure, and *Azospirillum rugosum* on growth and nutrient contents of *Lactuca sativa* L. – Biology and Fertility of Soils 45: 155-64.
- [37] Maguire, J. D. (1962): Speed of germination aid in selection and evaluation for seedling emergence and vigour. – Crop Science 2: 176-77.
- [38] McDonald, Jr. M. B. (1980): Assessment of seed quality. – Horticultural Science 15: 784-88.
- [39] Moore, R. P. (1973): Tetrazolium Stain for Assessing Seed Quality. – In: Heydecker, W. (eds.) Seed Ecology. The Pennsylvania State Univ., Univ. Park, PA, pp. 347-366.
- [40] Moosavi, A., Tavakkol Afshari, R., Sharif-Zadeh, F., Ayneband, A. (2009): Effect of seed priming on germination characteristics, polyphenoloxidase, and peroxidase activities of four amaranth cultivars. – Journal of Food, Agriculture and Environment 7: 353-58.
- [41] Muruli, C. N., Bhanuprakash, K., Channakeshava (2016): Impact of seed priming on vigour in onion (*Allium cepa* L.). – Journal of Applied Horticulture 18: 68-70.
- [42] Nego, J., Dechassa, N., Dessalenge, L. (2015): Effect of seed priming with potassium nitrate on bulb yield and seed quality of onion (*Allium cepa* L.) under rift valley conditions, Central Ethiopia. – International Journal of Crop Science and Technology 1: 1-12.
- [43] Osborne, D. J. (1983): Biochemical control systems operating in the early hours of germination. – Canadian Journal of Botany 61: 3568-77.
- [44] Owen, P. L., Pill, W. G. (1994): Germination of osmotically primed asparagus and tomato seeds after storage up to three months. – Journal of American Society of Horticultural Science 119: 636-41.
- [45] Patil, B. D., Manjare, M. R. (2013): Effect of seed priming on germination and bulb yield in onion (*Allium cepa* L.). – Ecology, Environment and Conservation 19: 243-46.
- [46] Ramadevi, V., Gopalkrishnan, P. K. (2001): Studies on the Effect of Pre-Sowing Hardening Treatment on Germination and Vegetative Growth of Cowpea (Var. V-118). – In: Dwivedi, R. S., Singh, R. S. (eds.) Plant Physiological Paradigm for fostering Agro and Biotechnology and Augmenting Environmental Productivity. Proc. Nat. Seminar. Indian Soc. Plant Physiol. Lucknow, 7-9 Nov., 2000, pp. 149-152.
- [47] Rood, S. B., Buzzell, R. I., Major, D. J., Pharis, R. P. (1990): Gibberellins and heterosis in maize: quantitative relationship. – Crop Science 30: 281-86.
- [48] Sadeghian, S. Y., Yavari, N. (2004): Effect of water-deficit stress on germination and early seedling growth in sugar beet. – Journal of Agronomy and Crop Science 190: 138-44.
- [49] Saranya, N., Renugadevi, J., Raja, K., Rajashree, V., Hemalath, G. (2017): Seed priming studies for vigour enhancement in onion CO onion (5). – Journal of Pharmacognosy and Phytochemistry 6: 77-82.
- [50] Selvarani, K., Umarani, R. (2011): Evaluation of seed priming methods to improve seed vigour of onion (*Allium cepa* cv. *aggregatum*) and carrot (*Daucus carota*). – Journal of Agricultural Technology 7: 857-67.
- [51] Shende, S. T., Apte, R., Singh, T. (1977): Influence of *Azotobacter* on germination of rice on cotton seeds. – Current Science 46: 675-76.
- [52] Singh, B. G. (1995): Effect of hydration-dehydration seed treatments on vigour and yield of sunflower. – Indian Journal of Plant Physiology 38: 66-68.
- [53] Taiz, L., Zeiger, E. (1991): Plant Physiology. – The Benjamin/Cumming Publishing Company. Inc., New York.

- [54] Taylor, A. G., Allen, P. S., Bennett, M. A., Bradford, K. J., Burris, J. S., Misra, M. K. (1998): Seed enhancements. – *Seed Science Research* 8: 245-56.
- [55] Weiss, D., Ori, N. (2007): Mechanisms of cross talk between gibberellin and other hormones. – *Plant Physiology* 144: 1240-46.
- [56] Yari, L., Khazaei, F., Sadeghi, H., Sheidaei, S. (2011): Effect of seed priming on grain yield and yield components of bread wheat (*Triticum aestivum* L.). – *Journal of Agriculture and Biological Sciences* 6: 1-5.
- [57] Yarnia, M., Farajzadeh, E., Tabrizi, M. (2012): Effect of seed priming with different concentration of GA₃, IAA and kinetin on Azarshahar onion germination and seedling growth. – *Journal of Basic and Applied Science Research* 2: 2651-61.

TREND ANALYSIS OF STREAMFLOW AND ITS RELATION TO RAINFALL IN THE LOWER TAMIRAPARANI SUB-BASIN OF TAMILNADU, INDIA

MARTINA ISABELLA, M. * – AMBUJAM, N. K. – SANTHANA KRISHNAN, P. T.

College of Engineering, Anna University, Chennai, Tamilnadu 600025, India

**Corresponding author
e-mail: isabella789@gmail.com*

(Received 11th Jul 2019; accepted 25th Nov 2019)

Abstract. Trend analysis of streamflow and its linkages to rainfall can facilitate the development of water resource management plans for watersheds. The present study focuses on trends in observed streamflow of the lower Tamiraparani river sub-basin in Tamilnadu, India using Mann – Kendall test and Sen’s slope estimator for a period of 30 years. From this analysis, both the annual streamflow, annual rainfall increased very marginally at the rate of 0.1799 m³/s/year and 4.3741 mm/year, respectively. Similarly, in the northeast monsoon period, both the rainfall and streamflow were increased very minimally during the analysis period. However, the observations made during the southwest monsoon showed declining trends for most of the rainfall stations and no significant trend was observed for streamflow. The calculated Spearman’s Rho correlation factor (ρ) between rainfall and streamflow showed weak correlation during summer (0.26) and very strong correlation during northeast monsoon (0.83), strong correlation during southwest monsoon (0.53) and moderate correlation during winter (0.40). From this analysis, using Mann – Kendal test and Spearman’s correlation it implies that other than precipitation and temperature, urbanization, watershed and ecological development of the catchment area could have also influenced the trends of streamflow.

Keywords: *climate variables, climate change, hydrological environment, Mann – Kendal, Sen’s slope*

Introduction

Water is a vital element for both natural and artificial environments and it is provided by the rivers of the country offering life generating fuel to ecology (Islam and Sikder, 2012). Rainfall serves as one among the major sources of flow in the rivers while others include melting of glaciers, base flow from groundwater, return flow from agricultural areas etc. (Raghunath, 2006). Streamflow assessment plays a vital role in guiding the decision makers for better planning and providing accurate information towards the future research. Due to the climate change and anthropogenic activities, most rivers are altering their streamflows on a global scale and present rivers are under severe threats (Gautam and Acharya, 2012). So, it is vital to analyse the changing phenomenon of various climatic variables mainly rainfall and temperature. The work by Jayadas and Ambujam (2019) studied the trend patterns of rainfall in lower Vellar sub-basin in Tamil Nadu which indicated that there has been an early onset of monsoon in the last three decades. Jain and Kumar (2012) reviewed about the trend analysis of rainfall and temperature of many studies and explained about the estimation procedure of trend analysis and magnitude of trend by Mann – Kendal and Sen’s slope estimator.

Mann – Kendal test is one of the best methods for rainfall and temperature trend analysis to study the impacts of climate change and Mann – Kendal test can be used as the best water management tool for proper watershed protection (Nouri, 2017). Palaniswami and Muthiah (2018) analysed the trends in annual, seasonal maximum and minimum temperature in the Vellar river basin in Tamilnadu and found out that there is

a significantly increasing trend in the basin. Punyawardena and Premalal (2013) using the Mann – Kendal test in central Sri Lanka observed that there was increasing trend patterns in the very heavy rainfall data series. Chakraborty et al. (2013) observed there was decreasing trends in both annual and seasonal rainfall in the Seonath river basin and they estimated the decreased rainfall as -13.8mm/year for Bodala river basin and 0.1 mm/year in sigma station using Sen’s slope estimator test. Chand et al. (2019) analysed the temperature trends in the river basin in Nepal and they observed that there were the highest warming trends in the summer season followed by winter, pre monsoon and post monsoon. It is well understood that globally there is an increasing pattern of trends in temperature and decreasing patterns in rainfall. In addition to this, the work done by Panda et al. (2013) on streamflow trends in the Mahanadi river basin, India, estimated that there was a declining rate of $3388 \times 106/\text{decade}$ in the river which suggested the possible environmental measures for the protection of the river basin. Various research works (Yadav et al., 2014; Ahmad et al., 2015; Javari, 2017; John and Brema, 2018) highlighted the importance of Mann – Kendal and Sen’s slope estimator to detect the trend and Magnitude of trends and outlined the effectiveness of the statistical tests in finding out the trend of rainfall, temperature and streamflow in several areas worldwide. Hydro-climatic conditions assessment at a larger regional scale may lead to the loss of the spatial information of the particular variable. Therefore, it is logical to analyse hydro climatic variables at a small scale rather than at larger scale. So the objective of the study is framed to analyse the trend patterns in the measured stream flow and rainfall at the sub-basin level. Also, to investigate the correlation of upstream catchment rainfall over the streamflow of the lower Tamiraparani sub-basin which is one among the sub-basins of perennial Tamiraparani River basin in India.

Materials and Methods

Study area

The lower Tamiraparani sub-basin is one among the seven sub-basins of Tamiraparani river basin in Tamilnadu, India as shown in *Fig. 1*. The lower Tamiraparani sub-basin lies between geographic coordinates N. lat $8^{\circ}26'53.14''$ to $9^{\circ}12'00''$ and E. long $77^{\circ}29'19.91''$ to $78^{\circ}07'52.31''$. The entire sub-basin covers an area of about 1891.64 km². Tamiraparani River originates from Agastya malai on the Western Ghats of India, at an altitude of about 2000 m. River Tamiraparani has a number of tributaries named Servalar, Manimuttar, Gadanadhi, Pachaiyar and Chittar. The river flows towards north east initially and towards east in the middle and at the end it confluences with Bay of Bengal near Palaya Kayal as shown in *Fig. 2*. All the sub-basins along with Lower Tamiraparani basin lies within the tropical monsoon zone. Among all the basins, lower Tamiraparani sub-basin has the highest concentration of population, about 45 percent of the entire basin population lives here. It covers almost 37 percent of the total command area of the entire basin (Report on Micro level Reappraisal study of Tamiraparani River basin, 2015). Based on the hydro meteorological features of the basin, the entire year is divided into two periods 1) Monsoon period from June to December and 2) Non-monsoon period spanning from January to May. The monsoon period of the sub-basin is further sub-divided into southwest monsoon period from June to September and northeast monsoon period from October to December. Similarly, the non-monsoon period is further sub-divided into winter period from January and February and summer period from March to May. For

the rainfall trend analysis, Point rainfall from rain gauges maintained by PWD were used. There are totally 16 rain gauge stations available, out of these 13 rain gauge stations located upstream to the stream gauge station were considered for the analysis. As these stations influence the streamflow measured in the lower Tamiraparani sub-basin, the rainfall data from these stations were considered based on availability and reliability as shown in Fig. 2. As per the PWD appraisal report, the maximum annual rainfall is 1237.2 mm and the minimum annual rainfall is 236.30 mm in the study area. There is a gauge station named Murappanadu in the lower Tamiraparani sub-basin to measure the streamflow variations in the river. In the entire river basin, there are a total of two weather stations to measure temperature, relative humidity, wind speed and solar radiation.

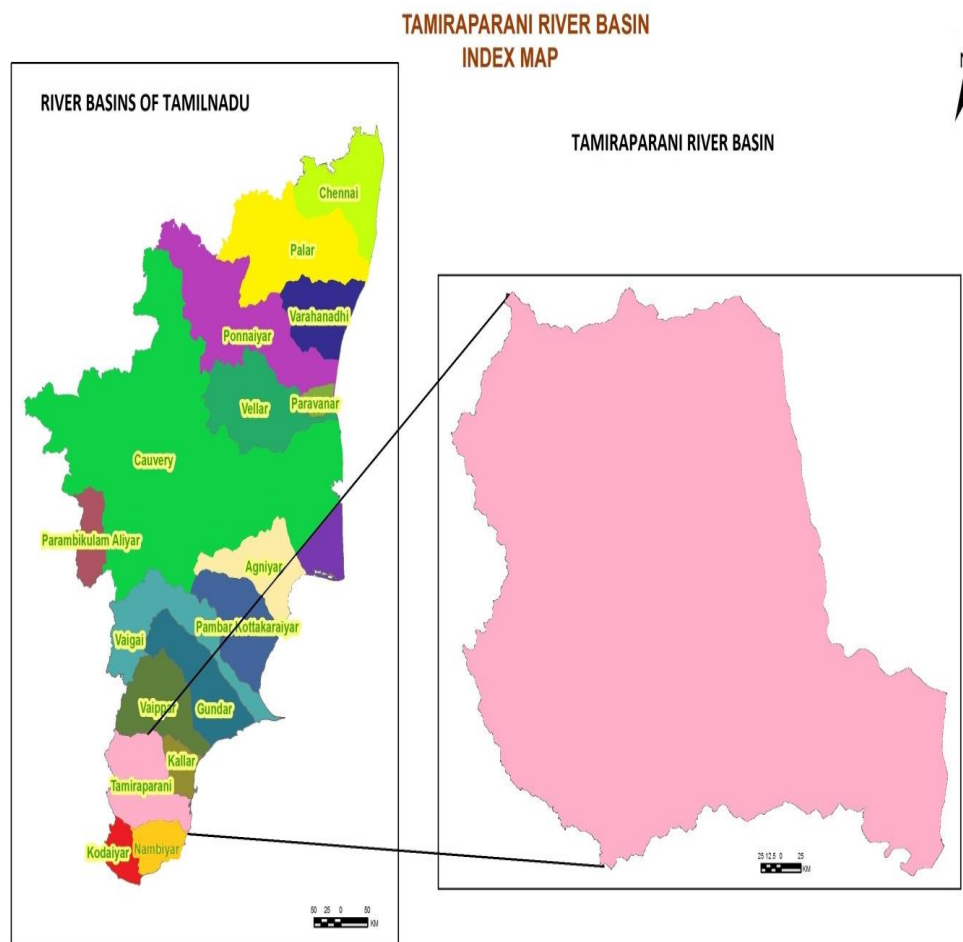


Figure 1. Index Map of Tamiraparani River basin

Data set

Streamflow data of the river were collected from the gauging station named Murappanadu as shown in Fig. 2, which is maintained by the Central Water Commission, Government of India. This is the nodal department in India to observe, calculate, quality check and archive all the hydrologic data of the river. All the meteorological parameters such as rainfall, wind speed and humidity and solar radiation were collected from the Institute of Water Studies, Public Works Department, and

Tamil Nadu. Due to the insufficient availability of the observed temperature data, the temperature data was extracted from the gridded data collected from the Indian Meteorological department at the resolution of $1^{\circ} \times 1^{\circ}$. The duration of the data sample collected was from 01-Jan-1985 to 31-Dec-2015. For the proper assessment of all climate change observations and to compare the spatial distribution of trend of streamflow and rainfall, it is normally necessary to have the sample duration of a minimum of 30 years of data. For the study, lower Tamiraparani river sub-basin is delineated using 30 m resolution ASTER data in ArcGIS 10.3. The total area of the sub-basin is estimated to be 1891.64 km². For the rainfall trend analysis, annual and seasonal rainfall from all influencing rain gauge stations contributing the streamflow in the study area from upper and middle reaches considered for the study as depicted in *Fig. 2*. The location details and period of data records of influencing and non-influencing rain gauges considered are given in *Table 1*.

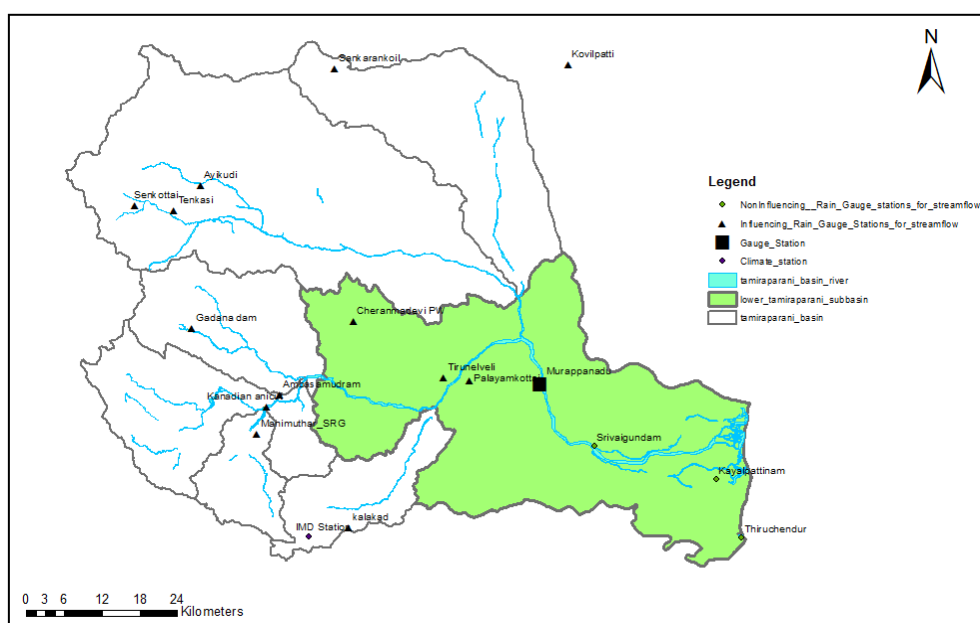


Figure 2. Geographical distribution of major stream network, streamflow gauging station and the influencing and non-influencing Rain gauge stations for streamflow of gauging station of Lower Tamiraparani sub-basin

Analysis of data

The following indicators were estimated and subjected to trend analysis.

- Inter - annual monthly mean streamflow which was calculated by estimating the monthly mean streamflow values for the same month of all the years.
- Annual mean streamflow which was estimated by taking the mean streamflow values for all the months of the gauging station.
- Seasonal mean streamflow, which was calculated by taking the mean of monthly streamflow values for summer, winter, northeast monsoon and southwest monsoon separately.
- Monthly maximum and minimum streamflows which were calculated by considering the maximum and minimum streamflow values recorded in a month for the gauging station.

- Monthly and annual rainfall for all the rain gauges at the upstream of gauging station.
- Weighted annual, seasonal and monthly average rainfall for the rain gauges at upstream of the gauging station.
- Annual and seasonal maximum and minimum mean temperature for the weather station.

Theissen polygon method is one of the normally used methods in computing average rainfall for all hydrological studies. Through this theissen polygon method in the ArcGIS environment, the weights of each rain gauge stations were calculated with respect to the entire basin area and the annual and seasonal rainfall of the rain gauges which is at the upstream side of the gauge station was calculated.

Table 1. Geographical Coordinates and period of data records of the Rain Gauge stations

Rain gauge station	Latitude	Longitude	Period of records
Ambasamudram	08°42'09"N	77°27'26"E	1985 – 2015(30 years)
Ayikudi	09°00'03"N	77°20'34"E	1985 – 2015(30 years)
Cheranmadevi	08°41'17"N	77°33'49"E	1985 – 2015(30 years)
Gadana dam	08°47'46"N	77°19'53"E	1985 – 2015(30 years)
Kalakadu	08°30'48"N	77°33'27"E	1985 – 2015(30 years)
Kanadian Anicut	08°41'08"N	77°26'22"E	1985 – 2015(30 years)
Kovilpatti	09°10'27"N	77°52'28"E	1985 – 2015(30 years)
Manimuthar	08°38'45"N	77°25'32"E	1985 – 2015(30 years)
Palayamkottai	08°43'23"N	77°43'55"E	1985 – 2015(30 years)
Sankarankoil	09°10'04"N	77°32'12"E	1985 – 2015(30 years)
Senkottai	08°58'18"N	77°14'54"E	1985 – 2015(30 years)
Tenkasi	08°57'52"N	77°18'17"E	1985 – 2015(30 years)
Tirunelveli	08°43'40"N	77°41'41"E	1985 – 2015(30 years)
Kayalpatinam*	08°34'56"N	78°05'19"E	1985 – 2015(30 years)
Srivaigundam*	08°37'45"N	77°54'44"E	1985 – 2015(30 years)
Tiruchendur*	08°29'56"N	78°07'30"E	1985 – 2015(30 years)

*Non-influencing rain gauge stations to the stream flow

Statistical analysis

While analyzing the trends in the data series, the monotonic trends of all the hydro – climatic data series was tested using non parametric Mann – Kendall test using XLSTAT program. Initially all the time series data of the study were tested for lag one autocorrelation. If the time series data did not show any auto correlation, then Mann – Kendall test was adopted for the trend analysis. If auto correlation was detected in the time series data then modified Mann – Kendall as suggested by Hamed-Rao using XLSTAT program should be used since Mann – Kendall test did not account for the serial auto correlation existing in the hydro – climatic series (Abeysingha et al., 2014). Then in order to compare the spatio-temporal variability between the rainfall and stream flow over the basin, the standardized anomaly was calculated for the time series data of both rainfall and streamflow. The standardized anomaly is calculated by subtracting the mean value of the data series from each observation and then divides the following with the standard deviation of the series.

Mann – Kendall test

Monotonic trend analysis for rainfall, temperature and streamflow have been effectively done with non-parametric Mann – Kendall test in the studies (Mondal et al., 2012; Sharif et al., 2013; Silva et al., 2015). Mann – Kendall test is a statistical method which is being used for studying the variations of spatial regions and temporal trends of hydro climatic series. Mann – Kendall test had been formulated by Mann (1945) as non-parametric test for trend detection and the test statistic distribution had been given by Kendall (1955) for testing non-linear trend and turning point. Mann – Kendall test is a two tailed test. The test statistics S is calculated by

$$S = \sum_{i=1}^{n-1} \sum_{j=i+1}^n \text{sgn}(X_j - X_i), \quad (\text{Eq.1})$$

$$\text{sgn}(X_j - X_i) = \begin{cases} 1 & \text{if } (X_j - X_i) > 0 \\ 0 & \text{if } (X_j - X_i) = 0 \\ -1 & \text{if } (X_j - X_i) < 0 \end{cases} \quad (\text{Eq.2})$$

$$\sigma^2 = \frac{1}{18} \left[n(n-1)(2n+5) - \sum_p^q t_p(t_p-1)(2t_p+5) \right], \quad (\text{Eq.3})$$

$$Z = \begin{cases} \frac{S-1}{\sigma} & \text{if } S > 0, \\ 0 & \text{if } S = 0, \\ \frac{S+1}{\sigma} & \text{if } S < 0. \end{cases} \quad (\text{Eq.4})$$

In the above equations X_i and X_j are the time series observations, n is the length of time series, t_p is the number of ties for p th value and q is the number of tied values. The test hypothesis for Mann – Kendall analysis of trend is as follows:

- H_0 : There is no trend in the series.
- H_a : There is a trend in the series.

Positive Z values indicate an increasing trend in the hydrologic time series and negative Z values indicate a decreasing trend. The statistic Z has a normal distribution. For testing the increasing or decreasing trend at α level of significance H_0 was rejected if $|Z| > Z(1-\alpha/2)$, where $Z(1-\alpha/2)$ was obtained from the standard normal cumulative distribution.

Sen's Slope estimator test

Many research studies (Jayawardene et al., 2015; Samo et al., 2017; Gedefaw et al., 2018) estimated the magnitude of changing trends of the meteorological parameters well using Sen's slope estimator test. This test calculates both the slope and intercept using Sen's method (Sen, 1968). Initially a set of linear slope is calculated using

$$T_i = \frac{X_j - X_k}{j - k} \quad \text{For } i = 1, 2, 3 \dots N \quad (\text{Eq.5})$$

where, X_j and X_k are considered as data value at time j and k ($j > k$), respectively. The median of these N values of T_i is represented as Sen's estimator of slope which is given as:

$$Q_i = \begin{cases} \frac{T_{N+1}}{2} & N \text{ is odd} \\ \frac{1}{2} \left(\frac{T_N}{2} + \frac{T_{N+1}}{2} \right) & N \text{ is even} \end{cases} \quad (\text{Eq.6})$$

Positive value of Q_i indicates upward or increasing trend and a negative value of Q_i represents a presence of downward or decreasing trend in the time series of the data. Using the median based non-parametric slope estimator method suggested by Theil-Sen method (Theil, 1950). The magnitude of the trend is calculated using Equation 7

$$\beta = \text{median} \frac{x_j - x_k}{j - k} \dots \forall \dots k < j \quad (\text{Eq.7})$$

where X_j and X_k are the consecutive data values of series in year j and k , and β is the magnitude of the trend slope of data values.

Spearman's Rho correlation

Then non-parametric Spearman's Rho correlation coefficient (ρ) was used to test the relation between rainfall and streamflow. The Spearman's rank-order correlation is considered as the non-parametric method of the Pearson product-moment correlation. Spearman's Rho correlation coefficient, (ρ , also signified by r_s) estimates the strength and path of connotation between two ranked variables. Normally the co-efficient of Spearman's Rho correlation is calculated to determine the dependency rate of dependent variable which is streamflow in the river to the independent variable rainfall.

Results and Discussions

Rainfall and stream flow behaviour of the lower Tamiraparani sub-basin

To study the overall behaviour of the stream flow and rainfall of the influencing rain gauges, mean monthly stream flow and rainfall, annual streamflow and annual rainfall for the basin was calculated for the period of 30 years. Through the analysis, it was observed that both the maximum streamflow and maximum rainfall were observed during the month of November for most of the years. This indicates that almost all the rainfall occurring during November contributes to the streamflow of the river. In the lower Tamiraparani sub-basin bimodal rainfall pattern was observed, similar pattern was also observed in the streamflow of the river. The observed anomaly between the catchment rainfall and streamflow is depicted in Fig. 3. Both the annual mean streamflow and theissen weighted catchment rainfall of the basin showed no significant trends at both 5% and 10% level of significance as depicted in Table 2. The calculated Spearman's Rho correlation coefficient between two parameters showed that annual stream flow and annual rainfall have a very strong positive correlation existing between each other. The work observed in the river basin of Sri Lanka suggested that positive correlation between the annual rainfall and streamflow implied that annual mean streamflow of the river is mainly contributed by the catchment rainfall (Abeysingha et

al., 2017). So in the lower Tamiraparani sub-basin the value of ($\rho = 0.72$) implied that streamflow is mainly contributed by the annual catchment rainfall from all influencing rain gauges from upper reaches of the gauge station. The results are in well agreement with the study by Sharannya et al. (2018), which also observed that changes in annual streamflow is directly correlated to the changes in annual rainfall for past and present scenarios.

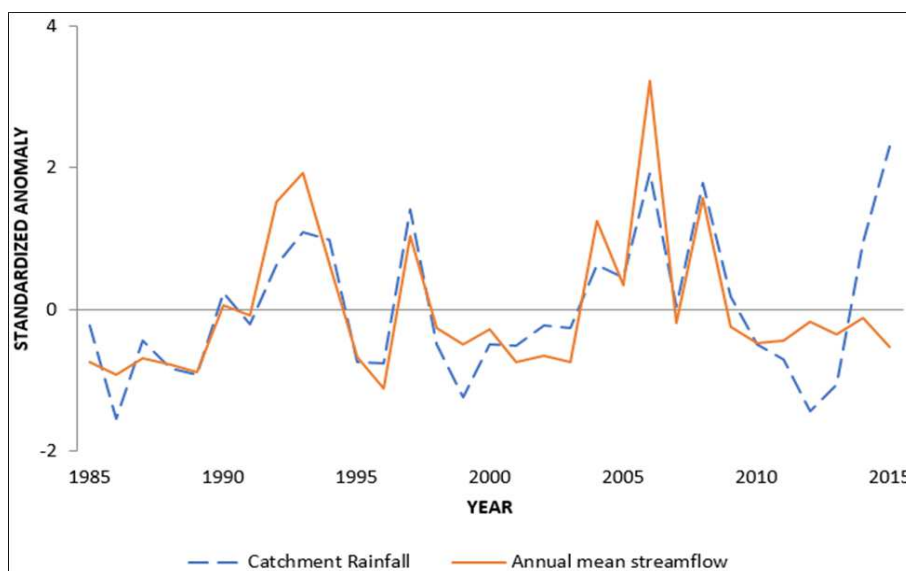


Figure 3. Temporal distribution of Standardized anomaly of catchment rainfall and annual mean stream flow for the period of 30 years

Table 2. Summarized results of Mann – Kendall test with Sen’s slope estimator for annual mean streamflow and Catchment rainfall

Sen’s slope	Annual mean stream flow(m ³ /s)	Catchment Rainfall(mm)
S	0.1799	4.3741

Trends in seasonal streamflow and seasonal rainfall

Monotonic trends in streamflow and rainfall for the observed four seasons were analysed for the sub-basin and the Sen’s slope estimator for all the seasons was calculated and given in *Table 3 and 4*. The calculated Sen’s slope estimator for all the influencing rain gauges for all the seasons depicted that almost more than 50% of the influencing rain gauges showed no significant trends as depicted in *Table 2*. Most of the major river basins in northern India showed decreasing trends in the streamflow due to the decreasing of trends in rainfall and due to the anthropogenic activities in the basin level (Jain et al., 2017). However, the sub-basin level analysis of the study of the lower Tamiraparani showed marginally increasing trends in streamflow for all the seasons. While for the calculated weighted average seasonal rainfall, both the winter and southwest monsoon periods showed minimally declining trends, which is only of about 0.7477 mm/year and 1.1091 mm/year as depicted in *Table 4*. The observed rainfall trends during the southwest monsoon and winter periods showed a decreasing trend in the last 30 years of the study area, which is well linked with the trend analysis in the

other major Indian river basin (Sharma and Singh, 2019). The calculated Spearman's rho correlation coefficient ($\rho = 0.53$) between the rainfall and streamflow in the southwest monsoon showed well correlation and during winter ($\rho = 0.40$) showed moderate correlation between the parameters as depicted in *Table 5*. In spite of the declining trends in the rainfall, minimal increase in streamflow implies that streamflow in lower Tamiraparani basin is not fully influenced by the rainfall during the periods instead partially influenced by others like anthropogenic activities which includes agricultural return flow, release water from hydro-electric power plant and rainfall in the upper hilly areas.

Table 3. Summarized results of Mann – Kendall test with Sen's slope estimator for seasonal rainfall (mm) of the influencing rain gauge stations of the streamflow in the sub- basin

Rain Gauge Stations	Summer	Winter	Northeast	Southwest
Ambasamudram	-0.009	0.0017	0.03	-0.0243
Ayikudi	0.0183	0.0001	0.0791	0.0038
Cheranmadevi	0.0191	0.0035	0.0804**	-0.0009
Gadana dam	-0.0187	-0.0442**	-0.0849	-0.0224
Kalakadu	0.0053	0.0059	0.03	-0.0131
Kanadian Anicut	0.0164	0.0122	0.034	-0.0028
Koilpatti	0.0024	-0.029*	-0.0016	-0.0403*
Manimuthar	0.0244	0.0429	0.1687	-0.0048
Palayamkottai	0.0237	-0.0117	0.0526	-0.0017
Sankarankoil	0.0524	-0.0009	0.0953*	0.0033
Senkottai	0.0131	-0.0008	0.0842	0.0312
Tenkasi	0.0284*	-0.0001	0.0511	-0.0096
Tirunelveli	-0.0119	-0.0199*	0.0128	-0.0217*

* - 5% level of significance, ** - 10% level of significance

Table 4. Summarized results of Mann – Kendall test with Sen's slope estimator for seasonal mean stream flow (m³/sec/year) and weighted average seasonal rainfall (mm/year) for the stations

Station	Summer	Winter	South West Monsoon	North East Monsoon
Murappanadu	0.0976	0.0778	0.0419	0.3337
Influencing rain gauges	1.1291	-0.7477	-1.1091	3.6938

Table 5. Calculated Spearman's Rho Correlation Coefficient between rainfall and stream flow

Seasons	Summer	Winter	Northeast	Southwest
P	0.26	0.40	0.82	0.53

These observations were following the same pattern in the study of trend assessment (Nune et al., 2013) between the rainfall and stream flow in Himayat Sagar catchment in southern India in which they observed a change in stream flow without significant change in rainfall, and then they endorsed the changes in stream flow trends to anthropogenic influences in the particular catchment. The observed trends for the

northeast monsoon for both streamflow and the rainfall showed minimal increase at a rate of 0.3337 m³/sec and 3.6938 mm/year but very strong positive correlation exists between the rainfall and stream flow ($\rho = 0.82$) during that period. The variation of the stream flow during North East Monsoon in the catchment is mainly attributed to the rainfall as evident by the significant positive correlation. The similar increasing trend pattern in the northeast monsoon rainfall was also observed in Amaravathi river basin one of the main river basins in Tamilnadu (Sridhar et al., 2017).

The observed trends between rainfall and stream flow during summer periods showed no significant trends which is of about 1.1291 mm/year and 0.0976 m³/sec and also there was weak correlation ($\rho = 0.26$) between the rainfall and stream flow which implies that influence of rainfall to the streamflow is very minimum during the summer periods. Vidhya and Arulkumar (2017) predicted that there will be increase in streamflow up to the period of 2040 due to climate changes and decrease in streamflow will be observed with the combined effects of streamflow and climate changes which is well correlated with the present study with observed increasing trends in streamflow with the act of climate change. Then the observed decrease in the summer monsoon rainfall implied the weakening of westerlies in lower troposphere and formation of easterly jet stream in the upper troposphere as mentioned in the study for the Indian region (Naidu et al., 2009). In order to compare the spatio-temporal variability of the seasonal rainfall and streamflow, standardized anomaly was calculated and given in *Fig. 4a-d* for all the seasons.

Trends in monthly mean streamflow

To study the monthly behaviour of streamflow in the river, trends using Mann – Kendall test and Sen's slope were analysed for inter-annual monthly mean streamflow values as depicted in *Table 6*. Inter-annual monthly mean streamflow showed significantly positive trends for some of the months as quoted in the work carried out in the Gomati river basin which is the perennial river in Northern India (Abeysingha et al., 2016). The trend patterns of Tamiraparani streamflow also followed the same significantly increasing trends at 5% and 10% level of significance for the months of February, March, May, September, November and December. The significantly increasing trends of the following months September, November and December showed the influence of northeast monsoon rainfall to the streamflow in the sub-basin. For the months of February, March and May, the significantly increasing trends are due to the influence of climate change in the upper reaches of the sub-basin.

Trends in monthly rainfall of the influencing rain gauge stations

Monotonic trends for the inter-annual mean monthly rainfall for all the influencing stations of the streamflow in the sub-basin were analysed and it is shown in *Table 7*. From the results, mixed trend was observed for all the months for all the rain gauges for the lower Tamiraparani sub-basin but none were significant. For all the influencing rain gauges, no significant trends were observed for some of the months. During the month of February which is the winter season, very minimum change rate of rainfall was observed for all the rain gauges studied. In the study analysed by Arthi et al. (2014) no significant trends were observed for the weekly and monthly rainfall in the Coimbatore district of Tamilnadu. The similar pattern of no significant trend was also observed in the present study for the monthly rainfall pattern in all rain gauges of the sub-basin which covers the Tirunelveli and Thoothukudi districts of Tamilnadu.

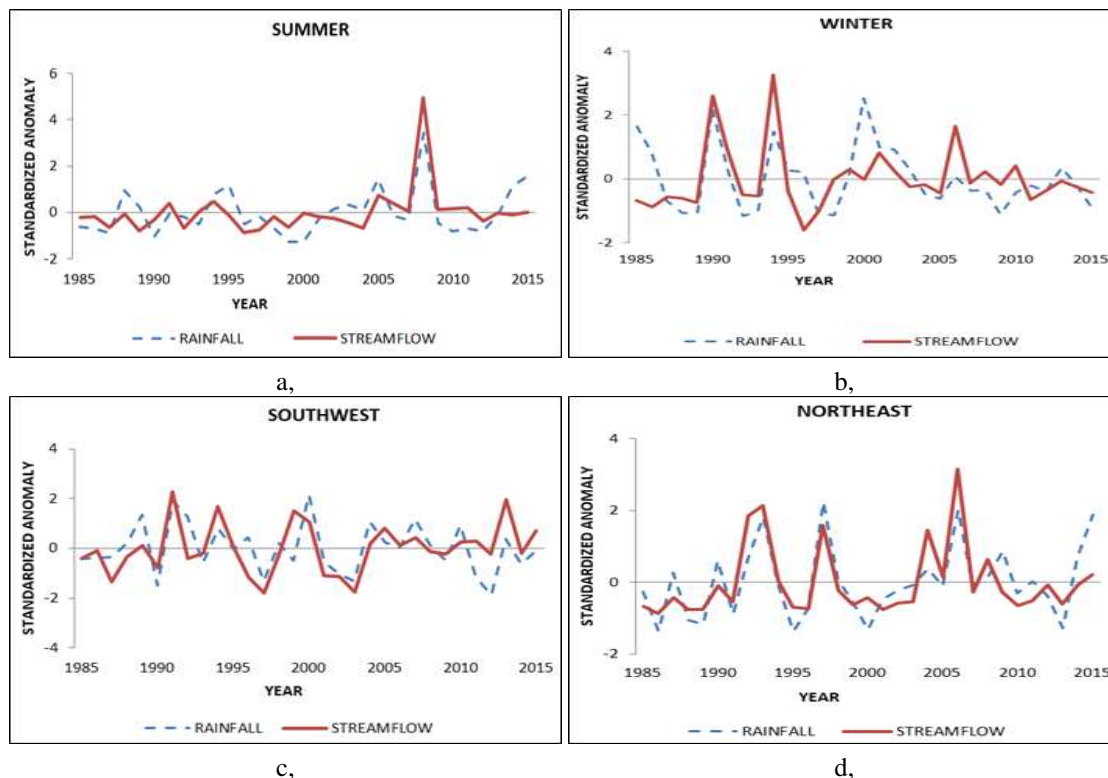


Figure 4. Temporal distribution of standardized anomalies of a: summer; b: winter; c: Southwest monsoon; d: Northeast monsoon streamflow and rainfall for all influencing rain gauges

Table 6. Summarized results of Mann – Kendall test with Sen’s slope estimator for mean monthly stream flow (m³/sec/year)

Month	Mean monthly streamflow
January	0.0896
February	0.1568*
March	0.0969**
April	0.0699
May	0.1332
June	0.0666
July	0.0899
August	0.0082
September	0.1104*
October	0.0443
November	0.6954**
December	0.6043**

* - 5% level of significance, ** - 10% level of significance

Trends in temperature

Table 8 showed the trends in annual, seasonal maximum and minimum temperature of the entire sub-basin for the study period. Annual temperature has increasing trends for both the maximum and minimum temperature. The results are well in agreement with the studies (Khavse et al., 2015; Ozgur et al., 2017), which analysed the long-term

temperature trends for the periods of 100 years in the study and they identified increasing trends in annual temperature and decreasing trends in the monthly temperature. Zarenistanak (2014) analysed the trend patterns of temperature in Iran and they found non-significant trends in rainfall and significant trends in the temperature during summer and they observed that maximum temperature was more stable than minimum and mean temperature very precisely. The similar pattern was also observed in the present study with the stable increasing trends at a rate of 0.01°C/year in the maximum temperature while the minimum temperature showed no stable trends. In the seasonal analysis, both the seasonal maximum and minimum temperature showed no significant trends for all the seasons except southwest monsoon and winter season. During the northeast monsoon period, both maximum and minimum temperature showed marginal increase during the analysis. The summer period of the study area showed decrease in summer temperature at a minimal rate of -0.0049°C and -0.0062°C for both maximum and minimum temperature, respectively. However, in the southwest monsoon and winter, significantly increasing trend for maximum temperature is observed. Even a small change in the temperature can affect the agricultural patterns in the area largely (Sharma and Chaudhary, 2014). Since this sub-basin covers the majority of agricultural land use patterns, it is advisable to take appropriate measures to protect the crop yield by reducing the drying tendency especially during the southwest monsoon period and winter periods.

Table 7. Summarized results of Mann – Kendall test with Sen’s slope estimator for Inter Annual monthly mean rainfall

Rain gauge station	January	February	March	April	May	June	July	August	September	October	November	December
Ambasamudram	-0.007	0.013	0.000	-0.015	-0.016	-0.022	-0.001	-0.020	0.013	0.011	0.101	0.023
Ayikudi	0.002	0.001	0.022	0.040	0.001	0.018	-0.003	-0.004	0.0252*	0.083	0.185*	0.047
Cheranmadevi	0.004	0.000	0.007	0.025	0.016	0.000	0.000	0.000	0.001	0.059	0.182	0.019
Gadana dam	-0.020	0.000	-0.016	-0.050	-0.012	-0.048	-0.016	-0.029	0.002	-0.155	-0.097	-0.037
Kalakadu	0.000	0.000	0.007	0.021	0.003	-0.020	-0.017	0.005	-0.005	0.018	0.143	-0.006
Kanadian Anicut	0.000	0.000	0.008	0.003	0.000	0.000	0.001	0.006	0.001	-0.046	0.077	0.058
Koilpatti	0.000	0.000	-0.009	-0.025	0.004	0.000	-0.018	0.000	-0.127	-0.063	0.073	-0.002
Manimuthar	0.007	0.032	0.027	0.002	-0.007	-0.018	-0.005	0.001	0.019	0.154	0.178	0.135
Palayamkottai	0.005	0.000	0.000	0.039	0.004	0.000	0.001	0.010	-0.010	-0.013	0.166	0.013
Sankarankoil	0.000	0.000	0.016	0.081	0.011	0.000	0.001	0.002	-0.004	0.047	0.257	0.024
Senkottai	0.000	0.000	-0.008	-0.013	-0.047	-0.035	0.030	0.012	0.087	0.041	0.143	0.046
Tenkasi	0.000	0.007	0.022	0.047	-0.001	-0.032	-0.029	-0.015	0.020	0.077	0.093	0.030
Tirunelveli	-0.0088**	0.000	-0.009	0.006	-0.016	0.000	0.001	0.001	-0.033	-0.027	0.086	-0.002

* - 5% level of significance, ** - 10% level of significance

Table 8. Summarized results of Mann – Kendall test with Sen’s slope estimator for annual and seasonal maximum and minimum temperature (°C/year) of station in Lower Tamiraparani sub-basin

Station	Annual	Summer	Winter	Southwest	Northeast
Max	0.01*	-0.0049	0.0149**	0.019*	0.004
Min	0.009	-0.0062	0.0122	0.012	0.009

* - 5% level of significance, ** - 10% level of significance

Conclusions and Recommendations

The analysis on the annual, seasonal and mean monthly streamflow observed at the Murappanadu gauge station for the period of 30 years, which is in the lower Tamiraparani sub-basin showed that there is less drying tendency of the downstream catchments of the entire Tamiraparani river basin. The annual rainfall contributed mainly to the annual streamflow as evident by the positive correlation. The observed rainfall trends during the Southwest monsoon and winter periods showed a nominally declining trend in the last 30 years of the study area and slightly increasing trends during northeast and summer season. The present study mainly concluded that variation of streamflow in the basin is partly attributed by the rainfall during southwest monsoon and the variation of streamflow during the Northeast monsoon is mainly attributed by the rainfall during the analysis period with the calculated correlation coefficient. Since the study area lies in the downstream side of river, the marginal increase in the streamflow with the decrease in rainfall during the southwest monsoon and winter indicates that other factors such as anthropogenic activities and other exogenous and ecological changes may contribute to changes in streamflow in the downstream areas. Decrease in rainfall and increase in temperature during these periods suggests that proper management measures ought to be adopted to avoid the detrimental effects of drying tendency of the area to provide proper agricultural production and ecosystem sustainability in the future. These sub-basin level seasonal observations from the present study are thus helpful in developing the holistic water management planning within the sub – basin particularly during the southwest monsoon and winter by taking the managerial practices at different spatial scales based on the needs, which may be useful to conserve the water to meet the demands in the drying trends by increasing water use efficiency of the river water in various sectors of the hydrological environment. From those observations, it is further recommended to carry out detailed analysis of rainfall, temperature and streamflow with the higher temporal resolution to develop a very precise relation among all the parameters. The decreased rainfall trends with increased trend in the temperature during southwest monsoon and winter season create a critical need to perform more detailed analysis to study the impacts on groundwater and surface water resources. Furthermore, this work can also be extended to study the impacts of projected land uses and future climatic projections over the streamflow to develop suitable policy and plans to maintain sustainability in available natural resources.

Acknowledgements. We acknowledge Dr. Arun Babu E, Assistant Professor, Centre for Water Resources, Anna University, Chennai, for his valuable guidance throughout the research period. The authors would also like to acknowledge the reviewers for their valuable guidance and suggestions to refine the manuscript.

REFERENCES

- [1] Abeyasingha, N. S., Singh, M., Sehgal, V. K., Kanna, M., Pathak, H. (2014): Trend analysis of Rainfall and Temperature of Districts of Gomati River Basin in North India. – J. Agri. Phy 14: 56-66.
- [2] Abeyasingha, N., Singh, M., Sehgal, V. K., Khanna, M. (2016): Analysis of trends in streamflow and its linkages with rainfall and anthropogenic factors in Gomati River basin of North India. – Theoretical and Applied Climatology 123(3-4): 785-799.

- [3] Abeysingha, N. S., Jayasekara, J. M. N. S., Meegastenna, T. J. (2017): Streamflow trends in up and midstream of Kirindi Oya river basin in Srilanka and its linkages to rainfall. – *Maussam* 68(1): 99-110.
- [4] Ahmad, I., Tang, D., Wang, T. F., Wang, M., Wagan, B. (2015): Precipitation trends over time using Mann-Kendall and Spearman's rho tests in Swat river basin, Pakistan. – *Advances in Meteorology*, Article ID 431860.
- [5] Anand, J., Gosain, A. K., Khosa, R., Srinivasan, R. (2018): Regional scale hydrologic modelling for prediction of Water balance, analysis of trends in streamflow and variations in streamflow: The case study of the Ganga river basin. – *Journal of Hydrology: Regional studies* 16: 32-53.
- [6] Anie John, S., Brema, J. (2018): Rainfall trend analysis by Mann-Kendall test for Vamanapuram River Basin, Kerala. – *International Journal of Civil Engineering and Technology* 9(13): 1549-1556.
- [7] Arthi, B., Manikandan, N., Narayanan, M. (2014): Trend analysis of Rainfall and Frequency of rainy days over Coimbatore. – *Mausam* 65(3): 379-384.
- [8] Chakraborty, S., Pandey, R. P., Chaube, U. C., Mishra, S. (2013): Trend and Variability analysis of rainfall series at Seonath River Basin, Chhattisgarh (India). – *International Journal of Applies sciences and Engineering research* 2.
- [9] Chand, M. B., Bhattarai, B. C., Baral, P., Pradhananga, N. S. (2019): Trend analysis of Temperature data for Narayani River Basin, Nepal. – *Sci* 1(1): 21.
- [10] Gautam, M. R., Acharya, K. (2012): Streamflow trends in Nepal. – *Hydrological Sciences Journal* 57(2): 344-357.
- [11] Gedefaw, M., Wang, H., Song, X., Yan, D. M., Dong, G. Q., Wang, J. W., Girma, A., Aijaz Ali, B., Batsuren, D., Abiyu, A., Qin, T. L. (2018): Trend analysis of Climatic and Hydrological Variables in the Awash River basin, Ethiopia. – *Water* 10: 1554.
- [12] Institute for Water studies. (2015): Report on Micro level Reappraisal study of Tamiraparani River basin. – Vol. 1, Public Works Department, Tamil Nadu.
- [13] Islam, S., Sikder, B. (2012): Hydrological Characteristics Analysis of Surma River in North-eastern Bangladesh: A Quantitative approach. – *Daffodil International University, Journal of Science and Technology* 11(2): 39-47.
- [14] Jain, S. K., Kumar, V. (2012): Trend analysis of Rainfall and Temperature data for India. – *Current science* 102(1): 37.
- [15] Jain, S. K., Nayak, P. C., Singh, Y., Chandniha, S. K. (2017): Trends in rainfall and peak flows for some river basins in India. – *Current science* 112(8).
- [16] Javari, M. (2017): Trend Analysis of Rainfall over Atrak River basin, Iran. – *International journal of Applied Environmental Sciences* 12(7): 1411-1448.
- [17] Jayadas, A., Ambujam, N. K. (2019): Observed trends in indices for daily rainfall extremes specific to the agriculture sector in Lower Vellar River sub-basin, India Extreme rainfall trends over Lower Vellar sub-basin. – *J. Earth Syst. Sci.* 128(3): 1-15.
- [18] Jayawardene, H., Jayawardene, D., Sonnadara, D. (2015): Interannual Variability of Precipitation in Sri Lanka. – *Journal of National Science Foundation of Srilanka* 43(1): 75-82.
- [19] Kendall, M. G. (1995): Rank correlation methods. – Hafner Publishing Co., New York.
- [20] Khavse, R., Deshmukh, R., Manikandan, N., Chaudhary, J. L., Kaushik, D. (2015): Statistical Analysis of Temperature and Rainfall Trend in Raipur District of Chhattisgarh. – *Current World Environment* 10(1): 305-312.
- [21] Mann, H. B. (1945): Non-parametric tests against trend. – *Econometrica* 3: 245-259.
- [22] Mondal, A., Kundu, S., Mukhopadhyay, A. (2012): Rainfall trend analysis by Mann-Kendall test: a case study of north-eastern part of Cuttack district, Orissa. – *International Journal of Geology, Earth and Environmental sciences* 2(1): 70-78.
- [23] Naidu, C. V., Durgalakshmi, K., Muni Krishna, K., Ramalingeshwara Rao, S., Sathyanarayana, G. C., Lakshminarayana, P., Malleswara Rao, L. (2009): Is summer

- monsoon rainfall decreasing over India in the global Warming era? – *J. Geophys. Res.* 114: D24108. <http://dx.doi.org/10.1029/2008JD011288>.
- [24] Naidu, C. V., Dharma Raju, A., Satyanarayana, G. Ch., Vinay Kumar, P., Chiranjeevi, G., Suchitra, P. (2015): An observational evidence of decrease of Indian summer monsoon rainfall in the recent three decades of global warming era. – *Global and Planetary Change* 127: 91-102.
- [25] Nouri, M., Homae, M., Bannayan, M. (2017): Quantitative trend, sensitivity and contribution analysis of reference evapotranspiration in some arid environments under climate change. – *Water resources Management* 31(7): 2207.
- [26] Nune, R., George, B. A., Teluguntla, P., Western, A. W. (2012): Relating trends in Stream flow to anthropogenic influences: a case study of Himayat Sagar catchment, India. – *Hydrol Earth Syst Sci.* Doi: 10.5194/hessd-9-9295.
- [27] Ozgur, K. I. S. I., Okan, E. R. A. Y., Cihan, M. E. R. T. (2017): Trend analysis of long term temperatures in Tbilisi, Georgia. – *Journal of Technical Science & Technologies* 5(2): 59.
- [28] Palaniswami, S., Muthiah, K. (2018): Change point detection and Trend analysis of Rainfall and Temperature series over the Vellar river basin. – *Pol.J.Environ.Stud.* 27(4): 1673-1681.
- [29] Panda, D. K., Kumar, A., Ghosh, S., Mohanty, R. K. (2013): Streamflow trends in the Mahanadi river basin (India); linkages to tropical climate variability. – *J. Hydrol* 495: 135-149.
- [30] Panda, R. K., Singh, G. (2016): Analysis of trend and Variability in the Mid-Mahanadi river basin of Eastern India. – *International scholarly and scientific Research & Innovation* 10(6).
- [31] Punyawardena, B. V. R., Premalal, K. H. M. S. (2013): Do trends in extreme positive rainfall anomalies in the central highlands of Srilanka Exist? – *Annals of Sri Lanka department of Agriculture* 15: 1-12.
- [32] Raghunath, H. M. (2006): *Hydrology: principles, analysis and design.* – New Delhi: New Age International.
- [33] Samo, S. R., Bhatti, N., Saand, A., Keerio, M. A., Bangwar, D. K. (2017): Temporal analysis of Temperature and precipitation trends in Shaheed Benazir Abad Sindh, Pakistan. – *Engineering technology and Applied Science research* 7(6): 2171-2176.
- [34] Sen, P. K. (1968): Estimates of the regression coefficient based on Kendall's tau. – *J. Am. Stat. Assoc.* 63: 1379-1389.
- [35] Sharannya, T. M., Mudbhatkal, A., Mahesha, A. (2018): Assessing climate change impacts on river hydrology- A case study in the Western Ghats of India. – *J. Earth syst. Sci.* 127: 78.
- [36] Sharif, M., Archer, D. R., Fowler, H. J., Forsythe, N. (2013): Trends in timing and magnitude of flow in the Upper Indus Basin. – *Hydrol. Earth Syst. Sci.* 17: 1503-1516.
- [37] Sharma, G. K., Chaudhary, J. L. (2014): Time trends in temperature of Bastar plateau agro climatic zones of Chhattisgarh. – *Mausam* 65(1): 29-36.
- [38] Sharma, S., Singh, P. K. (2019): Spatial trends in rainfall seasonality: a case study in Jharkhand, India. – *Weather* 70(1).
- [39] Silva, R., Santos, C., Moreira, M., Corte-Real, J., Silva, V., Medeiros, I. (2015): Rainfall and river flow trends using Mann-Kendall and Sen's slope estimator statistical test in Cobras River Basin. – *Nat hazards* 77(2): 1205-1221.
- [40] Sridhar, S. I., Raviraj, A. (2017): Statistical trend analysis of rainfall in Amaravathi River basin using Mann-Kendall. – *Current World Environment* 12(1): 89-96.
- [41] Taxak, A. K., Murumkumar, A. R., Arya, D. S. (2014): Long term spatial and temporal trends and Homogeneity analysis in Wainganga basin, Central India. – *Weather and Climate Extremes* 4: 50-61.

- [42] Theil, H. (1950): A rank - invariant method of linear and polynomial regression analysis. – Part I, II, III, In Proceedings of Koninklijke Nederlandse Akademie van Wetenschappen A.53, 386, 512, 1397.
- [43] Vidhya, R., Arulkumar, T. (2017): Geospatial Assessment Of Land Use and Climate change impacts on Hydrology of the Tamiraparani river basin, India. – Ecology, Environment and Conservation Paper 23(2): 992-1002.
- [44] Yadav, R., Tripathi, S. K., Pranuthi, G., Dubey, S. K. (2014): Trend analysis by Mann-Kendall test for precipitation and temperature for thirteen districts of Uttarakhand. – Journal of Agrometeorology 16(2): 164-171.
- [45] Zarenistanak, M., Dhorde, A. G., Kripalani, R. H. (2014): Trend analysis and Change point detection of annual and seasonal precipitation and temperature series over southwest Iran. – Journal of earth system science 123(2): 281.

IN-VITRO REGENERATION AND DEVELOPMENT FOR THE CONSERVATION AND PROPAGATION OF TOMATO PLANT (*SOLANUM LYCOPERSICUM*) AND CURRANT TOMATO (*S. PIMPINELLIFOLIUM*) FROM TWO DIFFERENT EXPLANTS

RAZA, M. A.^{1,2} – NAWAZ, A.² – ALI, M.¹ – ZAYNAB, M.³ – MUNTHA, S. T.⁴ – ZAIDI, S. H. R.⁵ – KHAN, A. R.⁵ – ZHENG, X.-L.^{1*}

¹College of Food Science and Biotechnology, Key Laboratory of Fruits and Vegetables Postharvest and Processing Technology Research of Zhejiang Province, Zhejiang Gongshang University, Hangzhou 310018, PR China

²Department of Horticulture, Faculty of Agricultural Sciences and Technology, Bahauddin Zakariya University, Multan 60000, Pakistan

³College of Life Sciences and Oceanography, Shenzhen University, Shenzhen 518060, PR China

⁴Laboratory of Germplasm Innovation and Molecular Breeding, Institute of Vegetable Sciences, Zhejiang University, Hangzhou 310058, PR China

⁵Zhejiang Key Laboratory of Crop Germplasm, Department of Agronomy, College of Agriculture and Biotechnology, Zhejiang University, Hangzhou 310058, PR China

*Corresponding author
zheng9393@163.com (Zheng, X.-L.)

(Received 12th Jul 2019; accepted 29th Nov 2019)

Abstract. While the contribution of stable tomato cultivars to ecological balance and environmental preservation has been recognized, two tomato cultivars have developed methods for tissue culture. For two tomato cultivars *Solanum lycopersicum* and *Solanum pimpinellifolium*, the regeneration capacity of two types of explants (cotyledons and stem node segments) was compared. Explants were cultured on five different regeneration media (½ MS and BAP) for stem node and MS for callus induction with a combination of 6-benzylaminopurine (BAP) and α -naphthaleneacetic acid (NAA). It was found that ability to regenerate was substantially dependent on both the cultivars and the type of explant. Stem nodes, followed by cotyledons, were the best explants to induce shoot regeneration. It was noticed that the best formulation of the medium for this regeneration from cotyledon explants used was MS with 1 mg/L BAP and MS+1BAP+0.25 NAA mg/L for callus induction in *S. pimpinellifolium* and for stem node explant the best formulation used was ½ MS and 7 mg/L BAP in *S. lycopersicum* was observed. All these data raised the possibility that to preserve and propagate wide hybrids of tomato materials *in vitro*, the regeneration ability of two explants was compared in *Solanum lycopersicum* and *S. pimpinellifolium*.

Keywords: tomato, explants, benzylaminopurine (BAP), α -naphthylacetic acid (NAA), stem node

Introduction

Tomato (*Solanum lycopersicum*, $2n=2x=24$), is an economically important crop worldwide. Moreover, this vegetable appears as a model plant for the introgression of agronomically crucial genes into the genome of dicotyledonous crop plants (Bhatia et al., 2004). The introduction of qualitative traits into commercial tomato cultivars is substantial, the aim being to ameliorate their nutritional value, productivity, abiotic stress resistance and application in molecular farming (Gerszberg et al., 2015). These crop species exhibited

extraordinary nutritional value that's why it is considered to be preventive food (Raiola et al., 2014).

Recently, this crop has gained huge popularity due to its anti-cancer and antioxidant characteristic (Khuong et al., 2013). Elaboration of the aforementioned system is essential for positive results in a broad range of techniques, including micro propagation, mutation selection, somatic hybridization or germplasm preservation of the ecological balance (Benson, 2000).

Numerous studies pointed out that the process of tomato regeneration via the organogenesis pathway is influenced by various elements, including media composition, environmental conditions, genotype, explant origin and its age (Ishag et al., 2009; Rashid and Bal, 2010; Zhang et al., 2012; Wayase and Shitole, 2014). So far, several procedures were developed concerning *in vitro* tomato plants regeneration from diverse explants through organogenesis and tomato transformation (Gerszberg et al., 2015).

These findings pointed out the intractability of *S. lycopersicum* explants (fragmentary or even complete incapability to react to *in vitro* culture impulses) (Bhatia et al., 2004). Consequently, the improvement of a suitable recovery system exploiting tissue culture techniques of *S. lycopersicum* plants has a great potential if we consider the fact that various genotypes differ in regards to their morphogenic potential.

Traditional methods for tomato breeding can be expensive and tedious due to the time and facilities required by each breeding generation and to the problems with the selection of suitable standards for cultivating (Gerszberg et al., 2015). Therefore, as an alternative, the creation of effective regeneration protocols is an essential step for exploiting of tissue or cell culture for genetic amelioration.

Tomato *in vitro* culture has been used successfully in various biotechnological applications including clonal propagation of high-value commercial cultivars, virus-free plants, and genetic transformation (Hanus-Fajerska, 2005; Li et al., 2011; Yarra et al., 2012; Namitha and Pradeep, 2013).

The current research was focused on the impact of different media formulations on the regeneration of two tomato inbred lines of *S. lycopersicum* and *S. pimpinellifolium*. We used two inbred lines for *in vitro* culture to establish the best system of tissue culture in tomato, to conserve F₁ plants from wide hybridization for the balance of ecology.

Materials and methods

Plant materials

The present research work was conducted at Department of Horticulture, Faculty of Agricultural Sciences and Technology, Bahauddin Zakariya University Multan, Pakistan. Two different inbred lines of *Solanum lycopersicum* cv. Micro-Tom (2n = 24) and *S. pimpinellifolium* line WVa700 (2n = 24) were used as a plant material in this study. The seeds of these varieties were surface sterilized with 70% (v / v) ethanol for 1 minute; subsequently they were dipped in a commercial bleach solution comprising 5.5% (w / v) of sodium hypochlorite for 10 minutes accompanied by 5 times rinsed with sterilized distilled water (3 minutes for each).

Culture conditions

The seeds were placed in a sterilized glass jar containing MS medium and then transferred to the growth room under controlled conditions at a temperature of 25±1°C

under 16 hours of photoperiod light intensity (1500 lux) and relative humidity (60-70%). Sterilized seeds were placed in jars on the seed germination medium. Four seeds were inoculated in each jar. The culture was then incubated in the incubation room until seed germination. It was observed that seeds began to grow in the dark and were later transferred to light.

The explants, both cotyledon and stem node, were taken from sterile seedlings (young seedlings) and placed on two media types: MS with different concentrations of benzylaminopurine (BAP i.e. cytokinin) and α - naphthaleneacetic acid (NAA i.e. auxin) for callus induction and $\frac{1}{2}$ MS and BAP with different concentrations for stem node induction respectively to conserve F₁ plants as shown in (Table 1 and Table 2). Experiment was repeated three times, with a total of 150 explants (50 explants per replicate).

Table 1. Composition of culture media used for stem node induction and plant regeneration of *Solanum lycopersicum* and *Solanum pimpinellifolium*

Medium	Composition
MS ₁	without plant growth regulators
MS ₂	$\frac{1}{2}$ MS + 1 mg/L BAP
MS ₃	$\frac{1}{2}$ MS + 3 mg/L BAP
MS ₄	$\frac{1}{2}$ MS + 5 mg/L BAP
MS ₅	$\frac{1}{2}$ MS+ 7 mg/L BAP

MS= Murashige and Skoog medium, BAP= benzyloaminopurine

Table 2. Composition of culture media used for callus induction and plant regeneration of *Solanum lycopersicum* and *Solanum pimpinellifolium*

Medium	Composition
MS ₁	without phytohormones
MS ₂	1 mg/L BAP + 0.25 mg/L NAA
MS ₃	1mg/L BAP + 0.50 mg/L NAA
MS ₄	2mg/L BAP + 0.25 mg/L NAA
MS ₅	2 mg/L BAP + 0.50 mg/L NAA

BAP= benzyloaminopurine, NAA= α - naphthaleneacetic acid

Experimental data for stem node induction and callus bud induction was collected after 15, 30 and 45 days, respectively. All the regeneration parameters (e.g. callus bud induction frequency and axillary bud frequency or growth features) were evaluated constantly. Explants of the two varieties were grown on 5 different media to evaluate their regeneration capacity.

Statistical analysis

The data collected was statistically analyzed following the analysis of the variance (ANOVA) technique and the mean differences were assessed by Duncan's Multiple Range Test (DMRT) using the statistical computer package program MSTATC (Gomez and Gomez, 1984).

Results

The purpose of this study was to investigate the performance of the two tomato explants, one explant (cotyledon) for callus induction and another explant (stem node) for axillary bud induction from two different cultivars i.e. inbred lines of *S. lycopersicum* cv. (Micro-Tom) ($2n = 24$) and *S. pimpinellifolium* line (WVa700) ($2n = 24$) were used as parents. The seed germination rate on MS media was 80% where 1.5% of the seeds were contaminated and the remainder was unable to grow. The impact of different levels and combinations of PGRs in both cultivars was noted in MS and $\frac{1}{2}$ MS media for tomato explant for callus proliferation and stem node induction.

In the present experiment, the capability of two types of tomato explants (cotyledons and stem nodes) for the regeneration through indirect organogenesis was tested. Both explants cut from tomato seedlings (young seedlings) were cultured on various media: $\frac{1}{2}$ MS+BAP (at different concentrations) for stem node and BAP (cytokinin), together with NAA (auxin) (at different concentrations) for cotyledon for the production of callus and multiple shoots (Table 1 and Table 2).

Generally, callus induction was noticed in the aforementioned type of explant culture. Among the 5 media tested, no substantial variation was observed in the frequency of callus induction except *S. pimpinellifolium* at BAP, together with NAA (at different concentrations) for cotyledon for the production of callus but the highest callus bud induction frequency was noticed with the concentration of MS+ 1BAP+0.25 NAA (Fig. 1).

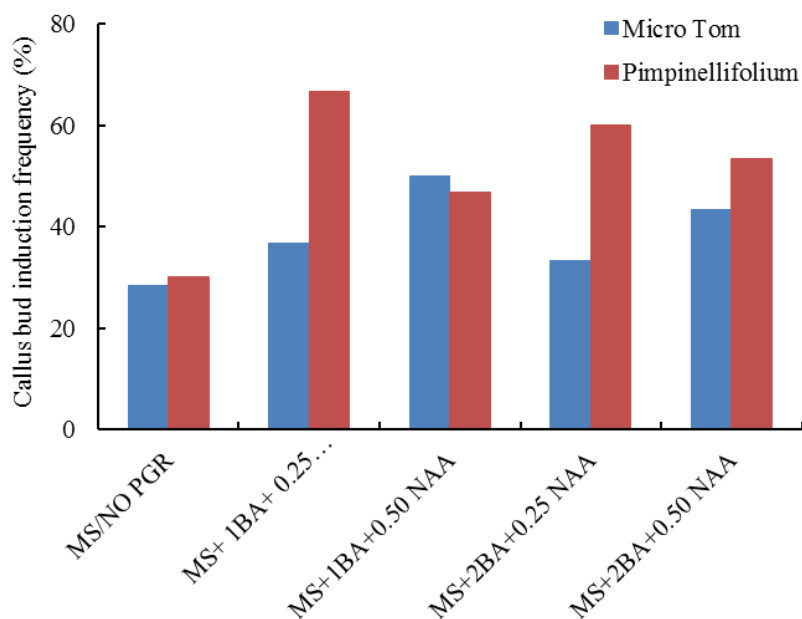


Figure 1. Callus bud induction frequency of *Solanum lycopersicum* cv. Micro-Tom and *S. pimpinellifolium* line WVa700

Callus formation began within ~12 days and shortly thereafter buds occurred. The origination of calli and shoots was noticed in the middle part of explants and on cut edges. In terms of morphology, the callus was fragile and characterized by a pale yellow or green color. In general, stem node explant showed high frequency of axillary bud regeneration in comparison to the callus originating from cotyledons because callus

induction took a long time to regenerate while stem node usually took less time. Shoot regeneration frequency changed with medium composition, the variety and also with explant type.

Despite the fact the plant regeneration could be caused with BAP only, combining with NAA enhanced the frequency of plant regeneration significantly. Based on our results, MS with 1mg/L BAP and 0.25 mg/L NAA is the best formulation of the medium for regeneration from the cotyledon explants used in this research. The regeneration of plants from axillary buds or shoots has been shown to be the most generally applicable and reliable method of *in vitro* true-to-type propagation (Fig. 2).

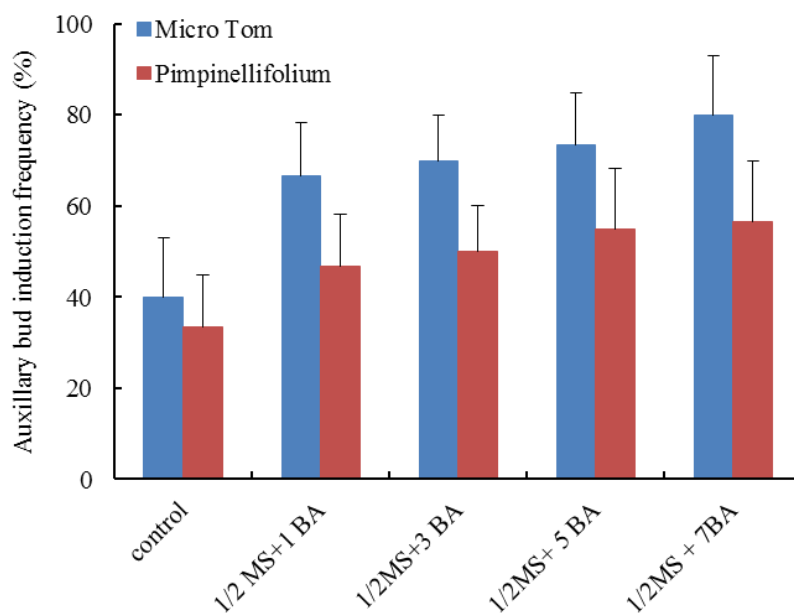


Figure 2. Axillary bud formation percentage of *Solanum lycopersicum* cv. Micro-Tom and *S. pimpinellifolium* line WVa700

We observed high regeneration axillary bud frequency from the stem node explants used in this study with the following concentrations $\frac{1}{2}$ MS and 1BA, $\frac{1}{2}$ MS and 3BA, $\frac{1}{2}$ MS and 5BA and $\frac{1}{2}$ MS and 7BA.

Our data showed the highest axillary bud regeneration frequency (80%) in *S. lycopersicum* (Micro-Tom) and (56.6%) in *S. pimpinellifolium* (WVa700). Moreover, by comparing two cultivars, highest germination rate was observed in Micro-Tom and lower in Pimpinellifolium (WVa700). It has therefore been noted that $\frac{1}{2}$ MS and 7 mg/L BA in Micro-Tom are the best formulation of the medium used for this stem node explant regeneration (*S. lycopersicum*) (Fig. 2).

According to recent findings, in callus induction, *S. pimpinellifolium* (WVa700) showed high callus bud induction and multiple shoot regeneration as compared to *Solanum lycopersicum* (Micro-Tom) (Fig. 1) while in stem node induction, *Solanum lycopersicum* (Micro-Tom) showed high axillary bud regeneration frequency over *S. pimpinellifolium* (WVa700) (Fig. 2 and Fig. 3).

Plants with a well-developed root system were moved to pots with a soil and perlite compound (3:1) and subsequently successfully acclimated and grown in a glasshouse. All *in vitro* plants were characterized by normal phenotypic appearance.

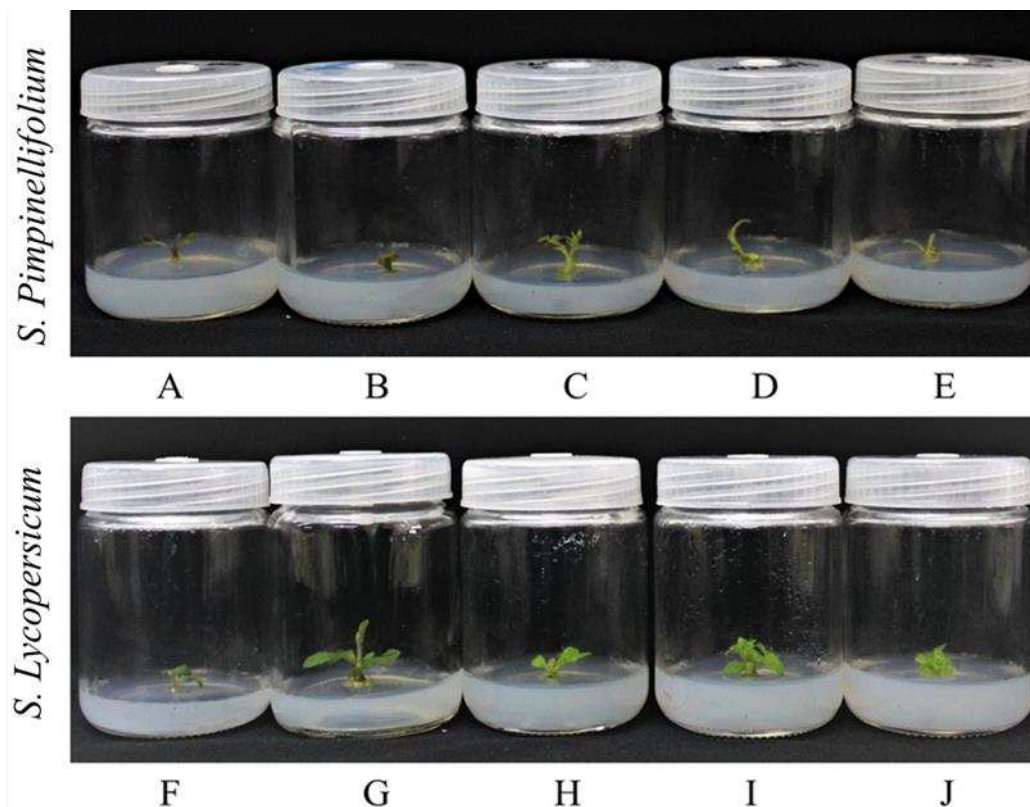


Figure 3. Axillary bud regeneration from stem node explant of *Solanum lycopersicum* cv. *Micro-Tom*, *S. pimpinellifolium* line *WVa700*, **A.** control, **B.** $\frac{1}{2}$ MS +1BA, **C.** $\frac{1}{2}$ MS +3BA, **D.** $\frac{1}{2}$ MS +5BA, **E.** $\frac{1}{2}$ MS +7BA for *S. pimpinellifolium* (*WVa700*), **F.** control, **G.** $\frac{1}{2}$ MS +7BA, **H.** $\frac{1}{2}$ MS +5BA, **I.** $\frac{1}{2}$ MS +3BA, **J.** $\frac{1}{2}$ MS +1BA, for *S. lycopersicum* (*Micro-Tom*)

Discussion

The seeds of both cultivars *Solanum lycopersicum* and *S. pimpinellifolium* were germinated on plant growth regulator-free MS medium. Fifteen days after germination, seedlings were harvested for use as explant. The use of *in vitro* methods is useful for many cultivars and the individuals who rely on them. It has been noted that plant regeneration by *in vitro* technologies is usually associated with the existence of variability among regenerants (Duncan, 1996).

In our previous studies, phenotypic traits of parents and their hybrids in terms of plant height (6.866 cm for M_W and 5.966 cm for W_M) at 6 leaf stage, plant height (56.66 cm for M_W and 74.33 cm for W_M) at 8 leaf stage (70 days old leaf), fruit shape index (0.953 for M_W and 0.985 for W_M) and single fruit weight (3.622 g for M_W and 4.352 g for W_M) were observed at 6 leaf stage (45 days old leaf) respectively (*Fig. 4* and *Fig. 5*) (Raza et al., 2017). The present experiment was performed to conserve F₁ generation used in our previous studies by using *in vitro* technique.

Plant growth regulators (PGRs); have influenced the morphogenic response by modifying various physiological processes. In the case of tomato regeneration, a broad range of different phytohormones (e.g. BAP, zeatin, 2iP (isopentenyl adenine), KIN (Kinetin), IAA, NAA (α -Naphthaleneacetic acid) IBA (Indole-3-butyric acid), 2, 4-D (2, 4-Dichlorophenoxyacetic acid) at varying concentrations have been used so far (Koleva Gudeva and Dedejski, 2012; Jehan and Hassanein, 2013; Koul et al., 2014).

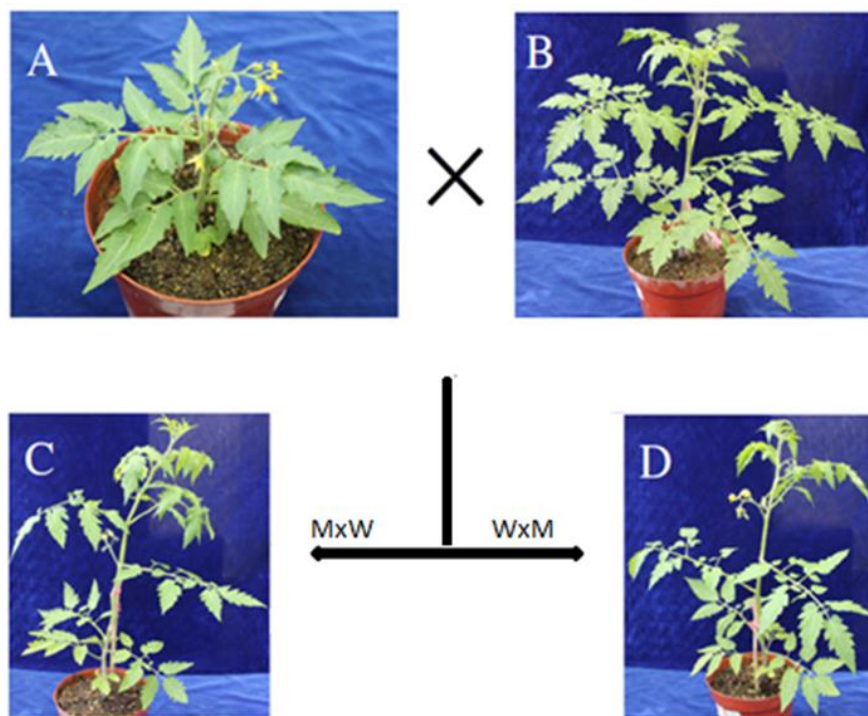


Figure 4. Parents and their reciprocal hybrids, **A.** *Solanum lycopersicum* cv. Micro-Tom, **B.** *S. pimpinellifolium* line WVa700, **C.** Micro-Tom_WVa700 i.e. (Micro-Tom X WVa700) **D.** WVa700_Micro-Tom i.e. (WVa700 X Micro-Tom)

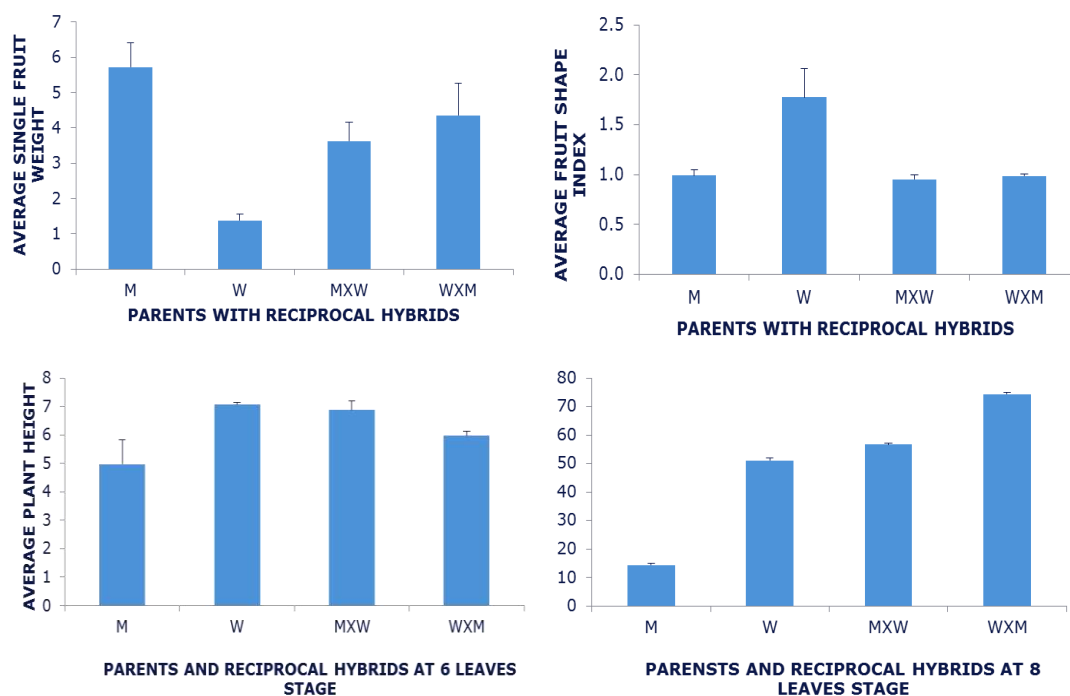


Figure 5. Phenotypic traits of parents *Solanum lycopersicum* cv. Micro-Tom, *S. pimpinellifolium* line WVa700, and their reciprocal hybrids (Micro-Tom X WVa700) and (WVa700 X Micro-Tom)

Moreover, the nature and concentration of PGRs used in the medium proven to be dependent on the cultivar being cultured and especially on the auxin or cytokinins applied (Koleva Gudeva and Dedejski, 2012; Bahurupe et al., 2013; Jehan and Hassanein, 2013; Koul et al., 2014; Wayase and Shitole, 2014). Majority of *in vitro* methods depend on induction of the regeneration process exploiting different explants cultured *in vitro*. Various types of explants were used by others: seed-cut cotyledon, hypocotyl, leaf, stem sections, nodes, internodes, pedicels, petioles, apical meristem, shoot apex/tip and inflorescences for organogenesis (Gerszberg et al., 2015).

A substantially higher range of BA (22.2 μM) was used for *Hedeoma multiflorum* micro propagation (Koroch et al., 1997). Slightly lower values were recorded for *S. lycopersicum* (Micro-tom) (Fig. 1). In many tree species, a range of auxin in combination with cytokinin played a vital role in multiple shoot regeneration (Vengadesan et al., 2002; Giri et al., 2004; Anis et al., 2011). Moreover, addition of low levels of auxin along with cytokinin is known to increase shoot numbers in many plant species like *Wrightia tinctoria* (Purohit et al., 1994).

Conclusion

The present study revealed an acceptable frequency of regeneration from two explants (cotyledons and stem node segments). Development of an effective *in vitro* regeneration protocol for crop species could be extremely beneficial in the process of cultivating and creating new varieties or in breeding lines in a relatively short period of time and for genetic improvement by exploiting biotechnology strategies. It is known that there are more than ten thousand tomato cultivars, and it is therefore impossible to establish a universal tomato regeneration protocol.

Hence, creating a tissue culture protocol for selected commercially important varieties is fully justified. This step should be preceded by wide screening of the above-mentioned varieties of morphogenic potential. Our study would provide novel valuable information about this very important issue. It can be concluded from the above findings that the regeneration protocol developed in this study is simple, reproducible and applicable.

Acknowledgements. The research was supported by Food Science and Engineering—the most important discipline of Zhejiang Province (No. 2017SIAR207) and Higher Education Commission of Pakistan (No: 21-1997/SRGP/ R&D/HEC/ 2018).

REFERENCES

- [1] Anis, M., Ahmad, N., Siddique, I., Varshney, A., Naz, R., Perveen, S., Khan, P. (2011): Biotechnological approaches for the conservation of some forest tree species. Forest decline: causes and impacts. – Nova Science Publishers Inc., New York, USA, 1-39.
- [2] Bahurupe, J., Patil, S., Pawar, B., Chimote, V., Kale, A. (2013): Callus induction and plantlet regeneration in tomato (*Solanum lycopersicum* L.). – Journal of Cell and Tissue Research 13(2): 3765.
- [3] Benson, E. E. (2000): Sepecial symposium: In vitro plant recalcitrance in vitro plant recalcitrance: An introduction. – In Vitro Cellular & Developmental Biology-Plant 36(3): 141-148.

- [4] Bhatia, P., Ashwath, N., Senaratna, T., Midmore, D. (2004): Tissue culture studies of tomato (*Lycopersicon esculentum*). – *Plant cell, tissue and organ culture* 78(1): 1-21.
- [5] Duncan, R. (1996): Tissue culture-induced variation and crop improvement. – *Advances in agronomy* 58: 201-240.
- [6] Gerszberg, A., Hnatuszko-Konka, K., Kowalczyk, T., Kononowicz, A. K. (2015): Tomato (*Solanum lycopersicum* L.) in the service of biotechnology. – *Plant Cell, Tissue and Organ Culture (PCTOC)* 120(3): 881-902.
- [7] Giri, C., Shyamkumar, B., Anjaneyulu, C. (2004): Progress in tissue culture, genetic transformation and applications of biotechnology to trees: an overview. – *Trees* 18(2): 115-135.
- [8] Gomez, K. A., Gomez, A. A. (1984): *Statistical procedures for agricultural research*. – John Wiley & Sons.
- [9] Hanus-Fajerska, E. (2005): Variation in Tomato Plants Regenerated from Cucumber Mosaic Virus Infected Tissue. – Paper presented at the XV Meeting of the EUCARPIA Tomato Working Group 789.
- [10] Ishag, S., Osman, M. G., Khalafalla, M. M. (2009): Effects of growth regulators, explant and genotype on shoot regeneration in tomato (*Lycopersicon esculentum* cv Omdurman). – *Int J Sustain Crop Prod* 4: 7-13.
- [11] Jehan, S., Hassanein, A. (2013): Hormonal requirements trigger different organogenic pathways on tomato nodal explants. – *American Journal of Plant Sciences* 4(11): 2118.
- [12] Khuong, T. T. H., Crété, P., Robaglia, C., Caffarri, S. (2013): Optimisation of tomato Micro-tom regeneration and selection on glufosinate/Basta and dependency of gene silencing on transgene copy number. – *Plant cell reports* 32(9): 1441-1454.
- [13] Koleva Gudeva, L., Dedejski, G. (2012): In vivo and in vitro production of some genotypes of cherry tomato *Solanum lycopersicum* var. *Cerasiforme* (DUNAL). – *International Journal of Farming and Allied Science* 1(4): 91-96.
- [14] Koroch, A. R., Juliani, H. R. Jr., Juliani, H. R., Trippi, V. S. (1997): Micropropagation and acclimatization of *Hedeoma multiflorum*. – *Plant cell, tissue and organ culture* 48: 213-17.
- [15] Koul, B., Srivastava, S., Amla, D., Sanyal, I. (2014): Establishment and optimization of agrobacterium-mediated transformation and regeneration of tomato (*Solanum lycopersicum* L.). – *International Journal of Biosciences (IJB)* 4(10): 51-69.
- [16] Li, T., Sun, J. K., Lu, Z. H., Liu, Q. (2011): Transformation of HBsAg (Hepatitis B Surface Antigen). – *Czech J. Genet. Plant Breed* 47(2): 69-77.
- [17] Namitha, K. K., Pradeep, S. N. (2013): Morphogenetic Potential of Tomato (*Lycopersicon esculentum*) cv.'Arka Ahuti' to Plant Growth Regulators. – *Notulae Scientia Biologicae* 5(2): 220.
- [18] Purohit, S., Kukda, G., Sharma, P., Tak, K. (1994): In vitro propagation of an adult tree *Wrightia tomentosa* through enhanced axillary branching. – *Plant Science* 103(1): 67-72.
- [19] Raiola, A., Rigano, M. M., Calafiore, R., Frusciante, L., Barone, A. (2014): Enhancing the health-promoting effects of tomato fruit for biofortified food. – *Mediators of inflammation* Vol. 2014: 139873.
- [20] Rashid, R., Bal, S. S. (2010): Effect of hormones on direct shoot regeneration in hypocotyl explants of tomato. – *Notulae Scientia Biologicae* 2(1): 70.
- [21] Raza, M. A., Yu, N., Wang, D., Cao, L., Gan, S., Chen, L. (2017): Differential DNA methylation and gene expression in reciprocal hybrids between *Solanum lycopersicum* and *S. pimpinellifolium*. – *DNA Research* 24: 597-607.
- [22] Vengadesan, G., Ganapathi, A., Amutha, S., Selvaraj, N. (2002): In vitro propagation of *Acacia* species—a review. – *Plant Science* 163(4): 663-671.
- [23] Wayase, U., Shitole, M. (2014): Effect of plant growth regulators on organogenesis in tomato (*Lycopersicon esculentum* Mill.) cv. Dhanashri. – *International Journal of Pure and Applied Sciences and Technology* 20(2): 65-71.

- [24] Yarra, R., He, S.-J., Abbagani, S., Ma, B., Bulle, M., Zhang, W.-K. (2012): Overexpression of a wheat Na⁺/H⁺ antiporter gene (TaNHX2) enhances tolerance to salt stress in transgenic tomato plants (*Solanum lycopersicum* L.). – *Plant Cell, Tissue and Organ Culture (PCTOC)* 111(1): 49-57.
- [25] Zhang, W., Hou, L., Zhao, H., Li, M. (2012): Factors affecting regeneration of tomato cotyledons. – *Bioscience Methods*, 3(4).

RAPID, NONDESTRUCTIVE AND SIMULTANEOUS PREDICTIONS OF SOIL CONTENT IN WULING MOUNTAIN AREA USING NEAR INFRARED SPECTROSCOPY

LUO, J.^{1,2§*} – WANG, Y.^{1§} – LOU, W. L.³ – ZHOU, X. L.^{1,2*} – TIAN, Y. X.^{1,2}

¹*Hunan Academy of Forestry, Changsha, Hunan Province, China*

²*Hunan Cili Forest Ecosystem State Research Station, Cili, Hunan, China*

³*Torch High Technology Industry Development Center, Ministry of Science & Technology, Beijing, China*

[§]*Contributed equally to this work.*

^{*}*Corresponding authors*

e-mail: luojia@hnlky.cn (Luo, J.); ZXI@hnlky.cn (Zhou, X. L.)

(Received 13th Jul 2019; accepted 25th Nov 2019)

Abstract. Estimating the soil content using near infrared (NIR) spectroscopy with an appropriate method of multivariate regression analysis, is a rapid and nondestructive testing technique with the virtue of high analysis speed and easy operation. Partial least squares (PLS) and least square support vector machine (LS-SVM) as the existing models widely used in other studies were improved and employed to develop an optimal regression model for the prediction of typical soil nutrient in Wuling mountain, Hunan Province, including total nitrogen, available phosphorus, and organic carbon. The performance of models established in this research was assessed by the coefficient of determination (R) and the root mean square error of calibration (RMSEC) and prediction (RMSEP). The result showed that the pre-processing method MSC+SG displayed the highest R values in PLS and LS-SVM models, which were 0.89 and 0.91, respectively. However, compared to the PLS model, LS-SVM displayed more desirable performance on the predictions. The RMSEC and RMSEP values of LS-SVM (4.84 and 4.75, respectively) were much better compared to PLS (6.15 and 6.58, respectively).

Keywords: *near infrared spectroscopy, chemometrics, soil nutrient analysis, prediction models, partial least squares*

Introduction

Soil nutrients are crucial for plant growth. The traditional analysis methods in laboratory restrict sample numbers due to the exhausting test time. Investigating the nutrient content in laboratory is time-consuming and demands considerable expenses. In the past decades, researches have been implemented to estimate the soil nutrient content from reflectance in the near infrared ranges (vis-NIR, 700-2500 nm) since spectrum data in the vis-NIR range has been proved to be reasonably accurate and fast in practical applications (Chung et al., 2015; Chen et al., 2017; Sampaio et al., 2018). With the development of chemometric methods and combination with NIR spectroscopy practices, these techniques have been

extensively applied to estimate soil nutrient content, such as total nitrogen, available phosphorus, and organic carbon (Pandit et al., 2010; Kwon et al., 2014; Sudarno et al., 2017; Yu and He, 2017). Compared with traditional test methods, the NIR spectroscopy techniques are not only cost- and time-effective, but also non-destructive, and demand no chemical reagents during the measurement (Al-Harrasi et al., 2017; Genisheva et al., 2018). Ecological environment monitoring requires rapid investigation and response to the drastic change of soil properties. Therefore, NIR spectroscopy techniques as promising test methods used in ecological environment monitoring will be effectively monitoring the change of soil properties in certain areas.

Partial least squares (PLS) regression is a statistical method, associated with principal component regression (PCR) (Yang and Ying, 2011). However, it is not to find the hyperplane of the minimum variance between dependent and independent variables, but to find a linear regression model by projecting predictive variables and observational variables into a new space. Under one algorithm, PLS can combine multiple linear regression (MLR), principal component analysis (PCA) and correlation analysis between two groups of variables together (Suykens and Vandewalle, 1999; Stella et al., 2015). PLS is a regression modeling method of multiple dependent variables for multiple independent variables, which can solve many problems that cannot be solved by ordinary multiple regression. Support vector machine (SVM) is a new general learning method proposed by Vapnik et al. (1997) according to statistical theory. It is based on the VC dimension (Vapnik Chervonenks Dimension) theory of statistical theory and the structural risk minimization principle. It can solve small sample, nonlinear, high dimension and local minima better. Practical problems such as classification, function approximation and time series prediction have become one of the hotspots in machine learning. Least square support vector machine (LS-SVM) is an improvement of SVM. Contrasted to the standard SVM model, this method has obvious advantages: (1) using equality constraints rather than inequality constraints in standard SVM algorithm; (2) transforming quadratic programming problem into solving linear equations directly (Suykens and Vandewalle, 1999; Li et al., 2017).

In China, a large sum of farmland has been converted to forests under the policy of returning farmland to forests in the past two decades. A lot of studies focused on the effects of this policy on ecosystem processes. However, little concerns were cast on the influence on the change of soil content, especially in hilly erosion areas. Therefore, the object of this paper is to evaluate the performance of PLS and LS-SVM modeling techniques to predict the typical nutrient content in soil, including total nitrogen, available phosphorus, and organic carbon content of soil sampled in the hilly erosion area of Cili where is located in Wuling mountain area of Hunan Province.

Materials and Methods

Soil sampling and laboratory analysis

The sample sites where the soil samples collected were in Liangxi Village, Wuling mountains of West Hunan Province in China (E111°12'42.836", N29°25'27.582"), about 7 km northwest of Cili County. The annual average temperature and precipitation in this location are 18.1°C and 1436 mm, respectively. The landscape mainly includes mountains, posts and plains, in which is dominated by red soil, and the layer of soil is more than 80 cm. The forest in the sample sites is a concentrated area of returning farmland to forest, due to its coverage rate in this area over 80%, and the vegetation types oriented at returning farmland to forests and secondary forests. In this area the soil parent rock is mainly sand shale, and the soil is primarily yellow-red soil and acid soil. *Pinus massoniana* forest, *Eucommia ulmoides* forest, *Citrus reticulata* and miscellaneous shrub forest are the dominant vegetation types in and around the sampled sites. All samples were taken randomly from 0-50 cm below the ground. In May 2018, the soil of this location was sampled in 29 different sites spanning mainly alongside the Li River, which was illustrated in *Fig. 1*. All soil samples of laboratory analysis were performed in accordance with Chinese Standards, including GB 9834, NY/T 1121.7, and HJ 615.

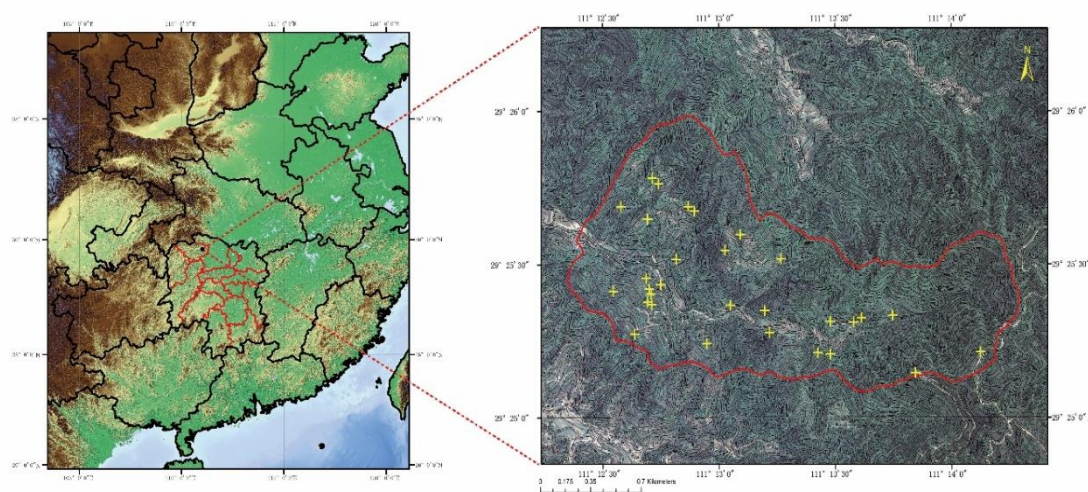


Figure 1. The location of the sites sampled: Cili, Hunan Province

Optical measurement

Vis-NIR spectra from 400 nm to 2500 nm, 2 nm/step with 1050 points was obtained by using Antaris II FT-NIR spectrometer (Thermo Fisher Scientific, the United States) charged with a sample cup. Every spectrum of all soil samples was collected with an average of 32 scans with 16 references scans before each sample.

Spectral data pre-treatment

It is prone to scatter effects for NIR spectroscopy when the samples are solid. The scattering effects are primarily caused by the distribution of sample size. Therefore, data pre-processing was crucial to establish the best models. The pre-processing techniques applied in this paper were standard normal variate (SNV), multiplicative scatter correction (MSC), 1st derivative using the Savitsky-Golay (SG) routine with 7 points and a 3rd order polynomial fitted to the data. All pre-processing steps were performed in Unscrambler X 10.4 (CAMO Software Inc., USA).

Comparison of calibration algorithms

In order to predict the of the soil nutrients content from the NIR spectrum data demands the calibration of the NIR spectra and the laboratory analysis values of soil nutrients. In our research, PLS and LS-SVM were used and compared to construct models to predict soil nutrient content. The data of the matrices are comprised of NIR spectra that was dominated by X and the values of soil content including total nitrogen, available phosphorus, and organic carbon that dominated by the vector Y.

Partial least squares regression

PLS regression is applied widely and considered as one of the most common multivariate methods for the establishment of predictive models. Usually, multiple linear regression (MLR) is utilized to build prediction models with a lot of factors. However, once the factor number is getting too large, the model will be defined as over-fitting which means that the model fits the sampled data perfectly but fails to predict the new sample data well. Under such circumstances, there are many dominant factors, but there may be few latent factors that account for most of the variation in the response. The primary concept of PLS is to attempt to extract these latent factors, accounting for as much of the dominant factor variation as possible while constructing the perfect models to fit the responses well. Therefore, PLS is also called “projection to latent structure” (Geladi and Kowalski, 1986; Tobias, 2017).

Least square support vector machine

LS-SVM is least squares version of SVM, which is a set of related supervised learning methods that analyze data and recognize patterns to be utilized for classification and prediction analysis. In these versions, the solution is obtained by solving a set of linear equations rather than a convex quadratic programming (QP) problem for classical SVMs (Suykens and Vandewalle, 1999). By this method, the improved LS-SVM avoids the complicated calculations of the classical SVMs. Also, it can also solve the problem of the multivariate calibration relatively fast and avoid over-fitting.

Evaluation of model performance

The quantitative models between NIR spectral data and soil content were built by PLS and LS-SVM, respectively. The modeling parameters were optimized and evaluated by the root mean square error of calibration (RMSEC) and prediction (RMSEP), and the coefficient of determination (R). RMSE and R are defined as follow (Eq. 1 and Eq. 2).

$$RMSE = \sqrt{\frac{\sum_{i=1}^n (y_i - \hat{y}_i)^2}{n}} \quad (\text{Eq.1})$$

The coefficient of determination is illustrated as below.

$$R = \sqrt{1 - \frac{\sum_{i=1}^n (y_i - \hat{y}_i)^2}{\sum_{i=1}^n (y_i - \bar{y})^2}} \quad (\text{Eq.2})$$

where n is the soil sample number in the validation test set, y_i and \hat{y}_i are the experimental data measured by laboratory analysis and the predictive results of the model for the corresponding test sample i, respectively.

Results

Soil content

Table 1 summarizes the laboratory analysis values of total nitrogen, available phosphorus, and organic carbon of all 306 soil samples, which displays the calibration set and the validation set, respectively. The total nitrogen content for all the sets ranging from 50.88 mg·kg⁻¹ to 648.93 mg·kg⁻¹, which has an average of 205.42 mg·kg⁻¹. The contents of available phosphorus and organic carbon for all sets are varying from 0.81 mg·kg⁻¹ to 90.45 mg·kg⁻¹ and 1.86 g·kg⁻¹ to 25.44 g·kg⁻¹, respectively. The average values of these two contents are 0.15 mg·kg⁻¹ and 13.72 g·kg⁻¹ separately. The mean values in these sets of total nitrogen, available phosphorus, and organic carbon content are similar to each other, while the standard deviations are also close to each other. Therefore, it can be confident in the validation.

NIR spectrum of soil samples

The original NIR spectrum (10,000-4000 cm⁻¹) of soil samples are represented in Fig. 2. NIR spectra displayed different degrees of migration or drift that made pretreatment

crucial for the establishment of prediction models with desirable performance. Moreover, the bands were broad and overlap, which made the spectrum difficult to interpret. Although the variables of the soil samples had quite a wide range of values, some useful information was represented in the vis-NIR region related to the total nitrogen, available phosphorus, and organic carbon of soil samples. There were mainly three absorption bands observed at 7083 cm^{-1} , 5205 cm^{-1} and 4532 cm^{-1} , among which 5205 cm^{-1} displayed the strongest absorption relevant with the combination of bending and stretching of hydroxyl group (O-H) of soil content (Cho et al., 1998; Cécillon et al., 2009; An et al., 2015). The absorption band observed at 7083 cm^{-1} was owing to the combination of C-H second overtone and the first overtone of O-H anti-symmetric stretching of soil (Cécillon et al., 2009; Viscarra Rossel and Hicks, 2015). The NIR spectrum of soil also displayed a major absorption band at 4532 cm^{-1} , due to the stretching and bending vibrations of C-H groups linked to organic carbon (Douglas et al., 2018).

Table 1. *Statistic description of soil nutrition content*

	Data set	Samples	Min.	Max.	Mean	Std dev.	CV (%)
Total nitrogen ($\text{mg}\cdot\text{kg}^{-1}$)	Calibration set	204	50.22	614.51	201.39	15.25	114
	Validation set	102	51.45	652.26	213.51	16.11	112
	All data	306	50.88	648.93	205.42	15.87	113
Available phosphorus ($\text{mg}\cdot\text{kg}^{-1}$)	Calibration set	204	0.84	89.54	52.13	9.84	108
	Validation set	102	0.79	91.21	53.25	9.68	106
	All data	306	0.81	90.45	52.43	9.79	106
Organic carbon ($\text{g}\cdot\text{kg}^{-1}$)	Calibration set	204	2.35	20.01	13.87	1.25	115
	Validation set	102	1.58	24.69	13.77	1.04	112
	All data	306	1.86	25.44	13.72	1.12	114

Min. is minimum, Max. is maximum, Std dev. is standard deviation, CV is coefficient variation

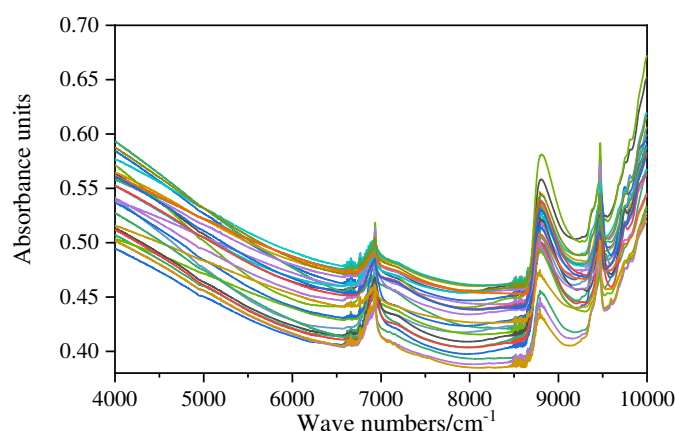


Figure 2. *Weak absorption peaks in NIR spectra of soil samples*

Performance of PLS and LS-SVM models

Pre-processing methods are quite crucial for the accuracy of models. For PLS, the most optimum calibration was obtained by applying the pre-processing method with MSC combined with SG pretreatment (RMSEC=6.15 and $R_c=0.89$). The validation results of MSC+SG pretreatment was also the best of all (RMSEP=6.58 and $R_p=0.90$).

For the spectra analyzed by LS-SVM, the most optimum calibration was achieved by using the pre-processing method also with MSC combined with SG pretreatment for prediction of total nitrogen, available phosphorus, and organic carbon content (RMSEC=4.84 and $R_c=0.91$), which maintained the best validation results (RMSEP=4.75 and $R_p=0.93$). The optimum calibrated PLS and LS-SVM models were employed to conduct predictions for total nitrogen, available phosphorus, and organic carbon content that the results confirmed the desirable accuracy of these selected models in bold in *Table 2*.

Table 2. Analysis of PLSR and LS-SVM models with selected pre-processing methods including SG, ANV+SG, MSC+SG and 1stD+SD

Model types	Data pre-processing	Calibration set		Validation set	
		R_c	RMSEC	R_p	RMSEP
PLSR	None	0.78	8.55	0.76	8.01
	SG	0.84	7.21	0.86	7.45
	SNV+SG	0.86	7.02	0.84	6.89
	MSC+SG	0.89	6.15	0.90	6.58
	1stD+SG	0.88	6.54	0.89	6.67
LS-SVM	None	0.86	6.21	0.87	6.34
	SG	0.88	5.98	0.86	5.74
	SNV+SG	0.90	5.25	0.91	5.12
	MSC+SG	0.91	4.84	0.93	4.75
	1stD+SG	0.86	4.97	0.87	4.87

The results emphasized in bold are selected models

Discussion

NIR spectra of solid samples is usually prone to scatter noise due to the uneven distribution of particle size of samples, for example soil samples (Casale and Simonetti, 2014; Acquah et al., 2015). To take full advantage of the spectra data re sample corded by NIR and to diminish the noise to the most extent, the data pre-processing methods are usually crucial to the establishment of the calibration model. The results of prediction are related to some uncertainties which mainly comprise environment conditions, measurement error, model selection and system settings. A simultaneous applications of data pre-processing methods and PLS models were applied to validate which model could

be more accurate in the predictions of soil nutrients including total nitrogen, available phosphorus, and organic carbon content. A large number of computer runs were required in order to establish different models derived from analysis of NIR spectrum data corresponding to different pre-processing methods. It is crucial to enhance the predictive ability of the analysis of the NIR spectroscopy data, particularly for batch samples of more sophisticated systems (Suykens and Vandewalle, 1999).

In addition, it is obvious that the optimal smoothing mode should be chosen in order to implement the pretreatment optimization for the following establishment of the best prediction models. The performance of PLS and LS-SVM was different to some extent when SG smoothing and the pre-processing method (MSC, 1stD or SNV) was applied separately or combined, respectively. Spectra could be normalized by SNV when there were variations of the effective path length among samples. Moreover, this kind of path length could emerge especially when investigating powdered samples. In this study, the particle size, structure and color were varying among the soil samples.

SG filter is widely used in data flow smoothing and de-noising. It is known as a smoothing method based upon the local polynomial least squares fitting in time domain (Tobias, 2017). The most important merit of this method is that it can keep the shape and width of the signal unchanged while filtering out the noise. When smoothing filter is used to filter the signal, the low-frequency components of the signal are fitted and the high-frequency components are smoothed out. If the noise is at high frequency, then the result of filtering is to remove the noise. Otherwise, if the noise is at low frequency, then the result of filtering is to leave the noise (Geladi et al., 1985; Norgaard et al., 2000). MSC is a multivariate scattering correction technique, which can effectively eliminate the baseline shift and offset caused by scattering between samples and improve the signal-to-noise ratio of the original spectra. This pre-processing method can be regarded as a suitable way to smooth the spectroscopy data of samples with different structure and size. It could be concluded from *Table 2* that the data pre-processing method (MSC+SG) displayed the highest R values in PLS and LS-SVM models, which were 0.89 and 0.91, respectively. This step of pre-processing methods could eliminate the spectrum differences in the same series of samples caused by the inhomogeneity of particle size. However, model effect could be different when the pre-processing methods were applied separately or combined. The R_c values of PLS and LS-SVM models used SG pretreatment method separately were both lower than SG combined with SNV, MSC or 1stD. Therefore, the appropriate combination should be screened for the pre-processing optimization.

Comparing the performances of PLS and LS-SVM, LS-SVM displayed better prediction ability. For PLS and LS-SVM models, all variables from the soil sample spectrum were applied to the calibration of the models. The values of RSMEC and RMSEP of LS-SVM (4.84 and 4.75, respectively) were better compared to PLS (6.15 and 6.58, respectively). LS-SVM uses the least squares linear system as the loss function to replace it, so the inequality constraint is replaced by the equality constraint method, and

the LS-SVM evolves into the solution of linear equations, which improves the speed of solution and the convergence precision of solution. Therefore, compared with PLS model, LS-SVM demonstrated more desirable ability of predictions on the content of soil nutrients.

Conclusions

Based on NIR spectroscopy and chemometrics, two quantitative prediction models of soil nutrients including total nitrogen, available phosphorus, and organic carbon were established, which were PLS and LS-SVM models. As the existing prediction models, these models were widely applied in other studies, which were improved and adopted in this study for the prediction of typical soil nutrient in Wuling mountain, Hunan Province, including total nitrogen, available phosphorus, and organic carbon. The results illustrated that these two models both had good predictive ability. The pre-processing methods could enhance the ability of prediction models. MSC+SG method displayed the highest R values in PLS and LS-SVM models, which were 0.89 and 0.91, respectively. However, compared with PLS model, LS-SVM displayed more desirable performance on the predictions. The values of RSMEC and RMSEP of LS-SVM (4.84 and 4.75, respectively) were much better compared to PLS (6.15 and 6.58, respectively). The proposed methods in this study demonstrated obvious superiority over traditional laboratory test. The results demonstrated that NIR spectroscopy combined with chemometric technique is a rapid, low cost and reliable method for the analysis of soil content in the soil monitoring and improvement along the area of Wuling mountain. Further studies will be performed to validate the model in another place located in Hunan Province. In addition, more predictive models will be developed for practical applications in future.

Acknowledgements. This work was supported by the grant of Forestry Science and Technology Innovation Project in Hunan (XLC201970), Forestry Science and Technology Plan Project in Hunan (XLC201701-2), Major Research and Development Program in Hunan (2017NK2223), Forestry Science and Technology Plan Project in Hunan (XLKPT201710), National Science and Technology Plan for Twelfth Five-Year in the Countryside (2015BAD07B04), National Key R & D Program of China (2017YFC0505506), and Forestry Science and Technology Project in Hunan (2012-HNLYKY-01), Forestry Science and Technology Key Innovation Project in Hunan (HNGYL-2019-01).

REFERENCES

- [1] Acquah, G. E., Via, B. K., Fasina, O. O., Eckhardt, L. G. (2015): Non-destructive prediction of the properties of forest biomass for chemical and bioenergy applications using near infrared spectroscopy. – *Journal of Near Infrared Spectroscopy* 23: 93-102.
- [2] Al-Harrasi, A., Rehman, N. U., Mabood, F., Albroumi, M., Ali, L., Hussain, J., Hussain, H., Csuk, R., Khan, A. L., Alam, T., Alameri, S. (2017): Application of NIRS coupled with PLS regression as a rapid, non-destructive alternative method for quantification of KBA in

- Boswellia sacra. – *Spectrochimica Acta Part A: Molecular and Biomolecular Spectroscopy* 184: 277-285.
- [3] An, X., Li, M., Zheng, L., Sun, H. (2015): Eliminating the interference of soil moisture and particle size on predicting soil total nitrogen content using a NIRS-based portable detector. – *Computers and Electronics in Agriculture* 112: 47-53.
- [4] Casale, M., Simonetti, R. (2014): Review: Near infrared spectroscopy for analysing olive oils. – *Journal of Near Infrared Spectroscopy* 22: 59-80.
- [5] Cécillon, L., Barthès, B. G., Gomez, C., Ertlen, D., Genot, V., Hedde, M., Stevens, A., Brun, J. J. (2009): Assessment and monitoring of soil quality using near-infrared reflectance spectroscopy (NIRS). – *European Journal of Soil Science* 60: 770-784.
- [6] Chen, Y., Delaney, L., Johnson, S., Wendland, P., Prata, R. (2017): Using near infrared spectroscopy to determine moisture and starch content of corn processing products. – *Journal of Near Infrared Spectroscopy* 25: 348-359.
- [7] Cho, R. K., Lin, G., Kwon, Y. K. (1998): Nondestructive analysis for nitrogens of soils by near infrared reflectance spectroscopy. – *Journal of Near Infrared Spectroscopy* 6: A87-A91.
- [8] Chung, I. M., Kim, J. K., Lee, J. K., Kim, S. H. (2015): Discrimination of geographical origin of rice (*Oryza sativa* L.) by multielement analysis using inductively coupled plasma atomic emission spectroscopy and multivariate analysis. – *Journal of Cereal Science* 65: 252-259.
- [9] Douglas, R. K., Nawar, S., Alamar, M. C., Mouazen, A. M., Coulon, F. (2018): Rapid prediction of total petroleum hydrocarbons concentration in contaminated soil using vis-NIR spectroscopy and regression techniques. – *Science of The Total Environment* 616-617: 147-155.
- [10] Geladi, P., Macdougall, D., Martens, H. (1985): Linearization and scatter-correction for near-infrared reflectance spectra of meat. – *Applied Spectroscopy* 39: 491-500.
- [11] Geladi, P., Kowalski, B. R. (1986): Partial least-squares regression: a tutorial. – *Analytica Chimica Acta* 185: 1-17.
- [12] Genisheva, Z., Quintelas, C., Mesquita, D. P., Ferreira, E. C., Oliveira, J. M., Amaral, A. L. (2018): New PLS analysis approach to wine volatile compounds characterization by near infrared spectroscopy (NIR). – *Food Chemistry* 246: 172-178.
- [13] Kwon, Y. K., Bong, Y. S., Lee, K. S., Hwang, G. S. (2014): An integrated analysis for determining the geographical origin of medicinal herbs using ICP-AES/ICP-MS and ¹H NMR analysis. – *Food Chemistry* 161: 168-175.
- [14] Li, Y., Zhang, J., Li, T., Liu, H., Li, J., Wang, Y. (2017): Geographical traceability of wild *Boletus edulis* based on data fusion of FT-MIR and ICP-AES coupled with data mining methods (SVM). – *Spectrochimica Acta Part A: Molecular and Biomolecular Spectroscopy* 177: 20-27.
- [15] Norgaard, L., Saudland, A., Wagner, J., Nielsen, J. P., Munck, L., Engelsen, S. B. (2000): Interval partial least-squares regression (ipls): a comparative chemometric study with an example from near-infrared spectroscopy. – *Applied Spectroscopy* 54: 413-419.
- [16] Pandit, C. M., Filippelli, G. M., Li, L. (2010): Estimation of heavy-metal contamination in soil using reflectance spectroscopy and partial least-squares regression. – *International Journal of Remote Sensing* 31: 4111-4123.
- [17] Sampaio, P. S., Soares, A., Castanho, A., Almeida, A. S., Oliveira, J., Brites, C. (2018): Optimization of rice amylose determination by NIR-spectroscopy using PLS chemometrics algorithms. – *Food Chemistry* 242: 196-204.
- [18] Stella, E., Moschetti, R., Haff, R. P., Monarca, D., Cecchini, M., Contini, M., Massantini, R. (2015): Review: Recent advances in the use of non-destructive near infrared spectroscopy for intact olive fruits. – *Journal of Near Infrared Spectroscopy* 23: 197-208.

- [19] Sudarno, Silalahi, D. D., Risman, T., Widyastuti, B. L., Davrieux, F., Yuan, Y. Y., Caliman, J. P. (2017): Rapid determination of oil content in dried-ground oil palm mesocarp and kernel using near infrared spectroscopy. – *Journal of Near Infrared Spectroscopy* 25: 338-347.
- [20] Suykens, J. A. K., Vandewalle, J. (1999): Least squares support vector machine classifiers. – *Neural Processing Letters* 9: 293-300.
- [21] Tobias, R. D. (2017): An introduction to partial least squares regression. – Sas Institute Inc., Cary, NC.
- [22] Vapnik, V. N. (1997): The nature of statistical learning theory. – *Technometrics* 38: 409-409.
- [23] Viscarra Rossel, R. A., Hicks, W. S. (2015): Soil organic carbon and its fractions estimated by visible–near infrared transfer functions. – *European Journal of Soil Science* 66: 438-450.
- [24] Yang, D., Ying, Y. (2011): Applications of Raman Spectroscopy in Agricultural Products and Food Analysis: A Review. – *Applied Spectroscopy Reviews* 46: 539-560.
- [25] Yu, X. L., He, Y. (2017): Challenges and opportunities in quantitative analyses of lead, cadmium, and hexavalent chromium in plant materials by laser-induced breakdown spectroscopy: A review. – *Applied Spectroscopy Reviews* 52: 605-622.

COMPARISON OF SINGLE AND COMPOUND WASHING OF REMEDIATING PB CONTAMINATED SOIL OF NON-FERROUS SMELTERS

GUO, W.^{1,2} – ZHANG, H. Z.^{1*} – YIN, X. X.^{1,3} – WANG, Z. L.^{1,4}

¹*School of Water Resources and Environment, China University of Geosciences
#29 Xueyuan Road, Haidian District, Beijing 100083, P. R. China*

²*Taiyuan Environmental Monitoring Center, Taiyuan Ecology and Environment Bureau
Taiyuan 030002, P. R. China*

³*Research Center for Eco-Environmental Sciences, Chinese Academy of Sciences
Beijing 100085, P. R. China*

⁴*Beijing Zhongdihongke Environmental Science and Technology Co. Ltd.
Beijing 100011, P. R. China*

**Corresponding author*

e-mail: huanzhen@cugb.edu.cn; phone: +86-10-8232-1068

(Received 13th Jul 2019; accepted 25th Nov 2019)

Abstract. Orthogonal and single factor experiments were used to investigate the remediation effect of single and compound washing on Pb contaminated soil from a typical non-ferrous metal smelter. The optimal washing conditions and speciation distribution of Pb were determined. The obtained removal efficiency of Pb from the soil is 68.35%, which could be remedied to less than "risk intervention values (Pb < 2500 mg·kg⁻¹) for soil contamination of the development land" in soil environmental quality standard China (GB36600-2018) when the compound ratio of HCl & Rhamnolipid is 1:1, the ratio of liquid-solid is 10:1 and the washing time is 1080 min. The removal efficiency of Pb are significantly higher when using compound eluents compared to single eluents, such as HCl, EDTA, oxalic acid and rhamnolipid. Moreover, compound eluents can effectively remove active Pb from soil, which greatly reduces their bioavailability and environmental risk.

Keywords: *heavy metal pollution, soil washing, rhamnolipid, speciation distribution, kinetic analysis*

Introduction

Global industrialization is accelerating at a continuous rate. The development of the non-ferrous metal mining, smelting and processing industry in particular has led to the severe degradation of soils due to heavy metal pollution, and such contamination incidents have also attracted much attention (Park et al., 2002; Li et al., 2013; de Andrade Lima and Bernardez, 2017). Many experimental remediation technologies for heavy metal contaminated soils, such as soil exchange, solidification and stabilization, vitrification, and phytoremediation microbial remediation, have been developed (Dermont et al., 2008; Voglar and Leštan, 2011; Reza et al., 2015). However, they are difficult to implement in practical remediation projects of heavy metal contaminated soil due to their limitations, characteristics, secondary pollution, cost end effect on contaminated soil (Moutsatsou et al., 2006; Chen et al., 2017).

Soil contaminated by heavy metals in non-ferrous metal smelters is characterized by its high pollution intensity, complex forms, and is often accompanied by other heavy metals, which brings great challenges to its remediation (Bacon and Dinev, 2005; Burges et al., 2017). However, chemical washing has a promising application prospect as it is highly efficient, low cost, and has a short cycle (Abumaizar and Smith, 1999; de Andrade Lima and Bernardez,

2017). The type of eluent is the key to the repair effect, and the mechanism and removal capacity of different types of eluents vary. Common eluents include: inorganic eluents, artificial chelating agents, natural organic acid, biological surfactant and compound eluents (Dermont et al., 2008). For example, inorganic eluents can quickly and effectively remove heavy metals from the soil, and is low cost, but may damage the soil structure and biology. Artificial chelating agents can effectively remove heavy metals by self-chelating, but they are not easily biodegradable, and therefore cause secondary soil pollution. The costs of biological surfactants are often too high, which limits their engineering applications (Chen et al., 2017). Compound washing can not only improve the removal efficiency of pollutants, but also avoids secondary pollution and high cost associated with a single eluent through the synergistic solubilization of compound reagents.

In this paper, Pb contaminated soil from typical non-ferrous metal smelter was selected as the research object, and remedial target is to satisfy with the requirement of the “Risk control standard for soil contamination of development land” in soil environmental quality standard China (GB36600-2018). Hydrochloric Acid (HCl), Oxalic Acid, Ethylene Diamine Tetraacetic Acid (EDTA) and Rhamnolipid were selected as eluents, and oscillating washing experiments were carried out on the contaminated soil by single and compound washing. The optimal combination of eluents and conditions of washing were determined, and the washing kinetics and washing mechanism were explored to establish the theoretical basis and technical support for the actual remediation project of heavy metal contaminated soil in non-ferrous metal smelters.

Materials and methods

Soil samples collection and preservation

Soil samples were collected from the surface layer (0-100 cm) of a typical non-ferrous metal smelter in Yunnan, China (103.329, 26.455). Remove the impurities, such as stones and plant roots, and air-dry naturally in the absence of light. After crushing, they are fully mixed and evenly stored in plastic bags. Subsequently, soil samples are screened according to the specific requirements of the experiment. Some of the soil samples were screened with 100 meshes for the determination of soil physical and chemical properties and heavy metals. Another part of the soil samples was screened with 20 meshes for washing experiments. The basic characteristics and test methods of the soil sample are shown in *Table 1* and *Fig. 1*.

Table 1. Basic characteristics of contaminated soil

Parameter	Detection method ^a	Value
Soil type	/	Red soil
Soil size (%)	LY/T 1225-1999	/
Clay (<0.002mm)	/	3.57
Silt (0.002~0.05mm)	/	57.41
Sand (0.05~2mm)	/	38.02
pH	NY/T 1377-2007	6.70
Organic matter content (g·kg ⁻¹)	LY/T 1237-1999	61.2
CEC ^b (cmol·kg ⁻¹)	LY/T 1243-1999	13.5
TN (g·kg ⁻¹)	LY/T 1228-2015	0.95
TP (g·kg ⁻¹)	LY/T 1232-2015	2.69
Total Pb (mg·kg ⁻¹)	GB/T 17141-1997	7500.00

^a China standard detection method for soil, ^b Cation exchange capacity



Figure 1. Soil samples collection and preservation

Experimental equipment

Inductively Coupled Plasma Optical Emission Spectrometer (ICP-OES-5100, Agilent Technologies), Thermostatic oscillator (THZ-82, Guohua electric appliance Co., Ltd., China), Ultraviolet spectrophotometer (Cary 4000, Agilent Technologies), electronic balance (CP-214, Ohaus instrument), High speed tabletop refrigerated centrifuge (LXJ-II B, Shanghai anting scientific instrument, China), Microwave digestion instrument (Mars-6, CEM Corporation) were used in the experiment. All experimental water is deionized water.

Method of washing experiment

The washing experiment conditions of single eluents are shown in *Table 2* according to the principle of an orthogonal experiment (Cui et al., 2007; Zhao et al., 2013; Zuo et al., 2016).

Table 2. Orthogonal experiment conditions for single eluents

Levels	HCl (M)	Oxalic acid (M)	EDTA (M)	Rhamnolipid (%)	Liquid-solid ratio	Washing time (min)
1	0.1	0.1	0.01	0.25	5:1	60
2	0.5	0.2	0.05	0.5	8:1	180
3	1.0	0.5	0.1	1.0	10:1	480
4	2.0	1.0	0.2	2.0	15:1	900

A single factor experiment was used for compound washing, and the basic specific experimental methods were carried out in the following order: (1) Determination of the optimum compound ratio: HCl was compounded with EDTA and Rhamnolipid (2%), respectively. The compound ratios were set as 3:1, 2:1, 1:1, 1:2, and 1:3. The liquid-solid ratio was 8:1, and the washing time was 480 min; (2) Determination of optimal liquid-solid ratio: The compound ratio of HCl & EDTA was 1:1, the compound ratio of HCl & Rhamnolipid was 1:2, and the washing time was 480 min. The liquid-solid ratio gradients were set to 3:1 5:1, 8:1, 10:1, 15:1, and 20:1; (3) Determination of the optimum washing time: The compound ratio of HCl & EDTA was selected for 1: 1, and liquid-solid ratio for 10: 1. The compound ratio of HCl & Rhamnolipid as 1: 2, and liquid-solid ratio for 15: 1. The washing times for the two compound eluents were set at 60, 180, 300, 480, 720, 1080, 1440, and 2160 min.

Soil samples of 3.00 g were weighed and packed into 100 mL centrifugal tubes. The eluents were added according to the experimental methods to oscillate for a given time at 210 RPM at room temperature, centrifuged at 5000 RPM for 6 min, and the supernatant was filtered with a 0.45 µm filter membrane. The contents of Pb were determined by ICP-OES.

All data were averaged by three groups of parallel experiments.

Determination method

In order to determine the distribution of heavy metal speciation in the soil before and after washing, the continuous extraction method of modified BCR was selected for the determination of Pb speciation in the soil (Tessier et al., 1979; Ashraf et al., 2012): (1) *Acid extractable*: add 40 mL of 0.1 M CH₃COOH to 1.00 g of soil samples, shaken at 210 RPM for 16 h at (22±5)°C, and centrifuged at 3000 RPM for 20 min; (2) *Reducible*: 40 mL of 0.5 M NH₂OH·HCl was added to the residue, and shaken at (22±5)°C for 16 h, centrifuged at 3000 RPM for 20 min; (3) *Oxidizable*: 10 mL of H₂O₂ was added to the residue at room temperature for 1 h, and 10 mL of H₂O₂ was added again at (85±2)°C and maintained for 1 h, evaporated to near dryness, then 50 mL of 1 M CH₃COONH₄ was added, shaken at (22±5)°C for 16 h, and centrifuged at 3000 RPM for 20 min; (4) *Residual*: residual residue of 0.10 g was weighted and 10 mL HNO₃, 1 mL HClO₄ and 1 mL HF were added. The residue was microwaved until clear and transparent.

The content of various forms of Pb was determined by ICP-OES.

Methods of data processing and analysis

In this study, the ratio of heavy metal content in washing solution to original heavy metal content in contaminated soil was used to calculate the removal rate of Pb; and the results of washing were analyzed by Origin 2017.

Method of washing kinetics

In order to better understand the process of Pb washing in soil, three different models, Elovich equation, Two-constant equation, First-order equation, were selected to analyze and evaluate the washing kinetics data by least squares regression.

Elovich equation (*Eq.1*) contains a series of reactions including solute diffusion and surface activation in the liquid phase. Two-constant equation (*Eq.2*) is applicable to the dynamic system process with relatively complex reaction. First-order equation (*Eq.3*) reflects the relationship between reaction equilibrium concentration and reaction rate. Their expressions are as follows:

$$S = A + Blnt \quad (\text{Eq.1})$$

$$\ln S = A + Blnt \quad (\text{Eq.2})$$

$$\ln S = \ln S_{max} + Bt \quad (\text{Eq.3})$$

where, S (mg·kg⁻¹) was the washing amount of Pb, S_{max} (mg·kg⁻¹) was the total washing amount at equilibrium, A and B were both constants, and t (min) was the washing time. The determination coefficient (R^2) is used to judge the significance and merits of the model. The larger R^2 indicating that the higher the fitting degree, the better the model.

Results and discussion

Effect of single eluent washing conditions

The experiment results are shown in *Table 3~Table 6*.

Table 3 shows that the concentration of HCl is the key factor affecting the removal rate of Pb. The higher the concentration, the higher the removal efficiency of Pb in soil, with the highest removal rate of 39.22%. However, there was no significant change in the removal rate of Pb in soil when HCl exceeds $1.0 \text{ mol}\cdot\text{L}^{-1}$, and increasing HCl concentration leads to the destruction of soil structure and physic-chemical properties, and increases the cost of remediating the contaminated soil (Moutsatsou et al., 2006). The washing process of HCl is mainly the result of the interaction of H^+ promoting the dissolution of solid heavy metals and Cl^- complexation promoting the formation of metal ion complexes.

Table 3. Orthogonal experiment and results of HCl washing

No.	HCl (M)	Liquid-solid ratio	Washing time (min)	Pb Removal rate (%)
1	0.1	5:1	60	5.22
2	0.1	8:1	180	7.94
3	0.1	10:1	480	10.40
4	0.1	15:1	900	12.43
5	0.5	5:1	480	16.94
6	0.5	8:1	900	18.71
7	0.5	10:1	60	23.35
8	0.5	15:1	180	29.34
9	1.0	5:1	900	12.03
10	1.0	8:1	60	16.96
11	1.0	10:1	180	27.53
12	1.0	15:1	480	31.20
13	2.0	5:1	180	19.43
14	2.0	8:1	480	21.74
15	2.0	10:1	900	24.73
16	2.0	15:1	60	39.22
<i>R(Pb)</i>	0.173	0.146	0.041	—

Oxalic acid is a kind of natural organic acid eluent, which has the characteristics of extensive existence and easy biodegradation. It can be seen from *Table 4* that the oxalic acid has little effect on removing Pb from soil, only about 1%, regardless of the concentration of oxalic acid. The main reason is that oxalic acid is one of the dicarboxylic acids, and has few reaction sites, which provides limited acidity and concentration of oxalate ion, and provides fewer reaction sites. In addition, oxalate ion reacts with Pb released from soil to produce insoluble compound $\text{C}_2\text{O}_4\text{Pb}$, whose standard solubility product constant is 4.8×10^{-10} (Wei et al., 2016), which further inhibits the migration of metal ions to the aqueous phase, resulting in a poor washing effect.

It can be seen from *Table 5* that EDTA has a strong extraction efficiency for Pb in soil, and removal effect increases with the increase of EDTA concentration, up to 43.41%. This is due to its strong complexing ability and easy formation of 1:1 soluble complex with metals. The equilibrium constant of Pb-EDTA complex is 19.0 (Zhang et al., 2010; Qiao et al., 2017), which can further promote the desorption of Pb from the surface of soil

particles and inhibit the re-adsorption of desorbed heavy metals. However, EDTA can easily cause secondary pollution to soil due to its own difficulty in degradation, and the instability of its chelates with heavy metals may bring potential environmental risks (Wei et al., 2016). Therefore, the optimal elution concentration of EDTA is 0.2 mol·L⁻¹.

Table 4. Orthogonal experiment and results of Oxalic acid washing

No.	Oxalic Acid (M)	Liquid-solid ratio	Washing time (h)	Pb Removal rate (%)
1	0.1	5:1	60	0.10
2	0.1	8:1	180	0.10
3	0.1	10:1	480	0.13
4	0.1	15:1	900	0.19
5	0.2	5:1	480	0.07
6	0.2	8:1	900	0.11
7	0.2	10:1	60	0.58
8	0.2	15:1	180	0.41
9	0.5	5:1	900	0.02
10	0.5	8:1	60	0.46
11	0.5	10:1	180	0.61
12	0.5	15:1	480	0.92
13	1.0	5:1	180	0.42
14	1.0	8:1	480	0.65
15	1.0	10:1	900	1.11
16	1.0	15:1	60	1.34
<i>R(Pb)</i>	0.007	0.006	0.002	—

Table 5. Orthogonal experiment and results of EDTA washing

No.	EDTA (M)	Liquid-solid ratio	Washing time (h)	Pb Removal rate (%)
1	0.05	5:1	60	8.81
2	0.05	8:1	180	10.59
3	0.05	10:1	480	13.36
4	0.05	15:1	900	10.02
5	0.1	5:1	480	24.29
6	0.1	8:1	900	18.34
7	0.1	10:1	60	29.50
8	0.1	15:1	180	26.82
9	0.2	5:1	900	36.84
10	0.2	8:1	60	40.17
11	0.2	10:1	180	31.50
12	0.2	15:1	480	36.46
13	0.5	5:1	180	29.88
14	0.5	8:1	480	41.57
15	0.5	10:1	900	43.41
16	0.5	15:1	60	37.94
<i>R(Pb)</i>	0.275	0.045	0.044	—

Rhamnolipid, an environmentally friendly anionic biological surfactant, can complexes with heavy metal ions by its own special hydroxyl and carboxyl structure, and can also reduce the surface tension of eluent and weaken the adhesion of heavy metal ions

to soil (Nitschke et al., 2010). However, as shown in *Table 6*, rhamnolipid washing alone is less effective in removing Pb from contaminated soil, with a maximum efficiency of less than 2.0%. The reason is that rhamnolipid is a pH neutral substance and can only remove water-soluble heavy metal ions, which is consistent with the research results of Zhou et al. (Wen et al., 2009; Zhou et al., 2017). Therefore, it must be combined with other acid eluents in order to wash heavy metals in soil more efficiently and economically.

Table 6. Orthogonal experiment and results of Rhamnolipid washing

No.	Rhamnolipid (%)	Liquid-solid ratio	Washing time (h)	Pb Removal rate (%)
1	0.5	5:1	60	0.01
2	0.5	8:1	180	0.06
3	0.5	10:1	480	0.14
4	0.5	15:1	900	0.03
5	1.0	5:1	480	0.01
6	1.0	8:1	900	0.22
7	1.0	10:1	60	0.33
8	1.0	15:1	180	0.36
9	2.0	5:1	900	0.15
10	2.0	8:1	60	0.31
11	2.0	10:1	180	0.67
12	2.0	15:1	480	0.73
13	5.0	5:1	180	0.38
14	5.0	8:1	480	0.77
15	5.0	10:1	900	1.08
16	5.0	15:1	60	1.33
<i>R(Pb)</i>	0.008	0.005	0.001	—

In addition, by comparing the magnitude of the Range (*R*) of orthogonal experiments, the influence degree of washing conditions for single eluents on the removal rate of Pb can be shown as follows: *Eluent Concentration* > *Liquid-Solid Ratio* > *Washing Time*.

In summary, there are great differences in the removal efficiency of heavy metals in soil by four kinds of single eluents. Among them, HCl and EDTA had better removal efficiency of Pb in soil, optimum washing conditions of HCl and EDTA were 1 mol·L⁻¹, 0.2 mol·L⁻¹, respectively; the liquid-solid ratios were 15:1 and 8:1; the washing time of both was 480 min; Oxalic acid is not suitable for remediation of contaminated soil in this site because of its poor washing effect; rhamnolipid needs to be combined with acid eluents in order to fully play its role.

Effect of compound eluent washing conditions

Compound eluents are optimized by compounding different types of single eluents, which mainly utilize the synergistic effect of different agents to further improve the removal efficiency of pollutants, and can avoid the secondary pollution and high cost of the single eluent. HCl was compounded with EDTA and rhamnolipid according to the orthogonal experimental results of single eluent, and the elution conditions were optimized by single factor experiments of compound washing.

Effect of the compound ratio of eluent on washing efficiency

It can be seen from *Fig. 2* that with the increase of the compound ratio of HCl & EDTA, the removal rate of Pb first increase and then decrease. The removal rates of Pb are the highest (up to 60.36%) when the ratio of HCl & EDTA is 1:1. However, for HCl & Rhamnolipid, the higher the compound ratio, the better the removal efficiency of heavy metals, but when the compound ratio exceeds 1:2, the removal rate does not change much. In addition, the removal rate of Pb by compound eluents were better than that by single eluents.

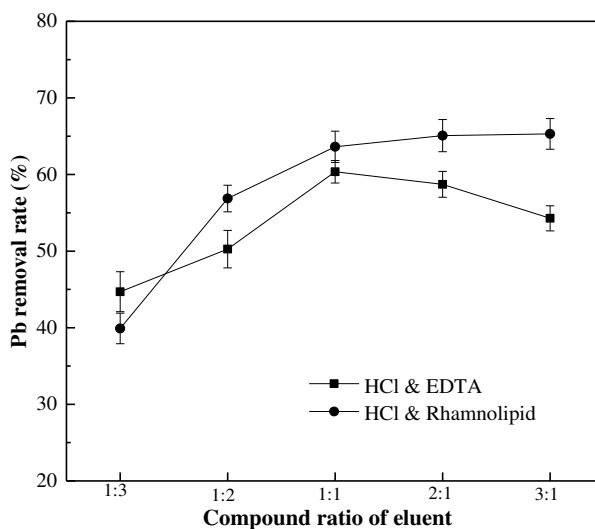


Figure 2. *Effect of compound ratio on Pb removal rate*

For HCl & EDTA combined elution, the elution mechanism is mainly as follows: (1) The acid solubility of H^+ and the complexation of Cl^- provided by HCl; (2) EDTA can not only reduce the surface tension of the eluent, but also form a stable complex Pb-EDTA with a coordination ratio of 1:1 with Pb; (3) the synergistic solubilization among different agents. However, for HCl & Rhamnolipid, besides (1) and (3), rhamnolipid is an anionic biosurfactant, which can not only reduce the surface tension of the eluent, but also form stable complexes with the special hydroxyl and carboxyl structures of the eluent and the Pb released from the soil.

Effect of liquid-solid ratio and washing time on washing efficiency

It can be concluded from *Fig. 3(a)* that with the increase of liquid-solid ratio, the removal rate of Pb in the soil of the two kinds of compound eluents are generally increasing; however, rate of removal increases slowly when it reaches a certain liquid-solid ratio. The essence of the increase of liquid-solid ratio is the increase of the amount of eluent, which leads to the increasing removal rate of heavy metals. The optimal liquid-solid ratio of both HCl & EDTA and HCl & Rhamnolipid was 10:1, according to the removal rate of Pb and the cost of remediation.

Washing time is a key factor that determines whether the eluent can interact adequately with the heavy metal pollutants in soil. Appropriate washing time can not only shorten the period of soil remediation, but also save costs. As can be seen from *Fig. 3(b)*, the longer the washing time, the higher the removal efficiency of the two kinds of compound

elutents. However, when washing time exceeds a certain limit, the removal efficiency of heavy metals does not exhibit much change. Therefore, the washing time of HCl & EDTA was 720 min, while that of HCl & Rhamnolipid was 1080 min.

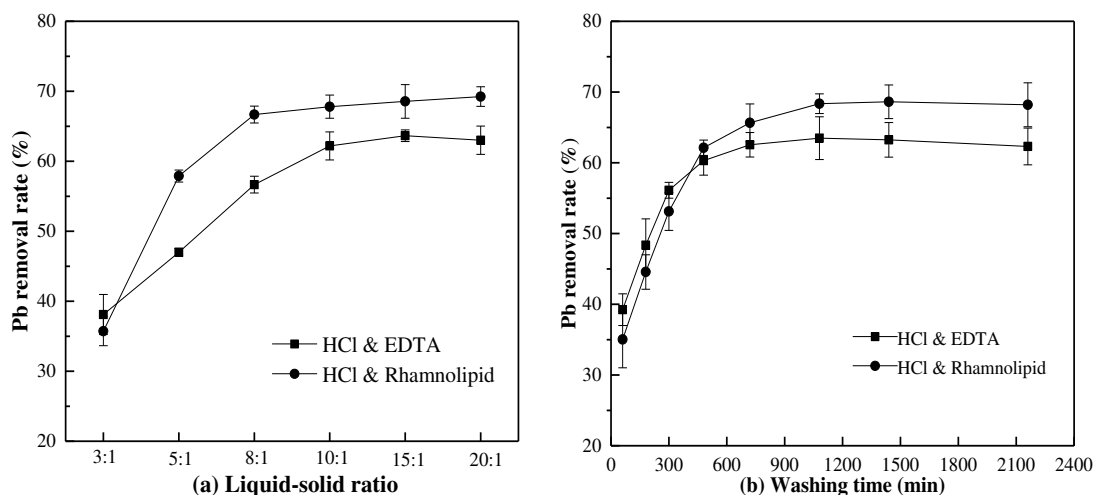


Figure 3. Effect of liquid-solid ratio and washing time on washing efficiency

Therefore, considering various factors of soil remediation, such as washing cost, secondary pollution, etc., HCl & Rhamnolipid compound washing effect is better, the optimum mixed ratio is 1:1, the liquid-solid ratio is 15:1, the washing time is 1080 min, and the removal rate of Pb in soil is 68.35%, which can be repaired to meet "risk intervention values (Pb content < 2500mg·kg⁻¹) for soil contamination of the development land" in soil environmental quality standard China (GB36600-2018).

Kinetics of compound washing

In order to better understand the process of Pb washing in soil, three different models, Elovich equation, Two-constant equation, First-order equation, were selected to analyze and evaluate the washing kinetics data by least squares regression, and the fitting results are shown in Table 7.

Table 7. Fitting results of three different models

Equation	Elovich equation $S = A + Blnt$	Two-constant equation $lnS = A + Blnt$	First-order equation $lnS = lnS_{max} + Bt$
Fitting result	$y = 10.391x - 6.3177$	$y = 0.2009x + 2.7916$	$y = 0.0003x + 3.8352$
R ²	R ² = 0.9339	R ² = 0.9199	R ² = 0.5468

By comparing R² of the three models, it can be seen that Elovich equation and Two-constant equation have a high fitting degree for the washing kinetics of heavy metal Pb in contaminated soil, while First-order equation is not suitable for describing the washing kinetics. Therefore, the washing desorption process of Pb in soil by HCl & Rhamnolipid is controlled by diffusion factors, and it is mainly a heterogeneous diffusion process.

Speciation distribution of Pb before and after washing

The risks of heavy metal pollution to soil is directly related to their total concentration as well as their speciation distribution. In this study, we further compare the speciation changes of Pb in the soil before and after compound washing. The results are shown in Table 8.

Table 8. *Speciation distribution of Pb in soil before and after washing*

Pb speciation	Before washing		HCl & EDTA		HCl & Rhamnolipid	
	Content (mg·kg ⁻¹)	Percentage (%)	Content (mg·kg ⁻¹)	Percentage (%)	Content (mg·kg ⁻¹)	Percentage (%)
<i>Acid extractable</i>	1426.50	19.02	350.35	12.47	240.70	10.14
<i>Reducible</i>	2058.00	27.44	233.75	8.32	141.24	5.95
<i>Oxidizable</i>	1192.50	15.90	272.52	9.70	190.14	8.01
<i>Residual</i>	2823.00	37.64	1952.88	69.51	1801.67	75.9
<i>Total</i>	7500.00	100.00	2809.50	100.00	2373.75	100

Table 8 shows that Pb in contaminated soils of the smelter exists mainly in the form of Residual and Reducible, accounting for 37.64% and 27.44%, respectively, indicating that Pb forms a stable crystal structure with soil or firmly binds with clay minerals. After compound washing, the speciation distribution of Pb in soil changed greatly, and the concentration of all forms decreased significantly, indicating that the compound eluents of HCl & EDTA and HCl & Rhamnolipid could release Pb in various forms.

The Acid extractable is the most susceptible metal form to washing, and it is very sensitive to pH changes, and can be easily eluted when the pH is reduced. Therefore, the addition of HCl among the compound eluent greatly reduced the content of acid extractable Pb in the soil. Reducible mainly refers to heavy metals bound by Fe and Mn oxides in soil (Shen et al., 2007). The content of reducible Pb in soil also decreased significantly, which is mainly due to the high content of Fe and Mn in the soil polluted by this smelting site. A large amount of Fe and Mn are extracted at the same time in the process of composite washing, which leads to the decrease of Pb content in the form of Fe and Mn oxides in soil. The Oxidizable mainly refers to heavy metals bound by organic matter and sulfide in soil. The higher the content of organic matter in soil, the better the extraction of Oxidizable (i.e. organic matter bound) (Li et al., 1996). The content of organic matter in the soil used in this study is relatively high, so the content of Oxidizable Pb has also decreased significantly after complex washing. The properties of Residual are usually stable, and they usually exist in silicate, primary minerals and secondary minerals (Barona et al., 2001). The residual Pb in soil also decreases to some extent after complex washing, which may be due to the release of some residual Pb accompanied by silicate dispersion.

Conclusion

In this study, single and compound eluents were applied to washing remediate the soils with Pb contamination intensity of 7500 mg·kg⁻¹ in an abandoned non-ferrous metal smelter in Yunnan China. The results showed that when the compound ratio of HCl (1 mol·L⁻¹) & Rhamnolipid (2%) was 1:1, the liquid-solid ratio was 10:1, and the washing

time was 1080 min, the removal rate of Pb in the soil was 68.35%, which met "*Risk screening value for soil contamination of the development land*" ($\text{Pb} < 2500 \text{ mg}\cdot\text{kg}^{-1}$) in "soil environmental quality standard China (GB36600-2018)". The washing desorption process of Pb in soil conforms to Elovich model and is mainly a heterogeneous diffusion process. In addition, from the distribution of Pb forms in soil, the main forms of Pb in the waste smelter soil are acid extractable and reducible. The active Pb was effectively removed, which greatly reduced the biological toxicity and environmental risk of the soil.

The heavy metals in the contaminated soil are eventually transferred to the washing waste liquid, so the recovery and treatment of the washing waste liquid should be further studied in the future. In addition, this study mainly simulated the ectopic washing process of contaminated soil, and the amount of soil used in the experiment was less. Therefore, the soil column washing experiment could be conducted by simulating the in-situ washing process in the future.

Acknowledgements. This work was financially supported by the National Water Pollution Control and Treatment Science and Technology Major Project (2015ZX07406005), and Preparation Project of Education Material for Soil Environmental Protection Publicity of Ministry of Ecology and Environment of People's Republic of China (H201606).

REFERENCES

- [1] Abumaizar, R. J., Smith, E. H. (1999): Heavy metal contaminants removal by soil washing. – *Journal of Hazardous Materials* 70(1-2): 71-86.
- [2] Ashraf, M. A., Maah, M. J., Yusoff, I. (2012): Chemical Speciation and Potential Mobility of Heavy Metals in the Soil of Former Tin Mining Catchment. – *The Scientific World Journal* 2012: 1-11.
- [3] Bacon, J. R., Dinev, N. S. (2005): Isotopic characterisation of lead in contaminated soils from the vicinity of a non-ferrous metal smelter near Plovdiv, Bulgaria. – *Environmental Pollution* 134(2): 247-255.
- [4] Barona, A., Aranguiz, I., Elías, A. (2001): Metal associations in soils before and after EDTA extractive decontamination: Implications for the effectiveness of further clean-up procedures. – *Environmental Pollution* 113(1): 79-85.
- [5] Burges, A., Epelde, L., Blanco, F., Becerril, J. M., Garbisu, C. (2017): Ecosystem services and plant physiological status during endophyte-assisted phytoremediation of metal contaminated soil. – *Science of The Total Environment* 584-585: 329-338.
- [6] Chen, F., Luo, Z., Liu, G., Yang, Y., Zhang, S., Ma, J. (2017): Remediation of electronic waste polluted soil using a combination of persulfate oxidation and chemical washing. – *Journal of Environment Management* 204(Pt 1): 170.
- [7] Cui, W., Li, X., Zhou, S., Weng, J. (2007): Investigation on process parameters of electrospinning system through orthogonal experimental design. – *Journal of Applied Polymer Science* 103(5): 3105-3112.
- [8] de Andrade Lima, L. R. P., Bernardes, L. A. (2017): Characterization of the soil contamination around the former primary lead smelter at Santo Amaro, Bahia, Brazil. – *Environmental Earth Sciences* 76: 470.
- [9] Dermont, G., Bergeron, M., Mercier, G., Richer-Lafllèche, M. (2008): Soil washing for metal removal: A review of physical/chemical technologies and field applications. – *Journal of Hazardous Materials* 152(1): 1-31.
- [10] Li, Z., Shuman, L. M. (1996): Redistribution of forms of zinc, cadmium and nickel in soils treated with EDTA. – *Science of The Total Environment* 191(1-2): 95-107.
- [11] Li, Z., Ma, Z., van der Kuijp, T. J., Yuan, Z., Huang, L. (2013): A review of soil heavy metal

- pollution from mines in China: Pollution and health risk assessment. – *Science of The Total Environment* 468-469: 843-853.
- [12] Moutsatsou, A., Gregou, M., Matsas, D., Protonotarios, V. (2006): Washing as a Remediation Technology Applicable in Soils Heavily Polluted by Mining-Metallurgical Activities. – *Chemosphere* 63(10): 1632-1640.
- [13] Nitschke, M., Costa, S. G., Contiero, J. (2010): Rhamnolipid surfactants: An update on the general aspects of these remarkable biomolecules. – *Biotechnology Progress* 21(6): 1593-1600.
- [14] Park, J., Jung, Y., Han, M., Lee, S. (2002): Simultaneous Removal of Cadmium and Turbidity in Contaminated Soil-Washing Water by DAF and Electroflotation. – *Water Science and Technology* 46(11-12): 225-230.
- [15] Qiao, J., Sun, H., Luo, X., Zhang, W., Mathews, S., Yin, X. (2017): EDTA-assisted leaching of Pb and Cd from contaminated soil. – *Chemosphere* 167: 422-428.
- [16] Reza, S. K., Baruah, U., Singh, S. K., Das, T. H. (2015): Geostatistical and multivariate analysis of soil heavy metal contamination near coal mining area, Northeastern India. – *Environmental Earth Sciences* 73(9): 5425-5433.
- [17] Shen, J., Liu, E., Zhu, Y., Hu, S., Qu, W. (2007): Distribution and chemical fractionation of heavy metals in recent sediments from Lake Taihu, China. – *Hydrobiologia* 581(1): 141-150.
- [18] Tessier, A., Campbell, P. G. C., Bisson, M. (1979): Sequential extraction procedure for the speciation of particulate trace metals. – *Analytical chemistry* 51(7): 844-851.
- [19] Voglar, G. E., Leštan, D. (2011): Efficiency modeling of solidification/stabilization of multi-metal contaminated industrial soil using cement and additives. – *Journal of Hazardous Materials* 192(2): 753-762.
- [20] Wei, M., Chen, J., Wang, X. (2016): Removal of arsenic and cadmium with sequential soil washing techniques using Na₂EDTA, oxalic and phosphoric acid: Optimization conditions, removal effectiveness and ecological risks. – *Chemosphere* 156: 252-261.
- [21] Wen, J., Stacey, S. P., McLaughlin, M. J., Kirby, J. K. (2009): Biodegradation of rhamnolipid, EDTA and citric acid in cadmium and Zn contaminated soils. – *Soil Biology Biochemistry* 41(10): 2214-2221.
- [22] Zhang, W., Huang, H., Tan, F., Wang, H., Qiu, R. (2010): Influence of EDTA washing on the species and mobility of heavy metals residual in soils. – *Journal of Hazardous Materials* 173(1-3): 369-376.
- [23] Zhao, P., Ge, S., Yoshikawa, K. (2013): An orthogonal experimental study on solid fuel production from sewage sludge by employing steam explosion. – *Applied Energy* 112: 1213-1221.
- [24] Zhou, D., Li, Z., Luo, X., Su, J. (2017): Leaching of rare earth elements from contaminated soils using saponin and rhamnolipid bio-surfactant. – *Journal of Rare Earths* 35(9): 911-919.
- [25] Zuo, W., Jiaqiang, E., Liu, X., Peng, Q., Deng, Y., Zhu, H. (2016): Orthogonal Experimental Design and Fuzzy Grey Relational Analysis for emitter efficiency of the micro-cylindrical combustor with a step. – *Applied Thermal Engineering* 103: 945-951.

DECODING SPATIOTEMPORAL PATTERNS OF URBAN LAND SPRAWL IN ZHUHAI, CHINA

LI, L. Y.¹ – QI, Z. X.^{2*} – XIAN, S.³

¹*Department of Urban Planning, College of Architecture and Urban Planning, Tongji University, Shanghai 200092, China; e-mail: lilingyue929@gmail.com*

²*Guangdong Provincial Key Laboratory of Urbanization and Geo-simulation, School of Geography and Planning, Sun Yat-sen University, Guangzhou 510275, China*

³*School of Geographical Sciences, Guangzhou University, Guangzhou 510006, China*

**Corresponding author*

e-mail: qizhixin@mail.sysu.edu.cn; phone/fax: +86-20-84115833

(Received 13th Jul 2019; accepted 25th Nov 2019)

Abstract. Urban sprawl is a major factor that threatens the loss of arable landmass, and its evolving morphology has long interested numerous scholars. However, existing research on this study has not been concerned with the cases of ordinary cities, particularly their intra-urban land and urban sprawl. This study goes beyond mega-/super-cities and takes Zhuhai, an ordinary large city in China's Pearl River Delta (PRD) region, as a case. Through remote sensing and GIS technology, this research identifies the increasing built-up areas and its sub-typologies (infill, outlying and edge-expansion), distinguishes the reclamation area and the decreasing arable landmass and evaluates the rate of land-use inside its five districts from 1980 to 2015. The growth of urban areas and loss of arable landmass are uneven inside Zhuhai. The most uneven outlying and infill growth were observed from 1990 to 1995 and from 2013 to 2015, respectively. Edge-expansion is the least imbalanced typology and reached its minimum from 2010 to 2013. The extent of variability of the total urban sprawl generally accords with that of edge-expansion and imbalance of arable landmass loss that reached a peak from 2005 to 2008. However, policy, planning and other factors that matter in urban sprawl are also discussed.

Keywords: *land reclamation, arable land loss, variability, Landsat, ArcGIS*

Introduction

The term sprawl originated from the U.S. and its rapid suburbanisation (Leichenko and Solecki, 2014). However, the definition of urban sprawl varies among researchers and policymakers as this politically charged terminology lacks precision in the narrative of policy documents. In addition, the characteristics of sprawl differ from place to place (e.g. Sprawl in American cities is much less dense than that in Asian cities) (Shahraki, 2011; Hamidi and Ewing, 2014). Thus, contextualised case studies, especially from the global South, are needed to offer insights. In this research, we specifically deploy urban land sprawl denoting the adjacent sprawl of urban land, away from existing built-up area to undeveloped rural area. With the breakthrough of urban margins, this type of urban activity is often criticised for encroaching arable land, causing environmental degradation and undermining the natural landscape. Thus, sprawl represents an uncoordinated growth without thinking about the random effects, the additive urban growth that results in inefficient resource utilisation and ecological destruction (Bhatta et al., 2010). This unsustainability has already been revealed in fast-expanding cities. For instance, in India, under unprecedented urban sprawl, land use has changed rapidly in fringe towns and cities along the rapid transportation corridor (Theobald, 2001). Indicators used to identify urban

sprawl include the loss of arable landmass and forest habitat and the increase of impervious surface.

Urban sprawl is a spatial process along with complex changes in land use (Bhatta et al., 2010). This process is influenced by urban policy and planning. Urban sprawl morphology and its spatiotemporal characteristics have attracted the attention of scholars. Old theories, such as concentric zones and sectors and multiple nuclei theories (Burgess, 1925; Hoyt, 1939; Harris and Ullman, 1945) are unable to capture long-term and multi-temporal sprawl patterns. Recent research has benefitted from the advancement of remote sensing. However, data assemblage and interpretation have always been an enormous task before quantifying land-use change (Batty, 2002; Herold et al., 2003; Peng et al., 2010; Xian et al., 2019). Moreover, researchers have focused on the sprawl patterns of cities (especially mega city-regions) across macro-scale regions, nations and even the world (Grainger, 1995; Li et al., 2004; Hamidi and Ewing, 2014; Scheuer et al., 2016; Li and Li, 2019; Aniekwe and Igu, 2019). For instance, Hamidi and Ewing (2014) have stated that the growth of infill increases the density of metropolitan areas (often in coastal areas). However, they have identified that the density of urbanised areas in the U.S. decreases with the increase of metropolitan sprawl between 2000 and 2010, leading to overuse of automobiles. In an up-to-date study exploring the spatiotemporal patterns of urban sprawl in China from 2006 to 2014 (Li and Li, 2019), the growth rates of built-up areas outweighing the population are most significant in the Western region, followed by the Eastern and Central regions and least significant in the Northeast. The rates of urban sprawl in mega and super cities are minimum, sometimes even negative. However, these rates are still notable in large and medium cities. The sprawl is also found related to population and economic growth. Nevertheless, the manner in which ordinary, large, medium and small cities sprawl, including the patterns and typologies in intra-urban sprawls, remains unclear. Do these cities sprawl with different patterns or rules? How does sprawl take place inside the city? What are the specific causes?

This current study aims to address the questions by giving special attention to the volume, structure and forms of land use (Long and Li, 2012). Furthermore, the trend, rates and variability of urban land sprawl in a non-mega-/super-city is examined. Zhuhai, located in the Southern coast China, is selected as the study area for two main reasons. Firstly, urban China is an interesting subject matter, exhibiting different sprawl patterns from the American model. These patterns are revealed in numerous up-to-date studies (Chen, 2016; You, 2016; Ding and Wang, 2018; Yang et al., 2018; Liu, 2020). Secondly, different from mega-/super-cities (according to the National Statistical Bureau, cities with permanent residents more than 10 million are megacities; between 5 and 10 million are super cities; between 1 and 5 million are large cities; between 500 hundred thousand and 1 million are medium cities and fewer than 500 hundred thousand are small cities), Zhuhai is a large city embracing a green environment and eco-city ideology. From a small county to a sizable metropolis, the specific trajectory and forms of sprawl can update existing understanding beyond economic star megacities, e.g. Shenzhen, Guangzhou, and Shanghai. However, in what patterns city grows is still unclear. Unravelling the spatiotemporal transition of land can provide a comprehensive picture and produce invaluable implications for the ongoing urban development in China. Using Zhuhai as a case, this research distinguishes and quantifies different land use (e.g., urban built-up area and arable land); evaluates the rate of land-use change to economic and population growth; measures the extent of sprawl variability and discusses how policy, planning and other factors matter in urban sprawl. Edge-expansion, outlying, and infilling as different sprawl typologies of built-up area are also computed (Budd, 1996; Liu et al., 2010; Shi et al., 2010).

Materials and methods

Area of research

Zhuhai, known as a city of hundred islands, has been reputed for its appeal, windy coastline, diverse tropical vegetation, green ambiance for liveability and stretched urban structure in Pearl River Delta (PRD) in China. Adjacent to Jiangmen, Zhongshan and Macau, Zhuhai is situated at the estuary of South Guangdong (*Fig. 1*). The city has Xiangzhou, Doumen, Jinwan districts under its jurisdiction. Gaoxin district, which are known as the city's High-tech Zone, and Hensqin vitalise local economic growth. Zhuhai is a typical fast-growing immigrant city evolving from a traditional Cantonese-speaking region of Guangdong province to a Mandarin-based area with a large influx of immigrants from inland provinces.

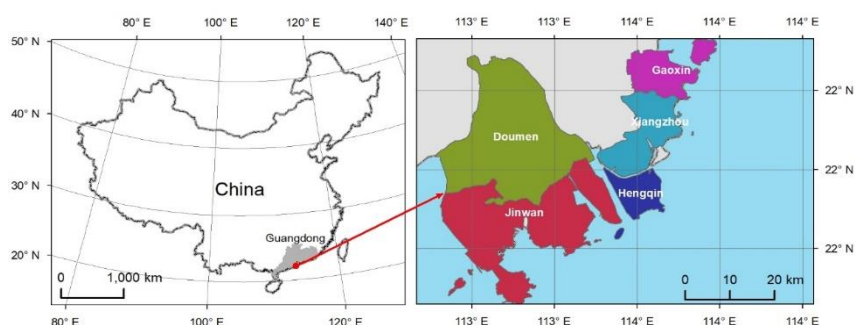


Figure 1. Zhuhai's Location and its districts

Data sources

Land cover and land-use change identification are essential for ecological environment analysis and planning. The information is commonly extracted from satellite images by using supervised classification methods, which require classified reference samples to train the classifier and subsequently classify unknown data (Qi et al., 2012). Given the availability of the data and pre-research on Zhuhai, remote sensing images spanning nine years from Landsat satellites are acquired from the United States Geological Survey, with a time span of 35 years (*Table 1*). Except for the earliest 1980 image provided by the Multispectral Scanner Sensor (MSS), which have 78 m coarse resolution, the rest of the images of the Thematic Maps (TM) and Operational Land Imager (OLI) all have 30 m resolution.

Table 1. Dataset of landsat images

Acquisition time	Satellite	Sensor	Resolution (m)
1980	Landsat-3	MSS	78
1990	Landsat-5	TM	30
1995	Landsat-6	TM	30
2000	Landsat-7	TM	30
2005	Landsat-5	TM	30
2008	Landsat-5	TM	30
2010	Landsat-7	TM	30
2013	Landsat-8	OLI	30
2015	Landsat-8	OLI	30

As the expansion rate became increasingly rapid, the later the periods, the shorter the time, such that the urban land change can be accurately captured

Methods

Identifying land use types

Diverse methods are used to determine the different types of land use. In this research, support vector machines (SVMs) (Chang and Lin, 2011), which are one of the most widely used supervised classifiers, are used for Landsat image classification to extract land cover information. Radial basis function (RBF) is selected as the mapping kernel of SVM. A grid search strategy is used to derive the optimal parameters of the RBF kernel SVM (Chang and Lin, 2011). To collect ground truth data in assessing the accuracy of identifying urban sprawl features, fieldwork is conducted using high-resolution Google Earth images. Based on experience with multinomial distribution (Congalton and Green, 2009), a minimum of 50 samples are collected for each land cover class. Different categories of land use are identified. The built-up area is the main parameter quantifying urban sprawl (Shahraki, 2011). Reclamation is a special parameter to complement the understanding of coastal urban expansion. The built-up area is visually interpreted through the software of ArcMap and reviewed by qualified technicians (Akbari et al., 2003) as visual form performs better than spectral signal in distinguishing land use characteristics. Furthermore, visual form avoids misclassifications and guarantees preciseness.

Evaluating the rate of change

In assessing the growth of the economy and population relates with urban land sprawl, standardised sprawl efficiency of GDP (LSGDP_s) and permanent residents (LSPE_s) (calculating the growth rate of the GDP and the permanent resident population to that of urban built-up areas) is applied to each district in different periods. This article also calculates the annual loss rate of arable land, which partially transited to the increase of the built-up areas.

Measuring the extent of variability

The coefficient of variation (CV) is calculated to reveal the extent of variability in relation to the mean of land sprawl, arable land and forest loss within a city. The CV is defined as the ratio of the standard deviation to the mean value and is calculated as

$$(C \cdot V)_{ij} = \frac{S_{ij}}{\bar{X}_{ij}} \times 100\%, S_{ij} = \sqrt{\sum (\bar{G}_{ijk} - \bar{X}_{ij})^2 / n} \quad (\text{Eq.1})$$

where $(C \cdot V)_{ij}$ is the variation score of sprawl/loss type j during time period i , \bar{X}_{ij} and S_{ij} denote the sample mean and standard deviation of sprawl type j during time period i , and n represents the number of the sample. A larger value of CV signifies a greater level of dispersion around the mean. Conversely, a smaller value of CV entails a lower level of dispersion around the mean. This research also measures the CV of different typologies of land sprawl, which are calculated by the Landscape Expansion Index (LEI) (Liu et al., 2010; Xian et al., 2019). In LEI, different value intervals denote various sprawl typologies: newly built patches that spread from the boundary of existent areas are identified as edge-expansion (0–50). Enclave new patches detaching from the existent areas is categorised as outlying (0). Newly developed urban patch stuffing an existing land parcel is infill (50–100). The typologies further detail the sprawl trajectory of the case city.

Results

The general trend of urban land sprawl

The general change of urban land use is identified through visual interpretation based on Landsat data and presented in Fig. 2. The left vertical axes indicate data sets of forest, urban and arable land in square kilometers while the right vertical axes shows urban land per capita (with unit of km²/person). Among the identified categories, arable land and forest land gradually decrease over time. Until 2015, almost 300 km² of arable land and 50 km² of forest land has been encroached, a substantial part of which has turned into urban built-up area. From 1980 to 2015, the proportion of Zhuhai's arable land to the total landmass dropped from 44.64% to 23.88%, with the urban built-up area expanding to 240.48 km². The urban built-up area has increased from 35.19 to 275.67 km², whereas the per capita area has fluctuated significantly, surging from 96.32 m² in 1980 to 168.53 m² in 1995; this area declined to 144.13 m² in 2000 and increased again to 169.73 m² in 2013 (Figs. 2 and 3).

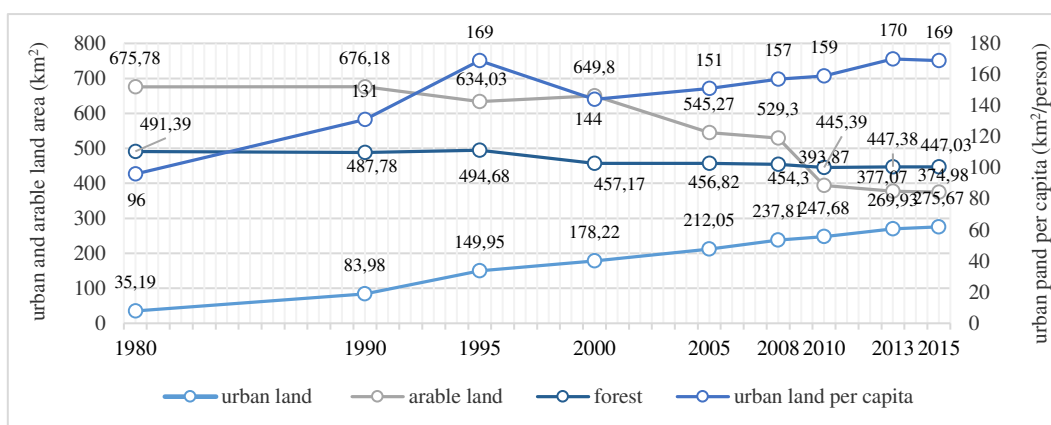


Figure 2. Change of urban and arable land (per capita) in Zhuhai (1980–2015)

The coastline in Zhuhai was reshaped from 1980 to 2015 (Fig. 3). From 1980 to 1990, artificial land reclaimed along the coastlines reached a peak of 108.4 km², which happened along the Western coast of Jinwan. From 1990 to 1995, reclamation projects decreased but remained considerable at 11.27 km² in areas scattered around Northeast Hengqin. From 1995 to 2000, Northwest Hengqin and the Western Coast of Jinwan witnessed visible reclamation. However, the amount reduced to 7.35 km². From 2000 to 2005, the reclamation mainly took place in South Jinwan and North Gaoxin and slightly increased to 8.12 km². Between 2005 and 2008, lands were reclaimed along the Southwest coast of Jinwan but shrank sharply to 1.45 km². From 2008 to 2010, three pieces of land up to 10.16 km² were reclaimed in South Jinwan and Northwest Hengqin. However, from 2010 to 2013, the reclamation area dropped to 8.96 km². From 2013 to 2015, these areas were reduced to 0.45 km², which all occurred in the Jinwan District.

The gains and loss rates of urban land sprawl

The intra-urban spatiotemporal patterns, the annual sprawl area of Zhuhai and the five districts are calculated (Fig. 4). Jinwan overwhelmingly expanded over 700 ha in 1990 and 1995, 270 ha in 2000 and 2005, 480 ha in 2005 and 2008, 250 ha in 2010 and 2013,

followed by Xiangzhou, expanding 290 ha in 1980 and 1990, 340 ha in 1990 and 1995, 250 ha in 1995 and 2000. The least sprawled district is Hengqin with a less than 10 ha annual increase before 2010. The annual sprawl areas of Doumen and Gaoxin districts were among the average.

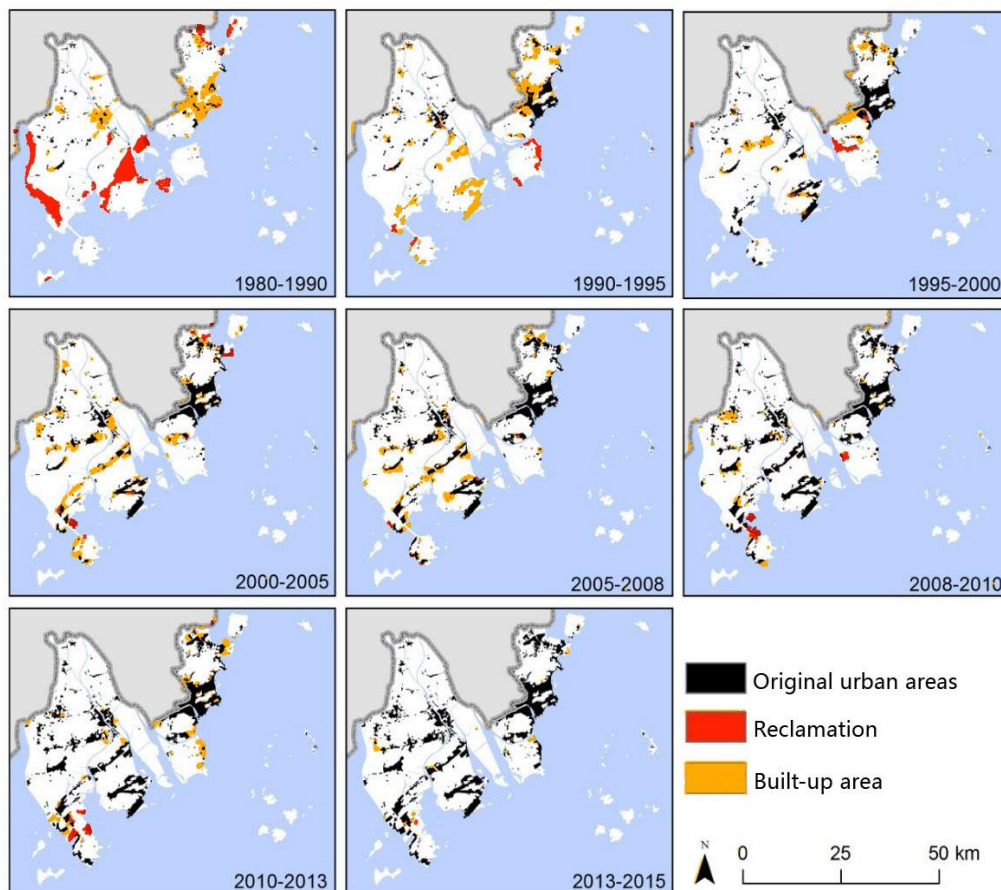


Figure 3. Urban land sprawl and coastal land reclamation in Zhuhai (1980-2015)

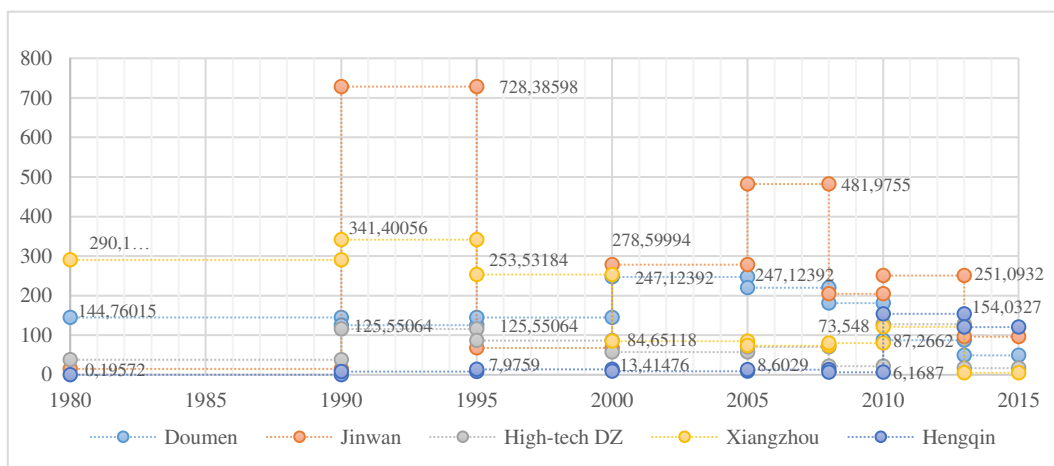


Figure 4. Annual sprawl area of Zhuhai's five districts in eight periods (1980-2015) (unit: hectare)

LSGDP_s was generally higher than LSPE_s during 2008 and 2015. Xiangzhou's LSGDP_s is highest in 2008-2010 (36.66) but declined thereafter (*Fig. 5*). Jinwan's LSGDP_s declined first in 2010-2013 and increased again in 2013-2015. Doumen's LSGDP_s was negative in 2008-2010 (-0.98) but had a significant increase throughout 2010-2013 (10.87) and 2013-2015 (13.86). All the districts' LSPE_s decreased in 2010-2013 and increased in 2013-2015, but Xiangzhou's LSPE_s in 2008-2010 (6.19) remains most significant and Jinwan's LSPE_s is minimum in 2010-2013 (0.13).

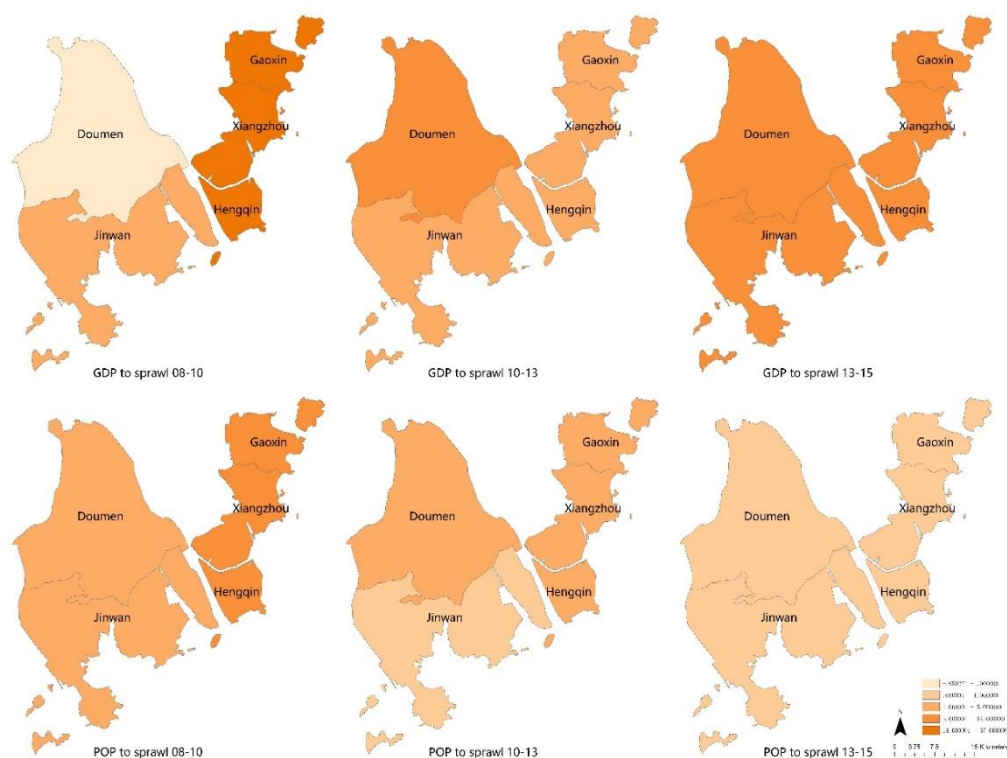


Figure 5. Standard sprawl efficiency of GDP and permanent residents in Zhuhai's five districts (2008-2015)

Loss rate of arable land is greater after 2000 than in previous years but varies across periods and districts (*Fig. 6*). In *Fig. 6*, the shallow the colour, the greater loss of the arable land. The most intensive loss of arable land occurred between 2000 and 2005, and 2010 and 2013, with each district losing more than 0.9% arable land except Gaoxin (2010-2013). Xiangzhou (1990–1995, -5.17%; 2008–2010, -11.38%; 2010–2013, -8.21%) and Gaoxin (1990–1995, -4.76%; 2008–2010, -21.73%) were the top districts that experienced intensive arable land decrease with over a 4.5% loss rate. Hengqin gained arable lands in 1980–1990 (7.48%) and 1990–1995 (60.42%). A similar increase was also observed in Gaoxin (1995–2000, 4.12%), Doumen (1995–2000, 2.23%) and Jinwan (1980–1990, 1990–1995, 1.08%).

Imbalance of urban land sprawl

From 1980 to 2015, the CV of arable land loss was higher and greater than forest loss (*Fig. 7*). However, both lands experienced three rounds of increase (1990–1995, 2005-2008, 2013–2015). The lowest value was in 2010 and 2013, with both CVs reaching

zero, thus indicating a highly balanced loss of arable land and forest. The imbalance of arable loss reached a peak in 2005–2008, with a CV of 0.87 and forest loss in 1990–1995, with a CV of 0.76.

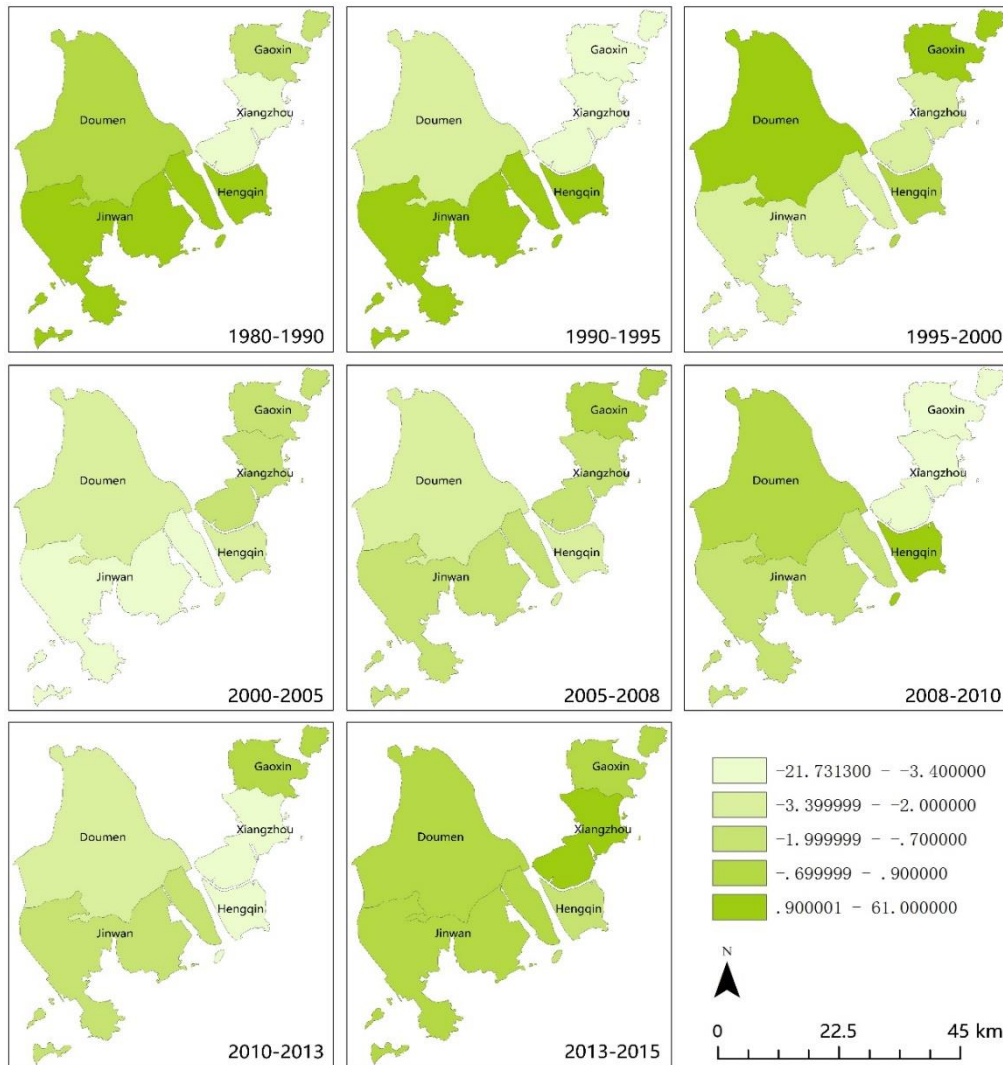


Figure 6. Annual loss rate of arable land in Zhuhai's five districts (1980–2015)

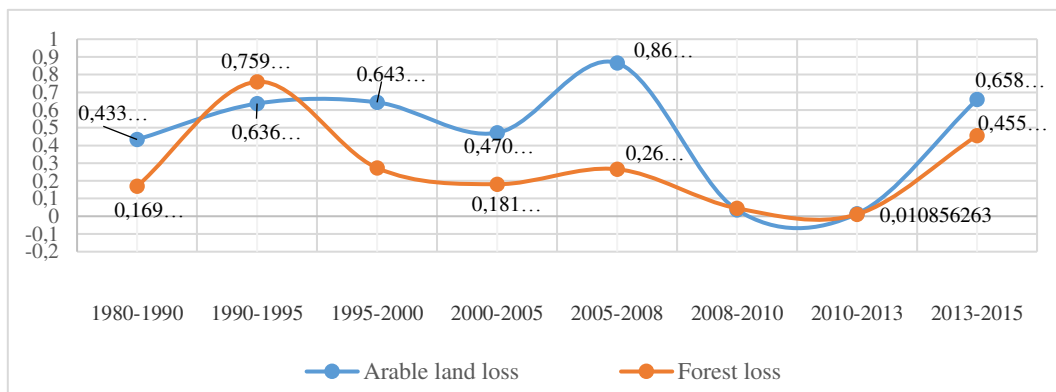


Figure 7. The CV of arable land and forest loss throughout eight periods (1980-2015)

To get a clearer picture of intra-urban sprawl patterns, sprawl typologies of eight periods in Zhuhai's five districts are explored (Table 2). Edge expansion has played a major role for 35 years and was mainly distributed across former centres of Doumen and Xiangzhou in the initial period. Outlying growth mainly took place in the Jinwan District and surpassed edge expansion in the early 1990s. Though much lesser than the other two types, infill growth was significant from 1995 to 2000, 2000 to 2005 and 2010 to 2013. In addition, this growth occasionally occurred in the Gaoxin District before 2005. Sprawl in Hengqin gained speed in 2010 with edge expansion and outlying growth representing the main types. Three typological sprawls stabilised from 1995 to 2010. Between 1995 and 2000, the growth amount decreased to 28.30 km² with the outlying growth suddenly dropping to 5.47 km² and hardly increasing in large numbers afterwards. Between 2000 and 2005, the sprawl area fairly reached 34.1 km² in which edge expansion and infill growth made up certain vacant spaces along Zhuhai Avenue. From 2005 to 2008, westward sprawl increased with edge sprawl continued completing the main transport corridor. The outlying growth and infill growth supplemented the sprawl but did not take the main role. The subsequent sprawl from 2010 to 2013 and from 2013 to 2015 experienced a downward trend. The edge expansion continued to drop, but the outlying growth became substantial, especially in Hengqin.

Table 2. *Sprawling typologies in Zhuhai's different districts (1980-2015) (unit: m²)*

		1980-1990	1990-1995	1995-2000	2000-2005	2005-2008	2008-2010	2010-2013	2013-2015
Doumen	Outlying	5184557	1189280	915297	1309671	759685	880705	574847	40500
	Edge-expansion	8913359	3630740	5838817	10323974	4776961	2672469	1446939	938700
	Infill	378099	1457512	469337	722551	1072585	64060	596200	0
Jinwan	Outlying	1010176	30702779	0	2526234	2702522	490649	4724333	1476000
	Edge-expansion	467954	5315060	1034900	9076057	11038427	3433755	912238	218700
	Infill	2669	401460	2350281	2327706	718316	170826	1896225	223200
Gaoxin	Outlying	931459	998320	788522	723320	0	0	696991	0
	Edge-expansion	1757827	4225096	3397747	785622	2072209	396116	3132133	333900
	Infill	1108498	576432	132170	1370461	33095	30844	3417	0
Xiangzhou	Outlying	2231989	1235465	3089352	0	330952	591960	259663	0
	Edge-expansion	2678734	11942536	6805385	3768557	1309109	876399	2655624	98100
	Infill	0	3892027	2781855	464002	566379	134644	732011	0
Hengqin	Outlying	19572	383696	670738	357813	54156	0	2192617	2412900
	Edge-expansion	0	15099	0	72332	330200	122188	2428364	0
	Infill	0	0	0	0	1504	1186	0	0
Zhuhai	Total	48793500	65965500	28274400	33828300	25766100	9865800	22251600	5742000

The imbalance of infill growth reached its peak (2013–2015) with a CV of 2.24 (Fig. 8). The CV of outlying growth fluctuated the most before 2010 and became the most uneven from 1990 to 1995 with a CV of 1.93 and from 2005 to 2008 with a CV of 1.46. Overall, edge expansion is the least imbalanced growth type and reached its minimum from 2010 to 2013 with a CV of 0.42. The extent of variability of total sprawl generally accords with that of edge expansion.

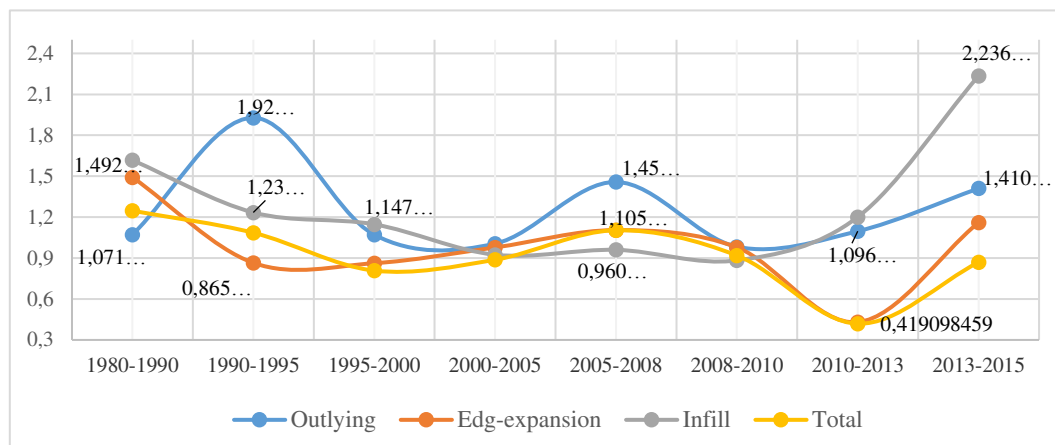


Figure 8. The CV of urban land sprawl throughout eight periods (1980-2015)

Discussion

Environmental policies/discourses regulating sprawl rates and typologies

The Zhuhai's remarkable growth and 35-year sprawl is only half of Guangzhou's growth (from 1978 to 2005) and less than 35% of Shenzhen's (from 1980 to 2010). Loss of arable land is particularly striking in Shenzhen, shrinking from 354.73 km² in 1979 to 39.77 km² in 2015 and decreasing to 88.8% in the same period (Li et al., 2004). Most of Shenzhen's arable land designated for vegetable use became polluted and surrounded by urban areas. The relatively smaller sprawl in Zhuhai is due to its pro-environmental policies/discourses. Zhuhai was prudent in the early 1980s, when numerous PRD cities prioritised industrialisation as their development strategy for economic growth. Balancing the economy and the environment was central to Zhuhai's early development pathway. Having labelled itself as a coastal garden city and favouring tourism as its key industry for development, Zhuhai did not jeopardise its ecological environment. Suppressing industrial development to retain the city's environmental quality and beautiful landscape affected Zhuhai's economy. This phenomenon was reflected not only in the smaller expansion area of its urban land but also in its slower economic growth than its counterparts, such as Shenzhen. Zhuhai's average GDP growth rate was only 20% of Shenzhen from 1979 to 1984. Similar to Shenzhen, Zhuhai put industrialisation as part of its agenda since 1984 to address the economic backwardness. Zhuhai's GDP began to accelerate, and more than 3,000 cooperative firms were set up. In this period, Zhuhai's urban growth ran into a fast track, and its urban construction land experienced an upsurge until the early 1990s. Similar to other cities in the PRD, Zhuhai's industrialisation had low technology and was labour-intensive, which led to environmental degradation. Manufacturing firms sprouted and contaminated the soil, water and air. Land reclamation between the 1980s and the early 1990s also reached its peak (Fig. 3). Most of the reclaimed land was used for agricultural purposes, such as paddy fields, fishponds and cropland, to support local industrial development. These early large-scale reclamation projects were approved by the Ministry of Water Resources, but none of them obtained a permit for ocean use from the State Oceanic Administration nor evaluated environmental and ecological effects. This scenario threatened local ecological sustainability. A series of environmental regulations, such as the Eight Prohibitions for Environmental Protection, legislated in 1992, were legitimised. This legislation proposed numerous

prohibitions to improve the quality of the natural environment. For instance, buildings that exceeded 25 m above the hillside, less than 30 m approaching the riverbank or 50 m along the estuary bank were prohibited. Noise higher than 45 decibels was also forbidden to nurture a quiet and peaceful environment. Other regulations were made available to control pollution and carbon emission. This pro-environment mentality slowed Zhuhai's expansion rate. From 1995 to 2000, the expanded urban construction land area was 42.3%, and from 1990 to 1995, the outlying growth declined. In Zhuhai's pursuit of a garden city, the city followed the policies of Singapore, a world renowned model for learning environment-friendly initiatives such as vegetation planting (Orff, 2001). Adopting these practices were important to strengthen the role of Zhuhai as an ecologically sustainable pioneer in PRD. The idea of an eco-city protected urban landscapes and environments. It also transformed Zhuhai into a liveable garden city. Zhuhai's economy was overshadowed by Shenzhen and Guangzhou, but Zhuhai's pleasant environment showcased its achievements in eco-city building and were in favour of the city's long-term sustainability.

High-tech industrial development was integrated into Zhuhai's pro-environment strategy, in which eco-sustainability and urban growth became interdependent. Zhuhai was a fishing village with a weak technological foundation; it started to develop as a high-tech city in the early 1990s. The local government invested over one billion yuan to build Zhuhai University Town to attract science and technology talents. The college students and talents played a large role in Zhuhai's high-tech development, especially in the growth of industrial parks. Built in 1992, the Zhuhai National High-Tech Industrial Development Zone expanded in 1999, nurtured several high-tech firms and generated considerable output values. High-tech city development balanced economic growth and ecological sustainability. This development also played a positive role in the sustainable development of Zhuhai.

Ecological landscape steering sprawl balance and typologies

The ecological landscape of Zhuhai is significant to determine the typologies and (im)balance of urban land sprawl. Zhuhai's distinctive mountainous terrain fosters initial sprawl surrounding the boundary of mountains and hills. From 1980 to 1990, urban land around the Fenghuang and Banzhang mountains in the Xiangzhou District expanded prominently and was mainly characterised by edge expansion. In the Doumen District, areas along the Huangyang mountains were urbanised mostly with edge expansion as the main form supplemented by infill growth. Some sporadic expansion took place around other small hills, and the mountain-oriented expansion persisted until the early 2000s. Zhuhai grew in harmony with its natural surroundings and captured the idea of an eco-city. Thus, Zhuhai strategically selected eco-city as its development model. Unlike numerous Chinese cities, Zhuhai did not destroy mountains for expansion. Its sprawl is fast and rational. Given that Xiangzhou and Doumen county centres were naturally developed around green mountains, this type of infill growth also emerged occasionally in matured built-up areas. This scenario was particularly evident from 1990 to 2000.

The coastal landscape enriches Zhuhai's sprawl, and this land reclamation has lasted until today. Reclamation creates new land over oceans, riverbeds or lakebeds. As a key mechanism accommodating urban growth, reclamation is popular in many harbour cities (Ng, 2011). Zhuhai has been reclaiming land for years and remains keen on expanding over the waters. Most of the reclamation took place in Jinwan District and Hengqin Island. Coastal reclamation in the first decade was tremendous, with 108.4 km²

area having been infilled. However, a considerable proportion of the reclamation was not for urban growth but for agricultural use, thus aligning with Zhuhai's policies for sustainability in its early reform period. These reclamation activities result from an integrated thinking toward ecology and socioeconomic development, maximising the benefits that can be brought to local development and minimising the damage to local sustainability. In the early 1990s, Hengqin was recognised as one of the four key development zones by the Guangdong provincial government, for which the land area almost doubled by reclamation. This change has propped up the upscaling of Hengqin as a national new area. In 2013, the State Council approved to reclaim an approximately 20-km² seaside land area in Jinwan, creating new land for competitive industrial development, such as a yacht base and for the aviation industry. In 2015, the adjustment of the Hengqin Ocean Functional and Reclamation Plan was approved, granting 27.9 km² more reclamation quotas in South Hengqin. This reclamation largely resolved the land resource constraints for free trade zone. Given the negative ecological impacts, the municipal government launched several rounds of environmental evaluation before project delivery to mitigate its adverse effects on nature. Harbour reclamation was part of Zhuhai's marine urban economic strategy. However, the cost and benefits of its reclamation are difficult to determine. Moreover, the ecological consequences of the reclamation also prompted substantial concerns from experts, scholars and officials. Large-scale reclamation is detrimental to sustainability in the long run and should best be practiced with caution in the future.

Geolocation is also influential. Similar to Shenzhen bordering Hong Kong, Zhuhai is close to Macau. However, Macau is not as competitive as Hong Kong; its tiny economic scale hardly benefits Zhuhai. This circumstance partly explains why Zhuhai did not follow Shenzhen's targeted strategy for industrialisation and why the city turned to eco-city development. Nevertheless, this difference did not prevent Zhuhai's cross-border land sprawl. From 1980 to 1990, Zhuhai started its urban land sprawl near Macau, mainly in the form of edge expansion supplemented by outlying growth. In all the increased 48.79 km² area in the first decade, more than 29 km² was in Xiangzhou District, which borders Macau. Land sprawl in Hengqin also benefitted from Zhuhai's cross-border location. In the early stage, Hengqin grew extremely slowly but cross-border vantage helped this area gain particular attention from the central government. In 2009, Hengqin was upgraded to a national new area, and its growth reached a peak of 4.62 km² from 2010 to 2013 and 2.41 km² in a short period between 2013 and 2015.

Conclusion

In deploying technical tools of remote sensing and GIS, this article investigates the general change of urban built-up area in the hinterlands and reclamation in the coast of Zhuhai, an ordinary large city in China's PRD region. It unravels spatiotemporal characteristics of urban land sprawl and discusses how the land of Zhuhai evolves under citywide pro-environment policies/discourses. The results corroborate that Zhuhai's urban land has expanded 1.06% annually for the past 35 years. Furthermore, the sudden growth of urban built-up area in total and per capita in 1995 (*Fig. 2*) was interpretable from local, regional, and national levels. At the local level, Zhuhai airport was officially built into navigation. As most advanced and modern airports at that time, Zhuhai airport not only racked up air passage between the city and other parts of China but also drove local construction profoundly. At the regional level, industrial investment from Hong

Kong to PRD reached 25.2 billion HKD in 1995, leading to massive industrialisation in PRD. Regional urbanisation driven by this type of industrialisation has brought considerable growth opportunities for cities in PRD. At the national level, the number of cities experienced a surge from 193 in 1978 to 622 in 1994. With the huge influx of rural immigrants, urban population reached 343 million in 1994 and imposed an urgent demand for urban construction. The urban sprawl slowed down in the last five years of the 1990s and accelerated again in the 2000s with the construction of new towns in the Western part of the city. The rate slowed down from 2008 to 2010 but accelerated again from 2010 to 2013 with the promotion of Hengqin to a national new area in 2009. The findings of Zhuhai's three typologies of sprawl confirm the following information. Firstly, edge expansion has dominated each period and is prominent along the boundary of mountains and hills. Secondly, enclave development zones and new towns contribute to outlying growth. Thirdly, infill, as a supplement, mainly appears in well-developed city centres and is less common than the other two. The rate and intensity of three typologies have varied over time.

This study contributes to the understanding of urban sprawl in high density, rail transit-oriented area beyond the 'American model' and provides a view on a modest growing city. Different from U.S. metropolitan areas or China's mega-/super-cities where rates of outlying or expansion are less significant (than infill) or even negative (Hamidi and Ewing, 2014; Li and Li, 2019), Zhuhai's sprawl remains dominated by edge expansion with infill playing a negligible role. It also offers a clearer picture of urban land sprawl inside a city. The growth of urban built-up areas is uneven inside Zhuhai. Outlying was most uneven from 1990 to 1995 with a CV of 1.93. The unbalance of infill reached its peak recently (2013–2015) with a CV of 2.24. Edge expansion is the least unbalanced typology reaching the minimum of 0.42 CV from 2010 to 2013. The CV of arable land loss was higher and fluctuated greater than that of forest loss. The unbalance of arable land loss reached a peak from 2005 to 2008 with a CV of 0.87. In addition, extent of intra-urban land sprawl imbalance significantly fluctuates because local urban sprawl is sensitive to policy makings from local political leaders who are frequently reposted under China's floating cadre appointment system (He et al., 2018). Leaders of each tenure are likely to propose new potential areas, leading to great variability of urban sprawl inside the city. This city-level pattern is distinct from the macro-level one that regional differences (among the east, west, central, and northeast) have long been well-noted and that the backward west region has long sprawled more extensive than the developed east.

Furthermore, Zhuhai's growth amount is not as resplendent as that in star cities, such as Shenzhen and Guangzhou. From 1980 to 2015, the expanded urban area in Zhuhai was only one-third of that in Shenzhen and half of that in Guangzhou. This prudential growth has prevented Zhuhai's natural ambience from damage and has led the city to embrace a sustainable garden city ideology. Without sacrificing the environment, Zhuhai has gained several awards nationally and internationally for its ecological merits since 1997. Furthermore, its specific sprawl trajectory sheds some light on policy implications. Firstly, a pro-environment policy may reconcile contradictions between ecological environment and urban growth. It distinguishes cities with ecological merits from others. Secondly, environmental policy suppresses urban land growth to preserve high-quality environments for sustainable long-term development, thereby reaching a compromise between environmental sustainability and urban land growth. Thirdly, growth typology, despite circumstantial differences, conforms with environmental development in which natural mountains, rivers, and harbours are of utmost respected. Zhuhai did not stagnate

but developed at a slow pace, which brought the city's natural environment into play. This study argues to conduct more in-depth case studies to enrich the understanding of intra-urban sprawl patterns, especially those invisible land sprawl, in small to medium sized cities and relate local policy and politics with the interpretations of sprawl patterns. Future research can also benefit from quantifying conversion between urban built-up area and other land uses so that the sources of sprawl can be tracked and monitored.

Acknowledgements. The work is funded by the National Natural Science Foundation of China [Grant No. 51808391, 41601445, 41701189] and Open Projects Fund of Key Laboratory of Shanghai Urban Renewal and Spatial Optimization Technology [Grant No. 2019020202].

REFERENCES

- [1] Akbari, H., Rose, L. S., Taha, H. (2003): Analyzing the land cover of an urban environment using high-resolution orthophotos. – *Landscape & Urban Planning* 63(1): 1-14.
- [2] Aniekwe, S., Igu, N. (2019): A Geographical Analysis of Urban Sprawl in Abuja, Nigeria. – *Journal of Geographical Research* 2(1): 13-19.
- [3] Batty, M. (2002): Thinking about Cities as Spatial Events. – *Environment and Planning B-Planning & Design* 29: 1-2.
- [4] Bhatta, B., Saraswati, S., Bandyopadhyay, D. (2010): Urban Sprawl Measurement From Remote Sensing Data. – *Applied Geography* 30: 731-40.
- [5] Budd, W. W. (1996): Land mosaics: The ecology of landscapes and regions: Richard T. T. Forman, Cambridge University Press, 1995, 632 pp. – Book review. *Landscape & Urban Planning* 36(3): 229-231.
- [6] Burgess, E. W. (1925): The Growth of the City. – In: Park, R. E., Burgess, E. W., McKenzie, R. (eds.) *The City: Suggestions of investigation of Human Behavior in the Urban Environment*. University of Chicago Press, Chicago.
- [7] Chang, C. C., Lin, C. J. (2011): LIBSVM: a library for support vector machines. – *ACM Transactions on Intelligent Systems and Technology* 2(3): 1-27.
- [8] Chen, J. (2016): Urban land expansion and the transitional mechanisms in Nanjing, China. – *Habitat International* 53: 274-83.
- [9] Congalton, R., Green, K. (2009): *Assessing the Accuracy of Remotely Sensed Data: Principles and Practices*. – CRC Press, Boca Raton.
- [10] Ding, J., Wang, K. (2018): Spatio-temporal evolution of industrial production space and its driving mechanisms in Pearl River Delta urban agglomeration. – *Geographical Research* 37(1): 53-66.
- [11] Grainger, A. (1995): National Land Use Morphology: Patterns and Possibilities. – *Geography* 80: 235-45.
- [12] Hamidi, S., Ewing, R. (2014): A longitudinal study of changes in urban sprawl between 2000 and 2010 in the United States. – *Landscape & Urban Planning* 128: 72-82.
- [13] Harris, C. D., Ullman, E. L. (1945): The Nature of Cities. – *Annals of the American Academy of Political & Social Science* 242: 7-17.
- [14] He, S., Li, L., Zhang, Y., Wang, J. (2018): A Small Entrepreneurial City in Action: Policy Mobility, Urban Entrepreneurialism, and Politics of Scale in Jiyuan, China. – *International Journal of Urban and Regional Research* 42(2): 286-302.
- [15] Herold, M., Goldstein, N. C., Clarke, K. C. (2003): The spatiotemporal form of urban growth: measurement, analysis and modeling. – *Remote Sensing of Environment* 86: 286-302.
- [16] Hoyt, H. (1939): *The Structure and Growth of Residential Neighborhoods in American Cities*. U.S. – Government Printing Office, Washington.

- [17] Leichenko, R. M., Solecki, W. D. (2005): Exporting the American Dream: The Globalization of Suburban Consumption Landscapes. – *Regional Studies* 39(2): 241-253.
- [18] Li, W., Wang, Y., Peng, J., Li, G. (2004): Landscape spatial changes in Shenzhen and their driving factors. – *Journal of Applied Ecology* 15: 1403.
- [19] Li, G., Li, F. (2019): Urban sprawl in china: differences and socioeconomic drivers. – *Science of The Total Environment* 673: 367-377.
- [20] Liu, X., Li, X. Y., Chen, Y., Tan, Z., Li, S., Ai, B. (2010): A new landscape index for quantifying urban expansion using multi-temporal remotely sensed data. – *Landscape Ecology* 25(5): 671-682.
- [21] Liu, T. (2020): *China's Urban Construction Land Development*. – Springer, Singapore.
- [22] Long, H., Li, T. (2012): The coupling characteristics and mechanism of farmland and rural housing land transition in China. – *Journal of Geographical Sciences* 22: 548-62.
- [23] Ng, M. K. (2011): Power and rationality: the politics of harbour reclamation in Hong Kong. – *Environment and Planning C-government and Policy* 29: 677-92.
- [24] Orff, K. (2001): Great leap forward. – In: Chung, C. J., Inaba, J., Koolhaas, R., Leong, S. T. (eds.) *Great leap forward / Harvard Design School Project on the city*. Koln.
- [25] Peng, J., Wang, Y., Zhang, Y., Wu, J., Li, W., Li, Y. (2010): Evaluating the effectiveness of landscape metrics in quantifying spatial patterns. – *Ecological Indicators* 10: 217-23.
- [26] Qi, Z., Yeh, A. G. O., Li, X., Lin, Z. (2012): A novel algorithm for land use and land cover classification using RADARSAT-2 polarimetric SAR data. – *Remote Sensing of Environment* 118: 21-39.
- [27] Scheuer, S., Haase, D., Volk, M. (2016): On the Nexus of the Spatial Dynamics of Global Urbanization and the Age of the City. – *Plos One* 11(8): e0160471.
- [28] Shahraki, S. Z., Sauri, D., Serra, P., Modugno, S., Seifoddini, F., Pourahmad, A. (2011): Urban sprawl pattern and land-use change detection in Yazd, Iran. – *Habitat International* 35: 521-528.
- [29] Shi, Y., Sun, X., Zhu, X., Li, Y., Mei, L. (2010): Characterizing growth types and analyzing growth density distribution in response to urban growth patterns in peri-urban areas of Lianyungang City. – *Landscape & Urban Planning* 98: 425-33.
- [30] Theobald, D. M. (2001): Land-Use Dynamics beyond the American Urban Fringe. – *Geographical Review* 91: 544-64.
- [31] Xian, S., Li, L., Qi, Z. (2019): Toward a sustainable urban expansion: A case study of Zhuhai, China. – *Journal of Cleaner Production* 230: 276-85.
- [32] Yang, Y., Liu, Y., Li, Y., Du, G. (2018): Quantifying spatio-temporal patterns of urban expansion in Beijing during 1985–2013 with rural-urban development transformation. – *Land Use Policy* 74: 220-30.
- [33] You, H. (2016): Quantifying megacity growth in response to economic transition: A case of Shanghai, China. – *Habitat International* 53: 115-22.

ADSORPTION AND DEGRADATION BEHAVIOR OF METHANOL IN PRODUCED WATER IN THE SOILS OF NORTHERN SHAANXI GAS FIELD, CHINA

MA, Y.^{1,2*} – LI, Y.³ – GAO, L.³ – XIE, J.⁴

¹*College of Petroleum Engineering, Shaanxi Province Key Laboratory of Advanced Stimulation Technology for Oil & Gas Reservoirs, Xi'an Shiyou University, Xi'an, Shaanxi 710065, China
(phone: +86-29-8838-2673; fax: +86-29-8823-4429)*

²*Engineering Research Center of Development and Management for Low to Ultra-Low Permeability Oil & Gas Reservoirs in West China, Ministry of Education, Xi'an, Shaanxi 710065, China
(phone: +86-29-8838-2683; fax: +86-29-8823-4429)*

³*No.2 Gas Production Plant, Changqing Oilfield Company, Yulin, Shaanxi 710200, China
(e-mail: lyao3_cq@petrochina.com.cn, gliang1_cq@petrochina.com.cn
phone: +86-29-8650-3011; fax: +86-29-8658-2076)*

⁴*College of Chemistry and Chemical Engineering, Shaanxi Province Key Laboratory of Environment Pollution Control Technology of Oil Gas and Reservoir Protection, Xi'an Shiyou University, Xi'an, Shaanxi 710065, P. R. China
(e-mail: Xie_juan@xsyu.edu.cn, 1007724077@qq.com
phone: +86-29-8838-2706; fax: +86-29-8823-4429)*

**Corresponding author
e-mail: mayun9401@xsyu.edu.cn*

(Received 13th Jul 2019; accepted 25th Nov 2019)

Abstract. Injection of methanol as a thermodynamic inhibitor is a common approach in the petroleum industry. Due to the volatility and recovery process of methanol, it could be found in natural waters, sediments, soil, and so on. This study focused on adsorption and degradation behavior of methanol in produced water (PW) at northern Shaanxi oil and gas fields soil, China. Through dynamic tests, the results showed that the pH, gas condensate, salinity of PW and temperature have weak influences on methanol adsorption on the soil. Through the simulated degradation experiments, the chemical oxidation, photo and thermal degradation were found not to be the main mechanism of methanol degradation (MD) in nature. The methanol in some soil could not be degraded completely by Nitrate-reducing bacteria (NRB) in the soil within 60 days unless methanol content was less than 600 mg/L with NRB medium. The Griess detection verified that there were NRB in five soils. Even without the NRB medium, there are great differences in MD of the soils. If the concentration of methanol was more than 1000 mg/L, the MD efficiencies were obviously slowing down, nearly 0. The longer the gas development time of the study region, the stronger the MD ability of the region's soil.

Keywords: *methanol, adsorption, degradation, sandy soil, Nitrate-reducing bacteria (NRB)*

Introduction

In economic and safety hazards points of view, it is crucial to avoid the formation of clathrate hydrate of gases in oil and natural gas transportation/production systems (Muromachi, 2019). Injection of methanol as a thermodynamic inhibitor is a common approach in industry to shift the hydrate phase boundary to higher pressures/lower temperatures. Because of its high volatility, methanol is lost in the vapor phase, which lead its toxicity to the environment and human beings (Aziz et al., 2002). Although methanol in aqueous solution was generally treated by biological treatment and advanced oxidation processes (AOPs), in which the most

commonly used approaches were the up flow anaerobic sludge bed (UASB), supercritical water oxidation (SCWO), bio-filtration and plasma degradation (Ma et al., 2009, 2013; Fujii et al., 2011; Barcón et al., 2012; Zhen et al., 2017; Wu et al., 2019), but few studies focused on adsorption and degradation behavior of the methanol in produced water (PW) in the soil. The northern Shaanxi oil and gas fields is located in Ordos plateau (Semi-arid region), China. The surface layer of the soil is the quaternary aeolian sandy soil or brown desert soil, among which aeolian sandy soil is in the majority. Because of the special soil composition, the methanol will show special adsorption and degradation behavior in the soil. Through temperature oscillation dynamic tests and the simulated degradation of methanol in the five kinds of typical soil, the behavior of adsorption and degradation have been discussed, which lead to a better understanding of the influence of methanol on the north Shaanxi gas field environment.

Material and Method

Soil Sample collection and pre-treatment

The five kinds of soil samples were collected from five different sites located in Northern Shaanxi gas field, respectively is Jingbian gas field (1#), Jingbian farmland (2#), Zizhou gas field (3#), Zizhou farmland (4#) and Wuding river (5#) in Mizhi county, Yunlin city. The map of study area were showed as in *Fig. 1*. The surface layer is the quaternary aeolian sandy soil or brown desert soil, among which aeolian sandy soil is in the majority (Ma et al., 2013). The sampling date was April to May, 2018. The sampling depth is 0 ~ 20 cm. After the soil sample is naturally dried, ground and sifted with a 2 mm sifter, then stored in five bottles at low temperature.

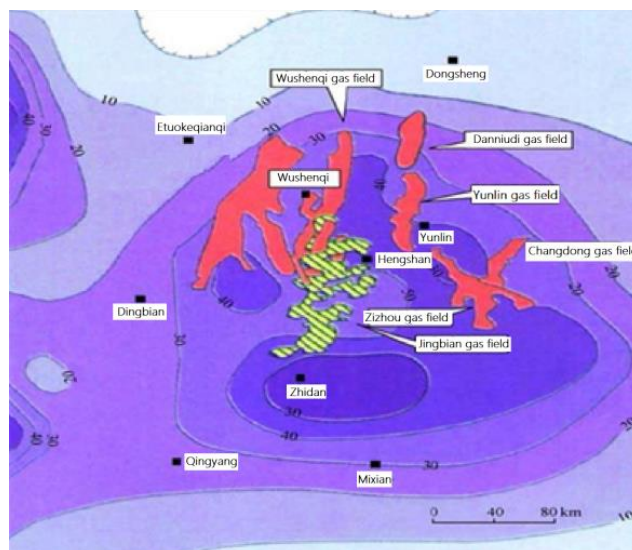


Figure 1. The map of study area

Measurement of soil parameters

The physiochemical analysis (pH, moisture, organic matter content and mass size distribution) of five samples was respectively refer to “Soil dry matter and moisture determination - gravimetric method” (HJ 613-2011), “Soil test part II: determination of pH” (NY/T 1121.1 – 2006), “Determination of forest soil organic matter and calculation

of carbon - nitrogen ratio” (LY/T 1237 – 1999) and the Wu’s method (Ghasemy et al., 2019).

Adsorption test

Adsorption of methanol in different soils

Due to the strong adsorption capacity of bentonite and activated carbon, these two materials were selected as the experimental reference in order to facilitate the study of the adsorption capacity of methanol in five soil samples. The seven samples were taken respectively in the experiment and 20.00 g were put into a 250 mL glass bottle, and 100 mL methanol concentration of 1000 mg/L solution with 10000 mg/L salinity and a certain amount of microbial inhibitors were added. Then, the sealed 250 mL bottle were settled in the thermostatic oscillator (TS-200B, Shanghai Tiancheng co. LTD) under the condition of 25°C for 24 h, later transferred to the soil suspension in the centrifuge tube at 4000 r/min centrifuge for 10 min after taking centrifugal supernatant on 2 mL for methanol concentration. The concentrations of methanol was determined by gas chromatography (Agilent HP 6890). A packed column (Agilent Porapak N G3591-80036) was used. The retention time of methanol was 5.652 min (Ma et al., 2013). The adsorption capacity and samples site were compared, and 3# was selected as the representative for future research.

Adsorption equilibrium and isotherm of methanol in soil

In Adsorption equilibrium test, the 2 mL supernatant was samples after 0.5, 1, 2, 4, 6, 8, 10, 12, 24 h. In Adsorption isotherm test, the methanol concentration, respectively is 0, 20, 40, 60, 80, 100, 200, 500 and 1000 mg/L. Other test conditions are consistent with conditions detailed above.

Affecting factors of methanol adsorption in soil

The range of PW pH, temperature, gas condensate, salinity were according to the quality of gas PW from Northern Shaanxi gas field (The quality of gas PW from North Shaanxi gas field had analyzed by our lab in the past 10 years). Other test conditions are consistent with conditions detailed above.

Degradation behavior of Methanol in soils

Physicochemical factors on degradation of methanol in different simulation conditions

When the gas PW with methanol is treated and injected back into the stratum, it will directly or indirectly enter the soil environment because of evaporation and leakage. According to the possible factors affecting degradation of methanol in the possible environment, ammonium persulfate and hydrogen peroxide (used as oil-field chemicals), high temperature and pressure (re injection into some formations), strong ultraviolet (direct solar radiation) were selected to make a series of simulation experiments to study the degradation degree of methanol in gas PW under different conditions. A temperature and pressure reactor (Parr 4578, Parr instrument company, USA) was used to stimulate the condition of reinjection formation (200°C and 15 MPa). The 50 g core powder was added into the reactor, and the methanol equilibrium concentration after 12 hours adsorption in core powder was the baseline concentration for degradation. A UV light (80W, Xinbao Environmental Products Co., Ltd., CHN) was used to stimulate rapid solar

radiation. The source of radiation was located 25 cm from samples and positioned horizontally. All solution is 1 L and 1000 mg/L methanol, and other experimental temperature is 25°C unless it is specifically requested.

Stimulated degradation experiment in different soils

Nitrate reducing bacteria (NRB) are very common in nature, most of which are facultative. When methanol (CH₃OH) is used as the carbon source in wastewater treatment, the reaction formula for synthesis of exogenous denitrifying cells was shown in Eq.1 (Ma and Wei, 2009).



According to the above theory, if methanol is degraded by NRB in nature, the degradation rate would increase. Therefore, the difference between with or without the medium of NRB (M_{NRB}) was compared in different salinity water with different methanol concentration under 25°C and the proportion of 1# soil to methanol (20%) after 60 days. Table 1 is the composition of M_{NRB}.

Table 1. The composition of M_{NRB}

Composition	KH ₂ PO ₄	KHCO ₃	MgSO ₄	FeCl ₃	CaCl ₂	CH ₃ COONa	(NH ₄) ₂ SO ₄	NaNO ₃
Concentration (mg/L)	30	500	200	100	30	860	660	850

According above studies, the different soils was respectively soaked in the simulated water containing 200 ~ 2200 mg/L methanol (salinity: 100000 mg/L) for 120 d with the proportion of the soils to methanol (20%). In order to verify the effect of NRB, NRB was enriched, separated and screened from five soils samples, respectively. Two strains in every solid mediums plate were selected, which grow faster, colony moist, roundness, surface smooth, edge tidy, bulging and larger colonies. After many times of separation and purification, a strain was selected out of every two in the soil, which were 1S#, 2S#, 3S#, 4S# and 5S# strain. The five strains of bacteria were tested with Griess reagent (García-Robledo et al., 2014).

Each experiment was performed three times, and the average value is calculated by three parallel experiments.

Results and discussions

Physiochemical analysis results of five samples

The physiochemical analysis results of five samples were shown in Table 2. The minimum moisture of five soils was 0.30% (w/w) while the maximum is 1.45% (w/w). The pH values of the tested soil samples were all around 8.0 ~ 9.0, belonging to weakly alkaline soil. The organic content of the tested soil samples was also relatively small, among which the organic matter content of 4# was the highest, 0.655% (w/w) and that of 1# was the lowest, 0.266%(w/w). All soils are sandy soil, except 4# soil is loam sandy soil, which would lead that it was easy for the methanol to infiltrate into the groundwater through them.

Table 2. *Physiochemical analysis results of five soil samples*

No.	pH	Moisture (w/w%)	Organic matter (w/w%)	Mass size distribution (w/w%)					Type
				2-50µm	50-100µm	100-250µm	250-1000µm	1000-2000µm	
1#	8.34	0.30	0.266	0.0000	0.2413	0.7354	0.2330	0.0000	sandy soil
2#	8.61	0.55	0.307	0.0000	0.1911	0.7616	0.4730	0.0000	sandy soil
3#	8.78	1.10	0.410	0.0000	0.3149	0.4809	0.2042	0.0000	sandy soil
4#	8.88	1.45	0.655	0.0000	0.5623	0.2014	0.2363	0.0000	loam sandy soil
5#	8.66	0.50	0.366	0.0000	0.1659	0.7407	0.9340	0.0000	sandy soil

Adsorption of methanol in different soils

The results of methanol adsorption capacity (MAC) in different soils are shown in Fig. 2. The MAC in the five tested soil samples was significantly different from that of activated carbon and bentonite. The largest adsorption capacity of activated carbon was up to 2.38 mg/g, that of bentonite took second place, reached about 1.37 mg/g, and those of five soils are between 0.45 mg/g and 0.60 mg/g. Among five soils, the soil from Zizhou had higher adsorption capacity than those of other soils. The reasons should be that the soil from Zizhou has higher organic content which lead to higher adsorption capacity. The experimental results are consistent with the characteristics of small activated carbon/bentonite particles, large specific surface area of particles and large adsorption capacity. Therefore, it can be concluded that the five soils have a certain adsorption capacity for methanol, but the adsorption amount is relatively small. All that also should lead that most of methanol could infiltrate into groundwater through them easily and not be degraded in the soils.

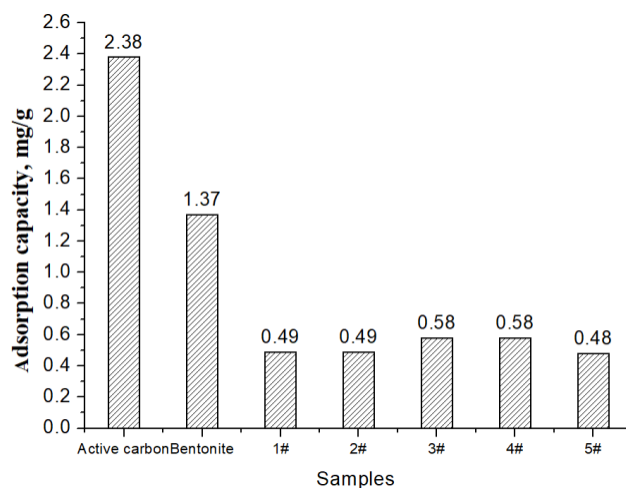


Figure 2. *MAC in different samples and soils*

Adsorption equilibrium and isotherm of methanol in soil

The adsorption equilibrium curve and isotherm curve of methanol in 3# soil respectively was shown in Fig. 3 and Fig. 4.

From Fig. 3, when the adsorption time was less than 10 h, the adsorption capacity of methanol in the 3# soil increased rapidly, but when the adsorption time was more than

10 h, the adsorption capacity tended to be stable, and the maximum adsorption amount was about 0.55 mg/g. This reason is that the opportunity for the soil to fully contact methanol increases with the gradual extension of time, and the amount of methanol adsorption in the soil increases. From Fig. 4, when the methanol concentration is smaller than 200 mg/L, the adsorption capacity increases sharply with the increase of methanol concentration. When the methanol concentration is higher than 200 mg/L, the adsorption capacity tends to be balanced, about 0.5 mg/g, which indicated that the adsorption capacity of methanol in the soil had reached a saturated state.

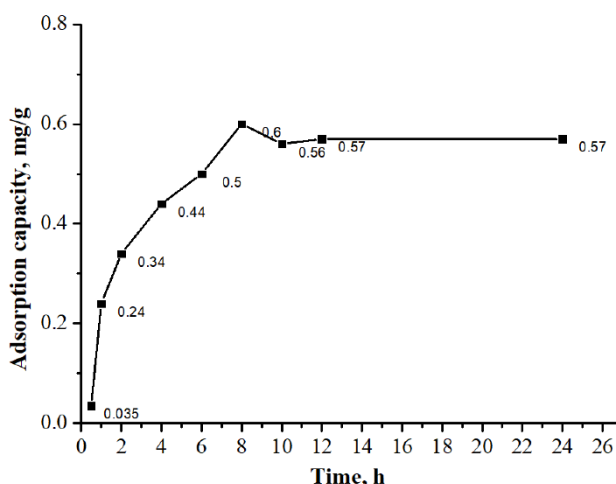


Figure 3. Adsorption equilibrium curve of methanol in 3# soil

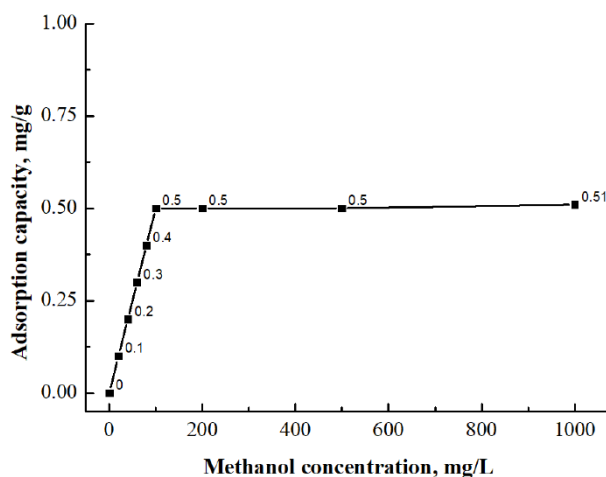


Figure 4. Isotherm curve of methanol in 3# soil

Affecting factors of methanol adsorption in soil

pH values

The influence of different pH values on the methanol adsorption amount (MAA) was shown in Fig. 5. As can be seen from Fig. 5, with the increase of pH value of solution, the MAA in soil gradually decreases from 0.458 mg/g to 0.007 mg/g. In the alkaline environment, the sediments and organic matter in the soil may undergo flocculation

changes, leading to the fact that methanol molecules cannot be uniformly adsorbed on the soil sediments and organic matter (Viotti et al., 2000). Lopez et al. (1996) believe that at low pH, strong hydrogen bonds are formed between organic pollutants and O, N, and H atoms in some materials in the soil, but they are completely different under alkaline conditions, and the resistance to hydrogen bond formation increases, leading to hydrogen bond dissociation. Some scholars also reached the conclusion that the adsorption amount of an organic compound in alkaline soil was low, while that in acidic soil was high (Ertli and Marton, 2004; Goh and Lim, 2004). With the increase of pH value, the increase of OH⁻¹ content on the surface of soil particles leads to the increase of electrostatic repulsion force, the decrease of charge density on the surface of soil, and the decrease of adsorption force on the surface of soil particles. The pH value is an important factor affecting the variable charge, and the change of pH value has an important impact on the electrostatic adsorption of anions. With the decrease of pH value, the positive charge increases, and the amount of electrostatic adsorption of anions increases. In the case of pH > 7, even the variable charge soil with kaolinite and iron and aluminum oxides as the main colloidal substances has a relatively low electrostatic adsorption capacity of anions (Zhang, 2009).

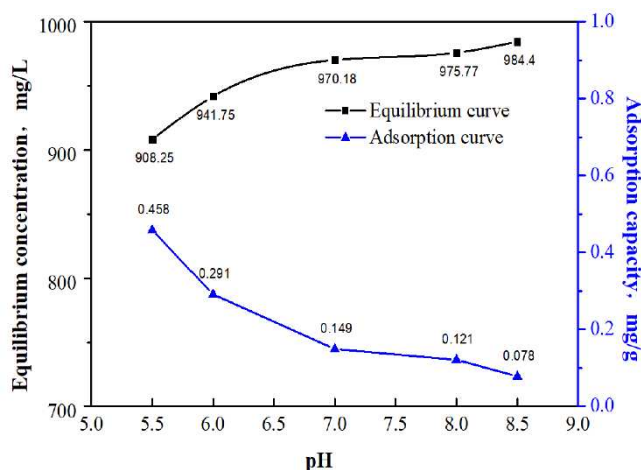


Figure 5. Influence of different pH values on the MAA in 3# soil

Salinity

The effects of water quality with different salinity on the adsorption of methanol in soil was shown in Fig. 6.

The MAA in soil increases from 0.373 mg/g to 0.487 mg/g with the increase of salinity in solution from 0 mg/L to 100000 mg/L. This was due to the adsorption coefficient (K_p) is defined as follows Eq.2 (Pena et al., 2019):

$$K_p = \frac{\text{Adsorption capacity of organic compounds in the solid phase, mg/g}}{\text{dissolved amount of organic matter in aqueous solution, mg/L}} \quad (\text{Eq.2})$$

From Eq.2, the K_p is related to the adsorption amount in solid phase and the solubility of organic matter in water phase. With the increase of salinity in soil solution, the solubility of organic matter in water decreases, which is mainly due to the influence of "salting out". Salting out, in which salts are added to an aqueous solution of a substance, results in a decrease in the solubility of the substance. In this experiment, the soil adsorption increased with the increase

of salinity, indicating that methanol was affected by "salting out". Since "salting out" reduced the value in the denominator of the above equation, Kp value increased (Zhao et al., 2000). The lower the solubility, the higher the solid adsorption. The adsorption capacity is closely related to the hydrophilicity of the adsorbed substance. Although salinity cannot change the nature of the adsorbed substance in the soil, it does change its solubility. Therefore, it is basically the same as increasing its hydrophobic effect, so the solid phase adsorption increases. It can be seen from the above analysis that the adsorption of pollutants by salinity mainly affects the solubility of pollutants (Gennadiev et al., 2015).

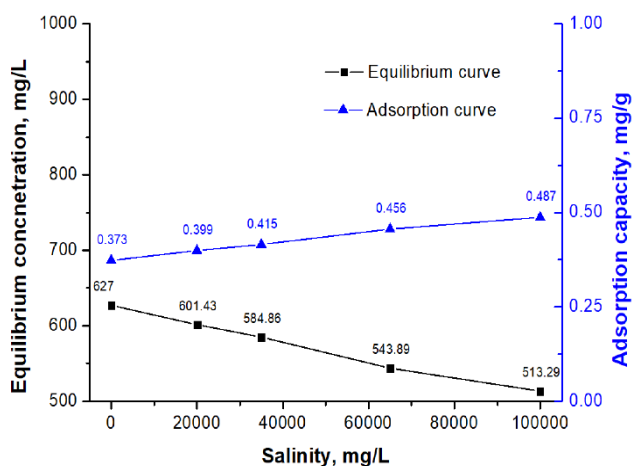


Figure 6. Influence of different salinity on the methanol adsorption amount in 3# soil

Condensate oil

The effect of condensate oil content on the methanol adsorption in soil was shown in Fig. 7.

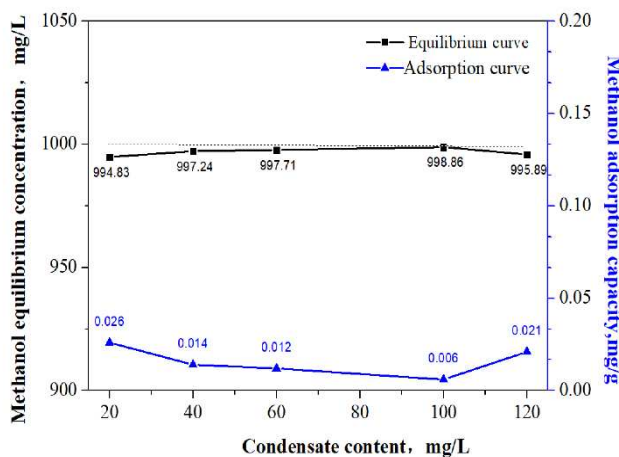


Figure 7. Effect of condensate oil content on the methanol adsorption in 3# soil

With the increase of the condensate concentration, the equilibrium concentration of methanol in the soil did not change much, between 994.83 mg/L and 995.89 mg/L, indicating that the condensate could not be adsorbed by the sediments or organic matters

in the soil after entering the soil environment. Some scholars also found similar phenomena in soil-water system (Jonker et al., 2003, 2006). They called the minimum concentration of oil in sediments or soil in independent form as critical separate phase concentration (CSPC), and pointed out that this concentration was related to organic matter content. Generally, the higher the organic matter content is, the higher the CSPC is, which is 11% (Khan et al., 2018) or 15% (Li et al., 2019) of the soil organic carbon content. The soil organic matter content of 3# sandy soil is 0.41%, which should be 1100 or 1500 mg/kg according to the theoretical value of CSPC in previous studies. The practical significance of CSPC is that when the condensate oil concentration in the soil is greater than this value, the condensate oil can exist in the soil in the form of free state (independent phase), as a "adsorbent" to enhance the overall adsorption (distribution) ability of the soil to other organic pollutants. When the value is less than that, the condensate oil is absorbed by the soil organic matter in the form of "adsorbent", which may compete with other organic pollutants for the adsorption position on the organic matter. In the study of Jonker et al. (2003, 2006) this competitive adsorption was more obvious.

Temperature

The influence of environmental temperature on the MAA in the soil was shown in Fig. 8. With the increase of temperature from 10 °C to 35 °C, the MAA in the soil also increases obviously (from 0.330 mg/g to 0.975 mg/g) when the temperature was below 35 °C. When the temperature rises to 35 °C, the adsorption curve begins to be smooth, methanol adsorption capacity is essentially unchanged. It indicates that the adsorption reaction rate of methanol in soil increases with the increase of temperature. When the adsorption capacity of methanol in soil reaches a balance, the MAA in soil does not increase, indicating that the adsorption of methanol in soil is an endothermic process. Li et al. (2019) believed that soil adsorption is a kind of biphasic adsorption, and mineral as a traditional solid adsorbent, organic matter as a distribution medium. As the temperature rises, water molecules are more affected by molecules than organics, and the relative adsorption competitiveness of organic matters increases, and the adsorption capacity on the mineral surface increases (Pena et al., 2019).

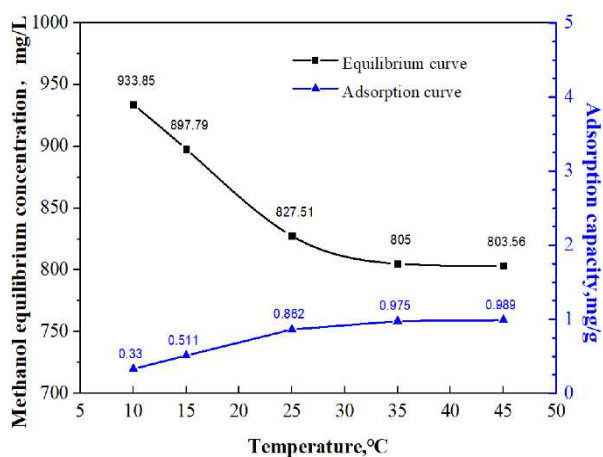


Figure 8. Influence of environmental temperature on the MAA in 3# soil

Degradation behavior of methanol in soils

Physicochemical factors on degradation of methanol in different simulation conditions

Degradation degree of methanol in different simulated extreme environment was shown in Table 3. The degradation efficiency (η) of methanol in extreme environment (200°C, 15 Mpa) after 30 days was only 10.18%. The η of strong ultraviolet radiation and the chemical oxidation were 23.94%, 21.69% and 11.84%, respectively. The radiation intensity and the concentration of chemical oxidant were usually more than their value in nature. The results showed that among the factors on degradation of organic matter in nature, the physicochemical factors, such as thermal degradation relying solely on temperature, chemical oxidation degradation and photo-degradation could not be found the main factors of methanol degradation (MD).

Table 3. Degradation degree of methanol in different simulated environment

Simulated extreme environment (200°C, 15 MPa)			Strong ultraviolet radiation (Power: 80W)			Chemical oxidation (Reaction time: 30 min)			
Reaction time (day)	Concentration (mg/L)	η (%)	Reaction time (h)	Concentration (mg/L)	η (%)	Reaction dosage (mg/L)	Concentration (mg/L)	η (%)	
0	933	0	0	1000	0	0	1000	0	
4	886	5.04	10	942	5.78	Ammonium persulfate (NH ₄) ₂ S ₂ O ₈	300	858	14.21
6	861	7.72	20	901	9.86	500	846	15.39	
8	859	7.93	40	827	17.31	800	783	21.69	
10	857	8.15	60	803	19.72	Hydrogen Peroxide (H ₂ O ₂)	0	1000	0
12	854	8.47	80	799	20.12	5000	1093	2.51	
14	841	9.86	100	781	21.87	10000	1025	6.89	
30	838	10.18	120	761	23.94	20000	882	11.84	

Nitrate reducing bacteria influence on methanol degradation

NRB influence on (MD) in 1# soil was shown in Fig. 9. Obviously, the ability to degrade methanol of 1# soil with M_{NRB} was much higher than that of 1# soil without M_{NRB}, up more than 50%, which indicated that NRB could significantly promoted the degradation methanol ability of the soil.

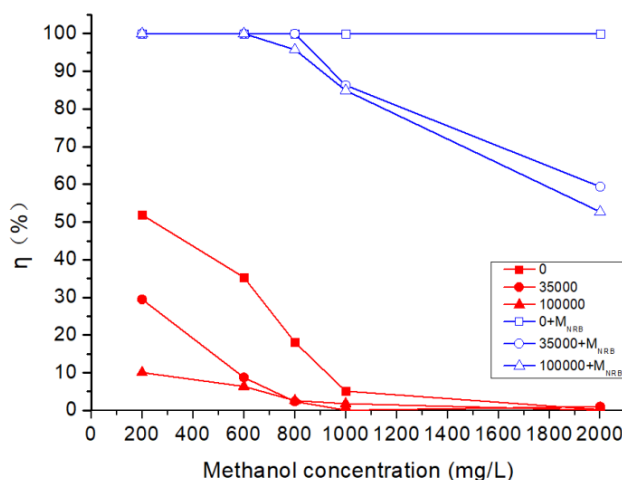


Figure 9. NRB influence on MD in 1# soil (60 days)

In the presence of M_{NRB} , methanol concentration in fresh water was less than 2000 mg/L, the methanol can be completely degraded in 1# soil. In the absence of M_{NRB} , methanol cannot be completely degraded within the range of 200 ~ 2000 mg/L, the highest η was only 51.9% and the lowest one was 0.07%, nearly 0. In the presence or absence of M_{NRB} , the degradation rate began to decline when the salinity increased, and the degradation rate decreased significantly when the methanol concentration was more than 1000 mg/L. The reason should be that both salt and methanol have inhibitory effect on soil microorganisms and affect the biodegradation of methanol.

Methanol degradation in different soils

MD efficiency in different soils was shown in Fig. 10.

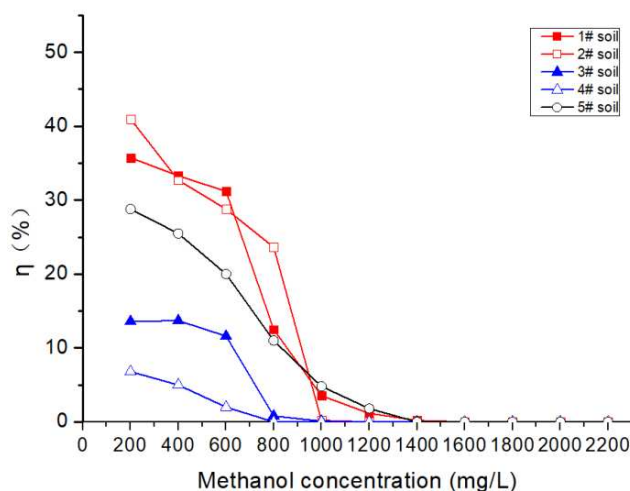


Figure 10. Different MD in different soils (Salinity: 100000 mg/L, Without M_{NRB} and 120 days)

When the salinity is 100000 mg/L in the absence of M_{NRB} , the degradation degree of methanol was obviously different when the initial concentrations were different. The highest η was 2# soil, 41.0%. The degradation rate decreased rapidly when the methanol concentration was greater than 1000 mg/L. The lowest one was nearly 0 when the methanol concentration is more than 1400 mg/L. There were great differences existing in degradation rate of different soil. The 1# and 2# soil from Jingbian had the best degradation ability of methanol, followed by the 5# from the Wuding river, the worst were that of 3# and 4# soils from Zizhou. The main reasons should be the Jingbian region had the longest history of developing gas, so it is the earliest blocks where the methanol was first used among the three regions. The microbes in Jiangbian surrounding soil has more superiority strains capable of degrading methanol. The 5# sediments was from Wuding river, so the microbial content in it was relatively high. Therefore, 3# soil and 4# soil had the lower degradation ability of methanol than other's.

The Griess detection result of five strains was showed in Fig. 11. Compared with the control, all the bacterial solutions immediately changed from colorless or pale yellow to red after the addition of Griess reagent, which indicated that all strains were NRB. Under the same culture conditions, the color of the reaction between strain 3S# and Griess reagent was lighter than that of other strains, while that of strains 1S# and 4S# was faster and darker. This may be related to the quantity of nitrate reductase and nitrite reductase

produced by each strain. The higher the concentration of nitrate reductase and nitrite reductase in the bacterial solution, the deeper the color rendering, which indicated that the denitrification ability of each NRB is different (Ma and Wei, 2009). Compared with the degradation results, the denitrification ability of five NRB strains from five soils did not correspond to the MD capacity of five soils. The reason should be that the MD in the soil was not entirely dependent on NRB, but the NRB significantly promoted the degradation methanol ability of the soil.



Figure 11. Griess detection photo of five strains from five soils

Conclusion

Five kinds of soils in the study region are sandy soil or loam sandy soil, and the MAA of them are relatively small, which would lead that the methanol to infiltrate into groundwater through them easily not be degraded in the soils. The pH, gas condensate, salinity of PW, temperature have the weak influences on methanol adsorption on the soil. Through the simulated degradation experiment of methanol, the chemical oxidation degradation, photo-degradation and thermal degradation are not the main mechanism of MD. But when the methanol comes into contact with the soil, the methanol in some soils could not be degraded completely by NRB in the soil within 60 days unless methanol content is less than 600 mg/L with NRB medium. The NRB significantly promoted the degradation methanol ability of the soil. Even without the NRB medium, there are large differences among the soils although five soils had the certain capability to degrade methanol. When the methanol content increase or the salinity of the water increased without M_{NRB} , the MD rate decreased. The Griess detection verified there were NRB in five soil. The longer the gas developing time of the studying region, the stronger the methanol degrading ability of the region's soil. If the concentration was more than 1000 mg/L, the MD efficiencies were obviously slow after 120 days. Both salt and methanol have inhibitory effect on soil microorganisms and affect the biodegradation of methanol. The conclusion led to a better understanding of the influence of methanol on the north Shaanxi gas field environment, and suggested that the biodegradation of methanol in nature should be considered, especially NRB.

Funding. This research is supported by the Key laboratory Research Project of Shaanxi Education Department (CHN) under grant numbers 15JS090 and 17JS112.

Conflicts of Interests. The authors declare no conflict of interests.

REFERENCES

- [1] Aziz, M. H., Agrawal, A. K., Adhami, V. M., Ali, M. M., Baig, M. A., Seth, P. K. (2002): Methanol-induced neurotoxicity in pups exposed during lactation through mother: Role of folic acid. – *Neurotoxicol. Teratol.* 24(4): 519-527.
- [2] Balseiro-Romero, M., Monterroso, C., Casares, J. J. (2018): Environmental Fate of Petroleum Hydrocarbons in Soil: Review of Multiphase Transport, Mass Transfer, and Natural Attenuation Processes. – *Pedosphere* 28(6): 833-847.
- [3] Barcón, T., Alonso-Gutiérrez, J., Omil, F. (2012): Molecular and physiological approaches to understand the ecology of methanol degradation during the biofiltration of air streams. – *Chemosphere* 87: 1179-1185.
- [4] Ertli, T., Marton, A., Földényi, R. (2004): Effect of pH and the role of organic matter in the adsorption of isoproturon on soils. – *Chemosphere* 57(8): 771-779.
- [5] Fujii, T., Hayashi, R., Kawasaki, S., Suzuki, A., Oshima, Y. (2011): Water density effects on methanol oxidation in supercritical water at high pressure up to 100 MPa. – *J. Supercrit. Fluids* 58(1): 142-149.
- [6] García-Robledo, E., Corzo, A., Papaspyrou, S. (2014): A fast and direct spectrophotometric method for the sequential determination of nitrate and nitrite at low concentrations in small volumes. – *Marine Chemistry* 162: 30-36.
- [7] Gennadiev, A. N., Pikovskii, Yu. I., Tsibart, A. S., Smirnova, M. A. (2015): Hydrocarbons in Soils: Origin, Composition, and Behavior (Review). – *Eurasian soil Sci.* 48(10): 1076-1089.
- [8] Ghasemy, A., Rahimi, E., Malekzadeh, A. (2019): Introduction of a new method for determining the particle-size distribution of fine-grained soils. – *Measurement* 132: 79-86.
- [9] Goh, K. H., Lim, T. T. (2004): Geochemistry of inorganic arsenic and selenium in a tropical soil: effect of reaction time, pH, and competitive anions on arsenic and selenium adsorption. – *Chemosphere* 55: 849-859.
- [10] Jonker, M. T. O., Sinke, A. J. C., Brils, J. M., Koelmans, A. A. (2003): Sorption of Polycyclic aromatic hydrocarbons to oil contaminated sediment: Unresolved complex? – *Environmental Sci. Technol.* 37(22): 5197-5203.
- [11] Jonker, M. T., Barendregt, A. (2006): Oil is a sedimentary superabsorbent for polychlorinated binhenyls. – *Environmental Sci. Technol.* 40(12): 3829-3835.
- [12] Khan, M. A. I., Biswas, B., Smith, E., Naidu, R., Megharaj, M. (2018): Toxicity assessment of fresh and weathered petroleum hydrocarbons in contaminated soil- a review. – *Chemosphere* 212: 755-767.
- [13] Li, M. F., Wang, L. J., Guo, D. (2019): Effect of land management practices on the concentration of dissolved organic matter in soil: A meta-analysis. – *Geoderma* 344: 74-81.
- [14] Lopez, A., Mascolo, G., Földényi, R., Passino, R. (1996): Disinfection by-products formation during hypochlorination of isoproturon contaminated groundwater. – *Water. Sci. Technol.* 34: 351-358.
- [15] Ma, F., Wei, L. (2009): Research on molecular ecology and activities regulation of oilfield sulfate reducing bacteria. – Science Press.
- [16] Ma, R. S., Wang, L. F., Jiao, J. (2009): Treatment of high concentration methanol Wastewater by micro-electrolysis-catalytic oxidation Process. – *Environ. Protect. Chem. Ind.* 29: 51-53. (in Chinese).
- [17] Ma, Y., Chen, J. R., Wu, X. M. (2013): Assessment of heavy metals contaminations from solidified waste drilling mud landfilling pond in Ordos plateau (Semi-arid region), China. – *Environ. Eng. Manag. J.* 12(9): 1837-1842.
- [18] Ma, Y., Chen, J. R., Yang, B., Yu, Q. S. (2013): Degradation of high concentration methanol aqueous solution by dielectric barrier discharge. – *IEEE T. Plasma Sci* 41(7): 1716-1724.
- [19] Maletic, S. P., Beljin, J. M., Roncevic, S. D., Grgic, M. G., Dalmacija, B. D. (2019): State of the art and future challenges for polycyclic aromatic hydrocarbons in sediments: sources, fate, bioavailability and remediation techniques. – *J. Hazardous Materials* 365(5): 467-482.

- [20] Muromachi, S. (2019): Phase equilibrium for clathrate hydrates formed in the (methane, carbon dioxide or ethane) + water + ammonium chloride system. – *Fluid Phase Equilibria* 485: 234-238.
- [21] Pena, A., Delgado-Moreno, L., Rodríguez-Liébana, J. A. (2019): A review of the impact of wastewater on the fate of pesticides in soils: Effect of some soil and solution properties. – *Science of The Total Environment*: 134468.
- [22] Viotti, P., Petrangeli Papini, M., Chiulli, C. (2000): A laboratory experimental set-up for the study of organic compounds transport through unsaturated soils. – *Waste Manag. Series* 1: 525-532.
- [23] Wu, J., Liu, Q., Feng, B., Kong, Z., Jiang, B., Li, Y.-Y. (2019): Temperature effects on the methanogenesis enhancement and sulfidogenesis suppression in the UASB treatment of sulfate-rich methanol wastewater. – *International Biodeterioration & Biodegradation* 142: 182-190.
- [24] Zhang, B. G. (2009): *Environmental chemistry*. – Huazhong university of science and technology press: 204-205.
- [25] Zhen, G. Y., Lu, X. Q., Kobayashi, T., Su, L. H., Kumar, G., Bakonyi, P., He, Y., Sivagurunathan, P., Nemestóthy, N., Xu, K., Zhao, Y. (2017): Continuous micro-current stimulation to upgrade methanolic wastewater biodegradation and biomethane recovery in an upflow anaerobic sludge blanket (UASB) reactor. – *Chemosphere* 180: 229-238.

STUDY OF NITROGEN AND PHOSPHORUS FLOW IN WATER, AQUATIC PLANTS AND SEDIMENT

ZHU, X.^{1,2} – CHEN, Y. P.^{1,2*} – GAN, M.^{1,2} – ZHOU, J. J.^{1,2} – HU, X. D.³

¹*State Key Laboratory of Hydrology-Water Resource and Hydraulic Engineering, Hohai University, 1 Xikang Road, Nanjing 210098, China*

²*College of Harbour, Coastal and Offshore Engineering, Hohai University, 1 Xikang Road, Nanjing 210098, China
(phone: +86-138-1390-6122; fax: +86-25-8378-7708)*

³*Jiangsu Hydraulic Research Institute, 97 Nanhu Road, Nanjing 210017, China
(phone: +86-189-3600-6564; fax: +86-25-8645-5646)*

**Corresponding author
e-mail: ypchen@hhu.edu.cn*

(Received 13th Jul 2019; accepted 25th Nov 2019)

Abstract. Using aquatic plants to control nitrogen (N) and phosphorus (P) loads and restore eutrophic lakes has been put into practice since the 1980s. However, existing studies can hardly illustrate the law of N&P flow in water, aquatic plants and sediment during the growth of plants. In this study, three typical aquatic plants, two emerged plants and one submerged plant from Lake Gehu, China, were chosen to study the rule of N&P flow. The N&P contents and some related parameters in the water, sediment and plant samples were measured and the correlations between them were analyzed. The results show that the flow of N&P is generally controlled by the growth of plants, and N can flow directly between plants and sediment while P transfer is more significant in water and sediment. In emerged plants, 70-75% total nitrogen (TN) and over 50% total phosphorus (TP) is concentrated in leaves at early and medium stages of growth, and at the decline stage N&P transfer to roots. Results also show that reaping plants around August and purifying sediment after plants decay can make nutrient removal efficiency.

Keywords: *eutrophication, lakes restoration, nutrient removal, Lake Gehu, experimental study*

Introduction

Eutrophication has been a worldwide water pollution problem for decades. In the lower reaches of the Yangtze River basin, China, eutrophication has been affecting people's daily life. For example, algal bloom occurred in Lake Taihu around the end of May and lasted for 2 months in 2007. It affected the nearby city Wuxi where more than 2 million people were short of drinking water (Guo, 2007). From 2011 to 2013, cyanobacteria have comprised over 99% of total phytoplankton biomass in Lake Chaohu during the whole summer which affected water supply for 7.6 million people (Zhang et al., 2015). Although the Chinese government has taken actions to restore the aquatic ecosystem, the annual surveys of water quality of lakes, from 2006 to 2016, show a high proportion of eutrophicated lakes at around 78%. In short, eutrophication is still a serious problem in China.

For a long time, phosphorus (P) has been considered as the elemental factor to stimulate excess growth of phytoplankton and further trigger algae bloom (Hilton et al., 2006). However, some experiment results show that only controlling P loads does not have a significant effect on eutrophic status. Meanwhile, nitrogen (N) was discovered as another essential factor that contributes to eutrophication process (Dodds, 2007). Also, it

is now commonly accepted that reducing both N&P loads can reduce water nutrient level (Conley et al., 2009).

Using aquatic plants to control N&P loads and restore eutrophic lakes is widely recognized in ecology (Qiu et al., 2001; Xiao et al., 2009) since aquatic plants can absorb and assimilate nutrients, and also stimulate the microbial action of the rhizosphere (Hans, 1997). There are many studies on aquatic plants in eutrophic environment. Periphyton and phytoplankton together with macrophyte are indicators of a eutrophic environment (Hilton et al., 2006). Furthermore, the coexistence of snails and submerged plants can decrease concentrations of N&P in water (Mo et al., 2017), but various species of plants have different abilities of removing excess nutrients (Wen and Recknagel, 2002). However, aquatic plants growing environment is complex, it also contains water and sediment, which both have impact on nutrient loads. For example, physical and chemical properties of water can make enormous difference, like calcium phosphate (Ca-P) dissolved very easily at low pH while aluminium phosphate (Al-P) dissolved more easily at high pH (Smil, 2000); ferric ion (Fe^{3+}) will reduce to ferrous ion (Fe^{2+}) when water is anaerobic which can cause ferric phosphate (Fe-P) to dissolve (Liu et al., 2002). Hydraulic dynamics is also a significant factor of nutrient transfer, like the retention time of water (O'Hare et al., 2018) and flow velocity (Hilton et al., 2006). Besides, adsorption and desorption of sediment have essential effects in transferring N&P (Wang et al., 2018; Meghdadi, 2018) since mineral composition and some other sediment characteristics play key roles in this process (Smil, 2000). As indicated above, existing studies make good explanations on factors affecting N&P transferring, but lack showing the process of N&P flow in the whole aquatic environment system.

Although lake ecological restoration is carried out by cultivating aquatic plants, surveys revealed that the lake eutrophication in China hadn't been alleviated significantly in recent years (China water resources bulletin 2010-2016). The result does not meet expectations due to the lack of scientific management, which further indicates the importance of learning the rule of N&P flowing between water, aquatic plants and sediment. This will therefore serve as a guide to form a rational and systematic management of aquatic plants for effective restoration of eutrophic lakes. Furthermore, diversity of aquatic plants varies a lot with time and space (Rooney et al., 2011; Bolpagni et al., 2018). Such perspective can be reflected in Lake Gehu. From 1970 to 2007, the total aquatic plants coverage had a sharp decline (Xu et al., 2013). Since 2012, several types of emerged plants were cultivated in shallow areas (Wu et al., 2017). This means surveys of aquatic plants species should be conducted before learning the rule of N&P flowing in water, aquatic plants and sediment.

Hence, the present work has been undertaken with the following objectives: (1) Figuring out the changing processes of N&P concentration in water, aquatic plants and sediment during aquatic plants growth, respectively. (2) Learning the rule of N&P flowing in water-aquatic plants-sediment within a life cycle of aquatic plants. (3) Giving suggestions on using aquatic plants to restore eutrophic lakes.

Materials and Methods

Study area

This study is based on the background of Lake Gehu, China. The coordinates of the lake are 119°44'E-119°52'E and 31°28'N-31°44'N (Fig. 1). Lake Gehu, the main source of drinking water for nearby residents, is an important shallow lake in the south of Lake

Taihu in Jiangsu province, China (Fig. 1a), which belongs to the Taihu basin. It is a typical shallow aquatic vegetation lake. The water storage area is 144.1 km² and the average water depth is 1.31 m. The lake has a moderate and humid climate and also has sufficient sunlight. And the annual mean temperature is around 16.7°C. It plays an essential role in protecting the water quality of Lake Taihu, forming the most important natural defense line for Lake Taihu (Xu et al., 2013). Around 16 rivers enter into it from west, while 15 others divert from south-east (Fig. 1b). Lake Gehu has been eutrophic for over a decade with a strong adverse influence on local freshwater supply, and aquaculture. Since 2009, the local government carried out many measures to restore Lake Gehu including aquatic plant restoration (Wu et al., 2017). However, the algal bloom still occurs in high frequency, especially in summer.

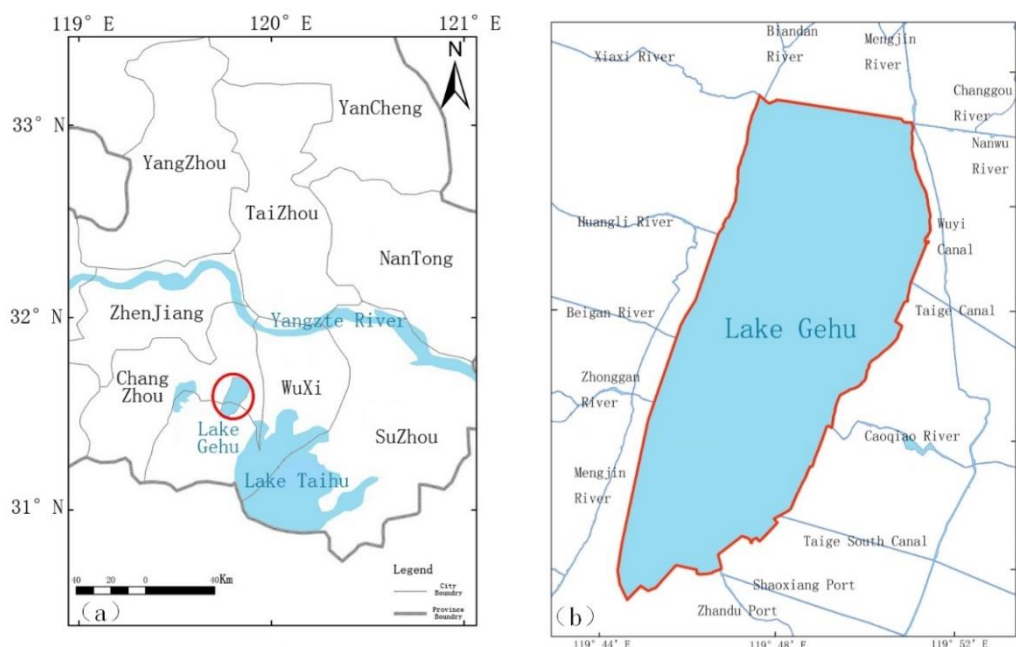


Figure 1. Location (a) and River system (b) of Lake Gehu

Experiment materials

Materials for experiments and relative value settings are based on the results of a field investigation, which are shown in the results section.

Aquatic plants: Two emerged plants *Phragmites australis* (Ph.a.), *Zizania latifolia* (Z.l.), and one submerged plant *Hydrilla verticillata* (H.v.) were collected at the same time from Lake Gehu, in the early of April when plants were at their initial stage of growth, for indoor cultivating experiment particularly.

Water: NH_4Cl and KH_2PO_4 were used to formulate experimental water. Initial N&P concentration were set at 2.0 mg/L and 0.2 mg/L, respectively.

Sediment: Experimental sediments were from areas around aquatic plants in Lake Gehu, to replicate the original growing environment for aquatic plants.

Indoor experiment

The indoor cultivating experiments were conducted in 70 L (0.5*0.35*0.4 m) cubic plastic containers. In each container, there were about 50 L water with initial N&P

concentration, moderate sediment at bottom (around 0.12 m depth), and 500 g submerged plants or 5 emerged plants. The total water depth was around 0.3 m. Besides, control experiments (no plants) were also arranged. Each container had a duplicate (Fig. 2). All containers were settled together to ensure other environmental conditions unified. The experiment was conducted in a ventilated indoor area. The temperature was set at room temperature. The average temperature was around 20°C while it reached 7-8°C in December and was over 30°C in July and August. The sunny weather contained 60% of experimental days, thus the sunlight was abundant. The initial pH and the dissolved oxygen content (DO) of the water were around 6.7 and 9 mg/L, respectively.

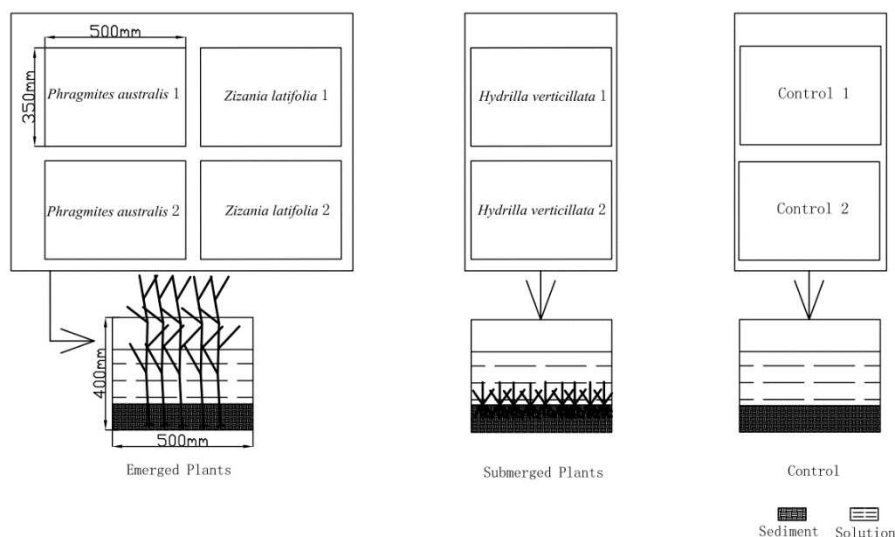


Figure 2. Experiment arrangement. *Phragmites australis* and *Zizania latifolia* are emerged plants showed in the left, *Hydrilla verticillata* is the submerged plant showed in the middle and control groups with no plants are showed in the right. Each experimental container has a duplicate

Sampling and analysis

The indoor cultivating experiment initiated from May and ended at the end of December 2016, covering a life cycle of aquatic plants. The frequency of taking plants and sediment samples was twice per month, around the 10th and the 20th of each month. Around 10 g plants samples and 50 g sediment samples were taken synchronously from every container every time. Emerged plant samples were separated into leaves, stems and roots, while submerged plant samples were analyzed as a whole since they were too small to separate. Samples were operated orderly by freeze-drying, grinding and sieving. Then total nitrogen concentration (TN) and total phosphorus concentration (TP) of samples were analyzed in a timely manner. TN of samples were analyzed by persulfate digestion (Smarta et al., 1983) while TP of samples were analyzed by SEDEX method (Ruttenberg, 1992). Analysis experiments of all parameters at different time were repeated 3 times. Around 200 ml water samples were taken from each container once a week. Samples were saved in fridge with the temperature around 5°C. Analysis experiments were conducted within 24 h after sampling. The following water parameters were analyzed: pH, dissolved oxygen content (DO), chemical oxygen demand (COD), TN, TP, ammonia nitrogen ($\text{NH}_4^+\text{-N}$) and nitrate nitrogen ($\text{NO}_3^-\text{-N}$). pH and DO were recorded by a multi-parameter

data logger (YSI 6820). Analysis experiments of other parameters were proceeded according to standard techniques (APHA, 1980; Valderrama, 1981; Jin and Tu, 1990). Analysis experiments of all parameters at different times were repeated 3 times.

Statistical analysis

First, parameters of water, aquatic plants and sediment samples were sorted by time, plant species and organs. Prior to statistical analysis, the normality of data sets was tested with Shapiro–Wilk test (Wang et al., 2012). Then, the T test was applied for statistical comparison of measured values among different times, plant species and organs for judge whether a detected trend was statistically significant or not. Last, parameters of water, aquatic plants and sediment samples were analyzed by Spearman correlation analysis (IBM statistic, version 22) to learn the flow progress of N&P in water-aquatic plants-sediment. A p-value of <0.05 was considered statistically significant.

Result

To obtain up-to-date distribution of aquatic plants and N&P loads in Lake Gehu, surveys were conducted in 2016. There are about 15 species of aquatic plants: 3 submerged macrophyte, 7 emerged plants, 3 floating plants and 2 floating-leaved macrophyte. Among these species, two emerged plants *Phragmites australis* (*Ph.a.*), *Zizania latifolia* (*Z.l.*), and one submerged plant *Hydrilla verticillata* (*H.v.*), have evidently high coverage, frequency and abundance which are critical parameters to calculate the Simpson index (Magurran, 1988). TN in water was 2.343 mg/L while TP was 0.245 mg/L. Both TN&TP reach the V level (TN=2.0 mg/L; TP=0.2 mg/L) according to the Chinese environment quality standard (*Environment quality standard for surface water-GB 3838-2002*) which indicates that Lake Gehu is still highly eutrophicated.

N and P in plants

In the experiment, May, August and December represent the germination, flourish growth and decay periods of aquatic plants. Values of TN&TP in plants in August are significantly higher than in May and December ($p < 0.05$); There is a significant difference between emerged plants and submerged plants ($p < 0.05$). A significant difference is also found between different organs of emerged plants ($p < 0.05$). Changing trends of TN&TP in plants with time, organs and species are shown in *Figures 3 and 4* in detail.

Curves of TN&TP in two emergent plant leaves are unimodal in general, while peaks mainly lie between July and September (*Fig. 3*). No significant difference is observed for TN between two emerged plant leaves ($p = 0.258$). The variation range starts from around 10 mg/g, gradually increases and reaches the maximum at 25 mg/g, and finally decreases to about 1 mg/g. TP of two emerged plants have similar start and end values, around 1.3 mg/g and 0.1 mg/g, respectively. However, the TP peak of *Ph.a.* reaches 2.5 mg/g while that of *Z.l.* is relatively lower at 1.8 mg/g. From May to October, leaves contained the most nutrient, with TP accounting for over 50% of total and TN accounting for nearly 70-75%. Values in leaves are significantly higher than in stems and roots ($p < 0.05$). TN&TP in emerged plant stems both show a continuous downward trend with fluctuation, but value ranges are significantly different ($p < 0.05$). In April and May, when peaks appeared, TN is around 10 mg/g while TP is around 1.5-1.8 mg/g. TN&TP then decrease to 1.0

mg/g and 0.1 mg/g respectively at the end of experiment. Besides, in this two periods, TN&TP in stems and leaves are close (TN: $p=0.637$; TP: $p=0.542$). TN&TP in emerged plant roots are generally steady but fluctuate near the end of the experiment. TN&TP in *Ph.a.* roots are higher than those in *Z.l.*, although the difference is not significant (TN: $p=0.071$; TP: $p=0.062$). During May-September, TN&TP in roots account for less than 10% of total. However, in October-December, TP in roots is significantly higher than in stems and leaves ($p<0.05$), the proportion increase with over 50%. Changes of TN&TP in emerged plant leaves, stems and roots indicate that leaves absorb large amount of nutrient and act as the main organ to store nutrient at early and medium stages of plant growth. However, when plants decay, nutrient in roots increases while that in leaves and stems both decreases. Therefore, roots are the main organ to store nutrient when emerged plants decay. In conclusion, in emerged plants, nutrients are absorbed from outside and stored mainly in leaves at early and medium stages of growth but gradually transferred to roots when decay.

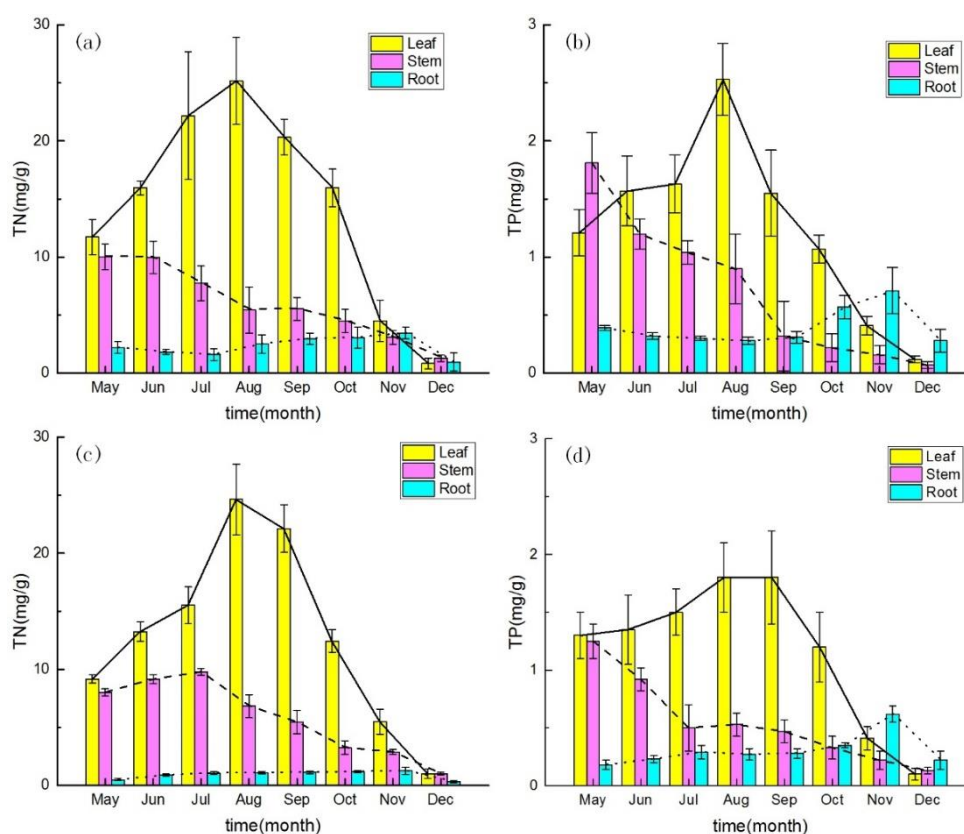


Figure 3. Total nitrogen (TN) in *Phragmites australis* (*Ph.a.*) (a), *Zizania latifolia* (*Z.l.*) (b) and total phosphorus (TP) in *Ph.a.*(c), *Z.l.*(d). In total 4 samples are collected for each month, of which 2 samples are collected at the 10th of the month and the other 2 collected at the 20th of the month. The mean values for each month are presented by color bars and the standard deviations are presented by error bars

Although curves of TN&TP in *H.v.* are both unimodal (Fig. 4), values of TN are significantly higher than TP ($p<0.05$). TN increases from around 15 mg/g to around 36 mg/g, then decreases to around 5 mg/g. While TP increases from around 3 mg/g to about 6 mg/g, then decreases to less than 1 mg/g. Peaks appear in July and August. The

ratio of TN to TP of *H.v.* is around 5:1 to 7:1, and this ratio of *Ph.a.* and *Z.l.* is the most around 15:1. It indicates that the growing of *H.v.* is limited by N while the growing of *Ph.a.* and *Z.l.* is limited both by N and P (Tessier et al., 2003).

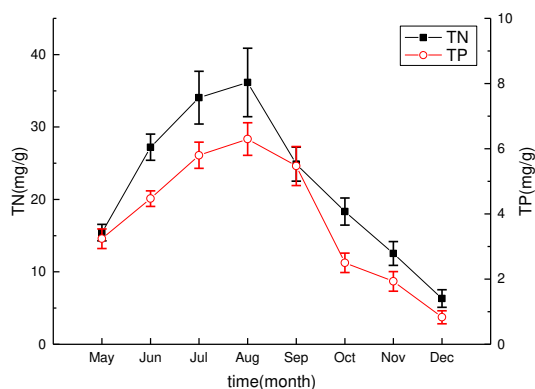


Figure 4. Total nitrogen (TN) and total phosphorus (TP) in *Hydrilla verticillata* (*H.v.*). In total 4 samples are collected for each month, of which 2 samples are collected at the 10th of the month and the other 2 collected at the 20th of the month. The standard deviations are presented by error bars

N and P in sediment

Values of TN&TP in sediments in May and December are significantly higher than in August ($p < 0.05$). There is a significant difference between control groups (no plants) and plant groups ($p < 0.05$). Changing trends of TN&TP in sediments with time are shown in Figure 5 in detail.

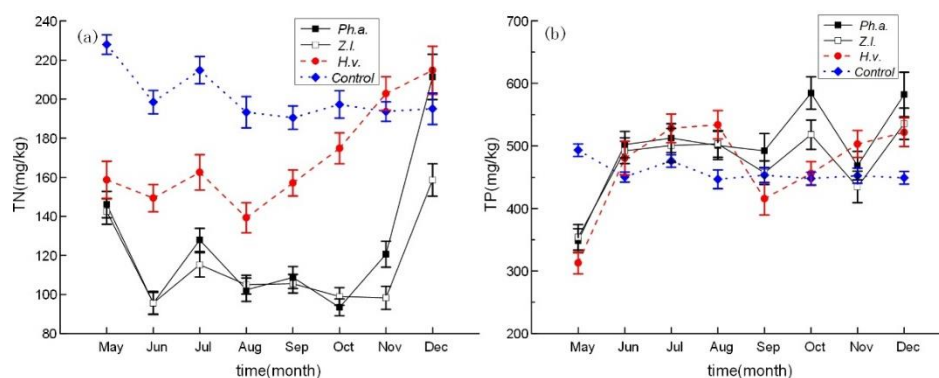


Figure 5. Changing trends of total nitrogen (TN) (a) and total phosphorus (TP) (b) in sediment with time. 'Ph.a.', 'Z.l.' and 'H.v.' represent sediment samples from *Phragmites australis* groups, *Zizania latifolia* groups and *Hydrilla verticillata* groups, respectively. In total 4 samples are collected for each month, of which 2 samples are collected at the 10th of the month and the other 2 collected at the 20th of the month. The standard deviations are presented by error bars

No significant difference is observed for the TN&TP in control groups sediment among different times (TN: $p = 0.061$; TP: $p = 0.057$), changing trends are basically in stable state with slight fluctuations (Fig. 5). TN ranged from 190.54 to 227.93 mg/kg,

while TP ranged from 446.72 to 453.27 mg/kg. TP decreased at the beginning because the concentration between water and sediment tended to equilibrate phosphorus concentration (EPC₀) (Zhou et al., 2005). Slight fluctuations might be caused by temperature variation. Changing trends of TN in the sediment of the container with emerged plants are similar (Fig. 5a). And variation ranges are close (p=0.457), 93.43-211.35 mg/kg. In the first two months, the value sharply decreased by 50.45 mg/kg (p<0.05), while in the last two months, it dramatically increased by 90.72 mg/kg (p<0.05). However, it was relatively stable around 93-125 mg/kg during other months. It indicates adsorption and desorption effects of sediments are not obvious when aquatic plants exist in the system. Changing trends of TP in three aquatic plants sediment are similar, rising first and then fluctuating (Fig. 5b). The value range is close (p>0.05). The minimum at the beginning was around 350.00 mg/kg, then the value increased by around 150.00 mg/kg during the first month. The maximum value appeared in the end, around 550 mg/kg.

Water parameters

All water parameters, except NH₄⁺-N, show significant difference in May, August and December (p<0.05; NH₄⁺-N: p=0.242). All water parameters, except NH₄⁺-N, show significant difference between control groups (no plants) and plant groups (p<0.05; NH₄⁺-N: p=0.463). However, to show the transforming of different forms of N in water, NH₄⁺-N concentration was still contained in Fig. 6.

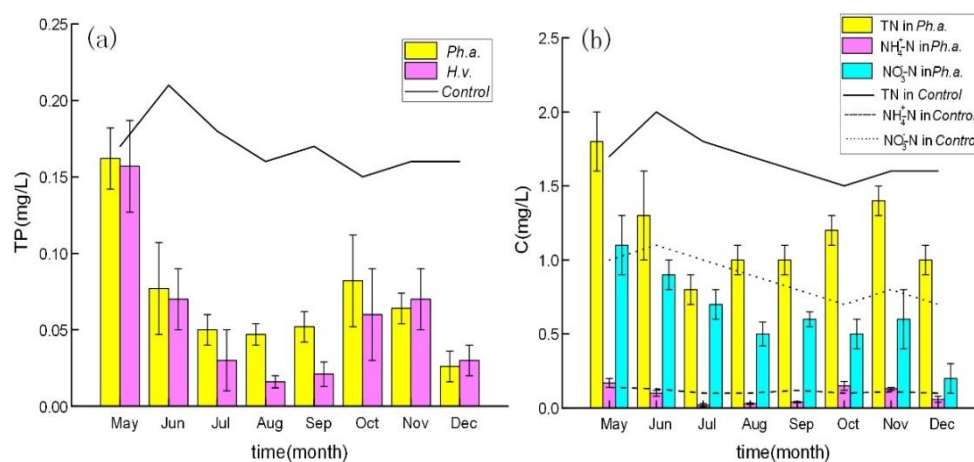


Figure 6. Changing trends of total phosphorus (TP) (a) and three forms of nitrogen (N) (b) in water samples with time. 'Ph.a.' and 'H.v.' represent water samples from *Phragmites australis* groups and *Hydrilla verticillata* groups, respectively. 'TN', 'NH₄⁺-N' and 'NO₃⁻-N' represent concentration of total nitrogen, ammonia nitrogen and nitrate nitrogen, respectively. In total 8 samples are collected for each month, of which 2 samples are collected every week. The mean values for each month are presented by color bars and the standard deviations are presented by error bars

pH, DO and COD

pH, DO and COD in control groups show no significant difference with time (p>0.05). Control groups pH was between 8.0 and 8.5, water was alkalescence. DO fluctuated in 8.0-11.0 mg/L. COD was below 5.0 mg/L all the time and stayed at a relatively low level.

In general, water quality of control groups is good (*Table 1*). Values of these 3 water parameters in aquatic plants are close and no significant difference is found ($p>0.05$). pH decreased from 8.0 to around 6.5 first, and then increased to 8.0, so the water changed from alkaline to faintly acidic and resumed to alkaline. It might have a relation with concentrations of phosphate radical (PO_4^{3-}) and ammonium radical (NH_4^+). DO kept low level in aquatic plant groups, the average was below 2.0 mg/L. COD increased first then declined. These two parameters are both affected with plants biomass.

Table 1. pH, dissolved oxygen (DO) and chemical oxygen demand (COD) in the water samples of aquatic plants and control groups

Month	Control			Ph.a.			Z.l.			H.v.		
	pH	DO	COD	pH	DO	COD	pH	DO	COD	pH	DO	COD
May	8.5	7.7	2.7	8.1	3.8	5.6	8.0	4.0	6.5	7.3	2.7	6.3
Jun	8.3	8.0	2.6	7.7	3.3	9.9	7.8	3.3	9.6	7.5	1.3	13.6
Jul	8.1	8.2	2.8	7.5	2.5	13.7	7.5	2.1	13.4	7.3	0.5	19.4
Aug	8.2	8.4	2.5	7.6	2.0	15.8	7.2	1.0	15.0	7.3	0.3	23.3
Sep	8.5	8.7	2.3	7.2	0.8	11.9	7.3	1.3	10.6	7.1	0.1	16.0
Oct	8.3	8.7	2.6	6.7	1.2	9.0	6.6	0.7	8.5	6.5	0.2	12.7
Nov	8.0	8.5	2.7	6.9	1.4	7.3	7.0	0.9	6.8	7.1	0.3	9.5
Dec	8.2	8.0	2.5	7.6	2.0	6.0	7.4	1.4	5.5	7.7	0.5	6.6

The unit of DO and COD are both mg/L. ‘Ph.a.’, ‘Z.l.’ and ‘H.v.’ represent water samples from *Phragmites australis* groups, *Zizania latifolia* groups and *Hydrilla verticillata* groups, respectively. In total 8 samples are collected for each month, of which 2 samples are collected every week

N&P in water

Values of TN&TP in water have no significant difference in emerged plants (TN: $p=0.534$; TP: $p=0.730$). Also the changing trends are similar. Therefore, *Ph.c.* is selected as representative of emerged plants for plots (*Fig. 6*).

The TP in water of control groups ranged from 0.15 mg/L to 0.21 mg/L, with a continuously declining trend. Range of TN (NO_3^- -N, NH_4^+ -N) in water of control groups was 1.5-2.0 mg/L (0.7-1.1 mg/L, 0.10-0.14 mg/L). TN and NO_3^- -N both declined with fluctuations, while NH_4^+ -N maintained a steady state with slight fluctuations. This reflects the process of nutrient exchange between water and sediment forced by concentration gradient. The TP in water of plant groups decreased at the beginning and near the end of the experiment. The range of TN (NO_3^- -N, NH_4^+ -N) was 1.00-2.00 mg/L (0.20-1.10 mg/L, 0.03-0.17 mg/L), which were all lower than those in control groups ($p<0.05$). NH_4^+ -N accounts for less than 10% of TN on average while NO_3^- -N accounts for more than 50% of TN on average.

Comparing control groups and plant groups, it can be concluded that plants can stimulate nutrient flowing, and biochemical action is a more powerful force than concentration gradient. NO_3^- -N is the main form of N existing in water and transform between NO_3^- -N and NH_4^+ -N are controlled by nitrification and denitrification (Reddy et al., 1990). From May to August TN&TP in water of emerged plants decreased by 0.800 mg/L and 0.115 mg/L, respectively while those of submerged plants decreased by 1.000 mg/L and 0.141 mg/L, respectively. Declines of TN&TP in water of submerged plants

are greater than those of emerged plants ($p < 0.05$). Submerged plants act better in removing N&P loads than emerged plants.

Correlation analysis

The experiment lasted 8 months (May-December). Plants and sediment samples were collected twice per month (at 10th and 20th), while water samples were collected 4 times per month (including 10th and 20th). Besides, each experimental container had a duplicate (Fig. 2). Thus, parameters of samples at 10th and 20th every month are used for spearman correlation analysis, and the number of samples were 32.

Correlations of TN, TP in plants and sediment are shown in Table 2. There is a significant negative correlation between TN in roots of emergent plants and TN in sediment. TN in submerged plants has a significant negative correlation with TN in sediment. TP in plants and sediment does not present strong correlation. It indicates that N flow mainly occurred between plants and sediment directly by biochemical action of roots.

Table 2. Spearman's rank correlation coefficient of N&P between aquatic plants and sediments

<i>Ph.a.</i>						
Sediment	Leaf		Stem		Root	
	TN	TP	TN	TP	TN	TP
TN	-0.692	-0.167	-0.095	-0.079	-0.903**	-0.733
TP	-0.429	-0.396	-0.381	-0.245	-0.123	-0.054
<i>Z.l.</i>						
Sediment	Leaf		Stem		Root	
	TN	TP	TN	TP	TN	TP
TN	-0.214	-0.108	-0.214	-0.095	-0.819*	-0.524
TP	-0.046	-0.180	-0.333	-0.476	-0.167	0.024
<i>H.v.</i>						
Sediment	Plants TN			Plants TP		
TN	-0.833*			-0.810*		
TP	0.381			0.286		

'Ph.a.', 'Z.l.' and 'H.v.' represent samples from *Phragmites australis* groups, *Zizania latifolia* groups and *Hydrilla verticillata* groups, respectively. TP and TN represent for total nitrogen concentration and total phosphorus concentration, respectively. $n=32$ (number of samples). Statistical significance codes: * $p < 0.05$; ** $p < 0.001$

Correlations of TN&TP in plants and sediment with water parameters are shown in Table 3. There is no significant correlation in control groups. TN&TP in emerged plant leaves and submerged plants have a strong positive correlation with water COD. There is a significant negative correlation between TP in water and sediment. These suggest plant growth may increase the content of organic matters in water, which can be a hazard of aquatic plants restoring eutrophicated lakes. P flow mainly relies on water since it shows no strong correlation between plants and sediments but presents a significant negative correlation between water and sediments.

Table 3. Spearman's rank correlation coefficient of N&P in aquatic plants and sediment with water parameters

			pH	DO	COD	TP	TN	NH ₄ ⁺ -N	NO ₃ ⁻ -N
Control	Sediment	TN	0.000	-0.185	0.354	0.536	0.607	0.350	0.590
		TP	0.068	-0.202	0.110	0.647	0.479	0.595	0.513
Ph.a.	Leaf	TN	-0.060	-0.072	0.922**	-0.180	-0.552	-0.627	-0.078
		TP	0.683	0.683	0.19	0.452	0.268	-0.060	0.659
	Stem	TN	0.587	0.635	0.119	0.524	0.220	0.012	0.755*
		TP	0.647	0.719*	0.167	0.476	0.220	-0.024	0.719*
	Root	TN	-0.647	-0.623	0.024	0.429	0.415	0.335	0.096
		TP	-0.373	-0.133	-0.455	-0.310	0.761*	0.819	0.548
	Sediment	TN	0.371	0.347	-0.476	-0.333	-0.073	-0.120	0.048
		TP	-0.323	-0.204	0.190	-0.826*	-0.537	0.012	-0.671
Z.l.	Leaf	TN	-0.048	-0.084	0.952**	-0.299	0.335	-0.623	0.060
		TP	0.132	0.125	0.886**	-0.211	0.380	-0.584	0.211
	Stem	TN	0.643	0.643	0.524	0.431	0.671	-0.275	0.743*
		TP	0.643	0.594	0.357	0.491	-0.695	-0.060	0.719*
	Root	TN	-0.810*	-0.841*	0.333	0.024	-0.144	0.275	-0.144
		TP	-0.762*	-0.793*	0.310	-0.048	-0.395	0.108	-0.180
	Sediment	TN	0.381	0.314	-0.310	-0.359	-0.252	-0.347	-0.156
		TP	-0.357	-0.344	0.071	-0.874**	-0.371	-0.515	-0.554
H.v.	Plant	TN	-0.012	-0.096	0.905**	-0.482	0.096	-0.619	-0.466
		TP	-0.025	-0.096	0.857**	-0.518	0.084	-0.690	-0.479
	Sediment	TN	-0.074	-0.036	-0.619	0.265	-0.252	0.429	0.184
		TP	0.356	-0.024	0.548	-0.778*	-0.299	-0.690	-0.675

Explanation of abbreviations: Phragmites australis groups (Ph.a.), Zizania latifolia groups (Z.l.), and Hydrilla verticillata groups (H.v.), total nitrogen concentration (TN), total phosphorus concentration (TP), dissolved oxygen concentration (DO), ammonia nitrogen concentration (NH₄⁺-N) and nitrate nitrogen concentration (NO₃⁻-N). n=32 (number of samples). Statistical significance codes: * p<0.05; ** p<0.001

Discussion

Difference of nitrogen and phosphorus flow

The difference of N&P flow is that N transfers mainly between sediments and plants, while P needs water to realize cycling. P in water is diversified into the total particle phosphorus (TPP) and the total dissolved phosphorus (TDP). Large amount of TPP can transfer in a short time. Most of P release during the eluviation (Liu et al., 2018) is one phenomenon caused by this. It implies P flow is mainly a physical process. Biochemical actions of plants have minor effect on P flow (Smil, 2000). It can explain the strong correlation of P in sediment and water, also the conclusion of P flow relying on water. In addition, this conclusion applies to some natural catchments. For example, TPP is the main form of P in many rivers (Meybeck, 1982). N is identified as the organic nitrogen (ON) and the inorganic nitrogen (IN). The latter is the main form of N in water and sediment. IN can be known as NH₄⁺-N, NO₃⁻-N, and NO₂⁻-N. But plants need to transform IN to ON to meet growing requirements. It indicates N flow is mainly through

biochemical reaction, which is also concluded in other research (Rattray et al., 1991). For example, NO_3^- -N can be transformed to NH_4^+ -N through catalytic reduction by nitrate reductase (May et al., 2011); nitrification and denitrification, influenced by plants growth, can make mutual transformation of NH_4^+ -N, NO_3^- -N, and NO_2^- -N (Reddy et al., 1990). Thus there is a significant negative correlation between N in plant roots and sediment, and N flow is mainly between plants and sediment rather than between sediment and water.

Emerged plants vs submerged plants

Emerged plant leaves and stems are usually above water surface, while roots and part of stems are under water surface. Therefore, emerged plants have properties of both land and aquatic plants. Their roots are the main organ absorbing nutrient from sediments, meanwhile they can get abundant sunlight. Thus they usually show large biomass. Besides, emerged plants can weaken hydraulic dynamics and prevent sediment suspended (Hans, 1997). Furthermore, it can reduce sediments desorption effects. To sum up, emerged plants have significant effects on N&P in sediment, which is also showed in the correlation analysis of this study. Submerged plants are usually entirely under water surface, so they have larger biomass within water than emerged plants. Large biomass is likely to make water turn to anaerobic state which will stimulate the release of N&P (Reddy et al., 1990; Liu et al., 2002). In this study, sharp decrease of TN&TP in *H.v.* during Aug.-Oct. (*Fig. 4*) verifies the conclusion mentioned above. The submerged plants have roots degraded due to the limitation of light intensity (Phillips et al., 1978; Jones et al., 1999), but their other parts all have the ability of absorbing water and nutrient. Thus submerged plants have strong connections with N&P in water. In natural lakes, commensalisms and competitions between emerged and submerged plants are ubiquitous, and it is worthy of consideration in further studies.

Some suggestions for aquatic plants restoration

According to *Fig. 6*, N&P in water show a sharp decline during plants growth, which indicates aquatic plants do have the ability of removing excess nutrient in water. Moreover, submerged plants act better than emerged plants in removing nutrient, so submerged plants are the superior choice in restoring eutrophicated lakes. And some studies, focusing on effects of submerged plants restoration, have already verified the practicability of this suggestion (Gao et al., 2017). However, the results also show aquatic plants can release a large amount of N&P when they decay. Therefore, it may cause a secondary pollution unless aquatic plants are reaped scientifically. For saving cost, it's essential to know the time and main plant organs to reap. Reaping the 3 aquatic plants around August and September is a proper timing. At this time around 70-75% TP and 80% TN of water can be removed according to *Fig. 6*. However, this value could be lower in lakes since hydrodynamics and some other conditions are not considered in this study. Besides, emerged plant leaves need to be reaped by times, since leaves fall easily in natural environment and the residue can release nutrient directly into sediment and water. Although emerged plant roots contain most nutrient when plants decay, it is not suggested to reap roots, because they are the key of plant regeneration and moderate residues are helpful to remove N (Gessner, 2000; Hernes et al., 2001). If controlling P loads is the main purpose, it is imperative to reap plants before P in plants reach the peak. The reason is the amount of P release is large within a short time when plants decay (Liu et al., 2018).

On the other hand, if controlling N loads is the main purpose, reducing content of NO_3^- -N by enhancing denitrification would be an effective action.

In *Fig. 6*, there is another low value occurring around November and December, because N&P are adsorbed by sediments after plants decay. Thus, purifying sediments at this time can remove around 90% N&P in water. Although this value could be lower in lakes where water and sediment interactions are strong, purifying sediment is still necessary to prevent sediment become the source of N&P. However, it is too costly to initiate a project specifically for such purpose. As a result, the purification can be combined and included within some other engineering projects like dredging and reclamation at the appropriate time. As this experimental study has simplified some complicated environmental conditions, further studies could be done to find more integrated solutions for restoring the highly eutrophicated lakes.

Conclusion

For increasing the efficiency of using aquatic plants to restore eutrophic lakes and learning the rule of N&P flow between water, aquatic plants and sediment, indoor experiments were conducted. The general process of N&P flow in the system is from water and sediments to plants, then back to water, and finally they are adsorbed by sediments. However, N flow is mainly between plants and sediment, while P flow is mainly between water and sediment. Generally, N flow is a biochemical process, while P flow is a physical process. N&P in emerged plants are stored in leaves at early and medium stages of growth (May-October) and transferred to roots at the decline stage (November-December). Submerged plants act better in removing excess nutrient in water, but harvesting them before N&P contents reaching peak is indispensable (August). Purifying sediments after plants decay (December) can be helpful to decrease N&P loads, which can be combined and included within some other engineering projects.

Competition and promotion exist between different species of aquatic plants in nature, which may reduce or improve effects of using aquatic plants to restore eutrophic lakes. Thus, learning competition and promotion between different aquatic plants species is a meaningful direction for further study.

Acknowledgements. This work was partly supported by the National Key R&D Program of China (2017YFC0405401), the National Natural Science Foundation of China (51620105005), the Jiangsu Science and Technology Program (SBK2015040816) and Jiangsu Water Conservancy Science and Technology Project (2016028). We would also like to thank Jiangsu Hydraulic Research Institution for providing equipment and place for the experiment.

REFERENCES

- [1] American Public Health Association (1980): Standard Methods for the Examination of Water and Wastewater. – 15th edn. APHA, Washington, DC. 642 p.
- [2] Bolpagni, R., Laini, A., Stanzani, C., Chiarucci, A. (2018): Aquatic Plant Diversity in Italy: Distribution, Drivers and Strategic Conservation Actions. – *Frontiers in Plant Science* 9: 1-12.
- [3] Conley, D. J., Paerl, H. W., Howarth, R. W., Boesch, D. F., Seitzinger, S. P., Havens, K. E., Lancelot, C., Likens, G. E. (2009): Controlling eutrophication: nitrogen and phosphorus. – *Science* 323(5917): 1014-1015.

- [4] Dodds, W. K. (2007): Trophic state, eutrophication and nutrient criteria in streams. – *Trends in Ecology and Evolution* 22(12): 669-676.
- [5] Gao, H. L., Qian, X., Wu, H. F., Li, H. M., Pan, H., Han, C. M. (2017): Combined effects of submerged macrophytes and aquatic animals on the restoration of a eutrophic water body—A case study of Gonghu Bay, Lake Taihu. – *Ecological Engineering* 102: 15-23.
- [6] Gessner, M. O. (2000): Breakdown and nutrient dynamics of submerged *Phragmites* shoots in the littoral zone of a temperate hardwater lake. – *Aquatic Botany* 66(1): 9-20.
- [7] Guo, L. (2007): Doing battle with the green monster of Taihu Lake. – *Science* 317(5842): 1166.
- [8] Hans, B. (1997): Do macrophytes play a role in constructed treatment wetlands. – *Water Science & Technology* 35(5): 11-17.
- [9] Hernes, P. J., Benner, R., Cowie, G. L., Goni, M. A., Bergamaschi, B. A., Hedges, J. I. (2001): Tannin diagenesis in mangrove leaves from a tropical estuary: a novel molecular approach. – *Geochimica et Cosmochimica Acta* 65(18): 3109-3122.
- [10] Hilton, J., O'Hare, M., Bowes, M. J., Jones, J. I. (2006): How green is my river? A new paradigm of eutrophication in rivers. – *Science of The Total Environment* 365(1-3): 66-83.
- [11] Jin, X., Tu, Q. (1990): *The standard Methods for Observation and Analysis in Lake Eutrophication*. – 2nd edition. Chinese Environmental Science Press, Beijing. (in Chinese).
- [12] Jones, J. I., Young, J. O., Haynes, G. M., Moss, B., Eaton, J. W., Hardwick, K. J. (1999): Do submerged aquatic plants influence their periphyton to enhance the growth and reproduction of invertebrate mutualists. – *Oecologia* 120(3): 463-474.
- [13] Liu, M., Hou, L. J., Xu, S. Y., Ou, D. N., Zhang, B. L., Liu, Q. M., Yang, Y. (2002): Characteristics of phosphate adsorption in tidal flat surface sediments of the Yangtze river estuary. – *Acta Geographica Sinica* 57(4): 397-406.
- [14] Liu, S. L., Jiang, Z. J., Zhou, C. Y., Wu, Y. C., Arbi, I., Zhang, J. P., Huang, X. Q., Trevathan-Tackett, S. M. (2018): Leaching of dissolved organic matter from seagrass leaf litter and its biogeochemical implications. – *Acta Oceanologica Sinica* 37(8): 84-90.
- [15] Magurran, A. E. (1988): *Ecological Diversity And Its Measurement*. – Springer, Croom Helm Ltd.
- [16] May, S. K., Gu, L. J., Chen, H. M. (2011): The Role of Nitrate Reductase and Nitrite Reductase in Plant. – *Current Biotechnology* 3: 159-164.
- [17] Meghdadi, A. (2018): Characterizing the capacity of hyporheic sediments to attenuate groundwater nitrate loads by adsorption. – *Water Research* 140: 364-376.
- [18] Meybeck, M. (1982): Carbon, nitrogen, and phosphorus transport by world rivers. – *American Journal of Science* 282(4): 401-450.
- [19] Mo, S. Q., Zhang, X. F., Tang, Y. L., Liu, Z. W., Kettridge, N. (2017): Effects of snails, submerged plants and their coexistence on eutrophication in aquatic ecosystems. – *Knowledge & Management of Aquatic Ecosystems* 418: 44.
- [20] O'Hare, M. T., Baattrup-Pedersen, A., Baumgarte, I., Freeman, A., Gunn, I. D. M., Lázár, A. N., Sinclair, R., Wade, A. J., Bowes, M. J. (2018): Responses of Aquatic Plants to Eutrophication in Rivers: A Revised Conceptual Model. – *Frontiers in Plant Science* 9: 451.
- [21] Phillips, G. L., Eminson, D. Moss, B. (1978): A mechanism to account for macrophyte decline in progressively eutrophicated freshwaters. – *Aquatic Botany* 4: 103-126.
- [22] Qiu, D. R., Wu, Z. B., Liu, B. Y., Deng, J. Q., Fu, G. P., He, F. (2001): The restoration of aquatic macrophytes for improving water quality in a hypertrophic shallow lake in Hubei Province, China. – *Ecological Engineering* 18(2): 147-156.
- [23] Rattray, M. R., Howard-Williams, C., Brown, J. M. A. (1991): Sediment and water as sources of nitrogen and phosphorus for submerged rooted aquatic macrophytes. – *Aquatic Botany* 40(3): 225-237.
- [24] Reddy, K. R., D'Angelo, E. M., Debusk, T. A. (1990): Oxygen Transport through Aquatic Macrophytes: The Role in Wastewater Treatment. – *Journal of Environmental Quality* 19(2): 261-267.
- [25] Rooney, R. C., Bayley, S. E. (2011): Relative influence of local- and landscape-level habitat

- quality on aquatic plant diversity in shallow open-water wetlands in Alberta's boreal zone: direct and indirect effects. – *Landscape Ecology* 26(7): 1023-1034.
- [26] Ruttenberg, K. C. (1992): Development of a sequential extraction method for different forms of phosphorus in marine sediments. – *Limnology and Oceanography* 37(7): 1460-1482.
- [27] Smarta, M. M., Rada, R. G., Donnermeyer, G. N. (1983): Determination of total nitrogen in sediments and plants using persulfate digestion. An evaluation and comparison with the Kjeldahl procedure. – *Water Resource* 17(9): 1207-1211.
- [28] Smil, V. (2000): Phosphorus in the environment: Natural Flows and Human Interferences. – *Annual Review of Energy and The Environment* 25: 53-88.
- [29] Tessier, J. T., Raynal, D. J. (2003): Use of Nitrogen to Phosphorus Ratios in Plant Tissue as an Indicator of Nutrient Limitation and Nitrogen Saturation. – *Journal of Applied Ecology* 40(3): 523-534.
- [30] Valderrama, J. C. (1981): The simultaneous analysis of total nitrogen and total phosphorus in natural waters. – *Marine Chemistry* 10(2): 109-122.
- [31] Wang, H., Edwards, M., Falkinham, J. O., Pruden, A. (2012): Molecular Survey of the Occurrence of *Legionella* spp., *Mycobacterium* spp., *Pseudomonas aeruginosa*, and *Amoeba* Hosts in Two Chloraminated Drinking Water Distribution Systems. – *Applied and Environmental Microbiology* 78(17): 6285-6294.
- [32] Wang, J. B., Xu, J., Xia, J., Wu, F., Zhang, Y. J. (2018): A kinetic study of concurrent arsenic adsorption and phosphorus release during sediment resuspension. – *Chemical Geology* 495: 67-75.
- [33] Wen, L., Recknagel, F. (2002): In situ removal of dissolved phosphorus in irrigation drainage water by planted floats: preliminary results from growth chamber experiment. – *Agriculture, Ecosystems and Environment* 90(1): 9-15.
- [34] Wu, X. D., Li, W. C., Pan, J. Z., Ma, S. Z., Chen, B. F., He, S. W. (2017): Restoration in northern Lake Gehu, a eutrophic lake in China. – *Chinese Journal of Oceanology and Limnology* 35(6): 1417-1431.
- [35] Xiao, L., Yang, L. Y., Zhang, Y., Gu, Y. F., Jiang, L. J., Qin, B. Q. (2009): Solid state fermentation of aquatic macrophytes for crude protein extraction. – *Ecological Engineering* 35(11): 1668-1676.
- [36] Xu, L. G., Pan, J. Z., Jiang, J. H., Zhao, H. B., Liu, C. H. (2013): A history evaluation modelling and forecastation of water quality in shallow lake. – *Water and Environment Journal* 27(4): 514-523.
- [37] Zhang, Y. C., Ma, R. H., Zhang, M., Duan, H. T., Loiselle, S., Xu, J. D. (2015): Fourteen-Year Record (2000–2013) of the Spatial and Temporal Dynamics of Floating Algae Blooms in Lake Chaohu, Observed from Time Series of MODIS Images. – *Remote Sensing* 7(8): 10523-10542.
- [38] Zhou, A. M., Tang, H. X., Wang, D. S. (2005): Phosphorus adsorption on natural sediments: Modeling and effects of pH and sediment composition. – *Water Research* 39(7): 1245-1254.

SPACE DISTRIBUTION OF BACTERIAL COMMUNITIES AND SUBSTRATE ENZYMES IN VERTICAL FLOW CONSTRUCTED WETLANDS

XU, Q. L.* – CAI, X. J. – FU, L. – HU, Y.

*Department of Resources & Environmental Engineering, Anshun University
Anshun 561000, China*

**Corresponding author*

e-mail: amy.198510@163.com; phone: +86-1898-4089-040

(Received 13th Jul 2019; accepted 25th Nov 2019)

Abstract. Microbial communities and substrate enzymes play a key role in constructed wetlands (CWs), therefore it's important to understand the diversity of microbial communities and activities of enzymes therein. In this study, System A (planting with *Pennisetum sinense* Roxb); System B (planting with *Pennisetum purpureum* Schum.); and System C (no plant) -- were set to investigate the variation of species richness, community equitability and substrate enzymes. It showed that Betaproteobacteria were most abundant in these three systems. The number of microorganisms species in system A, system B and system C were 60-90 cm > 30-60 cm > 0-30 cm, 60-90 cm > 0-30 cm > 30-60 cm and 30-60 cm > 60-90 cm > 0-30 cm, respectively. But urease, phosphatase and cellulase were all reduced with the increase of matrix depth. The results showed that the enzyme activity was not necessarily related to the number of microorganisms species, but enzyme activity could be related to the population of corresponding functional bacteria. In conclusion, Proteobacteria, Bacteroidetes, Firmicutes, Acidobacteria, Chloroflexi, Verrucomicrobia, Actinobacteria, TM7, Nitrospira, and OP11 were detected in these three constructed wetlands. However, there are still about 10% unknown bacteria at class level. The specific relationship between microorganisms, enzymes and wetland pollutant removal remains to be further studied in the future indicating that wetland microbial research has great potential in the future.

Keywords: *vertical flow constructed wetland, microbial communities, substrate enzymes, Pennisetum sinense* Roxb, *Pennisetum purpureum* Schum

Introduction

Constructed wetland (CW) is a prospective sewage purification technology (Kadlec and Knight, 1996; Cui et al., 2013). Compared with traditional sewage treatment methods, CW has the simple technology, relatively low operation and maintenance requirements (Zurita et al., 2009; Tang et al., 2017). CWs mainly include 2 types, which are surface flow CW and subsurface flow CW (IWA, 2000; Kadlec and Wallace, 2008; Vymazal and Kröpfelová, 2008). Vertical flow constructed wetland (VFCW) is a kind of subsurface flow wetland (Xu et al., 2015). In the last two decades, VFCW technology has become a popular choice for sewage treatment (Prochaska and Zouboulis, 2006; Abou-Elela et al., 2012), because it is high-efficiency not only for mitigation of biochemical oxygen demand and total suspended solids (Vymazal, 2009) but also for nitrification even in winter (Arias et al., 2005; Cooper, 2005; Prochaska et al., 2007). The VFCW with unsaturated flow has stronger oxygen carrying capacity than horizontal underground flow and is more effective for the mineralization of biodegradable organics (Kantawanichkul et al., 2009). As we all know, the main mechanism of CW sewage purification is the interaction of substrate, vegetation and microorganism through a series of biological, physicochemical reactions (Truu et al., 2009; Fu et al., 2013). Wetlands vegetation can affect enzyme activity and microbial

species structure and diversity that in turn indirectly affect enzyme activity (Zhang et al., 2010). Therefore, it's important to see the activities of enzymes and diversity of microbial population in constructed wetland. Wang (2009) proposed that the number of microorganisms, bacterial diversity and dominant community in the wetland system are closely relevant to the removal of phosphorus, nitrogen and organic compounds. Zhang et al. (2010) wetlands contains a wide range of cellulose and glycosidase, protease, urease, phosphatase, phenol oxidase and other enzymes. In our preliminary study, based on the study of the microbial enzyme activity in the artificial wetland system, the urease activity in the root system of aquatic plants was considered as an important index of nitrogen purification (Cui et al., 2013). In this study, several important bacterial communities (Proteobacteria, Bacteroidetes, Chloroflexi, Nitrospira, and OP11 etc.) and activities of substrate enzymes related to C, N and P cycle was analyzed, employing Illumina high-throughput sequencing technology and zymological means. The objective of this study is to estimate the space distribution of bacterial community and enzyme activities in the VFCW system. It is expected to provide a theoretical basis for microbial regulation of VFCW.

Materials and methods

Construction of VFCW

Three vertical wetlands were established and maintained in the greenhouse facility of South China Agriculture University (SCAU) in Guangzhou city. Each system was structured at 200 cm x 100 cm x 130 cm (length x wide x height). These three systems were constructed as followed: System A planted with *Pennisetum sinese Roxb*, System B planted with *Pennisetum purpureum Schum.*, and System C planted nothing. The sketch map of the CW systems was seen in *Figure 1*. The vegetation types of *Pennisetum sinese Roxb* and *Pennisetum purpureum Schum.* were transplanted into A, B system respectively, and the density is 10 plant/m².

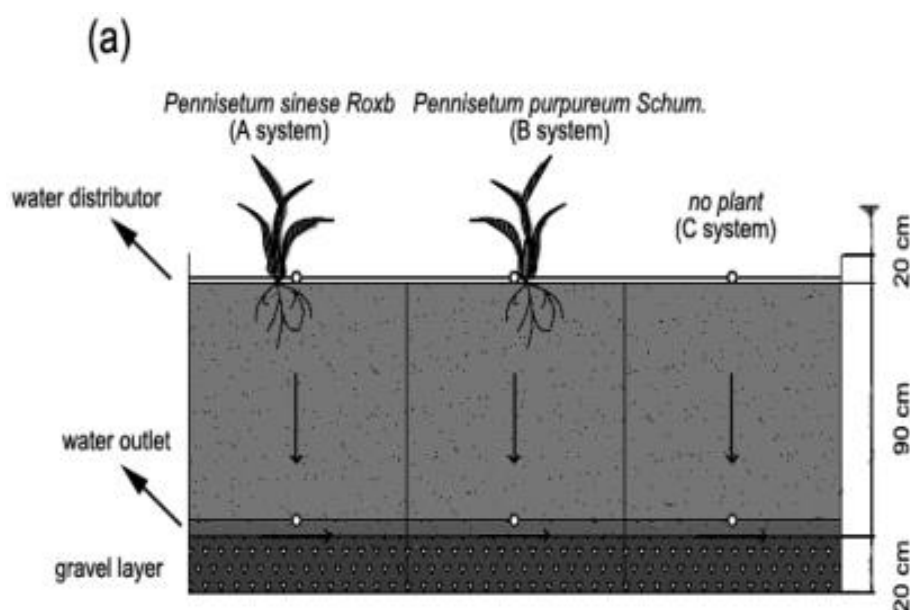


Figure 1. The profile of wetland system

Synthetic sewage

The synthetic wastewater is prepared from 400 litres of tap water, 70 g milk powder, 60 g soluble starch, 18 g urea, 10 g (NH₄)₂SO₄, 6 g MgSO₄, 6 g KH₂PO₄, 60 g NaHCO₃, and 50 ml 1% FeCl₃. Water quality indicators were as follows: the average values of TN, TP and COD were 40 mg/L, 4 mg/L and 330 mg/L. The pH value was 6.39-6.7 and the DO value was 4-6.

Operation of constructed wetland

Each CW system was constructed in mid-March, then started to operate on 28th of March and at last ended on 26th of September. These three systems carried out at 20 cm/d hydraulic loading. The sewage was feeded on 28th of March, these three systems were irrigated continuously with sewage for 8 hours every day. On 11th of April, we collected the water from the outlet position and analyzed once a week. The water monitoring indexes include TN, TP and COD etc. The over ground part of system vegetations were reaped once a month. By the end of the trial, five substrate samples were collected individually from 0–30 cm layer, 30–60 cm layer and 60–90 cm layer in every constructed wetland. These five samples were blended to get one typical sample for each layer. The community structure and diversities were monitored, by using High-throughput Sequencing Techniques and the enzyme activities were measured by zymological methods. The basic information of soil samples are shown in *Table 1*.

Table 1. Basic information of sample (DNA samples)

Sample number	Constructed wetland	Depth(cm)	Code
1	A (planting with planting <i>Pennisetum sinense Roxb</i>)	0-30	A1
2	A (planting with planting <i>Pennisetum sinense Roxb</i>)	30-60	A2
3	A (planting with planting <i>Pennisetum sinense Roxb</i>)	60-90	A3
4	B (planting with <i>Pennisetum purpureum Schum.</i>)	0-30	B1
5	B (planting with <i>Pennisetum purpureum Schum.</i>)	30-60	B2
6	B (planting with <i>Pennisetum purpureum Schum.</i>)	60-90	B3
7	C(no plant)	0-30	C1
8	C(no plant)	30-60	C2
9	C(no plant)	60-90	C3

Note: A (1,2,3) indicates that the sampling depth in system A is 0-30 cm (top layer), 30-60 cm (middle layer), and 60-90 cm (bottom layer), respectively. B (1, 2, 3), C (1, 2, 3) were set in the same way

DNA extraction

DNA was extracted from matrix samples using the Power Soil DNA separation kit (Mobio Laboratories Inc., Carlsbad, CA, USA) in accordance with the manufacturer's protocol. The extraction quantity and quality of DNA were determined by spectrophotometry. The extracted DNA before further analysis is stored in - 80°C.

PCR detection

The V3-V4 region (338F-806R) of 16S rRNA was amplified by PCR with the primers 338F (5'-ACTCCTACGGGAGGCAGCA-3') and 806R (5'-GGACTACHVGGGTWTCTAAT-3') (Wang et al., 2014; Lin et al., 2018).

These PCR reactions were proceed in a 30 ul reaction mixture, including 0.75 units Ex Taq DNA polymerase, 1× Ex Taq loading buffer, 0.2 mM dNTP mix, 0.2 μM of each primer, and 100 ng template DNA.

The amplification of each specimen was carried out in triplicate in an Eppendorf Master cycler PC.

94°C	30 s	35 cycles
50°C	1 min	
72°C	1 min	
72°C	10 min	

The PCR production was replicated and its concentration was monitored in a 2% agarose gel, Amplicons of all specimen were collected at the same ratio and the mixture was purified using the Gel Extraction Kit (E.Z.N.A.TM). Purified and mixed PCR products meet the requirements and were sequenced based on Illumina Miseq PE (paired end) 280bp.

Statistical analysis

Microbiological information analysis: the purified mixed PCR products were used for high throughput sequencing. Using Mothur (V.1.36.1) the original DNA sequence was filtered to remove chimeras and obtain the optimized sequence; According to 97% similarity, the optimized sequence is divided into Operational Taxonomic Units (OTU). Species taxonomy: A total of 6752 OTUs were obtained from 9 soil samples. Of the 6751 OTUs species in the sample, 5693 (84.3%) were at least accurate to phylum level and 5173 (76.6%) were at least to class level. Venn diagram analysis: It can be used to count the number of common or unique OTU in multiple samples, and can intuitively show the degree of similarity of OTU composition among environmental samples. water quality and soil enzymes were analyzed by EXCEL2007 and SPSS17.0. A one-way analysis of variance was conducted for constructed wetland: system A (planting *Pennisetum sinense Roxb*), system B (planting *Pennisetum purpureum Schum.*) and system C (no plant), to be detected the statistical significance of differences ($p < 0.05$) between means of treatments, and the Duncan test was performed.

Enzymes activities measured

Urease activity was measured by phenol-sodium hypochlorite method. The determination of urease activity in soil is based on the amount of ammonia produced after the enzymatic reaction with urea as the substrate, and can also be obtained by measuring the amount of unhydrolyzed urea. In this method, the urease liveness was analyzed by taking urea as the zymolyte, and the blue indophenol was produced by the reaction of the enzyme product ammonia with phenol-sodium hypochlorite. Phosphatase was measured by disodium phenyl phosphate method. In this method, the activity of the enzyme is expressed by the amount of phenol produced by hydrolyzing the substrate with phosphodisodium phosphate as the substrate under the action of phosphatase (Guan, 1986).

Results

Microbial community composition

At the phylum level, 26 phyla of bacterial, 523 genera were identified in this study. Among 9 substrate samples, Proteobacteria (averaging 55.1%) was the most abundant phyla, followed by (averaging 10.2%), unclassified (averaging 8.0%), Firmicutes (averaging 6.6%), Acidobacteria (averaging 5.3%), and Chloroflexi (averaging 4.7%). The other predominant phyla (>1%) were Verrucomicrobia (averaging 1.9%), Actinobacteria (averaging 1.8%), TM7 (averaging 1.6%), Nitrospira (averaging 1.4%), and OP11 (averaging 1.1%). Furthermore, their relative abundance of these predominant bacterial populations usually exhibits significant spatial variability in every system.

From *Figure 2(a)*, it showed that there was a large difference in bacterial flora among the three constructed wetlands. Proteobacteria was dominant in 9 studied samples. The spatial variation of the proportion of proteobacteria in VFCW has rarely been studied. In this experiment, the analysis on community of wetland microorganisms showed the advantage of proteobacteria in vertical flow to CW. However, a relatively high proportion of proteobacterial was found in the systems of planting with planting *Pennisetum sinese Roxb* and with *Pennisetum purpureum Schum.*, while the system with no plants showed a decrease. The abundance of the Chloroflexi in system A (planting with *Pennisetum sinese Roxb*) and B (planting with *Pennisetum purpureum Schum.*) was higher than that of system C (no plant). At the same time, the abundance of Chloroflexi phylum increased as the substrate depth deepen. Chloroflexi is a facultative anaerobic bacterium, which has been proved to be effective in eliminating chloride pollution in the environment. In this study, the results showed the following rule: The Nitrospira of the planting system was stronger than that not plant system, but decreased with the increase of substrate depth, Nitrospira on the top layer of system B is remarkably the highest (planting with *Pennisetum purpureum Schum.*), while the abundance of firmicutes, Bacteroidetes and OP11 in system C were higher than system A and system B.

At the class level, in total, 53 bacterial taxa were observed. Most predominant bacteria (>1%) were ascribed to Betaproteobacteria (averaging 24.1%), followed by Deltaproteobacteria (averaging 13.4%), Alphaproteobacteria (averaging 10.5%), Gammaproteobacteria (averaging 5.8%), Clostridia (averaging 4.8%), Bacteroidia (averaging 4.6%), Anaerolineae (averaging 4.2%), Actinobacteria (averaging 1.84%), Sphingobacteria (averaging 1.80%), Acidobacteria_Gp7 (averaging 1.63%), and Nitrospira (averaging 1.4%). Furthermore, the relative abundance of these groups indicates that the spatial variations of wetland systems are large.

Figure 2(b) showed that proteobacteria mainly was composed of Alpha-, Beta-, Delta- and Gammaproteobacteria. Betaproteobacteria was most richest in these three systems. The distribution of the Deltaproteobacteria showed the following trends: as the substrate depth increased, the Deltaproteobacteria abundance also increased, and this bacterium were the most abundant in system C (the abundance of C3 was up to 22.5%). Compared to Deltaproteobacteria, Alphaproteobacteria was adverse, and it was most abundant in top layer substrate of these 9 constructed wetlands, while the distribution rule is that the bacterial abundance decreased as substrate depth increased. It showed that the depth of substrate has a strong impact on microbial community structure.

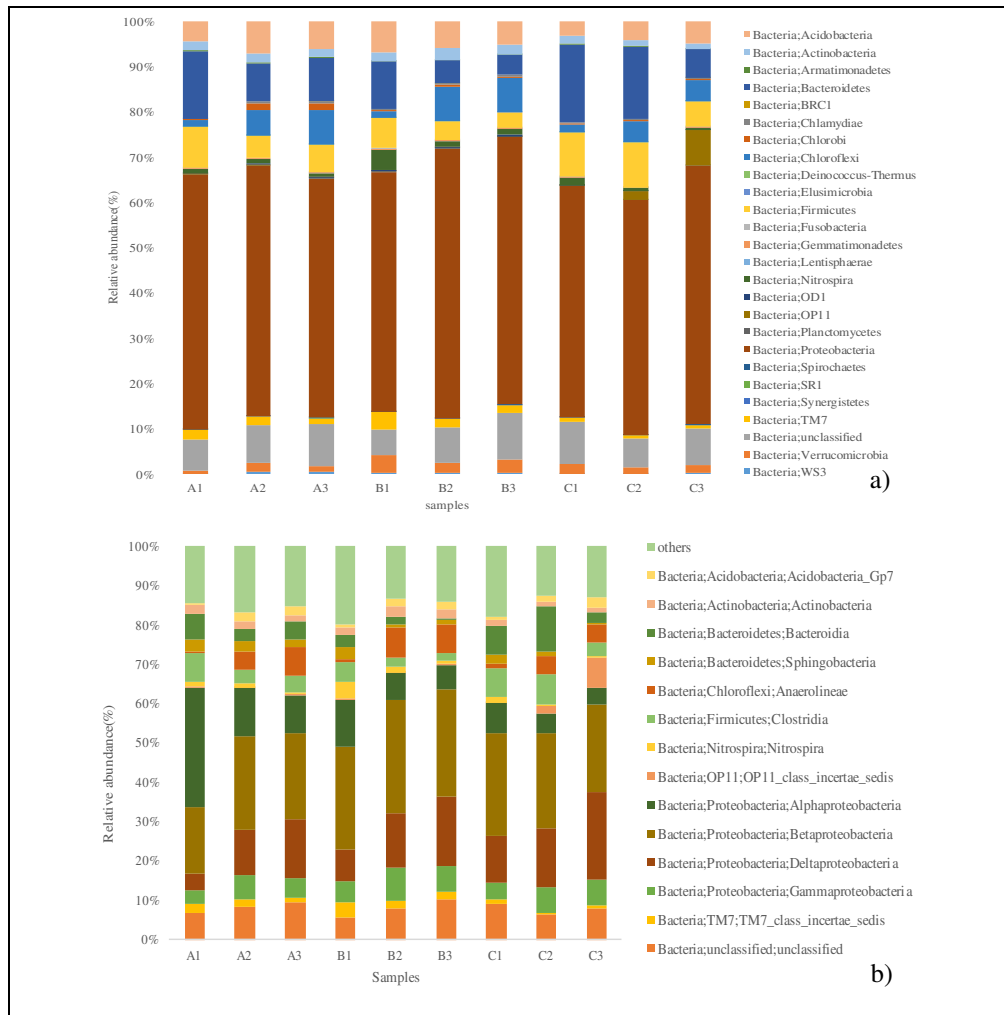


Figure 2. Bacterial community composition in three vertical flow constructed wetland. *a)* Phylum-level distribution of bacteria; *b)* Class-level distribution of bacteria (Others include the bacteria class with the relative abundance less than 1% in each sample)

Venn analysis

The common number of OTU (operational taxonomic units) among multiple samples can reflect the similarity and overlap of environmental samples. The statistical results are obtained in the form of Venn diagram. In general, 97% of OTU at similar levels was selected for analysis, and the number of OTU can also represent the number of bacterial species. From *Figure 3*, there were some results as followed: The number of bacterial species in system A, system B and system C were 60-90 cm > 30-60 cm > 0-30 cm, 60-90 cm > 0-30 cm > 30-60 cm and 30-60 cm > 60-90 cm > 0-30 cm, respectively.

Enzymes activities

Figure 4 illustrated that the changes of urease, phosphatase and cellulase are consistent, and they all reduced with the increase of matrix depth. The rule was shown as followed: 0-30 cm > 30-60 cm > 60-90 cm. This is consistent with previous research results. The comparison between this result and *Fig. 3* indicates that the number of microorganisms is not necessarily related to the enzyme activity.

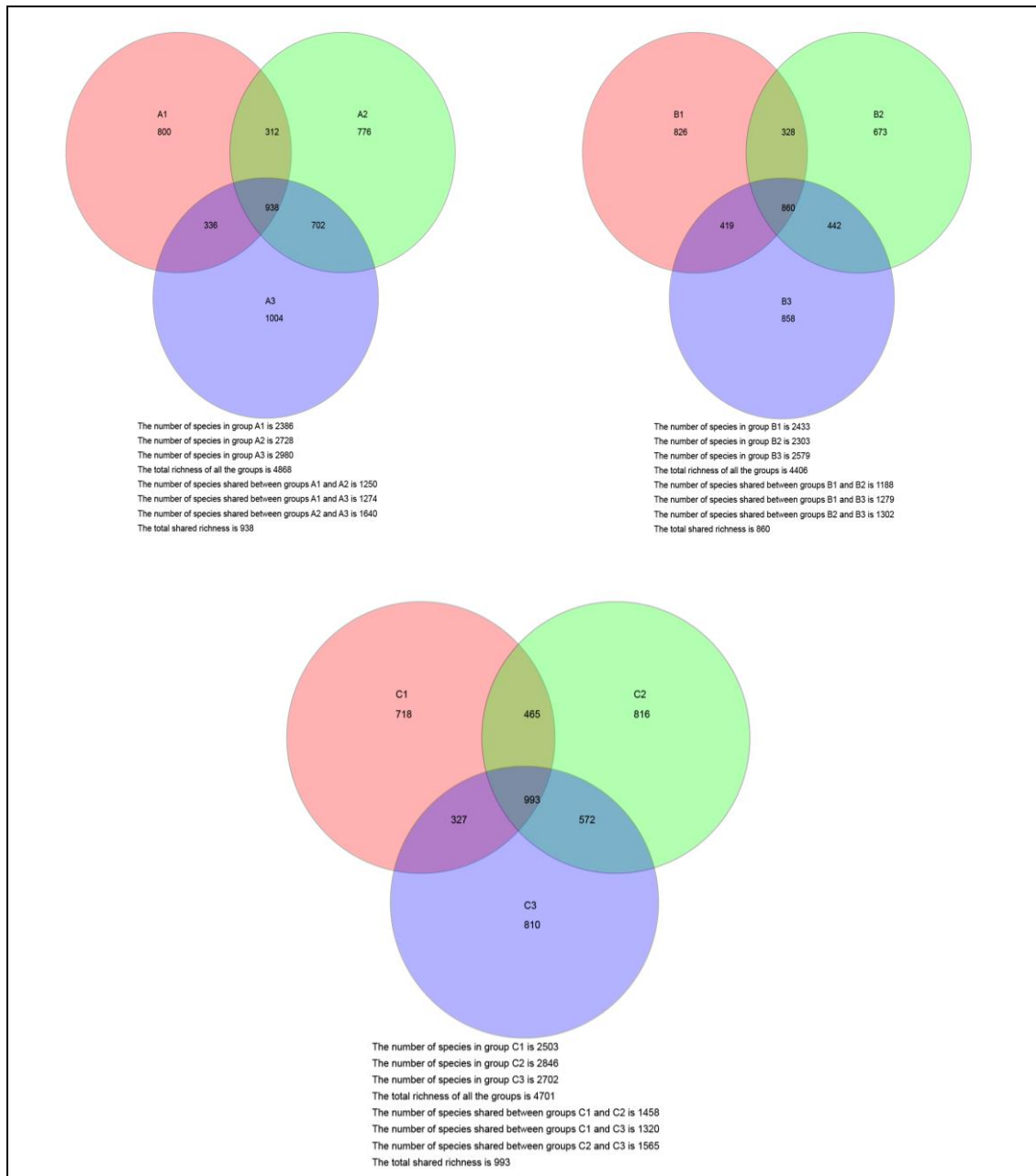


Figure 3. Venn diagram

Water quality change

Figure 5 illustrated that the changes of TN, TP and COD. The N removal efficiency in these three CW systems was about 50–70%. With the operation of the system, the removal rate of TP basically presents a downward trend. After August 15, the P removal efficiency patterns from the three CW systems were in the following order: B > A > C, and showed a significant difference in September 12 ($p < 0.01$). The average removal efficiency of COD was higher than 85% and COD removal performed was satisfied.

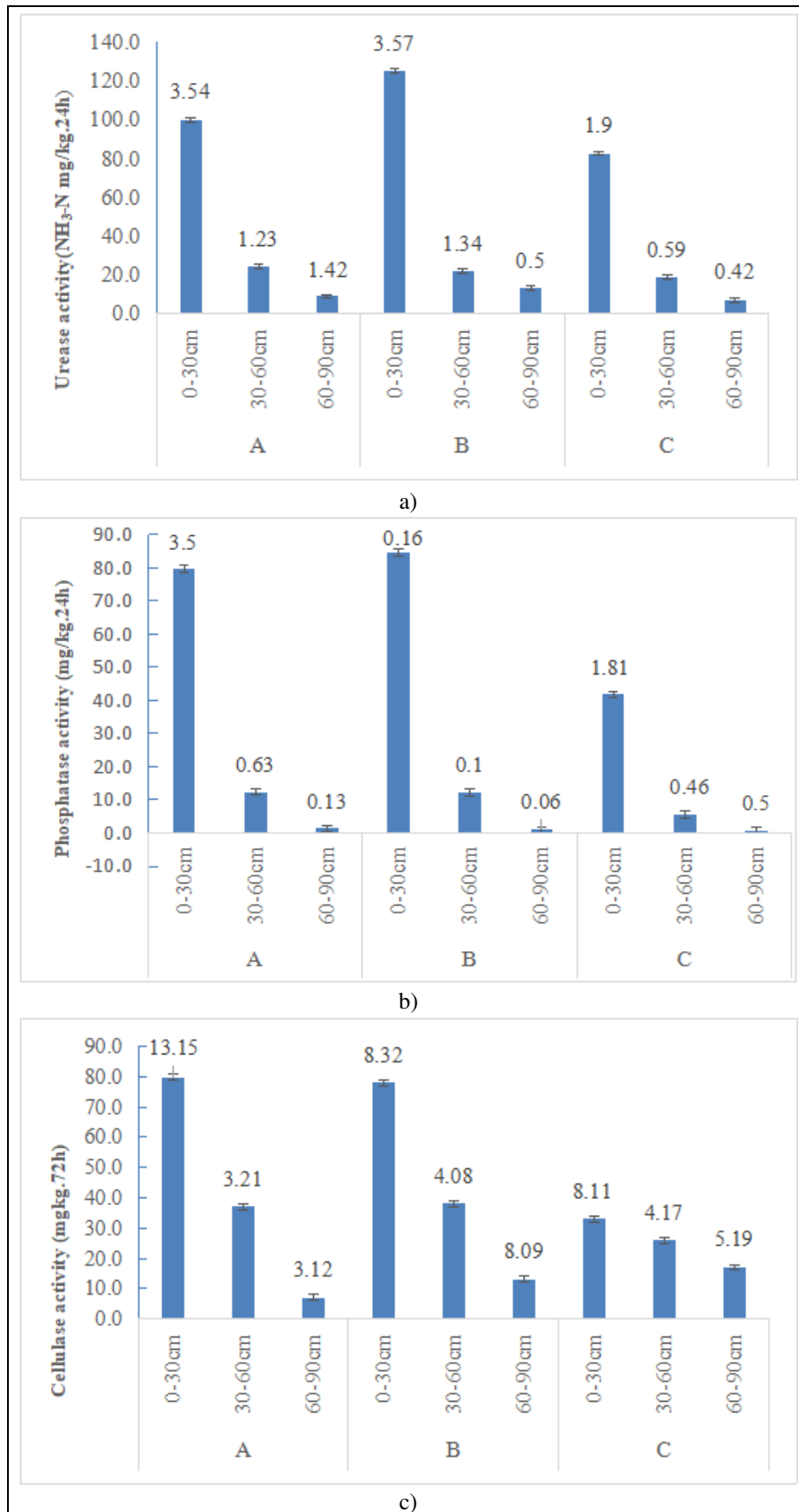


Figure 4. Substrate enzymes dynamic change in three systems

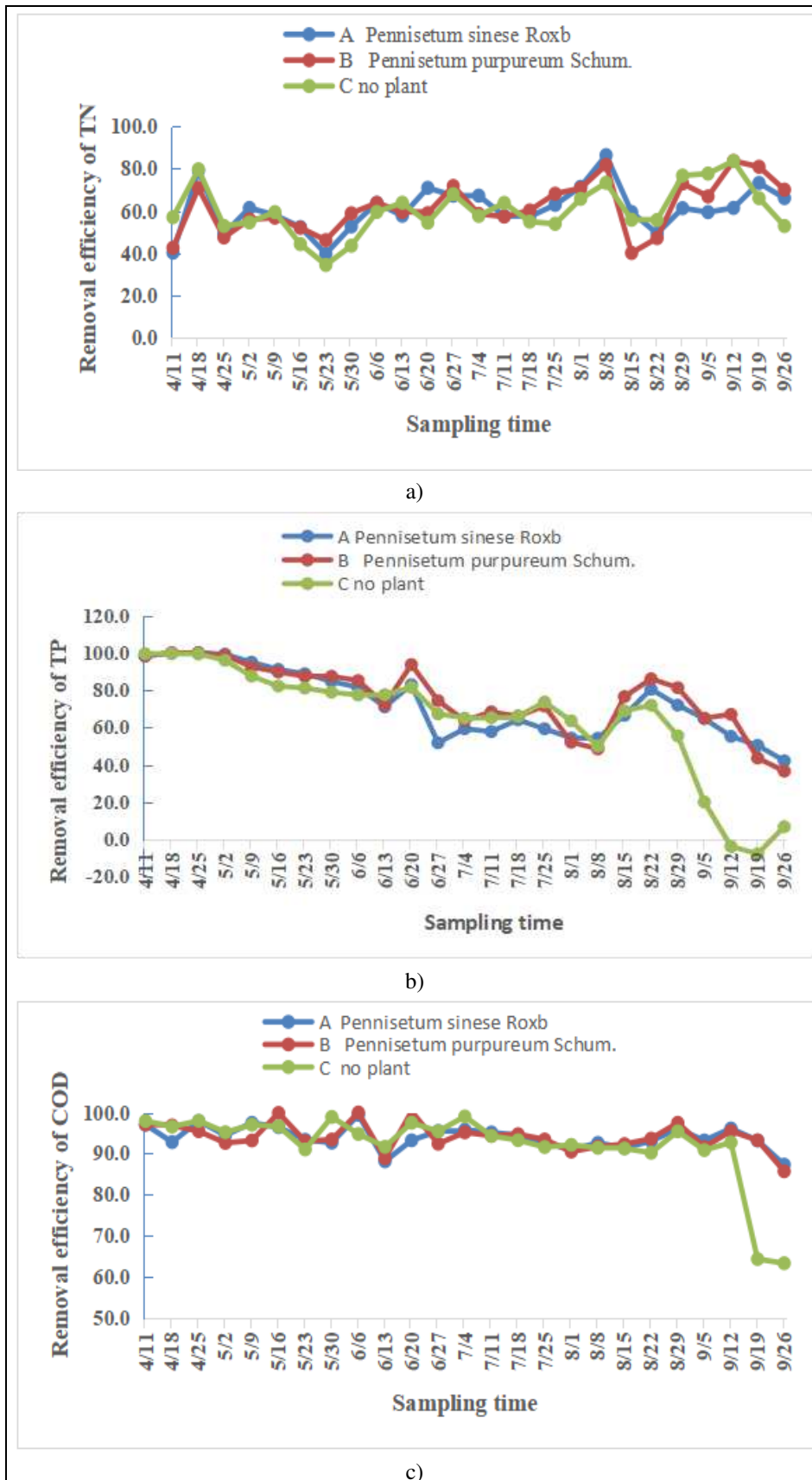


Figure 5. Water monitoring indexes change in three systems

Discussion

Microbial community in constructed wetland

Species diversity is a prerequisite for maintaining the normal function of an ecosystem (Ansola et al., 2014). The richness and diversity of bacterial communities make wetlands play an important ecological role in nutrient cycling, organic degradation, heavy metal morphological transformation and greenhouse gas emissions (Conrad, 1996). Among the 9 soil types of wetland plants in this study area, the abundance and diversity of soil bacterial communities are consistent: Proteobacteria was dominant in 9 studied samples. Proteobacteriagate is a kinds of bacterial community, in the study of many wetland bacteria have the highest relative abundance, such as the Yellow River delta wetland (Yu et al., 2012), China Hong Kong mangrove wetland (Jiang et al., 2013), the United States Olentangy river wetland (Ligi et al., 2014) and artificial wetland (Ansola et al., 2014), etc. The proteobacteria mainly was composed of Alpha-, Beta-, Delta- and Gammaproteobacteria. Betaproteobacteria was most richest in these three systems. Chloroflexi and Nitrospirae in system A and B are remarkably higher than system C, however, the abundance of firmicutes, Bacteroidetes and OP11 in system C were higher than system A and system B. These results proved that the presence of vegetation, types of vegetation all can affect the microbial community structure. The regulation of plant collocation could vary the microbial structure distribution, and eventually optimize the decontamination ability of the wetland system. The results can provide theoretical basis for the selection and matching of constructed wetland plants in the future.

Enzyme activity

The number of microorganisms in system A, system B and system C were 60-90 cm > 30-60 cm > 0-30 cm, 60-90 cm > 0-30 cm > 30-60 cm and 30-60 cm > 60-90 cm > 0-30 cm, respectively. But urease, phosphatase and cellulose were all reduced with the increase of matrix depth. The results showed that the enzyme activity was not necessarily related to the number of microorganisms. Guo (1997) found that the relationship among urease, phosphatase, cellulose activities and microbial biomass were as followed: Enzymes activities increased with the increase of microbial biomass. However, our research was not consistent with it, which may be related to the structure of the VFCW (Aon and Colaneri, 2011) or some function bacterial. Due to the special structure, the oxygen in the upper matrix of the VFCW was relatively sufficient, which was only conducive to the reproduction of aerobic microorganisms. In addition, the enzyme activity of rhizosphere in system A was different from that in system B. Both urease and phosphatase showed that the activity of planting *Pennisetum purpureum Schum.*'s enzyme was higher than that of planting *Pennisetum sinense Roxb*'s enzyme. Enzyme activity around rhizosphere can not only reflect the bacteria activities in plant root zone, but also reflect the effect of plant spices. Different plants have different influence on secretion of enzymes and microorganisms' growth. *Pennisetum sinense Roxb* and *Pennisetum purpureum Schum.* both have large biomass. Therefore, the rhizosphere microorganism quantity and activity are slightly higher. Consequently, *Pennisetum sinense Roxb* and *Pennisetum purpureum Schum.* should be the better vegetation choices for construct wetland to remove pollution.

Water quality changes

The high removal efficiency of TN and COD in this experiment might be attributed to the higher temperature in summer, resulting in higher microbial activities. Temperature indeed has a great effect on the nutrients removal efficiency of CWs (Fan et al., 2013). It could be related to some functional bacteria, for example the *Nitrospira* are known for their role in nitrite oxidation (Feng et al., 2013), and the proteobacteria often take advantage of ammonia gas produced by the decomposition of organic matter and may have participated in the biological reaction of various organic matters in nature or artificial systems (Madigan et al., 1997; Liao et al., 2013; Liu et al., 2014). It may indirectly explain the effective removal of TN and COD in these three VFCWs. In addition, a previous study also showed that proteobacterium was dominant in the large-scale CW purification and polluted river system (Wei et al., 2015).

Above all, the variation in microbial structure are most likely to reflect the impact of changes in microbial community of constructed wetland in the balance wetland ecosystem. In future studies, we must focus on the potential mechanisms driving community variation and elucidation of how these variations affect the microbial community function of constructed wetlands.

Conclusion

(1) There was no direct relationship between microbial species population and enzyme activity. Meanwhile, planting vegetation whether or not, vegetation type and substrate depth may have a great influence on the bacterial community and substrate enzyme in VFCW. This suggests that we could improve pollutant removal by planting different wetland plants and designing different substrate depths to regulate wetland microorganisms.

(2) Proteobacteria predominated in these three systems, which was mainly included Alpha-, Beta-, Delta- and Gammaproteobacteria, and among them Betaproteobacteria was most abundant. Enzyme activity is independent of microbial populations, but could be related to the populations of corresponding functional bacteria, for example *Nitrospira* may be related to urease. In future studies, we will further research the specific relationship between enzymes and microorganisms in wetland decontamination, and use genetic engineering to study the decontamination mechanism of microorganisms deeply.

Acknowledgements. The authors wish to thank researcher Lin Jingxing of Chinese Academy of Geological Sciences for scientific discussion and comments on earlier versions of the manuscript. This study was also supported by Guizhou normal colleges and technology top-notch talent support program project (qianjiaohe KY [2016]097), Guizhou provincial science and technology plan project (qiankehe LH [2016]7283), Doctoral fund project (asubsjj201607), National Natural Science Foundation of China (41271245) and Construction project of SCAU sewage ecological treatment and water body restoration engineering technology research center (2012gczxA1004) for their financial support.

REFERENCES

- [1] Abou-Elela, S. I., Hellal, M. S. (2012): Municipal wastewater treatment using vertical flow constructed wetlands planted with *Canna*, *Phragmites* and *Cyperus*. – *Ecological Engineering* 47: 209-213.

- [2] Ansola, G., Arroyo, P., Sáenz de Miera, L. E. (2014): Characterisation of the soil bacterial community structure and composition of natural and constructed wetlands. – *Science of The Total Environment* 473-474: 63-71.
- [3] Aon, M. A., Colaneri, A. C. (2011): II. Temporal and spatial evolution of enzymatic activities and physico-chemical properties in an agricultural soil. – *Applied soil Ecology* 18(3): 255-270.
- [4] Arias, C. A., Brix, H., Marti, E. (2005): Recycling of treated effluents enhances removal of total nitrogen in vertical flow constructed wetlands. – *Journal of Environmental Science Health* 40(6-7): 1431-1443.
- [5] Conrad, R. (1996): Soil microorganisms as controllers of atmospheric trace gases (H₂, CO, CH₄, OCS, N₂O, and NO). – *Microbiological Reviews* 60(4): 609-640.
- [6] Cooper, P. (2005): The performance of vertical flow constructed wetland systems with special reference to the significance of oxygen transfer and hydraulic loading rates. – *Water Science Technology* 51(9): 81-90.
- [7] Cui, L. H., Ouyang, Y., Gu, W. J., Yang, W. Z., Xu, Q. L. (2013): Evaluation of nutrient removal efficiency and microbial enzyme activity in a baffled subsurface-flow constructed wetland system. – *Bioresource Technology* 146: 656-662.
- [8] Fan, J. L., Liang, S., Zhang, B., Zhang, J. (2013): Enhanced organics and nitrogen removal in batch-operated vertical flow constructed wetlands by combination of intermittent aeration and step feeding strategy. – *Environmental Science & Pollution Research* 20: 2448-2455.
- [9] Feng, S., Chen, C., Wang, Q. F., Yang, Z. Y., Zhang, X. J., Xie, S. G. (2013): Microbial community in a full-scale drinking water biosand filter. – *J. Environ. Biol.* 34: 321-324.
- [10] Fu, G. P., Zhang, J. H., Chen, W., Chen, Z. R. (2013): Medium clogging and the dynamics of organic matter accumulation in constructed wetlands. – *Ecological Engineering* 60: 393-398.
- [11] Guan, S. Y. (1986): *Soil enzyme and its research method*. – Agriculture Press, Beijing.
- [12] Guo, J. X., Jiang, S. C., Lin, H. J., Jin, L. (1997): Enzymic activity of alkaline meadow soil with different grassland vegetations. – *Chinese Journal of Applied Ecology* 8(4): 412-416.
- [13] IWA. (2000): *Constructed Wetlands for Pollution Control: Processes, Performance, Design and Operation*. – Scientific and Technical Report No. 8. International Water Association, London, UK.
- [14] Jiang, X. T., Peng, X., Deng, G. H., Sheng, H. F., Wang, Y., Zhou, H. W., Tam, N. F. Y. (2013): Illumina Sequencing of 16S rRNA Tag Revealed Spatial Variations of Bacterial Communities in a Mangrove Wetland. – *Microbial Ecology* 66(1): 96-104.
- [15] Kadlec, R. H., Knight, R. L. (1996): *Treatment Wetlands*. – Lewis Publishers, Michigan Boca Raton, FL.
- [16] Kadlec, R. H., Wallace, S. D. (2008): *Treatment Wetlands*. – Second ed. CRC Press, Boca Raton, USA.
- [17] Kantawanichkul, S., Kladpraserta, S., Brix, H. (2009): Treatment of high-strength wastewater in tropical vertical flow constructed wetlands planted with *Typha angustifolia* and *Cyperus involucratu*s. – *Ecological Engineering* 35: 238-247.
- [18] Liao, X. B., Chen, C., Wang, Z., Wan, R., Chang, C. H., Zhang, X. J., Xie, S. G. (2013): Changes of biomass and bacterial communities in biological activated carbon filters for drinking water treatment. – *Process Biochem.* 48: 312-316.
- [19] Ligi, T., Oopkaup, K., Truu, M., Preem, J. K., Nölvak, H., Mitsch, W. J., Mander, Ü., Truu, J. (2014): Characterization of bacterial communities in soil and sediment of a created riverine wetland complex using high-throughput 16S rRNA amplicon sequencing. – *Ecological Engineering* 72: 56-66.
- [20] Lin, Z., Ye, W., Zu, X. P., Xie, H. S., Li, H. K., Li, Y. P., Zhang, W. D. (2018): Integrative metabolic and microbial profiling on patients with Spleen-yang-deficiency syndrome. – *Scientific reports* 8: 1-11.

- [21] Liu, Y., Zhang, J. X., Zhao, L., Zhang, X. L., Xie, S. G. (2014): Spatial distribution of bacterial communities in high-altitude freshwater wetland sediment. – *Limnology* 15: 249-256.
- [22] Madigan, T. M., Martinko, J. M., Parker, J., Brock, T. D. (1997): *Brock Biology of Microorganisms*. – Upper Saddle River, NJ: Prentice Hall.
- [23] Prochaska, C. A., Zouboulis, A. I. (2006): Removal of phosphates by pilot vertical-flow constructed wetlands using a mixture of sand and dolomite as substrate. – *Ecological Engineering* 26: 293-303.
- [24] Prochaska, C. A., Zouboulis, A. I., Eskridge, K. M. (2007): Performance of pilot-scale vertical-flow constructed wetlands, as affected by season, substrate, hydraulic load and frequency of application of simulate urban sewage. – *Ecological Engineering* 31: 57-66.
- [25] Tang, P., Yu, B. H., Zhou, Y. C., Zhang, Y., Li, J. (2017): Clogging development and hydraulic performance of the horizontal subsurface flow storm water constructed wetlands: a laboratory study. – *Environmental Science and Pollution Research* 24: 9210-9219.
- [26] Truu, M., Juhanson, J., Truu, J. (2009): Microbial biomass, activity and community composition in constructed wetlands. – *Science of the total environment* 407: 3958-3971.
- [27] Vymazal, J., Kröpfelová, L. (2008): *Wastewater Treatment in Constructed Wetlands with Horizontal Sub-Surface Flow*. – Series of Environmental Pollution, Vol. 14. Springer, Germany.
- [28] Vymazal, J. (2009): Horizontal sub-surface flow and hybrid constructed wetlands systems for wastewater treatment. – *Ecological Engineering* 25: 478-490.
- [29] Wang, X. D., Zhai, Y. H., Zhao, S., Li, R. Q., Ma, W. L., Li, Y. H. (2009): Effect of free surface flow wetland and subsurface flow wetland on bacterial diversity in Beijing cuihu wetland park. – *Environmental Science* 30: 280-288. (in Chinese).
- [30] Wang, P., Chen, B., Zhang, H. (2017): High throughput sequencing analysis of bacterial communities in soils of a typical Poyang lake wetland. – *Acta Ecologica Sinica* 37(5): 1652-1658.
- [31] Wei, G., Yin, M., He, T., Xie, S. G. (2015): Influence of substrate type on microbial community structure in vertical-flow constructed wetland treating polluted river water. – *Environmental Science and Pollution Research* 22(20): 16202-16209.
- [32] Xu, Q. L., Huang, Z. J., Wang, X. M., Cui, L. H. (2015): Planting *Pennisetum sinense* Roxb and *Pennisetum purpureum* Schum. as vertical-flow constructed wetland vegetation for removal of N and P from domestic sewage. – *Ecological Engineering* 83: 120-124.
- [33] Yu, Y., Wang, H., Liu, J., Wang, Q., Shen, T. L., Guo, W. H., Wang, R. Q. (2012): Shifts in microbial community function and structure along the successional gradient of coastal wetlands in Yellow River Estuary. – *European Journal of Soil Biology* 49: 12-21.
- [34] Zhang, C. B., Wang, J., Liu, W. L., Zhu, S. X., Liu, D., Chang, S. X., Chang, J., Ge, Y. (2010): Effects of plant diversity on nutrient retention and enzyme activities in a full-scale constructed wetland. – *Bioresource Technology* 101: 1689-1692.
- [35] Zurita, F., De Andab, J., Belmonte, M. A. (2009): Treatment of domestic wastewater and production of commercial flowers in vertical and horizontal subsurface-flow constructed wetlands. – *Ecological Engineering* 35: 861-869.

NUTRIENT DISTRIBUTIONS IN THE EAST CHINA SEA AND CHANGES OVER THE LAST 25 YEARS

YE, L. A.^{1,2} – ZHANG, H. B.¹ – FEI, Y. J.¹ – LIU, L.¹ – LI, D. L.^{2,3,4*}

¹*Ningbo Environmental Monitoring Center, SOA, Ningbo 315040, China*

²*Department of Geography and Spatial Information Techniques, Ningbo University, Ningbo 315211, China*

³*Laboratory for Marine Geology, Qingdao National Laboratory for Marine Science and Technology, Qingdao 266061, China*

⁴*State Key Laboratory of Estuarine and Coastal Research, East China Normal University, Shanghai 200062, China*

**Corresponding author*

e-mail: lidongling@nbu.edu.cn; phone: +86-574-8760-5546; fax: +86-574-8760-5546

(Received 13th Jul 2019; accepted 25th Nov 2019)

Abstract. A survey of seasonal variations in the distribution of nutrients along a standard section of the East China Sea was carried out between 1991 and 2015. Here, interannual variations of five key nutrients are analyzed and discussed in the context of possible controlling factors, with special attention given to seasonal variations recorded over the year 2015. Results indicate that concentrations of dissolved inorganic nitrogen (DIN), phosphate (DIP) and silicate (DSi) exhibit gradual increases over this period. Measured concentrations of DIN, DIP and DSi were 5.34–11.87 $\mu\text{mol/L}$, 0.31–0.53 $\mu\text{mol/L}$ and 11.12–23.15 $\mu\text{mol/L}$, respectively. Since 1996, concentrations of DIN, DIP and DSi have increased significantly. The annual average concentration of DIN, DIP and DSi in the East China Sea were ~2 times greater in 2015 than in 1991, respectively. The N/P ratio exhibits an increasing trend followed by steady-state asymmetric M-type fluctuations. Conversely, the Si/N ratio is generally stable and exhibits an asymmetric W-type fluctuation. The distribution of nutrients in the East China Sea exhibits clear seasonal variations, with phosphate and inorganic nitrogen contents generally higher in autumn and winter than in spring and summer. Silicate content is higher in summer and winter than in autumn and spring. The main source of nutrients into the East China Sea is the Yangtze River plume, with the Taiwan Warm Current providing an additional, secondary source. The combined effects of the Yangtze River plume and the Taiwan Warm Current enforce a decreasing trend in nutrient concentrations from west to east.

Keywords: *inorganic nitrogen, phosphate, silicate, interannual change, seasonal variation*

Introduction

The East China Sea is bordered by the Yangtze River estuary in the west, the Pacific Ocean in the east, the Taiwan Strait in the south and the Yellow Sea in the north. The boundary between the East China Sea and the Yellow Sea is defined by the line between the northern end of the Yangtze River estuary and the southernmost point of Jeju Island. The eastern boundary of the East China Sea with the Pacific Ocean is defined by the Ryukyu Islands. The East China Sea is fed by more than 40 rivers exceeding 100 kilometers in length (Yanzgi et al., 1993; Chu et al., 2005). These rivers add nutrients to the East China Sea which, in turn, supports one of the most highly productive marine ecosystems in the world (Li and Dag, 2004). As a

result, the distribution and variations in nutrient concentrations in the East China Sea is a topic of great importance that has inspired numerous scientific investigations.

For example, Wang et al. (2008) studied the three-dimensional distribution and seasonal variation of nutrients in the East China Sea. Wang et al. (2019) then improved on these studies by incorporating a three-dimensional low-trophic ecosystem model that reevaluated budgets of nutrients and biogenic particles (phytoplankton and detritus) in the East China Sea and found that export of biogenic particles through the Tsushima Strait is greater than that through the continental shelf break.

Based on surveys of nutrient concentrations along three sections in the East China Sea, Cao et al. (2014) compared profiles collected during the relatively wet period of 1989–2010 to more typical profiles along the same sections to identify long-term changes in the concentrations and distributions of inorganic nitrogen, active phosphate and silicate. To evaluate the contribution of each source of nutrients to the nutrient inventory and primary production over the continental shelf, Zhang et al. (2019) tracked the behavior of all of the state variables incorporated into a low-trophic ecosystem model. Using this technique, Zhang et al. (2019) discovered strong seasonal variations in the spatial distribution of nutrient sources attributable to seawater circulation, mixing, and stratification. The ecological effect of these nutrients is in turn affected by the level of nutrient limitation, light availability and water temperature at the locations of each of these sources (Zhang et al., 2019). Mi et al. (2011) used the survey data collected between April and August, 2011, to analyze and discuss the distribution of nutrients in the East China Sea and adjacent Yellow Sea over the spring and summer seasons, as well as various influencing factors. Based on survey data collected over four voyages conducted in the East China Sea (120°–128°E, 25°–33°N) over the spring, summer, autumn and winter of 2013, Ye et al. (2015) analyzed the spatiotemporal distribution and structure of nutrients in the East China Sea and discussed limitations to the growth of phytoplankton.

Excess nutrients can lead to pollution of water in the East China Sea. Moreover, the concentrations and distributions of these nutrients vary from year to year. Therefore, to promote the rational exploitation and utilization of the marine resources in the East China Sea it is important to generate accurate and timely understandings of the distribution, spatiotemporal variations and influencing factors of nutrients in the East China Sea.

In this study, we analyze the results of nutrient monitoring surveys conducted between 1991 and 2015 and evaluate interannual trends and variations in nutrient concentrations and distributions. Additional survey data collected from 30 stations in the East China Sea in the spring (May), summer (August), autumn (November) and winter (February) of 2015 to determine the distribution of nutrients in East China Sea and possible influencing factors are likewise discussed and analyzed. The goal of this study is to systematically investigate the distribution of nutrients in the East China Sea and to identify seasonal, interannual and long-term variations in the distributions of these nutrients over the past 25 years, thereby providing fundamental data by which to advance scientific study of the East China Sea and to promote rational development and utilization of marine resources in this region.

Materials and methods

Sample collection

Samples were collected during a series of four oceanographic research cruises conducted by the Ningbo Marine Environmental Monitoring Center along standard sections of the East China Sea (27–33°N, 121–128°E), China, between 1991 and 2015. The total of 30 survey stations are arranged into 3 oceanographic sections supplemented by four auxiliary stations. A map of the relevant survey stations is presented in *Fig. 1*.

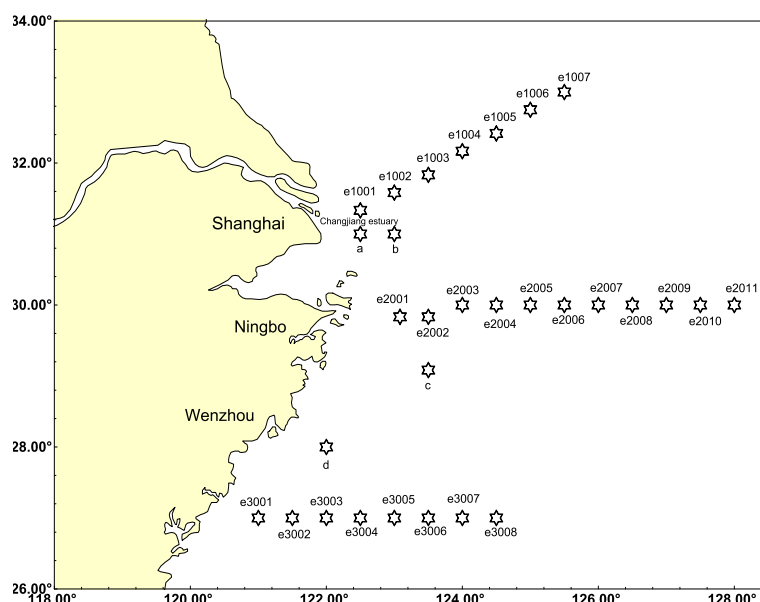


Figure 1. Sampling sites in the East China Sea

Sampling and analysis

Full water-depth sampling of seawater was conducted using a CTD self-capacitive sampler (Seabird, USA). Samples were filtered using a HCl acid-washed neutral pH cellulose acetate fiber filtration membrane (0.45 µm). After filtration, nutrient assays were conducted using the methods outlined in the fourth volume of the marine survey code (GB17378.4-2007): the investigation of the chemical elements in sea water (Xu et al., 2005). The analytical methods and detection limits for dissolved inorganic phosphate (DIP), nitrite (NO₂-N), nitrate (NO₃-N), ammonium salt (NH₄-N) and silicate (DSi) are presented in *Table 1*. Dissolved inorganic nitrogen is the sum of the nitrate, nitrite and ammonia nitrogen components (*i.e.*, DIN = NO₃-N + NO₂-N + NH₄-N). Data interpolations between sampling locations, statistical data processing and visualization were carried out using the Surfer software (Golden Software, USA).

Table 1. Analytical methods by component

Project	NO ₂ -N	NO ₃ -N	NH ₄ -N	DIP	DSi
Analysis method	Naphthalene ethylenediamine spectrophotometric method	Zinc and cadmium reduction	Hypobromate oxidation	Phospho molybdenum blue method	Silicon molybdenum yellow method
Instruments	723C visible spectrophotometer				

Data processing

Long-term trends in nutrient concentrations were evaluated by performing a linear regression on monitoring results obtained in August and calculating the Pearson correlation coefficient, R . (Eq. 1)

This coefficient was defined as the correlation coefficient between the time series $\{X\}$ and the integers $\{n\}$, $i=1,2,3,\dots,n$. In this study, n is the total span of years of the data. The coefficient was computed from the following equation:

$$R = \frac{\sum (x - \bar{x}) \cdot (y - \bar{y})}{\sqrt{\sum (x - \bar{x})^2 \cdot \sum (y - \bar{y})^2}} \quad (\text{Eq.1})$$

where $y=(n+1)/2$. Its significance level is determined from the Student's t -test. A positive (negative) value of R indicates that the time series $\{X\}$ has a linear positive (negative) trend (Liu et al., 2005).

Results and discussion

Interannual variations in nutrient concentrations

Analyses of dissolved nutrient concentrations indicate that concentrations of DIN in the East China Sea gradually increased over the study period, from 5.34 $\mu\text{mol/L}$ in 1991 to 11.87 $\mu\text{mol/L}$ in 2015 (Fig. 2). Concentrations of DIP likewise gradually increased, from 0.31 $\mu\text{mol/L}$ in 1991 to 0.49 $\mu\text{mol/L}$ in 2015 (Fig. 3). Concentrations of DSi exhibit high levels of interannual variability (Fig. 4). However, with the exception of a large increase in 1999, the trend is generally increasing, from 11.12 $\mu\text{mol/L}$ in 1991 to 23.15 $\mu\text{mol/L}$ in 2015. Since 1996, the average concentration of DIN, DIP and DSi in the East China Sea have increased significantly. The annual average concentration of DIN in the East China Sea in 2015 was ~ 2 times greater than that measured in 1991, the annual average concentration of DIP increased ~ 1.6 times, and the annual average concentration of DSi increased ~ 2 times.

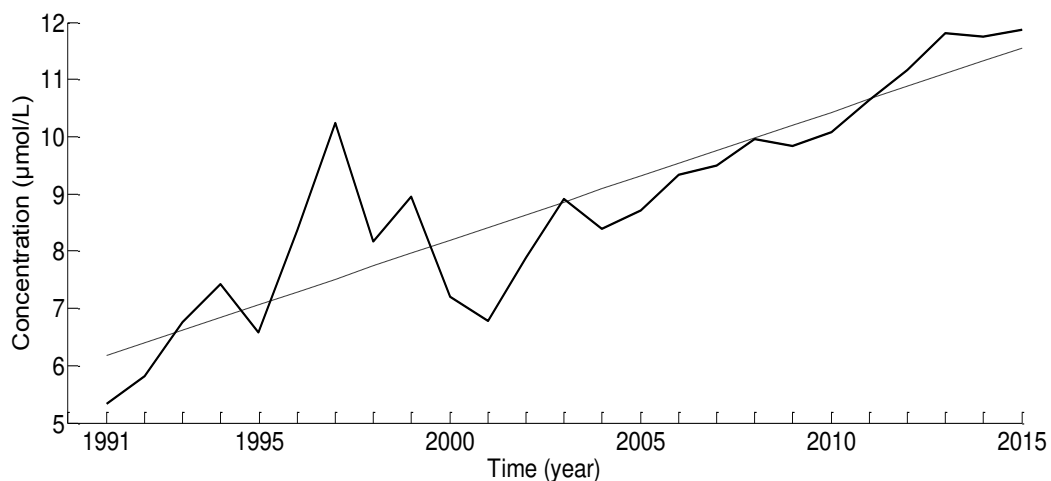


Figure 2. Interannual variations and long-term trends in DIN concentrations in the East China Sea

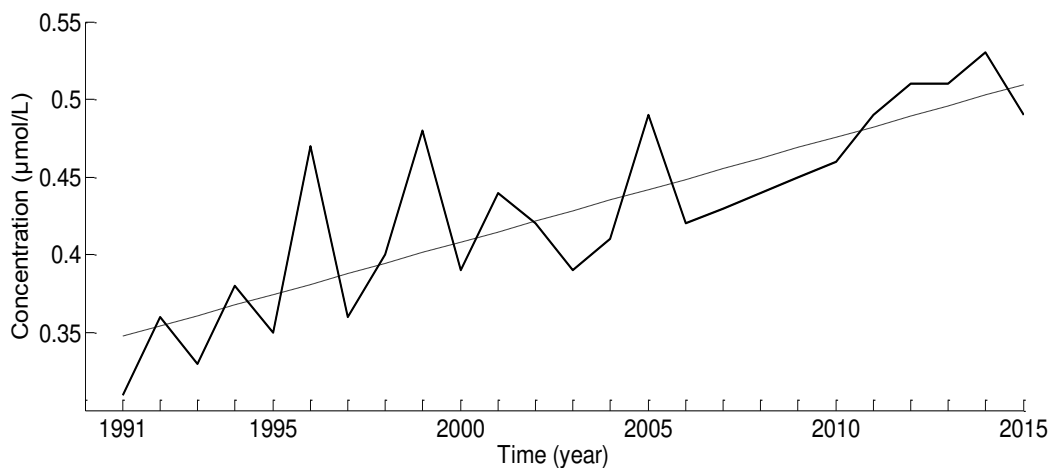


Figure 3. Interannual variations and long-term trends in DIP concentrations in the East China Sea

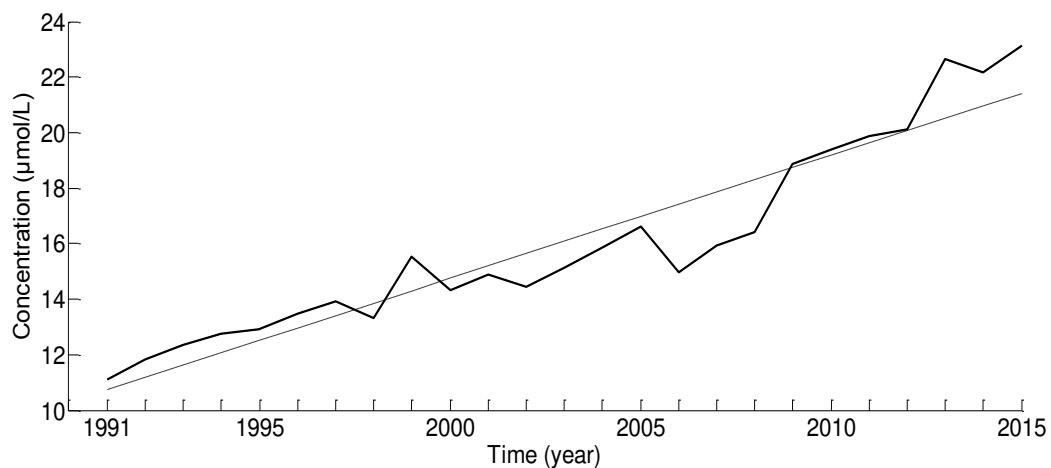


Figure 4. Interannual variations and long-term trends in DSi concentrations in the East China Sea

The nutrient content of samples collected at Datong Station on the Yangtze River exhibit a similar historical change to that of the East China Sea (Li et al., 2007), suggesting that annual variations in DIN and DIP in the East China Sea are synchronized with those of the Yangtze River estuary (Chen et al., 2011). As a result, we propose that the increase of DIN and DIP in the East China Sea is primarily attributable to runoff from the Yangtze River. Since 1996, the concentration of DIN and DIP in the East China Sea has increased significantly (Cao et al., 2014). Bing et al. (2019) analyzed velocity and nutrient data collected from satellite images and *in situ* measurements between 1993 and 2014 to study spatiotemporal variations in cross-shelf nutrient exchanges at the 200 m isobath. Average integrated nitrate transport (FQ) over this 22-year period is 22.0 ± 12.4 kmol/s (Bing et al., 2019). Furthermore, the on- and off-shelf components of FQ are roughly twice that of FQ itself, such that variations in FQ over time are primarily determined by the on-shelf component (Bing et al., 2019).

While interannual variations in FQ are greater than seasonal variations, no persistent interannual signal was identified (Bing et al., 2019). Our results show that this increase is also in line with a longer term gradual trend, which would suggest that these increases in nutrient concentrations are caused by long-term environmental changes. For example, the development of agriculture and the establishment of chemical industrial facilities along the coast and along the Yangtze River would tend to increase the input of nutrients from land sources, including runoff from the Yangtze River. Acting in contrast to this trend, the expansion of sewage processing facilities would tend to decrease the amount of coastal industrial pollutants and related inorganic nutrient directly discharged into the sea. Processes within the ocean, such as physical dilution by oceanic seawater and the absorption of nutrients by marine phytoplankton would also serve to modify nutrient concentrations in the East China Sea (Luo, 2006).

As concentrations of DIN, DIP and DSi change, derivative ratios such as N/P and Si/N also change (Li et al., 2007). It is generally considered that the proportion of C: Si: N: P suitable for diatom growth is 106: 16: 16: 1 (Xia et al., 2007), and that changes in nutrient concentrations affect the cell size and community composition of phytoplankton (Pätsch et al., 1997; Egge et al., 1998). Between 1991 and 2015, the N/P ratio of nutrients in the East China Sea increased gradually and then stabilized after 2009, exhibiting an asymmetric M-type pattern (Fig. 5). The maximum and minimum values of N/P appeared in 1997 and 2001, respectively, and their values were 28.44 and 15.41. Between 1991 and 2009, the average Si/N ratio in the East China Sea exhibited an asymmetric W-type fluctuation (Fig. 6). The maximum and minimum values of Si/N appeared in 2001 and 1997, respectively, and their values were 2.20 and 1.36. After 2009, the Si/N ratio gradually stabilized between 1.80 and 1.95.

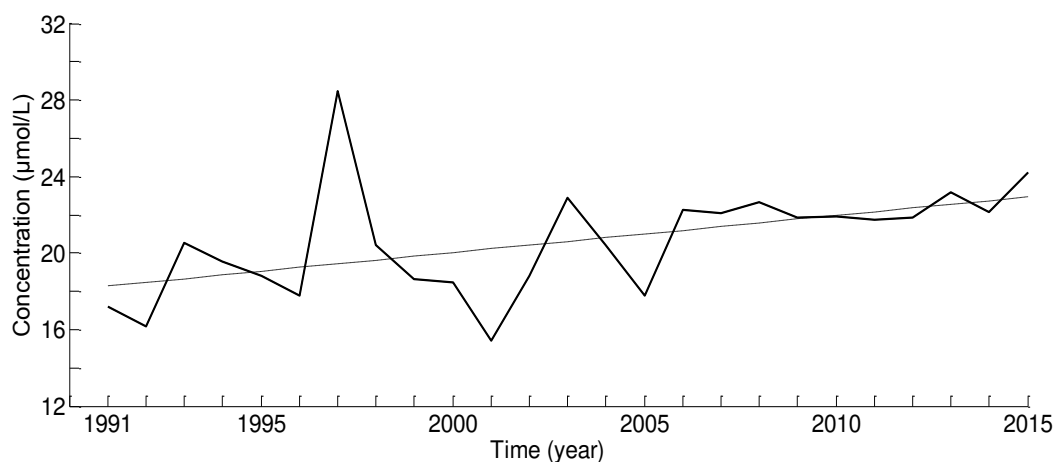


Figure 5. Interannual variations and long-term trends in the N/P ratio in the East China Sea

A large number of studies have shown that the value of N/P is closely related to the growth of phytoplankton (e.g., Chen et al., 2011). When plankton masses proliferate, although nitrogen and phosphorus are consumed in large quantities, inorganic nitrogen still maintains a high concentration. However, the proportion of N/P in the East China Sea was basically maintained at 21.93 ± 6.51 . This ratio is only slightly higher than that reported by Redfield (1958) and is largely attributable to the high concentration of inorganic nitrogen.

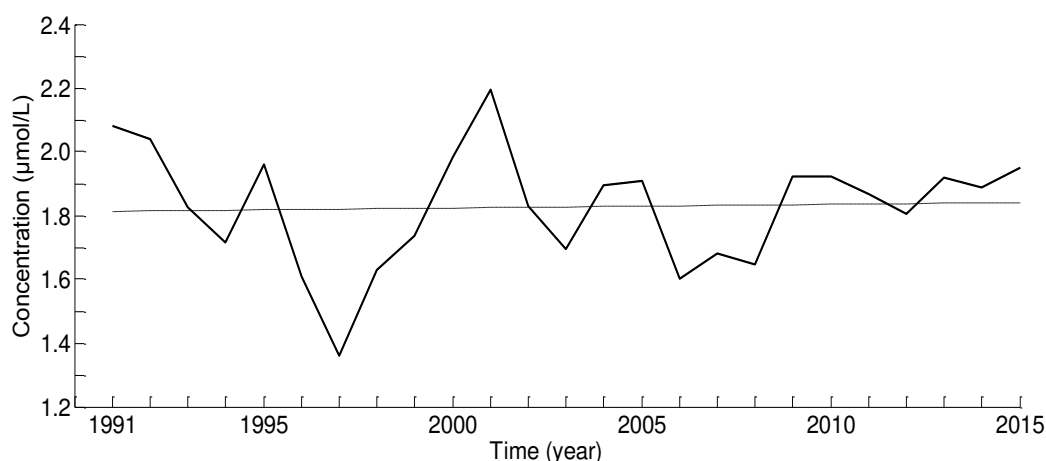


Figure 6. Interannual variations and long-term trends in the Si/N ratio in the East China Sea

The Si/N ratio in East China Sea is greater than 1. Therefore, DSi is not a limiting factor in the growth of diatoms. In recent years, changes in sediment transport have had a direct effect on the flux of dissolved silicate to the ocean (Humborg et al., 1997). However, our data show that despite high levels of interannual variation, the Si/N ratio of the East China Sea has been generally stable. Over the past twenty-five years, the N/P and Si/N ratios of seawater in the East China Sea show a trend of roundabout rise, and all tend to be stable. The interannual variation of nutrients in the East China Sea is becoming much more stable, which may be related to changes the runoff, sediment transport and the structure of N and P use in chemical fertilizers (Chen et al., 2011). This apparent stabilization is closely related to the relevant policies of the total pollution control of the marine environmental and the protection of the marine environment.

Distribution of nutrients in East China Sea District surface waters

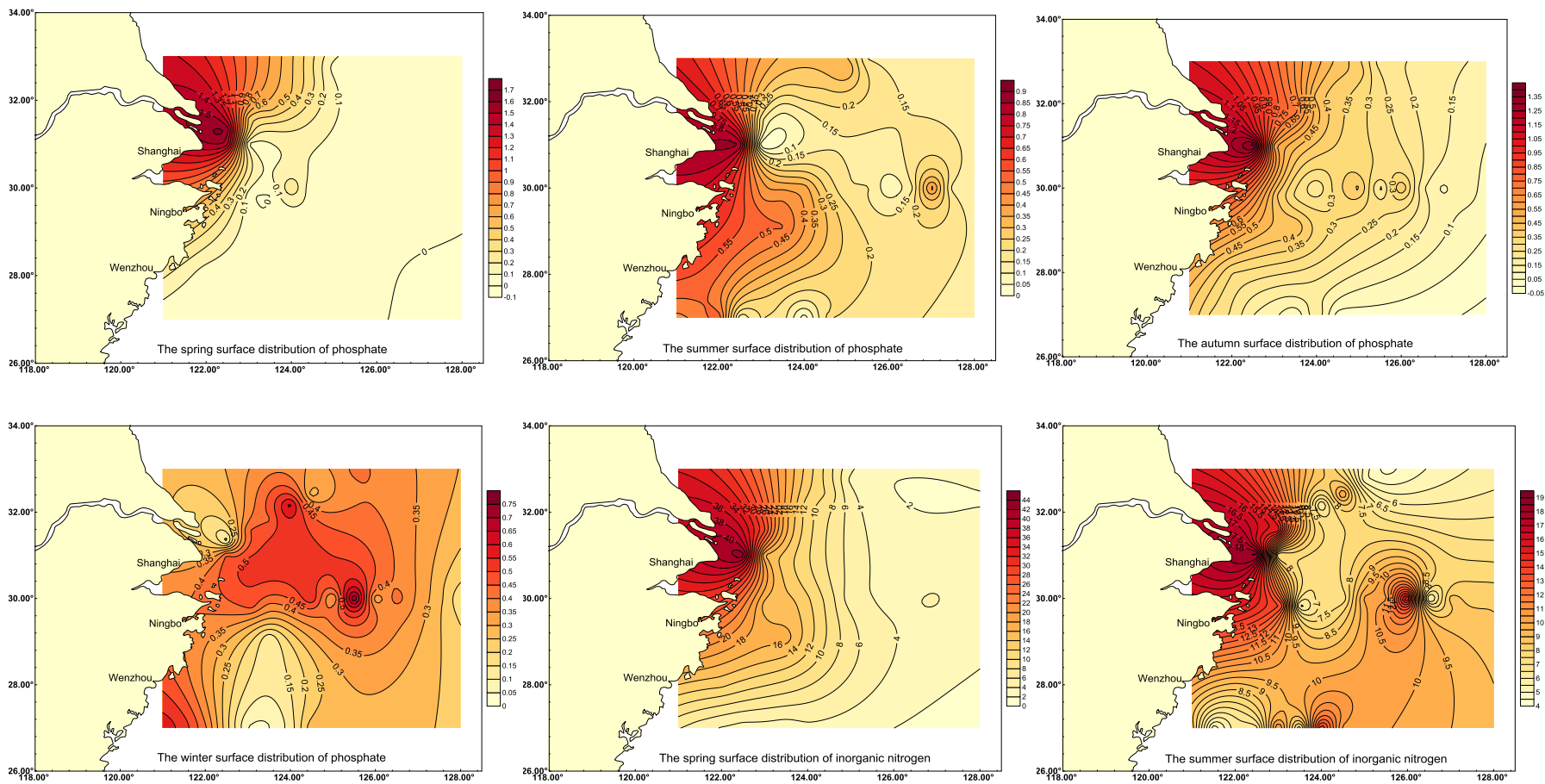
Figure 7 shows the planar distribution of phosphate, inorganic nitrogen, and silicate in the surface waters based on samples collected during the four research cruises. It can be seen from the figure that high surface concentrations of phosphate, inorganic nitrogen, and silicate in the East China Sea in the spring (May), summer (August), autumn (November) and winter (February) of 2015 appear in the waters of the Yangtze River estuary, and expand to form dense isolines. As the importance of oceanic waters increases with distance offshore, surface concentrations of phosphate, inorganic nitrogen, silicate gradually decrease. Controlling for location, surface concentrations of phosphate are higher in winter and autumn than in summer and spring. This pattern may be related to the gradual growth of surface water phytoplankton in the in the spring and the associated large amount of phosphate absorption. Surface concentrations of inorganic nitrogen were likewise higher in winter and autumn than in spring and summer. Surface concentrations of inorganic nitrogen increased in autumn and reached the highest value in winter before decreasing in spring, and reaching the lowest value in summer. Concentrations of DIN may be affected by the expansion of runoff from the Yangtze River. Areas of high DIN concentrations are centered around the Yangtze River estuary, whereas DIN concentrations generally decrease with distance from the estuary. The main reason for this structure of nutrients is the segregations of surface

waters from nutrient-rich deep waters over the summer and subsequent depletion of biogenic nutrients in surface waters (Ning et al., 1998). Surface concentrations of DSi are higher in summer and winter than in autumn and spring. The distribution of silicate in the waters of the Yangtze River estuary is basically the same as that of the Yangtze River, which extends as two tongues, one to the northeast and a second to the southeast, with a wide range of influence (Zhu et al., 2005).

Analysis of changes in nutrients

Changes in the distribution of nutrients in the East China Sea are closely related to seasonal variations in marine biological activities and internal biogeochemical nutrient cycling mechanisms. Nutrient concentrations are additionally controlled by complex circulation patterns in the East China Sea, which are strongly affected by seasonal variations in Yangtze River discharge and associated nutrient transport (Gao et al., 2004; Ye et al., 2017). Previous studies of nutrients in the East China Sea have indicated that the Kuroshio, Taiwan warm current, the Yellow Sea warm current and the Yangtze River estuary plume with its associated freshwater input greatly affect the distribution of nutrients and that substantial exchanges occur between these contrasting water masses (Wang et al., 2002; Chen et al., 2007).

The East China Sea is located in the East Asian monsoon region, which has exhibited a high rate of global environmental change. This leads to challenges in researching the dynamics of nutrient concentrations and related biogeochemical processes and marine ecosystems, which are strongly affected by complex monsoon-driven physical and chemical conditions (Liu et al., 2003). The outer sea area of the East China Sea is strongly influenced by the western side of the Taiwan warm current. Hence, contrasting concentrations of nutrients occur in the surface water and the bottom water. The invasion path of the Taiwan warm current into the East China Sea is characterized by a high level of nutrients in the bottom water (Wang et al., 2008). Nutrient concentrations in East China Sea surface water are primarily influenced by the input of freshwater from the Yangtze River, and high concentrations of nutrients occur in coastal surface waters of the Yangtze River estuary, as well as off the coasts of Zhejiang and Fujian provinces. Surface waters in the open ocean are greatly affected by the influence of the Kuroshio Current, where nutrient concentrations are generally low. Deeper waters are affected by the decomposition of organic matter, and nutrient concentrations generally increase with depth (Mi et al., 2012). The concentration of nitrate in the freshwater of the Yangtze River is high (the highest concentration is up to 100 $\mu\text{mol/L}$), but the concentration of phosphate is relatively low (Liu et al., 2008). As a result, the concentrations of nutrients in the sea area near the Yangtze River estuary is significantly larger than that of the middle and bottom layers. This further indicates that the main source of the nutrients into the East China Sea is the Yangtze River, and that phosphate concentrations in the East China Sea are primarily controlled by concentrations in the Yangtze River and the Taiwan warm current (Shi et al., 2003). Nutrient concentrations exhibit a decreasing trend from west to east or, alternatively, with distance offshore. The nutrient concentrations of DIN, DIP and DSi in the Kuroshio Subsurface Water and Kuroshio Intermediate Water are additionally quite high, indicating that these water masses, together with Changjiang Diluted Water (CDW), are probably important contributors to the nutrients inventories of the northeastern section of the East China Sea (Liu et al., 2017).



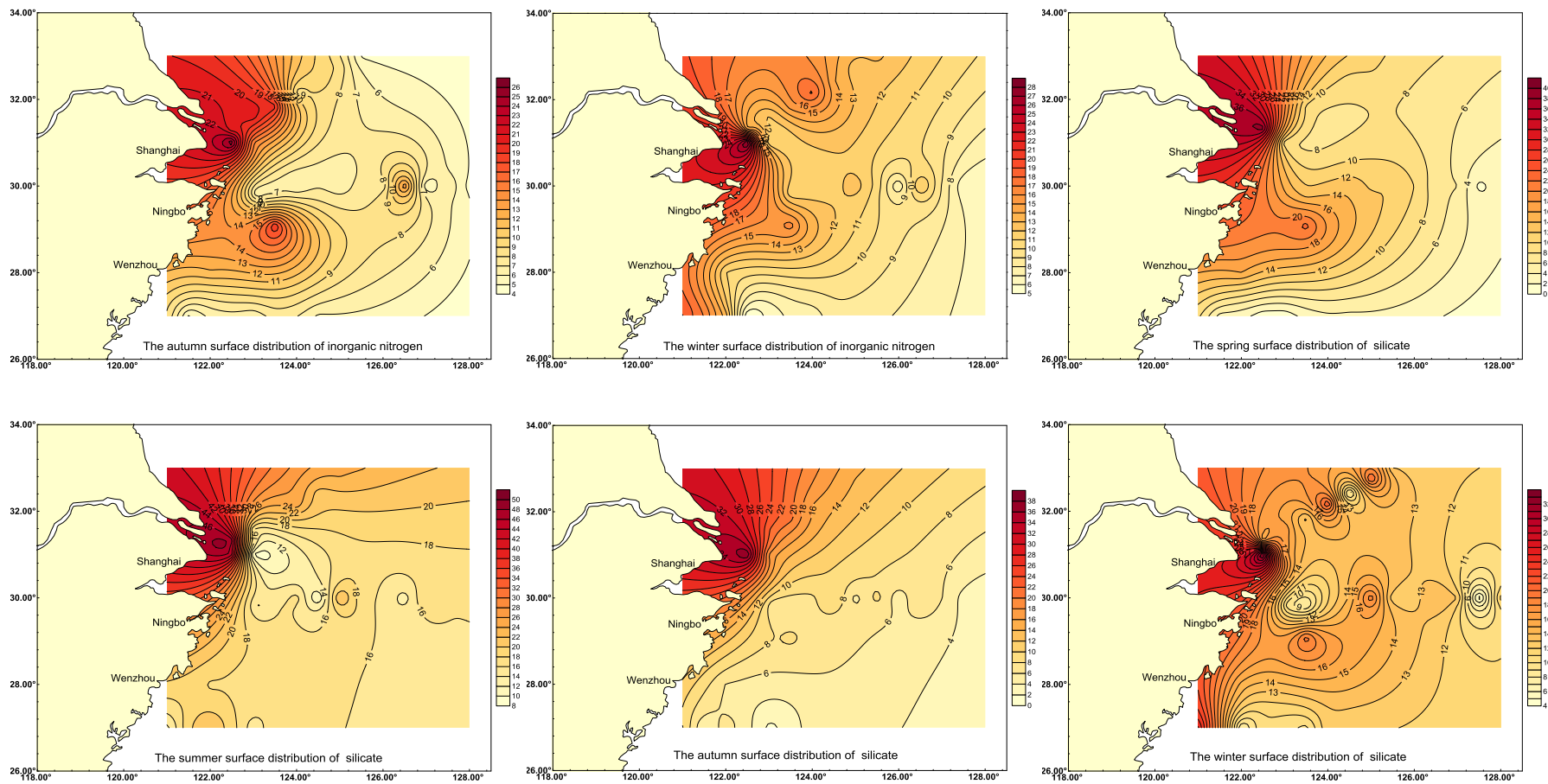


Figure 7. Seasonal distribution of phosphate, inorganic nitrogen and silicate in the East China Sea during the spring, summer, autumn and winter, 2015

Conclusion

Based on the analysis of nutrient concentrations in seawater samples taken along standard oceanographic sections in the East China Sea for nearly 25 years, we conclude that concentrations of DIN, DIP and DSi exhibit a gradual increase characterized by interannual variability. Concentrations of DIP, DIN and DSi range from 5.34–11.87 $\mu\text{mol/L}$, 0.31–0.53 $\mu\text{mol/L}$ and 11.12–23.15 $\mu\text{mol/L}$, respectively. From 1996, the concentrations of DIN, DIP and DSi increased significantly. In 2015, the annual average concentration of DIN in the East China Sea was ~ 2 times greater than in 1991, the annual average concentration of DIP was ~ 1.6 times greater, and the annual average DSi concentration was ~ 2 times greater. This increase in nutrient concentration primarily reflects increases in land-source emissions, physical dilution by ocean water and absorption of nutrients by phytoplankton. The N/P ratio of the East China Sea is generally stable and exhibits an asymmetric M-type fluctuation. The Si/N ratio is likewise generally stable and exhibits an asymmetric W-type fluctuation. This may be related to changes in runoff and sediment transport as well as changes in the N and P structure of chemical fertilizer over recent years. Certain policy changes, such as China's recent efforts to control China's total marine pollution and protect marine environments may also play a significant role.

The distribution of nutrients in the East China Sea exhibits clear seasonal variations. Concentrations of phosphate and inorganic nitrogen are higher in winter and autumn than that in summer and spring. Silicate concentrations are higher in summer and winter than in autumn and spring. The major source of nutrients into the East China Sea is the Yangtze River estuary plume. Consequently, nutrient concentrations decrease from west to east.

Despite the scale of this study, we advocate for the adoption of continued annual marine environmental monitoring, which will provide reliable data support for decision-making by China's marine environmental management departments. We additionally propose strengthening marine environmental monitoring and early warning systems and adherence to the strategy of sea and land pooling. Recognizing that data alone will not solve any environmental issues, we additionally advocate for the strengthening marine protection efforts and promoting these efforts through more widespread awareness and environmental education.

Acknowledgements. This work was supported by the Open Research Fund of State Key Laboratory of Estuarine and Coastal Research under contract No. SKLEC-KF201708; the Laboratory for Marine Geology, Qingdao National Laboratory for Marine Science and Technology under contract No. MGQNL201707; basic research program through the National Key Research and Development Program of China No. 2016YFC1402405; National Oceanic Administration East China Sea Branch Youth Marine Science of China No. 201803; the Natural Science Foundation of China under contract Nos 41776193 and 41876215; the Natural Science Foundation of Zhejiang Province under contract Nos LY17D060001 and LQ15D020001. This work was also supported by the K. C. Wong Magna Fund in Ningbo University. Finally, we thank Guy Evans, PhD, from Liwen Bianji, Edanz Editing China, for editing the English text of a draft of this manuscript.

REFERENCES

- [1] Cao, W., Cai, Y. H., Zhang, H. B. (2014): Analysis of nutrient distributions and potential eutrophication in seawater of the East China Sea nearly two decades. – *Journal of Zhejiang Ocean University (Natural Science)* 33: 251-256. (in Chinese).
- [2] Chen, C. C., Gong, G. C., Shiah, F. K. (2007): Hypoxia in the East China Sea: One of the largest coastal low-oxygen areas in the world. – *Marine Environmental Research* 64: 399-408.
- [3] Chen, H. M., Shun, C. X., Wu, Y. Q. (2011): Analysis on the change trend and influencing factors of nutrient structure in the Yangtze Estuary and its adjacent waters over the past 23 years. – *Marine Environmental Science* 30: 551-553. (in Chinese).
- [4] Chu, P., Chen, Y. C., Kuninaka, A. (2005): Seasonal variability of the yellow sea/east china sea surface fluxes and thermohaline structure. – *Advances in Atmospheric Sciences* 22(1): 1-20.
- [5] Ding, R. B., Huang, D. J., Xuan, J. L., Zhou, F., Thomas, P. (2019): Temporal and Spatial Variations of Cross-Shelf Nutrient Exchange in the East China Sea, as Estimated by Satellite Altimetry and In Situ Measurements. – *Journal of Geophysical Research: Oceans* 124: 1331-1356.
- [6] Egge, J. K. (1998): Are diatoms poor competitors at low phosphate concentrations? – *Journal of Marine Systems* 16: 191-198.
- [7] Gao, S. Q., Lin, Y. A., Jin, M. M. (2004): Distribution features of nutrients and nutrient structure in the East China Sea and the Yellow Sea in spring and autumn. – *Donghai Marine Science* 22: 38-50. (in Chinese).
- [8] Humborg, C., Ittekkot, V., Cociasu, A. (1997): Effect of Danube River dam on Black Sea biogeochemistry and ecosystem structure. – *Nature* 386: 385-388.
- [9] Li, D. J., Dag, D. (2004): Ocean pollution from land-based sources: East China Sea, China. *Ambio*. – *A Journal of the Human Environment* 33: 107-113.
- [10] Li, Y., Li, D. J., Tang, J. L. (2007): Distribution and change of phytoplankton in the Yangtze Estuary and adjacent sea area. – *Environmental science* 28: 719-729. (in Chinese).
- [11] Li, M. T., Xu, K. J., Watanabe, M. (2007): Long-term variations in dissolved silicate, nitrogen, and phosphorus from the Yangtze River into the East China Sea and impacts on estuarine ecosystem. – *Estuarine Coastal and Shelf Science* 71: 3-12.
- [12] Lin, C., Ning, X., Su, J. (2005): Environmental changes and the responses of the ecosystems of the Yellow Sea during 1976–2000. – *Journal of Marine Systems* 55: 223-234.
- [13] Liu, K. K., Tang, T. Y., Gong, G. C. (2000): Cross-shelf and along-shelf nutrient fluxes derived from flow fields and chemical hydrography observed in the southern East China Sea off northern Taiwan. – *Continental Shelf Research* 20: 493-523.
- [14] Liu, X. Q. (2001): Distribution features of TS and chemical constituents at the PN section in the East China Sea during summer. – *Oceanologia Et Limnologia Sinica* 32: 204-212. (in Chinese).
- [15] Liu, K. K., Peng, T. H., Shaw, P. T. (2003): Circulation & biogeochemical processes in the East China Sea and the vicinity of Taiwan. – *Deep Sea Research II* 50: 6-7.
- [16] Liu, Y. L., Gao, L., Liu, Y. L., Gong, G. C. (2017): Dynamics of nutrients in the Northeastern East China Sea in summer. – *Oceanologia Et Limnologia Sinica* 48: 733-744. (in Chinese).
- [17] Luo, R. X. (2006): Study on the ecological amplitude of nutrient limiting factors in the intersection of the Jialing River of the Changjiang River. – Master's thesis of Chongqing University 27: 65-66. (in Chinese).
- [18] Mi, T. Z., Yao, Q. Z., Meng, J. (2012): Distributions of nutrients in The Southern Yellow Sea and East China Sea in spring and summer 2011. – *Oceanologia Et Limnologia Sinica* 43: 678-68. (in Chinese).

- [19] Ning, X. R., Vaulot, D., Liu, Z. S., Liu, Z. L. (1988): Standing stock and production of phytoplankton in the estuary of Changjiang (Yangtze River) and the adjacent East China Sea. – *Marine Ecology Progress Series* 49: 141-150.
- [20] Pätsch, J., Radach, G. (1997): Long-term simulation of the eutrophication of the North Sea: temporal Development of nutrients, chlorophyll and primary production in comparison to observations. – *Journal of Sea Research* 38: 275-310.
- [21] Shi, X. Y., Wang, X. L., Han, X. R. (2003): Nutrient distribution and its controlling mechanism in the adjacent area of Chanjiang River estuary. – *Chinese Journal of Applied Ecology* 14: 1086-1092.
- [22] Wang, B. D., Zhan, R., Wang, J. Y. (2002): Distributions and transportation of nutrients in Changjiang River Estuary and its adjacent sea areas. – *Acta Oceanologica Sinica* 24: 53-58. (in Chinese).
- [23] Wang, X. L., Sun, X., Han, X. R. (2003): Comparison in macronutrient distributions and composition for high frequency hab occurrence areas in the East China Sea between summer and spring 2002. – *Oceanologia Et Limnologia Sinica* 35: 323-331. (in Chinese).
- [24] Wang, F., Shou, S. Z. (2008): Nitrate and phosphate conditions and fishery resources in the offshore area of the East China Sea. – *Resources Science* 30: 1592-1599.
- [25] Wang, Y. C., Guo, X. Y., Zhao, L., Zhang, J. (2019): Seasonal variations in nutrients and biogenic particles in the upper and lower layers of East China Sea Shelf and their export to adjacent seas. – *Progress in Oceanography* 176: 102138 (1-18).
- [26] Xia, P., Lu, D. D., Zhu, D. D. (2007): The trend and characteristics of the occurrence of red tide in the coastal waters of Zhejiang. – *Journal of Marine Sciences* 25: 47-56. (in Chinese).
- [27] Xu, H. Z., Ma, Y. A., Yu, T. (2007): Specifications for marine monitoring. – Beijing, China: 109-119. (in Chinese).
- [28] Yanzgi, T., Takahashi, S. (1993): Seasonal variation of circulations in the East China Sea and the Yellow Sea. – *Journal of Oceanography* 49: 503-520.
- [29] Ye, R., Liu, Y. Y., Cui, Y. P. (2015): Temporal and spatial distributions of nutrient structure and limitation on phytoplankton in The East China Sea. – *Oceanologia Et Limnologia Sinica* 46: 311-320. (in Chinese).
- [30] Ye, L. A., Wang, L. B., Jiang, Z. F. (2017): Seasonal variations in distribution characteristics of nutrients in the East China Sea in 2015. – *Journal of Shanghai Ocean University* 26: 354-361. (in Chinese).
- [31] Zhang, J., Guo, X. Y., Zhao, L. (2019): Tracing external sources of nutrients in the East China Sea and evaluating their contributions to primary production. – *Progress in Oceanography* 176: 102122 (1-18).
- [32] Zhu, J. R., Wang, J. H., Sheng, H. T. (2003): Observation and analysis of the mid to late 6 off the Changjiang River Estuary fresh water and red tide in 2003. – *Chinese Science Bulletin* 50: 59-65. (in Chinese).

MICROBIAL COMMUNITY STRUCTURE AND SEASONAL VARIATIONS IN MUDFLAT SEDIMENTS OF SANSHA BAY, CHINA

YANG, Z.¹ – WANG, Y. Z.¹ – WU, Z. C.¹ – REN, L. R.¹ – XIONG, C. J.² – MA, Y.^{1*}

¹*Key Laboratory of Healthy Mariculture for the East China Sea, Ministry of Agriculture, Fisheries College of Jimei University, Xiamen 361021, China*

²*College of Foreign Language, Hunan University, Changsha 410006, China*

**Corresponding author*

e-mail: maying@jmu.edu.cn; phone: +86-1896-5423-006; fax: +86-0592-6181-476

(Received 13th Jul 2019; accepted 25th Nov 2019)

Abstract. Illumina high-throughput sequencing was applied to study the microbial community structure and seasonal variations in the mudflat sediments of Sansha Bay, China. Significant seasonal differences of microbial communities were observed, and pH, total P, total N, and organic carbon concentration were important factors affecting the microbial communities. A total of 52 bacterial phyla were detected in the sediments, dominated by *γ-Proteobacteria* (27.78%), *δ-Proteobacteria* (20.16%) and Bacteroidetes (10.58%). A total of 717 bacterial genera were detected, and among the top 100 genera with the highest abundances, 48 genera changed significantly ($p < 0.05$) with seasons. The microbial community structure in summer was significantly different from others, and the environmental factors driving the changes were mainly temperature, organic carbon and total N concentration. The bacteria with higher abundances in summer were mainly attached bacteria, thermophilic bacteria, anaerobic bacteria, and those involved in carbon and nitrogen cycling, while in other seasons, those with higher abundances were mainly aerobic bacteria, which could adapt to low temperatures and are involved in the degradation of cellulose and chitosan. However, the physicochemical indexes didn't change significantly, which indicated that the bacterial communities are more sensitive and can serve as a good sentinel for environmental changes.

Keywords: *Illumina high-throughput sequencing, bacterial genetic diversity, seasonal changes, intertidal sediments, physicochemical characteristics, Sansha Bay*

Introduction

Traditionally, marine environmental quality is assessed by physical-chemical and biological indexes, such as dissolved oxygen (DO), chemical oxygen demand (COD), nitrogen (N), phosphorus (P), heavy metal, persistent pollutant, and so on (Arsad et al., 2012). However, such static indexes have difficulties characterizing the structure and function of the marine ecosystem (Viswanathan et al., 2010). At present, most of the biological indicators used to characterize ecosystem structure and function are large animals, plants or benthos (Cabana et al., 2013; Hannah, 2015; Wang et al., 2018), or some microscopically visible single-celled organisms, such as diatoms and cyanobacteria (Daby, 2006). Nevertheless, when the impact of the disturbance has caused obvious changes in these biological indicators, the time of early warning is long gone.

Microorganisms are one of the most important components of the intertidal zones of mudflat ecosystems, and are involved in nutrient cycling, energy flow, organic matter degradation, and pollutant removal. Microbial communities are sensitive to environmental variation, which makes them ideal biological indicators for environmental pollution and ecosystem changes (Sun et al., 2012). Total coliforms,

fecal coliforms (*Escherichia coli*) and enterococci have been commonly used as indicators to assess the microbiological safety of water resources (Lage and Bondoso, 2011). Previous studies also showed that there was a positive and strong association of total phosphorous, total nitrogen, and ammonium-nitrogen contents with microeukaryotes and Gram-positive bacteria (Zhao et al., 2010), and several metals are also strongly associated with microbial community composition (Cao et al., 2006). Although microorganisms are more sensitive to environmental changes and are better indicators for environmental quality, they have not been adopted as environmental quality indexes yet due to our poor understanding of them and the difficulty of detection. The emergence of molecular biological technique, especially the high-throughput sequencing, has provided us important opportunity for fully and deeply understand environmental microbes because of the high data throughput (10^3 – 10^6 sequences per sample), high accuracy and low cost. This technique enables us to identify the dominant and rare populations within a community simultaneously, thus it could reveal a significantly greater level of microbial diversity than conventional molecular tools (Binladen et al., 2007; Caporaso and Gordon, 2011).

Sansha Bay is a typical enclosed bay, which is located on the southeastern coast of Ningde City, Fujian Province, and includes Dongwuyang, Guanjingyang, and Sanduao. The streams and rivers from the eight surrounding cities, with a basin area of 8,700 km², flow into this harbor, containing the domestic sewage of over 2 million people (Tang et al., 2018). In recent years, due to the high discharge of domestic sewage and industrial wastewater as well as the large inflow of residual breeding bait, the mudflat environment has been subjected to substantial pollution. The main goals of the study are to investigate the community structure and seasonal variations of organisms in mudflat sediments of Sansha Bay, and their relationship to physicochemical indexes. The results present here will provide microbial parameters for assessing the environment quality, and to lay a foundation for further illumination of the ecological functions of microorganisms in mudflat sediments.

Methods

Sample collection and physicochemical index analysis

The study was performed in the Northern Yantian port of Sansha Bay (*Fig. A1*). The total area was about 2.6 acre, at an east longitude from 119.7975 to 119.7986 and a northern latitude from 26.8411 to 30.8422. The study area was divided into four plots, and sediment samples of each plot were collected on 10 October, 2014 (autumn), 2 January, 2015 (winter), 6 April 2015 (spring), and 2 July 2015 (summer). The sediments of the surface layer (top 3-5 cm) were removed and about 200 g subsurface sediments from three different sites within the same plot were collected and mixed as one sample, resulting in a total of 16 samples in four batches. The samples were termed as Oct-P1 to Oct-P4, Jan-P1 to Jan-P4, Apr-P1 to Apr-P4, Jul-P1 to Jul-P4, according to sampling time and sampling plots.

All the 16 sediment samples were used for the determination of the physicochemical indices, 10 g sediments of each sample were freeze-dried in a lyophilizer (Labconco, Kansas City, MO, USA). The following parameters were analyzed, and each sample was measured twice. Total nitrogen (TN) was determined via the Kjeldahl method (Bradstreet, 1954) and total phosphorus (TP) via the ammonium molybdate spectrophotometric method (GB11894-89, China; Huang,

2000). Organic matter contents (OrgC and OrgS) were determined via a Vario Max CNS analyzer (Elementar, Hanau, Germany). For the determination of pH, sediment and water were mixed at a ratio of 1:5 (W/V). Water temperature (T_m) was measured on the site.

DNA extraction, PCR amplification, and Illumina sequencing

For DNA extraction with the PowerSoil DNA Isolation Kit (MOBIO-Laboratories, USA), we used 0.25 g of the sediment samples. The V4 variable region in the bacterial 16S rRNA gene was amplified with the primer pair 515F (5'- GTG CCA GCM GCC GCG GTA A-3') and 806R (5'- GGA CTA CHV GGG TWT CTA AT-3'). The PCR products of the different samples were mixed with equimolar concentration and sent to the Majorbio Co. Ltd. (Shanghai) for paired-end sequencing through the Illumina Miseq platform.

Bioinformatic analysis

Post-processing of the Illumina sequence reads included quality control and clustering of the operational taxonomic unit (OTU) with 97% sequence identity. The QIIME was applied to collect the OTUs for sequence clustering, the chimeras were removed, and OTU abundance was defined. The RDP Bayesian classifier was applied to conduct taxonomic analyses on OUT-representative sequences with 97% similarity level; the classification was identified in the Silva database (Release128 <http://www.arb-silva.de>), and the community composition of each sample was analyzed at each classification level, including phylum, class, order, family, genus, and OTU.

Mothur software was used to analyze alpha diversity. Community diversity was estimated by Shannon (Magurran, 1988) and Simpson (Simpson, 1949) indices. The total number of species in each sample was estimated with Chao1 and Ace. Phylogenetic diversity (PD) whole tree was used to analyze the relationships among observed species. Sampling coverage was used to evaluate whether the sequencing quantity is enough.

Hierarchical clustering was analyzed by the unweighted pair group method with arithmetic (UPGMA). Student's *t*- test was used to test the significant difference of alpha diversity in different season, and one-way ANOVA was used to test the differences of physicochemical factors or bacterial communities at the phylum and genus levels. All statistical analyses were carried out using software SPSS 18.0 or stats packages in the R environment (version 3.2.2, <http://www.r-project.org>) (R Development Core Team, 2008).

Redundancy Analysis (RDA) was used to reveal the relationship between physicochemical factors and bacterial community composition (Wollenberg, 1977). Forward selection of physicochemical factors was performed by Monte Carlo test with 999 permutations. The Partial Mantel test was also applied to distinguish the relative contribution of time variables (Legendre et al., 2016). RDA was carried out using rda packages in R environment. The original sequence data obtained was submitted to the NCBI SRA database with the registration number PRJNA505598.

Results

Sequencing results and alpha diversity analysis

We obtained a total of 533,568 effective high-quality sequences, which were classified into 65,517 OTUs, with an average of $4,095 \pm 346.52$ OTUs in each sample. Sequence homogenization was conducted to obtain 30,000 sequences in each sample, followed by alpha diversity analysis; the results are shown in *Table 1*. The coverage of each sample was over 96%, indicating that most bacterial groups could be determined. However, the sequencing depth did not reach saturation, which indicates that the microflorae in the sediment of Sansha Bay was highly abundant. The Shannon index values ranged from 6.31 to 7.02, while the PD index varied between 179.61 and 242.73. The diversity index variations in each sample were not significantly different ($p > 0.05$, *Table A1*) among the different seasons.

Table 1. Alpha diversity indicators (OTU, Shannon, Simpson, ACE, Chao1, PD and coverage) of bacterial communities in mudflat sediments of Sansha Bay

Sample name	OTUs	Shannon	Simpson	ACE	Chao1	PD	Coverage	Sampling date
Oct-P1	4056	6.70	0.0050	5717.53	5640.81	218.68	0.96	October 10, 2014
Oct-P2	4388	6.85	0.0042	6145.69	6067.05	232.08	0.96	
Oct-P3	3877	6.57	0.0057	5537.69	4987.95	207.8	0.96	
Oct-P4	3662	6.61	0.0048	5073.19	5384.34	195.33	0.97	
Average	3996	6.68	0.0049	5618.53	5520.04	213.47	0.96	
Jan-P1	4366	6.84	0.0041	6065.44	6336.64	229.15	0.96	January 2, 2015
Jan-P2	4074	6.61	0.0065	5654.31	6266.61	215.66	0.96	
Jan-P3	4093	6.65	0.0055	5719.33	5590.49	214.78	0.96	
Jan-P4	4695	7.02	0.0036	6220.91	5766.58	242.73	0.96	
Average	4307	6.78	0.0049	5915.00	5990.08	225.58	0.96	
Apr-P1	3615	6.37	0.0073	5344.25	5611.13	187.63	0.96	April 6, 2015
Apr-P2	4199	6.73	0.0053	5628.99	5205.31	218.65	0.96	
Apr-P3	4349	6.70	0.0060	6031.25	5981.72	226.72	0.96	
Apr-P4	3875	6.63	0.0052	5620.25	5765.90	207.17	0.96	
Average	4010	6.61	0.0060	5656.19	5641.01	210.04	0.96	
Jul-P1	4332	6.83	0.0044	5990.67	6200.28	226.44	0.96	July 2, 2015
Jul-P2	4363	6.92	0.0038	5853.22	6056.11	223.84	0.96	
Jul-P3	4218	6.87	0.0037	5990.22	6040.11	220.84	0.96	
Jul-P4	3355	6.31	0.0077	4816.68	4801.49	179.61	0.97	
Average	4067	6.73	0.0049	5662.70	5774.49	212.68	0.96	

Oct, Jan, Apr and Jul indicate sampling times; P1, P2, P3 and P4 represent four different sampling plots. OUT represent operational taxonomic unit, PD represent phylogenetic diversity

Beta diversity

According to the beta diversity distance matrix, hierarchical clustering analysis was conducted at different classification levels, and the UPGMA algorithm was used to construct the tree structure (*Fig. 1*). *Figure 1* shows that the clustering results were not stable at the phylum and class levels. However, from the order to the OTU level, except for sample Jan-P4, the other samples were clustered into four categories according to the sampling time; the most significant difference was observed between the summer sample and other samples, while the differences were lower among spring, autumn, and winter samples.

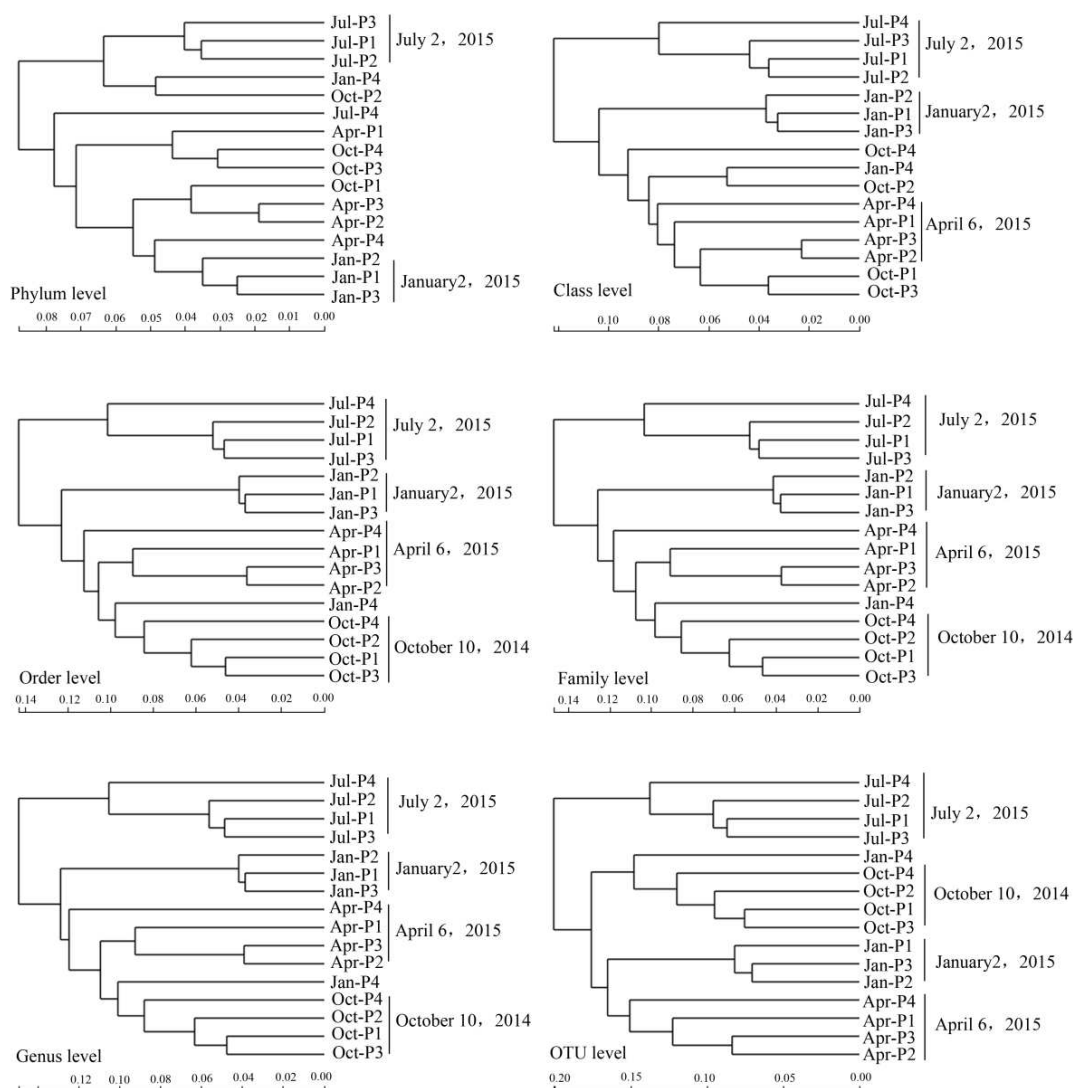


Figure 1. Clustering analysis diagram of mudflat sediment samples from Sansha Bay, China (Oct, Jan, Apr and Jul indicate sampling times; P1, P2, P3 and P4 represent four different sampling plots)

Microbial community structure and seasonal changes in mudflat sediments in Sansha Bay

Microbial community structure and dynamic changes at the phylum level

We detected a total of 52 bacterial phyla in the mudflat sediments of Sansha Bay (Fig. 2). The dominant microbial phylum was *Proteobacteria*, and the proportions of γ -*Proteobacteria*, δ -*Proteobacteria* and α -*Proteobacteria* in the total sequences were 27.78, 20.16 and 4.36%, respectively. The subdominant phylum *Bacteroidetes* accounted for 10.58% of the total sequences. The other abundant phyla were *Planctomycetes* (5.09%), *Chloroflexi* (4.95%), *Acidobacteria* (3.65%), *Nitrospirae* (2.38%), *Cyanobacteria* (2.10%), *Gemmatimonadetes* (1.94%), *Verrucomicrobia* (1.59%), and *Latescibacteria* (1.01%). The proportions of the other 42 bacterial phyla, including *Spirochaetae*, *Actinobacteria*, and *Ignavibacteriae*, were always below 1%.

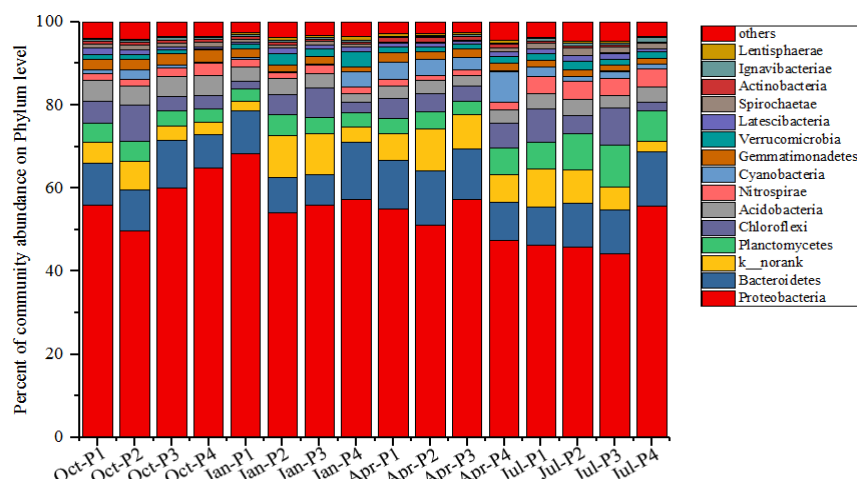


Figure 2. Microbial communities in mudflat sediments of Sansha Bay, China, at the phylum level (Oct, Jan, Apr and Jul indicate sampling times; P1, P2, P3 and P4 represent four different sampling plots)

Of the 52 bacterial phyla, 14 showed significant differences ($p < 0.05$, Table A2) among the different sampling seasons. Compared with the other seasons, the abundances of nine phyla were significantly increased in summer, including *Planctomycetes*, *Nitrospirae*, *Spirochaetae*, *Ignavibacteriae*, *Hydrogenedentes*, *KSB3_Modulibacteria*, *Chlorobi*, *Tenericutes*, and *PAUC34f*. In contrast, the abundances of two phyla, *Actinobacteria* and *Armatimonadetes*, were significantly increased in winter.

Microbial community structure and dynamic changes at the genus level

A total of 717 bacterial genera were detected in the sediments of Sansha Bay. The dominant microbial genus that could be identified was *Desulfobulbus*, which occupied 4.97%. The subdominant genera were *Nitrospira* (2.34%) and *Sva0081_sediment_group* (1.73%). Most of the genera occupied less than 1%, including *Halioglobus*, *Draconibacterium*, *Deferrisoma*, *Spirochaeta*, *Urania-1B-19_marine_sediment_group*, *Haliaea*, *Desulfatiglans*, *Aquibacter* and so on. In addition, unclassified genera also occupied a large proportion, such as *c_Gammaproteobacteria* (occupied 6.69%), *f_JTB255_marine_benthic_group* (6.22%) and *o_Gammaproteobacteria_Incertae_Sedis* (4.32%), etc.

Among the top 100 genera with the highest abundances, 48 genera showed significant variations ($p < 0.05$, Table A3). The clustering results of the heat map (Fig. 3) also indicated significant seasonal differences in the microbial community structures, with more significant differences between summer and other seasons and smaller differences among spring, autumn, and winter. Compared with the samples from the other seasons, in summer, 13 genera showed significantly higher abundances, including *Nitrospira*, *f_Flammeovirgaceae*, *Deferrisoma*, *Spirochaeta* and *f_Lentimicrobiaceae*, etc., while in winter, genera *Aquibacter*, *Kangiella*, *Lutibacter* and other 9 genera increased significantly. In autumn, 14 genera increased significantly, including *Haliaea*, *Desulfatiglans*, *Sulfurovum*, *Robiginitalea*, and *Haliangium*, etc., while only *Halioglobus* and other 8 genera increased significantly in spring.

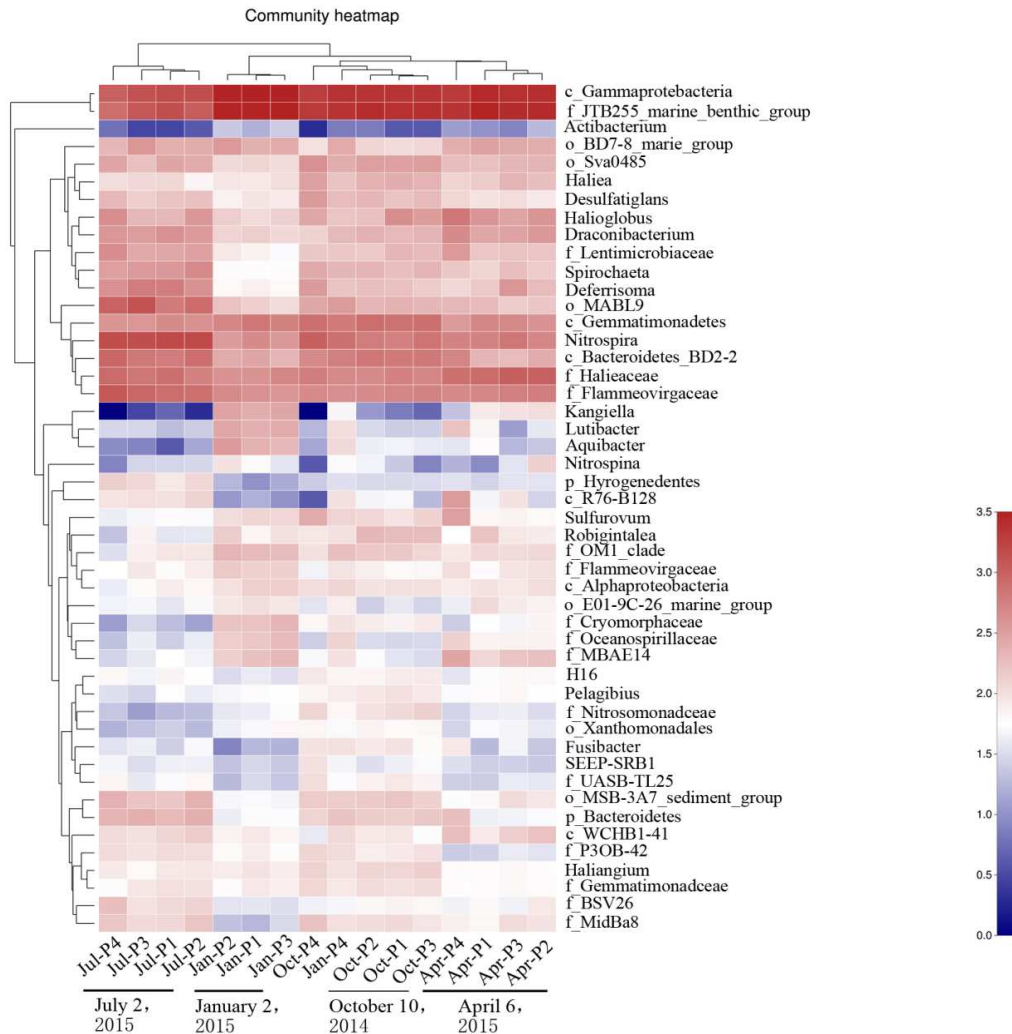


Figure 3. Heatmap of the microbial communities in mudflat sediments of Sansha Bay, China, at the genus level. (Oct, Jan, Apr and Jul indicate sampling times; P1, P2, P3 and P4 represent four different sampling plots)

Physicochemical indices of mudflat sediments in Sansha Bay and the relationships with microbial communities

The values of the physicochemical indices are shown in *Figure 4*. In the different sampling seasons, pH ranged from 8.37 to 8.59, with highest values in spring and lowest values in winter. Temperature varied between 12.61 and 30.06°C, with highest values in summer and lowest values in winter, and the difference between summer and winter had reached a significant level ($p < 0.05$, *Table A4*). Furthermore, organic carbon, total nitrogen, and total phosphorus concentrations were also highest in summer, while the organic sulfur levels were lowest in summer and highest in winter. However, except for the temperature, all these differences among other physicochemical indices were not statistically significant.

At the genus level, the microbial communities were used as indicators for environmental changes applying redundancy analysis (RDA), and six physicochemical indices of the sediment, including TP, TN, OrgC, OrgS, Tm, and pH, were used as

explanatory variables (Fig. 5). The RDA1 and RDA2 explained 76.48 and 3.74% of the total variance, respectively. At the genus level, the microbial community structure in summer differed most significantly from those of the other seasons, followed by the community structure in spring. In contrast, the communities in winter and autumn showed a higher similarity. TP, TN, OrgC, Tm, and pH were important factors affecting the microbial community structure and were correlated ($p < 0.05$) or highly correlated ($p < 0.01$) with microbial community structure (Table A5).

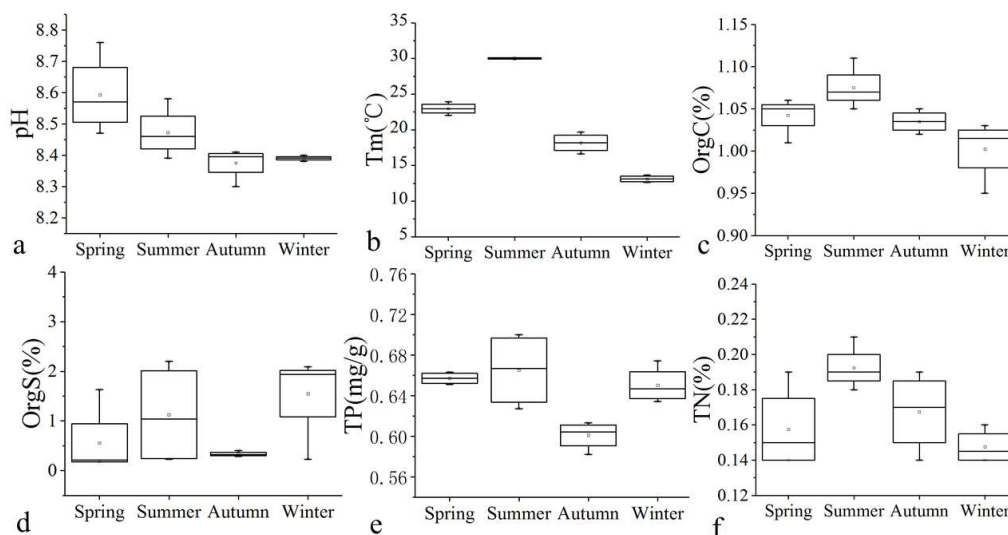


Figure 4. Physicochemical indices of mudflat sediments in Sansha Bay, China. (a) pH, (b) Temperature ($^{\circ}\text{C}$), (c) Organic carbon (%), (d) Organic sulfur (%), (e) Total phosphorus (mg/g), (f) Total nitrogen (%)

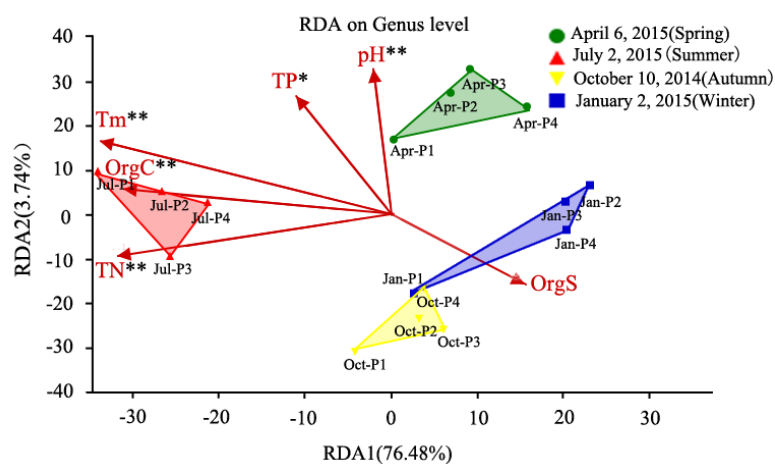


Figure 5. Relationships between microbial communities and environmental factors in Sansha Bay sediments (TN, TP, OrgC, OrgS and Tm represent total nitrogen, total phosphorus, Organic carbon, sulfur contents and water temperature, respectively. Oct, Jan, Apr and Jul indicate sampling times; P1, P2, P3 and P4 represent four different sampling plots. Arrow direction represents the direction of increasing environmental factors. * and ** represent significance levels of 0.05 and 0.01, respectively)

Discussion

Previous studies have indicated temperature is an important factor influencing microbial diversity in mudflat sediments (Hicks et al., 2018). The seasonal differences of microorganisms in mudflat sediments of Sansha Bay were significant, and the summer samples most significantly differed from the samples taken in the other seasons. This was consistent with the significantly higher water temperature in Sansha Bay at summer, indicating a highly significant correlation between temperature and microbial communities. Temperature was also an important factor affecting phytoplankton communities, and in a previous study, the phytoplankton density increased with increasing water temperatures (Wang et al., 2015). While, the higher phytoplankton density results in the release of higher amounts of dissolved organic matter, directly affecting the microbial community structure (Shabarova et al., 2017). Also it can be seen in Fig. 5, TN and OrgC were significantly correlated with the microbial community structure and had the highest impacts on microbial communities in summer.

In terms of microbial community composition, the abundance of *Planctomycetes* was significantly higher in summer, and most of them are attached bacteria (Caporaso and Gordon, 2011). The significant increase of such bacteria in summer might be related to the generally higher biomass levels in summer. Bacteria which were significantly increased in summer included those involved in nitrogen or carbon cycles, such as *Nitrospirae* and *Nitrospira*, which are important nitrite-oxidizing bacteria. The phylum *Spirochaetae* is mainly composed of anaerobic heterotrophic microorganisms, which are involved in lignocellulose degradation and nitrogen fixation (Chen et al., 2017a). *Chlorobi* is a strictly anaerobic photoautotrophic bacterium and able to fix CO₂. The higher input rates of N and P, the lower the relative abundance of *Chlorobi* (Ling et al., 2017). The phylum *Ignavibacteria* consists of strictly organotrophic, facultatively anaerobic bacteria which are divided from *Chlorobi*. They play an important role in the degradation of polycyclic aromatic hydrocarbons (PAHs) and in the removal of organic matter (Kadnikov et al., 2013). Some bacteria in *Hydrogenedent* are involved in key geochemical processes including sulfur, nitrogen, and carbon cycles and generally survive in dark and hypoxic sub-surface biospheres (Momper et al., 2018). Most of the genera with significantly increased abundances in summer are thermophilic microorganisms. For example, the optimum growth temperature of *Deferrisoma* is 50°C, while both *Nitrospira* and *Draconibacterium* can survive temperatures above 30°C, corresponding to the relatively high temperatures in summer (Du et al., 2015; Hoshino et al., 2016; Daims and Wagner, 2018).

The bacterial species with increased abundances in the other seasons were mainly aerobic bacteria and involved in the degradation of cellulose and chitosan. In winter, the abundance of *Actinobacteria*, which can adapt to lower temperatures, was significantly increased, and they played important roles in carbon cycling and the decomposition of cellulose and chitosan (Aparicio et al., 2018). *Armatimonadetes*, a group of aerobic oligotrophic soil bacteria with a wide distribution, was chemoautotrophic and involved in the degradation of photosynthetic biomass (Hu et al., 2014). Previous studies have found that *Armatimonadetes* might also be involved in hydrolysis-fermentation and the degradation of cellulose (Lee et al., 2014). The abundance of genera *Lutibacter* and *Aquibacter* in the family *Flavobacteriaceae* are also significantly increased in the winter. *Flavobacteriaceae* can degrade high-molecular-weight organic polymers, including cellulose, chitosan, and proteins (Wissuwa et al., 2017), while *Kangiella* can

use lignocellulose degrade by-products derived from it, facilitating the degradation of rhizome residues in sediments (Darjany et al., 2014). The increased abundances of these bacteria in winter might be related to the lower temperatures, decreased organic nutrient content, increased dissolved oxygen levels, as well as the relatively higher contents of animal and plant residues. *Gemmatimonadetes*, with a significantly higher abundance in autumn, are common soil bacteria and can adapt to low humidity levels; they are an indicator for semiarid ecosystems (Genderjahn et al., 2018); this corresponds to the decrease in relative humidity in autumn. *Halioglobus*, with a significantly increased abundance in spring samples, is a Gram-negative aerobic bacterium and can reduce nitrate into N₂ (Chen et al., 2017b).

Conclusion

The microbial community structure in the Sansha Bay sediments presented significant seasonal variations, with the most significant differences in summer. The environmental factors driving this microbial community variation were mainly temperature, but also organic carbon and total nitrogen concentrations. However, no significant differences were observed in physicochemical indexes among different seasons, this indicated that the bacterial communities are more sensitive and can serve as a good sentinel for environmental changes. The results present here provide microbial parameters for assessing the environment quality, and to lay a foundation for further illumination of the ecological functions of microorganisms in intertidal sediments. However, most of our discussions regarding the bacterial functions derived from previous studies, clearly a combination of the high throughput sequencing approach presented here and isolation and characterization of the indicator bacteria will both be required in the future to better understand microbial functionality. Furthermore, numerous microbial groups detected in this study were uncategorized or unidentified, and their physiological functions needed to be further investigated.

Acknowledgments. The authors would like to thank the NSFC project (31272669) and the Public Science and Technology Research Funds Projects of Ocean (201205009-4) for funding support for the present research.

REFERENCES

- [1] Aparicio, J. D., Saez, J. M., Raimondo, E. E., Benimeli, C. S., Polti, M. A. (2018): Comparative study of single and mixed cultures of actinobacteria for the bioremediation of co-contaminated matrices. – Journal of Environmental Chemical Engineering 6(2): S2213343718301519.
- [2] Arsad, A., Abustan, I., Rawi, C. S., Syafalni, S. (2012): Integrating Biological Aspects into River Water Quality Research in Malaysia: An Opinion. – Social Science Electronic Publishing.
- [3] Binladen, J., Gilbert, M. T. P., Bollback, J. P., Panitz, F., Bendixen, C., Nielsen, R., Willerslev, E. (2007): The use of coded PCR primers enables high-throughput sequencing of multiple homolog amplification products by 454 parallel sequencing. – Plos One 2(2): e197.
- [4] Bradstreet, R. B. (1954): Kjeldahl Method for Organic Nitrogen. – Analytical Chemistry 26(1): 185-187.

- [5] Cabana, D., Sigala, K., Nicolaidou, A., Reizopoulou, S. (2013): Towards the implementation of the Water Framework Directive in Mediterranean transitional waters: the use of macroinvertebrates as biological quality elements. – *Advances in Oceanography & Limnology* 4(2): 212-240.
- [6] Cao, Y., Cherr, G. N., Córdova-Kreylos, A. L., Fan, T. W.-M., Green, P. G., Higashi, R. M., LaMontagne, M. G., Scow, K. M., Vines, C. A., Yuan, J., Holden, P. A. (2006): Relationships between Sediment Microbial Communities and Pollutants in Two California Salt Marshes. – *Microbial Ecology* 52(4): 619-633.
- [7] Caporaso, J. G., Gordon, J. I. (2011): Global patterns of 16s rRNA diversity at a depth of millions of sequences per sample. – *Proc Natl Acad Sci USA* 108.
- [8] Chen, C., Xu, X. J., Xie, P., Yuan, Y., Zhou, X., Wang, A. J., Lee, D. J., Ren, N. Q. (2017a): Pyrosequencing reveals microbial community dynamics in integrated simultaneous desulfurization and denitrification process at different influent nitrate concentrations. – *Chemosphere* 171: 294-301.
- [9] Chen, Z., Wuang, G., Dan, W., Fang-Kun, S. I. (2017b): Analysis on Change Characteristic of Autumn Relative Humidity in China. – *Modern Agricultural Science & Technology*.
- [10] Daby, D. (2006): Coastal Pollution and Potential Biomonitors of Metals in Mauritius. – *Water Air & Soil Pollution* 174(1-4): 63-91.
- [11] Daims, H., Wagner, M. (2018): Nitrospira. – *Trends in Microbiology* 26(5): 462-463.
- [12] Darjany, L. E., Whitcraft, C. R., Dillon, J. G. (2014): Lignocellulose-responsive bacteria in a southern California salt marsh identified by stable isotope probing. – *Frontiers in Microbiology* 5(6): 263.
- [13] Du, J., Lai, Q., Xie, Y., Liu, Y., Shao, Z., Dong, C. (2015): *Draconibacterium sediminis* sp. nov., isolated from river sediment. – *International Journal of Systematic & Evolutionary Microbiology* 65(7): 2310.
- [14] Genderjahn, S., Alawi, M., Mangelsdorf, K., Horn, F., Wagner, D. (2018): Desiccation- and Saline-Tolerant Bacteria and Archaea in Kalahari Pan Sediments. – *Frontiers in Microbiology* 9.
- [15] Hannah, T. I. (2015): Influence of landscape- and stand-scale factors on avian communities in open pine ecosystems. – *Dissertations & Theses - Gradworks*.
- [16] Hicks, N., Liu, X., Gregory, R., Kenny, J., Lucaci, A., Lenzi, L., Paterson, D. M., Duncan, K. R. (2018): Temperature driven changes in benthic microbial diversity influences biogeochemical cycling in coastal sediments. – *Frontiers in Microbiology* 9.
- [17] Hoshino, T., Kuratomi, T., Morono, Y., Hori, T., Oiwane, H., Kiyokawa, S., Inagaki, F. (2016): Ecophysiology of Zetaproteobacteria Associated with Shallow Hydrothermal Iron-Oxyhydroxide Deposits in Nagahama Bay of Satsuma Iwo-Jima, Japan. – *Frontiers in Microbiology* 6(386): 1554.
- [18] Hu, Z. Y., Wang, Y. Z., Im, W. T., Wang, S. Y., Zhao, G. P., Zheng, H. J., Quan, Z. X. (2014): The First Complete Genome Sequence of the Class Fimbriimonadia in the Phylum Armatimonadetes. – *Plos One* 9(6): e100794.
- [19] Huang, X. F. (2000): *Survey, Observation and Analysis of Lake Ecology*. – China Standard Press, Beijing.
- [20] Kadnikov, V. V., Mardanov, A. V., Podosokorskaya, O. A., Gavrilov, S. N., Kublanov, I. V., Beletsky, A. V., Bonch-Osmolovskaya, E. A., Ravin, N. V. (2013): Genomic analysis of *Melioribacter roseus*, facultatively anaerobic organotrophic bacterium representing a novel deep lineage within Bacterioidetes/Chlorobi group. – *Plos One* 8(1): e53047.
- [21] Lage, O. M., Bondoso, J. (2011): Planctomycetes diversity associated with macroalgae. – *Fems Microbiology Ecology* 78(2): 366-375.
- [22] Lee, C. Y., Morgan, X. C., Dunfield, P. F., Tamas, I., McDonald, I. R., Stott, M. B. (2014): Genomic analysis of *Chthonomonas calidirosea*, the first sequenced isolate of the phylum Armatimonadetes. – *Isme Journal* 8(7): 1522-1533.

- [23] Legendre, P., Fortin, M., Borcard, D. (2016): Should the mantel test be used in partial analysis? – *Methods Ecol. Evol.* 6(11): 1239-1247.
- [24] Ling, N., Chen, D., Guo, H., Wei, J., Bai, Y., Shen, Q., Hu, S. (2017): Differential responses of soil bacterial communities to long-term N and P inputs in a semi-arid steppe. – *Geoderma* 292: 25-33.
- [25] Magurran, A. E. (1988): *Ecological diversity and its measurement.* – Princeton, NJ: Princeton University Press.
- [26] Momper, L., Aronson, H. S., Amend, J. P. (2018): Genomic description of ‘Candidatus Abyssobacterium’ a novel subsurface lineage within the candidate phylum Hydrogenedentes. – *Frontiers in Microbiology* 9.
- [27] Okeke, B. C., Thomson, M. S., Moss, E. M. (2011): Occurrence, molecular characterization and antibiogram of water quality indicator bacteria in river water serving a water treatment plant. – *Science of The Total Environment* 409(23): 4979-4985.
- [28] R Development Core Team (2008): *R: A language and environment for statistical computing.* – In: R Foundation for Statistical Computing, Vienna, Austria, (ISBN 3-900051-07-0).
- [29] Shabarova, T., Kasalický, V., Šimek, K., Nedoma, J., Znachor, P., Posch, T., Pernthaler, J., Salcher, M. M. (2017): Distribution and ecological preferences of the freshwater lineage LimA (genus *Limnohabitans*) revealed by a new double hybridisation approach. – *Environmental Microbiology* 19(3): 1296.
- [30] Simpson, E. H. (1949): Measurement of diversity. – *Nature* 163: 688.
- [31] Sun, M. Y., Dafforn, K. A., Brown, M. V., Johnston, E. L. (2012): Bacterial communities are sensitive indicators of contaminant stress. – *Marine Pollution Bulletin* 64(5): 1029-1038.
- [32] Tang, F. Y., Wang, J. H., Chen, H., Hang, B. L., Chen, Y. (2018): Community structure of phytoplankton and its relationship with environmental factors of Sansha Bay in spring. – *Journal Of Shanghai Ocean University* 04: 522-530. (in Chinese).
- [33] Van den Wollenberg, A. L. (1977): Redundancy analysis an alternative for canonical correlation analysis. – *Psychometrika* 42(2): 207-219.
- [34] Viswanathan, S., Voss, K. A., Pohlman, A., Gibson, D., Purohit, J. (2010): Evaluation of the biocriteria of streams in the San Diego Hydrologic Region. – *Journal of Environmental Engineering* 136(6): 627-637.
- [35] Wang, L., Wang, C., Deng, D. G., Zhao, X. X., Zhou, Z. Z. (2015): Temporal and spatial variations in phytoplankton: correlations with environmental factors in Shengjin Lake, China. – *Environmental Science & Pollution Research* 22(18): 1-13.
- [36] Wang, N., Xiong, J. Q., Wang, X. C., Zhang, Y., Liu, H., Zhou, B., Pan, P., Liu, Y., Ding, F. (2018): Relationship between phytoplankton community and environmental factors in landscape water with high salinity in a coastal city of China. – *Environmental Science and Pollution Research* 25(28): 28460-28470.
- [37] Wissuwa, J., Le Moine Bauer, S., Steen, I. H., Stokke, R. (2017): Complete genome sequence of *Lutibacter profundus* LP1 T isolated from an Arctic deep-sea hydrothermal vent system. – *Standards in Genomic Sciences* 12(1): 5.
- [38] Zhao, L., Zhu, L., Liu, G. (2010): Relationships between Sedimentary Microbial Communities and Nutrient Factors in Luoma Lake. – *International Conference on Bioinformatics & Biomedical Engineering.*

APPENDIX

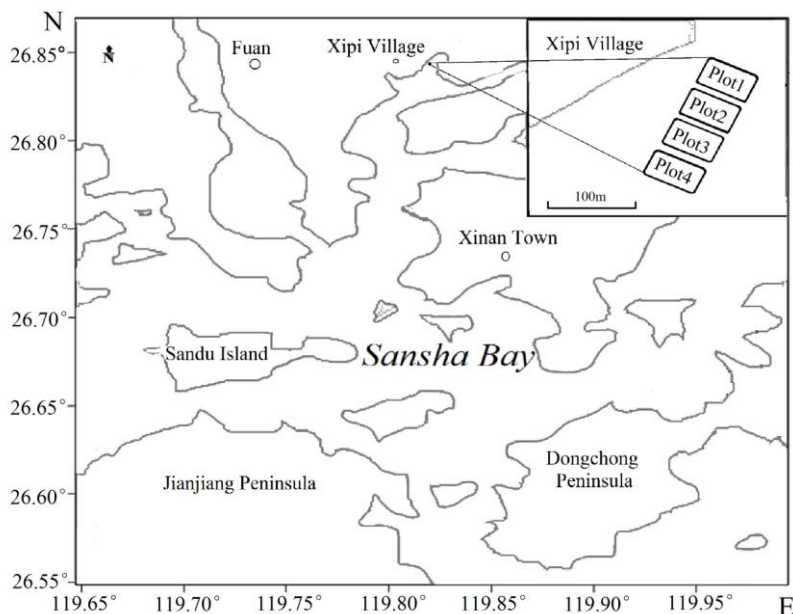


Figure A1. Location map of the sampling

Table A1. *P* values of diversity indices of bacterial communities in mudflat sediments of Sansha Bay

Estimators	P value (autumn-spring)	P value (autumn-winter)	P value (autumn-summer)	P value (spring-winter)	P value (spring-summer)	P value (summer-winter)
OUT	0.872	0.06539	0.4479	0.1103	0.5368	0.4972
Shannon	0.5452	0.3713	0.7071	0.2127	0.467	0.7874
Simpson	0.1555	0.9517	0.9806	0.2721	0.4066	0.9868
ACE	0.8695	0.1894	0.6641	0.191	0.7384	0.5481
Chao1	0.6803	0.1583	0.5454	0.2064	0.7273	0.5859
Coverage	0.9778	0.07192	0.1153	0.3892	0.08455	0.8638
PD	0.8402	0.1099	0.659	0.1079	0.5739	0.4257

OUT, Shannon, Simpson, ACE, Chao1, PD, Coverage represent operational taxonomic unit, the Shannon diversity index, the Simpson diversity index, the ACE estimator, the Chao1 estimator, Phylogenetic diversity, and the Good's coverage, respectively. A *p*-value less than 0.05 was considered statistically significant differences

Table A2. *P* values of significantly different microbial communities in mudflat sediments of Sansha Bay, phylum level

Species name	P value	Species name	P value	Species name	P value
Nitrospirae	1.26E-05	Hydrogenedentes	0.001225	Planctomycetes	0.02849
Lentisphaerae	0.000177	Tenericutes	0.001299	Chlorobi	0.03041
Acidobacteria	0.000496	Spirochaetae	0.001386	PAUC34f	0.03488
Gemmatimonadetes	0.001011	Ignavibacteriae	0.01015	Armatimonadetes	0.04917
Actinobacteria	0.001032	KSB3_Modulibacteria	0.01223		

Table A3. *P* values of significantly different microbial communities in mudflat sediments of Sansha Bay, genus level

Species name	P value	Species name	P value	Species name	P value
Nitrospira	1.26E-05	c__R76-B128	0.005521	f__Flammeovirgaceae	0.021896
Draconibacterium	0.000204	f__UASB-TL25	0.005604	f__MidBa8	0.022372
f__P3OB-42	0.000224	o__MSB-3A7_sediment_group	0.005799	f__Flammeovirgaceae	0.022533
f__JTB255_marine_benthic_group	0.000369	Pelagibius	0.007134	H16	0.022659
f__Nitrosomonadaceae	0.000449	Haliaea	0.007633	Fusibacter	0.02294
Gammaproteobacteria	0.000968	f__BSV26	0.007774	c__WCHB1-41	0.03256
f__Cryomorphaceae	0.001018	f__MBAE14	0.009141	Desulfatiglans	0.03713
Deferrisoma	0.001846	o__Sva0485	0.009547	Lutibacter	0.039
Spirochaeta	0.001886	p__Bacteroidetes	0.021101	Nitrospina	0.04354
f__Xanthomonadales_Incertae_Sedis	0.002456	Haliangium	0.021237	Actibacter	0.049079
c__Alphaproteobacteria	0.003124	c__Bacteroidetes_BD2-2	0.0213	SEEP-SRB1	0.049361
o__BD7-8_marine_group	0.00314	f__Lentimicrobiaceae	0.021342	c__Gammaproteobacteria	0.049369
c__Gemmatimonadetes	0.003308	Kangiella	0.021679	f__Nitrospinaceae	0.049734
f__Oceanospirillaceae	0.003574	Robiginitalea	0.021688	f__Hydrogenophilaceae	0.049901
Sulfurovum	0.003582	o__MSBL9	0.021718		
f__OM1_clade	0.004208	Aquibacter	0.021727		
o__E01-9C-26_marine_group	0.005462	Halioglobus	0.021768		

Table A4. *P* values of physicochemical indices of mudflat sediments in Sansha Bay

Estimators	P value (autumn-spring)	P value (autumn-winter)	P value (autumn-summer)	P value (spring-winter)	P value (spring-summer)	P value (summer-winter)
pH	0.0574	0.5801	0.0837	0.0571	0.1535	0.0840
OrgC	0.5801	0.1396	0.0500	0.1070	0.1007	0.0563
OrgS	0.4003	0.5565	0.1755	0.1318	0.5527	0.0534
TP	0.0503	0.0545	0.0572	0.5966	0.6832	0.5979
TN	0.5598	0.1488	0.0975	0.4626	0.0599	0.0513
Tm	0.0559	0.0594	0.0503	0.0519	0.0503	0.0212

TN, TP, OrgC and OrgS, Tm represent total nitrogen, total phosphorus, Organic carbon and sulfur contents, Water temperature, respectively

Table A5. *P* values and envfit of Physicochemical indices in Sansha Bay

Estimators	RDA1	RDA2	r ²	P value
pH	-0.1782	0.984	0.5437	0.004
OrgC	-0.9734	0.2292	0.6121	0.001
OrgS	0.7598	-0.6501	0.2965	0.097
TP	-0.5014	0.8652	0.4572	0.016
TN	-0.9868	-0.1622	0.6171	0.002
Tm	-0.9042	0.4272	0.8758	0.001

TN, TP, OrgC and OrgS, Tm represent total nitrogen, total phosphorus, Organic carbon and sulfur contents, Water temperature, respectively